Handbook of Applied Hydraulics

THIRD EDITION

Calvin Victor Davis, Editor-in-Chief • Kenneth E. Sorensen, Co-Editor

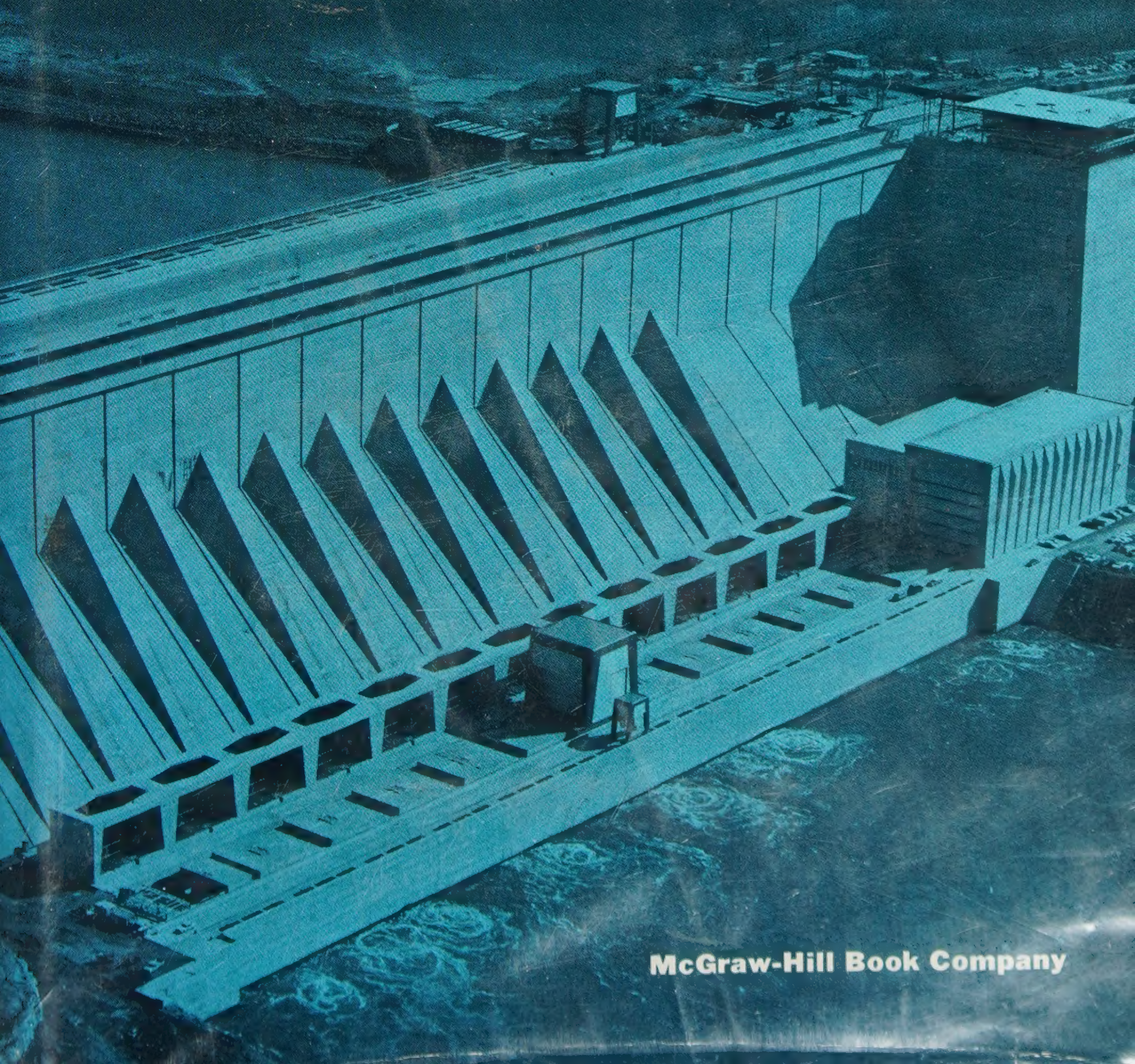

McGraw-Hill Book Company

1584 pages • 978 illustrations

Handbook of Applied Hydraulics

THIRD EDITION

Calvin Victor Davis, Editor-in-Chief,
Consulting Hydraulic Engineer,
Harza Engineering Company
Kenneth E. Sorensen, Co-Editor,
Vice President, Harza Engineering Company

Here is the latest edition of a classic reference for the design of hydraulic structures and water-using systems. Revised from cover to cover, this monumental handbook is your key source for the practical applications of these tested principles.

Reflecting the collective experience of over 40 experts, this master reference is the only complete volume of hydraulics facts for every specialized area of hydraulic engineering. But more than a fact-finding guide, the book closely coordinates field measurements of actual prototype behavior with theoretical analysis. In this way you have access to the full range of problem solutions, as well as a unique opportunity to develop good engineering judgment.

In the past decade a series of rapid changes has revolutionized hydraulics engineering, rendering time-honored policies and practices obsolete. This all-new third edition fully records the tremendous impact of such dynamic changes as the correlation of field and laboratory testing programs . . . new design methods . . . and the use of digital computers to predict and check results.

Many sections in the book are completely new while others are fully revised to conform to today's requirements. Supplementing this wealth of material are design examples of actual structures drawn from the records of recent construction projects. In many instances significant advances are featured in print for the first time. For example:

- the latest design methods for approaching field measurements in prototypes, and their adaptation to computerized procedures.
- practical guides, based on U.S. agency experience, in the hydraulic planning and design of river navigation systems and flood control works.
- basic principles of tidal energy development.
- the behavior of prototype structures, particularly

(continued on back flap)

HANDBOOK OF APPLIED HYDRAULICS

OTHER McGRAW-HILL HANDBOOKS OF INTEREST

American Society of Mechanical Engineers · ASME Handbook—Metals Properties
American Society of Mechanical Engineers · ASME Handbook—Engineering Tables
American Water Works Association · Water Quality and Treatment
Baumeister and Marks · Standard Handbook for Mechanical Engineers
Brady · Materials Handbook
Callender · Time-Saver Standards
Carrier Air Conditioning Company · Handbook of Air Conditioning System Design
Conover · Grounds Maintenance Handbook
Crocker and King · Piping Handbook
Croft, Carr, and Watt · American Electricians' Handbook
Emerick · Handbook of Mechanical Specifications for Buildings and Plants
Emerick · Heating Handbook
Factory Mutual Engineering Division · Handbook of Industrial Loss Prevention
Fink and Carroll · Standard Handbook for Electrical Engineers
Gaylord and Gaylord · Structural Engineering Handbook
Harris · Handbook of Noise Control
Harris and Crede · Shock and Vibration Handbook
Havers and Stubbs · Handbook of Heavy Construction
Heyel · The Foreman's Handbook
Hicks · Standard Handbook of Engineering Calculations
Huskey and Korn · Computer Handbook
Katz · Handbook of Natural Gas Engineering
King and Brater · Handbook of Hydraulics
Klerer and Korn · Digital Computer User's Handbook
Korn and Korn · Mathematical Handbook for Scientists and Engineers
La Londe and Janes · Concrete Engineering Handbook
Magill, Holden, and Ackley · Air Pollution Handbook
Manas · National Plumbing Code Handbook
Mantell · Engineering Materials Handbook
Merritt · Building Construction Handbook
Merritt · Standard Handbook for Civil Engineers
Moody · Petroleum Exploration Handbook
Morrow · Maintenance Engineering Handbook
Mulligan · Handbook of Brick Masonry Construction
Myers · Handbook of Ocean and Underwater Engineering
Perry · Engineering Manual
Rossnagel · Handbook of Rigging
Staniar · Plant Engineering Handbook
Streeter · Handbook of Fluid Dynamics
Timber Engineering Co · Timber Design and Construction Handbook
Urquhart · Civil Engineering Handbook
Watt · NFPA Handbook of the National Electrical Code
Woods · Highway Engineering Handbook

HANDBOOK OF APPLIED HYDRAULICS

CALVIN VICTOR DAVIS *Editor-in-Chief*

Chief Technical Advisor, Harza Engineering Company, Chicago

KENNETH E. SORENSEN *Co-Editor*

Vice President, Harza Engineering Company, Chicago

1969

THIRD EDITION

McGRAW-HILL BOOK COMPANY

New York St. Louis San Francisco Auckland Düsseldorf

Johannesburg Kuala Lumpur London Mexico

Montreal New Delhi Panama São Paulo

Paris Singapore Sydney Toronto

KŌGAKUSHA COMPANY, LTD.

Tokyo

HANDBOOK OF APPLIED HYDRAULICS

 Library of Congress Catalog Card Number 67-25809

15538

23456789-MAMM-765

CONTRIBUTORS

JAMES W. BALL *Vice President and Managing Director, Western Canada Hydraulic Laboratories, Ltd., Port Coquitlam, B.C., Canada; formerly Bureau of Reclamation Hydraulic Laboratory, Denver, Colo.*

RAY J. BANYS *Fish Facilities Department Head, Harza Engineering Company, Chicago*

W. J. BAUER *President, Bauer Engineering, Inc., Chicago*

EARL J. BECK *Vice President, Harza Engineering Company, Chicago*

JOSEPH R. BOWMAN *Project Engineer, Langley, McDonald and Overman, Consulting Engineers, Virginia Beach, Va.*

EDGAR H. BURROUGHS (Retired) *formerly President, Ambursen Engineering Corporation, New York*

THOMAS R. CAMP *Senior Partner, Emeritus, Camp, Dresser & McKee, Consulting Engineers, Boston*

FRANK B. CAMPBELL *Consultant; formerly Chief, Hydraulic Analysis Branch, and Assistant Chief, Hydraulics Division for Coordination of Research, U.S. Army Engineer Waterways Experiment Station, Vicksburg, Miss.*

J. BARRY COOKE *Consulting Engineer, Kentfield, Calif.*

CALVIN V. DAVIS *Chief Technical Advisor; formerly President and Chairman, Harza Engineering Company, Chicago*

JOHN P. DAVIS *Chief, Inland Navigation Section, Engineering Division, Office, Chief of Engineers, Corps of Engineers, U.S. Army, Washington, D.C.*

WILLIAM W. DONNAN *Branch Chief, Southwest Branch, Soil and Water Conservation Research Division A.R.S., U.S. Dept. of Agriculture, Riverside, Calif.*

JACOB H. DOUMA *Chief, Hydraulic Design Branch, Engineering Division, Office, Chief of Engineers, Corps of Engineers, U.S. Army, Washington, D.C.*

SIR THOMAS FOY *Consultant, Haigh, Zinn & Associates, London*

ARTHUR P. GEUSS *Executive Vice President, Harza Engineering Company, Chicago*

SAMUEL A. GREELEY *Late Partner, Greeley and Hansen, Chicago*

H. SPENCER GREEN *Associate and Assistant Chief Civil Design Department, Harza Engineering Company, Chicago*

RICHARD D. HARZA *Vice President, Harza Engineering Company, Chicago*

NICHOLAS M. HERNANDEZ *Civil Department Head, Harza Engineering Company, Chicago*

KENNETH V. HILL *Partner, Greeley and Hansen, Chicago*

IVAN E. HOUK *Consultant (Retired); formerly U.S. Bureau of Reclamation, Denver, Colo.*

WENDELL E. JOHNSON *Chief, Engineering Division, Civil Works, Office, Chief of Engineers, Corps of Engineers, U.S. Army, Washington, D.C.*

ROLLAND F. KASER *Associate and Chief Resources Engineer, Harza Engineering Company, Chicago*

PHILLIP Z. KIRPICH *Hydraulic Engineer, International Bank for Reconstruction and Development, Washington, D.C.*

VICTOR A. KOELZER *Vice President, Harza Engineering Company, Chicago*

WARREN H. KOHLER *Consultant, formerly Head of the Large Gates and Valves Section, Mechanical Branch, Bureau of Reclamation, Denver, Colo.*

JOSEPH C. LAWLER *Partner, Camp, Dresser & McKee, Consulting Engineers, Boston, Mass.*

KENNETH R. LEONARDSON *Civil Engineer and Section Head, Harza Engineering Company, Chicago*

DAVID S. LOUIE *Associate and Chief Hydraulic Engineer, Harza Engineering Company, Chicago*

JOHN LOWE III *Partner, Tippetts-Abbett-McCarthy-Stratton, New York*

CLAUDIO MARCELLO (Deceased) *Consulting Engineer; formerly General Manager of the Power Plants Construction Department of EDISON Group, Milan*

PAUL R. MAYER *Head of Gate Department, Harza Engineering Company, Chicago*

LEWIS F. MOODY *Late Professor of Hydraulic Engineering, Emeritus, Princeton University*

DONALD NEWTON *Partner, Greeley and Hansen, Chicago*

ELLIS B. PICKETT *Chief, Hydraulic Analysis Branch, U.S. Army Engineer Waterways Experiment Station, Vicksburg, Miss.*

RUSSELL W. REVELL *Chief Hydrologist, Harza Engineering Company, Chicago*

GEORGE R. RICH *Vice President, Chas. T. Main, Inc., Boston; Partner, Uhl, Hall & Rich, Boston*

FRANKLYN C. ROGERS *Vice President, Harza Engineering Company, Chicago*

KENNETH E. SORENSEN *Vice President, Harza Engineering Company, Chicago*

WILLIAM E. STANLEY *Professor Sanitary Engineering, Emeritus, Massachusetts Institute of Technology; Senior Associate, Ryckman, Edgerley, Tomlinson and Assoc., St. Louis; Staff Consultant, Sunn, Low, Tom and Hara, Inc., Honolulu*

I. C. STEELE *Consultant (Retired), Piedmont, Calif.*

JOHN C. STEVENS *Consulting Engineer (Retired), Portland, Ore.*

JAMES H. STRATTON (Brig. Gen. U.S. Army Retired) *formerly partner Tippetts-Abbett-McCarthy-Stratton, New York*

A. RYLANDS THOMAS *Consultant, Binnie & Partners, London*

WILLIAM L. VOORDUIN *Consulting Engineer; formerly Vice President and Director of Engineering, Development & Resources Corp., New York*

ROMAN P. WENGLER *Head, Structural Division, Harza Engineering Company, Chicago*

GORDON R. WILLIAMS *Associate and Chief Hydrologist, Tippetts-Abbett-McCarthy-Stratton, New York*

ERIC M. WILSON *Reader in Civil Engineering, University of Salford, England*

OLGIERD C. ZIENKIEWICZ *Professor, Head of Civil Engineering, University of Wales, Swansea*

THADDEUS ZOWSKI *Vice President and Chief Mechanical Engineer, Harza Engineering Company, Chicago*

PREFACE TO THE THIRD EDITION

The objectives of the third edition are identical with those of the first and second: (1) to present clearly and concisely the fundamental principles which are basic to each subdivision of hydraulic engineering, and (2) to demonstrate the practical applications of these principles by examples which have been drawn largely from the actual practice of hydraulic engineering.

Since the publication of the second edition in 1952, many time-honored practices have been made obsolete by revolutionary advances. In preparing the third edition, the Editors were confronted with the task of bringing the book up-to-date in a period of rapid and dynamic change. Three factors of primary importance are: (1) The correlation of extensive field and laboratory testing programs; (2) the development of new designing methods which now brings the results of theoretical analyses closer to those obtained from field observations; and (3) the rapid increase in the use of the digital computer.

Recent advances in dam design illustrate the interrelations between these three factors. As one example, field measurements to determine the actual behavior of large gravity-type dams have revealed characteristic patterns of vertical normal stress distribution which vary widely from the straightline distribution as obtained by conventional analytical methods. Concurrently there has been developed the finite-element method of analysis. The pioneer exploratory work of several investigators, as described in Sections 9 and 10, resulted in patterns in stress distribution which in many cases approached those obtained from tests of both prototype structures and structural models. The application of the finite element method would not be practical without the aid of the digital computer.

In a similar manner these changing practices have resulted in improvements in designing methods for arch dams. The trial-load method of analysis, as presented in the first and second editions, is now almost universally accepted as a basis for the design of arch dams. During recent years, however, some trial-load procedures have been changed to adapt them to computer programming.

These improvements in designing methods have been paralleled by the development of improved structural types. Several notable advances have been made in Europe during the past decade. To illustrate, dams of the flexible-concrete-block type, the cored-gravity type, and the wide-span multiple-arch type have been developed by Italian and French engineers.

Another example of progress is afforded by improved criteria for the design of large water conductors, spillways, canals, and other hydraulic works. Here again, definite advances have resulted from the close coordination of field and laboratory experimental programs. By way of example, field tests to measure the discharge capacities of large tunnels, and other water conductors, operating under velocities ranging up to 90 feet per second, are described in Sections 2 and 3. From the data thus obtained, friction coefficients have been related to Reynolds numbers of unprecedented magnitude. As a result, a substantial element of heretofore theoretical fluid mechanics now enters the realm of practical applied hydraulics.

These recent observations have furnished designers with more realistic criteria for the giant river projects which are being built in response to the rapidly growing food requirements of many developing nations. Vast programs of civil works, involving hydraulic structures of unprecedented magnitude and cost, are being equated directly to average increases in per capita caloric intake and also to the nation-wide economic benefits which result from multipurpose systems operations for irrigation, flood control, power, domestic and industrial water supplies, and other water uses. More than ever before the work of the hydraulic engineer is now related to the achievement of national goals.

In response to many requests, the Editors have added new sections on basic hydraulics, reservoir hydraulics, natural channels, regime canals, river diversion, basic principles of concrete dam design, cored-gravity and massive-buttress dams, prestressed dams, barrages and dams on soft foundations, fish passing facilities, pumped storage, flood control, navigation, groundwater, drainage, and tidal energy development. Many other sections have been completely rewritten.

For convenience in reference, the third edition has been divided into four parts: I, Hydrology and Basic Hydraulics; II, Water Conveyance; III, Dams; and IV, Water Use, Control, and Disposal.

Calvin V. Davis
Kenneth E. Sorensen

ACKNOWLEDGMENTS

The completion of the third edition brings together professional writings which have been produced over a period of nearly forty years. The Editors express their appreciation for the guidance and assistance of many friends and associates who have pioneered advances in hydraulic engineering during these four decades. Some have passed away; others have reached advanced ages. The names of many do not appear elsewhere in this book.

The initial inspiration to undertake the Handbook was given to the Senior Editor by the late Edward Wegmann, well known consulting engineer and author of "Design and Construction of Dams" (Wiley). The eighth and final edition of this monumental treatise appeared in 1927.

The late Boris A. Bakhmeteff, then Professor of Civil Engineering, Columbia University, and also eminent statesman, industrialist, and hydraulic engineer, furnished counsel and guidance throughout the preparation of the first and second editions.

Some of the creative thinking of the late André Coyne has found its way to this book from records of many personal conversations with Mr. Coyne in his Paris office, and from the generous contributions of Mr. Jean Bellier of the firm of Coyne and Bellier, Consulting Engineers, Paris, France.

The Editors express their deep gratitude to all who have made contributions to the third edition. Reference to the list of contributors will reveal the eminent position which each occupies in his respective field.

The Editors wish to give special acknowledgment to the senior contributors, some of whom have worked on the book over the entire period of production of the three editions. By way of example, Mr. Ivan Houk made outstanding contributions to the early development of the trial-load method as applied to arch dams. Mr. I. C. Steele did pioneer work both in creating improved designs and in recording the structural behavior of rockfill dams. The late Mr. Samuel A. Greeley was a world-renowned expert in the field of sanitary engineering. Professor William E. Stanley joined Mr. Greeley in producing sections for each of the three editions. Mr. Julian Hinds has been a leader in engineering water conveyance systems of unprecedented magnitude. Mr. J. C. Stevens is noted for his achievements in the fields of hydraulic design and water measurement. The Senior Editor also had associations, dating as far back as 1921, with the late Mr. Lewis F. Moody, who later made classic contributions on hydraulic machinery to the first and second editions. This roster of early contributors would not be complete without giving special tribute to Mr. Thomas R. Camp for his widely used sections on water supply.

The Senior Editor's long association with the late Mr. L. F. Harza, consulting hydraulic engineer of Chicago, Illinois, had made a definite impact on this book. Mr. Harza's dynamic and creative approaches to hydraulic engineering left a priceless heritage to those of us who worked with him.

Finally, the Editors warmly thank Miss Ellen Crigley for her assistance in the preparation of the manuscripts. It is worthy of special mention that Miss Crigley has now worked on these manuscripts over a period of some twenty years, thus possibly setting an all-time record for secretarial endurance, patience, and faithfulness.

Calvin V. Davis
Kenneth E. Sorensen

CONTENTS

Index follows Section 42.

SECTION 1

HYDROLOGY

By Phillip Z. Kirpich and Gordon R. Williams

A brief discussion of engineering hydrology is presented in this section. The scope of this book, together with space limitations, does not permit a complete treatment of the subject, for which reference is made to several comprehensive texts published during recent years on the broader applications of the subject.

PRECIPITATION

1. Measurement. Nonrecording precipitation gages of good design provide a means of magnifying precipitation depth so that it is more easily observed. The standard U.S. Weather Bureau gage,[1,*] for example, with a receiver area of 50.3 sq in. (8 in. diameter) and a measuring tube area of 5.03 sq in. (2.53 in. diameter), provides a magnification of 10. Automatic recording gages, which produce a chart record, are manufactured by several instrument companies. Results obtained from recording-gage charts should be checked by making periodic volumetric measurements in order to guard against faulty operation of the gage mechanism.

To minimize error, gages should be located to avoid poor exposure. The ideal location is a large, flat, open area free from large trees or structures which might intercept precipitation. On the other hand, to reduce wind effects, low barriers such as bushes or fences are desirable at a distance from the gage not less than twice their height.

Observers at nonrecording gages usually report only daily amounts of precipitation and depths of snowfall on the ground. It is often advantageous to instruct them to record, in addition, the times of beginning and ending of heavy precipitation. Used in conjunction with the record of a nearby recording gage, this information is of great use in delineating both areal and time distribution of precipitation. There are at present in the United States 10,270 nonrecording gages and 3,204 recording gages.

2. Sources of Data. In the United States, the principal source of precipitation data is the U.S. Weather Bureau. Many other agencies, both public and private, maintain gages. However, in a given locality it is always best to obtain data first from the appropriate regional office of the Weather Bureau, as this agency often publishes data obtained from other agencies. An excellent series of river basin maps, locating both precipitation- and stream-gaging stations, is available.[2]

3. Adjustment of Records. A precipitation record is often obtained from a poorly exposed gage or from one whose location has been changed during the period of record. If the exposure was satisfactory for part of the record (at least 5 years or more), an adjustment of the remainder of the record can be made. The adjustment should be made by comparing the ratio between the recorded values of the annual or seasonal precipitation with the corresponding average value for a group of base stations in the vicinity. Compute the ratios for each year or season, and examine them for indications of any sharp changes or trends, which, if present, indicate modifications in the

* Superior numbers refer to items in the Bibliography at the end of this section.

regime of the station. In lieu of computing the ratios, the *double-mass-curve* technique[3] may be used. Either of these two methods is based on the fact that seasonal precipitation figures at stations in the same general locality are usually consistent with one another. However, this is not true for short-period precipitation, for which this type of adjustment is not recommended.

4. Estimates for Missing Records. Ratios established as described in Art. 3 can be used to estimate the missing portion of a record. As an example, available records for Stations A and B in the same general locality are as follows:

Period	Station A	Station B
1930	41.0 in.	
1931	40.2 in.	
1932	36.0 in.	
1933–1949 (avg)	37.5 in.	39.0 in.

The precipitation at Station B for the years 1930, 1931, and 1932 are estimated by proportion to be 42.6, 41.9, and 37.4 in., respectively.

5. Geographical Distribution. The following basic factors determine the amount of mean annual precipitation at a station on the earth's surface:[4] (1) latitude, (2) position and size of the continental land mass in which the station is located, (3) distance of the station from the coast or other source of moisture, (4) temperature of ocean and coastwise currents with respect to adjacent land masses, (5) extent and altitude of adjacent mountain ranges, *i.e.*, *orographic effects*, (6) altitude of the station.

Considering latitude alone, the generalized world pattern is composed of a series of belts resulting from the circulation of the atmosphere. At the equator, there is a belt of relatively low pressure known as the doldrums, where intense solar radiation heats the air and causes it to expand and rise. Warm moisture-laden winds converge on the region and produce high precipitation from frequent thunderstorms. At about 30° north and south latitude, there are high-pressure belts, called the horse latitudes, where warm, dry air descends and precipitation is low. From about latitudes 35° to 65° interaction of the moisture-laden prevailing westerlies with cold, dry polar air generates storms of the frontal type (see Art. 9) and produces abundant precipitation. Convection-type thunderstorms also occur in this zone in summer, but produce less total precipitation than the frontal storms even though the short-duration intensities at individual points are generally much higher. From latitude 65° to the poles, dry polar air predominates increasingly and causes a decrease in precipitation.

The wide variations in mean annual precipitation in the United States (Fig. 1) are an example of the large departures from the generalized world precipitation pattern caused by factors (2) through (6). The latter factors produce even greater variations in Asia. High pressure builds up in winter over the cold continental land mass and produces a dry wind (winter monsoon) blowing outward to the Indian Ocean. The summer monsoon is wet and blows in the reverse direction. Thus the normal planetary circulation of the atmosphere is greatly modified by the large size of the Asiatic continent. The combined effects of the wet summer monsoon and the high altitude of the Himalayas in northern India, which it crosses, explain why this region is one of very high precipitation. For example, the mean annual precipitation at Cherrapunji, India, is 428 in.

6. Seasonal Distribution. The belts of different atmospheric pressure described in the preceding article move north in summer and south in winter (opposite seasons in

Prepared from Isohyetal Map by U S Department of Commerce, Weather Bureau data based on 30 year normals, 1921–1950 of 276 stations, supplemented by approximately 1800 long-term station averages in western and coastal mountain areas

FIG. 1. Normal annual amount of precipitation in the United States. (*From V. T. Chow, "Handbook of Applied Hydrology," McGraw-Hill Book Company, New York*, 1964.)

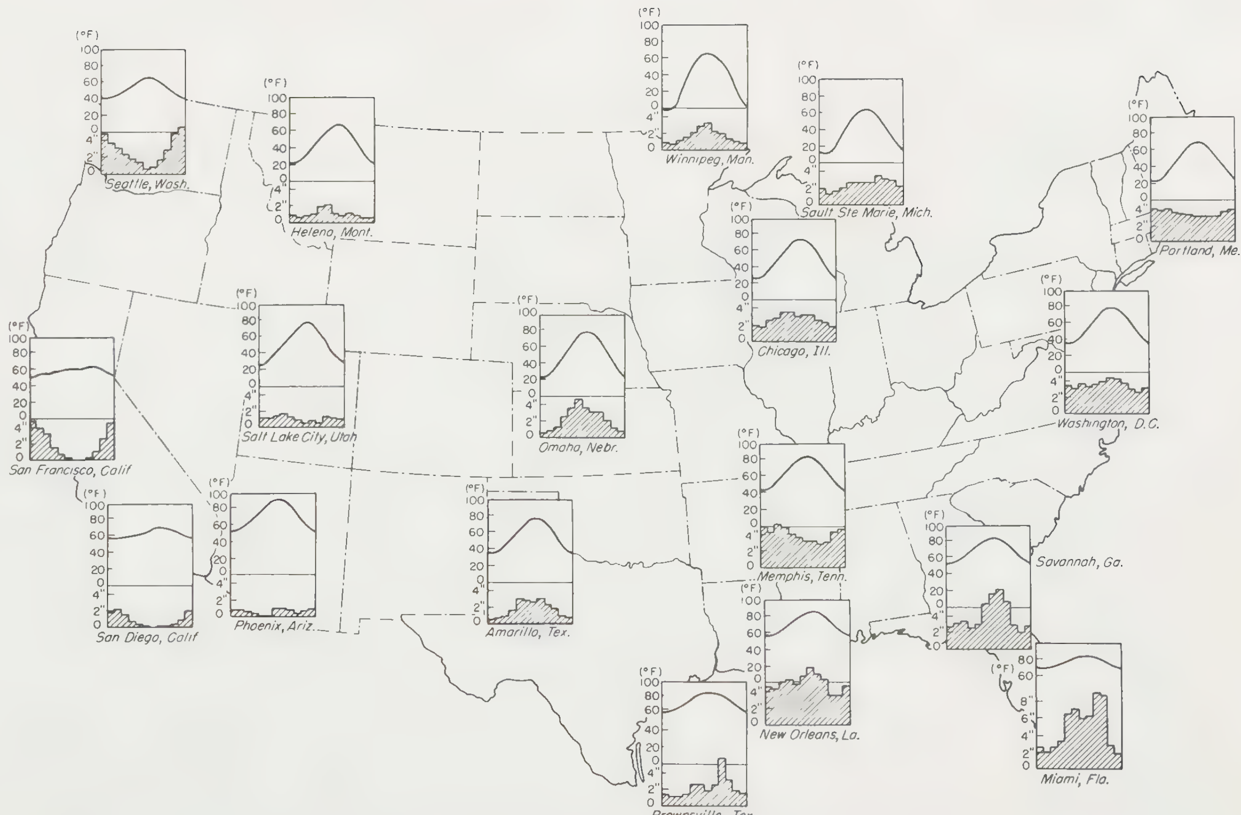

FIG. 2. Monthly mean temperature and precipitation for selected stations in the United States.

the Southern Hemisphere), causing marked changes in the depth and type of precipitation for the various seasons of the year. In the United States, the variation in depth between summer and winter is greatest on the West Coast (Fig. 2) because of two principal factors: (1) the northward movement in summer of the dry high-pressure belt of the horse latitudes and (2) the presence of cool coastal water. The latter lowers the temperature below the dew point and hence reduces the moisture content of air carried landward by the prevailing westerlies. Subsequently, when this air strikes the warm land mass, dehumidification takes place, and almost all opportunity for precipitation is lost.

The East Coast, on the other hand, shows a fairly uniform seasonal depth of precipitation. The origin of precipitation is distinctly different, however, in summer and winter. Summer precipitation is mostly of the convectional thunderstorm type and increases toward the south owing to increased summer convectional activity in that direction. Winter precipitation is almost entirely of the cyclonic or frontal type caused by the interaction of polar and tropical air masses. A further description of storm types is given in Art. 9.

In the interior of the country, particularly west of the 95th meridian, still other seasonal patterns exist. In the Great Plains region, as at Omaha, Neb., summer thunderstorms produce high precipitation as compared with winter, when the region is covered by cold, dry polar air. In the Plateau Region, as at Salt Lake City, Utah, mountain ranges seal off incoming moist air during all seasons.

Figure 3 gives monthly temperatures and precipitation for selected stations throughout the world representative of climatic conditions varying from subarctic to tropical. Climatic types are after Trewartha.[4]

7. Snow. Investigations to date are insufficient for the determination of adequate relationships among the many variables involved in snow problems. However, satisfactory empirical relations can often be derived if there are sufficient snow-cover measurements and precipitation, temperature, and runoff records.

Figure 4 shows correlations between (1) a snow-survey index for April 1 and the ensuing April–July runoff, and (2) the basin winter precipitation and the ensuing April–July runoff. It is noted that the first correlation is much the better of the two. The snow-survey index is the estimated water equivalent on the basin in inches determined as follows:

1. Average water equivalents were measured along 11 snow courses, each at a constant elevation from 5,700 to 10,300 ft in the Sierra Nevada (see Ref. 6 for snow-surveying methods).
2. The basin was divided into three zones according to altitude.
3. The average water depth for each zone was computed by averaging the courses in that zone.
4. The average basin depth, or snow-survey index, is the weighted average of the zones, the weights being taken as proportional to the area of the zone.

Another type of correlation, shown in Fig. 5, gives the "degree-day factor" for use in short-period predictions. The degree-day factor multiplied by the weighted degree-days gives snowmelt in inches. Degree days are measured from 32 F as a base; a day having an average temperature of 44 F would be equivalent to 12 degree-days. In Fig. 5*a*, the mean temperature at an index station (Blue Canyon) and the elevation of the snow line (the lower limit of snow cover) are used as parameters to get "weighted" degree-days. The latter, multiplied by the degree-day factor, which is a function of the date, gives snowmelt in inches.

The setting up of design storms of storm rainfall is described in Art. 11. Rainfalls

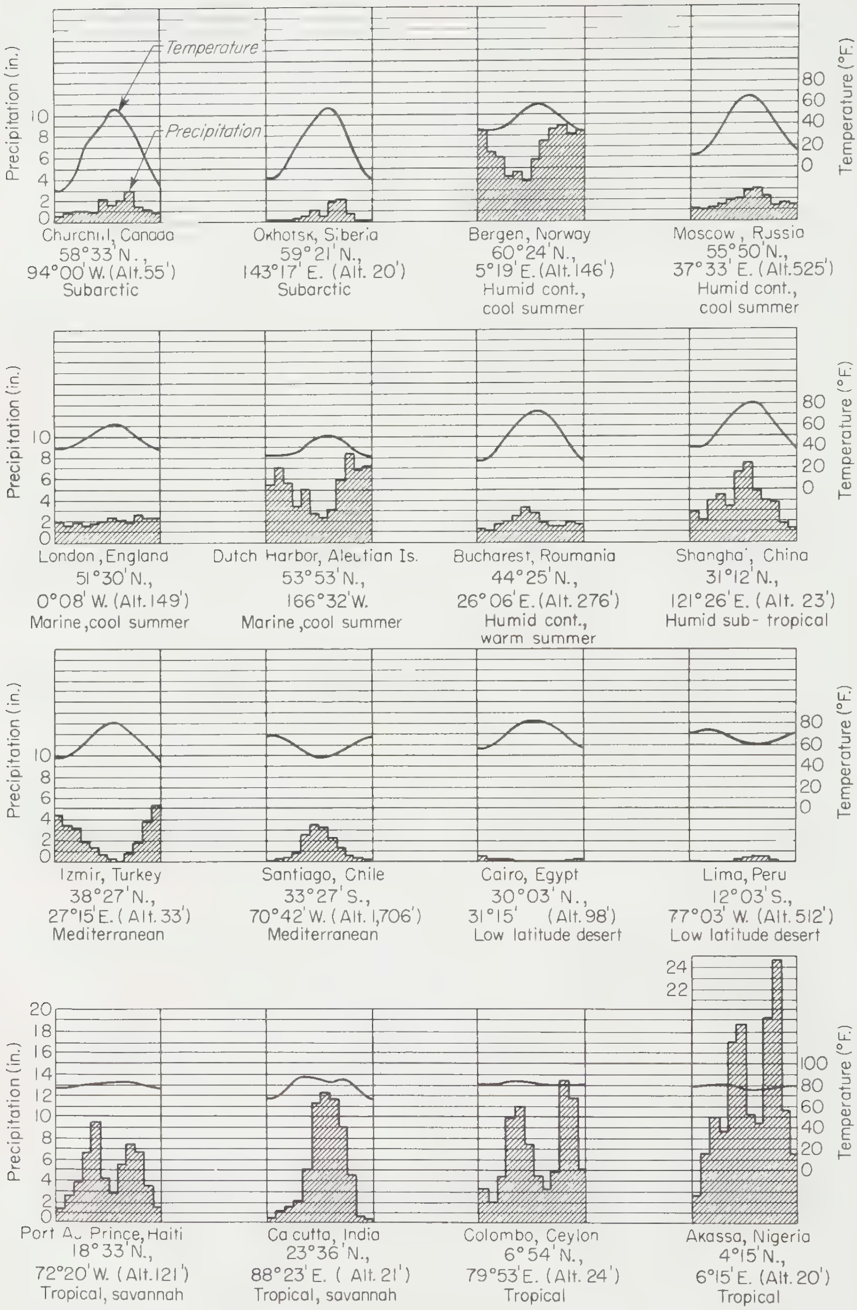

FIG. 3. Monthly mean temperature and precipitation for selected world stations outside the United States.

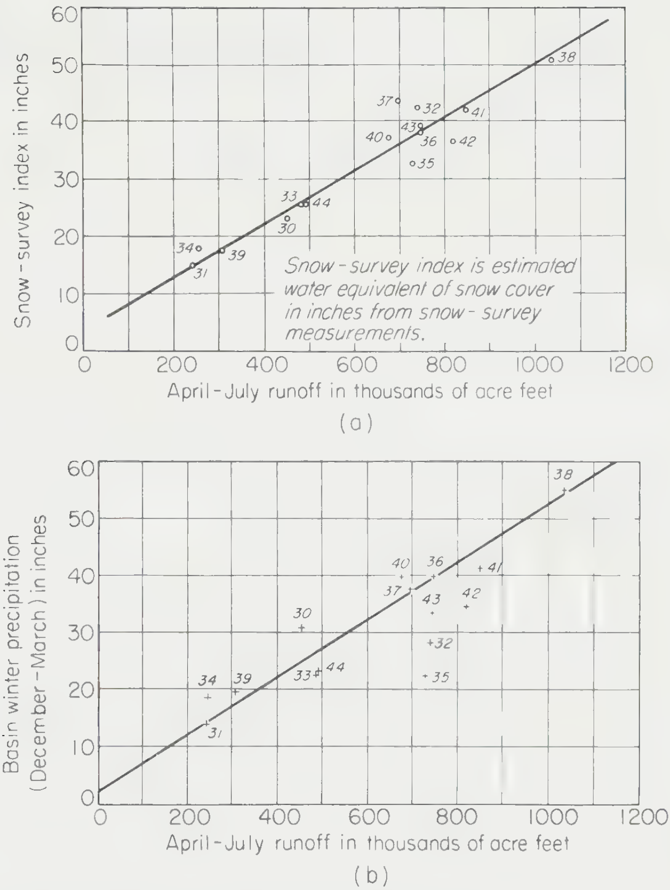

FIG. 4. Comparison of runoff correlations for the Tuolumne River at Hetchy Hetchy, Calif.[5] (*a*) Snow-survey data. (*b*) Precipitation data.

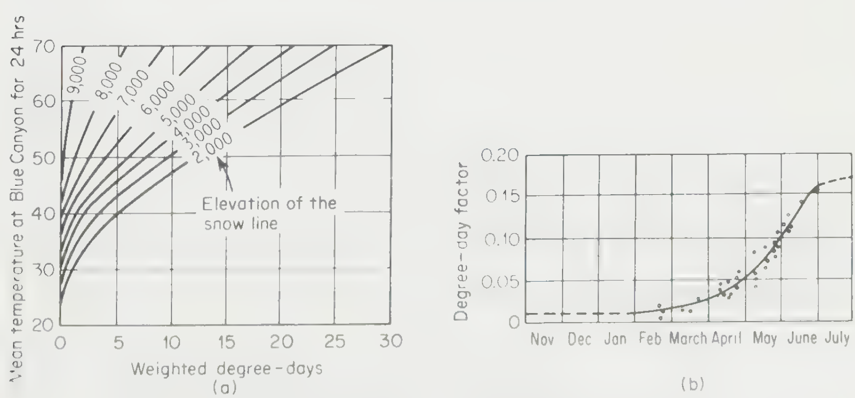

FIG. 5. Snowmelt correlations utilizing degree-day factors.[44]

from winter storms are often critical for large areas, particularly if augmented by snowmelt. Because in this case we are interested in maximum rather than in average conditions, the degree-day method described in the preceding paragraph would give too low a value of the snowmelt, and it is necessary to study the physics of melting snow more closely.

Light[7] and Wilson[8] have done this, Light presenting the formula

$$D = V[0.00736(T - 32)10^{-0.0000156Z} + 0.0231(e - 6.11)]$$

in which D is the snowmelt in 6 hr in inches, V is the wind velocity 50 ft above the snow surface in miles per hour, T is the air temperature 10 ft above the snow surface in degrees Fahrenheit, e is the vapor pressure in millibars, and Z is the station elevation in feet above mean sea level. If Z is less than a few thousand feet, its effect may be neglected, and the formula reduces to

$$D = V(0.0074T + 0.023e - 0.37)$$

Light's formula, which is empirical in part, evaluates snowmelt caused by turbulent heat exchange between the air (including water vapor in the air) and the snow.

Snowmelt by rainfall can be computed from

$$D_r = \frac{P(T_w - 32)}{144}$$

derived from the fact that the heat of fusion of ice is 144 Btu/lb, in which D_r is snowmelt in inches, P is rainfall in inches, and T_w is the wet-bulb temperature, assumed equal to the rain temperature. D_r is usually small compared with D; the wind, high humidity, and temperature accompanying warm rains cause more snowmelt than the rain.

Studies of storms with large depths of snowmelt in the Ohio River basin in western Pennsylvania showed D to be only 60 to 72 percent of that indicated by the formula.[9] Unfortunately there are insufficient determinations at present to evaluate the percentages for general application. Studies for a particular basin, if justified, should include detailed meteorologic and hydrologic analyses of past storms and the resulting runoff to establish values of the variables in the formula for D during successive time periods. The runoff hydrographs should be analyzed to determine variation in infiltration (see Art. 23) with time, runoff due to rainfall, and runoff due to snowmelt. If K is the percentage of snowmelt D, given by the theoretical formula, the variation of its value with time can be determined and applied later in setting up design storms (see Art. 11) for maximum conditions. A value of K of zero during the early part of the storm might be logical, as ripening of the snow cover takes place before the maximum rate of snowmelt is reached. By "ripening" is meant the process prior to the occurrence of melting, in which the temperature of the snow is brought up to the melting point and the capacity of the snow to hold liquid water is exhausted.

8. Droughts. The safe (or "firm") capacity of projects depending on streamflow must, as discussed in Art. 20, be based on records sufficiently long to include low-flow or drought periods. The word "drought" as used here is merely a descriptive term, denoting a period of lower than average flow. If the streamflow record is too short, it may be extended by developing correlations with precipitation records as described in Arts. 18 and 19.

Thornthwaite,[10] in a discussion of the definitions of drought from an agronomical point of view, points out that it cannot be defined merely as a shortage of rainfall, because both the demand of vegetation for water (which varies according to the time of the year) and the moisture available in the soil must be taken into account. He has developed curves for "potential evapotranspiration," or the amount of water that would be evaporated and transpired by plants, if it were available. Figure 6 is an example showing that at Columbus, Ohio, in an average year there is a surplus of rain from December to May; from May to July the excess of potential evapotranspiration over precipitation is withdrawn from soil moisture; from July to October there is moisture deficiency, *i.e.*, drought; and from October to December precipitation again exceeds potential evapotranspiration, causing soil moisture accretion. It is seen that the magnitude of drought depends not only on the quantity of precipitation, but also

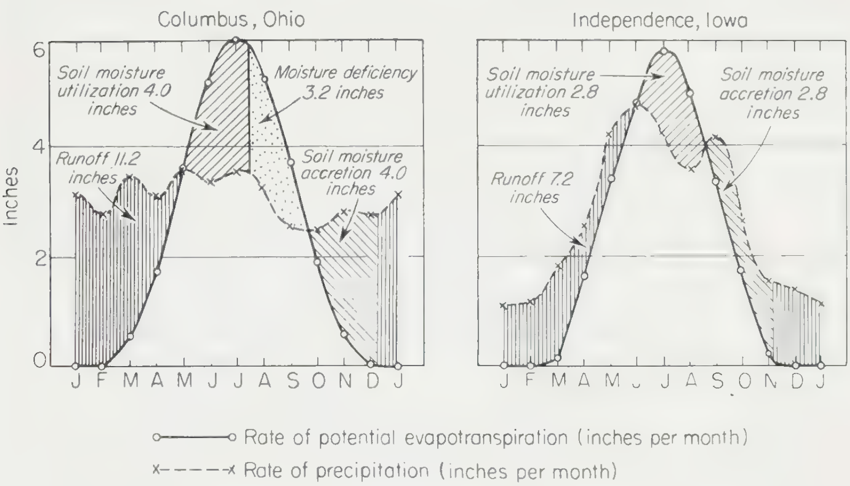

FIG. 6. Potential evapotranspiration and concurrent precipitation.[10]

on its relative timing with respect to potential evapotranspiration. At Independence, Iowa, during an average year, owing to better relative timing, there is no moisture deficiency, even though the total annual rainfall is less than at Columbus.

While the moisture deficiency at Columbus does not mean crop failure during an average year, it does indicate that crop yields would be increased if the deficiency were eliminated. The possible countermeasures listed by Thornthwaite are supplemental irrigation and improved farming practices, which include adjustment of the crop calendar so that harvest will precede drought, and crop rotation to improve the soil structure and increase its water-storage capacity.

Acquaintance with the agronomist's point of view is of increasing importance to the hydrologist for two principal reasons: (1) If future scientific research and economic studies demonstrate the value of supplemental irrigation, even in "humid" regions like eastern United States and western Europe, it will be necessary to develop sources of supply to meet the new demand for water. (2) If farming practices are improved, actual evapotranspiration prevailing at present will be increased so as to equal potential evapotranspiration. Although crop yields will benefit, the net runoff to streams will be reduced (see Art. 16).

STORM RAINFALL

9. Storm Types. Certain features of the various types of storm should be considered in the design of flood-control and drainage structures, and spillways for dams.

These features include season of probable occurrence, areal extent, duration, frequency, and possibility of rapid succession of two or more storms.

Cyclones. The term cyclone denotes a storm area of low atmospheric pressure, generally circular in shape, in which the winds blow spirally inward counterclockwise in the Northern Hemisphere, clockwise in the Southern. There are two main types of cyclones each associated with a distinct storm type: the tropical cyclone (also called hurricane or typhoon) and the extratropical cyclone or frontal-type storm.

Tropical cyclones[11a] are comparatively small, violent storms originating in the doldrums belt about 15° of latitude from the equator. Hurricane winds, which often reach velocities greater than 100 mph, blow spirally inward about the center or eye of the storm. The resulting rapid convergence of warm, moist air causes heavy precipitation. A total of 96.5 in. of rain fell at Silver Hill, Jamaica, W.I., in 4 days, during the passage of a hurricane. The diameter of a tropical cyclone varies from 100 to 600 miles. For data on frequencies and paths of hurricanes, see Ref. 12.

The *frontal-type storm* is associated with the extratropical cyclone. In fact, as stated by Bjerknes,[11b] the extratropical cyclone is formed, initially, by an unstable wave or eddy in the polar front, which forms the boundary of separation between northern polar air and southern tropical air. Extratropical cyclones vary greatly in size up to 1,000 miles in diameter and move generally eastward across the United States at a speed of 300 to 700 miles/day. As stated in Art. 6, almost all precipitation in winter on the East Coast of the United States is caused by frontal storms.

Thunderstorms are local atmospheric disturbances of short duration characterized by violent vertical air currents, gusty surface winds, torrential rain, lightning, thunder, and sometimes hail. The necessary conditions for thunderstorm formation are three: (1) the presence of a body of warm, moist air, (2) atmospheric instability in the zone overlying this body of air, and (3) an initial lifting agent. By "atmospheric instability" is meant a condition wherein the rate of decrease in temperature with height (lapse rate) exceeds the rate at which the warm, moist air mass cools by adiabatic expansion. The intensity of the storm depends on the magnitude of the three factors. The initial lifting agent is most commonly local thermal convection. Quiet, humid surface air over an intensely heated land area becomes warmer than the surrounding air and causes an unstable condition in which the warm air rises and is replaced at the ground by cooler descending air. The latter also becomes heated and rises. If this unstable convective condition continues, towering cumulus clouds form and thundershowers occur. Local convectional storms usually occur following the hottest part of the day and produce a large percentage of the summer rainfall in the middle-latitude continents and almost all the annual rainfall in the tropics.

A second cause of initial lifting is a well-developed cold front. A series of cold-front thunderstorms may develop as a continuous line (called a squall line) along the front. Unlike the convectional type, cold-front thunderstorms can occur at any time of the day and any season of the year, although they are rare during the winter months. If conditions are favorable, such a storm can produce large amounts of rainfall over a relatively wide area such as the storm of July 7–8, 1935, which caused record-breaking floods in the upper Susquehanna River basin in south central New York.

Another cause of thunderstorms is orographic lifting in mountainous areas, a factor tending to increase the frequency and intensity of thunderstorms in such areas. Intensity-duration relations for thunderstorms are discussed in Art. 10.

10. Point Rainfall. By point rainfall is meant rainfall at a single station as distinguished from rainfall over an area. Point rainfall is applicable in design to small areas up to about 10 sq miles.

Time Distribution. The time distribution of precipitation can be shown graphically by either a hyetograph or a mass curve, as shown in Fig. 7. The former shows the depths during a selected time period (½ hr in this case); the latter shows the cumulative depth vs. time, the slope at any point giving the rate of rainfall. In many storms, precipitation expressed as a percentage of storm totals is the same at widely distributed points; hence the mass curve for a nonrecording gage can be determined by plotting the observed points and then sketching in the curve by comparing it with

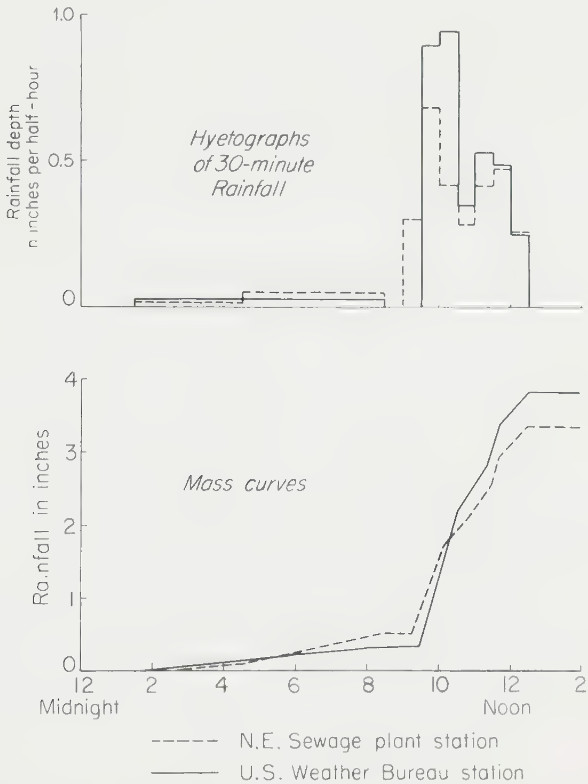

Fig. 7. Hyetographs and mass curves for the storm of Aug. 3, 1950, at Philadelphia, Pa.

the known curve for a nearby recording gage. With complex storms of long duration, meteorologic studies may be justified to give a closer approximation.

Design Storms. In setting up a hypothetical storm for design conditions, the most critical features of several past storms are often combined, for a given frequency of occurrence, into a single design storm, thereby simplifying design computations. This involves, first, establishment of the intensity-duration relation, for the design frequency selected, as follows: The maximum 5-min rainfall intensities during the storms of record are arranged in order of magnitude. If the record is 50 years long, the highest rainfall intensity has a return period of 50 years, the second 25 years, the third 16.7 years, and so on. A smooth curve is plotted from which the intensity for any return period can be determined. A similar computation is made for 10-min, 15-min, and other durations. Cross plots are then made giving curves of intensity vs. duration, with return period as a parameter. Chow[13a] has made an extensive compilation of formulas for rainfall intensity, most of which have the form

$$I = \frac{a}{t + b}$$

in which I = rainfall intensity, in./hr
t = duration of rainfall, min
a and b = empirical constants for area under study

but since 1935 such formulas have been largely superseded by Yarnell's studies[14] as supplemented, more recently, by those of Hershfield.[15] The latter reference contains a series of 54 outline maps of the United States showing point-rainfall depths for various frequencies and durations. Figure 8 shows the 6-hr rainfall depths determined in Ref. 15 to have an average return period of 10 years. A study of the outline maps indicates that the 6-hr depths for other frequencies bear the relation to the 10-year depth shown in Table 1. The maximum deviation from the average for a particular location is less than 10 percent for return periods of 5 years or more. For shorter return periods, the maximum deviation is no greater except for areas in the Southwest where the 1-year rainfall is only 40 to 45 percent of the 10-year rainfall. An error of 10 percent will still be tolerable for most design purposes; if not, the maps in Ref. 15 should be consulted. With the 6-hr depth established, the depths for other durations can be determined from the percentages in Table 2, obtained, as were the values in Table 1, from a study of the outline maps in Ref. 15.

Table 1. Frequency of 6-hr Rainfalls

Return Period, Years	Depth, % of 10-year Depth
1	53
2	64
5	85
10	100
25	120
50	135
100	148

Table 2. Rainfall Amounts for Durations Other than 6 Hr*

Percent of 6-hr rainfall

Duration	Zone A	Zone B	Zone C
5 min	9	14	18
15 min	19	30	38
30 min	25	40	50
1 hr	35	55	62
2 hr	55	70	76
6 hr	100	100	100
12 hr	130	124	118
24 hr	165	150	140

* Zone A is the area in the states of California, Oregon, and Washington west of the Sierra Nevada and Cascade Mountains; Zone B, between Zones A and C; Zone C, east of the Continental Divide. Values are fairly accurate (within 10 percent) in Zone A except that (1) in the northwest portion (roughly north of the 35th parallel and west of the 95th meridian) the percentages for durations over 6 hr should be multiplied by the factor 0.90 and those under 6 hr by 1.10; (2) in the higher parts of the Appalachian range, values tend to approach those of Zone A. Values in Zones B and C may vary from the averages given above by 25 percent. See Ref. 15 when greater accuracy is required.

FIG. 8. Six-hour rainfall, in inches, to be expected once in 10 years in the United States.

With the depth-duration relation established, the rainfall pattern is next determined, as in Table 3. The assumption in this case, namely, that the 5-year, 15-min, 30-min, and other-duration rainfalls would all occur in the same storm, is a severe one and therefore conservative when used as a design criterion. The frequency of this storm would actually be less than once in 5 years. The sequence of depths, shown in the last column of Table 3, has been chosen so as to place the greatest intensities in the early part of the storm in accordance with a Weather Bureau study[16] of heavy thunderstorms. Figure 9, taken from this study, shows that, as the depth for the total storm duration increases, the rates for partial durations become more uniform.

TABLE 3. COMPUTATION OF HYPOTHETICAL 5-YEAR DESIGN STORM FOR VICINITY OF LOUISVILLE, KY.

6-hr 10-year rainfall = 3.3 in. (Fig. 8)
6-hr 5-year rainfall = 0.85 × 3.30 = 2.80 in. (Table 1)

Duration, min	Depth, in.*	Depth increment, in.	Design-storm depths, in.
0	0		
		1.06	
15	1.06		0.25
		0.34	
30	1.40		1.06
		0.25	
45	1.65		0.34
		0.17	
60	1.82		0.17
		0.14	
75	1.96		0.14
		0.12	
90	2.08		0.12
		0.09	
105	2.17		0.09
		0.07	
120	2.24		0.07

* From factors in Table 2 for Zone C; intermediate values were interpolated.

11. Areal Rainfall. As stated in Art. 10, for areas greater than about 10 sq miles, the point rainfall and the areal rainfall are usually different. If areal rainfall is defined as the average precipitation over an area during a given time period, there are two types of problems, as in the case of point rainfall: (1) analysis of past storms to give, for a selected area, areal rainfall as a function of time, and (2) determination of areal rainfall vs. time for design conditions.

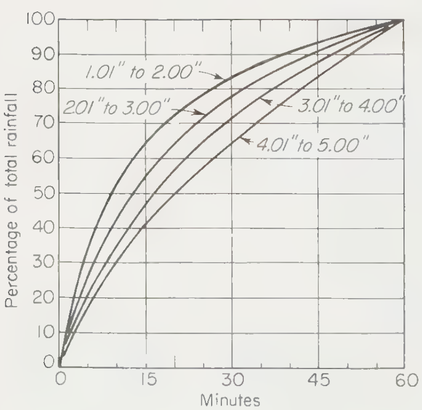

FIG. 9. Typical mass curves of 1-hr thunderstorm rainfall over a basin.[16]

The first problem is best analyzed with the use of the mass curve for point rainfall described in Art. 10. Various methods are used for weighting the point rainfalls to get the areal rainfall, including simple arithmetic averages, the Thiessen method, and the isohyetal method. Simple averages are of satisfactory accuracy only when rainfall varies slightly or when stations are equally spaced. In the Thiessen method, the weight of each station is proportional to its area of influence, determined by plotting perpendicular bisectors to the lines joining adjacent stations and measuring the portion of the area falling within the resulting polygon. Thiessen polygon lines are shown in the example in Fig. 22. In the isohyetal method, lines of equal rainfall are drawn by interpolating the station values (see Fig. 22). Straight-line interpolations are generally used unless known topographic influences indicate otherwise. From the isohyetal map, the average areal rainfall is computed by measuring the areas within successive isohyets. As a repetition of this process for many storms is laborious, the Thiessen method is often preferred even though it may not be so accurate. In some cases a successful compromise may be effected by modifying the Thiessen-method weights so as to give results in accordance with the isohyetal method as applied to only a sampling of the total number of storms to be analyzed.

The second problem, that of setting up a design storm for a given drainage basin, is approached by detailed studies of past storms of record. These rainfall values are then used in design-flood computations for important structures, as explained in Art. 24. The underlying principle in these studies is that of *storm transposition*, in which it is assumed that past storms in a region can recur in a transposed position, which is critical with respect to the basin being studied. Unless the basin is narrow and elongated or has some other unusual shape, a further assumption is often made, namely, that the storm shape and orientation will conform sufficiently closely to the shape of the basin so that reductions in the precipitation values need not be made. In mountainous regions where orographic effects are pronounced, modifications can be introduced, as described in Art. 13.

For areas up to about 400 sq miles and durations up to about 2 hr, thunderstorm-type rainfall produces the governing values. Figure 10 gives average area-depth curves, as determined for 20 dense gage networks up to 400 sq miles from various regions in the United States.[15]

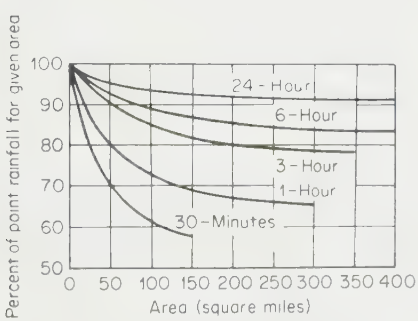

Fig. 10. Area-depth curves.[15]

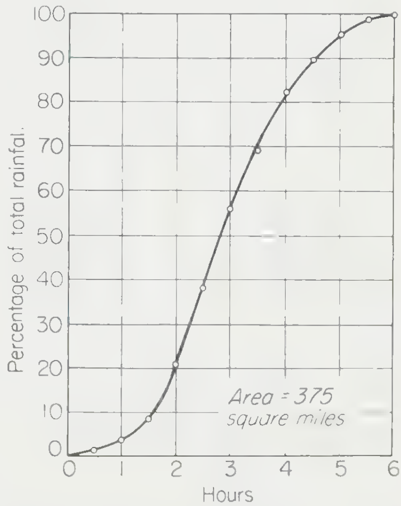

Fig. 11. Typical mass curve of thunderstorm rainfall over a basin.

Duration-depth relations for point rainfall, previously discussed, showed that in thunderstorms the higher intensities occur in the early part of the storm. However, when areal thunderstorm rainfall is considered, the effect of storm movement, causing nonsynchronization of the mass curves of rainfall at various points in the area, results in a more uniform rainfall pattern. A typical mass curve of thunderstorm rainfall for an area of 375 sq miles is shown in Fig. 11.

For areas greater than about 400 sq miles, the governing values are produced by frontal cyclonic storms rather than by thunderstorms. In regions subject to tropical hurricanes that type of storm usually causes the greatest depths for a wide range of areas. The task of analyzing in a comprehensive manner the precipitation data for large-area storms requires too great an expenditure of labor to be justified in the investigations for a single project. Fortunately, however, the extensive projects for flood control and river-basin development of agencies of the Federal government have greatly stimulated studies of large-area storms. These studies, started in 1937 by the Corps of Engineers in cooperation with the Hydrometeorological Section of the Weather Bureau, have included detailed examinations of original precipitation records for both recording and nonrecording gages, and meteorological studies of the storm history to aid in the plotting of mass curves. Following the plotting of the mass curves, isohyetal maps and depth-area-duration curves, similar to those shown in Fig. 12, were drawn. To January, 1958, the results for 527 major large-area storms have been published in Ref. 17, which is continually being revised and supplemented as additional studies are completed. Data for 150 of these storms are also presented by Bernard in Ref. 18, which includes a description by Hathaway of the methods of analysis used.

12. Probable Maximum Precipitation. For structures the failure of which would be disastrous to human life or to important economic values, a design storm based on 50-year or even 100-year rainfall amounts may be inadequate. The U.S. Weather Bureau has therefore developed the concept of *probable maximum precipitation*, abbreviated PMP. The PMP for a given area is the amount of rainfall resulting from the most critical meteorological conditions that are considered probable of occurrence.[19,20] Figure 13 gives ratios of the 6-hr PMP to the 100-year 6-hr rainfall, for areas of 10 sq miles or less (point rainfall), as determined from data in Refs. 19 and 20 and as published in Ref. 15. East of the 105th meridian, the point PMP's for other durations are about as follows:

Duration, hr	Rainfall, % of 6-hr
1	50
2	65
6	100
12	110–120
24	118–128
48	128–143

Where a range is indicated, higher values should be used for southerly locations. West of the 105th meridian, Ref. 21 gives the following for Zones A and B as defined in Table 2:

Duration, hr	Rainfall, % of 6-hr	
	Zone A	Zone B
1	26	47
2	57	76
6	100	100
12	143	143
24	180	180
48	238	238

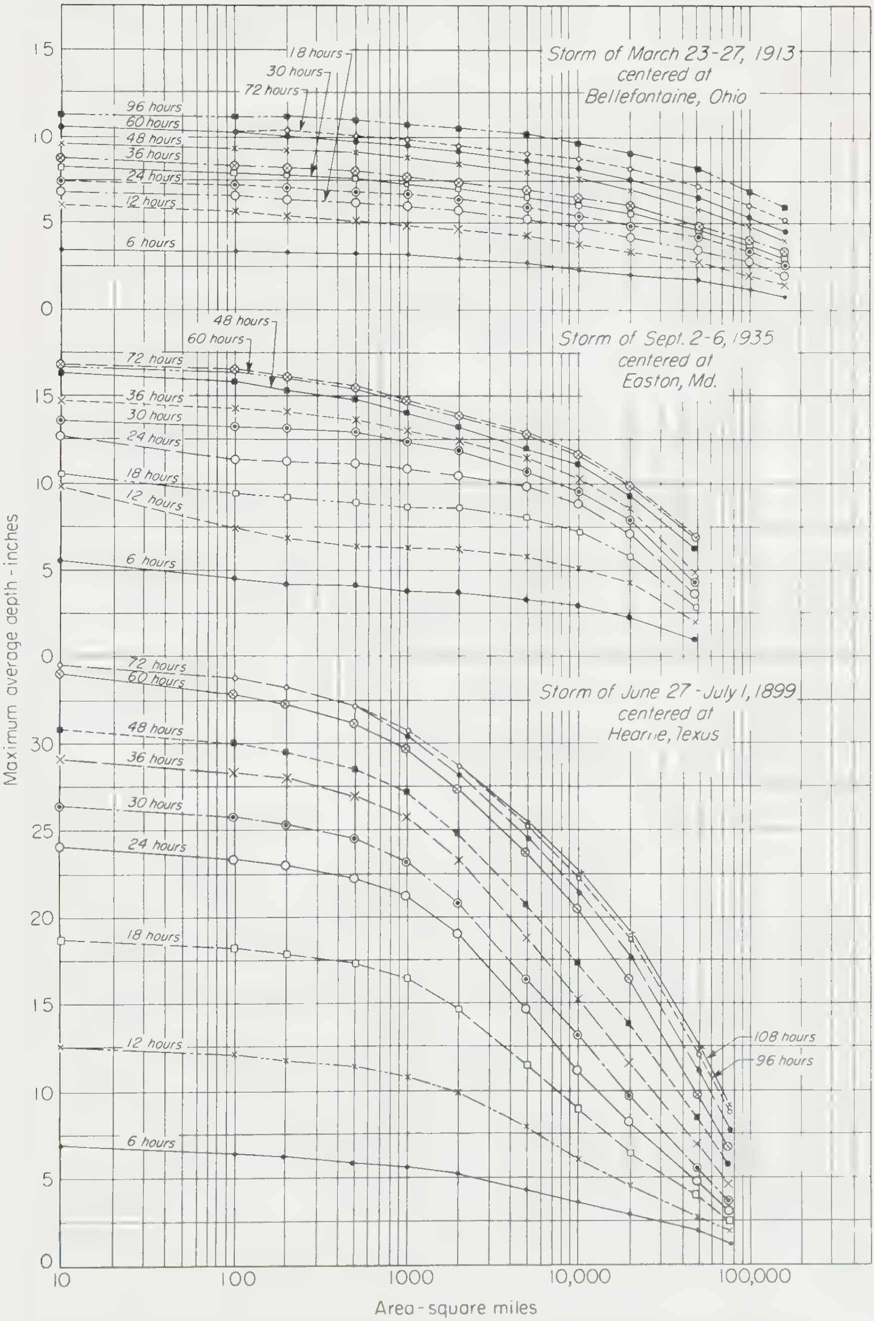

FIG. 12. Depth-area-duration curves for three large-area United States storms.

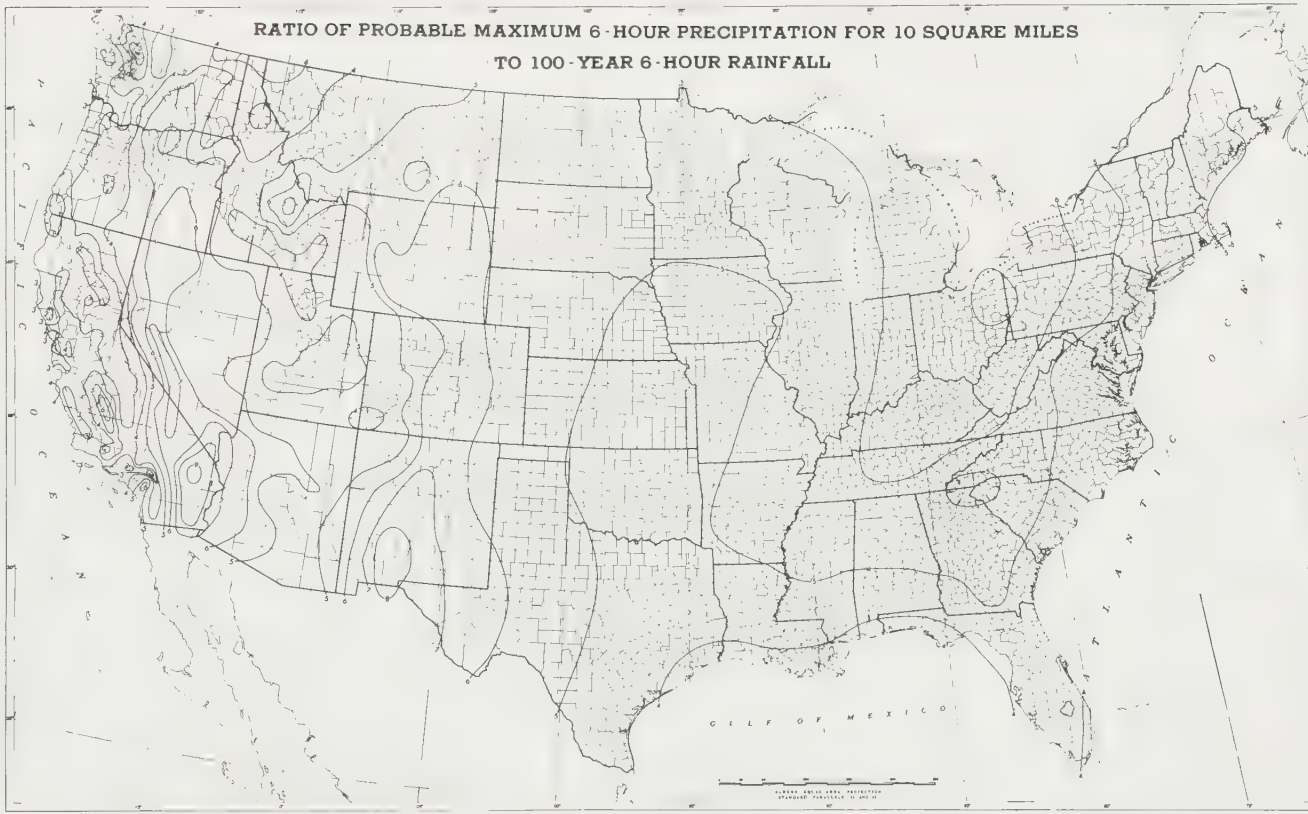

FIG. 13. Ratio of 6-hr PMP to 6-hr 100-year rainfall.[15]

Reduction factors to obtain average rainfall depths as a function of area are as follows (in percent of point rainfall):

Duration, hr	East of 105th meridian*		West of 105th meridian†	
	100 sq miles	1,000 sq miles	100 sq miles	400 sq miles
1	...	...	72	61
6	77	55	89	80
12	80	59	92	83
24	82	62	93	87
48	83	66		

* These are average values derived from charts in Ref. 19, which divides the area into eight zones. Maximum deviation from the average for a particular zone is 10 percent.

† From chart, Ref. 20, p. 54.

13. Orographic Effects. The orographic effect, or lifting of air passing over a mountain barrier, was listed in Art. 5 as one of the factors governing the depth of annual precipitation. When associated with thunderstorms or cyclonic activity, the orographic effect may greatly influence the areal distribution of storm rainfall. Therefore, in mountainous regions it is necessary to modify the simple procedure of storm transportation described in the preceding article.

A method[32a] that has been used with some success is to express storm rainfall at various stations in the basin as a percentage of the mean annual precipitation. If this is done, it is often found that the recorded rainfall depths tend to be equal percentages of the mean annual rainfall in spite of the orographic effects which cause large differences in the depths of both storm rainfall and mean annual precipitation. Isopercential lines (lines of equal percentage) can be drawn, and in the storm transposition, the pattern of the isopercential lines, rather than of the isohyetal lines, can be transposed. Linsley[22] lists the following minimum meteorological conditions before consideration of the foregoing theory can be applied: (1) the inflow directions of storms crossing the area do not vary excessively; (2) the air-mass characteristics are reasonably the same from storm to storm; and (3) the area under consideration is small enough so that variation in latitude of storm tracks does not affect the distribution within the zone.

RUNOFF

14. The Nature of Runoff. Runoff, which results from precipitation, is not directly proportional to precipitation but is a residual phenomenon which takes place only after certain demands (termed "losses") have been satisfied. The most important loss is termed "evapotranspiration" and denotes water returned to the atmosphere as (1) evaporation from land surfaces; (2) evaporation from "interception," which refers to precipitation intercepted by vegetation and not reaching the ground; and (3) transpiration, whereby water, drawn from the soil by the roots of plants as part of their life process, is then released through pores into the atmosphere. The term "consumptive use" is often used interchangeably with evapotranspiration, and its determination is of prime importance in the design of irrigation projects (see Sec. 33). Let P denote the volume of annual precipitation on a drainage basin, E the evapotranspiration, and R the runoff. Then

$$P = E + R \qquad \text{and} \qquad R = P - E$$

From this equation, called the equation of the hydrologic cycle, it is seen that, from the point of view of runoff, evapotranspiration is a loss. Hence, it is often referred to as "water loss." For drainage basins having large water areas in lakes or swamps, water loss equals the sum of evapotranspiration plus the evaporation from the water areas. Subterranean flow, or "deep seepage," sometimes occurs to or from a basin in sufficient magnitude to require adjustment of the runoff factor (see Art. 16).

By subtracting mean annual runoff from mean annual precipitation, Williams[23] has compiled mean annual water losses for many drainage basins in humid parts of the United States, with results as shown in Fig. 14. He also found (Fig. 15) an approximate correlation between mean annual water loss (evapotranspiration) and mean annual temperature. A noteworthy feature of Fig. 14 is the fact that the water-loss lines are approximately parallel to the temperature lines east of longitude 95°. West of this longitude, the water-loss lines turn sharply and become perpendicular to the temperature lines. This is explained by the rapidly decreasing precipitation westward, which fails to satisfy the evapotranspiration demands that would otherwise occur at the prevailing temperature. The actual demands of vegetation under adequate water supplies can be determined from computed values of potential evapotranspiration[10,24] (see also Art. 8).

Quantitative data on consumptive use of water by various crops[25] and by forest and range lands under various systems of management are necessary not only for determination of water-supply requirements for irrigation systems (see Sec. 32) but also to determine what the effect on basin annual and seasonal runoff will be of large-scale schemes for irrigation or watershed management.

15. Short-term Runoff. Although the total runoff over a long period of time, such as a year, may be known, for example, by deducting evapotranspiration from basin precipitation, fluctuations over shorter periods of time require a more detailed analysis of mechanics of the runoff process. Referring to Fig. 16, it is seen that, from the total rainfall measured by a gage on the ground, the amount necessary to wet vegetation must be deducted. This amount, measured in inches over the drainage basin, is called *interception* and is returned to the atmosphere by evaporation. Rainfall reaching the ground moves through the soil surface, a process which is called *infiltration*. Infiltration occurs both prior to and during the occurrence of surface runoff. The infiltration capacity or rate at which the soil is able to absorb rainfall is a variable depending on many factors. Water which has infiltrated the surface passes first through the *belt of soil water*. In this belt, water is withdrawn by the transpiration of plants and by evaporation from the soil, which in arid climates may reach depths as great as 20 ft.[26] Proceeding downward under the action of gravity, water leaving the belt of soil water passes through an intermediate belt and reaches the *water table*. The water table is a surface marking the upper limit of a zone or underground reservoir in which the soil is completely saturated. If water is added from above, the volume in the underground reservoir increases, causing a rise in the water table. This addition of water from above is called *groundwater* recharge. The relatively slow movement of water from the groundwater reservoir or zone of saturation to a stream channel is called groundwater or *base flow*. When the rate of rainfall exceeds the infiltration capacity, water accumulates on the ground surfaces as a thin film or sheet, and *overland flow* begins. A volume of water required to fill small surface depressions, termed *depression storage*, is abstracted, following which the depressions overflow and overland flow enters one of the myriads of channels and subchannels

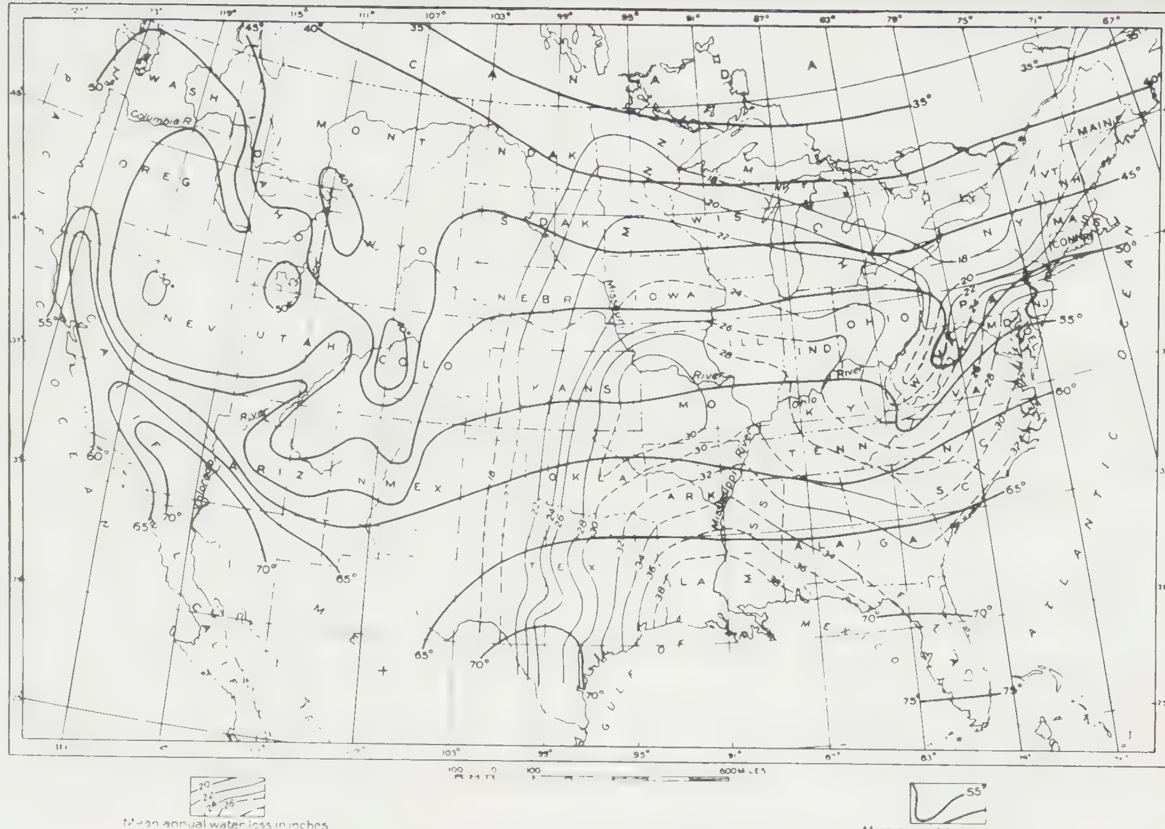

FIG. 14. Generalized lines of mean annual water loss and temperatures in the United States.[23]

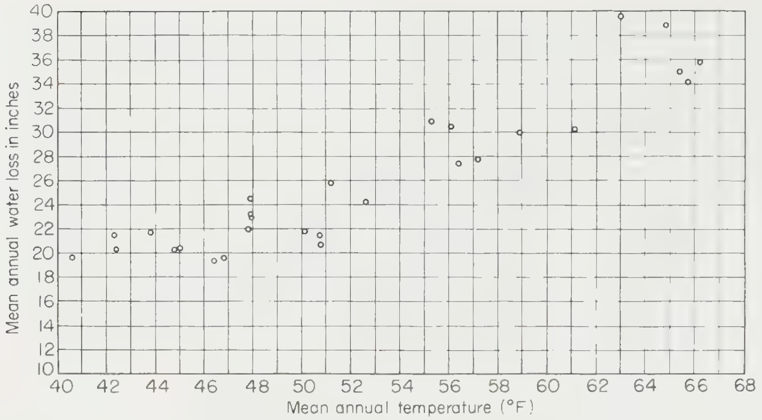

FIG. 15. Mean annual evapotranspiration vs. mean annual temperature for selected basins with the mean annual precipitation exceeding 20 in.[23]

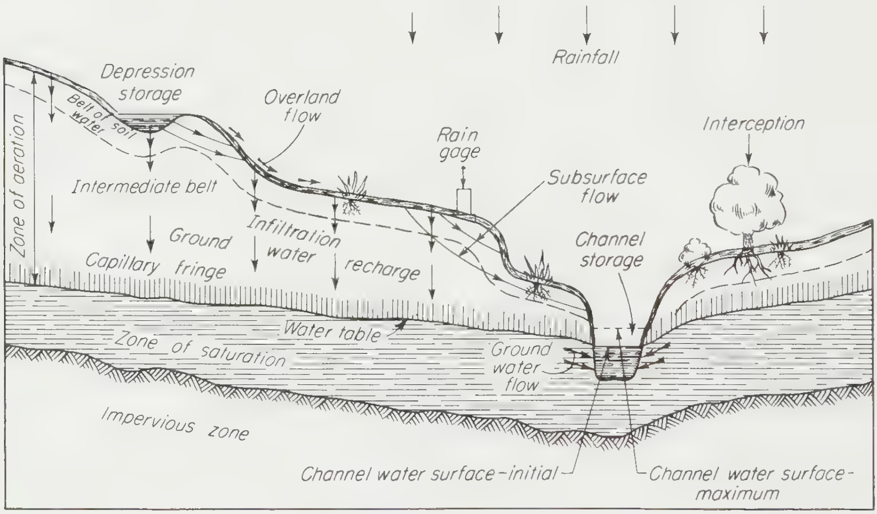

FIG. 16. Generalized cross section defining runoff terms.

found throughout the drainage basin. The volume of water in transit in the overland-flow sheet is called *surface detention*. The sum of interception and depression storage is called *initial abstraction*. The term *rainfall excess* denotes the total volume (expressed in inches over the basin) of overland flow; or from the preceding definitions, it is precipitation less initial abstraction less infiltration. Local geological and soil conditions in some basins permit another path of movement to the stream channel, namely, through upper soil layers (see Fig. 16), when the term *subsurface* flow or *interflow* is applied. The term *direct runoff* denotes the sum of the overland and subsurface flow. Increasing rates of runoff (direct plus base) reaching a stream channel cause a rise in water surface and an increase in *channel storage*, which is the

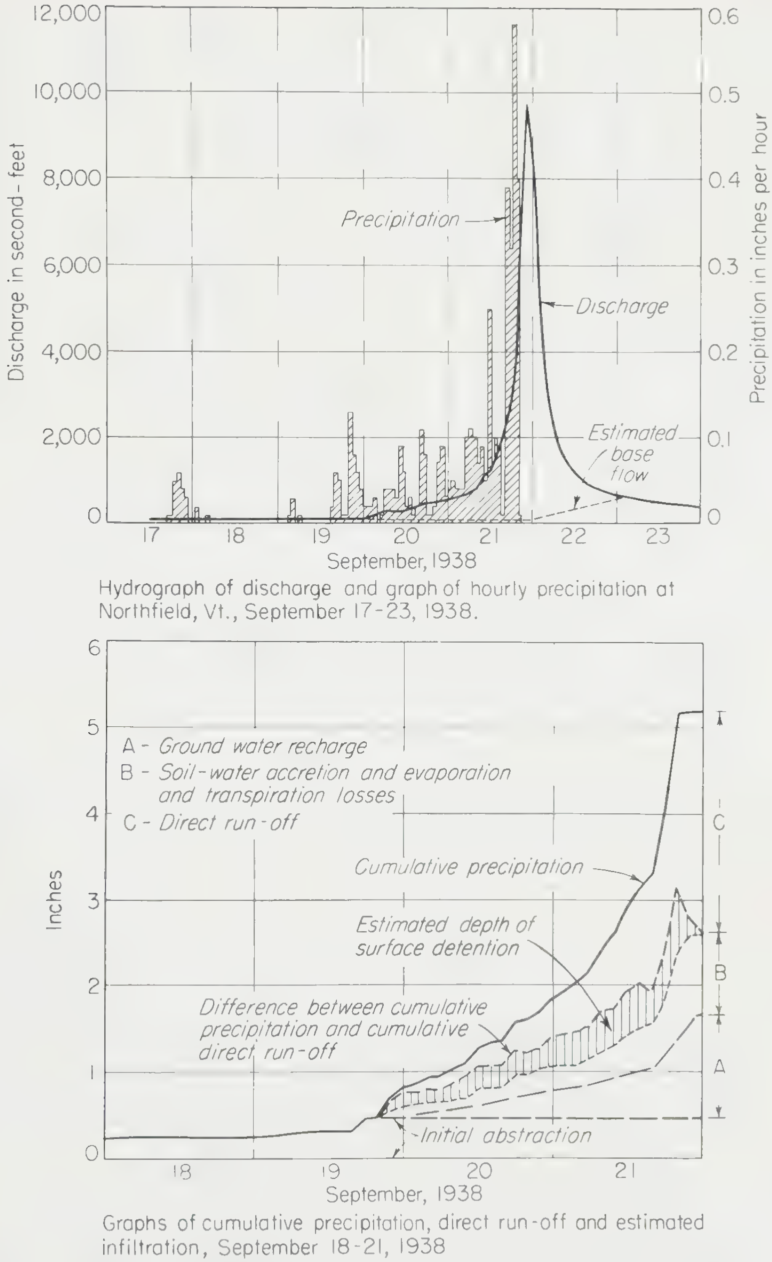

FIG. 17. Analyses of rainfall and runoff in the basin of Dog River at Northfield Falls, Vt.[27]

volume under the water-surface profile (see Sec. 5). This volume becomes large during floods, particularly when streams have wide flood plains. Figure 17, showing the discharge hydrograph of a stream and the graph of rainfall at a nearby recording gage, serves to illustrate further the above definitions.

16. Groundwater Runoff. Although water is present in the ground within all the belts between the impervious zone and the surface (Fig. 16), the term "groundwater" as used in hydraulic engineering refers only to water recoverable by springs and wells. The development of wells as a source of water supply is treated in Sec. 35.

The space between the ground surface and the water table is called the *zone of aeration* and includes the *capillary fringe* where water is held in the soil pores by capillarity, the *intermediate belt* where suspended water (called "vadose" water) is held by molecular attraction, and the belt of soil water. Plants extend their roots into the intermediate belt to various depths, while trees usually extend their roots into the zone of saturation.

The term *aquifer* refers to a water-bearing geologic formation, *i.e.*, one that is saturated with water. If confined between impervious strata, aquifers may contain water under pressure, in which case they are called *artesian*.

After the occurrence of direct runoff accompanying a stream rise, stream flow during the descending limb or *recession* side of a flow hydrograph occurs as outflow from channel storage and outflow from groundwater storage (groundwater or base flow). The former outflow occurs relatively rapidly, following which flow is entirely from groundwater storage. From studies of many hydrographs it has been found[28] that groundwater-depletion curves for a given drainage basin are nearly always the same; hence the term *normal groundwater-depletion curve* is used. It has been found further that this curve, or at least segments of it, follows a simple inverse exponential function[29] of elapsed time of the form

$$Q_t = Q_0 K^{-t}$$

where Q_0 is the discharge at any instant, Q_t is the discharge t days later, and K is the "daily depletion factor." As Q_t is the derivative of storage with respect to time, integration of this equation gives

$$S_0 = \frac{Q_0}{\log_e K}$$

where e is the base of natural logarithms and S_0 is the groundwater storage available for runoff at the time of Q_0. From this, it is seen that the discharge at any time is proportional to the water remaining in storage. The value of K can be determined by plotting observed recession curves on semilogarithmic paper, taking care to select periods of little or no direct runoff. In Fig. 18, the recession constant K is the average slope of the streamflow hydrographs, plotted on semilogarithmic paper, for 3 years during which typically low summer flows were preceded by periods of relatively high direct runoff.

17. Annual Runoff. Figure 19 is a map of the United States showing lines of equal average annual runoff. The indicated mean annual runoff for a given region is a generalized one, local variations due to geology and soil cover, especially to topography, causing departures from the average for the region. A detailed study of variations in mean annual runoff in the Connecticut River Basin in New England[31b] showed differences of 100 percent between valleys and nearby mountain peaks, with values for the basin as a whole ranging from 18 to 40 in. The principal reason for the variations in this case is the difference in precipitation caused by the mountainous terrain. It is apparent, therefore, that the values indicated in Fig. 19 give the average

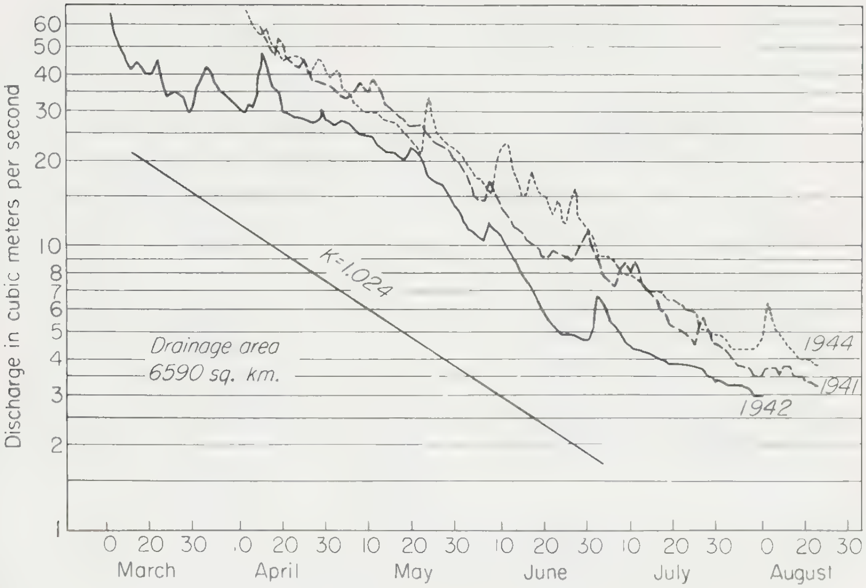

FIG. 18. Semilogarithmic plotting of stream flow and derivation of the recession constant K. Gediz River at Kizkoprusu, Turkey.

runoff over large areas and that there may be substantial errors if the values are applied to small ungaged areas, especially in mountainous regions.

It is of interest to compare mean annual precipitation and runoff over the United States as shown in Figs. 1 and 19. In central Nebraska, the mean annual runoff of about 1 in. is only about 5 percent of the precipitation of 20 in., whereas in Pennsylvania the runoff is 20 in., or 50 percent of the precipitation of 40 in. Note that in both cases the difference between precipitation and runoff or evapotranspiration is approximately the same—20 in.

18. Seasonal and Long-term Variations. Figure 20 shows the seasonal variations in the United States and a stream in the Caribbean area in terms of average monthly percentages of the annual runoff. The United States data are from Ref. 32*a*. In the autumn and winter, runoff is generally low in most of the United States as soil moisture, depleted during the summer, is replenished and as much precipitation occurs in the form of snow. Spring and early summer are periods of high flow, caused by melting snow in northern and high-altitude areas and the high moisture content of the soil as a result of accumulations during the winter.

Long-term variations in streamflow are best studied by computing 10-year moving averages and plotting them against the terminal or midyear. A series of 16 such plotted graphs for various streams in the United States, having records for 40 or more years, is described on page 68 of Ref. 32. The principal conclusion to be drawn from these studies is that there is no definite trend in the quantity of runoff, either upward or downward, for the United States as a whole. The graphs for some of the streams have seemingly regular cyclic variations; however, graphs for other streams showing similar periodic variations for part of the record do not repeat the periodicities with sufficient regularity to enable forecasting of future streamflows.

19. Estimates for Missing Records. Estimates of daily, monthly, or annual streamflow, when records are incomplete or even entirely lacking, may sometimes be

Fig. 19. Average annual runoff in the United States.[30]

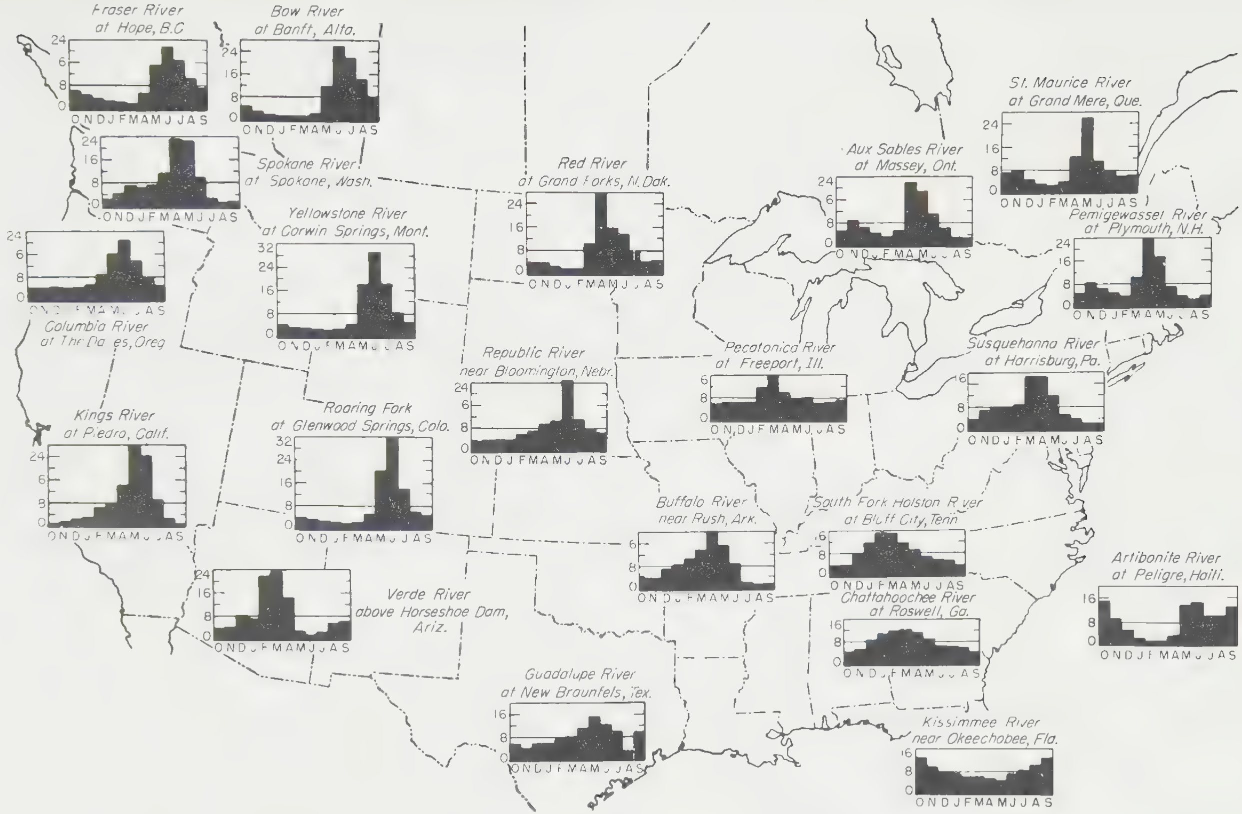

FIG. 20. Average percentage distribution of annual runoff by months.

made; however, the problem is one requiring great caution and judgment and thorough familiarity with the hydrologic characteristics of the region and drainage basin being studied.

If a partial record is available, it may be completed by making correlations with nearby records for concurrent periods. Periods of overlapping records may be plotted with an arithmetic time scale and a logarithmic discharge scale. The vertical distances between the plots, which are a measure of the ratios between the two discharges, will be found to vary, being greater for low flows and less for high flows. This is because low-water flows tend to vary as the first power of the drainage areas while flood flows vary as a fractional power, usually the square root (see Art. 24). The above procedure is applicable to estimating missing periods or extrapolating short records of daily, monthly, or annual runoff.

Values for missing periods in monthly and annual runoff records may be estimated by using ratios to normals as recommended for precipitation records in Arts. 3 and 4.

Attempts to derive direct correlations between annual runoff and annual basin precipitation are generally unsuccessful. In addition to the methods described above, annual runoff may be estimated from evapotranspiration and precipitation, using the equation of the hydrologic cycle (see Art. 14). Year by year, variations in evapotranspiration may be estimated from adjacent river basins,[23] but in lieu of individual values the average annual value may be computed from the average annual temperature (see Figs. 15 and 16). As annual evapotranspiration is the most stable term in the equation of the hydrologic cycle, use of average values is a reasonable approximation. Individual annual runoff values are computed by subtracting the estimated evapotranspiration from basin precipitation computed as outlined in Art. 11.

Estimates of monthly and annual runoff at a place entirely lacking in stream-gaging measurements should be approached with great caution, particularly in arid and semiarid regions where the quantity of flow during drought periods is greatly affected by climatic and physiographic features. A possible solution is to obtain spot discharge measurements several times a year and then estimate the runoff by comparison with a long-term station in the same general locality. However, for important projects a gaging station should be installed as an essential first step in the project investigations. In humid regions such as the Eastern United States, where fairly uniform conditions prevail, it may be permissible to compute runoff as being proportional to the drainage area. A sufficient number of gages should be available in the region to establish whether or not seasonal runoffs are in fact proportional to the drainage area; estimates for drought periods should be made with caution as described above for arid regions.

20. Utilization Studies. The various techniques for determining reservoir storage requirements to meet water-utilization demands are described in Sec. 4. These techniques, which include the flow-duration curve, the mass curve, and the residual mass curve, are based on stream-gaging records with corrections applied for evaporation from the reservoir surface (see Art. 27). Inasmuch as future operation of the reservoir and the expectation of safe yields are based on past records, it is apparent that these records must be of sufficient length to include samples of extremely dry and wet periods that occur at infrequent intervals. Where streamflow records are short, it will be necessary to extend them, as described in Art. 19. Ordinarily only runoff quantities for periods longer than a month can be obtained by this method but such data would be ample in studying a reservoir of relatively large storage capacity. On the other hand, with small reservoirs taking run-of-the-river flow it would be necessary to know the expected instantaneous (or possibly average daily) minimum. Studies of groundwater-depletion curves, correlated with minimum flows during the period of observed runoff records, may be useful in this connection.

FLOODS

21. The Flood Hydrograph. The runoff hydrograph for a stream covering a time interval during which a period of direct, *i.e.*, storm, runoff occurred, was shown and discussed in Art. 15 and will now be examined in greater detail.

An essential first step in flood-hydrograph analysis is the separation of storm runoff and base runoff, following which it is sometimes desirable to separate the storm runoff into surface and subsurface runoff. In Fig. 21, lines AC and DE are normal groundwater-depletion curves. Groundwater recharge occurs in the time interval AB, the points A and B defining, respectively, the beginning and the end of the flood hydrograph. While the form of the groundwater hydrograph between A and B is largely indeterminate, it need not ordinarily be established exactly, as the groundwater flow is usually a small part of the total flow. Furthermore, if a consistent procedure is followed in separating the groundwater flow, in both analyzing and synthesizing flood hydrographs, results will be accurate enough for practical purposes. In Fig. 21, the groundwater hydrograph has been drawn arbitrarily as a reverse curve with the point of inflection about midway between A and B. The hydrograph of direct runoff is then APB. Barnes[29] has developed an analytical method for separation of the direct-runoff hydrograph into surface and subsurface flow. However, while desirable for research, this refinement is not usually made in design studies.

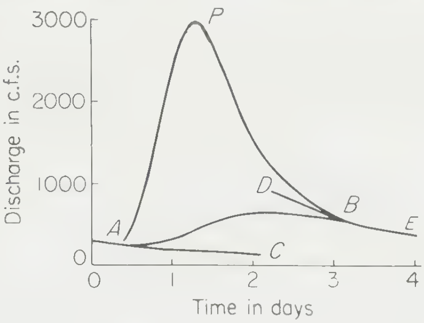

FIG. 21. Separation of direct and base runoff.

The factors determining the magnitude and time of the peak and the shape of the direct-runoff hydrograph can be placed in two groups: meteorological factors and drainage-basin characteristics. The meteorological factors include intensity of rainfall and its variation with time and place, depth and condition of snow on the ground, and temperature. The drainage-basin characteristics include a subgroup of topographic factors comprising size, shape (including length and width), drainage density (length of all stream channels in the basin divided by the area of the basin), land slope, channel discharge capacity and slope, and a second subgroup of geological and agronomical factors comprising surface and subsurface soil characteristics and vegetal cover. While almost all these factors can be expressed in quantitative terms,[34,35] a satisfactory explicit function for the direct-runoff hydrograph involving these factors has never been derived. However, a long step forward in flood-hydrograph analysis occurred with the introduction in 1932 by Sherman[36] of the unit hydrograph.

22. The Unit Hydrograph. Suppose that rainfall excess on a given drainage basin has a volume of 1 in. of depth, that it is uniformly distributed throughout the basin, and that it occurs at a constant rate with respect to time, beginning at time = 0 and ending at time = t_R. The resulting observed hydrograph of direct runoff would also have a volume of 1 in. and would represent the integrated effect of all the drainage-basin characteristics described above. Let this hydrograph be called a *unit hydrograph* for duration t_R. If the rainfall-excess volume is n in., uniformly distributed as before, ordinates of the resulting discharge hydrograph can be obtained simply by multiplying ordinates of the unit hydrograph by n. If rainfall excess is reasonably uniform throughout the basin, here is a powerful tool for synthesizing flood hydrographs.

The preceding theory has some limitations. As discharge rates increase, overland and channel velocities increase and tend to produce a more sharply peaked hydrograph. On the other hand, valley storage and overland detention also become greater, these factors having a dampening effect on the hydrograph. In a given drainage basin, if the velocity effects are greater than the storage effects, unit hydrographs based on minor observed flood rises are apt to have low peak values and should not be used. If, with rising flood stages, storage effects become pronounced, the final flood hydrograph should be corrected as described in Ref. 37. Experience with observed flood hydrographs permits the generalization that unit hydrographs should not be used for drainage areas greater than about 2,000 sq miles, when valley storage effects, as well as variations in rainfall excess in the drainage basin, tend to become too great to be reflected in the unit hydrograph alone.

Hydrologists are coming to recognize a lower limit as well in applicability of the unit-hydrograph principle.[32b] For very small areas of less than about 1 sq mile, the relative importance of overland flow detention is very great and other methods of flood-hydrograph determination are recommended (see Art. 26).

The techniques of unit-hydrograph derivation are summarized briefly in the following steps with references made to the example in Fig. 22:

1. Study the rainfall and runoff records and select for analysis storms which are isolated, intense, and occurring uniformly over the basin. A storm having all these characteristics will obviously be rare, particularly in a short record, and it will be necessary to select storms approaching that ideal as closely as possible.
2. Plot mass-rainfall curves, an isohyetal map for the storm, and hyetographs showing time distribution of rainfall loss and rainfall excess. Determination of the loss and its distribution is partly a matter of judgment. The total volume of the loss equals the basin rainfall minus the volume of direct runoff (see step 3). The rate of loss is greatest in the early part of the storm, but it may be rather uniform, particularly with wet soil conditions from antecedent rainfall. A fuller discussion of loss rates is contained in Art. 23.
3. Plot the observed discharge hydrograph and separate and subtract the base flow (see Art. 21), giving the hydrograph of direct runoff with a volume of 1.40 in. Dividing the ordinates by 1.40 gives the unit hydrograph for rainfall-excess duration t_R of 12 hr, this time interval being the duration of rainfall excess indicated by the hyetographs.
4. To obtain a unit hydrograph for other values of t_R, proceed as shown in Fig. 23 and Table 4.
5. Repeat the process with additional storms and develop unit hydrographs for the same value of t_R so that they can be compared and averaged. If a storm has characteristics too complex for unit-hydrograph development it may be necessary to estimate a trial unit hydrograph and reconstitute the hydrograph as described in the following paragraph.

Application. Two examples, each illustrating the computation of a flood hydrograph by use of the unit hydrograph, are given in Table 5 and Fig. 25. Within the limitations cited above, the unit hydrograph has become an invaluable aid in the

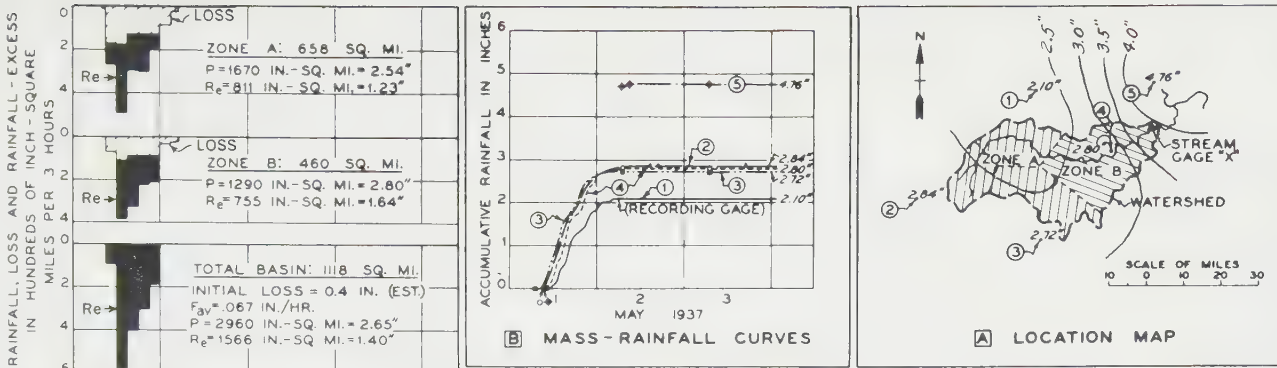

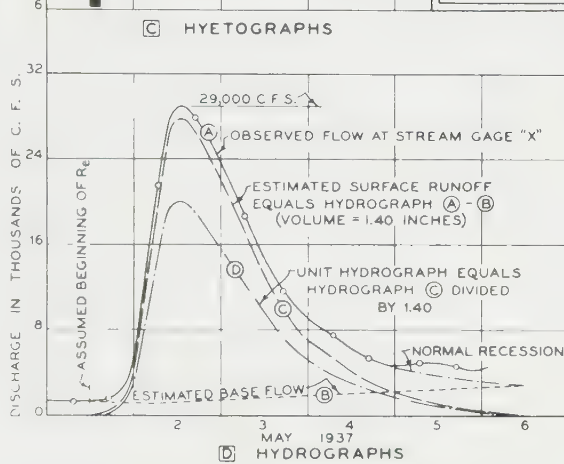

E TABULATION OF 12-HR. UNIT HYDROGRAPH D

TIME FROM BEGINNING OF R_e, IN HRS.	INSTANTANEOUS DISCHARGE, IN C F S.
6	300
12	3,100
18	13,300
24	20,000
30	18,600
36	15,900
42	12,600
48	9,600
54	6,800
60	5,300
66	4,000
72	3,000
78	2,300
84	1,800
90	1,300
96	1,000
102	700
108	430
114	230

SPECIAL NOTES

FIG. A

CIRCLED NUMBERS 1, 2 ETC. REFER TO PRECIPITATION STATIONS; STATION 1 WAS EQUIPPED WITH RECORDING RAIN GAGE, ALL OTHERS WITH NON-RECORDING GAGES.

FIG. B:

MASS-CURVE NUMBERS CORRESPOND TO PRECIPITATION-STATION NUMBERS IN FIG. A. OBSERVED RAINFALL VALUES ARE INDICATED BY LEGENDS o, ▪, ▴ ETC

FIG. C:

F_{av} = AVERAGE INFILTRATION INDEX FOR ENTIRE BASIN.

P = VOLUME OR AVERAGE DEPTH OF PRECIPITATION OVER AREA DESIGNATED.

R_e = VOLUME OR AVERAGE DEPTH OF RAINFALL-EXCESS OVER AREA DESIGNATED.

= (P) - (LOSS BY INFILTRATION, EVAPORATION ETC.)

FIG. D:

DISCHARGE VALUES COMPUTED FROM OBSERVED GAGE HEIGHTS ARE INDICATED BY LEGEND, o.

THE "UNIT-RAINFALL DURATION" OF UNIT HYDROGRAPH D IS ASSUMED EQUAL TO 12 HOURS.

FIG. 22. Computation of a unit hydrograph from an isolated storm.[38a]

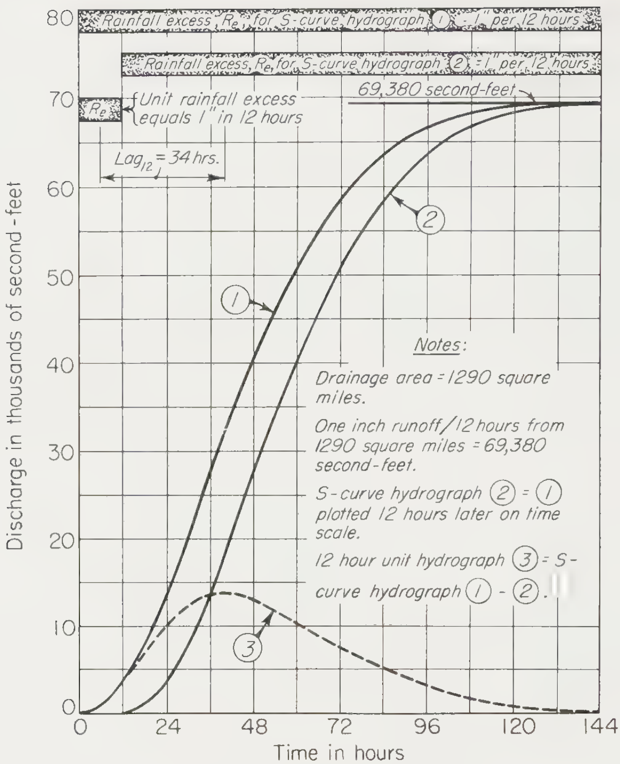

FIG. 23. *S*-curve hydrographs.

determination of flood hydrographs required in the design and operation of spillways, flood-control and multiple-purpose reservoirs, drainage pumping stations, and other water-control structures. Coupled with the principles of storm transposition (see Art. 24), the unit-hydrograph method permits much more reliable estimates of design-flood discharges than was formerly possible.

Synthetic Unit Hydrographs. Since the introduction in 1932 of the unit hydrograph, its use has become widespread in the United States, particularly among agencies of the Federal government. Certain characteristics of observed unit hydrographs and of the drainage basins producing them have been compiled in the form of standard data sheets by participating agencies of the Subcommittee on Hydrologic Data of the Federal Inter-agency River Basin Committee. The purpose of the compilation, which is still continuing, is to permit exchange of basic information on unit hydrographs among interested agencies in order to obtain means of evaluating and comparing observed unit hydrographs and of deriving synthetic unit hydrographs for drainage basins having little or no streamflow measurements. Drainage-basin characteristics compiled include the drainage area; the length L along the longest watercourse from the gaging station to the head of the stream (not to the divide); the length L_{ca} along the stream from the gaging station to a point opposite the center of gravity of the drainage basin; the drainage density or total length of all streams (including intermittent streams) divided by the drainage area; the average stream slope or total fall of the longest watercourse divided by L; the average slope of trib-

TABLE 4. COMPUTATION OF UNIT HYDROGRAPH OF ONE DURATION FROM UNIT HYDROGRAPH OF ANOTHER DURATION[38d])

Time, hr	Computation of *S*-curve hydrograph from known 12-hr unit hydrograph			Computation of 6-hr unit hydrograph from 12-hr *S*-curve hydrograph		
	12-hr unit hydrograph 3 in cfs	12-hr *S*-curve hydrograph 2 in cfs	12-hr *S*-curve hydrograph 1 in cfs	12-hr *S*-curve hydrograph 1 shifted 6 hr	Runoff from 0.5 in. R_e in 6 hr (col. 4 − col. 5)	6-hr unit hydrograph, 2 (col. 6) in cfs
(1)	(2)	(3)	(4)	(5)	(6)	(7)
6	900		900		900	1,800
12	3,400		3,400	900	2,500	5,000
18	6,900	+ 900	7,800	3,400	4,400	8,800
24	10,100	3,400	13,500	7,800	5,700	11,400
30	12,300	+ 7,800	20,100	13,500	6,600	13,200
36	13,600	13,500	27,100	20,100	7,000	14,000
42	13,900	20,100	34,000	27,100	6,900	13,800
48	13,200	27,100	40,300	34,000	6,300	12,600
54	11,800	34,000	45,800	40,300	5,500	11,000
60	10,300	40,300	50,600	45,800	4,800	9,600
66	8,950	45,800	54,750	50,600	4,150	8,300
72	7,650	50,600	58,250	54,750	3,500	7,000
78	6,400	54,750	61,150	58,250	2,900	5,800
84	5,250	58,250	63,500	61,150	2,350	4,700
90	4,200	61,150	65,350	63,500	1,850	3,700
96	3,200	63,500	66,700	65,350	1,350	2,700
102	2,280	65,350	67,630	66,700	930	1,860
108	1,580	66,700	68,280	67,630	650	1,300
114	1,100	67,630	68,730	68,280	450	900
120	750	68,280	69,030	68,730	300	600
126	500	68,730	69,230	69,030	200	400
132	300	69,030	69,330	69,230	100	200
138	150	69,230	69,380	69,330	50	100
144	50	69,330	69,380	69,380	0	0

All discharges are instantaneous values at the end of the hour designated in column (1). Drainage area equals 1,290 sq miles.

Given: 12-hr unit-hydrograph values in columns (1) and (2).

Procedure: 1. Compute *S*-curve hydrographs 1 and 2, which is the sum of a series of 12-hr unit hydrographs spaced 12 hr apart. Computation procedure is indicated by the arrows in the table.

2. Shift *S*-curve hydrograph 1 6 hr as in column (5) and subtract from column (4) giving, in column (6), the runoff from a rainfall excess of ½ in. in 6 hr.

3. Multiply values in column (6) by 2 to get the rainfall-excess volume of 1 in.

utary streams (a tributary stream being defined as one whose drainage area is less than 10 percent of the total drainage area); the average slope of the main streams (a main stream being defined as one whose drainage area is more than 10 percent of the drainage area); and the maximum, minimum, and mean elevations of the drainage basin. Unit-hydrograph characteristics, compiled as originally suggested by Snyder,[39] include the duration of rainfall excess (also called unit duration); peak of the unit hydrograph Q_p in cubic feet per second and q_p in cubic feet per second per square

TABLE 5. COMPUTATION OF HYPOTHETICAL HYDROGRAPH*

Time, hr	12-hr unit hydrograph, cfs	Rainfall excess, in. per 12 hr	Surface runoff from rainfall-excess units, cfs					Base flow, cfs	Total discharge, cfs
			Rainfall-excess, in.				Subtotal		
			0.7	3.8	10.9	1.8			
(1)	(2)	(3)	(4)	(5)	(6)	(7)	(8)	(9)	(10)
6	800	0							
12	2,900								
18	5,900	0.7	560	......	....	......	560	2,200	2,760
24	8,600	....	2,030	......	....	......	2,030	2,200	4,230
30	10,500	3.8	4,130	3,040	....	......	7,170	2,200	9,370
36	11,600	....	6,020	10,200	....	......	16,220	2,200	18,400
42	11,800	10.9	7,350	22,400	8,720	......	38,470	2,200	40,700
48	11,300	....	8,120	32,700	31,600	......	72,420	2,200	74,600
54	10,100	1.8	8,260	39,900	64,300	1,440	113,900	2,200	116,000
60	8,800	....	7,910	44,100	93,700	5,220	150,930	2,200	153,000
66	7,600	....	7,070	44,800	114,400	10,600	176,870	2,200	179,000
72	6,500	....	6,160	42,900	126,400	15,500	190,960	2,200	193,000
78	5,500	....	5,320	38,400	128,600	18,900	191,220	2,200	193,000
84	4,500	....	4,550	33,400	123,200	20,900	182,050	2,200	184,000
90	3,500	....	3,850	28,900	110,100	21,200	164,050	2,200	166,000
96	2,700	....	3,150	24,700	95,900	20,300	144,050	2,200	146,000
102	1,960	....	2,450	20,900	82,800	18,200	124,350	2,200	127,000
108	1,330	....	1,890	17,100	70.800	15,800	105,590	2,200	108,000
114	940	....	1,370	13,300	60,000	13,700	88,370	2,200	90,600
120	630	....	930	10,300	49,000	11,700	71,930	2,200	74,100
126	430	....	660	7,450	38,200	9,900	56,210	2,200	58,400
132	250	....	440	5,050	29,400	8,100	42,990	2,200	45,200
138	130	....	300	3,570	21,400	6,300	31,570	2,200	33,800
144	50	....	180	2,390	14,500	4,860	21,930	2,200	24,100
150	......	....	90	1,630	10,200	3,530	15,450	2,200	17,700
156	......	....	40	950	6,870	2,390	10,250	2,200	12,500
162	......	....	.....	490	4,690	1,690	6,870	2,200	9,070
168	......	....	.....	190	2,730	1,130	4,050	2,200	6,250
174	......	....	.....	......	1,420	770	2,190	2,200	4,390
180	......	....	.....	......	550	450	1,000	2,200	3,200
186	......	....	.....	......	....	230	230	2,200	2,430
192	......	....	.....	......	....	90	90	2,200	2,290

* Drainage area = 1,100 sq miles. All discharges are instantaneous values at the end of the hour given in column (1).

mile; time t_p from the center of rainfall excess to the peak; time t_v from the center of rainfall excess until 50 percent of the runoff volume has occurred; coefficient $C_t = (t_p/LLca)^{0.3}$; and coefficient $640C_p = q_p t_p$.

It has been found that, if adjacent streams have similar characteristics, the values of C_t and $640C_p$ are about the same; in the absence of streamflow records, therefore, these coefficients can assist in the derivation of a synthetic unit hydrograph. The

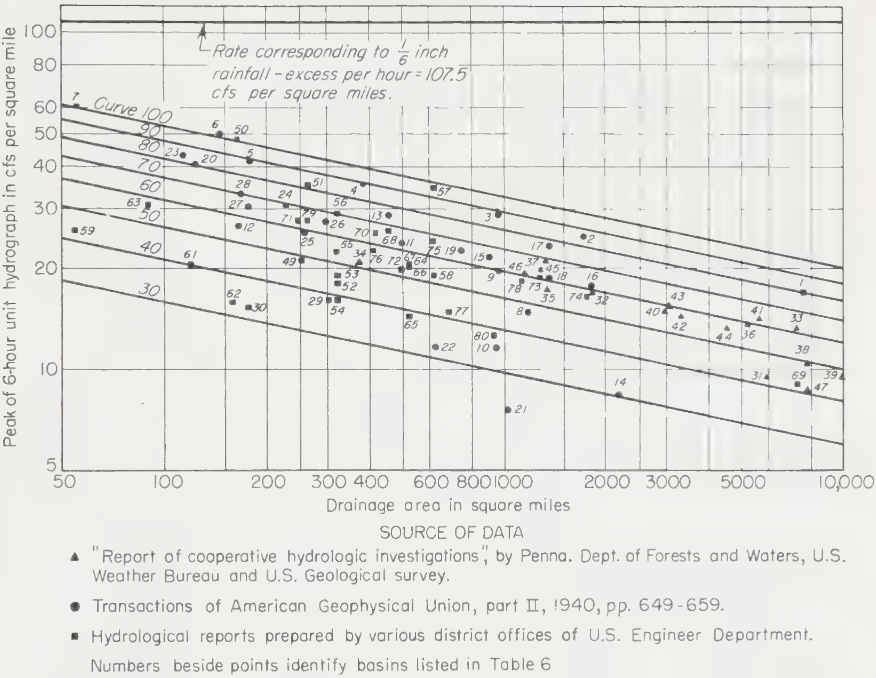

FIG. 24. Six-hour unit hydrograph peaks vs. drainage area.[38d] Numbers beside points identify basins listed in Table 6.

curves in Fig. 24 were taken from Ref. 38*d* (also given in Ref. 45*a*), which describes curve 100 as being an enveloping curve of the plotted points and of some additional points (not shown) for drainage areas larger than 10,000 sq miles. The curves parallel to curve 100 correspond to percentages of the latter, as indicated. These curves and Table 6 can be used to assist in estimating the synthetic unit-hydrograph peak.

Reference 40 contains about 60 unit hydrographs for drainage basins throughout the state of Illinois.

23. Infiltration Theory. Infiltration was defined in Art. 15. It is necessary to estimate the total volume of infiltration and its distribution in determining rainfall excess, as described in Art. 22. Infiltration has been measured directly on small plots of land and related to soil type, vegetal cover, and antecedent soil-moisture conditions.[32c] These measurements, having been made under laboratory conditions, cannot be applied directly to natural drainage basins of varying soil, cover, and topography; however, they have been very useful in studying means by which agronomic methods can increase infiltration capacity (the maximum rate at which the soil can absorb rainfall), thereby reducing surface runoff and soil erosion.

Other basic differences between small plots and natural drainage basins include (1) the presence of channelization in the latter, which increases the speed of water particles compared with the overland flow velocities of small plots, and (2) quick subsurface flow, which may be present in natural areas. Despite these differences, which tend to make indicated loss rates much smaller than those obtained from experimental plots, the infiltration approach has been furthered persistently by many investigators[32c] who have introduced the term *infiltration index* to denote the computed

Table 6. Identification of Basins in Fig. 24

Point No.	Stream	Location
1	Washita River, Okla.	Near Mouth
2	Youghiogheny River, Pa.	Sutersville, Pa
3	Black River, Ark.	Leeper, Ark.
4	Casselman River, Pa.	Markelton, Pa.
5	So. Fk. Ten Mile Creek, Pa.	Jefferson, Pa.
6	Turtle Creek, Pa.	E. Pittsburgh, Pa.
7	Canacadea Creek, N.Y.	Almond dam site, N.Y.
8	Tygart River, W.Va.	Tygart dam site, W.Va.
9	Cheat River, W.Va.	Rowlesburg, W.Va.
10	Allegheny River, Pa.	Kinzua, Pa.
11	L. Beaver Creek, Pa.	E. Liverpool, Pa.
12	Sugar Creek, Pa.	Sugar Creek, Pa.
13	Redbank Creek, Pa.	Redbank Cr. dam site, Pa.
14	Allegheny River, Pa.	Above Kinzua, Pa.
15	Clarion River, Pa.	Clarion, Pa.
16	Kiskiminitas River, Pa.	Vandergrift, Pa.
17	Cheat River, W.Va.	Beaver Hole, W.Va.
18	Conemaugh River, Pa.	Bow, Pa.
19	West Fork River, W.Va.	Enterprise, W.Va.
20	Laurel Hill Creek, Pa.	Ursina, Pa.
21	French Creek, Pa.	Utica, Pa.
22	French Creek, Pa.	Saegerstown, Pa.
23	Buffalo Creek, W.Va.	Barrackville, W.Va.
24	Dunkard Creek, Pa.	Bobtown, Pa.
25	Chartiers Creek, Pa.	Carnegie, Pa.
26	Oil Creek, Pa.	Rouseville, Pa.
27	Raccoon Creek, Pa.	Moffatts Mills, Pa.
28	Yellow Creek, Pa.	Hammondsville, Pa.
29	Brokenstraw Creek, Pa.	Youngsville, Pa.
30	Millers River, Mass.	Birch Hill, Mass.
31	Allegheny River, Pa.	Franklin, Pa.
32	Allegheny River, Pa.	Vandergrift, Pa.
33	Monongahela River, Pa.-W.Va.	Dam No. 2, Pa.
34	West Fork River, W.Va.	Clarksburg, W.Va.
35	Tygart River, W.Va.	Fetterman, W.Va.
36	Monongahela River, Pa.-W.Va.	Charleroi, Pa.
37	Youghiogheny River, Pa.-W.Va.	Connellsville, Pa.
38	Susquehanna River, Pa.	Towanda, Pa.
39	Susquehanna River, Pa.	Wilkes-Barre, Pa.
40	W. Br. Susquehanna River, Pa.	Renova, Pa.
41	W. Br. Susquehanna River, Pa.	Williamsport, Pa.
42	Juniata River, Pa.	Newport, Pa.
43	Delaware River	Port Jervis, N.Y.
44	Delaware River	Belvidere, N.J.
45	Lehigh River, Pa.	Bethlehem, Pa.
46	Schuylkill River, Pa.	Pottstown, Pa.
47	Susquehanna River, Pa.	Towanda, Pa.
48	Canisteo River, N.Y.	Arkport Dam, N.Y.
49	Otselic River, N.Y.	Whitney Pt., N.Y.
50	Westfield River, Mass.	Knightville dam site, Mass.
51	Loyalhanna Creek, Pa.	New Alexandria, Pa.
52–56	Mahoning Creek, Pa.	Dayton, Pa.
57–58	Coldwater River, Miss.	Coldwater, Miss.
59	Saddle River, N.J.	Lodi, N.J.
60	Whippany, N.J.	Morristown, N.J.
61	Ramapo River, N.J.	Mahwah, N.J.
62	Ramapo River, N.J.	Pompton Lakes, N.J.
63	Wanaque River, N.J.	Wanaque, N.J.
64–68	Redbank Creek, Pa.	Pa.
69	Washita River, Okla.	Durwood, Okla.
70	Strawberry River, N.Y.	Poughkeepsie, N.Y.
71	Petit Jean River, Ark.	Boonville, Ark.
72	Petit Jean River, Ark.	Blue Mt. dam site, Ark.
73	N. Br. White River, Mo.	Tecumseh, Mo.
74	N. Br. White River, Mo.	Norfolk dam site, Ark.
75	Eleven Pt. River, Mo.	Bardley, Mo.
76	Fourche la Fave River, Ark.	Gravelly, Ark.
77	Fourche la Fave River, Ark.	Nimrod dam site, Ark.
78	Little Red River, Ark.	Greer's Ferry, Ark.
79	Row-Willamette River, Ore.	Dorena (Star), Ore.
80	Illinois River, Okla.	Tahlaquah, Okla.

loss rate for natural basins. Although it might appear that the two differences noted above would tend to vitiate the infiltration approach, there may be value in its use in a practical case if it is found, for example, that the records for several flood periods for a drainage basin can be resynthesized by using a constant unit hydrograph and consistent values of the infiltration index. The example given in Art. 24 under Past Floods illustrates the use of the infiltration index. The results of a large number of determinations of the infiltration index for drainage basins in various parts of the United States are given in Refs. 38*e* and 45*b*.

24. Flood Discharge Estimates. Methods are summarized in this article for making discharge estimates for (1) past floods and (2) design floods.

Past Floods. Reliable stream-gaging observations, if available, form the best basis of determining the discharge of a past flood; however, if such observations are faulty or incomplete, other methods can provide a check on the discharge determinations. The general procedure is to assemble all known facts regarding the flood, including the areal and temporal distribution of precipitation, temperature, soil conditions, river stages, and flood discharges in adjacent river basins or in the same basin at upstream and downstream points. With all these facts, along with a knowledge of pertinent characteristics of the various drainage basins involved, it is possible, in many cases, to piece together the history of a past flood occurrence including a hydrograph giving the desired peak discharge.

Figure 25 is an example of such a determination. The mass rainfall curve in (*a*) was derived by plotting an isohyetal map of rainfall for the basin, computing the total basin rainfall (7.1 in.), and determining the time distribution by comparison with mass curves (not shown) at nearby stations. The mass infiltration curve, the slope of which equals the infiltration index, was developed in the course of comprehensive studies of the storm of July, 1942, and the concurrent runoff, covering a large area and many drainage basins in northwestern Pennsylvania and southwestern New York. In (*b*) are shown hyetographs for rainfall, infiltration, and rainfall excess. The rainfall rate equals the slope of the mass rainfall curve in (*a*). During the time interval 11 P.M. to midnight, July 17, the rainfall rate exceeded the infiltration rate (average); hence, the volume of infiltration is as given in curve 1. From midnight to 3 A.M., July 18, the rainfall was less than the indicated infiltration rate in curve 1. The volume of infiltration during this period is therefore the same as the rainfall. This is shown in (*a*) by shifting curve 1, as indicated by the arrow, giving curve 2. From 3 to 5 A.M. the rainfall rate again exceeded the infiltration rate, as indicated by a segment of curve 1 shifted to curve 2. A similar procedure is followed during the remainder of the storm period. The shifting of the infiltration curve follows a suggestion made by C. F. Izzard.[41] The 1-hr synthetic unit hydrograph has the Snyder coefficients indicated in the figure, as determined from observed coefficients for similar drainage basins in the same region. The 2- and 3-hr graphs were derived from the 1-hr graph utilizing the *S*-curve procedure (not shown) described in Art. 22. Finally, the flood hydrograph in (*d*) was computed from the unit hydrographs in (*c*) and the rainfall excess volumes in (*b*).

Design Floods. Design-flood hydrographs are needed in the design of reservoirs, spillways, flood channels, and other water-control structures. Methods applicable to drainage systems, including small natural areas of a few square miles or less, and to urban drainage are described in Art. 26. Economic factors are of prime importance in the selection of a design flood. For example, it may be found in the case of a local flood-protection project that physical limitations make it uneconomical to set the design capacity higher than the maximum flood of record. In this instance, the design flood equals the maximum past flood; it should of course be established concurrently that the project is economically justified even with the limited protection. As a second example, the severity of the design flood for a reservoir spillway should be related to the economic loss resulting from the possible failure of the impounding dam or from downstream inundation.

The procedure for developing a design flood is the same as that described in the previous example relating to a past flood, except that the magnitude of the three main components—precipitation, infiltration index, and unit hydrograph—is changed to correspond to more critical conditions. Just how critical these conditions must be is related to the economic problem as previously discussed. Taking the infiltration index first, the most severe condition might be to use the minimum values observed in the region for similar physiographic conditions, or a value of zero would be used in the case of melting snow. The peak of a unit hydrograph derived from observations of a minor flood may have to be increased as much as 50 percent to reflect conditions during a major flood.[38f,39] The determination of the design precipitation or design storm may require considerable meteorological research, as summarized in Art. 11. Snowmelt problems in connection with design floods are discussed in Art. 7.

Prior to the development of current techniques based on the unit hydrograph and flood routing analysis, a large number of empirical formulas were used to estimate

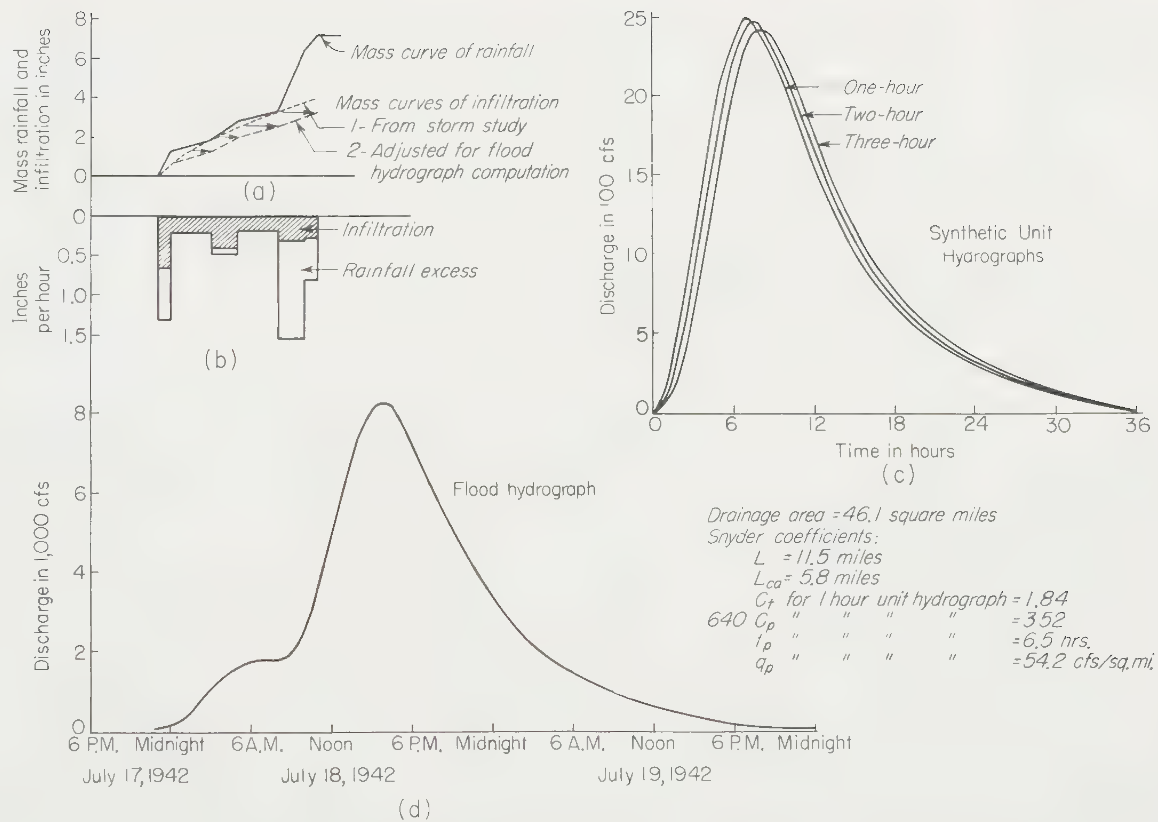

FIG. 25. Computation of a hydrograph for a past flood. Dodge Creek at Portville, N.Y.

flood discharges for design purposes. The formulas, many of which are given and evaluated in Ref. 42, make use of various combinations of factors such as drainage area, average width of the basin, average basin slope, and frequency. These formulas generally have only local application, but they may be useful in extrapolating the available data. A second method, and one that still has value, is to plot for a given region all known maximum discharges in csm (cubic feet per second per square mile) against drainage area in square miles. If plotted on logarithmic paper, a straight line will usually define the envelope of maximum points. As the only factor here considered is drainage area, it is obvious that such a plot provides only another basis of comparing the design-flood discharge with the past flood history of the region being studied. Studies of maximum flood discharges throughout the United States have shown the slope of the envelope curve to be 0.5 in most cases, giving a formula of the type

$$Q = C\sqrt{A}$$

where Q is the discharge in cubic feet per second, A is the drainage area in square miles, and C is a coefficient known as the *Myers rating*. The equations of envelope curves for various regions will indicate that the exponent of the drainage area may be more but rarely less than 0.5. Where the indicated exponent is less than 0.5, the usual conclusion is that portions of the drainage basin are not contributing to flood flows and therefore the formula is not applicable. This is true of very large river basins or for those in semiarid regions. In both cases, major flood-producing storms do not encompass the entire basin defined by the topographic boundaries. If a sufficient number of station-years of river records are available, the envelope curve is a measure of the flood-producing potential of a region, and provides only a general index of flood intensity. Because of peculiar physical features, the flood-producing potential of drainage basins will vary widely even though the meteorological characteristics may be similar. It is inadvisable to apply envelope curves with coefficients of 0.5 to drainage areas less than about 10 sq miles. Flood discharges for drainage areas of a few square miles tend to vary more nearly as the first power of the drainage area. Discharge values estimated from high Myers rating on small drainages indicate rates of runoff that are higher than known rainfall rates for point rainfall.

The Myers ratings of the envelope curves for various regions of the United States are given in Table 7.

25. Frequency Analyses. Flood-frequency analyses are generally made for one of two purposes: (1) as a guide to judgment in determining the capacity of a structure, such as a highway bridge opening or cofferdam where it is considered permissible to take a calculated risk, and (2) as a means of estimating the probable flood damage prevented by a system of flood-protection works over a period of years, usually equal to the estimated economic life of the works. In the first case, the magnitude of the flood discharge that will be equaled or exceeded in a certain period of years is desired. In the second case, it may be necessary to consider, in addition to the peak-flood discharge, factors such as duration of flooding, time between flood peaks, and month of occurrence (agricultural damage, for example, might be significant only during the growing season). In both cases, the reliability of the frequency estimates depends on the length of the observed record rather than on the specific method of mathematical analysis used to obtain the frequency relation. Thus, if a 50-year record is available, the peak discharge of a 10-year flood based on this record might be stated with assurance; however, the peaks of the 50- or 100-year floods could be estimated only approximately.

The procedure followed in deriving a frequency relation for peak discharges consists of three steps: (1) compilation of flood peaks in order of magnitude, (2) com-

Table 7. Envelope Curves of Maximum Flood Discharges in the United States

Region	Approx range of drainage areas, sq miles	Myers rating
North Atlantic and Middle Atlantic slope basins	10–400	7,000
	500–30,000	5,500
South Atlantic slope and Eastern Gulf of Mexico	10–10,000	6,000*
Ohio River basin	10–900	7,000
	1,000–4,000	6,000
	5,000–200,000	4,300
Eastern Great Lakes and Eastern St. Lawrence River basins	10–60	6,000
	70–1,000	3,500
Upper Mississippi River and Western Great Lakes basins	10–150	4,000
	200–800	2,700
	900–15,000	1,800
Lower Missouri and Western Mississippi River tributaries	10–5,000	7,500
	6,000–15,000	4,000
Western Gulf of Mexico basins	50–3,000	14,000*
	4,000–9,000	10,000
	10,000–40,000	5,000
Pacific Slope basins in California	10–3,000	6,000*
	4,000–12,000	4,000
Pacific Slope and Lower Columbia River basins in Washington and Oregon	10–8,000	7,000*
Great Basin and Rocky Mountains	10–700	4,000*
	800–6,000	3,000

* Higher estimates available, but subject to further confirmation.

putation of recurrence intervals, and (3) plotting. In compiling the flood peaks, either the "annual-flood" method or the "partial-duration series" method is used. In the former, only the highest peak in each water year is listed. In the latter, all floods above a base are compiled. This eliminates an objection to the annual-flood method, namely, that the second highest peak during a given year may be greater than the highest peak during another year. However, in selecting peaks for the partial-duration series, caution should be exercised so as not to include consecutive peaks caused by storms which are not independent meteorological events. If flood damage is of primary concern, the time interval between peaks affects the amount of the damage and hence is a factor in deciding on which peaks to include in the compilation. "Historic floods" are severe floods that occurred prior to the beginning of the continuous stream-gaging record but whose peaks are established on the basis of satisfactory evidence. They should be included in the compilation, but their recurrence interval is computed differently, as described subsequently.

The recurrence interval of each flood peak is computed by one of the following formulas:

$$T_r = \frac{N}{M} \tag{1}$$

$$T_r = \frac{N}{M - 0.5} \tag{2}$$

$$T_r = \frac{N + 1}{M} \tag{3}$$

where T_r is the recurrence interval in years, N is the length of continuous record in years, and M is the order of magnitude of the flood peak. Reference 43 discusses these formulas and shows that the shape of the final curve, particularly in the frequent-flood range, is little affected by the choice of the formula. The writers prefer formula (1) because of its simplicity and because refinements in making frequency estimates do not appear justified, considering the degree of accuracy of the basic data and the fact that, for the less frequent floods, the length of record is generally too short to make any positive predictions with regard to frequency.

When historic floods are included, the recurrence intervals for all floods equal to or greater than these floods are computed in the same way except that the value of N is made equal to the time in years between the earliest historic flood and the end of the continuous record. The final plot of peak discharge vs. recurrence interval can be made on probability or semilogarithmic paper. It is convenient in flood-damage studies to use percent chance of occurrence rather than the recurrence interval T_r in years. The percent chance of occurrence $P = 100/T_r$.

More reliable flood-frequency determinations, as well as estimates of flood frequency from ungaged areas, may be made by combining the results of flood-frequency analyses of all available runoff records in a region, thereby developing a generalized frequency relation supported by all available data. The U.S. Geological Survey, in cooperation with state agencies, has made studies of this kind in a number of states, and the procedure is outlined in Ref. 33. Briefly the method utilizes the fact that, in hydrologically homogeneous regions, floods of selected frequencies bear an essentially constant relation to the mean annual flood. For example, floods having a 25-year recurrence interval may be equivalent to 2.2 times the mean annual flood. The latter flood is determined from the individual frequency curves to be that occurring at a recurrence interval of 2.33 years. A reference or index flood determined in this manner is more dependable than one determined from an arithmetic mean of the known flood events. In a homogeneous region, a satisfactory relation can usually be developed between size of drainage area and the magnitude of the mean annual flood.

26. Storm Runoff from Small Areas. The term "small area" is a qualitative one indicating that, for the area in question, surface detention is high relative to channel storage. Such is the case of flat areas drained artificially such as airfields and agricultural drainage districts, and natural areas of less than a few square miles.

Urban built-up areas drained by storm sewers may also be classed under "small areas." See Sec. 39, Drainage, for methods of estimating storm runoff for such areas.

Current practice with respect to airfield drainage design is based on the *overland-flow hydrograph* method, described in Refs. 32*f* and 46, and on the *rational method*, described below (see also Ref. 47).

In agricultural drainage work, ditch capacities are usually based on empirical factors called "drainage moduli," giving runoff per unit of drainage area. Obviously, such factors must be based on experience in the region and judgment must be exercised, particularly if some of the runoff is from an adjacent natural area that is not drained artificially. In the case of projects involving large canals and pumping stations, and possibly also pondage to reduce pumping requirements (as an example see Ref. 48), it may be necessary to develop flood hydrographs based on extensive analyses of many related factors such as rainfall, consumptive use of crops and other vegetation, soil moisture and storage, and groundwater.

With respect to floods from small natural areas, the effort expended on analysis should be related to (1) the importance of the structure being designed and (2) whether the complete hydrograph is needed as well as the peak discharge.

An excellent summary of current practice for estimating peak discharges for highway culvert design is given in Ref. 13. Reference 49 presents a method based on a statistical study of 96 watersheds from 1 acre to 25 sq miles in size, all located east of the 105th meridian, but excluding the Atlantic and Gulf Coastal Plain and certain other areas where drainage-basin characteristics are difficult to define. The so-called "rational method" described in Sec. 39, Drainage, can be used where empirical formulas based on local experience are lacking; data on coefficients and a critique of this method are in Ref. 50. No matter which method is used, the following statement is pertinent: "The results obtained . . . must be considered as aids to engineering judgment rather than proven figures."[49]

If the complete hydrograph is required, such as for design of spillways and outlets of dams, an analysis based on observed floods or on an application of the unit-hydrograph principle can be made. In the absence of stream-gaging records, the unit hydrograph can be synthesized from a procedure given in Ref. 21*b*.

27. Evaporation. In this article only evaporation from free-water surfaces is discussed. The readily measurable factors affecting the rate of evaporation are[32d] air and water temperature, relative humidity, wind velocity, barometric pressure, and salinity of the water. The last two factors normally have a minor effect on evaporation.

Measurements of evaporation in the United States have most commonly been made with the standard U.S. Weather Bureau Class A pan consisting of an unpainted galvanized iron pan 4 ft in diameter, 10 in. deep, and set on a wood grillage 6 in. above ground to permit circulation of air under the pan.

Formulas for computing evaporation from meteorologic data utilize Dalton's law, according to which the rate of evaporation is a function of the differences in the vapor pressures at the water surface and in the atmosphere. Experimental evidence[51,52] substantiates the following formula for pan evaporation:

$$E = (e_0 - e_a)^{0.88}(0.37 + 0.0041u)$$

where E is the daily evaporation in inches, e_0 is the saturation vapor pressure in inches of mercury at the water temperature, e_a is the actual vapor pressure in inches of mercury of the air 2 m above the ground, and u is the wind velocity in miles per day measured 6 in. above the rim of the pan.

Reservoir evaporation may be estimated from pan measurements by applying coefficients which vary with season of the year and with the climatological characteristics of a region. For example, the coefficients for converting annual pan evaporation to evaporation from shallow lakes and reservoirs varies from a maximum of 0.81 in the northeastern states to a minimum of 0.60 in the southwestern states. Figure 26*a* is a map[53] of the United States showing variations in the coefficient for converting annual pan evaporation to evaporation from shallow lakes and reservoirs. Average annual lake and reservoir evaporation in the United States for the 10-year period 1946–1955 is given in Fig. 26*b* and has been computed from pan evaporation data, which have in turn been reduced by appropriate coefficients.

The term "shallow," when applied above to lakes and reservoirs, is intended to limit the coefficients and evaporation depths to bodies of water with maximum depths of about 180 ft. Deeper bodies of water have different evaporation characteristics because of the longer time lag required for the water temperature to adjust to the seasonal changes in air temperature. Data on the differences in evaporation between deep and shallow reservoirs are meager, but it is probable that the differences in seasonal totals are more significant than differences in annual totals.[54]

The relative importance of evaporation in water-resources planning depends entirely on the climatological characteristics of the region in which a reservoir is located. In humid regions water surface evaporation may be little different from evapotranspiration in the reservoir area, and therefore the creation of a reservoir will not materially change the water yield of the reservoir area. In semiarid regions, where the depth of evaporation may be many times the depth of runoff per unit of area,

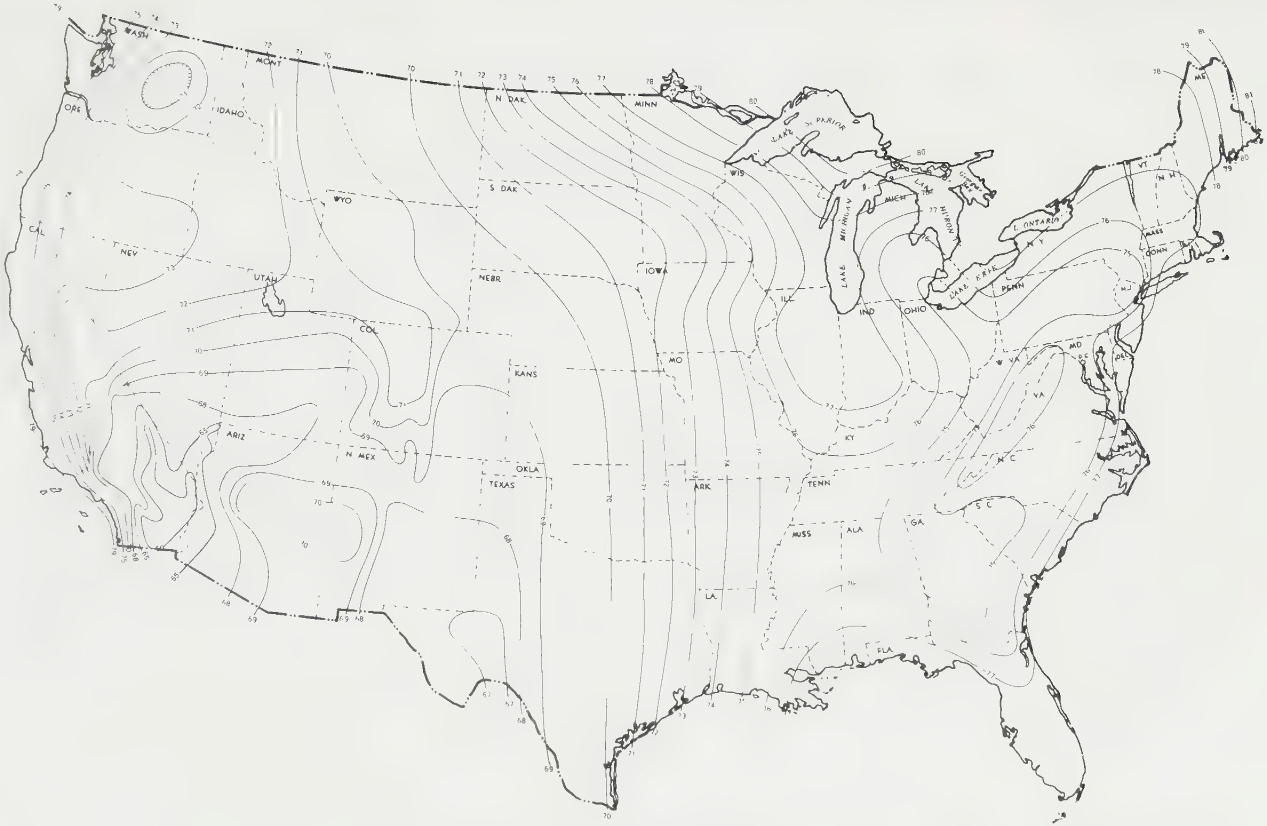

FIG. 26a. Evaporation data for the United States: average annual Class A pan coefficient in percent.[53]

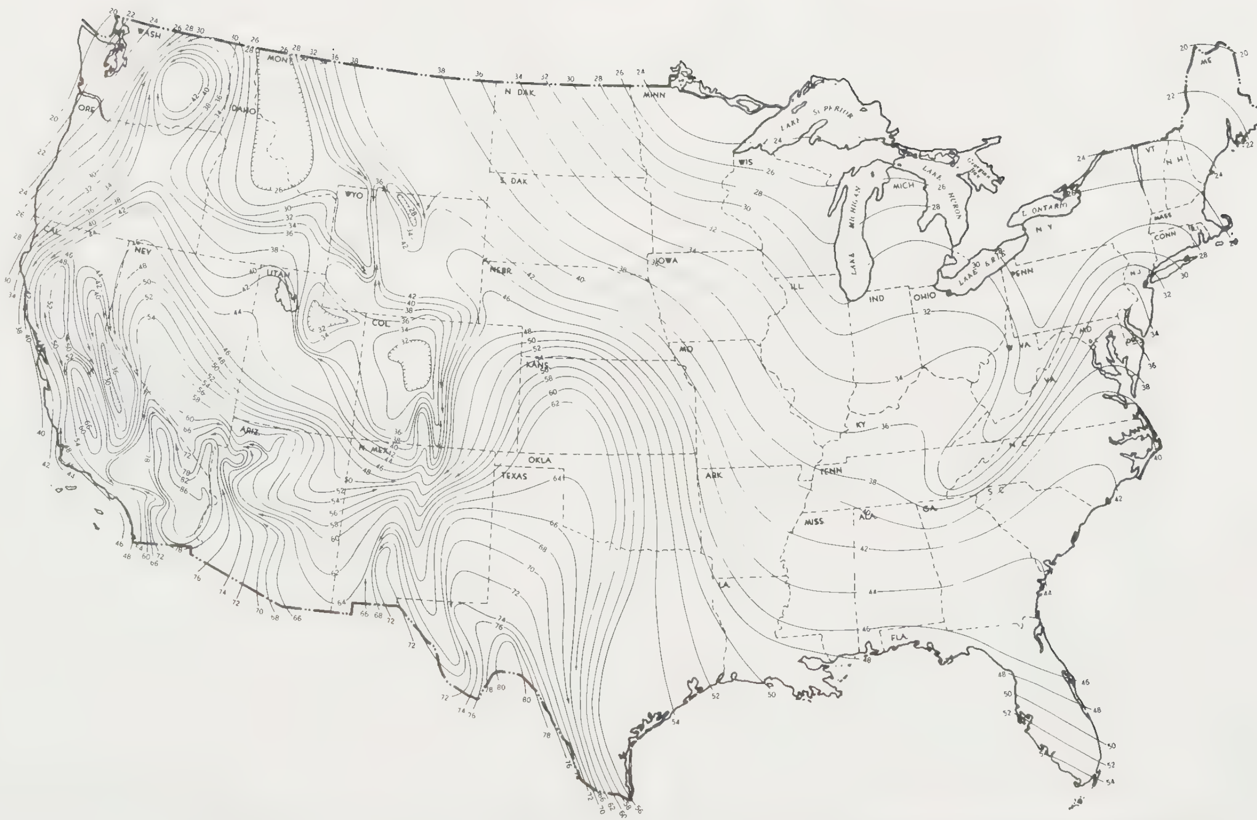

FIG. 26b. Evaporation data for the United States: average annual lake evaporation in inches (period 1946–1955).[53]

conversion of only a small percentage of a drainage basin to water area may seriously deplete the water yield available below the reservoir.

On large projects where evaporation is an important consideration, extensive investigations may be justified including supplemental pan measurements and meteorological measurements at a proposed reservoir site. Such supplemental measurements, even though of short duration, may be compared with similar long-term observations at regular Weather Bureau stations, thus enabling a more reliable estimate of evaporation at the reservoir site.

Bibliography

1. Instructions for Climatological Observers, *U.S. Weather Bur. Circ.* B, 11th ed., 1962.
2. "River Basin Maps Showing Hydrologic Stations," prepared under the supervision of the U.S. Weather Bureau, Washington, D.C., and compiled under the auspices of the Inter-Agency Committee on Water Resources, Sub-committee on Hydrology, 1961.
3. Searcy, J. K., and C. H. Hardison, Double-mass Curves, Manual of Hydrology, Part I, General Surface-water Techniques, *U.S. Geol. Survey Water Supply Paper* 1541-B, 1960.
4. Trewartha, Glenn T., "An Introduction to Climate," 3d ed., p. 225, McGraw-Hill Book Company, New York, 1954.
5. Boardman, H. P., Snow Survey versus Winter Precipitation for Forecasting Runoff of the Tuolumne River, California, *Trans. Am. Geophys. Union*, **28** (5,752–5,765), October, 1947.
6. Snow Surveying, *U.S. Dept. Agr. Misc. Publ.* 380, Washington, D.C., 1940.
7. Light, Phillip, Analysis of High Rates of Snow Melting, *Trans. Am. Geophys. Union*, Part I, pp. 195–205, 1941.
8. Wilson, W. T., An Outline of the Thermodynamics of Snowmelt, *Trans. Am. Geophys. Union*, Part I, pp. 182–195, 1941.
9. Maximum Possible Precipitation over the Ohio River Basin above Pittsburgh, Pa., *U.S. Weather Bur. Rept.* 2, Hydrometeorological Section, in cooperation with Corps of Engineers, U.S. Army.
10. Thornthwaite, C. W., Climate and Moisture Conservation, *Ann. Assoc. Am. Geograph.*, **37** (2), 87–100, June, 1947.
11. Petterson, Sverre, "Introduction to Meteorology," McGraw-Hill Book Company, New York, 1941. (*a*) p. 159, (*b*) p. 153.
12. Tannehill, Ivan Ray, "Hurricanes—Their Nature and History," 7th ed., Princeton University Press, Princeton, N.J., 1950.
13. Chow, Ven Te, Hydrologic Determination of Waterway Areas for the Design of Drainage Structures in Small Drainage Basins, *Univ. Illinois Eng. Expt. Sta. Bull.* 442, Urbana, Ill., 1962. (*a*) pp. 78–82, (*b*) Chap. 2.
14. Yarnell, David L., Rainfall Intensity-Frequency Data, *U.S. Dept. Agr. Misc. Publ.* 204, Washington, D.C., 1935.
15. Hershfield, David M., Rainfall Frequency Atlas of the United States, *U.S. Weather Bur. Tech. Paper* 40, Washington, D.C., 1961.
16. Thunderstorm Rainfall, *U.S. Weather Bur. Rept.* 5, Hydrometeorological Section, 1947.
17. "Storm Rainfall in the United States, Depth-Area-Duration Data," Corps of Engineers, U.S. Army.
18. Bernard, Merrill, Primary Role of Meteorology in Flood Flow Estimating, *Trans. ASCE*, **109,** 311–382, 1944.
19. Seasonal Variation of the Probable Maximum Precipitation East of the 105th Meridian for Areas from 10 to 1000 Square Miles and Duration of 6, 12, 24 and 48 Hours, *U.S. Weather Bur. Hydrometeorological Rept.* 33, Washington, D.C., 1956.
20. Generalized Estimates of Probable Maximum Precipitation for the United States West of the 105th Meridian for Areas to 400 Square Miles and Durations to 24 Hours, *U.S. Weather Bur. Tech. Paper* 38, Washington, D.C., 1960.
21. "Design of Small Dams," *U.S. Bureau of Reclamation*, 1960. (*a*) pp. 28, 32, (*b*) pp. 41–48.
22. Linsley, Ray K., Jr., Frequency and Seasonal Distribution of Precipitation over Large Areas, *Trans. Am. Geophys. Union*, **28** (3), 445, June, 1947.
23. Williams, G. R., Natural Water Loss in Selected Drainage Basins, *U.S. Geol. Survey Water Supply Paper* 846, Washington, D.C., 1940.
24. Thornthwaite, C. W., and J. R. Mather, "Instructions and Tables for Computing Potential Evapotranspiration and the Water Balance," Drexel Institute of Technology, Laboratory of Climatology, Centerton, N.J., 1957.
25. Blaney, Harry F., and Wayne D. Criddle, Determining Consumptive Use and Irrigation Water Requirements, *U.S. Dept. Agr. Tech. Bull.* 1275, December, 1962.
26. Terzaghi, Karl, Soil Moisture in "Hydrology," Vol. 9, p. 361, of "Physics of the Earth," Dover Publications, Inc., New York, 1942.
27. Hurricane Floods of September 1938, *U.S. Geol. Survey Water Supply Paper* 867, p. 469, Washington, D.C., 1940.
28. Horton, Robert E., "Surface Runoff Phenomena," Part I, Analysis of the Hydrograph, pp. 42–43, Edwards Brothers, Inc., Ann Arbor, Mich., 1935.
29. Barnes, Bertram S., The Structure of Discharge-Recession Curves, *Trans. Am. Geophys. Union*, **20,** 721–725, 1939.

30. Langbein, Walter B., Annual Runoff in the United States, *U.S. Geol. Survey Circ.* 52, Washington, D.C., June, 1949.
31. Williams, G. R., Hydrology, Chap. 4, in "Engineering Hydraulics" edited by Hunter Rouse, John Wiley & Sons, Inc., New York, 1950. (*a*) pp. 286–288, (*b*) pp. 259–261.
32. "Hydrology Handbook," ASCE Manual of Engineering Practice 28, American Society of Civil Engineers. (*a*) p. 67, (*b*) p. 90, (*c*) Chap. 2, (*d*) Chap. 4, (*e*) p. 126, (*f*) p. 92.
33. Dalrymple, Tate, Flood Frequency Analyses, *U.S. Geol. Survey Water Supply Paper* 1543-A, pp. 25–47, 1960.
34. Langbein, W. B., Topographic Characteristics of Drainage Basins, *U.S. Geol. Survey Water Supply Paper* 968-C, 1947.
35. Horton, R. E., Drainage Basin Characteristics, *Trans. Am. Geophys. Union*, **13,** 350–361, 1932.
36. Sherman, L. K., Stream Flow from Rainfall by the Unit Graph Method, *Eng. News-Record*, **108,** 501-505, 1932.
37. Gilcrest, B. R., Flood Routing, Chap. 10 in "Engineering Hydraulics," pp. 635–710, edited by Hunter Rouse, John Wiley & Sons, Inc., New York, 1950.
38. "Hydrologic and Hydraulic Analyses, Flood Hydrograph Analyses," Engineering Manual, Civil Works Construction, Part 114, Chap. 5, Department of the Army, Corps of Engineers, March, 1948. (*a*) Plate 6, (*b*) Plates 10 and 11, (*c*) Plate 16, (*d*) Plate 7, (*e*) Plate 5, (*f*) p. 16.
39. Snyder, F. F., Synthetic Unit Graphs, *Trans. Am. Geophys. Union*, **19** (Part 1), 447–454, 1938.
40. Mitchel, W. D., "Unit Hydrographs in Illinois," Division of Waterways, Illinois Department of Public Works and Buildings, 1948.
41. Izzard, C. F., Discussion of Drainage of Airport Surfaces—Some Basic Design Considerations, *Trans. ASCE*, **113,** 831, 1948.
42. Jarvis, C. S., and Others, Floods in the United States, Magnitude and Frequency, *U.S. Geol. Survey Water Supply Paper* 771, 1936.
43. Linsley, Ray K., Jr., Max A. Kohler, and Joseph L. H. Paulhus, "Applied Hydrology," p. 546, McGraw-Hill Book Company, New York, 1949.
44. Linsley, Ray K., A Simple Procedure for the Day-to-day Forecasting of Runoff from Snowmelt, *Trans. Am. Geophys. Union*, **24** (Part III), 62–67, 1943.
45. Creager, W. P., J. D. Justin, and J. Hinds, "Engineering for Dams," Vol. I, John Wiley & Sons, Inc., New York, 1945. (*a*) p. 164, (*b*) p. 148.
46. "Surface Drainage Facilities for Airfields," Engineering Manual for Military Construction, Part 13, Chap. 1, Department of the Army, Corps of Engineers, June, 1955.
47. "Airport Drainage," Federal Aviation Agency, 1960.
48. Kirpich, P. Z., and C. S. Ospina, Flood Control Aspects of Cauca Valley Development, *J. Hydraulics Div. ASCE*, September, 1959, pp. 28–33.
49. "Peak Rates of Runoff from Small Watersheds," U.S. Bureau of Public Roads, Washington, D.C., 1961.
50. Kirpich, P. Z., Rational Theory of Surface Runoff for Drainage Design, in "Engineering Hydraulics," pp. 309–318, edited by Hunter Rouse, John Wiley & Sons, Inc., New York, 1950.
51. Water-loss Investigations: Lake Hefner Studies, *Tech. Rept. Geol. Survey Prof. Paper* 269, pp. 127–148, 1954.
52. Kohler, M. A., T. J. Nordenson, and W. E. Fox, Evaporation for Pans and Lakes, *U.S. Weather Bureau Research Paper* 38, May, 1955.
53. Kohler, M. A., T. J. Nordenson, and W. E. Fox, Evaporation Maps for the United States, *U.S. Weather Bur. Tech. Paper* 37, 1959.
54. Horton, Robert E., in collaboration with C. E. Grunsky, Hydrology of the Great Lakes, *Rept. Engr. Bd. of Review, Sanitary District of Chicago*, Part III, Appendix II, 1927.

SECTION 2

BASIC HYDRAULICS

By W. J. Bauer, David S. Louie, and W. L. Voorduin[1]

PART I. CLOSED CONDUITS

FLUID PROPERTIES

1. General. Applied hydraulics is concerned with the physical action and the interaction of particular masses of fluid in either the static or kinetic states. These actions and interactions are analyzed by attributing to the fluid certain physical properties each of which is defined to be the controlling property for a particular type of action. Viscosity plays an important role in the problem of hydraulic friction. Mass density is important in nonuniform flow. Unit weight is of great concern in stratified flow. Surface tension is a factor in model experiments. Compressibility is a factor in water hammer. Vapor pressure is a factor in high-velocity flow.

2. Conservation of Mass. The fundamental law of continuity is frequently expressed as

$$Q = AV \tag{1}$$

in which Q = discharge in volume per second
A = cross-sectional area of the flow
V = average velocity normal to the flow section

In a more general sense, the temporal mean velocity may be constant at a point, but it usually varies from point to point in a section so that

$$Q = \int_0^{A_0} v\, dA \tag{2}$$

in which v = temporal mean velocity
dA = an element of area for which v is the velocity
A_0 = total area of the flow cross section

Because the mean of the values of v is equal to the average velocity, Eq. (1) is exact for all distributions of velocity. Written between two sections 1 and 2 through which the same steady discharge is passing, Eq. (1) also provides the familiar

$$A_1V_1 = A_2V_2 \tag{3}$$

3. Conservation of Momentum and Energy. Equations similar to Eq. (2) are written to define the flux of momentum and energy past a flow cross section as follows:

Momentum flux

$$\rho \int_0^{A_0} v^2\, dA = \beta\rho V^2 A_0 \tag{4}$$

[1] Material in addition to formulas and charts, prepared by W. L. Voorduin, which appear in the first, second, and third editions, was contributed by W. J. Bauer and David S. Louie.

Energy flux

$$\frac{\rho}{2}\int_0^{A_0} v^3\,dA = \frac{\alpha\rho V^3 A_0}{2} = \alpha Q\,\frac{V^2}{2}\,\rho \tag{5}$$

in which ρ = mass density
α = kinetic-energy factor
β = momentum factor

If v is constant across the section both α and β are unity. If v is variable across the section, both α and β are greater than 1.

4. Bernoulli Equation. One of the equations used in the analysis of one-dimensional, steady, incompressible flow is the Bernoulli equation, a special form of the law of conservation of energy. For a constant discharge in a closed conduit the theorem

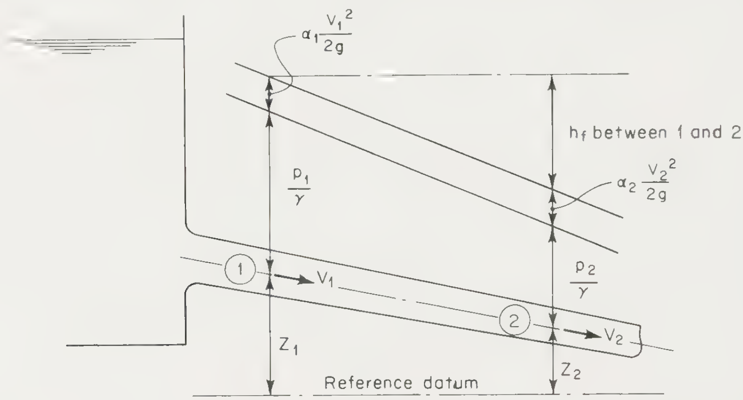

$$\frac{p_1}{\gamma} + Z_1 + \alpha_1\frac{V_1^2}{2g} = \frac{p_2}{\gamma} + Z_2 + \alpha_2\frac{V_2^2}{2g} + h_f\ \text{(between 1 and 2)}$$

where p = average pressure
Z = distance above reference datum
V = velocity
α = kinetic - energy factor
γ = specific weight

FIG. 1. Bernoulli equation.

states that the energy head at any cross section must equal that in any other downstream section plus the intervening losses. Figure 1 shows these relationships for a typical closed conduit.

It is a common practice to determine the velocity head at a section by means of the average velocity of the flow. In the usual case, the velocity distribution is nonuniform and the energy head so computed is somewhat less than the true value. A kinetic-energy factor, as defined in Eq. (4), should be applied to the velocity head of the mean velocity in order to obtain the correct energy head. That is,

$$h_v = \alpha\,\frac{V^2}{2g} \tag{6}$$

If the velocity distribution is known, the distribution coefficient may be determined as follows:

$$\alpha = \frac{\int_0^A v^3\,dA}{V^2\int_0^A v\,dA} = \frac{\sum^A v^3\,\Delta A}{A V^3} \tag{7}$$

where v is mean velocity through the elementary area and V is the mean velocity for the cross section.

For turbulent flow at medium and high Reynolds number in straight conduits of established regimen, α commonly varies from 1.02 to 1.10; in viscous flow and at bends and similar nonuniformities, it may be 2.0 or greater. Because it usually has a small effect and is tedious to evaluate, the effect of α is usually neglected in practical engineering. The Bernoulli equation then becomes

$$\frac{p_1}{\gamma} + Z_1 + \frac{V_1^2}{2g} = \frac{p_2}{\gamma} + Z_2 + \frac{V_2^2}{2g} + h_f \tag{8}$$

Although α is neglected in design, its use may be required when analyzing the results of field investigation of prototype structures in order to provide a logical explanation of certain hydraulic behavior.

FRICTION LOSSES

5. General. Application of the Bernoulli equation requires a clear understanding of the factors which affect the head loss H_L. The head losses are commonly classified as boundary losses and form losses. Boundary losses are those arising from shear forces between the fluid and the boundary materials. In addition, cross-sectional shapes are significant to boundary losses because they affect the ratio of the flow area to the wetted perimeter. The effects associated with the cross-sectional shape of a uniform conduit are not classified as form losses. Form losses arise from recirculating eddies produced by the geometry of the containing vessels such as bends and either expanding or contracting transitions.

Two types of flow must be considered: laminar flow in which the fluid may be envisioned as flowing in parallel layers and turbulent flow in which the particles are moving in all directions causing a complete mixing of the fluid. The concept of laminar flow as moving in parallel layers is actually an artificial one which is useful as an aid to theoretical analyses—for engineering practice, conditions of turbulent flow are encountered more frequently than those of laminar flow. As will be shown elsewhere in this section, different laws govern the two types of flow. The principles and equations of fluid resistance, as developed by Chezy, Manning, Kutter, Darcy-Weisbach, Scobey, and Hazen and Williams, apply to turbulent-flow conditions.

6. The Chezy Formula. Friction losses h_f are usually determined by formulas which have a long background in use. Of fundamental importance is the Chezy formula

$$V = C\sqrt{RS} \tag{9}$$

where V = mean velocity, fps
R = hydraulic radius, ft
S = slope of hydraulic gradient
C = a coefficient

7. The Manning Formula. The Manning expression

$$C = \frac{1.486}{n} R^{1/6} \tag{10}$$

where n = a coefficient of frictional resistance which, under many conditions, is common to both the Kutter and Manning formulas.

As will be shown elsewhere in this section, n is a function of roughness, viscosity, diameter, and velocity. Figure 2 shows a chart for the solution of the Manning formula using average values of n. Figure 2 may be applied to both open and closed conduits.

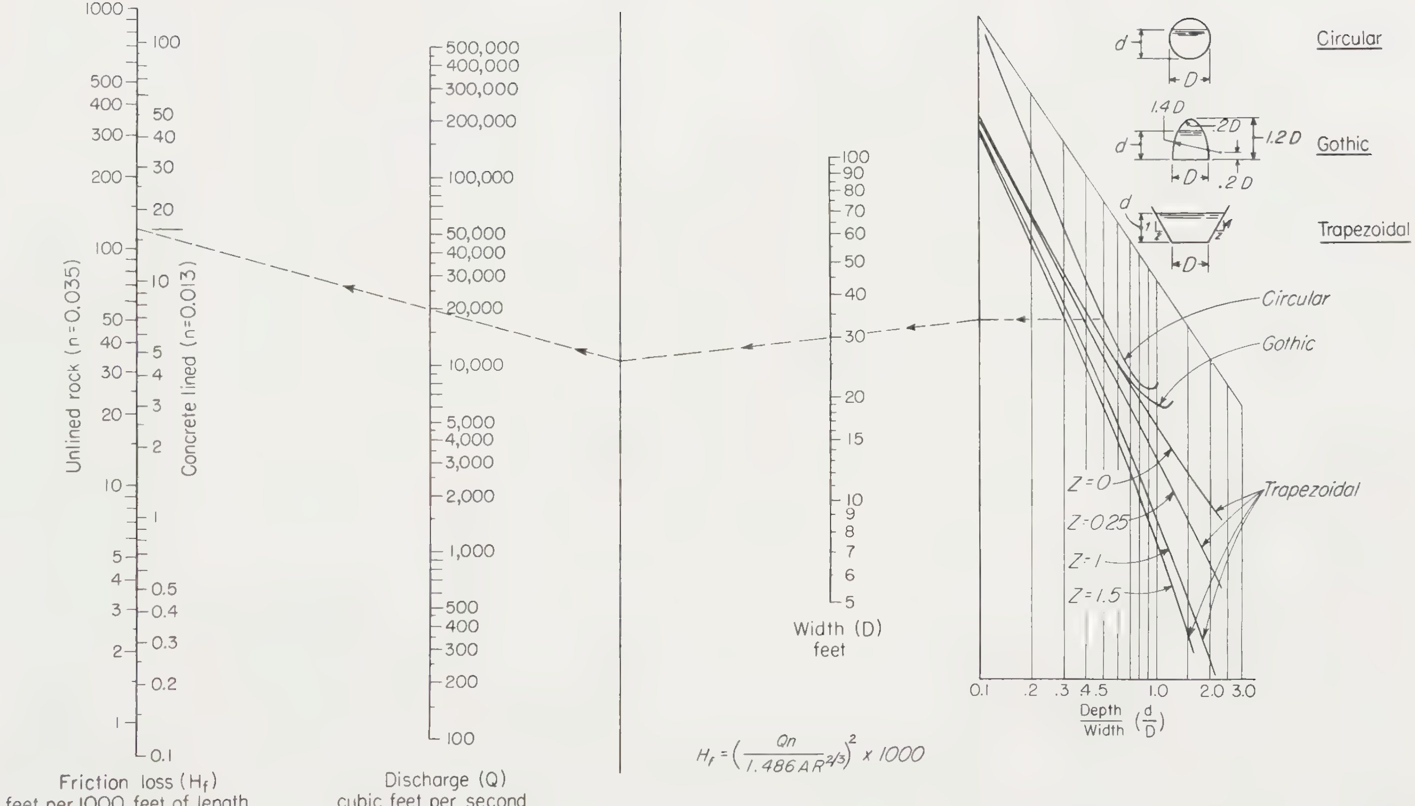

FIG. 2. Friction loss, tunnels and channels.

In computing the flow in pipes, the formulas which result from combining the Manning and Chezy formulas may take several forms:

$$V = \frac{0.590}{n} d^{2/3} S^{1/2} \tag{11}$$

$$Q = \frac{0.463}{n} d^{8/3} S^{1/2} \tag{12}$$

$$h = 2.87 n^2 \frac{l V^2}{d^{4/3}} \tag{13}$$

$$h = 4.66 n^2 \frac{l Q^2}{d^{16/3}} \tag{14}$$

$$d = \left(\frac{2.159\ Qn}{S^{1/2}} \right)^{3/8} \tag{15}$$

Figure 3 shows a chart which may be used in applying Manning's formula to the computation of flow in pipes flowing full. Table 1 gives average values of n in Manning and Ganguillet and Kutter formulas in common use for various materials.

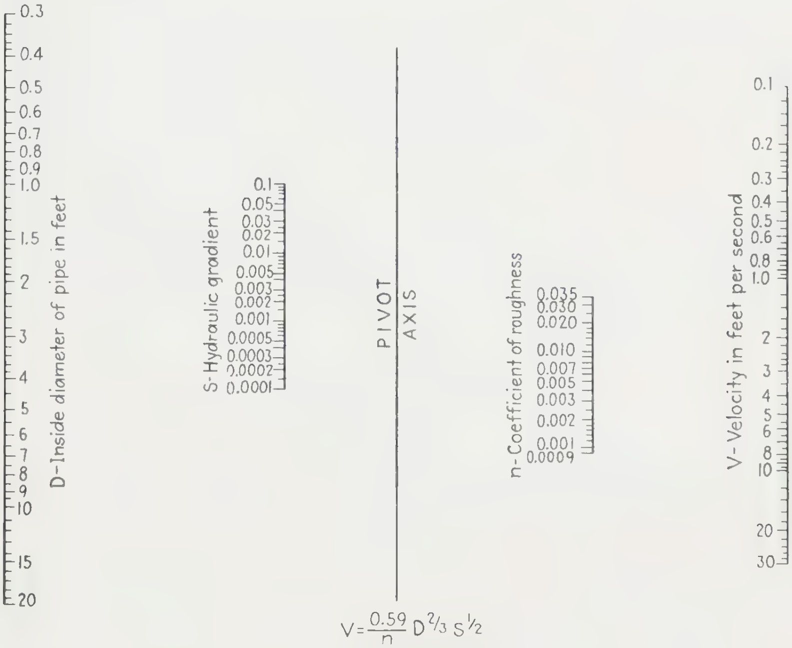

Fig. 3. Manning's formula for pipes flowing full.

These values may be used for preliminary investigations. It should be kept in mind, however, that n is not a constant but a variable, as will be shown elsewhere in this section.

8. The Kutter Formula. The historic Kutter formula is still widely used to determine the value of C in the Chezy formula. Ganguillet and Kutter determined

TABLE 1. VALUES* OF COEFFICIENT OF ROUGHNESS n IN MANNING AND GANGUILLET AND KUTTER FORMULAS

Type of pipe	Condition	n			
		Best	Good	Fair	Bad
Cast iron	Clean, uncoated	0.012	0.013	0.014	0.015
	Clean, coated	0.011	0.012	0.013	
	Dirty or tuberculated	.....	.....	0.015	0.035
Wrought iron	Commercial, black	0.012	0.013	0.014	0.015
	Commercial, galvanized	0.013	0.014	0.015	0.017
Lock bar or welded	Smooth and clean	0.010	0.011	0.013	
Brass or glass	Smooth	0.009	0.010	0.011	0.013
Riveted steel or spiral steel	Clean	0.013	0.015	0.017	
Vitrified sewer pipe	....	0.011	0.013	0.015	0.017
Common clay drainage tile	....	0.011	0.012	0.014	0.017
Concrete	Rough joints	.....	0.016	0.017	
	Dry mix, rough forms	.....	0.015	0.016	
	Wet mix, steel forms	.....	0.012	0.014	
	Very smooth	.....	0.011	0.012	
Wood stave	....	0.010	0.011	0.012	0.013

* Values are based on tables by Horton and values recommended by King. See H. W. KING and E. F. BRATER, "Handbook of Hydraulics," 5th ed., McGraw-Hill Book Company, New York, 1963.
Values given under good or fair may be used for designing.

empirically in 1869 that

$$C = \frac{41.6 + 0.00281/S + 1.811/n}{1 + \dfrac{(41.6 + 0.00281/S)n}{\sqrt{R}}} \tag{16}$$

9. The Darcy-Weisbach Formula. Still in use at the present time (1967) is the hundred-year-old Darcy-Weisbach formula

$$h_f = f \frac{l}{d} \frac{V^2}{2g} \tag{17}$$

where h_f = friction loss, ft
l = length of pipe, ft
d = inside diameter, ft
f = coefficient of frictional resistance

Like n in the Kutter and Manning formulas, f is a function of roughness, viscosity, diameter, and velocity.

10. The Scobey Formulas. Scobey's formulas have had an extensive use in the design of irrigation and hydroelectric works. As a result of field measurements Scobey arrived at the relationships shown by Table 2. Values of C_s and K_s are given in Tables 3 and 4. Figures 4, 5, and 6, respectively, show diagrams for the solution of the wood-stave, concrete, and steel pipe formulas.

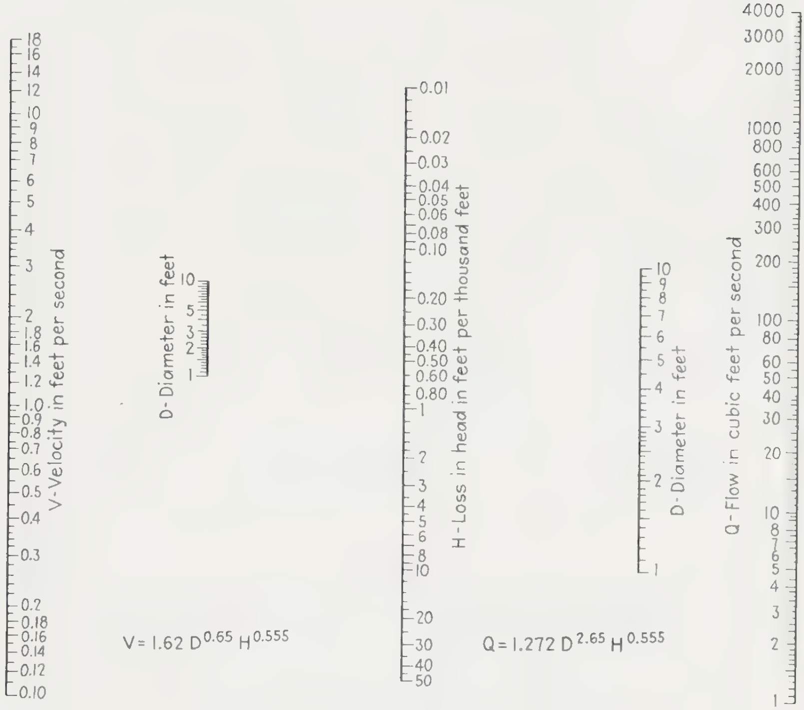

FIG. 4. Solution of Scobey's formula for wood-stave pipe.

TABLE 2. SUMMARY OF SCOBEY FORMULAS

Function	Wood-stave pipe	Concrete pipe	Steel pipe
$V =$	$1.62D^{0.65}h_f^{0.555}$	$4.73D^{0.625}h_f^{0.50}$	$\dfrac{D^{0.58}h_f^{0.526}}{K_s^{0.526}}$
$Q =$	$1.272D^{2.65}h_f^{0.555}$	$3.72C_sD^{2.65}h_f^{0.50}$	$\dfrac{0.785D^{2.58}h_f^{0.526}}{K_s^{0.526}}$

in which D = inside diameter, ft
h_f = friction loss, ft/1,000 ft
C_s = a coefficient
K_s = a coefficient

11. The Hazen and Williams Formula. The Hazen and Williams formula for the flow in pipes has been used extensively in the design of water-distribution systems. This formula is usually expressed as

$$V = 1.318CR^{0.63}S^{0.54} \tag{18}$$

in which C = a coefficient
R = hydraulic radius
S = slope of hydraulic gradient

TABLE 3. VALUES OF C_s IN SCOBEY'S FORMULA FOR CONCRETE PIPES

Class	Condition	C_s
1	Old California cement pipes; generous supply of mortar in joints, mortar squeeze not removed Also: class 2 pipes conveying sewage	0.267
2	Dry-mix precast in short units, washed inside with cement mortar, moderate care; monolithic pipe over rough wood forms; cement-gun finish, not troweled	0.310
3	Wet-mix precast in short units; dry-mix precast in long units; monolithic pipe on steel forms; small cement-lined iron pipe; concrete pipe made under pressure and mechanically troweled with neat cement. Also: class 4 pipes conveying sewage or detritus-laden water	0.345
4	Glazed-interior pipes; large cement-lined iron pipes; monolithic pipes with joint scars or surface irregularities removed; highest quality precast pipe, made against oiled steel form, with joints as smooth as remainder, untouched with brush or "wash" process	0.370

TABLE 4. VALUES OF K_s IN SCOBEY'S FORMULAS FOR STEEL PIPES

Class	Condition	Type	K_s
1	Full-riveted pipe, having both longitudinal and girth seams held by one or more lines of rivets with projecting heads from capacity standpoint; pipe with countersunk rivetheads on interior belongs in class 3	*a.* New sheet metal up to $\frac{3}{16}''$ thick	0.38
		b. New plate metal $\frac{3}{16}''$ to $\frac{7}{16}''$ thick, with either taper or cylinder joints	0.44
		c. New plate metal $\frac{1}{2}''$ up, with either taper or cylinder joints, and for plate $\frac{1}{4}''$ to $\frac{7}{16}''$ thick, when butt-jointed	0.48
		d. New butt-strap pipe of plate, $\frac{1}{2}''$ up	0.52
2	Girth-riveted pipe, having no retarding rivetheads in the continuous-seamed longitudinal joints, but having the same girth seams as full-riveted pipe	New sheet- and plate-metal pipe, such as lock-bar and hammer-weld pipe with lap or flange-riveted field (girth) joints; electric weld, hammer-weld and drawn pipe with riveted bump joints; and all other types with surface continuous except for girth belt of rivetheads between field units	0.34
3	Continuous interior pipe, having interior surface unmarred by plate offsets or by projecting rivetheads in either longitudinal or girth seams. Not necessarily described as smooth	New sheet- and plate-metal pipe such as pipe with full-welded crimped slip joint, lock bar with welded flange or leaded sleeve connections, bell and spigot, bolted coupling pipes all belong to this class	0.32

Figure 7 shows a nomographic chart for the solution of this equation, and Table 5 gives values of C for pipes of various ages and materials.

EVALUATION OF FRICTION COEFFICIENTS

12. General. It has been pointed out previously that the friction factors f, in the Darcy-Weisbach formula, and n in the Manning and Kutter formulas, both vary with roughness, viscosity, diameter, and velocity. The evaluation of friction factors under the widely varying conditions usually encountered in practice has been made

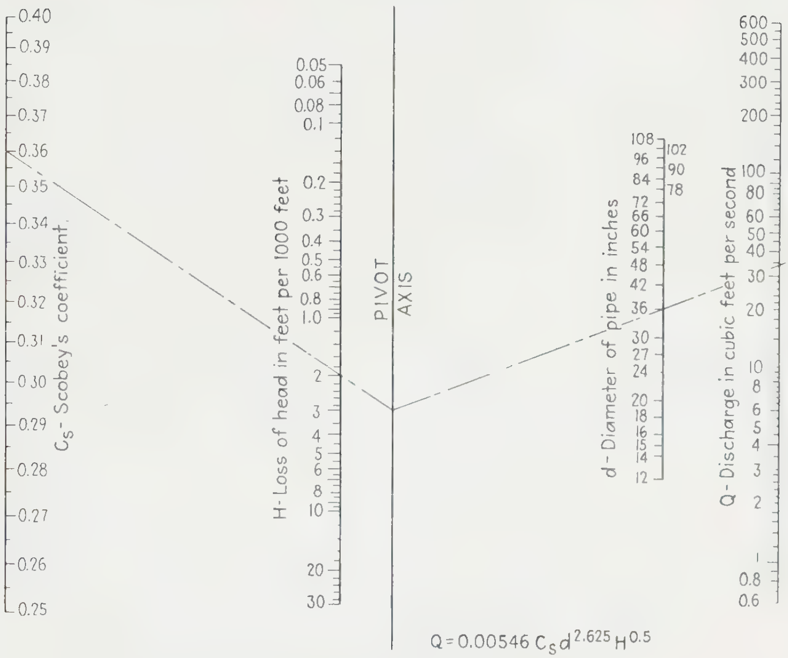

Fig. 5. Scobey's formula for concrete pipe.

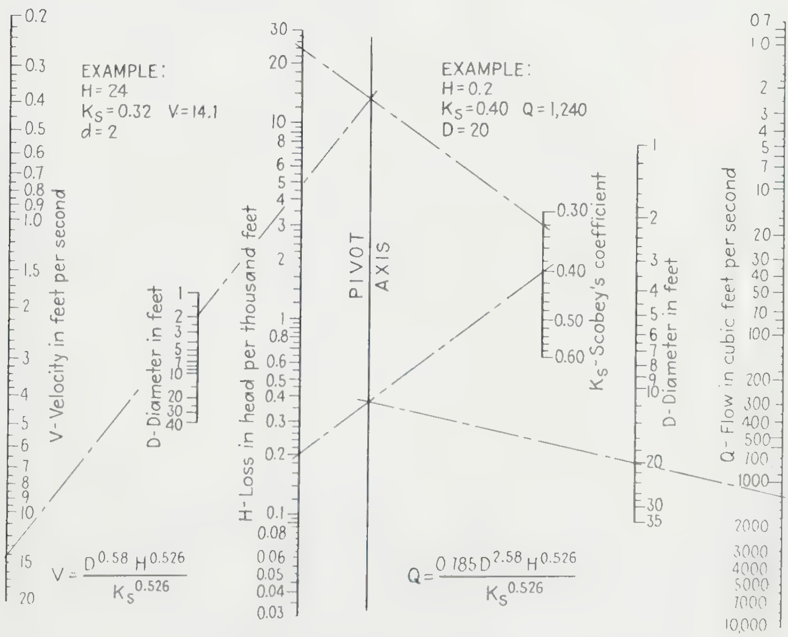

Fig. 6. Solution of Scobey's formulas for steel pipe.

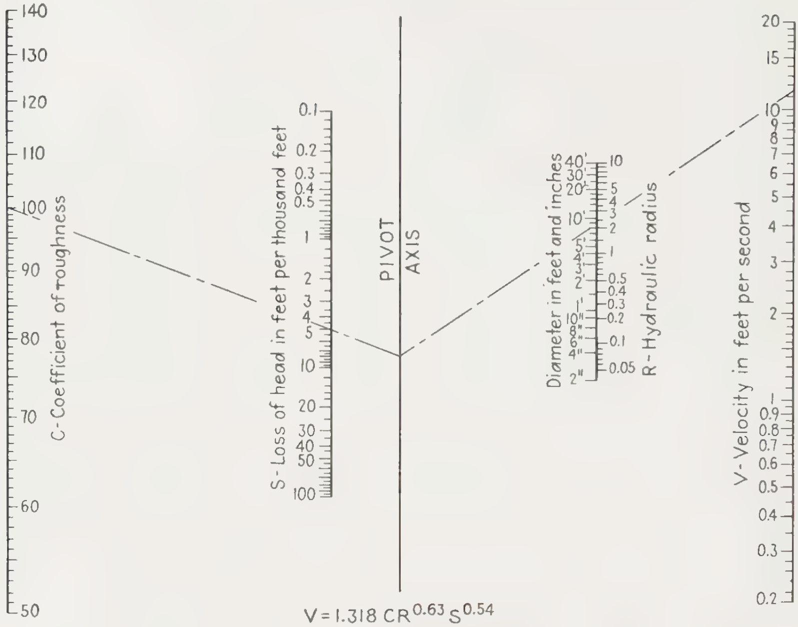

FIG. 7. Solution of the Hazen and Williams formula.

TABLE 5. VALUES OF *C* IN HAZEN AND WILLIAMS FORMULA

Type of pipe	Condition		"C"
Cast iron	New	All sizes	130
	5 years old	12″ and over	120
		8″	119
		4″	118
	10 years old	24″ and over	113
		12″	111
		4″	107
	20 years old	24″ and over	100
		12″	96
		4″	89
	30 years old	30″ and over	90
		16″	87
		4″	75
	40 years old	30″ and over	83
		16″	80
		4″	64
		40″ and over	77
		24″	74
		4″	55
Welded steel	Values of *C* the same as for cast-iron pipe, 5 years older		
Riveted steel	Values of *C* the same as for cast-iron pipe, 10 years older		
Wood-stave	Average value, regardless of age		120
Concrete or concrete-lined	Large sizes, good workmanship, steel forms		140
	Large sizes, good workmanship, wooden forms		120
	Centrifugally spun		135
Vitrified	In good condition		110

possible by the contributions of Reynolds, Nikuradse, Von Karman, Prandtl, and Colebrook-White.

13. The Contribution of Reynolds. The Reynolds criterion, developed by Sir Osborne Reynolds late in the nineteenth century, relates the inertial forces per unit of volume to the viscous forces per unit of volume. This relationship provides a rational basis for establishing the dynamic similarity of fluid motion in closed conduits.

As an approach to his analysis, Reynolds considered the Newtonian concept that the tangential stress between contiguous strata of the fluid should be proportional to the rate dv/dy at which the velocity varies across the section of flow. This proportionality has been adopted as a measure of the fluid viscosity. The relationship may be expressed as

$$\tau = \mu \frac{dv}{dy} \tag{19}$$

in which τ = intensity of shear
μ = dynamic viscosity

In accordance with the Newtonian equation for shear a typical viscous force per unit of volume may be written as

$$\mu \frac{V}{L^2} \tag{20}$$

in which L is a length parameter sometimes expressed as D, the diameter of the conduit.

A typical inertial reaction per unit of volume may be designated by

$$\rho \frac{V^2}{L} \tag{21}$$

in which ρ is the mass density. The ratio of the inertial force per unit of volume to the viscous force per unit of volume reduces to the form

$$\rho \frac{VL}{\mu} \tag{22}$$

The factor μ/ρ, known as the kinematic viscosity ν, may be compared with the gravitational factor $\gamma/\rho = g$. The introduction of the kinematic viscosity factor ν into the expression $\rho(VL/\mu)$ yields

$$\mathbf{R} = \frac{VL}{\nu} \tag{23}$$

which is known as the Reynolds number. The kinematic viscosity of water relative to temperature is shown by Fig. 8. The basic relationship between boundary shear stress τ_0 and friction factor f is

$$v_* = \sqrt{\frac{\tau_0}{\rho}} = V\sqrt{\frac{f}{8}} \tag{24}$$

where v_* = shear velocity or friction velocity
ρ = density of the fluid (for water, ρ = 1.935 slugs/cu ft)

Using the Newtonian definition of laminar flow, Eq. (19) may also be expressed as

$$\tau = -\mu \frac{dv}{dr} \tag{25}$$

For a circular pipe the shearing stress at the boundary developed by equating shear and pressure forces acting on a cylindrical body of fluid at radius r and

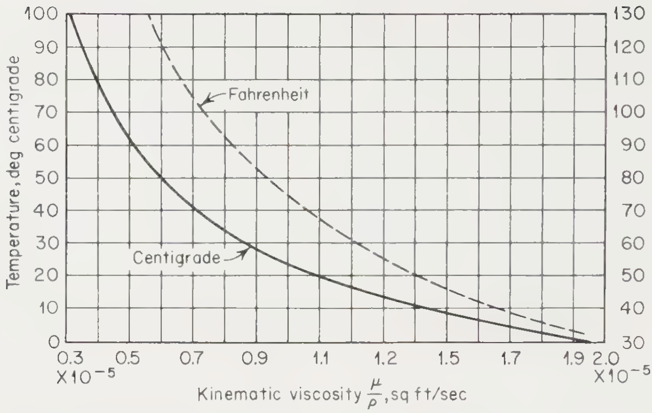

FIG. 8. Kinematic viscosity of water relative to temperature. (*J. N. Bradley and L. R. Thompson, "Friction Factors for Large Conduits Flowing Full," U.S. Dept. of Interior, Bureau of Reclamation.*)

length L would be

$$\tau_0 = \frac{\gamma h_f r}{2L} \tag{26}$$

The equation for velocity distribution in laminar flow is

$$v = 2V\left[1 - \left(\frac{r}{R}\right)^2\right] \tag{27}$$

where R is the radius of the pipe. Using Eqs. (25), (26), and (27), it follows that

$$h_f = \frac{32\mu l V}{\gamma d^2} \tag{28}$$

From this it can be developed that the Darcy-Weisbach coefficient of friction in the laminar regime is

$$f = \frac{64}{\mathbf{R}} \tag{29}$$

Equation (29) is valid for values of **R** up to about 2,000. The work of Blasius and Nikuradse verified Eq. (29) and showed that head loss in this flow regime is independent of boundary-surface roughness.

14. The Contribution of Nikuradse. During 1932 and 1933, Nikuradse, working under the direction of Drs. Prandtl and Von Karman, published the results of his now famous experiments on artificially roughened pipe. Small, smooth pipes of different diameters were coated with sand grains of uniform size and subjected to a wide range of velocities. The resistance to flow represented by the Darcy-Weisbach friction factor f was plotted with respect to the Reynolds number for various values of the relative roughness r_0/k where r_0 represents the radius of the pipe and k the average diameter of sand grains. The Nikuradse k is not the absolute roughness or rugosity ϵ, as the term is defined by more recent writers. The results of these experiments are shown by Fig. 9. The Nikuradse criterion offers a means of grouping pipes having similar roughness characteristics for partially and fully developed turbulent flow. The straight line A in Fig. 9 represents laminar flow where $f = 64/\mathbf{R}$ for values of **R**.

Line C represents the results obtained for turbulent flow in smooth brass pipe. The lines denoted as D are for turbulent flow in pipes coated with uniform sand grains. The size of the pipe and diameter of the sand-grain coating were varied in the experiments. The results were then plotted in terms of the relative roughness r_0/k.

15. The Colebrook and White Contribution. Referring to Fig. 9, the lines marked B represent a transition zone between laminar and turbulent flow in smooth brass pipe. The lines marked D are for turbulent flow. The curves of Nikuradse consistently show a sharp drop followed by a reverse curve in the transition zone. The analyses of Von Karman and Prandtl, based on the Nikuradse experiments, showed some disagreement in the transition zone. This disagreement was not explained satisfactorily until 1939, when Colebrook and White developed a practical form of transition to bridge the gap.

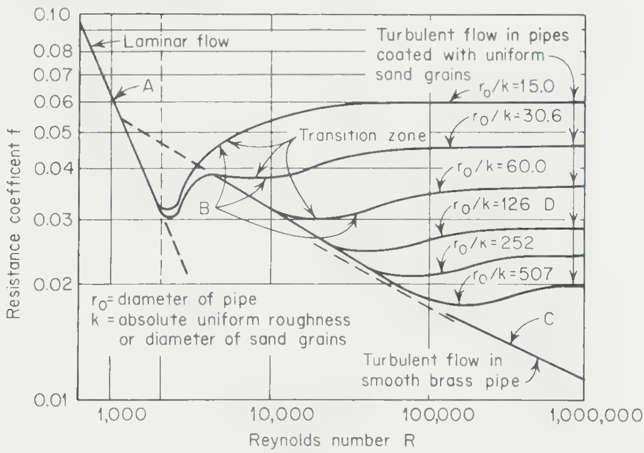

FIG. 9. Variation of the resistance coefficient with the Reynolds number for artificially roughened pipes. (*Bradley and Thompson, "Friction Factors for Large Conduits Flowing Full," Engineering Monograph, No. 7, U.S. Dept. of Interior, Bureau of Reclamation, March,* 1951.)

Colebrook and White demonstrated that the deviation of the Von Karman–Prandtl analyses from those of Nikuradse stemmed from the fact that resistance to flow for uniform sand is different for equivalent, nonuniform roughness, such as that which exists in commercial pipes. The coarser grains disturbed the laminar sublayer before the smaller irregularities became effective. The resulting formula, as proposed by Colebrook and White, follows the trend of experimental results and is asymptotic to both the smooth and rough pipe equations of Von Karman and Prandtl.

The Colebrook and White formula is

$$\frac{1}{\sqrt{f}} - 2\log_{10}\frac{r_0}{k} = 1.74 - 2\log_{10}\left(1 + 1.87\,\frac{r_0/k}{\mathbf{R}\sqrt{f}}\right) \tag{30}$$

The U.S. Army Engineers, Waterways Experiment Station, after careful study of several large prototype structures concluded that Eq. (30) could not be verified for large Reynolds numbers.

16. The Von Karman and Prandtl Contribution. Concurrently with the Nikuradse experiments, Von Karman and Prandtl developed a theoretical analysis for pipe flow with suitable formulas for smooth and rough pipe. Smooth pipes are defined as those having small irregularities when compared with the thickness of the boundary layer.

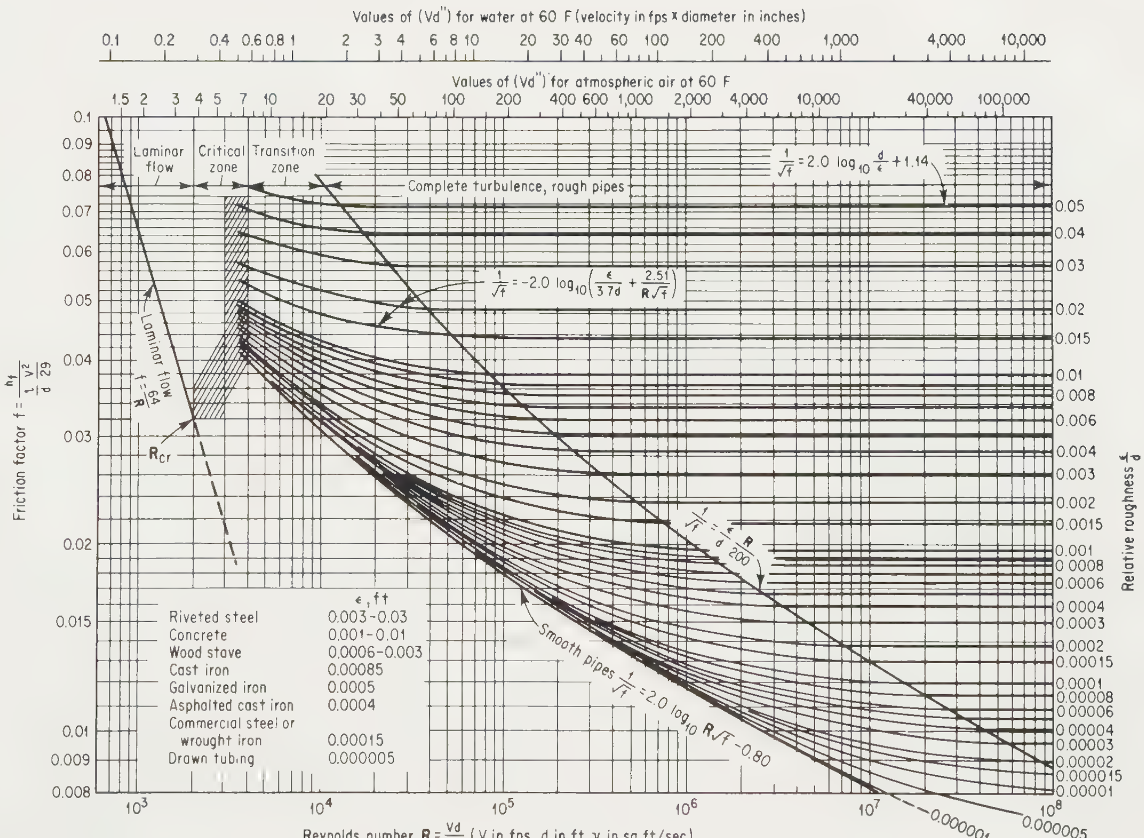

FIG. 10. Friction factors for any kind and size of pipe.

Rough pipe is defined as having irregularities in the walls which break up the laminar boundary layer, with the result that completely turbulent flow is developed.

The Von Karman–Prandtl resistance equation for turbulent flow in smooth pipe is

$$\frac{1}{\sqrt{f}} = 2 \log_{10} (\mathbf{R} \sqrt{f}) - 0.8 \tag{31}$$

which corresponds to line C of Fig. 9. The equation for rough pipes is

$$\frac{1}{\sqrt{f}} = 2 \log_{10} \frac{r_0}{k} + 1.74 \tag{32}$$

17. The Moody Chart. The Prandtl–Von Karman experiments and the contribution of Colebrook and White were finally brought together by Moody in a com-

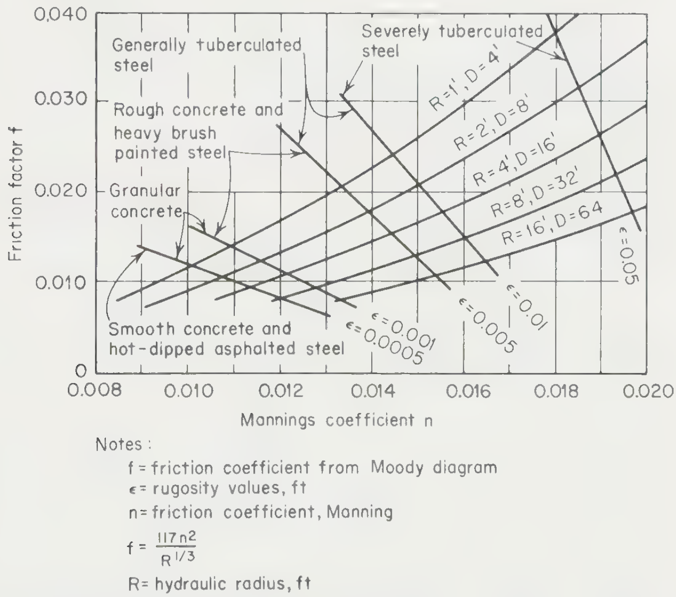

FIG. 11. Relationship between the Darcy-Weisbach f, Manning's coefficient n, and the value of ϵ.

prehensive chart (Fig. 10) which may be superimposed on all the experimental f vs. $\mathbf{R}$ curves for larger pipes. In contrast to the Nikuradse sand roughness, the roughness elements of commercial pipe are not uniform. The protuberances vary not only in sizes but also in pattern of spacing. As a means of differentiating the Nikuradse uniform sand-grain roughness k, the nonuniform roughness or rugosity of commercial pipes will be designated as ϵ. This is a practical simplification of more complex definitions of roughness. In practice, the measurement of natural roughness has been based upon the use of twice the root-mean-square height of the roughness elements ϵ, which is measured by moving a small probe across a rough surface or a plaster cast of that surface. Figure 11 shows the relationship between the Darcy-Weisbach f, Manning's coefficient n, and values of ϵ corresponding to various surfaces. The difference between the Nikuradse k and twice the root mean square of projection ϵ is sometimes overlooked but it should not be if the most accurate understanding is to be achieved.

In actual flow, the shear is influenced by both turbulent and viscous actions. In the central portion of a conduit where the mixing process has a freedom of action, viscosity has virtually no influence on the shear. At high Reynolds numbers, the flow can be considered totally turbulent action. However, at low Reynolds numbers, the effect of viscosity is quite important. Near the wall, the momentum exchange between layers apparently does not take place, and on this basis, it is reasoned that there must be a laminar film or sublayer. This assumption was verified experimentally by Hagen and Poiseuille. The velocity distribution in the laminar film is linear. Next to the thin laminar film is the transition zone; beyond this lies the turbulent zone.

18. Laminar Film or Sublayer. The concept of laminar film provides a physical picture of the difference between "rough" and "smooth" pipe surfaces. If the thickness of laminar film δ is greater than the roughness ϵ the surface is smooth; however, if δ is less than ϵ then the surface is rough. Von Karman gave the following experimentally derived value for δ:

$$\delta = \frac{11.6\nu}{\sqrt{\tau_0/\rho}} = \frac{11.6\nu}{\sqrt{RSg}} \tag{33}$$

where R = hydraulic radius

S = hydraulic slope

Equation (33) may be rewritten in the form

$$\delta = \frac{32.8d}{\mathbf{R}\sqrt{f}} \tag{34}$$

This equation clearly states that the film thickness decreased with increase in velocity. Therefore, the same pipe may have a hydraulically smooth boundary surface at low velocity and a hydraulically rough boundary surface at higher velocity.

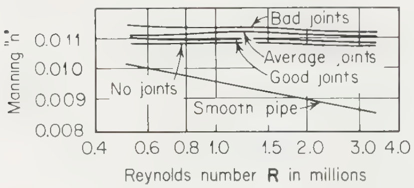

(a) Friction coefficients for 36-in tamped pipe with various joint conditions

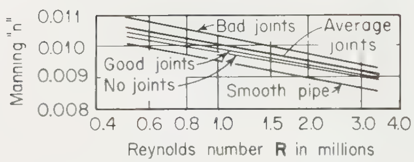

(b) Friction coefficients for 36-in cast pipe with various joint conditions

FIG. 12. Friction coefficients for 36-in. tamped and cast pipe with various joint conditions. (*Lorenz G. Straub, Charles E. Bowers, and Meir Pilch, Resistance to Flow in Two Types of Concrete Pipe, Technical Paper no. 22, Series B, St. Anthony Falls Hydraulic Laboratory, University of Minnesota.*)

19. Variations of Friction Coefficients with Reynolds Numbers as Observed in Prototype Experiments. It is of interest to note the relationships between friction coefficients and Reynolds numbers which have been observed during prototype experiments. To demonstrate this previously mentioned variation, only four examples will be given. For a more complete discussion of prototype behavior reference should be made to Sec. 3.

Reference to Fig. 12 shows the variations of Manning's n with $\mathbf{R}$ for 36-in.-diameter concrete pipe with various joint and surface conditions. Figure 13 shows the variations of the Darcy-Weisbach f and Manning n for unlined rock sections of the Apalachia tunnel, TVA. Figure 14 shows the variations of the Darcy-Weisbach f with $\mathbf{R}$ for various sizes and lining conditions of corrugated-metal pipe. Figure 15 shows the results of flow tests at high Reynolds numbers in three coated-steel pen-

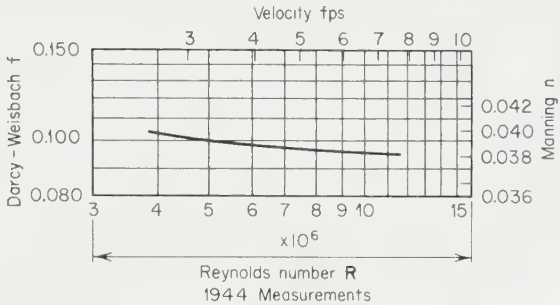

Characteristics of Unlined Tunnel Section

Nominal diam ft	Area sq ft			Diameter Equiv circle ft	Hydraulic radius ft		Average Overbreak ft
	Max	Min	Avg		Equiv	Measured	
20	419	335	375.3	21.86	5.47	5.36	0.93
22	504	368	430.8	23.42	5.86	5.68	0.71

FIG. 13. Apalachia tunnel—Tennessee Valley Authority. (*Rex A. Elder, Friction Measurements in Apalachia Tunnel, Proc. ASCE, paper* 1007, *June*, 1956.)

stocks at San Gabriel Dam in California. The resulting friction factors seemed to coincide with the smooth-pipe curve of Nikuradse and Von Karman.

20. Partly Lined Conduits. Tunnels and conduits constructed with different materials along their length due to geologic and other reasons will have different head losses in each reach. In this case an effective friction coefficient is a direct weighted average of the component factors, depending simply on the relative proportion of each type of roughness. This method is quite useful in preliminary design where numerous combinations of conduit sizes and materials must be studied in order to arrive at an economical design. However, when the results of the economical design, or when the materials for various portions of the conduit are better known, then the boundary-friction loss of each part can be determined separately to provide a more accurate estimate.

In the case of conduits partially lined circumferentially, it is believed that the linear assumption may not be valid because of the interplay between two flow regimes. An expression that has been used for such conduits is

$$n_e = n_r \left[\frac{P_r + P_s (n_s/n_r)^{3/2}}{P_t} \right]^{2/3} \tag{35}$$

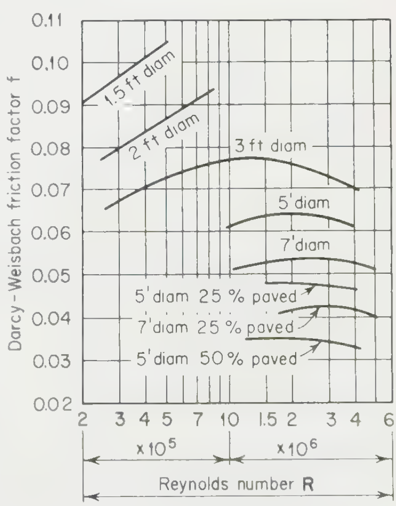

FIG. 14. Friction factors, corrugated-metal pipe. (*U.S. Army Corps of Engineers, Waterways Experiment Station, Hydraulic Design Criteria, Chart* 224-½.)

where n = Manning's coefficient
P = perimeter
r = subscript for the rough section
s = subscript for the smooth section
t = subscript for the whole section
n_e = weighted Manning coefficient for the partially lined section

Tests conducted at the Imperial College, England, indicated that at low Reynolds numbers and low absolute roughness, the composite friction coefficient was closer to the smooth-pipe factor than to the arithmetic proportions as shown. Furthermore,

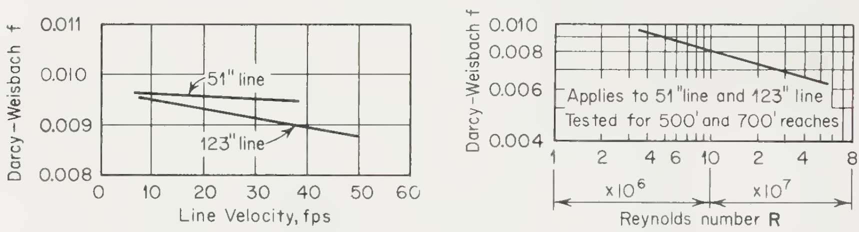

Fig. 15. Results of flow tests—San Gabriel Dam in California. (*Maxwell F. Burke, High-velocity Tests in a Penstock, Trans. ASCE, paper* 2766, *vol.* 120, *p.* 863, 1955.)

tests indicated that at high Reynolds numbers and at high absolute roughness, the converse is true.

21. Unlined Tunnels. The size and shape of any unlined rock tunnel may vary considerably from one section to another, thus resulting in large surface irregularities. Field investigations of unlined tunnels made by Rahm[1] show that a definite relationship exists between the Darcy-Weisbach f and variations in cross-section area.

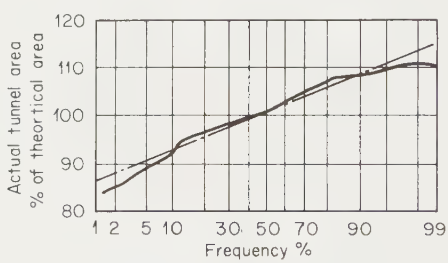

Fig. 16. Distribution curve for cross-sectional areas, unlined tunnels—Tasan tunnel, Sweden. (*Lennart Rahm, Friction Losses in Swedish Rock Tunnels, Water Power, London, p.* 461, *December*, 1958.)

Rahm related the friction factor f to variations in the cross-sectional areas along the tunnel which were arranged in a series according to their order of magnitude and then plotted in a normal-distribution logarithmic diagram, as shown for a typical tunnel by Fig. 16.

The slope of the straight line in Fig. 16 represents the variation in the cross-sectional area of the tunnel by the relation

$$s = \frac{A_{99} - A_1}{A_1} \times (100 \text{ percent}) \tag{36}$$

[1] Rahm, Lennart, Friction Losses in Swedish Rock Tunnels, *Water Power*, London, December, 1958.

in which s = slope, as defined by Eq. (36)

A_{99} = cross-sectional area corresponding to a frequency of 99 percent

A_1 = cross-sectional area corresponding to a frequency of 1 percent

As determined from Fig. 16, $s = 33$ percent.

Figure 17 shows the relationship between the percentage variation in area s and the friction coefficient f. For practical design purposes, Rahm expressed this as a

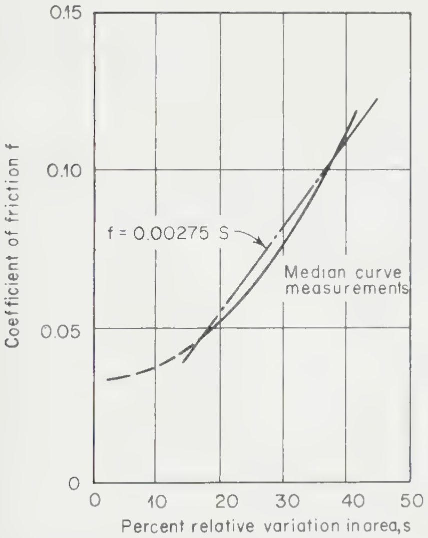

FIG. 17. Relationship between f and s, unlined tunnels. (*Rahm, Water Power, p.* 462.)

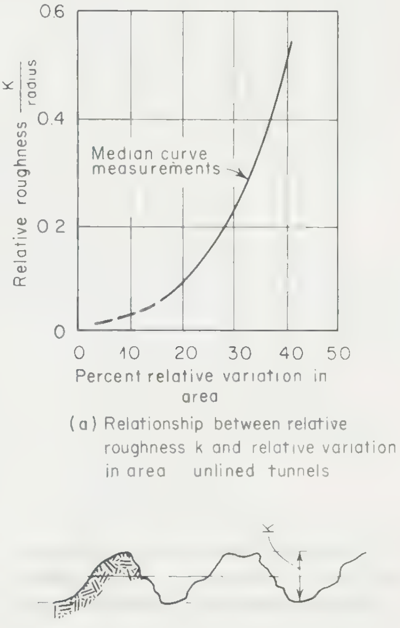

FIG. 18. (*Rahm, Water Power, p.* 462.)

straight-line relationship which may be expressed as

$$f = 0.00275s \tag{37}$$

Furthermore, it was found that approximately

$$s = \frac{200tm}{R_t} \tag{38}$$

in which tm = average excess overbreak

R_t = hydraulic radius of the theoretical section

Rahm also determined the relationships between relative roughness and relative variation in area, as shown by Fig. 18*a*. A definition sketch defining the value k is shown by Fig. 18*b*. The relationship between various values of k, f, and actual tunnel area is shown by Fig. 19.

22. Deposits and Organic Growth. The discharge capacities of tunnels and other water passages may decrease with aging because of deposits and organic growths on the interior surfaces. These accumulations increase boundary-friction losses with resulting decreases in discharge capacities.

Corrosion on the interior surface of water-conveyance structures reduces carrying capacity in water-supply mains, produces discolored water, and creates taste and odor problems. In metal pipes, corrosion gives rise to tubercules on the interior surface, and these in turn decrease the carrying capacity by roughening of the interior of the pipe surface. Improper filtration of water or operation of treatment plants beyond their capacities may result in floc passing through filters, depositing aluminum hydroxide on the pipe walls. Even a thin coating will reduce the carrying capacity materially. Other coatings may consist of calcium carbonate and silica slime.

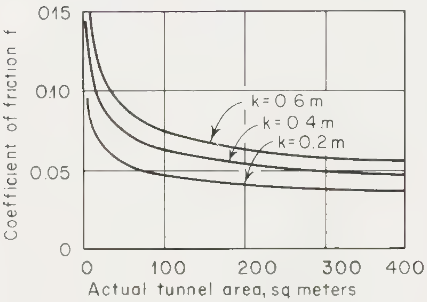

Fig. 19. Relationship between f and actual cross-sectional area corresponding to varying values of k. (*Rahm, Water Power*, p. 463.)

In a number of tunnels in Chicago, an analysis of the gelatinous material showed that it was principally aluminum hydroxide and silica. Measurement of the fric-

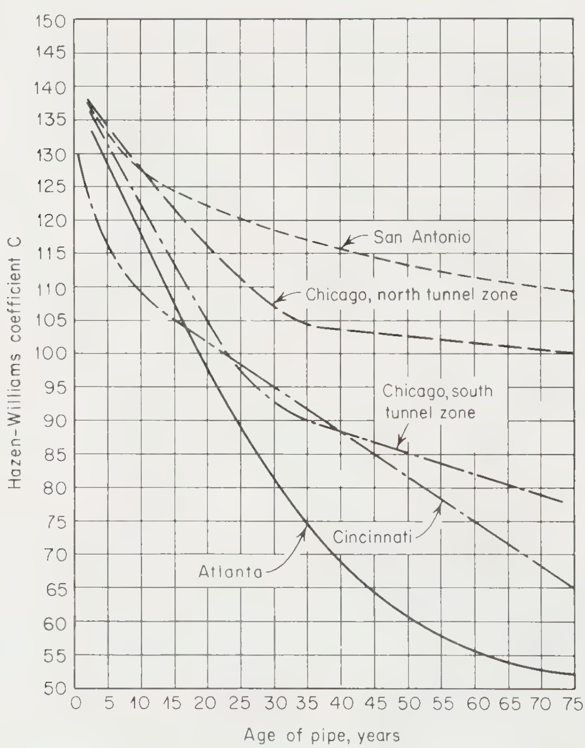

Fig. 20. Trend curve, head-loss tests. (*W. D. Hudson, Studies of Distribution System Capacity, J. Am. Water Works Assoc., February*, 1966.)

tion loss in these tunnels indicated that the Manning's coefficient of friction n had increased from 0.014 when new to as high as 0.0196 for some tunnels after 7 years of service.

After 10 years of service, the 18-ft-diameter tunnel leading to the Apalachia hydroelectric plant (TVA) was found to have the following changes in roughness: the average values of Manning's n rose from 0.011 to 0.018 for the concrete section, from 0.010 to 0.018 for the steel section, and from 0.030 to 0.038 for the unlined rock section.

After only 3 years of service, the 10 ft-0 in.-by-10 ft-0 in. concrete fish-passing conduit at the Priest Rapids hydroelectric project, Columbia River, accumulated from ½ to ⅝ in. of algae and sponge sliming, which increased the value of n from 0.0104 to 0.0187. After cleaning, this value dropped to 0.0108.

Figure 20 shows the effect of aging of water-supply mains in several large cities in the United States as measured by increases in the Hazen and Williams coefficient C. The loss in capacity may range between 25 and 30 percent.

FORM LOSSES

23. General. Generally, between intake and exit, the flow encounters a variety of shape configurations in the flow passageway such as changes in section from rectangular to circular, partial obstacles, branches, bends, slots, expansions, and contractions. These impose losses in addition to those resulting from frictional resistance. Form losses are the result of fully developed turbulence and thus can be expressed in the general form

$$H_L = K_e \frac{V^2}{2g} \tag{39}$$

in which K_e = coefficient of form loss

H_L = form loss

There follow discussions of a few of the commoner types of form losses encountered in engineering practice.

24. Sudden Enlargements. A sudden enlargement, such as that shown by Fig. 21, results in intense shearing action between the incoming high-velocity jet and the surrounding water. As a result, much of the kinetic energy of the jet is dissipated by eddy action. Most of the turbulence disappears and the velocity becomes practically uniform across the section of the enlarged pipe at a distance of about five diameters from the enlargement. Rapid pressure fluctuations accompany the enlargement.

Using the symbols shown by Fig. 21, the loss of head at a sudden enlargement is

$$H_L = \frac{(V_1 - V_2)^2}{2g} \tag{40}$$

Practical applications of this principle may be found in several high-head outlets which are designed to release discharges at velocities which will not damage the water-passage linings. The proposed sudden-enlargement energy dissipator for Mica Dam, to be constructed on the Columbia River in British Columbia, offers one example.

One of the two 45-ft diversion tunnels at Mica was selected as the most logical and economic location for a gate-controlled expansion chamber which would serve to reduce the velocities of the discharge into the tunnel during the filling period of the reservoir. With outlets of conventional design, the maximum velocity would have been 170 fps. The most promising arrangement provided for a sudden-enlargement energy dissipator in the tunnel upstream of the main plug which would contain three gated outlets.[1]

[1] Russell, Samuel O., and James W. Ball, Sudden-enlargement Energy Dissipator for Mica Dam, *Proc. ASCE, J. Hydraulics Div.*, July, 1967, p. 41.

Possible cavitation of the concrete tunnel lining was an important consideration. As shown by the hydraulic gradient (Fig. 21) pressures in the fast-moving eddies are lower in the surrounding water and under certain conditions can fall as low as the vapor pressure. If pressures fall sufficiently low, the collapse of vapor bubbles may occur

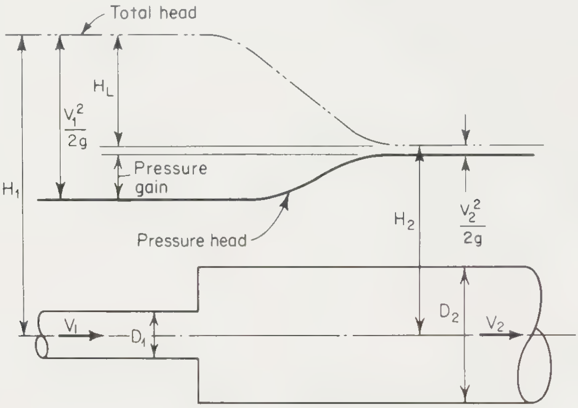

FIG. 21. Sudden enlargement.

at the boundary of the tunnel lining, with resulting damage to the surface. From comprehensive model tests, including one made on a concrete-lined steel pipe under approximately prototype discharge conditions, it was determined that the design

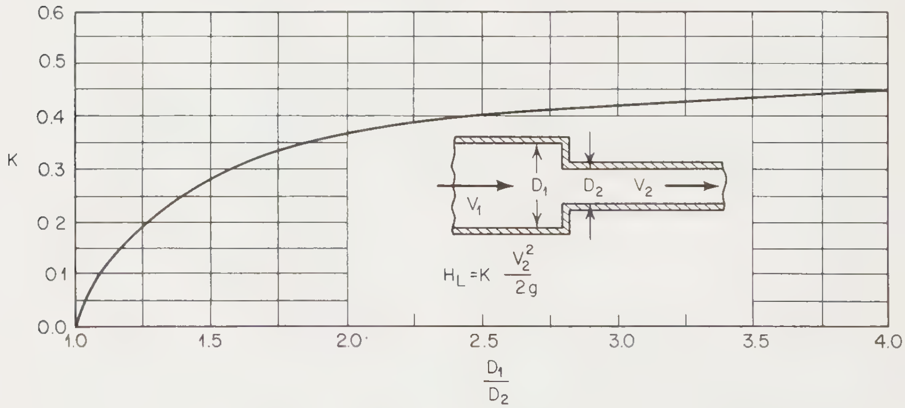

FIG. 22. Head loss, sudden contraction. (*Pipe Friction Manual, Hydraulic Institute.*)

cavitation number K for the Mica expansion chamber, as expressed by the formula

$$K = \frac{H_2 - H_v}{H_t - H_2} \tag{41}$$

in which H_v = vapor pressure of water, H_t = total head of flow entering enlargement, and H_2 = pressure head downstream from the enlargement, should be approximately 3. The value of K at the point of incipient cavitation damage was less than 1.

25. Sudden Contraction. The head loss resulting from a sudden contraction may be expressed as

$$H_L = K \frac{V_2^2}{2g} \tag{42}$$

Values of K for various ratios of D_1 to D_2 are shown by Fig. 22.

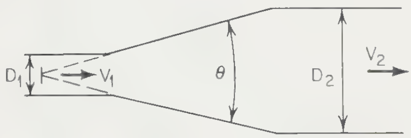

Fig. 23. Gradual conical expansion.

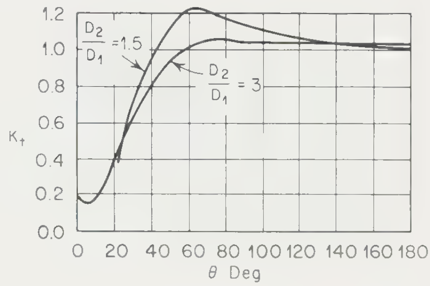

Fig. 24. Loss coefficients for gradual conical expansion.

26. Gradual Conical Expansion. The losses resulting from gradual expansion, such as shown by Fig. 23, may be expressed in the following form:

$$H_t = K_t \frac{(V_1 - V_2)^2}{2g} \tag{43}$$

where V_1 and V_2 are velocities in the upstream and downstream sections, respectively, H_t the transition head loss, and K_t the transition loss coefficient.

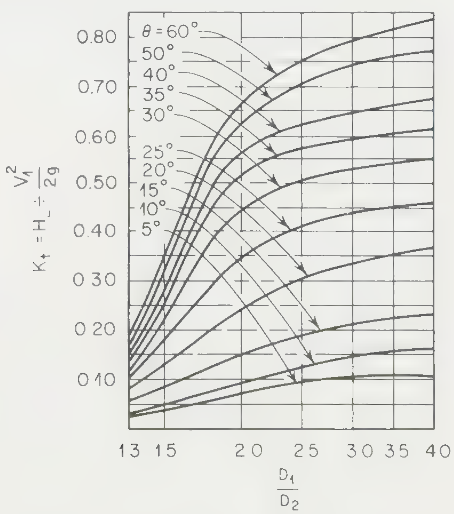

Fig. 25. Head loss in conical expansion

Early experiments by Gibson[1] show that the loss coefficient K_t is a function of the central angle θ of the truncated cone. The tests show that the loss coefficient is also a function of the ratio of areas A_1 and A_2. The results of the Gibson tests[2] are shown by Fig. 24.[3]

[1] Department of the Army, Office of the Chief of Engineers, Engineer Manual EM 1110-2-1602, p. 7, August, 1963.

[2] Gibson, A. H., The Conversion of Kinetic to Pressure Energy in the Flow of Water through Passages Having Divergent Boundaries, *Engineering*, **93,** 205, 1912.

[3] Streeter, Victor L., "Fluid Mechanics," 2d ed., p. 188, McGraw-Hill Book Company, New York.

Figure 24 shows that the loss coefficient increases rapidly as θ increases up to about 60°.

The results of more comprehensive tests published by V. Tatarinov, which appear in *Product Engineering*, May, 1946, are shown by Fig. 25. These tests confirm some of the earlier results obtained by Gibson.

27. Gradual Conical Contraction. There is less laboratory information available on the loss in contraction transitions, such as shown by Fig. 26, than for expansion transitions. Tatarinov also presented the results of tests on gradual conical contractions shown by Fig. 27.

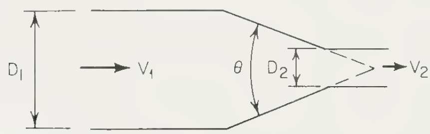

FIG. 26. Gradual conical contraction.

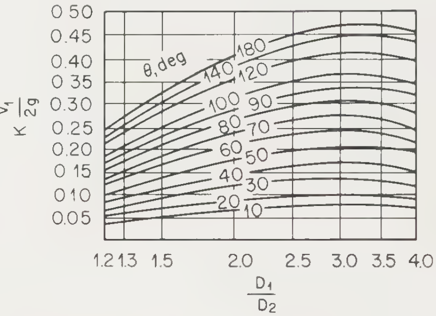

FIG. 27. Head loss in conical contraction. (*V. Tatarinov, Product Engineering, May, 1946.*)

28. Bend Losses. The bend loss excluding friction loss for a circular conduit is a function of the bend radius, pipe diameter, and deflection angle of the bend. Bend losses for pipes having 90-deg bends and varying degrees of rugosity ϵ/D are shown

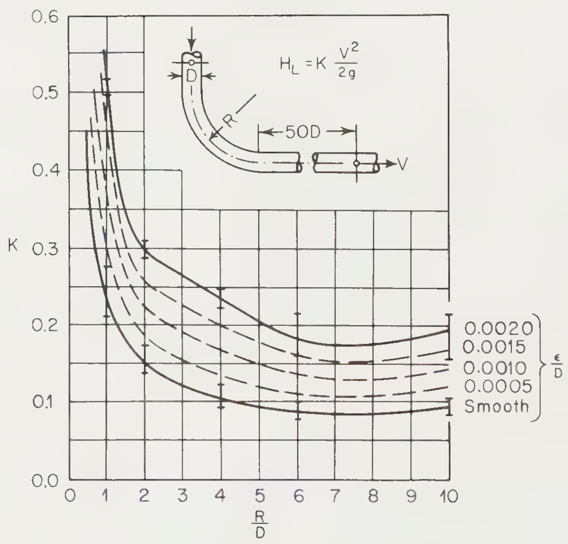

FIG. 28. Resistance coefficients for 90-degree bends of uniform diameter. (*Pipe Friction Manual, Hydraulic Institute.*)

by Fig. 28. Curves showing recommended bend-loss coefficients for R/D ratios from 1 to 10 and for deflection angles from 0 to 90 deg are given in Fig. 29.[1]

[1] Factors Influencing Flow in Large Conduits, Report of Task Force on Flow in Large Conduits, Committee on Hydraulic Structures, *Proc. ASCE*, *J. Hydraulic Div.*, November, 1965, p. 138. See also Ito. Hand Imai K., Energy Losses at 90° Junctions, *Proc. ASCE J. Hydraulics Div.*, September, 1973, p. 1373.

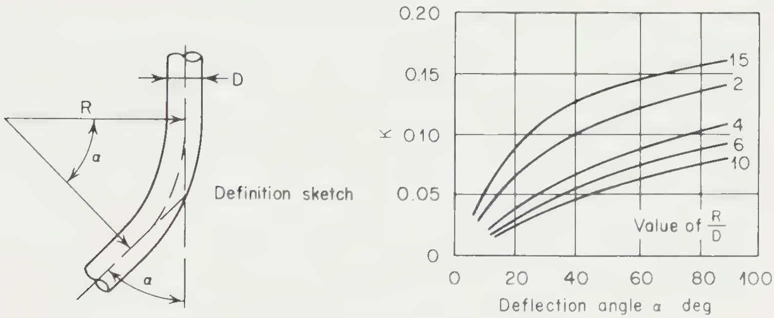

FIG. 29. Friction losses at bends.

MEASUREMENT OF FLOW IN CLOSED CONDUITS

29. Differential Head Meters. The flow of a fluid through a constriction in a closed conduit results in a lowering of pressure at the point of minimum sectional area. This drop in pressure is a function of the rate of flow. Differential head meters have been used in many forms. To illustrate the principle, two will be described: the Venturi meter and the diaphragm orifice.

30. Venturi Meters. The Venturi meter is an instrument which makes practical use of Bernoulli's theorem in measuring the quantity of liquid flowing through a pipe. The meter, as shown by Fig. 30*a*, consists of a short length of pipe tapering to a narrow throat in the middle. Tubes entering the enlarged end and at the throat make it possible to measure pressures at these points.

31. Venturi Meter Formulas. Referring to Fig. 30*a*,

$$Q = CA_1 \frac{1}{\sqrt{r^2 - 1}} \sqrt{2gh} \qquad \text{or} \qquad Q = CA_2 \sqrt{\frac{r^2}{r^2 - 1}} \sqrt{2gh}$$

$$M = \text{meter constant} = \frac{A_1}{\sqrt{r^2 - 1}} = A_2 \sqrt{\frac{r^2}{r^2 - 1}}$$

$$Q = CM \sqrt{2gh} = K \sqrt{2gh} \tag{44}$$

where Q = rate of discharge, cfs

r = ratio of area at entrance to area at throat = A_1/A_2 or for circular areas $D_1{}^2D_2{}^2$ if D_1 and D_2 are diameters at entrance and at throat (usually r is greater than 4, smaller than 16)

g = acceleration due to gravity

h = difference in level (ft) at which a liquid stands in two vertical tubes, which are connected to the side holes at entrance and throat, respectively, and are either open to the atmosphere or under equal pressure or connected through a closed space *in vacuo*

C = discharge coefficient, which varies between 0.97 and 1.00 for well-made Venturi tubes of suitable size for conditions of operation

Figure 30*b* also shows a graph for values of the discharge coefficient C in terms of meter size and throat velocities. Figure 31 shows the variation of C with Reynolds numbers for Venturi meters having a ratio of throat diameter to entrance diameter of 0.50.

32. Diaphragm Orifice. If properly calibrated by tests, a diaphragm inserted in a conduit may also be used to measure flows. Figure 32 shows such an arrangement

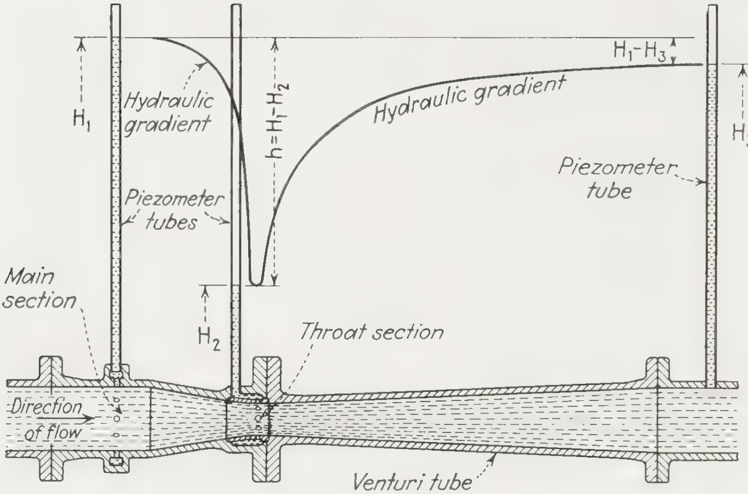

FIG. 30*a*. Section of Venturi tube.

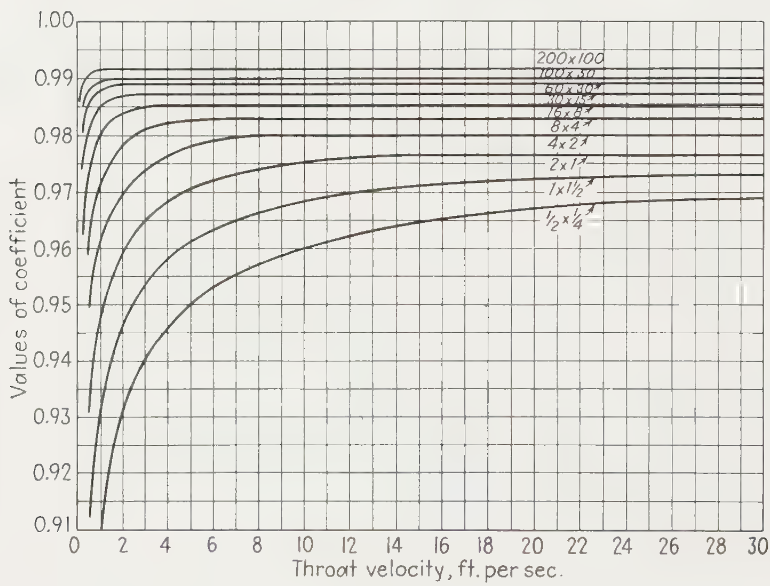

FIG. 30*b*. Values of discharge coefficient C (Venturi meter).

and the symbols which appear in the equation for determining the discharge

$$Q = KA_d \sqrt{\frac{2gh}{1 - (d/D)^4}} \tag{45}$$

Values of K which were determined experimentally by Johansen are shown by Fig. 33.

33. Minor Losses. Minor losses may be expressed in the equivalent length of pipe that has the same energy loss for the same discharge. The chart in Fig. 34 offers a convenient method of estimating these losses.

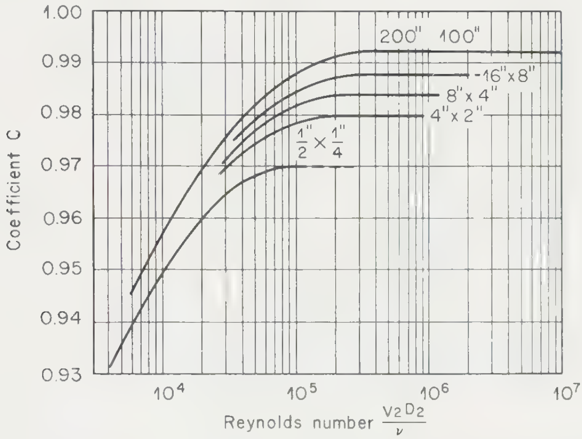

FIG. 31. Venturi meter—discharge coefficients. (*ASME Power Test Code.*)

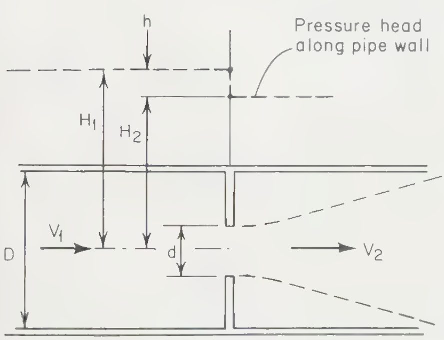

FIG. 32. Diaphragm orifice.

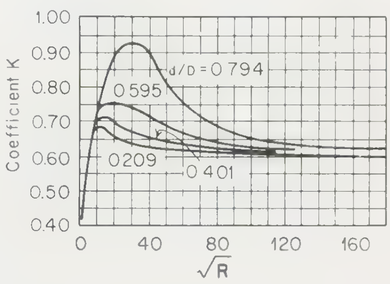

FIG. 33. Diaphragm orifice—coefficients of discharge.

ORIFICES

34. High Head. When the head is relatively large, as compared with the size of the orifice, the following equation will apply:

$$Q = CA\sqrt{2gH} \tag{46}$$

in which Q = discharge, cfs
H = head on center line of orifice, ft
A = area of orifice, sq ft

Sharp-edged circular orifices, as shown by Fig. 35 and the accompanying table of discharge coefficients, will operate through a wide range of heads with a value of C of approximately 0.60. Rectangular orifices, such as those which are formed by opening

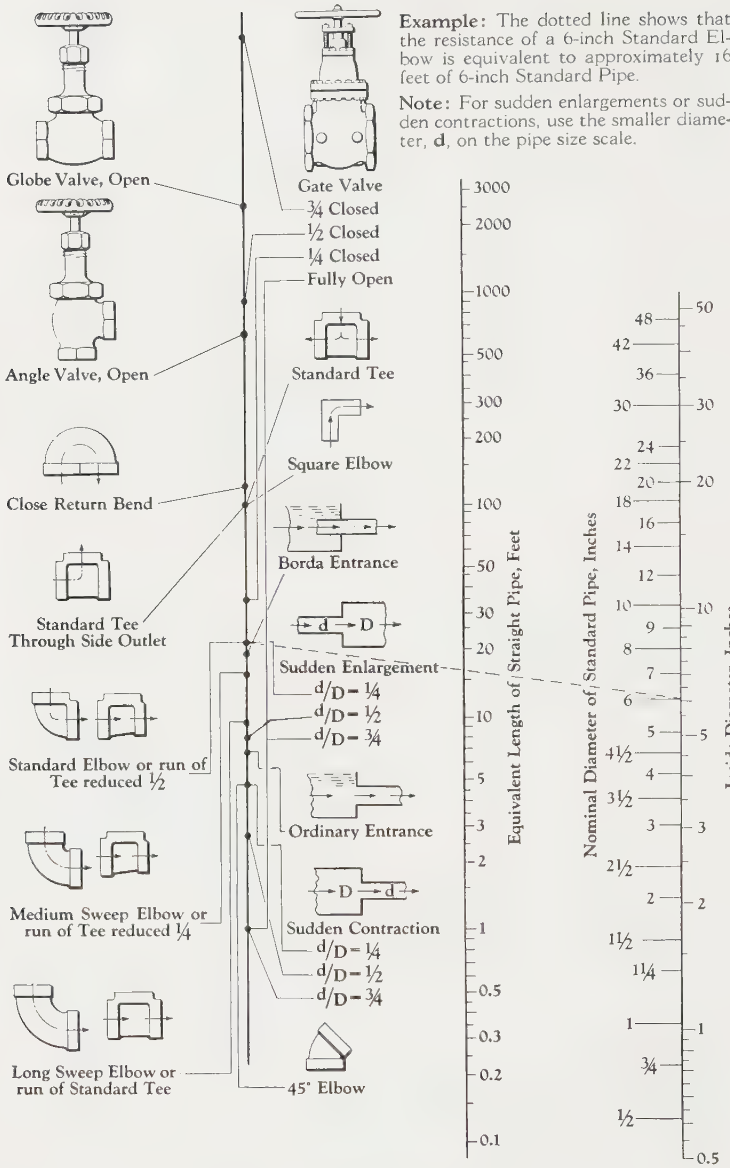

FIG. 34. Resistance of valves and fittings to flow of fluid.

a gate having a shape such as that shown by Fig. 36, will have much higher discharge coefficients. Discharge coefficients for submerged orifices of varying forms are shown by Fig. 37.

35. Low Head. When the dimensions of the orifice are large, as compared with the head, the discharge formula may be written

$$Q = \tfrac{2}{3}C\sqrt{2g}\,L(H_2^{3/2} - H_1^{3/2}) \tag{47}$$

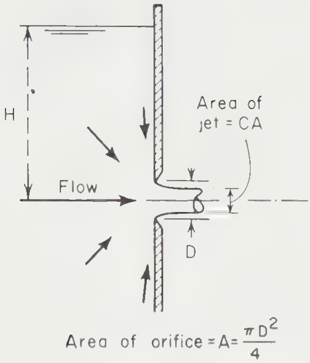

H, ft	Orifice diameter D, inches			
	0.50	1.00	2.00	4.00
	Values of C			
10	0.604	0.597	0.596	0.595
20	0.602	0.596	0.595	0.594
30	0.600	0.595	0.594	0.594
40	0.600	0.595	0.594	0.593
50	0.599	0.595	0.594	0.593
60	0.599	0.594	0.593	0.593

FIG. 35. Discharge coefficients, circular sharp-edged orifices, varying heads. (*F. W. Medaugh and G. D. Johnson, Civil Engineering, p. 424, July,* 1940.)

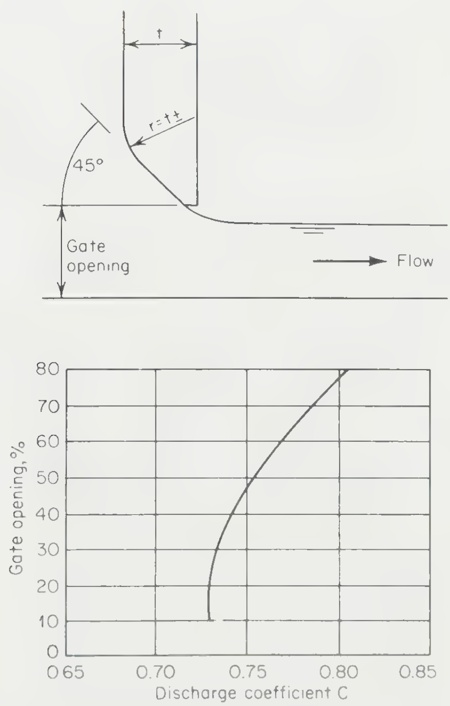

Source: Hydraulic Design Criteria, Waterways Experiment Station, Corps of Engineers U.S Army, Sheet 320-1

FIG. 36. Discharge coefficient *C*.

with dimensions and symbols as indicated by Fig. 38. The expression $\frac{2}{3}C\sqrt{2g}$ may be designated as the overall coefficient m which appears in the equations and coefficients determined by prototype measurements of the spillway discharge capacity of Wilson Dam. These and other prototype experiments are described more fully in Sec. 20.

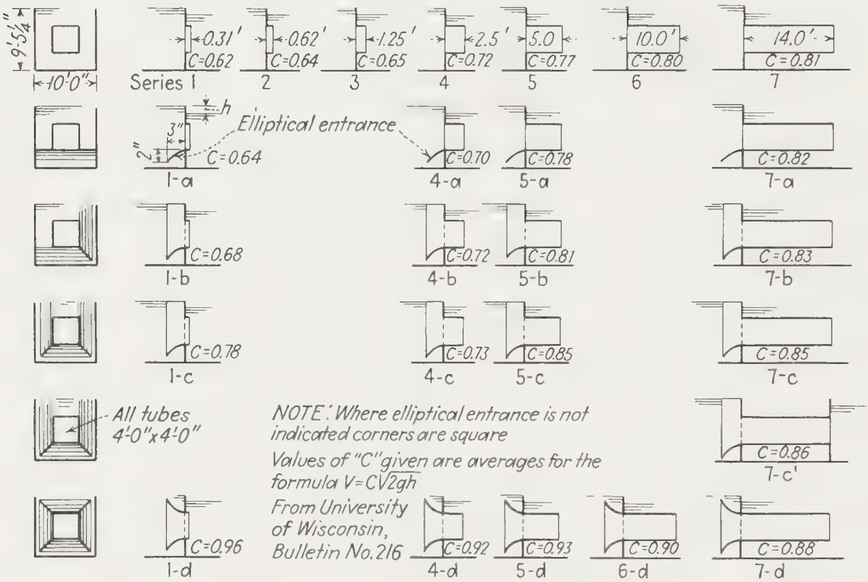

FIG. 37. Discharge through orifices and tubes.

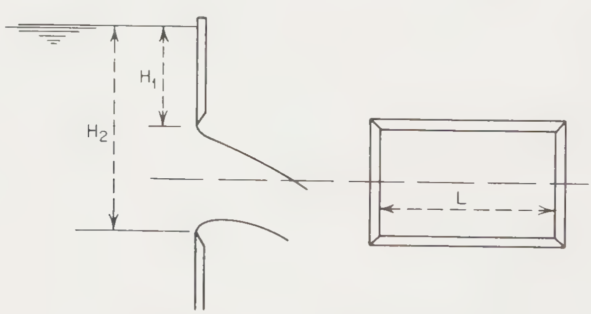

$$\text{Discharge} = \frac{2}{3} C\sqrt{2g}\, L\,(H_2^{\frac{3}{2}} - H_1^{\frac{3}{2}})$$

FIG. 38. Discharge for large vertical orifice compared with head.

PART II. OPEN CHANNELS

36. Critical Flow. Flow in open channels is governed primarily by the action of gravity upon the moving fluid. The acceleration of gravity g or the slope S is expressed or implied in all open-channel flow formulas. In most problems the acceleration of gravity may be considered to be a constant. This makes possible its implicit presence in some flow formulas, even though it is not expressed.

The dimensionless parameter used to describe and classify open-channel flow is the Froude number

$$F = \frac{V}{\sqrt{gy}} \tag{48}$$

where F = Froude number
V = average velocity of the flow
g = acceleration of gravity
y = depth of flow

Flows are classified as follows:

$F < 1$: flow is subcritical
$F = 1$: flow is critical
$F > 1$: flow is supercritical

Critical flow requires the least energy for a given rate of discharge. Assuming a hydrostatic distribution of water pressure within the moving fluid,

$$y_c = \sqrt[3]{\frac{q^2}{g}} \tag{49}$$

in which y_c = critical depth
q = unit discharge per lin ft width
g = acceleration of gravity

The critical velocity is the average velocity of flow at the critical condition and is expressed by

$$V_c = \frac{q}{y_c} = \sqrt[3]{gq} = \sqrt{gy_c} \tag{50}$$

In uniform flow in a rectangular channel at critical depth, the velocity head $V^2/2g$ is exactly half the depth of the flow. For other prismoidal sections, Eq. (50) may be used without appreciable error by using the average depth of flow. The average depth is the area of flow divided by the surface width of the flow. Figure 39 defines terms and notations commonly used in analysis of open-channel flow.

As shown by Fig. 39, the velocity is a variable throughout the section, being typically low near a boundary and high at some distance from a boundary. The square of the average velocity is used in calculating the velocity head, which is considered to be a measure of the total kinetic energy of the moving fluid. In reality the total kinetic energy is made up of the sum of the kinetic energies of all the filaments comprising the flow. As the square of the mean is not equal to the mean of the squares, a correction is in order if more precise calculations are required, and the kinetic-energy factor must be applied, as is explained in the preceding portion of this section on closed conduits.

37. Classification of Flow Profiles. The concept of critical depth serves as a useful tool for the classification of all possible water-surface profiles for flow in open channels. Flow at velocities greater than critical is called supercritical flow, and flow at velocities less than critical is called subcritical flow. A convenient way to determine whether flow is subcritical or supercritical is to compare the average depth of the flow with the critical depth. It can be demonstrated that the critical depth is equal to two-thirds of the specific energy. For example, with a specific energy of 3 ft, all

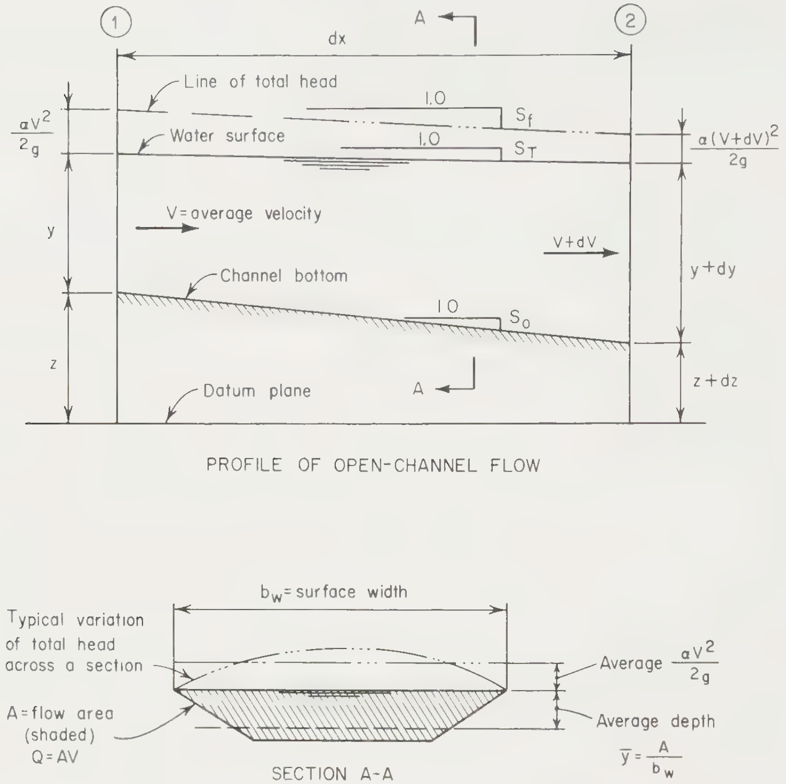

FIG. 39. Profile of open-channel flow and terms and notations for open-channel flow.

flows at greater than 2 ft of depth are subcritical, and all flows at less than 2 ft of depth are supercritical.

The normal depth of flow in an open channel is that depth at which the slope of the water surface and the slope of the bottom are parallel. Gravitational forces and friction forces are in balance. Flow is steady and uniform.

Slopes are classified according to the relationship between the critical depth and the normal depth. The critical depth is dependent upon the unit discharge of the flow; the normal depth is dependent upon the unit discharge and the slope and roughness of the channel. Classification of slopes is as follows:

Mild slope. The normal depth is greater than the critical depth. Only subcritical flow can be sustained on a mild slope for an indefinite length.

Steep slope. The normal depth is less than the critical depth. Only supercritical flow can be sustained on a steep slope for an indefinite length.

Adverse slope. Any slope adverse to the direction of flow. The normal depth is infinite. In a channel of uniform width but variable slope there are only a limited number of possible water-surface profiles which can be developed for a given unit discharge. Combinations of these water-surface profiles may be used to describe the shape of the water surface in transitions between one slope and another. Figure 40 shows the various combinations which are possible.

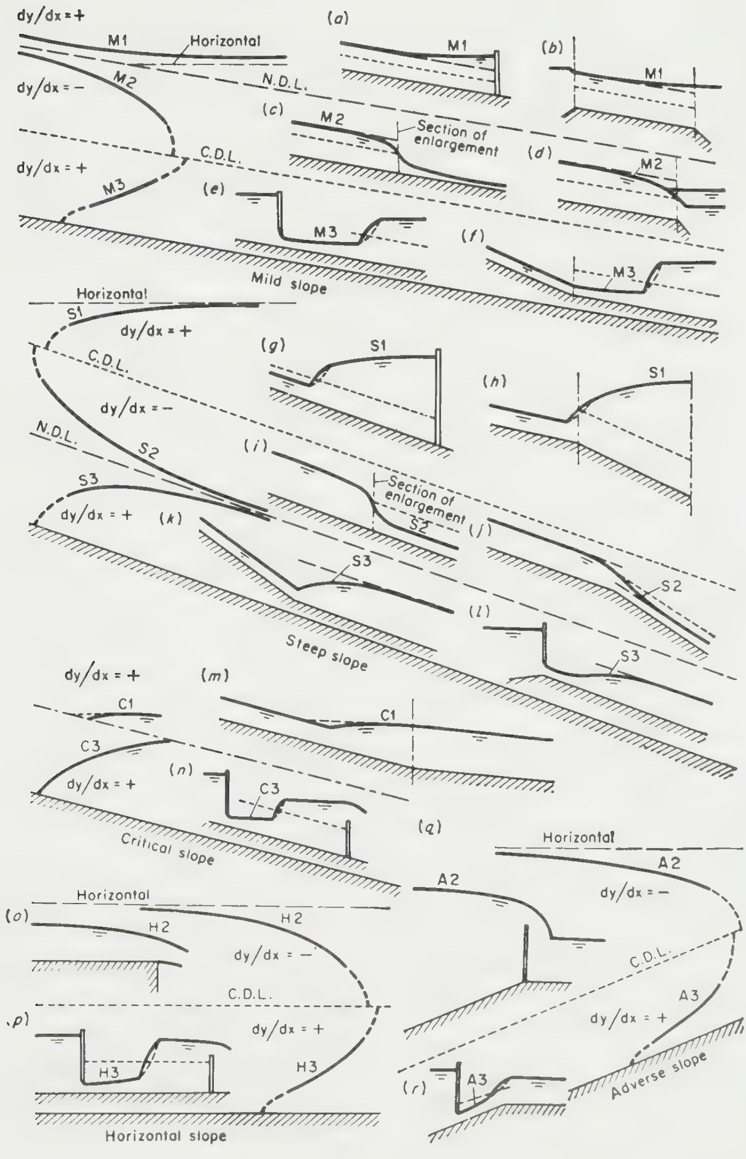

S_o = channel bottom slope

S_c = critical slope

Y_n = normal depth

Y_c = critical depth

NDL = normal depth line

CDL = critical depth line

M profiles $S_o < S_c$ and $Y_n > Y_c$

S profiles $S_o > S_c$ and $Y_n < Y_c$

C profiles $S_o = S_c$ and $Y_n = Y_c$

FIG. 40. Examples of flow profiles. (*Ven Te Chow, "Open-channel Hydraulics," McGraw-Hill Book Company, New York,* 1959.)

38. Steady Uniform Flow. This is flow in which identical conditions prevail from point to point and from time to time within the flow. The depth, cross section, discharge, velocity distribution, density, viscosity, turbulence, and all other aspects of the flow remain constant from point to point and from instant to instant. Steady uniform flow in open channels is rare, even in the laboratory.

Under usual field conditions, flow is nonuniform and unsteady. Nevertheless, the hypothetical simple condition of steady uniform flow is frequently substituted for the more complex real condition because it is easier to handle mathematically. Although not strictly correct, it is sometimes convenient to analyze nonuniform and unsteady flows by considering the behavior to be comprised of basic steady uniform flow upon which the effects of unsteadiness and nonuniformity are superimposed.

39. Flow Formulas and Frictional Resistance. The most widely used formulas for determining the flow in open channels are those of Chezy, Kutter, Darcy-Weisbach, and Manning, as set forth respectively in Eqs. (9), (16), (10), and (17).

For most of the small channels and conduits used in irrigation works, the Kutter-Chezy formula will yield conduit sections comparable with those computed by the Manning formula. Using an n of 0.014 hydraulic radii between 2 and 6, and with slopes between 0.01 and 0.0001, both formulas give approximately the same average velocity. Outside these limits different values of n must be used in one or the other of these formulas to obtain the same results. For example, in a reach of one canal tested with a hydraulic radius of 11.3 and a slope of 0.00061, a value of n of 0.0152 is required in Manning's formula to provide the same average velocity given by Kutter's formula with an n of 0.014.[1]

The coefficient of friction of the Darcy-Weisbach formula may be related to the size of the roughness comprising the bed and banks of the open channel through the assumption that the Von Karman–Prandtl equation for flow in rough pipes may be adapted to open-channel flow through the substitution of $4R$ for the diameter of the pipe. The symbol k is used for the effective roughness spacing in feet, and the Darcy-Weisbach, Chezy, and Manning open-channel flow formulas are shown in their relationships to each other in Fig. 41. For example, this figure shows that a Manning n of 0.030 and a hydraulic radius of 10 ft would correspond to a Darcy f of 0.050, a Chezy C of 72, and k equal to about 0.8 ft.

In addition to Fig. 41, the design chart for the solution of the Manning formula (Fig. 2) may be used for determining the flow in open channels.

In Fig. 41 the dashed lines of constant k are seen to run nearly vertically in the vicinity of $n = 0.020$, $k = 0.1$ ft. In this range of roughness the n value appears to be relatively independent of the hydraulic radius. Both above and below this range of n values, however, the lines of constant k are seen to diverge to one side or the other of the vertical. If one assumes that a given surface texture has a constant k and also that the Von Karman–Prandtl equation for flow in rough pipes can be applied as it was in deriving Fig. 41 to give accurate predictions of the effect of roughness, then one can reason as follows:

1. For a given roughness (k = constant), the n value is dependent upon the hydraulic radius.

2. In the range of n values for smooth concrete, for a k of 0.001 ft, the n values for concrete pipes of 1 ft and 8 ft in diameter are seen to be about 0.010 and 0.012, respectively. In this range, increasing R produces higher values of n and lower values of f.

3. In the range of n values for cobble-lined canals, say $k = 0.5$, there is little dependence of n upon R in the range of $R = 10$ ft and above, but a significant dependence upon R in the range of $R = 10$ ft and below.

[1] Tilp, Paul J., Capacity Tests in Large Concrete-lined Canals, *Proc. ASCE*, May, 1935.

4. The choice of the proper n values for comparing alternative designs with different values of R should take into account the effect of R upon n as evidenced in Fig. 41.

Steady uniform flow in open channels which are made up of surfaces with differing roughnesses can be calculated using a weighted average n value calculated on the basis of the portion of the wetted perimeter made up of each material.

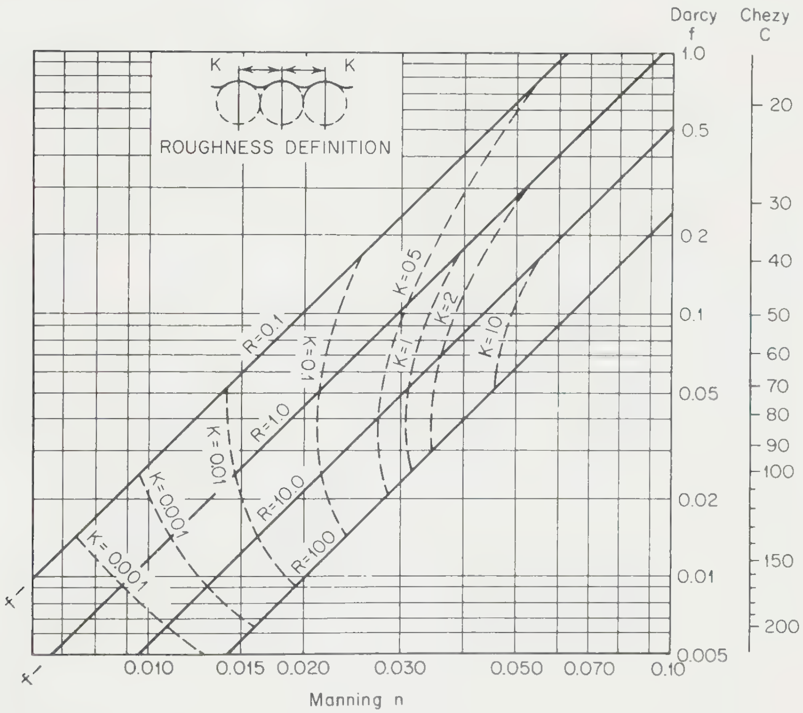

Notes:

1. Chart solves $n = \frac{1.486\ R^{1/6}}{C}, = 0.0926\ R^{1/6},\ f^{1/2}$

2. Dashed lines for roughness K in feet are based on:

$$\frac{1}{\sqrt{f}} = 2 \log_{10} \frac{R}{K} + 2.34 \text{ (Karman - Prandtl equation)}$$

3. Values of hydraulic radius R are in feet

4. Chart applies only to fully turbulent flow.

FIG. 41. Plot relating roughness coefficients.

40. Steady Nonuniform Flow. Steady nonuniform flow remains constant with time but varies in velocity from point to point within the fluid. Steady nonuniform flow in an open channel is complicated by the fact that the pressure at the free surface must remain atmospheric. This requirement results in pronounced changes in the configuration of the free surface in zones of rapid convergence or divergence in open channels.

The dynamic equation for steady nonuniform flow involves a direct application of the principles of conservation of mass, momentum, and energy. Application of the equations for flow without friction is illustrated in Fig. 42. At each section A, B, C, D, E, and F, the total head above the floor line—the specific head—must be exactly equal to the vertical distance from the floor to the horizontal line of total head. For each specific energy there is only one maximum unit discharge assuming hydrostatic distribution of water pressure inside the flow. Letting H equal the specific head at a point,

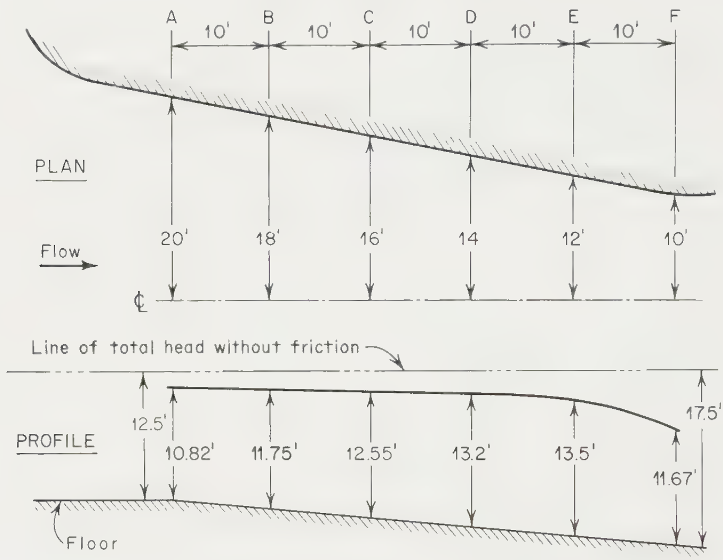

Section	A	B	C	D	E	F
Specific energy = H	12.5'	13.5'	14.5'	15.5'	16.5'	17.5'
Unit q	136	152	170	188	206	225
Flow width	20	18	16	14	12	10
Q	2,720	2,740	2,720	2,630	2,470	2,250
Governing Q	2,250	2,250	2,250	2,250	2,250	2,250
Unit Q	112.5	125	141	161	188	225
Depth	10.82	11.75	12.55	13.2	13.5	11.67
$V^2/2g$	1.68	1.75	1.95	2.3	3.0	5.83
V	10.4	10.6	11.2	12.2	13.9	19.4
Check q	112.5	125	141	161	188	225

FIG. 42. Steady uniform flow, sample computation.

the maximum or critical discharge per foot of width with hydrostatic pressure distribution for rectangular channel is

$$q_c = 3.1H^{3/2} \tag{51}$$

Using this equation, the maximum unit discharge is calculated for each section A through F. This unit discharge is then multiplied by the width of flow at the section to obtain a maximum discharge at that section. Section F is found to govern, as the maximum discharge of 2,250 cfs calculated for that section is less than the maximum calculated at any other section. Dividing this discharge of 2,250 cfs by the widths of flow at the various sections gives a unit discharge at each section. Then by trial and error a combination of velocity head and depth is found for each section which adds to the specific energy available at that section and also gives the unit discharge required by the principle of conservation of mass. Plots of specific energy, unit discharge, and depth may be constructed as illustrated in Fig. 43.

It is to be noted that only the principles of conservation of energy and matter were utilized in the foregoing illustrative computation of steady nonuniform flow. Only these two principles were necessary, as the loss in energy was known, being zero in the

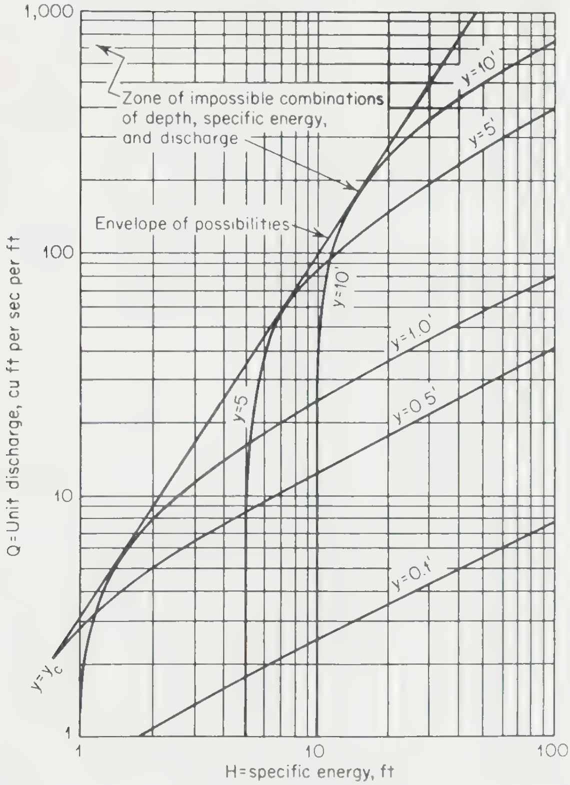

FIG. 43. Specific energy, depth, and unit discharge for hydrostatic pressure distribution.

example. For any other energy loss which might be assumed, there would likewise be a definite solution to the problem using only the principles of conservation of energy and mass. One could, on the basis of a first trial, using the assumption of zero energy loss, construct the water-surface profile and calculate the velocity along the flow as in the preceding example, and then refine the calculation by calculating an energy loss in each reach according to the velocity in the reach.

The method used to calculate the energy loss could be that of a developing boundary layer. However, if the surfaces are relatively smooth, a useful answer can be obtained by assuming the friction loss in a reach to be that of uniform flow in a channel of average cross section flowing at the average velocity, in the reach between sections

E and F, for example, the average of 13.9 and 19.4, or 15.65 fps. Using an f value of 0.016 (corresponding to $R = 6$ ft and $k = 0.008$) the loss in the reach would be $0.016 \times {}^{10}\!/\!_{24} \times 15.65^2/2g$, or 0.025 ft. Losses in other reaches are less, so that the overall loss in head would be about 0.08 ft. This is seen to be relatively small compared with the 17.5 ft of specific head at F, so that the assumption of zero energy loss appears to give reasonably accurate results.

41. Backwater Curves. The general approach to the solution of the problem of backwater curves is presented in Sec. 5 as it pertains to natural channels. The same approach is applicable to prismatic open channels. However, certain simplifications are possible in prismatic channels which can simplify the calculation of backwater curves. The general equation for nonuniform steady flow in open channels is used as a beginning:

$$S_0 - \frac{\partial y}{\partial x} - S_f = \frac{\alpha V}{g}\frac{\partial V}{\partial x} \qquad (52)$$

in which S_0 = bottom slope

$\frac{\partial y}{\partial x}$ = rate of change of depth y with distance x

S_f = friction slope

α = kinetic-energy factor

g = acceleration of gravity

V = average velocity

$\frac{\partial V}{\partial x}$ = rate of change of velocity with respect to distance x

Both S_f and $V(\partial V/\partial x)$ can be expressed in terms of a constant q and the depth y, producing an equation in which only x and y are variables. This permits integration of the equation, usually with the aid of some tabulated numerical values of some of the more complex functions. Bresse's backwater functions are among the better known of this type of function.

42. Slug Flow. Slug flow and flow with roll waves occur at very low Reynolds numbers on steep slopes. Channel slopes are 2 percent, or steeper, and the Reynolds number is, roughly, 400 or less for roll waves and between 1,000 and 4,000 for slug flow. Flow at 1 fps at a depth of ½ in. has a Reynolds number on the order of 4,000. Thus the greater velocities and depths which occur in most civil engineering structures place the flow outside the ranges for slug flow and roll waves.

Wind-generated waves in a reservoir may pass over a spillway crest and be transmitted on down the chute. Such waves would ordinarily be rapidly attenuated as the average velocity of the flow in the chute would be greater than the wave celerity. Such disturbances are not included in the definition of slug flow or roll waves given above.

43. Unsteady Flow. Unsteady, nonuniform flow is a general type of flow commonly analyzed in two-dimensional forms. The fundamental idea is that water-surface slope not only offsets friction but also produces acceleration:

$$\text{Total slope} - \text{friction slope} = \text{acceleration slope}$$

Let terms be defined as shown in Fig. 39. The dimensionless form of the terms is

$$\text{Total slope} = S_0 + \frac{\partial y}{\partial x}$$

$$\text{Friction slope} = S_f$$

$$\text{Acceleration slope with distance} = \frac{\alpha V}{g}\frac{\partial V}{\partial x}$$

$$\text{Acceleration slope with time} = \frac{1}{g}\frac{\partial V}{\partial t}$$

The equation becomes

$$S_0 + \frac{\partial y}{\partial x} - S_f = \frac{\alpha V}{g}\frac{\partial V}{\partial x} + \frac{1}{g}\frac{\partial V}{\partial t}$$

Care must be taken with signs. Slopes S_0 and S_f are called positive when sloping down in the direction of flow as in the usual case. The term $\partial y/\partial x$ produces forces in this same direction when y is decreasing. Therefore, if a reduction in y is called negative, the sign of $\partial y/\partial x$ becomes negative and the equation becomes

$$\begin{aligned} S_0 - \frac{\partial y}{\partial x} - S_f &= \frac{\alpha V}{g}\frac{\partial V}{\partial x} + \frac{1}{g}\frac{\partial V}{\partial t} \\ A - B - C &= D + E \end{aligned} \qquad (53)$$

Term D contains the kinetic-energy factor α and also the average velocity V. This term is present even in *steady* nonuniform flow.

Term E contains the time t. It is the only term which accounts for changes with time.

All five terms are dimensionless slopes. It is significant to examine the magnitude of each in any real problem to evaluate the relative significance of each. An example follows.

Example: A river in flood is found to have the following characteristics:

$$\text{Bottom slope} = S_0 = 0.0002$$
$$\text{Usual friction slope at observed discharge} = S_f = S_0$$

Velocity V increased from 1.5 to 2.0 fps in period of 1 hr while depth y increases 8 to 10 ft in the same period. Since $S_0 = S_f$, the equation becomes

$$-\frac{\partial y}{\partial x} = \frac{\alpha V}{g}\frac{\partial V}{\partial x} + \frac{1}{g}\frac{\partial V}{\partial t}$$

Evaluate the time effect as follows:

$$\frac{1}{g}\frac{\partial V}{\partial t} \approx \frac{1}{g}\frac{\Delta V}{\Delta t} = \frac{1}{g}\frac{2.0 - 1.5}{3{,}600 \text{ sec}} = 4.3 \times 10^{-6}$$

This is seen to be rather small compared with the friction slope and bottom slope, being only 2.15 percent as large. As a first trial, neglect it so that

$$-\frac{\partial y}{\partial x} = \frac{\alpha V}{g}\frac{\partial V}{\partial x}$$

which when integrated merely says that the change in depth is equal to α times the change in velocity head. As a refinement the 4.3×10^{-6} slope effect can be added by multiplying this slope by the length of reach involved.

44. Wave Profiles and Velocities. Unsteady flow in open channels involves waves of one sort or another. The shape of these waves is an important factor in the analysis, as are wave velocities which are related to wave shape. The first trace of a wave is transmitted with a celerity $c = \sqrt{gy}$ with respect to the moving fluid. Thus the absolute propagation velocity is the vector sum of the fluid velocity V and the celerity c. As the wave front builds up, it moves at wave velocity V_w with respect to the moving fluid, this V_w being considerably less than the celerity c.

With reference to Fig. 44 the wave velocity for a constant shape of wave front is

$$V_w = \frac{V_1 y_1 - V_2 y_2}{y_1 - y_2} \qquad (54)$$

The moving waves of Fig. 44 can be transposed with a steady flow situation by the device of subtracting V_w from all velocities, causing the wave front to remain stationary with respect to the observer. This gives rise to a unit discharge $q = y_1(V_w - V_1) = y_2(V_w - V_2)$ which is useful in comparing wave shapes. Just as in steady flow, the shape of the water surface (wave front) depends upon the Froude number. The critical depth $y_c = \sqrt[3]{q^2/g}$ is used as a criterion. If the depth y_2 is greater than y_c then the water surface is a gentle curve. If y_2 is less than y_c then the water surface resembles a hydraulic jump. This then becomes a moving hydraulic jump, or hydraulic bore.

This technique of transposing the moving-wave problem into a steady-flow problem is very useful as a first approximation. If the friction slope is parallel to the bottom slope, accurate results are obtained. However, the passage of a wave front changes the discharge and depth and consequently the friction slope. A more elaborate

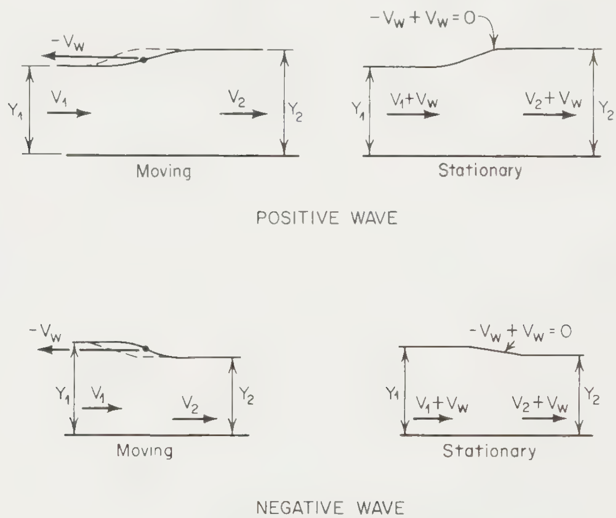

FIG. 44. Positive and negative waves.

analysis can be used if more precision is required, as it would be in relatively long channels.

45. Rating-curve Adjustments. One useful result of wave analyses assuming a constant shape of wave front is an equation for calculating the normal discharge Q_n at a particular river stage when a discharge measurement Q and time rate of change of stage j are known. Using V_w as the wave velocity and S_0 as the bottom slope,

$$Q = Q_n \sqrt{1 + \frac{j}{V_w S_0}} \tag{55}$$

For example, assume Q is measured by current meter during a rising flood stage, the rate of stage rise being 1 ft/hr. Assume the slope S_0 is 0.0002 and the wave velocity V_w is 3 fps. Then the quantity under the radical sign becomes $1 + 1 \div (3{,}600)(3)(0.0002)$ or $1 + 0.465$. The ratio $Q/Q_n = 1.21$. Therefore, the normal discharge would be 82.5 percent as large as the measured discharge under these conditions.

46. Typical Wave Velocities. Based on the assumption of a constant shape of wave front, wave velocities V_w in typical channel cross sections have been computed as follows:

	By Manning	By Chezy
Wide rectangular channel	$1.67\ V$	$1.50\ V$
Wide parabolic channel	$1.44\ V$	$1.33\ V$
Triangular channel	$1.33\ V$	$1.25\ V$

The average channel velocity is symbolized by V.

The actual channel shape is seen to have a significant effect, so that the calculation of a V_w in real channel can be approximate at best. Large-scale model studies and detailed observations along a particular reach of real channel are required to set up working procedures which involve accurate values of V_w. In the absence of such information, the usual practice is to exercise judgment in the selection of V_w with the aid of the typical factors given above.

47. Solitary Waves. Solitary waves of small height in rectangular channels have celerities approximated by

$$c = \sqrt{g(y + h)} \tag{56}$$

where c = celerity, fps, with respect to the fluid beneath the wave
y = depth
h = wave height above the average depth

48. Bores. The hydraulic bore is analyzed by the technique of Fig. 44, which transforms it into an ordinary hydraulic jump.

49. Surges in Power Canals. A long power canal flowing at maximum discharge will produce a positive surge when a sudden interrupting of the electrical load occurs. The governors automatically shut down the turbines, the flow through the plant suddenly stops, and a positive surge develops which travels upstream. Figure 45 illustrates this condition. The principle of conservation of momentum leads to the following:

$$\frac{(V_1 - V_2)^2}{g} = \frac{(y_1 - y_2)^2}{2} \frac{y_1 + y_2}{y_1 y_2} \tag{57}$$

This equation can be solved by trial and error. In the case in which $V_2 = 0$, the equation may be greatly simplified by the following approximation:

$$\frac{y_1 + y_2}{2} = \bar{y} \qquad \text{the average depth}$$

$$y_1 y_2 \approx \bar{y}^2$$

Making these substitutions and letting $V_2 = 0$ and $F_1 = V_1/\sqrt{gy_1}$

$$y_1 - y_2 = \bar{y}F_1 \tag{58}$$

The initial surge height is then approximately equal to the product of the average depth and the initial Froude number. If the average initial depth is assumed equal to y_1 for a first trial, successive trials made rapidly on a slide rule will give a reasonably accurate answer for the initial surge height.

Example: $V_1 = 6.8$ fps, $y_1 = 43$ ft, $V_2 = 0$. Find the initial surge height.

$$F_1 = \frac{V_1}{\sqrt{gy_1}} = \frac{6.8}{\sqrt{32.2 \times 43}} = 0.183$$

Assume $\bar{y} = y_1 = 43$ ft.

$$y_2 - y_1 = 0.183 \times 43 = 7.88 \text{ ft}$$

Reuse $\bar{y} = 43 + 7.88/2 = 47$ approximately.

$$y_2 - y_1 = 0.183 \times 47 = 8.6 \text{ ft}$$

Reuse $\bar{y} = 43 + 8.6/2 = 47.3$.

$$y_2 - y_1 = 0.183 \times 47.3 = 8.6 \text{ ft} \qquad \text{O.K.}$$

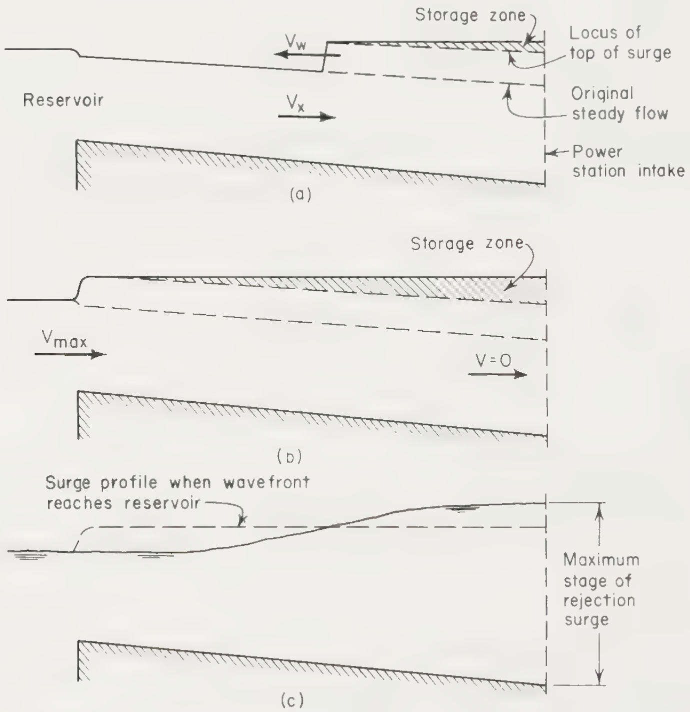

FIG. 45. Rejection surge in power canal. *(Ven Te Chow, "Open-channel Hydraulics," p. 569.)*

An important effect of the sloping channel must be taken into account for a more accurate prediction of surge height. The shaded zone labeled "storage zone" in Fig. 45 must be filled with water as the wave progresses upstream. Although this area is small when the surge begins, and V_2 is essentially zero, it becomes increasingly significant as the wave moves farther upstream, giving rise to an appreciable V_2. The trial-and-error stepwise solution of the more exact equation for surge height gives smaller and smaller surge heights as the surge approaches the reservoir. However, at the instant the surge reaches the reservoir, there is now an appreciable V_2 which produces a secondary surge over the level surface calculated on the basis of the initial shutdown.

The height of this secondary surge is less than V_2^2/g, which may be sufficiently precise for most design purposes. The velocity V_2 is calculated on the basis of the time rate of filling of the "storage zone," which in turn depends upon wave velocity, which comes from a step-by-step solution of the more exact equation for surge height.

50. Negative Surges. Small negative surges in power canals (or in tail tunnels of underground hydroelectric plants) are treated in much the same manner as are positive surges. Again the principle of conservation of momentum is used to write the equation relating surge height, depths, and velocities. Again, a trial-and-error solution is necessary, and again one must take into account the effects of slope and the requirements of continuity.

If the surge height is large, however, the fact that the top of the negative surge moves more rapidly than the bottom causes a significant change in wave-front shape.

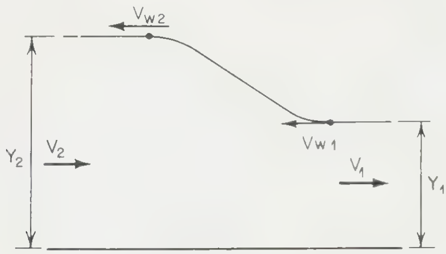

$$V_{w2} = \sqrt{gy_2} - V_2$$

$$V_{w1} = \sqrt{gy_1} - V_1 = 3\sqrt{gy_1} - 2\sqrt{gy_2} - V_2$$

$$q_1 = \left(\frac{V_{w2} + V_{w1}}{2}\right)(y_2 - y_1) + V_2 y_2$$

$$V_1 = q_1 \div y_1$$

Example: $y_2 = 10$, $y_1 = 5$, $V_2 = 0$ are given.

Then $V_{w2} = 18 - 0 = 18$

$$V_{w1} = 3\sqrt{161} - 2\sqrt{322} - 0 = 2.2$$

$$q_1 = \left(\frac{18 + 2.2}{2}\right)(10 - 5) + 0 = 50.5$$

$$V_1 = 50.5 \div 5 = 10.1 \text{ fps}$$

FIG. 46. Negative surge. (*Ven Te Chow, "Open-channel Hydraulics," p. 567.*)

More elaborate analyses are required to evaluate this effect. An approximate solution which is usually adequate for design purposes is shown in Fig. 46.

51. Long Tail Tunnels. A sudden load rejection produces, in a long tail tunnel, a negative surge which travels in the direction of flow, then returns as a positive surge. If the tunnel is not flowing full the problem is that of surges in an open channel. If the tunnel is flowing full, it becomes a surge-chamber problem, the reflected positive surge being the one which requires the surge chamber.

The air flow to and from the surge chamber tends to maintain the pressure at the top of the wave at atmospheric levels. The wave fronts then move as in ordinary open channels, the negative one moving at $\sqrt{gy}$ with respect to the main body of the flow. Again the top of the negative surge moves more rapidly than the bottom, so that the surge face flattens. The deceleration gradient causes the velocity V_1 to change continuously so that a step-by-step solution to the problem is required, the height of the wave becoming increasingly smaller. The movement of the negative surge is significant to the solution of the problem, as the magnitude of the deceleration gradient is dependent upon the wave position, as is the amount of the water to be decelerated.

52. Hydraulic Jump on Horizontal Floor. The hydraulic jump on a horizontal floor may be analyzed on the basis of the conservation of momentum. The momentum of the flow entering the jump, plus the hydraulic force of this flow, must equal the sum of the momentum of the flow leaving the jump, plus the hydrostatic force of that flow. Such an analysis ignores the friction forces on boundaries of the flow and additional forces introduced by piers, baffles, sills, and other energy-dissipating structures in the channel.

The depth and energy relationships of a jump on an unobstructed horizontal floor are shown by Fig. 47. Equating momentum and hydrostatic relationships for points

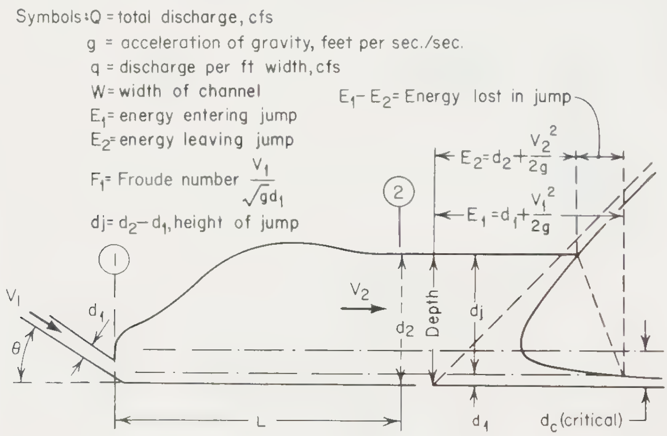

FIG. 47. Hydraulic jump on horizontal floor.

1 and 2 in Fig. 47 gives

$$d_2 = -\frac{d_1}{2} + \sqrt{\frac{d_1^2}{4} + \frac{2V_1^2 d_1}{g}} \tag{59}$$

in which d_1 = depth of channel at point 1
d_2 = depth of channel at point 2
V_1 = average velocity at point 1
V_2 = average velocity at point 2
g = acceleration due to gravity

The depths d_1 and d_2 may also be expressed in terms of the Froude number at point 1, designated as F_1, as follows:

$$\frac{d_2}{d_1} = \frac{1}{2}\left(\sqrt{1 + 8F_1^2} - 1\right) \tag{60}$$

This relationship is shown graphically by Fig. 48. The lengths of the jump L, expressed in terms of d_1, d_2, and F_1 are shown by Fig. 49 and the loss of energy in length L by Fig. 50. The relationships shown by Figs. 49 and 50 have been confirmed experimentally.

53. Hydraulic Jump on Sloping Apron. Several expressions have been developed for the hydraulic jump on a sloping apron as typified by Fig. 51. The following expression presented by Kindsvater has had wide acceptance:

$$\frac{d_2}{d_1} = \frac{1}{2\cos\phi}\left(\sqrt{\frac{8F_1^2\cos^3\phi}{1-2K\tan\phi}+1}-1\right) \tag{61}$$

All symbols have been referred to previously except K, a dimensionless parameter called the shape factor, which varies with F_1 and the slope of the apron. Figure 52 shows values of K which were determined experimentally.

It was found that the Froude number F_1 affected K only slightly; therefore, K may be related directly to $\tan\phi$ in making preliminary determinations. Figures 53,

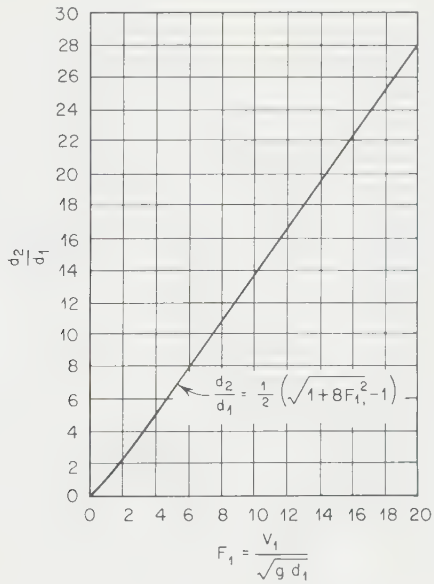

FIG. 48. Ratio of tail water depth to d_1.

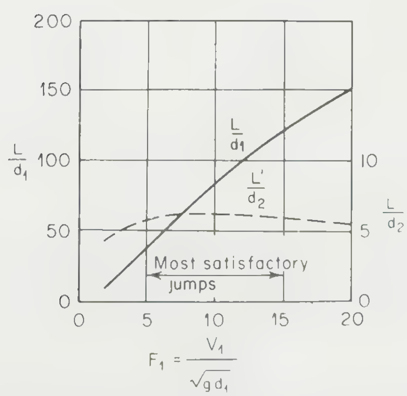

FIG. 49. Length of hydraulic jump in terms of d_1 and d_2.

54, and 55 were plotted from the results of the Bradley and Peterka experiments. Figure 53 shows the relationships between d_1 and d_2, tail-water depths, apron slopes, and F_1. Figure 54 shows the relationships between length of jump L, F_1, and apron slopes. Figure 55 shows the relationships between length of jump, tail-water depth, apron slope, and F_1.

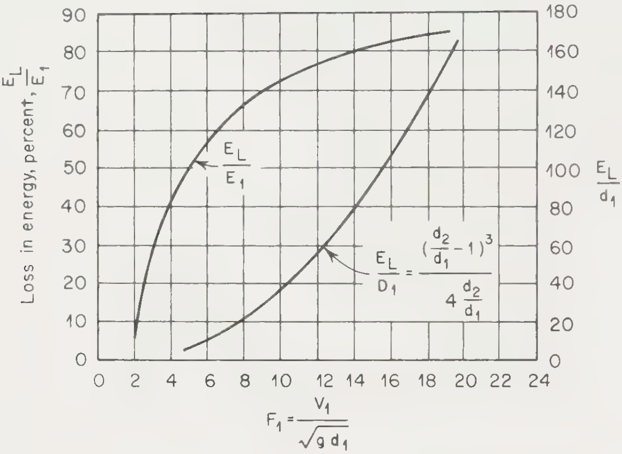

FIG. 50. Loss of energy in jump on horizontal floor.

These charts should be used as aids in the preparation of preliminary designs only. Final designs for important hydraulic structures should be verified by model tests. Further reference to application of the sloping-apron principle will be found in Sec. 20.

A small triangular sill is usually placed near the end of the apron. This serves to lift the flow as it leaves the apron and thus acts to control scour.

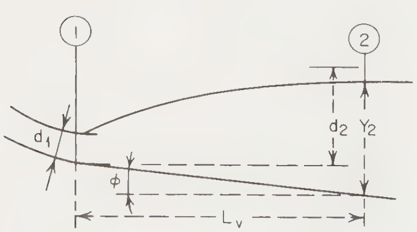

FIG. 51. Hydraulic jump on sloping apron.

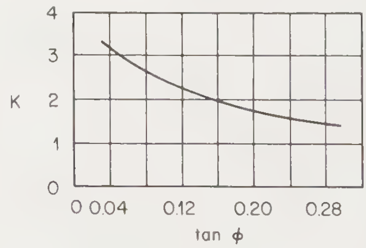

FIG. 52. K as function of tan ϕ.

54. Sharp-crested Weirs. Figure 56 shows a typical sharp-crested weir with two-dimensional flow. If the underside of the nappe is well-ventilated, the flow over such a weir without end contractions may be analyzed by

$$Q = KLh^{3/2} \qquad (62)$$

in which Q is the discharge, cfs, L is the length of the weir crest, and h is the difference between the elevation of the water surface upstream from the weir and the elevation

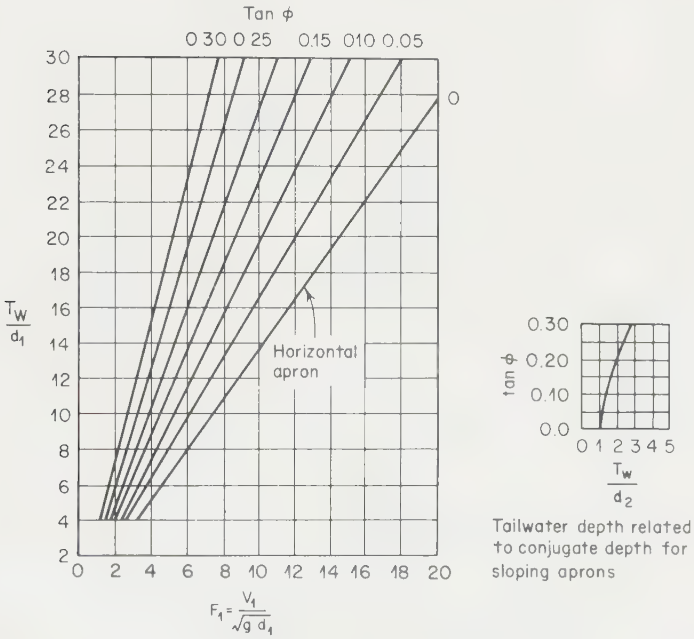

FIG. 53. Tail water depth for jump on sloping apron.

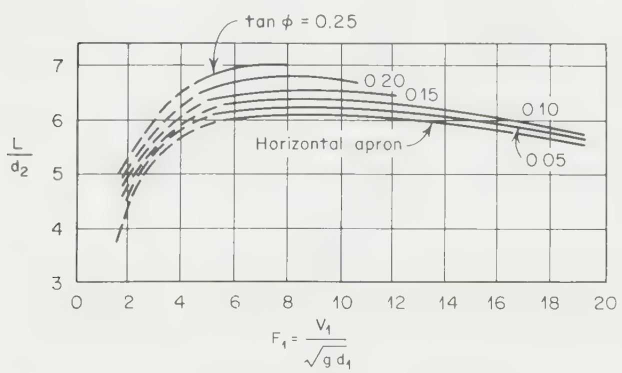

FIG. 54. Length of jump on sloping apron.

of the sharp crest. Note that h does not include the velocity head of the approach flow at the section where the elevation of the water surface is taken.

The coefficient K has been evaluated as follows by the experiments indicated:

Francis $$K = 3.33\left[\left(1 + \frac{h_v}{h}\right)^{3/2} - \left(\frac{h_v}{h}\right)^{3/2}\right] \tag{63}$$

Bazin $$K = \left(3.248 + \frac{0.079}{h}\right)\left(1 + 0.55\,\frac{h^2}{y_1^2}\right) \tag{64}$$

Rehbock $$K = 3.228 + 0.435\,\frac{h}{P} \tag{65}$$

The submerging of a sharp-crested weir, illustrated in Fig. 57, has the effect of reducing the flow over the weir to Q_1 as compared with the free flow Q determined from Eq. (62). Villemonte has found the following equation will evaluate this effect

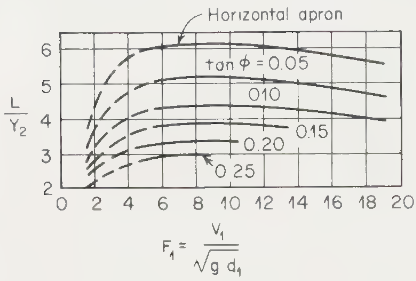

FIG. 55. Length of jump on sloping apron.

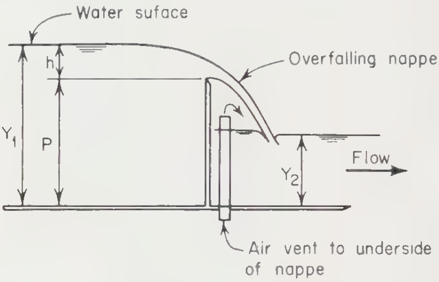

FIG. 56. Sharp-crested weir with ventilated two-dimensional overflow.

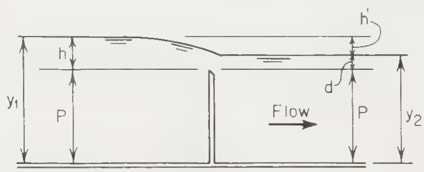

FIG. 57. Sharp-crested weir with submerged two-dimensional overflow.

with useful accuracy, the maximum deviation probably being 5 percent:

$$\frac{Q}{Q_1} = \left[1 - \left(\frac{d}{h}\right)^n\right]^{0.385} \tag{66}$$

The terms d and h are defined in Fig. 57. The exponent n is 1.5 for sharp-crested horizontal weirs without end contractions, and 2.5 for 90 deg triangular vee-notch weirs in which flow may be calculated by means of

$$Q = 2.5h^{2.5} \tag{67}$$

SECTION 3

PROTOTYPE PERFORMANCE AND MODEL-PROTOTYPE RELATIONSHIP

By Frank B. Campbell and Ellis B. Pickett

GENERAL

1. Model-Prototype Relationships. The word "prototype" has a special meaning in experimental hydraulics which does not follow the classical connotation of an original type of a class of things. The expression is used by hydraulic engineers to designate a full-scale structure or watercourse as contrasted with a reduced-scale model as used in a laboratory.

The concept of model-prototype relationship belongs to the recent era of hydraulic-model testing which is generally considered to have originated with Hubert Engles' work on river models in Dresden at the beginning of this century. Soon thereafter, Theodor Rehbock started his investigations of small-scale models of hydraulic structures at Karlsruhe.[1*] In America, the Alden Hydraulic Laboratory at Worcester, Mass., and the Alabama Power Company Laboratory at Mitchell Dam began testing models of hydraulic structures in the early 1920s.[2] Some 10 years later, the U.S. Corps of Engineers initiated their river-model testing at Vicksburg, Miss., and the U.S. Bureau of Reclamation started testing models of hydraulic structures at Ft. Collins, Colo. Each has developed into a valuable activity for their respective organizations.

The first model-prototype comparisons in the United States were the tests on discharge over the Keokuk Dam spillway by the State University of Iowa.[3] Much of the prototype testing effort in the fourth and fifth decades of this century was directed toward demonstrating that hydraulic models can predict the flow characteristics of the prototype.[4,5,6] After World War II, prototype testing began to evolve from a phase of proof of similarity between model and prototype behavior to a search for information on certain flow phenomena which cannot be obtained in the laboratory. In the meantime, the hydraulic model became recognized as a valuable design tool in many types of problems. The U.S. Army Engineers began installing prototype testing facilities in hydraulic structures and the U.S. Bureau of Reclamation made extensive collections of prototype test results.[7,8]

Froude Number—Gravity. The most basic of the model-prototype relationships are those in which the gravity forces are dominant in the model. The dimensionless ratio of inertial to gravity forces is called the Froude number in honor of William Froude.[1] This ratio is expressed as

$$\mathbf{F} = \frac{V}{(gL)^{1/2}} \tag{1}$$

where V is the velocity, g is the acceleration of gravity, and L is a significant length.

* Superior numbers refer to items in the Bibliography at the end of this section.

The model is geometrically similar to the prototype when the length ratio is

$$L_r = \frac{L_m}{L_p} \tag{2}$$

where length in the model is L_m and length in the prototype is L_p. For example, when the length ratio is 1/25, the linear scale ratio of the model is usually expressed as 1:25.

The Froude number in the model must be equal to that of the prototype if dynamic similarity is to be achieved in this type of model:

$$\frac{V_m}{(g_m L_m)^{1/2}} = \frac{V_p}{(g_p L_p)^{1/2}} \tag{3}$$

where V is the velocity and g is the acceleration of gravity with the proper subscripts. As the acceleration of gravity is essentially the same in model and prototype, the velocity ratio is

$$V_r = \frac{V_m}{V_p} = \frac{(L_m)^{1/2}}{(L_p)^{1/2}} = L_r^{1/2} \tag{4}$$

From Eqs. (2) and (4), it can be shown that the time scale ratio is

$$T_r = L_r^{1/2} \tag{5}$$

Recognizing that the volume ratio is the cube of the linear ratio, the discharge ratio is

$$Q_r = L_r^{5/2} \tag{6}$$

Therefore, when the linear scale ratio is established, the velocity and discharge scale ratios can be determined from Eqs. (4) and (6), insofar as the Froude law for dynamic similarity is applicable.

Reynolds Number—Viscosity. The effect of viscosity is important in establishing the physical limitations of model studies and in interpreting the results of certain types of prototype studies. Reynolds number is dimensionless and expresses the ratio of inertial to viscous forces as follows:

$$\mathbf{R} = \frac{VL}{\nu} \tag{7}$$

where ν, the kinematic viscosity, is the ratio of dynamic viscosity γ to density ρ of the fluid. The value of ν for water at 60 F is 1.21×10^{-5} sq ft/sec.[9]

The Reynolds number is of interest where surface resistance and form resistance are of an appreciable magnitude. The relationship of pressure-conduit resistance to Reynolds number is discussed in Art. 4. The drag coefficient of a cylinder, for example, is also a function of Reynolds number.[9]

Weber's Number—Surface Tension. The surface tension of water is not significant in as many problems as are gravity and viscosity. Nevertheless, in certain problems of similitude, it can become very important. Because of the relatively greater occurrence of the significances of other forces, surface tension may often be ignored in the interpretation of laboratory studies. Weber's number can be expressed as

$$\mathbf{W} = \frac{V}{\sqrt{\sigma/\rho L}} \tag{8}$$

where σ is the surface tension of the liquid. As the Weber number decreases, the effect of surface tension increases. The surface tension for water at 60 F is 0.00503 lb/ft.[9]

It has long been recognized that the spray from high-velocity jets as generated by flip buckets or Howell-Bunger valves cannot be simulated in the laboratory with water. Spray can cause icing on nearby highways and troubles in power-plant switch yards unless proper provisions are made. Air entrainment in steep chutes cannot ordinarily be predicted from a small-scale model.

The increase of the coefficient of discharge over thin-plate laboratory weirs[10] and spillway models, at very low heads, has often been observed. Although the cause of this phenomenon has not been fully explored, surface tension may be involved. In any case, spillway-model discharge coefficients with heads less than about 0.15 ft should not be interpreted as applicable to the prototype based on the Froude law alone.

2. Usefulness of Models. Hydraulic models may be classified roughly into structures and natural watercourses. Models of hydraulic structures have been employed extensively for specific projects and have been the subject of considerable basic research and generalization. However, many problems remain to be investigated. Models of natural watercourses have been studied for the effects of proposed artificial modification. Since a natural watercourse involves individual characteristics for each project, basic research and generalization have been scanty. Hydraulic machinery models are beyond the scope of this treatment. Hydraulic models have been found useful in the types of problems discussed briefly in the following paragraphs. This treatment is not intended to cover all such problems but rather to indicate the general types of problems where hydraulic-model testing has been found useful in design. The saving in construction costs alone is normally many times the cost of the model study.

Hydraulic Structures. Hydraulic-model studies of spillways and outlet works have constituted a fruitful field of endeavor, resulting in large savings in the cost of construction and improvement in operation.

Spillway Models. The hydraulic design of overflow spillways in connection with large concrete dams involves a number of problems where adequate criteria are lacking. The approach channel may be curved in plan, and three-dimensional flow nearly always develops in approaching the drop through critical depth at the overflow spillway. The effect of the abutment on the head-discharge relationship depends upon the approach conditions as well as upon the geometric and hydraulic variables. The contraction coefficient for crest piers of various cross sections and locations can be studied in the laboratory. A section model of larger scale ratio in a flume is of value in the study of the head-discharge relationship for various types of crest gates and degrees of submergence.

Chute spillways with low control crests of different cross sections have been studied in the laboratory. The wave patterns caused by disturbances at the trailing ends of crest piers can be reproduced qualitatively in the model. Chute spillways with converging and diverging side walls, in plan, involve three-dimensional flow which usually requires a model for solution. Important details of numerous other flow problems can be investigated with a hydraulic model. The free-surface vortex is a difficult problem in which the laws of similitude are not well known.

Outlet-works Models. Relatively short sluices through a concrete dam cannot be expected to have as large an effect of surface resistance as do longer conduits and tunnels. In general, the hydraulic model is of value in studying local pressures at boundary changes. Although the cavitation index cannot be transferred directly to the prototype, the tendency for low pressures to form at certain boundary locations is an indication that curvature away from the direction of flow is too severe.

The relative efficiency of different entrance shapes and gate chamber transitions can be evaluated in the laboratory. The effectiveness of and local pressures on tetrahedral deflectors designed to spread the jet at the exit portal can be studied in models. Reliable discharge coefficients of partly opened gates can be readily determined in the model.

Energy-dissipator Models. Hydraulic models are especially valuable in designing effective and economical energy dissipators. Gravity forces can be expected to be dominant. The behavior of the roller bucket has been studied in the laboratory[11] and in numerous models.[12] This type of problem can be investigated with a section model in a flume. The trajectory of a flip bucket can be studied in a model but prototype losses on the overflow section or in the tunnel should be estimated from prototype test results. The disintegration or fraying of the prototype jet with the attendant spray and mist cannot be simulated in the model because of the Weber-number effect. A qualitative study of scour tendencies of the plunging jet for various tail-water depths can be made with a movable-bed model.

Stilling-basin models are normally a profitable investment in hydraulic design for major projects. As the hydraulic jump is involved, the Froude law is applicable. Models have been used to advantage in the design of stilling basins as energy dissipators for both spillways and outlet works. The formation of the hydraulic jump requires that the pressure plus momentum upstream and downstream from the jump be equal. In a rectangular channel, this can be expressed as

$$\frac{d_2}{d_1} = \frac{1}{2}\left(\sqrt{1 + 8\mathbf{F}_1^2} - 1\right) \tag{9}$$

where d_1 and d_2 are the upstream and downstream depth, respectively, and $\mathbf{F}_1$ is the entering Froude number. It is common practice to use baffle blocks and end sills to permit a higher floor elevation of the basin or to reduce its length. As little is known of the entering distribution of velocity and the drag coefficients of baffle piers of various shape, size, and spacing, the hydraulic model becomes a valuable design tool. The bottom velocity at the termination of the structure is an important criterion of safe operation for the particular resistance to erosion of the unprotected channel bottom. These bottom velocities can be measured in the hydraulic model.

Natural Waterways. The design problems of concern with engineering works in natural waterways generally involve artificial modification of the natural condition. As each problem has its specific, commonly irregular boundaries, the hydraulic model study is very valuable. The types of such model studies can be loosely classified into rivers, estuaries, and harbors. However, a single model may be used at times for more than one purpose.

A river model may have flood problems as its principal objective where it is used to study levee and flood wall heights. The effect of a cutoff across the neck of a meander loop on the lowering of flood stages can be studied successfully in a model. The result of a navigation lock and dam or other constriction upon the increase of flood stages has been investigated in models. Problems of inland navigation in connection with locks and dams include lock-approach currents and shoaling in the navigation channel.

Models of estuaries are used to study the movement of the salt-water wedge with the ebb and flow of the tides for various fresh-water inflows. The deposition of sediment in estuaries may result in costly dredging to maintain navigation channels. The pollution of water supply by the salt-water wedge or by raw sewage can be studied in an estuary model. The effect of and protection against hurricane-generated tidal waves in an estuary have been successfully studied in hydraulic models.

Models of harbors are normally used to investigate wave-action problems. The optimum location of breakwaters to protect against heavy wave action within the harbor is a common objective of harbor models. The stability of the breakwater itself has been studied extensively in the laboratory. The effect of tsunamis or waves generated by seismic action can be studied in harbor models. With the rapid increase in pleasure craft, more emphasis is being placed on model studies of small-craft harbors.

Model Adjustments. Although gravity forces are expected to be dominant in hydraulic models, it has been found necessary and practical to make adjustments in some types of models to account for the effects of viscosity. Such adjustments are occasionally made in models of hydraulic structures and more often in models of natural waterways.

In the case of a chute spillway with a stilling basin, the model should be operated so that the sum of the pressure and momentum per foot of width entering the model basin simulates that of the prototype. As the loss in the model chute is normally higher than that for the corresponding flow in the prototype, a greater discharge in the model can be selected which simulates the pressure plus momentum entering the basin. A similar problem is encountered in the study of local pressures in a gated intake or central control shaft for a conduit or tunnel. Even a hydraulically smooth tunnel model will have a higher resistance coefficient than that of the prototype because of viscous effects. However, the pressure at the downstream end of a gate chamber or transition can be simulated by shortening the tunnel to a length based on resistance coefficients previously measured in model and prototype tunnels.

Whereas hydraulic models of structures with the Froude law applicable are normally undistorted; the natural waterway model where Reynolds law becomes important often involves linear distortion. The vertical scale is made large compared with the horizontal scale. Thus, there is a greater bottom slope and a greater flow depth in the model than would exist in an undistorted model. Both distortions tend to offset the effect of viscous forces inherent in a model of this type.

The pioneering work of Osborne Reynolds was conducted with distortions of horizontal to vertical scales of 1:33 and 1:27.[2.13] Such large distortions probably affected hydraulic laboratory practice for the next half century. Modern practice has tended toward a larger horizontal scale with less distortion, progressing from a distortion of 1:10 to 1:4 or even to undistorted models, where the potential construction and operations savings justify the cost of the larger-size model.

There are two general types of natural waterways models: the fixed-bed and the movable-bed. The first is used when bottom scour is not germane to the problem and the second when scour is important. For example, if the model is a fixed-bed type, an undistorted model may be justified; whereas in the case of the movable-bed model a 1:1½ or 1:2 distortion ratio has been successfully used. The larger vertical distortion produces a greater boundary shear on the bed of the model in order to simulate the natural bed-load movement with the attendant scour and deposition involved. Further, the engineer designing the model has recourse to two independent variables in selecting the model bed material. The grain size and the density of the bed material can be selected to give the desired results. Crushed bituminous coal with a specific gravity of approximately 1.3 is an economical bed-load material. Bed material made of plastic has been used but, in general, such manufactured particles are much more expensive.

Prototype verification is a necessary procedure in the model technique of natural watercourses. For example, in a fixed-bed flood-control model, certain adjustments are made in the model so that a prototype stage hydrograph can be simulated in the model. After the adjustments are made, the proposed artificial modifications are built in the model to determine their effect upon the hydrograph. In the prototype-verification process, the engineer may choose to adjust the boundary roughness, the water-surface slope, and perhaps the discharge itself. Experience and skill play a large part in the judgment required for an expeditious prototype-verification process.

Model adjustments for forces other than viscosity have not been well explored, although it appears possible to adjust *surface tension* in the model. As previously mentioned there may be a surface-tension effect for very low heads over weirs and overflow crests. The possible surface-tension effect upon the incipiency of a core of air being drawn into a free-surface vortex needs to be investigated. Modern wetting agents such as Aerosol and Santomerse are powerful surface-tension depressants. Certain precautions must be taken as the surface tension varies not only with concentration of the wetting agent but also with temperature and time after mixing. The experimenter must therefore be equipped to measure surface tension and adjust the concentration of the aqueous mixture. Exploratory tests with Aerosol have shown that excessive foaming may be a nuisance. However, with care, the Weber number may be adjusted in the laboratory.

A model to adjust the speed of travel of a water-hammer wave involves the *Mach number*. The speed of a pressure wave is dependent upon the moduli of elasticity of both the fluid and the pipe material, as well as the pipe diameter and thickness. Such model adjustments have been successfully made[14] by using plastic pipe of known elasticity. However, most clear plastics change their modulus of elasticity with time. Provision should therefore be made to conduct stress-strain tests on samples of the plastics used.

3. Necessity for Prototype Data. As mentioned in Art. 2, the prediction of prototype behavior from laboratory studies depends principally upon the Froude law. In cases where viscosity effects become substantial, the geometry or other independent variables must be distorted to simulate the prototype, as discussed above under Model Adjustments.

Viscosity. In the case of models representing natural watercourses, prototype observations of stage-discharge relationships are needed in order to conduct the prototype-verification tests of the model. If length adjustments are made in an outlet works model, prototype tests on conduit resistance are necessary to estimate the amount of length adjustment. It is therefore important to obtain prototype-test results for models where similitude is affected by viscosity. The same is generally true of open-channel flow, although precise field measurements in this category are difficult.

Of more direct concern to the designer are coefficients involved with surface resistance and form resistance. Economic studies of power penstocks and pressure conduits, in general, require reliable prototype information on the resistance coefficient to be expected. Prototype-test results are therefore necessary for direct use by the designer. There are thus two general objectives requiring prototype tests. When the flow phenomena are substantially affected by viscosity, prototype data are needed for both the laboratory and the design office.

Surface Tension. Surface-tension effects enter into a few special problems of model-prototype similitude. It has long been recognized that small-scale models cannot be used to determine the amount of air entrainment to be expected in a chute spillway. In such a case, both the development of the turbulent boundary layer, involving viscosity, and the entrainment of air from the surface, involving surface tension, may be expected to affect the quantity of air entrained and the bulking of the flow. In the problem of spray generated by jets from flip buckets or high-head valves surface tension suppresses the spray in the small-scale model. Prototype observations are needed in these cases and quantitative field tests are difficult. The effects of surface tension on the incipiency of a free-surface vortex with an air core in an intake model need further study in the field and laboratory.

Cavitation. The transfer of laboratory tests of the cavitation phenomena to the prediction of occurrence in the prototype is an unsolved problem. Until further progress is made, the designer of high-head projects should familiarize himself with the boundary conditions where cavitation has occurred in the prototype.

Vibration. Much theoretical and experimental work has been done on the vibration of elastic bodies. However, little is known of the disturbing frequency and force amplitude of various phenomena of flowing water. Again, as in the case of cavitation, the designer should familiarize himself with prototype observations of the vibration of gates and structural elements in contact with the flow.

CLOSED CONDUITS

4. Resistance Coefficients. *General Equations.* The total energy head H_M in a conduit may be expressed by the equation

$$H_M = (K_e + K_f + K_t + 1.0)\frac{V_c^2}{2g} \tag{10}$$

in which the coefficient K_e is for entrance losses; K_f is for surface resistance (friction); K_t is for transitions and other losses; 1.0 is for loss of the velocity head at the exit portal; and V_c is the mean velocity of the conduit flow. Prototype data have been obtained in varying amounts at different projects for surface resistance and entrance losses, but very little prototype information is available for losses from other elements of the conduit system.

The conduit-resistance loss coefficient K_f can be expressed in terms of the Darcy[15]-Weisbach[16] resistance coefficient f by the relation

$$K_f = f\frac{L}{D} \tag{11}$$

where L is the length of the reach and D is the conduit diameter. The variation of f with Reynolds number is given on the Moody[17] diagram shown in Fig. 1, which is extrapolated from the small pipe tests and analyses of Nikuradse,[18] Von Karman and Prandtl,[19,20,21] and Colebrook.[22]

The Manning formula has been used extensively in the computation of surface-resistance losses in both open and closed conduits. Empirical formulas developed by Scobey, Hazen-Williams, and others also have proved applicable to the determination of pipe-surface resistance in limited ranges of Reynolds numbers. The principal objections to these formulas are the dimensional character of the coefficients involved and the limited extent to which the coefficients may be extrapolated. The Darcy-Weisbach resistance coefficient, however, is dimensionless and is favored for use with the modern concepts of conduit resistance. Manning's n and the Darcy-Weisbach f for circular conduits can be related by the equation

$$f = \frac{185n^2}{D^{1/3}} \qquad \text{in English units} \tag{12}$$

Conduit pressure gradients determined from these equations are for fully developed turbulent flow in the conduits. In the upstream part of the conduit (the first 50 to 100 diameters) the effects of the conduit entrance and the development of the turbulence will result in a steeper gradient and give the appearance of a higher resistance coefficient.

Lined Tunnels and Conduits. Available prototype-test data for the large, lined tunnels and conduits listed in Table 1 are shown in Fig. 1. The concentration of the data from each test about its mean line is indicated by the standard-deviation values given in the tabulation. The prototype resistance-coefficient data include both smooth and rough concrete surfaces and steel surfaces with both smooth and rough

TABLE 1. CONDUIT-RESISTANCE TESTS

Curve		Project name	Test section			Tests			Range of data				Data source
Symbol	No.		Surface	Diam, ft	L/D	Year	Age, years	No.	Velocity, fps	R_e	f	Standard error	
○	1	Fort Randall Penstock 1, Missouri River, S.D.	Coal-tar enamel on steel	22	22	....	....	20	10.5 14.7	1.25×10^7 1.75×10^7	0.01053 0.01045	0.00023	General Design Memorandum G-7, 1955, U.S. Army Engineer District, Omaha
○	2	Fort Randall Penstock 8, Missouri River, S.D.	Vinyl paint on steel	22	22	1956	....	29	6.4 14.6	8.11×10^6 1.84×10^7	0.00833 0.00739	0.00017	General Design Memorandum G-9, 1956, U.S. Army Engineer District, Omaha
△	3	Fort Randall Tunnel 10, Missouri River, S.D.	Coal-tar enamel on steel	22	29	1959	....	5	21.0 65.8	4.67×10^7 1.46×10^8	0.00881 0.00869	0.00098	Unpublished data, U.S. Army Engineer Waterways Experiment Station
○	4	Denison Dam Tunnel, Red River, Okla. and Tex.	Concrete	20	32	1947–57	....	3	65.3 71.6	1.20×10^8 1.40×10^8	0.00764 0.00762	0.00034	Unpublished data, U.S. Army Engineer Waterways Experiment Station
△	5	Pine Flat Dam Conduit, Kings River, Calif.	Concrete	Rect. 5 × 9	54	1952	....	7	61.5 68.4	2.80×10^7 3.43×10^7	0.01318 0.01317	0.00037	Unpublished data, U.S. Army Engineer Waterways Experiment Station
○	6	Pine Flat Dam Conduit, Kings River, Calif.	Concrete	Rect. 5 × 9	54	1954–58	....	6	80.5 91.5	3.54×10^7 4.49×10^7	0.01750 0.01750	0.00073	Unpublished data, U.S. Army Engineer Waterways Experiment Station
△	7	Ontario Power Co. Tunnel, Niagara Falls, Canada	Concrete	18	361	....	8	5	4.0 20.0	5.88×10^6 2.94×10^7	0.00889 0.00733	0.00059	Scobey *Bull.* 852, 1924, USDA, Washington, D.C.
○	8	Umatilla River Siphon, Umatilla Project, Ore.	Concrete	3.83 3.83	2,550 2,565	....	5 2	5 2	1.4–3.2 4.0–4.2	3.80×10^5 1.14×10^6	0.01481 0.01310	0.00164	Scobey *Bull.* 852, 1924, USDA, Washington, D.C.
△	9	Umatilla Dam Siphon, Umatilla Project, Ore.	Concrete	2.5	2,011	....	New	3	3.4 3.6	6.00×10^5 6.40×10^5	0.01406 0.01396	0.00075	Scobey *Bull.* 852, 1924 USDA, Washington, D.C.

TABLE 1. CONDUIT-RESISTANCE TESTS (*Continued*)

Curve		Project name	Test section			Tests			Range of data				Data source
Symbol	No.		Surface	Diam, ft	L/D	Year	Age, years	No.	Velocity, fps	R_e	f	Standard error	
□	10	Prosser Pressure Pipe, Yakima, Wash.	Concrete	2.54	896	....	4	7	4.9 5.8	1.01×10^6 1.20×10^6	0.01768 0.01761	0.00151	Scobey *Bull.* 852, 1924, USDA, Washington, D.C.
▽	11	Deer Flat Conduit, Boise Project, Idaho	Concrete	3.0	2,427	....	6	5	5.4 9.1	1.32×10^6 2.20×10^6	0.01368 0.01333	0.00123	Scobey *Bull.* 852, 1924, USDA, Washington, D.C.
△	12	Chelan Station Conduit, State of Washington	Concrete	14.0	659	....	New	17	1.2 14.8	3.40×10^6 1.69×10^7	0.01123 0.01056	0.00039	Fosdick, *Trans. ASCE*, Vol. 101, 1936
○	13	Enid Dam Tunnel, Yocona River, Miss.	Concrete	11.0	5	1958	6	8	37.0 38.9	2.58×10^7 2.71×10^7	0.01290 0.01290	0.00062	Unpublished data, U.S. Army Engineer Waterways Experiment Station
□	14	Oahe Dam Tunnel, Missouri River, S.D.	Concrete	18.25	36	1960–62	....	4	36.7 44.4	7.37×10^7 9.17×10^7	0.00690 0.00682	0.00079	Unpublished data, U.S. Army Engineer Waterways Experiment Station
□	15	San Gabriel Penstock, Los Angeles County, Calif.	Enameled steel	4.23	118	1953	....	30	6.0 36.0	1.82×10^6 1.17×10^7	0.01162 0.01037	0.00066	Burke, *Trans. ASCE*, Vol. 120, 1955
▽	16	San Gabriel Penstock, Los Angeles County, Calif.	Enameled steel	10.23	49	1953	....	26	7.3 49.9	5.57×10^6 3.81×10^7	0.00880 0.00653	0.00031	Burke, *Trans. ASCE*, Vol. 120, 1955
□	17	Garrison Dam Penstock, Missouri River, N.D.	Vinyl paint on steel	24	32	1956	New	26	8.0 15.5	1.54×10^7 2.96×10^7	0.00761 0.00698	0.00019	Friction Loss Tests in Penstock 1, 1957, U.S. Army Engineer District, Garrison
○	18	Niagara–Sir Adam Beck Tunnel, Canada	Concrete	45	624	1954	New	6	8.4 15.1	3.25×10^7 5.66×10^7	0.00769 0.00747	0.00019	Bryce and Walker, *Eng. J.*, August, 1959
○	19	Louisville Sewer Model	Plastic	0.490 and 0.330	508 762	1949	New	16	1.18 4.15	4.80×10^4 1.13×10^5	0.0206 0.0168	....	Unpublished data, U.S. Army Engineer Waterways Experiment Station

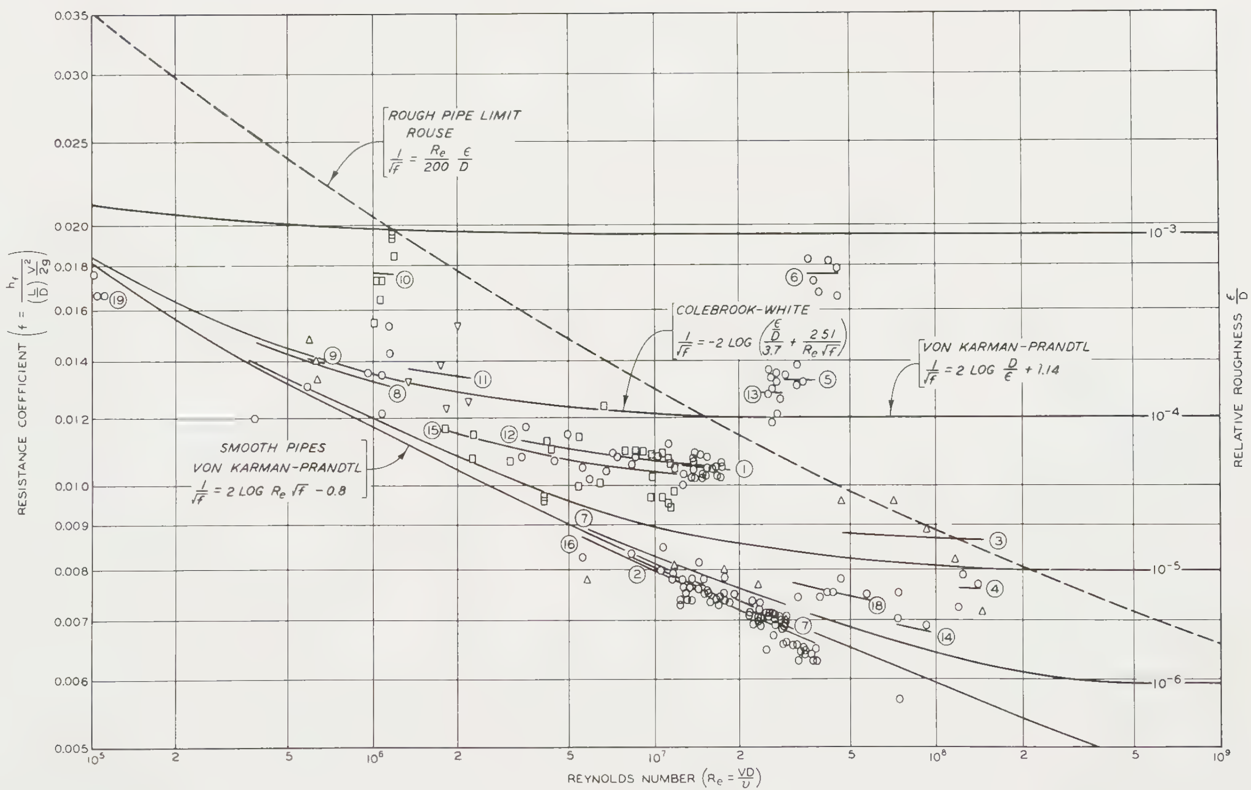

FIG. 1. Lined conduit and tunnel resistance coefficients. (h_f = resistance loss, ft; L = length of conduit, ft; D = conduit diameter, ft; ϵ = absolute roughness, ft; V = velocity, fps; ν = kinematic viscosity, sq ft/sec; and g = gravitational acceleration, ft/sec².)

finishes. The Pine Flat data are for a rectangular conduit and are plotted for a diameter based on equivalent hydraulic radius. The Louisville sewer data are from a smooth-plastic-model test. The smooth-pipe curve usually can be used in the design of smooth plastic models with appropriate adjustments for the anticipated prototype resistance coefficient.

The U.S. Army Engineers have obtained plaster replicas of conduit surfaces in a number of prototype tests in an attempt to correlate the physical roughness of the surface with the hydraulic roughness. A value of 2 times the standard deviation of the surface-profile fluctuations from the mean was assumed equivalent to a uniform sand grain diameter k. The results of these studies are given in Fig. 2 (after Rouse[23]),

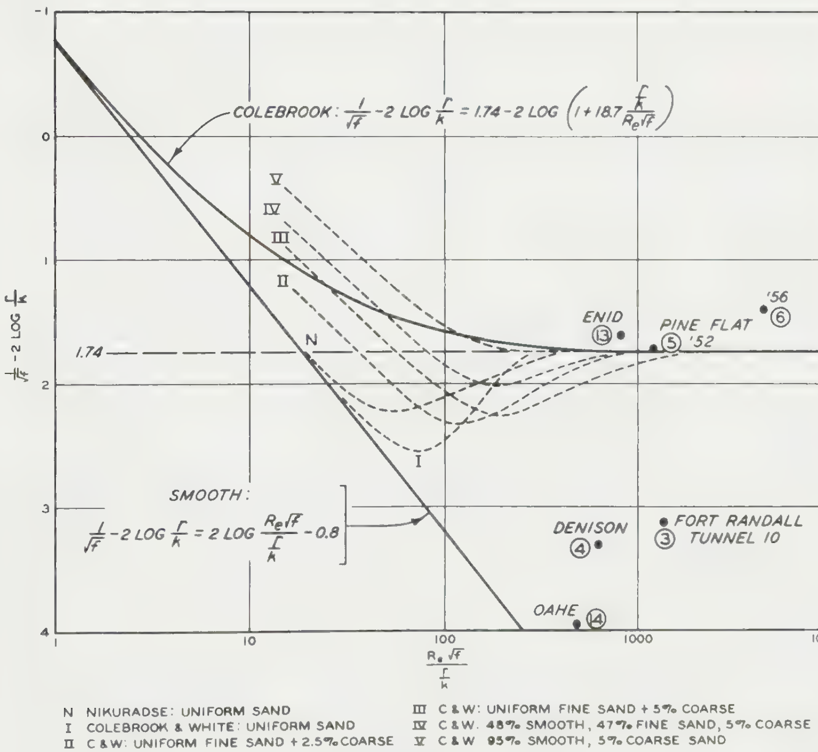

FIG. 2. Conduit-resistance transition functions for different types of surface roughness (after Rouse[23]). (f = resistance coefficient; r = conduit radius, ft; k = sand grain diameter, ft; and R_e = Reynolds number = VD/ν, where V = velocity, fps; D = conduit diameter, ft; and ν = kinematic viscosity, sq ft/sec.)

which shows a comparison of transition functions between smooth- and rough-pipe conditions for several kinds of surface roughness. There is fairly good agreement for the rough-pipe flow, but more tests are needed to confirm or develop the transition between smooth and rough for prototype structures. The transition function in Fig. 1 was developed by Colebrook and White from data on commercial steel pipe. However, a different transition may be more representative of flow conditions in large prototype conduits and tunnels.

Transition curves for several geometric patterns of roughness were developed by

Miller,[24] and all lie below the rough-pipe flow curve shown in Fig. 2. It appears that the shape of the transition depends upon the size, relative roughness, and relative spacing of the elements as well as upon the Reynolds number.

The data from the Army Engineers tests have been analyzed[25] in an attempt to correlate construction practices in forming concrete conduits and treating the interior surfaces. Table 2 is a summary of the results. The values of n were determined from the values of f by means of Eq. (12) and therefore would not be applicable to a conduit with a different diameter at the same Reynolds number.

Table 2. Observed Resistance Coefficients

Surface character	Coefficient	
	f	n
Near $R_e = 10^8$:		
Concrete, wood forms, joints ground (Oahe)	0.0068	0.0098
Concrete, steel forms (Denison)	0.0072	0.0103
Steel, coal tar (Ft. Randall)	0.0085	0.0114
Near $R_e = 10^7$:		
Steel, vinyl (Ft. Randall)	0.0075	0.0107
Concrete, wood forms (Enid)	0.0130	0.0125
Concrete, wood forms (Pine Flat)	0.0132	0.0115
Concrete, wood forms, roughened with use (Pine Flat)	0.0181	0.0135

Unlined Tunnels. The design decision as to whether to line a water-carrying tunnel or to leave it unlined involves a number of factors which affect the economic aspects of a project. The matter of structural stability of an unlined tunnel in rock depends on the findings of subsurface exploration, a study of the rock mechanics, and is beyond the scope of this section. The prospect of loss of flow through faults or fissures can be forecast only by thorough subsurface information, geological studies, and a knowledge of the groundwater features. In an opposite sense, the possibility of heavy flows into the tunnel during construction can be forecast only by studies similar to those just mentioned.

This treatment is concerned only with the probable loss of hydraulic head in a tunnel for a given discharge. Experience indicates that there is a wide variation in the resistance coefficient f depending upon the nature of the rock through which the tunnel is driven and the techniques of blasting used during construction. The literature reveals very little information on either aspect for those tunnels where discharge and head-loss measurements are available.

It can be expected that the friction factor in an unlined tunnel would be independent of the Reynolds number but would depend upon a ratio of an effective diameter to an average roughness size of the wall. The Von Karman–Prandtl type of equation can be expressed as

$$\frac{1}{\sqrt{f_t}} = 2 \log \frac{D_e}{K_e} + 1.14 \tag{13}$$

where f_t is a theoretical resistance coefficient, D_e an effective diameter, and K_e an effective roughness size.

Information on field measurements of the tunnel boundaries and head loss was not generally available until the publication of Rahm's[26] study. Colebrook[27] presented a study of Rahm's observations along with other information on lined tunnels.

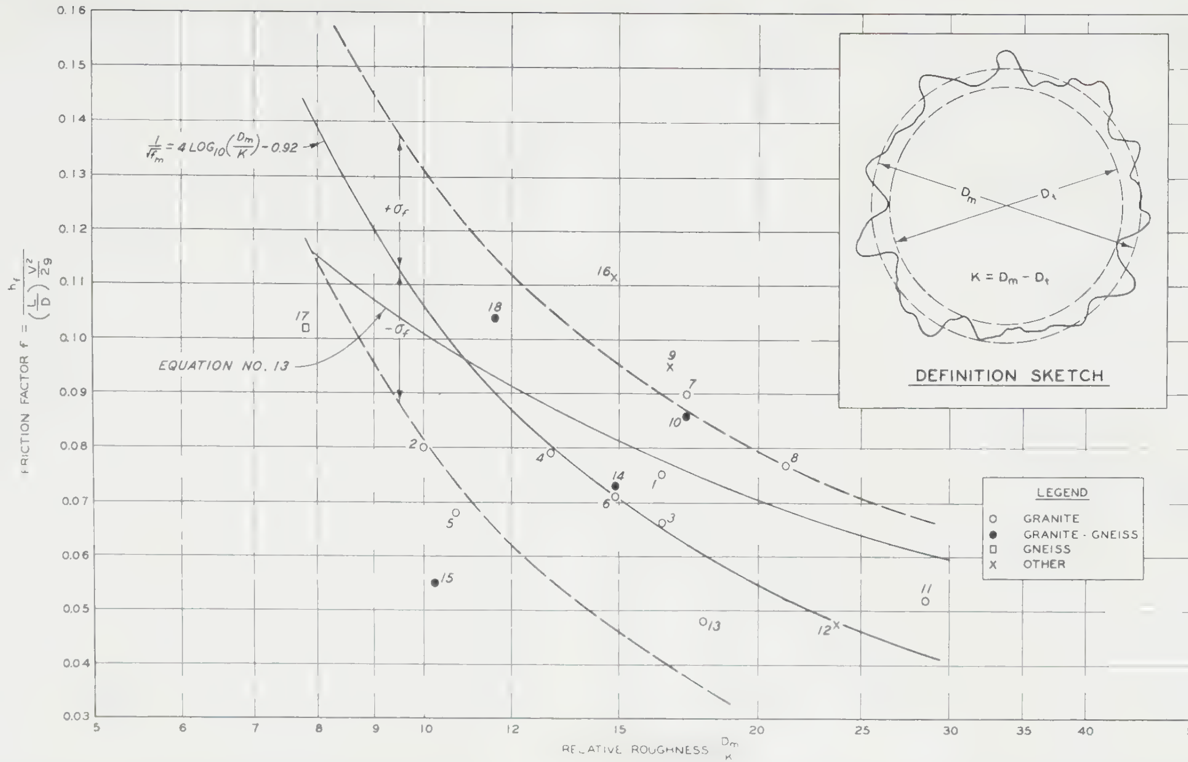

FIG. 3. Resistance coefficients for unlined tunnels. (f_t = resistance coefficient; D_m = mean diameter of completed tunnel, ft; D_t = theoretical diameter of tunnel, ft; K = effective roughness height, ft; h_f = resistance loss, ft; L = length of tunnel, ft; D = diameter, ft; V = velocity, fps; and g = gravitational acceleration, ft/sec^2.)

Colebrook recommended a mean roughness size of 6 in. to be used with the theoretical or specified diameter for smooth limits.

A restudy has been made of Rahm's observations along with data on American tunnels collected by Schumann.[28] This treatment is based on an average diameter and an average roughness size determined from the percent of cross-sectional overbreak area measured in the field. In most construction, it is required that blasting be performed so that no rock or only a very small percentage of the rock may protrude inside the theoretical or specified cross-sectional line.

Reference is made to the definition sketch in Fig. 3. The field measurements from tunnels of a horseshoe shape are treated as circular tunnels of equivalent cross-sectional area. The ratio of overbreak area to theoretical area can be expressed as

$$r_0 = \frac{A_m - A_t}{A_t} \tag{14}$$

Since the theoretical area is specified and the overbreak is measured, the mean effective area can be calculated from

$$A_m = A_t(1 + r_0) \tag{15}$$

The diameter of a circle with area A is

$$D = 1.128A^{1/2} \tag{16}$$

If it is assumed that the effective roughness height is

$$K = D_m - D_t \tag{17}$$

then the relative roughness is

$$\frac{K}{D_m} = 1 - \frac{D_t}{D_m} = 1 - \left(\frac{A_t}{A_m}\right)^{1/2} \tag{18}$$

It should be noted that the roughness K, calculated as the difference between the mean actual diameter and the theoretical diameter, is twice the mean overbreak thickness. Therefore, the nature of the K dimension is similar to the Nikuradse sand-grain-diameter concept.

The values of D_m, K, and D_m/K have been calculated from the areas available and are included in Table 3. The relative roughness was plotted on a semilogarithmic graph against the measured friction coefficient as seen in Fig. 3. The curve of best fit was found to be

$$\frac{1}{\sqrt{f_m}} = 4 \log \frac{D_m}{K} - 0.92 \tag{19}$$

The von Karman–Prandtl equation (13) is drawn for comparison with the data points described below.

It is not surprising that the plotted data exhibit considerable scatter in view of the variable nature of rock characteristics and blasting techniques. A comparison of the theoretical friction factor f_t with the f_m measured is shown in Table 3. The standard error is $\sigma_f = 0.0247$. Two curves representing $+\sigma_f$ and $-\sigma_f$ are drawn in Fig. 3.

It is recommended that the values of K shown in Table 3 be used as a guide for estimating the relative roughness. The value of f_t can in turn be estimated by Eq. (19) for a design basis or for an economic comparison with lined tunnels. If surge-tank design is involved, the $-\sigma_f$ curve can be used for the "load off" or decelerating flow.

Pressure Gradient at Exit Portal. The vertical location of the intersection of the pressure gradient with the exit-portal plane is important in design problems where

TABLE 3. FRICTION FACTORS—UNLINED ROCK TUNNELS

No.	Project	Rock	D_m, ft	K, ft	D_m/K	f_t	f_m
1	Cresta	Granite	28.9	1.8	16.4	0.0645	0.075
2	West Point	Granite	16.8	1.7	10.0	0.1053	0.080
3	Bear River	Granite	10.9	0.7	16.4	0.0645	0.066
4	Balch	Granite	14.7	1.2	13.0	0.0802	0.079
5	Haas	Granite	15.3	1.5	10.7	0.0980	0.068
6	Kings River	Granite	15.9	1.0	14.7	0.0704	0.071
7	Cherry	Granite	13.8	0.8	17.3	0.0614	0.090
8	Jaybird	Granite	15.7	0.7	21.3	0.0519	0.077
9	Apalachia	Quartzite and slate	23.4	1.4	16.7	0.0634	0.095
10	Alfta	Granite-gneiss	21.2	1.0	17.3	0.0614	0.086
11	Harsprånget	Granite	52.8	1.8	28.6	0.0416	0.052
12	Järpstrommen	Slate	39.5	1.6	23.8	0.0476	0.048
13	Krokstrommen	Granite	37.2	2.1	17.9	0.0598	0.048
14	Porjus I	Granite-gneiss	28.1	1.9	14.9	0.0704	0.073
15	Porjus II	Granite-gneiss	29.0	2.8	10.2	0.1031	0.055
16	Selsfore	Slate-granite	33.2	2.3	14.9	0.0704	0.114
17	Sillre	Gneiss	9.5	1.2	7.8	0.1425	0.102
18	Sunnerstaholm	Granite-gneiss	22.2	2.0	11.6	0.0885	0.104

NOTE: Projects 1 to 9 are American tunnels. Projects 10 to 18 are Swedish tunnels. Basic data are from Schumann.[28]

the length-diameter ratio is relatively small. Such may be the case for a large flood-control conduit or for a highway culvert.

The ratio of the height of the pressure-gradient intersection Y to the conduit diameter D is a function of the Froude number of the issuing flow based on mean velocity and diameter or height of the conduit. Experiments by Rueda-Briceno[29] at the University of Iowa determined the relationship between Y/D and $\mathbf{F}_r$ for a freely issuing jet unsupported by an apron or floor downstream from the exit portal. The effect of an apron support is to increase the Y/D ratios. A study was made of model results at the U.S. Army Engineer Waterways Experiment Station and a curve was presented in Chart 225.1 of Ref. 12. Various types of bottom support included floors which were level, sloping, and with a parabolic drop. A single prototype observation gave approximate confirmation of the model results, as would be expected with Froude number dominant. Although the curve of best fit for all supported jets was nonlinear on a log-log plot, the following equation appears to be adequate for design purposes within the range $1.0 < \mathbf{F}_r < 3.0$:

$$\frac{Y}{D} = 0.82\mathbf{F}_r^{-0.27} \tag{20}$$

No systematic investigation of the various cross-sectional shapes of conduit and of the various profiles of bottom support has been conducted.

5. Entrance Losses. The importance of the entrance loss depends on the shape of the intake and the length of the conduit. In very long tunnels or conduits the magnitude of the entrance loss becomes minor compared with the friction loss of the conduit. However, for the case of short conduits such as sluices through a concrete dam or culverts under roadways, the energy loss attributed to the entrance can be substantial relative to that caused by the conduit resistance. The shape of the entrance, the Reynolds number, and the relative roughness affect the entrance loss.

Shape of Entrance. The square-edge entrance is the simplest shape and is adequate for the intake of a pipe where entrance loss is unimportant and the maximum mean velocity head is well below 32 ft of head. A curved entrance where the boundary is circular in profile will have a loss coefficient depending upon the ratio of entrance radius to conduit diameter. A well-streamlined entrance should be used for a velocity head greater than, say, 25 ft.

The streamlined entrance shape has often been based on an approximation of the Kirchhoff conformal-mapping solution for the shape of a jet from a slit orifice of infinite width.[30] The equations in parametric form are

$$\frac{Y}{D} = \frac{2}{\pi}\sin^2\frac{\theta}{2} \tag{21}$$

$$\frac{X}{D} = \frac{1}{\pi}\left[\log\tan\left(\frac{\pi}{4}+\frac{\theta}{2}\right) - \sin\theta\right] \tag{22}$$

where D is the orifice breadth and θ varies from 0 to $-\pi/2$. The center of coordinates is located at the sharp edge of the slit orifice. Presumably, the pressure on a solid boundary would be atmospheric, if the boundary shape fits the theoretical shape of the jet.

The Kirchhoff equation is asymptotic to the Y/D value of 0.611 and would not become tangent to the parallel walls of a rectangular sluice. A compound curve of two ellipses was devised by the Waterways Experiment Station[31] to provide an approximate fit to the Kirchhoff curve. The equations for the two curves as shown in Fig. 4 are

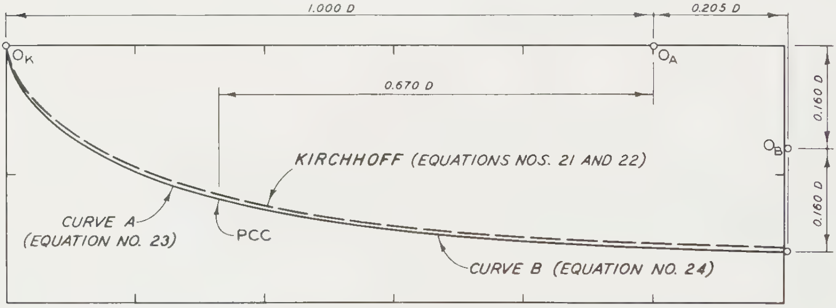

FIG. 4. Streamlined entrance curves. (D = conduit dimension, ft; O = origin of curve; and PCC = point of compound curvature.)

Curve A:

$$\frac{Y_A}{D} = 0.32\sqrt{1-\left(\frac{X_A}{D}\right)^2} \tag{23}$$

Curve B:

$$\frac{Y_A}{D} = \sqrt{1-\left(\frac{X_A+C_X}{D}\right)^2} + \frac{C_Y}{D} \tag{24}$$

The constant C_Y has a value of $0.160D$. For small-scale laboratory work, a value of C_X equal to $0.20D$ is adequate. However, for the prototype of large intakes, a more accurate value, $C_X = 0.205D$, may be needed for ordinary concrete construction tolerances. For example, if a sluice is 10 ft high, the former approximate value would produce an error of 0.05 ft in the X-coordinate of the curve B origin.

In the case of multiple parallel gate chambers in bottom intakes for outlet works, it is often uneconomical to provide adequate space between intakes for full streamlining of the side-wall intake curves. In any event the intake shape to the vertical side wall should be given as much rounding as is practical. Such a design would benefit from a model study with the tunnel or sluice foreshortened to give the proper pressure at the downstream end of the intake-structure complex. This can be estimated by using a realistic lower resistance coefficient to simulate the intake-structure exit pressure. Piezometers can then be used to determine whether there may be dangerously low pressures on the intake boundary.

Model-Prototype Comparison. As the model conduit commonly has a resistance coefficient higher than simple Froude relations would indicate, the entrance-loss

SHAPE	PROJECT (1)	CONDUIT PROPER: LENGTH / DIAM (2)	REYNOLDS NUMBER (2)	VELOCITY HEAD (1)	AVERAGE INTAKE COEFFICIENT K_e
	SINGLE INTAKE (CONCRETE DAM CONDUITS)				
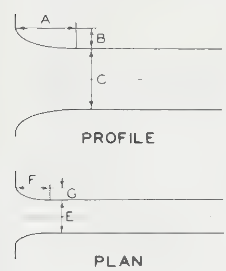	PINE FLAT (PROTOTYPE) A = 9.0, B = 3.0, C = 9.0, E = 5.0, F = 5.0, G = 1.7	54	$2.9-3.6 \times 10^{7}$ (PROTOTYPE)	65–81	0.16
	ES 802 (1:20 MODEL) A = 7.5, B = 2.5, C = 10.0, E = 5.7, F = 4.3, G = 1.4	83	6.7×10^{5} (MODEL)	97	0.07 (3)
	DOUBLE INTAKE (EARTH DAM TUNNEL)				
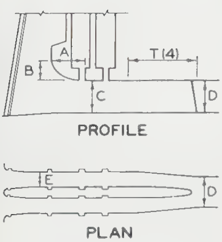	DENISON (5) (PROTOTYPE) A = 25.0, B = 39.0, C = 19.0, D = 20.0, E = 9.0, T = 53.0	40	1.2×10^{8} (PROTOTYPE)	66	0.19
	DENISON (1:25 MODEL) (SEE ABOVE)	47	$8.2-9.6 \times 10^{5}$ (MODEL)	61–82	0.12
	FT RANDALL (PROTOTYPE) A = 24.0, B = 16.0, C = 23.0, D = 22.0, E = 11.0, T = 49.0	39	$0.7-1.5 \times 10^{8}$ (PROTOTYPE)	16–72	0.25
	FT RANDALL (1:25 MODEL) (SEE ABOVE)	39	$0.9-1.0 \times 10^{6}$ (MODEL)	46–86	0.16

FIG. 5. Entrance-loss coefficients for concrete conduits (from Hydraulic Design Chart 221-1[12]). (1) Dimensions are in prototype feet. (2) Equivalent diameter for noncircular section based on hydraulic radius. (3) Does not include gate slot losses. (4) Length of transition. (5) Roof curve major axis vertical.

coefficient based on an extension of the pressure gradient upstream from its lower portion would be smaller than can be expected in the prototype.

A comparison of entrance-loss coefficients for the model and prototype is shown on Fig. 5. The Army Engineers had observed the piezometric pressure in both the laboratory and the field. The figure is adapted from Hydraulic Design Chart 221-1 of Ref. 12. The entrance losses for the Pine Flat sluice and the Denison and Fort Randall intakes are shown. None of the models tested had a length which was reduced the proper amount to account for the higher conduit resistance of the model.

It may be seen that the entrance-loss coefficient K_e in the prototype is higher in each case than that which was measured in the model.

It has been shown in the laboratory by Rao[32] that the entrance-loss coefficient is a function of the Reynolds number. Actually, the plot of K_e vs. R_e shows the loss decreasing with an increase of Reynolds number in the same manner as does the resistance coefficient of conduits. This can be fully explored by prototype measurements of the development of the turbulent boundary layer. The boundary roughness of the intake curve is also a factor, and prototype measurements are needed before the phenomenon can be adequately simulated in the laboratory.

It should be emphasized that the entrance loss is important with short conduits but becomes relatively unimportant with long tunnels. For example, values of $K_e = 0.20$ and $f = 0.007$ may be assumed. The ratio of entrance loss to total loss through the system is approximately 10 percent for an $L/D = 120$; whereas the ratio is only 5 percent for an $L/D = 400$.

Abrupt Entrances. An entrance is considered here as abrupt if not fully streamlined as discussed above. A pipe entrance with a circular rounding was investigated by Hamilton.[33] The ratio of radius of rounding to diameter of pipe was expressed as R/D. Hamilton found the entrance-loss coefficient K_e approaching zero for an R/D of 0.14. The loss coefficients for various radius-diameter ratios are shown in Table 4. Low head tests on full-size culvert pipe at the State University of Iowa[34] showed approximate agreement with Hamilton's tests. A value of K_e of 0.50 is commonly assumed for square-edged pipe entrances for conservative flow-capacity design. Reliable prototype-test results for abrupt entrances are not available.

TABLE 4. LOSS COEFFICIENTS FOR ENTRANCES OF CIRCULAR ROUNDING

R/D	K_e
0.00	0.45
0.045	0.14
0.10	0.03
0.14	0.0

Cavitation. Severe cavitation occurred at the abrupt entrances to the Madden Dam sluices. Hickox[35] reported this damage as well as some damage to the Norris Dam sluice entrances during river diversion. In the case of Norris, the pressure at the intake was increased by constricting the outlet end of the rectangular sluice. The cross-sectional area at the outlet end was reduced by 15 percent.

Cavitation at a fairly abrupt entrance to a temporary concrete diversion sluice caused damage 1.5 to 2.0 ft deep at Blakely Mountain Dam.[36] The entrance had a circular rounding with the ratio R/D of 0.18 and the sluices were 5.5 ft square. The operating head which caused the cavitation damage varied from 29 to 85 ft. Although Hamilton, as quoted above, indicates a near-zero loss coefficient for R/D ratios greater than 0.14, the Blakely Mountain experience indicates separation on the circular curve with consequent cavitation. As separation of the flow from the wall occurred, there must have been a substantial head loss.

6. Terminal Structures. The problem of terminating the artificial conveyance of high-velocity flow into a natural or unlined channel deserves special attention in design. The major objective is to make certain that the water-impounding structure is not endangered or that the water-conveying structure itself does not suffer serious damage. Model studies are usually required for major projects. However, because of the variability of natural materials and the lack of knowledge of their resistance to erosion, field observations of past failures and operating difficulties serve as important guides in design decisions.

The terminal structure may be a simple concrete apron, a stilling basin, a flip bucket, or a roller bucket. A concrete apron is often used downstream from a stilling basin. A concrete toe wall carried deep into the foundation is usually required to prevent scour from undermining the terminal structure. Riprap in a trench across the end of a terminal structure has been frequently used where the natural material is alluvium or an easily erodible formation.

A concrete apron is the simplest device used at the end of an outlet works or culvert. The functions of the apron are to permit partial transition to the normal flow of the natural channel beyond and for purposes of safety, to extend the distance from the exit portal to the location of erosion of the foundation material. A toe wall and riprap are often employed at the end of the paving. A simple apron will seldom suffice for a high-head outlet unless the foundation material is sound rock without closely spaced fractures, joints, and bedding planes. Many of the older dams, constructed before the principles of the hydraulic jump and stilling basins were fully recognized, employed aprons for spillways. Much can be learned from the rock erosion experienced at these projects.

The flip bucket as used in American practice is similar to the "ski jump" spillway of recent European parlance. A vertical curve of the floor, usually circular, throws the high-velocity jet into a trajectory which strikes the plunge pool some distance from the exit portal of an outlet works or the toe of an overflow spillway. The concrete boundary is sometimes shaped to form a lateral-throw flip bucket to cause the jet to impinge in the natural stream rather than upon the side of the valley where heavy erosion would result. The lateral-throw bucket is commonly developed in a model study. A simple flip bucket can cause eroded material from the bed of the plunge pool to be deposited downstream. The effect is to raise the tail water for normal operation of any power plant which may be a part of the project. The flip-bucket jet can be expected to disintegrate or fray in the course of the trajectory and in some cases cause heavy spray. Such spray may involve difficulties in power-plant electrical switch yards. In the case of the Lucky Peak Dam outlet works, the spray caused heavy icing on an adjacent highway during the winter.

If a circular bucket is submerged below tail water so that the issuing jet does not spring free, it is known as a roller bucket. The empirical design principles developed in the laboratory by McPherson and others are shown in Hydraulic Design Criteria Charts 112-6 and 112-6/1 of Ref. 12. One of the hazards of roller-bucket operation is the abrasion of the concrete caused by rock being entrained in the roller. Heavy abrasion damage and costly repair were experienced in the Grand Coulee Dam roller bucket. Another type of abrasion may be caused when a side roller of vertical axis forms at one end of the bucket. Such action introduced gravel from a cofferdam at Center Hill Dam, and potholes 8 ft deep developed in the concrete during construction. Model studies can normally be expected to indicate whether or not rock from downstream sources would be introduced and retained in the bucket. Furthermore, care should be exercised during construction and operation to prevent rock or metal fragments from entering the bucket.

Stilling basins are used as energy-dissipating devices for both outlet works and spillways. Their action depends upon the energy loss in the hydraulic jump. In a simple stilling basin the floor is set low enough so that the tail water for the design discharge causes the jump to form in the basin [see Eq. (9)]. Model studies have shown that baffle piers* and end sills protruding above the floor elevation can cause the jump to be formed with only 0.85 or 0.90 of the required d_2. The latter ratio is more conservative. Substantial economies may be involved in the use of these devices

* Also called "baffle blocks" or simply "baffles."

if the excavation for the basin floor is of an expensive type. Model studies are normally desirable to establish the most economical length and depth.

It is often necessary to excavate the floor of the stilling basin below the elevation of the natural stream bed, in which case a stepped end sill is commonly used. The steps direct the flow upward away from granular material or riprap just downstream from the end sill. In this case, a bottom roller usually forms with high upstream velocities near the bed. A model study can be used to advantage to study this action. Velocities across the end sill and in the bottom of the roller as measured in the model can be expected to simulate the prototype. The scour pattern of alluvium can be studied qualitatively in a movable-bed model. Furthermore, if the model scale is sufficiently large, a rough quantitative determination of the size of riprap needed can be made. In such a study, a section model in a laboratory flume is inexpensive and is adequate if side effects are not to be studied.

Stilling-basin Elements. The integrity and stability of certain stilling-basin elements are important. Although measurements of value can be obtained in the laboratory, knowledge of damage and malfunctioning of the prototype is needed in the design of such structures. Damage to the stilling-basin baffle piers, end sills, and even the floor and side walls has been caused by various phenomena of the prototype. Baffle blocks are particularly vulnerable to damage from cavitation and abrasion.

Cavitation. The severe damage to the Bonneville Dam[37] baffle blocks is one example of numerous such instances. More modern baffles have been streamlined and studies of various shapes were made in the laboratory at the U.S. Army Engineer Waterways Experiment Station.[38] The tendency of the basin floor near baffles to exhibit cavitation damage was also discussed in the paper. Baffle piers are commonly placed transversely across the basin in a single or double row. The clear spacing between the baffles is usually not less than the width of the block. If two rows are used, the baffles of the downstream row are centered on the clear space of the upper row.

The simplest shape of a baffle block is a cube. Concrete can be saved by sloping the downstream side, in which case the longitudinal dimension at the floor is greater than the lateral dimension. The drag of a baffle and hence its effectiveness depend upon the area presented to the flow. The drag coefficient is also dependent upon the shape. Very little systematic research has been performed on the force produced by baffles.

The side walls of some baffle piers have been streamlined in order to reduce the tendency toward separation and cavitation in the prototype. The incipient cavitation indexes studied in Ref. 38 reveal the effects of certain shape modifications but the scaling laws to interpret prototype behavior are unknown.

It should be emphasized that streamlining reduces the drag coefficient of a baffle pier and therefore its effectiveness in producing the hydraulic jump with a given available tail water. Nevertheless, experience has shown that streamlined baffles are less subject to cavitation damage and are therefore a practical compromise between effectiveness and permanency.

As the entering jet expands vertically within the hydraulic jump, the farther downstream the baffles are placed, the less liable they are to cavitation damage. Baffles placed well downstream are in an area of lower velocities and of higher static pressure. If baffles are moved upstream into the entering jet they are called chute blocks and are very vulnerable to cavitation. The chute blocks of Glendo Dam outlet works stilling basin suffered severe damage. Martin and Wagner[39] described laboratory studies made in an attempt to redesign the Glendo chute blocks by streamlining to eliminate severe cavitation. A model study will indicate the velocities and transient pressures to which baffles would be subjected at different locations in the longitudinal direction. Again, the engineer may seek a compromise between effectiveness and permanency. Baffle piers located about two-thirds the distance from the toe of the jump to the end sill are often safe from cavitation damage and show marked advantage in producing low velocities across the end sill. Model studies can be employed to advantage in such a determination of longitudinal location.

The use of removable steel armor plate has been suggested for elements subject to cavitation. If bolts are used to retain the armor plate, nuts should be tack-welded so that they may be cut loose if damaged plates must be replaced. The economic problem involves a comparison of the cost of armoring and replacement of damaged steel armor plates.

Abrasion. Severe damage to concrete surfaces can be caused by waterborne sand, gravel, and rock in high-velocity flow. An example of such abrasion is the invert of the tunnel at Mud Mountain Dam. In anticipation of abrasion, steel rails had been embedded longitudinally in the concrete of the invert. Inspection of the invert after operation revealed that the concrete had been deeply eroded between the rails. A determination as to whether the concrete has been damaged by abrasion or cavitation is sometimes a cause of misunderstanding. In general, damage by abrasion exhibits a smooth or rounded surface with resistant aggregate protruding. Damage caused by cavitation presents a ragged and angular surface as does concrete fractured by repeated blows of a hammer. In some cases, damage may be caused by a combination of abrasion and cavitation.

The prevention of damage by abrasion involves the elimination of the causes. Rock or pieces of scrap metal remaining from construction operations can cause abrasion. Rock thrown into stilling basins or left by fishermen who have used rock for anchors can cause abrasion. Fences on stilling-basin walls and the restriction of boats from terminal structure areas can sometimes eliminate sources of abrasion.

Side-wall Forces. The side walls of stilling basins may be subjected to random pulses of high pressure because of the violent nature of the hydraulic jump in the stilling basin. The center wall of the stilling basin at Texarkana Dam failed during operation as reported by Berryhill.[37] The top of the basin wall at Glendo Dam has been observed to move laterally about 1 in. during operation.[39] The nature of the pulsating forces on a side wall has been studied by the Bureau of Reclamation[40] in the laboratory. These studies indicate that a local pressure up to 1.5 times the velocity head of the entering flow may be expected near the bottom of the wall. The areal extent of these instantaneous pressure extremes is not known.

Bibliography

1. Rouse, H. and S. Ince, "History of Hydraulics," Iowa Institute of Hydraulic Research, Iowa City, 1957.
2. Freeman, J. R., Editor, "Hydraulic Laboratory Practice," American Society of Mechanical Engineers, New York, 1929.
3. Nagler, F. A., and A. Davis, Experiments on Discharge over Spillways and Models, Keokuk Dam, *Trans. ASCE*, **94,** 777–820, 844, 1930.
4. Vogel, H. D., Hydraulic Laboratory Results and Their Verification in Nature, *Trans. ASCE*, **101,** 597–629, 1936.
5. Randolf, R. R., Jr., Hydraulic Tests on the Spillway of Madden Dam, *Trans. ASCE*, **103,** 1080–1132, 1936.
6. Symposium, Conformity between Model and Prototype, *Trans. ASCE*, **109,** 1–193, 1944.
7. Campbell, F. B., and E. B. Pickett, The Value of Prototype Tests to Hydraulic Design, *Proc. 7th Hydraulics Conf.*, pp. 273–300, State University of Iowa, 1958.
8. Bradley, J. N., and L. R. Thompson, Friction Factors for Large Conduits Flowing Full, Engineering Monograph No. 7, U.S. Bureau of Reclamation, March, 1951.
9. Rouse, H., Editor, "Engineering Hydraulics," Iowa Institute of Hydraulic Research, John Wiley & Sons, Inc., New York, 1950.
10. Schoder, E. W., Precise Weir Measurements, *Trans. ASCE*, **93,** 999–1190, 1929.
11. McPherson, M. B., and M. H. Karr, A Study of Bucket Type Energy Dissipator Characteristics, *J. Hydraulics Div., ASCE*, Paper 1266, HY 3, June, 1957.

12. U.S. Corps of Engineers, "Hydraulic Design Criteria," prepared for Office, Chief of Engineers, Waterways Experiment Station, issued serially since 1952.
13. Reynolds, O., On Certain Laws Relating to the Regimen of Rivers and Estuaries, and on the Possibility of Experiments on a Small Scale, *Proc. 3d Intern. Navigation Congr.*, Frankfort-on-the-Main, Sec. II, 6th question, 1888.
14. Model Studies of Hydraulic Characteristics of Power Tunnel, Ft. Peck Dam, U.S. Waterways Experiment Station, *Tech. Mem.* 185-1, November, 1941.
15. Darcy, H. P. G., Recherches experimentales relatif au mouvement de l'euax dans les tuyaux (in French), Paris, 1857.
16. Weisbach, J., "Theoretical Mechanics" (1st German ed., 1846), p. 864, translation by E. B. Coxe of 4th German ed., D. Van Nostrand Company, Inc., Princeton, N.J., 1878.
17. Moody, L. F., Friction Factors for Pipe Flow, *Trans. ASME*, **66,** 671–684, 1944.
18. Nikuradse, J., Gesetzmassigkeiten der turbulenten Stromung in glatten Rohren (in German), *VDI-Forschungsh.* 356, Vol. 3, September–October, 1932.
19. Von Karman, T., Mechanische Aehnlichkeit und Turbulenz (in German), *Proc. 3d Intern. Congr. Appl. Mech.*, **1,** 85–93, 1930.
20. Prandtl, L., Zur turbulenten Stroemung in Rohren und Langs Platten (in German), *Ergeb. Aerodynamischen Versuchsanstalt Goettingen*, IV Lieferung, R. Oldenbert, Munich and Berlin, 1932.
21. Von Karman, T., Mechanische Aehnlichkeit und Turbulenz (in German, different paper from Ref. 19 of same title), *Nachr. Ges. Wiss. Goettingen*, 1930, pp. 58–76.
22. Colebrook, C. F., Turbulent Flow in Pipes with Particular Reference to the Transition Region between Smooth and Rough Pipe Laws, *J. Inst. Civil Engrs.*, **12** (4), 133–156, 1939.
23. Rouse, H., Evaluation of Boundary Roughness, *Proc. 2d Hydraulics Conf.*, 1942, pp. 105–116.
24. Miller, W. A., Jr., "Effects of Velocity Distribution and Resistance of Cylindrical Roughness in Turbulent Pipe Flow—An Analysis," Thesis, University of Tennessee, August, 1963.
25. U.S. Corps of Engineers, "Hydraulic Design of Reservoir Outlet Structures," Engineer Manual EM 1110-2-1602, Aug. 1, 1963, p. 10.
26. Rahm, Lennart, Flow Problems with Respect to Intakes and Tunnels of the Swedish Hydroelectric Power Plants, Sec. III, Friction Losses in Unlined Swedish Rock Tunnels, Institution of Hydraulics, Royal Institute of Technology, *Bull.* 36, 1953.
27. Colebrook, C. F., The Flow of Water in Lined, Unlined, and Partly Lined Rock Tunnels, *Proc. Inst. Civil Engrs.*, Paper 6281, **11,** 103–132, 1958.
28. Factors Influencing Flow in Large Conduits, Report of Task Force on Flow in Large Conduits, *J. Hydraulics Div., ASCE*, **91** (HY 6), 123–152, November, 1965.
29. Rueda-Briceno, D., "Pressure Conditions at the Outlet of a Pipe," State University of Iowa, Master's Thesis, February, 1954.
30. Lamb, H., "Hydrodynamics," 6th ed., p. 99, Dover, New York, 1945.
31. U.S. Army Engineer Waterways Experiment Station, Entrances to Conduits of Rectangular Cross-section—Investigations of Entrance Flared in Four Directions, *Tech. Mem.* 2-428, Vicksburg, Miss., March, 1956.
32. Rao, P. V., Boundary-layer Development at Curved Conduit Entrances, *J. Hydraulics Div., ASCE*, **93** (HYI), 195–217, January, 1968.
33. Hamilton, J. B., Suppression of Pipe Intake Losses by Various Degrees of Rounding, *Univ. Washington Eng. Expt. Sta. Bull.* 51, Seattle, 1929.
34. Yarnell, D. L., F. A. Nagler, and S. M. Woodward, The Flow of Water through Culverts, *Univ. Iowa, Studies in Eng. Bull.* 1, Iowa City, 1926.
35. Hickox, G. H., Experiences of the Tennessee Valley Authority—Cavitation in Hydraulic Structures —A Symposium, *Trans. ASCE*, **112,** 59–67, 1947.
36. Unpublished memoranda on Blakely Mountain Dam Cavitation, USAE Waterways Experiment Station, December, 1952.
37. Berryhill, R. H., Stilling Basin Experiences of the Corps of Engineers, *J. Hydraulics Div., ASCE*, **83** (HY 3), Paper 1264, June, 1957.
38. U.S. Corps of Engineers, Cavitation of Baffle Piers, CWI 806, Conducted for Office, Chief of Engineers, Waterways Experiment Station, Miscellaneous Paper 2-154, March, 1956.
39. Martin, H. M., and W. E. Wagner, *Proc. 9th Convention, Intern. Assoc. Hydraulic Res.*, pp. 153–172, Dubrovnik, Yugoslavia, 1961.
40. U.S. Bureau of Reclamation, Fontenelle Dam Spillway Model, *Hydraulic Lab., Rept.* HYD 486, Denver, Feb. 19, 1962.

SECTION 4

RESERVOIR HYDRAULICS

By Victor A. Koelzer

INTRODUCTION

1. General Discussion. A reservoir site is a natural resource. As such, it is important that it not be wasted by using it to less than its optimum potential. In this sense the word "optimum" may include the economic limit for a particular purpose or the inclusion of a variety of purposes to be served by a single reservoir.

In the present state of river development in the United States, reservoirs are seldom of single purpose. Even where one purpose dominates the situation, lesser purposes must be considered. U.S. Federal Power Commission regulations prescribe that functions other than power must be considered in the licensing of power projects. Practically all the legislation authorizing specific water-resource investigations requires consideration of a variety of purposes. The recent emphasis in the United States on recreation, pollution control, and preservation of open space makes such purposes, while possibly of secondary importance in the amortization of a project, of great importance in the overall planning of the nation's water resources. Hence, it may be said that, in the United States at least, practically all reservoirs must be planned with multiple purposes in mind.

Reservoir planning involves consideration of hydrology, hydraulics, design, economics, and sociology. This section is concerned with the hydrologic and hydraulic aspects of reservoir planning.

2. Definitions. An understanding of the reservoir-planning process requires a precise definition of terms. The following terms, considered generally acceptable, are used in this section:

Dead storage, sometimes called unusable storage, represents that portion of the reservoir volume below the elevation of the lowest outlet. Water in this portion of the reservoir can be evacuated only by pumping or by evaporation.

Inactive storage represents the portion of the reservoir volume which, by agreement or by legislation, will not be evacuated. Such storage may coincide with dead storage, but not necessarily.

Active storage, sometimes called usable or effective storage, represents the volume of the reservoir between the top of the inactive storage and the normal maximum operating level of the reservoir.

Conservation storage represents the part of the reservoir volume dedicated to impoundment of water for later release to serve some beneficial purpose, such as municipal supply, power, irrigation, or public health. It frequently coincides with active storage.

Flood-control storage represents the part of the reservoir volume to be utilized for impoundment of floodwaters. Such storage may be *inviolate*, in which case the dedicated volume can be used only for flood-control operations, or it may be *joint-use*, where the storage volume is used to serve both conservation and flood-control operations.

Surcharge storage represents that portion of the reservoir volume above the normal maximum operating level.

Normal maximum operating level is the maximum level at which the reservoir is operated to serve any of its planned purposes. Generally, this corresponds to the elevation of the top of the spillway gates. Operation of the reservoir to protect against a spillway design flood ordinarily will cause the reservoir level to rise above the normal maximum operating level.

Freeboard, as used here, represents the vertical distance between the maximum elevation reached in routing of the spillway design flood and the top of the dam. Some authors have used this term to represent the vertical distance between the normal maximum operating level and the top of the dam.

BASIC DATA FOR RESERVOIR PLANNING

3. Reservoir Area-Volume Curves. Sometimes referred to as "area-capacity curves," these curves are typified by Fig. 1. The curves show total reservoir volume (or storage capacity) and the reservoir area plotted against reservoir elevation. The best basis for such curves is a topographic map of the reservoir area.

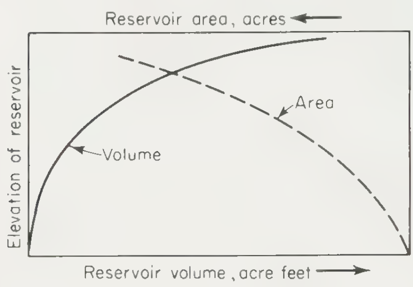

FIG. 1. Typical reservoir area and volume curves.

In the United States suitable topographic maps may be available in the form of "quadrangle sheets" prepared by the U.S. Geological Survey, which are publicly available. Frequently, however, it is necessary to prepare such maps especially for the reservoir study, by either photogrammetric or ground-survey methods. The desired scale and contour interval will depend on the size of reservoir and type of topography. The selected scale and contour interval should produce values of area and volume which are accurate within at least 5 percent. If such a map cannot be made available, a preliminary estimate of the available storage volume may be obtained from river profiles and valley cross sections.

4. Streamflow. A reliable estimate of the available streamflow is essential to reservoir planning. Such estimates can best be made from records of streamflow at the reservoir site, if available. In the absence of such records, estimates of streamflow may be made from records of streamflow at another location on the same stream, from records of another stream in the same area, or from records of precipitation.

It is important that estimates of streamflow at the reservoir site be as long as possible, in order that the reservoir design may be tested throughout a range of conditions. Therefore, such estimates frequently are obtained by a combination of the methods discussed above. The availability of records and the methods of estimation of streamflow are given in Sec. 1.

When applicable, corrections must be applied to recorded streamflow at a reservoir site (or to estimates obtained by correlation methods) to reflect a common level of development. For example, upstream reservoirs may have been introduced during the period of record which would, by regulation, modify the flow pattern. Similarly, evaporation in the reservoirs or upstream diversions for water use may deplete the natural flow. In such cases it is generally desirable to correct all records to the common base of natural, or "virgin," flow, *i.e.*, the flow that would have been available if no development had taken place. Such corrections involve the use of records on storage, diversion, or evaporation, which usually are available from the operating entities involved.

In special cases, where heavy losses of runoff are experienced along the streambed, because of evapotranspiration or accretion to groundwater, it may be necessary to estimate the gain or loss in streamflow that will occur as a result of a change in flow regime or as a result of inundation of valley areas by the reservoir. The "salvage" of natural streamflow losses has been found to be a significant factor in reservoir planning on the Colorado River.

5. Climatological Data. The climatological data that may be needed in reservoir planning include data on precipitation, temperature, humidity, wind velocity, and evaporation. The availability of this information is discussed in Sec. 1.

6. Sedimentation. Estimates of the sediment load of a stream are essential in reservoir planning to determine the rate of depletion of reservoir storage that can be anticipated through accumulation of sediment. Sediment records collected by the U.S. Geological Survey are published periodically in its "Water Supply Papers." Much unpublished data have been collected by various government agencies, which are inventoried periodically by a Federal interagency committee.[1]

Various government agencies periodically survey reservoirs which have been in operation for some time. Frequently, special reports on such surveys are made, which include data on rate of sediment accumulation, distribution of the sediment in the reservoir, and trap efficiency on density of sediment deposits. Summaries of such surveys also are issued periodically by the Inter-Agency Committee.[2]

SEDIMENT-STORAGE REQUIREMENTS

7. Rate of Sedimentation. Estimation of the rate of reservoir depletion by sediment accumulation usually involves three basic steps. The estimates required are (1) sediment inflow, (2) trap efficiency of the reservoir, and (3) density of the sediment deposits. In some instances the method of distribution of the sediment in the reservoir also is a required step. The estimation of sediment inflow offers the greatest opportunity for variation in procedures and results.

Sediment Inflow. The inflow of sediment to a reservoir consists of suspended load and bed load. Generally, suspended load is computed from available sediment records or by comparison of the basin in question with watersheds having sediment records. Bed-load records normally are too difficult to collect; hence bed-load estimates usually are made on the basis of judgment and are expressed as a percent of suspended load.

Several methods of estimating suspended load are used, as follows:

1. Use of average recorded sediment load
2. Computation by flow duration—sediment-rating-curve method
3. Estimates by unit yield of watershed
4. Estimates of erosion

The use of average recorded sediment load is restricted to instances in which the sediment load is measured at frequent enough intervals to establish what is essentially a continuous record. Even where such records are available, the period of sediment record is usually not as long as the streamflow records at the site, and adjustments to the historical average sediment load are desirable because it is not apt to be representative.

[1] "Inventory of Published and Unpublished Sediment Load Data in the U.S.," April, 1949, and supplements of later dates, prepared for Inter-Agency Committee on Water Resources by U.S. Department of the Interior.

[2] Summary of Reservoir Sediment Deposition Surveys Made in the U.S. through 1960, *U.S. Dept. Agr. Misc. Publ.* 964, May, 1964.

Sediment concentration usually increases rapidly with discharge, with the result that the load carried during the highest flood of a year may be as much as the total load carried for the remainder of the year. This highlights the necessity of obtaining as reliable a reflection of the influence of peak flood periods as possible, which is usually accomplished only if the entire period of streamflow record is considered.

The flow-duration–sediment-rating-curve method of analysis is the most desirable method of giving appropriate attention to the entire period of streamflow record. In this method a sediment-rating curve is first prepared from historical records, relating sediment discharge (expressed usually in tons per day) to the water discharge. A flow-duration curve is then prepared for the entire period of streamflow record (or by procedures described later in this section). The computation of average annual load is then made by combination of these curves.[1]

Figure 2 shows a typical sediment-rating curve. Preparation of the rating curve involves plotting all measured values of sediment discharge against the corresponding values of water discharge. The scatter in the plotted points in Fig. 2 is typical of most of such plottings. Some of the scatter frequently can be reduced by developing separate curves for different seasons of the year, when differences in sediment-runoff characteristics can be expected. In extrapolation of rating curves care should be taken to avoid extending the curves to an unreasonable value of concentration. For this purpose, plotting of lines of equal concentration frequently is useful.

The average annual sediment load is computed in the flow-duration–sediment-load method by using an incremental process. The water-discharge values of the mid-ordinate of increments of the flow-duration curve are used to obtain matching values of sediment load from the sediment-rating curve. The values of sediment load are multiplied by the percentage of time represented by the increment, and a summing of these products gives the total load. Table 1 gives an example of the method of computation used by the U.S. Bureau of Reclamation.

Where sediment records are not available (or as a check on other methods of computation), the sediment load may be estimated by estimating the sediment yield from a unit of area of the watershed. This may be done by selecting a unit value from a watershed believed to have similar characteristics of sediment runoff. The previously referred to Inter-Agency publication on reservoir surveys gives summaries of sediment yields in different watersheds.

Sediment yield also may be estimated by computing rates of erosion. A method developed by the U.S. Department of Agriculture[2] may be used for this purpose. This procedure uses the so-called "universal equation," which involves a number of variables related to localized conditions. The variables include storm energy, rainfall intensity, soil erodibility, land slopes, cropping patterns, and extent of conservation practices.

Only in rare instances is bed load known to exceed 25 percent of suspended load. In such instances special methods of computation of total load may be used.[3]

Bed load is usually estimated as a percentage of suspended load, on the basis of inspection of the load-carrying characteristics of the system.

Trap Efficiency. Trap efficiency represents the percentage of sediment inflow which is deposited in the reservoir. In major reservoirs this is frequently near enough

[1] Miller, Carl R., "Analysis of Flow Duration, Sediment-rating Curve Method of Computing Sediment Load," U.S. Bureau of Reclamation, April, 1951.

[2] Chow, Ven Te, "Handbook of Applied Hydrology," pp. 17-6 to 17-9, McGraw-Hill Book Company, New York, 1964. A Universal Equation for Predicting Rainfall-erosion Losses, *U.S. Agr. Res. Ser. Spec. Rept.*, March, 1961, pp. 22–26.

[3] Schroeder, K. B., and D. B. Raitt, "Total Suspended Load from Vertical Transport Distribution," U.S. Bureau of Reclamation, November, 1952. Koelzer, V. A., and M. Bitoun, "A Review of Sediment Problems and Possible Solutions," West Pakistan Engineering Congress, Lahore, April, 1962.

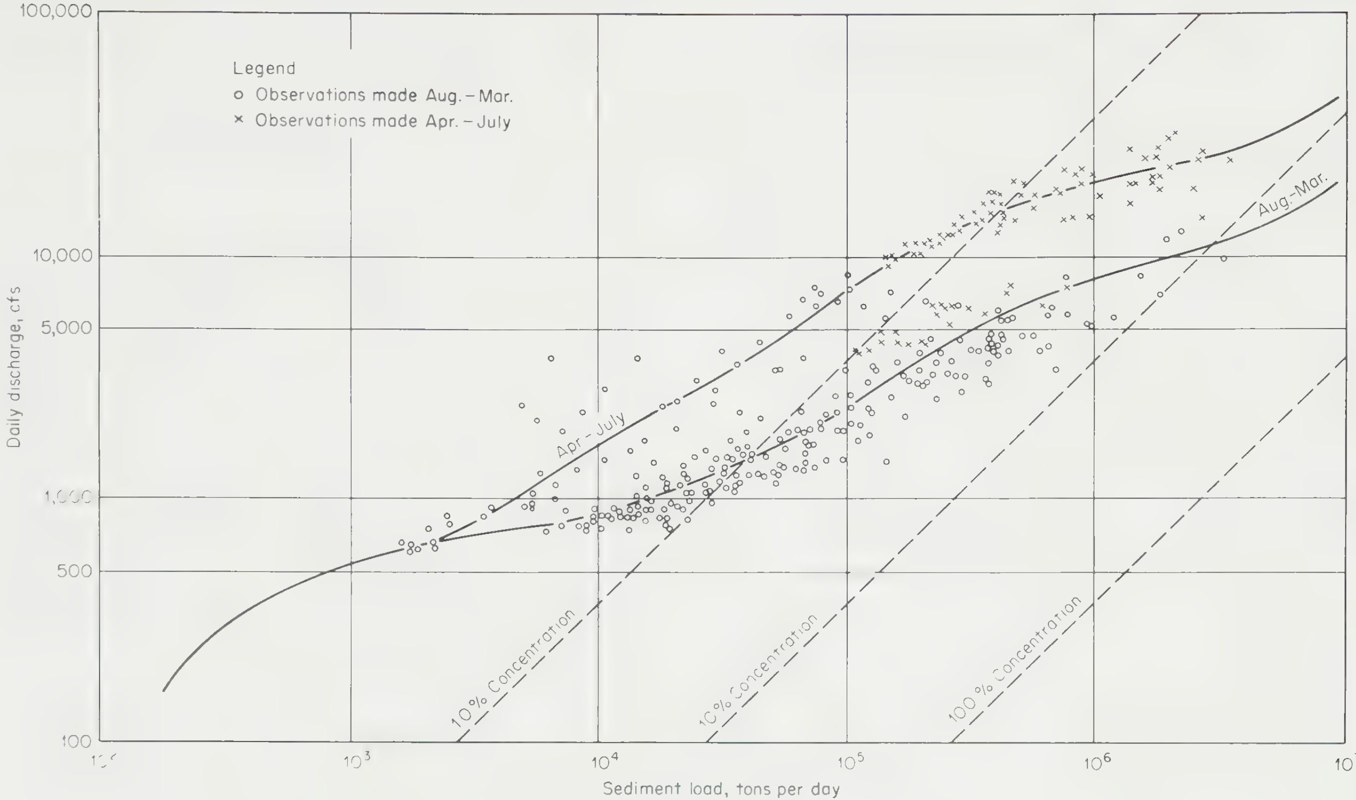

FIG. 2. Sediment-rating curve.

to 100 percent to allow use of such a value. However, there may be instances on major reservoirs in which a portion of the sediment load is passed through the reservoir. This may occur where the reservoir volume is small with respect to the maximum rates of water discharge through the reservoir.

TABLE 1. COMPUTATION OF SUSPENDED SEDIMENT LOAD

Limits of % of time	% interval	% mid-ordinate	Instantaneous water discharge, cfs	Instantaneous sediment discharge, tons/day	Daily sediment discharge [(2) × (5)], tons/day
(1)	(2)	(3)	(4)	(5)	(6)
0.00–0.02	0.02	0.01	13,000	2,700,000	540
0.02–0.1	0.08	0.06	8,100	1,600,000	1,280
0.1–0.5	0.4	0.3	4,600	820,000	3,280
0.5–1.5	1.0	1.0	2,700	425,000	4,250
1.5–5.0	3.5	3.25	1,400	185,000	6,470
5–15	10	10	830	93,000	9,300
15–25	10	20	420	39,000	3,900
25–35	10	30	250	19,500	1,950
35–45	10	40	190	13,600	1,360
45–55	10	50	155	10,200	1,020
55–65	10	60	127	7,500	750
65–75	10	70	105	5,700	570
75–85	10	80	81	3,800	380
85–95	10	90	51	1,720	172
95–98.5	3.5	96.75	25	325	11
98.5–99.5	1.0	99.0	13.5	17.5	
99.5–99.9	0.4	99.7	7.0		
99.9–99.98	0.08	99.94	2.75		
99.98–100	0.02	99.99			

Total average daily load [Col. (6)], in tons = 31,953.
Average annual suspended sediment load = 31,953 × 365 = 11,600,000 tons.

For smaller reservoirs, data developed by Brune[1] are useful. He relates trap efficiency to the capacity-inflow ratio (ratio of reservoir capacity to annual inflow), as shown in Fig. 3. The capacity-inflow ratio can be considered to be equivalent to the period of detention in the reservoir. For large reservoirs, data developed by the TVA[2] allow estimates of trap efficiency to be made on the basis of the relationship between the period of detention and the mean velocity of flow through the reservoir. Consideration of velocity of flow is desirable because deposition of sediment cannot take place if the velocity and resulting turbulence are too high. The TVA curve is shown in Fig. 4.

Density of Deposited Sediments. The procedures described for estimating sediment deposited in the reservoir, after applying the trap efficiency to the rate of sediment inflow, will result in a value expressed in terms of weight. It then will be necessary to convert the result to a volume basis by estimating the space occupied by a unit of weight of sediment. This conversion factor is referred to as specific weight, unit weight, or density.

Many published data are available on the many observations that have been

[1] BRUNE, GUNNAR M., Trap Efficiency of Reservoirs, *Trans. Am. Geophys. Union,* June, 1953. *U.S. Dept. Agr. Misc. Publ.* 970, p. 884.

[2] Proceedings of the Federal Inter-Agency Sedimentation Conference, May, 1947, U.S. Bureau of Reclamation, Denver, Colo.

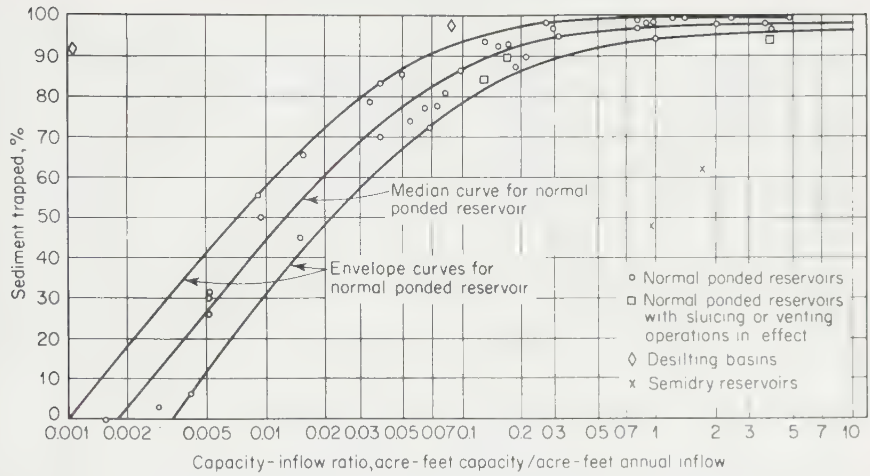

FIG. 3. Trap efficiency as related to capacity-inflow ratio. (*After Brune. From Ven Te Chow, "Handbook of Applied Hydrology," pp.* 17–23, *McGraw-Hill Book Company, New York,* 1964.)

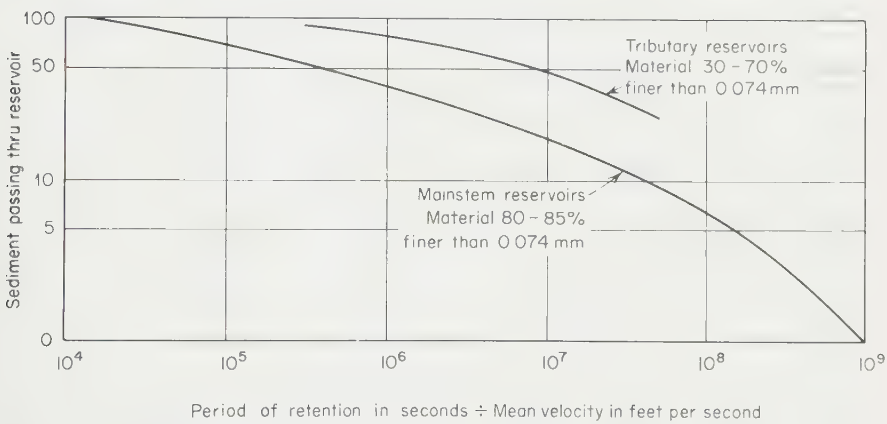

FIG. 4. Trap efficiency in TVA reservoirs. (*Proceedings of Federal Inter-Agency Sedimentation Conference, May,* 1947, *and correspondence from TVA.*)

made of the density of deposited sediment.[1] It has been found to vary from 18 to 125 lb/cu ft, depending on the sediment size, the depth of deposit, and the degree of submergence or exposure of the deposit. The density also depends on the length of time the material has been deposited, since the rate of consolidation greatly affects the sediment density.

The procedure presented by Lane and Koelzer[2] has gained general acceptance.

[1] LANE, E. W., and V. A. KOELZER, Density of Sediments Deposited in Reservoirs, *U.S. Interdepartmental Comm. Rept.* 9, St. Paul District, Corps of Engineers, St. Paul, Minn., November, 1943. HEMBREE, C. H., B. R. COLBY, H. A. SWENSON, and J. R. DAVIS, Sedimentation and Chemical Quality of Water in the Powder River Drainage Basin, Wyoming and Montana, *U.S. Geol. Survey Circ.* 170, Washington, D.C., 1952.

[2] *Op. cit.* KOELZER, V. A., and JOE M. LARA, Density and Compaction Rates of Deposited Sediments. *Proc. ASCE, J. Hydraulics Div., Paper* 1603, April, 1958.

The equation is

$$W = W_1 + K \log_{10} t \tag{1}$$

where W = density after t years, lb/cu ft
W_1 = density after 1 year, lb/cu ft
K = a constant for each sediment class and operation condition, to reflect consolidation
t = number of years of consolidation

The values of W_1 and K vary with the method of operation and the size of sediment material. The values are:

Reservoir operation	Sand (>0.05 mm)		Silt (0.005 to 0.05 mm)		Clay (0.005 mm)	
	W_1	K	W_1	K	W_1	K
Sediment always submerged or nearly submerged	93	0	65	5.7	30	16.0
Normally a moderate reservoir drawdown	93	0	74	2.7	46	10.7
Normally considerable reservoir drawdown	93	0	79	1.0	60	6.0
Reservoir normally empty	93	0	82	0.0	78	0.0

For materials covering a range of particle sizes, it was recommended that the equation be used with appropriate weights, applied in proportion to the percent by weight in each size classification.

Using the above procedure, the average density of deposits W_{av} after t years is

$$W_{av} = W_1 + 0.434K \left[\frac{t}{t-1} (\log_e t - 1)\right] \tag{2}$$

The U.S. Bureau of Reclamation[1] uses the above procedure but considers that the values of W_1 are too high. It prefers to use the initial densities determined by Trask[2] which are as follows:

Classification	Size range, mm	Initial density, lb/cu ft
Sand	0.5–0.25	89
Sand	0.25–0.125	89
Sand	0.125–0.064	86
Silt	0.064–0.016	79
Silt	0.016–0.004	55
Silt	0.004–0.001	23
Clay	0.001–0	3

8. Distribution of Sediment Deposits. The sediment deposited in a reservoir will deposit on a slope, so that the area-volume relationship will be affected throughout by deposition of sediment. Where sediment load is a significant factor, the dis-

[1] Miller, Carl R., Determination of the Unit Weight of Sediment for Use in Sediment Volume Computation, *U.S. Bur. Reclamation Mem.*, Feb. 17, 1963.

[2] Trask, Parker, Compaction of Sediments, *Bull. Am. Assoc. Petrol. Geologists*, **15**, 271–276.

tribution of deposits should be estimated, to allow determination of the extent to which different allocations of storage are affected by sediment accumulation. The Bureau of Reclamation[1] has developed procedures for estimating the distribution of deposits, based on observations of historical deposition in different types of reservoirs.

9. Density Currents and Stratifications. Differences in temperature of water at various locations and depths in a reservoir will occur with changing ambient temperatures. The differences in temperature, resulting in differences in density, will cause stratification within the reservoir, as well as exchange of water between areas of different densities.

The use of density currents to pass through a reservoir the fine sediments which tend to remain in suspension has been suggested on many occasions as a means of reducing deposition. The science of density currents and stratification is not well developed, and even the most sophisticated treatises[2] are hesitant to predict the conditions that will occur in given situations. The most extensive data on density currents and stratification in natural reservoirs have been collected in Lake Mead.[3]

RESERVOIR EVAPORATION

Reservoir planning requires consideration of the losses to be expected in evaporation from the reservoir surface. This can be quite significant in some instances. In Lake Mead, for instance, the annual evaporation loss at full reservoir approaches 1 million acre-feet, compared with an average annual water supply in the order of 10 million acre-feet. Methods of estimating reservoir evaporation are given in Sec. 1.

ANALYSIS OF WATER REQUIREMENTS

The design of a reservoir must be based on considerations of water availability as related to water requirements, since both generally vary throughout the year. The development of water requirements for various uses is discussed individually in Secs. 24, 30, 31, 33, 36, 39, and 40.

ANALYSIS OF WATER AVAILABILITY

Various techniques have been used to analyze water availability. Among the well-established methods are flow-duration analyses, mass-curve analyses, and period-by-period simulated reservoir operation through the historical period of streamflow record. The latter two methods are the commonest traditional approaches used in reservoir planning, and involve examination of the most critical combinations of historical streamflow in relation to the water demands expected to be placed on the reservoir. Recently, stochastic procedures, which are basically probability approaches, have gained increasing acceptance for reservoir planning.

10. Flow-duration Analyses. The procedures for flow-duration analyses of the records for a given stream are presented in Sec. 1. Duration curves are useful in computing sediment load, in establishing the degree of flood control to be provided, in establishing urban, highway, and agricultural drainage requirements, and in evaluating the power capabilities of a river.

[1] "Interim Report—Distribution of Sediment in Reservoirs," Project Investigations Division, U.S. Bureau of Reclamation, June, 1954.

[2] FRY, A. S., M. A. CHURCHILL, and R. A. ELDER, Significant Effects of Density Currents in TVA's Integrated Reservoir and River System, *Proc. Minnesota Intern. Hydraulics Conv.*, September, 1953, p. 335. TASK COMMITTEE ON PREPARATION OF SEDIMENTATION MANUAL, Sediment Transportation Mechanics: Density Currents, *Proc. ASCE, J. Hydraulics Div.*, September, 1963. HARLEMAN, D. R. F., and REX A. ELDER, Withdrawal from Two Layer Stratified Flows, *Proc. ASCE, J. Hydraulics Div.*, *Paper* 4398, July, 1965.

[3] "Lake Mead Density Current Investigations, 1937–40," U.S. Bureau of Reclamation, October, 1941.

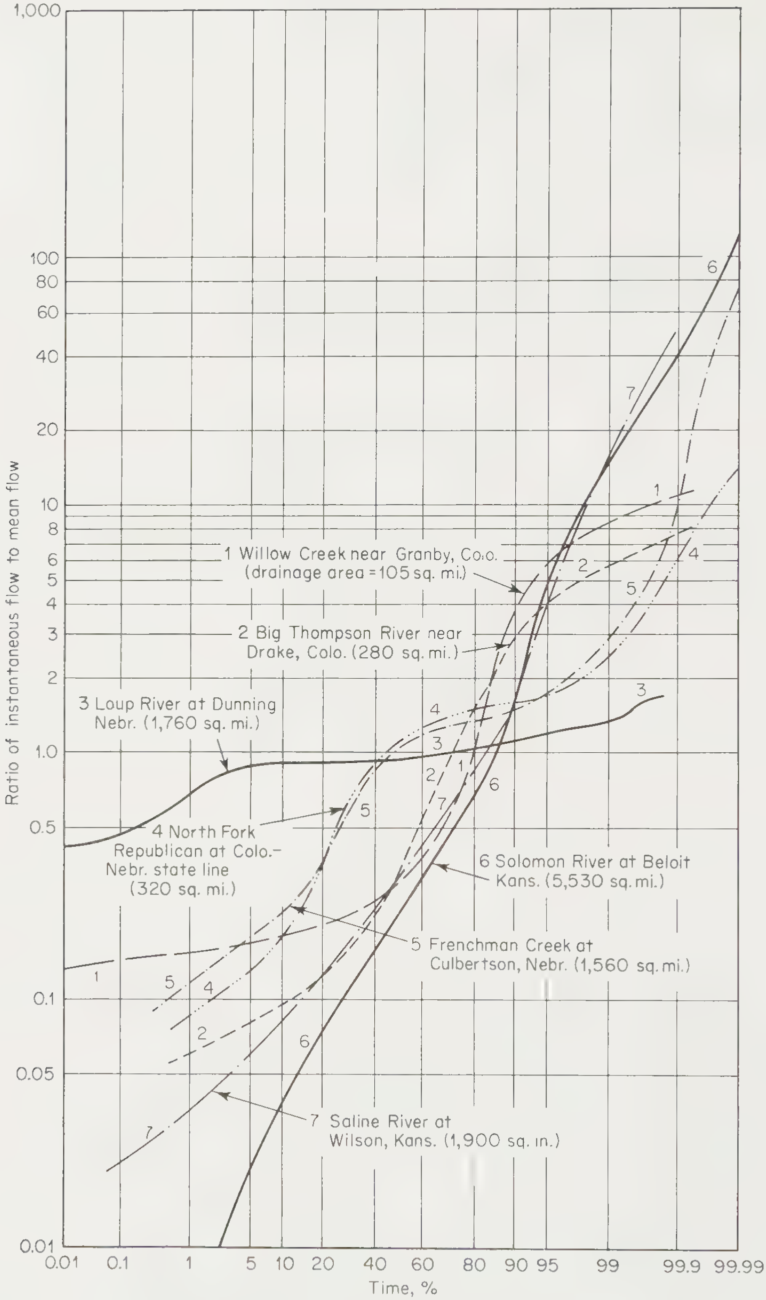

FIG. 5. Dimensionless flow-duration curve.

Where records for a given stream are not available, it sometimes is possible to synthesize a flow-duration curve. It has been found that the shape of the flow-duration curve is indicative of the runoff characteristics of the stream if the flow occurrences are converted to a dimensionless basis. This can be done by expressing the observed flow corresponding to a given percentage of time as a percentage of the average flow of the stream.

Figure 5 demonstrates this principle.[1] It shows flow-duration curves in dimensionless form from streams of varying size and characteristics. The watershed of the Loup River has low relief and is composed entirely of "sandhills," in which practically all streamflow originates from groundwater, with practically no surface runoff. The North Fork Republican and Frenchman Creek are intermediate-type streams, in which part of the basin is in sandhills and part is a moderately rolling area with normal type of surface runoff. The Solomon and Saline rivers are all of the surface-runoff type, from moderately rolling topography. Willow Creek and Big Thompson River originate in the rugged topography of the highest part of the Colorado Rockies, with much of the annual streamflow being from snowmelt.

It will be noted that the dimensionless flow-duration curves for the sandhills stream is extremely flat; that is, there is little variability in streamflow. The more normal surface-runoff type of watershed, on the other hand, has a high variability. The curves for the partly sandhills, partly normal surface runoff and the snowmelt are in between. Further, it will be noted that the curves for similar types of drainage areas are of very similar shapes, even though the drainage areas vary in size.

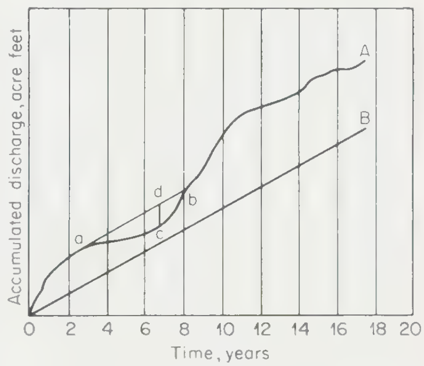

FIG. 6. Typical mass curve.

The similarity in shape of curve for basins of similar runoff characteristics suggests that a flow-duration curve for an ungaged stream can be synthesized. A flow-duration curve can be developed from data available on a stream considered to have the same runoff characteristics. It will be necessary, of course, to estimate the average flow at the ungaged stream location. This is generally possible, on the basis of relationships in drainage areas similar to that of the gaged stream.

11. Mass-curve Analysis. The mass-curve method of water-availability analysis is well established and is extremely useful. It can be utilized to great advantage for the complete analysis of a single reservoir having a simple pattern of water requirements. On a more complicated system, it can be used for preliminary analytical purposes, to identify periods that are apt to be most critical and in need of more detailed study.

Mass curves show cumulative flow and can be used to indicate cumulative utilization and storage requirements. Adjustments for evaporation and other losses must be made in determining the net volume available from accumulated streamflow. This may be done by subtracting from the natural flow the losses anticipated in order to ensure the required net yield. To illustrate, Fig. 6 shows an accumulation of streamflow OA and an accumulation of demand OB. The curve OA has been adjusted by subtracting the expected losses before the plot was made. If a line parallel to OB

[1] The assistance of Ivan Bauer and Norman Beck in the development of basic data utilized in Fig. 5 is gratefully acknowledged.

is drawn tangential to point *a*, the beginning of the longest dry period of record, the ordinate *dc* will represent the volume of storage required to maintain a rate of flow not less than that represented by the slope of the line *OB*.

The mass curve of water utilization need not be a straight line. Figure 7 shows a curve of irregular demand plotted with a curve of reservoir inflow for a typical dry period. The upper curve shows the cumulative requirements for water use from Oct. 1. The lower curve shows the total natural flow in acre-feet from Oct. 1 to May 7 to be 110,000. On Dec. 15 the total was 15,000 acre-ft; on Apr. 1 it was 40,000 acre-ft; likewise the total flow from Oct. 1 to other dates may be read from the curve. The maximum vertical distance between the curves is the storage required to meet the needs of the project. If the worst period of record is selected for the study, the storage requirements are obtained from the mass curve. In the illustration, it was assumed that the reservoir was full on Oct. 1, the beginning of the period. The greatest amount of storage was used on Jan. 31, 74,000 acre-ft. The reservoir was full again on May 4, when the two curves intersected.

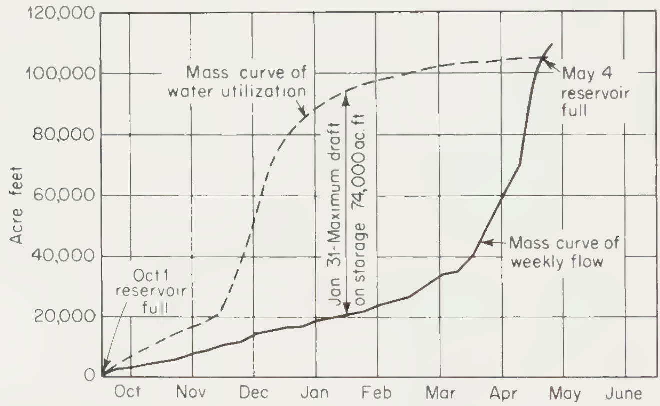

FIG. 7. Mass curves of water utilization and weekly flow.

12. Tabular Reservoir-operation Analysis. Where the relation between supply and demand is complicated, reservoir planning usually is accomplished by a tabular accounting of inflow, reservoir evaporation, release requirements, and reservoir storage. In a complex system where several reservoirs, water uses, and points of water diversion are involved, this becomes a complicated process.

Table 2 shows a reservoir-operation study of the critical period for a large reservoir. This is a multiple-purpose reservoir, planned for irrigation, power, and such incidental flood control as may be possible. The study was on a monthly basis and represented the final of several trial-and-error studies to develop the required reservoir size to meet specified water-delivery requirements.

A more complex study is frequently required for a number of alternative proposed reservoirs in a major river basin. This is particularly true if some of the reservoir sites are alternative to other sites and are for a variety of purposes, such as flood control, irrigation, and incidental power. Table 3 shows summarized results from such an actual system, with hypothetical names substituted for the actual names of reservoirs.

The results of Table 3 were obtained by detailed system-operation studies carried out on a digital computer. It involved a great many more columns of computation

TABLE 2. RESERVOIR-OPERATING STUDY FOR CRITICAL PERIOD

All values in 1,000 acre-ft

Year	Month	Inflow to reservoir	Total irrigation-water demands at diversion dam	Usable inflow between reservoir and diversion dam	Required reservoir release to meet irrigation demand	Evaporation	Required reservoir release for power demands	Change in reservoir storage	Reservoir storage at end of month	Reservoir spill
1950	May	106.7	41.2	11.5	29.7	0.3		+ 30.1	190.0	46.6
	June	76.9	37.7	1.5	36.2	1.2		0	190.0	39.5
	July	33.7	34.3	2.9	31.4	1.2		0	190.0	1.1
	August	19.0	32.9	1.0	31.9	1.2		− 14.1	175.9	
	September	13.6	31.1	1.6	29.5	0.9		− 16.8	159.1	
	October	13.1	24.6	1.0	23.6	0.6		− 11.1	148.0	
	November	12.9	22.3	0	22.3	0		− 9.4	138.6	
	December	11.9	22.0	0	22.0	0		− 10.1	128.5	
1951	January	12.0	22.5	0	22.5	0		− 10.5	118.0	
	February	13.2	21.1	0	21.1	0		− 7.9	110.1	
	March	21.5	23.3	6.4	16.9	0	19.2	+ 2.3	112.4	
	April	40.5	36.0	3.7	32.3	0.3		+ 7.9	120.3	
	May	52.4	41.2	5.1	36.1	0.3		+ 16.0	136.3	
	June	35.9	37.7	0.8	36.9	1.2		− 2.2	134.1	
	July	19.1	34.3	1.0	33.3	1.2		− 15.4	118.7	
	August	15.6	32.9	0.6	32.3	1.2		− 17.9	100.8	
	September	12.4	31.1	0	31.1	0.9		− 19.6	81.2	
	October	16.3	24.6	3.8	20.8	0.6	21.5	− 5.8	75.4	
	November	22.6	22.3	6.8	15.5	0	20.9	+ 1.7	77.1	
	December	15.3	22.0	3.4	18.6	0	21.8	− 6.5	70.6	
1952	January	14.3	22.5	2.5	20.0	0	21.6	− 7.3	63.3	
	February	20.2	21.1	5.9	15.2	0	21.0	− 0.8	62.5	
	March	34.5	23.3	10.4	12.9	0	22.1	+ 12.4	74.9	
	April	129.5	36.0	14.3	21.7	0.3		+107.5	182.4	
	May	191.1	41.2	21.8	19.4	0.3		+ 7.6	190.0	163.8
	June	113.0	37.7	2.1	35.6	1.2		0	190.0	76.2

TABLE 3. SUMMARY OF OPERATION STUDIES OF RESERVOIR SYSTEMS

System designation	Additions to existing system	Total dead storage of system additions ($AF \times 10^6$)	System active storage ($AF \times 10^6$)	Peak of reservoir design flood routed to diversion dam, cfs	Peak flood at Mid City, cfs	Annual system firm irrigation yield		Min flow at diversion dam for power, cfs
						Total ($AF \times 10^6$)	% of basin potential developed	
	Natural flow with no reservoirs	...	0	185,000	150,000	17.3	45.5	1,500
1	Existing system of three reservoirs	...	8.8	158,000	150,000	23.1	60.8	2,360
2	High Jones Reservoir	3.0	19.0	113,000	50,000	32.2	84.7	3,020
		0.5	21.5	113,000	50,000	33.7	88.7	3,410
3	Intermediate Smith Reservoir	4.0	22.8	99,000	150,000	34.3	90.3	3,470
		2.0	24.8	99,000	150,000	34.7	91.3	3,510
4	High Smith Reservoir	4.0	28.9	98,000	150,000	35.1	92.4	3,550
5	Low Jones and Low Smith Reservoirs	7.0	21.3	96,000	50,000	32.9	86.5	3,110
		5.0	23.3	96,000	50,000	33.9	89.2	3,180
6	High Brown Reservoir	3.5	26.8	97,000	50,000	35.2	92.6	3,310
7	Intermediate Smith and High Brown Reservoir	4.5	30.6	96,000	150,000	35.6	93.7	3,630

than shown in Table 2, since several reservoirs had to be considered in each operation. Nevertheless, the mechanics of study were basically the same, with accounting of such factors as inflow, water requirements, evaporation losses, reservoir storages, and outflows.

The studies made for the mammoth Indus River Basin investigations in West Pakistan represent a vast expansion of the type of studies described above. The studies involved five major tributaries, two major storage reservoirs, pumped supply of groundwater into numerous locations of an irrigation distribution system, five points of diversion, and many interconnected canals. The conjunctive operation of all these facilities required a method of operation that could only be carried out by computer, because of the sheer magnitude of work involved in manual studies and the impossibility of eliminating errors in the manual process.

13. Use of Historical Critical Period. The historical period is frequently useful as a basis for analyzing reservoir performance. It affords a demonstration of how a project or system has functioned under the various conditions that have been experienced historically. It has the advantage of being easily understood by the layman, since he can visualize what the reservoir will do under the worst historical conditions. However, the simplicity of this concept introduces pitfalls which should be avoided.

Reservoir-operation studies of historical flow sequences generally produce considerable volumes of computations, the very bulk of which may be so impressive that it is difficult to retain perspective regarding the limitations inherent in the method. However, the dependable yield of a reservoir cannot be more than an informed estimate and should not be treated as a precise quantity.

In using the historical critical period as a basis for design of a reservoir, there is a tendency to consider that, because a worse situation has not been experienced historically, the reservoir will meet the requirements for all time. This obviously is not true; a worse situation is always a possibility. There is a tendency also to attach undue significance to the sequence of runoff events in the historical critical period. This is dangerous because the greatest proportion of runoff is generally a chance occurrence of nature. In some streams the runoff of a preceding year or month may have some influence, but usually the influence is relatively small. It follows, therefore, that the probability of recurrence of a historical sequence is usually small.

Investigations should be made whenever possible to determine whether the magnitude or sequences of runoff in the critical period are comparable in severity with other rivers in comparable areas. If the situation is unique, adjustments may be necessary. Such adjustments usually have been made in the past on the basis of judgment. Recently, however, several investigators have proposed the use of parameters which allow area-wide runoff characteristics to be introduced, to influence the results obtained from analysis of the records of a single stream. This approach is under intensive investigation and development.[1]

14. Stochastic Analyses. While it may be possible to use parametric approaches to adjust historical flows to obtain a better basis of average yield or of yield for a single drought year, it leaves a question with respect to sequences of flow. The most promising approach to the hydrologic design of reservoirs for such cases appears to be through stochastic analysis. In this procedure the historical inflow data for a particular reservoir are utilized to develop certain statistical parameters and indexes, which allow different sequences of inflow to be "generated" by the use of stochastic (basically probability) procedures. The statistically generated sequences of flow data are then analyzed by any of the traditional evaluation methods (mass curve,

[1] Stall, John B., Low Flow of Illinois Streams for Impounding Reservoir Design, *Illinois State Water Survey Bull.* 51, 1964. Gooch, Robert S., Design Drought Criteria, *Proc. ASCE, J. Hydraulics Div.*, March, 1966.

tabular methods, etc.). Thus a variety of sequences of monthly and annual inflows may be considered, the sum total of which gives an evaluation of the probabilities involved.

There is an inherent psychological advantage to the stochastic approach, since the results must be expressed in terms of probabilities. This discourages a false sense of security that the design drought period will not be exceeded in severity—a feeling which can easily be obtained when the basis of design is the most critical period of record.

The stochastic approach is under rapid development. Although the basic philosophy, theories, and some procedural matters have been worked out, much remains to be done in the development of specific procedures before the approach can be considered to be fully operational. The classic work in this field was performed by Hurst,[1] followed by highly significant work by Langbein[2] and Fiering.[3]

To utilize the stochastic approach, it is necessary to develop several statistical parameters. These include the values of mean flow, measures of the variability of individual occurrences from the mean, and correlations between flows during previous periods and the flow during following periods. Although techniques for these analyses are undergoing rapid change, reference by the reader to the writings of the pioneer investigators referred to will provide basic background on the details of procedures that may be used.

After the statistical parameters are developed, they may be used to select random values of streamflow. This is the equivalent of "pulling historically observed streamflows from a hat," with proper constraints being applied to assure that unrealistic results will not be obtained. These constraints include such factors as the limitation on minimum flow that will be randomly selected (obviously it cannot be less than zero and usually it will be more) and the effect of the runoff from a previous period on the otherwise randomly selected runoff of a following period.

In using the stochastic approach it is necessary to decide on the number of years of record that should be generated and analyzed. While the number of years required to produce a result which has a certain probability of accuracy is undoubtedly subject to mathematical analysis, procedures have not yet been developed for this determination. Some investigators have arbitrarily utilized a 100-year generated record, but in some instances comparison of two separately generated 100-year periods has resulted in substantially different storage requirements.

Whatever the period of record that may be generated, it can be done most expeditiously and economically by use of a digital computer. Programs are available for this purpose, and these usually can be combined expeditiously with programs for analysis of the performance of the reservoir in meeting a variety of storage and delivery requirements.

The use of stochastic procedures, through development of a stochastic model, should not be interpreted as ignoring of historical data. Historical data are used to develop means, parameters of variability of flow, and relationships between successive flow periods. The only element of historical occurrences which is given small importance is the sequence of flows. This, however, is highly desirable since the historical sequence represents only one of many possibilities of sequence. The stochastic approach attempts, therefore, to put the historical sequence into proper perspective as to its probability of recurrence.

[1] Hurst, H. E., Long Term Storage Capacity of Reservoirs, *Trans. ASCE*, 1951, pp. 770–808.

[2] Langbein, W. B., Queuing Theory and Water Storage, *Proc. ASCE*, *Paper* 1811, October, 1958. Langbein, W. B., and N. C. Matalas, Information Content of the Mean, *J. Geophysical Res.*, August, 1962.

[3] Fiering, Myron B., Queuing Theory and Simulation in Reservoir Design, *Trans. ASCE*, 1962, pt. I, pp. 1114–1144.

15. Application of Stochastic Approach. The use of the stochastic approach can be demonstrated by studies for a river in the Philippines. In that basin there were no runoff or precipitation data available for a large portion of the 1941–1949 period, with appreciable periods of record both before and after that time. Accordingly, the normal procedure for bridging of the gap in data by correlating runoff with precipitation was not possible.

The storage reservoir proposed for this basin is of the holdover type, with several years of drawdown between reservoir fillings. Because of this, it was essential that the sequence of runoffs for consecutive years be representative. The assumption that the record prior to 1941 would be continuous with the record starting in 1949 would be open to serious question. Accordingly, it was concluded that the best procedure would be to consider water supply on a stochastic basis.

In the stochastic analysis new sequences of historical flows were generated, utilizing the historical flow data as the basis. Normal distribution of the historical values about the mean was assumed in this analysis, except for certain controls that were placed on the sequence of monthly events. This control was developed by plotting successive monthly flows, one against the other, to develop serial correlations of successive monthly flows.

The generation of monthly streamflows, as well as operation studies necessary to estimate the dependable outflow, was by use of the digital computer. The drawdown was determined for four assumed controlled outflows by the digital computer, for several 100-year series of generated streamflow, and the resulting drawdowns were averaged. The results, expressed in terms of 0.1 percent, 1.0 percent, and 5.0 percent probabilities of occurrence, are shown in Fig. 8. These curves furnished a basis for selection of the probabilities of a shortage in water supply that could be tolerated in design of the reservoir.

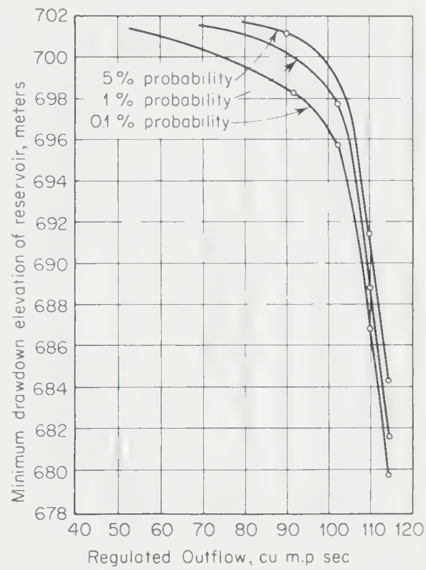

Fig. 8. Reservoir drawdown in critical period.

RESERVOIR WAVE ACTION

16. Freeboard Allowances. The term "freeboard" is frequently used in different ways. As defined previously, freeboard must include consideration of the following:

1. Height of wind tide (referred to also as setup)
2. Height of waves in deep water generated by winds
3. Effect of wave run-up on sloping embankments on height of waves
4. Any additional margin of safety considered necessary

Final design decisions on freeboard allowances usually involve consideration of the type of dam, the situation governing the spillway design flood, and the effect of waves. This section is concerned only with wave action. An excellent article by Saville, McClendon, and Cochran[1] and a manual by the U.S. Corps of Engineers[2] form the basis of procedures given in this section for computing waves.

17. Basic Assumptions. A number of formulas have been developed for computation of heights of wind tide, waves, and run-up. Most of these involve use of wind velocity and fetch as basic parameters. While the different formulas will yield different results, the variation between formulas is frequently not so great as the variation possible in results that are due to assumptions as to wind velocity and fetch. Thus, the development of reasonable assumptions is of prime importance.

Wind. The magnitude of wind tide, wave height, and run-up will vary with the magnitude of wind velocity and the duration of that velocity. Thus, it is desirable to develop wind data on a duration basis, if possible. The proper combination of velocity and duration is not always subject to precise determination, although procedures are available in the computation of wave heights for determining the minimum required time to reach maximum wave heights. Frequently, maximum wave conditions will not result unless the duration is in the order of 1 hr. Therefore, in wind-tide calculations the maximum observed 60-min average wind is frequently taken as the first trial for design. This assumption then can be checked against the values of wind tides derived as described later.

Care should be taken to utilize only those wind conditions considered possible of occurrence at the same time or immediately following the meteorological conditions causing the pool level under consideration. For example, if the spillway design storm is not of the hurricane type, the winds used to compute freeboard allowances should not be of the hurricane type.

Fetch. Fetch length is the horizontal distance of open water surface over which the wind blows. The use of the greatest straight-line distance over open water in wave computations will result in computed wave heights that are too high, since the amount of adjoining open water having shorter but significant fetches influences the waves. Observations on artificial reservoirs have indicated that use of an "effective fetch" is more reliable. The effective fetch is computed by dividing the 45° angle on either side of the maximum fetch line into about 15 equal segments, multiplying the fetch length for each segment by the cosine of the angle of deviation from the maximum fetch line, and dividing the sum of the products by the sum of the cosines.

Wind velocities over water are generally higher than over land under comparable meteorological conditions, because of lesser roughness. The following values represent averages observed on artificial reservoirs:

Fetch, miles	0.5	1.0	2.0	3.0	4.0	5.0 (or over)
Wind ratio $\frac{\text{over water}}{\text{over land}}$	1.08	1.13	1.21	1.26	1.28	1.30

The maximum potential wind velocity may not always coincide in direction with the direction of maximum fetch. If observations of maximum winds of given directions are available, the use of the effective fetch length can be carried one step further, utilizing the appropriate design wind velocities with the fetches indicated.

18. Wind Tide. Wind tide, or "setup," is the piling up of water at the leeward end of an enclosed body of water, as a result of the horizontal stress on water exerted by the wind. The magnitude of wind tide can be expressed by the following modifi-

[1] SAVILLE, THORNDIKE J., ELMO W. MCCLENDON, and ALBERT L. COCHRAN, Freeboard Allowances for Waves in Inland Reservoirs, *Trans. ASCE*, 1963, pt. IV, pp. 195–226.

[2] Waves in Inland Reservoirs, *Tech. Mem.* 132, Beach Erosion Board, U.S. Corps of Engineers, November, 1962.

cation of the Zuider Zee formula:

$$S = \frac{U^2F}{1{,}400D} \tag{3}$$

in which S is the wind tide (in feet) above still water, U is average wind velocity (in statute miles per hour) over the fetch distance F (in miles), and D is the average depth of water along the fetch line (in feet).

19. Wave Height and Other Characteristics. Wind-generated waves in a large body of water are not uniform in height. Successive waves will not be identical—each wave will be preceded and succeeded by a higher or lower wave. Data obtained from recordings of 45 storm periods at Fort Peck and Denison reservoirs have shown a very close comparison between the observed frequency distribution of wave heights on inland reservoirs with observed data on oceans. The following characteristics have been observed for the spectrum of waves observed at a given time and place:

% of total number of waves averaged to compute specific wave height H	Ratio of H to average wave height H_{av}	Ratio of H to significant wave height H_s	% of waves exceeding H
1	2.66	1.67	0.4
5	2.24	1.40	2
10	2.03	1.27	4
33⅓	1.60	1.00	13
50	1.42	0.89	20
100	1.00	0.62	46

The significant wave height H_s is defined as the average height of the highest one-third of all waves in a spectrum. As will be seen from the above tabulation, 13 percent of all waves can be expected to exceed H_s. These values would be reached at the end of a buildup period and give measures of the variations that can be expected in wave-height distributions. H_s may be computed by the set of curves in Fig. 9. Knowing the effective fetch and the wind velocity, the curve can be entered with these values to give the minimum time duration and value of H_s.

Once the value of H_s is computed, the occurrence frequency of a wave of any height can be computed from the preceding tabulation. The design height for waves H can be selected on the basis of consideration of frequency of winds of a given magnitude, duration of winds, and frequency of waves of given size. The finally selected design height must be a judgment value, involving consideration of the type of dam involved, as well.

20. Wave Run-up on Slopes. A wind-generated wave will be influenced when it runs up the slope of an embankment. The effect may be either to increase or to decrease the height of the wave in relation to the still-water surface, depending on wave characteristics and the slope, roughness, and permeability of the embankment. Therefore, the effect of run-up is usually combined with the actual wave height in computing allowances for wave action, into a single item designated as wave run-up height R.

In this sense R is the vertical distance between the maximum elevation obtained by a wave running up an embankment and the water elevation at the toe of the slope. The water elevation at the toe of the slope is the still-water elevation plus wind tide. Because of the relationship between wave height and run-up, it usually is convenient to compute run-up as a function of wave height.

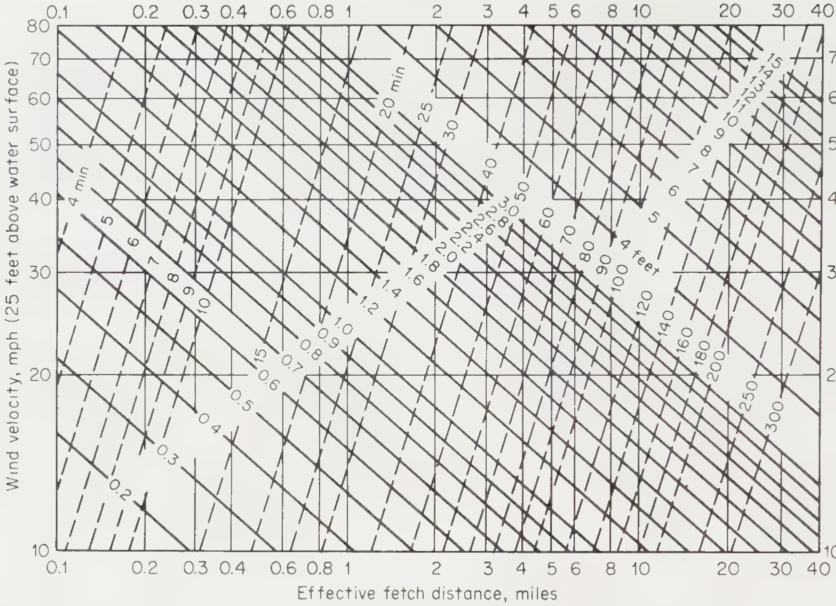

FIG. 9. Generalized correlations of significant wave heights H_s with related factors (deep-water conditions). Solid lines represent significant wave heights, in feet; dashed lines represent minimum wind duration, in minutes, required for generation of wave heights indicated for corresponding wind velocities and fetch distance. (*Beach Erosion Board, U.S. Corps of Engineers, Tech. Mem.* 132.)

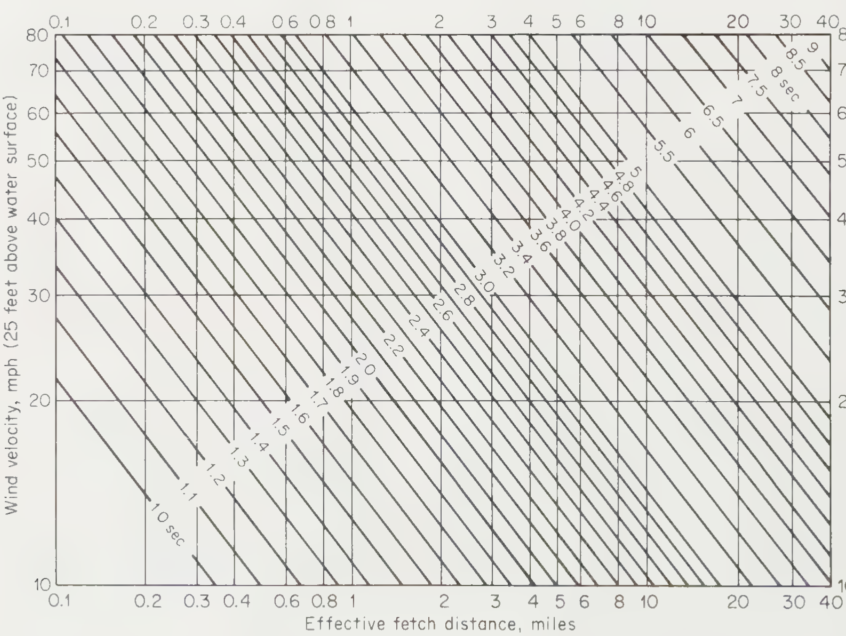

FIG. 10. Generalized relations between wave periods (T) and related factors (deep-water conditions). (*Beach Erosion Board, U.S. Corps of Engineers, Tech. Mem.* 132.)

The wave characteristics are represented by the wave steepness ratio H_0/L_0, where H_0 = specific wave height and L_0 = wave length, measured from crest to crest, in deep water. H_0 may, for practical purposes in deep reservoirs, be taken as equal to H. L_0 may be computed from the following formula:

$$L_0 = 5.12T^2 \tag{4}$$

where T is the wave period, which may be determined from Fig. 10. This wave period is approximately the same for waves ranging between the significant wave H_s and

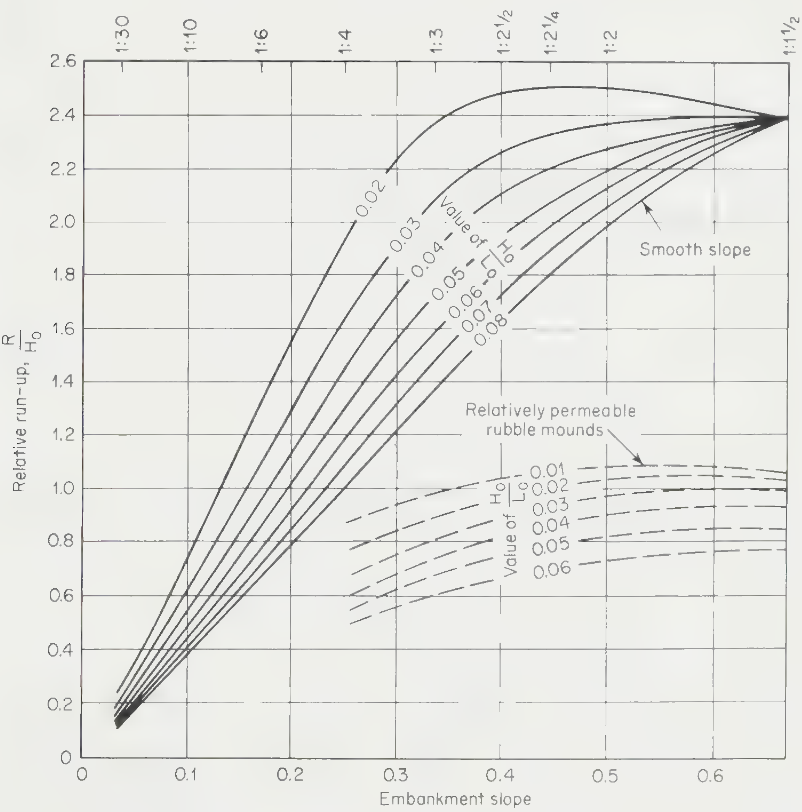

FIG. 11. Wave run-up ratios vs. wave steepness and embankment slopes. (*Trans. ASCE*, *vol.* 128, 217, 1963.)

the maximum wave H_{max}. Thus, in deep water the L_0 determined for the wave steepness ratio can be used for any value of H between H_{max} and H_s. Deep-water conditions can be considered to be present when the depth at the toe of the slope is more than one-third of the calculated wave length.

Using the values of H_0 and L_0, the effect of run-up on wave height may be computed from Fig. 11. Curves are shown for smooth slopes and for rubble mounds. Smooth slopes include surfaces such as well-graded earth embankments covered with sod and asphalt or concrete facing. Run-up on hand-placed riprap slopes approaches that computed for smooth slopes. Run-up on dumped riprap slopes can be considered to be about 50 percent of computed run-up on smooth slopes.

21. Total Allowance for Wave Action. The total allowance for wave action is the sum of the following:

1. Wind tide, computed as in Art. 18
2. The combination of wave height and wave run-up, utilizing wave height as computed in Art. 20 and the ratios shown in Fig. 11

RESERVOIR FLOOD ROUTING

Routing of floods through reservoirs is far simpler than through river channels, because of the unique relationship existing between reservoir stage and discharge. This relationship is established from the discharge characteristics of the reservoir outlets and the spillway, as they relate to reservoir elevation.

A number of methods have been developed for flood routing. Two methods, each of which has advantages, are presented here. The arithmetic method has the advantage of easy checking and filing. Also, because it utilizes curves developed from small differences, it possesses greater accuracy in reading of curves than most arithmetic methods. The graphical method has the advantage that variable time periods can be used, which is not easily possible with the arithmetic method.

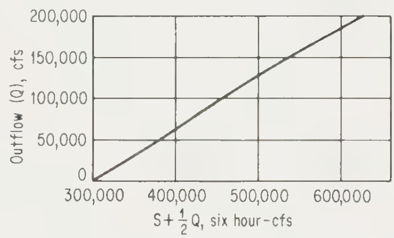

Fig. 12. Working curve for reservoir flood routing. Routing interval, 6 hr.

22. Arithmetic Method. For any time interval, the storage equation can be expressed as

$$I = (S_2 - S_1) + \left(\frac{Q_1}{2} + \frac{Q_2}{2}\right) \tag{5}$$

in which I = average inflow during period
S_1 and S_2 = storage at beginning and end of period
Q_1 and Q_2 = outflow at beginning and end of period

This may be rewritten as

$$\left(S_1 - \frac{Q_1}{2}\right) + I = S_2 + \frac{Q_2}{2} \tag{6}$$

If we let $S - Q/2 = (S + Q/2) - Q$, then, substituting, in the first step,

$$\left(S_1 + \frac{Q_1}{2}\right) - Q + I_1 = S_2 + \frac{Q_2}{2} \tag{7}$$

Also, in the second step,

$$\left(S_2 + \frac{Q_2}{2}\right) - Q + I_2 = S_3 + \frac{Q_3}{2} \tag{8}$$

If S and Q for the first step are known, and I for all steps also is known, the equations can be solved by a curve relating $(S + Q/2)$ to Q (for a given time interval). A typical curve for this purpose is shown in Fig. 12. This curve is constructed from data on reservoir volume and spillway discharge, as related to reservoir elevation. Since Q is small with respect to $(S + Q/2)$ the routing can be carried out utilizing a much smaller sheet of graph paper than would be required to obtain similar accuracy with the usual graphs relating $(S + Q/2)$ to $(S - Q/2)$.

Utilizing Fig. 12, the routing can be carried out in the following manner:

6-hr period	Item in routing	Volume, 6 hr, cfs	Origin of value
1	$S + \frac{Q}{2}$	300,000	Known
	$-Q$	0	Known
	$+I$	40,000	Given
2	$S + \frac{Q}{2}$	340,000	Algebraic sum
	$-Q$	23,000	From Fig. 12
	$+I$	80,000	Given
3	$S + \frac{Q}{2}$	397,000	Algebraic sum
	$-Q$	60,000	From Fig. 12
	$+I$	150,000	Given
4	$S + \frac{Q}{2}$	487,000	Algebraic sum
	$-Q$	118,000	From Fig. 12
	$+I$	90,000	Given
	$S + \frac{Q}{2}$	459,000	Algebraic sum

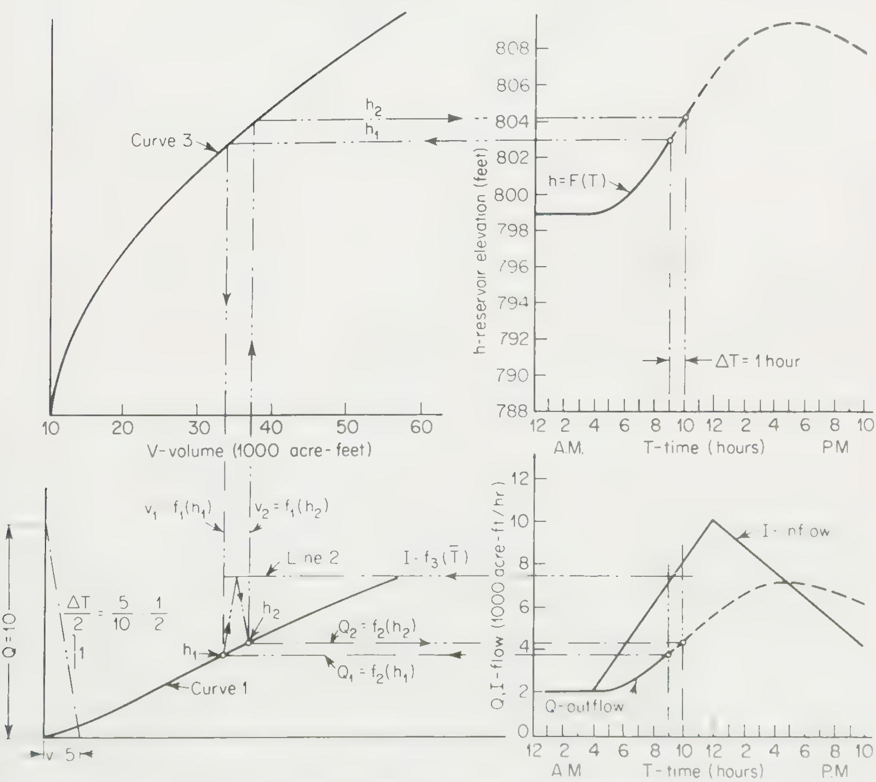

FIG. 13. Sorensen graphical method for routing floods.

23. Graphical Method. The equation for reservoir flood routing also may be expressed as

$$\frac{dV}{dT} = I - Q \tag{9}$$

in which reservoir volume $V = f_1(h)$
inflow $I = f_3(T)$
outflow $Q = f_2(h)$

so that

$$\frac{df_1(h)}{dT} + f_2(h) = f_3(T) \tag{10}$$

Figure 13 shows the graphical solution of Eqs. (9) and (10). Curve 1 is plotted with coordinates Q and V. Curve 3 is plotted with coordinates h and V (reservoir

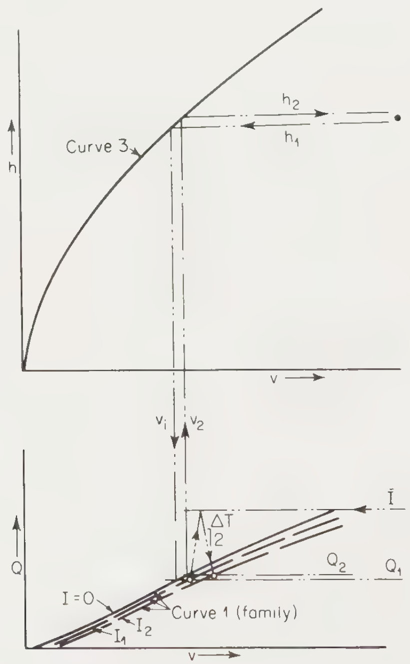

FIG. 14. Graphical adjustment for wedge storage.

volume curve). Both h and Q can be plotted as functions of time as the graphical solution progresses. As $f_3(T) = I$, it is convenient to plot the inflow hydrograph to the same scale as Q. Then line 2 can be drawn by projecting horizontally from the average value of I for each period ΔT.

If wedge storage is to be considered and is known, a family of curves may be drawn for curve 1, each labeled with the appropriate value of I. Then, as shown in Fig. 14, the curve corresponding to I_1 is used for the initial point h_1 and the curve corresponding to I_2 is used for the final point h_2. However, curve 1 corresponding to zero wedge storage must be used for projecting to curve 3 in obtaining the plot of h against time.

SECTION 5

NATURAL CHANNELS

By Russell W. Revell

INTRODUCTION

1. Flow Characteristics. Of the several types of open-channel flow, only those commonly found in natural channels are discussed here.

Flow in natural channels is varied because the depth changes along the channel. It is gradually varied if the change in depth is gradual and rapidly varied if the change is abrupt. Flow in natural channels is almost always turbulent flow with water particles moving in an irregular pattern. Viscous forces are small compared with inertial forces. The Reynolds number is less significant than the Froude number **F** (Sec. 2), which expresses the relationship between inertial forces and gravity forces. In the case of natural streams, the length characteristic L is the hydraulic mean depth.[1]

The commonest flow in natural channels is subcritical flow in which $V < \sqrt{gD}$ and **F** is less than unity. The flow is termed tranquil and the velocity is less than the velocity of gravity waves so that downstream conditions affect the depth of flow. In critical flow $V = \sqrt{gD}$ and the water-surface profile is usually marked by standing waves. In supercritical flow $V > \sqrt{gD}$ and the flow is described as rapid or shooting. Downstream conditions cannot affect the depth of flow. This section is concerned with subcritical flow.

HYDRAULICS OF NATURAL STREAMS

2. Discharge Formulas. Bernoulli's theorem applied to open channels states that the sum of the water-surface elevation and velocity head at any section is the same as at any upstream section minus the intervening loss in head. In Fig. 1,

$$Z_1 + h_{v_1} = Z_2 + h_{v_2} + h_f + \text{other losses} \tag{1}$$

where Z = elevation of the water surface above some datum
h_v = velocity head at the indicated cross section
h_f = head loss in reach due to friction
l = length of reach

Although the velocity head is usually assumed to be $V^2/2g$, where V is the mean velocity and g is the acceleration of gravity, this is not strictly true where velocity distribution is nonuniform. The true velocity head, in energy computations, is $\alpha V^2/2g$ where α is the energy coefficient. Kolupaila[2] proposed values of α for natural channels ranging from 1.15 to 1.50 with an average of 1.30. This refinement is frequently omitted where velocities are low.

Water flowing in a channel continually loses energy to its surroundings. This loss is expressed as the slope of the energy gradient. In Fig. 1 the energy gradient is $(h_f + \text{other losses})/l$. Discharge formulas define the relationship between the

[1] Chow, Ven Te, "Open-channel Hydraulics," McGraw-Hill Book Company, New York, 1959.
[2] Kolupaila, Steponas, Methods of Determination of the Kinetic Energy Factor, *The Port Engineer*, Calcutta, India, **5** (1), 12–18, January, 1956.

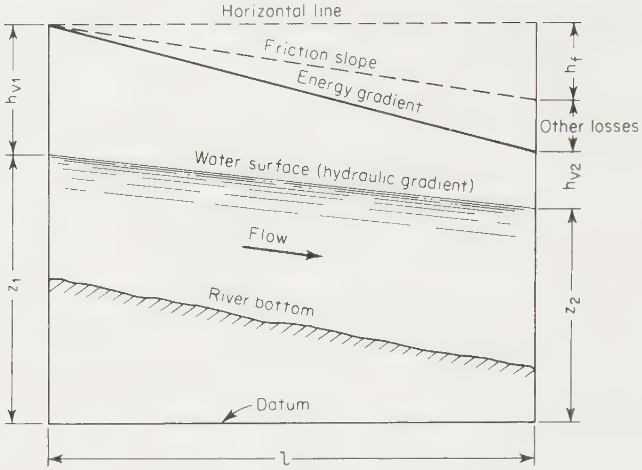

FIG. 1. Energy profile in open-channel flow.

friction slope h_f/l, the discharge, channel roughness, and the geometry of the channel cross section.

The other losses shown in Fig. 1 may result from stream curvature, form factors, contractions at bridges, and other channel obstructions. If these losses are fairly uniformly distributed along the channel, they are included in the friction head h_f. If not, they must be computed separately, as explained in Art. 5.

The Manning formula (Sec. 2) is by far the most commonly used in the United States for determining flow in natural channels. The Chezy formula (Sec. 2), the Ganguillet and Kutter formula (Sec. 2), and the Darcy-Weisbach formula (Sec. 2) are also in use. The values represented by the terms of these discharge formulas all vary from place to place in natural channels and also vary with discharge. Therefore, application of discharge formulas to natural channels is usually less accurate than for artificial channels. For this reason, their use for natural channels usually is restricted to relatively short reaches where reliable average values of the terms can be determined.

3. Roughness Factor. In the discharge formulas referred to in Art. 2, the resistance to flow is evaluated by roughness factors: n in Manning's and Kutter's formulas, C in the Chezy formula, and f in the Darcy-Weisbach formula.

Energy losses in turbulent flow are due primarily to skin friction, internal distortion, and impact. Roughness factors cover all these losses. Discharge formulas are empirically derived. The roughness factors are adjusted to make the formulas fit observed data. The formulas then will give reliable results for flow conditions having a similar roughness factor. For most flow conditions, impact will be small, and it is not too difficult to select a roughness coefficient that will account for the skin friction and the internal distortion. In natural streams having steep slopes and high velocities, large impact losses result from channel irregularities or obstructions that would cause only negligible impact losses for lower slopes and velocities. In such case, the n values must be substantially increased unless the additional impact losses are otherwise accounted for.

The effective roughness of a channel depends as much on the concentration of the roughness elements as it does on the size of the elements. The greatest effective roughness is found when the roughness elements cover from 15 to 25 percent of the channel.[1] Greater concentrations reduce rather than increase the distortion of the flow caused by the roughness elements.

A comprehensive discussion of roughness factors is given in a report of the American Society of Civil Engineers.[2]

4. Values of n for Natural Streams. Manning's formula is convenient to use with natural streams. Its n value can be computed if all the other terms are known. An n determined for one stage might not be usable at a significantly different stage because of differences in impact losses and changes in configuration, and because n varies slightly with hydraulic radius. When the bed is moving sand, dunes are formed on its bottom which significantly increase the n value over what it would be at lower velocities when the bed is not moving. There are no adequate criteria as to when the bed movement starts.

Where n cannot be computed directly, it must be estimated. This can be done by visually comparing the roughness of the channel with that for other channels of known roughness, or from descriptive tables of n values. Errors in estimating n values result in equal and opposite percentage errors in computing velocity and discharge. Therefore, care in selecting n values should be consistent with desired accuracy. Values of n for natural channels are given in Tables 1 and 2.

TABLE 1. VALUES OF n IN MANNING'S FORMULA FOR NATURAL STREAMS DETERMINED BY R. E. HORTON*

Natural-stream channel	Condition of stream bed			
	Best	Good	Fair	Bad
1. Clean, straight bank, full stage, no rifts or deep pools..	0.025	0.0275	0.030	0.033
2. Same as 1 but some weeds and stones................	0.030	0.033	0.035	0.040
3. Winding, some pools and shoals, clean................	0.033	0.035	0.040	0.045
4. Same as 3, lower stages, more ineffective slopes and sections..	0.040	0.045	0.050	0.055
5. Same as 3, some weeds and stones..................	0.035	0.040	0.045	0.050
6. Same as 4, stony reaches..........................	0.045	0.050	0.055	0.060
7. Sluggish river reaches, rather weedy or with very deep pools..	0.050	0.060	0.070	0.080
8. Very weedy reaches.............................	0.075	0.100	0.125	0.150

* CORBETT, DON M., and OTHERS, Stream-gaging Procedure, *U.S. Geol. Survey Water Supply Paper* 888.

Although Horton's n values originally were intended for use with the Kutter formula, they are also applicable to Manning's formula.[3]

Another approach to the determination of n values is the one used by the U.S. Soil Conservation Service, as shown on page 461 of "Design of Small Dams" by the U.S. Bureau of Reclamation.[4] This method, shown in Table 2, gives a much clearer definition of just what kind of energy losses is included in the roughness coefficient n.

[1] ROUSE, HUNTER, Critical Analysis of Open Channel Resistance, *Proc. ASCE, J. Hydraulics Div.*, July, 1965.

[2] Task Force on Friction Factors in Open Channels of the Committee on Hydromechanics of the Hydraulics Division of the American Society of Civil Engineers, Friction Factors in Open Channels, Progress Report, *Proc. ASCE, J. Hydraulics Div.*, **89** (HY2), pt. 1, March, 1963.

[3] CORBETT, DON M., and OTHERS, Stream-gaging Procedure, *U.S. Geol. Survey Water Supply Paper* 888.

[4] U.S. BUREAU OF RECLAMATION, "Design of Small Dams."

TABLE 2. SOIL CONSERVATION SERVICE METHOD OF DETERMINING n VALUES

Steps:

1. Assume basic n
2. Select modifying n for roughness or degree of irregularity
3. Select modifying n for variation in size and shape of cross section
4. Select modifying n for obstructions such as debris deposits, stumps, exposed roots, and fallen logs
5. Select modifying n for vegetation
6. Select modifying n for meandering
7. Add items 1 through 6

Aids in Selecting Various n Values:

1. Recommended basic n values

Channels in earth	0.010	Channels in fine gravel	0.014
Channels in rock	0.015	Channels in coarse gravel	0.028

2. Recommended modifying n value for degree of irregularity

Smooth	0.000	Moderate	0.010
Minor	0.005	Severe	0.020

3. Recommended modifying n value for changes in size and shape of cross section

Gradual	0.000	Frequent	0.010–0.015
Occasional	0.005		

4. Recommended modifying n value for obstructions such as debris, roots

Negligible effect	0.000	Appreciable effect	0.030
Minor effect	0.010	Severe effect	0.060

5. Recommended modifying n values for vegetation

Low effect	0.005–0.010	High effect	0.025–0.050
Medium effect	0.010–0.025	Very high effect	0.050–0.100

6. Recommended modifying n value for channel meander

L_s = straight length of reach $\qquad$ L_m = meander length of reach

L_m/L_s	n
1.0–1.2	0.000
1.2–1.5	0.15 times n_s
>1.5	0.30 times n_s

where n_s = items 1 + 2 + 3 + 4 + 5

5. Curvature, Form Factors, and Other Losses. The n in Manning's formula normally accounts for the friction from the roughness of the channel boundary and for normal internal distortion. Other losses in natural channels result from velocity disturbances caused by curvature of the channel, bank irregularities, expansion or contraction of the channel, and obstructions in the channel. These cause abnormal internal distortion and impact losses. Before applying additional corrections for such losses, the selected n value should be carefully reviewed to determine whether or not it already accounts for these losses.

Losses not covered by the n value usually are expressed as percentage of velocity head or percentage of changes in velocity head. Bends in natural channels induce energy loss in addition to that from an equal length of straight channels. Spiral flow is induced in and below the bend, with the water near the surface being deflected toward the outside of the bend and water near the bottom being forced toward the inside of the bend. Also, the water-surface elevation on the outside of the bend is somewhat higher than on the inside, because of the centrifugal force.[1]

Few quantitative data are available on the head loss in bends in natural channels. Experimental observations on losses in bends are largely restricted to artificial channels where variables can be controlled. Adapting head losses for artificial channels to natural channels requires considerable judgment.

Yen and Howe[2] list three sources of additional head loss due to bends: internal

[1] BLUE, F. L., JR., J. K. HERBERT, and R. L. LANCEFIELD, Flow around a River Bend Investigated, *Civil Eng.*, **4** (5), May, 1934.

[2] YEN, C. H., and J. W. HOWE, Effects of Channel Shapes on Losses in a Canal Bend, *Civil Eng.*, **12** (1), January, 1942.

friction from secondary currents in and below the bend, reduction of effective cross-sectional area due to eddies accompanying separation of flow from the bank, and loss of head due to repeated velocity changes. These combined effects can exceed those of boundary friction. They found the energy loss due to a 90-deg bend with uniform width of 11 in. and 5-ft radius of curvature to be

$$H_b = 0.380 \frac{V^2}{2g} \tag{2}$$

where H_b = head lost in the bend, ft
V = mean velocity in the approach section, fps
g = acceleration of gravity

Experiments by Scobey[1] on the flow of water around bends in flumes indicated that Manning's n value should be increased by 0.001 for each 20 deg of curvature per 100 ft.

Yarnell and Woodward[2] found the loss in 180-deg bends in flumes to be

$$H_b = 0.21 \frac{\text{channel width}}{\text{inner radius}} \frac{V^2}{2g} \tag{3}$$

A rough empirical guide for energy loss due to expanding or contracting sections follows: In a contracting section the energy loss due to contraction is considered to vary from 10 percent of the difference in velocity head where the contraction is gradual and smooth to 50 percent where the contraction is abrupt. For expanding sections, the energy loss is considered to vary from 20 percent of the difference in velocity head where the expansion is gradual and smooth to 50 percent where the expansion is abrupt.

Other sources of energy losses are channel obstructions such as bridge piers, which have been covered in technical literature.[3] Such losses are discussed in Art. 11.

DETERMINATION OF DISCHARGE

6. Methods. Discharge in natural channels usually is determined from current-meter measurements, from evaluating the terms in formulas for turbulent flow, as in the slope-area method, by special indirect methods utilizing known hydraulic properties, or for small streams, from weir measurements.

7. Weir Measurements. Weir formulas are derived from experiments; so the geometry and approach conditions of the weir must be similar to those of the experimental weir from which the formula was derived. In addition, the underside of the nappe must be well ventilated so that the pressure will be atmospheric.

The use of weirs for determining discharge of natural channels is limited by the difficulty of obtaining free overflow conditions for the ranges in discharge usually experienced and, for larger streams, by installation cost. In addition, variable approach conditions often cause the discharge to vary appreciably from that indicated by weir formulas. Therefore, where accuracy is required, weirs in natural channels should be rated frequently by current-meter measurements rather than depend on a weir formula.

An outgrowth of the weir for natural channels has been the artificial control whose purpose is to stabilize the stage-discharge relationship rather than to fit a standard weir formula. The artificial control creates supercritical velocity up to the stage at

[1] Scobey, Fred C., The Flow of Water in Flumes, *U.S. Dept. Agr. Tech. Bull.* 393.

[2] Yarnell, David L., and Sherman M. Woodward, Flow of Water around Bends, *U.S. Dept. Agr. Tech. Bull.* 526.

[3] Yarnell, David L., Bridge Piers as Channel Obstructions, *U.S. Dept. Agr. Tech. Bull.* 442, 1934. Liu, H. K., J. N. Bradley, and E. J. Plate, "Backwater Effects of Piers and Abutments," prepared by the Civil Engineering Section, Colorado State University, Fort Collins, Colo., in cooperation with the U.S. Bureau of Public Roads, October, 1957.

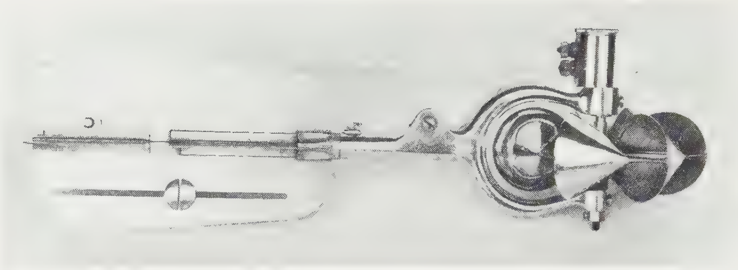

Fig. 2. Price-type current meter (U.S. Geological Survey).

which it becomes "drowned out," thereby eliminating any effects of changing channel conditions downstream for such stages. The control must be rated by discharge measurements or model studies. It is subject to the same inaccuracies due to changing upstream pool conditions as are weirs.

8. Current-meter Measurements. Current-meter measurements offer a relatively accurate method of determining flow in natural channels. Current meters have a rotating element actuated by the current, a device for indicating rotations of this element, and usually fins for orienting the meter with the current. The rate of rotation of the rotor indicates the velocity of the water. There also must be a device for lowering the current meter to the desired depth below the water surface. The commonest current meter in the United States is the Price-type meter shown in Fig. 2. It gives reliable results for velocities ranging from about 0.1 to more than 15 fps.

With this meter, an electric circuit is completed with each rotation, or each fifth rotation, of the rotor by a cam touching an electrical contact. The closing of the circuit causes an audible signal in an earphone. The circuit consists of a dry-cell battery, the meter, and the earphones connected in series.

Current-meter measurements in shallow water can be made by wading with the current meter mounted on a sliding support on a graduated wading rod which indicates the water depth. One electrical lead is attached to one of the electrical contacts of the current meter and the other to the wading rod. The circuit is completed through the metallic body of the current meter and the wading rod.

Discharge measurements for deeper rivers are made from a cableway, bridge, or boat with the meter mounted above a streamlined sounding weight. The meter is supported by a thin steel cable with an inner insulated conductor. The outer part of the cable is connected, through a special connector, to the current-meter body and the inner conductor is connected to the electrical contact of the meter. The sounding cable can be paid out from a graduated sounding reel or handline. These and other auxiliary items of equipment are described in U.S. Geological Water Supply Paper 888.[1]

If a double-conductor cable is not available, a separate insulated conductor can be attached to the contact point of the meter, but this increases the drag in swift water. Another solution is to use a single-conductor sounding cable insulated from the body of the current meter. A short electrical conductor connects the cable to the contact point of the meter. A separate bare wire is trailed in the river, completing the circuit by the conductivity of the river water. For this circuit the sounding cable must not be grounded. A rating table is furnished with each current meter.

In making a current-meter measurement, it is essential to measure the cross-sectional area of the river with an accuracy comparable with that used in determining

[1] Corbett, Don M., and Others, Stream-gaging Procedure, *U.S. Geol. Survey Water Supply Paper* 888.

velocities. The cross section should be as nearly at right angles with the current as possible and far enough downstream from tributaries or channel obstructions for normal velocity distribution to be fully developed. The depth is measured at known distances from a reference mark on shore. A convenient method for wading or boat measurements is to string a tagline across the river with markers at convenient intervals. For measurements from a cableway or bridge, the cable or bridge railing can be marked with paint at convenient intervals.

The average velocity, from top to bottom, is determined at each sounding point. When velocity distribution is normal, as will be found at a well-located measuring section, the average of the velocities at 0.2 and 0.8 of the distance from the water surface to the bottom will represent the average velocity in that particular vertical within close limits. Where shallow depths do not permit placing the current meter at 0.8 depth or where reduced accuracy can be tolerated, the velocity at a single point 0.6 of the distance from the surface to the bottom can represent the average velocity in the vertical. Where vertical velocity distribution is abnormal, it is advisable to measure the velocity at 0.2, 0.6, and 0.8 of the distance from the water surface to the bottom and let the average of the three velocities represent the average velocity in the vertical. In positioning the current meter, it is the axis of the meter that must be at the indicated depths, not the bottom of the sounding weight.

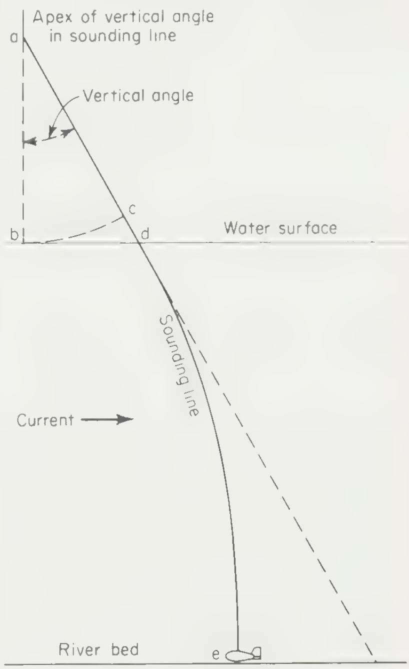

FIG. 3. Position of sounding weight and sounding line. (*U.S. Geological Survey.*)

Verticals are selected across the river so that the discharge represented by each vertical is a reasonably uniform percentage of the total discharge. A good rule is to keep this percentage from exceeding 5 percent. This usually can be accomplished with about 30 verticals. The probable error of a measurement with 30 verticals is only about two-thirds that for a measurement with 15 verticals.[1]

Two common causes of inaccuracies in discharge measurement are failure to compensate for elements of the current not being at right angles to the measuring section and failure to compensate for the vertical angle of the sounding cable when the meter is cable-supported.

The horizontal-angle correction, when required, is made at each subarea. It is most conveniently made by multiplying the mean velocity in the vertical by the cosine of the deviation of the current from a perpendicular to the measuring cross section.

In discharge measurements from a bridge, boat, or cableway, the depth is commonly determined by positioning the bottom of the sounding weight at the water surface, then lowering it to the river bottom and noting the amount of sounding cable paid out. The sounding weight will be carried downstream by the current, causing the sounding cable to be slanted as shown in Fig. 3.

[1] CARTER, ROLLAND W., and IRVING E. ANDERSON, Accuracy of Current Meter Measurements, *Proc. ASCE, J. Hydraulics Div.*, **89** (HY4), July, 1963.

The amount of cable paid out *ce* will be greater than the depth of the water by the amount *cd*, called the dry-line correction, plus the difference between the curved length *de* and the true water depth, called the wet-line correction. These corrections may be determined from tables of correction which are available in U.S. Geological Survey publications.[1]

Dry-line corrections can be dispensed with, even with the meter supported from a considerable distance above the water, if the tag method is used. In this method, tags of fabric or other material are firmly attached to the sounding cable at fixed distances above the bottom of the sounding weight. The sounding weight is lowered to the bottom of the river. It then is raised until the highest submerged tag is at the water surface. The sounding weight is again lowered to the bottom and the additional sounding line that is paid out is measured with the sounding reel or other device. Since the vertical angle changes little when the sounding weight is close to the bottom, the wet line will have been measured in its entirety, it being the distance from the bottom of the weight to the tag plus the additional line paid out. It is still necessary to measure the vertical angle to obtain the wet-line correction.

The amount of the sounding corrections can be reduced with the accuracy of the discharge measurement increased by using heavier sounding weights, thereby reducing the vertical angle.

It is sometimes necessary to measure the discharge under an ice cover on a river. The effective depth is the distance from the underside of the ice cover to the river bottom. If the effective depth is sufficient, the mean velocity in the vertical can be found by averaging the velocity at 0.2 and 0.8 of the effective depth. For smaller effective depths the mean velocity in the vertical is found by multiplying the velocity at 0.5 of the effective depth by 0.88.

Discharge measurements in winter sometimes encounter anchor ice, which is a slushy type of ice attached to the streambed. Since the sounding weight and current meter will sink through this layer of anchor ice, care must be used in noting its top surface. This surface should be considered to be the river bottom for purpose of computing the discharge measurement. Its surface can be detected as the point at which the current meter ceases to register any velocity.

9. Area-Velocity Method. Computation of discharge from a current-meter measurement is most conveniently performed by the area-velocity method, as shown in Fig. 4. The cross-sectional area is divided into many small areas of measured size,

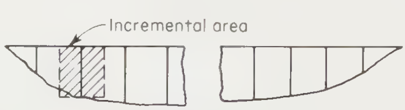

Fig. 4. Subdividing the cross section.

as explained in Art. 8, and the mean velocity is determined for each area. The sum of the incremental products of area and velocity is the total discharge.

An incremental area is found by multiplying the depth at each vertical by the sum of half the distances to each adjacent vertical. The average velocity in the vertical is taken to represent the average for the entire incremental area.

10. Slope-Area Method. Practical considerations sometimes prevent making discharge measurements during floods. The slope-area method is useful for determining such flood discharges from field data. It is essentially the reverse of computing n from field data as explained in Art. 4. It makes use of an open-channel formula,

[1] Corbett, Don M., and Others, Stream-gaging Procedure, *U.S. Geol. Survey Water Supply Paper* 888.

usually Manning's formula. The following conditions are desirable for a slope-area reach:

1. Sufficient high-water marks to determine the flood-crest profile along each bank
2. A single, fairly uniform channel with no significant gain or loss in the reach
3. No significant erosion or deposition in the reach during or following the flood

Cross sections, at least two and preferably three, are surveyed. They are so spaced that the fall between them can be measured accurately, but close enough together so that uniformity of conditions in the reach is not sacrificed unduly. Elevations in the cross sections should be to the nearest tenth of a foot, and in the profiles to the nearest hundredth of a foot. Where there are pronounced breaks in the slope or roughness of a cross section, such as between main channel and overbank areas, the conveyances are computed separately for each subsection.

The discharge will not be reliable without an accurate determination of n; so considerable care should be given to its selection. A contracting section is preferable to an expanding section because the effects of errors in determining n are reduced.

Since the submerged cross sections almost certainly will have different areas, velocity-head corrections must be made to determine the energy gradient. If there are large variations of velocity in a cross section, the velocity head must be determined from weighted velocity heads for different parts of the cross section.

In making the computations, approximations of discharge will have to be tried until the proper discharge is found that will give compatible values of energy gradient and surface gradient.

11. Indirect Determinations. A contracted section in a channel causes an abrupt drop in water surface due to conversion of static head to velocity head. A contracted bridge opening is a typical example. This drop can be used to determine discharge, using Bernoulli's theorem of continuity of head. The equation for discharge through the contracted opening is

$$Q = kA\sqrt{2g\left(H + \frac{V^2}{2g} - h_f\right)} \tag{4}$$

where Q = discharge
k = a coefficient for sharp-edged or square entrances, usually ranging from 0.90 to 0.95
A = effective area of the most contracted section (eliminating parts of the cross section not contributing to the flow)
g = acceleration due to gravity
H = drop in water surface due to the contraction
$V^2/2g$ = velocity head in the approach section
h_f = loss in head due to friction

A sketch of the site will aid materially in making the computations. Longitudinal profiles upstream and downstream from the contraction, when extended to the point of contraction, will give the value of H. If the determination is made later from flood marks, care must be exercised to eliminate the effects of standing waves in the downstream profile. Velocity head in the approach section can be determined from the cross-sectional area by trial and error. The friction loss h_f can be determined from Manning's formula using for the average velocity the square root of the average of the squares of the velocities in the approach section and in the contracted section. The value of h_f has a minor effect in short, abrupt contractions.

STREAMFLOW RECORDS

12. General Requirements. Unlike many other resources, streamflow is an ever-varying quantity. Consequently, records of streamflow must be kept over a long period before average streamflow and streamflow variability at a particular place can be evaluated accurately. Therefore, if streamflow records are not available at or near a site, a stream-gaging program should be initiated as soon as the need for records becomes apparent. Fortunately most important rivers in the United States have some kind of flow record. The U.S. Geological Survey alone operates approximately 7,500 stream-gaging stations, and many others are operated by various public and private agencies.

Frequently a streamflow record is too short to provide the required information. Usually it is possible to extend a short record by correlating it with a much longer record at some other point on the river or on a nearby river. Sometimes recourse must be had to correlating a short streamflow record with a much longer precipitation record, although this is usually less satisfactory.

For some purposes, such as power studies or reservoir-operation studies, it is important to have a long sequence of streamflow data. It is common practice to assume the historical sequence of streamflows, but this limits the length of the sequence to the length of the record and may not adequately reflect the probabilities of unusual events. If the record is sufficiently long to define average conditions and variations, it can be extended to any length by stochastic procedures using statistical parameters, as explained in Sec. 4.

The accumulation of streamflow records requires three steps: (1) the collection of stage or gage-height records, (2) the determination of the relationship between stage and discharge, and (3) the computation of discharge from stage using this relationship.

13. Gage-height Records and Recorders. The record of river stage is derived from periodic readings of a nonrecording gage, usually a graduated vertical staff gage, or obtained continuously from a water-stage recorder. The site for a river gage should be selected carefully. For best results:

1. There should be a good control section, such as a rocky riffle, a short distance downstream of the gage to provide a stable relationship between stage and discharge.
2. The gage should be on a reach which is fairly straight and with a stable cross section.
3. The site should not be subject to variable backwater such as would result from a confluence with another river a short distance downstream.
4. There should be a section fairly near the gage suitable for current-meter measurements.
5. Conditions for installation of the gage should not be difficult.
6. The site should be accessible under all weather and river conditions.
7. Suitable personnel to serve as gage readers and to perform minor services should be available nearby.
8. The site should be as near as practicable to the site for which streamflow records are required.

Frequently it is impossible to obtain all desired features. For instance, large rivers usually do not have suitable control sections.

Nonrecording gages are adequate for rivers where the stage changes gradually, provided a reliable gage reader is available. On the other hand, flashy streams would require very frequent gage readings to provide a good record of stage. Therefore, most river gages are provided with an automatic water-stage recorder.

Water-stage recorders make a continuous ink or pencil trace of stage on a moving graduated chart or print the stage on moving tape. Cylindrical charts mounted on revolving drums commonly provide a record of stage for a day, week, or month. Long strip charts passing over rollers will provide a record for up to a year at normal rate of chart movement. Some continuous recorders will operate unattended for several months. For every recording gage installation there should be a nonrecording gage to which the recorder is referred.

Water-stage recorders usually are actuated by a float in a stilling well in which the water level is maintained at the same level as in the river by connecting intake pipes or openings through the wall of the stilling well. The size of the intake or opening should be such as to dampen out waves and surges in the river, yet allow the water surface in the stilling well to follow every change in stage of the river.

Stilling wells embedded in the river bank are fitted with intake pipes, usually two or more at different levels in case one becomes clogged with sediment. The lowest intake pipe should be lower than the minimum expected stage. The stilling well should extend far enough below the lowest intake pipe to provide a sump for the accumulation of sediment, which should be removed periodically. The intake pipes should be fitted with flushing devices for streams carrying sediment.

If the stilling well is large enough for access there should be a staff gage attached to the inside wall. The recorder should be set to read the same as this gage. For smaller stilling wells the recorder should be actuated by a graduated tape reading the same as the outside staff gage. Differences in elevation between the river surface and the water surface in the stilling well indicate faulty intake action or drawdown of the gage well due to the velocity of the water past the end of the intake pipe.

Stilling wells sometimes are attached to bridge piers or abutments or to river walls. In such cases a small opening allows access of river water but dampens out waves and surges. Small-diameter stilling wells in deep water sometimes are fitted with a cone at the bottom with a small hole which serves as an intake and also permits escape of sediment that otherwise would accumulate in the well.

In cold climates, precautions must be taken to prevent the float from freezing to the water surface. One method is to set the stilling well deep in the river bank and then construct a floor as a frost barrier across the gage well below the freezing level of the ground with provisions for the float cable, and sometimes for the float, to pass through the floor. Another solution is to place the float in a vertical cylinder open at both ends. A light oil or kerosene is poured into the cylinder. The recorder float then floats in the oil. The water in the stilling well outside the cylinder is allowed to freeze.

Where range in stage or sediment makes use of a stilling well difficult or expensive, a servomanometer, sometimes referred to as a bubble gage, usually will overcome the difficulty. Dry nitrogen gas from a high-pressure tank is reduced in pressure and allowed to escape very slowly from the end of a tubing firmly anchored to a point below the lowest low water. The pressure of the gas will equal the water pressure over the end of the tubing. There is a mercury manometer with a reservoir at one end moved by a motor so that the mercury pressure and gas pressure balance. The movement of the mercury reservoir is transmitted through gearing to a water-stage recorder. Figure 5 shows a servomanometer gage connected to both a continuous recorder and a printer.

All gages should be checked periodically by levels to assure that they are at correct datum. Therefore, there should be at least one, and preferably more, bench marks at known elevation and completely separated from the gage structure so that they will remain unaffected by any casualty to the gage.

14. Stage-Discharge Relationships. The second step in determining streamflow is to establish the relationship between river stage and discharge. This requires the

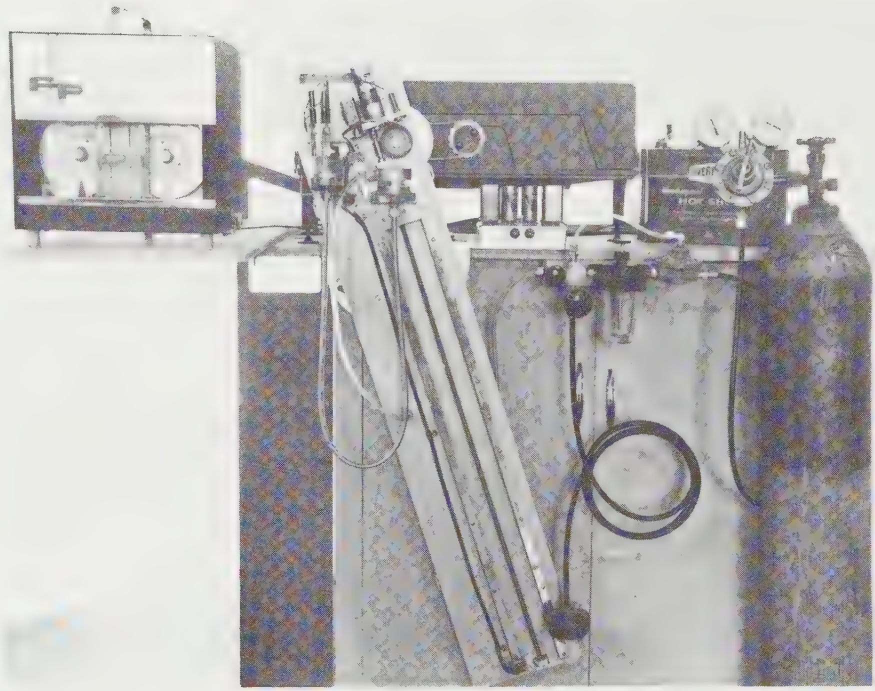

FIG. 5. Servomanometer gage. (*U.S. Geological Survey.*)

simultaneous observation of river stage and measurement of river discharge. Except for the unusual case of a completely stable channel, the relationship between stage and discharge will not long remain constant. Therefore, the determination of the stage-discharge relationship is a continuing process.

Stage is plotted as ordinate against discharge as abscissa on either rectangular or logarithmic coordinates, and a representative curve is drawn through the plotted points. Where a rating curve is used for a considerable period of time, it is convenient also to express the relationship in tabular form. The curve and/or table are referred to as the station rating.

The daily discharge is computed directly from daily average gage heights and the rating. In cases of rapidly changing stage, the day should be subdivided into several shorter periods and discharge computed for each period and averaged.

Where the stage-discharge relationship is unstable, different ratings should be used from time to time. Where a large number of ratings otherwise would be required, the "shifting control" method can be used. In this method a variable-shift adjustment is applied to the gage reading for each discharge measurement to make the measurement plot close to a reasonably representative rating curve. Similar shift adjustments are applied to daily average stages before applying the rating to determine daily discharge. The shift will be known for each day on which a discharge measurement is made but must be interpolated or otherwise estimated for days between measurements. Therefore, frequent discharge measurements are required where the stage-discharge relationship shifts badly.

Stations affected by variable backwater present complications since a third variable, slope, must be considered. This requires two river gages separated a sufficient distance to permit accurate determination of the fall in water-surface elevation yet sufficiently close to provide an essentially plane water surface between them. Both gages should avoid areas of distorted water surface, such as bends. If there is appreciable difference in cross-sectional areas, both gage heights should be corrected for velocity head.

If only intermittent backwater is experienced, a standard rating curve can be derived for periods of no backwater and a second curve drawn showing the relationship between the fall and percent reduction in discharge for periods of backwater. Where backwater is experienced a large part of the time, or on large rivers of low slope where changing discharge results in changing slope, a standard slope or fall is selected and all measurement discharges are corrected to this standard slope or fall. This is done by multiplying the discharge by the ratio of the square root of the standard slope or fall to the square root of the slope or fall for the measurement. A rating curve is then drawn for these corrected discharges. The use of the curve is the reverse of its derivation. The discharge read from the curve is multiplied by the ratio of the square root of slope or fall for that particular time to the square root of the standard slope or fall.

An ice cover on the river or "anchor" ice clinging to the bottom will change the stage-discharge relationship. The surface in contact with the flowing water, and hence the resistance to flow, is increased. Therefore, the river stage for a given discharge is increased. This increase in stage is termed the "backwater due to ice." Frequent discharge measurements and a plotting of air temperatures help to interpret this backwater when computing daily discharges.

BACKWATER CURVES

15. Problem and Purpose. A common problem in river hydraulics is to determine what the water-surface profile of the river would be under specific river-discharge and channel conditions. The term "backwater curves" is applied to such profiles.

Backwater curves are used to determine grade lines for flood-protection works, highways, and bridges. They are used to determine tail-water ratings for hydroelectric power plants and elevations for pumping plants, canal headworks, and energy dissipaters. They are often used to determine areas subject to flooding.

16. Theory and Principles. It has been shown that there are 12 possible types of backwater curves,[1] but as used herein, the term applies to low-gradient profiles in rivers or other open channels with subcritical velocities. Such conditions are found above dams or other obstructions. River backwater curves usually are derived by one of many step methods, in which the reach of river in question is subdivided into many short subreaches and the change in water-surface elevation is determined for each subreach, either analytically or graphically.

Figure 1 shows the energy profile for open-channel flow. Equation (1), based on that figure, can be rearranged to read

$$Z_2 = Z_1 + h_f + \text{other losses} + h_{v1} - h_{v2} \tag{5}$$

where the subscripts 1 and 2 have been reversed because backwater computations for subcritical velocities proceed in an upstream direction.

Determination of a backwater curve for a specific discharge consists of successively computing Z_2 for the upstream end of a reach from known values of Z_1 at the downstream end and the physical characteristics of the reach. The value Z_2 then becomes Z_1 for the next upstream reach. This continues until the desired backwater curve has been computed.

[1] Woodward, Sherman M., and Chesley J. Posey, "Hydraulics of Steady Flow in Open Channels," John Wiley & Sons, Inc., New York, 1941.

The key to the computations is the determination of the friction loss h_f, and other losses if significant, usually with Manning's formula. This formula, when used for backwater curves, usually is written in the form

$$S_f = \frac{Q^2}{K^2} \tag{6}$$

where S_f = friction slope
Q = discharge, cfs
K = conveyance = $(1.486/n)AR^{2/3}$ for English units

The value of K is found by trial and error. Details of computations are covered in Art. 18.

17. Basic Data. All step methods of deriving backwater curves require a knowledge of the shape and elevation of cross sections at each end of the various subreaches and also of the channel roughness and the water-surface elevation at the starting point.

Backwater curves start at a point where the water-surface elevation is known for the particular discharge and proceed upstream. If there are no such points of known water-surface elevation, then a starting elevation must be assumed for a point well downstream from the reach for which the backwater curve is desired. A good procedure for such cases is to assume two different starting elevations, one higher and one lower than the elevation normally expected for such a discharge. Backwater curves are computed from each starting point. If the two curves merge downstream from the reach for which the backwater curve is desired, then the procedure is acceptable. If not, the computations should be started at a point farther downstream.

Field surveys are required unless accurate large-scale topographic maps showing water depths are available. Cross sections should extend up both banks to above the expected backwater elevation and should be approximately at right angles to the current. The field survey determines the values in the Manning formula.

Where several backwater curves are to be computed, it is convenient to plot the hydraulic radius and the cross-sectional area at each section against water-surface elevation as shown in Fig. 6.

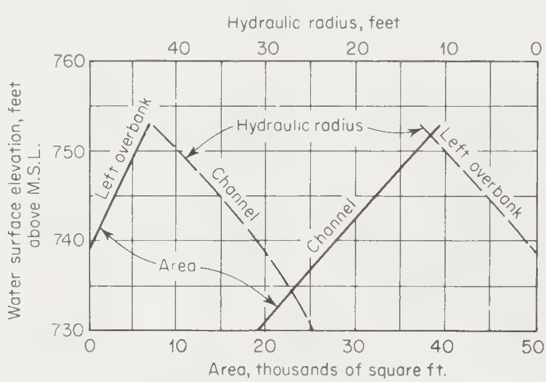

FIG. 6. Elements of cross section No. 1, Missouri River at Kansas City, Mo. (*U.S. Army Corps of Engineers.*)

The distance between cross sections depends on the uniformity of the channel and on the desired accuracy. Cross sections should be located at transitions between expanding, contracting, or uniform sections. Preferably, they should be spaced so that average velocities will not vary by more than 20 percent between adjacent cross sections. On large rivers, cross sections spaced at an average interval of a mile or more may be adequate, while on small rivers the spacing might be a few hundred feet. Distances between cross sections should be measured along the main part of the current. In some cases, such as overbank flow at a river bend, the distance between cross sections, and hence the slope, will be different for the main channel and the overbank flow. If pronounced, this will require special procedures.[1]

Cross sections should represent conditions for a significant length of reach. Therefore, purely local irregularities should be disregarded. When taking cross sections, soundings should be taken to establish shape of the underwater part of the cross section, and water elevation noted.

Where there are large variations in depth or roughness in different parts of the cross section, the cross section should be subdivided and the conveyances for the cross sections added. A common situation requiring subdivision is the case of the flow extending onto a flood plain.

An index map should be prepared showing the river channels, overbank areas, cross sections, and any structures that might affect the flow of the river. An example of such a map is shown in Fig. 7.

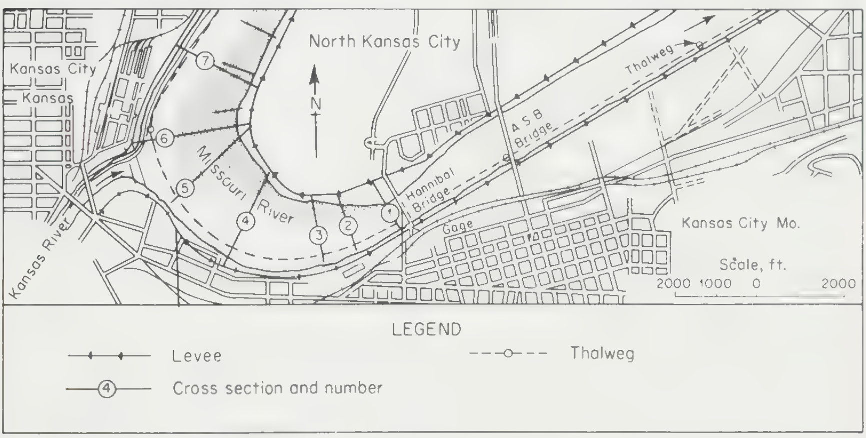

FIG. 7. Missouri and Kansas rivers at Kansas City, Mo. (*U.S. Army Corps of Engineers.*)

18. Mathematical Solutions. The standard step method is particularly suited to natural channels and is illustrated here. It is convenient to prepare a table of hydraulic elements such as shown in Table 3.

The actual steps in determining the backwater curve are carried out in Table 4. The functions of the columns of the table follow:

Column (1) identifies the cross section. Locations of cross sections for the example are shown in Fig. 7.

Column (2) shows the trial elevation from which the characteristics of the cross section are determined.

Column (3) shows the distance of the cross section from some reference.

Column (4) is the length of the reach in feet.

Column (5) shows the cross-sectional area of each part of the cross section.

Column (6) shows the wetted perimeter of each part of the cross section.

[1] U.S. CORPS OF ENGINEERS, "Engineering Manual," Civil Works Construction, Part 114, Chap. 9, Hydrologic and Hydraulic Analyses, Computation of Backwater Curves in River Channels, p. 9, May, 1952.

Table 3. Hydraulic Elements*
Missouri and Kansas rivers at Kansas City, Mo.

Section No. (1)	River mile (2)	Reach, ft (3)	W.S. El., ft MSL (4)	Description of area (5)	From station (6)	To station (7)	Width, ft (8)	Wetted perimeter, ft (9)	Area, sq ft (10)	Remarks (11)
				Missouri River						
1	377.58		745.1	Left overbank	0 + 35	5 + 05	470	470	2,650	Levee 1 on 3
				Channel	5 + 05	13 + 90	885	900	31,900	Bank 1 on 1
		1,060								
2	377.78		745.3	Left overbank	0 + 62	2 + 40	178	181	1,190	Levee 1 on 4
				Channel	2 + 40	14 + 97	1,260	1,290	32,500	Bank 1 on 5
		845								
3	377.94		745.5	Left overbank	0 + 61	1 + 50	89	92	580	Levee 1 on 4
				Channel	1 + 50	16 + 72	1,520	1,550	38,300	Bank 1 on 4
		2,060								
4	378.33		745.9	Channel	2 + 91	23 + 72	2,080	2,110	48,500	Levee 1 on 4 Bank 1 on 4½
		1,690								
5	378.65		746.2	Left overbank	4 + 62	11 + 80	720	720	3,020	Levee 1 on 4
				Channel	11 + 80	32 + 24	2,040	2,080	47,300	Bank 1 on 1
		1,580								
6	378.95		746.2	Left overbank	4 + 62	11 + 80	720	720	3,020	Levee 1 on 4
				Channel	11 + 80	32 + 24	2,040	2,080	47,300	Bank 1 on 1
		2,430								
7	379.41		746.9	Left dike	0 + 61	9 + 40	880	880	8,270	Levee 1 on 4
				Channel	9 + 40	22 + 35	1,300	1,320	34,700	Levee 1 on 3
				Kansas River						
1K	0.00	1,430	757.0	Channel			840	860	29,400	Levee 1 on 3 both sides
		298								
2K	0.056		757.0	Channel			840	860	29,400	Levee 1 on 3 both sides
				Missouri River						
10	383.54		750.3	Left overbank	32 + 80	44 + 50	1,170	1,180	12,900	Levee 1 on 3
				Channel	44 + 50	57 + 40	1,290	1,310	34,600	
				Dike	57 + 40	62 + 29	490	490	5,700	Levee 1 on 4
		2,430								
Fairfax bridge	384		750.3	Left overbank			560	640	5,010	1 level surface and 3 pier surfaces
				Channel			1,400	1,580	36,600	7 pier surfaces
				Right overbank			125	130	1,100	Bank 1 on 4
		8,290								
11	385.57		751.6	Left overbank	59 + 60	81 + 10	2,159	2,150	13,900	Levee 1 on 3
				Channel	81 + 10	89 + 32	820	840	22,300	Bank 1 on 1

* U.S. Army Corps of Engineers.

Column (7) shows the hydraulic radius for each part of the cross section. It is found by dividing the area by the wetted perimeter.

Column (8) shows the two-thirds power of the hydraulic radius. Columns (6) and (7) could be dispensed with if $R^{2/3}$, instead of wetted perimeter, were plotted against water-surface elevation in Fig. 6.

Column (9) is Manning's roughness factor n.

Column (10) shows the conveyance K for the various parts of the cross section. It is equal to $(1.486/n)AR^{2/3}$ in the Manning formula.

Column (11) shows the square root of the slope at the cross section. It is found by dividing the discharge by K.

Column (12) shows the slope at the cross section. It is the square of the value in Column (11).

Column (13) is the mean slope in the reach.

Column (14) is the friction head in the reach. It is the mean slope multiplied by the length of the reach.

Column (15) shows the discharge in each part of the cross section. This is required for the computation of velocity head in Columns (16) to (19). The total discharge is distributed between the subsections in proportion to the conveyance of the subsections shown in Column (10).

Column (16) shows the velocity in each part of the cross section.

Column (17) is velocity squared times discharge. It is computed for each part of the cross section and the values totaled.

Column (18) is found by dividing the total value for the cross section in Column (17) by the total discharge.

Column (19) is the velocity head and is found by dividing the value in Column (18) by twice the acceleration of gravity.

Column (20) shows the difference in velocity head. It is found by subtracting the value in Column (19) from the similar value for the previous (downstream) cross section.

Column (21) shows the total difference in head between the cross section and the previous (downstream) cross section.

Column (22) shows the elevation at the cross section. It is the previous value plus Column (21). If it differs materially from the assumed value in Column (2), a new value must be assumed and the computations for the entire line repeated. The elevation in Column (22) is a point on the desired backwater curve.

Where energy losses not covered by the roughness factor n are significant, as discussed in Art. 5, they must be taken into account in computing backwater curves. This will require additional columns in the computation table.

Bridges that obstruct the flow of the river must be considered in computing backwater curves. Table 4 illustrates an approximate method that is suitable for low velocities where the bridge presents only a minor obstruction. Cross sections are taken through the bridge and 50 ft upstream and downstream from the bridge. The wetted perimeter for the bridge section is increased by the water depth on the sides of the piers. In the illustration, the curves of hydraulic elements for section 10 are used for the cross sections 50 ft upstream and downstream from the bridge.

19. Effect of Tributaries. In carrying a backwater curve past a sizable tributary, it is necessary to compute the water-surface elevation of both streams immediately above the confluence. These two cross sections are designated 6 and 1K in Fig. 7 and Tables 3 and 4. The discharge above the confluence consists of 350,000 cfs from the Missouri River and 81,000 cfs from the Kansas River. The friction slope is computed for each of the two cross sections using the flows at the respective cross sections. The friction head for the Missouri River is computed using the mean slope of sections

Table 4. Determination of Backwater Curve*

Missouri and Kansas rivers at Kansas City, Mo., for discharge of 431,000 cfs

	Identification			Characteristics of cross sections							Friction losses			Velocity-head corrections						Elevations	
Sec. no.	Trial el., ft	River mile	Reach L, ft	Area A, sq ft	Wetted perimeter P, ft	Hydraulic radius R, ft (5) ÷ (6)	$R^{2/3}$	Roughness factor n	Conveyance K, million cfs $(1.486/n) AR^{2/3}$	$S^{1/2}$ $Q \div K$	Friction slope S_f [Col. (11)]^2	Mean friction slope S_m	Friction head h_f 4 × 13 ft	Discharge Q cfs	Velocity V 15 ÷ 5 cfs	V^2Q $16^2 \times 15$	V_{av}^2 17 ÷ Q	Velocity head h_v ft	Diff. in velocity head $h_{v1} - h_{v2}$ ft	Total diff. in head H 14 + 20 ft	Water-surface el. ft
(1)	(2)	(3)	(4)	(5)	(6)	(7)	(8)	(9)	(10)	(11)	(12)	(13)	(14)	(15)	(16)	(17)	(18)	(19)	(20)	(21)	(22)
River Gage																					
1	752.2	377.58		6,060	497	12.2	5.30	0.05	0.95					14,300	2.36	79,650					
				38,600	910	42.2	12.1	0.025	27.76					416,700	10.80	48,590,000					(start)
									28.71	0.0150	0.000225			431,000		48,669,650	112.9	1.76			752.25
2	752.5	377.78	1,060	2,580	210	12.3	5.33	0.05	0.41					7,000	2.71	51,000					
				41,600	1,310	31.8	10.04	0.025	24.73					424,000	10.19	44,028,000					
									25.14	0.0171	0.000292	0.000258	0.27	431,000		44,079,000	102.3	1.59	0.17	0.44	752.69
3	753.3	377.94	845	1,400	123	11.4	5.06	0.05	0.21					3,000	2.14	13,900					
				50,300	1,570	32.0	10.08	0.025	30.20					428,000	8.53	31,000,000					
									30.41	0.0142	0.000202	0.000247	0.21	431,000		31,013,900	72.2	1.12	0.47	0.68	753.37
4	754.0	378.33	2,060	65,400	2,170	30.2	9.70	0.025	37.70	0.0114	0.000130	0.000166	0.34	431,000	6.59		43.4	0.67	0.45	0.79	754.16
5	754.5	378.65	1,690	9,040	754	12.0	5.24	0.05	1.41					15,700	1.74	47,500					
				64,200	2,100	30.6	9.78	0.025	37.32					415,300	6.47	17,384,900					
									38.73	0.0111	0.000123	0.000126	0.21	431,000		17,432,400	40.5	0.63	0.04	0.25	754.41
Balance section: 350,000 cfs from Upper Missouri, 81,000 cfs from Kansas River																					
Mouth of Kansas River																					
1K	755.0		1,430	27,700	844	32.8	10.25	0.025	16.88	0.00480	0.000023	0.000073	0.10	81,000	2.93	695,000			0.28	0.38	754.79
Missouri River																					
6	754.8	378.95	1,540	9,300	755	12.4	5.36	0.05	1.48					13,200	1.41	26,200					
				64,900	2,100	30.9	9.85	0.025	38.02					336,800	5.19	9,070,000					
									39.50	0.00886	0.000078	0.000101	0.16	350,000							
														431,000		9,791,200	22.7	0.35	0.28	0.44	754.85

Table 4. Determination of Backwater Curve* (*Continued*)

Sec. no.	Trial el., ft	River mile	Reach L, ft	Area A, sq ft	Wetted perimeter P, ft	Hydraulic radius R, ft (5) ÷ (6)	$R^{2/3}$	Roughness factor n	Conveyance K, million cfs $(1.486/n) AR^{2/3}$	$S^{1/2}$ $Q \div K$	Friction slope S_f [Col. (11)]^2	Mean friction slope S_m	Friction head h_f 4 × 13 ft	Discharge Q cfs	Velocity V 15 ÷ 5 cfs	V^2Q $16^2 \times 15$	V_{av}^2 17 ÷ Q	Velocity head h_v ft	Diff. in velocity head $h_{v1} - h_{v2}$ ft	Total diff. in head H 14 + 20 ft	Water-surface el. ft
Identification				Characteristics of cross sections							Friction losses			Velocity-head corrections						Elevations	
(1)	(2)	(3)	(4)	(5)	(6)	(7)	(8)	(9)	(10)	(11)	(12)	(13)	(14)	(15)	(16)	(17)	(18)	(19)	(20)	(21)	(22)
Proceeding up the Missouri River. Discharge is 350,000 cfs																					
7	754.9	379.41	2,430	15,400	914	16.9	6.59	0.04	3.77					41,300	2.68	297,000					
				45,100	1,330	34.0	10.50	0.025	28.15					308,700	6.84	14,444,000					
									31.92	0.0110	0.000121	0.000100	0.24	350,000		14,741,000	42.1	0.65	−0.30	−0.06	754.79
10	758.6	383.54		22,800	1,200	18.9	7.10	0.050	4.81					46,700	2.05	196,000					
				45,300	1,310	34.6	10.62	0.025	28.60					277,800	6.13	10,439,000					
				9,900	519	19.0	7.12	0.040	2.62					25,500	2.58	170,000					
									36.03	0.0097	0.000094	0.000108		350,000		10,805,000	30.8	0.48			758.77
Fairfax Bridge, −50 ft (use curves for section 10)																					
	759.2		2,380	23,500	1,200	19.5	7.24	0.050	5.06					47,600	2.03	196,000					
				46,100	1,310	35.2	10.74	0.025	29.43					276,600	6.00	9,958,000					
				10,200	521	19.6	7.27	0.040	2.75					25,800	2.53	165,000					
									37.24	0.0094	0.000088	0.000091	0.22	350,000		10,319,000	29.5	0.46	0.02	0.24	759.01
Fairfax Bridge																					
	759.0	384.0	50	9,910	730	13.8	5.75	0.050	1.69					19,700	1.99	78,000					
				48,800	1,640	29.7	9.59	0.025	27.82					324,400	6.65	14,346,000					
				2,340	165	14.2	5.86	0.050	0.51					5,900	2.52	37,500					
									30.02	0.0117	0.000137	0.000113	0.01	350,000		14,461,500	41.3	0.64	−0.18	−0.17	758.84
Fairfax Bridge + 50 ft (use curves for section 10)																					
	759.2		50	23,500	1,200	19.5	7.24	0.050	5.06					47,600	2.03	191,000					
				46,100	1,310	35.2	10.74	0.025	29.43					276,600	6.00	9,958,000					
				10,200	521	19.6	7.27	0.040	2.75					25,800	2.53	165,000					
									37.24	0.0094	0.000088	0.000112	0.01	350,000		10,314,000	29.5	0.46	0.18	0.19	759.03
11	760.0	385.57	8,240	32,100	2,180	14.7	6.00	0.050	5.72					83,200	2.59	558,000					
				29,200	852	34.3	10.56	0.025	18.33					266,800	9.14	22,288,000					
									24.05	0.0146	0.000213	0.000150	1.24	350,000		22,846,000	65.3	1.01	−0.55	0.69	759.72

Note: Sections 8 and 9 deleted from table to save space.

* U.S. Army Corps of Engineers data.

5 and 6 for the Missouri River and sections 5 and $1K$ for the Kansas River. The velocity head at sections 6 and $1K$ is determined from the combined flow of 431,000 cfs at the two sections through the combined area of the two sections. The values in Columns (15) and (17) are totaled for the two cross sections to obtain a velocity-head value, 0.35 ft. The difference in velocity head between section 5 and the combined sections is 0.28 ft. This is added to the 0.16-ft friction loss for the Missouri River to obtain a total head difference of 0.44 ft and the 0.10-ft friction loss for the Kansas River to obtain a total head difference of 0.38 ft. These values are added to the elevation at section 5 to obtain the elevations at sections 6 and $1K$, respectively.

FLOW ROUTING

20. Definition and Methods. Flow routing is the determination of the timing and shape of a flow wave in an open channel or reservoir. Since flow routing is frequently used for predicting or reconstructing the progress of a flood, it is often referred to as "flood routing" regardless of the magnitude of the flows involved.

Flow-routing methods include mathematical, graphical,[1] and computer[2] methods. A common mathematical method is described in Art. 24. Most flow-routing methods will work to a degree for either a river or a reservoir. The choice depends on convenience and required precision. This article is concerned with flow routing through open channels, such as natural rivers, in which there is no significant backwater from tributaries.

21. Practical Applications. Routed streamflows are used to provide flood warnings, to determine benefits from existing or proposed flood-control works, to determine the effects of upstream power-plant operation on downstream plants, for scheduling irrigation deliveries, etc. They also can be used to reconstruct natural flood hydrographs on regulated rivers to extend the period of flood-frequency data and to check the consistency of streamflow records at different points on a river.

22. Theory and Principles. Flow routing has two basic aspects, time displacement of the flood wave, and the reduction of the peak and spreading out of the wave base. Complex procedures utilizing all the known factors affecting open-channel flow[3] are used where there are tidal influences or where the quality of the basic data and the required accuracy of the results warrant the considerable additional work involved. For most problems, approximate methods that keep the computations within manageable limits are indicated. These methods ascribe the change in shape of the flood wave to channel storage.[4] A common method is described in Art. 24.

The solution of flow-routing problems must conform to the law of continuity. In any time interval and using comparable units,

$$O = I - \frac{\Delta S}{\Delta t} \tag{7}$$

where O = mean outflow during period Δt
I = mean inflow during period Δt
ΔS = change in storage during period Δt
Δt = length of period

[1] LAWLER, EDWARD A., Hydrology of Flood Control, Part II, Flood Routing, in "Handbook of Applied Hydrology" by Ven Te Chow, McGraw-Hill Book Company, New York, 1964. LINSLEY, RAY K., JR., MAX A. KOHLER, and JOSEPH L. H. PAULHUS, "Applied Hydrology," McGraw-Hill Book Company, New York, 1949.

[2] KOHLER, MAX A., Electrical Analogies and Electronic Computers: A Symposium, Application to Stream-flow Routing, *Trans. ASCE*, **118**, 1953. ROCKWOOD, DAVID M., Columbia Basin Streamflow Routing by Computer, *Proc. ASCE*, *J. Waterways Harbors Div.*, Paper 1874, WW 5, December, 1958.

[3] U.S. CORPS OF ENGINEERS, "Engineering Manual," Civil Works Construction, Part 114, Chap. 8, Hydrologic and Hydraulic Analysis, Routing of Floods through River Channels, p. 2, September, 1953. THOMAS, H. A., "Hydraulics of Flood Movement in Rivers," Carnegie Institute of Technology, Pittsburgh, Pa., 1934.

[4] CARTER, R. W., and R. G. GODFREY, Storage and Flood Routing, *U.S. Geol. Survey Water Supply Paper* 1543-B, 1960.

The above equation can also be written as follows:

$$S_2 - S_1 = \tfrac{1}{2}(I_1 + I_2)\,\Delta t - \tfrac{1}{2}(O_1 + O_2)\,\Delta t \tag{8}$$

where subscripts 1 and 2 denote values at the beginning and end of a period, respectively.

Figure 8 shows a typical drainage area for which the flow is to be routed from A to B. A tributary is gaged at C, and the remaining inflow between A and B is ungaged.

Tributaries present a special complication. There is no exact direct solution for the case in which the flow of one stream induces significant backwater in the other stream. Gilcrest[1] presents a trial-and-error procedure for such a case. Where the backwater induced by the confluence is small, a simple procedure is adequate. If the tributary enters the reach near the upstream end as in Fig. 8, its flow can be

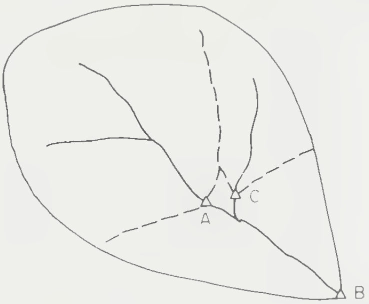

FIG. 8. Location of flow-routing reach.

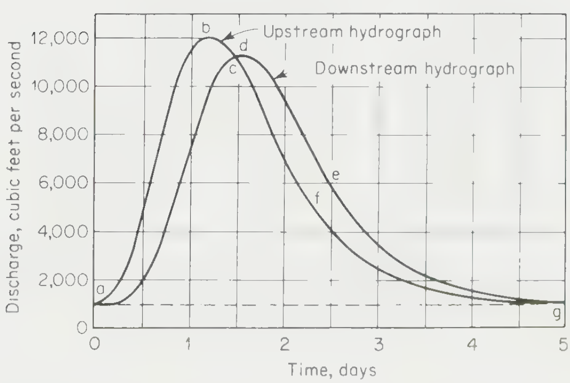

FIG. 9. Change in flood wave due to channel storage.

combined with the inflow from the main channel. If it enters near the downstream end of the reach, its flow can be added to the outflow after completing the routing. For tributaries entering midway in the reach and for ungaged inflow, the inflow can be distributed between the two ends of the reach or, for greater accuracy, treated as an independent variable.[2] Ungaged inflow can be determined from rainfall data using a synthetic unit hydrograph or by assuming it to be a percentage of the gaged flow at a nearby gaging station.

[1] GILCREST, B. R., Flood Routing, Chap. 10 in "Engineering Hydraulics," edited by Hunter Rouse, John Wiley & Sons, Inc., New York, 1950. U.S. CORPS OF ENGINEERS, "Engineering Manual," Civil Works Construction, Hydrologic and Hydraulic Analysis, Routing of Floods through River Channels, Part 114, Chap. 8, September, 1953.

[2] U.S. CORPS OF ENGINEERS, "Engineering Manual," Civil Works Construction, Hydrologic and Hydraulic Analysis, Routing of Floods through River Channels, Part 114, Chap. 8, September, 1953.

Figure 9 shows typical hydrographs at the upstream and downstream ends of a reach of channel. The inflow to the reach is denoted by *abcfg* and the outflow from the reach by *acdeg*. The downstream or outflow hydrograph has a lower peak and is more spread out than the upstream hydrograph. These changes result from the volume *abca* going into channel storage during the period *ac* and an equal volume *cdegfc* being released from channel storage during the period *cg*.

23. Basic Data Requirements. All methods of flow routing require knowledge or assumptions regarding the river channel. The most basic requirement is the relationship between discharge and channel storage.

Surveys, including cross sections for various discharges, will give this storage. Such surveys usually are not available. An alternate, and more common, method is to compute channel storage from inflow and outflow records of an observed flood. Figure 9 will serve as an example of effective inflow and outflow for the river reach *AB* shown in Fig. 8.

TABLE 5. DETERMINATION OF CHANNEL STORAGE

Day (1)	Hours (2)	Avg inflow (3)	Avg outflow (4)	Change in channel storage ¼ SFD (5)	Total channel storage (end of period) ¼ SFD (6)
1	0–6	1,300	1,000	300	300
	6–12	2,600	1,400	1,200	1,500
	12–18	6,000	2,600	3,400	4,900
	18–24	9,800	5,300	4,500	9,400
2	0–6	11,700	8,500	3,200	12,600
	6–12	11,700	10,600	1,100	13,700
	12–18	10,400	11,200	−800	12,900
	18–24	8,300	10,400	−2,100	10,800
3	0–6	6,300	8,800	−2,500	8,300
	6–12	4,900	7,000	−2,100	6,200
	12–18	3,700	5,400	−1,700	4,500
	18–24	2,900	4,100	−1,200	3,300
4	0–6	2,300	3,200	−900	2,400
	6–12	1,900	2,600	−700	1,700
	12–18	1,600	2,100	−500	1,200
	18–24	1,400	1,800	−400	800
5	0–6	1,200	1,500	−300	500
	6–12	1,100	1,300	−200	300
	12–18	1,000	1,200	−200	100
	18–24	1,000	1,100	−100	0

The first step in determining channel storage from inflow and outflow records is to determine the average inflow and outflow by periods for the entire flood event. The computations are shown in Table 5. In this example, the flood event is divided into 6-hr periods. The average inflow and outflow for each period, $\frac{1}{2}(I_1 + I_2)$ and $\frac{1}{2}(O_1 + O_2)$, respectively, in Eq. (8), are shown in Columns (3) and (4), respectively, of the table. Column (5) shows the change in channel storage during the period, and Column (6) shows the total channel storage at the end of the period above an arbitrary base. The computations should cover a period such that the beginning and ending discharges are about the same. If the resulting beginning and ending storage values are not approximately equal, then either the inflow or the outflow, or both, should be adjusted.

Another basic data requirement is the time of travel of the flood wave through the reach. The time of travel of the flood wave will be the time between the center of mass of the flood hydrographs for A and B. This time will be somewhat greater than the time interval between the peaks at the two points.

Gilcrest[1] has shown by the Manning formula that the velocity of the flood wave is 1.67 times the average velocity of flow for a wide rectangular channel, 1.44 times the average velocity for a wide parabolic channel, and 1.33 times the average velocity for a triangular channel. Another method of determining time of travel of the flood wave through the reach is given in Art. 24.

24. Mathematical Solution. One of the most satisfactory mathematical methods of flow routing is the Muskingum method, described in this section, developed by G. T. McCarthy and others in 1934–1935 during studies of the Muskingum Conservancy District Flood Control Project of the Corps of Engineers in Ohio.

In the Muskingum method, storage is related by a weighting process to both inflow and outflow. It is convenient to consider the storage in the reach as being composed of both prism storage and wedge storage as shown in Fig. 10. A reservoir

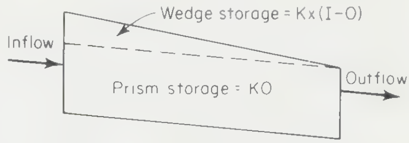

FIG. 10. Flood-wave storage.

has no wedge storage; so the discharge for a given gate opening is a function only of the reservoir stage. In a river channel the outflow is a function of both stage at outflow point and slope at the outflow point. The slope at the outflow is related to difference in flow within the reach. During the rising phase of a flood wave, inflow exceeds outflow, creating the wedge storage and increasing the slope of the water surface. During the falling phase the wedge storage is negative. The total storage is expressed mathematically by the Muskingum equation as follows:

$$S = K[xI + (1 - x)O] = KO + Kx(I - O) \tag{9}$$

where S is storage volume and I and O are simultaneous instantaneous values of inflow and outflow, respectively. K is a coefficient with the dimension of time and is equal to the time of passage of the centroid of the flood wave through the reach. The parameter x weighs the relative effects of inflow and outflow on storage within the reach.

The Muskingum method assumes that K and x are constant throughout the flood and that there is a unique relationship between storage and weighted discharge at the two ends of the reach. This is not strictly correct in most cases, but the method usually gives adequate results and the simplifying assumptions greatly reduce the computations.

The actual flow routing is performed for reaches and time intervals of predetermined length. The objective is to determine outflow from the reach at the end of successive time intervals. The general equation for outflow is

$$O_2 = C_1'I_2 + C_2'I_1 + C_3'O_1 \tag{10}$$

where subscripts 1 and 2 to the O and I terms denote values at the beginning and end,

[1] GILCREST, B. R., Flood Routing, Chap. 10 in "Engineering Hydraulics," edited by Hunter Rouse, John Wiley & Sons, Inc., New York, 1950.

respectively, of the routing time intervals, and where

$$C_1' = \frac{-(Kx - 0.5\Delta t)}{0.5\Delta t + K(1 - x)} \tag{11}$$

$$C_2' = \frac{Kx + 0.5\Delta t}{0.5\Delta t + K(1 - x)} \tag{12}$$

$$C_3' = \frac{-0.5\Delta t + K(1 - x)}{0.5\Delta t + K(1 - x)} \tag{13}$$

Adding these equations shows that

$$C_1' + C_2' + C_3' = 1 \tag{14}$$

An alternate and somewhat simpler form of the equation follows:

$$O_2 = O_1 + C_1(I_1 - O_1) + C_2(I_2 - I_1) \tag{15}$$

where

$$C_1 = \frac{\Delta t}{K(1 - x) + 0.5\Delta t} \tag{16}$$

$$C_2 = \frac{0.5\Delta t - Kx}{K(1 - x) + 0.5\Delta t} \tag{17}$$

It will be noted that all the C values in the above equations are dimensionless. K and Δt must be in the same units. Equation (15) is used in the routing example in this section.

Before computing the C values, it is necessary to determine Δt, K, and x. The first step in flow routing is to select the routing period Δt. Flow-routing procedures

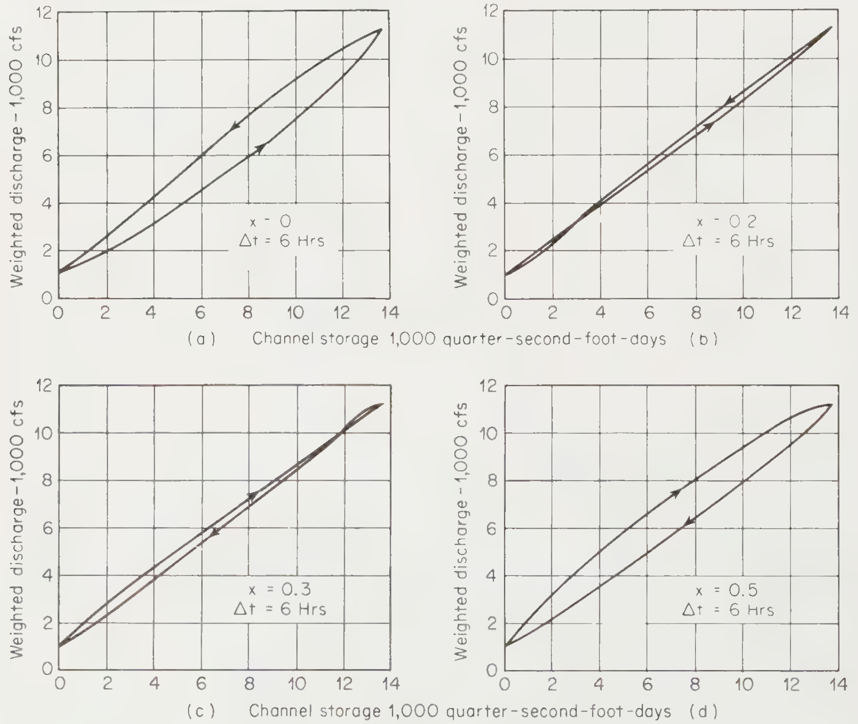

FIG. 11. Discharge-storage loops.

give the ordinate of the outflow hydrograph at the end of each routing period. The periods should be sufficiently short to define that hydrograph adequately. Also the period should be not longer than the time of travel of the flow through the reach and not less than $2Kx$.

If the length of the reach is such that the flood is at an appreciably different phase at the two ends of the reach, the reach should be subdivided into two or more subreaches. The value of K must be reduced accordingly. The flow is routed successively through each subreach, the outflow for the upstream subreach becoming the inflow for the next downstream subreach.

A value of x is chosen so that the storage will be the same for a given weighted discharge for rising and falling stages [see Eq. (9)]. Its value will be between zero and 0.5. It will be zero for a reservoir and 0.5 for uniformly progressive flow. Its determination for a natural river requires inflow and outflow records. In the absence of such records a value of 0.25 often is used. A lower value should be used where the reach is constricted at the lower end. A higher value should be used for steep fairly uniform channels where the flow is confined within well-defined banks or levees at all stages.

The values of K and x can be found simultaneously where dependable records of storage vs. discharge are available. In the example, inflow and outflow are taken from Fig. 9. Weighted discharge, $xI + (1 - x)O$, is plotted as ordinate against storage for that instant [Column (6) of Table 5] in Fig. 11 using several values of x. It will

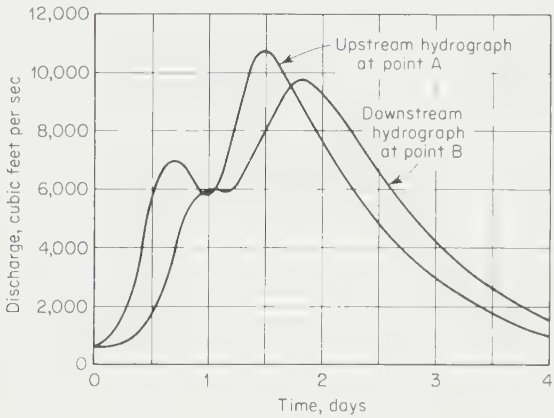

FIG. 12. Routed hydrograph.

be noted that curves b and c for x values of 0.2 and 0.3, respectively, have the smallest loops; that is, the relationship for rising and falling stages is most nearly the same. Therefore, 0.25 would be an acceptable value for x. The corresponding value of K is the reciprocal of the slope of the curve, or 8 hr.

With the values of Δt, K, and x determined, the coefficients C_1', C_2', and C_3' in Eq. (10) or the coefficients C_1 and C_2 in Eq. (15) are computed. The latter equation is used for illustration.

Figure 12 shows a new hydrograph for the upstream end of the reach AB in Fig. 8. This hydrograph is routed in Table 6, and the routed downstream hydrograph is also shown in Fig. 12.

In Table 6, Columns (1) through (4) can be computed first. Since the flow wave starts at zero hour on the first day, the inflow [Column (1)] and the outflow [Column (8)] are the same at that instant. Column (5) is found by subtracting Column (8)

TABLE 6. ROUTING COMPUTATIONS

$O_2 = O_1 + C_1(I_1 - O_1) + C_2(I_2 - I_1)$

Units: 1,000 cfs $C_1 = 2/3$, $C_2 = 1/9$

Day and hour (1)	I (2)	$I_2 - I_1$ (3)	$C_2(I_2 - I_1)$ (4)	$I_1 - O_1$ Col. (2) − Col. (8) (5)	$C_1(I_1 - O_1)$ (6)	$C_1(I_1 - O_1) + C_2(I_2 - I_1)$ Col. (4) + Col. (6) (7)	O (8)
1—0	0.6	1.0	0.11	0	0	0.11	0.6
6	1.6	3.9	0.43	0.89	0.59	1.02	0.71
12	5.5	1.4	0.16	3.77	2.51	2.67	1.73
18	6.9	−1.1	−0.12	2.50	1.67	1.55	4.40
24	5.8	2.6	0.29	−0.15	−0.10	0.19	5.95
2—6	8.4	2.3	0.26	2.26	1.51	1.77	6.14
12	10.7	−1.2	−0.13	2.79	1.86	1.73	7.91
18	9.5	−1.7	−0.19	−0.14	−0.09	−0.28	9.64
24	7.8	−1.6	−0.18	−1.56	−1.04	−1.22	9.36
3—6	6.2	−1.4	−0.16	−1.94	−1.29	−1.45	8.14
12	4.8	−1.1	−0.12	−1.89	−1.26	−1.38	6.69
18	3.7	−0.7	−0.08	−1.61	−1.07	−1.15	5.31
24	3.0	−0.6	−0.07	−1.16	−0.77	−0.84	4.16
4—6	2.4	−0.6	−0.07	−0.92	−0.61	−0.68	3.32
12	1.8	−0.4	−0.04	−0.84	−0.56	−0.60	2.64
18	1.4	−0.4	−0.04	−0.64	−0.43	−0.47	2.04
24	1.0						1.51

from Column (2). Column (7) is found by adding Columns (4) and (6). Column (8) for the next line (O_2 for the first period or O_1 for the second period) is computed next. It is found by adding Columns (7) and (8) for the line above. Column (5) for that line is then computed. This routine is then followed until the routing is completed.

SECTION 6

REGIME CANALS

By Franklyn C. Rogers and A. Rylands Thomas

CHANNELS IN ALLUVIUM

1. Stable and Regime Channels. Channels formed in alluvial soils and other erodible materials may be lined with nonerodible materials such as concrete or with materials which increase resistance to erosion such as gravel, or they may be designed so that their unprotected banks and beds will not be eroded by the flow. The relative economy of lined and unlined canals depends on the particulars of each case. Channels lined with nonerodible materials are dealt with in Sec. 7. Channels lined with gravel are similar to unlined channels excavated in gravel and may be designed by the tractive-force method described in Art. 3. Channels with unprotected beds and banks formed of alluvial materials in the silt-sand range may be designed by the regime-channel formulas given in Art. 4.

As is generally the case with canals drawing supplies from rivers, the flow carries sediment in suspension and as bed load. Suspended load is sediment which is supported and distributed by the turbulence of the flow. It is subdivided into bed-material load, comprising particles of a size range found also in the bed, and wash load comprising smaller particles generally absent from the bed. Bed load is sediment which is transported by rolling and sliding along the bed or by intermittent entrainment in the turbulent flow near the bed. It is important to prevent deposits of sediment which would reduce the discharge capacity of a canal. It is equally important to avoid erosive velocities which would attack banks and the foundations of structures. The regime formulas have been derived for this case. Also they provide guidance for the design of lined canals which are to carry sediment-laden flow.

2. Channels in Alluvium. Channels formed in alluvial or other granular material are said to be "stable" if their geometry remains substantially unchanged by scour or sediment deposit. Such stability will be achieved if (1) the materials forming the boundaries are sufficiently coarse to resist scour from flow in the channel and (2) the sediment carried by the flow does not exceed in size or quantity the transport capability of the channel.

Channels are said to be "in regime" when scour and deposition occur, but the balance of these is such that the boundaries remain essentially in equilibrium over a period of time. In this condition the materials transported by the flow and forming the boundaries are of similar origin and accordingly have generally the same physical characteristics.

Formulas for the design of stable and regime channels have been derived by two different approaches: one, based on the effect of shear stress (or tractive force) at the boundary (applying primarily to stable but not necessarily regime channels) and the other, a more empirical approach, based on observations of channels seen to be in regime.

3. Tractive Force. The tractive-force formulas are useful for the design of channels with erodible boundaries carrying clear water and also channels in which the material forming the boundaries is appreciably coarser than the transported sediment. Typical of the latter are channels with gravel boundaries carrying fine sand as suspended sediment and channels with rigid boundaries conveying flow with sediment of any size.

Tractive-force Formula. The mean shear stress or tractive force per unit area may be obtained by resolution of forces along the wetted boundary of the channel, assuming that the component of weight of water acting in the direction of the channel slope is balanced by the total shear resistance of water acting on the wetted perimeter

$$\tau_0 P = \gamma A S_0 \tag{1}$$

where τ_0 is the mean shear stress on the bed, P the wetted perimeter, γ the unit weight

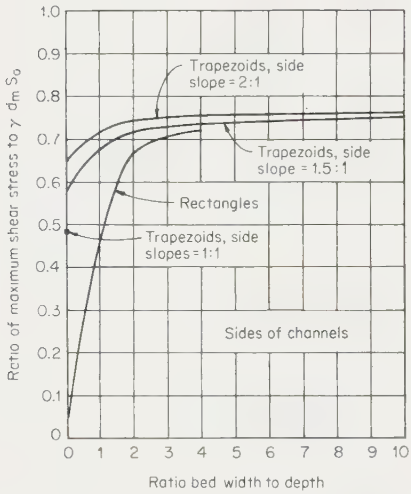

FIG. 1. Maximum shear stress on sides of channel.

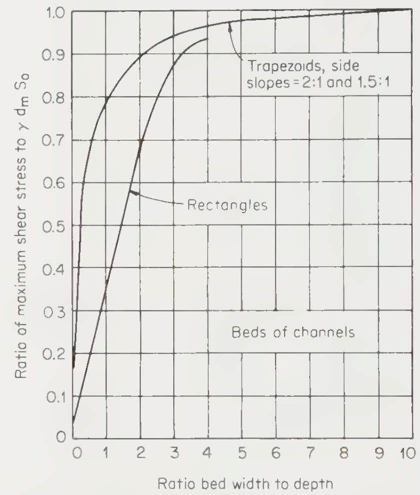

FIG. 2. Maximum shear stress on channel bed.

of water, A the cross-sectional area, and S_0 the longitudinal slope of the bed. The mean shear stress is expressed as

$$\tau_0 = \frac{\gamma A S_0}{P} = \gamma R S_0 \tag{1a}$$

where R is the hydraulic radius. In relatively wide channels the mean shear stress on the bed is given by

$$\tau_0 = \gamma d_m S_0 \tag{1b}$$

where d_m is the mean depth.

Maximum Shear Stress. Shear stress generally varies over the wetted perimeter. In natural channels, it tends to be maximum in the bed and minimum on the slopes. Correspondingly, the boundary material is often coarser in the bed and finer near the banks. Figures 1 and 2 show the maximum shear stress acting on the sides and beds of rectangular and trapezoidal channels.[1,*]

Limiting Tractive Forces. To avoid erosion of the material forming the boundary the shear stress should not exceed certain limiting values which are related to the grain size of the material and to the angle of side slope. The theory is directly

* Superior numbers refer to items in the Bibliography at the end of this section.

applicable to the side slopes of noncohesive granular material and to the beds of channels consisting of smooth (plane) surfaces formed in such material where there is no bed load. Such conditions may prevail in channels formed in coarse gravelly material.

The tractive-force formula is also applied to channels in fine material transporting sediment as bed load. In such cases accumulation of transported sediment may occur unless the shear stress at the bed exceeds the limiting value for the material transported (but to avoid erosion of the sides the shear stress should be within the given limits). Where there is bed load, however, it is preferable to use the regime-channel formulas given in Art. 4.

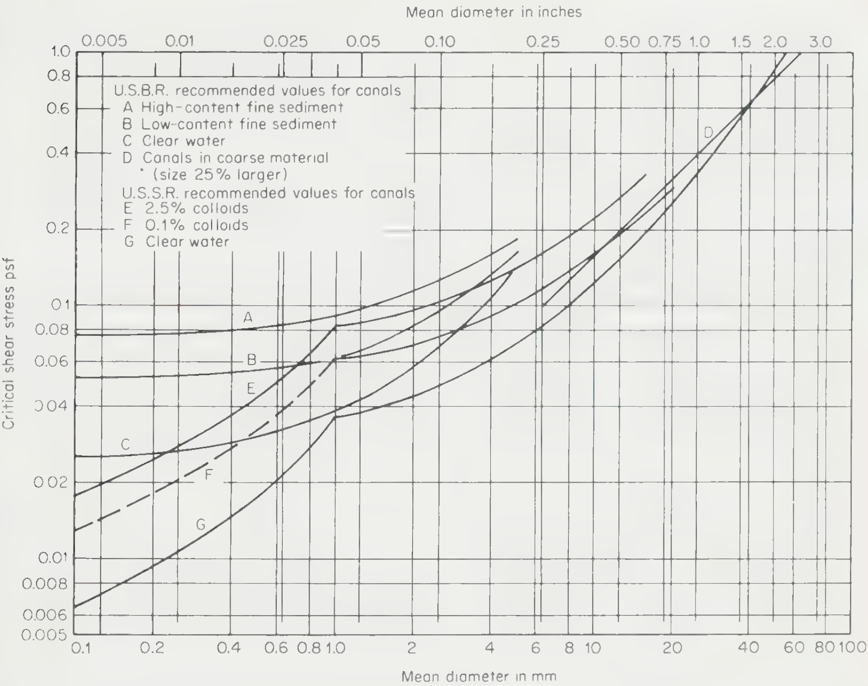

FIG. 3. Recommended values of limiting shear stress. *(From American Society of Civil Engineers.)*

Figure 3 shows the limiting shear stress or tractive force recommended for the design of stable channels by the U.S. Bureau of Reclamation. The values in Fig. 3 apply to horizontal or near horizontal beds. For sloping banks or sides of channels a reduction of factor K should be used, depending on the angle of repose of the material. Values of K may be determined from Fig. 4.

Slope Formulas. The formula in most general use is that of Manning

$$V = \frac{1.486}{n} R^{2/3} S_0^{1/2} \tag{2}$$

where V is the mean velocity and n a roughness factor.

There are no precise means of determining n, and an estimate has to be based on judgment and records of similar channels. n depends on the particle or grain size of the boundary material and on larger-scale form roughness. For example, n is affected by ripples in the bed, by channel geometry such as bends and changes in cross sections, and also in some cases by the sediment load. Plant growth increases the value considerably. A wide range of n values appears in Tables 1 and 2 in Sec. 5.

Channels with Gravel Beds. Channels with beds of gravel, shingle, or boulders may be considered in two categories according to whether or not there is bed movement.

If there is no bed movement and the banks are stable (which may be verified by Figs. 1 to 4), the relation of slope to grain size is indicated approximately by the following formula:

$$V = 8.2 \left(\frac{R}{k_s}\right)^{1/6} (gRS_0)^{1/2} \tag{3}$$

where k_s is the equivalent grain roughness, which is taken as the mean size of the material forming the boundary, and g is the gravitational constant. g, R, and k_s are

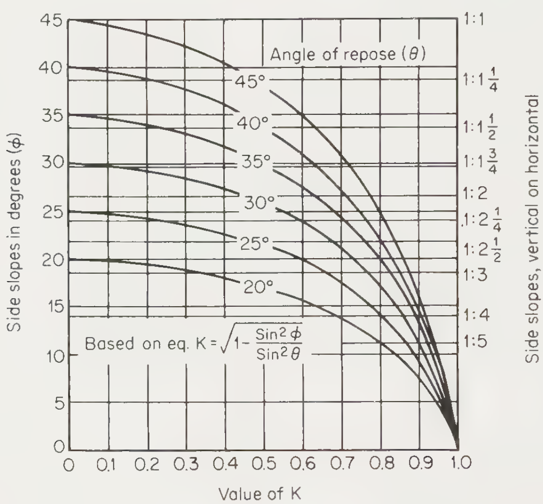

FIG. 4. Critical shear stress on inclined slopes.

in the same units. Equation (3) approximates the Nikuradse rough-pipe formula over a range of R/k_s from 10 to 150.[2]

In terms of the Manning formula this is equivalent to

$$n_g = 0.021 k_s^{1/6} \tag{4}$$

where n_g is the coefficient for grain roughness when k_s is in inches. In nearly all cases, however, because of irregularities in bed and banks, grain roughness is superimposed on form roughness and the value of n is higher than indicated by Eq. (4). The Manning roughness factor is expressed as

$$n = (n_g^2 + n_f^2)^{1/2} \tag{5}$$

where n_f is the coefficient for form roughness based only on the irregularities. Values of n_f are given in Fig. 5, which shows curves based on Eqs. (4) and (5) and data of the San Luis Valley canals, Colorado.[3] It will be seen that in gravel of representative size ¾ to 4 in., n_f ranged, with few exceptions, from 0 to 0.02 and n from 0.022 to

0.033. It is stated that there was bed movement in some of these canals, which may explain the wide range of n_f. Elsewhere n values of 0.023 (Upper Jhelum Canal, Pakistan, 10,000 cfs) and 0.025 (Dun Canal, India, 80 cfs) have been observed in canals with gravel beds.

If there is general movement the bed becomes irregular and n is consequently increased. This is very marked in the case of natural streams with a wide range of discharge and considerable bed movement at high stages. The value of n may vary considerably with stage, often being maximum at low stages when the large formations resulting from flood flows create discontinuities and surface waves. The value of n in the river Beas, India, where the mean size of bed material was between 3 and 6 in., ranged from 0.023 with 56,000 cfs to 0.037 with 3,300 cfs.[4] When designing a canal with a low value of n it is therefore important to check that the bed and side slopes will be stable under all possible conditions.

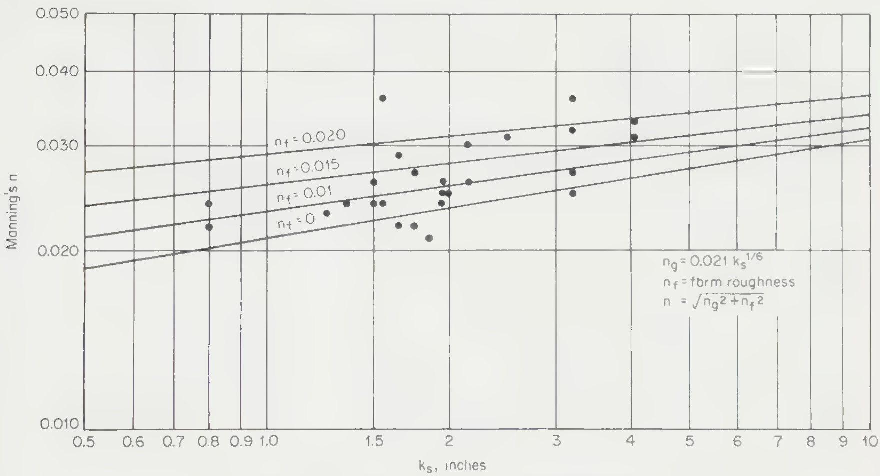

FIG. 5. Manning's n for gravel channels.

Channels with Sand Beds. Although there is a tendency for Manning's n to be higher with coarse sand than with finer materials, the predominant factor is the degree of roughness resulting from formation of ripples or dunes on the bed. In the case of small channels, the condition of the side banks has some influence. The following values of Manning's or Kutter's n have been used for many years as a guide in India and Pakistan:[5]

Condition of Channel	n
Above average	0.0225
Tolerably good	0.025
Below average	0.0275
Bad	0.030

Actual values observed have ranged from 0.011 with nearly plane bed to 0.039 with bed of large dunes of coarse sand.

THEORY OF REGIME CHANNELS

4. Regime-channel Formulas. The regime formulas of Kennedy, Lacey, and others apply to channels with erodible boundaries in alluvial soils carrying small sediment loads. They were derived mainly from data of irrigation channels in the alluvial plains of India and Pakistan where the canals draw supplies directly from large rivers and in the flood season carry sediment consisting of silt and fine and medium sand, the load generally not exceeding 2,000 ppm.

Unless the dimensions and slope of a channel are constructed to regime requirements, the geometry will suffer gradual change and performance will deteriorate. Inadequate slope leads to siltation and loss of discharge capacity, excessive slope to scour, endangering structures. Inadequate width leads to bank scour, excessive width to meandering.

Kennedy's Formula. Now mainly of historic interest, Kennedy's formula[6]

$$V_0 = 0.84 d_b^{0.64} \tag{6}$$

where V_0 = nonsilting, nonscouring, mean velocity and d_b = average depth over the bed (excluding the side slopes), was widely used for many years. The coefficient and exponent were developed for the Bari-Doab canal system, Punjab, where the channel bed materials were medium sand approximately 0.32 mm mean diameter.

Lindley's Regime Concept. It was later recognized that for stability a channel must also have the correct width and slope. Lindley[7] advanced a "regime" concept embracing all channel dimensions and slope, which he believed were fixed by nature for given conditions. Lindley stated, "when an artificial channel is used to convey silty water, both bed and banks scour or fill, changing depth, gradient and width, until a state of balance is attained at which the channel is said to be regime."

Lacey's Formulas. Lacey[8–12] analyzed data from irrigation channels and rivers, mainly in India and Pakistan, but also some in Egypt, Europe, and America. His results supported Lindley's regime concept and permitted quantitative evaluation. They were obtained by the correlation of dimensions and slopes of apparently stable channels with discharges and size of bed material. The Lacey formulas express three primary relationships. All three must be satisfied to achieve true regime:

Velocity-to-depth relationship

$$V = 1.15 f^{1/2} R^{1/2} \tag{7}$$

Velocity-to-slope relationship

$$V = 16 R^{2/3} S_0^{1/3} \tag{8}$$

Width-to-discharge relationship

$$P = 2.67 Q^{1/2} \tag{9}$$

where V = mean velocity, R = hydraulic mean depth, S_0 = longitudinal slope, P = wetted perimeter, Q = discharge, and f = a silt or sediment factor, all in foot-second units. Lacey proposed an approximate relationship of f to the grade of bed materials:

$$f = 1.76 D_g^{1/2} \tag{10}$$

where D_g = mean diameter, mm. Plots of Eq. (8) are shown in Figs. 6 and 7 and of Eq. (9) in Fig. 8.

From Eqs. (7), (8), and (9), others can be derived, each relating three of the various factors. For example, in terms of discharge and sediment factor,

$$R = 0.47 \left(\frac{Q}{f}\right)^{1/3} \tag{11}$$

$$A = \frac{1.26 Q^{5/6}}{f^{1/3}} \tag{12}$$

$$V = 0.79 f^{1/3} Q^{1/6} \tag{13}$$

$$S_0 = \frac{f^{5/3}}{1{,}859 Q^{1/6}} \tag{14}$$

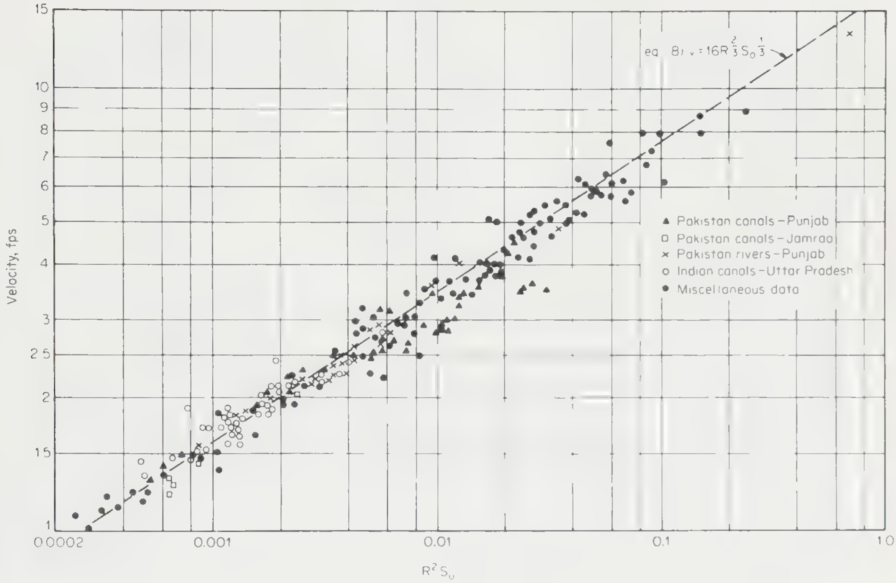

FIG. 6. Regime channels—velocity vs. hydraulic radius and slope.

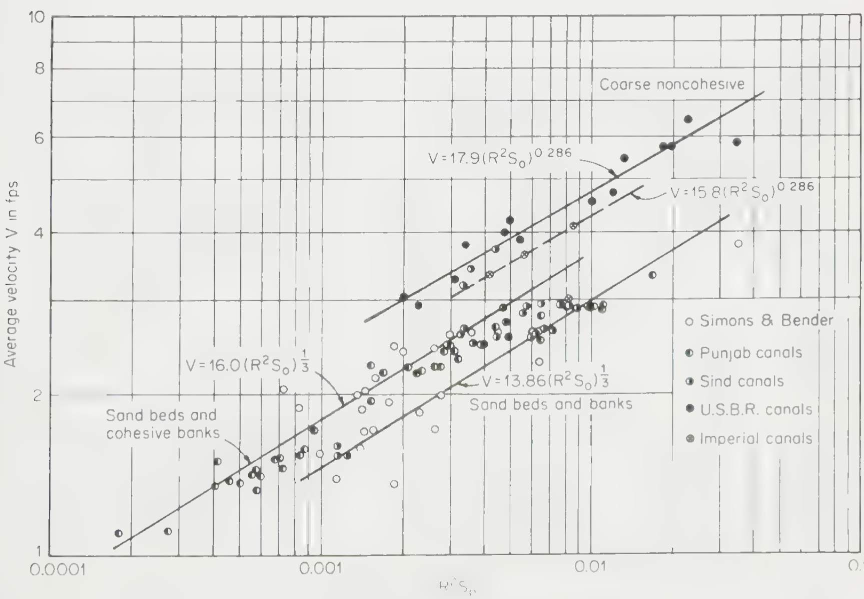

FIG. 7. Variations of average velocity with hydraulic radius, slope, and type of channel. *(From Proc. ASCE, Vol. 86, paper 2484, 1960.)*

where A = cross-sectional area. These together with Eq. (9) are useful in the preliminary design of a channel to carry a given discharge. Formulas (11) to (14) apply only if (9) is satisfied; otherwise (7), (8), and the following formula derived from (7) may be used:

$$R = \frac{0.91q^{2/3}}{f^{1/3}} \tag{15}$$

where $q = Q/P$. Lacey's general slope formula (*i.e.*, for both regime and nonregime conditions) is

$$V = \frac{1.346}{N_a} R^{3/4} S_0^{1/2} \tag{16}$$

where N_a is a coefficient of rugosity equal to $0.0225f^{1/4}$. Equation (16) is similar in form to Manning's formula, but according to Lacey, N_a is more representative of the

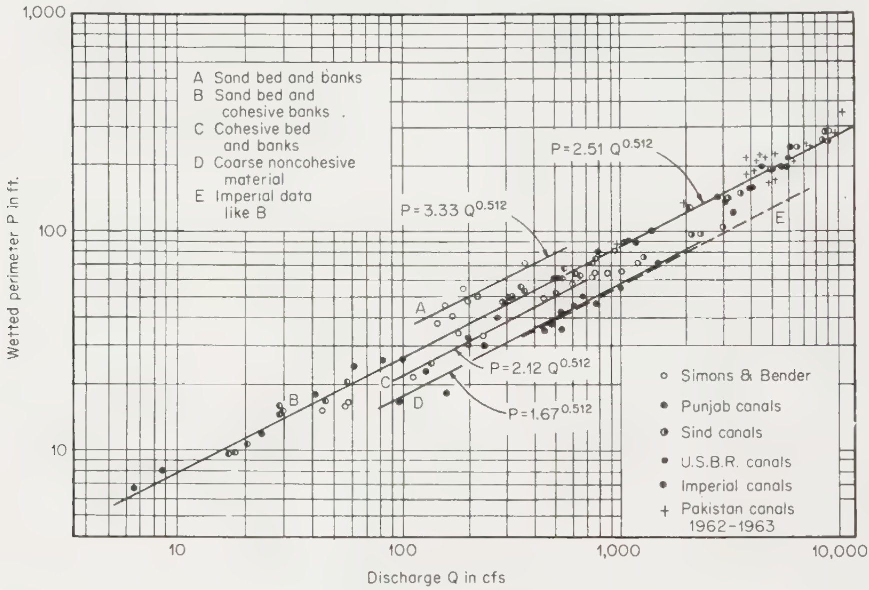

FIG. 8. Variations of wetted perimeter with discharge and type of channel. (*From Proc. ASCE, Vol.* 86, *paper* 2484, 1960.)

variable boundary roughness of an alluvial channel. The Lacey coefficient may be related to the Manning roughness factor:

$$N_a = 0.9nR^{1/12} \tag{17}$$

The two formulas will not be found inconsistent if it is recognized that both factors are variables in alluvial channels.

Equation (16) can be derived from Eqs. (7) and (8) in terms of f or N_a; Eq. (8) is essentially a regime formula whereas Eq. (16) is valid over a wider range of conditions. The formula in terms of q corresponding to Eq. (14) is

$$S_0 = \frac{f^{5/3}}{2{,}580q^{1/3}} \tag{18}$$

In his later papers Lacey substituted mean depth d_m for R in Eq. (7) and surface width W for P in Eq. (9). R remained in the slope formulas. While d_m and W are often more convenient to use, the formulas utilizing the revised notation have not so far been fully substantiated by data. However, except in small channels, the differences are not very significant, and either system may be used. Using d_m instead of R in Eq. (7), and rearranging,

$$f^{1/2} = \frac{4.9V}{(gd_m)^{1/2}} = 4.9\mathbf{F} \tag{19}$$

where $\mathbf{F}$ is the Froude number and g is the gravitational constant. This relationship between f and $\mathbf{F}$ is important and useful in connection with models. If tests on models of alluvial channels are performed with sand of the same grade and equal Froude number in model and prototype, the results will conform to the Lacey velocity-depth relationship.

The Lacey formulas provide a quantitative evaluation of some of the characteristics of natural channels. Among channels having similar bed material those of greater discharge will have greater ratio of width to depth and flatter longitudinal slopes. Among channels of the same discharge those with coarser bed material have higher velocity, greater width-to-depth ratio, and steeper longitudinal slope.

5. Variations in Regime. The early regime formulas included no provision for variation in sediment load and were derived from data of channels where bed and suspended load were small—usually less than 2,000 ppm. Performance of canals in India, Pakistan, and elsewhere indicates that many apparently stable channels operate with a regime differing somewhat from the Lacey relationships [Eqs. (7), (8), and (9)], as may be seen, for example, from Figs. 6 to 8. In particular, wide variations can occur in the slope.

Deviations are frequently due to variation in bed-material transport and consequently in bed form. Laboratory studies of flow in flumes have shown that with increasing velocity or tractive force the configuration of sand beds changes through phases of ripples, dunes, plane bed, and antidunes (dunes which move upstream). The incidence of these phases is illustrated in Fig. 9 based on a diagram by Simons and Miller.[13] The friction factors n and N_a are found to increase through the ripple and dune phases but decrease sharply in the plane-bed phase. In regime and near-regime channels only the ripple and dune phases occur.

The dimension given by Eq. (9) is intended to indicate the width of channels where side berms have formed by natural deposition of fine sediment carried in suspension. Such berms are more resistant to erosion than artificially compacted soil and should be encouraged to form by setting the artificial banks back from the excavated slopes.

Excess bed and suspended sediment loads have different effects. An increase of bed load (coarser fractions) generally leads to a change in bed formation, an increase in the number or size of ripples or dunes, with a resultant increase in frictional resistance to flow. The channel compensates by increasing (or attempting to increase) longitudinal slope and by scouring (or tending to scour) the banks to form a wider channel. These results may persist, even when the bed load is later reduced; so the sediment factors and channel configuration reflect to some degree the previous history. Inglis[14,15] held that because of variations in bed load the values of f were not the same in the various formulas; generally f_{RS} in Eq. (15) tended to exceed f_{VR}, the value in Eq. (7), where

$$f_{RS} = 192R^{1/3}S^{2/3} \tag{20}$$

$$f_{VR} = \frac{0.75V^2}{R} \tag{21}$$

Inglis suggested that the normal or true value of f was the geometric mean of the two.

An increase in the finer fractions of suspended sediment can reduce resistance to flow. This was discovered from observations at Beleida on the Nile where n was found to decrease as suspended sediment increased.[16] In laboratory experiments Vanoni[17] observed a reduction of 15 percent in n with an increase in suspended load from zero to 7,500 ppm, but the effect of further increasing the concentration was less. Vanoni later[18] concluded that the effect of bed configuration could be much greater than that of suspended sediment, which was of minor importance where there were dunes on the bed. Experience in India and Pakistan, however, is that increase in suspended load drawn from rivers in flood tends to reduce the friction factors.

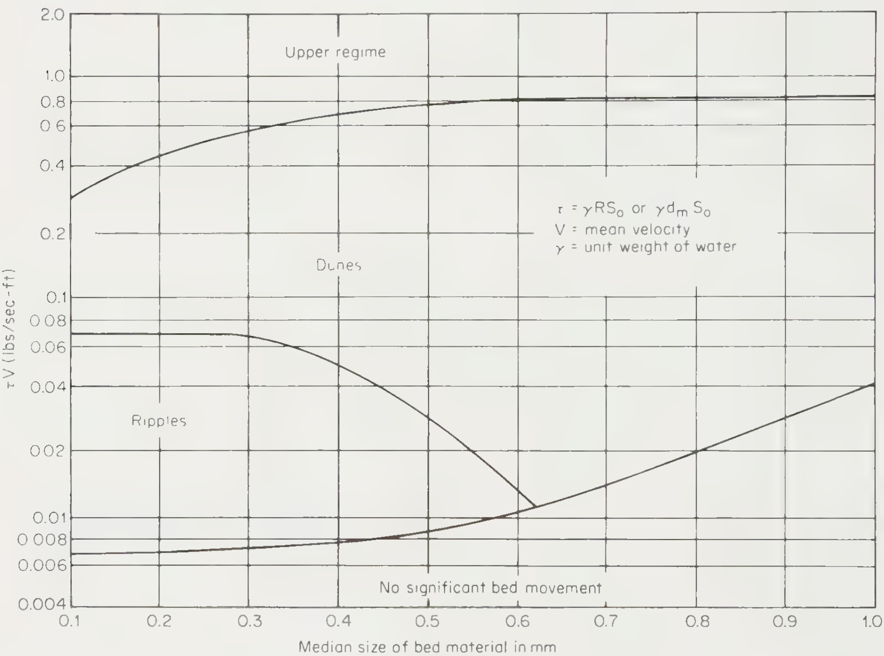

FIG. 9. Bed form roughness in channels.

Some rivers and large canals in very fine sand or silt and transporting fine sediment in suspension have been observed to flow with very flat slopes approaching values consistent with the smooth-pipe formulas adjusted for channel flow. On the other hand, a very heavy load of fine sediment can demand a slope nearer the normal. An interesting case is the Wei Pei Main irrigation canal,[19] which with a maximum discharge of 575 cfs carried a load of 0.1 to 10 percent of sediment finer than 0.03 mm at a slope of 0.43 per 1,000, mean velocity up to 3.3 fps. For this case f_{RS} and f_{VR} are approximately equal at 1.8 (much higher than would be expected for the grade of sediment in low concentrations), but the coefficient in Eq. (8) is almost exactly the Lacey value of 16.

Some examples of canal data from the Punjab (West Pakistan) are given in Table 1.[20] The Lower Jhelum (3a, 1962) is a canal approximating Lacey regime in longitudinal section though rather wider; f_{VR} and f_{RS} are nearly equal. The Sidhnai Canal (4a, 4b, 1962) was subject to a seasonal change in August (Q = 3,780) when the total suspended load temporarily increased to nearly 6,000 ppm; f_{VR} increased

TABLE 1. IRRIGATION CANALS, WEST PAKISTAN, 1962

Q, A, V, P, R in foot-second units, D_g in millimeters, C_c in parts per million

No.	Canal	Q	A	V	$S_0 \times 1{,}000$	P	R	f_{VR}	f_{RS}	n	D_g	C_c
1962:												
1a	Abbasia	972	430	2.26	0.086	84	5.1	0.75	0.64	0.018	0.198	195
1b	Abbasia	878	442	1.90	0.108	81	5.5	0.53	0.78	0.024	0.167	70
2a	Rangpur	1,900	810	2.35	0.120	139	5.8	0.71	0.85	0.022	0.180	70
2b	Rangpur	1,960	787	2.49	0.111	139	5.7	0.82	0.79	0.020	0.176	450
3a	Lower Jhelum	3,870	1,410	2.74	0.132	214	6.6	0.85	0.93	0.022	0.257	180
3b	Lower Jhelum	3,030	1,170	2.59	0.142	215	5.4	0.93	0.92	0.021	0.220	270
4a	Sidhnai	3,800	1,510	2.52	0.073	183	8.3	0.57	0.68	0.021	0.03	10
4b	Sidhnai	3,780	1,330	2.84	0.070	185	7.2	0.84	0.63	0.016	0.05	810
5a	Lower Chenab	5,360	1,730	3.10	0.182	207	8.4	0.86	1.26	0.027	0.330	135
5b	Lower Chenab	5,540	1,760	3.14	0.200	209	8.4	0.88	1.35	0.028	0.305	350
6a	Upper Gugera	5,300	1,760	3.01	0.149	216	8.1	0.84	1.07	0.024	0.277	345
6b	Upper Gugera	6,200	1,880	3.30	0.159	223	8.4	0.97	1.15	0.023	0.231	466
7a	Panjnad	9,860	3,280	3.00	0.089	282	11.6	0.58	0.86	0.024	0.197	110
7b	Panjnad	9,230	3,279	2.81	0.087	281	11.7	0.51	0.87	0.028	0.175	100
7c	Panjnad	7,320	2,530	2.89	0.089	255	9.9	0.63	0.83	0.022	0.163	85
7d	Panjnad	6,850	2,580	2.65	0.112	255	10.1	0.52	0.96	0.028	0.139	265
8a	Upper Chenab	14,400	4,110	3.50	0.189	356	11.5	0.80	1.43	0.030	0.230	225
8b	Upper Chenab	14,000	4,010	3.49	0.197	362	11.1	0.82	1.43	0.030	0.230	245
1963:												
1a	Abbasia	358	248	1.44	0.100	78	3.2	0.49	0.61	0.022	0.182	<10
1b	Abbasia	267	227	1.18	0.123	75	3.0	0.35	0.69	0.029	0.170	<10
2a	Lower Jhelum	3,850	1,407	2.74	0.146	212	6.6	0.86	1.00	0.023	0.212	35
2b	Lower Jhelum	3,970	1,468	2.70	0.134	217	6.8	0.80	0.96	0.023	0.194	410
3a	B.R.B.D.	4,250	1,290	3.29	0.246	212	6.1	1.33	1.37	0.024	0.190	175
3b	B.R.B.D.	4,710	1,495	3.15	0.213	213	7.0	1.06	1.30	0.025	0.174	390
3c	B.R.B.D.	3,700	1,565	2.36	0.069	188	8.3	0.50	0.65	0.021	0.075	10
3d	B.R.B.D.	4,110	1,589	2.59	0.079	186	8.5	0.60	0.73	0.021	0.072	15
4a	Dipalpur	4,480	1,714	2.61	0.110	208	8.2	0.63	0.89	0.024	0.178	40
4b	Dipalpur	4,250	1,617	2.63	0.115	206	7.8	0.67	0.90	0.024	0.160	25
5a	Muzaffagarh	5,030	1,849	2.72	0.095	226	8.2	0.68	0.81	0.021	0.084	80
5b	Muzaffagarh	5,000	1,565	3.19	0.100	219	7.1	1.08	0.80	0.026	0.072	115
5c	Muzaffagarh	4,540	1,606	2.83	0.092	213	7.5	0.80	0.77	0.018	0.072	30
5d	Muzaffagarh	3,670	1,326	2.77	0.089	188	7.0	0.82	0.73	0.018	0.182	115
6a	Upper Gugera	5,280	1,713	3.08	0.172	223	7.6	0.94	1.17	0.025	0.142	145
6b	Upper Gugera	6,170	1,905	3.24	0.175	223	8.5	1.24	1.23	0.025	0.260	105
6c	Upper Gugera	4,880	1,456	3.35	0.150	174	8.4	1.01	1.10	0.023	0.235	125
6d	Upper Gugera	5,630	1,710	3.29	0.173	177	9.6	0.85	1.26	0.027	0.212	165
7a	Lower Chenab	4,890	1,562	3.13	0.179	211	7.4	0.99	1.19	0.024	0.295	100
7b	Lower Chenab	4,910	1,624	3.02	0.177	206	7.9	0.87	1.20	0.026	0.290	140
7c	Lower Chenab	5,160	1,792	2.88	0.171	222	8.1	0.77	1.18	0.027	0.350	30
7d	Lower Chenab	6,300	1,821	3.46	0.196	221	8.2	1.10	1.31	0.024	0.350	160
8a	Lower Bari Doab	7,480	2,436	3.07	0.079	241	10.1	0.70	0.77	0.021	0.235	70
8b	Lower Bari Doab	7,390	2,444	3.02	0.127	240	10.2	0.89	1.05	0.026	0.205	340
9a	Balloki-Sulleimanki	12,800	3,348	3.83	0.118	331	10.1	1.04	1.00	0.020	0.120	320
9b	Balloki-Sulleimanki	12,200	2,913	4.19	0.152	327	8.9	1.48	1.13	0.019	0.136	270
9c	Balloki-Sulleimanki	10,300	3,018	3.41	0.078	323	9.3	0.94	0.74	0.017	0.141	120
9d	Balloki-Sulleimanki	7,430	2,548	2.92	0.128	319	8.0	0.80	0.98	0.023	0.135	75
10a	Upper Chenab	13,900	4,103	3.39	0.193	366	11.2	0.77	1.43	0.031	0.240	150
10b	Upper Chenab	14,100	4,095	3.44	0.178	366	11.2	0.79	1.35	0.028	0.305	580
10c	Upper Chenab	13,900	3,576	3.89	0.181	335	10.7	1.06	1.35	0.025	0.194	205
10d	Upper Chenab	14,000	3,706	3.78	0.162	336	11.0	0.98	1.27	0.025	0.228	305

while f_{RS} and n decreased. This is an example of the effect of a heavy load of fine sediment temporarily blanketing the normal bed material. The Lower Chenab (5a, 5b, 1962) is a canal which had drawn excessive bed load for many years before a sand excluder was provided; f_{RS} exceeds f_{VR} and n is rather high, an indication that slope is excessive.

The regime characteristics are generally more marked in the head reaches of a canal system where the bed load in excess of the transport capability is usually deposited. The mean grain size of bed material frequently decreases continuously from the head to the tail of a canal.[14] This should be recognized in design and the values of f and n adjusted accordingly.

In a comparison of the Lacey formulas, with data from canals and laboratory tests, Simons and Albertson[21] put forward separate relationships between velocity, depth, and slope for channels having different boundary materials. These are shown in Fig. 7, from which it will be seen that the coefficient in Eq. (8), to which Lacey gave the value of 16 for regime, appears to be 14 for sand bed and banks and 16 for sand bed and cohesive banks. The high coefficient of 20 for the Imperial canals data may be a result of the high concentration of fine sediment of 4,000 to 8,000 ppm.

The width of stable channels also shows some variation from the Lacey formula, Eq. (9). Channels carrying a high concentration of bed load tend to be wider; channels constructed narrower in cohesive soils may remain narrow because of the resistance to scour of the banks. The derived Lacey formula relating width to velocity is

$$P \text{ or } W = \frac{5.37V^3}{f} \tag{22}$$

This is derived from Eqs. (7) and (9), and consequently f is f_{VR}, Eq. (21). Blench[22,23] found it more reasonable to separate these two factors, putting

$$W_m = \frac{V^3}{F_s} \tag{23}$$

where W_m = mean width and F_s is a side factor depending on the bank materials, given as 0.1, 0.2, 0.3 for "loams of very slight, medium, and high cohesiveness." It will be appreciated that the effect of variation in bed load is implicit in the mean velocity. In view of the lack of extensive supporting data, the values to be used in design should be verified from observations of existing channels. The Lacey value for channels with beds of fine to medium sand is approximately 0.2.

Simons and Albertson[21] confirmed the trend of the Lacey $P:Q^{1/2}$ relation, Eq. (9), but the value of the coefficient varied from 1.67 for USBR canals with beds and banks of coarse noncohesive material to 3.33 for canals with sand beds and banks. These are shown in Fig. 8. The variation should not be regarded as a negation of the Lacey coefficient of 2.67. The low values are explained by the values of V^3/W, which approximate Blench's lowest value; the high values generally apply to canals originally constructed to the widths existing at the time of observation.

EFFECTS OF SEDIMENT AND SEEPAGE

6. Sediment Transport. The balance of erosion and deposition which characterizes regime channels is closely related to the sediment-transport capabilities of the flow. The sediment forming the bed and banks of the regime channel originates from the rivers and streams from which the supplies are drawn and to a lesser degree from the beds and banks.

Sediment content exceeding 50 percent by weight has been observed for the Ching River in China.[24] A maximum of 40.8 percent has been reported for a tributary of the

Colorado River.[25] But the sediment load in streams from which regime canals are fed seldom exceeds 5,000 ppm with an annual average measured in hundreds of ppm. Concentrations of sediment coarser than 0.075 mm diameter for various locations along the Chenab River in West Pakistan are plotted in Fig. 10. The individual lines are visually placed averages of hundreds of readings which show wide scatter in the extremes. The effect of curvature in the river is demonstrated by comparing values for the Trimmu 1961 left (outside) bank with those for the Trimmu 1961 right bank. A gradual change in curvature may account for the difference between the Trimmu left-bank values for 1939 and 1961.

The behavior of sediment depends on the specific gravity, size, and shape of the particles and on the size distribution. A typical sample of sediment consists of a

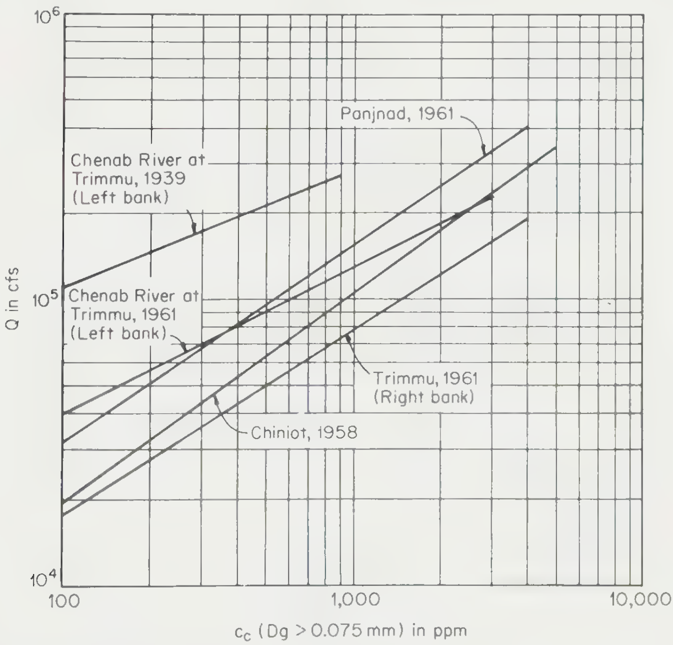

FIG. 10. Sediment concentration vs. discharge—Chenab River, West Pakistan.

mixture of particles of various densities, sizes, and shapes. The variation of density is generally small, and for practical purposes the mean density may be used for all the sediment. The density is in most cases so near the density of quartz (specific gravity 2.65) that this value may be used without significant error in the formulas for sediment transport which follow.

Sediment is classified according to size. The classification proposed by the Subcommittee on Sediment Terminology of the American Geophysical Union[26] is given in Table 2.

Particle size is determined by sieving (coarser particles) or sedimentation (finer particles). For the study of the mechanics of sediment transport and computation of sediment load both size and shape are conveniently defined by the fall velocity, *i.e.*, the terminal velocity of fall of a particle in water. The relation of size to fall velocity for quartz spheres at various temperatures is shown in Fig. 11.[27] Flat (e.g., micaceous)

TABLE 2. SEDIMENT GRADE SCALE

Class name	Size range		Approx sieve mesh openings per inch	
	Millimeters	Inches	Tyler	United States standard
Very large boulders	4,096–2,048	160–80		
Large boulders	2,048–1,024	80–40		
Medium boulders	1,024–512	40–20		
Small boulders	512–256	20–10		
Large cobbles	256–128	10–5		
Small cobbles	128–64	5–2.5		
Very coarse gravel	64–32	2.5–1.3		
Coarse gravel	32–16	1.3–0.6		
Medium gravel	16–8	0.6–0.3	2½	
Fine gravel	8–4	0.3–0.16	5	5
Very fine gravel	4–2	0.16–0.08	9	10
Very coarse sand	2.000–1.000	....	16	18
Coarse sand	1.000–0.500	....	32	35
Medium sand	0.500–0.250	....	60	60
Fine sand	0.250–0.125	....	115	120
Very fine sand	0.125–0.062	....	250	230
Coarse silt	0.062–0.031			
Medium silt	0.031–0.016			
Fine silt	0.016–0.008			
Very fine silt	0.008–0.004			
Coarse clay	0.004–0.0020			
Medium clay	0.0020–0.0010			
Fine clay	0.0010–0.0005			
Very fine clay	0.0005–0.00024			

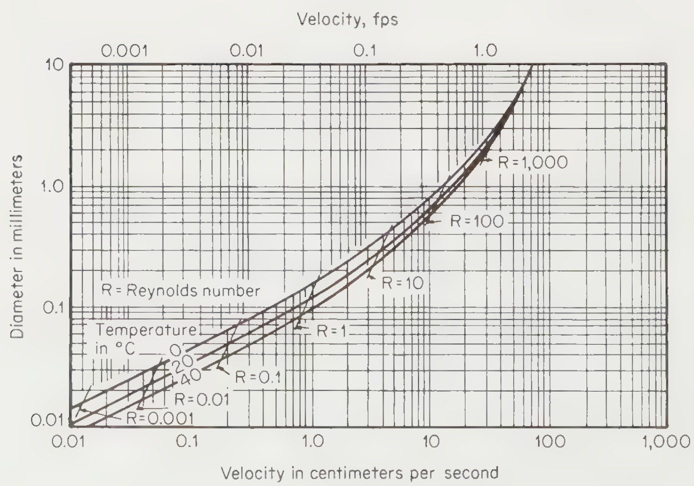

FIG. 11. Fall velocity of quartz spheres in water.

particles have lower fall velocities than shown, the effect being small for particles up to 0.1 mm, but it may be 25 percent for 1-mm particles.

The size distribution of a sediment mixture can be represented by a frequency diagram as in Fig. 12, which shows characteristic grain sizes for typical sandy suspended sediment and bed materials. The mean or effective diameter of a mixed sediment is often described by its median or 50 percent size. For further information on the properties of sediment see Ref. 28.

Sediment is transported partly in suspension and partly as bed load. Transport results from the action of turbulent flow on the bed. Basically this consists of drag on individual particles due to relative velocity. Transport action is complicated by variations in velocity, bed forms, presence of particles of a wide size range, action of the flow in sorting and lifting particles of various sizes into suspension, and variation of fluid properties with varying concentration of suspended sediment. The mechanics

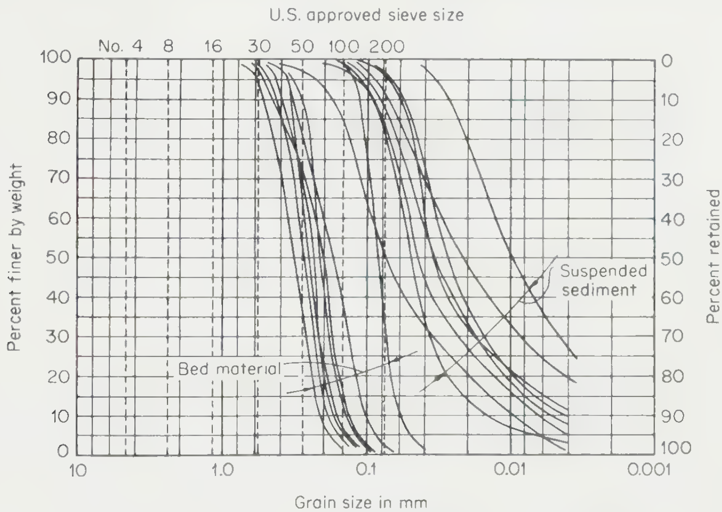

FIG. 12. Grain size of suspended and bed sediments in regime canals.

of entrainment are very complex and are not yet adequately understood. Continuous interchange of sediment occurs between bed and suspended load, but because sand and finer particles are more easily entrained than coarser material there is a marked difference in behavior between active channels in which the bed material is sand or finer and those in which it is gravel or coarser. In the former the suspended load is composed of particles representing the whole range of bed-material size, though the fine grades generally predominate. In the latter, with normal velocities, the suspended load consists only of sand and finer particles without any of the dominant sizes of bed material. In both cases the volume of suspended load may greatly exceed the bed load.

Typical grain sizes of suspended and bed load, sampled in eight regime canals in West Pakistan, are shown in Fig. 12. The effect of alluvial sorting is indicated by the narrow range of grain sizes of the bed material. In most regime canals the sizes of the bed material and suspended sediments usually show a marked seasonal variation.

Although the finer suspended sediments (less than about 0.06 mm) have a measurable effect on the performance of a canal (see Art. 5), the impairment of canal performance usually results from an excess of coarser materials (greater than about 0.06 mm). Accordingly, it is the concentrations of the coarser sizes and the variation in such concentrations that are significant in canal operation. A typical annual variation, as measured near the head of the Upper Chenab Canal, West Pakistan, is shown in Fig. 13.

The transport capability of a channel is a function of capacity, measured as the quantity of sediment which will be moved, and competence, measured by the maximum size of bed particles which will be moved. Capacity increases with decrease in particle size, and transport capability in any given size range can be far greater than the volume of sediment available.

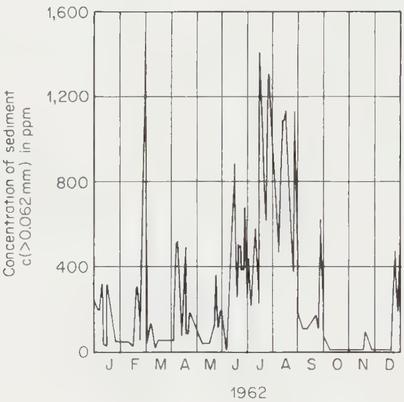

Fig. 13. Annual variation of sediment concentrations—Upper Chenab Canal, West Pakistan.

The size of transportable grain is indicated by the tractive force [Eq. (1) and Fig. 3]. In a regime channel the bed material is usually composed of sediment which deposited during periods of decreased competency or insufficient transport capacity.

No precise formula for the rate of sediment transport in an alluvial channel is available, and it is doubtful whether any single formula can cover the whole range. Several formulas, however, give fair indications of transport capability within the range of the data used in their derivation. Yet the sediment load of a channel can often be varied by 10 or 100 times without resulting in immediate change in flow conditions. This is one reason for the wide scatter obtained when testing formulas against observed data in the field. Another reason is the generally inaccurate means of sampling, especially in the case of bed load.

The earliest bed-load formula is probably that of Du Boys:

$$q_s = C\gamma s_s \tau_0(\tau_0 - \tau_c) \tag{24}$$

where q_s is the weight of bed load per unit time per unit width of channel, C is a coefficient related to grain size, γ is specific weight of water, s_s is specific gravity of bed material, τ_0 is the bed shear stress (see Art. 3), and τ_c is the critical bed shear stress (see Fig. 3). Values of C and τ_c given by Straub[29] are as follows:

Particle size, mm	0.25	0.5	1	2	4
C	0.48	0.29	0.17	0.10	0.06
τ_c, psf	0.017	0.022	0.032	0.051	0.09

Equation (24) is useful only for a rough indication of the volume of uniform-sized quartz granular material under flume-flow conditions.

Shields' formula[30] provides for materials of different density:

$$\frac{q_s(s_s - 1)}{q\gamma s_0} = 10 \frac{\tau_0 - \tau_c}{\gamma(s_s - 1)D_g} \tag{25}$$

where q is discharge of water in volume per unit time per unit width, S_0 is energy slope, and D_g is particle size.

Relative movement of particles in fluid is evidently more directly a function of fall velocity than of size and density. It was therefore a logical step to include the fall velocity (see Fig. 11) as a parameter of particle behavior; no additional parameter for density is then required. Whether a further parameter for particle size is required probably depends on its importance in relation to boundary roughness. In the case of sand beds the bed forms (ripples or dunes) are of greater importance but particle size could be a factor where the bed consists of gravel or coarser material.

Suspended sediment load requires separate consideration from bed load. A considerable advance resulted from the application of the theories of turbulence to the distribution of sediment on a vertical. Sediment falls relative to the fluid surrounding it, but the fluid is mixed by turbulence. A state of equilibrium results when the rate of sediment falling by gravity is balanced by the net rate of sediment lifted by turbulence. This approach was due largely to O'Brien[31] and to Rouse,[32] who produced an equation for the distribution of sediment within a moving fluid. A detailed presentation and discussion of the distribution function are given by the American Society of Civil Engineers Committee on Sedimentation.[33]

Einstein[34] used both bed-load and suspended-load functions in his method of computation of total bed-material load. This is a rational step-by-step method based on probabilities of turbulent velocities and particle exposure. An imaginary distinction is made between cross-sectional area and hydraulic radius contributing to shear stress on bed particles and those concerned with shear stress due to bed forms. Sediment load of each size range is computed separately, and a "hiding factor" is introduced to allow for the availability of particles in a mixture. A relationship is derived between a function ϕ concerned with rate of movement of bed load and Ψ concerned with bed shear stress. Suspended load is computed as a function of bed load.* The method is complicated and is perhaps the most highly refined method available so far. It represents the first serious attempt to compute bed and suspended load of graded sediment. An example of its application to a natural channel with sandy bed material is given by Einstein. Application to a canal in medium-fine sand is given by Shieh-Wen Mao and Rice.[35]

An approximation to the Einstein formula for bed load is the earlier formula of Meyer-Peter modified by Chien:[36]

$$\phi = \left(\frac{4}{\Psi} - 0.188\right)^{3/2} \tag{26}$$

The variables in Eq. (26) are defined as

$$\phi = \frac{q_s}{\rho_s g}\left(\frac{1}{s_s - 1}\right)^{1/2}\left(\frac{1}{gD_{35}{}^3}\right)^{1/2} \tag{27}$$

$$\Psi = (s_s - 1)\frac{D_{35}}{R'S_0} \tag{28}$$

* Suspended load includes that part of bed-material load that is transported intermittently in suspension. It does not include wash load, i.e., sediment of grain sizes finer than those of the bed.

where D_{35} is the diameter of particle in a mixture, 35 percent by weight being finer, and R' is hydraulic radius relating to the part of the cross-sectional area contributing to shear stress on the bed particles. Equation (26) may be used for ϕ values from 0.0001 to 10.

Bishop, Simons, and Richardson[37] compared computations using the Einstein method with results of numerous measurements in laboratory flumes using sand mixtures of median diameters of 0.93, 0.47, and 0.19 mm, also some canal data. The general trend of experimental results was indicated by Einstein's formula, but the agreement was far from perfect. Einstein's factors were reevaluated to give better conformity with the data and curves produced for use in bed-load computations.

Colby[38] analyzed experimental flume data to compare the relationship of bed-material load to four parameters: mean velocity, stream power, and two forms of effective bed shear. He concluded that each of these could be used but no one was satisfactory for all flows, nor was total shear a satisfactory parameter. The relationship of load to mean velocity was found to be as good as the others (except where antidunes persisted, which is unlikely in controlled canals) and was convenient to apply.

Mean velocity was used by Dixon and Westfall,[39] who summarized more than a thousand sediment measurements taken in flumes, canals, and rivers representing discharges ranging from 0.09 to 95,200 cfs with sediment concentrations (fraction coarser than 0.062 mm) ranging from 1 to 133,000 ppm. From these data the authors derived the following general relationship:

$$V = 6.8(q_s\omega)^{1/4} \tag{29}$$

when q_s is the transported sediment load, lb/sec/ft of channel width, and ω is the fall velocity of the median-sized grain. In Eq. (29), q_s represents only the sand fraction taken as coarser than 0.062 mm. A representative selection of the data used by Dixon and Westfall and the graph of Eq. (29) is shown in Fig. 14. For specific channels the coefficient in Eq. (29) may be slightly higher or lower than the indicated value of 6.8.

A simple empirical formula which has been shown to conform moderately well with sediment-load data of flumes and canals in medium-fine sand is that of Ahmad and Rehman:[40]

$$\frac{1{,}000q^{2/3}S_0}{\omega^{1/2}} = 1 + 5c^{2/3} \tag{30}$$

where q is discharge per unit width, S_0 is energy slope, ω is mean fall velocity of the sediment, and c is the concentration of sediment by weight in parts per 1,000, excluding sediment finer than 0.06 mm.

7. Sediment Control. The introduction of excessive sediment into a canal frequently results in deposition in the canal with loss of capacity. If available head is sufficient to increase velocity and carry the sediment through the canal, the problem must be dealt with at the point where the water is discharged from the canal. Usually either or both aspects are objectionable and provisions are made for excluding the sediment from the canal.

A canal drawing supplies at an angle from a river will tend to draw bed water and therefore a heavy load of coarse sediment. The most effective way of excluding coarse material is conversely to locate the offtake on the outer bank of a bend in the river so that it draws mainly surface water. This method, which has been successfully used by Inglis,[41] requires smooth approach-flow conditions. Divide walls, which are provided at most canal headworks in India and Pakistan, can ensure proportional distribution of sediment where the approach is straight. Sediment excluders with

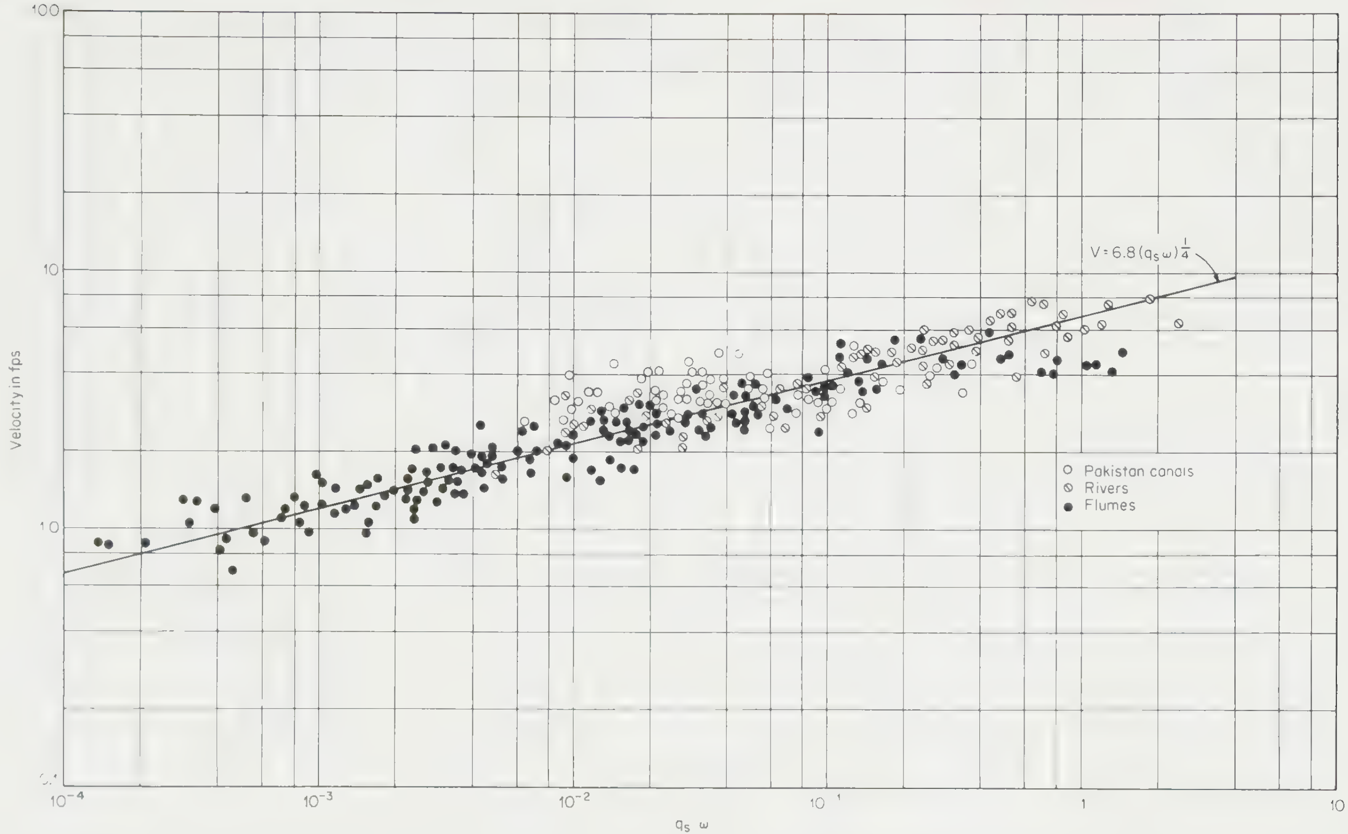

FIG. 14. Velocity vs. sediment load and grain-size parameter. (*Adapted from unpublished report by Dixon and Westfall, Harza Engineering Company*, 1966.)

tunnels discharging downstream[42,43] are sometimes provided between the divide wall and the canal-head structure; these also require smooth approach conditions to avoid mixing bed and surface flow. The canal-head structure should be given a crest high above the river bed and the canal should be designed with energy level below that of the river, thus providing a margin of head so that a slight steepening of slope in the canal will not drown the head control.

A form of sediment excluder in operation on a number of large canals in Pakistan employs a depressed area or pocket to collect the coarser sediments before the flow enters the canal-head regulator. Sediments are flushed intermittently from the pocket through low-level culvert-type tunnels which extend past the face of the regulator to a point downstream from the canal intake.

The flow approaching the pocket and head regulator should be guided so as to minimize turbulence through the entire range of canal operation. Guide walls are usually provided to assure a short length of straight approach channel leading to the regulators. Observations have established that sediment excluders utilizing pockets and tunnels can keep out 30 to 70 percent of the coarse sediment.[43]

The desilting works built in 1938 at the headworks of the All-American Canal on the California bank of the Colorado River uses six stilling basins 269 by 769 ft by 12.5 ft deep to precipitate sediment down to 0.075 mm diameter.[44] Sediment is collected from the basin floors by seventy-two 125-ft-diameter electrically driven rotary scrapers and flushed to a sluiceway through sludge discharge pipes varying from 15 to 36 in. in diameter. The works are designed to remove 80 percent of the incoming sediment load, which is estimated as 60,000 tons/day for a flow of 12,000 cfs. The sediment control is sufficient to achieve successful operation of the unlined canal on a slope of 1 to 19,000 at a flow of 15,000 cfs.

Another type of basin is used to desilt the flow entering the 34-mile-long unlined channel which supplies 3,000 to 3,500 cfs to the hydroelectric plants of the Loup River Public Power District, Nebraska.[45] The basin is a widened canal section 10,000 ft in length, 16 ft deep, 200 ft in bed width, and 264 ft wide at the water surface. The flow, at velocities of 0.8 to 0.9 fps, deposits all material including medium sand down to 0.25 mm diameter and about half of the fine sand (0.25 to 0.075 mm). A dredge with a 24-in. pump powered by a 1,200-hp electric motor (nominal dredge capacity 62.5 cfs) removes about 1.8 million tons of silt per year, which is equivalent to an average of 1,100 ppm for the flow passing through the basin. The canal has operated for 25 years without appreciable deposition or scour on a slope of 1 to 20,000.

When desilting works are provided, a means of control is required to allow some fine sediment to enter the canal to avoid serious erosion downstream.

8. Seepage Losses. The loss of water by seepage from unlined canals can be a significant factor in selecting a design and appraising the economic value of a canal. Seepage losses have been measured in Pakistan as ranging from 2 cfs per million square feet of wetted area in canals cut in clayey soils to as high as 15 cfs per million square feet in coarse sand. Values of 6 to 8 cfs per million square feet are common for fine to medium sand.

In the United States seepage losses are usually estimated (roughly) by the Moritz formula.[46]

$$O = 0.2C_0\left(\frac{Q}{V}\right)^{1/2} \tag{31}$$

in which O is the loss in cfs per mile of canal, Q is the discharge of the canal in cfs, V is the mean velocity in fps, and C_0 is the rate of water loss in cubic feet per 24 hr per square foot of wetted area. Average observed values of C_0 are listed in Table 3.

TABLE 3. AVERAGE OBSERVED VALUES OF LOSSES IN EARTH CANALS

Type of Material	C_0, cu ft in 24 hr for 1 sq ft Wetted Area
Cemented gravel and hardpan with sandy loam	0.34
Clay and clayey loam	0.41
Sandy loam	0.66
Volcanic ash	0.68
Volcanic ash with sand	0.98
Sand and volcanic ash or clay	1.20
Sandy soil with rock	1.68
Sandy and gravelly soil	2.20

DESIGN OF REGIME CANALS

9. Design Procedure. The design of a regime canal is developed from two given values: Q, the discharge, and f, the sediment factor. When these are known, the main dimensions of the canal, such as wetted perimeter (or the width), the hydraulic radius (or depth), and the longitudinal slope, may then be calculated.

Most canals are operated over a wide range of flow conditions which must necessarily match the demand pattern at the point of delivery. It is not possible to design a channel to be in regime for more than one discharge. Since the sediment deposited at low flows will usually be scoured by subsequent high flows, the canal is designed for the maximum or near maximum expected discharge. Low flows with little or no sediment load would not, however, be objectionable. A channel may be designed for a discharge less than the maximum if higher flows occur rarely and banks of sufficient height are provided.

The selection of sediment factors requires careful consideration. The best guide is provided by existing channels which are operating satisfactorily under similar conditions. The value or values of f may be determined from observations of the channel dimensions, using Eqs. (7) and (11) through (15), depending on the completeness and reliability of the data. In the absence of suitable observations on channels operating under similar conditions, or where conditions will differ especially in respect to sediment load, the following criteria should be taken into account. Generally, it is desirable to exclude the heavy bed load, but this cannot always be ensured. In Eq. (7), f is dependent mainly on the size of bed material and may be assumed equal to the f calculated from Eq. (10) using the mean diameter of bed material. In the head reaches of a canal, this material may be derived from bed or suspended sediment drawn from a river or parent channel. In the lower reaches, it may consist of the finer fractions of the upstream load or of the coarser fractions of the material through which the channel is excavated. Samples from the source of flow and from the channel bed materials should be analyzed and the mean diameter size determined after excluding the fine material unlikely to affect the bed. If the bed material is mainly fine sand, material finer than 0.05 mm should be excluded when determining mean diameter. The value of f, related to hydraulic radius and slope, for use in the combination of Eqs. (11) and (14), depends considerably on sediment load. If the total load rarely exceeds 2,000 ppm this factor may be assumed the same value as the factor computed from Eq. (7). If the load exceeds 2,000 ppm and contains a significant proportion of coarse material, the value of this factor should be greater than that determined from Eq. (7).

A forecast of sediment mean diameter also permits correlation and interpolation with canals which are not necessarily equivalent in all respects. Data in Table 1 present a wide range of values useful as guides.

The following are suggested steps in design using the Lacey formulas:

1. The design values of Q, f, and Manning's n are selected. f_{RS} may differ from f_{VR} [see Eqs. (20) and (21)].
2. P is determined from Eq. (9).
3. R is determined from Eq. (11) and $A = P \times R$.
4. V is determined from Q/A and checked by Eq. (7).
5. S_0 is determined by Eq. (14) using f_{RS} and checked by Eq. (20). Manning's n is calculated by Eq. (2) and S_0 adjusted if considered necessary.
6. Slope required is checked with slope available. Where available slope exceeds S_0 head can be absorbed in drop structures. Where it is deficient, realignment may be necessary. Head can sometimes be conserved by adopting a rather deeper canal section and taking steps to exclude coarse bed material so that the deep section can be maintained; a lower value of f_{RS} is then possible.
7. Width and depth are reconsidered in the light of step 6, sediment load, and type of bank material. Width may differ from that given by Eq. (9) and Figs. 7 and 9. Side slopes in cut and bank are determined.
8. Design values of f_{VR}, f_{RS}, and Manning's n are reviewed.

The formulas used for the foregoing steps are considered preliminary. The design may then be refined by the following steps:

9. The discharge q is recalculated using Q/b_w, where b_w is surface width of channel.
10. Mean depth is checked by Eq. (15) using f_{VR}.
11. A and V are recalculated.
12. S_0 is recalculated from Eq. (18) using f_{RS} and checked by Eqs. (2) and (8).
13. f_{RS} is checked by Eq. (20), and S_0 is adjusted if necessary.
14. If the sediment load is appreciable the design may be checked by one or more of the sediment-load formulas given in Art. 6.

Except in the case of small channels (discharge less than say 50 cfs) top width may be used instead of wetted perimeter and mean depth instead of hydraulic radius, with little or no modification of the f values.

Example: A canal for maximum discharge of 2,000 cfs is to be located upstream of Rangpur Canal, West Pakistan (see Table 1, item 2, 1962), where the bed load is expected to be similar except that it may be somewhat coarser.

Taking the mean diameter as 0.20 mm, by Eq. (10), $f = 0.79$ compared with 0.74 for the Rangpur, for which f_{VR} was 0.82 and f_{RS} 0.79. On consideration with the data of the Lower Jhelum Canal (Table 1, item 3, 1962) f_{VR} is taken as 0.85 and f_{RS} as 1.0. Manning's n may be about 0.22, as on the Lower Jhelum.

From Eq. (9), $P = 120$ ft. From Eq. (11), $R = 6.3$ ft. $A = P \times R = 760$ sq ft. $V = Q/A = 2.63$ fps. From Eq. (7), $V = 2.66$ fps. From Eq. (14), $S_0 = 0.00015$, and using this in Eq. (2), $V = 2.82$ fps, which is near enough to the previous value. From Eq. (8), $V = 2.9$ fps. It appears that the slope is slightly high but suitable for the preliminary design. This slope is available, and the design proceeds to step 7.

A cross section with 110-ft bed width, 6.6-ft depth, and 1 on 1 side slopes is chosen. Excavated side slopes will be sufficiently resistant for a normal channel width. Banks above ground level will be set back by 10 ft each side, but this is ignored in the calculations. Top width is taken as 123 ft, area $A = 770$ sq ft, mean depth 6.3 ft, and R 6.0 ft. f_{VR} and f_{RS} are reviewed and considered reasonable, and the design proceeds to step 9. $q = 2{,}000/123 = 16.3$ sq ft/sec. By Eq. (15), R or mean depth $= 6.2$ ft which is sufficiently near the design value. $A = 770$, $V = 2{,}000/770 = 2.60$ fps. By Eq. (18), $S_0 = 0.00015$. By Eq. (2), $V = 2.72$ fps and by Eq. (8), $V = 2.71$ fps, which are near enough. By Eq. (20), $f_{RS} = 0.98$, which checks.

As a check on the sediment-load capability Dixon and Westfall's Eq. (29) and Ahmad and Rehman's Eq. (30) are used, taking ω as 0.1 fps corresponding to the mean diameter of 0.20 mm (see Fig. 11). According to the former, transport capability is 250 ppm by weight, and according to the latter it is

260 ppm, which are considered acceptable if measures are taken to control the intake of coarse material. Both figures refer to that component of sediment coarser than 0.06 mm.

Bibliography

1. Lane, E. W., Progress Report on the Results of Studies on Design of Stable Channels, *U.S. Bur. Reclamation Hydraulic Lab. Rept.* Hyd-352, Denver, 1952.
2. Keulegan, G. H., Laws of Turbulent Flow in Open Channels, *J. Res. Natl. Bur. Std.*, Vol. 21, Washington, 1938.
3. Lane, E. W., and E. J. Carlson, Some Factors Affecting the Stability of Canals Constructed in Coarse Granular Materials, *Proc. IAHR*, Minneapolis, 1953.
4. Malhotra, J. K., Hydraulic Data for a Boulder River (Beas at Sujanpur Tira), Central Board of Irrigation, *Ann. Rept. (Tech.)*, Simla, 1943.
5. Buckley, R. B., "Irrigation Pocket Book," p. 178, Spon, London, 1928.
6. Kennedy, R. G., The Prevention of Silting in Irrigation Canals, *Proc. Inst. Civil Engrs.*, **119**, 281, 1895.
7. Lindley, E. S., Regime Channels, *Proc. Punjab Eng. Congr.*, Lahore, **7**, 1919.
8. Lacey, G., Stable Channels in Alluvium, *Proc. Inst. Civil Engrs.*, **229**, 259, 1929–1930.
9. ———, Uniform Flow in Alluvial Rivers and Canals, *Proc. Inst. Civil Engrs.*, **237**, 421, 1933–1934.
10. ———, "Regime Flow in Incoherent Alluvium," Central Board of Irrigation, India, Publication 20, Simla, 1939.
11. ———, A General Theory of Flow in Alluvium, *J. Inst. Civil Engrs.*, **27**, 16, 1946.
12. ———, Flow in Alluvial Channels with Mobile Sandy Beds, *Proc. Inst. Civil Engrs.*, **9**, 145, 1958.
13. Simons, D. B., and C. R. Miller, Sediment Discharge in Irrigation Canals, *Trans. ICID, 6th Congr.*, New Delhi, 3, 20.263, 1966.
14. Inglis, Sir C. C., Divergence from Regime in Stable Channels in Alluvium, Central Board of Irrigation, India, *Ann. Rept. (Tech.)*, p. 90, Simla, 1941.
15. ———, The Behavior and Control of Rivers and Canals, Central Waterpower Irrigation and Navigation Research Station, Poona, India, *Res. Publ.* 13, pp. 99 et seq., 1949.
16. Buckley, A. B., The Influence of Silt on the Velocity of Water Flowing in Open Channels, *Proc. Inst. Civil Engrs.*, **226**, 183, 1922–1923.
17. Vanoni, V. A., Transportation of Suspended Sediment by Water, *Trans. ASCE*, **111**, 67, 1946.
18. ———, Resistance Properties of Sediment-laden Streams, *Proc. ASCE*, **85**, paper 2020, 1959.
19. Eliassen, S., Discussion on Stable Channels in Erodible Material, by E. W. Lane, *Trans. ASCE*, **102**, 155, 1937.
20. West Pakistan Water and Power Development Authority, "Canal and Headworks Data Observation Programme, 1962 Data Tabulation," 1963. Also "1963 Data Tabulation" published 1964.
21. Simons, D. B., and M. L. Albertson, Uniform Water Conveyance Channels in Alluvial Material, *Proc. ASCE*, **86**, paper 2484, 1960.
22. Blench, T., and C. King, Effect of Dynamic Shape on Lacey Relations, Central Board of Irrigation, India, *Ann. Rept. (Tech.)*, p. 75, Simla, 1941.
23. Blench, T., "Regime Behaviour of Canals and Rivers," p. 32, Butterworth & Co. (Publishers), Ltd., London, 1957.
24. Todd, O. J., and S. Eliassen, The Yellow River Problem, *Trans. ASCE*, **105**, 346, 1940.
25. Stevens, J. C., The Silt Problem, *Trans. ASCE*, **101**, 207, 1936. Discussion by E. W. Lane, p. 255.
26. Lane, E. W., Report of the Subcommittee on Sediment Terminology, *Trans. Am. Geophys. Union*, **28** (6), 936, 1947.
27. Rouse, H., "Nomogram for the Settling Velocity of Spheres," Division of Geology and Geography Exhibit D of the Report of the Committee on Sedimentation, 1936–37, National Research Council, Washington, D.C., October, 1937, pp. 57–64.
28. Sediment Transportation Mechanics: Introduction and Properties of Sediment, Progress Report, Task Committee on Preparation of Sedimentation Manual, *Proc. ASCE*, paper 3194, July, 1962.
29. Straub, L. G., "The Missouri River," 73d Congress, 2d Session, p. 1135, Government Printing Office, Washington, D.C., 1935.
30. Brown, C. B., Sediment Transportation, p. 795 in "Engineering Hydraulics," edited by H. Rouse, John Wiley & Sons, Inc., New York, 1950.
31. O'Brien, M. P., Review of the Theory of Turbulent Flow and Its Relation to Sediment Transportation, *Trans. Am. Geophys. Union*, **14**, 487–491, 1933.
32. Rouse, H., Modern Conceptions of the Mechanics of Fluid Turbulence, *Trans. ASCE*, **102**, 463, 1937.
33. American Society of Civil Engineers, Sediment Transportation Mechanics: Suspension of Sediment, Progress Report, Committee on Sedimentation, *Proc. ASCE*, paper 3636, September, 1963.
34. Einstein, H. A., The Bed Load Function for Sediment Transportation in Open Channel Flows, *U.S. Dept. Agr. Soil Conserv. Serv. Tech. Bull.* 1026, 1950.
35. Shieh-Wen Mao and L. Rice, Sediment-transport Capability in Erodible Channels, *Proc. ASCE*, paper 3569, July, 1963.
36. Chien, Ning, The Present Status of Research on Sediment Transport, *Proc. ASCE*, separate 565, December, 1954.
37. Bishop, A. A., D. B. Simons, and E. V. Richardson, Total Bed-material Transport, *Proc. ASCE*, paper 4266, March, 1965.

38. Colby, B. R., Practical Computations of Bed-material Discharge, *Proc. ASCE*, paper 3843, March, 1964.
39. Dixon, John H., and David E. Westfall, "A Simplified Method of Computing Bed Material Transport," unpublished report, Harza Engineering Company, 1966.
40. Ahmad, Mushtaq, and Abdul Rehman, Appraisal and Analysis of New Data from Alluvial Canals of West Pakistan in Relation to Regime Concepts and Formulae, *Proc. West Pakistan Eng. Congr.*, 1963, p. 69.
41. Inglis, Sir C. C., The Behaviour and Control of Rivers and Canals, Central Waterpower Irrigation and Navigation Research Station, Poona, India, *Res. Publ.* 13, pp. 217–279, 1949.
42. International Association for Hydraulic Research, *Proc. 4th Meeting*, Bombay, 1951, several papers on Q.2.
43. Haigh, F. F., The Emerson Barrage, *J. Inst. Civil Engrs.*, December, 1941, p. 107.
44. Forester, D. M., Desilting Works for All-American Canal, *Civil Eng. (N.Y.)*, October, 1938, p. 649.
45. Information supplied by Loup River Public Power District, Columbus, Nebr.
46. U.S. Bureau of Reclamation, "Canals and Related Structures," Design Standard No. 3, January, 1961.

SECTION 7

CANALS AND CONDUITS

By Calvin V. Davis and Kenneth E. Sorensen*

INTRODUCTION

1. Introductory Statement. Artificial channels for the conveyance of fluids fall into two primary divisions: those which merely guide the fluid as it flows down a sloping surface, and those which confine and guide its movement under pressure, commonly referred to as free-flow and pressure conduits. Free-flow conduits may be simple open channels or ditches, or they may be pipes or other enclosed structures, flowing partly full. In size, they may vary from enormous irrigation water supply, power, or navigation canals to a single furrow which guides the farmer's water or the small gutters and troughs found around the home or factory. Pressure conduits may be of wood, metal, glass, steel, concrete, ceramics, plastic, or other suitable substance and although usually circular in cross section may be of any form. Consideration is to be given here only to those types of conduits commonly utilized in the civil works of hydraulic projects.

HYDRAULIC FACTORS

2. Effect of Slope. The velocity at which the water flows depends on the steepness of the slope, the size and shape of the channel, the roughness of its walls, and the viscosity and density of the water. Reference should be made to Sec. 2 for the flow formulas in common use. For the problems of this section, and within the usual temperature range, the effect of viscosity is negligible.

Resistance to the flow of fluids is usually referred to as frictional resistance, although it has little relation to ordinary friction between solids. A solid body sliding down an inclined plane in a vacuum will accelerate indefinitely. In contrast, fluid resistances increase with velocity and rapidly approach equality with the component of gravity parallel to the slope. Consequently, for any set of conditions there is a maximum velocity, which will not be exceeded, however long the channel may be.

In solving problems involving resistance to fluid motion, reliance is placed on experimentally derived coefficients for empirical formulas, a variety of which has been proposed. In Secs. 2 and 3 will be found the summarized results of both laboratory and prototype field observations.

3. Mean Velocity. The velocity used in most flow formulas is equivalent to the quantity of flow divided by the area of the water prism and is called the mean velocity. The actual velocity varies throughout the water prism in some manner that depends on the conditions of flow. In certain problems, this variation must be taken into account, but its effect is usually hidden in empirical coefficients. Only turbulent flow will be considered in this section. Reference is made to Secs. 2 and 3 for the principles governing turbulent flow and for tables and diagrams useful in the design of both free-flow and pressure conduits.

4. Best Hydraulic Shape. The wetted perimeter offers resistance to flow and generally, for "hard" conduits, contributes to cost. Hence, it should be held to the

*Grateful acknowledgment is made to Julian Hinds for material in this section which appeared in the first edition (1942) and the second edition (1952).

minimum value consistent with the conditions. The degree to which a conduit conforms to this criterion is a measure of its hydraulic efficiency.

The most hydraulically efficient of all possible sections on this basis is a semicircle, open at the top and flowing full. The best closed section, flowing full, is a circle. The best polygonal section is one circumscribed about a semicircle for free flow, or about a circle for a closed conduit flowing full. For a specified number of sides, a regular polygon or half polygon is better than an irregular one, and the greater the number of sides, the greater the hydraulic efficiency. A circle flowing full is less efficient than any reasonably shaped open channel.

Although minimum area and perimeter contribute to economy, they may be overshadowed by practical considerations. Figures 1 and 2 show, respectively, typical sections of aqueducts and tunnels which are now in service. A square closed conduit is obviously hydraulically inefficient, and its flat sides are structurally undesirable, for either internal or external load. Yet such conduits are occasionally used to meet practical conditions.

Both unlined and lined canals have traditionally been trapezoidal, for construction reasons. With recent development of mechanical trimming and lining machines (see Art. 42) this reason is no longer always valid, and curved bottoms are appearing,

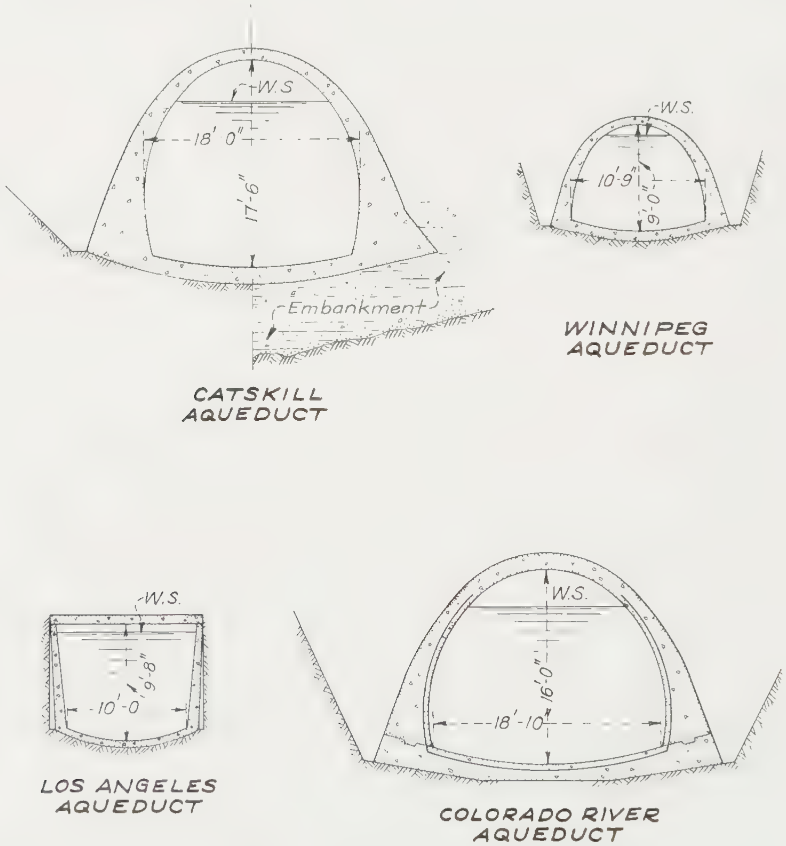

Fig. 1. Typical aqueduct sections.

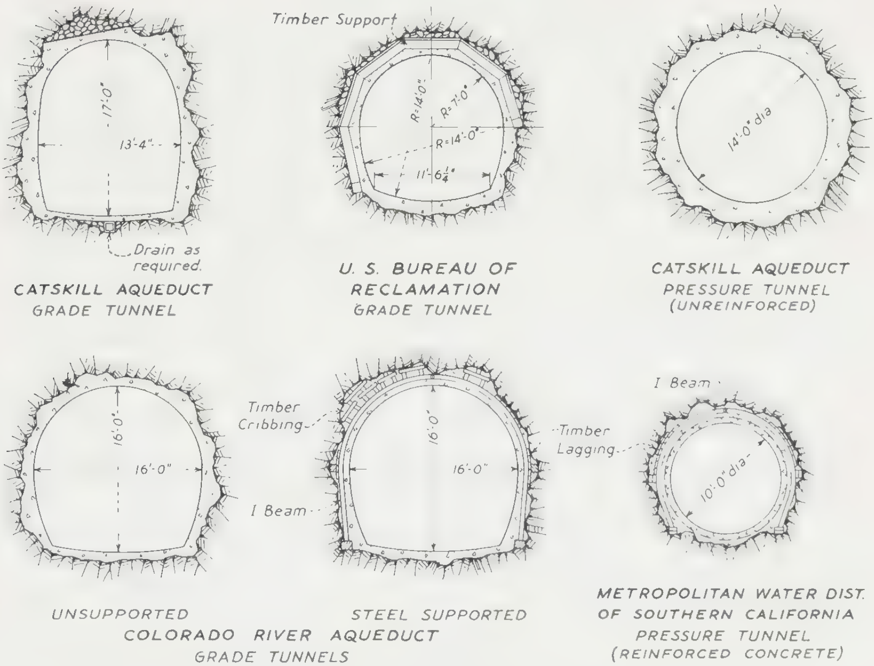

FIG. 2. Typical tunnel sections.

particularly with membrane linings (Arts. 61 to 69). The best shape for a lined tunnel usually is a circle, but the section is frequently modified to provide increased floor space for hauling equipment, and for other purposes. Figure 3 shows the proportions of a standard horseshoe tunnel. Tables 1 and 2 summarize the principal geometric hydraulic design parameters for partially filled circular and horseshoe conduit sections.

5. Allowance for Critical Flow. As explained in Sec. 2, flow in an open channel, at or near the critical depth (Froude's number $\mathbf{F} = 1.0$), is in indifferent equilibrium, and slight boundary irregularities may produce marked irregularities in flow. The relation of designed depth to critical depth should always be known, and where a safe

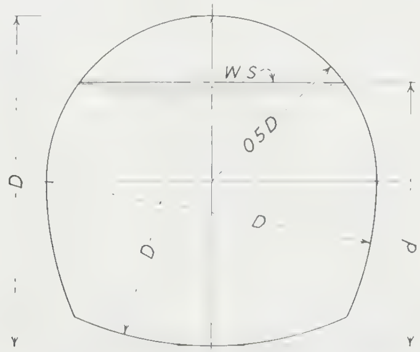

FIG. 3. Standard horseshoe tunnel.

Table 1. Area, Wetted Perimeter, and Hydraulic Radius of Partially Filled Circular Conduit Sections

$\frac{d}{D}$	$\frac{\text{Area}}{D^2}$	$\frac{\text{Wet. per.}}{D}$	$\frac{\text{Hyd. rad.}}{D}$	$\frac{d}{D}$	$\frac{\text{Area}}{D^2}$	$\frac{\text{Wet. per.}}{D}$	$\frac{\text{Hyd. rad.}}{D}$
0.01	0.0013	0.2003	0.0066	0.51	0.4027	1.5908	0.2531
0.02	0.0037	0.2838	0.0132	0.52	0.4127	1.6108	0.2561
0.03	0.0069	0.3482	0.0197	0.53	0.4227	1.6308	0.2591
0.04	0.0105	0.4027	0.0262	0.54	0.4327	1.6509	0.2620
0.05	0.0147	0.4510	0.0326	0.55	0.4426	1.6710	0.2649
0.06	0.0192	0.4949	0.0389	0.56	0.4526	1.6911	0.2676
0.07	0.0242	0.5355	0.0451	0.57	0.4625	1.7113	0.2703
0.08	0.0294	0.5735	0.0513	0.58	0.4723	1.7315	0.2728
0.09	0.0350	0.6094	0.0574	0.59	0.4822	1.7518	0.2753
0.10	0.0409	0.6435	0.0635	0.60	0.4920	1.7722	0.2776
0.11	0.0470	0.6761	0.0695	0.61	0.5018	1.7926	0.2797
0.12	0.0534	0.7075	0.0754	0.62	0.5115	1.8132	0.2818
0.13	0.0600	0.7377	0.0813	0.63	0.5212	1.8338	0.2839
0.14	0.0668	0.7670	0.0871	0.64	0.5308	1.8546	0.2860
0.15	0.0739	0.7954	0.0929	0.65	0.5404	1.8755	0.2881
0.16	0.0811	0.8230	0.0986	0.66	0.5499	1.8965	0.2899
0.17	0.0885	0.8500	0.1042	0.67	0.5594	1.9177	0.2917
0.18	0.0961	0.8763	0.1097	0.68	0.5687	1.9391	0.2935
0.19	0.1039	0.9020	0.1152	0.69	0.5780	1.9606	0.2950
0.20	0.1118	0.9273	0.1206	0.70	0.5872	1.9823	0.2962
0.21	0.1199	0.9521	0.1259	0.71	0.5964	2.0042	0.2973
0.22	0.1281	0.9764	0.1312	0.72	0.6054	2.0264	0.2984
0.23	0.1365	1.0003	0.1364	0.73	0.6143	2.0488	0.2995
0.24	0.1449	1.0239	0.1416	0.74	0.6231	2.0714	0.3006
0.25	0.1535	1.0472	0.1466	0.75	0.6318	2.0944	0.3017
0.26	0.1623	1.0701	0.1516	0.76	0.6404	2.1176	0.3025
0.27	0.1711	1.0928	0.1566	0.77	0.6489	2.1412	0.3032
0.28	0.1800	1.1152	0.1614	0.78	0.6573	2.1652	0.3037
0.29	0.1890	1.1373	0.1662	0.79	0.6655	2.1895	0.3040
0.30	0.1982	1.1593	0.1709	0.80	0.6736	2.2143	0.3042
0.31	0.2074	1.1810	0.1755	0.81	0.6815	2.2395	0.3044
0.32	0.2167	1.2025	0.1801	0.82	0.6893	2.2653	0.3043
0.33	0.2260	1.2239	0.1848	0.83	0.6969	2.2916	0.3041
0.34	0.2355	1.2451	0.1891	0.84	0.7043	2.3186	0.3038
0.35	0.2450	1.2661	0.1935	0.85	0.7115	2.3462	0.3033
0.36	0.2546	1.2870	0.1978	0.86	0.7186	2.3746	0.3026
0.37	0.2642	1.3078	0.2020	0.87	0.7254	2.4038	0.3017
0.38	0.2739	1.3284	0.2061	0.88	0.7320	2.4341	0.3008
0.39	0.2836	1.3490	0.2102	0.89	0.7384	2.4655	0.2996
0.40	0.2934	1.3694	0.2142	0.90	0.7445	2.4981	0.2980
0.41	0.3032	1.3898	0.2181	0.91	0.7504	2.5322	0.2963
0.42	0.3130	1.4101	0.2220	0.92	0.7560	2.5681	0.2944
0.43	0.3229	1.4303	0.2257	0.93	0.7642	2.6061	0.2922
0.44	0.3328	1.4505	0.2294	0.94	0.7662	2.6467	0.2896
0.45	0.3428	1.4706	0.2331	0.95	0.7707	2.6906	0.2864
0.46	0.3527	1.4907	0.2366	0.96	0.7749	2.7389	0.2830
0.47	0.3627	1.5108	0.2400	0.97	0.7785	2.7934	0.2787
0.48	0.3727	1.5308	0.2434	0.98	0.7816	2.8578	0.2735
0.49	0.3827	1.5508	0.2467	0.99	0.7841	2.9412	0.2665
0.50	0.3927	1.5708	0.2500	1.00	0.7854	3.1416	0.2500

TABLE 2. AREA, WETTED PERIMETER, AND HYDRAULIC RADIUS OF PARTIALLY FILLED HORSESHOE CONDUIT SECTIONS

$\frac{d}{D}$	$\frac{\text{Area}}{D^2}$	$\frac{\text{Wet. per.}}{D}$	$\frac{\text{Hyd. rad.}}{D}$	$\frac{d}{D}$	$\frac{\text{Area}}{D^2}$	$\frac{\text{Wet. per.}}{D}$	$\frac{\text{Hyd. rad.}}{D}$
0.01	0.0019	0.2830	0.0066	0.51	0.4466	1.7162	0.2602
0.02	0.0053	0.4006	0.0132	0.52	0.4566	1.7362	0.2630
0.03	0.0097	0.4911	0.0198	0.53	0.4666	1.7562	0.2657
0.04	0.0150	0.5676	0.0264	0.54	0.4766	1.7763	0.2683
0.05	0.0209	0.6351	0.0329	0.55	0.4865	1.7964	0.2707
0.06	0.0275	0.6963	0.0394	0.56	0.4965	1.8165	0.2733
0.07	0.0346	0.7528	0.0459	0.57	0.5064	1.8367	0.2757
0.08	0.0421	0.8054	0.0524	0.58	0.5163	1.8569	0.2781
0.0886	0.0491	0.8482	0.0578	0.59	0.5261	1.8772	0.2804
0.09	0.0502	0.8513	0.0590	0.60	0.5359	1.8976	0.2824
0.10	0.0585	0.8732	0.0670				
0.11	0.0670	0.8950	0.0748	0.61	0.5457	1.9180	0.2844
0.12	0.0753	0.9166	0.0823	0.62	0.5555	1.9386	0.2864
0.13	0.0839	0.9382	0.0895	0.63	0.5651	1.9592	0.2884
0.14	0.0925	0.9597	0.0964	0.64	0.5748	1.9800	0.2902
0.15	0.1012	0.9811	0.1031	0.65	0.5843	2.0009	0.2920
0.16	0.1100	1.0024	0.1097	0.66	0.5938	2.0219	0.2937
0.17	0.1188	1.0236	0.1161	0.67	0.6033	2.0431	0.2953
0.18	0.1277	1.0448	0.1222	0.68	0.6126	2.0645	0.2967
0.19	0.1367	1.0658	0.1282	0.69	0.6219	2.0860	0.2981
0.20	0.1457	1.0868	0.1341	0.70	0.6312	2.1077	0.2994
0.21	0.1549	1.1078	0.1398	0.71	0.6403	2.1297	0.3006
0.22	0.1640	1.1286	0.1454	0.72	0.6493	2.1518	0.3018
0.23	0.1733	1.1494	0.1508	0.73	0.6582	2.1742	0.3028
0.24	0.1825	1.1702	0.1560	0.74	0.6671	2.1969	0.3036
0.25	0.1919	1.1909	0.1611	0.75	0.6758	2.2198	0.3044
0.26	0.2013	1.2115	0.1662	0.76	0.6844	2.2431	0.3050
0.27	0.2107	1.2321	0.1710	0.77	0.6929	2.2666	0.3055
0.28	0.2202	1.2526	0.1758	0.78	0.7012	2.2906	0.3060
0.29	0.2297	1.2731	0.1804	0.79	0.7094	2.3149	0.3064
0.30	0.2393	1.2935	0.1850	0.80	0.7175	2.3397	0.3067
0.31	0.2489	1.3139	0.1895	0.81	0.7254	2.3650	0.3067
0.32	0.2586	1.3342	0.1938	0.82	0.7332	2.3907	0.3066
0.33	0.2683	1.3546	0.1981	0.83	0.7408	2.4170	0.3064
0.34	0.2780	1.3748	0.2023	0.84	0.7482	2.4440	0.3061
0.35	0.2878	1.3951	0.2063	0.85	0.7554	2.4716	0.3056
0.36	0.2975	1.4153	0.2103	0.86	0.7625	2.5000	0.3050
0.37	0.3074	1.4355	0.2142	0.87	0.7693	2.5292	0.3042
0.38	0.3172	1.4556	0.2181	0.88	0.7759	2.5595	0.3032
0.39	0.3271	1.4758	0.2217	0.89	0.7823	2.5909	0.3020
0.40	0.3370	1.4959	0.2252	0.90	0.7884	2.6235	0.3005
0.41	0.3469	1.5160	0.2287	0.91	0.7943	2.6576	0.2988
0.42	0.3568	1.5360	0.2322	0.92	0.7999	2.6935	0.2969
0.43	0.3667	1.5561	0.2356	0.93	0.8052	2.7315	0.2947
0.44	0.3767	1.5761	0.2390	0.94	0.8101	2.7721	0.2922
0.45	0.3867	1.5962	0.2422	0.95	0.8146	2.8160	0.2893
0.46	0.3966	1.6162	0.2454	0.96	0.8188	2.8643	0.2858
0.47	0.4066	1.6362	0.2484	0.97	0.8224	2.9188	0.2816
0.48	0.4166	1.6562	0.2514	0.98	0.8256	2.9832	0.2766
0.49	0.4266	1.6762	0.2544	0.99	0.8280	3.0667	0.2696
0.50	0.4366	1.6962	0.2574	1.00	0.8293	3.2670	0.2538

margin above or below critical cannot be maintained by changing the shape of the channel, or otherwise, ample freeboard to care for possible disturbances should be provided.

6. Permissible Velocities. The cost of a conduit varies with its size. Therefore, if available slope permits, the cost of the initial construction may be reduced by using the highest safe velocity. However, if the velocity is made too high, the conduit or open channel may be damaged or destroyed by erosion. This must be avoided by limiting velocities according to the boundary materials.

For clear water in smooth concrete or other hard-surfaced water conductors, the limiting velocity is beyond practical requirements, except perhaps in very steep chutes. Velocities above 40 fps for clear water in concrete channels have been found to do no harm. If the water carries abrasive materials, damage may occur with lower velocities. Unless the abrasive material is particularly bad, velocities up to 10 or 12 fps should not prove injurious to wood or concrete. Thin metal flumes may be damaged by coarse sand or gravel at 6 to 8 fps, and the galvanizing may be injured by lower velocities. The abrasive materials may be in the water at its source or may enter along the channel. No definite relation has been established between the nature of abrasive material, material of channel bank, and permissible velocity. Such materials should be excluded as far as practicable.

In unlined earthen channels, the limiting velocity involves many factors. Generally, a fine soil is more easily eroded than a coarse one, but the effect of grain size may be obscured by the presence or absence of a cementing or binding material. The tendency to erode is reduced by seasoning. Groundwater conditions exert an important influence. Seepage out of the channel, particularly if the water is turbid, tends to toughen the banks; infiltration reduces resistance to erosion. Erosion can be reduced or avoided by designing for low velocities. If carried to an extreme, this results in large and costly canals, encourages the growth of aquatic plants, and increases seepage and evaporation.

If the water carries an appreciable amount of silt in suspension, too low a velocity will cause the canal to fill up until the capacity is impaired. It is necessary to choose a velocity that will keep the silt in motion but that will not erode the banks of the canal. The margin of permissible velocities depends on the amount and nature of the silt in the water, the nature of the bank material, the size and shape of the canal, and many other factors. The silt content of most turbid waters varies with the season, as does also the demand for water and the resultant velocity of the flow. Thus, as demonstrated in Sec. 6 (Regime Canals), a canal that will scour at one season may silt at another.

The determination of nonscouring, nonsilting velocities for earth canals has attracted the attention of many investigators over a long period of time, and a considerable mass of data and formulas have been accumulated. Because of its complexities and importance this problem is discussed separately in Sec. 6. Reference should be made to this section for design information on all important canal projects in alluvium soils.

However, for preliminary purposes, and for design in many cases, use may be made of the approximate values proposed by Fortier and Scobey, in 1926, as shown in Table 3.[1] Where the silt burden is important, it is better to make the slope a little too steep rather than a little too flat. A gradient that proves to be too steep can be controlled by checks. In hard-surfaced channels silting is easily controlled if fall for scouring velocity is available.

The values in columns (3) and (4) apply only to particles in suspension and not to coarser particles, usually referred to as the *bed load,* which are rolled along the bottom.

[1] Fortier and Scobey, Permissible Canal Velocities, *Trans. ASCE*, **89**, 940, 1926.

Table 3. Permissible Canal Velocities

Original material excavated for canal	Velocity, fps, after aging, of canals carrying		
	Clear water, no detritus	Water transporting colloidal silts	Water transporting noncolloidal silts, sands, gravels, or rock fragments
(1)	(2)	(3)	(4)
Fine sand (noncolloidal)	1.50	2.50	1.50
Sandy loam (noncolloidal)	1.75	2.50	2.00
Silt loam (noncolloidal)	2.00	3.00	2.00
Alluvial silts when noncolloidal	2.00	3.50	2.00
Ordinary firm loam	2.50	3.50	2.25
Volcanic ash	2.50	3.50	2.00
Fine gravel	2.50	5.00	3.75
Stiff clay (very colloidal)	3.75	5.00	3.00
Graded, loam to cobbles, when noncolloidal	3.75	5.00	5.00
Alluvial silts when colloidal	3.75	5.00	3.00
Graded, silt to cobbles, when colloidal	4.00	5.50	5.00
Coarse gravel (noncolloidal)	4.00	6.00	6.50
Cobbles and shingles	5.00	5.50	6.50
Shales and hardpans	6.00	6.00	5.00

Every precaution should be taken to exclude these coarser particles, and where this cannot be fully accomplished, means for removal should be provided.

CONVEYANCE LOSSES

7. Explanatory. There is an inevitable loss of water from all forms of conduits, possibly excepting a pipe perfectly constructed of metal or other nonporous materials. Losses are caused by leakage, absorption, and evaporation. The greatest loss usually results from seepage in unlined channels. The value of water lost is an important factor in all economic problems concerning the conveyance of water.

8. Losses from Concrete, Metal, and Wood Conduits. The leakage from well-constructed and well-maintained concrete, metal, and wood conduits is relatively small. Where such conduits occur in short lengths in systems composed chiefly of earthen channels, losses from them are negligible by comparison. However, no conduit is completely tight, and in long lined systems the accumulation of even small leakage may be important. An example is the Colorado River Aqueduct, bringing water from the Colorado River to Los Angeles. The main line of this aqueduct is 242 miles in length, made up as follows: tunnel (16 ft) 92.0 miles, cut-and-cover conduit (18 ft) 55.0 miles, lined canal (20 ft) 62.4 miles, pressure conduits 29.7 miles, unlined canal 1.0 mile, reservoir passage 2.2 miles. The specifications required that all visible leaks be closed, yet an appreciable loss was allowed in economic studies. Using data available at the time, the loss for final full operation, including reservoir seepage and evaporation for some 3,000 acres of canal and reservoir surfaces, was set at about 80,000 acre-ft/year, or 7.5 percent of the designed annual capacity. This allowance has been found adequate.

Data on losses from large aqueduct conduits are scarce. Such leakage is frequently expressed in terms of gallons per inch diameter of conduit per mile per day. Tests on 17 ft by 17 ft 6 in. concrete horseshoe conduits in the New York City water system showed leakage of 167 to 463 gal per inch diameter, with an average of 283. An average leakage allowance of 300 to 400 gal per inch diameter is liberal for any well-constructed concrete, steel, or timber free-flow conduit. Leakage from new concrete conduits may exceed this allowance, but if visible leaks are repaired, the loss reduces as the concrete swells and as small openings fill with silt or algae.

9. Losses from Canals. The losses discussed in Arts. 7 and 8 are applicable primarily to substantially built channels of structural materials, or excavated in rock or firm earth. The boundary materials of canals, both lined and unlined, are subject to wide variations in permeability, as discussed elsewhere in this section.

FLOW RESISTANCE

10. Basic Data. The subjects of flow resistance and flow formulas for computing it are discussed in Secs. 2 and 3. Flow formulas are to varying degrees empirical. Their application depends on experimental coefficients or constants of which many published lists are available. Such data are usually derived from tests on newly constructed or well-maintained channels, the designer being left to use his judgment of any allowance needed to provide for deterioration with use.

This situation is not newly discovered. Mossy channels and encrusted pipes have caused trouble for many years. Because of the random nature of such occurrences, as to both frequency and severity, attempts to codify them are fairly recent.

11. Unlined Earth Channels. An unlined earth channel is generally more subject to progressive deterioration than other waterways. It is easy to compute, with reasonable accuracy, the hydraulic performance of a newly constructed channel. However, once put into service, resistance begins to change because of erosion, silting, aquatic growths such as weeds, grass, tules, willows, moss, Crustacea, and other reasons. Aquatic growths increase flow resistance and reduce the effective waterway area. If left unattended, the usefulness of the channel may be seriously impaired. The speed with which choking growth may appear is difficult to predict. Some channels require only occasional weeding. Others, more exposed to seeding opportunities, may deteriorate rapidly.[1]

In the case of very light annual growth, a liberal design friction factor may largely eliminate the trouble. For rapid, or choking, growth, a liberal allowance for friction is not a complete remedy. It is not practicable to tabulate a friction value for a "mossy" or otherwise fouled canal. The ultimate remedy is cleaning, which in serious cases must start early and proceed continuously and may be expensive. A more liberal design or freeboard may extend the time between cleanings and reduce costs. Cleaning may be accomplished mechanically, by fallowing, or chemically. The cost is uncertain and variable.

12. Hard-surface Conduits. The effects of fouling in hard-surface conduits usually are less pronounced and more easily controlled than in earth channels. Several examples of the effects of sliming and other capacity-reducing factors will be found in Sec. 2. In many cases flow capacity has been tested and found to be less than the designed capacity.

Three or four decades ago, flow formulas and tables for cast-iron and steel pipes were generally accompanied by tables of aging factors, to allow for the gradual accumulation of tubercules on the interior surface. With modern coatings this difficulty has been mitigated. As a result, the aging factors are frequently ignored. Severe tuberculation is unlikely, unless the coating fails or spalls off. Such failures are relatively rare, making it cheaper to clean and repair occasionally than to provide excessive capacity initially. However, modern linings do not completely inhibit deterioration

[1] Stephens, J. C., R. D. Blackburn, D. E. Seaman, and L. W. Weldon, Flow Retardance by Weeds and Their Control, *Proc. ASCE, J. Irrigation Drainage Div.*, June, 1963.

by organic slimes and other aquatic growth which may affect any hard-surfaced conduit. Diversity of conditions almost defies specific rules. It would be difficult to specify a set of flow factors for "slimy" conduits.

13. Recent Studies. Recognizing the need for a codification of information on flow resistances from fouling, the Bureau of Reclamation has under way a continuing study of flow conditions in several of its important concrete-lined canals.[1]

14. Scope of Bureau Studies. A series of hydraulic-capacity tests were conducted in some 170 miles of subcritical flow in nine of the largest concrete-lined irrigation canals in the Western United States. Several unusual aspects of flow resistance were revealed by the tests, which were made between 1957 and 1962. The tests had four objectives: (1) determination of maximum discharge capabilities of new canals built with modern equipment, (2) documentation of seasonal changes in flow resistance resulting from aquatic growths, (3) verification of estimated head losses across canal structures, and (4) documentation of increased flow resistance caused by horizontal curves in canal alignment.

15. General Findings. Disclosure of the variety and extent of aquatic growths on concrete lining surfaces was a surprising result of the tests. The occurrence of algae, fresh-water clams, sponges, amphipods, bryozoa, and fish was unexpectedly deleterious and generally varied seasonally and with water source and geographical location.

The results were compared with standard tabulated values of Manning's n and with Reynolds number friction factors. Although the effects of these sometimes minor and sometimes major factors have at times been surprising, procedures normally applied by experienced engineers are by and large yielding acceptable results. However, notable deviations of sufficient frequency and severity to warrant a more conservative approach to the design of lined canals have been observed. Tests on the Delta-Mendota and Friant-Kern canals (California, 1957–1958) showed a water depth over considerable lengths 10 percent greater than assumed in design. In the 48-ft-bottom-width Delta-Mendota Canal, the depth was 18.1 ft in a section designed for 16.6 ft. A systematic study program has been initiated in an attempt to find the mechanism of the resistance and, if possible, to predetermine its occurrence.

16. Conclusions. From the results of these field investigations, it was found that:

1. On the five largest canals (hydraulic radius 9 to 15 ft) the retardation was greater than expected. Design values of Manning's n ranging from 0.0137 to 0.0152 increased to 0.015 to 0.019.

2. On four small canals ($r = 3$ to 7 ft) the effect was less, n changing from 0.0141 and 0.0145 to 0.013 and 0.016.

3. Values of friction factor f from straight reaches of the concrete-lined open canals were generally 30 percent higher than usually measured by others in large circular concrete closed conduits at the same Reynolds number. Aquatic growths, coatings on the lining, construction methods, or other factors may account for this variation.

4. Flow resistance caused by "filamentatious" algae growths (presumably moss) vary seasonally in clear-water canals, peaking at the time of peak demand.

5. Biweekly treatments of 2 lb of copper sulfate per cfs applied throughout the delivery period controlled but did not eradicate such growths.

6. In most large lined canals extensive cleaning is not required, but in the Delta-Mendota Canal some 50,000 cu yd of silt-clam materials were found on the invert of

[1] Tilp, Paul J., Capacity Tests in Large Concrete Lined Canals, *Proc. ASCE, J. Hydraulic Div.*, May, 1965, p. 189.

1960 after 7 years of continuous operation. These deposits contributed to increased hydraulic resistance, and their removal involved an unexpectedly large expense.

7. Hydraulic friction losses in the inverted siphon sections of the test canals were generally less than anticipated in the original design.

DESIGN OF CANALS

17. General Approach. Earth canals have traditionally been trapezoidal in form, but with modern materials and construction facilities curved bottoms are possible for specific jobs. Side slopes are determined by stability of the bank materials, on

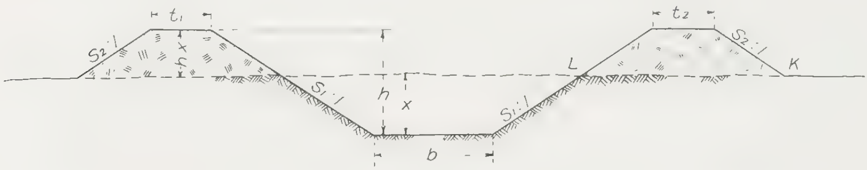

Fig. 4. Typical canal section.

the basis of experience. The dimension of the channel and its setting in the ground are governed by costs and practical considerations. Hydraulic efficiency is not usually a determining factor. The heights and widths of banks are determined by freeboard and stability requirements. Typical unlined trapezoidal canal sections are shown in Figs. 4 to 7, inclusive. A curved bottom section for buried membrane is shown in Fig. 12, Art. 59.

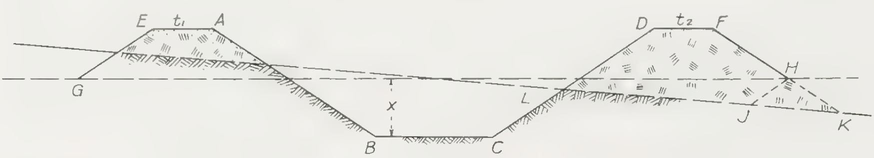

Fig. 5. Typical canal section.

18. Bank Slopes. The side slopes of cuts and fills not exposed to the action of water must conform to the angle of repose of the materials, with allowance for possible saturation by seepage. The steepest safe slopes are usually most economical. If the slopes within the waterway of an unlined canal are made too steep, the banks will erode or slough. Etcheverry and Harding[1] suggest slopes within unlined waterways as shown in Table 4.

[1] Etcheverry and Harding, "Irrigation Practice and Engineering," vol. 2, p. 124, McGraw-Hill Book Company, New York, 1933.

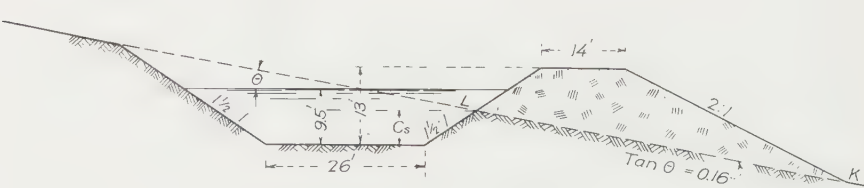

Fig. 6. Typical canal section.

FIG. 7. Typical deep-cut canal section.

These suggested slopes, based on judgment and experience, have been proved by many years of use and are generally adequate for normal canal work. For long, large canal embankments, however, it is advisable to resort to more scientific procedures as discussed in Arts. 30 to 35.

TABLE 4. CANAL-BANK SLOPES

For cuts in firm rock	¼ : 1
For cuts in fissured rock, more or less disintegrated rock, tough hardpan	½ : 1
For cuts in cemented gravel, stiff clay soils, ordinary hardpan	¾ : 1
For cuts in firm, gravelly, clay soil, or for side-hill cross section in average loam	1 : 1
For cuts or fills in average loam or gravelly loam	1½ : 1
For cuts or fills in loose sandy loam	2 : 1
For cuts or fills in very sandy soil	3 : 1
For banks not within the waterway:	
Rock and gravel fills	1¼ : 1
Fills of average loam, gravelly loam	1½ : 1
Sandy loam and sandy soil	2 : 1

Lining protects the banks of the waterway from weathering and from the action of the water in the canal, but for bank slopes steeper than 1:1 or 1.5:1, the lining may have to act as partial retaining wall and unless specially designed may fail. Almost any coherent, free-draining material can be maintained on a 1:1 slope if substantially lined.

19. Freeboard. An inadequate friction coefficient, accumulation of sand or silt, the growth of moss or other vegetation, centrifugal force on curves, wave action, increase in flow resulting from error at diversion, or the inflow or storm waters may raise the water level above that computed for a normal flow. Therefore, canal banks must extend above the designed water level to provide a factor of safety. The lower limit for freeboard is usually 1 ft for small canals, and 4 ft is a usual upper limit for a canal having a capacity of 2,000 or 3,000 cfs. Between these limits, the freeboard may be made about 1 ft plus 25 percent of the depth, with special allowance for unusual conditions.

The top of the lining, in lined canals, is not usually extended for the full height of the bank freeboard. Figure 8 shows the U.S. Bureau of Reclamation recommendations for bank height for canals and freeboard for hard-surface, buried-membrane, and earth linings.[1]

20. Top Width and Thickness of Banks. A canal bank must have sufficient thickness and strength to withstand the water pressure against it and to prevent too free an escape of water by seepage. The top width is usually made about equal to the depth of the water with a minimum of 4 ft, or 12 ft if a patrol road is required. If the embankment is to be exposed to the water pressure for a considerable height, it should be widened as required and carefully compacted. For first-class gravelly soil with just sufficient clay to ensure cohesion, the horizontal distance from L to K

[1] U.S. BUREAU OF RECLAMATION, "Linings for Irrigation Canals," p. 36, 1963.

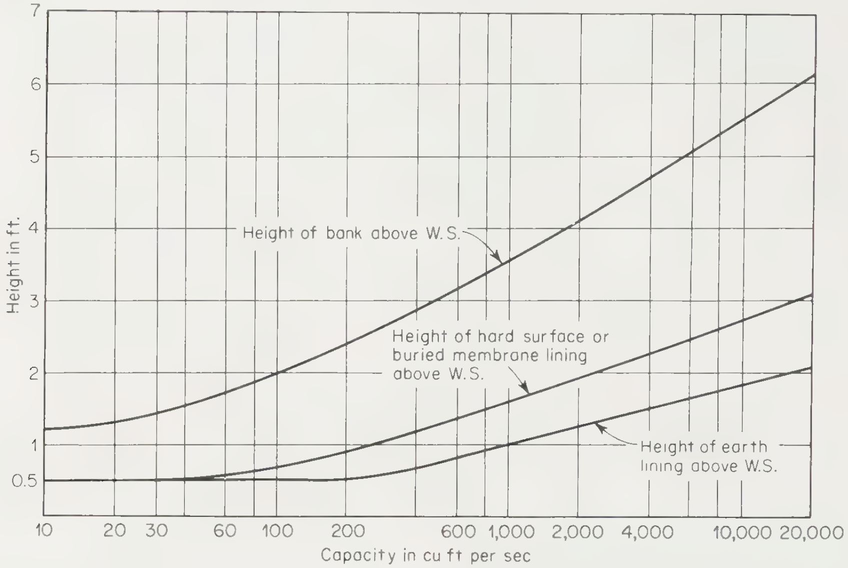

FIG. 8. Bank height for canals and freeboard for hard-surface, buried membrane, and earth linings. (*Reproduction of Fig. 7, p. 36, "Linings for Irrigation Canals," U.S. Department of Interior, Bureau of Reclamation.*)

(Figs. 4, 5, and 6) may be as little as four or five times the depth of water above *L*. For less stable soils this distance should be increased to a ratio of 8 or 10. The bank thickness must be sufficient to avoid piping along the outer toe.

21. Spoil Banks and Berms. Deep cuts may yield more materials than needed for banks. If the excess materials are deposited adjacent to the canal, a level space, or berm, should be provided to protect the waterway from sloughing materials. Berms are also desirable in excavated slopes above the freeboard level. Spoil banks should be regular in form and roughly level. Waste materials may be used to construct an embankment along the uphill side of the canal to exclude cross drainage or, if not needed for this purpose, may be used to reinforce the downhill bank. A typical deep-cut canal section is shown in Fig. 7. Berms usually vary from 5 to 10 ft in width, depending on the height of fills or cuts. Where practical the tops of banks should slope away from the canal.

22. Shape and Size of Waterway. In an unlined canal, the area of the waterway is determined by the permissible velocity or by the available slope if the maximum permissible velocity is not to be attained. In a lined canal, the area and velocity are usually determined by the available slope, unless some other condition controls. A steep hydraulic slope and high velocity reduce the size and cost of the canal but may use up head needed for other purposes. Where such factors can be evaluated, the canal velocity may be made such that the cost of the canal, plus the loss due to steepened slopes, is a minimum. In large canals, it may be necessary to limit the depth to avoid the expense of making high banks safe against water pressure or to minimize the danger of a bank failure. For moderate-sized canals, depths in excess of 10 ft are usually avoided, but appreciably greater depths are permissible where required. In rock cut or other firm material, the danger resulting from increased depth is negligible. In unlined canals where topographic conditions make the use of flat hydraulic slopes difficult, wide shallow sections may be used to reduce velocities, but this device should not be carried to an extreme.

If the canal is to be constructed across a nearly level terrain, without restriction as to the relation of water level to ground surface, the banks become lower and hence of smaller volume as the base is widened, decreasing the volume of earthwork. If the width is made extreme, the cost per cubic yard of excavation and the cost for foundation trimming increase, and the cost of the whole project may be greater. A bottom width in excess of six times the water depth is seldom justified.

A usual procedure is to choose arbitrarily a ratio of base to depth b/d and find the value of d from the equation

$$d = \sqrt{\frac{A}{b/d + S{:}1}} \tag{1}$$

where d = depth of water, b = bottom width and A = area of the water prism found by dividing the flow by the permissible mean velocity, and $S{:}1$ is the side slope. The bottom width is usually chosen to the nearest foot or 2 ft, and the depth is adjusted as required.

Equation (1) applies only to trapezoidal sections. Similar equations may be derived for other fixed shapes.

HYDRAULIC COMPUTATIONS

23. Basic Procedures. It will be necessary, as the discussion proceeds, to illustrate hydraulic computations for various types of conduits. Appropriate flow formulas and basic constants are chosen from Sec. 2. Once the required formula is selected and adjusted if necessary to Arts. 10 to 16, the computations are conceptionally simple, but the combinations of fractional exponents in flow formulas and algebraic complexities of some conduit shapes produce cumbersome arithmetic.

24. Computation Aids. This difficulty has led to the development of computation aids. In repetitive work such aids are indispensable. Tabular aids for fixed-shape conduits, such as circles and horseshoes, appear in Tables 1 and 2, respectively. For canals it is not customary to hold the water prism to an exact fixed shape; hence tabular or diagrammatic aids are sometimes complicated. In any event, their intelligent use is helped by an understanding of the basic procedures. For this reason the following examples will be solved with minimum use of such aids.

25. Example 1. The simplest and most basic problem is the computation of the flow capacity in an existing canal. Assume such a problem with the following information:

1. *Data*
Trapezoidal, unlined, firm, loam, good repair, clear water
Bottom width b = 12.00 ft
Flow depth d = 5.60 ft
Side slopes $s{:}1$ = 1.5:1
Hydraulic slope s = 0.000144
Manning's n (Sec. 2) = 0.0225
Wanted: velocity v and discharge Q

2. *Symbols.* Symbols used in this and in subsequent examples are as follows:

A = area of waterway, sq ft
b = bottom width of canal, ft
d = water depth, ft
p = wetted perimeter, ft
r = hydraulic radius = A/p, ft
s = hydraulic slope
v = mean velocity, fps
n = flow-resistance factor in Manning's formula
Q = discharge, cfs

3. *Canal Properties.* From the specified data find the physical canal properties as follows:

$$A = (b + 1.5d)d = (12.00 + 8.4)5.6 = 114.24 \text{ sq ft}$$
$$p = b + 2d\sqrt{3.25} \text{ (for } S{:}1 = 1.5{:}1) = 32.19 \text{ ft}$$
$$r = \frac{A}{p} = 3.55 \text{ ft}$$
$$r^{2/3} = 2.33$$
$$s = \sqrt{0.000144} = 0.012$$

4. *Computing Flow from Manning's Formula, Sec. 2.*

$$v = \frac{1.486}{n} r^{2/3} s^{1/2} = 1.85 \text{ fps}$$
$$Q = Av = 114.24 \times 1.85 = 211 \text{ cfs}$$

The flow Q was not specified; hence 211 merely indicates what to expect.

26. Example 2. Assume that the actual flow in the canal of Example 1 is measured and found to be only 200 cfs, indicating $n = 0.0225$ to be low. From the given data find the correct value of n. This is a problem of frequent occurrence in investigational work.

1. *Procedure.* Find A, r, $r^{2/3}$, and $s^{1/2}$, as in Example 1. Then find the actual value of v by dividing the known flow by A, thus:

$$v = \frac{200}{114.24} = 1.75 \text{ fps}$$

2. *Computation of n.* Insert this value of v into the Manning formula, Example 1, leaving n as an unknown, and solve as follows:

$$1.75 = \frac{1.486}{n} r^{2/3} s^{1/2}$$
$$n = \frac{1.486}{1.75} \times 2.33 \times 0.012 = 0.0237$$

the answer desired.

27. Example 3. Find dimensions and hydraulic slope for a new canal in firm loam, for a flow of 1,020 cfs, at maximum permissible velocity.

1. *Data and Assumptions.* From Table 3, Art. 6, the maximum allowable velocity in firm loam is $v = 2.50$ fps. From Sec. 2, assume Manning's formula, with $n = 0.0225$. From Art. 18, assume side slopes of 1.5:1. Assume a desirable bottom width-to-depth ratio of $b/d = 4$ with b restricted to the nearest foot.

2. *Canal Properties.* Compute the physical properties of the canal as follows:

$$A = \frac{Q}{v} = \frac{1{,}020}{2.50} = 408 \text{ sq ft}$$

From Eq. (1) with $b/d = 4$,

$$d = \sqrt{\frac{A}{b/d + S{:}1}} = \sqrt{\frac{408}{5.5}} = 8.61 \text{ ft}$$
$$b = 4d = 34.44 \text{ ft}$$

3. *Correcting to $b = 34.00$ ft.* Rounding b out to the nearest foot (34.00 ft), a few trial repetitions of the computation lead to $d = 8.68$ ft, giving a value of 408.13 sq ft for A, close enough to the specified 408 sq ft.

4. *Computation of s.* The computations for s are as follows:

$$p = 34 + 2 \times 8.68\sqrt{3.25} = 65.30 \text{ ft}$$
$$r = \frac{A}{p} = \frac{408}{65.3} = 6.25$$
$$r^{2/3} = 3.39$$

With these values and the specified values of n, Manning's formula yields

$$2.5 = \frac{1.486}{0.0225} \times 3.39 \times s^{1/2}$$

from which

$$s = 0.000125$$

28. Example 4. As a further illustration, assume that in Example 3 the terrain makes it impossible or impracticable to use a slope flatter than 0.00015 without relocation or costly checks. Investigate the possibility of velocity control by a change in canal shape.

Enter Manning's equation with the specified values of n and s, leaving r unknown, thus:

$$2.50 = \frac{1.486}{0.0225} r^{2/3} \sqrt{0.00015}$$

from which

$$r^{2/3} = 3.09$$
$$r = 5.43$$

The wetted perimeter is

$$p = \frac{A}{r} = \frac{408}{5.43} = 75.14$$

From a trial or two it is found that $b = 50$ ft and $d = 6.8$ ft satisfies the values of $v = 2.50$ fps and $s = 0.00015$. This width is excessive. Whether it should be used depends on factors not specified in this example.

29. Example 5. A more usual condition, particularly in lined canals, is to have only the slope and flow prescribed, the velocity and canal dimensions being optional. Assume a flow of 1,000 cfs in trapezoidal lined canal, Manning's $n = 0.014$, side slopes 1.5:1, hydraulic slope 0.0004.

On the basis of experience, with or without published aids, the designer must start with trial dimensions. A pure trial-and-error approach will be illustrated.

1. *Assumptions.* As a first basic assumption a value of $b/d = 2$ is arbitrarily chosen.

2. *First Trial.* As a start, try $b = 16.00$, $d = 8$, and proceed thus:

$$A = (b + 1.5d)8 = 224 \text{ sq ft}$$
$$p = 2 \times 8 \sqrt{3.25} + 16 = 44.85 \text{ ft}$$
$$r = \frac{224}{44.85} = 4.99 \text{ ft}$$
$$r^{2/3} = 2.92$$

From Manning's formula, with $n = 0.014$,

$$v = \frac{1.486}{0.014} r^{2/3} s^{1/2}$$
$$= 106.14 \times 2.92 \times 0.02 = 6.20 \text{ fps}$$
$$Q = Av = 224 \times 6.20 = 1{,}389$$

which misses the required $Q = 1{,}000$ cfs by a wide margin.

3. *Added Trials.* The excess capacity of 389 cfs indicates a substantial reduction in size. A second trial of $d = 7$ and $b = 14$ appears reasonable, and repeating the computation yields results $A = 171.5$, $v = 5.68$, $Q = 974$, which is reasonably close. If a closer value is desired a trial of $b = 14$ and $d = 7.1$ will yield $Q = 999.4$.

These examples do not cover all eventualities but are illustrative of procedures.

LOCATION AND CONSTRUCTION

30. Locating the Canal on the Ground. If there is no restriction as to depth of cutting or in the relation of the water surface to the ground level, the canal prism may be set into the ground a distance such that the excavated materials will just suffice for the construction of the banks. If the ground surface is smooth or regular, this can be accomplished precisely for each foot of canal, but surface irregularities make it necessary to resort to averages. Balancing the cut and fill at any particular section may be accomplished algebraically or by trial. For a trapezoidal canal in level ground, as illustrated in Fig. 4, algebraic expressions for the area in cutting and the area of the two banks may be equated, giving the relation

$$bx + x^2S_1 = [(t_1 + t_2)(h - x) + (S_1 + S_2)(h - x)^2](1 + k) \tag{2}$$

where k is the percentage of shrinkage between area of cutting and area of compacted fill, and all other symbols are as indicated in the figure. This equation may be solved for x, the only unknown.

If the canal is on gently sloping ground but still requires an uphill bank as in Fig. 5, the economic cut for level section can be found approximately by setting the canal so that the intersection of the top of the level cutting with the ground surface comes halfway between the points G and H.

In Fig. 6, the ground slope is such that the upper bank has disappeared. Algebraic expressions for the cut and fill can be devised and solved, or the solution may be made by trial.

The foregoing applies to the economic cut for a straight canal at a single station. On curves, allowance must be made for the effect of curvature. Contours are usually too irregular to be followed minutely. Consequently the depth of cutting must depart from the theoretical at many points, and economy requires that portions of the materials be transported along the canal. The excess or deficiency in excavated material in each station or fractional station is computed and an algebraic summation is carried forward in the form of a table or is plotted on a profile as a differential mass diagram. The location is moved uphill or downhill as required to keep the summation close to zero. Materials may be moved either backward or forward, and the distance of transportation must be considered in computing the cost of the work. Excessive haulage should be avoided by wasting and borrowing. The permissible length of haul depends on the equipment used for excavation. For important canals, particularly on sidehill locations, it is sometimes required as a condition of safety that the water prism be set wholly within the original ground, as far as practical, which removes the possibility of balanced cut and fill. Smaller canals with frequent turnouts may be set in shallow cutting to facilitate diversions, the resulting deficiency in excavated material being made up by borrowing.

31. Construction of Embankment. Canal banks must be placed on adequate foundations and constructed with care. For high banks, subject to water pressure, or for important canals in "thorough fill," the rules for selection and compaction of earth-dam materials (Sec. 18) should be followed. The strict application of such rules to sections like those shown by Figs. 4 and 5 obviously would be extravagant. However, some compaction is required for any bank, especially those dumped in place by draglines or similar mechanical means.

32. Embankment Foundations. Economy dictates that the canal embankments be placed on the foundation materials at hand. If weak, the embankment is spread to compensate. Soft or leaky spots should be avoided by alternative locations, or removed and replaced. Surfaces should be scarified, and excessive vegetation should be removed.

In certain arid and semiarid regions, extensive areas of light alluvium or windblown materials are sometimes found which have never attained their full natural subsidence. When waterlogged by a canal such materials may settle disastrously; hence they should be avoided or presettled, or the design should provide for compensation. A stable but leaky foundation may be remedied by a sheetpile or slurry trench cutoff or by a lined section.

33. Embankment Materials. Any good well-graded earth material can be used for canal embankments, but swampy muck, soft wet clay, quicksand, fine silt, and blow sand are unsuitable. For high wet banks and for deep center fills, reference should be made to Sec. 18. If obviously unsuitable materials are rejected and reasonable moisture control is used, canal cut materials generally can be used in embankments.

34. Placing and Compacting. Embankment may be placed on the fill with dump trucks, loaded by shovels or other devices or by power-driven scrapers or dragline. The dump truck or scraper is usually followed by a bulldozer, which spreads the load in an even, relatively thin layer. For well-graded, properly moistened materials, this operation usually provides sufficient compaction for water depths up to from 2 or 3 ft. For greater depths added compaction by tamping rollers or other devices may be required (Sec. 18). The inclusion of lenses of sand, gravel, and soft materials passing through the fill must be avoided.

35. Failure by Sloughing. Complete saturation of an appreciable part of an outer slope may cause failure by sloughing or sliding. Also, a too high escape velocity for seepage on the face, at the toe, or from the foundation presents a danger of failure by piping. These conditions are not usual in canal banks but are possible.

THE LINING OF EARTH CANALS

36. Purposes of Lining. There are thousands of miles of all kinds and sizes of unlined earth canals in satisfactory service throughout the world. They are economical to construct and will continue to be used where suitable. However, on occasion, for one or more of many reasons, it is desirable or necessary to provide canals with a lining. A partial list of reasons is:

1. To avoid excessive loss of water by seepage
2. To avoid piping through or under banks
3. To provide needed stability
4. To avoid erosion
5. To promote the continued movement of sediments
6. To facilitate cleaning
7. To help in the control of weeds and aquatic growths
8. To reduce flow resistance
9. To avoid waterlogging of adjacent lands
10. To promote economy by a reduction in excavation

37. History and Progress of Lining. The active history of canal lining probably began in the nineteenth century. In the early part of this period water was relatively plentiful, and a moderate waste was unimportant. Where lining was used, it was likely to be for some reason other than the simple value of the water lost.

This situation gradually changed over the years as demands for water encroached upon available supply. At first shortages were met by going afield for added supplies, but in many places this is becoming impossible or impracticably expensive. Where perennial streamflow is inadequate, storage is required which is often expensive. For an extensive system of long unlined canals, losses sometimes have been known to run as high as 30 to 40 percent. However derived the wasted water is just as costly as the used water. Also, the upper reaches of the works must be oversized to carry the water destined to be wasted. Thus water has achieved a value, seepage has become expensive, and the need for an economical means for sealing conduits is emphasized.

This need has developed gradually and has been accompanied by an increasing search for better and cheaper canal linings. The search for materials went through many stages: masonry, hand-placed concrete, machine-placed concrete, mortar and plaster, asphaltic concrete, asphaltic membranes, rubber and plastic sheets, compacted soils, solid and chemical sealants.

The U.S. Bureau of Reclamation of the Department of the Interior, and other water-transporting agencies, have been working on the problem of effective canal lining at minimum cost since the beginning of the present century, and about 1945 began an intensive study, giving particular attention to newly developed materials and to the cost reductions which would be made possible by improvement in the design and construction of conventional types.

The accomplishment of this study up to 1963 is effectively analyzed in a report entitled "Linings for Irrigation Canals."[1] This report is drawn on freely for essential information in the following discussion of alternative lining materials and procedures.

[1] U.S. Bureau of Reclamation, "Linings for Irrigation Canals," Denver, Colo., 1963.

PORTLAND-CEMENT-CONCRETE LINING

38. Desirable Qualities. Because of its many desirable qualities, Portland-cement concrete has long held a dominant place in the canal-lining field. It meets more of the requirements of Art. 36 than any other material so far developed, and meets them more effectively. However, as generally used in the past, it has been relatively expensive, and in this respect it fails to meet the ever-increasing need for low-cost linings.

39. Cost Factors. The high cost of concrete lining is due in part to the inherent cost of the concrete itself, but there are controllable factors, especially applicable to canals, which can be improved. Among these are thickness, reinforcement, placing procedures, and design and construction tolerances. Because of the need of codified information on these and other items, the possible improvement of concrete lining has high priority on the Bureau of Reclamation's current canal-study program.

40. Thickness Requirements. The required thickness of a concrete lining is determined by the purpose to be served and by operating conditions. If seepage control were the only purpose, a relatively thin lining (if uncracked, or if cracks are closed) would suffice. Because of lack of data, the choice of thickness is often arbitrary.

As an extreme example, consider the 62-mile length of lined canal on the Colorado River Aqueduct, bringing domestic water to southern California. This 20-ft-bottom-width canal with 10.2 ft water depth could not readily be taken out of service for repairs. Hence the bottom lining was made 8 in. thick, the sides tapering to 6 in. at the top. Twenty-five years of operation have proved this thickness to be ample, but there is no proof that a thinner lining might not have sufficed. Thinner linings have been successfully used under comparable circumstances.

A brief discussion of thicknesses for use in cement concrete, asphaltic concrete, and shotcrete is given on page 33 of "Linings for Irrigation Canals," followed by a diagram of the relation of thickness to canal capacity, derived from Bureau practice. The data on this diagram are transposed into Table 5. The values shown are somewhat arbitrary but are based on long experience under a wide variety of conditions and are valuable as guides.

If surface deterioration from alkali, freezing and thawing, or other cause, or if

TABLE 5. SUGGESTED THICKNESSES OF PORTLAND-CEMENT AND ASPHALTIC CONCRETE LININGS*

Thickness, in.	Flow, cfs
Unreinforced concrete:	
2.00	0–200
2.50	200–500
3.00	500–1,500
3.50	1,500–3,500
4.00	Above 3,500
Asphaltic concrete:	
2.00	0–200
3.25	200–1,500
4.00	Above 1,500
Reinforced concrete:	
3.50	0–500
4.00	500–2,000
4.50	Above 2,000
Gunite:	
1.25	0–100
1.50	100–200
1.75	200–400
2.00	400 up

* U.S. BUREAU OF RECLAMATION, "Linings for Irrigation Canals," Denver, Colo., 1963.

heavy icing or other extraneous influences are possible, the indicated thicknesses may need to be increased.

41. Minimum Reinforcement. The requirement for reinforcement for other than structural purposes is indeterminate. Returning to the Colorado River Aqueduct for an extreme example, it was important that this canal be free from breakage and as nearly bottle-tight as possible. Nominal reinforcement in conjunction with adequate jointing, or continuous reinforcement, adequate to preclude any wide-open cracks, were indicated alternatives. The latter was chosen using 0.6 percent of high-elastic-limit steel. The result sought was many closely spaced surface cracks with no through cracking. This objective was achieved, but there is nothing to indicate whether it was overdesigned.

The Bureau of Reclamation has found that for usual irrigation requirements, much lighter reinforcement or none at all provides adequate strength and seepage control and recommends that reinforcement on irrigation canals be used only where required for structural reasons. For thin linings, nominal reinforcement may defer complete collapse by holding cracked segments together.

42. Mechanical Trimming and Placing. The trimming of banks and actual placement and finishing of the concrete are important cost items in lining a canal. To avoid waste of concrete, the banks must be fine-graded. Laborsaving means of accomplishing this and of placing the concrete, which can greatly reduce cost, have been developed gradually and improved over more than a quarter century. A distinct impetus was given to this development on the previously mentioned Colorado River Aqueduct, where mechanical trimming of the canal and placement of concrete were adopted. The procedure was as follows:

1. The canal was excavated slightly undersize, by dragline.
2. Fine grading, following the dragline, was done by a trimmer consisting of a series of small dredger-type buckets traveling on a trapezoidal frame set to trim to exact neat lines. The trimmer was supported on carefully aligned steel rails on the two banks.
3. Reinforcing steel was placed and tied by hand.
4. Concrete was hauled to the site in trucks or transit mixers and delivered to a placer consisting of a slip form exactly fitting the finished canal surface, supported on the same rails as the trimmer, and drawn forward by winches. Concrete fed into vibratile hoppers at the leading edge emerged as a perfectly formed lining. From a light following scaffold workmen hand-troweled the surface and applied a curing compound. This was an eminently successful operation, but too costly for general irrigation work.

The Bureau of Reclamation has improved these machines over the ensuing 30 years and has lightened and tailored them to irrigation-canal needs. By experimentation it has been found that the guide rails often can be eliminated, the equipment being supported from the subgrade.

43. Relaxed Tolerances. Canal surfaces must be maintained smooth and regular, without abrupt changes, and large-scale sinuosity should be avoided, but experience has shown that there is no need to hold sections and surfaces precisely to prescribed dimensions. Good judgment and experience will dictate how far relaxation may go.

44. Joints and Grooves in Concrete and Mortar Lining. A concrete or mortar canal lining is subject to swelling and shrinkage under varying temperature and moisture conditions. In concrete lining of normal thickness swelling is unimportant. For uncracked thin concrete or mortar, swelling can cause buckling. Buckling is generally not a serious problem, and expansion joints usually can be omitted except at junctions with rigid structures. Short of very heavy and costly reinforcement (see Art. 41), concrete lining cannot be designed to overcome cracking. Partial control can be secured by contraction joints at proper intervals, with or without light reinforcement.

The use of reinforcement steel for this purpose, except in special cases, such as for high-velocity channels, has been practically abandoned. For continuously placed lining a weakened-plane-type joint, or "sidewalk" groove, formed in the concrete to a depth of about one-third of the lining thickness is effective in controlling the spacing and consequently the width of cracks. For a canal perimeter of more than 30 ft, longitudinal as well as transverse joints are advisable. Recommended spacing of transverse grooves in unreinforced concrete varies from 10 to 15 ft, depending on the size of canal and the thickness of lining. Figure 9 and the accompanying table show

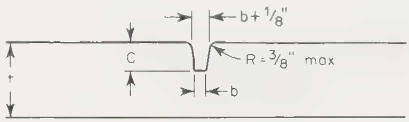

t, inches	b, inches	c, inches	Approximate groove spacing, center to center (feet-inches)
2	1/4 to 3/8	5/8 to 3/4	10-0
2 1/2	1/4 to 3/8	3/4 to 7/8	10-0
3	3/8 to 1/2	1 to 1 1/8	12-0 to 15-0
3 1/2	3/8 to 1/2	1 1/8 to 1 1/4	12-0 to 15-0
4	3/8 to 1/2	1 1/4 to 1 3/8	12-0 to 15-0

Dimensions b and c show allowable tolerance

FIG. 9. Recommended groove dimensions for unreinforced-concrete canal linings and accompanying table. (*Reproduced from Table* 6, *p.* 35, "*Linings for Irrigation Canals*," *U.S. Department of Interior, Bureau of Reclamation.*)

recommended spacing and groove dimensions. A more detailed discussion of the spacing of grooves and methods of forming them is contained in the Bureau's "Concrete Manual." Similar grooves may be provided in gunite linings. Expansion joints also may be required for gunite linings if placed in cold (less than 50 F) weather. One-inch-wide joints at 100-ft centers have been found to be effective.

For thick concrete linings, particularly in high-velocity channels such as spillway chutes, thicker linings and more substantial joints, designed to permit limited slippage without leakage, may be required. Typical examples are shown in Fig. 10. Figure 11 indicates a type of grooving that may be used around precast slab lining.

THIN PORTLAND-CEMENT-MORTAR LININGS

45. Span of Experience. The use of relatively thin cement-mortar canal lining as a means of reducing cost has a long history. However, until recently little effort was made to collect and publish information on effectiveness, durability, and cost. Recently compiled data show excellent performance.

46. Service History, Hand-placed Thin Linings. Some linings of thin Portland-cement mortar in mild climates are known to have been in service for more than 60 years. More than 20 miles of ¾-in.-thick unreinforced mortar linings placed between 1880 and 1890 in southern California are still in service. A total of 37 miles of 1½-inch-thick, hand-troweled, unreinforced, mortar lining placed in canals of the Okanogan Project, Washington, between 1912 and 1917, is still in good, serviceable condition, somewhat cracked and in need of some maintenance, but only about ½ mile in a severe-frost area needs to be replaced.

47. Pneumatically Applied Mortars. Hand plastering has largely given way to pneumatic placement of cement-mortar linings, usually referred to as gunite or shotcrete.

Pneumatic placement has many advantages. The equipment is light, inexpensive, and mobile, making gunite attractive for remote locations and for scattered small jobs. However, the rate of placing is slow, the cement content is high, and aggregates require careful selection and processing, for which reasons gunite is not always so cheap as slip-form concrete on large jobs. Gunite 1½ in. thick may be expected to cost about as much as 2.0 in. of unreinforced slip-form concrete.

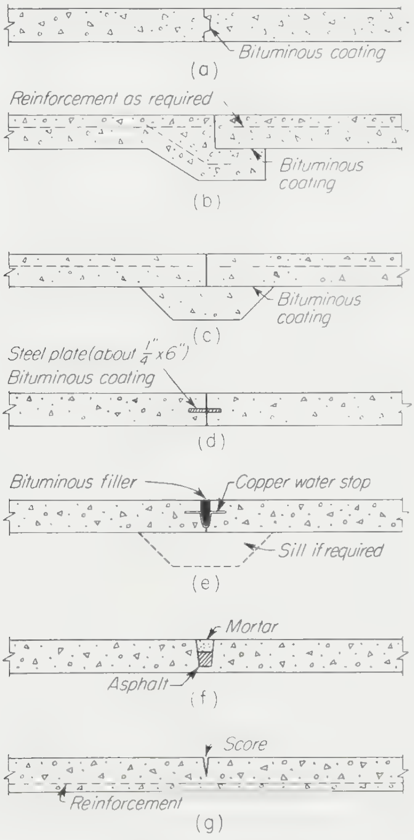

FIG. 10. Typical canal-lining joints.

48. Thickness and Reinforcement of Pneumatic Lining. Gunite linings placed by the Bureau of Reclamation are usually 1½ in. or more in thickness, sometimes reinforced with wire mesh, where structural safety is involved, using 4- by 4-in. or 6- by 6-in. mesh of No. 9 or 10 gage wire. Under adverse conditions such lining may crack, heave, and break, but particularly if reinforced, complete failures are rare and prompt repairs are possible, ensuring a satisfactory low-cost long-life lining.

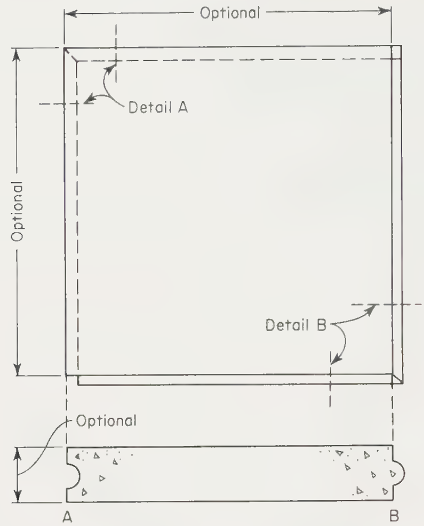

FIG. 11. Suggested precast slab details.

49. Repair of Portland-cement Concrete and Mortar Linings. Shrinkage cracks in Portland-cement concrete or mortar may be filled with brushed-in cement grout or with a stiff mastic. Damaged areas may be removed and replaced with concrete, gunite, or hot-mixed asphaltic concrete. An extensively deteriorated lining may be repaired by a full-area overlay, 1 to 2 in. thick, of hot-mixed asphalt. A similar layer of gunite could be used.

ASPHALTIC LININGS

50. Objectives. The successful and economical use of asphaltic concretes for the pavement of roads, driveways, and other areas has drawn attention to its possible use for canal linings. Sporadic use, particularly for lining small reservoirs, dates back to the early 1900s. Systematic evaluation of its use for canal lining was begun by the Bureau of Reclamation in the 1940s. As an exposed-surface lining it generally has not been found superior, if equal, to Portland-cement concrete and mortar linings; hence its value largely depends on relative costs.

51. Hot-mixed Asphalt Concrete. Hot-mixed asphalt used for canal linings is similar in general appearance to that used for road surfacing, but its performance requirements are different. To assure its value for seepage control, its density should be high. This calls for careful selection and proportioning of materials and thorough compaction. Early installation of hot-mixed lining was placed and finished by hand, but slip-form machines, adapted from those developed for Portland-cement concrete, are being found to yield superior results at a low cost.

To 1963, the Bureau of Reclamation had in service 330,000 sq yd of hot-mixed linings in various areas, particularly on the Contra Costa Canal in California and the Snipe Mountain Canal in Washington. This was followed by an 88,000-sq-yd installation on the Pasco Pump Lateral, Washington, which was laid with the first slip-form machine to be specifically designed for asphaltic concrete.

52. Subgrade Problems. Asphalt-concrete linings, having less structural strength, are somewhat more sensitive to subgrade weakness than comparable thicknesses of

Portland-cement concrete or mortar but being more flexible are less subject to rupture from yielding soils.

53. Weed Problems. Asphaltic concrete, even of fair thickness, is subject to penetration by weeds, roots, willows, and other plant growths. Where conditions are favorable to such growths, it is advisable that the soil be chemically sterilized in advance of construction. Various sterilants and their effectiveness are being studied by the Bureau of Reclamation. Some have been found to be only temporarily effective; others give promise of longer life. All are under continuing study. A prospective user of asphaltic lining should consult a dealer in agricultural chemicals for latest data on soil sterilants.

54. Reinforcement. Steel reinforcement in asphaltic-concrete canal lining has been tested but so far has been found to be of little or no value.

55. Thickness and Mixture. Recommended thicknesses for asphaltic-concrete linings are indicated in Table 5, Art. 40. Adequate thickness is, of course, intimately related to the composition of the lining and the care with which it is placed. Of two experimental reaches laid by the Bureau in 1963, one, with thicknesses of 1.0 to 2.0 in., used a fine pit-run sand, hot-mixed and hand-placed. The mix lacked stability and performed poorly. An alternative reach, hand-placed, hot-mixed with well-graded aggregate, laid in 1-, 2-, and 3-in. thicknesses, gave excellent performance, except for some willow penetration and slight buckling of the 1.0-in. lining.

In 1944, 11,000 sq yd of 2.0-in. asphalt-concrete lining, using a coarse (but graded) aggregate and a heavy asphalt, produced a rough open surface. A squeegeed seal coat was temporarily successful, but deterioration continued, and in 1957 a need for rehabilitation became apparent.

EXPOSED MEMBRANE LINING

56. General Features. A sheet of plastic, even a very thin one, is essentially watertight, as long as it remains perfect. However, experience to date, as subsequently explained, indicated that the element of perfection disappears when such membranes are spread over the extensive areas involved in canal linings. However, these products are relatively new and are rapidly being improved. If used, careful consideration should be given to ability to meet the rigors of the installation. Exposed membranes should not be used on structures which are not structurally safe without lining.

57. Exposed Asphaltic Membranes. Thin sprayed-in-place, hot or cold, exposed asphaltic cements have been tried experimentally but with limited success, as they are very subject to injury. Tests are continuing.

Considerable experimentation is being done with prefabricated asphaltic membranes, following the pattern of the well-established use of asphaltic felts for roofs. The membranes, received in rolls or sheets, are laid with lapped joints shingle fashion, or with butt joints closed with cemented-on strips. The felt filler may be composed of organic, asbestos, or glass fibers, and may be from $\frac{1}{16}$ to $\frac{1}{2}$ in. thick. Experience to date with such exposed sheets has been only partially successful.

58. Exposed Plastics and Synthetic Rubber. Membrane films of plastics and synthetic rubber suitable for canal linings have been and still are under test. Many of the plastics tested and installed experimentally as exposed membrane linings have shown low resistance to puncture, and some types disintegrate upon exposure. Thicker plastics and synthetic rubber, with greater resistance, are more expensive. Butyl-rubber sheets 30 and 60 mils thick have been installed and, although costly, are proving serviceable as canal and pond liners. Membrane linings should not be laid on rocky surfaces or on gravelly soils containing sharp particles that might promote puncturing. Vandalism has been a problem in some areas.

BURIED MEMBRANE LININGS

59. Advantages and Disadvantages. The vulnerability of exposed membrane lining to damage can be partially mitigated by a cover of earth or of earth and gravel. Such protection adds greatly to the security of the lining against mechanical damage and vandalism. However, it is not enough simply to spread a thin layer of earth on the lining surface. The cover must be of substantial thickness. The lined section may be conventionally trapezoidal, or the bottom may be rounded, as suggested in Fig. 12. It has been found that the side slopes should be flatter than for unlined canals, because of the plane of weakness introduced by the membrane surface, and usually should not be steeper than 2:1.

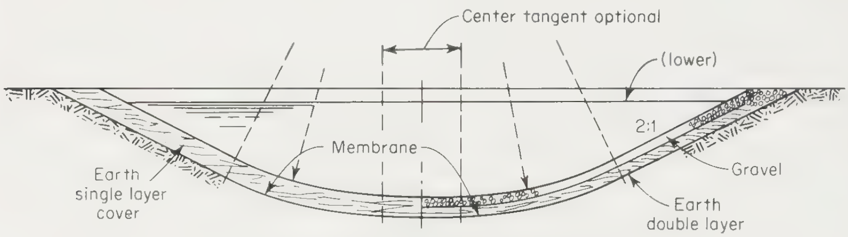

FIG. 12. Round-bottom buried membrane.

A minimum thickness of about one-twelfth the water depth plus 10 in. is indicated for a cover of clayey or gravelly surfaced soil, or other equally erosion-resistant material. Otherwise it may need to be thicker. The erosion resistance could be improved by compaction, but compaction would need to be done with great care, to avoid rupture of the membrane. A canal with a buried lining is subject to the same difficulties from aquatic growths, the same limitation of velocity and flow resistance, and the same (if not greater) maintenance difficulties as on unlined canals.

OTHER TYPES OF LINING AND SEALANTS

60. Possible Types. In addition to concrete, asphalt, plastic, and rubber types of linings, there are numerous other types that deserve mention. Among these are masonry, compacted earth, loose earth, soil cement, and waterborne sealants.

61. Masonry Linings. Stone and brick masonry were the earliest hard-surfaced types of lining. They were laid by hand, with dry or mortared joints. With dry joints they are of little value for seepage control but may serve other purposes. With carefully mortared joints such paving can be made reasonably watertight. Surfaces can be left rough, or smoothed with mortar to reduce flow resistance. These linings are substantial and permanent, but not particularly cheap, and in many parts of the world have been rendered obsolete by the rising cost of manual labor. Dumped-in-place rock, or riprap, is still in general use in special locations for erosion control.

62. Earth Linings. A properly selected, well-graded, and thoroughly compacted earth material can rival a lean concrete in impermeability and has an advantage in flexibility. One disadvantage is that a canal lined with earth is still an "earth canal," subject to low erosion resistance, high flow resistance, and aquatic growths. Nevertheless, in some situations there is a net advantage to earth linings. The most abundant source of coordinated information on earth lining is the Bureau of Reclamation's report of "Linings for Irrigation Canals," from which the following information on thick-compacted, thin-compacted, loosely placed earth linings, and soils with admixtures, is abstracted.

Compacted earth linings designated as "thick" are usually 3 ft horizontally on the sides and 12 to 24 in. vertically on the bottom. The normal-to-surface thickness of so-called "thin" lining usually runs from 6 to 8 in.

63. Thick-compacted Earth Linings. Where suitable materials for the construction of a thick-compacted earth lining are readily available, this is likely to be the lowest-cost permanent lining for large canals. A thick-compacted earth lining, because of its weight and plastic characteristics, can withstand considerable hydrostatic pressure; in many instances it can be used in high-groundwater areas without drains and is useful for constructing partially lined sections or reaches, where required to cut off permeable areas. Careful inspection and construction control are required. The soil must be homogeneous when placed, of proper thickness, and compacted at proper moisture content to a prescribed density.

Except for thin surface layers frost action has not destroyed the compacted density in severely cold climates. Field tests are now being made to determine the effects of frost. Frost-susceptible soils should be avoided in cold climates. Even in mild climates weathering can in time cause some loss of density, but to date this has not been found serious. Just as in an unlined canal, attention must be given to maximum velocities, erosion possibilities, high flow resistance, aquatic growth, and cleaning.

64. Thin-compacted Earth Linings. Thin-compacted earth linings have some of the characteristics of the thicker linings of the type discussed above. They are susceptible to severe frost action and scour. The thickness in this classification varies from 6 to 12 in.

65. Loosely Placed Earth Blankets. Loosely placed earth blankets, unless the soil used is highly impermeable and stable, have limited use. The blanket must be protected from scouring and eroding action of the flowing water and the elements by use of stable gravel or gravelly materials. Its usefulness is generally limited to emergency or temporary situations.

66. Soils with Admixtures. Where it is necessary to use substandard embankment materials, impermeability and stability may be improved by adding bentonite or other materials such as Portland cement and asphalt emulsions to the soils, but the cost is usually high and may be prohibitive. Very few linings of this type have been placed.

67. Soil-cement Lining. A mixture of Portland cement and naturally sandy soil, if available at the site, usually called "soil cement," has been used for canal linings in mild climates with good results. Such mixtures have been widely used for other purposes, including road subgrades and earth-dam facing. Thickness required for canal lining has not been standardized, and cost records are scarce.

68. Soil Sealants and Stabilizers. Many water-borne, mixed-in-place, spray-applied, and subgrade-injected sealants have been considered as a means of waterproofing or sealing soils to reduce their permeability as well as provide stability, and some have been tried, with limited benefits. Manufacturers are studying such materials as resins, petroleum-based emulsions, plastics, and other related compounds. The future development of a suitable product is a possibility, but nothing fully satisfactory is now available.

69. Other Means of Seepage Control. Emulsified or hot liquid asphalts and Portland-cement grouts have been injected under pressure into crevices and joints in rock, shattered shale, gravel, sand, and other water-permeable materials. Cutoffs of Portland-cement concrete, asphalt, and plastic sheets may be installed in trenches. These measures are used primarily to correct individual problems. Unreinforced, cast-in-place concrete pipe 24 to 48 in. in diameter, for heads up to 15 ft, costs little more than concrete lining for a canal of equal capacity and has numerous incidental advantages. Chemical grouting is also useful but to date is relatively expensive.

SEEPAGE FROM CANALS

70. Need for Information. A canal may require lining for any of many reasons, including those listed in Art. 36. The reduction of seepage is usually a prime item, calling for advanced knowledge of seepage losses, before and after lining. The value of water at point of loss is needed, also relative construction costs. The determination of seepage losses may be approached statistically, theoretically, or by direct measurement.

71. Unlined Canals. Seepage loss from an unlined canal depends on the canal's dimension, the gradation of the materials of which its perimeter is composed, groundwater conditions, and other geological factors.

72. Historical Unlined-canals Data. A very simple and reasonably reliable procedure for unlined canals is based on historical statistics. An example is shown in Table 6, which was compiled and published by Etcheverry and Harding in 1933. The values shown were carefully compiled from many field measurements and are still usable. However, these simple visual graduations should be used as a guide in preliminary investigations. They do not meet the growing need for accurate estimates.

TABLE 6. STATISTICAL LOSSES FOR CANALS NOT AFFECTED BY THE RISE OF GROUNDWATER

Character of Material	Cu ft/sq ft in 24 hr
Impervious clay loam	0.25–0.35
Medium clay loam underlain with hardpan at depth of not over 2 to 3 ft below bed	0.35–0.50
Ordinary clay loam, silt soil, or lava-ash loam	0.50–0.75
Gravelly clay loam or sandy clay loam, cemented gravel, sand, and clay	0.75–1.00
Sandy loam	1.00–1.50
Loose sandy soils	1.50–1.75
Gravelly sandy soils	2.00–2.50
Porous gravelly soils	2 50–3.00
Very gravelly soils	3.00–6.00

73. Theoretical Approach. Frequent attempts have been made to reduce the element of judgment by the development of a theoretical approach to seepage problems. A recent promising attempt is a paper by Herman Bouwer, *Proc. ASCE, J. Hydraulic Div.*, May, 1965. It starts with a thorough environmental field study, covering soil classification and gradation, groundwater levels, and general geology. Electrically analogous conditions established at selected stations are subjected to voltage drops. The flow of current is measured and translated mathematically into water flow.

Assuming adequate analogies at a sufficient number of points, the results should be dependable. However, as with other indirect approaches, care must be taken to see that sampling is representative.

74. Tracers and Electric Logs. As a part of its canal-lining program the Bureau of Reclamation, with the aid of the University of California, is making a thorough study of the determination of seepage by means of dyes and other tracers, combined with electrical logging. It is hoped that these devices will be particularly helpful in identifying areas of high losses.

75. Direct Measurement of Seepage. As a more direct approach, seepage losses may be measured in the field. The Bureau of Reclamation, working with other agencies, has developed at least three types of tests: ponding, inflow-outflow, and seepage meters.

76. Ponding Method, Existing Canals. For an existing canal, lined or unlined, selected reaches may be isolated by dikes into basins from which the rate of loss can be measured. The canal must be out of service for a reasonably long period. If the tests are performed off season, care must be taken to see that percolation conditions are reasonably normal, particularly as to groundwater and frost.

This procedure can be applied to the full length of a canal or to several test reaches, thus avoiding the spotty results possible with other procedures. The ponds may be held at full or partial canal depth.

77. Ponding Method, Proposed Canals. For a proposed canal the ponding method can be used by excavating well-selected ponds along the right of way, making sure that the ponds penetrate all porous layers and that the test period and the ponded area are adequate to simulate normal operating conditions. Seepage rates from proposed lined canals may be estimated by lining the ponds, being careful to assure that the lining is neither more nor less perfect than it will be in the prototype.

78. Inflow-Outflow Method. As an alternative, a careful record may be kept for a reasonable length of time of all flows into and out of a selected reach of canal. This method is perhaps less accurate than the ponding method but has compensating factors. The canal need not be taken out of service.

TABLE 7. SEEPAGE FROM LINED CANALS*

Item No.	No. tests	Thickness, in.	Range of C_s†	Avg depth, ft	Avg C_s, cu ft/day
Unreinforced concrete:					
1	1	3.5	....	17.2	0.07
2	3	4.0	....	.....	0.53
Concrete blocks:					
3	1	....	....	2.55	0.20
Gunite mortar:					
4	2	1.5	....	14.0	0.30
Exposed prefabricated membrane:					
5	11	½	0.01–0.53	0.82	0.12
6	3	¼	0.05–0.48	0.75	0.20
Buried hot applied asphalt:					
7	1	3⁄16–¼	....	2.10	0.16
Buried prefabricated organic fiber:					
8	5	⅛	0.03–0.39	0.69	0.16
9	4	⅛–3⁄16	0.09–0.54	0.91	0.35
Buried prefabricated asphalt asbestos fiber:					
10	13	3⁄32	0.02–0.13	0.86	0.07
Buried prefabricated asphalt glass fiber:					
11	22	1⁄16	0.01–1.57	0.77	0.23
12	19	1⁄16	Fig. 8	0.82	0.14
Thick compacted earth:					
13	1	2.0–2′8″	....	3.76	0.08
14	1	2.0–3.0	....	17.2	0.07
15	2	1.0–3.0	....	7.0	0.10
16	1	1.5	....	2.79	0.05
Loose earth:					
17	4	12	0.54–1.47	0.68	0.83
Soil cement:					
18	7	3	0.03–0.20	2.20	0.09
Sedimentation:					
19	7	....	0.54–1.06	1.89	0.76

* Condensed and rearranged from Table 4, "Linings for Irrigation Canals," U.S. Bureau of Reclamation.

† C_s = cubic feet per square foot per day.

79. Seepage Meter. A third approach is the seepage meter, a device which when inserted in a borehole measures the rate of flow past it, yielding data from which seepage may be computed. The results reported seem to conform with reasonable accuracy to ponding tests. The meter has a decided cost advantage and can be used at frequent points to determine variation of leakage along the line. It may thus reveal that a leaky canal can be sufficiently controlled by lining or sealing a few selected reaches. If points of installation are carefully chosen and if an analogous source of seepage water to be measured can be supplied, a seepage meter can be used for a new canal.

80. Leakage from Lined Canals. In lined canals seepage can be determined by the means described for unlined canals, or the permeability of lining materials may be tested in the laboratory. Because of variation in installation and maintenance factors, laboratory tests are less dependable than field tests.

81. Statistical Leakage Data, Lined Canals. In connection with its canal-lining studies, the Bureau of Reclamation has performed hundreds of seepage tests on existing and proposed canals, lined and unlined. Selected data from these tests are tabulated in Table 7.

ECONOMICS OF CANAL LINING

82. General Consideration. Predominating factors in determining the need for lining in a specific canal are likely to be economic, although other values may play a part. An exposition, by example, of all the various influences, including those listed in Art. 36, would be cumbersome. Some of the influences, such as waterlogging of land and influence on cleaning, depend on local conditions, capable of being evaluated for specific cases but difficult to state hypothetically. A simplified case will be examined.

83. Illustrative Example. Assume that choice is to be made, on the basis of cost alone, between a lined and an unlined section for a proposed canal, under the following conditions:

1. Flow Q = 1,000 cfs, constant throughout the year, irrigation service, canal-side value of water $10 per acre-foot.
2. Soil, gravelly to sandy loam, seepage factor C_s = 2.50 cu ft/day, Manning's n = 0.0225.
3. Lining, 3.0 in. unreinforced concrete (arbitrary choice), C_s = 0.10 cu ft/day, Manning's n = 0.014.
4. Topography, gently sloping, slope optional up to 0.0009, economic cutting acceptable.
5. Allowable velocity, unlined 2.50 fps; lined limited by slope only.
6. Assumed construction costs,[1] excavation, including replacement in fills, $0.60 per cubic yard. Concrete, $2.25 per square yard, trimming $0.60 per square yard.

Value of head involves the cost of bringing the water to its initial heights, by whatever means. If by pumping, the total capitalized cost includes original cost of facilities, the annual cost of power, maintenance operation, and other cost factors. The annual costs must be "capitalized" for combination with plant costs. Actual examples are complicated; however, for the purpose of this exercise an arbitrary value of $60 per cfs per ft of lift has been chosen. This value is slightly escalated from past experience and is perhaps on the low side when compared with present values.

84. Canal Properties. The dimensions and other canal properties are computed

[1] These assumed costs are for illustrative purpose only. They should not be accepted as a basis for cost estimates.

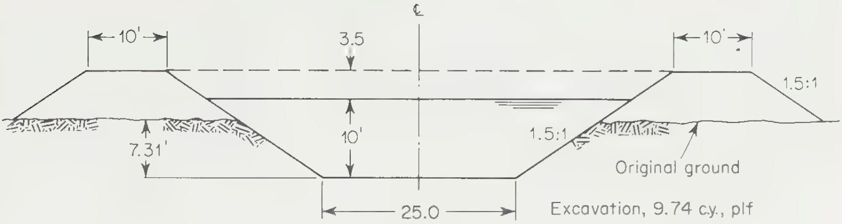

Q = 1,000 cfs, n = 0.0225, s = 0.000117, p = 61.0 ft

FIG. 13

in accordance with Arts. 17 to 29. The computations are not shown. The results are shown graphically in Figs. 13 and 14.

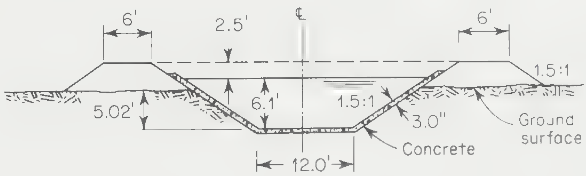

Q = 1,000 cfs, n = 0.014, s = 0.0009, p = 34.0

P_{con} = 39.0'

Excavation, 3.63 c.y. plf

FIG. 14

85. Cost Computations. With the cost data from Art. 83 and the quantities from Figs. 13 and 14, comparative costs may be computed. The results are as follows:

1. *Construction Costs*

Item	Unlined	Lined
Excavation, cu yd	9.74	3.63
Cost at \$0.60	\$5.85	\$2.18
Lining and trimming, sq yd	. . .	4.33
Cost lining at \$2.25	. . . . .	\$9.74
Cost, trimming at \$0.60	. . . . .	\$2.60
Total construction cost	\$5.85	\$14.52

2. *Capitalized Value of Water*

Unlined, C_s = 2.50 cu ft/day
Loss, cu ft/day/sq ft wetted area = C_s = 2.50
Loss, cu ft/day/ft of canal = pC_s = 61 × 2.5 = 152.5
Loss, cu ft/year/ft = $365pC_s$ = 55,662
Loss, acre-ft/year/ft = 1.28
Annual value, at \$10 = \$12.80
Capitalized at 4 percent = 12.80 × 25 = \$320
Lined, C_s = 0.10 cu ft/day, following an identical procedure
Capitalized value = \$7.13 per foot of canal

3. *Capitalized value of head,* for 1.0 ft of head, for full flow, equals 60 × 1,000 = \$60,000, and head per foot equals hydraulic slope (Figs. 13 and 14).

Value, unlined = 0.000117 × 60,000 = \$7.02
Value, lined = 0.0009 × 60,000 = \$54

4. *Summary of Costs*

Item	Unlined	Lined
Construction cost	\$ 5.85	\$14.52
Capitalize, water	320.00	7.13
Capitalize, head	7.02	54.00
Comparative costs	\$332.87	\$75.65

86. Comments. Note that the construction cost for the lined canal, even with its reduced size, is 2.5 times that for the unlined canal and that its head-loss value is 7.7 times higher. However, even for moderate-value irrigation water, the water costs are \$320 for unlined to \$7.13 for lined, raising the total capitalized cost of the unlined canal to 4.50 times that for the lined canal, a very decisive difference.

A less permeable original soil would reduce the disadvantage of an unlined canal, but its permeability would have to be less than $C_s = 0.50$ to give equality. Such soils are possible (see Table 6, Art. 72).

For present high values of domestic, industrial, and irrigation water, an unlined conduit is usually out of the picture.

ECONOMIC CONDUIT SIZES

87. Basic Principles.[1] If the slope is abundant and of little value, water conduits are made steep and small to save cost. However, elevating the water to provide slope is frequently expensive, or head already in existence may have value for the production of power or for other purposes. In such cases, economic design requires a balancing of conduit cost against the cost or value of head.

A simple case is illustrated in Fig. 15, where a *stated discharge* is to be elevated from

Fig. 15. Illustrating economic analysis.

a natural stream at A by a dam B and conveyed through a tunnel CD to a fixed level in reservoir E. A graphical solution is illustrated in Fig. 16, where curve AB represents the cost of the tunnel, CD the cost of the dam, and EF the cost of both combined. The best slope is that corresponding to point G, the low point on the combined cost

[1] For a more detailed discussion of economic slopes see Julian Hinds, Economic Water Conduit Size, *Eng. News-Record*, Jan. 28, 1937; Economic Sizes of Pressure Conduits, *Eng. News-Record*, Mar. 25, 1937.

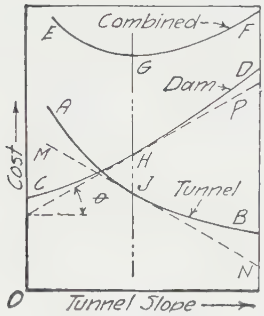

FIG. 16. Illustrating economic analysis.

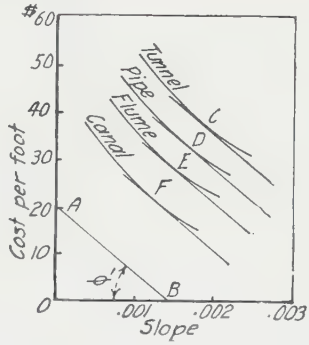

FIG. 17. Illustrating economic analysis.

curve. This is an easy solution for a single conduit but is inadequate for more complicated problems.

In Fig. 15 the water is elevated by a dam. The same principle of analysis can be applied if it is elevated by pumping or other means, a cost-of-lift curve being substituted for the cost-of-dam curve (Fig. 16). The cost of lift must include the cost of equipment plus the *capitalized cost* of perpetual operation. If the elevation at the inlet is predetermined, the outlet elevation being subject to variation, the slope is determined by the *value of head* at the outlet, as for the production of power, or for furnishing a gravity supply to domestic or irrigation consumers. The value of fall for the production of power is equal to the *capitalized net return* from power sales less the cost of the power installation. For convenience, the term *value of a foot of head* is used to designate either the cost of its production at the inlet or its value at the outlet.

88. Cost-slope Tangent Method. Evidently the slopes for the two cost curves at H and J (Fig. 16) must be numerically equal, but opposite in direction, as otherwise the tangent, at G, would not be horizontal. Usually the region of uncertainty in height of dam is limited, and the curve CD is approximately straight within that region; hence, the economic slope may be located as follows: Take a trial height of dam corresponding to some arbitrarily chosen tunnel slope, as at H, and draw the tangent HP to the cost curve CD. Draw tangent MN with slope equal to slope of HP but reversed. If point of tangency J is on same vertical as H, then J marks the economic slope; otherwise, assume a new height of dam and repeat. Satisfactory adjustment is not difficult to make, as points of tangency are more or less indefinite.

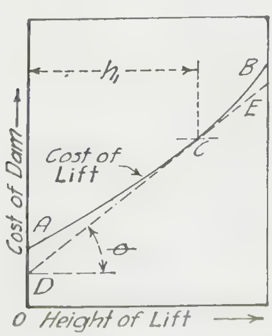

FIG. 18. Illustrating economic analysis.

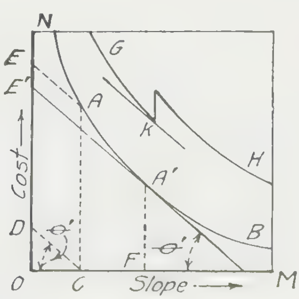

FIG. 19. Illustrating economic analysis.

The significance of the slope-tangent method is shown by Fig. 19. Curve AB represents the cost-slope relationship for a foot of conduit for a specified flow. Slopes are measured on the horizontal OM and costs on the vertical ON. A trial slope OC gives a cost per foot of conduit equal to CA. If CD is drawn so that tan θ' is equal to the value of a foot of head, the distance OD will represent the cost (or value) of the fall in a foot of conduit on slope C. If AE is drawn parallel to CD, OE represents the combined cost. The lowest position of the point E occurs when A reaches A'; hence the economic slope is OF. In case of an irregular cost curve, as GH, the economic slope is marked by the lowest possible contact with the slope line, as at K.

89. Application to Composite Conduits. The procedure for a conduit composed of many types is illustrated in Figs. 17 and 18. In Fig. 17, a cost-slope curve is plotted for each conduit type. If conditions vary, two or more curves may be required for a single type. These curves are on a linear-foot basis. The cost-of-lift curve is plotted separately, as in Fig. 18, and may represent the cost of a dam, capitalized cost of pumping, or the value of head at an outfall, as conditions require. A trial lift is assumed as h_1 (Fig. 18), and the corresponding tangent ED is drawn, having an inclination θ to the horizontal. A line AB is then drawn on Fig. 17, tan θ' being made numerically equal to tan θ, each measured in the terms of its own diagram. Tangents parallel to AB are drawn, the economic slopes for the various conduits being marked at C, D, E, and F. These slopes are applied to the corresponding known conduit lengths, starting from some point of known elevation to give a computed height of lift to replace the assumed height h_1. If the slope of the line DE for the new height is essentially different from that for h_1, the solution should be repeated.

90. Application to High-head Pipes. In pipelines under high head, the pressure introduces an additional variable. A simplified example of a high-head steel pipe is illustrated in Fig. 20. Such pipes are limited by available plate thicknesses and usually by standard diameters. Cost-slope curves, based on constant plate thicknesses, take the form of curves 1, 2, 3, and 4. The ability of the pipes represented by any one of these curves to withstand head is variable. Another set of curves 5, 6, 7, 8, and 9 may be drawn, representing the cost of pipe designed for constant head, without regard to standard plate thickness or pipe diameter.

Diameters, as well as slopes, are shown in Fig. 20 for convenience. The primary plotting, however, must be in slope coordinates, which must be rectangular.

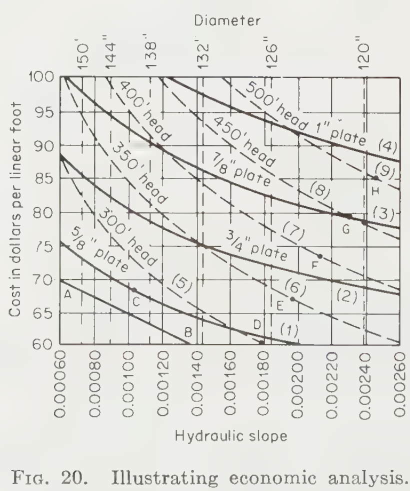

Fig. 20. Illustrating economic analysis.

For low pressures, the economic slope tangent parallel to AB is applied to the lowest permissible plate-thickness curve, the economic slope being marked as at C. For higher pressures, the tangent is applied to the constant-head lines as at D, E, F, G, and H. If these points fall on odd plate thicknesses or diameters, the nearest standard section of sufficient strength may be used.

Instead of plotting the constant-head lines, the permissible heads may be noted at the intersection of commercial plate thickness and standard diameters. The best practical size for any required head is the one of sufficient strength showing the lowest position of the sloping index line.

The best diameter decreases as the head increases. This is a well-known characteristic of deep inverted siphons. If the pipe is to be supported on a bridge, the cost of the bridge, or at least such part of the cost as is dependent on pipe size, must be included in the cost curve.

91. Controlling Elevations. Frequently, the controlling elevation is at neither the outlet nor the inlet but at some intermediate point, as at F (Fig. 21). Economic slopes upstream and downstream from the control are separately determined from the value of head at the inlet and outlet, respectively.

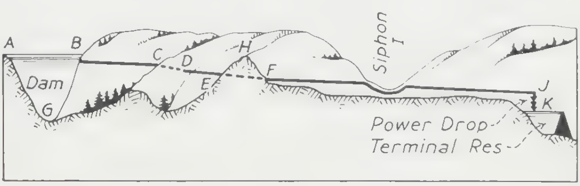

Fig. 21. Illustrating economic analysis.

On the assumption that these slopes have been correctly determined for a tentatively chosen trial position of the control, it is then necessary to determine whether this choice is correct or whether the whole line should be raised or lowered from its trial position. The cost of the lift at the inlet can be reduced by lowering the entire line. The drop at J will be correspondingly reduced, a loss being thus introduced depending on value of head at the outlet. If the cost of head at the inlet exceeds the value of fall at the outlet, lowering the line will effect a net saving in these two items. However, any appreciable lowering will increase the length and cost of the tunnel EF, and the result may be an increase in the total. Raising the line will have an opposite effect. If the trial control is incorrectly chosen, the line must be raised or lowered until some definite change in topographic conditions is encountered. For the conditions illustrated, the tunnel would be shortened only slightly by raising the line but would be greatly increased if the line were lowered. This indicates the pocket at F as a possible control.

The control need not be at the end of a tunnel but may be any point marking a sharp division in construction conditions or costs. For a canal system, it may be a saddle, the boundary of a swampy region, a parcel of expensive right of way, or any of a number of similar obstacles. Raising or lowering the line may increase the cost of features other than the critical feature. Change of ground conditions, due to raising or lowering the line, may change costs throughout. All such factors must be taken into account. This seldom can be done mathematically because of irregularity of physical factors. The procedure is to select a trial control, determine economic slopes, and prepare an estimate to be compared with similar estimates for slightly higher and lower elevations and for other apparent controls.

Sometimes both inlet and outlet elevations are predetermined. If both the height of dam and water-surface elevation at E (Fig. 16) are fixed, the tunnel should utilize all the available slope. The same is true of a long composite line, except that there exists the problem of distributing the slope between the various conduit types. To do this, plot cost-slope curves for all types, as in Fig. 17, then assume a trial value for tan θ' and locate points C, D, E, F, etc., which mark a coordinated set of economic slopes. Apply these slopes to the known conduit lengths, and compute the required fall. If the required fall differs from the available fall, assume a new value for tan θ' and repeat the analysis, continuing until satisfactory agreement is secured. An intermediate control between fixed inlet and outlet levels may divide the line into two parts, for which the slopes are determined separately.

The principles herein outlined are of great assistance in the proportioning of long waterways, but they should not be applied with too great mathematical precision. Cost curves never can be precise. Also, the location of the point of tangency, as at G (Fig. 16) or C, D, E, or F (Fig. 17), is indefinite, and an appreciable variation from the exact value has little effect on the overall economy.

SECTION 8

RIVER DIVERSION

By Arthur P. Geuss

GENERAL

1. Site Limitations. Construction of a dam in a river channel requires that the site be unwatered. The scheme used for the diversion and cutting off the flow often will rank in importance with other project features and may be a major cost item.

Each site will have some limitations. A stream channel may be narrow and deep, wide and shallow, or some combination of these. Depths of alluvium vary widely and these variations must be known. Topography and types of materials are important factors in the selection of a scheme. For example, deep weathering of abutments may preclude the use of tunnels. If tunnels are used, they must have an adequate cover of rock.

2. Type of Dam. Many concrete dams require diversion tunnels of minimum length and capacity with seasonal high flows passed through or over portions of the structures. Some rock-fill dams have been designed so that seasonal flood flows overtop the partially completed fill. With proper design the partially completed fill can stand a certain degree of overtopping without severe damage or failure. The overtopping flow can be maximized by ensuring uniform depth of flow and by the use of cabled mats or fencing anchored to the downstream face and top of the fill. This latter operation may require flattening of the downstream face. In addition, consideration must be given to the differential height of fill and river stage downstream of the fill dam. This type of operation may be feasible during the first season but may entail too much risk of major damage or complete loss of the completed fill if used during the second or subsequent high-flow seasons.

3. Staging. The length of time required for construction, diversion flow capacity, maximum expected stream flow, and layout of structures is a factor that will govern the number of stages or phases of the diversion operations during construction. In some cases only three phases are involved, such as (1) construction of diversion channel, conduit, or tunnel; (2) construction of cofferdams and diversion of stream; and (3) closure of diversion facilities and removal of cofferdams.

Construction on large rivers usually has been accomplished by the in-channel method whereby the cofferdam is extended into the stream to permit construction of a portion of the concrete structures. This cofferdam is then removed to permit flow through the partially completed structure. The remaining portion of the channel is then cofferdammed to allow construction in the river to continue to completion. The seasonal-flow pattern will, in some cases, permit construction of this first cofferdam as two enclosed areas with one area protected against the highest flood flow expected and the other area designed for overtopping of the cofferdam during the flood period. This would cause some interruption of construction operations. However, this would be reduced to the time required for the flood period, pumping out, and clean-up.

DISCHARGE CAPACITIES

4. Limiting Factors. Expected river-flow pattern, length of construction period, limitations of the site, and type of diversion schemes are the principal factors which will influence the selection of diversion capacity. Requirements for passage of upstream fish migrants may limit velocities through diversion facilities and require intermediate resting areas. Maintenance of minimum downstream releases for power, navigation, water supply, recreation, or fish may be required after the diversion facilities are closed.

Capacity and the risk of overtopping must be evaluated. Frequently the entire diversion scheme can become so much a part of the design of the permanent works that the contractor will have little choice except to increase the height of the cofferdam or capacity of the tunnel or channel so as to meet both diversion and ultimate requirements.

TUNNELS

5. Permanent Use of Diversion Facilities. Diversion tunnels or conduits are sometimes designed so that they are utilized as part of the permanent facilities. The conversion to penstocks of the diversion tunnels for Mangla Dam, as described elsewhere, furnishes an example of such use.

Use of a diversion tunnel as a permanent spillway (see Sec. 20) is often controlled by the slope and the resulting limitations on discharge capacity. Preferably the inclined shaft connecting the spillway and the diversion tunnel should have a slope which is not flatter than 45 deg so as to permit excavation by stoping. The head drop from the spillway crest to the tunnel invert will generate velocities that require sufficient slope in the tunnel so that a hydraulic jump will not occur.

Diversion tunnels are frequently adapted to permanent use to supply water to hydraulic turbines or release valves. The grade line of the tunnel for diversion purposes will, in some instances, be found to be higher than that desired if a short connection to the turbines is contemplated. Diversion tunnels have also been adapted to permanent use as a tail tunnel to receive the discharge from the hydraulic turbines in an underground power plant.

6. Diversion-tunnel Hydraulics. Practice varies widely in selecting the design flood. The risk which the contractor and owner are prepared to take is the principal factor in determining diversion capacity. A situation where overtopping during construction would have disastrous results calls for greater conservation than one in which only nominal damage would result. Accordingly, a high concrete dam which could accommodate a substantial amount of overtopping without failure would require relatively less diversion capacity than would an embankment dam of equivalent height. Several examples will illustrate:

The Dworshak Dam, now under construction (1968) on the North Fork of the Clearwater River in Idaho, will be a concrete gravity-type dam having a height of approximately 700 ft. The design of the diversion facilities had three basic requirements:[1,*] (1) to pass a river flow of 68,000 cfs, which is a flood with a 25-year recurrence level; (2) to accommodate the annual log drive which occurs during the high-water period each spring; and (3) to pass upstream migratory fish during construction.

The characteristics of the valley walls indicated that diversion should be accomplished by the construction of a single tunnel through the left abutment. The general plan is shown by Fig. 1, a section through the tunnel by Fig. 2, and a profile by Fig. 3.

It was assumed that logs with a maximum length of 40 ft would be passed between 10,000 and 44,000 cfs with approximately 6 ft of minimum clearance between the

* Superior numbers refer to items in the Bibliography at the end of this section.

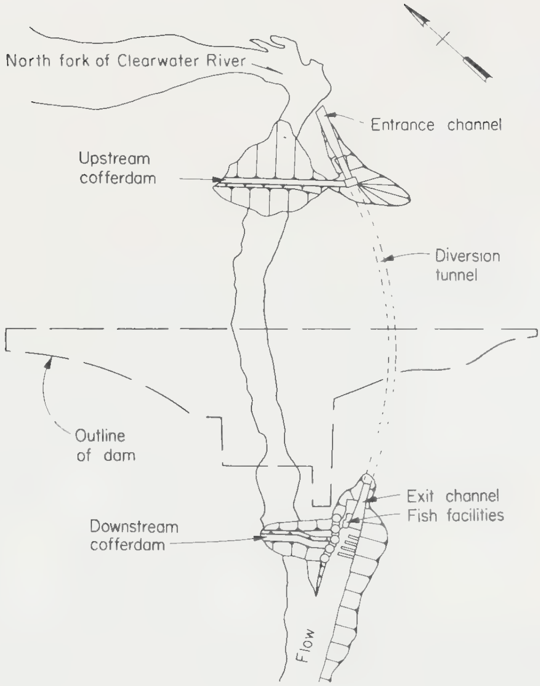

FIG. 1. General plan of diversion facilities.

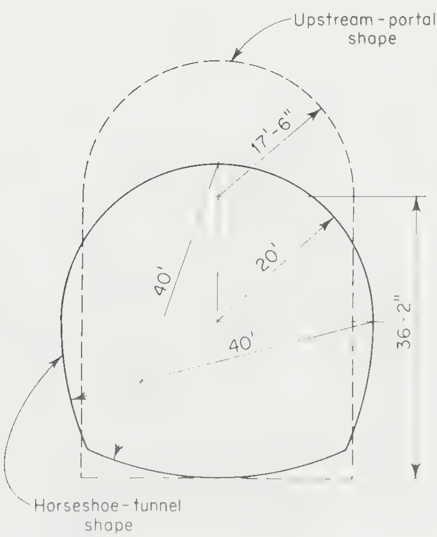

FIG. 2. Cross section of tunnel.

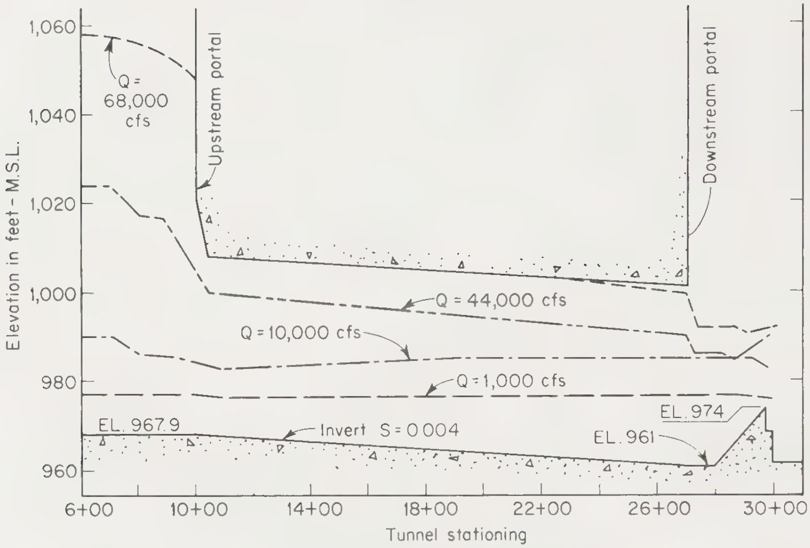

FIG. 3. Diversion-tunnel water-surface profiles.

water surface and the roof along the center line of the tunnel. The smooth concrete lining is expected to reduce any erosion resulting from high-velocity flow or abrasion from passing logs. Mean velocities as high as 52 fps are anticipated for the conditions of design flow. In computing the head loss due to friction in the tunnel a value for Manning's n of 0.011 was used for concrete. The pool elevation was computed for the design discharge of 68,000 cfs with an n value of 0.013. It is recognized that a period of service may increase the value of n. Generally, energy-dissipation works should be designed for the discharge conditions arising from a low friction coefficient resulting from the most favorable conditions, whereas discharge capacity should be designed for the most unfavorable conditions that will exist after the tunnel has been in service for a time and perhaps roughened by the passage of logs or gravel.

Prototype experience in passing large floods through both concrete-lined and unlined diversion tunnels has revealed that average discharge velocities ranging from 50 to 75 fps have resulted in little or no damage to the contact surfaces. A few examples of prototype performance will illustrate.

Of especial interest is the performance of the diversion tunnels of the 770-ft-high embankment dam now (1968) nearing completion on the Feather River in California.[2]

The left abutment of this dam will contain an underground power plant which will have a total capacity of 644 mw. Two concrete-lined, 35-ft-diameter diversion tunnels will parallel this underground structure and following diversion will be converted to tailraces for the power plant. Each of these tunnels is approximately 4,500 ft long. Figure 4 shows a plan of the tunnels. The reservoir surface will normally vary between elevation 730 and 790. The reservoir has a total capacity of 3,484,000 acre-ft.

When all power-plant units are operating at the maximum total discharge of 16,500 cfs, the velocity in each tunnel will be 11 fps. During diversion, however, velocities in excess of 75 fps were encountered. As a basis for design, the rugosity value ϵ (epsilon) of concrete was selected as 0.0004 and the Darcy-Weisbach f of 0.0083.

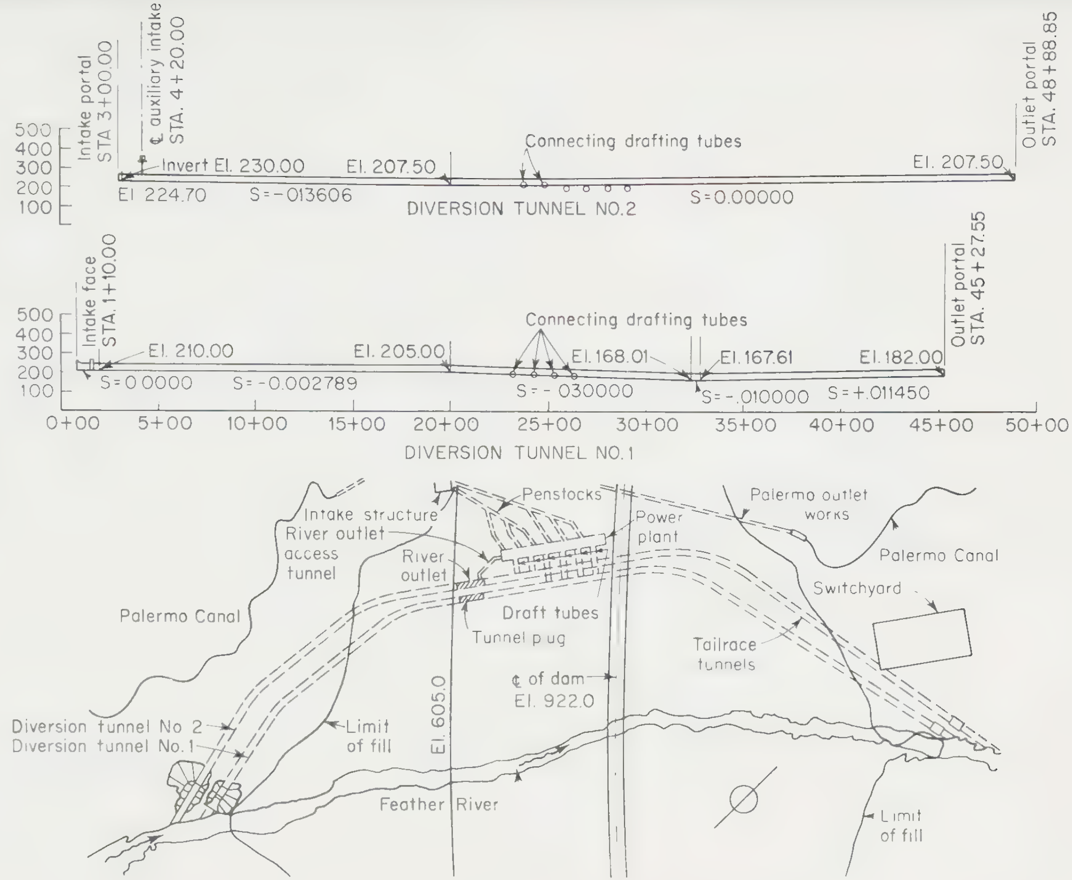

FIG. 4. Plan and profile of Oroville Dam diversion tunnels.

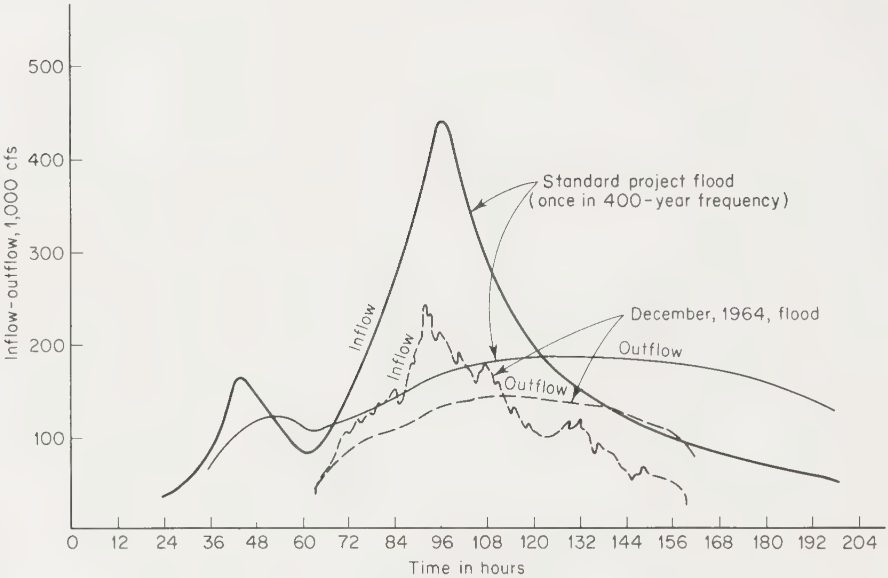

FIG. 5. Oroville Dam and reservoir—estimated and actual flood.

Initial entrance losses were assumed to be $0.20(V^2/2g)$. Measurements from model tests, however, revealed that these losses would be $0.10(V^2/2g)$ for tunnel 1 and $0.05(V^2/2g)$ for tunnel 2. In the model tests the entrance loss in tunnel 1 rose to $0.13(V^2/2g)$ when vortices formed between 30,000 and 60,000 cfs in the tunnel. The entrance to tunnel 1 is provided with a rectangular to circular bellmouth 95 ft long. A central dividing pier is designed to accommodate a pair of steel bulkhead gates for closure. The entrance to tunnel 2 is a circular bellmouth placed 20 ft higher than that of tunnel 1.

During December, 1964, the partly completed dam was subjected to a flood greater than any known flow on the Feather River for a period in excess of 100 years. At that time, the upstream section of the embankment, essentially a 415-ft-high diversion dam, and the two diversion tunnels were in operation. At the peak of the flood the two diversion tunnels were discharging a combined flow of 145,000 cfs at an average velocity of about 75 fps. Figure 5 shows a comparison of the computed inflow and outflow of the standard project flood with those of the December, 1964, flood. Figure 6 shows a comparison of rating curves for reservoir elevations and discharge as developed from preliminary estimates, hydraulic-model studies, and prototype operations. It will be noted that the reservoir level required to discharge the 1964 flood was substantially lower than the levels indicated by either the design calculations or the model tests. The amount of overall damage to the tunnel was found to be extremely light, with probably 90 percent or more of the tunnel's surface texture substantially intact.

During operations the emerging water remained in a cylindrical jet for some distance past the end of the side walls. Extreme turbulence existed at least 500 ft downstream from the tunnels.

The 15-m- or 50-ft-diameter concrete-lined diversion tunnel of the Shihmen Reservoir project, located in the northern end of Taiwan, discharged 3,800 cms (134,000 cfs) at a velocity of about 72 fps during typhoon Pamela on Sept. 12, 1961.

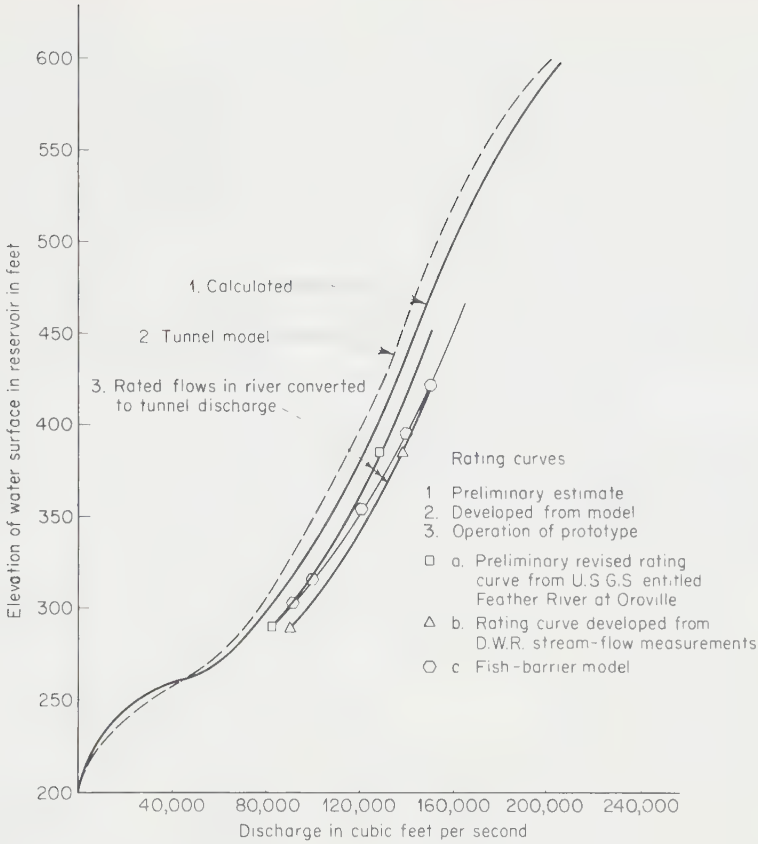

FIG. 6. Oroville Dam and reservoir; diversion-tunnel discharge rating curves.

The concrete lining of the tunnel was not damaged. A section through the tunnel is shown by Fig. 7 and a photograph of the discharge conditions during the Pamela flood by Fig. 8. The tunnel was designed to pass the maximum recorded flood having an estimated peak discharge of about 5,170 cms, or 183,000 cfs. Routing this flood through the tunnel resulted in a maximum pool level of 181 m. The top of the upstream cofferdam was elevation 190 m. Overtopping this cofferdam would require a flood of about 5,500 cms, or 194,000 cfs, which had a return period falling between 50 and 60 years according to recorded peak flows.

The Shihmen project consists of a 420-ft-high cobble-gravel embankment dam, a gated chute spillway, two individually controlled 15-ft-diameter tunnel penstocks, irrigation and river outlets, and a powerhouse with two 50,000-kva units.

The satisfactory results obtained during the prototype operations of concrete-lined diversion tunnels discharging at high velocities appear to be related to the acceptance in several proposed projects of design velocities ranging from 75 to 100 fps. Design criteria based on high-velocity discharge, however, must also be related to the relative smoothness of the tunnel lining. With workmanship of poor quality resulting in offsets at the lining joints and rough tunnel surfaces, such high velocities could result in the destruction of the tunnel lining.

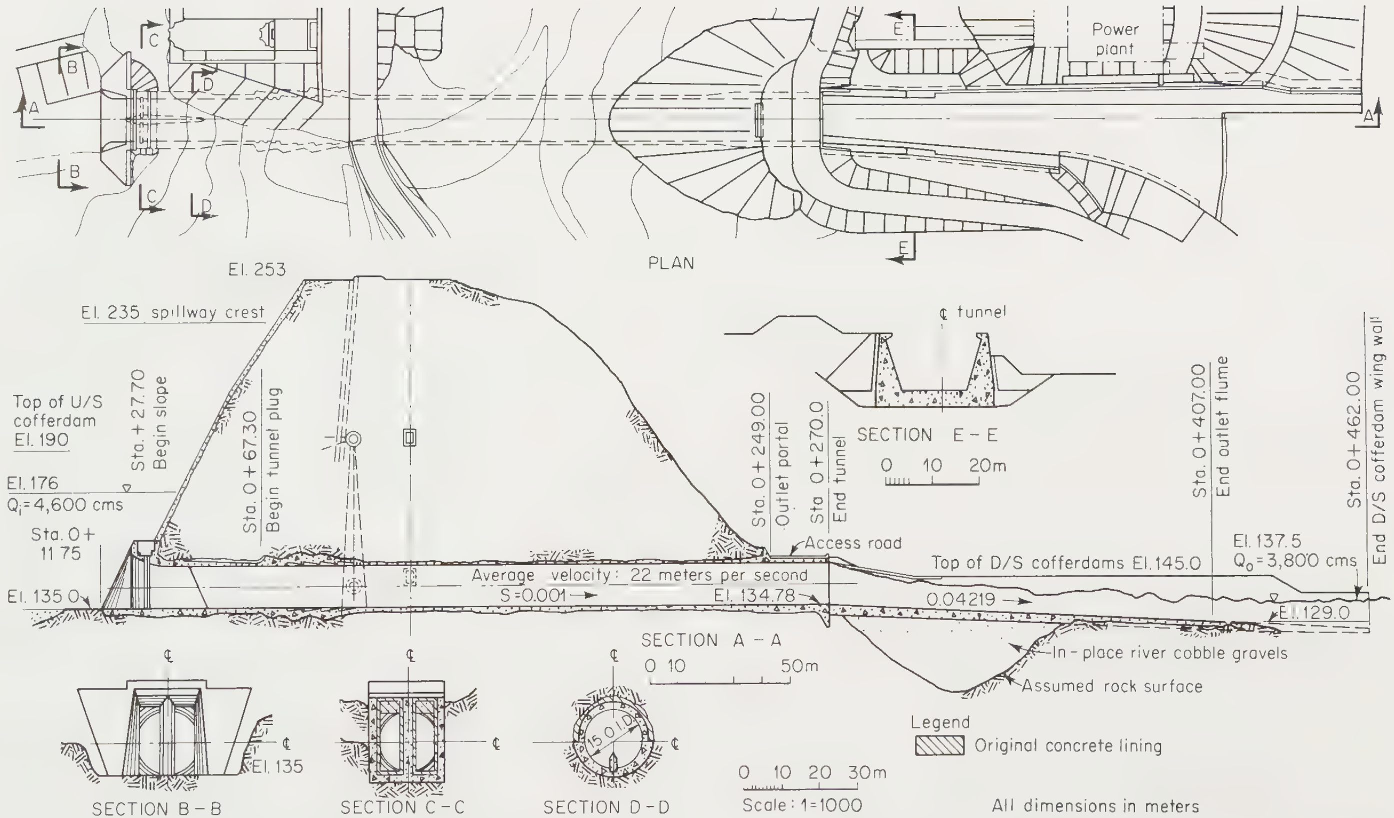

FIG. 7. Shihmen Reservoir project—section through tunnel. (*Courtesy of Tippetts-Abbett-McCarthy-Stratton, Consulting Engineers, New York.*)

FIG. 8. Shihmen Reservoir project—typhoon Pamela, discharge conditions. (*Courtesy of Tippetts-Abbett-McCarthy-Stratton, Consulting Engineers, New York.*)

Quality of workmanship was an important factor in designing the diversion tunnels for the 400-ft-high Mangla dam, an embankment-type structure completed in 1967 on the Jhelum River, West Pakistan, by the West Pakistan Water and Power Development Authority.[3,4]

A study of recorded discharges of the River Jhelum disclosed that flood peaks in excess of 1 million cfs could occur during the months of July and August. It was determined that a flood of 1,240,000 cfs, having a return period of approximately 73 years, could be passed by five 30-ft-diameter diversion tunnels, each about 1,900 ft ong, located in the left abutment, with a closure dam level of 1,080 (approximately

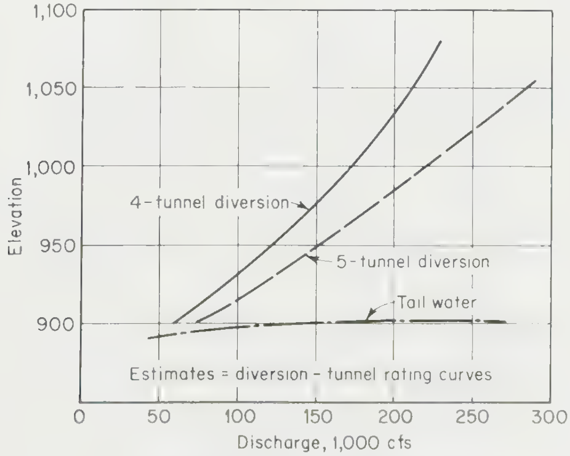

FIG. 9. Mangla Dam—estimated rating curves.

65 ft above the stream bed) before the cofferdam would be overtopped. Estimated rating curves are shown by Fig. 9.

To meet power-production requirements, tunnels 1 and 2 were lined with steel during the diversion period, thus reducing their diameters from 30 to 26 ft. For design purposes discharge rating curves had been calculated on the basis of both high and low loss coefficients to indicate the possible range. According to the computations, an occurrence of the design flood would result in a discharge of approximately 300,000 cfs, through five tunnels, before the embankment would be overtopped. The tail-water level at this discharge was approximately 900. Tunnels 1 and 2 were steel-lined. After being in service for a short period, tunnel 1 was closed and the remainder of the construction was completed with four tunnels in service.

During diversion a rating curve was derived from observation of pressures in concrete-lined tunnel 3 through flows in the river which ranged from 100,000 to 130,000 cfs. These observations indicated an overall discharge coefficient for the four tunnels in operation, with the minimum loss coefficients taken for design. The results of these measurements were consistent with a friction coefficient f of 0.006 in the Darcy-Weisbach formula (see Sec. 2). Reynolds number was approximately 1.2×10^8. Because it was impossible to isolate the steel-lined tunnel 2 from the remaining concrete-lined tunnels 3, 4, and 5, the foregoing observations must be considered as approximations.

The dual use of the Mangla tunnels for both irrigation and power introduced several hydraulic problems which would not be dealt with ordinarily in designing tunnels for diversion alone. To meet the power requirement the slope of the tunnels was such that high-energy hydraulic jumps would form under low- and intermediate-flow conditions. To control the resulting undesirable effects and to keep the tunnels under positive pressure under all flow conditions, an inflatable dam was constructed in the tailrace. During river closure this dam was deflated to give the lowest possible tail-water level, thereby easing the actual closure operation.

Surprisingly high velocities have been passed without damage by unlined tunnels in rock. For example, the 25-ft-diameter horseshoe, 530-ft-long diversion tunnel for the Mayfield Dam, a 200-ft-high concrete dam constructed on the Cowlitz River in the state of Washington, passed during the flood of Apr. 7, 1962, a flood of 30,000 cfs. The average area of the tunnel, including overbreak, was about 600 sq ft. The average velocity was approximately 50 fps. The rock through which the tunnel was driven was a sound basalt. No damage was observed.

7. Diversion-tunnel Plugs. In many cases temporary tunnel closure is effected by lowering gates or stop logs at the upstream portal. This operation is followed by pouring concrete plugs some distance down. Two types of plugs are illustrated by Fig. 10*a* and *b*. Figure 10*a* shows longitudinal and transverse sections of the plug in the diversion tunnel for the 600-ft-high Mossyrock Dam on the Cowlitz River. Figure 10*b* shows a longitudinal section of the diversion tunnel built at Angat (Philippines) through which gate-controlled irrigation releases can be made. Where concrete lining is provided, it is customary to serrate a section of the lining, as shown by Fig. 10*c*, to provide increased shearing resistance against water pressure.

COFFERDAMS

8. Design. A cofferdam must be designed as a temporary dam. The type used is governed by the materials available and by foundation and placement problems.

In the past many cofferdams have been constructed in the form of timber cribs. Earth or rock fill or filled sheetpile cells are at present used most frequently. Timber cribs are usually floated into place and then filled with rock or cobbles. Watertightness is achieved by the use of wood plank and canvas. Alluvium overlying the top of

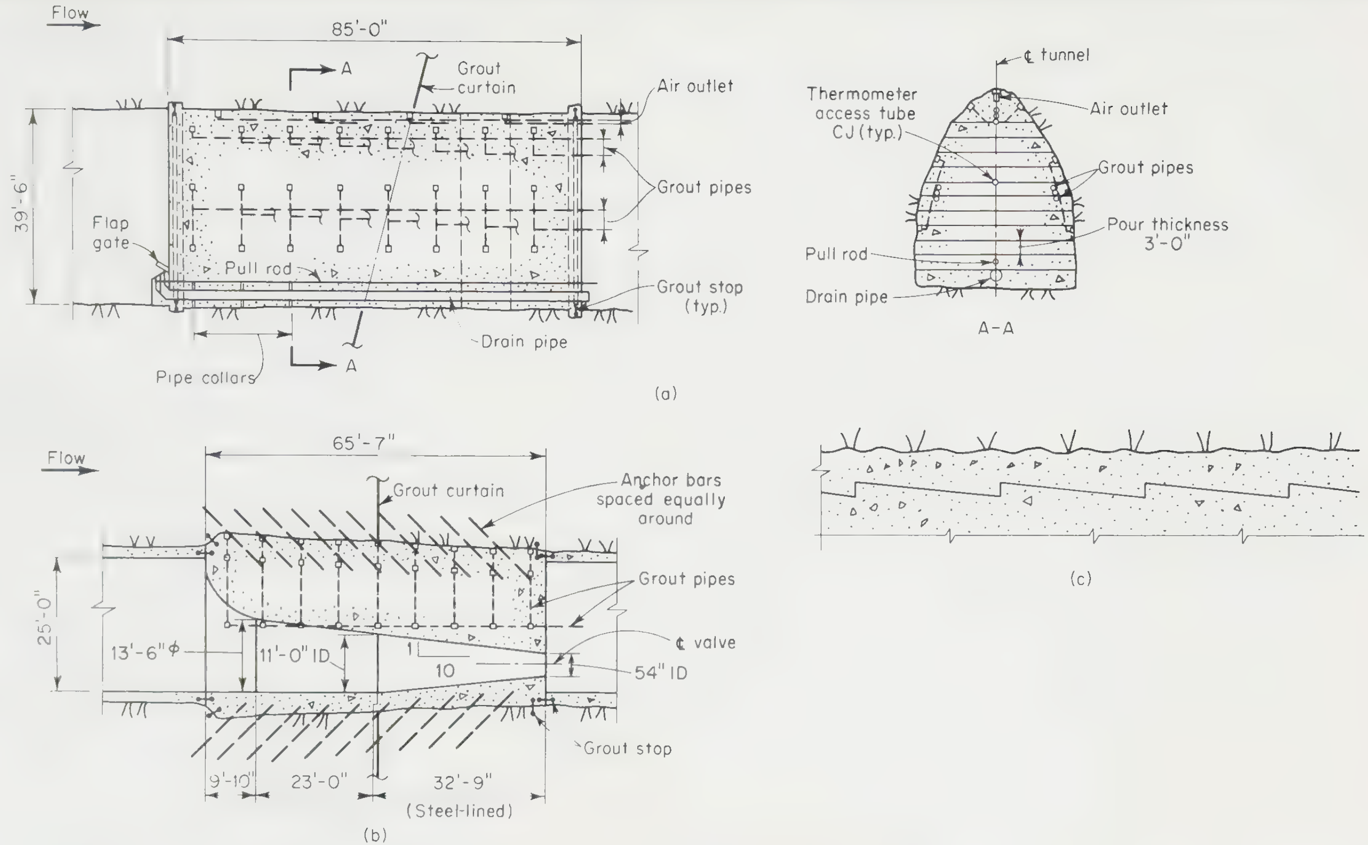

FIG. 10. (*a*) Mossyrock Dam—longitudinal and transverse sections of the plug in diversion tunnel. (*b*) Angat (Philippines)—longitudinal section of the diversion tunnel. (*c*) Serrated tunnel lining in vicinity of closure plug.

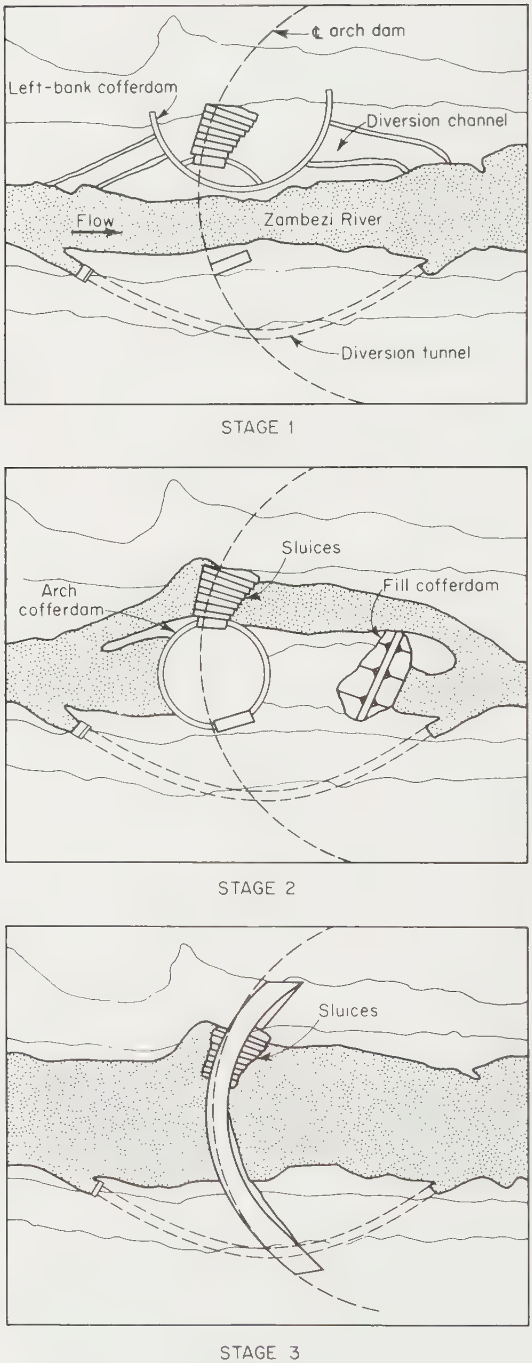

Fig. 11. River diversion at Kariba Gorge Dam.

a rock foundation should be removed prior to placement of the cribs, which are constructed with a bottom that approximately fits the rock surface. Fill or blanketing material is then placed at the upstream heel to reduce leakage through this contact.

Steel sheetpiling is most commonly used to construct circular cells which are connected to one another to form a barrier. Filling material is usually gravel or sand which has sufficient shear strength and can be readily removed. When filled, the pressure of the fill material will develop tension in the interlocks sufficient to provide watertightness. Proportions of the cells are determined by strength of the interlocks and shear resistance of the fill material. A straight single row of sheetpiling will serve as a cofferdam, if adequately braced. Seepage through the interlocks can be minimized by the application of mastic in the interlocks prior to driving. A cellular cofferdam, placed in a hard foundation that will not permit driving, must be sealed on the bottom to prevent piping of fill material. Frequently a layer of tremie concrete is placed prior to placement of the fill material. Measures also must be taken to ensure that the cofferdam is adequately tied to the abutments.

Seepage through or under the cofferdam and through the abutments will, of course, dictate the rate and extent of pumping required during construction. Crib and cellular cofferdams are usually protected against overtopping by placement of large stone or rock on top of the fill, since finer materials will be removed by the overtopping flow. The top portion of the fill material can be designed as a layered filter, which will minimize the loss. Occasionally, cellular cofferdams are capped with concrete for this purpose.

Large rock on the top and downstream slope of a fill cofferdam will resist erosion to some extent. This loss can be minimized by placing a heavy netting on these surfaces. The netting is held in place by anchors in the fill. Damage will be greater if the overtopping flow is concentrated rather than spread over the longest possible length of the cofferdam.

Debris should be controlled to minimize the damage of plugging of diversion tunnels or conduits. The upstream watershed may produce considerable quantities of debris during high-flow periods, particularly if clearing of the reservoir is in progress. Floating drift and debris can be controlled to some extent by long booms extending

FIG. 12. Closure of river at Fort Randall Dam (South Dakota).

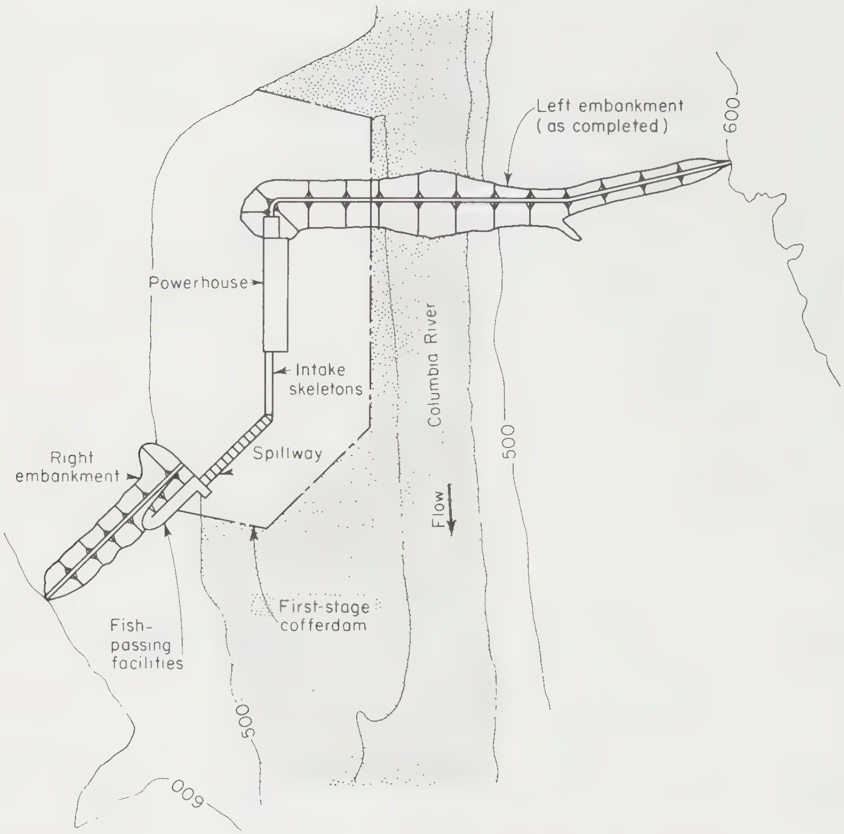

FIG. 13. Wanapum Dam project (Washington)—river diversion.

across the river channel. If placed in a reach of the river where velocities are lower, a log beam can be very effective. A log beam will not control debris that is moved along the river bottom.

DIVERSION SCHEMES

9. Illustrative Examples. Because each project requires individual treatment, it is difficult to illustrate the basic principles of river-diversion planning and design with descriptions of actual schemes. Outlines of several may be of interest, however, as an indication of the wide variety of designs which must be developed in response to the conditions which were encountered at specific sites.

Figure 11 shows river diversion at Kariba (Rhodesia). During stage 1, the Zambezi River was not diverted from its natural channel while work proceeded on both banks of the river. On the left bank a diversion channel was excavated and a thin arch cofferdam built to protect the construction of several blocks of the dam on the bank. On the right bank, a diversion tunnel was excavated and a block of the dam concreted. During stage 2, the river was diverted through the sluice openings and the diversion tunnel. A circular concrete-arch cofferdam was built to permit placement of concrete in the river bed. During stage 3, the diversion tunnel was

FIG. 14. Wanapum Dam project (Washington)—river diversion.

closed while river diversion continued through the sluice openings. Placement of concrete then proceeded on all blocks of the dam.

Closure of the river at Fort Randall (South Dakota) (Fig. 12) was made by hydraulic placement of a combination sill-weir section of dredged chalk fill up to about 1 ft above water level. The diversion dam thus created was then built up to about 20 ft above upstream water level by end-dump trucks. The entire flow of the river was then diverted through the power tunnels previously excavated and concreted on the left bank of the river. The sill-weir section was built up at a uniform rate along the entire length of about 1,000 ft. This method avoided the classic choking of the stream with the attendant scouring action. All material was pumped into place by a 30-in. dredge; sizes of chalk rocks were up to 18 in. with about 30 percent larger than 6 in. River flow at time of closure was about 30,000 cfs.

At the Wanapum project (Washington) (Fig. 13), during stage 1, the Columbia River was not diverted from its natural channel. A fill cofferdam was built on the right bank to protect the area on which the major elements of the project are built (right-bank embankment and fish-passing facilities, spillway, intake skeletons, power plant, and part of the left-bank embankment).

During stage 2, the river was diverted through the completed facilities on the right bank and the natural channel was dammed by a fill embankment (see Fig. 14). Large rocks were dumped into the flow to complete closure of the river (left foreground). The first-stage cofferdam is shown removed by dragline (left center). Part of the river flow is being passed through six skeleton intakes provided for future extension of the powerhouse (center).

Bibliography

1. PEARCE, ROBERT O., Hydraulic Design of Dworshak Dam Diversion Facilities, *Proc. ASCE, J. Hydraulics Div.*, January, 1968.
2. LANNING, CORTLAND C., Oroville Diversion Tunnels, *Proc. ASCE, J. Power Div.*, October, 1967.
3. THOMAS, A. R., and J. R. GWYTHER, Diversion of the River Jhelum during Construction of Mangla Dams, Ninth International Congress on Large Dams, Istanbul, 1967, Q 33, R9.
4. BINNIE, F. M., et al., Mangla Dam, Paper 7063, *Proc. Inst. Civil Engrs.*, November, 1967.

SECTION 9

CONCRETE DAMS, BASIC PRINCIPLES OF DESIGN

By Calvin V. Davis

STRUCTURAL CHARACTERISTICS

1. Gravity and Buttress Dams. Certain basic principles of design which are common to the concrete types are discussed in this section. In some cases, with successive modifications, one structural type may be evolved into another. To illustrate, starting with the typical gravity type (Fig. 1), the evolutionary process has followed three paths: The first has led to the buttress type with its many variations. The second has led to the arch-gravity and to the various arch types. The third has led to the recently developed flexible gravity dam.

The stability of the gravity-type dam depends principally upon the weight of the concrete. The usual steep batter on the upstream face does provide a relatively small stabilizing vertical water load as shown by Fig. 1. Transverse joints frequently are not grouted. In such cases each block is able to adjust to its own load, and the small openings between blocks provide some opportunity for drainage and for the reduction of uplift pressures.

If each block is free to act independently there is no reason why the openings should not be made larger and thus provide even more positive relief from uplift. The 370-ft-high Albinga Dam, constructed in 1959 for the city of Zurich, Switzerland, offers a

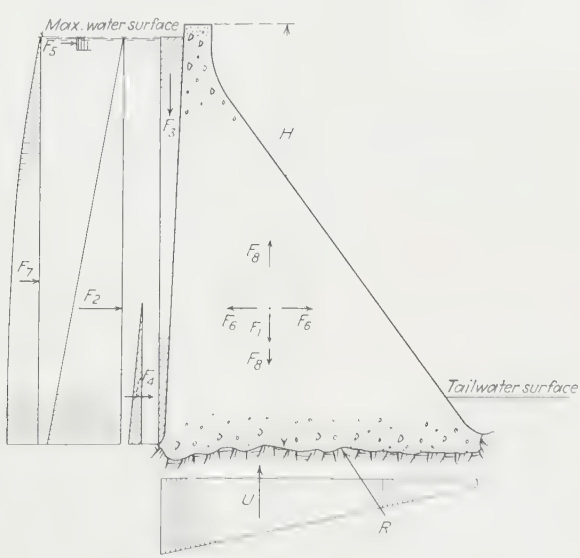

Fig. 1. Typical gravity dam.

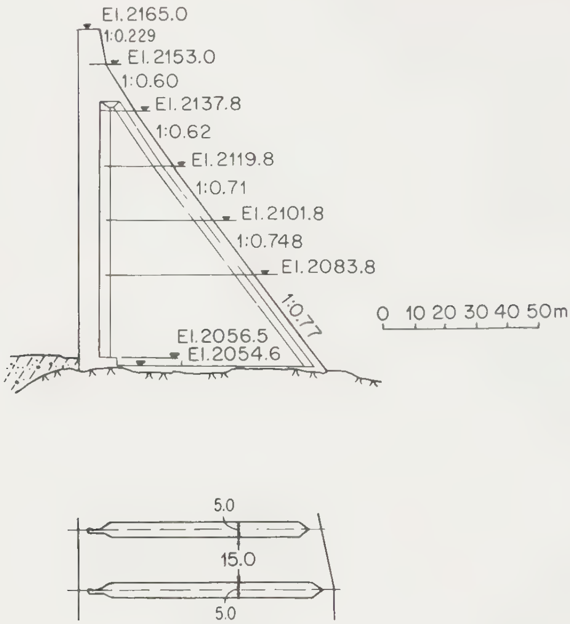

FIG. 2. Albinga Dam vertical and horizontal cross section. (*From "Behavior of Large Swiss Dams," p.* 116, *Swiss National Committee on Large Dams,* 1964.)

good illustration of a feature which has been incorporated in several dams in Switzerland. Figure 2 shows typical sections. The blocks are spaced 66 ft on centers. The openings between the blocks are approximately 16 ft wide. In 65 drainage boreholes drilled in the foundation between the hollow spaces of the joints and from the galleries the uplift pressure has been measured monthly. Most of the measuring points show little or no uplift pressure.

The Albinga design illustrates the first step in the evolutionary process which leads to the development of the buttress type. Should the openings between the blocks be made substantially wider there would result a cored-gravity or massive-buttress-type dam, as shown by Fig. 3 and further described in Sec. 12. In this case some compensation would be provided for the loss of weight of the concrete by sloping the upstream face.

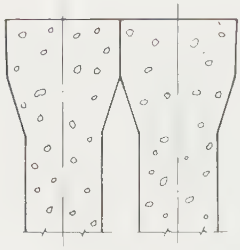

FIG. 3. Typical cored-gravity type.

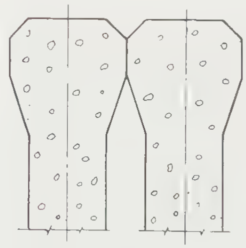

FIG. 4. Typical cored-gravity type.

The water-bearing upstream face may take several forms. In one, the massive buttresses are flared to form contiguous heads which are provided at midspan with adequate contraction joints and water stops. Three variations are shown by Figs. 3 to 5, inclusive.

Another provides a deck which spans the buttresses. For example, Fig. 6 shows the deck and haunch construction which is typical of the Ambursen type (see Sec. 13) and Fig. 7 shows the multiple-arch type (see Sec. 15).

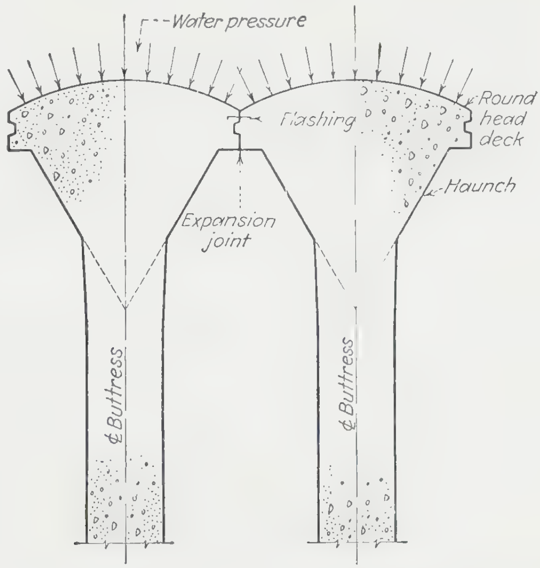

FIG. 5. Typical round-head buttress type.

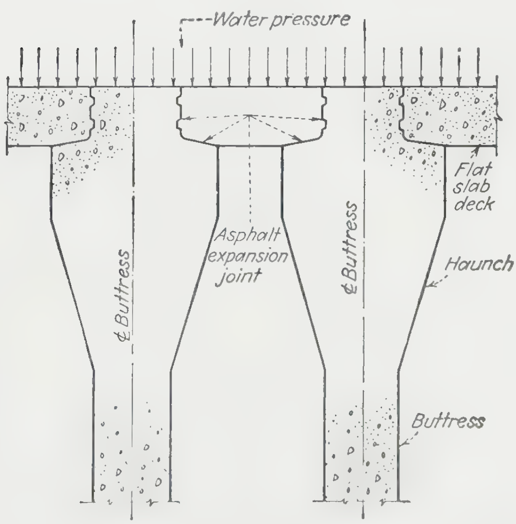

FIG. 6. Typical Ambursen massive-buttress type.

By continuing this evolutionary process, buttresses may be made progressively thinner with compensating stabilizing vertical water loads provided by flattening the upstream buttress slopes. There are economic limitations. For example, buttresses having slopes flatter than 7 horizontal to 10 vertical may develop tensional stresses in planes of second principal stress, which are nearly parallel to the upstream face just below the bearing surface. As the buttresses become progressively thinner, steel and form costs increase. Buttress spacings have ranged from 18 ft center to center for Ambursen dams to 250 ft center to center for multiple-arch dams. For the 200- to 600-ft-height range it has been found to be more economical to provide buttress spacings from 50 to 60 ft center to center for the cored-gravity or massive-buttress head types. For multiple-arch dams falling within this height range, comparative studies have demonstrated that wide spans, ranging from 200 to 300 ft, are the most economical.

2. Gravity and Buttress Dams, Relative Economy. Reference to Fig. 8 will demonstrate the principles discussed previously, as applied to dams ranging up to 250 ft in height. The comparison is based on the concept that both the gravity dam and the buttress dam may be envisioned as consisting of contiguous elementary

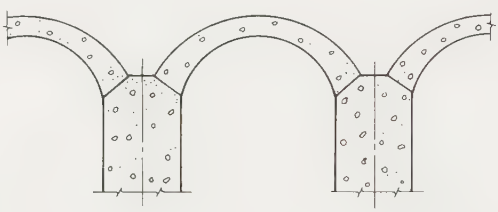

Fig. 7. Typical multiple-arch type.

inclined columns, each of which transmits an increment of the water load from the upstream face through the dam to the foundations. The force polygon for the column *A*, *B*, *C*, *D*, *E* (Fig. 8*a*) illustrates how the horizontal water pressure against the face of a gravity dam must be counterbalanced by a relatively large concrete weight in order to direct the load line close to the axis of the column.

In contrast, the direction of the inclined water load supported by column *A*1, *B*1, *C*1, *D*1, *E*1 (Fig. 8*b*) of the buttress dam falls very close to the axis of the column, with the result that the concrete serves efficiently to transmit, through the dam to the foundations, its increment of load in compression, and the incremental vertical weight of the water load replaces a large part of the weight of the concrete.

The effects on the volume of concrete are shown by Fig. 8*c*. In regard to the Ambursen type, it will be noted that there is little difference in concrete quantities between design *A*, having a buttress spacing of 40 ft center to center, and design *B*, having a buttress spacing of 18 ft center to center. Design *C*, a round-head type (see Fig. 5) with a buttress spacing of 50 ft center to center, contains more concrete per lineal foot of dam than either of the two Ambursen designs (designs *A* and *B*) but will require little or no reinforcing steel. The radial surfaces of the round heads minimize bending moments and resulting tensional stresses. There would be little difference in the cost of designs *A*, *B*, and *C*, but each would cost less than the typical gravity dam, design *D*. The conclusions that may be drawn from these and other studies made within the 250-ft-height range are (1) the massive-buttress designs, with thick buttresses and wide buttress spacings, will be more economical to build than the thin-buttress designs with close buttress spacings; and (2) the cost of the

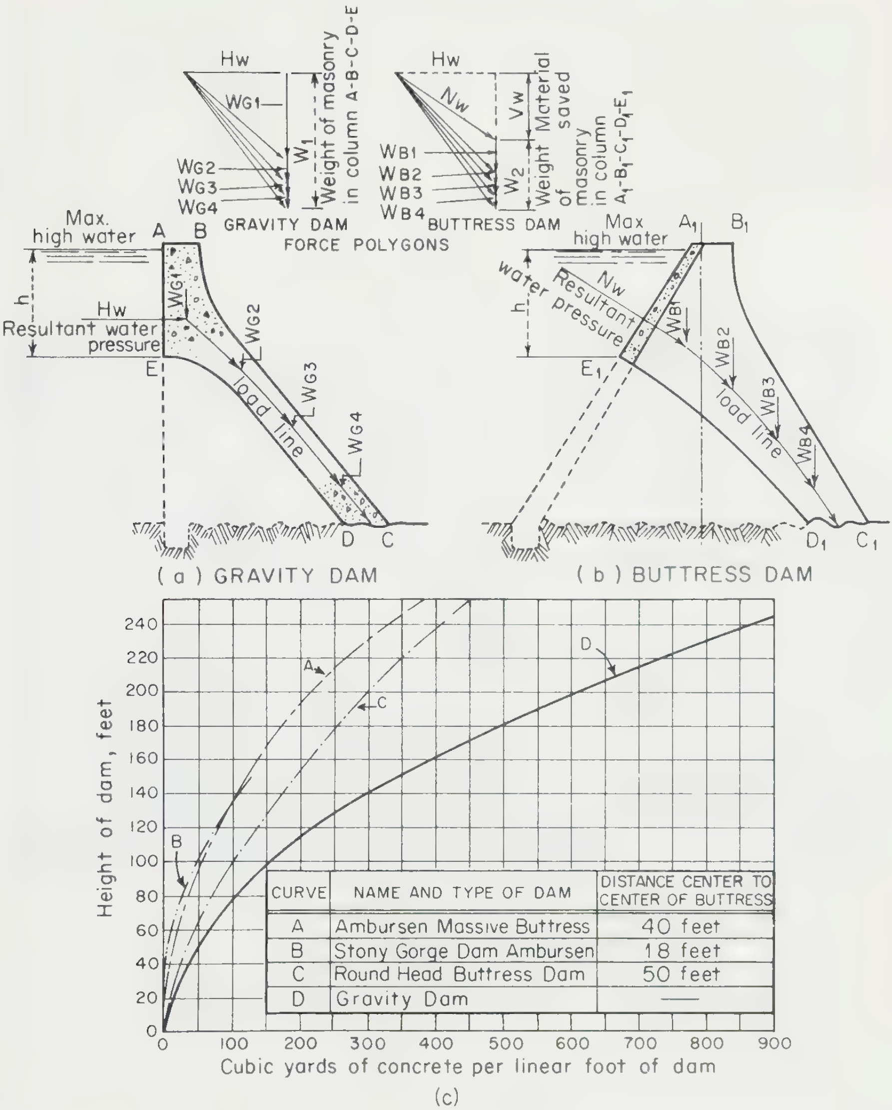

FIG. 8. Comparison of loading action and quantity of materials in gravity and buttress dams.

buttress designs, both thin and massive, will be less than that of an equivalent gravity dam.

The structural and economic merits of the massive-buttress principle have received wide recognition in Europe and the British Isles. For example, the Nant-y-Moch Dam of the Afon Rheidol River in Wales illustrates the application of this principle to the design of a dam having a maximum height of 172 ft and an overall crest length of 1,150 ft.[1]

[1] The Rheidol Scheme, *Water Power*, December, 1963, p. 491.

Figure 9 shows the upstream elevation and Fig. 10 a section at maximum height. The dam consists of 10 buttresses, spaced 65 ft center to center, which vary in thickness from 23 ft at the crest to 26 ft at maximum height. Except for the very steep batter on the upstream face, the outlines shown by Fig. 10 approximate those of a gravity dam. The buttress heads have elliptical downstream faces.

Comparative studies for gravity- and massive-buttress-type dams having heights ranging from 250 to 600 ft reveal that the massive-buttress types will have concrete volumes which fall somewhere between 65 to 75 percent of the volume of an equivalent gravity dam. To illustrate, Fig. 11 shows the outlines of a cored-gravity-type structure having a maximum height of nearly 600 ft and a base width of 570 ft. The buttress heads are placed on a flat arc and are spaced 65 ft 6 in. center to center at the

FIG. 9. Nant-y-Moch Dam. (*The Rheidol Scheme, Water Power, December*, 1963, *p.* 491.)

crest. Buttress thicknesses vary from 20 ft at the top to 43 ft at the foundation. The maximum principal stress of 700 psi occurs at the downstream face at the foundation.

The massive multiple-arch structure shown by Fig. 12 is of the same height but has buttresses spaced 200 ft center to center. These vary in thickness from 40 ft at the top to 104 ft at the foundation. The maximum principal stress occurs near the foundation at the downstream face and is also about 700 psi. Both structures approximately meet the same design criteria. Admittedly both are conservatively designed, and the use of thinner sections would have been permissible under different site conditions.

Figure 13 shows quantity curves which compare the concrete quantities per lineal foot of dam for the structures shown by Figs. 11 and 12 with those of the Grand Coulee Dam (Sec. 11) which may be characterized as a conventional, conservative gravity-type dam which meets approximately the same design criteria.

In recent years there has been a tendency to increase the maximum allowable principal stresses to as high as 1,500 psi in arch and multiple-arch-type dams. If advantage were taken of this higher allowable stress the volume of concrete in the multiple-arch dam would be less than half of that in the gravity dam.

3. Gravity, Curved-gravity, and Arched Dams. Curving the axis of a gravity-type dam introduces a three-dimensional effect on the distribution of loads: some part of the loading is transferred to the horizontal arch elements, with the result that the loads on the vertical cantilever elements are lessened. The effects of introducing increasing degrees of curvature in the axis of a gravity dam may be illustrated by the results of a comparative study shown by Fig. 14 for design A, a conventional gravity

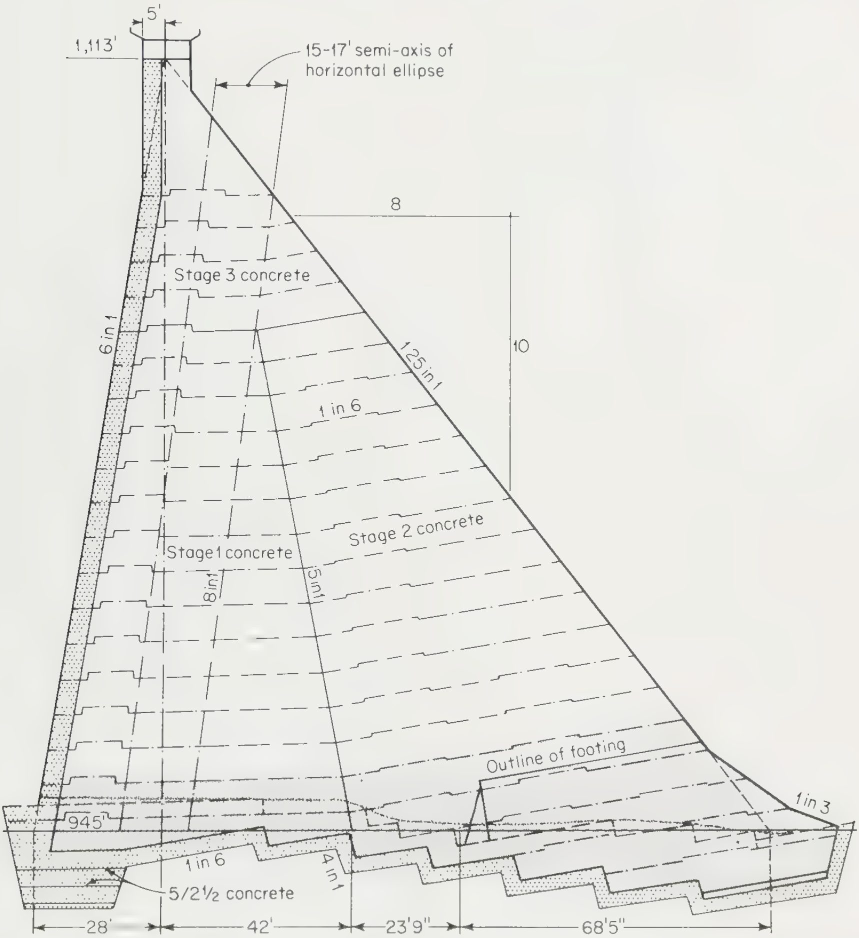

FIG. 10. Section of typical buttress at Nant-y-Moch showing concreting details. (*The Rheidol Scheme, Water Power, December*, 1963, *p.* 495.)

dam; design B, a curved- or arched-gravity dam; and design C, an arch dam supplemented by thrust blocks. Ordinarily, this site would be considered more suitable for a gravity or curved-gravity dam than for an arch. The gravity dam (design A) has a maximum height of 600 ft and an overall crest length of approximately 2,400 ft.

The transfer of water loads from vertical cantilever elements to horizontal arch elements permits the batter of the downstream face of the arched-gravity dam to be reduced from 7.5 horizontally to 10 vertically for design A, to 5 horizontally to 10 vertically for design *B*. The total volume of concrete was correspondingly reduced from 4.2 million cu yd in design *A* to 3.7 million cu yd in design *B*. The corresponding reduction in cost was only about 5 percent. Within present limits of estimating accuracy, designs *A* and *B* could be considered equal in cost.

In design *C* the radii of curvature have been shortened and the central angles

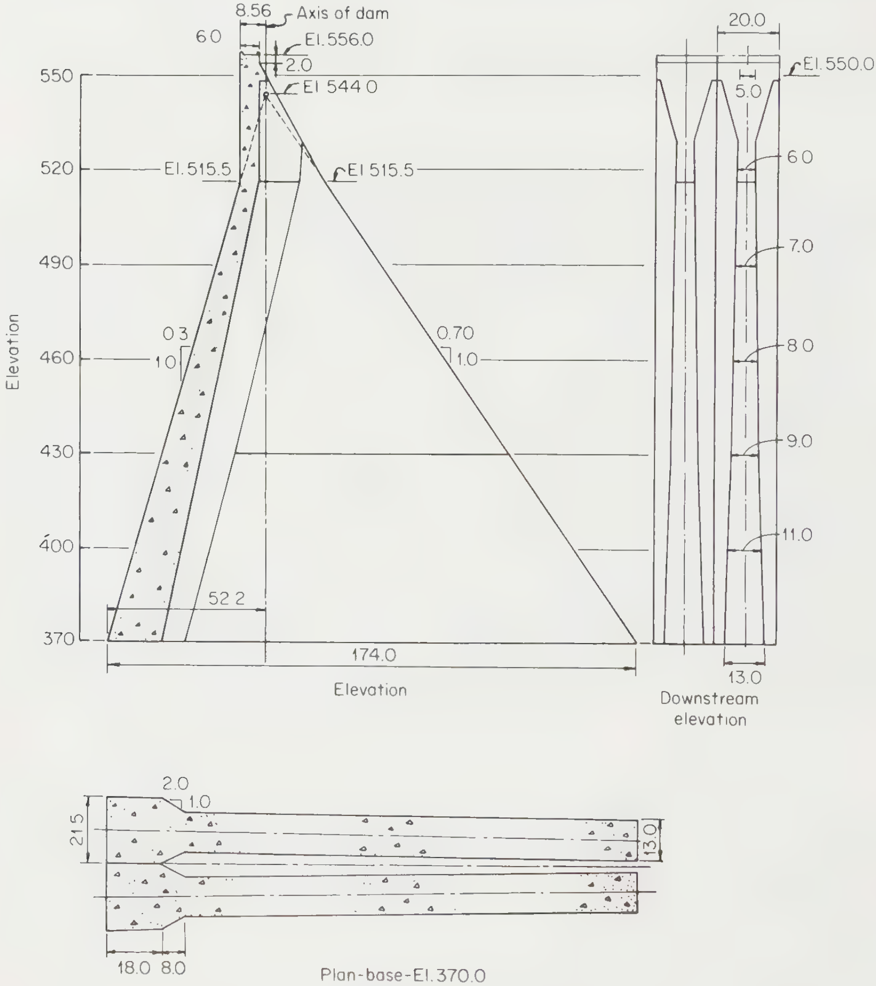

FIG. 11. Cored-gravity dam. *Note:* dimensions in meters.

increased. Supplementary thrust blocks flanked by gravity sections were required at the abutments. The total concrete required for design *C* was 2.7 million cu yd or about 64 percent of the concrete required for a straight gravity dam. Because of more complicated formwork there was little saving in cost when compared with that of the gravity dam. In this particular study the characteristics of the profile were dominating factors in cost determination. These characteristics required the introduction of compensating structural elements, which largely offset the savings inherent in the arch and arch-gravity types.

With topography more favorable for the arch type than that shown by Fig. 14 much greater savings, as compared with a conventional gravity dam, can be achieved. In relatively narrow U- or V-shaped canyons the arch may be shaped to transfer the greater part of the water loads to the horizontal arch elements and thus achieve

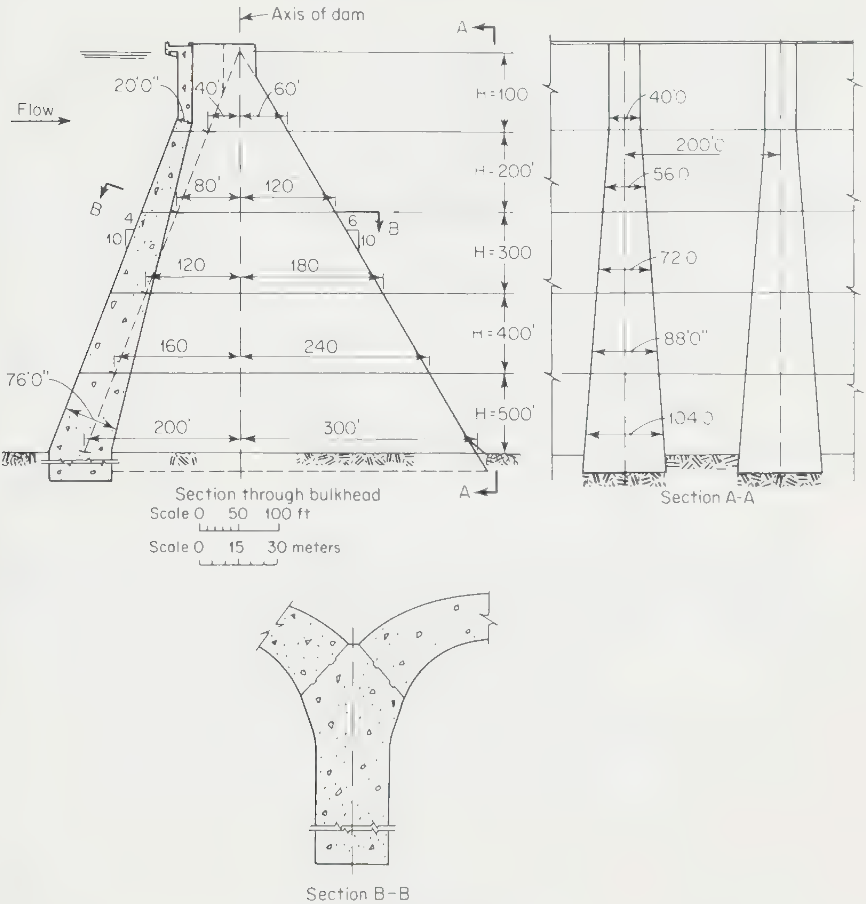

FIG. 12. Massive multiple-arch dam.

maximum economy by utilizing the concrete in direct compression. In such cases the volume of concrete in the arch dam may be as low as 25 percent of the volume of an equivalent gravity dam.

If the shape of the profile were a perfect U with a length-height ratio less than 2, maximum economy could be obtained by using a triangular section of dam having both a constant radius and a constant central angle of about 133 deg.

A V-shaped axis profile presents more difficult problems. Either a constant radius or a constant angle in V-shaped canyons can result in arches which are unnecessarily thick at some levels. It has been demonstrated that the horizontal loads at

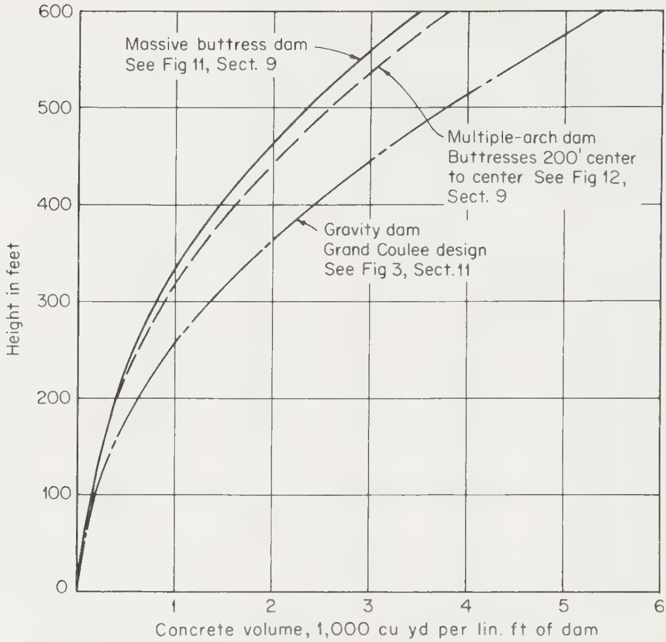

FIG. 13. Concrete volumes.

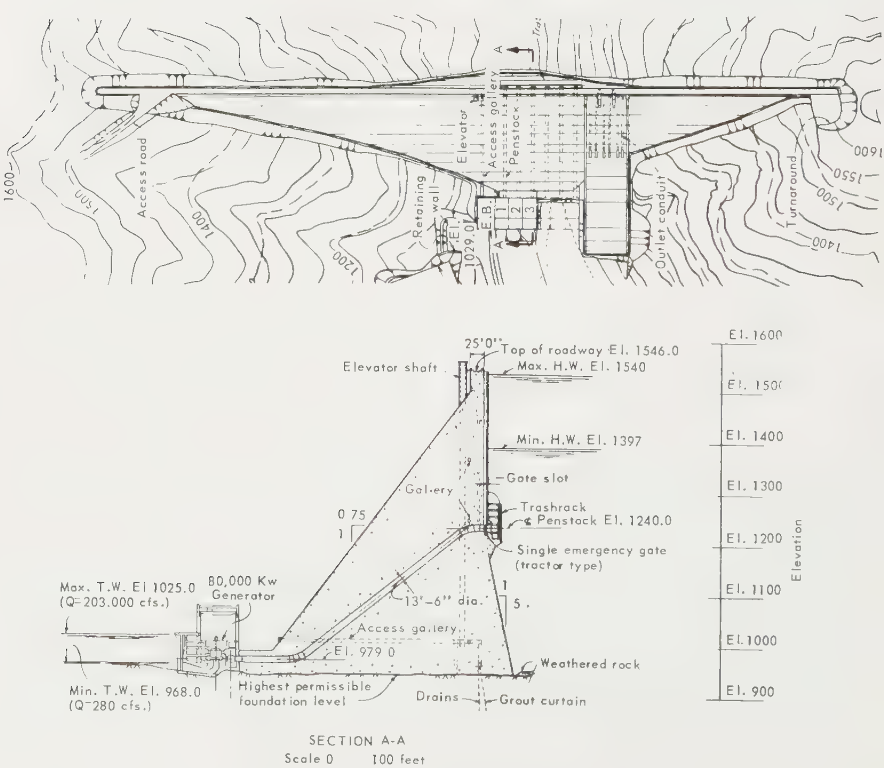

FIG. 14a. Gravity dam.

these levels are transferred to the abutments by interior arches which are defined by exterior zones of tension.

In recent years more efficient designs have been obtained by shaping the arch so that these zones of tension are eliminated. This procedure results in a double-curvature arch as shown by design C, Fig. 14. More detailed descriptions of large, double-curvature arch dams will be found in Sec. 14.

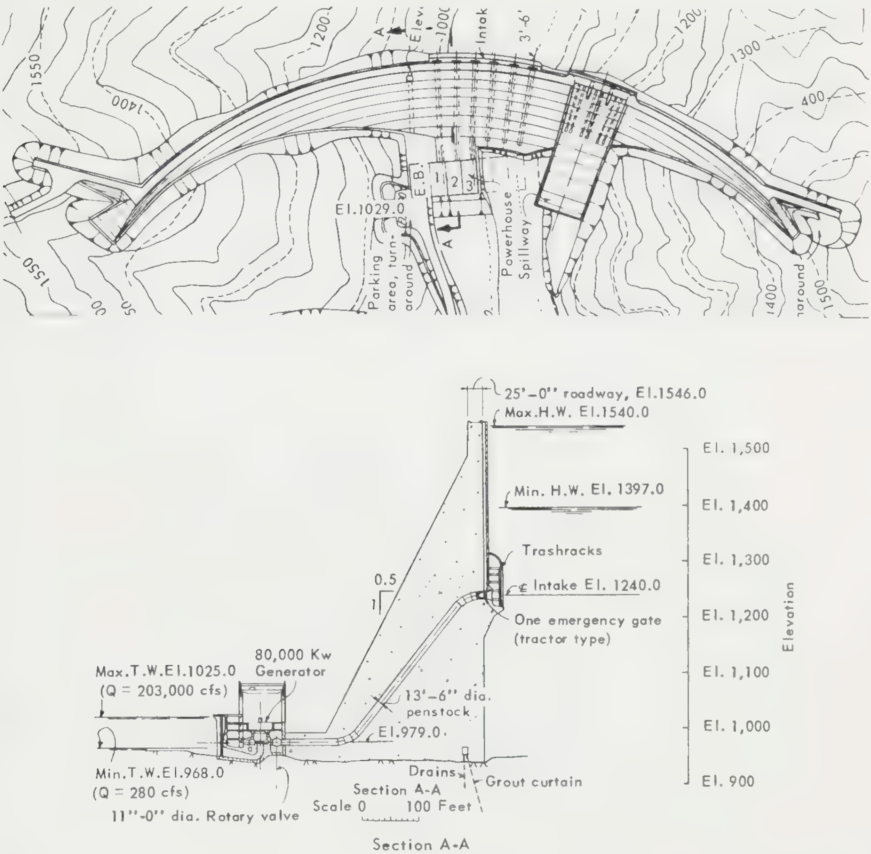

FIG. 14b. Arched-gravity dam.

It has also been demonstrated that arch dams may be constructed economically at sites having relatively high ratios of crest lengths to maximum heights. A single example will demonstrate: Fig. 15 shows a section and profile of the 420-ft-high Kariba Gorge Dam constructed recently on the Zambezi River in Rhodesia. The developed length is about 2,000 ft. It will be noted that the dam is thicker near the central portion than it is near the base. The increased flexibility near the foundation transfers a substantial part of the water load from the lower arch rings to the higher and thicker sections above. As the arch attempts to deflect near the foundations the central section comes into action and takes the additional load.[1] Kariba is a double-

[1] COYNE, HON. M. ANDRE, "Arch Dams: Their Philosophy," ASCE Paper 959, April, 1956. PATON, T.A.L., New Kariba Dam: Ready to Harness the Zambesi, *Eng. News Record*, Nov. 20, 1958, p. 30.

curvature arch. At the base the dam is 80 ft thick. The principles of design applied to Kariba were developed by the late Andre Coyne, consulting engineer of Paris, France.

The site topography may be adaptable to other recent innovations in design. Consider, for example, the Roselend Development, a 500-ft-high dam, constructed in the Isere River Basin in the southeastern part of France.[1] At this site a gorge in

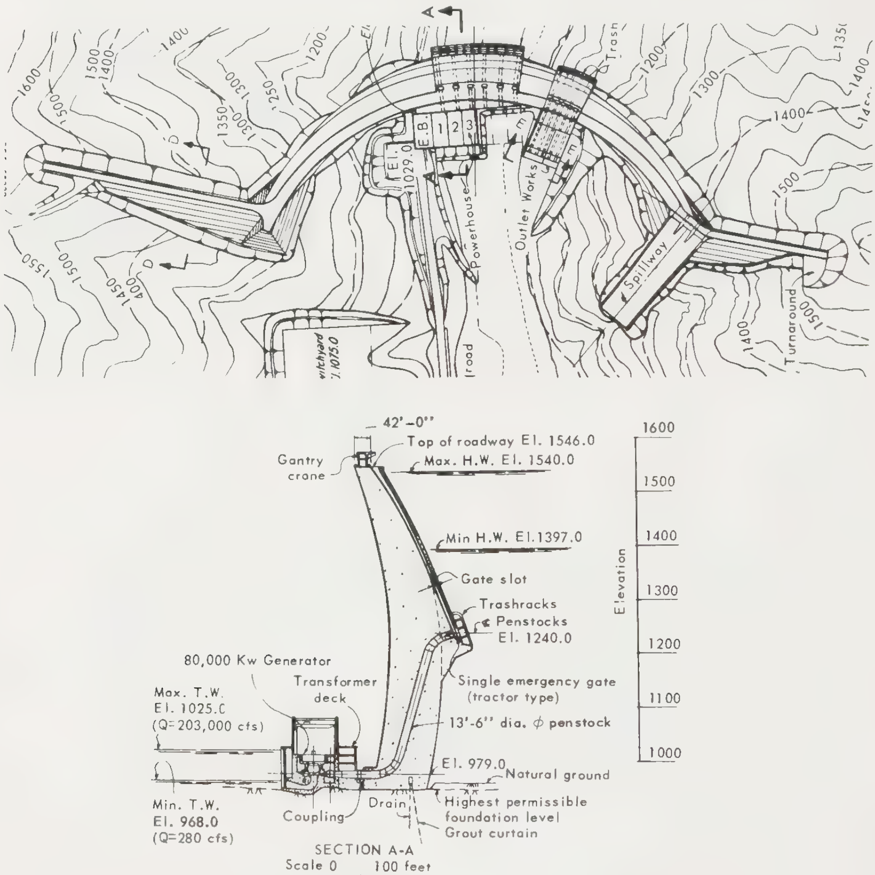

FIG. 14*c*. Double-curvature arch dam.

the river is not deep enough to accommodate the full height of the dam.[2] The structural type selected is a composite one: a truncated arch having a 200-m span in the gorge section is flanked on both abutments by a hammerhead, massive-buttress type of dam. This scheme also was the concept of the late Andre Coyne. Figure 16 shows the completed structure. Advantage is taken of the savings inherent in both the arch and the buttress types. The principal features (Figs. 17 and 18) show how the truncated central arch supports the flanking buttress-type structure. Figure 18

[1] The Roselend Development, *Water Power*, January, 1961, p. 5.
[2] French Dam Combines Arch and Buttresses, *Eng. News Record*, Jan. 18, 1962.

shows the buttress-type dam which extends across the valley on each side of the gorge. These buttresses are 9 m thick and are spaced 20 m center to center. It will be noted that the outlines of the buttress dam are approximately those of an equivalent gravity dam. It will also be noted that each buttress contains two inclined contraction joints. The merits of these joints will be discussed elsewhere in this section.

4. Flexible Gravity Dams. The preceding discussions demonstrate that masonry and concrete dams can no longer be classified in distinct and separate categories; in some cases composite structures, which bring together the advantages of several types,

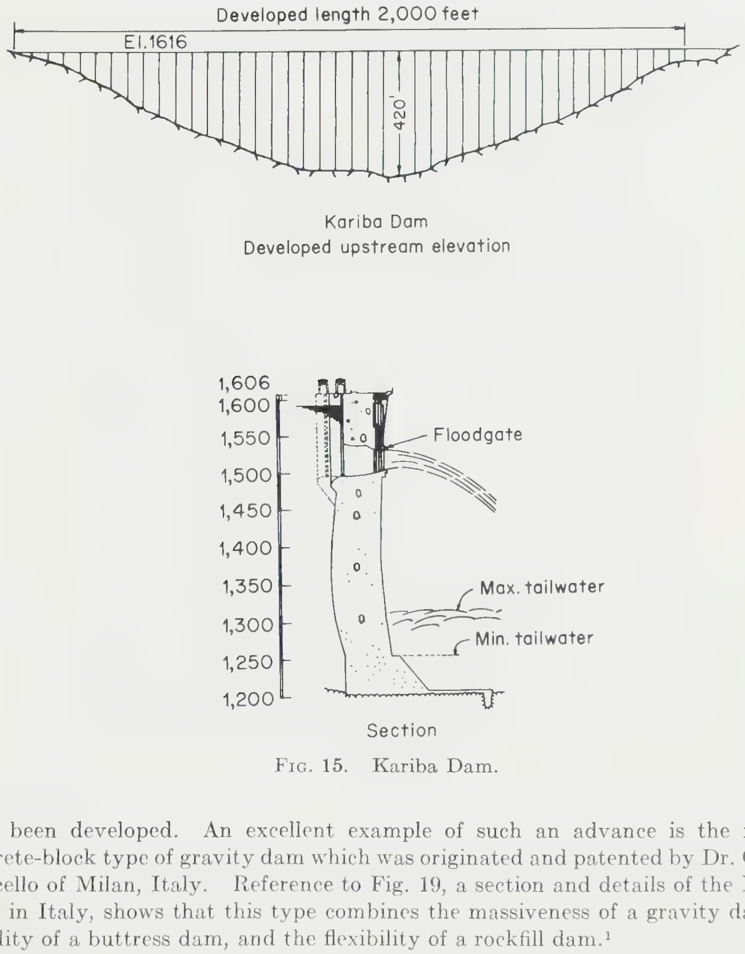

Fig. 15. Kariba Dam.

have been developed. An excellent example of such an advance is the flexible, concrete-block type of gravity dam which was originated and patented by Dr. Claudio Marcello of Milan, Italy. Reference to Fig. 19, a section and details of the Pozzillo Dam in Italy, shows that this type combines the massiveness of a gravity dam, the stability of a buttress dam, and the flexibility of a rockfill dam.[1]

Essentially, this structure consists of 13-ft cubic concrete blocks which are poured in place with an intermediate lift joint. In cross section the columns of blocks are built up in contact to form triangular-profile buttresses normal to the facings. In effect, the dam consists of a series of 13-ft-wide buttresses the thickness of the blocks, which are separated by 6-in.-wide gravel-filled gaps. The gravel acts as a lubricant,

[1] Marcello, Dr. Claudio, Concrete Block Dams for Highly Compressible Foundations, *Water Power*, June and July, 1961.

which permits each buttress to adjust to differential foundation settlements. The vertical block joints are staggered, as shown by Fig. 19, and the horizontal joints are sloped to increase resistance to horizontal shear and sliding.

Flexibility is provided in three dimensions: the 13-ft-thick buttresses provide both transverse and vertical flexibility and the 5-in. gravel-filled joints provide both longitudinal and vertical flexibility. A dam constructed in this manner also has many of the characteristics of a rockfill dam and is suitable for a foundation in which unequal settlements are likely to occur. At sites where the elastic properties of the foundation vary widely it would be advisable to place, as a first step, a highly reinforced foundation slab which would be designed to obtain a more uniform distribution of the foundation pressures.

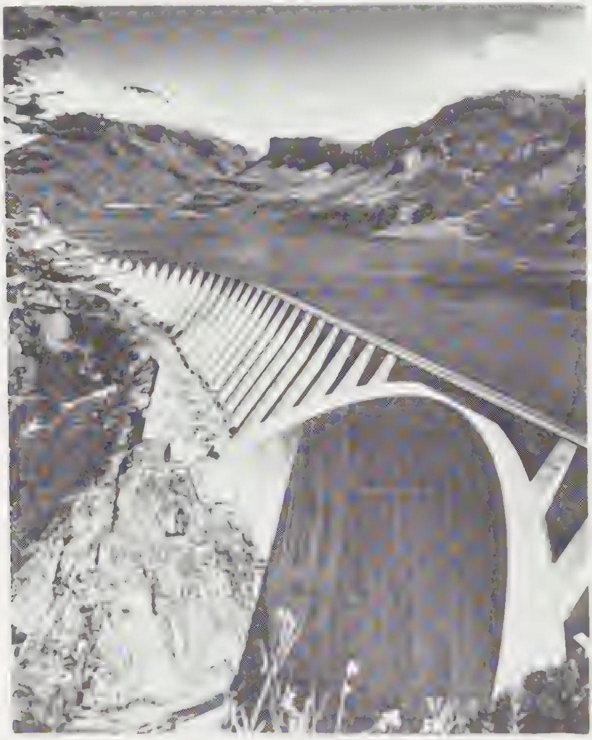

FIG. 16. Roselend Dam. (*Courtesy of Coyne and Bellier, Paris, France.*)

Figure 20 shows the details of a plate steel membrane which provides a watertight upstream face. This membrane could also be constructed as a reinforced-concrete deck slab spanning the 13-ft-thick concrete-block buttresses.

BASIC ASSUMPTIONS

5. Standards. Houk and Keener[1] list 25 basic assumptions which are generally standard for all concrete types:

1. The rock that constitutes the foundation and abutments at the site is strong

[1] HOUK AND KEENER, Masonry Dams; A Symposium, Basic Design Assumptions, *Proc. ASCE*, May, 1940, p. 813.

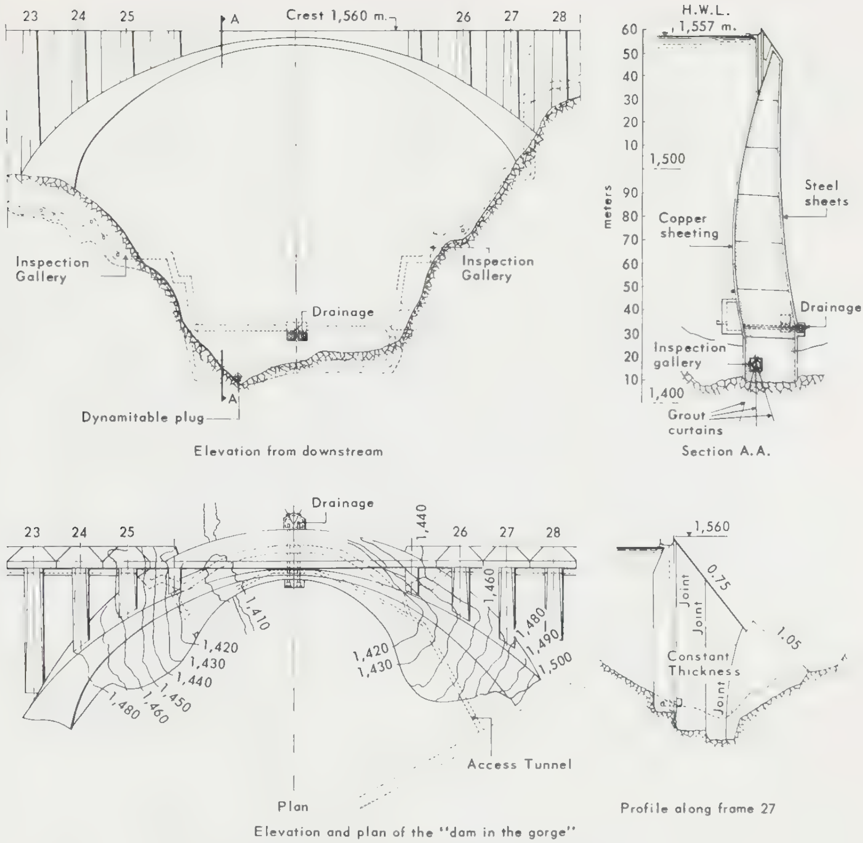

FIG. 17. Roselend Dam, central portion.

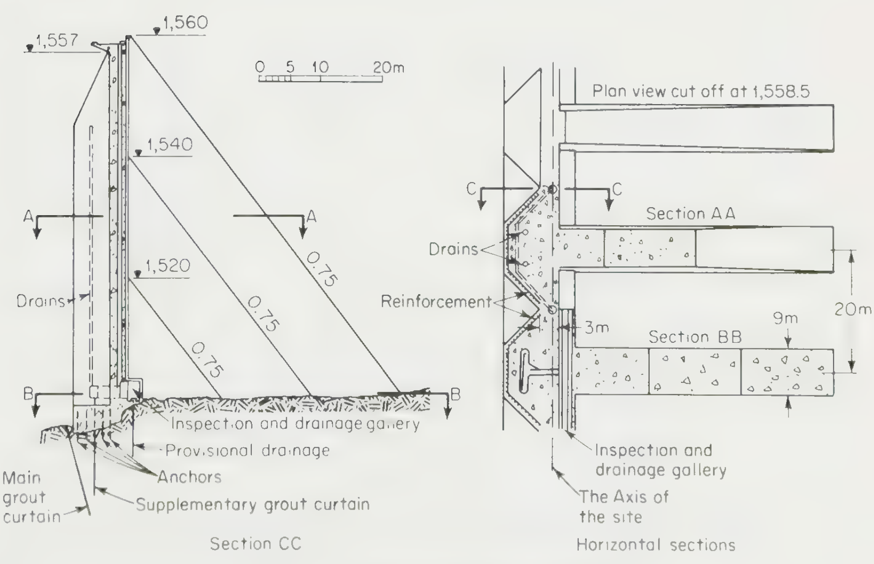

FIG. 18. Roselend Dam, side portions.

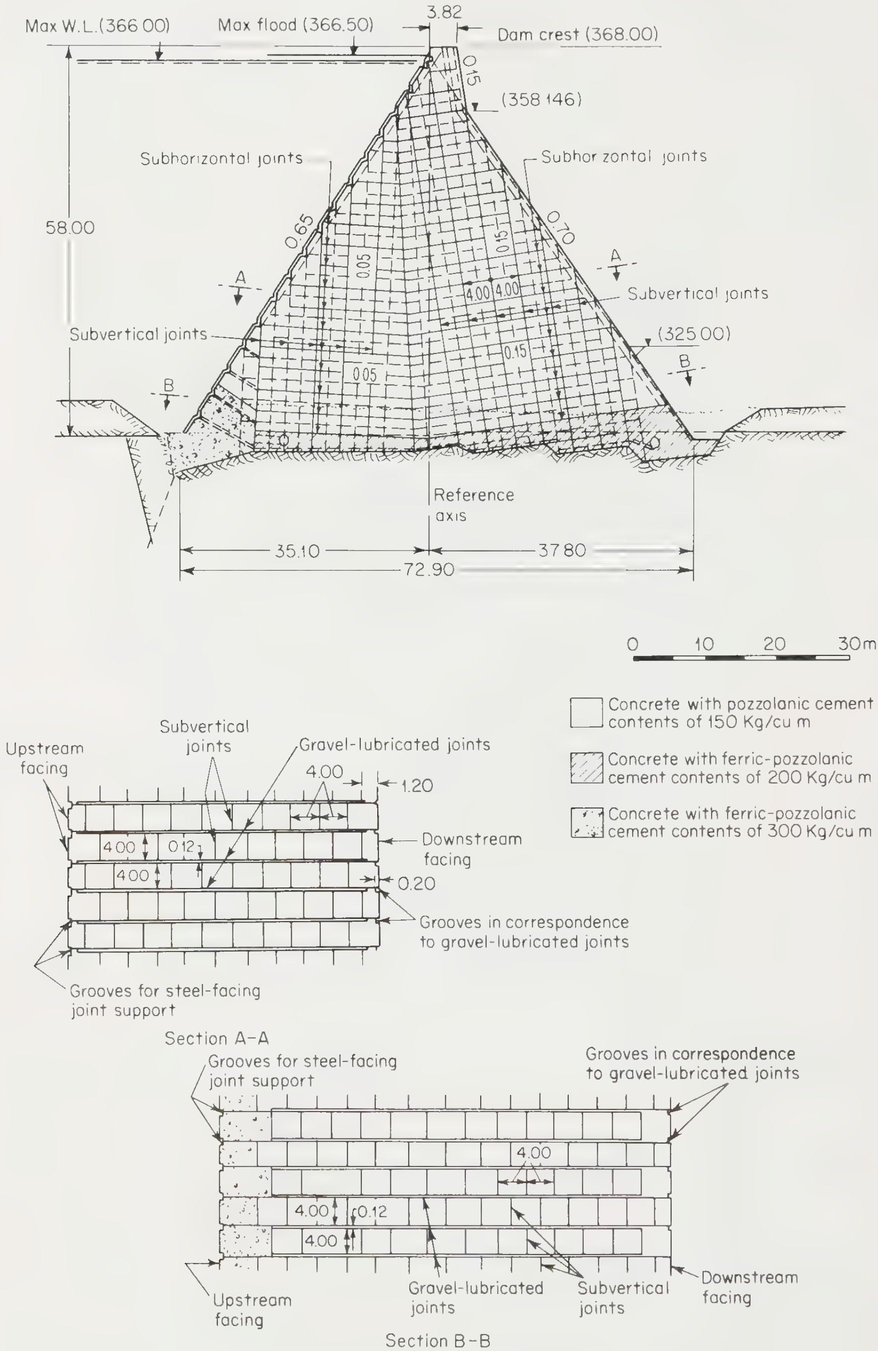

Fig. 19. Typical cross section through Pozzillo Dam, together with sketches showing the system of joints.

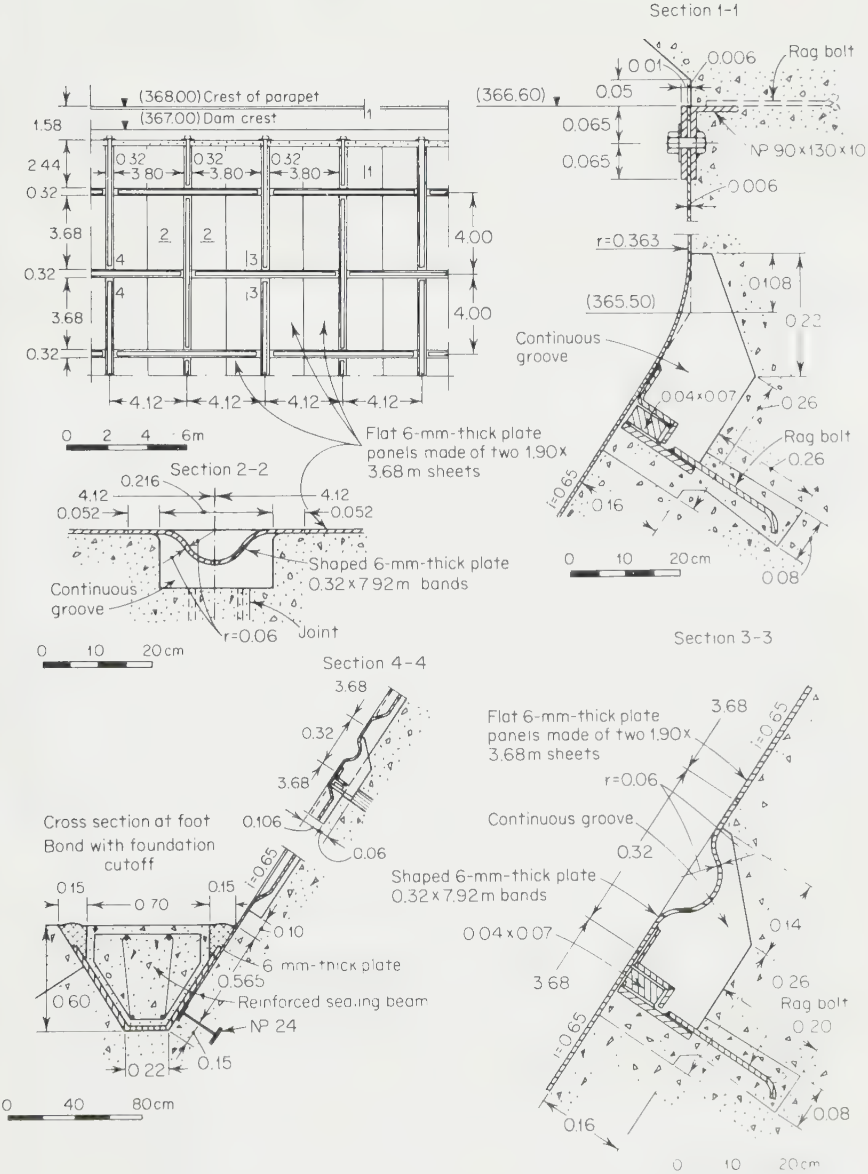

FIG. 20. Details of steel membrane on the upstream face of Pozzillo Dam.

enough to carry the forces imposed by the dam with stresses well below the elastic limit at all places along the contact planes.

2. The bearing power of the geologic structure along the foundation and abutments is great enough to carry the total loads imposed by the dam without rock movements of detrimental magnitude.

3. The rock formations are homogeneous and uniformly elastic in all directions, so that their deformations may be predicted satisfactorily by calculations based on the theory of elasticity, by laboratory measurements on models constructed of elastic materials, or by combinations of both methods.

4. The flow of the foundation rock under the sustained loads that result from the construction of the dam and the filling of the reservoir may be adequately allowed for by using a somewhat lower modulus of elasticity than would otherwise be adopted for use in the technical analyses.

5. The base of the dam is thoroughly keyed into the rock formations along the foundation and abutments.

6. Construction operations are conducted so as to secure satisfactory bond between the concrete and rock materials at all areas of contact along the foundation and abutments.

7. The concrete in the dam is homogeneous in all parts of the structure.

8. The concrete is uniformly elastic in all parts of the structure, so that deformations due to applied loads may be calculated by formulas derived on the basis of the theory of elasticity or may be estimated from laboratory measurements on models constructed of elastic materials.

9. Effects of flow of concrete may be adequately allowed for by using a somewhat lower modulus of elasticity under sustained loads than would otherwise be adopted for use in the technical analyses.

10. Construction joints are properly grouted under adequate pressures, or open slots are properly filled with concrete, so that the dam may be considered to act as a monolith.

11. Sufficient drains are installed in the dam to reduce such uplift pressures as may develop along areas of contact between the concrete and rock materials.

12. Effects of increases in horizontal pressures caused by silt contents of floodwaters usually may be ignored in designing high-storage dams but may require consideration in designing relatively low diversion structures.

13. Uplift forces adequate for analyzing conditions at the base of the dam are adequate for analyzing conditions at horizontal concrete cross sections above the base.

14. Internal stresses caused by natural shrinkage and by artificial cooling operations may be adequately controlled by proper spacing of contraction joints.

15. Internal stresses caused by increases in concrete temperature after grouting are beneficial.

16. Maximum pressures used in contraction-joint grouting operations should be limited to such values as may be shown to be safe by appropriate stress analyses.

17. No section of the United States may be assumed to be entirely free from the occurrence of earthquake shocks.

18. Assumptions of maximum earthquake accelerations equal to one-tenth of gravity are adequate for the design of important masonry dams without including additional allowances for resonance effects.

19. Vertical as well as horizontal accelerations should be considered, especially in designing gravity dams.

20. During the occurrence of temporary abnormal loads, such as those produced by earthquake shocks, some increases in stress magnitudes and some encroachments on usual factors of safety are permissible.

21. Effects of foundation and abutment deformations should be included in the technical analyses.

22. In monolithic straight gravity dams, some proportions of the loads may be carried by twist action and beam action at locations along the sloping abutments, as well as by the more usually considered gravity action.

23. Detrimental effects of twist and beam action in straight gravity dams, such as cracking caused by the development of tension stresses, may be prevented by suitable construction procedure.

24. In monolithic curved gravity and arch dams, some proportions of the loads may be carried by tangential shear and twist effects, as well as by the more usually considered arch and cantilever actions.

25. The distribution of loads in masonry dams may be determined by bringing the calculated deflections of the different systems of load transference into agreement at all conjugate points in the structure.

These assumptions do not apply uniformly in all cases. For example, assumption 3, stating that "rock formations are homogeneous and uniformly elastic in all directions," applies to very few sites. With modern design methods, such as the "finite-element" method, as described elsewhere in this section, it is possible to evaluate the effects on stress distribution of a foundation having varying elastic characteristics.

DESIGN CRITERIA, GENERAL

6. Introduction. There are three principal criteria: (1) loading, (2) design method, and (3) allowable stresses. These are closely related. The manner in which the structure is loaded often determines designing methods. The limitations of these methods must be understood in evaluating allowable stresses and safety factors. To illustrate, applying the cylinder formula (see Sec. 14) alone to determine the preliminary thickness of an arch ring might reveal a maximum compressive stress of 500 psi. An experienced designer would know that rib shortening, temperature, and other stresses could easily double this stress. The results of preliminary analyses, therefore, must be evaluated in the light of experience and the allowable stresses adjusted accordingly.

Of primary importance is the manner in which loads are transmitted from the upstream face through the dam to the foundation. The assumptions which are made in this respect affect every other step in design.

7. Nomenclature. The following symbols are used in this and other sections:

H = total height of dam from base to crest
h = height of section considered to water surface, depth of water
h_s = depth of silt above foundation
b = base or thickness of dam from the face to the back measured horizontally
e = eccentricity, distance from point of application of resultant to center of base
y_1 = distance from center of base to downstream face
y_2 = distance from center of base to upstream face
w = density of water, 62.5 lb/cu ft
w_s = submerged weight of silt
R = resultant, foundation reaction, or equilibrant
F = total force; see Fig. 1 for subscripts
U = total uplift force
ΣH = algebraic summation of all active horizontal forces
ΣV = algebraic summation of all active vertical forces
ΣM = algebraic summation of all moments
σ_x = vertical normal stress
σ_1 = first principal stress
σ_2 = second principal stress
τ_{xy} = horizontal and vertical shearing stress
θ = angle made by downstream face with vertical

α = angle made by upstream face with vertical
ϕ = angle of internal friction
a = ratio of acceleration due to earthquake forces to the acceleration of gravity
f = sliding factor
f' = coefficient of maximum static friction between two surfaces
q = unit shear resistance of foundation material
Q = shear-friction factor of safety

CRITERIA—LOADING

8. Weight of Concrete. The relative weights of structures for concrete and buttress dams and their effects on loading have been demonstrated by Fig. 8. By the use of modern construction methods, a concrete weight of 155 lb/cu ft is frequently attained. In preliminary designs, it is conservative to assume that the weight will be 150 lb/cu ft. Foundation pressures with an empty reservoir are proportional to the density of the material. Vertical weight likewise influences the magnitude and direction of stress when the reservoir is full. Consequently, tests should be made to determine in advance of design the weight and strength of the concrete or masonry that could economically be made available for construction at the site of the particular dam under consideration.

The application of the concrete loads to the various buttress types is not well understood. By way of example it is demonstrated in Sec. 13 that the weight of the concrete deck of an Ambursen dam may be partially transferred to the foundation, with the result that the stabilizing concrete load is decreased and the horizontal overturning load is increased. The same effect could result from a small downward movement in the arch barrel of a multiple-arch-type dam. Furthermore, the extent to which the horizontal section of the arch barrel acts integrally with the buttresses is not known. It is advisable to make assumptions which will result in a safe structure under all possible conditions of concrete-load application.

9. Water Pressure. The unit pressure of water increases in proportion to its depth. The horizontal force due to water pressure can thus be represented by a triangular load whose resultant is at two-thirds of the distance from the water surface to the base of the section under consideration. The formula for this water pressure is

$$F_2 = \tfrac{1}{2}wh^2$$

The vertical water load F_3 is of course proportional to the horizontal pressure if the slope of the upstream face is constant. When the slope of the upstream face is not a constant, the total vertical load on any section is represented by the area of water vertically above that section, and the resultant of the vertical load is through the centroid of that area.

10. Silt Pressure. In most reservoirs, finely divided silt or clay is deposited in substantially horizontal layers against the upstream face of the dam. These deposits are produced by flows of muddy water along the bottom of the reservoir and are to be distinguished from the deltas of silt and sand that form in the upper end of reservoirs. The total pressure F_4 that may develop from this cause and the location of the resultant are quite indeterminate.

When such fine clayey material is first deposited, the percentage of solid matter by weight is relatively small. Under the load of subsequent deposits, the excess water is progressively displaced. At the point of complete saturation, the weight of the clayey material in any unit volume is substantially equal to the weight of the water. If it is assumed that at this point of saturation the mixture is completely fluid, the resulting pressure is equivalent to that of a liquid having a unit weight of 90 lb/cu ft. In order for the weight of a unit volume of such deposits to be greater than about 90 lb/cu ft, water must be expelled by reduction of the void ratio under the weight of overlying deposits. It will then act as a true fluid only under abnormal conditions. At considerable distances below the surface of a silt deposit, the unit pressure against the dam may become less than the pressure of water at the same depth.

More precise calculations can be made by determining the horizontal component of the silt load from the Rankine formula, neglecting cohesion:

$$F_4 = \frac{W_s h_s^2}{2}\left(\frac{1 - \sin\phi}{1 + \sin\phi}\right)$$

11. Ice Pressure. In the colder sections of the world, ice pressure F_5 must likewise be considered. The amount of this pressure naturally varies greatly, depending upon the thickness of the ice that will form on the reservoir and upon other factors, including the slope of the banks of the reservoir and the shape of the upstream face of the dam itself. The magnitude of ice pressure has been variously estimated from zero to 50 kips/lin ft of contact with the vertical face of a dam.

Ice of substantial thickness forms slowly even during extreme low temperatures. Consequently, the greatest ice pressure will develop from the expansion of an ice sheet as a result of a temperature rise after a cold wave. Recent studies indicate that probable maximum ice thrusts for continental United States range from 5 to 20 kips/lin ft.[1]

12. Uplift. Regardless of the measures taken to prevent percolation, some water under pressure will find its way between the dam and the foundation, along pour joints in the dam or in horizontally bedded joints under the foundation. Whenever this occurs part of the weight of the dam is supported by the water and the foundation reaction is correspondingly reduced. The total uplift force U to be allowed for in any design is largely a matter of judgment based upon the character of the foundation, the steps taken to eliminate percolation, the probable efficiency of the foundation drains, and the method of construction to be used. Prototype performance offers our most reliable guide.

There are two constituent elements of uplift pressure: the area factor and the intensity factor. The area factor, or the percentage of the foundation area over which uplift is exerted, has been assumed by various designers to fall somewhere between 66⅔ and 100 percent. Many designers are now turning to the more conservative assumption that uplift pressures actually are exerted over 100 percent of the area.

The discussions relating to Figs. 21 to 25, inclusive, are concerned largely with the uplift forces under gravity dams. Many excellent papers and books have been written on this subject. By way of example, the late L. F. Harza offered a mathematical demonstration[2] which leads to the conclusion that uplift pressures are effective over 100 percent of the area of the base.

Dr. Leliavsky, in a comprehensive treatise,[3] concludes that uplift pressures act over somewhat less than 100 percent of the base but exceed greatly the 66⅔ percent area factor which had been assumed for many earlier designs.

The largest builders of dams in the United States, the U.S. Corps of Engineers, the U.S. Bureau of Reclamation, and the Tennessee Valley Authority, use similar assumptions, as illustrated by Fig. 21. These are (1) a straight-line drop from reservoir level at the heel of the dam to a fraction of the difference in head between reservoir and tail water along the line of the drains and (2) from there another straight-line drop to tail

[1] Rose, Edwin, Thrust Exerted by Expanding Ice, *Trans. ASCE*, **112**, 871, 1947. U.S. Bureau of Reclamation, Design of Small Dams, p. 235.

[2] Harza, L. F., The Significance of Pore Pressures in Hydraulic Structures, *Trans. ASCE*, **114**, 193.

[3] Leliavsky, "Uplift in Gravity Dams," Constable & Co., Ltd., London.

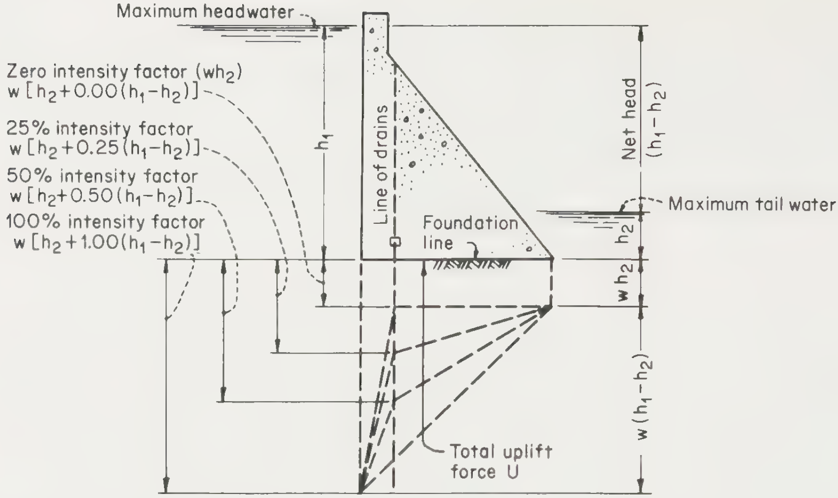

FIG. 21. Uplift assumptions. (*From Uplift in Masonry Dams, Final Report of the Subcommittee on Uplift in Masonry Dams of the Committee on Masonry Dams of the Power Division* 1951, *Trans. ASCE, Paper* 2531, *vol.* 117, 1218, 1952.)

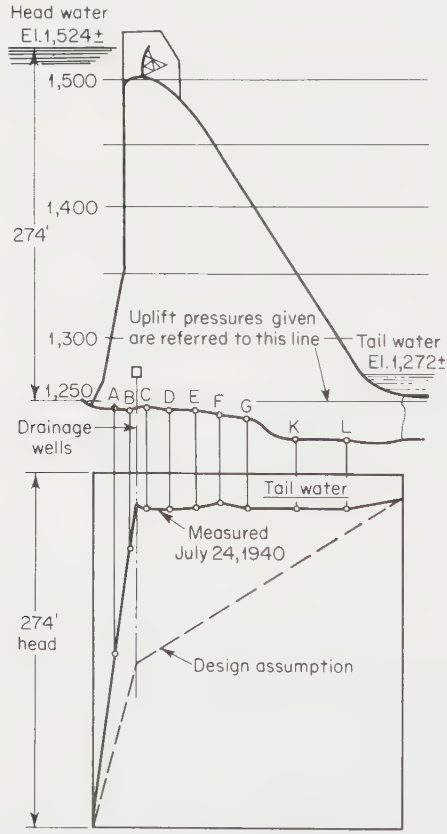

FIG. 22. Uplift pressures at the base of Hiwassee Dam. (*C. E. Pearce, Design of Hiwassee Dam, Basic Considerations, Civil Eng., June,* 1940, *p.* 340.)

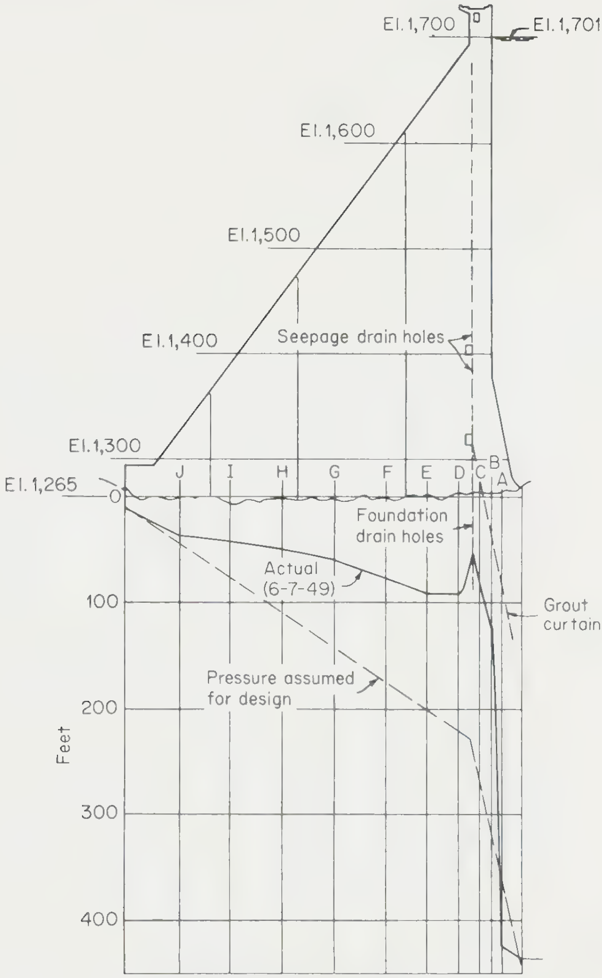

Fig. 23. Fontana Dam, uplift-pressure diagram, block 19.

water at the downstream toe.[1] This pressure is assumed to be effective over 100 percent of the area of the base.

The value of that fraction now (1968) used by the Tennessee Valley Authority is $\frac{1}{4}$ and that used by the Bureau of Reclamation is $\frac{1}{3}$. These reductions from the earlier, more conservative assumptions have resulted from observations on existing dams. Four will be discussed: Hiwassee Dam (Fig. 22) and Fontana Dam (Fig. 23) built by TVA, and Shasta Dam (Fig. 24) and Hoover Dam (Fig. 25) built by the Bureau of Reclamation. Grout curtains and drainage wells were features of all four.

There is no agreement among designers on the relative merits of grout curtains and drainage wells; the principal reliance appears to be placed on drainage wells. From

[1] Casagrande, Arthur, First Rankine Lecture, delivered Jan. 25, 1961, at the Institution of Civil Engineers, London, England.

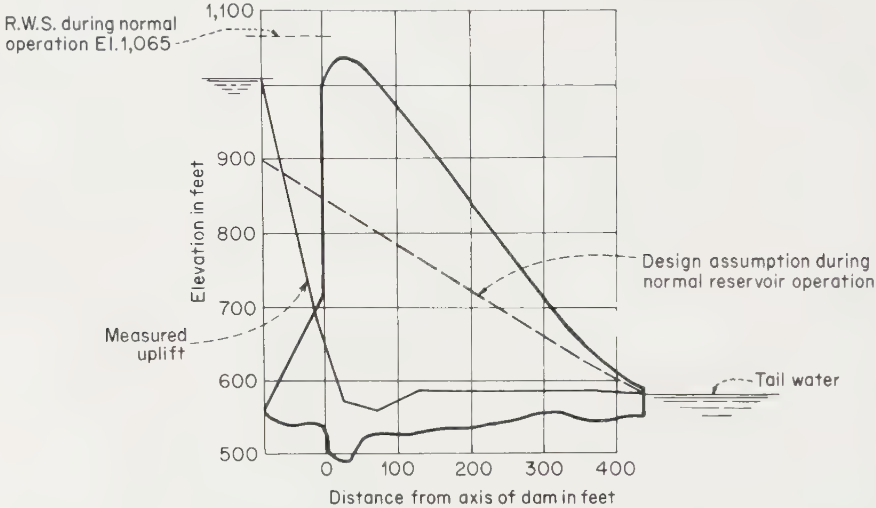

FIG. 24. Uplift pressures at foundation of Shasta Dam in California from measurements made during 1947. (*From Kenneth B. Keener, Uplift Pressures in Concrete Dams, Trans. ASCE, vol.* 116, 1218, 1951.)

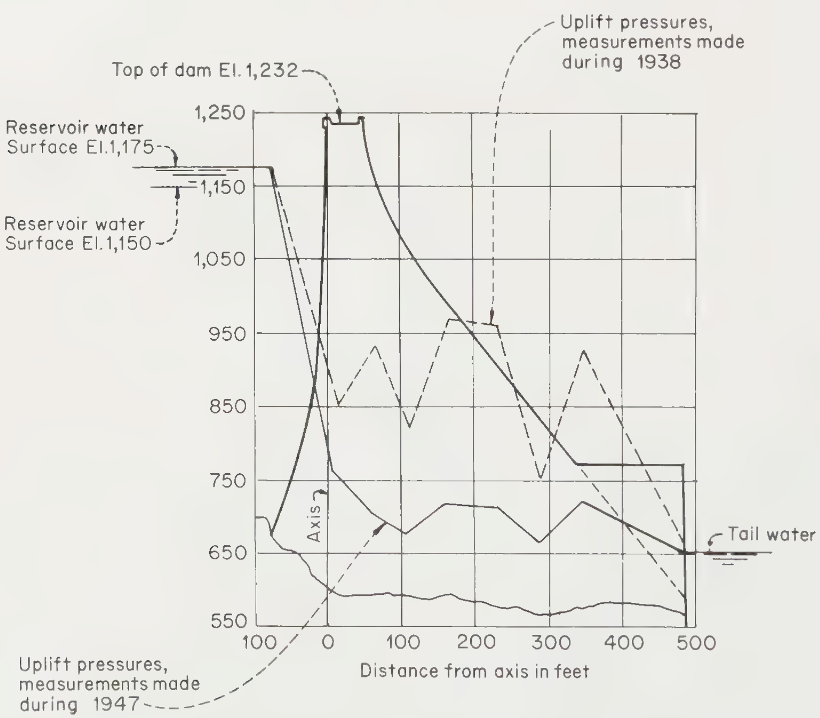

FIG. 25. Hoover Dam. (*From Kenneth B. Keener, Uplift Pressures in Concrete Dams, Trans. ASCE, vol.* 116, 1218, 1951.)

field observations it has been concluded that the pressure gradient decreases in a straight line from reservoir pressure at the heel to some fraction of this pressure at the foundation drains. Figures 22, 23, and 24, showing, respectively, the uplift pressure gradients for Hiwassee, Fontana, and Shasta, show that the actual pressures at the drains fall well below the present design assumptions and also that the present design assumptions are much less conservative than the original design assumptions.

As a general philosophy of design it is suggested that the safety of such large structures should not depend on the proper functioning of grout curtains and drains. Calculations which give credit to properly functioning drains may reveal what may be expected under normal operating conditions. It must be remembered that large dams may be in existence for hundreds of years. No one can predict proper maintenance over such a long period. Drains have been known to clog. Dams should still have a large margin of safety against failure if they do. The original design assumptions for Hiwassee, Fontana, Hoover, and Shasta provide this reserve.

The need for conservation is demonstrated by a study of the case history of Hoover Dam.[1] Figure 25 compares the uplift gradients measured during 1938 with those made during 1947 after remedial measures had been undertaken to provide more drain holes and further foundation grouting.

The field measurements of uplift at Hoover Dam again illustrate the wisdom of designing the structure to be safe with uplift pressures greatly in excess of those based upon the effectiveness of drains.

Uplift under buttress dams does not present such a serious problem. In the case of massive-buttress-type dams it would be conservative to assume that uplift pressure varied from 100 percent of the difference between headwater and tail-water pressure to tail-water pressure at the downstream site of the deck or water-bearing structure. Because the pressure gradient is so steep it is of primary importance to provide an adequate grout curtain at the upstream heel and a system of drainage wells penetrating into the foundation between buttresses.

Barrages and buttress dams constructed on poor or soft foundations must have foundation structures which furnish adequate water travel to flatten the gradient sufficiently to prevent failure by underseepage or piping.

The same uplift criteria which apply to gravity dams may also be applied to arch- and gravity-arch-type dams. In designing both arch- and gravity-arch types consideration must also be given to the short path of water travel between the upstream and downstream faces in relation to the foundation characteristics.

13. Seismic Forces. No part of the world is entirely free from earthquakes; hence adequate allowance should be made for seismic forces. The magnitude of such forces depends upon both the amplitude and the frequency of the indirect waves. Seismic forces act in all directions. Horizontal forces are produced by the inertia of the dam and the momentarily increased pressure of the water as the foundation shifts laterally. Any upward acceleration opposes the acceleration of gravity, and the effective weight of the dam upon which its stability depends is thereby momentarily reduced.

In order to determine the seismic forces it is necessary to know the acceleration or the earthquake intensity. A joint committee of the American Society of Civil Engineers and Structural Engineers Association of California has suggested that the maximum value of the horizontal intensity expressed as a coefficient of g shall be 0.10.[2]

The U.S. Bureau of Reclamation has consistently used a horizontal intensity $\alpha = 0.10$ along with a vertical intensity of equal or smaller magnitude.[3]

[1] Keener, Kenneth B., Uplift Pressures in Concrete Dams, *Trans. ASCE*, **116**, 1218, 1951.

[2] Lateral Forces of Earthquake and Wind, *Proc. ASCE*, **77**, 1951.

[3] Zanger, C. N., "Hydrodynamic Pressures on Dams Due to Horizontal Earthquake Effects," U.S. Bureau of Reclamation Engineering Monograph 11.

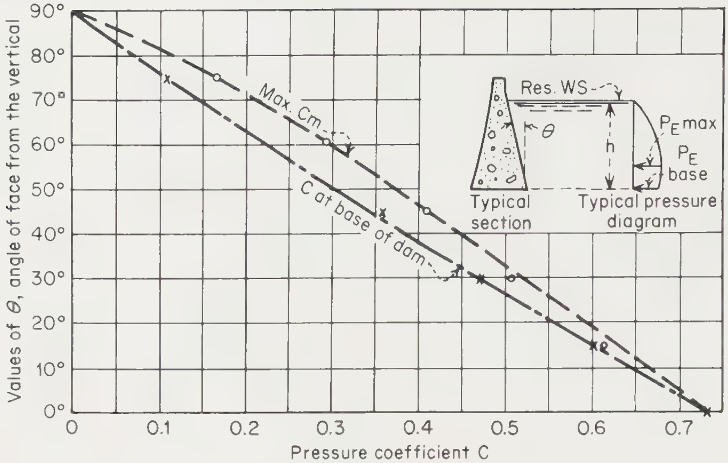

FIG. 26. Pressure coefficients for constant sloping faces.

In 1953, Zanger presented formulas for computing the hydrodynamic pressures exerted on vertical and sloping faces by horizontal earthquake. The effect of inertia on the concrete should be applied at the center of gravity of the mass. For dams with vertical or sloping faces the increase in water pressure P_e in pounds per square foot at any elevation, with earthquake intensity λ, is given by the following equation:

$$P_e = C\lambda wh$$

where C is a dimensionless coefficient giving the distribution and magnitude of pressures. The maximum value of C for a given constant slope is shown by Fig. 26, and

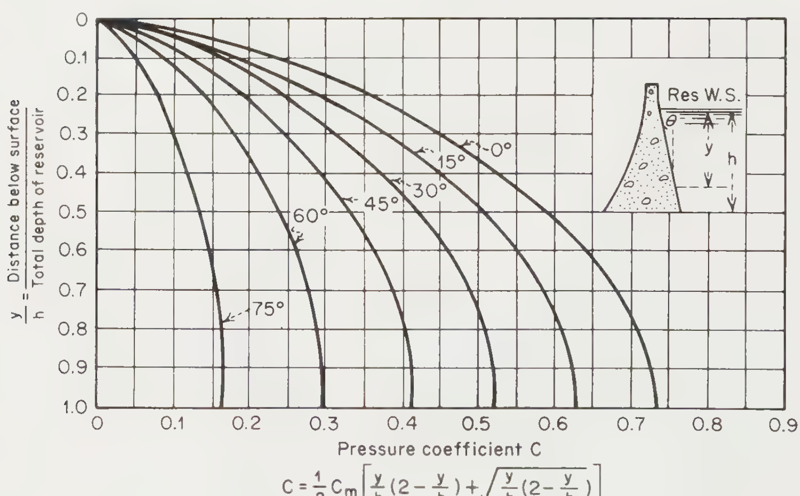

$$C = \frac{1}{2} C_m \left[\frac{y}{h}\left(2 - \frac{y}{h}\right) + \sqrt{\frac{y}{h}\left(2 - \frac{y}{h}\right)} \right]$$

where: C_m is maximum C value from fig 26

FIG. 27. Coefficients for pressure distribution for constant sloping faces.

the values of C for various degrees of slope and relations of depth y to total head h are shown by Fig. 27. Zanger's equation is also shown by Fig. 27.

It may be shown analytically that the total horizontal force F_7 (see Fig. 1) above any elevation or distance below the reservoir surface and the total overturning moment M_e above that elevation are[1]

$$F_7 = 0.726P_e y \qquad \text{and} \qquad M_e = 0.299P_e y^2$$

The Zanger formulas may be applied, with reasonable accuracy, to dams of all heights. It is recognized, however, that they may give results which are less accurate for high dams than for low dams.

CRITERIA—METHODS OF ANALYSIS

14. Trapezoidal Law. Stresses normal to horizontal planes, designated σ_x, are usually assumed to have straight-line or trapezoidal distribution. The formulas expressing the trapezoidal law and its application to different structural forms will be found in Secs. 11 to 15, inclusive. The assumption of straight-line distribution simplifies greatly the analysis of shearing and principal stresses. As illustrated by the examples in Sec. 13, the differences of total normal pressures on two horizontal planes will yield the total shear on the vertical sectional area between these planes, and differences of shearing-stress intensities between two horizontal planes will yield the total horizontal load between these planes. From these differences may be found horizontal normal stresses. With shearing, vertical normal, and horizontal normal stresses known, it is possible to determine the magnitude and direction of the first and second principal stresses and of maximum shearing stresses. Numerical examples illustrating this procedure will be found in Secs. 12 and 13.

Stress measurements on structural models and on existing dams reveal that the distribution of vertical normal pressures is not rectilinear but curvilinear. Figure 28 *a* and *b* shows the results of stress measurements on an aluminum model of the high-buttress design shown by Fig. 11. These measured stresses are compared with those computed by the trapezoidal law. It is important to note that the measurements on the model reveal tension at the upstream face near the foundation line. At this point, the trapezoidal-law computations indicated compression. Figure 29 shows the trajectories of the first and second principal stresses as derived from the model tests. Prototype measurements which have been taken over a period of years show an even greater variation from straight-line distribution. Figure 30, for example, shows a comparison of measured and calculated foundation pressures for Hiwassee Dam under both low and high reservoir levels.[2]

Figure 31 shows the foundation pressures under the Shasta Dam as measured on Jan. 1, 1954. The reservoir was nearly full. The actual distribution of pressures follows closely the load line of the concrete. The measured maximum pressure was 600 psi at a point close to the center of the base. The sharp reduction in pressures near the downstream face to about 125 psi indicates that about the downstream third of the concrete is taking a relatively minor part of the load.

It will also be noted that maximum shearing stresses occur near the downstream face in an area of minimum vertical pressure. The average factor of safety Q against shear-friction failure (Sec. 11) for the dam as a whole is not representative of shear-friction safety in this area.

A somewhat different pattern of stress distribution was observed during the field testing program for the Grand Coulee Dam. Figure 32 shows the normal and shearing

[1] U.S. Bureau of Reclamation, "Design of Small Dams," Figs. 164, 165, pp. 237, 238.

[2] Pearce, C. E., Design of Hiwassee Dam, Basic Considerations, *Civil Eng.*, June, 1940, p. 340.

stresses as measured under full-reservoir conditions on July 1, 1952. There is a characteristic rise in pressure under the upstream third of the base over that shown by the trapezoidal diagram. From the upstream maximum calculated at this point the pressure declines to about the quarter point of the base, as measured from the downstream toe. From this point it again rises to a maximum at the downstream toe. Unlike Shasta, the shear-friction factor of safety would rise to a maximum in the downstream third of the base.

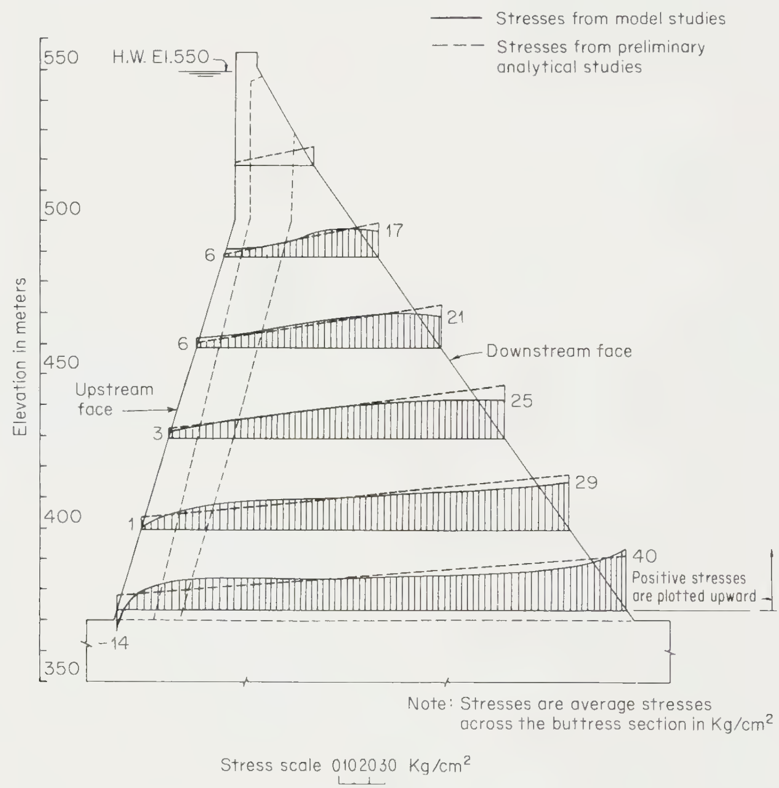

Fig. 28a. Vertical stresses σ_x on horizontal planes. (Numbers refer to stresses from model studies at up- and downstream faces, in kg/sq cm.)

15. Finite-element Method. The structural behavior of high gravity dams, as determined by field measurements, leads to the conclusion that the classic trapezoidal law produces stress patterns which do not even remotely resemble those obtained from field measurements. Recent research has given the designer new tools of analysis which hold the promise of yielding more realistic results.

The finite-element method, as described under Sec. 10 by Dr. Zienkiewicz, is now recognized as an important advance. By this method the structure and its foundations may be divided into elementary, contiguous triangles, and the elastic properties of each may be analyzed and linear simultaneous equations formulated for each nodal point. The solution of these equations is made possible only by the use of the digital computer. The results obtained from a preliminary analysis of the foundation pressures under a 700-ft-high gravity dam are shown by Fig. 33 and have some of the characteristics of the previously described prototype measurements. It will be noted that the upstream half of the base takes a greater percentage of the load than that indicated by the trapezoidal distribution. It will also be noted that the maximum stresses do not occur at the downstream toe and that there may be tension instead of compression at the upstream heel. It will also be noted that the results of the structural-model tests shown by Fig. 28 indicated some tension at the upstream heel. The

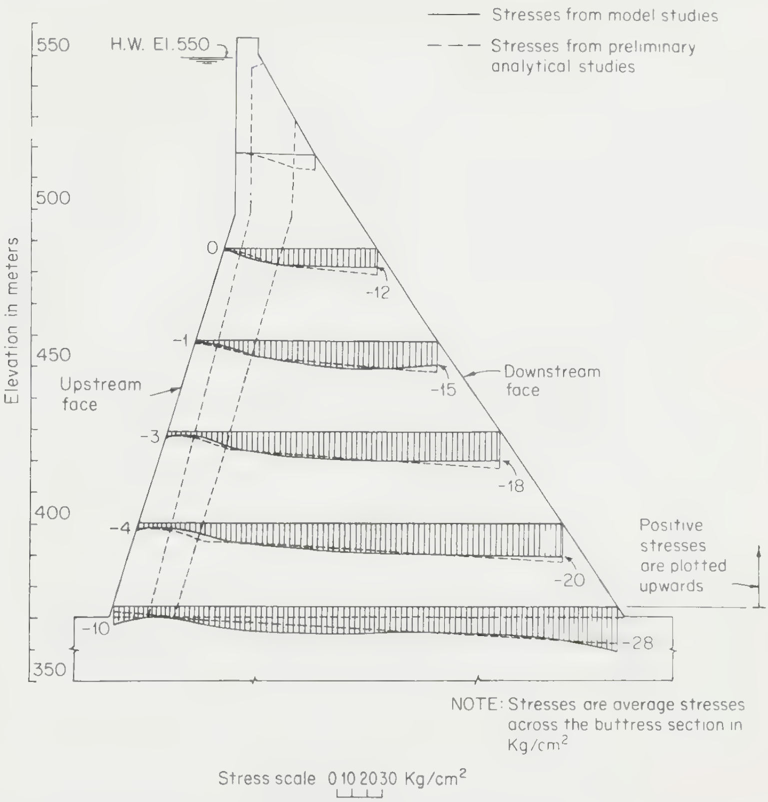

FIG. 28*b*. Shear stresses τ_{xy} on horizontal planes. (Numbers refer to stresses from model studies at up- and downstream faces, in kg/sq cm.)

finite-element method makes it possible to analyze the stresses in dams on foundation material having elastic characteristics which are different from those of the concrete.

It is doubtful if any analytical method will be devised which will do more than approximate the stresses measured in prototype structures. Measured stresses are affected by such factors as the rate of placing concrete, the spacing and arrangement of construction and contraction joints, the temperature of the reservoir, and the lift of the concrete pours.

Contraction joints affect materially the stress distribution. Vertical longitudinal joints which are keyed and grouted do not always give the assurance that the structure

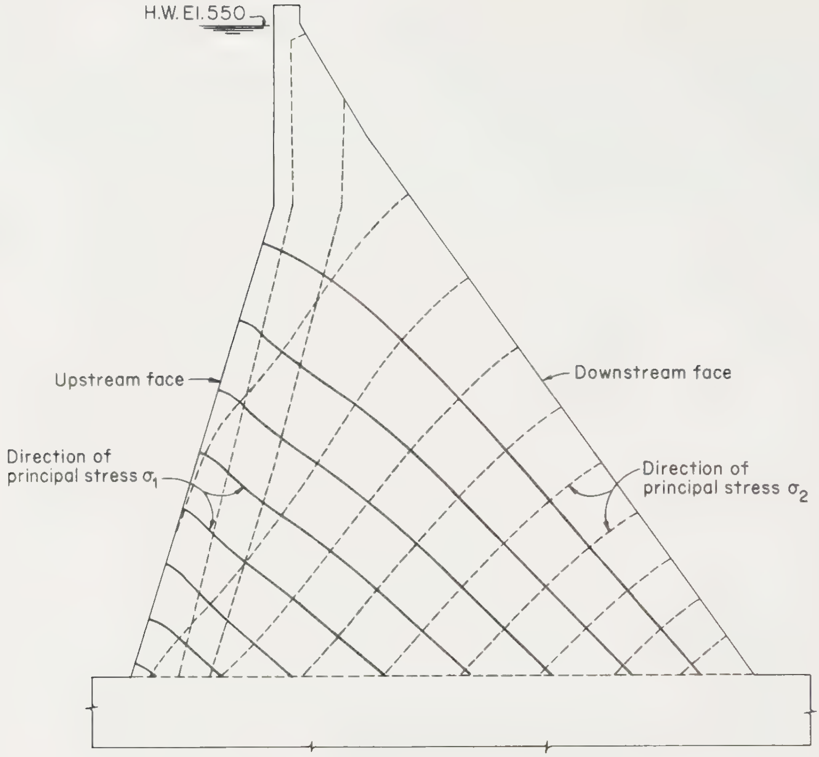

FIG. 29. Principal stress trajectories.

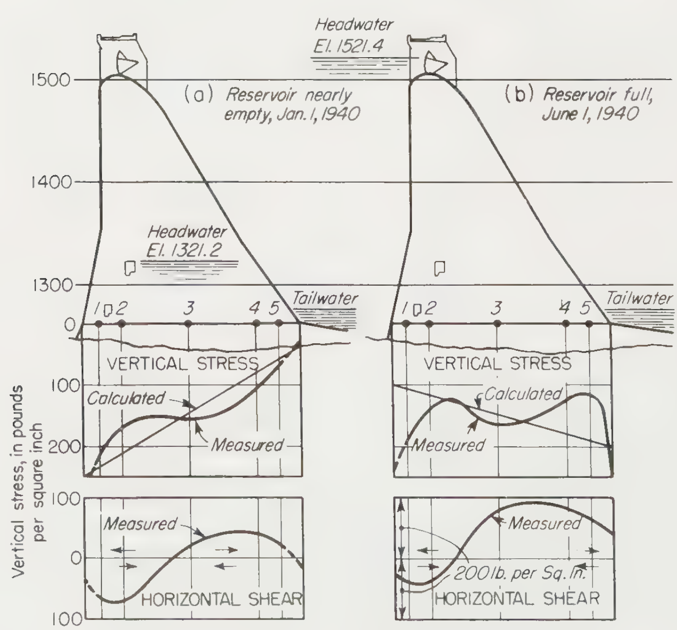

FIG. 30. Hiwassee Dam foundation pressures.

will act as a monolith. The structural behavior of the 500-ft-high Fontana Dam,[1] for example, indicated that the four vertical columns had a degree of structural independence even though the joints were keyed and grouted and the concrete cooled before grouting.

The stress patterns measured at Fontana indicated that the dam showed some evidence that it acted partially as four contiguous columns.

The structural behavior of the 564-ft-high Hungry Horse Dam,[2] constructed on the

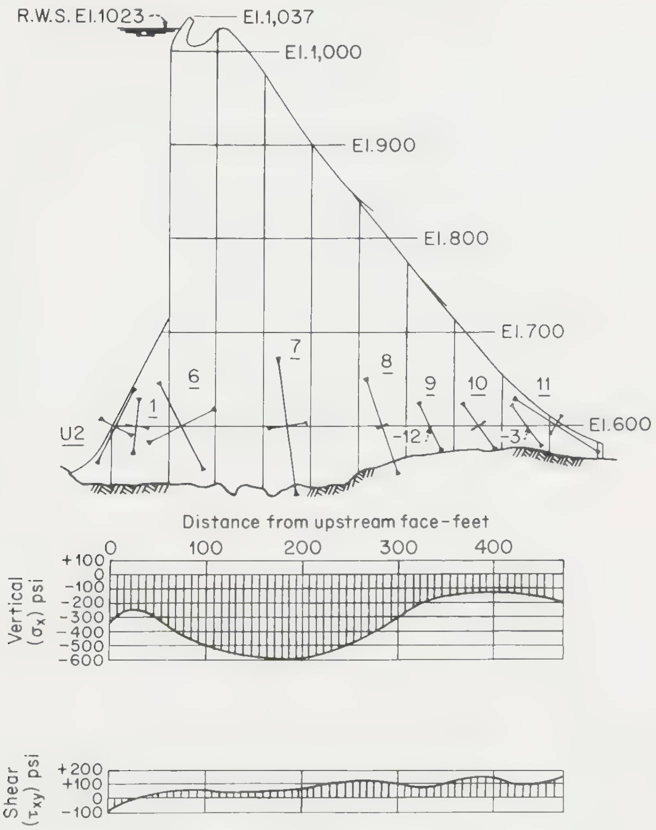

FIG. 31. Shasta Dam. Stresses measured Jan. 1, 1954. (*William T. Lockman, The Structural Behavior of Shasta Dam, U.S. Bur. Reclamation, Tech. Mem.* 656, *Fig.* 6.)

south fork of the Flathead River in Montana, is also of interest in respect to the effect of a vertical contraction on the distribution of stresses.

The Hungry Horse dam is an arch-gravity-type structure having the general proportions shown by Fig. 34. The crest of the dam is 2,100 ft long and the base thickness is 330 ft on the plane of the centers at the foundation. It will be noted that there is only one longitudinal contraction joint. The concrete was cooled during construc-

[1] "Measurements of the Structural Behavior at Fontana Dam," Tennessee Valley Authority Technical Monograph 69.

[2] RICHARDSON, JOE T., "The Structural Behavior of Hungry Horse Dam," U.S. Bureau of Reclamation Engineering Monograph 24.

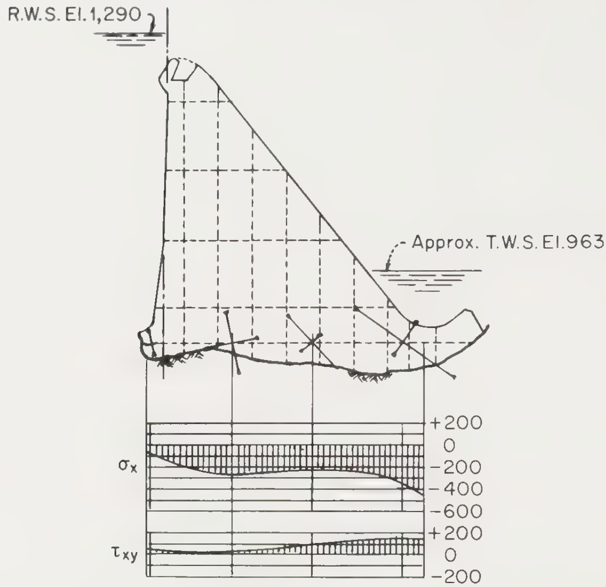

FIG. 32. Grand Coulee Dam. Measurements, July 1, 1952. (*William T. Lockman, Structural Behavior of Grand Coulee Dam, U.S. Bureau of Reclamation 15 Year Report, Tech. Mem.* 652, *March*, 1955.)

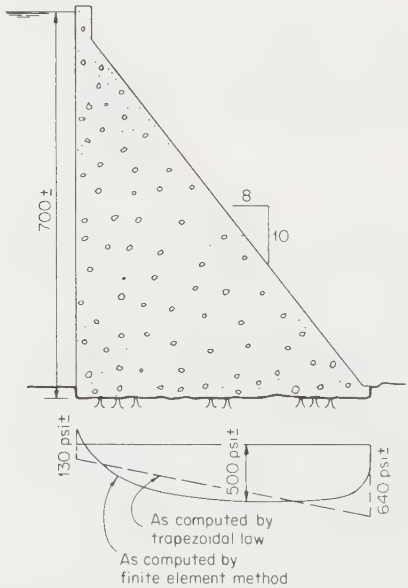

FIG. 33. Gravity dam. Normal stresses at foundation line σ_x. Load condition: dead, live, horizontal, and vertical earthquake loads.

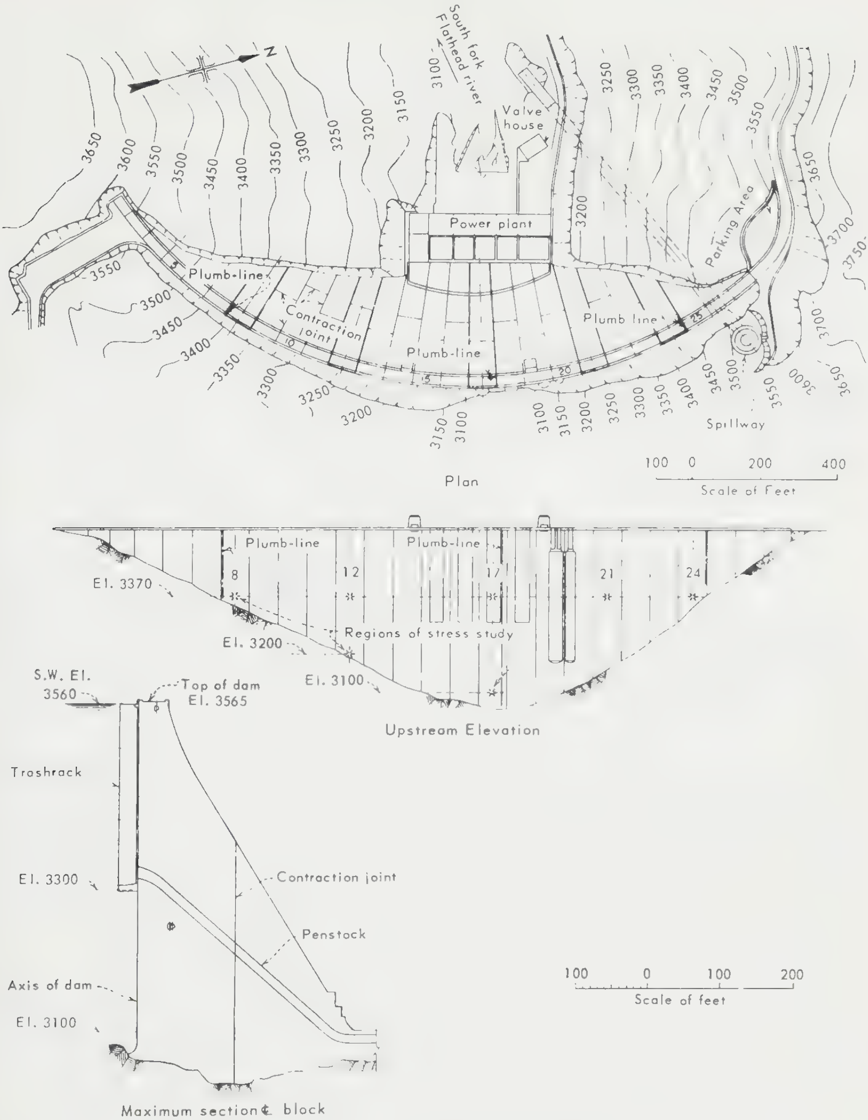

FIG. 34. Hungry Horse Dam.

tion and the longitudinal joint was grouted. Regardless of these precautions the field measurements revealed that the two sections of the dam, separated by the joint, acted to some extent as contiguous rings. At some points there was a marked discontinuity of stress patterns at the plane of the joint. Actually, this discontinuity of stress patterns could be a favorable factor. It can be demonstrated that a series of contiguous arches separated by low-friction joints will have a more favorable stress distribution than that in a massive arch.

Some designers have preferred inclined contraction joints which parallel approximately trajectories of first principal stress under full-load conditions. Inclined contraction joints were used in connection with the flanking abutment sections of the Roselend Dam, the Coolidge Dam, the Big Dalton Dam, and other large structures of the buttress type.

16. The Trial-load Method. The problems dealt with previously were mostly two-dimensional. Dams with keyed and grouted transverse joints, both gravity and arch, can be subjected to both vertical cantilever action and beam or arch action, depending upon the type of structure. Basically the process of analysis in this case, known as the trial-load method, consists of equating vertical and horizontal deflections at a number of points in the structure. This method, which was first developed nearly 40 years ago, has gone through successive refinements, the latest being its adaptation to computer operations. The trial-load method, as applied to arch dams, is described fully in Sec. 14. In this section also the results obtained by trial-load method as applied to Karadj Dam in Iran are compared with the stresses as obtained from experiments with a structural model and prototype measurements obtained during a field testing program.

CRITERIA—STRESSES

17. Allowable Unit Stresses. Allowable unit stresses have increased with height. We know, for example, that a gravity dam some 500 ft high would have a maximum dead-load pressure near the heel of approximately 500 psi and that a dam 1,000 ft high would have a dead-load pressure of about double that intensity. The water load tends to shift the maximum vertical pressure to some point downstream from the center of the base. At this point the maximum first principal stress is of primary interest.

Maximum compressive stresses falling between 1,000 and 1,500 psi under dead load, water load, and earthquake conditions are now being accepted by some designers. A word of caution should be introduced in connection with the design of high arch dams. Stresses double those computed can result from even a moderate break in the profile, according to the results obtained from testing structural models. Changes in the moduli of the foundation rock can result in the transfer of loads with resulting increases in stresses. Any factor which shifts the load line in the arch may also increase stresses.

With field strengths between 4,000 and 6,000 psi being attained by modern construction methods, higher unit stresses are permissible if consideration is given to the contingencies which may increase these stresses.

Shearing stresses are being increased proportionally. Maximum shearing stresses falling between 250 and 350 psi or even higher intensities are safe provided these are not in the presence of tension. A common error in the design of buttress dams is to neglect second principal stresses which may be in tension if the slope of the upstream face is relatively flat. In such cases the combination of shearing and tensioned stresses must be treated much the same as diagonal shear in the design of beams and girders.

The compressive and shearing strengths of the foundation materials are of equal importance. The shear-friction factor of safety (see Sec. 11) combines frictional and shearing resistance to downstream movement. As pointed out previously, an overall average value for this factor may be meaningless if there are high shearing stresses in the presence of low compressive stresses at the foundation level.

Comprehensive programs of testing foundation strengths and elastic properties are commonly undertaken as a first step in the design of high concrete dams.

SECTION 10

THE FINITE-ELEMENT METHOD

By O. C. Zienkiewicz

1. Introduction. The rapid development of large digital computers is changing drastically the approach to problems of structural engineering. This impact is particularly strong in the area of dam design where the complex two- and three-dimensional stress distributions have up to this time had to be crudely approximated. Now, with a suitable formulation of the problem, it is possible to perform a two- or three-dimensional analysis of a dam on a large computer within a matter of minutes, stating only the *fundamental* assumptions about the behavior of material. As the preparation of the necessary data is usually no more time-demanding than for the crude analysis processes, the *cost* of this more accurate approach is at least comparable—an important factor from the view of the practicing engineer.

The full analysis of the form mentioned is often based on precisely the same premises as *model tests* which the engineer often uses to check out his preliminary calculations. In such cases the cost saving becomes important as the model test can be eliminated. Indeed, in computation, it becomes possible with no additional difficulty to deal with such aspects as pore-water effects and temperature. These factors are either impossible or very costly to model.

Many of the computer approaches (though by no means all) are based on the assumption of elastic behavior, which, however, need not imply isotropy and homogeneity as in classical elasticity. Indeed in this section this assumption only will be invoked. An immediate reaction of some engineers is that this assumption, being only an approximation to the real behavior of concrete, may be no more valid than their traditional ones (such as, for instance, a specification of a linear-stress variation in a buttress dam). Such an attitude can easily be shown to be inconsistent, as indeed the assumption of elasticity is usually invoked in *addition* to the *further* simplifications. Understanding of the true nature of the assumptions, of their range of applicability, and of the problems in which more elaborate assumptions have to be introduced is the only way progress can be achieved.

Various computer methods are today available for stress analysis. Finite-difference procedures or various integral methods are often used. Most promise and versatility lie, however, in the so-called "finite-element" method, and this section will describe its use.

2. Finite-element Analysis. The origins of the finite-element analysis of a continuous two- or three-dimensional structure stem from the classical approaches of structural analysis. The *infinite* degree of freedom of the continuous medium is made finite by:

1. Dividing the whole region into a series of subregions or *elements* assumed to be interconnected at a finite number of *nodal points*
2. Specifying certain simple displacement patterns dependent on the displacements of the nodes and the relationships between *nodal forces* to obtain *nodal displacements*
3. Assembling the "elements" together by imposing *equilibrium* condition at all the

nodes in a straightforward "structural" manner and, by solution of the resulting simultaneous equations, finding the *nodal displacements*

4. Finally, computing all the stresses by step 2 from the now known nodal displacements

This "structural" concept, first introduced by Turner, Clough, et al.,[1,*] is easily visualized and instinctively appealing. Much further work has served to extend the

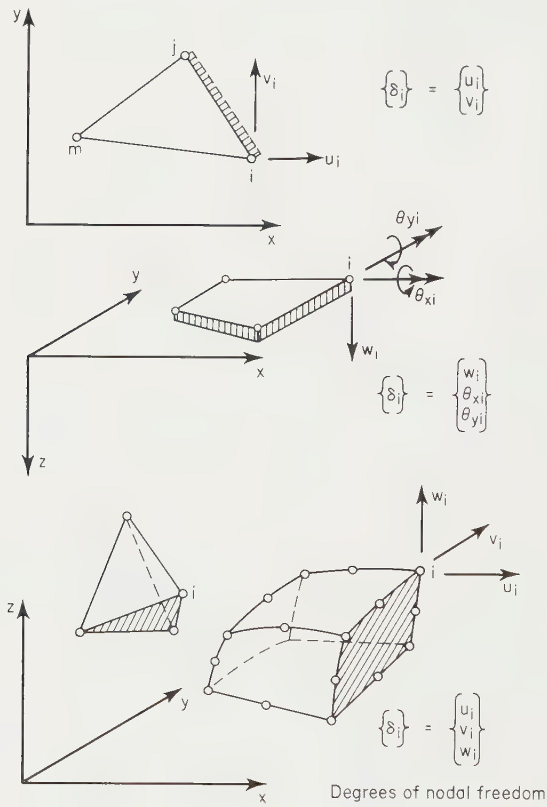

FIG. 1. Some finite elements for plane, bending, and three-dimensional problems.

full mathematical implications of the process, and indeed it is now well established that the method is a particular case of the general Ritz procedure. For details of the formulation many original papers can be consulted or reference made to a full textbook on the matter.[2] In the space of this section it is impracticable to give more than the briefest details. These will be relegated to the Appendix, where the essentials are summarized.

Much variety can be expected in the shape of elements and the number of interconnecting nodes. These can range from the simplest triangle interconnected at the corners for two-dimensional problems, through plate elements with rotational degrees of freedom, to complex three-dimensional elements with many nodes (Fig. 1). In some cases elements with curved sides have been used with success.

* Superior numbers refer to items in the Bibliography at the end of this section.

Whatever the shape, number of nodes, or elastic properties of the element we can always write for each node the displacement as $\{\delta_i\}$, a "listing" of the nodal degrees of freedom, and for the whole element

$$\{\delta\}^e = \begin{Bmatrix} \delta_i \\ \delta_j \\ \cdot \\ \cdot \\ \cdot \end{Bmatrix} \tag{1}$$

listing all the nodal displacements. The calculation of stage 2 will result in the listing of the forces associated with each node in the appropriate direction of displacement in the form

$$\{F\}^e = \begin{Bmatrix} F_i \\ F_j \\ \cdot \\ \cdot \\ \cdot \end{Bmatrix} = [k]^e\{\delta\}^e + \{F\}_T{}^e + \{F\}_q{}^e \tag{2}$$

In this $[k]^e$ is the "stiffness" matrix of the element while $\{F\}_T{}^e$ and $\{F\}_q{}^e$ are forces contributed to the nodes by thermal changes and distributed weight or pore pressure. Calculation of these factors is the basic step of the method, and the general principles are given in the Appendix. A large number of different elements have been computed and programs written for their derivation. All, however, will be in the basic form given above.

The assembly of the overall "equilibrium" equation consists simply of adding up all the (internal) forces $\{F\}$ acting at each node and equating these to the external nodal forces which may be imposed on the structure $\{R\}$. This results in a system of equations which can be written in matrix form as

$$\{R\} = \begin{Bmatrix} R_1 \\ \cdot \\ \cdot \\ \cdot \\ R_n \end{Bmatrix} = [K]\begin{Bmatrix} \delta_1 \\ \cdot \\ \cdot \\ \cdot \\ \delta_n \end{Bmatrix} + \begin{Bmatrix} F_{T1} \\ \cdot \\ \cdot \\ \cdot \\ F_{Tn} \end{Bmatrix} + \begin{Bmatrix} F_{q1} \\ \cdot \\ \cdot \\ \cdot \\ F_{qn} \end{Bmatrix} \tag{3}$$

Now *all* the nodes are considered, and it is easy to show that the various components of the matrices are given by simple addition of all element contributions. Thus

$$\begin{aligned} K_{rs} &= \Sigma k_{rs}{}^e \\ F_{Ts} &= \Sigma F_{Ts}{}^e \\ F_{qs} &= \Sigma F_{qs}{}^e \end{aligned} \tag{4}$$

The equations for the complete solution are thus known, and though their number may in a typical problem reach several hundred or even two or three thousand in special cases, no difficulties in solution are presented if large computers are available. (At this stage all the prescribed displacements or support conditions obviously have to be inserted.)

Once all the displacements for each element are found, stresses are easily obtained by equations quoted in the Appendix.

The derivation of full computer programs is a process demanding a considerable amount of experience. Nevertheless once these are written (and many are now available) a very simple set of data (such as the coordinates of nodal points, their numbers, elastic properties of each element together with applied forces) can be assembled by an engineer not necessarily familiar with the details of the process. Some experience is nevertheless required in the original idealization of the mesh, as obviously the process involves a mathematical approximation. Previous experience and the use of progressively smaller meshes will indicate for practical purposes the amount of approximation involved.

3. Loads and Criteria of Analysis. Assuming that suitable finite-element computer programs are available some general matters of the assumptions regarding loading conditions, initial stress, etc., have to be considered *before* an analysis is carried out. In addition, *after* the results become available some criteria concerning their interpretation will be needed.

As most of the factors are common to all dam problems, it is convenient to discuss them jointly.

Foundations. The foundations of the dam are an integral part of the structure, and their deformability can be included in the analysis without difficulty. As the stresses caused by the dam within the foundations "dissipate" rapidly it is possible to use elements of a very large size there, grading into the smaller dam subdivision where the stresses are more important and their variation greater.

Initial stresses due to weight and various kinds of tectonic action exist within the foundation rock *prior* to the construction of the dam. It is a general rule (which can only be violated in exceptional cases) that these stresses are estimated (or computed) *before* the interconnection with the dam. This means that no gravity loads within the foundation should be applied to the analysis of the dam-foundation complex.

The same comment applies to the loads caused by pore-water pressure. Only the *difference* between the pore-pressure state after and before the construction can be applied as loading to the whole assembly of dam and foundation.

The initial gravity, tectonic, and pore-water-pressure stresses are obviously simply *superposed* on the additional effects of dam stresses.

In the analysis it is important to know at least the approximate elasticity constants of the rock material. With the finite-element process no difficulty arises in dealing with nonhomogeneity or anisotropy, as will be shown in later examples. However, the knowledge of rock properties is usually limited and only approximate values can be put into the analysis. It is extremely fortunate that the stresses in most dams are relatively insensitive to the exact values of foundation constants—and often the true solution can be "bracketed" by extreme assumptions of their values. This generally involves very little additional computation labor.

Water Loading. All water forces on a concrete (or rock) structure are applied effectively as volume-*body force* action. Thus if p is the pore pressure, the forces per unit volume of material in the x, y, and z directions are[3]

$$X = -\frac{\partial p}{\partial x} \qquad Y = -\frac{\partial p}{\partial y} \qquad \text{and} \qquad Z = -\frac{\partial p}{\partial z} \tag{5}$$

respectively.

The "fiction" of surface-water-pressure load can be still approximately true if, say, internal drainage or configuration such as occurs in buttress dams prevents the buildup of any pore pressure close to the water-supporting face. If, there, the variation of pressure from the full head on the outside to zero at a line of elements close to the face is assumed, the effect will be almost identical to a surface pressure. Thus all computer programs written specifically for dam analysis should possess the faculty of dealing with pore pressures.

For example, in the simple two-dimensional element in Fig. 1 (see also Appendix) it is convenient to assume pressure to vary linearly between the nodal values, *i.e.*,

$$p(x,y) = N_i p_i + N_j p_j + N_m p_m$$

in which N_i, etc., are as defined in the Appendix.

Differentiating, we have simply

$$X = -\frac{b_i p_i + b_j p_j + b_m p_m}{2\Delta}$$

$$Y = -\frac{c_i p_i + c_j p_j + c_m p_m}{2\Delta}$$

By the last equation of the Appendix it will be seen that as these forces are constant they simply result in allocating to each node one-third of the total force which would be acting on the element of Fig. 2, with external distribution of pressures shown.

It is important to repeat here the point already mentioned in the previous article. Within the foundation only the effect of the difference between the initial and final states of pressure distribution will produce forces which can influence the dam stresses. Typically pressures in foundations of a valley in which a river is present can be such as those represented in Fig. 3*a*, while the state of pressure after the dam construction approximates the pattern given in Fig. 3*b*. The approximate forces acting on the dam-foundation complex are given in Fig. 3 by the direction of the arrows.

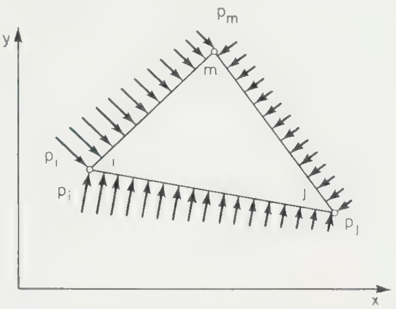

FIG. 2. Pore-pressure body forces on a two-dimensional element.

It is quite clear that in no circumstances will the foundation be subject to anything approaching a downward surface water load, a fact often ignored and by no means obvious.

Gravity Loading. It has already been mentioned that in the complete analysis the gravity of the foundation should be excluded (and effectively reintroduced by superposition of the initial stress system which is in equilibrium with it).

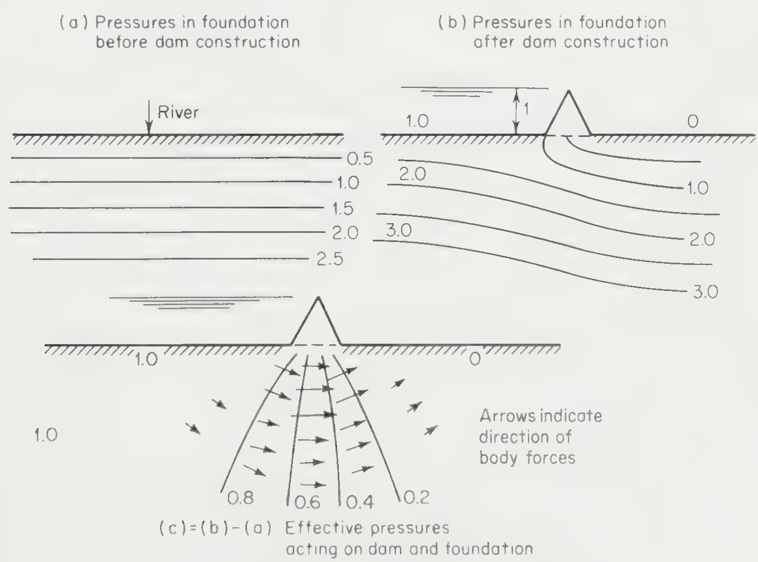

FIG. 3. The action of foundation pore pressure.

In the dam itself it is often accurate enough to consider the gravity as if it were applied externally to the completed, weightless structure. This assumption is manifestly not true, and for special cases the step-by-step construction process can be followed in the finite-element analysis, just as is often done in model analysis.[4] This process is obviously more expensive in computer time, and the approximation of applying gravity to the whole structure gives results which do not differ by a large amount from those of the more exact process.

Creep of concrete will usually make the true gravity stresses lie between the two alternative assumptions.

For simple elements like the plane triangle of Fig. 1, the application of expressions (D) of the Appendix gives the intuitive result, i.e., that the weight of each element is transmitted equally to each node.

Inertia Loads. If the dam is subject to a known prescribed acceleration in any direction this can be treated in a similar manner to gravity loads. The only special remark which should now be made is that this acceleration may well have to be applied to some portion of the foundation to approximate the earthquake effects.

In a complete study of earthquake shocks the true dynamic behavior of the structure must be considered. In the finite-element process it is relatively simple to include the inertia forces, which will result in an additional force in Eq. (2).

$$\{F\}_m^e = -[M]\{\ddot{\delta}\}^e \tag{6}$$

where the "dots" indicate differentiation with respect to time² and $[M]$ a suitable mass matrix.

With the aid of such a formulation one can study natural frequencies of the structure and predict its response to earthquakes.[5,6]

Thermal "Loads." Temperature effects on stresses are treated easily in the general formulation as simply one of the load systems.

The two types of temperature distribution which arise (1) from *external* causes such as seasonal cycles and (2) from heat of hydration present somewhat different problems.

In the first case a reasonably elastic behavior of the concrete can be assumed without serious error.

The second acts on the concrete during its early life when creep effects are most serious. While again the solution of such creep problems is possible by the finite-element method, it is subject to certain uncertainties and indeed is quite costly.[7,8] By the time the dam construction is completed it will usually introduce a system of *initial stresses.* These constitute probably the largest unknown in stress analysis of dams, though the magnitude of such stresses is limited and can be reduced by proper construction processes.

Prestressing and Other Loads. It is quite common in modern dam design to introduce cables prestressing the structure. The cable loads must obviously be treated as concentrated forces acting at a suitable node of the element subdivision. Local effects can be studied simultaneously with the general stress distribution by using a fine subdivision in the region of such load concentrations.

Similar problems of concentrated loads arise in gate support loads, etc.

General Comments and Design Criteria. From the remarks already made, it is clear that for maximum efficiency computer programs for finite-element analysis of dams should have certain special characteristics.

1. A system of initial stress specified externally must form part of the input.
2. Different elastic properties should be capable of being specified for each element.
3. Gravity, water-pore pressure, and temperature loads should be automatically calculated for all nodes from specified values of density, pressure, and temperature.
4. Additional concentrated loads should form a special input.

It is usually no more expensive to obtain separate solutions for each load and obtain totals by automatic addition. The separate effects can thus be studied individually or in sum.

The input will generally require an intelligent element subdivision and a specification of coordinates of a large number of nodal points. The latter part is undoubtedly tedious and provides a possible source for introduction of mistakes. Much effort has recently been given to at least a partial automation of this process. In a typical procedure the mesh is automatically generated by interpolation from the specification of boundary-point coordinates only.

All programs should be capable of computing the principal stress system acting at various points of the structure. It is these stresses which will finally decide whether a suitable safety is ensured, and decisions on modification of the *design* will be taken on that basis.

One of the basic criteria usually introduced is that *no tensile stress* should be present in the final structure. Certainly this must apply in the rock, which is usually fissured, and probably it is desirable to extend this to the concrete mass, where cracking could have occurred by thermal or shrinkage action.

In elastic stress analysis it is almost impossible to design a dam structure with no tension in any part. The criterion must therefore be modified. A reasonable approach is to consider the criterion as applicable after a *limited amount of cracking has occurred.*

A dam structure in which tensile stresses cannot be eliminated by limited cracking must be considered unsafe.

Introduction of cracks into finite-element analysis presents little difficulty by a "trial-and-error" process. Recently automatic methods of introducing such cracking have been attempted with success.[9]

While the *elastic* stress analysis gives a good picture of working stresses and makes it possible to estimate the *least factor* of safety against failure, the true failure load can only be obtained by the introduction of plastic nonlinearities into the analysis. This is a complicated process, and while much work has been done in the direction,[2] at the moment this matter must be considered as being in the research, rather than application, stage.

4. Some Applications of Static Finite-element Analysis. *Buttress and Gravity Dams.* In both these types of dam a *two-dimensional* state of stress can generally be assumed without much error. (An appreciable error may occur where the cross section changes rapidly—but this will be localized and only in special cases will it be necessary to go to a full three-dimensional analysis.)

The first example[10] is that of a massive-head buttress dam. Figure 4 shows the dam section, its foundation in which various inhomogeneities exist, and the division into triangular elements. Around the perimeter of the foundation zero displacements are prescribed.

Figure 5 shows the vertical stresses due to gravity and water loading and indicates how far the "conventional" linear assumptions can err.

In Fig. 6*A* the plot of the principal stresses is shown and indicates the tensile region developed. In Fig. 6*B* the introduction of a crack eliminates the tension from the dam. (The tensions remaining in the foundation are here less than the "initial" stress in the rock, which in fact eliminates them.) Figure 7 shows some thermal stresses in the same dam.

In the second example of Fig. 8 a thin Ambursen dam is analyzed. The buttresses are here linked in pairs for lateral stability. As the foundation conditions were variable, different assumptions regarding it were made. In Fig. 8*a*, for instance, the whole foundation is taken as having a modulus of elasticity equal to 0.25 of that of the modulus of concrete. In Fig. 8*b* a stepwise variation of modulus between an upstream value of $0.25Ec$ and a downstream value of $0.025Ec$ was assumed. The results indicate the relative insensitivity of stresses near the base of the dam to such radical conditions. As a result of such analysis the design of the dam was modified and a considerable saving of concrete made.

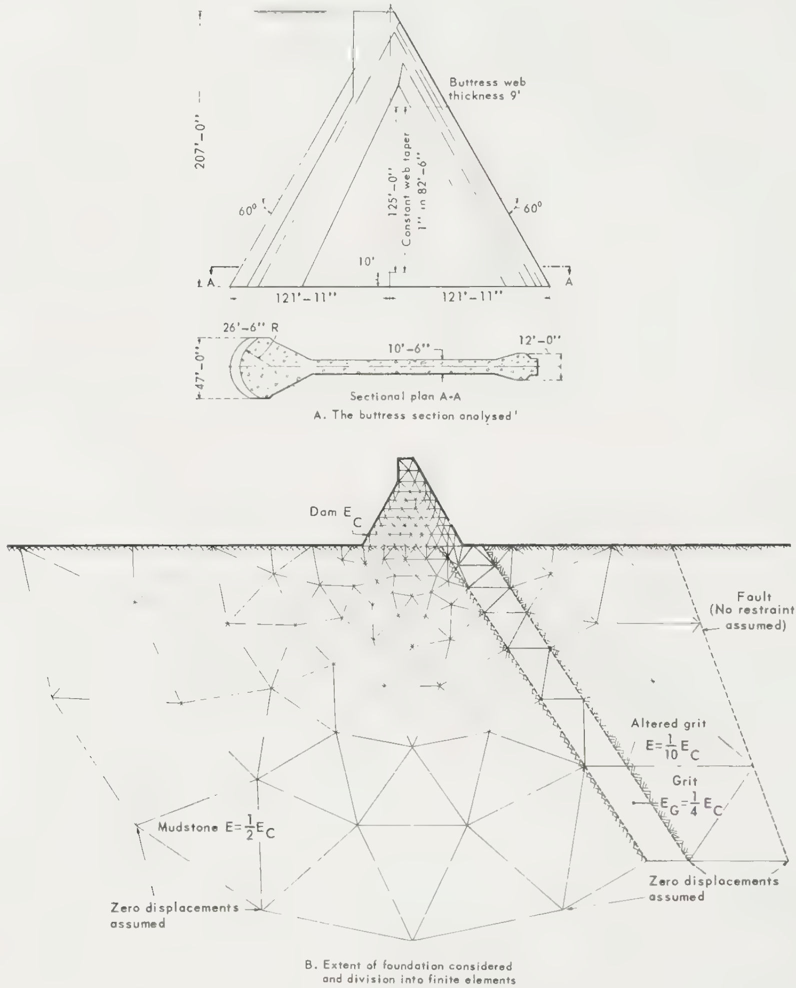

Fig. 4. Massive-head buttress-dam analyses by the finite-element method (Clywedog Dam—Wales).

In this problem the cross walls are simply approximated by a two-dimensional stiffening. Clearly the stress distribution in their vicinity is not accurate. For the solution here quadrilateral elements are used, derived by linking pairs of simple triangles. The technique results in a better stress averaging and reduces considerably the input data for computation.

Examples of Figs. 9 and 10 show two gravity dams. In the first the point of interest is the study of localized cable stresses simultaneously with that of the overall distribution. In the second an unusual hollow dam construction is indicated. Here a model study supplemented the numerical investigation, and the differences between the resulting stresses were of the order of errors inherent in the model study. Clearly both present problems to which adequate results could not be obtained by conventional theory.[11]

Arch Dams as Three-dimensional Problems. While full three-dimensional analysis by finite elements is still relatively expensive, it is at the present stage of development clearly more economical than such processes as full trial-load analysis.

The complex three-dimensional element shown in Fig. 1 and possessing 60 degrees of freedom has proved to be efficient for this purpose.[12,13] By the use of such an

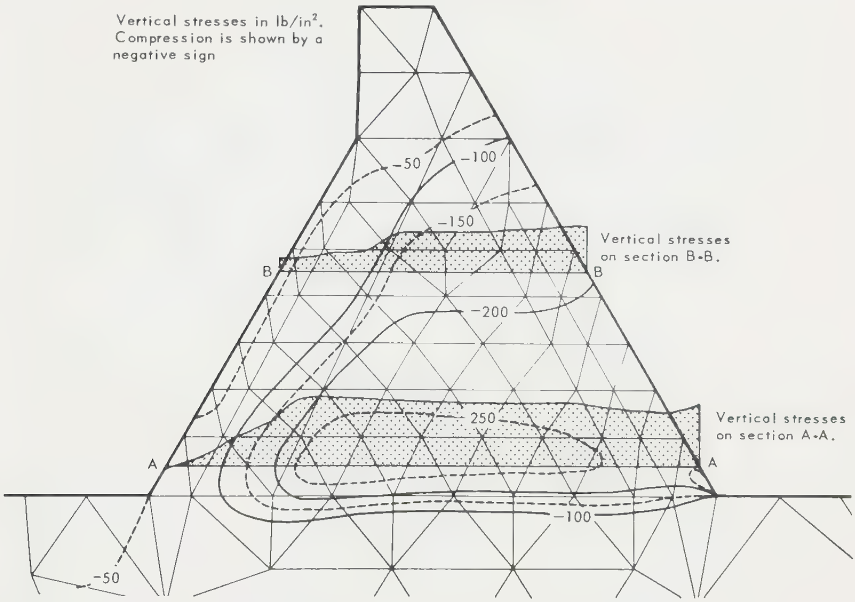

FIG. 5. Distribution of vertical stresses due to gravity and water pressure for buttress dam of Fig. 4.

elaborate finite element quite complex states of stress can be represented and a considerable accuracy gained over simpler elements for the same total number of nodes involved. This permits the total number of simultaneous equations involved in a given accuracy of representation to be reduced to reasonable proportions. (With 500 to 1,000 total unknowns very accurate solutions can be obtained.)

As the element nodes can be placed in any position and as the sides can be curved (to a parabolic shape), quite large elements may be used and yet fit the geometry of the problem well. By making two sides of each element parallel to each other the process of determining nodal coordinates becomes simplified, and it is possible to work from parallel sections arranged in either horizontal or vertical planes. The geometric definition of the dam can be arbitrary, and openings or spillway cutouts present no difficulties.

The element division can be extended into the foundation, and appropriate moduli can be used whether the situation is homogeneous or not. This avoids the need for the introduction of the approximate Voigt assumptions there.

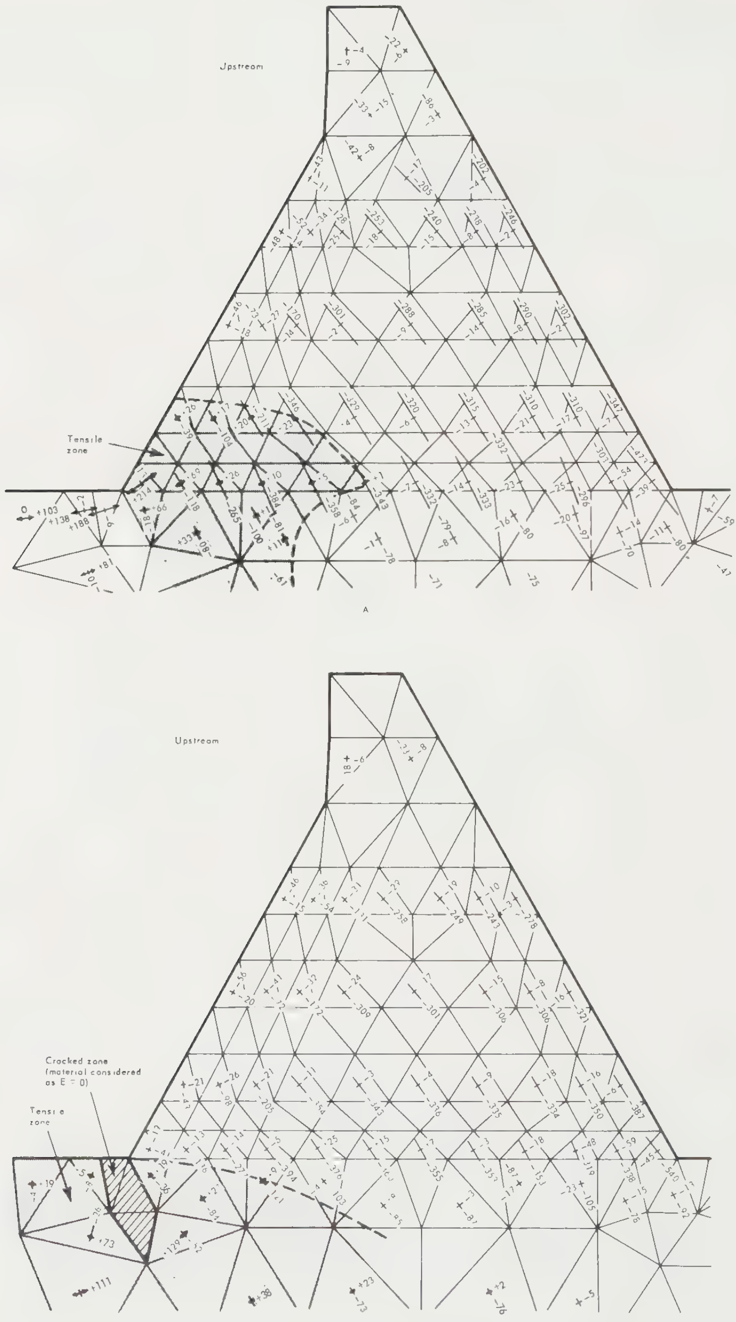

Fig. 6. Principal stresses in dam of Fig. 4 before and after the introduction of a crack (gravity and pore-water pressures).

For relatively simple cylindrical shapes the full trial-load analysis and three-dimensional finite-element solutions give comparable answers. In doubly curved dams of the modern type the trial-load assumptions are somewhat dubious, and recent comparisons[14] show that in fact considerable differences exist between its results and those of full three-dimensional treatment. It is therefore to be anticipated that such solutions will displace "trial-load" approaches and indeed the *elastic* types of models to which they are a more economic and versatile alternative.

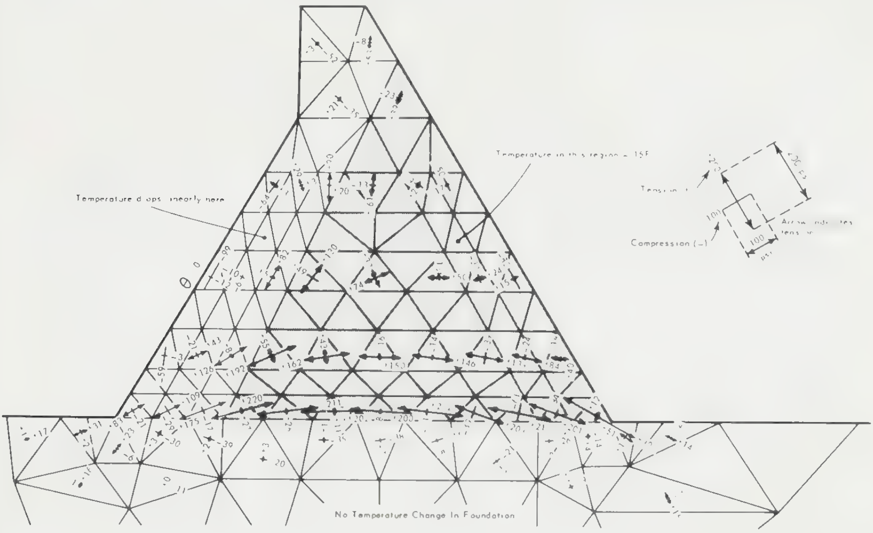

Fig. 7. Thermal stresses due to a temperature drop in the web area of the buttress of Fig. 4.

Figure 11 shows an isometric view of a typical doubly curved dam* and its division into elements. A nonhomogeneous foundation condition is included here by way of illustration.

Figures 12 and 13 show some of the results of an analysis. Here the effect of valley elasticity is shown on the deflection and stresses of the center-line section.

Thin Arch Dams—Shell-type Solution. When an arch dam is thin it is possible to introduce into its analysis the basic assumptions of the shell theory and thus treat the problem as "two-dimensional." This reduces the total number of unknowns needed for a finite-element solution and makes this approach obviously cheaper.

The essential assumption of shell theory introduced here will be the one[16] involving the normals to the middle surface remaining straight and normal to it during deformation. This, in engineering terms, presumes a linear distribution of stresses through any section.

Two difficulties arise. The first is that all "shear deformation" is thus suppressed—a factor which is not serious for thin sections, however. The second difficulty concerns the introduction of foundation deformation. Here it is necessary to reintroduce the Voigt assumptions in common with trial load.

Various approaches to shell solutions are being studied. In the simplest of these the surface of the shell is divided into flat elements of rectangular or triangular shape. The stiffness of such an element is considered in terms of (1) "in-plane" (plane stress)

* A shape currently studied by the Arch Dams Committee of the Institution of Civil Engineers.[15]

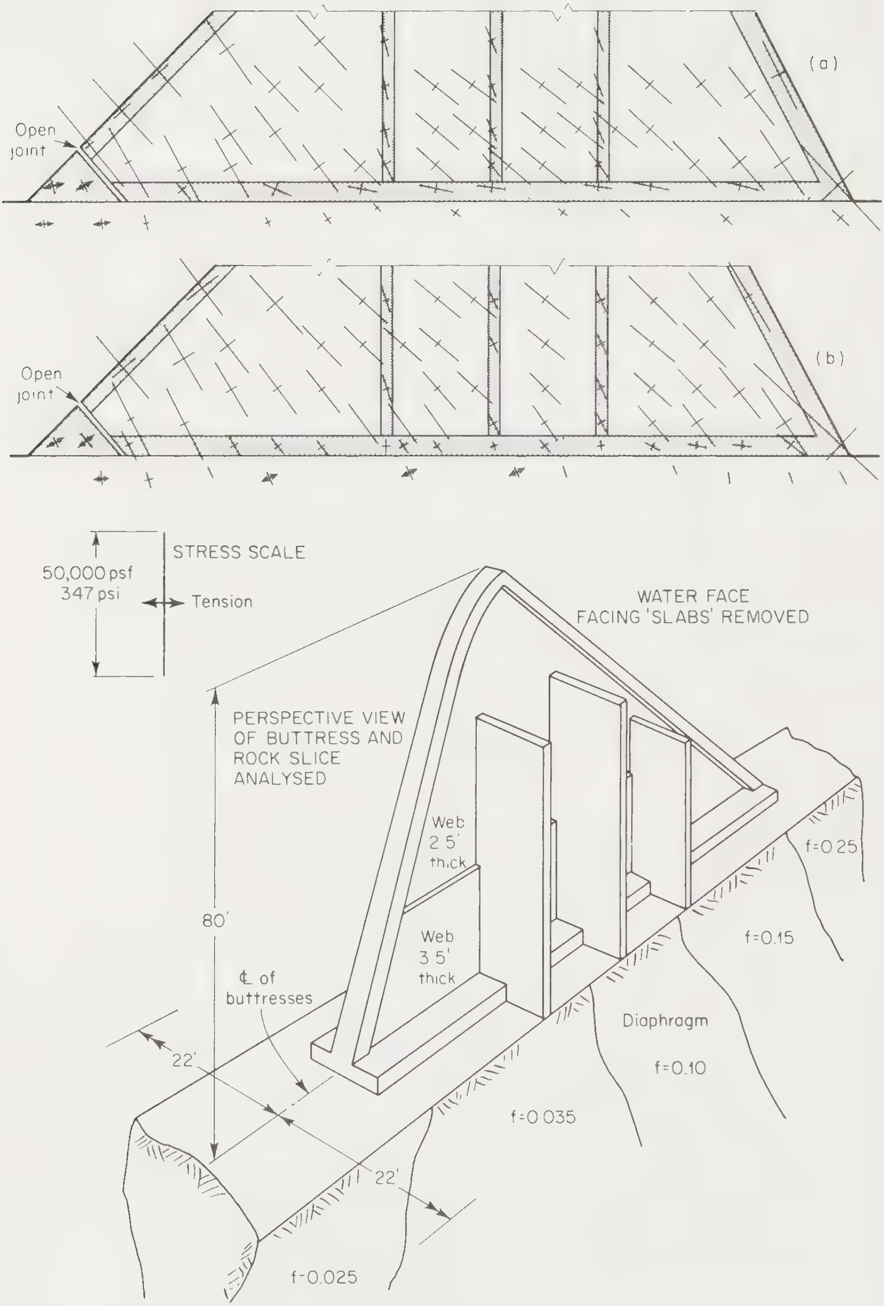

FIG. 8. A thin-section buttress dam (Muda Dam—Malaya). $f = E$ rock/E concrete. (a) $f = 0.25$ throughout foundation. (b) $f = 0.25$ to 0.025 varying as shown.

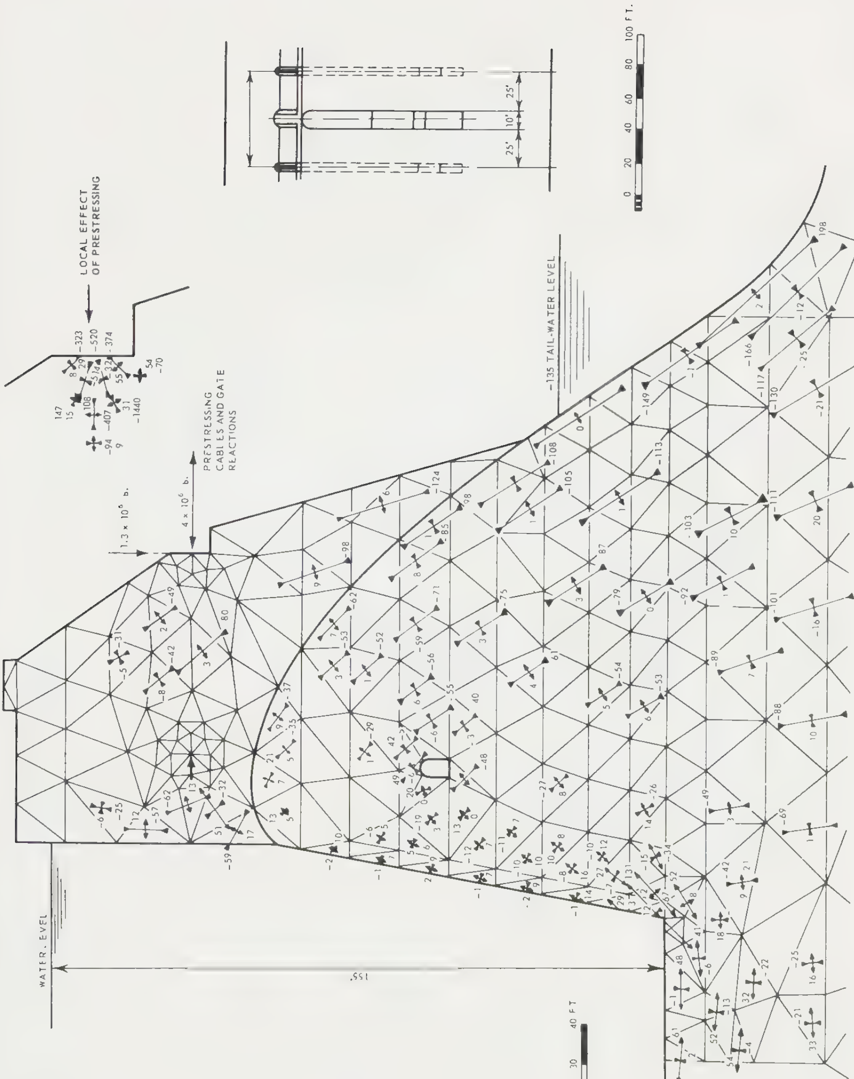

FIG. 9. Some stress studies for a massive gravity dam with piers (Kainji Dam—Nigeria).

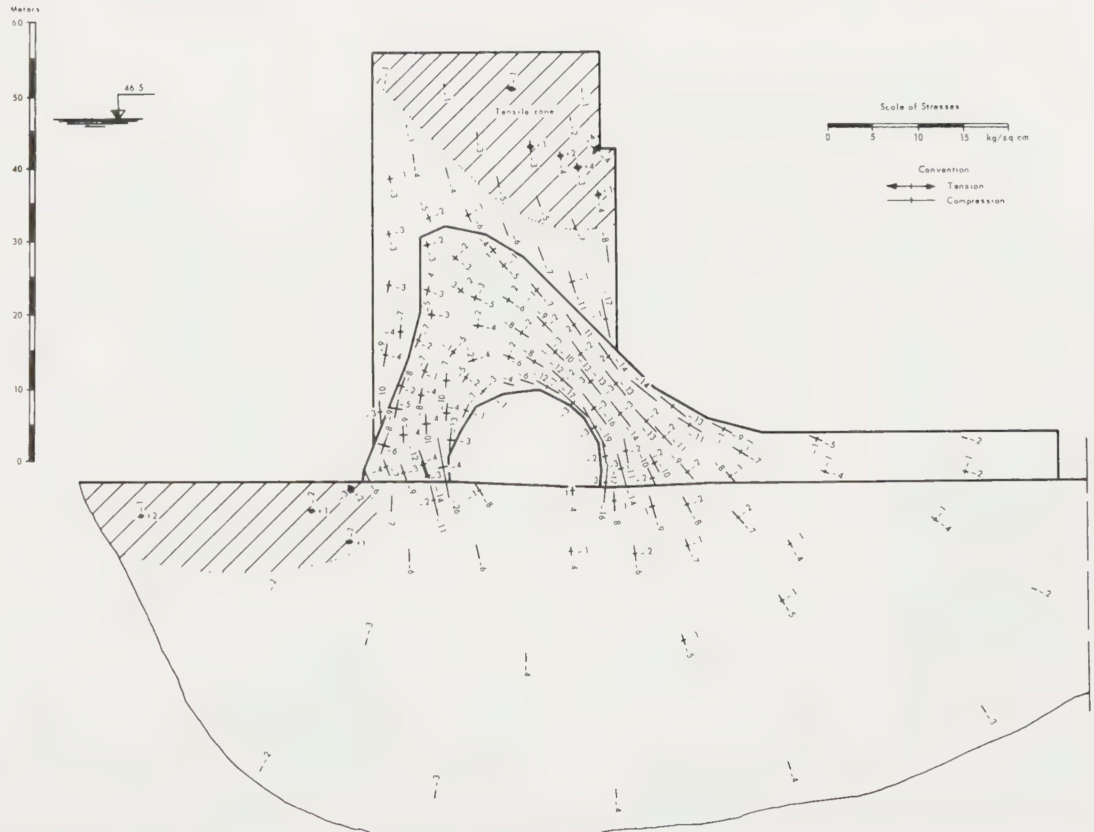

FIG. 10. A hollow gravity dam. Results of a finite-element analysis for gravity and water-pressure forces. (Carrapatelo Dam—Portugal).

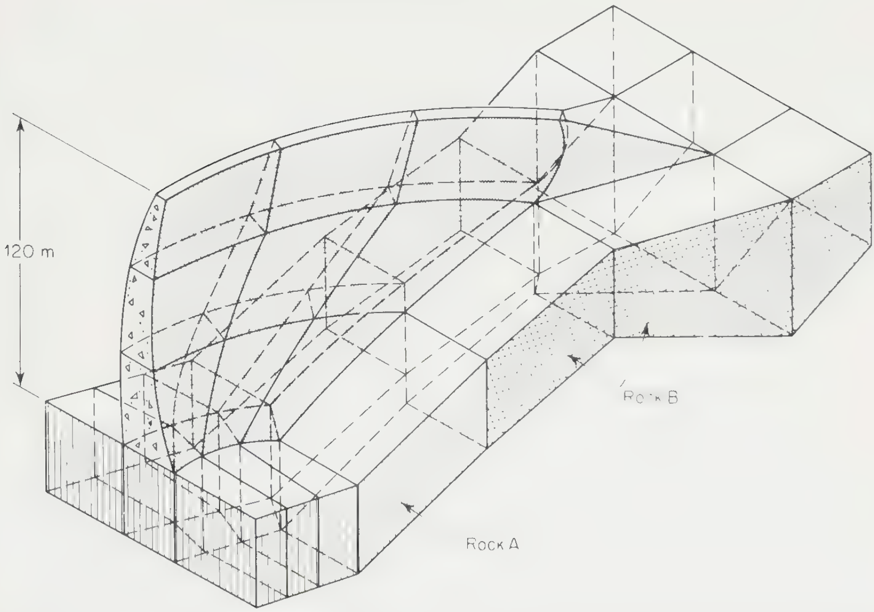

FIG. 11. A three-dimensional analysis of a doubly curved arch dam and its nonhomogeneous foundation. Elastic moduli: concrete, 2.00×10^5 kg/cm²; rock A, 0.25×10^5 kg/cm²; rock B, 1.00×10^5 kg/cm²; Poisson's ratio 0.15 for all materials.

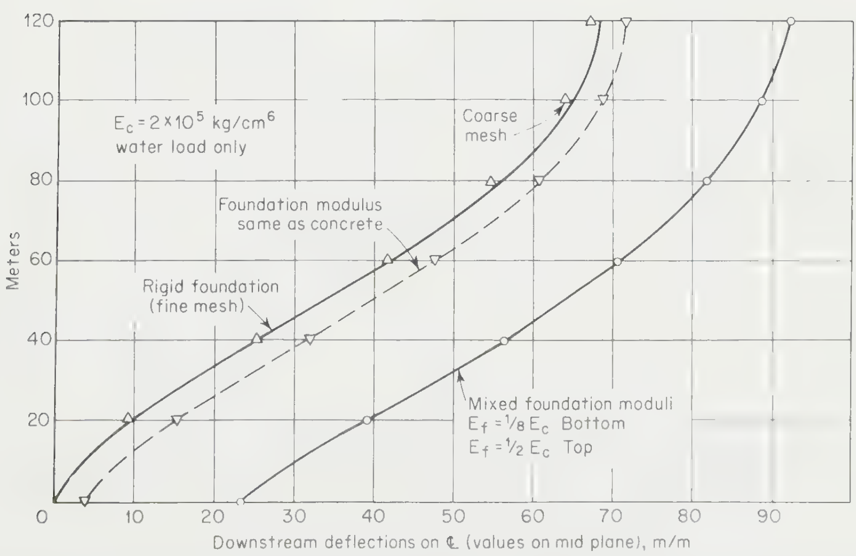

FIG. 12. Downstream deflections on the midplane of the arch dam of Fig. 11 for various foundation deformabilities. Note that pore-pressure action in the foundation causes an overall movement of the whole structure.

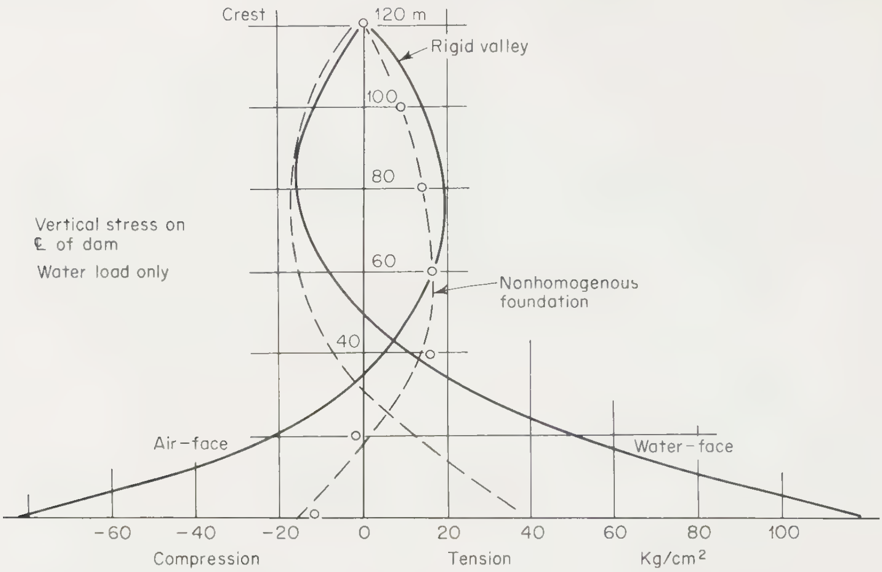

FIG. 13. Vertical (cantilever) stresses for the center section of the dam of Fig. 11 (for two extreme foundation conditions).

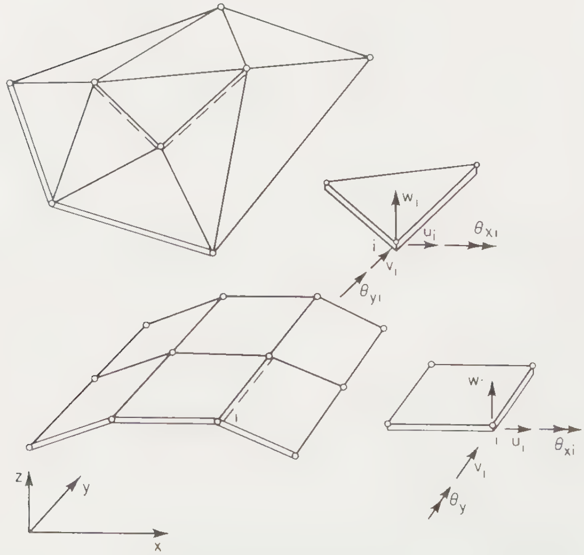

FIG. 14. Representation of curved surfaces by flat plate elements.

action and (2) "bending" action based on standard plate theory. Figure 14 shows such divisions of curved shell surfaces into flat "elements" and the degrees of freedom which have to be considered at nodal points. Again for details of various stiffness matrices involved the reader is referred to the text of the subject[2] or original papers.[17,18]

For doubly curved dams the use of triangular elements is obviously necessary to be able to represent the surface (even approximately) while for singly curved shapes

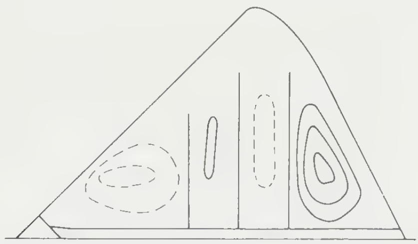

FIG. 15. First mode of vibration of the buttress dam of Fig. 8. Frequency found is 16.7 cps.

rectangular elements suffice. The results of such shell analysis are remarkably close to those obtained three-dimensionally.[19]

Some Special Problems for Which Finite-element Methods Are Applicable.

Vibration Frequencies. It has already been mentioned that for a study of earthquake response a knowledge of free vibration frequencies is essential. Such a typical study is shown for the example of the dam illustrated in Fig. 8. With a thin dam of this kind it is clear that the lowest frequencies of vibration will occur because of plate-type motion in direction transverse to the valley.[6] A typical buttress was therefore

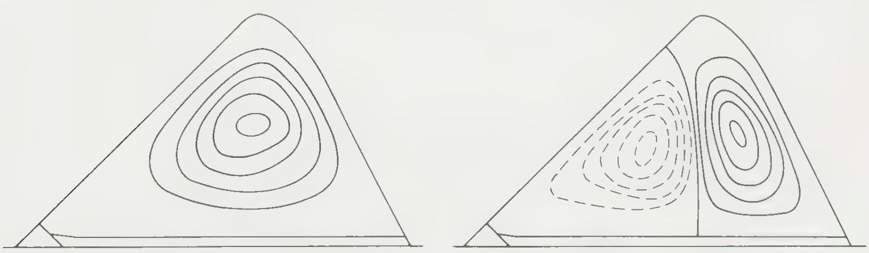

(a) (b)

FIG. 16. First and second modes of vibration of buttress dam of Fig. 8 on removal of cross walls. Frequencies found are 4.3 and 7.8 cps.

divided into triangular plate (bending) elements, and it was assumed that the cross walls provided an immovable lateral support. Figure 15 shows the contours of the first mode and the value of the lowest frequency. In Fig. 16 the effect of the removal of the cross walls is shown. The dangerous lowering of the fundamental frequencies is to be noted.

Other vibration problems have been studied—for instance, in a similar manner arch-dam and gravity-dam frequencies can be obtained.[20,21]

For all the basic theory details the reader should consult Ref. 2.

Buckling Stability of Buttresses. With thin buttress sections various rules are used to limit the stresses in relation to the "unsupported column" length in order to ensure

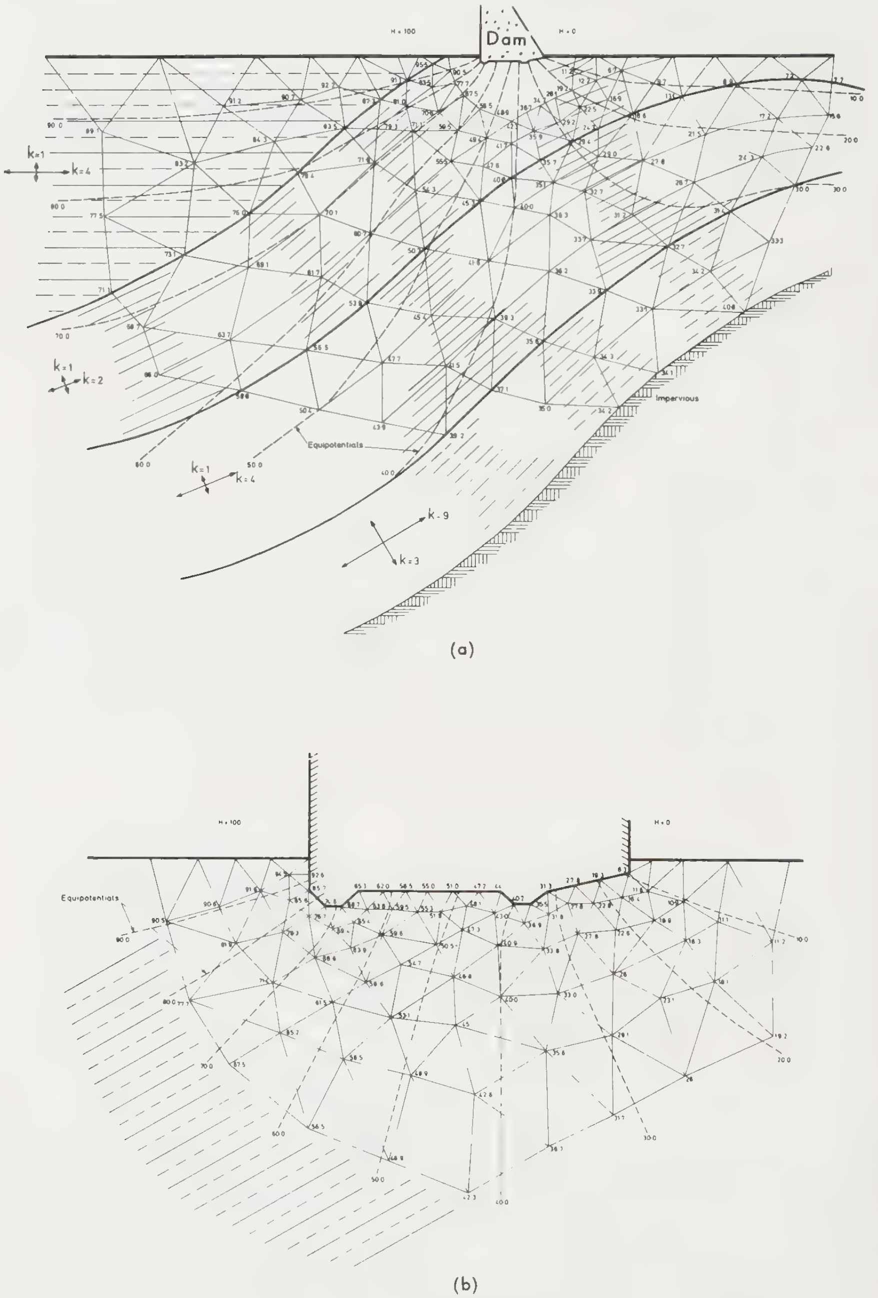

Fig. 17. Seepage flow below a dam through a highly anisotropic and contorted foundation rock.

safety against buckling. By a suitable formulation of the finite-element analysis[2] it is possible to determine the factor by which an increase of all the "in-plane" stresses would cause buckling failure. This factor can thus be considered as a safety factor against buckling, and it would be reasonable if in future specifications a given number were attached to it.

Such an analysis carried out for the thin, low dam in Fig. 8 shows a surprisingly high safety factor. This was 160 for situations without and 460 with cross walls.

Nonstructural Applications of the Finite-element Method. As the finite-element process is in essence a variational method of approximate solution of boundary-value problems, its applications range well beyond the few structural examples quoted here.

Two nonstructural problems which are of interest in dam design are (1) the development of pore pressures in a porous mass of concrete or rock and (2) the distribution of temperatures.

To both, the finite-element process can be simply applied, and indeed the same element division can be used so that the first solution provides data for the stress-distribution analysis. Details will again be found in Ref. 2 or in Refs. 22 and 23. Figure 17 shows a seepage solution for an imaginary and extremely complex rock configuration involving inhomogeneity and anisotropy. It may well be said that no other methods could have tackled problems of such complexity with such ease.

Concluding Remarks and a Glance at the Future. From this survey and the examples shown it is evident that many of the difficult problems of stress analysis posed to the dam designer can now be rapidly solved. The computer times (and therefore costs) are small. Preparation of data, though demanding meticulous care, can be handled by relatively unskilled personnel once the programs are prepared.

This rapidity of solution allows the engineer to concentrate his attention on design. Introduction of design changes (such as modification of thicknesses of a buttress or arch dam) or investigation of unknown parameters (such as effects of different rock properties) is easy and can often be accomplished by replacement of only a few data cards and an additional computer run. The picture is therefore much different from the situation where computations for a changed design demanded weeks or even months of additional work and if models were involved proved very costly. It is hoped that improved designs will now be possible.

While the above introduction of changes has already proved advantageous, much development work is at present in process in many organizations for an *automatic optimization process.* Perhaps the time is not too far off when a design of say an arch dam with minimum volume (subject to constraints such as shape of valley or rock properties) can be produced automatically.

APPENDIX

Brief Details of the Finite-element Displacement Formulation

We shall illustrate the process by considering the triangle element in plane strain (Fig. 1). The displacements within the triangle can be defined in terms of the displacements at the nodes by a linear relationship. Writing, for instance,

$$u = \alpha_1 + \alpha_2 x + \alpha_3 y$$

one can solve for all the constants in terms of prescribed values of u at the three nodes i, j, n. Performing such a solution we have for displacement at any point

$$\{f\} = \begin{Bmatrix} u \\ v \end{Bmatrix} = \frac{1}{2\Delta}[IN_i, IN_j, IN_m] \begin{Bmatrix} \delta_i \\ \delta_j \\ \delta_n \end{Bmatrix} = [N]\{\delta\}^e \qquad (A)$$

in which $I = \begin{bmatrix} 1 & 0 \\ 0 & 1 \end{bmatrix}$, $\{\delta_i\} = \begin{Bmatrix} u_i, \\ v_i \end{Bmatrix}$ etc.

$$N_i = a_i + b_i x + c_i y \qquad \text{with} \qquad a_i = x_j y_m - x_m y_j$$
$$2\Delta = \det \begin{vmatrix} 1 & x_i & y_i \\ 1 & x_j & y_j \\ 1 & x_m & y_m \end{vmatrix} = 2\,(\text{area of } i, j, m) \qquad \begin{aligned} b_i &= y_j - y_m \\ c_i &= x_m - x_j \end{aligned}$$

N_j and N_m are given by changing suffixes in order *i-j-m*. The assumed displacement pattern preserves continuity between elements and includes all constant strain states—two necessary conditions for convergence.[2]

The strains in the element are now given as

$$\{\epsilon\} = \begin{Bmatrix} \epsilon_x \\ \epsilon_y \\ \epsilon_{xy} \end{Bmatrix} = \begin{Bmatrix} \dfrac{\partial u}{\partial x} \\ \dfrac{\partial v}{\partial y} \\ \dfrac{\partial u}{\partial y} + \dfrac{\partial v}{\partial x} \end{Bmatrix} = [B]\{\delta\}^e \tag{B}$$

in which by appropriate differentiation we have from (A)

$$[B] = [B_i, B_j, B_m] \qquad \text{and} \qquad [B_i] = \frac{1}{2\Delta} \begin{Bmatrix} b_i, 0 \\ 0, c_i \\ c_i, b_i \end{Bmatrix} \qquad \text{etc.}$$

The stress-strain relations can be written as

$$\{\sigma\} = \begin{Bmatrix} \sigma_x \\ \sigma_y \\ \tau_{xy} \end{Bmatrix} = [D](\{\epsilon\} - \{\epsilon_0\}) \tag{C}$$

where $[D]$ is the elasticity matrix which, for example, in plane strain of an isotropic material is

$$[D] = \frac{E}{1 - \nu^2} \begin{bmatrix} 1 & \nu & 0 \\ \nu & 1 & 0 \\ 0 & 0 & (1 - \nu)/2 \end{bmatrix}$$

with usual elastic constants, while $\{\epsilon_0\}$ represents thermal strain

$$\{\epsilon_0\} = \begin{Bmatrix} \alpha T \\ \alpha T \\ 0 \end{Bmatrix}$$

in which α is the expansion coefficient.

If the nodal "forces" are in equilibrium then the *work done externally* on an element during a virtual displacement is equal to the *internal* work. Taking a virtual displacement of the nodes or $\{\delta^*\}^e$ we thus have

$$\{\delta^*\}^{eT}\{F\} = \int \{\epsilon^*\}^T \{\sigma\} d\,(\text{vol}) - \int \{f^*\}^T \{q\} d\,(\text{vol})$$

if $\{q\}$ are the *body* forces per unit volume corresponding with the u and v directions. By substitution of (B) and (C) we have finally the relation of form (2) in which

$$\begin{aligned} [k]^e &= \int [B]^T [D][B] d\,(\text{vol}) \\ [F]_T{}^e &= -\int [B]^T [D] \{\epsilon_0\} d\,(\text{vol}) \\ [F]_q{}^e &= -[\int N]^T \{q\} d\,(\text{vol}) \end{aligned} \tag{D}$$

Noting that for plane stress only the matrix $[N]$ contains the x and y coordinates, that d (vol) $= dx\, dy$ for a unit thickness, and that its integral is simply the triangle area, the above become

$$[k]^e = [B]^T[D][B]\,\Delta$$
$$[F]_T{}^e = -[B]^T[D]\{\epsilon_0\}\,\Delta$$
$$[F]_q{}^e = \frac{\Delta}{3}\begin{Bmatrix} X \\ Y \\ X \\ Y \\ X \\ Y \end{Bmatrix}$$

if $\{q\} = \begin{Bmatrix} X \\ Y \end{Bmatrix}$ and is constant through the element. It is not necessary to evaluate any of the above products explicitly for a computer program (although this can in fact be simply done).

While the above derivations were made for a particular case of plane stress, the relationships (A) to (D) are quite general for any finite-element problem or type of element. The process is dependent only on the suitable choice of the shape function $[N]$—and beyond this point all steps of the calculation are pretty well automatic. For some more complex shapes of elements the integration in the volume becomes very difficult, and it may on occasion be necessary to use numerical-integration methods. This, for instance, is the case of the general three-dimensional element of Fig. 1.

Bibliography

1. Turner, M. J., R. W. Clough, H. C. Martin, and L. I. Topp, Stiffness and Deflection Analysis of Complex Structures, *J. Aeronaut. Sci.*, **23**, 805–823, 1956.
2. Zienkiewicz, O. C., and Y. K. Cheung, "The Finite Element Method in Structural and Continuum Mechanics," McGraw-Hill Book Company, New York, 1967.
3. Zienkiewicz, O. C., Stress Analysis of Hydraulic Structures Including Pore Pressure Effects, *Water Power*, **15**, 104–108, 1963.
4. Brown, C. P., and I. P. King, Automatic Embankment Analysis. Equilibrium and Instability Conditions, *Geotechnique*, 1966, pp. 204–214.
5. Clough, R. W., and A. K. Chopra, Earthquake Stress Analysis in Earth Dams, *Structures and Materials Res. Rept.* 65-8.
6. Zienkiewicz, O. C., G. Anderson, and B. Irons, Vibration and Stability Analysis of Buttress Dams with Particular Reference to Earthquake Loads, *Water Power*, September, 1967.
7. King, I. P., J. M. Raphael, and R. W. Clough, Finite Element Analysis of Two Dimensional Time Dependent Stress Problems, *Structures and Materials Rept.* 65-1, January, 1965. Construction Stresses in Dworshak Dams, *Structures and Materials Rept.* 65-3, April, 1965.
8. Zienkiewicz, O. C., and M. Watson, Some Creep Effects in Stress Analysis with Particular Reference to Concrete Pressure Vessels, *J. Nuclear Eng. Design*, **4**, 406–412, 1966.
9. Zienkiewicz, O. C., S. Valliapan, and I. P. King, Stress Analysis of Rock as a "No Tension" Material, *Geotechnique*, March, 1968.
10. Zienkiewicz, O. C., and Y. K. Cheung, Buttress Dam on Complex Rock Foundations, *Water Power*, **16**, 193, 1964; Stresses in Buttress Dams, *Water Power*, **17**, 69–75, 1965.
11. Zienkiewicz, O. C., Y. K. Cheung, A. A. Ribeiro, M. C. Azevedo, M. T. E. Ferreira, and J. O. Pedro, Comparison of Analytical and Experimental Results in the Design of a Hollow Gravity Dam, International Congress on Large Dams, Istanbul, 1967.
12. Irons, B., Numerical Integration Applied to Finite Element Methods. Conference on Use of Digital Computers in Structural Engineering, University of Newcastle, July, 1966.
13. Ergatoudis, J., B. M. Irons, and O. C. Zienkiewicz, Three Dimensional Stress Analysis of Arch Dams by the Finite Element Method, part I, *Research Rept.*, Division of Civil Engineering, University of Wales, Swansea, C/R/58/66, November, 1966.
14. Ergatoudis, J., B. M. Irons, and O. C. Zienkiewicz, Three Dimensional Stress Analysis of Arch Dams by the Finite Element Method, part II, *Research Rept.*, Division of Civil Engineering, University of Wales, Swansea, C/R/60/66, November, 1966. Also, by the same authors, Three Dimensional Analysis of Arch Dams and Their Foundations, *Symp. on Arch Dams, Inst. Civil Eng.*, London, 1968.
15. Research into the Design of Arch Dams, *1st Interim Rept.*, Civil Engineering Research Association, London, 1963.
16. Timoshenko, S. and S. Woinowsky-Krieger, "Theory of Plates and Shells," 2d ed., McGraw-Hill Book Company, New York, 1959.

17. Clough, R. W., and T. L. Tocher, Analysis of Thin Arch Dams by the Finite Element Method, *Proc. Symp. Theory of Arch Dams*, Southampton University, 1964 (Pergamon Press, New York, 1965).
18. Zienkiewicz, O. C., and Y. K. Cheung, Finite Element Method of Analysis for Arch Dam Shells and Comparison with Finite Differential Procedures, *Proc. Symp. Theory of Arch Dams*, Southampton University, 1964 (Pergamon Press, New York, 1965).
19. Zienkiewicz, O. C., C. Parekh, and I. P. King, Arch Dams Analyzed by a Linear Finite Element Shell Solution Program, *Symp. on Arch Dams, Inst. Civil Eng.*, London, 1968.
20. Dungar, R., R. V. Severn, and P. R. Taylor, "Earthquake Effects in Arch Dams," International Congress on Large Dams, Istanbul, 1967.
21. Clough, R. W., and A. K. Chopra, Earthquake Stress Analysis in Earth Dams, Structures and Materials, *Res. Rept.* 65-8, University of California, Berkeley, Calif., 1965.
22. Zienkiewicz, O. C., and Y. K. Cheung, Finite Elements in the Solution of Field Problems, *The Engineer*, 1965, pp. 507–510.
23. Zienkiewicz, O. C., P. Mayer, and Y. K. Cheung, Solution of Anisotropic Seepage Problems by Finite Elements, *Proc. ASCE*, **92** (EM 1), 111–120, 1966.

SECTION 11

GRAVITY DAMS

By Calvin V. Davis

STRUCTURAL FEATURES

1. Profile Characteristics. Any dam that does not depend upon arch or beam action to resist the forces imposed upon it may be termed a gravity dam. The term, however, is customarily restricted to solid masonry or concrete dams which are straight or only slightly curved in plan.

The basic philosophies of design are set forth in Sec. 9. There are several distinguishing characteristics, however, which should be emphasized. A gravity dam should be constructed on a sound, hard-rock foundation. Soft or yielding foundations require some other structural type. Assuming an adequate foundation, the slope of the downstream face will usually fall somewhere between 7 and 8 horizontally to 10 vertically.

The highest gravity dam in the United States, Dworshak, now (1968) being constructed on the North Fork of the Clearwater River in Idaho, will have a maximum height of 693 ft. A section through the completed dam would show a vertical upstream face, a downstream face with a slope of 8 horizontally to 10 vertically, and a 30-ft-wide public roadway at the crest.[1]

The profile of the 940-ft-high Grand Dixence[2] Dam furnishes another example of modern design. Figure 1 shows that the slope of the downstream face is 6.8 horizontally to 10 vertically for a height of about 75 m below the maximum reservoir level. Below, the slope changes to 8.1 horizontally to 10 vertically.

It will be noted that the upstream face is vertical down to elevation 2,200; below that elevation the face slopes 3 horizontally to 100 vertically in a downstream direction.

Grand Dixence was built in stages. The first-stage profile, shown by the heavy line, was topped in 1956; the second and final stage was topped in 1961. Construction extended over a period of 8 years.

The profiles of the Shasta, Grand Coulee, Detroit, and Fontana dams, shown by Figs. 2 to 5, inclusive, are representative of modern American practice. The curved, theoretical profiles of the gravity-type dams of a generation or so ago have been replaced by the clean, straight lines shown by these illustrations.

2. Concrete. Reduction in cement has been a primary objective in the construction of modern gravity dams. Not only does cement produce the heat that causes the cracking, but it is also the most expensive ingredient of the concrete. The introduction of air entrainment has saved up to 47 lb of cement/cu yd and resulted in concrete with superior weathering resistance.

Improvement in aggregate gradings and the substitution of pozzolans for cement have resulted in further savings. The loss of strength has been negligible and the heat yield is reduced greatly.

[1] *USCOLD Newsletter*, September, 1965.
[2] Grand Dixence, *Water Power*, April, 1963, p. 145.

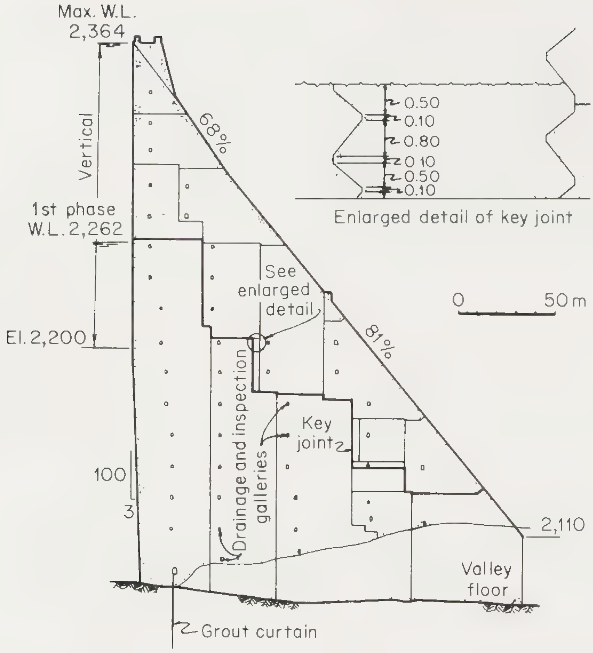

Fig. 1. Section through Grand Dixence Dam. The first-phase profile is shown by a heavier line. (*From Grand Dixence, Water Power, April,* 1963.)

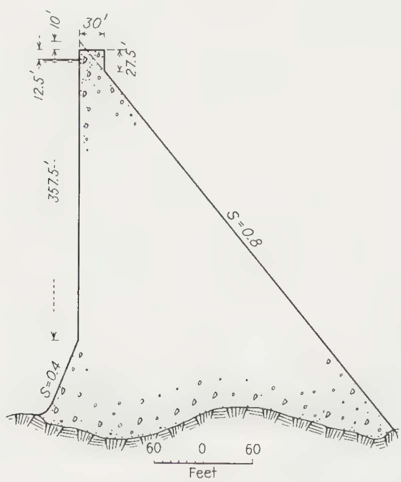

Fig. 2. Shasta Dam, Sacramento River, California.

3. Transverse Joints. Transverse contraction joints are usually spaced between 50 and 60 ft. Details vary widely. There are two schools of thought concerning the use of keys. One urges the complete elimination of all keys on the ground that they have no structural value; the other favors keys on the principle that the structure as a whole should be as nearly monolithic as possible and that keys assist materially in this direction. Examples of both types are plentiful. Some U.S. government agencies favor keying and grouting throughout the entire height. Others prefer ungrouted joints having plane surfaces.

In the Hiwassee Dam, keys were placed in the lower third of the area of vertical joints as shown by Fig. 6. The parts of the joints that were keyed were grouted according to usual practice; the plane surfaces above the keys were open and ungrouted. The transverse joints in the Fontana Dam were keyed and grouted in the

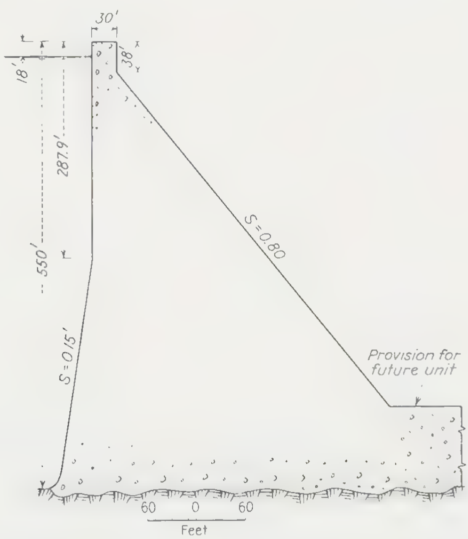

FIG. 3. Grand Coulee Dam, Columbia River, Washington.

lower 25 percent of the height. The upper 75 percent had plane surfaces and were not grouted. In contrast, the transverse joints of the Grand Dixence Dam (Fig. 1) were keyed and grouted throughout.

4. Longitudinal Joints. Vertical, longitudinal contraction joints must necessarily be keyed in order to transmit vertical shearing stresses across the section. To minimize shearing stresses along these keys, alternate surfaces are placed approximately in the planes of principal stress trajectories under full reservoir conditions. Figures 7, 8, and 9 show the typical details of a longitudinal joint for the Fontana Dam.

There appears to be no standard practice governing the size and spacing of keys in contraction joints. Extreme variation is revealed by an examination of existing designs, indicating that the judgment of the designer is the principal factor in determining the size and spacing of keys.

The present trend is toward either increasing the spacing of longitudinal joints or eliminating these joints entirely. To illustrate, the spacing in the Shasta and Grand Coulee dams is 50 ft. The Hungry Horse Dam in Montana has a single joint (see Sec. 9). The spacings of the three joints in the Fontana Dam (Fig. 5) measured from the upstream heel are as follows: 103 ft, 103 ft, and 83 ft. No longitudinal joints were used in the Detroit Dam (Fig. 4).

5. Drainage. Drainage is provided primarily to relieve uplift pressure. Details vary widely. The transverse joints of the Grand Dixence Dam are spaced 53 ft apart.[1] These joints are drained by a series of vertical shafts, the first shaft being 23 ft from

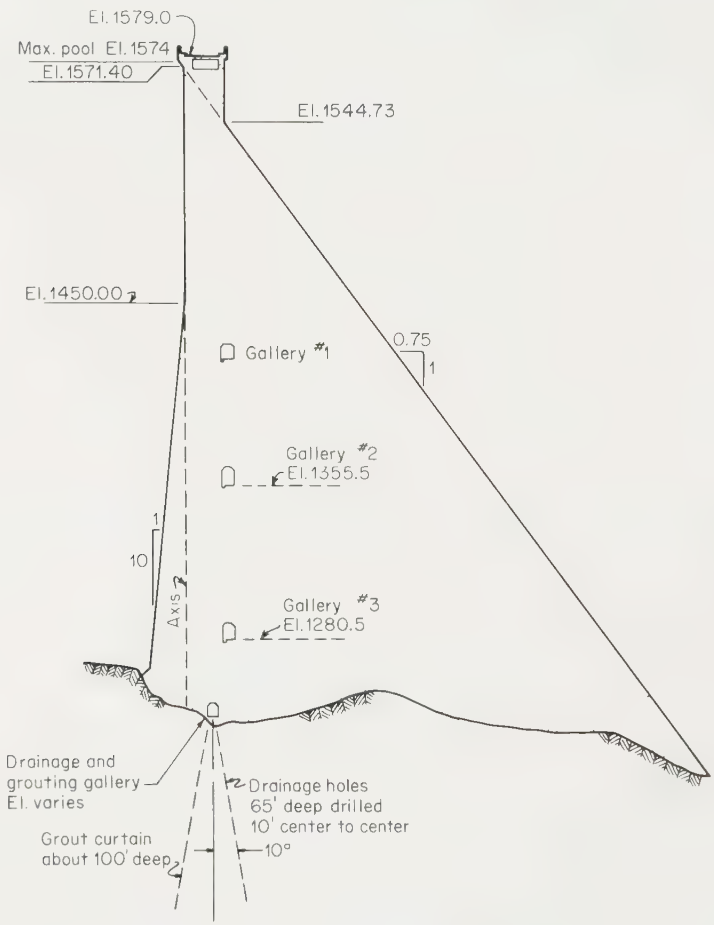

FIG. 4. Detroit Dam—typical nonoverflow section; scale: 1 in. = 50 ft.

the upstream face. A series of drainage galleries, spaced approximately 130 ft apart, was placed along the foundation line. The bedrock was left bare. In the body of the dam numerous inspection galleries provided additional relief. Finally, the drainage was completed under the dam by a horizontal gallery located about 950 ft below the storage level. The observed uplift pressures varied from 100 to 40 percent of the hydrostatic head upstream from the grout curtain and from 30 to 10 percent downstream of the curtain in a distance of approximately 200 ft from the upstream face.

[1] "Behaviour of Large Swiss Dams," p. 132, Swiss National Committee on Large Dams, 1964.

Downstream from this point there were no measurable pressures. The grout curtain penetrates the foundation 650 ft below the deepest part of the lake.

The 500-ft-high Guri Dam, now (1968) being constructed on the Caroni River by the Corporacion Venezolana de Guayana, Electrificacion del Caroni, offers an example of a high gravity dam which like Grand Dixence is being constructed in stages. Unlike Grand Dixence, however, the transverse joints are not keyed and grouted and are continuous plane surfaces. Figure 10 shows a section through the final intake

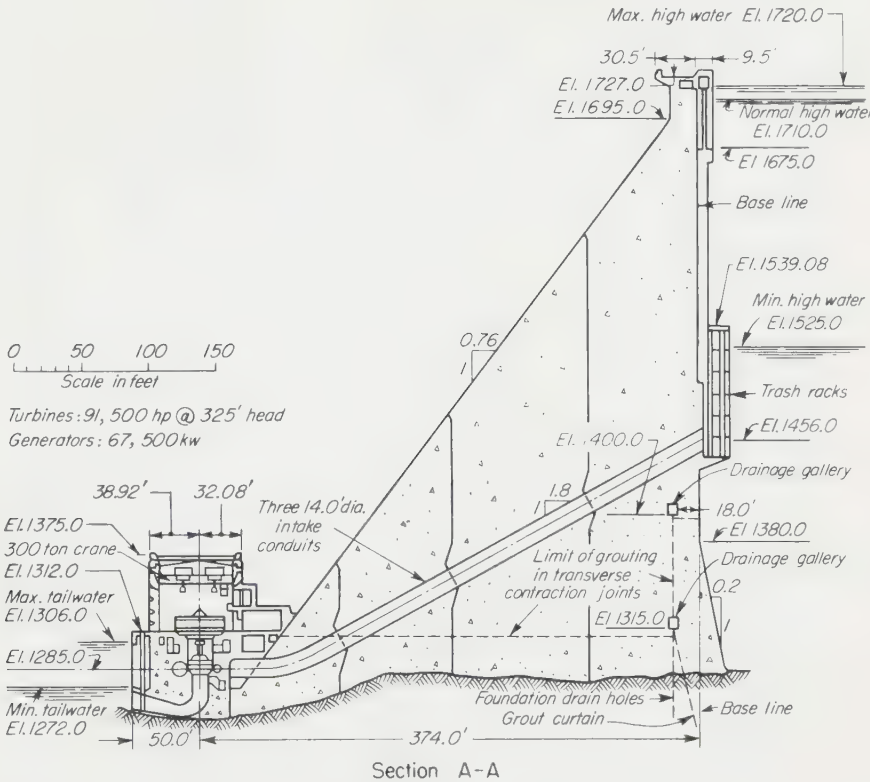

FIG. 5. Fontana Dam and powerhouse, Little Tennessee River, North Carolina. (*Civil Eng., July*, 1943, *p.* 306.)

structure with dotted lines indicating the first and second stages. Figure 11 shows an enlarged section through the transverse joints and details of the water stops and drains. Table 1 shows the foundation characteristics, depths of grout curtains, depths of drainage wells, and the spacing of these wells for a selected list of dams which have been constructed by the Bureau of Reclamation, the Tennessee Valley Authority, and the Corps of Engineers.

It should be emphasized again, as it was in Sec. 9, that grout curtains and drainage wells serve to reduce uplift and, in general, increase the watertightness of the structure and the foundations. Because of the long life of these structures, the proper maintenance of drains cannot be assumed. The safety of the structure should not depend upon the proper functioning of these features.

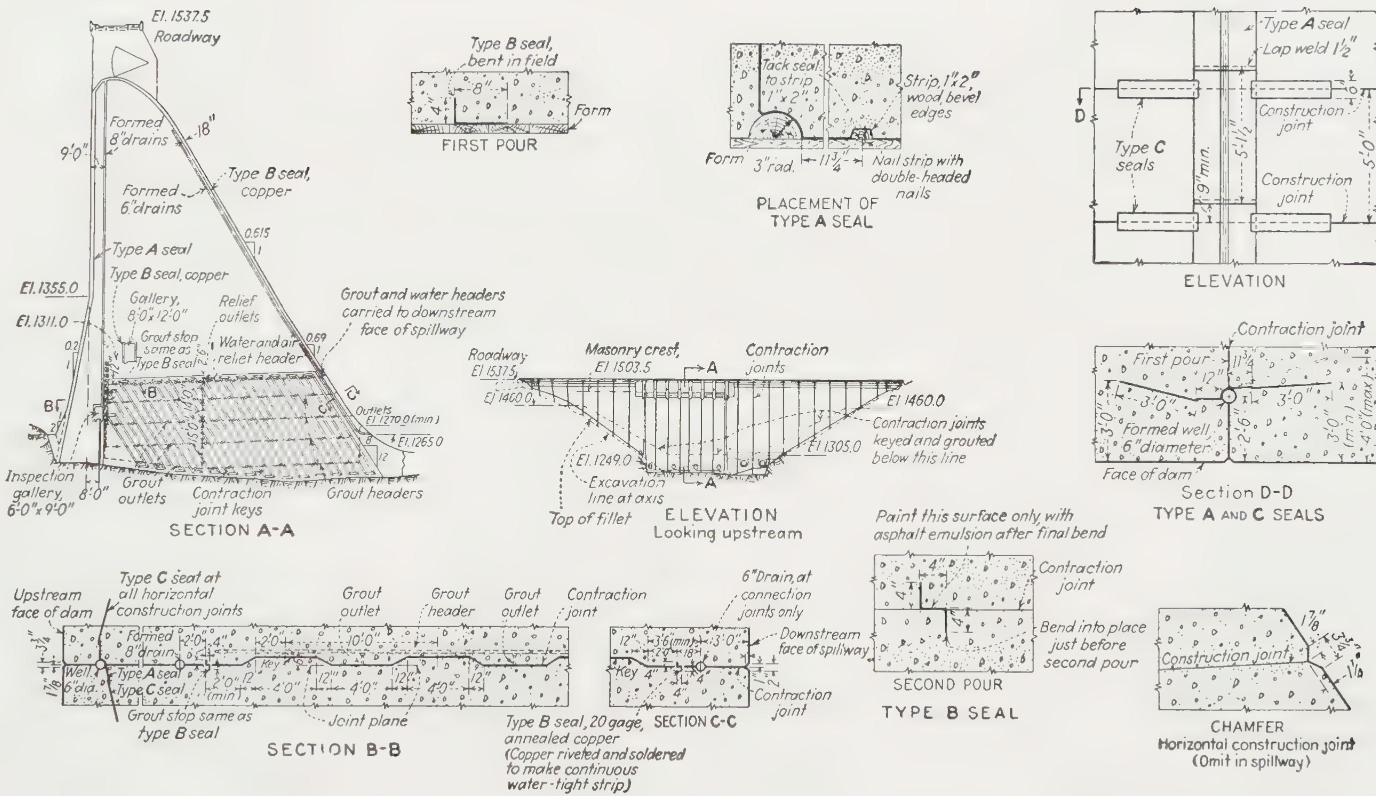

FIG. 6. Construction details, Hiwassee Dam. (*From Cecil E. Pearce, Design of Hiwassee Dam, Civil Eng., July, 1940, p. 433.*)

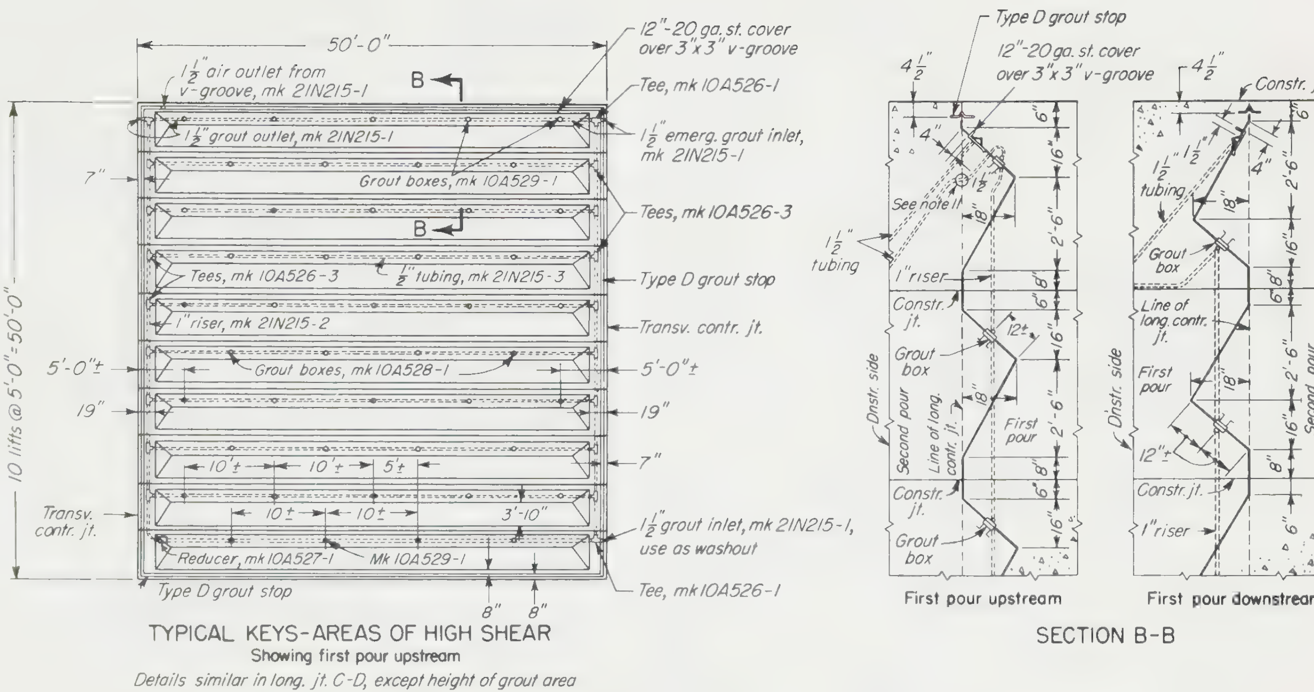

FIG. 7. Fontana Dam—typical keys, area of high shear.

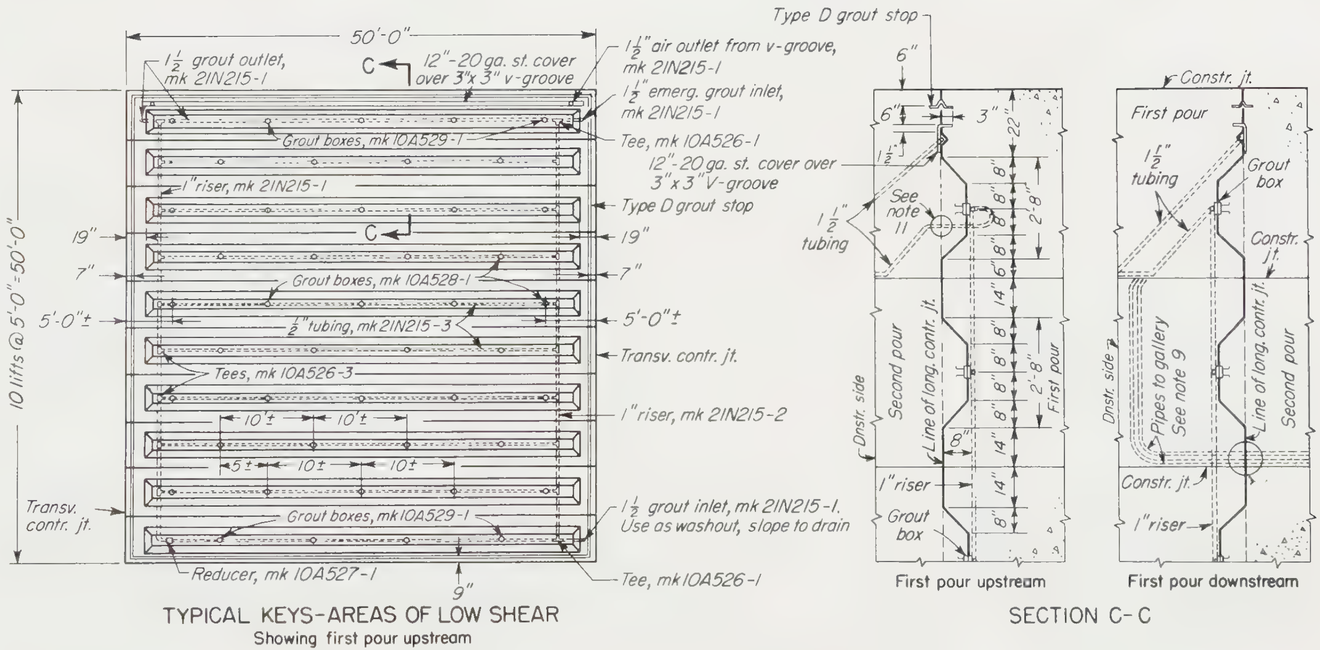

Fig. 8. Fontana Dam—typical keys, areas of low shear.

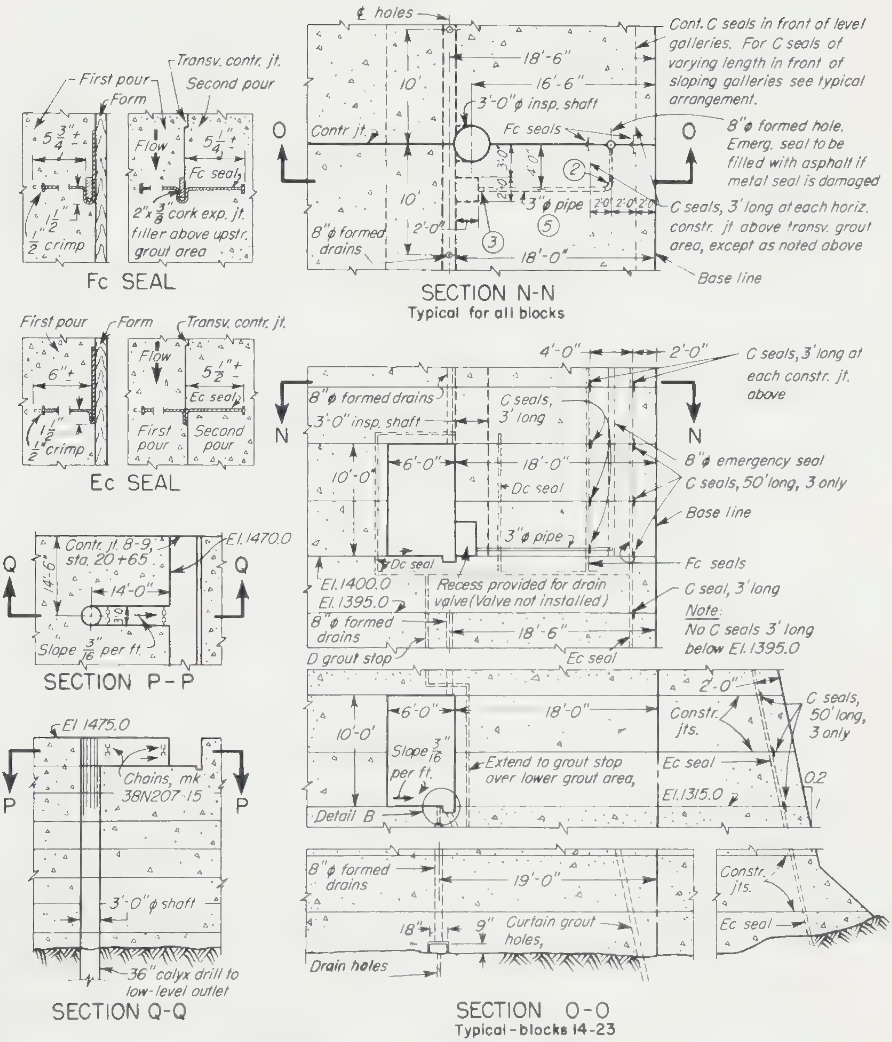

FIG. 9. Fontana Dam—typical arrangement of drains, seals, and water stop.

6. Water Stops. Metal water stops are used frequently as adjuncts of construction joints in order to deter the passage of water through these joints. In the United States, it was formerly standard practice to use 20-oz soft annealed copper for them. Monel metal is considered more durable, however, and for this reason it was selected for the water stops in Hoover Dam. Stainless-steel strips, 20 gage, were used for the Hiwassee Dam.

The ultimate effectiveness of any metal water stop is open to question. It is possible that in time the copper strips may become brittle and crack.

A yielding type of rubber or plastic seal has been used for a number of dams. Rubber should be used only in locations which are always wet and dark. Such seals

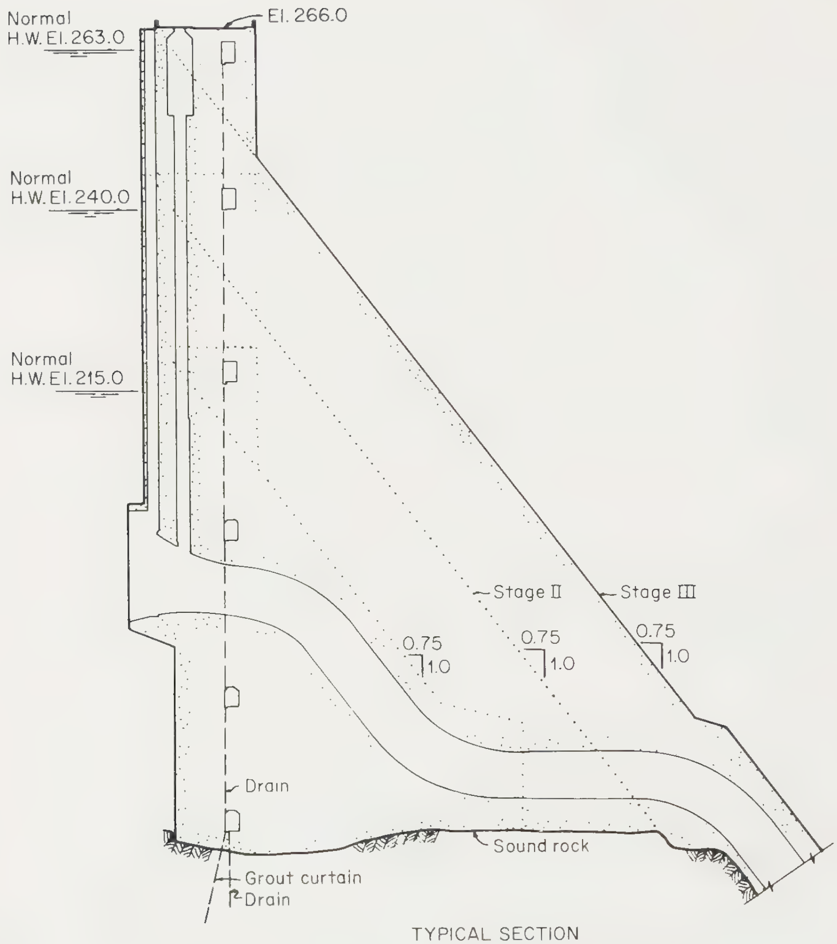

FIG. 10. Guri Dam, Caroni River, Venezuela.

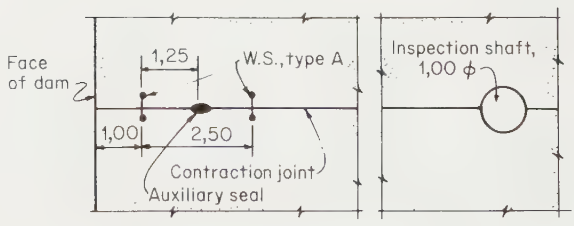

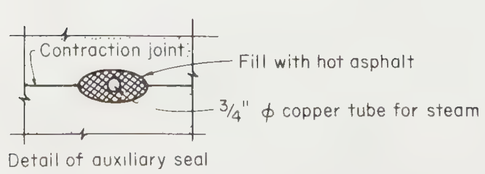

FIG. 11. Guri Dam, Caroni River, Venezuela. Transverse joints, details of water stops and drains.

TABLE 1*

Name of dam	Compressive strength, psi	Depth of grout curtain, ft	Depth of drainage, ft	Spacing of drains, ft
Bureau of Reclamation (USBR) Dams				
American Falls	Not available	20	20	5
Hoover	15,000	480	30–50	20
Friant	High	100	50	20
Grand Coulee	High	300	50	20
Gibson	Not available	40	40	4–7
Marshall Ford	Not available	125	40	20
Owyhee	400	270	110	10–20
Seminoe	Not available	100	100	5–10
Tennessee Valley Authority (TVA) Dams				
Wheeler	High	30		
Fontana	High	150	50	10
Douglas	High	200	40	8
Cherokee	Low	100	40	8
Hiwassee	Variable	80	40	8
Corps of Engineers (USED) Dams				
Clark Hill	....	80	30	12
Allatoona	1,900–44,000	75	20	5
Buggs Island	6,721–19,118	50	40	10
Philpott	3,210– 7,018	100	To be determined	
Tygart	200– 5,000	160	100	2.5
Bluestone	1,095– 8,810	150	100	10
Conemaugh	1,095– 8,810	To be determined		
Wolf Creek	2,840–13,100	75	65	10
Center Hill	6,180–13,860	100	80	10
Dale Hollow	3,110– 9,640	100	50	10
Stewarts Ferry	6,132– 7,050			
Narrows	913–34,900	100	40	10
Norfork	2,100–30,200	150	53	8
Bull Shoals	25,000 avg	200	60	8 and 9
Fort Gibson	813–13,200	75	40	10
Fall River	70– 5,000	30	20	10
Harlan County	1,227– 1,400	85	50–75	5 and 10
Conchas	1,067– 9,717	56	84	15
Caddoa	2,510– 6,150	52	35	10
Whitney	4,000	150	60	7
Chief Joseph	12,288–34,960	To be determined	To be determined	7
McNary	3,900–44,600	Varies from 60 to 100	50	10
Bonneville	370– 1,250	55	50	60
Detroit	6,000–48,000	150	To be determined	To be determined
Meridian	4,050– 7,250	150	100	10
Cottage Grove	1,100– 4,700	50	50	20
Dorena	None available	75	40	10
Folsom	Not available	50	40	10
Pine Flat	9,350–31,500	150	To be determined	10

* From *Proc. ASCE*, Separate 133, **78**, June, 1952. Uplift in Masonry Dams, Final Report of the Subcommittee on Uplift in Masonry Dams of the Committee on Masonry Dams, 1951.

are usually about ⅜ in. thick by 9 in. long with a ½-in.-radius bulb at each end and a cored ¾-in.-radius bulb at the intersection of the joint.

7. Crack Control. Properly designed contraction joints constitute only one provision for the control of cracks; other steps are as follows:[1]

1. The construction of shallow vertical lifts preferably not more than 5 ft high in large dams
2. The use of a low cement content
3. Refrigeration of mixing water
4. Allowance of sufficient time between the construction of vertical lifts to permit a large loss of heat from the surface
5. Cooling the concrete by circulating water through pipes embedded in the concrete

The construction of shallow lifts has been open to question. In the construction of the 200-ft-high Stewartville Dam, near Ontario, the highest lift that was practical to form—in the neighborhood of 50 ft—was poured. Rate of placing was the governing factor rather than height of lift.[2]

The cooling systems used in the construction of Grand Coulee, Shasta, and other high gravity dams built by the Bureau of Reclamation are made up of embedded coils, placed in parallel and served by supply and return headers. The coils consist of 1 in. outside diameter, thin-walled metal tubing about 800 ft long, coupled with expansion-type couplings.

The vertical spacing of the pipes is usually 5 ft, the tubing being placed on the top of each lift after the concrete has hardened. Horizontally the spacing varies between 2 and 6 ft, depending upon the extent of cooling required.

The velocity of flow through the embedded coils is not less than 2 fps, or about 4 gpm in the 1-in. tubing. Water may be either pumped through the coils or circulated by a gravity system. When river water is used, the warmed water, after passing through the coils, is wasted. When refrigerated water is used, the warmed water is returned to the refrigerating plant and used repeatedly. The cooling pipes in Fontana Dam are shown by Fig. 12.

The temperature of the concrete is determined by resistance thermometers either embedded in the concrete or inserted in pipes embedded in the concrete.

Basic to the design of any crack-control system is the formula for stress in any point in a dam due to temperature change[3]

$$f = CE_cR(t_p + t_r - t_f)$$

where f = stress in concrete, psi, resulting from thermal expansion
C = coefficient of thermal expansion of concrete, usually about 0.000005 in.
E_c = modulus of elasticity of concrete, usually between 4 and 5 million psi for 28-day concrete
R = restraint factor
t_p = placing temperature of the mix
t_r = temperature rise of concrete after placing due to heat of hydration of cement
t_f = final stable temperature of concrete

In the design of high-gravity dams, it is desirable to keep f below 200 psi.

[1] Steele, Byram W., Masonry Dams, A Symposium, Construction Joints, *Proc. ASCE*, May, 1940, pp. 908–941.

[2] Ontario Hydro Pushes Work on Power Dam at Stewartville, *Eng. News-Record*, Sept. 2, 1948, p. 65.

[3] Design of Fontana Dam for Stresses Caused by Temperature Change, *Report* 17-19, TVA.

In the time required to produce temperature stress, plastic flow and other factors may produce an effective value of E_c varying between 2 and 3 million psi.

The restraint factor R is 100 percent at the foundation. This decreases very rapidly above the foundation. In designing the Fontana Dam, the following relations were used: for a length of block L, R reduces to 50 percent for a height of $0.15L$ and to zero at a height of $0.5L$ above the foundation. R will increase appreciably above any level where concreting stops for more than 10 days or 2 weeks.

t_p is dependent mostly on the temperatures of the water, cement, and aggregates entering the mixing plant. With no special control except winter heating, it will approximate air temperatures with variations from 40 F in winter to 80 F in summer.

t_r depends upon the heat-generating characteristics of the cement. It will be about 36 F for a mix using 0.8 bbl of Type B cement per cubic yard and placed in

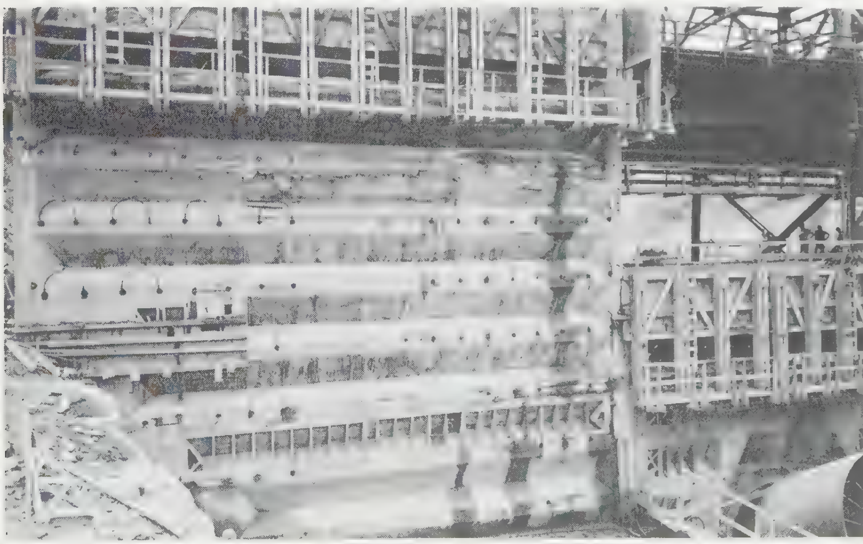

FIG. 12. Fontana Dam—vertical longitudinal joints, showing metal returns of cooling system. (*Tennessee Valley Authority.*)

5-ft lifts at 3-day intervals. Lower values may be obtained by other combinations of lifts and time intervals.

t_f is affected by climatical conditions, such as annual average air temperature, reservoir water temperature, foundation temperature, and exposure of the dam to the sun. At Fontana, t_f ranges from 45 F near the upstream face to 65 F near the downstream face. These temperatures are also approximated in Norris as shown (Fig. 13).

The problem of temperature control can be summarized as follows:

1. Lower the placing temperature t_p by cooling the mix, and reduce the temperature rise t_r through a proper arrangement of the pouring schedule and by circulating cooling water through the concrete immediately after a lift is poured.

2. Reduce the volume of concrete where high restraint occurs combined with a careful arrangement of pouring schedule and forced cooling. This method was adopted at Fontana.

8. Factors of Safety. Before the proper cross section of a gravity dam can be determined, certain minimum factors of safety consistent with the assumptions set forth in Sec. 9 must be adopted.

Overturning. The factor of safety against overturning is usually defined as the ratio of the righting moments to the overturning moments about the toe of the dam. When so defined, all forces, excepting the direct foundation reaction, are deemed active. Ordinarily the factor of safety against overturning is between 2 and 3.

Sliding. Clear distinction must be made between sliding factor and the factor of safety against sliding. The former is more accurately defined as the coefficient of friction required to prevent sliding of the dam upon its base under particular loading conditions. A third term, coefficient of static friction, is a limiting factor and is equal to the maximum horizontal force that can be applied to a body of unit weight without

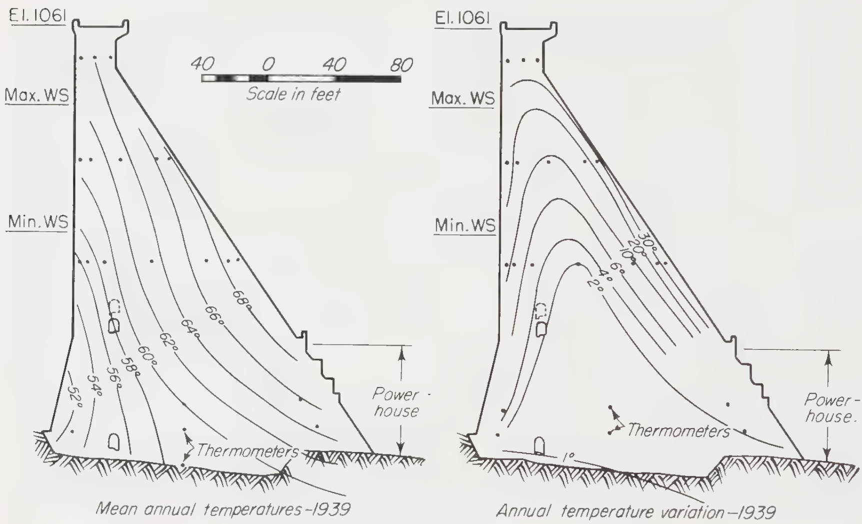

FIG. 13. Final temperatures, Norris Dam, concrete, blocks 30 and 36. (*Measurements of the Structural Behavior of Norris Dam, Technical Monograph No. 53, Tennessee Valley Authority.*)

causing sliding on a horizontal plane. If the plane upon which the unit weight rests is inclined gradually, the tangent of the angle between the horizontal and the maximum slope at which sliding does not occur is equal to this coefficient of static friction. The coefficient of static friction is variously reported from 0.65 to 0.75 for the materials ordinarily encountered in the construction of a gravity dam.

The sliding factor of a gravity dam, when the base is horizontal, is equal to the tangent of the angle between the perpendicular to the base and the direct foundation reaction under a given loading condition. When the sliding factor is greater than the coefficient of static friction, the dam is unsafe. The ultimate resistance of the dam to sliding varies, depending upon the loading condition, and is equal to the product of the net normal direct foundation reaction multiplied by the coefficient of static friction.

The factor of safety against sliding is properly defined as the ratio of the coefficient of static friction f' to the tangent of the angle between a perpendicular to the base and the direct foundation reaction.

The resistance of a gravity dam to sliding is primarily dependent upon the development of sufficient shearing strength. The factor of safety due to combined shearing and sliding resistance may be expressed by the formula

$$Q = \frac{[(\Sigma V - U) \times f'] + (b \times q)}{\Sigma H}$$

in which Q = shear-friction factor of safety
ΣV = algebraic summation of all active vertical forces
U = total uplift force
f' = coefficient of maximum static friction between two surfaces
b = length of base of dam measured horizontally
q = unit shear resistance of foundation material
ΣH = algebraic summation of all active horizontal forces

In practice, this resistance is attained in part by stepping the foundation and by measures taken to ensure bond between concrete and rock and successive pours of concrete. In a true masonry dam, adequate shearing strength results from the interlocking of the blocks of masonry; in a concrete dam, however, the resistance to shear on any approximately horizontal construction joint above the foundation depends entirely upon the bond developed between successive pours. The specifications for construction of a gravity dam thus are as much a matter of design as the analysis of stresses.

Shear. Regardless of the fact that the ability of a gravity dam to withstand the forces acting upon it depends largely upon the strength of the material in shear, little is known about the actual strength of concrete in shear.

The strength of concrete in compression is generally measured by the loads required to break test cylinders in a compression machine. Ordinary concrete suitable for placing in a gravity dam should test at least between 3,000 and 5,000 psi at the end of 28 days; much stronger concrete is customary. It is generally assumed that the unit shearing strength of concrete is about one-fifth of the breaking stress of standard cylinders. This would indicate shearing strength of 600 to 1,000 psi for concrete of the character used in the construction of gravity dams.

The distribution of shear along a horizontal plane of a gravity dam is from about zero at the heel to a maximum near the toe, so that the intensity of shear at the toe is roughly twice the average. Furthermore, bond may not be developed uniformly between successive concrete pours. The average shear on any construction joint should thus be limited to about one-twentieth of the compressive strength of the concrete as determined by standard crushing tests.

9. Structural Analysis. In final designs for high gravity dams, consideration should be given to combined beam and cantilever action, the effect of rock movements, and the effects of twist and beam action along sloping abutments in addition to the conventional stability and stress analyses. Only the more conventional analysis for a vertical section having a width of 1 ft is considered in this section.

Ordinarily the following steps are taken:

1. Compute the righting and overturning moments on selected horizontal planes, taking into consideration all the forces which may act on the section.

2. Compute the vertical normal stresses σ_x on each selected plane of analysis by the formulas

$$\sigma_x \text{ max (at downstream face)} = \frac{\Sigma V}{144b}\left(1 + \frac{6e}{b}\right)$$

$$\sigma_x \text{ min (at upstream face)} = \frac{\Sigma V}{144b}\left(1 - \frac{6e}{b}\right)$$

in which σ_x = vertical normal pressure

e = eccentricity (distance from point of application of resultant load to center of base)

Vertical normal stresses may be assumed to have straight-line variation between the toe and the heel. Usually these stresses are computed on the assumption that no uplift pressure is acting on the base.

3. Compute the principal and shearing stresses at the downstream face. The first principal stress $\sigma_1 = \sigma_x/\cos^2\theta$ in which θ = the angle between the downstream face and the vertical. The horizontal shearing stress at the toe is $\tau_x = \sigma_x \tan\theta$.

4. Estimate the probable distribution of uplift pressure on the foundation, and determine its effects upon the stability of the section.

5. Considering the effects of uplift on the sliding factor, compute the shear-friction factor of safety and the factor of safety against overturning.

In important structures, it may be desirable to determine the intensities and directions of the principal and maximum shearing stresses at various points throughout the section. The usual procedure in analyzing these stresses is to divide the section into elementary prisms and consider each prism to be held in equilibrium by the stresses acting upon it. By starting with vertical normal stresses acting on the upper and lower surfaces of each elementary prism, it is possible to determine by successive integration the vertical and horizontal shearing-stress intensities, the horizontal normal stresses, and the first and second principal stresses.

Case 1 and Case 2 illustrate the principles of stability computation applied to the section through Norris Dam shown by Fig. 14. These computations apply only to a horizontal plane at El. 800. Forces due to earthquakes are not included. The results of the analysis for other planes are also shown by Fig. 14. For a complete structural analysis of the Norris Project see *Technical Report* 1, The Norris Project, Tennessee Valley Authority, Government Printing Office, 1940.

Case 1. Reservoir Empty

Dimensions	*Volume of concrete, cu ft*	*Moment arm, ft*	*Righting moment*
$\frac{1}{2} \times 75 \times 15$ =	563	193.09	109,000
260×20 =	5,200	178.09	926,000
$240.13 \times 168.09 \times \frac{1}{2}$ =	20,182	112.06	2,262,000
	25,945	127.05	3,297,000
	150 lb/cu ft		150 lb/cu ft
Weight of concrete =	3,892,000 lb	127.05	494,437,000 ft-lb

$$\text{Eccentricity } e = 127.05' - \frac{203.09'}{2} = 25.50'$$

$$\text{Average vertical normal stress} = \frac{3{,}892{,}000 \text{ lb}}{203.09' \times 144} = 133 \text{ psi}$$

$$\text{Maximum vertical normal stress at upstream face } \sigma_{x\,\max} = 133 \text{ psi}\left(1 + \frac{6 \times 25.50'}{203.09'}\right)$$

$$= 233 \text{ psi, upstream face}$$

$$\text{Minimum vertical normal stress at downstream face } \sigma_{x\,\min} = 133 \text{ psi}\left(1 - \frac{6 \times 25.50'}{203.09'}\right)$$

$$= 33 \text{ psi downstream face}$$

Case 2. Reservoir Full

Water surface El. 1,052, tail water El. 847, no uplift on base

	Force, lb	*Moment arm, ft*	*Righting moment, ft-lb*
Weight of concrete =	3,892,000	127.05	494,437,000
Vertical water load:			
Upstream face			
$177 \times 15 \times 62.5$ =	166,000	195.59	32,456,000
$75 \times 15 \times \frac{1}{2} \times 62.5$ =	35,000	198.09	6,964,000
Downstream face			
$47 \times 32.9 \times \frac{1}{2} \times 62.5$ =	48,000	10.97	530,000
ΣV =	4,141,000	129.05	534,387,000

Horizontal water pressure:			
Upstream face			
$\frac{1}{2} \times \overline{252}^2 \times 62.5 =$	1,985,000	84.00	166,698,000
Downstream face			
$\frac{1}{2} = \overline{47}^2 \times 62.5 =$	69,000	15.67	1,082,000
$\Sigma H =$	1,916,000	86.44	165,616,000
Sliding factor $f =$	$\frac{1,916,000}{4,141,000} = 0.463$		368,771,000

Point of application of resultant, distance from downstream face $= \frac{368{,}771{,}000 \text{ ft-lb}}{4{,}141{,}000 \text{ lb}} = 89.05$ ft

$$e = \frac{203.09'}{2} - 89.05' = 12.50'$$

$$\sigma_{x\,\text{av}} = \frac{4{,}141{,}000 \text{ lb}}{203.09 \times 144} = 142 \text{ psi}$$

$$\sigma_{x\,\text{max}} = 142\left(1 + \frac{6 \times 12.50'}{203.09'}\right) = 194 \text{ psi at downstream face}$$

$$\sigma_{x\,\text{min}} = 142\left(1 - \frac{6 \times 12.50'}{203.09'}\right) = 89 \text{ psi at upstream face}$$

First principal stress σ_1 parallel to downstream face

$$= \sigma_x(1 + \tan^2\theta) = \sigma_x/\cos^2\theta$$
$$= 194 \text{ psi } (1 + 0.49) = 289 \text{ psi}$$

Maximum horizontal shearing stress $= \tau_x = (\sigma_x - \text{uplift pressure}) \tan\theta$

$$= (194 \text{ psi} - 20 \text{ psi} = 174 \text{ psi}) \times 0.7 = 122 \text{ psi}$$

Effect of uplift pressure on sliding factor

(Assume uplift varies from full static head at upstream face to tail water at downstream face applied to two-thirds of area of face)*

$$\text{Uplift } U = \frac{2}{3} \times 62.5 \text{ lb/cu ft} \times 203.09 \text{ sq ft/ft} \times \frac{252' + 47}{2} = 1{,}265{,}000 \text{ lb}$$

ΣV with uplift $= 2{,}876{,}000$ lb

Sliding factor $f = \frac{1{,}916{,}000 \text{ lb}}{2{,}876{,}000 \text{ lb}} = 0{,}666$

Shear friction factor of safety, considering effect of uplift

$$-Q = \frac{(2{,}876{,}045 \times 0.65\dagger) + (203.09 \text{ sq ft/ft} \times 400\ddagger \text{ psi} \times 144 \text{ psi})}{1{,}916{,}000 \text{ lb}} = 7.1$$

Figure 15 shows the results of the stability analysis of a typical section of Fontana Dam. The designer has been cautioned in Sec. 9 and elsewhere that the results of stability analyses, made by conventional methods, may not be indicative of the actual stresses in the dam. For a detailed comparison of the results of field measurements of the stresses in Fontana Dam with those obtained from theoretical analysis, reference should be made to "Measurements of the Structural Behavior at Fontana Dam," Technical Monograph 69, Tennessee Valley Authority, 1953. The findings in this report indicated that:

1. There are indications that shear displacements took place along at least two of the joints under certain loading conditions.
2. The pattern of stresses indicates that at least one column separated by the longitudinal joint may function largely independently of the others.
3. There may be at work a temperature thrust near the downstream face. The stress distribution at the base of the structure supports the correctness of this assumption.
4. A maximum compressive stress of about 1,800 psi is indicated.

* The author recommends that this factor be increased to 1 in future designs.
† Coefficient of internal friction.
‡ Unit shear resistance of foundation rock.

STRESSES AT UPSTREAM FACE IN POUNDS PER SQUARE INCH

Elev.	Reservoir Empty: Vertical Found. Pressure	Reservoir Empty: Conc. Stress Parallel to Face	Reservoir W S Elev. 1052: Water Pressure	Reservoir W S Elev. 1052: Vertical Found. Pressure	Reservoir W S Elev. 1052: Conc. Stress Parallel to Face	Reservoir W S Elev. 1052: Shear Stress on Horiz. Plane
1000	76	76	23	49	49	0
950	127	127	44	61	61	0
900	179	179	66	69	69	0
850	211	219	88	78	81	2
800	233	242	109	89	93	4

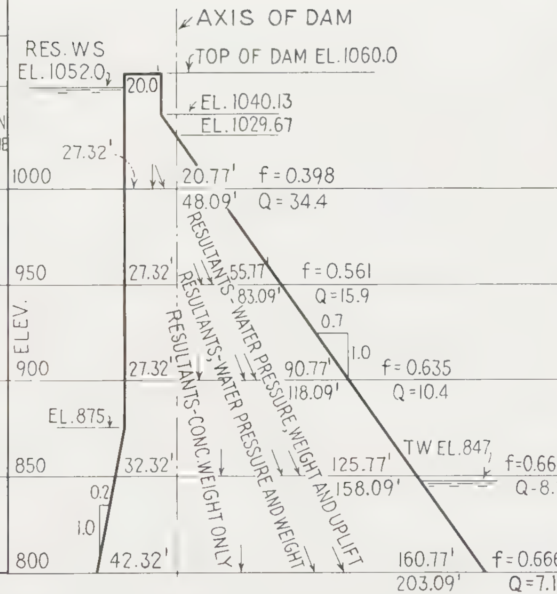

STRESSES AT DOWNSTREAM FACE IN POUNDS PER SQUARE INCH

Elev.	Reservoir W S Elev. 1052: Vertical Found. Pressure	Reservoir W S Elev. 1052: Conc. Stress Parallel to Face	Reservoir W S Elev. 1052: Shear Stress on Horiz. Plane	Reservoir Empty: Vertical Found. Pressure	Reservoir Empty: Conc. Stress Parallel to Face
1000	27	40	19	0.8	1.1
950	66	98	46	-0.9	-1.4
900	108	161	76	-1.0	-1.6
850	151	224	105	12	18
800	194	289	122	33	49

MAXIMUM ABUTMENT SECTION

FIG. 14. Structural analysis, bulkhead section, Norris Dam.

CASE	EL	ΣH KIPS	ΣV KIPS	STRESSES LB. SQ. IN			SHEAR SAFETY FACTOR
				σ_x max. TOE	σ_x min. HEEL	AVG SHEAR	
I	1475	–	3,600	–4	270	–	–
	1380	–	6,860	–3	369	–	–
	1265	–	12,400	48	417	–	–
	1255	–	12,970	52	422	–	–
II	1475	1,870	3,020	181	43	69	9.70
	1380	3,610	5,790	253	57	97	7.26
	1265	6,410	10,570	324	73	120	6.06
	1255	6,680	11,030	329	74	122	5.99

NOTES.
Weight of concrete – 153 lbs per cubic foot
Weight of water 62.5 lbs per cubic foot
Case I: Dead load only. Reservoir empty
Case II: HW El. 1720, TW El. 1306.
Analyses made for 1.0' length of dam.

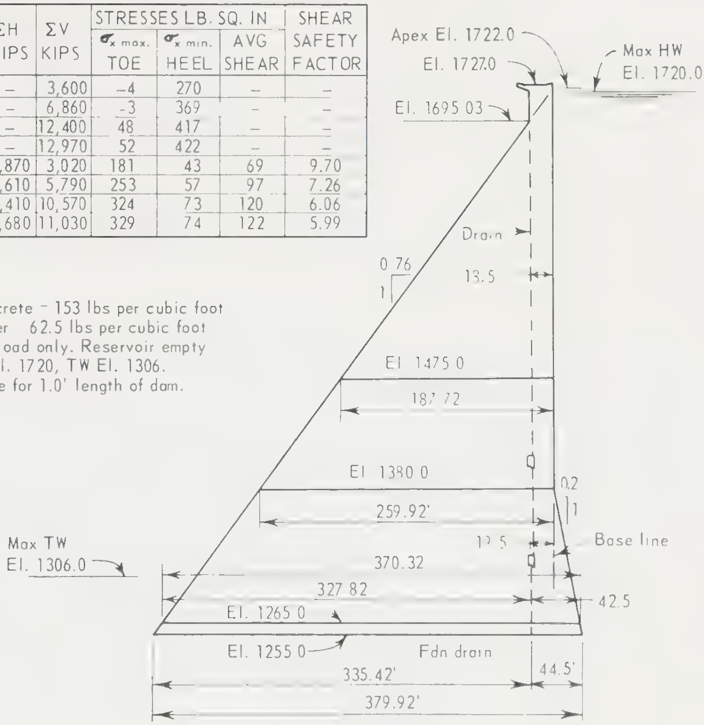

FIG. 15. Final stability analysis—typical section. (*Reproduced from p.* 63, *Fig.* 18, *The Fontana Project Technical Report* 12, *Tennessee Valley Authority*, 1949.)

SECTION 12

HOLLOW GRAVITY DAMS

By Claudio Marcello

INTRODUCTION

1. Evolution. The conventional gravity-type dam, as described in Secs. 9 and 11, depends for its stability primarily upon the weight of the concrete contained within its approximately triangular profile. The section is proportioned to provide an adequate factor of safety (usually about 2) against the overturning forces of water pressure, uplift, silt loads, ice loads, and seismic forces. It also provides sufficient shear-friction resistance at the plane of contact with the foundation to provide a satisfactory factor of safety against sliding or shearing failure.

Depending upon the criterion selected, the volume of concrete required to counterbalance the effects of uplift would fall somewhere between one-quarter and one-third of the total volume of the section. This suggests the removal of that part of the concrete which by its very presence creates a substantial part of the uplift within a gravity dam. The partial elimination of uplift pressures by the creation of internal cavities within a gravity dam is therefore the first important factor in the development of the hollow gravity dam.

A second factor is the manner in which water, concrete, and other loads are transmitted through the structure to the foundation. This subject is treated comprehensively in Secs. 9, 11, 13, and 14. It will suffice here to point out that, depending upon assumed allowable stresses, somewhere between two-thirds and three-quarters of the volume of a gravity dam is required as a counterweight to overcome overturning and shear-friction forces and that only between one-quarter and one-third of the concrete is required to transmit the loads, at acceptable stresses, through the structure to the foundations.

It has been demonstrated elsewhere that the replacement of the resisting moment of this counterweight concrete with that of the weight of water on an inclined upstream face resulted in increased safety factors and improved stress patterns.

Applications of these principles produce a variety of structural types ranging from massive concrete buttress-type dams to thin-sectioned Ambursen and multiple-arch-type dams. Savings in concrete volume, however, do not necessarily result in corresponding savings in construction costs. Decreases in concrete volumes may result in high unit costs of placement and in increases in form and reinforcement costs.

During the past 30 years European engineers have developed a hollow gravity type which eliminates redundant concrete, provides massive unreinforced-concrete sections, and has adequate lateral bracing for the buttresses. Form costs are approximately comparable with those of the gravity dam. Uplift pressures are largely eliminated, stress patterns are improved, and as compared with gravity dams of equal height, safety factors are increased. Construction costs compare favorably with those of the thin-buttress types.

The hollow gravity type, as described in the following paragraphs, carries the evolutionary process (which resulted in the massive or gravity-buttress type, Sec. 9)

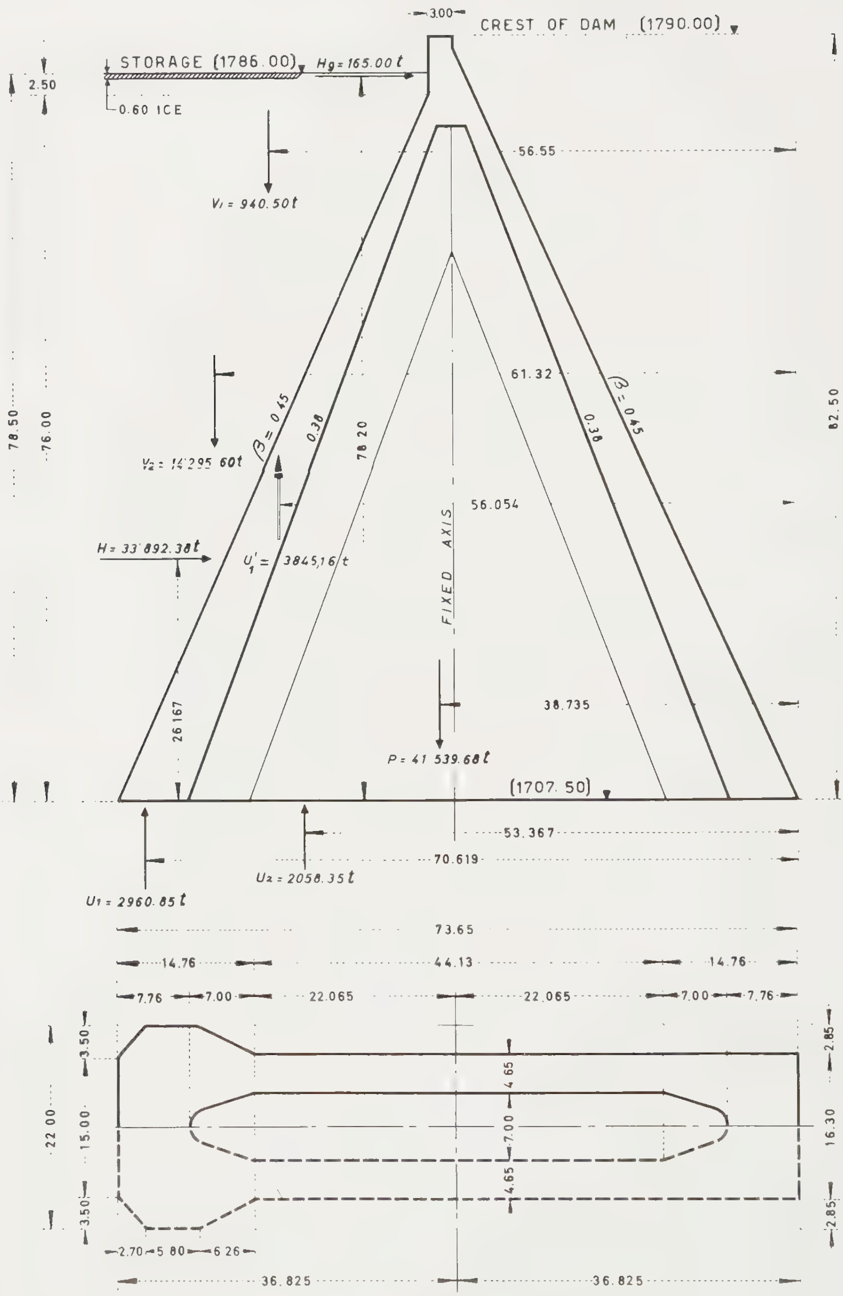

FIG. 1. Typical buttress, hollow gravity-type dam.

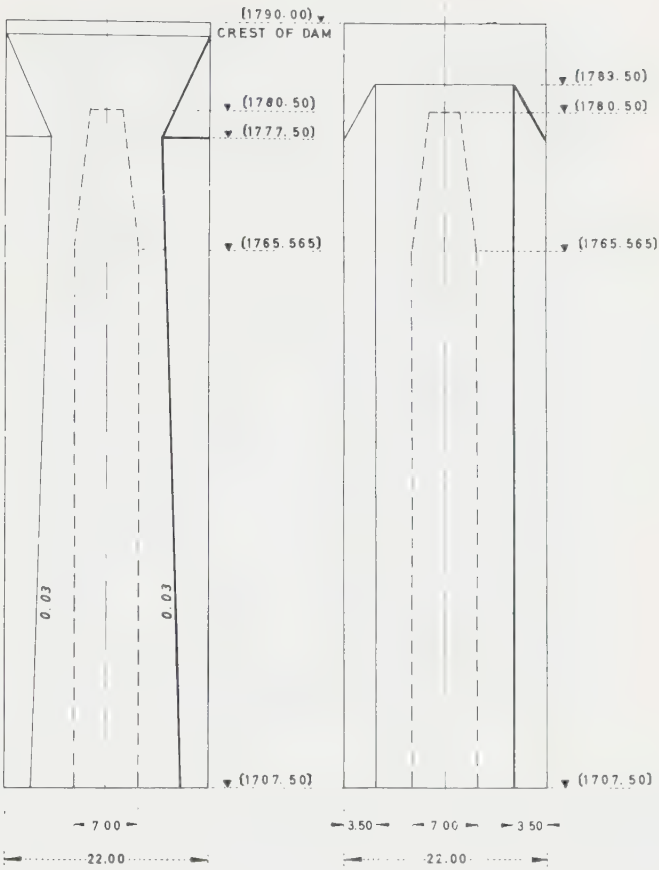

FIG. 1. (*Continued.*)

one step further. Further benefits were obtained by providing cavities within the massive buttress monoliths. Figure 1 shows a typical structure of this type.

2. Structural Features. Figure 1 shows a hollow gravity-type dam having features typical of those which have been designed and constructed principally by Italian engineers. Figure 2 shows the detailed dimensions of a horizontal section at El. 1,707.5 which is analyzed as a typical example elsewhere in this section. The upstream and downstream face slopes are each 4.5 horizontal to 10.0 vertical. The base width of 73.65 m is 0.90 of the height at the point of intersection of the upstream and downstream faces. This compares with base widths varying between 0.75 and 0.80 of the heights as commonly used for gravity dams.

The 7.0-m-wide internal cavity creates two buttresses, each having a maximum thickness of 4.65 m. To increase lateral stability, these buttresses are joined by flared sections at both the upstream and downstream faces.

The stabilizing effect of the vertical water load, introduced by providing a sloping upstream face, more than compensates for the loss of weight which results from coring the monoliths. Figures 3 and 4 showing, respectively, the Ancipa Dam and the Bissina Dam (Table 1), both in Italy, demonstrate the structural features and two

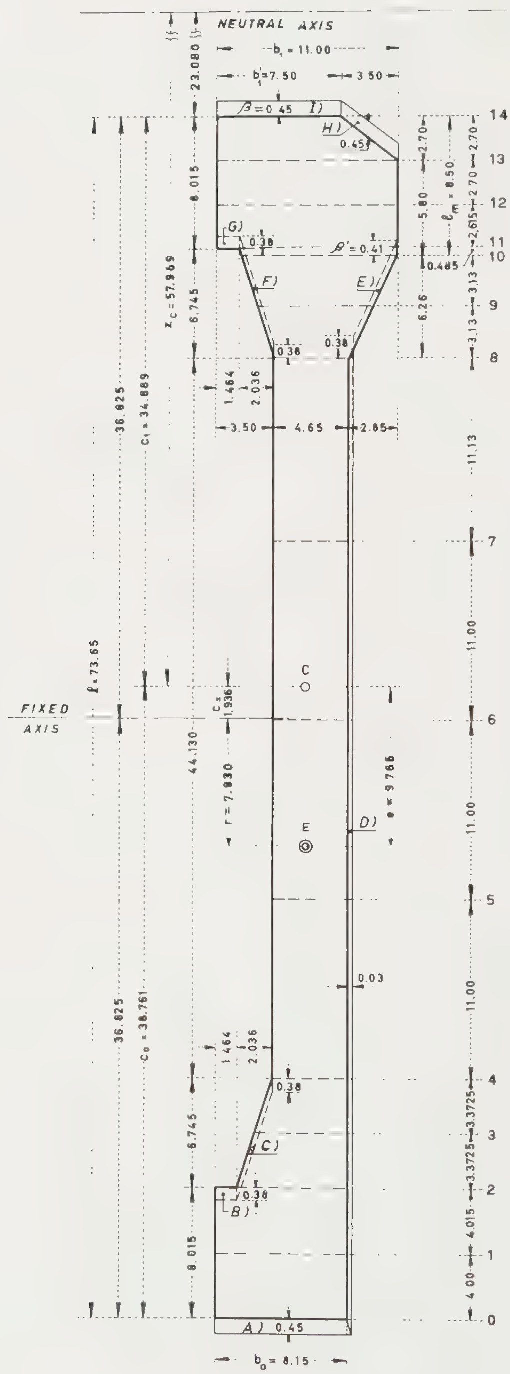

FIG. 2. Detailed geometric data.

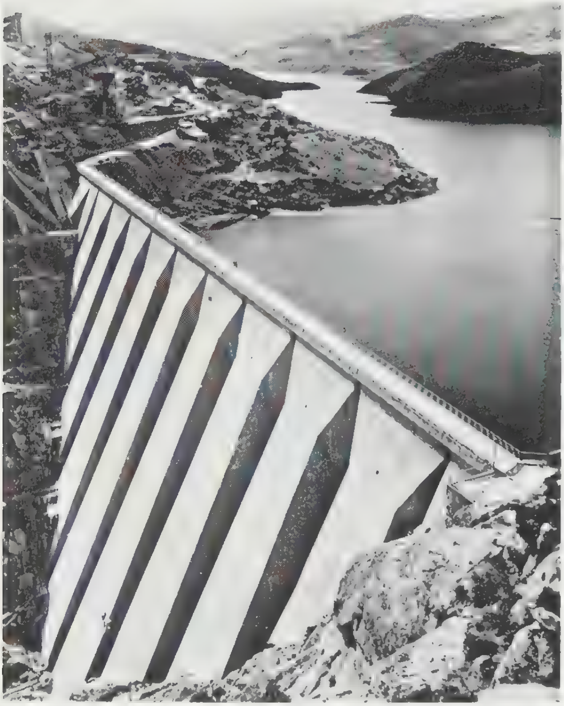

Fig. 3. Ancipa Dam.

Fig. 4. Bissina Dam.

Table 1. Hollow Gravity Dams with Hollow Elements*

Name and period of construction	Stream (basin)	Max height, m	Crest length, m No. of elements	Volume of dam, 10^3 cu m	Crest elevation, meters above sea level
In Italy:					
Lago di Trona† (1939–1942)....	Bitto di Gerola (Adda)	58.40	182.00 6‡	84.10	1,808.00
Lago dell'Inferno† (1941-1944)..	inferno (Adda)	41.20	151.00 7§	39.00	2,088.00
Bau Muggeris (1948–1949).....	Flumendosa	63.00	235.00 7	131.73	802.00
Poglia (1949–1950)............	Poglia (Oglio)	50.00	137.10 4	34.60	632.40
Ancipa (1949 1952)............	Troina (Simeto)	111.50	253.00 9	318.00	952.00
Sabbione (1949 1953).	Rio del Sabbione (Ticino)	63.60	279.00 11	135.00	2,461.60
Pantano d'Avio (1949–1956)....	Coleasca (Oglio)	65.00	400.00 15	200.00	2,379.00
Ponte Vittorio (1954–1955).....	Strona (Ticino)	38.50	125.00 4	24.20	710.00
Boazzo (1954–1956)............	Chiese (Oglio)	57.10	439.91 5	79.00	1,226.50
Bissina (1955–1957)............	Chiese (Oglio)	87.00	563.40 22	440.00	1,790.00
Venerocolo (1956–1958)........	Outflow from lake (Oglio)	31.40	362.68 8	42.00	2,539.40
Calamaiu (1958–1961).........	Liscia	69.00	278.50 9	135.00	180.00
Greece:					
Pidima (1951–1954)...........	Ladhon	56.00	106.00 3	34.00	422.40
Brazil:					
Cachoeira do França (1953–1958)	Rio Juquià	48.00	206.75 6	69.00	642.00
Cachoeira da Fumaça..........	Rio Juquià	54.60	163.65 6	90.00	533.00

* Designed by the author.

† Triangular profile with subvertical upstream face.

‡ Width of the head of each element 24.00 m.

§ Width of the head of each element variable.

types of architectural treatment. Table 1 presents a list of existing dams of this general type and pertinent data on their principal features.

DESIGN PROCEDURES

3. Stability. Many of the criteria which appear in Sec. 9 may also be applied to the hollow gravity-type dam. In general the factor of safety against overturning should not be less than 2.0.

The resistance to shearing and sliding may be expressed by the formula

$$Q = \frac{f(\Sigma V - U) + A\tau_0}{\Sigma H} \tag{1}$$

in which Q = shear-friction factor of safety

f = coefficient of maximum static friction between the concrete and foundation surfaces

ΣV = algebraic summation of all active vertical forces
U = total uplift force
A = area of foundation in contact with structure
τ_0 = unit shear resistance of foundation material
ΣH = algebraic summation of all active horizontal forces

These forces and their moment arms are shown by Fig. 1.

In applying this formula to the hollow gravity-type dam, it must be kept in mind that Q represents the average factor of safety for the area of contact between the dam and the foundation. Should contraction joints be required in the buttresses, the relationship between vertical loading and shear at the foundation line may vary throughout the base. In this case the shear-friction factor of safety should be analyzed separately for each column bounded by the joints.

4. Stresses. The analytical methods described in Secs. 9, 10, and 13 also may be applied to the hollow gravity-type dam. Of fundamental importance is the pattern of distribution of vertical normal stresses on horizontal planes, heretofore designated as σ_x. It is usually assumed that σ_x will have linear distribution on a horizontal plane and that it may be computed from the well-known law of the trapezoid

$$\sigma_x = \frac{\Sigma V}{A} \pm \frac{MY}{I} \tag{2}$$

in which ΣV = algebraic sum of all active vertical forces
A = sectional area of base
M = moment = $(\Sigma V)e$
e = eccentricity (distance from point of application of resultant force on base to center of gravity of the section)
Y = distance from center of gravity to most remote fiber
I = moment of inertia of horizontal section

As shown by Sec. 9, the determination of stress patterns in structural models and in prototype field measurements indicates only slight curvilinear distribution in dams having heights falling between 60 and 80 m. The trapezoidal law, therefore, can be applied, without substantial error, to dams in the medium-height range. In cases involving significant differences between the elastic properties of the concrete and foundation materials, more exact methods of analysis, such as the finite-element method, as described in Sec. 10, may be required.

The horizontal and vertical shearing-stress intensities τ_{xy}, the horizontal normal-stress intensities σ_y, and the first and second principal stresses σ_1 and σ_2, respectively, may be determined from the distribution pattern of vertical normal stresses σ_x. In general, the principles of analysis and the design procedures would be similar to those applied to the Rodriguez Dam in Sec. 13.

The shearing and the horizontal normal stresses may be determined from arithmetic integration. Referring to Fig. 5, the vertical and horizontal shearing-stress intensities at point A, the center of an elementary slice having a thickness Δh, may be determined by calculating the total vertical normal loads N between points a and b and $N + \Delta N$ between points c and d. Therefore,

$$V = N + W - (N + \Delta N) \tag{3}$$

in which V = total shear across section ac
W = weight of concrete, elementary section a, b, c, d

Therefore,

$$\tau_{xy} = \frac{V}{\text{incremental area } \Delta A} \tag{4}$$

Because horizontal and vertical shearing-stress intensities are equal, horizontal shearing stresses may also be arithmetically integrated on two horizontal planes separated by the vertical increment of height Δh. Designating the total horizontal shear between a and b as V_1 and the total horizontal shear between c and d as V_2, the horizontal normal-stress intensity at point A would be

$$\sigma_y = \frac{V_1 - V_2}{\text{incremental area } \Delta A} \tag{5}$$

In computing the values of σ_y, the average values of τ_{xy} would be determined on horizontal plane A lying midway between planes ab and cd. The same process would then be repeated on horizontal plane B located Δh below plane A. Having deter-

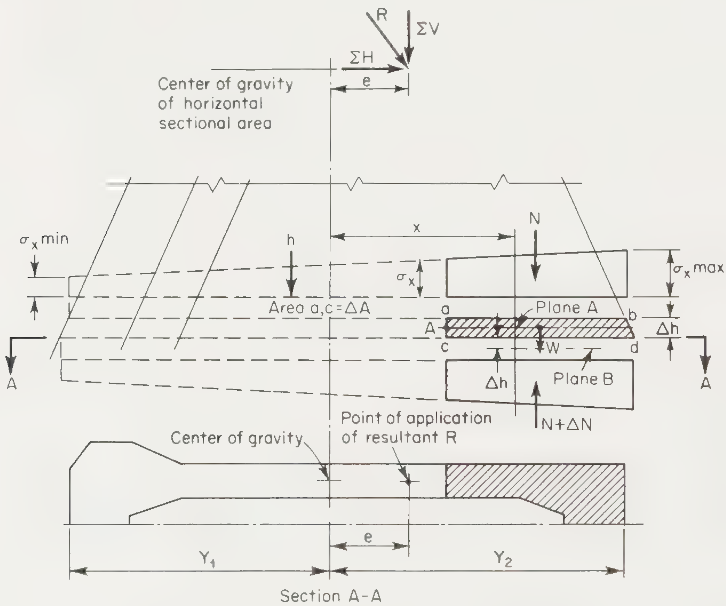

FIG. 5. Determination of shearing stresses.

mined the values of σ_x, σ_y, and τ_{xy} at a sufficient number of points, it is then possible to compute the first and second principal-stress intensities σ_1 and σ_2, which may be determined from the following equations:

$$\sigma_1 = \frac{\sigma_x + \sigma_y}{2} + \frac{1}{2}\sqrt{(\sigma_x - \sigma_y)^2 + 4\tau_{xy}^2} \tag{6}$$

$$\sigma_2 = \frac{\sigma_x + \sigma_y}{2} - \frac{1}{2}\sqrt{(\sigma_x - \sigma_y)^2 + 4\tau_{xy}^2} \tag{7}$$

Principal-stress intensities and their directions and shearing-stress intensities may also be analyzed graphically by the construction of Mohr's circles, as described in Sec. 13. Because the process of arithmetic integration involves small differences of very large numbers, it becomes a matter of some importance to select a value of Δh which will be practical for computation. For dams of medium height, say 60 to 80 m, it has been found that reasonably accurate results may be obtained by selecting a value

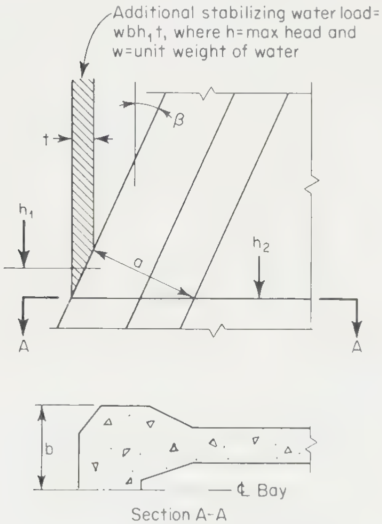

FIG. 6. Section AA water load.

of Δh which falls somewhere between 1.0 and 4.0 m. In the results of a numerical example presented elsewhere the value of Δh is 1.0 m.

Because of the massiveness of the structure it may be assumed that the entire horizontal area, as typified by section AA in Fig. 5, will act integrally in resisting overturning and shearing forces. This assumption introduces an additional stabilizing water load as shown by Fig. 6. This additional load will equal wbh_1t, in which h_1 equals the mean head of a water column having a thickness t. The overturning moment, on plane AA, from water pressure would result from head h_2.

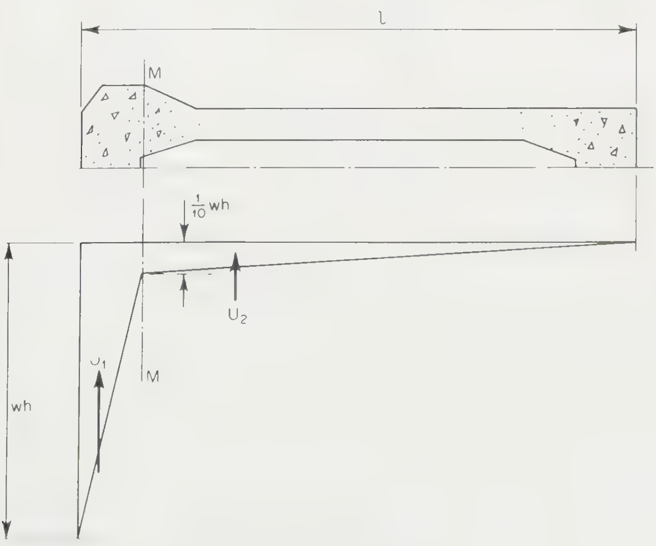

FIG. 7. Assumed uplift.

In this respect the cored gravity-type dam has a distinct advantage over the slab-and-buttress types and the multiple-arch type. Unless the deck, or upstream water-bearing member, acts integrally with the remainder of the structure, part of the weight of the deck may be transferred to the foundation. When this occurs the stabilizing loads on the dam are decreased and an additional overturning force, represented by a horizontal component of the deck load, may be introduced. In contrast, the extent to which the arches of a multiple-arch dam act integrally with the buttresses is not known.

These design procedures are of a generalized nature and may, in fact, be applied to both buttress- and gravity-type dams. The process of balancing the forces on elementary sections and computing the stresses on the incremental areas of these sections will give results which are just as accurate as the basic assumptions. This more comprehensive design procedure is applied in the final design stage in cases where

TABLE 2. VALUES OF COEFFICIENT n

Dead weight + water load + ice thrust − uplift

Abscissa	σ_x t/sq m	μ t/sq m	$\sigma_x - \mu$, t/sq m	τ, t/sq m	n
0	214.960	0	214.960	96.732	3.339
1	206.071	0.482	205.589	94.505	3.328
2	197.149	0.966	196.183	92.242	3.328
2′	197.149	0.966	196.183	96.036	3.196
3	189.654	1.372	188.282	98.826	3.042
4	182.160	1.778	180.382	104.326	2.821
5	157.715	3.104	154.611	103.043	2.656
6	133.270	4.429	128.841	100.811	2.510
7	108.825	5.755	103.070	97.631	2.381
8	84.091	7.096	76.995	93.449	2.264
9	77.135	7.473	69.662	48.935	4.204
10	70.179	7.850	62.329	26.735	7.476
11	69.102	11.881	57.221	25.476	7.684
11′	69.102	11.881	57.221	18.590	10.531
12	63.290	33.616	29.674	16.212	10.717
13	57.290	56.059	1.231	13.802	10.939
14	51.290	78.500	−27.210	12.244	10.473

it is important to determine principal and shearing stresses at critical points in the structure. Shearing stresses may be of especial importance if vertical construction or contraction joints are used in the buttresses.

In the preparation of preliminary designs, it will suffice ordinarily to compute vertical normal pressures and the principal and shearing stresses by the more approximate methods described in Secs. 12, 13, and 15.

STRUCTURAL ANALYSIS

5. Assumptions. The forces acting on a hollow gravity-type dam are normally:

1. The weight of the concrete w_c assumed in this example as 2.5 metric tons (t) per cubic meter for the case of empty reservoir and earthquake effects and the reduced figure 2.3t per cubic meter for full reservoir.

2. The unit weight of water w assumed to be $1.0t$ per cubic meter.

3. Ice thrust, estimated to be $2.5t$ per meter of length of the dam crest per each 10 cm of thickness of the ice field, with thrust applied at the middle point of that thickness.

4. Uplift pressure, as shown by Fig. 7, assumed as decreasing linearly from a value equal to that resulting from full head at the upstream face, to one-tenth of this pressure at the intersection of the upstream expansion with the buttress, and thence

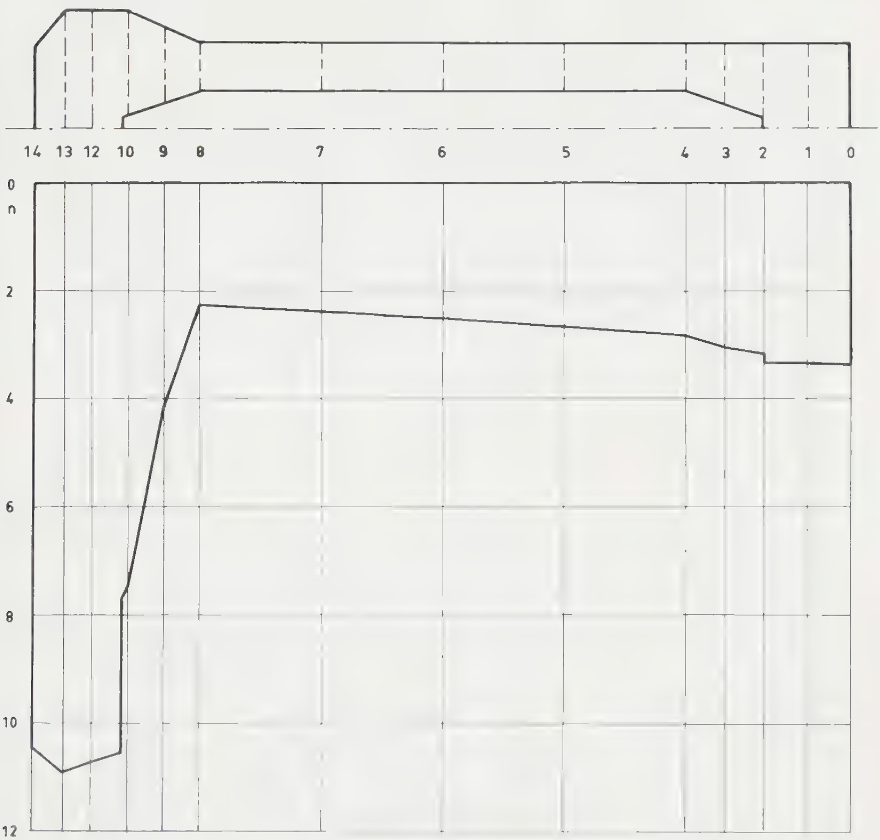

Fig. 8. Values of coefficients n at El. 1,707.50.

linearly to zero at the downstream face. It is assumed that these pressures will be applied to an area equal to 100 percent of the base.

5. Pore pressures are assumed to have the same values and the same distribution as those assumed for uplift pressures.

6. Earthquake effects are assumed:

   a. For vertical shocks, alternately to equal a 20 percent increase and decrease of mass.

   b. For horizontal shocks, equal to horizontal forces amounting to 10 percent of the mass of the individual parts affected.

TABLE 3. VALUES OF STRESSES

Dead weight + water load + ice thrust + pore pressure

Abscissa	σ_x, t/sq m	σ_y, t/sq m	τ, t/sq m	σ_I, t/sq m	σ_{II}, t/sq m
0	216.565	43.854	97.454	260.419	0
1	206.128	47.261	94.997	250.526	2.864
2	195.653	44.054	92.491	239.437	0.270
2′	195.653	53.911	96.383	244.416	5.148
3	186.852	62.821	99.065	241.712	7.961
4	178.054	78.020	104.511	243.900	12.174
5	149.351	91.419	102.325	226.731	14.039
6	120.650	103.994	99.009	211.681	12.963
7	91.947	115.789	94.564	199.180	8.556
8	62.907	127.267	88.916	189.647	0.527
9	54.740	84.976	47.686	119.883	19.833
10	46.572	66.251	27.194	85.331	27.492
11	45.307	67.805	26.494	85.339	27.773
11′	45.307	57.728	20.276	72.723	30.312
12	38.483	59.457	20.093	71.635	26.305
13	31.440	60.153	19.951	70.376	21.217
14	24.394	60.466	20.354	69.626	15.235

TABLE 4. VALUES OF STRESSES

Full reservoir + horizontal earthquake (upstream-downstream)

Abscissa	σ_v, t/sq m	σ_0, t/sq m	τ, t/sq m	σ_I, t/sq m	σ_{II}, t/sq m
0	253.910	51.417	114.259	305.327	0
1	239.619	54.025	111.415	291.821	1.823
2	225.276	49.138	108.555	276.994	−2.580
2′	225.276	60.108	113.500	283.057	2.327
3	213.225	69.053	117.149	278.690	3.588
4	201.178	84.868	124.442	280.383	5.663
5	161.877	97.438	122.155	255.990	3.325
6	122.579	109.180	118.669	234.738	−2.979
7	83.277	120.087	113.983	217.141	−13.777
8	43.514	130.581	108.020	203.510	−29.415
9	32.331	86.198	63.323	128.077	−9.548
10	21.148	65.841	41.585	90.703	−3.714
11	19.415	66.767	40.876	90.329	−4.147
11′	19.415	56.829	34.054	76.976	−0.732
12	10.073	57.524	34.235	75.451	−7.854
13	0.427	57.605	34.508	73.828	−15.796
14	−9.219	58.370	35.480	73.575	−24.424

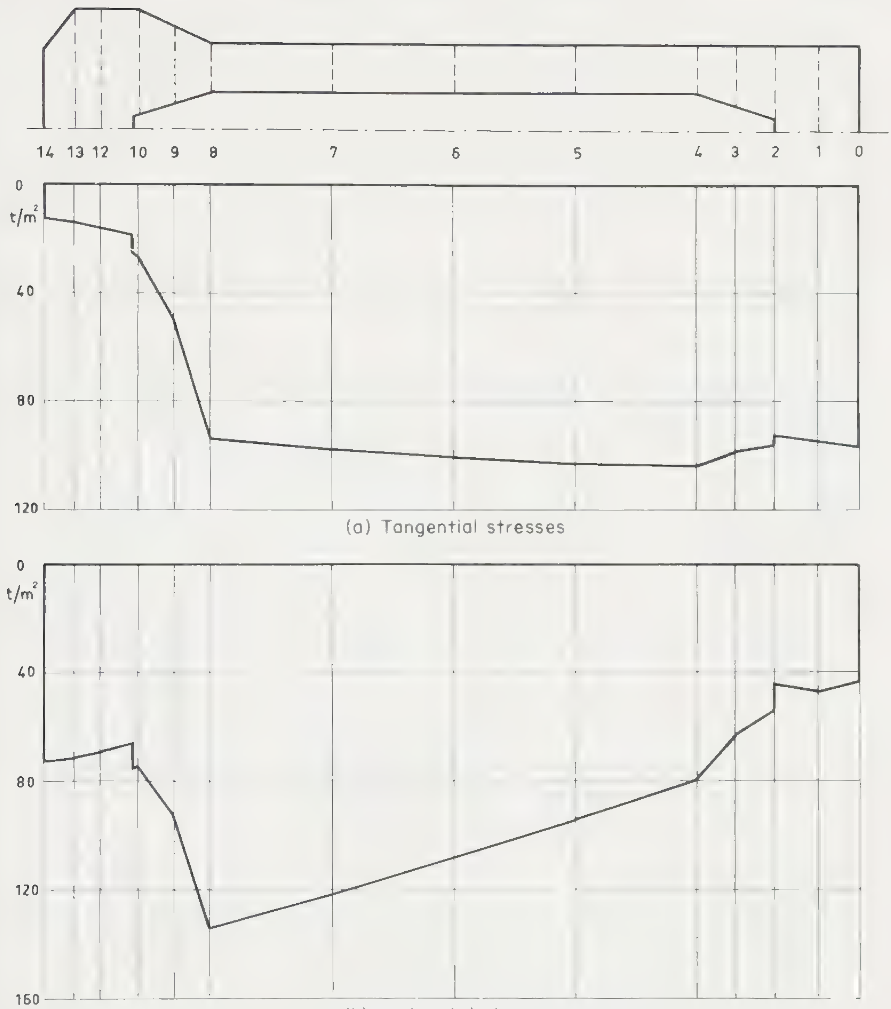

FIG. 9. Variation of shearing stresses.

c. For determining the effect of the inertia of the water against the face of the dam, the Westergaard equations should be applied. The diagram of load equivalent to the increased horizontal dynamic pressure is elliptical with vertical half axis equal to $h = 78.50$ m (maximum head) and horizontal half axis $p_0 = 0.6h$.

These assumptions have been found acceptable for the design of hollow gravity dams in Italy and other European countries. They may not be entirely consistent with American practice as set forth in Secs. 9 to 15, inclusive.

The section analyzed is that at El. 1,707.5, as shown in Fig. 1.

6. Overturning. Figure 1 shows the dimensions of the structure, the principal forces which act upon it, and the moment arms of these forces. Expressed in approxi-

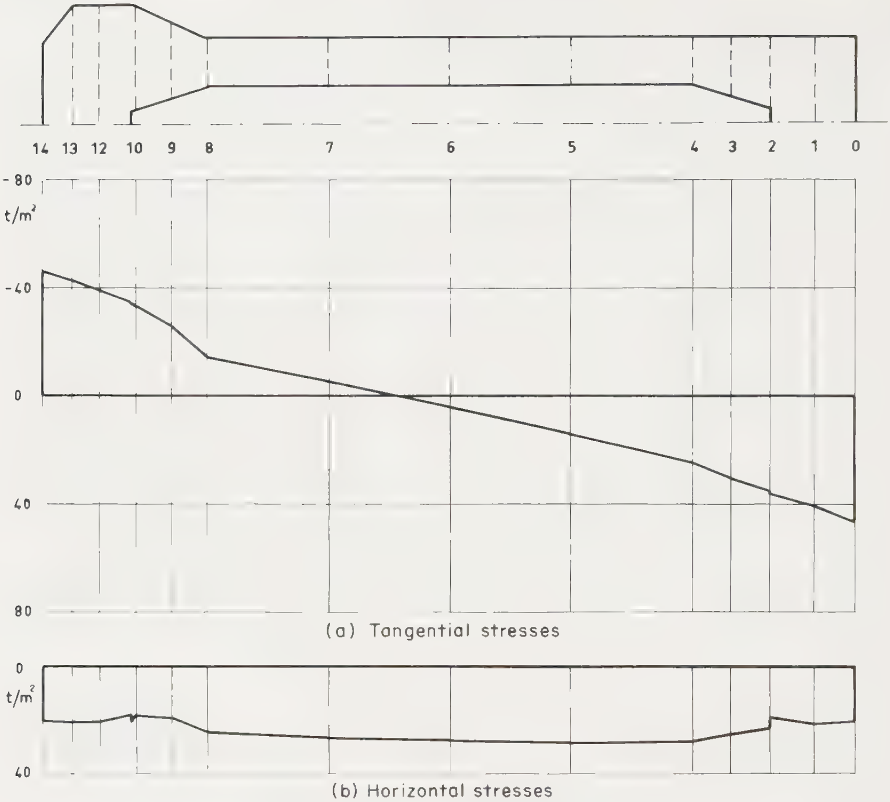

FIG. 10. Second condition of load.

mate terms the maximum stabilizing moment is 2.55 million metric tons and the maximum overturning moment is 1.22 million metric tons. The factor of safety against overturning is therefore $2.55/1.22 = 2.09$.

In the case of horizontal shock (earthquake) the factor of safety against overturning becomes $2.55/(1.22 + 0.24 = 1.46) = 1.75$.

7. Shear Friction. The vertical normal force would be, in metric tons (t),

Vertical water load	$15,250t$
Concrete	$41,540t$
	$56,790t$
Uplift	$-5,020t$
Total	$51,770t$

The horizontal normal pressure would be

Ice load	$165t$
Horizontal water load	$33,890t$
	$34,055t$

The sliding factor, ordinarily designated as f, would therefore be

$$\frac{34{,}055t}{51{,}770t} = 0.66$$

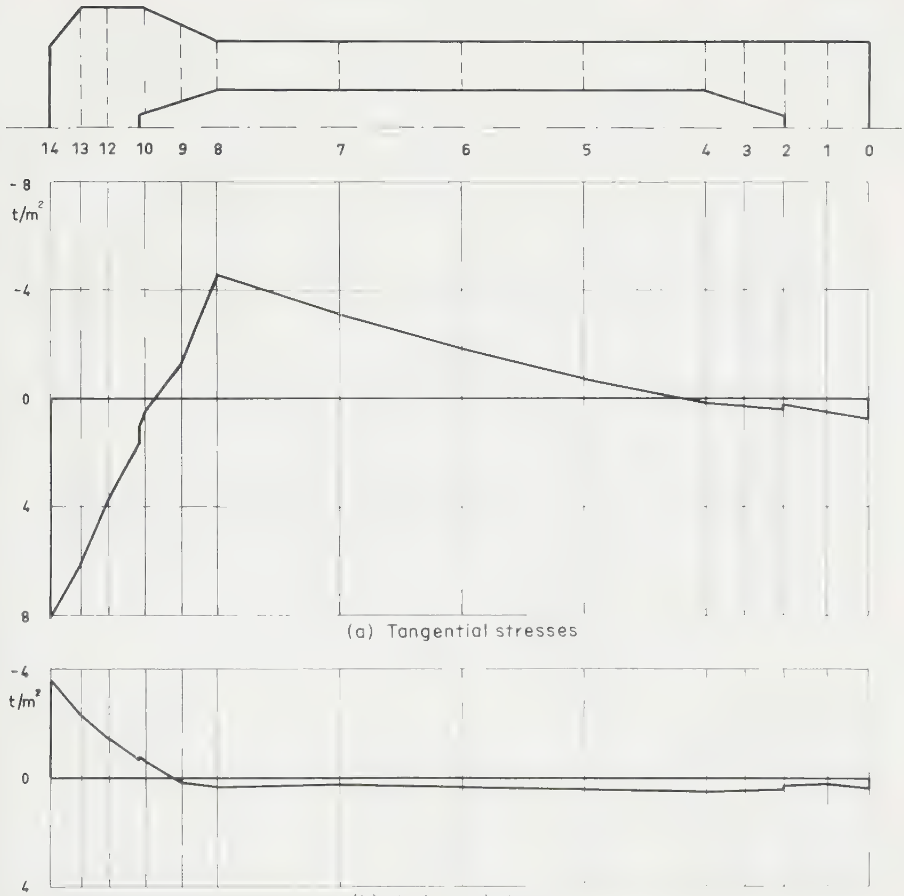

(a) Tangential stresses

(b) Horizontal stresses

Fig. 11. Third condition of load.

Frictional resistance is only one component of the factor of safety against downstream movement as expressed in Eq. (1). Assuming that the unit shear resistance of the rock-to-concrete bond is $\tau_0 = 150t$ per square meter and that a sliding factor f of 0.80 would not result in downstream movement, the overall factor of safety against shear-friction failure would be, according to Eq. (1),

$$Q = \frac{\{0.8[(\Sigma V - U) = 51{,}770t] = 41{,}300t\} + [150t \text{ per sq m} \times (A = 441 \text{ sq m}) = 66{,}000t] = 107{,}300t}{\Sigma H = (\text{water} + \text{ice}) = 34{,}055t}$$

$$= 3.2 \pm$$

In the case of a vertical earthquake shock, only a slight change in the value of Q would result. In the case of a horizontal earthquake shock, the horizontal pressure would be increased by $7{,}750t$, thus increasing the sliding factor f to 0.81 and decreasing the overall safety Q to 2.57. Both indicate that the structure would be safe from shear-friction failure under seismic-load conditions.

As has been mentioned previously, the overall factor of safety against failure by shear friction is not necessarily indicative of the safety of component parts of the structure, especially of columns separated by construction joints.

The shear-friction factors of safety at the points of reference shown by Fig. 2 may be determined by the formula

$$n = \frac{\tau_0 + 0.8(\sigma_x - \mu)}{\tau} \tag{8}$$

in which the following symbols apply to a specified point of reference:

n = shear-friction factor of safety
τ_0 = ultimate shearing stress for rock-to-concrete bond
σ_x = vertical normal-unit-stress intensity
μ = uplift pressure, unit intensity
τ = actual unit-shearing-stress intensity

Table 2 demonstrates the variation of n which occurs throughout the horizontal section at **El.** 1,707.50 as shown by Figs. 1 and 2. This variation is also shown by Fig. 8.

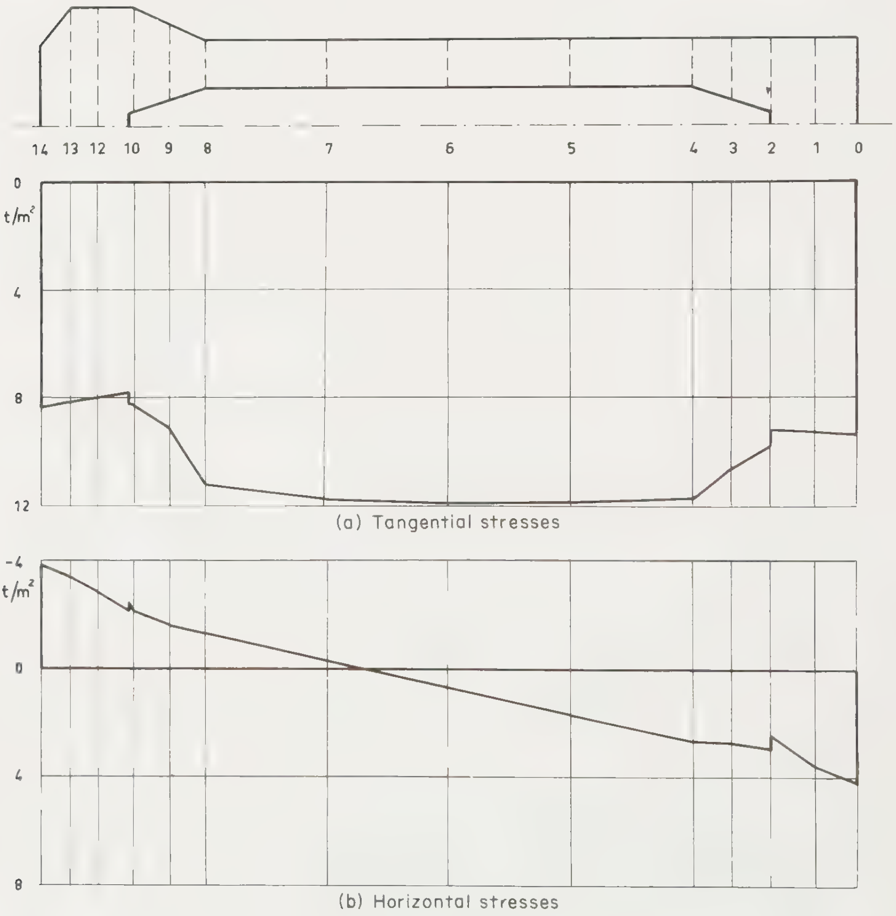

FIG. 12. Fourth condition of load.

8. Stresses. By following the design procedures, as described previously, it is possible to compute the vertical normal, horizontal normal, shearing, and first and second principal stresses for each of the reference points shown by Fig. 1. The results of typical analyses are summarized in Tables 3 and 4. Figures 9 to 13 show variation of shearing stresses τ_{xy} and horizontal stresses σ_y for five loading conditions. Figure 14 shows the first and second principal stresses σ_1 and σ_2 for three loading conditions.

It will be noted from Fig. 14 that, in all cases, the maximum principal stress occurs at the intersection of the upstream flare with the buttress. This stress approximates the total water pressure per linear meter at that point divided by the area of the buttress. For example, with a head of 78.5 m the water pressure would be 78.5*t* per square meter and the total pressure per linear meter would be 78.5×11 m $= 863.5t$. Dividing this by the area of a 1.0-m-wide strip of buttress, or 4.65 sq m, gives a value for σ_1 of 186*t* per square meter, which corresponds very closely to the value shown by Fig. 14 for the full reservoir plus dead weight of concrete plus ice pressure plus pore pressure.

9. Principal-stress Trajectories. From an analysis of principal-stress directions by the construction of Mohr's circles, the manner in which concrete and water loads are transmitted to the foundation may be clearly demonstrated. Figure 15 shows the directions of principal stresses resulting from the weight of the concrete only and Fig. 16 those which result from a combination of concrete and water loading.

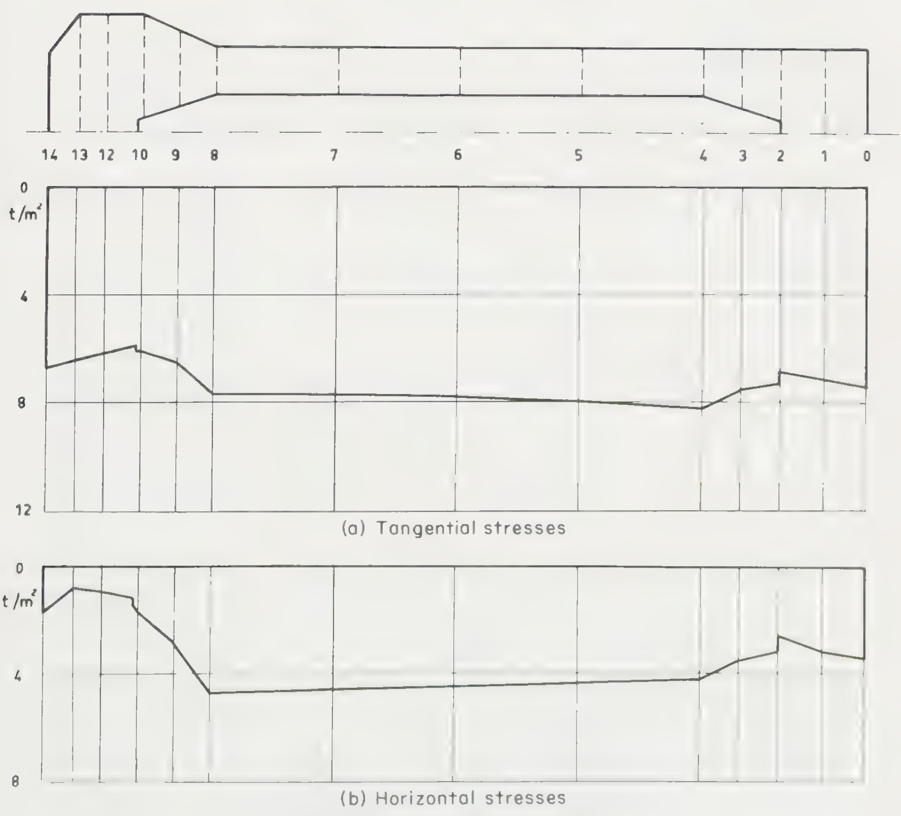

FIG. 13. Fifth condition of load.

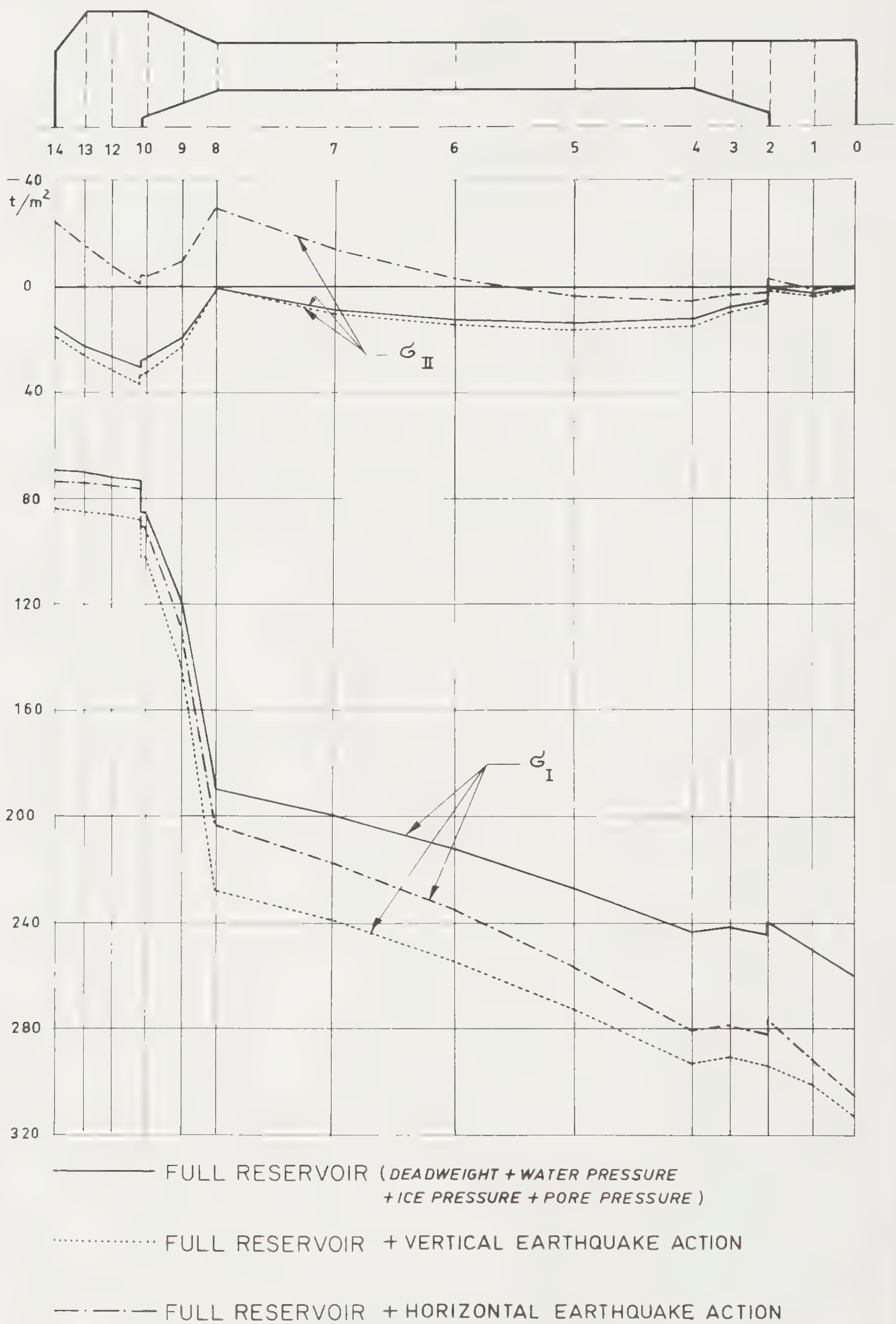

Fig. 14. Principal stresses, three combinations of loading.

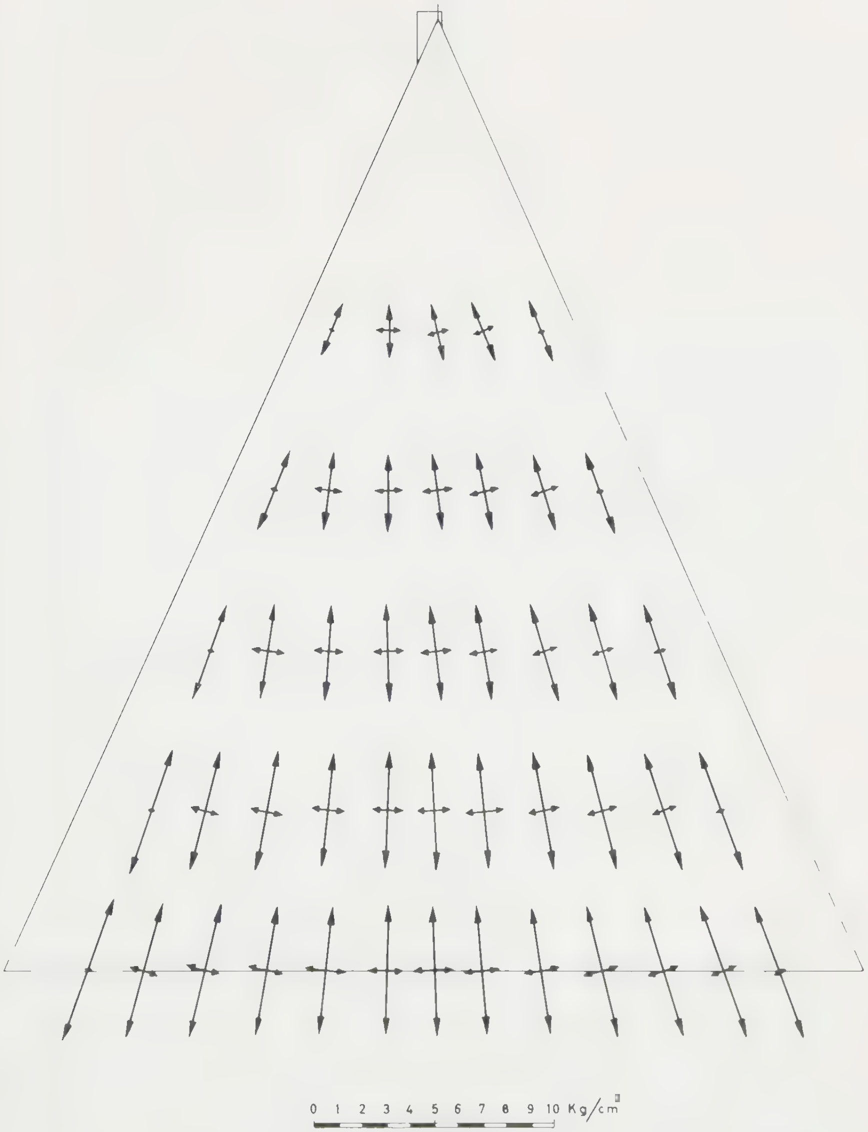

Fig. 15. Principal stresses and directions relative to weight (empty reservoir).

Regardless of the analytical approach, whether by the finite-element method, model testing, or the balancing of the forces on elementary sections as described here, the directions of principal-stress trajectories lead to the same concept: A concrete dam of either the buttress or gravity type may be envisioned as a series of contiguous, inclined elementary columns, each of which transmits a part of the water and concrete loads from the upstream face through the dam to the foundations.

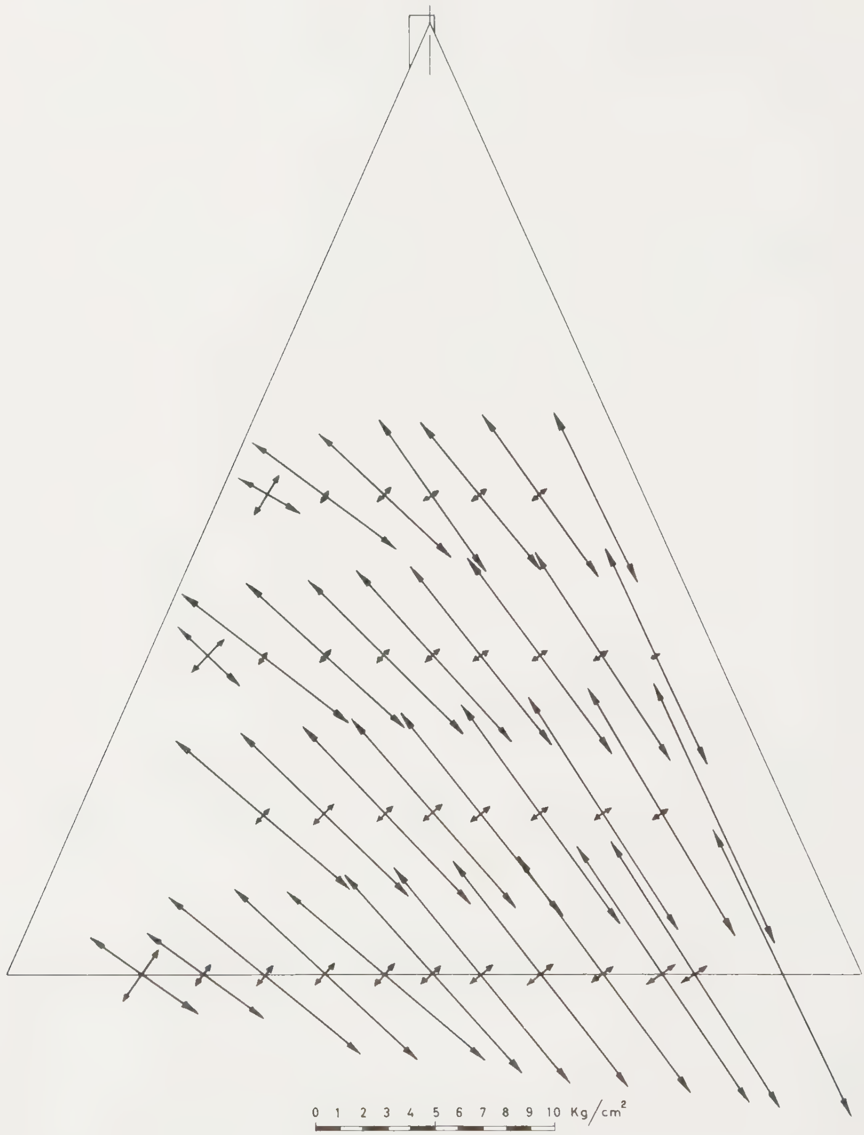

FIG. 16. Principal stresses and directions relative to weight and water load (full reservoir).

One of the principal merits of the design illustrated in this section is that these elementary loads are coincident with the column axes and that concrete is therefore used principally to convey loads in axial compression. The end results are:

1. Increased factors of safety
2. Savings in construction cost
3. A structure of striking architectural beauty

SECTION 13

AMBURSEN DAMS

By Edgar H. Burroughs

PRINCIPAL FEATURES

1. Characteristics of Type. The basic flat-slab and buttress type, as shown by Fig. 1, has borne the name of its inventor since 1903. These articulated, reinforced-concrete buttress dams are provided with expansion joints between the decks and the buttresses. The deck consists of reinforced-concrete water-bearing slabs, separated by buttress tongues and supported by reinforced-concrete haunches which are constructed monolithically with the buttresses. Nearly four hundred dams of this type have been constructed. The Rodriguez Dam (Fig. 1) on the Tijuana River, Lower California, with a maximum height of 267 ft, is the highest of record.

The designing methods described in this section are applicable to all types of buttress dams if appropriate treatment is given to the deck or water-bearing member. For example, in the design of either hammerhead or multiple-arch-type dams, the decks and buttresses are assumed to act integrally as described in Sec. 9. In the design of an Ambursen dam, the deck acts independently of the buttress.

FORCES ON AMBURSEN DAMS

Consideration must be given to the following forces:

1. Headwater pressure
2. Weight of structure
3. Tail-water pressure
4. Silt
5. Ice thrust
6. Temperature expansion and contraction
7. Earthquake accelerations

2. Headwater Pressure. The Ambursen dam, in common with other buttress types, utilizes the water load upon its inclined deck as a stabilizing force. Reference to Fig. 2 showing the principal forces will make this property clear. The resultant water load N_w, acting normal to the deck, may be resolved into a vertical component V_w, exerting a righting moment $V_w a_1$, and a horizontal component H_w, exerting an overturning moment $H_w a_2$. In addition to the moment effect of the various loads, there is a tendency to slide and shear across the foundation material. Resistance to horizontal movement is commonly expressed by the shear-friction factor of safety (see Sec. 9).

The headwater uplift pressure on an Ambursen dam is usually of insignificant proportions, varying in an arbitrary manner from the maximum pressure at the upstream face of the water-bearing member to either zero or tail-water pressure at the downstream face.

3. Weight of Structure. It is most convenient to treat the weight of the structure as divided into two parts: (1) the buttress load and (2) the deck load. The buttress

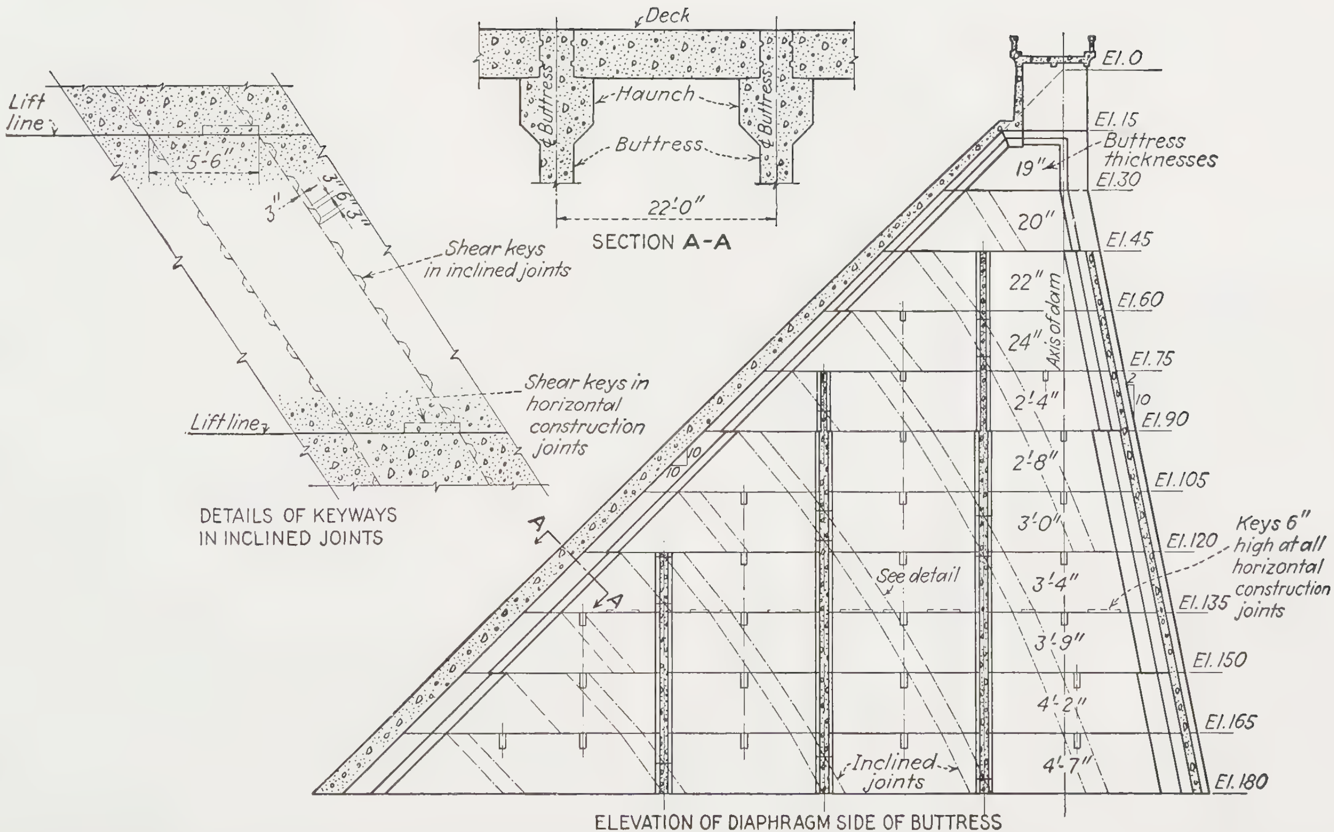

Fig. 1. Rodriguez Dam. Buttress elevation and sections (inclined joints).

load is transmitted down through masonry directly to the foundation material and is handled in computations in a manner similar to usual masonry loads. The manner in which the deck load is transmitted to the foundation depends entirely upon the way in which the slab is placed on the upstream end of the buttress. If the deck is constructed monolithic with, or properly keyed into, the buttress, the masonry weight is transmitted in its entirety down through the buttress to the foundation, in a manner similar to the buttress load. With reference to Fig. 2, it will be seen that the righting moment of the buttress is equal to Wa_3 and that of the deck is V_Da_4.

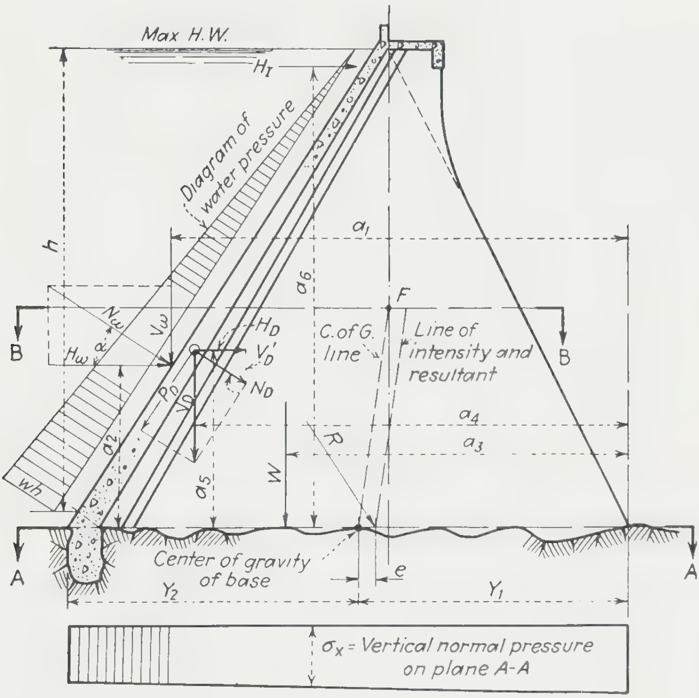

FIG. 2. Forces acting on buttress dams.

When the deck is completely articulated and merely rests against the upstream face of the buttress or upon the haunches, the weight of the deck is broken down into two components, one normal to the upstream edge of the buttress and the other parallel to the face. The normal component is transmitted down through the buttress masonry to the foundation, and the parallel component travels down through the deck slab directly to the foundation. Again with reference to Fig. 2, it will be noted that the righting moment of the buttress is equal to Wa_3. However, in this case the righting moment of the deck is equal to V'_Da_4. The overturning moment exerted by a completely articulated deck is equal to H_Da_5.

4. Tail-water Pressure. The force on the deck and the buttress due to tail water reduces the effective headwater pressure and, consequently, is beneficial in this respect. However, the loss of effective weight due to partial submergence of the structure frequently offsets whatever advantage is gained by the presence of tail water. It is usually advisable to analyze the structure for both maximum and minimum tail-water conditions.

5. Silt. An additional load due to silting of the reservoir will be placed on the deck near the bottom of the dam. The height to which the silt load may extend up the deck of the dam will depend on the quantity of suspended matter carried by the stream, the velocity of the water through the reservoir, and the size and shape of the reservoir. For streams bearing heavy silt loads, it is usual to assume that the depth of silt will build up from one-quarter to one-half the full height of the dam. Conventional methods of computing earth pressures with proper allowances for the effect of saturation should be applied in making the analysis (see Sec. 9).

6. Ice Thrust. The effects of ice thrust are illustrated in Fig. 3. The harmful overturning moment on the sloping upstream face of an Ambursen dam is minimized because there is insufficient frictional resistance or adhesion between the deck and the ice to overcome the component of ice thrust parallel to the deck. The result is a breaking up of the ice sheet adjacent to the deck.

7. Temperature Expansion and Contraction. Temperature changes both during and after construction are of major importance. To eliminate the effects of serious temperature stresses during construction, the buttress and deck concrete is poured and

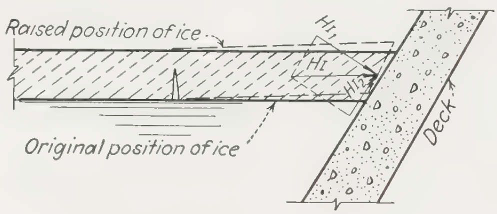

Fig. 3. Action of ice on deck slab.

cured in relatively small sections or blocks. Temperature stresses developing after construction are either carried by horizontal steel or relieved by contraction and expansion joints.

8. Earthquake Accelerations. The articulated flat-slab buttress-type dam offers an inherent resistance to earthquake forces. Two examples of the selection of this type of structure specifically for construction in earthquake zones are the Stony Gorge Dam built by the U.S. Reclamation Bureau and the Rodriguez Dam built by the National Irrigation Commission of Mexico. Each structure was built across a geological fault, the Rodriguez Dam being designed with alternate pairs of buttresses tied together by reinforced-concrete diaphragms so as to form a tower construction, heavy unanchored beams or struts being installed in the intermediate bays (see Sec. 9).[1]

A well-designed Ambursen dam has such a large factor of safety against overturning that the additional overturning force resulting from seismic loads will be negligible. This does not apply, however, to the lateral stability of the buttresses. If the earthquake hazard is severe, special lateral bracing in the form of either beams or diaphragms should be provided.

THEORY OF BUTTRESS DESIGN

The fundamental principles of design and analysis are applicable to all types of buttress dams. When judiciously applied, these principles can be extended to include, in addition to the usual solid-wall buttress, the hollow-buttress and the diaphragm-buttress types.

Design involves two steps: (1) the selection of a trial design, (2) the analysis of this

[1] *J. AWWA*, **25** (3), 355, 1933.

design to determine whether it satisfies stress and stability requirements. In selecting the proportions of the trial design, the buttress outline and thicknesses may be computed directly by using simplifying assumptions or determined from the results of previous experience with a similar structure.

9. Trial Design Using Simplifying Assumptions. Preliminary investigations are based on the simplifying assumption that a buttress consists of a system of columns (see Fig. 4), each carrying the incident water load by column action to the foundation. These columns are proportioned to develop a uniform compressive stress and curved to avoid any serious eccentricity on any normal or horizontal plane when the water and concrete loads are resolved. It is possible to determine, graphically,

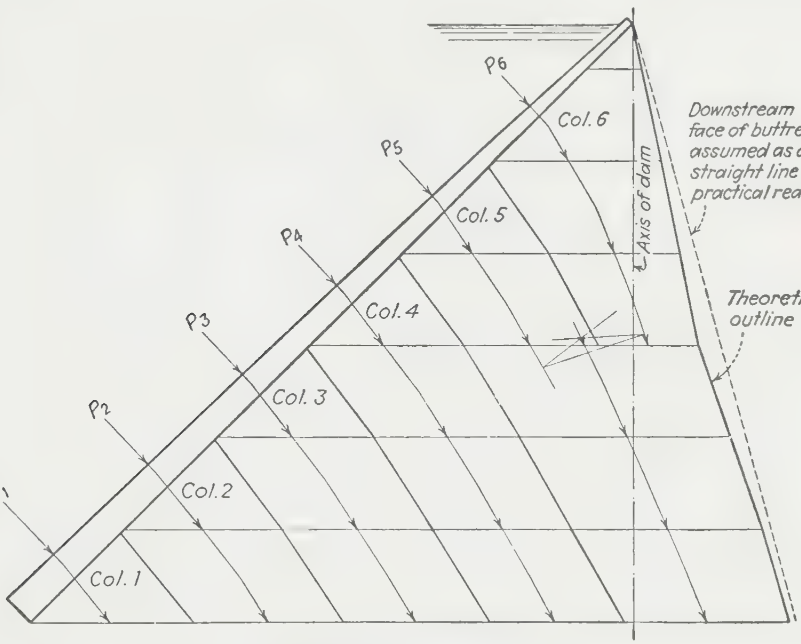

FIG. 4. Column design of buttress.

the approximate outline and thicknesses of a buttress by progressively designing a series of column sections, starting at the foundation and continuing to the crest, such that the load carried by the individual columns produces no shear between adjacent columns. This method of design is based on the assumptions (1) that the buttress columns are free to act independently of each other, and (2) that by placing all columns concentric with their respective loadings, the second principal stress will be zero for maximum load conditions. If the buttress is constructed as a monolith, the columns become merely hypothetical and cannot act independently. It is obvious that in this case deformations and, consequently, stress will be transmitted between adjacent (hypothetical) columns. However, for small dams the monolithic buttress offers the additional inherent stability of a larger and continuous member. Analysis indicates that in a monolithic buttress proportioned in strict accordance with the direct-design method the first principal stress will not remain uniform, nor

[1] *Trans. ASCE*, **98**, 418, 1933.

will the second principal stress be zero throughout the buttress. If the buttress is jointed so as to preserve the columnar structure (as shown in Fig. 5), the action and the stresses will more nearly approximate the theoretical. The decision as to whether the buttress should be jointed or monolithic rests with the designer. The jointed buttress has the advantages of (1) minimizing stresses due to setting and temperature, (2) eliminating the necessity of placing a substantial amount of horizontal or inclined

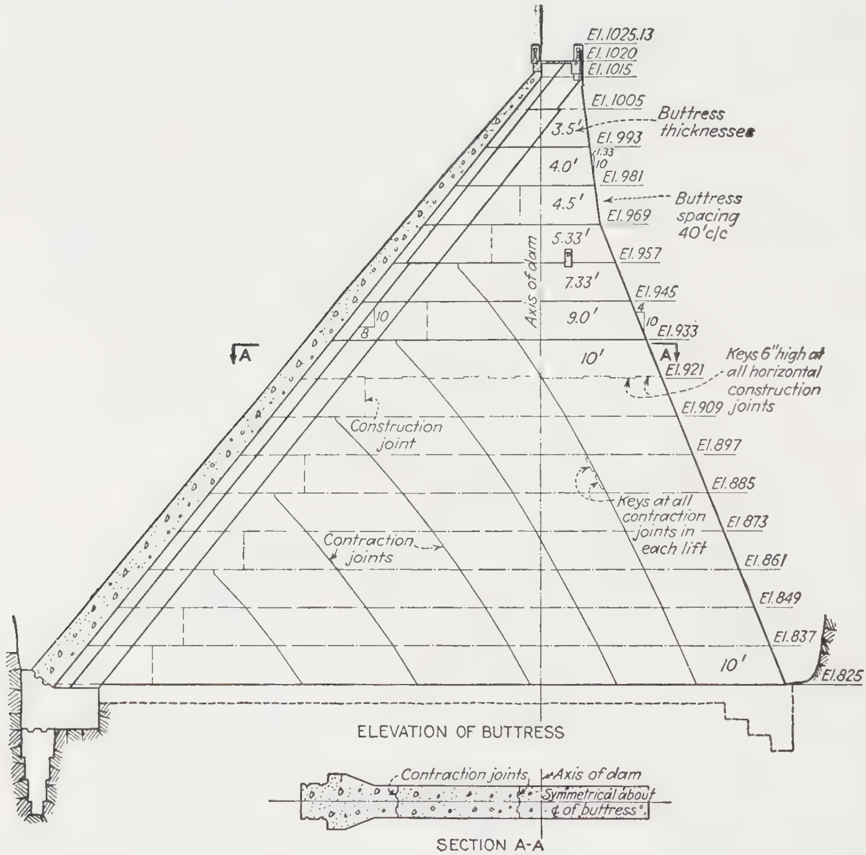

Fig. 5. Possum Kingdom Dam (renamed Morris Sheppard Dam). Bulkhead buttress and sections; keys in contraction joints (inclined joints).

steel in the main body of the buttress, (3) facilitating construction, and (4) approaching the theoretical action.

It is important to note that any variation from the buttress shape and thicknesses determined by the above-described trial-design method, such as the addition of haunches or corbels at the upstream edge of the buttress or the addition of pilasters at the downstream edge, will, in proportion to the relative size of the addition, alter the principal stress values from those used as a design requirement. In view of its many uncertainties, the direct-design results should be carefully checked by a thorough stress analysis except, perhaps, in the case of a low, simple buttress.

With reference to Fig. 4, which shows a simple buttress of approximately triangular shape, the incident water load is divided into six sections of approximately equal length along the water-bearing face. By starting at the foundation, the upper boundary of column 1 is determined so that the trajectory, described by resolving the water load P_1 and the masonry weight, passes through the center of gravity of either horizontal or normal sections through column 1. This procedure is repeated for columns 2, 3, 4, 5, and 6 in succession. The lower boundary for each column is the upper edge of the preceding column. A practical guide to the most desirable horizontal column width is the limitation of the horizontal length of pour that can safely be made without inviting shrinkage cracks. The limiting length is about 35 or 40 ft, proper curing of the green concrete being assumed. Thicknesses are determined so as to give uniform major compressive stress throughout the buttress. The maximum allowable stress is governed by the slenderness ratio as in the design of common columns. It is, usually, more economical to use struts or diaphragms to keep the unsupported length at the greatest allowable value (l/d = 15) with which the maximum compressive stress may be used.

10. Stability and Stress Investigations. After the trial design has been selected, subsequent detailed investigations will involve computations for the following:

1. Stability against overturning and sliding (movement downstream)
2. Normal foundation pressures and normal pressures on selected horizontal planes through the buttress at various elevations
3. Shearing, horizontal normal and principal stresses

Stability against overturning and sliding are determined in the conventional manner by summing all moments, vertical forces, and horizontal forces at the base of the dam.

For ordinary computations, it is sufficiently accurate to assume that normal stresses on horizontal planes have straight-line distribution, as shown for the plane AA (Fig. 2). This assumption is more nearly accurate when the median line of the buttress is normal, or nearly so, to the plane of analysis. When the angle formed by the median line and the plane of analysis approaches 45 deg, the distribution of the vertical normal stress varies noticeably from a straight line. The recently developed "finite-element" method, as described in Sec. 10, will yield curvilinear distribution of stresses. Normal foundation pressures or normal stresses having linear distribution on horizontal planes are obtained from the well-known law of the trapezoid.

$$\sigma_{x\binom{\max}{\min}} = \frac{N}{A} \pm \frac{MY}{I} \tag{1}$$

where σ_x = intensity of normal stress on horizontal plane
N = total vertical load on section
A = sectional area of base
M = moment = Ne
e = eccentricity (distance from point of application to center of gravity of section)
Y = distance from center of gravity to most remote fiber
I = moment of inertia of horizontal section

Location of resultants, sliding factors, and vertical normal pressures for Rodriguez Dam and for Possum Kingdom Dam are shown in Figs. 6 and 7, respectively.

11. Shearing, Horizontal, Normal, and Principal Stresses. Briefly stated, the method of computing the principal stresses in a buttress consists of dividing the buttress by horizontal and vertical planes into a number of elementary prisms which are then considered to be in vertical and horizontal equilibrium. Equations are written expressing the unknown stress functions in terms of the stresses which may be determined directly from Eq. (1).

If vertical normal stresses, horizontal normal stresses, and vertical shearing stresses are thus evaluated, both the principal stresses and their directions may be determined either analytically, by the principal-stress equations, or graphically, by Mohr's circle. In the following, this procedure is developed more fully. Assume,

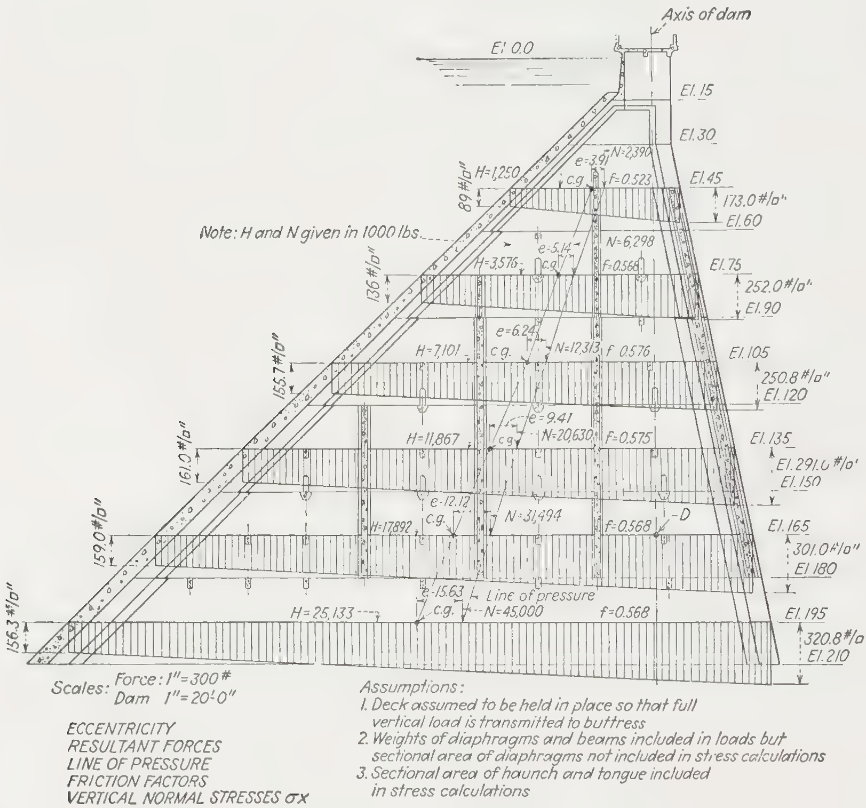

Fig. 6. Rodriguez Dam. Buttress elevation with e, H, N, f, etc.

for example, that it is desired to determine the intensities and directions of the principal stresses at point F, plane BB (Fig. 2). For convenience, an enlarged section of Fig. 2 is shown by Fig. 8. Horizontal planes CC and DD (Fig. 8) are plotted equal distances above and below plane BB, and the values of σ_x (max) and σ_x (min) are computed for each plane by Eq. (1). The distance between these planes must be relatively small if sufficient accuracy is to be maintained.

Next construct a vertical plane intersecting the three horizontal planes at E, F, and G. The elementary prism $ECBF$ may then be visualized as separated from the buttress as shown in Fig. 9 and to be held in equilibrium by the forces acting on it. These forces are the total vertical normal pressure on the plane EC, $\sum_C^E b_1\sigma_x\Delta x$; the

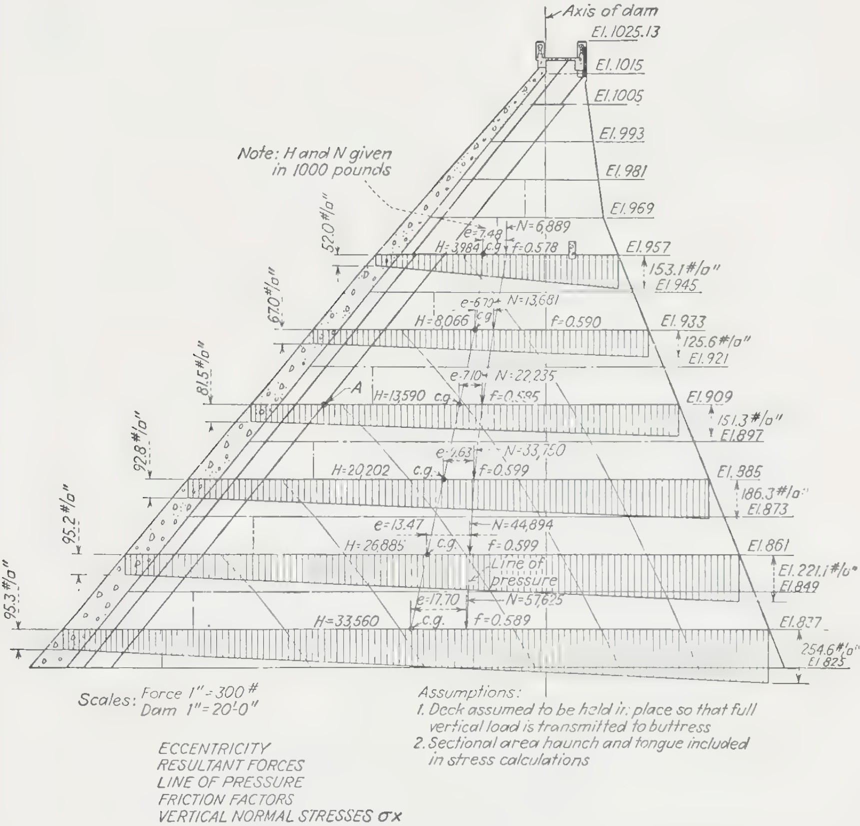

FIG. 7. Possum Kingdom Dam. Buttress elevation with e, H, N, f, etc.

SAMPLE COMPUTATIONS—HORIZONTAL SHEAR STRESS

$$pd = 217.87^k \qquad \gamma_t = 1.500$$
$$p'd = 2.312 \qquad m = 0.4$$
$$k = 0.7464 \qquad l_0 = 134.67'$$
$$k' = 0.00182 \qquad z = 9.6'$$
$$S_z = a + b_z - cz^2$$
$$a = mpd = 0.4 \times 217.87 \qquad = 87.1$$
$$b = p'd - mk - \gamma_t$$
$$= 2.312 - 0.4 \times 0.7464 - 1.500 \qquad = 0.513$$
$$c = \frac{k'}{2} = \frac{1}{2} \times 0.00182 \qquad = 0.00091$$
$$S = 87.1 \times 0.513 \times 9.6 - 0.00091 \times \overline{9.6}^2 = 91.9^k$$
$$\tau = \frac{S}{t} = 9.19^k/\text{sq ft or } 63.8 \text{ psi}$$

weight of the masonry in the prism W_m; and the total vertical normal pressure on the plane FB, $\sum_B^F b_2\sigma_x\Delta X$.

The total shear V across the plane EF may now be determined by writing the equation for vertical equilibrium for the prism $ECBF$:

$$V_{EF} = \sum_C^E b_1\sigma_x\Delta X + W_m - \sum_B^F b_2\sigma_x\Delta X \tag{2}$$

The average intensity of shear v_1 on the section EF is equal to V_{EF} divided by the sectional area between E and F. By a similar procedure, the average shearing stress

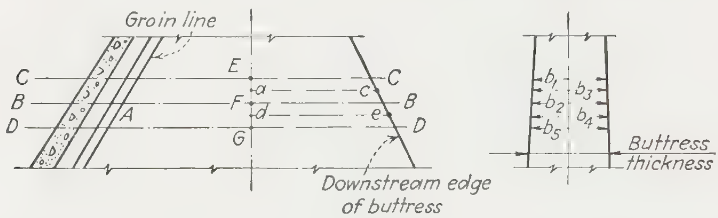

FIG. 8. Partial side elevation of buttress. Planes for principal stress analysis.

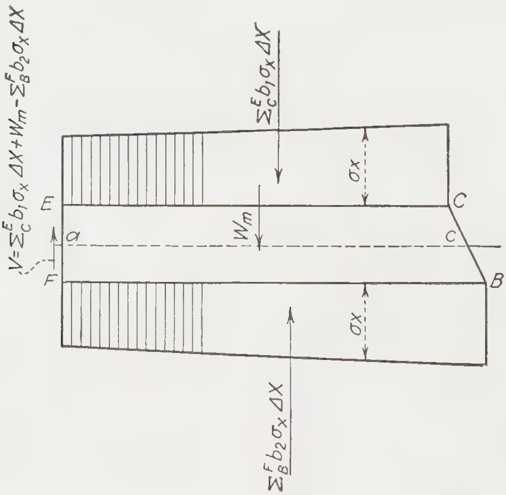

FIG. 9. Unit block removed from Fig. 8.

v_2 between F and G may be determined. The shearing stress at the point F on the plane BB is equal to

$$\tau_{xy} = \frac{v_1 + v_2}{2} \tag{3}$$

The next step is to separate the prism $acde$ from the buttress and consider it in horizontal equilibrium under the shearing forces acting upon it. As horizontal and vertical shearing stress intensities are equal, the total shear acting on the planes ac

and de may be determined by the procedure outlined above. The differences between these total shearing forces will be a horizontal force N_y over the area ad and normal to the plane EF. These forces are expressed in the following equation:

$$N_y = \sum_c^a b_3\tau_{xy}\Delta X - \sum_e^d b_4\tau_{xy}\Delta X \tag{4}$$

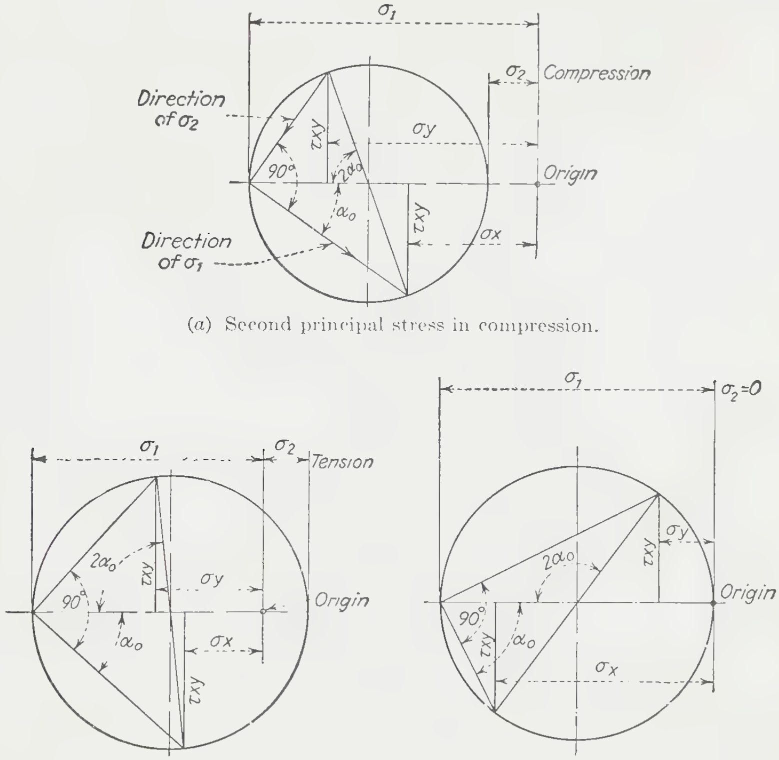

(a) Second principal stress in compression.

(b) Second principal stress in tension.

(c) Second principal stress zero.

FIG. 10. Analysis of principal stresses by Mohr's circle.

The average intensity of horizontal normal pressure σ_y equals N_y divided by the sectional area between a and d.

It is now possible to determine the principal stresses and the state of stress at the point F from the following principal stress equations:

$$\sigma_1 = \frac{\sigma_x + \sigma_y}{2} + \frac{1}{2}\sqrt{(\sigma_x - \sigma_y)^2 + 4\tau_{xy}^2} \tag{5}$$

$$\sigma_2 = \frac{\sigma_x + \sigma_y}{2} - \frac{1}{2}\sqrt{(\sigma_x - \sigma_y)^2 + 4\tau_{xy}^2} \tag{6}$$

$$\tan 2\alpha = \frac{2\tau_{xy}}{\sigma_y - \sigma_x} \tag{7}$$

Both the first and second principal stresses and their directions may be easily determined graphically by means of Mohr's circle as illustrated by Fig. 10. The construction of Mohr's circle is self-explanatory, and the derivation may be readily determined by inspection. Figure 10*a*,*b*,*c*, shows three cases: (1) the analysis of a point at the groin line with the second principal stress in compression, (2) the analysis of a point at the groin line with the second principal stress in tension, and (3) the analysis of a point at the downstream face of the dam where the second principal stress is zero. The fact that incorrect proportioning of the buttress may readily cause σ_2 to be a dangerously high tensional stress emphasizes the importance of computing the normal stresses on all planes through the point of analysis.

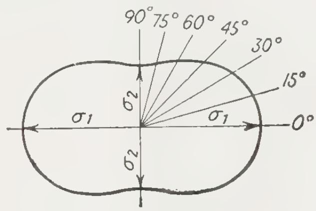

(*a*) Both principal stresses in compression.

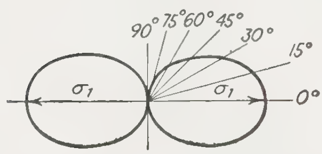

(*b*) First principal stress in compression and second principal stress zero.

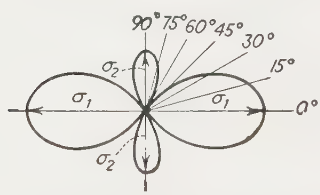

(*c*) First principal stress in compression and second principal stress in tension.

FIG. 11. Distribution of stresses around a point.

In Fig. 11 are shown three general cases of normal stress variation around a point: (*a*) for both principal stresses in compression, (*b*) for the first principal stress in compression and the second principal stress equal to zero, and (*c*) for the first principal stress in compression and the second principal stress in tension. After the intensities and directions of both the first and second principal stresses are computed, this variation may be determined at any point by the following equation:

$$\sigma = \sigma_1 \cos^2 \phi + \sigma_2 \sin^2 \phi \qquad (8)$$

in which σ is the normal stress on any plane acting at an angle of ϕ with the direction of σ_1.

If in a particular design, for purposes of economy, to secure a low sliding factor or to satisfy other design considerations, it is decided to allow tension in the second principal stress, inclined steel in an amount sufficient to take the entire tensional stress in the buttress should be provided.

Although the basic theory of buttress analysis is readily understandable, its application to a specific case offers several problems, the major of which is to determine the degree of accuracy required in the stress computations. The accuracy of the method described here depends on obtaining small differences of very large numbers. Computations should be carried forward on either a computer or calculating machine.

Two factors affecting the accuracy of stress-analysis computations are the shape of the buttress and the method of applying the theory of analysis. Stress computations are relatively simple for a triangular-shaped buttress of constant thickness and become increasingly difficult as the shape is complicated by changes in thickness, the addition of haunches or corbels, and the addition of flanges or pilasters at the downstream end. Further difficulty is experienced in the analysis of buttresses carrying spillway gate piers or having other special treatment. Unfortunately, it is usually the more complicated shapes that require the most accurate and exhaustive stress analysis.

The methods of applying the theory of principal stress analysis vary for the most part in the selection of the size of block or the distance between the planes in question (dimension *EF*, Fig. 8). In the general derivation of the theory, the planes are considered as being relatively close and it is on this close spacing that the claim to accuracy of the method is based. The use of a spacing of 1 ft between planes (total height of two blocks equals 2 ft) gives accurate results and is entirely satisfactory for use on a simple buttress shape. However, for extremely complicated shapes the computations may have to be carried with as many as 20 significant figures to ensure accuracy of the small differences used in the final substitutions. The method using small blocks is fully analytical, summing, in every case, the full distance from the downstream edge of the buttress to the point in question. It is necessary only to substitute constants derived from the vertical normal stress computations on each of the three planes in the equations to evaluate the vertical and horizontal shears (τ_{xy}) and the horizontal normal stress (σ_y). This method has the advantage of being particularly applicable to analyzing isolated points and sections of the buttress. This advantage becomes a disadvantage when a complete buttress analysis is required because every portion of the buttress must be treated as an isolated area.

In order to avoid greatly extended computations, block heights greater than 2 ft are commonly used, the selection being influenced by the height of the dam. When using the greater height, it is frequently more convenient to subdivide the entire buttress into blocks of approximately square elevation and carry the necessary summations as numerical rather than analytical operations. The horizontal summations are extended as with the smaller blocks by successive steps from the downstream end toward the upstream end of the buttress. The use of larger blocks in combination with numerical summation relies on linear interpolation for accuracy, and in many cases the variation of stresses from the assumed linear distribution is sufficient to introduce appreciable error in the final principal stress determination. Because of the size of the blocks, the summation cannot be carried up under the haunch (point *A*, Fig. 8) where the stress conditions tend to be most critical.

A typical example will illustrate the application of the principal stress analysis using larger blocks to a practical design. The problem, illustrated by Figs. 6 and 12, is to determine the principal stresses at point *D* in the buttress of a 210-ft-high Ambursen dam having buttresses spaced 22 ft center to center. As indicated by Fig. 6, the buttress is constructed in 15-ft vertical lifts, or pours. The vertical normal pressures, as determined from stability computations, are also shown by

Fig. 6. These stresses may be computed readily by an application of Eq. (1) and involve no unusual difficulties.

To determine the principal stresses, the first step is to separate from the buttress the prisms $A\ B\ C\ D$ and $C\ D\ E\ F$ as shown in Fig. 12. Each prism is then assumed to be held in equilibrium by the normal and shearing stresses and by the weight of the masonry within the boundaries of the prism. Figure 12 illustrates the successive steps in computing the principal stresses.

If the directions of principal stresses are determined at a large number of points, it will be observed that the trajectories of principal stresses follow definite mathematical relations as illustrated by Fig. 13. These trajectories indicate that the water

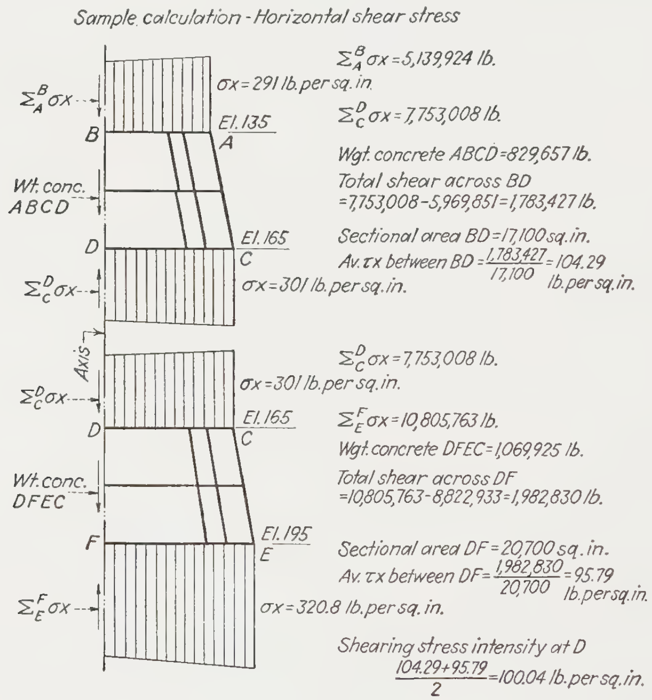

Fig. 12. Rodriguez Dam. Unit block with sample calculation. Horizontal shear stress.

load normal to the deck is transmitted through the buttress to the foundation by means of a series of elementary curved, inclined columns substantiating, in general, the theory presented under Trial Design Using Simplifying Assumptions. Each of these elementary columns is in equilibrium under the influence of the water load, the second principal stresses on each side, and the weight of masonry in the column.

These trajectories of the principal stresses have an important bearing on buttress-dam design as they represent planes on which construction or contraction joints may safely be placed so that under maximum loading the monolithic action of the buttress as a whole will not be destroyed. The reason for this monolithic action is that the shearing stresses along the planes of principal stress are zero, and there is no tendency for relative motion between the columns along the joints when the reservoir is full. However, under partial reservoir loading, the trajectories will vary from the pattern for full reservoir loading and the continuance of monolithic action depends on the transmittal of light shearing stresses across the joints. For this reason, keys (as shown in Fig. 5) are placed in the joints An additional benefit derived from the use of keys along the joints is the stiffening effect that the shorter columns have on the adjacent longer columns.

The inclined-column concept is illustrated further by Figs. 14a and b, which show graphically the relationship between the forces acting on a column visualized as separated from the buttress (illustrated by Fig. 4) along a trajectory of principal

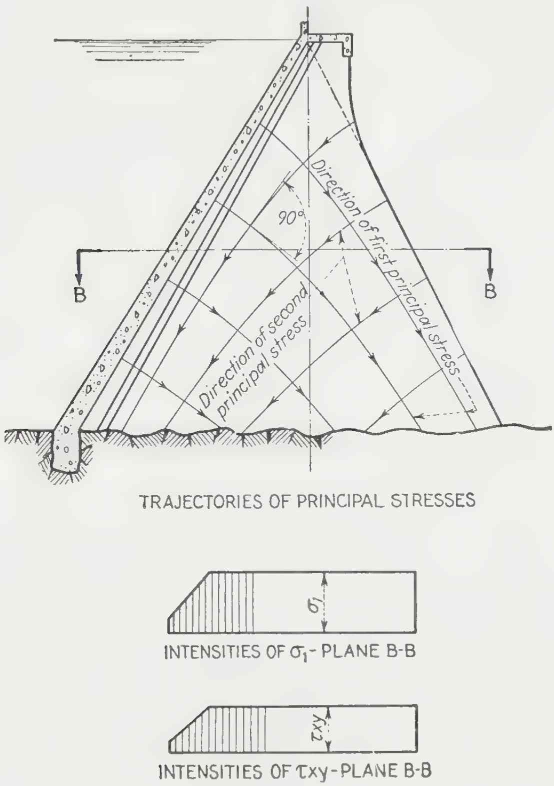

Fig. 13. Trajectories of principal stresses.

stress. It will be noted that the column is held in equilibrium by the weight of the masonry, the water load on the upstream face, and the second principal stresses. A graphical analysis of this type offers a convenient method of checking the stability of sections of buttress separated by joints.

The disadvantage of using small blocks lies in the handling of the extremely large values of the vertical normal pressures necessary to evaluate correctly the small stress differentials across a 1-ft height. The advantage with small blocks is the ease with which any point, including the area directly under the haunch, may be analyzed. The use of larger blocks facilitates the basic computations of the vertical normal stresses but then introduces undesirable errors by extending the use of linear interpolation to include not only the vertical normal stresses but also the horizontal normal and the

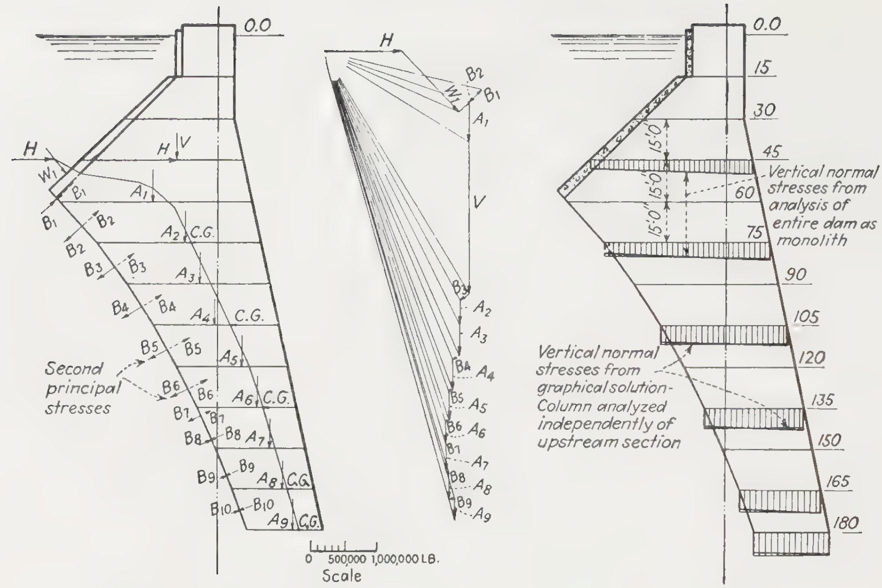

FIG. 14a. Rodriguez Dam. Graphic analysis of inclined column including effect of second principal stresses.

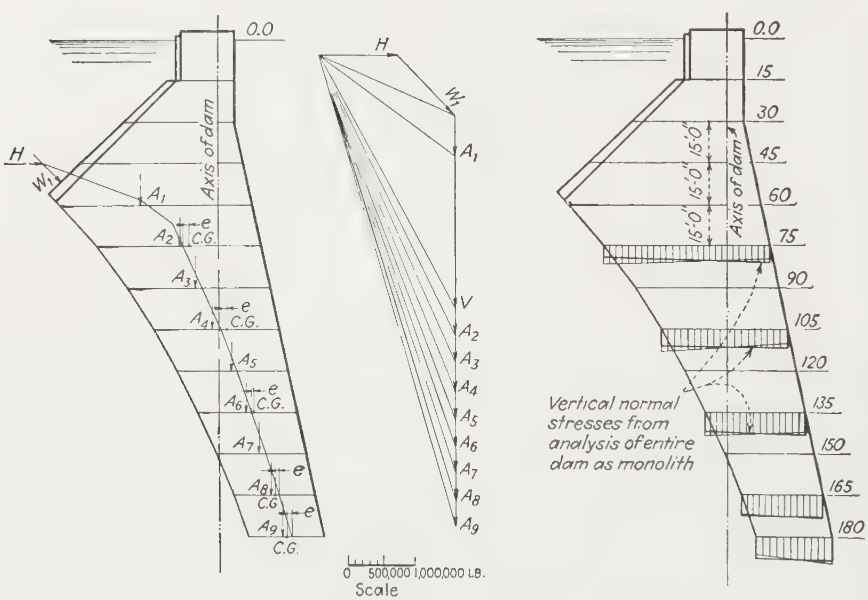

FIG. 14b. Rodriguez Dam. Graphic analysis of inclined column assuming no second principal stresses.

vertical and horizontal shearing stresses. This method becomes inaccurate to the point of being unreliable in the area just under the upstream haunch. A combination of the desirable features of both methods by using blocks of medium height (6- to 15-ft blocks have been found satisfactory) and then evaluating the vertical normal stress by interpolation offers a more rapid and accurate analysis particularly applicable to triangular-shaped buttresses. The general equations of internal equilibrium [Eqs. (2) and (4)] are written in the differential form.

$$\frac{d\sigma_y}{dx} + \frac{d\tau_x}{dy} = 0 \tag{9}$$

$$\frac{d\sigma_x}{dy} - \frac{d\tau_y}{dx} + w_m = 0 \tag{10}$$

$$\tau_x + \tau_y = 0 \tag{11}$$

In order to include the influence of the variable buttress thickness t, the values of the normal and shearing stresses are expressed as a value per unit length (equal to the stress in an imaginary buttress of uniform thickness, $t = 1$).

$$p_x = t\sigma_x \tag{12}$$

$$p_y = t\sigma_y \tag{13}$$

$$s_x = t\tau_x \qquad s_y = t\tau_y \tag{14}$$

$$w_{mt} = tw_m \tag{15}$$

Then Eqs. (9), (10), and (11) become

$$\frac{dp_y}{dx} + \frac{ds_x}{dy} = 0 \tag{16}$$

$$\frac{dp_x}{dy} - \frac{ds_y}{dx} + w_{mt} = 0 \tag{17}$$

$$s_x + s_y = 0 \tag{18}$$

After evaluating p_x, p_y, s_x, and s_y, and thereby σ_x, σ_y, and τ_{xy}, the principal unit stresses σ_1 and σ_2 are easily determined by Mohr's circle or by Eqs. (5), (6), and (7). As a further refinement, Eqs. (16), (17), and (18), by expanding and grouping terms, are reduced to expressions of constants and variables. The variables are evaluated for the entire buttress elevation and the results plotted in curve form. It is then possible to determine rapidly the principal stresses at any point by selecting the proper values from the curves and substituting in the basic equations.

Figure 7 shows an Ambursen bulkhead buttress 178 ft high used for the Possum Kingdom Dam on the Brazos River, Texas. The vertical normal stresses [as computed by Eq. (1)], eccentricities, and sliding factors are given in Fig. 7 for six planes or lift lines. Values of p_d, the intensity of the vertical normal (trapezoidal) stress at the downstream end of any horizontal section; of k, the rate of change of the vertical normal stress; and of the first and second differentials of both p_d and k are determined from the stress diagrams shown in Fig. 7. The shear s and the horizontal normal stress p_y are evaluated by Eqs. (19) and (20) in which m expresses the slope of the downstream edge of the buttress, w_{mt} the masonry weight as previously explained, and z the distance from the downstream edge of the buttress to the point being analyzed.

$$s = m(p_d) + (p_d' - mk - w_{mt})z - \frac{1}{2}k'z^2 \tag{19}$$

$$p_y = m^2(p_d) + m(2p_d' - mk - w_{mt})z + \frac{1}{2}(p_d'' - 2mk' - w_{mt}')z^2 - \frac{1}{6}k''z^3 \tag{20}$$

SECTION 14

ARCH DAMS

By Ivan E. Houk and Roman P. Wengler

An arch dam is a curved dam that carries a major part of its water load horizontally to the abutments by arch action, the part so carried being primarily dependent on the amount of curvature. Massive masonry dams, slightly curved, are usually considered as gravity dams, although some parts of the loads may be carried by arch action. Many early arch dams were built of rubble, ashlar, or cyclopean masonry. However, practically all arch dams constructed during recent years have been built of concrete.

Arch principles have been used in bridges and buildings since about 2000 B.C. Apparently, Pontalto Dam, built in Austria in 1611 A.D., was the first arch dam recorded in engineering history.[1] The 64-ft Bear Valley Dam, built in the San Bernardino Mountains of southern California in 1883, was the first arch dam constructed in America. It was followed by the 95-ft Sweetwater Dam, in 1888, and the 88-ft Upper Otay Dam, in 1900, both built near San Diego, Calif. Lake Cheesman Dam, a 236-ft curved gravity dam constructed near Denver, Colo., in 1904, was the first high dam for which a careful attempt was made to analyze arch action. Since 1904, many arch dams have been built in the United States and abroad.

ARCH-DAM TYPES

Arch dams are usually classified on the basis of thickness, symmetry with respect to the crown section, or characteristics of extrados and intrados curves. For instance, they may be referred to as constant-thickness, variable-thickness, symmetrical-arch, nonsymmetrical-arch, single-arch, compound-arch, constant-radius, single-curvature, double-curvature, or variable-radius types, or by other more or less self-explanatory designations. Typical examples of actual designs are given later.

1. Constant-radius Dams. A constant-radius arch dam generally has a vertical upstream face. However, an unusually high structure, such as Hoover Dam, may have extrados curves of gradually increasing radii in the lower part of the canyon, to provide a vertical batter near the base of the higher cross sections. Intrados curves may be concentric or nonconcentric with reference to extrados curves. They usually have decreasing radii as the depth below the crest increases, to provide the increased thickness needed for the higher reservoir pressures. Constant-radius arch types are particularly adapted to U-shaped canyons, where relatively large proportions of the water load at the lower elevations are carried by cantilever action.

2. Variable-radius Dams. A variable-radius arch dam, also known as a constant-angle arch dam, usually has extrados and intrados curves of gradually decreasing radii as the depth below the crest increases.[2] This is to keep the central angle as large and as nearly constant as possible, so as to secure maximum arch efficiency at all elevations. Variable-radius arch dams are often also doubly curved, that is, curved

[1] Noetzli, Fred A., Pontalto and Madruzza Arch Dams, *Western Construction News*, Apr. 10, 1932, pp. 451–452.

[2] Jorgensen, Lars R., The Constant-angle Arch Dam, *Trans. ASCE*, **78**, 685–733, 1915.

in both the horizontal and vertical planes. The resulting overhangs are generally upstream near the foundation contact and downstream in the upper central part of the dam. The dead-load bending stresses in the cantilevers thereby tend to counteract the water-load bending stresses. The variable-radius type of arch dam is frequently adapted to narrow V-shaped canyons.

GENERAL THEORY OF ARCH DAMS

The general theory of arch dams now used in design constitutes a comparatively recent development in engineering science. The mathematical principles, laws of mechanics, and theories of elasticity involved in an arch-dam analysis have been known for many years. Summarized arch-dam formulas are given later. This section is confined to the general theory of arch-dam action.

3. Arch Action Only. Many arch dams have been designed on the theory that all horizontal water loads are carried horizontally to the abutments by arch action and that only the dead-load weights, plus the vertical water loads in the case of a sloping upstream face, are carried vertically to the foundations by cantilever action. In some of the earlier designs, arch thicknesses were determined by the unreliable thin-cylinder formula $t = RP/S$, where t is the thickness of the arch, R the radius of the upstream face, P the water load, and S the allowable concrete stress. In other cases, thicknesses were determined by analyses of elastic arches, formulas being used such as those developed by the late William Cain.[1]

Designs that ignore centilever action can seldom be considered wholly satisfactory. The vertical cantilevers that make up the dam are restrained at the foundation. They must bend until their deflected positions coincide with the deflected positions of the arch elements. Since the cantilever bending can be produced only by the transfer of water load through the cantilever elements to the foundation, the theory that the entire water load is carried horizontally to the abutments by arch action is obviously incorrect.

4. Cantilever and Arch Action. The most commonly accepted method of analyzing arch dams assumes that the horizontal water load is divided between the arches and cantilevers so that the calculated arch and cantilever deflections are equal at all conjugate points in all parts of the structure. During the development of this method and for many years thereafter, the load distribution required to satisfy this criterion was determined by trial. Consequently, the method was called the trial-load method. At the present time, the load distribution is often obtained directly through the use of flexibility matrices and computers. However, the analysis is still generally called the trial-load method. After the load distribution between arches and cantilevers is found, whether by trial or directly, the stresses of the arches and cantilevers are subsequently calculated and are considered to be the true stresses in the dam.

The first analyses are usually made on the theory that any element can move in a radial direction without being restrained by adjacent elements and without being subjected to tangential or twisting deformations. Since this theory is inaccurate, the discrepancies must be corrected by subsequent trial-load adjustments which make adequate allowances for tangential shear and twist effects.

The cantilever elements are assumed to be fixed at the foundation and the arch elements fixed at the abutments. However, the rock formations may be moved by loads transferred through the dam and by direct reservoir pressures. Although foundation and abutment materials are probably never uniformly elastic, owing to the presence of cracks, fissures, faults, and bedding planes, their movements may be roughly calculated by elastic formulas and included in the analyses of arch and canti-

[1] Cain, William, The Circular Arch under Normal Loads, *Trans. ASCE*, **85**, 233–283, 1922.

lever deflections. Since the dam is curved, the cantilever elements are vertical slices, bounded by vertical radial planes. Arch elements are horizontal slices, with constant vertical thicknesses from abutment to abutment.

5. Basic Assumptions. The basic assumptions usually made in designing arch dams may be briefly listed as follows:[1]

1. The foundation and abutment rock is homogeneous, isotropic, and uniformly elastic.
2. The concrete is homogeneous, isotropic, and uniformly elastic.
3. The stresses are well within the elastic limit, and Hooke's law applies.
4. Stresses vary as a straight line between the upstream and downstream faces of the dam in both arch and cantilever elements.
5. Plane surfaces in the unloaded structure remain plane after the load is applied.
6. Temperature changes in the arches vary with the horizontal thickness but are constant throughout each element.
7. Temperature strains and stresses are proportional to temperature changes.
8. Effects of flow of concrete and rock materials may be neglected.
9. Tension stresses are relieved by cracking, so that all loads are carried by compressive and shearing stresses in the uncracked portions of the dam.
10. Radial construction joints are grouted or open slots filled, so that the dam acts as a monolith.
11. Vertical shrinkage is completed before the joints are grouted or the slots filled, so that no loads are transferred laterally by vertical arching.

LOADS ON ARCH DAMS

Loads on arch dams are essentially the same as loads on gravity dams, except that temperature changes, which usually are not important considerations in straight dams, cause important deflections and stresses in curved dams. The principal dead load is the concrete weight. The principal live load is the reservoir water pressure. Additional loads may be imposed by tail-water pressure, uplift pressure, upward water pressure under overhanging sections, deposition of silt on sloping faces, presence of silt in flood flows, and formation of ice surfaces. Earthquake accelerations cause momentary changes in water pressure and an additional live load due to the inertia of the concrete.

The general subject of forces on dams is treated in Secs. 11 and 12. Discussions presented here are confined to additional considerations required in designing arch dams.

6. Uplift Pressure. Uplift pressure seldom has an important bearing on the safety of an arch dam. If no cracking occurs, it can be neglected. If cracking occurs, uplift pressure in the cracks causes increases in downstream deflections, changes in load distribution, and increases in maximum compressive stresses in both arch and cantilever elements. Uplift in horizontal cantilever cracks usually has a greater effect on stress conditions than uplift pressure in vertical arch cracks.[2]

7. Ice Pressure. Ice pressure causes a continuous concentrated load along the arch element at the elevation of the ice. This load is carried partly by arch action and partly by cantilever action. The actual distribution can be determined by a trial-load analysis. The transference of ice loads to the foundation and abutments can be facilitated by placing vertical reinforcing at the faces of the dam. Concentration of

[1] HOUK, IVAN E., and KENNETH B. KEENER, Masonry Dams—Basic Design Assumptions, *Trans. ASCE*, **106**, 1115-1130, 1941.

[2] HOUK, IVAN E., Uplift Pressure in Gravity Dams, *Western Construction News*, July 25, 1930, pp. 344-349.

reinforcing at the downstream face, along the elevation of the ice, increases the proportion of ice load carried by arch action.

8. Temperature Loads. Temperature changes cause internal forces that move the dam upstream during the summer and downstream during the winter, the former condition working against the reservoir load and the latter with it. Consequently the winter condition is usually the more important in the stress analysis.

Since zero temperature stresses occur at the time of closing the arches, the closures should be made after the setting heat has been developed and dissipated. Most high arch dams are now cooled artificially with refrigerated-pipe cooling. This generally allows the designer to make closure by grouting the contraction joints at the opportune time. Unless the concrete is artificially cooled,[1] it may be necessary to include some of the setting-heat effects in analyzing temperature stresses.[2]

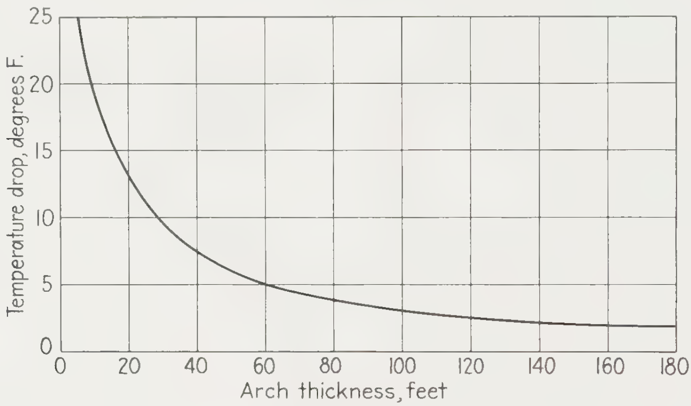

FIG. 1. Maximum drop in average concrete temperature, below mean annual.

If closure can be deferred until the setting heat has been fully developed and completely dissipated, the designer may assume that the temperature changes to be considered in the arch analyses will be the reductions from mean annual to minimum concrete temperatures expected during full reservoir load. Figure 1 shows the maximum drop in average concrete temperature, below mean annual, which may occur in arches of different thickness. This curve is based on actual observations. It was drawn so as to be well above the average of all actual measurements.

STRESS DISTRIBUTION IN ARCH DAMS

The distribution of stress in an arch dam varies with the horizontal curvature, shape of vertical cross sections, general dimensions of the structure, and uniformity of canyon profile. Pronounced humps in the rock surface cause stress concentrations in adjoining concrete, sometimes resulting in the formation of diagonal cracks. Maximum cantilever stresses often occur at such humps, even though the elevations are appreciably higher than the base of the maximum cross section.

9. Cantilever Stresses. Maximum cantilever stresses in arch dams, built at sites free from pronounced irregularities, usually occur at the base of the highest cantilever. During full reservoir load, maximum compressive stresses usually occur at the downstream edge of the base, but may occur at the upstream edge in comparatively high

[1] STEELE, BYRAM W., Cooling Boulder Dam Concrete, *Eng. News-Record*, **133**, 451–455, 1934.

[2] HOUK, IVAN E., Setting Heat and Concrete Temperature, *Western Construction News*, Aug. 10, 1931, pp. 411–415.

and thick dams provided with an upstream batter. Tension often occurs at the upstream edge of the base in relatively thin arch dams and at the downstream face in the upper central portion of the dam.

10. Arch Stresses. Arch stresses in the central and upper portions of arch dams are commonly higher than in the lower portions. Maximum arch stresses usually occur at the crown and abutment sections. At the crown section, relatively high compressive stresses usually occur at the upstream face of the dam and relatively low compressive or tension stresses at the downstream face. At the abutment sections, stress conditions are usually reversed in accordance with the change in moment sign which generally takes place near the quarter points. Stress conditions at the abutments may be somewhat different in the top arches of long thin dams, owing to the upstream deflections that sometimes occur near such locations. Shearing stresses at the crown section are zero in symmetrical arches symmetrically loaded.

11. Principal Stresses. Major principal stresses along the contact between concrete and rock usually act in planes approximately horizontal at the top of the dam, practically vertical at the base of the maximum cross section, and at gradually varying inclinations along the intervening parts of the profile. The principal stresses for water load only are shown in Fig. 2 for Mossyrock Dam. Mossyrock Dam is a 606-ft-high variable-radius dam located on the Cowlitz River in Washington. These stresses were obtained by trial-load analysis including tangential and twist adjustments.

12. Stress Examples. Figure 3 shows the stress distribution in Seminoe Dam, central Wyoming, under full reservoir load combined with horizontal earthquake accelerations, construction joints grouted at concrete temperatures 5 deg below mean annual being assumed. Seminoe Dam is a 261-ft constant-radius arch dam, located on the Kendrick Irrigation Project.

Figure 4 shows the stress distribution in Stewart Mountain Dam, central Arizona, determined by a trial-load analysis for maximum flood conditions, the arch elements being assumed closed at mean annual concrete temperatures. Stewart Mountain Dam is a 212-ft variable-radius arch dam, located on the Salt River Valley Irrigation Project. This dam was designed for a maximum stress of 650 psi, the full water load being assumed to be carried by the arch elements.

Figure 5 shows the dead load, water load, and temperature stress distribution for Mossyrock Dam. The dam was designed for a maximum concrete stress of 1,200 psi.

DESIGN OF ARCH DAMS

The design of an arch dam is a cut-and-try problem. Preliminary plans must be prepared, stresses analyzed, and costs compiled. The best design will have the stresses as uniformly distributed as possible, tension stresses as low as possible, maximum compressive and shear stresses kept within allowable limits, and the total cost of the structure held to a minimum. The following sections briefly discuss technical problems involved in determining the best design.[1] Details of structural features and construction methods are not considered.

13. Allowable Stresses. Stresses in arch dams analyzed by trial-load methods, on the assumption of a straight-line distribution of stress, should not exceed one-fourth of the mass concrete strength at 1 year as determined on 18- by 36-in. cylinders or from correlation with 6- by 12-in. cylinders. Increases up to 33 percent may be permissible, momentarily, during intense earthquake shocks. However, decreases of 25 to 35 percent should be made if the dam is analyzed by approximate methods, such as

[1] HOUK, IVAN E., Technical Design of High Masonry Dams, *Engineer*, Aug. 4, 1933, pp. 105–106; Aug. 11, 1933, pp. 128–130.

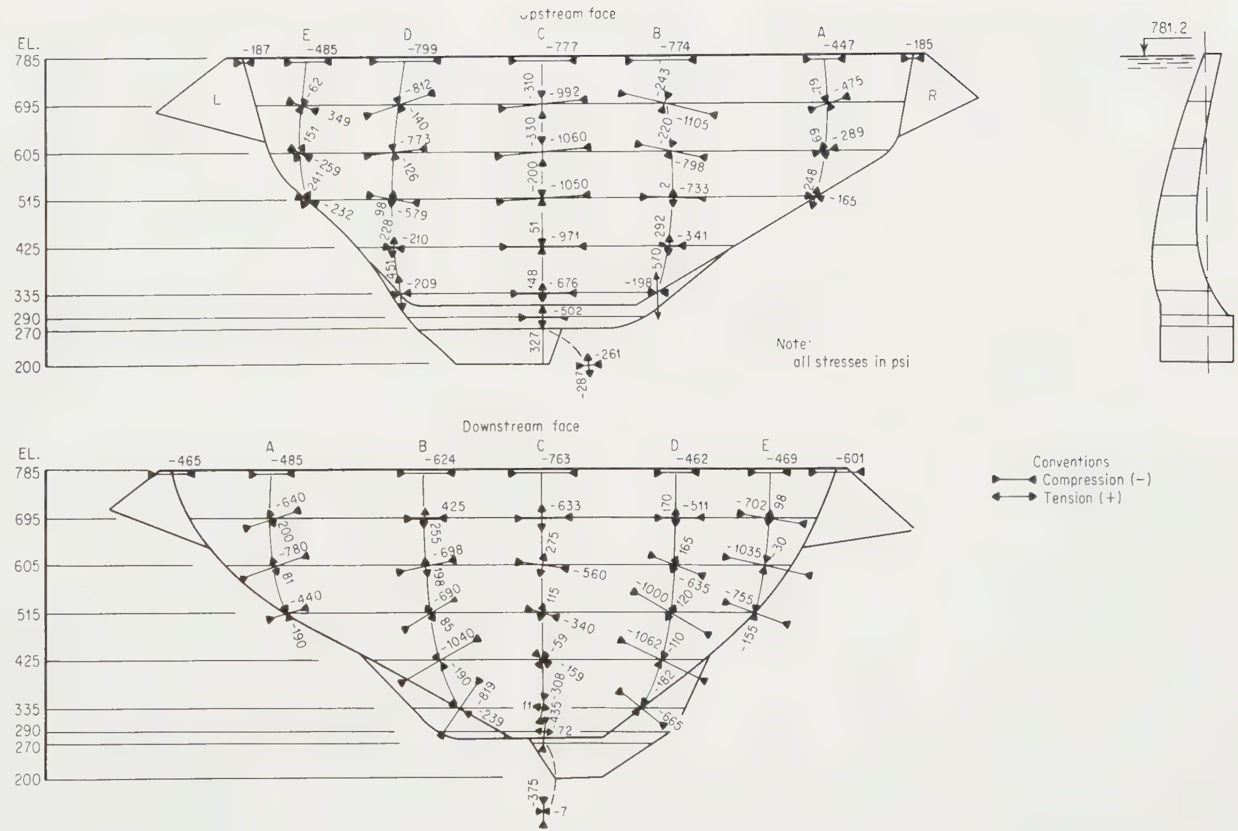

FIG. 2. Principal stresses in Mossyrock Dam.

Cantilever stress at A	B	C	D	Arch stress at abut	Principal stress at abutment P_2	P_1	Location of direct stress	Maximum shearing stress Rock plane	Arch abut	Elev
				-93	0	-193	U.S.	+37	+45	6361
				-22	0	-22	D.S.			
+63	+88	+96	+99	-73	+92	-102	U.S.	+63	+64	6300
+3	+[illegible]	-4	8	+367	-50	+451	D.S.			
	+00	+20	+136	-82	+95	-96	U.S.	+87	+81	6250
	+26	+75	+8	+410	+8	+485	D.S.			
	+3[illegible]	-4	-45	46	+01	62	U.S.	+124	+103	6200
	+[illegible]	+[illegible]	+[illegible]	+324	+49	+43	D.S.			
		+[illegible]		[illegible]	+10	-31	U.S.	+34	+94	6150
		+92	+[illegible]	+8[illegible]	+[illegible]	+395	D.S.			
			+34				U.S.			6100
			+272				D.S.			

STRESSES AT LEFT OF CROWN

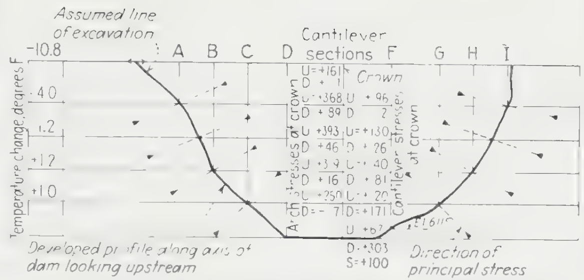

STRESSES AT CROWN AND DIRECTION OF MAJOR PRINCIPAL STRESS AT DOWNSTREAM FACE AT ABUTMENTS

Elev	Maximum shearing stress Arch abut	Rock plane	Location of direct stress	Principal stress at abutment P_1	P_2	Arch stress at abut	Cantilever stress at F	G	H	I
6361	+44	+36	U.S.	-101	0	101				
			D.S.	+225	0	+225				
6300	+50	+46	U.S.	-43	+121	-99	+98	+97	+84	+77
			D.S.	+457	-12	+429	-7	-5	+8	+15
6250	+75	+76	U.S.	-106	+110	-84	+132	+123	+99	
			D.S.	+457	+28	+411	+23	+31	+57	
6200	+00	+.9	U.S.	-55	+113	34	+136	+117	+92	
			D.S.	+415	+43	+310	+84	+107	+131	
6150	+93	+34	U.S.	26	+111	4	+106	+89		
			D.S.	+396	+8	+178	+189	+203		
6100			U.S.				+64			
			D.S.				+290			

STRESSES AT RIGHT OF CROWN

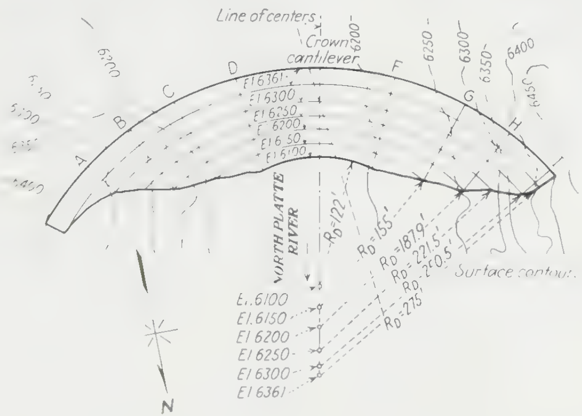

PLAN

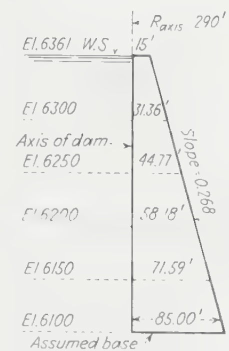

MAXIMUM SECTION

NOTES

Upstream and downstream cantilever stresses act parallel to edges of cantilevers

Upstream and downstream arch stresses act parallel to edges of arches

U = Upstream stress D = Downstream stress

+ = Compression − = Tension

S = Maximum shearing stress

+S means downstream shear

All stresses are pounds per square inch

Assumed earthquake shock has acceleration = 0.10 gravity, period of vibration = 1.0 second, and acts horizontally along line of centers

Arches closed at concrete temperatures 5°F. below mean annual

Effects of twist, tangential shear and abutment deformations included

U.S = Upstream face D.S = Downstream face

FIG. 3. Stress distribution in Seminoe Dam.

CANTILEVER STRESS AT A	B	C	D	ARCH STRESS AT ABUT	PRINCIPAL STRESS AT ABUTMENT P_2	P	LOCATION OF DIRECT STRESS	MAXIMUM SHEARING STRESS ROCK PLANE	ARCH ABUT	ELEV
				C			U.S.		+35	1530
				+611			D.S.			
+55	+71	+92	+140	C			U.S.	+68	+66	1490
+7	C	C	C	+488	−41	+540	D.S.			
+37	C	C	+44	C			U.S.	+95	+88	1450
+76	[illegible]	+203	[illegible]	+490	−58	+626	D.S.			
C	C	C	C	C			U.S.	+331	[illegible]	1410
+187*	+591*	+859	+238	+304	+202	+96[illegible]	D.S.			
			C	−22			U.S.	+305	+122	1370
			+862	+237	+145	+990	D.S.			
							U.S.			1325
							D.S.			

STRESSES IN LEFT PART OF DAM

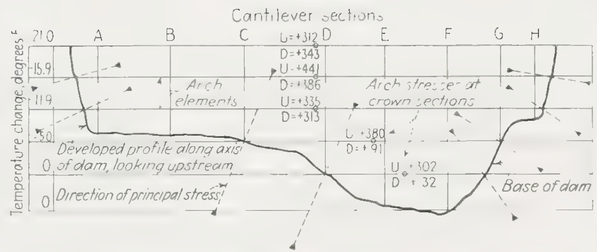

ARCH STRESSES AT CROWN SECTIONS AND DIRECTIONS OF MAJOR PRINCIPAL STRESSES AT DOWNSTREAM FACE OF ABUTMENTS

ELEV	MAXIMUM SHEARING STRESS ARCH ABUT	ROCK PLANE	LOCATION OF DIRECT STRESS	PRINCIPAL STRESS AT ABUTMENT P_1	P_2	ARCH STRESS AT ABUT	CANTILEVER STRESS AT E	F	G	H
1530	+41		U.S.			C				
			D.S.			+625				
1490	+48	+49	U.S.			C	+116	+78	+17	+39
			D.S.	+493	−13	+475	C	C	+50	+23
1450	+92	+102	U.S.			−57	+57	+36	C	C
			D.S.	+520	65	+270	+88	+90	+152	+144
1410	+82	+197	U.S.			−49	C	C	C	C*
			D.S.	+605	−9	+340	+228	+154	+181	+245
1370	+4	+73	U.S.			−9	C	C		
			D.S.	+654	+18	+229	+429	+293		
1325			U.S.				C	C		
			D.S.				+735	+453		

STRESSES IN RIGHT PART OF DAM

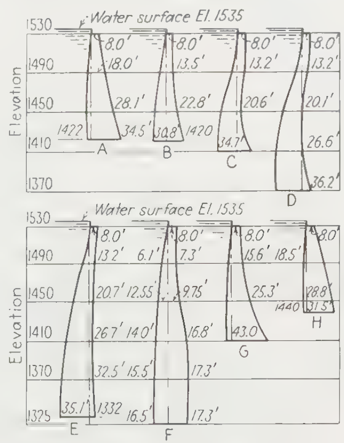

CROSS SECTIONS AT CANTILEVERS

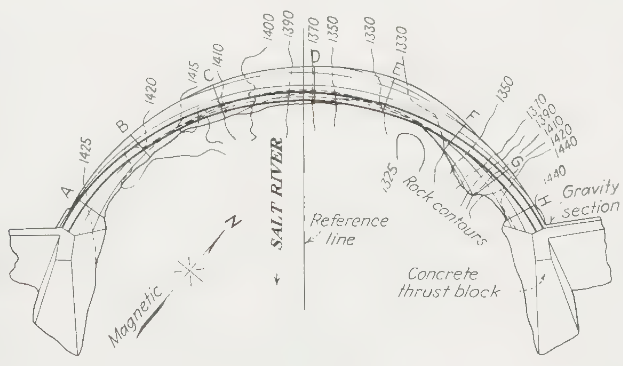

NOTES

Upstream and downstream cantilever stresses act parallel to edges of cantilevers
Upstream and downstream arch stresses act parallel to edges of arches
U = Upstream stress D = Downstream stress
+ = Compression − = Tension
C Cracked to point of zero stress
∗ Stress at base of cantilever
+ Shearing stress means downstream shear
All stresses are pounds per square inch
∘ Location of arch crown
Reservoir water surface at top of parapet
Tailwater surface at elevation 1413
Uplift pressures vary from reservoir head at upstream face to zero or tailwater head at downstream face
Uplift pressures are applied over 50 per cent of the area
Effect of twist, tangential shear, and abutment deformations included
U.S = Upstream face D.S = Downstream face

FIG. 4. Stress distribution in Stewart Mountain Dam.

Cantilever stress at		Arch stress at			Location of stress	Shear stress at abt	Elev
A	B	ABT	A	B			
0	0	100	471	811	U.S.	-4	785
0	0	549	504	610	D.S.		
190	241	153	375	1137	U.S.	47	695
-21	-57	616	576	394	D.S.		
93	190	260	222	884	U.S.	61	605
186	149	417	754	54	D.S.		
194	-38	110		799	U.S.	92	515
58	518	435		440	D.S.		
	-83	258		261	U.S.	118	425
	643	482		926	D.S.		
	71	219			U.S.	145	335
	483	337			D.S.		
		97			U.S.	176	290
		300			D.S.		

STRESSES AT LEFT OF CROWN

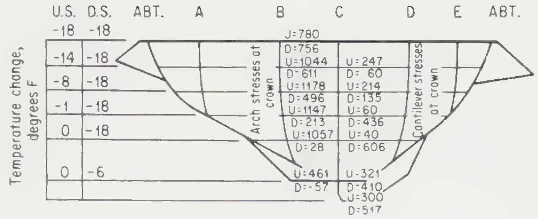

ARCH AND CANTILEVER STRESSES AT CROWN

Elev	Shear stress at abt	Location of stress	Arch stress at			Cantilever stress at	
			D	E	ABT.	D	E
785	-9	U.S.	800	438	107		
		D.S.	432	474	675		
695	32	U.S.	827	280	28	152	161
		D.S.	481	676	961	-13	51
605	61	U.S.	869	180	167	43	2
		D.S.	509	1031	846	296	298
515	89	U.S.	469		172	-47	78
		D.S.	797		666	512	249
425	135	U.S.	144		146	43	
		D.S.	890		582	472	
335	145	U.S.			205	199	
		D.S.			312	343	
290	157	U.S.			211		
		D.S.			156		

STRESSES AT RIGHT OF CROWN

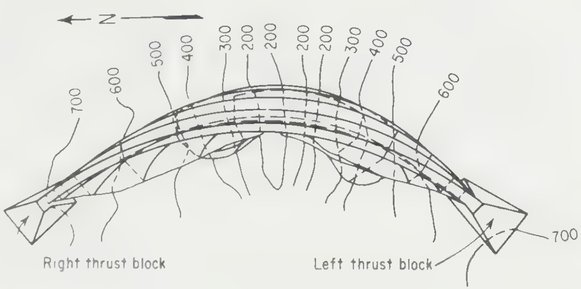

PLAN

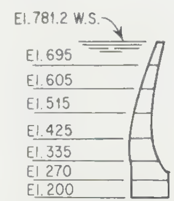

CROWN CANTILEVER SECTION

NOTES

Upstream and downstream cantilever stresses act vertically.
Upstream and downstream arch stresses act parallel to arch centerline.
U = Upstream stress   D = Downstream stress
+ = Compression   − = Tension
All stresses are in pounds per square inch
Arches are closed at mean annual temperature.
Effects of twist tangential shear and abutment deformations are included.
U.S. = Upstream face   D.S. = Downstream face

FIG. 5. Stress distribution in Mossyrock Dam.

TABLE 1. MAXIMUM STRESSES IN ARCH DAMS DETERMINED BY TRIAL-LOAD ANALYSES
Psi

Name of dam	Type[c]	Max height, feet	Cantilever stresses			Arch stresses			Principal stresses[e]			Loading condition
			Comp.	Tens.	Shear	Comp.	Tens.	Shear	Comp.	Tens.	Shear	
Hoover	C.R.	731	565	None	154	231	31	120	565	16	160	Full reservoir, 5 deg subcooling
Owyhee	C.R.	421	358	6	86	294	242	175	413	344	143	W.S. at top of dam[f]
Arrowrock[a]	C.R.	356	466	39	164	305	314	128	496	314	207	Full reservoir with earthquake
Parker	C.R.	335	289	C[d]	65	542	1	76	451	C	95	Full reservoir with earthquake 7 deg subcooling
Ariel	V.R.	313	808	C	...	560	107	...	.....	...	...	W.S. at top of parapet
Horse Mesa	V.R	305	956	C	250	1,061	C	273	1,074	C	297	W.S. at top of parapet
Seminoe	C.R.	261	303	8	100	429	193	103	485	193	134	Full reservoir with earthquake, 5 deg subcooling
Mormon Flat	V.R.	229	633	C	74	893	C	181	1,095	C	322	W.S. at top of parapet
Stewart Mountain	V.R.	212	862	C	56	625	C	182	990	C	331	W.S. at top of parapet
Gibson[b]	C.R.	199	605	C	...	364	66	...	.....	...	...	W.S. at top of parapet
Deadwood	C.R.	168	472	C	...	360	184	...	.....	...	...	W.S. at top of parapet
Cat Creek	V.R.	118	413	C	...	277	114	...	.....	...	...	W.S. 1.5′ above top of dam
Mossyrock	V.R.	606	643	−83	...	1,178	57	...	1,062[g]	570[g]	...	Full reservoir
Mayfield	C.R.	245	647	0	...	726	149	...	.....	...	...	Full reservoir
Karadj	V.R.	590	845	131	...	1,003	13	...	1,220[g]	356[g]	...	Full reservoir

[a] Analysis for 5-ft increase in height.
[b] Tangential shear and twist not included.
[c] C.R., constant radius; V.R., variable radius.
[d] C, cracked, no load carried by tension.
[e] Along abutment planes.
[f] W.S., water surface.
[g] Water load only.

placing the full water load on the arch elements or bringing the arch and cantilever deflections into agreement at the crown section only.

Ordinarily, vertical tension at the upstream face may be as high as 100 psi without analyzing secondary cantilevers, when the corresponding compression at the downstream face does not exceed 500 psi. Horizontal tension at the upstream face may be as much as one-third the corresponding compression at the downstream face without analyzing secondary arches, when the sum of the tension and compression does not exceed 600 psi.

14. Maximum Stresses. Table 1 gives maximum arch, cantilever, and principal stresses in some arch dams recently designed or analyzed by trial-load methods. Effects of tangential shear and twist action were included in all cases except Gibson Dam. Effects of rock deformations were considered in all cases.

15. Constants Needed in Analyses. Table 2 gives general values of constants needed in analyzing arch dams. These values may be used in preliminary studies where more accurate information is not available. They should be replaced by data based on field and laboratory measurements before adopting final designs. Tabulated values of modulus of elasticity are for sustained load conditions. Great accuracy in determining elastic properties of canyon rock is not necessary since effects of foundation and abutment movements are of a secondary nature. The modulus of elasticity for direct stress may be assumed to be the same for tension and compression, for both rock and concrete materials. The modulus for shear can be computed by the formula $E_s = E/2(1 + \mu)$, where μ is Poisson's ratio, E the modulus for direct stress, and E_s the modulus for shear.

TABLE 2. CONSTANTS NEEDED IN ANALYZING ARCH DAMS

Constant	Material	Values	Units
Weight, saturated	Concrete	150	lb per cu ft
Weight, saturated	Silt	110–120	lb per cu ft
Weight, saturated	Sand	110–120	lb per cu ft
Temperature coefficient	Concrete	0.0000040–60	ft per ft per deg F
Poisson's ratio	Concrete	0.15–0.22	
Poisson's ratio	Rock	0.10–0.30	
Modulus of elasticity	Concrete	2–3.0 million	psi
Modulus of elasticity	Limestone	1–2 million	psi
Modulus of elasticity	Granite	2–4 million	psi
Modulus of elasticity	Sandstone	1–1.5 million	psi

16. Preliminary Plans. In preparing preliminary plans for an arch dam, the engineer should study designs adopted for similar sites, where dimensions and curvature were accurately determined by trial-load analyses. Published descriptions of constructed dams and data are helpful in preliminary investigations. In order to avoid high-tension stresses at the reservoir face and to secure maximum arch efficiency, central angles should be as large as possible. Theoretical considerations, based on the thin-cylinder formula, show that a central angle of 133°34′ is most advantageous from the viewpoint of economy.[1] However, practical considerations, together with topographical conditions, usually prevent the adoption of such angles for the lower arch elements.

The extrados and intrados curves should be located so that the ends of the arches converge in a downstream direction. Otherwise radial buttresses at the abutments

[1] JORGENSEN, *op. cit.*, p. 689.

may be needed to carry the loads transferred horizontally by radial shear. Such buttresses are often necessary where arch elements abut against gravity tangents. Radial arch ends are most desirable; but smaller amounts of convergence usually suffice where radial construction requires excessive excavation, as in large thick dams.

Top widths of arch dams are usually made constant from abutment to abutment. Arch thicknesses at lower elevations may be constant or may increase toward the abutments, depending on stress conditions. Abutment thickening should be warped between adjacent arch elements, so as to avoid undesirable appearances at the downstream face.

The ratio of length to thickness at the top of the dam should not exceed about 60. Usually the ratio will be smaller, owing to the desirability of stiffening the upper part of the structure or the necessity for providing a roadway along the top. Considerations of slenderness ratio are not important at the lower arches. The additional thicknesses needed from the stress viewpoint, together with the reduced widths of the canyon, will reduce the ratio to satisfactory values. Furthermore, the restraining effect of the cantilevers on the bending of the arch elements increases as the depth below the top increases.

17. Foundations and Abutments. Depths of required excavation must be estimated in determining dimensions for preliminary analyses. Sometimes humps in rock profiles, which may cause stress concentrations, can be removed in preparing rock surfaces. Sometimes deep holes, or relatively narrow gorges, can be plugged with concrete and treated as parts of the foundation instead of parts of the dam. Excavated surfaces should be gradually warped between adjacent elevations, pronounced stepping along abutment planes being avoided. Adequate grouting and draining should always be specified. Geological conditions at the dam site should be approved by competent foundation experts before proceeding with detailed designs.

ANALYSES OF PRELIMINARY PLANS

Analyses of preliminary plans for arch dams are usually made for full reservoir load plus maximum temperature drop. Analyses for other loads, which seldom require major changes in dimensions, can be made after general designs are tentatively adopted. Analyses of preliminary plans may be made by the following methods:

1. Assigning full horizontal loads to arch elements.
2. Dividing horizontal loads between arch and cantilever elements on the basis of a radial adjustment of deflections at the crown section.
3. Dividing horizontal loads between arch and cantilever elements on the basis of radial adjustments at several vertical sections.

The method to be used in a particular case depends on the shape of the canyon and the type, height, and importance of the structure. If the rock profile contains pronounced irregularities, or the shape of the canyon is not symmetrical, the analyses should be made by the trial-load method, listed as 3, regardless of the size of the dam. If the canyon is V-shaped, with comparatively uniform sides, and the dam of nominal size and importance, the second method may suffice. If the canyon is relatively regular and narrow, and the dam of low height, so that a symmetrical thin arch structure with large central angles can be adopted, the first method may be sufficient. However, with high-speed computers the time required to use method 2 is negligible, and the costs have been reduced sufficiently so that the first method is seldom used.

18. Full Load on Arches. Formulas for analyzing circular arches of constant thickness, under uniform radial loads, have been developed by various engineers. The studies made by William Cain were especially noteworthy.[1] Slightly modified forms

[1] CAIN, *loc. cit.*

of Cain's equations for thrust and moment at the crown and abutment sections, due to uniform water loads, are as follows:

Thrust at crown, $$H_0 = pr - \frac{pr}{D} 2\varphi \sin \varphi \frac{t^2}{12r^2} \tag{1}$$

Moment at crown, $$M_0 = -(pr - H_0)r\left(1 - \frac{\sin \varphi}{\varphi}\right) \tag{2}$$

Thrust at abutments, $$H_a = pr - (pr - H_0) \cos \phi \tag{3}$$

Moment at abutments, $$M_a = r(pr - H_0)\left(\frac{\sin \varphi}{\varphi} - \cos \varphi\right) \tag{4}$$

In the preceding formulas, r is the radius to the center line of the arch, p the normal radial pressure at the center line, t the horizontal arch thickness, and φ the angle between the crown and abutment radii. The center-line pressure p is the extrados

FIG. 6. Constant-thickness circular arch, fixed at abutments.

pressure times the ratio of the upstream radius to the center-line radius (see Fig. 6).

If shear is neglected, values of D are given by the equation

$$D = \left(1 + \frac{t^2}{12r^2}\right)\varphi\left(\varphi + \frac{\sin 2\varphi}{2}\right) - 2\sin^2\varphi \tag{5}$$

In order to simplify the formulas for crown thrust, D has been used in Eqs. (1) and (8), in lieu of the lengthy right-hand part of Eq. (5), which appears in the original formulas.

When shear is included, D is replaced by D_s, the value of which is given by

$$D_s = \left(1 + \frac{t^2}{12r^2}\right)\varphi\left(\varphi + \frac{\sin 2\varphi}{2}\right) - 2\sin^2\varphi + 3.00\,\frac{t^2}{12r^2}\varphi\left(\varphi - \frac{\sin 2\varphi}{2}\right) \tag{6}$$

Thrusts and moments having been calculated, intrados and extrados stresses may be found by the usual formula

$$S = \frac{H}{t} \pm \frac{6M}{t^2} \tag{7}$$

More complicated formulas, referred to the neutral axis, with water pressures referred to the extrados, were later developed by Cain.[1] Frederick Hall Fowler, using Cain's formulas as a basis, worked out diagrams from which intrados and extrados stresses at the crown and abutment sections may be easily obtained for different values of central angle and ratio of thickness to radius.[2] Philip Cravitz later prepared similar diagrams which included effects of abutment deformations.[3]

For temperature loads, Cain's equations, shear being neglected, are as follows:

$$H_0 = \frac{2\varphi \sin \varphi}{D} \times \frac{Et^3cT}{12r^2} \tag{8}$$

$$M_0 = H_0 r \left(1 - \frac{\sin \varphi}{\varphi}\right) \tag{9}$$

$$H_a = H_0 \cos \varphi \tag{10}$$

$$M_a = H_0 r \text{ vers } \varphi - M_0 \tag{11}$$

In the preceding formulas, E is the modulus of elasticity, c the coefficient of thermal expansion, and T the change in concrete temperature. Other quantities are the same as before. In the preceding equations, the moment of inertia I has been replaced by the quantity $t^3/12$ which applies to rectangular sections. Formulas for temperature thrusts and moments, including shear, are given in the subsequent section on arch analyses.

19. Radial Adjustment at Crown. In analyzing an arch dam by dividing horizontal loads between arch and cantilever elements on the basis of a radial deflection adjustment at the crown section, formulas for cantilever and arch deflections are needed. Since such methods assume the partial water loads on the arch elements to be constant from abutment to abutment, Cain's arch equations may be used. His crown deflection equations for constant thickness, circular arches, slightly modified, are as follows:

Water-load deflection, $$\Delta = \frac{PR_u rC}{ET} \tag{12}$$

Temperature deflection, $$\Delta = crTC \tag{13}$$

In these equations, P is the normal radial pressure at the extrados, R_u the radius of the extrados, and C a coefficient depending on r, t, and φ, previously defined. If shear is neglected, C is given by the formula

$$C = \frac{(\varphi - \sin \varphi)(1 - \cos \varphi)}{\left(\varphi + \frac{\sin 2\varphi}{2}\right) - \left[\frac{1 - \cos 2\varphi}{\varphi\left(1 + \frac{t^2}{12r^2}\right)}\right]} \tag{14}$$

When shear is included, C is replaced by C_s, the value of which is given by the formula

$$C_s = \frac{(1 - \cos \varphi)\left[\left(1 + \frac{t^2}{12r^2}\right)(\varphi - \sin \varphi) + \frac{t^2}{4r^2}(\varphi + \sin \varphi)\right]}{\left(1 + \frac{t^2}{12r^2}\right)\left(\varphi + \frac{\sin 2\varphi}{2}\right) - \left(\frac{1 - \cos 2\varphi}{\varphi}\right) + \frac{t^2}{4r^2}\left(\varphi - \frac{\sin 2\varphi}{2}\right)} \tag{15}$$

Figure 7 shows values of C_s for different values of φ and the ratio t/r.[4]

[1] Cain, William, Discussion of Stresses in Thick Arches of Dams by B. F. Jakobsen, *Trans. ASCE*, **90**, 522–547, 1927.

[2] Fowler, F. H., A Graphic Method for Determining the Stresses in Circular Arches under Normal Loads by the Cain Formulas, *Trans. ASCE*, **92**, 1512–1560, 1928.

[3] Cravitz, Philip, Analyses of Thick Arch Dams, including Abutment Yield, *Trans. ASCE*, **101**, 501–523, 1936.

[4] Houk, Ivan E., Arch Deflections and Temperature Stresses in Curved Dams, No. II, *Engineer*, Apr. 9, 1937, pp. 414, 415.

Cantilever forces, moments, deflections, and stresses may be calculated by methods described in the subsequent section on cantilever analyses. If the dam is relatively thin, cantilevers may be considered as vertical slices with parallel sides 1 ft apart. However, they generally should be considered as vertical slices with radial sides 1 ft apart at the upstream face or at a circular vertical plane passing through the upstream edge of the top, herein referred to as the axis of the dam. Analyses of cracked cantilevers seldom are necessary in preliminary studies.

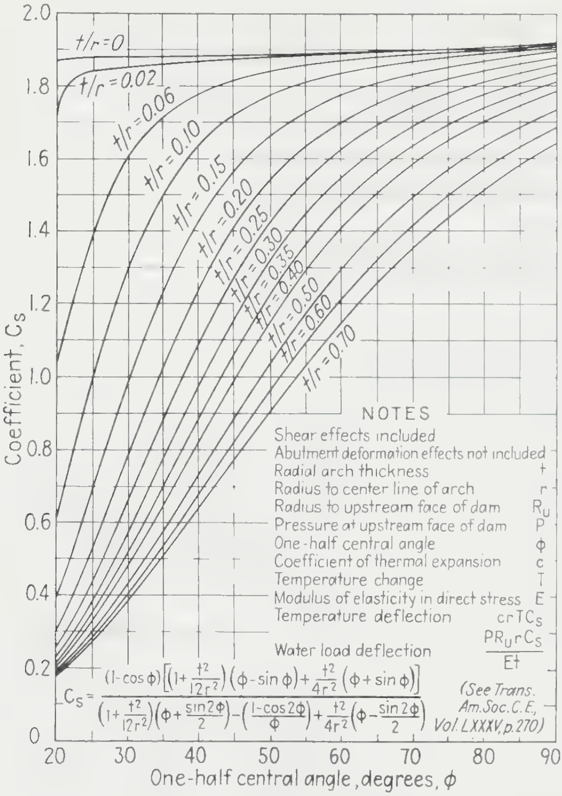

FIG. 7. Values of C_s, Eq. (15).

In determining the water-load distribution, temperature deflections must be added to water-load deflections in the case of the arch elements, but not in the case of the cantilever elements. The load distribution having been determined, arch stresses may be obtained from the Fowler or Cravitz diagrams. Arch stresses due to temperature changes may be calculated by formula (7), after thrusts and moments have been computed by Eqs. (8) to (11).

20. Radial Adjustment at Several Sections. In analyzing an arch dam by adjusting radial deflections at several vertical sections the division of the water load between the different horizontal and vertical elements can be done by trial and error or directly by use of simultaneous equations. Arch and cantilever stresses are then computed for the final load distribution. The analysis of five or six arch elements and an equal number of cantilever elements usually is sufficient in preliminary studies.

Cantilever elements may be analyzed by methods given later. Arch elements must be analyzed by more complicated methods than those given above, for the loads are not constant along the extrados curves. In preliminary trial-load calculations, arch elements may be analyzed by the voussoir summation process[1] or by theoretical formulas given in the subsequent section on arch analyses. In relatively thick dams, arch analyses should include radial shear effects. Effects of tangential shear, twist, rock deformations, and other secondary influences usually may be omitted in preliminary trial-load computations.

ANALYSES OF ADOPTED PLANS

General plans of arch dams, adopted on the basis of preliminary investigations, should be reanalyzed by detailed trial-load methods, including all important secondary effects. Necessary alterations in dimensions or curvature can then be made before beginning construction. Final analyses should consider all possible load conditions, including earthquake shocks, ice forces, silt pressures, maximum flood stages, and maximum temperature increases, as well as normal full reservoir loads plus maximum temperature reductions. However, special load conditions generally may be analyzed on the basis of radial adjustments of deflections. One complete analysis, including effects of tangential shear and twist action, usually is adequate. Repeated trial-load studies have shown that such effects for the same dam under different conditions of loading are of the same sign and very similar magnitude, unless the change in applied loads is sufficient to change the direction of the deflections, as may sometimes be true in the case of using maximum temperature increases instead of maximum temperature reductions. The consideration of eight or ten arch elements and an equal number of cantilever elements usually is sufficient in the final analyses.

Radial shear buttresses at the ends of the arched section, if needed, are analyzed by methods used for gravity dams. Radial shear forces are added to direct water pressures and are assumed to decrease uniformly from maximum values at the edge of the buttress, adjoining the arched section, to zero at the opposite edge.

THE TRIAL-LOAD METHOD

The development of the trial-load method was begun by the Bureau of Reclamation in 1923,[2] about the time a similar method was being investigated in Europe.[3] The Bureau's first use of the method included effects of thrust, moment, and temperature in the arch analyses and thrust, moment, and horizontal radial shear in the cantilever elements. The first analyses brought the deflections into adjustment in the radial direction only. The next step in the development was the inclusion of radial shear effects in the arch calculations. Since that time the method has been gradually amplified; so that now effects of rock deformations, tangential shear, twist action, and other secondary considerations may be included whenever necessary. The introduction of tangential shear and twist effects requires adjustments of deflections in circumferential and angular directions as well as in radial directions.[4]

21. Rock Movements. Considerations of rock movements and their effects on the action of arch dams may be based on approximate formulas.[5] If the ends of the arch elements are vertical, and the bases of the cantilever elements horizontal, rock rota-

[1] Howell, C. H., and A. C. Jaquith, Analysis of Arch Dams by the Trial Load Method, *Trans. ASCE*, **93**, 1191–1316, 1929.

[2] *Ibid.*

[3] Stucky, Alfred, Study of Arch Dams, *Bull. Tech. Suisse Romande*, Lausanne, 1922.

[4] Houk, Ivan E., Trial Load Analyses of Curved Concrete Dams, *Engineer*, July 5, 1935, pp. 2–5.

[5] Vogt, Fredrik, Ueber die Berechnung der Fundamentdeformation, *Det Norske Videnskaps-Akademi*, 1925.

tions and deflections of elements with parallel sides 1 ft apart may be calculated by the following equations:

Rotation due to moment, $$\alpha' = \frac{MK_1}{E_r t^2} \tag{16}$$

Deflection due to thrust, $$\beta' = \frac{HK_2}{E_r} \tag{17}$$

Deflection due to shear, $$\gamma' = \frac{VK_3}{E_r} \tag{18}$$

Rotation due to twist, $$\delta' = \frac{M_t K_4}{E_r t^2} \tag{19}$$

Rotation due to shear, $$\alpha'' = \frac{VK_5}{E_r t} \tag{20}$$

Deflection due to moment, $$\gamma'' = \frac{MK_5}{E_r t} \tag{21}$$

In the preceding equations, M and V are the arch and cantilever moments and shears, H the arch thrust, M_t the cantilever twisting moment, E_r the elastic modulus of the rock, t the radial thickness of the element, and K_1, K_2, K_3, K_4, and K_5, constants depending on Poisson's ratio and the ratio of the average length of the dam b to the average width a. Table 3 gives values of K constants for a Poisson's ratio of 0.20 and different values of b/a.

Equations (16), (18), (20), and (21) give movements at the ends of the arch and cantilever elements. Equation (17) gives horizontal movements caused by arch thrusts. Vertical movements at cantilever bases and twist movements at arch abutments are not needed. Equation (19) gives twist movements at cantilever bases. Rotations and deflections given by Eqs. (20) and (21) are of a secondary nature and relatively unimportant.

TABLE 3. VALUES OF K CONSTANTS IN EQS. (16) TO (21), FOR POISSON'S RATIO = 0.20

Values of b/a	Values of K				
	K_1	K_2	K_3	K_4	K_5
1.0	4.32	0.62	1.02	4.65	0.345
1.5	4.65	0.78	1.23	4.86	0.413
2.0	4.84	0.91	1.39	5.18	0.458
3.0	5.04	1.10	1.60	5.64	0.515
4.0	5.15	1.25	1.77	5.90	0.550
5.0	5.22	1.36	1.89	6.08	0.574
6.0	5.27	1.47	2.00	6.20	0.592
8.0	5.32	1.63	2.17	6.37	0.614
10.0	5.36	1.75	2.31	6.46	0.630
15.0	5.41	1.98	2.55	6.59	0.653
20.0	5.43	2.16	2.72	6.66	0.668

If pounds, feet, and radians are used as dimensional units, calculated deflections and rotations are feet and radians, respectively. Further discussions of rock movements in trial-load analyses are given in subsequent sections on cantilever and arch analyses.

CANTILEVER ANALYSES

In cantilever analyses, the vertical elements are divided into sections by horizontal planes at small increments of height, as shown in Fig. 8. Total loads, shears, and moments, acting on the horizontal planes, are then summated from the top downward to the foundation; and slopes of neutral axis, moment deflections, and shear deflections are summated from the foundation upward to the top, rock deformations being inserted as initial movements in beginning the upward summations. Radial deflections at assumed horizontal planes are then found by adding moment and shear deflections.

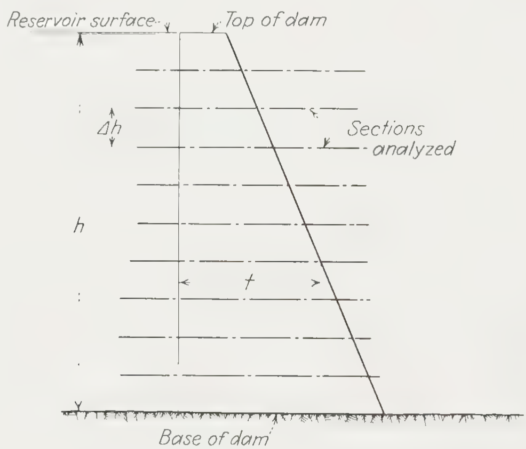

Fig. 8. Vertical element of arch dam.

In the following discussions, cantilevers with parallel sides, radial sides, and upstream cracking are treated from the viewpoint of radial loads. Effects of tangential shear and twist loads on uncracked elements with radial sides are then considered separately.

22. Cantilever with Parallel Sides. For an uncracked cantilever with parallel vertical sides, 1 ft apart, increments of concrete weight, vertical water loads on the upstream face, where sloped, horizontal water pressure, centers of gravity, shears, moments, and moments of inertia are easily calculated by usual methods. Slopes of the neutral axis, moment deflections, and shear deflections are then obtained by the following summation formulas:

$$\text{Slope of neutral axis,}\quad \frac{dy}{dh} = \alpha' + \alpha'' + \sum \frac{12M}{Et^3}\,\Delta h \tag{22}$$

$$\text{Moment deflection,}\quad \Delta_m = \sum \left(\alpha' + \alpha'' + \sum \frac{12M}{Et^3}\,\Delta h\right)\Delta h \tag{23}$$

$$\text{Shear deflection,}\quad \Delta_s = \left(\gamma' + \gamma'' + \sum \frac{KV}{tE_s}\,\Delta h\right) \tag{24}$$

In these equations, M is the resultant bending moment, V the total horizontal shear in the radial direction, Δh the increment of height, dy a differential movement in the horizontal radial direction, E_s the shearing modulus of elasticity, and K a constant allowing for nonuniform distribution of shear, usually taken as 1.25. Other quantities are the same as in preceding sections. The moment of inertia I has been replaced by its equivalent $t^3/12$.

Vertical stresses at the faces of the dam may be computed by Eq. (7), the vertical force W being used instead of the horizontal thrust H. Inclined stresses at the edges of the cantilever, acting parallel to the slopes, and unit shearing stresses on horizontal and vertical planes at the edges of the cantilever may be calculated by the formulas

Inclined stress, $$S_i = S \sec^2 \alpha - p \tan^2 \alpha \tag{25}$$

Shearing stress, $$N = \mp (S - p) \tan \alpha \qquad (-\text{ at upstream face}) \tag{26}$$

where S = vertical stress

p = water pressure

α = angle between the face of the dam and the vertical direction

If the face of the dam is vertical, the shearing stress at the edge of the cantilever is zero.

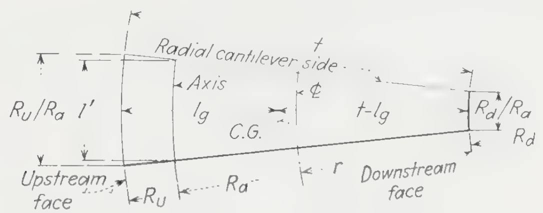

FIG. 9. Horizontal section of cantilever with radial sides.

23. Cantilever with Radial Sides. Properties of an uncracked cantilever with radial sides 1 ft apart at the axis of the dam, as shown in Fig. 9, may be calculated by the following formulas:

Area, $$A = \left(\frac{R_u + R_d}{2R_a}\right) t \tag{27}$$

Distance to center of gravity, $$l_g = \frac{t}{3}\left(\frac{R_u + 2R_d}{R_u + R_d}\right) \tag{28}$$

Moment of inertia, $$I = \frac{t^3}{36}\left(\frac{R_u^2 + 4R_uR_d + R_d^2}{R_a(R_u + R_d)}\right) \tag{29}$$

Vertical stress at upstream face, $$S_u = \frac{W}{A} - \frac{Ml_g}{I} \tag{30}$$

Vertical stress at downstream face, $$S_d = \frac{W}{A} + \frac{M(t - l_g)}{I} \tag{31}$$

In these equations R_u is the upstream radius, R_d the downstream radius, R_a the radius to the axis, and W the total vertical load. Other quantities are the same as before.

By using A, l_g, and I in their proper places and increasing upstream widths to R_u/R_a before calculating water pressures, loads, moments, shears, slopes of neutral axis, and deflections may be determined by summation methods, as in the preceding section. Rock movements at the cantilever base should be multiplied by R_a/r before being included in the summations.

24. Cracked Cantilevers. In analyzing cracked cantilevers as shown in Fig. 10, the depth of cracking may be calculated by the formula

$$\frac{R_u + l_g - c}{R_d} = \frac{1}{2}\left[\frac{1 + \dfrac{2R_d}{R_0} + 3\left(\dfrac{R_d}{R_0}\right)^2}{\dfrac{R_d}{R_0} + 2\left(\dfrac{R_d}{R_0}\right)^2}\right] \tag{32}$$

In this equation, R_0 is the radius to the upstream limit of the uncracked area, and e the distance from the center of gravity of the entire area to the location of the resultant. The equation is found by taking moments of the stress solid about the center of gravity. Values R_u and R_d are known; l_g is given by formula (28); and e is calculated by usual methods. These terms determine the fraction at the left of the equation.

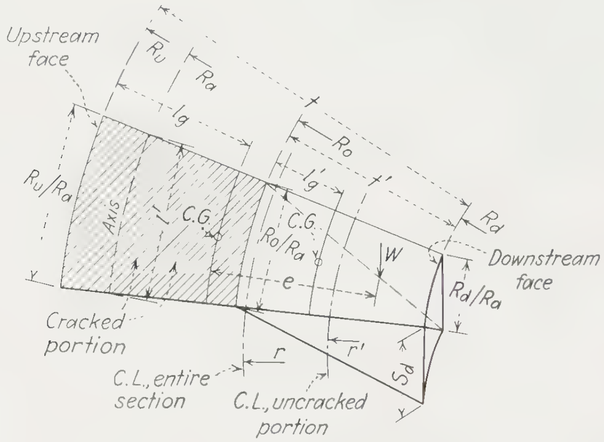

FIG. 10. Section of cracked cantilever.

Probably the best way to use Eq. (32) is to plot a diagram showing values of the function at the right for different values of R_d/R_0. Calculated values of the fraction at the left may then be used to obtain R_d/R_0 from the diagram. If R_d/R_0 is less than R_d/R_u, no cracking occurs. If R_d/R_0 is greater than R_d/R_u, the section is cracked.

Having determined R_d/R_0, the uncracked thickness t' may be obtained from the formula

$$t' = \frac{R_d}{\dfrac{R_d}{R_0}} - R_d \tag{33}$$

Equations for area A', distance from the point of zero stress to the center of gravity l_g', and moment of inertia I' for the uncracked part of the cross section may be obtained by substituting t' for t and R_0 for R_u in Eqs. (27), (28), and (29). The moment of the redistributed forces about the new center of gravity and the vertical stress at the downstream face may be computed by the following formulas:

Moment,
$$M' = \frac{Wt'}{6} \frac{1 + \dfrac{4R_d}{R_0} + \left(\dfrac{R_d}{R_0}\right)^2}{1 + \dfrac{3R_d}{R_0} + 2\left(\dfrac{R_d}{R_0}\right)^2} \tag{34}$$

Vertical stress,
$$S_d = \frac{W}{A'} + \frac{M'(t' - l_g')}{I'} \tag{35}$$

Deflections may be computed by formulas given in preceding sections, by using t', M', I', and other quantities pertaining to the uncracked portions of the cross sections. Rock movements should be multiplied by R_a/r', before being included in the summations, r' being the radius to the center line of the uncracked area.

25. Tangential Shear Loads. Tangential shear loads, equal and opposite to corresponding loads on the arch elements, are multiplied by r/R_a, to allow for the reduced width at the center line of a cantilever with radial sides, and are then applied along the center line. Shear loads are summated from the top downward to the foundation, and shear deflections, from the foundation upward to the top, as in the case of radial loads.

Deflections are computed by the summation formula

$$\Delta_s = \frac{R_a}{r}\gamma' + \sum \frac{V}{AE_s}\Delta h \qquad (36)$$

No correction factor is needed in the second term, for tangential shear is assumed to be uniformly distributed.

26. Twist Loads. Twist loads in foot-pounds per square foot, equal and opposite to corresponding loads on the arch elements, are multiplied by r/R_a and applied at the center line. The loads act in horizontal planes, as in the case of radial and tangential shear loads. Loads are summated from the top down, and resulting angular deflections from the foundation up, as before.

Angular deflections are computed by the summation formula

$$\Delta\theta = \frac{R_a}{r}\delta' + \sum \frac{M_t}{2E_sI}\Delta h \qquad (37)$$

All quantities in the formula are the same as previously explained. The moment of inertia I is taken about the same axis as in the case of radial loads. Consequently, its value is determined by Eq. (29). The foundation rotation δ' caused by the twisting moment M_t is computed by Eq. (19).

The equations for cantilever analysis as developed above can be solved manually or can be readily programmed for the computer.

ARCH ANALYSES

Moments, forces, and movements of arch elements, caused by radial, tangential, twist, and temperature loads, may be analyzed by flexure formulas for curved cantilever beams, amplified to allow for rib-shortening and transverse-shear effects. The method consists of cutting the loaded arch at the crown, introducing initial moments, thrusts, and shears to compensate for crown displacements, developing equations for crown movements for both parts of the arch, equating the two sets of formulas, and solving for crown forces. Equations for moments, thrusts, and shears may then be written in terms of crown forces, and moments, thrusts, and shears due to external loads. The moments, thrusts, and shears having been determined, stresses may be calculated by usual formulas.

The basic theory of analyzing the arch is identical whether done manually or by computer. However, since there can be a considerable difference in technique, the following treatment is divided into two parts: manual method and computer method.

Abutment movements, determined by Eqs. (16) to (21), may be inserted in the general deflection formulas. However, for the sake of simplicity, such movements are neglected in the following treatment. Temperature effects are discussed separately for the same reason.

27. Notation. The following notation is used, all quantities being measured in horizontal planes:

R_u = radius to upstream face
R_d = radius to downstream face
r = radius to center line

t = radial arch thickness
A = area of radial cross section
I = moment of inertia of radial cross section about axis along arch center line
s = length along center line
φ = angle from arch point under consideration to any point on arch
$x = r \sin \varphi$
$y = r \operatorname{vers} \varphi$
φ_a = angle from arch point where deflections are desired to abutment
φ_0 = angle from arch point where deflections are desired to beginning of external load
φ_1 = angle from beginning of external load to abutment
M = moment
H = thrust
V = shear
P = intensity of external load
E = modulus of elasticity of concrete in tension and compression
E_s = modulus of elasticity of concrete in shear
μ = Poisson's ratio
K = constant to allow for nonuniform distribution of shear
c = coefficient of thermal expansion of concrete
T = temperature change, positive when rising
θ = angular movement of arch center line
Δr = radial deflection of arch center line
Δs = tangential deflection along center line

The subscript 0 means at the crown, a at the abutment, L at the left of the crown, and R at the right of the crown. In the case of M, H, and V, subscripts L or R mean that the moment, thrust, and shear are due to external loads on the left or right portions of the arch, respectively.

If μ equals 0.20, and K 1.25, the ratio K/E_s in some of the subsequent equations may be replaced by $3/E$.

28. Signs. The convention of signs, shown in Fig. 11, is as follows:

Positive moments cause compression at the extrados.

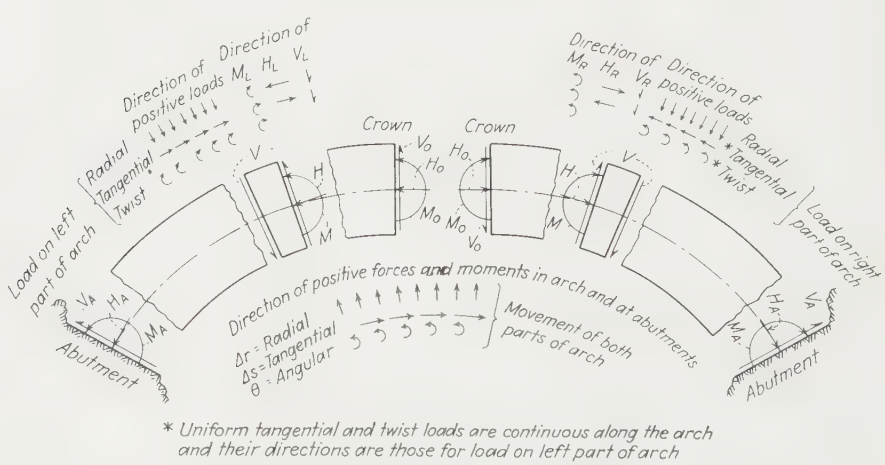

FIG. 11. Direction of positive loads, forces, moments, and movements.

Positive thrusts cause compression.

Positive shears produce positive moments on the section of the arch at the left in the case of the left part of the arch and positive moments at the right in the case of the right part, except V_0, which acts as shown in Fig. 11.

Radial loads are positive when acting toward the arch center. Uniform tangential loads are positive when acting from left to right, in both parts of the arch. Triangular tangential loads are positive when acting from the abutments toward the crown. Uniform twist loads are positive when acting clockwise in both parts of the arch. Triangular twist loads are positive when acting clockwise in the left part and counterclockwise in the right part.

Positive moments, thrusts, and shears (M_L, H_L, V_L, or M_R, H_R, V_R) due to external loads are in the same direction as the moments, thrusts, and shears of positive radial loads. Following this convention, moments, thrusts, and shears of all positive triangular loads are positive except thrusts of tangential loads, which are negative. Since the portion of the uniform tangential or twist load on the right part of the arch is applied in the same direction as the load on the left part, the M_R, H_R, and V_R of these loads will change sign.

Positive radial deflections are upstream.

Positive tangential deflections are toward the right.

Positive angular movements are counterclockwise.

MANUAL METHOD

General formulas are given for a circular arch subjected to symmetrical or nonsymmetrical loads. Special formulas for constant-thickness circular arches are then given for the terms that are functions of the arch properties, called *arch constants;* for the moments, thrusts, and shears due to external loads, called *load formulas;* and for the terms that are functions of both arch and load properties, called *load constants.* The formulas for load constants and for moments, thrusts, and shears due to external loads include equations needed in analyzing effects of uniform and triangular loads. The loads considered include tangential and twist loads as well as radial loads. Deflections for symmetrical or nonsymmetrical nonuniform loads may be obtained by adding deflections for different combinations of uniform and triangular loads.

Consider a differential element of length ds in the left part of an arch cut at the crown, as shown in Fig. 12. From mechanics, the equations for the arch movements

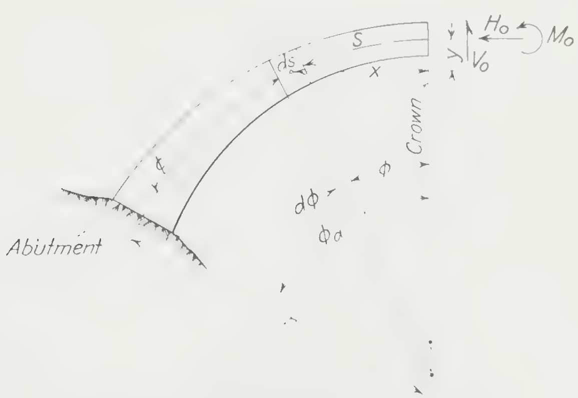

FIG. 12. Left part of arch cut at crown.

at the crown, due to a moment, thrust, and shear acting on the element, are

$$d\theta_0 = \frac{M\,ds}{EI} \tag{38}$$

$$d(\Delta r)_0 = \frac{Mx\,ds}{EI} - \frac{H \sin \alpha\,ds}{EA} + \frac{KV \cos \varphi\,ds}{E_sA} \tag{39}$$

$$d(\Delta s)_0 = -\frac{My\,ds}{EI} - \frac{H \cos \varphi\,ds}{EA} - \frac{KV \sin \varphi\,ds}{E_sA} \tag{40}$$

The first term in Eqs. (39) and (40) gives the movement caused by bending; the second term, the movement caused by rib shortening; and the third term, the movement caused by shear.

By integrating the preceding equations and using s to designate the total length along the center line from crown to abutment, the following equations are obtained for the left part of the arch:

$$\theta_0 = \int_0^s \frac{M\,ds}{EI} \tag{41}$$

$$\Delta r_0 = \int_0^s \frac{Mx\,ds}{EI} - \int_0^s \frac{H \sin \varphi\,ds}{EA} + \int_0^s \frac{KV \cos \varphi\,ds}{E_sA} \tag{42}$$

$$\Delta s_0 = -\int_0^s \frac{My\,ds}{EI} - \int_0^s \frac{H \cos \varphi\,ds}{EA} - \int_0^s \frac{KV \sin \varphi\,ds}{E_sA} \tag{43}$$

Quantities M, H, and V may be replaced by their equivalents in terms of moment, thrust, and shear at the crown (M_0, H_0, and V_0) and moment, thrust, and shear due to external loads between the differential element and the crown (M_L, H_L, and V_L):

$$M = M_0 + H_0y + V_0x - M_L \tag{44}$$

$$H = H_0 \cos \varphi - V_0 \sin \varphi + H_L \tag{45}$$

$$V = H_0 \sin \varphi + V_0 \cos \varphi - V_L \tag{46}$$

If these substitutions are made and the ratio K/E_s replaced by $3/E$, the following formulas are obtained:

$$\theta_0 = M_0 \int_0^s \frac{ds}{EI} + H_0 \int_0^s \frac{y\,ds}{EI} + V_0 \int_0^s \frac{x\,ds}{EI} - \int_0^s \frac{M_L\,ds}{EI} \tag{47}$$

$$\begin{aligned} \Delta r_0 = {} & M_0 \int_0^s \frac{x\,ds}{EI} + H_0 \left(\int_0^s \frac{xy\,ds}{EI} - \int_0^s \frac{\sin \varphi \cos \varphi\,ds}{EA} + 3 \int_0^s \frac{\sin \varphi \cos \varphi\,ds}{EA} \right) \\ & + V_0 \left(\int_0^s \frac{x^2\,ds}{EI} + \int_0^s \frac{\sin^2 \varphi\,ds}{EA} + 3 \int_0^s \frac{\cos^2 \varphi\,ds}{EA} \right) \\ & - \left(\int_0^s \frac{M_Lx\,ds}{EI} + \int_0^s \frac{H_L \sin \varphi\,ds}{EA} + 3 \int_0^s \frac{V_L \cos \varphi\,ds}{EA} \right) \end{aligned} \tag{48}$$

$$\begin{aligned} \Delta s_0 = {} & -M_0 \int_0^s \frac{y\,ds}{EI} - H_0 \left(\int_0^s \frac{y^2\,ds}{EI} + \int_0^s \frac{\cos^2 \varphi\,ds}{EA} + 3 \int_0^s \frac{\sin^2 \varphi\,ds}{EA} \right) \\ & - V_0 \left(\int_0^s \frac{xy\,ds}{EI} - \int_0^s \frac{\sin \varphi \cos \varphi\,ds}{EA} + 3 \int_0^s \frac{\sin \varphi \cos \varphi\,ds}{EA} \right) \\ & + \left(\int_0^s \frac{M_Ly\,ds}{EI} - \int_0^s \frac{H_L \cos \varphi\,ds}{EA} + 3 \int_0^s \frac{V_L \sin \varphi\,ds}{EA} \right) \end{aligned} \tag{49}$$

If symbols are substituted for the multipliers of M_0, H_0, and V_0 and for the terms depending on load, the preceding equations may be written

$$\theta_0 = A_1M_0 + B_1H_0 + C_1V_0 - D_1 \tag{50}$$

$$\Delta r_0 = C_1M_0 + B_2H_0 + C_2V_0 - D_2 \tag{51}$$

$$\Delta s_0 = -B_1M_0 - B_3H_0 - B_2V_0 + D_3 \tag{52}$$

Similar equations for the right part of the arch may be developed in the same manner. In this case, the values of M, H, and V are

$$M = M_0 + H_0 y - V_0 x - M_R \tag{53}$$
$$H = H_0 \cos\varphi + V_0 \sin\varphi + H_R \tag{54}$$
$$V = H_0 \sin\varphi - V_0 \cos\varphi - V_R \tag{55}$$

The resulting equations for the right part of the arch are

$$\theta_0 = -A_1'M_0 - B_1'H_0 + C_1'V_0 + D_1' \tag{56}$$
$$\Delta r_0 = C_1'M_0 + B_2'H_0 - C_2'V_0 - D_2' \tag{57}$$
$$\Delta s_0 = B_1'M_0 + B_3'H_0 - B_2'V_0 - D_3' \tag{58}$$

29. Crown Forces The moment, thrust, and shear at the crown, M_0, H_0, and V_0, may be obtained by equating the values of θ_0, Δr_0, and Δs_0 for the two parts of the arch as given by formulas (50), (51), (52), (56), (57), and (58). The equations so derived are

$$(A_1 + A_1')M_0 + (B_1 + B_1')H_0 + (C_1 - C_1')V_0 = (D_1 + D_1') \tag{59}$$
$$(C_1 - C_1')M_0 + (B_2 - B_2')H_0 + (C_2 + C_2')V_0 = (D_2 - D_2') \tag{60}$$
$$(B_1 + B_1')M_0 + (B_3 + B_3')H_0 + (B_2 - B_2')V_0 = (D_3 + D_3') \tag{61}$$

If the quantities in parentheses are replaced by a, b, c, and d, the equations may be written

$$a_1M_0 + b_1H_0 + c_1V_0 = d_1 \tag{62}$$
$$c_1M_0 + b_2H_0 + c_2V_0 = d_2 \tag{63}$$
$$b_1M_0 + b_3H_0 + b_2V_0 = d_3 \tag{64}$$

By solving Eqs. (62), (63), and (64) simultaneously and introducing an additional symbol K', the following equations for M_0, H_0, and V_0 are obtained:

$$M_0 = \frac{1}{K'}[d_1(b_3c_2 - b_2^2) - d_3(b_1c_2 - c_1b_2) - d_2(b_3c_1 - b_1b_2)] \tag{65}$$

$$H_0 = \frac{1}{K'}[-d_1(b_1c_2 - b_2c_1) + d_3(a_1c_2 - c_1^2) + d_2(b_1c_1 - a_1b_2)] \tag{66}$$

$$V_0 = \frac{1}{K'}[-d_1(b_3c_1 - b_1b_2) + d_3(b_1c_1 - a_1b_2) + d_2(a_1b_3 - b_1^2)] \tag{67}$$

The value of K' is given by the equation

$$K' = a_1(b_3c_2 - b_2^2) - b_1(b_1c_2 - c_1b_2) - c_1(b_3c_1 - b_1b_2) \tag{68}$$

In the case of a symmetrical arch, the preceding equations reduce to

$$M_0 = \frac{1}{K'}(d_1b_3 - d_3b_1) \tag{69}$$

$$H_0 = \frac{1}{K'}(-d_1b_1 + d_3a_1) \tag{70}$$

$$V_0 = \frac{d_2}{c_2} \tag{71}$$

$$K' = a_1b_3 - b_1^2 \tag{72}$$

The functions included in the a, b, c, and d terms of Eqs. (62), (63), and (64) are given in Table 4. These are the quantities needed in determining the moment, thrust, and shear at the crown. In the case of the b_2, c_1, and d_2 terms, the signs of the quantities for the right part of the arch are negative, in accordance with the signs in Eqs. (59), (60), and (61). Consequently, the algebraic sums of the a, b, c, and d terms in Table 4 may be substituted directly in Eqs. (62) to (72). Evaluations of the integrals in Table 4 are given in subsequent sections.

TABLE 4. FUNCTIONS NEEDED IN DETERMINING CROWN FORCES

Term	Functions: Left part	Functions: Right part
a_1	$\int_0^s \frac{ds}{EI}$	$\int_0^s \frac{ds}{EI}$
b_1	$\int_0^s \frac{y\,ds}{EI}$	$\int_0^s \frac{y\,ds}{EI}$
c_1	$\int_0^s \frac{x\,ds}{EI}$	$-\int_0^s \frac{x\,ds}{EI}$
b_2	$\int_0^s \frac{xy\,ds}{EI}$ $-\int_0^s \frac{\sin\phi\cos\phi\,ds}{EA}$ $3\int_0^s \frac{\sin\phi\cos\phi\,ds}{EA}$	$-\int_0^s \frac{xy\,ds}{EI}$ $\int_0^s \frac{\sin\phi\cos\phi\,ds}{EA}$ $-3\int_0^s \frac{\sin\phi\cos\phi\,ds}{EA}$
c_2	$\int_0^s \frac{x^2\,ds}{EI}$ $\int_0^s \frac{\sin^2\phi\,ds}{EA}$ $3\int_0^s \frac{\cos^2\phi\,ds}{EA}$	$\int_0^s \frac{x^2\,ds}{EI}$ $\int_0^s \frac{\sin^2\phi\,ds}{EA}$ $3\int_0^s \frac{\cos^2\phi\,ds}{EA}$

Term	Functions: Left part	Functions: Right part
b_3	$\int_0^s \frac{y^2\,ds}{EI}$ $\int_0^s \frac{\cos^2\phi\,ds}{EA}$ $3\int_0^s \frac{\sin^2\phi\,ds}{EA}$	$\int_0^s \frac{y^2\,ds}{EI}$ $\int_0^s \frac{\cos^2\phi\,ds}{EA}$ $3\int_0^s \frac{\sin^2\phi\,ds}{EA}$
d_1	$\int_0^s \frac{M_L\,ds}{EI}$	$\int_0^s \frac{M_R\,ds}{EI}$
d_2	$\int_0^s \frac{M_L x\,ds}{EI}$ $\int_0^s \frac{H_L \sin\phi\,ds}{EA}$ $3\int_0^s \frac{V_L \cos\phi\,ds}{EA}$	$-\int_0^s \frac{M_R x\,ds}{EI}$ $-\int_0^s \frac{H_R \sin\phi\,ds}{EA}$ $-3\int_0^s \frac{V_R \cos\phi\,ds}{EA}$
d_3	$\int_0^s \frac{M_L y\,ds}{EI}$ $-\int_0^s \frac{H_L \cos\phi\,ds}{EA}$ $3\int_0^s \frac{V_L \sin\phi\,ds}{EA}$	$\int_0^s \frac{M_R y\,ds}{EI}$ $-\int_0^s \frac{H_R \cos\phi\,ds}{EA}$ $3\int_0^s \frac{V_R \sin\phi\,ds}{EA}$

30. Deflections. The deflections at any point on an arch may be obtained by considering the portion of the arch between the given point and the abutment as a curved cantilever beam. The desired movements are the sum of the movements due to the moment, thrust, and shear at the point and the movements due to the external load between the point and the abutment. Consequently, the movements may be calculated by the general formulas given in the preceding section.

In calculating deflections at a point in the left part of the arch, the moment, thrust, and shear at the crown are first determined as previously explained. The moment, thrust, and shear at the point are then obtained from Eqs. (44), (45), and (46), by using formulas for M_L, H_L, and V_L given in the subsequent section on load formulas. The deflections at the point are then obtained from Eqs. (47), (48), and (49), the radial section through the point being considered as a new crown section and the moment, thrust, and shear at the point being used as new values of M_0, H_0, and V_0. Deflections at points in the right part of the arch may be determined by similar methods.

31. Arch Constants. The quantities A_1, B_1, B_2, B_3, C_1, and C_2 in Eqs. (50), (51), and (52) and the similar quantities in Eqs. (56), (57), and (58) consist of integrals or groups of integrals which are functions of the arch properties. Consequently, they are designated *arch constants*. These constants are really deflections at a point due to a unit force or moment at the point. Their meanings may be briefly stated as follows:

A_1 = angular movement due to a unit moment
B_1 = angular movement due to a unit thrust, or the tangential deflection due to a unit moment

C_1 = angular movement due to a unit shear, or the radial deflection due to a unit moment
B_2 = radial deflection due to a unit thrust, or the tangential deflection due to a unit shear
C_2 = radial deflection due to a unit shear
B_3 = tangential deflection due to a unit thrust

If the arch has a constant thickness and the center line is used instead of the neutral axis, quantities I, s, ds, and A in Eqs. (47), (48), and (49) may be replaced by $t_3/12$, $r\varphi$, $r\,d\varphi$, and t. Since E is a constant, the integrals of the arch constants, for either side of the arch, may then be evaluated and the constants determined by the following equations in which φ_a is the angle from the point where the deflections are desired to the abutment:

$$A_1 = \frac{12r}{Et^3}[\varphi_a] \tag{73}$$

$$B_1 = \frac{12r^2}{Et^3}[\varphi_a - \sin\varphi_a] \tag{74}$$

$$C_1 = \frac{12r^2}{Et^3}[\text{vers}\,\varphi_a] \tag{75}$$

$$B_2 = \frac{12r^3}{Et^3}\left[\text{vers}\,\varphi_a - \frac{\sin^2\varphi_a}{2}\right] + \frac{r}{Et}[\sin^2\varphi_a] \tag{76}$$

$$C_2 = \frac{12r^3}{Et}\left[\frac{\varphi_a - \sin\varphi_a\cos\varphi_a}{2}\right] + \frac{r}{Et}\left[\frac{(\varphi_a - \sin\varphi_a\cos\varphi_a)}{2} + \frac{3(\varphi_a + \sin\varphi_a\cos\varphi_a)}{2}\right] \tag{77}$$

$$B_3 = \frac{12r^3}{Et^3}\left[\varphi_a - 2\sin\varphi_a + \frac{(\varphi_a + \sin\varphi_a\cos\varphi_a)}{2}\right] + \frac{r}{Et}\left[\frac{(\varphi_a + \sin\varphi_a\cos\varphi_a)}{2} + \frac{3(\varphi_a - \sin\varphi_a\cos\varphi_a)}{2}\right] \tag{78}$$

Since the quantities contained in the brackets of Eqs. (73) to (78) depend only on the arch angle, suitable tables may be prepared for use in calculating arch constants.

32. Load Formulas. Formulas for moment, thrust, and shear due to external loads M_L, H_L, and V_L or M_R, H_R, and V_R must be obtained before the D terms in the preceding equations can be evaluated. Such formulas may be written in terms of the external load P, the upstream radius R_u, the center-line radius r, the total central angle subtended by the load φ_1, and different functions of the central angle φ from the beginning of the load to any point on the loaded section of the arch. Equations for the uniform and triangular radial, tangential, and twist loads shown on Figs. 13, 14, and 15 are given in Table 5. Equations for M_R, H_R, and V_R due to similar loads on the right side of the arch are the same as the equations for M_L, H_L, and V_L, except as noted in the section on signs.

P is usually expressed in pounds per square foot in the case of radial and tangential loads, and in foot-pounds per square foot in the case of twist loads. Since the twist loads are couples applied along the arch center line, they do not produce thrusts or shears. Consequently no formulas for H_L or V_L due to twist appear in the table. The load formulas may be used to calculate moment, thrust, and shear due to external loads at the right of any point between the beginning of the load and the abutment.

33. Load Constants. The quantities D_1, D_2, and D_3 in Eqs. (50), (51), and (52) and the similar quantities in Eqs. (56), (57), and (58) consist of integrals or groups of integrals that depend on both arch properties and external loads. These quantities are designated *load constants*. They are really deflections at a point due to the loads applied between the point and the abutment. D_1 is the angular movement, D_2 the

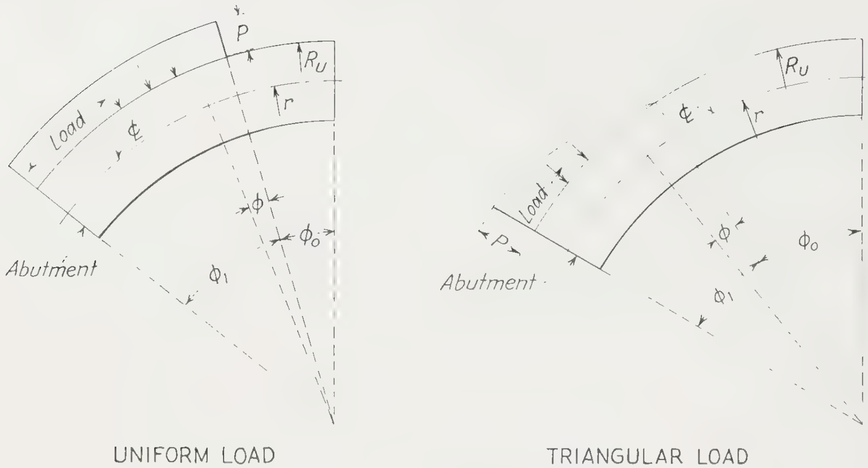

FIG. 13. Uniform and triangular radial loads.

radial movement, and D_3 the tangential movement. Their values for the left part of a constant-thickness arch, loaded from the abutment to an angular distance φ_1, as shown in Figs. 13, 14, and 15, again using the center line instead of the neutral axis, are given by the following formulas:

$$D_1 = \frac{12}{Et^3}\int_0^{\varphi_1} M_L r\, d\varphi \tag{79}$$

$$D_2 = \frac{12}{Et^3}\int_0^{\varphi_1} M_L r^2 \sin\varphi\, d\varphi + \frac{1}{Et}\int_0^{\varphi_1} H_L r \sin\varphi\, d\varphi + \frac{3}{Et}\int_0^{\varphi_1} V_L r \cos\varphi\, d\varphi \tag{80}$$

$$D_3 = \frac{12}{Et^3}\int_0^{\varphi_1} M_L r^2 \operatorname{vers}\varphi\, d\varphi - \frac{1}{Et}\int_0^{\varphi_1} H_L r \cos\varphi\, d\varphi + \frac{3}{Et}\int_0^{\varphi_1} V_L r \sin\varphi\, d\varphi \tag{81}$$

Formulas for the right side of the arch are the same as above except that M_L, H_L, and V_L are replaced by M_R, H_R, and V_R.

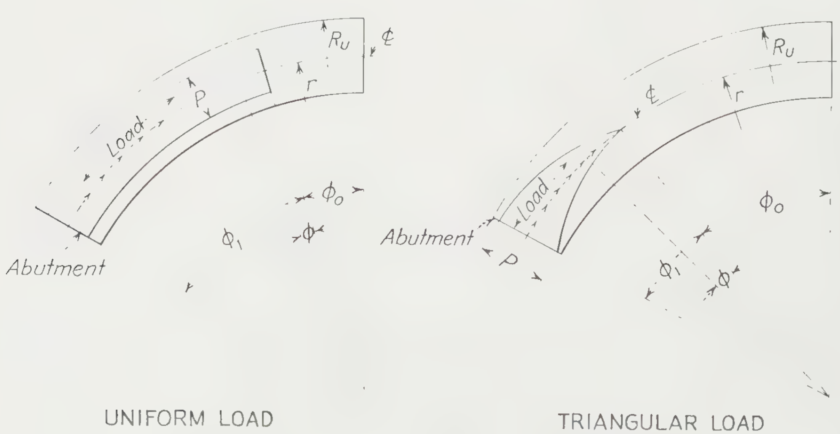

FIG. 14. Uniform and triangular tangential loads.

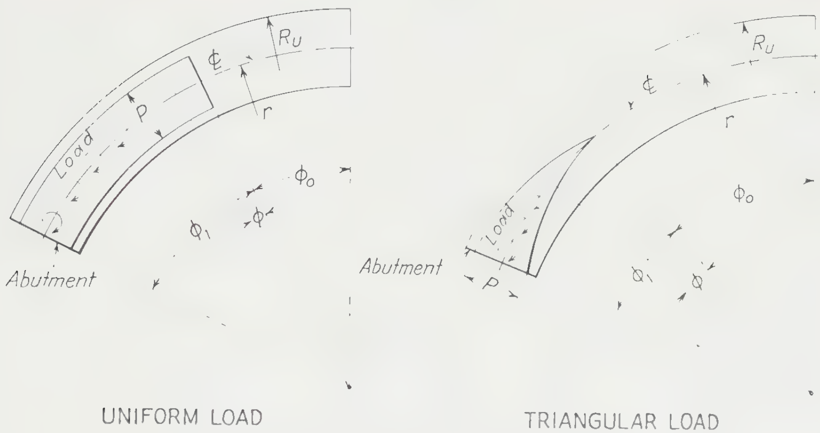

FIG. 15. Uniform and triangular twist loads.

By substituting M_L, H_L, and V_L from Table 5 in Eqs. (79), (80), and (81) and integrating between the limits of 0 and φ_1, equations for D_1, D_2, and D_3 at the point where the load begins may be obtained. By introducing proper functions of φ_0, the angular distance beyond the loaded section, the equations may be amplified to give D terms at points on the unloaded portion of the arch.

Formulas for load constants, for the uniform and triangular loads shown in Figs. 13, 14, and 15, may be compiled from data given in Tables 6 and 7. Table 6 gives data needed for radial and tangential load constants; Table 7 gives data needed for twist-load constants. Since some of the lengthy trigonometric functions appear in several of the equations, the trigonometric parts of the formulas are given in the first columns of the tables, and the places where they appear, together with their multipliers, are indicated in subsequent columns.

TABLE 5. FORMULAS FOR MOMENT, THRUST, AND SHEAR DUE TO EXTERNAL RADIAL, TANGENTIAL, AND TWIST LOADS

Loads	Force	Formulas for loads shown in Figs. 13, 14, and 15	
		Uniform loads	Triangular loads
Radial loads (see Fig. 13)	M_L	PR_ur vers ϕ	$\frac{PR_ur}{\phi_1}(\phi - \sin\phi)$
	H_L	PR_u vers ϕ	$\frac{PR_u}{\phi_1}(\phi - \sin\phi)$
	V_L	$PR_u \sin\phi$	$\frac{PR_u}{\phi_1}$ vers ϕ
Tangential loads (see Fig. 14)	M_L	$Pr^2(\phi - \sin\phi)$	$\frac{Pr^2}{\phi_1}\left(\frac{\phi^2}{2} - \text{vers}\ \phi\right)$
	H_L	$-Pr \sin\phi$	$-\frac{Pr}{\phi_1}$ vers ϕ
	V_L	Pr vers ϕ	$\frac{Pr}{\phi_1}(\phi - \sin\phi)$
Twist loads (see Fig. 15)	M_L	$Pr\phi$	$\frac{Pr}{\phi_1}\frac{\phi^2}{2}$

Table 6. Formulas for Load Constants for Uniform and Triangular Radial and Tangential Loads

Trigonometric part of formula*	Radial loads				Tangential loads			
	Uniform		Triangular		Uniform		Triangular	
	Designation	Multiplier	Designation	Multiplier	Designation	Multiplier	Designation	Multiplier
$\sin\phi_0\left(\frac{\sin^2\phi_1}{2}\right)+\cos\phi_0\left(\frac{\phi_1-\sin\phi_1\cos\phi_1}{2}\right)$	D_3 2d term 2d part	$\frac{PR_ur}{ET}$			D_2 2d term 1st part	$-\frac{Pr^2}{ET}$		
$\cos\phi_0\left(\frac{\sin^2\phi_1}{2}\right)-\sin\phi_0\left(\frac{\phi_1-\sin\phi_1\cos\phi_1}{2}\right)$	D_2 2d term 2d part	$\frac{PR_ur}{ET}$			D_3 2d term 1st part	$\frac{Pr^2}{ET}$		
$\phi_1-\sin\phi_1$	D_1 D_3 1st term 1st part	$\frac{PR_ur^2}{EI}$ $\frac{PR_ur^3}{EI}$						
$\sin\phi_0\left(\sin\phi_1-\frac{\phi_1+\sin\phi_1\cos\phi_1}{2}\right)+\cos\phi_0\left(\operatorname{vers}\phi_1-\frac{\sin^2\phi_1}{2}\right)$	D_2 1st term D_2 2d term 1st part	$\frac{PR_ur^3}{EI}$ $\frac{PR_ur}{ET}$	D_3 2d term 2d part	$\frac{PR_ur}{\phi_1ET}$	D_3 2d term 2d part	$\frac{Pr^2}{ET}$	D_2 2d term 1st part	$-\frac{Pr^2}{\phi_1ET}$
$\cos\phi_0\left(\sin\phi_1-\frac{\phi_1+\sin\phi_1\cos\phi_1}{2}\right)-\sin\phi_0\left(\operatorname{vers}\phi_1-\frac{\sin^2\phi_1}{2}\right)$	D_3 1st term 2d part D_3 2d term 1st part	$-\frac{PR_ur^3}{EI}$ $-\frac{PR_ur}{ET}$	D_2 2d term 2d part	$\frac{PR_ur}{\phi_1ET}$	D_2 2d term 2d part	$\frac{Pr^2}{ET}$	D_3 2d term 1st part	$\frac{Pr^2}{\phi_1ET}$
$\frac{\phi_1^2}{2}-\operatorname{vers}\phi_1$			D_1 D_3 1st term 1st part	$\frac{PR_ur^2}{\phi_1EI}$ $\frac{PR_ur^3}{\phi_1EI}$	D_1 D_3 1st term 1st part	$\frac{Pr^3}{EI}$ $\frac{Pr^4}{EI}$		
$\sin\phi_0\left(\phi_1\sin\phi_1-\operatorname{vers}\phi_1-\frac{\sin^2\phi_1}{2}\right)+\cos\phi_0\left(\sin\phi_1-\frac{\phi_1-\sin\phi_1\cos\phi_1}{2}-\phi_1\cos\phi_1\right)$			D_2 1st term D_2 2d term 1st part	$\frac{PR_ur^3}{\phi_1EI}$ $\frac{PR_ur}{\phi_1ET}$	D_2 1st term	$\frac{Pr^4}{EI}$	D_3 2d term 2d part	$\frac{Pr^2}{\phi_1ET}$
$\cos\phi_0\left(\phi_1\sin\phi_1-\operatorname{vers}\phi_1-\frac{\sin^2\phi_1}{2}\right)-\sin\phi_0\left(\sin\phi_1-\frac{\phi_1-\sin\phi_1\cos\phi_1}{2}-\phi_1\cos\phi_1\right)$			D_3 1st term 2d part D_3 2d term 1st part	$-\frac{PR_ur^3}{\phi_1EI}$ $-\frac{PR_ur}{\phi_1ET}$	D_3 1st term 2d part	$-\frac{Pr^4}{EI}$	D_2 2d term 2d part	$\frac{Pr^2}{\phi_1ET}$
$\sin\phi_1-\phi_1+\frac{\phi_1^3}{6}$							D_1 D_3 1st term 1st part	$\frac{Pr^3}{\phi_1EI}$ $\frac{Pr^4}{\phi_1EI}$
$\sin\phi_0\left(\frac{\phi_1^2}{2}\sin\phi_1+\phi_1\cos\phi_1-2\sin\phi_1+\frac{\phi_1+\sin\phi_1\cos\phi_1}{2}\right)+\cos\phi_0\left(\phi_1\sin\phi_1-\frac{\phi_1^2}{2}\cos\phi_1-2\operatorname{vers}\phi_1+\frac{\sin^2\phi_1}{2}\right)$							D_2 1st term	$\frac{Pr^4}{\phi_1EI}$
$\cos\phi_0\left(\frac{\phi_1^2}{2}\sin\phi_1+\phi_1\cos\phi_1-2\sin\phi_1+\frac{\phi_1+\sin\phi_1\cos\phi_1}{2}\right)-\sin\phi_0\left(\phi_1\sin\phi_1-\frac{\phi_1^2}{2}\cos\phi_1-2\operatorname{vers}\phi_1+\frac{\sin^2\phi_1}{2}\right)$							D_3 1st term 2d part	$-\frac{Pr^4}{\phi_1EI}$

* Trigonometric functions, times multipliers, give formulas for terms in designation columns.

TABLE 7. FORMULAS FOR LOAD CONSTANTS FOR UNIFORM AND TRIANGULAR TWIST LOADS

Trigonometric part of formula*	Twist loads: Uniform, Designation	Twist loads: Uniform, Multiplier	Twist loads: Triangular, Designation	Twist loads: Triangular, Multiplier
$\frac{\phi_1^2}{2}$	D_1 D_3 1st part	$\frac{Pr^2}{EI}$ $\frac{Pr^3}{EI}$		
$\frac{\phi_1^3}{6}$			D_1 D_3 1st part	$\frac{Pr^2}{\phi_1 EI}$ $\frac{Pr^3}{\phi_1 EI}$
$\sin\phi_0(\phi_1 \sin\phi_1 - \text{vers}\,\phi_1) + \cos\phi_0(\sin\phi_1 - \phi_1\cos\phi_1)$	D_2	$\frac{Pr^3}{EI}$		
$\cos\phi_0(\phi_1 \sin\phi_1 - \text{vers}\,\phi_1) - \sin\phi_0(\sin\phi_1 - \phi_1\cos\phi_1)$	D_3 2d part	$-\frac{Pr^3}{EI}$		
$\sin\phi_0\left(\frac{\phi_1^2}{2}\sin\phi_1 + \phi_1\cos\phi_1 - \sin\phi_1\right) + \cos\phi_0\left(\phi_1\sin\phi_1 - \frac{\phi_1^2}{2}\cos\phi_1 - \text{vers}\,\phi_1\right)$			D_2	$\frac{Pr^3}{\phi_1 EI}$
$\cos\phi_0\left(\frac{\phi_1^2}{2}\sin\phi_1 + \phi_1\cos\phi_1 - \sin\phi_1\right) - \sin\phi_0\left(\phi_1\sin\phi_1 - \frac{\phi_1^2}{2}\cos\phi_1 - \text{vers}\,\phi_1\right)$			D_3 2d part	$-\frac{Pr^3}{\phi_1 EI}$

* Trigonometric functions, times multipliers, give formulas for terms in designation columns.

In order to simplify the tabulations, the D_2 and D_3 constants are divided into two terms. The first term gives the effect of bending, and the second term the effects of rib shortening and shear. In order to still further simplify the tabulations, the first and second terms are sometimes subdivided into first and second parts. The subdivisions of the first terms have no special significance. In the case of the second-term subdivisions, the first part gives the effects of rib shortening, and the second part the effects of shear.

Since the D terms are deflections due to loads between the point considered and the abutment, D terms for intermediate points along a triangularly loaded arch cannot be obtained by integrating Eqs. (79), (80), and (81) up to values of φ less than φ_1. Values of D terms for such intermediate points must be calculated by integrating revised forms of the equations in which the M_L, H_L, and V_L parts apply to the uniform and triangular loads comprising the total external load from the abutment to the point considered.

COMPUTER METHOD

The arch constants and load constants developed in the previous section are for constant-thickness single-center circular arches. The integrations for these constants become considerably more complicated for variable-thickness multicenter circular arches and were not included here. When using a computer it becomes feasible to use a voussoir summation procedure. The voussoirs can be made small enough to be considered constant thickness with uniform load. The use of the voussoir method eliminates the need for integrating the rather complex formulas for the load and arch constants. Variable-thickness multicentered arches can therefore be analyzed almost as readily as the constant-thickness arches. The voussoir method does require, however, considerable geometrical manipulation in order to define the various voussoirs and their loading geometrically.

During the early development of the trial-load method, it was found convenient to use triangular loads which varied from maximum at the abutment to zero at some distance away from the abutment, as shown in Figs. 12 and 13. By varying the sign, magnitude, and distance from the abutment it was possible to approximate reasonably any varying distributed load. This load scheme made it possible to set up procedures and tables which facilitated calculation of the load constants by hand. With computers, these tables assume a position of lesser importance. Once the equations are

FIG. 16. Triangular radial loads.

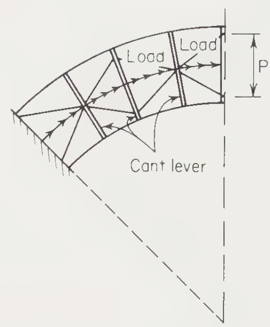

FIG. 17. Triangular tangential loads.

programmed, it becomes easier in some cases to use the computer than the tables. The computer programmer is therefore free to choose whatever shape of load he pleases. Shapes shown in Figs. 16, 17, and 18 are often used. The points of maximum load are located so as to coincide with the intersections of the cantilevers. The load then varies linearly to zero at the adjacent cantilever.

The geometry of a nonsymmetrical multicentered arch is defined in Fig. 19. The geometrical properties of the individual voussoirs can be derived to be as follows:

When $\phi < \phi_1$,

$$t_m = R_1 - (R_1 - r_1 - T_0)\cos\frac{m}{N_s}\phi_1 - \left\{r_1^2 - \left[(R_1 - r_1 - T_0)\sin\frac{m}{N_s}\phi_1\right]^2\right\}^{1/2}$$

where m is the voussoir number for which t is being computed.

$$X_m = \left(R_1 - \frac{t_m}{2}\right)\sin\frac{m}{N_s}\phi_1$$

$$Y_m = R_1 - \frac{t_0}{2} - \left(R - \frac{t_m}{2}\right)\cos\frac{m}{N_s}\phi_1$$

$$\delta_s = \left(R_1 - \frac{t_m}{2}\right)\frac{\phi}{N_s}$$

Similarly, values can be derived for t_m, X_m, and Y_m for $\phi > \phi_1$.

Having determined the required geometrical properties of the voussoirs, one can now proceed with the arch analysis. The basic equations (38), (39), and (40) as developed for the hand method still apply. However, the integral signs in Eqs. (41),

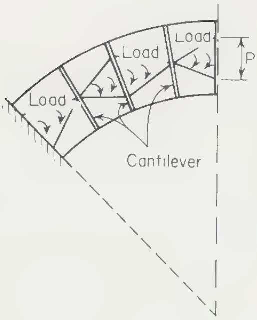

FIG. 18. Triangular twist loads.

(42), and (43) are replaced by summation signs. Equations (44), (45), and (46) remain the same. The integral signs in (47), (48), and (49) are replaced by summation signs. The development of Eqs. (50) through (72) remains unchanged. The functions needed in determining the crown forces shown in Table 4 remain identical except that the integral sign changes to a summation sign.

The values for the arch constants can now be obtained directly through summation. Formulas still need to be derived for obtaining moments, thrust, and shear due to external loads. Assume a typical triangular load as shown in Fig. 20. Assume the distributed load over any voussoir is a concentrated load P at the center of the voussoir. For a load with intensity of unity at cantilever 2, the value of P to the

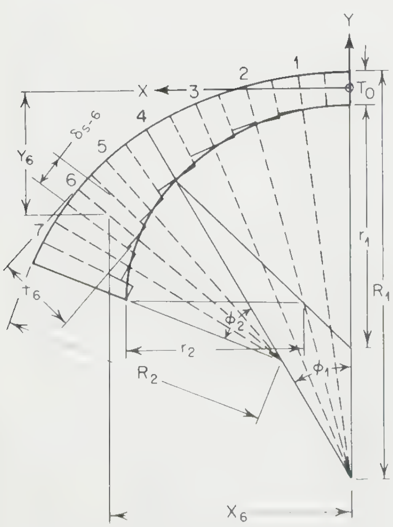

FIG. 19. Geometry of multicentered arch.

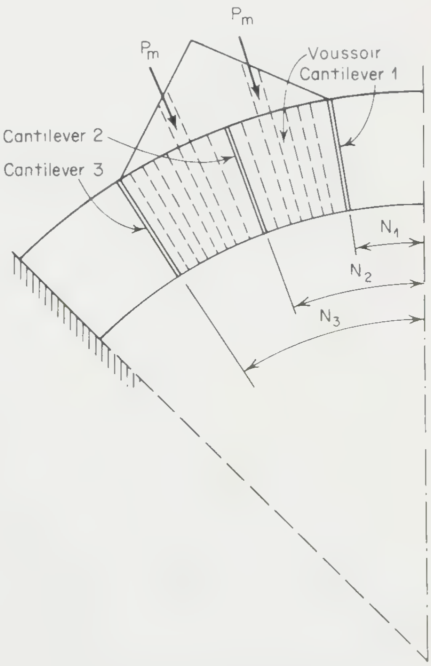

FIG. 20. Voussoir loading.

right of cantilever 2 is

$$P_m = \frac{m - N_1}{N_2 - N_1}\,\delta_s$$

To the left of cantilever 2,

$$P_m = \left(1 - \frac{m - N_2}{N_3 - N_2}\right)\delta_s$$

where m is the voussoir number for which P is being computed and $N_{1,2,3}$ are the number of voussoirs from the crown to the first, second, and third cantilevers, respectively. The formulas for moment, thrust, and shear due to external loads become

Radial loads,

$$\begin{aligned} M_L &= \Sigma P_n(\Delta x)\cos\phi + \Sigma P_n(\Delta y)\sin\phi \\ H_L &= \Sigma P_n \sin\Delta\phi \\ V_L &= \Sigma P_n \cos\Delta\phi \end{aligned}$$

Tangential loads,

$$\begin{aligned} M_L &= \Sigma P_n(\Delta y)\sin\phi + \Sigma P_n(\Delta x)\cos\phi \\ H_L &= \Sigma P_n \cos\Delta\phi \\ V_L &= \Sigma P_n \sin\Delta\phi \end{aligned}$$

Twist loads,

$$M_L = \Sigma P_n$$

where Δx, Δy, and $\Delta\phi$ are incremental values for x, y, and ϕ, respectively, between P_n and the point where M_L is being computed. All the load constants [Eqs. (79) through (81)] can now be evaluated and the crown reactions determined with Eqs. (47) through (49).

34. Adjustments. Having determined the deflections due to unit loads of the various arches and cantilevers, it is now possible to divide the external load by trial and error so that the deflections in the radial directions are equal. In the present use of the method, adjustments of deflections are first made in radial directions, including effects of radial shear and rock deformations in both arch and cantilever elements. If considerations of tangential shear and twist effects are necessary, adjustments are next made in circumferential directions, then in angular directions. In circumferential adjustments, equal and opposite tangential shear loads are introduced, by trial, to compensate for differences in tangential movements caused by radial loads, one set of loads being applied to the arch elements and the balancing set to the cantilever elements. In angular adjustments, equal and opposite twist loads are applied to arch and cantilever elements, to compensate for discrepancies in rotation caused by radial loads. Radial movements, caused by tangential shear and twist loads, are then considered in a radial readjustment and their effects considered in circumferential and angular readjustments, until resultant deflections are in agreement in all three directions.[1]

This procedure of determining the load distribution by trial and error was developed prior to the development of the electronic computer. It can also be adapted to a computer solution. It is probably more expedient, however, to write a set of equations which equate the deflections of the arches and cantilevers and to solve these equations for the unknown load distribution. Using the matrix notation, let $[A]$ be the deflection matrix of the independent arches and $[C]$ that of the cantilevers. The elements of these matrices, given in Tables 8 and 9, are obtained from the unit-load coefficient equations derived in the previous paragraphs. Let $[P_A]$ be a column matrix of the external load applied to the arches and $[P_C]$ that of the external load applied to the cantilevers. Let $[I_A]$ be an unknown column matrix representing

[1] Westergaard, H. M., Arch Dam Analysis by Trial Loads Simplified, *Eng. News-Record*, **106**, 141–143, 1931.

TABLE 8

Lds / Pts.	A_{10}	A_{11}	A_{21}	A_{12}	A_{22}	A_{32}	A_{13}	A_{23}	A_{33}	A_{43}	A_{14}	A_{24}
10	${}_{10}A_{10}$	${}_{10}A_{11}$	0	${}_{10}A_{12}$	0	0	${}_{10}A_{13}$	0	0	0	${}_{10}A_{14}$	0
11	${}_{11}A_{10}$	${}_{11}A_{11}$	0	${}_{11}A_{12}$	0	0	${}_{11}A_{13}$	0	0	0	${}_{11}A_{14}$	0
21	0	0	${}_{21}A_{21}$	0	${}_{21}A_{22}$	0	0	${}_{21}A_{23}$	0	0	0	${}_{21}A_{24}$
12	${}_{12}A_{10}$	${}_{12}A_{11}$	0	${}_{12}A_{12}$	0	0	${}_{12}A_{13}$	0	0	0	${}_{12}A_{14}$	0
22	0	0	${}_{22}A_{21}$	0	${}_{22}A_{22}$	0	0	${}_{22}A_{23}$	0	0	0	${}_{22}A_{24}$
32	0	0	0	0	0	${}_{32}A_{32}$	0	0	${}_{32}A_{33}$	0	0	0
13	${}_{13}A_{10}$	${}_{13}A_{11}$	0	${}_{13}A_{12}$	0	0	${}_{13}A_{13}$	0	0	0	${}_{13}A_{14}$	0
23	0	0	${}_{23}A_{21}$	0	${}_{23}A_{22}$	0	0	${}_{23}A_{23}$	0	0	0	${}_{23}A_{24}$
33	0	0	0	0	0	${}_{33}A_{32}$	0	0	${}_{33}A_{33}$	0	0	0
43	0	0	0	0	0	0	0	0	0	${}_{43}A_{43}$	0	0
14	${}_{14}A_{10}$	${}_{14}A_{11}$	0	${}_{14}A_{12}$	0	0	${}_{14}A_{13}$	0	0	0	${}_{14}A_{14}$	0
24	0	0	${}_{24}A_{21}$	0	${}_{24}A_{22}$	0	0	${}_{24}A_{23}$	0	0	0	${}_{24}A_{24}$
34	0	0	0	0	0	${}_{34}A_{32}$	0	0	${}_{34}A_{33}$	0	0	0
44	0	0	0	0	0	0	0	0	0	${}_{44}A_{43}$	0	0
54	0	0	0	0	0	0	0	0	0	0	0	0
15	${}_{15}A_{10}$	${}_{15}A_{11}$	0	${}_{15}A_{12}$	0	0	${}_{15}A_{13}$	0	0	0	${}_{15}A_{14}$	0
25	0	0	${}_{25}A_{21}$	0	${}_{25}A_{22}$	0	0	${}_{25}A_{23}$	0	0	0	${}_{25}A_{24}$
35	0	0	0	0	0	${}_{35}A_{32}$	0	0	${}_{35}A_{33}$	0	0	0
45	0	0	0	0	0	0	0	0	0	${}_{45}A_{43}$	0	0
16	${}_{16}A_{10}$	${}_{16}A_{11}$	0	${}_{16}A_{12}$	0	0	${}_{16}A_{13}$	0	0	0	${}_{16}A_{14}$	0
26	0	0	${}_{26}A_{21}$	0	${}_{26}A_{22}$	0	0	${}_{26}A_{23}$	0	0	0	${}_{26}A_{24}$
36	0	0	0	0	0	${}_{36}A_{32}$	0	0	${}_{36}A_{33}$	0	0	0
17	${}_{17}A_{10}$	${}_{17}A_{11}$	0	${}_{17}A_{12}$	0	0	${}_{17}A_{13}$	0	0	0	${}_{17}A_{14}$	0
27	0	0	${}_{27}A_{21}$	0	${}_{27}A_{22}$	0	0	${}_{27}A_{23}$	0	0	0	${}_{27}A_{24}$
18	${}_{18}A_{10}$	${}_{18}A_{11}$	0	${}_{18}A_{12}$	0	0	${}_{18}A_{13}$	0	0	0	${}_{18}A_{14}$	0

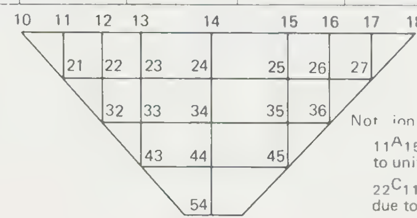

Notation

${}_{11}A_{15}$ = Arch deflection at point 11 due to unit arch load at point 15

${}_{22}C_{11}$ = Arch deflection at point 22 due to unit cantilever load at point 11

TABLE 8. (Continued)

Lds. / Pts.	A_{34}	A_{44}	A_{54}	A_{15}	A_{25}	A_{35}	A_{45}	A_{16}	A_{26}	A_{36}	A_{17}	A_{27}
10	0	0	0	$_{10}A_{15}$	0	0	0	$_{10}A_{16}$	0	0	$_{10}A_{17}$	0
11	0	0	0	$_{11}A_{15}$	0	0	0	$_{11}A_{16}$	0	0	$_{11}A_{17}$	0
21	0	0	0	0	$_{21}A_{25}$	0	0	0	$_{21}A_{26}$	0	0	$_{21}A_{27}$
12	0	0	0	$_{12}A_{15}$	0	0	0	$_{12}A_{16}$	0	0	$_{12}A_{17}$	0
22	0	0	0	0	$_{22}A_{25}$	0	0	0	$_{22}A_{26}$	0	0	$_{22}A_{27}$
32	$_{32}A_{34}$	0	0	0	0	$_{32}A_{35}$	0	0	0	$_{32}A_{36}$	0	0
13	0	0	0	$_{13}A_{15}$	0	0	0	$_{13}A_{16}$	0	0	$_{13}A_{17}$	0
23	0	0	0	0	$_{23}A_{25}$	0	0	0	$_{23}A_{26}$	0	0	$_{23}A_{27}$
33	$_{33}A_{34}$	0	0	0	0	$_{33}A_{35}$	0	0	0	$_{33}A_{36}$	0	0
43	0	$_{43}A_{44}$	0	0	0	0	$_{43}A_{45}$	0	0	0	0	0
14	0	0	0	$_{14}A_{15}$	0	0	0	$_{14}A_{16}$	0	0	$_{14}A_{17}$	0
24	0	0	0	0	$_{24}A_{25}$	0	0	0	$_{24}A_{26}$	0	0	$_{24}A_{27}$
34	$_{34}A_{34}$	0	0	0	0	$_{34}A_{35}$	0	0	0	$_{34}A_{36}$	0	0
44	0	$_{44}A_{44}$	0	0	0	0	$_{44}A_{45}$	0	0	0	0	0
54	0	0	$_{54}A_{54}$	0	0	0	0	0	0	0	0	0
15	0	0	0	$_{15}A_{15}$	0	0	0	$_{15}A_{16}$	0	0	$_{15}A_{17}$	0
25	0	0	0	0	$_{25}A_{25}$	0	0	0	$_{25}A_{26}$	0	0	$_{25}A_{27}$
35	$_{35}A_{34}$	0	0	0	0	$_{35}A_{35}$	0	0	0	$_{35}A_{36}$	0	0
45	0	$_{45}A_{44}$	0	0	0	0	$_{45}A_{45}$	0	0	0	0	0
16	0	0	0	$_{16}A_{15}$	0	0	0	$_{16}A_{16}$	0	0	$_{16}A_{17}$	0
26	0	0	0	0	$_{26}A_{25}$	0	0	0	$_{26}A_{26}$	0	0	$_{26}A_{27}$
36	$_{36}A_{34}$	0	0	0	0	$_{36}A_{35}$	0	0	0	$_{36}A_{36}$	0	0
17	0	0	0	$_{17}A_{15}$	0	0	0	$_{17}A_{16}$	0	0	$_{17}A_{17}$	0
27	0	0	0	0	$_{27}A_{25}$	0	0	0	$_{27}A_{26}$	0	0	$_{27}A_{27}$
18	0	0	0	$_{18}A_{15}$	0	0	0	$_{18}A_{16}$	0	0	$_{18}A_{17}$	0

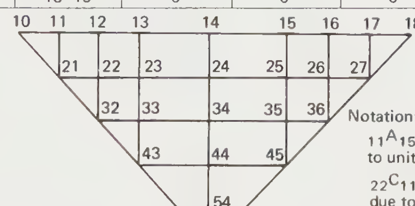

Notation:
$_{11}A_{15}$ = Arch deflection at point 11 due to unit arch load at point 15
$_{22}C_{11}$ = Arch deflection at point 22 due to unit cantilever load at point 11

TABLE 8. *(Continued)*

Lds. / Pts.	A_{18}	C_{10}	C_{11}	C_{21}	C_{12}	C_{22}	C_{32}	C_{13}	C_{23}	C_{33}	C_{43}	C_{14}	C_{24}
10	${}_{10}A_{18}$	${}_{10}C_{10}$	0	0	0	0	0	0	0	0	0	0	0
11	${}_{11}A_{18}$	${}_{11}C_{10}$	0	0	0	0	0	0	0	0	0	0	0
21	0	0	${}_{21}C_{11}$	${}_{21}C_{21}$	0	0	0	0	0	0	0	0	0
12	${}_{12}A_{18}$	${}_{12}C_{10}$	0	0	0	0	0	0	0	0	0	0	0
22	0	0	${}_{22}C_{11}$	${}_{22}C_{21}$	0	0	0	0	0	0	0	0	0
32	C	0	0	0	${}_{32}C_{12}$	${}_{32}C_{22}$	${}_{32}C_{32}$	0	0	0	0	0	0
13	${}_{13}A_{18}$	${}_{13}C_{10}$	0	0	0	0	0	0	0	0	0	0	0
23	0	0	${}_{23}C_{11}$	${}_{23}C_{21}$	0	0	0	0	0	0	0	0	0
33	0	0	0	0	${}_{33}C_{12}$	${}_{33}C_{22}$	${}_{33}C_{32}$	0	0	0	0	0	0
43	0	0	0	0	0	0	0	${}_{43}C_{13}$	${}_{43}C_{23}$	${}_{43}C_{33}$	${}_{43}C_{43}$	0	0
14	${}_{14}A_{18}$	${}_{14}C_{10}$	0	0	0	0	0	0	0	0	0	0	0
24	0	0	${}_{24}C_{11}$	${}_{24}C_{21}$	0	0	0	0	0	0	0	0	0
34	0	0	0	0	${}_{34}C_{12}$	${}_{34}C_{22}$	${}_{34}C_{32}$	0	0	0	0	0	0
44	0	0	0	0	0	0	0	${}_{44}C_{13}$	${}_{44}C_{23}$	${}_{44}C_{33}$	${}_{44}C_{43}$	0	0
54	0	0	0	0	0	0	0	0	0	0	0	${}_{54}C_{14}$	${}_{54}C_{24}$
15	${}_{15}A_{18}$	${}_{15}C_{10}$	0	0	0	0	0	0	0	0	0	0	0
25	0	0	${}_{25}C_{11}$	${}_{25}C_{21}$	0	0	0	0	0	0	0	0	0
35	0	0	0	0	${}_{35}C_{12}$	${}_{35}C_{22}$	${}_{35}C_{32}$	0	0	0	0	0	0
45	0	0	0	0	0	0	0	${}_{45}C_{13}$	${}_{45}C_{23}$	${}_{45}C_{33}$	${}_{45}C_{43}$	0	0
16	${}_{16}A_{18}$	${}_{16}C_{10}$	0	0	0	0	0	0	0	0	0	0	0
26	0	0	${}_{26}C_{11}$	${}_{26}C_{21}$	0	0	0	0	0	0	0	0	0
36	0	0	0	0	${}_{36}C_{12}$	${}_{36}C_{22}$	${}_{36}C_{32}$	0	0	0	0	0	0
17	${}_{17}A_{18}$	${}_{17}C_{10}$	0	0	0	0	0	0	0	0	0	0	0
27	0	0	${}_{27}C_{11}$	${}_{27}C_{21}$	0	0	0	0	0	0	0	0	0
18	${}_{18}A_{18}$	${}_{18}C_{10}$	0	0	0	0	0	0	0	0	0	0	0

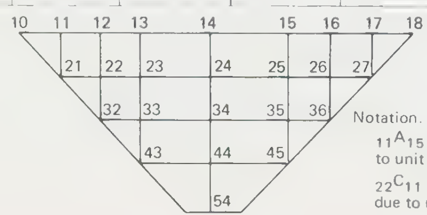

Notation.
${}_{11}A_{15}$ = Arch deflection at point 11 due to unit arch load at point 15
${}_{22}C_{11}$ = Arch deflection at point 22 due to unit cantilever load at point 11

TABLE 8. *(Continued)*

Lds. / Pts.	C_{34}	C_{44}	C_{54}	C_{15}	C_{25}	C_{35}	C_{45}	C_{16}	C_{26}	C_{36}	C_{17}	C_{27}	C_{18}
10	0	0	0	0	0	0	0	0	0	0	0	0	${}_{10}C_{18}$
11	0	0	0	0	0	0	0	0	0	0	0	0	${}_{11}C_{18}$
21	0	0	0	0	0	0	0	0	0	0	${}_{21}C_{17}$	${}_{21}C_{27}$	0
12	0	0	0	0	0	0	0	0	0	0	0	0	${}_{12}C_{18}$
22	0	0	0	0	0	0	0	0	0	0	${}_{22}C_{17}$	${}_{22}C_{27}$	0
32	0	0	0	0	0	0	0	${}_{32}C_{16}$	${}_{32}C_{26}$	${}_{32}C_{36}$	0	0	0
13	0	0	0	0	0	0	0	0	0	0	0	0	${}_{13}C_{18}$
23	0	0	0	0	0	0	0	0	0	0	${}_{23}C_{17}$	${}_{23}C_{27}$	0
33	0	0	0	0	0	0	0	${}_{33}C_{16}$	${}_{33}C_{26}$	${}_{33}C_{36}$	0	0	0
43	0	0	0	${}_{43}C_{15}$	${}_{43}C_{25}$	${}_{43}C_{35}$	${}_{43}C_{45}$	0	0	0	0	0	0
14	0	0	0	0	0	0	0	0	0	0	0	0	${}_{14}C_{18}$
24	0	0	0	0	0	0	0	0	0	0	${}_{24}C_{17}$	${}_{24}C_{27}$	0
34	0	0	0	0	0	0	0	${}_{34}C_{16}$	${}_{34}C_{26}$	${}_{34}C_{36}$	0	0	0
44	0	0	0	${}_{44}C_{15}$	${}_{44}C_{25}$	${}_{44}C_{35}$	${}_{44}C_{45}$	0	0	0	0	0	0
54	${}_{54}C_{34}$	${}_{54}C_{44}$	${}_{54}C_{54}$	0	0	0	0	0	0	0	0	0	0
15	0	0	0	0	0	0	0	0	0	0	0	0	${}_{15}C_{18}$
25	0	0	0	0	0	0	0	0	0	0	${}_{25}C_{17}$	${}_{25}C_{27}$	0
35	0	0	0	0	0	0	0	${}_{35}C_{16}$	${}_{35}C_{26}$	${}_{35}C_{36}$	0	0	0
45	0	0	0	${}_{45}C_{15}$	${}_{45}C_{25}$	${}_{45}C_{35}$	${}_{45}C_{45}$	0	0	0	0	0	0
16	0	0	0	0	0	0	0	0	0	0	0	0	${}_{16}C_{18}$
26	0	0	0	0	0	0	0	0	0	0	${}_{26}C_{17}$	${}_{26}C_{27}$	0
36	0	0	0	0	0	0	0	${}_{36}C_{16}$	${}_{36}C_{26}$	${}_{36}C_{36}$	0	0	0
17	0	0	0	0	0	0	0	0	0	0	0	0	${}_{17}C_{18}$
27	0	0	0	0	0	0	0	0	0	0	${}_{27}C_{17}$	${}_{27}C_{27}$	0
18	0	0	0	0	0	0	0	0	0	0	0	0	${}_{18}C_{18}$

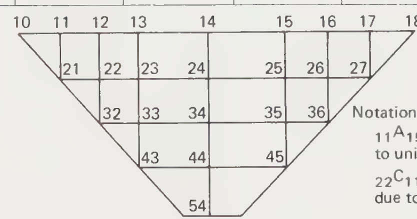

Notation:

${}_{11}A_{15}$ = Arch deflection at point 11 due to unit arch load at point 15

${}_{22}C_{11}$ = Arch deflection at point 22 due to unit cantilever load at point 11

TABLE 9

Lds / Pts	A_{10}	A_{11}	A_{21}	A_{12}	A_{22}	A_{32}	A_{13}	A_{23}	A_{33}	A_{43}	A_{14}	A_{24}
10	$_{10}A_{10}$	$_{10}A_{11}$	0	$_{10}A_{12}$	0	0	$_{10}A_{13}$	0	0	0	$_{10}A_{14}$	0
11	0	0	$_{11}A_{21}$	0	$_{11}A_{22}$	0	0	$_{11}A_{23}$	0	0	0	$_{11}A_{24}$
21	0	0	$_{21}A_{21}$	0	$_{21}A_{22}$	0	0	$_{21}A_{23}$	0	0	0	$_{21}A_{24}$
12	0	0	0	0	0	$_{12}A_{32}$	0	0	$_{12}A_{33}$	0	0	0
22	0	0	0	0	0	$_{22}A_{32}$	0	0	$_{22}A_{33}$	0	0	0
32	0	0	0	0	0	$_{32}A_{32}$	0	0	$_{32}A_{33}$	0	0	0
13	0	0	0	0	0	0	0	0	0	$_{13}A_{43}$	0	0
23	0	0	0	0	0	0	0	0	0	$_{23}A_{43}$	0	0
33	0	0	0	0	0	0	0	0	0	$_{33}A_{43}$	0	0
43	0	0	0	0	0	0	0	0	0	$_{43}A_{43}$	0	0
14	0	0	0	0	0	0	0	0	0	0	0	0
24	0	0	0	0	0	0	0	0	0	0	0	0
34	0	0	0	0	0	0	0	0	0	0	0	0
44	0	0	0	0	0	0	0	0	0	0	0	0
54	0	0	0	0	0	0	0	0	0	0	0	0
15	0	0	0	0	0	0	0	0	0	$_{15}A_{43}$	0	0
25	0	0	0	0	0	0	0	0	0	$_{25}A_{43}$	0	0
35	0	0	0	0	0	0	0	0	0	$_{35}A_{43}$	0	0
45	0	0	0	0	0	0	0	0	0	$_{45}A_{43}$	0	0
16	0	0	0	0	0	$_{16}A_{32}$	0	0	$_{16}A_{33}$	0	0	0
26	0	0	0	0	0	$_{26}A_{32}$	0	0	$_{26}A_{33}$	0	0	0
36	0	0	0	0	0	$_{36}A_{32}$	0	0	$_{36}A_{33}$	0	0	0
17	0	0	$_{17}A_{21}$	0	$_{17}A_{22}$	0	0	$_{17}A_{23}$	0	0	0	$_{17}A_{24}$
27	0	0	$_{27}A_{21}$	0	$_{27}A_{22}$	0	0	$_{27}A_{23}$	0	0	0	$_{27}A_{24}$
18	$_{18}A_{10}$	$_{18}A_{11}$	0	$_{18}A_{12}$	0	0	$_{18}A_{13}$	0	0	0	$_{18}A_{14}$	0

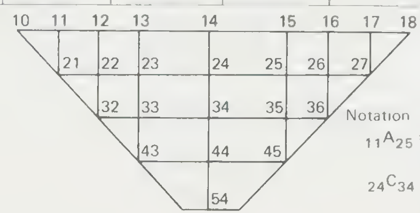

Notation

$_{11}A_{25}$ = Cantilever deflection at point 11 due to arch load at point 25

$_{24}C_{34}$ = Cantilever deflection at point 24 due to cantilever load at point 34

TABLE 9. *(Continued)*

Lds. / Pts.	A_{34}	A_{44}	A_{54}	A_{15}	A_{25}	A_{35}	A_{45}	A_{16}	A_{26}	A_{36}	A_{17}	A_{27}
10	0	0	0	${}_{10}A_{15}$	0	0	0	${}_{10}A_{16}$	0	0	${}_{10}A_{17}$	0
11	0	0	0	0	${}_{11}A_{25}$	0	0	0	${}_{11}A_{26}$	0	0	${}_{11}A_{27}$
21	0	0	0	0	${}_{21}A_{25}$	0	0	0	${}_{21}A_{26}$	0	0	${}_{21}A_{27}$
12	${}_{12}A_{34}$	0	0	0	0	${}_{12}A_{35}$	0	0	0	${}_{12}A_{36}$	0	0
22	${}_{22}A_{34}$	0	0	0	0	${}_{22}A_{35}$	0	0	0	${}_{22}A_{36}$	0	0
32	${}_{32}A_{34}$	0	0	0	0	${}_{32}A_{35}$	0	0	0	${}_{32}A_{36}$	0	0
13	0	${}_{13}A_{44}$	0	0	0	0	${}_{13}A_{45}$	0	0	0	0	0
23	0	${}_{23}A_{44}$	0	0	0	0	${}_{23}A_{45}$	0	0	0	0	0
33	0	${}_{33}A_{44}$	0	0	0	0	${}_{33}A_{45}$	0	0	0	0	0
43	0	${}_{43}A_{44}$	0	0	0	0	${}_{43}A_{45}$	0	0	0	0	0
14	0	0	${}_{14}A_{54}$	0	0	0	0	0	0	0	0	0
24	0	0	${}_{24}A_{54}$	0	0	0	0	0	0	0	0	0
34	0	0	${}_{34}A_{54}$	0	0	0	0	0	0	0	0	0
44	0	0	${}_{44}A_{54}$	0	0	0	0	0	0	0	0	0
54	0	0	${}_{54}A_{54}$	0	0	0	0	0	0	0	0	0
15	0	${}_{15}A_{44}$	0	0	0	0	${}_{15}A_{45}$	0	0	0	0	0
25	0	${}_{25}A_{44}$	0	0	0	0	${}_{25}A_{45}$	0	0	0	0	0
35	0	${}_{35}A_{44}$	0	0	0	0	${}_{35}A_{45}$	0	0	0	0	0
45	0	${}_{45}A_{44}$	0	0	0	0	${}_{45}A_{45}$	0	0	0	0	0
16	${}_{16}A_{34}$	0	0	0	0	${}_{16}A_{35}$	0	0	0	${}_{16}A_{36}$	0	0
26	${}_{26}A_{34}$	0	0	0	0	${}_{26}A_{35}$	0	0	0	${}_{26}A_{36}$	0	0
36	${}_{36}A_{34}$	0	0	0	0	${}_{36}A_{35}$	0	0	0	${}_{36}A_{36}$	0	0
17	0	0	0	0	${}_{17}A_{25}$	0	0	0	${}_{17}A_{26}$	0	0	${}_{17}A_{27}$
27	0	0	0	0	${}_{27}A_{25}$	0	0	0	${}_{27}A_{26}$	0	0	${}_{27}A_{27}$
18	0	0	0	${}_{18}A_{15}$	0	0	0	${}_{18}A_{16}$	0	0	${}_{18}A_{17}$	0

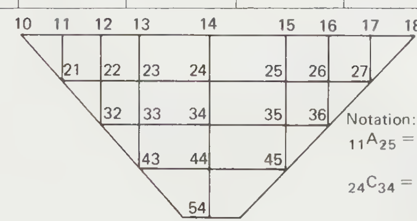

Notation:

${}_{11}A_{25}$ = Cantilever deflection at point 11 due to arch load at point 25

${}_{24}C_{34}$ = Cantilever deflection at point 24 due to cantilever load at point 34

Table 9. (*Continued*)

Lds / Pts	A_{18}	C_{10}	C_{11}	C_{21}	C_{12}	C_{22}	C_{32}	C_{13}	C_{23}	C_{33}	C_{43}	C_{14}	C_{24}
10	$_{10}A_{18}$	$_{10}C_{10}$	0	0	0	0	0	0	0	0	0	0	0
11	0	0	$_{11}C_{11}$	$_{11}C_{21}$	0	0	0	0	0	0	0	0	0
21	0	0	$_{21}C_{11}$	$_{21}C_{21}$	0	0	0	0	0	0	0	0	0
12	0	0	0	0	$_{12}C_{12}$	$_{12}C_{22}$	$_{12}C_{32}$	0	0	0	0	0	0
22	0	0	0	0	$_{22}C_{12}$	$_{22}C_{22}$	$_{22}C_{32}$	0	0	0	0	0	0
32	0	0	0	0	$_{32}C_{12}$	$_{32}C_{22}$	$_{32}C_{32}$	0	0	0	0	0	0
13	0	0	0	0	0	0	0	$_{13}C_{13}$	$_{13}C_{23}$	$_{13}C_{33}$	$_{13}C_{43}$	0	0
23	0	0	0	0	0	0	0	$_{23}C_{13}$	$_{23}C_{23}$	$_{23}C_{33}$	$_{23}C_{43}$	0	0
33	0	0	0	0	0	0	0	$_{33}C_{13}$	$_{33}C_{23}$	$_{33}C_{33}$	$_{33}C_{43}$	0	0
43	0	0	0	0	0	0	0	$_{43}C_{13}$	$_{43}C_{23}$	$_{43}C_{33}$	$_{43}C_{43}$	0	0
14	0	0	0	0	0	0	0	0	0	0	0	$_{14}C_{14}$	$_{14}C_{24}$
24	0	0	0	0	0	0	0	0	0	0	0	$_{24}C_{14}$	$_{24}C_{24}$
34	0	0	0	0	0	0	0	0	0	0	0	$_{34}C_{14}$	$_{34}C_{24}$
44	0	0	0	0	0	0	0	0	0	0	0	$_{44}C_{14}$	$_{44}C_{24}$
54	0	0	0	0	0	0	0	0	0	0	0	$_{54}C_{14}$	$_{54}C_{24}$
15	0	0	0	0	0	0	0	$_{15}C_{13}$	$_{15}C_{23}$	$_{15}C_{33}$	$_{15}C_{43}$	0	0
25	0	0	0	0	0	0	0	$_{25}C_{13}$	$_{25}C_{23}$	$_{25}C_{33}$	$_{25}C_{43}$	0	0
35	0	0	0	0	0	0	0	$_{35}C_{13}$	$_{35}C_{23}$	$_{35}C_{33}$	$_{35}C_{43}$	0	0
45	0	0	0	0	0	0	0	$_{45}C_{13}$	$_{45}C_{23}$	$_{45}C_{33}$	$_{45}C_{43}$	0	0
16	0	0	0	0	$_{16}C_{12}$	$_{16}C_{22}$	$_{16}C_{32}$	0	0	0	0	0	0
26	0	0	0	0	$_{26}C_{12}$	$_{26}C_{22}$	$_{26}C_{32}$	0	0	0	0	0	0
36	0	0	0	0	$_{36}C_{12}$	$_{36}C_{22}$	$_{36}C_{32}$	0	0	0	0	0	0
17	0	0	$_{17}C_{11}$	$_{17}C_{21}$	0	0	0	0	0	0	0	0	0
27	0	0	$_{27}C_{11}$	$_{27}C_{21}$	0	0	0	0	0	0	0	0	0
18	$_{18}A_{18}$	$_{18}C_{10}$	0	0	0	0	0	0	0	0	0	0	0

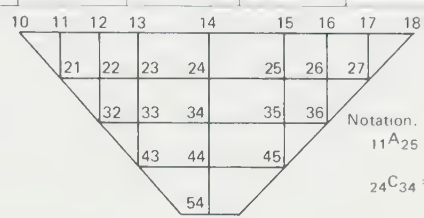

Notation.

$_{11}A_{25}$ = Cantilever deflection at point 11 due to arch load at point 25

$_{24}C_{34}$ = Cantilever deflection at point 24 due to cantilever load at point 34

TABLE 9. *(Continued)*

Lds. / Pts.	C_{34}	C_{44}	C_{54}	C_{15}	C_{25}	C_{35}	C_{45}	C_{16}	C_{26}	C_{36}	C_{17}	C_{27}	C_{18}
10	0	0	0	0	0	0	0	0	0	0	0	0	${}_{10}C_{18}$
11	0	0	0	0	0	0	0	0	0	0	${}_{11}C_{17}$	${}_{11}C_{27}$	0
21	0	0	0	0	0	0	0	0	0	0	${}_{21}C_{17}$	${}_{21}C_{27}$	0
12	0	0	0	0	0	0	0	${}_{12}C_{16}$	${}_{12}C_{26}$	${}_{12}C_{36}$	0	0	0
22	0	0	0	0	0	0	0	${}_{22}C_{16}$	${}_{22}C_{26}$	${}_{22}C_{36}$	0	0	0
32	0	0	0	0	0	0	0	${}_{32}C_{16}$	${}_{32}C_{26}$	${}_{32}C_{36}$	0	0	0
13	0	0	0	${}_{13}C_{15}$	${}_{13}C_{25}$	${}_{13}C_{35}$	${}_{13}C_{45}$	0	0	0	0	0	0
23	0	0	0	${}_{23}C_{15}$	${}_{23}C_{25}$	${}_{23}C_{35}$	${}_{23}C_{45}$	0	0	0	0	0	0
33	0	0	0	${}_{33}C_{15}$	${}_{33}C_{25}$	${}_{33}C_{35}$	${}_{33}C_{45}$	0	0	0	0	0	0
43	0	0	0	${}_{43}C_{15}$	${}_{43}C_{25}$	${}_{43}C_{35}$	${}_{43}C_{45}$	0	0	0	0	0	0
14	${}_{14}C_{34}$	${}_{14}C_{44}$	${}_{14}C_{54}$	0	0	0	0	0	0	0	0	0	0
24	${}_{24}C_{34}$	${}_{24}C_{44}$	${}_{24}C_{54}$	0	0	0	0	0	0	0	0	0	0
34	${}_{34}C_{34}$	${}_{34}C_{44}$	${}_{34}C_{54}$	0	0	0	0	0	0	0	0	0	0
44	${}_{44}C_{34}$	${}_{44}C_{44}$	${}_{44}C_{54}$	0	0	0	0	0	0	0	0	0	0
54	${}_{54}C_{34}$	${}_{54}C_{44}$	${}_{54}C_{54}$	0	0	0	0	0	0	0	0	0	0
15	0	0	0	${}_{15}C_{15}$	${}_{15}C_{25}$	${}_{15}C_{35}$	${}_{15}C_{45}$	0	0	0	0	0	0
25	0	0	0	${}_{25}C_{15}$	${}_{25}C_{25}$	${}_{25}C_{35}$	${}_{25}C_{45}$	0	0	0	0	0	0
35	0	0	0	${}_{35}C_{15}$	${}_{35}C_{25}$	${}_{35}C_{35}$	${}_{35}C_{45}$	0	0	0	0	0	0
45	0	0	0	${}_{45}C_{15}$	${}_{45}C_{25}$	${}_{45}C_{35}$	${}_{45}C_{45}$	0	0	0	0	0	0
16	0	0	0	0	0	0	0	${}_{16}C_{16}$	${}_{16}C_{26}$	${}_{16}C_{36}$	0	0	0
26	0	0	0	0	0	0	0	${}_{26}C_{16}$	${}_{26}C_{26}$	${}_{26}C_{36}$	0	0	0
36	0	0	0	0	0	0	0	${}_{36}C_{16}$	${}_{36}C_{26}$	${}_{36}C_{36}$	0	0	0
17	0	0	0	0	0	0	0	0	0	0	${}_{17}C_{17}$	${}_{17}C_{27}$	0
27	0	0	0	0	0	0	0	0	0	0	${}_{27}C_{17}$	${}_{27}C_{27}$	0
18	0	0	0	0	0	0	0	0	0	0	0	0	${}_{18}C_{18}$

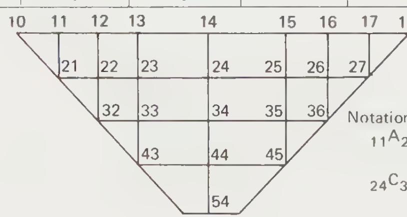

Notation:
${}_{11}A_{25}$ = Cantilever deflection at point 11 due to arch load at point 25
${}_{24}C_{34}$ = Cantilever deflection at point 24 due to cantilever load at point 34

internal arch loads and $[I_C]$ representing unknown cantilever loads required to bring the arches and cantilevers in agreement. Then

$$[A]\begin{bmatrix}P_A\\P_C\end{bmatrix} + [A]\begin{bmatrix}I_A\\I_C\end{bmatrix} = [C]\begin{bmatrix}P_A\\P_C\end{bmatrix} + [C]\begin{bmatrix}I_A\\I_C\end{bmatrix}$$

Because the internal loads have to be self-balancing

$$[I_A] = [-I_C]$$

Then

$$[A]\begin{bmatrix}-I_C\\I_C\end{bmatrix} - [C]\begin{bmatrix}-I_C\\I_C\end{bmatrix} = -[A]\begin{bmatrix}P_A\\P_C\end{bmatrix} + [C]\begin{bmatrix}P_A\\P_C\end{bmatrix}$$

It is now possible to solve for the adjusting loads $[I_C]$.

35. Arch Stresses. When the arch deflections have been brought into satisfactory agreement with the cantilever deflections in all parts of the dam, arch thrusts, moments, and shears, caused by the combined radial, tangential, twist, and temperature loads, are calculated for the locations where stresses are desired, usually the crown and abutment sections. Direct stresses at the extrados and intrados curves are then computed by Eq. (7). Stresses at different depths in the concrete may be computed on the assumption of a straight-line variation between the faces of the dam.

Average shearing stresses are the shearing forces divided by the areas on which they act. Shearing forces at crown sections of symmetrical arches, symmetrically loaded, are zero. Horizontal shearing stresses at the upstream and downstream edges of arch elements, acting in vertical tangential planes, may be computed by the formula

$$N = \mp (S - p) \tan \beta \qquad (- \text{ at extrados})$$

where S = direct stress acting normal to the plane
p = water pressure at the face of the dam
β = angle between the normal to the plane and a line tangent to the edge of the arch element

In circular constant-thickness arches, shearing stresses at the extrados and intrados are zero; and maximum shearing stresses in the interior may be estimated at $3/2$ the average shearing stress, a parabolic distribution being assumed. If tangential shear and twist effects are analyzed, Eq. (90) should include the correction $\pm N_t \tan \alpha$, where N_t is the tangential shear stress at the edge of the arch and α the angle between the edge of the cantilever and the vertical direction, as in Eq. (26), the plus sign being used for the extrados.

36. Temperature Loads. Formulas for temperature thrusts, moments, and shears at the crown and abutment sections of a constant-thickness arch, including effects of shear but not effects of abutment deformations, are as follows:

$$H_0 = \frac{cTr \sin \varphi}{\frac{12r^3}{Et^3}\left[(\varphi - 2\sin\varphi) + \frac{(\varphi + \sin\varphi\cos\varphi)}{2}\right] + \frac{r}{Et}\left[\frac{(\varphi + \sin\varphi\cos\varphi)}{2} + \frac{3(\varphi - \sin\varphi\cos\varphi)}{2}\right] - \frac{12r^3}{\varphi Et^3}[\varphi - \sin\varphi]^2} \tag{82}$$

$$M_0 = -\frac{r(\varphi - \sin\varphi)H_0}{\varphi} \tag{83}$$

$$V_a = 0 \tag{84}$$

$$H_a = H_0 \cos\varphi \tag{85}$$

$$M_a = -\frac{r(\varphi - \sin\varphi)H_0}{\varphi} + rH_0 \operatorname{vers}\varphi \tag{86}$$

$$V_a = H_0 \sin\varphi \tag{87}$$

Diagrams showing stresses caused by a 1-deg drop in temperature, including effects of abutment deformations, have recently been published for arch elements having different values of φ and t/r.[1]

Temperature deflections of the arch elements must be included with other arch-load deflections before adjusting with the cantilever deflections. Effects of temperature loads may be included in the general formulas for arch movements by adding the following terms to Eqs. (39) and (40), respectively:

$$d(\Delta r)_0 = \int_0^s cT \sin \varphi \, ds$$
$$d(\Delta s)_0 = \int_0^s cT \cos \varphi \, ds$$

T is the temperature change, positive when rising, and c the coefficient of thermal expansion.

The preceding additions to Eqs. (39) and (40) result in the following values of D_2 and D_3 for temperature loads:

$$D_2 = -cTy_a = -cTr \operatorname{vers} \varphi_1 \qquad (88)$$
$$D_3 = cTx_a = cTr \sin \varphi_1 \qquad (89)$$

INSTRUMENTATION OF ARCH DAMS

Most high arch dams being built today have an instrumentation program. The purpose of these programs is to give continuing assurance of the structural integrity of the dam and to furnish data leading to further refinements in design. The Stevenson Creek Dam was an early example of measuring stresses in dams. It was a constant-radius structure 60 ft high, and built solely for research measurements.[2] The measurements obtained were so accurate and comprehensive that research engineers were able to analyze satisfactorily the action of the structure. It gave an early verification that the trial-load analysis furnished a satisfactory basis for the design of arch dams.

The placement of instruments in the 600-ft-high Karadj Dam recently designed by Harza Engineering Company is shown in Fig. 21. Strain meters are embedded in locations of cantilever and arch intersection to simplify subsequent comparison with theoretical analysis. Joint meters are used to check on the extent of joint openings prior to grouting of the contraction joints. Foundation-deformation meters give an indication of stresses created in the foundation by changes in load.

To obtain principal stresses, strain meters are generally placed in groups of five (Fig. 22) at the faces of the dam and groups of nine (Fig. 23) in the interior. The interpretation of the strain-meter readings into stresses is a rather lengthy calculation. After the actual strains are obtained from all the meters in a group, they must be checked for compatibility. That is, the sum of the strains in any three mutually perpendicular directions must be equal. For the five-meter cluster,

$$e_1 + e_2 + e_3 = e_2 + e_4 + e_5$$

For the nine-meter cluster,

$$e_1 + e_2 + e_3 = e_2 + e_4 + e_5 = e_1 + e_6 + e_7 = e_3 + e_8 + e_9$$

As a rule, the strains as obtained from actual measurements do not satisfy this condition. The error must then be distributed among the meters in the group. For the five-meter group this is done by first taking the average of the sums of meters 1,2,3

[1] Houk, Ivan E., Arch Deflections and Temperature Stresses in Curved Dams, No. I, *Engineer*, Apr. 2, 1937, pp. 382–384.

[2] "Report on Arch Dam Investigation," Vols. I and III, The Engineering Foundation, 1927 and 1933.

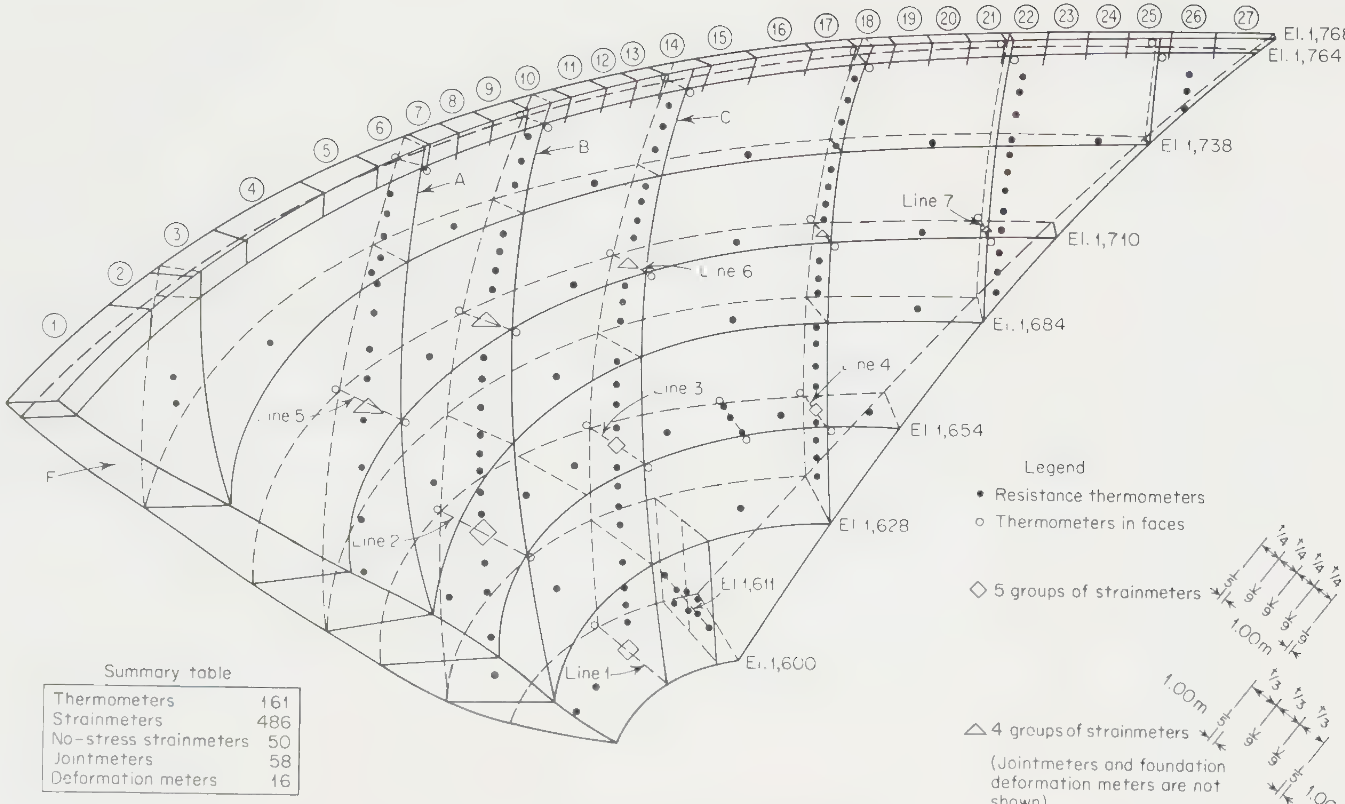

Thermometers	161
Strainmeters	486
No-stress strainmeters	50
Jointmeters	58
Deformation meters	16

FIG. 21. Instrument locations—Karadj Dam.

and 2,4,5:

$$\text{avg} = \frac{(e_1 + e_2 + e_3) + (e_2 + e_4 + e_5)}{2}$$

The difference between the first group (1,2,3) and the average is then divided by 3, giving the individual correction for each of the three meters in this group. As e_2 has now been corrected, the second group (2,4,5) is summed again. The difference between this sum and the average is divided by 2, thus giving the correction for meters

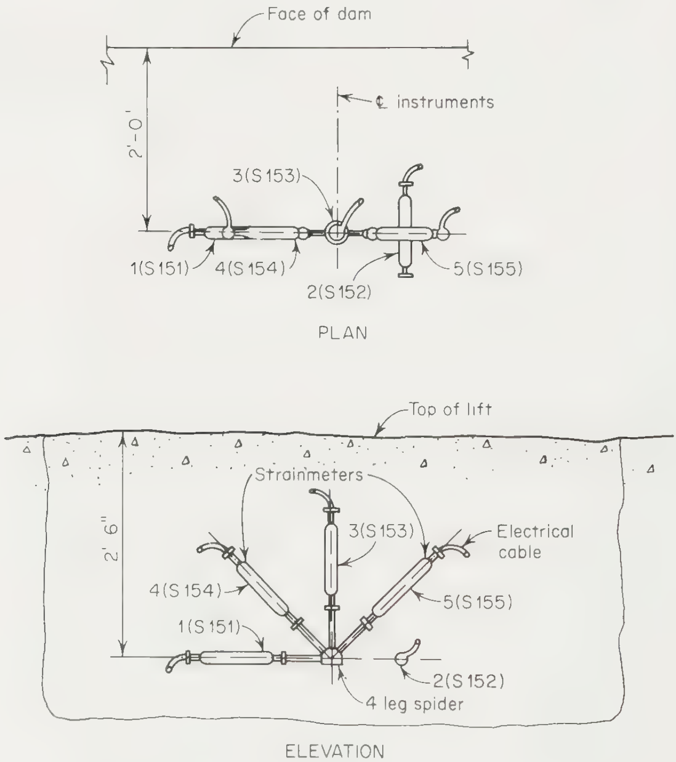

FIG. 22. Group of five strain meters.

4 and 5. As a check the corrected values are summed and compared for equality. A similar procedure can be developed for the nine-meter groups.

The next step is to correct for Poisson's ratio. This is necessary because elastic strains are altered by strains in other directions. The corrected values for the five-meter groups are

$$e_1' = Ae_1 + B(e_2 + e_3)$$

where

$$A = \frac{1 - v}{(1 + v)(1 - 2v)}$$

$$B = \frac{v}{(1 + v)(1 - 2v)}$$

$$e_2' = Ae_2 + B(e_1 + e_3)$$
$$e_3' = Ae_3 + B(e_1 + e_2)$$
$$e_4' = Ae_4 + B(e_2 + e_5)$$
$$e_5' = Ae_5 + B(e_2 + e_4)$$

The Poisson's-ratio corrections for a nine-meter group are similar.

In some cases a correction is required for concrete growth. The growth correction is obtained from a dummy no-stress strainmeter embedded near the cluster.

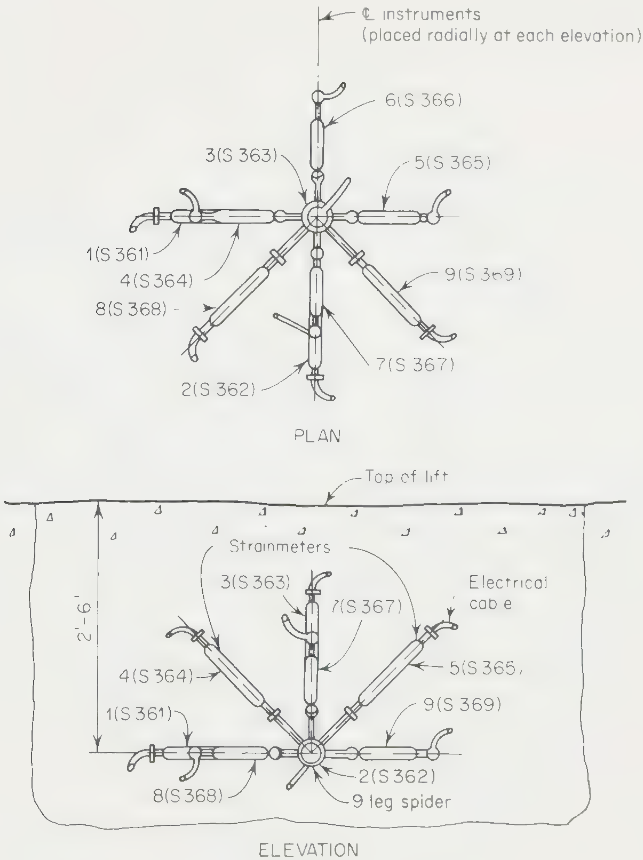

Fig. 23. Group of nine strain meters.

Having completed the correction of the strains, the stress can now be computed. This is a rather lengthy calculation because of the creep characteristics of concrete. Concrete, subjected to a constant stress, continues to deform with time. The properties of concrete undergo significant changes with time for some months immediately following placement. The Bureau of Reclamation has developed a mathematical method[1] to compute stress from strain.

[1] Jones, Keith, Calculation of Stress from Strain in Concrete, *U.S. Bureau of Reclamation Tech. Mem.* 653.

The concrete deformation for any one age at time of loading may be closely represented by the equation

$$\epsilon = \frac{1}{E'} + f(K) \ln (t + 1)$$

where ϵ = total strain due to unit stress at a period of time t after loading

$\frac{1}{E'}$ = instantaneous modulus of elasticity at time of loading

$f(K)$ = creep function

The change in deformation $\Delta\epsilon$, due to a change in stress $\Delta\tau$, is

$$\Delta\epsilon = \Delta\tau \left[\frac{1}{E'} + f(K) \ln (t + 1) \right] \tag{90}$$

or

$$\Delta\tau = \frac{\Delta\epsilon}{1/E' + f(k) \ln (t + 1)} \tag{91}$$

The values $1/E'$ and $f(K)$ are determined from laboratory tests. It is then possible to determine $\Delta\tau$ for each $\Delta\epsilon$. The summation of these values can be made to represent a

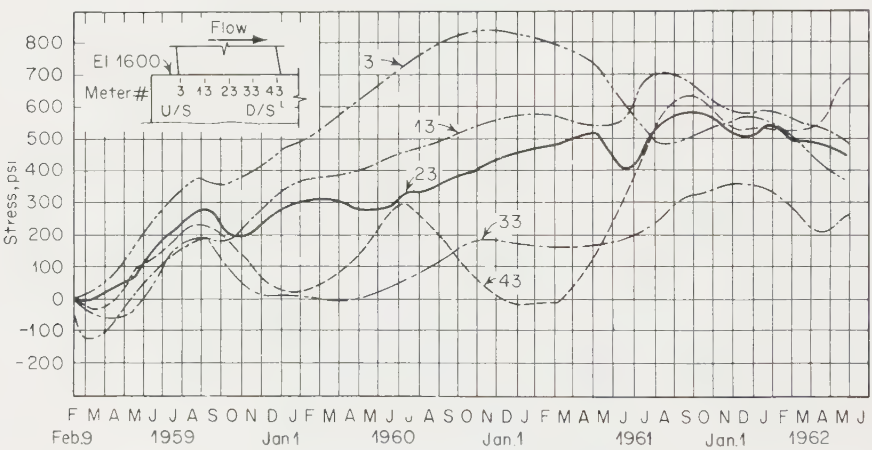

FIG. 24. Stress measurements—Karadj Dam.

stress curve that corresponds to a measured strain curve. Equation (90) can be expanded to

$$\epsilon = \sum_{i=1}^{n} \left[\frac{1}{E_i'} + f_i(K) \ln (t + 1) \right] \Delta\tau_i \tag{92}$$

The strain ϵ for all previous loads can be computed from Eq. (92) at any time t. The new load $\Delta\tau$ can then be computed from Eq. (91) assuming $\Delta\epsilon$ to be equal to the difference between measured strain and that computed by Eq. (92) for all previous loads. This is a very lengthy computation because the term ln $(t + 1)$ changes for each incremental load for each time period. The U.S. Bureau of Reclamation developed an equation in which the term ln $(t + 1)$ for each load was replaced by

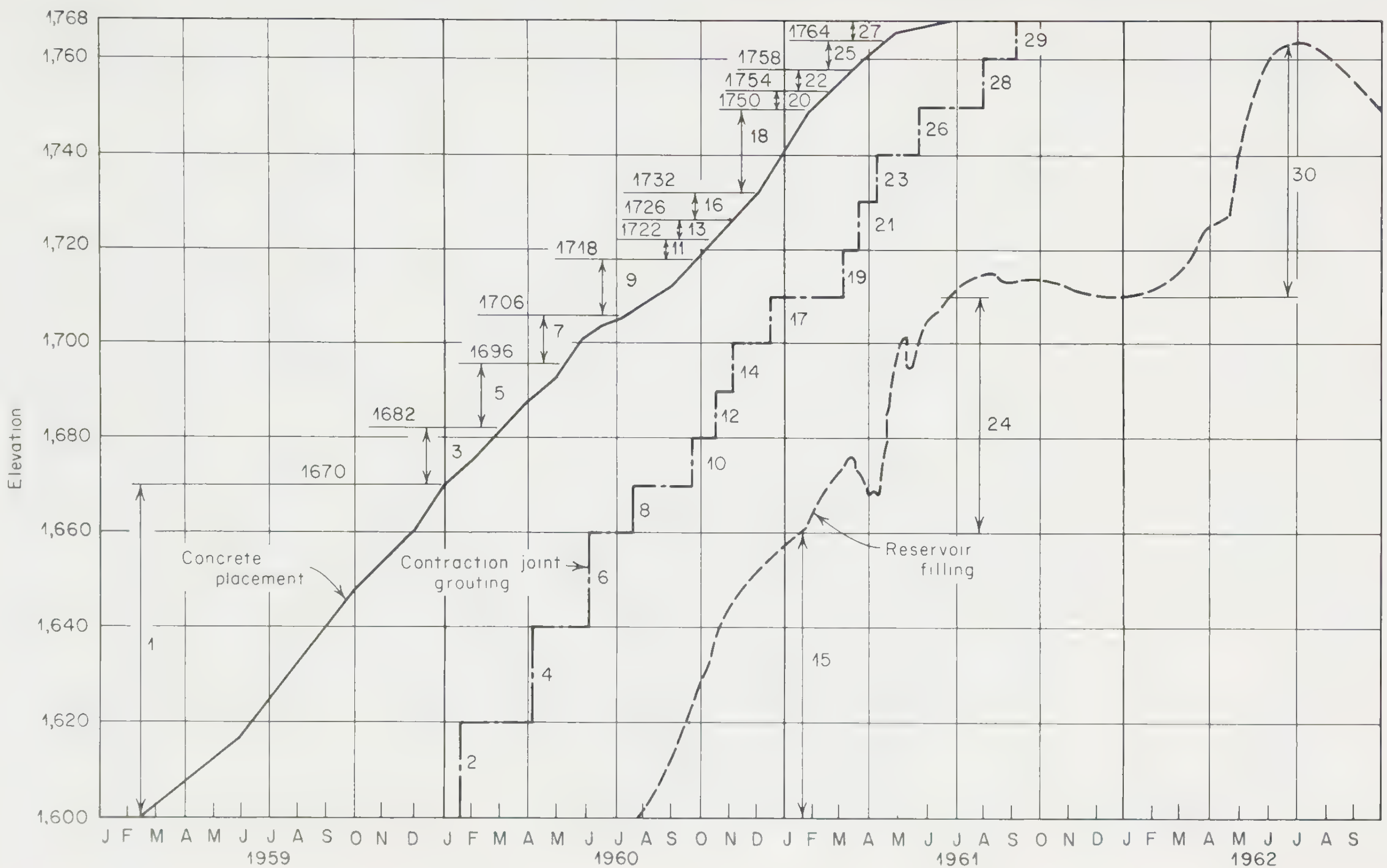

FIG. 25. Construction and reservoir-filling schedule—Karadj Dam.

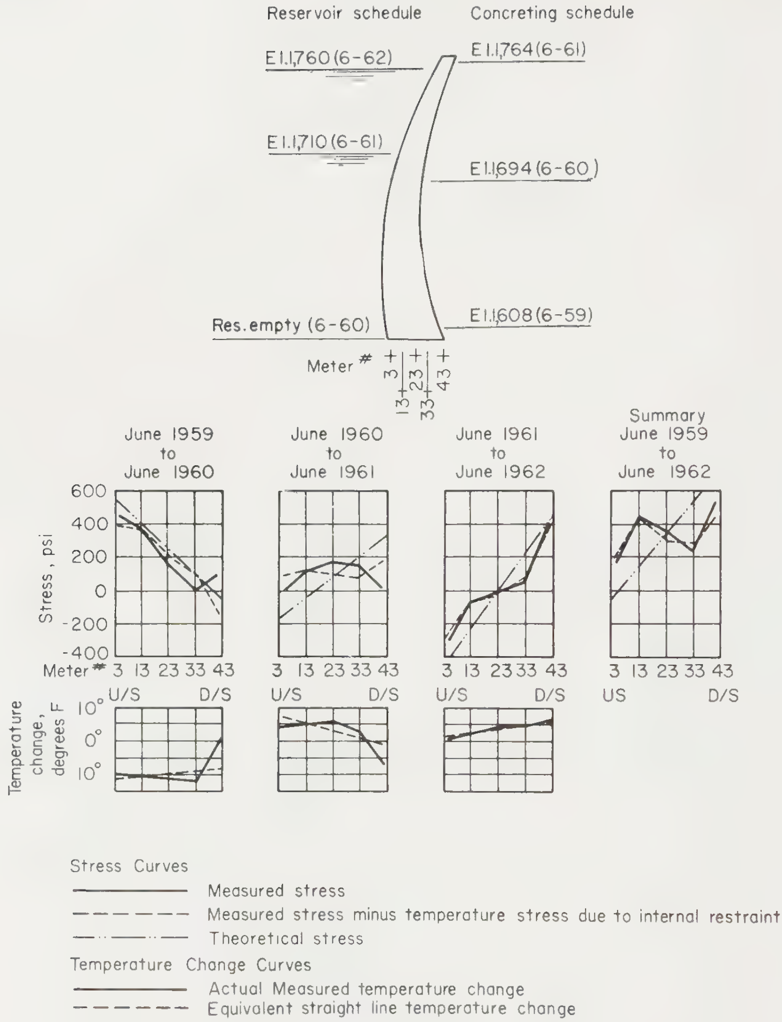

FIG. 26. Measured stress and theoretical stress—Karadj Dam.

In avg $(t + 1)$ for all loads. Equation (91) can then be rewritten as

$$\Delta\tau_n = E_s \left[\epsilon_n - \sum_{i=1}^{n} \frac{1}{E_i} \Delta\tau_i - \ln \text{avg } (t+1) \sum_{i=1}^{n} f_i(K)\, \Delta\tau_n \right]$$

in which E_s is the sustained modulus for the interval of time for which $\Delta\tau_n$ is being computed,

$$E_s = \frac{1}{1/E' + f(K) \ln (t+1)}$$

This equation can be readily programmed for solution with an electronic computer.

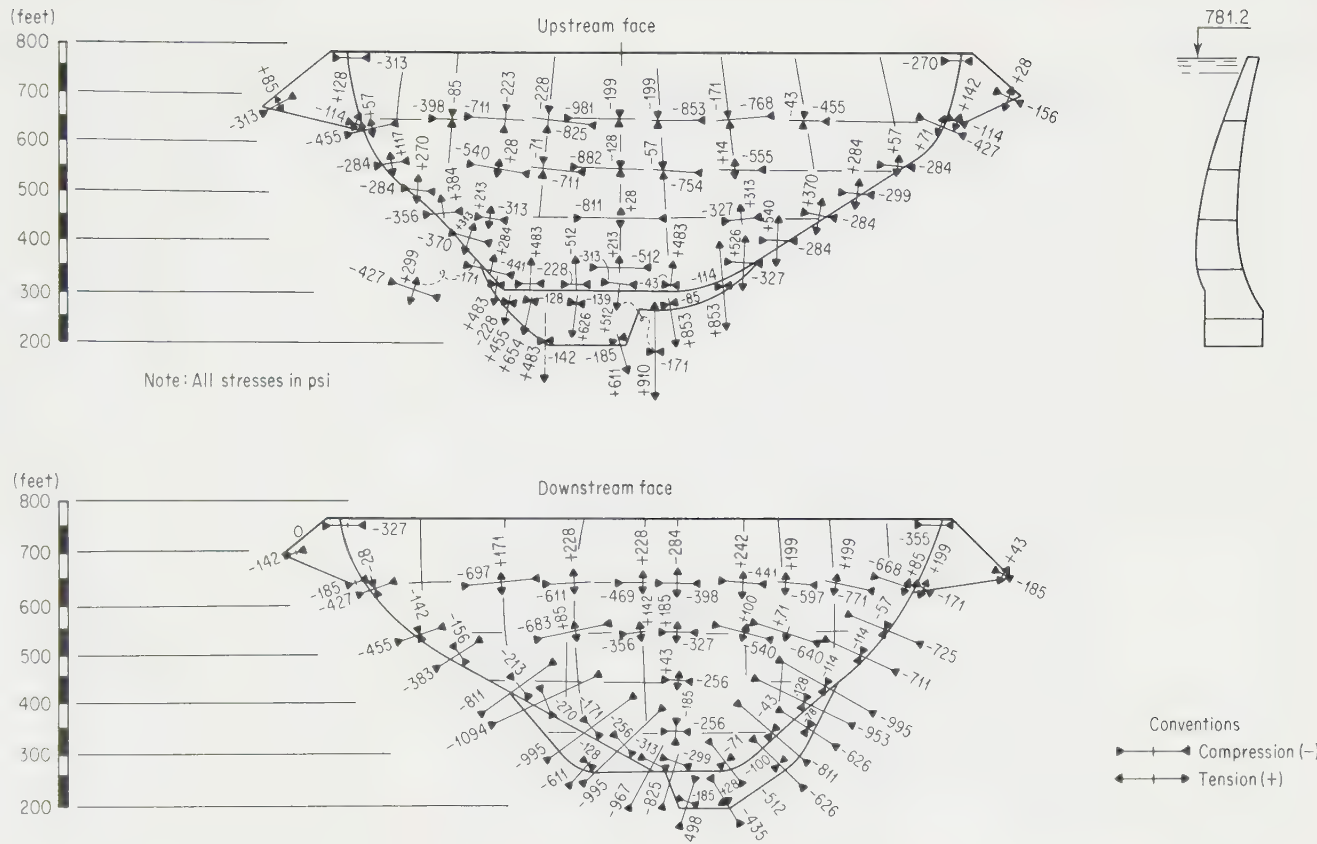

FIG. 27. Model-test stress results—Karadj Dam.

The stress history from day of embedment as determined by the above method for five vertical meters embedded in the base of Karadj Dam is shown in Fig. 24.[1] To evaluate these stresses, one needs to know the construction and reservoir-filling schedules. This is shown in Fig. 25. A comparison of measured stress with theoretical stresses for various time periods is shown in Fig. 26.

MODEL INVESTIGATIONS

Structural model tests are used extensively in arch-dam design. Certain designers prefer to carry out their design primarily with the aid of analytical tools using models only for verification of the analysis of the final shape. On the other hand, model testing techniques have been refined and simplified to the point where some designers now prefer to carry out the design primarily by models, using analytical tools only occasionally for checking purposes. Occasionally problems arise which are difficult if

Fig. 28. Model for hydrostatic load, Mossyrock Dam.

not impossible to analyze with existing mathematical tools. In these cases models are extremely valuable.

Mossyrock Dam, recently designed by Harza Engineering Company, was model-tested in the LNEC Laboratory in Lisbon. The results of test for water load are shown in Fig. 27. These can be compared directly with the analytical values shown in Fig. 2. The model generally shows somewhat higher stresses along the abutments. This was attributed to stress concentrations which can be expected where the intersection of the arch with the massive abutments forms a physical discontinuity. The modulus of elasticity of the concrete was assumed to be 3×10^6 psi, whereas the rock abutment was generally assumed to have a modulus of 1.5×10^6 psi and a small zone of 2.5×10^6 in the upper left abutment. As the foundation and arch were formed from the same plaster material, the variation in modulus of elasticity in the rock was obtained by drilling holes in the foundation according to a pattern determined experimentally that would reflect the difference. A picture of the model is shown in Fig. 28.

Figure 29 shows an ultimate-load test of the model after failure. As can be seen,

[1] Veltrop, J. A., R. P. Wengler, and S. Azri, "Structural Behavior of Karadj Dam," 8th Congress on Large Dams, Edinburgh, 1964.

failure occurred in the upper central portion of the model. Failure was caused by crushing of the model material.

Model tests are often used to investigate arch dams for earthquake. Either shaking tables or electromagnetic vibrators are used.[1] With the aid of models, one can determine the natural frequency of the prototype. The models can be subjected to specified accelerations. Considerable work has been done recently in analyzing available accelerograms of strong motion earthquakes. The various spectra such as

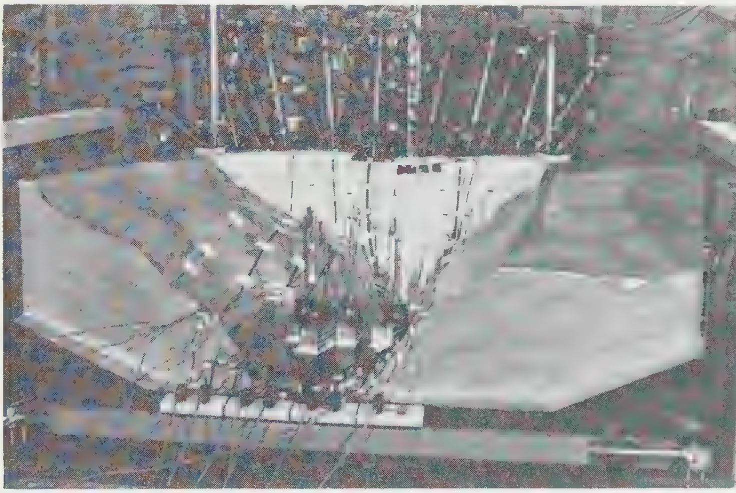

Fig. 29. Ultimate-load test, Mossyrock Dam.

velocity, acceleration, and power are obtained from these studies. Assuming an earthquake to be a random vibration, the strains can be measured in a model when subjected to the power spectrum of any historical earthquake.

EXAMPLES OF ARCH DAMS

The following examples illustrate practical design of arch dams that have been built and are operating satisfactorily. Hoover Dam represents an unusually high and massive arched-gravity type of constant-radius dam, whereas Karadj and Mossyrock are both high, variable-radius, double-curvature dams.

37. Hoover Dam. Hoover Dam, built by the Bureau of Reclamation, was completed on Colorado River near Las Vegas, Nev., in 1936. Figure 30 shows a general plan of the structure, a vertical cross section along the line of centers, and a tabulation of arch data at 100-ft intervals of elevation. The dam was designed on the basis of trial-load analyses. It is curved on a radius of 500 ft to the upstream edge of the crest, has extrados curves of gradually increasing radii as the depth below the crest increases, and is provided with long-radius fillets at the abutment ends of the intrados curves in the regions of pronounced arch stress. Short-radius fillets connect the dam with the abutment and foundation rock along the entire profile at the upstream face. Several articles describing its design and construction have been published.[2]

[1] Borges, J. F., J. Pereiva, A. Ravara, and J. Pedro, "Seismic Studies on Concrete Dam Models," Symposium on Concrete Dam Models, Lisbon, 1964.

[2] Houk, Ivan E., Technical Design Studies for Hoover Dam, *Western Construction News*, Apr. 10, 1932, pp. 187-193. Also see *Eng. News-Record*, **104**, Feb. 6, 1930; **109**, Dec. 15, 1932; **111**, Dec. 21, 1933; **115**.

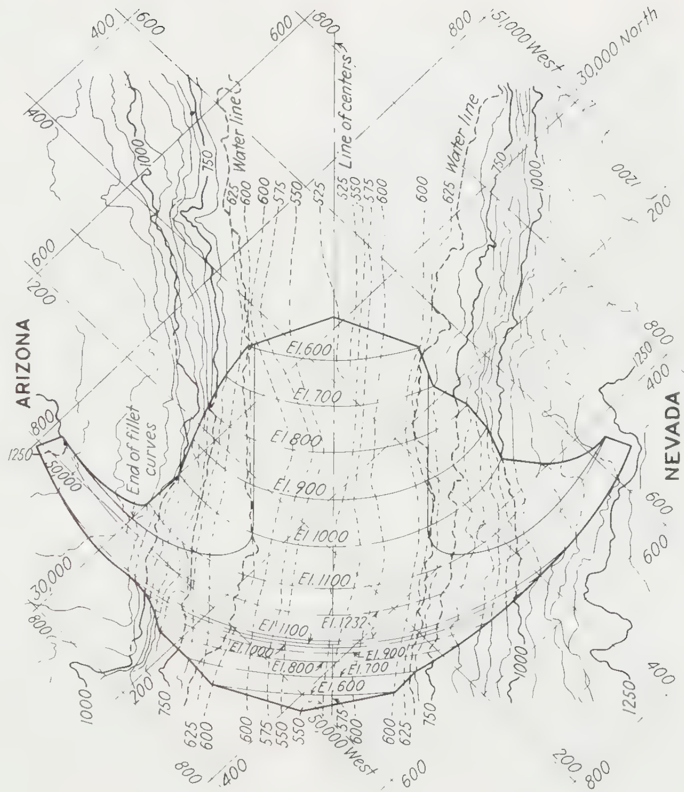

PLAN

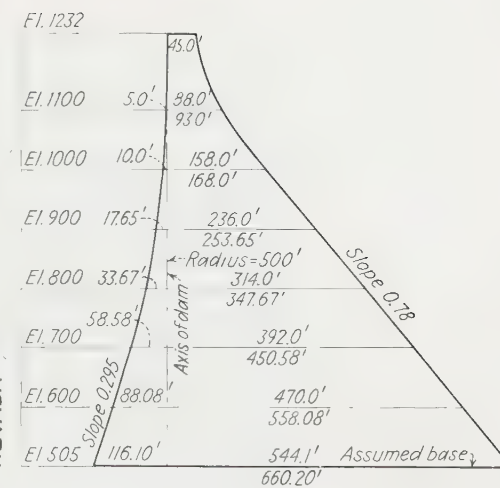

SECTION ON LINE OF CENTERS

ELEV.	RADII IN FEET				CENTER LINE LENGTH, FEET	CENTRAL ANGLE, DEGREES
	UP-STREAM	DOWN-STREAM	ARIZONA FILLET	NEVADA FILLET		
1232	500	455			1167	140
1100	505	412	215	262	896	112
1000	520	352	229	249	704	92.5
900	593	339	191	217	572	70.5
800	709	361	143	166	478	52.5
700	834	383	95	110	369	35.0
600	963	405	46	53	180	30.0

ARCH DATA

FIG. 30. Plan and maximum section of Hoover Dam.

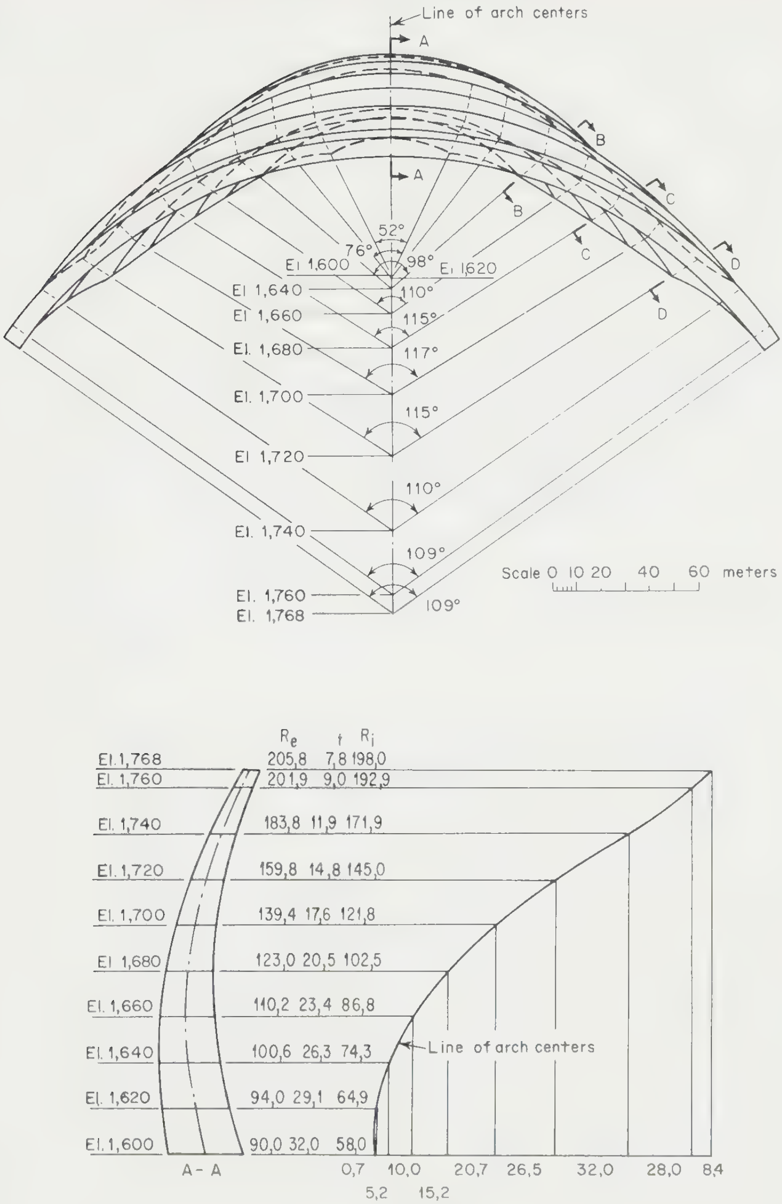

Fig. 31. Karadj Dam.

38. Karadj Dam. Karadj Dam, built by the Plan Organization of the government of Iran, was completed in 1962. It is located on the Karadj River approximately 25 miles northwest of Teheran. The dam is a multipurpose development that will serve the joint interest of water supply, irrigation, and power. Figure 31 shows a general plan of the dam and a cross section of the crown cantilever. A more complete description of the project features and its history, as well as significant data, has been published.[1]

39. Mossyrock Dam. Mossyrock Dam was built by the city of Tacoma. The project was completed in 1968. It is located on the Cowlitz River approximately 60 miles southwest of Tacoma, Wash. Figure 5 shows a general plan of the dam, a developed elevation, and vertical cross sections. The dam is 605 ft high with thrust blocks 140 and 125 ft high on the left and right side, respectively. An overflow spillway is provided with four 30- by 30-ft radial Tainter gates.

[1] Harza, R. D., and R. Edbrooke, Design of Karadj Hydroelectric Project, *Proc. ASCE, J. Power Div.*, **86,** (PO4), Proc. Paper 2579. Veltrop, J. A., and R. P. Wengler, Design of Karadj Arch Dam, *Proc. ASCE, J. Power Div.*, (PO1), Proc. Paper 3827.

SECTION 15

MULTIPLE-ARCH DAMS

BY CALVIN V. DAVIS[1]

INTRODUCTION

1. Type Characteristics. The multiple-arch dam has much in common with the other buttress types described in Secs. 9, 10, 12, and 13. Its distinguishing feature is that the water-supporting members consist of concrete arches which are supported by, and constructed integrally with, equally spaced, triangularly shaped buttresses. The deck or waterbearing member of the multiple-arch dam also has many of the characteristics of the arch dam (Sec. 14). Each type uses concrete efficiently in compression. Unlike the gravity type, the multiple-arch and the arch dam use concrete only partially as a counterweight to stabilize the structure.

In general, the multiple-arch dam is considered suitable for sound rock. There are, however, several notable exceptions. Only two will be mentioned. First, the Sherman Island Dam, built on the Hudson River in 1923, is a 75-ft-high multiple-arch structure supported by a continuously reinforced slab which transfers water and concrete loads to a sand and boulder foundation.[2] The buttresses have a uniform thickness of 3 ft 6 in. and are spaced 19 ft center to center. The length of the base slab in an up-and-downstream direction is 108 ft. Cutoffs of interlocking steel piles are provided. The maximum foundation pressure is less than 2.50 tons/sq ft. Backfill between buttresses was used to increase the resistance to sliding.

The second example, the 120-ft-high Cave Creek Dam[3] built in 1922, demonstrates notable exceptions to modern design criteria. This dam is supported on a foundation of cemented gravel. The buttresses extend through 60 ft of sand and gravel, are spaced 44 ft center to center, and vary in thickness from 1 ft at the top to about 5 ft 1 in. at a height of 80 ft. The lower portion of the buttress resting on the foundation has a uniform thickness of 10 ft. The length of the buttress at the base (not including the arches) is close to 90 ft. The sliding factor, at a height of 80 ft, is 1.07. There is no record of trouble having been experienced with this structure. The preceding examples should be regarded as exceptions, however, and not all attempts to build multiple-arch dams on poor foundations have been successful.

2. Early History. The Meer Alum Dam, built in Hyderabad, India, about 1802, is the earliest recorded example of a dam consisting of a series of arches supported by buttresses. This dam is approximately 3,500 ft long. The arches and buttresses are constructed of granite masonry in horizontal courses of roughly squared blocks. The maximum height is about 45 ft.

The mean average span, center to center of buttresses, is about 160 ft. The thickness of the buttress at the springing line of one of the larger buttresses is 23 ft 6 in., leaving a clear span of 136 ft 6 in. The length of the base of the highest buttress

[1] Grateful acknowledgment is made to Mr. J. Bellier, Coyne and Bellier, Consulting Engineers, Paris, France, for discussions and illustrations relating to Grandval Dam, France.

[2] NOETZLI, FRED A., Multiple-arch Dams, Part 4, p. 490 in "The Design and Construction of Dams," 8th ed., by Wegmann, John Wiley & Sons, Inc., New York.

[3] *Ibid.*, p. 485.

is about 45 ft or approximately equal to the maximum height. The thickness of the arch at the point of maximum height is approximately 10 ft.

This earliest known example of multiple-arch construction is of interest because of several features which have modern applications. The extent to which the buttresses and arches act integrally in transferring water loads from the upstream face through the structure to the foundations is unknown in multiple-arch design. A multiple-arch dam having these proportions would not be stable unless the arches and the buttresses acted integrally in resisting the water loads. The buttresses, acting alone, would either overturn or slide. Unwittingly, the designers demonstrated the advantages of using relatively wide spans in relation to height. The significance of this development will be discussed elsewhere.

3. Evolution. Following this very early start, a period of about 90 years elapsed before J. D. Derry, an Australian engineer, developed a masonry dam which is somewhat similar to the present-day multiple-arch dam. From this time onward there have been three distinct developments in multiple-arch design:

1. The standard type with buttress spacings falling between 20 and 80 ft center to center
2. The hollow-buttress type
3. The massive-buttress types, which have been developed largely by French engineers, with buttress spacings upward of 200 ft and with heights ranging between 200 and 700 ft

These developments cannot be placed in any chronological order as they have overlapped in point of time.

THE STANDARD TYPE

4. Buttress Spacing. A study of some of the earlier designs in the United States reveals the important principle that substantial economy can be achieved in designing dams above medium height (say 150 ft) by using relatively wide buttress spacings. A quantitative comparison of three dams (Fig. 4), Lake Hodges (Fig. 1), Florence Lake (Fig. 2), and Buchanan (Fig. 3), will illustrate this point.[1]

The Lake Hodges Dam (Fig. 1) was built in 1917 on the San Diequito River near San Diego, Calif. The maximum height is 136 ft and the overall length about 550 ft. The buttresses are spaced 24 ft center to center and vary in thickness from 1 ft 6 in. at the crest to 4 ft 1 in. at the bottom. The buttresses are stiffened by a T flange on the downstream face and are also braced by struts. The arches are circular in form and vary in thickness from 12 in. near the top to 2 ft 7 in. at the bottom. Neither the arches nor the buttresses are reinforced. A walkway through the dam invited buttress cracks, which extend roughly along trajectories of first principal stress from the upstream face of the buttresses to the foundations.

The Florence Lake Dam (Fig. 2), built by the Southern California Edison Company on the south fork of the San Joaquin River, has a maximum height of 160 ft and a total length of 3,300 ft. The buttresses are spaced 50 ft center to center and vary in thickness from 2 ft 3 in. at the crest to 7 ft 10 in. at a height of 150 ft. The arch barrels are semicircular in form and vary in thickness from 1 ft 6 in. at the crest to 4 ft 6 in. at a depth of 150 ft. As shown by Fig. 2, the buttresses and downstream face are stiffened by pilasters and T flanges. Both the buttresses and the arches are reinforced.

The Buchanan Dam (Fig. 3) (formerly named the Hamilton Dam) was built in 1936 on the Colorado River near Austin, Tex. The buttresses are spaced 70 ft center

[1] *Ibid.*, p. 476.

to center and buttress thicknesses vary from 3 ft 0 in. at the crest to 9 ft 0 in. at the foundations with variations occurring on the inclined planes. The arch deck is nearly semicircular in shape and varies in thickness from about 2 ft near the crest to 3 ft 4 in. at the foundation line. The buttresses are stiffened by a T flange on the downstream face and by intermediate pilasters. Both buttresses and arches are reinforced.

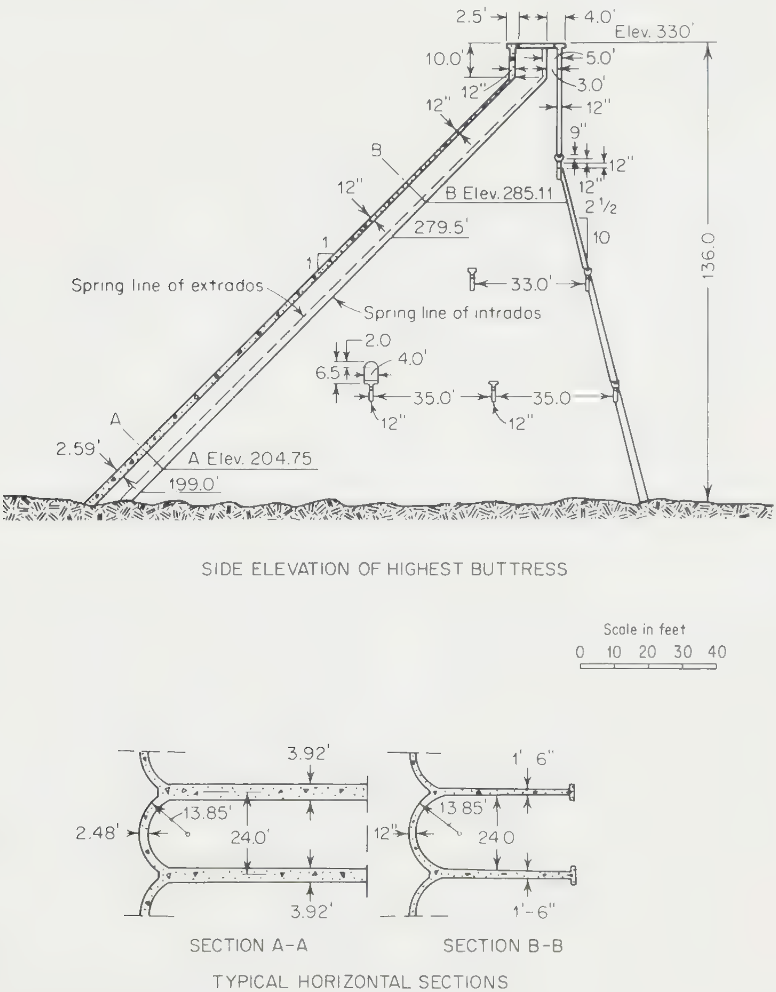

Fig. 1. The Lake Hodges Dam.

5. Comparison. A comparison of the concrete quantities per lineal foot dam in the Lake Hodges, Florence Lake, and Buchanan dams is shown by Fig. 4. There is only nominal variation of volume in relation to height for each of the three dams. It will be noted, however, that projections of the three curves come together at a height of 150 ft. All things being equal, the design having the widest buttress spacing would have the lowest unit cost of concrete because of the relative reduction of form surface and the increase in the massiveness of the structure.

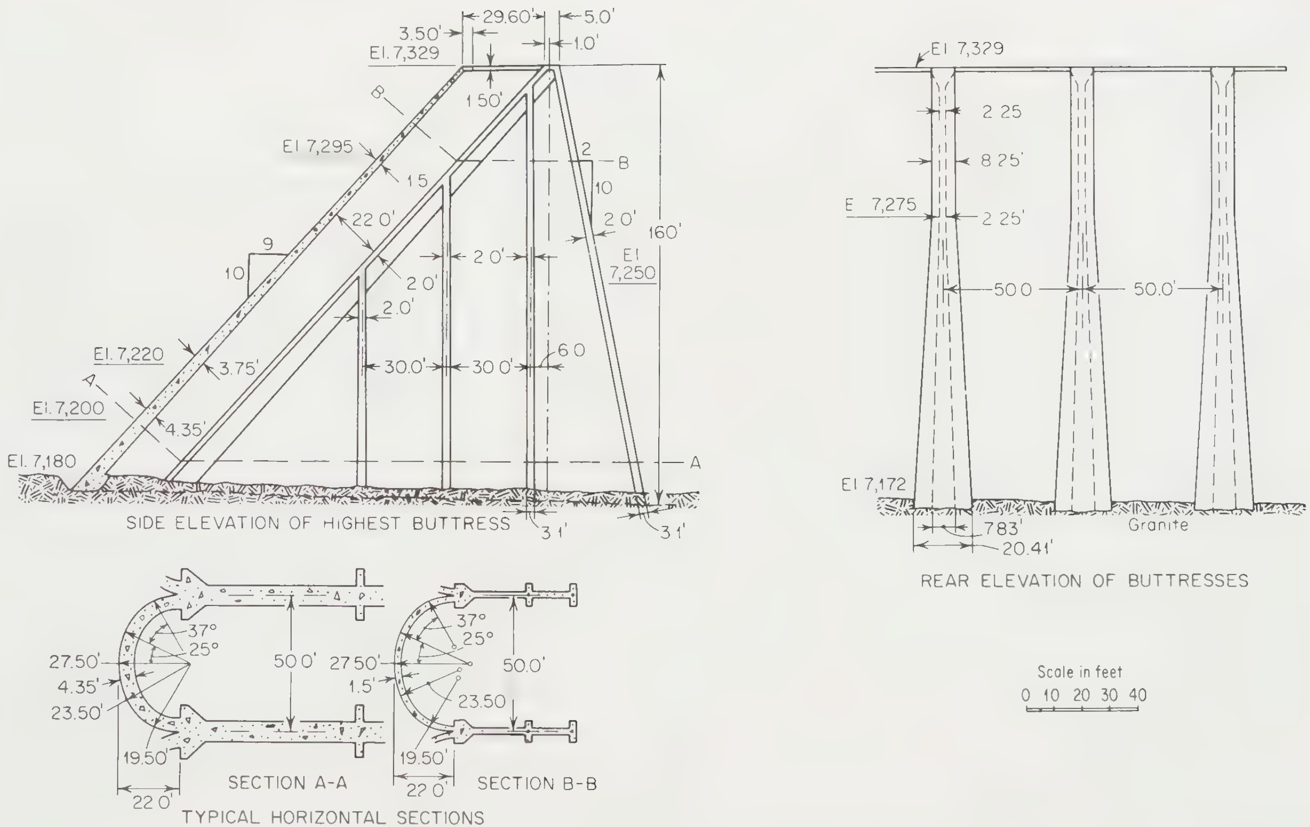

FIG. 2. The Florence Lake Dam.

The relative economy of using wide buttress spacings for dams over 200 ft high was also demonstrated by the 250-ft-high Coolidge Dam, a multiple-dome-type structure which was constructed on the Gila River in Arizona in 1928.[1]

The Coolidge Dam is a modified multiple arch. As shown by Fig. 5, the dam consists of two massive buttresses which, together with the abutments, support three

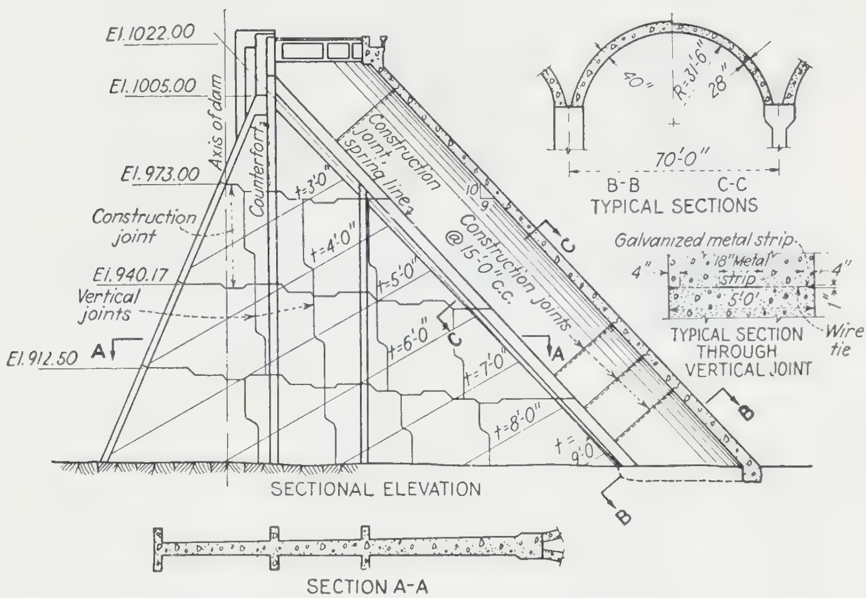

Fig. 3. The Buchanan Dam. Buttress elevation and sections.

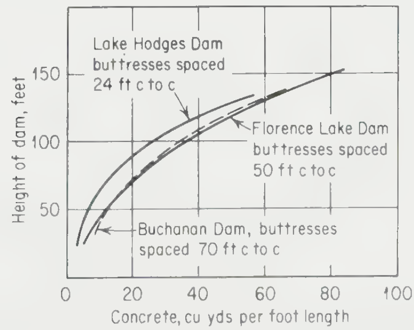

Fig. 4. Comparison of quantities (Figs. 1, 2, 3).

dome-type water-bearing members. The buttresses are spaced 180 ft center to center and vary in thickness from 20 ft at the top to 60 ft at a height of 250 ft. The domes vary in thickness from 4 ft at the top to 20 ft at a depth of 230 ft. Each buttress contains two inclined contraction joints positioned approximately along trajectories

[1] Features of Design, Coolidge Multiple Dome Dam, *Eng. News-Record*, Sept. 13, 1928. Wegmann, "The Design and Construction of Dams," 8th ed., p. 520, John Wiley & Sons, Inc., New York.

FIG. 5. Coolidge Dam, general view—multiple-dome type.

of first principal stress. The late Major C. E. Olberg, then Chief Engineer, U.S. Indian Service, demonstrated the following relationships between the multiple-dome and other structural types at the Coolidge site.

Type of dam	Relative cost, %	Relative volume, cu yd, %
Multiple-dome buttresses 180 ft center to center	100	100
Multiple-arch buttresses 60 ft center to center	102	67
Arched-gravity dam	120	192

It will be noted that buttress spacing had practically no effect on relative economy. It also could be stated, for estimating purposes, that although the arched-gravity dam had nearly twice the volume of concrete contained in the multiple-dome type, the relative saving in construction cost was about 20 percent. These relative savings, resulting from wide buttress spacings, compare very closely with those determined by the illustrative examples set forth in Sec. 9.

THE HOLLOW-BUTTRESS DAM

6. Development. The early, observable trend toward the use of wider spans, combined with the stiffening and bracing of the buttresses, led designers to attempt to minimize the volume of concrete further by developing the double-walled buttress with interior diaphragm bracing. The intent was to reduce buttress thicknesses to the absolute minimum required to take the maximum compressive stresses and at the same time provide adequate lateral stability. In an era of relatively low-cost formwork this feature helped to achieve overall economy. Almost concurrently, however, it was demonstrated by the designers of Coolidge Dam[1] and others that equal or greater economy could be achieved by the use of wide arch spans and massive structures.

[1] Features of Design, Coolidge Multiple-dome Dam, *Eng. News-Record*, Sept. 13, 1928. WEGMANN, *op. cit.*, p. 520.

The hollow-buttress dam was developed between 1925 and 1940. So far as is known, the Lake Pleasant Dam[1] completed in 1926 on the Agus Fria River was the first to be constructed. The maximum height is 250 ft and the overall length is 7,850 ft. The hollow buttresses, spaced 60 ft center to center, have a uniform distance between the outer faces of the walls of 16 ft. The side walls vary in thickness from 1 ft 6 in. at the crest to 5 ft 5 in. at a height approximately 50 ft above the lowest point in the foundations. The buttresses are stiffened by 16-in.-thick cross walls spaced 40 ft center to center and by intermediate struts between these walls. The arch barrel varies from 1 ft 6 in. thick at the crest to 5 ft 6 in. at the foundation line. Both arches and buttresses are reinforced.

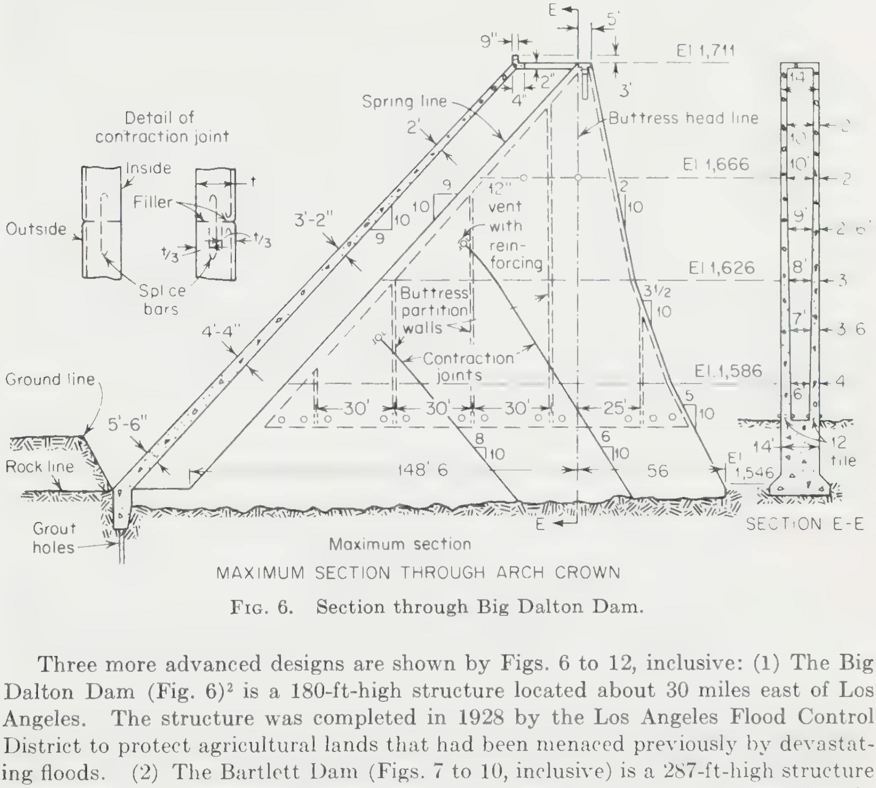

FIG. 6. Section through Big Dalton Dam.

Three more advanced designs are shown by Figs. 6 to 12, inclusive: (1) The Big Dalton Dam (Fig. 6)[2] is a 180-ft-high structure located about 30 miles east of Los Angeles. The structure was completed in 1928 by the Los Angeles Flood Control District to protect agricultural lands that had been menaced previously by devastating floods. (2) The Bartlett Dam (Figs. 7 to 10, inclusive) is a 287-ft-high structure built by the Bureau of Reclamation in 1939 near Phoenix on the Verde River in Arizona. (3) The Pensacola Dam (Figs. 11 and 12) is a 145-ft-high structure completed in 1940 by the Grand River Authority, on the Grand River near Vinita, Okla. The principal structure features and dimensions are shown by the illustrations. There are, however, important differences in the details which should be noted.

7. The Big Dalton Dam. The outer faces of the double-walled buttresses are 14 ft apart. These walls varied in thickness from 2 ft near the top to 5 ft near the base. Vertical stiffener walls 1 ft 6 in. thick spaced 30 ft center to center are provided between these walls. A concrete slab 2 ft thick closes the downstream end of the

[1] NOETZLI, FRED A., Multiple-arch Dams, Part 4, p. 499 in "The Design and Construction of Dams," 8th ed., by Wegmann, John Wiley & Sons, Inc., New York.
[2] *Eng. News-Record*, Dec. 26, 1929, p. 994.

buttress and provides additional stiffness. The buttresses are spaced 60 ft center to center. No additional bracing is required. Both the buttresses and the arches are reinforced.

A distinguishing feature is that two inclined contraction joints, paralleling trajectories of first principal stress under full load, are provided in each buttress. These

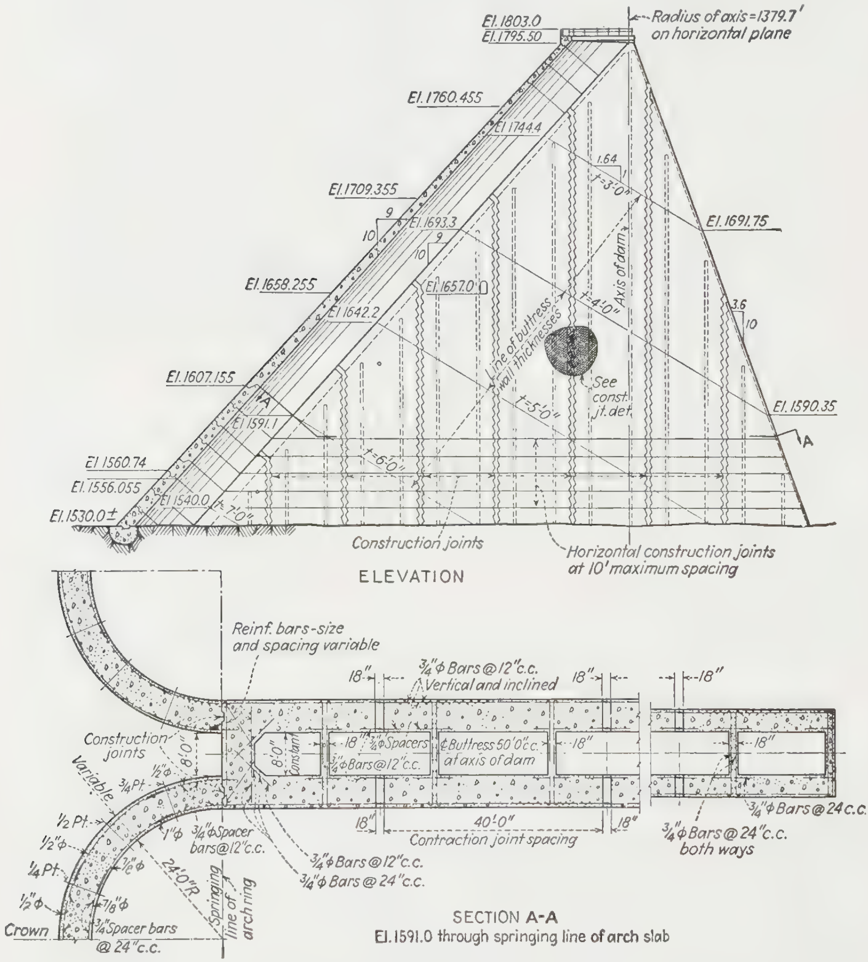

Fig. 7. Bartlett Dam, bulkhead buttress and sections (inclined faces in vertical joints).

weakened planes control buttress cracking. Two-thirds of the buttress thicknesses in the planes of the joints were separated by fillers. Reinforcing steel in the buttress faces was not continuous through the joints. Splice bars across the center of the joints were approximately one-half the area of the buttress reinforcement. Inclined contraction joints also have been used successfully in the Coolidge Dam and in other buttress dams built during this period. The merits of inclined contraction joints deserve consideration in the design of high buttress dams. There are minimum shearing stresses across these joints under full-load conditions and relatively light shearing stresses under partial-load conditions. The inclined columns, separated by the joints, are independently stable. For further discussion of joints of this type reference should be made to Sec. 13.

8. Bartlett Dam. Reference to Figs. 7 to 10, inclusive, will show interesting differences in details as compared with those of the Big Dalton Dam. The inside walls of the buttresses are vertical from top to bottom. To compensate for the decrease in arch resulting from buttress thickening and to simplify the arch formwork, the axis of the dam follows a curve with a radius of 1,379 ft. Buttress thicknesses vary from 3 ft near the crest to 7 ft at the foundation, with variations occurring on inclined planes having a slope of 1.64 horizontal to 1.0 vertical. Thus at the foundations, at maximum height, the buttresses taper and vary in thickness from 7 ft at the springing line of the arch to 4 ft 6 in. at the downstream face. Each buttress consists of a double wall separated by cross walls spaced 20 ft center to center.

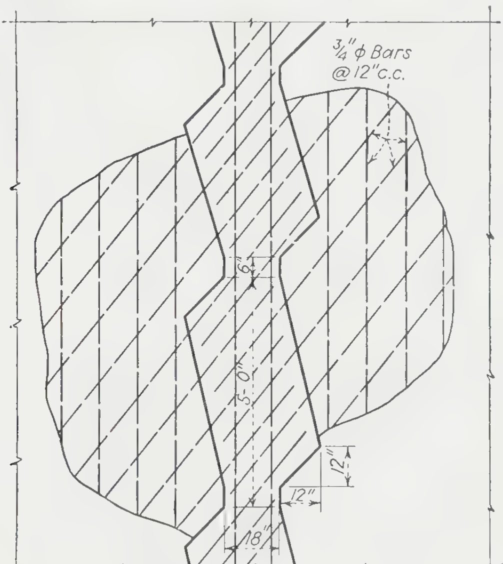

FIG. 8. Bartlett Dam, detail of vertical contraction joints.

Vertical, sawtooth contraction joints, spaced 41 ft 6 in., are provided in the walls as shown by Figs. 7 and 8. Filler pours separated by a maximum width of 1 ft 6 in. were provided between the joint faces. The planes of the sawtooth faces were placed alternately on approximate planes of first and second principal stress. This design is intended to combine the advantages of the inclined contraction joint, as described for the Big Dalton Dam, and the easier-to-construct vertical joint. The present trend is to control cracking by minimizing the number of joints and by depending to a greater extent upon temperature controls of both the aggregate and concrete.

The arch decks of the Bartlett Dam are formed, as shown by Fig. 9, to have a constant intradosal radius of 24 ft. These arches vary in thickness from 2 ft 4 in. at the crest to 7 ft 0 in. at the base. Both arches and buttresses are reinforced. Typical arch construction joints are shown by Fig. 9.[1]

[1] Building Bartlett Dam, World's Highest Multiple-arch, *Western Construction News*, November, 1938, pp. 389–395. KOPPEN, E. C., Building Bartlett Dam, *Construction Eng.*, The Reclamation Era, November, 1939, pp. 308–314.

9. The Pensacola Dam. The Pensacola Dam (Figs. 11 and 12) shows a third variation in detail. The designers recognized the economic advantages of wider buttress spacings as the hollow-buttress units are spaced 84 ft center to center. The maximum height is 145 ft. The constant buttress thickness, out to out, of the double-walled buttress is 22 ft at the arch springing lines, as shown by Fig. 12. The buttresses

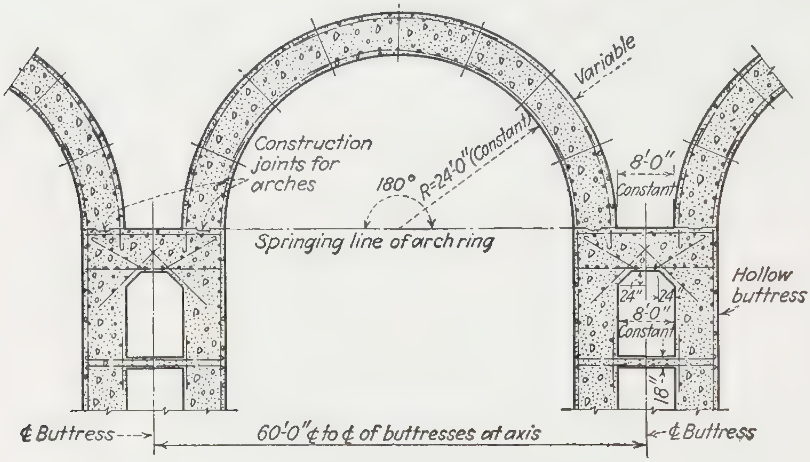

Fig. 9. Bartlett Dam, sections through arch.

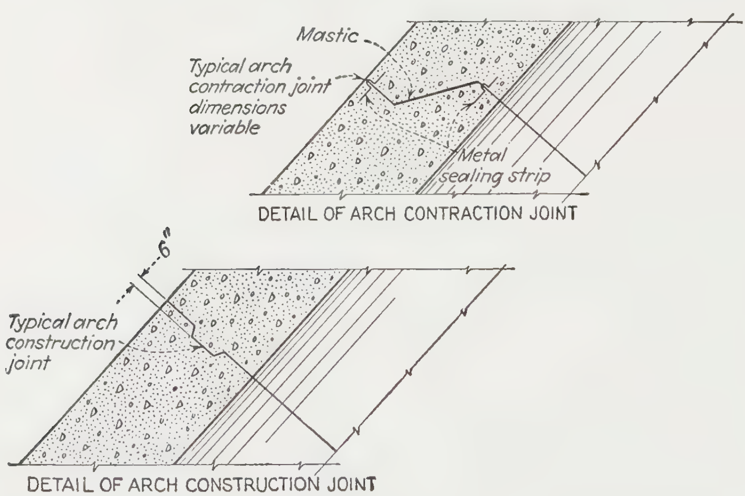

Fig. 10. Bartlett Dam, detail of arch construction and contraction joints.

vary in thickness from 2 ft near the crest to about 5 ft near the foundations. These variations occur along inclined planes sloping downwardly from the arch groin line on a slope of 1.5 horizontal to 7 vertical. The buttress side walls are braced by 1 ft 6 in. thick inclined cross walls spaced 28 ft center to center.

The cross walls are sloped as shown by Fig. 11. This arrangement provides, in effect, a series of inclined box columns which approximate in direction the columns

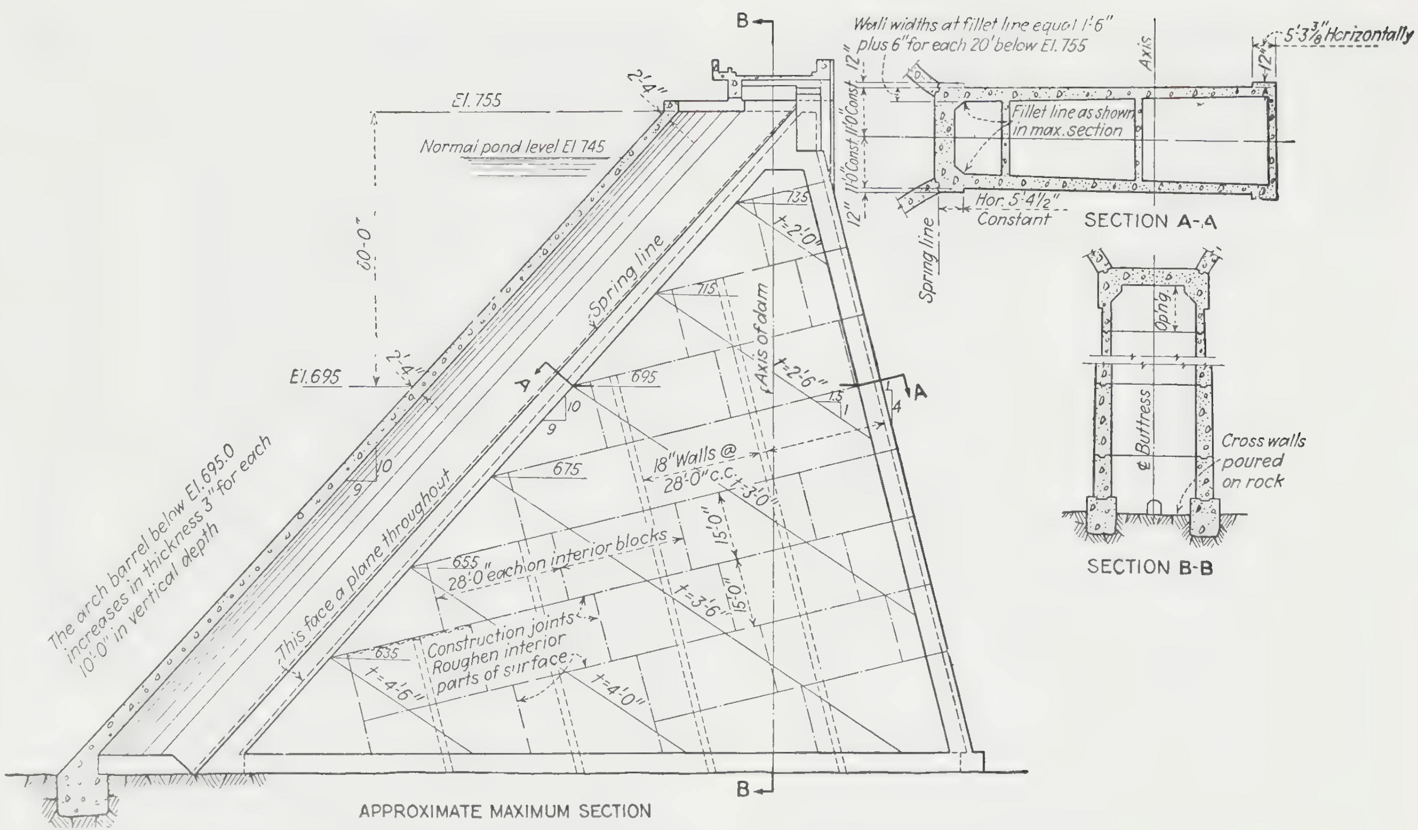

FIG. 11. Pensacola Dam, buttress elevation and sections (inclined joints).

created by the inclined joints in the Big Dalton buttresses. It will be noted that the Pensacola Dam combines some of the best features of both Big Dalton and Bartlett.

10. Structural Form as Related to Trends in Construction Cost. The precipitous rise in labor costs, following World War II, affected materially the cost of thin-walled buttress types. Even back in the 1920s and 1930s, as has been indicated elsewhere by Fig. 4, it was demonstrated that substantial savings in cost could result from the use of wide buttress spacings and relatively massive concrete sections. After 1940, few dams of either the Ambursen or multiple-arch type have been built with relatively thin concrete sections and close buttress spacings.

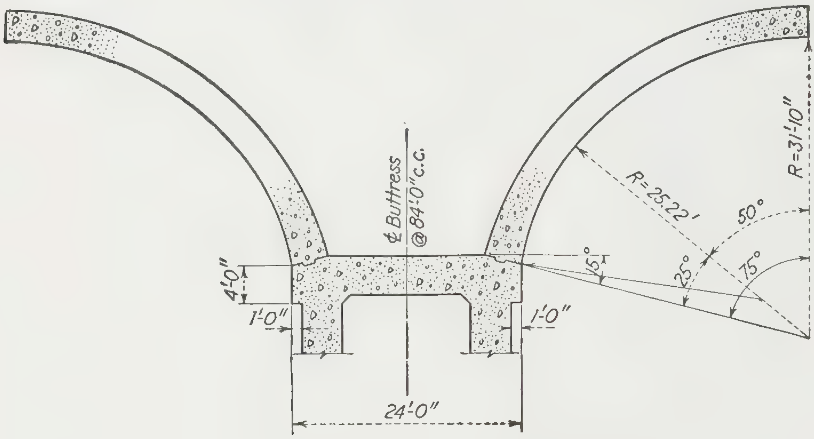

FIG. 12. Pensacola Dam, section through arch.

THE MASSIVE-BUTTRESS TYPE

11. The Modern Trend. Modern high multiple-arch dams are more massive than earlier structures of this type. Wider buttress spacings and thicker concrete sections bring together the inherent economy of the buttress dam with that of mass concrete construction.

Progress in multiple-arch design has been intermittent and sporadic. Great advances, made in the 1920s and early 1930s by such designers as the late Fred A. Noetzli and Major C. E. Olberg, went largely unrecognized for many years. The creative designs of the late Andre Coyne, Consulting Engineer, Paris, France, generated renewed interest in this type. The Coyne designs not only established firmly the economic merits of wide buttress spacing for multiple-arch dams having heights in excess of 150 ft but also introduced notable improvements in details.

To illustrate these more recent advances in design, two projects will be described: (1) the Grandval Dam,[1] 262 ft high, a multiple-arch structure built on the Truyere River in the mountains of central France, and (2) the nearly 700-ft-high Manicouagan 5 Dam[2] now being built by Hydro-Quebec on the Manicouagan River in the Province of Quebec. A brief description of each follows.

12. The Grandval Dam. This structure contains six inclined arches supported on seven buttresses spaced 164 ft apart. Figure 13 shows an elevation looking down-

[1] France's Newest Dam Has Novel Features, *Eng. News-Record*, Aug. 6, 1959, pp. 48, 49.

[2] JACOBUS, W. W., Hydro-Quebec's Big Beautiful Manicouagan 5 Hides in Bush, *Eng. News-Record*, Oct. 24, 1963, p. 38. The Manicouagen-Aux-Outardes Power Development, *Water Power Eng.*, October, 1964, p. 411.

stream and Fig. 14 shows an elevation looking upstream. The principal dimensions are shown by Fig. 15.

The arch thicknesses vary from 9 ft 9 in. at the crest to 14 ft 6 in. at the bottom. The buttresses, at maximum height, contain four inclined contraction joints which, in

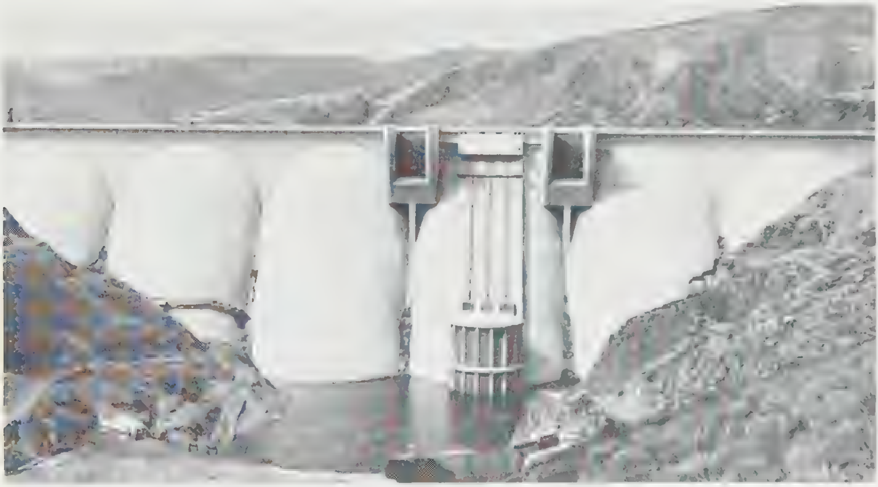

Fig. 13. Grandval Dam, view looking downstream.

Fig. 14. Grandval Dam, view looking upstream.

effect, create five contiguous, inclined columns. The downstream columns take the form of a variable-thickness flange or T section which is 18 ft thick at the top and about 32 ft at the point of maximum height. The remainder of the buttress is uniformly 18 ft thick.

Notable details of the Grandval Dam are the crests of the arches. Instead of being horizontal the slope downstream is at the same angle as the slope of the buttresses. The openings over the buttresses between adjacent arches are plugged with gravity section walls, as shown by Fig. 16, whose weight adds to the overall stability of the dam. Worthwhile savings in concrete result from this arrangement. The sloping crests impart a slight dome shape to the arches. As built, Grandval Dam required a

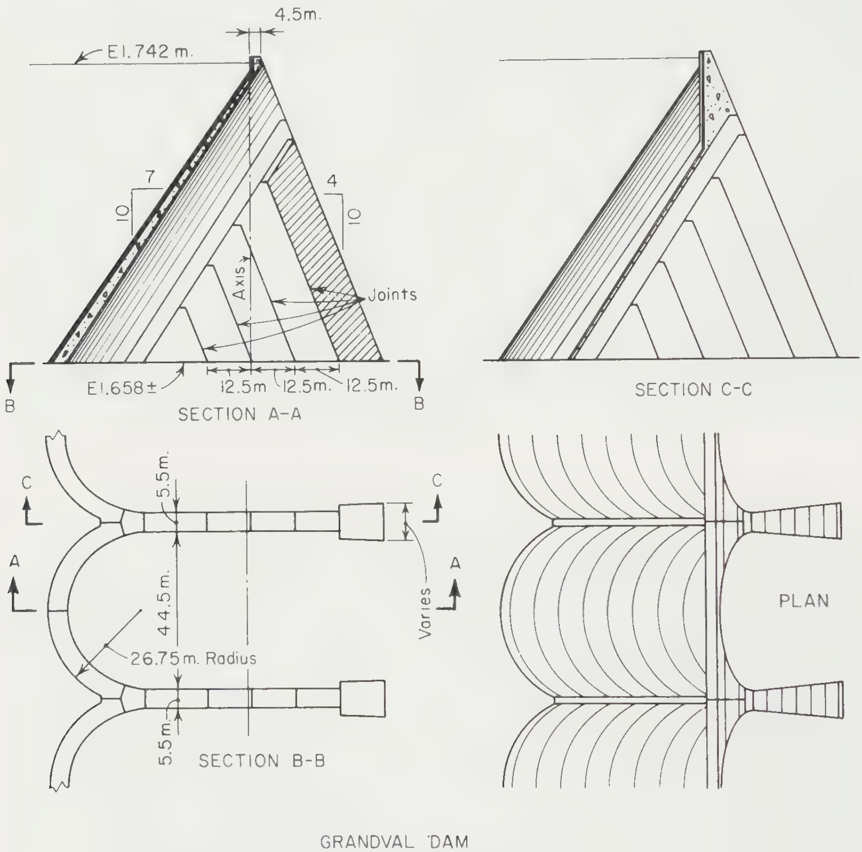

Fig. 15. Grandval Dam, sections.

total of 220,000 cu yd of concrete. This was about 37 percent of that required in an equivalent gravity dam. Only nominal reinforcing steel was used in the buttresses and arches.

13. The Manicouagan 5 Dam. This structure now (1968) under construction will be the highest multiple-arch dam in the world and the third highest dam of any kind in North America. Maximum economy was achieved by providing a large central arch supported by two massive buttresses that are oblique to the dam's axis. A general plan is shown by Fig. 17. The central arch has a span of 530 ft between buttress axes. The normal arches are defined by a cylinder on both downstream and upstream faces. This arch varies in cross-sectional thickness from 15 ft at the crest to 75 ft at the foundation. The slope of the upstream face of the arch and the downstream face of the buttress is 0.6. The main buttresses vary in thickness from 100 ft at the top to slightly less than 140 ft at the base. The cross-sectional thicknesses of the flanking multiple-arch spans vary from 10 ft at the crest to a maximum of 26 ft at the foundation line.

There is almost no reinforcing steel in the concrete arches. The monoliths have reinforcing only on the upstream and downstream faces to prevent hair cracking.

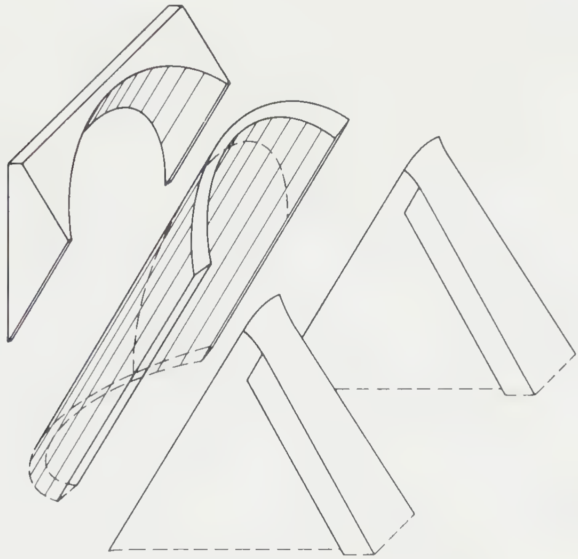

Fig. 16. Details of gravity crest.

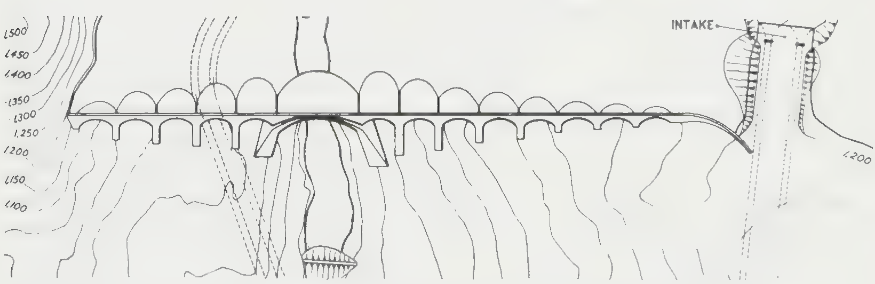

Fig. 17. Manicouagan, general plan. (*From The Manicouagan-Aux-Outardes Power Development, Part* 1, *Water Power, October*, 1964, *p.* 413.)

Where the arches and buttresses meet there is a mattress section of reinforcing steel that evenly distributes the load exerted by the arch between the buttress monoliths.

The relatively thin main arch and the two arches flanking it will be subject to stresses as high as 1,400 psi. The maximum stress in the remaining arches will be 700 psi.

Cooling coils cast in the monoliths control curing temperatures in the main arch dam and buttresses. Concrete specifications call for 4,500-psi concrete cast in 5-ft lifts in the side arches and 6-ft lifts in the main arch. Concrete temperatures are held at 55 F at the time of pouring.

DESIGN

14. Stresses. As pointed out in Sec. 9, many design criteria and designing methods are common to all the concrete types. Reference should be made to Sec. 9 for discussions of the classic design procedures which have been in use for many years and to Sec. 10 for the more recently developed finite-element method, which holds the promise of producing more realistic patterns of stress.

Reference should also be made to Sec. 13 for the techniques of stress analysis for determining the magnitudes and directions of first and second principal stresses and maximum shearing-stress intensities. The examples in Sec. 13 are based on rectilinear stress distribution. The method would apply, however, to any type of vertical normal stress distribution provided the variations could be expressed in mathematical terms. This method can be applied to both gravity and buttress dams.

The arches forming the upstream deck are subjected mainly to compressive stress and not to bending and shear stress. Therefore, these arches are largely in direct compression. The stresses in the arch barrels may be analyzed by the method of elastic analysis. Reference should be made to Sec. 14 for a comprehensive treatment of this method.

15. Stability. In common with other buttress dams the factor of safety of the multiple-arch dam against overturning usually falls somewhere between 3 and 4. There is no known record of any well-designed buttress dam having failed by overturning. Upstream buttress slopes as flat as 1 : 1 have been used to take full advantage of the stabilizing effect of the water load.

A word of caution must here be introduced. Flattening the upstream buttress slope beyond approximately 7 horizontally to 10 vertically has a tendency to introduce second principal stresses in tension in the buttresses. These tensional stresses attain maximum values just below the groin line of the arches. In this plane the first principal stresses are approximately parallel to the direction of the water loads.

As pointed out elsewhere, very little reinforcing steel is required in the buttresses and arches. It is good design practice, however, to place fairly heavy bands of reinforcing steel in the buttresses directly below the groin lines of the arches. This steel will help to distribute the tensional stresses which result from the longitudinal expansion of the arch barrels following a rise in temperature. These temperature stresses plus the tendency to develop second principal stresses in tension from loading may result in buttress cracking in this vicinity of the upstream face. When such cracks do form under maximum water loading as they did in the previously discussed Lake Hodges Dam, they usually follow roughly along a trajectory of first principal stress. In this case the dam can no longer be considered an integral structure but must be treated as a series of contiguous, inclined columns. The analysis of such columns is presented in Sec. 13. The same general method could be applied to multiple-arch dams.

Should tensional stresses near the upstream face occur when the reservoir is empty or only partially full, the resulting cracks may occur on vertical planes. In this case the contiguous columns, separated by the cracks, may not be independently stable. For these reasons designers in some cases, notably Coolidge, Big Dalton, Grandval, and others, have provided inclined contraction joints which, in a sense, have precracked the buttresses along planes which will not impair the stability of the structure.

As previously discussed in Sec. 9, little is known about the effect of the arch on the stability. If the arch is assumed to be supported on the buttress by a frictionless plane, then a large part of the weight of the concrete in the arch will be transferred to the foundation and in addition the arch will exert a horizontal overturning moment on the buttress. The mechanics of this action would be identical with that described for deck loads in Sec. 13.

If, however, the arch is completely integral with the buttress and is supported by appropriate joints and keys capable of transferring the deck loads to the buttresses, then the entire load of the arch and the vertical water load above the horizontal plane of analysis will act to stabilize the structure. A conservative procedure would be to design the structure to have acceptable factors of safety under each of these extreme conditions. If this procedure is followed the structure will be safe under all intermediate conditions.

Compressive stresses within the buttresses have not been a source of difficulty. These are within the control of the designer. Caution must be exercised, however, in the design of high buttress dams, when the first principal stresses in compression rise to somewhere between 500 and 700 psi. At these higher stresses maximum shearing stresses may rise to unacceptable levels. A comprehensive analysis should be made to determine the intensities, distribution, and directions of first and second principal stresses and maximum shearing stresses throughout the entire structure. The methods of analysis are discussed in Secs. 9, 10, and 13.

Safety against sliding is usually expressed in terms of the shear-friction factor of safety, as discussed in Sec. 9. For a sound rock design it is usual to provide at a given section a ratio of the sum of all horizontal loads to the sum of all vertical loads of 0.75. There are notable exceptions to this, however, as pointed out elsewhere.

The Cave Creek structure illustrates the importance of taking into consideration both shearing and frictional resistance to sliding. Ordinarily it is considered satisfactory if a multiple-arch dam has an overall shear-friction factor of safety which averages about 4. The average shear-friction factor of safety, however, may not be indicative of the actual factor of safety if there is a wide variation between the horizontal shearing stress, the vertical normal stress, and the actual shearing resistance of the foundation rock throughout the length of the base at the foundation line. It is important to come as close to uniformity as possible in the actual distribution of vertical normal pressures and shearing stresses.

In high multiple-arch dams the actual distribution of both vertical normal and horizontal shearing stresses may be curvilinear rather than rectilinear, as usually assumed. Furthermore, the elastic properties of the foundation rock may affect materially the patterns of stress distribution in the buttresses. For these reasons, the more advanced methods of analysis, supplemented by structural-model tests, must be used in designing high multiple-arch dam structures. For dams ranging in height up to approximately 250 ft the conventional trapezoidal law may be applied to stress analysis. Actual stress variation in medium- and low-height dams approximates linear distribution.

Uplift forces are usually not an important factor. Some uplift must be included under the surface of contact with the arches and in the upstream portion of the buttresses. The open spaces between the buttresses will prevent uplift from occurring within the buttress structures. It is good practice to provide drain holes between the buttresses extending at least 50 ft into the foundations. The extent of such drainage, of course, will depend upon the characteristics of the foundation material.

When the foundation structure consists of a continuous slab or monolithic concrete, uplift, of course, becomes a very important factor. At least one important failure has been attributed to this cause. The 143-ft-high Gleno Dam[1] built on the Oglu River at Darfo, Italy, was supported in a gorge by a concrete monolith which was subjected to full uplift pressures. The lighter multiple-arch structure and the vertical water load above this monolith did not possess enough weight to prevent a disastrous failure by sliding.

[1] Details of the Failure of an Italian Multiple-arch Dam, *Eng. News-Record*, Jan. 31, 1924, p. 182.

SECTION 16

PRESTRESSING IN DAMS

By O. C. Zienkiewicz

INTRODUCTION

1. Definition. Prestressing may be defined, in the broadest sense, as a controlled imposition of an initial state of stress on an unloaded structure which improves the final state of stresses under working-load conditions. Gravity stresses in a dam fall within the terms of this definition, and indeed suitable construction techniques may considerably improve the conventionally achieved stress distributions,[1,*] but within this section, consideration will be given only to prestressing induced by purely mechanical devices.

2. Methods. The mechanical methods of prestressing can be subdivided into two distinct categories: In the first, the force is applied to a tensioned steel cable, and

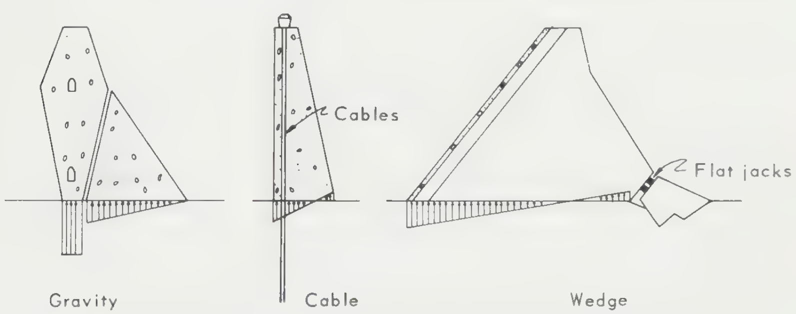

Fig. 1. Some methods of prestressing of dams.

it is this cable that maintains the prestressing force on the structure. In the second, no reliance is placed on steel and the jacking force is applied at some suitable internal point, the jack being then replaced by a "wedge" that maintains the imposed displacement. Both methods have their definite advantages, their own field of application, and, naturally, their opponents and advocates. Figure 1 illustrates some of the principles involved.

The method of prestressing by cables, which was originated by the late Andre Coyne in his, now classic, reinforcement and raising of the unsafe Cheurfas Dam in 1935,[2,3] has certainly a very wide field of applicability. The structural action is easily visualized, and it is probably true to say that in many practical cases it is the only possible solution for providing desirable initial stresses. The prestressing force, maintained by the elastic elongation of high-tensile steel cables, is not influenced appreciably by the creep of the concrete. On the other hand, the permanence of dam struc-

* Superior numbers refer to items in the Bibliography at the end of this section.

tures relying on steel reinforcement has often been questioned, and this may limit the range of application of the method until more experience is available. An additional drawback is the impracticability of applying very large forces necessary in high dams.

The "wedge" method of prestressing was originated by E. Freyssinet and first applied to the raising of the Beni Bahdel Dam in 1940.[4] Its application was essentially made possible by invention of the now famous "flat jacks" by Mr. Freyssinet. These jacks can be inserted in very narrow spaces (a few inches) and may, after inflation, be grouted to provide a permanent "wedge." Owing to the creep of concrete, which can reduce the prestress by as much as two-thirds of its initial value, several jacking operations are usually required and a suitable allowance must be made for future losses. This disadvantage combined with a particular type of buttress structure for which the method can be applied has somewhat limited its application in spite of the inherent advantage of no corrodible components. Two structures that are similar in type to Beni Bahdel have since been constructed, one being the Erranguene Dam and the other the Djen-Djen Dam.[5,6] The method can clearly be extended to arch dams in which grout under pressure or expansive cements could be used to provide the initial prestress.

In this section attention will be given only to the cable prestressing methods and the major part of the discussion will be focused on the design of straight, solid, or hollow dams.

GENERAL DESIGN OF PRESTRESSED DAMS

3. Design Criteria. A straight dam of solid or hollow section, in which prestressing is used, is subject to precisely the same forces as a similar gravity or buttress dam, and a reiteration of these here is not necessary. The essential design criteria are again of a similar nature and can be summed up as follows:

1. No tensile stresses in the concrete should be developed near the upstream face of the dam.
2. A certain amount of tensile stress in the concrete is permitted during the empty-reservoir stage at the downstream face of the dam. This tensile stress is to be limited to a reasonable figure of say one-tenth of the ultimate strength of the concrete. In some designs local reinforcement is introduced here to inhibit cracking.
3. Maximum compressive stresses in the concrete are not to exceed one-quarter of the ultimate strength of the concrete. (In computation of these, it is usual that the tensile resistance of the concrete is ignored.)
4. The cables should be securely anchored at a suitable depth to ensure safety against possible overturning.
5. Adequate safety factor against possible sliding or shear failure is to be ensured.

While the above conditions refer to the behavior of the dam under working-load conditions, additional requirements to ensure an adequate factor of safety against failure must be complied with.

4. The Dam Profile and Required Cable Forces. The principles governing the design of the profile and the determination of the required cable forces are similar to those used in the design of other prestressed-concrete structures as described in standard texts on this subject.[7]

To proceed with the determination of stresses in a typical profile some knowledge of the manner of stress distributions is required. Sufficient evidence from solutions based on the theory of elasticity is available to justify the usual assumptions of linear vertical stress distribution in the case of stresses caused by water pressures or gravity in the usual gravity- or buttress-dam profiles. This is true at least at sections of the dam some distance from the foundation level. When considering the stress distribution due to the prestressing force similar reasoning can be applied. For example, the exact elasticity solution available for an infinite wedge with a concentrated force at its apex is shown in Fig. 2 in which the distribution of vertical stresses is plotted on a typical section. This shows very small departures from linearity. Other elastic solutions for trapezoidal sections derived by Galerkin and summarized in Ref. 1 reinforce the validity of extending the usual "engineering" theory of bending to the case of prestressed dams.

The required cable force for a dam of an arbitrary profile can now be derived so as to satisfy the criteria of safety 1 to 3 with due consideration to criterion 5, which is usually expressed in terms of a permissible "friction coefficient" known as the "sliding

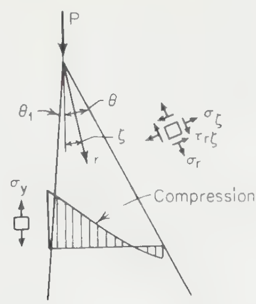

General solution

$\sigma_\zeta = \tau_{r\zeta} = 0$

$$\sigma_r = \frac{P}{r}\left\{\frac{[2(\theta+\theta_1) - \sin 2\theta - \sin 2\theta_1]\cos\zeta + [\cos 2\theta - \cos 2\theta_1]\sin\zeta}{\sin^2(\theta+\theta_1) - (\theta+\theta_1)^2}\right\}$$

FIG. 2. Wedge solution.

factor" f, such that

$$f \geq \frac{\text{sum of horizontal forces}}{\text{sum of vertical forces}}$$

acting on a section under consideration. Values of f similar to those used in gravity-dam design are usually adopted.

The problem of complying with requirements 1, 2, and 3 is illustrated in Fig. 3. In the simple profile shown, the forces P, W, U, and H represent, respectively, the prestressing force, weight of the dam, uplift force, and the external water thrust. If no prestressing force were present, calculations identical to those used in determining stresses in a gravity dam would result in the vertical stresses shown in Fig. 3*a* and *b* for the reservoir full and empty conditions, respectively. Similarly, the stresses due to the prestressing force are calculated and shown in Fig. 3*c*. Addition of these stresses results in the final distributions of vertical stresses shown in Fig. 3*d* and *e*. In the first of these, the design criteria require that

$$-(\sigma_y)_A \geq 0 \tag{1}$$

$$-(\sigma_y)_B \leq \frac{-\sigma_C}{1+n^2} \tag{2}$$

in which $-\sigma_C$ is the permissible compressive concrete stress. The second, i.e., the reservoir-empty condition, requires that

$$-(\sigma_y)_A \leq -\sigma_C \tag{3}$$

$$(\sigma_y)_B \leq \frac{\sigma_T}{1 + n^2} \tag{4}$$

in which σ_T is the permissible tensile stress.* The quantity $1/(1 + n^2)$ occurring in

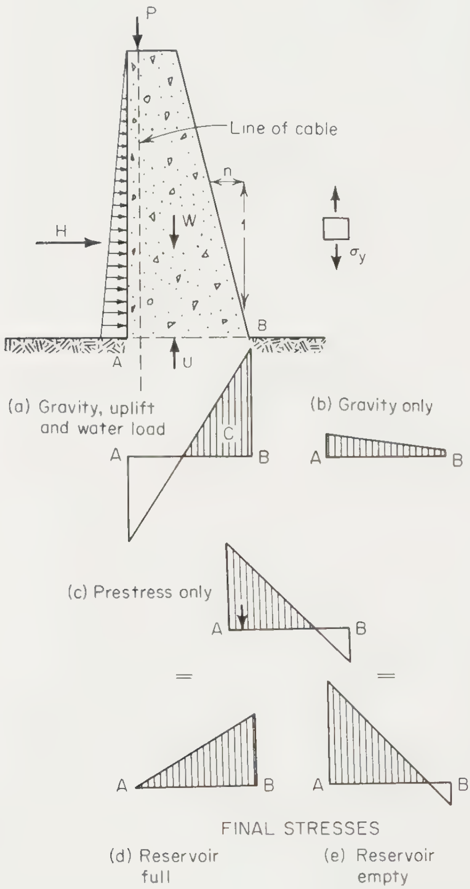

Fig. 3. Stresses on a horizontal section AB of a prestressed dam (compression areas shaded).

the above relations represents the ratio of the vertical stress component to the maximum principal stress on the downstream face.

It will be found generally that for small heights of the dam relation (1) will be the determining factor and the cable placed as close to the upstream force as possible will require the minimum force. For greater heights, however, condition (4) will place a limitation on the maximum cable force which may not be compatible with (1), and in such cases the cable has to be placed farther away from the upstream face to satisfy

* The usual convention of labeling tensile stress as positive necessitates the minus signs.

simultaneously both requirements. It is only for fairly high structures that relations (2) and (3) will govern the design.

While in all cases the sliding factor should be checked, it will usually be found that this exceeds that obtainable in an equivalent gravity profile and thus is seldom the determining factor for design.

The procedure outlined above is typical when the minimum required prestressing force is sought for ensuring the stability of an existing structure or when a dam is being raised by a simple addition to its height. If a profile is to be designed a priori to give the most economical structure the degree of freedom of the designer is much greater and a systematic investigation of alternatives must be undertaken. Such an investigation clearly invokes the relative costs of prestressing and mass concrete, and the possibility of using more than one line of cables to reduce the downstream tensions must be considered. Local conditions and designer's preference may lead to such a variety of profiles adopted as are illustrated in the section dealing with examples. Analytical studies of the economy of profiles are presented in Refs. 8, 9, and 10.

5. Depth of the Cable Anchorage. While the determination of the required cable forces discussed in the previous section presents no difficulties and can be dealt with rationally on the basis of the conventional beam theory, the question of the depth at which the cables are to be anchored in the rock is more complex.

In all cases, the dam is an essentially post-tensioned structure and there is a definite zone in the foundation to which the cable has to be attached while the stressing operations are in progress. Even if the cable is subsequently grouted, the major part of the transfer of the force from the cable to the rock occurs in the initial anchorage zone. Naturally, the anchor itself has to be so designed that pullout is impossible. This localized problem, to be discussed in the next section, does not influence, however, the decision regarding the depth at which this anchorage has to be placed. The rationale of the so-called "wedge theories" advanced from time to time, in which the cable wire is to be balanced by a certain weight of the overlying rock, is misleading in its concept as clearly it is possible, if not generally useful, to anchor the cable at any point of its length without incurring the pullout condition. The decision on the depth of the anchorage has, therefore, to be arrived at by other considerations. One obvious requirement is that previously stated as design criterion 5, *i.e.*, the requirement of overall stability of the dam and its foundation against overturning. An additional condition, which will later be seen to be automatically satisfied in most cases, is that the point of anchorage should be at a sufficient distance from the dam base to permit a stress distribution compatible with the assumption made by the conventional bending theory to be achieved. For example, an anchorage at the foundation level would obviously produce a very nonlinear stress distribution at all dam sections adjacent to it.

To answer some of the questions raised above, a more detailed method of stress analysis is required. A complete stress analysis based on the elastic two-dimensional behavior has recently been carried out by Zienkiewicz and Gerstner.[11,12] Although it is impossible and indeed unnecessary to go over the details of this solution here, some of its results are summarized in Figs. 4 and 5. In these the full stress distribution on various sections of the dam and its foundation is presented for two different depths of anchorage under the action of full water pressure.

The nonlinear distribution of the vertical stresses on the base section in the shallow anchorage is now evident as well as the rapid improvement in this distribution occurring when the anchorage is placed at a depth slightly exceeding the width of the dam base. As in most cases this depth at least is required, it is seen that the validity of the conventional assumptions even near the base of the dam can be taken to hold without much error.

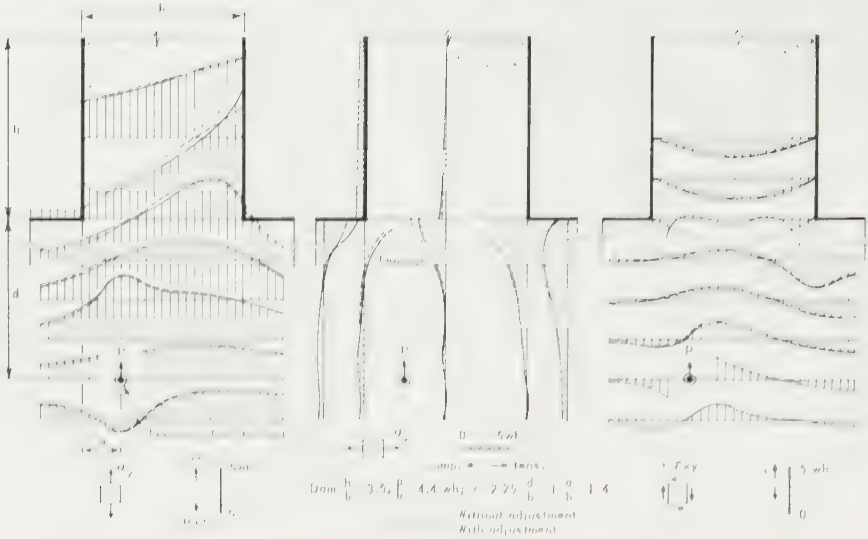

FIG. 4. Stresses near the foundation due to prestress, gravity, and water load (anchorage at depth = base width).

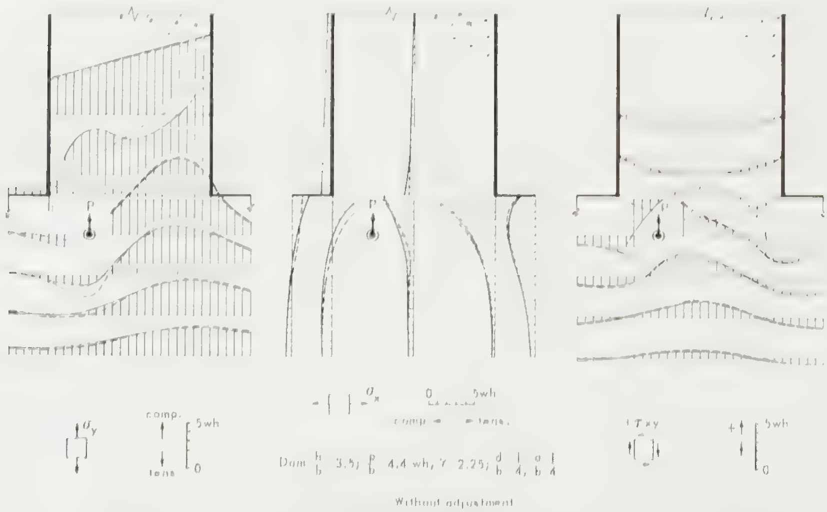

FIG. 5. Stresses near the foundation due to prestress, gravity, and water load (anchorage at depth = one-fourth base width).

While the distribution of vertical stress components presents an intuitively predictable picture, the occurrence of certain tensile regions within the foundation is less obvious. In Figs. 6 and 7, a more graphic presentation of the principal stresses and their trajectories is given. From these and also the preceding diagrams, it can be observed that tensile stresses tend to develop in all cases immediately below the anchorage. This will obviously tend toward opening up of fissures in the rock in the

FIG. 6. Principal stresses and their trajectories for case illustrated in Fig. 4.

FIG. 7. Principal stresses and their trajectories for case illustrated in Fig. 5.

vicinity of the anchor, which, however, by itself, is not a dangerous situation. Once this crack has opened up a short distance, a redistribution of the stress will occur which, combined with the stresses due to the weight of the rock, may still lead to a stable situation. In addition it should not be overlooked that in practice the cable load is transferred along an appreciable length and not at a point, a fact which will tend toward reducing the stresses from those of the idealized analysis.* However, the occurrence of tensile stresses at the upstream corner of the dam foundation and indeed along a large length of the line connecting this to the anchorage point is a more serious situation. A local weakness in the rock will initiate cracking which can proceed along the whole of this line as sufficient compressions do not exist in either of the cases illustrated to counteract the spread of this. In fact, the crack once opened permits an easy ingress of water under pressure, and failure can proceed further unless the resultant forces ultimately produce some compression to be overcome as is the case with deeper anchorages.

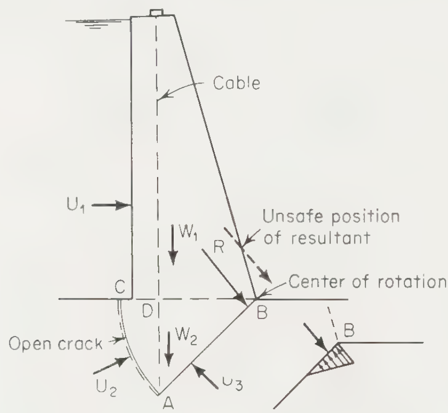

FIG. 8. A safety criterion.

The following conclusions result from the above discussion: either

1. Sufficient depth should be given to the anchorage to reduce the tensile stresses in the rock throughout to small or zero values; or
2. The design of the dam is made consistent with an ultimate behavior analysis which, while permitting a certain amount of cracking to occur, ensures a positive factor of safety against failure.

While the first criterion could be satisfied only by a somewhat elaborate stress analysis on the lines indicated in Ref. 11, it is possible to develop a rational design on the basis of a study of the possible ultimate behavior.[11] An outline of this procedure is given in Fig. 8. From point B, the downstream corner of the foundation, draw an arc AC passing through the anchorage point A. The position of point C will in general lie outside the upstream foundation corner D at which the highest tensile stresses tend to exist, but nevertheless the line AC will correspond approximately to the possible crack position. Assuming this line to correspond to an open fissure, *i.e.*, allowing full hydrostatic pressure to be developed along it, compute the effective uplift forces U_2 and U_3 acting along AC and AB, respectively (for calculation of the latter a linear decrease of uplift pressure between A and B can be assumed). Computing the

* That such cracks occur in actual practice is manifested by the additional grout absorption noted when grouting is carried out after the prestressing operations.

remaining forces acting on the dam and the portion of the foundation BAC, *i.e.*, the external water pressure on the upstream force U_1 and the weights of the dam and the portion ABC of the foundation W_1 and W_2, the magnitude and the position of the resultant force R acting on the section AB can be determined. Clearly if this falls outside the point B reliance must be placed on tensile stresses acting along AB, and stability is therefore endangered. The only possibility of resisting the overturning forces entirely by compressions is if this reaction R falls within the length AB, even so admitting a certain amount of cracking along this length if the reaction is close to this point B.

To ensure a certain factor of safety it is necessary to arrange the anchorage at such a depth that the reaction R passes well within the section AB. If the stresses occurring on the section AB are computed according to some reasonable assumption, such as linear distribution, and the maximum value of the principal stress is found to fall within permissible limits for the foundation material, an adequate factor will be assured. In this calculation, no allowance should be placed on tensile stresses and the section AB should be permitted to crack as far as is required.

The outlined method of analysis is somewhat similar to procedures used in earth-dam stability investigations. A criticism may be raised that AC does not represent the most obvious line at cracking; however, a consideration of the possible mechanism of failure will convince the reader that a crack along the line connecting, for instance, A to D would not permit overturning without calling in other resisting forces. The somewhat unpredictable nature of foundation rock and its initial state of stresses makes the above a reasonable and safe design guide. It is interesting to note that some model tests of a prestressed dam on a noncohesive granular foundation and others on test dams anchored into rock which were carried out in connection with the design of the Catagunya Dam[10] have indicated failure patterns somewhat similar to those assumed in the above analysis.*

The procedure outlined above has the merit of an easy extension to hollow or buttress sections. In Figs. 9 and 10 a design of an intake structure for the Wanapum Dam on the Columbia River is illustrated. The relevant forces, the magnitude of the resultant, and the estimated extreme stresses are shown here.

THE CABLE AND ITS ANCHORAGE

6. Types of Cable. In the general context of this section the term "cable" has been adopted to describe the prestressing member. Inspection of Table 1, in which some examples of prestressed dam construction are summarized, will show that in some cases the term "bars" would be more suitable to describe the elements, which are sometimes as thick as 1⅛ in. diameter. It is, however, a generally preferred practice to use smaller-diameter strands (5 mm or ¼ in.) in appropriately greater numbers. The reasons for this are several:

1. Greater flexibility of the cable, permitting the handling of complete lengths without couplings, which are always a potential source of weakness
2. Greater ultimate strengths available in cold-drawn wires than in larger-diameter sections
3. The decreased possibility of failure if corrosion attack on a single strand should occur
4. Smaller bond-length requirements in the anchorage zone

* The tests with an entirely noncohesive foundation show that in fact some passive resistance of the material increases slightly the failure load from the one which could be predicted by the above analysis. In the tests carried out on a larger model (of some 5 ft base width) anchored to solid rock, much larger failure loads were obtained, as indeed could be expected, but the general pattern of cracking observed followed the predictions made here closely.

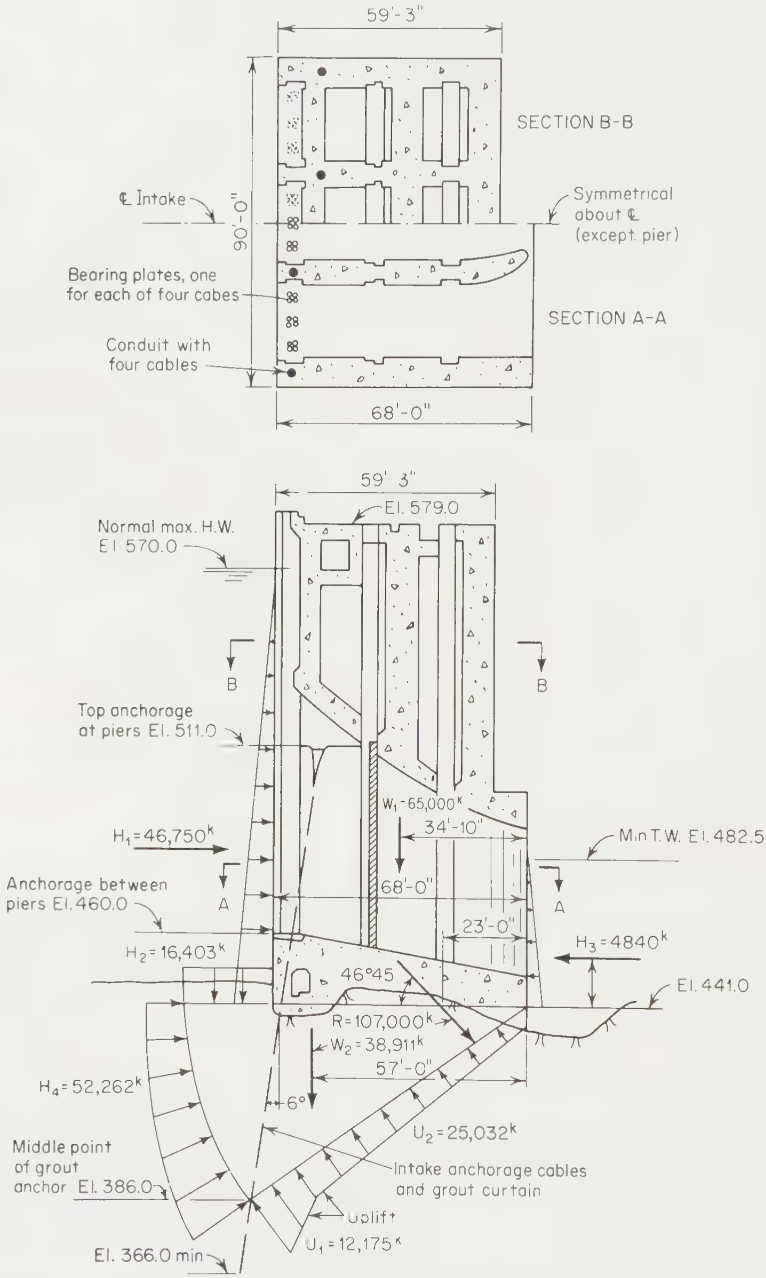

FIG. 9. Wanapum intake structure (Columbia River, 1961) and the stability considerations.

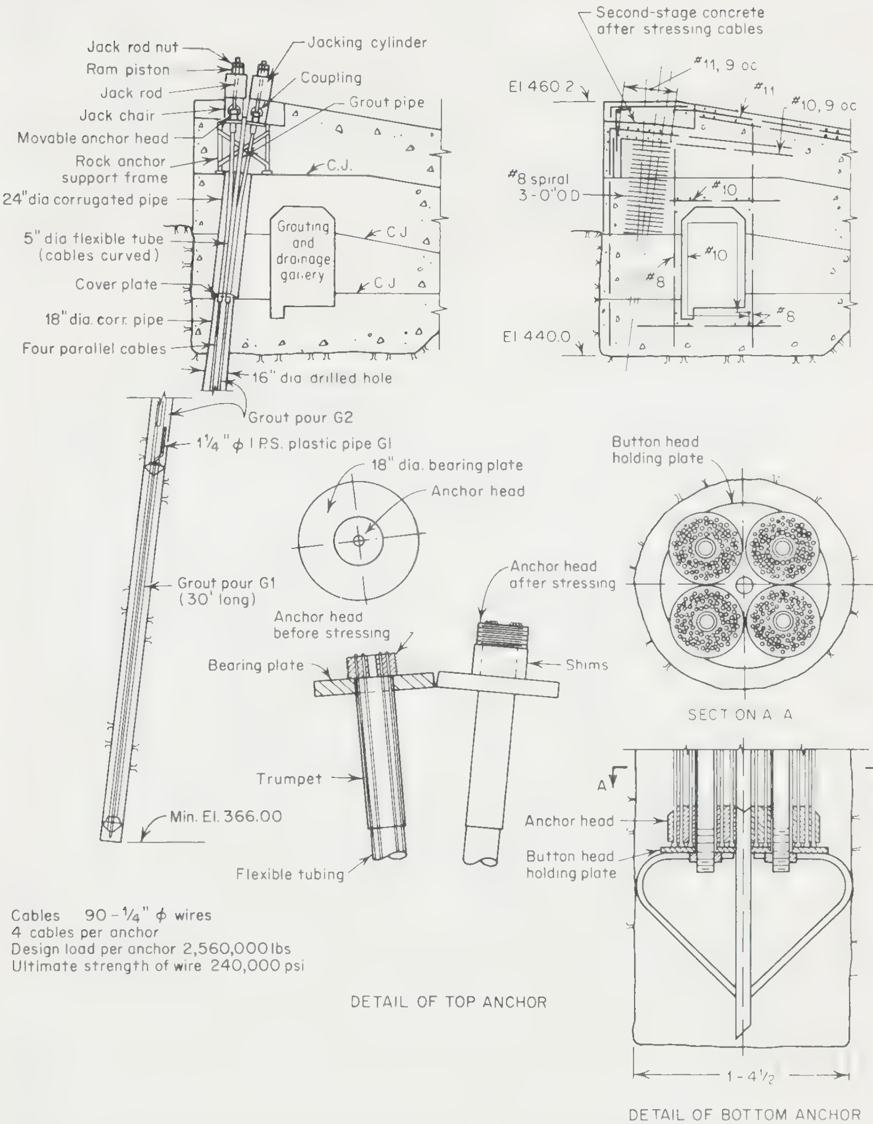

FIG. 10. Wanapum intake structure. Details of the cable and its anchorage. Installation procedure: *A*. Drill hole at foundation level. *B*. Form hole in concrete. *C*. Lower complete cable unit into hole and support from rock anchor support frame. Make grout pour GI and remove plastic pipe GI. *D*. Concrete 5-in. flexible conduits in formed hole. Enclose support frame. *E*. Stress cables. Place split ring shims. Remove jacks. Make grout pour G2.

TABLE 1

Name and country	Year of construction (c) and prestress (p)	Height (raising), ft	Cables				Reference	Remarks
			Duct size, in.	Composition	Force, tons per cable (max)	Force, tons per ft of dam		
Cheurfas (Algeria)	1882 (c) 1935 (p)	105 (10)	10 ϕ	630 wires at 0.197 in. ϕ	1,000	77	3,18	Strengthening and raising
L'Oued Fergoug (Algeria)	1873 1934 (p)	100	9–10 ϕ	Wires at 0.197 in. ϕ	125–285	22	18	Reconstruction after failure (1927)
Mareges (France)	1935	50	10 ϕ	555 wires at 0.197 in. ϕ	900		18	Wing of an arch dam
Tansa (India)	1892 (c) 1951 (p)	188 (2)	$2\frac{1}{2}$ ϕ	37 wires at 0.197 in. ϕ	70	25	17,8	Strengthening and raising
Steenbras (South Africa)	1921 (c) 1954 (p)	100 (6.5)	$2\frac{1}{2}$ ϕ	37 wires at 0.197 in. ϕ	77	20	7	Strengthening and raising
Henley (South Africa)	1958 (p)	(23)					20	Strengthening and raising
Gafarsa (Ethiopia)	1910 195(?)	35 (19)			70		25	Strengthening and raising
L'Oued Mellegue (Tunis)	1957	56	16 ϕ	610 wires at 0.197 in. ϕ	1,200	67	8,18	New dam
Jeux (France)	1905 (c) 195(?) (p)	(11)	12 ϕ		1,200		25	Strengthening and raising
Allt na Lairige (Scotland)	1957	73	48 × 28 shaft	28 bars at 1.125 in.	1,176	56	19,20	New dam
U.S.S.R.		80	16 × 24	10 bars at 1.4 in. ϕ	187		27	New dam
Howden (England)		(23)	16 ϕ		1,400		15	Strengthening and raising (proposed)
Ernestina (Brazil)	1954	50′		Freyssinet cased cables 12 at 0.197 in.			5	New dam
Catagunya (Tasmania)	1961	150	4 ϕ	102 wires at 0.2 in.	200	160	10	New dam

The size of the complete cable is governed by the total prestressing force required per unit length of the dam and the maximum spacing between individual cables required to approximate the design assumption of a line load. No hard-and-fast rules fixing this maximum spacing are available, but clearly this should be considerably less than, say, one-fourth the height of the dam, although, subject to a detailed stress analysis, such a requirement may be violated. The maximum sizes of cables placed in one duct to date appear to be those in the Wanapum intake structure on the Columbia River (Fig. 10) and in the Howden Dam. In both cases, the complete cable taking some 1,200 tons is accommodated in a 16-in. hole. Again the inspection of Table 1 will show the range of variation of the cables and of the duct sizes.

7. The Cable Ducts. In applications of prestressing to the raising of existing dams it is clear that drilling provides the only practicable method of constructing the cable duct and anchorage. Holes up to 4-in. diameter are usually drilled by percussive means to depths up to 200 ft. For larger-diameter or deeper holes, rotary drills of various types are preferred. As straightness of the hole is essential, great care has to be taken in the process, and if difficult rock strata are encountered it is necessary to use rotary drills even for smaller-diameter holes, as was the case in the Steenbras Dam.[14] It is generally felt that percussion-drilled holes provide a better bond than those resulting from rotary drilling, and site pullout tests should be carried out in most cases.

In new construction use has been made of excavated pits for the anchorage of the cable (Allt na Lairige[19,20]), but this practice has not been followed since. It appears that the practice of preforming the holes through the concrete of the dam and subsequent drilling through the foundation is the most advantageous.[10]

8. The Anchorage. The satisfactory anchorage of the cable in the foundation rock is one of the first problems to be overcome by the constructor. In the anchorages a transfer of stress from the steel through the surrounding concrete to the rock has to be effected. The first stage, that is, that of transference of the stress to concrete, can be accomplished by direct bond, and this appears to be the method originally used at Cheurfas and practiced most frequently. The provision of suitable mechanical anchorage devices is more difficult to accomplish and is adopted only where direct access to the anchorage zone is possible.

In the anchorage by direct bond the commonly adopted procedure is to feed the cables into grout previously deposited at the bottom of the anchorage hole. To ensure grout of good quality and a low water-cement ratio pregrouting of holes to reduce water infiltration and the deposition of grout in a hole previously filled with water are considered to be good practices.[14,15,10] The efficiency of such an anchorage is determined by a direct test. It was found by experiment that a length of about 2 ft is necessary for the anchorage of 5-mm wires in a cable with a 77-ton load anchored in a 2½-in.-diameter hole.[14] To provide a margin of safety, lengths of anchorage varying from 6 to 40 ft have been used.

A recently introduced system of anchorage using cold-formed buttons at the ends of the wires and anchor plates is shown in Fig. 10. Tests carried out on a trial anchorage with the wires embedded in approximately 38 ft of cement pozzolan grout showed no signs of failure with loads close to the ultimate strength of the wires.[13]

It should be noted here that the bond situation existing in an anchorage is less satisfactory than that in the so-called "pretensioned" system of prestressing. The application of the prestressing forces to the wires after these have been encased in the surrounding grout tends, by reducing their diameter because of the Poisson effect, to destroy the bond. The usual practice of regrouting of the cables after completion of the prestressing operations is to be recommended. If some slippage should occur the stresses will be transferred to a portion of the cable immediately above the original anchorage, now under more favorable circumstances as a certain expansion of the wire due to its decreasing tension will ensure a positive wedging action.*

The prestressing load transferred now to the surrounding grout must in turn be transmitted to the rock foundation. In the earliest examples an enlargement of the lower portions of the duct was executed to ensure a mechanical wedge (Fig. 10); it is more economical, however, to use holes of a constant diameter and rely entirely on the friction and certain wedging action developing on the walls of a simple concrete plug.

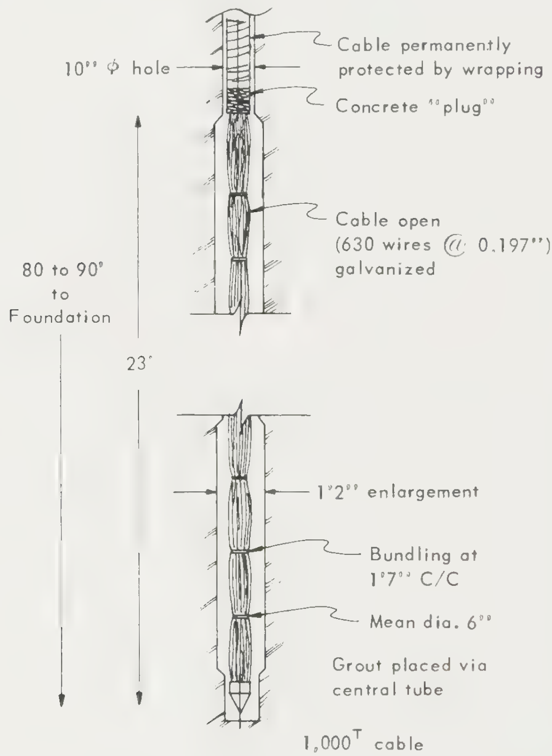

FIG. 11. Rock anchorage. Detail of cable at Cheurfas Dam (Algeria, 1935).

Percussion-drilled holes give a very good bond, but even with other methods of drilling a roughness seems to develop which apparently is always sufficient to prevent the pullout of the whole plug. An approximate method of determining the length of the plug is to assume that the shear stress on the walls of this does not exceed a certain safe value, usually assumed in the range of 150 to 250 psi.

As all the anchorages are effectively tested during the prestressing operation and are subsequently grouted a very large factor of safety against pullout exists.

9. Stressing the Cable. The stressing of the cables is generally one of the last construction operations to be carried out. The upper cable end is anchored into a suitably reinforced head block and stressed by insertion of jacks, which are replaced as

* The transfer of stress from the wires to the grout cannot be effected abruptly. A certain length of the wires is obviously involved in which gradually decreasing stresses will develop. The tests on the Wanapum anchorage[13] showed that there, with a ¼-in. wire, lengths up to 14 ft may be involved.

the elongation proceeds by steel or highly reinforced concrete packing wedges. Suitable reinforcement is required near the area of such an anchorage to prevent a local failure. In Fig. 11, detail of a typical stressing head is shown. An alternative arrangement, whereby the cables are stressed in pairs, avoids some of the anchorage problems. Such a scheme was used in the raising of the Steenbras Dam,[14] and the detail is shown in Fig. 12. Some other less orthodox arrangements which have been used are shown in Fig. 13. As in all prestressed construction, the possibility of relaxation of the initial prestress has to be allowed for. The relaxation is due primarily to the creep of concrete, which behaves under stress like a viscoelastic material,

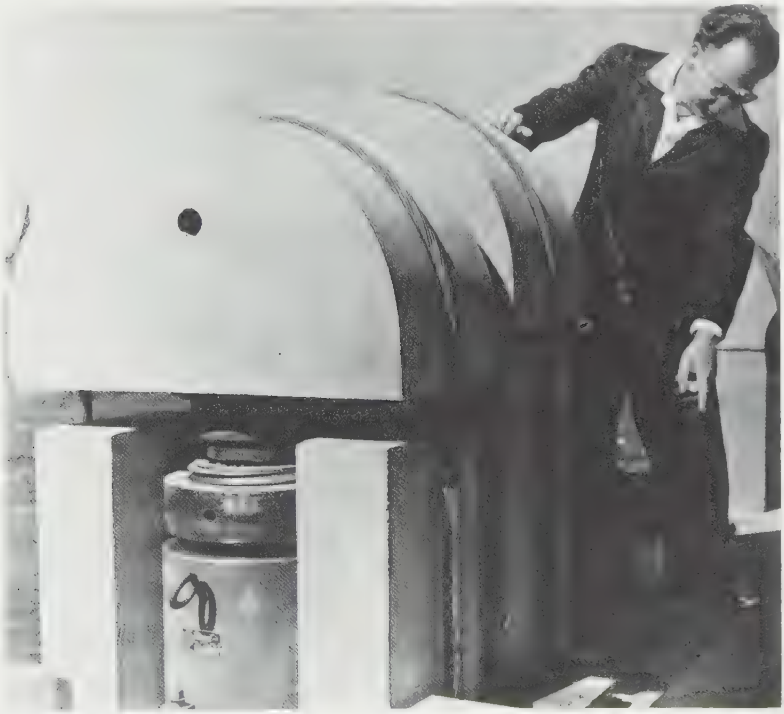

Fig. 12. Prestressing heads and jacks used at Steenbras Dam (South Africa, 1955).

and secondly to the creep of the steel itself. Allowance for these effects has been theoretically considered. R. Priscu and M. Constantinescu[9] computed a 9 percent ultimate prestress loss due to the creep of concrete (under the action of its own weight and the prestressing force) in a specific example of a dam some 120 ft high. In Allt na Lairige dam an allowance of 10 percent for prestress loss was made in the design. Similar allowances are usually adopted.

In most of the specifications applied to prestressed dams, a requirement of retesting the initial tension after a certain time lapse after prestressing has been included. It appears, however, that in no case was any detectable loss of prestress found with times varying from 28 days to 3 months. The tests on Cheurfas Dam show a relaxation of some 4.5 percent after a period of 9 years, with 4.0 percent occurring during the first

3 years. One could conclude from this rapidly decreasing rate that an allowance of 10 percent would be on the safe side.

10. Protection of the Prestressing Steel. The suitable protection of the prestressing steel against possible corrosion is clearly the crucial problem on which the feasibility of prestressing must depend. Inadequate protection at any point of the lower part of the cable may cause a failure, and this possibility is considered by some as precluding the use of prestressing in structures which must be able to perform their function for a considerable time.

It would doubtless be desirable to develop methods of suitable instrumentation by which the state of the cables at any time would be checked. This subject by itself forms a profitable field of research, and it is hoped that more work in this direction will soon be undertaken. At present investigations into the use of electric-resistivity methods are

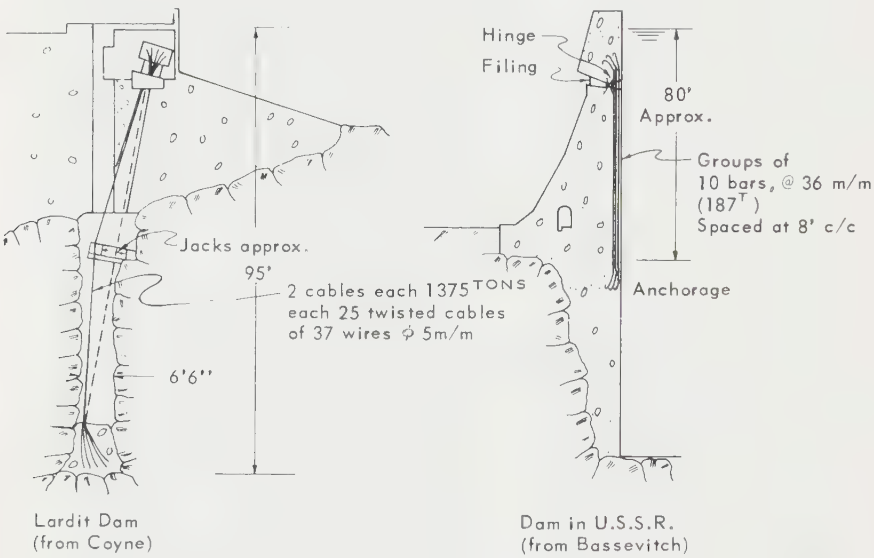

FIG. 13. Some unorthodox prestressing techniques.

in progress.[10] In the Catagunya Dam, several selected cables have permanent electrical connections at each end to insulated copper conductors. It is proposed to measure the resistance of these cables, and tests so far conducted show that the method may be of practical value, a deterioration or break in the cable being indicated by a slight increase of resistance. Obviously, however, further work in this direction is imperative.

The methods of cable protection practiced to date fall into two categories: In the first the cable is protected by a nonbonding plastic material such as grease or bitumen which, while preventing corrosion, effectively permits prestressing operations to be carried out at a later date. The technique was, to the knowledge of the author, attempted only on two early dams, Cheurfas and Fergoug.[3,17] In the first, an elaborate system of prewrapping of the cable enclosing a layer of a grease-bitumen mixture was adopted, while in the latter the cable duct was filled directly with hot bitumen some months after prestressing was completed.

In Allt na Lairige dam the lower portions of all bars were suitably wrapped, enclosing a greasy substance. However (with the exception of two bars), all the remaining lengths of the bars were grouted after prestressing, thus preventing any possible retensioning.

The second procedure, which appears to be almost universally adopted, is the complete enclosure of the cables by cement grouting. This method, while preventing restressing, has the advantage of providing an increased factor of safety against anchorage pullout, as mentioned earlier. In addition, the relative ease with which such grouting can be effectively performed in vertical holes with straight wires (as proved by tests carried out on the Steenbras Dam[14]) provides a uniform degree of protection and avoids the possibility of dangerous zones such as may develop at the junction of the concrete anchorage with the bitumen.

EXAMPLES OF PRESTRESSED DAMS

11. Existing Projects. Since the original application of the Cheurfas Dam the use of cable prestressing in dams has grown rapidly. The technique has been applied with success to the strengthening and raising of numerous old gravity dams and to the

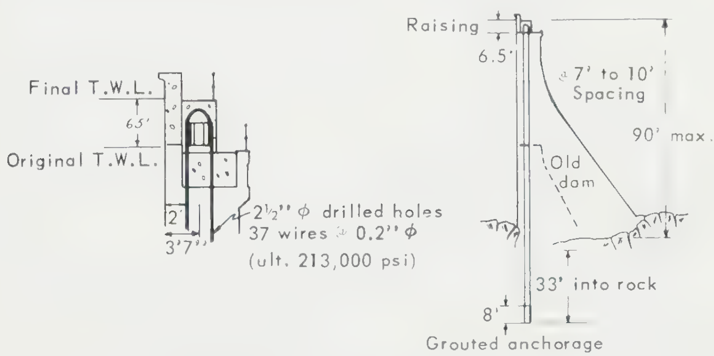

Fig. 14. Raising of Steenbras Dam (South Africa, 1955).

construction of several new dams of the straight-wall type. In both uses the result proved economical, with substantial savings in prime cost being achieved. Figure 14 shows the profile of Steenbras Dam[7] in South Africa which was raised recently, and in Figs. 15 and 16 profiles of some structures designed a priori utilizing the prestressing force are shown. The first of these is the side wall at Mareges (France) where the straight prestressed wall forms an extension of the main arch dam over a relatively short distance.[18] This wall, completed in 1934, is one of the earliest examples of the application of the method to a new structure. In the same diagram the profile of a similar extension constructed more recently in Tunsia is shown.[8] It is seen that the daring and confidence of the designer have increased considerably. In Fig. 16, two medium-height dams designed to rely entirely on the prestressing forces are shown. The first is the Allt na Lairige dam in Scotland[19,20] and the second the Ernestina Dam in Brazil.[5] The first is considerably higher than the latter and to the author's knowledge is the highest new dam presently utilizing the prestressing principle. A dam of considerably greater height is under construction in Tasmania.[35] This dam, with a cross section similar to that of Allt na Lairige, will reach a maximum height of some 150 ft. Figure 17 shows the profile of the spillway section of that dam. The Ernestina Dam is remarkable for the complicated arrangement of prestressing steel,

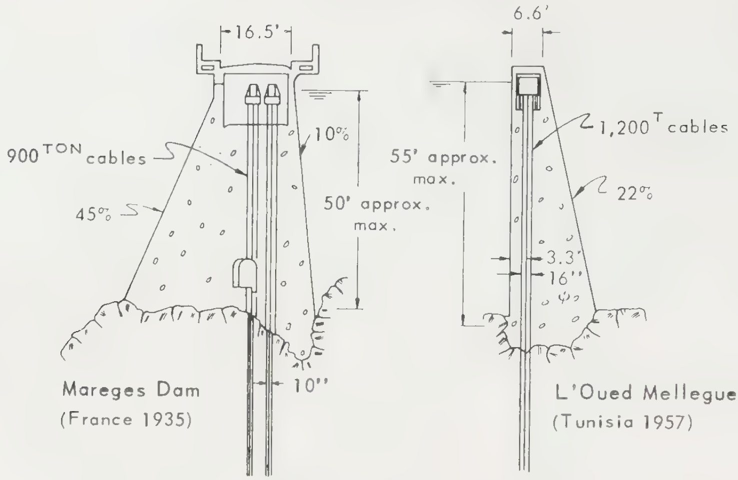

Fig. 15. Examples of prestressed wing dams.

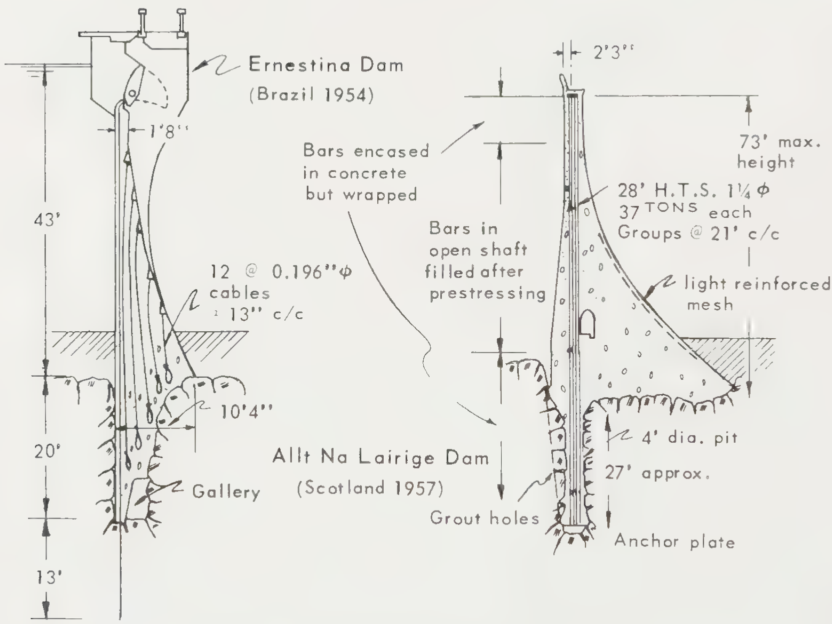

Fig. 16. Examples of prestressed dams.

which one would expect to be considerably more expensive in placement than the very simple scheme adopted in other structures.

In at least one recent dam constructed in England (Avon Dam) provision has been made for a raising anticipated in the future, and suitable cable ducts were incorporated into the original structure, which is of a conventional gravity type.[21,22] Such a procedure is likely to save considerable expense at a later date and is indeed a wise provision if a raising is anticipated.

In addition to straight dams with the cable action similar to that of a simple prestressed concrete cantilever, cable prestressing found an extensive use in construction of large-span buttress dams of the multiple-arch type. In these, several cables are frequently used to "tie" the buttress into their foundation rock and also to increase compressive stresses in planes normal to the principal stress trajectories. Examples of such applications are, to quote but a few, the L'Oued de Mellegue Dam,[8] St. Michel Dam,[18] La Girotte Dam,[23] and Mont Larron Dam.[24] Figure 18, which illustrates the last of these, shows this type of application clearly.

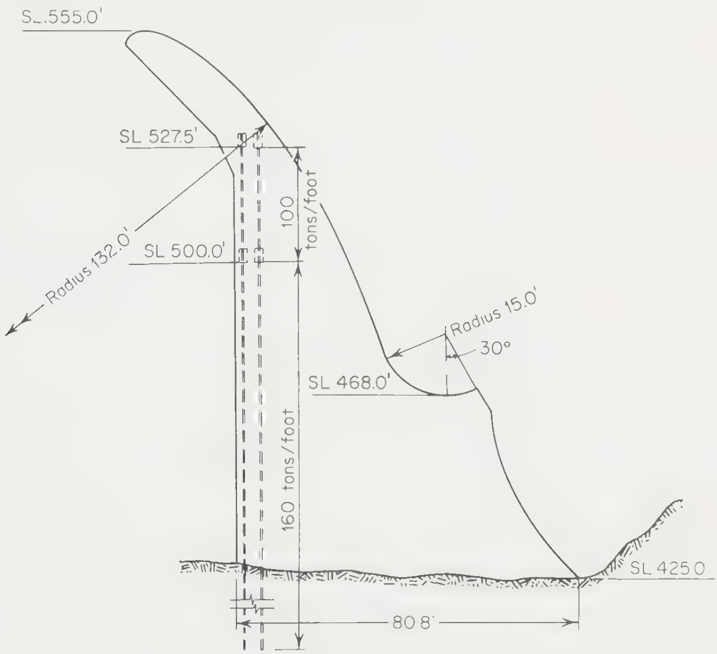

FIG. 17. Cross section and detail of the cables used in Catagunya Dam (Tasmania, 1961). *(From Water Power, December, 1960.)*

The advantageous use of prestressing cables for some parts of the permanent structure of a dam such as spillway piers or for temporary diversion walls, etc., is almost obvious, and a discussion of these is not included here, although the general principles to be elaborated here apply.

The interesting examples of such applications are presented in the various phases of the design of the Wanapum spillway. In addition to the intake structure, illustrated diagrammatically in Fig. 9, prestressing is used there for reinforcing of the piers which support large radial gates. The layout of the cables, in such a pier, is shown in Fig. 19. Complex problems of stress distribution naturally arise in such instances, and elaborate computations, together with the use of structural-model analysis, were needed in this particular design.

The use of prestressing cables in arch dams presents novel and interesting possibilities. It is beyond the scope of this section to discuss in detail the stress distri-

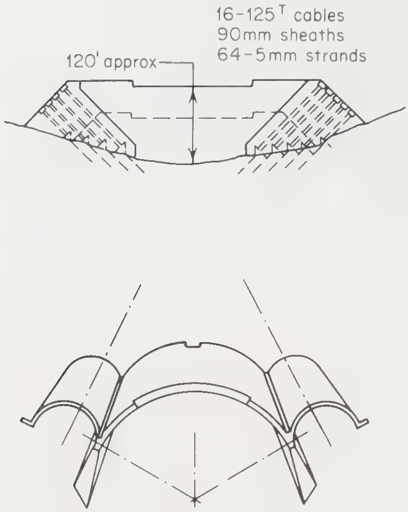

Fig. 18. Mont Larron Dam, France, 1958. Use of cable prestressing in multiple-arch dam.

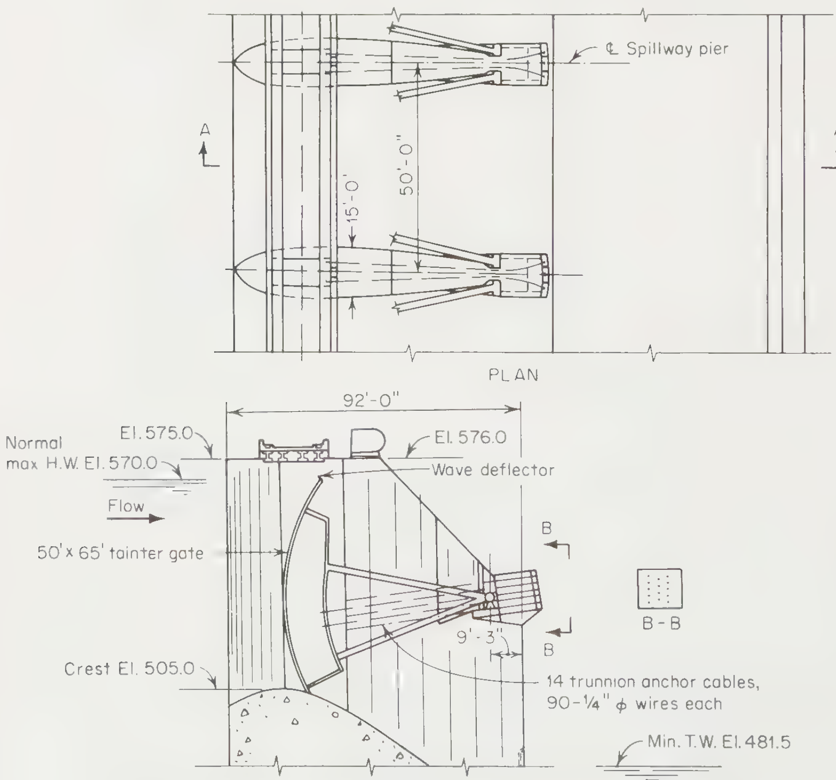

Fig. 19. Piers at the Wanapum Dam (Columbia River, 1960).

bution in such dams and the desired changes of stress which can be brought about by prestressing.

CONCLUDING REMARKS

Some of the possibilities of application of prestressing in dams have been illustrated, but the major problem of the durability of such structures, in common with other reinforced-concrete and prestress applications, deserves further study and research. It appears that the moderate amount of experience already available permits a reasonable degree of optimism, and it can be seen that the technique can already be considered as standard for the reinforcement and raising of old dams. Its use in temporary structures, spillway retaining walls, and structures of medium importance certainly deserves extension. The application to very high dams does not at the moment appear possible or indeed economical, because the prestressing force required increases, roughly, with the cube of the height while the volume of concrete increases with the square of the height.

Bibliography

1. Bassevitch, A. Z., Stress Redistribution in the Building and in Heightening of Concrete Dams, *6th C.L.D.*, R. 112, New York, 1958.
2. Coyne, A., Perfectionnements aux barrages-poids par l'adjonction de tirants en acier, *Genie Civil*, **97** (8), 186, 1930.
3. Drouhin, M., Consolidation de barrage des Cheurfas par tirants metaliques mis en tension, *Ann. Ponts Chaussees*, **105** (8), 253, 1935.
4. Freyssinet, E., Beni Bahdel, *Travaux*, November, 1941; also *Proc. 6th C.L.D.*, New York, 1958.
5. Muller, J., Various Applications of Prestressing to Dams, *Proc. World Conf. Prestressed Concrete*, p. A27-1, San Francisco, 1957.
6. Durand, M., Le barrage de Erranguene, *Travaux*, 1958, p. 744.
7. Lin, T. Y., "Design of Prestressed Concrete Structures," John Wiley & Sons, Inc., New York, 1955.
8. Montmarin, A. de, and W. Ter-Minassian, Interest economique des differents types d'ouvrages du barrage composite de l'oued Melleque, en Tunisie, *5th C.L.D.*, R. 67, **2**, 323, Paris, 1955.
9. Priscu, R., and M. Constantinescu, Considerations concernant la surelevation et la construction en etapes des barrages-poids par precontrainte, *6th C.L.D.*, R. 34, New York, 1958.
10. Wilkins, J. K., and J. Fidler, Design of Catagunya Prestressed Dam, *Trans. Inst. Engrs. Australia*, CE 1, p. 47, September, 1959. Also private report on third structural model of Catagunya Dam, 1961.
11. Zienkiewicz, O. C., and R. W. Gerstner, Stress Analysis and Special Problems of Prestressed Dams, *Proc. ASCE*, **87**, 0.1, January, 1961.
12. ——— and ———, The Method of Interface Stress Adjustment and Its Uses in the Solution of Some Plane Elasticity Problems, *Intern. J. Mech. Sci.*, **2**, 267, 1961.
13. Anon., "Wanapum Development Report on Pullout Test for Rock Anchorage," private report, Harza Engineering Co., Chicago, 1961.
14. Morris, S. S., and W. S. Garrett, The Raising and Strengthening of Steenbras Dam, *Proc. ICE*, **5**, pt. 1 (1), 23, 1956; discussion, **5**, pt. 1 (4), 399, 1956.
15. Parker, P. J., The Raising of Dams with Particular Reference to the Use of Stressed Cables, *6th C.L.D.*, R. 34, New York, 1958.
16. Swida, W., Über einige Anwendungsmöglichkeiten des Spannbetons im Tallsperrenbau, *Bautechnik*, **32** (6), p. 182, 1955.
17. Drouhin, M., Fermeture partiale de la breche du barrage de l'oued Fergoug, *Ann. Ponts Chaussees*, July, 1955.
18. Coyne, A., "Les Tirants Tendus," private report, 1959.
19. Banks, J. A., Allt-na-Lairige Prestressed Concrete Dam, *Proc. ICE*, **6**, 409, 1957.
20. Banks, J. A., The Employment of Prestressed Technique on Allt-na-Lairige Dam, *5th C.L.D.*, R. 68, **2**, 341, Paris, 1955.
21. Bogle, J. M. L., Provision for Future Raising of Avon Dam by the Method of Stressed Cables, *6th C.L.D.*, R. 2, New York, 1958.
22. Bogle, J. M. L., R. M. Ross, and T. McMillan, The Design and Construction of the Avon Dam, *Proc. ICE*, **12**, 83, 1959; discussion **13**, 601, 1959.
23. Bourgin, A., "Design of Dams" (translated from the French), Sir Isaac Pitman & Sons, Ltd., London, 1953.
24. Marchal, J. P., and H. Vieu, Le Barrage du Mont-Larron, *Travaux*, 1958, p. 663.
25. Bellier, J., Progrès récent réalise dans les methods de consolidation et de surélevation des barrages par tirants tendus, *6th C.L.D.*, R. 48, New York, 1958.
26. Toran, J., Raising of Existing Dams and Construction by Stages, *6th C.L.D.*, R. G.-A., New York, 1958.
27. Bassevitch, A. Z., Ouvrages hydrauliques en beton precomprime, *5th C.L.D.*, C 37, **4**, 1345, Paris, 1955.
28. ———, Argentat, *Water Power*, October, 1957, p. 364.

SECTION 17

BARRAGES AND DAMS ON PERMEABLE FOUNDATIONS

By Sir Thomas Foy and H. Spencer Green

BARRAGE AND THE RIVER

1. Introduction. The name "barrage" has been given to the relatively low head, diversion type of dam constructed chiefly in Pakistan, India, Egypt, Iraq, and other countries in the Middle East.

Such structures consist of a number of gated, flood-passing bays of masonry or concrete. The function of these structures is to raise the river level sufficiently to divert the river flow or a part of it into the main supply canal of an irrigation system.

Barrages include canal regulators, low-level sluices to maintain proper flow approach to the regulator, silt-excluder tunnels to control entrance of silt into the canal, and sometimes fish ladders.

Many barrages have been constructed on rivers flowing over deep beds of permeable sand. Engineering and construction records of such structures on this difficult type of foundation date back about 100 years. In this period, a considerable wealth of engineering knowledge has been gained, some of it through hard experience in the failure or partial failure of structures. Engineers in the Middle East have persistently applied themselves to the problems involved by observing, by recording and studying data, by testing models, and by developing mathematical analyses and formulas.

Out of this continued endeavor has come a body of special information, rules, and criteria applicable to the design of barrages or dams built on sand.

In this section, an attempt has been made to bring together the most useful and pertinent parts of this body of information and criteria. An excellent reference for further detail on this subject is Ref. 1.

2. Nomenclature. In order to acquaint the reader with the nomenclature usually applied to the various parts of a barrage, and which is used in the subsequent text, Figs. 1 and 2 have been included.

3. Siting. In selection of a barrage site, the location and elevation of the irrigation canal, or canals, which the barrage will command will play an important part. Adjustments in location of the canal to suit the barrage might be made to some extent, but the topography will generally limit this. The rivers on which barrages are constructed are generally very unstable, but if it is possible to find a relatively stable site, where the floodplain is locally comparatively narrow, within the general area determined by the canal location, it is desirable to adopt this for the barrage location. A study of old maps of the river may contain clues indicating such sites of relative stability. Other factors which will influence location are slope and curvature of the river, volume of pondage, interference with existing structures such as bridges, roads, railroads, or towns, and valuable farmland.

4. Orientation. If the river flows in a braided floodplain, the orientation and exact lateral location of the barrage must be carefully considered by an engineer or engineers of long experience before a final decision is made. The requirements are facility of construction and satisfactory operation after completion.

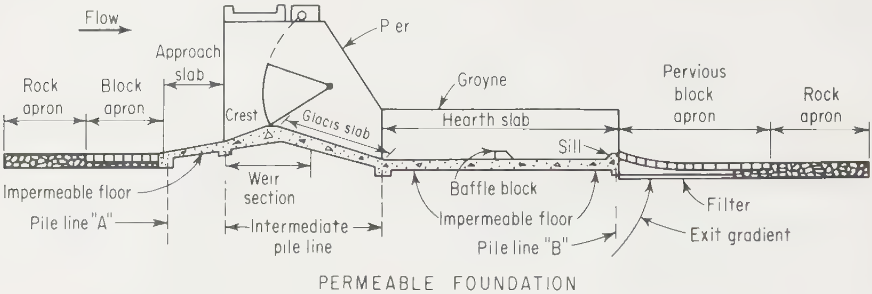

FIG. 1. Section through barrage.

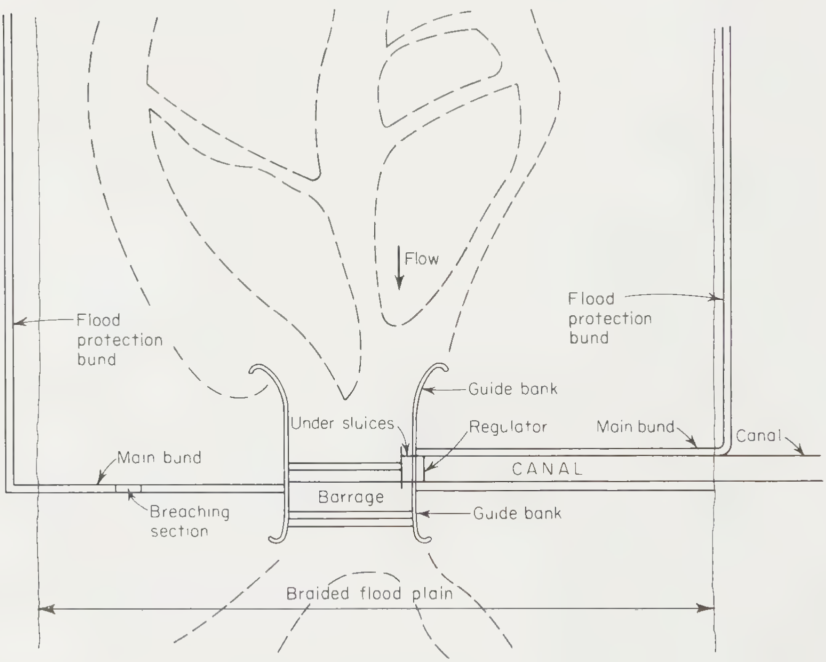

FIG. 2. Plan of barrage and bunds on a braided river.

To assist in the decision an aerial photomosaic of the river for several miles upstream and downstream, taken at low stage, showing the pattern of river channels is invaluable. Old maps of the river reaches under consideration may indicate regions, if any, of comparative channel stability.

In general, because the channels are unstable and a major channel which is on the right one year may in one flood shift to the left, and because of the general downstream progression of loops and meanders, the requirements are best met by selecting a tentative site for the barrage centrally in the floodplain and normal to the overall river axis in that reach.

One of the major considerations is the facility of diversion of river flows during construction. In a number of cases where the floodplain is wide enough, the barrage is constructed on high ground toward the canal side surrounded by earthen cofferdams, while the river continues to flow in the original deep channel. After completion of barrage construction, the river is diverted through leading cuts over the barrage with simultaneous closure of the deep channel.

A large comprehensive model is a useful tool that can be used as a final check and confirmation of the orientation selected. The model can be constructed by using data from recent topographic maps and aerial photographs, care being taken to reproduce in the model important vegetative cover such as forest growth, and differences in the nature of the soil such as a local occurrence of clay.

Practical consideration generally requires the model to be distorted in vertical scale. The scales used for the model, both vertical and horizontal, should be the largest which the available facilities afford.

The bed of the model should be sand particles which have hydraulic simulation close to that of the material of the river being studied. Direction and velocities of currents should be carefully observed, studied, and recorded by time-exposure photography of floating confetti. Scour effects in the riverbed near the structure can be obtained from the model after a sustained run; owing to the difficulty of ensuring the correct hydraulic simulation of the sand particles, these scour measurements should be regarded as having qualitative rather than absolute quantitative value.

5. Accretion and Retrogression. After a barrage has been constructed, the pond formed by it will act as a huge settling basin for the sediments carried by the river. The process of settling out of solids is called accretion. Accretion starts shortly upstream of the barrage just beyond the limit of the temporary scouring effects induced by the operation of the barrage gates during high river stages and gradually works its way upstream, eventually raising the river bottom parallel to the prebarrage slope.

For a number of years after construction of a barrage, because of accretion the water discharging from the barrage will be freer of silt and sediment than before construction. This clearer water, not having its normal load, will pick up silt and sediment from the riverbed downstream of the barrage, causing a lowering or retrogression of the bed. The amount of retrogression in some existing barrages has been between 4 and 7 ft. This is directly reflected in water surface for the lower levels of flow but reduces the water surface only 1.0 to 1.5 ft for the maximum flood flows.

After accretion upstream has ceased, the prebarrage amount of silt will pass through the barrage. The downstream flows, being charged with silt, will no longer pick up bed material, but the reverse will occur. Retrogression will gradually change to accretion, with the riverbed rising again to its original grade or perhaps even higher. This fact of accretion and retrogression is of great significance in design of barrages or dams on alluvial streams, and is never to be overlooked. Some reasonable estimate must be made of retrogression before the final level of a barrage hearth slab has been established. The hearth slab must be low enough so that the hydraulic jump stays on it for all stages of flow with the river in a retrogressed condition.

6. Afflux. Afflux is a term applied to the increase in the maximum flood level upstream of a barrage as a result of its construction. It is also the difference in elevation between the headwater and tail water at the time of maximum flood. The effect of afflux will extend upstream many miles, gradually tapering off to the prebarrage floodwater surface profile. In the rivers of the Punjab, where the sand is quite fine, designers have generally limited afflux to between 3 and 4 ft to obtain a discharge of 250 to 300 cfs per foot run of barrage width. A greater amount of afflux would result in a narrower barrage with higher discharges per foot run. This would necessitate lowering of the hearth slab, the pervious block apron, and the rock apron, and consequential increase in the dimensions of the works; the result could be uneconomic and could increase construction difficulties. In riverbeds of coarser-grained sand or consolidated or cohesive material, more than 3 or 4 ft of afflux could be permitted.

It must be remembered that the figures quoted, *i.e.*, 250 to 300 cfs per foot run, are average figures over the entire width of barrage. Owing to the inequalities of intensity of flow they will be greatly exceeded in certain bays during high floods, and this must be taken into consideration in the detailed design.

Top levels of guide banks will be determined by the afflux, and levels of flood-protection bunds will be determined by the backwater curve caused by the afflux. Over a number of years, accretion may increase the amount of afflux. The raised levels may occur for many miles upstream, but the effect diminishes as the distance increases. Additional freeboard on the guide banks and bunds may be constructed at the time of original construction. However, since the full effect will not take place for many years, the extra freeboard can be obtained when needed by adding a layer of compacted fill to the tops of these earth structures.

BARRAGE-TOPSIDE DESIGN

7. Barrage Width. Three considerations govern the width of a barrage. They are the design flood, the Lacey design width, and the looseness factor.

The design flood must be established from flood records; methods used are fully covered in Sec. 1. In Pakistan and India, barrages were formerly designed to pass the maximum flood previously experienced with some margin of safety. In terms of modern hydrology the designs in practice were capable of accommodating floods of about 40- or 50-year frequency. Larger floods were experienced in the course of time, and these breached the main earth bunds, which in effect became fuse plugs. Such a principle has been found to be more economical than providing a greater spillway capacity in the barrage, and can be permitted because no great amount of stored water is lost, as the barrage is primarily a diversion structure. To have the main bund breach at a predetermined location, a section of this bund is constructed with a slightly lower crest than the rest of the bunds. This section is located at a safe distance from the barrage so that there will be little chance of barrage washout when the bund breaches.

The weakness of this practice arises from the fact that the fuse plug cannot become operative until shortly before the flood peak so that erosion of the bund is limited. This combined with the fact that the channel approach to the fuse plug soon gets silted up and overgrown with brushwood reduces the capacity of the escapage so that the relief afforded by the fuse plug is only a small percentage of the maximum flood.

The second consideration governing the barrage width is the combined widths of the channels approaching the barrage. These channels flow in erodible material and tend to adopt the Lacey regime given by the formula

$$Pw = 2.67\sqrt{Q}$$

where Pw = wetted perimeter, ft
Q = discharge, cfs

For these large channels the formula may be modified with reasonable approximation to

$$W = 2.67\sqrt{Q}$$

where W = minimum stable width, ft, or Lacey width

The width W would be developed by the discharge Q flowing continuously for a length of time sufficient to develop regime conditions. The bed and banks of the channel, though erodible, have been formed by lesser discharges than the maximum flood, which never flows for long enough to establish regime conditions. While the bed adjusts fairly rapidly to the increasing discharge, the banks are often protected by a clay cover reinforced by vegetation. Away from the barrage the flood is carried partly by the existing channels and partly over the floodplain. The barrage is accordingly designed for a width exceeding W, partly to accommodate this floodplain discharge and partly to take advantage of the dispersion of the channel flow induced by the obstruction caused by the barrage itself.

This ratio of actual width to regime width is the "looseness factor," the third factor affecting barrage width. It has been used in the design of barrages generally to increase the minimum width indicated by the Lacey formula. Values used have varied from 1.9 to 0.9, the larger factor being applied in the earlier designs. The extra-wide barrage was advocated because of the convenience of construction resulting from not too low downstream floors and protections. At many of the "loose" barrages, sand islands developed immediately upstream, no doubt a direct result of too much width. The slower velocities permitted settling out of sediment and gradual accumulation until islands formed. Islands became anchored and fixed by growth of vegetation. They disturbed the flow patterns during floods, both upstream and downstream, resulting in undesirable cross currents and concentrations of flow. Very deep scour holes have been a consequence, sometimes causing failure or partial failure of the barrage. More recent designs have recognized this fault of too much width by using smaller looseness factors.

An additional reason for selecting a low value for the looseness factor is the increasing utilization of supplies in the upper reaches of a river for storage and diversion. These withdrawals reduce the low and medium supplies which shape and form the approach channels. The withdrawals have little, if any, effect on the size of the major floods. A barrage designed to suit a low looseness factor will have a larger margin of safety under the changed conditions.

8. Crest Level. Four factors determine the crest elevation of a barrage: the afflux, the pond level, the discharge per foot run, and the coefficient of discharge. The afflux is usually set at 3 or 4 ft, and the average discharge per foot run q is determined by dividing the design flood by the sum of the clear span distances. The coefficient of discharge varies between 2.5 and 2.8 depending on the degree of submergence. A value of 2.6 is usually satisfactory for first trials and can be refined as the design advances, using submergence factors given elsewhere in this book. By substituting the known values of q and C in the spillway discharge formula $q = Ch^{3/2}$, a value of head on crest h is obtained. Pond level is determined by adding the afflux to the natural flood stage at the location selected, and crest elevation is determined by subtracting h from the pond level. The maximum average discharge should be increased by some percentage to allow for unequal flow over the barrage. On the main tributaries of the Indus a figure of 20 percent has been adopted, which experience has shown to be inadequate. Unequal flow is a function of the ratio of the peak flood discharge to the dominant discharges which shape and form the river channels impinging on the barrage, and of the degree of dispersion caused by the barrage. it is preferable to allow for concentration on the following basis:

$$\text{Average discharge} = q \text{ (cubic feet per second/foot run)}$$
$$\text{Concentrated discharge} = q(1 + ab)$$

In which a = (Lacey P_w for maximum design flood) ÷ (Lacey P_w for mean of 3 successive lowest annual floods)

b = dispersion factor for which a value of 0.30 is appropriate for this type of structure

9. Width of Bays. Clear distance between piers is governed by the magnitude of the structure, type of structure, bridge requirements, and kind and size of flotsam. The larger barrages generally have clear distances of 60 ft and the smaller ones about 40 ft. If the barrage will have to pass large logs or trees, the larger spans are in order. A design with reinforced-concrete floor slabs may be more economical than mass concrete design with spans up to 60 ft, but extensions of the piers downstream to the sill, called groins, are required to provide the slab with weight against uplift.

10. Piers. Pier thickness has varied from 7 to 15 ft in different designs. However, 7 ft has been usually adopted and is considered to be adequate even for 60-ft spans with balanced vertical lift gates. For Tainter gates thicker piers may be necessary. Forces that must be considered in pier design are the thrust coming from the Tainter gates or wheeled gates, particularly when an adjacent bay is unwatered by stop logs; bridge forces; and earthquake forces.

11. Glacis. The glacis is the name given to the surface which slopes down from the crest to the hearth slab. It is on this surface that the upstream end of the hydraulic jump should occur. The glacis controls the location of the jump, keeping it in a well-defined zone for the full range of discharges. A jump forming on a horizontal surface is unstable and may move downstream with slight changes of discharge or tail water. If the jump moves off the hearth slab, the structure is in jeopardy. Glacis slopes designed to follow the theoretical trajectory from a 1-ft gate opening under a normal pool ending in a 2 horizontal to 1 vertical slope have been frequently adopted in recent practice.

12. Hearth Slab. With a properly designed glacis and hearth slab, the upstream end of the hydraulic jump will always occur on the glacis for all discharges. With the upstream end of the jump so confined, the downstream end of the hearth slab can be established. Length of hearth slab is made equal to length of jump. Although the length of jump cannot be precisely determined, experience shows that most of the turbulence has ended in a length which is equal to $5(D_2 - D_1)$. The hearth slab provides an erosion-resistant surface for the full length of the jump at all discharges. It is of paramount importance that the full length of the jump be contained on the hearth slab because, in this length, practically all the energy generated by the falling water is transformed into violent turbulence which could dislodge and remove blocks, stone, and all smaller particles.

A high quality of concrete is necessary in the top surface of the hearth slab. It should be resistant to the erosive action of the water carrying sand in suspension. In order to increase the resistance of the surface to erosion, hard particles are sometimes worked into the surface during the concrete-finishing operation. A suitable application of this kind, developed by "Master Builders," is known as "Master Plate," in which iron particles are worked into the top of the concrete. The utmost care must be taken that no cleavage plane develops between the surface concrete and the main mass of concrete.

The top surface of the hearth must be set deep enough so that the upstream end of the jump will always occur on the glacis. This depth is equal to D_2 ft below the surface of the tail water. As shown in Fig. 3, D_2 is the subcritical flow depth occurring downstream of the standing wave of the jump, and can be computed from the hydraulic-jump formula

$$D_2 = -\tfrac{1}{2}D_1 \pm \sqrt{\frac{2}{g} V_1^2 D_1 + \tfrac{1}{4}D_1^2}$$

in which D_1 = supercritical flow depth

V_1 = supercritical flow velocity

V_1 is computed by using the potential head h in the formula $V = \sqrt{2gh}$ where h

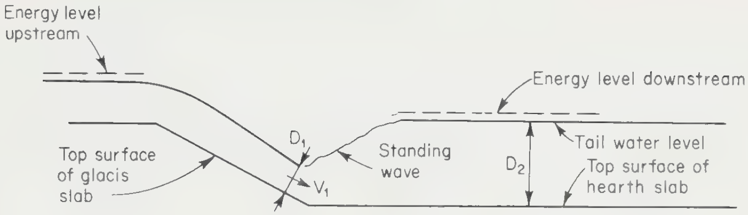

FIG. 3. Hydraulic jump.

equals the difference between the energy level upstream and the level of the glacis at the point where the standing wave forms. Potential head should include the effect of unequal flow described in Art. 8.

To be on the safe side, a small increment can be added to the computed D_2. However, this should not be overdone, since depth in excess of that actually required will cause unnecessary excavation, concrete, and unwatering costs. An addition of 10 percent to D_2 is desirable. Economy requires close determination of the optimum level, particularly for very wide barrages.

For making preliminary studies, the curves in Fig. 4 are very useful in quickly obtaining the elevation of the hearth slab. Elevations of hearth for several values of discharge and corresponding tail water should be obtained. The lowest elevation so obtained would be the correct level. In determining the tail-water level to use in these computations, possible retrogression of the downstream riverbed should be considered. As has been noted previously, it has been found in past experience on alluvial-sand rivers that retrogression over several years can lower tail water 1 to 1½ ft during maximum flood, but 4 to 7 ft during normal or low flow stages

The thickness of hearth slab and glacis must be sufficient to resist uplift and bending moments. Conditions of uplift with gates closed with low tail water and open with high tail water must be considered. In the latter condition, a large unbalanced load occurs under the trough in the hydraulic jump, requiring the thickest portion of

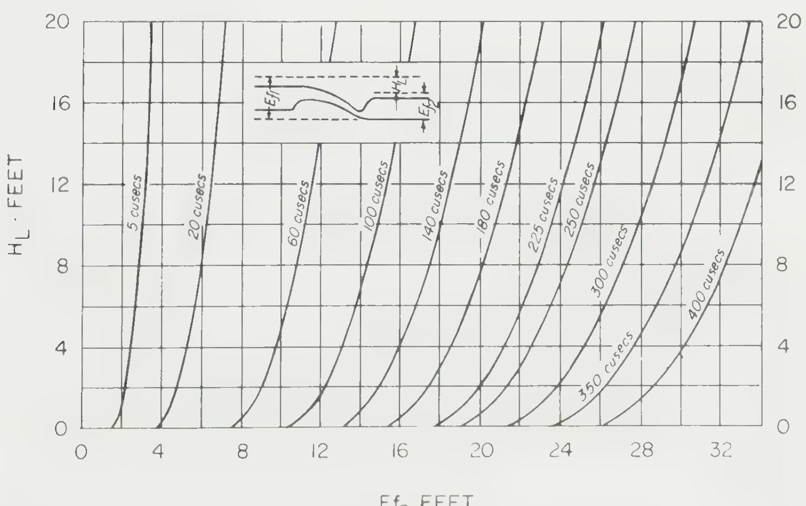

FIG. 4. Curves for setting the level of the hearth slab.

the hearth slab. Some reduction in thickness can be made by bridging this large load over an upstream-downstream length of slab which is longer than the length of the trough.

13. Baffle Blocks. Baffle blocks of proper design will assist in concentrating the center of turbulence of the jump close to the glacis, and so will permit reduction in the length of the hearth slab. Size, location, and spacing of blocks can best be determined during hydraulic-model studies. It is imperative that baffle blocks be thoroughly bonded into the underlying concrete.

Baffle blocks are very vulnerable to erosion, particularly if much sediment is carried by the water. For this reason, the blocks should be constructed of extra-strength concrete and should have a high percentage of reinforcing steel to prevent occurrence of cracks. If a crack develops in the upstream face of the block, the impinging water will cause a pressure buildup and fluctuation of pressure inside the concrete, which in time will cause spalling. All corners should be formed with round chamfers of about 6 to 9 in. radius, as sharp corners have always been one of the first points of erosion attack.

14. Hearth Sill. A concrete hearth sill at the downstream end of the hearth slab is essential to proper design. A well-designed sill will deflect the bottom currents of water off the hearth at an upward angle. The angle of this current will cause a horizontal vortex or ground roller immediately downstream of the sill. Desirable and undesirable patterns for the ground roller are shown in Figs. 5 and 6.

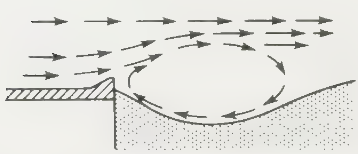

FIG. 5. Desirable ground-roller pattern —with end sill.

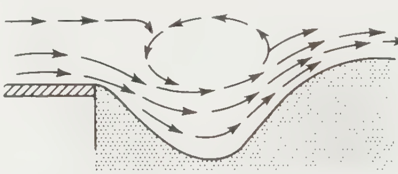

FIG. 6. Undesirable ground-roller pattern—without end sill.

With the sill shown in Fig. 5 the upstream movement of water along the bottom tends to move loose particles toward and against the sill. If no sill were provided, bottom currents downstream of the sill would be in a downstream direction, and the resultant action seen in Fig. 6 is transport of loose particles downstream and away from the sill. With no sill, a longer and deeper scour hole would form downstream than would be the case with a sill. This is well illustrated by results of a transverse sectional model taken with a 1-ft-high sill (Fig. 7) and a 4-ft-high sill (Fig. 8), both subject to the same conditions of flow.

Loss of material at this critical point will increase the exit-gradient pressures, which in turn will increase the tendency for loss of foundation material. Barrages have been badly damaged and have failed because material at the end has been removed by currents, permitting foundation material under the barrage to escape. Sheetpiling under the sill is necessary, as will be discussed in subsequent paragraphs. The final shape of sill should be obtained from observing results on a movable bed by several shapes and sizes of sills in a series of model runs.

15. Approach Slab. A concrete slab upstream of the weir section is a necessary feature. It will increase the seepage path and so reduce uplift pressures. It will provide a smooth erosion-resistant transition in an area where the velocity increases considerably.

The upstream end of the approach slab must be securely joined to the upstream

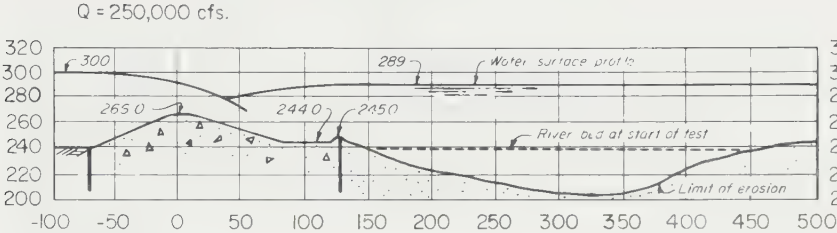

FIG. 7. Erosion pattern with a 1-ft sill.

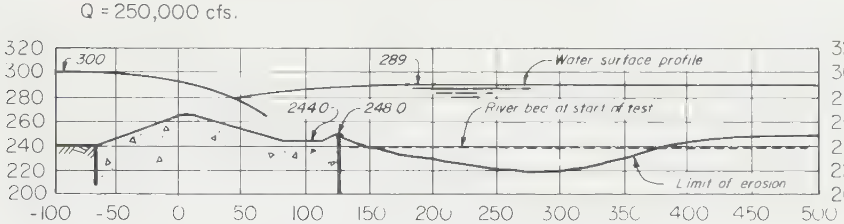

FIG. 8. Erosion pattern with a 4-ft sill.

line of sheetpiling or to the vertical concrete cutoff, if that is used. The downstream end is joined to the weir section in many designs with a flexible watertight joint. With this type of design the approach slab is provided with temperature reinforcement only.

Alternatively, if it is desired to make the approach slab monolithic with the weir section in order to utilize its potential capacity to provide the structure with additional resistance against sliding, it will be necessary to determine the uplift pressures, to establish a suitable coefficient of friction between the slab and the foundation sand, and to design the reinforcement to suit these conditions.

In determining the share of resistance to sliding that the approach slab contributes to the entire structure, the uplift and a suitable coefficient of friction must be established. Determination of uplift can be obtained by the method of independent variables as discussed under uplift. Maximum values of coefficients of friction are 0.45 for clay and 0.55 for sand and gravel, but values 15 or 20 percent higher than this should be used when computing the reinforcing that resists sliding and 15 to 20 percent lower when computing the sliding resistance contributed by the slab to the whole structure. The slab will slope down to the upstream end gradually from the 3 horizontal to 1 vertical slope of the crest section. The elevation of the upstream end should be made low enough, if economically feasible, so that the average maximum approach velocity on the upstream blocks and stone apron will not exceed 10 fps, which is considered to be the upper limit for water flow on loose-stone aprons. The level is also set below the crest level a minimum of 0.2 times the maximum head on the crest to achieve a good coefficient of discharge.

16. Design of Weir Section, Glacis, and Hearth Slab. The weir section, glacis, and hearth slab are required to withstand the uplift pressures, and this objective can be achieved in two ways:

1. By making the section at all points of sufficient thickness and weight equal to the maximum uplift pressure at the point under consideration. This design is known as a gravity section.

2. By designing the barrage slab as a reinforced-concrete raft and utilizing the weight of the piers and groins to assist the glacis and hearth slabs in resisting uplift. This design is known as the Raft design; where adopted, care should be taken to provide some positive pressure or weight in excess of the total uplift pressure.

Where the Raft design is adopted, the reinforcement will be designed in accordance with reinforced-concrete practice. Where the gravity design is used, the slab is often reinforced to prevent temperature and shrinkage cracks.

The selection of one type or the other is a matter of judgment, taking into consideration the comparative cost, facilities for construction, and available materials and skills.

17. Concrete-block Aprons and Scour. Aprons of unreinforced-concrete blocks are usually placed immediately upstream of the approach slab and downstream of the hearth slab. The blocks are cast in place, usually measuring about 3 by 5 ft in plan and 2 ft deep for those upstream, and 3 to 4 ft deep for those downstream. The 4-ft-deep blocks are preferable as being less likely to shift under swirling scour. Downstream blocks are cast with a 3-in. space between each and all adjoining blocks; upstream blocks are contiguous. The 3-in. space is to permit relief of uplift pressure. Between the upstream blocks, the direction of flow is downward. It is therefore better to have the blocks as close as possible to reduce water flow and uplift.

Immediately downstream of the hearth slab, an inverted filter is provided for a length of 1 to 1.5 times the normal scour depth without allowance for concentration in order to have an adequate cover for the downstream pile line to safeguard against the steepening of the exit gradient in case of scour downstream. The inverted filter consists of two or three layers designed for protection of the base soil and is weighted by concrete blocks with 3-in. open joints tightly packed with gravel. Downstream of these inverted filter blocks, flexible apron blocks laid on a 2-ft layer of rock are provided for about one-third the length of the total flexible protection mentioned in Art. 18.

It has been the practice in the Punjab to provide total lengths of block aprons equal to $1.5D$ to $2.0D$ downstream and about $1.0D$ upstream, where D is the design depth of scour below the top of a slab. Upstream the blocks are placed on a 2-ft thickness of loose stone, making a total thickness of 4 ft equal to the stone apron which continues farther upstream.

$D = XR$ minus depth of water above top of slab

$X =$ 1.25 to 1.75 for upstream aprons, 1.75 to 2.0 for downstream aprons (the factor X provides for the additional scour due to concentration and any local eddy formation)

$R = 0.9(q^2/f)^{1/3}$ = Lacey scour depth, ft below floodwater surface, based on unit flow without allowance for concentration

$f = 1.0$ for fine sand

q = average flow, cfs per foot run

The rules for designing block and stone aprons set out above and in Art. 18 were evolved by Dr. A. N. Khosla[1] and are still very widely followed. Experience has shown that the assumed concentration of 20 percent on which these rules are based can be inadequate. It is preferable to use the factor $(1 + ab)$ described in Art. 8 as X for the upstream apron and $(1 + ab + 0.25)$ as X for the downstream apron.

18. Stone Aprons. In addition to the concrete-block aprons, additional protection against scour is provided by means of stone aprons upstream and downstream. Where there is the combination of concrete-block and stone aprons, the total quantity per foot run required in either upstream or downstream pervious aprons is $10D$ minimum, which includes blocks, filter, and riprap.

Stone protective blankets are also placed on the compacted-earth guide-bank slopes and toes. Depth of scour is also the criterion used to determine the length of these aprons, and the quantity of stone needed per foot run is equal to $7D$. This is based on providing enough stone to cover a scoured slope of 2:1 with a 3.1-ft depth of rock, as shown in Fig. 9.

Table for X in $XR = D + Y$ in Fig. 9

Upstream of weir and concrete blocks	1.25–1.75*
Downstream of weir and concrete blocks	1.75–2.25*
Transition from nose to straight guide banks	1.25–1.75*
Straight reaches of guide banks	1.0 1.5*
Noses of guide banks	2.0 –2.5*

* These factors include allowance for concentration and are to be used when q does not include concentration allowance. Experience has shown that for the guide-bank aprons the upper limits of the suggested factors are preferable. A modified rule for the factors for the barrage upstream and downstream aprons has been suggested in Arts. 8 and 17.

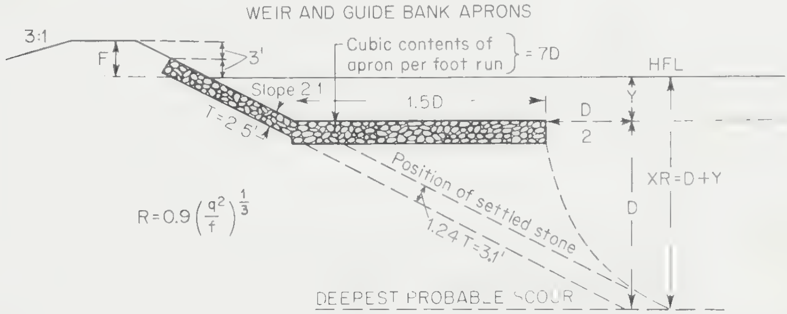

Fig. 9. Criteria for stone protective blankets and aprons on weir and guide banks.

BARRAGE—BOTTOM-SIDE DESIGN

19. Steel Sheetpiling. The principal function of sheetpiling under a barrage or dam on a permeable-sand or other soft foundation is to confine and hold secure the foundation material under the structure during all conditions of river flow and turbulence. Other functions are the increase of the seepage path to reduce uplift pressure and the exit gradient. A well-designed sheetpile system will make a continuous and closed circuit around the periphery of the entire structure. The lines under the flanking walls will guard against high subsoil water level on the flanks blowing up the hearth slab and will ensure confinement of the foundation if an adjacent bund is washed out when the barrage is outflanked by a superflood (Fig. 10).

The two lines of piling given most consideration during design are under the upstream end of the approach slab a and under the downstream end of the hearth slab b. These lines are the ones most frequently vulnerable to attack by the river.

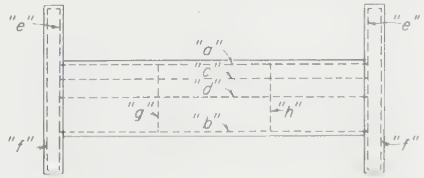

Fig. 10. Plan of pile lines.

Other lines include intermediate piles parallel to the center line of the structure *c* and *d*, which help to reduce uplift pressures, transverse lines under the toe and heel of the flanking structures *e* and *f*, and several transverse lines between the two flanks *g* and *h*.

The upstream line of piling *a* has two functions:

1. To prevent the loss of foundation material in case a scour hole should occur near the structure
2. To increase the seepage path and thus reduce the uplift force under the structure

The downstream line *b* also has two functions:

1. Same as 1 above
2. To minimize the exit gradient

Function 1 governs the depth of both lines *a* and *b*. Intermediate lines *c* and *d* are installed in some designs to act as a second line of defense against loss of the weir, piers, gates, and bridge in case of failure of the approach or hearth slab. The intermediate lines also effectively increase the seepage path to reduce uplift under the hearth slab.

Where the barrage is very long, transverse lines *g* and *h* are used to divide the foundation into sections. This is another precaution against progressive and total failure by undermining. Complete enclosure of the flanking-structure foundation material is recommended, as shown by pile lines *e* and *f*.

Perimeter piles are driven to a depth to prevent failure by scour. The Lacey formula, defined previously for scour depth, has been used as a guide in many barrage designs. In this application, *q*, the maximum discharge per foot run, is increased by some concentration factor usually in the order of 20 percent.

Scour holes are usually the result of concentrated flows that develop because gates are opened unevenly, because sand islands create disturbance in laminar flow, or because lack of river training or changed conditions result in cross flows upstream, producing a higher water level and discharge at one flank than at the other. To have the design recognize these possibilities, the concentration factor is applied to the discharge before the Lacey formula is solved. The upstream line *a* can be driven deeper than indicated by the formula to be extra safe. However, the downstream line *b* should not be driven any deeper than necessary for proper exit gradient, since increased depth would increase uplift under the hearth slab. Depth of downstream piles is primarily determined by the exit-gradient considerations. Protection against scour is provided by the inverted filter and blocks and by the downstream flexible protection.

If deep scour occurs next to a line of piles, it will cause an unbalanced load on the piles. There would be a water load on only one side and submerged earth plus water load on the other side. Piles must have sufficient strength to resist this unbalanced load. A working stress somewhat under the yield point of the steel can be used to determine the section modulus of the piles.

Steel for sheetpiles is often specified with about 0.2 percent of copper alloyed with the steel to increase resistance to corrosion. A minimum thickness of ⅜ in. should be specified. All handling holes or any other holes below the bottom of concrete should be covered with welded steel patches. Prior to driving, all interlocks should be given a good coating of pitch to seal the interlocks against passage of water and foundation particles.

The tops of the sheetpiling should be embedded in the concrete deep enough to hold against the reaction from the unbalanced load caused by a scour hole. A well-reinforced concrete longitudinal pile cap extending several feet below the bottom of the slab is usually provided to support the sheetpiling.

20. Foundations. The upper layers of sand in alluvial rivers are quite loose. Generally they are too loose to permit construction of a large, important structure thereon without some special treatment to increase bearing capacity and reduce potential settlement.

Consolidation of loose foundation material may be required to provide minimum bearing capacity. This can be done by compacting with sheeps-foot rollers or vibratory rollers or by the modern vibroflotation methods if the other methods are not sufficient. Use of bearing piles is not considered a sound practice. If settlement of the foundation occurs, a space opens between the concrete and foundation sand. This space will permit excessive uplift pressures and will greatly reduce resistance to sliding.

Table 1 gives data on the consolidation of sand foundations and bearing capacity by the vibroflotation method.

TABLE 1. TABLE OF VIBROFLOTATION COMPACTION

Design bearing capacity, psf	Min relative density, %	Triangular pattern of compaction point	Effective area of one compaction, sq ft
4,000	60	9′0″	70
6,000	70	7′6″	50
8,000	85	6′6″	35

Caisson or well foundations may be desirable in soils of low bearing capacity and have been used often.

21. Uplift. Since uplift is one of the principal factors governing the design of any dam, a realistic determination of this is basic. The first attempt at a rational procedure to determine uplift was developed by Bligh. It was called the Bligh creep theory and was based on linear loss of head along all contact surfaces between the structure and foundation. This was used extensively, but after actual pressures under several structures designed on this basis were checked it was found to be in error. Lane then modified this concept by giving three times more resistance to percolation along vertical contact surfaces than to that along horizontal contact surfaces. The result was known as the weighted creep theory and gave more correct results. Weaver, of the University of Wisconsin, initiated a mathematical solution which was developed and refined to an accurate method by Khosla, Bose, and Malhotra, of the Punjab Irrigation Research Institute. This is known as the method of independent variables. It is applicable for any shape structure having one or more lines of cutoffs. This method, along with the electric-analog method, has given results which are reasonably confirmed in prototype structures. Either of the last two methods is recommended for use in determining uplift under structures built on permeable homogeneous foundations without underdrainage.

If an electric-analog model is available, with personnel experienced in the technique of its use, accurate flow nets can be obtained quickly. It is particularly advantageous when quite a number of different solutions are being studied for one structure. The method of independent variables is recommended as the most practical means of obtaining uplift under a structure on sand, as it requires no special equipment or technique and an engineer can become familiar with the method quickly. Dr. Khosla has developed a set of curves to give pressures for particular elements to be used in the solution by the method of independent variables. These curves are given in Fig. 11. As an example of use of the curves, the uplift under a typical type of barrage as shown in Fig. 12 has been solved. Each foundation element is considered independently

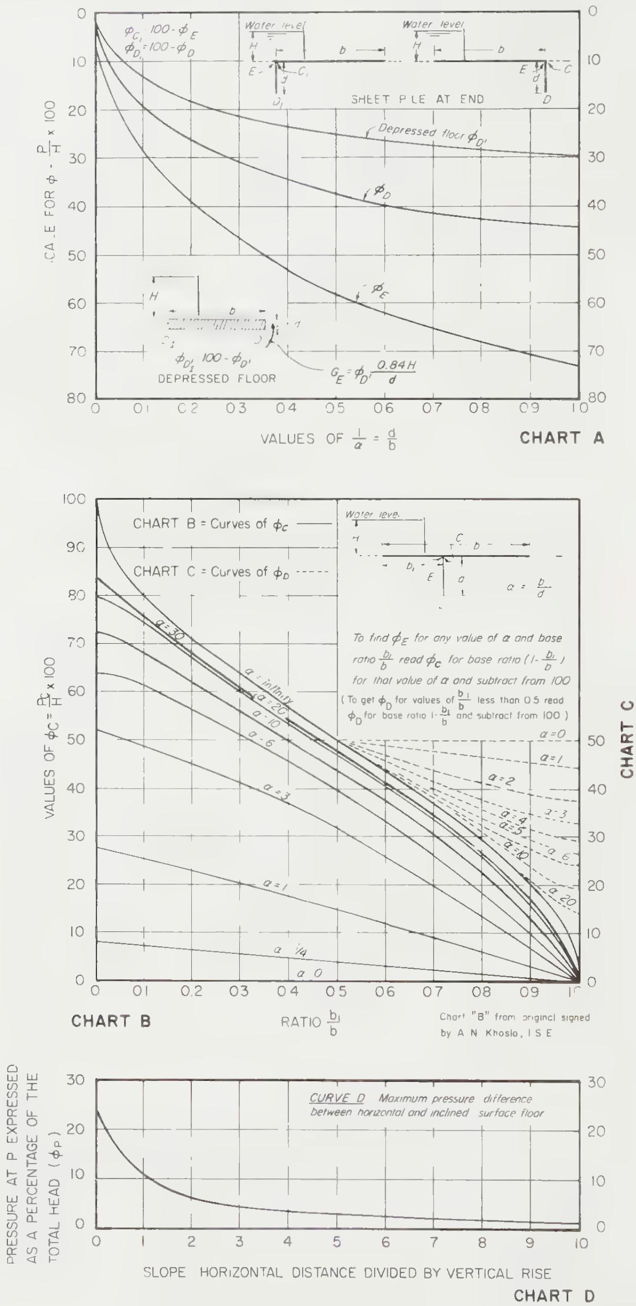

FIG. 11. Curves for solutions of uplift under barrages.

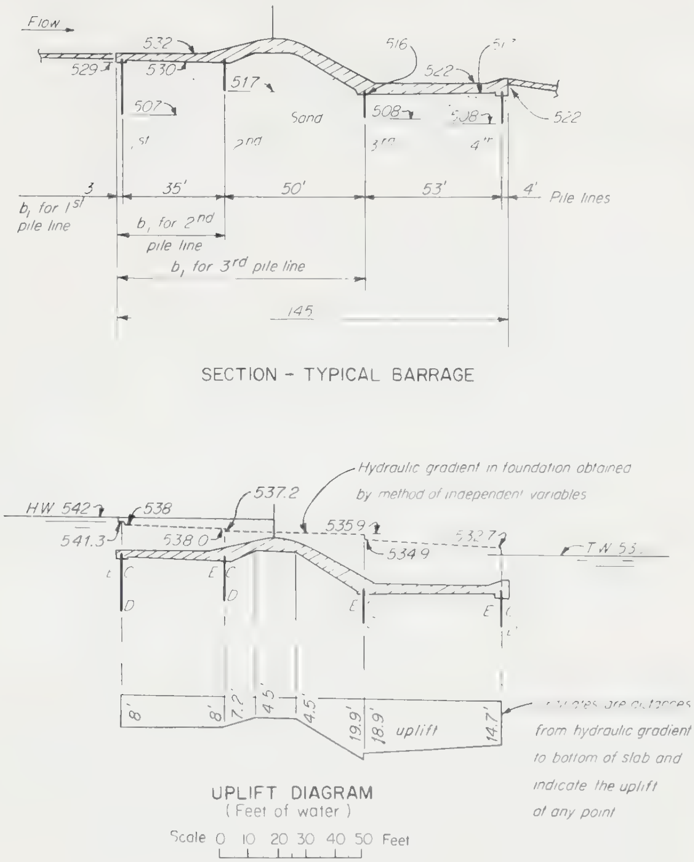

FIG. 12. Hypothetical barrage cross section in illustrative uplift problem.

with appropriate corrections as required by this method. Using Khosla's notation, the symbol ϕ denotes the proportion of head H at any point; $\phi = 100P/H$. The suffix D applies to the bottom of a pile line; E and C apply to the junction of the pile and floor upstream and downstream, respectively; α is the ratio of the length of floor b to the depth of pile d, and b_1 is the distance of the pile from the upstream end of the floor. It is strongly recommended that Dr. Khosla's book be studied thoroughly by anyone applying this method.

First Pile Line

$$b = 145 \text{ ft total length of monolithic slabs}$$
$$d = 532 - 507 = 25\text{-ft depth of pile below top of slab}$$
$$b_1 = 3 \text{ ft}$$
$$\alpha = \frac{145}{25} = 5.8$$
$$\frac{b_1}{b} = \frac{3}{145} = 0.027$$
$$\phi_E = 96.5 \text{ percent}$$

On Chart B, read $\phi_c = 3.5$ percent for $b_1/b = 1.0 - 00.27 = 0.97$ and for $\alpha = 5.8$. Then $\phi_E = 100.0 - 3.5 = 96.5$ percent.

$$\phi_D = 74.5 \text{ percent}$$

On Chart C, since b_1/b is less than 0.5, subtract it from 1.0 and read 25.5 percent on right scale for $\alpha = 5.8$; $\phi_D = 100 - 25.5 = 74.5$ percent.

$$\phi_c = 63.0 \text{ percent}$$

On Chart B, read 63.0 percent directly for $\alpha = 5.8$ and $b_1/b = 0.027$

Corrections to be applied to ϕ_E and ϕ_c:

$$\phi_E \text{ correction for depth } = \frac{532 - 529}{532 - 507} \times (\phi_E - \phi_D) = 2.6 \text{ percent}$$

$$\phi_c \text{ correction for depth } = \frac{532 - 530}{532 - 507} \times (\phi_D - \phi_c) = 0.88 \text{ percent}$$

Influence of second pile line on ϕ_c:

$$D_2 = 530 - 517 = 13 \text{ ft}$$
$$D_1 = 530 - 507 = 23 \text{ ft}$$

$$\text{Correction to } \phi_c = +19 \sqrt{\frac{D_2}{b'}} \times \frac{D_1 + D_2}{b}$$
$$= +19 \sqrt{\frac{13}{35}} \times \frac{23 + 13}{145} = +2.9 \text{ percent}$$

b' = distance between piles

This correction is added when the influencing pile is downstream and subtracted when it is upstream of the pile line in question. Then

$$\phi_E \text{ corrected} = 96.5 - 2.6 = 93.9 \text{ percent}$$
$$\phi_c \text{ corrected} = 63.0 + 0.88 + 2.9 = 66.8 \text{ percent}$$

Second Pile Line

$$d = 532 - 517 = 15 \text{ ft}$$
$$b_1 = 38 \text{ ft}$$
$$\alpha = \frac{145}{15} = 9.7$$
$$\frac{b_1}{b} = \frac{38}{145} = 0.26$$
$$\phi_E = 72.0 \text{ percent}$$

On Chart B, read $\phi_c = 28.0$ for $b_1/b = 1.0 - 0.26 = 0.74$ and $\alpha = 9.7$. Then $\phi_E = 100 - 28 = 72.0$ percent.

$$\phi_D = 64.0 \text{ percent}$$

On Chart C, since b_1/b is less than 0.5, subtract from 1.0 and read 36.0 percent on right scale for $\alpha = 9.7$, $\phi_D = 100 - 36.0 = 64.0$ percent.

$$\phi_c = 58.0 \text{ percent}$$

On Chart B, read 58.0 percent directly for $b_1/b = 0.26$ and $\alpha = 9.7$.

Corrections to be applied to ϕ_E and ϕ_c:

$$\phi_E = \text{correction for depth} = \frac{532 - 530}{532 - 517}(\phi_E - \phi_D) = -1.1 \text{ percent}$$

$$\phi_c = \text{correction for depth} = \frac{532 - 530}{532 - 517}(\phi_D - \phi_c) = +0.8 \text{ percent}$$

Influence of first pile line on ϕ_E:

$$\text{Correction to } \phi_E = -19\sqrt{\frac{D_2}{b'}} \times \frac{D_1 + D_2}{b}$$

$$= -19\sqrt{\frac{23}{35}} \times \frac{13 + 23}{145} = -3.9 \text{ percent}$$

$$D_2 = 530 - 507 = 23 \text{ ft}$$
$$D_1 = 530 - 517 = 13 \text{ ft}$$
$$b' = 35 \text{ ft}$$

Influence of third pile line on ϕ_c:

$$\text{Correction to } \phi_c = +19\sqrt{\frac{D_2}{b'}} \times \frac{D_1 + D_2}{b}$$

$$\text{Correction to } \phi_c = +19\sqrt{\frac{22}{50}} \times \frac{13 + 11}{145} = +2.1 \text{ percent}$$

$$D_2 = 530 - 508 = 22 \text{ ft}$$
$$D_1 = 530 - 517 = 13 \text{ ft}$$
$$b' = 50 \text{ ft}$$

Correction to ϕ_c for slope:

Slope is 1 vertical to 2 horizontal upward; from Chart D, correction is −6.5 percent (minus for slope upward with flow). Proportional length is $^{10}\!/_{50}$ correction = $6.5 \times \frac{1}{5} = -1.3$ percent. Then

$$\phi_E \text{ corrected} = 72.0 - 1.1 - 3.9 = 67.0 \text{ percent}$$
$$\phi_c \text{ corrected} = 58.0 + 0.8 + 2.1 - 1.3 = 59.6 \text{ percent}$$

Third Pile Line

$$d = 522 - 508 = 14 \text{ ft}$$
$$b_1 = 88 \text{ ft}$$
$$\alpha = \frac{145}{14} = 10.4$$
$$\frac{b_1}{b} = \frac{88}{145} = 0.61$$
$$\phi_E = 48.5 \text{ percent}$$

On Chart B, read $\phi_c = 51.5$ for $b_1/b = 1.0 - 0.61 = 0.39$ and $\alpha = 10.4$; then $\phi_E = 100 - 51.5 = 48.5$ percent.

$$\phi_c = 38.0 \text{ percent}$$

On Chart B, read 38 percent directly for $b_1/b = 0.61$ and $\alpha = 10.4$.

$$\phi_D = 43 \text{ percent}$$

On Chart C, since b_1/b is greater than 0.5, read 43 percent directly on right scale.

Corrections to be applied to ϕ_E and ϕ_c:

$$\phi_E \text{ correction for depth } = \frac{522 - 516}{522 - 508}(\phi_E - \phi_D) = -2.4 \text{ percent}$$

$$\phi_c \text{ correction for depth } = \frac{522 - 516}{522 - 508}(\phi_D - \phi_c) = +2.2 \text{ percent}$$

Influence of second pile line on ϕ_E is nil since bottom of second pile line is at elevation 517 and ϕ_E relates to elevation 516.

Influence of fourth pile line on ϕ_c:

$$\text{Correction to } \phi_c = +19\sqrt{\frac{D_2}{b_1}} \times \frac{D_1 + D_2}{b}$$

$$= +19\sqrt{\frac{8}{53}} + \frac{8 + 8}{145} = 0.8 \text{ percent}$$

$$D_2 = 516 - 508 = 8 \text{ ft}$$

$$D_1 = 516 - 508 = 8 \text{ ft}$$

$$b_1 = 53 \text{ ft}$$

Correction to ϕ_E for slope:

Slope is 1 vertical to 2 horizontal upward; from Chart D, correction is +6.5 percent (plus for slope upward against flow). Proportional length is $^{25}\!/_{50}$; therefore, correction = $+6.5 \times \frac{1}{2} = +3.25$ percent. Then

$$\phi_E \text{ corrected} = 48.5 - 2.4 + 3.25 = 49.35 \text{ percent}$$

$$\phi_c \text{ corrected} = 38.0 + 2.2 + 0.8 = 41.0 \text{ percent}$$

Fourth Pile Line

$$d = 522 - 508 = 14 \text{ ft}$$

$$\frac{1}{\alpha} = \frac{d}{b} = \frac{14}{145} = 0.097$$

$$b = 145 \text{ ft}$$

$\phi_E = 27.5$ by Chart *A*, reading directly

$\phi_D = 18.8$ by Chart *A*, reading directly

Corrections to be applied to ϕ_E:

$$\phi_E \text{ correction for depth } = \frac{522 - 516}{14}(\phi_E - \phi_D) = -3.8 \text{ percent}$$

$$\phi_E \text{ correction for influence of third pile line } C = -19\sqrt{\frac{8}{53}} \times \frac{8 + 8}{145} = -0.8 \text{ percent}$$

$$\phi_E \text{ corrected} = 27.5 - 3.8 - 0.8 = 22.9 \text{ percent}$$

Exit gradient (see Art. 22):

$$G_E = \frac{H}{d}\,\frac{1}{\pi\sqrt{\lambda}}$$

$$\lambda = \frac{1 + \sqrt{1 + (b/d)^2}}{2}$$

$$\lambda = \frac{1 + \sqrt{1 + (^{145}\!/_{14})^2}}{2}$$

$$\lambda = \frac{1 + 10.4}{2} = 5.7$$

$$G_E = \frac{12}{14}\,\frac{1}{\pi\sqrt{5.7}} = 0.114$$

Nearly all authorities on the subject of uplift have concluded that uplift pressures should be applied to 100 percent of the base area of the structure. This holds particularly true for structures constructed on permeable foundations where there is no adhesion between foundation and concrete.

It has been consistent practice in India and Pakistan to give no reliance to underdrainage systems to reduce uplift pressures. The conclusion reached is that underdrains might become choked up with fines as time goes by, rendering them inoperative and resulting in greater uplift pressures than the designs assumed. Without reliance on underdrains, designs are more conservative, resulting in thicker hearth slabs, more excavation, and somewhat greater cost.

American practice has not been so averse to the use of underdrains. Such structures as Petenwell and Castle Rock spillways, built in 1949 and 1950, on the Wisconsin River, and the Santee Spillway in South Carolina, built in 1940, are on deep fine-to-medium-sand foundations and have well-designed underdrains. These are subject to heads as great as or greater than similar structures in the Middle East.

If an underdrainage system is used, the uplift determination is simplified. With an upstream line of sheetpiling of adequate depth, it may be safely assumed that the uplift under the approach slab at the line of piling is about 80 percent of the difference between headwater and tail water. It may then be assumed that the uplift diminishes uniformly to tail water at the upstream end of the underdrainage system.

22. Exit Gradient. Loss of material from the riverbed at the end of the structure by "piping" may occur if the weight of the sand is overcome by the upward flow of water through it. Good design requires that pressure gradient in the foundation material at the end of the structure, causing this upward flow, be as low as possible consistent with other requirements of design. The gradient is an inverse function of the depth of the downstream line of sheetpiling and the length of the structure, and a direct function of the head. Deep downstream piling will reduce the gradient; however, it will also increase uplift and therefore increase concrete and excavation quantities. A depth should be used that is just sufficient for reducing the gradient to a proper value. Experiments with sands of various densities have shown that flotation can occur with gradients from $G_E = 0.44$ to 1.44, or with an average value of G_E of about 1.0. A factor of safety of between 4.0 and 6.0 may be applied for coarse to very fine sand, respectively. Dr. Khosla has derived the following formula for determination of the exit gradient at point C for a single row of downstream piling as illustrated in the upper right corner of Chart A.

$$G_E = \frac{H}{d}\frac{1}{\pi\sqrt{\lambda}} \qquad \text{with} \qquad \lambda = \frac{1 + \sqrt{1 + (b/d)^2}}{2}$$

in which G_E = exit gradient

H = head between headwater and tail water

d = depth of downstream sheetpiling below downstream bed level

b = length of concrete structure from upstream to downstream ends

23. Pressure Pipes. Since uplift is of such importance in a structure of this kind, there should be some way of measuring it after the structure is built. Pressure pipes with conventional well points have been used for this purpose; while in many cases some of the pipes have clogged, sufficient remain effective to give useful indications, and such pipes should always be fitted into new works. Pipes and well points of 1½ in. diameter are adequate for the purpose. All pipes should terminate at a convenient location in the piers near the bridge.

Systematic and regular readings of pressure show the condition of stability of the structure. If the measured uplift should be greater than the values used in design, advance warning will have been given so that remedial measures can be taken. Readings will also have the scientific value of providing more data for use in future designs.

The critical locations are:

1. Immediately downstream of the upstream pile under the approach slab
2. Under the toe of the glacis
3. At the downstream end of the hearth slab at the top of the pile
4. At the bottom of the downstream sheetpiles

At these locations, the pressure pipes are usually provided in all the bays. A few bays are, however, provided with a greater number at all the points used in theoretical calculations.

Each pipe must have a definite designation, which should be maintained throughout construction; otherwise their usefulness will be nullified if, after construction, it is not known which points correspond to the projecting pipes. The most satisfactory device for measuring the height of water in the pipes is known as a Bell sounder, as shown in Fig. 13. It is lowered into the pipe by a steel tape. When the cup hits the water in the pipe, a distinctive loud sound is produced. Readings accurate to $\frac{1}{16}$ in. can be made with this device.

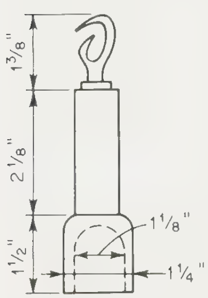

FIG. 13. Bell sounder.

24. Sliding Factor. In barrage design, as in any other dam design, a basic objective is to maintain a proper ratio of the total horizontal forces to the total net downward vertical forces. This ratio, known as the sliding factor, must be limited so that the frictional resistance of the foundation will not be exceeded. Since structures constructed on sand have no adhesion with the foundation, the shear-friction safety factor criterion is not applicable; only the friction or sliding factor can be used. In the case of fine sand, medium sand, coarse sand, or gravel foundations, a value of $\Sigma H/\Sigma V = f = 0.4$ is considered safe; and for clay the value should never exceed 0.3. Some English authorities recommend a more conservative 0.3 for sand and 0.2 for clay.

The condition of loading which causes the greatest tendency to slide is the normal condition with gates closed in which tail water is low and net uplift is high. In computing resistance to sliding of the whole structure, no credit is usually given to the anchoring effect of sheetpiling. However, reinforcement should be included in the approach slab and around the top of the piling, assuming an anchoring effect.

The discussion on the approach slab covers resistance to sliding of this particular part of the barrage.

BARRAGE APPURTENANT STRUCTURES

25. Gates and Hoists. Details of gate design can be found in Sec. 21. The varieties of gates normally used on barrages are the Stoney gate and the fixed-wheel gate, which are variants of the vertical-lift gate, and the Tainter gate. Each variety can be designed for power or hand operation. The vertical-lift gates may or may not be counterbalanced.

Selection of the type to be adopted will depend on the local conditions considered under the following heads:

1. Liability of the stream to carry heavy drift or logs
2. Flashiness or otherwise of the floods and the length of time of flood warning
3. Whether the pond must be carefully regulated
4. The need for a constantly maintained operating staff

Tainter gates have the advantage of economy as far as the cost of gates and hoisting gear is concerned. Their concentration of loading at the pins may require wider piers, and this with the consequential increased width of barrage may more than offset the economy of the gate. The radial struts are vulnerable to damage by logs.

The vertical-lift gates without counterbalances require power operation. They definitely require wider piers than balanced gates. Their use has advantages for very flashy rivers or where there is difficulty in recruiting operational staff, and where this staff is costly.

The vertical-lift counterbalanced gate, hand-operated, is suitable where the river is not unduly flashy and where a staff is required permanently for regulation and other purposes, and labor is relatively cheap. There are two varieties of this gate, *i.e.*, the fixed-wheel gate and the Stoney roller-train gate. While both types have their uses, it is easy to house the roller train in the grooves to protect against debris, trash, and logs. They are also easy to maintain and have been widely used in the past, particularly in the Punjab. The counterbalanced gates could also be power-operated, in which case they would be suitable for flashy rivers.

To prevent the formation of vortices occurring just off the spillway and hearth sill, uniform gate opening across the barrage is the ideal as vortices are likely to form when one bay is discharging materially more water than adjacent bays. This ideal is not attainable when regulation is necessary to remove shoals upstream of a barrage. When unequal flow is necessary, the difference in gate opening from one bay to the next should be limited. A differential discharge of 10 percent is generally safe, but this should be checked by visual observation. The standing wave must always be kept on the glacis.

26. Flank Walls. The barrage flank walls are primarily retaining walls which support the abutting earth bunds. Therefore, retaining-wall principles of design should be followed, but with these precautions:

1. Design should provide for good positive contact between the earth fill and the backs of the flank walls to prevent seepage of water along the plane of contact. Backs of walls should therefore have a definite batter to create better contact as the fill settles. Vertical cutoff walls on the back of the flank wall into the abutting earth structure are usually provided along the upstream and downstream sheetpile lines. Depths of cutoffs are determined by horizontal flow net at the back of the wall. A check is made for safe exit gradient at the downstream end along the back side of the wall.

2. Water levels in the abutting earth should be considered for various loading conditions. In the case of fast lowering of tail water, there can be a residual water level above tail water.

3. Scour possibilities along the upstream and downstream ends of the flank walls beyond the limits of the monolithic concrete aprons should be carefully investigated. This can best be determined by model studies. Adequate depth of steel sheetpiling should be provided to protect the structure from possible scour.

27. Regulators. Barrages are constructed to raise the level of a river sufficiently to permit diversion into a supply canal. The control structures at the point of diversion are referred to as regulators and are located at one or both ends of a barrage. Model tests have indicated that a slight inclination upstream gives better approach conditions than a normal takeoff.

Design of the regulators follows the same principles used in design of barrages. Regulators are smaller versions of barrages designed to pass several thousand cubic feet per second, whereas barrages are designed to pass up to several hundred thousand cubic feet per second. Openings and crest elevations must be set to permit passage of the maximum canal flow at various pond levels. Silt exclusion from the canals is a very important consideration in connection with regulator design. Quite often silt-excluder tunnels are constructed in the barrage bay or bays adjacent to the regulator. These tunnels discharge onto the downstream side of the barrage and are designed to bypass the heavier silt-laden bottom layers of water which would otherwise go through the regulator into the canal.

28. Guide Banks. For barrages on rivers with erodible beds and banks and very variable discharges, guide banks are necessary. The ideal aimed at is to direct the main current of the river normally onto the work as centrally as possible, and so to center the channel that the embankments upstream and downstream of the barrage are kept away from river attack and erosion. They may also be designed to induce a favorable curvature for silt exclusion from the canals.

The upstream guide banks should be at least equal to the width between the abutments of the barrage. In plan they may be normal to the barrage, may converge to form a funnel, or where silt exclusion is an important consideration may be given a curve concave to the river axis. At their upstream end they must be given a curve which is generally of 1,000 ft radius and is carried round through at least 135 deg to the river axis.

The downstream guide banks should not be less than 500 ft long and curved outward in plan.

The guide banks must be pitched on the side slope adjacent to the river and must be provided with an adequate self-launching stone apron in advance of the pitching. The apron should be laid at the lowest feasible level without excessive pumping.

Model tests are generally carried out to determine the optimum layout of the guide banks.

29. Marginal Embankments or Bunds. Barrages normally raise the pond levels above the level of the floodplains; flood levels are higher still, with the backwater curves extending many miles upstream. It is necessary to provide marginal embankments, which are sometimes called bunds in India and Pakistan.

The function of these embankments is to prevent outflanking of the barrage by the pond or during floods. Where there has been encroachment on the floodplain, the embankments are aligned to limit the flooding of valuable agricultural land or village sites.

The banks are aligned to connect from the abutments with land at elevations above the afflux level and backwater curve. They generally cross the floodplain more or less at right angles to the river axis in the vicinity of the barrage and are then turned parallel to the river axis to protect the valuable land, etc. In this portion of their length, which may extend for more than 10 miles, they should be set back far enough from the central river axis to avoid embayments, since it is usually not feasible from an economic aspect to protect the banks themselves against river scour. Setting back, however, in many cases is not practically feasible, so that it is often necessary to provide stone or brushwood armored spurs to protect the embankments, more particularly in the area immediately upstream of the barrage. Sometimes it is necessary to construct these spurs simultaneously with the barrage, but it is often possible to defer their construction until river attack develops. In the latter case it is desirable, if possible, to envisage the final line to which it is desired to train the river and to make financial provision for the spurs.

The design of the embankments follows the rules and practice for any water-containing bank as to geometry, freeboard, wave action, and resistance to seepage both through the bank and under it. By reason of their extent, local soil must be used and the design fitted to the available soil. A good growth of vegetation on the riverside should be encouraged as an antiwave measure.

The tops of all banks should be made wide enough and hard enough to provide a roadway for light vehicles for inspection and maintenance purposes.

DAMS ON PERMEABLE FOUNDATIONS

Many of the principles and criteria given above for barrages are equally applicable to dams on permeable foundations. Usually, in the case of a spillway for a dam, the afflux will be greater than for a barrage. This results in greater discharge per foot run, requiring a deeper and possibly longer hearth apron. Dams generally resist greater heads than barrages with attendant greater uplift, overturning, and sliding

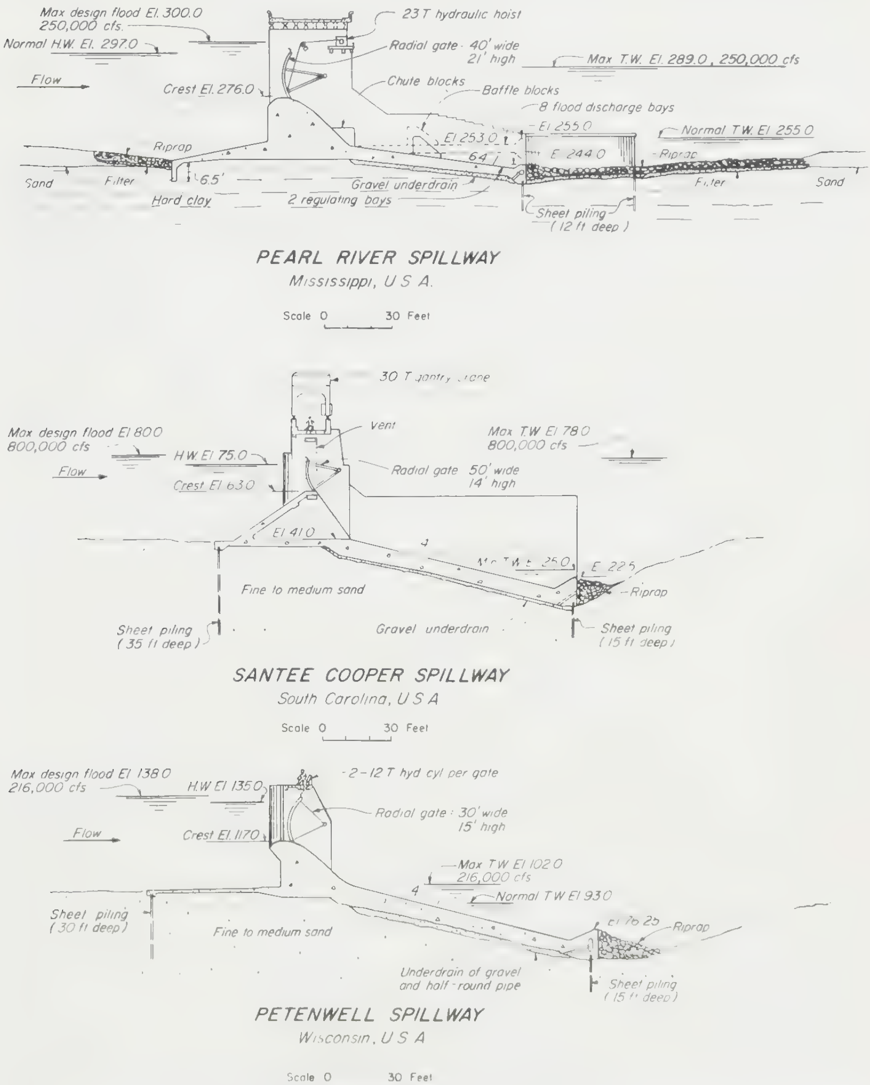

FIG. 14. Examples of spillways constructed in the United States on permeable foundations.

problems. Examples of dams on soft foundations are well illustrated in the transverse sections given in Fig. 14. Spillway capacities are proportioned for design floods more on the order of a 1,000-year recurrence rather than for 40- or 50-year recurrence, as used for barrages. Reference 2 has useful information on a concrete dam constructed on a deep sand foundation.

Bibliography

1. Khosla, A. N., N. K. Bose, and E. M. Taylor, "Design of Weirs on Permeable Foundations," Central Board of Irrigation, India, Publication 12.
2. Fucik, E. Montford, Petenwell Hydroelectric Project. *Trans. ASCE*, 1952.
3. Leliavsky, S., "Design of Dams for Percolation and Erosion," Vol. 3, Chapman & Hall, Ltd., London, 1965.
4. Weaver, W., "Uplift Pressure on Dams," *J. Math. Phys.*, June, 1932, p. 114.
5. Vaidhianathan, V. I., On the Electrical Method of Investigating the Uplift Pressure under Dams and Weirs, Research Publication, vol. V, no. 4, Punjab Research Institute, April, 1935.
6. Lane, E. W. "Security from Under-Seepage Masonry Dams on Earth Foundations," Trans. ASCE, Paper No. 1919, Vol. 100, 1935, p. 1235.
7. Haigh, F. F., Design of Weirs on Sand Foundations, Punjab Engineering Congress, Paper No. 182, 1935.
8. Pavlovsky, N. N., The Theory of Ground Waters Flow under Hydrotechnical Structures (in Russian), Leningrad, U.S.S.R., 1922. An English Summary appeared in Paper 36, Question 27, First Congress on Large Dams, Stockholm, 1933.
9. Terzaghi, C., Effect of Minor Geological Details on the Safety of Dams, Technical Publication of the Institute of Mining and Metallurgical Engineers, No. 215, February, 1929.
10. Harza, L. F., Uplift and Seepage under Dams on Sand, *Trans. ASCE*, Paper no. 1920, vol. 100, p. 1352, 1935.

SECTION 18

EMBANKMENT DAMS*

By John Lowe III

INTRODUCTION

Embankment dams, dikes, and levees have been used in the control of streams and rivers for thousands of years, and innumerable instances of their use exist in all parts of the world. The entire range of soils from clays to boulders and excavated rock has been used in their construction. The term embankment dam includes both earth dams and rock-fill dams as well as combinations of the two. Rock-fill dams with facings of materials other than earth fill are discussed in Sec. 19.

The choice of an embankment dam as compared with a concrete dam for a particular site depends upon several factors such as foundation conditions, the availability of construction materials, and topography. Embankment dams usually prove to be the most economical choice on soil foundations and frequently on rock foundations in wide valleys. Earth dikes and levees are usually the most economical structures for local flood-protection works unless space limitations prevent their use.

Natural soils vary to a great degree, and detailed field and laboratory investigations are necessary at each site to identify the soils at that site and to determine their engineering properties. In order to make best use of the soils at a particular site the designer of the embankment dam needs to be both imaginative and thorough. By using past experience and applying the latest developments in soil mechanics, he can make a safe design for an embankment dam for almost any site.

The purpose of Sec. 18 is to present:

1. The basic considerations that enter into embankment-dam design
2. Data and methods of analysis for uses in design
3. Examples of embankment-dam designs for various foundation conditions and for various conditions of availabilities of construction materials

A list of references is given for more detailed discussion of certain points and for alternative methods of analysis. Although the term embankment dam is used throughout the text, the discussions apply generally as well to dikes and levees.

GENERAL DESIGN PROCEDURE

1. Statement of the Problem. The problem of the design of an embankment dam may be expressed as follows:

Given: 1. Certain reservoir water-level and operating requirements and permissible leakage

* The author wishes to acknowledge the assistance of Kalman Szalay and other engineers of Tippetts-Abbett-McCarthy-Stratton in connection with the preparation of this section. Data obtained from other sources are acknowledged in the text.

2. Certain interrelationships with other features of the project
3. Certain foundation conditions
4. Certain available construction materials

Problem: Design a dam cross section and foundation treatment which will produce a safe and sufficiently watertight structure and which will result in a project of minimum cost.

The solution to the problem is made by trial. Different dam cross sections and foundation treatments are set up and checked for stability and watertightness. Several trials are needed for each different type of cross section and foundation treatment to find the slopes and dimensions which will give the required factors of safety. Cost studies can then be made to determine which cross section and foundation treatment result in the project of minimum cost. The most economic embankment-dam project would be compared with alternative schemes utilizing other types of dams. The effect of each of the four different sets of conditions listed above on the design of the embankment dam and its foundation treatment is discussed in the following paragraphs: (1) reservoir conditions, Art. 4; (2) interrelationships with other features, Art. 5; (3) foundation conditions, Arts. 6 to 10; and (4) construction materials, Arts. 11 to 13.

The design is usually carried out in three stages: reconnaissance report stage, economic and technical-feasibility report stage, and final-design stage where drawings and specifications for construction are prepared. In progressing from stage to stage the design becomes more refined. Also each stage indicates the additional field investigations and studies to be made in the following stage. Discussion of the effect which the different given conditions listed above have upon the choice of dam cross section and foundation treatment is given in Arts. 2 through 13.

2. Site and Laboratory Investigations. The program of field and laboratory investigations is normally carried out in three stages and in conjunction with the three cycles of design. In the first or reconnaissance stage, investigations are made to determine the general location and height of the dam and of the other features of the project. Small-scale topographic maps with scales of 500 to 1,000 ft to the inch generally have to suffice in this stage. Geological reconnaissance and a limited program of borings and/or test pits are utilized to check general foundation conditions and the availability of embankment materials. Samples of foundation and borrow soils are classified visually and by simple laboratory tests. Engineering properties of the soils such as permeability, shear strength, and compressibility usually can be estimated from these classifications with sufficient accuracy for use in preparing a rough design.

In this stage the design does not have to be proved; rather one or possibly two sites are chosen which appear to be economically and technically feasible. More detailed site investigations are then made for these sites in the second stage.

In the second or economic and technical-feasibility report stage, the types of structures as well as the basic dimensions and locations are established. The report should prove the technical feasibility of the project, and the design should be in sufficient detail so that a reliable cost estimate can be established for the project. This report is generally used as a basis for financing of the project. Topographic maps to a scale of 100 to 200 ft to the inch are required. Additional geologic studies, borings, test pits, and other subsurface investigations are made to establish the character of the foundations and to enable drawing of geologic profiles and sections close to all structures. Representative foundation and borrow samples are tested to determine engineering properties of the soil.

In the third stage, final design is made and plans and specifications for construction prepared. A topographic map to a larger scale and ground profiles and sections may be necessary. Additional borings and test pits are put down at the exact location of structures to fill the gaps in information disclosed by the second-stage design. Additional field tests and special investigations, such as the construction of a test embankment, may be necessary. Supplementary laboratory tests may be performed to expand and confirm the data collected in the second stage.

A description of methods of subsurface investigation is given in Arts. 43 through 49 and a description of laboratory investigations in Arts. 50 through 55.

3. Design Investigations. The following analyses should be made in connection with the design of an embankment dam:

1. Seepage analysis to determine the quantity of seepage through the embankment and its foundation and to establish the pattern of flow through the embankment and its foundation for use in stability analysis and piping analysis
2. Stability analysis of the embankment and of the dam and its foundation in combination
3. Settlement of the embankment and its foundation
4. Analysis of slope protection and freeboard requirements

4. Hydraulic Considerations. The general location of a dam, its height, the hydraulic conditions under which it must be stable, and the maximum leakage loss permissible are determined primarily by river planning. The total height of the dam is equal to the height of the spillway crest plus the surcharge height of the maximum spillway design discharge plus a freeboard height depending on wave action and seiche. The water conditions under which the dam must be stable are established from operation studies of the reservoir and include maximum and minimum design water levels and rates of filling and drawdown of reservoir. The amount of permissible leakage through the dam and its foundation depends upon the purpose of the reservoir, and whether the leakage represents a loss of water to power or domestic or irrigation water supply. The permissible leakage varies from project to project. In flood-control projects generally large leakages are permissible. In hydroelectric and water-supply projects leakage would be reduced to the point where the costs of design changes and/or foundation treatments to reduce water loss exceed the value of the water saved.

5. Interrelationship of Dam and Other Features. An embankment-dam project may include outlet works and powerhouse as well as spillway and diversion works. The design of the dam must take into account the interrelationship between the dam and all these other features. The location, cross section, and foundation treatment chosen for the dam should be the one which results in minimum cost of the total project, and this is not necessarily the location, cross section, and foundation treatment which would produce the dam of minimum cost.

Overtopping of an embankment dam usually results in washout of the dam; thus adequate spillway capacity is essential in an embankment-dam project. The most desirable type of spillway for an embankment dam is one located some distance from the dam in a saddle in the reservoir rim. If a distant spillway is not feasible, the alternative would be a chute or tunnel spillway in one of the abutments of the dam. A chute spillway in an abutment usually requires a large sidehill cut. The cut should be located far enough into the abutment so that a reasonable section of natural rock or, if rock is not present, natural ground is left between the spillway channel cut and the end of the dam. The side slopes of the spillway cut should be adequately safe against slides which might block the spillway channel. If it is difficult or costly to make a cut of sufficient size to accommodate a spillway for the full spillway design flood, consideration may be given to constructing a spillway designed to accommodate normal floods plus an emergency spillway through a saddle in the reservoir rim. At times a low-cost emergency spillway can be built at a remote location and occasional damage accepted whereas an operating spillway at the same location would be expensive since it would have to be built to avoid damage under frequent operation. When an abutment spillway is required, the location of the embankment dam in the valley is frequently governed to a large extent by the consideration of locating where the abutment topography is suitable for the spillway. Discharges from abutment chute or tunnel spillways must be made so as to avoid any erosion of the downstream toe of the dam.

For low-level outlets from embankment-dam reservoirs, the first choice is tunnels through the abutments; the next choice is a conduit constructed on a bench in rock cut in the abutment. As a last resort the conduit would be founded on natural earth or earth fill underneath the dam. In all three instances one set of gates should be located at or upstream of the core of the dam. In the case of a tunnel in rock this would mean a set of gates at or upstream of the grout-curtain extension of the core into the abutment. If the operation of the project requires that the outlet be under water pressure downstream of the core of the dam the water should be carried in a steel penstock inside the conduit. In this way any leakage can be noted and would be carried away without causing erosion of the dam or foundation. For similar reasons it is desirable that tunnels in the abutments which have to carry water pressure downstream of the core of the dam be lined with steel for watertightness or have an inner penstock like the conduit mentioned above.

When outlet works are required in connection with an embankment-dam project, the location of the dam in the valley is frequently governed to a large extent by consideration of topography suitable for tunnels or bench cuts in rock. Where conduits are used special measures are required to minimize seepage through the dam along the faces of the conduits. Seepage fins are usually used on the conduits and special compaction and filters used in the construction of the dam adjacent to the conduit. Where the conduit is founded on an earth foundation special articulated design may be necessary to permit the conduit to settle and change in length as the foundation settles under the load of the earth dam. Outlet works should not discharge at high velocity near the toe of the dam. Stilling basins, or Howell-Bunger-type valves, or other energy-dissipating devices are usually required. In order to keep the length and cost of the outlet tunnel or conduits as low as possible it is desirable to steepen the slopes of the dam at least in the vicinity of the outlet works. The use of more costly materials in the dam to permit steeper slopes frequently can be justified on the basis of savings which the steeper slopes permit in the cost of the conduit.

When a powerhouse is included at the site of an embankment-dam project consideration needs to be given to the topography and foundations condition for the power features in locating the dam in the valley. Steepening of the slopes of the dam is particularly desirable if by shortening the power waterways a surge tank can be eliminated.

The scheme of diversion of the river during construction of the embankment dam may affect both the location and the cross section of the dam. Certain locations in the valley may be better suited for construction of diversion channels and cofferdams than others. Savings in project cost can frequently be made by incorporating the diversion cofferdams in the upstream and downstream shells of the embankment dam. It is frequently desirable to use the outlet or power tunnels for diversion tunnels. In order to pass the construction-period floods it may be necessary that appreciable head be developed at the upstream end of these tunnels. In order to do this the dam would have to be constructed to some minimum elevation during the first dry season after diversion. Frequently only a portion of the dam cross section is built to this elevation, as in the case of Binga Dam described in Art. 61. A specially designed cross section is generally required to permit this procedure. In cases where the dam must be built to some minimum height during a single dry season, it is often helpful if the foundation treatment for the dam or a portion of it can be completed the previous dry season. In this case the foundation treatment must be such that it can withstand the wet-season flow over it without significant damage.

In the design of the cross section of an embankment dam, the maximum use of materials from required excavations for other features such as spillway, outlet works, powerhouse, and diversion channel usually results in a project of minimum cost. Generally there will be little difference in cost in materials from required excavations and similar materials from borrow. Thus within the limits of embankment requirements, the designer may plan features requiring large excavations without materially affecting the cost of the project. Sometimes the width and depth of such excavations can be varied and some control thereby obtained over the amounts of different types of material obtained. To make use of materials from required excavations at minimum cost the cross section of the dam should be zoned so that the materials can go directly into the dam from the excavations without stockpiling.

FOUNDATION TYPES AND TREATMENTS

6. General Considerations. The choice of type of embankment dam and the design of the dam are affected to a large extent by the foundation conditions at the site. Generally some treatment of the foundation is required to control seepage. These treatments may be in the form of cutoffs, impervious upstream blankets, or foundation-drainage measures. The cross section of the dam must be such as to accommodate or be compatible with the foundation treatment. For example, the impervious core of the embankment must connect with an upstream impervious blanket if one is used. Further the strength of the foundation will have an important effect on the slopes selected for the dam if the strength of the foundation material is less than the strength of the embankment material.

The stratification and properties of the foundation materials frequently are erratic and difficult to delineate. This is especially the case because subsurface conditions in valleys are generally the result of numerous geologic processes involving sequences of erosion and deposition. In contrast the materials in the embankment are placed by man, and all materials and their distribution may be a matter of record. The success or failure of a dam frequently depends upon the making of sufficient subsurface explorations to disclose all strata or lenses critical for stability or seepage and properly designing for them. The following description of foundation types treats with more or less homogeneous foundation conditions in order to illustrate various principles of foundation treatment. Actual foundation conditions generally are not homogeneous, and a combination of treatments may be required.

7. Rock Foundation. A sound rock foundation is the best possible type of foundation for an earth- or rock-fill dam from both stability and seepage considerations. Sound rock is of much greater shear strength than any earth or rock fill and will permit as steep slopes as the shear strength of earth- and rock-fill materials themselves will permit. Seepage through the fissures in sound rock is usually negligible and no problem of erosion of the rock by seeping water exists. The critical consideration in connection with rock foundations is the presence of planes and zones of weakness such as faults, joints, shear zones, bedding planes, and solution caverns and passageways. Such planes and zones of weakness may be critical with respect to both stability and seepage. Ascertaining the presence of planes and zones of weakness and delineating their location and characteristics are difficult. In coring rock, for example, cores are obtained of the sound rock, but generally no core recovery is made of critical materials in joints and zones of weakness. Water-pressure tests can be performed throughout the depth of borehole in increments. Although such tests provide some information on the openness of joints and fault zones, they provide no information on the strength characteristics of the material filling the joints and fault zones. Exploratory adits and trenches give good information on location of planes and zones of weakness and also permit in situ tests. Such tests are valuable aids in establishing seepage, strength, and compressibility characteristics for design.

Nominal foundation treatment for a good rock foundation consists of a Portland-cement grout curtain connected to the impervious core of the dam. Grout curtains are described in Art. 25. Foundation treatment for planes and zones of weakness varies greatly depending upon their location and characteristics. Treatments may include drainage measures and grouting, as well as excavation and replacements with concrete in critical places.

Most rock foundations consist of moderately to highly fractured rock and weathered rock; sound rock foundations are the exception rather than the rule. Highly fractured and weathered rock foundations grade into earth-type foundations, which are discussed below.

8. Pervious-soil Foundation. Where an embankment dam is founded upon a pervious-soil stratum the main requirement of foundation treatment generally is the control of underseepage. The preferred foundation treatment for control of underseepage is a cutoff through the pervious stratum to impervious material. Where the thickness of pervious material is not too great and where reasonable measures can be used to handle groundwater in the pervious stratum, the cutoff is made by excavating a trench to the underlying impervious foundation stratum and backfilling it with compacted impervious fill. An example of such a cutoff is the foundation treatment for Shihmen Dam, a cross section of which is shown in Fig. 62. In this case the pervious stratum was river alluvium consisting of sand, gravel, cobbles, and boulders and the underlying impervious foundation stratum, sandstone and mudstone bedrock. The cutoff was designed as the extension of the core below general ground level for the base of the embankment dam, the side slopes of the core extending down to bedrock. In this design the gradient through the cutoff is consistent with the gradient through the core.

Further, since seepage along the interface between cutoff and bedrock probably is easier than directly through the core itself, the length of contact between cutoff and bedrock should be no less than the length of seepage path through the core. This is the case where the cutoff is an extension of the core. Joints and fissures in the bedrock to which the cutoff is connected, particularly joints and fissures parallel to the direction of the seepage, should be cleaned and then pressure- and/or slush-grouted before placement of the impervious cutoff material.

Where it is difficult to excavate the cutoff trench to the underlying impervious stratum because of groundwater problems in overlying pervious stratum and because of the depth of the pervious stratum the slurry-trench method of cutoff may be considered. This method is described in Ref. 77. In essence the method consists of keeping the cutoff trench filled with bentonite slurry during excavation. Thus steep slopes can be used for the excavation. The slurry is then replaced with impervious material dumped into the trench to displace the slurry. Because of the poor compaction of the trench filling, slurry-trench cutoffs are generally located upstream of the body of the dam and connected to the core of the dam with a compacted impervious blanket. The cross section used for Wanapum Dam is shown in Fig. 55. Because the contact of the cutoff and the underlying impervious stratum is not exposed the tie of the slurry-trench cutoff to the underlying impervious stratum is less certain than the tie described above for the compacted fill placed in the open trench. Slurry-trench cutoffs are of particular advantage for cofferdams and levees.

Another type of cutoff which utilizes a slurry trench is the ICOS type of wall.

This method is described in Ref. 18. In this case a narrow trench is excavated in short sections using special buckets. The trench is kept filled with bentonite slurry, which maintains the vertical sides of the trench. After each section of the wall is excavated the slurry is displaced by concrete. The resulting cutoff consists of a concrete wall about 1 m wide extending from ground surface to a short distance into the underlying impervious stratum. Before the concrete is placed in the trench a grout curtain can be constructed in the underlying stratum if it is suitable. The ICOS wall cutoff is frequently located upstream of the main body of the dam and in this case it is connected to the impervious core by means of a compacted impervious blanket. ICOS cutoff wall has been used for Sesquile Dam, Colombia, and Manicouagan 5 Dam. The concrete wall must maintain its integrity under the lateral and drag loads imposed upon it by settlement of the dam and filling of the reservoir and because of earthquake. Also there must be no gaps in the continuity of the wall or in its contact with the underlying impervious stratum. The gradient across the wall is exceedingly high and can readily result in excessive leakage and possibly local internal erosion of the pervious stratum if the pervious stratum consists of stratified fine and coarse material. The ICOS concrete wall may be of particular advantage for cofferdams and levees where heads are generally low and high water is of short duration.

Grouted cutoffs have been considered for pervious soil foundations, but they offer many uncertainties and generally are expensive. The main problem centers around obtaining a continuous curtain. Several rows of close-spaced holes have been used; still there is no certainty that a continuous curtain has been obtained. Because of the high gradient across the curtain appreciable leakage will occur through any gaps; also possible local internal erosion might occur in stratified fine and coarse pervious material. Portland-cement grout, flocculated-clay grout, and chemical grouts have been proposed both alone and in combination. A grouted cutoff was used for the Serre Ponçon Dam Project described in Ref. 21.

When a positive cutoff to the underlying impervious stratum is expensive and some leakage is permissible or when the depth to the underlying impervious stratum is great and a positive cutoff is not feasible, reduction of overall seepage gradients may be accomplished by construction of an upstream impervious blanket; drain wells and/or a drainage blanket underneath the downstream shell of the dam may be used in addition to assist in control of exit gradients. The distance from the upstream edge of the blanket to the downstream toe of the dam should be at least fifteen times and preferably twenty times the head difference between these two points. An example of the use of an impervious upstream blanket is the proposed Tarbela Dam, West Pakistan, a cross section of which is shown in Fig. 63. Impervious upstream blankets for control of underseepage are frequently used in connection with levees.

9. Impervious Soil over Rock Foundation. Impervious-soil foundations may consist of alluvial silts and clays or well-graded glacial tills or residual soils. These soils generally present little difficulty from the standpoint of seepage but where silt or clay is present require careful investigation in connection with stability and settlement. Although the quantity of leakage is not a problem, careful control of exit gradients by drain wells and other means is required for cohesionless silts and rock flours which are susceptible to piping.

Where the shear strength of the impervious soil is less than the shear strength of the compacted embankment-shell material, either the faces of the dam should be concave or wide counterweight berms with heights up to half the height of the dam should be used. Methods of stability analysis involving composite surfaces of sliding have been developed for a dam on this type of foundation and are described in Art. 35.

Settlement analysis of dams on compressible foundations needs to be made to determine the camber to be provided at time of construction and also to determine whether differential settlements will be of such magnitude as to be detrimental to the behavior of the dam. Generally the most serious differential settlements occur where the foundation changes from relatively incompressible rock abutments to valley-bottom compressible impervious material. Appreciable differential settlement might cause transverse cracking of the dam, which could be dangerous to the safety of the structure.

In rare instances, sand drains and electro-osmosis have been installed in compressible soils to facilitate the rate of consolidation and thereby the rate of increase of shear strength. In this way the dam may be built to full height much more quickly. A sand-drain foundation treatment was used for the Selset Dam in Ref. 7 and electro-osmosis for West Branch Dam.[16,*]

10. Impervious Soil over Pervious-soil Foundation. This type of foundation presents the same foundation difficulties as the impervious soil over rock type described above. In addition there is the danger of boils or of piping at the downstream toe of the dam whenever the thickness of the impervious stratum is insufficient to resist the hydrostatic uplift which develops at its base. Frequently the pervious stratum connects somewhere to the water upstream of the dam or riverward of the levee. Little head is lost in flow through the pervious stratum so that practically the full hydrostatic head of the water upstream of the dam develops at the base of the impervious layer. To relieve this pressure, a relief trench or a series of relief wells may be installed at the downstream toe to penetrate into the pervious stratum. In cases where the pervious strata dip upstream and outcrop some distance downstream of the dam, the relief measure may best be placed just upstream of where the pervious strata outcrop. For levees relief trenches are usually more economical to construct where the depth of penetration required is less than about 10 ft. For greater depths, drainage wells are more economical. An example of relief drains is shown in Fig. 54, which presents a cross section of the Portville levee. The design of relief drains is discussed in Art. 23.

Where a foundation consists of varved silt or clay (alternate layers of fine sand and silt or silt and clay) excessive pore pressures may be developed in the compressible layers because of the weight of the dam. These hydrostatic excess pressures may then be transmitted laterally by the more pervious layers to locations where the pressures are inordinately high with respect to the weight of overlying material and may cause stability failure. A case of this type is described in Ref. 17, particularly pp. 1416–1421.

EMBANKMENT TYPES

11. General Considerations. The cross section of a dam as well as the method of its construction depends to large extent on the materials available from required excavations and borrow. Sufficient impervious material should be incorporated in the dam to reduce the seepage to the permissible limit for the given case, and sufficient pervious material should be incorporated to ensure stability with economical side slopes. Seepage analysis (Art. 19) can be made to determine the flow of water through a dam, and the uppermost line of seepage can be delineated. To protect the downstream slope against softening and sloughing, the uppermost line of seepage should be kept well within the dam. Upon drawdown of the reservoir, destabilizing forces are generated in the upstream portion of the dam. Features should be incorporated in the dam to minimize the effect of these forces and the upstream shell should be of sufficient strength to resist what increase in destabilizing forces occurs.

Ideal shell materials are free-draining well-graded gravels and cobbles or clean hard rock fill suitable for compaction in shallow lifts. Particles making up shell materials should remain hard and durable throughout the life of the dam. If free-

* Superior numbers refer to items in the Bibliography at the end of this section.

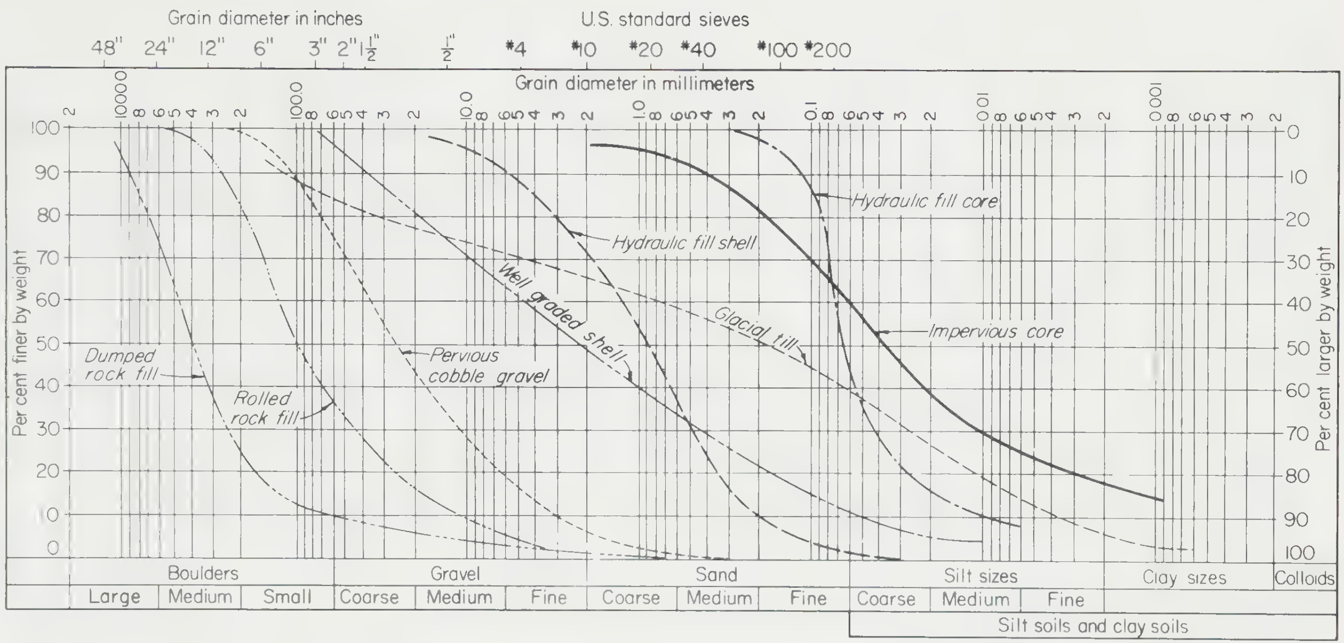

Fig. 1. Grain-size distribution curves of typical embankment materials.

draining shell material is not available the next best choice is granular nonplastic material which exhibits dilatency upon shearing.

Ideal core materials are well-graded glacial-till-type material and moderately plastic clay. The former is impervious, has high shear strength and low compressibility, and can be compacted to high density. The latter is impervious but has lower shear strength and higher compressibility than the till-type material. Both materials are resistant to piping, the till type because of the wide range of grain sizes up to gravels and cobbles and the clay because of its cohesion. Cohesionless low-plasticity silts are impervious, but they are readily susceptible to piping, require careful control of water during compaction, and may have low shear strength and high compressibility.

Grain-size curves of typical embankment materials are given in Fig. 1. The range in permeability of various embankment materials is given in Fig. 7. A permeability of 1 ft/day, 2.5×10^{-4} cm/sec, is commonly used as the dividing line between pervious and impervious materials.

Study of the cross sections of existing embankment dams in the vicinity of the project and of dams constructed of similar materials on similar foundation conditions is helpful in developing the cross section for a proposed dam. A list of existing dams throughout the world is given in Ref. 28; many embankment dams are described in Refs. 2 and 55. Cross sections of several typical embankment dams are given at the end of this section. A discussion of principles for selection of foundation types and embankment types is given in the two articles following.

The approximate slopes which may be used for an embankment of cohesionless

Table 1. Approximate Slopes of Cohesionless Embankment Materials

Shell material	Drained friction angle ϕ, deg	Approx slope	Qualifying conditions
		Downstream Face	
Sound rock fill	45	1 on 1.5	Sloping core
Sound rock fill	45	1 on 1.75	Center core
Sand and gravel	37	1 on 2.0	Slope protection: cobbles or rock fill
Sand	30	1 on 2.5	Slope protection: topsoil and grass
		Upstream Face, Rapid Drawdown Considered	
Sound rock fill	45	1 on 1.75	Center core
Sound rock fill	45	1 on 2.5	Sloping core: properties of core affect slope
Cobble gravel	37	1 on 2.25	Center core; shell: free-draining
Sand and gravel	37	1 on 3.25	Center core; shell: water retained by capillarity upon drawdown; dilatent upon shearing, free-draining slope protection
Sand and gravel	37	1 on 3.25	Center core; shell: relatively incompressible with seepage roughly parallel and out of upstream face upon drawdown; free-draining slope protection
Sand	32	1 on 4.0	Center core; shell: relatively incompressible with seepage roughly parallel and out of upstream face upon drawdown; free-draining slope protection

material on a foundation which is rock or which is much stronger than the embankment material is given in Table 1.

When the shells of an embankment dam are composed of clayey material the slopes of the upstream and downstream faces depend upon the height of the embankment. For low dams approximate slopes would be 1 on 2.5 downstream and 1 on 4.0 for an upstream slope subjected to rapid drawdown. For higher dams the faces are generally made concave with the steeper slopes mentioned above at the top and flatter slopes near the toe.

In the two following articles, different types of earth-dam sections are discussed for various conditions of availability of impervious and pervious materials at the site. Where only pervious materials are available, the reader is referred to Sec. 19. Impervious membranes may be placed on earth-fill materials as well as rock fill. Recently asphaltic-concrete membranes have been placed on gravel fill in Norway.

12. Impervious and Pervious Construction Materials Available at Site. Where ample quantities of impervious and pervious construction materials are available at the site, the usual section chosen is one with a central core of impervious material and shells of pervious material. Under certain conditions an inclined impervious core is more advantageous; these conditions will be discussed at the end of this article. The central core is usually placed directly in the center of the dam as in the case of Hanabanilla Dam (Fig. 59) and Shihmen Dam (Fig. 62) or slightly upstream as in the case of John Flanagan Dam (Fig. 61). The width of a central core increases with head on the core and generally should be no less than half the head. Since the shear strength of core material is generally much less than the shear strength of shell materials, for stability reasons the width of the core generally should not be more than about two times the head. In addition the width of core actually selected for a dam will depend upon the relative cost of core and shell material at the site.

Immediately upstream and downstream of the core should be transition zones or filter zones. If ample material to act as a filter between the core and the shells is available, a transition zone with width equal to about half the head is desirable. If filter material is limited, filter zones with at least 10 ft width should be used. As thick a filter as feasible generally should be used downstream of the core. If ample quantities of free-draining shell material are available, the situation is ideal and stable upstream and downstream slopes can be obtained readily. If the quantity of free-draining shell material is sufficient for only one shell, it should be used for the upstream shell; a chimney and horizontal drain together with non-free-draining material should be used for the downstream shell as described in Art. 13. The use of free-draining material for the upstream shell is desirable for two reasons. Water drains out of the shell concurrently with drawdown, and the destabilizing forces created by the drawdown are therefore less than if the water had not drained out freely. Even with the free-draining condition, however, the driving forces in stability analysis increase significantly because of the change in weight of the shell from buoyant weight before drawdown to drained weight after drawdown. Because of the increased driving forces, the shell must develop increased shear resistance. Volume changes of necessity will occur in the shell material accompanying the development of increased shear resistance. With free-draining shell material, no adverse pore pressures will build up in the shell material because of this volume change.

At times the available shell material is cohesionless and appreciably more pervious than the core material, yet not free-draining upon drawdown. In the use of such material for an upstream shell it is desirable that the material be placed at such a degree of compaction that it will tend to dilate during shearing. This will ensure against any decrease in shear strength below the strength obtaining before drawdown. Also with such compaction, the shell material would be more resistant to reduction of shear strength under repetitive earthquake loading. More economic design usually results if, in addition to the zones for impervious, pervious, and transition material or filters, zones for random fill are provided. Materials for such zones would have suitable shear and compressibility characteristics for use in the embankment section but would vary considerably in permeability characteristics and result in a zone with a high degree of stratification. Without a random zone, material from heterogeneous borrow and required excavations would have to be tediously differentiated truckload by truckload as suitable for core or shell or transition.

Where a dam is on a strong foundation and where a positive cutoff can be made to impervious material, a central-core dam generally provides the simplest and most economic choice.

Sloping-core earth dams have advantages over center-core earth dams under certain construction and site conditions. The first sloping-core earth dam constructed was Nantahala Dam, built under the direction of J. P. Growdon, chief hydraulic engineer of the Aluminum Company of America. A cross section of the dam is shown in Fig. 53. The dam consists of a large downstream section with upstream and downstream slopes close to the angle of repose of the rock-fill material used. A sloping impervious core together with filters is placed against the upstream face of the large downstream rock-fill section and is in turn overlain by an upstream rock-fill shell. The upper 40 ft of the dam is a central-core section. The advantage of the sloping-core section for construction is that it permits placement of rock fill in the large downstream section to lead placement of the core. During construction of a center-core dam it is desirable that the core and shells be maintained at close to the same level. In earlier rock-fill-dam construction, placement of rock fill in dumped lifts of 30 ft or more makes construction with a center core awkward. Even today, when placement of rock fill in 2- to 5-ft compacted lifts is becoming the rule, weather conditions may restrict placement of core, and in such cases the sloping-core section is more adaptable to having the rock fill or pervious shell material lead the core.

When a positive cutoff is not feasible at the site and an upstream impervious blanket is used for underseepage control, a sloping core is expedient for minimizing the amount of impervious material required for core and blanket. Tarbela Dam (Fig. 64) illustrates such a situation.

For the situation where an initial stage of the dam has to be constructed to maximum height in one season for construction-period flood control and diversion, a sloping-core dam may be advantageous also. In such a situation, all construction effort is directed to building the large downstream pervious section together with overlying filter layers and possibly some sloping core. Because of the steep slopes of the downstream pervious section, maximum height of dam is reached using a minimum amount of material. The filter layers together with at least the lower portion of the core should be placed so that seepage into the downstream section is reduced to an amount which the section can pass safely. Binga Dam (Fig. 57) is an example of the use of a sloping-core section for this purpose.

Sometimes, because of topographic and foundation conditions, it is desirable to locate the cutoff considerably upstream of the center line of the dam. In this case, a sloping core is advantageous. An example of such a case is Hirfanli Dam shown in Fig. 56. If the dam were moved upstream so that the axis of the dam were directly over the ideal location for the cutoff, the volume of the dam would have increased greatly.

The volume of a sloping-core dam on a strong foundation is about the same as the volume of a center-core dam, although for this to be true the strength characteristics of the sloping-core material need to be above average. Also the design of the filters downstream of the core is more critical than for a center-core dam since seepage through the sloping core is more in a downward direction. For the same quantity of core material, the sloping core would have the same horizontal width as a central core, but the thickness of the core measured normal to the plane of the sloping core would be less and the gradients through it somewhat higher.

13. Ample Impervious Material but Limited Pervious Available at Site. It sometimes happens that practically all the material for construction of a dam at a site is relatively impervious. Pervious material for shells and filters has to be imported from a long distance or produced from a quarry or by processing from a widely graded material.

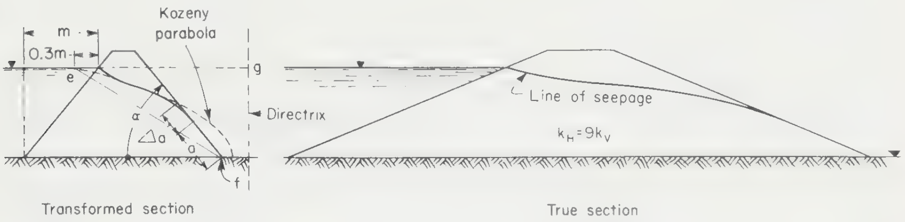

Fig. 2. Position of line of seepage in uniform embankment on impervious foundation.

For the case of a dam constructed of a single material, seepage of water out of the downstream slope would normally occur as illustrated in Fig. 2. To prevent this condition from occurring, rock-fill toes, horizontal drainage blankets, and chimney drains are installed in the dam. Drainage blankets (Fig. 4*a*) are usually several feet thick and extend from 25 to 100 percent of the distance from the downstream face to the center line of the dam. When an impervious embankment is placed on a foundation with an upper pervious layer, a natural drainage blanket is available, as shown in Fig. 4*b*. The advantage of the drainage blanket over the rock-fill toe is that in a homogeneous embankment, the blanket keeps the line of saturation farther away

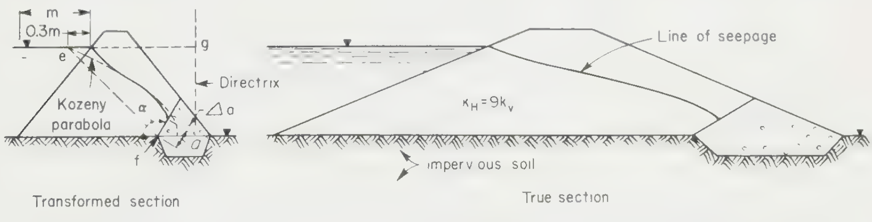

Fig. 3. Position of line of seepage in uniform embankment with rock-fill toe.

from the downstream face than a rock toe and thereby permits design of a section with somewhat steeper or more stable downstream slope. When pervious material is not available at the time of construction of the lower portion of the embankment or where an old dam or levee is to be stabilized, a section of pervious material is sometimes placed on top of the downstream face of the impervious material and acts like a rock toe.

The effectiveness of a horizontal drainage blanket is greatly improved by the addition of a "chimney" drain as shown in Fig. 5*a*. Stratification is practically unavoidable in construction of a so-called homogeneous embankment cross section because of normal variations in the permeability of the construction material. Even in the most uniform of construction materials a ratio of horizontal to vertical permeabilities of much greater than 10:1 may be expected. Also there is always the chance that a layer of relatively more impervious materials may overlie the horizontal drainage blanket. Such a layer would cut off drainage to the drainage blanket and cause water to emerge at the downstream face just above the more impervious layer. A chimney drain effectively intercepts seepage for the full height of the dam.

Occasionally in flood-control dams and levees, seepage may not penetrate far into the embankment because the reservoir will be against the upstream face for only a

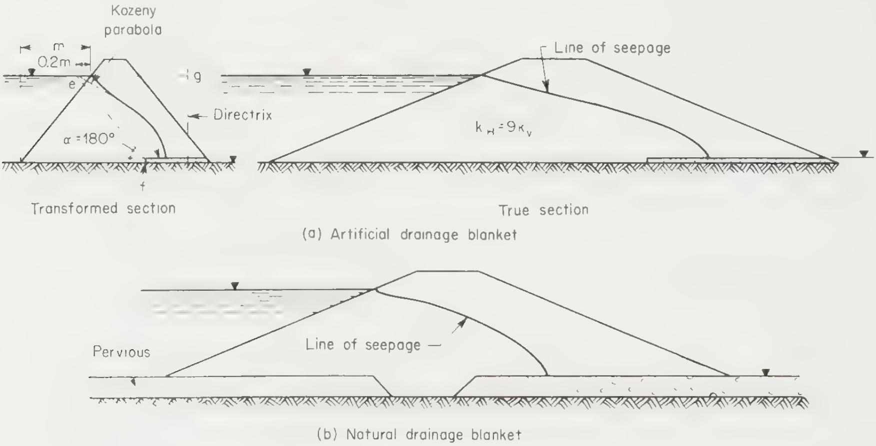

FIG. 4. Position of line of seepage in embankment with drainage blanket.

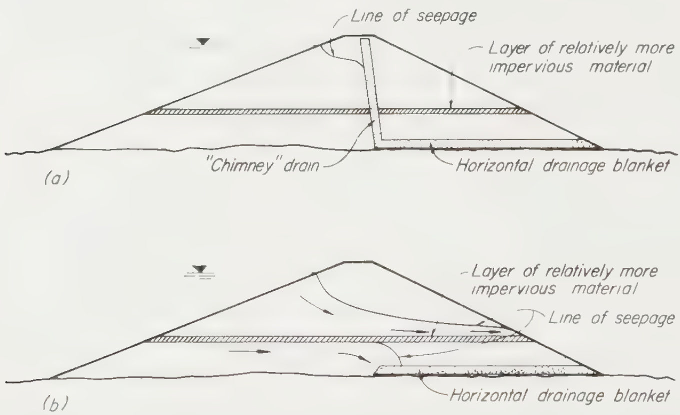

FIG. 5. Position of line of seepage in embankment containing a more impervious zone.

short period of time. Theoretically no rock toe, drainage blanket, or chimney drain is required in such cases, but usually nominal drainage measures are installed. For levees where seepage at the downstream face will occur only occasionally and for short periods, no drainage measures need be used, provided the downstream face is flat so that the exit gradient of the seeping water is small, about 0.2.

Horizontal drainage blankets are useful also at various levels in the upstream and downstream shell portions of embankment dams for dissipating pore pressures which tend to develop because of the weight of overlying fill. An example of such drains is shown in Fig. 62 for Shihmen Dam.

Horizontal drainage blankets may be used also to control the direction of seepage in the upstream shells of embankment dams upon drawdown of the reservoir. For the drainage blankets to be most effective the shells should be composed of relatively incompressible material. Typical relatively incompressible non-free-draining materials are well-compacted sand and gravel with fines and well-compacted weathered rock. If the height of capillary rise in the relatively incompressible material is equal to the height of the embankment, seepage will not develop and upstream drainage blankets would be of no use.

METHODS OF EMBANKMENT CONSTRUCTION

14. Preparation of Foundation. The foundation under the embankment dam or levee should be cleared, grubbed, and stripped of topsoil and any other undesirable material. Earthen foundations should be harrowed and moistened if necessary and then rolled as for a layer of the dam. If the foundation is below groundwater table, dewatering by means of well points, deep wells, or sheeted sumps should be used so that the embankment fill, especially impervious or semipervious material, can be placed in the dry. Care must be exercised in draining foundations that seepage forces do not loosen and weaken the foundation soils.

Abutments should be shaped so that there are no sharp changes in slope. All knobs and overhangs should be eliminated. If the overhang cannot be eliminated feasibly by excavation, lean concrete fill may be used to build out the abutment below the overhang. It is desirable that abutment slopes be no steeper than 1 on 1, especially in the area of the core. In rock canyons, however, it is sometimes necessary to have slopes as steep as 4 vertical on 1 horizontal. In such cases it is most important that the fill be compacted to a high degree to reduce its compressibility. Compaction to the maximum density indicated by the Modified AASHO compaction test is desirable.

Where the impervious core is placed on a rock foundation it is essential that the entire surface of contact be cleaned of all overburden material. Hand-excavation methods and air and water jets are usually required. Cracks and crevices need to be cleaned out and then backfilled with impervious material or dry-pack concrete by hand tamping, or slush-grouted with sanded grout. Where the impervious core is placed against impervious-earth foundation material it is desirable that a shallow trench extend into the impervious foundation to check the continuity of the impervious foundation layer in the area of contact with the core. In connection with levees in built-up areas such a trench is valuable for exploring the foundation for forgotten pipelines or drains.

Special treatments for earth foundations have occasionally been used or considered. At Franklin Falls Dam, explosives were used to compact a loose sand and incidentally to reduce its stratification.[43] Vibroflotation has been considered also for compaction of loose-sand foundations.[19] Sand drains[7] and electro-osmosis[16] have been used in rare instances to facilitate the consolidation of compressible clay foundations.

15. Degree of Compaction Required. As a soil is made more compact its undrained shear strength is increased significantly and its compressibility and permeability decrease. Increased compactive effort should be applied to the soil as long as the incremental benefits resulting from improvement of the soil properties exceed the incremental cost of compaction. On a strong foundation where the shear strength of the embankment material is critical in determining the embankment slopes, an increase in shear strength would permit an increase in steepness of the side slopes.

On the other hand, where the strength of the foundation is critical in determining the side slopes, an increase in the shear strength of the embankment material is not apt to be significant in permitting an increase in the steepness of the side slopes.

Many designers require compaction to about 95 percent of maximum unit weight determined by the Standard AASHO compaction procedure. Compaction to an appreciably greater unit weight, as 95 to 98 percent of maximum unit weight by Modified AASHO procedure, however, is desirable in many instances, such as the case of high dams where the granular material is subject to high pressures, where it is unavoidable that the dam be placed against steep abutments, and in areas subject to earthquake.

Where embankments are placed on weak foundation, usually only light compaction should be used in the lower portion of the embankment. The use of heavy equipment and many repeated passes of equipment tend to develop cracks and slickensides in the foundation and embankment and may result in excessive spreading of the foundation and failure.

Some expansive types of clay, if compacted according to usual procedures, will swell upon saturation under light loads. If it is necessary to use such material, cognizance must be taken of such swelling in designing the embankment section.

16. Rolled Fills. Materials for placement in a rolled-fill embankment dam may be excavated, hauled, compacted, and processed by a variety of equipment. Excavation equipment would include shovels, scrapers, draglines, bucket-wheel excavators, front-end loaders, and elevating scrapers. The shovel and wheel excavators are good for mixing material encountered in the full height of their cut. The other excavators are good for scraping off thin individual layers of material; by cutting on a slope across layers, however, they can also accomplish mixing of layers. Transportation of material to the embankment may be by various means including end- and bottom-dump trucks, scrapers if the haul is not too long, conveyor belts, and railroad. Placement of material on the fill is usually by trucks or scrapers, the material being transferred to them from the conveyor belt or railroad at some point close to the dam. On the fill, bulldozers or graders are used for spreading the fill from end-dump trucks and to a lesser extent for shaping material spread by bottom-dump trucks and scrapers. Processing consists primarily of passing the construction material over a grizzly or screen to separate coarse and fine fractions. Grizzlies generally have bar spacings of from 6 to 12 in. and are used to remove oversize particles which would interfere with compaction of the fill in layers as well as produce large-sized material suitable for upstream slope protection. Generally it is not feasible to use screens of smaller opening than about 1 in. They may be used to remove excess coarse fraction from a skip-graded material so that the fine fraction may be suitable for impervious zones in the dam.

For proper compaction, embankment material should be at close to the optimum water content for compaction. Laboratory tests give a good indication of what this optimum water content should be, but test embankments and analysis of the results of field density and water-content tests on the initial construction give most accurate information on the optimum water content for compaction by the particular equipment being used. If the material in its natural condition is not close to the optimum water content, the water content should be adjusted by drying the material or wetting it in the borrow pit. Drying may be accomplished by trenching the borrow area and/or by scarifying the surface on fair days. In order to minimize wetting of the material by rain in both the borrow pit and stockpile and on the fill, the surface of the borrow pit and fill should be shaped to drain, and before each rainstorm the surface should be rolled smooth. To increase the water content, the borrow pit may be irrigated or flooded. Water can be added also on the fill with sprinkler trucks; then discing or harrowing is required to distribute the water uniformly throughout the material to be compacted. Drying can be accomplished on the fill by discing and harrowing but is to be avoided since it slows down construction.

In the 1950s there was considerable discussion as to whether it was better to place material dry of optimum or wet of optimum. By placing the material dry of optimum there was less chance that undesirable pore pressures would be developed by the weight of overlying material. On the other hand material placed wet of optimum appeared more plastic than that placed dry of optimum and therefore was more desirable for core material since it would be less susceptible to cracking. Tests by Seed[49,50] show that at strains of 15 to 20 percent, the strength of a material at a particular unit weight placed dry of optimum is just about the same as the strength at the same unit weight placed wet of optimum. Strengths at strains of 15 to 20 percent are generally used in stability analyses for the design of earth dams. Thus from the point of view of stability analysis it is the unit weight of the material which is important and not so much whether it has been placed dry or wet of optimum. At low strains material compacted on the dry side of optimum is much stiffer than material compacted on the wet side and therefore for strain-stress analyses of the embankment for the condition below failure compaction dry or wet of optimum has significance.

Many different types of rollers are available for compaction. The sheepsfoot roller, the 50- to 100-ton rubber-tired roller, and the vibratory roller are the most important. A sheepsfoot roller consists of a steel drum on which are mounted tamping feet. The pressure on the feet vary from 250 to 500 psi depending on the size of the roller and how it is weighted. A heavy roller would have a weight of about 4,000 lb/lin ft. Sheepsfoot rollers are most suitable for compaction of impervious-type material with no particles larger than gravel sizes. Lifts are usually placed at about 8 in. loose measure and compacted with 8 to 12 passes of the roller, at which point the roller usually walks out of the lift; the feet ride on top of the material instead of penetrating it. The surface of a completed lift is rough and makes for good bonding with the next lift. Because the feet initially penetrate the lift at the beginning of compaction they have a tendency to homogenize the material of the lift by breaking down lumps and distributing moisture, and this may be of advantage in many instances. The roughness of the surface of the compacted lift facilitates soaking of the lift by rain and is therefore undesirable in this connection. Maximum unit weights are slightly higher than Standard AASHO compaction.

Heavy rubber-tired rollers may be used for compacting both impervious-type material and cohesionless material. Usually the roller consists of four large rubber tires similar to tires used on heavy hauling equipment. Tire pressures are in the range of 80 to 100 psi. Lifts for compaction are usually 12 to 18 in., loose measure. If full compaction is not required lifts up to 2 or 3 ft may be used. The number of passes is generally about 6. Maximum compacted unit weights are close to the maximum unit weights indicated by the Modified AASHO compaction test. Heavy rubber-tired hauling equipment can accomplish compaction similar to that of heavy rubber-tired rollers when tire pressures and loads are similar. At times the rear tire of a loaded truck can be used to accomplish compaction in hard-to-get-to places next to the abutment and next to structures. Moderate compaction can be accomplished by requiring hauling equipment to distribute their travels across the fill. In order to assure uniform compaction, however, it is best to require at least a minimum number of passes of a heavy rubber-tired roller.

In the field, a rough test for determining whether a soil is above or below the optimum water content for compaction is to roll a piece of it into a thread. If the thread breaks when rolled down to ¼ in., the soil is about at the optimum water content.

Since the early 1960s, 10-ton steel-drum vibratory rollers have been generally available. These rollers are good for compaction of cohesionless materials. Lifts up to about 2 ft have been used. It is expected that heavier vibratory rollers will become available in the future and that the vibratory roller will become a standard piece of equipment like the sheeps-foot and heavy rubber-tired rollers. In the past, cohesionless materials have been compacted with passes of a crawler tractor. One that was pulling another roller was more effective since the tractor vibrated more. Lifts used with the crawler tractor have varied from 6 in. for sand up to 2 or 3 ft with coarse-grained material. Flooding of cohesionless material during compaction with either the vibratory roller or tractor improves compaction.

In the past it has been common practice to place rock fill by end dumping in lifts of 30 ft or more. During dumping jet streams of water are directed at the rock fill to wash away fine material and permit the larger rock pieces to be in point-to-point contact. The volume of water used would be in an amount two to four times the volume of rock. The tumbling of the rock down 30 ft or higher dump slopes vibrates the rock already placed and to some extent improves compaction. Quarry-run rock up to the largest sizes which can be handled by the hauling equipment can be placed in this manner. Observation of the settlement of rock-fill dams as reported in Ref. 2 shows that dumped rock fill is quite loose. Rock fill placed in 2- or possibly 3-ft lifts and compacted with either heavy rubber-tired rollers or heavy vibratory steel-wheel rollers is much better compacted than dumped rock fill. When rock fill is placed in 2- or 3-ft lifts the maximum size should be no greater than the thickness of the lift and preferably two-thirds the thickness of the lift. Thus somewhat more blasting may be required for rolled rock fill than for dumped rock fill. In either case the rock-fill material should be such that the rock pieces will not break down with time and weathering nor will the points of contact crush. Hard and sound rock can be placed as rock fill; highly weathered rock can be placed as earth fill. Some intermediate-type rocks are not suitable for either rock fill or earth fill. Their use in embankment dams is limited to counterweight berms where weight is the only consideration for their use. For soft rock to be placed as earth fill, its gradation after placement must be such that there are no void spaces into which the products of further breakdown of the rock can go. Rock for either rolled or dumped rock fill should not contain flat and elongated pieces which will bridge at time of placement but later break down under the weight of overlying material or water loadings. Breakdown of the rock into smaller pieces by greater use of explosives in the quarry may reduce the amount of flat and elongated pieces.

17. Hydraulic Fills. In the western part of the United States, at the end of the nineteenth century, the hydraulic method of moving earth, which was developed in placer mines, was applied to earth-dam construction. With the recent developments in excavating, hauling, and compacting equipment, the hydraulic-fill method is not used much. The hydraulic-fill method was used not only to excavate and transport the fill material but also to separate it into fine and coarse fractions for the core and shells, respectively. Suitable material for segregation consists of sand and gravel with some silt and clay. The method of constructing such a hydraulic fill is illustrated in Fig. 6. The base of the shell sections is placed by rolled-fill methods, as is frequently the uppermost portion of the dam. The pipeline or sluiceway carrying the hydraulic-fill material is located near the outer slopes. As the material is discharged onto the fill the coarser materials settle out in the shell section and the finer materials in the pool which is maintained in the core area. The size of the pool is controlled by spillways. Material finer than about 0.01 mm is generally wasted over the spillways; by so doing the rate of consolidation of the core is enhanced. During construction, samples should be taken of both the core and shell to check the gradations of materials. Care should be taken that tongues of coarse pervious material do not extend beyond the minimum limits required for the core. Clay ball and lenses of impervious material should not be permitted in the shells. The gradations of typical core and shell materials for a hydraulic fill are shown in Fig. 1.

The main use of hydraulic-fill methods in earth-dam construction in recent years has been in cases where sand or sand and gravel are readily available from underwater borrow. Volgograd Dam in the U.S.S.R. is an example of the use of such hydraulic fill. In such cases no segregation of fine and coarse fractions is made; the borrow material is generally uniform in grain size. Sand hydraulic fill when deposited under water assumes a loose structure but when deposited above water becomes very dense. Compaction of sand under water by means of gangs of concrete-type vibrators has been used for fill inside cellular cofferdams, but no means appear to have been used for densifying sand placed under water in a dam.

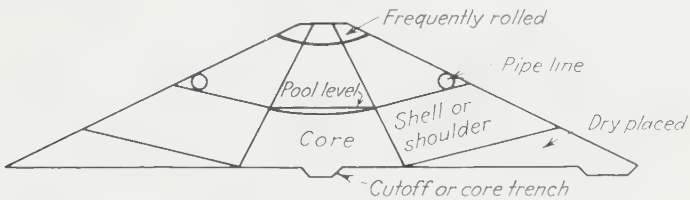

Fig. 6. Hydraulic-fill construction.

SEEPAGE ANALYSIS AND CONTROL

18. Permeability. The flow of water through soils except the coarser ones like gravels and rock fill is of the laminar type and in accordance with Darcy's law. This law states that the superficial velocity of flow is directly proportional to the pressure gradient through the soil. On the basis of this law we may write the following equation for flow:

$$Q = kiAt$$

where Q = quantity of flow in time t
k = coefficient of permeability
i = hydraulic gradient
A = superficial area of flow (total cross-sectional area for flow, not cross-sectional area of soil pores)
t = time during which flow takes place

The coefficient of permeability may be determined in the laboratory by tests on undisturbed samples or compacted specimens, as described in Art. 53, and by field seepage tests, as described in Art. 47. Various means are available also for making estimates of the coefficient of permeability on the basis of grain-size distribution of the soil. The range in permeability of various soil types on the basis of grain size is shown in Fig. 7 together with their embankment characteristics and methods for determining their permeability. Approximate determination of the coefficient of permeability may be made also by using Hazen's expression $k = CD_{10}^2$, where D_{10} is the grain-size diameter than which 10 percent of the material is finer by weight. Using cgs units of measure in the expression, the range in values of C reported by Hazen for tests on uniform fine sands as used in water-treatment filter plants is 41 to 146. Recent tests reported by Burmister[8] for a wider range of cohesionless soil types indicate a range in values of C from 20 to 600.

In both cases a mean value of about 100 was obtained for C.

Type of flow	Turbulent: $Q = k_t i^{2\pm} At$	Turbulent @ high i Laminar @ low i	Laminar: $Q = kiAt$	
Coefficient of permeability, k: ft./day	10^5, 10^4, 10^3, 10^2, 10^1, 10^0, 10^{-1}, 10^{-2}, 10^{-3}, 10^{-4}, 10^{-5}			
cm/sec.	10^2, 10^1, 1.0, 10^{-1}, 10^{-2}, 10^{-3}, 10^{-4}, 10^{-5}, 10^{-6}, 10^{-7}, 10^{-8}, 10^{-9}			
μ/sec.	10^6, 10^5, 10^4, 10^3, 10^2, 10^1, 1.0, 10^{-1}, 10^{-2}, 10^{-3}, 10^{-4}, 10^{-5}			
Embankment characteristics	Pervious free draining on rapid drawdown	Semi pervious, not free drainage on rapid drawdown	Material suitable for core	Practically impervious, core material
Soil types	Clean gravel	Clean sands, clean sand and gravel mixtures	Very fine sands, organic and inorganic silts, mixtures of sand silts and clay, glacial till, stratified clay deposits, etc.	Compacted clays
			Clays modified by effects of vegetation and weathering	Homogeneous clays below zone of weathering
Direct determination of k	Direct testing of soils in its original position pumping tests. Reliable if properly conducted. Considerable experience required			
	Constant-head permeameter. Little experience required			
		Falling-head permeameter, reliable. Little experience required	Falling-head permeameter, unreliable. Much experience required	Falling head permeameter, fairly reliable. Considerable experience required
Indirect determination of k	Computation from grain-size distribution Applicable only to clean cohesionless materials			Computation based on results of consolidation tests, reliable. Considerable experience required.
		Horizontal and vertical capillarity tests, fairly reliable Little experience required		

Fig. 7. Permeability and drainage characteristics of soils. (*After A. Casagrande and R. E. Fadum.*)

Natural soils almost invariably occur in a stratified condition, with the result that the permeability of the soil varies from a maximum in the direction of the strata to a minimum perpendicular to the strata. Even rolled fill of selected material will have some stratification because of the inevitable variation in density and composition of material from layer to layer. Casagrande[9] suggests that the ratio of $k_{\max}$ to $k_{\min}$ for rolled fills of selected material is probably at least 9:1. The maximum and minimum permeabilities for a stratified soil may be computed using the following formulas:

$$k_{\max} = \frac{k_1d_1 + k_2d_2 + \cdots + k_nd_n}{d_1 + d_2 + \cdots + d_n}$$

$$k_{\min} = \frac{d_1 + d_2 + \cdots + d_n}{d_1/k_1 + d_2/k_2 + \cdots + d_n/k_n}$$

where k_1, k_2, d_1, d_2, etc., are the corresponding permeabilities and thicknesses of the strata or layers composing the soil.

19. Flow Nets. The pattern of flow for steady seepage of an incompressible fluid through a porous soil of constant pore space can be expressed mathematically by a Laplacian equation. Direct solution of the Laplacian equation is generally difficult and has been made only for a limited number of cases. Examples of direct solutions as well as examples of solutions made using modern mathematical tools for close approximations are given by Harr.[22] For two-dimensional flow, graphical solution known as the flow net has been proposed by Forchheimer and is widely used. This method is described in detail by Casagrande[9] and in various textbooks on soil mechanics. Difficult flow nets can be determined using hydraulic or electrical models. When a hydraulic model is used a typical cross section is constructed of soils between the two glass plates of a narrow flume. The dimensions and permeabilities of the soils in the flume bear the same relationship to each other as in the prototype. Dyes are injected at points where water enters the soil to trace the flow lines of seepage through the soil. Model flumes are expensive and cumbersome and have been more or less displaced by electrical-analogy models. Methods of relaxation can also be used to develop flow nets as described by Southwell.[59]

A typical flow net for an isotropic embankment on an impervious foundation is shown in Fig. 8. The net consists of flow lines and equipotential lines which intersect

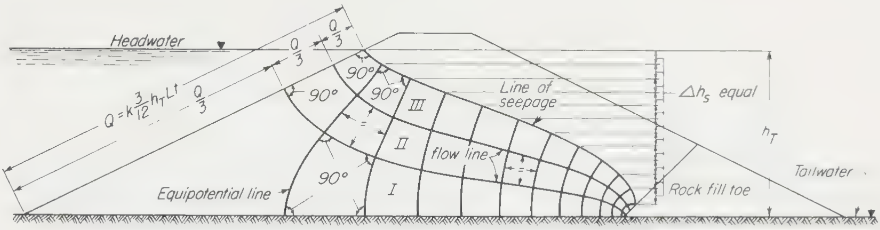

FIG. 8. Flow net for isotropic embankment on impervious foundation.

at right angles. For any particular problem there exist an infinite number of possible flow lines and possible equipotential lines. In constructing a flow net for the two-dimensional case in rectilinear coordinates, the lines are chosen so as to form "squares." Two adjacent flow lines of a flow net form a flow channel, and the quantity of flow through each channel of the net is the same. The equipotential lines connect points of equal total head and intersect the top flow line at equal increments of elevation. Suggestions for sketching flow nets are given by Casagrande[9] and Taylor.[64] In sketching, it rarely happens that the number of flow channels and number of equipotential drops both come out to be whole numbers. Usually there will be one fractional flow path or one fractional equipotential drop, as shown in Fig. 15. For the sake of appearance, many of the flow nets shown in this book have been specially chosen to have a whole number of flow channels and equipotential drops.

When the flow lines cross the boundary of two soil zones of different permeability the direction of the flow changes and the flow net deflects as shown on Fig. 16. Since each flow channel carries the same amount of water, this deflection provides a wider flow channel in material of lower permeability. When the flow channel widens the spacing of the equipotential lines will not be equal to the width of the new flow channel, and the flow net will not be composed of "squares" but of "rectangles" where the ratio of the longer side to the shorter equals the ratio of permeabilities.

Flow nets can be constructed for condition of radial flow and three-dimensional flow as described by Taylor.[64] Instead of the flow net being composed of "squares," "rectangles" are required and the ratio between the equipotential and flow-line sides of the rectangles depends upon the location of the rectangle.

In the case of material having different permeabilities in different directions, such as thinly stratified materials, the flow net of squares is drawn on a section transformed in such a manner that all dimensions in the direction of maximum permeability are reduced by dividing them by the square root of the ratio of $k_{\max}$ to $k_{\min}$ (or all the dimensions in the direction of minimum permeability are increased by multiplying them by the square root of the ratio $k_{\max}$ to $k_{\min}$). After the flow net has been drawn on the transformed section, the flow lines and equipotential lines are transposed back to the true scale section. This process is illustrated in Figs. 9 and 14.

The following procedure is valuable in connection with determining the position of the top flow line and is illustrated by Figs. 2, 3, and 4a. A parabola, called the basic parabola, is constructed through point e with point f as a focus. For flat

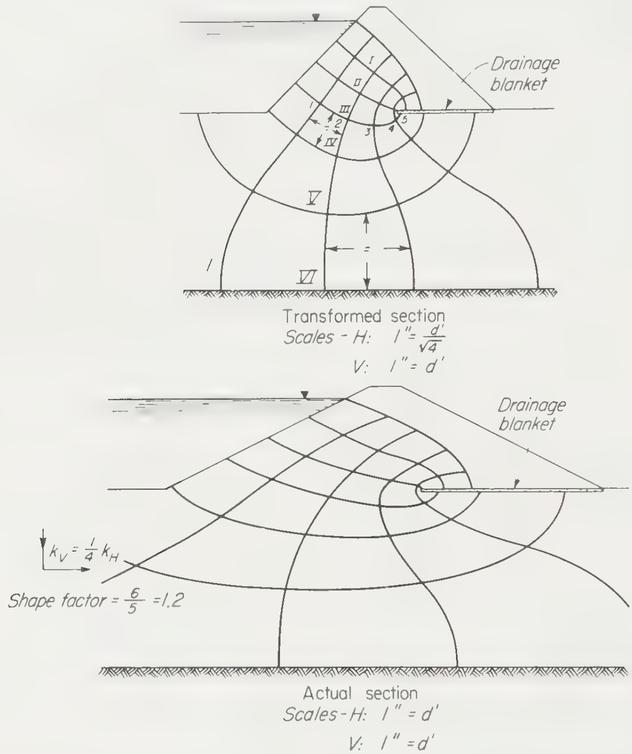

FIG. 9. Flow net for stratified embankment and foundation.

upstream slopes, the coefficient by which the distance of the figures must be multiplied to obtain point e is equal to ⅓, for average slopes ¼, and for steep slopes less than ¼. The directrix of the parabola is located at a distance ge from e. The distance ge equals the distance fe. Every point on the parabola is equidistant to the focus and the directrix by definition. For a dam with horizontal drainage blanket $\alpha = 180$ deg (Fig. 4a) the basic parabola gives the location of the exit point of the top flow line directly. For dams with rock toes and dams with ordinary downstream slopes, as shown in Figs. 3 and 2, respectively, the location of the exit point of the top flow line is determined by applying the correction $\Delta a/(a + \Delta a)$ to the basic parabola. A chart of values of $\Delta a/(a + \Delta a)$ slope angle has been prepared by Casagrande and is presented in Fig. 10.

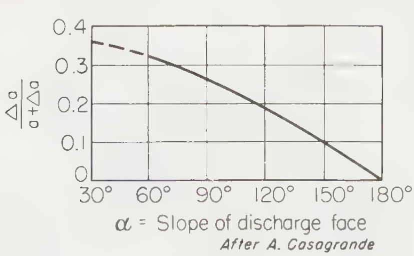

FIG. 10. Basic parabola correction.

20. Quantity of Seepage. The quantity of seepage can be computed directly from a flow net or, in certain instances, from charts or equations without the construction of a flow net. The equation for computation of the quantity of seepage from a flow net is as follows:

$$Q = k \frac{n_f}{n_d} h_t L$$

where Q = quantity of seepage in length of dam under consideration
k = effective coefficient of permeability which is $\sqrt{k_{\max} k_{\min}}$
n_f = number of flow channels of net
n_d = number of equipotential drops of net
h_t = head difference between headwater and tail water
L = length of dam to which the flow net applies

The ratio n_f/n_d is termed the shape factor of the flow net.

Both graphical and analytical methods are available for computation of the quantity of seepage through an earth dam on an impervious foundation. The results of such computations are presented in Fig. 11 as a family of curves. The chart is

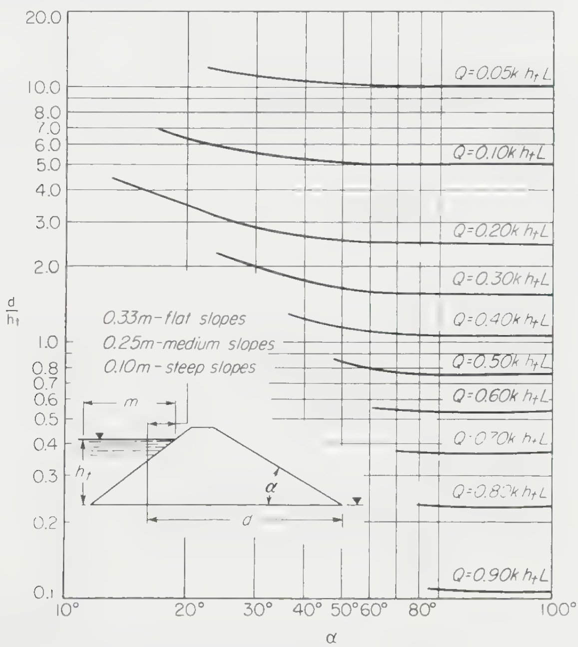

FIG. 11. Seepage through embankment on impervious foundation.

entered with the values of d/h_t and α as defined on the key sketch, and the seepage equation with the proper shape-factor coefficient is determined by interpolation from the family of curves. The quantity of seepage through an embankment overlying a foundation of approximately the same or lesser permeability can be estimated from the above chart, but to it must be added the seepage through the foundation in order to obtain the total seepage.

Approximate solutions for the quantity of seepage underneath an impervious embankment founded on a pervious foundation have been developed by Terzaghi. The definitions of terms for the equations are as given before or as defined in Fig. 12.

Case I. When $I > 2U$: $$Q = \frac{h_t k}{0.88 + I/U} L$$

Case II. When $I < 2U$: $$Q = \frac{h_t k (2U/I - 1)^{1/3}}{2} L$$

In both the chart and the solution by Terzaghi, the dimensions used should be those of the transformed section described above, and permeability should be the effective permeability.

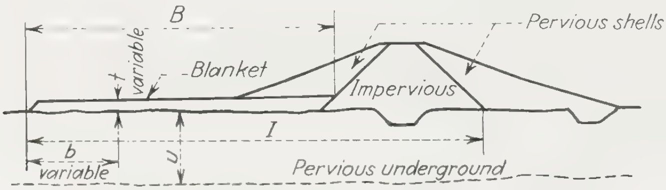

FIG. 12. Blanket diagram.

21. Piping. Piping occurs when the force exerted on the soil by seeping water exceeds the resistive force offered by the soil. Filters are provided at places where seeping water emerges from the soil when the resistive force of the soil does not have sufficient factor of safety against migration of fines. An earth dam and its foundation form a barrier that maintains a differential head between the water surface in the reservoir and the tail water below the dam. The potential energy represented by this difference in head is dissipated as frictional loss as the water flows through the soil. The seepage force J exerted on the soil by the water is equal to the unit weight of water γ_w times the hydraulic gradient i and is always in a direction perpendicular to equipotential lines. For either an isotropic or stratified soil, the hydraulic gradient is determined by dividing the head lost between two equipotential lines by the perpendicular distance between the lines measured on the true scale drawing. Where water flows into the upstream face of an embankment, the seepage force has a stabilizing effect, but where seepage is out of an embankment the seepage force has a destabilizing effect. When upward flow exists in a cohesionless soil and the head loss per foot of length exceeds the submerged effective weight of the material, movement of the soil particles will take place. For example, if the weight of a foot cube of saturated cohesionless soil is equal to 125 lb, the submerged weight will be 62.5; hence if there is an upward hydraulic gradient of 1, the seepage force will be equal to 62.5 lb and the material will be in a condition of unstable equilibrium, termed a quick condition.

Whenever water flows from a less pervious material to a more pervious one, or out onto ground surface, the possibility of migration of fines or piping should be considered. Even a very minor washing away of fines at the downstream side of a dam is serious. As soon as some fines are washed away, the resistance to seepage along the path of seepage is reduced and increased flow results. Owing to the increased flow, the rate of washing away of fines is increased.

In order to prevent piping, movement of soil particles under the action of seepage forces must be prevented. Where the soil subject to possible piping is exposed as at the downstream side of a dam or levee, piping can be prevented either by reducing the seepage gradient at the exit point so that the seepage force is too small to cause movement of particles or by holding the soil at the exit area in place mechanically. To prevent the movement of soil particles mechanically, the pores of the coarser soil must be so small that the larger particles of the finer soil cannot pass through the pores. When the coarser soil under consideration does not have sufficientiy small pores a filter or series of filters may be placed between the fine soil and coarse soil to accomplish the mechanical restraining action.

22. Filters. On the basis of research by Bertram reported in Ref. 4, the following criteria for designing filters are recommended: The D_{15} size of the filter should be (1) no larger than four to five times the D_{85} of the material to be protected and (2) preferably at least four to five times larger than the D_{15} size of the material to be protected. The D_{15} and D_{85} sizes are the particle sizes than which 15 and 85 percent of the soil are finer, respectively. The purpose of the first requirement is to prevent migration of fines and that of the second to ensure adequate permeability of the filter relative to the material being protected. An exception to the above criteria occurs when the material to be protected is skip-graded to the extent that the fine fraction can migrate readily in the pores of the coarse fraction. In this case the filter would be designed for the D_{85} size of the fine fraction instead of the D_{85} size of the entire material. Some engineers prefer to have the shape of the grain-size-distribution curve of the filter material similar to the shape of the grain-size curve of the material being protected. There is advantage, however, in having the filter uniformly graded since then there is little chance of segregation of the filter during placement; also the permeability of the filter is higher. When a filter is to be placed between fine core material and rock fill, not only must the D_{15} size of the filter be met as described above, but in addition the D_{85} size of the filter must be no less than one-fourth to one-fifth the D_{15} size of the rock fill. The design of such a filter is illustrated in Fig. 13. Sometimes the resulting filter gradation covers too wide a range in particle sizes. In such cases, the filter can be constructed in two or more layers, each layer satisfying the above criteria with respect to materials adjacent to it. A two-layer filter for the above case will be more pervious than a single-layer filter. The thickness of the filter layers varies from 12 to 18 in. per layer in drainage trenches and at rock toes to over 8 ft (horizontal measurement) for filters between the core and the shell sections of a dam. In the latter case the 8-ft width is the minimum for easy operation of spreading and compaction equipment. A wider filter or a transition zone is desirable, particularly if there is any possibility of cracking of the filter due to settlement or earthquake. Where the core material is fine-grained and has low or no plasticity a crack through it and a narrow filter may permit piping. By blending the fine-grained core material and the filter material any cracks which might develop would tend to be self-healing, since after a little core material had piped the coarse-grained fraction would cave into the crack and choke it. Adequate compaction of filters between core and shell sections is essential during construction to prevent excessive settlement and adjustment of the fill. Where filters are placed on natural soils, it is usually more economical to design the filter to protect most of the soil and then place an additional layer between the regular filter and the finer pockets of foundation soils where such pockets occur. Where filter packs come against well pipes and drainage pipes the following criteria apply: the D_{85} size of the filter should be greater than 1.0 times the size of perforations or 1.2 times the width of slots. Slots generally are more efficient than perforations.

23. Drainage Trenches and Relief Wells. Drainage measures are required frequently at the downstream toes of dams and levees to reduce uplift pressures and seepage gradients to tolerable magnitudes. An illustration of the uplift pressures and gradients which may develop is given in Fig. 14, which is a reproduction of an example presented by Cedergren in Ref. *3a*. In this example, a dam 70 ft high is founded on a 10-ft-thick layer of foundation material having an effective permeability of 5 ft/day which is underlain by a 40-ft-thick stratum having an effective permeability of 300 ft

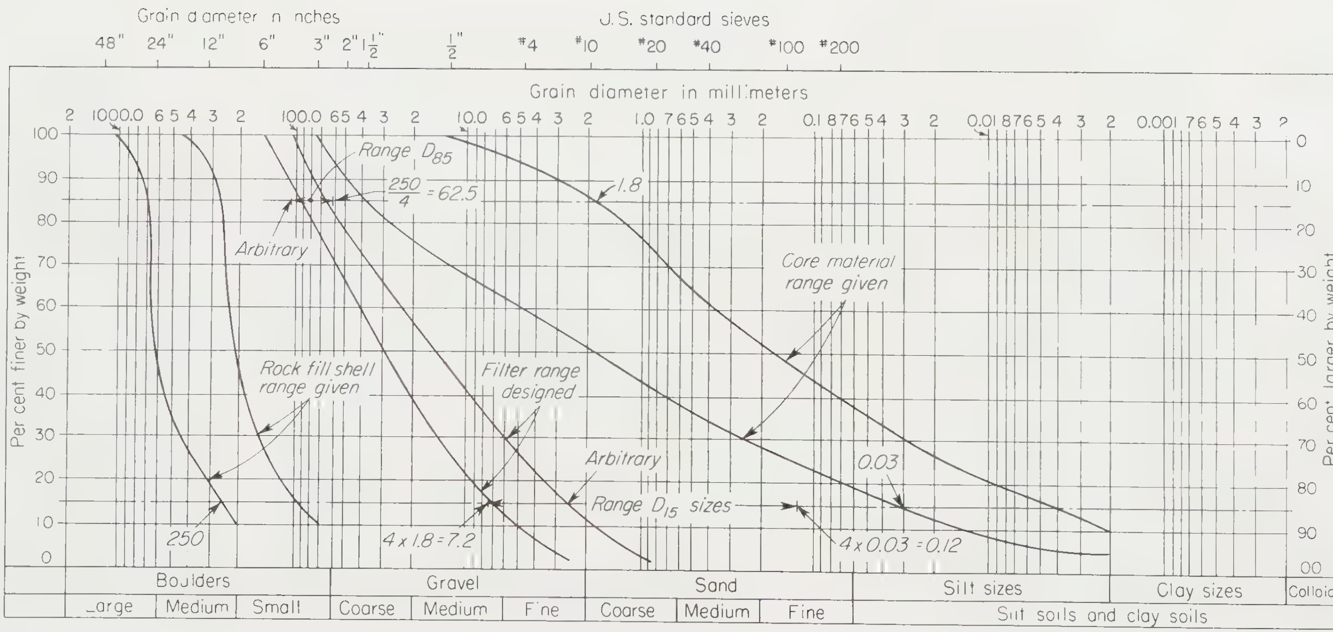

FIG. 13. Design of filter.

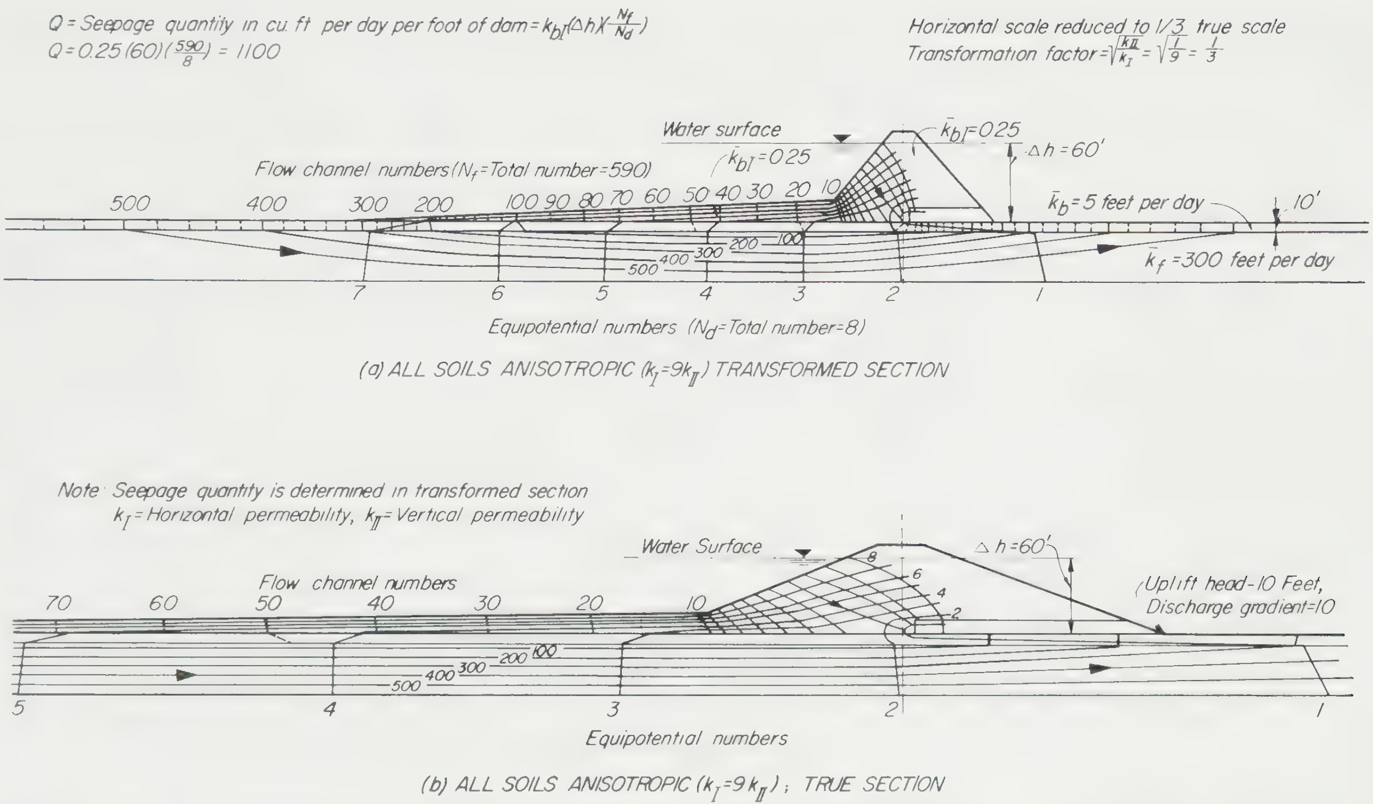

FIG. 14. Flow net for anisotropic embankment and blanket placed on anisotropic foundation. (*After H. R. Cedergren.*)

day. Below this level, the foundation material is impervious. An impervious blanket 1,100 ft long is provided upstream of the dam. The effective permeability of the dam and blanket is 0.25 ft/day. The ratio of horizontal to vertical permeability

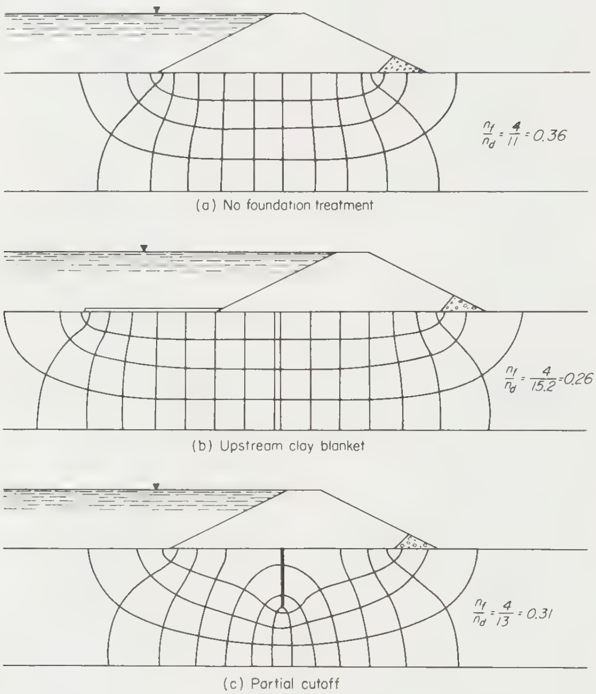

FIG. 15. Effect of foundation treatments on flow through pervious foundation.

is 9 for all soils. The transformed section is shown in Fig. 14a and the true section in Fig. 14b. Under a 60-ft head the uplift which develops underneath the 10-ft stratum at the downstream toe is 10 ft. Thus the seepage gradient through the 10-ft stratum is 1.0 and critical at this point. To reduce the exit gradient to a reasonable amount a drainage trench could be constructed through the 10-ft impervious stratum at the downstream toe. Seepage would be increased about 47 percent by construction of such a relief trench. Equations helpful in connection with designing the length and thickness of blankets in problems similar to the one mentioned above are given by Bennett in Ref. 3a. An example of a drainage trench is given in Fig. 54.

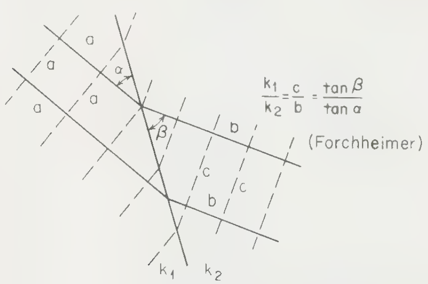

FIG. 16. Deflection of flow net at boundary of soils of different permeability. (*After A. Casagrande.*)

A row of relief wells may be used as an alternative to a relief trench, particularly where the pervious stratum to be tapped occurs at depth. The effect of different penetrations of a drainage curtain consisting of wells in a stratified foundation where the permeability of the strata increases with their depth is given in Fig. 17. The cross section of the levee, natural blanket, and foundation is shown in Fig. 17*a* and the effect of the drainage wells of different penetration on the hydraulic grade line beneath the uppermost impervious foundation stratum in Fig. 17*b*. If the head of water relative to ground surface at the land side of the levee is 50 ft, the uplift on the base of the impervious stratum for 10 percent penetrating wells is 33 percent of 50 ft, or 17 ft. This is excessive and the 10 percent penetration of wells is inadequate. A penetration of about 50 percent reduces the uplift to 8 ft, which is barely safe, and greater penetration of wells is required. Various methods of underseepage control are discussed in Ref. 68.

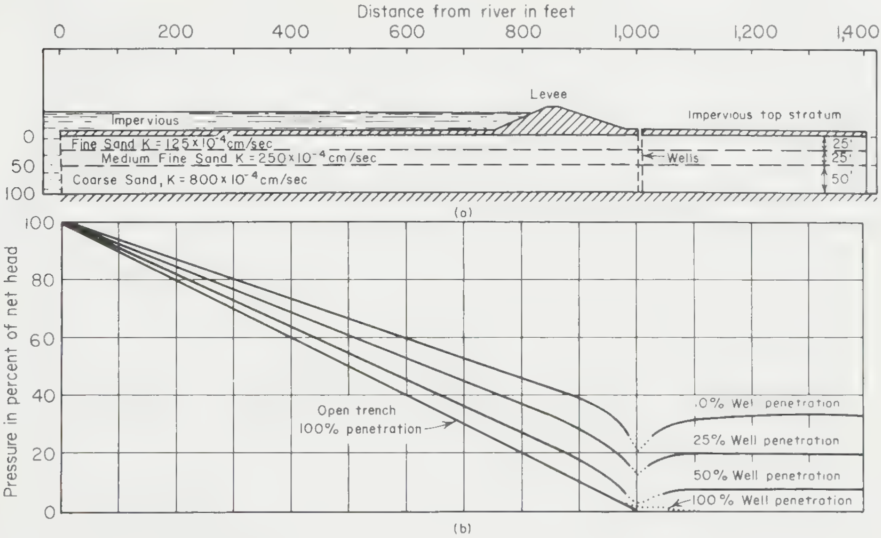

FIG. 17. Effect of penetration of relief wells on hydraulic grade line. (*After W. J. Turnbull and C. I. Mansur.*)

Relief wells are constructed in a manner similar to water wells. The outside diameter of the wells is usually 10 to 18 in. A filter pack of 4 to 6 in. is placed between the outside of the well and the filter screen and discharge pipe. The well screen and discharge pipe is usually 4 to 8 in. in diameter. To minimize the deposit of minerals such as calcium carbonate and iron oxide in the well the discharge point of the well should be under water continuously. This means that the wells should discharge into a channel or gallery below the water surface in that channel or gallery. Also the wells should be so located that a drill rig can readily be placed above them to flush them out or repair or replace them. Where the wells discharge into a gallery, a manhole above each well may be required to provide this access. The well screens should be made of material which will last indefinitely. Stainless steel, wood, and some plastics seem to offer the best possibilities for long life of screens. Information on the construction of drainage wells is given in Refs. 67, 69, and 73.

24. Drainage Curtains. Drainage curtains are installed in abutments for the purpose of intercepting water before it emerges on the lower face of the abutment. For the wells composing the drainage curtain it is necessary that a tunnel or adit be driven at about tail-water elevation and the wells discharge into it. Wells both above and below the collection adit may be required. The wells would be the same as the relief wells described above if the abutment is earth. If the abutment is rock without any erodible material in the fissures or erodible layers, plain 2- to 3-in.-diameter drill holes may be satisfactory. If the rock is highly fractured and there is possibility of caving of the walls of the drill hole, perforated casing of a material with an indefinitely long life should be installed to maintain the walls of the hole. Where the rock is erodible or has fissures which contain erodible material larger-diameter wells with a gravel pack would be required. Such holes might be 4 to 6 in. in diameter with a 2-in. drainpipe in the center. Drain holes in rock abutments usually are placed at about 10- to 30-ft spacing. Where the depth from ground surface to the collection adit in the abutment is about 200 ft or less the drain holes may be drilled from the surface to intercept the adit. The smaller-sized drain hole used in abutment drainage curtains is partly governed by the limitation in size of hole which can be drilled from the 5- by 7-ft adit normally used. Also it is frequently desirable to have close-spaced drain holes in the abutment drain curtains, particularly where there may be a concentration of flow. In such cases many small-diameter holes are preferred to a few large-diameter holes. Holes above the adit cannot be continuously submerged and so are subject to clogging with deposits. Careful periodic checking of such drainage-curtain holes is required. If clogging occurs and it cannot be removed by washing and surging, then replacement drain holes must be installed. Telltale piezometers should be installed at critical locations to indicate the buildup of excessive pore pressures due to clogging of drains.

25. Grout Curtains. Where the impervious core of an embankment dam is founded on rock, grout curtains into the rock are frequently used. Where the impervious core is founded upon overburden grout curtains through overburden have been used only occasionally. Grout curtains in rock will be discussed first and then some general comments will be given regarding grout curtains in overburden.

The purpose of a grouted curtain in rock is (1) to lengthen the path of seepage of water through the rock foundation and thereby reduce the seepage gradient in the rock and (2) to reduce the quantity of seepage either for conservation purposes or for alleviating the load on the drainage system. Generally seepage through rock is through joints and fissures or solution channels, although on occasion rocks with a porous structure are encountered. Where the joints and fissures are generally clean and the rock is sound a reasonably tight curtain 10 to 20 ft wide can usually be obtained with one, two, or three rows of grout holes. All weathered and disintegrated rock should be removed from under the base of the core and the core founded upon groutable rock. The entire base width of the core should be grouted to a depth of about 20 ft to form a grout platform. Both vertical and angle grout holes should be located to intercept joints and fissures as evident from the exposed surface of the foundation subsurface investigations and geological studies. At about the center line of the grout platform the grout curtain should be installed. The curtain plus the grout platform forms a T-shaped grouted zone. The depth of the grout curtain should be about one-half the differential head acting across the curtain; then the nominal gradient for the shortest path of seepage around the curtain will be 1. If an impervious rock layer is present at shallower depth or at reasonably deeper depth the grout curtain should be tied to that layer. The purpose of the grout platform is to prevent a high gradient from occurring in the core just above the vertical curtain. If no platform were present seepage would enter the base of the core from the foundation at the upstream face of the curtain at reservoir head and leave the core at the downstream face of the curtain at tail-water head, making for a much higher gradient in this part of the core than at any place else in the core. A second reason for the platform is to prevent seepage, through fissures and joints in the foundation upstream and downstream of the curtain, from eroding the base of the core. If it is not feasible to excavate the entire base of the core to groutable rock, a trench may be excavated to groutable rock for the construction of the curtain. This trench would then be backfilled with concrete and concrete paving 2 or 3 ft thick placed over the remainder of the base of the core, thus forming a T-shaped treatment similar to the one mentioned above utilizing a grout platform. Alternatively the concrete may be extended into the core as a seep-fin-type wall.

Grouting may be done by either the stage grouting method or the packer method, although the stage method is the one more commonly used. In the stage method the grout holes are drilled to a depth of about 30 ft and grouting is accomplished before the holes are deepened by another 30-ft stage. Depending upon the depth of the curtain, five or six or more stages may be required. In each stage, grouting is done generally by the split-spacing method. Initially grout holes are drilled at about 20-ft spacing and grouted. These initial holes are called primary holes. Then holes called secondary holes are drilled midway between the primary holes and are grouted. After the secondary holes are grouted, tertiary holes spaced midway between the secondary holes are drilled and grouted. Splitting of the spacing of the grout holes is continued until the grout and/or water takes in the final series of holes are substantially less than in the previous series and it is not expected that further splitting and grouting will further reduce the grout and water takes.

The maximum pressure to be used in grouting rock generally should not exceed 1 psi for each foot of cover of overlying rock and overburden. The grouting pressure is measured by pressure gage at ground surface. Assuming the unit weight of overlying material is 144 lb/cu ft, the above rule in effect limits the grout pressure to a pressure equivalent to that created by the weight of overlying material. If greater grout pressures are used there is the danger that bedding planes and fissures will be opened up because of heaving or distortion of the rock. Not only will more grout be required, probably unnecessary grout, but there is also the danger that later grout holes will cause heaving and distortion which will open cracks in previously grouted holes and so damage the effectiveness of the earlier grouting. By performing grout- and water-take tests at several pressures one can note whether the takes increase inordinately with pressure after some particular pressure is reached. If so such a pressure would be the limiting pressure above which opening of bedding planes and fissures might be expected to occur.

In grouting it is usual to start with a thin grout and increase the consistency of the grout as more and more grout is taken. An initial grout would consist of 1 part cement to 3 to 6 parts of water by volume. As a rough guide, on some jobs the author has specified that grouting start with a 1:4 mix. This mix is pumped until either practical refusal is met under the maximum allowable pressure or a take of 30 bags in a 30-ft stage has occurred. Practical refusal is defined as some small take, as 6 bags/30-ft stage/10 min. If refusal has not been met the grout is thickened to a 1:3 mix and the same procedure is repeated. The grout may be further thickened in steps until a 1:1 mix is reached; after that sanded grout is used.

After experience is gained at a site grouting may start with thicker grout mixes, if it is certain that refusal will not be met before the grout has traveled a reasonable distance. The purpose of grouting by the split-spacing method is to achieve a curtain about 20 ft wide. In connection with grouting with thin mixes it should be kept in mind that the Portland cement in the grout filters out at constrictions in the passageways through which the grout flows and forms a filter cake which hardens to seal the passageway; the space grouted is thus the volume of the filter cake and not the volume of the grout mix.

Washing of grout holes with water and with air and water removes silt and clay in the seams and fissures to be grouted. It is not at all possible to remove all the filling materials by surging from a single grout hole or even by washing between grout holes. However, washing does open up more passageways through the seams and fissures, and these passageways increase the probability of contacting other natural passageways and so improve the degree to which grout fills openings. Further such washing facilitates development of a crisscrossing series of grout streamers through the natural fillings in the seams and fissures and so tends to help confine the natural fillings against erosion.

Grouting is most successful in hard rocks which have clean fissures. Where the fissures are filled or partially filled with erodible material or where layers of the rock are erodible there is always the danger that when the gradient caused by more or less full reservoir head is being lost through a 10- to 20-ft-wide grout curtain, it will cause erosion and piping of the joint-filling materials with time. Because of this,. two, three, or four or more rows of grout holes may be required to widen the grout curtain to reduce the gradient across the curtain so that there is no longer any danger of erosion and piping. The nature of the natural joint-filling material or erodible layer such as the size of its particles and the degree of cementation or cohesion of the particles to each other and to the wall of the joint, as well as the width of the joints or erodible layer, determines what the allowable gradient across the grout curtain may be. When the joint filling is readily erodible material such as silt or rock flour and when the width of such joints is great, say several inches, then a very wide grout curtain is required. In such cases it probably is not economically feasible to use a grout curtain for foundation treatment.

Grouting of soil overburden is quite a different matter from grouting of rock. Instead of joints and fissures the pore space between soil particles requires grouting. Where the overburden to be grouted is openwork gravel Portland-cement grout can be used since the passageways through the soil are large enough to accept the cement particles readily. On the other hand, the passageways through a porous sand are too small to do so. In this case either especially fine grained Portland cement or clay with an agent to cause it to gel after it has penetrated the sand may be used for coarser sands. For fine sands chemical grouts are required. Alternatively special patented high-pressure methods as the Soletanche *tube à manchette* method may be used. In this method a casing is grouted into a hole drilled to the full depth of the proposed grout curtain. This casing has groups of perforations at about 1 m spacing. By means of a grout pipe with packers which is inserted inside the casing, grouting can be done separately from each group of perforations. Grouting pressures are high, 300 psi or more, so that bearing-capacity failure is caused in the initial grout surrounding the casing and in the soil surrounding the particular set of perforations being grouted. The spiral-shaped cracks formed in the soil because of the bearing-capacity failure provide passageways into which grout may flow. The concept is that these surfaces of grout will overlap to form a honeycomb type of grout structure and this structure will greatly reduce the permeability of the sand stratum. To be successful a honeycomb grout structure has to be achieved throughout 100 percent of the depth and width of the curtain.

Where all the layers of soil to be grouted are of such grain size that the coarsest soils satisfy filter requirements with respect to the finest soil layers present it is possible to create a grout curtain by one of the above appropriate methods and materially reduce seepage. Where such is not the case, as when both layers of fine uniform sand and layers of openwork gravel are present in the overburden, the same problem arises as mentioned above for joints filled with erodible material, but in this case the sand layers are the erodible material. Unless the grout curtain is exceedingly wide the gradients which will develop across the curtain will be sufficient to cause erosion and piping of the fine-sand layers into the adjacent openwork-gravel layers. The presence of natural filters between the fine-sand layers and openwork-gravel layers would prevent such piping, but it is necessary to prove that such natural filters are present at every place that they are required.

Whether in rock or alluvium where the grout curtain ties into an impervious layer at depth, the thickness of the grout curtain should be the same for the full depth of the curtain since the gradient across the curtain is the same for the full depth. Where the grout curtain does not tie into a more impervious stratum, the width of the curtain may decrease with depth since the head across the curtain becomes less and less with depth. Since higher grout pressures may be used increasing with depth sometimes fewer rows of grout holes are required to develop the same width of grout curtain at depth; the higher grout pressures force the grout farther away from the grout hole than lower pressures.

STABILITY ANALYSIS

26. Basic Concepts. Whenever the shearing force along any surface through the embankment and its foundation exceeds the shearing resistance along that surface, a stability failure occurs. The trace of the surface of sliding on a cross-sectional view generally may be approximated by either a straight line, the arc of a circle, a portion of a logarithmic spiral, or a composite of such lines. The stability analysis is made by considering various possible surfaces of sliding and computing the factor of safety against stability failure for each. The factor of safety is defined as the available shearing resistance divided by the shearing force. The sliding surface with the lowest factor of safety is the critical one. This is a limit-equilibrium type of approach.

The various cases of loading for which embankment slopes are analyzed together with the minimum factors of safety recommended for these cases are tabulated below.

Condition	Min Factor of Safety	
End of construction case, both upstream and downstream slopes	1.25	
With earthquake loading in addition		1.0
Steady seepage at partial pool, upstream slope	1.5	
With earthquake loading in addition		1.25
Steady seepage, downstream slope	1.5	
With earthquake loading in addition		1.25
Rapid drawdown, upstream slope	1.25	
With earthquake loading in addition		1.0

The shearing strengths of the embankment and foundation materials are different for each of the cases mentioned above. The differences are due primarily to differences in the conditions of consolidation and drainage which obtain in each of the cases. Four ways of expressing the shear strength are in general use.

1. In terms of *total* applied *stresses* at time of failure
2. In terms of *effective stresses* at time of failure
3. In terms of *consolidation stresses* at time of consolidation, for a condition prior to applying the increment of load which causes failure
4. As *in situ shear strength* (generally used for foundation)

Methods of testing soils to determine their shear strengths for different conditions of consolidation and drainage are described in Art. 54. Choice of the method of test and of the way of expressing the shear strength for analysis of a particular case is described in Arts. 31 through 35. More detailed discussion of these subjects by the author may be found in Refs. 39, 40, and 42.

For each condition of consolidation and condition of drainage during shear, the shear strength may be expressed in terms of the parameters c and ϕ according to the following expression:

$$s = c + \sigma \tan \phi$$

Either total stresses, effective stresses, or consolidation stresses may be used for the normal stress σ. The values of c and ϕ will be different for each condition of shearing and for each normal stress used. The linear relationship indicated by the expression is generally only an approximation of actual shear strength and applies generally only to a limited range of normal stresses.

Several methods are available for making stability analyses, including the ϕ circle method, the log-spiral method, the slices method, and the sliding-block method. When carried out using consistent assumptions and when the sliding surfaces approximate each other reasonably well all four methods give substantially the same results. The slices method and sliding-block method are the two most commonly used and are the only ones described here. The ϕ circle and log-spiral methods are described by Taylor.[62,64]

Another approach to the stability problem is to determine the ratio of shear resistance to shear stresses at points throughout the embankment and its foundation. The location of any overstressed zones as well as the average of the ratios of sheer resistances to shear stresses along some potential surface of sliding is of interest. The finite-element method of analysis using an electronic computer is a powerful tool in this connection. The method is described in Ref. 12. Use of this approach should be checked using one of the limit-equilibrium stability methods mentioned above.

Simplified methods of stability analysis such as the infinite-slope analysis can be made for cohesionless materials which are relatively incompressible since pore pressures which develop in them because of shear stresses are small and can be neglected. These methods are described in Arts. 27 and 28. The location of critical circles for analysis is given in Art. 29. The slices method of stability analysis is applicable to all types of soils and conditions of loadings. The method is described in Arts. 30 through 34. The sliding-block method is described in Art. 35. Stability charts for rapid analysis of simple embankment cross sections are presented in Art. 36.

27. Infinite-slope Analysis. The infinite-slope type of analysis is made by considering a typical vertical slice of a long shallow sliding mass. The length of the sliding mass is so great compared with the depth that end effects on the sliding mass are negligible. An illustration of a typical slice is shown in Fig. 18. The infinite-

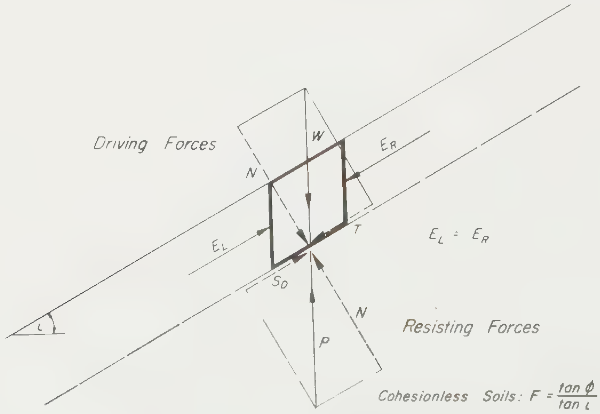

FIG. 18. Infinite slope. Forces acting on unit volume.

slope type of analysis is useful in connection with analyzing the stability of the faces of embankment dams where the shell is composed of cohesionless material. Analysis may be made for the case of no seepage or for the case where seepage is in one direction for the entire length of the long shallow potentially sliding mass. For the case of no seepage the factor of safety of the slope is as follows:

$$F = \frac{\tan \phi}{\tan i}$$

where i is the angle of the face of the slope

The required angle of friction for a factor of safety of 1.0 is called the developed angle of friction ϕ_D. In the above case ϕ_D equals i.

When seepage occurs additional frictional resistance is required for stability. For the case of seepage parallel to the face of the slope and in the downward direction the factor of safety may be expressed as follows:

$$F = \frac{\tan \phi \times \gamma_{\text{subm}}}{\tan i \times \gamma_{\text{sat}}}$$

where γ_{subm} = unit weight of material, submerged

γ_{sat} = unit weight of material, saturated = $\gamma_{\text{subm}} + \gamma_{\text{water}}$

The increase ω in developed friction angle which is required in case of seepage in various directions and at various gradients is given in the chart in Fig. 19. For the use

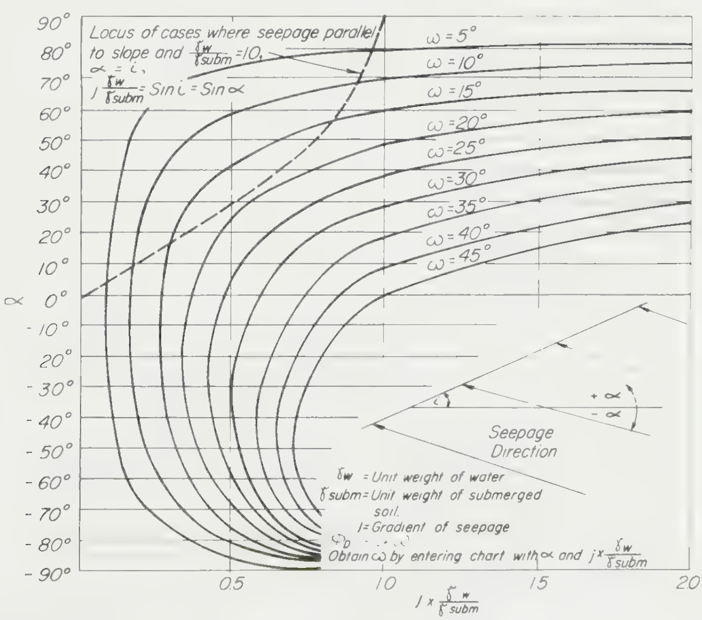

FIG. 19. Stability chart for infinite slope of cohesionless material.

of the chart the gradient j needs to be known. This may be determined from a flow net or, in certain simple cases as indicated below, may be estimated. When seepage is parallel to the face of an embankment dam the gradient is equal to the sine of the slope angle i. For the case of complete drawdown for an embankment dam on an impervious foundation seepage occurs horizontally out of the lower portion of the upstream slope as illustrated in Fig. 20*a*. The gradient for seepage in this case is equal to about tan i. If drawdown is not complete the flow net shown in Fig. 20*b* obtains. In this case seepage just below the water level of the reservoir is perpendicular to the face of the dam and at a gradient about equal to sin i.

When the gradient has been determined or estimated the term $j(\gamma_{\text{water}}/\gamma_{\text{subm}})$ as defined on the chart can be computed, and with this value the chart can be entered. The required friction angle ϕ_D is obtained by adding the slope angle and the angle ω obtained from the chart. This latter value is read from the chart utilizing the family of curves which represent the angle ω.

The locus of points representing cases where seepage is parallel to the slope and in a downward direction and the ratio of $\gamma_{\text{water}}/\gamma_{\text{subm}}$ equals 1 is shown in Fig.19. These are the cases that correspond to the equation given above for seepage parallel to the face of the slope.

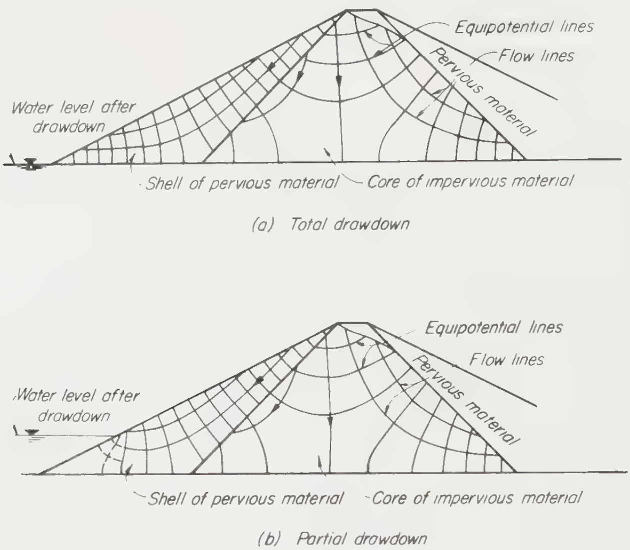

Fig. 20. Flow net in a dam with core of impervious material. Rapid drawdown. (*After E. Reinius.*)

Assuming that the gradient is equal to sin i, the most critical direction for seepage is upward at an angle α about equal to the angle of the slope i. For embankment dams with slopes flatter than about 15 deg, however, the factor of safety for a gradient equal to sin i is about the same whether seepage is downward parallel to the slope, horizontal, or upward perpendicular to the slope. Vertical seepage whether upward or downward has no effect on the ϕ_D. Of course, if the upward seepage force equals the submerged weight of the soil, a quick condition develops. Also any upward seepage reduces the resistance of the element considered to driving forces other than the driving forces created by weight of the element itself as the force created by seismic acceleration.

28. Reinius' Charts. A comprehensive analysis of the stability of the upstream slope of earth dams composed of cohesionless material under condition of seepage out of the upstream slope upon drawdown was made by Reinius and reported in Ref. 47. The result of his analyses with regard to the required or developed friction angle for different slopes with different effective thicknesses of slope protection is shown in Fig. 21. The type of circular sliding surface used is illustrated in Fig. 21*a*. This

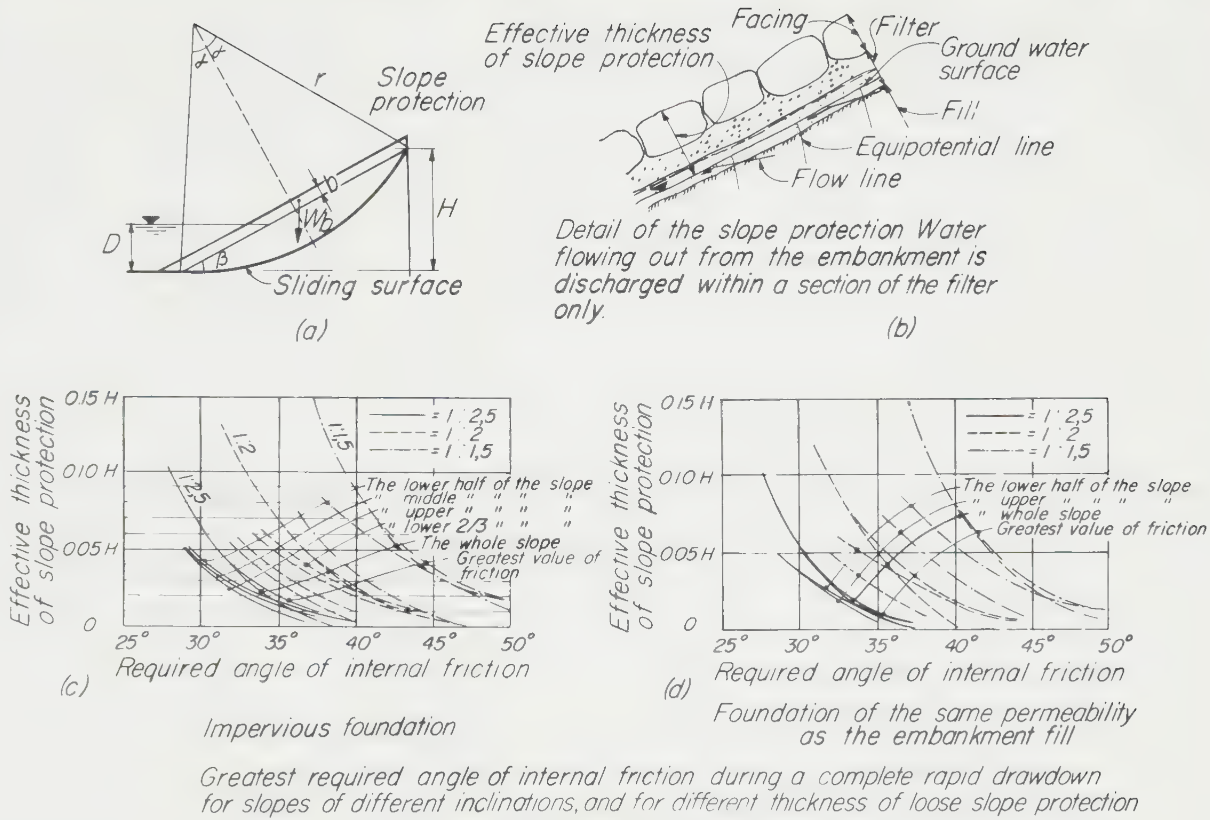

FIG. 21. Stability of the slope protection. Reinius charts.

figure shows the type of circle used for the full height of slope; similar circles were used for analyzing the lower, middle, and upper halves of the slope. The effective thickness of slope protection is illustrated in Fig. 21*b*. The slope protection consists of filters and riprap. Only the portion of the slope protection above the water surface in the slope protection is effective. The angle of friction of the slope protection is assumed to be the same as the underlying shell of the embankment. The required friction angle for an embankment dam on an impervious foundation is shown in Fig. 21*c* and for an embankment dam on a foundation with the same permeability as the embankment in Fig. 21*d*. The effective thickness of slope protection required for local stability of face of embankment is given as a fraction of the height of the embankment dam. From the curves of Fig. 21*c* and *d*, a design can be made for a concave slope having uniform thickness of slope protection or for a uniform slope having the slope protection thickening with distance from crest of dam.

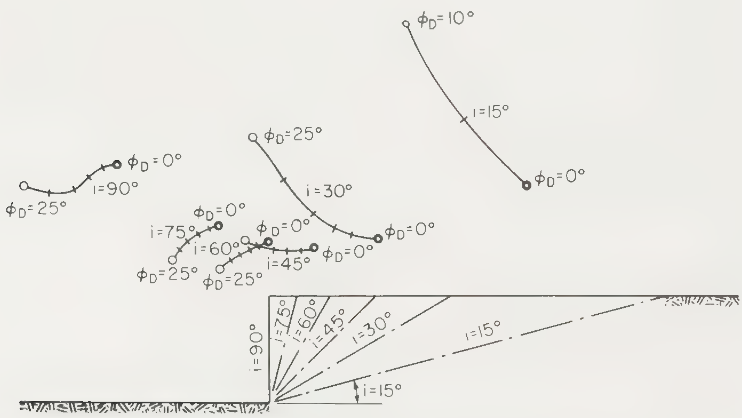

FIG. 22. Influence of value of developed friction angle ϕ_D on position of center of critical toe circle for different values of slope angle i.

29. Location of Critical Circles. Circular surfaces of sliding may be either toe circles, slope circles, or mid-point circles as illustrated in Fig. 25. In homogeneous material toe circles are the critical circles for steep slopes. For flat slopes mid-point circles are critical, but these may be restricted by the presence of a strong stratum at shallow depth or a counterweight a short distance from the toe. If the strong stratum is at very shallow depth the critical circle breaks out on the face of the slope as shown in Fig. 25*d*. The effect of the value of developed friction angle ϕ_D on the position of critical toe circle for different values of slope angle i is shown in Fig. 22. All the circles illustrated above are for the case where the top of slope extends for a long distance horizontally. For dams where the crest of the dam is of limited width the critical circle usually breaks out close to the edge of the crest on the opposite side from the face being analyzed for stability. This is illustrated in Fig. 29. In nonhomogeneous material, the critical circle is located so that a maximum portion of its length passes through the lowest-shear-strength material. The lowest-shear-strength material may be the core of the dam or a foundation layer. To facilitate circular-arc stability analyses where the face of the core is the lowest-shear-strength material it is permissible to assume a virtual cross section of the dam where the upstream face of the core has a curved shape matching the circular-arc surface under investigation. Such a virtual cross section is shown on Fig. 29.

30. Slices Method of Stability Analysis. The slices-method stability analysis was introduced by Fellenius in 1926 in Ref. 14 and also presented in 1936 in Ref. 15. Modifications have been made in details of the method, for example, by May in 1936[44] and by Bishop in 1955.[6] May's method does not consider earth forces on the vertical sides of the slices. Bishop's method assumes that the earth forces on the sides of the slices act in a horizontal direction. The variation presented here is one where earth forces generally having a direction which makes an angle with the vertical sides of the slices, as well as the water forces acting on the sides of the slices, are considered in the analysis. This variation is more elaborate than the original method or the variations mentioned above. Neglecting the earth forces on the sides of the slices makes it impossible to achieve static equilibrium in certain slices, but in many cases the errors resulting are self-compensating and in many instances negligible differences occur between the analyses neglecting earth forces on the sides of the slices and the more rational analysis where they are considered. Significant differences do occur in certain cases, however, as, for example, the case of analysis of a sloping-core dam where there is appreciable difference in shear strength between the shell material and core material. The factor of safety computed neglecting earth forces on the sides of the slices is lower than that computed considering earth forces, and an unnecessarily conservative design results. The variation considering earth forces on the sides of the slices is necessary when it is desired to analyze the stress conditions point by point along the failure surface. When the earth forces on the sides of the slices are neglected an improper distribution of stresses results. An alternative to the assumption that the earth forces on the vertical sides of slices are neglected is the assumption that lateral earth forces exist but their direction is parallel to the base of the slice. Although this alternative provides the equilibrium of individual slices, an unreasonable set of lateral earth forces will result. However, the accuracy of the analysis will not be affected. A more detailed discussion of the effect of the lateral forces by the author may be found in Ref. 42.

The first step is to divide the sliding mass into a number of vertical slices, as may be seen in Fig. 29. The sliding surface may be a circular arc or a combination of arcs and straight lines. The number of slices chosen usually is about 8 to 10. This number is consistent with the general accuracy of the method. The width of each slice need not be the same. Widths of slices are adjusted so that the entire base of each slice is located on a single material.

The forces acting on a typical slice are shown in Fig. 23 and consist of the following:

W_T = total weight of the slice
E_L, E_R = earth forces on left-hand and right-hand vertical faces
U_L, U_R, U_B = water forces on left-hand and right-hand vertical faces and bottom of slice
P = resultant earth force on base of slice

The water forces are determined from water-pressure diagrams on the sides and base of the slice determined from static water conditions if no seepage occurs or from flow nets if seepage occurs. The directions of water pressures are perpendicular to the surfaces on which they act. Sometimes a lateral force may be used which is a combination of an earth force and a water force on the side of the slice. Pressures generated in the pore water by consolidation and shearing in the embankment are taken into consideration in various ways depending upon the method used for expressing shear strength.

The resultant force on the base of the slice P can be represented by a component N normal to the base of the slice and a component S_D tangential to the base of the slice. The tangential component can be separated into two parts, namely, $N \tan \phi_D$ and c_D, as illustrated in Fig. 23.

$$\phi_D = \arctan \frac{\tan \phi}{F} \qquad \text{and} \qquad c_D = \frac{c}{F}$$

The resultant force of N and $N \tan \phi_D$ is P_f.

Different values of factor of safety may be used for F in the two expressions above, although the author prefers to use the same for both.

The force polygon for the forces acting on the typical slice of Fig. 23*a* is shown in Fig. 23*b*. The magnitude and direction of the forces W_T, U_B, U_L, U_R are determined from the geometry of the slice, the unit weight of the soil, and reservoir and groundwater conditions. The direction of each of the forces E_L and E_R may be assumed as midway between the directions of the face of the slope and the failure surface of the vertical plane on which the force E acts. The values of the soil parameters c and ϕ are known from soil testing.

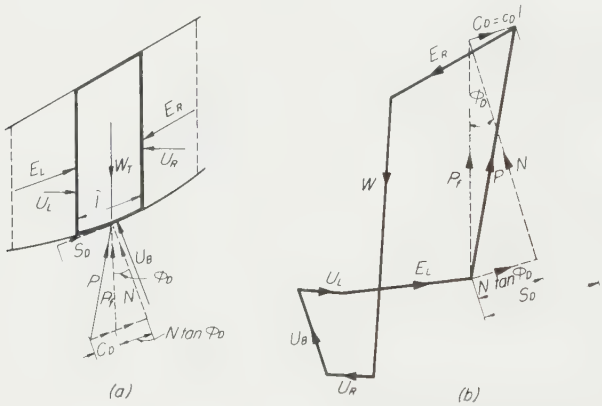

FIG. 23. Slices method of stability analysis. Force polygon for a slice.

The solution for the factor of safety is made by trial and error. The analysis is started at the topmost slice where only one E force is acting. A trial factor of safety is assumed and the force polygon for the topmost slice is constructed. On the basis of the assumed factor of safety the force C_D can be computed. The magnitudes of E_L, N, and $N \tan \phi_D$ are unknown, but the directions of E_L and that of the resultant force $N \tan \phi_D$ are known, and this permits the closure of the force polygon. Having determined E_L for slice 1, E_R for slice 2, which is the reaction of E_L on slice 1, is also determined. The force polygon for slice 2 is then completed in a similar manner as for slice 1, and similarly for the remainder of the slices. For the last slice as for the first, only one E force exists. Thus the force polygon for the last slice is overdetermined. If on using the E force, as obtained from the previous slice, the force polygon for the last slice does not close, a new trial is required using a different value of factor of safety. When the proper value of factor of safety has been assumed, the force polygon for the final slice will close.

31. End of Construction. The analysis is usually made on the assumption of hypothetical instantaneous construction. Some consolidation of materials in impervious zones in the dam undoubtedly occurs during construction, but no means are yet available to predict this consolidation. No theory is available for consolidation of soil with compressible fluid in its pores.

The shear strength used in the stability analysis for embankment materials for the end-of-construction case may be expressed in terms of either total stresses or effective stresses. In using the total-stress expression the shear-strength parameters are determined from tests performed on specimens compacted to the same water content and to the same unit weight as anticipated in the prototype embankment. The tests are performed with drainage lines closed both during application of the chamber pressure as well as during shear, *i.e.*, *UUU* or *Q* tests. Where the consolidated drained, *CD*, or *S* strength is less than the *UUU* strength, this strength is used as illustrated in Fig. 24. The reason for using the *CD* strength where such strength is less than the *UUU* strength is that the *UUU* strength is increased to greater than the *CD* strength by tensile pore pressure. Air may come out of solution from the pore water with time and reduce this tensile pore pressure. Thus it is conservative to use the *CD* strength where it is the lower of the two strengths.

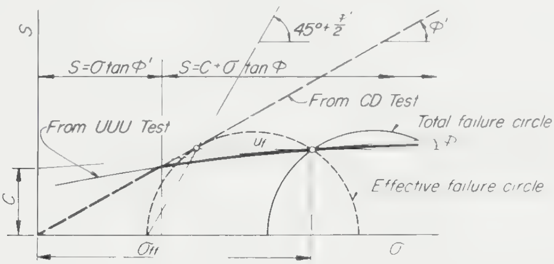

FIG. 24. Shear-strength parameters for end of construction stability analysis using total stresses.

For the foundation consisting of a saturated compressible soil, the *in situ* strength of the foundation before placement of the fill may be used. This, in effect, means that each point in the foundation has a particular strength in undrained shear which is independent of the loads applied by the fill. The *in situ* shear strength is the *CU* shear strength for condition of consolidation under the weight of overburden before placement of fill. If significant consolidation of the foundation will occur during construction, the *CU* strength of the foundation material would have to be determined for the particular consolidation which occurs.

When the shear strength used in the stability analysis is expressed in terms of effective stresses, it becomes necessary to predict the pore pressures which will develop along the failure surface because of both the weight of the overlying fill and the shear stresses which develop along the failure surface.

Methods for predicting the pore pressure in embankment materials are given by Bishop[5] and Hilf.[23,24] Bishop expresses the pore-pressure increment as

$$\Delta u = B[\Delta\sigma_3 + A(\Delta\sigma_1 - \Delta\sigma_3)]$$

where A and B, pore-pressure coefficients, are based upon empirical experience. For saturated soil B is 1.0; for partially saturated soil its value varies between 0 and 1.0. For a soil at maximum Proctor density and optimum water content, the usual values of B are between 0.1 and 0.5. The value of coefficient A, at failure, varies with soil types as follows:

Sensitive clays from +0.75 to 1.50
Normally consolidated clays from +0.50 to +1.0
Impervious granular soils from −0.25 to +0.25
Overconsolidated clays from −0.50 to 0.0

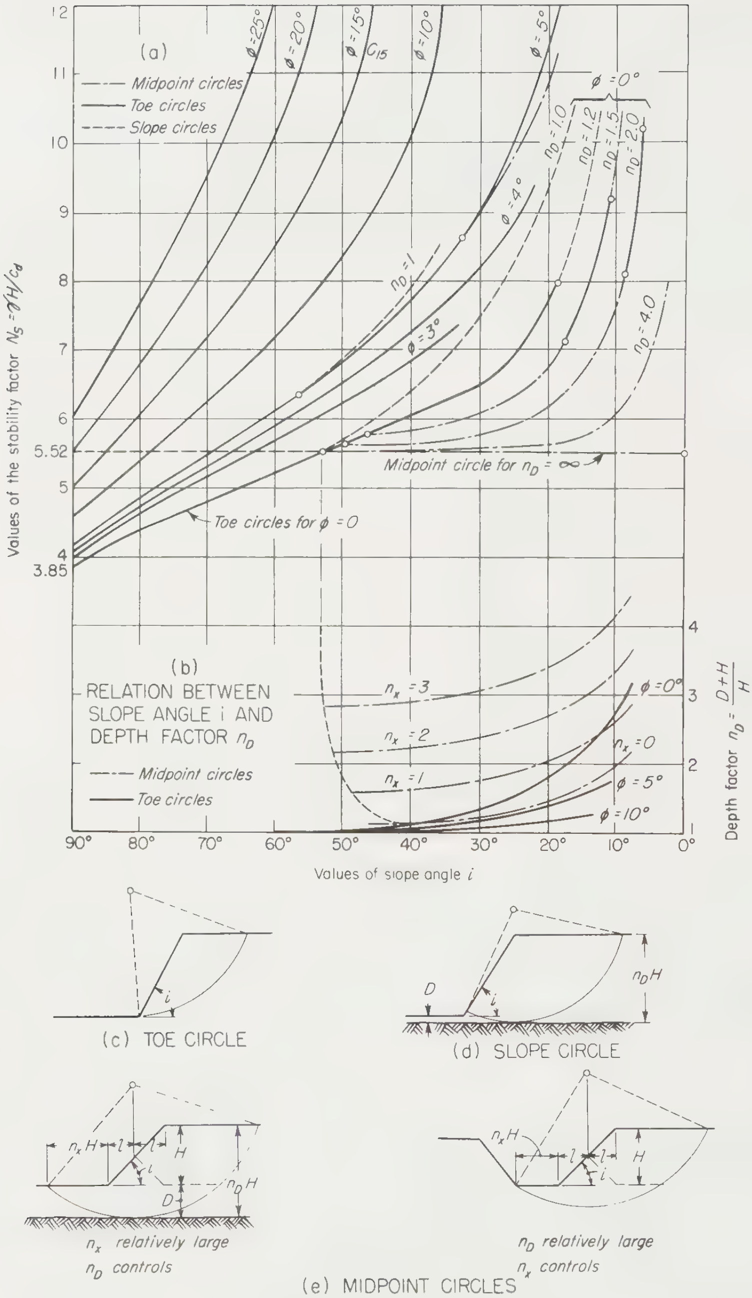

FIG. 25. Stability chart.

The pore-pressure coefficients A and B are further explained and additional values are given by Skempton in Ref. 57.

Hilf expresses the pore pressure as

$$u = \frac{P_a \times \Delta V}{V_a + hV_w - \Delta V} + u_c$$

This formula is based upon Henry's law and Boyle's law. In the above equation,

P_a = air-pore pressure after initial compaction, very close to atmospheric pressure
V = volume change of soil mass, expressed as percentage of initial volume
V_a = volume of free air in the voids after initial compaction in percentage of initial volume of the soil mass
V_w = volume of water, percentage of initial volume
h = Henry's constant of solubility of air in water by volume (0.0198 at 68 F)
u_c = capillary pressure due to curvature of meniscus; $u_c = 2T_s/r$
T_s = surface tension of water = 0.0764 g/cm
W_c = capillary pressure due to curvature of the meniscus
T_s = surface tension of water = 0.0764 g/cm
r = radius of effective meniscus; in soils, approximately equal to $D_{50}/2$

D_{50} is the grain size than which 50 percent of the soil is finer.

Hilf describes his method in Refs. 23 and 24.

Development of a stability-analysis procedure based upon laboratory tests of partially saturated embankment materials is required. One of the difficulties is the measurement of the pore pressures in the water in the pores of a partially saturated soil.

The stability of an embankment dam during construction and continuing until the end of construction can be a critical problem, particularly when weather and borrow conditions require that the impervious material in the dam be placed relatively wet. In such cases piezometer measurements should be taken frequently. It is then necessary that the stability analysis furnish the limiting values of pore pressure which can be tolerated for a particular factor of safety.

32. Steady Seepage. For steady seepage through the dam the critical condition for the stability of the upstream slope is the case of partial pool. Under the condition of partial pool the weight of the material in the upper part of the slope is moist weight, which results in the maximum driving force, whereas the weight of the material in the lower part of the slope is buoyant weight, which results in the development of minimum resistance at the toe. Stability analyses are made for different levels of pool to determine the critical level of pool for the minimum factor of safety. It is assumed that the embankment materials have reached equilibrium under the loading conditions along the failure surface; therefore, the author prefers to use in this analysis the consolidated drained strength for shear strength. The total stresses equal the effective stresses, and thus there is no distinction between the total-stress and effective-stress methods of expressing shear strength. The factor of safety provides a margin of safety for inaccuracies in the method of stability computation and location of the critical surface for sliding but primarily for inaccuracies in determination of the shear strength of the embankment materials.

The method of slices analysis is similar to that presented for high reservoir before drawdown in Fig. 29. A flow net is constructed to determine the water forces on the sides and bottom of the slice. The water forces are determined from the piezometric levels indicated by the equipotential lines of the flow net.

The stability analysis of the downstream slope is made in a manner similar to that for the upstream slope except that seepage from maximum reservoir level is generally critical.

33. Rapid Drawdown—Upstream Slope. In the rapid-drawdown case it is assumed that the reservoir has been at high level for a sufficiently long time so that the material along the proposed sliding surface has come to equilibrium under the buoyant weight and whatever seepage forces exist in the sliding mass. Generally hypothetical instantaneous drawdown is assumed. This means that there is no time for drainage to occur to relieve the pore pressures which develop in the soil along the sliding surface because of the increased load caused by the increase in weight of sliding mass from buoyant to saturated or moist weight or by the increase of seepage forces and the increase in shearing stresses so created. With usual core materials and drawdown taking place during a period of about 1 month, the assumption of instantaneous drawdown is reasonable.

The method of rapid drawdown analysis presented here is that proposed by Lowe and Karafiath.[36] An example of the method of analysis is given in Fig. 29 for a sloping-core dam with upstream rock shell. Under the condition of high reservoir, the face of the core is loaded to lesser degree than the remainder of the core. As seepage occurs through the core, the seepage force accumulates from zero at the upstream face of the core to a maximum at the downstream face. The upstream face of the core is thus under the least load before drawdown and the most critical for stability. The first step in the analysis is to make a stability analysis for the upstream slope for the case of steady seepage under high reservoir. The closure polygon for this analysis is shown in Fig. 29a. From this analysis the normal and shear stresses σ_{fc} and τ_{fc} developed along the failure surface are obtained for condition of high reservoir. The major and minor principal stresses σ_{1c} and σ_{3c} acting at this same time can be computed on the assumption that there is no rotation of principal stresses from high reservoir condition before drawdown to condition after drawdown. This assumption is reasonable for a dam with shell and core since the rapid drawdown loading is more or less equivalent to suddenly increasing the weight of the sliding mass throughout the drawdown zone from buoyant weight to saturated or moist weight, which amounts to about a doubling of the weight of the sliding mass; thus no change in the directions of driving forces occurs. The Mohr diagram illustrating this assumption and the equations for computation of σ_{1c} and σ_{3c} are given in Fig. 26. Proper laboratory testing to determine the shear strength of the core soil under rapid drawdown loading requires (1) compaction of the soil to the density anticipated on the field, (2) consolidation under major and minor stresses corresponding to high reservoir level with full saturation of the soil, (3) increase of all-around chamber pressure by an amount equal to change in σ_3 from high reservoir condition to low reservoir condition (this step is generally not significant and is usually omitted), and (4) shearing to failure under increasing major principal stress. In the Lowe-Karafiath method the shear strength so obtained is plotted against the normal stress on the failure plane at the time of consolidation σ_{fc}. This relationship varies depending upon the ratio of principal stresses at the time of consolidation. The available undrained shear strength for the case of major principal stress ratio $K_c = 1.92$ is shown in Fig. 29. In the lower stress range where tensile pore

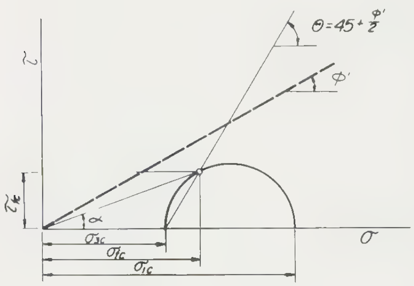

$$\sigma_{3c} = \sigma_{fc} - \frac{\tau_{fc}}{\tan\theta}$$

$$\sigma_{1c} = \sigma_{3c} + \frac{2\tau_{fc}}{\sin 2\theta}$$

$$K_c = \frac{\sigma_{1c}}{\sigma_{3c}} = 1 + \frac{2\tan\alpha/\sin 2\theta}{1-\tan\alpha/\tan\theta}$$

FIG. 26. Mohr diagram of stresses before drawdown.

pressures are observed in the laboratory test the shear strength is reduced to the line representing zero pore pressure. A discussion of the zero-pore-pressure line is presented in Ref. 42. The closure polygon (Fig. 29*b*) for the after-drawdown condition is made using a shear strength for each slice determined from the available undrained-shear-strength chart for the K_c ratio and the normal stress acting on the base of the slice at time of consolidation σ_{fc}. Trial factors of safety are assumed until the after-drawdown polygon closes.

Generally, in the past, shear tests have been performed using an equal all-around pressure for consolidation instead of a major principal stress greater than the minor principal stress as described. Also the shear strength is plotted against the total stress on the failure plane at time of failure of the consolidated undrained laboratory test. Using all-around consolidation instead of anisotropic consolidation results generally in using lower shear strengths than actually obtained. In the conventional stability analysis the plot of shear strength vs. total normal stress at time of failure is entered with the normal consolidation stress σ_{fc}. This is an inconsistent procedure but fortunately involves only a small error.

In the effective-stress method of analysis the pore pressures resulting from undrained shear from anisotropic consolidation properly should be used in the analysis.

34. Seismic Loading. The conventional method of making stability analysis of an embankment dam for earthquake loading is to add an outward-driving force in a horizontal direction to each slice. The magnitude of the horizontal force varies from 0.05 to 0.15 times the total weight of the slice depending upon whether light or severe earthquake conditions are anticipated. Generally no change in shear strength is made from shear strengths determined from standard laboratory tests. The author prefers to make the analysis in a manner similar to that described above for the rapid-drawdown case. Stability analysis is made for the steady-state condition prior to earthquake and the major and minor principal stresses are determined. The normal stress on the failure surface under steady-state condition together with the ratio of major to minor principal stress defines the shear strength which will obtain on the failure surface during undrained shearing under the earthquake loading. A force polygon similar to closure polygon *b* of Fig. 29 is made, including the earthquake forces on each slice.

Seed[52] has investigated the undrained shear strength of embankment materials under condition of pulsating loading starting from a condition of anisotropic consolidation. Initial indications are that serious loss of strength under a few cycles of pulsating load occurs only under light loadings on loose soils. When the loose soils are subjected to high consolidation loads, particularly anisotropic consolidation, they densify to such a degree that little decrease in strength occurs under many cycles of pulsating loading. For proper stability analysis of the earthquake condition, the shear strength based upon pulsating loading should be used particularly for fine-grained cohesionless material and for sensitive foundation soils. Improvement is still required in determination of the loads generated in the sliding mass by earthquake.

35. Sliding-block Method. This method is similar to the slices method of stability analysis except that only two or three slices, called blocks, are used and the surface of sliding is composed of two or three planar surfaces. Examples of sliding surfaces are shown in Figs. 27 and 28. The analysis of the stability of the upstream shell of a sloping-core dam by means of an active wedge and passive wedge is illustrated in Fig. 27. The analysis of the downstream shell of a dam with counterweight situated upon a foundation layer of low shear strength is illustrated in Fig. 28. In this analysis a central block is present between active and passive wedges. The analysis using either the two or three blocks can be made in exactly the same manner as with the method of slices. Alternatively the earth forces on the interfaces with the active and passive wedges may be computed by usual methods for determining active and passive forces. Use of tables for earth pressures as given by Ref. 30 facilitates such computations. In the computation of active and passive pressures and the resistance of the central block, $\phi_D = \arctan \phi/F$ and $c_D = c/F$ should be used. In this way the same factor of safety with respect to shear strength is used along the entire length of the failure surface and the method of analysis is directly comparable with the method

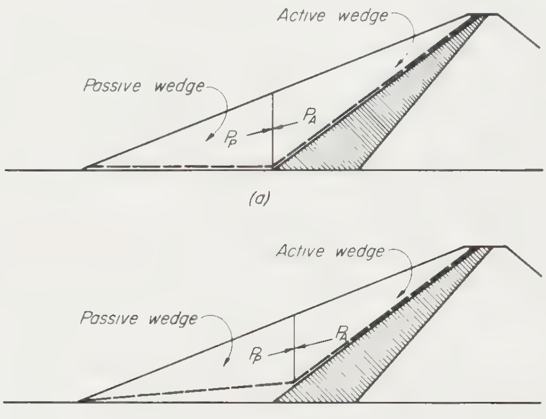

FIG. 27. Sliding-block method of stability analysis, sloping-core dam.

of slices for a circular sliding surface. Analyses are made assuming different factors of safety until the lateral force of the active wedge is exactly resisted by the lateral force of the central block plus the lateral force of the passive wedge. In the sliding-block method care must be exercised to determine the location of the most critical planes for sliding. For example, Fig. 27*a* shows the failure planes commonly used for analysis

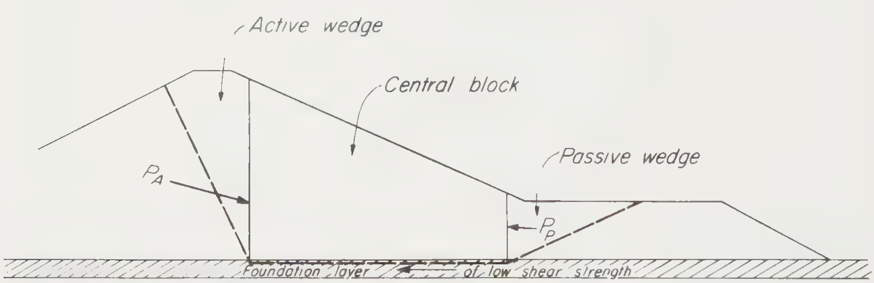

FIG. 28. Sliding-block method of stability analysis, dam with counterweight berm situated on foundation of low shear strength.

of stability of the upstream shell of a dam. Actually planes located about as shown in Fig. 27*b* result in a lower factor of safety and should be investigated. The inclination of the interface between blocks and the obliquity of earth forces on the interfaces between blocks are important. The obliquity depends upon the strain which occurs on the interface at the time of incipient failure on the failure surface. The order of magnitude of the obliquity may be ½ to ⅔ϕ_D.

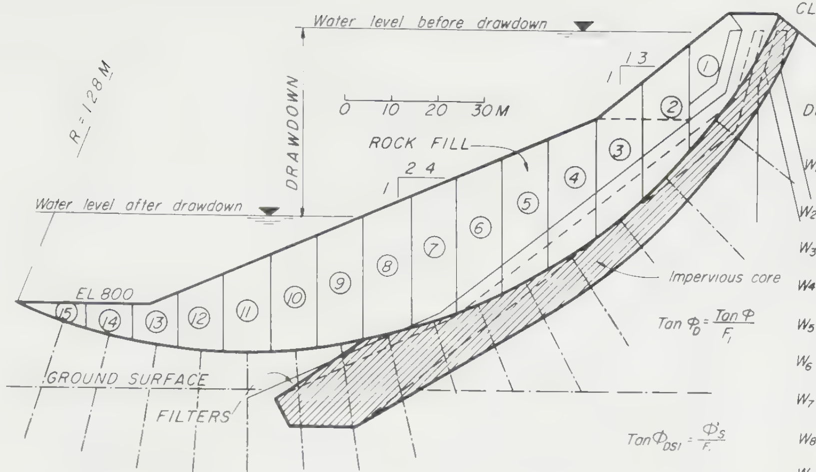

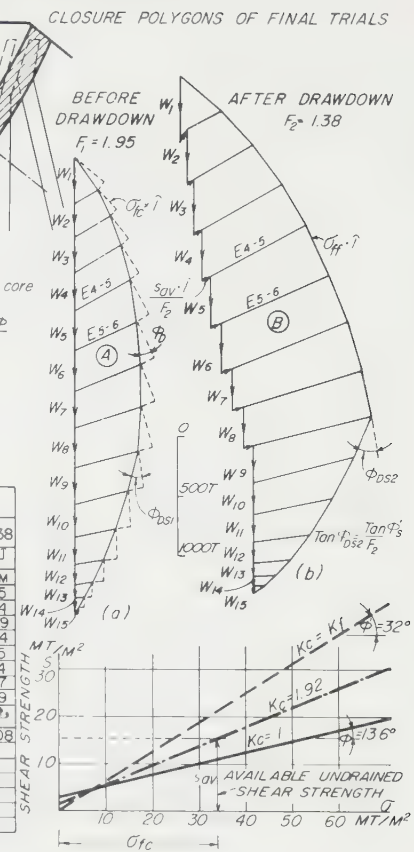

SLICE		RESERVOIR LEVEL: HIGH												LOW		
		FORCE POLYGON: A F_1=1.95						DETERMINATION OF K_c						FORCE P:B F_2=1.38		
		W MT/M	$\hat{l}$ M	Tan Φ'	F_1	N MT/M	T MT/M	σ_{fc} MT/M²	τ_{fc} MT/M²	σ_{3c} MT/M²	σ_{1c} MT/M²	K_c	S_{av} MT/M²	W MT/M	$S_{av} \cdot \hat{l}$ MT/M	$\frac{S_{av} \cdot \hat{l}}{F_2}$ MT/M
1	CORE	368	34 4	0625	1 95	298	95	870	273	718	13 63	1 92	50	541	172	125
2	CORE	286	13 8			230	74	1670	5 35	13 73	26 33		8 4	468	116	84
3	CORE	302	13 0			255	82	1960	6 30	16 10	30 95		9 4	486	122	89
4	CORE	312	12 0			275	88	2290	7 35	18 82	36 12		10 8	439	130	94
5	CORE	336	11 7			340	108	2900	8 55	24 25	44 45		12 4	435	145	105
6	CORE	347	11 0			345	110	31 20	10 00	25 65	49 25		13 0	421	143	104
7	CORE	304	10 8			340	108	31.50	10 00	25 95	49 55		13 6	350	147	107
8	CORE	334	10 6			350	112	33 10	10 60	27 20	52 20		14.2	344	150	109
				Tan Φ'_S											Tan Φ'_S	$\frac{Tan\ \Phi'_S}{F_2}$
9	ROCK SHELL	302	10.4	0839	1 95	325	140	31 2	13 5					304	0839	0608
10	ROCK SHELL	268	10 0			310	134	31 0	13 4					268		
11	ROCK SHELL	226	10 0			255	110	25 5	11 0					226		
12	ROCK SHELL	173	10 2			190	82	18.7	8 1					173		
13	ROCK SHELL	112	10 2			140	60	13 7	5 9					112		
14	ROCK SHELL	80	10 3			95	41	9 2	4 0					80		
15	ROCK SHELL	52	16 2			50	22	3 1	1.4					52		
COL		1	2	3	4	5	6	7	8	9	10	11	12	13	14	15

FIG. 29. Stability analysis of rapid drawdown.

36. Stability Charts. The stability-factor chart presented in Fig. 25 affords an accurate and simple method for determining the factor of safety against stability failure for a homogeneous dam and foundation in (1) the dry condition, (2) the completely submerged condition, (3) the condition of seepage parallel to the face of slope, and (4) the condition of complete rapid drawdown from crown to toe for an embankment with negligible drainage. Approximate solutions can be made also for nonhomogeneous dams and for the condition of seepage not entirely parallel to the face of the slope and for the condition of rapid drawdown over part of the slope. The chart gives the relationship between factor of safety F, height of slope H, angle of slope i, developed friction angle ϕ_D, and developed cohesion c_D. The effect of a firm stratum at shallow depth in the foundation and the effect of counterweights a short distance away from the toe of slope are also included by means of the terms n_D and n_x defined in Fig. 25. The shear-strength parameters and shear-strength expressions to use with the stability chart for the different cases of loading should be those recommended in Arts. 31 to 34. In summary these are:

End of construction: total stresses, *UUU* test

Consolidation under dry or submerged condition (no seepage): total or effective stresses, *CD* test

Rapid drawdown or seepage parallel to face, earthquake: consolidation stresses, *CU* or *ACU* test

The steps used to solve two typical stability problems are outlined below. The solutions are for embankments and foundations in which no seepage or consolidation is occurring. If the slope is above the freewater surface, the total unit weight is used for γ. If the slope is completely submerged, the submerged unit weight is used for γ. Modifications to the given solutions to solve other problems are also given.

Problem A. Determine the permissible slope for an embankment of prescribed height to satisfy a prescribed factor of safety.

1. Determine $C_D = c/F$ and $\phi_D = \arctan (\tan \phi)/F \approx \phi/F$.
2. Compute $N_s = \gamma_H/c_D$.
3. Determine n_x, and the minimum of the actual value of n_D, and the value of n_D from Fig. 25*b*.
4. Enter chart with N_s and ϕ_D using the proper n_D line when $\phi_D < 5$ deg and $i < 53$ deg, and determine the slope angle i.

Problem B. Determine the factor of safety for a slope of prescribed height.

1. Assume a value for the factor of safety.
2. Compute $\phi_D = \arctan (\tan \phi)/F \approx \phi/F$.
3. Compute n_x, and determine the minimum of the actual value of n_D and the value of n_D from Fig. 25*b*.
4. Enter chart with i and ϕ_D, using the proper n_D line when $\phi_D < 5$ deg and $i < 53$ deg, and determine the stability factor N_s.
5. Check the assumed factor of safety against F computed from

$$F = \frac{c}{c_D} = \frac{cN_s}{H}$$

6. Repeat this procedure until the assumed and the computed F agree.

As an alternate to problem B, the factor of safety may be prescribed and it may be desired to determine the permissible height of embankment. The solution is similar to that of problem B. For the third and fourth cases above where the face of the slope approximates the piezometric line for pore pressure along the critical circle, the three problems may be solved as indicated, except that

$$\phi_D = \frac{\gamma_{\text{subm}}}{\gamma_{\text{total}}} \times \arctan \frac{\tan \phi}{F}$$

Also γ_{total} is used in computations for N_s. When the embankment and foundation are composed of more than one material, an approximate solution can be made by obtaining weighted-average values for ϕ, c, and γ. The following steps may be followed in the solution:

1. Assume average values for ϕ, c, and γ.
2. Solve the problem as described above and determine ϕ_D and i.
3. Draw the critical circle, either the proper mid-point circle or the toe circle defined by Fig. 22 for ϕ_D and i.
4. Check the assumed average values; repeat the solution if necessary with more accurate average values.

In determining the proper average unit weight, particularly for the case where $\phi = 0$, only the weight of the net driving area should be considered. For example, for the mid-point circles shown in Fig. 25 only the weight above the dashed line is effective for driving; the center of gravity of the area below and to the left of the dashed line lies directly below the center of rotation and generates no driving moment.

Stability charts were first published by Taylor in 1937.[62]

A more elaborate series of charts for various slope configurations has been prepared by Janbu[29] and is frequently useful.

SETTLEMENT ANALYSIS

37. General Considerations. Prediction of the settlement which will occur in an embankment dam and in its foundation is required for several reasons. At the end of construction adequate camber must be provided so that after settlement the crest of the dam will be at such elevation as to provide sufficient freeboard. Generally after settlement some camber should remain for appearance. Differential settlement of the dam, particularly that caused by abrupt changes in foundation conditions, is critical in connection with developing transverse cracks through the dam. Construction methods and design measures must be used so as to protect the dam adequately against the development of such cracks. Where a conduit passes underneath or through an embankment dam on a soil foundation, the design of the conduit requires knowledge of the pattern of settlement along the conduit. In this case estimation of longitudinal movements along the conduit which will result in squeezing together or extension of the conduit is required also. Finally estimation of the settlement of the foundation and compression of the embankment during construction is needed for proper estimation of the required fill volumes.

The possible sources of settlement as listed by Seed[51] for cohesive materials apply also to embankment materials and include (1) immediate or elastic settlement, (2) volumetric compression resulting from consolidation, (3) axial and lateral strains induced by effective stress changes during consolidation, (4) secondary compression, and (5) plastic flow or creep at constant water content. Skempton and Bjerrum[58] suggest a method for computing the immediate settlement and also by utilizing the pore-pressure coefficients introduce a procedure for incorporating the effect of stress changes during consolidation. Lambe[34] introduces a method that by using the effective stress path gives solution for immediate settlement and also takes into account the effect of stress changes and axial and lateral strains during consolidation. The secondary compression is discussed by Taylor[63] and by Scott.[48] Although research has been done for determining the influence of creep on settlement no generally recognized design procedure has been developed. All these sources will not be significant in every instance.

Generally the settlement due to volumetric compression resulting from consolidation is most significant. The rate of reduction in hydrostatic excess pore pressures which results from consolidation is important also in connection with determining shear strength since the shear strength of a consolidating layer increases directly with decrease in the pore pressure. Of the four sources of settlement only one, volumetric compression resulting from consolidation, is discussed in some detail in Arts. 38 and 39.

38. Settlement from Consolidation of Foundation. When a compressive load is applied to a confined soil, the total volume of the soil decreases. For all practical purposes, this volume change is only a change in the void volume of the soil; the volume of soil particles remains constant. When the voids of a soil are filled with water, the rate at which the void volume can change depends upon the rate at which the water content of the soil can be changed.

When an increment of pressure is applied to a saturated soil in which the pore pressure is the natural hydrostatic pressure, the entire increment of pressure is at first carried by an increase in water pressure which is termed hydrostatic excess pressure. At the moment of application of load, the soil is considered to be at zero percent consolidation under the increment of pressure. Owing to the hydrostatic excess pressure, water is forced out of the soil and the soil structure compresses. As the soil structure compresses, it is able to carry part of the increment of load. As the intergranular pressures in the soil structure increase, the hydrostatic excess water pressures decrease. When the entire increment of pressure is carried as intergranular pressure, the soil is considered to be 100 percent consolidated under the particular increment of load. The portions of a soil stratum nearest the drainage faces drain first because the hydraulic gradients created by the hydrostatic excess pressure are greatest there. The variation of excess pressure with time t, the percent consolidation U, at various

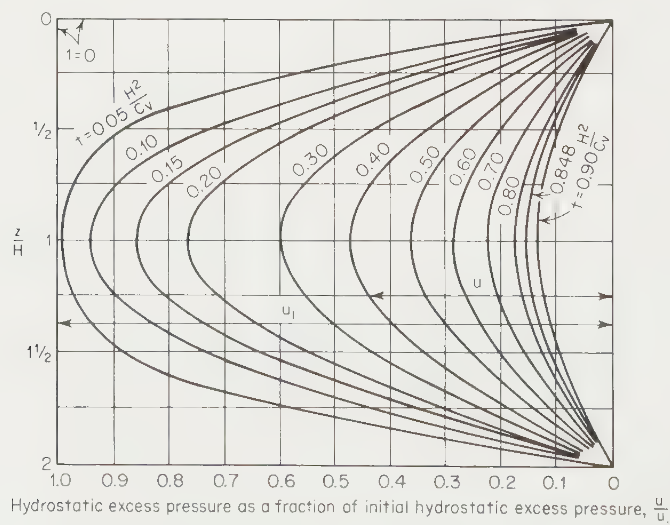

FIG. 30. Distribution of percent consolidation throughout a consolidating stratum, Case IA of Fig. 31.

depths z, in a stratum of thickness $2H$ with drainage at top and bottom and for the case when the hydrostatic excess pressure is constant with depth at time of application of load is given in Fig. 30. The average rate of consolidation throughout the stratum is given in Fig. 31 for three different types of initial hydrostatic excess pressure distribution which may be encountered. The hydrostatic excess-pressure diagram for curve IA is that for the case described above. Cases IB, II, and III represent other types of possible field loading.

The procedure of obtaining the magnitude of settlement and the time required for the settlement includes (1) determining the stresses that cause settlement, (2) determining compression characteristics of the soil, (3) computing total settlement, and (4) computing the time required for settlement.

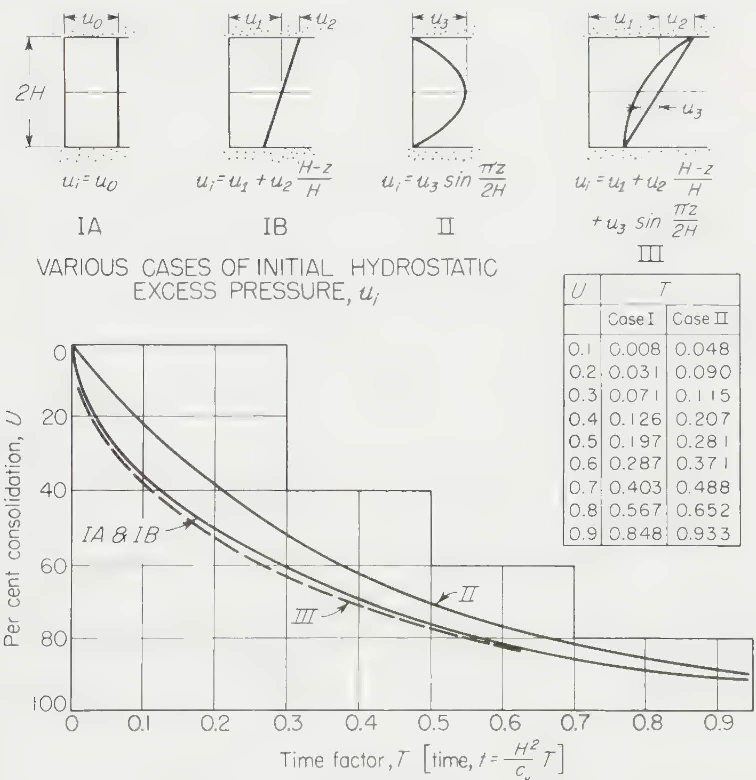

U	T	
	Case I	Case II
0.1	0.008	0.048
0.2	0.031	0.090
0.3	0.071	0.115
0.4	0.126	0.207
0.5	0.197	0.281
0.6	0.287	0.371
0.7	0.403	0.488
0.8	0.567	0.652
0.9	0.848	0.933

FIG. 31. Rate-of-consolidation curves.

1. Determining the stresses that cause settlement. At several depths throughout the foundation the increase of stresses due to the increment of load is determined using the theory of elasticity. Either the Boussinesq or Westergaard formula for distribution of vertical stresses may be used depending on whether the soil is homogeneous or varved. The distribution of vertical compressive stresses σ_z due to a point load is given in Fig. 32. The same curves may be used for determining stresses due to distributed load by dividing the loaded area into squares whose sides are not larger than one-third the depth to the point at which the stress is being computed. Each

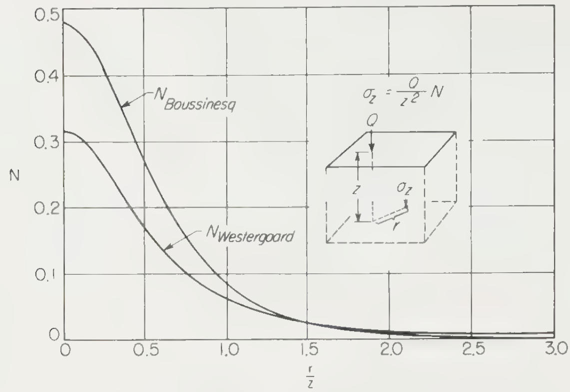

FIG. 32. Distribution of vertical stresses due to point load on surfaces of semi-infinite elastic solid.

loaded area fraction is considered as a concentrated load. The total stress increment for any desired point is the sum of the increments from each of the loaded areas. The decrease in stress due to release of load by excavation can be computed in a similar manner. Such decreases in stress should be considered in settlement analyses where applicable. Simpler methods for computing stresses due to various loadings are given in Refs. 31, 45, 46, and 65. These sources contain formulas, tabulations, and influence charts. The tabulations and charts are results of integration of formulas based on the theory of elasticity and give stresses due to various loadings for any point of the foundation.

2. Determining the compression characteristics of the soil. The soil properties required for settlement-analysis computations are determined by means of the consolidation test described in Art. 55. In the consolidation test, load is applied to the soil specimen and the volume change caused by this load is observed together with the time required for the volume change. The test provides the compression index C_c, which gives the relation between applied load and change in void ratio, and the coefficient of consolidation c_v, which expresses the rate of consolidation.

The compression index C_c, an indicator of soil compressibility, can be determined for any load range by the formula

$$C_c = \frac{e_1 - e_2}{\log p_2 - \log p_1}$$

where e_1, p_1, and e_2, p_2 are the void ratio and vertical stress before and after the application of a load increment.

The coefficient of consolidation c_v is computed by the formula

$$c_v = \frac{T_U H_1^2}{t_{1U}}$$

where T_U = time factor, as given in Fig. 31, for various U percent of consolidation
H_1 = length of seepage path in the laboratory sample, half of the sample thickness if double drainage is used
t_{1U} = time required for U percent consolidation in the laboratory

3. Computing total settlement. The change in void ratio in any foundation layer is determined by the equation

$$\Delta e = \frac{0.435 C_c \Delta p}{p_{\text{av}}}$$

where Δp = net increase in vertical stress at the center of the soil stratum
p_{av} = average vertical stress during the application of consolidation load $(p_1 + \Delta p/2)$

The ultimate settlement is computed from the equation

$$\Delta h = \frac{\Delta e}{1 + e_1} h$$

where h = thickness of the soil stratum

The total settlement of the foundation is obtained by summing the compressions of the various layers composing the foundation.

4. Computing the time required for settlement. The time t_U required for various percentages of settlement is expressed by the formula

$$t_U = \frac{H^2 T_u}{c_v}$$

In the laboratory test the first part of the compression under a particular load increment takes place at a rate governed by the rate of dissipation of hydrostatic excess pressure. This part of the compression is termed primary compression; the remaining part of the compression under the load increment is termed secondary compression. The prediction of what part of the compression of the prototype will take place as primary compression and what part as secondary is somewhat controversial, and the reader is referred to Refs. 48 and 63 for discussion of this matter.

39. Settlement from Compressions in Embankment. The embankment is divided into a series of horizontal layers. The load applied to a particular layer by the overlying layers is computed on the basis of stress distribution of the weights of each of the overlying layers by either the Boussinesq or the Westergaard formula. The stress-strain characteristics of each layer are determined by consolidation tests on material compacted at the same water content and to the same density as anticipated in the embankment. The ultimate settlement is then computed as for the foundation in Art. 38.

The consolidation theory presented in Art. 38 applies only to saturated soils; no theory is available for predicting the rate of consolidation of partially saturated soil.

SLOPE PROTECTION

40. General Considerations. The slopes of earth embankments must be protected against erosion by wave action, rainwash, frost, and wind action. Protection cannot economically be provided against the erosion which would occur if the dam were overtopped. A major cause of earth-dam failures has been overtopping; therefore, care must be exercised that freeboard and spillway capacity are ample to prevent it. A detailed discussion of slope protection is given in Refs. 1 and 75.

41. Freeboard. Freeboard is the vertical distance between the maximum water surface of the spillway design flood and the crest of the dam. This vertical distance should be ample to prevent overtopping of the dam due to wind setup (rise in water level at dam due to wind blowing toward dam), the height of waves above pool level, and run-up of waves on the face of the dam as illustrated in Fig. 33.

Wind setup may be computed by the Zuider Zee formula:

$$S = \frac{V^2 F}{1{,}400D} \cos A$$

where S = setup above normal pool level, ft
V = wind velocity, mph
F = fetch, miles
D = average depth of water, ft
A = angle between direction of waves and normal to face of dam

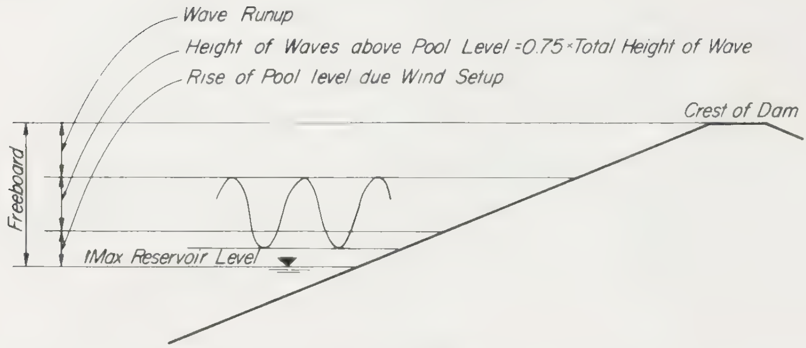

FIG. 33. Freeboard.

The height of waves may be computed using the Molitor-Stevenson equations given below.

For a fetch greater than 20 miles,

$$h_w = 0.17(VF)^{0.5}$$

For a fetch less than 20 miles,

$$h_w = 0.17(VF)^{0.5} + 2.5 - (F)^{0.25}$$

where h_w = height of wave from trough to crest, ft. Three-quarters of the height of wave is considered to be above the pool level.

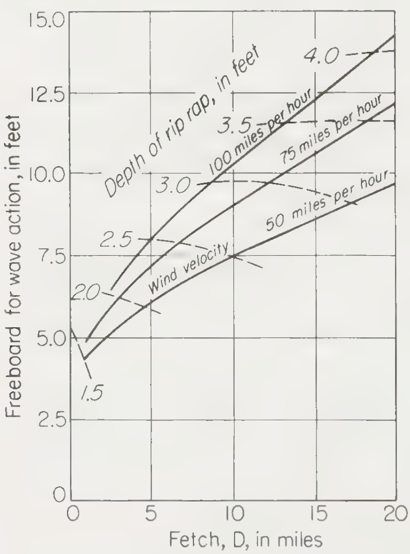

FIG. 34. Relationship between fetch, freeboard for wave action, and thickness of dumped riprap for slope protection.

The run-up of waves on the face of the dam may be computed by the formula

$$\text{Run-up of waves} = \frac{V^2}{2g}\, 1.5h_w$$

This formula does not contain a term expressing the roughness of the face and so is approximate.

Fetch is the distance from the dam to the opposite shore. Generally the straight-line distance is used. Where slight bends in the measured line will lengthen the fetch, however, such bends should be incorporated according to judgment.

The relationship between freeboard for wave action (omitting setup) and fetch for wind velocities of 50, 75, and 100 mph is shown graphically in Fig. 34. The freeboard for wave action plus the freeboard for setup almost always is greater than 5 ft. It is thus greater than the usual depth of frost penetration. If the depth of frost penetration is greater than the above computed distance, the depth of frost penetration should be used for the freeboard distance.

42. Types of Slope Protection. The types of slope protection used on earth dams and levees vary from sod to several feet of dumped riprap. The choice of slope protection for a particular slope depends upon the type of erosive action against which the slope is to be protected and the frequency of attack. The discussion below takes up the various types of slope protection which may be considered for the upstream and downstream faces of dams and levees.

The upstream slopes of dams are commonly protected with dumped riprap or its equivalent. The thickness of the riprap may vary from 1.5 to 5 ft, depending on the severity of wave action. Suggested values for thickness of riprap for various fetches and wind velocities are given in Fig. 34. The riprap should be founded on a filter or filters designed as described in Art. 22. The thickness of the filter should be about 12 in. The stone used for riprap should be hard and durable and be able to resist long exposure to weathering. Stone suitable for riprap generally should be able to pass the standard soundness tests used for concrete aggregate. However, occasionally rock which casehardens will not pass soundness tests and yet be satisfactory for riprap. Fifty percent of the stone by weight should have diameters about equal to the proposed thickness of riprap. The remaining 50 percent should be graded downward as quarry conditions permit for reasonable design of the underlying filter bed. The riprap should extend from the top of the dam to about 5 ft below the lowest normal pool level. To prevent raveling at the lower end, the riprap is usually abutted against a large stone embedded in the embankment. Also a berm is frequently located at the lower end of the riprap to assist in preventing raveling and to facilitate construction of the riprap. Where rock is expensive, a layer of hand-placed riprap about half the thickness of the dumped riprap may prove more economical, the cost of the additional labor required being compensated by the saving in quantity of rock used. Run-up of waves on the relatively smooth face of hand-placed riprap is greater than on dumped riprap. Other alternatives which may be considered where rock is expensive are cast tetrahedron blocks of concrete, ceramic blocks, or soil cement as described by Holtz and Walker.[25] Slope protection consisting of continuous concrete pavement has been used occasionally as at McKay Dam in Oregon and Lake Babcock in Nebraska.

The downstream face of an earth dam is usually protected with sod where the climate is suitable. In climates where sod cannot grow, a thin layer of stone or gravel riprap may be used. To develop a sod, 4 to 6 in. of topsoil is spread on the downstream face and the face seeded and strip-sodded. The grass or vine used for making the sod will depend on local conditions. Berms which intercept the runoff have at times been used on the face of the dam. Care must be exercised, however, in designing and maintaining the berms to see that the water which they intercept is safely conducted away; otherwise the berms may cause more difficulty than they prevent. Culverts are generally required at the intersection of the faces of the embankment with the abutments.

Where riprap is used on the downstream face, its thickness and permeability should be ample to conduct safely the rainwater flowing down the slope. The stability of such riprap against sloughing caused by the seepage force of the rainwash can be analyzed in a manner similar to the methods discussed in Arts. 27 and 28. Where the downstream slopes of earth dams are subject to tail water, they should be protected by riprap.

Both the riverside and landside slopes of levees are commonly protected with sod. Where river currents would cause erosion of the sod, as at the outside of bends, dumped riprap slope protection or its equivalent may be used. Other types of slope protection that have been used on levees include articulate concrete mats, asphalt pavement, and willow mats.

SUBSURFACE INVESTIGATIONS

43. General Considerations. Many methods are available for determining the nature of subsurface conditions at a dam or levee site. Methods for both soil and rock exploration are discussed in this article. The methods for soil exploration consist of three types: (1) indirect methods wherein no or only practically worthless samples are obtained, (2) methods wherein representative but disturbed samples are obtained, and (3) methods in which undisturbed samples are obtained. Seepage tests in soil and pressure tests in rock are also used. A general discussion of the program of subsurface investigation for an earth dam or levee is given in Art. 2. A thorough discussion of subsurface exploration programs and methods is given in Ref. 27. Only the more common and important methods of exploration are described below.

44. Indirect Methods. The *seismic method* is the most extensively used of the various geophysical methods in which no samples are obtained. It is described in Refs. 54 and 74. It consists essentially in observing the time required for shock waves, set off by a small explosive charge or the blow of a sledge hammer, to reach a detector. The waves travel either entirely through the soil overburden, or down through the overburden to rock, through the rock, and then up through the overburden to the detector. From observations of the time required for the shock waves to reach the detector by the two paths, the depth to rock can be computed. The depth so determined should be spot-checked by test boring since the depths determined by purely seismic methods may be considerably in error at times. In some instances determination can be made of the depth to groundwater table, or to the top of an underlying soil stratum having different velocity for transmission of shock wave from the overlying soil.

The *electrical-resistivity method* is similar to the seismic method except that electric current is used instead of shock waves. It is described in Ref. 74. The method has been used mainly for locating underlying gravel beds and depth to groundwater table.

45. Representative but Disturbed Sample Methods. *Auger borings* are used frequently for soil explorations of shallow depth, particularly in borrow areas. Because of the augering action the natural structure of the soil is disturbed, although the water content and relative proportion of the various soil constituents remain unchanged. Care must be exercised so that material from the sides of the auger hole is not mixed with the material from the bottom of the hole during augering.

Drive (or dry) sample borings are used very commonly in dam and levee subsurface exploration work. The borehole in which drive samples are obtained is generally put down by wash-boring methods, although at times auger or churn-drill methods are used. Casing is used as required to maintain the walls of the borehole. The drive sample is obtained by driving a thick wall sampler 1 to 3 ft into the natural soil below the bottom of the borehole. Samples may be taken continuously or at each change in soil strata, but at intervals no greater than about 5 ft. A split-barrel sampler similar to the one shown in Fig. 35 may be used. The sampler should be equipped at the top

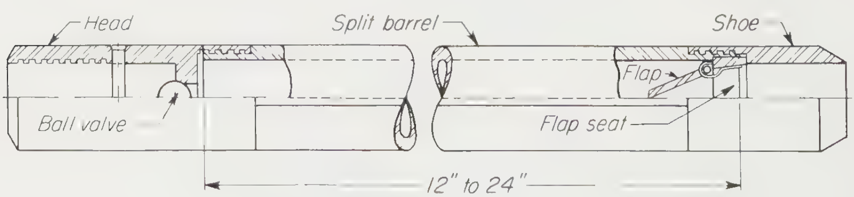

Fig. 35. Split-barrel sampler.

with a check valve, and when required to sample loose cohesionless soils or soft cohesive soils, it should be equipped at the bottom with a flap or conical spring trap. The sampler may vary from 1⅜ in. ID by 2 in. OD to 2½ in. ID by 3 in. OD or larger. The larger size is desirable for sampling soils containing gravel. Record should be kept of the number of blows of the drop hammer required for driving the sampler together with the weight of the hammer and the height of drop. Such data may be used to infer the relative density of cohesionless soils and the relative consistency of cohesive soils as described on pages 294 and 300 of Ref. 66 and pages 71 and 72 of Vol. II of Ref. 8. Continuous-drive sample boring is advantageous for exploring borrow areas where gravel in the soil prevents the use of auger borings. Such boreholes should be put down by the process of continuous sampling, and wash-boring methods should be avoided so that samples of material above the groundwater table may be obtained at their natural water content.

In connection with auger or continuous-drive sample borings in borrow areas, it is desirable to install observation wells and note the variation in groundwater-table level over a complete cycle of seasons. Borings should be put down during various seasons also to determine changes in the water content with the seasons.

46. Undisturbed Soil Sampling. The *Denison double-tube core barrel* shown in Fig. 36 is excellent for obtaining undisturbed samples of soils, especially those in a relatively compact state. The Denison sampler can obtain specimens of practically all soils except loose gravelly soils. The sampler consists of an inner core barrel and liner which remain stationary, and an outer core barrel and toothed bit which revolve. The length of bit used can be varied so that the cutting edge of the inner core barrel can follow, be flush with, or lead the bit as required to obtain the best sample. At the top of the inner core barrel is a cage check valve and at the bottom a basket spring trap. The size of samplers varies from 2.75 to 8 in. core diameter. The sample is shipped to the laboratory in the liner. Drilling fluid is used generally instead of water in the drilling to minimize the use of casing. Samples may be taken either continuously or intermittently. Drilling in between intermittent samples may be by tricone or fishtail bit.

In glacial till containing gravel and cobble-sized rock fragments and in shear zones in rock the use of a 6-in.-core-diameter double-tube core barrel with liner and diamond bit has been found to be more advantageous than the Denison double-tube core barrel, primarily because the diamond bit cuts the rock fragments much better than the Denison toothed bit.

The *stationary thin-wall piston-type sampler* with liners shown in Fig. 37 is suitable primarily for sampling soft cohesive soils and also some fine sands. Generally soils which can be sampled with it are not suitable for dam foundations because of the low shear strength of the material. Low dams and levees may be founded on such soils, and for these cases the sampling is valuable. As in the case of drive sample borings, the drill hole is put down by the wash-boring process. Before sampling, the drill hole is carefully cleaned of all disturbed soil. The sampler is lowered to the bottom of the drill hole with the piston held fixed at the bottom of the sampler. The piston rod is then held stationary with respect to ground surface and the thin-wall sample tube is forced into the natural soil at a rate of about 1 fps. The piston is then again made fixed relative to the sample tube and the sampler is withdrawn. The plastic liners are removed and capped and shipped to the laboratory. The liners come in short sections, 6 in. length for 2.8-in.-diameter sample, so that cutting of the sample tube in the laboratory is not necessary. The sample is suitable for all laboratory testing. For average soil conditions, the cutting edge of the thin-wall tube should be about 0.7 to 1.5 percent less in diameter than the inside of the tube in order that friction between the sample and walls of the tube may be reduced. Stationary-piston thin-wall samplers without liners may be obtained in diameters from 2 to 6 in.

The *thin-wall tube (Shelby) sampler*, shown in Fig. 38, is used for sampling soils similar to those sampled by the fixed-piston type of sampler. It is not so elaborate as the piston-type sampler, and somewhat less undisturbed samples are obtained. Its

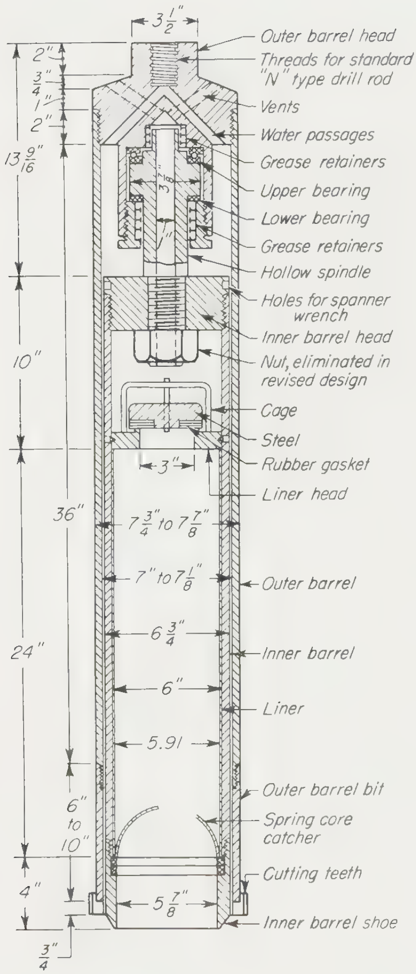

FIG. 36. Denison double-tube core barrel.

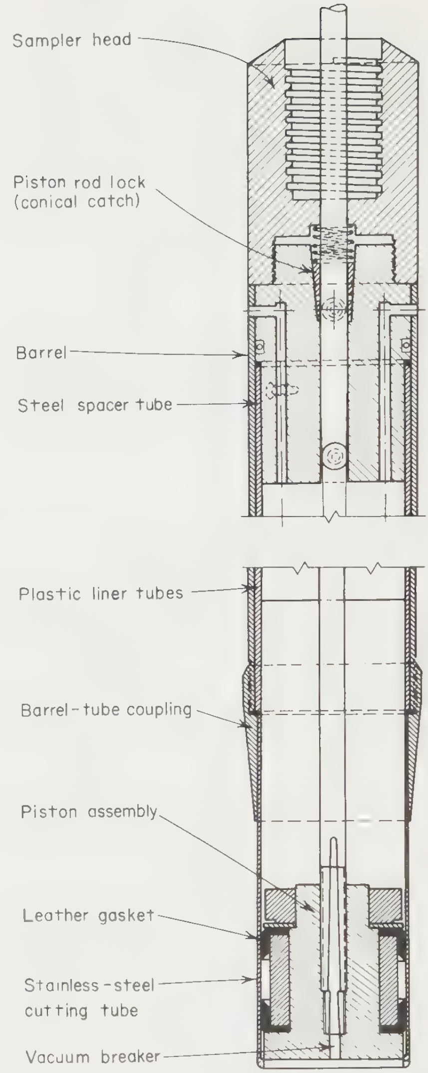

FIG. 37. Thin-wall stationary-piston sampler with liners.

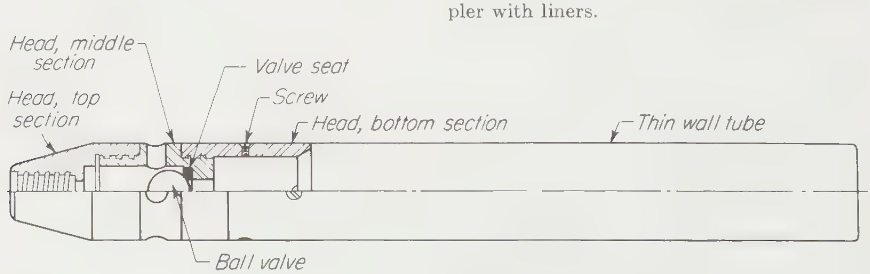

FIG. 38. Thin-wall (Shelby-tube) sampler.

cutting edge should be about 0.7 to 1.5 percent less in diameter than the inside diameter of the tube. Also a check valve should be located at the top. Diameters of samplers vary from 2 to 6 in.

Hand-carved samples from test pit or trench are obtained by careful carving from a bench at the bottom or side of the pit or trench. A detailed description of the procedure is given on pages 372–383 of Ref. 27. This method is particularly suitable for obtaining undisturbed samples of soils with gravel or boulders. Practically any size or shape of sample can be obtained, but the depth to which the method can be used is limited by the depth of the test pit or trench. Sampling cannot be done below groundwater table unless special dewatering of the area has been accomplished in advance of test pitting by well points or deep wells with submersible pumps.

47. Field Permeability Tests in Soil. These tests are of particular value in determining the in-place permeability of granular soils for which it is difficult, if not impossible, to obtain undisturbed samples. Two general types of seepage tests may be performed. One type is performed by utilizing a single borehole. In the other a central borehole and several surrounding observation holes or wells are used.

In the single-hole type of seepage test, casing is driven to the bottom of the borehole and the hole is cleaned out flush with the bottom of the casing. Any of three procedures may be used: the rising-, the falling-, or the constant-water-level procedure. In the rising-water-level procedure, the water level in the borehole is lowered by pumping or bailing to below the groundwater table, and the natural rate of rise of the water in the borehole is observed. If the material at the bottom of the borehole becomes quick in such a test, the falling-water-level procedure should be used. In this case the water level in the drill hole is raised above the groundwater table and the rate of fall of the water level is observed. In the latter case, care must be exercised to see that no fine material is suspended in the water in the drill hole. Upon settling, such material would form a relatively impervious skin at the bottom of the drill hole and vitiate the results of the test. The equation for computing the permeability from either of the above types of observations is as follows:

$$k = 1.8r_0 \frac{\log h_1 - \log h_2}{t_2 - t_1}$$

where r_0 = inside diameter of casing

h_1 and h_2 = difference in elevation between water level in casing and natural groundwater table at times t_1 and t_2, respectively

Where the permeability of the soil being tested is high and the rising- or falling-water-level procedures described above would not be satisfactory because of the fast rate at which the water level would change, the constant-water-level procedure may be used. In this procedure, observation is made of the rate at which water must be added to the borehole to maintain the water level at constant level, such as the top of the casing. The coefficient of permeability is computed from the following formula:

$$k = (0.25 \text{ to } 0.50) \frac{q}{hr_0}$$

where r_0 = inside diameter of casing

h = difference in elevation maintained between water level in casing and natural groundwater table

q = rate of pumping into or out of casing to maintain constant water level in casing

Formulas for computing permeability for the case where the borehole extends below the bottom of the casing are given in Refs. 71 and 72.

In the method wherein observation wells in a radial pattern from a central borehole are used, water is pumped either into or out of the central hole at a constant rate. The central hole should extend to the full depth of the pervious stratum; also the casings for the observation wells should be perforated. Observations are made of the water levels in the observation wells, and when flow conditions become steady, the permeability is computed by the following formula:

$$k = \frac{q \ln (r_2/r_1)}{\pi(z_2^2 - z_1^2)}$$

where q = rate of pumping

z_1, z_2 = heights of water above bottom of pervious stratum in observation wells at radial distances of r_1 and r_2, respectively

The observation-well method gives the average permeability of the material between the observation wells and is the more reliable of the two types of field methods. Methods of utilizing only a single borehole give the permeability of the material in the immediate vicinity of the bottom of the drill hole.

48. Rock Drilling. In subsurface investigations for a dam, it is essential to determine the depth to bedrock and the nature of the bedrock. Wherever rock is encountered, it should be core-drilled to determine whether it is actually bedrock or boulders. Usually $2\frac{1}{8}$-in. (NX) cores obtained with a diamond bit are satisfactory although 4- and 6-in.-diameter cores are used at times where the rock is fractured or where the holes are deep and telescoping is required. Occasionally smaller-diameter cores may be used. In some instances, 24- or 30-in.-diameter holes have been put down by Calyx drill methods. The latter holes are large enough to permit a man to be lowered into them for inspection of the rock *in situ*. Generally double-tube core barrels with core catcher and check valve should be used. Single-tube core barrels should be used only in massive sound rock when good core recovery may be obtained with them. A drill with hydraulic feed is preferred to one with screw feed. The rate of progress of a drill under a particular pressure is an indication of the nature of the rock. The location of all places of core loss should be noted as well as the percentage of core recovery. Unfortunately the places where core is not recovered are the places in the foundation which are critical for design. Every effort should be exerted to adjust the drilling technique to obtain maximum recovery of core. Also observation of the nature and of the percentage return of drilling fluid and of the behavior of the drill should be made to obtain as much information as possible on material in places where core losses occur. Sometimes the use of a borehole camera or borehole television will help to determine the nature of material in places of core loss.

49. Pressure Tests in Rock. Information on the permeability of rock in situ as well as some indication of the soundness of the rock may be obtained from pressure tests in drill holes in rock. A schematic diagram of a pressure-test apparatus is shown in Fig. 39. A more elaborate apparatus is described on page 35 of Ref. 32. The apparatus shown in Fig. 39 seals off a section of the drill hole by means of inflatable rubber packers. The water pressure in the sealed-off section is then raised above the piezometric level normally obtaining in the rock at this section. The leakage into the rock from the sealed-off section under various pressures such as 15, 30, and 45 psi above natural piezometric pressure is observed. A linear variation of leakage with pressure indicates stable passages for flow of water in the rock. If the leakage increase is less than the linear increase the passageways are plugging; if greater then the linear passageways are unplugging or perhaps enlarging by spreading apart under the increase in pressure. The maximum pressure for testing should be limited to 1 psi of pressure for each foot of rock and soil overlying the section being tested in order to ensure against possible heaving and damage to the foundation. For general information a loss of 2 gpm for a 5-ft test section of NX borehole under 30 psi excess pressure would indicate an equivalent permeability of about 1 μ/sec.

The packer test formula[71,72] is frequently used for computing the permeability of rock:

$$k = \frac{Q}{2\pi LH} \log_e \left(\frac{L}{r}\right) \qquad \text{if } L \geqq 10r$$

where k = permeability
Q = constant rate of flow into the hole
L = length of the portion of the hole tested
H = pressure head
r = radius of hole
$\log_e$ = natural logarithm

This formula gives an approximate value of k only because it does not take into account the effect of flow back to the borehole around the packer and includes several simplifying assumptions. These, however, do not change the order of magnitude of the permeability obtained; therefore, the formula is satisfactorily accurate for practical purposes. Figure 40 gives a graphical solution for the above formula. The chart gives the permeability k in centimeters per second if the value of Q is introduced in gallons per minute and the values of L, r, and H in feet.

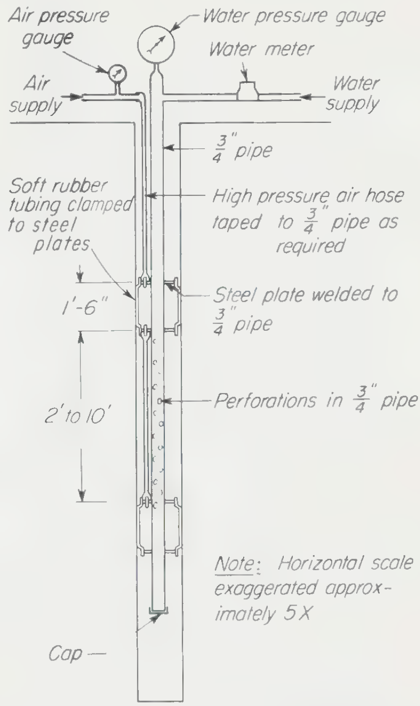

FIG. 39. Pressure-testing apparatus.

LABORATORY INVESTIGATIONS AND TESTS

50. General Considerations. There are three general types of laboratory tests which are performed on earth-dam materials: classification and identification tests, compaction tests, and physical-property tests. The classification and identification tests are simple and are performed on both foundation and borrow materials. They are used to amplify and impart exactness to the visual classification of materials. Also, they indicate roughly the physical properties to be expected for the soil. On the basis of the identification tests, samples can be chosen for the more elaborate compaction and physical-property tests so that the range in variation in the properties of a soil can be covered with a minimum amount of testing. The compaction tests are used to determine the optimum and allowable moisture contents for placing fill materials and for predicting the unit weight of such fill. Physical-property tests include shear strength, permeability, and compressibility tests and are performed on undisturbed samples of foundation materials and on compacted samples of borrow materials. It is essential that the procedures in the physical-property tests performed in the laboratory as well as the composition and condition of the test specimens duplicate field conditions as closely as possible.

Standard test procedures have been set up for the classification and identification tests and compaction tests. The physical-property tests are not standardized but are generally performed in about the same way by the various soil-testing laboratories. It

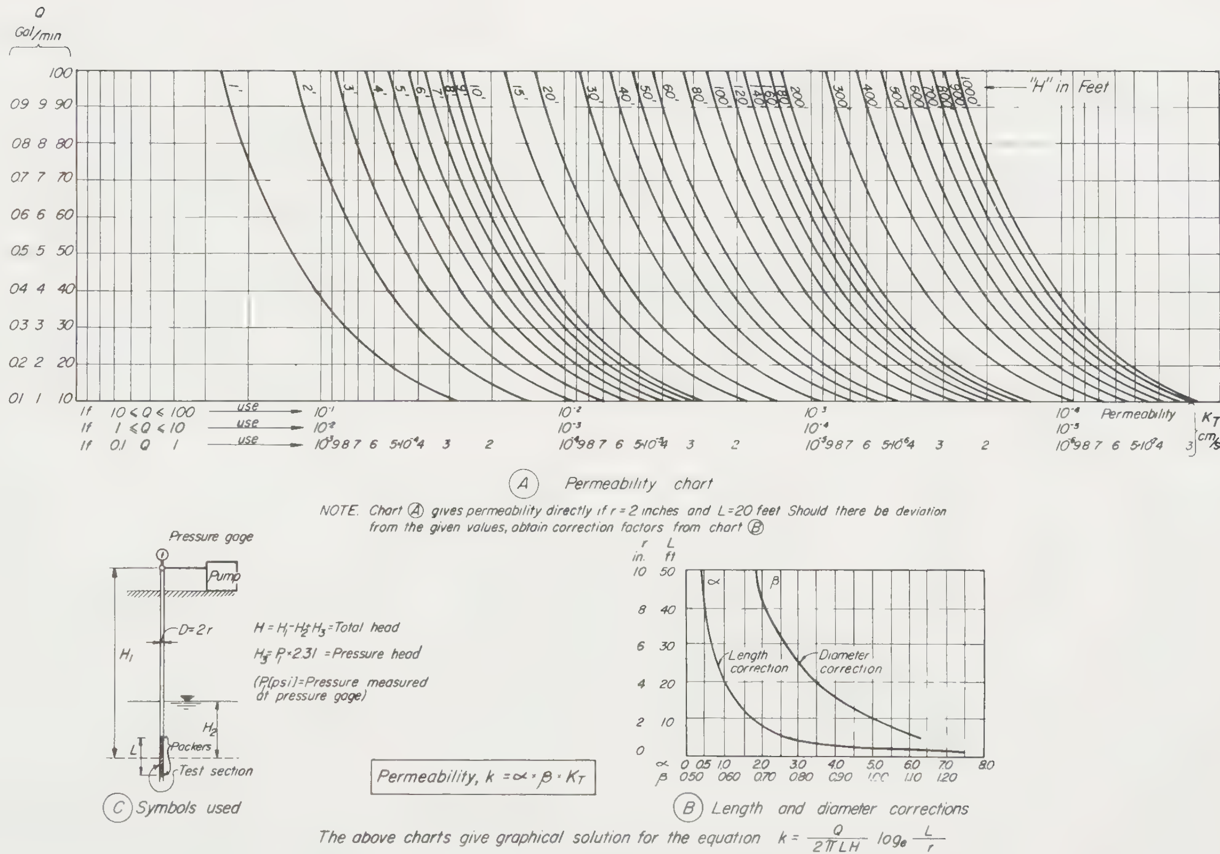

FIG. 40. Graphical solution for determining permeability from packer-type test.

is difficult to standardize the property tests because research is continually developing improved techniques for testing and because projects frequently require special modifications for the particular soil or conditions encountered at the site. Because soil-property tests are not standardized, it is essential that the designer know the particular test procedure used so that he can properly apply the results of the tests. Detailed information on soil-testing procedures is given in Refs. 13, 33, 70, and 72.

51. Identification Tests. The *water content* of a soil is expressed as a percentage and is defined as the ratio of the weight of water in the soil specimen (difference between the natural weight of the soil specimen and the ovendry weight) to the weight of soil particles (ovendry weight) times 100. The natural water content of a soil is of general assistance in soil classification and is useful as an index for the shear strength of normally consolidated clays. The relation between the natural water content of a soil and the optimum water content for compaction is a major consideration in choice of borrow materials.

The *unit weight* of a soil may be determined by any of several methods wherein the weight and volume of a particular mass of soil are determined. The natural unit weight is frequently useful in classification of foundation soils. The unit weight of soil particles (alternatively the specific gravity of soil particles) is required for void ratio or porosity determinations and is at times useful in connection with classification. Knowledge of the unit weights of embankment and foundation soils in the dry, drained, saturated, and submerged conditions is required in structural and hydraulic design.

The *grain-size distribution* of a soil is determined by sieves for particles larger than about 0.07 mm and by hydrometer or some type of sedimentation analysis for particles finer than 0.07 mm. Standard test procedures are given by the ASTM.[3] The results of grain-size analyses are usually presented as a plot of grain sizes vs. percent fines by weight as shown in Figs. 1 and 13. Grain-size analyses are useful for classification of cohesionless soils but rarely for plastic soils. They are required for filter design.

The *liquid and plastic limit* tests are performed on plastic soils and comprise the standard method of classification of such soils. The liquid limit w_L is the water content of the soil at an arbitrarily defined borderline condition between the semiliquid and plastic states. The plastic limit is the water content of the soil at an arbitrarily defined borderline condition between the plastic and solid states. Standard procedures for test are given by the ASTM.[3] The A-line chart in Fig. 41 is generally used as a basis for classification.[10] The liquid limit has been found[56] to be directly related to the compressibility of normally consolidated ordinary clays. Normally consolidated clays are those which have never been subjected to a pressure greater than their present overburden pressure. The liquid limit is related to the compression index by the equation

$$C_c = 0.009(w_L - 10 \text{ percent})$$

Chemical or mineralogical tests are performed on earth-dam materials to determine the presence of soluble minerals or of highly swelling clay minerals such as montomorillonite. Differential thermal analysis is used for identification of clay minerals. With the further development of the chemistry of soils and the chemical treatment of soils, it is likely that more tests of a physical-chemical nature will be made in the future.

The *relative density* test is a classification and index test used for cohesionless soils. The relative density D_R is defined as follows:

$$D_R = \frac{e_{max} - e}{e_{max} - e_{min}}$$

where e = void ratio, volume of voids to volume of solids

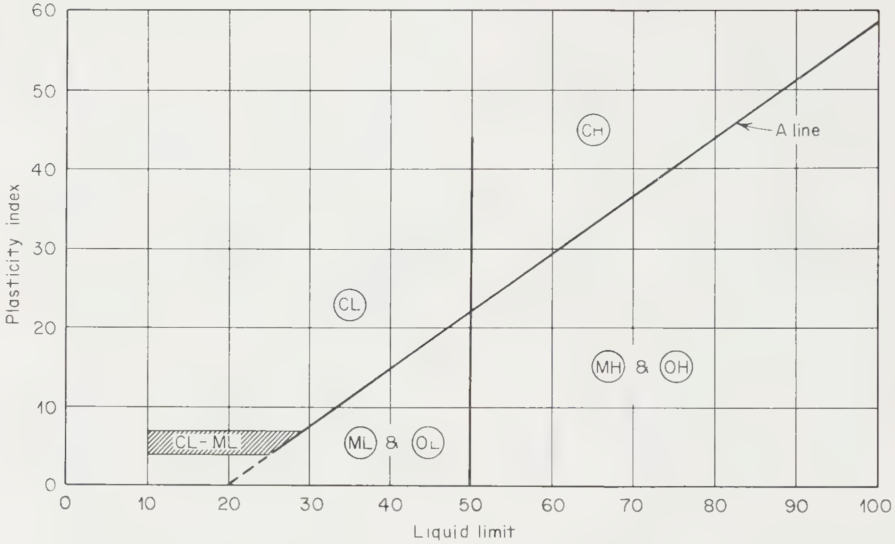

FIG. 41. Plasticity chart. *(After A. Casagrande.)*

For determining the maximum void ratio, the soil, in ovendry condition, is gently poured from a funnel at low height into a container of known volume. The minimum void ratio is determined according to the modified AASHO procedure or the vibratory compaction procedure mentioned in the following article, whichever produces a greater density. In reporting relative-density results, the procedure used for determining the maximum and minimum void ratios should be stated. Procedures for relative-density tests are suggested in Refs. 3 and 72.

52. Compaction Tests. Laboratory compaction tests are performed to predict the unit weight which can reasonably be expected to be obtained by compaction in the field and the optimum moisture content for compaction. The compaction tests indicate the range of densities to which specimens should be prepared for the physical-property tests. Also the compaction tests generally are used as a reference in setting up the specifications for field compaction. Three types of compaction tests are available: impact, kneading, and vibratory.

In the *impact-type compaction test* the soil is compacted in layers in a cylindrical mold by blows of a rammer of particular weight dropped a particular height. Three standards of impact compaction are in common use: Standard AASHO, Modified AASHO, and U.S. Bureau of Reclamation Large Scale Compaction. A summary of these methods is given in Table 2.

The results of compaction tests are usually presented as shown in Fig. 42. The higher the compactive effort, the higher the optimum unit weight and the lower the optimum water content for compaction. The portions of compaction curves for water contents above optimum usually are parallel to and close to the 85 percent saturation curve. The latter curve represents relation between water content and density when the given water content fills 85 percent of the air voids.

Kneading compaction may be performed in the Harvard miniature device developed by Wilson[78] or Seed's device.[50] In both cases the soil is compacted in layers in a cylindrical mold by tamps of a particular pressure. The area of the tamping foot is a fraction of the cross-sectional area of the layer. The Harvard miniature compaction

TABLE 2

	MOLD SIZE			WEIGHT OF HAMMER	NUMBER OF LAYERS	HAMMER DROP	NUMBER OF BLOWS	COMPACTIVE ENERGY	MAXIMUM PARTICLE SIZE	REFERENCES
	Height Inches	Diam Inches	Vol cu ft	lbs.		Inches		ft lb/cu ft		
Standard AASHO (Proctor mold)	4.6	4	$\frac{1}{30}$	$5\frac{1}{2}$	3	12	25	12,400	No 4	ASTM D698-64T
Standard AASHO (CBR mold)	4.5	6	$\frac{1}{13.33}$	$5\frac{1}{2}$	3	12	55	12,400	$\frac{3}{4}$ inches	ASTM D698-64T
Modified AASHO (Proctor mold)	4.6	4	$\frac{1}{30}$	10	5	18	25	56,300	No 4	ASTM D1557-64T
Modified AASHO (CBR mold)	4.5	6	$\frac{1}{13.33}$	10	5	18	55	56,000	$\frac{3}{4}$ inches	ASTM D1557-64T
Bureau of Reclamation (Large size)	9	20	1635	185.7	3	18	22	12,400	3 inches	Bureau of Reclamation Earth Manual E 38

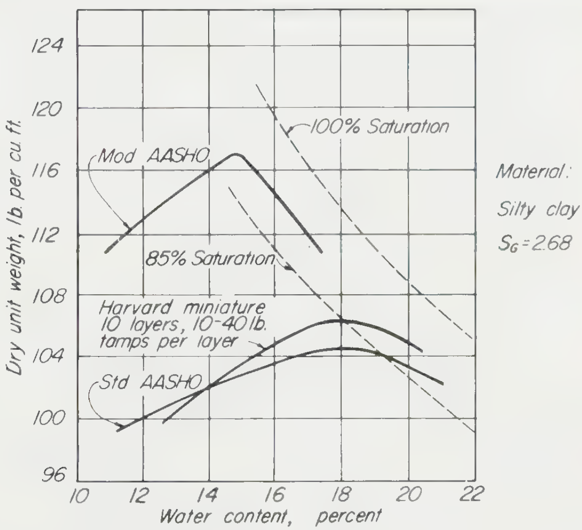

FIG. 42. Comparison between moisture-density curves obtained by various methods.

mold is 2.816 in. in height, 1.313 in. in diameter. Compaction may be in various numbers of layers, with various tamps per layer and with forces of 10 to 40 lb used on the circular tamping foot. The diameter of the tamping foot is ½ in. The compaction curve for a soil compacted using 10 layers each having 10 tamps of a 40-lb force is shown in Fig. 42. This tamping procedure usually produces a compaction curve close to the Standard AASHO compaction curve. The size of mold in Seed's kneading-compaction tests varies from 1.4 to 6.0 in. Usually 20 tamps on a triangle-shaped tamping foot are used for compaction. The kneading-type compactor probably duplicates field compaction conditions better than the impact compactor, but impact compaction is the type in general use. As described by Seed,[50] the structure of a compacted clay soil varies with the method of compaction and whether the moisture content of the soil is drier or wetter than the optimum for compaction. The structure of the compacted soil mainly affects the stress-strain characteristics of the soil at low shear strains. At high strains, as at 15 to 20 percent axial strain in a triaxial test, the shear strength of the soil is relatively independent of the compacted structure of the soil. Fortunately the shear strengths at 15 to 20 percent strain are the ones which are pertinent to the stability analyses described in Arts. 30 to 36. This indicates that for representative results attention has to be given to duplicating field soil structure in the laboratory.

Vibratory compaction is used for determining maximum density of granular materials. This type of compaction is performed by placing material in layers into a mold which is mounted on a vibratory table. A surcharge of 2 psi is placed on the material. The mold is then vibrated, usually at 3,600 cpm. When the soil ceases to densify, the process is repeated until the mold is completely filled. The Bureau of Reclamation test procedure described in Ref. 72 may be used for this test.

Static compaction is used frequently to prepare specimens for triaxial testing. This type of compaction is performed by placing material in layers into a mold and applying a known static pressure to each layer in succession. The static pressure used may

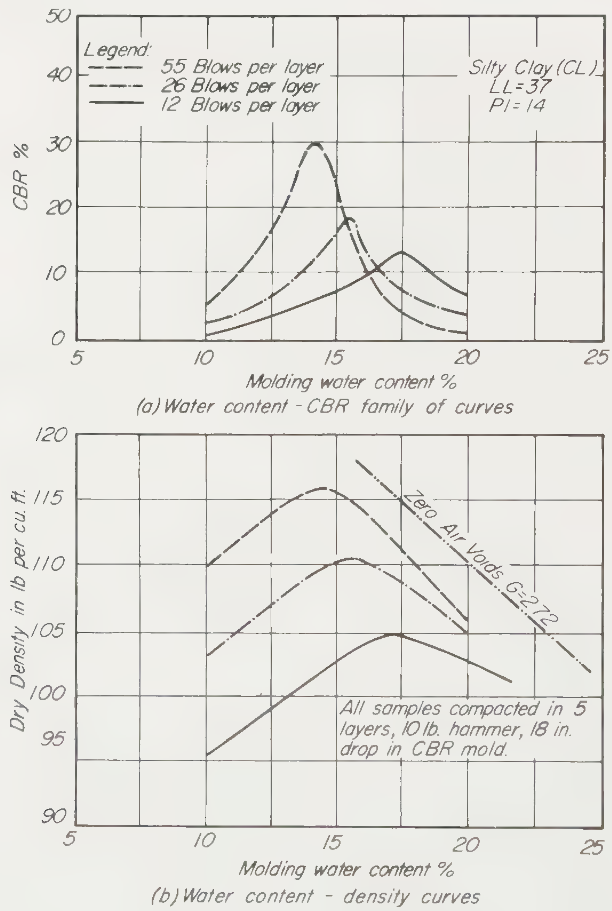

Fig. 43. CBR test results.

be of the order of 200 to 2,000 psi. The pressure and number of layers are adjusted to form a specimen which has the desired unit weight uniformly throughout the specimen.

As indicated in Table 2, the maximum size of particle for standard tests in the 4-in.-diameter mold is the No. 4 sieve size and in the 6-in.-diameter mold the ¾-in. size. When the material to be tested contains sizes larger than those specified the desirable procedure is to run tests in a larger-size mold so that the diameter of the mold is about six times the maximum size of particle. Alternatively, if the percentage of oversize particles is small, say no more than about 30 percent by weight, the oversize particles may be removed and the compaction test performed on the remaining fraction, or the percentage of oversize may be replaced by an equal weight of material in the No. 4 sieve to ¾-in. range. In the first alternative the water contents and unit weights determined in the test can be adjusted to apply to the total sample by the method

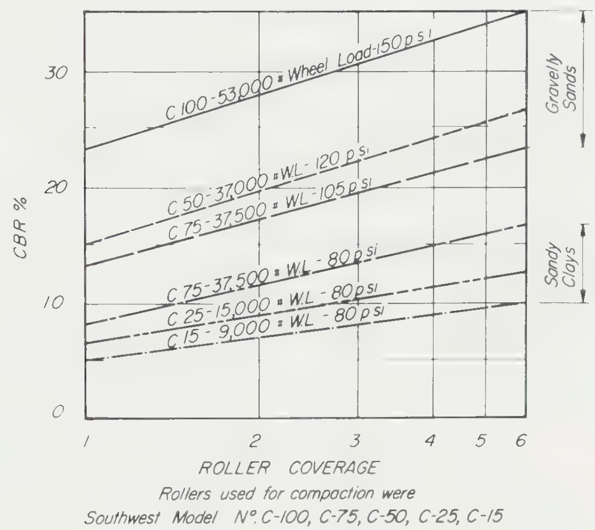

FIG. 44. Relationship between roller coverage and CBR value. (*After A. H. Hunter.*)

given in Ref. 72 considering that the oversize particles float in a matrix of the compacted remaining fraction. A second alternative is to predict the maximum and minimum densities of a soil from its grain-size distribution, particle shape, and particle specific gravity as suggested by Burmister.[8] When soils occur in the borrow area on the wet side of the optimum moisture content for compaction it is frequently of interest to determine the highest moisture content which can be tolerated before the soil is no longer trafficable by the construction equipment. The California Bearing Ratio test, *CBR test*, is useful in relating trafficability and water content. The method is described in Refs. 3 and 70. Typical test results are shown in Fig. 43. Three different compactive efforts are used, namely, 100 percent, 47 percent, and 22 percent of Modified AASHO. The approximate experimental relationship between CBR and number of passes of rollers is given in Fig. 44.

53. Permeability Tests. The permeability of coarse-grained soils is determined generally by constant-head permeability tests and the permeability of fine-grained soils by falling-head permeability tests, as indicated in Fig. 7 for various soils. In the constant-head type of test the difference in head between the ends of the test specimen is maintained constant and the rate of flow measured. The permeability is computed from the equation

$$k = \frac{ql}{\Delta h A}$$

where k = coefficient of permeability
q = rate of flow through the specimen
Δh = difference in head between ends of specimen
A = cross-sectional area of specimen perpendicular to flow

In the variable-head test the specimen is subjected to a variable head provided by the water level falling in a standpipe as water flows through the specimen. A schematic sketch of a variable-head permeameter is shown in Fig. 45. This permeameter provides for the specimen to be under back pressure during testing to ensure that the

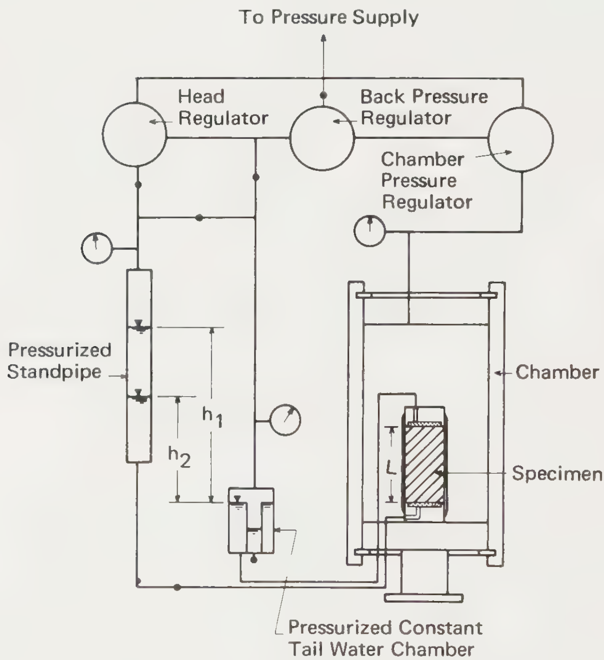

FIG. 45. Variable-head backpressure permeameter. Schematic diagram.

specimen is fully saturated during testing. The coefficient of permeability is computed from the following equation:

$$k = 2.3 \frac{aL \log (h_1/h_2)}{A(t_2 - t_1)}$$

where a = cross-sectional area of the standpipe
L = length of soil sample
A = cross-sectional area of the sample
t_1 = time at the beginning of the tests
t_2 = time at the end of the tests
h_1 = head at time t_1
h_2 = head at time t_2

In determining the permeability of soils which are fully saturated in the prototype it is necessary that the laboratory tests be performed on fully saturated specimens. About the only satisfactory method for achieving saturation of laboratory specimens, especially compacted specimens, is to apply high neutral all-around pressures to the water in the pores of the soil, thereby increasing the capacity of the water to dissolve air. The high neutral all-around pressure is termed "back pressure." This pressure must be sufficiently high to permit all air in the soil to be dissolved. For a test specimen having 85 percent saturation about 100 psi back pressure is required to effect saturation under condition of keeping the test specimen at constant volume and adding water to the soil by percolation to make up for the volume of air dissolved. Information on back-pressure saturation is given in Ref. 37. Further information on permeability tests is given in Refs. 33 and 72. Since back-pressure saturation of compacted embankment soils is required for consolidated undrained triaxial testing, it is frequently advantageous to conduct permeability tests on the specimens in the triaxial machine after saturation and prior to triaxial shearing. The tightly fitting membrane around the sides of the triaxial test specimen has the added advantage of minimizing the possibility of leakage along the sides of the specimen.

54. Shear-strength Tests. The most advanced and versatile test for determining shear strength of foundation and embankment soils is the triaxial shear test. Other shear tests have more limitations but are useful in particular circumstances. The *direct shear test* is particularly useful for determining the shear strength of the soil in the fully drained condition. Occasionally large-sized shear-strength boxes have been used for testing soils containing large particles.[60] The *annular ring shear test*[26] is useful for determining the shear strength under condition of large shearing displacements. The *unconfined compression test*[33] affords a rapid means of determining the approximate *in situ* shear strength.

The *triaxial test* normally is carried out as a compression test on a cylindrical specimen of soil which is encased in a thin rubber sheath and subjected to an all-

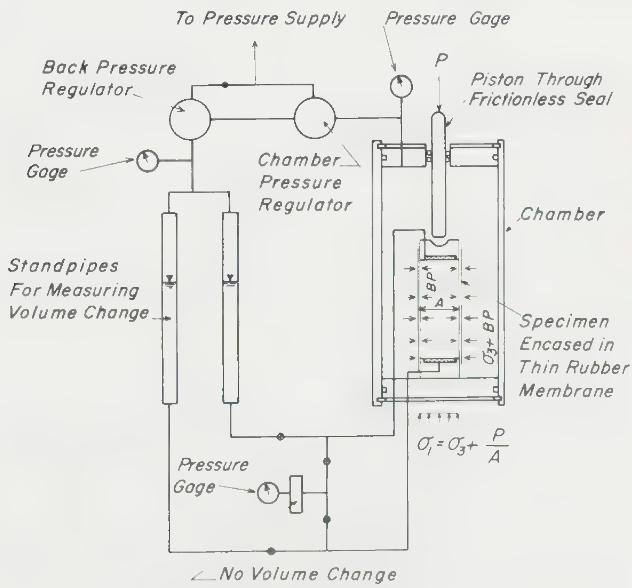

FIG. 46. Back-pressure triaxial apparatus. Schematic diagram.

around pressure. The diameter of the test specimen should be at least four and preferably eight times the maximum size of the particle in the test specimen. The length of the test specimen should be about 2.25 times the diameter. A schematic sketch of the apparatus is shown in Fig. 46. By increasing the axial compressive load shear failure can be brought about on planes making an angle of approximately 45 deg + $\phi'/2$ with the ends of the specimen. The angle ϕ' is the angle of friction of the soil as determined from a plot where the shear strength is plotted vs. effective normal stress on the failure plane at the time of failure. At times lateral-extension tests may be performed. In these tests failure of the cylindrical specimen is caused by reducing the all-around chamber pressure while maintaining the axial pressure constant. This test is pertinent to determining the *in situ* shear strength for cut slopes of excavations.

Since various conditions of consolidation, drainage during shear, and loadings obtain for embankment dams and their foundations, various types of procedures of triaxial test are required to duplicate these conditions in testing in the laboratory. The main types of test are (1) the unconsolidated undrained test, UU or Q test, (2) the consolidated undrained test, CU or R test, and (3) the consolidated drained test, CD or S test.

The procedure for testing in the UU or Q test is to place the specimen in the triaxial chamber, apply an all-around pressure without permitting any drainage from the specimen, then increase the axial load until failure again without permitting

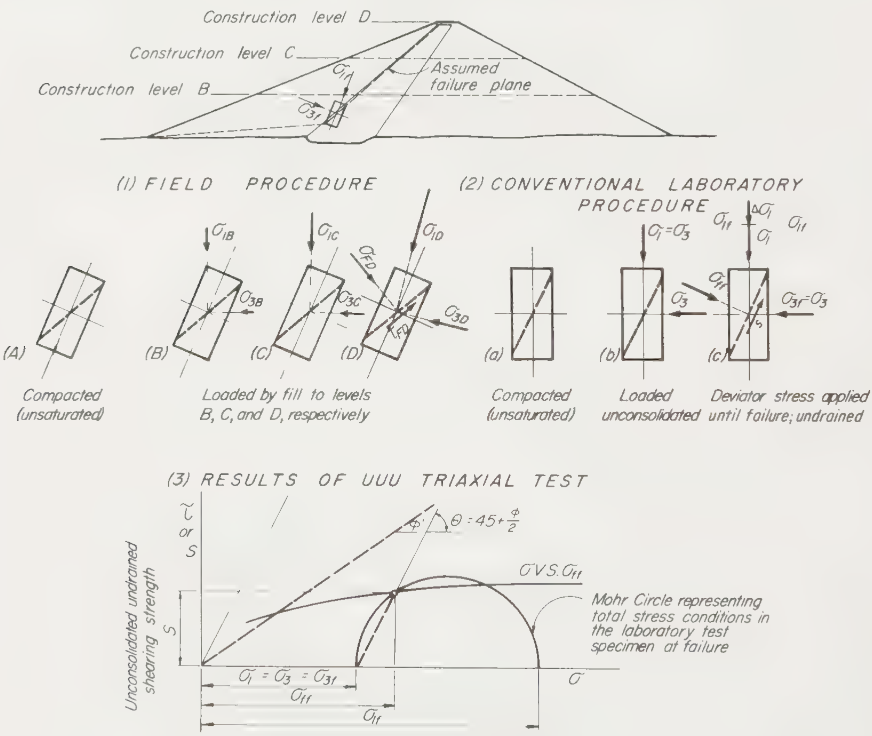

FIG. 47. Unconsolidated undrained triaxial test. Generally used for determining shear strength for stability analysis of the construction case. Comparison between field and test conditions, results of test.

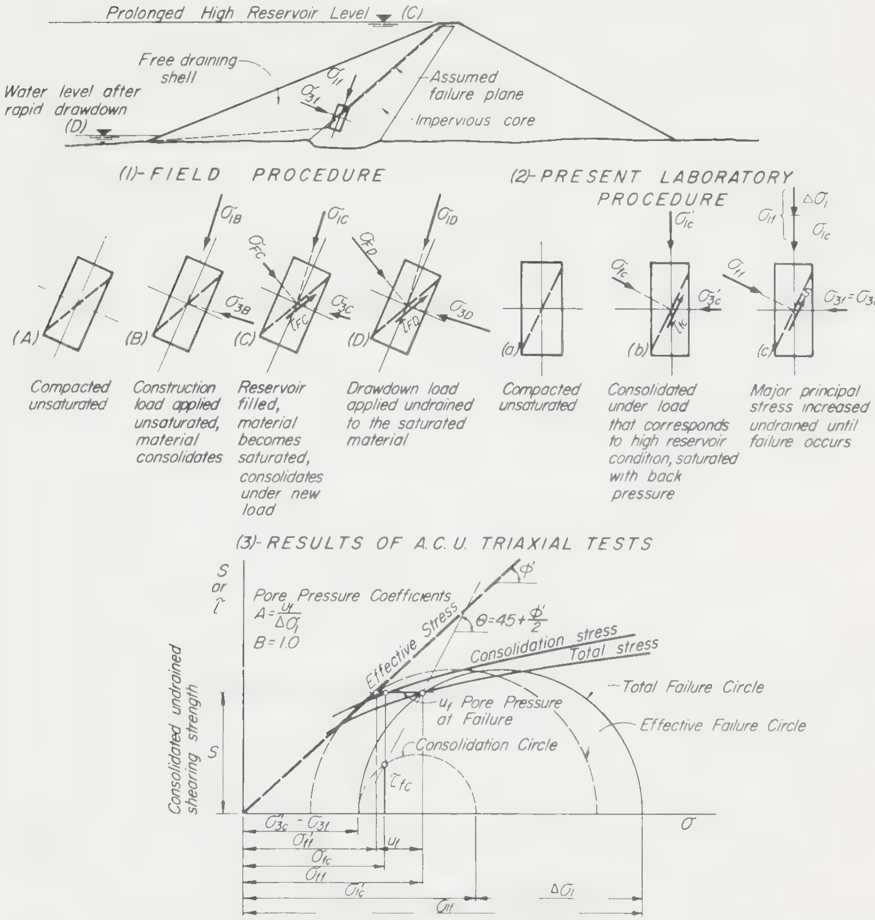

FIG. 48. Consolidated undrained triaxial test. Generally used for determining shear strength for stability analysis of rapid drawdown or earthquake cases. Comparison between field and test conditions, results of test.

drainage (Fig. 47). For embankment materials the specimen should be compacted to the unit weight and water content anticipated in the prototype. Tests on such materials are designated as *UUU* tests, which signifies unsaturated unconsolidated undrained condition. When *UU* tests are performed on undisturbed samples of saturated foundation soils, back pressure should be used to ensure saturation in the laboratory. In the *CU* or *R* test, the procedure after preparation of the specimen is to saturate it by means of percolation and back pressure. Following this an all-around equal pressure is used for consolidation in most laboratories. Generally anisotropic consolidation, where the axial pressure is greater than the lateral pressure, better represents prototype conditions of consolidation, and this type of test is preferred. The test is termed an *ACU* test. Drainage is permitted during application of the consolidation pressure, but after consolidation is achieved the drainage lines are closed and the sample is sheared undrained (Fig. 48). In the *CD* or *S* test drainage is permitted not only during consolidation but also during shearing.

The results of triaxial tests are presented by Mohr diagrams. The typical observations made during a test on a single specimen from beginning of test to failure are shown in Figs. 47(2), 48(2), and 49(2) for the three basic types of triaxial test. The corresponding Mohr diagrams for which each of the above tests provides a single circle, either total stress or effective stress, for the failure condition are shown in Figs. 47(3), 48(3), and 49(3). For failure condition stresses are frequently taken as the stresses at 15 to 20 percent axial strain. Sometimes peak stresses develop at low axial strains, about 5 percent; then the stresses decrease until at 15 to 20 percent strain the stresses are significantly lower than the peak stresses. Some designers use the peak stresses to define the strength of soil. Because of progressive failure conditions which probably obtain in the prototype and uncertainties as to how well the structure of laboratory-compacted specimens duplicates that of the compacted soil in the embankment, it

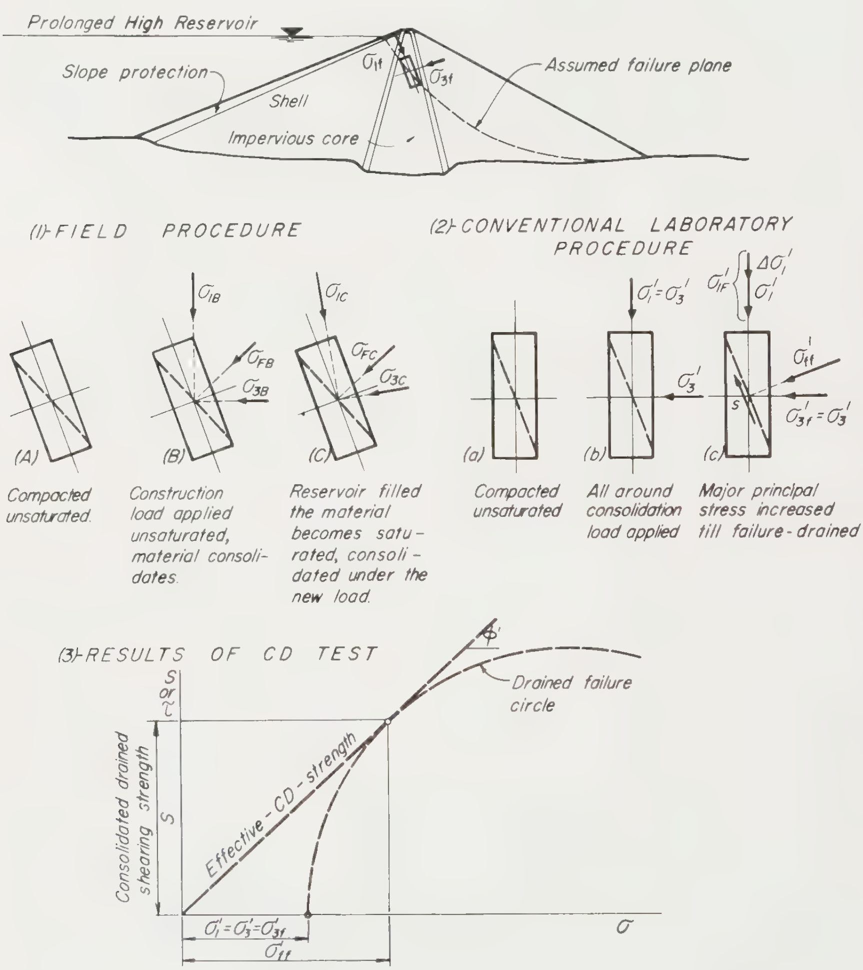

FIG. 49. Consolidated drained triaxial test. Generally used for determining shear strength for stability analyses where the material is consolidated and the new load is applied slowly. Comparison between field and test conditions, results of test.

appears more realistic to the use of stresses at 15 to 20 percent strain to define the strength.

In the *UU* or *Q* tests, because it is usually performed on partially saturated embankment materials, the Mohr envelope is generally plotted only in terms of total stresses (Fig. 47). To measure the pore pressures in the partially saturated soil during testing in order to determine the effective stresses, special techniques are required. For saturated soils pore pressures can readily be measured during *UU* or *Q* tests and the effective-stress as well as total-stress Mohr envelope determined.

In *CU* or *R* tests pore-pressure measurements are generally made and both total-stress and effective-stress Mohr circles and envelopes are plotted (Fig. 48). Effective-stress Mohr circles and envelopes are shown by dashed lines and total-stress circles and envelopes by full lines. The shear strength may be plotted against total stress at failure, consolidation stress, or effective stress at failure as shown in Fig. 48. The effective-stress envelope from a *CU* or *R* test closely approximates the *CD* envelope of the same soil tested at the same initial density for testing if the soil is not extremely loose or dense. Although both envelopes are based on effective stresses, because of the undrained condition no volume change takes place in the *CU* or *R* test, whereas volume change does take place in the *CD* or *S* test. Because of the long time required to permit full drainage during shearing in the *CD* test the amount of *CD* testing on a project is frequently limited and the effective-stress envelope from a *CU* or *R* test is used as a close enough approximation of the *CD* or *S* envelope.

In the *CU* or *R* tests full saturation of the test specimens is essential for proper test results and proper determination of pore pressures during testing. The back-pressure technique described in Art. 53 for permeability testing is the only procedure known to ensure full saturation, and it should be used in all *CU* or *R* tests as well as in *UU* tests on specimens of saturated foundation soils.

In the *CD* or *S* test no pore pressure develops; therefore, the total and effective Mohr circles representing failure are identical (Fig. 49). Alternatively the *CD* tests are performed in a direct shear machine where the sample can drain much more readily than in the triaxial machine.

55. Consolidation Tests. This test is used to determine the compressibility and consolidation characteristics of a soil. The results are used in connection with settlement analyses and with predicting the rate of increase in shear strength of foundation soils. Consolidation tests are usually performed in an apparatus called an oedometer or consolidometer, as illustrated in Fig. 50. A new type of oedometer designed by the

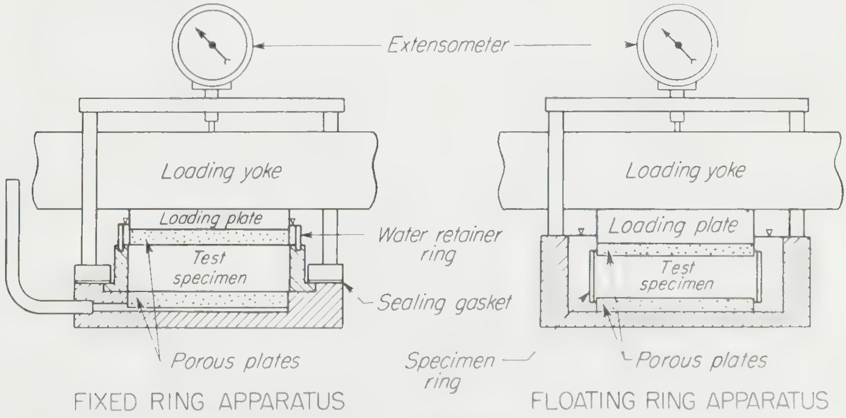

FIG. 50. Oedometers.

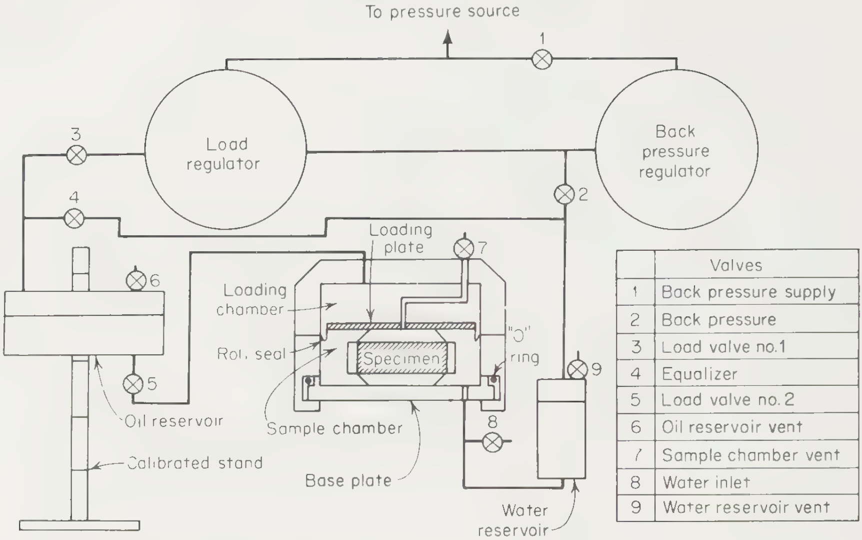

Fig. 51. Back-pressure oedometer. Schematic diagram.

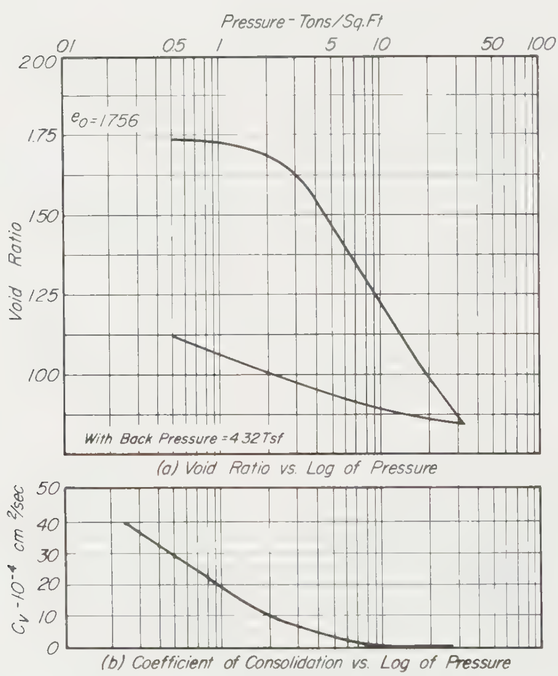

Fig. 52. Consolidation-test results.

author permits application of back pressure during testing. A schematic diagram of this apparatus is shown in Fig. 51. Further discussion of this apparatus and the back-pressure consolidation-test technique may be found in Ref. 41. The back-pressure apparatus is desirable for testing foundation soils in which gas bubbles come out of solution when the soil sample is removed from the ground. The back pressure will cause the bubbles to redissolve and thus permit testing of the soil in the fully saturated condition at which it exists *in situ*.

The procedure for testing in the oedometer consists in applying loads to the specimen in a sequence about as follows: 0.125, 0.25, 0.5, 1.0, 2.0, 4.0, 8.0, 2.0, 0.5, and 0.125 kg/sq cm. Each load is maintained generally for 1 day, and the time rate of compression under each load is determined. Typical consolidation-test results are shown in Fig. 52. A pressure-void-ratio curve plotted to semilog scale is shown in Fig. 52*a*, and the coefficient of consolidation c_v is plotted against the log of pressure in Fig. 52*b*.

Consolidation data can also be collected from a series of *CU*, *ACU*, or *CD* triaxial tests at various consolidation pressures; the tests in this case are three-dimensional.

FIELD OBSERVATIONS DURING AND AFTER CONSTRUCTION

56. Field Observations. Several types of field observations should be made during the construction of an embankment dam and after its completion. One series of observations consists of controls to confirm that the fill is placed so that it has the unit weight, gradation, and physical properties required by the design. Other observations are required to check vertical and horizontal deformations and earth and water pressures which develop.

At the beginning of construction a "test embankment" is usually constructed to establish the moisture-density relationship for compaction with the field equipment. The number of passes and thickness of lifts required to achieve proper compaction are investigated also. During construction, field density measurements are made at regular intervals, one for about each 3,000 cu yd of fill. Also undisturbed samples of the fill are taken of representative materials and physical-property tests, particularly shear-strength tests, are performed to check the design assumptions. When the fill contains large-sized particles field density checks must be made to a size so that the diameter of the test hole is no less than about four or six times the diameter of the maximum size of particle. Techniques for field density control are given in Refs. 20 and 72.

Standpipe piezometers[11] or remote-reading pore-pressure devices as, for example, that described in Ref. 76 are required when pore pressures may develop in the dam or its foundation. Pore pressures develop in embankment materials which are relatively impervious and particularly those which are placed on the wet side of the optimum water content for compaction. For observing pore pressures which develop in saturated relatively impervious and compressible embankment and foundation soils, remote-reading pore-pressure devices have several advantages over the standpipe piezometers. They can be placed under the upstream portion of the dam and be read after filling of the reservoir, whereas the standpipe would project into the reservoir. Leads from each of the remote-reading pore-pressure devices can be brought to one or two central reading stations, whereas each standpipe had to be read in place. The leader from the remote-reading devices can be led out of the fill horizontally at the lift where it is placed. The standpipes must be carried up vertically and frequently interfere with construction. The standpipe frequently is more foolproof and longer-lasting than remote-reading devices, but gas bubbles which develop sometimes at the tip of the standpipe can cause erroneous readings.

Every dam undergoes some settlement due to compression of the foundation of the dam and compression of the embankment material. Allowance has to be made for this settlement in the height to which the dam is constructed. Observation should be made of the actual settlement in the field to check the predicted settlement. For measuring settlement due to compression of the foundation, settlement plates are usually set at the base of the dam. Observation rods in telescoping casing may be brought up as construction of the dam proceeds, or at the end of construction boreholes may be put down through the embankment to the settlement plates and observation rods installed at that time. Information on the settlement due to the foundation permits more accurate determination of the volume of material actually placed in the embankment dam. This determination may be important in connection with payment for embankment material. Settlement contributed by compressions in the various lifts of the embankment dam itself may be determined by the U.S. Bureau of Reclamation type of crossarm device,[72] by devices such as Dr. Idel's electromagnetic location probe,[35] or by hydraulic devices like those used at Oroville Dam.[61]

Horizontal displacements in an embankment dam may be measured by installing horizontally instead of vertically devices similar to the crossarm and electromagnetic devices mentioned above. The measuring torpedo is moved through the device by cables and pulleys instead of by lowering it up and down. Observations of horizontal displacements are important, particularly in places where cracking of the embankment dam may occur as directly over the area where the foundation for the dam changes from, say, rock in the abutment to alluvium in the valley bottom.

For determining the distortion which may occur along a vertical line in the embankment dam and its foundation, the slope indicator may be used as described in Ref. 53. Devices used for observing earth stresses are described in Refs. 35, 53, and 79.

Failures of embankment dams and their foundations are preceded usually by surface movements of readily measurable magnitude. Thus it is worthwhile to set bench marks in a pattern over the faces and after completion along the crest of the embankment. Periodic observation should be made of the vertical and horizontal movements of these bench marks. Additional bench marks should be set in any areas where movements are noticed. In cases of foundation failure, a rapid increase in settlement occurs, closely followed by heaving at the toe of the embankment. Embankment failures are indicated by bulging of the slopes. When any question arises as to the stability of the embankment, raising of the embankment should be stopped and berms added or the height of fill reduced or both. Careful reanalysis of the stability of the dam must be made before construction is resumed.

In essence design of embankment dams depends upon the designer's being able to predict the field behavior of earth structures and their foundations. By successive trials he selects an embankment-dam cross section and foundation treatment which will meet the requirements of stability and leakage. Observations of actual field behavior of an embankment dam and its foundation are therefore essential for checking present design methods and for development of better methods. Every opportunity should be taken to observe the deformations, pore pressures, and seepage quantities in embankment dams and their foundations; where possible, observation of stresses is also of interest. Such observations to be of value must be carefully planned, executed, and analyzed.

TYPICAL DESIGNS OF EMBANKMENT DAMS

57. Nantahala Dam, Nantahala River, North Carolina. This dam exemplifies a rock-fill dam with sloping core. A cross section of the dam is shown in Fig. 53. The maximum height is 260 ft and the crest length 1,200 ft. The foundation is rock. All rock for the dam was obtained from the spillway excavation, and the rolled earth fill for the impervious core was obtained from a nearby borrow pit. The following quantities of material were used: 1,692,000 cu yd of quarry-run rock, 350,000 cu yd of processed rock for filters, and 223,000 cu yd of rolled earth fill. The maximum settlement at the end of 2 years was 1 ft and after 8 years 2½ ft. The seepage through the dam is approximately 2.75 cu ft/min under full reservoir. The spillway is constructed in a sidehill cut in the right abutment. A diversion tunnel and a power tunnel are located in rock in the left abutment.

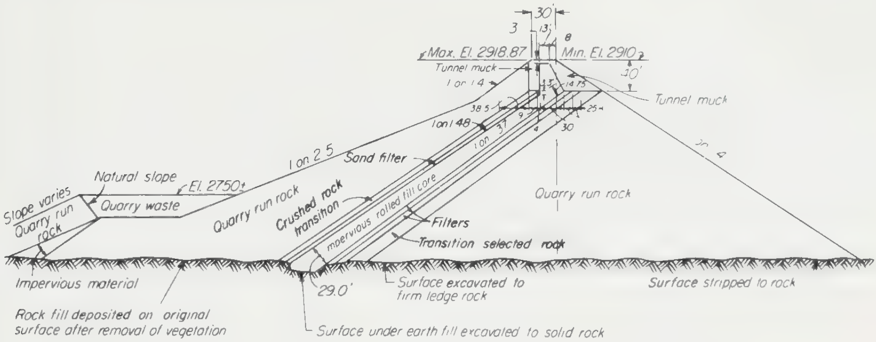

FIG. 53. Cross section of Nantahala Dam, North Carolina.

58. Portville Dikes, Allegheny River and Tributaries, New York State. The project is located about 80 miles south of Buffalo at the village of Portville. Its purpose is to give added flood protection to the village by constructing 22,950 ft of dikes, a pumping station, flood walls, and culverts. The dikes are mostly new structures but in small part are enlargements of existing ones and are located along the Allegheny River and its tributaries. The foundations are alluvial deposits and

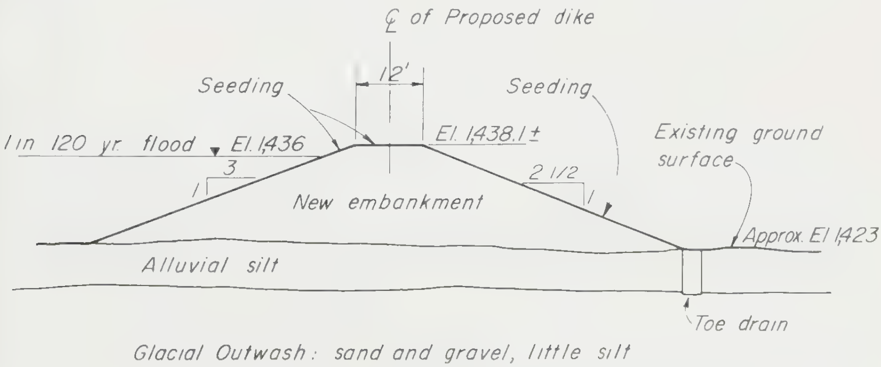

FIG. 54. Cross section of Portville Dike, New York State.

glacial outwash and in general are composed of two layers. The upper layer, which is up to 12 ft thick, is fine sand and silt, while the lower layer is silty sand and gravel. The permeability of the lower layer is about 1,000 times greater than that of the upper. The sand and gravel layer is generally exposed in the river channel. Uplift at the landside toe was reduced by installing drainage trenches through the silt to the underlying sand and gravel along the landside toe. The well-graded impervious material for the construction of the dikes was obtained from nearby borrow areas. A typical cross section of the dikes is shown in Fig. 54.

59. Wanapum Dam, Columbia River, Washington State. This 170-ft-high earth dam is built on highly pervious alluvial foundation which is composed of sand, gravel, and cobbles with "openwork" gravel zones. The depth of the alluvium is in excess of 80 ft at places. The embankment has a 9,400-ft crest length and includes 4.6 million cu yd of fill. The major problem in connection with the design and construction of this dam was the control of underseepage through the pervious alluvium, which has a permeability about 3,000 ft/day. This problem was solved by the construction of a 10-ft-wide slurry-trench-type cutoff. The slurry trench extends down to 80-ft depth and is located along the center line of the dam. Where the depth of alluvium is greater than 80 ft a Soletanche-type grout curtain consisting of three rows of grout holes was constructed below the slurry trench. Where the embankment crosses the riverbed, a pervious fill was placed below water level through which the slurry trench extends. The dam has a central impervious core; the shells are made of rolled pervious earth fill. The cross section of the embankment and cutoff trench is shown on Fig. 55. More information on this project may be found in Refs. 55 and 77.

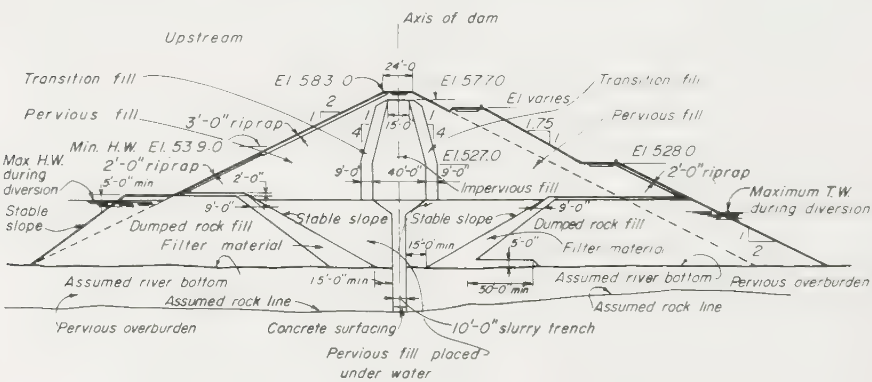

FIG. 55. Cross section of Wanapum Dam, Washington State.

60. Hirfanli Dam, Kizilirmak River, Turkey. The project is located about 80 air kilometers southeast of Ankara. The height of the embankment is 80 m and its crest length is 364 m. The amount of earth and rock materials used in the construction at the dam is slightly over 2 million cu m. The inclined core is built of sandy clayey silt which was obtained from a borrow in the floodplain upstream of the dam. For the construction of the shells sound to highly weathered gabbro was used from spillway excavation. The coarse sound gabbro was used as dumped sluiced rock fill, while the rest of the rock material was placed as rolled fill. In the riverbed 2.5 to 12 m of alluvial deposit lies above the generally sound gabbro bedrock. At one location, near the axis of the dam, a 15-ft-thick weathered-rock zone was found below the alluvium. The impervious core was brought into direct contact with sound foundation rock. A grout curtain is located below the core contact. The depth of the grout curtain is about one-third the height of the dam. A grouted platform in the entire area of the contact secures good contact between the core and the curtain. Vertical drain holes are located at the downstream quarter point of the dam and are designed to relieve water pressures in the foundation. The cross section at the dam is given in Fig. 56.

The other structures of the project are a spillway located in a cut in the right abutment, two power tunnels driven through the right abutment, and a powerhouse. The power tunnels were used for diversion. The powerhouse is located at the toe of the dam and contains three 46,000-kva units. Additional information on the dam is contained in Ref. 38.

61. Binga Dam, Agno River in Luzon, Republic of the Philippines. The Binga Project is primarily a power project and operates in conjunction with the Ambuklao Dam Project upstream. The dam has a height of 103 m and a crest length of 210 m.

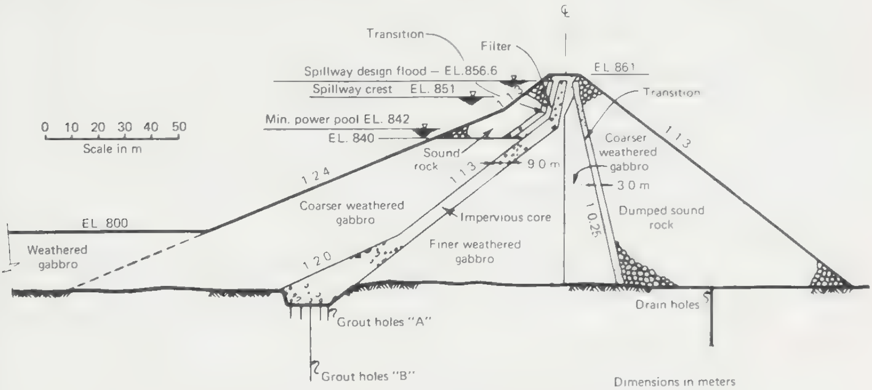

FIG. 56. Cross section of Hirfanli Dam, Turkey.

The embankment has an inclined impervious core constructed of disintegrated metamorphic rocks obtained from borrow near the power intake. The shells were constructed of rock fill obtained from the spillway excavation, much of which was placed as rolled rock fill, plus 12-in. sound rock raked from the rolled fill zones prior to rolling; some sound rock available directly from spillway excavation was placed in the shells,

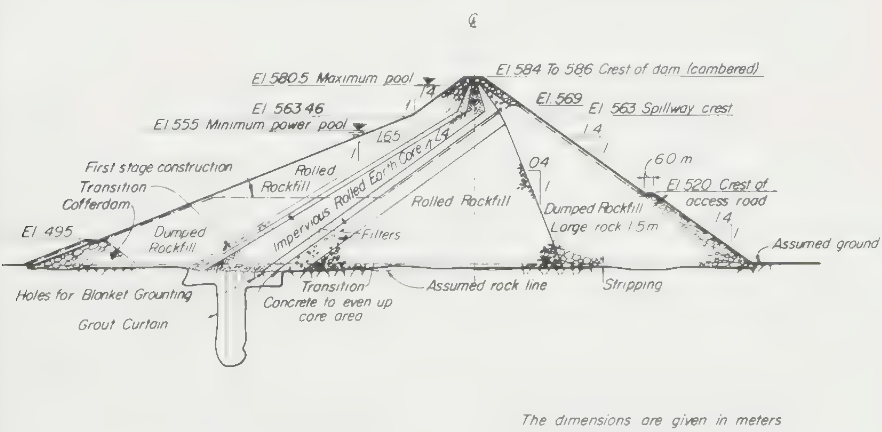

FIG. 57. Cross section of Binga Dam, Philippines.

as sluiced, dumped rock fill. The bedrock at the site is composed of a series of metamorphic rocks that contain numerous dikes and veinlets of igneous rock. The rock had no or only a thin cover of residual soil, but the weathering of the rock was generally deep. The inclined core is in contact with the bedrock, and in the contact area blanket grouting was performed. A grout curtain extends downward to a depth equal to one-half the reservoir head. The cross section of the dam is shown in Fig. 57.

The other structures composing the project are two diversion tunnels, a gated spillway in the left abutment, a power intake and pressure tunnel, an underground powerhouse, and a tailrace tunnel. Additional information on this dam is contained in Ref. 38.

62. Prompton Dam, Lackawaxen River, Pennsylvania. The primary purpose of this dam is to impound floodwaters, but it also provides a low-level permanent pool for recreation. The valley except for a shallow surface layer of alluvium is filled to depths of 140 ft by glacial deposits. The underlying rocks are well-cemented sandstones and siltstones. The glacial overburden material is a heterogeneous mass made up of many lenses and beds with wide range of composition. Most of these are well graded from gravel through silt, although a silt bed occurs near the right abutment and clean sands and gravels were found locally. The embankment, the cross section of which is shown in Fig. 58, consists of homogeneous compacted earth fill with riprap protection on the slopes, cutoff trench, inclined drain, horizontal drainage blanket, upstream uncompacted random fill and downstream dumped rock toe. The height of the embankment

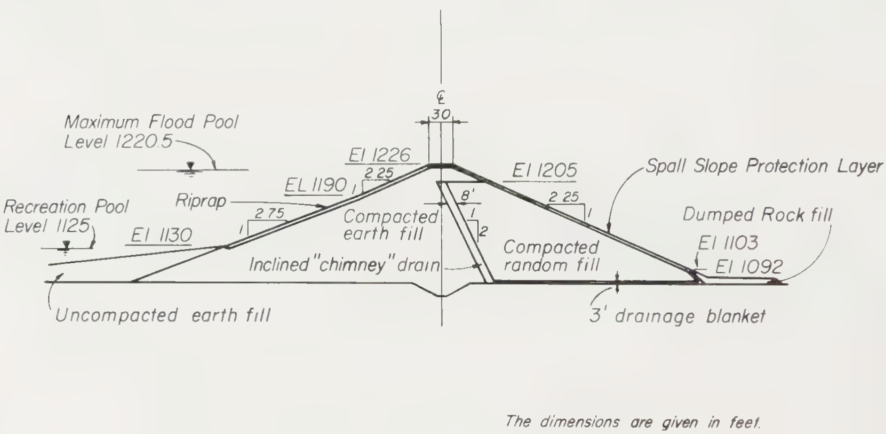

FIG. 58. Cross section of Prompton Dam, Pennsylvania.

is 140 ft and its crest length is 1,230 ft; the volume of fill used for its construction is 900,000 cu yd. The required excavations for spillway and outlet works provided approximately one-half the volume of the dam. The remainder was obtained from borrow excavations. The earth materials excavated in the borrow and also in the required excavations were similar in composition to the deposits filling the valley. The rock fill required in addition to that amount which was available from required excavations was quarried sound sandstone. The spillway of the project is a small unlined cut in the west abutment and the outlet works consist of a cut-and-cover-type conduit under the embankment. At the downstream toe relief wells are installed to reduce natural artesian pressures due to groundwater in the abutments as well as uplift pressures created by the reservoir.

63. Hanabanilla Dam, Hanabanilla River, Cuba. The Hanabanilla Project was constructed primarily for power-generating purposes. To create the reservoir, two dams were required: the Hanabanilla Dam and the Jibacoa Dam. The Hanabanilla Dam is located about 4 km north of the village of Siguanea. The bedrock, composed of gneiss and schist, was found at shallow depth below the recent surface deposits. The impervious material, lean clay, for the central-type core of the dam was obtained from a borrow area, located about 5 km east of the damsite. The shells are of rock fill, which was supplied by excavations for spillway, penstock, and tunnels. A grout curtain is provided under the core. The height of the dam is 46 m and its crest length is about 260 m. The volume of fill used for the construction of the embankment is 399,000 cu m. The cross section of the dam is given in Fig. 59.

64. Jibacoa Dam, Jibacoa River, Cuba. The second dam, which together with the Hanabanilla Dam creates the Hanabanilla Reservoir, is located approximately 150 m downstream from the place where the Negro and Guanayara rivers meet to form the Jibacoa River. The river valley is filled with alluvial deposits that extend to a depth of about 55 m at the deepest point. The alluvial deposits consist of lenses and interbeds of gravel, sand, and silt. The silt beds are of low shear strength and compressible. The rock of the left abutment is massive, metamorphosed limestone, whereas the right abutment is formed of calcareous schist. Because of the low-strength silt in the foundation it was necessary to use a counterweight-berm type of

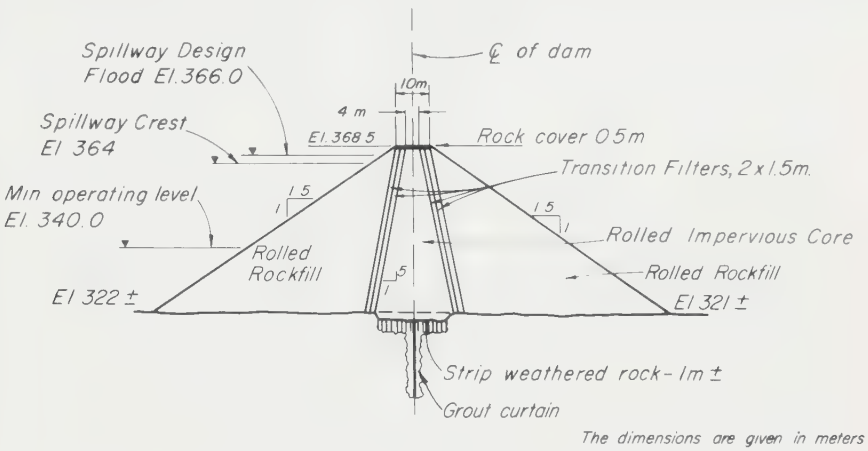

FIG. 59. Cross section of Hanabanilla Dam, Cuba.

construction, together with a minimum-sized top portion. Impervious materials were used in the counterweight berms and beneath the central portion in order to control underseepage gradients and quantities. The term "piggyback" has been applied to this type of cross section.

In the left abutment a grout curtain was constructed to limit seepage through the jointed limestone. The impervious material, a silty clay, for the construction of the core and berm came from a nearby borrow area while the rock was obtained partially from a quarry on the north side of the valley and partially from the spillway and tailrace tunnel excavation. The Jibacoa Dam has no spillway of its own; the reservoir is serviced by the one near the Hanabanilla Dam. The embankment of the Jibacoa Dam contains 1,490,000 cu m of fill; its crest length is 415 m and its height is 37 m. The cross section of the dam is given in Fig. 60.

65. John Flanagan Dam, Pound River, Virginia. This dam is located 1.8 miles upstream of the confluence at Pound River and the Russel Fork of the Big Sandy River and is primarily for the purpose of flood control. The foundation at the site consists of 0 to 5 ft of residual, sandy clay overlying predominantly sandstone bedrock. The sandstone is weathered near the surface, but in the area of the dam foundation the weathering does not extend deeper than a few feet. Within the sandstone there are minor members and seams of shale, siltstone, and coal. The embankment has a central core and its shells are constructed of rock fill and random fill. The height of the embankment is 245 ft, the length of the crest is 910 ft, and the total volume is 1.9 million cu yd. Overburden from the spillway excavation was used for the impervious core; rock from the spillway excavation was mostly shale and was used for the random zones of the embankment. Additional amounts of materials were obtained

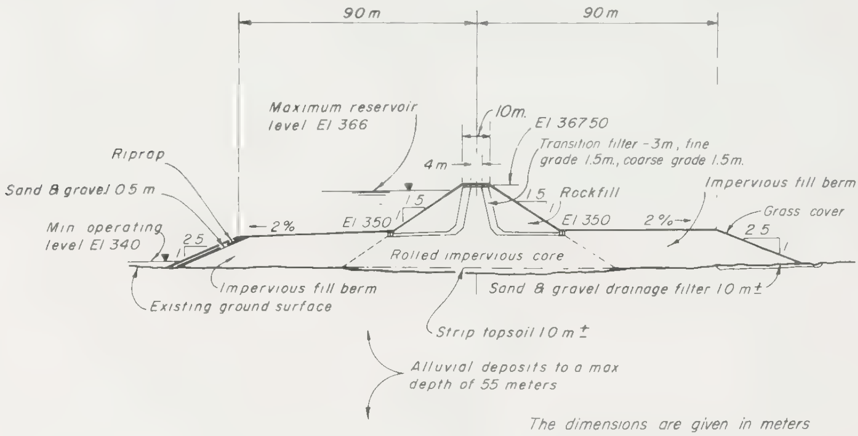

FIG. 60. Cross section of Jibacoa Dam, Cuba.

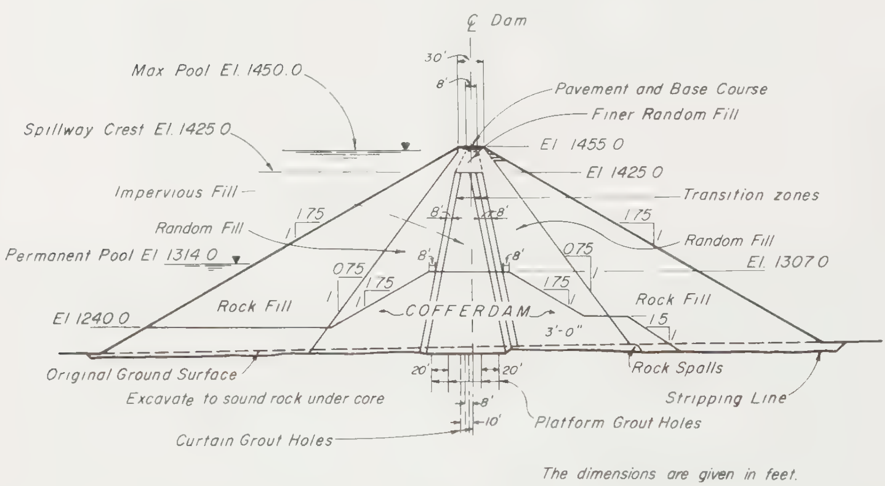

FIG. 61. Cross section of John Flanagan Dam, Virginia.

from nearby borrow areas: sandy and silty clay for the core, weathered sandstone for the random zones, and sound limestone for the rock fill. In the area of impervious core the alluvium and a few feet of weathered rock were removed and the core was placed in contact with sound rock. Shallow platform grouting was performed in the area of the core contact, and a grout curtain consisting of two rows of holes extended below this. The cross section of the dam is given in Fig. 61.

66. Shihmen Dam, Takekan Creek, Taiwan. This dam is located at the edge of the foothills of a mountainous area where the Takekan Creek enters the coastal plain about 60 miles south of Taipei. The island of Taiwan is located in the Pacific seismic belt and is subject to frequent earthquakes. The foundation of the dam consists of alluvial and colluvial deposits underlain by bedrock. The alluvial deposits which form the overburden in the river section consist of silt, sand, gravel, and boulders. The depth of these varies from 0 to 20 m. The colluvial deposits which form the overburden on the slopes include talus and slope wash. The bedrock consists of massive to thick bedded sandstones with some interbeds of siltstone and sandy shale. A cross section of the dam is shown in Fig. 62. The embankment has a vertical core which extends to bedrock. The shells were constructed of rolled cobble-gravel fill. The height of the embankment is 116 m above the riverbed; the length of the crest is 357 m. The total volume of fill used for the construction of the embankment is 6.43 million cu m. The construction materials were obtained from two sources, from cobble-gravel deposits in the riverbed immediately downstream of the damsite and from terrace deposits northwest of the dam. The first source supplied

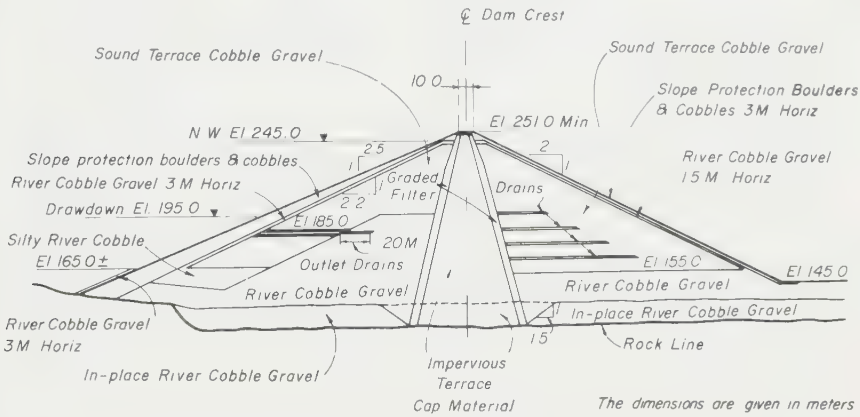

FIG. 62. Cross section of Shihmen Dam, Taiwan.

sound pervious fill for the shells while material from the second was used in both core and shells. The cap material in the terrace deposits varied from silty clay to clayey sand and was used for the core. The deposits below the cap were a mixture of slightly to highly weathered cobbles and gravel with some sand and fines; these materials were used in the zones of lower stress of the shells. The foundation treatment consists of a grout platform and a grout curtain. The depth of the grout curtain varies from one-third to one-half of the height of the dam. Other project components in addition to the embankment are a diversion tunnel, a powerhouse and two penstocks, gated spillway, low-level outlet, and irrigation outlet. Further information on the dam and the materials for its construction is given in Refs. 39 and 40.

67. Tarbela Dam, Indus River, West Pakistan. The project is located about 70 miles north of Rawalpindi. Construction is scheduled to start in 1968. The height of the embankment is 460 ft above the riverbed and the length of the crest is 8,700 ft. The foundation, in most part, is pervious alluvium with depths ranging up to 600 ft. The alluvium consists generally of boulder cobble gravel choked with sand. In some places limited-size lenses of sand and occasional lenses of boulder cobble gravel without sand, openwork gravel, occur. The rocks underlying the alluvium and composing the abutments are metamorphosed sedimentary rocks; limestone, phyllite, quartzite, and schists. An upstream impervious blanket about 4,600 ft long controls underseepage gradients and reduces seepage to a tolerable amount. A line of drainage wells, located along the downstream toe, together with a drainage blanket underneath the downstream shell, provides controlled exit for the water that seeps through the foundation. For the construction of the dam, 139 million cu yd of earth and rock fill is required and 20 million more for the construction of the impervious blanket. The

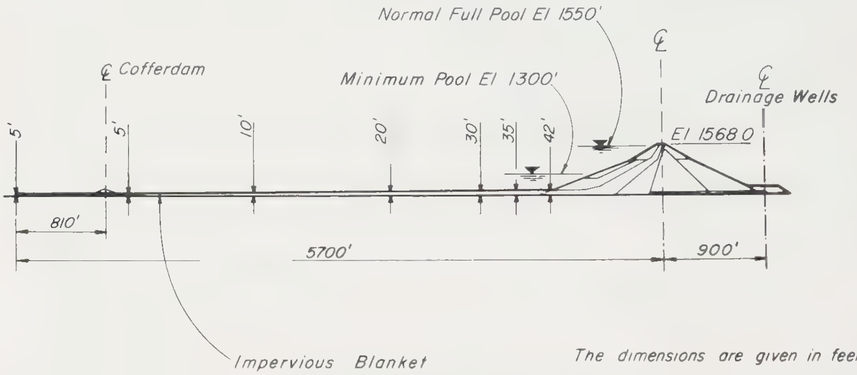

FIG. 63. Tarbela Dam, West Pakistan. Cross section of main embankment and blanket

inclined core of the embankment is built of a well-graded blend of silt, sand, and gravels; the shells are composed of rolled earth and rock fills. The construction materials are provided in about equal amounts from required excavations and borrow areas. Four 45-ft-diameter tunnels, located in the right abutment, serve diversion, irrigation, and power. Two gated spillways in the left-bank area have a combined

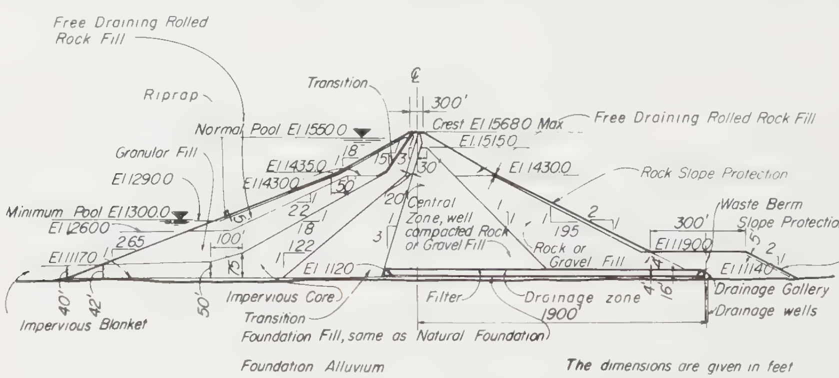

FIG. 64. Cross section of Tarbela Dam, West Pakistan.

capacity of 1,500,000 cfs. Two auxiliary dams, one of 18 million cu yd and the other of 1.7 million cu yd, are required to close the reservoir rim.

The cross section of the embankment and blanket is shown in Fig. 63, and a more detailed cross section of the embankment is given in Fig. 64.

Bibliography

1. AMERICAN SOCIETY OF CIVIL ENGINEERS, Report of the Subcommittee on Earth Dams of the Soil Mechanics and Foundation Division (1949), Review of Slope Protection Methods, *Proc. ASCE*, June, 1948; discussions, October, 1948, December, 1948, January, 1949.
2. ———, Symposium on Rockfill Dams, *Proc. Symposium Series 3*, reprinted from *Proc. ASCE, J. Power Div.*, 1958.

3. American Society for Testing and Materials, Procedures for Testing Soils, Philadelphia, 1964.
3a. Bennett, P. T., The Effects of Blankets on Seepage through Foundations, *Trans. ASCE*, 1946.
4. Bertram, G. E., "An Experimental Investigation of Protective Filters," Harvard University, Graduate School of Engineering, Soils Mechanics Series 7, 1940.
5. Bishop, A. W., The Use of Pore Pressure Coefficients in Practice, *Geotechnique*, **4** (4), 148, 1954.
6. ———, The Use of the Slip Circle in the Stability Analysis of Slopes, *Geotechnique*, **5** (1), 11, 7–17, 1955.
7. ——— et al., "Pore Pressure Observations at Selset Dam," Pore Pressure and Suction in Soil Conference, Butterworth & Co. (Publishers), Ltd., London, 1960.
8. Burmister, D. M., "Soil Mechanics," Vols. 1, 2, Columbia University Press, New York, 1948–1955.
9. Casagrande, A., "Seepage through Dams," reprinted in Contributions to Soil Mechanics, 1925–1940, Boston Society of Civil Engineers, 1937.
10. ———, Classification and Identification of Soils, *Trans. ASCE*, 1948.
11. ———, Soil Mechanics in the Design and Construction of Logan International Airport, *J. Boston Soc. Civil Engrs.*, April, 1949.
12. Clough, R. W., and R. J. Woodward III, Analyses of Stresses and Displacements in Embankments and Foundations, presented at ASCE Specialty Conference on Stability and Performance of Slopes and Embankments, University of California, Berkeley, 1966.
13. Dawson, R. F., "Laboratory Manual on Soil Testing," Pitman Publishing Corporation, New York, 1949.
14. Fellenius, W., Jordslatiska Beräkningar med Friktion och Kohesion för Cirkularcylindriska Glyditor, *Kungl. Vag-Och Vattenbyggnadskårens Årsskrift*, pp. 79–127, Stockholm (Earth Statistical Calculations with Friction and Cohesion and upon Supposition of Circular Cylindrical Sliding Surfaces), 1926.
15. ———, Calculation of the Stability of Earth Dams, *Trans. 2d Congr. Large Dams*, Washington, D.C., **4**, 445, 1936.
16. Fetzer, C. A., Electro-osmosis Stabilization of West Branch Dam, presented at ASCE Specialty Conference on Stability and Performance of Slopes and Embankments, University of California, Berkeley, 1966.
17. Fields, K. E., and W. L. Wells, Pendleton Levee Failure, *Trans. ASCE*, 1948.
18. Franke, R., The Concrete-pile Cutoff Wall According to the ICOS-Veder Patent [translated from the German, *Wasserwirtschaft*, **44** (3), 60, by the Army Engineers Research Center, Vicksburg, Miss., Translation 54-6], September, 1954.
19. Fruhauf, Bedrich, Wet Vibration Puts Strength in Sand, *Eng. News-Record*, June 23, 1949.
20. Gordon, B. B., and R. K. Miller, Control of Earth and Rockfill for the Oroville Dam Embankment, *Proc. ASCE*, **92** (SM 3), May, 1966.
21. Guelton, M., et al., The Serre-Ponçon Dam—Conception of the Project, *Travaux* (in English), May, 1961.
22. Harr, M. E., "Groundwater and Seepage," McGraw-Hill Book Company, New York, 1962.
23. Hilf, J. W., Estimating Construction Pore Pressures in Rolled Earth Dams, *Proc. 2d Intern. Conf. Soil Mech. Foundation Eng.*, Rotterdam, **4**, 6.5, 1948.
24. ———, "Estimating Pore Water Pressure in Earth Embankments, Construction Stage," USBR Design Memorandum on Earth Dams, No. 2, 1961.
25. Holtz, W. G., and F. C. Walker, Soil Cement as Slope Protection for Earth Dams, *Proc. ASCE*, **88** (SM 6), 3361, December, 1962.
26. Hvorslev, M. J., A Ring Shear Apparatus for the Determination of the Shearing Resistance and Plastic Flow of Soils, *Proc. Intern. Conf. Soil Mech. Foundation Eng.*, Cambridge, Mass., **2**, 125, 1936.
27. ———, "Subsurface Exploration and Sampling of Soil for Civil Engineering Purposes," U.S. Waterways Experiment Station, Vicksburg, Miss., 1949.
28. International Commission on Large Dams: World Register of Dams, Paris, 1964.
29. Janbu, N., Stability Analysis of Slopes with Dimensionless Parameters, Harvard Soil Mechanics Series 46, 1954.
30. Jumikis, A. R., "Active and Passive Earth Pressure Coefficient Tables," Bureau of Engineering Research, Rutgers State University, New Brunswick, N.J., 1962.
31. Jurgenson, G., "The Application of Theories of Elasticity and Plasticity to Foundation Problems," reprinted in Contributions to Soil Mechanics, 1925–1940, Boston Society of Civil Engineers, 1937.
32. Justin, J. D., J. Hinds, and W. P. Creager, "Engineering for Dams," John Wiley & Sons, Inc., New York, 1945.
33. Lambe, T. W., "Soil Testing for Engineers, MIT," John Wiley & Sons, Inc., New York, 1951.
34. ———, Methods of Estimating Settlement, *J. ASCE*, SM5, 4060, p. 43, September, 1964.
35. Lauffer, H., and W. Schober, The Gepatsch Rockfill Dam in the Kauner Valley, *Proc. 8th Congr. Large Dams*, Edinburgh, **2**, 635, 1964.
36. Lowe, J., III, and L. Karafiath, Stability of Earth Dams upon Drawdown, *Proc. First Panamerican Conf. Soil Mech. Foundation Eng.*, Mexico City, 1959.
37. ——— and T. C. Johnson, Use of Back Pressure to Increase Degree of Saturation of Triaxial Test Specimens, *ASCE Proc. Conf. Shear Strength Cohesive Soils*, Boulder, Colo., pp. 819–836, 1960.
38. ———, Discussion of paper, Rockfill Dams: Dams with Sloping Earth Cores, by James Growdon, Paper 1743, *Proc. ASCE, J. Power Div.*, **86** (PO5), October, 1960.
39. ———, Shear Strength for Embankment Dam Design, *Proc. Golden Jubilee Convention of the Chinese Institute of Engineers*, Taipei, Taiwan, 1961.
40. ———, Shear Strength of Coarse Embankment Dam Materials, *Trans. 8th Intern. Congr. Large Dams*, Edinburgh, Scotland, 1964.

41. ———, P. F. Zaccheo, and H. S. Feldman, Consolidation Testing with Back Pressure, *ASCE Proc. Conf. Design of Foundations for Control of Settlement*, Evanston, Ill., June, 1964, published in *J. ASCE*, **90** (SM 5), 4058, September, 1964.
42. ———, Stability Analysis of Embankments, state of the art paper, presented at ASCE Specialty Conference in Stability and Performance of Slopes and Embankments, University of California, Berkeley, 1966.
43. Lyman, A. K. B., Compaction of Cohesionless Foundation Soils by Explosives, *Trans. ASCE*, 1942.
44. May, D. R., Application of the Planimeter to the Swedish Method of Analyzing the Stability of Earth Slopes, *Trans. 2d Congr. Large Dams*, Washington, D.C., **4,** 540, 1936.
45. Newmark, N. M., Influence Charts for Computation of Stresses in Elastic Foundations, *Univ. Illinois Eng. Expt. Sta. Bull.* 338, Urbana, Ill., 1942.
46. ———, Influence Charts for Computation of Vertical Displacements in Elastic Foundations, *Univ. Illinois Eng. Expt. Sta. Bull.* 367, Urbana, Ill., 1947.
47. Reinius, E., The Stability of the Upstream Slope of Earth Dams, Swedish State Committee for Building Research, *Bull.* 12, Victor Pettersons Bokindustriaktiebolag, Stockholm, 1948.
48. Scott, R. F., "Principles of Soil Mechanics," Addison-Wesley Publishing Company, Inc., Reading, Mass., 1963.
49. Seed, H. B., and C. K. Chan, Structure and Strength Characteristics of Compacted Clays, *Proc. ASCE*, **85,** (SM5), 2216, p. 87, October, 1959.
50. ———, J. K. Mitchell, and C. K. Chan, The Strength of Compacted Cohesive Soils, *Res. Conf. Shear Strength Cohesive Soils*, pp. 877–964, ASCE, Denver, 1960.
51. ———, Settlement Analysis, A Review of Theory and Testing Procedures, *Proc. ASCE*, SM2, 4275, 39, March, 1965.
52. ———, A Method for Earthquake Resistant Design of Earth Dams, *Proc. ASCE*, SM1, 4616, 13–41, 1966.
53. Shannon, W. L., et al., Field Measurements, Chap. 13 in "Foundation Engineering," by G. A. Leonards, McGraw-Hill Book Company, New York, 1962.
54. Shepard, E. R., and R. M. Haines, Seismic Subsurface Explorations on the St. Lawrence River Project, *Trans. ASCE*, 1944.
55. Sherard, J. L., R. J. Woodward, S. F. Gizienski, and W. A. Clevenger, "Earth and Earth-Rock Dams," John Wiley & Sons, Inc., New York, 1963.
56. Skempton, A. W., Notes on the Compressibility of Clays, *Quart. J. Geol. Soc., London*, **C,** 119–135, 1944.
57. ———, The Pore Pressure Coefficients A and B, *Geotechnique*, **4** (4), 143, 1954.
58. ——— and L. Bjerrum, A Contribution to the Settlement Analysis of Foundations on Clay, *Geotechnique*, **7,** 168, 1957.
59. Southwell, R. V., "Relaxation Method in Engineering Science," Oxford University, England, 1942.
60. Sowers, G. F., and C. E. Gore, Large Scale Preconstruction Tests of Embankment Materials for an Earth-rockfill Dam, *Proc. 5th Intern. Conf. Soil Mech. Foundation Eng.*, Paris, **2,** 718, 1961.
61. State of California Department of Water Resources, Oroville Dam, papers prepared for ASCE Specialty Conference on Stability and Performance of Slopes and Embankments, 1966.
62. Taylor, D. W., Stability of Earth Slopes, reprinted in Contribution to Soil Mechanics, 1925–1940, Boston Society of Civil Engineers, 1937.
63. ———, Research on Consolidation of Clays, Department of Civil and Sanitary Engineering, MIT, Serial 32, Cambridge, Mass., August, 1942.
64. ———, "Fundamentals of Soil Mechanics," John Wiley & Sons, Inc., New York, 1949.
65. Terzaghi, K., "Theoretical Soil Mechanics," John Wiley & Sons, Inc., New York, 1943.
66. ——— and R. B. Peck, "Soil Mechanics in Engineering Practice," John Wiley & Sons, Inc., New York, 1948.
67. Thorfinnson, S. T., Underseepage Control at Fort Randall Dam, *Trans. ASCE*, **125,** 792, 1960.
68. Turnbull, W. J., and C. I. Mansur, Underseepage and Its Control, A Symposium, *Trans. ASCE*, 3247, **126** (pt. I), 1427–1568, 1961.
69. ——— and ———, Construction and Maintenance of Underseepage Control Measures, *Trans. ASCE*, **126** (pt. I), 1540, 1961.
70. U.S. Army, Material Testing, Technical Manual, TM 5-530, Government Printing Office, Washington, D.C., 1957.
71. U.S. Department of the Interior, Bureau of Reclamation, "Design of Small Dams," Government Printing Office, Washington, D.C., 1960.
72. ———, "Earth Manual," Government Printing Office, Washington, D.C., 1963.
73. U.S. Army Engineer Waterways Experiment Station, Field and Laboratory Investigation of Design Criteria for Drainage Wells, *Tech. Mem.* 195-1, Vicksburg, Miss., 1942.
74. ———, Seismic and Resistivity Geophysical Exploration Methods, *Tech. Mem.* 198-1, Vicksburg, Miss., 1943.
75. ———, Slope Protection for Earth Dams, preliminary report prepared by office, Chief of Engineers, U.S. Army, Vicksburg, Miss., 1949.
76. Warlam, A. A., and E. W. Thomas, Measurement of Hydrostatic Uplift Pressure on Spillway Weir with Air-piezometers, *ASTM Spec. Publ.* 392, Instruments and Apparatus for Soil and Rock Mechanics, 1965.
77. Willey, C. K., Wanapum Hydroelectric Development, *Civil Eng.*, September, 1960, p. 65.
78. Wilson, S. D., Small Soil Compaction Apparatus Duplicates Field Results Closely, *Eng. News-Record*, November, 1950.
79. Wilson, S. D., Investigation of Embankment Performance, state of the art paper, presented at ASCE Specialty Conference in Stability and Performance of Slopes and Embankments, University of California, Berkeley, 1966.

SECTION 19

CONCRETE-FACE ROCK-FILL DAMS

By I. C. Steele and J. B. Cooke

INTRODUCTION

1. Definition of Rock-fill Dams. A now obsolete definition of a rock-fill dam, used in an ASCE Symposium[1,*] as recently as 1939, is "A dam consisting of a loose (dumped) rockfill with slopes on both faces closely approximating natural slopes, with an impervious facing on the upstream side between which and the rockfill there should be placed a cushion of dry rubble." The definition properly defined the rock-fill dam of that time, 1939. Since that time the rapid development of the earth-core rock-fill dam and compacted rock have made the definition obsolete.

A current definition is "A dam that relies on rock, either dumped in lifts or compacted in layers, as a major structural element." This definition embraces both impervious-face and impervious earth-core rock-fill dams. It is the definition used in the ASCE Rockfill Dam Symposium of 1960[2] and in the Eighth International Congress on Large Dams at Edinburgh in 1964.[3]

Section 18 on Embankment Dams includes the earth-core rock-fill dam; this section covers only concrete-face rock-fill dams. Among the impervious-face type of rock-fill dams, the concrete-face type is the most commonly used. Asphalt is the next most frequently used impervious face, the use of gunite, steel, timber, and masonry being infrequent.

2. History of Rock-fill Dams. The origin of rock-fill dams was in the Sierra Nevada Mountains of California. In the 1850s, gold miners needed dams in inaccessible locations in the glaciated granite of the Sierra where no earth was available. Available were trees and solid rock. Those circumstances, combined with the miner's knowledge of the use of explosives, logically resulted in rock-fill dams. The first dams were rock-fill log-crib dams which permitted steep slopes and a minimum amount of rock; English Dam in 1856 was 79 ft high. Later, rock-fill dams with a face of timber or concrete developed.

Prior to 1925, only eight rock-fill dams were higher than 100 ft, Morena, Strawberry, and Swift Dams all being highest at about 160 ft. The eight dams were all in the United States and most in California. In 1925, the 275-ft-high Dix River concrete-face rock-fill dam was constructed in Kentucky. Through the 1930s a number of concrete-face rock-fill dams in the 200- to 300-ft height were constructed, the highest being the 328-ft-high Salt Springs Dam.[2]

The 1940s saw the continued use of concrete-face dams and the beginning of high earth-core rock-fill dams:[2] the 375-ft-high thick-central-core San Gabriel No. 1 Dam in 1938, the 260-ft-high thin-sloping-core Nantahala Dam in 1942, the 318-ft-high thick-central-core Watauga Dam in 1948, and the 400-ft-high thin-central-core Mud Mountain Dam in 1948.

Since 1950, development of both the earth-core and concrete-face types of rock-fill dams has proceeded exceptionally rapidly. This is understandable since, in compari-

* Superior numbers refer to items in the Bibliography at the end of this section.

son with the history of other types of dams, the history of rock-fill dams is relatively short.

In the period 1950–1963, about 30 earth-core rock-fill dams of 250- to 510-ft height were completed, and in 1963 about 40 dams of 280 to 980 ft were under construction or proposed.[4] Rapidly increasing knowledge of the use of rock fill and of its excellent performance has made this possible.

Since 1950, concrete-face dams have generally been of 100- to 250-ft height, the highest being Paradela in Portugal at 365 ft, Wishon and Courtright in California at 290- and 310-ft height, and Exchequer in California at 500-ft height. Recent progress in the concrete-face dam has been due to increased knowledge of rock fill and to major improvements in design.

3. Traditional Design of the Concrete-face Rock-fill Dam. Design is empirical and is based on experience and judgment. There is little that can be computed for

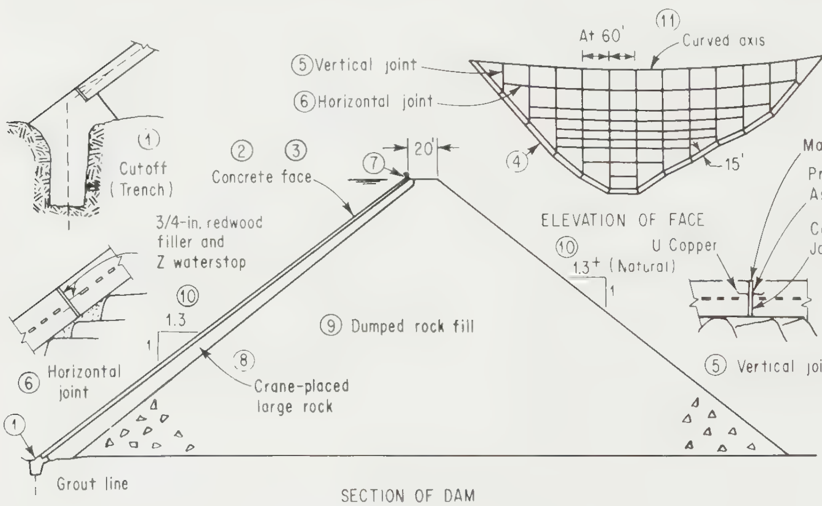

FIG. 1. Typical traditional design of concrete-face rock-fill dam.

the concrete-face rock-fill dam. Between 1925 and 1960, there were improvements in design, with objectives of economy and of minimum cracks, joint maintenance, and leakage. However, there was little major change.

Features of the typical traditional design (Fig. 1) were (1) a cutoff trench into bedrock with a notched recess in the concrete to receive the slab, (2) a face-slab thickness of 1 ft plus 8 in. for each additional 100 ft of dam height, (3) face-slab reinforcing of 0.5 percent in center both ways, (4) a joint system that permitted relative movement of the individual face slabs, (5) vertical joints of 1- to 2-in. dimension with compressible premolded asphalt material, (6) horizontal joints of ½- to ¾-in. dimension with wood filler, (7) a wave-deflector coping wall, (8) a zone of crane-placed selected large rock to support the concrete face, (9) dumped rock fill, (10) natural dumped rock slopes, 1.3:1 to 1.4:1, and (11) a curved axis.

Dams of the traditional design of less than 250-ft height performed well. The higher dams had face-crack and leakage problems. The troubles were associated with the movements in the face slab and the joints. Though the troubles in no way affected safety and were of nominal cost, they called for design improvements.

The use of crane-placed rock in the traditional design required the availability of suitable rock, involved high labor costs, and controlled the construction schedule. These factors made the concrete-face dam unfeasible or uneconomical at many sites.

4. Recent Design Trends. Since 1960, substantial improvements in all features of concrete-face rock-fill dam design have occurred. The new design features (Fig. 2) are (1) a cutoff slab doweled to bedrock; (2) thinner face slab; (3) variable percent reinforcing; (4) minimum joints; (5) tight vertical construction joints; (6) no horizontal joints other than cold construction joints; (7) a simple rectangular-section coping wall; (8) a special zone of compacted rock to support the face; (9) zoned rock fill of compacted rock and dumped rock, as dictated by available rock sources, acceptable movements, permeabilities, and economics; (10) slopes of 1.3:1; and (11) a straight axis.

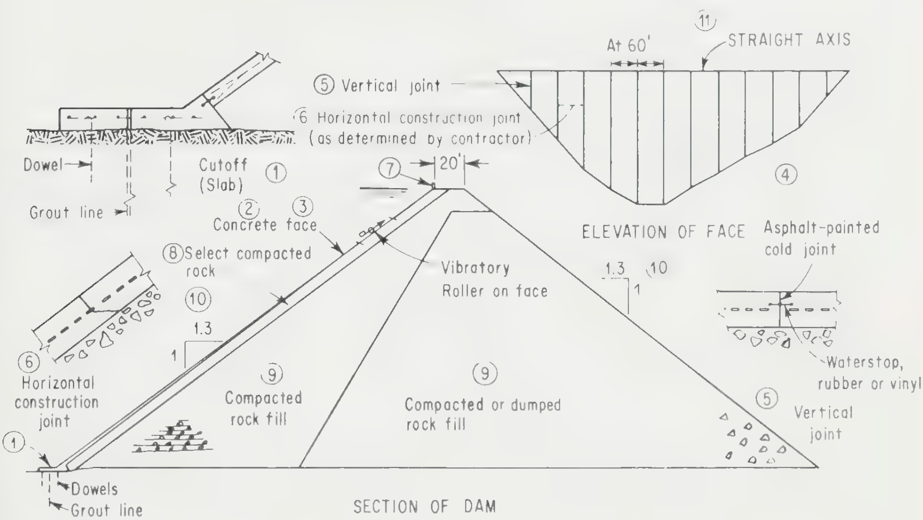

FIG. 2. Typical recent design of concrete-face rock-fill dam.

FACTORS IN SELECTION OF THE CONCRETE-FACE TYPE OF ROCK-FILL DAM

5. Foundation. Foundation requirements are the same as for an earth-core rock-fill dam, they are less severe than for concrete dams, and they are usually more severe than for earth dams. Hard bedrock is desirable for the cutoff to permit a cutoff with a short seepage path.

Potentially pervious or erodible zones, such as seams, faults, and soft zones, can be accepted crossing the cutoff. For watertightness and safety, treatment can consist of grouting, excavating and plugging with concrete, or upstream blanketing. River gravels and rock talus are often acceptable in the foundation. Erodible zones and weathered or small fractured rock zones are covered by filters or compacted rock layers to prevent any possibility of the foundation's being piped into the rock fill.

6. Available Materials. For the concrete-face rock-fill dam, the necessary material is rock. Nearly all concrete-face dams were constructed of dumped rock fill until 1960, dumped rock fill requiring sound high-compressive-strength (15,000 to 30,000 psi) rock. The advent of compacted rock has permitted the use of weaker rock and has made rock-fill dams feasible at more sites. The use of gravels or weathered-rock random zones can be economical.

The earth-core rock-fill type of dam requires earth and filter material as well as rock. Where earth is not available, the core rock fill is not feasible, though usually earth is available at some distance, which in a comparison is reflected in cost. The absence of natural sands and gravels increases the cost of the earth-core rock-fill alternative, since manufactured filters are expensive.

7. Spillway and Diversion Tunnel. The development of zoning of rock fill, and of the use of poorer rock as compacted rock, has resulted in spillway excavation being usable more frequently, improving the economy of rock-fill dams.

The concrete-face design has a base width of $2.6H$ in comparison with $3.6H$ for a core design, where H is the height of the dam. This can result in a lower spillway and tunnel cost for the concrete-face design.

8. Topography. If the site has one or more narrow ridge abutments, the lesser base width of the concrete-face design can be important. If the site has unfavorable downstream-downhill slopes under the core or rock fill, it is unfavorable to the earth-core rock fill in cost or inherent safety. The concrete-face rock fill is independent of the up-downstream abutment slope at cutoff, whereas the earth-core rock-fill dam is not and can require substantial excavation to obtain proper core contact. For the concrete-face design, steep downward and downstream slopes can be accepted under the rock fill.

In placing the dam on the site, the optimum axis is generally not that giving minimum rock-fill volume, but that giving minimum face area.

9. Crest Details. The concrete-face design has a narrower crest and less freeboard than an earth-core design. Crest width is usually 20 ft in comparison with 30 to 40 ft for an earth-core type of rock fill. For purposes of freeboard, the dam crest is the top of the coping wall. As a reinforced-concrete extension of the face slab, the coping wall is a rugged and nonerodible element of the dam. Being vertical, wave ride-up is not involved; splash is harmless.

At Wishon Dam water is stored to the dam crest level, the 4-ft coping providing freeboard. As an example of the competence of a coping wall, at Taum Sauk pumped storage dam water is stored 8 ft up on a 10-ft-high coping wall. The requirement for freeboard is that the wall not be overtopped by the level of the reservoir under any circumstances. To assure this, the freeboard dimensions are directly related to the type of spillway; that is, a spillway that takes greatly increased discharge as freeboard is encroached on requires less freeboard.

10. Diversion and Care of River. Large embankment dams that are constructed through one or more construction seasons present serious problems in handling floods during construction. The problems involve risk and expenditure to minimize risk. When the dam is low and can store no water, losses are limited to the site. When the dam is high enough to store water, its overtopping and failure during construction can create a flood from the sudden release of stored water.

Flows of several thousand cubic feet per second can safely pass through rock fill that has large rocks in the downstream toe, but it should be assumed that rock fill will fail when overtopped, unless specially designed for overtopping. In 1939–1941, Weiss,[5] on several concrete-face rock-fill dams in Mexico, used reinforcing in the downstream face to withstand overtopping by floods. It was successful and has since been widely used.[6,7,8]

For embankment dams with river-handling problems, the concrete-face rock fill has an advantage—the rock fill can be raised faster and on a schedule not affected by rainfall. This permits a smaller diversion tunnel or gives less risk of overtopping failure. Water can be temporarily stored in flood routing before the concrete face is constructed, with some flow passing through the rock fill. Flow through rock fill requires large rock in the downstream toe of the rock fill, which can be economically and reliably obtained by a zone of dumped rock fill.

Low flows can be taken through the dam, which can be economical in eliminating a diversion tunnel or permitting economical permanent outlet construction while water passes through the rock fill. A low slab is not placed until the outlet is ready for operation.

11. Construction Schedule and Rainfall. The concrete-face rock-fill dam usually has a smaller yardage of rock than does the earth-core rock-fill type. It can be constructed faster, essentially in the time it takes to place the rock fill. There is no wait for core-contact-surface preparation and grouting. The concrete-face cutoff work can be accomplished independently of the rock-fill placement. Rainfall affects reliable scheduling and cost of a core rock-fill dam, whereas it does not affect the concrete-face dam. The concrete face can be constructed concurrently with rock placement and not govern filling of the reservoir; concrete slip-form placement is rapid.

12. Reservoir Operation. The high concrete-face dam is subject to leakage more than any other type of dam. It can be watertight, can leak 1 or 2 cfs, or can leak tens of cubic feet per second. After the first filling if there is trouble, leakage can temporarily be 20 to 100 cfs or greater. Leakage does not impair safety but is a matter of economics. The movements that cause joint leakage occur principally during and soon after the first filling. When repairs have been made, they have been final except for dams over 250 ft high.

Underwater leak detection is accomplished by a simple audio device or by closed-circuit TV which shows the concrete face and the movement of a semibuoyant streamer. When the leak locations are determined, the leakage can be reduced either by underwater work or by work in the dry when the water level is lowered.

Experience has been that, when leakage has occurred, it has been technically embarrassing, but its cost has been negligible when compared with the saving in cost of the dam. Though it is expected that the recent design improvements will give improved performance, there has not been enough experience to verify that.

13. Future Raising. The concrete-face dam is well adapted to being raised by adding rock fill and extending the face slab. The face thickness would be designed for the ultimate height, or in the event of unexpected raising, a higher ratio of head to thickness would need to be accepted.

14. Height. Since compacted rock settles less and is less compressible than dumped rock, concrete-face rock-fill dams with a zone of compacted rock can be constructed to greater heights.

Dumped rock fill has been a major contributing factor to face movements and cracks near the base and near the abutments of the dumped rock-fill concrete-face dam. A dumped rock-fill lift is well graded and dense in the upper portion and of large rock with a high percentage of voids in the lower portion. The lower portion is the most compressible part of the fill and is the location where water pressure is greatest. These factors combine to give trouble with the concrete face for the dumped rock-fill dam of more than about 200-ft height. The use of compacted rock fill will give better performance as well as permit the construction of higher dams.

15. Economics. In comparing an earth-core rock-fill design with a concrete-face rock-fill design, complete studies would be made for each. The auxiliary features for the concrete-face layout will cost less, principally because of the lesser base width. An approximate comparison can be visualized. The core design usually requires more rock fill, which is a credit to the concrete-face design as is the saving in auxiliary features. The basic comparison is then of the cost of the impervious features: for the core design, there is foundation excavation, area and curtain grouting, surface treatment, the core, and the filters; for the concrete-face design, there is foundation excavation, cutoff slab, curtain grouting, face slab, and the cost above that of the rock fill for the special zone of rock to support the slab.

16. Design Progress. Since 1960, the improvements in design of the concrete-face rock fill have decreased the cost of the impervious feature by about one-half of previous cost. The main changes are:

1. Change from crane-placed large rock to special zone of compacted rock for supporting concrete face. This reduced cost from \$10 to \$12 per cubic yard to \$3 per cubic yard. It also expedited the work. The more regular surface reduces excess face-slab concrete from about 15 to 4 to 6 in.
2. Change from cutoff trench and wall to a reinforced and doweled cutoff. This eliminated expensive rock-trench excavation and backfill concrete, resulting in scheduling as well as cost savings.
3. Change to thinner slab and fewer and simpler joints.

EVOLUTION OF CONCRETE-FACE ROCK-FILL DAM DESIGN

17. Design Evolution and Recent Trends. Since design of the concrete-face rock-fill dam is empirical, precedent has played an important part in design. This has restricted progress in design. However, since 1960, the accumulated experience, the construction of many dams, and the emergence of layered rock-fill construction (compacted rock) have combined to stimulate recent important progress. Design can best be reviewed by examples of selected dams that have contributed to progress, with emphasis on recent dams.

18. Meadow Lake, California, 1903. Meadow Lake Dam[9] is one of several early California dams of about 75-ft height with steep slopes and a surface layer of dry masonry rock. The upstream slopes are 0.50:1 for the top 25 ft and 0.75:1 for the lower 50 ft. The downstream slopes are 0.50:1 for the top 25 ft and 1:1 for the lower 50 ft. These are much steeper than the nominal 1.3:1 "angle of repose" and have performed satisfactorily.

Such dams, with steeper than natural dumped slopes, provide evidence that the shearing strength is substantially greater than that based on the 1.3:1 natural dumped slope. For example, on a basis of infinite slope a slope of 0.5:1 requires a minimum tan ϕ of 2.0, whereas a 1.3:1 natural slope indicates a tan ϕ of 0.77. Experience with these dams and higher dams with 1:1 slopes justifies the use of natural slopes of 1.3:1 for the slopes of impervious-face rock-fill dams.

The cutoff for Meadow Lake Dam is only 1 to 2 ft into granite. Since the wood face was replaced in 1930 by a 2- to 4-in. gunite face with no joints, there has been negligible leakage. There has been no significant deterioration of the thin gunite in 37 years of service.

19. Bucks Creek, California, 1928. This 128-ft-high dam[9] was unique. The reinforced-concrete face had no joints. In its first 39 years there have been no cracks, leakage has been negligible, and no maintenance has been required. In looking back, it is regrettable that the favorable experience with the unjointed face slab was not utilized in design of subsequent dams.

20. Salt Springs, California, 1931. The 328-ft-high Salt Springs Dam was constructed in 1931. It established a precedent for many other high concrete-face rock-fill dams, culminating in Paradela (360 ft) in Portugal and Wishon (290 ft) and Courtright (310 ft) in the United States in 1950. Design, construction, and performance of these and other high rock-fill dams are well presented in the literature.[2]

The basic features of Salt Springs were included in other designs all over the world for the 30-year period to 1960. Those features were dumped rock, placed rock, thickness and reinforcing of concrete slab, face joints, and cutoff trench and wall. Modifications were minor.

Salt Springs experience provided important data still useful in both earth-core and concrete-face rock-fill dam design. Among the data are the movements of the rock fill, the performance of the concrete face, the stabilizing of settlement of the high dumped rock fill to a negligible amount, and the permanence of a concrete slab under a hydraulic gradient of 100. However, future dams should be patterned after more recent experience and practice.

21. Cogoti, Chile, 1940. Cogoti Dam, 250 ft high, is one of 17 concrete-face rock-fill dams built in Chile in the 1930s. This type was selected as being earthquake-resistant. Contrary to the usual design using placed rock as the layer supporting the concrete face, a screened and washed gravel zone was used. To allow for the natural slope of gravel and for earthquake, a 1.6:1 upstream slope was adopted. The downstream slope was exceptionally flat, 1.8:1, as an arbitrary recognition of the earthquake hazard in Chile. The use of the gravel zone was progressive. Cogoti Dam demonstrated its earthquake resistance in a severe shock on Apr. 7, 1943. The fill settled 1.38 ft with no damage and no increase in leakage.

The use of gravel at a slope of 1.5:1 was studied as an alternative design for Wishon Dam in 1957. A design using thin placed rock at steeper slopes of 1.3:1 to 1:1 was estimated to cost less and was adopted. High labor and equipment cost, and the adverse effect of placed rock on the scheduling of the work, pointed out that placed rock was not an appropriate type of construction in the economy of 1960 in the United States.

22. Quioch, Scotland, 1956. The 126-ft-high concrete-face dam was conventional except for two features: (1) the rock fill was compacted in 2-ft layers by a drum vibratory roller (3.5-ton), and (2) the face was 12 in. thick at a point 100 ft below crest instead of the conventional 1.67 ft at that elevation.[2] Both features were progressive and have become a part of modern designs. The use of the vibratory roller for a dam of this height was not necessary; its importance was in introducing the technique to rock-fill dams. The settlement of Quioch of less than 1 in. is negligible and much more would be acceptable.

The use of the vibratory roller on rock-fill dams followed German and Swedish use and soon after extended to the United States. The need of heavier than 3.5-ton units for rock fill soon became evident, and available units increased in capacity to 4.5, 6, 8, 10, and 15 tons, 10 tons being commonly used in 1967.

23. Sassiere, France, 1959. Sassiere Dam (128 ft) was constructed of one lift of dumped rock fill.[10] Supporting the concrete face (1.4:1 slope) was a zone of vibratory-rolled rock of 11-ft horizontal width instead of the conventional placed rock. It was placed in 2-m layers. Settlement has been only 1 in. and leakage negligible.

Another progressive feature of Sassiere was the use of a 12-in. slab for the full height.

24. Taum Sauk, Missouri, 1963. The reservoir for Taum Sauk pumped storage project was formed by excavating the top of the mountain to reservoir floor level and using the excavated rock for an encircling dam (Fig. 3). The dam is a concrete-face dumped rock fill of particularly economical design.

The concrete-face type of rock fill with its minimum base width and maximum resistance to sliding was best adapted to encircle the top of the mountain. The slope of the foundation dips steeply downstream. To avoid excessive stripping and replacement rock fill, the downstream rock-fill foundation was stripped to a control line at 1:1 slope. The dam section (Fig. 3) is of one lift of dumped rock except for four 4-ft layers of rock to top off the dam to the narrow 12-ft-wide crest. Sluicing of the dumped rock was by monitor at 70 psi and 2 volumes of water to 1 of rock. The 4-ft layered rock fill was compacted by spreading and hauling equipment and thoroughly flooded with water. The rock was a rhyolite porphyry which quarried as small rock with excessive fines, a smaller-size grading than generally used for dumped rock.

Settlement after 2.5 years of service has been between 0.25 ft for 73-ft height and 0.71 ft for 116-ft height. This high settlement is probably due to the small-sized dumped rock and the repeated cycling of the pumped storage reservoir. Water is stored to 8 ft above the crest on the 10-ft parapet wall. The walls have remained vertical, and differential movement between the 60-ft panels has been slight.

The parapet wall and the toe are of poured concrete. The concrete face is sprayed concrete, with vertical joints at 60 ft and no horizontal joints. It was delivered by transit mix to a compressed-air gun at the upstream toe of the dam, conveyed by pipe up the face, and blown onto the face. The face of the dumped rock fill was ironed out

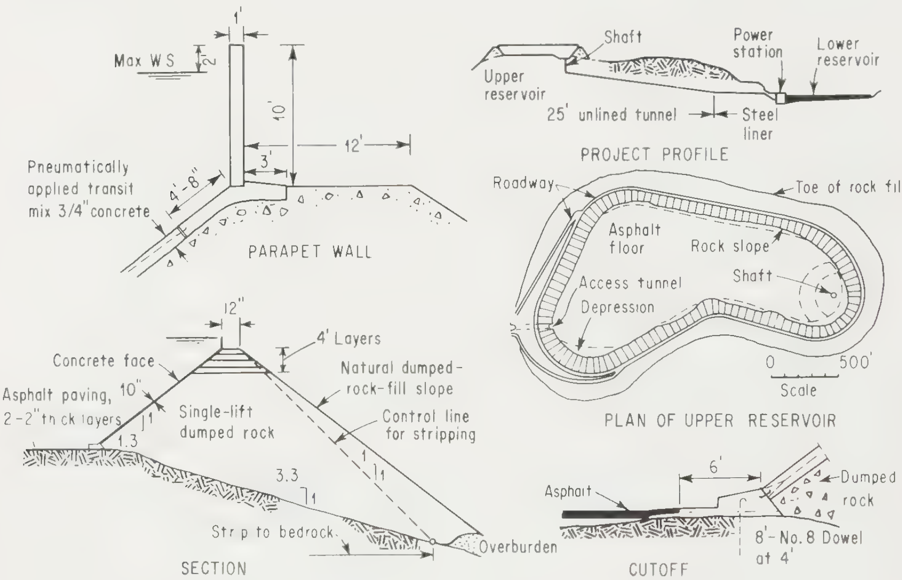

FIG. 3. Taum Sauk Dam. (*Union Electric Co., St. Louis, Mo.*)

by a 3.5-ton vibratory roller being pulled up and down the face. It was mounted in a ¾-in. plate with the roller projecting 3 in. below the steel plate. The cutoff is a doweled slab rather than the conventional trench and cutoff wall.

There have been leakage problems at Taum Sauk.[11] They have been due principally to blast-damaged bedrock and, to some extent, to the sprayed concrete causing segregation at the copper water stops. Leakage from the reservoir and the 6,000-ft-long dam had stabilized at 8 cfs in 1967.

25. New Exchequer, California, 1966. New Exchequer Dam (Figs. 4, 5, and 6) is a 490-ft-high concrete-face rock-fill dam. It was constructed to raise a 310-ft-high concrete gravity dam and in effect is a 305-ft-high concrete-face dam constructed on a 185-ft-high rock-fill foundation (Fig. 5). For essential irrigation water, it was necessary to operate the gravity dam during construction of New Exchequer and to store water on the new dam as it was being constructed. The concrete-face rock fill permitted this and was substantially economical and unquestionably safe. However, in initial filling there have been leakage and face-repair problems.

Zone of Rock Supporting Concrete Face. Zone 1 of Fig. 4 was scalped quarry-run rock of 2- to 15-in. size, placed dry in 2-ft layers and compacted by three passes of a 10-ton vibratory roller. The face was compacted and smoothed by pulling a 10-ton vibratory roller up the face. Fines were removed to make a zone that would accept high-velocity flows from a leak in the face without deterioration. Fines manufactured by the vibratory roller would fall into voids between rocks already in contact. During construction it was found that the grading was too coarse to give a firm face and a smaller grading was used. The clean rock has the advantage of stability, but a disadvantage in being highly permeable.

Rock Fill. All rock came from a quarry in high-strength 30,000-psi meta-andesite rock. The quarry was just downstream on the left abutment. The spillway was in a low saddle and did not provide rock for the dam; the saddle required a small central-core rock-fill wing dam of 1.75:1 outer slopes. The quarried rock met the grading for

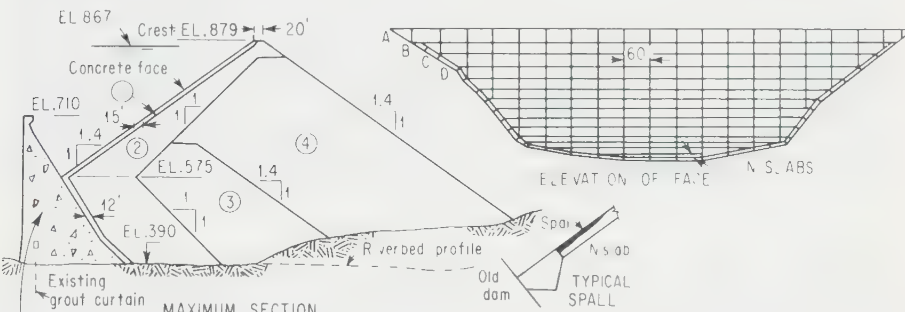

Zone	Sluicing water : rock	Max size	Layer thickness, ft	No. of passes
1	None	2–15 in.	2	3
2	0.5 : 1.0	4 ft	4	4
3	0.5 : 1.0		10	
4	2.0 : 1.0		Dumped	

10 TON VIBRATORY ROLLER

FIG. 4. New Exchequer Dam (Merced irrigation district).

Zone 2 compacted rock, but not for Zone 4 dumped rock. As a result, most of Zone 4 (Fig. 4) actually was Zone 3, which is rock of either grading placed in 10-ft layers.

The thin well-compacted Zone 2 is located to minimize differential settlement in the vicinity of the abutments. Smooth settlement in the balance of the face is acceptable and permits the economy of 10-ft layers and dumped rock for the rest of the rock fill. In the first filling of the reservoir, June, 1967, crest settlement was 1.3 ft (0.27 percent height), which is very low for a 490-ft rock-fill dam. For the concrete-face rock fill, settlement of the rock is not masked by settlement of the core and transitions as it is for the earth-core type of rock-fill dam.

Cutoff. The joint between the concrete face and the gravity dam is essentially a concrete rib floating on rock fill with asphalt-filled voids.[12] The cutoff on the abutments (Fig. 4) is a doweled reinforced slab which acts as a grout cap for the grout curtain. The cutoff slab is placed on groutable rock and is warped to the general shape of the rock.

Concrete Face. The concrete face is of traditional design, in part because the exceptional height made it difficult to break precedent. Concrete was placed by slip form.[13] Each row of slabs was placed as the rock-fill height permitted. Actually,

Fig. 5. General view of New Exchequer Dam (engineer—Tudor Engineering Co.; contractor—Dravo Corp.).

Fig. 6. View of New Exchequer Dam—rock-fill construction.

slabs were placed, with rock fill in the downstream part of the dam being 100 ft below the top of slab (Fig. 6). It subjected the slabs to movements during construction, about 2 ft normal to face in the lower central portion of the dam. Another unfavorable condition was the opening and closing of joints during construction; this had not happened on previous dams. The early placing of slabs and the unprecedented height both contributed to the slab movements during construction. These problems were accepted to achieve a demanding and valuable filling and completion schedule. Only leakage and maintenance cost, not safety, were possible consequences.

As for other dams, the face-slab forms were set on the rock face without regard to the design location, since some settlement occurs and minimum excess concrete beyond the design line is economical. At New Exchequer, and also at Cabin Creek, the excess concrete averaged about 6 in.

Concrete-face Joints. Similar to Lower Bear River, Paradela, Wishon, Courtright, and other dams of the 1950s, there was a hinge joint, horizontal joints were 1-in. redwood, and vertical joints were premolded asphalt, 1 in. in general and 2 in. in the central joints. When the D slabs (Fig. 4) were being poured, it was observed that vertical joints in the central third of the dam were closing excessively and joints near the abutments opening; one opened several inches. The central seven joints in the remaining top three slabs were changed to redwood instead of asphalt joints. This stopped further movement during construction. Neither these vertical joints nor the horizontal redwood joints crushed during construction. With no water load on the slab, the rock can readjust in the zone under the slab without developing significant compressive stress in the slab.

Face Damage—Leakage Repair. The reservoir was filled to 125 ft from full reservoir level in 1966. Leakage was 13 cfs. When the reservoir lowered below the crest of the gravity dam, the complete face was inspected. Spalling had occurred at the joint at the bottom of the N slab for about 30 percent of its length. The spalling usually began at corners of the N slabs and progressed upward. Spalls went down to the water stop and were sources of leakage (Fig. 4). The slabs were restored with additional reinforcing steel and concrete.

In June, 1967, the reservoir was completely filled. When the reservoir reached the same level as in 1966, the leakage reached 40 cfs; and for full reservoir in June, 1967, it reached about 400 cfs. The gradient within the rock fill for the 400-cfs leakage was 3 percent. This was determined from the gallery in the gravity dam. Underwater audio detection indicated several points of leakage at hinge joints on lower abutments. These were caulked by divers. A closed-circuit TV was used to view the face below a practical diving limit of 150 ft. The spalling had recurred in the N slab and had extended to the two joints above. The joint between the concrete face and the gravity dam was not damaged. The TV camera had a ribbon attached that would show visually the direction of flow and leakage. The pictures were recorded on tape so that they could be reviewed in conference later.

Having a full reservoir in July, 1967, normal operation will not draw the reservoir down to below the crest of the gravity dam for several years. Underwater placement of 18,000 cu yd of a slurry-trench backfill material, a well-graded mix of gravel-sand-earth with bentonite, was begun in July, 1967, to cover the lower three joints, spalling having occurred on those joints. This work reduced leakage from 400 to less than 10 cfs.

Conclusions. The rock-fill settlement is exceptionally small. The cutoff slab was economical and satisfactory. The supporting rock zone for the face should have been of smaller-sized grading. The construction of face slabs during rock-fill placement was essential to the project, but not compatible with the joint system that was used. The movements of slabs during and after construction invited the spalling that occurred.

26. Cabin Creek, Colorado, 1966. The Upper Reservoir for the pumped storage project[14] of Public Service Company of Colorado is formed by a 250-ft-high concrete-face rock-fill dam (Fig. 7).

Rock-fill Zones. The dam is constructed of weathered rock from required excavations and fresh rock from a quarry within the operating level of the reservoir. The three zones of rock are all compacted in 2-ft layers by three passes of a 3.5-ton

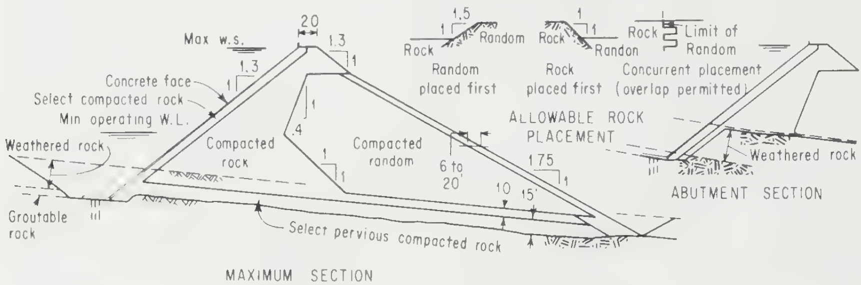

FIG. 7. Cabin Creek Dam. (*Public Service Company of Colorado.*)

FIG. 8. View of Cabin Creek Dam—placing of concrete face (engineer—Stone & Webster Engineering Corp.; contractor—J. A. Jones and P. Harrison).

vibratory roller without application of water. The gneiss was deeply weathered or loosened and was predicted to produce small-sized rocks. For the height of dam and the rock, the 3.5-ton vibratory roller and 2-ft layers were arbitrarily selected. The 1.3:1 upstream slope was compacted by pulling the vibratory roller up the face by a crane. The downstream 1.75:1 slope allows for badly weathered rock in the random zone.

Cutoff and Concrete Face. The doweled cutoff slab is broad and the grout curtain is of three lines to avoid excavating more deeply into badly weather-stained and jointed rock. The face slab is thinner than that of earlier designs; it is 1 ft to a maximum of 1.5 ft. Vertical asphalt-filled joints at 50-ft spacing and horizontal joints at 80-ft slope distance spacing were used, but not a hinge joint paralleling the abutments. The slip form used for the face was simple and efficient (Fig. 8). Concrete was distributed by a conveyor, fed by a hopper at one end. The form contacted only 8 in. of the face and was in effect a screed. Some of the lower slabs were covered with a backfill of impervious waste material.

Axis. The axis is straight, which gives lowest surveying and construction cost.

Performance. Maximum crest movement for the first 6 months of service (to July, 1967) has been 0.17 ft vertical and 0.06 ft horizontal. One abutment vertical joint has opened 0.25 in., and two central joints have closed enough to produce slight extruded asphalt. Total foundation and dam leakage for the full reservoir was 1.8 cfs.

27. Piedras, Spain, 1967. Piedras Dam (Fig. 9) is of only 130-ft maximum height but its crest length is 2,000 ft, and economy is important. It is an annual-carryover

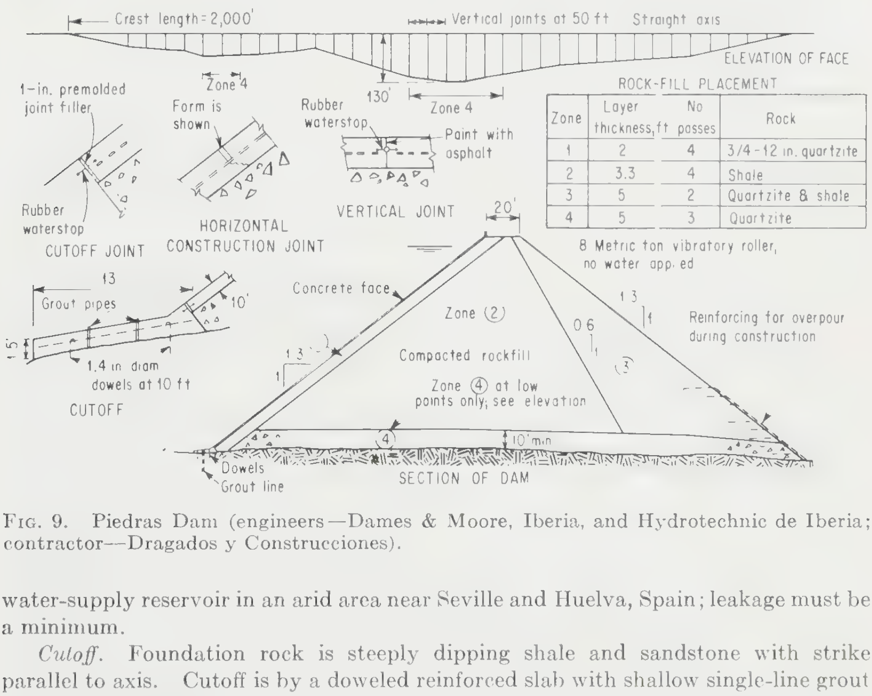

FIG. 9. Piedras Dam (engineers—Dames & Moore, Iberia, and Hydrotechnic de Iberia; contractor—Dragados y Construcciones).

water-supply reservoir in an arid area near Seville and Huelva, Spain; leakage must be a minimum.

Cutoff. Foundation rock is steeply dipping shale and sandstone with strike parallel to axis. Cutoff is by a doweled reinforced slab with shallow single-line grout curtain, conforming to the existing rock surface. There is little overburden or weathering of rock. The axis is straight and is located on abutments and over a knoll to give minimum face area, that being more economical than minimum yardage for the concrete-face dam.

Rock Fill. Five zones of rock are used (Fig. 9). All rock placement is without application of water, since water is not reliably available. Zone 1, supporting the concrete face, is of minimum width, 3 m, and of graywacke sandstone. Zone 2, the main body of the dam, is of slaty shale, the predominantly available rock and the lowest-cost rock to handle. Zones 3 and 4 are for larger rock. Zone 5 is a reliably free-draining zone of graywacke sandstone rock and is only in the two low points in the profile (Fig. 9). An 8-ton vibratory roller is used.

Concrete Face. The concrete face is 10 in. thick and reinforced with 0.5 percent reinforcing both ways. There are no horizontal joints. Vertical joints, at 50-ft spacing, are asphalt-painted cold joints with a rubber water stop. No joint filler is used.

Diversion. River handling is by a minimum-sized diversion tunnel with a low cofferdam. To provide for safe overtopping of the rock fill in the early construction period, the downstream rock face is reinforced with reinforcing steel.[6]

28. Barrage Des Fades, France, 1967. This 230-ft-high dam is of traditional design, except for the use of a compacted clean-rock zone supporting the face and a change from cutoff trench to cutoff slab made during construction. The slopes are 1.3:1. Face-slab joints include a hinge slab joint 15 ft from cutoff joint, vertical joints at 45 ft, and nine horizontal joints. Rock placement is in two zones, 3.3- and 6.6-ft layers, with compaction by 8.5-ton vibratory roller.

29. Pindari, New South Wales, Australia, 1969. Pindari is a two-stage dam, 150 ft high in first stage and 250 ft high when completed (Fig. 10). It embodies all

Zone	Layer thickness, ft	*No. passes	Grading
1	2	4	Max 6" To 12", < 7%-1", < 2%-#200
2	3	3	Max 1' To 3', < 25%-1", < 5%-#200
3	6	6	Max 1' To 6', < 25% 1" < 5%-#200
4	6	0	Max 3' To 6', 90% > 150-lb Size

10 Ton vibratory roller

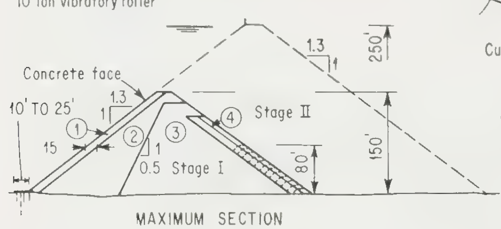

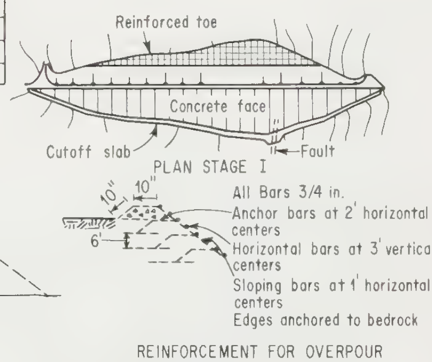

Fig. 10. Pindari Creek. (*The Water Conservation and Irrigation Commission of New South Wales.*)

recent design features except the use of a thinner than traditional slab, *i.e.*, thinner than 1 ft + 0.0067H, where H equals height of dam (Fig. 10).

Rock Fill. Rhyolite porphyry from spillway and from an additional quarry is being used. Zone 1 grading is 6- to 12-in. maximum size and not more than 7 percent minus 1 in. It is smaller-sized than used previously and will provide a denser, less pervious, and smoother-surfaced zone. Water is applied to this finely graded Zone 1 during placement, whereas it has not been used on coarser and cleaner Zone 1 rock. Zones 2 and 3 are placed without water in 3- and 6-ft layers. Zone 4 is a zone which includes reinforcing for probable overtopping during construction, the diversion tunnel being of minimum size. All compaction is by 10-ton vibratory roller.

Cutoff and Face Slab. Cutoff is a doweled and grouted reinforced slab. A fault (Fig. 10) crosses the cutoff line. The slab is extended upstream and filters cover the fault under the rock fill. Vertical joints are asphalt-painted polyvinyl chloride water-stop joints at 60-ft spacing, and there are no horizontal joints.

30. Kangaroo, South Australia, Australia, 1968. Kangaroo Dam, 210 ft high (Fig. 11), is similar to Pindari. A feature of economic importance is the use of a poor schist rock from spillway excavation as the main body of the dam. The Zone 3 rock is schist compacted in 3-ft layers by three to four passes of an 8- to 10-ton vibratory roller sluiced with not less than 180 gal of water per cu yd of rock. Adjacent to Zone 3 are free-draining zones of gneiss, Zones 2 and 4. All rock is from the spillway excavation. The spillway site is in a schist formation with one wide zone of gneiss which can furnish the sound rock for Zones 1, 2, and 4.

Zone	Layer thickness, ft	Rock
1	2	1"-12" gneiss
2	3	<20%, 1" gneiss
3	3	<30%, 1" schist
4	4	Gneiss

10-ton vibratory roller, w th water

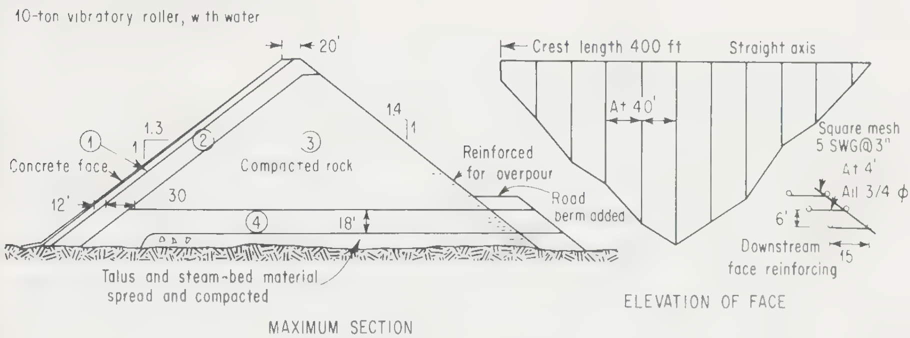

FIG. 11. Kangaroo Creek Dam. (*The Engineering and Water Supply Department, South Australia.*)

31. Cethana, Tasmania, Australia 1973. The 360 ft high dam was filled in May 1973. Movement during filling and first 9 months full was 3 inches vertical at crest and 4 inches normal to central face area, no cracks have occurred, dam and foundation leakage was 1.2 cfs. The design embodies recent design trends including: 1.3H:1V slopes, no horizontal joints, tight vertical joints, and thin slab of $t = 1 \text{ ft} + 0.002H$ (where H equals vertical distance from crest). Design and performance are presented in Proceedings of Eleventh Congress on Large Dams, Volume III, Madrid, 1973.

32. Alto Anchicaya, Colombia, 1974. The Corporacion Autonoma Regional del Cauca will complete a 500 ft high dam in 1974. Acres International Ltd. has selected the concrete face rockfill type on the basis of lowest cost and feasibility in this area of high rainfall. The design embodies recent design trends.

Bibliography

1. GALLOWAY, J. D., The Design of Rockfill Dams, *Trans. ASCE*, **104**, 1939; includes discussions by 25 engineers.
2. Rockfill Dams, *Trans. ASCE*, **125** (II), Rockfill Dams, 1960.
3. "Question 31—High Rockfill Dams," Eighth International Congress on Large Dams, Edinburgh, vol. III, 1964.
4. COOKE, J. BARRY, "Design, Methods of Construction, and Performance of High Rockfill Dams (above 80 m)," Eighth International Congress on Large Dams, Edinburgh, **4**, 595, 1964.
5. WEISS, Construction Technique of Passing Floods over Earth (Rockfill) Dams, *Trans. ASCE*, **116,** 1951.
6. WILKINS, J. K., The Stability of Overtopped Rockfill Dams, *Proc. 4th Austrian Congress Soil Mechanics Foundation Engineering*, 1963.
7. PARKIN, ALAN K., DAVID H. TROLLOPE, and JOHN D. LAWSON, Rockfill Structures Subject to Water Flow, ASCE Paper 4973, *J. SM Div.*, November, 1966.
8. OLIVER, H., Through and Overflow Rockfill Dams—New Design Techniques, *Proc. Inst. Civil Engrs.*, Paper 7012, 1967.

9. Steele, I. C., and J. B. Cooke, Salt Springs and Lower Bear River Concrete Face Rockfill Dams, *Trans. ASCE*, **125** (II) 74, 1960.
10. "Question 27—Sealing of Earth and Rockfill Dams with Bitumen or Other Materials," Seventh International Congress on Large Dams, Rome, vol. IV, p. 159, 1961.
11. Vencill, J. G., "Operating Experience at Taum Sauk," Conference Papers, ASCE Power Division Specialty Conference, Denver, Colo., August, 1965.
12. Old Gravity Dam Is Part of New Rockfill, *Eng. News-Record*, Nov. 18, 1965.
13. Form Climbs 72% Slope to Pave Dam Face, *Construction Methods*, December, 1965.
14. Robertson, L. M., P. W. Kiesling, and C. Waselkow, High-altitude Pumped-storage Plant to Develop 325 MW at 1190 ft Head, *Elec. World*, July 26, 1965.
15. Boughton, N. O., and G. E. A. Hale, "Foundation Studies for Cethana Arch Dam," Ninth International Congress on Large Dams, Turkey, 1967.

SECTION 20

SPILLWAYS AND STREAM-BED PROTECTION WORKS

By William J. Bauer and Earl J. Beck

DISCHARGE CAPACITY

1. Design Flood. The hydrological determination of the flood for which a spillway is to be designed is treated in Sec. 1. The operation of spillways and the methods of routing are treated in Sec. 4.

The spillway design flood is generally determined by transposing great storms, which have been known to occur in the region, over the drainage area. The resulting flood hydrographs are then determined by rational methods.

In determining discharge capacity consideration should be given to all possible contingencies. For example, one or more gates may become inoperative. Under some flood conditions operational errors may actually increase the discharge at the dam above the natural peak flow of the river. By storing too early on the rising side of the flood hydrograph, available storage space may be filled in advance of the peak inflow. Under these circumstances, it may be necessary to release a discharge in excess of the natural peak inflow.

Emergency capacity, in excess of that required to discharge the spillway design flood, may be obtained by (1) encroaching on the freeboard, which under design-flood conditions, would make adequate provision for wave action, reservoir tilt, and run-up; (2) providing emergency spillways; and (3) providing a total freeboard which would permit a sizable flood, say the flood of record, to pass over the top of the gates, if they become inoperative, without overtopping the dam. Emergency spillway capacity may be an especially important consideration in designing high fill dams which might be subject to overtopping if one or more spillway gates became inoperative. In evaluating the possible effects of emergency capacity, it must be remembered that the concurrence of maximum peak inflow, maximum wave heights, and reservoir tilt and run-up is an extremely remote possibility and that this additional freeboard may be brought into service under such conditions. In the case of fill dams requiring chute spillways, the end walls of the chutes should be high enough to convey the discharge which would result from the corresponding increase in reservoir level.

2. Approach Conditions. The term "approach conditions" as used here denotes the hydraulic properties of the water passages leading to the point of control in the spillway. For example, a chute spillway cut in one abutment at a damsite has the crest and control gates set back at some distance from the main body of the reservoir. Upstream of this control section is an excavated channel to convey water from the reservoir to the control section of the spillway. The hydraulic properties of this excavated channel would constitute the approach conditions for this case. Spillways of large capacity can produce discharges with great momentum in the approach channel. Undesirable conditions in the approach channel can reduce the spillway capacity, produce troublesome disturbances, contribute to the possibility of cavitation, prevent the satisfactory passage of floating debris through the spillway, and even produce erosion and undesirable undermining of the upstream portions of the spillway structure itself. It is important, therefore, to evaluate the approach conditions very carefully.

Analyses of approach conditions are of two general types—those performed in the design office and those performed in the hydraulic laboratory. Both are required for a large and important project as the benefits in the form of improved performance and reductions in construction costs which may be achieved through both analytical and model studies far outweigh the cost of these studies. On the other hand, for small structures it may be more economical to provide generous low-velocity approach conditions rather than invest in a model study.

The following basic principles should be given consideration when designing the approach to a spillway control structure:

1. The maximum velocity of approach under the most critical combination of reservoir elevation and discharge must not exceed the scouring velocity of the material of which the approach channel is constructed.

2. Curvature of flow in a horizontal plane should be gradual such that the central

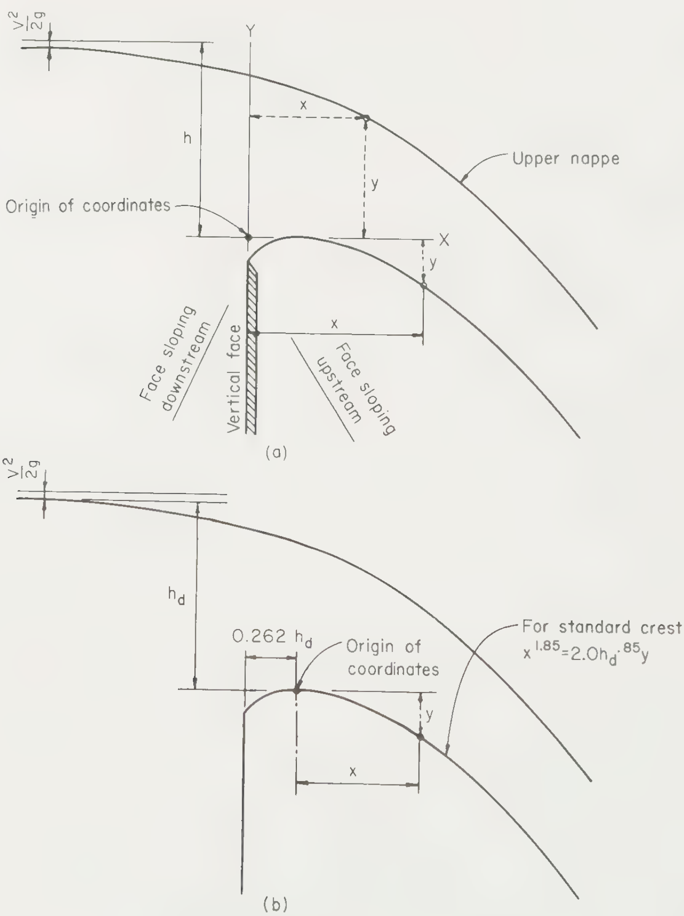

FIG. 1. Geometry of spillway crests.

acceleration would not produce an excessive differential in the water-surface elevations on opposite sides of the spillway. Excessive unbalance generates waves in the water conductors downstream from the control section which may present problems in their operation.

3. End walls which guide flow to the control structure should extend upstream from the crest to points where the velocity is low enough to avoid the development of strong vortices which would be carried over the crest. Walls can also be flared or curved at this upstream end to form, in plan, a streamlined entrance to the channel, thus avoiding the formation of vortices.

4. The depth of an approach channel should be established in combination with the design of the control structures so as to develop the most economical combination for the design capacity.

SPILLWAY CRESTS

3. Types. Nearly all spillways fall into one of six types or are made up of a combination of them: (1) overfall, (2) gates and orifice, (3) trough or chute, (4) side chan-

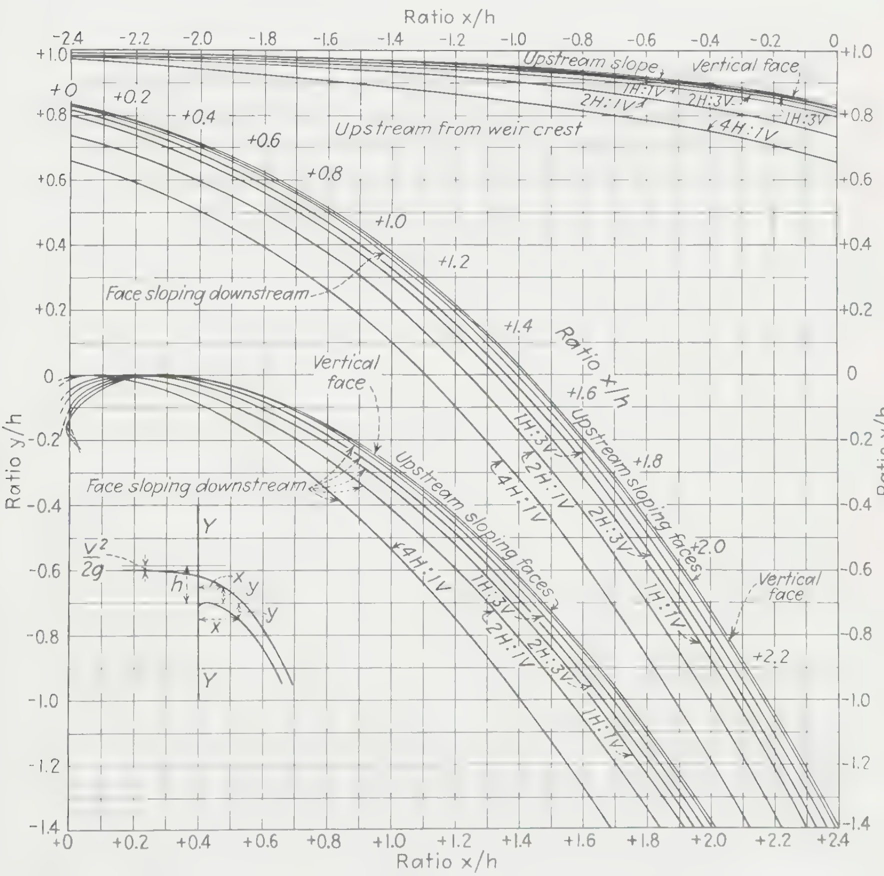

FIG. 2. Shape of upper and lower nappe for weirs with faces of various slopes.

nel, (5) shaft or glory hole, and (6) siphon. Stream-bed protection works, more or less common to all these types, are described under a separate heading.

The overfall type is by far the most common and is adapted to masonry dams that have sufficient crest length to provide the desired capacity.

Overfall spillways provided with crest gates will act as orifices under partial gate openings and as open-crest weirs under full gate openings. The same basic formulas applying to partially open Tainter and leaf gates will also apply to orifice-type gates located close to the crest.

Trough or chute spillways are commonly used for earth dams. Side-channel and shaft-spillway types are most frequently found in narrow canyons. The siphon spillway is usually used to provide automatically a nearly constant headwater level under varying flow.

OVERFALL SPILLWAYS

4. Shape of Crest. The crest of an overflow dam is frequently formed to fit the shape that the overflowing water would take for the selected design head h, as shown by Fig. 1a. Table 1 gives the ordinates of the upper and lower nappe for various slopes of the upstream face. Figure 2 shows the shape of the upper and lower nappes which correspond to the values given in Table 1. Figure 3 isolates the upper and lower

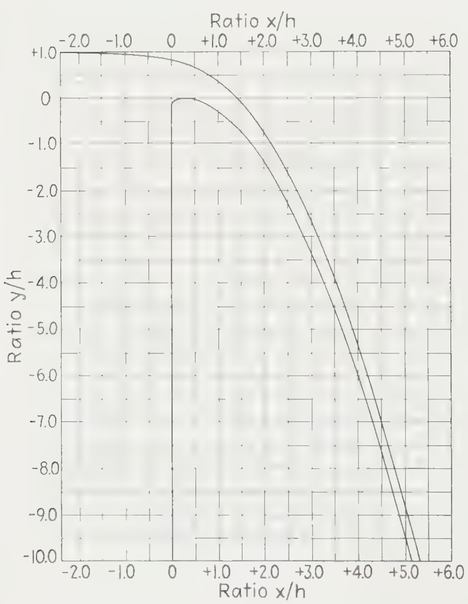

FIG. 3. Shape of upper and lower nappe for weir with vertical face.

nappes for a weir with a vertical face, for a dam of sufficient height so that the velocity of approach is negligible. Table 1 and Fig. 2 are derived from an analysis based on studies of the U.S. Bureau of Reclamation on the results of experiments by Bazin and Scimemi. As an example, if the head on the crest is 10 ft, all values taken from the curves shown by Fig. 3 should be multiplied by 10. The curves shown by Figs. 2 and 3 are expressed in terms of the design head measured from the highest point of the rounded crest. When the actual head on the crest is equal to the head for which the crest is designed, the pressure along the crest would be atmospheric for a frictionless fluid. However, with a real fluid slightly greater than atmospheric pressure results because of the developing boundary layer.

A design head greater than the actual head will push the crest surface into the

TABLE 1. NAPPE COORDINATES FOR SPILLWAY DESIGN
Lower Nappe

Horizontal coordinates x/h	Vertical coordinates y/h								
	Vertical	Weir face slope							
		Downstream					Upstream		
		$1H:3V$	$2H:3V$	$1H:1V$	$2H:1V$	$4H:1V$	$1H:3V$	$2H:3V$	$1H:1V$
0.0	− 0.125	− 0.098	− 0.066	− 0.045	− 0.012	− 0.004	− 0.159 − 0.136	−0.176 −0.136	−0.191 −0.136
0.05	− 0.066	− 0.051	− 0.032	− 0.021	− 0.002	− 0.000	− 0.080		
0.10	− 0.033	− 0.026	− 0.015	− 0.008	0.000	− 0.003	− 0.044		
0.15	− 0.014	− 0.011	− 0.005	− 0.001	− 0.002	− 0.010	− 0.022		
0.20	− 0.004	− 0.003	− 0.001	0.000	− 0.007	− 0.020	− 0.009		
0.25	0.000	0.000	− 0.001	− 0.003	− 0.014	− 0.033	− 0.002		
0.30	0.000	− 0.001	− 0.004	− 0.009	− 0.023	− 0.049	0.000		
0.35	− 0.004	− 0.005	− 0.010	− 0.018	− 0.038	− 0.068	− 0.003		
0.40	− 0.011	− 0.012	− 0.019	− 0.030	− 0.053	− 0.090	− 0.010		
0.45	− 0.021	− 0.022	− 0.031	− 0.045	− 0.072	− 0.115	− 0.020		
0.50	− 0.034	− 0.035	− 0.046	− 0.062	− 0.093	− 0.143	− 0.033	Same as 1:3 upstream slope	Same as 1:3 upstream slope
0.55	− 0.049	− 0.051	− 0.064	− 0.082	− 0.117	− 0.173	− 0.048		
0.60	− 0.066	− 0.069	− 0.084	− 0.104	− 0.141	− 0.206	− 0.065		
0.65	− 0.085	− 0.090	− 0.106	− 0.128	− 0.168	− 0.240	− 0.084		
0.70	− 0.106	− 0.113	− 0.131	− 0.154	− 0.197	− 0.277	− 0.105		
0.75	− 0.129	− 0.138	− 0.158	− 0.182	− 0.228	− 0.315	− 0.128		
0.80	− 0.157	− 0.165	− 0.187	− 0.212	− 0.261	− 0.356	− 0.153		
0.85	− 0.185	− 0.195	− 0.218	− 0.244	− 0.297	− 0.400	− 0.180		
0.90	− 0.216	− 0.227	− 0.251	− 0.278	− 0.333	− 0.443	− 0.210		
0.95	− 0.249	− 0.261	− 0.286	− 0.314	− 0.373	− 0.490	− 0.242		
1.0	− 0.283	− 0.297	− 0.323	− 0.352	− 0.413	− 0.538	− 0.277		
1.1	− 0.358	− 0.375	− 0.403	− 0.434	− 0.501	− 0.641	− 0.351		
1.2	− 0.441	− 0.461	− 0.491	− 0.524	− 0.597	− 0.752	− 0.433		
1.3	− 0.532	− 0.555	− 0.587	− 0.622	− 0.701	− 0.871	− 0.523		
1.4	− 0.631	− 0.657	− 0.691	− 0.728	− 0.813	− 0.998	− 0.621		
1.5	− 0.738	− 0.767	− 0.803	− 0.842	− 0.933	− 1.133	− 0.727		
1.6	− 0.853	− 0.885	− 0.923	− 0.964	− 1.061	− 1.276	− 0.841		
1.7	− 0.976	− 1.011	− 1.051	− 1.094	− 1.197	− 1.427	− 0.963		
1.8	− 1.107	− 1.145	− 1.187	− 1.232	− 1.341	− 1.586	− 1.093		
1.9	− 1.246	− 1.287	− 1.331	− 1.378	− 1.493	− 1.753	− 1.231		
2.0	− 1.393	− 1.437	− 1.483	− 1.532	− 1.653	− 1.928	− 1.377	Same as 1:3 upstream slope	Same as 1:3 upstream slope
2.2	− 1.711	− 1.761	− 1.811	− 1.864	− 1.997	− 2.302	− 1.693		
2.4	− 2.061	− 2.117	− 2.171	− 2.228	− 2.373	− 2.708	− 2.041		
2.6	− 2.443	− 2.505	− 2.563	− 2.624	− 2.781	− 3.146	− 2.421		
2.8	− 2.857	− 2.925	− 2.987	− 3.052	− 3.221	− 3.616	− 2.833		
3.0	− 3.303	− 3.377	− 3.443	− 3.512	− 3.693	− 4.118	− 3.277		
3.2	− 3.781	− 3.861	− 3.931	− 4.004	− 4.197	− 4.652	− 3.753		
3.4	− 4.291	− 4.377	− 4.451	− 4.528	− 4.733	− 5.218	− 4.261		
3.6	− 4.833	− 4.925	− 5.003	− 5.084	− 5.301	− 5.816	− 4.801		
3.8	− 5.407	− 5.505	− 5.587	− 5.672	− 5.901	− 6.446	− 5.373		
4.0	− 6.013	− 6.117	− 6.203	− 6.292	− 6.533	− 7.108	− 5.977		
4.2	− 6.651	− 6.761	− 6.851	− 6.944	− 7.197	− 7.802	− 6.613		
4.4	− 7.321	− 7.437	− 7.531	− 7.628	− 7.893	− 8.528	− 7.281		
4.6	− 8.023	− 8.145	− 8.243	− 8.344	− 8.621	− 9.286	− 7.981		
4.8	− 8.757	− 8.885	− 8.987	− 9.092	− 9.381	−10.076	− 8.713		
5.0	− 9.523	− 9.657	− 9.763	− 9.872	−10.173	−10.898	− 9.477		
5.2	−10.321	−10.461	−10.571	−10.684	−10.997	−11.752	−10.273		
5.4	−11.151	−11.297	−11.411	−11.528	−11.853	−12.638	−11.101		

TABLE 1. NAPPE COORDINATES FOR SPILLWAY DESIGN (*Continued*)

Upper Nappe

Horizontal coordinates x/h	Vertical coordinates y/h								
	Vertical	Weir face slope							
		Downstream					Upstream		
		$1H:3V$	$2H:3V$	$1H:1V$	$2H:1V$	$4H:1V$	$1H:3V$	$2H:3V$	$1H:1V$
−2.4	0.989	0.988	0.985	0.983	0.980	0.973	0.990	Same as 1:3 upstream slope	Same as 1:3 upstream slope
−2.2	0.987	0.986	0.981	0.977	0.972	0.957	0.988		
−2.0	0.984	0.983	0.977	0.971	0.964	0.940	0.985		
−1.8	0.980	0.979	0.971	0.964	0.955	0.922	0.981		
−1.6	0.975	0.974	0.965	0.957	0.945	0.904	0.976		
−1.4	0.969	0.968	0.958	0.949	0.934	0.885	0.970		
−1.2	0.961	0.959	0.950	0.941	0.921	0.865	0.962		
−1.0	0.951	0.948	0.939	0.930	0.904	0.842	0.953		
−0.8	0.938	0.935	0.926	0.917	0.883	0.817	0.940		
−0.6	0.921	0.918	0.908	0.899	0.858	0.788	0.923		
−0.4	0.898	0.895	0.885	0.875	0.826	0.754	0.900		
−0.2	0.870	0.865	0.853	0.841	0.786	0.712	0.872		
0.0	0.831	0.826	0.811	0.796	0.737	0.659	0.833		
0.05	0.819	0.814	0.798	0.783	0.723	0.643	0.822		
0.10	0.807	0.802	0.785	0.768	0.708	0.627	0.810		
0.15	0.793	0.788	0.770	0.752	0.692	0.610	0.796		
0.20	0.779	0.774	0.755	0.736	0.675	0.591	0.782		
0.25	0.763	0.758	0.739	0.719	0.657	0.572	0.766		
0.30	0.747	0.742	0.721	0.700	0.638	0.550	0.750		
0.35	0.730	0.724	0.702	0.680	0.617	0.528	0.733		
0.40	0.710	0.704	0.681	0.659	0.596	0.504	0.713		
0.45	0.690	0.683	0.659	0.636	0.572	0.480	0.693		
0.50	0.668	0.661	0.637	0.613	0.549	0.452	0.671		
0.55	0.646	0.638	0.613	0.588	0.523	0.424	0.650		
0.60	0.621	0.612	0.587	0.562	0.497	0.394	0.625		
0.65	0.596	0.586	0.560	0.535	0.470	0.363	0.600		
0.70	0.568	0.558	0.531	0.505	0.439	0.330	0.572		
0.75	0.539	0.529	0.501	0.475	0.408	0.298	0.543		
0.80	0.509	0.498	0.470	0.442	0.375	0.261	0.513		
0.85	0.478	0.466	0.438	0.409	0.340	0.223	0.482		
0.90	0.444	0.431	0.402	0.373	0.303	0.183	0.449		
0.95	0.410	0.395	0.366	0.337	0.264	0.141	0.415		
1.0	0.373	0.358	0.327	0.297	0.223	0.098	0.379		
1.1	0.295	0.278	0.245	0.214	0.135	0.005	0.302		
1.2	0.210	0.191	0.156	0.124	0.039	−0.096	0.218		
1.3	0.118	0.097	0.060	0.026	−0.065	−0.205	0.127		
1.4	0.019	−0.005	−0.044	−0.080	−0.177	−0.322	0.029		
1.5	−0.088	−0.115	−0.156	−0.194	−0.297	−0.447	−0.077		
1.6	−0.203	−0.233	−0.276	−0.316	−0.425	−0.580	−0.191		
1.7	−0.326	−0.359	−0.404	−0.446	−0.561	−0.721	−0.313		
1.8	−0.457	−0.493	−0.540	−0.584	−0.705	−0.870	−0.443		
1.9	−0.596	−0.635	−0.684	−0.730	−0.857	−1.027	−0.581		
2.0	−0.743	−0.785	−0.836	−0.884	−1.017	−1.192	−0.727		
2.2	−1.061	−1.109	−1.164	−1.216	−1.361	−1.546	−1.043		
2.4	−1.411	−1.465	−1.524	−1.580	−1.737	−1.932	−1.391		
2.6	−1.793	−1.853	−1.916	−1.976	−2.145	−2.350	−1.771		
2.8	−2.207	−2.273	−2.340	−2.404	−2.585	−2.800	−2.183		
3.0	−2.653	−2.725	−2.796	−2.864	−3.057	−3.282	−2.627		
3.2	−3.131	−3.209	−3.284	−3.356	−3.561	−3.796	−3.103		
3.4	−3.641	−3.725	−3.804	−3.880	−4.097	−4.342	−3.611		
3.6	−4.183	−4.273	−4.356	−4.436	−4.665	−4.920	−4.151		
3.8	−4.757	−4.853	−4.940	−5.024	−5.265	−5.530	−4.723		
4.0	−5.363	−5.465	−5.556	−5.644	−5.897	−6.172	−5.327		
4.2	−6.001	−6.109	−6.204	−6.296	−6.561	−6.846	−5.963		
4.4	−6.671	−6.785	−6.884	−6.980	−7.257	−7.552	−6.631		
4.6	−7.373	−7.493	−7.596	−7.696	−7.985	−8.290	−7.331		
4.8	−8.107	−8.233	−8.340	−8.444	−8.745	−9.060	−8.063		
5.0	−8.873	−9.005	−9.116	−9.224	−9.537	−9.862	−8.827		
5.2	−9.671	−9.809	−9.924	−10.036	−10.361	−10.696	−9.623		
5.4	−10.501	−10.645	−10.764	−10.880	−11.217	−11.562	−10.451		

theoretical nappe and result in greater pressure along the curved surfaces and in lower discharge capacities. Conversely, a design head lower than the actual head pulls the crest surface below the theoretical nappe, resulting in subatmospheric pressures over some portion of the crest curve. At the same time the discharge capacity of such a crest curve is increased. Excessive subatmospheric pressures can result in pulsating, inefficient spillway operation, and possibly damage to the structure as a result of cavitation. A certain amount of subatmospheric pressure can be attained without

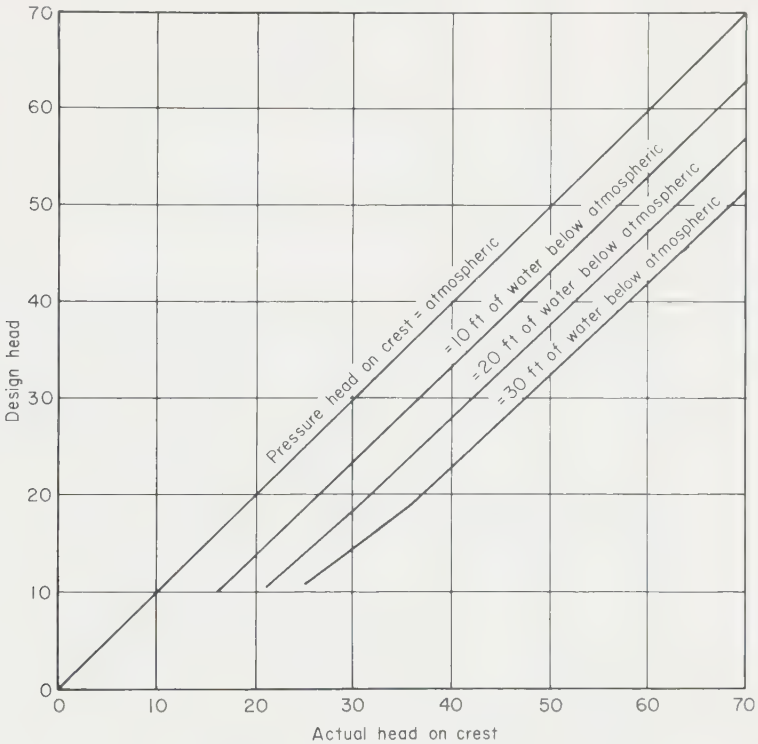

FIG. 4. Minimum pressure on crest as function of heads.

undesirable effects. Figure 4 provides a guide for determining the minimum pressures on the crest for various ratios of design head and actual head on the crest.

Designing the crest shape to fit the nappe for a head less than maximum head expected often results in economies in construction. The resulting increase in unit discharge may make possible a shortening of the crest length, or a reduction in freeboard allowance for reservoir surcharge under extreme flood conditions.

Because the occurrence of design floods is usually so infrequent, several water-control agencies design spillway crests which are fitted to the lower nappe of a head which is 75 percent of that resulting from the actual discharge capacity. Tests have shown that the subatmospheric pressures on a nappe-shaped crest do not exceed about one-half of the design head when the design head is not less than about 75 percent of the maximum head.[1] An approximate diagram of the subatmospheric pressures, as

[1] "Design of Small Dams," p. 282, U.S. Bureau of Reclamation.

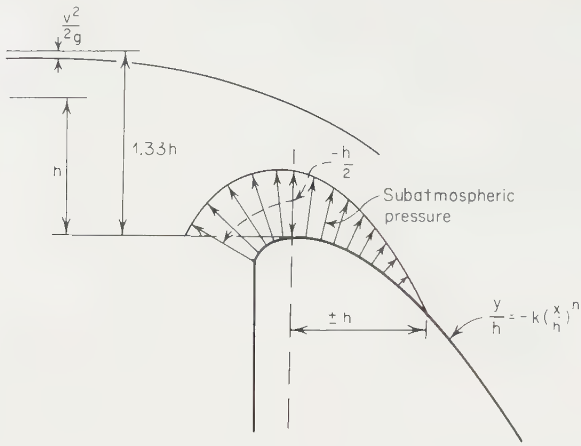

Fig. 5. Subatmospheric crest pressures ratio.

determined from model tests, is shown by Fig. 5. Figure 4 shows the manner in which the minimum pressure varies with the particular actual and design heads adopted for a given spillway. The minimum crest pressure must be greater than cavitation pressure. It is suggested that the minimum pressure allowable for design purposes be 20 ft of water below sea-level atmospheric pressure and that the altitude of the project site be taken into account in making the calculation. For example, assume a site where the atmospheric pressure is 5 ft of water less than sea-level pressure, and in which the maximum head contemplated is 60 ft; then, only 15 additional feet of subatmospheric pressure is allowable. Entering Fig. 4 with an actual head of 60 ft and an allowance of 15 ft of subatmospheric pressure, read the design head to be 50 ft. This is seen to be greater than the 45 ft which would be used under the $0.75 = h_d \div h_a$ rule; so that consideration of cavitation potential governs in this instance.

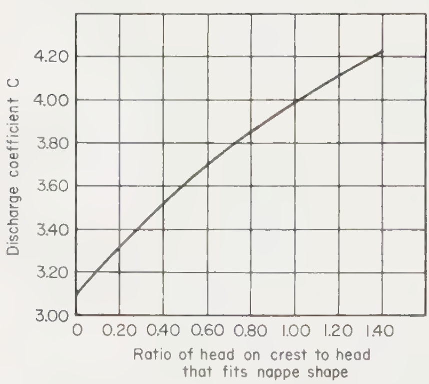

Fig. 6. Discharge coefficients.

An overfall spillway crest which approximates closely the lower portion of a jet issuing from a sharp-crested weir is designated as a standard crest. A curve plotted from the formula

$$x^{1.85} = 2.0h_d^{0.85}y \tag{1}$$[1]

as shown by Fig. 1b, fits very closely to the curve of the standard crest.

5. Overfall Spillway, Discharge Coefficients. The discharge for an overfall spillway of nappe shape varies as the following equation:

$$Q = CLh^{3/2} \tag{2}$$

[1] Hydraulic Design Criteria, Sheets 111-1 and 2, Corps of Engineers.

in which Q = total discharge over the spillway, cfs
L = net length of spillway, ft
h = total head on crest including velocity head, $V^2/2g$
C = coefficient of discharge

The results of model tests (Fig. 6) show that the discharge coefficient starts at 3 and reaches approximately 4 at the design head. End contractions at spillway piers reduce the net length between the pier faces. Equation (2) would then be modified as follows:

$$Q = C(L - kNh)h^{3/2} \tag{3}$$

in which k = pier-contraction coefficient
$h = h_d + V^2/2g$
L = net length between piers
V = velocity of approach
N = number of complete pier contractions (two per pier)

Figure 7[1] shows the effect of three commonly used pier shapes on the coefficient of

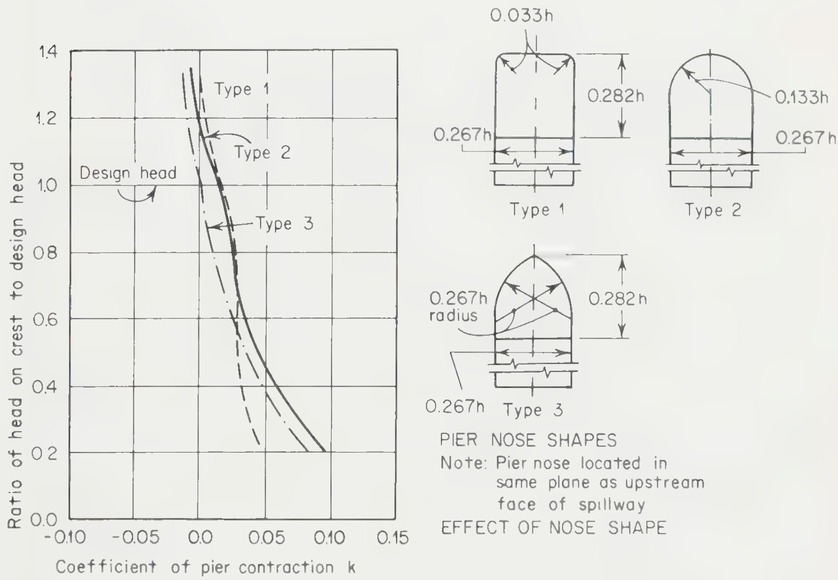

FIG. 7. Effect of pier nose shape.

pier contraction k for various ratios of head on crest to design head.

As a basis for design, spillway discharge coefficients are usually determined by model tests. Figure 8 shows the results of such tests for the spillway of the Chief Joseph Dam and Fig. 9 for those of the McNary Dam. Both these dams are on the Columbia River. The spillway of the Chief Joseph Dam is a concrete, gravity, ogee section with 19 bays, 40 ft wide, separated by piers 9 ft wide. The drop from the crest at elevation 901.5 to the stilling-basin floor is 158.5 ft. The spillway is designed to pass 1,250,000 cfs with a maximum head of 55.4 ft. The McNary spillway consists of

[1] Hydraulic Design Criteria Hydraulic Design Chart 111-5, Corps of Engineers.

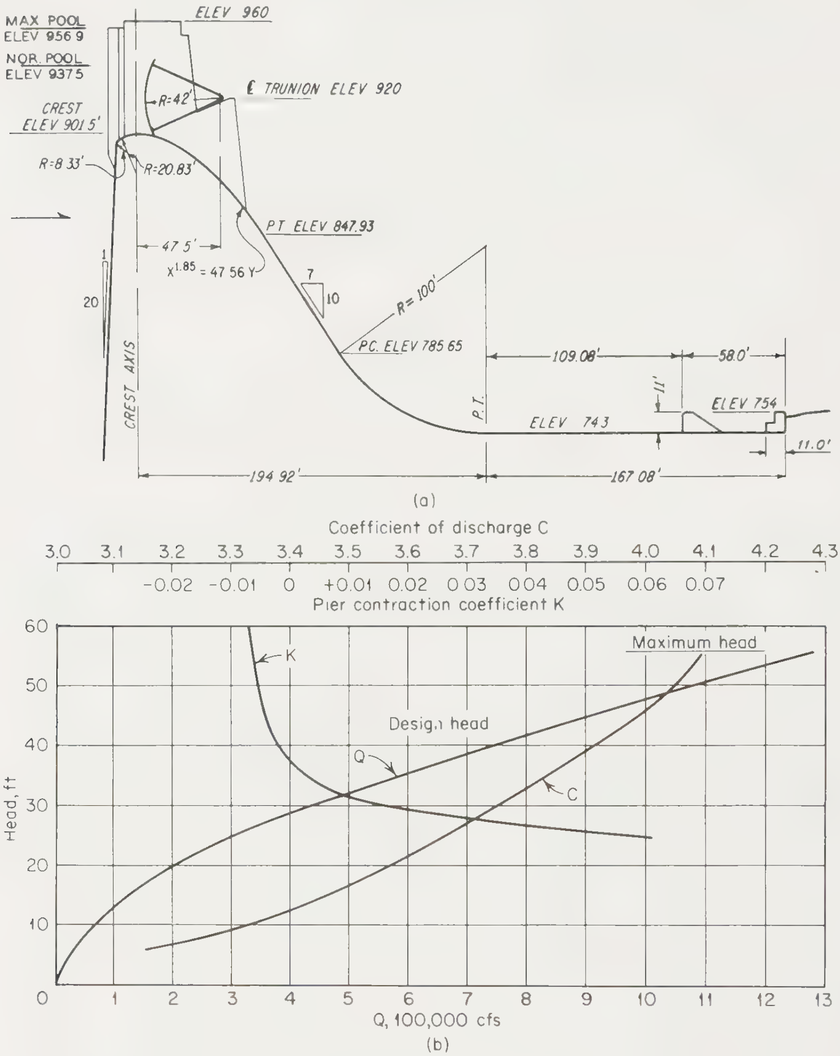

FIG. 8. Chief Joseph spillway. (*a*) Section of spillway. (*b*) Characteristics.

twenty-two 50-ft-wide bays with 10-ft-wide piers. It is designed to pass 2.2 million cfs with a maximum head of 65.5 ft on the spillway crest.[1]

Figure 10 shows the discharge coefficients obtained by model tests of the spillways of the Tennessee Valley Authority dams, and Fig. 11 shows the principal features of these spillways.[2]

Flow conditions both upstream and downstream from the controls are also factors

[1] WEBSTER, MARVIN J., Spillway Design for Pacific N.W. Projects, *Proc. ASCE, J. Hydraulic Div.*, August, 1959.

[2] KIRKPATRICK, KENNETH W., Discharge Coefficients for Spillways at TVA Dams, *Trans. ASCE*, **122**, 190, 1957.

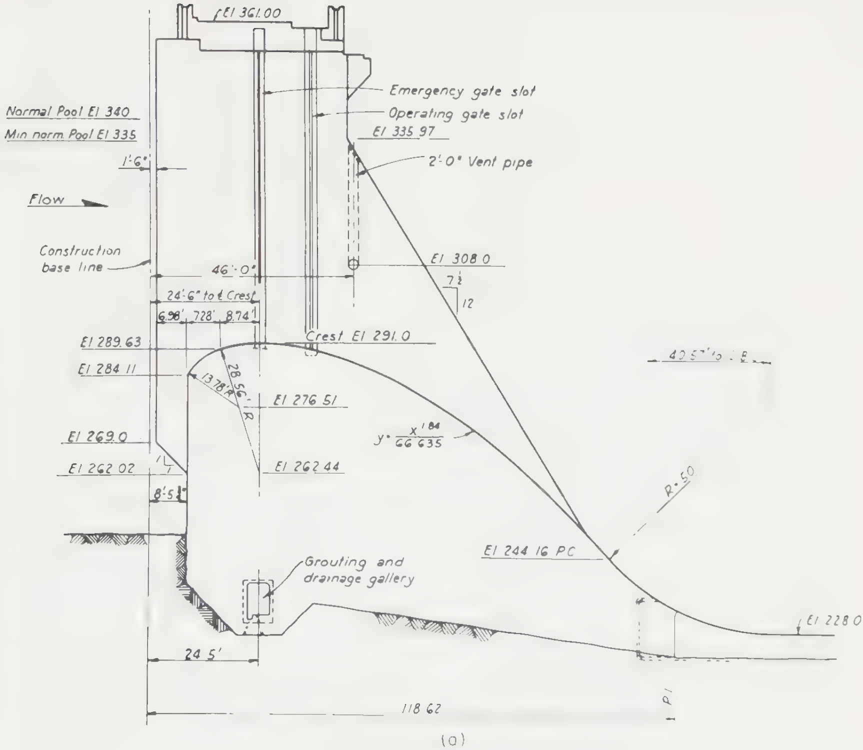

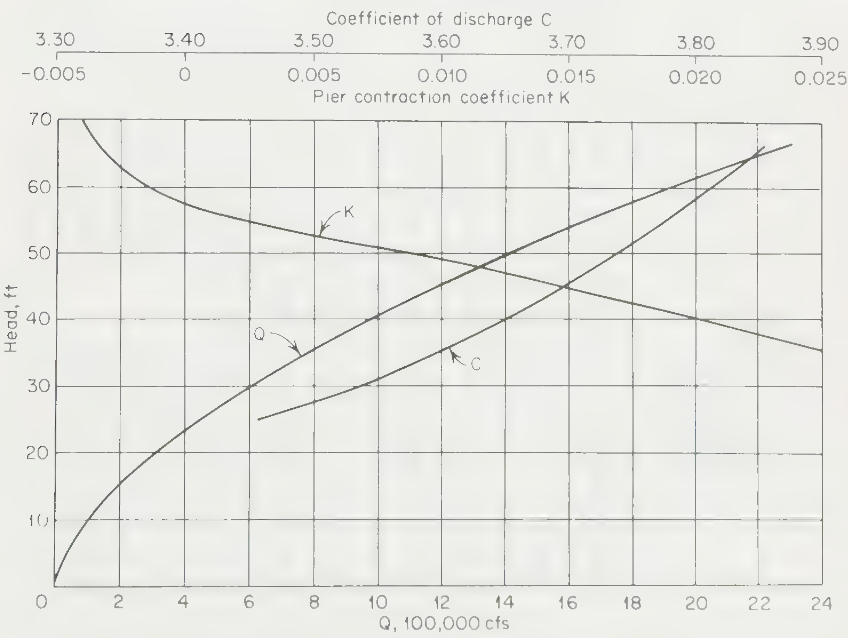

FIG. 9. McNary spillway. (*a*) Section of spillway. (*b*) Characteristics.

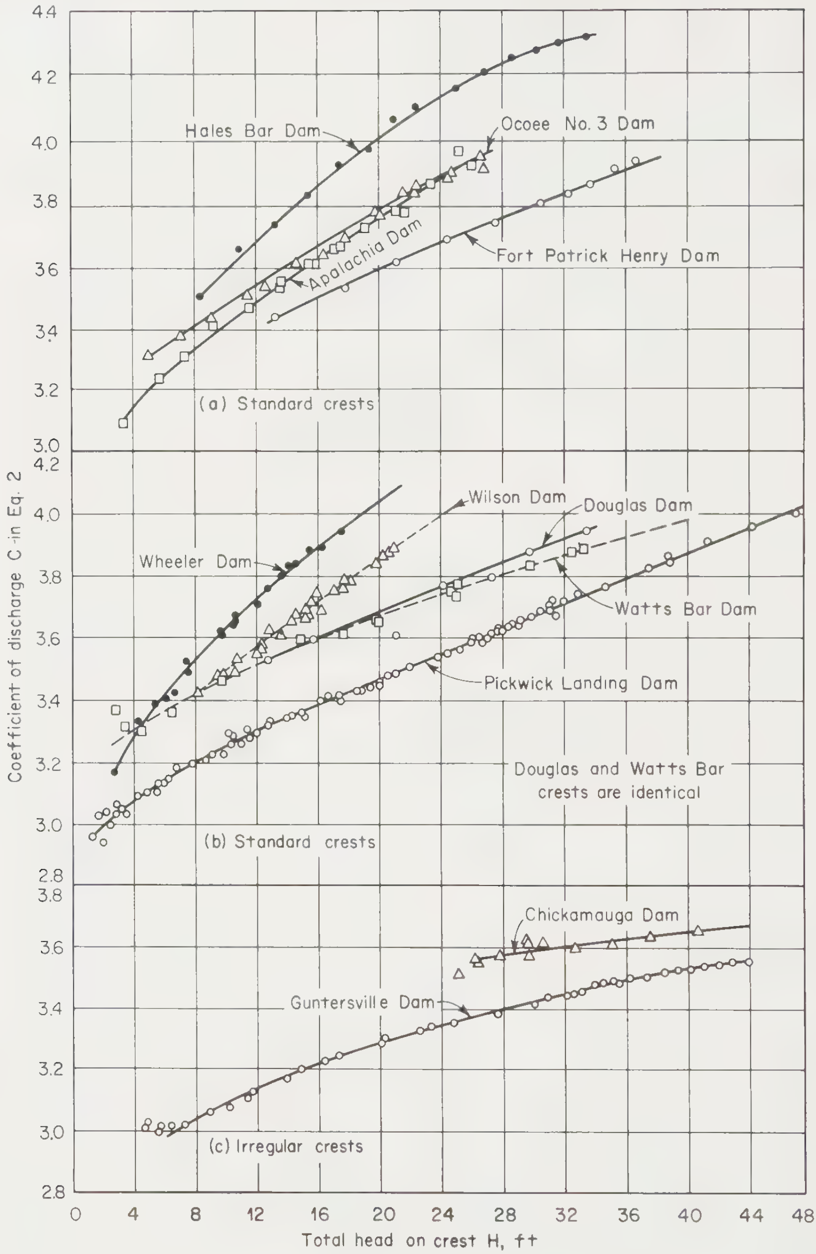

FIG. 10. Tennessee Valley Authority spillways. (*From Trans. ASCE, vol.* 122, 1957.)

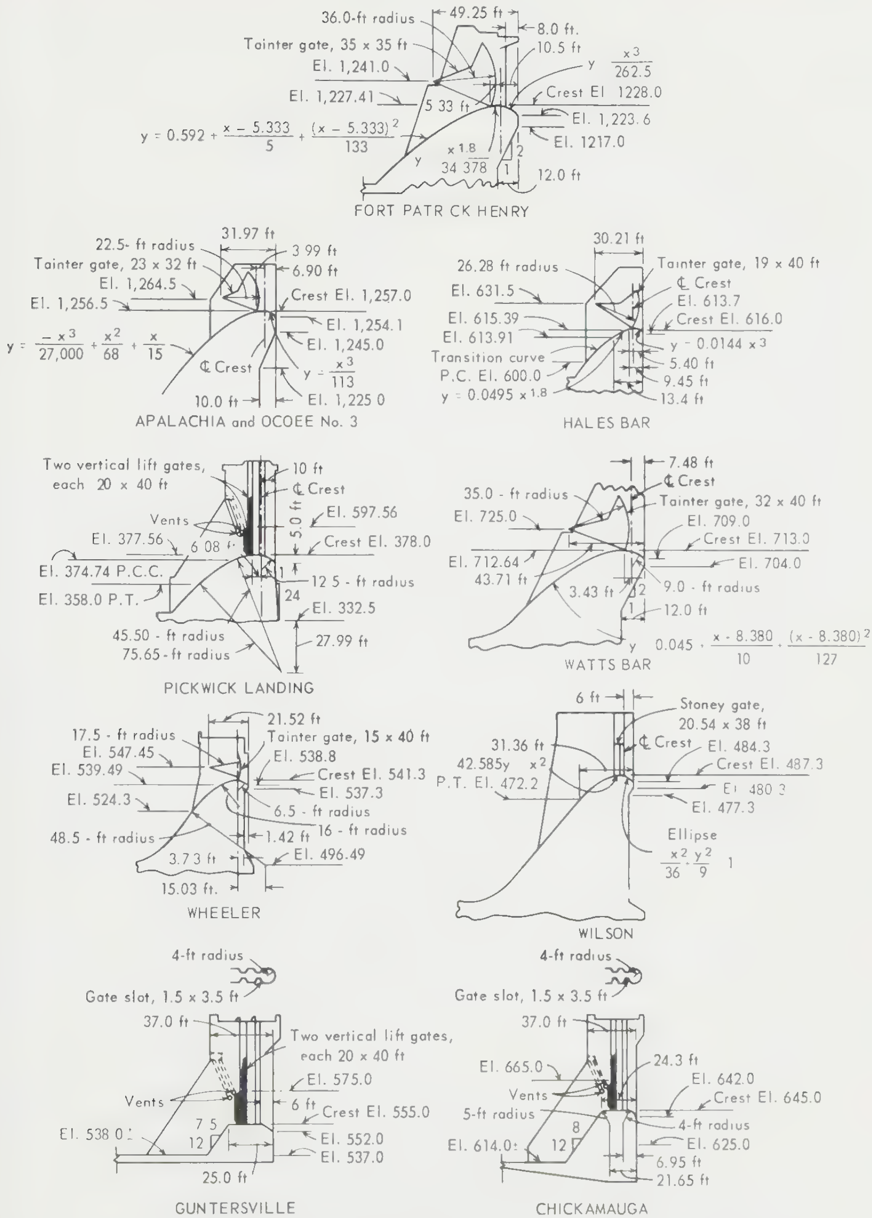

FIG. 11. Tennessee Valley Authority spillway crests. (*From Trans. ASCE vol.* 122, 1957.)

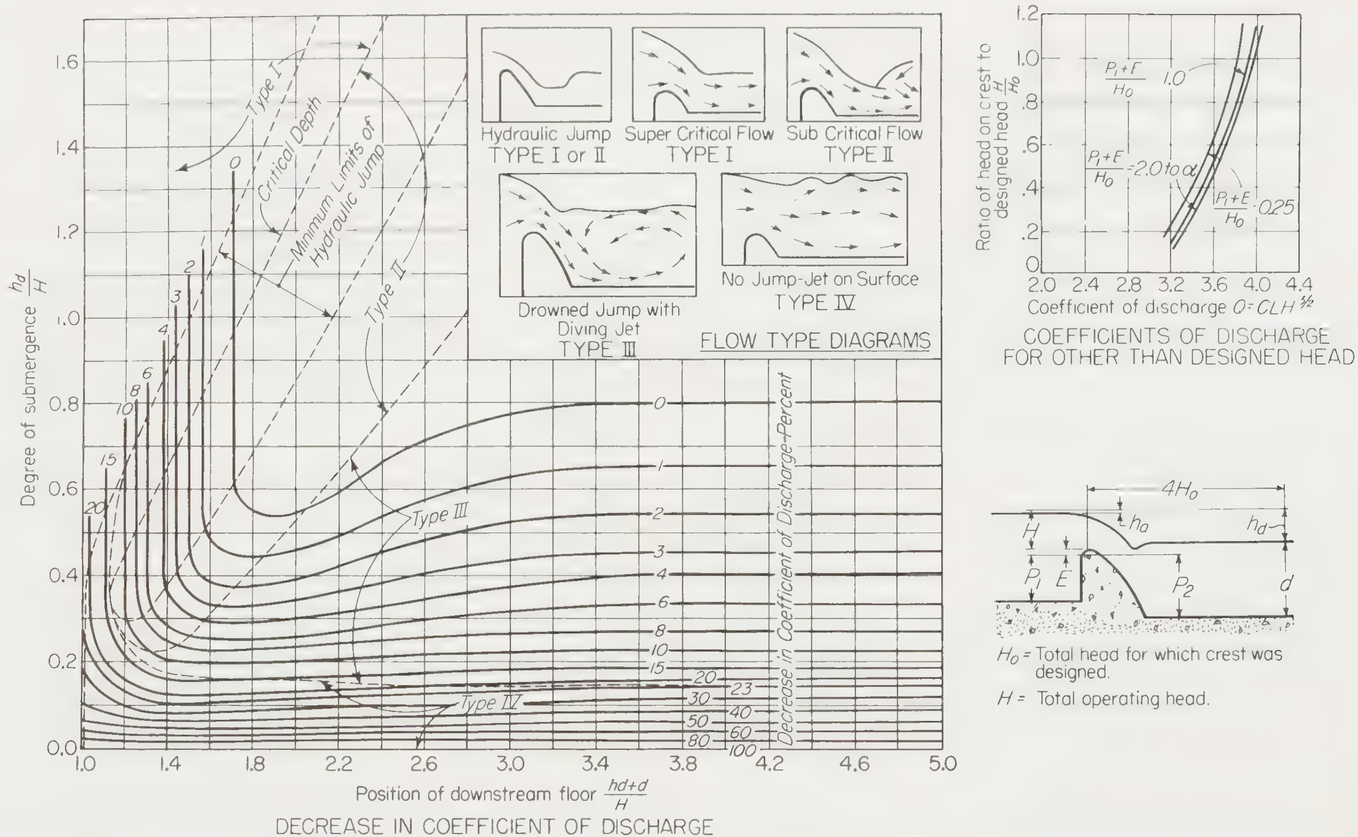

FIG. 12. Discharge coefficients for various approach depths and degrees of submergence. (*From "Boulder Canyon Projects, Final Reports," Part VI, Hydraulic Investigations, Bulletin 3, Studies of Crests for Overfall Dams, Fig. 44, p. 150, U.S. Bureau of Reclamation.*)

which may influence the discharge capacity. The depth of approach, friction losses in approach channels, downstream convergence, and downstream submergence are examples of factors which must be taken into consideration. Figure 12 shows the effect on discharge coefficients for various depths of approach and for downstream submergence.

GATED AND ORIFICE SPILLWAYS

6. Gate-controlled Ogee Crests. Releases for partial openings of gates controlling the discharge over ogee crests will occur as orifice flow. With the gate open a small amount under full head, the path of the jet can be expressed by the parabolic equation

$$-y = \frac{x^2}{4h} \tag{4}$$

where h is the head on the center of the opening.

For an orifice inclined at an angle θ from the vertical, the equation will be

$$-y = x \tan\theta + \frac{x^2}{4h \cos^2\theta} \tag{5}$$

The adoption of a jet-trajectory profile rather than a nappe profile will result in a wider ogee and in reduced discharge efficiency for full gate opening. Where the ogee is shaped to the ideal nappe profile, subatmospheric pressures may be reduced by placing the gate sill a short distance downstream from the crest.

The discharge for a gated ogee crest at partial gate openings, in cases where the openings are large, may be computed by the equation

$$Q = \tfrac{2}{3}\sqrt{2g}\, cL(h_1^{3/2} - h_2^{3/2}) \tag{6}$$

In some cases it may be convenient to express $\left(\frac{2}{3}\sqrt{2g}\, c\right)$ as an overall coefficient m as in Eq. (7).

The orifice discharge coefficient c will differ with different gate and crest arrangements. This coefficient is also affected by the approach and downstream conditions as they influence the jet contractions. Thus the contractions for a vertical leaf gate will differ from those for a curved inclined radial gate. Figure 13 shows the approximate

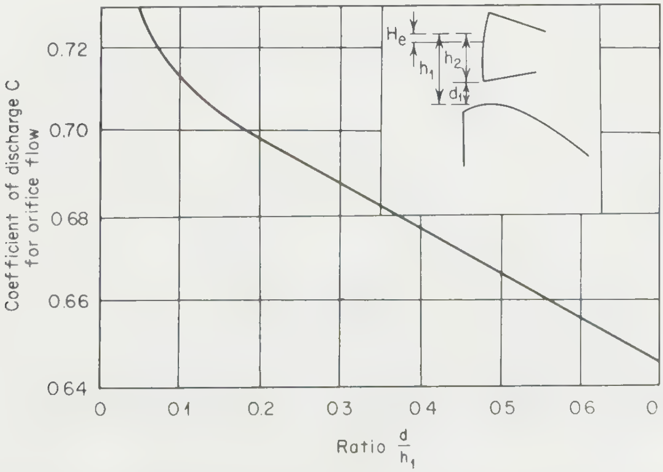

FIG. 13. Approximate coefficients of orifice discharge. *(From "Design of Small Dams," p. 284, U.S. Bureau of Reclamation.)*

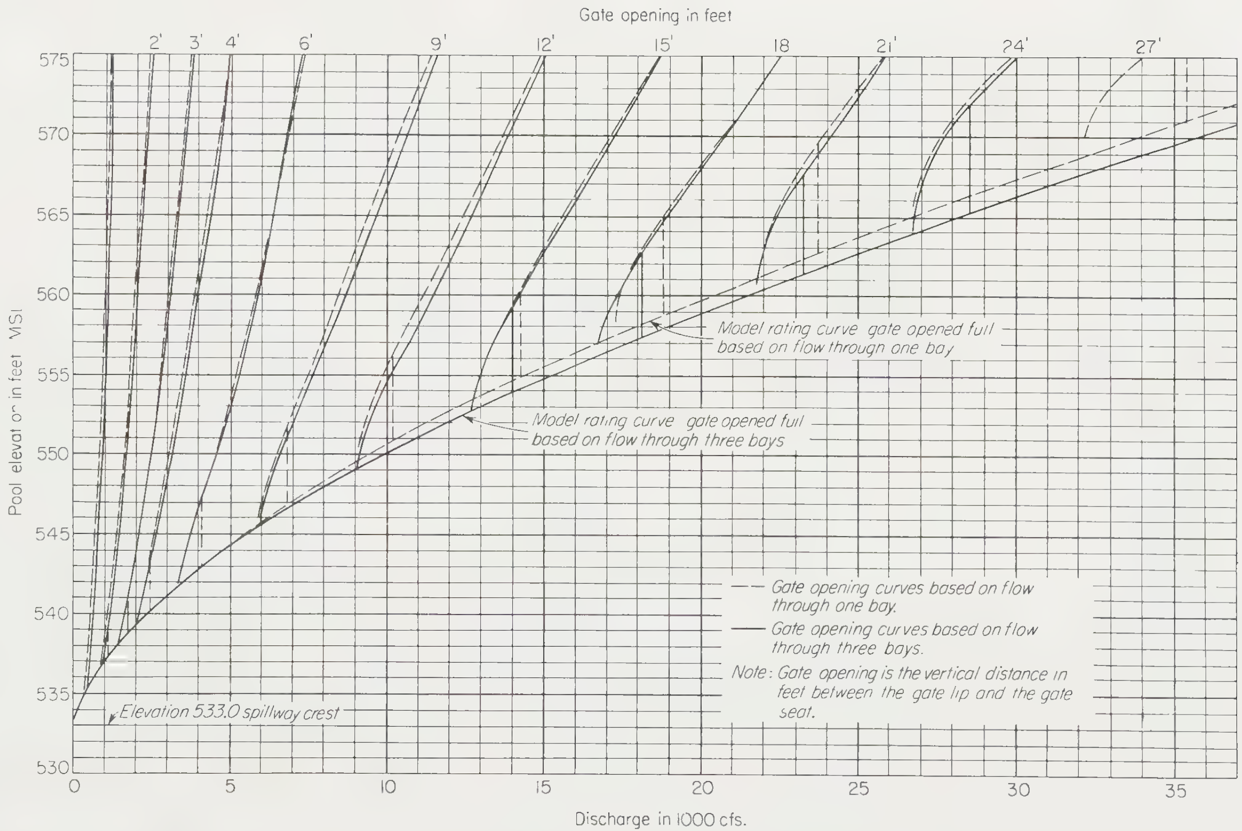

FIG. 14. Discharge rating curves from hydraulic-model study of one 40- by 38-ft Tainter gate.

coefficients of orifice discharge c for various ratios of gate openings d to total head h_1.

The rating curves for gate-controlled crests with partial gate openings are usually determined from model tests. Figure 14 shows typical discharge rating curves from a hydraulic model study for a 40-ft-wide by 38-ft-high Tainter gate.

The basic formula for spillway discharge, used in analyzing prototype measurements for a spillway, with a vertical leaf gate operating at partial opening, is

$$Q = mL(h_1^{3/2} - h_2^{3/2}) \tag{7}$$

in which h_1 = head on upper edge, ft
h_2 = head on lower edge, ft
L = net length, ft
m = coefficient of discharge = $\frac{2}{3}\sqrt{2g}\,c$ [in Eq. (6)]

m will not be identical with C in Eqs. (2) and (3) except where there is free overfall.

Interesting prototype experiments were conducted at Wilson Dam, Alabama, to determine the values of m.[1] These measurements were made at the dam with various heights of gate openings and with various combinations of gates in operation.

The spillway section of the Wilson Dam consists of a gravity overflow dam with the permanent crest about 80 ft above the stream bed. Flow is controlled by 58 gates 18 ft high by 38 ft wide. The piers are 8 ft thick. The pier noses are circular in form and flush with the upstream face of the dam.

Figure 15 shows the rating curve and discharge coefficients for two operating conditions: (1) with adjacent gates completely closed and (2) with adjacent gates completely open. Both sets of tests were made with the pool surface held constant at 18 ft above the permanent crest. The value of h_1 should not be taken as the distance

[1] PULS, LOUIS G., Spillway Discharge Coefficients of Wilson Dam, *Trans. ASCE*, **91**, 316, 1931.

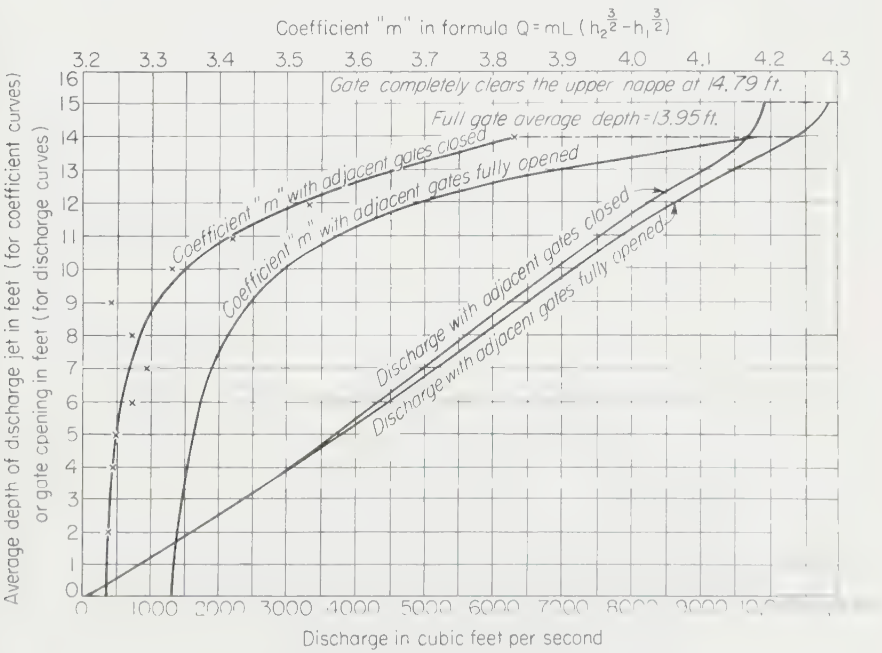

FIG. 15. Spillway rating curve, Wilson Dam.

from the pool level down to the point where the gate clears the water, but rather it should be equal to the head on the crest minus the depth of the discharging jet.

7. Design of Piers. The hydrostatic water pressures acting on the pier sides resulting from one gate discharging under maximum head, and with one or more adjacent gates closed, will result in lateral loadings which must be transferred to other parts of the structure. The thickness and reinforcement of the piers must be adequate to withstand, at acceptable factors of safety, the resulting bending and shearing stresses. Pier thicknesses usually range between 9 and 15 ft. The anchorages which transfer water loads to the piers from the crest gates will also be a factor in determining pier widths. Piers may also contain aeration ducts and serve other purposes such as supporting highway bridges and hoist or crane structures.

It is sometimes desirable to taper the downstream ends of spillway piers to provide for the gradual spreading of the discharge. When this is done, care must be taken to avoid negative pressures which could result in cavitation along the pier sides.

The possibility that cavitation may occur under high-velocity conditions at pier slots should be given consideration. Comprehensive studies of pier-slot design have been made by the U.S. Army Engineers and the Bureau of Reclamation.[1]

Figure 16 shows the design of the slots adopted for the McNary Dam on the Columbia River.

8. Orifice Spillways. One means of providing a submerged control is with an orifice-type spillway. This type may be designed to discharge as an orifice under

[1] BALL, J. W., Hydraulic Characteristics of Gate Slots, *Proc. ASCE, Hydraulics Div.*, October, 1959.

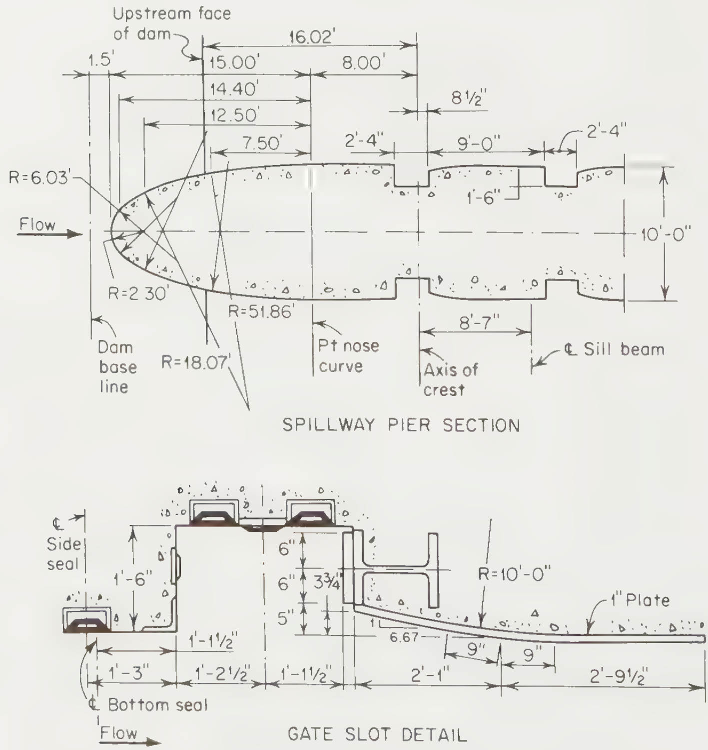

FIG. 16. Design of slots adopted for the McNary Dam. (*From Marvin J. Webster, Spillway Design for Pacific N.W. Projects, Proc. ASCE, J. Hydraulic Div., August, 1959.*)

partial gate openings and as an overflow spillway with an ogee crest under full gate opening. By moving the gate downstream from the axis and providing an adequate headwall, the spillway gate may be designed to control a head much higher than the gate height. By way of illustration, a 50-ft-high gate could be designed to control the discharge from a 100-ft head on the crest of an ogee-type spillway. The discharge resulting from this orifice-overflow combination would be approximately 4,000 cfs per lin ft of opening. In comparison with 50-ft gates mounted on the crest, assuming 10 ft surcharge, the discharge would be approximately half of that of the orifice-overflow combination. The length of the spillway could be reduced proportionately. At sites such as that at Mangla Dam on the Indus River (described elsewhere), where only a limited area and relatively short length of suitable foundation material are available for the spillway structure, the orifice-type spillway offered the most economic means of passing the design flood. It should be noted, however, that the orifice type results in high flow concentration, which will increase the size and cost of energy-dissipation works below.

The gates controlling orifice discharge would be opened fully only under the extremely rare occurrence of design-flood conditions. Under all other conditions the partially opened gates would discharge as orifices. The orifice-type gate offers the advantages of permitting a deep reservoir drawdown in advance of floods. In some situations these gates may be designed to serve both as spillway gates and as reservoir outlets. Either radial or vertical lift gates are usually used to control the discharge from the orifice-type spillway. Because of higher heads the gates are much heavier than a crest gate of equal size.

The spillway of the Roseires Dam on the Blue Nile River, constructed for the Republic of Sudan, is provided with seven 10-m-wide by 13-m-high spillway radial control gates operating under a design head of 28.5 m as shown by Fig. 17,[1] and by five 6.0-m-wide by 11.1-m-high sluice radial control gates which operate under a design head of 55.1 m as shown by Fig. 18. The high-level spillway will operate as an orifice during partial gate openings and as an ogee spillway when the gates are opened fully. The concrete headwall reduces the height of the radial gates by 4.5 m and increases the range of flows discharged by orifice action.

The water passages leading to the orifice outlet must be formed so as to minimize entrance vortices and negative pressures. The water passages for the Mangla orifice-type spillway (Fig. 19) were shaped after extensive model tests had been made on the headworks structure. Mangla Dam is located on the Jhelum River in West Pakistan.

[1] Ten-mile-long Dam Will Reinforce Sudan's Cottonpicking Economy, *Eng. News-Record*, June 3, 1965.

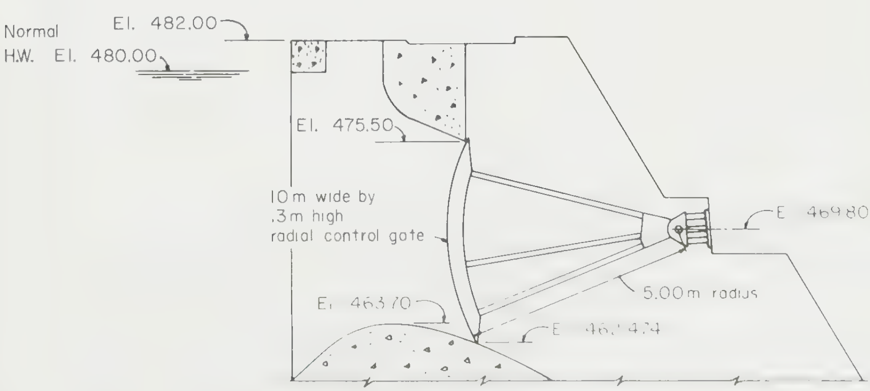

FIG. 17. Spillway, Roseires Dam, Blue Nile River, Republic of Sudan.

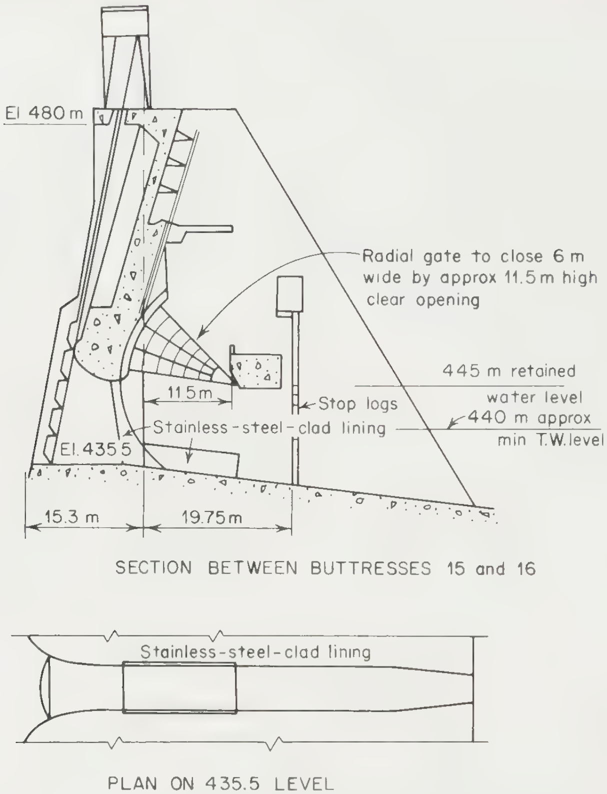

FIG. 18. Low-level outlet, Roseires Dam, Republic of Sudan. (*Courtesy of Sir Alexander Gibb and Partners, London.*)

The location and length of the spillway structure were limited by foundation conditions. The design flood assigned to the orifice structure of 1.1 million cfs will be controlled by nine 40-ft-high by 36-ft-wide radial gates. For a discharge of 1 million cfs mean velocity of flow in the water passage increases from 11 fps at the entrance to 66 fps at the exit from the gate openings. It may be noted in Fig. 19 that the concave-upward curvature of the streamlines is accomplished in the lower-velocity zones upstream from the gate, followed by a zone in which the streamlines curve concave downward, thus overcoming in the higher-velocity zones a tendency to form sub-atmospheric pressures on the roof. Model tests revealed that pressures on the sides, floor, and roof of the water passage were positive under all operating conditions.

TROUGH OR CHUTE SPILLWAYS

9. Features. The chute is the commonest type of water conductor used for conveying flow between control structures and energy dissipators. Chutes can be formed on the downstream face of gravity dams, cut into rock abutments and either concrete-lined or left unlined and built as free-standing structures on foundations of rock or soil.

One of the commonest causes of spillway failures has been the improper design of chutes. The flow in a chute is usually supercritical; in many cases the velocity is

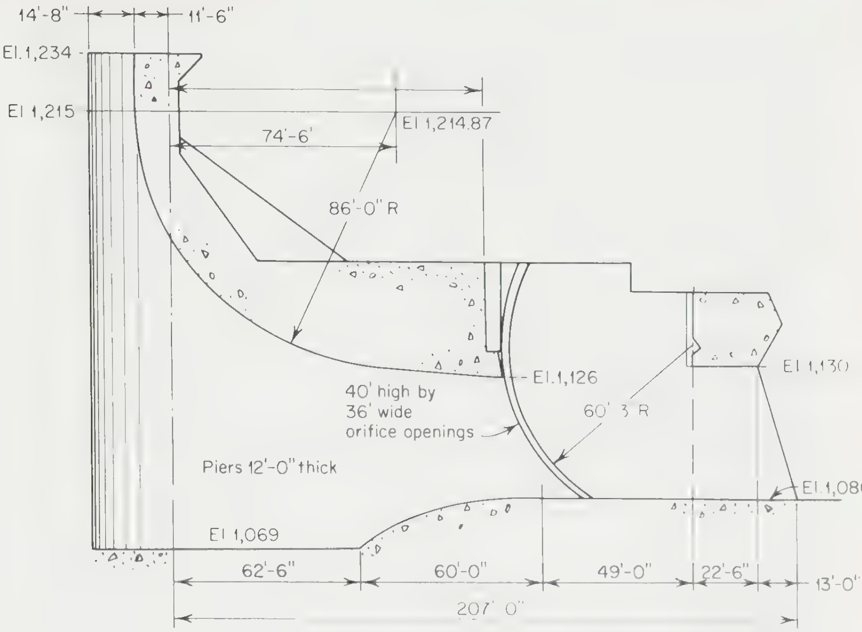

FIG. 19. Mangla Dam spillway, West Pakistan.

greater than 100 fps. As a result of the large dynamic forces, the structural and hydraulic design of the chute is a critical factor. Criteria governing the profile of the ogee are well known and commonly adhered to, but the necessity of correct shaping of the guide walls in plan is often overlooked.

10. Principles of Design. Water flowing down a steep chute and colliding with an improperly aligned guide wall will produce standing waves, piling up of water against walls, overtopping, excessive dynamic impact, cavitation, poor bucket action, and other adverse effects.

In general, the following principles should govern design: (1) nearly all guiding or changing direction of water should be limited to locations upstream from the control structure where velocities are comparatively low; (2) the alignment of the flow should usually be as straight and symmetrical as possible once the water is accelerated.

The velocity of water increases rapidly as it passes over the control structure. Downstream of the ogee crest the velocities become supercritical and increase with drop in elevation. Therefore, any changes in alignment of the walls downstream of the crest must be handled with extreme caution. Chute alignment for high-velocity flow can be curved in the lower reaches only if the chute floor and walls are shaped adequately to force water into a turn without overtopping the walls.

Since the width of a spillway is established by the required discharge at the controlling section near the crest, quite often the control section will be larger than the remaining chute, requiring a transition section between the two. In other cases, it is possible to limit the width of the control section by providing deep gates or submerged orifice gates with headwall. The width of the chute is limited by topography, construction cost, and width of the river channel into which it discharges. The transition between the control section and the chute should be governed by the following considerations: (1) the convergence should be symmetrical to balance hydraulic forces;

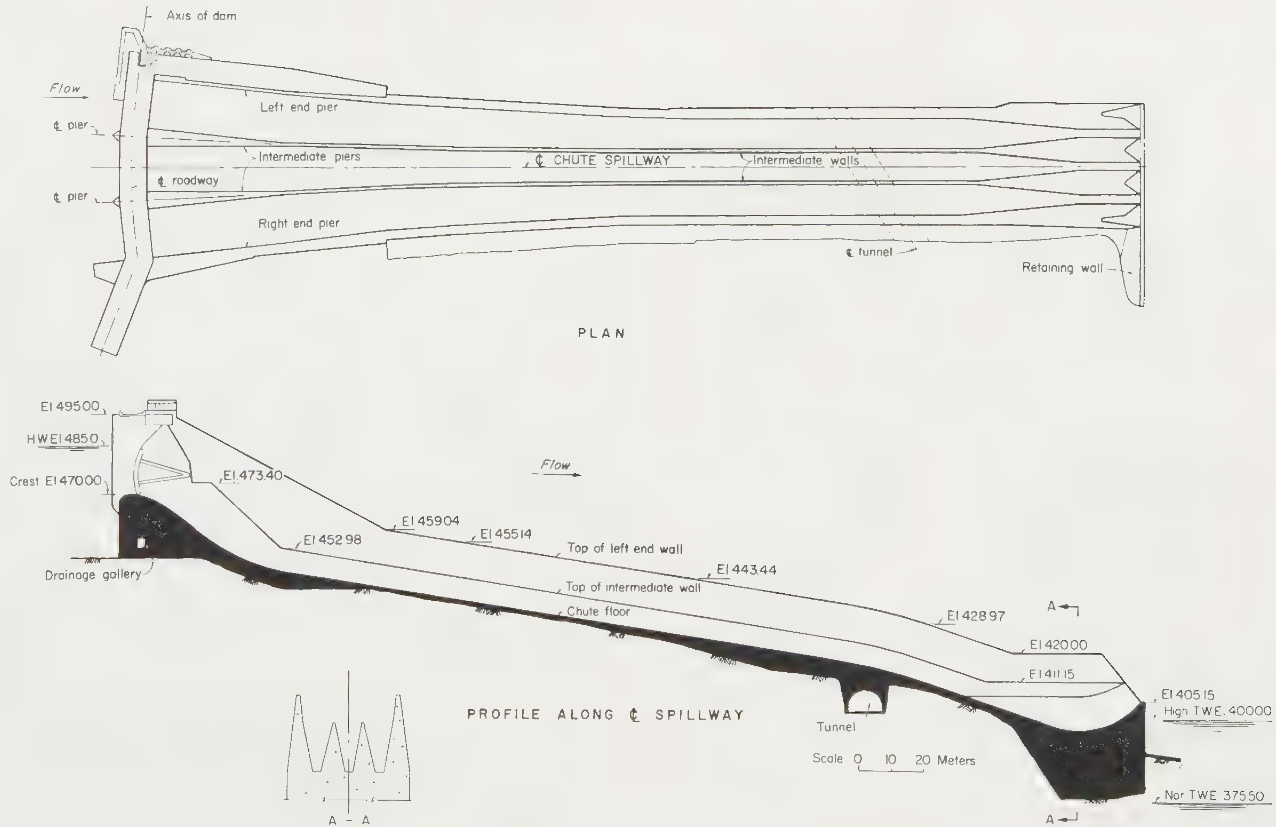

FIG. 20. Derbendi Khan Dam.

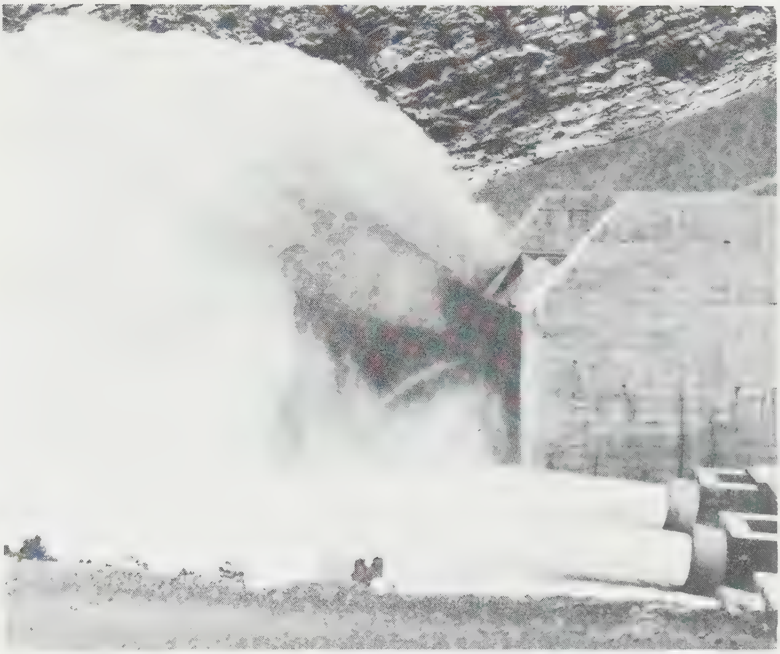

FIG. 21. Derbendi Khan Dam—spillway and bucket in action.

(2) the transition should be as far up the chute as practical, since velocities will be least at the upstream end; (3) the transition should be smooth and gradual and should be so proportioned that supercritical flow would be maintained throughout; (4) where the chute is narrower than the ogee, spillway openings should be arranged radially to eliminate a reverse curve in the guide walls.

FIG. 22. Derbendi Khan Dam—spillway and bucket in action.

These principles are illustrated by Fig. 20, which shows the spillway chute at the Derbendi Khan Dam on the Diyala River in northern Iraq. The main dam is a rock-fill structure about 430 ft high. Spillway discharges are controlled by three 49- by 49-ft radial gates. Under design-flood conditions, both the control structure and chute are designed to pass a flood of 400,000 cfs. The maximum concentration of flow at the crest is about 2,700 cfs/lin ft. The maximum concentration of flow in the chute is close to 4,000 cfs.

At maximum capacity the coefficient C in the discharge formula $Q = CLh^{3/2}$ was 4.09, indicating low negative pressures at the crest.

To attain satisfactory individual operation of each of the three spillway gates, internal training walls were extended down the chute to the bucket. The bucket type which showed the best characteristics was the V-channel type shown by Fig. 20. Figures 21 and 22 show the spillway and bucket in action.

In testing the models of the Derbendi Khan spillway, measurements of pressure and water-surface profiles were made for various flows. The increased pressures in the bucket locations must be given consideration in designing both the side-wall and floor structures. Centrifugal forces in these locations actually have an effect equivalent to that of increasing the density of the water. At the downstream bucket the actual pressure on both the walls and floor for a discharge of 400,000 cfs is approximately three times the hydrostatic pressure resulting from the depth of water on the bucket.

11. Side Walls. In addition to these centrifugal forces the design of the side walls is predicated on calculations of the following variables:

1. The average depth of flow called for by the simultaneous application of the law of continuity and the law of conservation energy.
2. The effect of changes in direction of flow which result in the formation of standing waves. This can occur where flow impinges upon a side wall, or it can occur upstream at a pier or some other obstruction. These waves are then reflected back and forth between the side walls of the chute.
3. The effect of the development of the boundary layer on the side walls and on the bottom of the spillway chute which requires flow area in addition to that which would be called for by the application of the laws of conservation of matter and energy.
4. The effect of the entrainment of air by the turbulent high-velocity flow which produces a general bulking, particularly along the side walls.
5. An arbitrary allowance of additional freeboard over and above that required by the preceding four considerations.

Hydraulic-model studies are useful in addition to the analytical studies which could be made to evaluate all the foregoing criteria except the one pertaining to air entrainment. Model studies are not applicable to the determination of air entrainment because the air-entrainment process depends upon the absolute magnitude of the velocity involved. For this reason guidance in estimating the amounts to be made for bulking, because of air entrainment, must depend upon observations in full-sized operating spillways. Figures 21 and 22 show the kind of bulking that takes place.

The entrainment of air results from the falling back into the flow of droplets turbulently ejected which then entrain the adjoining air in much the same way as does a plunging jet. If the water surface is not turbulent, air entrainment does not occur. In deeper portions of the flow at considerable distance from the side walls, turbulence is confined to the boundary layer along the bottom of the chute. At some point the thickness of the growing boundary layer becomes equal to the depth of flow. This point, called the critical point, marks the location of the division between the nonturbulent water surface upstream and the turbulent so-called white water downstream. Along the side walls white water appears much farther up in the spillway because the edge of the boundary-layer development along the side walls is continuously exposed to the atmosphere. Air entrainment along the walls then begins at the point where the intensity of turbulence is sufficient to project small masses of water required to entrain the air.

Calculation of the development of the boundary layer on the floor and side walls of a spillway chute can be made by the method given in the U.S. Army Corps of Engineers Hydraulic Design Criteria, Sheets 111-18 to 111-18/5. Also available from the Waterways Experiment Station is a publication describing the studies made to develop this design criterion. Presented here are some approximations which are useful in preliminary design:

1. The typical rate of growth of boundary-layer thickness in concrete-lined chutes is shown in Fig. 23.

2. The amount of energy lost in flow down spillway chutes may be taken to be the potential head multiplied by the boundary-layer thickness divided by five times the depth of flow at the point in question. For example, assume a spillway with a length of 200 ft, a drop of 100 ft at a point where the thickness of the flow is 2 ft. The

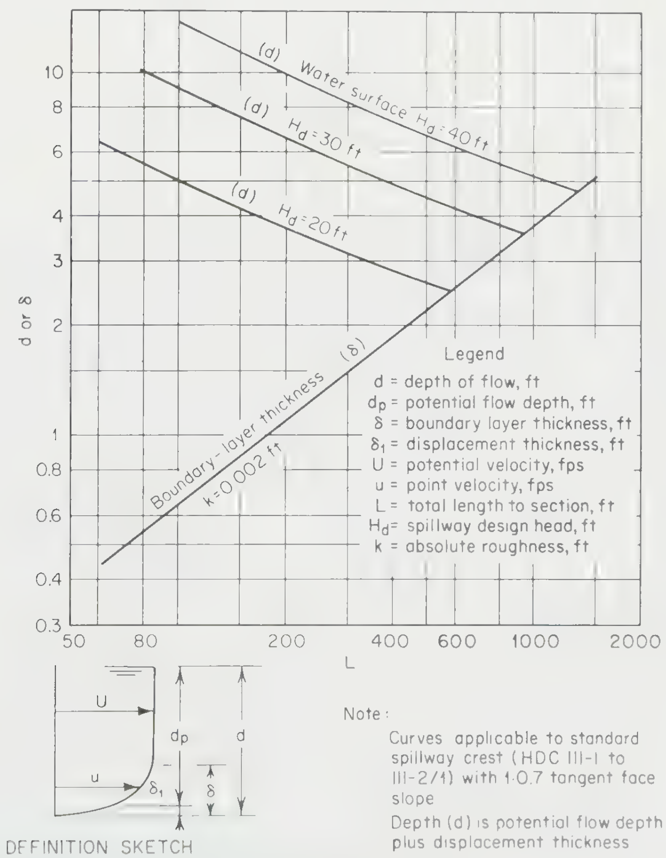

FIG. 23. Boundary-layer thickness in concrete-lined chutes. (*By U.S. Army Engineer Waterways Experiment Station, Vicksburg, Mississippi.*)

thickness of the boundary layer at this point could be on the order of 1 ft; the head loss at this point would be 100×1 ft divided by 5×2 ft $= 10$ ft, leaving an average of 90 ft of dynamic head.

3. The allowance to be made for wave action and surface bulking produced by piers on the spillway crest should be approximately 25 percent of the estimated thickness of the flow at the downstream edge of the piers at maximum discharge. Actual model tests might produce better estimates of the amount of the wave action, but additional bulking produced by air entrainment is presently a matter of judgment. It is believed that the provision of 25 percent of the thickness of the flow at the downstream edge of the piers would be sufficient to accommodate all bulking along the side walls of the spillway assuming that the alignment was carefully made.

4. The amount of additional freeboard above the sum of the potential thickness of the flow, 10 percent of the boundary-layer thickness and 25 percent of the thickness of the flow at the downstream edge of the piers, should be an additional 2 to 5 ft, depending upon the size of the spillway involved.

12. Floor Slabs. The possibility of the development of stagnation pressures beneath the slab as a result of impingement of high-velocity jet on offsets at joints must be considered. Should such large forces develop, the slab would in all probability be torn from its place as would all the spillway floor downstream from this point. Such failures have occurred in a large number of chute spillways. This type of failure can be guarded against by the following procedures:

1. Joints in floor slabs would be designed to accommodate possible differential movements without the formation of an abrupt surface upon which the high-velocity flow may impinge.

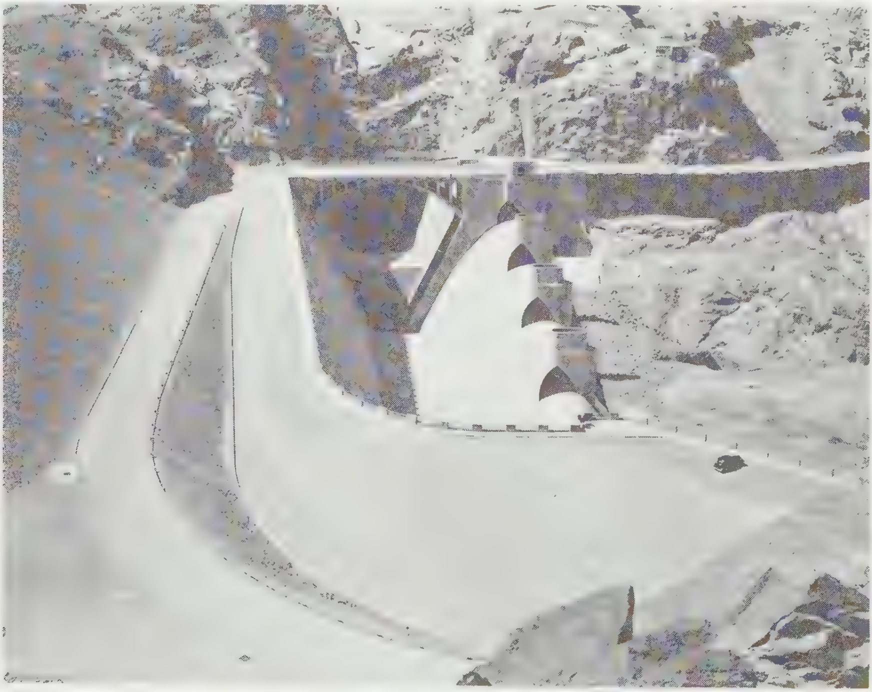

Fig. 24. Hoover Dam spillway.

2. Joints between sections of floor slab should be keyed or sloped to minimize differential motion.

3. Forces under floor slabs which could develop by underseepage from the headwater or from high tail water must be resisted structurally, or reliable underdrainage must be provided to eliminate the development of such high underpressures. The design of floor slabs depends a great deal on the nature of the foundation materials and the overall layout of the spillway, as well as the headwater and tail-water relationship. If failure of floor slabs is to be avioded, a design must be carefully executed by an experienced designer. Surface tolerances in floor slabs, and on side walls for that matter, are important from the standpoint of elimination of cavitation and other damage.[1]

SIDE-CHANNEL SPILLWAYS

13. General. The side-channel spillway is commonly used in sites where the sides are steep and rise to a considerable height above the dam. In this form, the water falls over the spillway crest into a channel, in which the flow is parallel to the crest. This channel leads eventually to the stream below the dam. A complete

[1] BALL, JAMES W., Construction Finishes and High-velocity Flow, *Proc. ASCE, J. Construction Div.*, September, 1963.

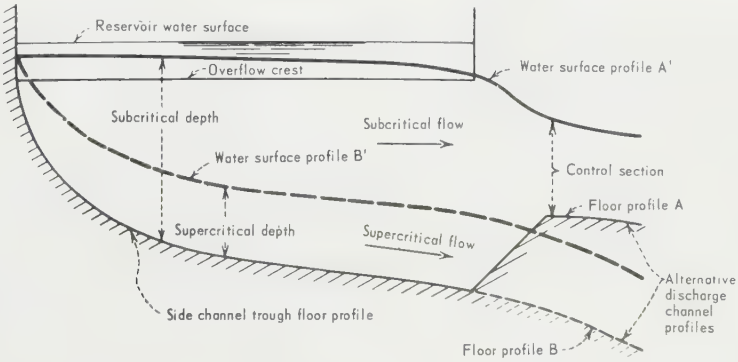

(a) Side-channel profile

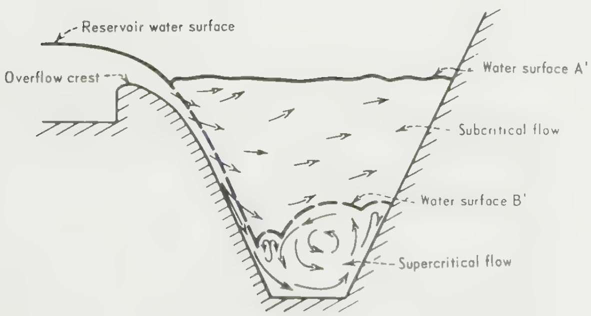

(b) Side-channel cross section

FIG. 25

explanation of the hydraulics is given by Hinds.[1] This analysis is based on the assumption that all the energy of the overfalling water is dissipated in turbulence and that the slope in the side channel must be sufficient to accelerate the overfalling water in the direction of flow down the channel. Observations on many spillway models have confirmed the essential accuracy of this analysis. In the spillways of Hoover Dam (Fig. 24), a cross weir was constructed at the downstream end of the channel section, to provide at all flows a considerable depth of water in which the energy of the overflowing water could be dissipated without causing excessive turbulence in the tunnel that carried the water back to the river. In this case, it was very desirable to avoid turbulence in order that the water might flow through the long tunnels without undesirable effects due to entrained air. The increase in the size of channel required with this weir was negligible. Extensive model experiments on the Hoover Dam spillways indicated that turbulence in the side channel can probably be reduced at less expense by such a device than by any form of baffles that might be used. Attempts to divert the overfalling water in a downstream direction, the velocity of flow in the channel being thus increased and the necessary size decreased, were unsuccessful in evolving any practical method. The tests demonstrated that the flow conditions in the channel downstream from the overflow section will be improved if the channel is narrowed, downstream from the overflow section, by offsetting the side toward the dam in by an amount equal to the thickness of the stream of water falling over the weir.

In connection with the design of the spillways of the Hoover Dam, extensive studies were made of crest shapes and discharge coefficients. These are much more extensive than are feasible to give in this book. Detailed information will be found in the Bureau of Reclamation reports.[2]

14. Flow Characteristics. Basic side-channel-flow characteristics are illustrated by Fig. 25. The theory of flow is based on the law of conservation of linear momentum. For any short reach of the side channel, the momentum at the beginning of the reach plus any increase due to external forces must equal the momentum at the end of the reach.[3]

Consider a short reach Δx in length, with a velocity and discharge at the upstream section of v and Q, respectively. At the downstream section the velocity and discharge will be $v + \Delta v$ and $Q + q(\Delta x)$ where q is the inflow per foot of length of the weir crest.

By applying the law of conservation of linear momentum, it can be demonstrated that change in the water elevation Δy in the reach Δx can be expressed in the following formulas:

$$\Delta y = \frac{Q}{g} \frac{v + \frac{1}{2}(\Delta v)}{Q + \frac{1}{2}(\Delta Q)} \left[\Delta v + \frac{g(\Delta x)}{Q} (v + \Delta v) \right] \tag{8}$$

If Q_1 and v_1 are values at the beginning of the reach and Q_2 and v_2 are the values at the end of the reach, Eq. (8) can be written

$$\Delta y = \frac{Q_1}{g} \frac{v_1 + v_2}{Q_1 + Q_2} \left[(v_2 - v_1) + \frac{v_2(Q_2 - Q_1)}{Q_1} \right] \tag{9}$$

This derivation can also be developed so that

$$\Delta y = \frac{Q_2}{g} \frac{v_1 + v_2}{Q_1 + Q_2} \left[(v_2 - v_1) + \frac{v_1(Q_2 - Q_1)}{Q_2} \right] \tag{10}$$

[1] Hinds, Julian, Side Channel Spillways, *Trans. ASCE*, **89**, 881, 1926. "Design of Small Dams," p. 293, U.S. Bureau of Reclamation.

[2] Studies of Crests for Overfall Dams, Boulder Canyon Project, Part VI, *Bull.* 3, U.S. Bureau of Reclamation.

[3] "Design of Small Dams," p. 283, U.S. Bureau of Reclamation.

By the use of Eqs. (9) and (10) the water-surface profile can be determined for any particular side channel by assuming successive short reaches of a channel once a starting point is found. Commonly a control section where critical flow occurs is the starting point. The solution of Eqs. (9) and (10) is obtained by a trial-and-error procedure.

MORNING-GLORY SHAFT AND TUNNEL SPILLWAYS

15. General. In morning-glory or shaft spillways, the water flows over the lip of a funnel-shaped spillway and discharges down a shaft or tunnel. This form of spillway is adapted to narrow canyons where room for a spillway is restricted. A disadvantage of this type is that the discharge beyond a certain point increases only slightly with increased depth of overflow and therefore does not give so great a factor of safety against underestimation of flood discharge as do most other forms.

The morning-glory type has been tested extensively in models, and some limited observations have been made of prototype performance.[1]

Because in ordinary model tests the air-entraining effects cannot be reproduced to scale, for the surrounding air pressure is not reduced to a magnitude corresponding to the model size, the degree of agreement of model tests with the prototype action is uncertain. The Davis Bridge spillway[2] (Fig. 26) is typical of the form. Since the spillway is placed on the side of the hill, it is usually provided with channels leading to it from both sides. Unless these channels are very deep, the water does not flow over the spillway crest in a radial direction, but owing to the tangential component of the water as it approaches the weir, it is more or less deflected from a radial path in the direction of the path of approach. It tends to pass over the lip, therefore, with a component toward the bank side of the spillway, which results in a concentration of flow about the middle of the bank side and causes an unequal flow down the spillway shaft, which gives rise to considerable turbulence. The undesirable condition can be largely eliminated by placing piers on the crest to guide the water.

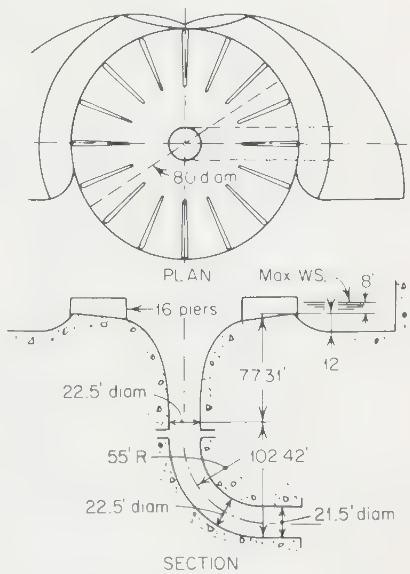

FIG. 26. Davis Bridge Dam spillway. (*From Trans. ASCE, vol.* 121, *p.* 313.)

Considerable turbulence occurs at the bend at the bottom of the vertical shaft. For comparatively low heads this is probably not serious, but the action under high heads is uncertain. For high dams, it would seem to be advantageous to begin to incline the tunnel as short a distance as possible below the intake and provide ample access of air to the inclined section.

The form of the spillway is largely controlled by the discharge to be accommodated and the depth of overflow permitted, for the length of crest must be sufficient to provide for the required discharge at the maximum head permitted. Thus large

[1] BRADLEY, JOSEPH N., Shaft Spillways Prototype Behavior, *Trans. ASCE*, **121**, 312, 1956.

[2] KURTZ, FORD, The Hydraulic Design of the Shaft Spillway for the Davis Bridge Dam and Hydraulic Tests on Working Models, *Trans. ASCE*, **88**, 1925.

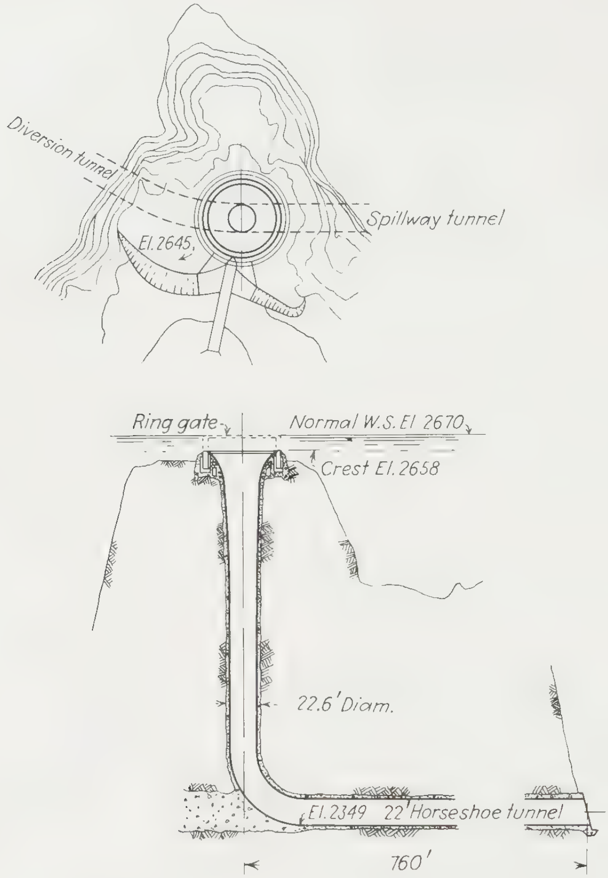

FIG. 27. Owyhee morning-glory and shaft spillway.

discharges and small depths of overflow give rise to large diameters of the intake section. The size of the outlet tunnel is determined by the discharge and fall and is commonly constructed so that the tunnel will flow full throughout its length but not cause a backwater action on the spillway crest under conditions of maximum discharge.

Three examples of structures in service will illustrate the principal features of this type: (1) the Davis Bridge spillway, (2) the Owyhee spillway, and (3) the Hungry Horse spillway.

16. Typical Morning-glory Spillways. *Davis Bridge.* The first morning-glory spillway in the United States was constructed at the Davis Bridge Dam on the Durfield River near Whittingham, Vt. The dam was completed about 1926. This spillway was designed for a maximum discharge of 27,000 cfs with a head on the crest of 8 ft and a drop of 188 ft from the reservoir to the invert of the horizontal tunnel. The principal features of the spillway are shown by Fig. 26. The computed discharge during the hurricane period of 1938, when the water reached 6 ft on the crest, was 19,400 cfs.

Owyhee Spillway. The Owyhee spillway in Idaho was completed by the U.S. Bureau of Reclamation in 1932. Figure 27 shows the principal features of this

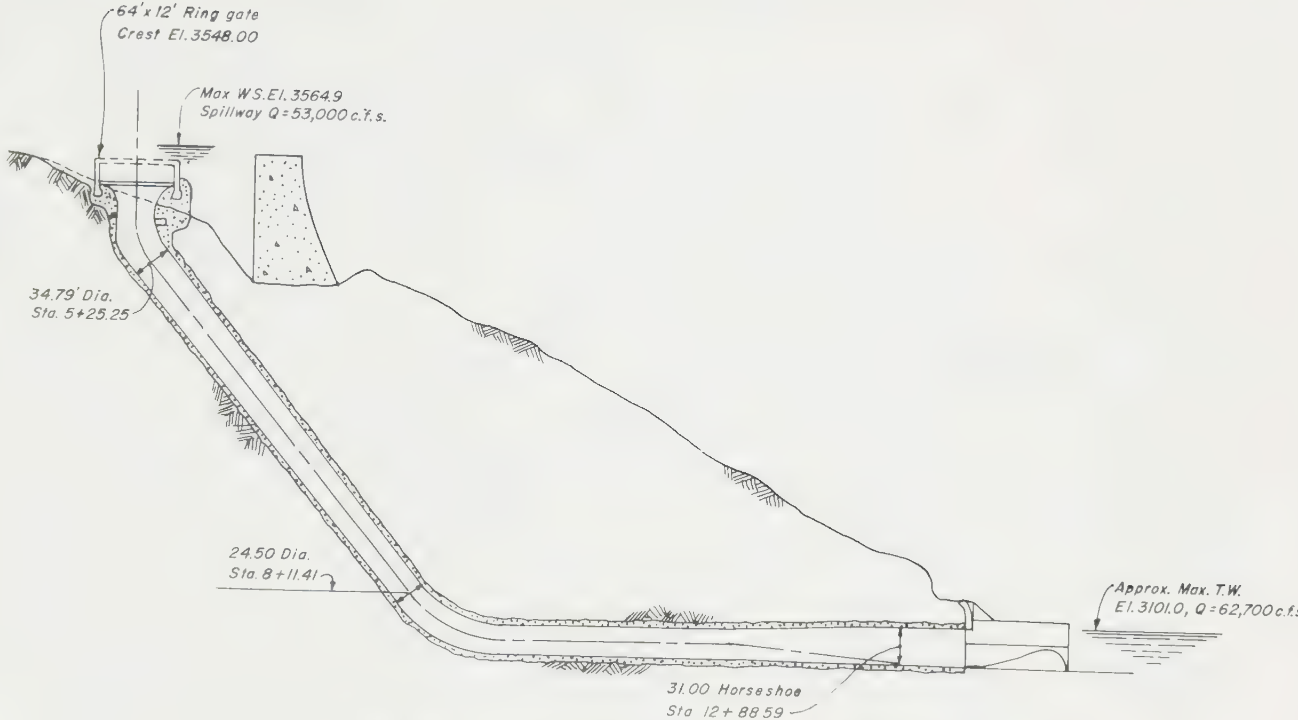

FIG. 28. Hungry Horse morning-glory and shaft spillway.

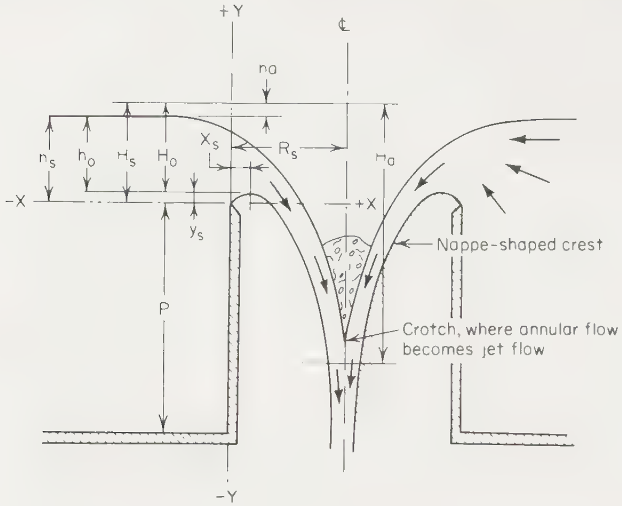

Fig. 29. Elements of nappe-shaped profile for circular weir.

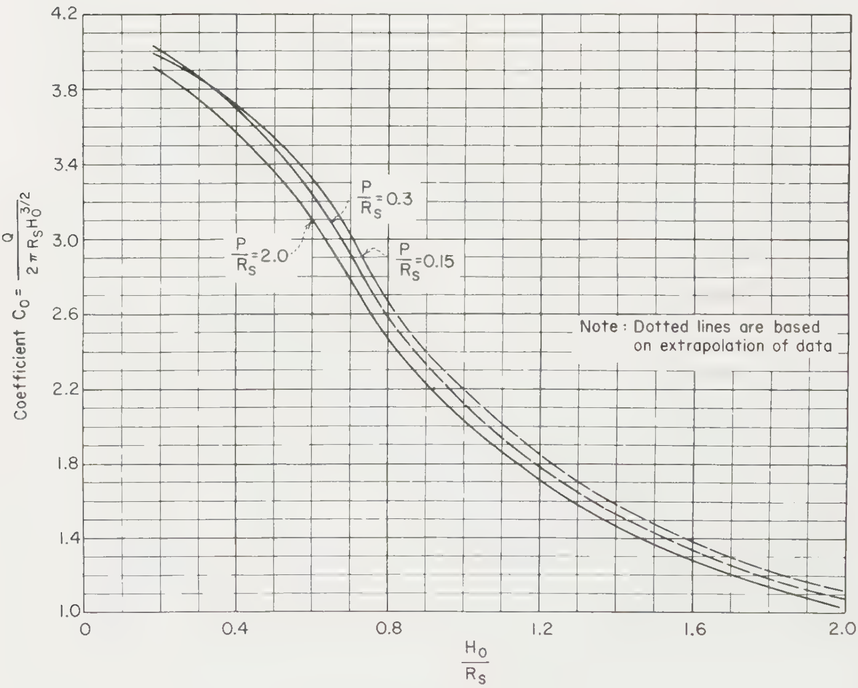

Fig. 30. Hoover Dam side-channel spillway.

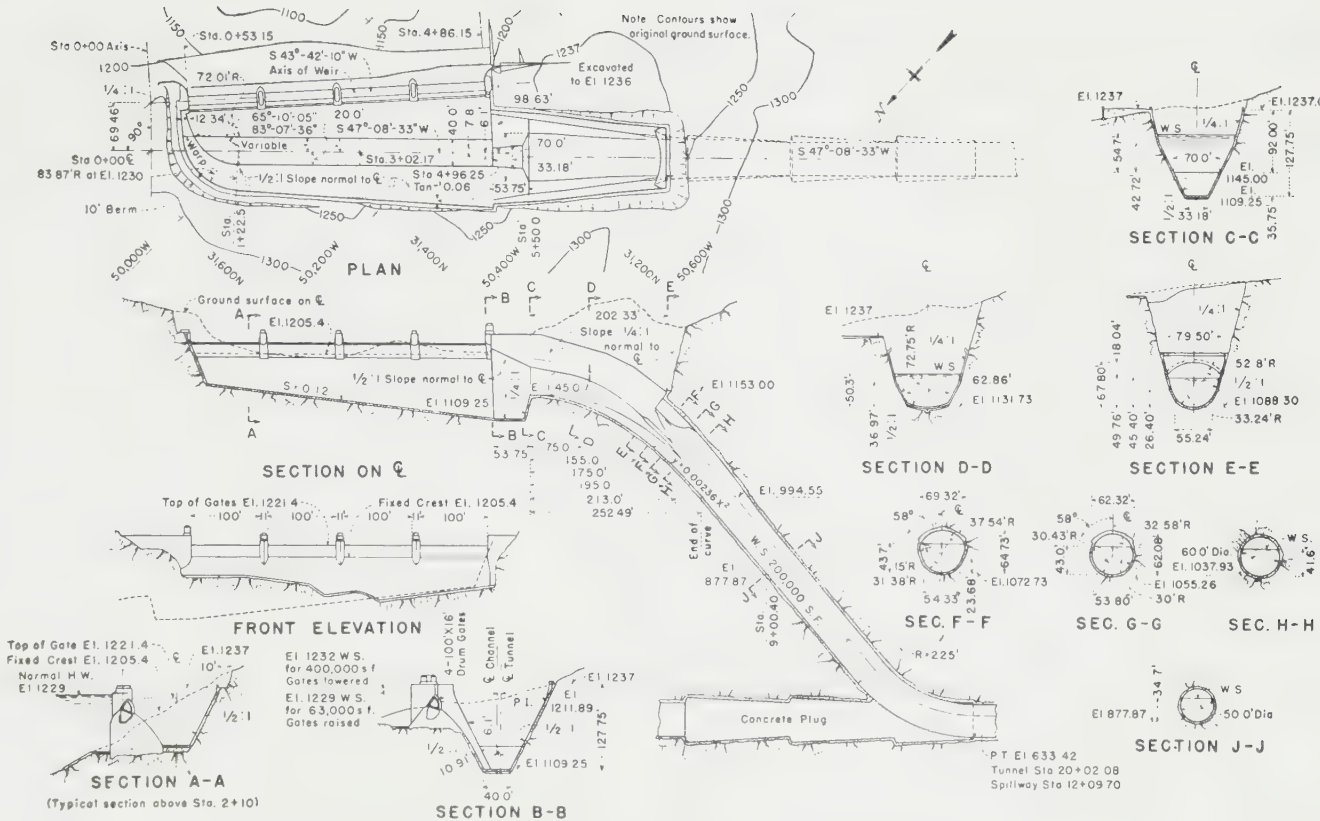

Fig. 31. Hoover Dam—general plan of Nevada spillway.

structure. The design flood is 30,000 cfs. The maximum head on the crest for this discharge is 12 ft and the water is dropped 320 ft through a vertical shaft. During 1952, this spillway operated for more than a month. The maximum discharge during this period was 20,000 cfs.

Hungry Horse Spillway.[1] The Hungry Horse Dam was completed in 1953 by the Bureau of Reclamation. It is located on the South Fork of the Flathead River near Columbia Falls, Mont. The principal features of the spillway are shown by Fig. 28. Discharges are controlled by an adjustable 64-ft-diameter by 12-ft-high ring-gate structure which releases into a tapering and sloping tunnel. The throat of the converging section, as shown by Fig. 28, is 37 ft in diameter. This tapers to a diameter of 34.79 ft at the upstream end of the inclined tunnel.

The incline has a vertical drop of 341.3 ft and tapers to a diameter of 24.5 ft at the downstream end. A vertical bend connects the inclined tunnel to the nearly horizontal tunnel which continues to the outlet portal at a slope of 0.0019. The tunnel is 24.5 ft in diameter throughout the lower bend and for a distance of 219 ft downstream then is transformed through a 166-ft-long transition section to a 31-ft-diameter horseshoe tunnel.

The spillway is designed to pass a flow of 53,000 cfs. In discharge tests, made in July, 1954, the reservoir release through the spillway was 30,000 cfs.

17. Hydraulics. The morning-glory shaft spillway may operate under three conditions: (1) *With crest control.* Under this condition there is accelerating flow in the vertical and transition sections of the shaft and decelerating open-channel flow in the outlet leg of the conduit. (2) *With tube or orifice flow.* Under this condition the morning glory acts under a partially submerged inflow with orifice control at the throat of the transition. (3) *With full pipe flow.* Under this condition the morning-glory intake is completely submerged and the entire conduit runs full. The control then moves to the downstream portal of the outlet leg of the conduit.

Using the nomenclature shown by Fig. 29,[2] the basic equation for the discharge of a nappe-shaped circular weir is

$$Q = C_0(2\pi R_s)H_0^{3/2} \tag{11}$$

It is apparent that the coefficient of discharge for a circular crest differs from that of a straight crest because of the effects of submergence and back pressure incident to the joining of convergent flows. Thus C_0 must be related to H_0 and R_s and, expressed in terms of H_0/R_s, is shown in Fig. 30[2] for three conditions of approach depth.

18. Typical Tunnel Spillways. Three notable spillways of this type will be described—Hoover, Fontana, and Glen Canyon. The Hoover Dam side-channel spillways (Figs. 24 and 31) are designed to pass a flow of 400,000 cfs, 200,000 cfs through each tunnel, with a fall in excess of 500 ft. The discharge from the side-channel spillways passes over weirs which discharge into 50-ft-diameter tunnels. The general plan and principal features of the spillway on the Nevada side are shown by Fig. 31.[3] The spillway tunnels are free-flowing, as shown by Fig. 31. The maximum theoretical velocity is 175 fps. Early operations resulted in some cavitation at the bend. This was apparently caused by some slight irregularities in the concrete surface.

The principal features of the Fontana spillway are shown by Figs. 32 and 33. The Fontana Dam, located on the Little Tennessee River in western North Carolina, was completed by the Tennessee Valley Authority in 1944. The concrete structure containing the main spillway is a gravity dam about 255 ft long forming an integral part of

[1] Donelman, Bernard, Discussion, Morning-glory Shaft Spillways, A Symposium, Paper 2802, *Trans. ASCE*, **121**, 334.

[2] "Design of Small Dams," pp. 311–314, U.S. Bureau of Reclamation.

[3] Model Studies of Spillways, Hydraulic Investigations, Boulder Canyon Reports, Fig. 2, Plan of Nevada Spillway, Bureau of Reclamation, *Bull.*

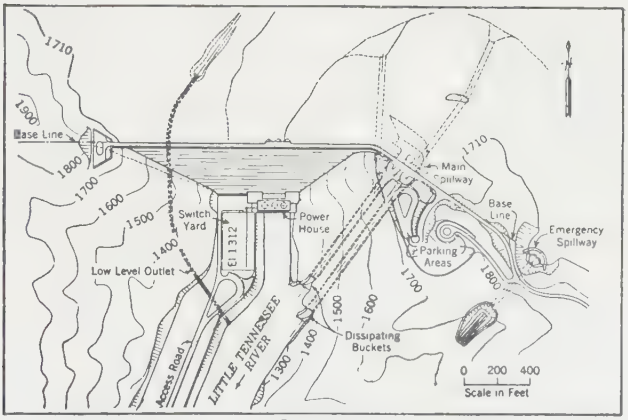

PLAN

Fig. 32. Fontana spillway.

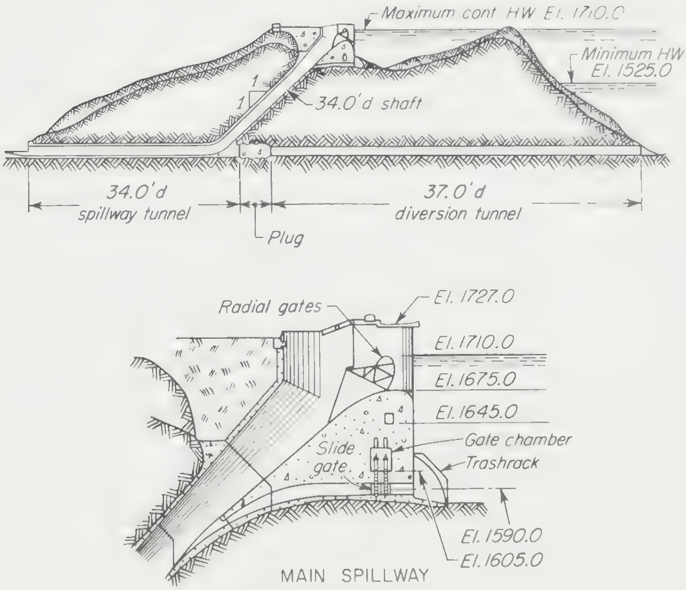

MAIN SPILLWAY

Fig. 33. Fontana spillway.

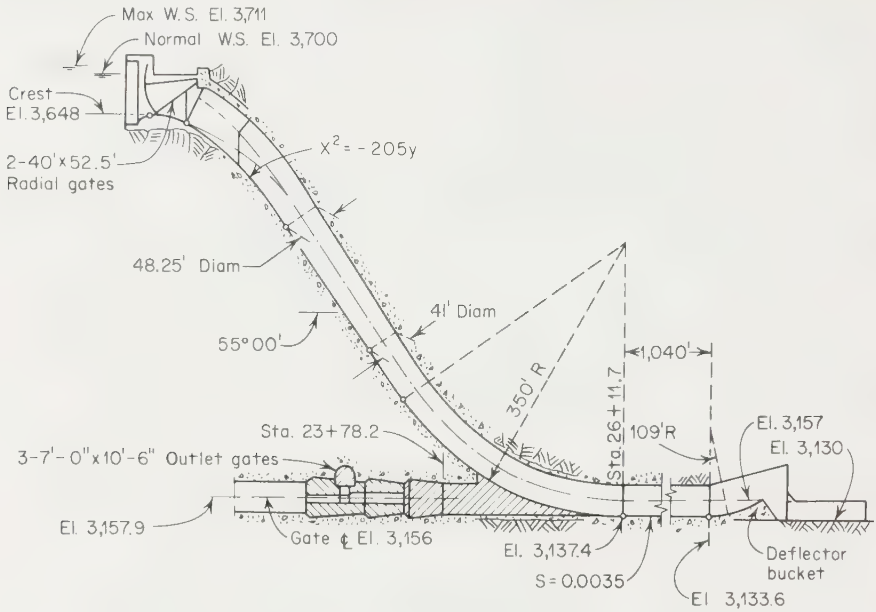

FIG. 34. Glen Canyon Dam, profile of left spillway and tunnel plug.

the low rim dam on the ridge of the left abutment. Its location on the rim dam was closely coordinated with the layout of the diversion tunnels, which were also used as discharge tunnels for the spillway.

The spillway discharges are controlled by two groups of two 35-ft-wide by 35-ft-high radial gates. Each pair is positioned on the chords of an arc to provide for the smooth convergence of the discharge into the 34-ft-diameter tunnels.

Supplementing the radial gates on the crest are three slide gates placed in three sluice openings, 5 ft 8 in. wide by 10 ft high. Each tunnel is designed to discharge 100,000 cfs flowing free.[1]

The largest and most important feature of the Colorado River storage project is the Glen Canyon Dam, located on the Colorado River in Arizona, 13 miles south of the Utah border. The main dam consists of a concrete arch which rises over 700 ft above the bedrock foundation.

Identical spillways in each rock abutment will discharge into inclined tunnels connecting with each diversion tunnel downstream from the plug. The principal features of the spillway are shown by Fig. 34. The total spillway capacity is 276,000 cfs. The discharge is controlled by two 40-ft-wide by 52.5-ft-high radial gates in each spillway.

SIPHON SPILLWAYS

19. General. Where the available space is limited and where the discharge is not extremely large, siphon spillways are often superior to other forms. They are also useful in providing automatic surface-level regulation within narrow limits. Because the siphon spillways prime rapidly and bring into action their full capacity, they are especially useful at the powerhouse end of long power canals with limited forebay capacity where the power may go off and the turbines shut down rapidly, the provision

[1] The Fontana Project, Tennessee Valley Authority, *Tech. Rept.* 12, 1949.

of a considerable discharge capacity being made necessary within a very short time in order to avoid overflow of the canal banks.

Figure 35 shows a cross section of one of 18 siphon spillways in the O'Shaughnessy Dam (as initially constructed), which have a combined capacity of about 20,000 cfs. Siphon spillways are often built with a basin at the lower end so that the discharge end will be submerged, but this is not necessary, as an ejector action can be introduced by placing a bend or lip in the downstream leg, which deflects the water when flowing over the crest at a slight depth to the opposite side of the siphon barrel. The lower end of the siphon barrel will thus be sealed, and the flowing stream, by carrying along bubbles of air from the inside of the siphon, will reduce the pressure inside enough to cause the siphon to start.

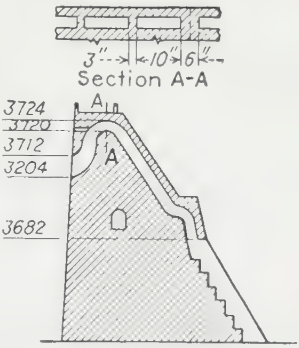

Fig. 35. Siphon spillway in O'Shaughnessy Dam.

After the siphon action is started, unless the siphon is vented, the upstream water level will be drawn down to the level of the entrance before flow ceases. The magnitude of the drawdown can be controlled by means of a vent, as shown in Fig. 35, through which the air enters the siphon and destroys the prime as soon as the water level has fallen below the vent.

The siphons should be made with gradually contracting entrances and curves of as large radius as possible. The capacity can sometimes be increased by gradually expanding the downstream section of the tube. It is not possible to compute accu-

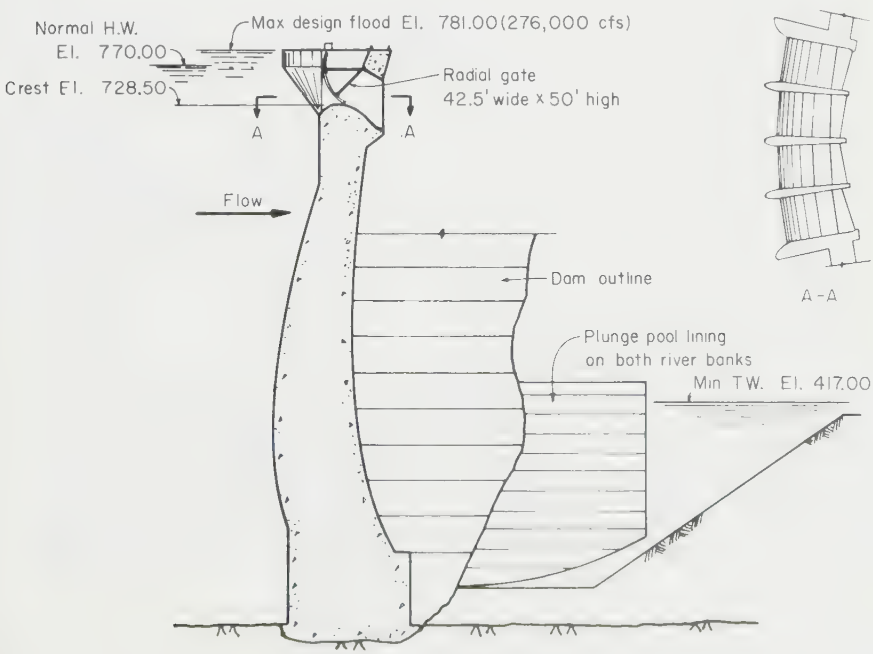

Fig. 36. Mossyrock spillway.

rately the action of siphon spillways. Much better results can be obtained by model tests. For further discussion on siphon spillways, reference should be made to Sec. 34, Irrigation Structures.

SCOUR PROTECTION BELOW OVERFALL DAMS

20. Plunge Pools. A plunge pool frequently offers a simple and effective means of dissipating the energy of falling water. Natural waterfalls usually erode a pool having a depth of approximately one-third the head above the pool. Thus nature offers a rough guide in determining pool depths. Figure 36 shows a plunge pool of this type below the overfall spillway of the 600-ft-high double-curvature arch dam now (1968) being constructed by the city of Tacoma on the Cowlitz River in Washington.

The spillway discharge for the design flood would be 276,000 cfs. This discharge is controlled by four 42 ft 6 in. wide by 50 ft 0 in. high radial crest gates. During the period of the design flood the maximum depth of the pool below the overfall spillway would be approximately 260 ft.

In the design of plunge pools, model tests are usually required to determine that the energy of the spillway discharge is dissipated before it reaches the foundation. For example, in some cases, the discharge over an ogee-type spillway with a radial bucket at the toe, into a relatively deep pool, may follow the submerged face of the dam and travel horizontally along the foundations as a submerged jet. In such cases the energy of the submerged jet will be diminished only slightly by frictional losses and undercutting of the stream-bed protection works may result.

21. Deflector Buckets. Where the spillway discharge may be delivered directly to the river without providing additional stream-bed protection works the jet may be projected beyond the structure by a deflector bucket. Flow from these deflectors leaves the structure as a free-discharging upturned jet.

The trajectory of the jet depends upon the energy of the flow at the lip and the angle at which the jet leaves the bucket. With the origin of the coordinates taken at the end of the lip, the path of the trajectory may be expressed by the equation

$$y = x \tan \theta - \frac{x^2}{K[4(d + h_v) \cos^2 \theta]} \qquad (12)^1$$

in which θ = angle of edge of lip with horizontal

K = a factor usually assumed as 0.9 to compensate for loss of energy

d = depth of water on bucket

h_v = velocity head of discharging jet

Ordinarily the exit angle should not exceed 30 deg and the minimum radius of curvature should not be less than five times the depth of the water on the bucket. Figures 21 and 22 show the deflector bucket for the Derbendi Khan spillway operating under free-discharge conditions.

In cases where the defector bucket discharges under submerged or partially submerged conditions model tests are usually required to finalize the design. More complete discussion of the hydraulics of deflector buckets can be found elsewhere.[2]

Under some conditions of submergence large eddy currents may circulate around the guide walls and possibly undercut the bucket and terminal structures. Model tests show that the omission of the guide walls near the end of the bucket will introduce eddies which will counteract this effect. These eddies result from the centrifugal force acting on the bucket, which spreads laterally some part of the spillway discharge.

[1] "Design of Small Dams," p. 291, U.S. Bureau of Reclamation.

[2] "Design of Small Dams," U.S. Bureau of Reclamation. McPherson, M. B., and M. H. Karr, A Study of Bucket Type Energy Dissipator Characteristics, *Proc. ASCE*, Paper 1266, Symposium on Spillway Basins and Energy Dissipators, June, 1961.

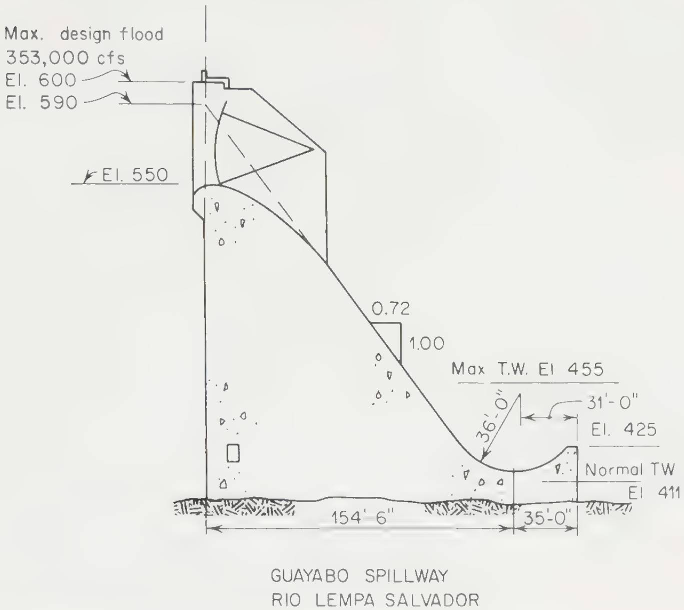

Fig. 37. Guayabo spillway.

Fig. 38. Guayabo spillway discharging under approximately design-flood conditions.

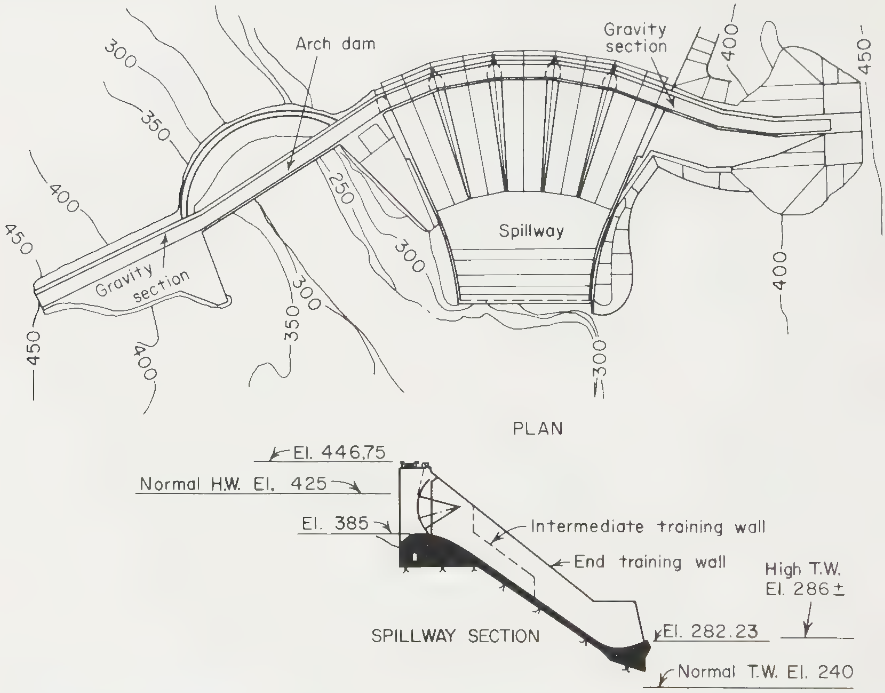

Fig. 39. Mayfield spillway.

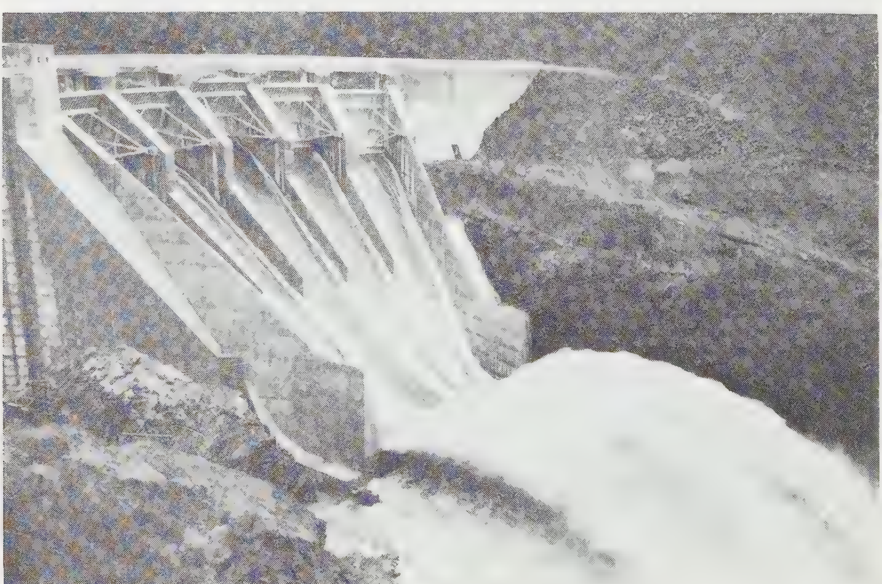

Fig. 40. Mayfield—initial operation under partial gate openings.

The prototype performance of two existing structures having deflector buckets which will operate under conditions ranging from free jet discharge to deep submergence will be described.

Figure 37 shows a section through the Guayabo spillway, a 200-ft-high gravity dam, located on the Lempa River in El Salvador, Central America. The spillway discharge is controlled by seven 39-ft-high by 40-ft-wide radial gates. The narrow canyon below limited the width of the spillway. With a surcharge of 10 ft the design flood of 350,000 cfs would cause a tail-water rise of 65 ft. Figure 38 shows the Guayabo spillway discharging under approximately design-flood conditions.

Figure 39 shows a plan and section of the 180-ft-high Mayfield spillway, constructed by the city of Tacoma on the Cowlitz River in Washington. Mayfield is a run-of-river project constructed a short distance downstream from Mossyrock (Fig. 36). The spillway is located in a saddle in the left abutment. The discharge is controlled by five 40-ft-wide by 40-ft-high crest gates which are capable of passing a design flood of 314,000 cfs. Figure 40 shows the initial operation under partial gate openings.

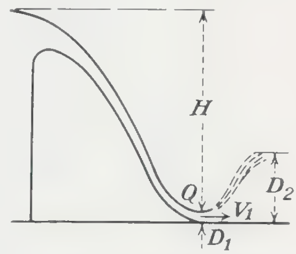

Fig. 41. Elements of hydraulic jump.

The model tests for both Guayabo and Mayfield indicated that there would be aggradation of foundation material against the downstream face of the deflector bucket. To date (1967) the hydraulic performance of both spillways has conformed closely to that of the models.

Reference to Fig. 39 shows that the Mayfield spillway chute narrows down to a width of 120 ft at the lip of the bucket. Model tests showed that this sharp convergence could be achieved (1) by placing the upstream faces of the radial gates on the chords of an arc, (2) by tapering the piers, and (3) by extending the piers well down the chute. The benefits obtained from these features are illustrated by Fig. 40.

22. Stilling Basins. Unless proper precautions are taken, the velocity of the spillway discharge may erode the stream-bed material and undermine the dam until failure occurs. The hydraulic jump, in many cases, is the most effective way of preventing this erosion, as it quickly reduces the velocity of the water to a point where it is incapable of damaging the stream bed.

The simplest kind of protection could be used if a jump would form at all stages on a horizontal floor, at the stream-bed level, extending from the dam to the downstream end of the jump. The formula for the hydraulic jump in a horizontal channel of rectangular section is

$$D_2 = -\frac{D_1}{2} \pm \sqrt{\frac{2V_1^2D_1}{g} + \frac{D_1^2}{4}} \quad (13)$$

where, as shown by Fig. 41, D_1 and D_2 are the depths upstream from the jump

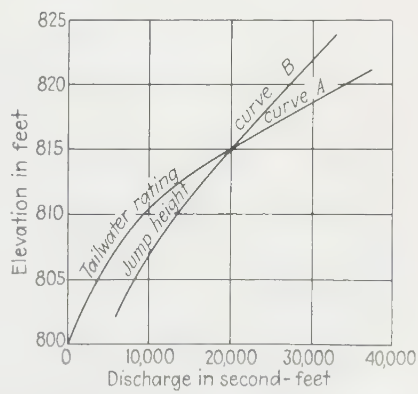

Fig. 42. Tail-water rating curve vs. jump height.

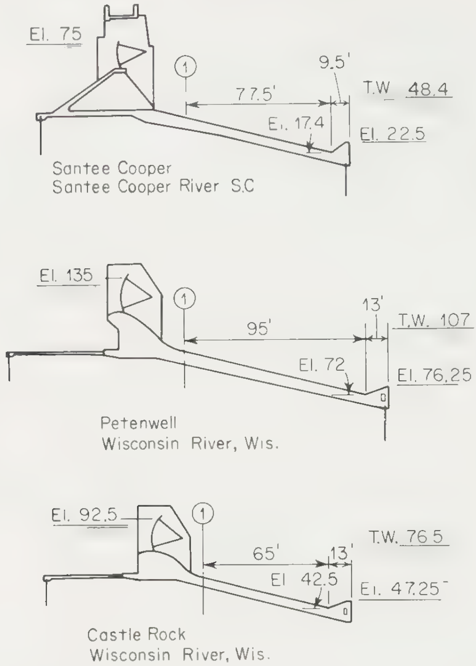

FIG. 43. Sloping aprons of Santee Cooper, Petenwell, Castle Rock.

and V_1 and V_2 are the corresponding velocities. A more complete discussion of the hydraulic jump on both horizontal and sloping aprons will be found in Sec. 2.

The height of the tail water for each discharge seldom corresponds to the height of a perfect jump. Frequently the elevation discharge curve of the tail water or the tail-water rating curve is as shown by Fig. 42. The relations between the positions of these curves fall into four classes: (1) jump-height curve above tail-water rating curves, (2) jump-height curve below tail-water rating curve, (3) jump-height curve

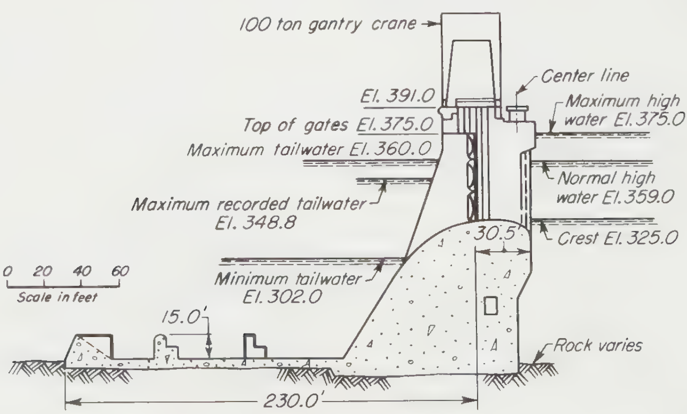

FIG. 44. Section through Kentucky Dam spillway, TVA.

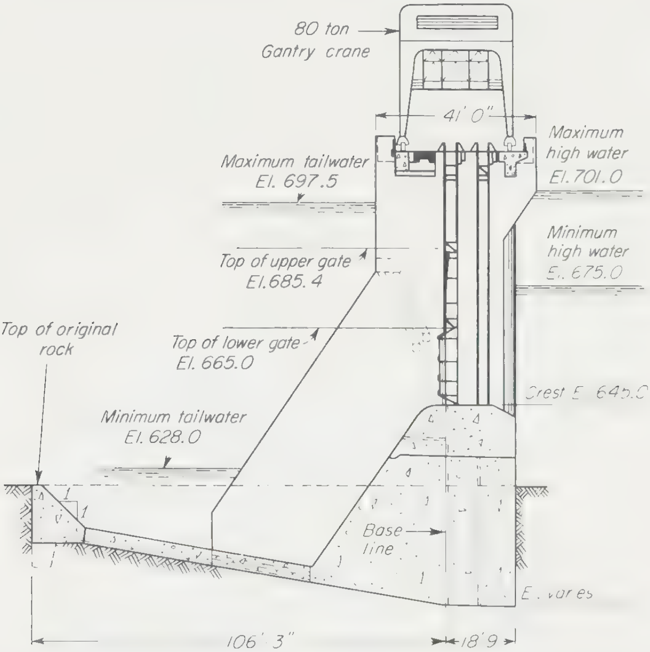

FIG. 45. Section through spillway at Chickamauga Dam, TVA.

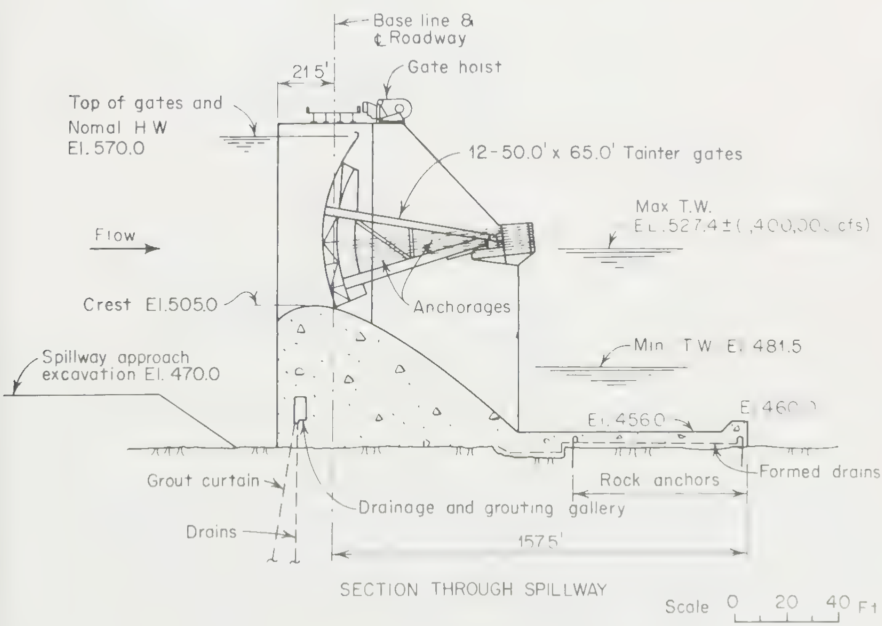

FIG. 46. Section through spillway at Wanapum.

above tail-water rating curve at low discharges and below at high discharges, (4) jump-height curve below tail-water rating curve at low discharges and above at high discharges. The best form of protection depends largely upon which of these four conditions exists.

In some cases the sloping apron of the general type shown by Fig. 43 will permit a hydraulic jump to form at the proper depth within the limits of the apron throughout the entire range of spillway discharges and corresponding tail-water depths. It will be noted that each of these sloping aprons terminates in a deflector sill which directs the discharge upward toward the surface of the tail water where the residual energy is dissipated.

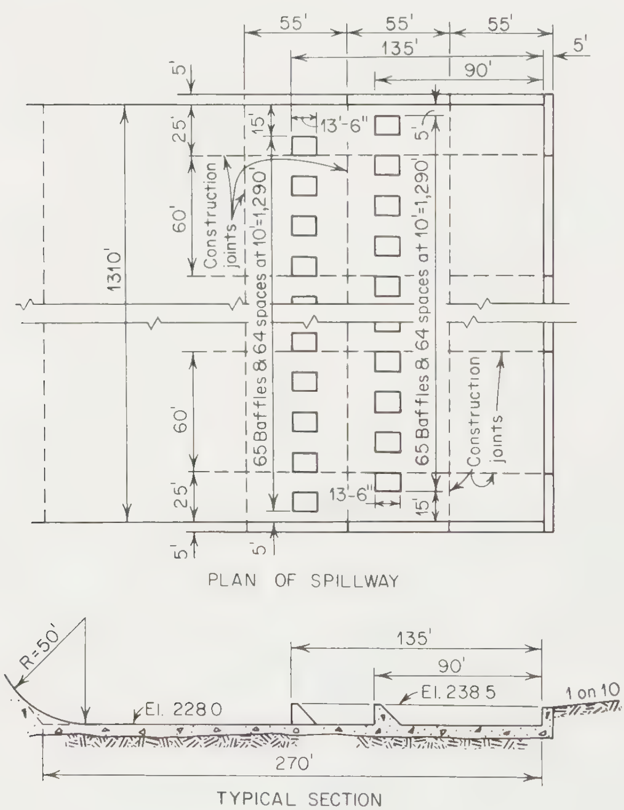

Fig. 47. Typical section—stilling-basin dimensions, McNary Dam.

Another type of stream-bed protection structure which has operated successfully under a wide range of discharge and tail-water conditions is shown by Figs. 44 to 46, inclusive. Features which are common to these three structures are stilling basins formed by plane surfaces with deflector sills at the end of the hearth. In connection with the Kentucky Dam (TVA) a dentated sill was used as the terminal structure in conjunction with intermediate baffle blocks.

Model tests for the Wanapum project, completed in 1964 on the Columbia River by the Grant County Public Utility District Number 2, revealed that a relatively short hearth and low terminal sill would be adequate to deflect a large part of the discharge upward and dissipate the energy on the surface of the tail water. These tests showed a high localized positive pressure at the junction of the ogee and the horizontal apron

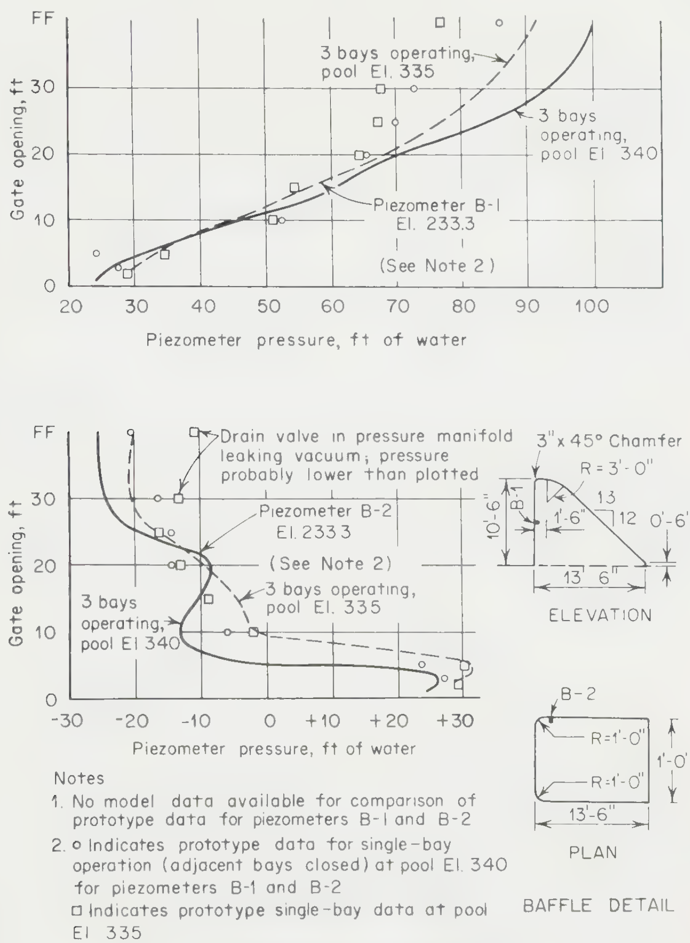

FIG. 48. Baffle-pier pressures, McNary Dam.

slab. Model tests indicated that the introduction of a curved bucket at this intersection required a substantial increase in the length of the hearth. Apparently a substantial amount of energy is dissipated at this point and part of the discharge is reflected upward to the surface. The residual flow is directed upward to the surface by the deflector sill.

Stilling-basin designs have varied widely. As one example of an earlier design,

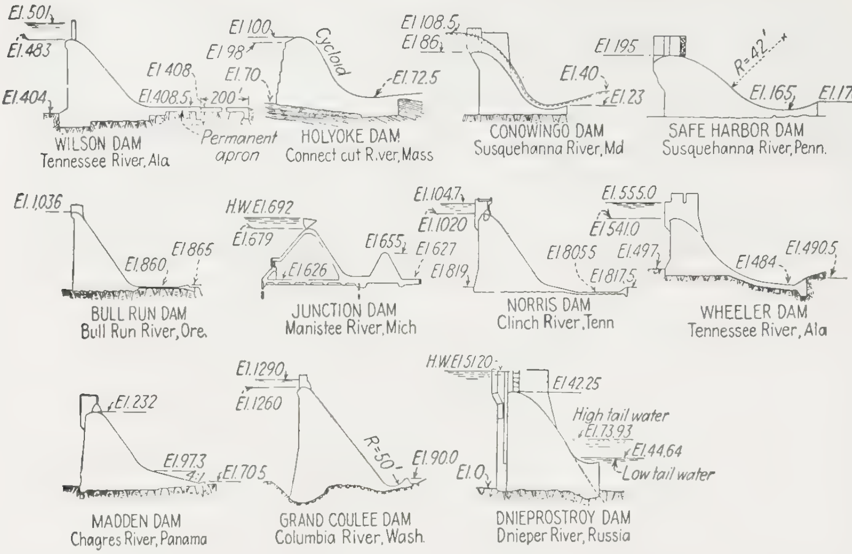

FIG. 49. Cross sections of dams showing various methods of protection against scour.

Fig. 47 shows the stilling-basin dimensions of the McNary Dam and Fig. 48 shows baffle-pier pressures observed during prototype observation tests made in 1955.[1]

The stilling basin is of the conventional hydraulic-jump type. Flood flows are passed through twenty-two 50-ft by 50-ft gates each of which is capable of discharging 100,000 cfs. Model tests for this arrangement indicated that the apron length should

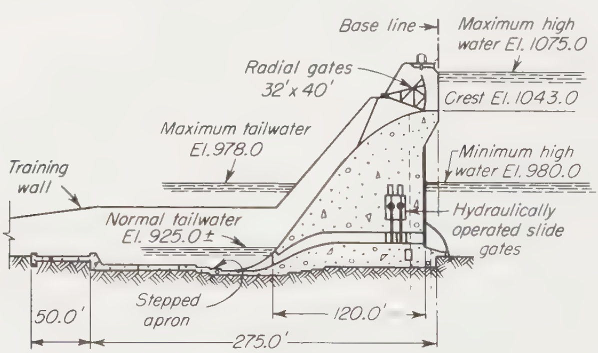

FIG. 50. Spillway section at Cherokee Dam.

be 3.2 D_2, where D_2 is the maximum conjugate depth after the hydraulic jump. The apron elevation was set so that the maximum tail-water depth of 75.5 ft was equal to 0.90 D_2 because of the anticipated effect of the baffle piers. The Froude number

[1] BERRYHILL, R. H., Stilling Basin Experiences of the Corps of Engineers, *Proc. ASEC*, Paper 1624, Symposium on Stilling Basins and Energy Dissipators, June, 1961.

$V_1/\sqrt{gD_1}$ at design discharge is 3.3, where V_1 and D_1 are the velocity and depth, respectively, upstream from the hydraulic jump.

Prototype operation tests were made in June and July, 1955, with normal pool operations of 335 and 340 (see Fig. 9) and with spillway bays 15, 16, and 17 discharging together and with bay 16 discharging alone. The results of the piezometer tests on the baffles and the baffle details are shown by Fig. 48. The low pressures shown for piezometer B_2 indicate that cavitation pitting on the sides of the baffles may be expected.

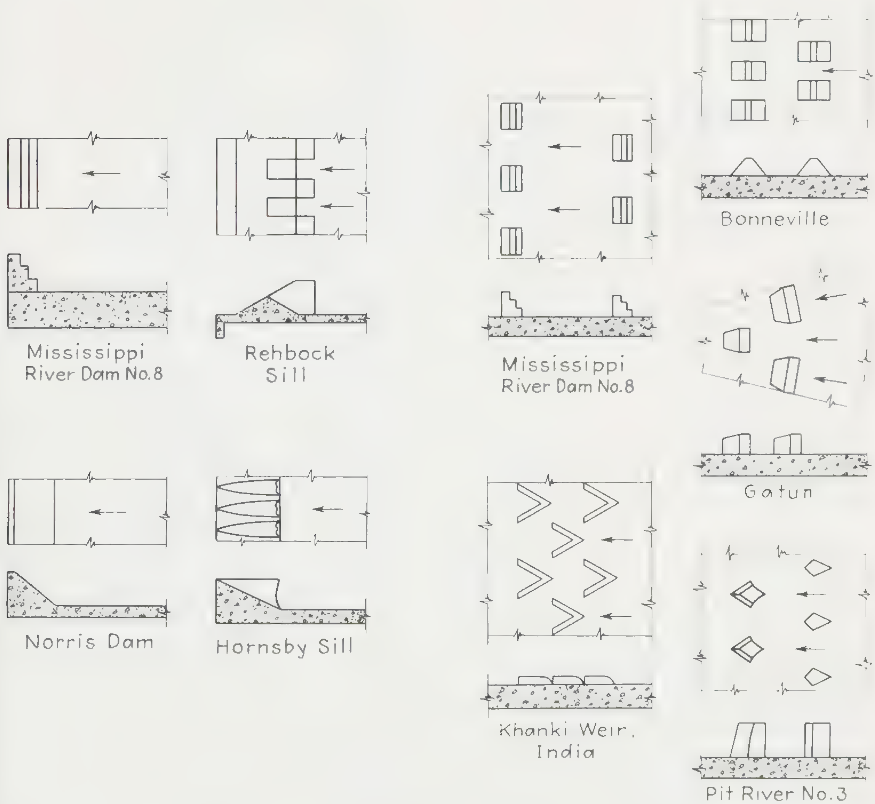

Fig. 51. Typical forms of baffle piers and sills.

Cavitation damage on the sides of baffle piers has occurred on several high-head projects. In one instance the sides were deeply cut away during floods, leaving the blocks in the rough form of large I beams.

In general, piers with rounded edges have sustained less damage than those with sharp edges. However, this measure reduces to some extent the ability of the pier to dissipate energy. Nine baffle piers at Bonneville Dam on the Columbia River were repaired in 1947 with a 9 in. radius on each leading edge and a 2.5 ft radius connecting top and back slope.

Other examples of the various methods of protecting against scour are shown by

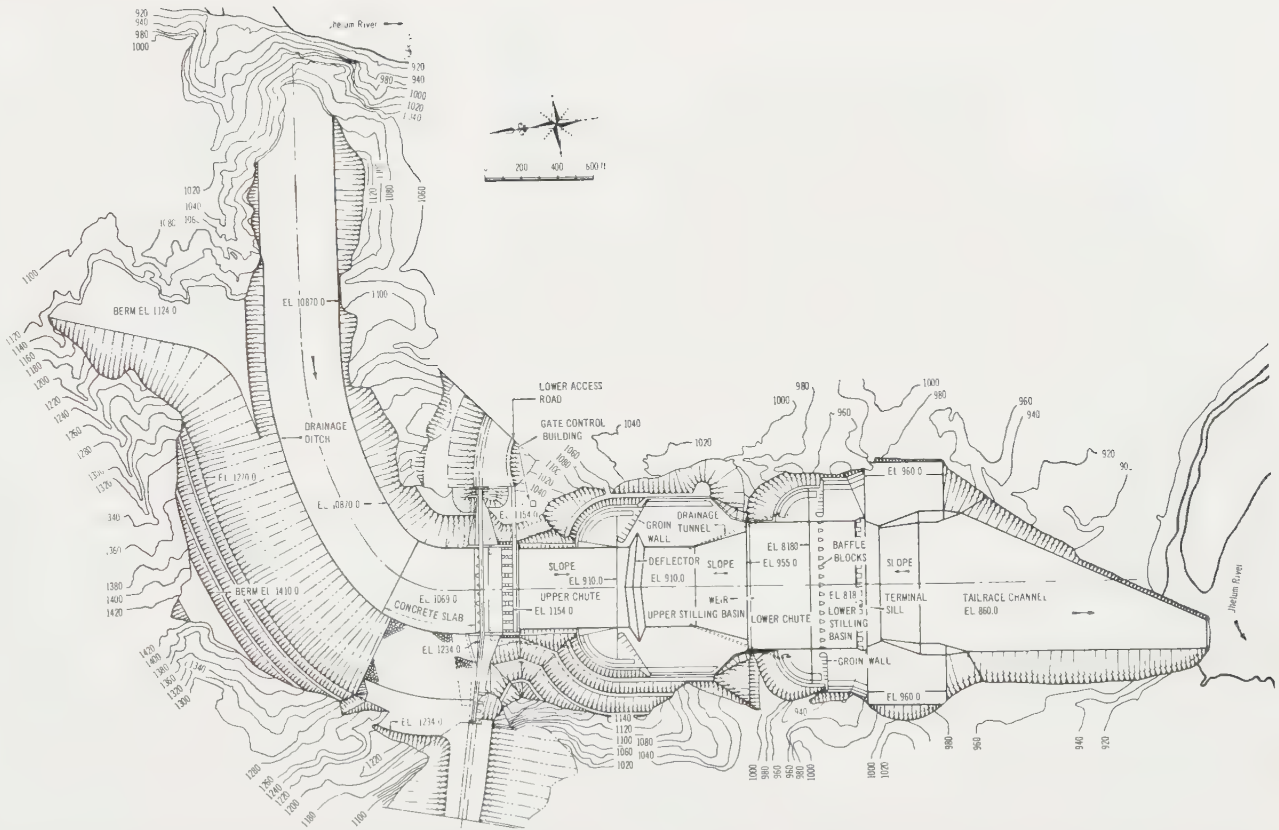

FIG. 52. Mangla Dam—plan of the main spillway designed for a maximum discharge of 1,080,000 cfs.

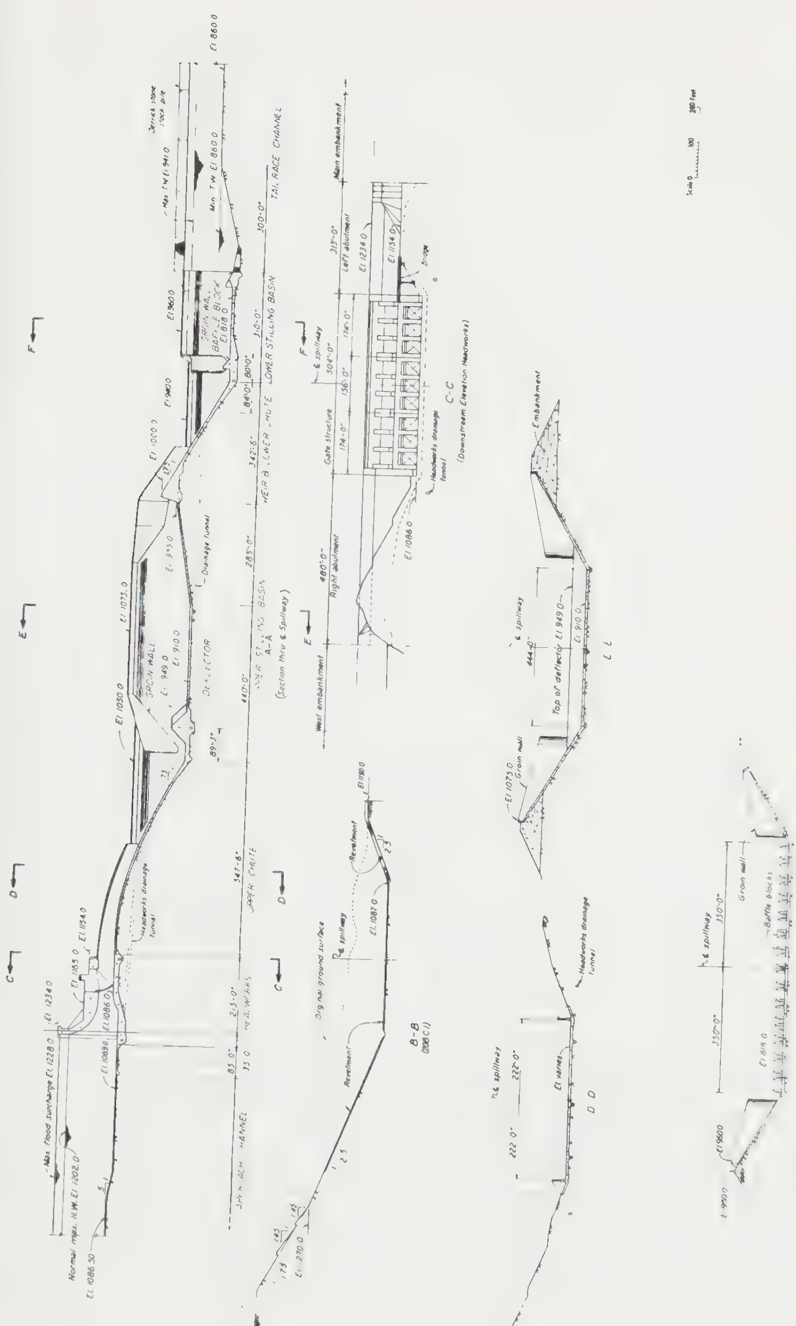

FIG. 53. Mangla Dam—spillway general sections.

Figs. 49 to 51, inclusive. These are principally of historic interest as continuous research by the U.S. Army Engineers, the U.S. Bureau of Reclamation, and other water-control agencies and private firms is resulting in continuous improvement. The problems vary from structure to structure. Each is unique and seldom may the feature of one design be applied to another. Designs for important spillways passing large amounts of water must be checked by model tests if reliable results are to be obtained.

The Mangla spillway which is now being constructed by the government of West Pakistan offers one example of a spillway structure which was designed to meet very special conditions. The headworks and orifice gates for this structure are shown by Fig. 19. A plan of the spillway is shown by Fig. 52 and a section by Fig. 53.

The Mangla spillway is designed to discharge 1,100,000 cfs, as shown by Figs. 52 and 53. To eliminate the effects of tail-water uplift two stilling basins were required. Energy dissipation in the upper basin will be achieved by a hydraulic jump which will be induced by a 39-ft-high deflector sill.[1]

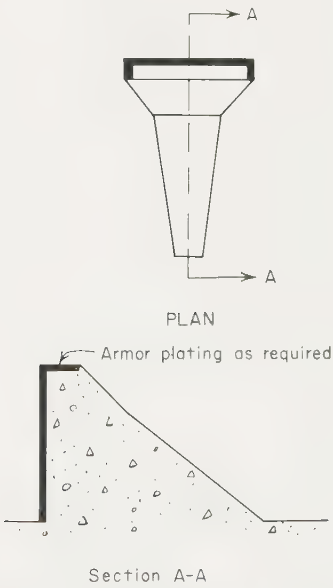

FIG. 54. General type of lower stilling-basin baffle blocks—Mangla Dam project.

The required depth of water in the upper stilling basin is provided by a weir of ogee shape at the downstream end of the basin. The maximum depth of flow over this weir will be approximately 45 ft.

From this weir water is next conveyed down a second chute to the lower basin. The maximum drop from the upper stilling basin to tailrace elevation will be 125 ft. The energy of this drop will be dissipated in the lower stilling basin where a second hydraulic jump will be formed. Model tests indicated that a combination of baffle blocks and terminal dentated sills would offer the best means of dissipating the residual energy. With the arrangement shown by Figs. 52 and 53 about two-thirds of the energy would be dissipated in the upper basin and about one-third in the lower basin.

To avoid the formation of negative pressures and resulting cavitation the blocks were constructed with T-shaped sections, as shown by Fig. 54. The block faces were heavily armored with steel. The results of model tests showed that each block could be subjected to a longitudinal force of 7.2 million lb.

The poor sandstone foundations at Mangla precluded the use of high vertical training walls. To overcome the unfavorable effects of the sloping sides of the stilling basins, groin walls and guides were used as shown by Figs. 52 and 53.

As a guide to the design of stilling basins for small dams the Bureau of Reclamation presents three charts in "The Design of Small Dams" which are reproduced in Figs. 55, 56, and 57. Figure 55 applies to jump phenomena where the incoming flow depths and velocities are in the Froude-number range between 2.5 and 4.5.[2]

[1] Progress at Mangla, *Water Power Eng.*, May, 1966, p. 173.

[2] "Design of Small Dams," pp. 294–298, U.S. Bureau of Reclamation.

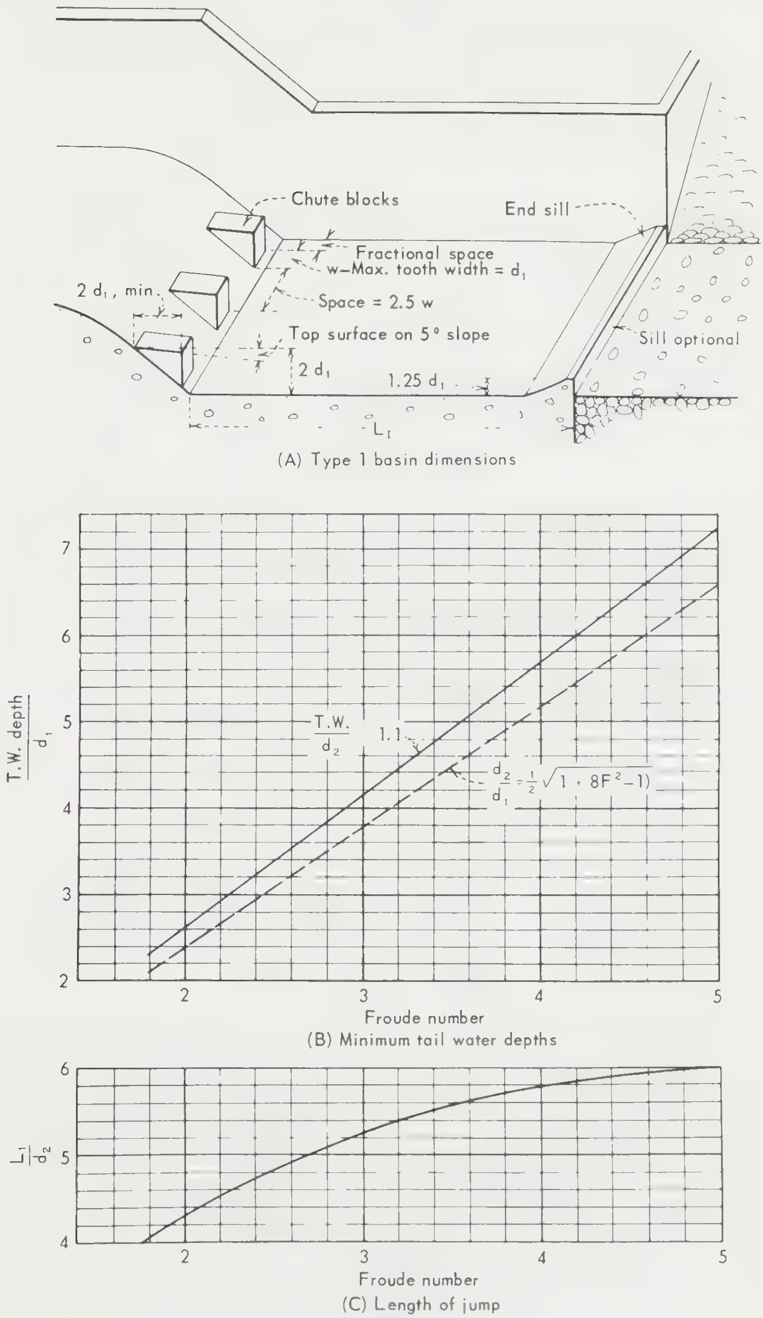

FIG. 55. Stilling-basin characteristics for Froude numbers between 2.5 and 4.5.

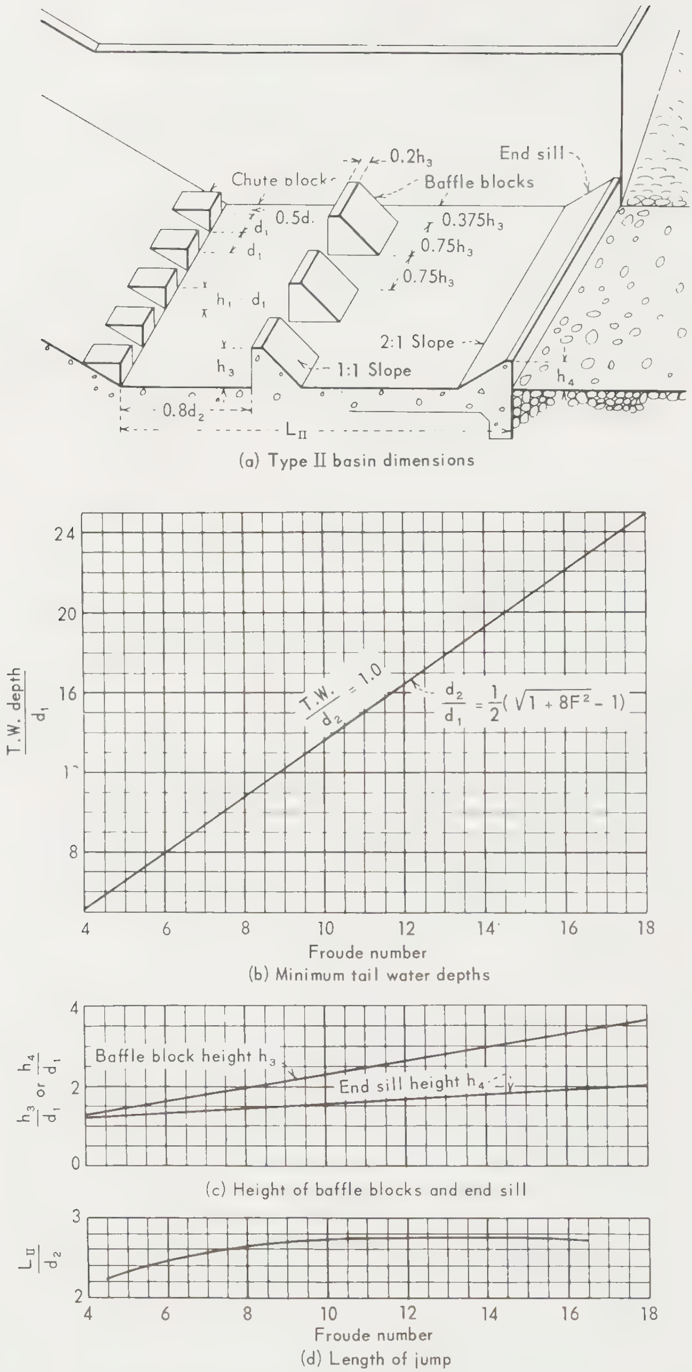

FIG. 56. Stilling-basin characteristics for Froude numbers above 4.5 where incoming velocity does not exceed 50 fps.

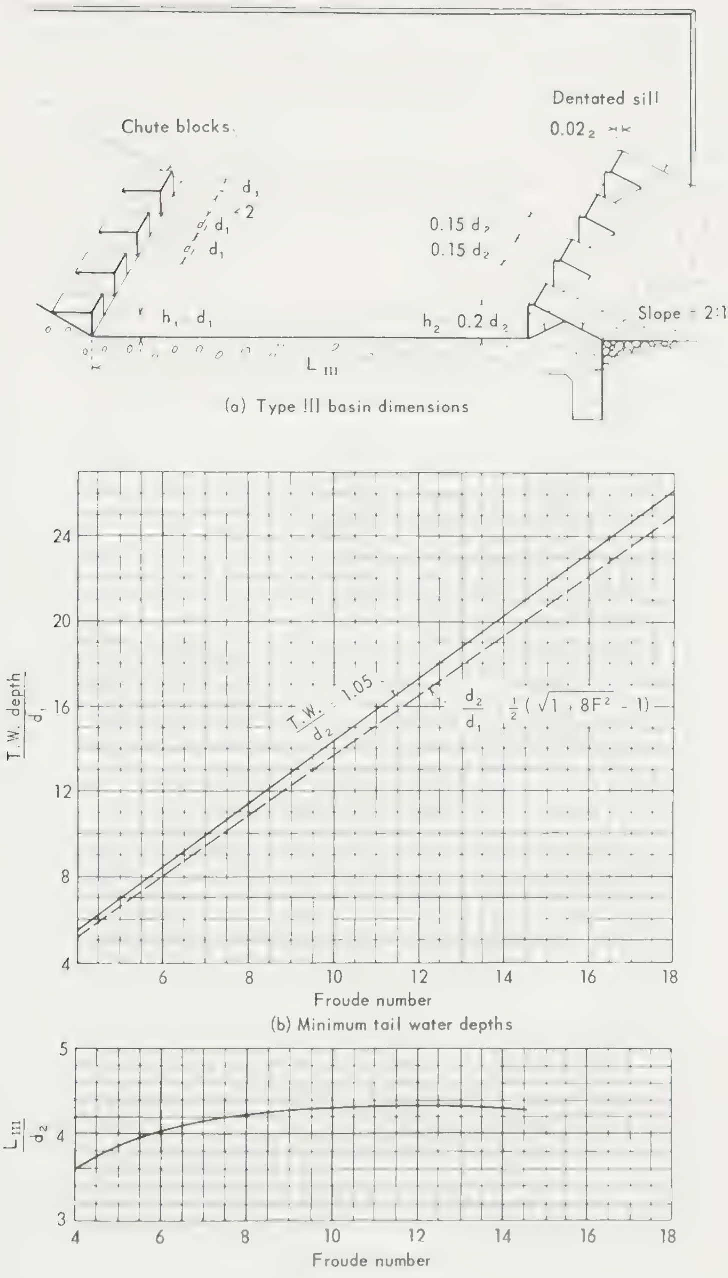

FIG. 57. Stilling-basin characteristics for Froude numbers above 4.5.

Figure 56 applies to Froude numbers above 4.5 where the incoming velocity does not exceed 50 fps. Where velocities exceed 50 fps or where impact baffle blocks are not employed the type of basin shown by Fig. 57 can be used.

It must be emphasized that these three charts should be used only in the formulation of preliminary designs. The whole subject of stream-bed protection is a complex one, and in most cases, no single chart can offer a complete solution.

SECTION 21

SPILLWAY CREST GATES

By P. R. Mayer and Joseph R. Bowman*

1. Introduction. However advantageous a fixed-crest free overfall spillway may be from the operating standpoint, the great value of property and improvements in many reservoir sites prohibits the backwater stages resulting above such a dam during flood. At the same time, the desirable storage or head requirements on projects concerned with the conservation of water or control of floods may often approach the limit that can be obtained at the feasible damsites.

The solution of this problem lies in some form of movable crest, by means of which increases in flood stage above the dam may be materially lessened within the limits of backwater effect, without seriously curtailing the low-water storage or head normally available.

Many types of movable crests are in successful operation. However, relatively few of these many types may be suitable or economical for a given situation. The problem of the engineer is to select and design the proper type and size of crest gate that will pass the maximum flood without appreciable damage to the dam and other structures and in which there is proper economic balance between the cost of structures and operation and the costs due to the resulting flood stages upstream.

The degree of success with which this problem is solved depends on knowledge of the local conditions under which the spillway gates must be operated and an appreciation of the features of any type which are fundamentally suitable or unsuitable for these conditions.

2. Conditions under Which Gates Must Be Operated. Generally speaking, the local physical, hydrological, climatic, and operating conditions must be properly evaluated in selecting the most suitable size and type of spillway gate. Consideration must be given as to whether:

1. The foundation is susceptible to serious erosion or is very resistive.
2. Surface turbulence downstream is objectionable.
3. The stream carries heavy drift or logs.
4. Floods are flashy or rise gradually.
5. Floods are frequent throughout the year or are confined to a few occurrences at definite seasons.
6. Intense floods occur frequently or only at long intervals.
7. The stream is subject to severe ice floes.
8. The gates will freeze in during the winter and, if so, whether they may be expected to be frozen or clear at the time of the first spring floods.
9. The pool level must be closely regulated.
10. Water can be wasted or must be conserved.
11. The spillway must be operated and maintained by other personnel or will have its own operating force.

* Parts of this section appearing in the First and Second Edition were contributed by Joseph R. Bowman and the late James S. Bowman. The additional material appearing here was contributed by P. R. Mayer.

12. Some operating force will be available at all times or only occasionally.
13. The reservoir must be lowered rapidly to provide flood-control storage.

The study of many of these conditions falls under a special subject, such as hydrology, and therefore will not be treated in detail in this section.

From the fact that a spillway usually concentrates the discharge in a much narrower width below the dam than was occupied by flood flow under natural conditions, every consideration should be given to the possible consequences of this change in regimen. This fact argues for as long a spillway as feasible. Particularly where foundations are susceptible to serious erosion, lengthening of the crest, with corresponding reduction in depth of overflow, reduces the energy to be dissipated per unit length. The economics of this problem may be approached by comparing the cost of various spillway lengths with the cost of providing the required stilling pool or other protection downstream. The persistence of surface turbulence for considerable distances downstream is often objectionable from the standpoint of navigation or because of serious bank erosion. Although this is largely a problem of spillway design, the effects may often be minimized by proper consideration of the size and arrangement of the gates.

Heavy runs of ice or drift necessitate long gates from the fact that piers must not offer sufficient obstruction to cause jams. If the ice goes out with a moderate rise, a number of gates of the overflow type or a length of open spillway should be provided. However, on many large reservoirs, the ice melts in place and but little passes the spillway. A study of this condition should be made on adjacent existing reservoirs.

Frequent flashy or intense floods require gates with mechanism that can be readily and conveniently operated at any time with minimum operating labor. When gates must be constantly available for use in cold climates, a type should be selected that will reduce the leakage to a minimum and avoid the dangers of freezing which are inherent in some types. The design should be such that various methods of heating and ice removal can be readily provided.

Where pool levels must be closely maintained or fluctuated within certain limits, it is advisable to provide a number of gates designed particularly for this service as well as for other purposes. These gates should be arranged for close adjustment and may be operated from fixed hoists controlled from the powerhouse or other point if frequent attention is required. However, if the incremental volume of the reservoir is large, compared with the variation in discharge, small inaccuracies in gate adjustment are usually of no consequence. Automatic operation is largely related to this question by way of the attendance required to maintain constant pool levels. However, a considerable amount of attendance and a high degree of maintenance are required for any so-called automatic gate, and the additional cost of this equipment is rarely justified by any actual saving in operation.

It is fortunate that proper provision can usually be made to meet any of these conditions without detriment to others. Great ingenuity is often required, however, to meet an abnormal condition in a small development where the more elaborate provisions possible on a large development cannot be justified as to either investment or cost of operation. The question often arises as to how far provision against extremely improbable circumstances or combinations of circumstances should be carried. Except where loss of life or great property damage might result from possible inadequacy, this question may often be resolved by comparing the additional charges with the possible damage, such as overtopping of masonry structures or the flooding of land, that would occur at an estimated frequency. Such estimates should, however, be used only as a guide in the exercise of the soundest judgment in each case and not as a justification for inadequate works. Frequency studies do not fix the time of occurrence, and the possible consequence of serious damage during the first few years of operation must be considered.

FLASHBOARDS, STOP LOGS, AND NEEDLES[1,*]

3. Flashboards.† Flashboards, stop logs, and needles are the simplest and probably the oldest types of movable-crest devices. Where the size and type of installation are such that they can be readily handled by the operating force available, they are efficient and economical. However, where the installation is large or where frequent freshets require continual manipulation, the operation becomes laborious and hazardous. They may often be adopted with considerable saving in cost for portions of the spillway that will be in use only during the most extreme floods.

Flashboards are water-retaining devices placed on top of a fixed crest to provide an extra depth of storage, but which may be quickly removed at times of flood. The means of removal may be by deliberate failure of the flashboards or of their supporting members when the boards are overtopped to a predetermined height or by providing some simple tripping device that may be operated when necessary.

Flashboards have the advantage of providing an unobstructed crest when lowered. Where possible, a regulating gate, of sufficient capacity to pass the normal flow, should be provided so that the headwater may be temporarily lowered to allow the flashboards to be set up. This may conserve water and head for a considerable period after the recession of high water, during which it might otherwise be impossible to restore the flashboards. Such a gate may also be utilized for passing small rises which would otherwise trip the boards. Automatic flashboards have been a fertile field for invention. However, the wear and corrosion of moving parts with the accompanying change in frictional resistance, fouling with trash, and similar troubles have in time spelled the failure of many of these schemes that were alluring on paper.

4. Stop Logs. The customary stop logs are dimension timbers spanning horizontally between vertical grooves in adjacent piers. They are built up one on another, a vertical bulkhead being formed from the crest of the spillway to the headwater level. They may vary in size from short lengths, which can be handled by one man, to sizes limited only by the span and the capacity of a power winch to raise them. A means of handling is provided by cutting a longitudinal slot vertically through the timber near each end. A bolt is then passed transversely through this slot on the horizontal center line of the timber. A pike pole having a special hook with a line attached is lowered down the groove in the pier until the hook enters the slot and engages the bolt, after which the line may be hoisted by hand or by a power winch.

Since the logs must be handled through overflowing water, it is imperative that the grooves in the piers be made amply deep to protect the hoisting device from the current during the fishing operation. This depth is usually deeper than the allowable bearing stress of the timber requires and, for any considerable depth of overflow, should be not less than 12 to 16 in. The groove should not be wide enough to permit the timber to turn sufficiently to bind. The outer downstream corner of the groove should be protected by a continuous steel angle to provide ample bearing area, to give greater watertightness, and to minimize frictional resistance in moving the timber.

Stop logs may prove an economical substitute for more elaborate gates where relatively close spacing of piers is not objectionable and where variations in flow require the removal of only a few logs, except at infrequent intervals. They are adaptable to deeper openings than are flashboards, and where a bridge is available, shallow stop logs are often substituted for flashboards on account of the greater facility of operation.

* Superior numbers refer to items in the Bibliography at the end of this section.

† In this section flashboards are distinguished from stop logs, or other devices, as not being supported in grooves at the ends or having a permanent hoisting mechanism attached.

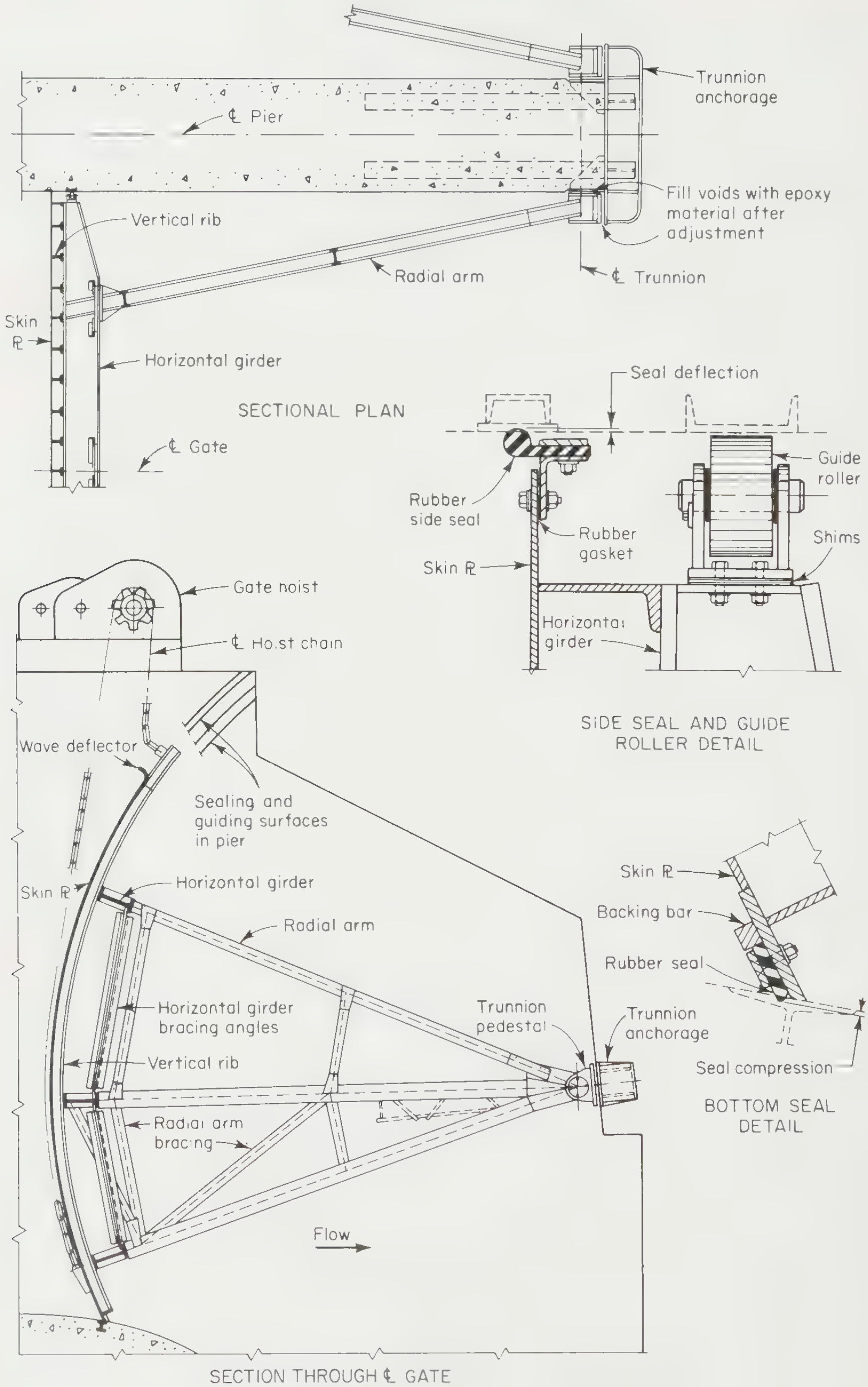

Fig. 1. Details of a conventional Tainter gate.

5. Needles. Needles are set on end side by side to close an opening. They are supported at the top by a runway, from which they are handled, and are supported at the bottom by a ledge on the sill or spillway crest. They are usually made of dimension timbers.

Needles are somewhat difficult to place in swift water of considerable depth. Hence, their use is largely confined to emergency spillways where they are seldom raised and where they can readily be replaced after floodwaters have receded. For emergency bulkhead construction in still water, needles are preferable to stop logs for the reason that they sink readily and can be staunched as placed. On the other hand, it is difficult to hold stop logs down and force them into proper sealing contact without differential head. After the entire bulkhead has been placed and a differential head established, the frictional resistance may become so great that the logs cannot be forced into position to close the leaks between them.

TAINTER GATES

6. Principal Features. The conventional form of Tainter gate consists of a skin plate formed to a segment of a cylinder, the vertical elements being circular arcs, which

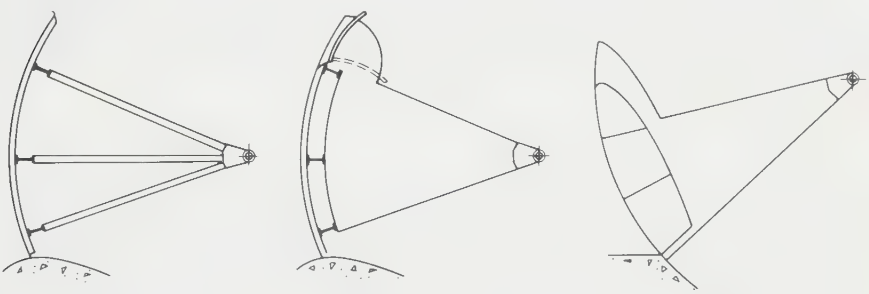

Fig. 2. Types of Tainter gates.

is supported by a framework of horizontal or vertical purlins and stiffeners. The purlins in turn may be supported by vertical or longitudinal girders from which two or more radial struts converge downstream to horizontal shafts or pins that are anchored in the piers and carry the entire thrust of the water load. The skin plate is made concentric to this pin, and hence the resultant of the water pressure passes through the pin, creating no moment to be overcome in hoisting the gate. This is the fundamental principle of the gate. The hoisting load consists solely of the weight of the gate, the friction between the side seals and the piers, and the small force necessary to overcome the moment of the frictional resistance at the pins.

Tainter gates are probably the simplest, most reliable, and least expensive type of crest gate for passage of large floods. They require no slots in the piers and have good discharge characteristics. They have become the most widely used crest gate in the United States[2] and are being used with increased frequency in other countries.

The conventional Tainter gate is not suited for the passage of floating material unless fully open, which may involve waste of water. This drawback may be overcome by altering the conventional gate by adding a flap to the top of the gate (Fig. 2*b*) or by making the gate submergible (Fig. 2*c*) so that water may be passed over the top of the gate. For larger discharges, both these types are raised in the same manner as the conventional gate. The gate at the right of Fig. 3 is a conventional 40-ft-wide by

FIG. 3. Priest Rapids Spillway. (*Harza Engineering Co.*)

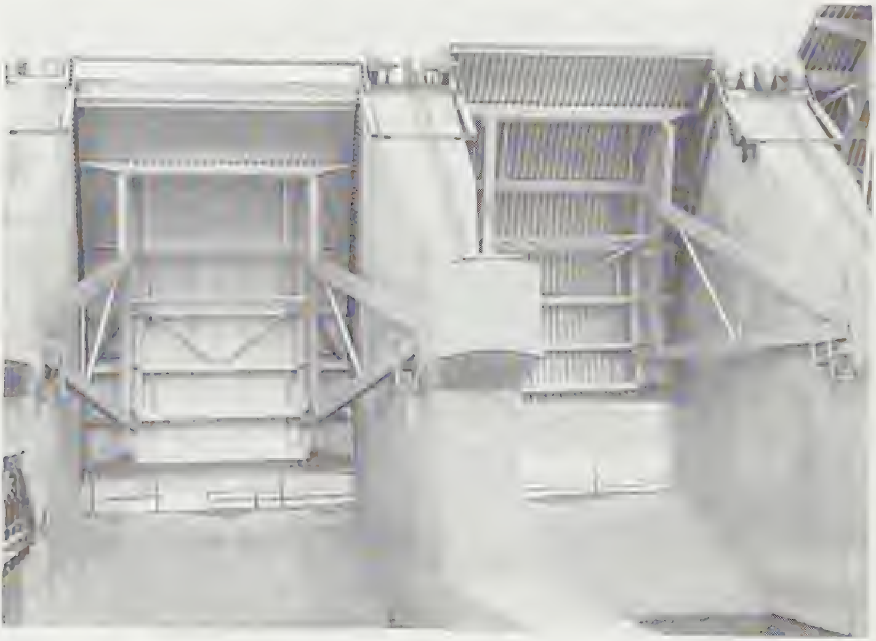

FIG. 4. Wanapum Spillway Gates. (*Harza Engineering Co.*)

50-ft-high Tainter gate with a 25-ft-wide by 12-ft-high flap mounted in the top central portion.

Tainter gates are usually operated by chains or cables attached near the bottom of the gate at each side on either the upstream or downstream side of the skin-plate assembly. Some gates also have been made to be operated by trunnion-mounted hydraulic cylinders where piston rods are attached to the gate.

Since the early fifties there has been a marked increase in the maximum size of Tainter gates. Gates 50 ft wide with a damming height of 65 ft above the spillway crest are in use at the Wanapum Dam on the Columbia River (Fig. 4) and on the Guri Dam in Venezuela. There are a number of dams on the Ohio River with gates 100 ft wide with a damming height of 42 ft above the spillway crest. The large concentrated loads brought to the trunnions of these large gates have led to the increased use of prestressed steel and concrete anchorages to transfer these loads to the spillway piers.[3]

FLAP GATES

7. Principal Features. This type of gate is a leaf hinged at bearings along its lower edge. The leaf may be flat or curved to give better discharge characteristics when rotated to its open position. The position of the leaf may be controlled by hoisting attachments that pull or push at one or both ends or by hydraulic or screw-stem hoists that push at selected locations under the gate. This type of gate can be built to great lengths and is well suited for passing floating material and for close regulation. Counterweights and/or floats may be incorporated in the hoisting mechanisms of relatively small flap gates to provide automatic operation with little or no other source of power.[6]

As with flashboards, the flap gate has been a fertile field for invention and ingenious arrangements. Figure 5 shows two of the many possible arrangements. Unlike flashboards, however, which are either fully closed or fully opened, the flap gate which operates at partially opened conditions must be designed for the hydrodynamic effects of the overflowing sheet of water. If not properly designed and vented, destructive vibration forces may occur.[10] It is recommended that hydraulic-model studies simulating all expected opening conditions of the prototype gate be carried out before proceeding with the fabrication of flap gates of any importance. The designer also should not be too optimistic about the reliability of any automatic scheme of operation.[6] Many a scheme that appeared foolproof on paper proved to be not so reliable when corrosion and misalignment of functioning parts upset the assumed theoretical balance.

DRUM GATES

8. Principal Features. The drum gate fundamentally is an acute circular sector in cross section, formed by skin plates attached to internal bracing. It is hinged at the center of curvature, which may be either upstream or downstream, in such manner that the entire sector may be raised above the masonry crest or may be lowered so the upper surface becomes coincident with the crest line. These gates are controlled by the application of headwater pressure underneath. Figure 6 shows the two principal arrangements of this type of gate. Section *a* in the figure shows that developed by the U.S. Bureau of Reclamation, which is hinged on the upstream side and is enclosed on all three faces and at the ends to form a watertight vessel. This gate has been used on many projects designed by the Bureau of Reclamation and has been built as large as 135 ft long by 28 ft high. Figure 6*b* shows the type that is hinged on the downstream side and that usually is enclosed only on the upstream and downstream surfaces.

Drum gates are not adapted to low dams having low substructures on account of the deep excavation required and the liability of flooding of the recess in which the

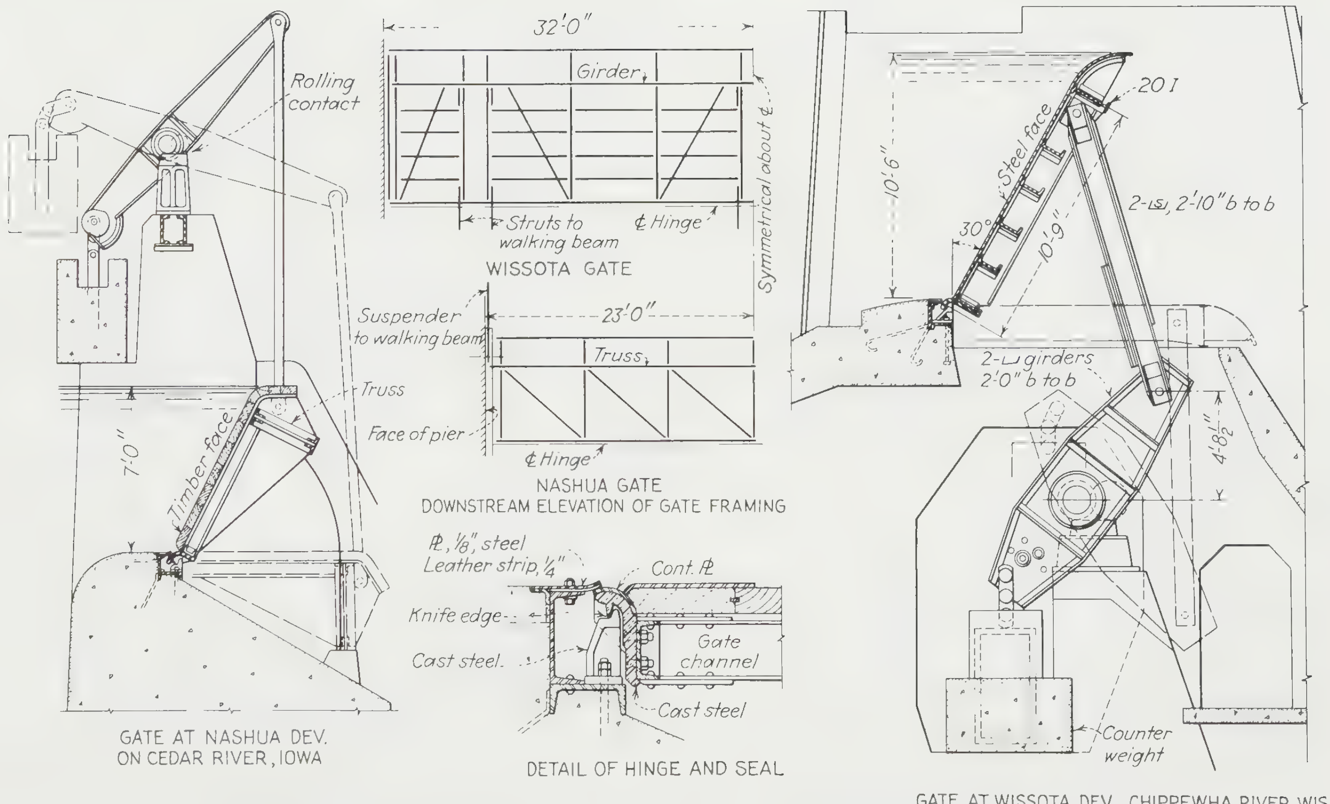

Fig. 5. Stauwerke automatic counterweighted gates. (*Fargo Engineering Company, Engineers.*)

gates float. The operating mechanism for controlling water pressure beneath the gates may be placed in the abutments, or in the piers with access through a gallery, the necessity of an overhead bridge being eliminated and the pier height being reduced to a minimum. They are very well adapted for surface regulation and, on account of the lengths to which they can be constructed, are suitable for passing debris. Sheet ice causes no damage because of the upstream slope, and the seals can be easily protected against freezing under usual winter conditions. With extremely low temperatures, special provision would have to be made for insulation and heating of the downstream seals.

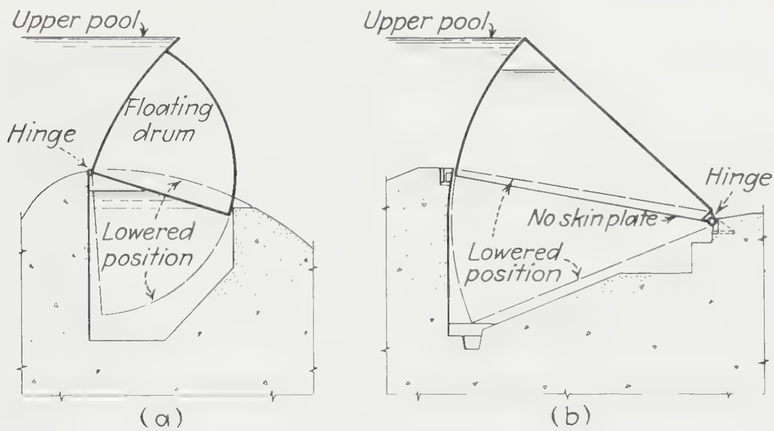

Fig. 6. Drum gates.

Because they are relatively more costly than Tainter or flap gates, and their operational features may be achieved by judicious combined use of Tainter and flap gates, the use of drum gates is becoming increasingly rare.

VERTICAL-LIFT GATES

9. General Description. The designation vertical-lift gates is here used to include all rectangular gates supported by vertical guides in which the gates move vertically in their own plane. The hoist is usually mounted on a runway overhead, and the gate is either raised or lowered, depending on the particular design, from its normally closed position by means of cables or stems. The gate proper consists of a framework to which a skin plate is attached, normally on the upstream face. This presents no unusual difficulties in design, the principal problem being the determination of the arrangement of beams and girders and skin-plate thickness which will result in the most economical construction. However, such features as seals, lifting mechanisms, dogging devices, rollers, guides, and similar appurtenances require meticulous care in design and warrant a careful study of the operating behavior of such features under similar conditions on existing projects.

10. Sliding Gates. In this type, the frame of the gate bears directly on the downstream guide member, the seal being formed by contact between the two. The coefficient of friction in sliding may vary from 0.5 to 0.9, which requires large hoist capacity not only for raising but for lowering as well, for only in the smaller sizes will the weight of the gate exceed the frictional resistance when the gate is near the position of maximum water loading.

This fact rather definitely limits the size of this type to such dimensions that the additional cost for wheels or rollers to lessen the frictional resistance is greater than the additional hoist capacity. As a practical matter, this limits the use to small spillways, wasteways, log flume inlets, and similar purposes, and in these uses it is particularly adapted to being lowered for passing the discharge over the top.

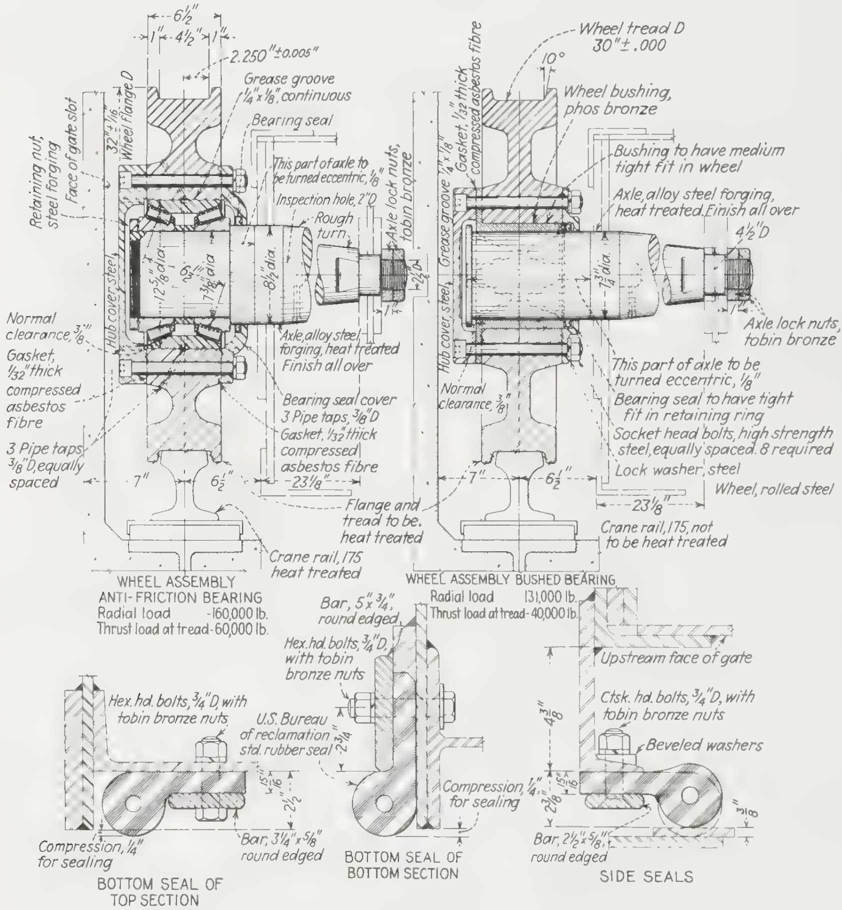

FIG. 7. Wheels and seals for spillway gates. Pickwick Landing Dam.

11. Fixed-wheel Gates. This type differs from the sliding gate in having a series of fixed wheels mounted along each end to carry the water load to a vertical track on the downstream side of the gate groove. The wheels substitute rolling friction for sliding friction, which allows the gate to be self-closing under its own weight. The wheel shafts are located between the main horizontal girders and are supported either by two vertical members of the frame or in pedestal bearings bolted to the frame.

As with the conventional Tainter gate, the fixed-wheel gate is not suitable for the passage of floating material without a considerable waste of water. Greater headroom also is required for hoisting this type of gate above the water surface. Two general methods have been used to overcome these drawbacks:

1. To split the gate horizontally into sections that travel in the same guides with the upper sections setting directly on top of the lower sections. The top section is made a suitable height for surface spilling or regulation. The upper sections are progressively raised and removed from the guides, and the lower sections are grappled and raised to the required position. This method also considerably reduces the hoisting load. Figure 8 shows gates 40 ft wide and 62 ft high. Three of these gates are sectionalized into three leaves each 20 ft 8 in. high. The top leaf of the fourth gate is further sectionalized into two 10 ft 4 in. high leaves. The top leaves of the gates in

FIG. 8. Box Canyon Dam Downstream view of spillway. (*Harza Engineering Co.*)

Fig. 8 are shown stored, while the center leaves are raised to allow water to discharge under them and over the bottom leaves.

2. To divide the gate into two leaves arranged so that the upper leaf may be lowered alongside the lower leaf to allow small flows over the top of the gate. The top leaf is supported at its top by a crossbeam mounted on wheels that travel on the same tracks that the wheels for the lower leaf travel on. The bottom of the top leaf is supported by wheels that roll on the lower leaf. This type of gate has been used quite extensively in Europe, where it is called a "hook gate" because the cross section of the top leaf resembles a hook owing to its being shaped for the overflowing water.

STONEY GATES

12. General Description. Stoney gates, so called because of their inventor F. G. M. Stoney, are mentioned here as a matter of historical reference since the writer is not aware of their use on any projects built within the last 30 years. The fundamental difference between Stoney and fixed-wheel gates is that in the former a moving train of rollers is substituted for the fixed wheels in the latter. The roller train, composed of horizontal rollers held in position by shafts bolted into continuous vertical bars on each side, is attached to neither the gate nor the guide, but rolls vertically between the two as the gate is moved. As the rollers transmit the entire load from a bearing strip on the gate to a roller path on the guide, there is no axle friction, and only rolling friction is developed. Since the gate moves on the roller diameter while the roller revolves on its radius, the roller moves only one-half the

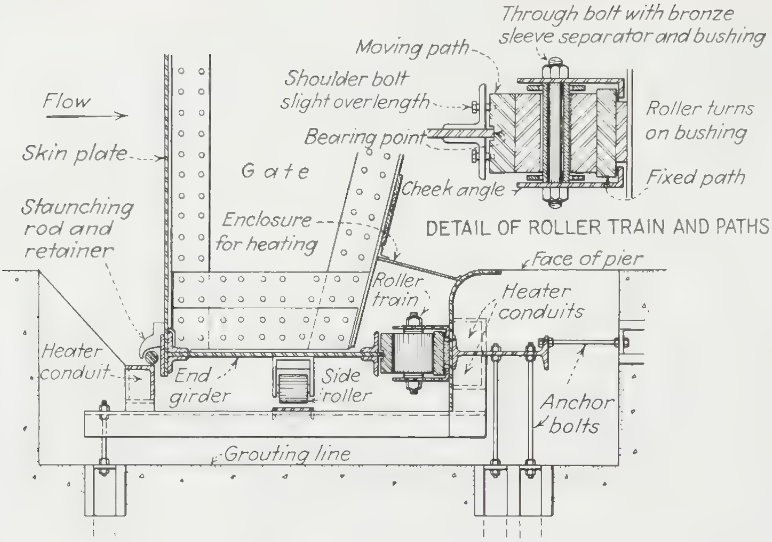

FIG. 9. End section of Stoney gate. (*From F. Newell, Dominion Bridge Company, Ltd.*)

distance of the gate movement and the bottom of the roller train always lags the gate by one-half the distance the gate is opened.

Figure 9 shows details of the end of a Stoney crest gate and the roller train. The gate leaf is constructed much the same as any other vertical-lift single-leaf gate.

Vertical-lift gates have been generally used where it was necessary to store a high head of water and to obtain large discharges in narrow confines. Since severe hydraulic conditions prevail at the slots in the piers and since these gates require powerful hoisting machinery, large piers, and hoist housing structures, they are seldom specified in the United States since the advent of large Tainter gates.

BEAR-TRAP GATES

13. General Description. A bear-trap gate consists essentially of two leaves, an upstream leaf hinged and sealed along its upstream edge and a downstream leaf hinged and sealed along its downstream edge. When the gate is lowered, the leaves are in horizontal position with one leaf lying on top of the other. The two leaves have a sliding seal or hinge at their juncture and are sealed against the piers at each end. When pressure from headwater is applied in the chamber underneath, the gate can be raised to any desired height so long as the two leaves remain in contact. The water pressure under the gate is regulated by an adjustable weir or by the setting of inlet and outlet valves in a control chamber in the abutment of the spillway. This was probably the first gate involving the principle of the application of headwater pressure for its operation.

Bear-trap gates have been used in the United States for over a hundred years as regulating gates in movable navigation dams and for log-sluicing operations. An improved form of bear trap has been developed and widely used in central Europe as an automatic spillway crest, and a number of gates of this type have been installed in the United States.

14. American Bear-trap Gates. In American engineering practice, a large number of variations from the simple bear-trap form have been designed. The principal forms of these are shown in Fig. 10. The purposes of these variations have been to eliminate friction between the leaves, to close the reentrant angle to trash accumulation, to economize on substructure width, and to make it possible to raise the gate with small differential head.

In designing a bear-trap gate, great care should be used in determining the external water load in various positions, and calculations should usually be checked by experiments. This fact is of particular importance in determining (1) the differential head required to raise the gate and (2) the water level underneath required to establish equilibrium when the gate is partly raised. For automatic operation, it is essential to determine the conditions of equilibrium for all positions.

Large logs and trees may cause severe damage to a partly lowered bear trap, because when part way over the crest the head end may fall to the downstream leaf with sufficient impact to break the planking and the rear end will drag over the crest timbers. To meet this condition, heavy transverse skid timbers may be bolted to the surface of the downstream leaf at about 2-ft intervals and a heavy steel angle should be anchored to the ends of the purlins to cover the edge of the upstream leaf.

The accumulation of silt under bear traps set on the riverbed has been a source of considerable trouble and expense. The U.S. Engineer Department has now developed methods for removal of this silt by sluicing.

Bear-trap gates are well suited for surface regulation and passing drift and ice. They can be built in almost any length usually required, and as no overhead structure

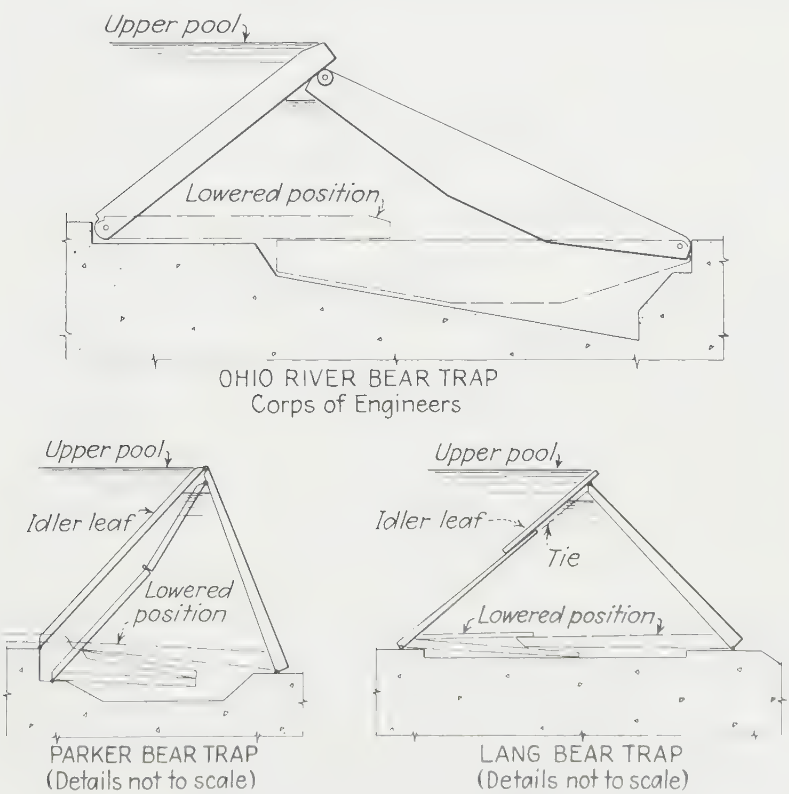

FIG. 10. American bear-trap gates.

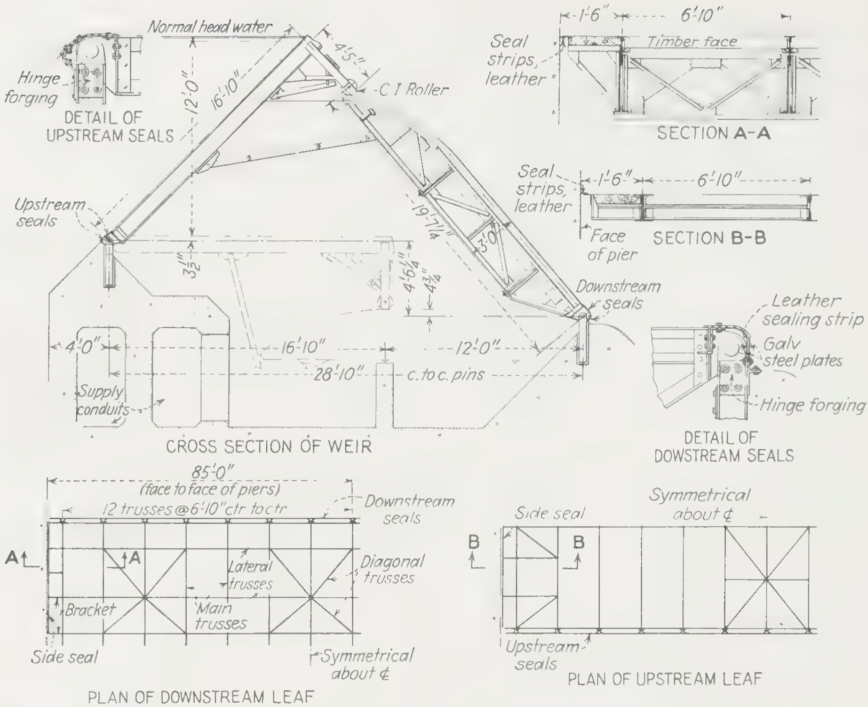

Fig. 11. Huber and Lutz roof weirs for Texas Hydro-Electric Corporation. (*Fargo Engineering Company, Engineers.*)

Fig. 12. Types of rolling gates.

is needed, they offer little obstruction to flood flow. In low-head dams, there is considerable saving in the cost of substructure owing to elimination of a deep recess or gate chamber. They are not seriously affected by ice, for the leaves drop away from ice accumulation on the piers when being lowered and the overflowing sheet cuts the ice away as the gate is raised.

The major objection to a bear-trap gate is the low coefficient of discharge resulting from the broad flat crest when the gate is lowered. This is, of course, not objectionable in low dams with the sills practically at riverbed level.

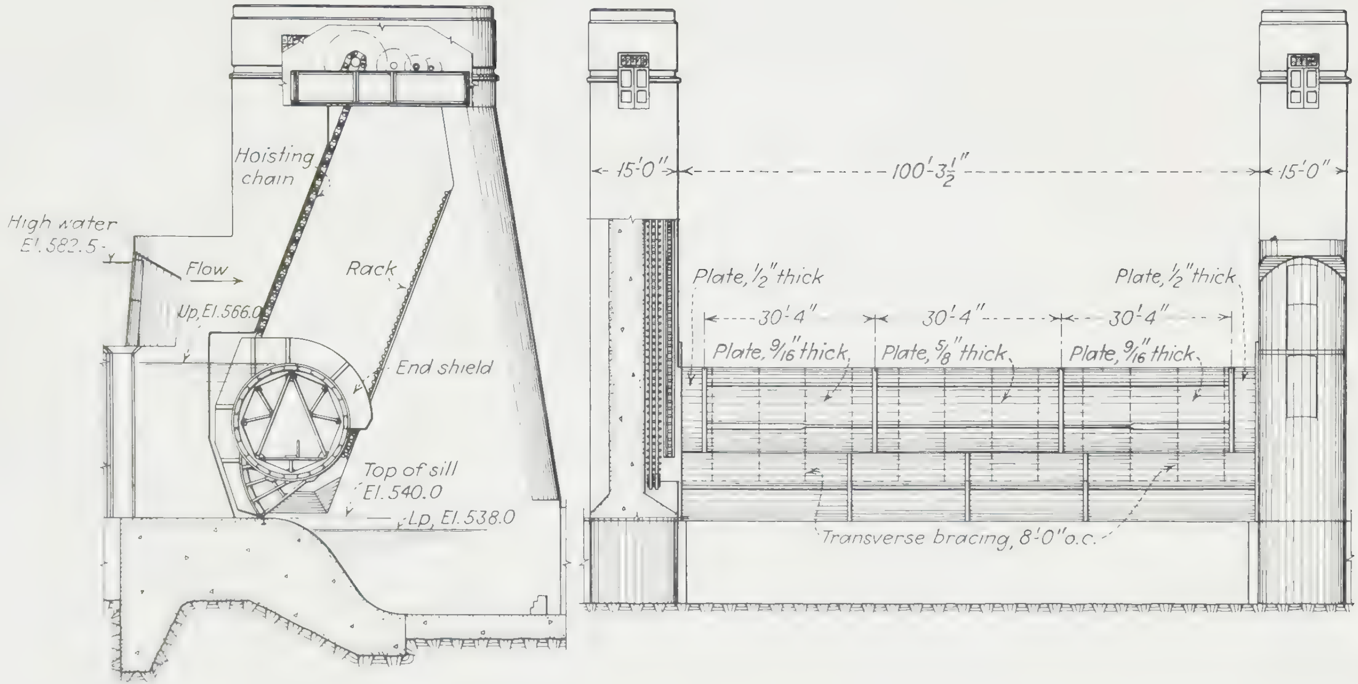

SECTIONAL ELEVATION

UPSTREAM ELEVATION

FIG. 13. Rolling gate at Lock and Dam No. 1, Kanawha River. (*U.S. Corps of Engineers.*)

15. European Bear-trap Gates. The most prevalent European type of bear trap is that developed by Huber and Lutz of Zurich, Switzerland. This type, known as the *roof weir*, is shown in Fig. 11. It adds a vertical lip to the upstream leaf that carries rollers bearing on the downstream leaf, reduces friction and eliminates the reentrant angle, and introduces curvature in the downstream leaf, thus eliminating the objections to the original bear trap.

ROLLING GATES

16. General Description. The conventional rolling gate consists of a cylindrical plate-steel roller, approximately as large in diameter as the height of opening to be closed and spanning between piers. Encircling each end of the roller is a heavy annular rim casting with peripheral teeth and a bearing surface which transfer the loads to similar teeth and a bearing surface on a sloping rack supported by a ledge in the piers. The gate is raised or lowered along this rack by means of a heavy chain which winds around and over the top of the gate at one end and pulls upward, parallel to the rack. This gate was developed in Europe, but a number of large installations have been made in the United States.

There are two principal variations of the conventional type: (1) where the roller is greatly reduced in size and merely forms the rolling member on which the water face, composed of a sector of considerably greater height and radius, is supported, and (2) the Greisser gate in which light trusses span between load disks with toothed rims of the required circumferential length and support the curved sector of the water face. The conventional type may be also arranged so it can be lowered a small distance for passage of drift, or an ice shutter may be hinged on top for the same purpose. Figure 12 shows these various arrangements diagrammatically.

The rolling gate has been extensively used by the Corps of Engineers on the upper Mississippi and on past Ohio River improvements. Figure 13 shows the gate installed at Lock and Dam 1 on the Kanawha River. This gate has a total height of 26 ft, the roller being 19.5 ft in diameter and the lower lip being 6.5 high, and may be considered as the conventional type, for the roller carries directly over one-half the horizontal water load and a lip is always required to support the bottom seal. The transverse stiffening consists of three segmental trusses, the inner chords of which intersect at the main splice points, forming an extremely effective and economical arrangement. These support longitudinal purlins at an angular interval of 15 deg. The internal diameter of the roller is constant throughout, but the shell thickness varies from end to end as required by the bending and torsional moments. As with drum gates, the use of rolling gates is becoming increasingly rare because of their high cost.

Bibliography

1. "Spillway Gates on or Adjacent to Dams," Serial Report of the Hydraulic Power Committee 1928–1929, N.E.L.A.
2. Tommerup, Carl C. H., *Proc. ASCE, Power Div.*, December, 1962, paper 3348.
3. Prestressing in Tainter Gate Dam Construction, *Tech. Bull.* 15, September, 1964, Stresssteel Corporation.
4. Buzzel, D. A., "Tainter Gates of Simplified Design," E.N.R., Apr. 1, 1948, p. 80.
5. Osipovich, A. A., The Design of Tainter Gates, *Modern Designing with Steel*, **7** (1), March, 1961, Kaiser Steel Corporation.
6. Blackmore, W. E., "Control of Flood Gates," I.A.H.R. Congress, London, 1963.
7. Holliday-Hoffman, "Types of Gates, Valves and Control Equipment Used for Bureau of Reclamation Spillways and Outlets," Question 12, Quatrième Congres des Grands Barrages, New Delhi, 1951.
8. Hines, Julian, Automatic Spillway Gates of Black Canyon Dam, *Eng. News-Record*, June 25, 1935, p. 1046.
9. Newell, F., "Hydraulic Regulating Gates," Engineering Institute of Canada, Oct. 8, 1925.
10. Petrikat, Dr. K., *M. A. N. Tech. Bull.* D552524/E, "Model Tests" on Weirs, Bottom Outlet Gates, Lock Gates and Harbour Moles.
11. Technical Reports, Bulletins, Nomographs, and Memoranda of the TVA, U.S. Bureau of Reclamation, U.S.A.C.O.E.

SECTION 22

HIGH-PRESSURE OUTLETS, GATES, AND VALVES

BY WARREN H. KOHLER AND JAMES W. BALL

BASIC PRINCIPLES

1. Scope and Purpose. Only the basic general principles which apply to outlet works and to gates and valves are covered in this section. Although some detailed guidelines and data pertaining to the design of gates and valves are included, this section is not intended to be a gate and valve design manual. Its purpose is to set forth and discuss the various arrangements of high-pressure outlets and the types of gates, valves, and associated equipment which are used for such outlets. The application, desirable and undesirable features, operating characteristics, and the principal hydraulic and structural factors involved in the design and operation of various categories and types of equipment used for high-pressure outlets are covered. The general factors to be considered in determining the arrangement and selecting equipment for outlet works are discussed to provide understanding and knowledge on which to base selections for specific installations. Attempting to set rigid categorical rules for the selection of a specific gate, valve, or outlet arrangement is neither a sound nor a practical approach. The general-information approach is used, as normally more than one basic arrangement and type of gate or valve can be used to perform the basic outlet function. The engineer must make the selection after due consideration of the overall arrangement, structural factors, operating requirements, and cost, as related to a specific case, to ensure getting the best possible installation.

In the discussion of gate and valve designs, the information given is of a general nature except where experience has shown specific details to be critical from a hydraulic, structural-design, or operation standpoint. Basic design considerations from the hydraulic, material-selection, fabrication, installation, and maintenance standpoints are covered to provide basic background information about equipment selection and design.

2. History and Development. Except for a few noteworthy exceptions, such as Roosevelt, Arrowrock, Pathfinder, Buffalo Bill, and Owyhee Dams, most of the gate and valve installations before the building of Hoover Dam were for relatively low heads of less than 150 ft. In the case of the low-head outlet works, the conventional "high-pressure" slide gates were found to give satisfactory operation at heads to about 100 ft without excessive cavitation. When gates which operated satisfactorily at low heads were installed in some of the higher-head dams, serious cavitation-damage problems developed. These problems were due primarily to a lack of knowledge of cavitation phenomena and destructiveness. Discontinuities and projections into the high-velocity fluid flows which produced only minor, tolerable cavitation damage at low heads resulted in massive damage at high heads. Costly repairs and maintenance, radical modification, or abandonment proved necessary in several of these early high-head installations.

One such outlet works, involving several 5- by 10-ft slide gates, was installed in 1908 to regulate flows at a design head of 220 ft at Roosevelt Dam in Arizona. When placed in service for regulation at considerably less than design head, very serious damage occurred to the gate parts and the conduits downstream from the gates. After the damage was repaired, additional use of the gates resulted in further damage, so that the gates were judged unsafe for use and were abandoned. The gate tunnel was filled with concrete, and a new outlet works using slide-type guard gates and needle valves for regulating releases was installed.

At Pathfinder Dam in Wyoming, where slide gates like those used at Roosevelt Dam were installed in 1909, similar cavitation-damage problems developed. In this case the use of the gates for regulation was stopped but the gates were retained for use as guard gates. The gates provide protection for a new outlet control works which was added to the tunnel downstream from the original slide-gate installation. Slide-type guard gates and needle valves for regulation were installed in the new outlet works which was added.

In contrast to these early problems, 7- by 10.5-ft slide gates of modern design were used for free discharge release of over 2 million acre-ft of water at nearly 350 ft of head at Glen Canyon Dam in 1965. Only relatively minor cavitation damage resulted. Slide gates are also giving satisfactory performance in other installations at heads which were once considered far beyond those suitable for this type of gate.

Another early valve which has had a significant influence on the design of regulating valves for high-pressure outlets is the needle valve. The basic design was invented in 1908 by H. O. Ensign, who was then Chief Electrical Engineer at the Bureau of Reclamation. The Ensign-type needle valve proved to be better than the slide gates of that time for regulation. However, the design did not eliminate cavitation problems, and the method of mounting the valve on the face of a dam made valve repairs impossible without drawing the reservoir level below the elevation of the outlets. These shortcomings have led to the abandonment of most of the Ensign-type needle-valve installations. However, the valves installed in 1915 at Arrowrock Dam in Idaho are still in use, despite considerable annual maintenance which is required.

Of greater importance were the numerous developments and modifications which have been evolved from the basic Ensign design. The needle-type valve was modified to mount on the exit rather than the entrance to an outlet conduit and became the standard valve for regulating high-head discharges for about 30 years. Some of the widely used types of needle valves which followed were the Larner-Johnson valve, and the "internal" and "interior differential" types which were developed principally by the late Phillip A. Kinzie of the Bureau of Reclamation. The "internal differential" type of needle valve had proved to be satisfactory on a number of Bureau installations and was installed at Hoover Dam. Under the high head at Hoover Dam, however, the slight divergence in the cone angles of the body and needle produced rapid cavitation damage on the needle and required frequent repair by overlaying with stainless steel and grinding. Hydraulic studies were successful in developing the proper geometry for a noncavitating needle, but at the cost of a considerable reduction in the discharge capacity as compared with the divergent-cone type of needle-valve design.

In addition to solving the cavitation problem on the Hoover Dam needle valves, the laboratory tests resulted in the development of the tube valve. A tube valve is essentially a needle valve with the downstream conical needle portion of the closure member omitted. Elimination of the conical needle did remove a surface on which cavitation had been occurring; but it was found that jet stability was also being sacrificed, although the instability was within tolerable limits for most installations. The relatively few tube-valve installations which the Bureau of Reclamation has made have been satisfactory in general, despite a few operating problems. The 102-in.-diameter valves in the lower tier of outlets at Shasta Dam were designed to regulate within a conduit. These valves required very large air-admission ducts, and one valve vibrated considerably at openings above about 96 percent. The high cost of the Shasta tube valves resulted in design studies being made of alternative methods of regulating flow in the remaining 14 middle and upper tier conduits. The jet-flow gate was developed as a result, and the 96-in. size has given satisfactory service at Shasta Dam. Jet-flow gates of similar design have been installed at Canyon Ferry and Trinity Dams, Bhakra Dam in India, and Tumut Pond Dam in Australia.

Further modification and rearrangement of the needle-valve elements led to the invention of the fixed-cone valve by C. H. Howell and Howard Bunger. In this valve the conical needle remains fixed and regulation is effected by sliding a cylindrical closure member axially across radial openings upstream from the cone. The invention of the hollow-jet valve by B. H. Staats and G. J. Hornsby of the Bureau of Reclamation in 1940 produced another type of valve which evolved from the needle valve. In the hollow-jet valve a needle closure member moves upstream axially to regulate or stop the outflow from a conduit. Both the Howell-Bunger fixed-cone and the Staats-Hornsby hollow-jet valves have proved to be excellent and reliable flow-regulating devices.

This brief outline of historical experiences and developments of gates provides some background on the problems which have been met and overcome. It should not be presumed, however, that new ideas and further development are not necessary. From this historical background of experience some basic criteria for use in the design of outlet works which will function satisfactorily in the transporting and controlling of water flow under high pressures have been established. Some of these basic criteria are as follows:

1. The fluidway and gate- or valve-closure device must be carefully designed for the required operating conditions to ensure that the installation is hydraulically sound and will not be subject to cavitation damage or have undesirable flow conditions. Model tests to verify the foregoing conditions are almost mandatory for new developments and for designs which differ to a considerable degree from previously tested installations.
2. Gates or valves must be simple and rugged, and must be provided with a reliable seal.
3. Conduits must be suitably vented, and an adequate supply of air must be provided for regulating types of gates and valves.
4. Adequate means of servicing and maintaining gates and valves must be provided.

These broadly stated fundamental criteria will be inherent in the development of improved outlets and of gates and valves. Much improvement remains to be made in design. The history of outlet-works designs is valuable in avoiding a repetition of past mistakes in striving to develop improved designs.

3. Definitions. The terminology used to describe the various types of closure devices and to differentiate between high and low heads is subject to individual differences in understanding and interpretation. To avoid confusion in the use of terminology in this section, the following general definition of terms will be followed:

1. Gate. A gate is a closure device in which a leaf or closure member is moved across the fluidway from an external position to control the flow of water.
2. Valve. A valve is a closure device in which the closure member remains fixed

axially with respect to the fluidway and is either rotated or moved longitudinally to control the flow of water.

3. Guard gates or valves. Guard gates or valves operate fully open or closed and function as a secondary device for shutting off the flow of water in case the primary closure device becomes inoperable. Guard gates are usually operated under balanced-pressure no-flow conditions, except for closure in emergencies.

4. Regulating gates and valves. Regulating gates and valves operate under full pressure and flow conditions to throttle and vary the rate of discharge.

5. Bulkhead gates. Bulkhead gates are usually installed at the entrance and used to unwater fluidways for inspection or maintenance, and are nearly always opened or closed under balanced pressures.

6. Stop logs. Stop logs are installed in the same manner and perform the same function as bulkhead gates. A stop log may be considered as a section of a bulkhead gate which has been made of several units to permit easier handling.

7. High pressure. The term "high pressure" is very indefinite as it is based on comparison. For this reason the meaning has changed considerably through the years, as what was considered high pressure in the early days of outlet works is now considered low pressure. Nevertheless, as used here, to avoid confusion with past usage, the term "high pressure" will be arbitrarily applied to all heads in excess of 100 ft.

In addition to the foregoing definitions which provide a framework, additional discussion, definitions, and terminology will be included as appropriate under the various paragraphs on specific equipment and subjects in the section.

4. Outlet Functions, Arrangements, and Considerations. The basic purpose of a dam is to create a reservoir of sufficient capacity and head so that the water stored can be used economically to satisfy downstream requirements, such as irrigation, domestic uses, flood control, navigation, and power. The basic function of any outlet from a reservoir is to provide an efficient, economical means of releasing water from a reservoir to obtain the desired downstream use or uses. Figures 1 to 3 show schematically some of the typical arrangements of outlets for dams. Figure 4, showing the tower intakes of the San Luis Dam in California, illustrates the tower intake scheme with rectangular gates shown by Fig. 3.

The conduits, pipes, or penstocks for high-head outlets are usually metal, and have gates or valves located at the upstream entrance, at an intermediate point, or at the downstream end. Such outlets may also utilize a combination of these arrangements, and have a guard gate at the entrance or at an intermediate point with a regulating gate or valve at the downstream end.

There are six basic elements to be considered in the design of outlets: (1) the entrance; (2) the conduit, pipe, or penstock; (3) the reservoir head; (4) the velocity of flow; (5) the type and arrangement of the gates or valves to be used for controlling the flow; and (6) the means of dissipating the outlet energy. No categorical rules can be set forth to permit designing outlets which will ideally integrate all these basic elements.

Entrances for outlets should be properly proportioned and have the surfaces as smooth and free of discontinuities as possible. Conduits, pipes, and penstocks should be aligned as nearly straight as possible, should have smooth surfaces without offsets, and should have a fluidway configuration which avoids abrupt cross-sectional changes. Each outlet should be provided with two gates or valves capable of closing under flow. An upstream guard gate or valve is required primarily to ensure the safety of the conduit and equipment downstream and secondarily to permit inspection and maintenance of the downstream pipe and equipment. Guard gates must be capable

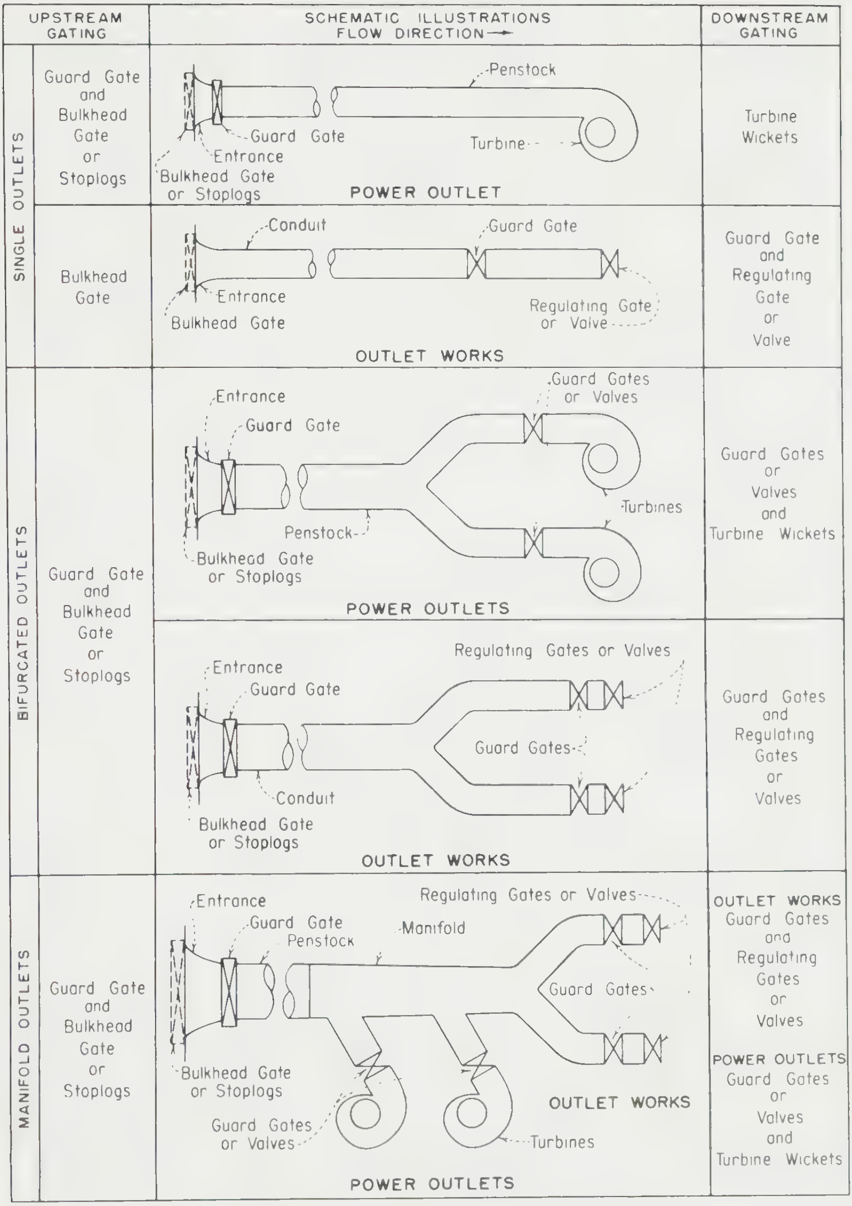

Fig. 1. Schematic of typical outlet arrangements.

of closing under the full head and the maximum possible flow, but are normally operated under balanced-pressure no-flow conditions. A bypass line is usually provided for balancing pressure before opening a guard gate.

In addition to gates or valves which can be closed with water flowing, most outlets are provided with a bulkhead gate or stop logs at the upstream end to permit inspec-

<table>
<tr><th>TYPE</th><th>SCHEMATIC ILLUSTRATION
FLOW DIRECTION ⟶</th><th>NOTES AND COMMENTS</th></tr>
<tr><td>VERTICAL INTAKE ON DAM OR ABUTMENT</td><td>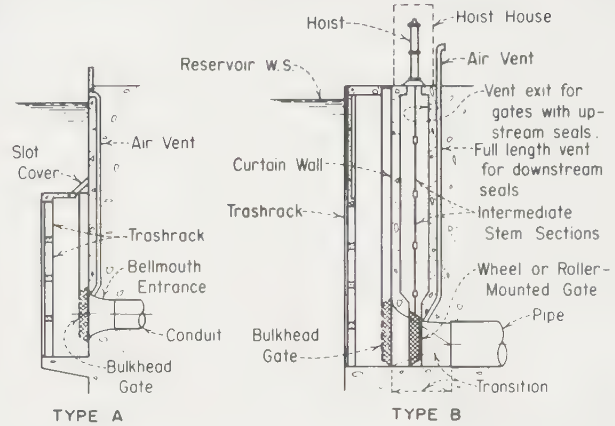
</td><td>Intake types used principally on concrete dams and on earth dams with abutment intakes. Type A used primarily for single line outlet works. Type B used for all types of power outlets and for branched and manifold type of outlet works</td></tr>
<tr><td>SMALL SLOPE INTAKE ON DAM</td><td>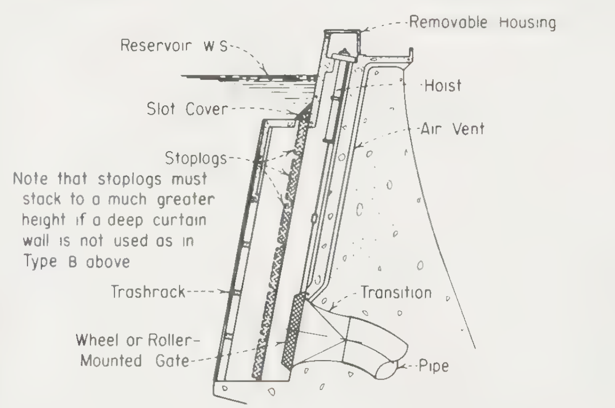
</td><td>Type of intake frequently used on thin-arch concrete dams. Used for all types of power outlets and for branched and manifold outlet works. Gantry crane is usually provided for handling gate and stoplogs for multiple outlet installations</td></tr>
<tr><td>LARGE SLOPE INTAKE ON ABUTMENT</td><td>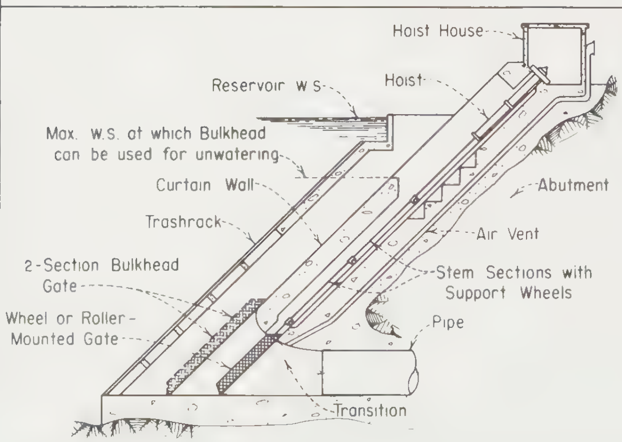
</td><td>Intake used mainly for abutment intakes on earth dams. Hoist stems must be provided with support wheels. Reduction in effective weight for gravity closing may require the provision of closing thrust by the hoist, or the use of roller-mounted gates.</td></tr>
</table>

Fig. 2. Typical intake gating arrangements.

TYPE	SCHEMATIC ILLUSTRATION FLOW DIRECTION ⟶	NOTES AND COMMENTS
TOWER INTAKE (RECTANGULAR GATE)	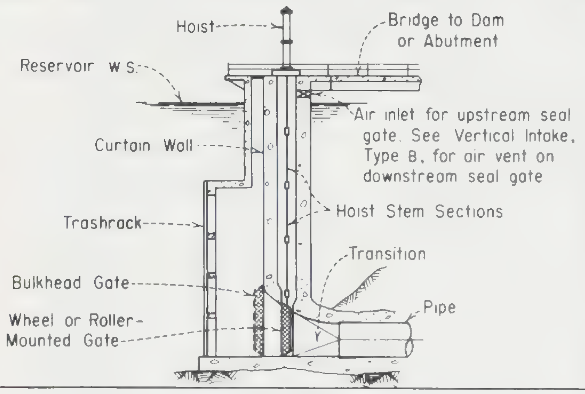	Tower intakes are used principally on earth dams where abutments are not suitable for intake structures Also used for concrete dams where intakes must be located on abutments and other types are not suitable Basic arrangement is similar to vertical abutment intake Bridge is usually provided to dam or abutment
TOWER INTAKE (CYLINDER GATE)	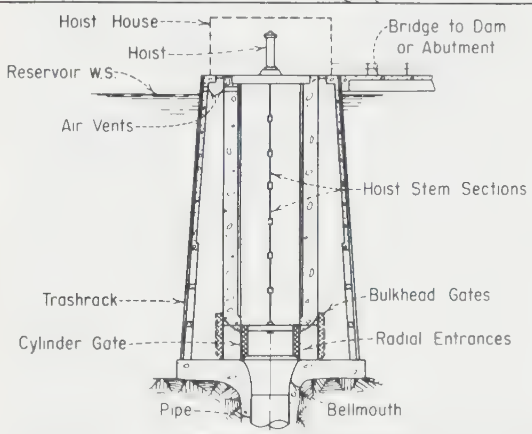	Tower intake used primarily where intake entrance is vertical Other selection factors are similar to those stated above for vertical towers for rectangular gates
SHAFT (SUBMERGED UPSTREAM INTAKE)	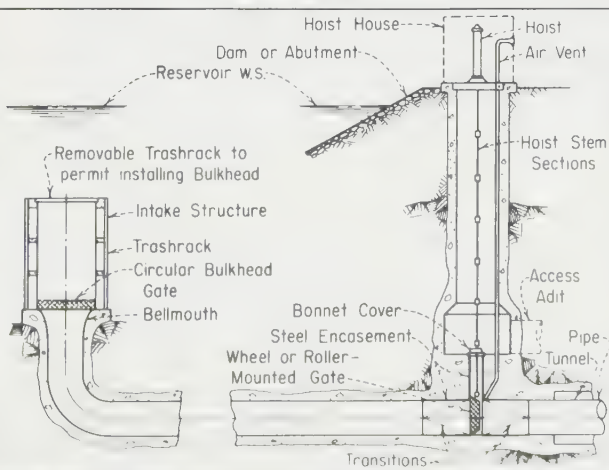	Intake arrangement used principally on earth dams Shaft usually located near axis of dam, either in dam or abutment. Abutment location is preferable to avoid joint between abutment rock and dam fill Intake Bulkhead installation requires drawing reservoir down or placement from a barge and the employment of divers

FIG. 3. Typical intake gating arrangements.

FIG. 4. Tower intakes at San Luis Dam in California. Note lifting frame and bulkhead gate section being hoisted by gantry crane for storage on the tower service deck.

tion or repair of the entrance to a conduit. Bulkhead gates and stop logs are normally designed to be placed and removed under balanced-head no-flow conditions.

GATES

5. General. Through the years a great many types of gates have been designed and built, but only a relatively few types have survived and are presently in use. The gates which have survived the test of time have several characteristics in common: they are simple, rugged, easy to maintain, and economical to build. This section is limited to some of the successful basic types.

Of those discussed, the conduit slide gates and jet-flow gates are the only ones which are specifically designed for throttling conditions to regulate flows. Wheel, roller-mounted, and cylinder gates are also sometimes used for regulation but are normally used only as fully opened or closed guard gates. Ring-follower gates, ring-seal gates, bulkhead gates, and stop logs are never used for throttling and regulating flow.

6. Conduit Slide Gates. In the early 1900s so-called "high-pressure" slide gates, as shown in Fig. 5, became the standard means for regulating and shutting off the flow of water in the outlet works in dams. With the increase in heads above 100 ft, problems in design and operation increased.

The early limitation on the use of slide gates for regulation under high heads left the needle valve as practically the only suitable device for regulating flow. The need for high-head flow regulators was largely filled by the needle valve until the development of the tube valve, the fixed-cone valve, the hollow-jet valve, and the jet-flow gate in the 1940s.

The success of the jet-flow regulating gate which was developed for Shasta Dam led to further studies by the Bureau of Reclamation to see if the flow-contraction principle could be applied to square or rectangular gates to make the flow jump past the gate slots. The studies involved designing and testing various modifications of

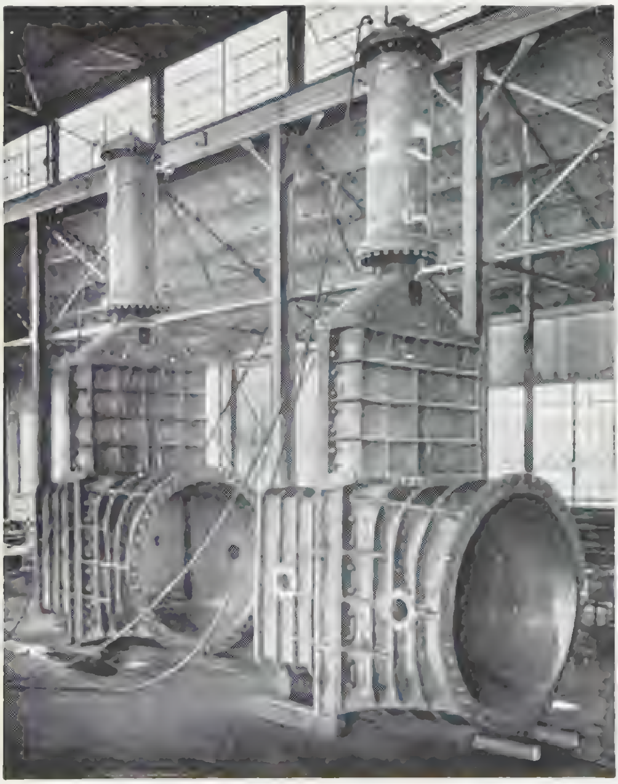

Fig. 5. 5- by 5-ft "high-pressure" slide gates with built-in square-to-round transition on downstream bodies for attaching 60-in. needle valves.

conventional "high-pressure" gates. The studies also led to reviewing the developments which had been made on slide gates by the U.S. Army Corps of Engineers. Numerous ideas were tried, such as putting contraction slopes on the conduit upstream from the gate slots to cause the flow to jump the slots. The tests eventually resulted in the development of a slide gate having narrow slots at the sides of the conduit. The conduit opening on the upstream side of the gate slot has no contraction, but there is a slight outward offset at the sides and top of the gate slot on the downstream side. The leaf has a sloping upstream face and a narrow seat surface on the bottom. See Art. 25 for further discussion of gate slots.

These developments and improvements have resulted in the successful use of

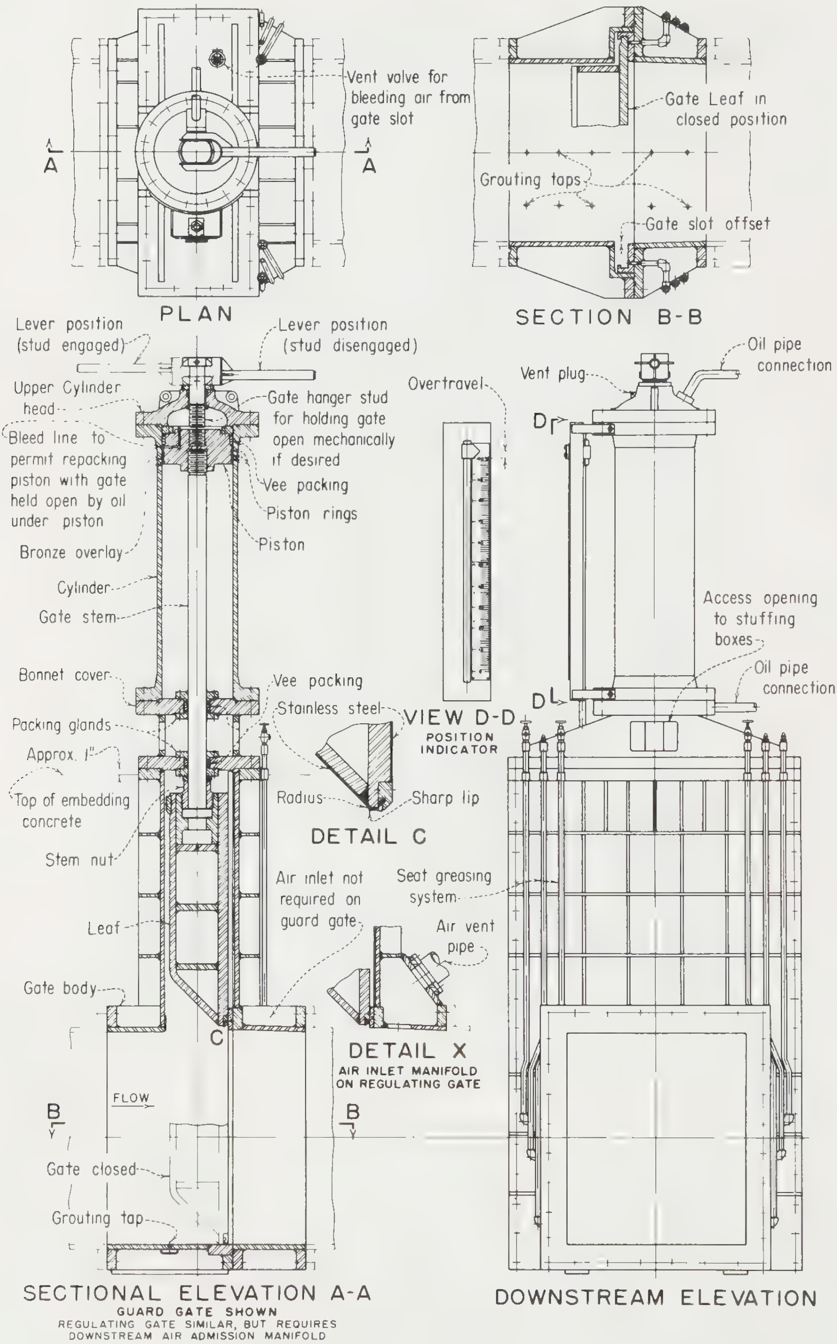

FIG. 6. General assembly and details of improved type of slide gate suitable for regulation at heads to at least 300 ft.

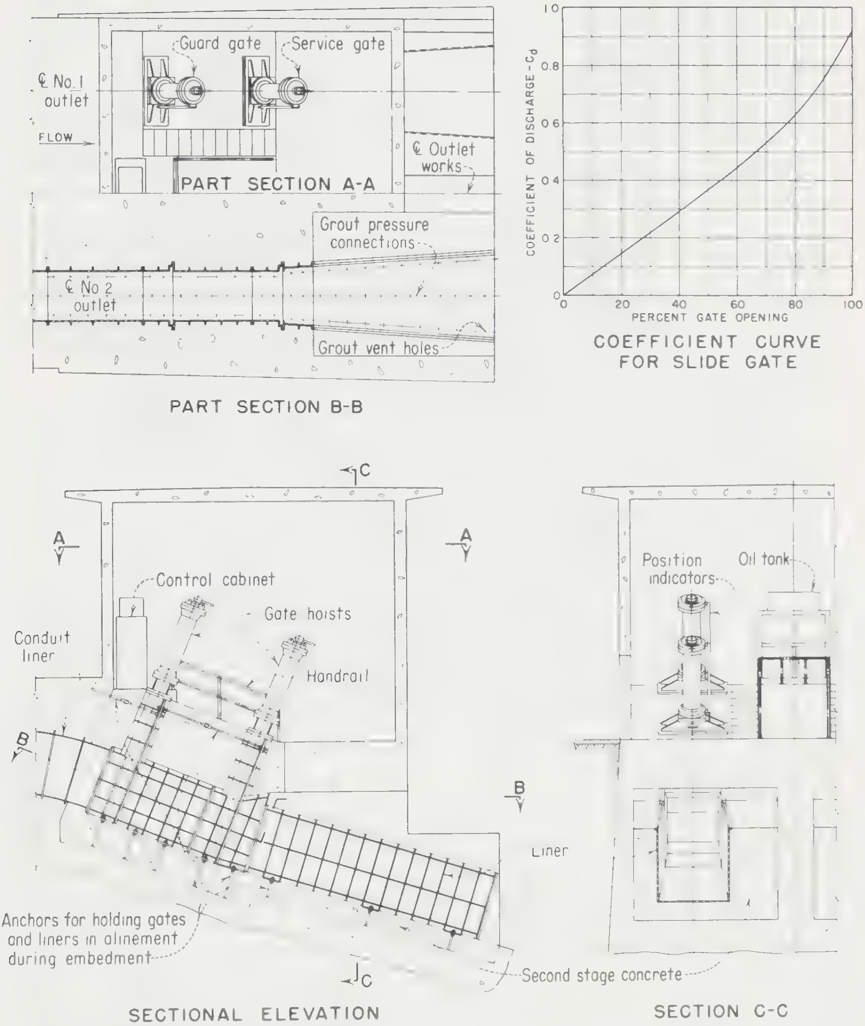

FIG. 7. Typical tandem slide-gate installation and discharge-coefficient curve.

specially designed slide gates for regulation at heads of over 300 ft, which was previously considered unthinkable (see Fig. 6). The incorporation of some of the features in the standardized "high-pressure" gates of the Bureau of Reclamation has led to increasing the operating heads of these gates for regulation to 200 ft.

The primary use of slide gates is for the control of discharges from outlet conduits in dams. Slide gates are used for both guard and regulating service. Frequently two practically identical gates are bolted together in tandem as shown in Figs. 7 and 8. In such cases the upstream gate functions as the guard gate for the downstream regulating gate. Slide gates are also used singly as guard gates. Some gate installations are made on a slope so that the discharge is downward into the stilling basin.

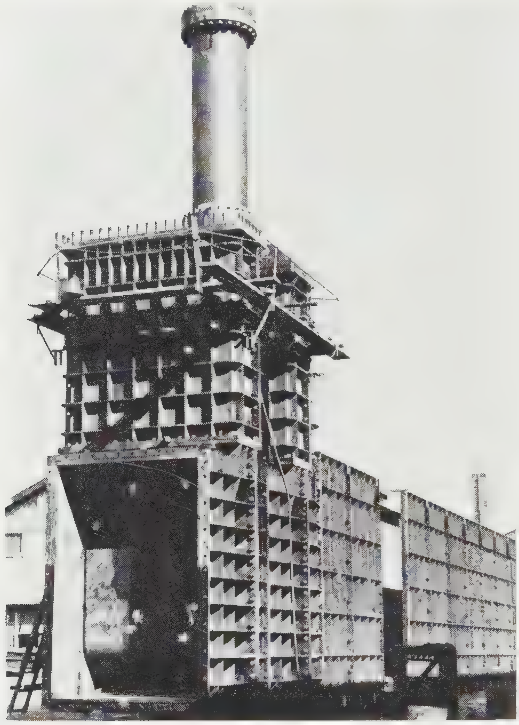

FIG. 8. Shop assembly of 7- by 10.5-ft slide gate and conduit liner for operation under 350-ft head at Glen Canyon Dam.

This arrangement reduces the required length and cost of the stilling basin. There is an increasing use of metal liners, as shown in Fig. 9.

Slide gates discharge smoothly at all openings but should not be operated at very small openings. The configuration of the flow, both at partial and at full openings, is well defined and can be readily handled by stilling basins. The gates can be used either for free discharge into atmosphere or for submerged discharge in water. The latter case requires more care to be sure adequate water can circulate and flow readily to the critical regions around the gate orifice. Laboratory model tests are very helpful for studying the flow patterns and pressures and in avoiding problems in the prototype installation.

There appears to be no definite size or head limitation for correctly designed slide gates. The successful use of such gates with only minor cavitation damage at heads of nearly 350 ft at Glen Canyon indicates that 500-ft heads are not unreasonable and that possibly considerably higher heads can be used. At heads above 200 ft, fluidway surfaces and the bottom seating and sloping surfaces of the gate leaf should preferably be stainless steel for better cavitation-damage resistance. The only practical limitation in the operation of slide gates for throttling is that they must not be operated at openings which are so small that flow beneath the gate does not spring clear of the lip on the bottom of the gate. At small openings the "short-tube effect" of the issuing flow may result in flow contact at the downstream edge of the gate lip and produce cavitation damage on the bottom sealing surfaces of the gate. To ensure that this

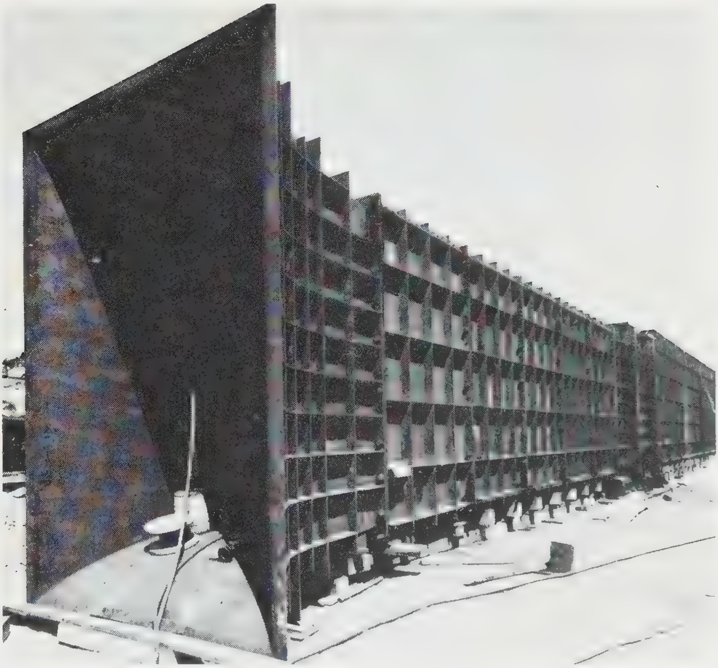

FIG. 9. Bellmouth entrance and conduit liners for 7- by 10.5-ft slide gates at Glen Canyon Dam.

condition will not occur, the minimum opening for regulation is limited to not less than one-half the width of the seating lip on the bottom of the gate.

Basically, a slide gate consists of a leaf which is either closed by being positioned across the fluidway in the body or opened by being withdrawn into the bonnet by a hoist mounted on the bonnet cover. The mating seats on the gate leaf, body, and bonnet serve both as the sliding surfaces for carrying the hydrostatic load on the leaf and as the sealing surfaces when the gate is closed. The body and bonnet are made in halves and are heavily ribbed to minimize distortion when the gate is embedded in concrete. The body and bonnet are not designed to withstand the internal fluid pressure, and the embedding concrete must be suitably reinforced to withstand the pressure. Only the bonnet cover, on which the hoist is mounted, and the top flange of the bonnet are designed to resist the internal water pressure. In addition to the internal water pressure, the bonnet cover and flange connections must resist the full load of the maximum hoisting effort as the gate leaf contacts the bottom seat when the gate reaches the closed position. Care must be taken to provide adequate bolting and flange thickness on the cover and bonnets for these loads. Only sufficient bolting to ensure that flange faces can be drawn into watertight contact is necessary for the flanges on embedded parts. Flange joints for high pressures are usually provided with square or round rubber gaskets, although only a mixture of white lead and linseed oil is sometimes used for low pressures.

With few exceptions, slide gates are operated by hydraulic hoists. The hoists are oil-operated and are mounted directly on the upper flange of the bonnet cover. The general design and arrangement of typical hydraulic hoists are covered in Art. 34.

In the design of slide gates for high pressures and velocities, several critical design and fabrication requirements must be met. The first critical requirement from a hydraulic standpoint is the smoothness, straightness, and lack of offsets at joints in the fluidway (see Art. 24). Other critical requirements are proper leaf-slot geometry (see Art. 25) and the design of the bottom of the leaf to minimize downpull and provide a converging fluidway and definite spring point for flow discharge.

The bottom of gate leaves is usually made with a slope of about 45 deg to provide a convergence of the flow passage when the gate is used partially open for regulating flows. The sloped surface has positive pressures which reduce downpull and ensure positive control at the spring point at the bottom of the leaf. The essential features of the bottom of a well-designed gate leaf and the spring joint at the junction of the sloping face and bottom lip are shown in Fig. 6, detail *C*. The sloping surface on the bottom of the leaf should preferably be stainless steel to ensure a smooth surface for high-velocity flows and avoid cavitation damage to the surface.

It is of prime importance that the seating and sealing surfaces on the downstream side of the body and bonnet be held closely to plane when the gate is installed so that the mating surface on the leaf will slide smoothly, bear and distribute the leaf load uniformly, and produce an effective seal when the gate is closed. For small relatively rigid gates, embedment in first-stage concrete is feasible provided special care is exercised to anchor the gates properly and place the concrete slowly and uniformly to minimize distortion. Unless the gate bodies and bonnets are made quite heavy and rigid, it is usually necessary to embed gates larger than about 5 ft in second-stage concrete, so that the gates can be securely anchored to existing concrete and can be adjusted to retain alignment during concrete placement. It is desirable to check the seating surfaces frequently during concrete placement to ensure that the minor displacements and distortions which occur do not exceed the permissible tolerance for the plane of the seating surface. As a "rule of thumb" for determining the acceptable tolerance for contact between the seating and sealing surfaces on the body and leaf, the surfaces should match well enough so that with the gate closed a feeler gage, having a thickness in thousandths of an inch approximately equal to the square root of the gate area in feet, cannot be inserted between the mating surfaces.

It is also important that care be taken to ensure that all spaces around the gate body and bonnet are filled with concrete. Some method of grouting to fill the voids under the bottom of the fluidway is usually provided for gate bodies and liners.

7. Ring-follower Gates. Before the 1930s the "high-pressure" slide gate (see Fig. 5) was commonly used as the guard gate for needle valves which regulated the flow from outlet works. This arrangement usually required the use of an upstream transition to change the fluidway cross section from circular to rectangular. A similar transition was always required downstream from the gate to return the cross-sectional shape to circular for the needle-valve connection. Such transitions added expense and hydraulic losses to outlet works, and led to the development and use of several gates of the ring-follower type as guard gates for needle valves. In present usage, the term ring-follower gate has arbitrarily been limited to the slide type. Other ring-follower types include the Paradox gate, which is a roller-mounted wedge-sealing type, and the ring-seal gate, which uses both antifriction roller trains and wheels and which has a movable, hydraulically actuated seal ring. The Paradox gate is no longer used because of the complexity and cost of fabrication, but the ring-seal gate is still used to a limited extent.

Basically, a ring-follower gate consists of a leaf, the body and bonnet parts, and a bonnet cover on which the hoist is mounted for moving the leaf to the open or closed positions (see Figs. 10 and 11). The leaf is composed of a bulkhead portion which blocks the fluidway through the body when the gate is closed, and a follower portion

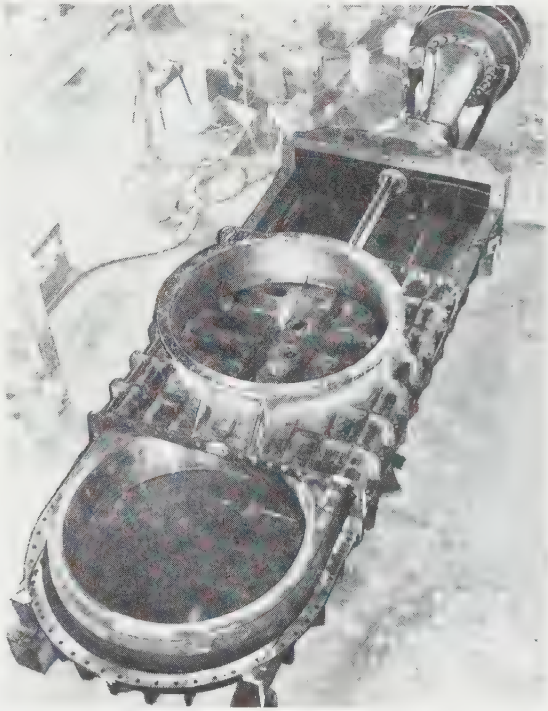

FIG. 10. Partial shop assembly of 96-in. ring-follower gate for Glen Canyon Dam.

having a circular opening which aligns concentrically with the fluidway through the body when the gate is open. The characteristic of having a ring portion which follows the movement of the bulkhead portion accounts for the name ring-follower gate.

As the follower ring on a ring-follower gate is essentially the same size and aligns with the pipe when the gate is open, there is practically no hydraulic loss for this type of gate. The gate can be installed at any location in a pipe and is suitable for high-velocity flows because the fluidway matches the pipe diameter closely and avoids pronounced boundary discontinuities. Ring-follower gates are simple and rugged, and make excellent, highly efficient guard gates. See Figs. 15 and 34 for typical guard-gate installations of ring-follower gates. These gates are not suitable for operation at partial openings for throttling to regulate flows; and if used for such service, severe cavitation damage will result. Other than manufacturing-plant capability, there is no size limitation for ring-follower gates. Likewise, there is no head limitation other than permissible bearing pressures on the sliding seats.

The gate leaf requires a lower bonnet below the fluidway into which the follower ring on the leaf can move when the gate is closed. The upper bonnet has a similar function for the bulkhead portion when the gate is open. It is important that a pipe connection be provided at the bottom of the lower bonnet. This connection will serve as a drain, but the primary function is to permit flushing out silt or debris which sometimes accumulates in the lower bonnet of such gates. The size of the connection is usually determined by considering the gate size and reservoir water conditions. Normally the size will vary between 3- and 8-in. pipe.

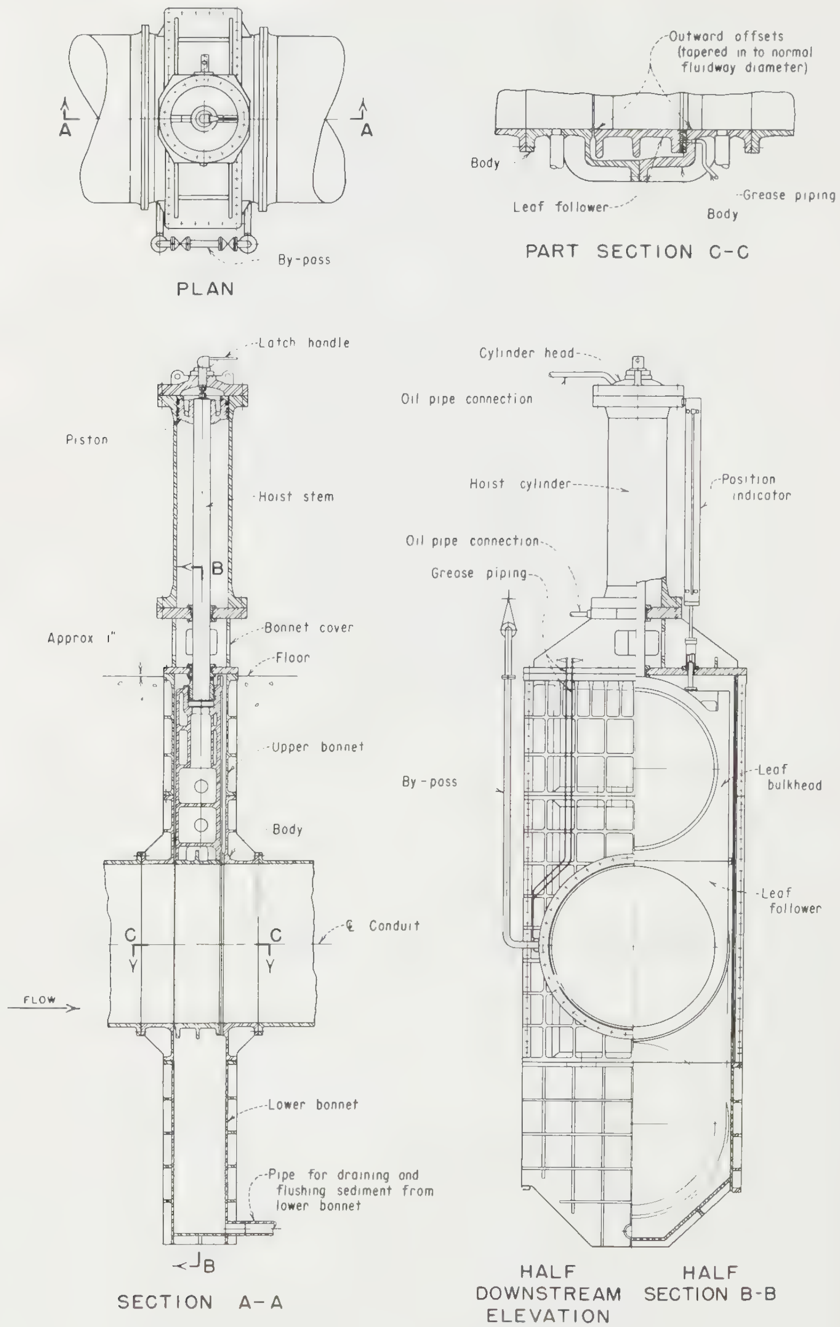

FIG. 11. General assembly and details of ring-follower gate.

The body and upper bonnet of ring-follower gates are made in halves and are heavily ribbed to minimize distortion and avoid misalignment of the seat and guides when the gate is embedded in concrete. The lower bonnet is also heavily ribbed and may be made in one piece as there are no stationary seats or other surfaces requiring machining on the interior of the lower bonnet. The body and bonnets are not designed to withstand the internal water pressure, and the embedding concrete surrounding these parts must be suitably reinforced to withstand the internal pressure. The top flange of the upper bonnet and the upper bonnet cover must be designed to resist not only the internal water pressure but also the full hoist thrust, which will occur during closure of the gate with water flowing in the conduit. Hydraulic hoists are usually used for operating ring-follower gates and are described in Art. 34.

Except for gate sizes of less than about 72 in., ring-follower gate leaves are usually made in two pieces for manufacturing convenience and economy. For the two-piece leaf construction, the bulkhead and follower halves of the leaf must be securely bolted together and the seats on the downstream side should be machined with the leaf sections bolted and doweled together. The mating seats on the body and bonnets should likewise be finished with the parts bolted and doweled together.

Cast steel is most commonly used for gate leaves, but gray-iron castings and weldments are also used. Because the complex shape involves numerous fitting and welding problems, welded construction is not usually economical for gate leaves, unless only one or two gates are required and the cost for patterns is an important factor. Gate bodies are frequently made of gray-iron castings, although steel castings are sometimes used. The lower bonnet is usually either gray iron or a weldment, and the upper bonnet is cast steel or a weldment. While some bonnet covers are made of gray iron or cast steel, the welded-steel bonnet cover is preferable because of the simplicity and the avoidance of porosity which sometimes occurs in cast covers.

Air-inlet manifolds are usually provided on the downstream side of ring-follower gate bodies when the gates are located at some distance upstream from the outlet end of the conduit. For gates which are directly coupled, or are located very close to the regulating gate or valve, air manifolds are frequently omitted; however, a small vent, which is usually manually operated, is always provided to permit releasing the air which is trapped during filling of the conduit between the ring-follower gate and the downstream gate or valve.

The function of an air vent on guard gates is not primarily to prevent cavitation damage but is to release air during filling of the downstream conduit and to avoid a high vacuum and reduce the noise and vibration which will result from emergency closure with flow through the conduit. The vent lines need only be large enough to serve these functions. It is unnecessary for such vent lines to be as large as those required for free-discharge regulating gates (see Art. 26).

Because ring-follower guard gates are usually designed to be closed, but never opened, under unbalanced pressure, a bypass for filling the pipe downstream from the gate is normally provided. The bypass line size is selected on the basis of an acceptable time limit for filling the conduit, and usually a 6-in. or smaller size is adequate. The bypass connections are frequently provided on the upstream and downstream bodies, so that a simple U-loop piping arrangement can be used. The loop extends above the floor level at the top of the upper bonnet and is provided with two shutoff gates or valves.

Because of the high conduit velocities it is important that the fluidway through ring-follower gates be smooth and that no inward offsets into the flow be present when the gate is open. To ensure smoothness the fluidway through ring-follower gates is finished to about 250 μin. roughness. To avoid abrupt inward offsets the fluidway may be designed as described in Art. 25 and shown in Fig. 51. This design arrangement avoids the necessity of having the leaf and body fluidways exactly the same size and in perfect alignment.

The metal combinations which are used for slide-gate seats are also used for the sliding seats on ring-follower gates. The recommended materials are discussed and specified in Art. 30. Gate seats should preferably be provided with a lubrication system.

While it may appear to be unnecessary to have position indicators on gates which are used only in the fully open or closed positions, experience has shown that full-scale position indicators are desirable. Such indicators are particularly useful in determining the precise gate position in case of malfunctions, and in checking to be sure the gate is operating properly at other times.

Usually downpull is not of particular importance in ring-follower gates as they are not normally operated under unbalanced conditions. For emergency closure under flow conditions, the downpull which occurs assists in closing the gate. In general it can be stated that liberal clearances in the body and bonnets should be allowed. The clearances will permit the free circulation of water to all leaf surfaces and minimize the unbalanced pressures on the leaf surfaces which produce downpull. Further discussion of downpull forces on gates is contained in Art. 34.

In the installation of ring-follower gates it is extremely important that seating surfaces on the gate body and bonnet be held to plane to provide an accurate mating surface for the leaf. The same requirements and procedures as specified for slide gates under Art. 6 also apply to the installation of ring-follower gates. The thickness of feeler-gage thousandths of an inch which can be inserted between the mating surfaces of the leaf and body seats should not exceed the number derived by taking the square root of the conduit area in feet. For example, the feeler-gage thickness for a 100 sq ft area would be 0.010 in.

8. Ring-seal Gates. A ring-seal gate is a ring-follower type of gate which has roller trains and wheels to reduce friction and which has a movable, hydraulically actuated seal ring. The primary purpose of these features is to reduce the friction and hoist capacity from that required for sliding-type ring-follower gates. The hoist capacity required was of considerable concern in the 1930s when these gates were invented by the late P. A. Kinzie of the Bureau of Reclamation. At that time mechanical rather than hydraulic hoists were preferred for gates. As mechanical hoists designed for capacities exceeding 100 to 150 tons are quite cumbersome, friction-reducing means, such as wheels or roller trains, were commonly used to minimize required hoist capacities.

The major initial use of the ring-seal type of gate was for the 40 outlets in the two upper tiers at Grand Coulee Dam (see Fig. 12). Each outlet has two identical gates, and there are a total of eighty 102-in. gates in these outlets. The upstream gate functions as the guard gate for the downstream service gate. While ring-follower-type gates are not normally operated under unbalanced conditions to open and close, the ring-seal gates at Grand Coulee Dam are unusual in that they are opened and closed under unbalanced conditions to release or shut off the flow through the outlets. The gates are never used at partial openings for throttling. The ring-seal gate has given excellent service at Grand Coulee, and also in other installations where it has been used primarily as a guard gate for turbines.

The first gate designs used twin screw-stem mechanical hoists and the movable ring seal was mounted on the leaf. This seal arrangement required complicated telescoping tubes to control the seal-actuating water pressure. At Green Mountain Dam the need for telescoping tubes was eliminated by locating the seal in the body. The two 126-in. gates at Boysen Dam (see Fig. 13) are the largest gates of either the ring-follower or ring-seal type which have been built by the Bureau of Reclamation, and are also the first ring-seal gates to be hydraulically hoisted. The hydraulic operation

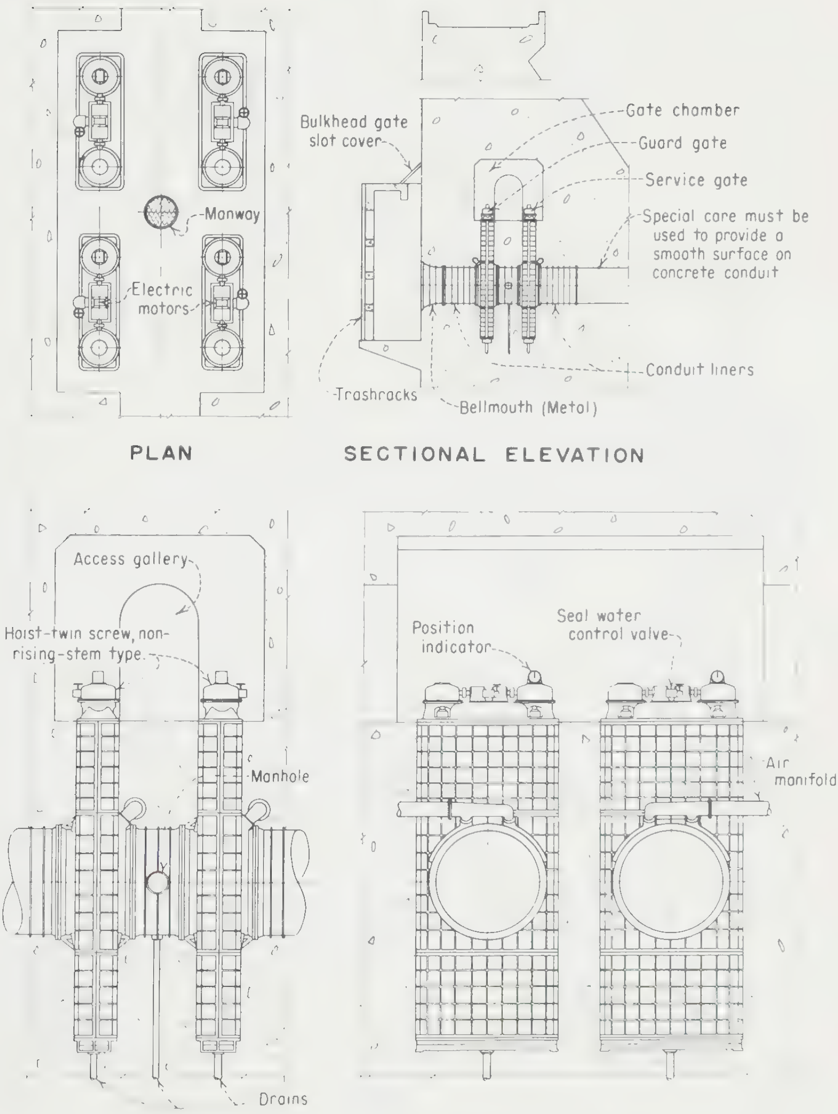

Fig. 12. Typical tandem installation of ring-seal gates. This general arrangement was used for the twenty 102-in.-diameter outlets in both the middle and upper tiers at Grand Coulee Dam.

of these gates permits closure in 30 sec. The rapid closure is achieved by having the gates close by gravity and controlling the speed by a throttle valve in the bypass line from the bottom to the top of the cylinder. The feature of being able to close a ring-seal gate by gravity without power, plus the negligible loss for this type of gate, makes it well suited for a turbine-guard gate.

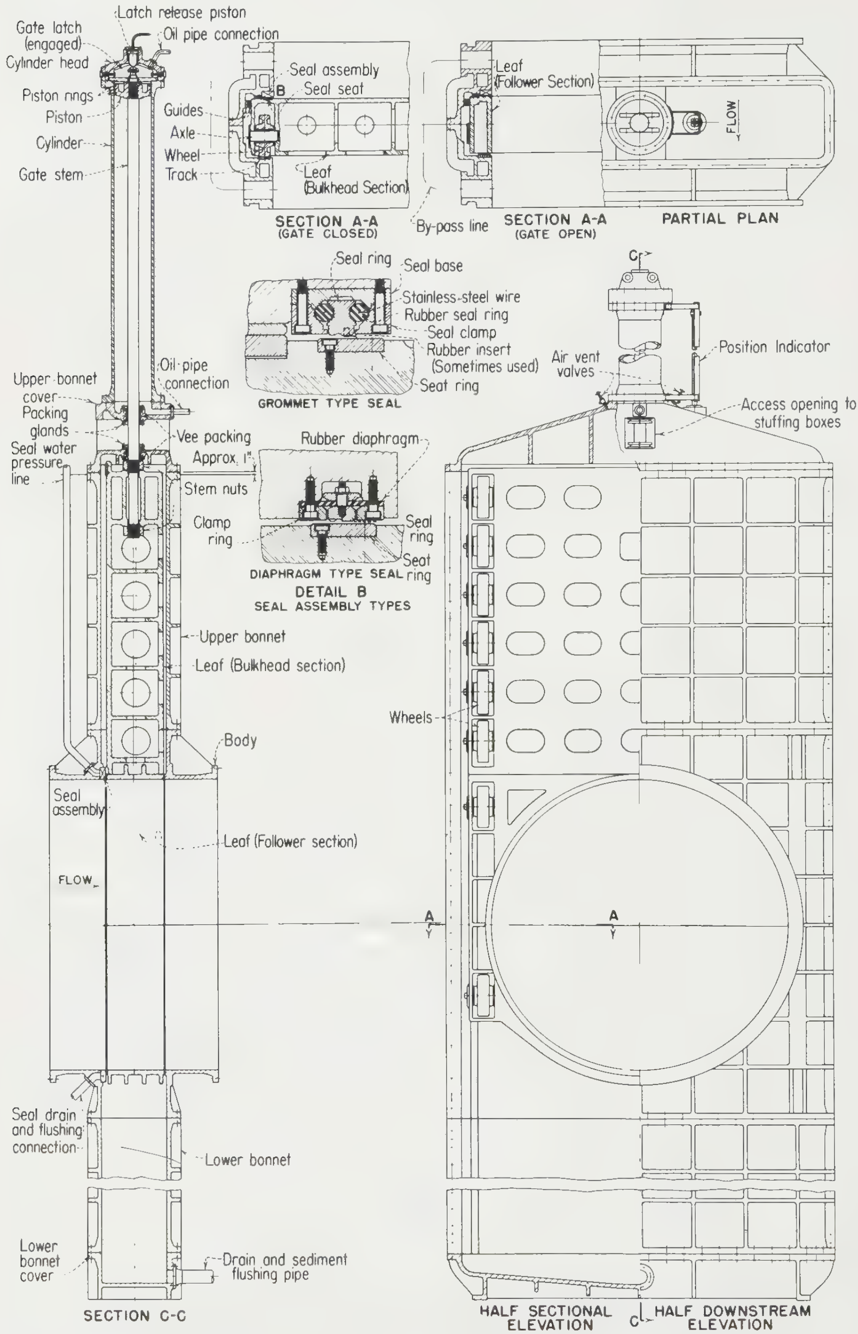

FIG. 13. Assembly and details of 126-in. hydraulically operated ring-seal gate which was used at Boysen Dam.

The general design and installation requirements are substantially the same for ring-seal gates as for ring-follower gates. The principal difference is in the wheels, roller trains, and seals which have been added. Both diaphragm- and "grommet"-type seals, as shown in the enlarged detail in Fig. 13, have been used on ring-seal gates. The "grommet" type is simpler and operates better. It is also cheaper to make because of the fewer parts and the relatively low rubber-molding costs as compared with the diaphragm type.

Further discussion and information on the design of roller trains and wheels are contained in Arts. 32 and 33.

9. Jet-flow Gates. The jet-flow gate was developed in the mid-1940s by K. L. Waltermire and Frank Lowe at the Bureau of Reclamation to be used as a substitute for the 14 tube valves which were originally scheduled for installation in the two upper tiers of outlets at Shasta Dam. The principal reason for the substitution was to reduce the cost of the installation. The development of a new type and design of gate which was radically different from any existing gates and would provide a better and less costly alternative to the tube valve was accomplished as a coordinated result of design and laboratory development and testing. The most recent design of a jet-flow gate which evolved from the original development is shown in Fig. 14. The fundamental features of the jet-flow gate are the truncated conical nozzle, a floating seal ring which forms a circular discharge orifice at the downstream end of the nozzle, and a flat-bottomed leaf which contacts and is moved across the seal-ring orifice to regulate flow discharges. The basic features produce a contracted, jet-type discharge which is responsible for the name of the gate.

In addition to Shasta Dam, 96-in. jet-flow gates of similar design are installed in the river outlets for Bhakra Dam in India. A design having a slightly modified seal and a flat-bottom, inverted U-shaped downstream conduit, similar to a "horseshoe" conduit, was used for the four 77-in. jet-flow gates which are installed at Canyon Ferry Dam. Other jet-flow-gate installations include 84-in. gates at Tumut Pond Dam in Australia and an 84-in. gate in the auxiliary outlet works at Trinity Dam in California. The jet-flow gate at Trinity Dam is installed as shown in Fig. 15 and has operated satisfactorily at full design head of nearly 390 ft.

The simplicity and excellent flow-regulation characteristics of jet-flow gates have resulted in the development of standard designs in 10-, 12-, and 14-in. sizes (Fig. 16) by the Bureau of Reclamation. These sizes are used for discharging small amounts of water to meet minimum stream-flow requirements. These small gates avoid the damage which frequently occurs when large gates are just "opened a crack" for small discharges.

No damage has been noted or reported at the jet orifice or in the gate slots on jet-flow-gate installations. Some minor damage in the downstream conduit has occurred at both Bhakra and Trinity Dams. In neither case was the extent or rate of damage deemed to be serious, although some paint and concrete repairs were required at Trinity Dam. Jet-flow gates operate very satisfactorily at all openings, although some minor pressure pulsation was noted in the operation of the gate at Trinity Dam. In general, however, jet-flow gates operate smoothly without vibration or serious cavitation damage at any opening. For partial openings there is considerable air demand under free-discharge conditions. The gates have also operated satisfactorily discharging submerged when wide open.

On the basis of successful operation at a head of nearly 400 ft, it appears that jet-flow gates can be used at considerably greater heads. Certainly operation at 500-ft heads appears reasonable, and heads considerably higher may prove feasible. It is possible that strength requirements in the design of the seal ring may prove to be the head-limiting factor for jet-flow-gate usage rather than the flow characteristics. The

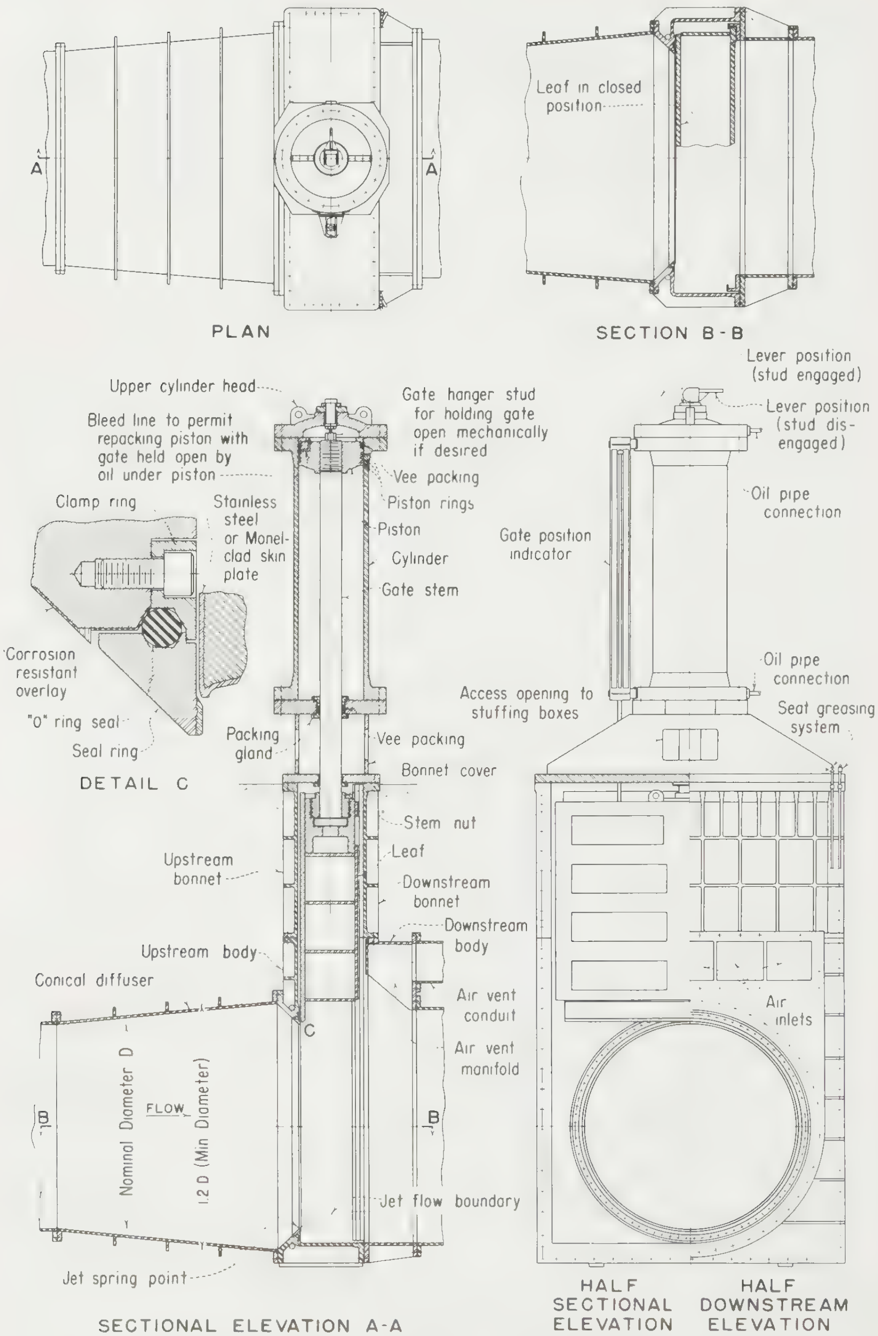

FIG. 14. Assembly and details of 84-in. jet-flow gate.

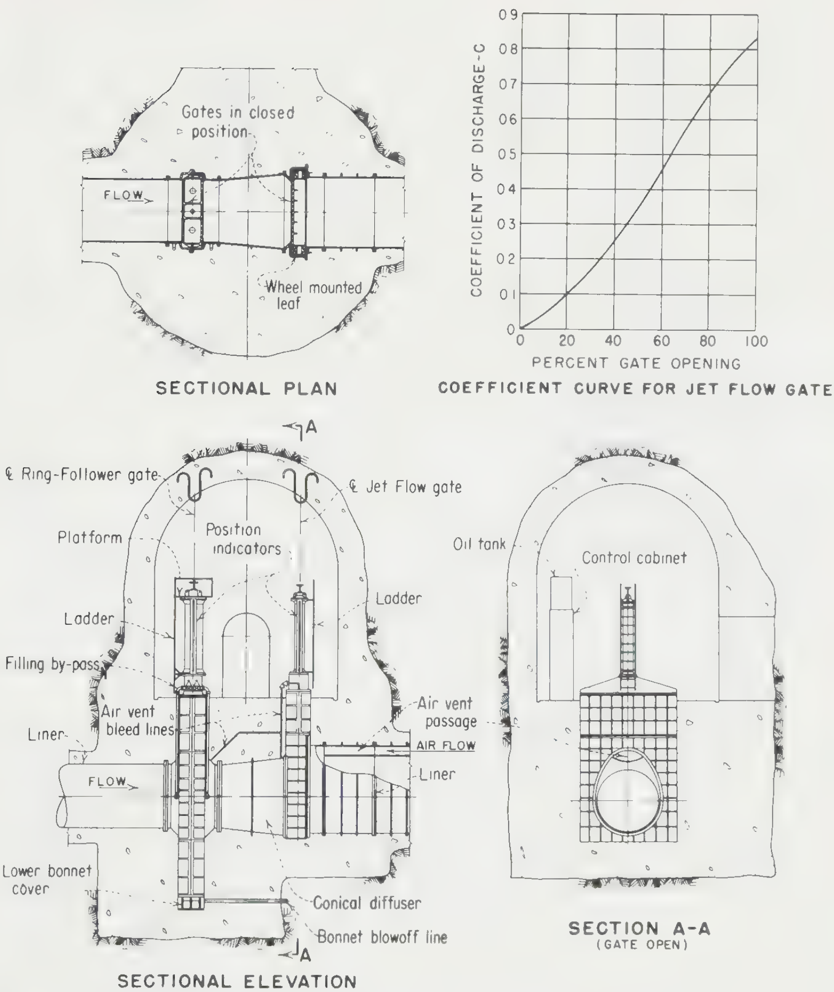

FIG. 15. Installation arrangement used at Trinity Dam for 84-in. jet-flow gate. Note ring-follower guard gate upstream.

size of jet-flow gates is limited primarily by manufacturing or shipping capabilities.

As shown in Fig. 14, a jet-flow gate consists of a flat-bottomed leaf, a body and bonnet, and a bonnet cover on which the operating hoist is mounted. The unusual characteristic of the jet-flow gate is the shape of the fluidway just upstream from the jet spring point, as shown in Fig. 52. The fluidway upstream of the spring point is the frustum of a 45-deg cone which forms a nozzle and causes the discharging jet to contract and spring free of the gate leaf slots. The small diameter of the nozzle forms the jet orifice. The large diameter of the nozzle is made at least 1.2 times the diameter of the jet orifice so that proper contraction of the jet will occur. The upstream conduit may be made the same diameter or larger than the jet orifice; however, if the upstream conduit is smaller than the large diameter of the jet nozzle, a conical diffuser which will

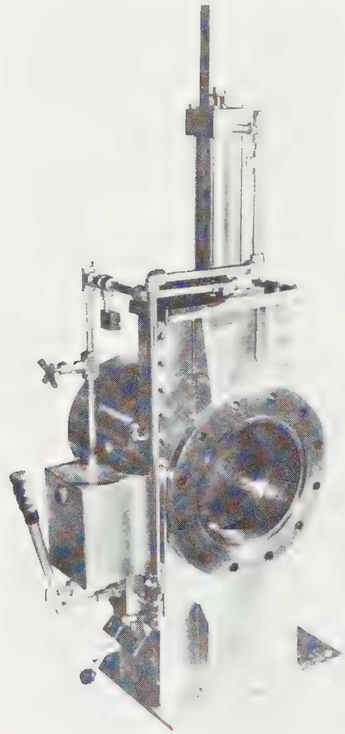

FIG. 16. 10-in. jet-flow gate used for regulating small releases from outlet works.

expand the size to the required 1.2 times the orifice diameter must be provided. The included angle for the conical diffuser should be about 7 deg for the best hydraulic efficiency, but angles to 12 or 15 deg can be tolerated if necessary.

It is essential that the 45-deg conical nozzle be machined to provide smoothness and accuracy. It is also necessary that the orifice boundary be designed to provide a definite spring point on both the conical nozzle and the bottom of the leaf. The basic features for the nozzle, leaf, and seals for jet-flow gates are shown in Fig. 14.

As only the circular upstream fluidway is under reservoir pressure, it is not necessary to provide heavy reinforcement around the body and bonnet in the embedding concrete. The interior spaces of the body and bonnet are rarely subjected to even very low water pressure, and usually the pressure will be atmospheric or slightly subatmospheric. As the bonnet cover is not subjected to reservoir pressure, the cover needs to be designed only for the closing thrust capacity of the hoist which is mounted on the cover.

The area of the downstream conduit is usually made 15 to 20 percent larger than the jet orifice. The flat bottom, inverted U-shaped downstream conduit eliminates jet impingement and flow turbulence in the gate slots which occur in gate openings up to about 25 percent for circular downstream conduits. This impingement does not seem to be critical, however, as no gate-slot damage has been noted in gates having circular downstream conduits. Shaping and sizing the downstream conduit to be certain that adequate air can be delivered around the entire periphery of the jet are important. While specified design data for computing air-vent size are lacking, the data given in Art. 26 provide a basis for estimating a size. In any case it is desirable to favor generously sized rather than minimum-sized air vents.

It is essential that the upstream face of the gate leaf which is in sliding contact with the seal be made of corrosion-resistant material. Steel plate, clad with either monel metal or 18-8 stainless steel, has been used to provide a corrosion-resistant surface. Preference has been given to monel metal because it is closer electrochemically to the bronze seal surface which rubs on the plate and consequently should be less susceptible to electrolytic corrosion. In the initial designs gate leaves were wheel-mounted to minimize the hoist capacity required for screw-stem-type mechanical hoists. High hoist capacities are readily obtainable with hydraulic hoists, and simple slide surfaces can replace the more complicated and costly wheel-mounted gate leaf. The increase in the cost of a somewhat larger hydraulic hoist is more than compensated for by the simplification of the gate parts. Also the overall width of the body and bonnets can be made less, which reduces the weight and machine work. Metals for the gate sliding surfaces should be the same as for slide gates, and the surfaces should be greased.

10. Wheel- and Roller-mounted Gates. In gate terminology, names such as "tractor," "caterpillar," "coaster," and "fixed-wheel" have been used to describe roller-mounted and wheel-mounted gates. There is need for clarification of terms and the adoption of more rational names.

Some of the common names which are used to describe roller-mounted gates are "Stoney," "tractor," and "coaster." It is perhaps fitting that the widely used term Stoney gate be retained as a tribute to the originator for describing roller-mounted-type spillway gates. There is no reason, however, for the confusion caused by applying the terms "tractor gate" and "coaster gate" to roller-mounted gates which are used for high-pressure outlets. The terminology does not describe or even suggest the features of the gate to which it is applied. Such gates will be referred to here as roller-mounted.

Similarly, although the name "fixed-wheel" gate is widely used and is generally understood, it is unfortunate that this contradictory terminology is so commonly used to describe a type of gate. Such gates may be accurately called wheel-mounted gates, and this terminology will be used here.

Wheel- and roller-mounted gates normally serve the same function when used in high-pressure outlets, namely, that of providing the primary shutoff gate for a conduit or penstock. Both gates are also usually designed to close by gravity. Determination of whether to use a wheel or a roller-mounted gate is basically the result of determining if the weight of the gate is sufficient to overcome friction forces. To ensure gravity closure of such gates, the design is usually made so that the net weight of the gate exceeds the sum of all friction forces by at least 25 percent. As the seal and guide frictions are essentially the same for either type of gate, the type of gate selected is usually determined by the friction of the wheels or rollers. Because wheel-mounted gates are somewhat simpler and more economical to build, they are usually given first preference. As the head on such gates increases, the size of the wheel pin must be increased to carry the bearing and bending load. The wheel diameter usually must also be increased to obtain a wheel-to-pin diameter ratio as large as possible and minimize the vertical force required to overcome the sliding friction on the wheel pin bearing. As heads increase, this combination of factors results in wheel sizes which become excessive in terms of the gate framing. These factors therefore limit the size and head for which wheel-mounted gates can be used from a practical and structural standpoint. The use of roller bearings or equivalent types of antifriction bearings instead of sleeve bearings increases the feasible heads for wheel-mounted gates by reducing frictional resistance of the wheel bearings. The cost and capacity of antifriction bearings impose economic and practical limitations on their use and establish the head limitation for which wheel-mounted gates are suitable.

When the maintenance of suitable proportions and enough excess weight to ensure gate closure is not attained in a basic wheel-mounted gate design, either excess ballast weight in the form of cast-iron pigs is added to the gate or a roller-mounted gate design is used. The low friction of roller trains and their high load-carrying capacity permit using roller-mounted gates for gravity closure at very high heads.

Wheel- or roller-mounted gates are usually installed at the entrance to conduits or penstocks. Such gates are frequently located on the face of a dam, in dam abutments, or in intake towers located in the reservoir. Typical installations are shown in Figs. 17 to 20, inclusive. Installation on the face of a dam is usually feasible only in the case of a concrete dam. Such gates are also sometimes installed in shafts near the axis of earth-fill dams where installation at an entrance is infeasible or too costly. As the primary use and function of wheel- and roller-mounted gates are usually to provide emergency shutoff of water for guarding the safety of the pipe and downstream equipment, the preferable location of such gates is at or near the entrance.

Such gates are usually used only in the fully open or closed positions and are

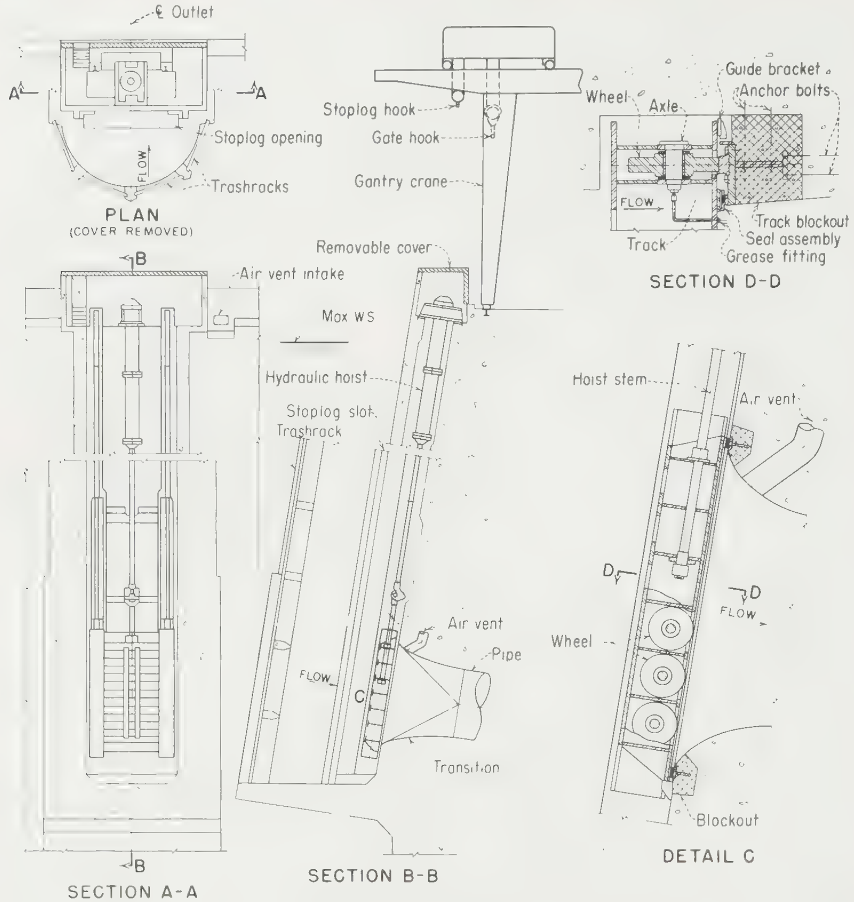

Fig. 17. Typical installation of wheel-mounted gate on the sloping upstream face of a dam.

suspended just above the intake, as shown in Fig. 17, so that closure can be made rapidly in case of an emergency. Hydraulic hoists, as shown in Fig. 19, are commonly used for operating such gates, although mechanically operated wire-rope hoists are also used. One important advantage of the hydraulic hoist is that the connection to the gate is made by a series of large stem sections which are easily protected by painting and are not materially weakened by corrosion of a degree which would seriously impair a wire rope. The wire ropes on mechanical hoists must either be made of stainless steel or, if made of carbon steel, be replaced frequently to ensure the safety of gate operation. The closure speed for wheel- and roller-mounted guard gates is usually set at 15 to 20 fpm, although faster or slower speeds are readily attainable. Except for remote-control circuits, no power is required to close gates having hydraulic hoists, and closure speed can be readily set as desired by adjusting the throttle valve which controls the oil being bypassed from the underside to the top of the piston. Opening speeds for such gates are not critical and opening times of 10 to 30 min are frequently used to avoid large oil pumps and electric motors. Figure 19 shows the general arrangement of a hydraulic hoist, such as may be used to operate a wheel- or roller-

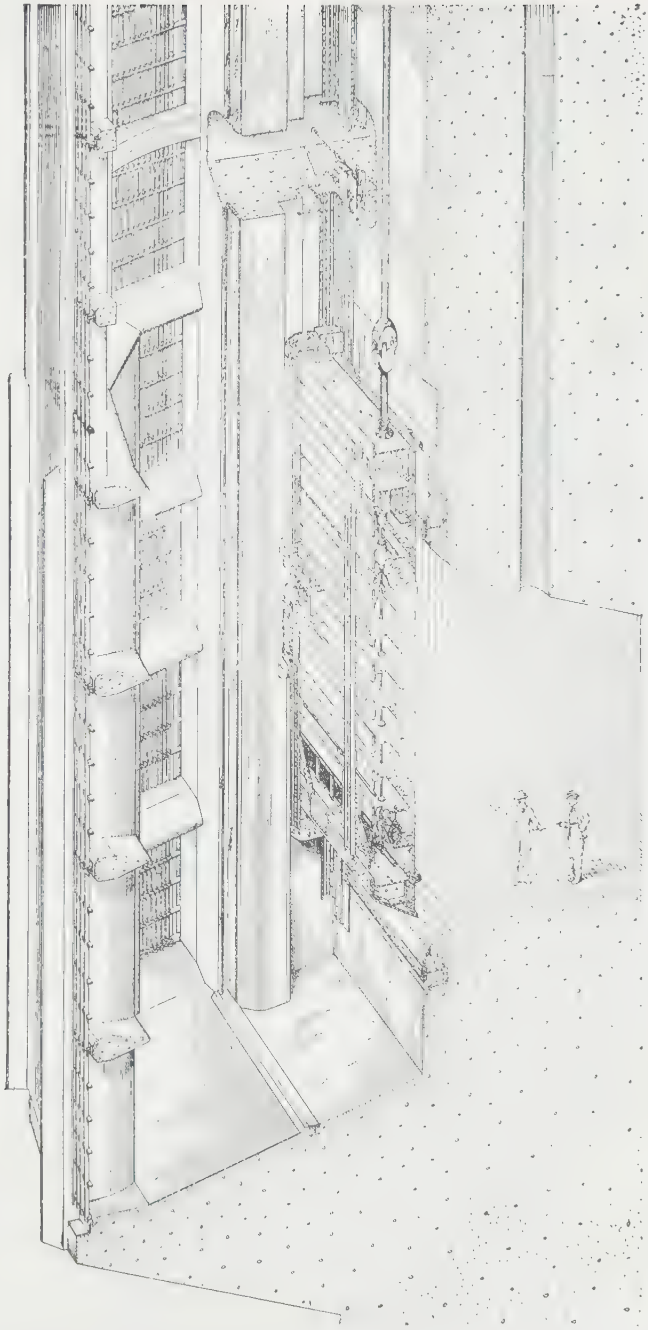

FIG. 18. 15- by 29.65-ft stem-operated coaster (roller-mounted) gate guarding penstock intake to 150,000-hp turbine at Grand Coulee Dam.

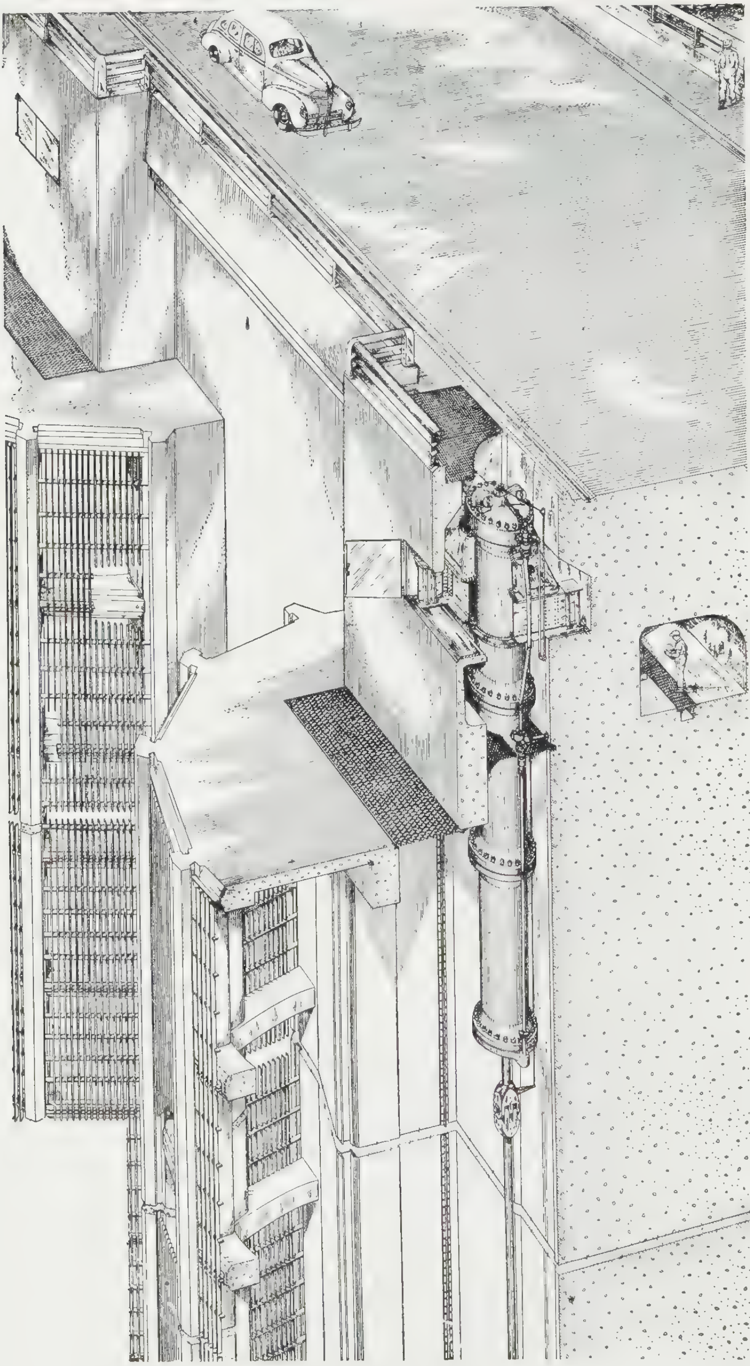

Fig. 19. Perspective illustration of the general arrangement of the hoists for the 15- by 29.65-ft penstock guard gates at Grand Coulee Dam.

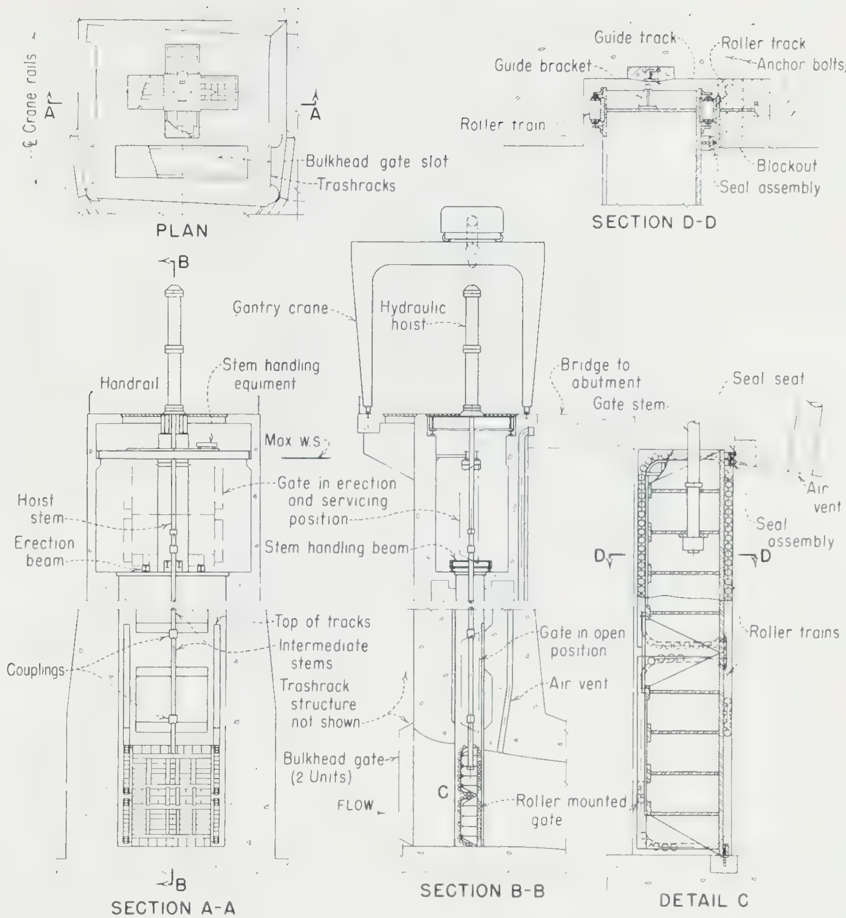

FIG. 20. Typical installation of roller-mounted gate in a tower-type intake.

mounted gate. The design details for such hoists are covered in Art. 34. The present general practice for hydraulic hoists, which are used to operate guard gates, is to hold the gates open by confining the oil under the piston and not to use mechanical devices to hold the gate open.

Figures 17 and 21 show a wheel-mounted gate, and Fig. 20 shows a roller-mounted gate. These figures illustrate designs which are practically all welded, except for parts which must be field-assembled. The 9.93- by 18.98-ft gate for Yellowtail Dam (Fig. 21) was fully shop-fabricated and shipped as a unit. The fabricated gate was stress-relieved as a unit before being machined. No critical distortion or machining problems were encountered in manufacture. The successful fabrication of this gate verifies the feasibility and desirability of making gates in the largest possible unit which can be fabricated and shipped.

The 17.5- by 22.89-ft roller-mounted gate for San Luis Dam (Fig. 20) is likewise an all-welded design. It was necessary, however, to make this gate in two sections because of shipping limitations. The connection between the two sections is made so

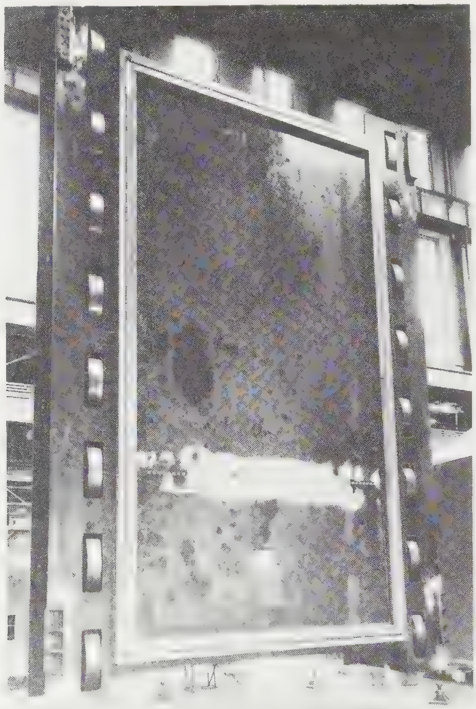

Fig. 21. Downstream view showing wheel and seal arrangement on 9.93- by 18.98-ft wheel-mounted, all-welded gate for Yellowtail Dam.

that the skin-plate splice acts as a hinge to permit the upper and lower sections to rotate slightly and accommodate minor deviations in the straightness of the tracks. This feature of articulating the two gate sections avoids the possibility of high bending stresses in the vertical plane at the joint between the sections and likewise helps to avoid excessive roller loads which could result from long, imperfectly aligned roller tracks. The rubber pads under the roller tracks also serve to distribute and equalize the load on the rollers by providing some flexibility of the support under the tracks.

The basic components of wheel- and roller-mounted gates are essentially the skin plate, transverse beams which frame into vertical girders, wheels or rollers, and the gate seal. The principal structural difference in wheel- and roller-mounted gates is in the arrangement of the vertical girders. For wheel-mounted gates the vertical girder is usually made of two continuous members to provide a slot for straddle-mounting the gate wheels. In some wheel-mounted gates a single vertical girder is used and the wheels are mounted on cantilevered shafts on the sides of the gate. For roller-mounted gates the vertical girder is usually a single member and is frequently not made continuous so that long roller trains, which are not desirable, can be avoided. The design of gate roller trains, wheels, and tracks is covered in more detail in Arts. 32 and 33.

If the structure in which a gate is installed will permit, it is usually preferable to have the gate skin plate and seal on the upstream side. This preference is based on the fact that downpull is usually absent on gates with upstream skin plates; consequently, savings in the gate stems and hoist result. It must not be assumed arbitrarily, however, that downpull is not possible on gates with upstream skin plates, as such gates operating under submerged conditions on the downstream side can have very substantial downpull unless the gate leaf is carefully designed to avoid low pressures under the bottom beam on the gate. The amount of upstream projection on the gate seal should also be carefully checked as this projection will produce an uplift on the gate which might prevent it from closing and seating by gravity. This force is particularly important because it becomes a maximum at the same time that the seal and wheel frictions are also at the maximum.

Upstream skin plates and seals also result in making it possible to inspect the wheels, rollers, or tracks when the gate is closed and the downstream side is unwatered. Despite the foregoing advantages of upstream skin plates, it should not be assumed that downstream skin plates are not satisfactory.

Practically all wheel- and roller-mounted gates which are installed on the face of a dam, as well as numerous other installations, have downstream skin plates and seals. For gates having downstream skin plates, downpull is always an important consideration. No easy solution is available which can be applied to all gate downpull problems. A general discussion on downpull and some of the critical factors involved are outlined in Art. 34.

The design of a suitable seal is usually the most critical and difficult problem. A number of designs seal well enough to be called satisfactory. The perfect seal has not yet been designed. The principal problem is that the seals must be strong enough to resist high pressures, while retaining flexibility to conform to irregularities on sealing surfaces. The detail design of rubber seals such as are frequently used on wheel- and roller-mounted gates is covered in Art. 31.

Seals on wheel- and roller-mounted gates frequently surround the opening like a picture frame. The second seal configuration which is frequently used has a picture-frame-type seal across the top and at the sides of the gate, but seals across the bottom by compression of a seal on the sill on which the gate rests when closed. The "picture-frame" seal has some advantage because the seal contact is all in one plane; however, the second type works very well and the right-angle corner at the bottom can be sealed satisfactorily.

The embedded frames on which the seal seats and tracks are mounted must be made and installed to close tolerances. It is especially important that the surfaces of the tracks be in plane and that the plane of the track surfaces and the plane of the seal seats be substantially parallel. It is also important that joints in the seal seats be flush and butt tightly. In addition to aligning and securing the track and seal seat frames, the anchor bolts are normally designed to withstand any hydrostatic separating force which can occur between the first- and second-stage block-out concrete in the gate slots.

Gate slots for wheel- and roller-mounted gates do not usually pose any hydraulic design problems, because the velocities are usually low. Such gates are not ordinarily used for throttling except as required occasionally for filling a conduit or penstock. A general discussion of gate slots is contained in Art. 25.

11. Cylinder Gates. In general cylinder gates are used primarily as shutoff gates for conduit and penstock intakes; however, cylinder gates are also used sometimes for regulating discharges. Cylinder gates provide a relatively simple and effective installation for vertical intakes where the controlling gates must operate in a shaft or intake tower. Although cylinder gates are not widely used, they are fundamentally a sound type of gate and merit serious consideration where vertical-shaft intakes are required.

Basically a cylinder gate is composed of a cylindrical shell which is raised and

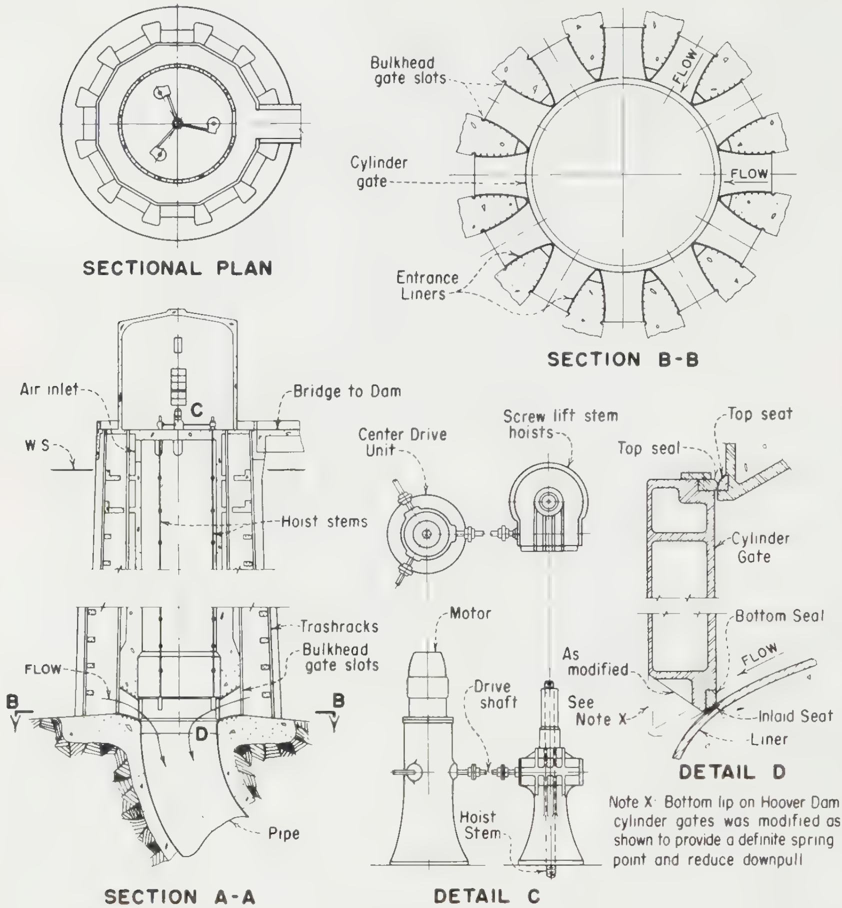

FIG. 22. Pertinent features of a cylinder-gate installation, based on the 32-ft-diameter cylinder-gate installation at Hoover Dam.

lowered to control flow through radial openings into a circular vertical-intake structure for an outlet works or power plant (see Figs. 22 and 23). Cylinder gates have been located on both the inside and the outside of the circular structure, but an inside location is preferable for maintenance reasons. Seals at the top and bottom of the cylinder contact mating seats when the gate is closed. Three equally spaced stems have usually been used for hoisting, although with proper gate guidance a single hoisting stem should also be satisfactory for gates on the interior of the tower.

Except for low heads, most intakes equipped with cylinder gates have had a low-level gate and a high-level gate. The basic purpose in providing an upper and lower gate has been to limit the maximum unbalanced operating head on the gates. A dual gate installation permits using the upper gate for high reservoir levels and the lower gate only at lower reservoir levels. In view of operating experience it is doubtful that the added expense of dual gating is justified on the basis of minimizing the operating head on a cylinder gate. It appears that a single, properly designed gate would be preferable from the operating, servicing, and economic standpoints. Certainly the use of a single gate would greatly simplify the maintenance problem which is inherent in most cylinder-gate installations. With a single cylinder gate the problem of raising the gate to the top of the tower for inspection and maintenance would be greatly simplified as the stems for only one gate would be involved. If there is a problem of getting water at desired temperatures from different depths in a reservoir, dual gating may be justified.

Although mechanically driven screw-lift hoists have been commonly used, there appears to be no reason why hydraulic hoists cannot be adapted to operate cylinder gates. It would appear desirable that a single cylinder be used and that it be arranged so that the gate can be picked up by one or three stems. The principal advantage of hydraulic operation, in addition to basic simplicity, is the ease with which rapid closure can be effected. The relatively long closure time for screw-stem hoists is particularly objectionable when cylinder gates are used as guard gates for penstock intakes.

Another feature of existing designs which appears to merit reconsideration is the practice of designing stems for column loading to force a gate closed. Operating experience does not indicate that thrust is necessary to close a cylinder gate. Basically there is no operating friction for a cylinder gate except for the very minor rubbing which may occur on the guides during raising and lowering. The fact that such friction is very low has been borne out by rather strong vertical vibrations which have occurred on some installations, especially where cylinder gates have been used at small openings for throttling flows. In the case of the gates which have vibrated, there was very little friction to produce a damping effect, and the gates vibrated at the natural frequency of the gate and stem system. These operating experiences indicate that thrust to overcome friction and close a cylinder gate is not necessary. In fact, a means of providing some guide friction in a design for damping possible vibrations may be desirable, particularly for regulating-type cylinder gates.

The exciting force for vibration of a cylinder gate is generated by the flow variations in the spaces beneath or around the gate. Usually the tendency to vibrate is most critical when the gate is nearly closed. In this position the downpull forces on a cylinder gate can be subject to considerable and rapid change in magnitude and tend to set up vertical vibrations. To minimize downpull and possible vibrations, it is important that the spring point on the bottom of cylinder gates be well defined, particularly on regulating gates. It is also necessary to provide adequate fluid circulation to the spring point. Detail *D* in Fig. 22 shows the modifications which were made to the bottom of the cylinder gates at Hoover Dam to eliminate vibration and excessive downpull.

Cylinder gates, such as those at Cle Elum Dam (Fig. 23) which are used for throttling to regulate flows, require vents to admit air. Modification and enlarging of the air vents have not resulted in fully satisfactory operation. When large amounts of air are entrained in the discharges, rather heavy and objectionable surging has resulted because of the unstable conditions which result when the air is released in the downstream tunnel. Objectionable air entrainment and bad surging conditions occur primarily when the upper gate is used for throttling flows and the free-falling discharge entrains air as it plunges into the water some distance below the upper gate. The entrained air is released in slugs downstream from the gate structure and creates an unstable surging condition at the gate shaft. In test operations where only the lower gate was used for releases and was discharging under submerged conditions, no air entrainment or surging occurred. If the lower gate at Cle Elum Dam had been designed for full-head operation, the problem of air demand and surging would probably have been avoided.

These operating experiences indicate that, when a cylinder gate is to be used at partial openings for regulation, special care must be used in considering the structural

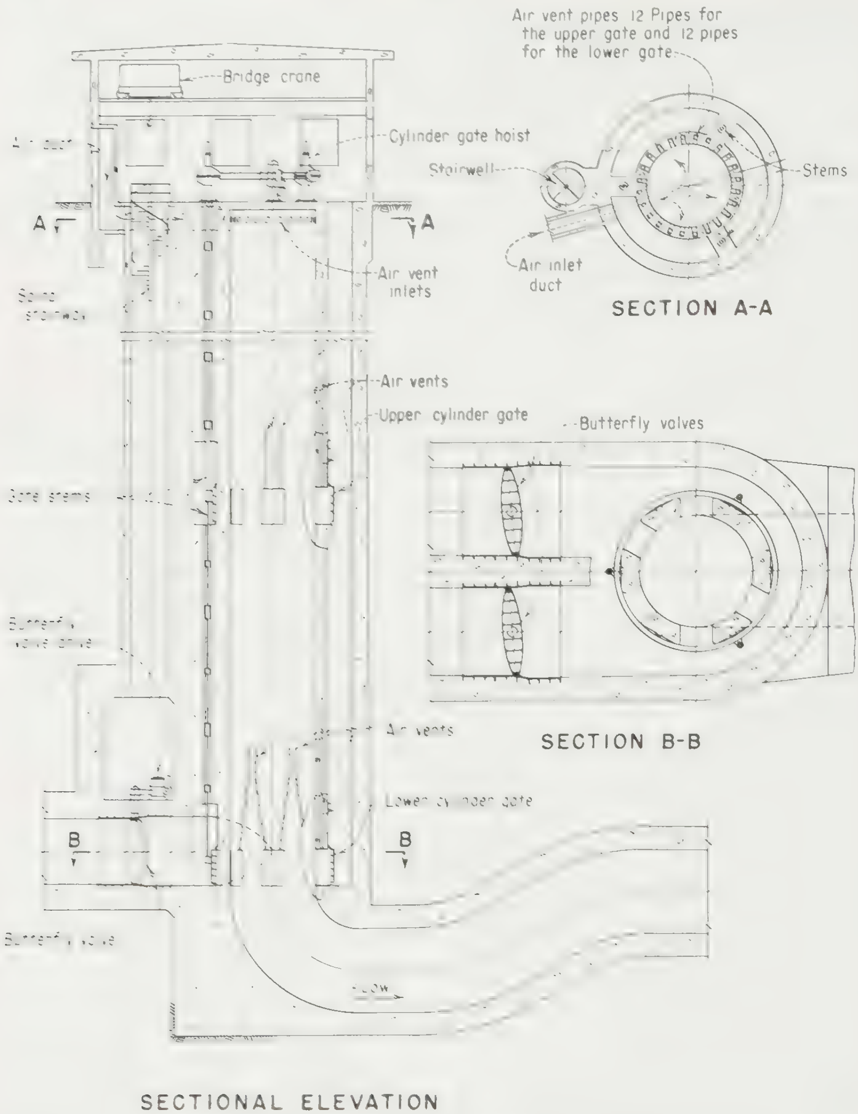

Fig. 23. Arrangement of 20-ft-diameter cylinder gates in outlet works at Cle Elum Dam. Note 11-ft-diameter butterfly guard valves at inlet and the air-supply ducts.

and hydraulic features of the installation. Gates used for regulating under submerged discharge conditions must have defined spring points and adequate fluid recirculation to the discharge orifice boundaries. A proper gate arrangement could eliminate the continuous need for large volumes of air and the objectionable effects attendant on the release of entrained air in the discharge. The need for adequate air vents to supply air during the draining or filling of a penstock or conduit would remain.

12. Bulkhead Gates and Stop Logs. Both bulkhead gates and stop logs are

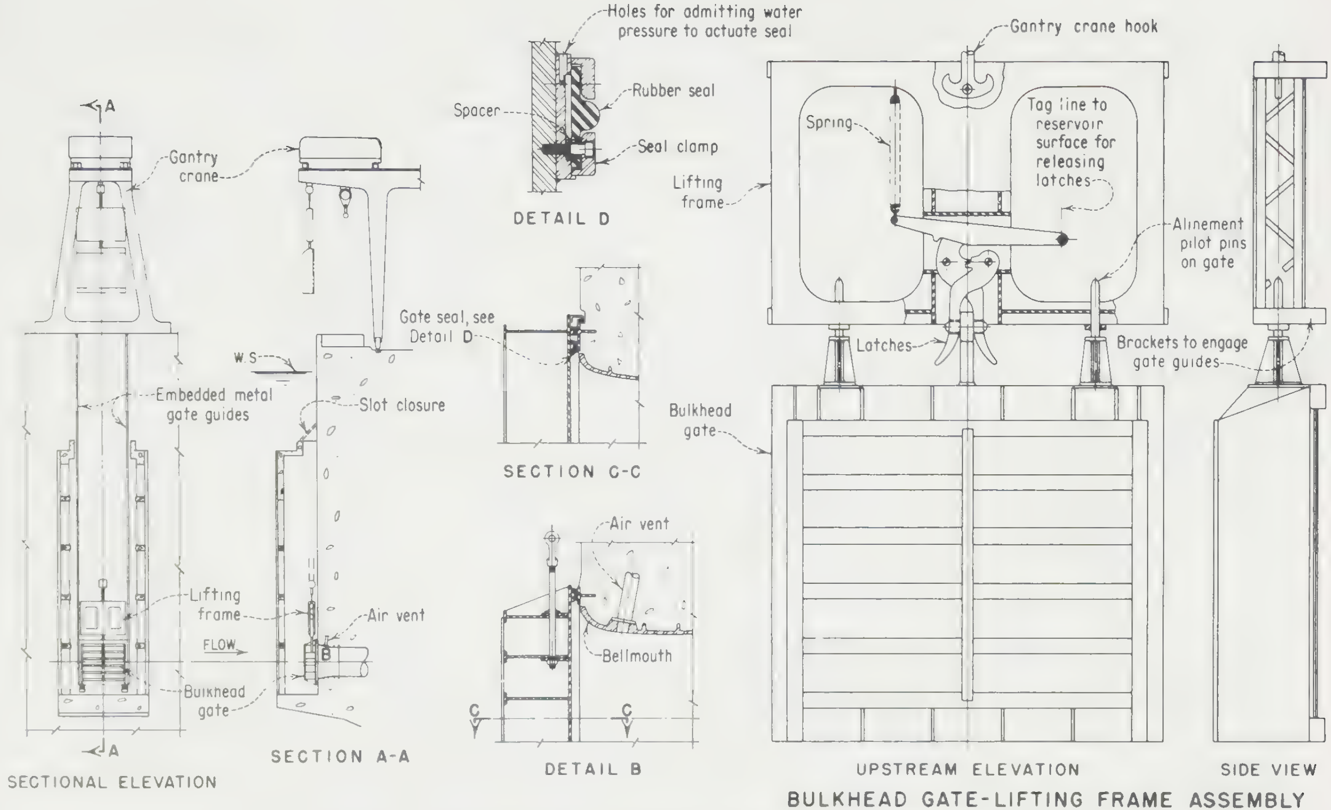

FIG. 24. Typical bulkhead installation and lifting-frame arrangement.

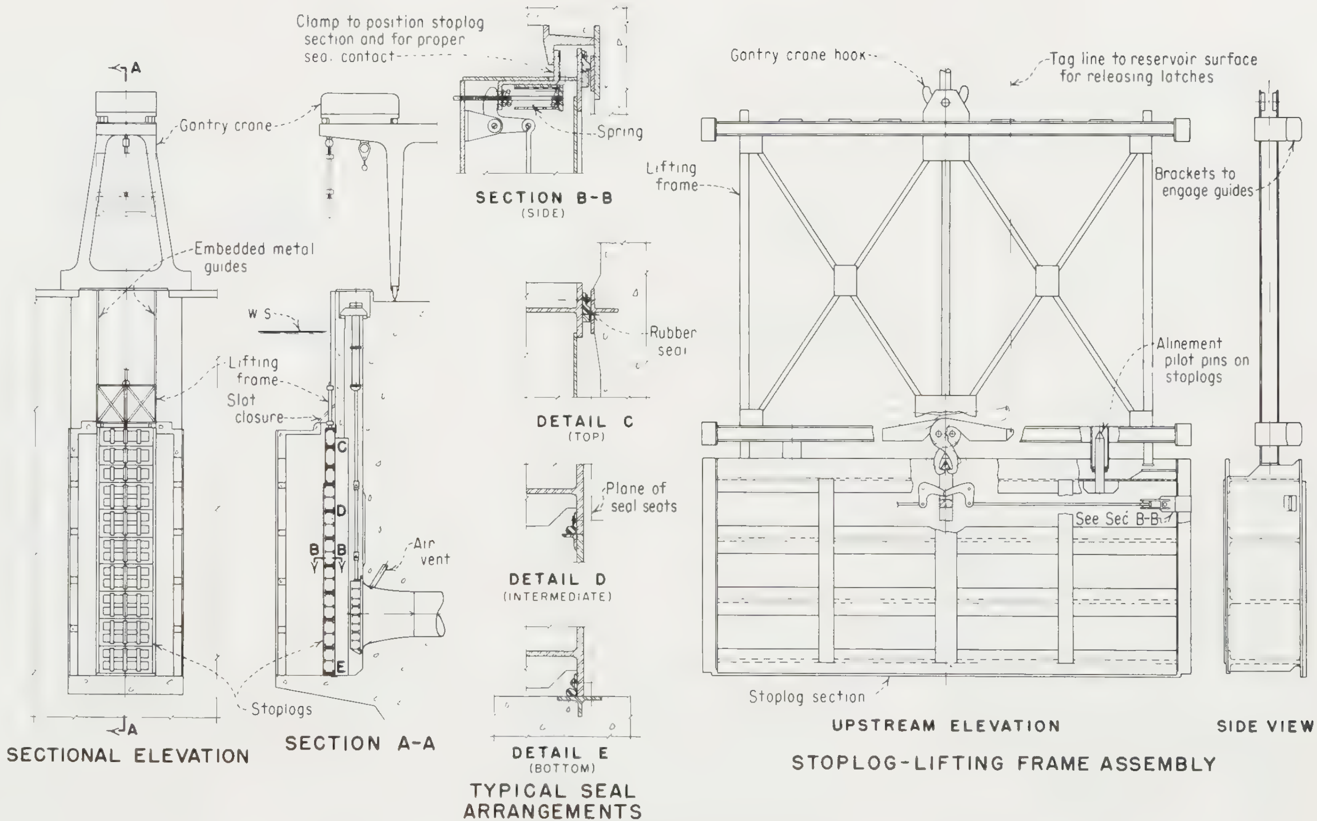

FIG. 25. Typical stop-log installation and lifting-frame arrangement.

usually placed over outlets under balanced-pressure no-flow conditions, and function to permit inspection or repair of the downstream fluidway and gate or valve parts. Bulkhead gates and stop logs are located as far to the upstream end of a conduit as possible to permit almost complete unwatering of a fluidway.

Modern stop logs and bulkhead gates frequently look very much alike and cannot be differentiated readily on the basis of general appearance. Stop logs no longer resemble the rough-hewn timbers from which the name originated, and the only remaining similarity between modern structural-steel stop logs and the original wooden stop logs is the fact that a number of substantially identical parts are placed in a slot at the entrance to a fluidway.

The general appearance of modern rubber-sealed structural-steel stop logs and bulkhead gates no longer provides a means of identifying these closure devices. For this reason the installation arrangement frequently determines whether the closure devices are called bulkhead gates or stop logs. In general, when there are not more than two closure sections, and only the entrance opening is covered, the name bulkhead gate is normally used. If more than two closure sections are used and the units fill a slot to a height above the existing reservoir surface, the name stop logs is commonly used.

Most conduit and penstock entrances are horizontal and have substantially vertical slots for placing of bulkhead gates or stop logs. Typical general arrangements are shown in Figs. 2 and 3. In the placement of such bulkheads or stop logs, a crane and lifting frame are usually used, as shown in Figs. 24 and 25. The lifting frame is equipped with a latching device having a tag line to permit connecting and disconnecting the bulkheads or stop-log sections under water. Automatic latching devices have been used, but tag-line operation is generally preferred. In addition to permitting the placement of multiple units, the lifting frame permits hoisting the frame above the reservoir surface to avoid rusting of the hoist ropes after a bulkhead has been placed. In cases where the top of a trashrack structure is below the upper reservoir surface, a cover over the bulkhead gate or stop-log slot opening is usually provided. Such covers are either removed with the lifting frame before bulkheading or stop-logging an outlet or with lifting ropes attached to the covers by divers.

In case conduits or penstocks have bellmouthed intakes on vertical-intake shafts, circular bulkheads are used. See the shaft-type intake in Fig. 3. For small, low-head intakes, either concrete or steel bulkheads are used. Elliptical and hemispherical circular steel bulkhead designs have also been used for vertical-intake shafts; but except for some savings in weight, such designs do not have any particular advantage in cost over a flat bulkhead of conventional beam and skin-plate design. For large intakes where field welding is required, the flat bulkhead has a definite advantage in avoiding field welds which are subjected to critical tension stresses as is the case for large elliptical and hemispherical bulkheads. For these reasons the conventional beam and skin-plate design is usually preferred for flat circular bulkhead gates.

Wooden seals are sometimes used for the sealing surfaces of stop logs and bulkhead gates; however, because wooden seals dry out, crack, and do not seal well, rubber seals are usually preferable. The "music-note" or "J" seal is the most widely used type of rubber seal for this equipment, and the use of wooden seals has largely been discontinued where rubber seals can be readily obtained.

The seal seats which are embedded in concrete at the intakes are normally fabricated with a corrosion-resistant contact surface, such as 18-8 stainless steel, for supporting and sealing bulkhead gates or stop logs. The provision of corrosion-resistant surfaces is especially important for such surfaces as they are usually permanently submerged after the reservoir has filled, and are not accessible for maintenance unless the reservoir is drawn down considerably below normal operating levels.

It is convenient to have permanent crane facilities available for placing and removing bulkhead gates and stop logs. Because of the infrequent usage, however, it is frequently not economically justifiable to provide permanent hoisting equipment. It is important, however, that fairly complete handling studies be made at the initial design stage to be sure that handling procedures using temporary equipment such as an A frame, a truck-mounted crane, or a barge-mounted crane, are feasible and are, in fact, the most economical. The fact that bulkheads and stop logs will be used only infrequently should not lead to the neglect of careful design. Proper design and facilities to permit easy handling will be found to be invaluable in assuring economical and adequate maintenance of outlets.

VALVES

13. General. The trend in valve designs has been the same as for gates, in that a relatively few simple and rugged types are being most widely used. The needle valve has been largely supplanted by Howell-Bunger fixed-cone or the Staats-Hornsby hollow-jet-type valves for regulating high-head releases. The slide gate and the jet-flow gate are also being used successfully for regulation at heads where needle valves were once the only suitable type. This trend has been spurred by the fact that the newer types of gates and valves are less costly and have a higher discharge capacity than a comparable size of needle valve. In addition, the later designs have fewer parts and require less service and maintenance than needle valves.

Mechanical or oil-pressure hydraulic systems are usually preferable to reservoir water-pressure hydraulic systems for operating valves. In some cases, reservoir water pressure is still used to avoid standby power units for emergency closure of power-plant guard valves, but this practice is commoner in Europe than elsewhere. The primary objections to using reservoir water as the hydraulic fluid are the problems involved in avoiding corrosion in the control system and the problems associated with the scale deposits from raw reservoir water. Minerals in untreated reservoir water have a tendency to come out of solution and be deposited on the surfaces of operating cylinders or in the small clearances of control valves. The oil-hydraulic operation and direct mechanical drives are most commonly used.

Various types of rotary shutoff valves are being used, but the butterfly- and sphere-type valves are most commonly used. Although the butterfly valve is somewhat less costly to build, there is an increasing use of sphere- or analogous-type valves, such as plug valves, which also have "straight-through" fluidways, because of their very low losses and less difficult sealing problems. The butterfly valve is still the most widely used valve for such service, particularly in the United States.

14. Needle Valves. A properly designed needle valve is an excellent device for regulating high-velocity flows, as is amply demonstrated by the almost universal use of such valves for controlling high-head flow for impulse turbines. However, the use of needle valves for the regulation of flow from outlet works has been supplanted to a large extent by more economical and hydraulically efficient types of gates and valves. Although the use of needle valves for outlet works is greatly diminished, this type of valve cannot be ignored as many needle valves are presently in service and the valve is fundamentally an excellent regulating device.

Figure 26 shows the principal stages of evolution for the needle valve from Ensign's original type through the interior differential type. It will be noted that all these valves are hydraulically operated by reservoir water. This method of operation normally requires that the valves be disassembled at periods ranging from 2 to 6 years to remove accumulated scale. In some installations, such as Hoover Dam where the water has extremely high scaling characteristics, it is necessary to drain the water completely from the valve controls when not in use and to fill the Paradox control with

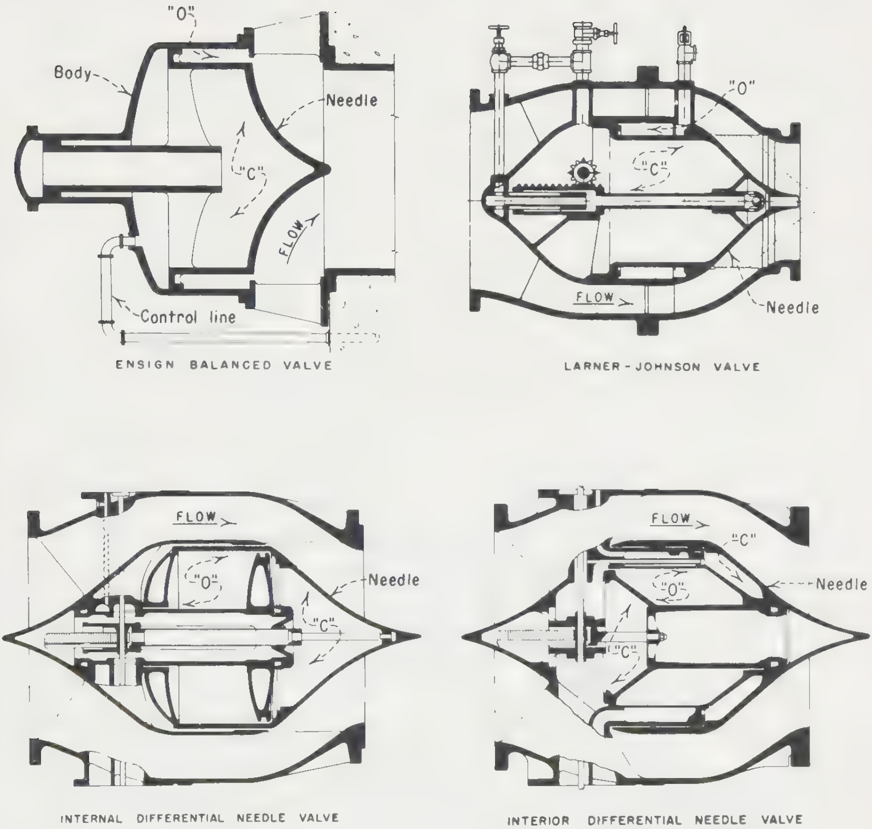

NOTE: All valves are hydraulically operated by conduit water pressure. Valves open by water pressure in chambers "O" and releasing water from chambers "C". Valves close by reversing the pressures in chambers "O" and "C".

FIG. 26. Evolutionary types of needle valves.

an oil, similar to kerosene, to avoid very frequent disassembly for removing scale. Obviously the relatively frequent diassembly for cleaning needle valves is costly and imposes considerable wear and tear on the parts.

Figure 27 shows a typical installation arrangement and cross sections through an interior differential needle valve and a Paradox control. The valve is closed by admitting water pressure to chambers C and C_1 and connecting chamber O to drain through the Paradox control. To open the valve, water pressure is admitted to chamber O and chambers C and C_1 are opened to drain. The control stand serves only to position the spool valve in the Paradox control for opening and closing the needle valve hydraulically. The control stand has no capability or connection for producing direct mechanical movement of the needle. The Paradox control is a compensating type of valve which will hold the needle in any position. Rotation of the handwheel turns the internal threaded member and moves the spool up or down, depending on the direction of rotation. As the needle responds and starts to move, the rack-and-pinion drive in the valve turns the external threaded member and drives the spool in an

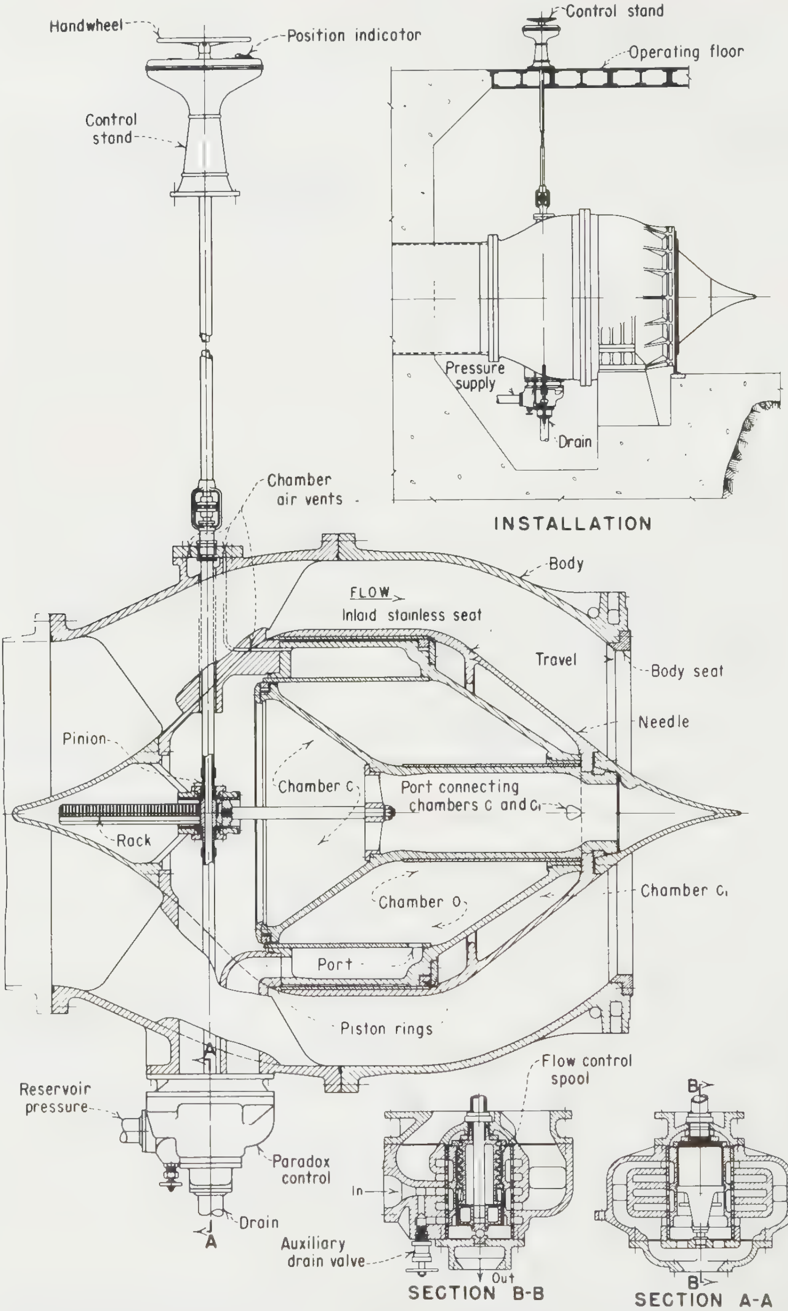

INTERIOR DIFFERENTIAL NEEDLE VALVE AND PARADOX CONTROL

FIG. 27. Interior differential-type needle valve with Paradox control.

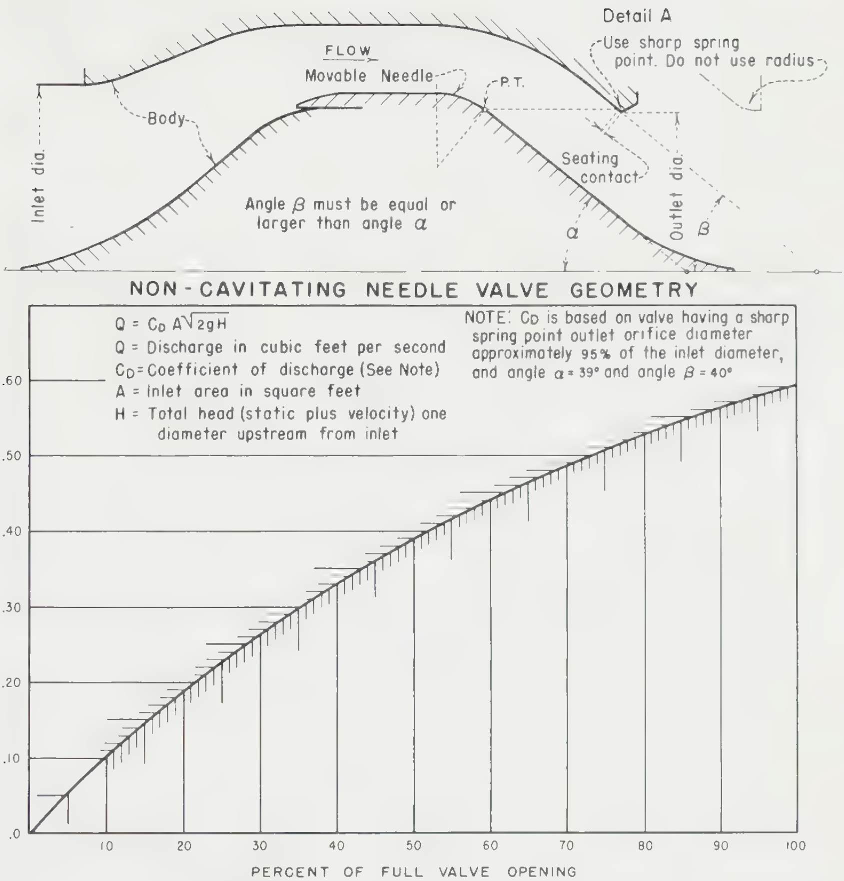

FIG. 28. Fluidway geometry for noncavitating needle valve—discharge-coefficient curves.

opposite direction from that produced by control-stand operation. Unless rotation of the handwheel is continued, the needle will stop when it has traveled a sufficient distance to return the Paradox control spool to the neutral center position. Any tendency of the valve to creep either open or closed from the set position will be automatically corrected by the spool valve being moved up or down so that pressure is directed into the proper valve chambers to counteract the needle creep.

Fundamental fluidway geometry to produce a noncavitating needle valve, and discharge curves for such a valve are shown in Fig. 28. In addition to the basic geometry and configurations shown, it is also important that the valve surfaces which will be in contact with high-velocity water be smooth and free of offsets (see Art. 24) to avoid cavitation.

In the valve fluidway geometry it is essential that the downstream cone angle of the needle be less than the downstream cone angle on the body to avoid cavitation at high heads. On some early designs which were used for moderate heads, a divergence rather than convergence of these cone angles appeared to be desirable as the discharge coefficient was increased and cavitation damage was not excessive. However, when similar valves were used under the higher head at Hoover Dam, rapid and excessive cavitation damage that required frequent and expensive weld repairs occurred. This problem resulted in hydraulic investigations being made and in the development of the fluidway geometry shown for a noncavitating needle valve.

Another important detail in fluidway geometry is shown in detail *A* of Fig. 28. The principal feature illustrated by the detail is the sharp, well-defined orifice and spring point which is necessary for the needle-valve jet. The rounded seat as shown in the phantom outline will produce cavitation and should not be used.

Although specially designed needle valves are being used successfully for discharge under submerged conditions, the conventional outlet-works valves are not usually suitable for such service. Outlet-works valves are normally installed completely above the downstream water surface, although operation with tail-water level to the horizontal center line can be tolerated. Needle valves should not be used for regulation within a pipe unless the operating chambers are designed to prevent the needle from slamming shut. Without proper design, reduced pressure on the needle surface can cause the needle to slam when nearly closed and set up undesirable and possibly dangerous water hammer.

In the operation of needle valves it is important that all air be vented from the interior pressure chambers and the high point of the fluidway before the valve is placed in service. Failure to vent valves properly can result in severe hydraulic shocks. These shocks are due to the rapid expansion of air compressed in the valve chamber and to the sudden needle movement which may occur when a chamber under high pressure is opened to low drain pressure for operating the valve. A gooseneck overflow having the high point above the maximum chamber elevation is usually provided to ensure that the operating chambers remain full of water.

15. Tube Valves. The tests which were conducted by the Bureau of Reclamation to develop a cavitation-free needle valve were also largely responsible for the invention and development of the tube valve. As cavitation was occurring on the conical surface of the needle, it was reasoned that elimination of the conical needle would eliminate the cavitation problem. Although elimination of the conical needle tip avoided a cavitation problem, it also resulted in a considerable instability of the jet at openings of less than about 35 percent. This instability is characterized by the jet no longer remaining concentric with the valve orifice and by having the direction of discharge of the jet change position in an unpredictable pattern around the valve orifice. Except for creating some minor problems of spray from the discharge, the jet instability is not objectionable and does not pose any vibration or hydraulic problems.

In free-discharge installations tube valves have given excellent service. Four 102-in. special long-body tube valves which were installed in the lower tier of outlets at Shasta Dam have had very limited use because of some undesirable operating characteristics. The amount of spray in the outflow discharge is objectionable at the adjacent switchyard. One valve had a tendency to vibrate severely at openings above 96 percent and some noise and rumble were evident in all valves toward the closed position of travel. Because of these operating characteristics and because the tube valves proved quite costly to build, the possible use of an alternative type of regulating gate was studied. The studies resulted in the development of the jet-flow gate which was installed in the middle and upper tiers of outlets instead of tube valves as originally planned.

Because of the basic configuration, tube valves can be used to discharge under submerged conditions. In one such installation, made to bypass the pump turbine at Flatiron power plant, the Bureau of Reclamation found no evidence of cavitation on a 42-in. tube valve after considerable operation.

As shown in Fig. 29, the fluidway configuration of a tube valve is quite similar to that of a needle valve without a downstream needle tip. Only relatively small unbal-

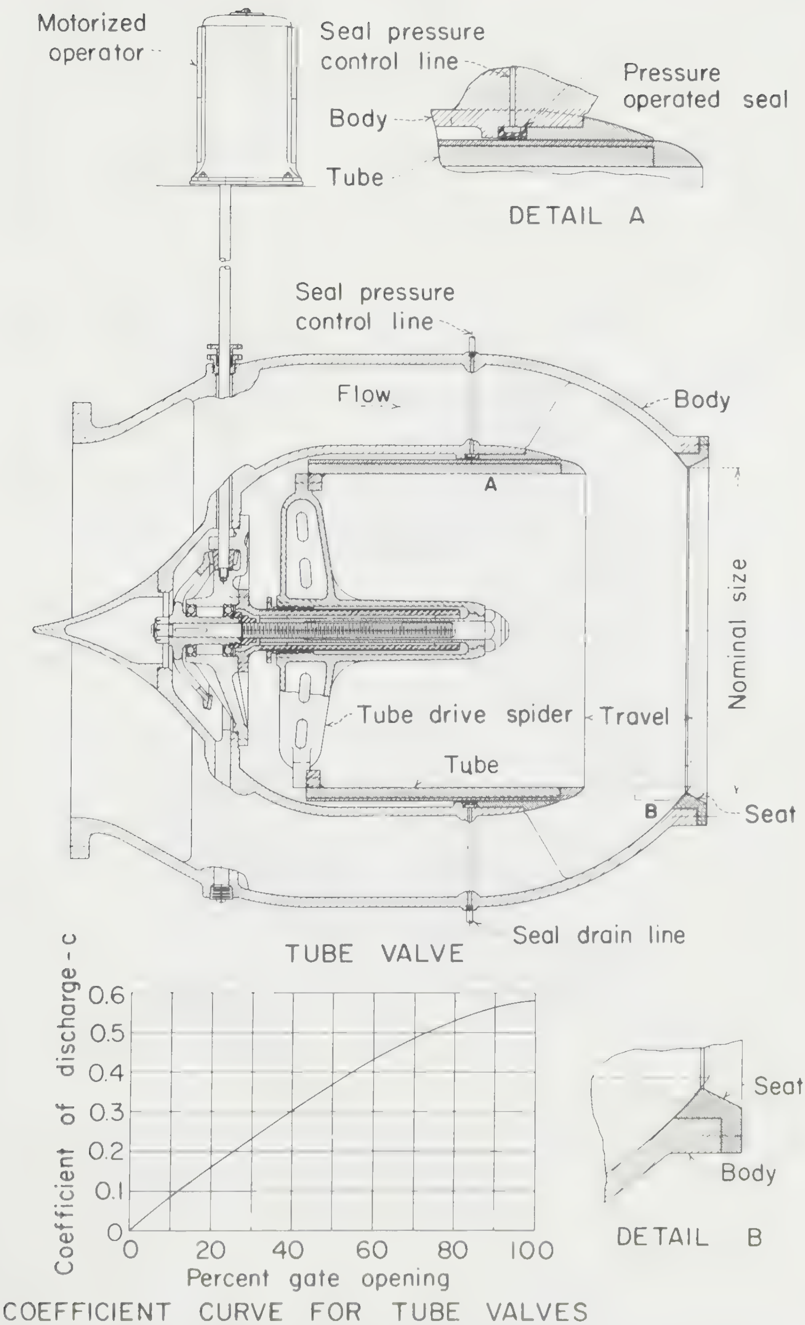

FIG. 29. General arrangement and discharge-coefficient curve for tube valves.

anced hydraulic thrust loads exist on the cylindrical tube as compared with the large thrust loads on a needle valve. It is therefore feasible to operate a tube valve by a relatively simple mechanical drive to move the cylindrical tube longitudinally for controlling flow. It would also be possible to use a small oil cylinder for operation.

The general seal and seat details, as well as discharge curves, are also shown in Fig. 29. In the design of tube valves no particular problems arise, except that an effective seal must be provided for the tube in the body bore. Both simple packings and water-pressure-actuated seals, as shown on detail *A*, have been used for the seal between the body and tube. Care must also be used to provide a well-defined control orifice between the tube and body seat as shown on detail *B*.

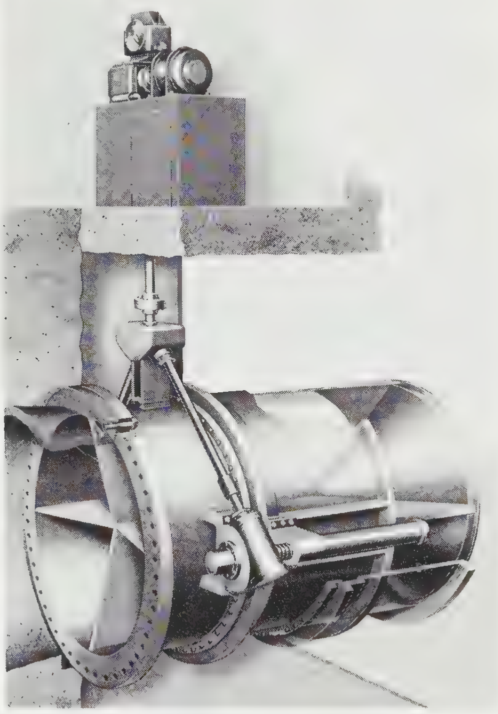

FIG. 30. Phantom view of Howell-Bunger valve installation. (*Allis-Chalmers Manufacturing Company.*)

16. Fixed-cone Valves (Howell-Bunger). The fixed-cone valve, which is more commonly known by the surnames of the inventors, C. H. Howell and Howard Bunger, has proved to be an excellent and widely used regulating valve. Although the primary use of the valve has been for free discharge into the atmosphere, the valves have also been used for submerged-discharge operation. Unless spray is objectionable, free discharge into atmosphere poses no particular problems; but for submerged discharges very careful design usually involving model testing is required. The basic arrangement and typical features of a Howell-Bunger valve installation are shown in Fig. 30 and in Fig. 31, which includes a set of discharge curves. The discharge curves are based on a wide-open discharge coefficient of $C = 0.85$, in accordance with the

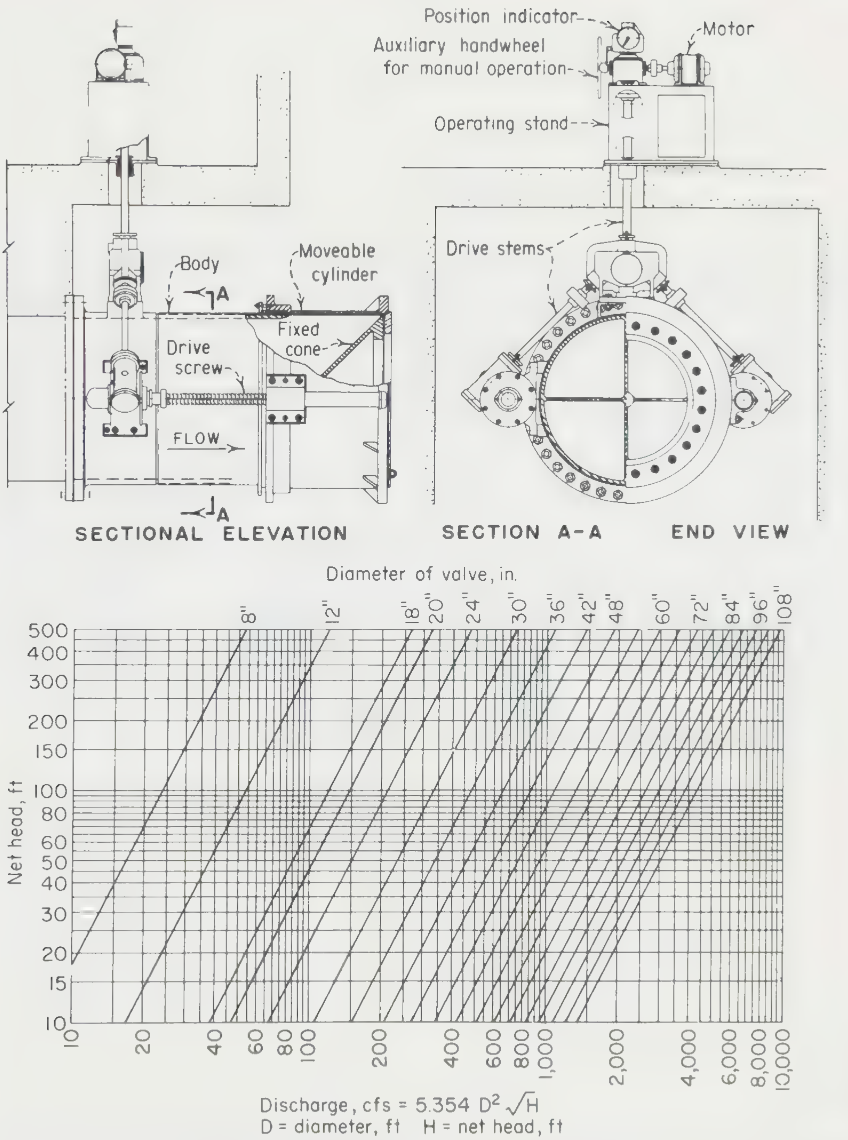

Fig. 31. General arrangement and discharge curves for Howell-Bunger valves. (*Allis-Chalmers Manufacturing Company.*)

following formula:

$$Q = CA\sqrt{2gH}$$

where Q = discharge, cfs
A = area of valve, sq ft based on nominal inside diameter
g = gravitational acceleration of 32.2 ft/sec²
H = net head, ft

By combining the constants the formula can be simplified and rewritten as shown in the following form in Fig. 31:

$$Q = 5.354D^2\sqrt{H} \qquad \text{(as shown on discharge curves)}$$

where D = nominal valve diameter, ft

The expanding cone-shaped discharge pattern of Howell-Bunger valves does an excellent job of aerating the water and dispersing the energy. Where the resulting

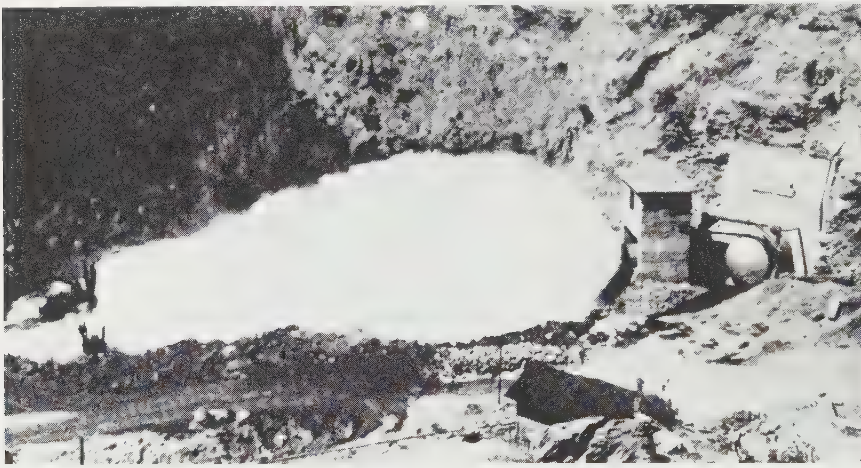

Fig. 32. Free discharge from 54-in. Howell-Bunger valve under 138-ft head. (*Allis-Chalmers Manufacturing Company.*)

spray from this type of discharge is not objectionable, the valves are usually allowed to discharge freely into air, as shown in Fig. 32. Where the spray from a widely dispersed jet is not acceptable, a downstream hood is used to confine and redirect the discharge, as shown in Fig. 33. Because of the wide dispersion of the jet, stilling basins are not normally used for these valves. In all installations it is important that adequate air be supplied to the region upstream from the jet. This requires large ducts on hooded-type installations. Because of the large air demands, the entrances to the ducts should be located and protected to avoid the danger of persons being sucked into the duct.

The basic Howell-Bunger valve is composed of four essential elements: (1) the body, (2) a cylindrical gate member, (3) the seals, and (4) the operating mechanism. The inside diameter of the cylindrical portion of the body is the same as the upstream pipe or conduit to which it is attached by a bolted flanged connection. Radial ribs, which are attached to the cylindrical portion of the body and which extend downstream from the end of the cylindrical shell, support the concentric conical head on the end of the valve. The apex of the cone is pointed upstream, and the cone angle with respect to the center line of the fluidway is about 45 deg. Flow from the radial discharge ports, formed by the arrangement of the body cylinder, ribs, and cone, is controlled by a cylindrical gate member on the outside of the valve body. The mating surfaces on the body and cylindrical gate member are made of corrosion-resistant material. An operating mechanism moves the cylindrical gate downstream to cover the radial discharge ports in the body and close the valve. In opening the valve the amount of discharge is governed by the varying area of the orifice between the cylindrical gate and the fixed cone as the cylinder is moved longitudinally.

The upstream end of the cylindrical gate is provided with a seal which slides and seals on the exterior cylindrical portion of the body. The sealing surface on the downstream end of the cylindrical gate is made of corrosion-resistant material and contacts the corrosion-resistant seat ring on the periphery of the conical portion of the valve body. The mating metal seats on the cylinder and cone are frequently made of stainless steel to resist corrosion and cavitation damage.

FIG. 33. 66-in. Howell-Bunger valve discharging at 265-ft head through a hood. (*Allis-Chalmers Manufacturing Company.*)

Although hydraulic cylinders, bell cranks, and other types of operators are used to operate these valves, the twin-screw type of operator shown in Figs. 30 and 31 is most commonly used.

Howell-Bunger valves are available in sizes from 8 to 108 in. Large-sized valves have been installed for heads up to 420 ft and smaller sizes for heads up to 900 ft. Special designs can be made to meet almost any size and head requirements. The relatively small force required to move the cylindrical sleeve permits manual operation up to about the 42-in. size; however, all sizes from 18 in. upward are available with motor operators.

17. Hollow-jet Valves (Staats-Hornsby). The hollow-jet valve, which was developed at the Bureau of Reclamation, is also known by the names of the inventors, B. H. Staats and G. J. Hornsby. The hollow-jet valve is an excellent and widely used valve for regulating high-pressure outlets. The valve is designed to be used for free discharge into the atmosphere, and should not be installed where discharge under fully submerged conditions can occur. It is permissible, however, to operate the valve partially submerged provided the tail water is not higher than the center line of the valve.

A typical outlet-works arrangement with a hollow-jet valve and a ring-follower-type guard gate upstream is shown in Fig. 34. For some installations the ring-follower

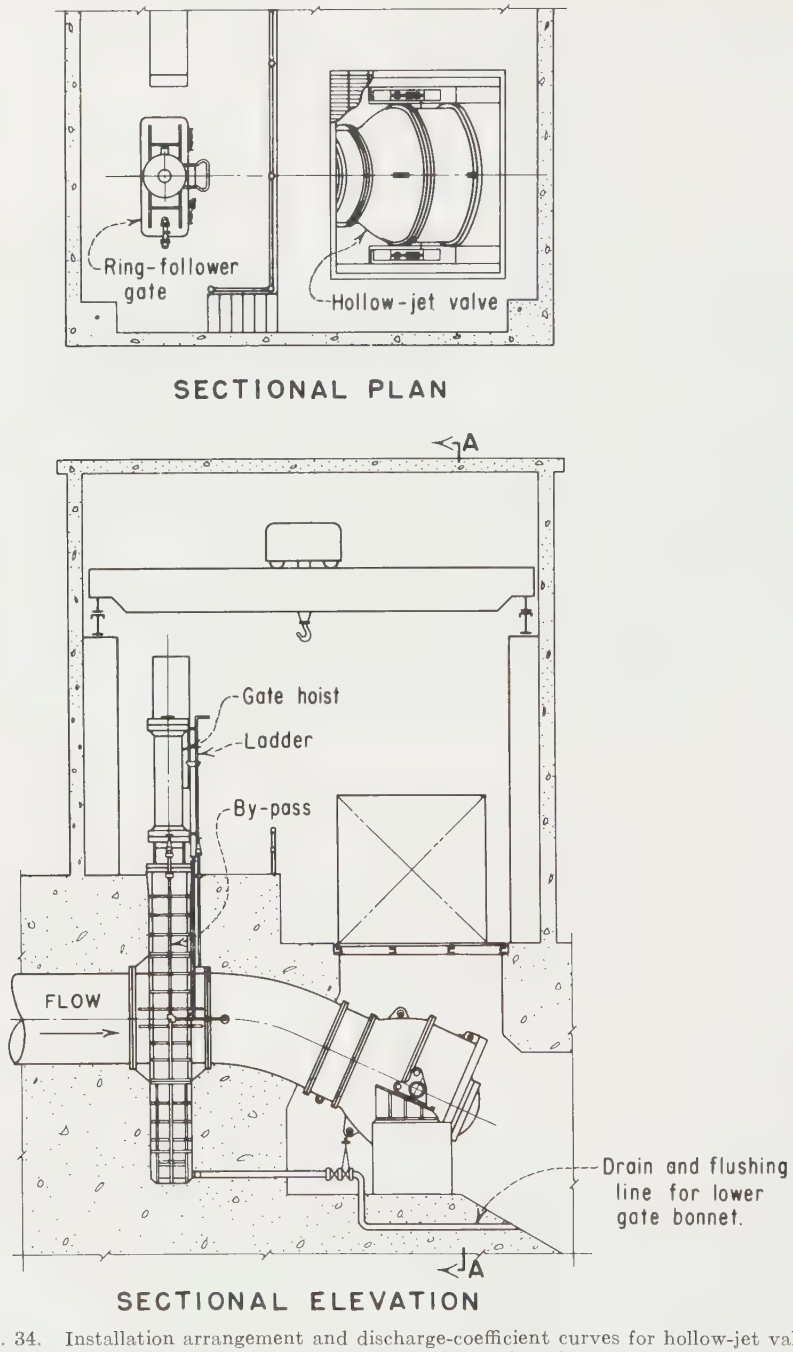

FIG. 34. Installation arrangement and discharge-coefficient curves for hollow-jet valves. A single hydraulic control system with appropriate valves is used to operate both the hollow-jet valves and the ring-follower guard gates.

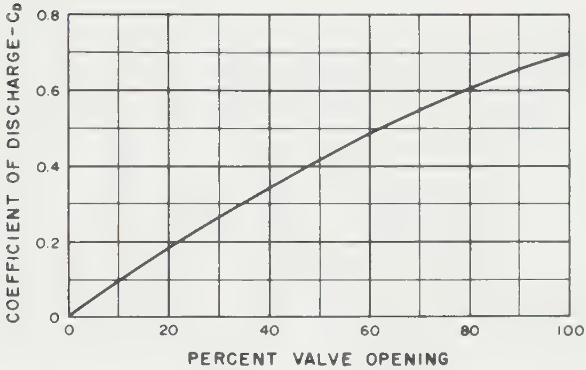

COEFFICIENT CURVE FOR HOLLOW-JET VALVES

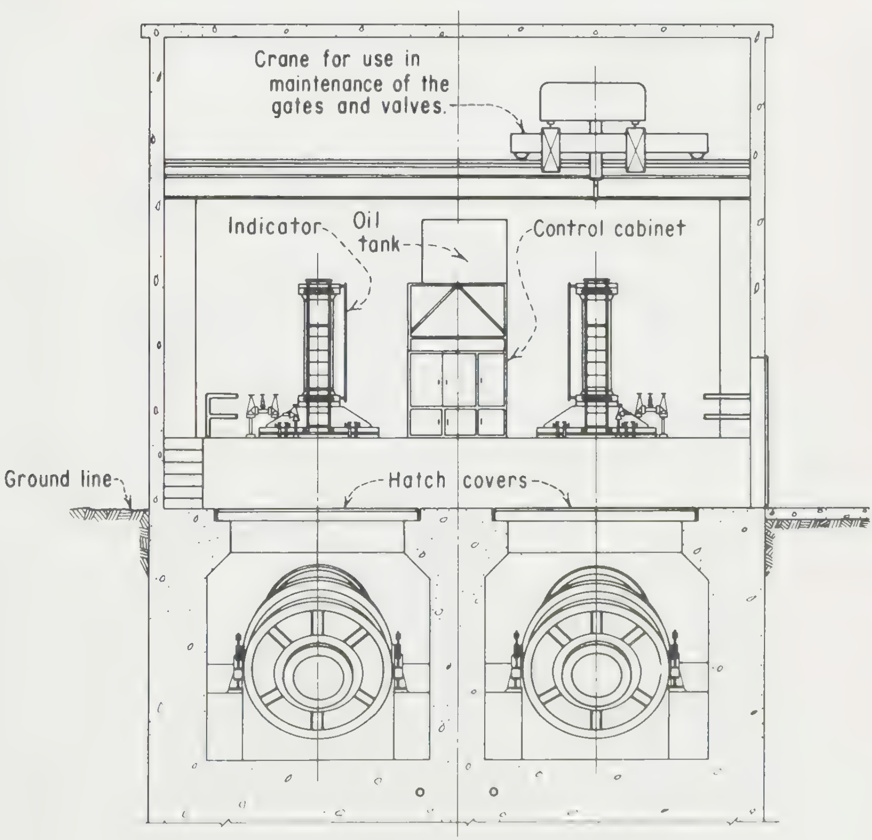

SECTION A–A

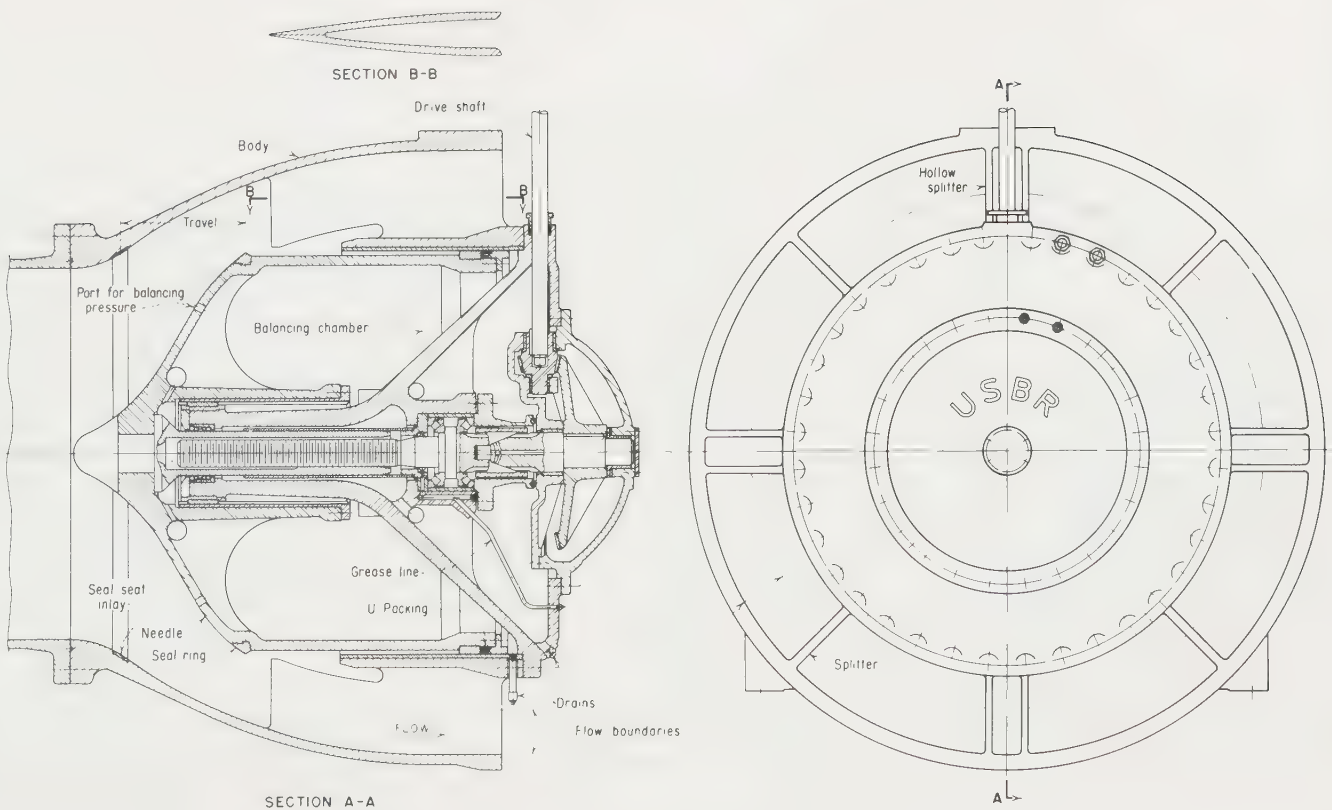

FIG. 35. General assembly of a mechanically operated hollow-jet valve.

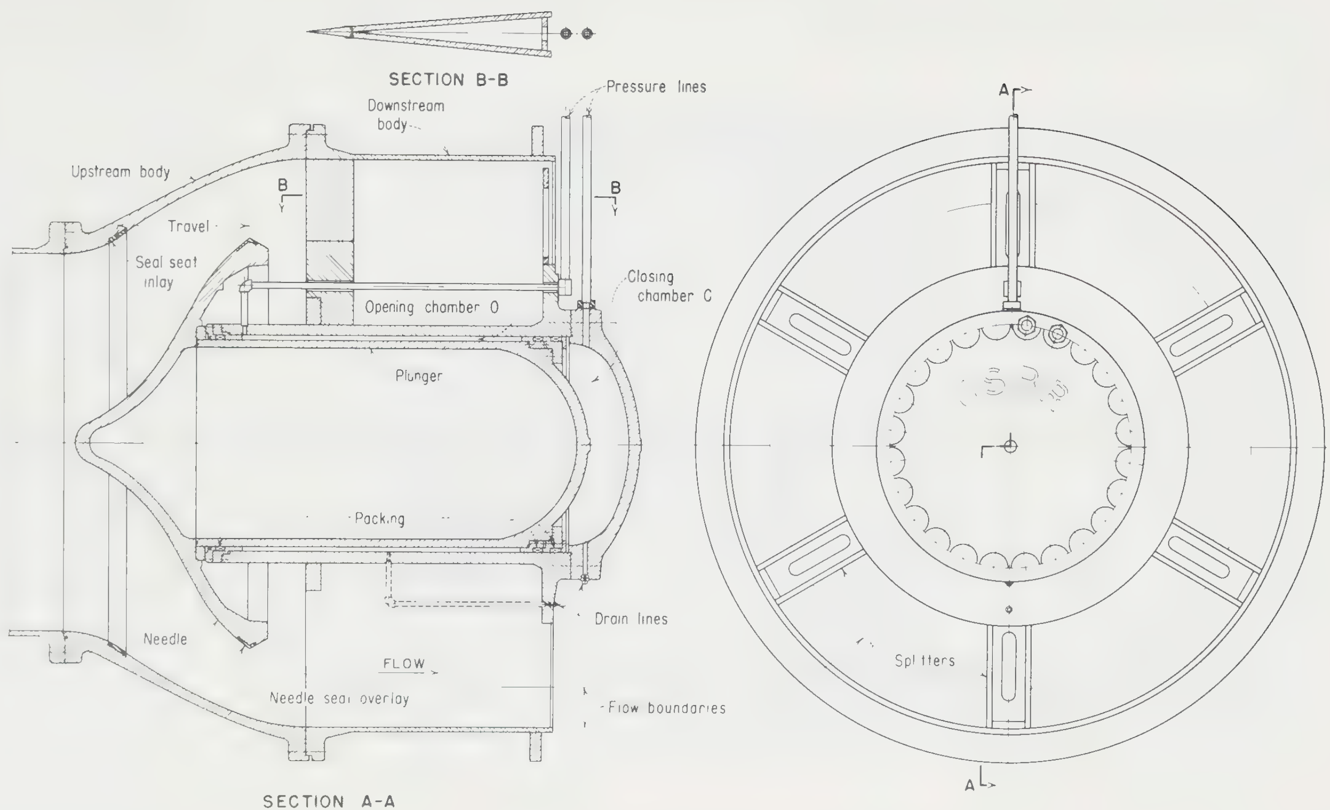

FIG. 36. General assembly of a hydraulically operated hollow-jet valve.

gate is installed on the same slope as the hollow-jet valve. Installing the ring-follower gate on a slope permits using a somewhat smaller enclosing building, but a vertical gate installation is simpler to install and easier to handle for maintenance. The hollow-jet valve is frequently mounted on trunnion supports so that it can be rotated easily to simplify handling and maintenance.

A discharge-coefficient curve as shown in Fig. 34 may be used to compute valve discharges in accordance with the following formula:

$$Q = CA\sqrt{2gH}$$

where Q = discharge, cfs
A = area of valve inlet, sq ft
g = gravitational acceleration of 32.2 ft/sec^2
H = total head (static plus velocity) at inlet flange of valve

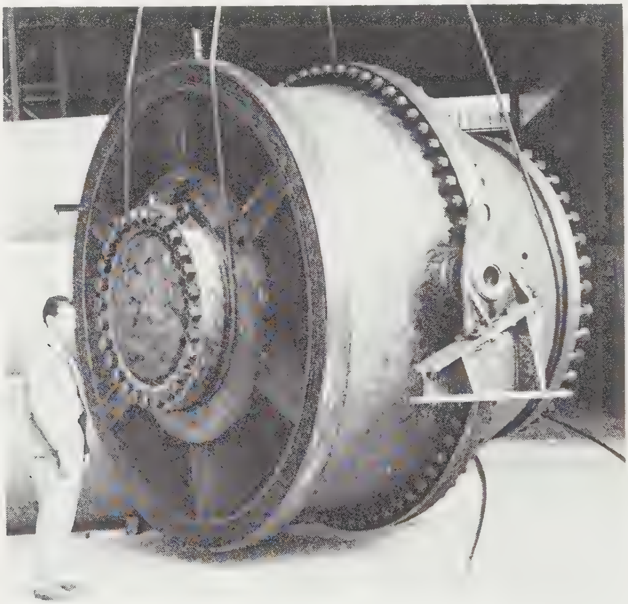

Fig. 37. Downstream view of 72-in. hydraulically operated hollow-jet valve for Navajo Dam.

Essentially, a hollow-jet valve is half a needle valve in which the needle closure member moves upstream toward the inlet end of the valve to shut off flow. There is no converging fluidway on the downstream end of the valve body; consequently the flow emerges in the form of an annular cylinder which is segmented by the splitter ribs as shown in Figs. 35 to 37. The fact that the issuing jet is a hollow cylinder, as contrasted with the solid jet of the needle valve, was the basis for adopting the name hollow-jet valve.

The splitter ribs perform two functions. In addition to supporting the central structure which contains the needle, they also provide openings for admitting air into the jet interior. The admission of air to the interior of the jet is essential to avoid excessive subatmospheric pressures and jet instability. There is a considerable degree

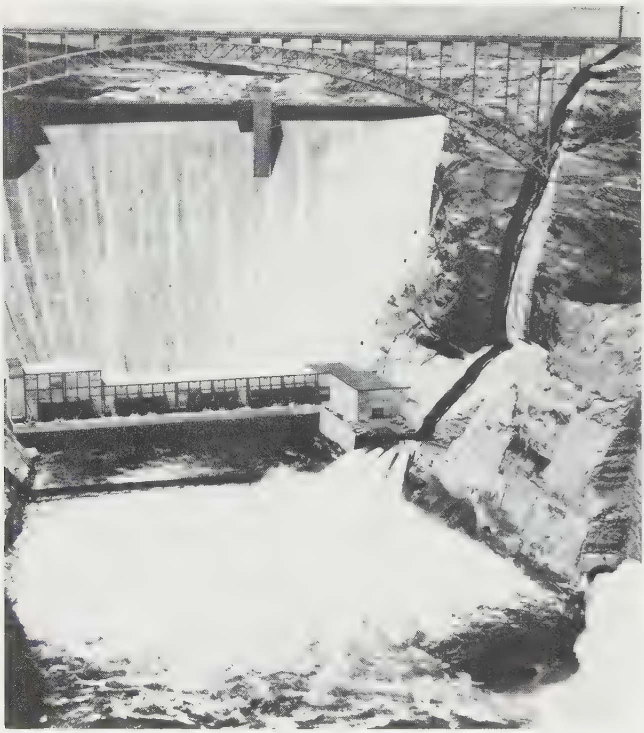

FIG. 38. Four 96-in. hollow-jet valves discharging about 3,500 cfs each at Glen Canyon Dam. Note also the 30,000 cfs from the three sets of 7- by 10.5-ft slide gates being discharged over the tunnel flip bucket in the lower right of the picture.

of air entrainment around the jet periphery, and an adequate supply of air must be provided to this region. The assurance of an adequate air supply must be carefully checked for installations where the valve is discharging into a tunnel.

The discharge of hollow-jet valves is dispersed and aerated considerably more than that of a needle valve but not so much as that of a Howell-Bunger valve. As shown in Fig. 38, the discharging jet has a fairly clean, well-defined cylindrical shape and does not require a hood to confine the discharge and avoid spray dispersion. However, unless there is sound rock or a deep pool into which the valve can discharge, a stilling basin is usually required.

A hollow-jet valve consists basically of a body, a needle, and the operating means for moving the needle upstream or downstream to vary the area of an annular orifice between the needle and body for controlling discharges.

The general arrangement of a mechanically operated valve is shown in Fig. 35. Figure 36 shows a comparable hydraulically operated valve. Both types have similar needle and body configurations and have an inlet diameter equal to the conduit diameter. The principal difference lies in the method of operating the needle.

In the mechanically operated valve it would be almost prohibitive physically and economically to design a screw-stem drive to withstand the total unbalanced hydrostatic load on the end of the needle. The necessity for such design was avoided by admitting fluidway water pressure through ports in the needle face to the balancing chamber in the valve to minimize the unbalanced hydraulic load on the needle. By properly locating the balancing ports on the face of the needle, it is possible to limit the unbalanced water load on the needle to approximately plus or minus 12 percent of the total water load on the needle at any opening. The resulting operating forces are not a problem and are low enough that manual operation can be used satisfactorily for valves up to 36 in. in diameter. Most valves, however, are supplied with motor-driven operators of a type which limits the maximum driving torque.

The hydraulically operated hollow-jet valve was developed in 1958 by B. H. Staats at the Bureau of Reclamation, and has been used as the standard design since then. The principal advantages of a hydraulically operated valve using oil as the hydraulic medium are that it is simpler and more economical to build and requires less maintenance after installation. The successful operation of this type of valve is dependent upon making the cylinder and hydraulic system sufficiently oiltight that a mechanical system is not required to prevent the needle from creeping open from a set position. Successful operation of these valves at Trinity, Glen Canyon, and other dams has proved that needle creep, because of hydraulic-system leakage, is not an operating problem. To facilitate maintenance or replacement of the main packing on the operating plunger it is made readily accessible and requires only removing the cover on the plunger cylinder.

The hydraulically operated valve eliminates the necessity of periodic disassembly of the valve for maintenance as was necessary for the mechanically operated valve. This disassembly was necessary primarily to remove water-deposited scale from the sliding surfaces in the balancing chamber to prevent damage to the valve seals. Inaccessible sliding surfaces which could collect scale have been entirely eliminated from the hydraulically operated valve and all sliding surfaces are lubricated by the hydraulic oil. For this reason major field disassembly for maintenance should rarely be required.

The operation of the hydraulic-type valve is very simple and does not require a balancing chamber to reduce the hydrostatic thrust on the needle. Oil pressure is directed to chamber *C* to close the valve. When the conduit upstream from the valve is filled with water under pressure, the valve can be opened by releasing oil from chamber *C*. If no conduit water pressure is available, the needle can be moved to the open position by admitting oil pressure to the annular chamber *O*.

The use of hollow-jet valves at openings of less than 5 percent may result in cavitation and damage downstream from the seat region and should be avoided if possible. No other cavitation, except that due to obvious surface imperfections in the valve fluidways, has been noted in these valves. As is the case with all surfaces over which high-velocity water passes, it is essential that the surfaces be smooth and have no pronounced offsets.

Hollow-jet valves have been built in sizes from 24 to 96 in. The highest head valves are the 96-in. hydraulic-type valves which are designed for discharging under a 535-ft head at Glen Canyon Dam. The 96-in. mechanical-type valves at Hungry Horse Dam are designed for a head of 460 ft.

18. Sleeve-type Valves. To utilize the excellent energy-absorbing capabilities of vertical stilling wells, it is necessary to have a valve capable of regulating under fully submerged conditions. This led to the development of a sleeve-type valve by the Bureau of Reclamation. The basic regulating member is a cylindrical sleeve, and the valve is similar in some respects to the cylinder gate and to the Howell-Bunger valve. It differs in operation from the usual cylinder gate in that the flow is from, rather than into, a central pipe. It differs from the Howell-Bunger valve in that the sleeve is internal rather than external and in that the issuing jet discharges at 90 deg with respect to the axial center line of the sleeve rather than at about 45 deg, as is the case

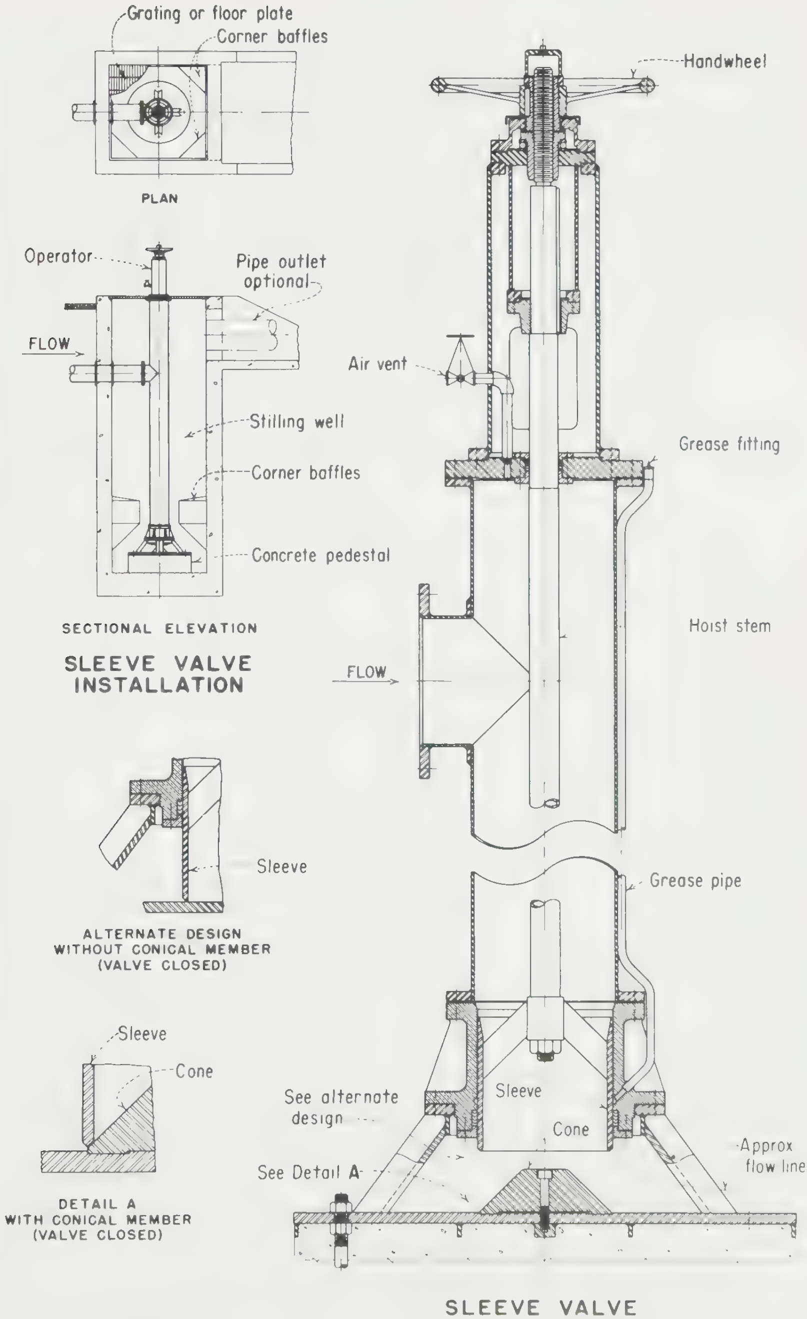

FIG. 39. Bureau of Reclamation type of sleeve-valve installation and details.

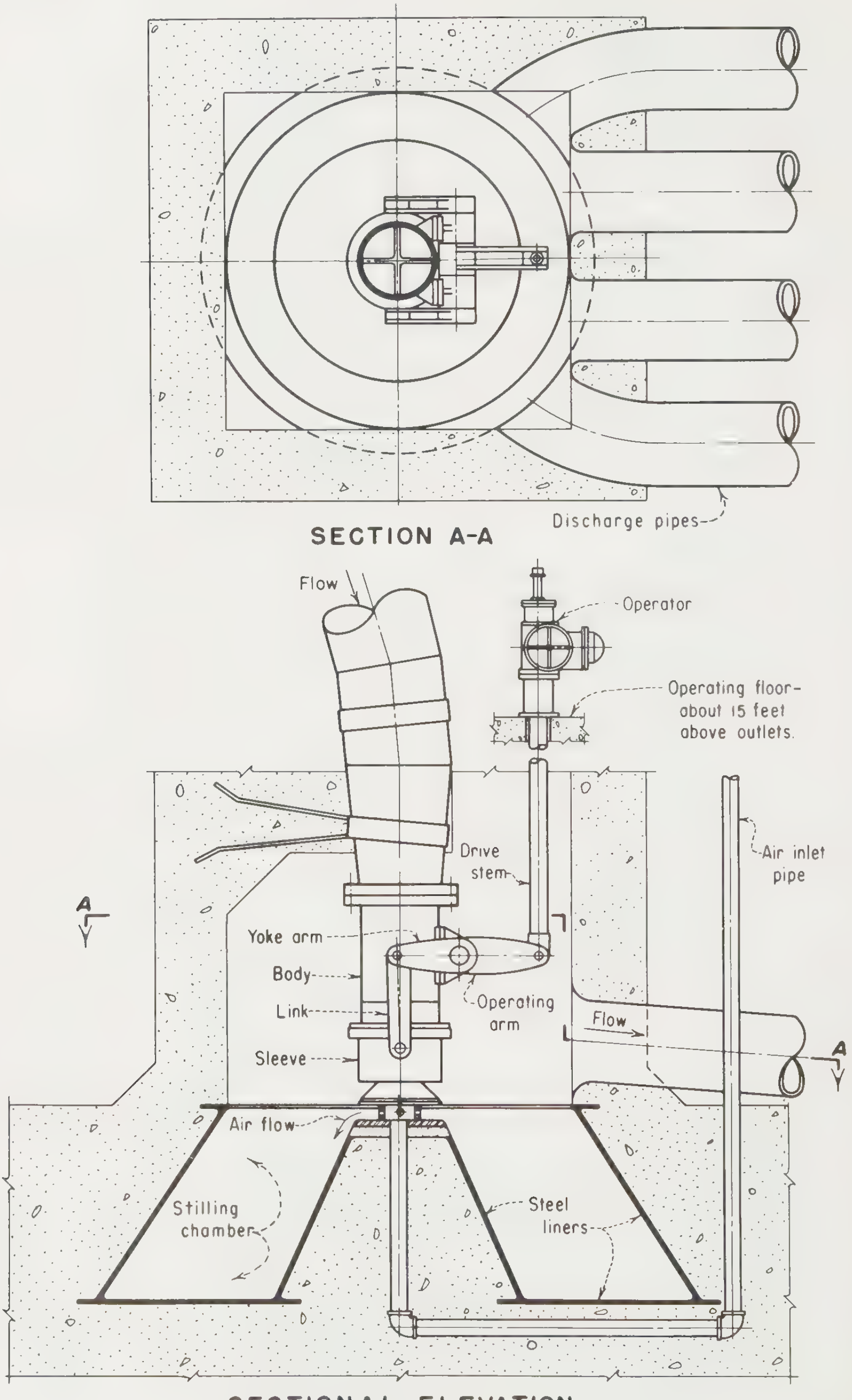

FIG. 40. Howell-Bunger-type sleeve-valve installation in a vertical stilling well. (*Allis-Chalmers Manufacturing Company.*)

with the Howell-Bunger valve. Both the Bureau-type sleeve valve and the Howell-Bunger-type sleeve valve are suitable for use in vertical stilling wells. Both types of valves embody the basic principle of the "sudden enlargement" and are designed to release the high-velocity discharge into an enlarged, water-filled chamber for dissipating the energy.

The installation and details of a typical Bureau-type sleeve valve are shown in Fig. 39. The outflow from the square stilling well is not under a large back pressure and either a conduit or open flume may be used. No air supply is required. Manual operation is suitable for valves up to about 36 in. in diameter, but motor operation can also be used if desired. Bureau-type sleeve valves have been made both with and without a central conical member mounted on the base plate. Various shapes and angles of central members have also been used to vary the discharge-rate characteristics.

The valve discharge is controlled by moving the sleeve axially with the control-stand operator to vary the orifice between the sleeve and cone (or the base plate if no cone is used). The base plate, cone, and sleeve are usually made of stainless steel to provide corrosion and cavitation-damage resistance. The tip of the sleeve must be designed to provide a definite spring point for the issuing flow to avoid cavitation damage (see detail *A* in Fig. 39).

Figure 40 shows a somewhat analogous vertical installation of a 17-in. Howell-Bunger-type valve which was made by the Allis-Chalmers Manufacturing Company for regulation under a head of 975 ft on the Tolt River Regulating Basin. This installation differs from the Bureau-type sleeve-valve installations in the shape of the stilling chamber and in the provision for air admission at the downstream periphery of the conical portion of the valve.

Although the use of submerged valves in vertical stilling wells has been somewhat limited, the satisfactory results reported indicate that suitable valve designs are available and that more extensive use of this type of design is feasible.

19. Butterfly Valves. The simple, rugged, and economical butterfly valve has stood the test of time. It is commonly used as the primary guard valve for turbines in power outlets, and frequently as the guard valve for regulating gates or valves in outlet works. Butterfly valves have also been used to some extent for regulating free discharges in outlet works. Standard valves in the small to medium sizes, built according to American Water Works specifications, are also widely used in water-distribution systems and outlet works.

The principal problem in the design and use of butterfly valves has been the seals. The main difficulty in sealing a butterfly valve is due to the fact that for most valves the seal must be designed to provide a continuous effective seal around the trunnions and the periphery of the leaf. Numerous seal designs have been made to cope with the leakage problem. In some designs the seal has been offset from the trunnions so that a single circular seal ring can be used to avoid the problem of sealing around the trunnions. Most butterfly-valve seals, however, are designed to seal around both the leaf and trunnions. For a number of years butterfly valves generally used only metal-to-metal seals. One notable early exception to the all-metal seals was the inflatable rubber seal which was provided on the 27-ft butterfly valves for Conowingo power plant.

The development and standardization of rubber-seated butterfly valves in the 1950s resulted in widespread use of rubber seats and a large reduction in the use of metal-seated valves. However, for large or specially designed valves for high-pressure outlet works and penstocks, a basic metal seal is still widely used. Rubber inserts are sometimes added to metal sealing faces to reduce the seal leakage.

The type of valve which is commonly used by the Bureau of Reclamation for large turbine guard valves is shown in Figs. 41 to 43. The valve illustrated has a 156-in.

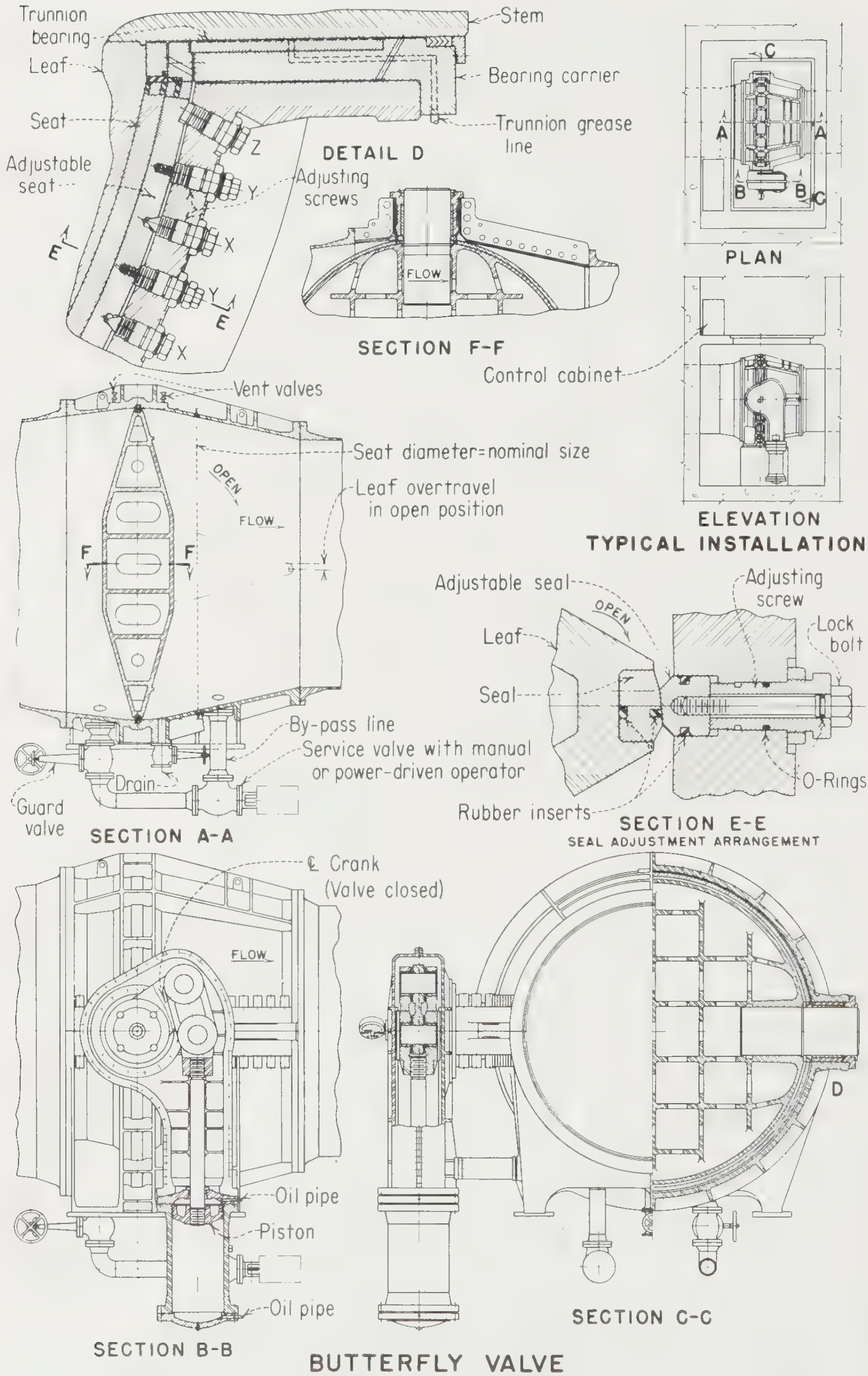

FIG. 41. General arrangement and details of butterfly valve, based on the 13-ft-diameter valves designed by the Bureau of Reclamation for the Central Valley project power plants.

seal diameter and is designed to operate under a maximum head of slightly over 400 ft. This design utilizes the conventional piston and crank mechanism for rotating the leaf, and is arranged so that all operating forces for the leaf are internal with respect to the valve unit. This arrangement avoids the problems of anchorage and alignment which are encountered when the operating unit and valve are mounted on the floor separately.

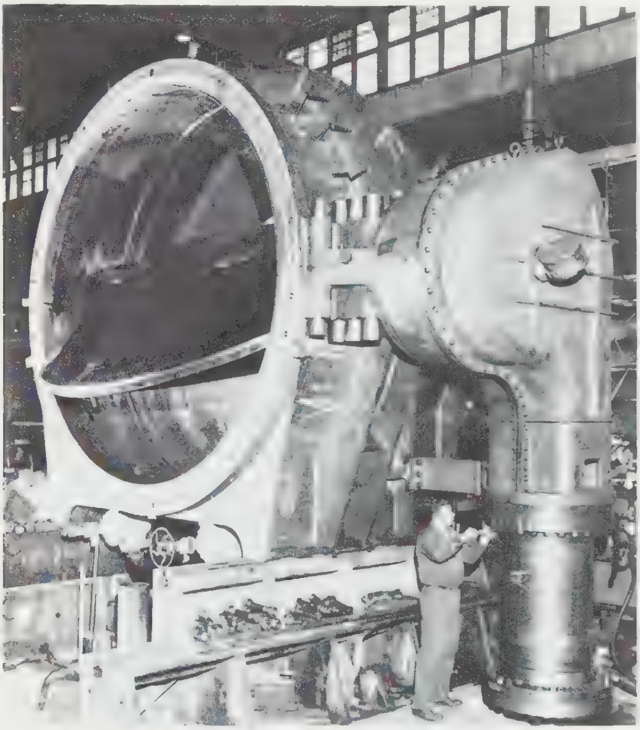

FIG. 42. Shop assembly of 13-ft butterfly valve.

Numerous types of operating units have been used for butterfly valves through the years. The crank arm was probably the first type used, and the crank or similar type of operator is still the most widely used. One novel and interesting operating unit was the hydraulic rotor drive, which was invented and developed primarily by Phillip A. Kinzie for use on the 120- and 168-in. turbine guard valves for Hoover power plant (see Fig. 44). Valves having this type of operator, as illustrated in Fig. 45, have many excellent characteristics. They are pleasing in appearance and very compact in terms of the torque delivered, and all operating forces are symmetrical and integral with respect to the valve unit. The operators have given very satisfactory service on the 17 butterfly valves in Hoover power plant. The cost of building the rotor-type operators is considerably more than for conventional crank operators, and for this reason operators of this type have not been widely used. Unless space is at a considerable premium and extreme compactness is required, as was the case for Hoover power plant, the rotor-type operator is not competitive economically. Improved types and knowledge of seals would probably permit a considerably more economical design of a rotor-type operator than was possible when the Hoover butterfly valves were designed in 1933. In fact, a standard line of commonly used sizes of torque devices involving the rotor principle has been marketed commercially.

Usually no mechanical locking device is provided for the operating units on turbine guard valves, as such devices have proved to be unnecessary in either the open or closed positions. If it is desired or necessary to block the valve open or closed, shutting off the oil-line valves to the top and bottom of the cylinder provides a powerful and effective locking method. In some cases where butterfly valves are used in high-velocity outlet-works installations, a leaf-holding method to ensure that unbalanced turbulent flow past the leaf does not induce closure may need to be considered.

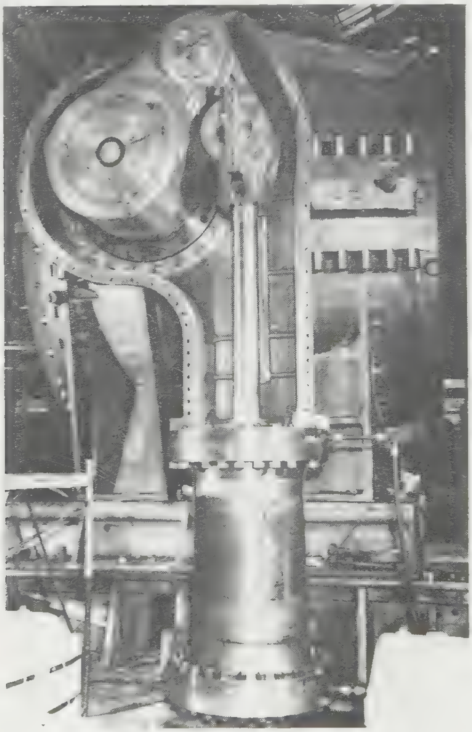

FIG. 43. Operating cylinder and crank arrangement for 13-ft butterfly valve.

A mechanical lock and the providing of a piston and control system which are practically leakproof are two methods which can be used to lock a leaf in position. Another method is to rotate the leaf slightly beyond the open position (see section *AA* in Fig. 41) so that flow-induced torque will tend to hold the leaf open rather than tend to close the leaf. In the closed position the trunnion friction from the water load on the leaf provides an effective brake on leaf movement. Arranging the leaf rotation so the bottom portion seats in the direction of flow results in a positive sealing torque on the leaf. The torque is developed by the differential pressure on the top and bottom halves of the valve leaf.

The tendency of butterfly valve leaves to be self-closing is a hydraulic operating characteristic which is not too obvious from the general configuration and operation of the valve. The dynamic closing torque produced by the flowing water must be considered for all butterfly valves in designing the operator. For valves which have relatively low velocities and high pressures, such as turbine guard valves, the dynamic closure torque is usually less than the torque required to overcome the seal and trunnion friction as the valve seats. For valves which must be either opened or closed under conditions approaching free discharge, the dynamic torque becomes very large and nearly always governs the torque capacity of the operator.

While formulas for the dynamic torque on butterfly valves are shown in various forms, the general relationships expressed in the following formula are usually inherent

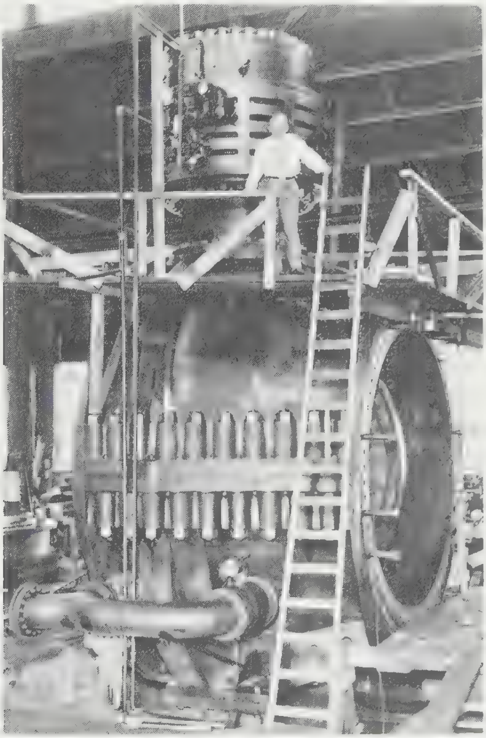

FIG. 44. Shop assembly of 14-ft-diameter butterfly valve for Hoover Dam. The late P. A. Kinzie, inventor of the novel hydraulic rotor used on these valves, is standing on the platform.

in all:

$$T = KV^2D^3$$

where T = operating torque, in. or ft-lb, depending on the units of the K factor
K = a constant determined by the leaf position and the units of torque as defined for T
V = velocity of flow through valve, fps
D = diameter of leaf, ft

The constant K will vary somewhat with the geometry of various valves and is usually determined by test of a specific shape by the valve manufacturer. The maximum value of K for free discharge will occur with the valve leaf about 20 deg from the fully open position. The variation of torque as the square of the velocity indicates the need for care in determining what the maximum velocity may be to ensure adequate operator capacity is provided. For valves which are relatively close-coupled to turbines, the maximum turbine discharge is usually assumed for determining the velocity. For valves which are used to guard considerable lengths of exposed conduits or penstocks, the assumption of free-discharge conditions which could occur with a line break is usually used for determining the operator torque capacity. Free-discharge valves require the most operating torque.

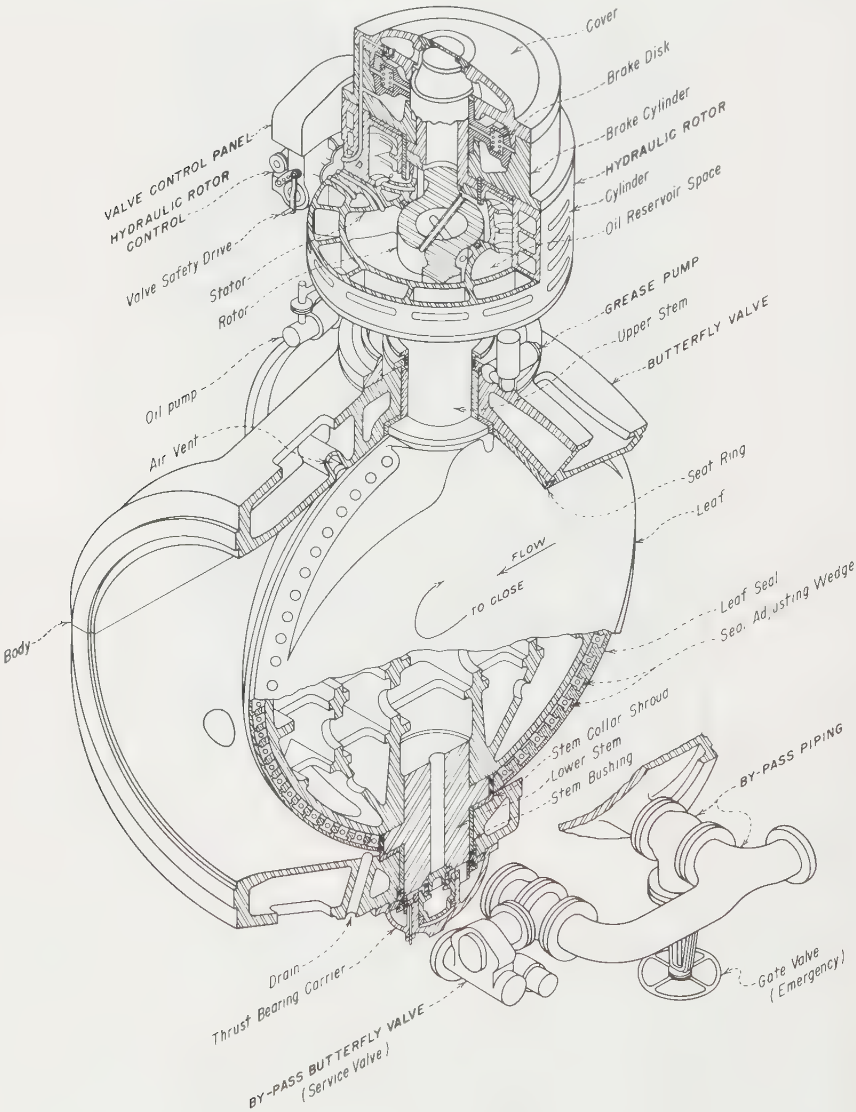

Fig. 45. General assembly of the 10- and 14-ft-diameter butterfly-valve design used at Hoover Dam.

Normally, butterfly guard valves are opened and closed under no-flow pressure-balanced conditions; however, such valves are always designed for closure under flow conditions. One or two bypass lines are usually provided on guard valves for balancing upstream and downstream pressures. Such bypasses frequently have a power-operated service valve and a manually operated guard valve. A drain to carry off seal leakage should also be provided just downstream from the leaf. This drain should be of adequate size to remove the maximum expected seal leakage. Making the drain diameter about 5 percent of the leaf diameter will normally ensure ample drain capacity.

The externally adjustable seal design shown in Fig. 41 has been used on a number of 13-ft valves for heads from 300 to 500 ft. Shop test leakages ranged from 3 gpm to a maximum of 15 gpm. Most of the valves were in the 5- to 10-gpm range. These leakages are well within tolerable limits. Although higher seal leakage can be tolerated, leakage should preferably be less than 25 gpm to avoid excessive spray and paint-application problems downstream. Such leakages can be attained by careful workmanship on all-metal seals and are readily attained if rubber inserts are added to the metal seals as shown in section *EE* in Fig. 41. All-rubber valve seals can be made droptight; but as the leakage from seals of metal or of metal plus rubber can be tolerated, the more rugged and durable metal seals are considered by many designers to be preferable for important primary guard valves.

Section *EE* in Fig. 41 shows the typical seal and adjusting arrangement. It will be noted that the seal is basically a metal-to-metal seal and would function quite effectively even though the rubber insert in the leaf seal were lost. It is essential that the seal-adjusting arrangement provide both circumferential and radial adjustment of the seals. The conical-nosed screws *X* shown on detail *D* provide circumferential adjustment for butting the seal tightly against the trunnion. The push-pull adjusting screws *Y* as well as the unidirectional push screw *Z* provide radial adjustment of the seal. Except for the initial circumferential adjustment of the seal bearing on the trunnion, all final adjusting of the seal may be made with the seal under pressure.

The junction between the circumferential and trunnion seals is critical, and special care must be exercised to avoid excessive leakage. To avoid excessive leakage the seal design should theoretically be such that no leakage can occur. In fabricating such a seal, minor inaccuracies will usually result in some tolerable amount of leakage. Some of the complexity of seal design for butterfly-valve design is obvious from the foregoing description, but in addition, it should be remembered that the seals must also be able to accommodate leaf deflections.

Butterfly valves are deceptively simple in appearance, but many complex hydraulic and mechanical problems are involved in design. A thorough study and understanding of the problems, particularly the seals, should be made before attempting a design.

20. Sphere Valves. The general name sphere valve is applied to valves having a circular fluidway through the valve body which is approximately spherical in shape. Various trade-name designations are also used for such valves, and there are several different arrangements for the closure member. Two of the commonly used arrangements are shown in Fig. 46. In the Type A valve, the cylindrical fluidway through the valve is an integral part of the rotating member and closure is effected by rotating the member 90 deg. In Type B, the circular fluidway is made an integral part of the body except for a narrow annular slot at one end. When the valve is open the slot is bridged by the surface of a hole through the spherical shell of the closure member. Closure is effected by rotating the spherical shell approximately 90 deg so that the solid bulkhead portion blocks the fluidway.

Both types of valves in the open position have a fluidway which is essentially a straight cylinder and has hydraulic losses approximately the same as would occur in an equivalent length of pipe. As practically no losses or flow disturbances are produced by sphere valves, they are well suited for installations where a turbine and the guard valve are very close together and turbulence must be minimized. Such valves are also suited hydraulically for use as the guard valve for high-velocity outlet works.

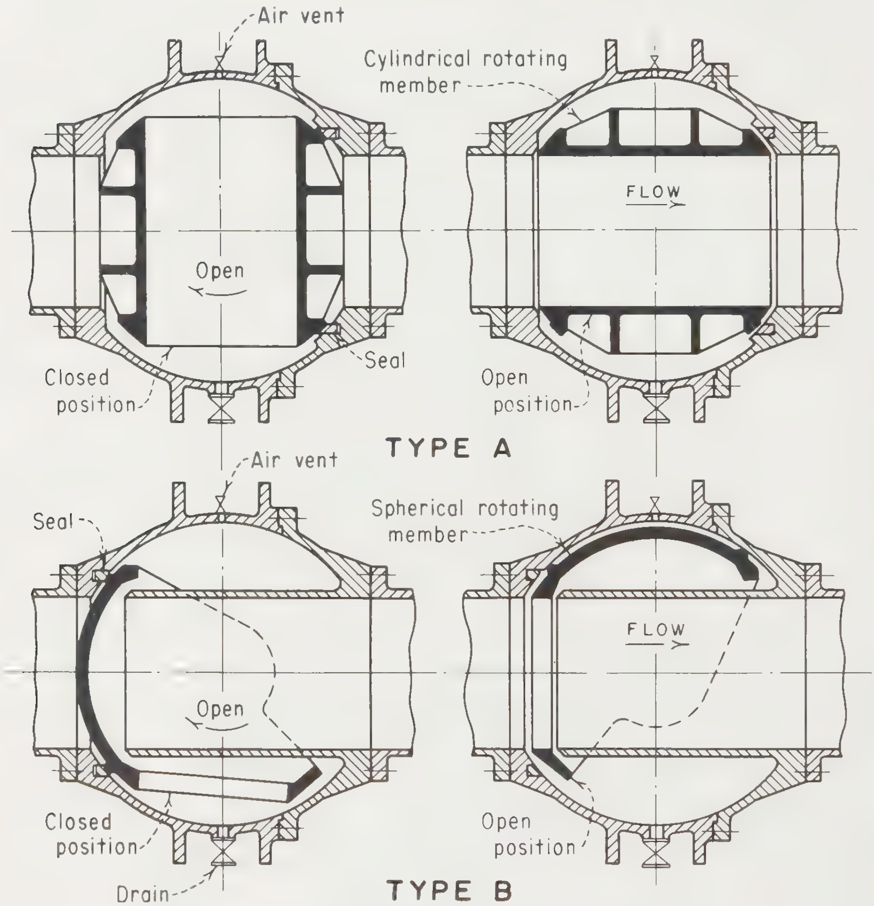

FIG. 46. Sphere-valve types (type B shown by courtesy of the English Electric Company).

Sphere valves can be readily sealed to provide practically droptight closures, even at very high heads. The sealing contact surfaces are usually made of corrosion-resistant metals such as bronze or stainless steel. Metal-to-metal sealing is the most common, particularly for high-head valves, but rubber on stainless-steel seals is also used. Most, but not all, seals are of the hydraulically actuated type which are retracted and not in contact during rotation of the valve. Hydraulic actuation of the seals by the water pressure in the pipe is used in some designs. In other designs an independent oil-pressure source is used for seal operation.

Although mechanical operators are frequently used on small valves, hydraulic pistons are used almost universally on the larger sizes as shown in Fig. 47. Normally a single operating cylinder powered by oil pressure is used, but sometimes dual cylinders powered by reservoir water pressure are used. The operating torques for sphere valves in which the central fluidway rotates will have dynamic torques which tend to close the valve, and which are similar in some respects to the torque characteristics of butterfly valves. Valves having spherical shell-type rotating members do not have a pronounced dynamic-closure torque characteristic, and the torque required for operation will be governed principally by the trunnion friction. In the case of the rotating fluidway valves subject to high-velocity flow, the dynamic-torque characteristic must be considered as well as friction torques in determining operator capacity.

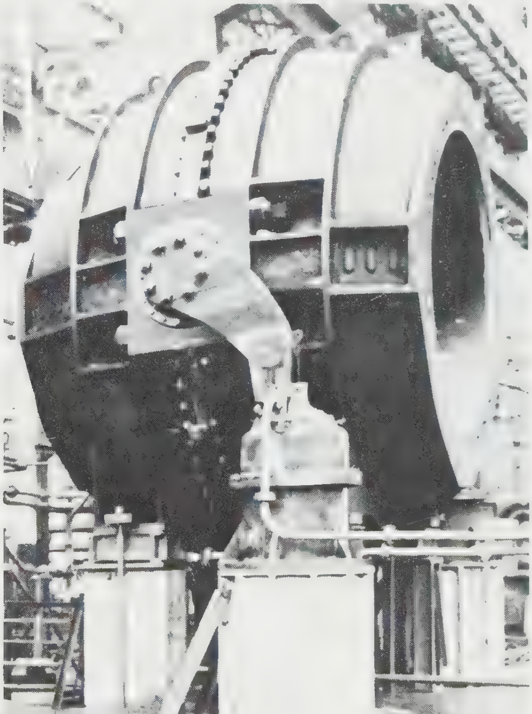

FIG. 47. Shop assembly showing general arrangement of hydraulically operated sphere valve. (*English Electric Company.*)

Sphere valves have been made in sizes considerably more than 10 ft in diameter and for heads in excess of 1,000 ft. Except for limitations imposed by shipping or manufacture, it appears that sphere valves could be made in any desired size and for practically any head. A large partially assembled valve is shown in Fig. 48.

The use of sphere valves and other analogous types, such as plug valves, which have straight-through fluidways is increasing because of their high hydraulic efficiency and avoidance of turbulence in flows. The question arises at times as to why such valves have not rendered the butterfly valve obsolete. The answer lies primarily in the overall economy of an installation. The value of the somewhat better hydraulic efficiency of the sphere valve must be evaluated against the lower weight and cost, as well as the shorter length and less diametral clearance required for a butterfly valve. Both types of valves have proved to be excellent and reliable guard valves.

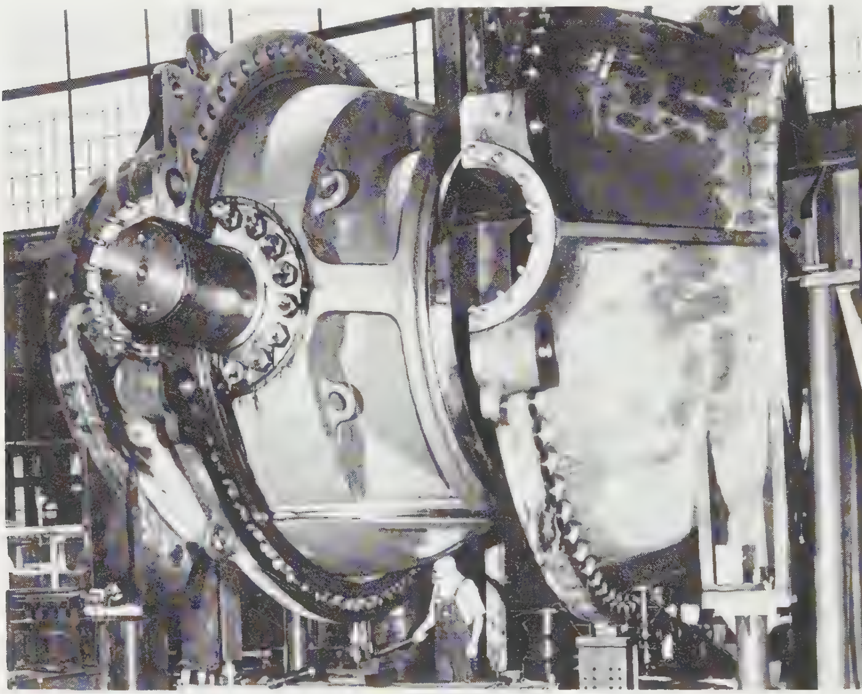

Fig. 48. Partial assembly of large sphere valve. (*Allis-Chalmers Manufacturing Company.*)

HYDRAULIC DESIGN FACTORS

21. General. The ideal outlet hydraulically would have (1) a perfectly shaped inlet, (2) a practically straight alignment, (3) smooth fluidway boundaries with no offsets, gate slots, or surface irregularities, (4) no cavitation, and (5) a discharge coefficient approaching unity. The practical factors of fluidway alignment, gating, and manufacturing limitations prevent attaining the ideal. However, in the design of outlets the ideal should be kept in mind to minimize the undesirable aspects of the practical factors which are involved.

In the design of high-velocity outlets, the entrance shape, the fluidway alignment, and surface discontinuities such as gate slots are critical. Only some of the basic general requirements can be pointed out and discussed here. For more complete data and information, cited references should be procured and studied in detail. In addition, publications of the Bureau of Reclamation, the U.S. Army Corps of Engineers, and the Hydraulics Division of the American Society of Civil Engineers are excellent sources of information on the hydraulic and equipment developments for outlet works.

Another very important source of information in the design of outlet works is model testing. While the basic quantities and overall flow characteristics of water can be readily calculated, the effect of various changes in boundary surfaces cannot be predicted or determined mathematically with reliable accuracy except in cases which are geometrically similar and have been verified by repeated tests. Model testing of new types of gates and valves and of outlet-works arrangements should always be performed to provide a basis for predicting full-scale performance. Model tests are especially useful in determining and studying flow patterns, estimating air demand, determining hydraulic forces such as downpull on gates, avoiding fluidway geometry which could cause cavitation, and providing discharge-coefficient and calibration information.

22. Cavitation. Cavitation may be defined as the formation of vapor-filled cavities in a liquid at substantially constant temperature by a dynamic action which reduces the pressure in localized regions to the vapor pressure of the liquid. Cavitation in the flow of water through high-pressure outlets may occur without causing fluidway damage when the collapse of the cavities occurs within the fluid and away from the fluidway surfaces. When the cavities collapse near or against a fluidway surface, extremely high local pressures and stresses in the fluidway surfaces result and cause pitting and erosion of the surface. The accepted terminology for such pitting and erosion is cavitation damage, although it is often referred to improperly as "cavitation."

Cavitation is an important factor which must be considered in the design of high-velocity outlet works where the fluidway alignment and every surface discontinuity are potential sources of producing cavitation and cavitation damage. The basic design approaches for the avoidance of cavitation damage are as follows:

1. Keep the fluidway alignment and boundary surfaces as straight and free of irregularities as possible.
2. Hold the pressure gradient as high as possible, particularly at points of alignment or surface boundary variations.
3. Introduce air, if possible, at points where subatmospheric pressures exist in the flowing water.
4. Provide definite and adequate spring points for flow separation, such as in a sudden enlargement.

In addition to basic design approaches, the use of cavitation-damage-resistant materials, such as stainless steels or epoxy concrete, is also effective in many cases. Neoprene paint has also been used with some success. In fact, the use of resistant materials, although it does not eliminate the basic cause, appears to be the only satisfactory method of dealing with cavitation-damage problems for some conditions.

Entrances, bends, flow-surface discontinuities and irregularities, and gate slots are critical points in the design of most outlet-works fluidways. These key points should be carefully studied and designed to minimize the dangers of cavitation.

Any cavitation damage which develops on installations should be repaired promptly, as it is usually a self-aggravating type of damage, and relatively minor roughening can develop into very serious damage if not corrected promptly. Stainless-steel welding carefully ground to remove surface irregularities is commonly used for repair of ferrous metals. Epoxy concrete is frequently used for repair of surface damage to concrete.

As a key to determining the cavitation potential of various types of geometrically similar gates and valves, the following formula has been found to be useful:

$$K = \frac{H_2 - H_{VP}}{H_T - H_2}$$

where K = cavitation index
H_T = total head (static plus velocity head) in upstream conduit
H_2 = static pressure head downstream from gate or valve
H_{VP} = vapor-pressure head of water

The incipient cavitation indexes K_i which have been determined are as follows:

Gate valves	1.5
Butterfly valves (discharging in a pipe at openings of more than 15 percent)	4

23. Bellmouth Entrances. Bellmouth entrances commonly used for high-velocity outlet works may be any of four types: (1) circular, (2) rectangular, flared all around, (3) rectangular, flared top and sides, or (4) rectangular, flared top only. The four types of entrances are shown in Fig. 49. The use of properly shaped entrances is

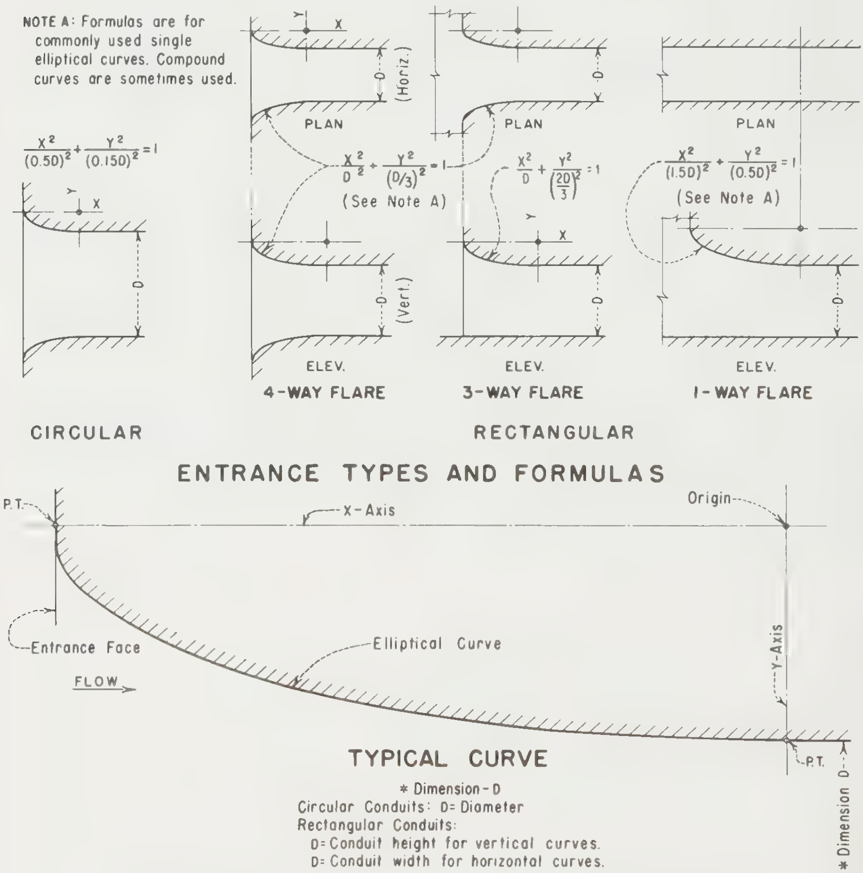

FIG. 49. Entrance types and formulas for high-velocity outlets. (*Rectangular outlet data from Corps of Engineers Tech. Mem.* 2-428, *Reports* 1 *and* 2.)

desirable in all outlet conduits. At high velocities it is imperative to use properly shaped entrances and to have appreciable back pressures in some cases to prevent cavitation.

To operate satisfactorily, bellmouths for high-velocity flow must be both designed and built properly. The curvature of the elliptically flared surfaces must not vary materially from the outline specified. It is important that there be no enlargement of the conduit immediately downstream from the point of tangency with the entrance ellipse, particularly when conduit pressures are low. Pressures in the zone can be critical and divergence of the conduit surfaces can cause flow separation and produce serious cavitation damage. There must be no pronounced waviness, and the entrance surface must be free of offsets, projections, or pronounced depressions. Surfaces should be smoothed by filling and grinding as necessary to remove irregularities. Special care must be taken in rectangular conduits to grind the corner welds or fillets smooth.

Tests indicate that the normal gate-seat projections or gate slots on the face of an intake structure are not critical for entrance flows, provided they lie outside the tangency boundary of the bellmouth flare. Tests of rectangular entrances flared in four directions also indicate that having the entrance face of the bellmouth tilted at angles up to 10 deg with respect to the conduit center line does not affect bellmouth pressures significantly. It is probable that similar tilting of the entrance face would have little effect on circular bellmouths or on rectangular entrances flared in one or three directions.

For circular bellmouths the following elliptical formula developed by the Bureau of Reclamation is commonly used and has given satisfactory service:

$$\frac{x^2}{(0.5D)^2} + \frac{y^2}{(0.15D)^2} = 1$$

where x = axis parallel to flow
y = axis normal to flow
D = diameter of pipe

The Corps of Engineers[1] conducted tests on entrances flared in one, three, and four directions. The tests were made on a 20:1 model under heads to 15 ft for a prototype conduit size of 5 ft 8 in. wide by 10 ft high, which gives a width-to-height ratio of 0.567. It has been assumed that profiles of jets through rectangular-shaped entrances of varying width-to-depth ratios would be similar and that the formulas can be used for other ratios; however, the accuracy of this assumption has not been verified by model or prototype tests.

The reports indicate that single elliptical curves can be used for most cases, but for high heads and low back pressures compound curves are recommended. The terms high heads and low back pressures are not defined; but as a general criterion on the basis of indicated pressure gradients, it would appear desirable to use compound curves when the static conduit pressure at the downstream end of the entrance is less than about one-tenth of the velocity head. On this basis the approximate minimum back pressures for various conduit velocities for single elliptical curves would be as follows:

Velocity, fps	Back Pressure, ft of water
0–50	Not required
60	5
80	10
100	15
120	23
140	30
160	40
180	50
200	63

[1] Report 1, Investigation of Entrance Flared in Four Directions, *Tech. Mem.* 2-428 CE WES, March, 1956. Report 2, Investigation of Entrances Flared in Three Directions and in One Direction, *Tech. Mem.* 2-428 CE WES, June, 1959.

For entrances flared in three or four directions which meet the velocity back-pressure criteria for single elliptical curves, the following formula may be used:

$$\frac{x^2}{D^2} + \frac{y^2}{(D/3)^2} = 1$$

where x = axis parallel to flow
y = axis normal to flow
D = conduit height for vertical curves at top or bottom of conduit, or conduit width for horizontal curves at sides of conduit

For conduits flared in three or four directions which do not meet the criteria for single ellipses, the following compound elliptical curves are recommended:

Flared in four directions:

(Upstream portion) $\quad\frac{x^2}{D^2} + \frac{y^2}{(0.32D)^2} = 1$

(downstream portion) $\quad\frac{x^2}{D^2} + \frac{y^2}{(0.16D^2)} = 1$

Flared in three directions:

	(Upstream portion)		(downstream portion)
Top:	$\frac{x^2}{(2D)^2} + \frac{y^2}{(0.64D)^2} = 1$	and	$\frac{x^2}{(2D)^2} + \frac{y^2}{(0.32D)^2} = 1$
Sides:	$\frac{x^2}{D^2} + \frac{y^2}{(0.32D)^2} = 1$	and	$\frac{x^2}{D^2} + \frac{y^2}{(0.16D)^2} = 1$

For rectangular entrances flared in only one direction, such as might occur in an entrance located between two training walls, a minimum flare of $1.5D$ is recommended. For entrances which are within the criteria cited for rectangular entrances with single-ellipse flares, the following curve may be used:

$$\frac{x^2}{(1.5D)^2} + \frac{y^2}{(1.5D/3)^2} = 1$$

For conditions where use of the foregoing formula is not appropriate, either of the following formulas may be used:

$$\frac{x^2}{(2D)^2} + \frac{y^2}{(2D/3)^2} = 1$$

	(Upstream portion)		(downstream portion)
or	$\frac{x^2}{(2D)^2} + \frac{y^2}{(0.64D)^2} = 1$	and	$\frac{x^2}{(2D)^2} + \frac{y^2}{(0.32D)^2} = 1$

NOTE: The second curve is only slightly better than the first, which shows a small dip in the pressure gradient.

24. Fluidway Surfaces. The necessity of having fluidway surfaces which are within acceptable limits of smoothness, waviness, and alignment becomes increasingly important as velocities increase and back pressures decrease. Laboratory tests on an abrupt sharp-cornered 5/16-in. offset into the streamflow showed incipient cavitation at a velocity of only 29 fps under no-back-pressure conditions. Laboratory tests and prototype installations show that under higher velocities, offsets as small as 1/32 in. can produce cavitation and damage.

It is especially important to have smooth surfaces immediately downstream from regulating gates and valves because an effective boundary layer has not developed in such regions. With the reestablishment of an effective boundary layer in the flow downstream from a gate or valve, the lower velocities near the boundary make irregularities in the fluidway surface less critical. However, it is not possible to predict precisely where an effective boundary layer will be reestablished, or to determine the relative increase in permissible surface roughness. For these reasons, it is prudent to assume that an effective boundary layer does not exist and to treat all fluidway surfaces for some distance downstream from regulating gates and valves accordingly. Various criteria for treating such surfaces are contained in a publication by the American Society of Civil Engineers.[1]

It is desirable that fluidway surfaces, particularly just downstream from gate or valve control orifices, have a smoothness of 250 μin. or better. This degree of smoothness is readily attainable by machining a surface. The surface roughness of unmachined rolled-steel plate with the mill scale removed will also meet this degree of smoothness. Smooth-troweled or ground concrete surfaces can also be made to this degree of smoothness; however, as producing this quality of concrete surface presents problems in mass-concrete placement schedules, it is more common practice to provide metal linings for some distance downstream from gates or valves. Surface damage which occurs on metal surfaces can be readily repaired by welding and grinding. Damaged concrete surfaces can be repaired satisfactorily with epoxy concrete. Before making repairs of cavitation damage, the cause should be sought and removed if possible.

Stainless-steel-clad plate liners are sometimes used to provide smooth surfaces in fluidways because of the additional cavitation damage resistance which stainless steel provides, and because it is not necessary to impair the basic smoothness of the plate with paint coatings. The use of stainless-steel fluidway surfaces is particularly desirable in the critical regions near a regulating gate where cavitation and damage are most likely to occur.

Any waviness of a fluidway surface, particularly in the direction of flow, should be such that the waves are sweeping gradual curves. For machined surfaces the normal methods of finishing will produce surfaces without objectionable waviness. For fluidway surfaces made of unfinished rolled-steel plates, care must be taken in the selection and fabrication of the plates to ensure acceptable flatness after manufacture and installation. As a general criterion, the flatness of fluidway surfaces, particularly in the direction of flow, should be such that the high point to high point on gentle sweeping waves is not less than 16 in. and that a feeler gage no thicker than 1/16 in. can be inserted under a 3-ft-long straightedge held in any position on the fluidway surface. This degree of flatness on welded-plate liner design can best be obtained by careful selection of plates for flatness and by performing the rib and flange welding carefully to minimize distortions. Experience shows that using 1-in.-thick plate and keeping the fillet welds on ribs between 3/16 and 1/4 in. avoids undue "cupping" distortion of the fluidway surface by the rib welds, and permits holding the plate flatness to the tolerances specified without difficulty. The use of thinner plates is possible, but considerably more care is required in fabrication to avoid unacceptable distortion of the fluidway surface.

Special care must be taken to avoid abrupt offsets in the fluidway alignment at flanged or other joints. Ideally the fluidway surfaces across joints should be straight and flush, but in practice this ideal is difficult to attain. Experience at Glen Canyon Dam with velocities of about 130 fps showed no fluidway surface damage downstream from joints offset outwardly from the flow by not more than 1/16 in. At 1/8-in. outward offset, some damage occurred, and at 1/4-in., considerable damage occurred. The foregoing data apply to joint offsets but do not apply to large offsets, such as sudden enlargements in fluidways. On the basis of these observations on an actual installation, outward offsets in fluidway alignment at joints should be limited to about 1/16 in.

[1] Ball, J. W., Construction Finishes and High-velocity Flow, *Proc. ASCE, J. Construction Div.*, September, 1963.

Offsets which exceed this dimension should be reduced to a maximum of $\frac{1}{16}$ in. by grinding off the excess offset and fairing with adjacent surfaces in the same manner hereafter specified for offsets into the flow.

An inward offset into the flow as small as $\frac{1}{32}$ in. in a fluidway surface downstream from a joint can produce cavitation damage. Therefore, all projections into the fluidway at joints should be ground flush and have the offset faired smoothly into the adjacent fluidway at a slope in accordance with the criteria in Fig. 50. It is also important that the junction of sloped surfaces with the normal fluidway surfaces be blended smoothly to avoid any marked outline of the intersection point.

In addition to the foregoing general requirements for boundaries of high-velocity fluidways, there are several types of localized surface discontinuities which can cause

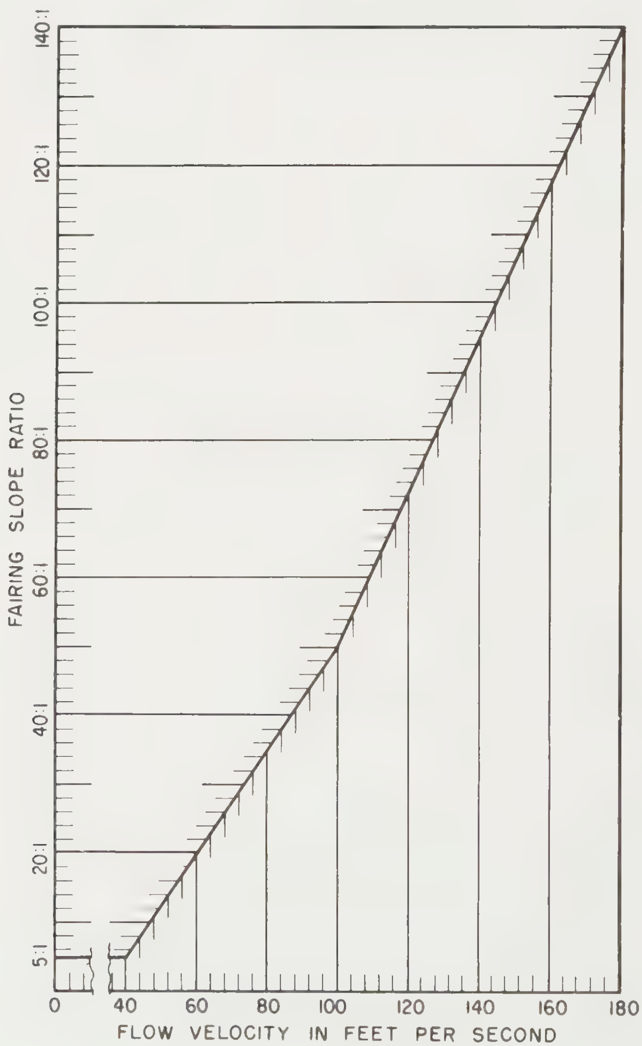

Fig. 50. Fairing-slope ratios for fluidway offsets.

damage. Paint on fluidways must be smooth. Fairly small ridges not parallel to the flow and localized projections on a painted surface can produce cavitation damage. For this reason painted surfaces should be checked to be sure that any discernible points, ridges, or pronounced roughness are removed after painting. Welding or casting fillets in the corners of conduits can likewise trigger cavitation unless ground smooth.

Another surface defect which can produce cavitation damage under high-velocity discharges is the small void which occurs in the surface of concrete fluidways. Such defects ("bug holes") are caused by air bubbles in the concrete, and should be filled and finished smooth and flush to avoid the danger of being the focal point for cavitation damage when subjected to high-velocity flow.

Manhole and pipe openings in fluidways should preferably be located in regions where the pressure gradient is well above atmospheric. In such regions the edges of holes need only be ground smooth to a small radius. Under conditions where the pressure gradient approaches atmospheric and velocities are 60 fps or more, manholes should be provided with a fairing surface which will be flush with fluidway surface. Piping connections in low-pressure-gradient regions should be faired into the fluidway very carefully using a liberal radius.

25. Gate Slots. Gate slots disrupt the smooth boundary lines for fluidways. This disruption of boundary-surface continuity increases the losses, and if the slots are not properly designed serious cavitation and damage can result. For high-pressure outlets where the velocities are low and the back pressures are high, such as is the case for power outlets, only the losses are important. For high-velocity discharges with low back pressures, such as a free-discharge gate, the problems of flow and possible cavitation damage are critical. Only slots for high-velocity types of conduit gates will be covered.

Figure 51 shows various methods which have been used to cope with the hydraulic problems created by gate slots in high-velocity outlets. The use of fillers which bridge the slots, such as the ring on a ring-follower gate, is one method. In the use of filler members, special care must be taken to be sure no part of the filler forms a sharp offset into the flow. For this reason it is good practice in such cases to have a slight outward offset on the upstream side of the leaf fluidway at the slot, and a similar offset in the body at the downstream side of the slot. These offsets must be sloped inwardly and faired smoothly to the basic fluidway surface dimensions.

Another method of avoiding the problems of gate slots is to force a contraction in the flow so that the discharge jumps across the gate slots. This arrangement is used for jet-flow gates and on the Type A slide-gate slot as shown in Fig. 51. Problems sometimes arise where the jet impinges on the conduit walls downstream from the slots; but if adequate air is provided downstream from the spring point, experience shows that some paint erosion may occur but that no cavitation damage will occur in the impingement area. It should be pointed out that the deflectors ordinarily do not prevent water from entering the gate slots under all conditions, as the lateral spread of the jet at some gate positions while regulating will usually result in some flow impinging and entering the gate slots. Such impinging flows have not been found to be critical. These flows into the gate slots could be avoided by increasing the degree of forced contraction at the upstream face of the slot. This increase in contraction would further reduce the discharge capacity, which is the undesirable feature of the forced contraction design for coping with the problems of flow past gate slots.

Another approach to the problem of gate slots is to set the size and geometry so that neither fillers nor jumps are necessary to avoid the hydraulic problems of high-velocity flows past the slots. The highly efficient Type B slide-gate slot shown in Fig. 51 accomplishes this objective.

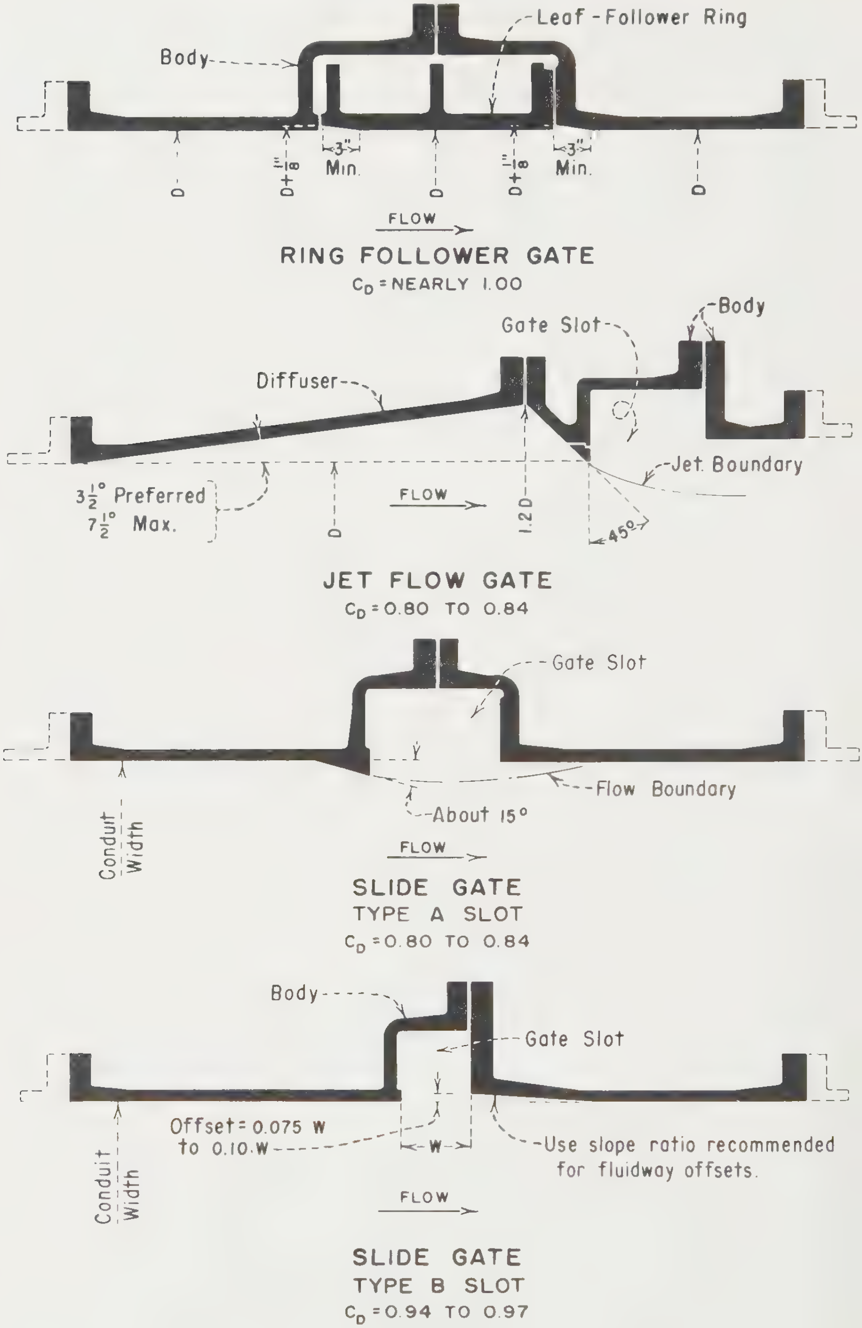

FIG. 51. Gate-slot types for high-velocity outlets.

In general, the Type B gate slot should be made as narrow as possible, the upstream slot face should have a sharp (not rounded) corner at the fluidway, and the downstream corner of the slot should also have a sharp or only slightly rounded corner at the fluidway. The outward offset of the fluidway at the downstream side of the slot should be within definite limits and should be sloped inwardly gradually and faired smoothly with the fluidway surfaces.

The amount of slot offset is closely related to the slot width. Variations in the depth of the slot do not appear to be critical. In general the use of a downstream offset of about 0.075 to 0.1 of the slot width will be satisfactory. The slope of the converging surface from the slot offset to the nominal fluidway size should follow the criteria given in Fig. 50.

It is especially important that there be no surface irregularities or imperfections in the regions of gate slots. This region is critical and merits special care to ensure that proper alignment and smoothness of the fluidway surfaces are maintained.

The testing and development work for the various types of gate slots are covered in greater detail in the referenced publications.[1]

26. Air Vents. Air vents fall into two basic categories: (1) those which act primarily as "breather" lines to vent or admit air during filling or draining a pipe, and (2) those which must deliver a continuous supply of air to a discharging gate or valve. Usually the problem is to determine the minimum size.

In the absence of specifically determined requirements for the size of filling-draining-type air vents, making the air-inlet area from ½ to 1 percent of the area of the fluidway being vented provides a convenient "rule-of-thumb" guide. Vents should preferably not be controlled with valves and should be extended above the maximum water surface to ensure positive venting during filling and draining. The factors of vent-line length, pipe-filling rate, and allowable subatmospheric pressure in the pipe or penstock may require that larger vent lines be used.

High filling rates for pipes and penstocks can produce very large water-hammer pressures at the time the fluidway is just filled if adequate air vents are not provided. To avoid water-hammer problems, the vent line should be made as large or larger than the filling line. Special care must also be used to fill pipes and penstocks slowly enough to vent all air during filling. If an appreciable volume of air is trapped during filling, the ultimate release of such pressurized air can cause disturbances approaching explosive violence.

Where vents are provided of only sufficient size for venting during the normal filling-draining operations, closure of the upstream guard gate under emergency conditions may result in substantial subatmospheric pressures in a conduit or penstock. The low pressures may be principally around the throttling gate or valve and be due to the high-velocity flow patterns during closure, or the subatmospheric pressure may be general in character throughout the pipe and be due to the rapid outflow of water during the upstream gate closure. The occurrence of low pressures and cavitating conditions because of the flow patterns at a gate or valve during emergency closure is usually not critical, as the occurrence is infrequent and of short duration so that only minor paint damage will probably occur. In the second case where a pipe is subjected to a considerable subatmospheric pressure throughout, a careful check should be made, particularly if the pipe is exposed, to be sure the low pressure is not sufficient to cause collapse of the pipe.

The size of air vents required for gates and valves which regulate and discharge at supercritical velocity is dependent on the type of discharge and the general characteristics of the downstream flow. Air demand is produced by entrainment in the water

[1] Bureau of Reclamation, *Hydraulic Lab. Rept.* HYD-387: Hydraulic Characteristics of Gate Slots, *Proc. ASCE, J. Hydraulics Div.*, 2224 HY10, October, 1959, and 2456, April, 1960.

AIR DEMAND DESIGN CRITERIA

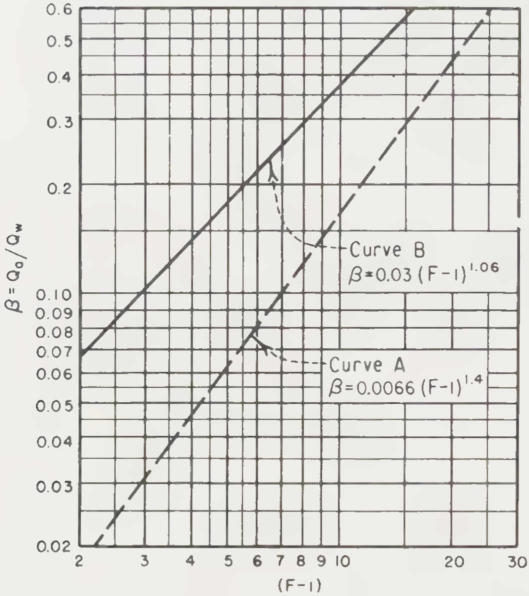

TERMINOLOGY

Y = Water depth in feet at vena contracta.
D = Height of gate opening in feet.
C_d = Discharge coefficient.
V = Velocity in feet per second.
G = Gravitational acceleration = 32.2 ft./sec.^{2}
H = Head across valve in feet. (For short conduits with fairly small losses, use the difference in head from the reservoir surface to the top of the vena contracta.)
W = Gate width.
Q_w = Water discharge in cubic feet per second.
F = Froude number.
Q_a = Estimated air demand in cubic feet per second.
β = Ratio of estimated air demand to water flow.

Curve A – Kalinske and Robertson tests – Use where a hydraulic jump forms in the downstream conduit.

Curve B – U.S. Army Engineers – Suggested curve for free surface flow discharges. (No jump)

AIR VENT SIZE DETERMINATION PROCEDURE:

1. Determine depth of water (Y) at vena contracta
   $Y = D\,(C_d)(\text{gate opening})$
   (See Note 1.)
2. Calculate spouting velocity (V)
   $V = \sqrt{2GH}$
3. Calculate discharge of water (Q_w)
   $Q_w = (V)(Y)(W)$
4. Determine Froude number (F) at vena contracta
   $F = V/\sqrt{GY}$
5. Evaluate (F − 1)
6. Determine β on curves A or B using (F − 1)
7. Determine air demand (Q_a)
   $Q_a = Q_w\,\beta$
8. Determine vent area based on allowed air velocity.
   (See Note 2.)
9. Check losses in vent to be sure they are less than 5 feet of water head.

NOTES

Note 1. Use 0.8 for 45° gate bottom and 0.6 for sharp bottom lip. Assume gate opening is 0.8.

Note 2. Allowable air velocities range from 150 fps to 300 fps.

FIG. 52. Air-demand design criteria. (*Based on data from Engineer Manual EM* 1110-2-1602, *Department of the Army, Office of the Chief of Engineers.*)

and by the jet-pump effect which results from the drag between surfaces of the high-velocity water and the air.

If a conduit fills downstream from a gate or valve, the air demand is governed by the amount of air which is entrained in the water and passes through the conduit. Comparison of prototype air demand with computed air demand based on curve *A* of Kalinske and Robertson in Fig. 52 shows good agreement, and it is recommended that this curve be used to calculate air demand for sizing vents in this case.

When water is released freely and does not fill a conduit, the air demand is produced by the jet-pump action of surface drag by the flowing water. Some entrainment will also exist. The condition of drag from free surface of water flowing to the exit of a pipe or conduit will produce considerably greater air demand than when a conduit fills. Although various studies have been made, no precise solution to the complex air-demand problem for free-surface discharges in conduits or tunnels has been developed. The Corps of Engineers suggests the use of various design assumptions to arrive at the size of air vents.[1] These assumptions appear to be conservative; and although the sizes derived may not be precise, the calculations should produce air-vent sizes which will be adequate.

The Corps of Engineers method of computing air demand for rectangular gates is based on the observation that maximum air demand for free-surface discharges occurs at about 80 percent gate openings. Gate-contraction coefficients of 0.80 for a 45-deg leaf bottom and 0.60 for a sharp bottom lip are assumed. The cross-sectional area of the vent is based upon the assumptions that the calculated air demand can be delivered without requiring an air velocity of more than 150 fps or producing a pressure drop of more than a 5-ft water head. In most cases, the pressure drop will be considerably less than 5 ft. It may be necessary at times to exceed these assumed limits. At the discretion of the designer, air velocities to 300 fps may be used. In such cases special care should be taken in evaluating vent-line losses and subatmospheric pressures for possible conditions which could cause cavitation damage in the fluidway. Curve data and procedures for computing air demand for free discharges either with or without a filled conduit are shown in Fig. 52.

Under conditions where there is a high degree of entrainment in addition to the jet-pump demand, as would be the case with a fixed-cone-type (Howell-Bunger) valve discharging in a tunnel, the amount of air required will be quite large. No specific method of calculating the air demand has been developed for this mixed-flow condition. Model tests indicate the advisability of providing large air vents, as air demand of more than double the water discharge was indicated in some cases where subatmospheric pressures were limited to about a 2-ft water head. Additional study and prototype tests will be necessary for establishing adequate criteria for mixed-flow air vents. Until definite criteria are established, it is suggested that air vents be provided which will deliver a volume of air at least equal to the volume of water discharged with air-vent velocities not exceeding 300 fps and negative pressures not greater than a 2-ft head of water.

Because of the high velocities involved, air intakes should be located and protected with screens or grills so that human life is not endangered by the air rushing into the vents.

27. Losses and Discharge Coefficients. In an outlet works the primary loss-producing elements which must be considered and evaluated to assure the required discharge are (1) trashracks, (2) entrances, (3) pipe friction, (4) transitions, (5) alignment or size changes, such as bends, junctions, expansions, or contractions, (6) gates or valves, and (7) exit losses.

[1] "Hydraulic Design of Reservoir Outlet Structures," EM 1110-2-1602, Department of the Army, Office of the Chief of Engineers.

Trashrack losses are usually quite small because velocities through the net area are usually limited to about 1 to 2 fps. Experience has shown that higher velocities frequently cause excessive trash buildup. The following loss values may be used:

Velocity, fps	Loss, ft
1.0	0.10
1.5	0.30
2.0	0.50

Only suitably shaped elliptical entrances are recommended for high-velocity conduits. Based on the velocity head H_V in the conduit proper, the following values may be used for entrance losses:

Circular bellmouths	$0.05H_V$
Square or rectangular bellmouths	$0.1H_V$

Any of the numerous well-known acceptable methods and formulas may be used for calculating pipe-friction losses.

Transition losses will range from 0.1 of the change in the velocity head H_V for gradual contractions to 0.2 of the change in H_V for gradual expansions. For abrupt changes in cross section the value of 0.5 of the change in H_V will apply. The Borda loss is often used for sudden enlargements. For specific information on transition losses refer to hydraulic texts and handbooks.

For alignment and size changes the loss coefficients for the various conditions may be calculated from the data available from hydraulic tests and handbooks.

The free-discharge coefficients C_D based on the total head immediately upstream from the various types of gates and valves are about as follows:

Slide gates	0.95–0.97
Ring-follower and ring-seal gates	Nearly 1.00
Jet-flow gates	0.80 0.84
Cylinder gates	0.80 0.90
Needle valves	0.45–0.60
Tube valves	0.50 0.55
Fixed-cone valves (Howell-Bunger)	0.85
Hollow-jet valves (Staats-Hornsby)	0.70
Sleeve valves (submerged discharge)	0.85
Butterfly valves	0.60–0.80
Sphere valves (full-diameter fluidway)	Nearly 1.00

Head loss through gates and valves at the ends of conduits may be determined by using the C_D of the gates or valves in the following formula:

$$H = \left(\frac{1}{C_D^2} - 1\right) H_V$$

The value of the exit loss is usually taken as unity based on the velocity-head loss with free discharge into atmosphere.

EQUIPMENT DESIGN FACTORS

28. General. The scope and variety of the designs used in high-pressure outlets preclude describing anything but some of the important fundamental structural factors and requirements which must be considered to ensure safe and effective designs for outlet works.

For the gates and valves used in outlet works, safety and reliability are paramount considerations. Any failure of gates or valves is usually a major disaster, and it is far better to err on the side of overdesign rather than underdesign. It must also be kept in mind that the time for doing maintenance work or making repairs on outlet works is usually limited seasonally to periods when reservoir releases can be interrupted. For these reasons outlet-works equipment should be as simple, rugged, and maintenance-free as possible, so that possible failures or operational breakdowns requiring unscheduled repairs or maintenance will be avoided.

The useful life required for the equipment is another factor which must be considered in selecting and designing gates and valves for outlet works. Such equipment should be selected and designed on the basis that, with proper maintenance, it will have the same useful life as the dam. This criterion will require a useful life of at least 100 years in most cases and considerably longer periods in some cases. Designing gates and valves for short lengths of service life and assuming replacement in 50 to 75 years have proved to be false economy. In addition to the reduced reliability of operation, the rising manufacturing and installation costs make replacement almost prohibitively expensive in 50 to 75 years, even though replacement is technically feasible. For these reasons the small additional incremental first cost to ensure a long life for equipment is basically a sound expenditure.

As corrosion is one of the principal problems encountered in the life of gates and valves, corrosion-resisting materials, such as brass, bronze, stainless steels, and monel metal, are rather widely used for all critical areas which cannot be adequately or economically protected with paint. It should not be assumed, however, that the use of materials which are normally corrosion-free in atmosphere will solve the problems of corrosion when such materials are submerged in water. Special care and consideration must be given when such materials are used in gates and valves to avoid conditions and combinations which will result in serious galvanic corrosion. In general, materials which are fairly close in the galvanic series are the most compatible.

Another critical factor in the design of outlet works is the need for suitable means to install and maintain the gates and valves. Handling equipment and procedures should be considered and designed as an integral part of every gate and valve installation. Failure to make adequate provisions for handling is dangerous and costly, as it will require the use of improvised means and inefficient procedures in the field. The lack of suitable handling equipment for servicing and maintaining gates and valves may also result in the work's being done so infrequently that excessive damage by deterioration may result. In most cases the life of gates and valves can be prolonged almost indefinitely if adequate means and programs for servicing and maintenance are provided.

29. Safety Factors, Stresses, and Friction Coefficients. The selection of safety factors and friction coefficients for gates and valves is a somewhat arbitrary design decision. Experience and testing provide some insight and basic guidance in setting these design factors, but the actual values used for design must also be tempered by prototype experience. In general, the use of rather conservative safety factors and friction coefficients is recommended because of the indeterminate structural, and variable operational, characteristics of gates and valves. The assurance that gates will operate and that there will be no structural failure in service is far more important than the slightly greater cost which may result at times from using conservative safety factors and friction coefficients. The discussion of safety factors and friction coefficients here will be limited to the special cases where information is not readily available in texts or reference handbooks.

In cases where specific codes or other accepted design criteria are not available, the following broad general rules are used by the Bureau of Reclamation for setting the design stresses for gates and valves:

1. The allowable design stress in tension for the following general categories of materials is the lower value derived by applying the percentages given to the minimum yield and ultimate strengths of the materials:

Materials	% of yield point	% of ultimate strength
Rolled or forged steel, monel metal, or allied materials	40	25
Rolled or forged steel and allied materials for bolts	25	16.5
Cast steel	33	20
Gray iron	...	12.5
Cast, forged, or rolled brass or bronze	33	16.5

2. The allowable compressive stresses for the foregoing materials are the same as for tensions except that the allowable compressive stress for gray iron is three times the allowable tensile stress.

3. The allowable shear stresses for the foregoing materials are 0.6 of the allowable tensile stress, except that for gray iron the allowable shear stress is equal to the allowable tensile stress.

Wherever practical in the design of gates fabricated of structural steel, the stress and fabrication standards of the American Institute for Steel Construction and the American Welding Society are used. The equivalent stress resulting from beam and skin-plate bending in a gate leaf of ASTM A36 steel is ordinarily limited to 20,000 psi maximum, so that any minor corrosion which may occur will not result in excessive stresses.

The foregoing criteria are cited to give a general idea of the range of design stresses which have been found to be satisfactory. The criteria should not be considered as setting absolute values of stress for all cases. Variations in the precision with which stresses are computed and variations in material and fabrication reliability must also be considered for specific cases. In addition, quality of maintenance, the expected useful life, and the degree of "calculated risk" which can be tolerated on specific installations must also be considered.

In setting design figures for friction coefficients, the results determined by laboratory tests must be used with caution. In checking friction coefficients in prototype designs, higher values than shown by laboratory tests are usually the case. For this reason friction coefficients which are somewhat higher than laboratory values are usually assumed for design purposes. The related factor of permissible bearing loads is also subject to considerably higher safety factors when setting permissible design stresses.

Although individual cases may warrant variations in values, the following coefficients of friction and bearing stresses are cited as a guide, and are frequently used for gate and valve designs.

1. Gate seats. Laboratory tests show sliding-friction coefficients as low as 0.15 for bronze on bronze or bronze on stainless steel, but prototype tests on unlubricated seats have shown apparent friction coefficients of slightly over 0.50. For this reason 0.60 is recommended as a minimum friction factor for slide gates with unlubricated seats. Factors as high as 1.0 are used by some designers, but the 0.6 factor has proved to be adequate at numerous slide-gate installations which have been made by the Bureau of Reclamation. If a good grease-lubrication system is provided, and gates are used frequently enough to retain a reasonable amount of lubrication on the seats, a friction factor of 0.50 may be used. For ungreased seats, loads should be limited to 1,000 to 1,500 psi. For well-greased seats, loads to 3,000 psi may be used.

2. Bushings. Friction coefficients of 0.15 to 0.20 are adequate for commonly used bronze bushings which are properly protected and greased. The loads on the pro-

jected area of such bearings are usually limited to about 3,500 psi. For bronze bushings which have self-lubricating inserts, friction coefficients of considerably less than 0.10 are consistently attainable in laboratory tests. Friction coefficients of 0.10 and bearing pressures to 6,000 psi are commonly used for prototype designs, after laboratory verification of friction and load characteristics.

3. Rolling resistance (friction). A conservative value frequently used for gate wheels and rollers is 0.01 for each rolling contact surface.

4. Rubber seals. Rubber seals are rarely used where they must slide on seats under loads unless a friction-reducing material covers the rubber where the seal makes contact with the mating-seal seat. Brass has been widely used to clad seal contact surfaces and permits assuming a friction coefficient of 0.30 to 0.35. Where fluorocarbon cladding is used on the contact surfaces of rubber seals, a friction coefficient of 0.15 may be assumed for design purposes.

30. Basic Materials and Uses. The kinds and number of materials available for fabricating gates and valves are almost unlimited. This variety of materials makes possible the selection of a material having almost any desired properties. The great variety of materials available also creates the problem of selecting suitable and economical materials for gate, valve, and conduit designs. Selection of suitable materials is of critical importance to ensure reliability and long life for the equipment in outlets.

The purpose of this discussion is to clarify the selection and use of materials for gate and valve designs, and to provide references to basic specifications, such as ASTM,[1] wherever possible. A relatively small number of basic materials is normally adequate for most designs. Normally the readily available, more economical, moderate-strength materials are used in preference to higher-strength materials, as extra thickness is an advantage for corrosion, and the slight extra weight is not usually critical. This practice does not apply, however, to the higher-cost corrosion-resistant materials.

The commonly used specifications will be cited and the materials will be discussed under the following broad general categories: gray-iron castings, steel castings, steel forgings, rolled steels, stainless steels, nickel-copper alloy (monel[2] metal), bronze and brass, and bolting materials. Except where otherwise noted all specification numbers refer to ASTM designations.

Gray-iron Castings. A48, Gray-iron Castings. Castings ranging from 20,000 to 60,000 psi tensile strength are available under this specification. The most readily available and commonly used castings are in the 30,000- to 40,000-psi classes. Annealing is normally specified for castings to be machined. When higher strengths are required, cast steel is frequently used. Gray iron is commonly used for low- to medium-head ring-follower and slide-gate leaves, bodies, bonnets, and conduit liners. The material should not be used where gates or valves may be subjected to heavy shock loading or water hammer.

Cast Steel. A27, Mild to Medium-strength Carbon-steel Castings for General Application; A148, High-strength Steel Castings for Structural Purposes; A487, Low-alloy Steel Castings for Pressure Service. Steel castings ranging in ultimate tensile strengths from 60,000 to 175,000 psi and yield strengths from 30,000 to 145,000 psi are available under these specifications. Carbon-steel castings (A27) having an ultimate strength of 65,000 psi and a yield strength of 35,000 psi in the annealed or normalized condition are readily available and are widely used for a variety of gate and valve parts. Where higher strength is required, A148 castings are used; and when hydrostatic testing is required, A487 castings are frequently specified.

[1] American Society for Testing and Materials, 1916 Race Street, Philadelphia, Pa. 19103.

[2] Monel is the International Nickel Company copyright name.

Steel Forgings. A235, Carbon Steel Forgings for General Industrial Use; A237, Alloy Steel Forgings for General Industrial Use; A504, Wrought Carbon Steel Wheels; A105, Forged or Rolled Steel Pipe Flanges, Forged Fittings, and Valves and Parts for High-temperature Service; A181, Forged or Rolled Steel Pipe Flanges, Forged Fittings, and Valves and Parts for General Service. Specification A235 covers seven classes of carbon-steel forgings ranging from ultimate tensile strengths of 47,000 to 90,000 psi and yield strengths of 30,000 to 55,000 psi. For parts requiring higher strengths, one of the nine grades of alloy-steel forgings under specification A237 may be used. In general, forgings are used when the greater homogeneity of wrought steel as compared with cast steel is deemed essential for the safety of a part.

Specification A504 is used for wheel-mounted gates which use wrought-carbon-steel wheels. Class AE, which has the entire wheel heat-treated and a rim hardness of 255 to 321 Brinell, is frequently specified for gate wheels.

Specifications A105 and A181 are specified for rolled-steel pipe flanges which are used in the design of welded gates and hydraulic hoists. In pressure ratings above 300 psi, manufacturers commonly produce the rolled flanges only to the A105 specification.

Rolled Steels. A29, General Requirements for Hot-rolled and Cold-finished Carbon and Alloy Steel Bars; A36, Structural Steel; A515, Carbon Steel Plates of Intermediate Tensile Strength for Fusion-welded Pressure Vessels for Intermediate and Higher Temperature Service. Specification A29, in addition to covering the general requirements, lists a number of reference specifications encompassing practically all types and strengths of hot-rolled and cold-finished steel bars which might possibly be used in gate or valve fabrication.

The most widely used steel in the "as-rolled" condition is covered by specification A36 for structural-steel shapes, bars, and plates. A36 steel has a minimum yield strength of 36,000 psi, and the ultimate strength varies from 58,000 to 80,000 psi. Normally the carbon content of this steel will not exceed 0.30 percent, although in some of the heavier plates a maximum of 0.33 percent is permissible. The weldability of this steel makes it ideally suited for fabricating all types of gates as well as other parts. No heat-treatment, except for stress relieving of welded parts which are to be machined, is used for this material.

One of the four grades of the firebox-quality steel in specification A515 is normally used for welded valve bodies, hoist cylinders, and other parts in the pressure-vessel category. Steels having ultimate tensile strengths from 55,000 to 85,000 psi and yield strengths from 30,000 to 38,000 psi are available under this specification.

Stainless Steels. A167, Corrosion-resisting Chromium-nickel Steel Plate, Sheet, and Strip; A176, Corrosion-resisting Chromium Steel Plate, Sheet, and Strip; A276, Hot-rolled and Cold-finished Stainless and Heat Resisting Steel Bars; A473, Stainless and Heat Resisting Steel Forgings; A461, Precipitation Hardening Alloy Bars, Forgings, Forging Stock for High Temperature Service; A264, Corrosion-resisting Chromium-nickel Steel Clad Plate, Sheet, and Strip. Stainless steels which are commonly used for gates and valves fall into three general categories: austenitic chromium-nickel alloys in the 18-8 category; martensitic, straight chromium types having 11.5 percent or more chromium; and the precipitation-hardening chromium-nickel alloys. The physical properties, corrosion resistance, and uses of these types vary considerably.

In the austenitic stainless steels, Types 304 and 304L are frequently used where high corrosion resistance and moderate strengths are required. In the annealed state most Type 300 stainless steels have ultimate and yield strengths of 75,000 and 30,000 psi, respectively. As higher physical properties require cold working, there is a considerable variation depending on the thickness of the material.

In the martensitic stainless steels, Types 410 and 416 are widely used where high physical properties are more important than the higher corrosion resistance obtainable in Type 300 stainless steels. Types 410 and 416 steels are commonly used for gate rollers, links, tracks, and wheel rims. Rolling surfaces are usually heat-treated to a Brinell hardness of about 255 to 320. This steel is also widely used for other parts such as gate stems. By appropriate heat-treatment ultimate strengths of 120,000 psi and yield strengths of 90,000 psi are readily attainable with the 410 and 416 type steels.

Of several grades of precipitation-hardening stainless steel under specification A461, Grade 630, which has a nominal composition of 17 percent chromium and 4 percent nickel plus other elements, is widely used because of the excellent physical properties, the simplicity of heat-treatment, and the high corrosion resistance. Where higher physical properties and better corrosion resistance than is afforded by Type 410 stainless steel justify an additional cost, Grade 630 is ordinarily used for gate rollers, links, and tracks. In Condition H1150 this grade has an ultimate strength of 135,000 psi, a yield strength of 105,000 psi, and minimum Brinell hardness of 277.

Specification A264 covers stainless-clad carbon-steel plates which are frequently used for gate parts and fluidway surfaces. Type 304 (18-8) stainless steel is most commonly used as the cladding material for gates. A36 steel is commonly used for the carbon-steel backing, although other steels are also available if desired. In the use of stainless-clad carbon steel it is desirable that the cladding be at least 0.05 in. thick. It is necessary to use care in design to avoid joints with both the carbon and stainless steels in close contact while submerged in water. Such a condition can result in severe "crevice corrosion" and damage to the carbon steel. This condition as well as pinholes from welding must be carefully avoided in designs which use stainless-clad plates.

All types of stainless steels should be carefully cleaned to remove carbon-steel contamination from the surfaces and to ensure maximum corrosion resistance by passivation of the surfaces before being placed in use.

Nickel-copper Alloy (Monel Metal). B127, Nickel-copper Alloy Plate, Sheet, and Strip; B164, Nickel-copper Alloy Rod and Bar; A265, Nickel and Nickel-base Alloy Clad Steel Plates. Although nickel-copper alloy is somewhat more expensive than stainless steels, the closeness to the brass and bronze alloys in the galvanic series and better corrosion resistance in saline waters justify the extra cost and make it preferable to the stainless steels in some cases. It has been extensively used for gate stems and other parts which are submerged in water and are in contact with brass and bronze.

Specification B127 covers a variety of conditions for plate, sheet, and strip. Typical annealed properties are 70,000 psi ultimate and 28,000 psi yield strengths. In other conditions considerably higher strengths are available, but only as-rolled plate properties of 75,000 psi ultimate and 40,000 psi yield strength would be of significance for usual designs.

Specification B164 covers a wide variety of strengths which are available for various conditions and sizes. Hot-finished rounds are available to 12 in. in diameter with an ultimate strength of 80,000 psi and a yield strength of 40,000 psi. In the cold-drawn and stress-relieved condition, diameters to 4 in. are available with ultimate strengths of 84,000 psi and yield strengths of 55,000 psi. Although higher physical properties are attainable in smaller sizes because of the greater effectiveness of work hardening, gate stems and other parts are commonly made from materials having properties in the strength ranges cited.

Specification A265 covers the cladding of carbon-steel plate with nickel-copper alloy. The basic general remarks which have been made about stainless-clad plate also apply to nickel-copper alloy.

Bronze and Brass. B144, High-leaded Tin Bronze Sand Castings; B145, Leaded Red Brass and Leaded Semi-red Brass Sand Castings; B148, Aluminum Bronze Sand

Castings; B21, Naval Brass Rod, Bar, and Shapes. The leaded bronzes covered in specification B144 are primarily bearing bronzes. The most widely used in gate designs is alloy 3A, which is nominally an alloy of 80 percent copper, 10 percent tin, and 10 percent lead. This alloy is substantially the same as Society of Automative Engineers Standard 64 for Phosphor Bronze Castings. The material is widely used for bearings of all kinds. Bronze seats of this material in combination with mating seats of 18-8 stainless steel or nickel-copper alloy have nearly replaced the class C and D bronzes which were practically standard for nearly 40 years. Tests have proved that a substantial percentage of lead is essential for slide-gate seats which are not lubricated, and the use of higher-strength bronzes with lower lead content is not recommended. Experience shows that lubrication of gate seats is desirable regardless of the materials used.

Alloy 4A in specification B145 (ounce metal) is widely used as a general-purpose low-strength corrosion-resistant material. Although it contains 5 percent lead, it should not be used as a bearing material except for very light loads. The ultimate strength of alloy 4A is 30,000 psi and the yield strength is 14,000 psi.

Alloy 9A in specification B148 is an excellent structural bronze and is also suitable where a strong material is necessary for highly loaded, lubricated bearings. It is not considered so good a bearing material as leaded bronze and its use as a bearing should be limited to cases where need for high strength exists. The 9A alloy has an ultimate strength of 65,000 psi and a tensile strength of 25,000 psi in the as-cast condition. Because aluminum bronze is suitable for bearings and is weldable, it is generally preferred to manganese bronze. Although higher-strength aluminum bronzes can be obtained by altering the composition and by heat-treatment, the resulting loss of ductility is undesirable. To avoid the increased stress-corrosion cracking which occurs with low ductility, the use of higher-strength bronzes should be avoided if possible.

Specification B21 covers four alloys of naval brass which are available in a number of tempers. In general, avoidance of the "hard" temper is recommended to minimize the stress-corrosion-cracking potential. In the softer tempers the ultimate tensile strengths will range from 50,000 to 60,000 psi with yield strengths from 20,000 to 27,000 psi.

Bolting Materials. The Bolt, Nut, and Rivet Standards of the Industrial Fasteners Institute[1] list practically all the standards which apply to bolts, nuts, and the materials for their manufacture. In the fabrication of gates and valves, it is recommended that bronze or brass bolting be avoided for principal load-carrying connections, as experience has shown that stress-corrosion failures in rolled alloys of copper and zinc or aluminum frequently occur. Likewise, brass nuts have been known to split from stress corrosion. Such failures in stainless steel or monel are not common, and the use of these materials for heavily loaded, critical bolts is recommended.

31. Rubber Seals. One of the critical elements in the design of any gate or valve is an effective seal. In gates and valves which are of moderate size and can be economically machined to close tolerances, various types of metal-to-metal seals have proved to be satisfactory. In large gates a seal which has the capability of accommodating to inaccuracies in gate alignment and seating surfaces is necessary to avoid very stringent and costly manufacturing tolerances.

Rubber seals provide the necessary flexibility to meet the alignment problem. But coupled with flexibility there is also a need for strength at high heads, and this fact creates the contradictory requirement and problem of making seals which are both flexible and strong. Acceptable seals which meet these requirements reasonably well have been designed, but further research and development will be necessary to attain the ideal solution.

[1] 1517 Terminal Tower, Cleveland, Ohio.

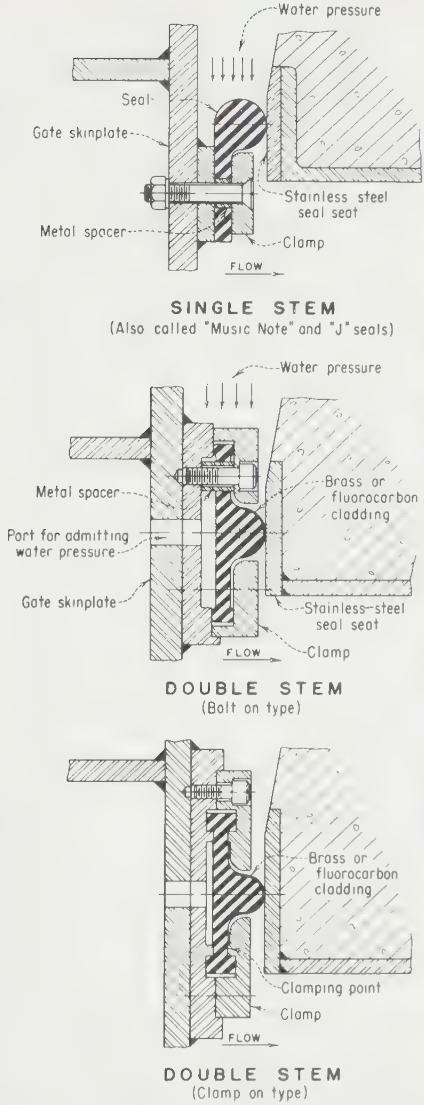

Fig. 53. Single- and double-stem seal assembly arrangements.

Two of the basic types of rubber seals for gates, the single-stem "music note" or "J" seal and the double-stem seal, are shown in Fig. 53. There are also numerous variations, such as the square bulb and different methods of attachment which have been developed from these basic designs. The bolt-on type of mounting, which involves drilling the rubber seal stems, is a satisfactory and common method of attaching seals. The bolt-on arrangement provides good resistance to seals being torn from a gate in severe service conditions. Various clamp-on methods of mounting gate seals are also used. The use of clamp-on mountings is increasing because more flexible and economical seal arrangements are possible.

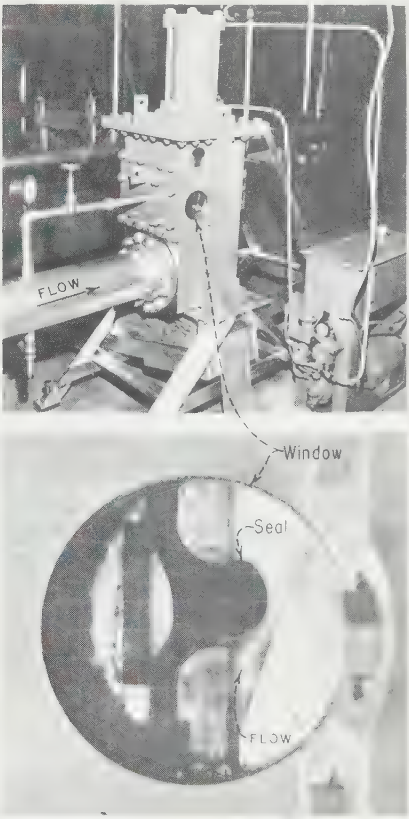

Fig. 54. Seal-test rig showing double-stem clamp-on seal being tested under 300-ft head.

In the mounting of gate seals, it must be kept in mind that rubber displaces rather readily under pressure. For this reason spacers must be used to limit the compression of rubber seals which are attached to gates with clamp bars. This arrangement is normally used for single-stem seals. For double-stem seals, spacers are necessary to ensure maintaining clearances to permit seal movement. Space must also be allowed for lateral displacement of rubber during clamping of seals as rubber has very little volumetric compressibility.

The single-stem seals are commonly used for outlet bulkhead gates and stop logs which are normally closed under balanced-pressure no-flow conditions. Where greater strength and resistance are required for gates which are closed under flow, the double-stem seal is used. Single-stem seals are usually all rubber, but double-stem seals are normally molded with a cladding material on the contact surface.

Brass cladding which is vulcanized to the seal during molding has been widely used on rubber seals. The principal reason for cladding seals is to reduce the high friction coefficient which rubber has on metal seal seats. The brass cladding also strengthens the seals and prevents distortion of the seal bulb into the clearance between the gate and seal seats. The disadvantage of the brass cladding on rubber seals is the loss of flexibility and capability for conforming to seating-surface imperfections. The reduced flexibility results in increased leakage.

Developments and tests (see Fig. 54) indicate that rubber seals having the bulb portion clad with an opaque fluorocarbon reinforced with glass fibers have many desirable characteristics and may replace brass cladding. The fluorocarbon material has a much lower coefficient of friction than brass, and for this reason will slide and not bind on slopes which would damage brass-clad seals. Because the fluorocarbon material is relatively soft and flexible, the sealing capability is excellent. Although wear resistance is very good, special care should be used to be sure the seal seats are smooth and free of sharp projections which could cut and damage the relatively soft cladding material. The rigidity of fluorocarbon-clad seals is somewhat less than for brass cladding, but tests show that these seals may be used for heads to at least 200 ft. It is probable that fluorocarbon-clad rubber seals can be developed to withstand heads to more than 500 ft; but until further tests verify that use for higher heads is safe, brass-clad seals should be used for heads over about 200 ft.

Single-stem seals are actuated directly by pressure on the bulb portion. For double-stem seals the use of control valves to admit reservoir pressure for sealing and to release sealing pressure when the gate was moving was common practice at one time. Although controlled actuation is still used in critical cases, it is commoner to have permanently open ports which admit reservoir pressure at all times to the space behind the seals. This design eliminates the complication of a seal control valve, but increases the friction which a gate must overcome for gravity closure.

Rubber seals are normally molded from compounds of natural and synthetic rubbers but can also be made of a single type of rubber if desired. The use of cotton fibers or cords as reinforcement in rubber seals is not recommended, as experience has proved that deterioration of the cotton results in shorter life than rubber seals without such reinforcement. If reinforcement is absolutely necessary, the use of synthetic, rot-resistant fiber, rather than cotton, is recommended.

Typical physical test[1] properties for rubber seals are as follows:

Tensile strength	3,000 psi (min)
Elongation	450 % (min)
Durometer hardness (Shore Type A)	60–70
Water absorption by weight	5 % (max)
Compression set	30 % (max)
Tensile strength after oxygen-bomb aging	80 % (min) of tensile strength

[1] Test methods for the various properties are described in the American Society for Testing and Materials Specifications D395, D412, D471, and D572.

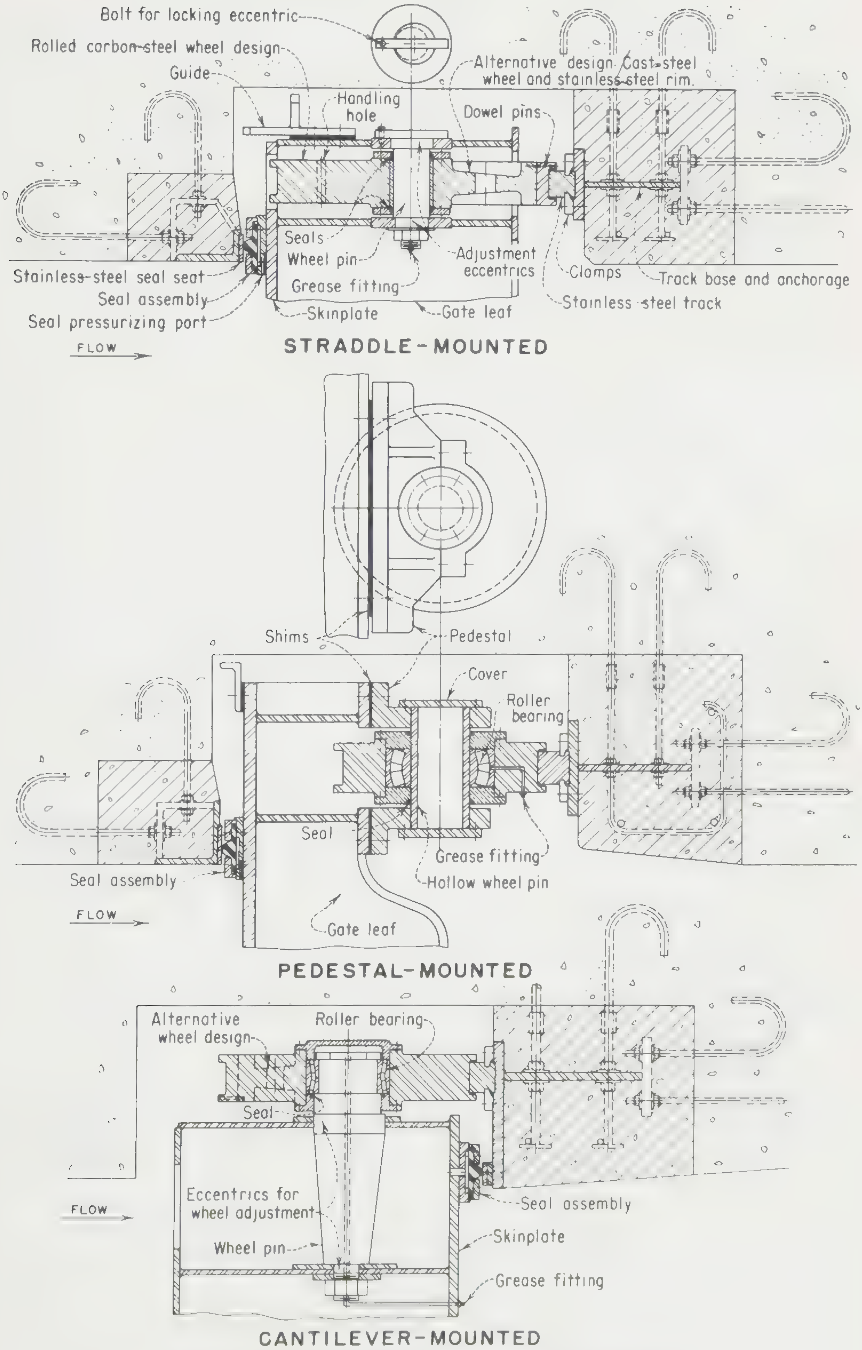

FIG. 55. Typical gate-wheel-mounting arrangements.

This brief summary of critical design and operation of rubber seals covers only a few of the many types of seals which are used for gates. The technical journals and publications of leading seal manufacturers[1] provide further information on the design and manufacture of rubber seals.

32. Gate Wheels. Three basic gate-wheel-mounting arrangements are shown in the gate-slot sections in Fig. 55. Each type has some advantages and disadvantages. All types have been used on successful gate designs.

The straddle-mounted type has the advantage of minimizing the required wheel-pin size. A small wheel pin permits the use of smaller wheels, because wheel-to-pin diameter ratios of about 5:1 are usually used for wheels with sleeve bearings. This ratio is used to keep the wheel-rotation forces small so that the gate weight will be enough to effect gravity closing. The straddle-mounted arrangement requires more complex gate-leaf framing and machining, and the need to remove the wheels for painting the wheel recesses makes maintenance more difficult.

The pedestal-mounted type which has one or two wheels mounted on a pedestal simplifies the gate-leaf framing and machine work. The wheel-pedestal assemblies can be fabricated as identical units and be easily assembled and aligned on the gate. The pedestal arrangement poses more limitations on wheel diameters than other types, and may require using roller bearings where sleeve bearings might otherwise be used.

The cantilever-mounted wheels provide a maximum of accessibility for inspection and maintenance. Cantilever-mounted wheels require fairly large wheel pins; consequently, antifriction bearings are frequently necessary. The framing for this type of mounting is comparable with the straddle-mounted type but the machine work on the gate is somewhat simpler. The units can be subassembled before being installed on the gates. The cantilever type requires an eccentric portion on the wheel pin, the same as straddle-mounted wheels do, to obtain proper alignment of the wheel tread faces.

Both sleeve and antifriction bearings are used for the wheels on all three types of mountings. Sleeve bearings are usually used for the straddle-mounted type; either sleeve or roller bearings are used for the pedestal-mounted type; and self-aligning roller bearings are frequently used for the cantilever-mounted wheels. Sleeve bearings are usually of the self-lubricating types, although leaded bronze bearings are also sometimes used. It is usual practice to provide seals on the ends of the bearings to minimize the entrance of water and silt.

When roller bearings are used on wheels, it is important that the bearing seals be effective, especially when gates are submerged for long periods of time between inspection and servicing. In some cases the use of stainless-steel antifriction bearings, even at considerably higher cost, may be well justified to avoid rusting and bearing damage which could prevent closure of critical gates.

In all cases the provision of grease fittings is recommended. Although not essential for lubrication of self-lubricating bearings, the grease performs the dual functions of lubricating and of filling the spaces around the bearing to help prevent the entrance of water and silt. This latter function is just as important as lubrication and justifies greasing all bearings.

The curves and data given in Figs. 56 and 57 provide means for making a quick determination of wheel sizes after the loads have been established. The curves also will provide a pin size after the desired wheel-to-pin diameter ratio has been established. As the cited University of Illinois reference and other sources are readily

[1] Catalogues of standard "Gate Seals" and "Engineering Information and Specifications for Rubber Gate Seals," Huntington Rubber Mills, Portland, Ore.

available for reference in making detailed calculations of permissible wheel loadings under various conditions, no detailed description of the procedure will be given.

Typical track-base and anchorage details are shown for the various types of gate-wheel mountings in Fig. 55. The track and tee sections are frequently designed using data from the following sources: *University of Illinois Bulletin* 212, "Beams on an Elastic Foundation,"[1] and Bending of an Infinite Beam on an Elastic Foundation.[2]

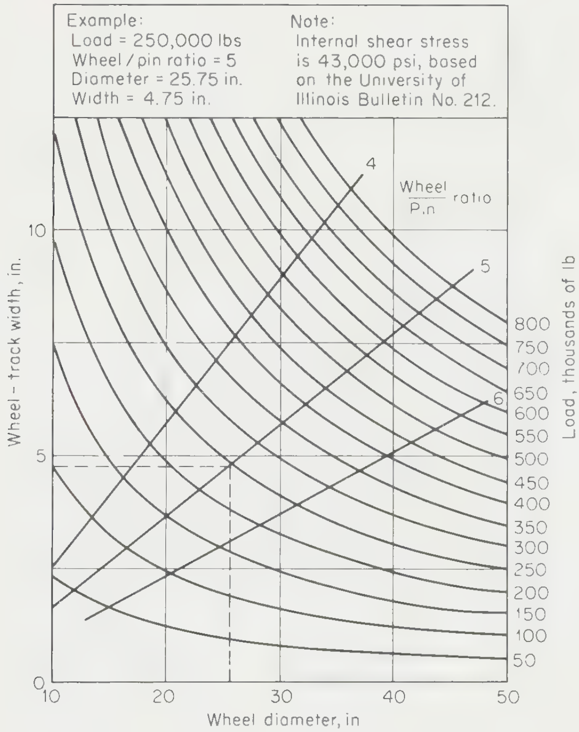

FIG. 56. Design chart for uncrowned 255 Bhn wheels on flat tracks.

The foundation modulus k is calculated using the following formula in Biot's paper:

$$k = 1.29 \left[\frac{1}{C} (1 - v^2) \frac{Eb^4}{E_b} I \right]^{0.11} \frac{E}{C} (1 - v^2)$$

The shear Q, bending moment M, and deflection y are calculated in accordance with the following formulas in M. Heyteni's book:

$$Q = -\tfrac{1}{2} P D_{\lambda x}$$

$$M = \frac{P C_{\lambda x}}{4\lambda}$$

$$y = \frac{P \lambda A_{\lambda x}}{2k}$$

The cited references should be consulted for the meanings of the nomenclature in the

[1] HEYTENI, M., The University of Michigan Press, Ann Arbor, Mich.
[2] BIOT, M. A., *J. Appl. Mech.*, March, 1937.

formulas cited and calculation procedures. The allowable shear stress in the track would be the same as for the wheels if the Brinell hardness were the same.

Rolled-carbon steel wheels similar to ASTM Designation A504 have been widely used on gates for about 30 years. The wheel treads on a number of gates show rather serious rusting and pitting, despite the use of paint, grease, and other protective tread coatings. In some cases the need for major refinishing and repairs is imminent.

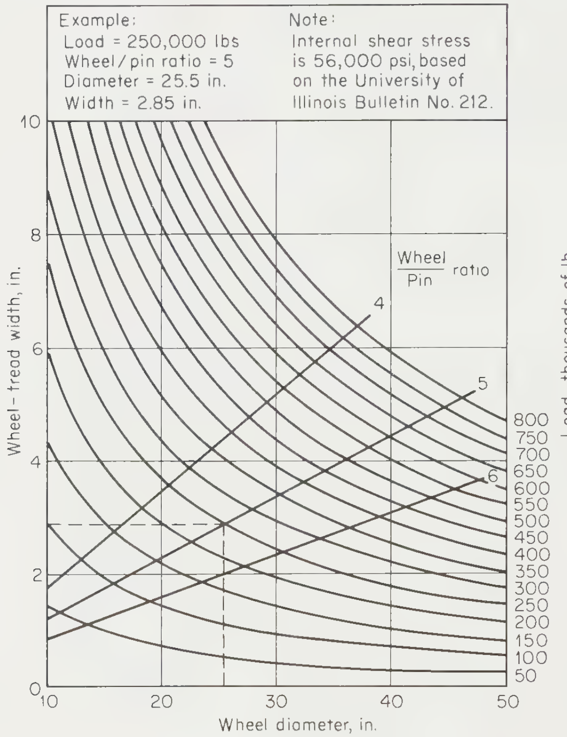

FIG. 57. Design chart for uncrowned 302 Bhn wheels on flat tracks.

Investigation of possible repair methods indicates that machining the outside diameters of the existing wheels and adding stainless-steel rims with a light shrink fit is the most desirable and feasible method of repair. The rim thickness should be great enough to contain the heavy shear forces under the Hertz area. Type 410 martensitic stainless steel, with a Brinell hardness of about 255 to 320, and a precipitation-hardening alloy corresponding to ASTM A461, Grade 630, appear to be the most suitable materials for the rims.

On the basis of past experience, the use of stainless rims for gate wheels should be considered for new designs where long life, reliability, and avoidance of future maintenance costs are of importance. Stainless steel has commonly been used for gate tracks because of their inaccessibility for repair. It is recommended that the stainless rims which are used to repair pitted wheels, as well as rims for new wheels, be made of the same stainless steel as the tracks to minimize the danger of galvanic corrosion. Some savings can be effected in new wheel designs having stainless-steel rims, by using cast-steel hubs instead of steel forgings.

33. Roller Trains. A typical roller-train design for a large, high-head gate is shown in Fig. 58. For large, multiple-section gates separate roller trains are usually mounted on each gate section as shown in Fig. 59. This design arrangement is simpler to fabricate and the flexibility at the gate-section joints permits each unit to distribute the loading to the embedded track much more uniformly than would be

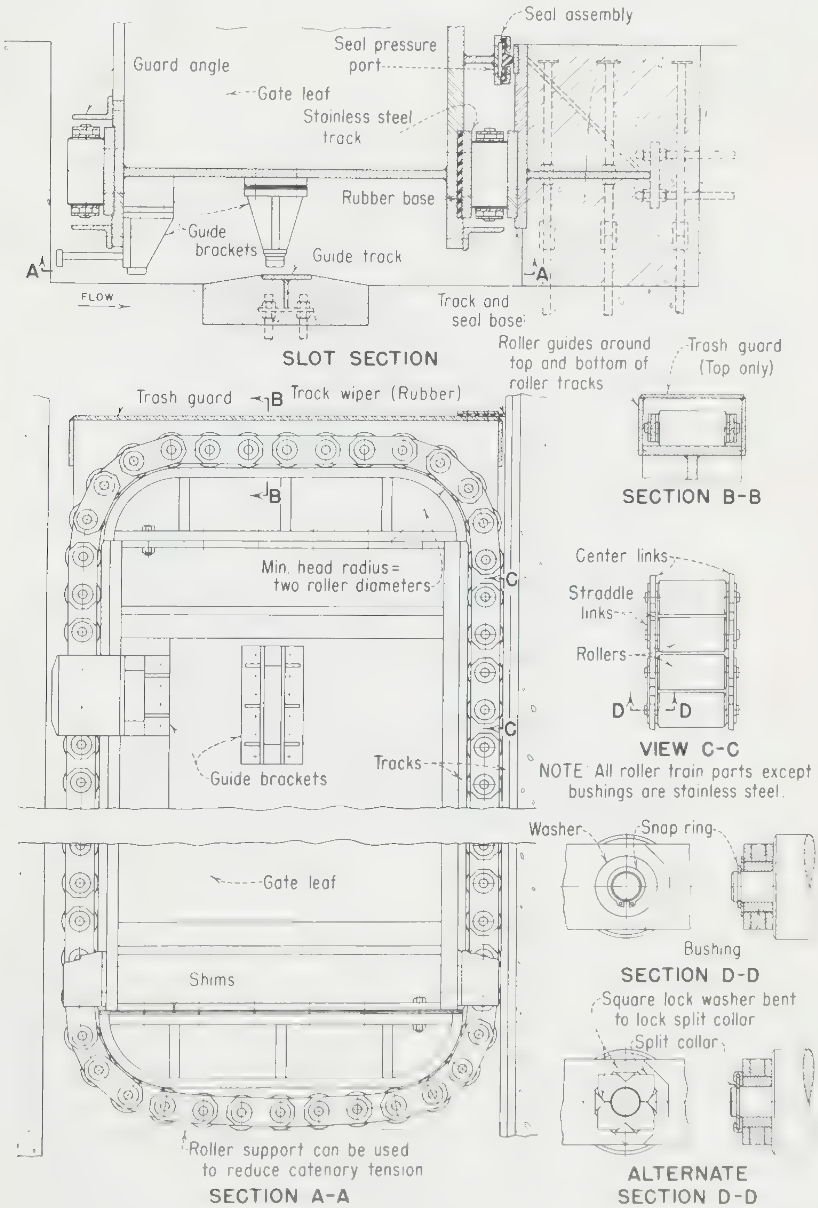

FIG. 58. Typical roller-train details and mounting arrangement.

possible with roller trains extending the full height of a gate. The shorter roller chains are also an advantage in reducing the loading on the link bushings.

Some early designs of roller trains caused trouble because the track radius for the top and bottom of the trains was made too small. Experience and the forces involved indicate that the radius should not be less than two roller diameters. The track radius may be a full semicircle or may be made in quadrants as shown in Fig. 58. The quadrant arrangement is used for large fairly thick gate leaves so that the maximum length for vertical distribution of the leaf load to the embedded track can be obtained. Semicircular tracks at the ends of roller trains are commonly used on the smaller gates.

Fig. 59. Lower half of 17.5- by 22.9-ft roller-mounted gate leaf for San Luis Dam in California.

Another critical element in the design of roller trains is the link arrangement. The straddle-mounted link design illustrated, which requires two thicknesses of links, should be used in preference to other types of design. The balanced loading on the chain bushings and the avoidance of binding of the bushing on the roller trunnions result in smooth operation of roller trains and justify the additional cost for the straddle-mounted design. To ensure that roller trains will roll straight, it is essential that the link centers between a pair of rollers be practically identical. For this reason it is good practice to jig-ream the links in matching sets and mark them for selective assembly.

To ensure even distribution of loading it is essential that roller diameters be held to as nearly a uniform size as is economically feasible. As a "rule of thumb" it is suggested that a tolerance of about 0.0002 times the roller diameter in inches be used as a tolerance. It is also important that the trunnions on each roller be substantially the same diameter to ensure that the rollers in a train will be parallel.

Both self-lubricating bronze bushings and leaded-bearing bronze bushings have been used with success on roller trains. For the more heavily loaded chains the self-lubricating bushings are used. It should be noted that with straddle link-chain construction the bushing load is primarily the load of the chain and the principal friction is due to the knee action of the links as the chain travels around the curved tracks.

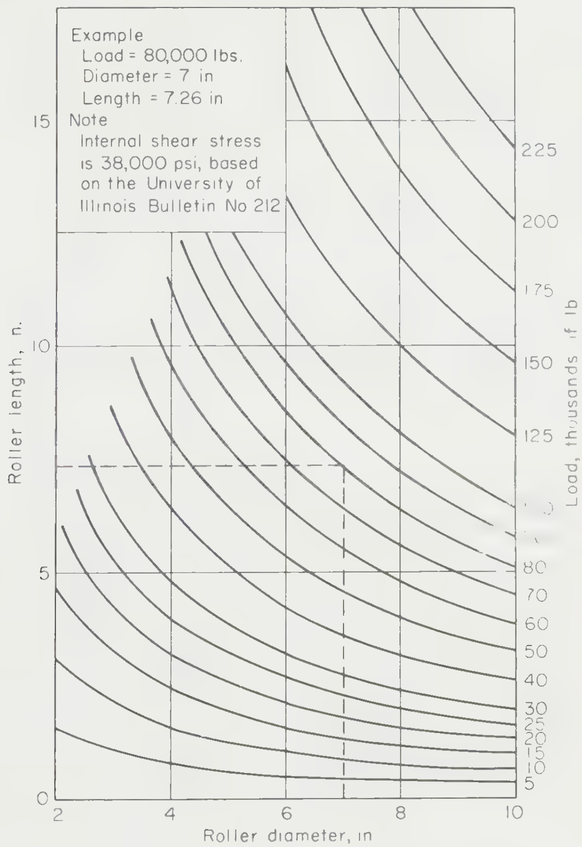

Fig. 60. Capacity chart for 255-Bhn rollers.

The roller trunnions theoretically carry only the weight of the roller and serve to position the roller accurately in the chain bushings. Bushing tolerances must be closely held to ensure satisfactory chain operation.

Two types of locking devices for holding the link and bushing assemblies on rollers are illustrated. The stainless-steel snap ring is the simplest. The split collar which is held in place by bending over the four corners on a square washer is a more rugged and positive type of locking device. This type is also more expensive but may be justified in some cases.

The rollers, tracks, and track bases for roller-mounted gates are designed on the same basic principles and formulas used for wheel-mounted gates. The charts in Figs. 60 and 61 show allowable loads in relationship to hardness for various sizes of steel rollers. The type 410 martensitic stainless steel in a Brinell hardness range from 255 to 320 is frequently used for rollers and tracks. The same type of steel is also used for the links. Precipitation-hardening steels are also used for rollers, tracks, and links.

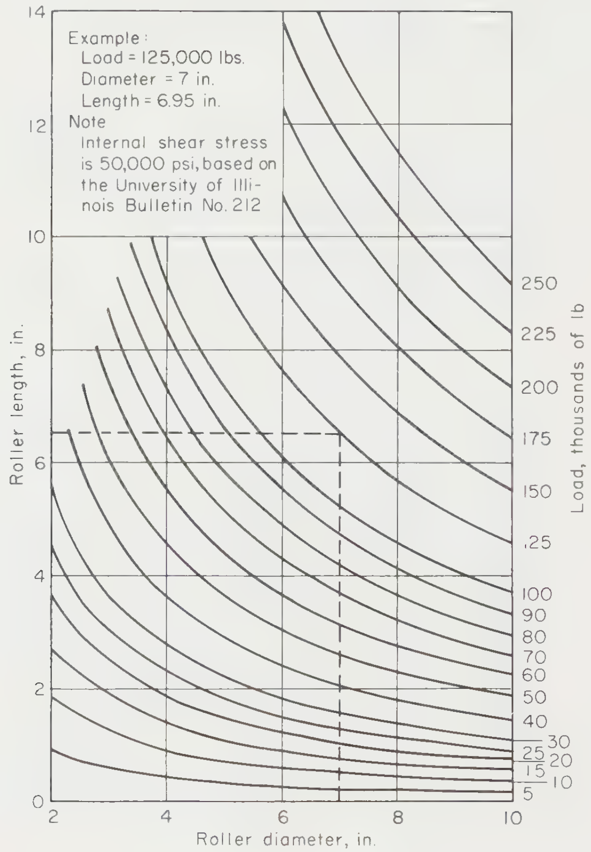

FIG. 61. Capacity chart for 302-Bhn rollers.

As shown in the slot section in Fig. 58, the track on the gate is sometimes mounted on a rubber base to allow movement of the track for adjusting to the slope at the sides of the leaf. This arrangement eliminates the hazard of getting high edge loadings on the rollers, but special care must be used to confine the rubber so that it cannot flow from under the track. This added complication is justified only where large loads and end slopes make it infeasible to accommodate to the slope elastically by other types of design.

Tests indicate that the force required to move an unloaded chain around a track is quite small, provided the catenary sag at the bottom end is not too tight. If the bottom rollers are supported on a guide track, the tension in the links due to catenary action can be eliminated. Arbitrarily assuming 20 percent of the roller train weight as the force required to move a roller should provide an ample operating-force allowance. The roller train and rolling friction forces plus the seal friction would be of primary importance in checking to be sure a gate will close by gravity.

It is desirable that a trash guard be placed over the top of roller trains as shown in section *AA*, Fig. 58. Considerable damage has sometimes resulted when foreign articles get between the rollers and tracks. Movement of the roller trains results in crushing the material and damage to both the roller and track surfaces.

34. Hydraulic Hoists and Operators. Although geared drives of the torque-limiting type are still widely used on many small- to medium-sized gates and valves, hydraulic operation has widely superseded the screw lift and geared drive units for large, high-head gates and valves. One of the big factors in this change through the years has been the need for higher hoist capacities and the ease with which such capacities can be attained with a hydraulic hoist. Other factors such as design simplicity, ease and flexibility of control, and operating reliability have also contributed to the increased use of hydraulic operation.

Hydraulic hoists have been the standard operating method for slide gates for many years, but until relatively recently it was thought necessary to provide a mechanical device to hold a gate leaf in intermediate positions. When it was proved in the mid-1950s on the 7.5- by 9-ft slide gates at Palisades Dam that a hydraulic hoist with a packed piston was reliable for holding a gate leaf in any position for long periods of time with practically no movement, a whole new field of application was opened for the use of hydraulic hoists. Regulating gates of all types which had previously been limited to mechanical hoists, as well as hollow-jet valves, were redesigned for direct hydraulic operation. The requirement for mechanical latches was eliminated from new designs for gate hoists, and the use of existing latches to hold the intake gates open has been discontinued on some older installations.

A typical hydraulic hoist for a penstock gate is shown in Figs. 62 and 63. The arrangement of similar hydraulic hoists for other types of gates is shown in Figs. 6, 11, and 14. Figure 36 shows a hydraulically operated hollow-jet valve, and Fig. 41 shows a conventional arrangement for operating a butterfly valve.

Basically a hydraulic hoist consists of a cylinder, upper and lower cylinder heads, a piston, and a stem. In Fig. 62 it will be noted that there is a hanger stud. This stud is provided primarily to hold the piston and stem within the cylinder during servicing and handling. The hanger stud is not engaged during normal hoist operation, and the gate is held in the fully open position by blocking the outflow of oil from the space under the packed piston.

The piston is fitted with three hydraulic-type piston rings and also with a stuffing box having V-packing rings. The V-packing rings practically eliminate all leakage past the piston and permit holding the piston in any position for long periods of time when outflow of oil from the bottom cylinder connection is blocked. The piston rings serve as a reserve seal in case of packing damage, and will permit deferring repacking until a convenient time, as the leakage past good-quality hydraulic rings is quite low. Repacking the piston requires only removal of the upper head for access and does not require removal of the hoist.

Pistons are made of bronze in the smaller sizes. Gray cast iron is frequently used for intermediate sizes and pressures to 1,000 psi. For large sizes and pressures above 1,000 psi, cast- or welded-steel pistons are usually used. The outside diameter of steel pistons is always provided with an overlay of aluminum bronze, so that the finished piston will not score the smooth cylinder walls which are normally honed to a 16-μin. finish. Overlays are not normally provided on cast-iron pistons.

Cylinders are usually fabricated from rolled-plate and forged-steel flanges. Small-sized cylinders are sometimes forged as a unit. In general, the standards of the

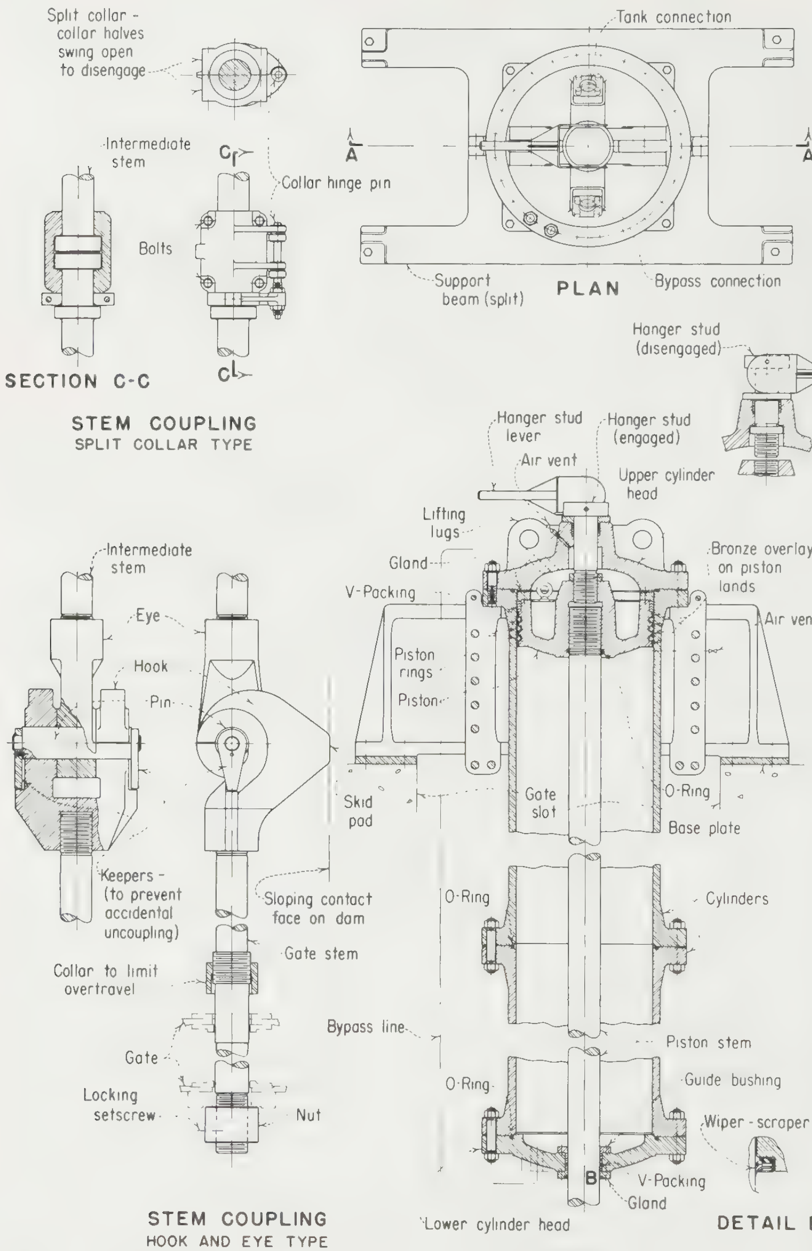

FIG. 62. Typical arrangement and details of hydraulic hoist and stems for large intake gates.

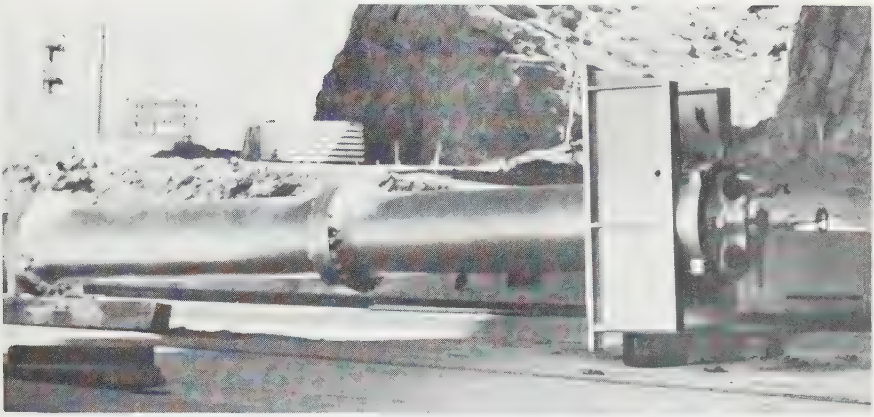

FIG. 63. Hydraulic hoist for 13.96- by 22.45-ft penstock intake gate at Glen Canyon Dam in Arizona.

Unfired Pressure Vessel Code of the American Society of Mechanical Engineers are followed in the design of cylinders. Radiographic examination of all welds is required. All cylinders and cylinder heads are also required to pass a hydrostatic test of 150 percent of design pressure. In multiple-cylinder hoists, the joints between the cylinders must be carefully matched for size, and any roughness which could damage the packing must be removed. Cylinder heads are usually made of cast steel although plates or fabricated heads are sometimes used.

Piston stems in diameters to about 5 in. are usually made of solid stainless steel or nickel-copper alloy (monel metal). In larger sizes it is frequently more economical to

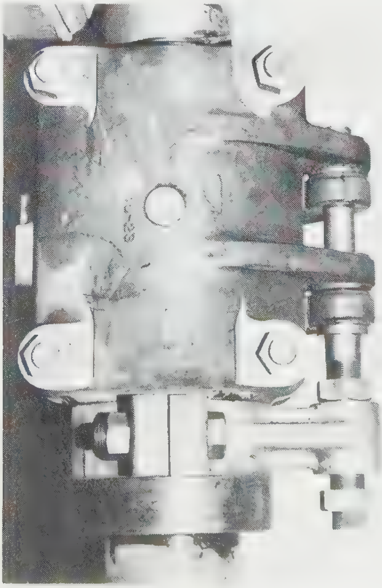

FIG. 64. Split-collar-type stem coupling.

use a steel stem having formed sheets of these corrosion-resisting materials welded around the stem. The thickness of the corrosion-resisting sheath should always be enough so that if a leak should develop in a weld, the hoist pressure will not be sufficient to cause yielding and "ballooning" of the sheath where the stem extends outside the cylinder.

Several types of couplings have been used for connecting the intermediate stems between the gate and hoist on intake gates. The clevis type was used originally but was rather expensive to make and cumbersome to connect and disconnect in the field. The split-collar type, shown in Figs. 62 and 64, was developed later and proved to be far less costly and more convenient to assemble and disassemble. For these reasons the split-collar-type coupling is preferred for all vertical-stem gates. This type of coupling is also used for gates on slopes of more than about 15 deg with the vertical, where the stem sections are aligned and supported on carriage brackets having wheels which run on tracks.

Fig. 65. Hook-and-eye couplings on the penstock intake gate at Glen Canyon Dam in Arizona.

For slopes to about 15 deg with the vertical, which are common on the curved faces of arch dams, the split-collar type of coupling poses some difficult assembly-alignment problems. The difficulty in getting the angularity accommodation required for coupling nonvertical-stem sections led to the development of the hook-and-eye type of stem coupling. This coupling is similar to the original clevis-type coupling but does not require the disassembly or manual handling of heavy parts for coupling the stems. See Figs. 62 and 65. The addition of skid pads on the loop of the hook provides an easy method of holding the stems in alignment on a slope. As the load on the skid pads is light, a smooth concrete surface on the face of the dam provides an adequate bearing surface for the pads.

It is recommended that the steel castings for both the split collar and for the hook-and-eye-type couplings be carefully checked for cracks or defects by suitable nondestructive methods, such as magnetic-particle testing. In addition, each stem unit with couplings attached should also be given a full-load proof test.

For static seals the use of O rings is recommended. For sealing moving parts, V-type packings have given very satisfactory service and are recommended. As V-packings can be damaged badly by overtightening, conventional gland adjustment is usually omitted and the packings are preset to the proper degree of snugness in the stuffing box. Care should be taken to specify mica finish instead of graphite for packings which are in contact with stainless steel and water. It is good practice to provide a wiper-scraper to remove foreign matter from exposed stems and prevent damage to the packing as the stem enters the cylinder.

The design capacity of a hoist is usually determined by four elements: the weight of the parts to be lifted or lowered, friction forces, downpull forces, and an arbitrary design factor. The calculation of weight and friction forces poses no unusual problems; but despite numerous tests which have been made, no really simple general method of computing downpull is available. Model tests provide the most accurate method of determining downpull for a given design. Although exact methods for computing downpull on the various types of gates may not be available, the various tests on specific gates and analyses which have been made do provide bases for making a reasonable estimate of the downpull forces for most cases.[1]

In determining the hoist capacity required, it should be borne in mind that the weight, friction, and downpull are additive only for gates which are opened under unbalanced conditions. For guard gates which are closed, but not opened, under unbalanced conditions, friction subtracts from weight and downpull in establishing hoist capacity.

Hoists are commonly designed for rated oil pressures of 1,000 or 2,000 psi, as pumps, valves, and other hydraulic operating-system components are readily available in these ratings. Selection of the pressure to be used for a specific design is largely a matter of judgment and of keeping the hoist size physically in balance with the size of the gate or valve structure. When hoists at 1,000-psi ratings require cylinders which are larger than desired, the design pressure should be increased to 2,000 psi or even to higher pressures if necessary to obtain required design features.

After the estimated net operating capacity for a hydraulic cylinder has been calculated, this capacity is usually multiplied by an arbitrary design factor of 1.33 to 1.50. The net area of the cylinder is then determined by dividing the total capacity by the rated design pressure. The arbitrary factor is added primarily to provide a pressure range for operating pressure-control devices. The factor also provides some margin of safety for variations in calculated oil-line friction losses and hoist capacity. For example, in a system rated for 1,000 psi the hoist cylinder pressure for the actual calculated load would be between 650 and 750 psi. The selection of an arbitrary design factor to use in a specific case is a matter of judgment based on the known factors for specific cases. In no case should the design factor be eliminated, and a 1.25 factor is considered the minimum which is acceptable for good design.

[1] Warnock, J. E., and Howard J. Pound, Coaster Gate and Handling Equipment for River Outlet Conduits in Shasta Dam, *Trans. ASME*, **68** (3), Feb. 3, 1946. "Hydraulic Design of Reservoir Outlet Structures," Department of the Army (USA), Office of the Chief of Engineers, Engineer Manual, EM 1110-2-1602, August, 1963. Colgate, Donald, Hydraulic Downpull Forces on High Head Gates, *Proc. ASCE, J. Hydraulics Div.*, **85**, November, 1959. Murray, R. I., and W. P. Simmons, Jr., Hydraulic Downpull Forces on Large Gates, U.S. Department of the Interior, Bureau of Reclamation, *Research Rept.* 4, 1966.

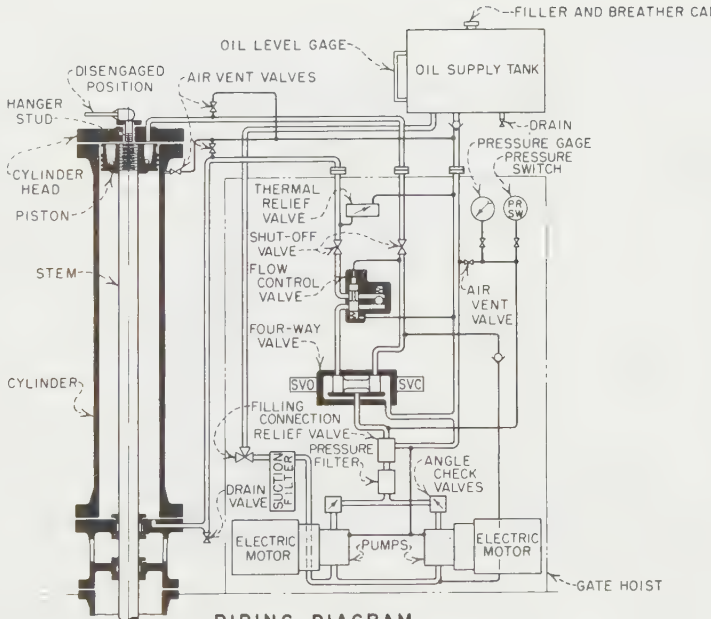

PIPING DIAGRAM

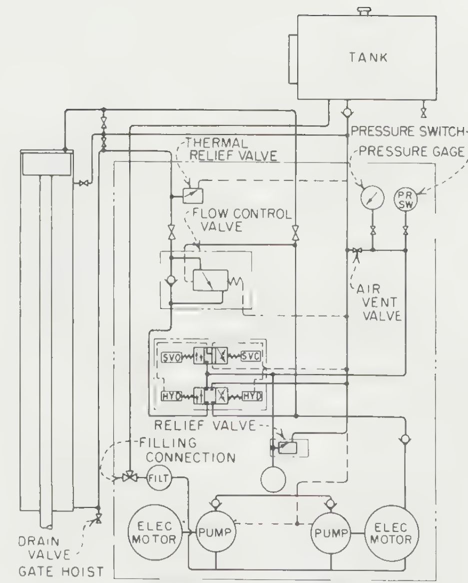

SCHEMATIC HYDRAULIC DIAGRAM

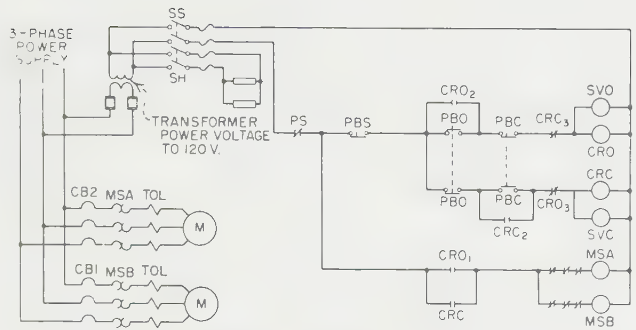

SCHEMATIC WIRING DIAGRAM

ELECTRICAL DEVICE DESIGNATIONS

CRC	Control relay-Close
CRO	Control relay-Open
PBC	Push button-Close
PBO	Push button-Open
SVC	Solenoid valve-Close
SVO	Solenoid valve-Open
CB1, CB2	Circuit breakers
MSA, MSB	Magnetic motor starters
TOL	Thermal overloads
PBS	Push button-Stop
PS	Pressure switch, normally closed
SS	Selector switch
SH	Heater switch

FIG. 66. Diagrams of typical operating system for gates and valves.

In case of doubt about hoist size, the use of a slightly larger cylinder diameter is the recommended practice, as the incremental increase in cost is quite small and the capacity increase for an inch or two on a cylinder diameter is quite large. The available sizes of standard flanges should be kept in mind in selecting a hoist cylinder size. It is poor economy to save an inch or two on a cylinder size at the cost of buying special nonstandard flanges. The available sizes of standard hydraulic piston rings is another practical factor which should be considered in selecting hoist sizes.

35. Hydraulic Operating Systems. The hydraulic systems for operating gates and valves require careful coordination of the various hydraulic- and electrical-system

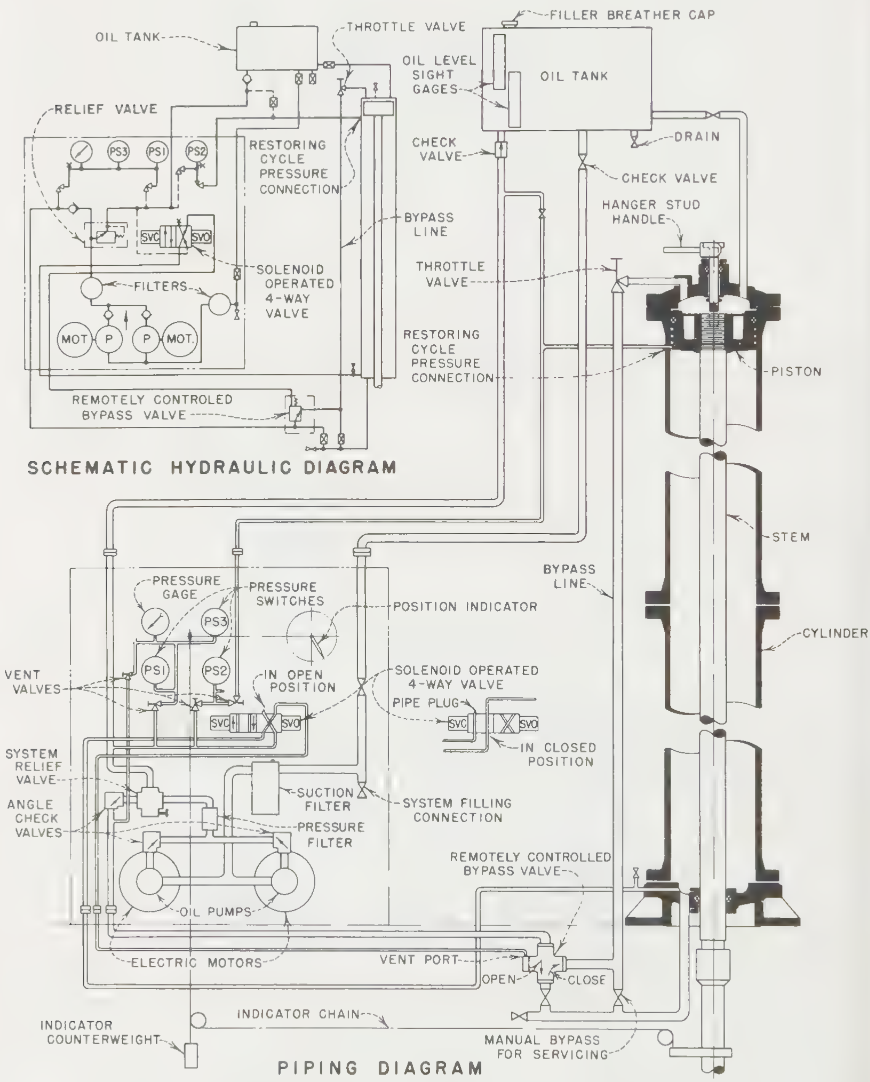

FIG. 67*a*. Piping and hydraulic diagrams for gravity-closing guard gates.

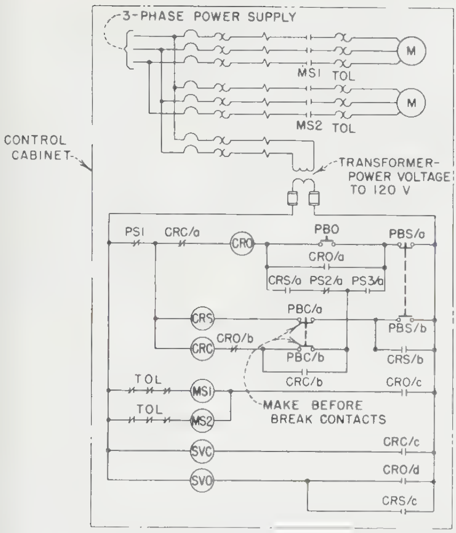

ELECTRICAL DEVICE DESIGNATIONS

CRC	Control relay-Close
CRO	Control relay-Open
CRS	Control relay-Stop
PBC	Push button-Close
PBO	Push button-Open
PBS	Push button-Stop
PS1, PS2, PS3	Pressure switches
SVC	Solenoid valve-Close
SVO	Solenoid valve-Open
MS1, MS2	Magnetic motor stater
TOL	Thermal overload

SCHEMATIC WIRING DIAGRAM

FIG. 67*b*. Wiring diagram with restoring cycle for gravity-closing guard gates.

functions and components. A relatively small number of basic components are required for most systems, but care must be used in selecting and arranging the components to ensure proper system functioning.

The basic components of hydraulic-electrical operating systems are the oil tank; filters; pumps with motors and starting equipment; flow-directing valves which are either manually, electrically, or hydraulically operated; a pressure-relief valve; piping; pressure gage; pressure-operated switches; and push buttons, relays, and other electrical equipment necessary for actuating and controlling the system. Figure 66 shows the schematic arrangement of a typical operating system commonly used for operating gates or valves which require the hoist piston to be positively driven in both directions. Figure 67 shows the schematic arrangement of an operating system for a gate that is opened by pumping but is closed by gravity when oil is bypassed from the underside to the top of the piston. The basic components in both systems are similar but the second type has the added complication of automatic operation to compensate for leakage and restore the gate to the fully raised position. Figure 69 shows a typical control-cabinet arrangement.

Several factors in hydraulic operating systems are of critical importance. One of the primary requirements is that the system be clean. Special care must be exercised in the manufacture and installation of hydraulic systems to ensure cleanliness. Oil tanks should be properly painted or made of stainless steel to ensure cleanliness and avoid rusting. Tanks should be provided with screened filler and breather openings. A filter with a screen no coarser than 100 mesh should be provided in the pump suction line, and the use of pressure filters in the pump discharge line to remove particles above a 10-micron size is recommended. Provision should be made to drain water accumulations from the low points in the oil tank and the hoist cylinder. If filled with very light oil, hydraulic systems will work in cold ambient temperatures; but as a general rule, it is desirable to maintain ambient temperatures of 40 F or higher. When cold temperatures for winter operation will be encountered, the hydraulic hoist and operating components should be protected by a heated enclosure.

Oil tanks should have a normal storage capacity equal to about three times the pump capacity in gallons per minute. Additional capacity must be provided for the volumetric displacement of the hoist stem and for temperature-produced volume changes. All return lines to the tank should be located below minimum oil level and be adequately separated from the pump suction by a baffle.

Two motor-driven oil pumps are commonly provided for each operating system to ensure the operation of a gate or valve. In effect, this arrangement provides a working spare which is immediately available in case one motor-pump unit fails. The single unit can be used until the faulty unit is repaired, as the only effect on the system is to double the normal pumping time. Electric motors are normally used to drive both pumps, but in some cases one of the pumps is driven by an internal-combustion engine to ensure operation where loss of power supply might be critical. The combined pump capacities are usually selected to operate hoists at a rate of about 1 fpm.

Unless some other type of pump is definitely required and specified, vane-type pumps, which are usually less expensive than other types, are normally furnished for hydraulic systems. Vane pumps have proved to be very satisfactory and reliable.

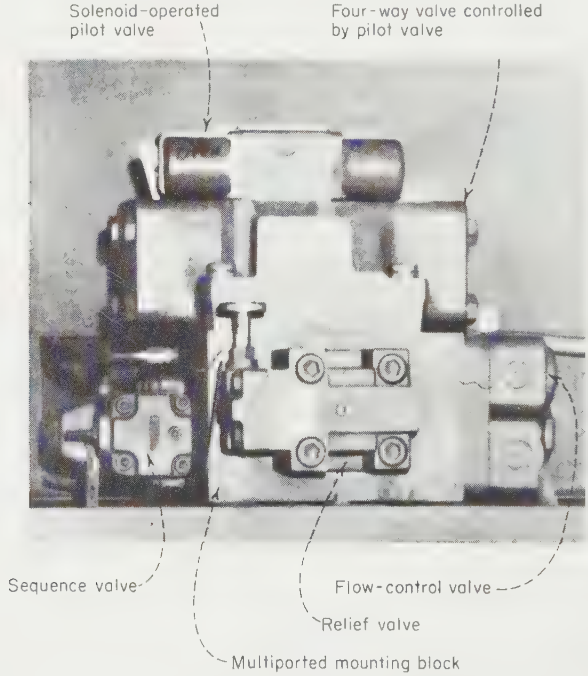

FIG. 68. Hydraulic control valves assembled on a multiported mounting block.

Subplate mounting-type valves are recommended for all four-way, relief, and similar types of valves which have spools or close-fitting operating elements. This type of mounting facilitates installation or removal of valves and also avoids piping strains which can cause malfunctioning of such valves. Figure 68 shows a multiported block which is large enough to accommodate subplate mounting-type valves on the top and sides. Suitably located and arranged passageways which communicate between the valve ports are drilled in the block. This design arrangement is efficient and compact, and eliminates a considerable amount of external piping. However, the return line from the relief valve must always be piped directly to the tank and never to the pump suction line.

One important requirement in hydraulic systems is to have the piping joints oil-tight. The use of standard tapered pipe threads for high-pressure oil piping nearly always results in some leaky joints. If pipe threads must be used, specifying "dryseal"-type threads is recommended. Various types of O-ring connectors, flared tubing connections, and socket-welded connections are most commonly used to ensure oil-tight hydraulic systems. Rugged, welded construction using socket-welding fittings, O-ring flange-type unions, and heavy-walled tubing is preferred for high-pressure piping above a ¾-in. size on gate and valve hydraulic systems. For ¾-in. and smaller sizes, standard hydraulic tubing and O-ring-type connectors are preferred. A smooth inner wall free of mill scale is essential for hydraulic-system pipes. To ensure this condition and provide piping which is easy to clean, cold-drawn, seamless steel tubing is frequently used for fabricating socket-welded piping. Hydraulic systems should always be tested to the full rated design pressure to check for leaks.

The flow losses should be carefully calculated in hydraulic systems. Unless known conditions indicate otherwise, assuming an ambient temperature of 40 F and limiting losses to a maximum of 150 psi are recommended.

Electrical control equipment, such as motor starters, relays, and breakers, which may be subject to arcing must be physically separated in control cabinets from the hydraulic system and mounted in a separate compartment to avoid fire hazard. Where complete separation of electrical equipment, such as motors and pressure switches, is not feasible, special care should be used to minimize fire hazards. It is desirable to provide a 75- or 100-watt heater in the electrical compartment of the cabinet to prevent moisture from condensing on the electrical equipment. Operation of the typical system shown in Fig. 66 is fairly simple and only a few aspects need clarification. To open or close the gate, the pump motor is started and the solenoid-operated four-way valve is shifted. When the gate reaches the open or closed position, the rise in pressure will actuate the pressure switch and deenergize the electric circuit. The gate may also be stopped at any intermediate position with the stop push button.

The flow-control valve in the line to the bottom of the cylinder contains both a check valve and a pilot-controlled spool valve. When the gate is being opened, oil is pumped through the check valve to the underside of the piston. For closure under balanced-pressure conditions, no force is required to drive the gate leaf closed, and the weight of the gate leaf could cause a rapid outflow of the oil from the bottom of the cylinder. Under these conditions it is necessary to control the rate of outflow of oil from the bottom of the cylinder, so that the closure speed does not exceed the rate at which oil is being pumped to the top of the cylinder. This condition would result in flooding the oil tank. A controlled rate of closure is ensured by connecting the pilot line for opening the spool valve in the flow-control valve to the top of the cylinder. As pilot pressure to operate the spool valve and release oil from the bottom of the cylinder will not exist unless there is a positive pressure on top of the piston, any tendency of the gate to close faster than the pumping rate will cause the pressure in the upper cylinder to drop and close the spool valve. This feature ensures that the closure speed will be directly controlled by the pumping rate. This same basic arrangement is also used for preventing butterfly valves from slamming closed.

Means of venting all air from a hydraulic system is necessary to avoid erratic operation. In the general piping diagrams in Figs. 66 and 67 it will be noted that all the air vents are piped back to the oil tank. This arrangement is recommended as it is more convenient and positive than attempting to bleed air at open connections.

The basic features of the gravity-closing-type hoist are shown in Fig. 67. To open the gate, the oil pumps are started and the solenoid-controlled four-way valve is shifted so that the pump pressure under the piston will hold the remotely controlled bypass valve closed and cause the piston to rise and open the gate. When the gate is fully open, the pressure rise will actuate the pressure switch PS1 and deenergize the electric

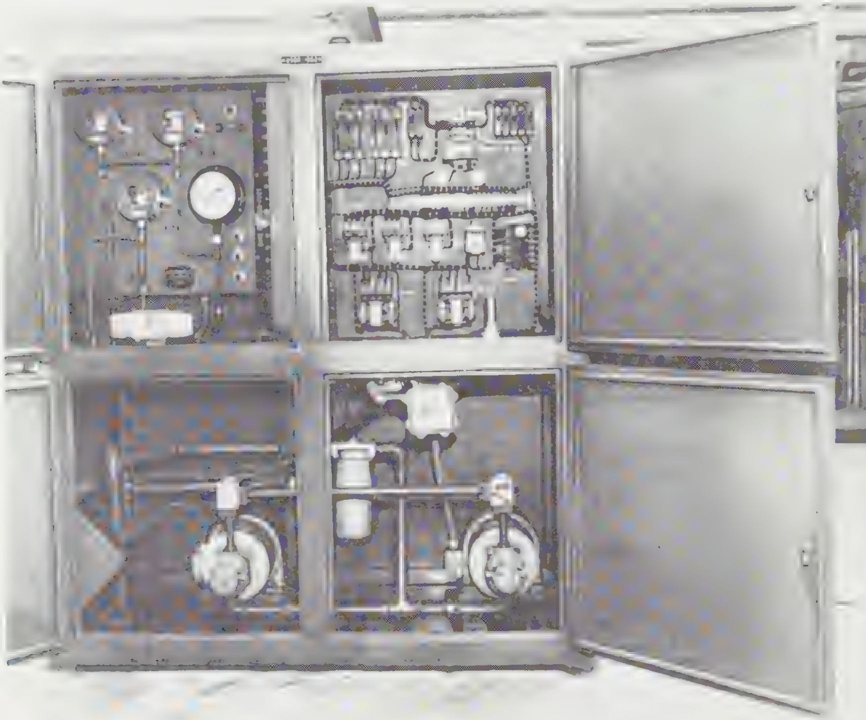

Fig. 69. Typical control-cabinet arrangement.

circuit. If leakage from under the piston allows the piston to lower enough that pressure is lost on the restoring-cycle pressure connection, pressure switch PS2 will restart the oil pumps and restore the gate to the fully opened position.

To close the gate it is only necessary to shift the solenoid-operated four-way valve for releasing the pilot pressure on the remotely controlled bypass valve. This action will allow oil to flow through the bypass line from the bottom to the top of the cylinder and cause the gate to close. The closure speed is regulated by the setting of the throttle valve. Normally closing speeds are set at 15 to 20 fpm.

With the gravity-closing system oil pumps are not required for closing and only shifting the four-way valve is necessary. In case of power failure the four-way valve can be readily shifted manually. These features permit gate closure with a complete loss of power and make the system ideal for guard gates. When used for penstock guard gates, the solenoid valve and emergency closing electric circuit are frequently powered by the 125-volt power-plant storage batteries to make the closure system completely independent of an outside source of a-c power.

36. Oils and Greases. The oil used in hydraulic systems should preferably be an oil specially compounded for such use. If hydraulic oil is not available, good-quality motor oils may be used. The use of high-viscosity oils should be avoided as the pressure losses in pumping heavy-bodied oil can be very high, especially at low temperatures.

Hydraulic oil which is specially compounded to inhibit rust formation, oxidation, and foaming should be used. Oils having the following physical properties have

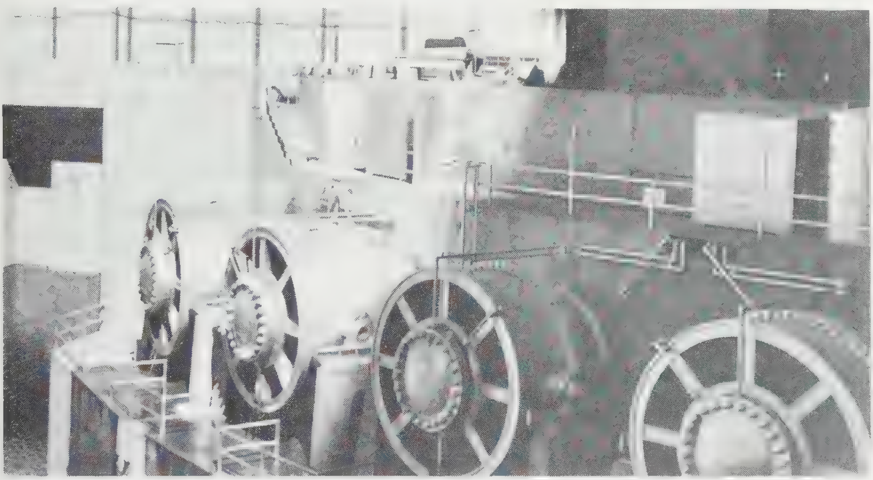

FIG. 70. 96-in. hollow-jet valves at Glen Canyon Dam in Arizona, showing control cabinets and piping for hydraulic operating systems.

proved satisfactory in a great many installations operating under widely varying ambient conditions:

Viscosity, SSU at 100 F	150 (approx)
Viscosity index	90 (min)
Pour point	−20 F

SAE 10W motor oil has viscosity and pour-point characteristics which are similar to those of this hydraulic oil and could be used as a substitute. In no case, however, should hydraulic and motor oil be mixed, and motor oil should not be used to replace small quantities of hydraulic oil which has leaked from a system.

The greases used for slide-gate seats and bearings on wheel-mounted gates and butterfly valves should be waterproof, calcium- or lithium-base types. The grease should be fairly soft, preferably National Grease Lubricating Institute Grade 2. Sodium-base greases should not be used for lubricating submerged bearing surfaces.

Hydraulic oils and greases having the properties specified can be obtained from practically all major oil companies. Such companies can also supply valuable information concerning special problems involving petroleum products.

37. Paints. The question of which paint is best for protecting gates and valves is subject to a wide variety of changing ideas, opinions, and answers. Most paints which are used have some desirable and some undesirable characteristics. No attempt will be made to discuss the pros and cons of the various paints which are available. To provide some guidance for consideration in the selection of paints, a brief summary of some commonly used paints and painting practices which have produced good results will be given.

A relatively small number of paint types have proved to be necessary for protecting gates, valves, and outlet conduits. These paints are of three basic types: red lead, vinyl resin, and coal tar.

Red-lead priming paints conforming to Federal Specifications TT-P-86c, Type II or Type IV[1] are widely used. Type II is used as a primer mainly on exterior surfaces which are subjected to normal atmospheric exposure and are not located in damp humid places. One or more coats of Type IV red-lead paint should be used as priming paint where exterior surfaces are located in highly humid atmospheres. Red-lead paints normally should not be exposed to sunlight without protective color coats. Several coats of Type IV paint have been used as the entire protection for continuously submerged surfaces, but other paints are normally preferable.

The vinyl-resin paints, VR-3 and VR-6,[2] have given excellent service. The VR-3 is nominally a three-coat system producing a 5-mil minimum dry-film thickness. The three-coat system may be used for atmospheric exposures and for painting the interiors of oil tanks and other surfaces in contact with oil. For surfaces which will have alternate or continuous submergence in fresh water, four coats should be applied to provide a 6-mil minimum dry-film thickness.

VR-6 paint is used for surfaces which are alternately exposed or submerged and for surfaces which require a smooth, durable paint coating. The minimum dry-film thickness for this system is 10 mils. The extra thickness and good abrasion-resistance characteristics of VR-6 paint provide a very durable coating, and make it a desirable paint to use where accessibility makes repainting difficult and costly. Typical applications in this category are wheel- and roller-mounted gates, gate frames, intermediate gate stems, and stem couplings. This paint is also used on the high-velocity conduits and the fluidway surfaces for hollow-jet valves. When used for high-velocity fluidways, the surface should be lightly sanded after the final coat to remove any roughness, laps, or slight protrusions which could start cavitation damage.

Coal-tar enamel conforming to American Water Works Association Standard AWWA C203 is frequently used as the interior coating for penstocks and outlet pipes. When properly applied to pipes which are located in suitable environment, coal-tar enamel provides excellent long-life protection.

When the enamel can be shop-applied by a spinning process, a glossy smooth surface having low hydraulic friction can be obtained. Because the enamel is thick and must be applied hot, smooth surfaces cannot be obtained by hand methods, nor can the enamel be readily applied to complex or irregular surfaces. Hand-applied coal-tar enamel should not be used in pipes where the velocity and pressure conditions are such that minor surface roughness might cause cavitation damage. Coal-tar enamel is commonly used in the higher pressure-gradient regions of outlet pipes. It is not used on gates or valves or on outlet pipes in high-velocity low-back-pressure regions. Enamel should not be used on pipe where temperatures above 150 F or below 0 F will be encountered.

Coal-tar epoxy paint conforming to MIL-P-23236, Type I, Class 2,[3] is widely used for painting all types of submerged metalwork. The paint is commonly applied by spray or roller. Two or more coats to produce a 16-mil or greater dry-film thickness are used. Coal-tar epoxy-painted surfaces should be protected from extended exposure to direct sunlight. This paint is generally used for painting ring-follower gates, slide gates, and other analogous types. It may also be used on wheel- and roller-mounted gates and other equipment provided direct exposure to sunlight will not occur. As coal-tar epoxy paint can be hand-applied to produce a fairly smooth coating as com-

[1] United States government specification.
[2] U.S. Bureau of Reclamation specifications.
[3] United States Military specification.

pared with hand-applied coal-tar enamel, it is frequently used in hand-painted regions of conduits to minimize surface roughness which might cause cavitation damage.

The preparation of surfaces for painting is of equal importance to the selection of good paint for long life. For all coatings on submerged surfaces, solvent cleaning, followed by blast cleaning to base metal using dry, hard, sharp sand or steel grit to produce a gray-etched surface, is mandatory. For Type II red lead the same preparation may be used but solvent cleaning, followed by chipping, scraping, wire brushing, or commercial-grade grit or sand blasting, is acceptable.

It is important to protect cleaned surfaces and apply paint before the surfaces become contaminated; otherwise recleaning must be performed. The surfaces must be free of moisture, and metal and air temperatures and other requirements recommended by the paint suppliers should be followed in applying paint.

The small additional cost that may be entailed in using top-quality paints and in applying the paints correctly on properly prepared surfaces will be repaid many times by reduced maintenance and equipment-damage expenses. Careful adherence to practices prescribed by recognized authorities is recommended.[1]

38. Operation and Maintenance. The keystone of proper operation and long service life of gates and valves is adequate inspection and maintenance. Because of the rugged nature of the equipment, the need for periodic inspections and maintenance is sometimes overlooked. With a proper schedule of testing, inspection, and maintenance the useful life of such equipment is practically unlimited. Without such a program, gates and valves can be junk in 30 to 50 years.

When gates and valves are installed, the operation should be carefully checked to be sure they work as intended. A schedule of testing should be established for checking the equipment periodically to be sure it continues to operate properly. The time interval for making such operational tests will vary with the nature, importance, and frequency of use of the equipment. Where no specific factors indicate otherwise, an annual operating check is recommended. It is also recommended that all gates and valves be given a full operating test after every major maintenance overhaul.

During initial operation of gates and valves the performance should be carefully observed to check for possible malfunctions. The parts of the gates, valves, and conduits which are visible should be checked frequently for any evidence of paint defects or cavitation damage. Any damaged areas should be repaired. The cause of cavitation damage should be removed. Careful checking during initial operation may save costly major repairs later.

No specific time interval for major inspection and maintenance work can be established for all cases, as there is a wide difference in the operation and characteristics of reservoir waters in different installations. Normally the period between major inspections and maintenance is about 10 to 15 years, but in some cases a shorter interval is necessary to avoid excessive deterioration. For this reason, scheduling the first major maintenance inspection is recommended after an outlet works has been in service about 5 to 7 years. On the basis of the condition of the outlet at the first inspection, a desirable interval for scheduling future maintenance of the equipment at a specific dam can be established.

At the first major maintenance inspection, arrangements should be made to have all parts and surfaces of gates and valves accessible for checking. Painted surfaces on all gates, valves, and conduits should be carefully checked for deterioration and damage. All moving parts, such as rollers, wheels, and gate seals, should be checked. Sliding surfaces on gate stems and seal seats should be inspected for deposits of scale from

[1] "Paint Manual," U.S. Department of the Interior, Bureau of Reclamation. "Steel Structures Painting Manual," vols. I and II, Steel Structures Painting Council.

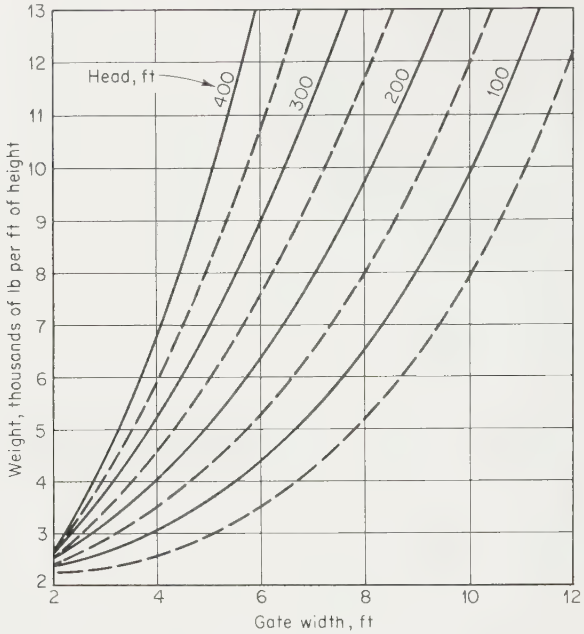

FIG. 71. Weight-estimating curves for welded-type slide gates.

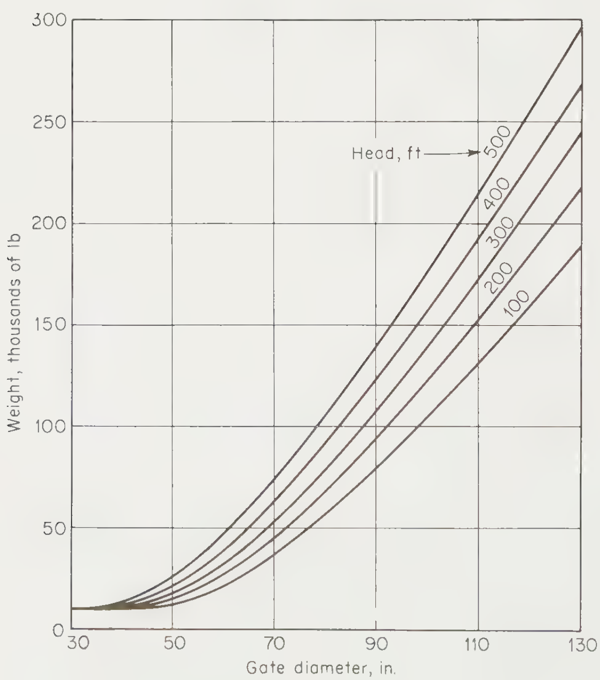

FIG. 72. Ring-follower and ring seal gate weight-estimating curves.

the water. The normally inaccessible regions around regulating gates and valves should be checked for cavitation damage.

Damaged paint should be repaired, or the surfaces should be completely repainted if necessary. Any other necessary repairs should be made. A careful record should be kept of all repairs for future reference and for establishing a periodic maintenance schedule.

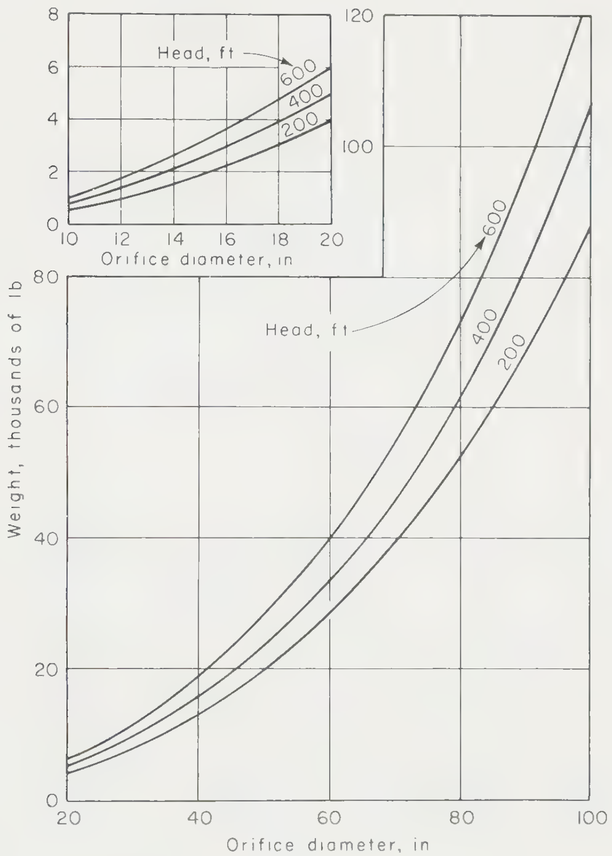

FIG. 73. Jet-flow gate weight-estimating curves.

39. Weight Estimates. Weight-estimating curves for various types of gates, valves, and associated equipment are shown in Figs. 71 through 79. These curves do not cover all types of gates and valves, and are based primarily on Bureau of Reclamation designs. The equipment produced by other design and manufacturing organizations may vary considerably from the weights shown on the curves. Despite the variations which may exist, these curves do provide a consistent basis for making comparative estimates when various types of equipment are being considered in the design of an outlet works. Although the accuracy of the curves is sufficient to provide a valid comparison between types of equipment, the curves should not be used when precise estimates of actual weights are necessary. Precise weight estimates can be

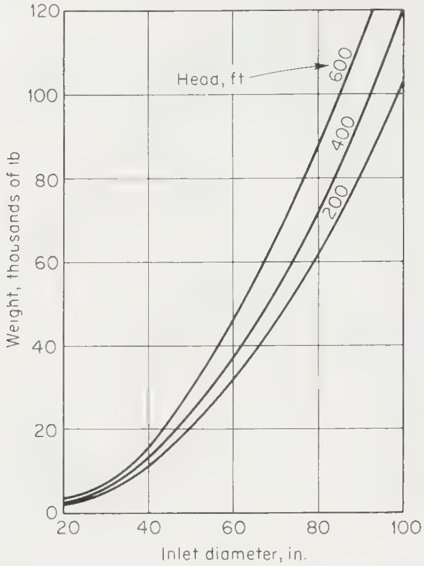

FIG. 74. Hollow-jet valve weight-estimating curves.

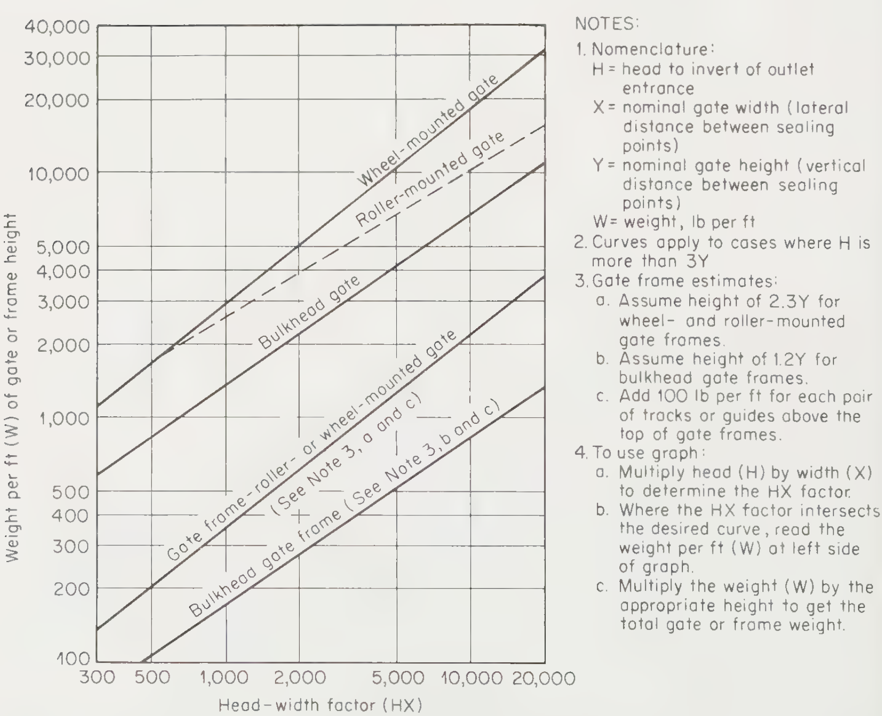

FIG. 75. Gate and frame weight-estimating curves for wheel-mounted, roller-mounted, and bulkhead gates.

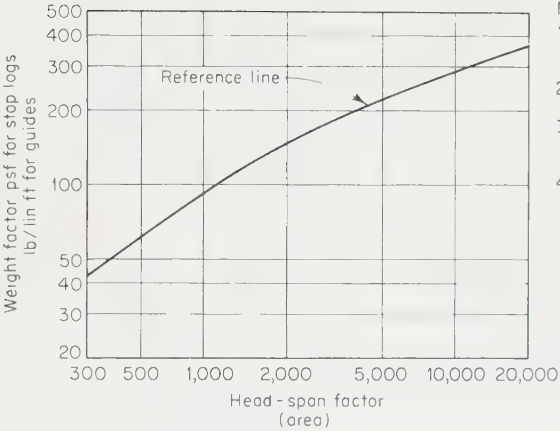

NOTES:

1. Weight data applies to cases where stop logs are placed from the outlet to the top of the dam.
2. Curve applies for slopes of less than 10 deg from vertical
3. Use bulkhead gate data for weights of stop logs which cover only a submerged opening
4. To use graph:
   a. Multiply head to invert of outlet entrance by stop-log span to determine the head-span factor (Use this figure also as stop-log area.)
   b. Where the head-span factor intersects the reference line, read the weight factor at left side of graph
   c. For total weight of stop logs, multiply the stop-log area in square feet by the weight factor.
   d. For total weight of a pair of guides, multiply the length (head) in feet by two and by the weight factor

FIG. 76. Stop log and guide weight-estimating curve.

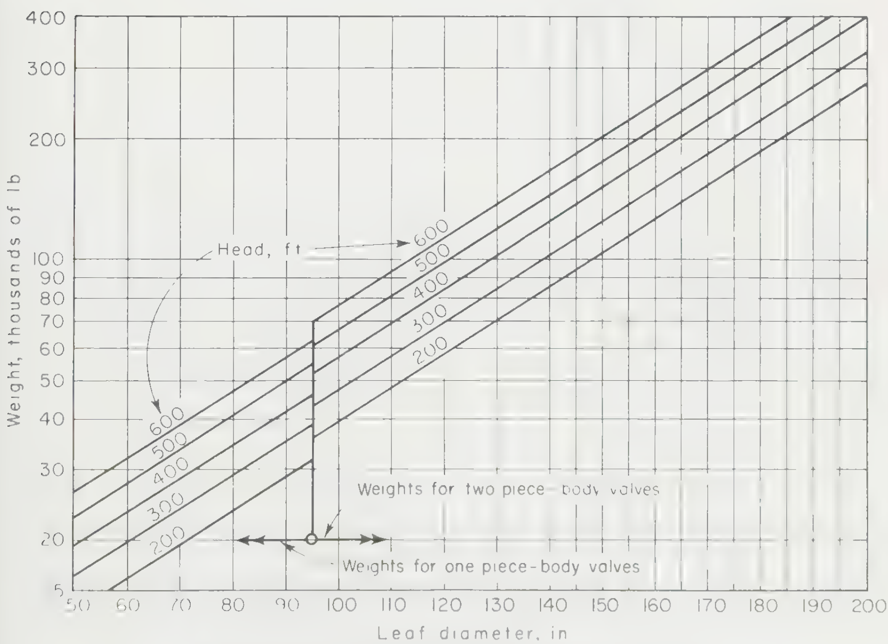

FIG. 77. Butterfly-valve weight-estimating curves.

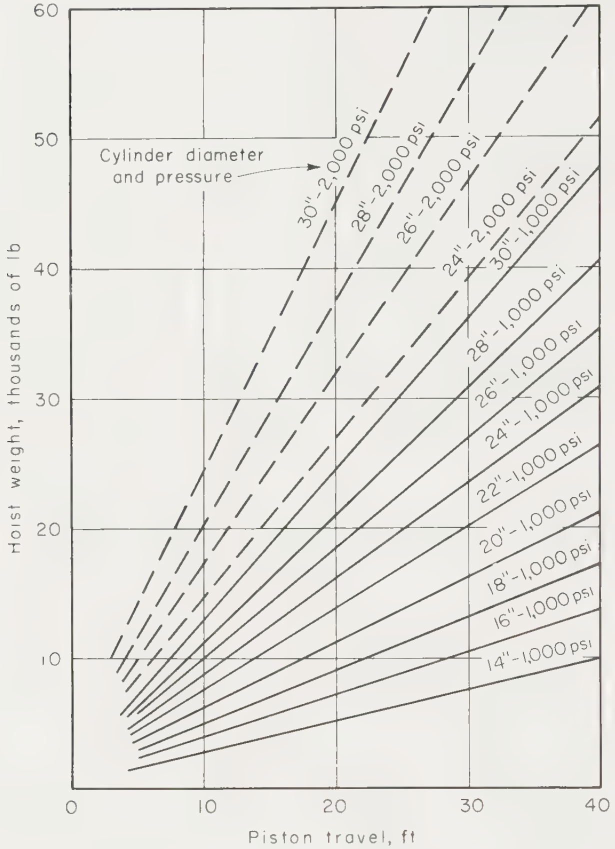

FIG. 78. Weight-estimating curves for intake-gate hydraulic hoists.

obtained only by carefully computing the weight of an actual design. In addition to the weight curves, tabulations of estimated weights are included for standard slide gates made from castings and for hydraulic control systems.

Estimated weights for standard cast-design slide gates, for 250-ft head, are shown in the following tabulation. The weights include the hoist but no upstream or downstream conduit.

Width*	Height	Weight	Width	Height	Weight
2.25	2.25	6,500	5.0	5.0	35,000
2.75	2.75	10,000	5.0	6.0	42,000
3.25	3.25	14,000	5.0	9.0	63,000
3.5	3.5	17,000	6.0	7.5	58,000
3.5	6.5	30,000	6.5	8.0	65,000
4.0	4.0	25,000	6.5	10.0	80,000
4.0	5.0	28,000			

* Width and height in feet, weight in pounds.

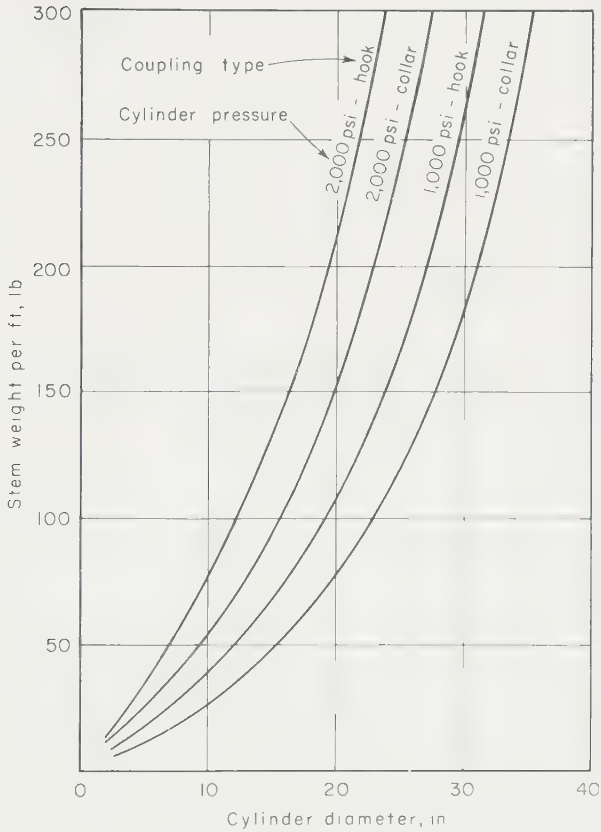

FIG. 79. Intake-gate stem weight-estimating curves.

For hydraulic operating systems having dual pumps and control components housed in a cabinet, the following tabulation of estimated weights may be used, provided the control cabinet is located reasonably close to the hoist and the hoisting speed is about 1 fpm. For remote cabinets additional piping weights must be added.

Cylinder diam, in.	Weight, lb	Cylinder diam, in.	Weight, lb
12	1,800	24	3,000
16	2,200	27	3,500
20	2,600	30	4,000

REFERENCES AND ACKNOWLEDGMENTS

A limited number of basic references have been cited in this section. No bibliography has been included as the many new developments in engineering tests and research would render any bibliography incomplete within a very short time. The best sources for obtaining current technical data and references are the Hydraulics

Division publications of the American Society of Civil Engineers, 345 East 47th Street, New York, N.Y. 10017; the Department of the Army, Office of the Chief of Engineers, Washington, D.C.; and the Bureau of Reclamation, Denver Federal Center, Denver, Colo. 80225. Computerized information retrieval will undoubtedly become the prime method of securing pertinent reference information within a few years. The Water Resources Scientific Information Center, Office of Water Resources Research, Washington, D.C., established in 1967, will provide a central source for references in the water-resources field when it becomes fully developed with a data bank responsive to detailed search questions.

Appreciation is acknowledged to the late Phillip A. Kinzie, who wrote the section "High-pressure Outlet Works" for previous editions of this handbook. Sincere thanks are due to the Bureau of Reclamation for the facilities afforded in the preparation of this section. All drawings, photographs, and illustrations are reproduced by courtesy of the Bureau of Reclamation, except where credit is otherwise specifically given. Thanks are due also to many individuals for their contributions, and especially to H. E. Sheda, W. E. Wagner, and E. E. Gonzales for their counsel and assistance.

SECTION 23

FISHWAYS AT DAMS

By R. Banys and K. R. Leonardson

GENERAL

1. Introduction. Fishways in dams or other hydraulic structures have a long history. Several hundred years ago, European engineers were designing fish-passing facilities as an integral part of dams, thereby recognizing the importance of conserving the salmon by allowing them to continue their upstream passage to their spawning grounds.

Many states and countries have passed conservation laws protecting the anadromous fish whenever a dam is constructed. In the United States, the dams authorized under license by the Federal Power Commission may be required to provide fish-passing facilities. Where this requirement is part of the license, the design of the fish facilities and their operation will come under the control of Federal and state fisheries. Dams not licensed may also be required by state or local government authority to provide fish facilities. The layout, design criteria, and all features of the facilities will therefore be reviewed and subject to approval by governmental agencies. In many cases hydraulic-model testing is required to demonstrate the performance of proposed fishways.

2. Migratory Characteristics. In order to understand better how fishways are designed, it is well to know the life cycle of the migratory Pacific salmon.

Fully grown salmon, after spending 3 to 4 years in the ocean, return to the river or stream of their origin to spawn. These fish cease feeding upon leaving salt water. During the journey upstream to their spawning grounds, they live on the food that has been stored in their bodies in the form of fat. Some salmon travel hundreds of miles to reach their destinations. As they ascend their chosen river or stream, they may pass rapids, falls, and manmade fishways in dams, until they reach the place their migratory instinct tells them is the right spawning ground. There, the females with their tails dig nests in the gravel and deposit their eggs. Males immediately fertilize them with a sperm-bearing liquid. Soon after that, the adult salmon die. For periods ranging from a few months to a year, depending upon the species, the young salmon start their downstream migration to the ocean. After maturing in the ocean, they return to the stream or river of their origin.

3. Types of Fish-passing Facilities. There are many types of fish-passing facilities constructed to enable migrants to travel either downstream or upstream past hydroelectric plants or natural river barriers. These facilities can be divided into two major groups: upstream and downstream migrant-passing facilities.

Upstream migrant-fish-passing facilities consist of the following types of fishways: fish ladders, fish locks or elevators, tramways, and trapping and trucking arrangements.

To provide a safe passage downstream for the young migrating fingerlings across higher-head dams, several types of fish-passing facilities are in use. These facilities, in general, tend to collect the migrants in the forebay for safe passage to the tailrace.

These facilities include fine-mesh screens of fixed or traveling type used to direct the fingerlings to a safe bypass system, louver deflectors, air bubblers, electrical fields, skimmers, and floating "gulpers."

The above-mentioned upstream and downstream migrant-passing facilities do not include all the existing types of passing facilities. Only the most commonly used facilities are mentioned.

UPSTREAM PASSING FACILITIES

4. General. Upstream fish-passage facilities are constructed to enable migratory fish, especially anadromous species, to travel past dams or natural obstructions in rivers. They are also installed near artificial propagation facilities, such as hatcheries and spawning channels, for the purpose of collecting and transporting the fish to these facilities.

The need for upstream passage of anadromous fish is to permit them to migrate to those areas of a river where they spawn. The most valuable fish of this type is the salmon. Facilities intended for this species of fish and the steelhead (a rainbow trout which migrates to the sea) will be described in this section.

Fish ladders are probably the most important and most used method to provide an artificial upstream fish passage. Their design is based on a fundamental characteristic of upstream migratory fish, which is to swim against the current of flowing water. They have been constructed at dams where great numbers of fish pass. The most elaborate system of fish ladders exists at nine dams on the Columbia River in the Pacific Northwest of the United States.

A great deal of research on fish passage in ladders and attraction to them has been done and is continuously in progress. Fish-ladder design at present is still in a stage of development. Over a period of a few years certain design concepts have changed. Experience with operating ladders has also contributed very much to the planning and design of fish facilities. It is important, in fact absolutely necessary, to make use of such research and experience in design of ladders in order to obtain successful fish passage.

5. Components. Fish ladders consist of several components. The basic components into which a fish-ladder system may be divided are (1) fish entrance, (2) fish passages, (3) fish exit, and (4) auxiliary water supply. The last of these, auxiliary water supply, has been omitted at some fish ladders. All the modern, large fish ladders on the Columbia River have very extensive provisions for auxiliary water supply.

6. Fish Entrances. Fish entrances are basically openings through which water is discharged, generally under a head of 1 ft, in order to attract fish into the ladder or a collection channel.

Three basic types of entrances are in common use. These are (1) weirs, (2) orifices, and (3) slots.

The weir entrance consists of a steel gate automatically controlled to follow tail-water fluctuations. Usually the depth of water flowing over the weir gate will be 6 ft. The width of the weir will depend on the number of fish to be passed and may be as wide as 15 ft. Several weirs may be needed at a single ladder entrance in order to obtain a directional effect from the attraction water discharged. The discharge over the weir may be assumed to be flowing at an average velocity of 4 fps when a 1-ft head is maintained at the weir. Therefore, a 15-ft-wide entrance with a 6-ft depth of flow would require 360 cfs (Fig. 1).

An orifice entrance also consists of a steel gate automatically controlled to maintain its top above the water surface. The orifice, usually of rectangular shape, is submerged. The orifice should be a few feet below the tail-water surface. This type of entrance is used in the powerhouse collection systems in hydroelectric plants on the Columbia River. Two orifice entrances have been installed above the draft tubes of each unit at Priest Rapids and Wanapum dams. It has been found that this type has effectively attracted fish. The common orifice-entrance discharge is 60 cfs under a head of 1 ft.

A slotted entrance consists of a vertical slot through which water is discharged, usually under a 1-ft head. With rising tail-water levels an increasing flow of water has to be provided, because of the increase in area of flow. The width of the slot is sometimes made variable, although parallel sides are also effective, and is based on the number of fish to be passed. The smallest slot to be effective for salmon would probably be 1 ft wide where few fish are to be attracted. A more usual design would be about 4 ft wide (Fig. 2).

Fig. 1. Priest Rapids, weir fish entrance.

The fish entrances described above are obviously the openings through which the fish are attracted into the entrance structure. The fish must then proceed into the ladder or a transportation channel leading to the ladder. The entrance structure must serve another purpose, however. In a facility of modern design, far more water is discharged through the entrance openings to attract fish than is required for the fish ladder. The difference between these two flows must be provided in the entrance structure. This flow is called the auxiliary water supply. It may be taken from headwater and flow by gravity through a conduit leading into the entrance structure. Another method used either by itself or in addition to a gravity system is to pump water from the tailrace into the entrance structure. These auxiliary water systems are described in Art. 9.

The method of addition of auxiliary water into the entrance structure is quite important. The two primary objectives to be attained are the proper placement and diffusion of the water into the entrance. Diffusion of the water is accomplished by the use of chambers in the floor or walls or by a combination of both. These diffusion chambers are located at the outlet of the auxiliary water-supply conduits. Extensive hydraulic-model testing has been done in order to ensure that the velocities at the outlets of the chambers are very nearly uniform. These studies have led to practically standard designs. Gratings are placed at the outlet surface of the diffusion chamber to prevent fish from entering. They also provide more uniform flow distribution. The velocity through the gross area of the floor gratings is usually limited to 0.25 to 0.50 fps and the wall gratings to 0.50 to 1.0 fps. These low velocities generally eliminate any tendency toward fish attraction. The spacing of grating bars should provide a clear opening of 1 in. Smaller openings would cause clogging by debris, whereas larger openings may cause the risk of fish entrapment or less uniform velocity distribution.

7. Fish Passages. At hydroelectric plants the fish passages consist of collection and transportation channels and the fish-ladder channel, which contains weirs or baffles.

The collection channel in a powerhouse is located above the draft tubes and receives the fish that pass through the entrances. Water supplied to the collection and transportation channels is generally sufficient to maintain a velocity of 2 fps in order to

FIG. 2. Wanapum, slotted fish entrances.

induce fish to travel up the channel. Diffusion chambers are required in collection channels to supply water for the fish entrances. Each orifice entrance discharging 60 cfs needs a diffuser with a gross area of grating of 240 sq ft (assuming mean velocity 0.25 fps through grating). The collection channels in the Priest Rapids and Wanapum powerhouses are 15 ft wide. The minimum water depth in channels of this type is 6 ft (Fig. 3).

Fish ladders of many variations have been constructed and model-tested. The best type to adopt for a specific installation depends on many factors and must be given careful consideration. There exists no one type which is ideal for use at every situation.

Some of the variables in ladder designs are the following:

1. Dimensions, width and depth
2. Slope

Fig. 3. Priest Rapids powerhouse, fish-collection channel.

3. Type of baffle, weir or vertical slot
4. Construction material

Examples of a few fish ladders for passing Pacific salmon and steelhead are given below.

Dam	Width, ft	Slope, horizontal to vertical
Bonneville	2 at 40 and 37 ft	16:1
Dallas	24	16:1
John Day	30	16:1
McNary	30	20:1
Priest Rapids	20 and 16	16:1
Wanapum	16	10:1
Wells	12	10:1

The slope on ladders at the newer dams has been increased to 10:1 from that used at older dams of 16:1. It appears that the steeper slope does not adversely affect fish passage.

Weirs are constructed across the fish-ladder channel, and the water-surface drop at each weir is generally 1 ft. The lower weirs will become submerged during periods of high tail water. When this occurs, additional water must be added in the lower portion of the ladder in order to provide velocities adequate to induce fish travel. This additional water is supplied by the auxiliary supply system through diffusion chambers in the lower portion of the ladder.

Orifices are provided in weirs, and nearly all the fish swim through them. This is preferable because it reduces possible injury to fish jumping weirs and probably requires a smaller expenditure of energy by the fish.

Newer designs of ladder weirs have baffles on the crest which reduce the overflow width of the weir. Earlier weir designs had an overflow crest extending across the entire ladder channel. The weir with baffle was developed by the U.S. Army Corps of Engineers for the Ice Harbor Dam fishway on the Snake River. Its hydraulic

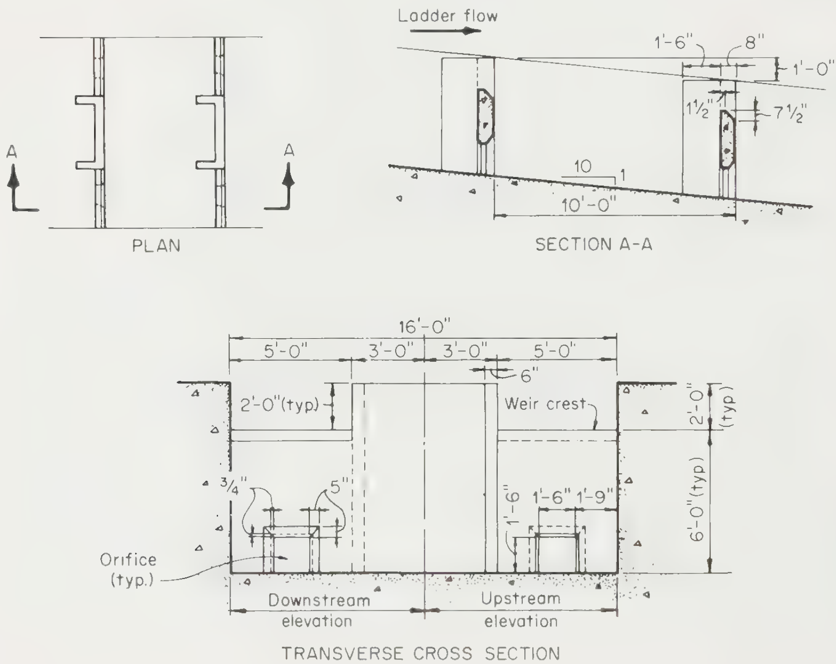

Fig. 4. Typical weir used in the fish ladder at Wanapum Dam, Columbia River, Washington.

characteristics have been advantageous, and this type of weir has been used at Wanapum and other dams (Fig. 4).

The discharge over fish-ladder weirs where the water differential is 1 ft is very close to 4 cfs/ft of weir. The discharge through the orifice in these weirs may be determined by assuming a coefficient of discharge of approximately 0.8 (Figs. 5 and 6).

8. Fish Exits. The fish-ladder exit is the upstream section of the ladder where fish leave the ladder and enter the reservoir of a dam. The exit section is designed to perform the following functions: (1) to admit the correct discharge of water for the fish ladder, (2) to maintain this correct discharge during fluctuations of headwater levels, and (3) to protect the fish ladder from large debris by installation of trash racks. It has been found that a 6-in. spacing of rack bars does not impede fish travel.

Two devices used to control the intake of water through the fish exit section are orifice walls and tilting weirs. The fish ladders at Priest Rapids and Wanapum dams have the orifice-wall system, and their performance has been good as well as economical. The orifice-wall concept is a fairly new development that probably originated in the Ice Harbor fish-facilities design by the U.S. Army Corps of Engineers. The purpose of these two systems is to maintain a constant discharge for the fish ladder when the headwater pool is fluctuating.

The orifice-wall system consists of a series of fixed walls across the fish channel. Each wall has two orifices large enough to discharge the entire water requirement of the ladder section under the maximum head differential across each wall which will occur under the maximum headwater level. It is assumed that the differential, under any conditions, is equal at each wall. When the headwater level is less than maximum, the head differential is also reduced across each orifice, which causes a deficient discharge. The deficiency is made up by drawing water from the reservoir through a conduit and discharging it through a diffuser immediately downstream of the last orifice wall above the fish-ladder weirs. The "make-up" water supply varies from

FIG. 5. Priest Rapids, right-bank fish ladder.

zero at maximum headwater to its maximum at low headwater. It is desirable to regulate this "make-up" flow by use of an automatically controlled valve.

The tilting-weir scheme has been installed at the McNary Dam. This system consists of weirs that are adjustable either manually or automatically to control the flow for the fish ladder as the reservoir level changes.

9. Auxiliary Water Supply. The purpose of auxiliary water supply is to provide water in addition to the flow down the ladder, in order to attract fish into the entrances, and also to induce them to swim up the deeply submerged collection or transportation channels. The addition of this water supply has been briefly described in Art. 6.

A characteristic of auxiliary water (also called attraction water) is that the demand increases with rising tail water. This is partially due to greater water depths in the fish-transportation channels. Greater discharges are also required by the entrances.

As mentioned previously, the two methods used to obtain auxiliary water are pumping from the tailrace and gravity flow from the headwater. The use of water supplied from headwater for large attraction discharges is economically justifiable only during periods of spill. The expenditure of energy to pump auxiliary water is less than the energy lost by discharging an equal flow from headwater. In many fish facilities it is only necessary to pump the auxiliary water about 6 ft above tail water.

Two types of pump drives have been used for the auxiliary water-supply pumps, electric and hydraulic-turbine-driven. In the latter, a small discharge from headwater runs the turbine, which in turn operates an axial-flow pump. Automatic controls, based on tail-water level, may be used to control the pumps.

The distribution of water into a transportation channel and an entrance structure is accomplished by the use of either gates or valves or fixed overflow weirs, sometimes called chimneys. These weirs, set at graduated levels, feed variable discharge into the ladder with varying water depths.

10. Fish Locks. The main use of fish locks is in Scotland and Ireland for passage of Atlantic salmon. A few fish locks have been constructed within some of the Columbia River dams; however, their use has been discontinued. Apparently the fish ladders also constructed at these dams handle fish passage more capably. This is probably because of the enormous fish run in the Columbia River.

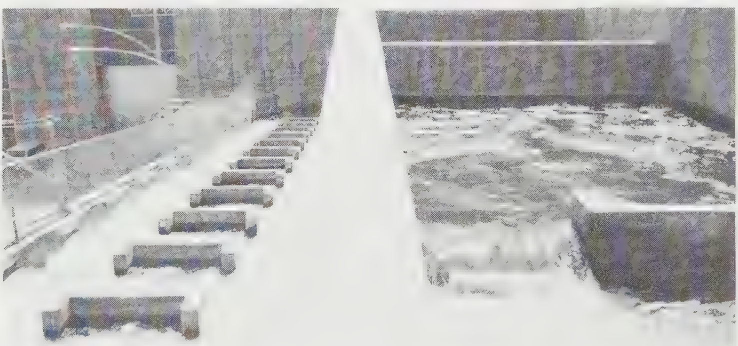

Fig. 6. Wanapum, left-bank fish ladder.

The construction of fish locks in small rivers under certain circumstances may be more economical than fish ladders. There is not complete agreement, however, that the two would be of equal efficiency in fish passage. The success of locks with Atlantic salmon does not imply an equal success with Pacific salmon.

The method of operation of fish locks is somewhat similar to navigation locks, with the exception that flow is maintained to induce fish into the chamber and out of it. Water is discharged through the chamber into tail water in order to attract fish into the lock. Then, the lock chamber is filled and the fish are induced to swim out into the reservoir by flow through the exit. Flow through the lock can be accomplished by the use of bypass pipes. The cycle is then repeated. The time for each cycle is variable. The success of the fish lock at a specific installation would depend on operating experience.

11. Mechanical Methods of Fish Transportation. At dams in excess of 100 ft in height, the use of fish ladders is generally neither economical nor practical. In such cases, other means are used for fish passage: tramways, cableways, or tank trucks. A pipeline can also be used in combination with a tramway.

Fish are carried in hoppers by tramway or cableway. The installation is designed so that fish swim into the hopper. The hopper is then transported to the reservoir or may be unloaded into a tank truck.

Tank trucks are used to convey fish to either the reservoir or a hatchery. The water in these tank trucks is aerated and may be refrigerated. The unloading device requires careful design to avoid injury to ripe female fish.

12. Fish-barrier Dams. Fish-barrier dams are low weirs constructed across rivers to stop the upstream migration of fish. Immediately downstream of the weir a fish-entrance structure is located in a manner to attract fish. These fish will then be induced to swim into a fish ladder or hopper pools for eventual transport by tank trucks. A fish ladder of this type, for example, leads the fish directly to Cowlitz Salmon Hatchery 1½ miles downstream of Mayfield Dam in Washington.

The design criteria adopted for the fish barrier at the Cowlitz Salmon Hatchery were as follows:

1. The height of the weir crest above tail water should not be less than 4 ft up to certain river discharges.
2. The differential between headwater and tail-water levels should not be less than 8 ft up to certain river discharges.
3. Electrified field should be provided to prevent fish migration past the barrier dam.

In some cases the headwater to tail-water differential is set at a 10-ft minimum. On the Baker River in Washington, a fish barrier has been constructed with a weir crest adjustable in height.

DOWNSTREAM PASSING FACILITIES

13. General. The protection of the seaward-migrating salmon from the spillways and turbines of high-head dams has become one of the most difficult problems to solve. Extensive studies have been made and are still being continued to find positive ways of deflecting or collecting these migrants in the forebay for a safe passage to the tailrace. Several methods, with varying degree of success, have been used in deflecting these migrants, the commonest of which are screens and louvers.

At low-head dams it is unnecessary to divert them away from spillways and power intakes, and they are allowed to pass with comparatively low mortality.

14. Screens. Various types of screens have been used in small hydroelectric plants, irrigation canals, or water-supply projects to divert or deflect the downstream migrants into a safe bypass. Some of them proved to be impractical because of large maintenance and operating costs or impingement of fish on the screens, others because of various biological reasons. Usually, screens should be used only where the flows in the river, creek, or canal are comparatively small.

Until further studies and research prove it otherwise, no attempt is being made to install screens in the forebays of large dams. To exclude the fingerlings from the intakes or spillways of large dams, it would be necessary to utilize fine-mesh screens, maintaining them clean and providing the required screen area and approach velocities. Because of this large capital investment and the operating and maintenance costs involved, these types of facilities become economically prohibitive and are not being constructed on a large scale.

Fish screens of many different types are being used today to deflect, divert, or screen the migrants within the small hydraulic structures. Some projects utilize fixed vertical wire-mesh screens. In this case it is advantageous to provide a duplicate number of screens and slots for screen installation. When the screen panel becomes plugged, a second panel is installed and the plugged panel is removed to be cleaned with a high-pressure water jet.

Another type of screen used is the rotating-drum screen. This type of screen is mostly used in irrigation intakes. However, in the Priest Rapids spawning channel rearing-pond control structure, a drum screen of 6 ft 0 in. diameter is operating to screen the fingerlings out of the 25-acre rearing pond. The same purpose will be served by the same size of screen for the city of Tacoma's large steelhead rearing pond near the Mossyrock Dam on the Cowlitz River. These wire-drum screens are self-maintaining. Floating debris is carried by the rotating drum and deposited downstream of the screen. On the White River in Washington, screens of 14 ft diameter are used for fish diversion.

Moving screens of the vertical type are being used in water-supply intakes. They are usually of standard design, consisting of an endless belt of wire-screen panels traveling upward on the upstream side and downward on the downstream side, and are manufactured commercially. Three screens of such type have been installed in the Cowlitz Salmon Hatchery pumping-plant intake for flows up to 200 cfs.

Within the last several years screens of the perforated-plate type have been used to screen the fries or fingerlings quite effectively. In the Priest Rapids spawning channel, two perforated-plate screens, called "inclined planes," with hole openings of $\frac{3}{16}$ in. diameter spaced $\frac{19}{64}$ in. on center, have been operating successfully for flows up to 100 cfs. Another has been installed in the city of Tacoma Swofford Valley rearing-pond control structure, to handle flows up to 25 cfs.

One of the most important aspects in fish-screen design is the approach-velocity criterion. To allow fish either to swim across the screen or not to become impinged upon it, low approach velocity must be maintained. Where rotating screens of drum or vertical type are used, this becomes especially important. If the approach velocity is too high, these migrants, upon contact with the wire screen, could be carried over the top of these rotating screens. For the self-cleaning type of screen such as drum or vertical rotating screens, approach velocity should not exceed 1.5 fps.

15. Louvers. A louver diverter or deflector is a fairly new concept used for downstream-migrant collection. It was developed and improved within the last 15 years by J. E. Kerr of Antioch, Calif., D. W. Bates of the U.S. Fish and Wildlife Service, and R. Vinsonhaler of the U.S. Bureau of Reclamation. A louver deflector does not physically prevent entry of fish but only discourages them from entering. It consists of vertical, flat-plate steel bars, spaced at intervals of 2 to 4 in. apart, aligned at a very acute angle (10 to 15 deg) to the direction of flow with the exception of the flow through the bypass. The individual bars are aligned perpendicular to the flow. The water flow passes between the individual bars. The migrants, however, tend to avoid them and follow the line of the louvers and are diverted into a bypass opening at an apex of the louver angle that is connected to either pipes or conduits. Confined to a very small flow quantity and isolated from the main flow, the migrants can easily be diverted by pipes or other means into the tailrace.

Louvers have been constructed and are operating in several installations within the United States and Canada with varying degrees of success. The first large-scale installation for flows up to 5,000 cfs occurred at Tracy, Calif., in the Delta-Mendota Canal. In this installation efficiencies of 93 to 100 percent were achieved by deflecting fish safely into the bypasses. At the Gold Hill hydroplant on the Rogue River in Oregon, louvers were arranged in inverted V pattern, with bypasses placed at the tip of each V. These louvers handle approximately 1,500 cfs flow. This design has an advantage of compactness and probably lower initial construction cost. A similar type of installation has been operating at the city of Tacoma Mayfield Dam power intakes on the Cowlitz River. These louvers were designed to divert fish into the bypasses for flows up to 12,000 cfs.

Other louver installations occur at Puntledge River in British Columbia, Maxwell Irrigation Canal in Umatilla River, Oregon, and Robertson Creek on Vancouver Island, British Columbia.

From tests conducted on existing louver installations and from past operating experiences, it can be stated that louvers are not able to divert the migrants with 100 percent efficiency and that minor migrant losses could therefore be expected.

In louver operation one of the most serious problems involved is trash. Large debris can be intercepted by upstream trashracks, but small trash such as leaves and weeds generally collects on the louvers and requires frequent maintenance.

ARTIFICIAL METHODS OF PROPAGATION

16. General. Experience has shown that the survival rate of eggs deposited under natural conditions is extremely low. Mortalities may be caused by either incomplete spawning of females, flash floods, inefficient fertilization of eggs, pollution, predatory birds, or animals, and even cold weather. Methods, therefore, were sought by biologists and engineers to increase the survival rate by artificial means, such as utilization of hatcheries and, within the last decade, use of artificial spawning channels.

17. Hatcheries. Throughout the world hatcheries for various species of fish are in existence. This section, however, will deal only with salmon hatcheries operating in the Pacific Northwest.

Salmon migrating upstream to spawn are trapped at the hatcheries and kept in the holding ponds until they become sexually mature. Their eggs are stripped, fertilized, and placed in incubation troughs containing clear flowing water. After the eggs hatch and the yolk sac is absorbed, these fries are placed in the rearing ponds, where they remain and are fed until released for seaward migration.

To obtain significant results in the fry production, many facets of hatchery operation have to be considered. Good water quality may control hatchery production. The dissolved oxygen content of the water must satisfy the biological requirements. If the water supply contains supersaturated nitrogen, artificial means should be used to eliminate it. Water-temperature requirements should range between 45 and 60 F, as the lower and upper limits.

Dietary requirements for hatchery culture also play a significant part in the success of rearing fry. It has been found that hatchery-fed fish are chemically different in the natural environment and somewhat less able to survive than wild fish. Therefore, experimenting and research still remain to be done regarding dietary foods for artificial rearing of fish.

Artificially raised salmon are also subject to a wide range of diseases. The majority of these diseases occur in water temperatures around 60 F or higher. "Warm-water" disease, known as columnaris, is quite prevalent and is a major problem on the Columbia River fish runs. Others, such as bacterial gill disease, tuberculosis, and external and internal protozoan diseases, are common among hatchery-raised fish. Methods of combating these various hatchery diseases are only partially effective, and much has to be done to find means of controlling them.

Generally speaking, fish reared in hatcheries are less able to survive in nature than wild fish. However, since larger numbers of young fish are released from hatcheries, even with their high mortality rates the total production as a whole increases. Hatcheries can be used as natural-production substitutes on rivers or streams supporting small salmon migrations and where rearing and spawning areas available are limited.

18. Spawning Channels. Within the last decade, spawning channels have shown promise as a method for artificially increasing the salmon production. It is believed that fry produced in the spawning channels are as viable as the ones produced in nature.

In the spawning channels, the fish spawn, incubate, and emerge into fries naturally. Environmental conditions within the channel, however, are improved and more stable than in nature. Resembling natural streams, these channels are constructed such that spawning gravels are of only certain graded size; velocities, depths, and flow quantities are stable and considered optimum for spawning and egg incubation. Criteria used in designing fall chinook salmon-spawning channels are as follows:

1. Spawning-channel bottom area should provide approximately 60 sq ft per pair of fish.
2. Width of channel should be in the vicinity of 25 ft.
3. Average channel velocity should be held at 2.3 fps.
4. Minimum water depth over spawning gravels should be 1 ft 6 in.
5. Minimum depth of spawning gravels should be 2 ft 6 in.
6. Provisions should also be made to incorporate, within the channel, fish resting pools at approximately 250- to 300-ft intervals. The resting pools should be designed to control water-surface elevations of the channel.

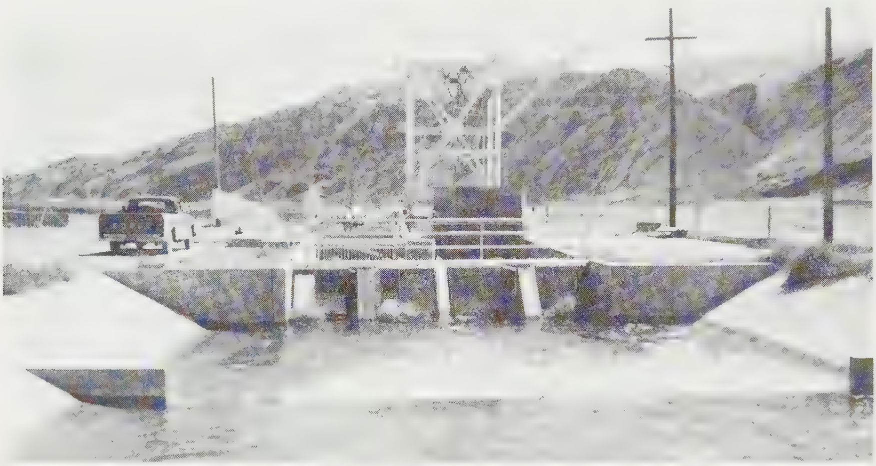

Fig. 7. Priest Rapids spawning channel fish-sorting facilities.

7. Minimum and maximum flows required in the channel are 25 to 100 cfs, respectively.
8. The holding pool should be sized assuming 20 cu ft of volume per fish.

The above-mentioned criteria were obtained from the Washington Department of Fisheries and were used as a guide in designing the Priest Rapids fall chinook-spawning channel on the Columbia River, constructed between 1963 and 1964.

Other existing and operating spawning channels are Jones Creek Channel, on the tributary of the Fraser River near Hope, B.C., the McNary Dam channel, Rocky Reach Dam channel, both on the Columbia River, and the Robertson Creek channel on Vancouver Island near Alberni. There are many other channels either under construction or operating in Oregon, California, and British Columbia.

Operation and maintenance costs of spawning channels in comparison with hatcheries are fairly low. Once the required flows within the channel are stabilized, little operation or maintenance is required. Most of the operating work is done during the periods of spawning and releasing of fry, where marking and counting of fries by weighing may be required.

One of the problems encountered in spawning-channel operations is silting up of spawning gravels. Silt could deposit by either flooding, bank erosion, or wind action. Egg-to-fry survival has definitely been adversely affected by these phenomena.

Occasionally, ice jams within the channel may block the flow through gravels, thereby impairing the chance of egg survival.

In maintaining silt-free gravels, one of the methods used has been a rake attached to a rubber-tired tractor. The tractor, traveling along the channel, lifts the gravels, and the channel flow washes the silt into the resting or control pools, from which it is easily removed.

Egg-to-fry survival in artificial spawning channels is showing promise of success. Also, from what has been known, fry produced by artificial channels are as viable as the ones produced in nature. It is possible, therefore, that the survival to the adult stage of fry produced in artificial channels might be greater than in hatcheries (Fig. 7).

SECTION 24

HYDROELECTRIC PLANTS

By J. C. Stevens and Calvin V. Davis

1. General. Sections 1 to 34, inclusive, are all more or less common to the subject of hydroelectric development. Multipurpose river-development projects may involve all water uses. Space requirements do not permit more than a broad treatment of hydroelectric-plant types with the approach made largely from the viewpoints of hydraulic design and project planning.

POWER FROM FLOWING WATER

2. Energy and Work. Energy is the capacity to perform work. It is expressed in terms of the product of weight and length. The unit of energy is the product of a unit weight by a unit length, *i.e.*, the foot-pound, the gram-centimeter, the kilogram-meter.

Work is utilized energy and is measured in the same units as energy. The element of time is not involved.

The energy of water exists in two forms; (1) potential energy, that due to position or elevation, and (2) kinetic energy, that due to its velocity of motion. These two forms are theoretically convertible one to the other. Energy may be measured with reference to any datum. The maximum potential energy of a pound of water is measured by its distance above sea level.

The potential energy of a given volume of stored water with reference to any datum is the product of the weight of that volume and the distance of its center of gravity above that datum. For example, a rectangular tank of water of 100 sq ft surface and 20 ft deep whose water surface is 100 ft above sea level has a potential energy of $100 \times 20 \times 62.5 \times 90 = 1{,}125 \times 10^4$ ft-lb. This potential energy cannot perform work until it is set in motion. If a stream flows out of that tank and connects with a pipe supplying water to a perfect turbine, $1{,}125 \times 10^4$ ft-lb of work may be performed by the turbine as the tank empties—the potential energy has been converted to kinetic energy.

3. Power is utilized energy per unit of time, or the rate of performing work, and is expressed in horsepower, 550 ft-lb/sec, or kilowatts, 737 ft-lb/sec. The power from the tank of the preceding example will be at a decreasing rate because the head and flow diminish as the tank empties. Assume the outflow for the first second is 100 cu ft. The surface of the tank would be lowered 1.0 ft, and the center of gravity (head) of that 100 cu ft is 99.5 ft. The energy utilized in this first second, therefore, is 621,000 ft-lb, or 1,130 hp.

Now assume that a stream flows into the tank as fast as it is drawn off—a constant discharge of 100 cfs may then be passed through the turbine under a constant head of 100 ft, for the surface is not lowered and a constant output of 625,000 ft-lb/sec may be realized from our perfect turbine, equivalent to 1,136 hp, or 848 kw.

The potential energy of a stream of water at any cross section must be measured in terms of power, in which time is an indispensable element. It is the weight of water passing per second $\times$ the elevation of its water surface (not center of gravity) above the datum considered. The kinetic energy of a unit weight of the stream is measured by its velocity. It must also be measured in terms of power since velocity involves time. It is the weight per second times the velocity head, *i.e.*, the height the water would have to fall to produce that velocity.

If the water of the preceding example were drawn off at a velocity of 10 fps, the surface elevation of the outlet channel would have to be $V^2/2g = 1.55$ ft lower than that in the tank in order to produce that velocity and the kinetic energy would be $6{,}250 \times 1.55 = 9{,}650$ ft-lb/sec. The total energy of a stream is the sum of its potential and kinetic energies. Thus the outlet stream has a total energy of 6,250 lb/sec $\times$ 98.45 = 615,350 potential plus 9,650 kinetic, or a total of 625,000 ft-lb/sec of total energy. At the perfect turbine, all the potential energy has been converted to kinetic energy and the velocity head is 100 ft.

Of course the perfect turbine does not exist. Some of the potential energy is converted into heat by friction and turbulence so that the useful part is less than the theoretical potential.

4. Energy Line. The energy head is a convenient measure of the total energy of a stream of constant discharge at any particular section. It is the elevation of the water surface, potential energy, plus the velocity head, kinetic energy, of a unit weight of the stream. Although every unit of the stream has a different velocity, that usually considered is the velocity head corresponding to the mean velocity of the stream.* If the stream is flowing in a pipe, the energy head is the elevation of the pressure line, or the height to which water would stand in risers, plus the velocity head of the mean velocity in the pipe.

A line joining the energy heads at all points is the energy line. The energy lines would be horizontal if the energy converted to heat were included. Energy converted to heat, however, is considered lost; hence the energy line always slopes in the direction of flow and its fall in any length represents losses by friction, eddies, or impact in that length. Where sudden losses occur, the energy line drops more rapidly. Where only channel friction is involved, the slope of the energy line is the friction slope.

Figure 1 illustrates the principles of the foregoing example. The potential energy head of the water in the forebay without inflow or outflow is that of the center of gravity Z. With inflow and outflow equal, however, the potential energy head is H. As the water passes into the canal, a drop of the water surface equal to the velocity head in the canal $V_1^2/2g$ must occur. At the entrance to the pipeline, an entrance loss h_1 is encountered as well as an additional drop for the higher velocity in the pipe. At any point in the pipeline, the pressure head h_p will be shown in a riser. The energy head at any point is the pressure head plus the velocity head, and the line joining the energy heads is the energy line. The energy lost (converted to heat) is the sum of friction, entrance, bend, and other losses in all the conduits, including the turbine and draft tube. The useful energy is that of the power developed by the turbine. The sum of the useful energy and the lost energy must equal the original potential energy.

* Owing to the variable velocity distribution, an energy coefficient should be applied to the velocity head of the mean velocity in order to determine the true energy head. That is,

$$H_e = C_e \frac{V^2}{2g}$$

If the velocity distribution is known, the energy coefficient may be found from

$$C_e = \frac{\int v^3\, dA}{AV^3}$$

where v is mean velocity through the elementary area dA and V is the mean velocity for the stream $= Q/A$. This coefficient is always positive. In straight conduits of established regimen, it may vary from 1.02 to 1.10; at bends or where otherwise disturbed, it may reach a value as high as 2.0 or greater. Because of the lack of knowledge concerning velocity distribution, it has generally been ignored.

5. The Bernoulli theorem expresses the law of flow in conduits. For a constant discharge in a closed or open conduit, the theorem states that the energy head at any cross section must equal that at any other downstream section plus the intervening losses. Thus above any datum

$$Z_1 + \frac{V_1^2}{2g} = Z_2 + \frac{V_2^2}{2g} + h_c \tag{1}$$

In Fig. 2, Z is the elevation of a free water surface above datum whether it be in a piezometer tube or a quiescent or moving surface of a stream, V is the mean velocity, h_c the conduit losses between the two sections considered, and e the energy head above the chosen datum.

Obviously Z may be made up of a number of elements such as elevation of stream bed or pipe invert above datum k, pipe diameter D, depth in open channel y, or pressure

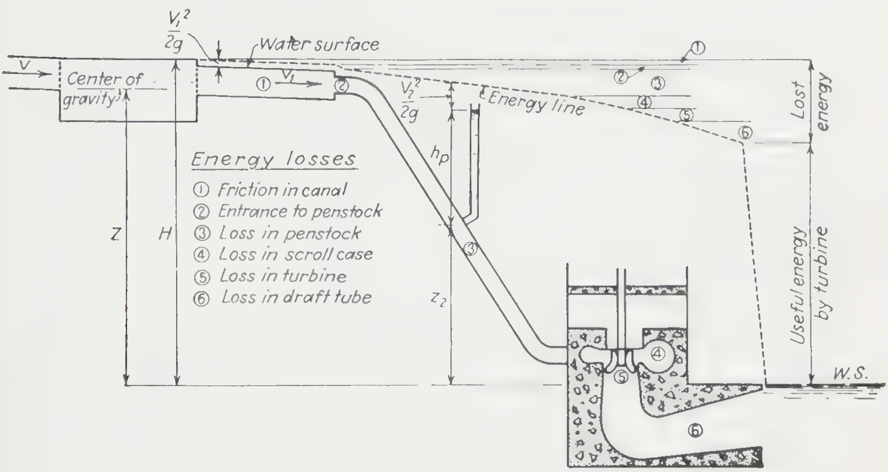

FIG. 1. Energy relations in a typical hydroelectric plant.

head above crown of pipe h. Frequently k and h are measured to the center line of the pipe, but if the pipe is large a distinction is necessary.

6. Head. There are several heads involved in a hydroelectric plant which are defined as follows:

Gross head, simultaneous difference in elevation of the stream surfaces between points of diversion and return.

Operating head on the plant, simultaneous difference of elevations between the water surfaces of the forebay and tailrace with allowances for velocity heads.

Net or effective head on the turbine has different meanings for different types of development as follows:

1. For an open-flume turbine, the difference in elevation between (1) headwater in the flume at a section immediately in advance of the turbine plus velocity head and (2) the tail water plus velocity head.

2. For an encased turbine, the difference between (1) elevation corresponding to the pressure head measured at entrance to the turbine casing plus velocity head at the same point of measurement and (2) the elevation of the tail water plus velocity head at a section beyond the disturbances of exit from draft tube.

3. For an impulse turbine, the difference between (1) elevation corresponding to

the pressure head at entrance to the nozzle plus velocity head at that point and (2) the elevation of the lowest point of the pitch circle of the runner buckets (to which the jet is tangent).

Strictly speaking, the various heads above are the differences in energy heads. For the gross head, the velocities in the stream are generally disregarded, as are the velocity heads in the tailrace for the operating head. The net head, however, is important in determining efficiency tests of a turbine in its setting; hence it is important to use the difference in energy heads at entrance and exit of the setting.

The net head includes the losses in the casing, the turbine proper, and draft tube, for they are charged to the efficiency of the turbine.

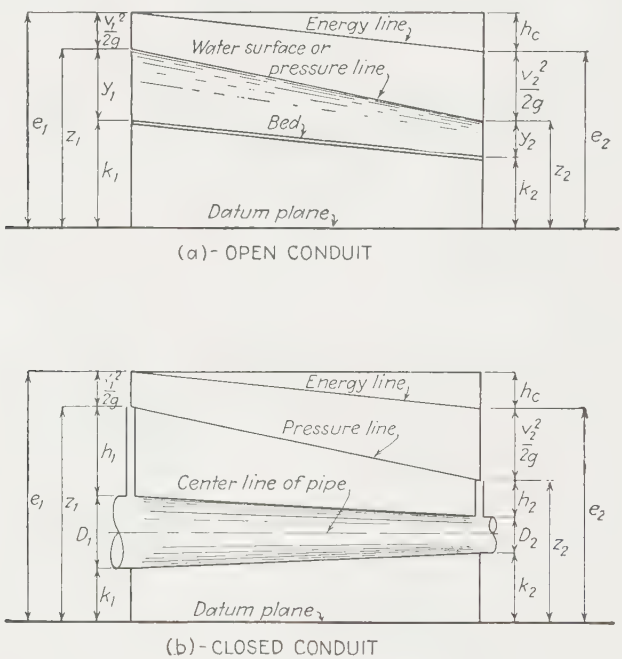

FIG. 2. Energy relations in open and closed conduits.

Formulas for the net head of the three cases above are as follows:

For one cased reaction wheel,

$$h = \left(Z_1 + \frac{V_1^2}{2g}\right) - \left(Z_2 + \frac{V_2^2}{2g}\right) = e_1 - e_2 \tag{2}$$

where Z_1 = elevation of pressure head at entrance of turbine casing
V_1 = mean velocity at entrance of turbine casing
Z_2 = elevation of tail water at draft-tube exit
V_2 = mean velocity in the draft tube at its exit
e_1 and e_2 = the respective energy heads

For an open flume setting of a reaction wheel, the expression is the same as in (2) but the quantities have slightly different meanings: Z_1 is the elevation of water surface in the open flume just upstream of the turbine, V_1 the mean velocity in flume at that section, Z_2 the elevation of water surface in the tailrace at draft-tube exit, and V_2 the mean velocity in the draft tube at its exit.

For the impulse turbine,

$$h = Z_1 + \frac{V_1^2}{2g} - Z_2 \tag{3}$$

in which Z_1 = elevation of pressure head at entrance to nozzle casing
V_1 = velocity at the same point
Z_2 = elevation of the lowest point of the pitch circle of the runner buckets
The elevation of the lowest point of the pitch circle above tailrace and the velocity head in the tailrace are lost as there must be clearance above the tail water for the runner to revolve.

7. Efficiency. *Efficiencies* of elements composing a hydroelectric system are all measured as the ratio of energy output to input or of useful to total energy.

No element is perfect; its functioning involves lost energy (conversion to heat). The efficiency of a plant or system is the product of the efficiencies of its several elements; thus

$$E_s = E_c E_t E_g E_u E_l E_d \tag{4}$$

where E_s is the overall system efficiency made up of the product of the several efficiencies of the conduits—canal, penstocks, tailrace, E_c; turbines, including spiral case and draft tube, E_t; generators, including exciters, E_g; step-up transformers, E_u; transmission lines, E_l; step-down transformers, E_d. Formula (4) expresses the overall efficiency from the river intake to the distribution switches at the substation. To this could be added the efficiency of the distribution system, even to the customer's meters, his lights, water heaters, ranges, motors, etc.

For a constant discharge, the hydraulic efficiencies of the several elements can be expressed in terms of elevations or head above a given datum, and since that datum may be arbitrary such efficiencies will have different values depending upon the datum of reference. If all such efficiencies were referred to sea level, plants at low levels would have higher efficiencies than those at higher altitudes. Such a condition is, of course, intolerable. In effect, the efficiency of an element is the ratio of (1) total energy less losses to (2) total energy, but the datum of reference must be stated.

For purposes of illustration, the following analysis is presented. For the headworks of a system, there is a loss through the control gates in passing from stream to canal, and the efficiency becomes

$$\frac{Z_1 + \dfrac{V_1^2}{2g}}{Z_o} = \frac{e_1}{Z_o} \tag{5}$$

For the canal, the loss is mostly channel friction:

$$\frac{Z_f + \dfrac{V_f^2}{2g}}{Z_1 + \dfrac{V_1^2}{2g}} = \frac{e_f}{e_1} \tag{6}$$

For the penstock, the loss is entrance and pipe friction:

$$\frac{Z_t + \dfrac{V_t^2}{2g}}{Z_f + \dfrac{V_f^2}{2g}} = \frac{e_t}{e_f} \tag{7}$$

For the turbine, the loss is entrance, friction, impact and eddies in casing and draft tub,

$$\frac{Z_d + \frac{V_d^2}{2g}}{Z_t + \frac{V_t^2}{2g}} = \frac{e_d}{e_t} \tag{8}$$

For the tailrace, the loss is eddying at draft-tube exits and channel friction,

$$\frac{Z_r + \frac{V_r^2}{2g}}{Z_d + \frac{V_d^2}{2g}} = \frac{e_r}{e_d} \tag{9}$$

In the foregoing expressions, Z represents elevation of water surface and e of energy heads above datum, subscript $_1$ refers to the head of the canal below control gates, f to forebay, t to the entrance of the turbine, d to the draft-tube exit, and r to the river at its junction with the tailrace.

Z_o is the elevation of the normal river surface at the intake before water enters the canal (river velocities are neglected), and as this may vary, the canal gates are manipulated to hold a given elevation in the canal intake for a given discharge. The efficiency of the headworks may therefore be variable even for a constant discharge. The elevation of the water surface at the head of the tailrace (exit of draft tube) Z_d may also be affected by the river stage, and this is reflected in variation in the efficiency of the turbine. The efficiencies of all the other elements will be sensibly constant for a constant discharge if canal, racks, etc., are kept clean and in good order.

Turbine efficiencies are specified for certain flows under certain heads and speeds and obviously must not vary arbitrarily with an arbitrary datum. The datum of reference is therefore considered to be moved to the water surface just downstream of the draft-tube exit where major turbulences have subsided.

The expression in Eq. (8) therefore must be modified by introducing a power head that represents the useful energy output of the runner and is determined by tests; thus

$$\frac{h_p}{\left(Z_t + \frac{V_t^2}{2g}\right) - \left(Z_d + \frac{V_d^2}{2g}\right)} = \frac{h_p}{e_t - e_d} \tag{10}$$

becomes the correct expression for the efficiency of the turbine and setting under constant discharge, the datum of reference being the water surface of the tailrace at exit of the draft tubes.

With the preceding notation, the efficiency of the entire plant may be expressed independently of an arbitrary datum; thus

$$\frac{h_p}{Z_o - Z_r} \tag{11}$$

velocity heads in the river at the headworks and at its junction with the tailrace being neglected.

The term *efficiency* is not often used for plant elements other than the generating equipment. It has been given here merely to illustrate the relationship of each element to the whole in this regard and to show the effect of the datum of reference on indicated efficiencies. In practice, the lost head in each such element is found and deducted from the gross head to obtain the net power head.

The efficiency of generators is generally greater the larger the unit, but it too depends upon the load carried. The efficiency of transformers increases rapidly with capacity and load within certain limits, whereas that of transmission lines increases with capacity but decreases with load.

The overall efficiency of a plant is the product of the instantaneous efficiencies of its several pieces of equipment referred to the gross head on the turbines. It obviously varies with capacity of units, head, load, and the number of units in service. Plant efficiencies are not always observed and frequently involve many complexities. In general, the plant efficiency is the ratio of the energy output of the generator to the water energy corresponding to the gross head (difference of forebay and tailrace levels) and that discharge through the turbines that results in the maximum efficiency, or it may be for that discharge and load for which the indicated efficiency of the turbine is a maximum. In any case, it should be clearly defined.

8. Power Formulas. A cubic foot per second of water at 62.5 lb/cu ft falling 8.8 ft is equivalent to 1 hp and falling 11.8 ft is equivalent to 1 kw; therefore

$$\text{Theoretical hp} = \frac{Qh}{8.8} \tag{12}$$

$$\text{kw} = \frac{Qh}{11.8} \tag{13}$$

If E is the efficiency of the plant, the power that can be realized is given by

$$\text{hp} = \frac{Qh}{8.8} E \tag{14}$$

$$\text{kw} = \frac{Qh}{11.8} E \tag{15}$$

In the expression, E is the plant efficiency and h is the head on the turbine defined by Eqs. (2), (3), or (4) as may be appropriate.

Useful energy is generally measured in terms of kilowatthours, occasionally in terms of horsepower-hours. Where the discharge and head are constant,

$$\text{hp-hr} = \frac{Qh}{8.8} Et \tag{16}$$

$$\text{kwhr} = \frac{Qh}{11.8} Et \tag{17}$$

where t is the time in hours for which the flow and head are constant or for which Q and h are average values. When the flow and head vary materially, the period considered is divided into smaller time intervals for which they are sensibly constant.

The horsepower-year and the kilowatt-year are terms sometimes used for power sales. On a 100 percent load factor the relationships are

$$1 \text{ hp-year} = 0.746 \text{ kw-year} = 8{,}760 \text{ hp-hr} = 6{,}540 \text{ kwhr}$$

9. Classifications of Power and Energy. Power from any particular plant may be limited by the capacity of the installed equipment, available water supply, head, and storage. There has, in the past, been much confusion in the definitions applied to the various classes of power and energy. The terms "firm capacity" and "dependable capacity" are interchangeable. For example, Creager and Justin[1,*] define the *firm capacity* of a hydroelectric plant as that portion of the total installed capacity which can perform the same function on that portion of the load curve assigned to it as alternative steam capacity could perform.

The Glossary of Important Power and Rate Terms, Abbreviations and Units of Measurement, 1949, prepared by the Federal Inter-Agency River Basin Committee

* Superior numbers refer to items in the Bibliography at the end of this section.

under the supervision of the Federal Power Commission, states: "Dependable capacity may be defined as the load carrying ability for the time interval and period specified when related to the load to be supplied."

Other definitions found in the Inter-Agency Glossary are as follows:

Firm Power. Power intended to have assured availability to the customer to meet his load requirements.

Primary Energy. Hydroelectric energy which is available from continuous power.

Secondary Energy. All hydroelectric energy other than primary energy.

Surplus System Capacity. The difference between assured capacity and the system peak load for a specified period.

Dump Energy. Energy generated that cannot be stored or conserved and is beyond the immediate needs of the electrical system producing energy.

The capacity of a power plant is not easily defined. Nameplate capacity or rated capacity of a turbine is usually given in horsepower for a given head, discharge, and speed at which the best efficiency obtains. Obviously each of these quantities may vary within definite limits. The rated capacity of a-c generators is usually stated in terms of definite speed, power factor, and temperature rise and is usually given in kilovolt-amperes. Each of these quantities may also vary within definite limits.

The IEEE definition of generating station capacity is "the maximum net power output that a generating station can produce without exceeding the operating limit of its component parts." The station or plant capacity can therefore be determined for a given station. It may be stated for a peak load over a given period as 15 min or 1 hr or for a continuous load. It would be higher for short periods than for continuous service if storage regulation exists but is limited by the temperature rise of generators. Until the station capacity has been fixed, the various factors having to do with capacity cannot acquire definite meanings. Where the capacity of a plant has not been fixed, it is customary to take nameplate capacity of generators as the plant capacity, which is often called *installed capacity.*

The average load of a plant or system during a given period of time is a hypothetical constant load over the same period that would produce the same energy output as the actual loading produced (IEEE).

The peak load is a maximum load consumed or produced by a unit or a group of units in a stated period of time. It may be the maximum instantaneous load or a maximum average load over a designated interval of time.

The maximum average load is generally used. In commercial transactions involving peak load, it is taken as the average load during a time interval of specified duration occurring within a given period of time, that time interval being selected during which the average power is greatest (IEEE).

The load factor is an index of the load characteristics. It is the ratio of the average load over a designated period to the peak load occurring in that period. It may apply to a generating or a consuming station and is usually determined from recording power meters. We may thus have a daily, weekly, monthly, or yearly load factor; it may apply to a single plant or to a system. Some plants of a system may be run continuously at a high load factor, whereas variations in load are taken by other plants of the system, either hydro or steam. Hydro plants designed to take such variations must have sufficient regulating storage to enable them to operate on a low load factor. They are often called *peak-load plants.* Operating on a 50 percent load factor, there must be sufficient storage to enable such a plant, in effect, to utilize twice the inflow for half the time: on a 25 percent load factor, the plant should be able to utilize four times the inflow for a quarter of the time, etc.—the lower the load factor, the greater the storage required.

As applied to the consumption of power, the load factor is the ratio of the average to maximum demand during any given period. It may apply to a single motor, an industrial plant, a city, or a consuming system. The maximum demand may be the highest consumer load during a 5-, 10-, or 15-min interval, the average of the two highest 5-min intervals, or otherwise as fixed by the management or by regulatory bodies. It is usually determined from a demand meter or taken from a graphic wattmeter. The period usually considered is a month for purposes of billing, although the sale rates of power are often based on the yearly load factor of the consumer.

The capacity factor is a measure of plant use. It is the ratio of the average load to the plant capacity. It may be computed for a day, month, year, or any other period of time. When the peak load just equals the plant capacity, the capacity factor and load factor are obviously the same. If the maximum demand is less than the plant capacity, the capacity factor may be either greater or less than the load factor, depending largely on the load factor itself.

The utilization factor is a measure of plant use as affected by water supply. It is the ratio of energy output to available energy within the capacity and characteristics of the plant. Where there is always sufficient water to run the plant at capacity, the utilization factor is the same as the capacity factor. A shortage of water, however, will curtail the output and may either decrease or increase the utilization factor according to the plant load factor. These several factors can be determined for any plant by analyzing past performance. They may also be forecast approximately by a complete analysis of stream flow and plant characteristics.

WATER CONDUCTORS

10. General. A hydroelectric development includes in some form a water-diverting structure, conduit to carry water to the turbines, the turbines and governors, generators, control and switching apparatus, housing for the equipment, transformers, and transmission lines to distribution centers. In most cases, a forebay or a surge tank is provided in which head regulation is effected. Trashracks and gates are placed at the head of penstocks. Connected to the waterwheel cases are the draft tubes which utilize the head below the wheels, recovering the kinetic energy of the water without undue losses. The draft tube delivers the water to the tailrace, through which it is returned to the stream.

11. The Forebay. The purpose of a forebay is to store water rejected when the load on the plant is reduced and to supply water for initial increments of an increasing load while the water in the canal or pipeline is being accelerated. Therefore, a forebay is essentially a storage reservoir at the head of the penstocks. It may be a canal, such as shown by Fig. 3 for the Box Canyon project on the Pend Oreille River in the state of Washington, and by Fig. 4 for the Brownlee project on the Snake River in Oregon.[2]

A canal-type forebay should be sized carefully to minimize losses and to equalize the flows into the turbines. Hydraulic-model tests are usually required.

12. The Intake. Intake structures vary widely depending upon the type of plant. In sharp contrast are the intake tower for the Watauga project (Fig. 5), the submerged intake for the South Holston project, TVA (Fig. 6), the intake structure at Fontana Dam (Fig. 7), and the integral intakes and powerhouse structures shown by Figs. 20, 21, 23, 24, and 26.

The South Holston intake (Fig. 6) is a concrete chamber which houses a 15-ft-diameter butterfly valve. This valve controls the flow into a tunnel approximately 1,200 ft long leading to a power plant containing one 35,000-kw unit acting under a rated net head of 180 ft. This intake chamber is completely submerged under all operating conditions. The roof of the chamber would be cut away during maximum drawdown should it become necessary to remove the butterfly valve.

The Fontana intake (Fig. 7) leads to water passages and structures which are built to accommodate three 67,500-kw generating units. These operate under a rated head of 330 ft. A short concrete transition leads from the 19 ft 2½ in. high by 11 ft 0 in. wide rectangular opening at the gate to a 14-ft-diameter steel-lined penstock. Each intake gate is of the tractor type. These gates are approximately 27 ft 10 in. high by 16 ft 6 in. wide and close openings which are 20 ft 10 in. high by 11 ft 6 in. wide. The reservoir serves as the forebay for a plant of this type.

The cylindrical-type intake should be given consideration at sites which do not provide sufficient room for more conventional types of structure. The cylindrical intake, in general, would consist of one or more large-diameter concrete cylinders with intakes located around the perimeter at such depths as may be required for control and

Fig. 3. Forebay, Box Canyon project, Pend Oreille River, state of Washington.

regulation. One or more tunnels, preferably through the abutments, would convey the water from the bottom of the intake cylinders to the turbines.

The cylindrical intake is adaptable to high-head structures. Because the cylinders are in direct compression, relatively thin walls and nominal steel reinforcement are factors which reduce construction costs.

An interesting application of a cylindrical intake is shown by Fig. 8.[3] A large concrete cylinder serves as an intake, a powerhouse, a spillway, and an irrigation-outlet structure.

13. Trashracks. Trashracks used in hydroelectric generating stations consist essentially of vertical or slightly inclined steel bars placed parallel to each other and spaced uniformly to permit the use of rakes. Bars are supported in water passages by horizontal supports which transmit loads developed by the flow, especially when partly clogged by trash, into side members or horizontal supporting beams.

By way of example, Fig. 7 also shows the arrangement of the trashracks and gates for the Fontana hydroelectric plant.[4] These precede three 14-ft-diameter steel-lined intake conduits leading to the units in the powerhouse at the foot of the dam. The

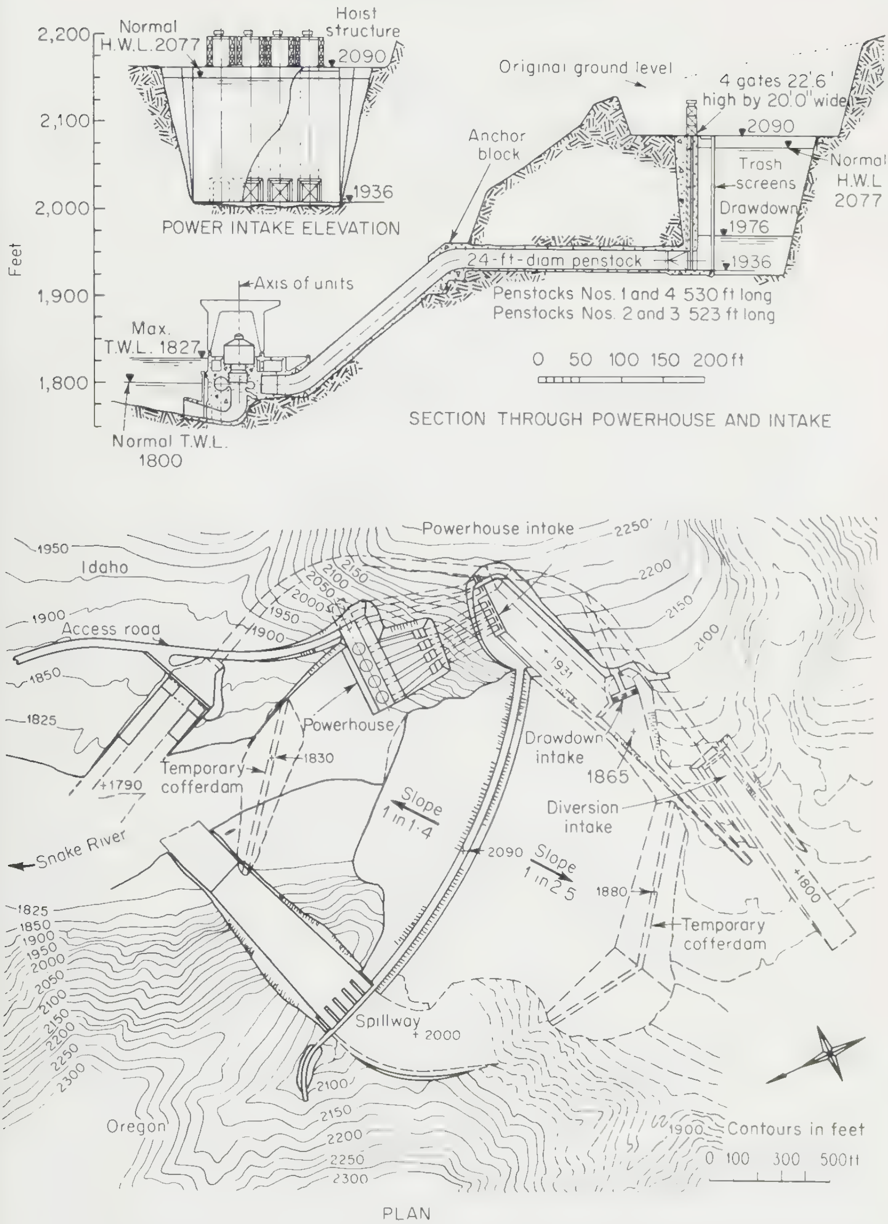

FIG. 4. Brownlee powerhouse and intake. (*Water Power*, April, 1957, pp. 140, 141.)

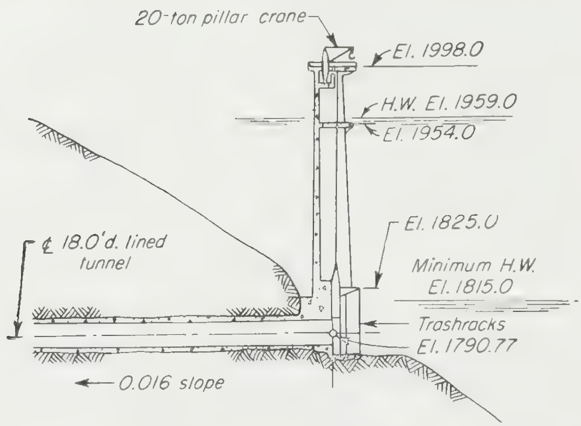

FIG. 5. Intake tower, Watauga project.

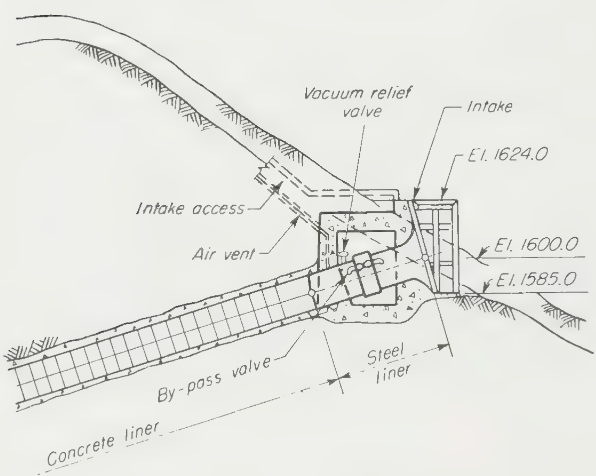

FIG. 6. Intake chamber, South Holston project.

powerhouse contains two 67,500-kw units with provision for a third. These units operate under a rated head of 330 ft. Each discharges 2,600 cfs at rated head and capacity.

Each of the three trashrack structures is supported on a concrete cantilever slab which projects 22 ft 2 in. from the face of the dam. In plan, the trashrack structure is of semicircular shape with a 13 ft 0 in. outside radius. The circumference of the semicircle is subdivided into four straight panels, framed by concrete columns with concrete-beam bracing. The column and beam structure has a total height of 97 ft, of which the lower 48 ft has the racks in the panel openings and the upper 49 ft is an extension for withdrawal and maintenance of the racks with the top 14 ft above minimum drawdown.

In the corner columns of the four panels, 7-in. guide channels are embedded. Four rack sections fit into each panel, each 12 ft 1½ in. high by 8 ft 4 in. wide. The

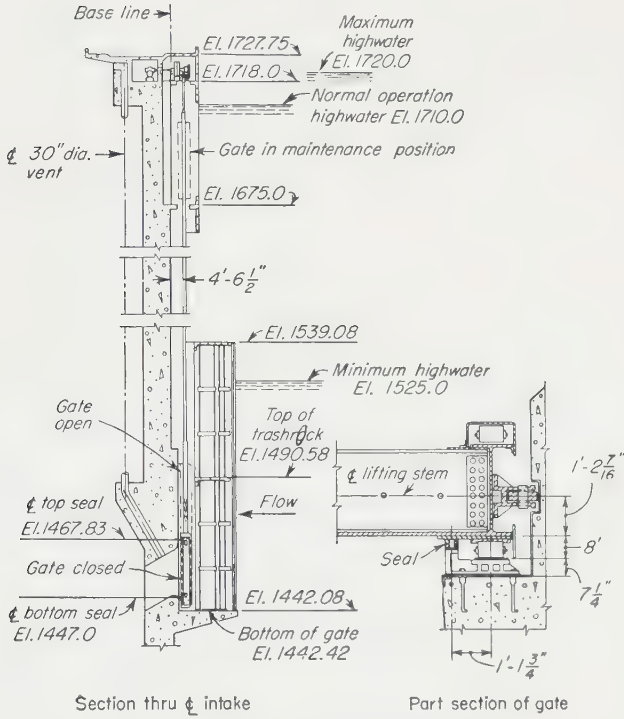

Fig. 7. Intake, Fontana project.

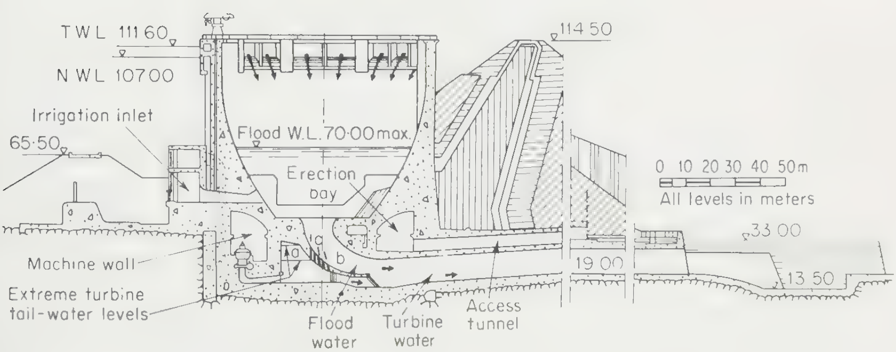

Fig. 8. Cross section through the circular power station showing the arrangement for handling flood discharges.

vertical rack bars are 4 by ⅝ in. and the horizontal supporting members are 6 by ¾ in., spaced to give openings 6 in. wide by 2 ft 4 in. high. The concrete structure is designed for a differential head of 10 ft and the steel rack sections are based on a differential head of 5 ft. The maximum velocity through the net trashrack area is 2.4 fps.

The head loss through trashracks is mainly due to the flow contraction at the entry and the sudden enlargement of the area at the exit from bar spaces. Among the many

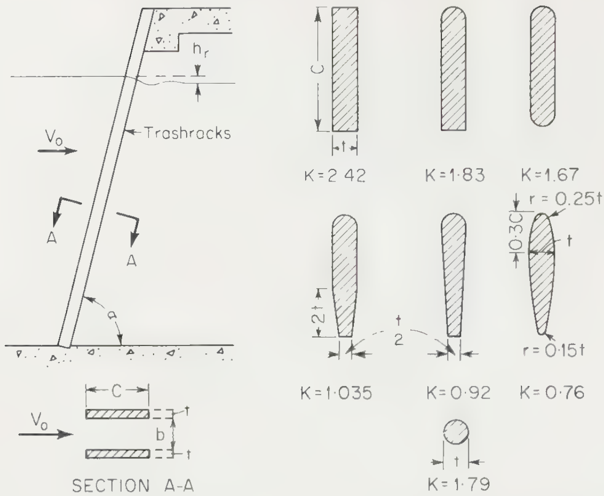

FIG. 9. Head loss in trashracks, values of factor K for various bar shapes.

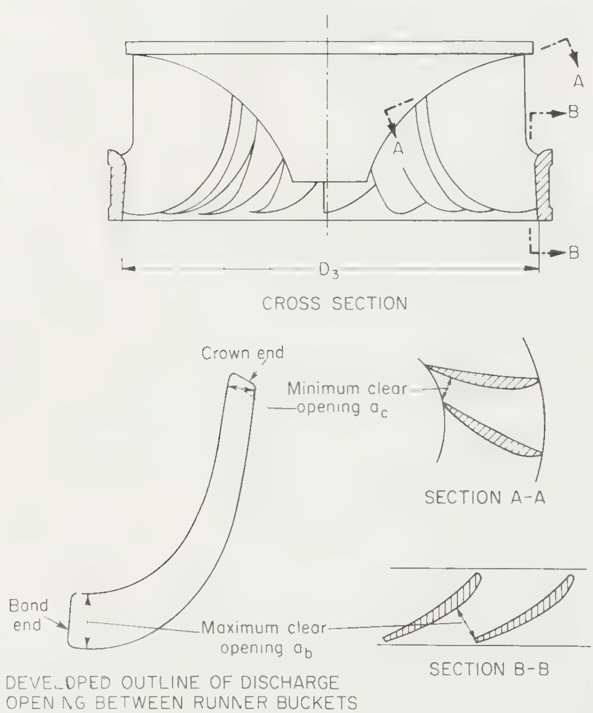

FIG. 10. Location of minimum clear opening in a Francis-type runner.

formulas for calculating head loss, the one developed by O. Kirchmer on the basis of experiments at the Munich Hydraulic Laboratory is in widespread use:

$$h_r = K \left(\frac{t}{b}\right)^{4/3} \frac{V_0^2}{2g} \sin \alpha \tag{18}$$

in which h_r = loss of head through racks, ft
t = thickness of bars, in.
b = clear spacing between bars, in.
V_0 = velocity of approach, fps
g = acceleration due to gravity
α = angle of bar inclination to horizontal, deg
K = a factor depending on bar shape in accordance with Fig. 9[5]

The losses determined from this formula apply to clean racks.

The spacing of the vertical or inclined rack bars depends primarily on the size and type of turbine to be protected and is also influenced by the size of the trash. In some localities an abnormally small spacing may be required by fish-conservation agencies.

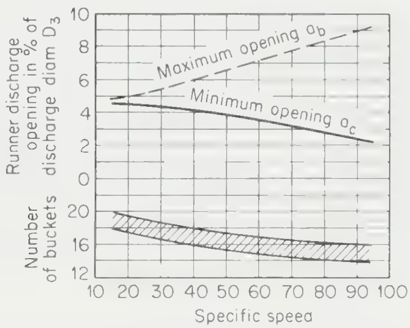

FIG. 11. Experience data for approximate determination of clear openings in Francis runners.

The rack bars are usually spaced so that the clear opening between them is not greater than the smallest fixed opening in the water passages of the turbine. In Francis turbines, the smallest fixed opening is located in the runner and is the shortest distance between the buckets or vanes of the runner, as is indicated by Fig. 10. Figure 11, which shows experience data for the approximate determination of clear openings in Francis turbines, may be used for preliminary investigations. Figure 12 shows the maximum recommended length of rack bars between lateral supports or stiffeners, as limited by vibration characteristics related to bar thickness and velocity through the net area. To avoid objectionable vibration, the length limits shown should not be exceeded.

Interesting innovations in design have resulted from the requirements for trash-rack structures for high dams. For example, the state of California is now (1968) building the 770-ft-high embankment-type Oroville Dam in north-central California. The intakes for this dam will convey water to the turbines of a 644-megawatt underground powerhouse.

A major innovation in the power-plant system is the intake structure shown by Fig. 13.[6,7]

In addition to performing the usual functions of an intake for a hydroelectric

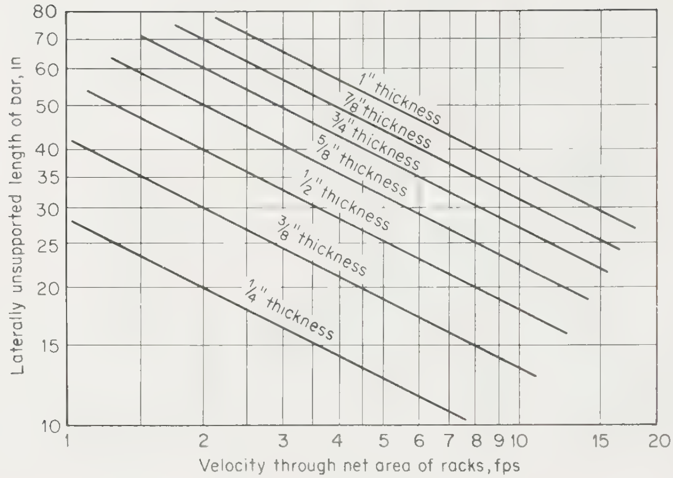

Fig. 12. Recommended limits of laterally unsupported length of steel rack bars to avoid vibration.

project, this structure is also intended to allow temperature control of the water through the power plant to meet agricultural and fish-conservation requirements.

The intake consists of two parallel, rectangular channels, approximately 650 ft in length open at the top and situated on a 1.9:1.0 slope along the side of the ridge comprising the left abutment of the dam. Figure 13 shows the general arrangement and Fig. 14 shows a photograph of the racks. It was found more economical to construct these racks of stainless steel. The trashracks system consists of 824 flat panels

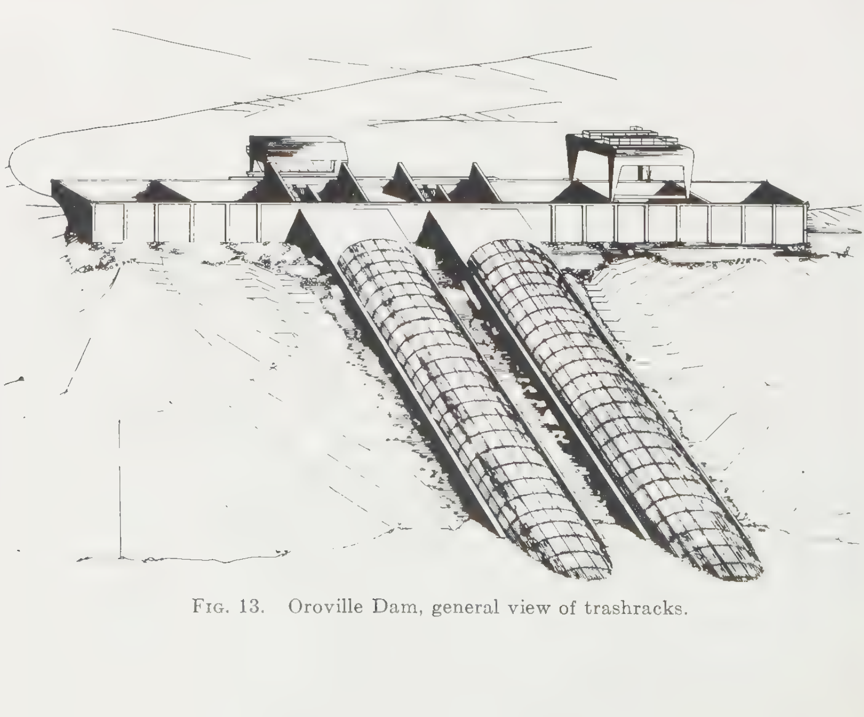

Fig. 13. Oroville Dam, general view of trashracks.

supported on 180 segmental arches. Temperatures of the tail water will be controlled by 26 shutters, 13 on each channel. These shutters consist of 40- by 44-ft fixed-wheel gates. The shutters span temperature levels which vary as much as 25 F between controlled reservoir levels.

The intake and trashrack arrangement for the 400-ft-high Mangla Dam[8] (Fig. 15) on the Jhelum River, West Pakistan, completed in 1967 by the Water and Power Development Authority, offers an interesting example of cage-type racks operating on the face of an embankment-type dam.

The 450-ft-wide intake structure is divided by contraction joints into five reinforced-concrete monoliths with each containing a power intake, as shown by Fig. 15. The gate opening of each power intake is 18 ft wide and 36 ft long on a slope of 1.0 on 2.5. The gate openings are followed by radius bends which showed a loss from intake to tunnel of 0.20 velocity head in the tunnel or approximately 0.62 ft at the design discharge of 10,000 cfs.

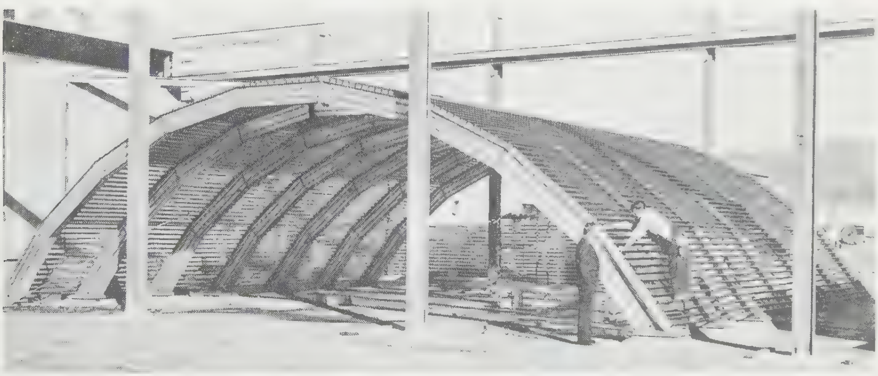

Fig. 14. Oroville Dam trashracks, shop assembly.

Each intake screen provides 3,000 sq ft net area and consists of $1\frac{1}{2}$-in. galvanized mild steel bars at 6-in. centers designed for 60 percent of the yield at a differential head of 10 ft. The supporting members of the bars are designed for a head of 20 ft.

14. Penstocks. Penstocks are designed to carry water to the turbines with the least possible loss of head consistent with the overall economy of the project. The various losses which occur between the reservoir and the turbine—trashrack, entrance, pipe friction, valves, and fittings—are discussed elsewhere (Secs. 2, 3, 22). Where there is an elbow in the penstock just ahead of the turbine and a reducer is required, minimum losses will usually result from shaping the elbow to serve also as a reducer.

The most economical penstock will be the one in which the annual value of the power lost in friction plus annual charges such as interest, depreciation, and maintenance will be a minimum. The variables entering the problem are (1) daily variation of flow through penstock, (2) estimated load factor over a term of years, (3) profile of penstock, (4) number of penstocks, (5) materials used in construction, (6) diameter and thickness, (7) value of power lost in friction, (8) cost of penstock installed, (9) cost of piers and anchors, (10) total annual charges of penstock in place, and (11) maximum permissible velocity.

It is extremely difficult to express these variables in a comprehensive formula, although several attempts have been made to do so. An interesting study by

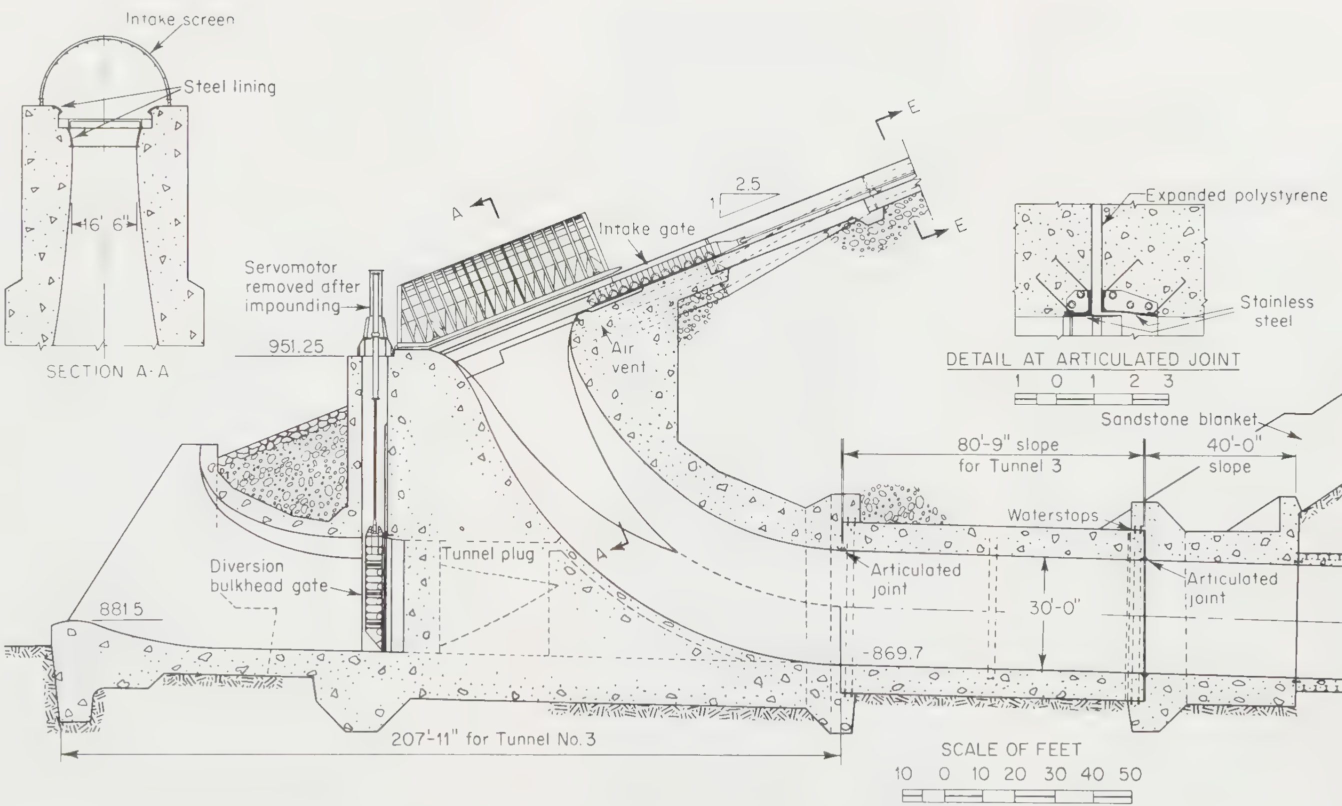

FIG. 15. Intake and trashracks, Mangla Dam, Indus Basin.

Sarkaria[9] resulted in a simple empirical formula, which applied to penstocks embedded in gravity intakes:

$$D = 4.44 \frac{P^{0.43}}{H^{0.65}} \tag{19}$$

in which D = economical diameter of penstock, ft
P = rated horsepower of turbine
H = rated head of turbine, ft

This formula is applicable primarily to power plants with Francis- and propeller-type turbines and gives fairly reliable results for penstocks 5 ft or more in diameter. By way of example, assume the following data for a steel penstock embedded in a gravity intake having a height of approximately 350 ft:

Type of turbine	Francis
Rated head	H = 280 ft
Rated hp	P = 155,000
Length of steel penstock	L = 300 ft
Average allowable stress in penstock plate	15,000 psi
Joint efficiency	90%
Load factor for power demand	60%
Assumed life of installation	50 years

Using Eq. (19), it will be found that D = 19.4 ft.

By going through a very lengthy investigation, which compared increases in construction cost with the capitalized value of power lost, it was determined that the economic diameter would lie somewhere between 19 and 20 ft. Figure 16 shows penstock velocities in selected existing plants having a wide range of heads.

Losses in bifurcations, which are usually located a short distance upstream from the control valves, may best be determined from model tests. Few prototype performance data are available. Hydraulic-model tests revealed that the maximum head loss for the bifurcation ahead of the Mangla turbines (Fig. 17) was approximately $0.40(V^2/2g)$.[8] The practice of the Corps of Engineers, U.S. Army, is to estimate bifurcation losses at $0.15(V^2/2g)$ and trifurcation losses at $0.50(V^2/2g)$. The results

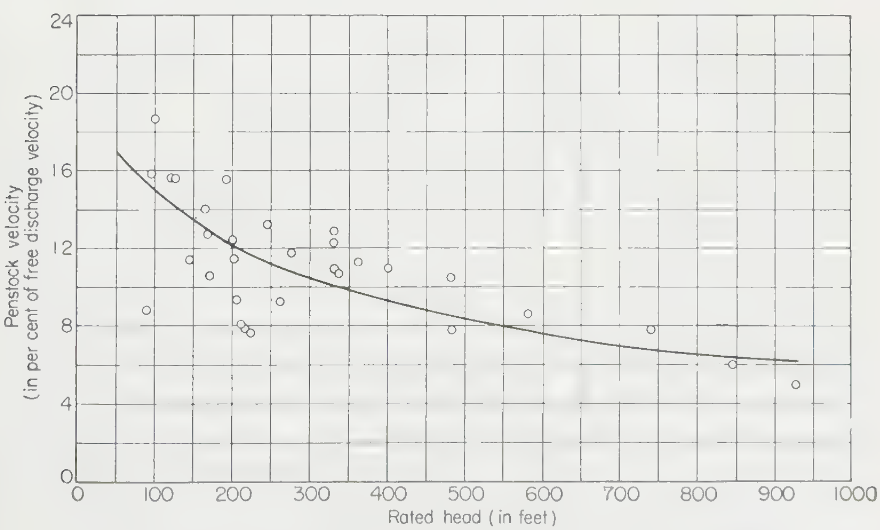

FIG. 16. Penstock velocities at full turbine discharge. Existing plants.

of a model study for a large trifurcation used in connection with the Round Butte hydroelectric project, Oregon, are shown by Fig. 18[10,23]. A 23-ft-diameter penstock was trifurcated into three 13 ft 7 in. diameter sections which feed three Francis turbines having a combined power capacity of 247,050 kw. With all tubes flowing and the flow equally divided, the head loss at maximum discharge varied from about $0.38(V^2/2g)$ to $0.53(V^2/2g)$.

Prototype tests were made to determine the hydraulic losses in the wye branch which divided the flow of the Chelan Station power tunnel.[11] A 2-mile-long 14-ft-diameter concrete-lined pressure tunnel converges below the surge tank to a steel-lined 14-ft-diameter penstock which divides through a bifurcation into two 12 ft 6 in. diameter water passages leading to the turbines. The head loss at this bifurcation, under full-flow conditions, was approximately $0.50(V^2/2g)$. In the foregoing, except the Round Butte trifurcation, V is the average velocity in the penstock before the flow is divided.

15. Turbines and Pumps. Reference should be made to Sec. 26 for a comprehensive presentation of the hydraulics of hydraulic machinery.

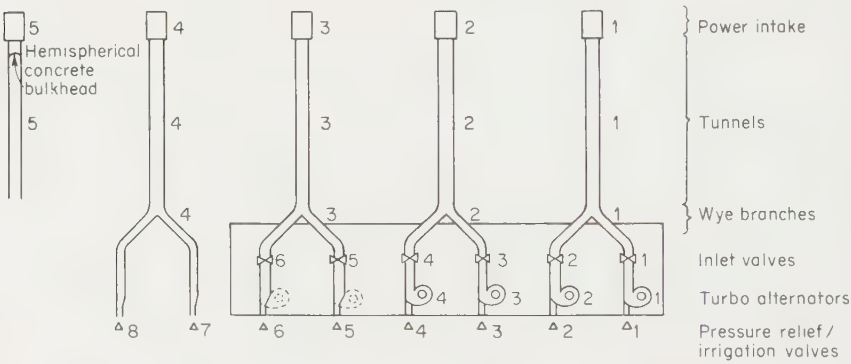

Fig. 17. Mangla Dam, West Pakistan, diagrammatic hydroelectric scheme.

16. Draft Tubes. The draft tube is usually a very essential part of a turbine installation. It supplements the action of the runner by utilizing most of the energy remaining in the water at the discharge from the runner.

The draft tube is designed as a diverging discharge passage connecting the runner with the tailrace. It is shaped to decelerate the flow with a minimum of losses so that the kinetic energy remaining in the flow at discharge from the runner may be efficiently regained by conversion into the suction head, thereby increasing the total pressure difference on the runner. This regain of kinetic energy is usually the primary function of a draft tube.

The draft tube frequently serves a second purpose, that of regaining static suction head in cases where the runner is located above tail-water level. When the vertical distance of the runner above tail water is well within an atmospheric head and when the outlet of the draft tube is sufficiently submerged to assure a water seal, the negative static draft head on the runner is added to the positive head from headwater to make up the total static head on the turbine. Although an atmospheric head is nearly 34 ft of water at sea level, the static draft head should never exceed 15 ft, and even this should not be reached except during low-water conditions of short duration with units of low specific speed and relatively high heads.

Draft tubes are not used with impulse wheels, and the head from the nozzle to tail water is necessarily lost.

Energy Relations. Using the tail-water level as datum, we can write the Bernoulli equation for the draft tube thus:

$$Z_1 + 2.3p_1 + \frac{V_1^2}{2g} = \frac{V_3^2}{2g} + h_f + h_i \tag{20}$$

where Z_1 = elevation of turbine exit above tail water equivalent to the draft head
p_1 = gage pressure, psi, at turbine exit
V_1 = velocity at turbine exit
V_2 = velocity at draft-tube exit
V_3 = velocity in tailrace beyond disturbance from draft-tube exit
h_f = friction loss in draft tube
h_i = eddy loss at draft-tube exit

For the vertical-tube type, the exit velocity head is lost, *i.e.*, $h_i = v_2^2/2g$. For the elbow or symmetrical type, some of the exit velocity is preserved in the direction

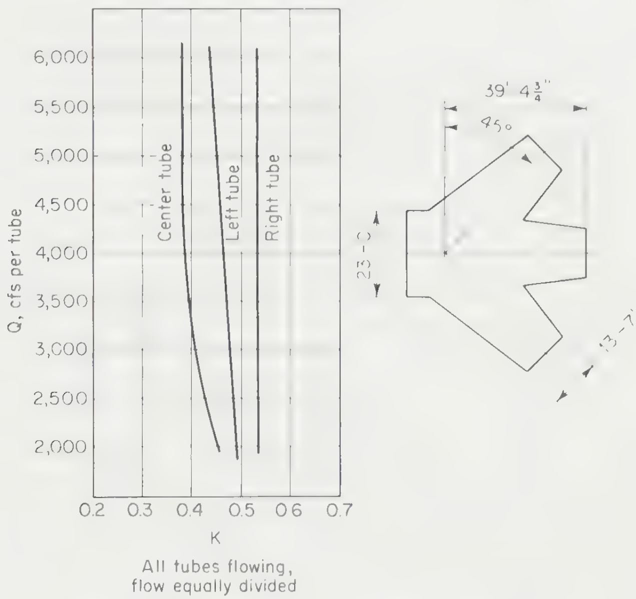

FIG. 18. Coefficient of loss, penstock trifurcation.

of flow in the tailrace; hence it may be considered as a sudden enlargement in a conduit for which the loss is

$$h_i = \frac{(V_2 - V_3)^2}{2g} \tag{21}$$

The right-hand member of Eq. (20) is a relatively small quantity, usually not over 2 ft. The exit velocity from the runner will depend on the specific speed of the turbine and may be anywhere between 20 and 40 fps; hence the greater V_1, the less the draft head, for the absolute pressure at the inlet to the draft tube cannot be less than the vapor pressure of water and should be substantially more.

The most efficient draft tube is a vertical tapered pipe expanding at the rate of about 8 deg central angle and approximately 4 to 5 inlet diameters in length. Rarely, however, is there space for such a tube, and the elbow-type draft tube is generally used.

The design of the draft tube is usually supplied by the turbine manufacturer and is

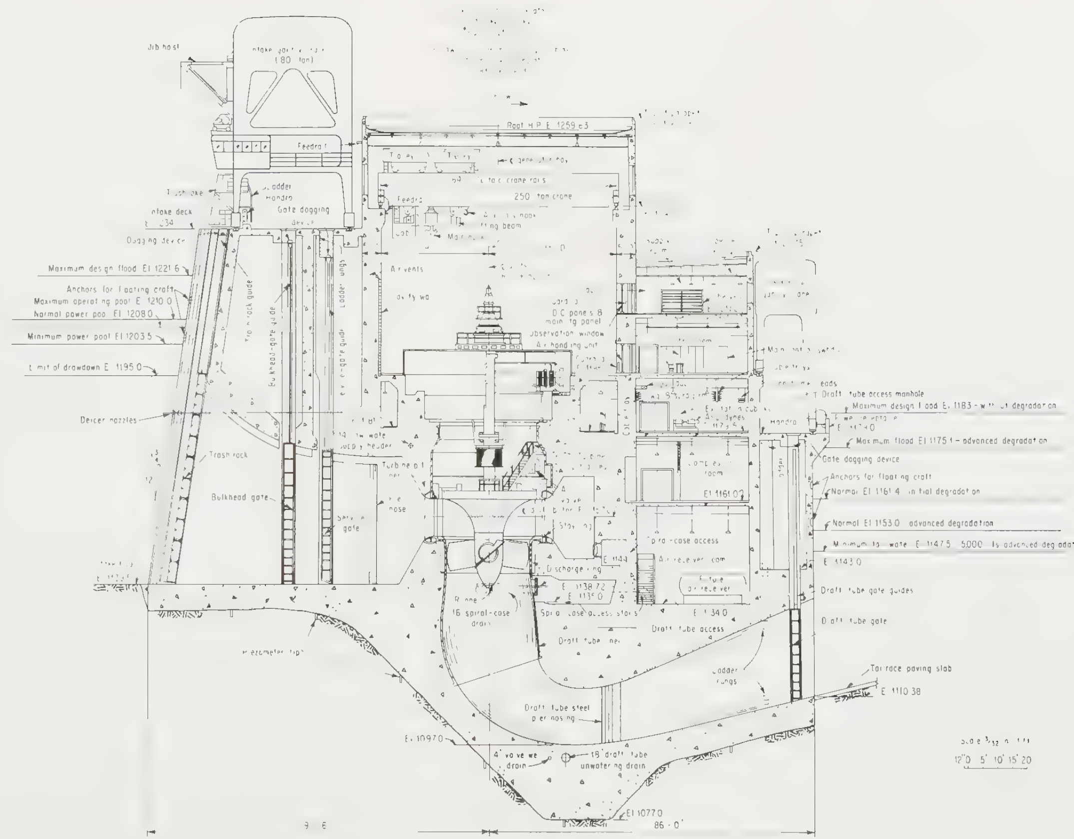

FIG. 19. Gavins Point powerhouse, Missouri River, Yanktown, S.D., transverse section through center line of unit.

an integral part of the turbine in determining turbine performance. Cavitation and pitting on the underside of runner blades may result with low-head high-specific-speed units if the draft head is too great or the rate of expansion too rapid.

The negative pressures at the head of the draft tube may be computed from Eq. (20).

17. The Tailrace. A careful study of tailrace conditions should be made. The first step is to obtain records showing the discharges at different elevations of tail water. Usually, downstream gages should be established to show the effects of projecting ridges which may influence tail-water elevations. The removal of such ridges may increase the operating head.

Elevated or chute spillways, located near the powerhouse, may erode deep plunge pools in the riverbed. Deposits of the eroded material downstream may raise the tail-water levels with a resultant loss of power.

A study of the hydraulics of the tailrace should reveal whether tail-water levels will become either lower or higher throughout the years of operation. A degrading tailrace usually results from the fact that the structures block the supply of deposits from the river upstream from the dam. Under those conditions, the river below the dam may continue to erode. In some cases this erosion has progressed to a point where the draft tubes have become unsealed. Reference to Fig. 19, a cross section of the Gavins Point powerhouse, will show the differences in tail-water levels which have been anticipated because of degradation.

Dams and power plants located in narrow gorges have been known to create tail-water problems. The concentration of spillway discharges may have several adverse effects: for example, tail-water levels may be raised by high hydraulic jumps. Resulting high-velocity eddies may undermine the canyon walls to a point where large rock falls will be deposited in the riverbed. This could result in a serious loss of head at the powerhouse and create a costly maintenance program.

A comprehensive study of tailrace conditions usually requires a coordination of hydraulic-model tests, hydraulic and power-output analyses, geological studies, and cost and economic-feasibility studies.

POWERHOUSE STRUCTURES

18. Classification. Powerhouse structures may be classified under five general types: (1) integral intake; (2) separate powerhouse constructed at the toe of the dam; (3) separate powerhouse structure connected to the intake by either penstocks or tunnels; (4) underground powerhouse; and (5) low-head powerhouse. Falling within these are plants which may be classified as indoor, outdoor, and semioutdoor. Typical examples of each are described.

19. The Integral Powerhouse. Representative of this type is the Wanapum powerhouse (Figs. 20 and 21). This project is located on the Columbia River near the center of the state of Washington.[12] The substructure is of mass concrete and the intake and semispiral case are of reinforced concrete. The superstructure is formed by the intake concrete wall, a downstream reinforced-concrete wall and a structural-steel roof deck. The reinforced-concrete intake roof is supported by the end walls and two intermediate piers in each bay. There are three wheeled gates, each 42 ft 6 in. high by 20 ft wide, one for each intake opening of one unit. Trashracks are designed for a maximum flow velocity of 4 fps through the gross area. Gates are provided for emergency or service closure of one unit. Draft-tube gates are provided for the emergency closure of two units. The powerhouse will contain, ultimately, 16 generating units and an erection bay. Generators are rated 87,500 kva at an 0.95 power factor, 13.8 kv, 60 cycle, 85.7 rpm. The turbines are of the vertical-shaft adjustable-blade propeller (Kaplan) type rated 120,000 hp at an 80-ft net head.

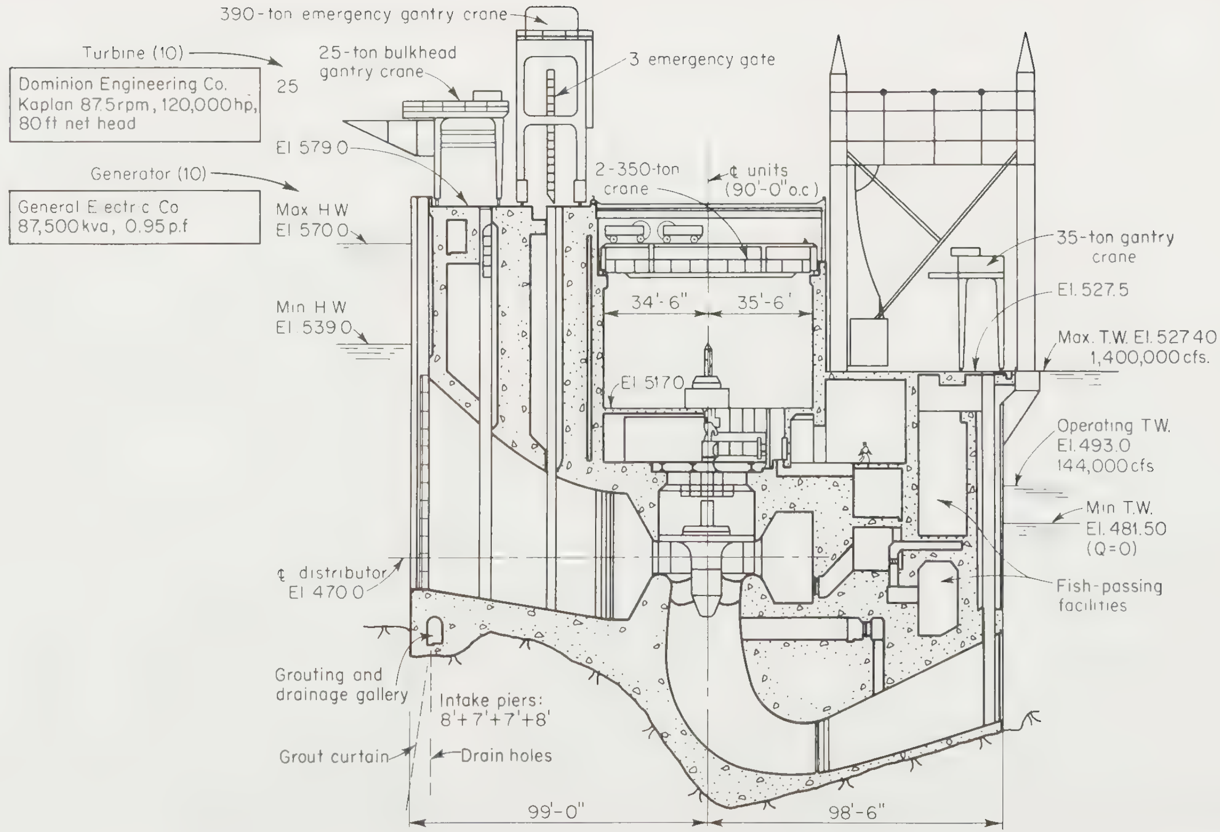

FIG. 20. Wanapum powerhouse (1963), 830-mw development on Columbia River, Washington.

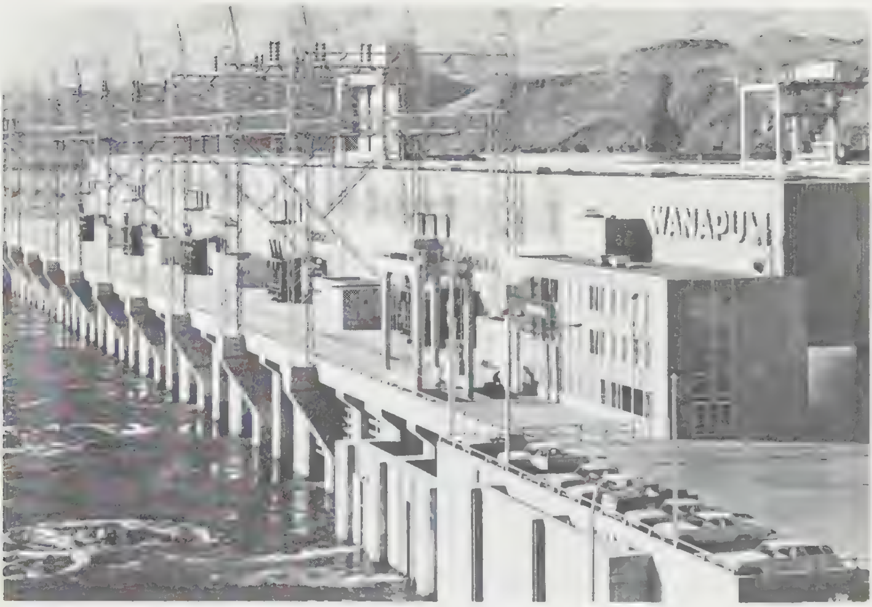

FIG. 21. Wanapum powerhouse (1963), 830-mw development on Columbia River, Washington.

FIG. 22. Gavins Point Dam and powerhouse, Missouri River, Yanktown, S.D. (*Courtesy of Corps of Engineers, U.S. Army.*)

The Gavins Point powerhouse on the Missouri River (Figs. 19 and 22) also is of the integral-intake type with an indoor powerhouse. The power installation consists of three vertical-shaft adjustable-blade Kaplan turbines having a 54,000 rated hp at 48 ft net head operating at a speed of 75 rpm. At 0.95 power factor the generators are rated at 33,345 kw. The intake roof is supported by the side walls and two intermediate piers. As shown by Fig. 19, provision has been made in the design to accom-

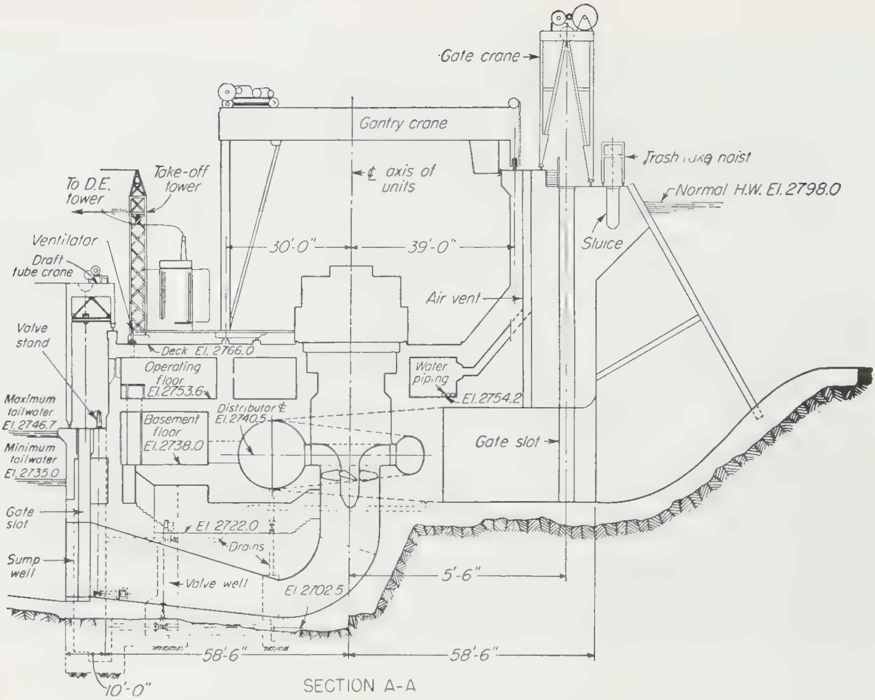

Fig. 23. Lower Salmon River plant, Snake River, Idaho. (*Ebasco, New York.*)

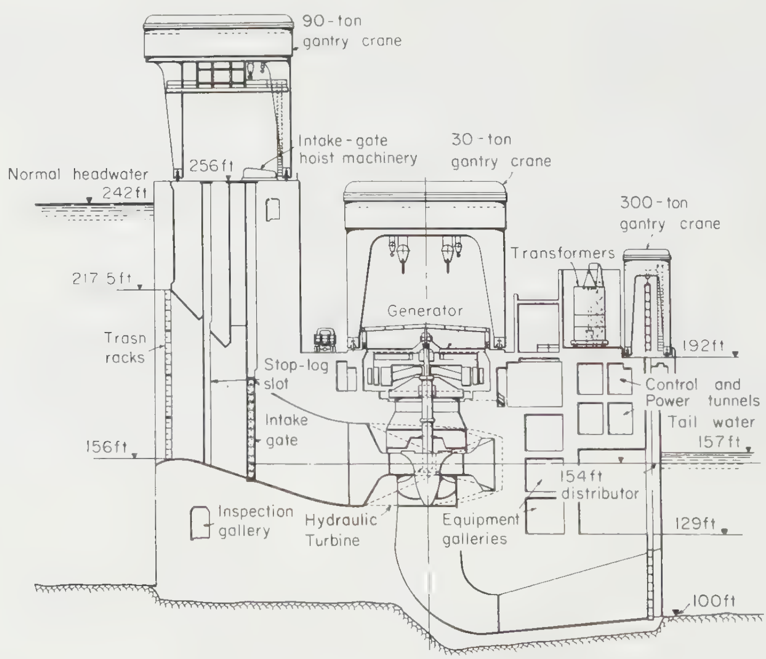

Fig. 24. Moses-Saunders hydroelectric plant, St. Lawrence River. Section, American side.

modate substantial changes in tail-water elevation resulting from the degradation of the stream bed.

Representative of practice in outdoor plant design is the Idaho Power Company's Lower Salmon station on the Snake River, Idaho, shown by Fig. 23. This plant is composed of four units, each of 15,000 kw capacity, operating under an average head of 56.5 ft. Three are driven by fixed-blade propeller turbines and one by a Kaplan turbine. Operating and service bays are located below the deck. The transformers are located on a deck downstream from the gantry crane. A metal housing is provided for the generators, thus eliminating the conventional superstructure of the indoor type.

In the early stages of development, it was thought that the outdoor type would not be suitable for severe climates. This notion has been largely dispelled by the Idaho Power Company. Temperatures at the Lower Salmon Station vary from 15 F below zero to 115 F.

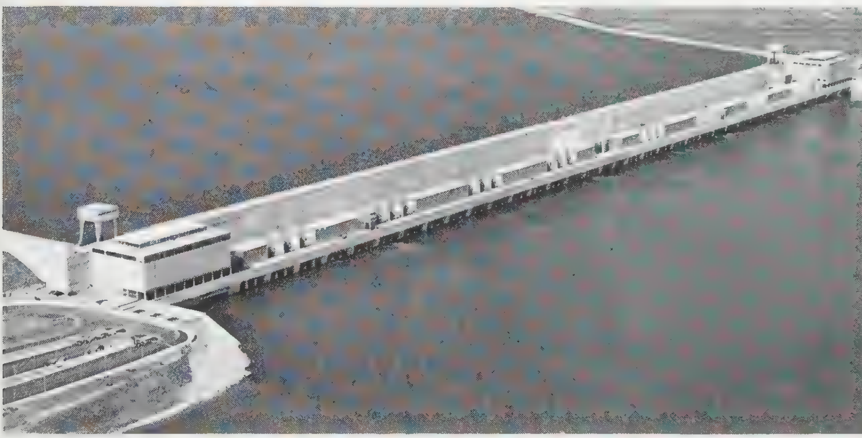

Fig. 25. Moses-Saunders hydroelectric plant, St. Lawrence River. (*Courtesy of New York State Power Authority. Uhl, Hall, and Rich, Consulting Engineers.*)

The Moses-Saunders project (Figs. 24 and 25) on the St. Lawrence River is a notable integral-intake structure with a modified outdoor-type powerhouse. This structure was built jointly by the New York State Power Authority and the Hydro-electric Commission of Ontario.[13,14]

The Moses-Saunders plant is located a short distance above Cornwall, N.Y., and connects the Canadian mainland with Barnhart Island. With it has been constructed a control dam which connects Barnhart Island with the United States mainland.

The powerhouse is approximately 3,200 ft long and contains 32 generating units. The turbines are of the fixed-blade propeller type and are rated at 79,000 hp each, at 81 ft head and a speed of 94.7 rpm. Three-phase 60-cycle generators are rated at 60,000 kva at 0.95 pf.

The intake and substructure form an integral dam and powerhouse which provide waterways for the 32 turbines. The powerhouse is divided into 32 blocks each of which is 80 ft long. Each intake passage is subdivided by two intermediate piers into three water passages.

Representative of semioutdoor design is the Kentucky power station structure (TVA) shown by Fig. 26.[15] This type combines some of the features of both the outdoor and indoor types. The generator room at Kentucky is 30 ft high, which is ample to clear the Kaplan head on the unit. The station houses four 32,000-kw units with provision for a fifth. The generators are driven by Kaplan adjustable-blade units which operate under a rated head of 48 ft. The head varies from a maximum of 58.5 ft to a minimum, during maximum flood conditions, of 6 ft.

20. Separate Powerhouse Constructed at Toe of Dam. Brief descriptions of three plants will illustrate the wide range of designs which fall under this classification: (1) the Karadj project, (2) the Hartwell project, and (3) the Kainji project.

The 600-ft-high Karadj Dam is located on the Karadj River about 25 miles from the city of Teheran, Iran. It was completed in 1961 by the Karadj Water and Power Authority, a division of the Plan Organization. Figure 27 shows a section of the dam and powerhouse and Fig. 28 a view of the powerhouse.

The powerhouse, an indoor-type structure, houses two Francis turbines rated at 55,230 hp at a head of 482.3 ft and a speed of 333 rpm. The generator rating is 40,000 kw.

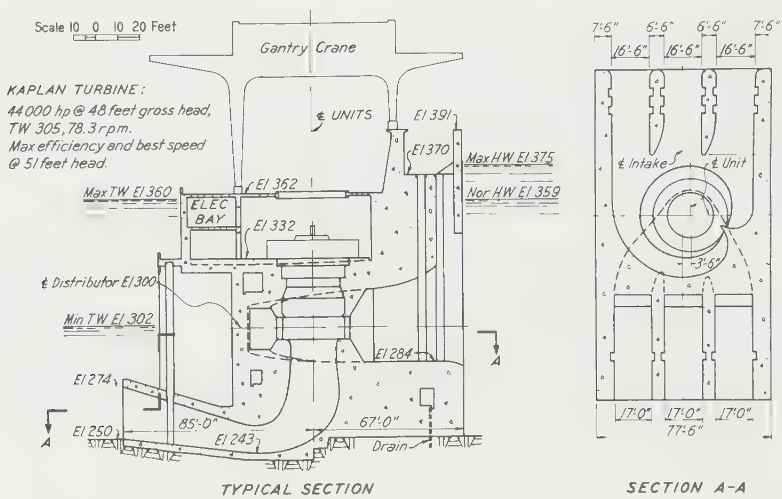

Fig. 26. Semioutdoor plant, Kentucky Dam, TVA.

The units are spaced 36.1 ft center to center. Provision is made for the later installation of a third unit. Steel-lined, 8 ft 6 in. diameter penstocks connect the intake, as shown by Fig. 27, with reducers which lead to 86.6-in. spherical-type turbine inlet valves.

The 200-ft-high Hartwell project, located on the Savannah River, Georgia, was completed in 1962 by the Corps of Engineers, U.S. Army. Figure 29 shows a section through the dam and powerhouse and Fig. 30 shows a view of the powerhouse. The dam and intake are of the conventional gravity type. An outdoor-type powerhouse contains four generating sets. The Francis-type turbines are rated 91,500 hp each at 170 ft head. The generators are rated at 66,000 kw each. The speed is 100 rpm. The units are 68 ft on centers.

The Kainji project (Fig. 31) is located in northern Nigeria on the Niger River.[16] The powerhouse is located at the toe of a conventional-type gravity intake. Initially the powerhouse contains four 80-mw generating sets. Provision has been made to increase the installation to 12 sets totaling 960 mw.

Each machine is contained in a separate block 78 ft wide. The rectangular intakes are divided by central splitter piers. The openings are controlled by fixed-wheel gates

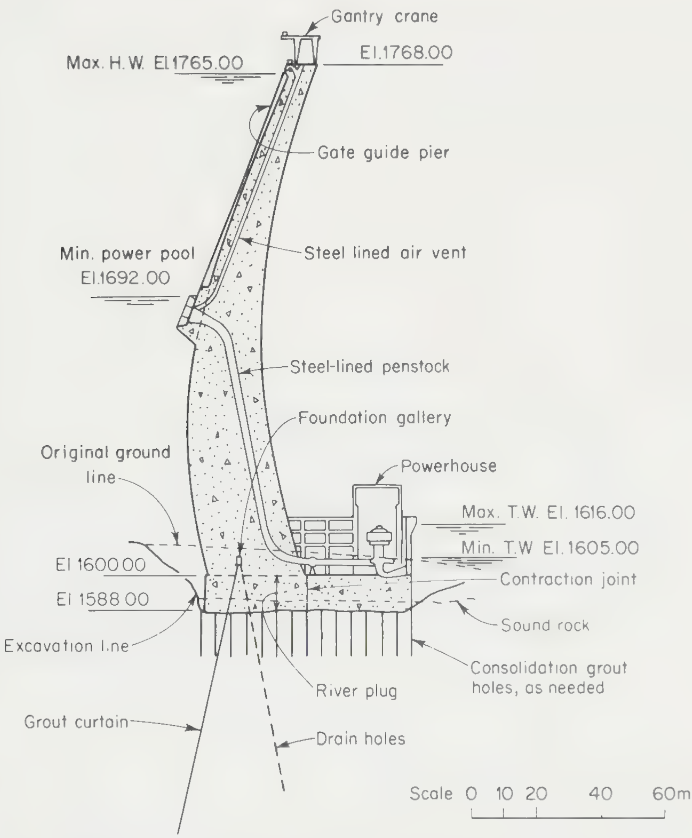

FIG. 27. Section of arch dam and powerhouse (Karadj).

FIG. 28. Karadj powerhouse, Karadj River, Iran. Plan Organization, Karadj Water and Power Authority.

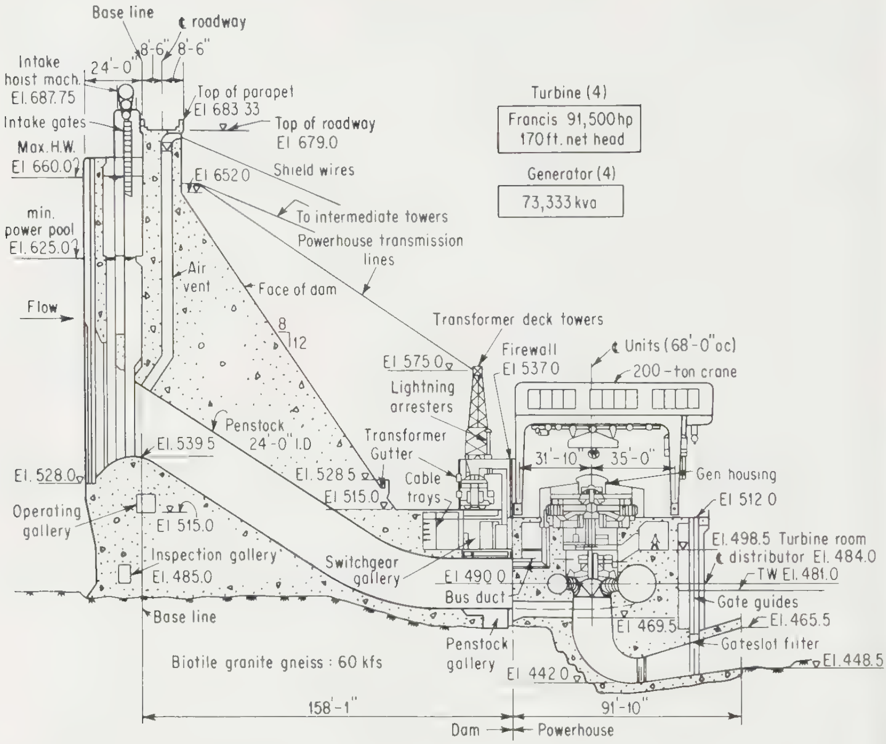

FIG. 29. Hartwell powerhouse (1962), 260-mw development on Savannah River. (*Courtesy of U.S. Army Engineers.*)

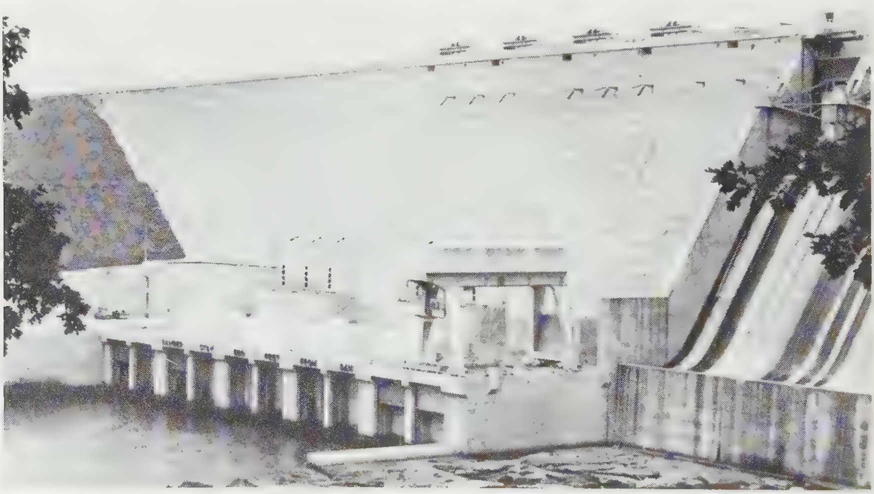

FIG. 30. Hartwell powerhouse, Savannah River, Georgia. (*Courtesy of U.S. Army Engineers.*)

16 ft wide by 34 ft 10 in. high. These rectangular intakes lead to 28-ft-diameter steel-lined penstocks. The draft tube from each turbine divides into two passages, each 28 ft wide by 16 ft deep at the draft-tube gate position.

Four Kaplan turbines, each rated to develop 110,000 hp at a net head of 97 ft, are designed to operate over a gross range between 77.5 and 135 ft. Each turbine contains six stainless-steel blades. The blade-tip diameter is 21 ft 2 in. The turbines are encased in plate-steel spiral cases.

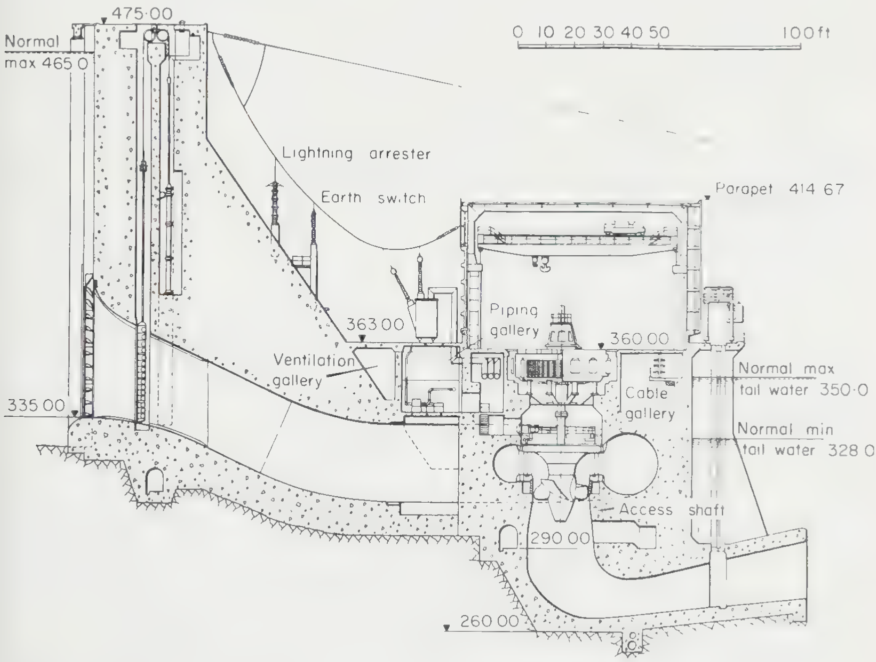

Fig. 31. Kainji power station.

21. Powerhouse Connected to Intake by Tunnels and Penstocks. The Appalachia powerhouse (Fig. 32) offers an interesting example of this type. A concrete dam 150 ft high, a tunnel nearly 8 miles long, and a powerhouse containing two 37,500-kw units operating under a 360-ft rated head are principal elements of the project. The units are spaced 44 ft center to center.

The substructure and outside walls of the superstructure are of concrete to levels above maximum tail-water elevation. The remainder of the superstructure consists of structural-steel framework with concrete floors and tile or concrete walls. The layout and design of the powerhouse were substantially influenced by the provision for tail water at elevation 882.[17]

The draft tube is of the plain elbow type. It has two outlet openings separated by a 4-ft-thick center pier. At the bottom of the runner, the draft tube is 8 ft 7 in. in diameter; at the discharge end it has a total clear width of 21 ft 9 in. and a height of 9 ft 8 in. The velocity head at the draft-tube exit at full gate discharge is 1.02 ft.

Cork-tar mastic is placed over the spiral case in the unit block and also over the upper half of the penstock where it goes through the east wall of the powerhouse. Between the unit block and the east wall, only the lower part of the penstock is embedded in concrete. These arrangements allow the penstock and the spiral case to expand and contract freely without causing undue stress in the concrete. Where the station is located at the toe of a dam, it is usual practice to provide a contraction joint between the dam and the powerhouse substructure. A flexible joint should be placed in the penstock where it crosses this contraction joint.

The Robert Moses Niagara power plant, completed on the Niagara River in 1961 by the Power Authority of the State of New York, is a medium-head plant of this type. Figure 33 shows a section through the plant and Fig. 34 shows a view from the downstream side. The structure is of the semioutdoor type. The plant is about 1,840 ft long and contains 13 unit blocks. The total installed capacity is 1,950,000 kw.

The Francis-type turbines are rated at 210,000 hp each at a net head of 300 ft. The normal operating head is 305 ft. The throat diameter of the runner is 205 in.

Welded-steel penstocks, approximately 462 ft long, connect the intake with the turbines as shown by Fig. 33. An upper elbow reduces the penstock from 28 ft 6 in. to 24 ft diameter. A lower elbow reduces it from 24 to 21 ft diameter at the spiral case extension.

The three-phase 60-cycle 150,000-kw generators operate at 120 rpm. The diameter of the stator frame is 40 ft.

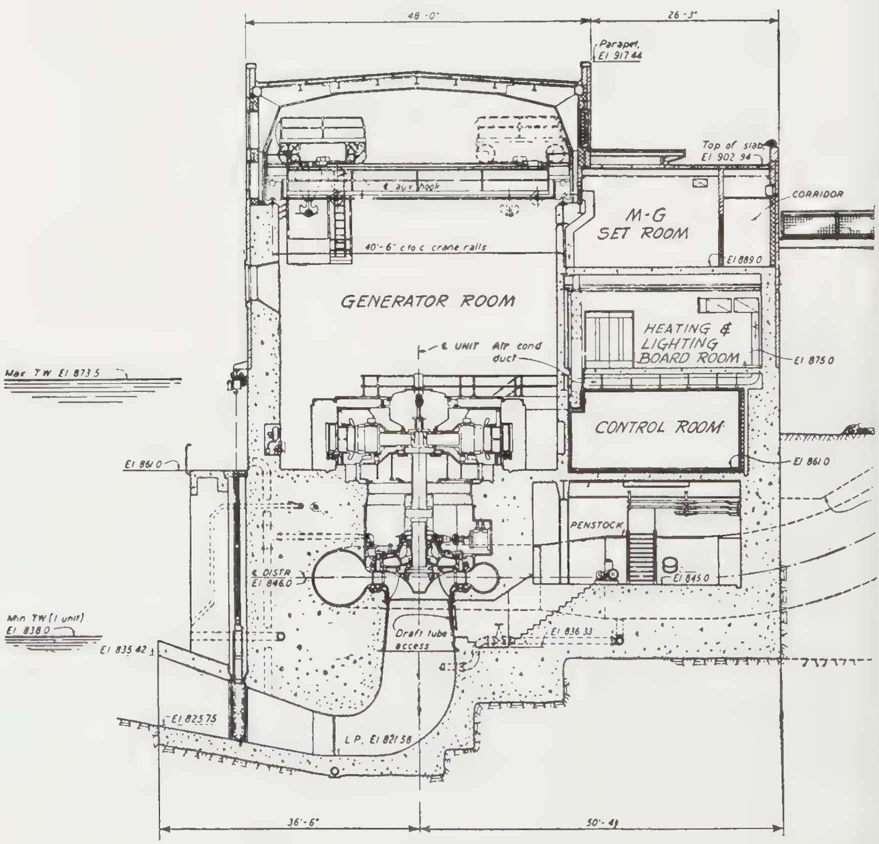

FIG. 32. The Appalachia powerhouse. *Left:* Section through

22. The Underground Powerhouse. Underground power plants are usually built in locations where the cost of excavating the caverns required to house the generating and electrical equipment will be less than that of constructing a powerhouse of another type. Where foundation conditions permit, the underground plant has many advantages at certain sites. For example, where space is lacking, as in a narrow gorge, to accommodate the structures, this type may be used to advantage. In some situations an additional advantage is obtained by cutting across one or more river bends with the tail tunnels and thus increasing the head on the plant and removing the tailrace from the influence of the spillway discharge.

Brief descriptions of two stations, the Kariba Gorge in Rhodesia and the Ambuklao in the Philippines, will illustrate the features of this type.

The Kariba Gorge project is located on the Zambezi River at a point where it flows through a narrow gorge some 250 miles downstream from Livingstone, Rhodesia. The project was built by the Rhodesian government and completed in 1960.[18,19] The scheme comprises a double-curvature arch dam 420 ft high and an underground powerhouse on the right bank designed to accommodate six hydro generating units, each of 100 mw capacity. The dam will raise the dry-weather water level in the river about 350 ft. Figures 35 and 36 show, respectively, a general plan and a cross section of the powerhouse.

The right-bank powerhouse is the first stage of power development. Provision has been made on the left bank to construct a future second stage.

The first stage consists of a concrete-lined underground machine hall 468 ft long, 75 ft wide, and 132 ft high and an adjacent transformer hall which is 537 ft long, 55 ft wide, and 60 ft high. Each turbine is supplied through an independent horizontal

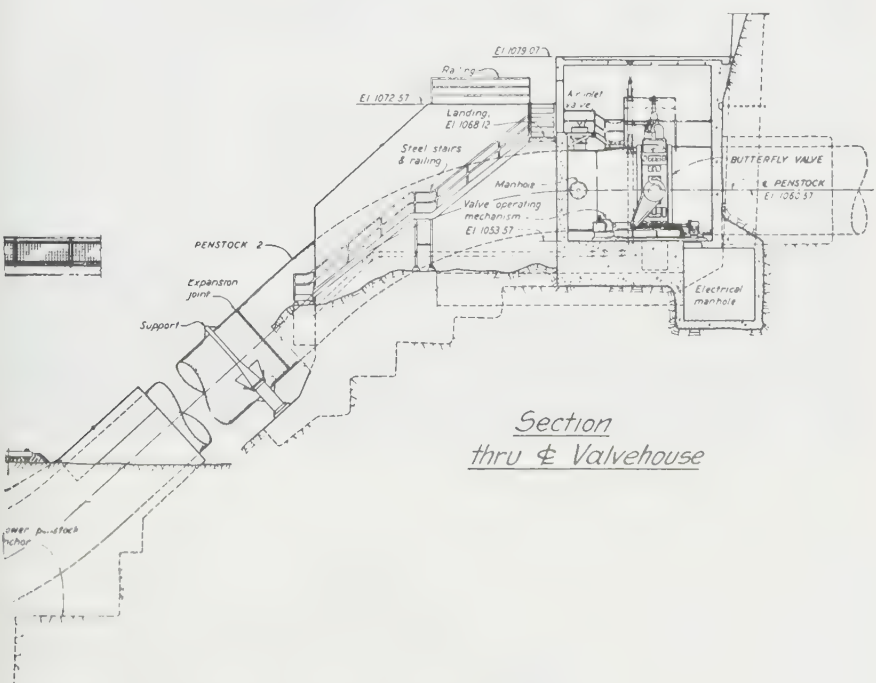

powerhouse. *Right:* Section through center-line valvehouse.

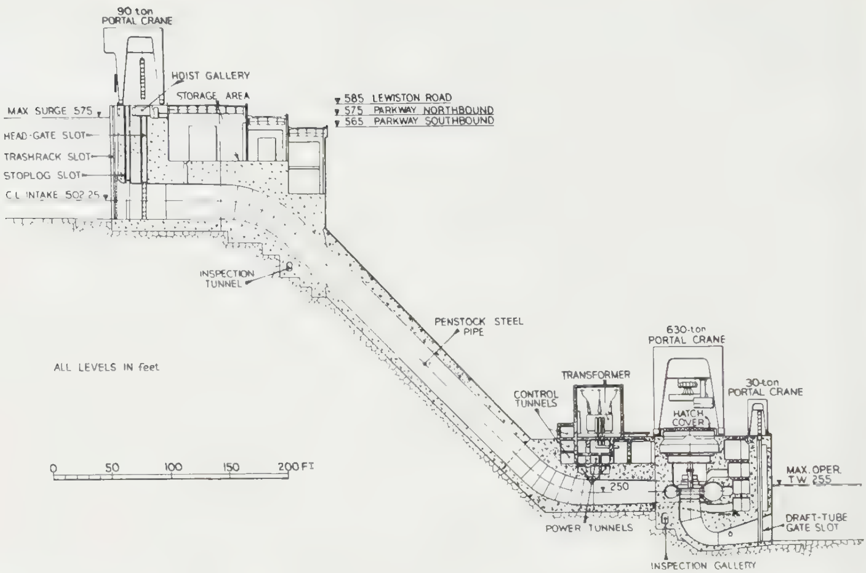

FIG. 33. Section through the Robert Moses Niagara power plant. (*Courtesy of New York State Power Authority. Uhl, Hall, and Rich, Consulting Engineers.*)

FIG. 34. Robert Moses Niagara power plant. (*Courtesy of New York State Power Authority. Uhl, Hall, and Rich, Consulting Engineers.*)

intake leading to a concrete-lined 20-ft-diameter vertical pressure shaft. Flow into these shafts is controlled by sector gates. Below elevation 1,780 the flow is carried to the turbines by vertical 17-ft-diameter steel-lined shafts.

Water is returned to the river by three tailrace tunnels, each 950 ft long and having an equivalent diameter of 34 ft each. Tailrace surges are controlled by 66-ft-diameter surge chambers.

The Ambuklao project, located on the Agno River near the city of Baguio in the Philippines, was completed by the National Power Corporation in 1955. The project

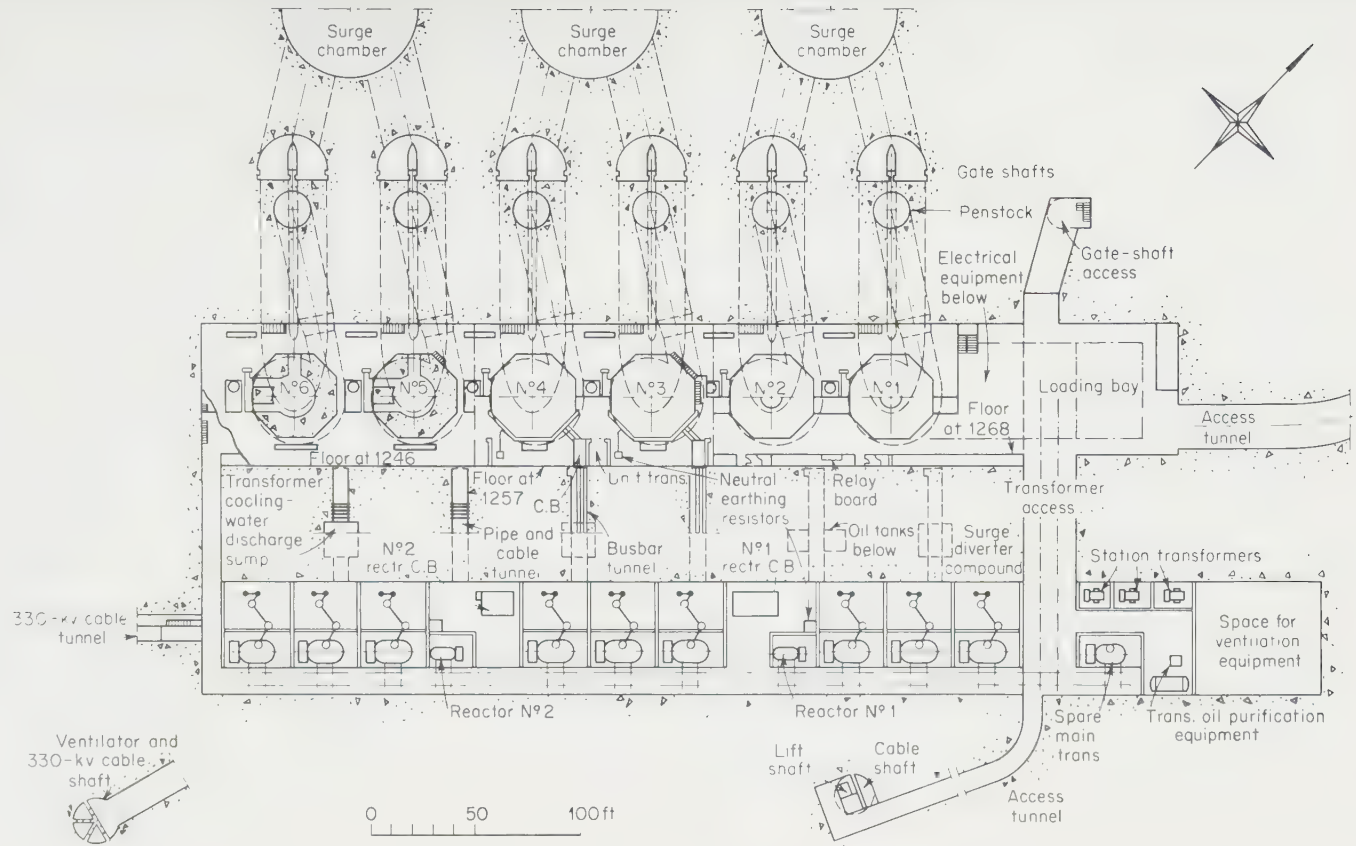

FIG. 35. Kariba Gorge powerhouse, general plan of underground powerhouse.

consists of a 430-ft-high rock-fill dam, a gated overflow spillway, low-level outlets, and the power features shown by Figs. 37 to 40, inclusive.[20]

A submerged 23-ft-diameter circular intake, shown by Fig. 37, has an operating platform placed at minimum drawdown level. A horizontal 23-ft-diameter concrete-lined horseshoe power tunnel connects the intake with a steel-lined manifold from which three 8.5-ft-diameter penstocks lead to the valve chambers shown by Fig. 38.

Each chamber houses a 102-in.-diameter butterfly valve and an 84-in.-diameter rotary valve. The butterfly valve serves as a guard for the rotary valve which is used in normal service. The valves control the flows to 7 ft 6 in. diameter steel-lined penstocks which make a 90-deg vertical turn and continue straight down to the spiral

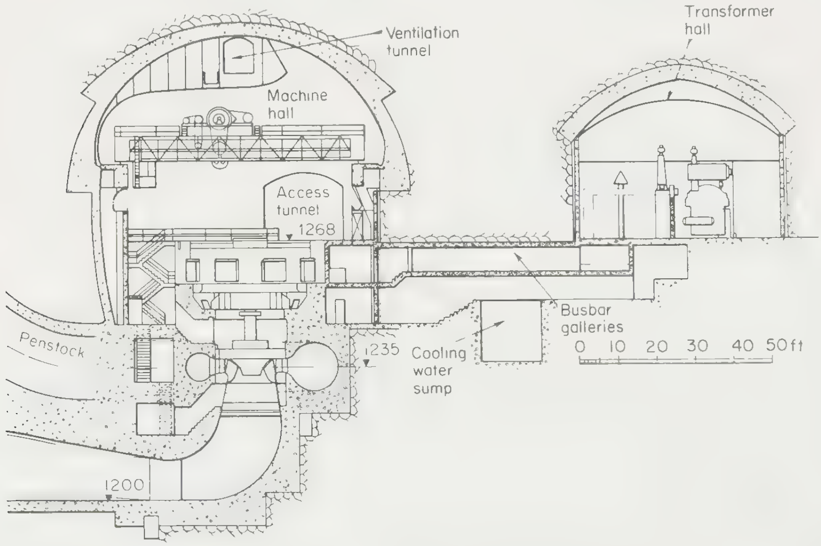

Fig. 36. Kariba Gorge powerhouse, vertical section showing arrangement of powerhouse and transformer hall.

case inlets. The steel liners are designed to take full internal pressure plus 23 percent of static head due to water hammer. The velocity in the penstocks is 15.1 fps at the rated discharge of 667 cfs per unit and 17.3 fps at the maximum discharge of 763 cfs.

The turbines are of the horizontal-shaft Francis type and are housed in cast-steel spiral cases embedded in concrete. The rated capacity of the turbines is 34,500 hp operating at 360 rpm under a net head of 505 ft. The corresponding generator rating is 25,000 kw. The turbines operate under a range of net heads varying between 380 and 572 ft.

The unit center lines are radial, as shown by Fig. 39. This arrangement permits the conical draft tubes to converge radially to the tailrace tunnel.

The concrete-lined tailrace tunnel is circular in section and 16.4 ft in diameter. It is 7,110 ft long and discharges, after crossing two river bends, about 5 miles downstream from the damsite. This extension increased the operating head on the plant by about 180 ft. The invert slopes upwardly from the draft tubes to assure the submergence of the turbines at low tail water. When the tunnel is flowing 0.90 full under the full plant discharge of 2,290 fps, the average velocity in the tunnel is 11.50 fps.

23. Low-head Plants. Many run-of-river stations such as Kentucky (Fig. 26) fall under this low-head classification. Improvements in the tubular-type generating units have resulted in the utilization of low heads which heretofore have not been economically feasible to develop.

The low-head hydroelectric stations on the Mosel River, Germany and France, illustrate a type of river development which may receive more attention in the future.[21]

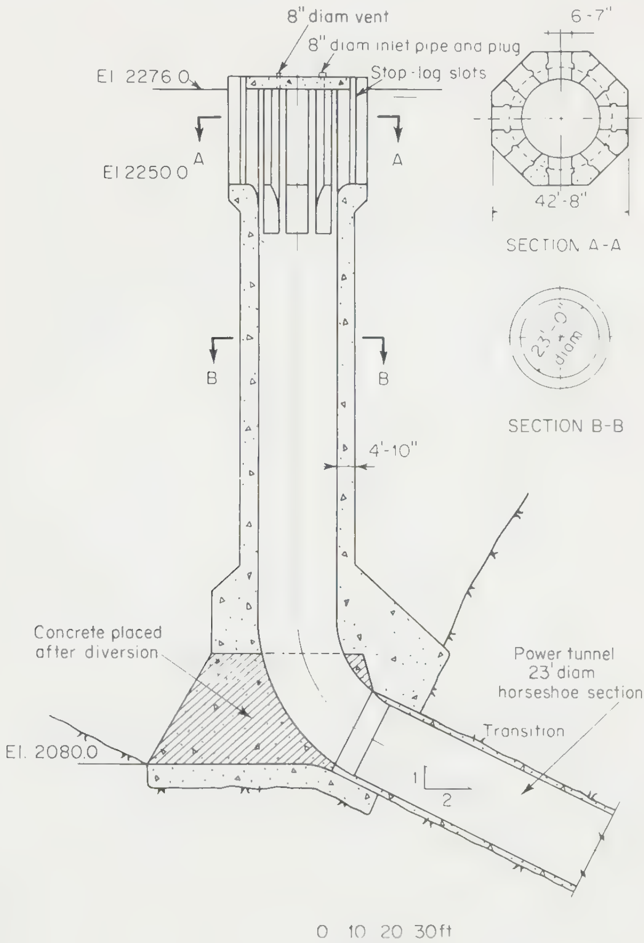

FIG. 37. Intake tower, Ambuklao project.

Figure 41 shows a map and profile of the Mosel River projects and water levels. The accompanying table in Fig. 41 shows some of the principal data for the 14 plants in Germany. It will be noted that the heads vary from 4 to 9 m.

The lowermost station at Coblenz (16 mw) is of conventional design with vertical-shaft Kaplan sets as opposed to the horizontal-shaft tubular sets used in the more recent stations constructed farther upstream.

The Trier station No. 10 (Fig. 42) illustrates the advantages of the tubular type. In addition to being a very low structure, with its roof only 2.4 m above the maximum

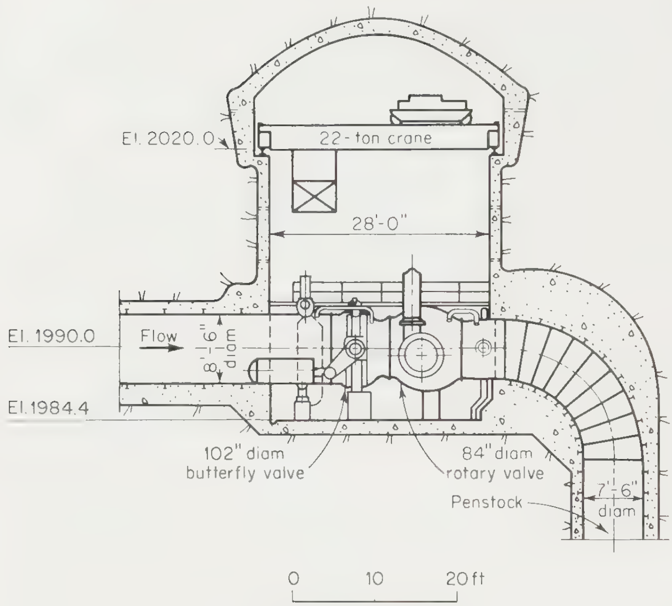

FIG. 38. Valve chamber, Ambuklao project.

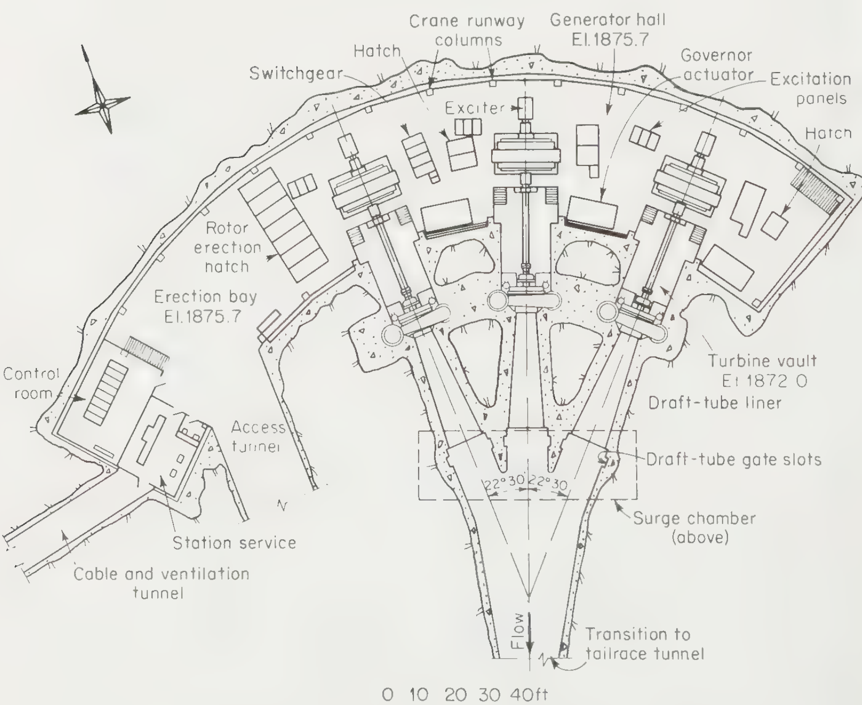

FIG. 39. Power station, plan, Ambuklao project.

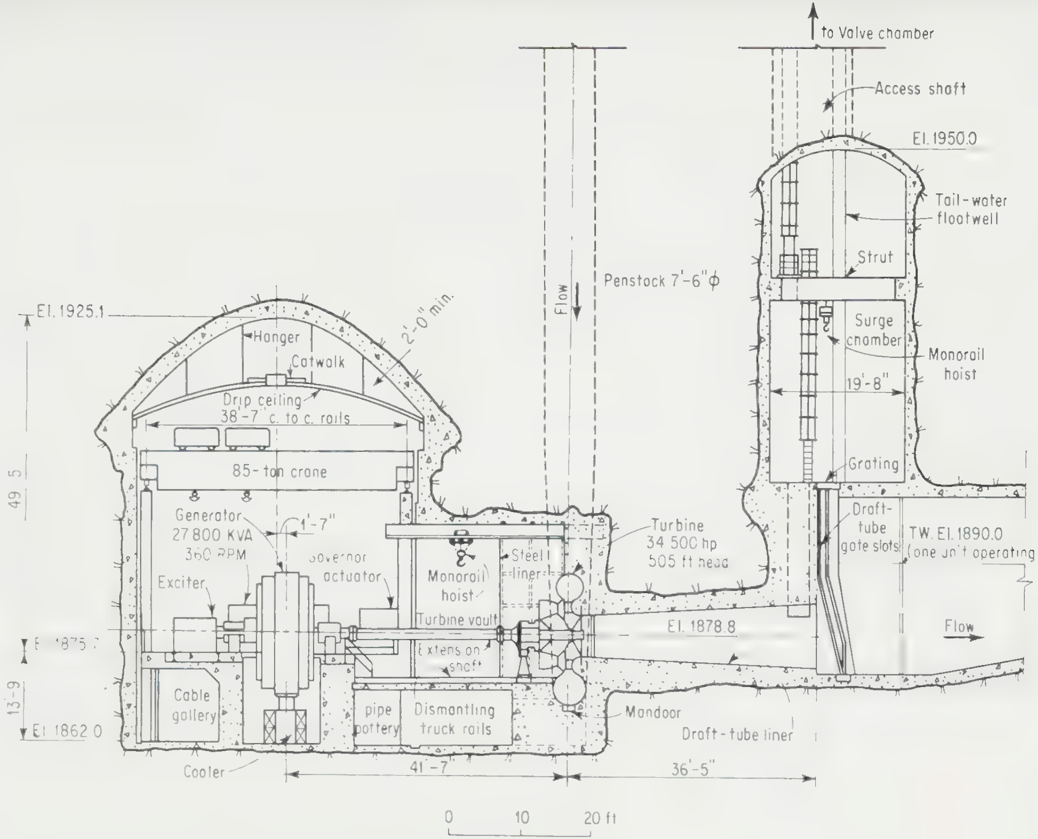

Fig. 40. Power station, transverse section, Ambuklao project.

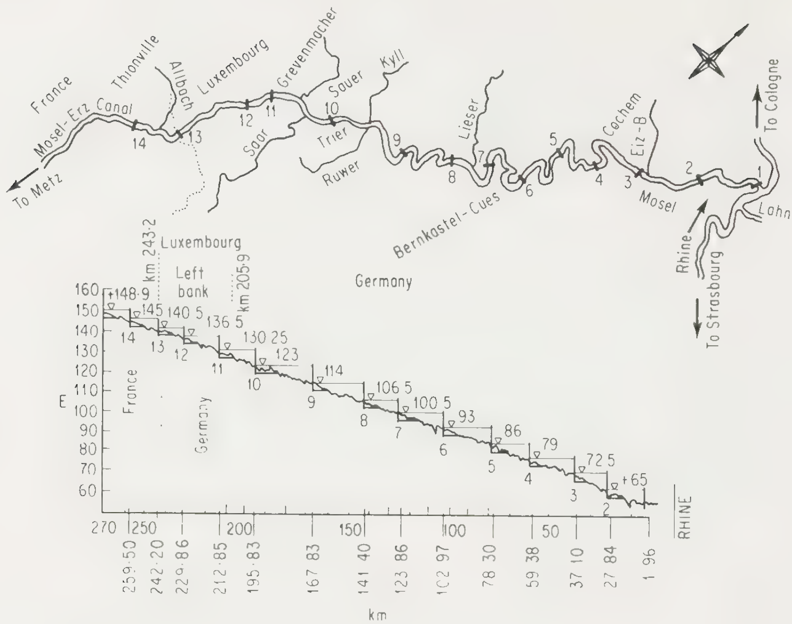

(a)

Station	No.	Pond elevation, m	Rated discharge, m³/sec	Head, m	Capacity, mw	Gross output, gwh	Construction dates
Coblenz	1	65.00	380	5.3	16.0	65.0	1941–1951
Lehmen	2	72.50	380	7.5	16.2	81.6	1960–1962
Müden	3	79.00	380	6.5	12.8	66.0	1963–1964
Fankel	4	86.00	380	7.0	14.72	71.6	1963–1964
St. Aldegund (Neef)	5	93.00	380	7.0	14.4	72.3	1962–1964
Enkirch	6	100.50	380	7.5	16.5	81.7	1964–1965
Zeltingen	7	106.50	380	6.0	12.2	61.7	1962–1964
Wintrich	8	114.00	380	7.5	17.7	87.0	1964–1965
Detzem	9	123.00	380	9.0	23.0	111.3	1960–1962
Trier	10	130.25	380	7.2	16.5	79.5	1959–1961
Grevenmacher	11	136.50	165	6.3	7.5	38.8	1963–1964
Palzem	12	140.50	150	4.0	4.1	19.6	1963–1964

(b)

FIG. 41. (a) Map and profile of Mosel River. (b) Principal features, Mosel plants. (*Water Power, July*, 1965.)

flood level of 132.31 m, the Trier station is much more compact longitudinally than a plant incorporating conventional Kaplan sets. At Coblenz, for example, the four vertical Kaplan units occupy a total length of 68.8 m, whereas the tubular sets at Trier are accommodated in only 45 m. The amounts of concrete used in the power stations were 25,100 cu m at Coblenz and 17,200 cu m at Trier.

24. Economic Design. Overall station economy must be the objective of the designer in selecting the size and spacing of the units, the elevation of the runner in

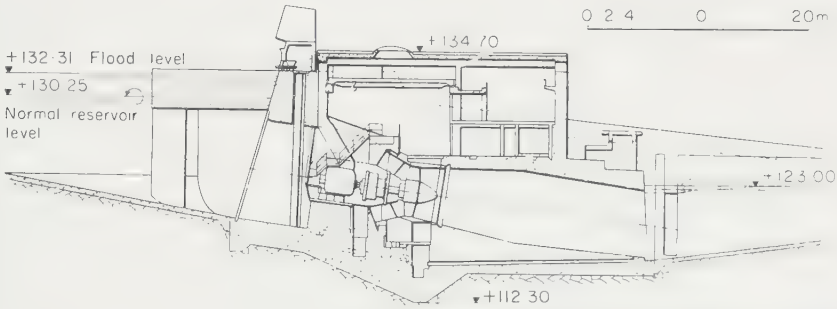

FIG. 42. Cross section through Trier power station showing arrangement of tubular generating set.

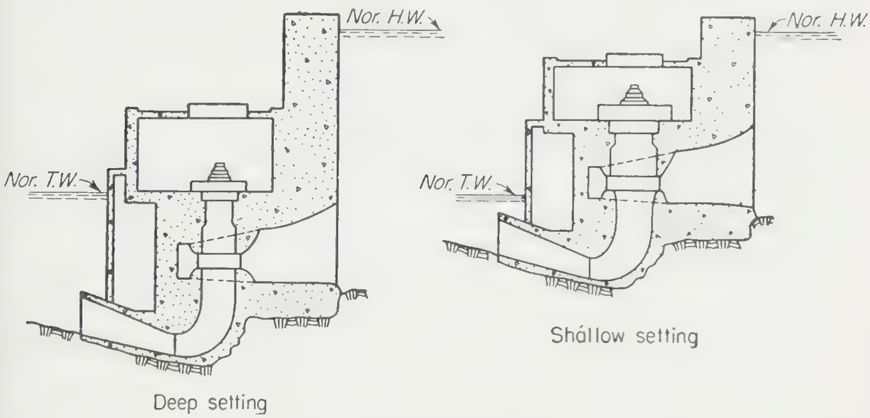

FIG. 43. Comparison of deep and shallow settings.

relation to tail water, and the specific speed. In order to achieve minimum station cost, the turbine setting must be tailored to the particular site and cannot be established by statistical or empirical methods. This is illustrated by Fig. 43,[22] which shows a somewhat exaggerated comparison of alternate deep and shallow settings for an integral intake and powerhouse substructure. In other words, the whole structure acts as a dam and both the overall proportions and the stability are affected materially by the choice of setting. For the same head, the same power, and the same margin of safety against cavitation, a relatively deep setting, with respect to tail water, means both deeper excavation and more expensive structures. This additional cost, however, is offset in part by a higher allowable operating speed which results in smaller physical dimensions and lower costs for the turbines and generators, and relatively less WR^2 will be required for a given degree of speed regulation.

The shallow setting, on the other hand, minimizes excavation and the structures. A slower operating speed, however, results in larger physical dimensions and costs for the generating units. The choice, therefore, will lie somewhere between the deep setting shown on the left of Fig. 43 and the shallow setting shown on the right. Where the rock is at low depth, the natural selection would be the smaller size, high-speed turbine, and conversely where the rock occurs at higher levels. For most sites, comparative estimates of several settings will be required to achieve the optimum.

It must be emphasized that the selection of the most economical turbine-generator set may not result in minimum overall powerhouse cost.

Bibliography

1. Creager, W. P., and J. D. Justin, "Hydroelectric Handbook," 2d ed., p. 261, John Wiley & Sons, Inc., New York.
2. Mackintosh, San B., Hells Canyon, *Water Power*, April, 1957, p. 138.
3. Bohn, M., and M. Hamon, The Djatiluhur Project, *Water Power*, August, 1967, p. 305.
4. The Fontana Project, *Tech. Rept.* 12, Tennessee Valley Authority.
5. Zowski, Thaddeus, Trashracks and Raking Equipment, *Water Power*, September, 1960, p. 342; October, 1960, p. 399.
6. Shiny Trash Racks Break Record, *Eng. News-Record*, July 20, 1967, p. 28.
7. Gilbert, Paul H., "Trashrack System Design for the Oroville Dam Power Plant Intake," paper presented to The National Association of Corrosion Engineers, Western Regional Conference, Corrosion Engineering Symposium, Honolulu, Hawaii, Nov. 9, 1965.
8. Binnie et al., Engineering of Mangla, *Proc. Inst. Civil Engrs.*, November, 1967, p. 449.
9. Sarkaria, G. S., Economical Diameter for Penstocks, *Water Power*, September, 1958, p. 352.
10. Gladwell, John S., and E. Roy Tinney, Hydraulic Studies of Large Penstock Trifurcation, *Proc. ASCE, J. Power Division*, May, 1965, p. 59.
11. Fosdick, Ellery R., Tunnel and Penstock Tests at Chelan Station, Washington, *Trans. ASCE*, **101,** 1409, 1936.
12. Willey, C. Keith, Wanapum Hydroelectric Development, *Civil Eng.*, September, 1960, p. 65.
13. Cochrane, H. G., The St. Lawrence Seaway and Power Project, *Water Power*, April, 1956.
14. New York State Power Authority, St. Lawrence Power, Aug. 10, 1954.
15. Palo and Marks, The Design of Hydroelectric Stations, *Trans. ASCE.*
16. The Kainji Project, *Water Power*, September, 1967, p. 347; October, 1967, p. 399.
17. The Appalachia, Ocoee No. 3, Nottley and Chatuge projects, *Tech. Rept.* 5, vol. 2, Tennessee Valley Authority.
18. Anderson, Paton, and Blackburn, Zambezi Hydroelectric Development, First Stage, *Proc. Inst. Civil Engrs.* **17,** 39, September, 1960.
19. Gibb, Sir Alexander, and partners, The Kariba Hydroelectric Scheme, *Water Power*, February, 1958, p. 45.
20. Eberhardt, Andrew, Ambuklao Underground Power Station, *Proc. ASCE, J. Power Div.*, April, 1958, paper 1598.
21. The Mosel Hydroelectric Stations, *Water Power*, July, 1965, p. 259.
22. Rich, G. R., Basic Hydraulics of Water Storage Projects, *Civil Eng.*, 1944, p. 351.
23. Williamson, J. V., and T. J. Rhone, Dividing Flow in Branches and Wye, *Proc. ASCE J. Hydraulics Division*, May, 1973, p. 747.

SECTION 25

PUMPED STORAGE

By Richard D. Harza

1. General. Pumped storage may be defined as any system which by means of a pump stores energy for use at a later time. By far the most important development in terms of energy stored is that in which water is pumped to an elevated reservoir for later use through turbines, and this is the type of development which is described here. It is appropriate to mention that many hydraulic machines, including hydraulic turbine governor actuators, involve "accumulator circuits," which are actually a miniature form of pumped storage utilizing compression of air.

The most obvious question about pumped storage is: why do it? Why build a power plant that actually consumes more energy than it produces? To appreciate the function and value of pumped storage consider the three basic factors common to all industry: production; inventory (warehousing, etc.); and sale or delivery. Production may be seasonal—as in agriculture—or it may be at a steady rate to achieve maximum efficiency. And sales or delivery may be at a steady or at an unpredictably changing rate, depending on many factors including human preference, the weather, changes in market conditions, etc. Hence it is the inventory-warehousing function which matches the production rate to the consumption rate. Note that inventory-warehousing does cost money and does not produce goods, yet it is amply justified because of the value it renders in reconciling production to consumption. Before pumped storage, the electric power industry was unique in that at any split second production exactly equaled consumption plus associated losses. Thus pumped storage has effected a major economic change in the electric utility industry by introducing the inventory-warehousing function into the business at a point between power generation (production) and distribution (consumption).

In operation, a pumped storage plant will consume excess energy from a large electric utility power system during periods when such energy is available. Then the pumped storage plant will deliver a part of this energy back into the system during maximum demand periods. Thus, low-value "off-peak" energy is converted into high-value "on-peak" capacity and energy.

There are many ways in which a pumped storage scheme can be developed in connection with conventional hydroelectric resources. All pumped storage schemes involve pumping water from a lower reservoir to an upper reservoir, and one of the most important types of pumped storage plant has always been the purely recirculating type in which the same water is reused during each cycle. The principal types of pumped storage schemes known today can be classified under four headings, as shown in Fig. 1: recirculating ("pure pumped storage") type, multiple-use type, water-transfer type, and tidal-power type. It is possible to combine these basic schemes in a great number of different ways, and some of the most complex hydro developments involve pumped storage features, as will be described later in this section.

The extent of pumped storage use is very widespread, and almost every industrialized nation can boast at least one such installation.

2. Principal Elements of Pumped Storage Developments. Because of their use of water, pumped storage schemes comprise the same major elements as conventional hydro power developments such as dams, reservoirs, spillways, conduits, and power plants. However, in pumped storage the emphasis on these elements is considerably different.

UPPER RESERVOIRS AND DAMS

The upper reservoirs of pumped storage projects fall into three general categories:

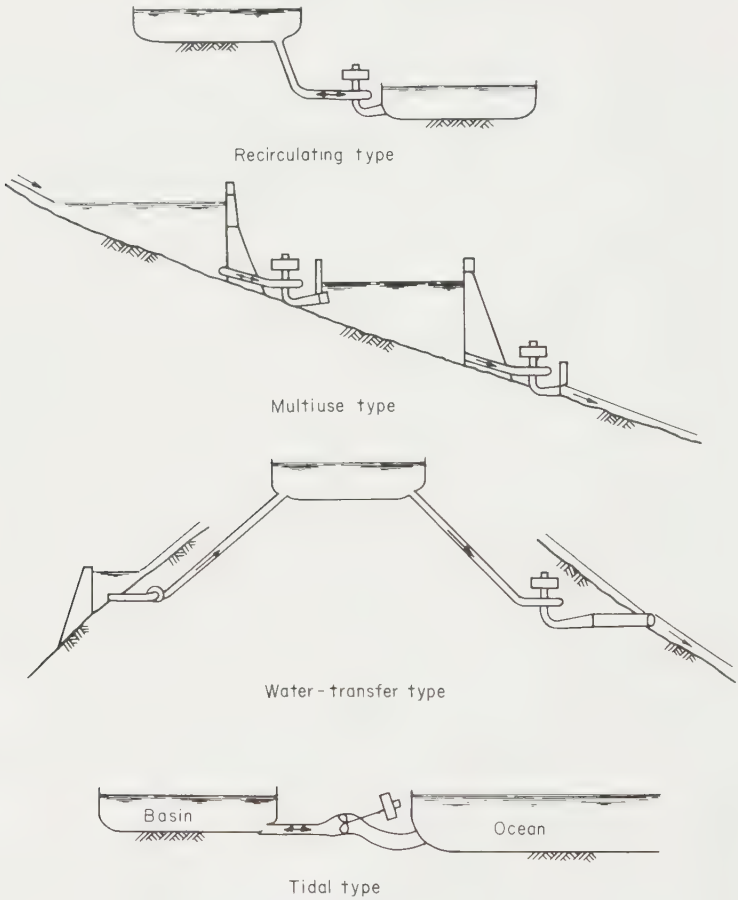

FIG. 1. Types of pumped storage development.

normal stream-valley reservoirs (Smith Mountain type), off-channel high-valley reservoir (Ffestiniogg type), and hilltop reservoirs (Taum Sauk) type. The first two types of reservoirs are normal in hydraulic practice and do not require special treatment here except to point out that all embankment slopes (and natural earth slopes at reservoir edges) must be stable under the very rapid and frequent drawdown conditions to which they will be subjected.

Large hilltop reservoirs are quite distinctive structures which are found only in connection with pumped storage projects. The design of hilltop reservoirs is generally determined by hilltop geology, hilltop topography, and quick-drawdown effects.

Geological conditions on hilltop areas generally include deep natural drainage, low groundwater, and deep weathering of soil and rock. Natural forces of gravity and weathering may cause progressively opening cracks in hilltop cap rocks as the adjacent process of valley formation tends to relieve stresses in and remove support from the cap rocks. Obviously, the ring dams which form hilltop reservoirs must be so situated that their foundations are absolutely stable. Sometimes this requirement reduces available storage capacity for a given height of embankment when the embankment cannot be located near the edge of the hilltop. Only careful geological studies and complete analyses of stability of embankments and foundations can resolve this problem. For economic reasons ring dams are always built from material excavated from the hilltop in such a way that the borrow pits become part of the reservoir capacity.

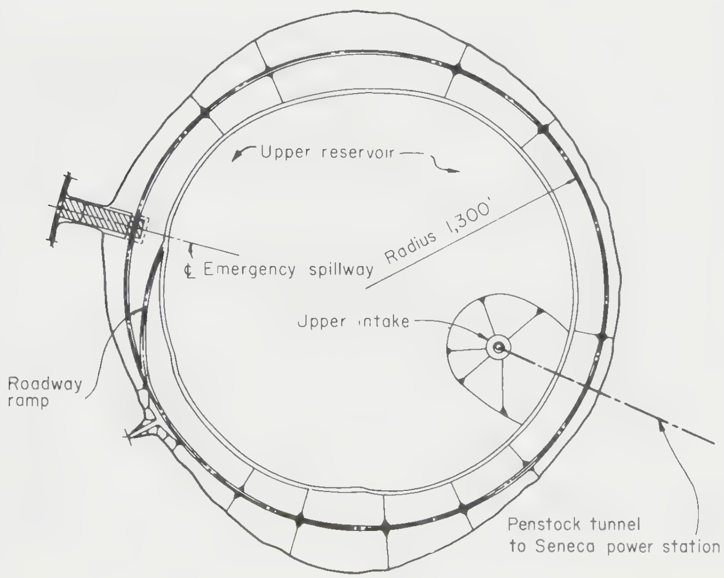

Fig. 2. Plan of Kinzua upper reservoir.

Because of the limitation of borrow area, and because of the deeper rock weathering on hilltops, a composite dam cross section including both rock fill and earth fill usually results.

3. Shape of Reservoir in Plan. Many shapes have been tried, but these categories dominate: circular, rectilinear, and kidney shape. Obviously the ideal economic shape for a reservoir on a flat surface is circular, because this gives the minimum excavation and embankment volume required to develop a given reservoir volume. Simple geometry shows that compared with a circular layout (on a flat surface) a square shape would require 12 percent more embankment length for the same storage, and an equilateral triangle would require a 28 percent increase in length. Actually, it has been found that even in relatively rough and irregular terrain, the circular (or ellipse) shape can often be the most economic solution. An example of the circular shape is shown in Fig. 2. If a circular layout can be positioned on the existing topography so that the maximum variation in embankment height is less than 1 to 2 percent of the developed length of embankment, then a circular layout may be the best solution. For a circular reservoir of 2,400 ft diameter, this would permit topographic height variation for short distances under the center line of the embankment of 150 ft. The noncircular shapes may be found necessary because of property lines, roads, or extreme irregularity of topography, but in most cases the starting point of upper-reservoir layouts should usually be a circle. Reentrant corners and angles are to be avoided because of the loss of reservoir volume without accompanying savings in embankment length.

4. Embankment Slopes and Reservoir Linings. Embankment slopes are necessarily determined by consideration of stability, and the trend is toward steep inner slopes, full impermeable lining of reservoirs and embankment faces, and elaborate drainage systems under the linings. Steep inner (wetted) slopes are particularly desired where heavy ice may form on the upper part of the embankment during draw-

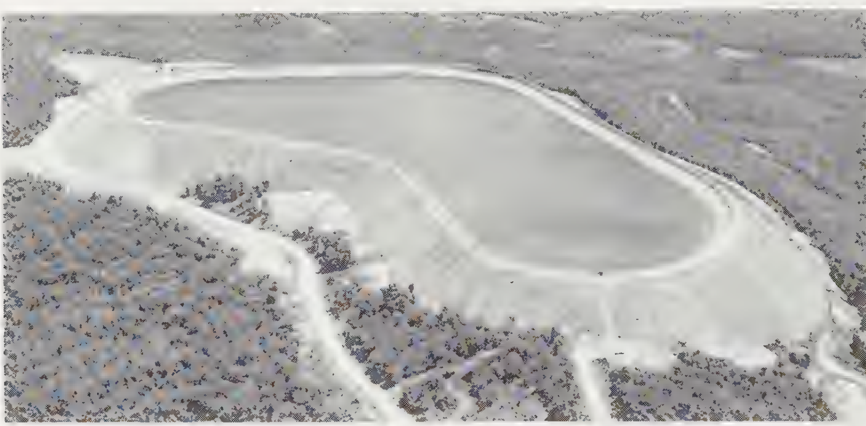

FIG. 3. Photo of Taum Sauk upper reservoir.

down and cause damage to the membrane of lining material. Economy of design also encourages steep slopes. At the Taum Sauk upper reservoir a 10-ft vertical parapet wall was designed and built on the crest of the embankment to gain additional storage capacity (Fig. 3). Various impermeable lining materials have been employed in upper reservoirs including concrete (both poured and pneumatically placed), earth, and bituminous concrete. The bituminous linings have proved to be remarkably watertight, durable, easily maintained, and generally successful. The watertightness can be ascribed to three things: the extremely low permeability of properly designed, dense (less than 2 percent voids) bituminous concrete; the effective hot sealing and lapping of joints; and continuity, plasticity, and flexibility of the lining. With the low leakage and effective underdrainage which can be achieved in bituminous concrete liners, uplift failures of membranes or embankment due to trapped leakage water and quick-drawdown operation can be avoided. It should be noted that some difficulties (which also serve to indicate the extreme impermeability of bituminous concrete) have been experienced when air trapped in the foundation rock and earth on the flat part of the reservoir bottom has raised large "bubbles" in the bituminous liner because of a sharp drop in barometric pressure shortly after placement of the liner. For this reason, adequate drainage (for both air and seepage water) must be provided under all flat and sloping parts of the bituminous liner. Some European upper reservoirs include elaborate underdrainage collection and measuring with accessible galleries and numbered collection drains covering the entire reservoir area.

The bituminous concrete itself is usually two layers (2 to 3 in. total thickness) laid on a prepared subdrain and working surface as shown in Fig. 4. Often a top seal coating is applied which contains asbestos fibers and is very rich in bitumen. This seal coat protects surfaces exposed to air and sunlight against weathering and further seals the joints, which are carefully staggered between the two basic layers.

5. Spillways. Spillways are not usually required on mountaintop ring dams. Normally, a double protective system to shut down pumps automatically when the water level reaches a safe limit provides adequate protection against overtopping of a dam by excess pumping. On certain projects where overtopping might cause unusu-

Fig. 4. Placing upper-reservoir bituminous lining at Vianden.

ally severe damage, spillways have been required (in addition to the normal measures) to direct any possible pumped overflows into "safer" areas. One example of this is the Kinzua project where a fuse-plug type of upper-reservoir spillway has been provided. Details are shown in Fig. 5.

6. Embankment Structures. All pumped storage mountaintop reservoirs to date have had embankments as the water-storage structures. Both rock-fill dams and earth-fill dams have been used. Economics usually dictate use of cut-and-fill operation and full utilization of whatever construction materials exist on the mountaintop. Frequently, the embankment is designed to be free-draining, and it requires a separate impermeable inner lining. At best, mountaintop reservoirs are expensive structures in terms of cost per acre-foot of storage. Thus, the upper reservoir at Kinzua required about 1 cu yd of embankment for each 4 cu yd of storage volume created, and together with its appurtenances it cost about $1,000 per acre-foot of storage.

7. Conduits, Valves, and Gates. Conduits for pumped storage schemes are similar to those for conventional hydro schemes, but certain special matters must be

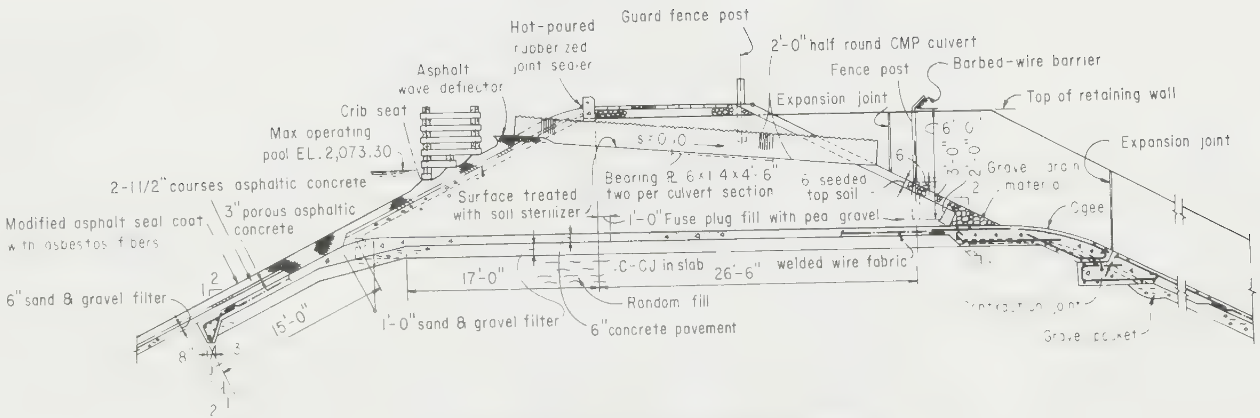

FIG. 5. Kinzua upper-reservoir fuse-plug spillway.

considered with pumped storage. Economy requires that, whenever possible, the main conduits be utilized for flow in both directions. Therefore, all elements of the conduit must be designed to accommodate flow in either direction. This is particularly important in manifolds and bifurcations, but it also applies to intakes, transitions, valves, gates, and all other elements. Tunnels seem to be preferred to exposed penstocks for pumped storage applications. This is doubtless due chiefly to economic consideration, but it also reflects the danger of penstock freezing, which could occur during an inactive period of pumped storage operations. It is interesting to note that some very high conduit velocities are under consideration for American pumped storage schemes. These contemplated velocities range up to 25 fps and are the result of a calculated sacrifice of efficiency in order to save capital investment in the pumped storage facility. Such efficiency losses can be tolerated in the pumped storage plant because it is designed for low-load-factor operation which is often in the 12 to 20 percent range.

Gates and valves utilized in pumped storage schemes are of the same basic type as used elsewhere. Roller gates and cylinder gates are common for the upper intake structures, although a number of American schemes will entirely omit the upper intake gates and have a simple, nongated "morning-glory" type of intake. Air-inlet valves in exposed penstocks to prevent collapsing are standard. Some pumped storage schemes utilize bypass values at the turbine to reduce overpressure.

In connection with pumped storage plants employing separate pumps and turbines, both the hydraulic elements will be protected by individual guard valves. The valves for the pump will generally be of the needle-valve type in order to permit throttling operations for starting and stopping pumps. The turbine is generally protected by a rotary valve or plug valve.

8. Draft Tubes. An important part of the conduit system in reversible-unit pumped storage plants is the draft tube. This must be designed for flow in both directions and therefore must have trash racks to protect the units while pumping. The usual case calls for a conventional elbow draft tube, but variations are starting to appear in American practice; for instance, the "double-draft tube" which is being used at the Kinzua project to permit draft-tube flows during generating to pass either to the reservoir area of the Allegheny Dam or to the tailrace area. The latter operation is used to obtain additional energy when downstream discharge can be scheduled. This draft tube is highly unconventional in design; as shown in Fig. 6, it consists of a vertical truncated cone with a center splitter cone, the draft-tube cone being supported on 12 solid steel columns of 3 ft 1 in. height.

9. Penstock Valves. Modern American practice calls for large, spherical valves immediately upstream of the spiral case where they can be serviced by the powerhouse crane. Some of these valves are of unprecedented size and weight, the largest to date being the 114-in. valves weighing 130 tons each (without operators) at Kinzua. These valves pose considerable problems in powerhouse layout and design because of their huge size (length 10 ft 9 in., height 15 ft, width 18 ft 4 in.). For this reason, a Belgian engineer, M. Greindl, has proposed reversible pump-turbines incorporating a cylinder valve into the turbine assembly and completely omitting other penstock valves of the conventional spherical type.

10. Powerhouses. Powerhouses for pumped storage projects resemble conventional hydroelectric powerhouses, and they may be located on the surface or underground. Pumped storage plants often require more extensive valving and auxiliaries. For instance, most reversible pumped storage installations require complete tail-water depression systems. In American practice, pumped storage power plants are often cut into the hillside of the lower reservoir area. A horizontal power-tunnel section leads to a sloping or vertical penstock shaft which reaches the upper reservoir. Normal reversible pump-turbines require a substantial submergence for pump operation, this submergence usually being in the range of 30 to 50 ft below minimum water level. Reversible pumps and pumps of high specific speed require deep submergence (as much as 150 ft at Cruachan), and this tends to favor underground powerhouse layouts.

An important consideration is aesthetics, and many steps are being taken to avoid unsightly or unharmonious outside appearances. Again, this favors underground power plants in scenic areas such as Hudson River Highlands (Cornwall plant) and Cruachan in the Scottish Highlands.

11. Lower Reservoirs. Lower reservoirs usually present the planner with fewer problems than their upper-reservoir counterparts. A lower reservoir is generally on a natural stream and may well be an existing reservoir built for flood control or other

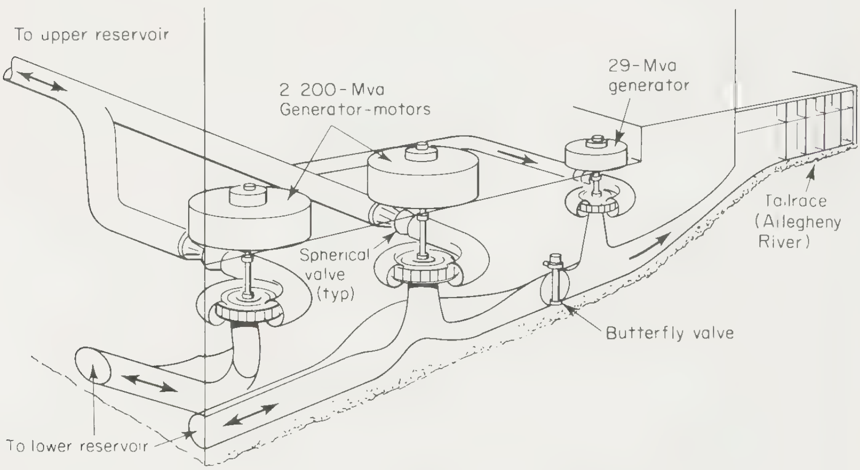

Fig. 6. Section of Kinzua double draft tube.

purposes. Lower reservoirs may have considerable catchment areas, and the expense of constructing an adequate spillway can be one of the major costs of the lower reservoir. Lower reservoirs tend to occupy valuable bottomland; so the cost of land acquisition and possible utility relocation is usually greater than for upper reservoirs. In recirculating pumped storage plants, make-up water to cover leakage and evaporation losses must generally come from natural inflow to the lower reservoir.

A number of unusual types of lower reservoirs have been proposed in addition to reservoirs on natural streams, although as yet no projects have been developed involving such novel lower reservoirs. In England and Taiwan pumped storage schemes are proposed using the sea as a lower reservoir. (All tidal schemes would do the same.) A scheme using Lake Michigan as a lower reservoir has been proposed, as has a scheme utilizing a disused mine in Ohio for a lower pumped storage reservoir. An urban drainage and pollution-abatement scheme under study for the Chicage area would use large galleries tunneled in hard rock 700 ft below the city as a pumped storage lower reservoir. It is of interest to note that the daily circulation of the partially contaminated storm-sewer water in pumped storage operation would have a beneficial effect from the standpoint of pollution abatement and raising the level of dissolved oxygen in the water.

MACHINERY

12. Reversible Pump-Turbines. These machines are covered in a separate section of this handbook under Turbines.

13. Separate Pumps and Turbines. The most frequently used machinery arrangements in all pumped storage projects completed to date (1968) are the separate pump and turbine assemblies common to European practice. An example of this arrangement is shown in Fig. 7. The trend today seems to be toward the reversible pump-turbine machines for reasons of economy, but the predominance of existing installations of separate pump and turbine installations to date indicates the great value of this arrangement. Separate pumps and turbines operate on opposite ends of a main shaft which has as its center a motor-generator which turns constantly in one direction. The constant speed and single direction of rotation permit very convenient and swift changeover between pump and generating modes. As shown in Fig. 8, this full changeover can be accomplished automatically in less than 2 min. When operating in the generating mode, the pump is brought quickly up to speed in the unwatered condition by the small synchronizing turbine on the main shaft; then an automatic coupling device connects the pump to the shaft of the motor-generator which is already at synchronous speed; the pump is watered; the pump shutoff valve is opened slowly and pumping starts; the turbine valve is closed; and the turbine is dewatered and it spins in air or vacuum during the pumping operation.

PLANNING FOR PUMPED STORAGE

14. Growth of Pumped Storage. Although pumped storage in Europe has experienced rather steady, progressive growth since its initial introduction in the late nineteenth century in Germany, it is only since 1960 in the United States that it has shown important growth trends. As of 1968 (Table 1), there are 15 major pumped storage projects in the United States in operation or under construction. These plants aggregate 3,765 megawatts of electrical capacity. The National Power Survey, pub-

TABLE 1. PUMPED STORAGE IN THE UNITED STATES, 1967, COMPLETED OR UNDER CONSTRUCTION

Project name	Date of operation	Generating capacity, megawatts
Rocky River, Conn.	1929	7
Buchanan, Tex.	1950	12
Flatiron, Colo.	1954	8
Hiwassee, N.C.	1956	59
Lewiston, N.Y.	1961	240
Taum Sauk, Mo.	1963	350
Smith Mountain, N.C.	1965	132
Yards Creek, N.J.	1966	337
Cabin Creek, Colo.	1967	325
Muddy Run, Pa.	1967	800
Thermalito, Calif.	1968	60
Oroville, Calif.	1968	261
San Luis, Calif.	1968	424
Kinzua, Pa.	1969	300
Keowee-Toxaway, S.C.	1971	450
		3,765

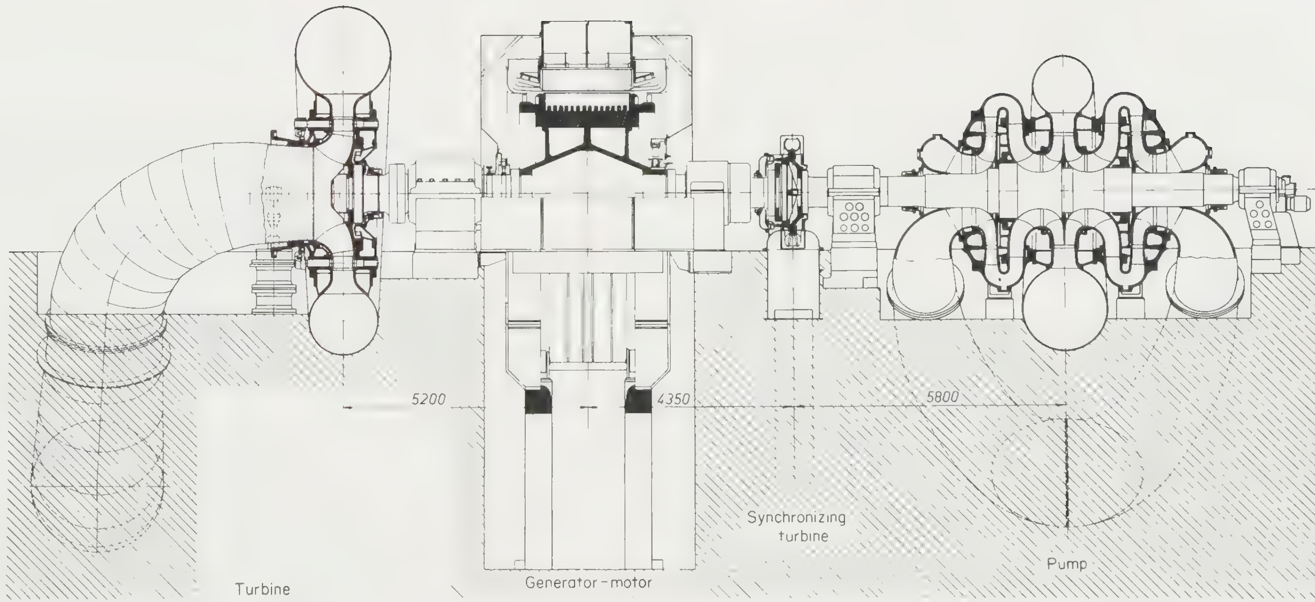

FIG. 7. Cross section of Vianden pump and turbine.

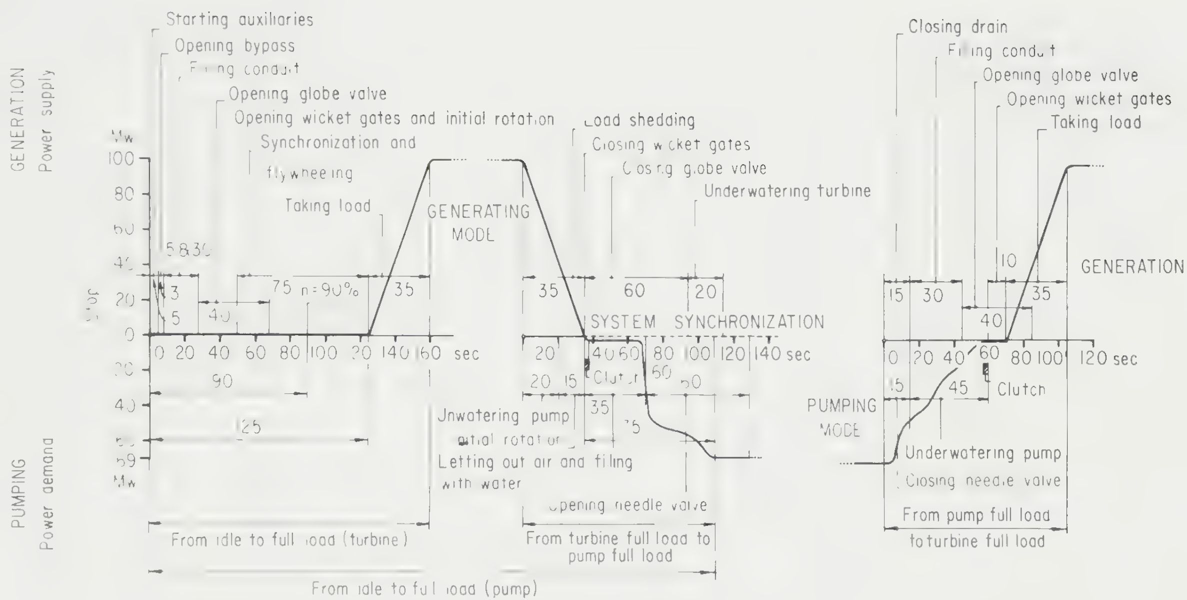

Fig. 8. Vianden unit starting and stopping time data.

lished by the Federal Power Commission in 1964, shows the projection of future pumped storage installations in the United States, indicating that 19 million kw will be installed by 1980, at which time pumped storage capacity would constitute 5.4 percent of the total electrical generating capacity in the nation. In view of this marked growth tendency, it is in order to review the principal considerations concerned with planning for pumped storage.

15. Supporting Electrical Generating System, Daily Peaking Service, and Seasonal Water Demands. Pumped storage is not a prime mover by itself but rather depends on other sources of generation to provide the power which pumped storage can store for later use. This fact rather severely limits the amount of pumped storage capacity which can be installed in any electrical generating system and at the same time can be considered firm generating capacity. The three things that pumped storage can do are: first, store energy during one part of the daily or weekly cycle for subsequent daily peaking; second, store energy during one part of the seasonal hydrological cycle for use during later parts of the season; and third, store water during one part of the seasonal hydrological cycle for use (and possibly basin transfer) during the season.

The first of these—daily peaking service—constitutes by far the largest use of pumped storage projects. Such installations are generally associated with generating systems that are dominantly or entirely thermal generation, with only a small hydroelectric component. Such systems are found in the flatter parts of Europe, that is, the northwestern part of Europe and the British Isles, as well as in the Eastern and Middle Western parts of the United States. Examples of seasonal energy storage are to be found in mountainous countries such as Switzerland and Austria, which are predominantly hydroelectric. Examples of seasonal water storage are to be found in arid areas where the value of water deliveries is great enough to justify elaborate water storage facilities, such as in California.

16. The Physical Site. Once the hydrological-system and power-system considerations have indicated the possibility for pumped storage installations, the next most important consideration is that of physical site. In general, the physical site should provide a head in the economical range, which is generally considered to be that adequately covered by reversible machines of economical size and speed. The optimum range would then be between 400 and 1,200 ft of head. Constant progress in reversible pump-turbine design is now permitting consideration of higher-head sites. Thus a 1,750-ft head at the Montezuma project in Arizona is now being planned (1968). Other important considerations for the physical site involve utilization of existing facilities and economics of water conductors. The most important single consideration for water conductors is that of total length. That is, the shorter the pressure conduit, the more economical the project. The pumped storage planner seeks sites with steep slopes which will shorten the water-conductor distance between the upper and lower reservoirs. The ratio of water-conductor length to head can vary anywhere from 2 up to 10. The optimum ideal ratio would be 1, wherein the upper reservoir was located directly over the lower reservoir, and several projects involving mines or specially created caverns have been proposed which would realize this unity ratio. The other site considerations common to hydroelectric plants also apply to pumped storage planning, and these include foundation conditions, transmission distance, sources of construction materials, effect of climatic conditions, etc.

17. Existing Project Facilities. Often a dominant consideration in planning pumped storage is the existence of transmission facilities or river reservoirs which can be incorporated into the pumped storage project, thus substantially reducing project costs. One of the larger inducements in the Eastern United States in recent years to construction of pumped storage has been the existence and development of hydroelectric and other multipurpose reservoirs which, when built, became the key factor in making an associated pumped storage development economically feasible. The Kinzua project, the Muddy Run project, and the Tocks Island project fall into this category.

18. Evolution of Machinery. This factor has had a great effect on pumped storage planning. The greatest single breakthrough was the reversible pump-turbine perfected in the 1950s and 1960s, although originally used at a much earlier date. A bold example of the first large-capacity reversible pump-turbine was the Taum Sauk installation of the Union Electric Company, where two 175-megawatt units were first operated in December, 1963. The possibilities of higher-head single-stage pumping have been developed rapidly with the reversible pump-turbine. Previous to the reversible-pump-turbine development, the maximum pumping head for a single-stage pump was generally considered to be in the range of 600 ft. There are now installations of single-stage reversible pump-turbines more than double this amount, and technology is constantly pushing up the head possible for reversible-pump-turbine installation. The perfecting of microwave and other remote-control techniques has permitted the planning of unattended pumped storage plants, and this has greatly enhanced their economic attractiveness.

19. Economic Comparisons with Alternative Power Sources. Although pumped storage planners have been accused of eying attractive pumped storage sites with the zeal of visionaries, it is almost without exception the case that cool and impartial economics must justify pumped storage developments. This fact necessitates complete analysis and comparison of a proposed pumped storage development with all possible alternative sources of the same electrical or water storage service. In general, sources of electrical peaking power would be from older existing thermal units; newly built steam units such as gas-turbine units; diesel units; and in some cases utilizing the demand-responsive characteristics of the more modern design of nuclear plants. If water storage for seasonal flow regulation is the primary purpose of a proposed pumped storage project, then alternative projects for cost-comparison studies would include groundwater storage, water storage in gravity-fed reservoirs, and reuse of existing water resources.

20. Economic Analyses. In the opinion of the author, the best form of economic analysis for a proposed pumped storage plant includes comparison with alternative installations and system fuel costs considering the alternative installations. For daily peaking the three greatest advantages for pumped storage will generally be found to be: first, low capital cost; second, ability to bring full power onto the line quickly (usually in less than 10 min); and third, progressively decreasing generating costs as lower-cost pumping energy becomes available in the system in future years. The greatest disadvantage to pumped storage is usually the limitation on energy availability from it. In those pumped storage installations which involve water transfer and seasonal distribution of water service, the economics of daily peaking will assume less importance, and the economics of water service will tend to dominate. It should be noted here that in certain pumped storage installations there are side uses which may have an influence on the economic decision. Such items would include potential use of upper reservoir for municipal water supply and, in certain cases, marginal flood-control benefits attributable to the pumped storage installation. At Keowee-Toxaway (South Carolina), a major consideration for an initial hydro and pumped storage installation of 610 megawatts is that its 18,400-acre reservoir will provide a future cooling pond for up to 7,000 megawatts of nuclear capacity to be added to the Duke Power Company system in future years. The present-worth value of this future cooling-pond benefit has been estimated to exceed \$2 million in this case.

EXAMPLES OF MODERN PUMPED STORAGE PRACTICE

21. Example A. San Luis Project—Pumped Storage in Water-conveyance System. A modern example of the incorporation of pumped storage into a major long-distance water-conveyance system is the San Luis pumping generating plant, a joint facility of the U.S. Bureau of Reclamation and the California Department of Water Resources. This plant, scheduled for operation in early 1967, essentially provides for seasonal off-channel storage of surplus waters being transferred from northern to southern California. Reversible pump generating units are employed, and off-peak pumping as well as on-peak generating will be used to the maximum extent consistent with the water-delivery schedule. A more detailed description of the plant follows. The pumping generating facility is housed in an outdoor powerhouse structure, approximately 480 ft in length by 90 ft in width and 110 ft in height. This is located in the left abutment of the San Luis Dam, a 78 million cu yd earth-fill structure. The plant will house eight vertical-shaft pump-turbine generator units. The pump-turbines are of the Francis type and have elbow draft tubes and spiral cases with fixed-stay vanes and no wicket gates. To accommodate the very large variations in operating heads ranging from 100 to 327 ft, the pump turbines are designed to pump or generate at either 120 or 150 rpm. Each unit will pump 1,375 cfs at 290 ft of static head at a speed of 150 rpm. Each unit will also, when generating, pass 1,640 cfs at the rate of 197 ft and a speed of 120 rpm. Each turbine is fitted on the upstream side with a butterfly valve, and each pair of units is further protected by a fixed wheel gate at the reservoir end of the high-head conduit tunnel.

The reversible motor-generator units are rated at 63,000 hp for motor operation and 150 rpm and 0.95 power factor, and are rated for 34,000 hp for motor operation at 120-rpm unit power factor. The generators are the synchronous type and will operate at 13.8 kv as generators and 13.2 kv as motors. Rated output of each generator will be 53 Mva at unity power factor and 150 rpm, or 34 Mva at unity power factor and 120 rpm. The motor-generators are designed to operate at 150 rpm as synchronous condensers. For starting of the pumps, the electrical across-the-line starting system will be used, and this can be employed either with water in the impeller zone or in the unwatered condition.

In operation, the surplus wintertime water in the north portion of the California aqueduct will be pumped from the San Luis forebay into the San Luis upper reservoir, a 2 million acre-ft seasonal storage facility. To the maximum extent possible, pumping will be done during off-peak hours. Later, during the irrigation season, water will be released from this San Luis reservoir back into the California aqueduct for transfer south. The stored energy will be reclaimed by the generating function of the pump generating plant.

22. Example B. Kinzua Pumped Storage Project. The Kinzua pumped storage project in northwestern Pennsylvania is basically a recirculating pumped storage project but has an additional flow-through hydro power feature to utilize the hydro potential of allowable downstream releases. The project, as shown in Fig. 9, is built in connection with a U.S. Army Corps of Engineers flood-control dam located on the Allegheny River. The project comprises the following elements: (1) low-head intake, (2) power plant, (3) high-head tunnel conduit, and (4) upper reservoir. The lower intake structure built in the pool of the Allegheny Dam permits flow in either direction between the Allegheny Reservoir and the power plant. This intake structure contains two fixed-wheel-type vertical gates, one for each of the conduits. These gates are capable of withstanding unbalanced pressure against either face of the gate, and each gate can be operated by hydraulic hoists. One closure bulkhead is provided which can operate in separate slots upstream of the intake gate. An interesting feature in connection with the lower intake is the two temperature-controlling bulkheads, which are provided to permit the withdrawal of low-temperature water for downstream release from various levels within the reservoir. Low-head conduits of 15 ft diameter lead from the lower intake to the power-plant structure. The power station itself houses two reversible pump-turbines and their associated motor-generators. In the generating direction the rated capacity of each of these units is 175 megawatts. A smaller pure hydro unit of 30 megawatts is included in the plant. Unit 1 nearest the Allegheny Dam is a pure recirculating unit and can handle water only between Allegheny Reservoir and the upper reservoir. Unit 2 in the center of the power plant can perform a similar function. In addition to this, it is also capable of drawing water from the upper reservoir and discharging into the Allegheny River downstream of Kinzua Dam. Thus, there is additional head benefit at times when water may be

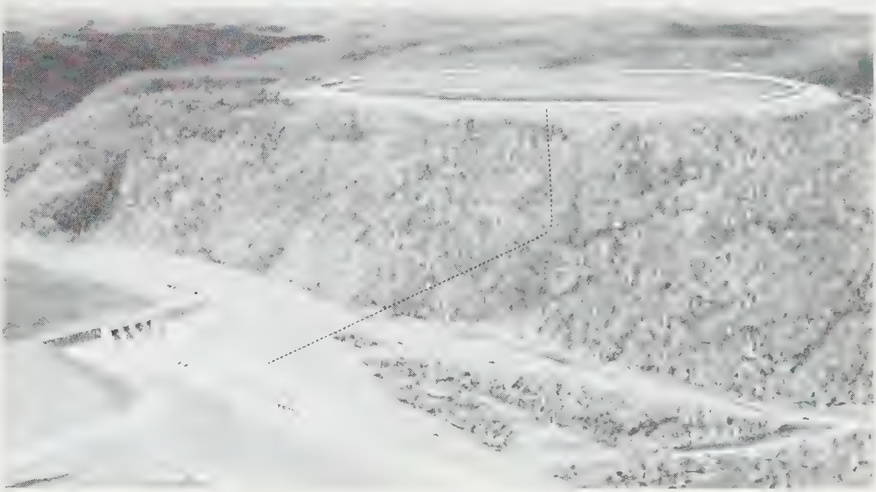

FIG. 9. Artist's conception of Kinzua project.

released downstream, in connection with the low-flow-augmentation operations of Allegheny Dam. Unit 3 operates only in a generating direction, receives its entire water supply from the upper reservoir, and discharges only into the Allegheny River downstream of the dam. This unit is sized to pass the basic 500-cfs minimum downstream release specified by the Corps of Engineers.

An additional function of the 30-megawatt Unit 3 is its starting duty. This unit provides a starting torque for the reversible units when they are being started in the pumping mode. The generator-motors will be started one at a time by connecting the armature of each to the armature of the Unit 3 generator at standstill. Using separate excitation the Unit 3 turbine will accelerate its generator and the electrically connected motor of the larger unit in synchronism up to rated speed. The time to bring the pump to operating speed will be less than 5 min.

The high-head conduit connects the pumping plant and the upper reservoir. On the horizontal run of approximately 2,300 ft, this conduit has 10 percent slope and is concrete-lined with an inside diameter of 22 ft 4 in. As the high-head conduit approaches the river valley it is steel-lined to take unbalanced pressures under the reduced rock cover. At this point the diameter is reduced to 21 ft 6 in. A vertical run leads up to the morning-glory-type intake in the upper reservoir.

The upper reservoir is located about 800 ft above Kinzua Dam and horizontal at a distance of approximately 2,000 ft from the dam. The upper reservoir is circular in plan, is fully lined with bituminous concrete, and is serviced by a single morning-glory-type intake. Over this intake a 100-ft-diameter flat-plate vortex suppressor is

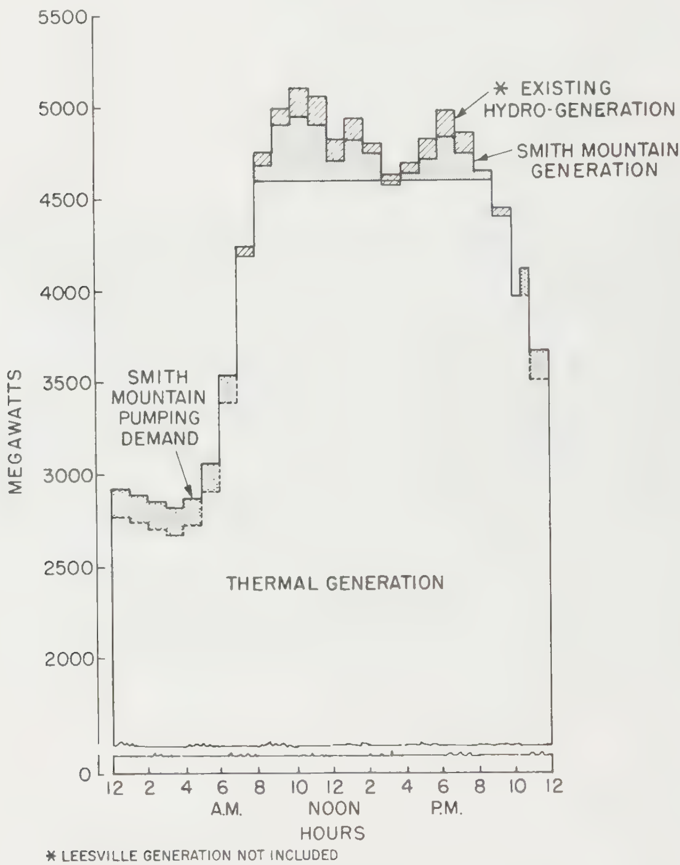

FIG. 10. Smith Mountain daily loading diagram.

provided to prevent vortex action which might draw in floating ice to the turbines during generating direction under adverse weather conditions. The upper reservoir contains an emergency spillway equal in capacity to the pumping capability of the two reversible units. The 6,000-acre capacity of the upper reservoir provides for 11 hr of continuous generation at full capacity. The 325-megawatt Kinzua project will be connected into an electric-utility power pool which contains more than 15 million kw total capacity and will have more than 1 million kw of pumped storage capacity at the time Kinzua is tied into the pool.

23. Example C. Smith Mountain Project. Smith Mountain project is an excellent example of the multiuse pumped storage project. It consists of two dams in tandem on the Roanoke River. By pumping backwater to the upper reservoir for reuse, the installed capacity of this project, which has been studied previously as a straight hydro two-stage development, was increased by a factor of 10. The total installed capacity of the project is 440 megawatts, of which 40 megawatts is in conventional hydro at the lower dam at Leesville. Provision is made for a fifth reversible 140-megawatt unit. Figure 10 illustrates how the Smith Mountain operation of pumping during off-peak and generating during on-peak hours fits with its intertied system of operations. It is noted here that the existing hydro generation of the system is accorded even higher position on the peak generation than is the pumped storage which came at a later date. By using weekend pumping, pumping energy is sufficient to ensure a firm peaking energy of 2 million kwhr per day.

Fig. 11. Lewiston pumped storage plant (background) and the Robert Moses hydroelectric plant (foreground).

A unique feature of the Smith Mountain project is the configuration of the power plant containing the reversible pump-turbine units with the 235-ft-high arch dam. Free-standing penstocks incorporating two 90-deg turns lead from a high-level intake on the dam face to the turbine units. This permits the release downstream of reservoir surface waters containing adequate dissolved oxygen for fish and wildlife requirements.

24. Example D. Lewiston Pumped Storage Project. This project is an excellent example of a low-head daily-peaking pumped storage project operating in connection with a large conventional hydroelectric plant. Thus, while the rated pumping head is only 85 ft, the effective generating head is 389 ft (75 ft at the Lewiston pumped storage plant plus 314 ft additional at the 2,190-megawatt Robert Moses hydroelectric plant located immediately downstream, as shown in Fig. 11).

Both these plants are on the American side at Niagara Falls, and by treaty larger flows can be diverted from the falls for power use at night than during the day. Although this treaty provision protects the scenic values of the falls, it results in the availability of the largest power flows at off-peak nighttime periods. Essentially the purpose of the Lewiston pumped storage plant is to reconcile the treaty flow pattern with the electrical-system demand pattern, and in this sense it is a special-purpose installation.

The Lewiston pumped storage plant contains 12 motor-generators directly connected to 12 reversible hydraulic pump-turbines. Each electrical unit is rated at 37,500 hp as a motor and at 20,000 kw as a generator operating at 112.5 rpm in either operation mode. Rated discharge of each pump is 3,400 cfs, 85 ft net head. Pumps are started "across the line." The plant, which includes a highway bridge on its lower deck, cost about $300 per kilowatt installed at Lewiston or about $30 per kilowatt installed at Lewiston and Robert Moses plant combined.

SECTION 26

HYDRAULIC MACHINERY

By Lewis F. Moody[1] and Thaddeus Zowski

HYDRAULIC TURBINES

1. General Classification. Hydraulic power-generating machines, or hydraulic prime movers, comprise most broadly the following: the early types of water wheels including the so-called current wheels utilizing the velocity of an open stream and gravity wheels, such as overshot, breast, and undershot wheels utilizing the elevation head of water, which are now obsolete; positive-displacement motors, utilizing pressure without significant effects of changes in the fluid velocity, such as reciprocating or rotary displacement motors which are used mainly in fluid-power applications other than water-power development; and hydraulic turbines. Turbines involve in their action a continuous transformation of the potential energy of the fluid into kinetic energy (and in reaction turbines a subsequent reconversion) and a conversion of kinetic energy, or of both kinetic and potential energy, into useful work. Turbines are the only prime movers of importance in modern hydraulic power development and are the only class that will be considered here.

Hydraulic turbines are divided according to their hydraulic action into two main classes: *impulse turbines* and *reaction turbines.* These terms should be regarded as names, having no special hydraulic significance in differentiating between their actions but being firmly established in general usage.

Impulse turbines are represented in modern practice by the Pelton-type water wheel, illustrated in Figs. 1 through 4. In an impulse turbine, all the available head is converted into kinetic energy or velocity head in one or more contracting nozzles (Fig. 4) by which the water is formed into one or more free jets before acting upon the runner. Throughout its action in the runner the water flows with free surfaces in buckets which it only partly fills, its flow thus being similar to that in an open channel. During this action, the water is in contact with the air, and although the Pelton wheel is provided with a housing to prevent splashing and to guide the discharge, this housing contains air usually at atmospheric pressure, through which the water discharged from the buckets falls freely into the tail water.

In reaction turbines, the entire flow from headwater to tail water takes place in a closed conduit system, being laterally constrained on all sides. At the entrance to the runner, only a part of the available head is converted into kinetic energy, a substantial part remaining in pressure head which varies throughout the passage through the turbine. The flow thus resembles that in a closed pipe system. In all modern forms of both impulse and reaction turbines, the water in entering the runner exerts upon it a force in the direction of flow, termed in hydraulics an impulse; and at discharge from the runner, it exerts a reaction opposite to its direction of flow.

Reaction turbines are represented in modern practice by two principal types, the Francis turbine, illustrated in Figs. 5 to 10, and the propeller turbine, illustrated in

[1] Deceased, April, 1953. This section has since been revised, updated, and supplemented for the Third Edition by Thaddeus Zowski.

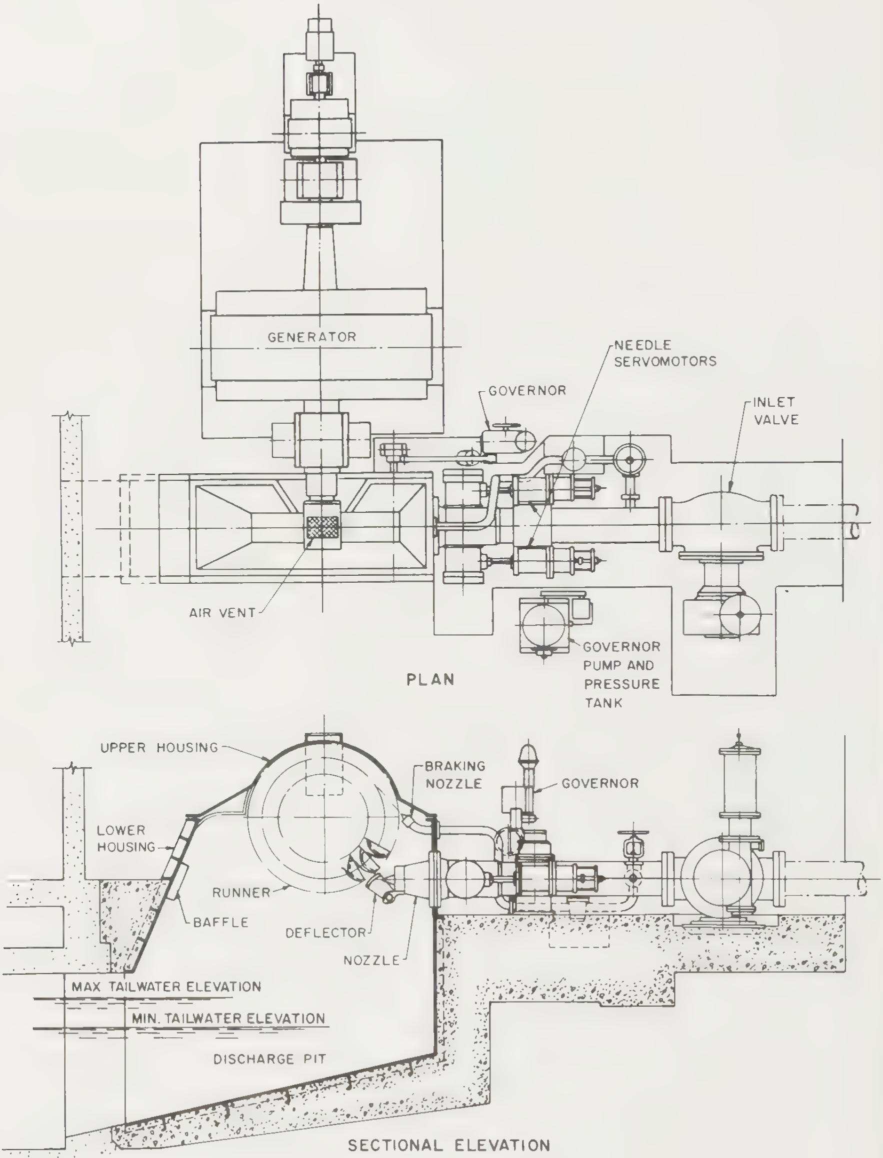

FIG. 1. Impulse turbine (Pelton type) rated 12,000-hp, 2,490-ft net head, 600 rpm. Typical horizontal-shaft single-jet arrangement with single overhung runner. Straight-flow nozzle with external needle servomotors. (*Allis-Chalmers Mfg. Co.*)

Figs. 11 to 18. Propeller turbines are subdivided into fixed-blade and adjustable-blade types; the latter are represented primarily by the Kaplan-type turbines. Intermediate types, such as diagonal-flow turbines, have also been developed. Adjustable-blade diagonal-flow turbines, known also as Deriaz-type turbines, came into commercial service in 1957.

Reaction turbines may operate with inward, outward, axial or mixed flow through the runner (these directions referring to the velocity components in a meridional plane, a plane containing the runner axis), and the general theory outlined later can be

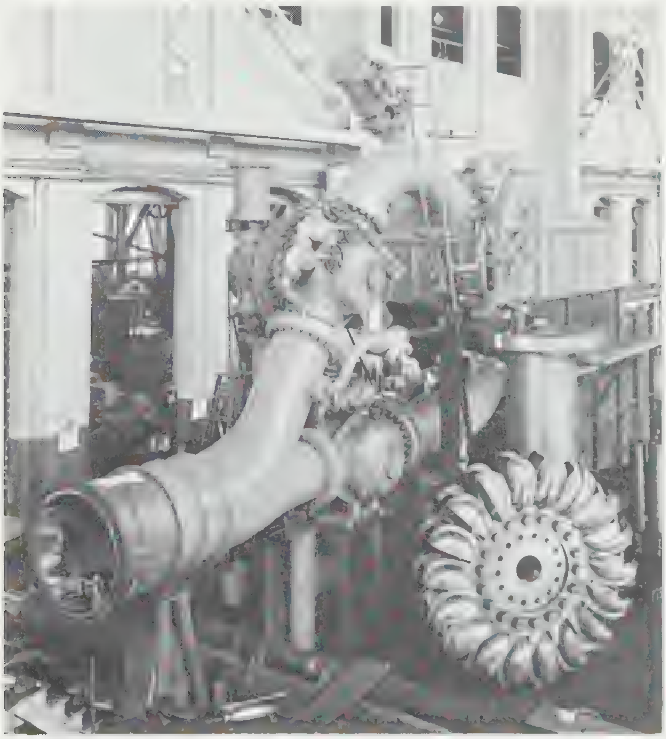

FIG. 2. Shop assembly of horizontal-shaft single overhung runner double-jet impulse turbine rated 28,000-hp, 1,580-ft net head, 450 rpm, for Paucartambo plant of Cerro de Pasco Corp., Peru. Runner with detachable buckets bolted on in pairs. (*Three units by Allis-Chalmers Mfg. Co.*)

applied to any of these cases. In the Francis turbine, the flow passes inwardly through a circular series of wicket gates, pivotally adjustable for regulation and forming contracting passages in which a part of the head is converted into velocity head. The streams issue from the wicket gates in a direction having both radial inward and tangential velocity components. The streams then merge within the space between the wicket gates and runner and form a continuous ring of revolving and inwardly progressing water. The water then enters the runner passages in which the radial component of motion is gradually turned between the hub and outer band into the axial direction, while the tangential or whirl component is gradually deflected by the vanes until at discharge from the runner only a small whirl component remains.

The flow then passes through a draft tube which by means of gradually increasing cross-sectional areas reduces the velocity, thus reconverting a large part of the residual kinetic energy remaining in the runner discharge into effective head, which is utilized through a reduction in the static pressure against which the runner discharges.

In the propeller turbine, the flow through the runner is axial in the meridional plane as it passes through the annular throat section of the water passage between the runner hub and discharge ring. The runner has relatively few blades, usually between three and ten, with free outer ends revolving within the stationary discharge ring with as small running clearance as is practical. The relative velocity between

Fig. 3. Impulse turbine runner (Pelton type) with buckets cast integrally with the hub. (*Allis-Chalmers Mfg. Co.*)

the blades and water is high, and undergoes comparatively little change as the water passes through the runner. In this last feature, the propeller turbine approaches the action in an impulse turbine in which the relative velocity remains practically constant in its passage through the runner buckets.

An important subdivision of the propeller turbine is the Kaplan adjustable-blade turbine in which the individual runner blades are pivotally mounted in the hub so that their inclination may be adjusted during operation, by governor action, simultaneously with the adjustment of the wicket gates, to meet changing power demands and changes in head. The blades are adjusted by means of a mechanism which connects them with a servomotor. The servomotor is usually operated by oil pressure admitted

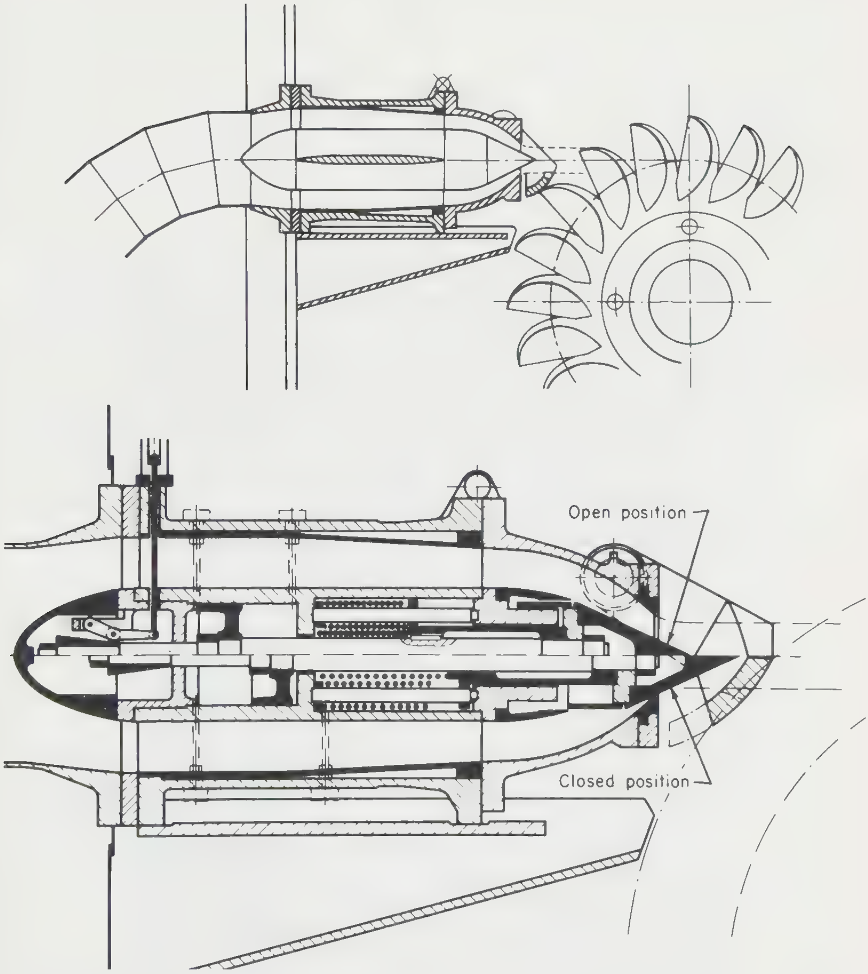

FIG. 4. Straight-flow-type nozzle with internal needle servomotor for Pelton-type impulse turbine. (*Escher Wyss Ltd.*)

from the governor through a blade control valve which is actuated from the wicket-gate movement by means of a cam and causes the runner-blade inclinations to correspond to the positions of the wicket gates.

Reaction turbines have been applied commercially for heads up to 2,205 ft.[1] Impulse turbines of the Pelton type have been used for heads up to 5,800 ft.[2] Propeller turbines have been employed for heads up to nearly 290 ft.[3]

Except for small installations under low heads, reaction turbines are equipped

[1] Francis turbines for the Rosshag power station, Austria; 58.4 Mw each under 672-meter maximum net head; built by Escher-Wyss and Maschinenfabrik Andritz, Austria.

[2] Impulse turbines at the Reisseck plant, Austria, 31,000 hp, 5,800-ft head; built by Charmilles, Geneva.

[3] Kaplan turbine at the Nembia plant, Italy, 18,000 hp, 288.7-ft (88-m) maximum head, built by Franco Tosi, Milan.

with spiral casings, these being usually of circular section and constructed of cast steel or plate steel. In low-head plants (less than about 100 ft), the spiral casings are usually of partly rectangular section, formed in the concrete substructure of the powerhouse. For small installations under very low heads (about 30 ft or less), open-flume settings have been used, the runner and wicket gates being placed in an open rectangular or partly spiral flume into which the free surface of headwater extends.

The foregoing statements regarding the absence of free surfaces exposed to air in reaction turbines should be qualified to this extent: many high-speed Francis and

Fig. 5. Francis-type runner for one of the turbines rated 204,000-hp, 179-ft net head, 100 rpm for the Smith Mountain Dam powerhouse. Runner fabricated by welding weighs 285,000 lb and has outside diameter exceeding 246 in., requiring splitting upon completion into halves for shipping. (*Baldwin-Lima-Hamilton Corp.*)

propeller turbines are equipped with automatically controlled valves for admitting air to the water passages in or near the runner during part-gate or light-load operation. This permits a portion of the flow to approach open-channel or free-jet characteristics, but the action takes place within completely enclosed spaces and the pressure of the air in the flow is not atmospheric. This admission of limited quantities of air improves the operation of Francis turbines under small loads, and the air is shut off progressively and automatically as the wicket gates are opened. In fixed-blade propeller turbines, air admission is frequently advantageous nearly up to normal gate opening.

Impulse turbines are regulated by needle nozzles, two types of which are shown in

Figs. 1 and 4. The straight-flow nozzle eliminates the disturbance of the jet caused by curvatures of water passages in an elbow-type nozzle. Since the flow in the penstock cannot be suddenly altered for quick regulation because of its great inertia, the needle nozzle is usually supplemented by either a jet deflector or an auxiliary nozzle. Upon load rejection, the governor acts immediately to bypass a part of the jet by means of either the deflector or auxiliary nozzle so that a part of the flow is removed from acting on the runner, after which a slow-closing action controlled by a dashpot permits the needle to close slowly while the deflector or auxiliary nozzle is simultaneously withdrawn from action.

FIG. 6. Francis-type runner for one of the Garrison Dam power-plant turbines rated 90,000-hp, 150-ft net head, 90 rpm. Runner is one of the largest cast in one piece in the United States. Outside diameter 223.5 in.; weight 150,000 lb. (*Baldwin-Lima-Hamilton Corp.*)

In reaction turbines having long penstocks, as in high-head installations, pressure regulators or relief valves are applied to bypass temporarily part of the flow from the turbine casing to the tailrace during quick closure of the wicket gates, in order to avoid too rapid deceleration of the penstock water column with consequent undue rise in pressure due to inertia effects or water hammer. Dashpot control permits the subsequent slow closure of the relief valve to minimize loss of water. Pressure regulators of several forms, principally of the angle-needle-valve type with matching energy absorbers, are in use. More recently, the Howell-Bunger conical hollow-jet-type valve has been applied to this service because of its relative simplicity combined with economy and good energy-dissipation capability.

For economical utilization of low heads up to about 50 ft, special axial-flow turbines of the tubular type have been developed. Conventional-type turbines with their spiral or semispiral cases and elbow-type draft tubes involve considerable costs in the structural features of the powerhouse because of the relatively large water passages needed to pass sufficient flow through the machines to develop significant power outputs under the low heads. This results in powerhouse structures which have large dimensions relative to the available head. Tubular turbines, by straightening the flow through them from forebay to tailrace, confining it to a substantially axial direction, and placing the shaft axis in a horizontal or slightly inclined position, enable the use of a more compact and simplified powerhouse structure. Furthermore, the straight axial flow enhances turbine performance, permitting increased operating speed

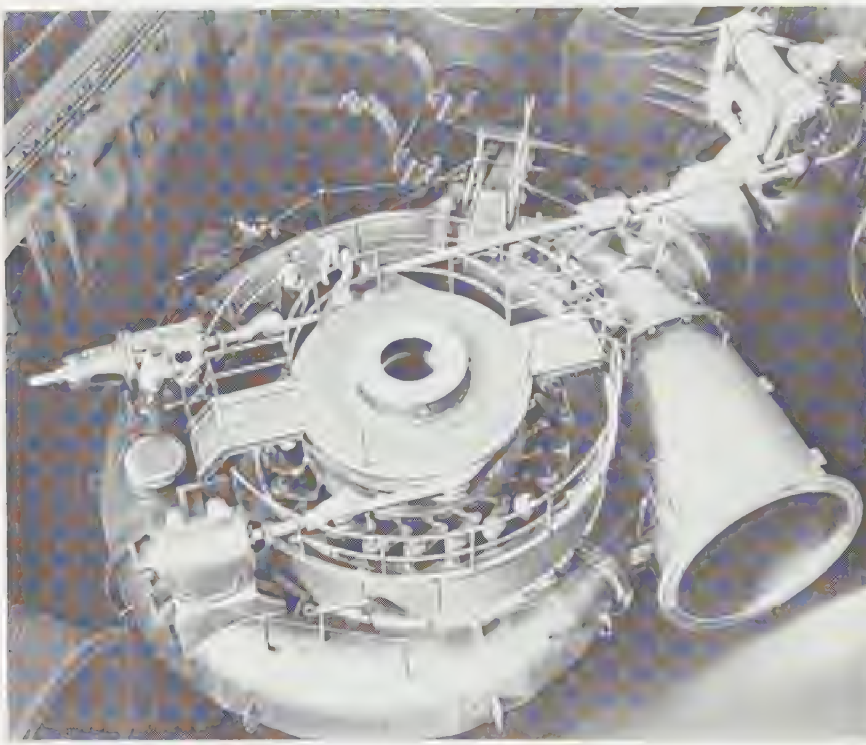

Fig. 7. Shop assembly of Francis turbine rated 115,000-hp, 440-ft net head, 180 rpm, for Hoover Dam power plant. Welded-plate-steel spiral casing with pressure regulator. (*Allis-Chalmers Mfg. Co.*)

and output, thereby reducing the size and cost of the machinery for a given output. The extensive research and development work on axial-flow turbines of the tubular type since their introduction in Europe in 1936 has produced highly efficient machines which are adaptable to an increased range of operating conditions, thereby opening up new prospects for economical development of low-head power sites and of tidal power.

Tubular turbines are a development of an idea originated and patented in America in the early 1920s by L. F. Harza, and utilized subsequently in a number of European low-head installations. The original design approached the ideal axial-flow machine by passing the water through a rim-type generator, which had its rotor attached to the periphery of the runner blades. Initial mechanical difficulties due to water leakage and excessive frictional losses in the water seals were overcome in later designs. Fifty-four of the modified units have been operating under remote control in Germany for many years (the first unit for more than 25 years) without undue maintenance problems. A more recent development is the bulb-type[1] turbine in which the generator is placed in a bulb-shaped watertight steel housing located in the center of an enlarged water passage (Fig. 17). Many variations of the bulb-turbine design, with generator driven by the turbine either directly or through gears, have been built and put into successful service. Bulb turbines built as reversible machines, with the generator designed so it can also operate as a motor to drive the turbine as a pump, are used in the world's first large-scale development of tidal power on the Rance River estuary in France, where 24 bulb pump-turbines are installed (Fig. 73)

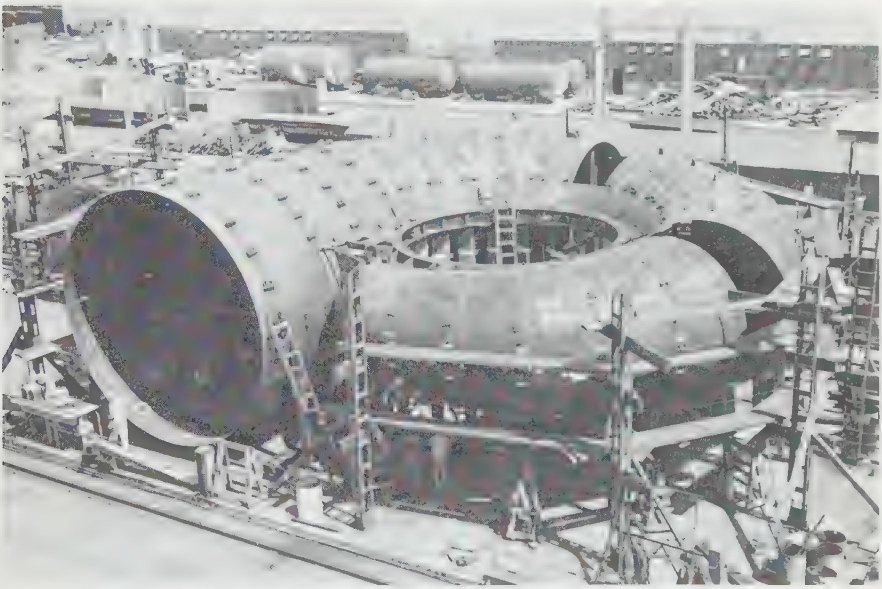

Fig. 8. Shop assembly of welded-plate-steel spiral case for one of Francis turbines rated 73,000-hp, 115-ft net head, 100 rpm for the Oxbow power plant of the Idaho Power Company. Casing inlet diameter 23 ft. (*Newport News Shipbuilding and Dry Dock Co.*)

The presence of the bulb-shaped generator housing in the center of the water passageway of the bulb-type turbine requires an enlarged water passage around the bulb; in this respect the bulb unit falls short of the earlier tubular design with rim generator, which virtually achieved the pure axial-flow-design objective. A type of tubular turbine developed in America and known by the copyrighted name of "TUBE" turbine avoids the use of a bulb in the water passageway and uses a conventional horizontal-type generator located outside the water passages where it is fully accessible.[2] By inclining the turbine-generator shaft, the generator can be placed above the water passageway without requiring deep excavation for the draft tube (Fig. 18). Comparative-cost studies for several low-head projects in America have shown that TUBE units offer a significant improvement in the economy of low-head installations.

[1] Casacci, S. X., and E. E. Chapus, "The Bulb Turbine," ASME Paper 64-WA/FE-27, 1964. Battegay, C. L., and H. Widdern, "Tubular (Bulb) Turbines," Escher Wyss News, No. 3, 1962.

[2] Mayo, H. A., Jr., "Tube Turbine Units and Their Application," ASME Paper 65-WA/FE-12, 1965.

2. Effective Head, Power, Efficiency. Figure 10 illustrates diagrammatically a reaction turbine supplied by a penstock and discharging through its draft tube into the tailrace. The turbine proper is, according to standard practice, taken to begin at the entrance to the turbine casing and to end at a section of the tailrace just beyond the physical end of the draft tube. The turbine thus comprises the casing, distributor, runner, and draft tube. The interdependence of the actions of the draft tube and the runner requires that the draft tube be considered an integral part of the turbine.

The effective head under which the turbine operates corresponds to the difference between the total energy contained in the water immediately before its entrance into the turbine and immediately after discharge from the turbine.

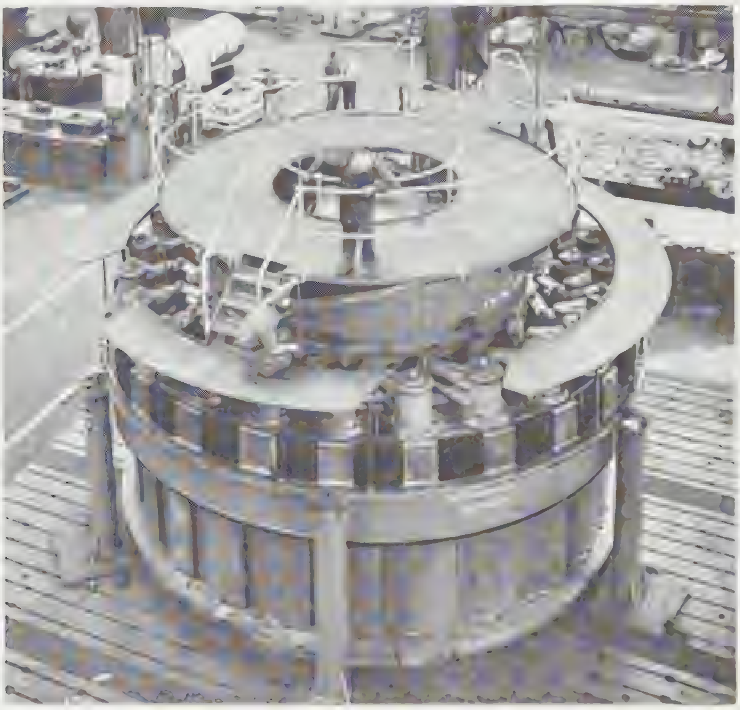

FIG. 9. Shop assembly of nonembedded parts of a Francis turbine rated 210,000 hp at best efficiency, 300-ft net head, 120 rpm, for the Robert Moses Niagara power plant. (*Baldwin-Lima-Hamilton Corp.*)

If we remember that an amount of water weighing W lb falling through a vertical distance H is capable of delivering WH ft-lb of work, an amount of head may be considered either as an elevation H above some selected datum of reference or as specific energy, *i.e.*, an amount of energy in foot-pounds per pound of water flowing, or WH/W. If a gage glass is connected to a piezometer orifice in the penstock adjacent to the inlet of the turbine casing, the potential energy in the water entering the turbine will be represented by the height to which the water rises in the gage glass. To this must be added the velocity head corresponding to the kinetic energy in the entering flow. This corrected elevation may be thought of as a virtual elevation equivalent to that of still water in a large forebay feeding the turbine directly. In the same way, on the tailrace side the tail-water elevation must be corrected by adding the velocity head at the point of measurement to give an equivalent still-water elevation representing the total energy remaining in the water at discharge from the turbine. The difference between these two equivalent elevations represents the effective head H; or in the words of the ASME Test Code for Hydraulic Prime Movers, PTC 18-1949:

"The effective head on the turbine shall be taken as the difference between the elevation corresponding to the pressure head in the penstock at the entrance to the turbine casing and the elevation of tailwater, the above difference being corrected by

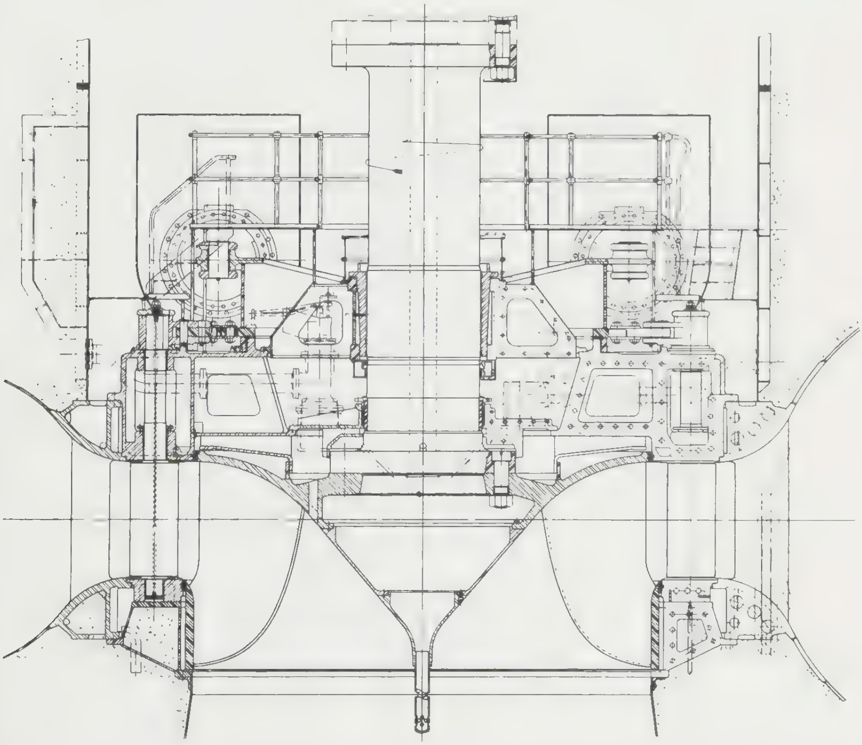

Fig. 10. Sectional elevation of 210,000-hp turbine for the Robert Moses Niagara power plant. *(Seven turbines by Baldwin-Lima-Hamilton Corp., six turbines by Newport News Shipbuilding and Dry Dock Co.)*

adding the velocity head in the penstock at the section of measurement and subtracting the residual velocity head at the section of measurement in the tailrace."

If the specific weight of the water is w lb/cu ft and the quantity passing through the turbine is Q cfs, the power available due to wQ lb of water falling H ft is wQH ft-lb/sec, and the available horsepower, or water horsepower, is

$$P_w = \frac{wQH}{550} \tag{1}$$

Not all this power can be delivered through the main shaft of the turbine to the electrical generator or other driven machine, because a portion is lost in hydraulic resistances and eddies within the turbine, in leakage around the runner, in frictional losses such as disk friction on a Francis runner crown and in bearing and seal friction on the shaft. By calling the turbine efficiency e, the delivered or brake horsepower is

$$P = \frac{wQHe}{550} \tag{2}$$

3. Fundamental Principles of Turbine Action. *Relative and Absolute Velocities.* In the simple inward-flow reaction turbine shown schematically in Fig. 20 the water passes through the contracting passages between the guide vanes from which it issues in an oblique direction having both radial and tangential components with respect to the turbine axis. When the water reaches the entrance tips of the runner

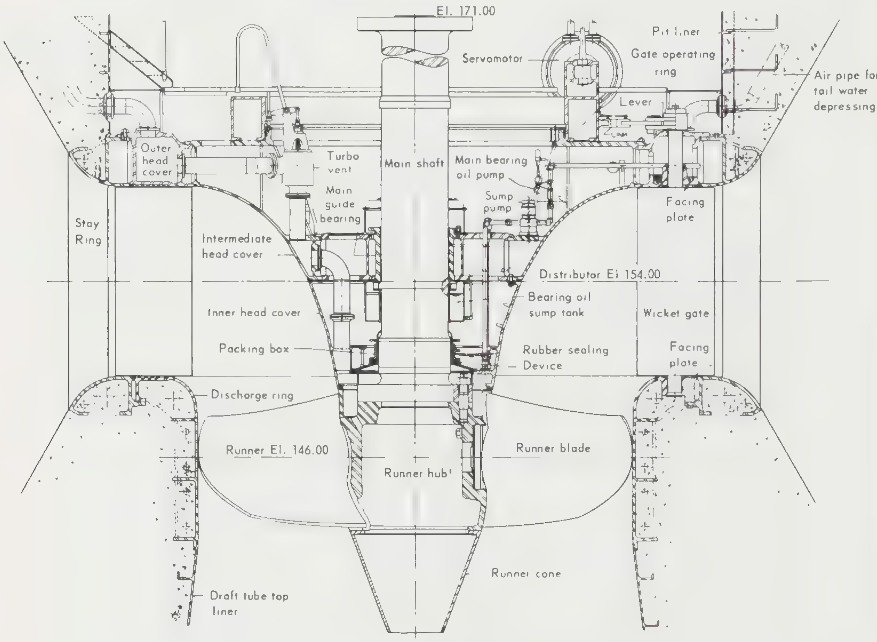

Fig. 11. Sectional elevation of 79,000-hp, 81-ft net head, 94.7-rpm fixed-blade propeller turbine for the St. Lawrence Power Dam powerhouse. Runner diameter 240 in. (*Eight turbines by Allis-Chalmers Mfg. Co.*)

vanes (buckets), it has a velocity V_1. Now consider the velocity both with respect to the stationary system and with respect to the revolving runner; the first, denoted by V_1, represents the motion as it would appear to a stationary observer and is termed the *absolute velocity*. The second, denoted by v_1, represents the motion as it would appear to an observer riding around on the runner and is termed the *relative velocity*. V_1 and v_1 are related by forming a vector triangle with u_1, the linear velocity of the corresponding point on the runner, here the runner-vane entrance tips. All velocities will be expressed in feet per second.

This relation may be understood by considering the movement of a particle in a small time interval Δt. Suppose Fig. 20*b* represents a plane revolving with the runner. A particle starts at *a* and moves to *b*, *ab* being the relative motion, or the motion as it would appear to an observer moving with the runner. If we now change our point of view to that of a stationary observer, the particle is seen to have started at a and moved to c, while the point b on the runner has moved from b to c. Thus bc is the movement of the runner and ac the absolute motion of the particle. The absolute motion ac is thus seen to be the resultant of ab and bc. The velocities are proportional to the movements in the given time, so that the absolute velocity V_1 is the resultant of the relative velocity v_1 and the linear velocity of the point of reference on the runner, u_1, the three forming a closed triangle. A similar relation applies at the exit from the runner, where v_2 is the exit velocity relative to the runner, u_2

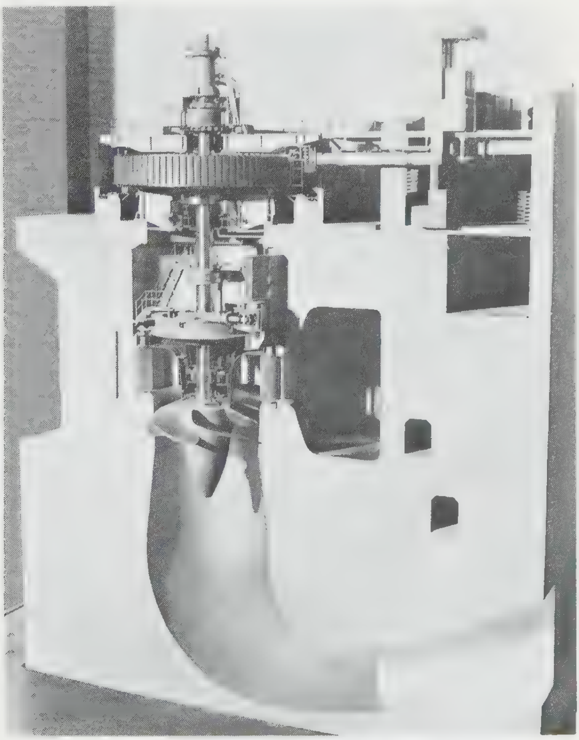

FIG. 12. Model of turbine and generator for Priest Rapids power plant. Kaplan-type turbine rated 114,000 hp, 78-ft net head, 85.7 rpm; runner diameter 284 in. (*Ten units by English Electric Company Ltd.*)

the linear velocity of the exit point on the runner, and V_2 their resultant, the absolute velocity of discharge from the runner. Since u_1 and u_2 are the circumferential velocities of two points on the same runner, they are proportional to their radial distances from the axis of rotation

$$u_1 = \frac{2\pi r_1 N}{60} \qquad u_2 = \frac{2\pi r_2 N}{60} \tag{3}$$

and $u_1/u_2 = r_1/r_2$, N being the rotational speed, rpm, and r_1 and r_2 the radii, ft.

It is convenient to extend the system of notation to include the angles of the inflow and outflow triangles and the tangential components of the velocities, or the whirl components. These designations are shown in Fig. 20c. The direction of v_2, *i.e.*, the angle β_2, is the direction imparted by the runner vanes at discharge, so that β_2 is substantially the inclination of the discharge portion of the runner vane. Similarly, when the turbine is running at its proper speed, the direction of v_1 should closely conform to the direction of the runner vane at the entrance, to avoid "shock" or eddy formation.

Force and Torque Relations. Let us now consider the forces exerted on the runner by the impulse and reaction of the entering and leaving water and the moments of

FIG. 13. A runner, shaft, and head cover assembly being lowered into the turbine pit of one of the 114,000-hp Kaplan turbines in the Priest Rapids powerhouse. Weight of assembly 750,000 lb. (*English Electric Company Ltd.*)

these forces upon the runner. At every point of the outer periphery of the runner, a cylindrical surface containing the entrance edges of the vanes, the flow enters with a velocity V_1, and every stream element comprising a flow of dq cfs exerts upon the runner a forward force or impulse $w(dq)V_1/g$, according to the momentum principle or that of the impulse of a jet. The tangential component of this force is everywhere $[w(dq)V_1/g] \cos \alpha_1$, or in our notation $w(dq)V_{u1}/g$, and its moment acting on the runner is $[w(dq)V_{u1}/g]r_1$. Hence the total moment of all the entering water is $wqV_{u1}r_1/g$, in which q is the total quantity of water passing through the runner per second. Similarly, at discharge from the runner, the total moment of the backward reaction

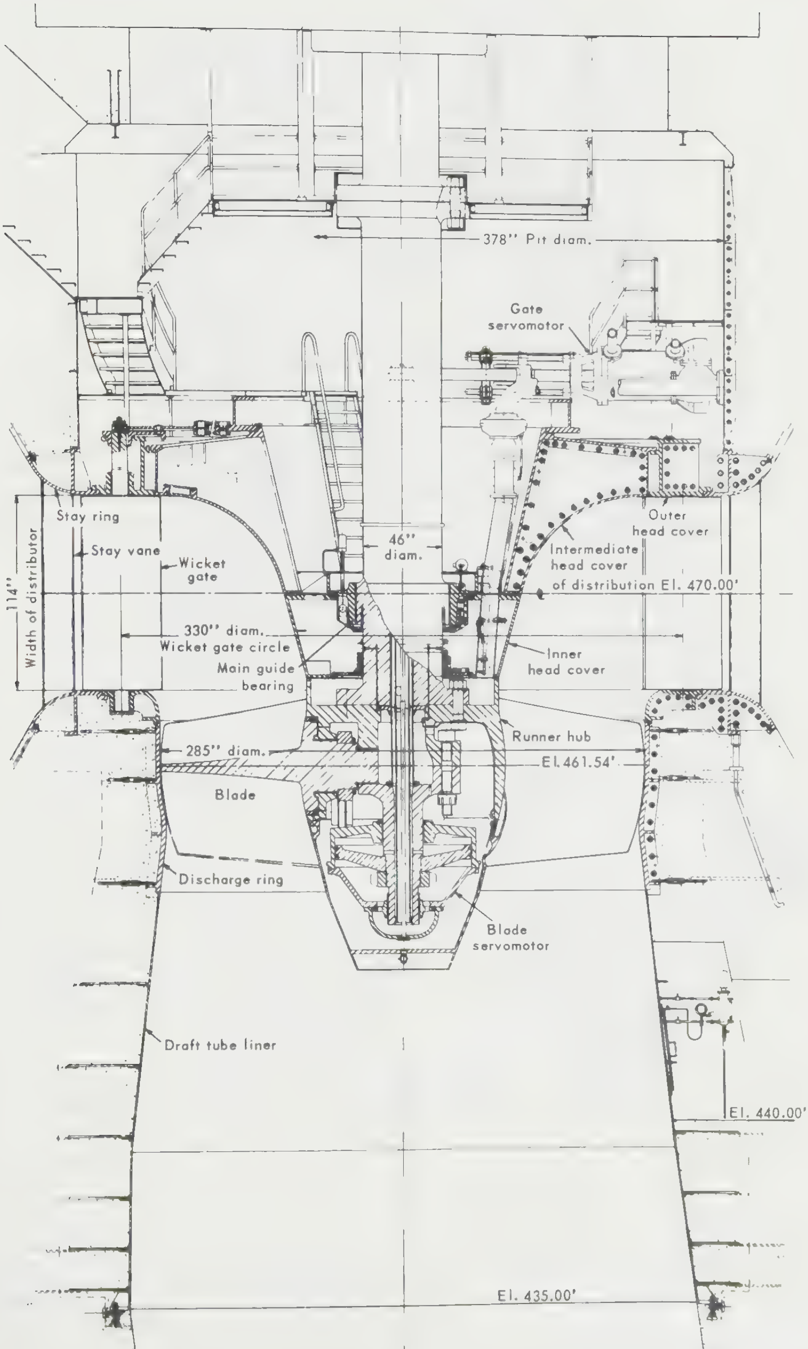

FIG. 14. Sectional elevation of 120,000-hp, 80-ft net head, 85.7-rpm Kaplan-type turbine for Wanapum power plant. (*Ten turbines by Dominion Engineering Works Ltd.*)

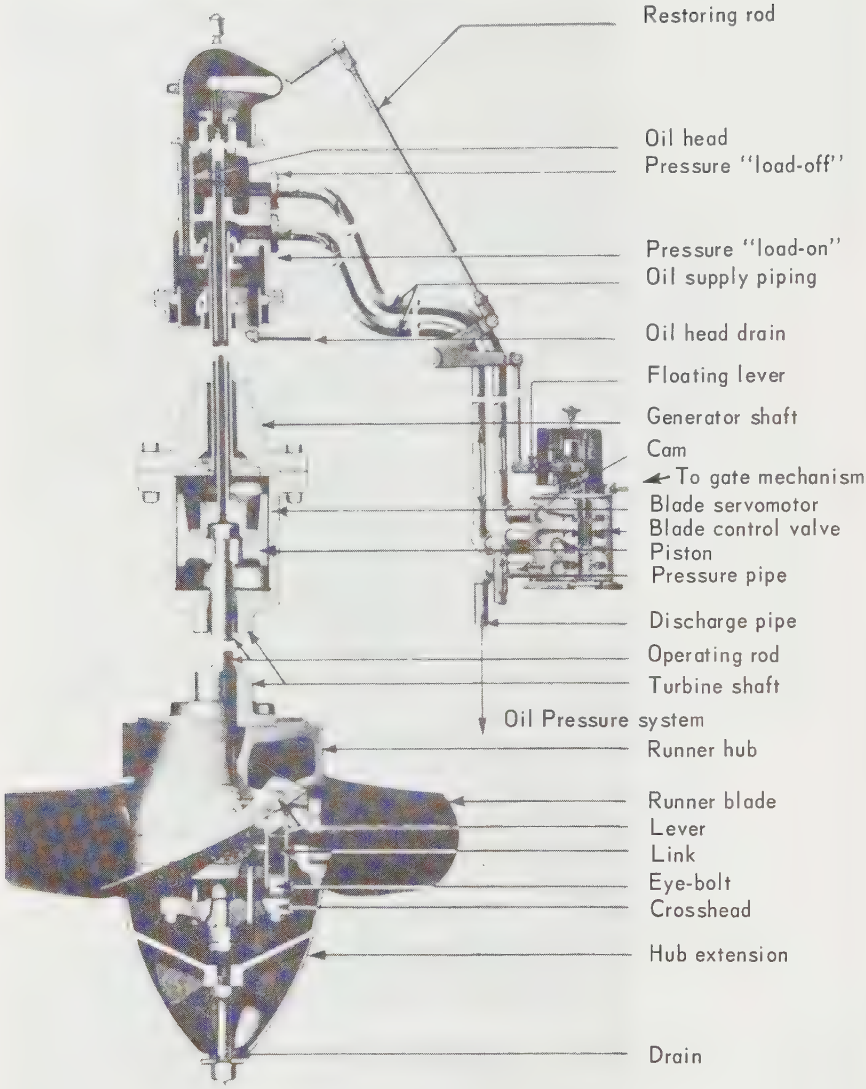

Fig. 15. Diagrammatic arrangement of the blade-operating mechanism, oil-supply head, and cam-operated blade-control valve of a Kaplan-type turbine. (*Allis-Chalmers Mfg. Co.*)

of the leaving water all the way around the inner periphery is $wqV_{u2}r_2/g$. Hence the net turning moment exerted on the runner is $(wq/g)(r_1V_{u1} - r_2V_{u2})$; and this is balanced by the resisting torque, due to the useful load on the shaft, and mechanical friction. If $q = Q - Q_L$, in which Q_L is the leakage loss, or flow that bypasses the runner through the clearance spaces, and e_v is the volumetric efficiency $(Q - Q_L)/Q$, we can put $q = e_vQ$.

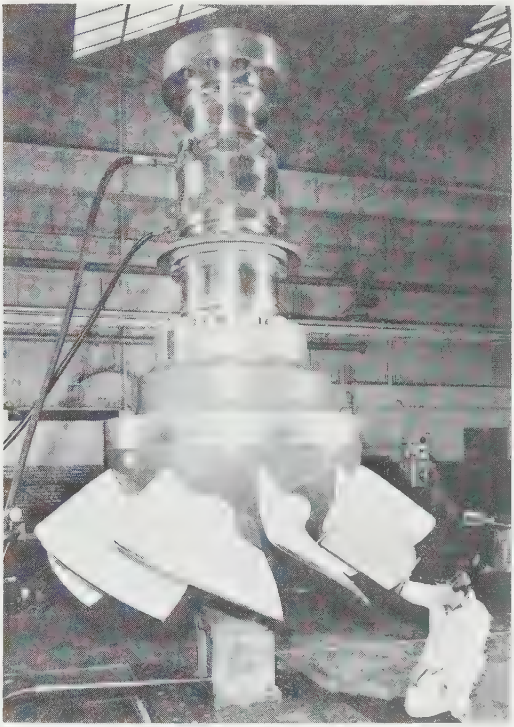

FIG. 16. Diagonal-flow adjustable-blade runner of the 30,500-hp, 180-ft net head, 300-rpm Deriaz-type turbine for the Culligran power station of the North of Scotland Hydro-Electric Board. (*English Electric Company Ltd.*)

This moment when multiplied by $2\pi N/(60 \times 550)$ gives the horsepower transmitted from the water to the runner; and this power multiplied by the mechanical efficiency e_m, to allow for the losses in bearing friction and in seal friction on the shaft, is equal to the power delivered by the shaft to the generator or other driven machine, *i.e.*, the delivered or brake horsepower. Hence,

$$\frac{2\pi N w Q e_v e_m}{60 \times 550 g}(r_1 V_{u1} - r_2 V_{u2}) = \frac{wQHe}{550}$$

If we subdivide the efficiency into volumetric efficiency e_v, mechanical efficiency e_m, and hydraulic efficiency e_h, then $e = e_v e_m e_h$; and if we remember that $2\pi r_1 N/60 = u_1$ and $2\pi r_2 N/60 = u_2$, the preceding relation becomes the Euler formula,

$$u_1 V_{u1} - u_2 V_{u2} = gHe_h \tag{4}$$

This is a relation of major importance in turbine design and analysis.[1]

The foregoing moment equation may be applied to the case of the flow in a vane-free space, such as the flow in the casing, in the transition space between the guide vanes and runner, and in the draft tube.

[1] Except in small turbines and those of the low-speed type, the bearing friction and seal friction are of small proportions, amounting usually to only a fraction of a percent, and the leakage loss seldom exceeds 1 or 2 percent, so that in the region of specific speeds greater than about 30 the hydraulic efficiency e_h will exceed the turbine efficiency e by an amount seldom greater than 1 or 2 percent.

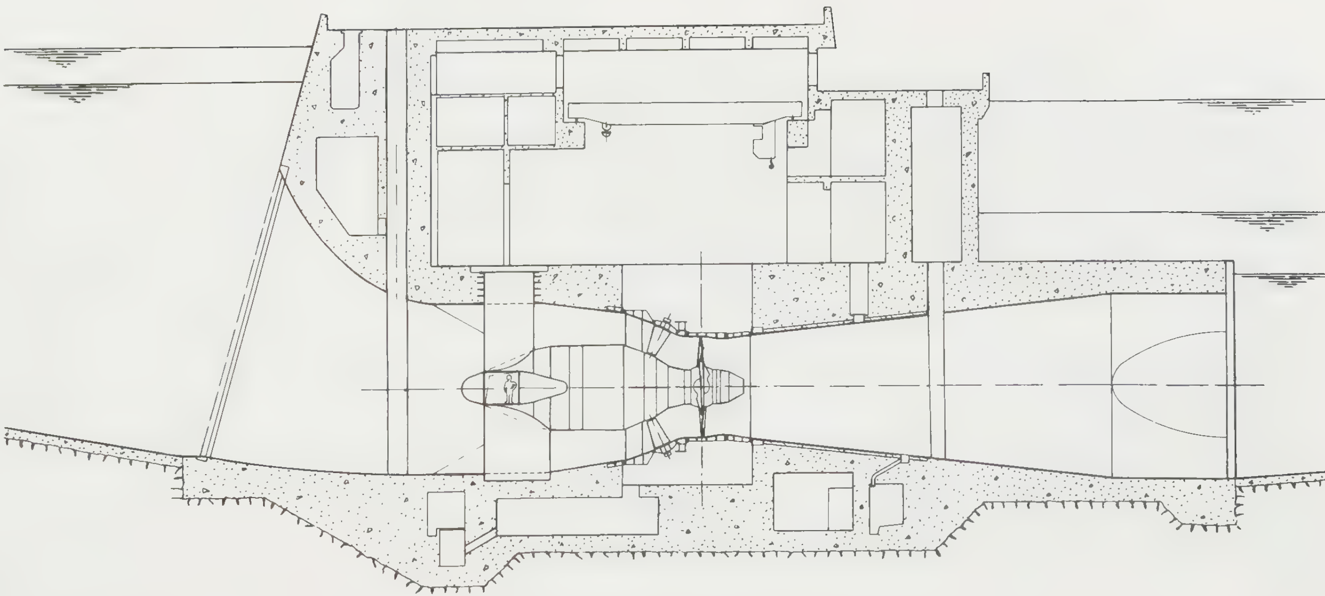

FIG. 17. Sectional elevation of one of four bulb units for Pierre Benite power plant in France. Nominal capacity 20,000 kw each at 26-ft net head, 83.3 rpm. Runner diameter 240 in. (*Turbines by Neyrpic, generators by Alsthom.*)

Consider the equilibrium of the ring of water occupying the doubly hatched annular space shown (Fig. 21) in a conduit bounded by surfaces of revolution. The space is free of vanes.

The moment exerted by the water entering and leaving the annular space must be equated to zero, for there are no vanes to resist it or to abstract power. Since steady flow is being considered, constant with respect to time, any moment exerted on the

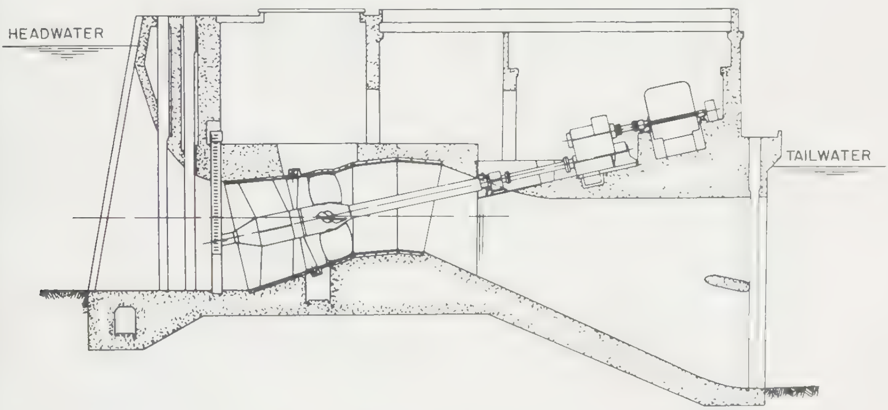

FIG. 18. TUBE turbine unit of 33,800-hp capacity at 26-ft net head (32.3-ft rated head), 60/514.3 rpm for the Ozark Lock and Dam powerhouse of the U.S. Army Corps of Engineers. Runner diameter approximately 315 in. (*Five units by Allis-Chalmers Mfg. Co.*)

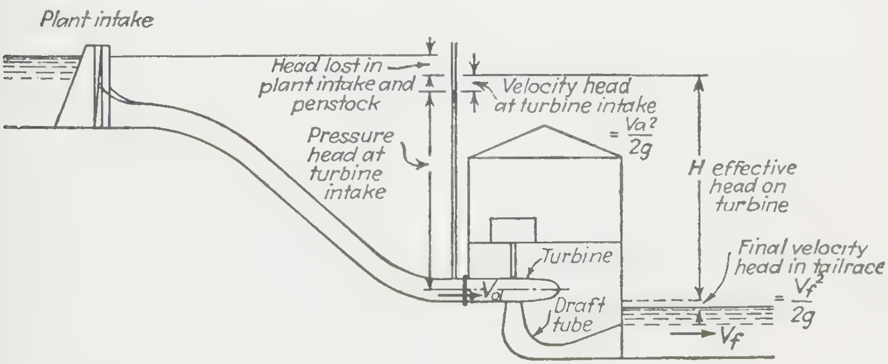

FIG. 19

free mass of water within the annular space would accelerate it indefinitely and destroy the balance of forces essential to steady flow. Hence in this case,

$$\frac{wq}{g}\,(r_1V_{u1} - r_2V_{u2}) = 0$$

and

$$r_1V_{u1} = r_2V_{u2}$$

If the flow enters at some radius r_0 with tangential velocity V_{u0}, then V_u at any point is given by

$$rV_u = r_0V_{u0} = \text{(a constant)} \tag{5}$$

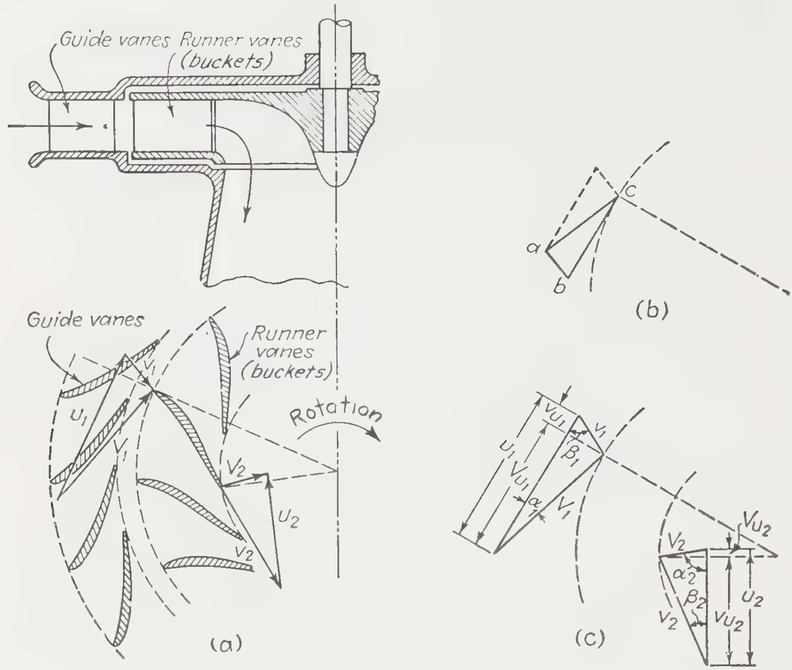

Fig. 20

i.e., the whirl component of the velocity varies inversely as the radius. This is the vortex law, or the principle of constancy of moment of momentum.

Although the principles just derived have been demonstrated for a purely radial inward-flow runner, they are equally applicable to the usual Francis runner (Fig. 22) in which the flow lines in the meridional section curve from a radial toward the axial

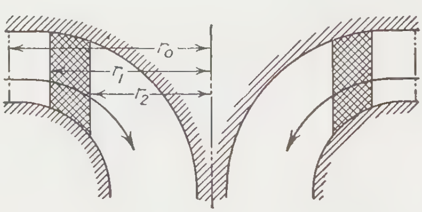

Fig. 21

direction. Here the inflow and outflow triangles for a given flow line cannot be drawn in one plane or surface; but the outflow triangle must be constructed, as in the case shown, on the development of a conical surface tangent to the flow line at the runner exit point 2. The preceding relations, however, apply unchanged.

Head or Energy Relations. It is also useful to trace the head or specific energy relations governing the flow by applying the Bernoulli theorem. With reference to Fig. 23, imagine a piezometer connected to the space at the entrance to the runner, at point 1, recording the pressure head h_{p1}. By taking the surface of tail water as

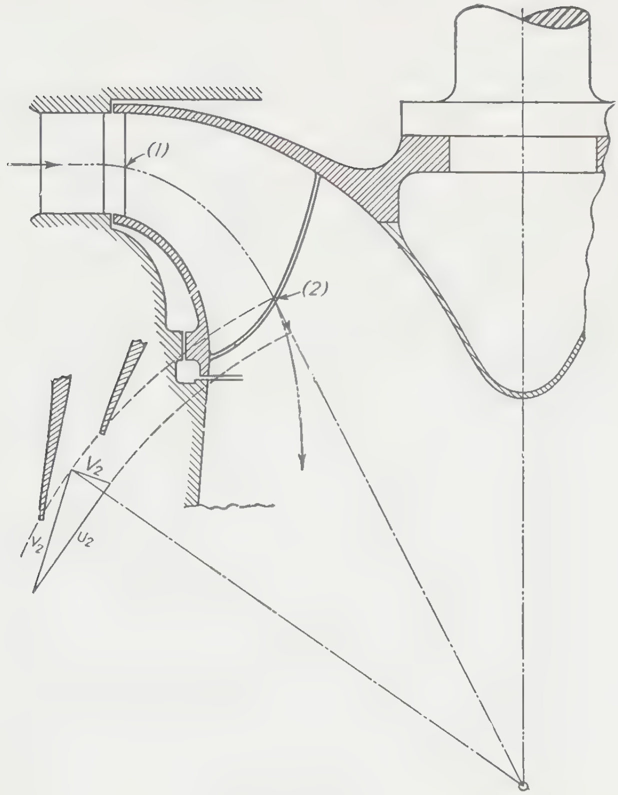

FIG. 22

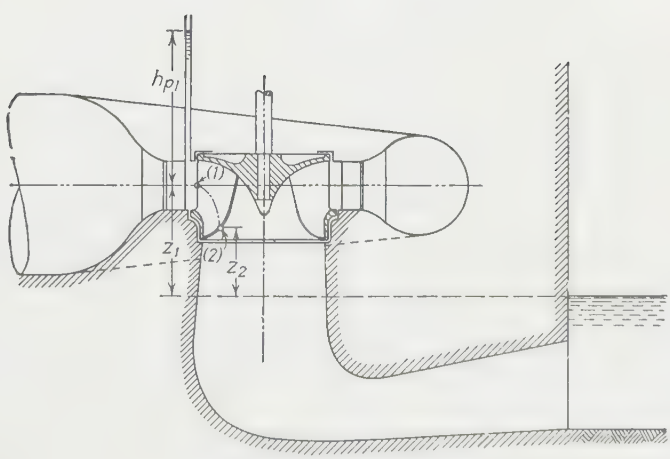

FIG. 23

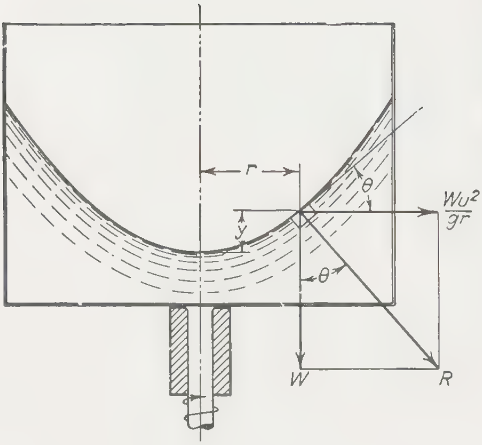

FIG. 24a

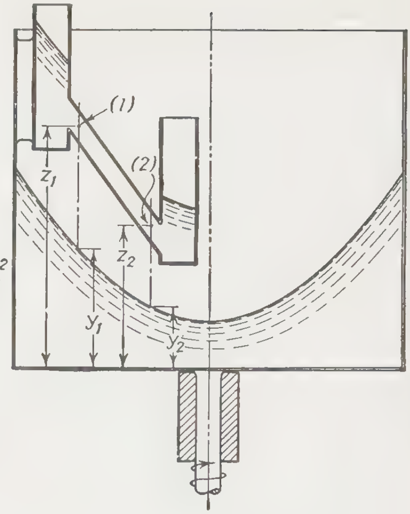

FIG. 24b

datum, the elevation of point 1 is z_1. The velocity at this point is V_1 and the velocity head $V_1^2/2g$. Hence the total dynamic head at 1, or the specific energy of the water flowing into the runner at this point, is $h_{p1} + z_1 + V_1^2/2g$. Of this energy or head, a certain portion h_L is lost in surface friction and eddies in the runner, another portion is transmitted to the runner to drive it against its useful load, and the remainder is the total dynamic head at point 2. The amount of head transmitted to the runner is the total foot-pounds per pound of water flowing, or

$$\frac{wqHe_h}{wq} = He_h$$

so that the Bernoulli formula takes the form

$$h_{p1} + z_1 + \frac{V_1^2}{2g} - h_L - He_h = h_{p2} + z_2 + \frac{V_2^2}{2g} \tag{6}$$

This is the Bernoulli formula expressing the energy balance with respect to the stationary system.

We can also imagine ourselves to be moving with the runner and can write the Bernoulli formula as it applies to the relative movement of the water in the runner. Let us first briefly review the principles of hydrostatics governing liquid at rest relatively to a rotating system turning uniformly about a vertical axis. In the open tank shown (Fig. 24a) rotating n revolutions per second, containing water with a free surface, a particle in the surface is subject to a downward force W, its weight, and a centrifugal force Wu^2/gr, u being the linear circumferential velocity of a point in the rotating system at radius r. Since the water is in equilibrium, at rest with respect to the tank, the resultant of the forces acting on the particle must be normal to the free surface, there being no force to resist motion along the surface. Hence the angle of inclination θ of the surface is such that

$$\tan\theta = \frac{Wu^2}{Wgr} = \frac{u^2}{gr} = \frac{dy}{dr}$$

as will be clear from the sketch. Putting $u = 2\pi rn$, $\frac{dy}{dr} = \frac{4\pi^2n^2r}{g}$, and $dy = \frac{4\pi^2n^2}{g} rdr$ is the differential equation of the surface curve. Integrating this, between $y = 0$ and $y = y$,

$$y = \frac{4\pi^2n^2r^2}{2g} = \frac{u^2}{2g} \tag{7}$$

which means that the surface is a paraboloid of revolution and the elevation of any point in the surface above that at the axis is equal to the velocity head corresponding to the linear velocity of the system at the point considered.

Now consider a pipe system such as shown (Fig. 24*b*), carried by the revolving tank and with water flowing with steady flow from one small tank into another through a pipe, revolving with the system. Let us write the Bernoulli formula between sections 1 and 2 of the pipe in terms of the relative velocities v_1 and v_2 of the flow in the pipe. Since a particle in the free surface of water at rest with respect to the large tank has no tendency to move relatively to the rotating system, it is the elevation of water above this surface which measures the head available to produce flow. Hence it is only necessary in applying the Bernoulli formula relatively to the system to replace our usual horizontal datum plane by a paraboloidal datum surface coincident with or parallel to an actual or imaginary water surface corresponding to the speed of rotation. That is, instead of the elevation heads z_1 and z_2, which would apply if the system were stationary, we must use

$$z_1 - y_1 = z_1 - \frac{u_1^2}{2g} \qquad \text{and} \qquad z_2 - y_2 = z_2 - \frac{u_2^2}{2g}$$

Our Bernoulli formula then becomes

$$h_{p1} + \left(z_1 - \frac{u_1^2}{2g}\right) + \frac{v_1^2}{2g} - h_L = h_{p2} + \left(z_2 - \frac{u_2^2}{2g}\right) + \frac{v_2^2}{2g}$$

This form of the Bernoulli formula for a rotating system applies directly to the turbine runner passages. By treating sections 1 and 2 as points on the revolving runner, it is clear that the pressure heads h_{p1} and h_{p2} merely measure intensities of the static pressure and are the same for points just outside the runner or just within it, or the same whether the observer is stationary or imagined to be moving with the runner. There is no need to introduce between points 1 and 2 on the runner any term representing the extraction of energy or the performance of work beyond the friction and eddy losses h_L within the passages, because between these points no relatively moving element is interposed. Hence we can write for the runner,

$$h_{p1} + z_1 - \frac{u_1^2}{2g} + \frac{v_1^2}{2g} - h_L = h_{p2} + z_2 - \frac{u_2^2}{2g} + \frac{v_2^2}{2g} \tag{8}$$

If we subtract this from the Bernoulli formula previously written with reference to the stationary system

$$h_{p1} + z_1 + \frac{V_1^2}{2g} - h_L - He_h = h_{p2} + z_2 + \frac{V_2^2}{2g}$$

we obtain

$$\frac{V_1^2 - v_1^2 + u_1^2}{2g} - \frac{V_2^2 - v_2^2 + u_2^2}{2g} = He_h \tag{9}$$

This is a useful relation connecting the absolute and relative velocities of the water, the velocities of the runner, the effective head on the turbine and its hydraulic efficiency.

If we now insert the trigonometric properties of the vector velocity triangles

$$v_1^2 = V_1^2 + u_1^2 - 2u_1V_1 \cos \alpha_1 = V_1^2 + u_1^2 - 2u_1V_{u1}$$

and

$$v_2^2 = V_2^2 + u_2^2 - 2u_2V_2 \cos \alpha_2 = V_2^2 + u_2^2 - 2u_2V_{u2}$$

we obtain

$$\frac{2u_1V_{u1} - 2u_2V_{u2}}{2g} = He_h$$

or

$$u_1V_{u1} - u_2V_{u2} = gHe_h$$

the same relation as previously derived from the balance of moments.

The foregoing principles are the fundamentals of turbine theory and should make clear the force relations and energy transformations involved and serve to explain the action. Although they are important in turbine design, the application of turbines to the conditions in a power installation and the problems of the user of turbines can be best handled by means of another series of principles based on dimensional relations and the laws of dynamic similarity, which will now be outlined.

4. Principles of Dynamic Similarity for Turbines. Consider a series of homologous turbines, or turbines that have geometrically similar water passages. Then imagine these to be operated under various effective heads. Any one of these turbines may of course be operated at various speeds; but there is one best speed at which the maximum efficiency will be developed, and if the design is correct this will be the designed speed or normal speed.

We have seen that at the proper speed the direction of the runner vanes at the entrance must agree with the relative direction β_1 of the entering flow. At any other speed, the flow will part from one side or the other of the vane, leaving an eddy-filled space which consumes energy and converts velocity head into heat, which is not utilized hydraulically. Hence only one fixed shape of inflow triangle is permissible to avoid this so-called *shock* loss.

In the same way, at discharge from the runner there is one relation between the velocities that is most favorable, and any other will be inconsistent with the highest efficiency. The important element here is the residual velocity head remaining in the water leaving the runner $V_2^2/2g$. A considerable portion of this, usually an amount of the order of some 80 percent, can be reconverted into effective pressure head by deceleration in the gradually enlarging draft tube, but it is inherent in the deceleration process that an appreciable part of this energy must be lost. Consequently, it is important that V_2 be held near a minimum value. The smallest value of V_2 would be secured by discharging the water perpendicularly to the surface of revolution generated by the discharge edges of the runner vanes, because the entire discharge must pass through this area and can do so at minimum velocity when the velocity is normal to the area. However, there are also internal losses in the runner, and the conduit friction or resistance of the vane surfaces must also be minimized. This frictional loss is closely proportional to the relative velocity head $v_2^2/2g$. The optimum condition requires the sum of these two losses to be a minimum and results in a small angle (90 deg $- \alpha_2$) of the absolute velocity of discharge V_2, this angle in most cases having values of 5 to 15 deg.

It is thus seen that for correct operation the shapes of the two vector velocity triangles are fixed and the angles must be kept unaltered. The values of the velocities may change but all in the same proportion. The scale of the triangles may be altered, but all velocities must retain the same ratios to each other. Thus if the velocity V_1 is doubled, u_1 must also be made twice as great and the speed of the turbine N must be doubled also, and all the remaining velocities will be increased in like ratio.

If a turbine of given geometric form is built in any size and operated under any head, we will suppose that the speed N has been adjusted to conform to a fixed shape of each velocity triangle. It would be reasonable to assume that the efficiency would then remain unaltered and independent of turbine size or head; but this conclusion is subject to a relatively small correction from the fact that the frictional losses may not vary in exact proportion to the velocity-head and eddy losses, as is well known in the case of pipe flow. As is known, to preserve strict dynamic similarity for conduit flow so that the flow patterns will be identical, the viscous forces must remain proportional to the inertia forces, which is possible only when the Reynolds number remains constant. This is considered to be of little importance in turbine calculations, because turbine conduits are large, even in the usual sizes of laboratory models, the velocities are high, and the surfaces exposed to the flow are relatively rough, so that the Reynolds numbers fall far beyond the region of the Reynolds critical velocity and the turbine passages fall into the class of rough conduits, in which the flow is completely turbulent and viscous forces are negligible. On the basis of this reasoning, variations of head on a given turbine should have negligible effect on the efficiency, a conclusion that seems to be in agreement with test data for turbines of usual sizes. There is a factor, however, that does effect the efficiency, namely, the lack of complete geometrical similarity. The similarity does not extend to the surface texture of the conduit walls, where there is more nearly a constancy of the degree of absolute roughness than of relative roughness necessary to complete homogeneity.

Consequently, the losses in hydraulic wall friction will not remain proportionately constant with change in size of turbine. However, the change in efficiency due to this cause is comparatively minor, and its effect on the validity of the relations about to be developed has been found to be negligible. In a later section, methods of correcting efficiencies for the effect of turbine size will be given.

If we assume that the efficiencies of homologous turbines of differing sizes and operating under different heads will remain substantially constant, or that the turbines are truly homologous even as to surface roughness, and assume that each turbine is operated at its correct speed for its size and head so that the velocity triangles will also be homologous, then all velocities will have a constant ratio to any one velocity selected as a reference value. Hence the relation between relative and absolute velocities derived above

$$\frac{V_1^2 - v_1^2 + u_1^2}{2g} - \frac{V_2^2 - v_2^2 + u_2^2}{2g} = He_h$$

can be expressed as constant $\times\ V_1^2/2g = He_h$; so that if e_h is substantially constant, it is seen that for correct similarity of operating conditions the velocity head corresponding to any velocity must be kept in constant ratio to the effective head on the turbine. The flow through the turbine will then follow the same laws as the flow through a nozzle, for example. These conclusions give us the following rules of similarity for turbines.

Any velocity head must vary as the effective head on the turbine $V^2/2g \propto H$.

Any velocity must vary as $\sqrt{H}$; $V \propto H^{1/2}$ (considering g as always practically the same).

The discharge must vary as velocity $\times$ area, $Q \propto VA \propto H^{1/2}D^2$, where D denotes any representative dimension of the turbine, such as the runner-throat diameter. (Any conduit area A varies as the square of the linear dimensions.)

Power output varies as QH; $P \propto H^{1/2}D^2H \propto D^2H^{3/2}$.

Since the velocity u of a point on the runner must vary in proportion to the other velocities, $u = \pi DN/60$ and $u \propto H^{1/2}$. Hence the turbine speed, rpm, varies as u/D and $N \propto H^{1/2}/D$.

These relations are convenient for use in the application of model tests to determine the expected performance of a large unit of the same design or to transfer the results obtained in one turbine to another of homologous form. For example, if a model of throat diameter D develops power P under a head H when running at a speed N, we can write

$$P \propto D^2H^{3/2} \qquad \text{or} \qquad P = P_1D^2H^{3/2} \tag{10}$$

in which P_1 is the power that would be developed by a homologous turbine of 1 ft throat diameter under 1 ft head as can be seen by putting $D = 1$ and $H = 1$ in the last relation. Knowing P, D, and H, we can compute P_1 from the model tests. Then a homologous turbine of D' throat diameter operating at the proper corresponding speed under a head H' would develop a power of $P' = P_1D'^2H'^{3/2}$. The proper speed can be found by the use of the relation $u \propto H^{1/2}$, or $u = (\text{const})\, H^{1/2}$, and using the customary notation the constant is called $\phi \sqrt{2g}$, so that

$$u = (\phi \sqrt{2g})H^{1/2} = \phi \sqrt{2gH} \tag{11}$$

i.e., ϕ is the ratio of the circumferential velocity of a point on the runner to the theoretical spouting velocity of the water, $\sqrt{2gH}$. Then ϕ may be computed from the model test and must remain the same for the large unit, *i.e.*,

$$\phi = \frac{u}{\sqrt{2gH}} = \frac{\pi DN}{60 \sqrt{2g}\, H^{1/2}} = \frac{\pi D'N'}{60 \sqrt{2g}\, H'^{1/2}}$$

from which N' is found.

5. Specific Speed. Modern practice in turbine design rests on the firm basis of actual results secured on laboratory models and large units, and each experienced manufacturer has available such test records for an extensive series of designs of progressively varying characteristics, each giving satisfactory performance. No matter how elaborate the method of design based on theory, no important installation would be carried out without confirming the calculations by tests on a model or closely similar field installation. The complexity of the flow conditions and the manifold factors involved make this procedure the sole source of assurance as to successful performance of the installation and also make it the most economical and timesaving method of design. Modified and radically new designs are continually being produced, however, and a sound theoretical basis of design cannot be dispensed with in favor of exclusively empirical methods.

One of the problems that arise early in planning a new hydroelectric project is the selection of the proper type of turbine and its proper speed to suit the given conditions of power capacity and effective head. This step has been greatly simplified by a relation of basic importance, which has systematized the entire field of turbine design and performance and in modified form also covers the field of pumps, and is applicable to hydraulic machinery in general. This is the specific-speed principle.

This may be viewed as a combination in a single expression of the foregoing principles of similarity and amounts to a definition of the rotary speed of the turbine N in dimensional form, the dimensions used being not the fundamental dimensions of length, mass, and time but those entering into the usual turbine problem, namely, head and power output.

We have just found that $P \propto D^2H^{3/2}$ when $N \propto H^{1/2}/D$. From the first expression, $D \propto \sqrt{P}/H^{3/4}$, and inserting this in the second, $N \propto H^{1/2}H^{3/4}/\sqrt{P} \propto H^{5/4}/\sqrt{P}$. By putting this in the form of an equation instead of a proportionality,

$$N = (\text{a constant})\, \frac{H^{5/4}}{\sqrt{P}}$$

To determine the constant, it is necessary only to put the head and power each equal to unity, from which it is seen that the constant is the speed (in revolutions per minute) of a homologous turbine of such size that it would develop 1 unit of power under 1 ft head. This is called the *specific speed* and is denoted N_s, so that the fundamental relation is simply

$$N = N_s \frac{H^{5/4}}{\sqrt{P}} \tag{12}$$

N_s is a constant for all geometrically similar turbines of any size under any head, each being operated at its proper speed corresponding to the head and size.

If the type or design is changed, we have another series of homologous turbines with a new value of the constant. N_s is therefore a quantity that sets forth in a single numerical value the inherent ability of a given form of turbine to develop speed for a given power and head; or if the expression is squared and solved for P, it is seen that N_s^2 represents the power capability of the design at a given head and speed.

Specific speed may be briefly defined as the speed of a homologous 1-hp turbine under 1 ft head. It is of course unnecessary actually to build a 1-hp model to find the value of N_s, for it can be readily computed from the tests of any size of model or installed unit by inserting the actual head, horsepower, and speed from the test in

$$N_s = N \frac{\sqrt{P}}{H^{5/4}} \tag{13}$$

Since the N_s value remains constant for all turbines of the same design, we can find the corresponding speed of another homologous turbine from Eq. (12) in which P and H will be those for the new installation.

In the metric system of units, with head expressed in meters, power in metric horsepower, and speed in rpm, the specific speed is 4.446 times the value with head expressed in feet and power in English horsepower units; with head expressed in meters and power in kilowatts, the specific speed becomes 3.813 times the value with head in feet and power in English horsepower units.

In a multiple-runner turbine, the specific speed is usually expressed as that of a single runner; and in a multiple-jet impulse wheel, the specific speed is normally based on the power of a single jet.

The entire field of turbines can be classified on the basis of the specific-speed values. This classification can be extended to include not only other prime movers such as steam turbines and gas turbines, but also such other hydrodynamic machines as pumps, centrifugal and axial-flow compressors or blowers, fans, aircraft and marine propellers. We shall here limit our consideration to hydraulic turbines.

As might be expected, there are some forms and proportions in turbine design that are particularly favorable to high efficiency with a corresponding range of specific speed values. Specific speeds that are abnormally high or low as compared with this normal range naturally entail impaired efficiencies.

Since for a given power capacity and head the actual speed is directly proportional to the specific speed, as shown by the specific-speed formula, and since high rpm results in reduced diameters and weights of the driven machine, and to some extent of the turbine itself, and also in reduced size and cost of the powerhouse structure, there is from economic considerations a strong attraction toward higher and higher specific speeds, even at the expense of some sacrifice in efficiency. It should be recognized, however, that in hydroelectric developments the major portion of the cost is usually in the dams, reservoirs, headworks pipelines, transmission lines, and similar fixed works and only a small portion in the powerhouse and machinery; so a saving in first cost of the latter elements must be justified in comparison with the sacrifice in earnings on the whole project entailed by a reduction in efficiency. In most cases a considerable increase in specific speed will be beneficial only when the impairment in efficiency is slight. These considerations are of special importance in low-head installations, where the actual speeds are low and the machinery large. The continual demand for the highest possible speeds has resulted in a wide range of specific speeds being available without significant sacrifice in efficiency, as seen from the curves of turbine efficiencies obtainable at various specific speeds (Fig. 25). The curves have been drawn to represent typical values of peak efficiencies attained under favorable conditions by modern large turbines of good design, where efficiency tests were conducted in accordance with generally accepted test codes. The curves are not intended to show the maximum efficiencies obtainable, as actually a growing number of large well-designed turbines are reported to have attained peak efficiencies exceeding those shown by the curves. However, the curves may serve as a guide which indicates the peak efficiency that can reasonably be expected in a new installation of medium- to large-sized turbines under favorable conditions. It will be noted that, over a wide

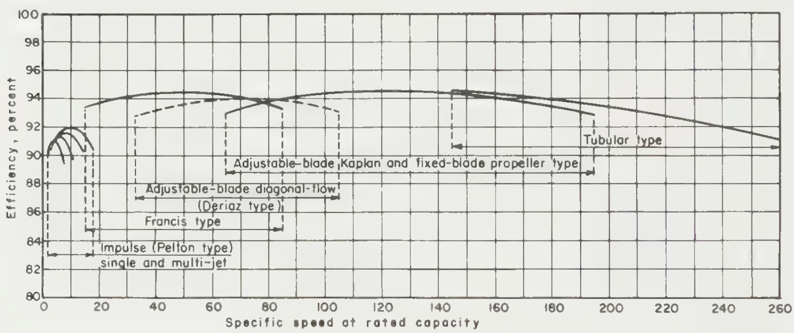

FIG. 25. Typical peak efficiencies of various turbines in relation to specific speed.

range of specific speeds, peak efficiencies in the range of 92 to 94 percent may reasonably be expected under favorable conditions.

In any turbine, as the gate opening is changed and the power output thus altered, the specific speed continually changes; there are two particular values of the specific speed for a given unit which may be taken as representative. The usual numerical value used in classifying turbines is the specific speed at the rated capacity or guaranteed power under the normal head for which the unit is designed. This may be called the *rated specific speed.* Except in the case of high-specific-speed Francis and fixed-blade propeller turbines, it is usual to have the point of highest efficiency occur at a power somewhat less than full rated load; the specific speed corresponding to the power at maximum efficiency may be called the *nominal specific speed.* The curves of Fig. 25 are based on the rated specific speeds.

The curve of efficiency vs. power output for a given turbine operated at varying gate opening has different characteristic forms for various turbine types and specific speeds, as illustrated in Fig. 26. The Pelton-type impulse wheel, having very low specific speeds, gives a flat-topped efficiency curve with high part-load and over load efficiencies and only small impairment of efficiency over a wide range of nozzle openings and outputs. The low-specific-speed Francis turbine has similar characteristics. Both types are therefore suitable for plants serving to regulate a power system and taking the load variations. High-specific-speed Francis turbines show poor part-load efficiencies and little overload capacity beyond the point of maximum efficiency; *i.e.*, they have a sharply peaked efficiency curve and are therefore best suited to operation under block load or within a narrow range of outputs. This characteristic is further intensified in fixed-blade propeller turbines. In run-of-river plants, such as low-head developments with limited pondage, where under reduced demand the unused flow is wasted over the spillway, the low part-gate efficiencies are of little consequence.

When a high degree of regulation is of importance in low-head plants, high part-gate and over-gate efficiencies may be secured in high-speed propeller turbines by

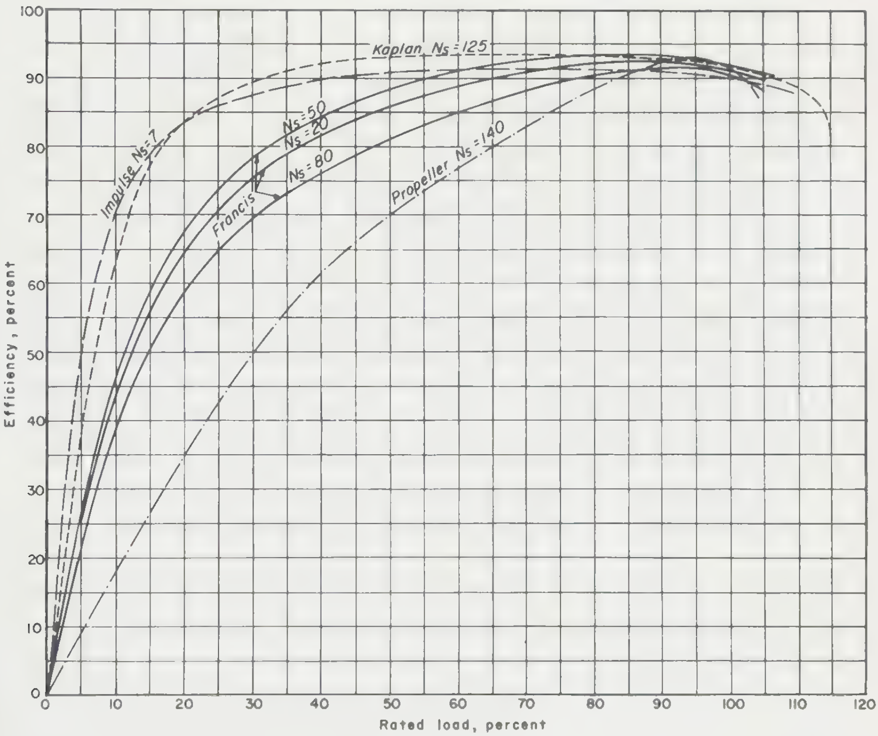

Fig. 26. Turbine-efficiency variation with load for turbines of various specific speeds

making the runner blades automatically adjustable in response to changes in the wicket gate openings, under governor control. This is the method of operation of the Kaplan type of turbine, which is capable of giving an efficiency-power curve of even more favorable form than low-speed Francis or Pelton units. Another advantageous characteristic of propeller and Kaplan units is their ability to operate under reduced heads while maintaining good power output, a fortunate property for low-head developments to which these types are suited, for such developments are usually subject to wide head variations.

In plants having high heads even a low specific speed in combination with the high head will usually give a reasonably high rpm. On the other hand, with low heads and large unit capacities, a low specific speed would result in extremely low rpm, very large diameters of turbine and generator, and large powerhouse structures. Consequently, high-specific-speed types are particularly desirable for low-head plants.

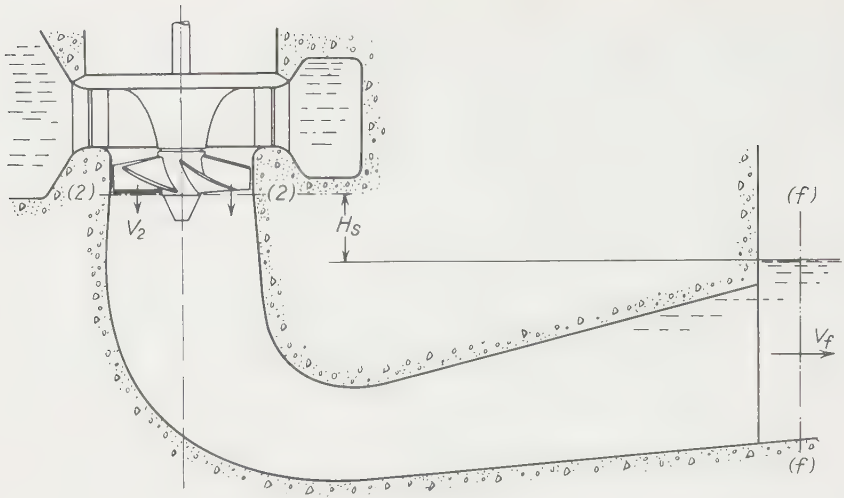

FIG. 27

In selecting the specific speed suitable for a given head, cavitation requirements are usually the controlling consideration, and this subject will now be taken up.

6. Cavitation. Let us write the Bernoulli formula for the draft tube of the turbine (Fig. 27) between section 2, at the outlet of the runner to section f, the point of final discharge into the tailrace, and take the tail-water surface as datum level. Then, by calling the elevation of section 2 above tail water H_s (the static draft head) and expressing all static pressure heads as absolute pressures, H_{p2} denoting the absolute pressure head at 2 and H_a the pressure head of the atmosphere,

$$H_{p2} + H_s + \frac{V_2^2}{2g} - H_L = H_a + O + \frac{V_f^2}{2g}$$

in which H_L is the loss of head in eddies and friction within the draft tube and V_f the final discharge velocity in the tailrace.

The total loss of energy is the internal loss plus the final residual velocity head rejected into the tailrace, $V_f^2/2g$. If the effective head on the turbine varies, and if the rotational speed of the runner is always adjusted to suit the head so that ϕ remains constant, V_2 will remain at constant angle of obliquity α_2 to the plane of section 2 and its axial component will remain in fixed ratio to V_2; and from the principle of continuity of flow, the velocity at any point in the tube and that at section f will likewise remain in fixed ratio to V_2. From the principles of similarity, the eddy losses within the tube and the final outflow loss $V_f^2/2g$ will then always be directly proportional to $V_2^2/2g$; if we make the reasonable assumption that the flow is completely turbulent, we can also take the frictional losses proportional to the velocity head at any point or to $V_2^2/2g$. The total loss can then be put equal to $K(V_2^2/2g)$, K being a constant coefficient for a given turbine.

Then the Bernoulli formula gives

$$\begin{aligned} H_{p2} &= H_a - H_s - \frac{V_2^2}{2g} + H_L + \frac{V_f^2}{2g} = H_a - H_s - \frac{V_2^2}{2g} + K\frac{V_2^2}{2g} \\ &= H_a - H_s - (1 - K)\frac{V_2^2}{2g} \end{aligned}$$

Now the head representing the total kinetic energy of the flow entering the draft tube is $V_2^2/2g$; it is the purpose of the draft tube, by gradually decelerating the velocity, to reconvert as much as possible of this kinetic energy into effective pressure head in order to reduce the back pressure H_{p2} against which the runner discharges. The efficiency of the draft tube can therefore be expressed as

$$e_d = \frac{V_2^2/2g - K(V_2^2/2g)}{V_2^2/2g} = 1 - K$$

so that the equation for H_{p2} becomes, simply,

$$H_{p2} = H_a - H_s - e_d \frac{V_2^2}{2g} \tag{14}$$

H_{p2} represents the average pressure head at the runner discharge. But on the runner vanes (blades) there will be a higher pressure on the vane faces and a lower pressure on the back surfaces; it is this pressure difference that drives the runner around and develops mechanical power on the shaft. Pressures at local points in section 2 will therefore alternately exceed and fall below the average pressure H_{p2}; at some local point on the back of a runner vane the pressure will fall below H_{p2}; and at the local point of minimum pressure we shall call the absolute pressure head H_m. The pressure difference $H_{p2} - H_m$, the local pressure drop, is due to the flow through the turbine and under dynamically similar conditions is proportional to the effective head producing the flow, *i.e.*, the effective head on the turbine, H. Hence we can write $H_{p2} - H_m = K_cH$, where K_c is a constant coefficient for a given turbine, its value depending on the particular shape of the vanes. The absolute pressure head at the point of minimum pressure in the turbine is then

$$H_m = H_{p2} - K_cH = H_a - H_s - e_d \frac{V_2^2}{2g} - K_cH$$

If we consider that when hydraulic similarity is preserved, by keeping the runner speed in proper relation to the head, $V_2^2/2g$ is proportional to H, we can combine the last two terms and put

$$e_d \frac{V_2^2}{2g} + K_cH = \sigma H$$

in which σ is a constant coefficient for a given turbine (or for any geometrically similar turbine) operating at a given ϕ. Then we have

$$H_m = H_a - H_s - \sigma H \tag{15}$$

Now suppose that both headwater and tail water are progressively lowered by equal amounts. The effective head H will remain constant, but H_s will increase so that H_m will be progressively lowered. There is, however, a limit to the possible reduction of H_m. When H_m reaches the vapor pressure of the water, the point at which the water boils, the pressure can go no lower as long as water is present as a liquid. Beyond this amount of reduction, the water cannot exist as a liquid. When H_m is reduced to this limiting value H_{vp}, the vapor pressure head, the water begins to boil and the passages become partly occupied by vapor cavities within the flowing stream. The formation of these vapor-filled cavities in the stream is called *cavitation*.

When the pressure at some point in the turbine reaches the vapor pressure, critical conditions ensue and the turbine becomes subject to the undesirable consequences of cavitation, namely, erosion (known as pitting) and noise and vibration of the machine and surrounding structures. When the extent of the cavitation increases, an impairment of power and efficiency results. This phenomenon is not limited to turbines but may also occur in pumps and in stationary conduits at points of low pressure and high velocity, as for example in sluiceways through dams. The guarding against its occurrence is a vital consideration in the selection of type and specific speed of a turbine and in fixing the runner elevation in relation to tail water.

The cavitation phenomenon can be explained as follows: Consider the flow through a turbine runner where the total draft head is excessive and where there is a failure of the vane (blade) contour to conform to the natural flow lines, because the curvature is too sharp for the pressure and velocity conditions. At such a point in the runner, usually on the back of the vanes near the discharge orifice and near the outer periphery, where the relative velocity is high, the flowing stream parts from the vane surface and leaves a void filled with eddies; and when the absolute pressure is reduced to the vapor pressure, this void or cavity becomes filled with water vapor, air, and other gases. As the flow continues downstream, the static pressure rises again and then exceeds the vapor pressure. Moreover the flow in large conduits at high velocities is never actually steady but is turbulent and subject to continual variations of velocity and pulsations of pressure. Hence, when a particle of the flowing liquid reaches a point where the local pressure just attains the vapor pressure limit, at one instant the particle will be under this pressure and vaporize, forming a cavity filled with vapor; at the next instant, the pressure will rise above the vapor pressure and the vapor will suddenly condense and return to liquid, producing a collapse of the cavity and an explosion or, more strictly, an *implosion*. This action is not confined to the larger cavities but extends into the pores of the metal. The water rushing in to fill the collapsed cavity will also enter the vapor-filled pores until instantaneously stopped by the bottom surface of the pore, where water-hammer action takes place. This is capable of producing pressure intensities on the areas of the same order as the tensile strength of the metal, and under the continual repetition of the shocks, the metal fails locally under fatigue and small particles are irregularly broken away, giving the surface a peculiar spongy appearance. The action, called *pitting*, is thus believed to be primarily mechanical, as just described; it was formerly thought to be mainly chemical, in the nature of rusting, or electrolytic; but it can be produced in wood, concrete, and even in glass, which points to a mechanical origin as outlined in the preceding theory.

It should be possible to prevent pitting by avoiding the occurrence anywhere in the turbine of a local pressure head so low as to approach the vapor pressure of the water. This method of avoiding cavitation and pitting has been found from experience to be effective.

In the formula for the minimum local pressure, we find that the critical point at which cavitation occurs is given by putting $H_m = H_{vp}$, the vapor pressure head, so that

$$H_{vp} = H_a - H_s - \sigma_c H \qquad \text{and} \qquad \sigma_c = \frac{H_a - H_{vp} - H_s}{H}$$

in which σ_c is the critical sigma, or the value of σ at which the undesirable effects of cavitation begin. We can call $H_a - H_{vp} = H_b$ the height of the barometric water column, or the height to which water may be drawn up in a water barometer. Then

$$\sigma_c = \frac{H_b - H_s}{H} \tag{16}$$

This is the Thoma formula for the critical value of the dimensionless ratio called the Thoma cavitation coefficient (known also as the Thoma cavitation number, factor, or parameter).

It will be readily perceived that if a turbine in a given plant is installed with excessive draft head H_s, *i.e.*, too high a setting of the runner in relation to tail water, so that the actual plant sigma is lower then the critical sigma σ_c, then portions of the water passages will be occupied by vapor instead of liquid. The stream areas and the lines of flow will be changed, and the principles of similarity will fail to apply, for we have no longer preserved complete geometrical similitude of the flow.

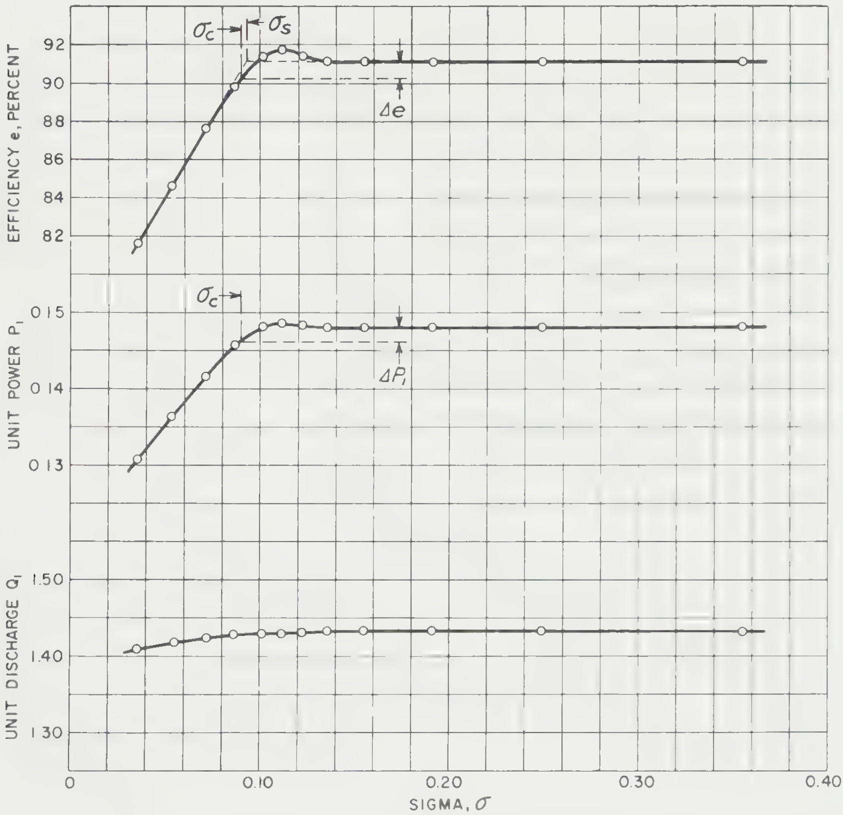

FIG. 28. Typical test curves of efficiency, unit power, and unit discharge vs. cavitation-coefficient sigma, showing evidence of cavitation at the critical value of sigma.

This gives us a method of determining the numerical value of σ_c for a given turbine. A homologous model may be tested by progressively increasing H_s while keeping H, N, and all other factors constant. So long as no cavitation occurs, the conditions of similarity will continue to be satisfied and no significant change in efficiency, power output, or discharge will occur. A drop in any or all of the quantities therefore indicates a departure from conditions of similarity, and the sigma at which the first significant drop in one of the quantities occurs is usually considered the critical sigma for the particular turbine. Figure 28 illustrates the method, utilizing the curves of efficiency e, unit power P_1, and unit discharge Q_1, plotted against σ.[1] To provide for cavitation-free turbine operation, we must be sure that in the actual installation the σ

[1] Curves of this type have sometimes been descriptively called "sigma break" curves.

for the plant is not less than this σ_c but exceeds it, some margin being thus allowed against cavitation.

It is possible in making the cavitation tests to vary H instead of H_s, the turbine speed N being always kept such that ϕ remains constant. We can then plot the values of e, P_1, and Q_1 against σ as abscissa, as before.

The shape of the cavitation test curves in some instances is such that it becomes difficult to establish precisely the points of drop in the quantities without the influence of individual judgment. Several different rules, based on somewhat varied criteria, have been devised for determining the critical sigma from the cavitation test curves, as illustrated in Fig. 28. One of the commonly used criteria establishes the critical sigma as that value of sigma, for decreasing values of sigma, at which the power drop ΔP_1 from the constant value is 1 percent. Another criterion establishes critical sigma as the value of sigma at which the efficiency drop Δe is a given amount, arbitrarily chosen by some as 1 percent of the constant value. Others have chosen a somewhat more conservative efficiency drop of 0.5 percent as the criterion, on the premise that the drop in the efficiency curve is often more acute than the drop in power and discharge. A proposed supplement to the International Code for Model Acceptance Tests of Hydraulic Turbines, Publication 193, First Edition, 1965, of the IEC[1] included a basis for determining the cavitation limit by use of a "standard sigma" value σ_s of the model, established by the intersection of the horizontal line of constant efficiency with the strongly dropping straight line along which the test points for substantially developed cavitation tend to align themselves. The proposed IEC basis provided further for determining the cavitation limit of the full-scale turbine by adding to the σ_s of the model a margin $\Delta\sigma$ based on experience acquired from model tests and their correlation with field cavitation data. It is quite evident that general agreement on a standard method of determining cavitation limits has yet to be reached, though progress toward standardization is being made.

The most reliable basis for determining critical sigma and the allowable value of H_s for the actual setting of a turbine is obtained by supplementing the cavitation tests on a homologous model with field-experience data from plants where pitting has actually occurred at certain values of sigma during operation. Since the most serious result of cavitation is pitting, we are most concerned with the value of σ where pitting begins. Some turbines are known to operate without measurable loss of power or efficiency but to develop distinct pitting; evidence of pitting is therefore a primary index of detrimental cavitation in field installations. The earlier phases of cavitation may usually be detected by audible indications such as the onset of cavitation noise.

7. Selection of Type and Speed of Turbine. Since the critical sigma and degree of resistance to cavitation of a particular turbine are greatly affected by its design, so that two turbines of the same specific speed may differ considerably in this respect, a cavitation test on a homologous model supplemented, if possible, by actual field experience from a nonpitting homologous installation is needed if a new installation is to be carried out safely without using a considerable margin in the value of the plant sigma, and therefore in the value of H_s.

Such information is of special importance in selecting Kaplan and fixed-blade propeller turbines for which the critical sigma is greatly dependent on the particular design, especially on the proportional blade area of the runner. Ample blade area is necessary to keep sigma within reasonable limits. In the absence of definite information, a fair degree of guidance for estimating the safe sigma may be obtained from curves based on pitting experience and available cavitation tests on representative turbines of various specific speeds.

The critical sigma of turbines is greatly dependent on their specific speed; therefore,

[1] International Electrotechnical Commission, Geneva, Switzerland (affiliated with ISO).

values of critical sigma of turbines of normal or conventional design plotted as a function of N_s provide a basis for plotting curves which are useful for preliminary selection of turbines. Figure 29 shows the range of critical sigma values found in practice for two of the principal types of reaction turbines. The existence of a considerable range of critical sigma values for each value of specific speed and type of turbine is due to variations in the cavitation characteristics of individual runner designs and also due to differences in the relative opening of the turbine wicket gates at which the rated capacity is obtained in individual cases. The curves shown in solid lines represent minimum values of plant sigma recommended as a guide for preliminary selection purposes. At these values of plant sigma, turbines of normal design, which are intended to develop their rated capacity at or near full gate opening, can reasonably be expected to have a small margin of safety against detrimental pitting or objectionable noise due to cavitation. The recommended minimum plant sigma vs. N_s curves represent the following empirical equations:

$$\sigma = 0.006 + 0.55\left(\frac{N_s}{100}\right)^{1.8} \qquad \text{for Francis turbines}$$

$$\sigma = 0.10 + 0.30\left(\frac{N_s}{100}\right)^{2.5} \qquad \text{for Kaplan turbines}$$

These curves are necessarily only approximations. If, in using them to determine static draft head for preliminary purposes, a reasonable margin of safety is desired, it is good practice to reduce the calculated static draft head by about 3 ft for Francis turbines and about 4 ft for adjustable-blade propeller turbines, to allow for some variations in runner characteristics and, especially in the case of regulating units, to allow for some transient pressure variations in the draft tubes of such units. For fixed-blade propeller turbines, plant sigma values about 5 to 8 percent lower than those indicated for Kaplan turbines may usually be used.

Although Fig. 29 is useful as a general guide, it should be recognized that specific speed is not a precise index of the cavitation characteristics of a runner, because different runners of the same specific speed may have substantially different values of peripheral speed coefficient ϕ and unit power P_1. A high unit-power runner has a relatively high discharge with consequent high velocity of flow through it. Since the velocity of flow strongly influences the cavitation conditions in the runner, unit power may be considered a better criterion than specific speed for determining the allowable value of plant sigma.[1] Therefore, in selecting the allowable static draft head for preliminary design purposes, it is advisable to supplement the approximate determination, based on data which relates critical sigma to specific speed, by using available data, such as published in the foregoing reference, which relates critical sigma values to unit power.

Using the N_s relation, the Thoma formula for cavitation coefficient, and curves relating cavitation coefficients to N_s, a preliminary selection of type, speed, and draft head of a reaction turbine can be made for any installation.

Other factors, such as form of efficiency curve, may also influence the selection, but the specific speed and draft head must be in proper relation to the effective head on the plant, if satisfactory performance and life of the vital parts are to be assured.

Since the designer of a hydroelectric plant usually wishes to avoid undue depth of excavation for the powerhouse foundation, a fairly large value of H_s is usually desired. On the other hand, the engineer of the turbine manufacturer is faced with the vital necessity of limiting H_s in accordance with a safe value of sigma and at the same time providing as high a specific speed as is feasible, in the interest of economy in cost of turbine, generator, and powerhouse. The economy secured by increase of specific

[1] "Hydraulic Turbine and Draft Tube Settings," Edison Electric Institute Publication 55-9, 1955.

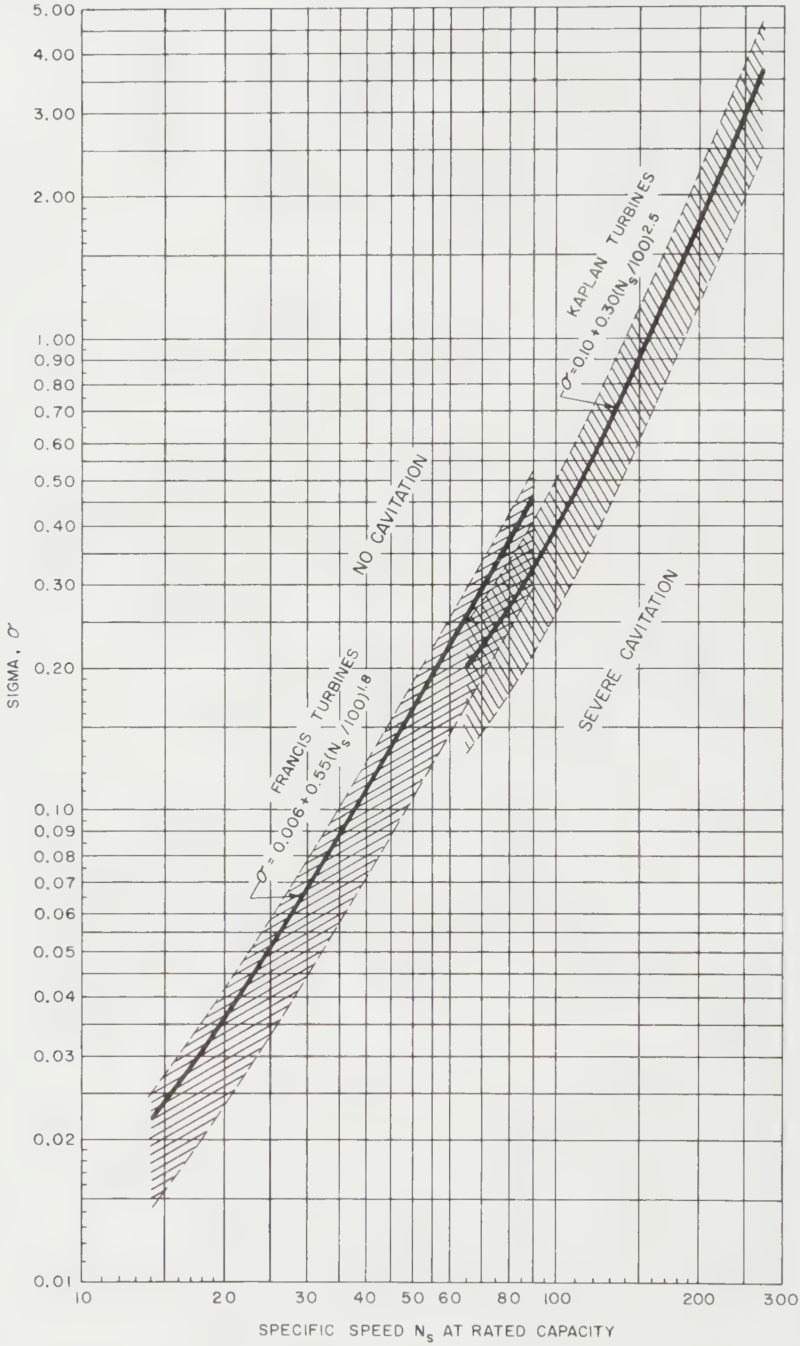

FIG. 29. Sigma values for various specific speeds. Shaded bands show approximate range of critical sigma of Francis and Kaplan turbines; curves indicate minimum plant sigma recommended as a guide for preliminary selection purposes.

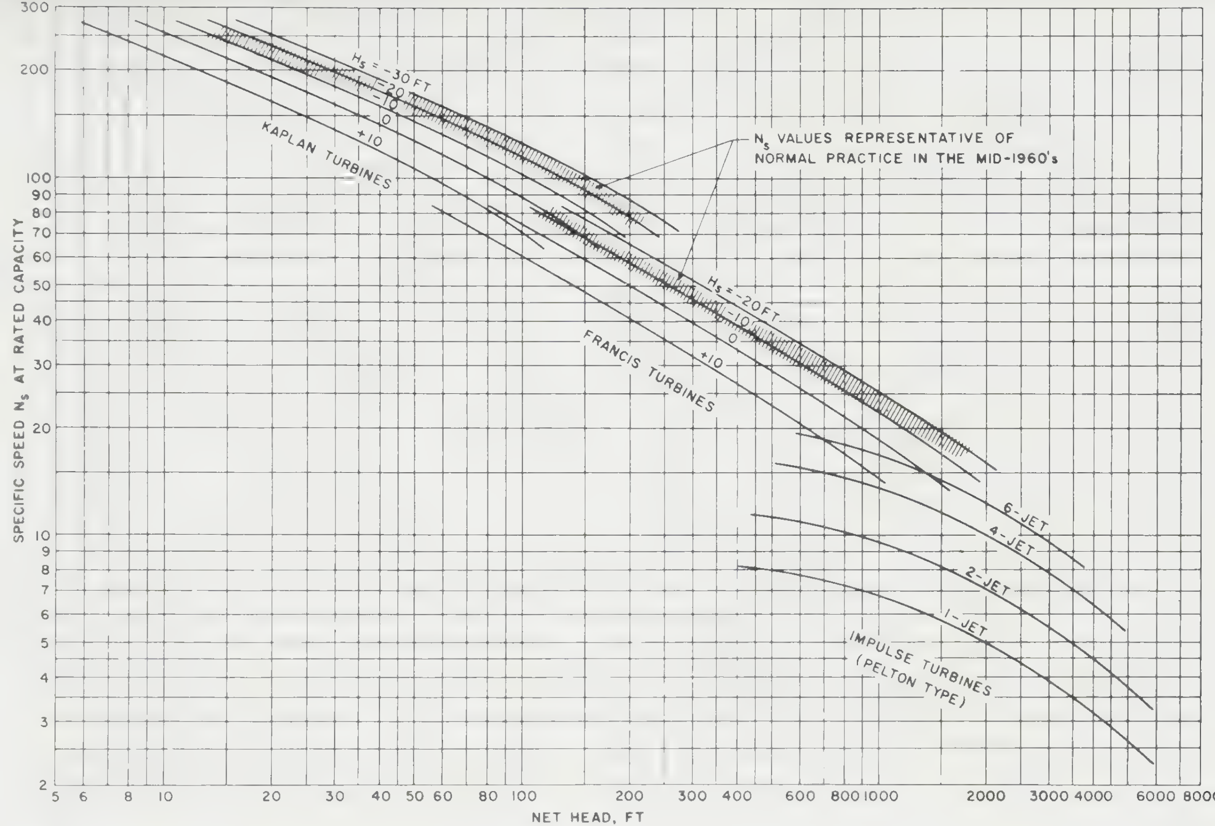

FIG. 30. Approximate limits of specific speed for various turbines and net heads. Effect of draft head H_s on maximum allowable N_s of Kaplan and Francis turbines and effect of number of jets on N_s of impulse turbines are illustrated. Shaded bands show range of N_s values representative of present normal practice for Kaplan and Francis turbines.

speed is so substantial and indeed necessary, in the case of low-head plants where the machinery is relatively large, that it becomes advantageous to adopt high-specific-speed turbines, and to secure the necessary plant sigma by setting the runner below the tail-water elevation, thus using a negative value of H_s.

An initial solution of the problem of selecting type, N_s and N, can be obtained from the chart of Fig. 30. Here the limits of N_s vs. head are shown for several values of H_s, calculated from the values of recommended plant sigma in Fig. 29.

For vertical Francis turbines, H_s is to be measured to the lowest point of the runner vanes or buckets; for propeller turbines, H_s is measured to the mid-height of the runner blades at the outer tips or runner periphery. This basis was used in constructing the curves of plant sigmas (Fig. 29). In the case of horizontal-shaft units, H_s should be

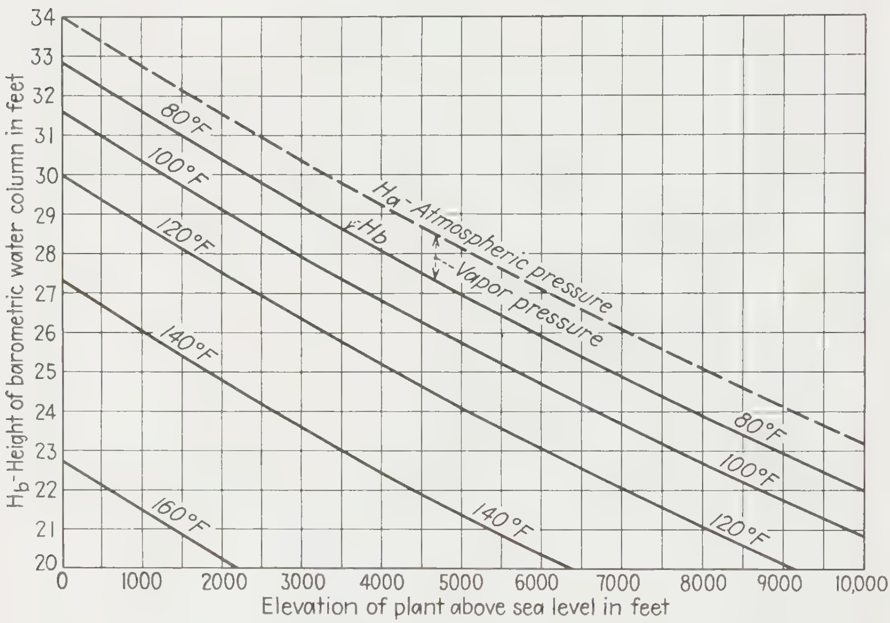

FIG. 31. Height of barometric water column H_b corresponding to atmospheric pressure at various elevations above sea level and various water temperatures.

measured to the upper end of the outlet diameter and not to the shaft center line, since the point of minimum pressure will be at the upper side of the water passage.

The chart is based on a value of H_b of 32.8 ft, corresponding to plants located at or near sea level and with water temperatures not exceeding about 80 F. For plants subject to higher water temperatures, the value of H_b must be reduced to allow for the increased vapor pressure. For plants to be erected at higher elevations, H_b must be reduced to allow for the corresponding decrease in atmospheric pressure H_a; this correction may be obtained from Fig. 31.

For Francis turbines, the lines of the chart plotted for several representative values of draft head H_s correspond to an equation for N_s obtained from the empirical equation for recommended minimum plant sigma and the Thoma formula, as follows:

$$\sigma = 0.006 + 0.55\left(\frac{N_s}{100}\right)^{1.8} = \frac{32.8 - H_s}{H}$$

from which

$$N_s = 139.4\left(\frac{32.8 - H_s}{H} - 0.006\right)^{0.555}$$

Similarly for Kaplan turbines, the lines on the chart plotted for several representative values of H_s correspond to an equation for N_s obtained from the empirical equation for recommended minimum plant sigma and the Thoma formula, as follows:

$$\sigma = 0.10 + 0.30\left(\frac{N_s}{100}\right)^{2.5} = \frac{32.8 - H_s}{H}$$

from which

$$N_s = 161.9\left(\frac{32.8 - H_s}{H} - 0.10\right)^{0.4}$$

The actual N used for a specific installation in a hydroelectric plant must be a synchronous speed for the generator. For 60-cycle frequency, $N = (7{,}200/n)$, in which n is the number of poles in the generator, which must be an even integer. For 50 cycles, used in Europe and South America, $N = (6{,}000/n)$.

To illustrate the use of these principles, let us apply them to a typical problem and select the type, speed, and draft head of a turbine rated 206,000 hp at or near full gate under a net head of 310 ft, to drive a 60-cycle generator. It is assumed that the plant is near sea level and that it is desired to provide for a possible water temperature of 80 F.

From the chart of Fig. 30 the N_s value representative of present normal practice for a net head of 310 ft is approximately 46. This corresponds to a Francis-type turbine of high attainable efficiency as seen from the curve of efficiencies in relation to N_s in Fig. 25. The permissible speed of the unit is

$$N = N_s \frac{H^{5/4}}{P^{1/2}} = 46\,\frac{310^{5/4}}{206{,}000^{1/2}} = 46\,\frac{1{,}301}{453.9} = 131.8 \text{ rpm}$$

The nearest synchronous speed that does not exceed this is

$$N = \frac{7{,}200}{n} = \frac{7{,}200}{56 \text{ poles}} = 128.6 \text{ rpm}$$

Then the N_s at rating will be

$$N_s = 128.6\,\frac{453.9}{1{,}301} = 44.8$$

The recommended static draft head H_s (referred to the lowest point of the runner buckets in a vertical Francis-type turbine) is read from the chart as approximately -9 ft. The numerical value calculated from the equation of recommended minimum plant sigma and the Thoma formula is

$$\sigma = 0.006 + 0.55\left(\frac{N_s}{100}\right)^{1.8} = 0.006 + 0.55\left(\frac{44.8}{100}\right)^{1.8} = 0.136$$

$$H_s = H_b - \sigma H = 32.8 - 0.136 \times 310 = -9.4 \text{ ft}$$

In the event the plant is to be located 1,000 ft above sea level, H_b would be 31.6 ft and the recommended draft head would be

$$H_s = 31.6 - 0.136 \times 310 = -10.6 \text{ ft}$$

In the field of impulse turbines, experience has shown that, as in other turbines, low specific speeds must be used for very high heads and the use of high specific speeds must be limited to low heads. This is consistent with the N_s curves for Francis- and Kaplan-type turbines.

In Fig. 30, the N_s values for Pelton-type impulse turbines at various heads and for various numbers of jets per turbine may be used as a guide reasonably representing maximum values used in present normal practice.

8. Characteristic Proportions of Turbine Runners. Figure 32 shows the typical forms of runner corresponding to various specific speeds. The three runners are plotted to the same scale, the dimensions being consistent with a constant output under a constant head, so that the figures show the great change in dimensions of a turbine of a given capacity involved in a change of specific speed. Since under a constant head the actual rpm is directly proportional to the specific speed, the values of N_s shown are a direct indication of the comparative speeds at which the various types would operate at a given power and head. Evidently, for example, a high-speed Francis turbine substituted for a propeller turbine would require a much heavier runner and larger turbine and would run only about one-half as fast, a generator of nearly twice the diameter of that needed for the propeller turbine being required. If a Pelton-type impulse wheel were substituted for the propeller turbine, it would require an enormous increase in dimensions and would run at a speed of the order of about one-fiftieth of that of the propeller unit.

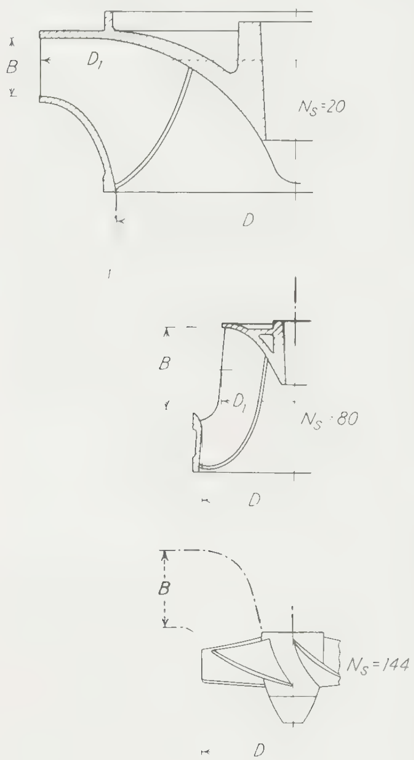

Fig. 32

The wide range of specific speeds available is obtained by altering the design proportions. Thus for a very low specific-speed Francis turbine, a large entrance diameter D_1 is used (see Fig. 32) and a small throat diameter D, the breadth B of the distributor being small. The disk friction on the runner hub and shroud ring and the leakage loss through the runner clearances are high, and the maximum efficiency is somewhat less than for a more normal specific speed; but the efficiency remains high for part loads and overloads, and the efficiency curve is flat and of favorable form for operation under widely varying load demands.

Increase in specific speed requires the reduction of D_1 to suit a higher rpm without going to a peripheral velocity u_1 out of proportion to the water velocities corresponding to the head. To accommodate the required quantity of flow, B must be increased to compensate for the reduced diameter and thus to maintain a proper entrance area. For a high-speed Francis turbine, D_1 becomes smaller than D, the runner vanes are large and are usually given a complex spoon formation, and the high relative velocity of the vanes through the water involves high surface friction. The restriction in D to suit the high rpm involves a high value of the kinetic energy discharged from the runner, and the performance becomes greatly dependent on the ability of the draft tube to regain as much as possible of this energy. Still higher specific speeds have been made possible by the development of the propeller turbine in which the shroud-ring friction is eliminated; the runner vanes become nearly flat blades inclined at a small angle to the tangential direction and have a high relative velocity through the water. These blades are few in number, usually four to eight, and of reduced length in the direction of flow, so that they normally overlap each other but little or not at all, their surface friction thus being kept from reaching inordinate amounts.

At the lower end of the specific-speed range, reduction below the speeds of low-speed Francis turbines is effected by going to partial admission; *i.e.*, instead of admitting water all the way around the runner periphery, it is admitted at only one to six points; and to reduce the friction and turbulence of the entering flow, this admission takes place through circular contracting nozzles equipped with adjustable needles for regulation, forming the flow into undisturbed jets with little loss of head. The most important and valuable feature of the Pelton-type wheel is the use of free jets, surrounded by air, and all the space in the runner not occupied by the flow is filled with air. The pressure through the runner space is not appreciably reduced at any point below the atmospheric value, and the possibility of cavitation is greatly reduced.

Although the proportions of turbines may be varied somewhat according to the choice of the designer, the general characteristics for any given specific speed are fairly determinate in ordinary practice, and the curve sheet of Fig. 33 gives values consistent with normal design and high efficiencies. The design calculations are carried out for the point of best efficiency, the velocity triangles being drawn, the runner vane angles fixed to suit the relative velocity at the runner entrance, and the areas of the discharge orifices of the wicket gates and runner vanes calculated so that at each point the velocity multiplied by the area and a coefficient of discharge is equal to Q, the discharge.

The coefficient of discharge of the wicket gates is nearly unity, and that of the runner outlet is usually of the order of, say, 0.85 to 0.90 but is dependent on the characteristics of the design. The most important magnitude controlling the discharge and therefore the power capacity is the outflow area of the runner, which is carefully checked during manufacture to ensure its conformity to the design calculations and to the value corresponding to the test model. Space does not permit the covering of the extensive subject of turbine design, but it is hoped that the general principles and approximate proportions will prove helpful to users of turbines.

The percentage of rated load at which the point of best efficiency is taken will depend largely on the requirements of the installation but is limited by the attainable turbine characteristics; in the absence of definite requirements, average figures for usual conditions may be taken within the approximate limits given in Fig. 34. The corresponding ratio of N_s at best efficiency to the N_s at rated capacity, at given head and speed, varies directly as the square root of the power,

$$\frac{N_s \text{ at best efficiency}}{N_s \text{ at rated capacity}} = \sqrt{\frac{P \text{ at best efficiency}}{P \text{ at rated capacity}}}$$

Kaplan and impulse turbines permit a wide degree of flexibility in this respect, and the values adopted will be governed largely by the plant conditions. The turbine builders usually allow about 5 or 6 percent margin in power beyond the guaranteed rated capacity to provide a range for governing and a margin for variations of actual from computed performance.

9. Pelton-type Impulse Wheels. In considering the design proportions of Pelton-type impulse wheels, space does not permit the inclusion of the complex subject of bucket design, and we shall limit ourselves to the determination of the leading dimensions of the wheel or runner and the jet. The most important dimensions are the pitch diameter D of the runner and the diameter d of the jet after it has reached its vena contracta, after which its diameter remains practically uniform until it enters the buckets. Both diameters are expressed here in feet. The diameter ratio (D/d) is an important factor and is the principal one in fixing the specific speed. We shall consider the most common type of Pelton wheel, that with a single jet, and shall consider a

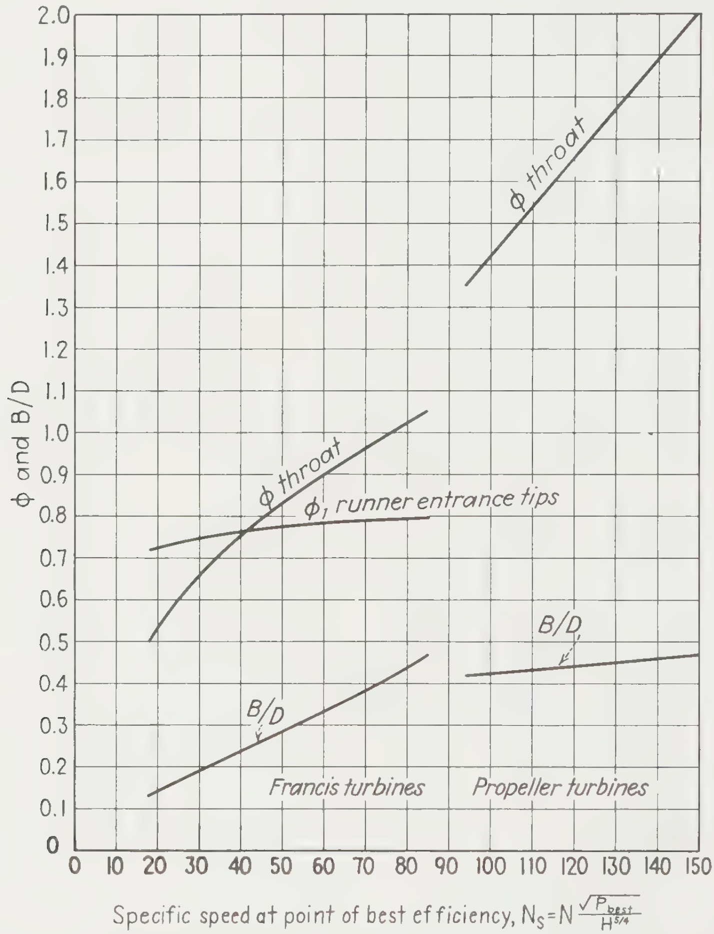

FIG. 33. Approximate runner proportions of reaction turbines of various specific speeds.

single runner. Naturally the effective specific speed of a unit having two single-nozzle runners or a single runner with two nozzles will be 1.41, or $\sqrt{2}$ times the specific speed of the single-nozzle runner, for the specific speed is proportional to the square root of the power. The pitch diameter of the runner is defined as the diameter of a circle tangent to the center line of the nozzle and jet; and the characteristic ϕ is the ratio of the velocity of the runner at the pitch diameter to $\sqrt{2gH}$, H being the effective head.

Before proceeding with the discussion of the Pelton-type wheel, the effective head should be defined. The following definition is quoted from the ASME Test Code for Hydraulic Prime Movers, PTC 18-1949:

". . . the effective head shall be taken as the elevation corresponding to the pressure head in the turbine inlet pipe immediately upstream from the nozzle if the pipe supplies only one nozzle, or immediately upstream from the upstream wye or branch diverging to the nozzles and furnished as part of the turbine if the pipe supplies more than one nozzle, plus the velocity head at this point, minus the elevation of the lowest point of the pitch circle of the runner buckets. The pitch circle is that circle which is tangent to the axis of the power jet."

This is the effective head on the machine and is the amount properly chargeable against it; if the tail-water level were brought up to the point where it would just clear the buckets, then, by disregarding the negligible depth of buckets beyond the pitch circle, it would be the available head at the powerhouse. Actually, however, the

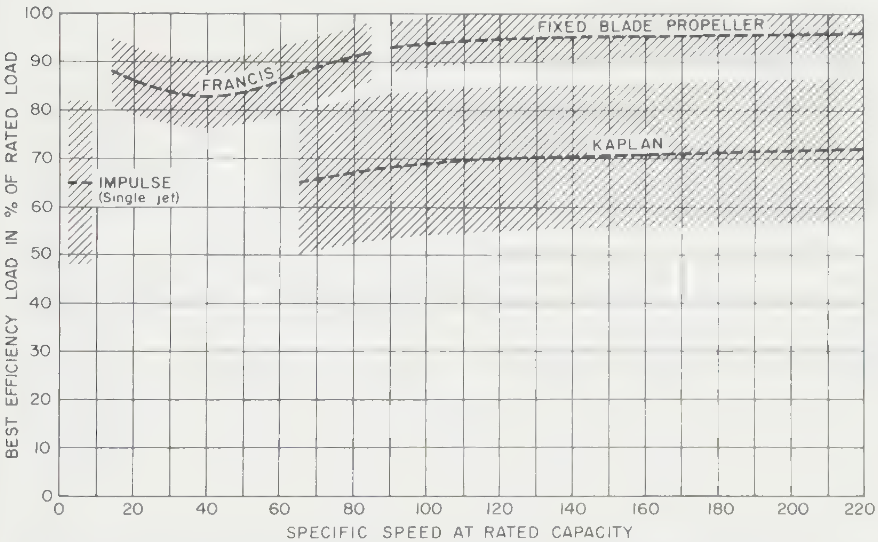

FIG. 34. Best efficiency load in percent of rated load. Shaded bands show approximate ranges found in practice; the curves show average values useful for preliminary purposes.

normal tail-water level must be some distance below the wheel to provide sufficient clearance between the runner and tail-water surface under all operating conditions, including those of high tail water occurring during periods of flood or surges in the tailrace. Hence there is always a free drop between runner and tail water which is entirely lost. Operation of the discharge passage as a draft tube, creating partial vacuum in the runner discharge pit to regain the head lost between the runner and the tail water, has not been found generally practical, because of the complications in regulating the free-water level and the relatively small amount of head thus saved in comparison with the high heads usually available at impulse-turbine installations. Furthermore, experiments have shown no perceptible gain attributable to draft-tube action through reduction of windage loss of the runner rotating in partial vacuum.

To allow development of the maximum head in impulse-turbine installations subject to considerable variation of the tail-water surface above normal level, it is sometimes economically justified to provide tail-water depression systems utilizing compressed air.[1] In those cases, the impulse runners are set with the necessary minimum clearance above normal tail-water level and this clearance is maintained during periods of higher tail water by admitting compressed air to the runner housing and discharge pit, which must be made airtight.

It should be pointed out that in comparing the installation efficiencies obtainable from impulse and reaction turbines, the impulse-turbine efficiencies should be discounted to allow for the free fall from runner to tail water, in order to obtain comparable values, because the reaction turbine is charged with the head down to tail water in computing its efficiency as already defined.

The water discharges from the nozzle under the effective head H, and the discharge is $Q = C_v \sqrt{2gH}\,(\pi/4)d^2$, C_v being the coefficient of velocity of the jet and d the diameter of the jet (vena contracta) and not that of the nozzle orifice. The horsepower is $P = wQHe/550$, and the linear velocity of the runner is $\pi DN/60 = \phi\sqrt{2gH}$, so that $D = 60\phi\sqrt{2gH}/\pi N$. Expressing d in terms of (d/D), we have

$$d = \left(\frac{d}{D}\right)\frac{60\phi\sqrt{2gH}}{\pi N} \tag{17}$$

We then have

$$P = \frac{wHeC_v}{550}\sqrt{2gH}\,\frac{\pi}{4}\left(\frac{d}{D}\right)^2\frac{(60)^2\phi^2 2gH}{\pi^2 N^2} \tag{18}$$

and collecting the constant terms

$$P = \frac{(60)^2 w(2g)^{3/2}}{550 \times 4\pi}\,eC_v\phi^2\left(\frac{d}{D}\right)^2\frac{H^{5/2}}{N^2} \tag{19}$$

Hence for geometrically similar units operating at correct speeds, *i.e.*, at constant ϕ, $P = (\text{const})H^{5/2}/N^2$, or $N = (\text{const})H^{5/4}/\sqrt{P}$. This is merely the specific-speed relation already derived from general considerations, or $N = N_sH^{5/4}/\sqrt{P}$. The specific speed is then

$$N_s = N\frac{\sqrt{P}}{H^{5/4}} = 30\sqrt{\frac{w}{550\pi}}\,(2g)^{3/4}\,\frac{\sqrt{eC_v}\,\phi}{D/d}$$

and putting $w = 62.4$ and $2g = 64.3$,

$$N_s = 129.3\sqrt{eC_v}\,\frac{\phi}{D/d} \tag{20}$$

It will be noted that homologous wheels of any size under any head, when running at their proper corresponding speeds and disregarding slight changes in relative friction, will have the same efficiency, C_v, ϕ, and D/d.

Hence this analysis shows that the factor N_s as just derived is a quantity that remains constant for a given design regardless of size or head. This fact specifically verifies the applicability of the specific-speed principle to impulse wheels, a conclusion that could have been foreseen since the original derivation was general. The last expression is, however, useful as showing the influence of the various factors on the value of N_s.

The value of C_v is subject to little variation in well-designed needle nozzles and can be taken as 0.97 to 0.99 as a good approximation. The following table gives typical values of ϕ for average practice:

N_s at best eff.	2	3	4	5	6	7
ϕ	0.48	0.465	0.45	0.44	0.433	0.425

[1] Dawson, P. B., "Multi-jet Impulse Turbines," ASME Paper 64-WA/FE-24, 1964. Osterwalder, J., Tailwater Depression of Multi-jet Impulse Turbines, *Water Power*, September, 1966.

With the aid of this table and the preceding formulas, the approximate leading dimensions D and d may be readily computed.

It will be noted that ϕ varies slightly, and since the efficiency does not vary greatly for moderate values of specific speed, it is seen that the specific speed is mainly dependent on the diameter ratio D/d. A convenient approximation can be obtained, for normal values of N_s, say 2 to 5, by using an average efficiency of 0.88 and an average ϕ of 0.46 and a C_v of 0.98, which give approximately

$$N_s = \frac{55}{D/d}$$

A normal diameter ratio, favorable to highest efficiency, is D/d = about 18 to 12. This corresponds to N_s of about 3 to 4.5. Good efficiency is obtainable with D/d = about 27 to 7, corresponding to N_s of about 2 to 8. Higher specific speeds involve a sacrifice of efficiency to an increasing extent.

With low specific speeds, the buckets can be cast separately and attached by lugs and bolts to the wheel hub (Fig. 2) or to a demountable rim, for easy replacement in the event of wear. With higher specific speeds, the buckets are large and closely spaced and must be cast integrally with the hubs (Fig. 3).

10. Scale Effect. By scale effect is here meant the effect of size of turbine on its efficiency, in a series of homologous turbines.

In the earlier section on dynamic similarity, it was noted that if the water passages in a turbine are considered to fall in the class of *rough conduits*, as termed by Karman and Prandtl, with high Reynolds numbers, the flow may be considered to be completely turbulent and the viscous forces negligible, so that the surface-friction losses in a given turbine may be expected to vary directly with the velocity heads and, therefore, with the effective head on the turbine. Hence a given turbine should have a substantially constant efficiency when operated at its proper speed under various heads. It was also noted, however, that so-called *homologous* turbines of different actual dimensions, geometrically similar in design and proportions, are not completely homologous with respect to the surface roughness. The variation in degree of relative roughness with change of size of turbine will cause a small, but appreciable, variation in the proportion of the effective head lost in hydraulic friction; therefore, the efficiency will change somewhat with change of size.

Of course, the hydraulic friction is not the entire source of loss in a turbine. There is also mechanical bearing friction, which, however, is very small in units of usual size, although appreciable in a laboratory model; and there are eddy or velocity head losses due to the final kinetic energy loss at the exit from the draft tube and at points of sudden enlargement in the turbine, as at the outlet from the wicket gates and runner where the vane thicknesses cause small eddy spaces at their ends. Such enlargement and outlet losses will tend to bear a fixed ratio to the velocity heads and therefore to the head on the turbine and consequently represent an unvarying element of proportional loss, not causing any change in efficiency.

In undertaking the formulation of the effect of change of size on efficiency, a sense of proportion makes it clear that any elaborate formulation would be uncalled for. In efficiency tests of turbines, there is a wide range of possible error in both the field and laboratory, owing, for example, to the difficulty in measuring the water quantity; and field measurements of efficiency are subject to considerable possible errors of the order of a percent or more even in well-conducted tests. In comparing the efficiencies of an installed unit and model, or even of two installed units of different size, there is rarely exact or complete geometrical similarity. Moreover, the proposed formula will be applied to model tests in different laboratories, and each laboratory will have a slightly different scale of efficiencies. Since the complexity of the factors involved in the problem makes a completely rational solution impractical, and the solution must be in part empirical, the degree of approximation involved in the data which must be relied upon will justify only a simple formulation of the desired relation.

As a first simplification, we shall not attempt to separate consideration of the various sources of loss, but shall treat all the losses in bulk and assume them to vary in the same manner, although not to the same degree, as the hydraulic friction, which will be considered to be of the same nature as pipe friction. Calling h_L the total loss of head in the turbine, and putting the efficiency as

$$e = \frac{H - h_L}{H} = 1 - \frac{h_L}{H}$$

we can write

$$1 - e = \frac{h_L}{H}$$

and using the Darcy formula for pipe friction:

$$1 - e = \frac{f(L/d)(V^2/2g)}{H}$$

in which L is an equivalent length of water passage, d the effective diameter of an equivalent pipe, and f a variable coefficient which is a function of the Reynolds number and of the relative roughness of the surfaces. As noted above, we can reasonably discard the dependence on Reynolds number. As a simple functional relationship we can use the well-established exponential relation between f and d, which has been found practically satisfactory for pipes over a wide range of sizes, namely,

$$f = \frac{\text{const}}{d^n}$$

giving the exponential formula $h_L = \text{const}(L/d^{1+n})(V^2/2g)$ for a given material or constant absolute roughness.

The value of $(1 + n)$ for pipes has been evaluated by many authorities, with values ranging from 1.25 to 1.33 and even to 1.4.

Considering the effect of the nonfrictional losses, the value $(1 + n) = 1.25$ was initially proposed as a good probable approximation, or $n = \frac{1}{4}$. We then have

$$1 - e = \frac{\text{const}}{d^n}\frac{L}{d}\frac{V^2}{2gH} \tag{21}$$

In two homologous turbines operating under dynamically similar conditions, distinguishing the values for one of them by the subscript 1,

$$\frac{1 - e_1}{1 - e} = \frac{(\text{const}/d_1^n)(L_1/d_1)(V_1^2/2gH_1)}{(\text{const}/d^n)(L/d)(V^2/2gH)}$$

From their geometrical similarity $L_1/d_1 = L/d$; and for dynamic similarity with the turbines operating at the proper corresponding speeds $V_1^2/2gH_1 = V^2/2gH$, so that

$$\frac{1 - e_1}{1 - e} = \left(\frac{d}{d_1}\right)^n \tag{22}$$

Here d and d_1 are the equivalent diameters representing the water passages. The ratio d/d_1 is merely a ratio of two corresponding linear dimensions and can be represented by any convenient characteristic lengths, such as the throat diameters.

From the comparison of field tests of large units with model tests, the average value of n was found to be approximately $\frac{1}{5}$ rather than $\frac{1}{4}$, for general application. The formula is therefore

$$\frac{1 - e_1}{1 - e} = \left(\frac{D}{D_1}\right)^{1/5} \tag{23}$$

When the efficiency e of a model is known, the efficiency e_1 of a full-sized homologous turbine can be readily calculated from this formula. Equation (23) has become generally known as the Moody formula for turbine-efficiency step-up. The step-up formula applies only to reaction turbines; for impulse-type turbines, which have very small frictional losses and frequently have more disturbed jets in large units than in models, an increase in efficiency with size cannot always be counted upon. In some cases, field efficiencies of impulse turbines were found to be slightly lower than model efficiencies. The Moody formula has been found to be reasonably applicable to centrifugal pumps under certain conditions, but its general application to pumps is limited since the relation between small and large pumps is not usually the same as that between model and full-sized turbines.

The efficiency step-up by the Moody formula

$$\Delta e = (1 - e)\left[1 - \left(\frac{D}{D_1}\right)^{1/5}\right]$$

is based on the maximum efficiency point of the model (peak of the efficiency hill) and the efficiencies of the full-sized turbine at all points are customarily obtained by uniformly adding to the corresponding model efficiencies the same increment Δe as for the point of maximum efficiency.

The Moody formula has been found to give somewhat excessive efficiency step-up between models and large modern turbines, especially Kaplan adjustable-blade and fixed-blade propeller turbines. Consequently, it has become common practice to apply only a part (about 0.6 to 0.75) of the Moody step-up to propeller turbines. Purchase specifications for Kaplan and fixed-blade propeller turbines in America now usually specify application of two-thirds of the Moody formula step-up in correcting the model efficiency to that which may be expected from the full-sized turbine. The trend in recent specifications for large Francis turbines, particularly those operating under relatively low to medium heads, is also toward application of two-thirds of the Moody step-up.

Although the efficiency of homologous reaction turbines changes rather consistently with change in size, their power output has not been found to change quite so consistently from proportional power, that is, proportional to the squares of the diameters and to the three-half powers of the heads. Therefore, it has become usual practice in America, when performance guarantees for full-sized turbines are to be verified by means of homologous model tests, to require that the model efficiency be corrected by the step-up formula, but that the principles of similarity be applied without correction to power.

Other forms of efficiency step-up formulas are used in various countries, and such formulas may be found in some of the national test codes for hydraulic turbines; space does not permit citing them here. However, it is of interest to note that the International Code for Model Acceptance Tests of Hydraulic Turbines, Publication 193, First Edition, 1965, recommends the use of the Moody formula for Francis-type turbines and the Hutton formula for Kaplan and fixed-blade propeller turbines, unless some other formula has been specified or agreed upon in advance. The applicable

Hutton formula is

$$\begin{aligned}\frac{1-e_1}{1-e} &= 0.3 + 0.7\left(\frac{R}{R_1}\right)^{1/5} \\ &= 0.3 + 0.7\left[\frac{D}{D_1}\frac{\nu_1}{\nu}\left(\frac{H}{H_1}\right)^{1/2}\right]^{1/5}\end{aligned} \tag{24}$$

where R = turbine Reynolds number $= VD/\nu = (2gH)^{1/2}D/\nu$
ν = kinematic viscosity of the fluid, sq ft/sec

11. Combined Operation of Several Turbine Units. When there are several units in a station, the question arises as to the best distribution of the station load among the units to give the best attainable station efficiency for any value of the station load. The notion was formerly held by some operators that with a number of similar units the load variation should be carried by one unit, while the other units are permitted to run at their points of best efficiency. This assumption is in error, and by a simple principle the best distribution can be readily prescribed for any load and between like or unlike units.

In stations having a small number of units and subject to considerable variation of load demand, the best solution of the problem of selection of units is frequently

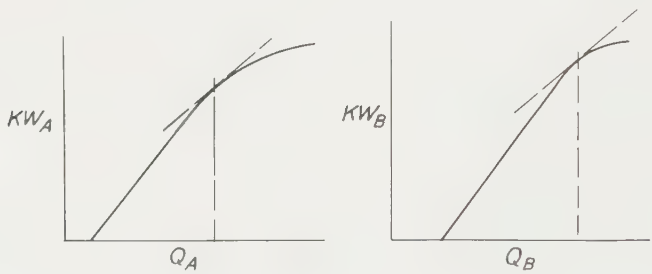

Fig. 35

the combination of one unit having a flat efficiency curve, such as a Kaplan or moderate specific-speed Francis turbine, with several high specific-speed turbines, the first unit being used to take the greater portion of the load variations.

Consider a plant containing two unlike units A and B. Curves are plotted giving the kilowatt output of the generator of each unit vs. the water quantity used at various gate openings, as shown in Fig. 35.

Suppose the units are running with discharges Q_A and Q_B and generator outputs KW_A and KW_B, respectively.

Let us find whether some other division of a given total quantity of water Q for the station will produce a greater total output KW, and let us determine the best division of load to give a maximum total output for a given total Q. Put the total discharge $Q = Q_A + Q_B$ with Q given and constant and Q_A and Q_B varying, and the total output $KW = KW_A + KW_B$. Using, say, Q_A as the independent variable, we should have $dKW/dQ_A = 0$, for maximum KW; or $(dKW_A/dQ_A) + (dKW_B/dQ_A) = 0$. Now to maintain Q constant, an increment of discharge dQ_A of unit A must be balanced by an equal decrement $-dQ_B$ of the discharge of unit B, or from the first equation above $dQ_A = -dQ_B$. Hence,

$$\frac{dKW_A}{dQ_A} - \frac{dKW_B}{dQ_B} = 0 \qquad \text{or} \qquad \frac{dKW_A}{dQ_A} = \frac{dKW_B}{dQ_B} \tag{25}$$

Therefore, for best economy the two units must be operated at points of equal slope on their output curves, as indicated in the figure. Since the same relation holds between any two units, as between A and a third unit C, all units in a station should be operated at any time at points of equal slope of their output vs. Q curves.

If all the units in a station are exactly similar, having identical curves, they must consequently share the load equally. Of course, as soon as the load drops to the extent of the capacity of one unit, it should for best economy be shut down completely and the load redistributed among the remaining units. It is assumed here that the curves are convex upward, the usual form. If one or both have concave portions, the preceding solution may correspond to a minimum rather than maximum output, and such cases require further consideration, the distinction between maximum and minimum being determined from the second derivative.

A method used by the late Prof. Pierre Danel will help to visualize this problem. Suppose curve sheet B is drawn on tracing paper, inverted, and placed over curve A with corresponding axes parallel, as in Fig. 36. At point 1 where the curves intersect, unit A is delivering KW_A with discharge Q_A and unit B is delivering KW_B with a discharge Q_B, so that the total output KW is the vertical height of the combined diagram between the two base lines and the total discharge Q is the horizontal width of the combined diagram between the vertical axes. The same relation holds for any other intersection as at 2, and so long as the curves intersect this relation is satisfied.

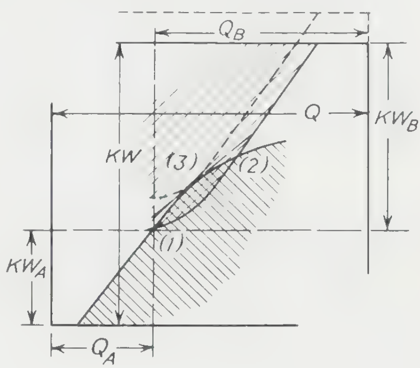

Fig. 36

To obtain maximum output for a given Q, we can move curve B upward until the two curves are just tangent, as shown dotted. For maximum economy, the units must therefore be operated at point 3, the point of tangency, the gates being adjusted so that the units discharge the corresponding quantities. At this point 3, the curves have a common tangent, so that the units are operating at points of equal slope on their output-Q curves, as previously found. This method can readily be applied to special cases, such as curves with concave portions. The method can also be applied to a plant containing three unlike units, in which case the KW vs. Q characteristics of two units are first combined, then matched with that of the third unit.

PUMPS

12. General Classification. Pumps are machines that convert mechanical energy into hydraulic energy, a process which is the reverse of that of prime movers. Considered broadly, pumps comprise classes corresponding to those mentioned under prime movers: gravity lift, such as chain pumps, rarely used; displacement pumps, of the reciprocating type or piston pumps, or rotary as in lobed-wheel pumps and blowers or gear pumps, in which the fluid is moved without change in velocity in the spaces between intermeshing rotors or gear teeth from a point of low pressure to one of high pressure; and pumps that utilize the reversed reaction-turbine process, involving transformations between pressure head and velocity head and conversion of mechanical into hydraulic energy.

Only the last class will be considered here. There is no conventional name for this class as a whole, which includes centrifugal pumps (Figs. 37 to 42), in which the flow through the runner or impeller is radially outward, and axial-flow propeller pumps (Figs. 54 and 55). Mixed-flow or diagonal-flow pumps, intermediate between these types (Figs. 49 to 53), are included under centrifugal pumps as a subclassification.

Centrifugal pumps thus correspond to Francis turbines with reversed flow direction, and propeller pumps correspond to propeller turbines reversed. It must not be mistakenly inferred that a turbine of normal design can be arbitrarily reversed in direction of rotation and employed as a pump; the changed conditions require fundamental changes in form so that the designs are essentially different. It is possible, however, to design a reversible machine with special design characteristics so that the same machine will operate as either a pump or turbine (see Reversible Pump-Turbines, Arts. 18 through 22).

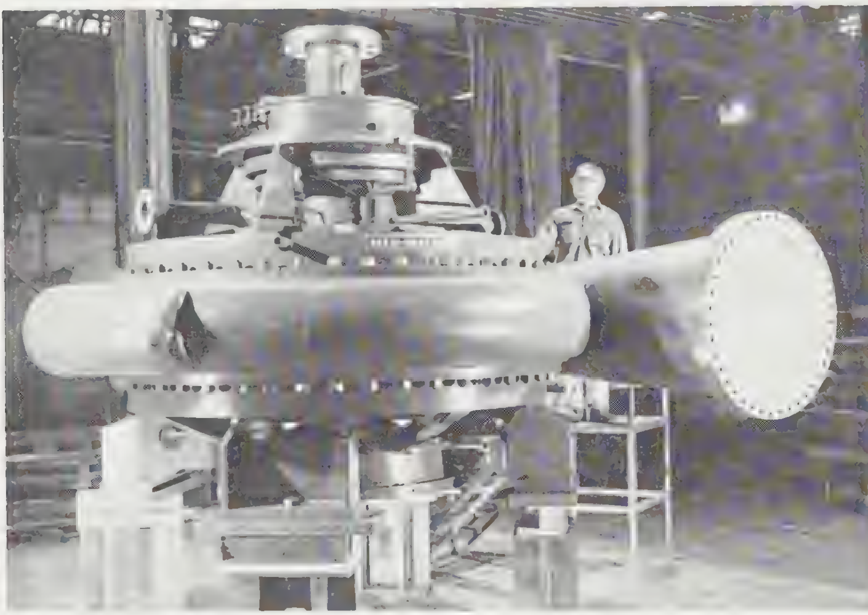

FIG. 37. Shop assembly of single-suction vertical-shaft centrifugal pump rated 72,000 gpm, 384-ft head, 9,000 hp, 400 rpm for Lamiero pumping station in Brazil. (*Three units by Allis-Chalmers Mfg. Co.*)

The form of centrifugal pump most frequently used is the simple combination of an axial inlet or suction pipe, a radial outward-flow impeller, and a volute or spiral casing. Usually no stationary guide vanes are used at either the inlet or outlet. The impeller tranforms mechanical energy into both pressure head and velocity head in the fluid, and the volute casing, often supplemented by a diverging conical discharge pipe, acts as a diffuser which gradually decelerates the flow velocity and converts most of the velocity head into pressure head at the discharge flange of the pump. Some special forms of pump use guide vanes at the entrance; and in some forms of multistage pumps used for high heads and small quantities of fluid and thus involving low specific speeds, the volute casing is replaced by discharge guide vanes or diffusion vanes, which provide decelerating passages between them. Such an arrangement is sometimes rather confusingly called a *turbine pump*, and it evidently corresponds in its relation of elements to a reversed Francis turbine, although as previously noted, the forms of the elements must be quite different from those of a turbine. Diffusion vanes are sometimes used in single-stage pumps (Fig. 38) and particularly in axial-flow propeller pumps of high specific speed (Figs. 54 and 55).

Pumps of small and moderate sizes are commonly arranged with horizontal shafts, and a wide range of sizes may be secured from the pump manufacturers as standardized or stock products with known performance characteristics as determined from shop tests. A common arrangement is with double-suction impellers, equivalent to two single-suction impellers placed back to back and made as a single casting; this arrangement gives balanced end thrust on the shaft (Figs. 40 to 42).

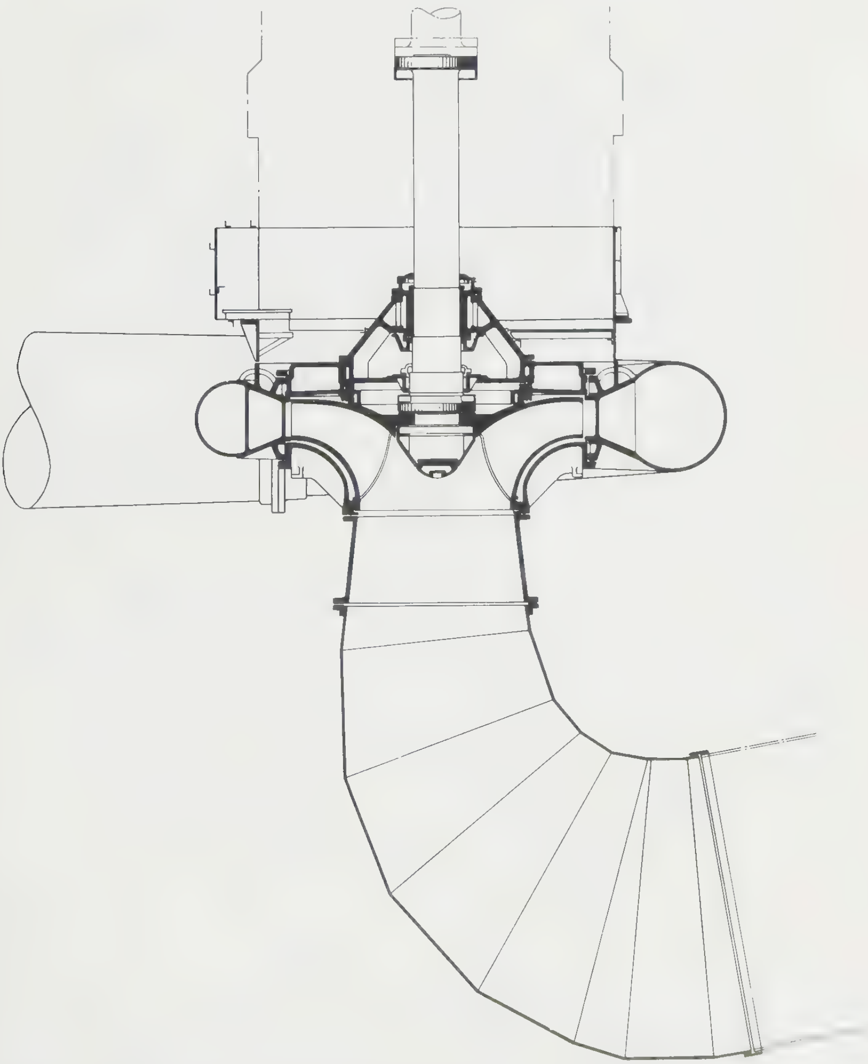

FIG. 38. Section of one of six pumps for Grand Coulee, rated 65,000 hp, 1,350 cfs each, 310-ft head, 200 rpm. (*Pelton–Byron Jackson.*)

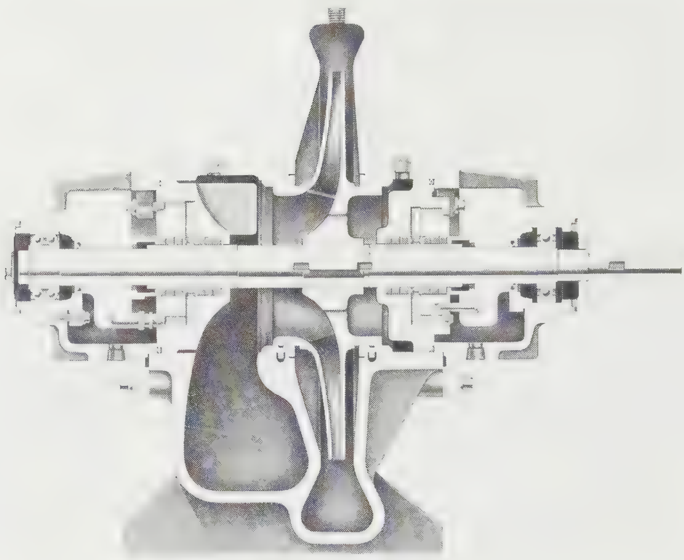

FIG. 39. Single-suction single-stage horizontal-shaft low-specific-speed pump. (*Allis-Chalmers Mfg. Co.*)

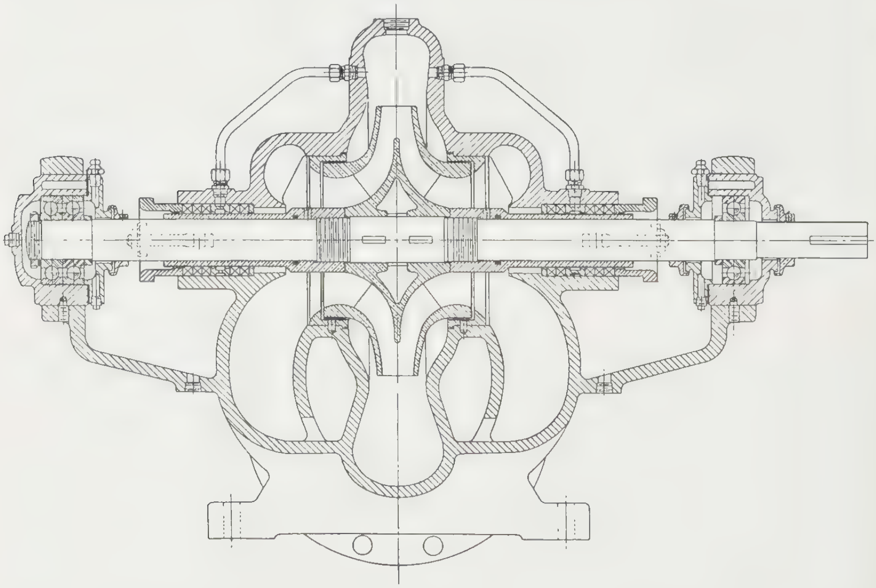

FIG. 40. Double-suction single-stage horizontal-shaft split-casing pump. (*Peerless Pump, FMC Corp.*)

For low and moderate heads and large capacities, as in water supply, drainage, and irrigation systems and condenser pumps, high specific speeds are needed, and here mixed-flow and propeller pumps are used often of large size and in vertical-shaft single-suction units. For low-head pumps required to operate under a widely varying head, adjustable-blade propeller pumps have been used to a limited extent. These are similar in construction to Kaplan turbines, but without the simultaneously adjustable wicket gates of the turbine.

At the other extreme requiring very low specific speeds, as in high-lift pumps such as mine drainage, deep-well pumps, and boiler-feed pumps, the method of placing a number of pumps in series is adopted, as many as 10 or 12 stages being frequently employed. The successive impellers are often placed in a single casing containing the proper water passages and forming a single multistage unit. Byron Jackson Pumps, Inc., have built some small pumps for oil-field application which have more than 200 stages.

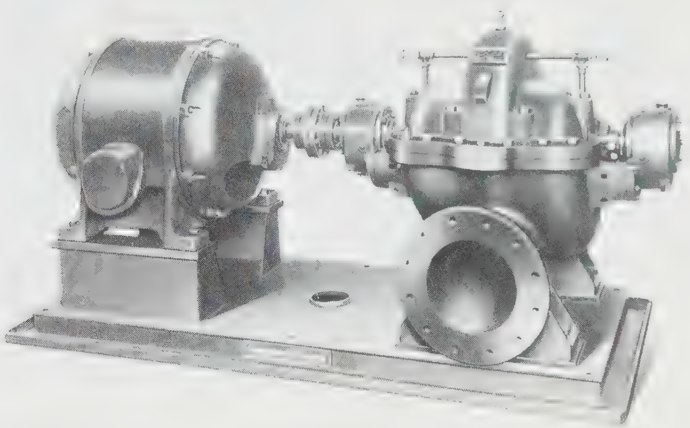

Fig. 41. Double-suction single-stage horizontal-shaft split-casing pump. (*Ingersoll-Rand.*)

13. Head, Power, Efficiency. The head against which a pump operates, called the *total head*, and here designated by H, is defined by the ASME Test Code for Centrifugal Pumps, PTC 8.1-1954, as follows:

"Pump total head (H) is the energy imparted to the liquid by the pump, expressed in foot-pounds per pound of liquid. It is the algebraic difference between the discharge head and the inlet head: $H = h_d - h_s$."

The definition is thus seen to be the same in substance as that of the effective head on a turbine.

This can be expressed as

$$H = \left(H_{pd} + \frac{V_d^2}{2g}\right) - \left(H_{ps} + \frac{V_s^2}{2g}\right)$$

in which H_{pd} is the absolute discharge pressure head in feet, H_{ps} the absolute suction pressure head in feet (both with respect to a fixed datum elevation), and V_d and V_s the discharge and suction velocities in feet per second.

When the suction pressure is measured close to the impeller and the flow direction is not controlled by fixed guide vanes, the centrifugal pressure due to rotating flow may cause serious error in the gage reading. This is particularly pertinent to vertical-shaft pumps in open sumps (Fig. 54) having short inlet passages. In such cases the total head should be taken as the reading of the discharge gage plus the velocity head at the gage section plus the elevation of the gage zero above the free-water surface in the pump.

The water horsepower is also defined exactly as for turbines, whp $= wQH/550$. The efficiency of a pump is the ratio of the water horsepower, which is the useful work

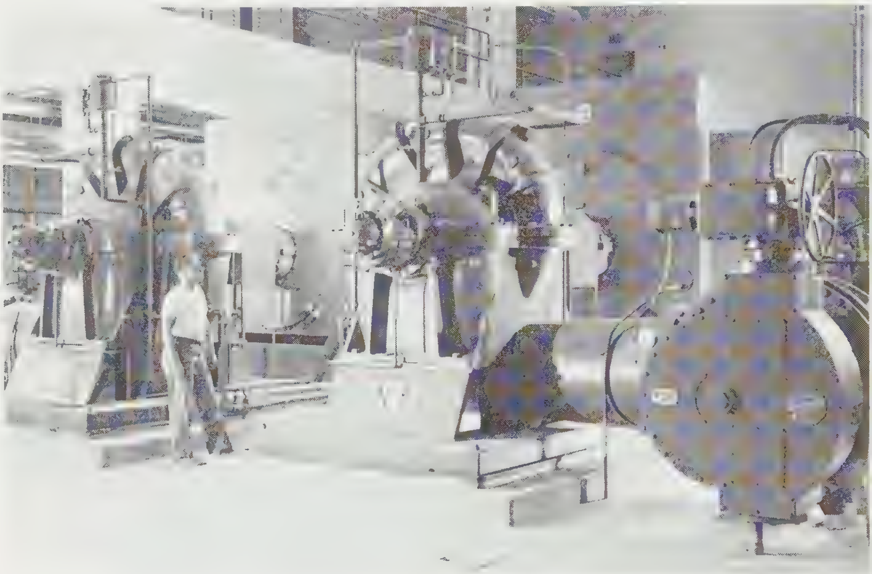

FIG. 42. Double-suction double-volute-type centrifugal pumps at Howard Avenue pumping station, city of Milwaukee. Each rated 50 mgd at 190-ft head and 40 mgd at 220-ft head; driven by 2,000-hp 600-rpm water-cooled synchronous motors. (*Allis-Chalmers Mfg. Co.*)

delivered, to the energy supplied to the pump by the shaft of the driving motor, or the input horsepower, bhp:

$$e = \frac{\text{whp}}{\text{bhp}} = \frac{wQH}{550\ \text{bhp}} \tag{26}$$

14. Fundamental Principles. The principles are the same as those explained above in the corresponding section for turbines. When applied to pumps, they take the following form. Referring to Fig. 20*a*, the subscript $_1$ will now represent the conditions at entrance to the impeller, and $_2$ those at discharge; and that figure will represent the pump action if the subscripts $_1$ and $_2$ are interchanged and all velocity directions reversed (Fig. 43).

If the same force and torque relations as developed for turbines are applied to pumps, the net turning moment exerted on the impeller is $(wq/g)(r_2V_{u2} - r_1V_{u1})$, where q is the quantity of water flowing through the impeller. Here Q, the discharge from the pump, is equal to q minus the leakage loss Q_L through the clearances, and we can put $Q = e_vq$, e_v being the volumetric efficiency, $e_v = Q/(Q + Q_L)$. The turning moment on the impeller multiplied by $2\pi N/(60 \times 550)$ gives the shaft horsepower multiplied by the mechanical efficiency e_m to allow for bearing and stuffing box friction.

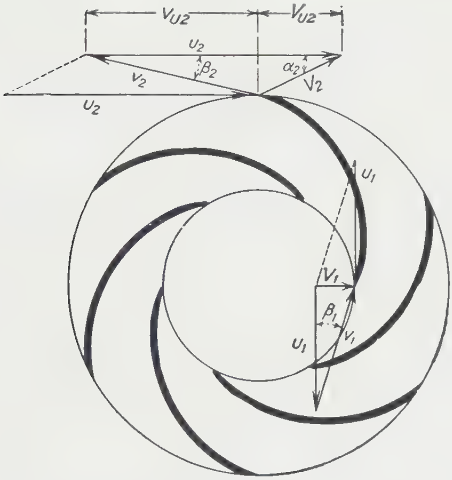

FIG. 43. Relative and absolute velocities in a pump impeller.

That is,

$$\frac{2\pi N w Q}{60 \times 550 e_v g}(r_2 V_{u2} - r_1 V_{u1}) = e_m \text{bhp} = e_m \frac{wQH}{550e}$$

Introducing as before $2\pi N r_2/60 = u_2$ and $2\pi N r_1/60 = u_1$, this relation becomes

$$\frac{u_2 V_{u2} - u_1 V_{u1}}{e_v g} = \frac{e_m H}{e}$$

and if we put $e = e_v e_m e_h$, in which e_h is the hydraulic efficiency, we have the Euler formula for pumps:

$$u_2 V_{u2} - u_1 V_{u1} = \frac{gH}{e_h} \tag{27}$$

This corresponds to Eq. (4) for turbines. For the usual centrifugal pump having no guide vanes at the entrance to the impeller to give initial whirl (Fig. 38) or having guide vanes to prevent initial whirl, $V_{u1} = 0$ and

$$u_2 V_{u2} = \frac{gH}{e_h} \tag{28}$$

The amount of head corresponding to the energy transmitted from the impeller to the water is $wqH/wqe_h = H/e_h$, and the Bernoulli formula applied to the pump, with reference to the stationary system [corresponding to Eq. (6) for turbines], is

$$h_{p1} + z_1 + \frac{V_1^2}{2g} - h_L + \frac{H}{e_h} = h_{p2} + z_2 + \frac{V_2^2}{2g} \tag{29}$$

Equation (8) applies unchanged to pumps, *viz.*,

$$h_{p1} + z_1 - \frac{u_1^2}{2g} + \frac{v_1^2}{2g} - h_L = h_{p2} + z_2 - \frac{u_2^2}{2g} + \frac{v_2^2}{2g} \tag{8}$$

and subtracting this from Eq. (29), we have

$$\frac{V_2^2 - v_2^2 + u_2^2}{2g} - \frac{V_1^2 - v_1^2 + u_1^2}{2g} = \frac{H}{e_h} \tag{30}$$

which corresponds to Eq. (9) for turbines.

Equations (27) and (28), although forming a sound basis for pump design, cannot be applied without taking account of some important distinctions. V_{u2} in Eq. (28) is the actual tangential velocity of flow and cannot be taken from an apparent velocity triangle constructed from the vane angle. If the impeller contained an infinite number of vanes, the relative direction of discharge could be properly taken as the direction of the vanes, and the discharge velocity could be taken as uniform around the circumference. Actually, with a finite number of vanes, the pressure intensity adjacent to the driving face of a vane is necessarily greater than that in the region of the rear surface of the preceding vane; and the velocity heads of the flow on opposite sides of an impeller channel therefore differ correspondingly but in reversed order, and the velocity is not uniform across the channel. Also although the flow adjacent to the vanes has rotational momentum effectively imparted to it, the portion of the flow intermediate between the vanes is less effectively acted upon and its flow lines near the discharge periphery of the impeller tend to approach the free path corresponding to a free vortex. Allowances for these considerations must be made by applying a coefficient (usually

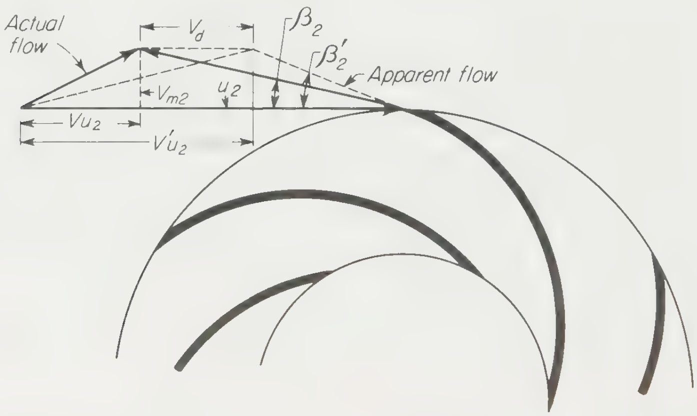

FIG. 44. Actual and apparent flow.

of the order of 0.7 to 0.8) to represent the ratio of actual momentum imparted to that realizable with an infinite number of vanes; *i.e.*, the apparent V_{u2} is multiplied by the coefficient K.

The following method for evaluating K, for radial- and mixed-flow pumps with overlapping vanes, has been developed by L. F. Moody with the cooperation of the Worthington Corp.

In Fig. 44 the dotted triangle represents the apparent flow based on the angle β_2' of the impeller vane. The solid triangle represents the actual flow based on the angle β_2 of the true average direction of discharge from the impeller. The meridional velocity component V_{m2}, or the radial component in a radial-flow impeller, remains unchanged, so that the actual flow triangle differs from the apparent triangle by a shift of the vertex parallel to u_2 through the distance V_d. The actual whirl component V_{u2} is calculated from the Euler formula

$$u_2 V_{u2} - u_1 V_{u1} = \frac{gH}{\epsilon_h}$$

V_d may be regarded as a differential velocity added vectorially to the apparent triangle to bring it into conformity with the actual triangle, changing the apparent whirl component V_{u2}' into the actual whirl component V_{u2} of the absolute flow. The ratio $V_{u2}/V_{u2}' = K$, the conversion coefficient. With an infinite number of vanes V_d is zero and $K = 1$.

The torque on the impeller

$$\frac{wq}{g}(r_2 V_{u2} - r_1 V_{u1})$$

may be equated to the average pressure difference between face and back of a vane multiplied by A_{mer}, the vane area projected in a meridional plane, and by its mean radius r_m to its center of gravity, and by the number of vanes n. If the pressure difference corresponds to a differential pressure head Δh_p,

$$\frac{wq}{g}(r_2 V_{u2} - r_1 V_{u1}) = wA_{\text{mer}} n r_m \, \Delta h_p$$

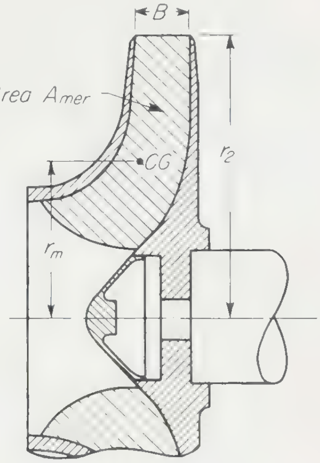

Fig. 45

Since V_d is a velocity, representing transverse flow in the circumferential direction across a vane passage from vane to vane, the corresponding velocity head $V_d^2/2g$ must correspond to a pressure head difference between the face of one vane and the back of the preceding vane, that is, Δh_p. We can therefore put $V_d^2/2g = (C/2)\,\Delta h_p$ in which C is a coefficient to be determined by test for any given type of impeller.

For normal operation with zero initial whirl

$$V_{u1} = 0 \qquad \text{and} \qquad \frac{V_d^2}{2g} = \frac{C}{2}\frac{q}{g}\frac{r_2 V_{u2}}{A_{\text{mer}} n r_m}$$

and putting $q = A_{\text{per}} V_{m2}$ in which A_{per} is the peripheral area of the impeller normal to V_{m2}, equal to $2\pi r_2 B$ − (vane thickness correction), we have

$$V_d = \sqrt{\frac{C}{n}\frac{A_{\text{per}}}{A_{\text{mer}}}\frac{r_2}{r_m} V_{m2} V_{u2}}$$

Here $A_{\text{per}} r_2$ and $A_{\text{mer}} r_m$ are the static moments of the two areas about the impeller axis.

Then since $K = V_{u2}/V_{u2}' = V_{u2}/(V_{u2} + V_d)$, we have

$$K = \frac{1}{1 + \sqrt{\dfrac{C}{n}\dfrac{A_{\text{per}}}{A_{\text{mer}}}\dfrac{r_2}{r_m}\dfrac{V_{m2}}{V_{u2}}}}$$

and

$$V_{u2}' = \frac{gH}{K\epsilon_h u_2}$$

A common practice combines $(K\epsilon_h)$ in a single coefficient sometimes called the manometric coefficient which we denote K_m (see Fig. 59).

The hydraulic efficiency ϵ_h may be estimated from the complete pump efficiency ϵ by an empirical relation:

$$1 - \epsilon_h = \frac{1 - \epsilon}{1 + \frac{1}{2}\sqrt{10{,}000{,}000/N_{SG}Q}}$$

in which N_{SG} is the specific speed based on gallons per minute and Q is in gallons per minute. In a double-suction pump both N_{SG} and Q are to be taken for the complete pump. The coefficient C, from an analysis by Osborne[1] of test data of the Worthington Corp., may be taken as $C = 0.4$ as a satisfactory average.

No attempt will be made here to cover the detailed methods of pump design, because excellent designs are available for a wide range of specific speeds, and pumps of satisfactory performance are standard products of the leading pump manufacturers. Attention will therefore be directed to the selection and application of pumps for various conditions of use.

15. Specific Speed. The principles of dynamic similarity explained in the case of turbines are equally valid when applied to pumps; and if a series of homologous pumps of various sizes are operated against various heads, we can say here as we did for turbines that $P \propto D^2H^{3/2}$ if each pump is operated at its proper speed for its size and head so that $N \propto H^{1/2}/D$. This leads to the same specific-speed relation as for turbines. However, this is not so convenient a relation in the pump field as another, which will be used instead. In specifying or designing a pump, the quantities in which we are most interested are not horsepower, head, and speed but discharge, head, and speed; *i.e.*, pumps are rated according to discharge capacity rather than power requirements. We shall therefore obtain a more convenient relation if we deal with Q instead of P. By applying the same principles of similarity as before $Q \propto D^2H^{1/2}$ when $N \propto H^{1/2}/D$. Eliminating D, we have

$$N \propto \frac{H^{1/2}}{\sqrt{Q/H^{1/2}}} \propto \frac{H^{3/4}}{\sqrt{Q}}$$

If this is expressed as an equation instead of a proportionality,

$$N = (\text{const})\,\frac{H^{3/4}}{\sqrt{Q}}$$

By putting H equal to 1 ft and Q equal to 1 cfs, the constant is seen to be the speed, in revolutions per minute, of a homologous pump of such size that it would deliver 1 cfs against 1-ft head. This is taken as the specific speed of a pump and is commonly denoted N_s. When it is desired to apply both specific-speed functions in the same problem, this new specific speed, based on quantity, may be distinguished by using the notation N_{sq}. This specific speed is equally applicable to turbines, although not so convenient in most turbine problems as the specific speed based on P. By expressing turbine specific speeds as N_{sq}, a comprehensive chart can be drawn showing both turbine and pump characteristics on a single diagram. When not otherwise noted, N_s will be used in this discussion to mean specific speed based on quantity, when dealing with pumps.

As in the case of turbines, this new N_s (or N_{sq}) is a constant for all geometrically similar pumps of any size and head, each being operated at its proper speed corresponding to the head and size. The type of pump can therefore be determined by inserting its values of Q, H, and N in

$$N_s = \frac{N\sqrt{Q}}{H^{3/4}} \tag{31}$$

and finding its N_s.

Some inconvenience, in centrifugal-pump calculations, results from lack of standardization of units of discharge. The United States pump industry customarily expresses the discharge capacity of standard or commercial-type pumps in gallons per minute (gpm). The Hydraulic Institute, a trade association of pump manufacturers in North America, has adopted gpm as the standard unit of pump discharge for deter-

[1] Osborne, W. C., A Method of Calculating the Degree of Flow Deviation at the Discharge of Centrifugal Pump Impellers, ASME annual meeting, Nov. 26–Dec. 1, 1950.

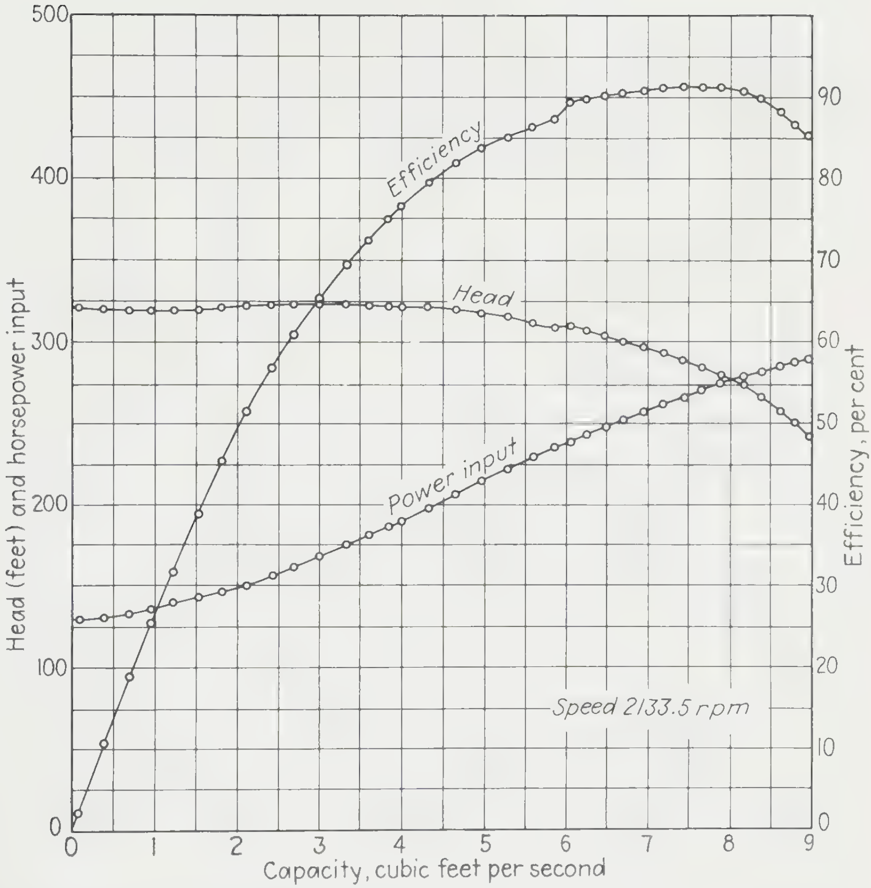

FIG. 46. Characteristic curves of a Pelton–Byron Jackson model pump tested at California Institute of Technology for Metropolitan Water District of Southern California.

mining specific speed. However, for large pumps, cubic feet per second (cfs) and million gallons per day (mgd) are often used as units of capacity. Specific speed stated on the basis of quantity in gallons per minute is

$$N_s = N \frac{\sqrt{Q_{\text{gpm}}}}{H^{3/4}} \tag{32}$$

This value of N_s will be distinguished here by the symbol N_{sG}. To convert N_{sG} into N_s (or N_{sq}), the following conversion factors are used: 7.48 U.S. gal = 1 cu ft; $7.48 \times 60 = 449$ gpm = 1 cfs.

$$N_s = \frac{N\sqrt{Q_{\text{gpm}}/449}}{H^{3/4}} = \frac{N}{\sqrt{449}} \frac{\sqrt{Q_{\text{gpm}}}}{H^{3/4}} = \frac{N_{sG}}{21.2}$$

The specific speeds here employed will be the values for a single-suction single-stage pump. Thus the quantity to be used in figuring the N_s for a double-suction pump is that for only one-half the double impeller, or one-half the total Q of the unit.

For a multistage pump, the head to be used in figuring N_s is the total head of the unit divided by the number of stages.

We shall also use for pumps the specific speed for the point of best efficiency, which should be the point of normal operation. Figures 46 and 47 show the efficiency and head characteristic curves for pumps of moderate specific speed and high efficiency.

As in the case of turbines, there are forms and proportions of pumps favorable to high efficiency, corresponding to a particular range of specific speeds; and abnormally

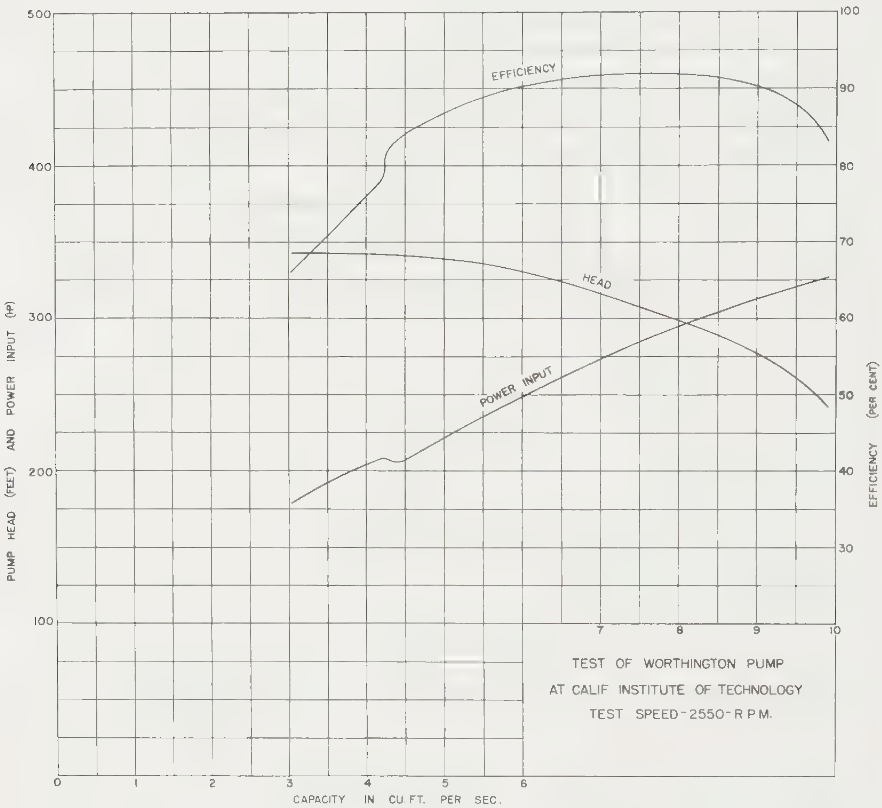

Fig. 47. Characteristic curves of a Worthington model pump tested at California Institute of Technology.

high or low specific speeds require abnormal proportions and are accompanied by impaired efficiencies. Figure 48*a* indicates the trend of maximum efficiencies, obtained in nearly every case from tests of large-capacity pumps. Small-capacity pumps and those of the usual commercial sizes cannot be expected to approach these values, since, just as in the case of turbines, efficiencies increase with an increase in dimensions. Comparative tests of homologous pumps have shown that an efficiency step-up formula of the same general form as the Moody turbine efficiency step-up formula

$$\frac{1 - e_1}{1 - e} = \left(\frac{D}{D_1}\right)^n$$

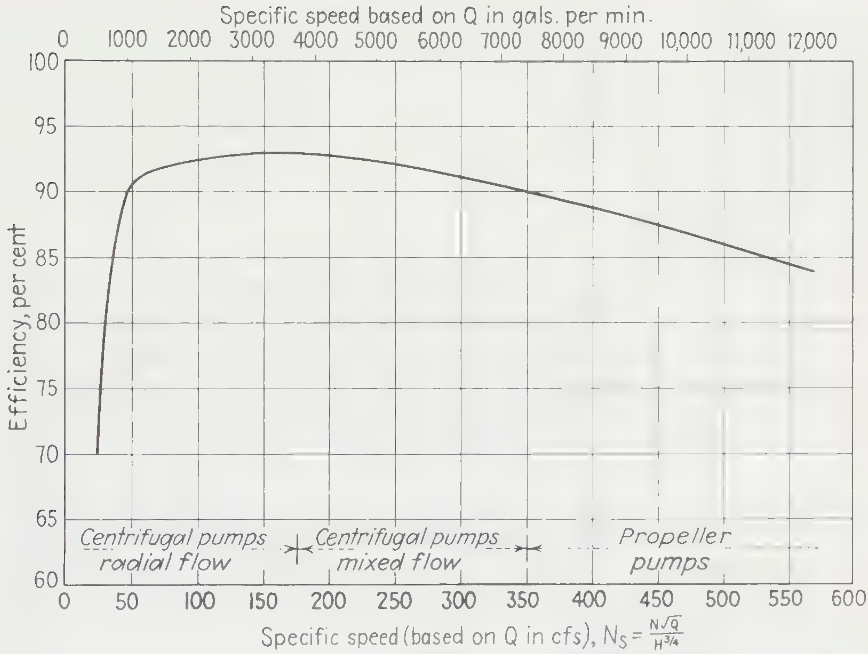

FIG. 48a. Typical maximum pump efficiencies obtained at various specific speeds.

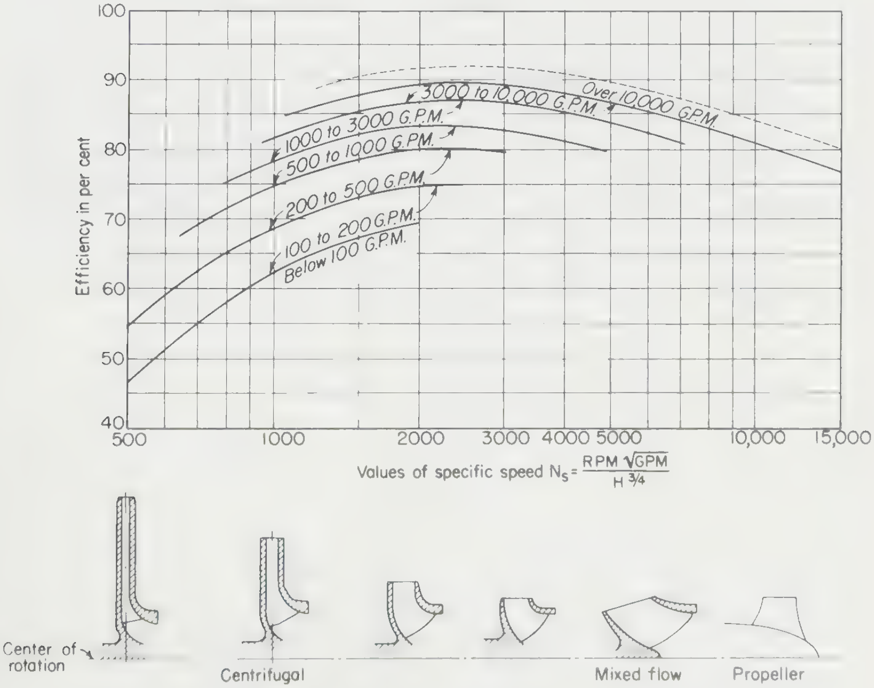

FIG. 48b. Effect of rated capacity on efficiency of good commercial pumps.

may conveniently be applied to pumps, if the proper value of exponent n is used, as explained further in Art. 17 under Model Tests. To show approximately the effect of size, in terms of capacity, on the efficiencies of commercial pumps, Fig. 48*b* is given. The curve of Fig. 48*a* will serve to indicate the region of specific speeds most favorable to high efficiencies and the comparative effect of variations of N_s. It will be noted that below a specific speed of 50 (cfs units) or 1,000 gpm units the efficiencies drop rapidly. This is mainly due to the absence of data for large pumps in this region. The efficiency of a radial-flow centrifugal pump of given unit capacity is practically unaffected by subdividing its inlet and changing from single-suction to double-suction

Fig. 49. Mixed-flow volute pump rated 70,000 gpm, 34.3-ft total head, 349 rpm, for a municipal sewage-treatment plant. Sketch shows one of bearing arrangements used in pumps of this design. (*Baldwin-Lima-Hamilton Corp.*)

design, so that for a double-suction pump of this type the specific speed in Fig. 48*a* is based on the total unit capacity.

For very high heads and small quantities to be pumped, as in boiler-feed pumps or mine pumps, the specific speed would work out far below the values for normal design and good efficiency, even when extremely high-speed driving motors are used. Instead of attempting to develop the head in a single impeller, the head is subdivided in a number of stages, and several pumps are placed in series, either as separate units or as a series incorporated in a single unit and with all the impellers on one shaft and within a common casing. For example, if s stages are used and the specific speed of the entire unit is $N_s = \sqrt{Q}/H^{3/4}$, the specific speed of one stage corresponding to a single impeller will be increased to $N_{s1} = N[\sqrt{Q}/(H/s)^{3/4}] = s^{3/4}N_s$, which can be increased to a value that will fall within the range of good design and normal proportions. For instance, suppose the specific speed for the total H and Q of a pump taken as a unit works out at a value of 10, which would require abnormal design and low efficiency. By using a number of stages such as 9, the specific speed of an individual impeller would be increased to $10(9)^{3/4} = 52$, which is within the region of normal design and good efficiency (see Fig. 48*a*).

On the other hand, the specific speed of a pump unit may be increased by placing a number of impellers on the same shaft arranged to pump in parallel. If the number of impellers in parallel is n, the specific speed of the unit will be

$$N_s = N\sqrt{nQ}/H^{3/4} = N_{s1}\sqrt{n}$$

where N_{s1} is the specific speed of a single-suction impeller. Thus the specific speed of a double-suction pump, having a double impeller, will be $N_s = N(\sqrt{nQ}/H^{3/4}) = 1.41N_{s1}$.

FIG. 50. Three 54-in. vertical-shaft mixed-flow pumps at Hyperion sewage-effluent plant of city of Los Angeles. Pump rating: 125,000 gpm at 64-ft head, 2,500 hp, 360 rpm. (*Allis-Chalmers Mfg. Co.*)

The value of the specific speed to be used in determining the form and characteristics of the impeller is that corresponding to one stage and single suction, which is the value used in the curves shown here.

Another reason for using a number of stages in a high-head pump is the desire not to exceed about 500 or 600 ft head per stage to avoid abrasion or wear of the parts exposed to high velocity; and frequently the head per stage is limited by cavitation requirements. The various design proportions of a pump may be expressed as functions of the specific speed. The impeller diameter, for example, can be fixed from $u_2 = 2\pi r_2 N/60 = \phi\sqrt{2gH}$; and Fig. 59 indicates reasonable values of ϕ as a function of N_s.

16. Cavitation. The same reasoning as set forth in Art. 6 for turbines applies equally to pumps, including the Thoma formula for the cavitation coefficient sigma $\sigma = (H_b - H_s)/H$, the criterion of cavitation. By plotting the sigma values of pumps as a function of specific speed, a basis is obtained for preparing charts corresponding to those given for turbines. An example of such charts is shown in Fig. 60 in which the solid line was drawn to indicate the approximate lower limit of sigma values for single-stage single-suction pumps with overhung impellers.

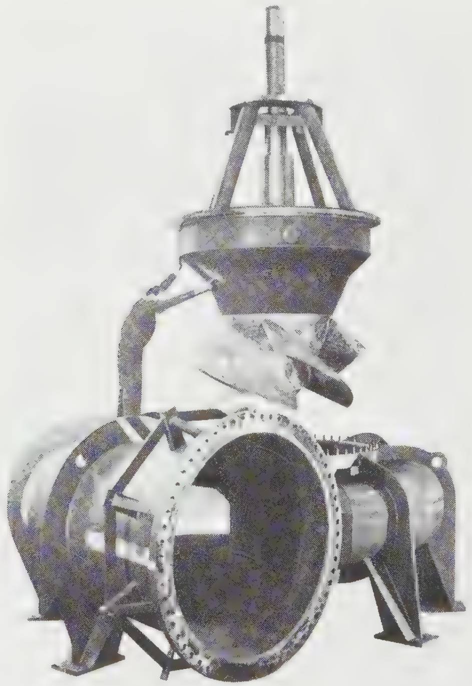

FIG. 51. Vertical-shaft mixed-flow volute pump rated 157,000 gpm, 36-ft total head, for condenser water circulation in nuclear-powered Dresden Station of Commonwealth Edison Co. *(Baldwin-Lima-Hamilton Corp.)*

The Hydraulic Institute has sponsored extensive studies of experience data accumulated by various pump manufacturers. Values of sigma were plotted against specific speed and the zones of safe and dangerous operation from the standpoint of cavitation were delineated. On the basis of these data, which indicated that, for any given total head and suction condition, the specific speed of the pump should be kept below a certain value to avoid cavitation, the Hydraulic Institute prepared a series of charts indicating the recommended limits of specific speed. The charts, reproduced here in Figs. 61 to 64, show the relationship between the total pump head and the recommended upper limits of specific speed under various conditions of suction lift and suction head. The first chart (Fig. 61) applies to double-suction single-stage pumps. The second chart (Fig. 62) applies to single-suction single-stage pumps with a shaft through the eye of the impeller. The third chart (Fig. 63) applies to single-

(a)

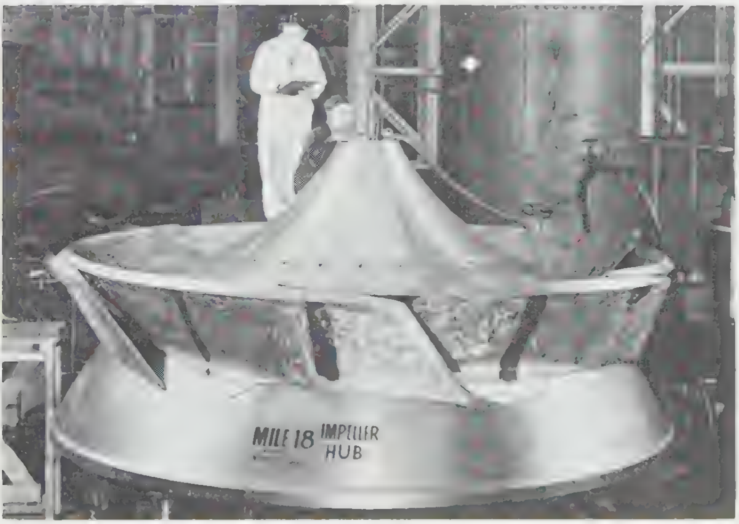

(b)

FIG. 52. Impeller of diagonal-flow adjustable-blade Deriaz-type pump rated 2,200 cfs, 125-ft total head, 120 rpm, for Mile 18 Pumping Plant of U.S. Bureau of Reclamation. (a) Blades fully opened. (b) Blades closed. (*Three pumps by English Electric Company Ltd.*)

suction overhung-impeller pumps. The types of pumps covered by these three charts find application principally in the medium- and high-head range. From a comparison of the first two charts against the third, it can be seen that for pumps in which the shaft extends through the suction space, the reduction of the effective eye or throat area due to the shaft requires a reduced specific speed, dependent on the size of the shaft and consequently on the head. The fourth chart (Fig. 64) applies to single-suction mixed-flow and axial-flow (propeller) pumps; these types of pumps are applied advantageously for low-head pumping. All four charts are based on pumping clear water at a temperature not exceeding 85 F at sea level. The charts are intended to apply to the normal rated operating conditions, on the assumption that the pump at rated conditions is operating at or near its point of maximum efficiency. Since pumps are normally applied for rated conditions near their maximum efficiency point, their rated specific speed is usually sufficiently close to the specific speed at point of best efficiency. However, when a pump is expected to operate at greater than normal discharges, as in cases where the operating head is subject to considerable variation, lower specific-speed values should be used.

Fig. 53. Shop assembly of one of two condenser circulating pumps for Joliet Station of Commonwealth Edison Company. Impeller and top plate of other unit in foreground. Pump rating: 230,000 gpm at 30-ft head, 212 rpm. (*Allis-Chalmers Mfg. Co.*)

The Hydraulic Institute specific speed–limit charts are revised from time to time to reflect advances in pump design. The charts have gained wide acceptance as a guide by pump manufacturers, users, and consulting engineers. The usual standard or commercial-type centrifugal mixed-flow and axial-flow pumps may be selected within the limits shown on the charts with reasonable assurance of freedom from cavitation under the conditions indicated. Values exceeding these limits should be used only for specially designed pumps.

The values of suction lift and suction head used in the charts are measured by pressure gage at the pump suction flange, corrected for velocity head, and referred to the elevation of the shaft center line for horizontal pumps, to the center line of the pump casing for vertical double-suction pumps, and to the entrance eye of the first-stage impeller for single-suction vertical centrifugal and mixed-flow pumps. For vertical-shaft axial-flow (propeller) pumps, the suction lift or suction head is measured to the mid-height of the impeller.

With reference to Fig. 65, h_p is the height of water column in a gage glass connected to the pump suction pipe at a point z ft below the shaft center line. h_p must be increased by the velocity head in the suction pipe at the section where the gage is connected. The top of the water column so corrected is the elevation of the equivalent or virtual sump elevation shown by the dashed line. The value of H_s referred to the pump axis is therefore $H_s = z - (h_p + v_a^2/2g)$. When the pump operates under positive suction pressure, this is termed *suction head,* which is merely $-H_s$. In applying the specific speed–limit charts to large horizontal-shaft installations,

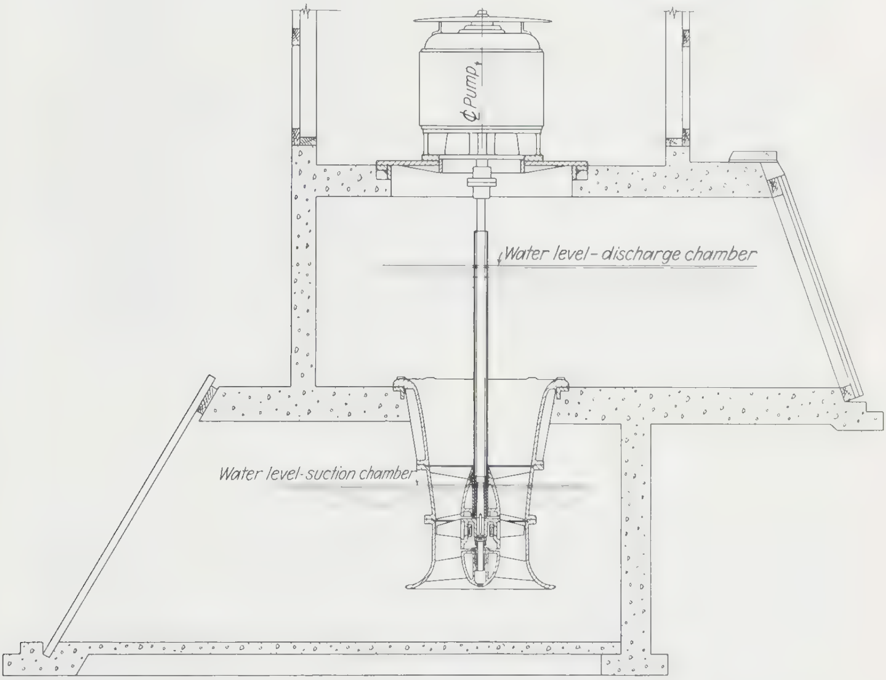

FIG. 54. Axial-flow propeller pump with diffusion vanes. (*Byron Jackson Pumps, Inc.*)

it is advisable to figure the suction lift or suction head in the large pump to the upper side of the impeller entrance diameter rather than to the shaft center line.

The Thoma cavitation formula $\sigma = (H_b - H_s)/H$ is usually expressed for pump application in the form $\sigma = H_{sv}/H$, in which H_{sv} is the excess of the absolute suction head above the vapor pressure, or the net positive suction head. The net positive suction head can also be introduced into the specific-speed relation. By using H_{sv} instead of H in the specific-speed formula, a useful parameter called the "suction specific speed" is obtained:

$$S = \frac{N\sqrt{Q_{\text{gpm}}}}{H_{sv}^{3/4}}$$

The suction specific speed expresses the combination of suction conditions which, if kept constant, will give similarity of flow and cavitation in pumps which are geomet-

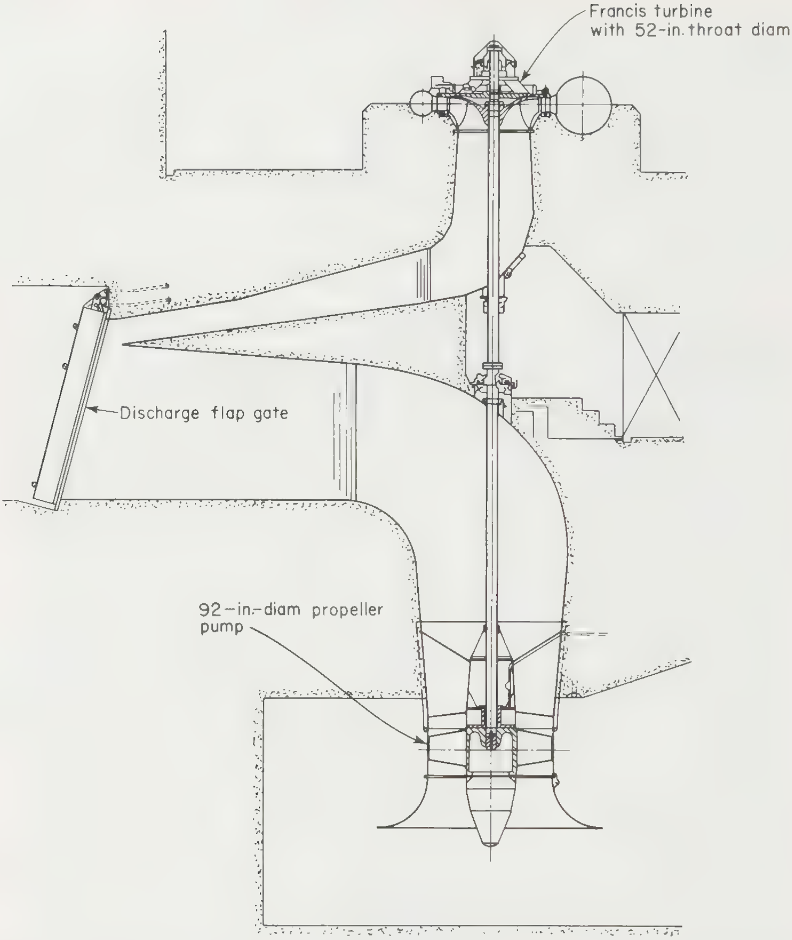

FIG. 55. Axial-flow propeller pump, direct-driven by hydraulic turbine, for supplying fish attraction water to fish-passing facilities at Wanapum hydroelectric power station. Rated 1,000 cfs total combined discharge of pump and turbine with pool-to-pool static heads of 6 ft on pump and 60 ft on turbine. (*Baldwin-Lima-Hamilton Corp.*)

rically similar in the suction passageways and in the low-pressure portions of the impeller. The suction specific speed and the Thoma cavitation coefficient are related as follows:

$$\sigma = \frac{H_{sv}}{H} = \frac{(N\sqrt{Q_{\text{gpm}}}/S)^{4/3}}{H} = \left(\frac{N\sqrt{Q_{\text{gpm}}}}{SH^{3/4}}\right)^{4/3} = \left(\frac{N_{sg}}{S}\right)^{4/3}$$

or

$$S = \frac{N_{sg}}{\sigma^{3/4}}$$

The solid line of Fig. 60 corresponds to a value of S of 8,990 or in round numbers

$$\sigma_c = \left(\frac{N_{sg}}{9{,}000}\right)^{4/3}$$

17. Shop and Model Tests of Pumps.[1] *Shop Test on Full-sized Pump at Full Head.* In order that a shop or laboratory test should correctly predict the results to be secured in the field installation, the setting as well as the pump proper should be duplicated. On the intake side the setting includes the passage between the impeller and a point in

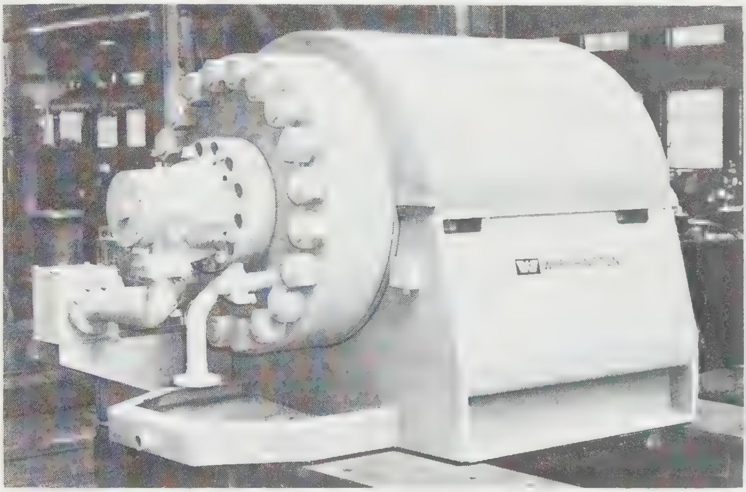

FIG. 56. Shop assembly of 10-in. six-stage barrel-type boiler-feed pump; driven by 9,700-hp, 5,500-rpm auxiliary turbine. (*Worthington Corp.*)

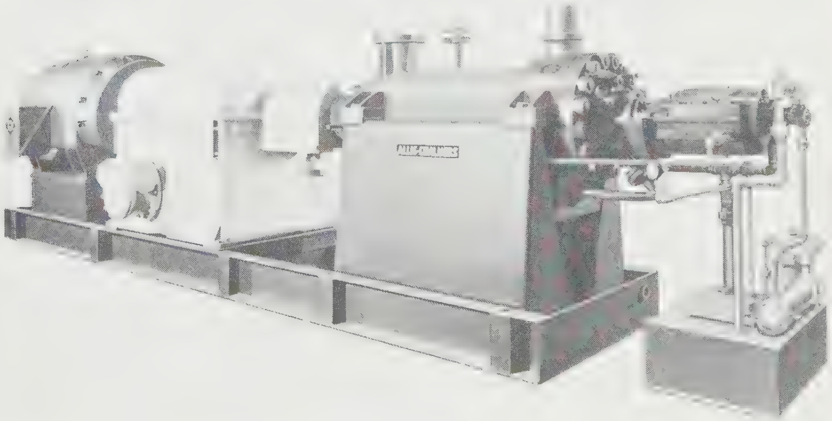

FIG. 57. Twelve-stage boiler-feed pump rated 685 gpm at 4,270-ft head, 3,500 rpm. Driven by a 1,000-hp motor through a fluid coupling. (*Allis-Chalmers Mfg. Co.*)

the supply piping or sump where the velocity head is so low that variations in passages beyond that point will have a negligible effect. On the discharge side it includes the passage between the pump casing and the point where the guaranteed head is to be

[1] Based in part on data contained in "Standards of the Hydraulic Institute," Centrifugal Pump Section, copyright 1965 by Hydraulic Institute, New York.

measured. To represent true pump performance, the discharge head should be measured, both in the shop or laboratory and in the field installation, in a straight section of discharge pipe a sufficient distance beyond the pump discharge flange to permit the flow to reach substantially normal distribution across the section of measurement, and thus to provide a "smoothing section" to overcome the distortion of flow caused by the pump volute or by a discharge elbow.

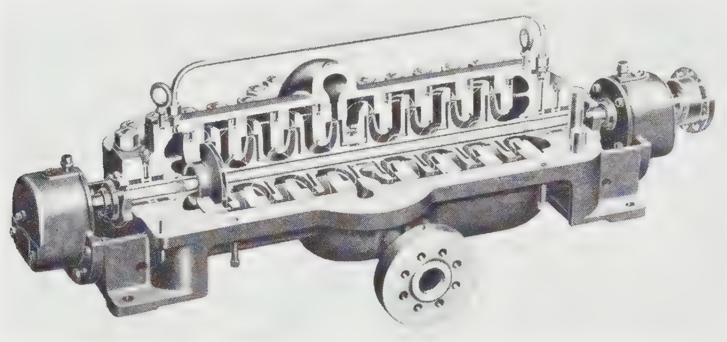

FIG. 58. Eight-stage split-casing pump. Diffuser-vane type. (*Ingersoll-Rand.*)

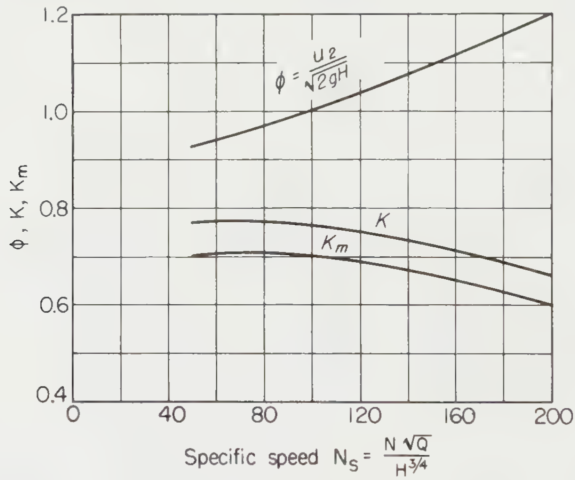

FIG. 59. Typical design factors for radial-flow centrifugal pumps.

If the shop or laboratory test is made at the same head and speed as the field installation, then, in the absence of a cavitation test, the suction head or lift must be the same if the atmospheric pressure and water temperature are the same. If the atmospheric pressure or water temperature is different, the suction head or lift must be such as to give the same cavitation factor $\sigma = (H_b - H_s)/H$, in which $H_b = H_a - H_{vp}$, the atmospheric pressure head minus the vapor pressure head of the water corresponding to its temperature. H_s is the net suction lift $= z - (h_p + Va^2/2g)$ as in Fig. 65; and H is the total pump head.

If, however, cavitation tests have been made on the pump and it has been established that the sigma of the installation is substantially in excess of the critical sigma throughout the range of operation, then if the sigma for the shop or laboratory tests is also kept well above the critical sigma, its exact value is of no significance.

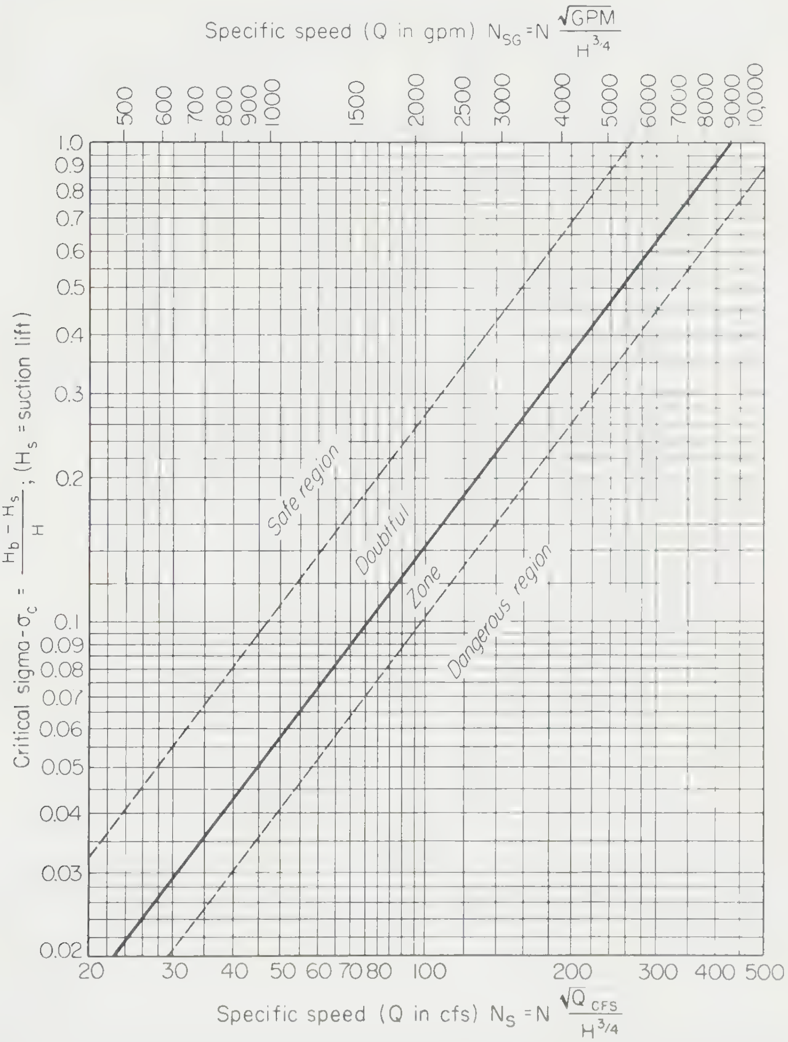

FIG. 60. Approximate limits of cavitation-coefficient sigma at various specific speeds for single-stage single-suction pumps with overhung impellers.

Example: A four-stage boiler feed pump rated at a capacity of 400 gpm is to operate against a total head of 900 ft, handling water at 250 F and running at 3,550 rpm. The suction gage pressure is to be 21 psi in a 4-in. suction pipe, at the elevation of the pump axis. The pump is to be tested in the shop under full head and at the same speed, handling water at 80 F. What suction head or lift should be applied in the shop test to make it correctly represent the field conditions?

The first condition is that the specific speed must be the same in the shop and the field operation, which will be secured with the head, speed, and capacity the same in both cases. The second condition is that the cavitation factor sigma must be the same in shop and field operations, to make the suction conditions in the shop test representative of the field conditions. Calling

$$H_{sv} = H_b - H_s = H_a - H_{vp} - H_s$$

in which H_{sv} is the "net positive suction head," or the excess of the absolute suction head over the vapor pressure head, then $\sigma = H_{sv}/H$.

In this example, from steam tables, at 250 F the specific volume of the water is 0.017 cu ft/lb, the specific weight is $w = 1/0.017 = 58.8$ lb/cu ft, and the vapor pressure is 30 psi absolute. The suction

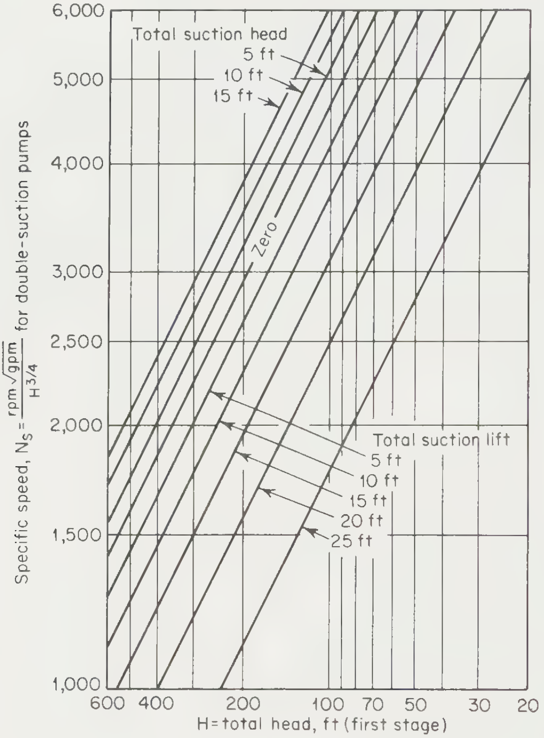

FIG. 61. Hydraulic Institute, upper limits of specific speeds, double-suction pumps, handling clear water at 85 F at sea level. (*Reprinted from "Standards of the Hydraulic Institute,"* 11*th ed., copyright* 1965 *by the Hydraulic Institute,* 122 *East* 42*nd Street, New York, N.Y.* 10017.)

pressure head is $h_p = (21)(144)/58.8 = 51.4$ ft, the pipe velocity V_a is 10.2 fps, and the velocity head is 1.6 ft, so that $H_s = z - (h_p + Va^2/2g) = 0 - 51.4 - 1.6 = -53.0$ ft (or 53 ft positive suction head).

Hence $H_{sv} = H_a - H_{vp} - H_s = [(14.7 - 30)/58.8](144) + 53.0 = 15.5$ ft. The head per stage is $H = 900/4 = 225$ ft, and $\sigma = H_{sv}/H = 15.5/225 = 0.069$.

To maintain the same σ in the shop test with the water temperature 80 F and the vapor pressure 0.5 psi, $H_{sv} = \sigma H$ must remain the same and the suction lift must be

$$\begin{aligned} H_s &= H_a - H_{vp} - H_{sv} \\ &= \frac{(14.7 - 0.5)(144)}{62.3} - 15.5 = 32.8 - 15.5 = 17.3 \text{ ft} \end{aligned}$$

Shop Test on Full-sized Pump at Reduced Head. When laboratory or shop limitations such as available power preclude full-head tests, reduced-head tests are permissible and are in general closely representative of tests at full head. However, in tests at reduced power the relative loss in mechanical bearing friction and stuffing-box friction may be increased (an effect which may be appreciable in small pumps); and the hydraulic friction losses may be relatively increased when the Reynolds number for the water passages is reduced (an effect which may be appreciable in small pumps of low specific speed). It is recommended that when reduced-head tests are used as acceptance tests, the guarantees specify the test head, and that the performance guarantees be based on the reduced-head conditions.

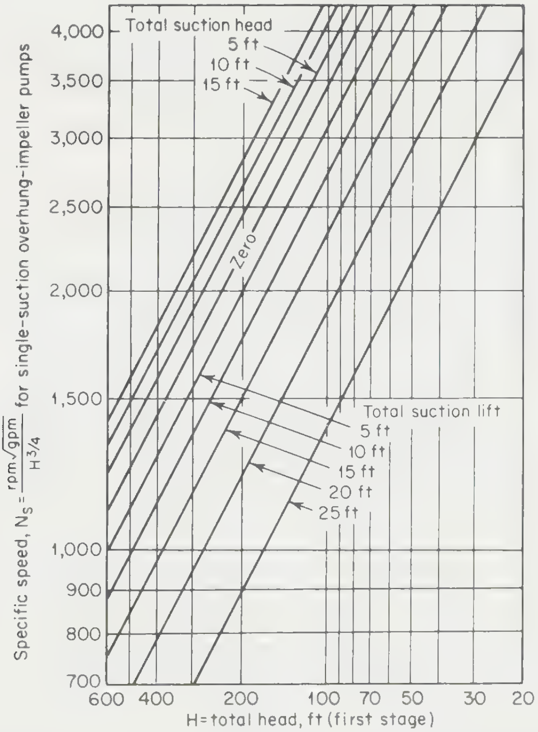

FIG. 62. Hydraulic Institute, upper limits of specific speeds, single-suction shaft through eye pumps, handling clear water at 85 F at sea level. *(Reprinted from "Standards of the Hydraulic Institute," 11th ed., copyright 1965 by the Hydraulic Institute, 122 East 42nd Street, New York, N.Y. 10017.)*

In any such reduced-head test, two conditions must be maintained: the operating speed must be such as to keep the specific speed the same as in the field installation, and the cavitation sigma must be the same. As noted, however, if it has been established by cavitation tests that sigma is substantially in excess of the critical sigma, then the second requirement is unnecessary.

In order to maintain hydraulic similarity with the field operation, the capacity Q_1 for the test and the test speed N_1 must be reduced below the installation capacity Q and speed N, respectively, in the ratio

$$\frac{Q_1}{Q} = \frac{N_1}{N} = \sqrt{\frac{H_1}{H}}$$

where H_1 and H are the pump heads for the test and installation, respectively.

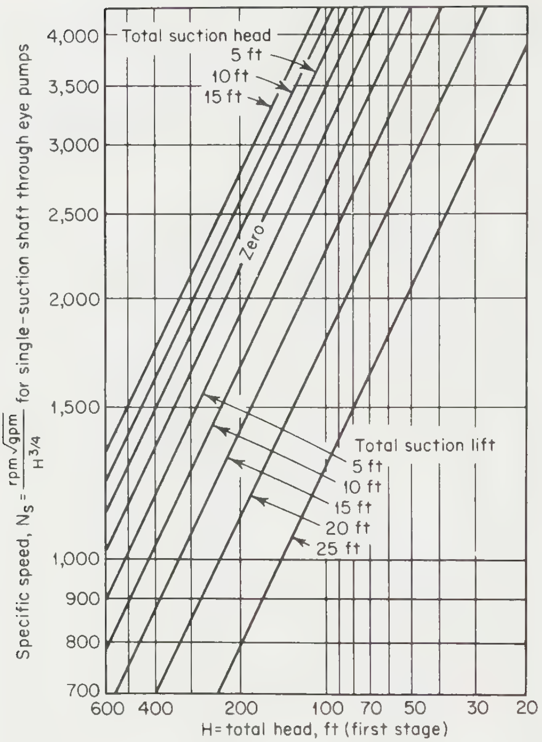

FIG. 63. Hydraulic Institute, upper limits of specific speeds, single-suction overhung impeller pumps, handling clear water at 85 F at sea level. (*Reprinted from "Standards of the Hydraulic Institute,"* 11*th ed., copyright* 1965 *by the Hydraulic Institute,* 122 *East* 42*nd Street, New York, N.Y.* 10017.)

Example: With the same field conditions as in the preceding example, the shop test on the same pump is to be made at a reduced head of 720 or 180 ft per stage with water at 80 F. What capacity, speed, and suction lift or head should be used in the shop test?

From the above relations, the capacity to be used in the shop test is

$$Q_1 = Q\sqrt{\frac{H_1}{H}} = 400\sqrt{\frac{180}{225}} = 358 \text{ gpm}$$

The speed to be used in the shop test is

$$N_1 = N\sqrt{\frac{H_1}{H}} = 3{,}550\sqrt{0.8} = 3{,}170 \text{ rpm}$$

The specific speed will now be the same in shop and field:

$$N_s = N\frac{\sqrt{Q}}{H^{3/4}} = 3{,}550\frac{\sqrt{400}}{(225)^{3/4}} = 3{,}170\frac{\sqrt{358}}{(180)^{3/4}} = 1{,}220$$

To keep the cavitation factor the same in shop and field, we found in the preceding example $\sigma = 0.069$ and $H_b = H_a - H_{vp} = 32.8$ for the shop test. Then for the shop test

$$H_s = H_b - \sigma H_1 = 32.8 - (0.069)(180) = 20.4 \text{ ft}$$

To reproduce the field conditions, the shop test must therefore be run with a suction lift of 20.4 ft.

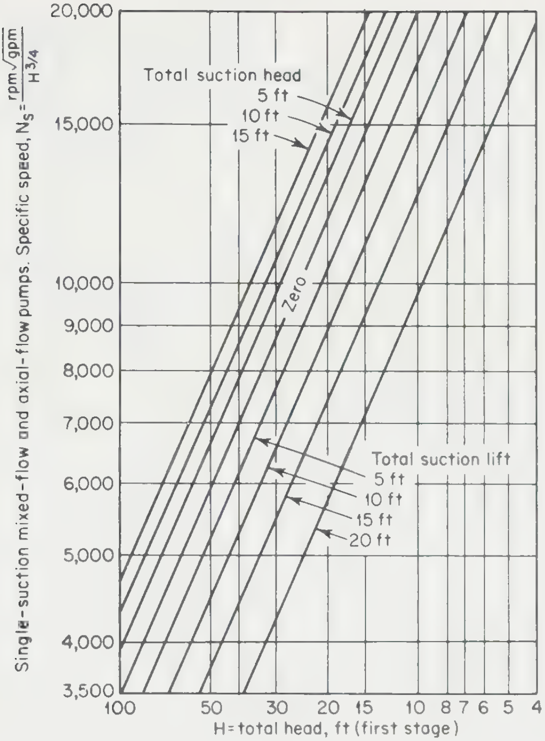

FIG. 64. Hydraulic Institute, upper limits of specific speeds, single-suction mixed- and axial-flow pumps, handling clear water at 85 F at sea level. (*Reprinted from "Standards of the Hydraulic Institute,"* 11*th ed., copyright* 1965 *by the Hydraulic Institute,* 122 *East* 42*nd Street, New York, N.Y.* 10017.)

Model Tests. In cases involving pumps of large size, model tests are of great utility. Even when it might be feasible to test the large pump in the shop, a model may often be tested with greater accuracy and thoroughness; and by adopting a standardized size of model for various pumps, properly comparable performances can be secured. Model testing in advance of final design and installation of a large unit, as standard procedure, not only provides advance assurance of performance but makes alterations possible in time for incorporation in the prototype. It is not essential that the model test head be the same as that in the prototype. Although the

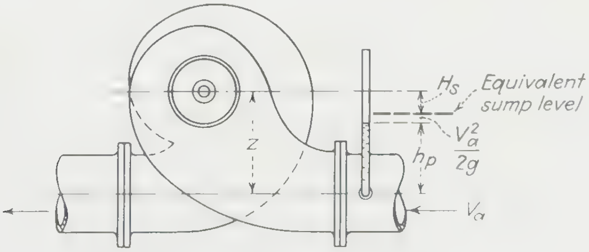

FIG. 65

current Eleventh Edition of the Hydraulic Institute Standards requires that the model test head be not less than 80 percent of the prototype head, there are differences of opinion concerning this requirement, because the necessity of performing the pump model test at no less than 80 percent of prototype head has not been clearly substantiated either by theoretical considerations or by comparisons of performance data from tests of models and their full-sized prototypes. There is evidence indicating that reliable results can be obtained with test heads no greater than about 50 to 65 percent of prototype head.

The model should have complete geometric similarity with the prototype, not only in the pump but in the intake and discharge conduits as specified for tests on full-sized pumps. The model should be run at such speed under the test head that the specific speed remains the same as that of the installed unit; and if cavitation tests are not available, the suction head or lift should be such as to give the same sigma value as in the installation.

If corresponding diameters of model and prototype are D_1 and D, respectively, then the model speed N_1 and capacity Q_1 under the test head H_1 must agree with the relations

$$\frac{N_1}{N} = \frac{D}{D_1}\sqrt{\frac{H_1}{H}} \qquad \text{and} \qquad \frac{Q_1}{Q} = \left(\frac{D_1}{D}\right)^2 \sqrt{\frac{H_1}{H}}$$

In testing a model of reduced size, the above conditions being observed, complete hydraulic similarity will not be secured unless the relative roughness of the impeller and pump casing surfaces is the same. With the same surface texture in model and prototype, the model efficiency will be lower than that of the larger unit; and greater relative clearances and shaft friction in the model will also reduce its efficiency.

The efficiency of a pump model can conveniently be stepped up to the prototype by applying a formula of the same general form as the Moody formula used for hydraulic turbines

$$\frac{1 - e_1}{1 - e} = \left(\frac{D}{D_1}\right)^n$$

The exponent n should be determined for a given laboratory and given type of pump on the basis of an adequate number of comparisons of the efficiencies of models and prototypes, with consistent surface finish of the models and prototypes. The Standards of the Hydraulic Institute state that the values for the exponent n have been found to vary from zero when the surface roughness and clearances of the model and of the prototype are proportional to their size, to 0.26 when the absolute roughness is the same in both model and prototype. Experience data accumulated from continued research and testing by leading pump manufacturers have enabled them to narrow the range of n values applicable to their individual laboratories and methods of finishing the surfaces of models and prototypes. Some manufacturers have found from tests of centrifugal-pump models and prototypes that the use of an exponent of $\frac{1}{5} = 0.20$, as used for hydraulic turbines, is reasonably justified; others have found that the average value of the exponent applicable to their test results is about $1/7.5 = 0.13$. Some European manufacturers consider an average exponent of $1/6.5$ reasonably justified for general pump application. In any case, it is apparent that, because the Moody step-up applies only to the friction losses, which are relatively small in pumps of modern design, reasonable differences in the value of the exponent have rather minor effect on the calculated efficiency of the prototype.

When model tests are to serve as acceptance tests, it is generally recommended that the efficiency guarantees be stated in terms of model performance, rather than in terms of calculated prototype performance. In the absence of such provision, the efficiency step-up formula and the numerical value of its exponent should be clearly specified, or agreed upon in advance of tests.

In pumps of high or medium specific speed, and in models of reasonable size, with correct relative clearances and with impeller and diffuser surfaces of smoother finish than in the larger prototype, a close approximation to the prototype efficiency may be secured if the model bearing and stuffing-box friction is minimized by a special design. In such models, operated under a head which is not too low, the Reynolds number of the flow passages is high enough to cause completely turbulent flow and to make viscous forces negligible and the Reynolds number without effect. In such cases little increase in prototype efficiency over model can be counted upon.

Not all pumps are well adapted for model testing. In installations in which free-water surface phenomena may affect the performance, complete hydraulic similarity prescribes constant Froude number, which requires a constant ratio of pumping head to the linear dimensions of the pump. To keep sigma the same, it is necessary to reduce the barometric pressure in the same ratio by enclosing the whole setting in a closed chamber. These conditions apply, for example, when a limited depth of free sump surface over the suction inlet may cause prerotation, or vortices drawing air into the pump. In pumps such as condensate pumps intended to operate under cavitating conditions, when vapor separation produces free surfaces within the pump, it is recommended that the pumps be tested in their full size at full head and speed.

Example: A single-stage pump to deliver 200 cfs against a head of 400 ft at 450 rpm and with a positive suction head, including velocity head, of 10 ft has an impeller diameter of 6.8 ft. The pump being too large for a shop or laboratory test, a model with 18-in. impeller is to be tested at a reduced head of 320 ft. At what speed, capacity, and suction head should the test be run?

Applying the above relations:

$$N_1 = N \frac{D}{D_1} \sqrt{\frac{H_1}{H}} = 450 \frac{6.8 \text{ ft}}{1.5 \text{ ft}} \sqrt{\frac{320}{400}} = 1{,}825 \text{ rpm}$$

$$Q_1 = Q \left(\frac{D_1}{D}\right)^2 \sqrt{\frac{H_1}{H}} = 200 \left(\frac{1.5}{6.8}\right)^2 \sqrt{\frac{320}{400}} = 8.73 \text{ cfs, or } 3{,}920 \text{ gpm}$$

To check these results, the specific speed of the prototype is

$$N_s = N \frac{\sqrt{Q}}{H^{3/4}} = 450 \frac{\sqrt{200}}{400^{3/4}} = 71.2 \text{ in the cfs system}$$

and that of the model is

$$N_{s1} = 1{,}825 \frac{\sqrt{8.73}}{320^{3/4}} = 71.2 \text{ (or 1,510 in the gpm system)}$$

The cavitation factor for the field installation, assuming a water temperature of 80 F as a maximum probable value and $H_b = 32.8$ ft as in the first example, will be

$$\sigma = \frac{H_b - H_s}{H} = \frac{32.8 + 10}{400} = 0.107$$

which should be the same in the test. With the water temperature approximately the same,

$$\sigma = \frac{H_b - H_{s1}}{H_1}$$

and

$$H_{s1} = H_b - \sigma H = 32.8 - (0.107)(320) = -1.45 \text{ ft}$$

Hence the model should be tested with a positive suction head of 1.45 ft, to reproduce the field conditions.

Test of Full-sized Pump or Model at Increased Head. Under some conditions it may be desirable to carry out shop or laboratory tests at a higher head than the installation head. This may be due, for example, to the limitations of test motors or electrical frequency. A more usual cause may be the inability to provide sufficient suction lift in the shop. The required sigma can then be obtained by an increase in the pumping head instead of an increase in suction lift.

Cavitation Tests. The critical value of sigma at which cavitation begins can be found by running the pump at constant specific speed and varying sigma by progressively altering the relation between suction lift and pumping head. The efficiency and the head corrected for constant speed can then be plotted against sigma. The point where the curves break away from the horizontal, as sigma is reduced, indicates the critical sigma. For pumps of abnormal design and those which are to operate close to or beyond the recommended limits of Figs. 61 to 64 cavitation tests are of great importance, sometimes of greater importance than accurate efficiency tests. Three typical arrangements are shown for determining the cavitation characteristics of pumps (Fig. 66).

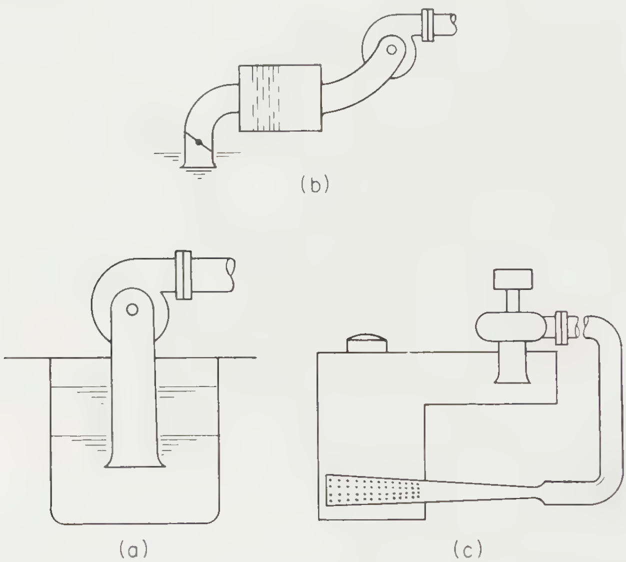

FIG. 66. Arrangements for determining pump cavitation characteristics.

In (*a*), the pump suction pipe simply draws from a sump in the form of a well in which the surface level can be varied in elevation over a fairly large range, thus varying the suction lift.

In arrangement (*b*), the suction is taken from a sump of fixed surface level through a throttle valve followed by an enlarged pipe forming a stilling chamber and containing screens or baffles to dissipate the turbulence from the throttle valve and to distribute the flow evenly, so that the pump takes a flow free from undue turbulence.

In arrangement (*c*), the pump is in a closed circuit in which the absolute pressure level can be drawn down to any desired extent without changing the pump head.

REVERSIBLE PUMP-TURBINES[1]

18. General Classification. *Definition.* A pump-turbine is a dual-purpose hydraulic machine that combines the functions of a pump and a turbine in a single machine; it is in a class distinct from both the pump and the turbine. Pump-turbines

[1] By Thaddeus Zowski.

are represented in current practice mainly by the reversible-type machine which operates in one direction of rotation as a pump and in the opposite direction of rotation as a turbine. Although pump-turbines of the nonreversible type have also been developed, they have not yet gained wide acceptance, and relatively little operating experience is available thus far from such machines.

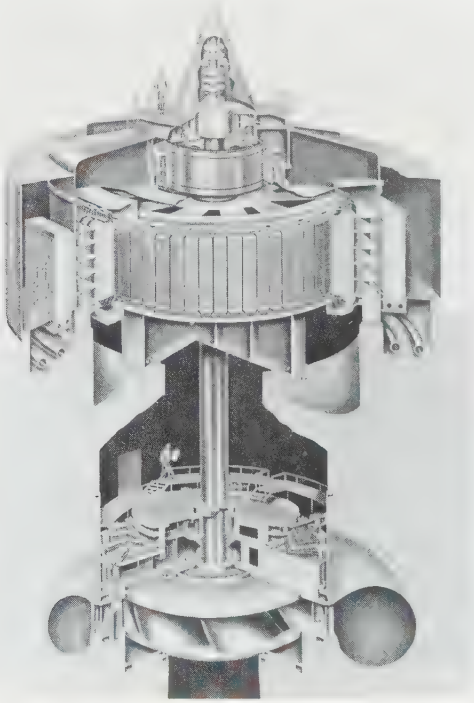

Fig. 67. Cutaway view of Francis-type pump-turbine and generator-motor. (*Allis-Chalmers Mfg. Co.*)

Classification. Pump-turbines may be divided into three principal types analogous to those of reaction turbines and pumps:

1. Radial-flow or Francis type (Figs. 67 through 70)
2. Mixed-flow or diagonal-flow type (Fig. 71)
3. Axial-flow or propeller type (Figs. 72 and 73)

The diagonal-flow and propeller types are subdivided into fixed-blade and adjustable-blade types. Pump-turbines are also classified according to the position of their main shaft as vertical-shaft and horizontal-shaft machines, and according to the number of stages as single-stage and multiple-stage units.

The Origins of Present Designs. The operating principle and possibilities of the reversible pump-turbine have long been known, but were not put into practice until the early 1930s, when the first two known reversible pump-turbine installations involving relatively small machines were placed in service in Europe. These were followed by two larger reversible pump-turbines installed in Brazil, one of which was of European manufacture (J. M. Voith) and was placed in service in 1939; the other was of American manufacture (Allis-Chalmers) and was placed in service in 1940. Subsequent extensive research and development work on reversible pump-turbines by the American hydraulic turbine industry produced designs of economical machines having good performance characteristics. The development of the reversible pump-turbine has greatly extended the field of economic development of pumped storage projects, because of the substantial saving in the cost of hydraulic machinery, valves, penstocks, and power-station structure that can be achieved in most cases by using single-unit reversible machines instead of separate pumps and turbines. The economy and good performance of this type of machine resulted in the adoption of reversible pump-turbines for a number of large installations in North America, beginning with the reversible Francis-type unit of Allis-Chalmers design and manufacture, which

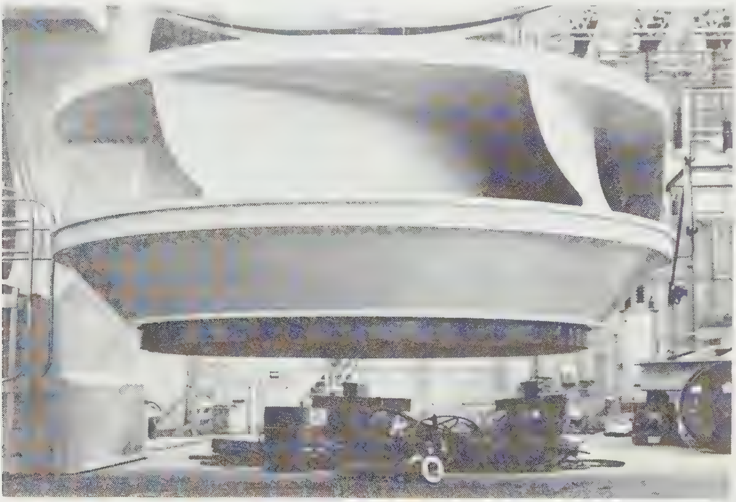

Fig. 68. Impeller runner of Francis pump-turbine for Hiwassee plant of TVA. Rated 83,000 hp at 190-ft net head as a turbine, 3,900 cfs at 205-ft total head as a pump, 105.9 rpm. Impeller-runner diameter 266 in. at distributor center line. (*Allis-Chalmers Mfg. Co.*)

was placed in service at the Flatiron power and pumping plant of the U.S. Bureau of Reclamation in 1954. All pumped storage projects in North America since that time have utilized reversible-type pump-turbines.

19. Basic Performance Relationships. *Interrelation of Pumping and Turbine Performance.* Since a reversible pump-turbine is both a pump and a turbine, a definite relationship exists between its pumping and generating capacities. Selection of a pump-turbine for a proposed installation ordinarily begins with the determination of the desired generating capacity at minimum net head. Establishment of the generating capacity for a machine of given type and specific speed substantially determines the pumping capacity also. Similarly, if a pumping capacity is established for a specified total head, the generating capacity for the corresponding turbine net head is also fixed within relatively narrow limits. The relationship of performances can be modified only slightly by design changes. Therefore, the prospective purchaser of a pump-turbine should not attempt to specify requirements rigidly fixed for both pumping and generating, unless he has had opportunity to study adequately the model-test data of pump-turbine manufacturers, or performance data from applicable existing installations.

Cavitation, Setting, and Speed. The operating duties of a pump-turbine are inherently less favorable from the cavitation standpoint when pumping than when generating, because head losses associated with flow through the suction-draft tube in the pumping direction always act to decrease the available net positive suction head. Furthermore, pump-turbine impellers are generally more sensitive to cavitation than turbine runners designed for the same specific speed. To avoid cavitation when pumping, it is necessary to set a pump-turbine lower in relation to tail water than would be required for turbine operation alone. As in the case of conventional turbines the selection of an appropriate specific speed for a pump-turbine depends not only on its operating head but also largely on the setting in relation to tail water; essentially,

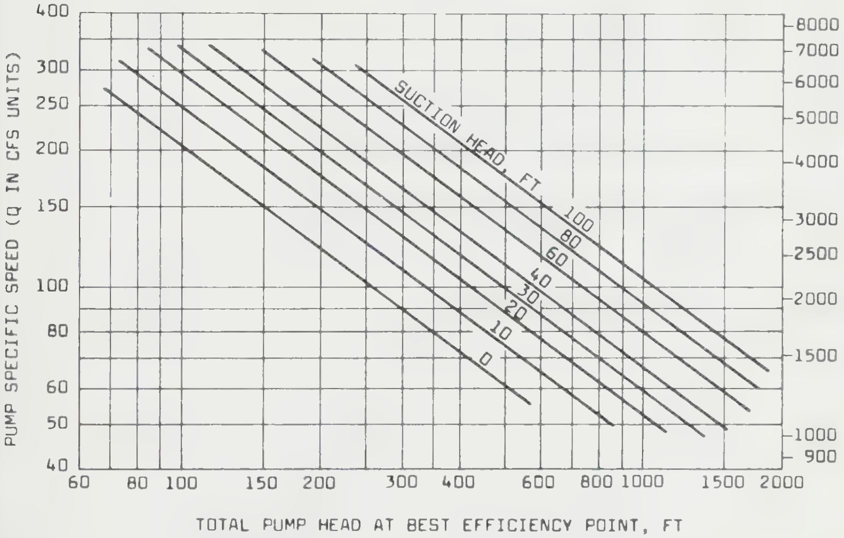

Fig. 69. General relationship between head, pump specific speed at point of best efficiency, and suction head of Francis pump-turbines.

it depends on the depth below tail water to which it is practical to submerge the pump-turbine. To utilize relatively high specific speeds and consequently smaller, more economical machines with higher operating speeds, pump-turbines require considerably deeper settings than turbines. Figure 69 shows the general relationship between pump total head, pump specific speed, and suction head of Francis-type pump-turbines. The chart is an approximation intended only as a general guide for preliminary purposes. It is based on a value of $H_a - H_v = 32.0$ ft and a suction specific speed $S = 10{,}000$ at the point of best efficiency (with discharge expressed in gpm units). The suction head refers to the lowest point of the impeller-runner blades of vertical-shaft pump-turbines.

The economics of pumped storage generally require that the pump-turbines have high efficiency both as a pump and as a turbine. It is also desirable, from the standpoint of design and cost of the generator-motor, that the pump-turbine have the same speed of rotation in both directions of operation. However, the hydraulic design of reversible pump-turbines with fixed blades is such that the point of best efficiency occurs at a higher value of peripheral-speed coefficient when pumping than when operating as a turbine. This means that, for operation of such machines at a single rotative speed, the head for pumping should preferably be lower than the head for operation as a turbine. Unfortunately, except in unusual installations, the effect of head losses in the penstock and related water-supply and discharge conduits is such that, for a given gross head, the total pump head will generally be higher than the net head during turbine operation by approximately twice the head losses for flow in one direction. However, through careful hydraulic design of reversible machines with fixed blades, the difference in heads required for optimum efficiency in both modes of operation at a single speed can be reduced appreciably. By use of adjustable blades, the best efficiency points for pumping and generating can be substantially brought together.

Transient Behavior. The operation of a pump-turbine involves hydraulic transient phenomena capable of producing substantial pressure variations at the machine and in the hydraulic system of upstream and downstream water conduits. For proper design of a pump-turbine installation, and for the selection of the most suitable governor time and amount of inertia in the rotating masses (WR^2), a thorough study must be made of the transient conditions following power failure when pumping and following load rejection when generating. Both conditions should be examined, because maximum water hammer and maximum speed changes could be caused by either power failure or load rejection. To analyze the transient behavior of the system, the complete hydraulic characteristics of the pump-turbine must be known. These characteristics are conveniently represented by a type of chart introduced by Theodor von Karman and commonly known as the four-quadrant characteristics. A complete four-quadrant characteristic shows the various possible combinations of head, discharge, and torque or power in the following regions of operation: (1) pump operation; (2) energy dissipation with rotation in the pumping direction and flow in the generating direction; (3) turbine operation; (4) energy dissipation with rotation in the turbine direction and flow in the pumping direction. The first three quadrants usually suffice for transient analysis of pumps, but reversible pump-turbines with adjustable wicket gates in some cases have been found to enter into a portion of the fourth quadrant during closure of wicket gates under runaway speed conditions.

Valuable information concerning methods of water-hammer analysis, design practices, and problems encountered after construction of pumped storage projects was presented at the winter annual meeting of the ASME, November, 1965, and published under sponsorship of the Fluid Transients Committee of the Fluids Engineering Division of ASME.[1]

20. Francis-type Pump-turbines. *General Design Characteristics.* Radial-flow or Francis-type single-stage reversible pump-turbines are being applied for operating heads from about 75 to 1,300 ft. The continuing development of their design may extend the upper limit to 1,700 ft or more. It is evident that the overall range of heads for which Francis pump-turbines are applied approaches that for which conventional Francis turbines are used. The upper limit exceeds the usual maximum for single-stage centrifugal pumps of conventional design.

Francis pump-turbines, though basically similar in construction to Francis turbines, differ from them significantly in the hydraulic design of their principal components. For a given head and power output, the reversible machine will be larger and will usually be set lower in relation to tail water than a conventional Francis turbine. Since it has been found that a good centrifugal pump will perform well as a turbine in the reverse direction of rotation, but a good Francis turbine will not perform satisfactorily as a pump, the impeller runner of a reversible Francis pump-turbine is designed

[1] International Symposium, Waterhammer in Pumped Storage Projects, ASME, New York, 1965.

essentially as a pump impeller rather than as a turbine runner. It has fewer blades than a Francis turbine runner, and the blades usually wrap around from throat to tip diameter by more than 90 deg, sometimes up to about 180 deg (Fig. 70). A conventional turbine runner, because of relatively short blades, is not well adapted to efficient deceleration of flow in its water passages, or to the cavitation requirements, when it is operated in the reverse direction for pumping. The ratio of tip to throat diameter of a reversible impeller runner is substantially larger than for an equivalent turbine runner. The relatively large tip diameter, approximately equal to that of an equivalent pump impeller and approximately 1.4 times that of an equivalent Francis

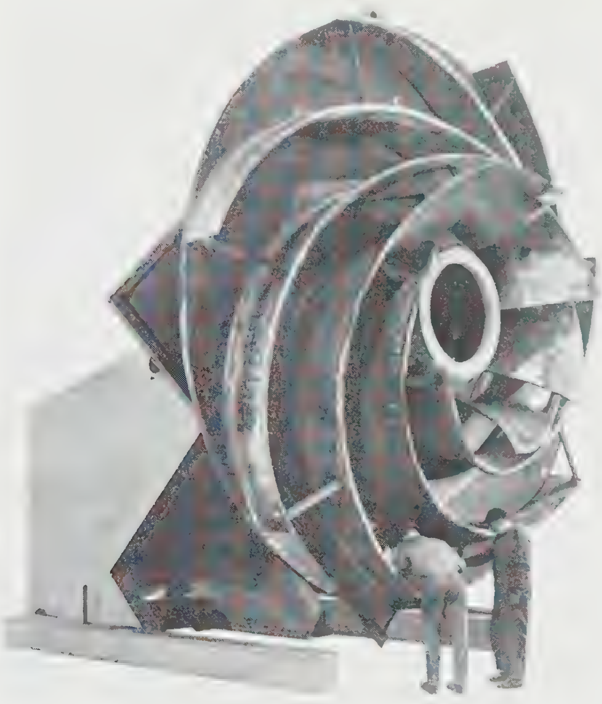

FIG. 70. Partially completed impeller runner of Francis pump-turbine. Blades being welded in assembly mounted on welding positioner. (*Baldwin-Lima-Hamilton Corp.*)

turbine runner, is necessary to obtain efficient diffusing passages and to reduce the velocity-head component of the total energy discharged from the impeller runner; it also provides a head-discharge characteristic favorable for starting of pump operation. The spiral case of a pump-turbine usually has its volute sections on a larger base circle than the casing of a centrifugal pump for the same rating. Since the impeller runner is larger than an equivalent turbine runner and the casing of a pump-turbine is larger than that of a pump, the resulting overall dimensions of the reversible pump-turbine are larger than those of either the equivalent turbine or the equivalent pump.

Because of the comparatively large tip diameter of the impeller runner, the Francis pump-turbine inherently has a lower runaway speed than a Francis turbine. Its runaway speed is generally in the order of 80 percent of that of the corresponding turbine. A further significant characteristic inherent in the hydraulic design of medium- to high-head (low-specific-speed) Francis pump-turbines is their decrease in discharge with increase in speed above normal operating speed. This characteristic, in installations involving long water conduits, can cause substantial water-hammer effects when runaway speed occurs.

Single-speed Operation. The majority of reversible Francis pump-turbines operate at a single speed. As previously indicated, to attain optimum efficiencies in both the pumping and generating cycle with single-speed operation, the head on a Francis pump-turbine should preferably be lower when pumping than when generating. The gap between the heads for peak efficiency is narrowed by careful hydraulic design but is difficult to eliminate entirely, as theoretical considerations indicate that the optimum efficiencies are not obtained with the same peripheral-speed coefficient in both pump and turbine operation. Nevertheless, good overall performance with efficiencies exceeding 90 percent is usually attainable when the ratio of maximum pumping head to minimum generating head does not exceed about 1.25. Since the difference in optimum efficiency heads diminishes somewhat with decreasing values of specific speed, high efficiencies in both modes of operation are attained more readily by Francis pump-turbines of low specific speed which are used for high operating heads.

Two-speed Operation. For those pump-turbines which must operate over a large range of heads, or where the pumping heads are considerably higher than the generating heads, two-speed operation to allow the maximum efficiency points for both cycles to be utilized may be justified. Specially designed two-speed synchronous generator-motors, which electrically change the effective number of poles for motor and generator operation, have been developed for pump-turbine application. Since a two-speed generator-motor is somewhat larger and its cost substantially greater than that of a single-speed generator-motor, a careful evaluation is usually necessary to determine whether the added cost of a two-speed machine is economically justified for a proposed installation. An example of a two-speed reversible Francis pump-turbine is provided by the Flatiron installation where the heads vary from 140 to 290 ft for turbine operation and from 170 to 300 ft for pump operation. The Flatiron unit operates normally at 257 rpm as a turbine and at 300 rpm as a pump, although it is capable also of operation at both speeds in both directions. A more recent example is provided by the San Luis Pumping-Generating Plant of the U.S. Bureau of Reclamation where the head on the eight pump-turbines varies from 110 to 330 ft when pumping and from 120 to 315 when generating. The San Luis machines operate at either 120 or 150 rpm as pumps and as turbines; the higher of the two speeds is used for heads exceeding 190 ft during pumping and for heads greater than 227 ft during generating. The Francis pump-turbines in these two examples do not have adjustable wicket gates.

Adjustable Wicket Gates. Reversible pump-turbines may be built with or without adjustable wicket gates. In the great majority of pumped storage applications, it is desirable to provide means for varying the power output of the pump-turbine. Adjustable wicket gates provide excellent regulation of power output and good control for starting and synchronizing the unit in turbine operation. In pumping operation, adjustable wicket gates are relatively ineffective for regulating discharge but enable operating at optimum efficiencies with varying heads. As the head increases with filling of the storage reservoir, the quantity of water pumped decreases; as the discharge decreases, the wicket-gate opening can be reduced to provide proper flow conditions for best efficiency. The use of adjustable wicket gates also facilitates starting and stopping in pump operation. Moreover, wicket gates provide a means of controlling the speed in the reverse direction after reversal of flow upon sudden loss of power to the generator-motor while pumping.

If adjustable wicket gates are not provided, the flow is usually controlled by means of the main shutoff valve. This valve usually opens and closes at a slower rate than adjustable wicket gates, because of its size and amount of travel as compared with wicket gates. Omission of adjustable wicket gates may be justified in some installations where the pump-turbine is used primarily for pumping service, and little adjustment of power and flow is required during turbine operation. Pump-turbines without wicket gates have the advantage of lower first cost, relative simplicity of operation, and reduced maintenance. They also are adaptable to slightly higher heads than those with wicket gates.

Starting Procedures. Starting a reversible pump-turbine for turbine operation does not present any special problems. If it is equipped with adjustable wicket gates, the machine can be started, brought up to speed, synchronized, and loaded in the same manner as a conventional turbine. If it does not have adjustable wicket gates, start-up is usually controlled by the main shutoff valve. However, starting the machine and bringing it up to speed in the reverse direction for pumping is associated with problems requiring special consideration.

Because of the water in the upper reservoir, the pump-turbine must obviously be started in the pumping direction with closed wicket gates, or with a closed shutoff valve or other device, if the machine does not have adjustable wicket gates. With the impeller runner submerged as necessary for pumping, the power input to start and accelerate the machine to synchronous speed and to develop shutoff head is quite high for large-capacity machines, despite the fact that the power for shutoff head on medium- and high-head pump-turbines is lower than at rated head and discharge. To reduce the power required for starting, compressed air is admitted to the space inside the wicket-gate circle to depress the water level below the bottom of the impeller runner so that it rotates in air. With the water level depressed, the machine is brought up to speed and synchronized. Means are usually provided to drain off the water that may leak from the spiral case through the wicket-gate clearances into the space between the outer periphery of the impeller runner and wicket gates, where it forms a rotating ring of water which increases the torque requirements. To minimize the starting torque due to bearing friction, the generator-motor thrust bearings for large pump-turbines are provided with high-pressure oil-starting equipment, which forces oil at high pressure between the stationary and rotating faces of the thrust bearing, thus lifting the rotating face free of metal-to-metal contact. Nevertheless, the power required for starting a large reversible Francis pump-turbine and its generator-motor from rest, and overcoming its inertia in accelerating it to synchronous speed, is considerable.

Several methods are in use for starting reversible pump-turbines for pumping operation; selection of the most suitable method depends largely on the size of the machine in relation to the capacity of the electrical-power system. The simplest method of starting consists of applying full voltage from the power system and letting the machine come up to speed as an induction motor, with the damper winding on the rotor acting as the squirrel-cage winding of an ordinary induction motor. However, this method will disturb the power system severely, unless the system and connecting transmission line are sufficiently large in relation to the generator-motor capacity. In some installations, a similar method is used, except that the voltage is reduced to limit the starting current. In other cases, including several recent installations with pump-turbines of large capacity, a starting motor of the wound-rotor type is provided on the generator-motor shaft for accelerating the unit from rest to synchronous speed. Another method employs so-called back-to-back synchronous starting in which a nearby generator or generator-motor is connected electrically to the generator-motor to be started with both machines at rest, then started and accelerated by means of its turbine, thereby starting and bringing the pump-turbine up to speed. A hydraulic starting method utilizing a starting turbine mounted on the shaft of the reversible machine is also available but has not found broad application thus far to reversible pump-turbines, mainly because of design complications arising from problems of setting in relation to tail water and properly accommodating the discharge from the starting turbine.

After the pump-turbine unit is synchronized to the power system while running in the pumping direction with the impeller runner rotating in air, the air must be released to admit water to the impeller runner. Proper procedures must be followed in releasing air and admitting the water, so as to control the rate of power increase up to the point where the unit is operating in water at shutoff head against closed wicket gates. The shutoff-power requirement of reversible Francis pump-turbines pumping against closed wicket gates can be from about 25 percent of full-load pumping power on high-head units to about 100 percent on low-head units. After full shutoff head is developed, the wicket gates are slowly opened. The increase in power demand is then controlled by the rate of opening the wicket gates to their normal operating position. The normal gate position for pumping should be kept at or near the best efficiency point; therefore, as the head on the pump-turbine increases during the pumping cycle, the wicket-gate opening should be gradually decreased. However, in some installations where the variation in pumping head is relatively small, operation of reversible Francis units at a single gate opening has been found practicable.

Reversible pump-turbines are normally shut down at the end of the pumping cycle by slowly closing the wicket gates to zero opening and disconnecting the generator-motor from the power system. When the speed of the machine has dropped to below half speed, the brakes on the generator-motor are applied to bring it to a complete stop.

21. Diagonal-flow Adjustable-blade Pump-turbines. Diagonal-flow adjustable-blade-type reversible pump-turbines, also called Deriaz[1]-type pump-turbines, are being applied for heads from about 35 to 250 ft. The upper limit of head is gradually being increased through advances in design and can be expected to exceed 300 ft in forthcoming applications. These machines are the reversible version of the diagonal-flow adjustable-blade turbine. Their hydraulic design is based primarily on mixed-flow pump practice. They usually have between five and nine blades, somewhat fewer than a corresponding turbine. The axes of the adjustable blades are inclined to the main shaft axis at an angle of about 30 to 60 deg. On several of the machines built thus far, an inclination angle of approximately 45 deg has been used. The blades are of simpler shape than those of Kaplan machines and can be designed so that adjacent blades touch one another along their entire length in the closed position. This is unlike Kaplan runner blades which, when closed, may be in contact at the periphery while a large gap remains between blades near the hub.

Owing to their adjustable blades, the diagonal-flow pump-turbines have greater operating flexibility and flatter efficiency curves than reversible Francis-type pump-turbines. They are suitable for low- to medium-head pumped storage applications where the head and discharge vary considerably. Their adjustable blades provide effective regulation of pumping discharge and power in contrast to the relatively ineffective regulation by adjustable wicket gates on Francis-type pump-turbines. By controlling simultaneously the blade angle and the wicket-gate opening of diagonal-flow machines, it is possible not only to vary the turbine output or maintain uniform output with varying head but also to vary the pump discharge while maintaining uniform head, without substantial decline in efficiency. Their ability to vary pump

[1] Name used in recognition of the development of the first successful commercial design of this type of machine in the early 1950s by Paul Deriaz, who was then Chief Water Turbine Designer of the English Electric Company, Ltd.

discharge while maintaining good efficiency permits these machines to follow system-load variations closely during pumping. Their high part-load efficiency in turbine operation, a feature which is always desirable, has special significance in connection with the present trend of selecting a small number of large units for pumped storage plants to gain economy in first cost and in annual cost of operation and maintenance. The high part-load efficiency may make it feasible in some cases to keep the units running as turbines at small load, in readiness for sudden increase in demand, thus providing highly valued instantaneous availability of power. These advantages should lead to increased application of adjustable-blade diagonal-flow pump-turbines

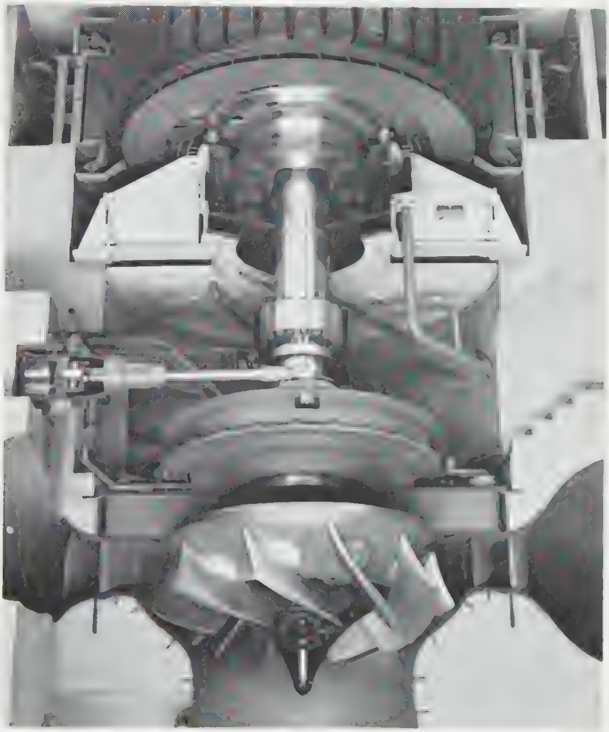

FIG. 71*a*. Model of diagonal-flow adjustable-blade-type pump-turbine for Valdecanas pumped storage plant in Spain. (*English Electric Company Ltd.*)

in the range of low to medium heads, below the range of best application of Francis-type pump-turbines.

However, the cost of adjustable-blade diagonal-flow pump-turbines is substantially higher than that of Francis pump-turbines, because of their greater complexity of design. Their cavitation characteristics are such that a deeper submergence is generally required than for Francis pump-turbines. Although their comparatively higher specific speed permits use of higher operating speeds, the ratio of their runaway speed to normal operating speed is substantially higher than that of Francis pump-turbines; therefore, a somewhat more expensive generator-motor is usually required. The relatively high runaway speed may, in some cases, become the limiting criterion in the selection of the operating speed, especially where the generator-motors are very large.

There is an important difference between the pumping characteristic of these machines and that of Francis-type pump-turbines. In contrast to the increasing discharge with decreasing head on Francis pump-turbines, the adjustable-blade diagonal-flow-type pump-turbines, when operated at best efficiency, have increasing discharge as head is increased. The increase in discharge with increasing head causes a pronounced rise in the power requirement, tending to increase the cost of the electrical installation.

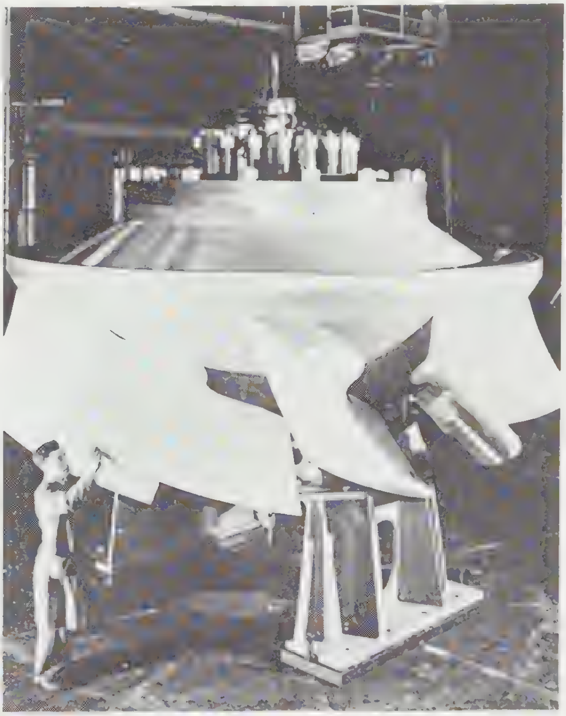

Fig. 71*b*. Shop assembly of diagonal-flow adjustable-blade Deriaz-type impeller runner of pump-turbine rated 108,500 hp, 243-ft head, 150 rpm for Valdecanas plant of Hidroelectrica Espanola S.A., Spain. (*Three units by English Electric Company Ltd.*)

The adjustable-blade diagonal-flow machines have a relationship of optimum blade angle to wicket-gate opening, known as the cam relationship, resembling that of Kaplan turbines. However, since the optimum relationship for turbine operation differs considerably from that for pump operation, an adjustable-blade diagonal-flow pump-turbine requires either two sets of cams or a somewhat more complex three-dimensional cam system suitable for both turbine and pump operation. As in the case of Kaplan turbines, diagonal-flow machines have both an on-cam and an off-cam runaway speed, the latter being the higher of the two.

The shape of the adjustable blades of a diagonal-flow pump-turbine is such that, when closed, they form a relatively smooth cone; consequently, a comparatively small torque is required for rotating the impeller runner in water. As a result, it has not been found necessary to depress the water level below the blades for pump starting, as is done with Francis-type pump-turbines. When the machine has been brought up to speed, the blades and wicket gates are gradually opened. The discharge increases smoothly to full pumping capacity. This procedure permits making a changeover from generating to pumping in less time than usually required for Francis pump-turbines.

Experience data available from the operation of adjustable-blade diagonal-flow reversible pump-turbines thus far are rather limited. The first machine of this type

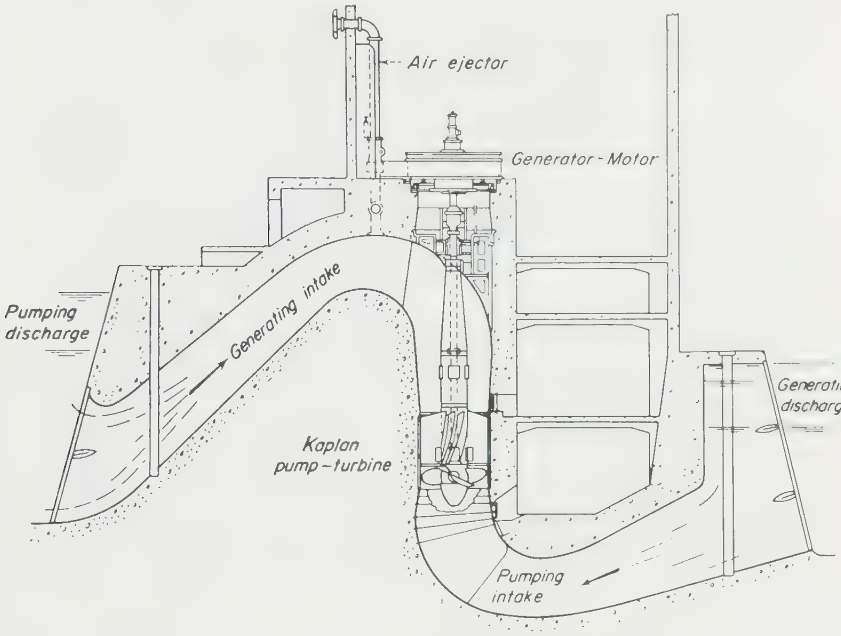

Fig. 72. Sectional elevation of axial-flow adjustable-blade propeller-type pump-turbine for Traicao pumping plant in Brazil. (*Three units by Allis-Chalmers Mfg. Co.*)

was placed in service in June, 1957, at the Sir Adam Beck No. 2 Niagara Pumping-Generating Station of the Hydro-Electric Power Commission of Ontario. The installation consists of six units which operate with heads varying from 59 to 90 ft in pump operation and from 45 to 85 ft in turbine operation. The machines operate at 92.3 rpm and are rated 45,500 hp under 83-ft net head (5,600 cfs) as a turbine and 4,600 cfs at 75-ft dynamic head (44,500 hp) as a pump. In 1965, three machines of this type, but of larger capacity, were placed in service at the Valdecanas pumped storage plant in Spain, where they operate at heads varying between 160 and 243 ft, each developing 108,500 hp under 243-ft head at 150 rpm (Fig. 71).

22. Axial-flow Pump-turbines. Axial-flow or propeller-type reversible pump-turbines are utilized for operating heads from about 3 to 45 ft. The axial-flow pump-turbines have impeller runners resembling those of propeller turbines, and usually have a tubular-type arrangement. When provided with adjustable blades, they permit substantial variations in head and discharge with good efficiency. The adjustable blades also permit a considerable reduction in the required torque for starting in pumping operation.

The first reversible pump-turbine of the adjustable-blade axial-flow type installed in the Western Hemisphere was placed in service in 1940 at the Traicao plant of the Sao Paulo Light S. A. in Brazil. The three pump-turbines at this plant are rated 3,450 hp each at 23-ft head as a turbine and 1,765 cfs at 23-ft head as a pump, operating at 150 rpm. The machines have a vertical-shaft siphon setting and S-shaped water passages (Fig. 72). These machines are the forerunners of the more recent designs of the Allis-Chalmers TUBE units.

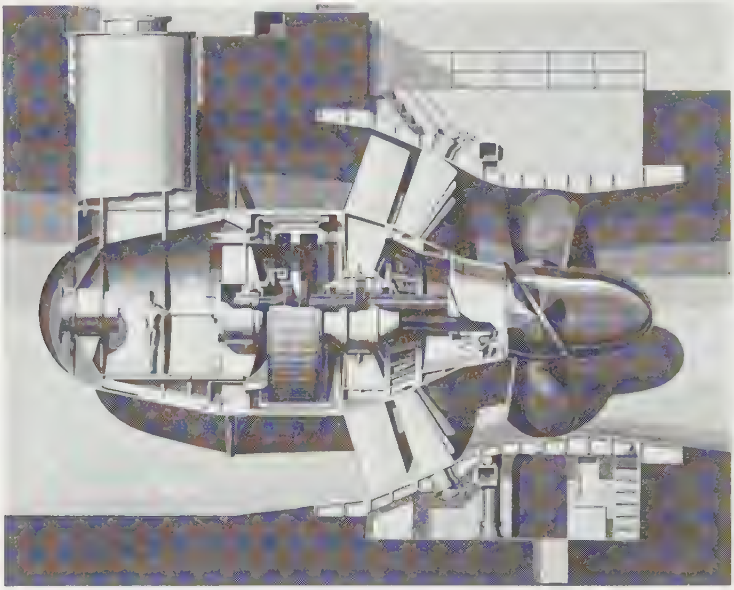

Fig. 73. Cutaway view of one of 24 axial-flow pump-turbines of the bulb type for the Rance tidal-power station in France. Nominal capacity 10,000 kw, 19-ft net head, 93.75 rpm. Runner diameter 211 in. (*Nine turbines by Neyrpic, with generators by Alsthom.*)

Axial-flow pump-turbines with horizontal-shaft arrangement are well adapted to tidal-power applications. To increase the flexibility of operation in tidal plants or for special cases of inland installations, the machines can be designed to operate as a pump or as a turbine with either direction of flow, giving them four-way operating capability. At the world's first large tidal-power development on the Rance River estuary in France, 24 reversible axial-flow pump-turbines of the bulb type have been installed (Fig. 73).

The extensive development work now under way in several countries on low-head pump-turbines for tidal-power applications can be expected to result in further significant advances in the design of axial-flow-type pump-turbines.

SECTION 27

WATER HAMMER

By George R. Rich

INTRODUCTION. WATER HAMMER—A TYPICAL TRANSIENT PHENOMENON

Water-hammer effects in closed conduits constitute one particular class of a broad family of electrical and mechanical wave movements which engineers have chosen to designate by the term transient phenomena. These disturbances may be said to mark the transition stage between any two successive steady states of the system. They are initiated by the application of a definite causative force or action, frequently but not necessarily applied with comparative suddenness, and are dissipated down to the level of the second steady state by the operation of some form of damping.

In the case of hydraulic pressure conduits, water hammer is the mechanism immediately responsible for every change in steady-state velocity, gradual or sudden. It is a wave movement propagated with the velocity of sound, usually initiated by a change in setting of the conduit control valve or its equivalent, and is attenuated down to the level of the second steady state by damping in the form of conduit friction. Because water-hammer pressures reach significant magnitudes only in the case of comparatively rapid valve operation, we are prone to lose sight of the fact that water hammer is, nevertheless, the direct means of effecting even the most gradual change in steady-state velocity.

Although it is assumed that most engineers have some acquaintance with water hammer, it may be advantageous, as a means of breaking ground for the essential differential relationships, to review just qualitatively, subject to subsequent mathematical confirmation, the salient steps of the water-hammer cycle for the elementary case of the simple conduit with instantaneous valve closure and with conduit friction and velocity head neglected. Referring to Fig. 1, upon closure of the valve, a wave of positive pressure travels upstream with the velocity of sound (in this particular case converting the conduit velocity to zero), compressing the water and stretching the conduit shell. Upon reaching the reservoir, the pressure wave obtains relief and drops down in intensity to the reservoir pressure. This in turn allows the compressed water stored in the stretched pipe to drop down to reservoir pressure again by means of the passage of a negative pressure wave traveling downstream with the velocity of sound and converting the conduit velocity from zero to minus V_1 in the reverse direction. When this negative wave has reached the closed valve at the downstream end of the conduit, all the water in the conduit is at that instant traveling upstream with a velocity minus V_1. Owing to the inertia of the water, this negative pressure wave traveling downstream will next be reflected at the valve so as to travel upstream with the same negative sign. Behind and downstream of the negative wave so reflected, the conduit velocity will again drop to zero, and the conduit shell will shrink a proportionate amount below the original size so as to furnish the volume of water necessary to maintain the velocity minus V_1 ahead of the traveling wave until the wave reaches the reservoir. When the reflected negative wave reaches the reservoir,

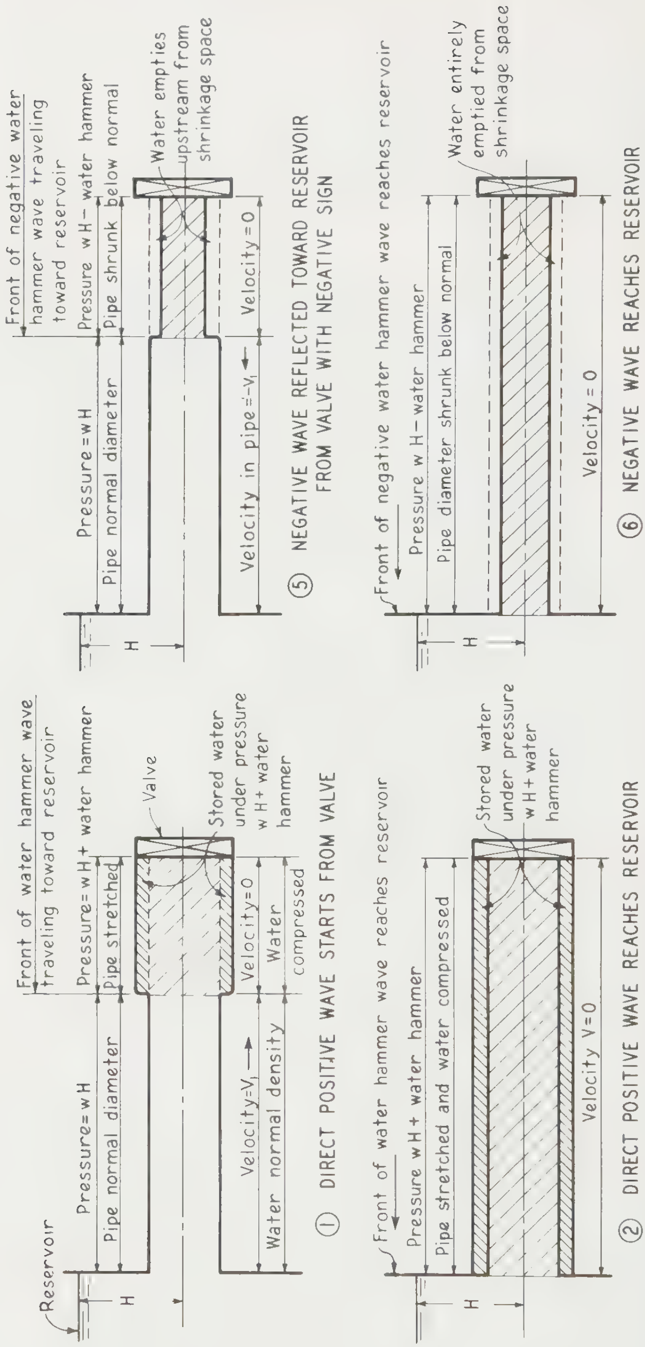
Reservoir
H
Pressure = wH
Pipe normal diameter
Velocity = V_1
Water normal density
Front of water hammer wave traveling toward reservoir
Pressure = wH + water hammer
Pipe stretched
Valve
Stored water under pressure wH + water hammer
Velocity = 0
Water compressed
① DIRECT POSITIVE WAVE STARTS FROM VALVE
Front of water hammer wave reaches reservoir
Pressure wH + water hammer
Pipe stretched and water compressed
Stored water under pressure wH + water hammer
Velocity V = 0
② DIRECT POSITIVE WAVE REACHES RESERVOIR
Pressure = wH
Pipe normal diameter
Velocity in pipe = $-V_1$
Front of negative water hammer wave traveling toward reservoir
Pressure wH − water hammer
Pipe shrunk below normal
Water empties upstream from shrinkage space
Velocity = 0
⑤ NEGATIVE WAVE REFLECTED TOWARD RESERVOIR FROM VALVE WITH NEGATIVE SIGN
Front of negative water hammer wave reaches reservoir
Pressure wH − water hammer
Pipe diameter shrunk below normal
Water entirely emptied from shrinkage space
Velocity = 0
⑥ NEGATIVE WAVE REACHES RESERVOIR

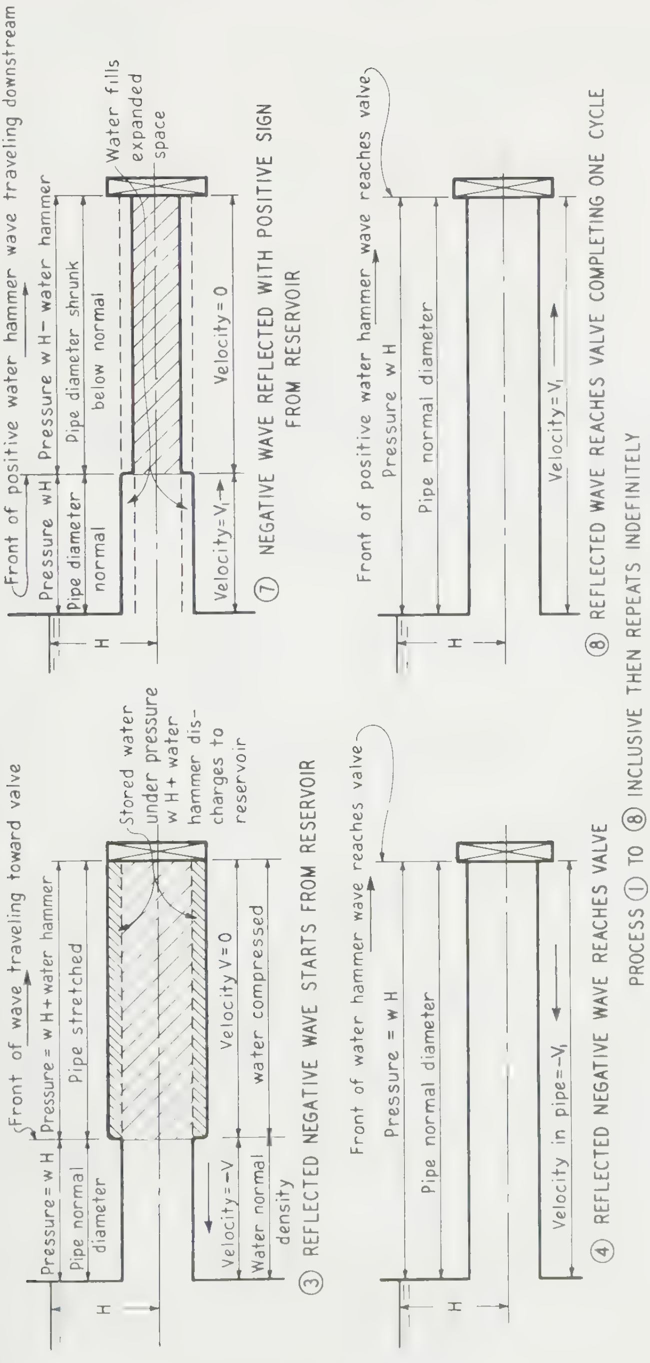

Fig. 1. Progress of water-hammer wave. Instantaneous valve closure.

the pressure will rise to reservoir level, and a positive pressure wave elevating the conduit pressure to normal reservoir head will be propagated downstream. The velocity upstream from and behind the wave will next be converted to plus V_1. This completes one cycle of the wave motion, and since the effect of friction in the conduit has been neglected, the procedure outlined will be repeated indefinitely and without diminution in intensity.

THE BASIC DIFFERENTIAL EQUATIONS

The physical process outlined in Fig. 1 has been so well substantiated by experiment and observation that we are justified in employing the fundamental concept of water hammer as a wave motion, compressing the water and stretching the conduit circumferentially, in formulating the primary differential equations of water hammer.

To facilitate cross reference with current literature, the basic derivations will be made in terms of pressure rather than head, and the origin of coordinates will be taken at the reservoir. Subsequently, in making application of the basic relationships to the various detailed methods of computation, appropriate changes in notation will be made where desirable to facilitate similar cross reference to the literature pertaining to these particular methods.

The following notation will be employed:

D = diameter of pipe, ft.
L = length of pipe, ft.
A = area of pipe, sq ft.
P = total pressure (surge plus steady state), psf.
V = total velocity (surge plus steady state), fps; positive in positive direction of x.
x = distance of section along axis of pipe, ft; measured from origin at reservoir.
K = volume modulus of compression of water, ft units.
b = thickness of pipe walls, ft.
E = modulus of elasticity of pipe wall, ft units.
F = friction force coefficient.
w = weight of unit volume of water, lb/cu ft.
g = acceleration of gravity, ft/sec.²
k = factor of proportionality in establishing linear approximation to conduit friction.
$W = \frac{w}{g}$.
$Q = \frac{1}{K} + \frac{D}{bE}$ (the reciprocal of the equivalent bulk modulus of water and pipe shell in combination).
t = time, sec.
$a = \frac{1}{\sqrt{WQ}}$ = water-hammer wave velocity, fps.

Referring to Fig. 2, as the water-hammer wave travels along the conduit, in each element of time ∂t, a length of water ∂x loses a decrement of velocity ∂V. The pressure behind the wave is greater than that ahead of the wave by an increment ∂P. In the figure the sign of ∂x must be plus to agree with the convention that x and V are both positive in the downstream direction. Since P and V depend upon x as well as t, the notation of partial derivatives is employed. A material simplification results from dropping second-order differentials at the outset of the analysis.

$$F = M\frac{\partial V}{\partial t} \qquad \text{Newton's second law}$$

$$\frac{\pi D^2}{4}(P + \partial P) - P = \frac{\pi D^2}{4}\frac{w}{g}\partial x\left(-\frac{\partial V}{\partial t}\right)$$

$$-\frac{\partial P}{\partial x} = W\frac{\partial V}{\partial t} \tag{1}$$

Under the effect of the increase in pressure due to water hammer ∂P, the diameter of the conduit increase by an amount ∂D.

$$\partial D = \frac{D^2\,\partial P}{2bE}$$

The volume per unit length of pipe made available by compression of the water under the increased pressure ∂P is

$$\partial\,(\text{volume}) = \frac{\pi D^2\,\partial P}{4K}$$

The total new volume to be filled in length ∂x by the discharge resulting from the

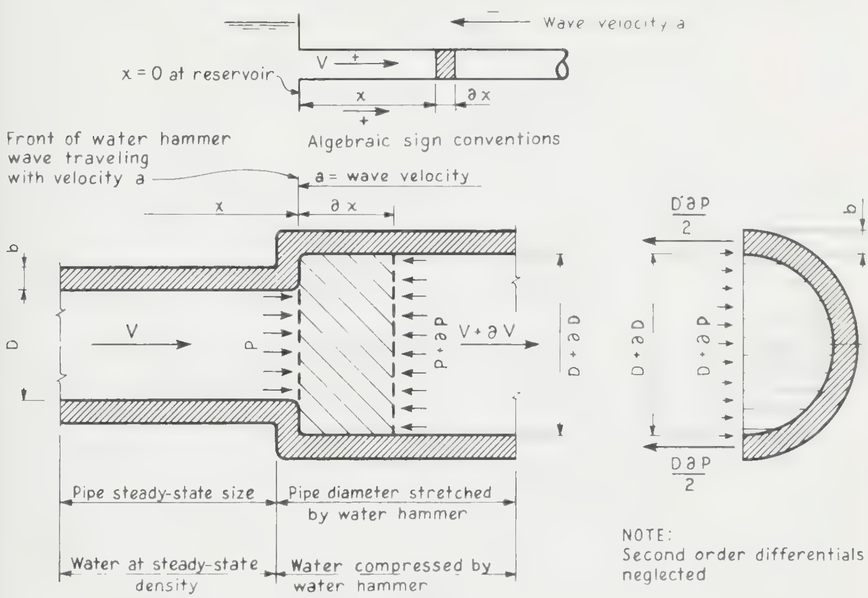

FIG. 2. Conditions during transit of water-hammer wave.

decrement of velocity ∂V is

$$\left[\frac{\pi D^2\,\partial P}{4K} + \frac{\pi(D + \partial D)^2}{4} - \frac{\pi D^2}{4}\right]\partial x = \frac{\pi D^2\,\partial P\,\partial x}{4K} + \frac{\pi D^3\,\partial P\,\partial x}{4bE}$$

But the volume of water resulting from the decrement of velocity ∂V, accumulated in time ∂t, is $\frac{\pi D^2}{4}\,\partial V\,\partial t$. Equating volumes for hydraulic continuity, and with due regard to sign conventions (Fig. 2), we obtain

$$-\frac{\pi D^2\,\partial P\,\partial x}{4K} - \frac{\pi D^3\,\partial P\,\partial x}{4bE} = \frac{\pi D^2}{4}\,\partial V\,\partial t$$

By definition,

$$Q = \frac{1}{K} + \frac{D}{bE}$$

and

$$-\frac{\partial V}{\partial x} = Q\,\frac{\partial P}{\partial t} \tag{2}$$

Now, if a is the velocity of propagation of the water-hammer wave, the velocity in a length of conduit having a length of adt will be decreased ∂V in the time ∂t.

$$F\,\partial t = M\,\partial V \qquad \text{Newton's second law}$$

$$\frac{\pi D^2}{4}\,\partial P\,\partial t = -\frac{\pi D^2}{4}\,\frac{wa\,\partial t\,\partial V}{g}$$

The minus sign of a is taken to agree with the sign convention of Fig. 2,

or
$$\partial P = -Wa\,\partial V$$

Substituting in (2)

$$-\frac{\partial V}{\partial x} = -\frac{QWa\,\partial V}{\partial t}$$

but
$$\partial x = a\,\partial t$$

and
$$a^2 = \frac{1}{WQ}$$

or
$$a = \frac{1}{\sqrt{WQ}} \tag{3}$$

By successive differentiation and combination of Eqs. (1) and (2), and using the notation of Eq. (3),

$$\frac{1}{WQ}\,\frac{\partial^2 V}{\partial x^2} = \frac{\partial^2 V}{\partial t^2} \tag{4}$$

$$\frac{1}{WQ}\,\frac{\partial^2 P}{\partial x^2} = \frac{\partial^2 P}{\partial t^2} \tag{5}$$

From their very form, the mathematical physicist[1] would immediately recognize Eqs. (4) and (5) as representative of a wave motion propagated in the x dimension with a velocity of propagation equal to the square root of $1/WQ$. These identical equations apply not only to water-hammer waves but also to the propagation of elastic stress waves in solid media and a wide variety of other mechanical and electrical transients. In each of these fields the essential character of the wave motion is the same, consisting basically of two subsidiary wave components traveling in opposite directions with the velocity $\sqrt{1/WQ}$ and without mutual interference. In other words, then, the existing fund of established knowledge regarding the general properties of Eqs. (4) and (5) gives us an independent check on the derivation of wave velocity expressed in Eq. (3).

In order to include the effect of conduit friction in our mathematical analysis, it will be necessary to introduce an approximation in order to obtain solvable differential equations. Instead of taking conduit friction proportional to the square of the velocity, we shall develop an equivalent device that permits us to express friction as proportional to the first power of the velocity.

Referring to Fig. 3, the pressure loss in length of conduit ∂x is $wckV_mV\,\partial x$.

The corresponding drop force due to friction in length ∂x is accordingly,

$$\frac{\pi D^2}{4}\,wckV_mV\,\partial x = \frac{\pi D^2}{4}\,FV\,\partial x$$

To include friction in Eq. (1) we write

$$\frac{\pi D^2}{4}\Big[(P + \partial P) - P\Big] + \frac{\pi D^2}{4}\,FV\,\partial x = \frac{\pi D^2}{4}\,\frac{w}{g}\,\partial x\left(-\frac{\partial V}{\partial t}\right)$$

and
$$-\frac{\partial P}{\partial x} - FV = W\,\frac{\partial V}{\partial t} \tag{6}$$

[1] Webster, Arthur Gordon, "Partial Differential Equations of Mathematical Physics," Chap. II, pp. 72–135, Teubner, Leipzig, 1933.

The pair of equations to be solved when friction is to be included is, therefore,

$$-\frac{\partial P}{\partial x} - FV = W\frac{\partial V}{\partial t} \tag{6}$$

$$-\frac{\partial V}{\partial x} = Q\frac{\partial P}{\partial t} \tag{2}$$

Equations (1), (2), (3), and (6) form the very foundation of the science of water hammer and are the basis of the development of every known method of computation.

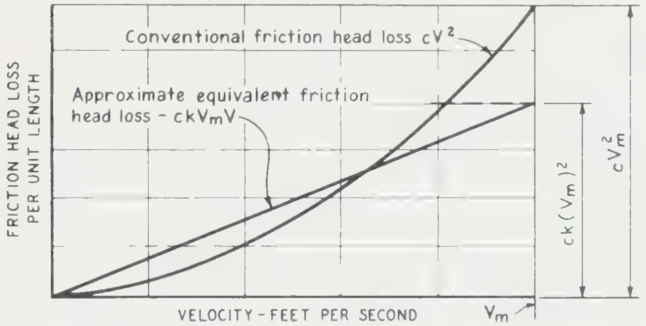

V_m = maximum velocity
k = factor assumed to fix position of best equivalent straight line

Straight line loss for any velocity $V = ck\,(V_m)^2\,\frac{V}{V_m} = ckV_mV$

Friction force drop per unit length $\partial x = \frac{\pi D^2}{4}\,wckV_mV\,\partial x = \frac{\pi D^2}{4}\,FV\,\partial x$

FIG. 3. Development of approximate equation for friction force term in water-hammer equations.

MECHANISM OF WAVE REFLECTION

With the basic differential relationships of water hammer at our disposal, we are now able to give independent mathematical confirmation to the wave reflection sequence outlined qualitatively in the introduction (Fig. 1). Referring to Fig. 4, the basic equations to be solved are

$$\frac{a^2\,\partial^2 P}{\partial x^2} = \frac{\partial^2 P}{\partial t^2} \tag{5}$$

$$-\frac{\partial P}{\partial x} = W\frac{\partial V}{\partial t} \tag{1}$$

The constants of integration are to be determined to comply with the two boundary conditions:

When $x = 0, \quad P = P_0$

and $x = L \quad V = 0$

Let us note very carefully at this point that no other boundary conditions whatever are adduced and in particular that no assumption whatever has been made regarding the genesis or character of reflections at the reservoir or at the valve. This means that the results we obtain regarding the internal mechanism of water hammer are exclusively the result of rigorous mathematical processes.

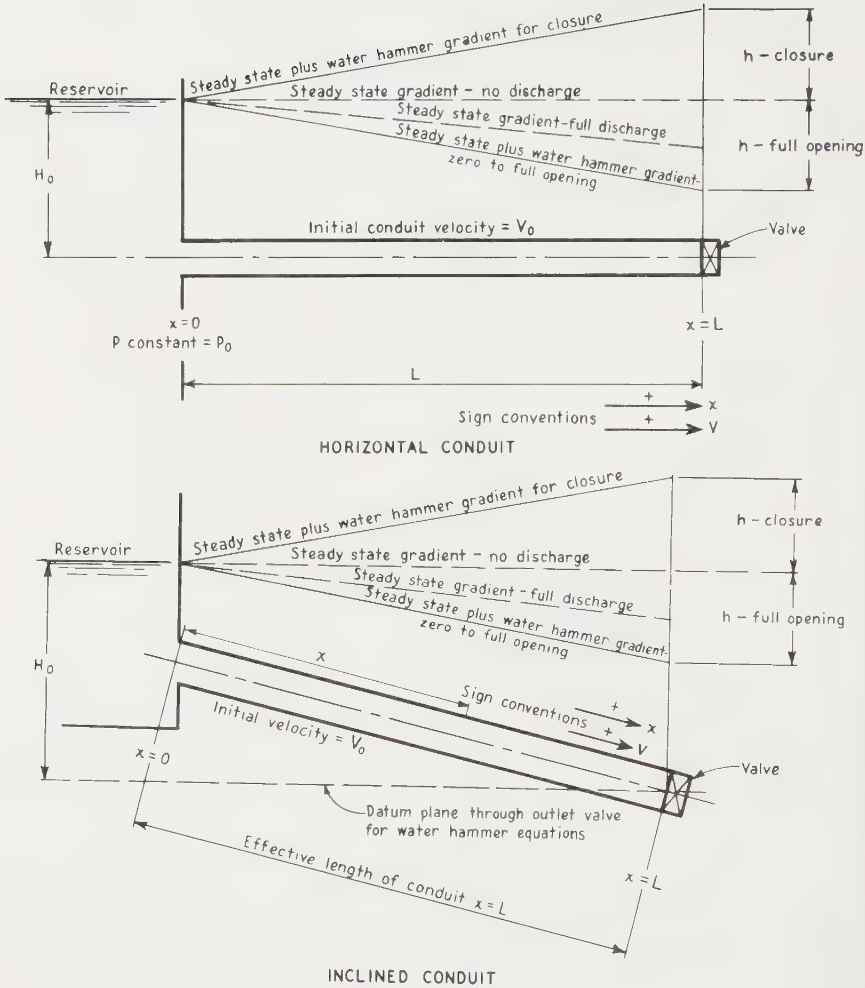

FIG. 4. Simple conduit with instantaneous valve closure.

For manipulative details of the solution the reader is referred to the current literature.[1]

The solution is given below in the form of an infinite summation of two wave components, the time of arrival of each successive component at the section x being denoted by the subscripts.

$$P = P_0 + \frac{waV_0}{g} \sum_{n=1}^{\infty} (-1)^{n+1} [1_{t > \frac{(2n-1)L - x}{a}} - 1_{t > \frac{(2n-1)L + x}{a}}] \tag{7}$$

$$V = V_0 \left[1 - \sum_{n=1}^{\infty} (-1)^{n+1} (1_{t > \frac{(2n-1)L - x}{a}} + 1_{t > \frac{(2n-1)L + x}{a}}) \right] \tag{8}$$

[1] RICH, GEORGE R., Water-hammer Analysis by the Laplace-Mellin Transformation, *Trans. ASME*, 1945, *Paper* 44–A38.

At the gate section $x = L$, the pressure equation becomes

$$P = P_0 + \frac{waV_0}{g}\left[1_{t>0} + 2\sum_{n=1}^{\infty}(-1)^n\, 1_{t>\frac{2nL}{a}}\right] \tag{9}$$

At the reservoir when $x = 0$, the velocity equation becomes

$$V = V_0\left[1_{t>0} - 2\sum_{n=1}^{\infty}(-1)^{n+1}\, 1_{t>\frac{(2n-1)L}{a}}\right] \tag{10}$$

The graphs of Eqs. (9) and (10) are given in Fig. 5 and, as will be seen immediately,

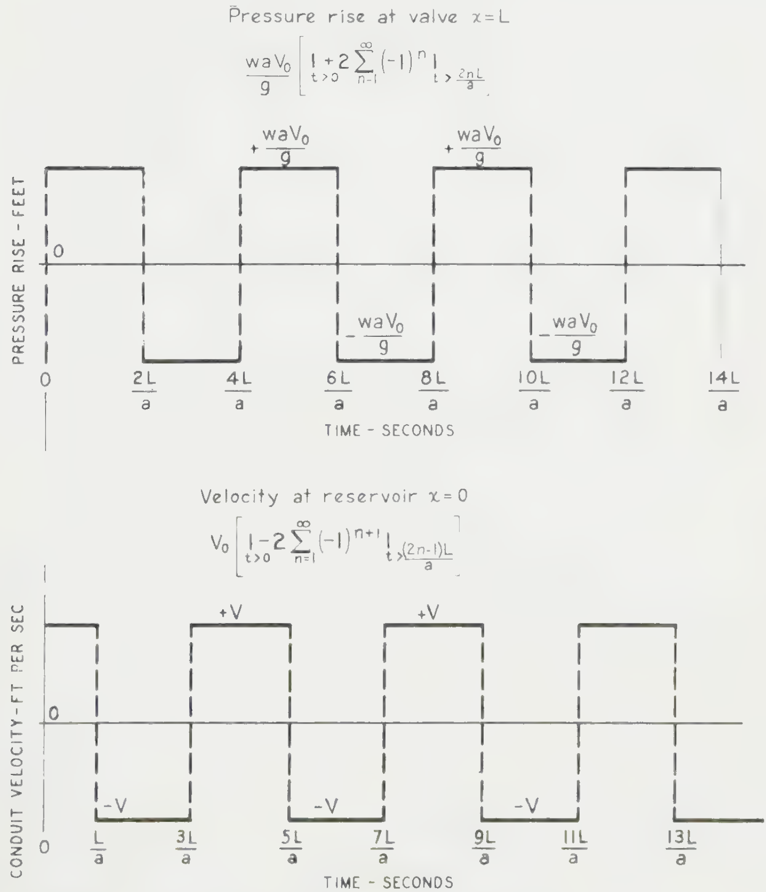

FIG. 5. Diagrams of pressure and velocity—simple conduit instantaneous valve closure. Conduit friction neglected.

are a complete confirmation of the physical process described qualitatively in the introduction (Fig. 1).

The sequence of wave propagation is summarized in the general rule that, at the reservoir, pressure waves are reflected with opposite sign and velocity waves with the same sign. At the control valve, pressure waves are reflected with the same sign and velocity waves with opposite sign.

Since the effect of the damping agent, friction, has not been included in the preceding analysis, the wave pattern shown in Fig. 5 will, as indicated by Eqs. (9) and (10), continue indefinitely with the time without attenuation. To illustrate the manner in which friction operates to damp down the wave motion, Fig. 6 has been calculated, based upon the solution of Eqs. (6) and (2),

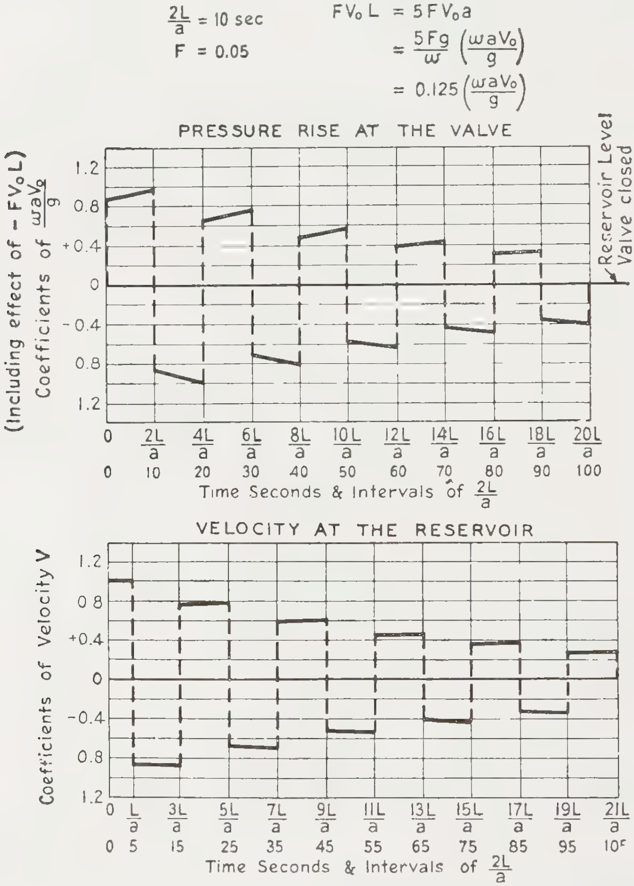

Fig. 6. Pressure rise and velocity—simple conduit instantaneous valve closure. Conduit friction included.

$$\frac{\partial P}{\partial x} + FV + W\frac{\partial V}{\partial t} = 0 \tag{6}$$

$$\frac{\partial V}{\partial x} + Q\frac{\partial P}{\partial t} = 0 \tag{2}$$

by the technique described in the current literature.[1] In this particular example, the conduit friction coefficient has been magnified far beyond any normal occurrence in order to accentuate the damping effect and make it more perceptible. In the great

[1] *Ibid.*

majority of cases ordinarily encountered in practice, the rate of attenuation would be so slow as to have no sensible effect upon the magnitude of water-hammer pressures and velocities, and it is of course for this very reason that it is almost invariably neglected in practical computation.

Unfortunately direct analytical solution of the basic differential equations for other than instantaneous closures is not possible when, as is customary, the time rate of decrease of valve opening with efflux velocity proportional to the square root of the steady state plus water-hammer head is specified as one of the boundary conditions. In fact it is because of this very impediment that the seemingly academic case of instantaneous valve closure becomes of such importance from the standpoint of practical detailed computation, by virtue of the assumption that the net actual pressure rise resulting from any gradual noninstantaneous closure may, with sufficient accuracy, be considered as consisting of a series of superimposed elemental square-topped waves, each generated by a small component element of valve movement in a correspondingly short interval of time.

The only difference then remaining for the case of more gradual closures is to take proper account of the effect of the partially open gate valve upon the reflected waves arriving from the reservoir at the downstream terminal section. As would naturally be expected under such conditions, the wave elements from the reservoir will be only partially reflected, the degree of reflection being dependent upon the relative amount of valve opening, the fully closed valve giving complete reflection.

The additional physical principle not yet utilized in our discussion, which controls and establishes the magnitude of wave reflection, is the discharge law corresponding to the setting at the particular instant of the terminal discharge mechanism. In the simplest case, that of a gate valve system in which the nozzle area is reduced according to a given function of the time, frequently a linear relation, the efflux velocity is assumed to follow the simple orifice law. When the terminal mechanism is a pump or turbine, the efflux velocity depends upon the machine speed, as well as the gate opening and total head, and must be taken from performance curves of the machine for conditions corresponding to the particular instant. In this case, algebraic formulation of the discharge law is not feasible.

The practical details of inserting this discharge mechanism law will be developed in greater detail in the illustrative examples given in the subsequent paragraphs. The only point to be emphasized at this juncture is that absolutely no additional compensation in the form of reflection factors is necessary. The truth of this statement can be verified by independent computation using the reflection factor method,[2] and also by deriving formulas for representative cases independently by the method of differential equations.[3] Since this feature has been one of the most troublesome in contemporary literature, it will not be superfluous to add that all derivations of reflection factors at the open control valve reduce simply to restatements of the orifice law and were introduced originally only in the attempt to obviate a portion of the trial-and-error detail in some forms of computation.

We have now forged all the basic tools required and may proceed to their application in various detailed methods of numerical calculation, the first, and in many respects the simplest, being that of arithmetic integration.

[1] *Ibid.* By prescribing the efflux velocity pattern, instead of the time rate of decrease of valve opening, direct analytical solution may be effected and general formulas obtained. Although this method appears to hold promise of future development, it cannot yet be considered to have advanced beyond the stage of research to general acceptance by practicing engineers.

[2] *ASME–ASCE Symposium on Water Hammer,* 1933. Glover, Robert E., Computations of Water-hammer Pressures in Compound Pipe, p. 66, Eq. (8), *et seq.*; *ibid.*, discussion of F. Knapp, p. 129 following Eq. (2); *ibid.*, High-speed Penstock Design, by A. W. K. Billings, O. H. Dodson, F. Knapp, and A. Santos, Jr., p. 38, Eq. (8), *et seq.*, and Fig. 4, p. 66.

[3] Rich, *op. cit.*

METHOD OF ARITHMETIC INTEGRATION

Water-hammer analysis by the method of arithmetic integration requires a comparative minimum of specialized technique and yet affords a direct and incisive means of studying every physical element of the process. To arrange the basic equations in the form most advantageous for step computation, we shall first write Eq. (1), using the notation of heads rather than pressures, and shall replace differentials by finite increments.

$$\Delta V = -g \frac{\Delta h \, \Delta t}{\Delta x} \tag{11}$$

$$Q = A(V_0 + \Sigma \, \Delta V) \tag{12}$$

For convenience, we shall select for the value of interval Δt some submultiple of L/a such as $L/4a$; then Δx will be the length of conduit traversed by the water-hammer wave in time Δt.

For the sake of simplicity in explanation, it will be assumed that the terminal mechanism is simply a gate valve in which the nozzle area is decreased linearly with the time. For the case of nonlinear decrease of valve area, an obvious appropriate modification will be made in the calculation; and for the case of a turbine or pump as a terminal mechanism the same general procedure will be followed except that the trial values of discharge would have to be taken from performance curves at the correct machine speed for the particular instant, head, and gate.

For linear reduction of valve area the discharge at the outlet at any instant will be

$$Q = \frac{Q_0 \times A_v \sqrt{H_0 + \Sigma \, \Delta h}}{A_{v_0} \sqrt{H_0}} \tag{13}$$

assuming constant values of discharge coefficients at all valve openings.

$\Sigma \Delta h$ is the sum of all direct and reflected (positive and negative) pressures up to and including the instant in question.

The mechanism of computation then follows directly from the conception of integration as a process of summation. By trial and error, we simply establish for each successive interval values of h and V that satisfy Eqs. (11), (12), and (13).

With respect to the pertinent question of partial reflections at the valve, we find that by arranging our intervals as even submultiples of L/a we shall, after time $2L/a$ has elapsed, have a reflection arriving from the reservoir at exactly each instant when we are completing the execution of one of our small gate movements. Since friction is neglected, every new elementary square-topped wave that is generated will continue its cycle of reflection according to Fig. 1, forever without diminution, except for the influence of partial reflection.

Now let us carefully examine the illustrative example, Table 1, in complete detail to satisfy ourselves that we actually do make the requisite correction to each reflected wave to compensate for partial reflection at the partly open control valve. For this purpose we select the interval at time 4.17 sec. At that time the wave originally generated at time 0.83 has returned to the valve with negative sign and we multiply it by 2 in column 7, because waves reaching the control valve are reflected upstream with the same algebraic sign.

If it were not for the arrival of this reflection, we should make the computation at time 4.17 sec exactly as we would in the case of the first four intervals. Then, to balance the trial-and-error computation, the value of Δh would be 80 instead of 105 and $\sqrt{H_0 + \Sigma \, \Delta h}$ would be $\sqrt{1{,}281 + 80}$ instead of $\sqrt{1{,}281 + 105 - 124}$. In other words, we have increased the value of Δh by 25 ft, and the negative wave reflected back upstream has the magnitude (62 − 25), or 37 ft instead of 62 ft; that is, about 60 per cent of the wave is reflected.

TABLE 1. ARITHMETIC INTEGRATION—SIMPLE CONDUIT (FOR LINEAR DECREASE OF VALVE AREA)

Conduit length L = 5,000 ft	Initial conduit velocity V = 12 fps
Conduit diameter = 15 ft	Wave velocity a = 3,000 fps
Conduit area = 177 sq ft	Initial head = 1,000 ft
Valve closure time = 10 sec	Initial Q = 2,120 cfs

For Δt = 0.83 sec,

$$\Delta V = \frac{\Delta h \times 32.2 \times 0.83}{2{,}500}$$

or

$$\text{Column (4)} = \frac{\text{Column (3)} \times 32.2 \times 0.83}{2{,}500}$$

$$\text{Column (8)} = \text{previous } (H_0 \Delta h) + \text{Column (3)} + \text{Column (7)}$$

$$\text{Column (10)} = \frac{2{,}120 \times \text{Column (9)} \times \sqrt{\text{Column (8)}}}{\sqrt{1{,}000}}$$

Note on calculation of reflection: Reflected wave component at time t = 4.17 sec equals direct wave component at time t = 0.83 sec × (−2).

Reflected wave component at time t = 7.50 sec equals direct wave component at time t = 0.83 sec × (+2), added to direct wave component at time t = 4.17 sec × (−2).

Reflected wave component at time t = 11.67 sec equals minus twice the sum of the direct wave component at time t = 0.83 sec plus the direct wave component at time t = 1.67 sec; plus twice the sum of the direct wave component at time t = 4.17 sec plus the direct wave component at time t = 5 sec; minus twice the sum of the direct wave component at time t = 7.50 sec plus the direct wave component at 8.33 sec.

(1) Time, sec	(2) Interval Δt, sec	(3) Δh at valve, ft	(4) Δv, fps	(5) V, fps	(6) $Q = 177V$, cfs	(7) $2\Delta h$ reflected from reservoir, ft	(8) Total head $H_0 + h$, ft	(9) Valve opening	(10) Cfs	(11) Column (8)—1,000 ft
0.00	....	.....	....	12.000	2,120	....	1,000.0	1.000	2,120	0
0.83	0.83	62.0	−0.661	11.339	2,010	....	1,062.0	0.916	2,008	62.0
1.67	0.84	65.0	−0.703	10.636	1,885	....	1,127.0	0.834	1,880	127.0
2.50	0.83	72.0	−0.770	9.866	1,745	....	1,199.0	0.750	1,747	199.0
3.33	0.83	82.0	−0.880	8.986	1,592	....	1,281.0	0.667	1,595	281.0
4.17	0.84	105.0	−1.140	7.846	1,390	−124.0	1,262.0	0.583	1,390	262.0
5.00	0.83	110.0	−1.175	6.671	1,180	−130.0	1,242.0	0.500	1,180	242.0
5.83	0.83	110.0	−1.175	5.496	973	−144.0	1,208.0	0.417	971	208.0
6.67	0.84	108.0	−1.171	4.325	764	−164.0	1,152.0	0.333	760	152.0
7.50	0.83	103.0	−1.102	3.223	571	− 86.0	1,169.0	0.250	573	169.0
8.33	0.83	100.0	−1.068	2.155	382	− 90.0	1,179.0	0.167	384	179.0
9.17	0.84	98.0	−1.058	1.907	194	− 76.0	1,201.0	0.083	194	201.0
10.00	0.83	102.5	−1.097	0	0	− 52.0	1,251.5	0	0	251.5
11.67	1.67	Valve closed at time t = 10.0 sec				−230.0	1,021.5	0	0	21.5
13.33	1.66	.....	....	......	.....	−273.0	748.5	0	0	−251.5
15.00	1.67	.....	....	......	.....	230.0	978.5	0	0	− 21.5
16.67	1.67	.....	....	......	.....	273.0	1,251.5	0	0	251.5
18.33	1.66	.....	....	......	.....	−230.0	1,021.5	0	0	21.5
20.00	1.67	.....	....	......	.....	−273.0	748.5	0	0	−251.5
21.67	1.67	.....	....	......	.....	230.0	978.5	0	0	− 21.5
23.33	1.66	.....	....	......	.....	273.0	1,251.5	0	0	251.5

If we chose, we could arrange the computation to show 80 − 37, or 43 ft, as the net head increment; carry it forward as 43 ft in the computation and enter the corresponding reflection $2L/a$ sec later at that value. We deliberately elect to make the entries separately and carry forward the reflection from each newly generated wave forever, simply because experience appears to indicate that we are better able to keep track of waves this second way and that fewer mistakes result. It will be apparent, upon examination, that the two methods of bookkeeping are in every respect equivalent; that is, 105 − 62 = 43 and 80 − 37 = 43.

One of the most important fields of application of water-hammer analysis by the arithmetic integration method is in the computation of speed variation[1] in turbines and pumps during opening or closure of the control valve. In a typical case, that of sudden loss of load by a hydroelectric generating unit, a certain definite interval of time is required to close the turbine gates; and during this time the energy of water flowing through the turbine is absorbed by the WR^2 of the generator and manifested as an increase in speed of rotation. As previously noted, this speed of rotation, head and gate opening at the particular instant determine the so-called setting of the turbine with respect to discharge. A solution of the problem reduces to a matter of trial-and-error balance between water hammer, power input to the machine, WR^2 of the generator, and instantaneous values of head, gate, and discharge.

In handling compound or branched pipes by the arithmetic integration method, the same general form of tabulation is applicable, and the only additional essential difference is that provision must be incorporated in the tabulation to facilitate keeping accurate track of wave reflections. It is believed that this is best arranged to suit the preferences of the particular computer. In this connection it has been the experience of the author that greater accuracy and much better understanding of the computation generally results from writing the actual basic relationships at each junction point rather than placing blind dependence upon general formulas for reflection and transmission coefficients. Only two elementary hydraulic principles are involved at junctions: (1) the total hydraulic pressure (steady state plus surge head) is the same for all branches and (2) to comply with hydraulic continuity, the sum of the discharges of the branches terminating in a junction point is zero, flows toward the junction point being counted positive, and flows away from the junction point being counted negative. The water-hammer wave velocities in each of the component elements terminating in a junction point will naturally reflect the diameters, wall thicknesses, and elastic moduli of the individual branches.

In general practice it has been customary in computation to substitute for the compound pipe a simple pipe of equivalent characteristics determined from the equations:

$$V = \frac{V_1L_1 + V_2L_2 + V_3L_3 + \cdots V_nL_n}{L}$$

$$a = \frac{a_1L_1 + a_2L_2 + a_3L_3 + \cdots a_nL_n}{L}$$

For comparatively slow rates of valve closure, this artifice does not appear to introduce any substantial error, but for rapid closures, particularly those approaching instantaneous closure, there is a marked discrepancy between the true magnitudes of water hammer and the superpressures yielded by use of the above equation.[2] In such cases it will generally be worth while to make more accurate determinations, taking full account of partial reflections at points in the conduit where the wave velocity changes.

[1] Strowger, E. B., and S. L. Kerr, Speed Changes of Hydraulic Turbines and Sudden Changes of Load, *Trans. ASME*, 1926, p. 220, Table I.

[2] Rich, *op. cit.* *ASME–ASCE Symposium on Water Hammer*, 1933. Billings, Dodson, Knapp, and Santos, *op. cit.*, p. 58, Fig. 8.

ANGUS GRAPHICAL METHOD

The graphical method developed by Prof. R. W. Angus and predicated upon the so-called interlocked series of Allievi furnishes an exceptionally rapid and easily understood means of solving the basic differential equations. To facilitate cross reference with basic literature, the differential equations in Art. 2 are based upon taking $x = 0$ at the reservoir and $x = L$ at the control valve. However, the literature dealing with the Allievi and Angus methods employs $x = L$ at the reservoir and $x = 0$ at the control valve, so that we shall use the latter convention in Arts. 5 and 6. This is equivalent in Eqs. (1) and (2), Art. 2, to replacing x by $L - x$, and since the literature for Arts. 5 and 6 uses the notation of heads rather than pressures, we shall also replace P by wH. This gives the basic equations in the following form:[1]

$$-\frac{\partial H}{\partial x} = \frac{1}{g}\frac{\partial V}{\partial t} \tag{14}$$

$$-\frac{\partial V}{\partial x} = \frac{g}{a^2}\frac{\partial H}{\partial t} \tag{15}$$

As can readily be verified by differentiation, the so-called general integral solution of this pair of partial differential equations[2] is

$$H - H_0 = F\left(t - \frac{x}{a}\right) + f\left(t + \frac{x}{a}\right) \tag{16}$$

$$V_0 - V = \frac{g}{a}F\left(t - \frac{x}{a}\right) - \frac{g}{a}f\left(t + \frac{x}{a}\right) \tag{17}$$

valid for every x along the entire conduit. It is well known that F and f[3] represent two traveling pressure heads propagated in the upstream and downstream directions with constant velocity a and without mutual interference.

Now, in these two preceding equations let us place $x = 0$ to obtain conditions at the control valve. Then, in view of the relatively high velocity of wave propagation, we may, with no practical sacrifice in accuracy, conceive the gate motion to consist of a series of partial gate movements executed at intervals $\frac{2L}{a}, \frac{4L}{a}, \frac{6L}{a}, \frac{8L}{a}$. Since, in the first interval $t_1 < \frac{2L}{a}$, no negative reflection will have returned from the reservoir, the pressure head will be due to the direct wave alone. Now, write Eqs. (16) and (17) to represent conditions at the control valve during these successive intervals.[3]

$$\begin{aligned} H_1 &= H_0 + F_1 \\ H_2 &= H_0 + F_2 - F_1 \\ H_3 &= H_0 + F_3 - F_2 \\ &\cdots\cdots\cdots \end{aligned} \tag{18}$$

$$\begin{aligned} V_1 &= V_0 - \frac{g}{a}F_1 \\ V_2 &= V_0 - \frac{g}{a}(F_1 + F_2) \\ V_3 &= V_0 - \frac{g}{a}(F_2 + F_3) \\ &\cdots\cdots\cdots \end{aligned} \tag{19}$$

[1] ALLIEVI, LORENZO, "The Theory of Water Hammer," translated by Eugene E. Halmos, Rome, 1925, Eqs. IV and V, p. IX.

[2] ANGUS, R. W., Simple Graphical Solution for Pressure Rise in Pipes and Pump Discharge Lines, *Eng. Jour.* of the Engineering Institute of Canada, February, 1935, p. 74, Eqs. (6), (7), and (8). Article 5 is very largely an abstract of this excellent paper.

[3] ALLIEVI, *op. cit.*, p. 6; WEBSTER, *loc. cit.*

Eliminating $F_1, F_2, F_3 \ldots$ from Eqs. (18) and (19), we obtain

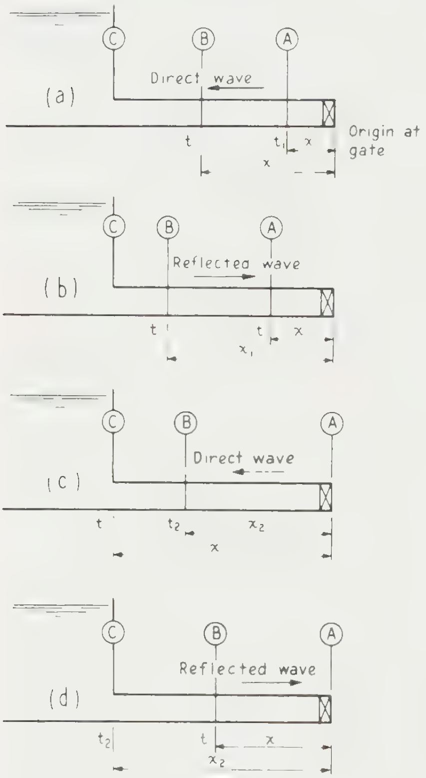

FIG. 7. Basic notation. Angus graphical method.

$$H_1 - H_0 = \frac{a}{g}(V_0 - V_1)$$
$$H_1 + H_2 - 2H_0 = \frac{a}{g}(V_1 - V_2)$$
$$H_2 + H_3 - 2H_0 = \frac{a}{g}(V_2 - V_3)$$
$$\cdots\cdots\cdots\cdots$$
$$H_n + H_{n-1} - 2H_0 = \frac{a}{g}(V_{n-1} - V_n) \tag{20}$$

Equation (20) gives the relation between values of pressure and velocity at the start of each successive interval $2L/a$. From the general character of the wave motion and Eqs. (16) and (17) we perceive that the function F, the sum of all direct or positive pressures at the time t taken at the section x along the conduit is identical with the same function F taken at the gate at a time x/a sec earlier. Correspondingly, the sum of all reflected or negative pressures at the section x for time t is the same as the function f at the gate x/a sec later. While Eq. (20) applies only to pressure rise at the valve at the ends of two successive intervals of $2L/a$, Eqs. (16) and (17) apply to any point on the pipe.

First, adding Eqs. (16) and (17), we obtain

$$H - H_0 = -\frac{a}{g}(V_0 - V) + 2F\left(t - \frac{x}{a}\right) \tag{21}$$

Second, subtracting Eqs. (16) and (17),

$$H - H_0 = +\frac{a}{g}(V_0 - V) + 2f\left(t + \frac{x}{a}\right) \tag{22}$$

Let A and B be any two sections on the pipe, as shown in Fig. 7a. Equation (21) then gives

$$H_{Bt} - H_{Bo} = -\frac{a}{g}(V_{Bo} - V_{Bt}) + 2F\left(t - \frac{x}{a}\right) \tag{23}$$

$$H_{At1} - H_{Ao} = -\frac{a}{g}(V_{Ao} - V_{At1}) + 2F\left(t_1 - \frac{x_1}{a}\right) \tag{24}$$

Since the conduit is of uniform diameter

$$V_{Ao} = V_{Bo}$$

and, since the velocity head is assumed negligible,

$$H_{Ao} = H_{Bo}$$

It is also apparent from Fig. 7*a* that

$$t - t_1 = \frac{x - x_1}{a}$$

so that

$$F\left(t - \frac{x}{a}\right) = F\left(t_1 - \frac{x_1}{a}\right)$$

We then obtain by subtracting Eq. (24) from Eq. (23),

$$H_{Bt} - H_{At1} = +\frac{a}{g}(V_{Bt} - V_{At1}) \tag{25}$$

By the same type of reasoning, the reflected wave Eq. (22) and Fig. 7*b* afford the following:

$$H_{Bt1} - H_{Bo} = +\frac{a}{g}(V_{Bo} - V_{Bt1}) + 2f\left(t_1 + \frac{x_1}{a}\right) \tag{26}$$

$$H_{At} - H_{Ao} = +\frac{a}{g}(V_{Ao} - V_{At}) + 2f\left(t + \frac{x}{a}\right) \tag{27}$$

From Fig. 7*b*,

$$t - t_1 = \frac{x_1 - x}{a}$$

or

$$t + \frac{x}{a} = t_1 + \frac{x_1}{a}$$

and subtracting Eq. (26) from Eq. (27) gives

$$H_{At} - H_{Bt1} = -\frac{a}{g}(V_{At} - V_{Bt1}) \tag{28}$$

If we are analyzing three points on the pipe, A, B, and C in Fig. 7*c*, the following equations may be written by means of Eqs. (28) and (25):

Direct wave, Fig. 7*c*: $$H_{Bt} - H_{Ct2} = -\frac{a}{g}(V_{Bt} - V_{Ct2}) \tag{29}$$

Indirect wave, Fig. 7*d*: $$H_{Ct} - H_{Bt2} = +\frac{a}{g}(V_{Ct} - V_{Bt2}) \tag{30}$$

Equations (29) and (30) are also applicable if the pipes AB and BC are of different diameters, the only change being in the value of a, which is different for each section, it being as usual assumed that the difference in velocity heads in the two sections is negligible compared to H_0.

Equations (25), (28), (29), and (30), used in conjunction with the law correlating gate motion, head H, and velocity V, permit us to solve all problems.

It is generally more convenient to use ratios H/H_0 and V/V_0 instead of H and V, so that we shall denote the former by h and the latter by v. Following Allievi's notation the quantity $aV_0/2gH_0$ will be designated ρ. Dividing Eq. (25) by H_0 gives

$$\frac{H_{Bt}}{H_0} - \frac{H_{At1}}{H_0} = \frac{aV_0}{gH_0}\left(\frac{V_{Bt}}{V_0} - \frac{V_{At1}}{V_0}\right)$$

or

$$\left.\begin{aligned} h_{At1} - h_{Bt} &= +2\rho(v_{At1} - v_{Bt}) && \text{Fig. 11}a \\ h_{Bt1} - h_{At} &= -2\rho(v_{Bt1} - v_{At}) && \text{Fig. 11}b \\ h_{Ct2} - h_{Bt} &= -2\rho(v_{Ct2} - v_{Bt}) && \text{Fig. 12}b \\ h_{Bt2} - h_{Ct} &= +2\rho(v_{Bt2} - v_{Ct}) && \text{Fig. 12}a \end{aligned}\right\} \tag{31}$$

Now the relation between gate setting and pipe velocity is obviously

$$\frac{V}{V_0} = E\sqrt{\frac{H}{H_0}} \qquad \text{or} \qquad v = E\sqrt{h}$$

where E varies only with the gate setting and is usually assumed to vary linearly with the time, starting with $E = 1$ for full gate.

Equations (31) are the loci of two series of parallel lines with slopes equal to $\tan + 2\rho$ and $\tan - 2\rho$. Conditions at the reservoir are always represented by some

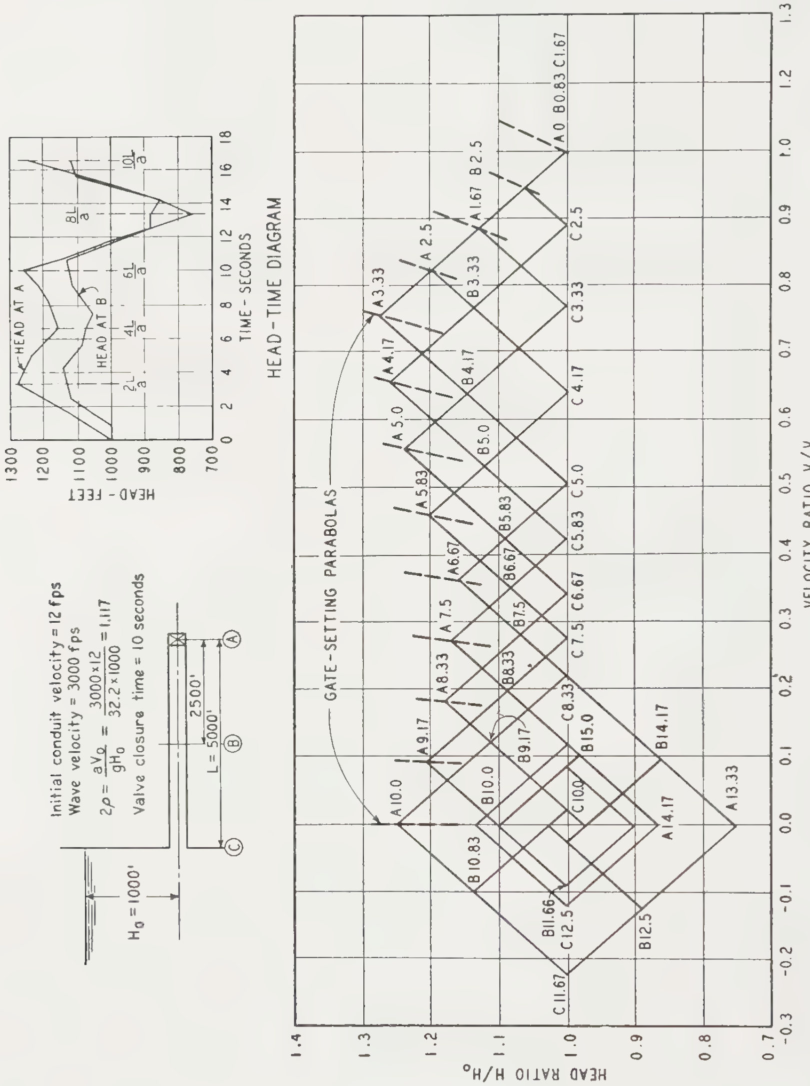

Fig. 8. Graphical analysis—simple conduit—gradual closure. Conduit friction neglected.

point on the horizontal line $Y = 1$, because there $\dfrac{H}{H_0} = 1$, if conduit friction is neglected. Conditions at the valve will be given by the intersection of the lines of negative slope with the curves representing the orifice discharge relationship.

Now let us apply the theory we have developed to solution of the identical problem solved by arithmetic integration in Table 1 of the preceding article, regarding the graphical construction, Fig. 8, not as an exercise in drafting but rather as applied analytic geometry, which enables us to make rapid solution of many pairs of simultaneous equations.

We first plot the parabolas correlating gate opening, head, and velocity for the times $t = 3.33$ sec or $2L/a$ and 6.67 sec or $4L/a$. Initial conditions are represented by the point $h = 1$, $v = 1$, and this will obviously hold true for $B_{0.83}$ and $C_{1.67}$ as well as A_0. Our first equation will be written between $C_{1.67}$ and $A_{3.33}$:

$$h_{C1.67} - h_{A3.33} = -2\rho(v_{C1.67} - v_{A3.33})$$

To plot this equation we draw a straight line of negative slope from the point $h = 1$, $v = 1$, or $C1.67$, to intersect the parabola covering all possible simultaneous values of head and discharge for the gate setting at time $t = 3.33$ sec or $2L/a$, the equation of this parabola being $v = 0.667\sqrt{h}$. The intersection then gives the simultaneous solution of the respective linear and second-degree equations and so establishes the correct relative values of head h and velocity v at $t = 3.33$. We mark the point $A_{3.33}$.

In similar fashion the second equation may conveniently be written between A at time $t = 3.33$ sec and C at 5.00 sec:

$$h_{A3.33} - h_{C5.00} = +2\rho(v_{A3.33} - v_{C5.00})$$

We draw the straight line representing this equation starting from $A_{3.33}$ and produce it downward with a positive slope until it intersects the horizontal axis, which, since conduit friction is neglected, represents all possible relative values of head $h = 1.00$ and velocity v. The intersection will establish conditions at the reservoir and of the line for $t = 5.00$ sec.

We next repeat the process for the equations

$$h_{C5.00} - h_{A6.67} = -2\rho(v_{C5.00} - v_{A6.67})$$

and

$$h_{A6.67} - h_{C8.33} = +2\rho(v_{A6.67} - v_{C8.33})$$

using the intersection of the first of these equations with the gate-setting parabola for $t = 6.67$ sec.

Finally we draw the line of negative slope from point $C8.33$, representing equation

$$h_{C8.33} - h_{A10.00} = -2\rho(v_{C8.33} - v_{A10.00})$$

to intersect the vertical axis, which is the gate-setting parabola for gate opening zero, giving us the relative head ratio at the gate at the instant of closure.

The equations governing the perpetual cycles of afterwaves following valve closure are

$$\begin{aligned}
h_{A10.00} - h_{C11.67} &= +2\rho(v_{A10.00} - v_{C11.67}) \\
h_{C11.67} - h_{A13.33} &= -2\rho(v_{C11.67} - v_{A13.33}) \\
h_{A13.33} - h_{C15.00} &= +2\rho(v_{A13.33} - v_{C15.00}) \\
h_{C15.00} - h_{A16.67} &= -2\rho(v_{C15.00} - v_{A16.67})
\end{aligned}$$

giving the closed diamond-shaped figure with corners $A10.00$, $C11.67$, $A13.33$, $C15.00$, and $A16.67$.

It will also be interesting to see how easily we may now obtain the transient values at the point B midway along the conduit.

The first step is to complete the gate-setting parabolas for all 12 intervals of 0.83 sec. As previously noted, the point $h = 1$, $v = 1$ will represent $A0$, $B0$, $C0$, $B0.83$, $C0.83$ and $C1.67$. To establish $A0.83$, we find the intersection of

$$h_{B0} - h_{A0.83} = -2\rho(v_{B0} - v_{A0.83})$$

with the parabola for $t = 0.83$. $A1.67$ is likewise found from the intersection of

$$h_{B0.83} - h_{A1.67} = -2\rho(v_{B0.83} - v_{A1.67})$$

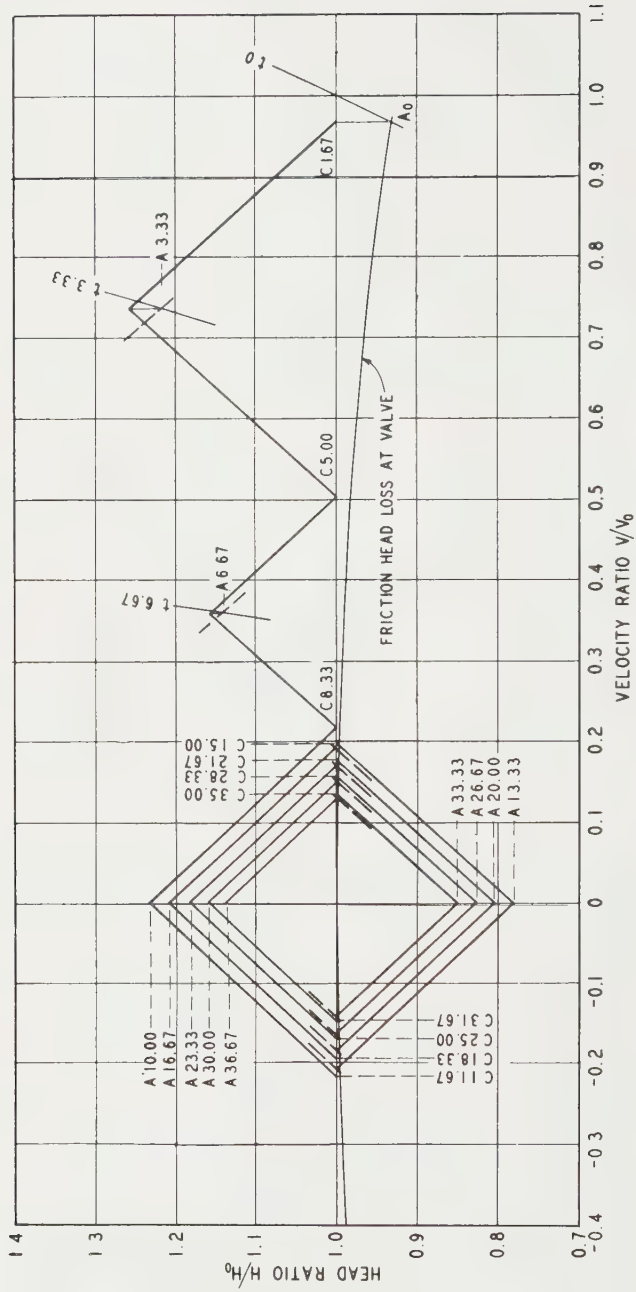

HEAD RATIO H/H_0
VELOCITY RATIO V/V_0
FRICTION HEAD LOSS AT VALVE
A_0
C 1.67
A 3.33
C 5.00
A 6.67
C 8.33
C 15.00
C 21.67
C 28.33
C 35.00
A 33.33
A 26.67
A 20.00
A 13.33
A 10.00
A 16.67
A 23.33
A 30.00
A 36.67
C 31.67
C 25.00
C 18.33
C 11.67

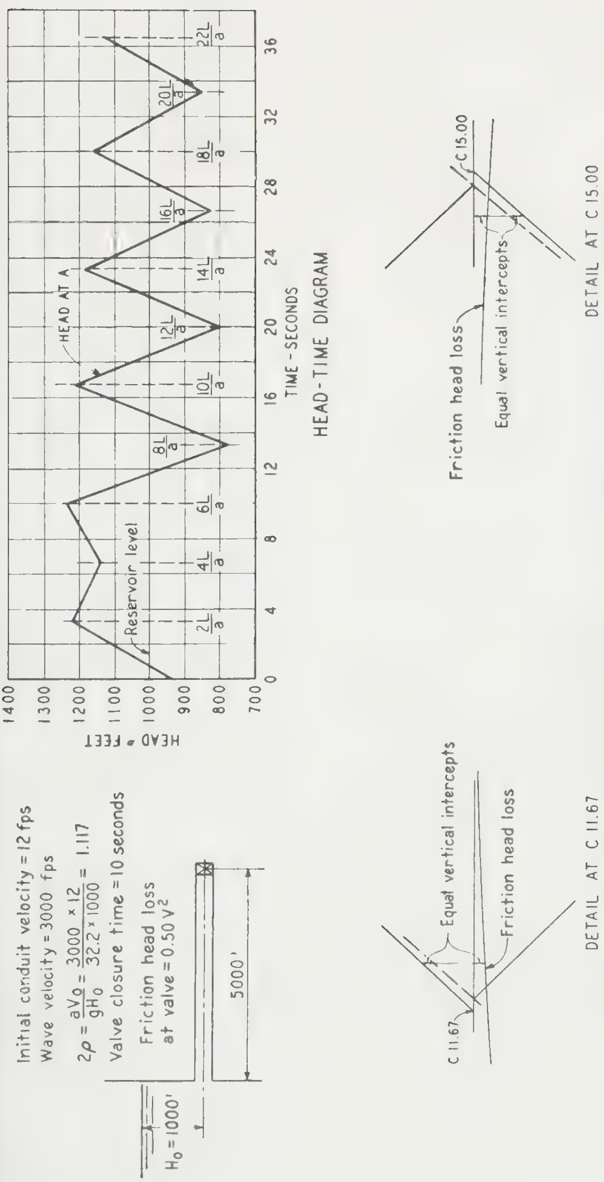

FIG. 9. Graphical analysis—simple conduit—gradual closure. Conduit friction included.

with the parabola for $t = 1.67$. Also, $A2.50$ is determined by the intersection of

$$h_{C0.83} - h_{A2.50} = -2\rho(v_{C0.83} - v_{A2.50})$$

$C2.50$ if found from the intersection of

$$h_{A0.83} - h_{C2.50} = +2\rho(v_{A0.83} - v_{C2.50})$$

and the horizontal axis.

It is evident that $B1.67$ is the same as $A0.83$ by drawing from $C2.50$:

$$h_{B1.67} - h_{C2.50} = +2\rho(v_{B1.67} - v_{C2.50})$$

$B3.33$ is obtained from the intersection of

$$h_{A2.50} - h_{B3.33} = +2\rho(v_{A2.50} - v_{B3.33})$$

and

$$h_{C2.50} - h_{B3.33} = -2\rho(v_{C2.50} - v_{B3.33})$$

and the remaining points of the charts are obtained by a continuation of the same process.

In the present state of our technique, the direct analytical solution of the basic differential equations is the only method capable of distributing the effect of friction along the conduit in accordance with nature. The graphical method, however, enables us to obtain very satisfactory and useful results by means of the artifice of lumping the cumulative effect of friction at certain selected points, most frequently at the control valve.

As an illustration of the method of application (Fig. 9), let us incorporate the effect of conduit friction in the previous example, assuming for simplicity that the aggregate friction head loss at the valve is represented by the expression $0.50v^2$, where v is the instantaneous value of total velocity at the valve. Next plot a curve of this equation below the horizontal axis, as indicated, so that the vertical intercept will represent the aggregate relative friction-head loss at the valve for various velocity ratios.

Then point $A0$, representing initial conditions at the valve, will be located at the intersection of the valve-setting parabola for the time $t = 0$, and the friction-head loss curve. Point $C1.67$, representing conditions at the reservoir for all times up to $t = 1.67$, will then be located on the horizontal axis directly above A, the intercept representing the aggregate steady-state friction-head loss along the conduit from C to A. But as our basic system of equations has been developed on the basis of neglecting friction, we shall continue to plot our fundamental network of solid lines as representing conditions with friction effect deducted, and shall apply dotted line corrections for friction at all points A. Obviously no such correction will be necessary until we reach the zone of afterwaves for all points C.

The method will be readily understood by explaining the true location of $A3.33$. The basic equation with friction neglected is

$$h_{C1.67} - h_{A3.33} = -2\rho(v_{C1.67} - v_{A3.33})$$

So starting at $C1.67$, produce the requisite solid line of negative slope beyond the intersection with the gate-setting parabola for $t = 3.33$. Then in the vicinity of this intersection transfer the range of intercepts from the friction-head loss curve to give the dotted line. The intersection of the dotted line with the gate-getting parabola gives the true location of $A3.33$.

To proceed in determing $C5.00$ we revert to our fundamental system of solid lines by drawing the vertical line upward from $A3.33$ to intersect the first solid line $C1.67$-$A3.33$. To locate $C5.00$ we draw the line of positive slope from the point so found to

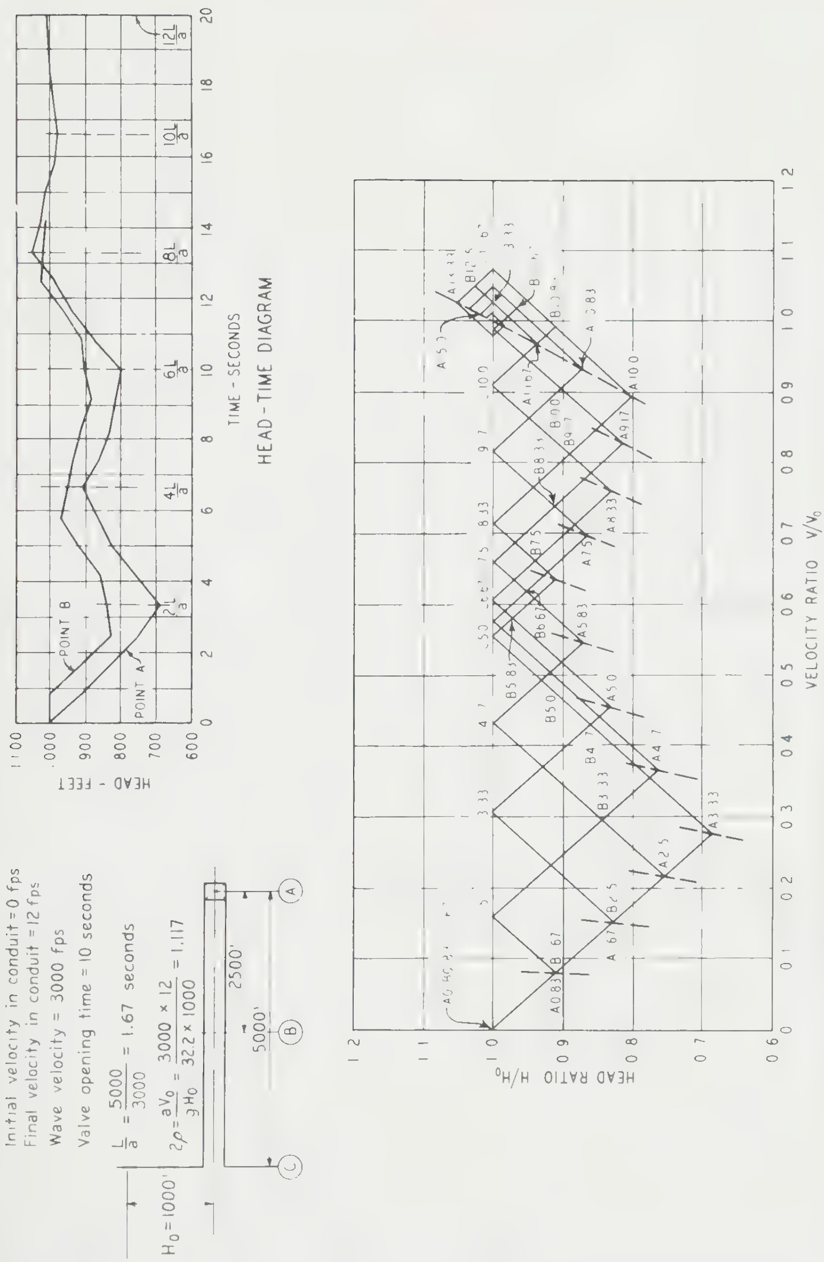

FIG. 10. Graphical analysis simple conduit gradual opening. (Conduit friction neglected.)

intersect the horizontal axis to give the true position according to the equation

$$h_{A3.33} - h_{C5.00} = +2\rho(v_{A3.33} - v_{C5.00})$$

The remaining points are established in similar fashion.

When we reach the zone of afterwaves, the most convenient place to apply the

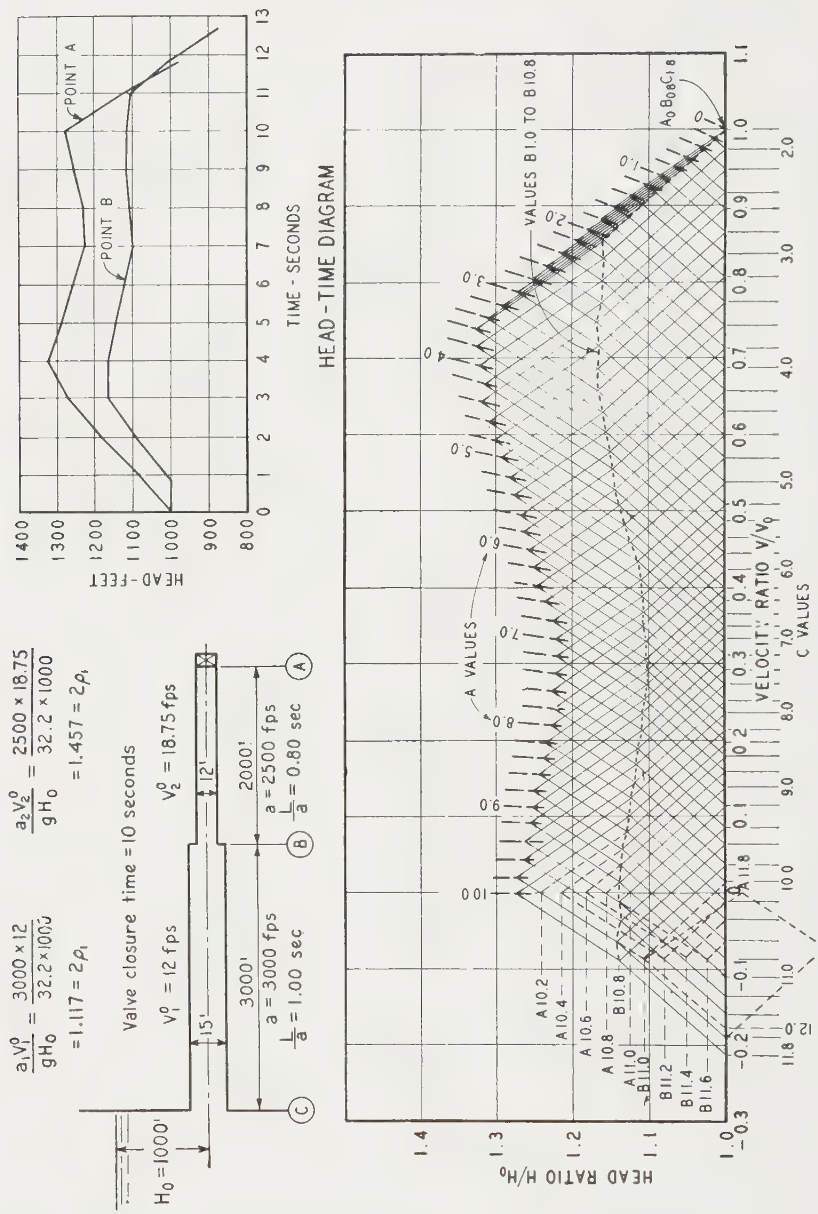

FIG. 11. Graphical analysis—compound conduit—gradual closure. Conduit friction neglected.

lumped friction correction is to the points C, fairly close to the friction-loss intercept curve. The key suggestion to keep in mind is that friction operates to decrease the conduit velocity at C, whether the conduit flow is in the positive or the negative direction. This explains why the dotted line is drawn below the solid for $C11.67$ and above the solid for $C15.00$. A very interesting exercise to develop better understanding of the method is to check Fig. 6, remembering, of course, to replace the curve cv^2 by the assumed straight-line friction loss.

Figure 10 shows the construction for the case of the simple conduit, friction neglected, under gradual opening; while Fig. 11 illustrates the solution of the compound pipe for gradual closure with friction neglected. It will be noted at once for the latter problem that the effect of differences in wave velocity or diameter of the component sections of the pipe is simply to change the values of slope of the corresponding straight lines. The number of intersections necessary to establish the solution is noticeably greater than would be expected from comparison with the illustrations for this case usually given in textbooks. This is because the latter examples are prefabricated so that the reflection times of the component sections of the conduit are even multiples. In actual practice this is seldom the case, so that Fig. 11 represents the degree of complexity normally to be expected. If only slight changes in the conditions of the given problem are sufficient to make the reflection times of the component sections even multiples, the resultant solution is obviously very greatly simplified; but more often than not changes of substantial magnitude would be necessary, and these could not be effected without introducing serious error. Before proceeding with the analysis of the more involved problems in branched and compound system, the engineer should consult Prof. Angus' excellent article.[1]

ALLIEVI CHART METHOD

By a combination of the so-called interlocked series equations and a rather cumbersome graphical device since superseded by the Angus method, the great pioneer investigator, Lorenzo Allievi, developed charts that are probably still the most widely used devices for the rapid solution of the elem ntary conventional cases of water-hammer analysis. It should be emphasized, however, that these charts have, strictly speaking, a comparatively limited field of applicability. Their derivation is predicated upon the fulfillment of two conditions that in many cases are not even remotely approached. These fundamental assumptions are that the nozzle area at the control valve is decreased or increased linearly with the time and that the efflux velocity at the nozzle at any instant is proportional to the square root of the sum of the steady-state plus water-hammer heads.

Obviously when the terminal mechanism is a centrifugal pump or hydraulic turbine operating through a transient range of speeds, the efflux velocity follows the law of the machine performance curve for the individual mechanism and departs markedly from the conventional orifice law. In commercial turbomachines not only is the discharge dependent upon the instantaneous speed but still further complication results from the fact that the gate motion is characterized by intervals of dead and cushioning time and is accordingly not at all a linear relationship. Results obtained by the application of Allievi charts to such cases may very naturally produce wide discrepancies from the true values of transient pressure and velocity.

Nevertheless, when used within their intended zone of application, the Allievi diagrams do effect an exceedingly great saving in time and labor for determining maximum or minimum point values. Allievi's great ingenuity in the use of his so-called Cartesian synopsis enabled him to summarize the entire field of uniform linear closure by means of two basic parameters, the pipe-line constant $\rho = \dfrac{aV_0}{2gH_0}$ and the valve operation or time constant $\theta = \dfrac{aT}{2L}$. The maximum rise or fall, as the case may be, is then taken from a single reading of the applicable chart, the dotted curved lines on the chart for closure indicating the interval in which maximum point pressure occurs. The charts do not enable us to plot a time history of the water-hammer wave.

[1] ANGUS, ROBERT W., Graphical Analysis of Water Hammer in Branched and Compound Pipes *Trans. ASCE*, 1939.

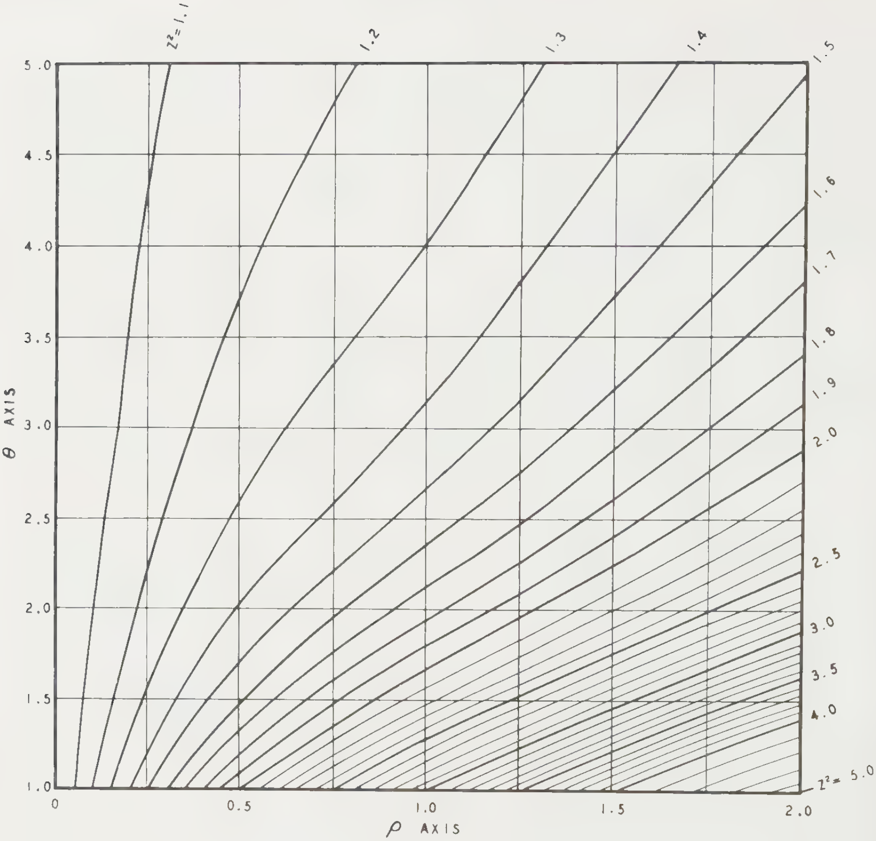

FIG. 12. Allievi diagram. Maximum pressure rise for uniform gate motion and simple conduits (for small values of ρ and θ).

As the first illustrative example in the use of the Allievi charts, let us establish the maximum values of pressure rise for the case covered by the arithmetic integration method in Table 1 and by the Angus graphical method in Fig. 8.

Simple Conduit—Gradual Closure
Conduit Friction Neglected

Initial head H_0	1,000 ft
Initial velocity in conduit	12 fps
Water-hammer wave velocity	3,000 fps
Valve closure time	10 sec
Length of pipe line	5,000 ft

$$\text{Pipe-line constant } \rho = \frac{aV_0}{2gH_0} = \frac{3{,}000 \times 12}{2 \times 32.2 \times 1{,}000} = 0.558$$

$$\text{Valve operation constant } \theta = \frac{aT}{2L} = \frac{3{,}000 \times 10}{2 \times 5{,}000} = 3.00$$

From Fig. 12 (small values of ρ and θ),

$$Z^2 = \frac{H_0 + h_{\max}}{H_0} = \frac{1{,}000 + h_{\max}}{1{,}000} = 1.280$$

Solving, maximum pressure rise at valve $= h_{\max} = 280$ ft. Since the point $\rho = 0.56$, $\theta = 3.00$ lies

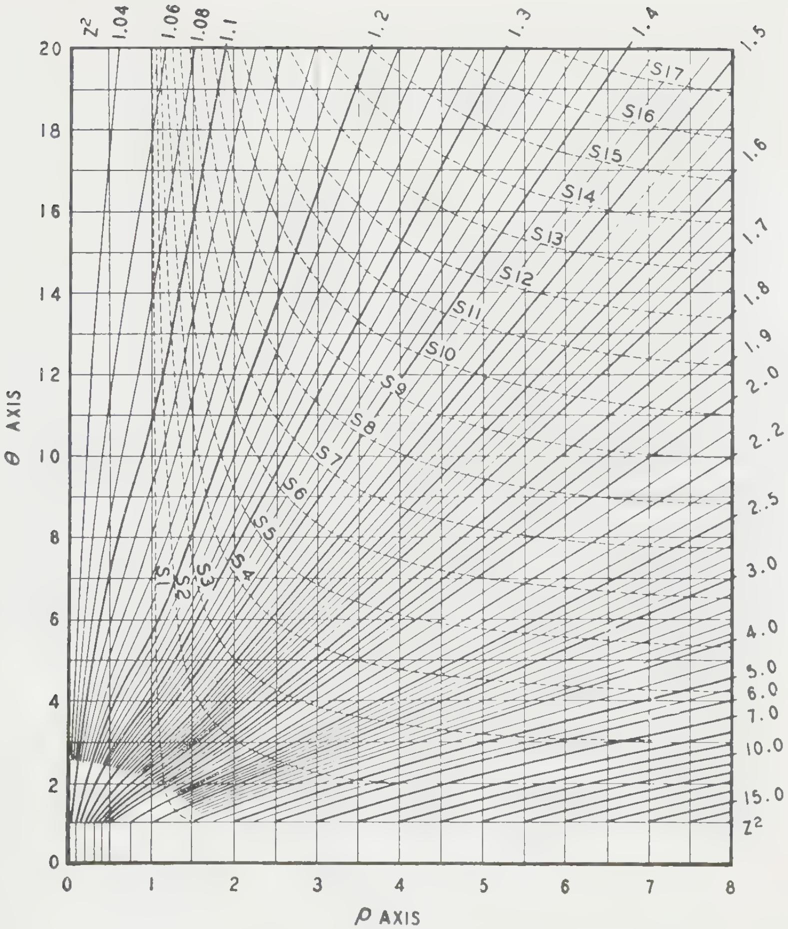

FIG. 13. Allievi diagram. Maximum pressure rise for uniform gate motion and simple conduits (for intermediate values of ρ and θ).

to the left of dotted line $S1$, Fig. 12, the maximum value of pressure rise occurs at some time during the first interval $2L/a$, or between $t = 0$ and $t = 3.33$ sec.

This checks very closely the values obtained by the arithmetic integration and graphical methods.

As a typical example of pressure drop during gradual opening by means of the Allievi charts, let us solve the problem given graphically in Fig. 10.

Simple Conduit—Gradual Opening
Conduit Friction Neglected

Initial head H_0	1,000 ft
Final velocity in conduit	12 fps
Water hammer wave velocity	3,000 fps
Valve opening time	10 sec
Length of pipe line	5,000 ft

$$\text{Pipe-line constant } \rho = \frac{aV_0}{2gH_0} = \frac{3{,}000 \times 12}{2 \times 32.2 \times 1{,}000} = 0.558$$

$$\text{Valve operation constant } \theta = \frac{aT}{2L} = \frac{3{,}000 \times 10}{2 \times 5{,}000} = 3.00$$

From Fig. 15,

$$Z^2 = \frac{H_0 - h}{H_0} = \frac{1{,}000 - h}{1{,}000} = 0.700$$

The pressure drop h is = 300 ft which checks quite closely the value obtained by the graphical method.

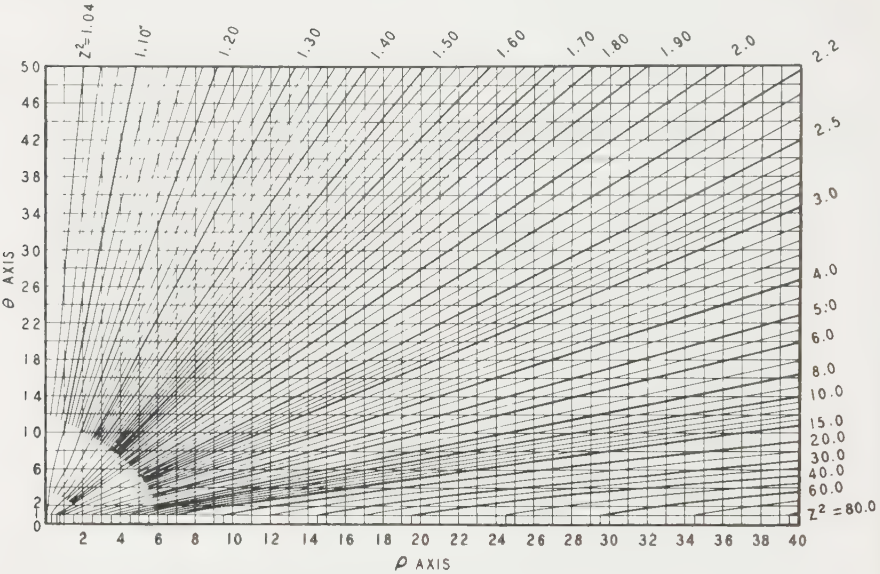

FIG. 14. Allievi diagram. Maximum pressure rise for uniform gate motion and simple conduits (for large values of ρ and θ).

As a third and final illustrative example in the use of the Allievi charts, let us check the compound pipe analyzed graphically in Fig. 11.

Compound Conduit—Gradual Closure
Conduit Friction Neglected
(See Fig. 11)

Initial head H_0	1,000 ft
Valve closure time	10 sec
V_1	12 fps
V_2	18.75 fps
Wave velocity a_1	3,000 fps
Wave velocity a_2	2,500 fps
Length L_1	3,000 ft
Length L_2	2,000 ft

$$\text{Equivalent conduit velocity } V = \frac{V_1L_1 + V_2L_2}{L_1 + L_2}$$

$$= \frac{12 \times 3{,}000 + 18.75 \times 2{,}000}{3{,}000 + 2{,}000} = 14.7 \text{ fps}$$

$$\text{Equivalent wave velocity } a = \frac{a_1L_1 + a_2L_2}{L_1 + L_2}$$

$$= \frac{3{,}000 \times 3{,}000 + 2{,}500 \times 2{,}000}{3{,}000 + 2{,}000} = 2{,}800 \text{ fps}$$

$$\text{Pipe-line constant } \rho = \frac{aV_0}{2gH_0} = \frac{2{,}800 \times 14.7}{2 \times 32.2 \times 1{,}000} = 0.64$$

$$\text{Valve operation constant } \theta = \frac{aT}{2L} = \frac{2{,}800 \times 10}{2 \times 5{,}000} = 2.80$$

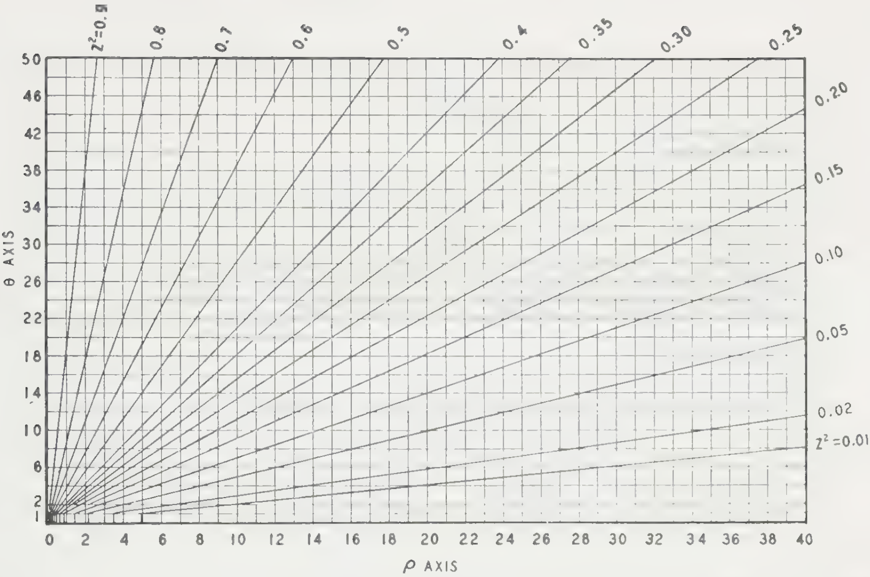

FIG. 15. Allievi diagram. Maximum fall in pressure for uniform gate motion and simple conduits.

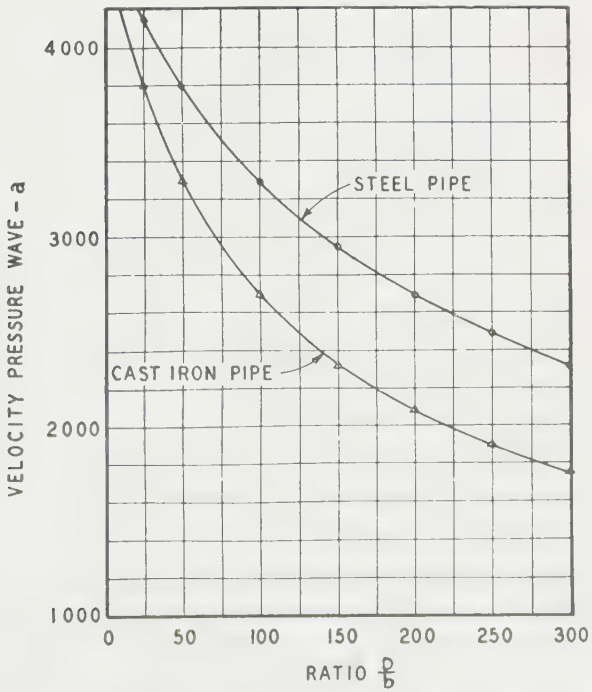

FIG. 16. Chart for calculation of velocity of pressure wave in cast-iron and steel pipe.

From Fig. 12 (small values of ρ and θ),

$$Z^2 = \frac{H_0 + h_{max}}{H_0} = \frac{1{,}000 + h_{max}}{1{,}000} = 1.320$$

Solving, the maximum pressure rise at the valve is 320 ft and occurs between the time 0 and 3.60 sec, giving a close check on the graphical analysis, Fig. 11.

There is one feature[1] of the Allievi charts that warrants particular emphasis. It will be noted that over the major portion of the diagram, Fig. 12, the radial lines giving value of Z^2 are straight, but that in the lower left-hand corner there is a pronounced break in slope. This means that in many cases closures starting from part gate with proportionally reduced velocity will produce higher water hammer than closure from the fully open position and full discharge velocity. For this reason, it is good practice to test all possible partial closures to establish the true maximum. The following example illustrates the procedure.

Simple Conduit—Gradual Closure
Conduit Friction Neglected

Initial head H_0	1,000 ft
Initial velocity in conduit	100 fps
Water-hammer wave velocity	3,000 fps
Valve closure time	33 sec
Length of pipe line	5,000 ft

First, for complete closure,

$$\text{Pipe-line constant } \rho = \frac{aV_0}{2gH_0} = \frac{3{,}000 \times 100}{2 \times 32.2 \times 1{,}000} = 4.65$$

$$\text{Valve operation constant } \theta = \frac{aT}{2L} = \frac{3{,}000 \times 33}{2 \times 5{,}000} = 9.90$$

From Fig. 12 (small values of ρ and θ),

$$Z^2 = \frac{H_0 + h_{max}}{H_0} = \frac{1{,}000 + h_{max}}{1{,}000} = 1.59$$

$$\text{Pressure rise } h_{max} = 590 \text{ ft}$$

Now, check closure from 10 per cent valve opening:

$$\text{Pipe-line constant } \rho = \frac{aV_0}{2gH_0} = \frac{3{,}000 \times 10}{2 \times 32.2 \times 1{,}000} = 0.47$$

$$\text{Valve operation constant } \theta = \frac{aT}{2L} = \frac{3{,}000 \times 3.3}{2 \times 5{,}000} = 0.99$$

From Fig. 12,

$$Z^2 = \frac{H_0 + h_{max}}{H_0} = \frac{1{,}000 + h_{max}}{1{,}000} = 2.00$$

And the pressure rise h_{max} = 1,000 ft as compared with 590 ft for closure from fully open poisition.

In foot units, the general expression for water-hammer wave velocity is from Eq. (3):

$$a = \frac{1}{\sqrt{WQ}} = \frac{1}{\sqrt{\frac{w}{g}\left(\frac{1}{K} + \frac{D}{bE}\right)}}$$

For steel pipes the value of E is 29,400,000 psi or 42.3×10^8 psf, while the bulk modulus of water is 294,000 psi or 42.3×10^6 psf. $\frac{w}{g} = \frac{62.5}{32.2} = 2.00$ closely enough.

[1] KERR, S. LOGAN, New Aspects of Maximum Pressure Rise in Closed Conduits, *Trans. ASME*, 1928, paper HYD-51-3.

The corresponding value of the wave velocity is

$$a = \frac{4{,}660}{\sqrt{1 + \dfrac{D}{100b}}}$$

which is plotted for convenience as the curve for steel pipe, Fig. 16.

For cast-iron pipe, the value of E is 15,000,000 psi or 21.60×10^8 psf, and the corresponding value of the wave velocity is

$$a = \frac{3{,}290}{\sqrt{0.51 + \dfrac{D}{100b}}}$$

the curve of which is plotted as cast iron, Fig. 16.

For concrete pipe with an assumed modulus of 2,500,000 psi $= 3.60 \times 10^8$ psf, the wave velocity becomes

$$a = \frac{1{,}340}{\sqrt{0.085 + \dfrac{D}{100b}}}$$

For a tunnel in solid rock the value of b becomes very large, and consequently the wave velocity approaches the velocity of sound in water, 4,660 fps.

For wood-stave pipe, Strowger[1] has developed the formula

$$a = \frac{4{,}660}{\sqrt{1 + \dfrac{KD}{E_w b + E_s \phi}}}$$

where b = stave thickness, ft.

ϕ = total cross-sectional area of steel bands, sq ft/lin ft of pipe.

E_s = modulus of elasticity of steel bands in tension, 4.23×10^9 psf.

E_w = modulus of elasticity of wood staves.

British Columbia or Douglas fir	2.30×10^8 psf
Redwood or cypress	1.92×10^8 psf
White pine	1.00×10^8 psf

For old deteriorated staves, tests show values as low as 0.60×10^8 psf.

FIELD OF APPLICABILITY OF VARIOUS METHODS

Although selection of the method best adapted to fit the various particular problems arising in practice is very largely a matter of preference of the individual engineer, it may be worth while in summary to indicate what the author believes to be the characteristic merits of the various devices.

For all but the cases of instantaneous valve operation, direct analytical solution of the basic differential equations is possible only by prescription of the efflux velocity extinction pattern rather than the conventional time rate of decrease of valve opening with discharge velocity determined from the orifice law. In spite of requiring this departure from tradition and also the command of relatively advanced technique, this method is still believed to be the most effective instrument for research investigation and for establishing in rigorous fashion the fundamental laws of water hammer. Once the manipulative technique has been mastered, the analytical solution does have the

[1] Strowger, E. B., Water-hammer Problems in Connection with the Design of Hydroelectric Plants, *Trans. ASME*, 1944, paper 44-A42.

additional advantage of affording a continuous time history of pressure and velocity in compact and perfectly general formulas. Development along such lines is believed to be incipient and affords definite promise for the future.

The author has found the arithmetic integration method to be particularly incisive in those cases in which the terminal mechanism is a turbomachine and in which, therefore, the discharge characteristics depend upon the instantaneous value of gate and speed. This method also is exceedingly valuable in teaching the computer the internal mechanism of water hammer and the synthesis of total pressures from direct and reflected wave components.

The graphical method, developed very largely on this continent through the efforts of Prof. Angus, is not only one of the greatest savers of time and labor in the hydraulic field, but it has the added advantage that the underlying theory is simple and readily understood. It handles with equal ease cases in which the valve closure is uniform or even nonlinear; and although it may be used effectively for those cases in which the machine speed passes either above or below normal, the author is slightly prejudiced in the case of the latter class in favor of arithmetic integration.

As already outlined, the Allievi charts, in spite of their limitations, continue to be the most popular and widely used of all water-hammer methods; but it should always be borne in mind that they were never intended to apply, even as a rough approach, to more highly specialized cases in which the efflux velocity depends upon the instantaneous setting and speed of the terminal mechanism.

One of the cases occurring most commonly in practice is that of a penstock, surge tank, and pipe line or tunnel. The standard method of analysis is to consider the free surface of water in the tank as an open reservoir and neglect the pressure wave traveling up the pipe line or tunnel. A more accurate determination of the system as a branched conduit problem may readily be effected by means of the graphical method, Ref. 4 in the Bibliography, or by the appropriate Calame and Gaden formulas, Ref. 6.

Bibliography

1. Allievi, Lorenzo, "The Theory of Water Hammer," Garroni, Rome, 1925. The original water-hammer classic, giving the development of the fundamental equations, description of the interlocked series, and presentation of the Allievi charts.
2. "Symposium on Water Hammer," published by the joint committee of ASME. Hydraulic and ASCE Power Divisions, 1933. A résumé of the principal modes of water-hammer analysis available up to that time.
3. Angus, Robert W., Simple Graphical Solution for Pressure Rise in Pipe and Pump Discharge Lines, *Eng. Jour.* of the Engineering Institute of Canada, February, 1935. An exceptionally clear treatment of the graphical method with valuable illustrative examples.
4. Angus, Robert W., Graphical Analysis of Water Hammer in Branched and Compound Pipes, *Trans. ASCE*, 1939. A valuable extension of graphical analysis to cover several more important illustrative cases.
5. Angus, Robert W., Air Chambers and Valves in Relation to Water Hammer, *Trans. ASME*, 1937, HYD-59-S.
6. Strowger, E. B., Water-hammer Problems in Connection with Design of Hydroelectric Plants, *Trans. ASME*, 1944. A concise résumé of the arithmetic integration and graphical methods brought up to date.
7. Rich, George R., Water-hammer Analysis by the Laplace-Mellin Transformation, *Trans. ASME*, 1945. Outlines the basic method of applying the complex variable operational calculus to the direct analytical solution of the basic differential equations.
8. Wood, F. M., The Application of Heaviside's Operational Calculus to the Solution of Problems in Water Hammer, *Trans. ASME*, 1937, HYD-59-15.
9. Strowger, Earl B., Relation of Relief Valve and Turbine Characteristics in the Determination of Water Hammer, *Trans. ASME*, 1937, HYD-59-14.
10. Rich, George R., "Hydraulic Transients," McGraw-Hill Book Company, Inc., New York, 1951.

SECTION 28

SURGE TANKS

By George R. Rich

INTRODUCTION

It is evident from Sec. 13 that adverse water-hammer effects may be mitigated easily and inexpensively only in the case of the shorter conduits or in installations in which very slow valve closure is no detriment; but it is likewise apparent that in hydraulic power installations which have any appreciable length of pipe line and which are required to hold frequency within commercial limits even when operating detached from the system, very slow turbine gate movement would not be compatible with practical economical speed regulation. If the expedient of synchronous by-pass valves were employed, which are in themselves a considerable item of expense, the conduit velocity would have to be maintained permanently at a rate sufficiently high to accommodate maximum load demand. In the case of plants having instantaneous load increases in the order of 50 per cent or higher, this last requirement would ordinarily involve a very expensive wastage of valuable water. Provision of a surge tank is the economical solution in such cases. As is well known, the tank has three primary and one concomitant functions: (1) to provide a free reservoir surface close to the terminal discharge mechanism as a quick source of compensating water-hammer reflections to limit penstock and materially reduce main conduit pressures, the initial reflections being negative in the case of closure and positive in the case of opening; (2) to supply the additional water required by the turbine during load demand until the conduit velocity has accelerated to the new steady-state value; (3) to store water during load rejection until the conduit velocity has been decelerated to the new steady-state value; (4) to make certain that the pendulation of water levels following even small as well as large load changes will be quenched positively and rapidly. In the language of the trade, the tank must pass the test for incipient stability.

Because inertia causes water to overtravel beyond the second steady-state position, the characteristic physical action of the surge tank is a pendulation of the water surface levels, although it is possible but usually not economical to obtain aperiodic or deadbeat action. Like water hammer, this mass acceleration in a surge tank is a transient phenomenon; but unlike water hammer, its periodicity is comparatively slow, requiring as much as 30 min or even longer to establish the second steady state for long conduits and large tanks, as compared to about 30 sec or less to damp out the significant portion of the water hammer under conditions commonly encountered in practice.

Because of this basic difference in periodicity, it is fortunately permissible for the purposes of computation to separate these two concurrent phenomena and to treat the surge by itself as a mass-acceleration problem. By this we mean that the velocity changes in the conduit occur so gradually that in computing the mass surge separately we may employ the simple momentum law and neglect the effect of stretching the conduit circumference and compression of the water. The water-hammer effects which are important only during the first 15 or 20 sec, and then principally in the penstock, and only to a secondary degree in the conduit, are segregated and handled as a detached second problem. Nevertheless, we should always remember that in nature the two actions occur simultaneously and that water-hammer effects, while of important magnitude only at the outset, are in reality the direct causative agent for the mass acceleration in the same fashion that they are the direct means of effecting the velocity changes in a simple pipe, even for the slowest rates of valve movement. As an extension of this same idea, it is sometimes helpful to consider water hammer as a rapid means of telegraphing the valve operation to the reservoir.

DIFFERENTIAL SURGE TANK

The salient feature of the differential surge tank invented by R. D. Johnson is the separation of the water-supply or water-storage function from the conduit acceleration or deceleration function, resulting in more rapid, efficient hydraulic action and reflecting sizable economy in tank diameter and capital cost. A very important second feature is the marked damping effect or throttling action afforded by the port arrangement which gives the differential tank pronounced ability to limit and suppress the surges due to synchronous load pulsations.

Accordingly, methods of analysis of the differential surge regulator will be given in detail with but passing reference to simple, restricted orifice, and compressed-air tanks at the close of this section. However, it will soon be apparent to the reader that this seeming deletion will in no way penalize the treatment of such alternative devices. The same principles of design will be found to hold in all cases; and if the analyst is thoroughly conversant with computations for the differential tank, he will have no difficulty with the simple, the restricted orifice, or the compressed-air regulator.

BASIC DIFFERENTIAL EQUATIONS

Although the differential equations for the Johnson regulator are not susceptible to direct conventional solution, it will be instructive to develop them as a means of crystallizing the principal elements of hydraulic action, particularly as a prerequisite to forming tabulations for arithmetic integration, the only method capable of effecting an exact solution.

Referring to Figs. 1 and 3 and the notation tabulated in Art. 4, the following equations are true at any instant, proper regard being given to algebraic sign:

Total head on conduit = friction and allied head losses + acceleration head

$$H - h_r = cv^2 + \frac{L}{g}\frac{dv}{dt} \tag{1}$$

Discharge from outer tank = discharge through ports

$$F\frac{dh_t}{dt} = a\sqrt{2g(h_t - h_r)} \qquad (2)^1$$

Turbine discharge Q_w

= conduit discharge Q_c + port discharge Q_t + riser discharge Q_R

$$Q_w = Av + a\sqrt{2g(h_t - h_r)} + A_r\frac{dh_r}{dt} \qquad (3)^1$$

Turbine discharge Q_w = function of head, efficiency, and gate or power

$$Q_w = f(h_r, P_w) \tag{4}$$

[1] The radical will be written $\sqrt{2g(h_r - h_t)}$ when $h_r > h_t$. The discharge coefficient is included in a in accordance with the notation of Art. 4.

By Eq. (4) we mean that the turbine discharge Q_w for any specified power output P_w or gate opening is a function of h_r and the turbine efficiency. Because of the variation in turbine efficiency with the gate, this function is not conveniently expressible in algebraic terms, and the value of Q_w at any instant must, as a practical matter, be selected from turbine performance charts.

The insuperable obstacle to direct conventional solution of the above system is, however, due to the fact that when the friction head loss is taken proportional to the square of the conduit velocity, there is no known solution for the resulting differential equations. In such cases, provided we have a sufficient number of equations to match the number of unknown quantities, the solution may always be effected by step-by-step calculation commonly known as arithmetic integration. The detailed procedure for an illustrative example will be given in Art. 8.

It can be readily appreciated that if we had to depend entirely upon mere guesswork for selecting fortuitous trial combinations of tank size and port area, determination of the correct design of tank by the arithmetic integration method would be hopelessly laborious. Thanks, however, to the genius of the inventor of the differential tank, we are equipped with a powerful method of obtaining very dependable trial values of tank dimensions so that the subsequent computation of performance curves, showing water levels and velocities by arithmetic integration, becomes largely confirmatory in purpose and seldom needs to be carried through more than one trial. The classic article[1] describing this method, which is abstracted in the following sections, will repay detailed study by surge-tank designers.

JOHNSON'S EQUATIONS FOR LOAD DEMAND

To avoid confusion, it will possibly be well to emphasize at the outset that the purpose of Johnson's equations is not to afford a means for computing performance

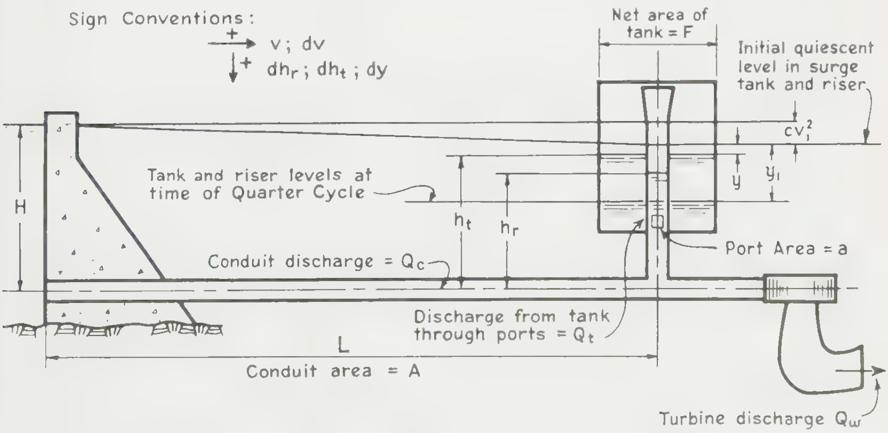

Fig. 1. Differential surge tank, load-demand condition.

curves of water levels and conduit velocities, but only rapidly to supply reliable trial values of port area, limiting upper and lower tank elevations, and tank and riser diameters for subsequent confirmation of performance by arithmetic integration.

The key to the simplification of Eqs. (1) to (4) in Art. 3, is shown in Fig. 2, in which the actual riser drop curve shown in dotted line is replaced by the assumed heavy solid rectangular curve. This assumption follows very naturally from an inspection of arithmetic integration performance curves for a wide variety of differ-

[1] Johnson, Raymond D., The Differential Surge Tank, *Trans. ASCE*, *Paper* 1324, vol. 78, 1915.

ential tanks. For most efficient action, the heel of the characteristic actual riser drop curve will come down initially so as to be level for a few seconds' duration with the subsequent common elevation of both tank and riser curves at the quarter cycle. If the port area is too small in relation to the tank area, the initial heel in the riser drop curve will lie appreciably below the levels at the quarter cycle; conversely, if the port area is too large in proportion to the tank area, the characteristic initial heel of the actual riser drop curve will lie some distance above the levels at the quarter cycle. In the first case, the instantaneous power capacity will be reduced because of excessively low elevation of the heel of the riser drop curve, and in the second instance the power output will be penalized by excessively low elevation of both levels at the quarter cycle. Maximum efficiency results when the riser drop curve has the char-

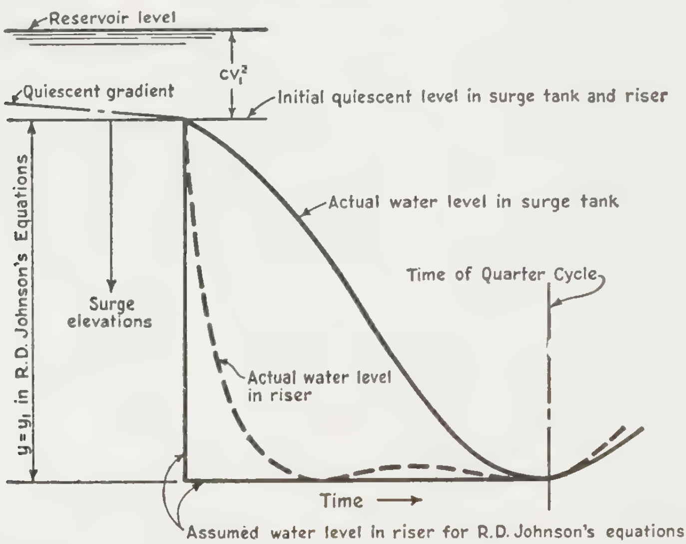

FIG. 2. Difference between actual and assumed rectangular riser drop curves for load-demand condition.

acteristic form given in Fig. 2, and it is reasonable to expect (and invariably confirmed in subsequent detailed computation) that the substitute rectangular outline gives a close workable approximation to the actual dotted form. This entire question (see Fig. 9) is clarified in detail in the discussion of Johnson's original article by Roy Taylor.[1]

Having established a reasonable and advantageous simplification of shape for the riser drop curve, let us next investigate what the concomitant physical actions in the tank must be to afford the desired rectangular configuration. It is quite obvious that the cross-sectional area of the riser must be considered negligible and equal to zero, and that the inertia of the water in the riser column must be neglected to ensure instantaneous drop of the riser curve to the quarter-cycle level immediately upon opening the turbine gates. Upon further reflection, it is also evident that to maintain the level of water in the riser constantly at the above fixed elevation throughout the quarter cycle, the area of the ports (though usually fixed in actual design) must be assumed to vary at each instant in just the right degree to ensure that, under dropping head on the port orifice, the discharge through the ports plus the increasing discharge from the main conduit is just sufficient to furnish the exact discharge required by the turbine at constant head up to the quarter cycle. Finally, it is quite evident, in

[1] *Ibid.*, Fig. 15, p. 803, discussion by Roy Taylor

view of the foregoing assumptions, that the equations derived on this basis will be valid only up to the time of the quarter cycle.

For convenient reference these assumptions are summarized as follows:

1. The analysis is valid only up to the time of the quarter cycle, that is, the time at which water levels in the riser and main tank approach coincidence.
2. The inertia of the water in the riser column is neglected.
3. In accordance with Fig. 2, it is assumed that upon initiating the opening movement of the turbine gates the water level in the riser drops immediately to its level at the quarter cycle, giving a rectangular shape to the riser drop curve.
4. The cross-sectional area of the riser is considered negligible and equal to zero.
5. The port area, though usually constant in any actual design, is, for the purpose of facilitating solution of the equations, assumed to vary with the time in just the right proportion to give the assumed rectangular shape of riser drop curve.

With these simplifying assumptions, Johnson's equations expressing a relationship between magnitude of surge and diameter of tank are obtained with comparative ease. In accordance with our usual practice, we shall adhere to Johnson's notation to facilitate cross reference with the original article.

The notation is as follows:

t = time in general, sec.
t_a = time of acceleration, sec.
t_r = time of retardation, sec.
T = time to complete one quarter cycle of the oscillation of tank levels, sec.
L = length of conduit, ft.
A = area of conduit, sq ft.
F = net area of tank, that is, in excess of riser area, sq ft.
H = difference in elevation between water surface in reservoir and center line of conduit, ft.
h_r = difference in elevation between water surface in riser and center line of conduit, ft.
h_t = difference in elevation between water surface in tank and center line of conduit, ft.
Q_w = turbine discharge, cfs.
A_r = area of riser, sq ft.
P_w = turbine output, hp.
a = area of restricted opening or port with 100 per cent coefficient of discharge, or the actual area times the discharge coefficient, sq ft.
a_0 = area of restricted opening when $t = 0$, sq ft.
a_1 = area of restricted opening when $t = T$, sq ft.
v = velocity in conduit at any instant, fps.
v_1 = initial conduit velocity before acceleration begins ($t_a = 0$), or = conduit velocity when $t_r = T$, or = constant-draft velocity between surge tank and water wheel, in terms of the conduit velocity during retardation.
v_2 = conduit velocity when $t_a = T$, or = initial conduit velocity before retardation begins ($t_r = 0$), or = constant-draft velocity between surge tank and water wheel, in terms of the conduit velocity during acceleration.
c = a coefficient such that cv^2 = total losses of head in the conduit (these losses may or may not include the velocity head, depending on the location of the surge tank).
y = departure of water level in tank from its initial quiescent position previous to a load change.
y_1 = y for $t = T$ = also, by hypothesis, the amount of initial sudden change of level in standpipe.
p = percentage of velocity change $= \dfrac{v_2 - v_1}{v_2}$ in acceleration.
$r = \dfrac{v_1}{v_2} = 1 - p$.
k = stability factor of surge $= \dfrac{y_1}{c(v_2^2 - v_1^2)}$.
log = natural logarithm to the base e.
$Z = \sqrt{\dfrac{y_1}{c} + v_1^2}$, or $y_{1_a} = c(Z^2 - v_1^2)$.
$Z_1 = \sqrt{v_2^2 - \dfrac{y_1}{c}}$, or $y_{1_r} = c(v_2^2 - Z_1^2)$.
$Z_0 = \sqrt{\dfrac{y_1}{c} - v_2^2}$, or $y_{1_r} = c(v_2^2 + Z_0^2)$.
$X = \dfrac{Z}{v_2} = \sqrt{k(1 - r^2) + r^2}$.

The resulting simplified differential equations for load demand are as follows:

$$dt = \frac{\frac{L}{g}\,dv}{y_1 - c(v^2 - v_1^2)} \tag{5}$$

$$Av_2\,dt = F\,dy + Av\,dt \tag{6}$$

Solving,[1] we obtain the tank diameter F for any specified surge y_1:

$$F = \frac{AL}{2gcy_{1a}}\left[\frac{v_2}{Z}\log_e\frac{(Z - v_1)(Z + v_2)}{(Z + v_1)(Z - v_2)} - \log_e\frac{Z^2 - v_1^2}{Z^2 - v_2^2}\right] \tag{7}$$

or

$$F = \frac{AL}{2gc^2v_2^2k(1 - r^2)}\left[\frac{1}{X}\log_e\frac{(X - r)(X + 1)}{(X + r)(X - 1)} - \log_e\frac{k}{k - 1}\right] \tag{8}$$

Equation (8) may be presented in the very convenient form of a chart for rapid computation (Fig. 6). For this purpose, in Eq. (8) let

$$\frac{2gc^2v_2^2F}{AL} = N^2 \tag{9}$$

and to obtain a scale convenient for reading, let

$$100N_a = 100v_2c\sqrt{\frac{2gF}{AL}} \tag{10}$$

Also, by definition,

$$y_{1_a} = k_ac(v_2^2 - v_1^2) \tag{11}$$

Then for any assigned values of y_{1_a} and v_2, we have corresponding values of p, k, and r, and may read the corresponding value of $100N_a$ from the chart (Fig. 6). The required net area of tank is then easily computed from Eq. (10).

In performing the arithmetic integration, it is useful to have an estimate of the time required to reach the quarter cycle. This is given by

$$T_a = \frac{L}{2gcZ}\log_e\frac{(Z - v_1)(Z + v_2)}{(Z + v_1)(Z - v_2)} \tag{12}$$

From Fig. 2 and the simple orifice law, the port area required at the start of the cycle will be

$$a_0 = \frac{A(v_2 - v_1)}{\sqrt{2gy_1}} \qquad \text{(for load demand)} \tag{13}$$

The theoretical[2] port area required at the quarter cycle will be

$$a_1 = \left[\frac{AFy_1}{L}\left(1 - \frac{1}{k}\right)\right]^{1/2} \tag{14}$$

which is always less than a_0.

JOHNSON'S EQUATIONS FOR LOAD REJECTION

The key assumption for the development of Johnson's equations for the load-rejection condition illustrated in Fig. 3 is, as would naturally be expected, the same as for load demand except that the water surface elevation in the riser rises (instead of falls) to the common elevation of both tank and riser levels at the quarter cycle.

[1] For complete intermediate steps in the solution, see Johnson, *op. cit.*, pp. 770*ff*.
[2] For details of the derivation see Johnson, *op. cit.*, p. 770, Eqs. (6), (7), (8), and (9).

As a secondary assumption, the depth of water overflowing the riser top as a weir crest is neglected.

Referring to Fig. 3, the fundamental differential equations for load rejection are

$$dt = \frac{\frac{L}{g}\,dv}{y_1 - c(v_2^2 - v^2)} \tag{15}$$

$$Av_1\,dt = F\,dy + Av\,dt \tag{16}$$

For the rejection condition two cases arise, depending upon whether or not the surge rises above the reservoir level, *i.e.*, whether $y_1 < cv_2^2$ or $y_1 > cv_2^2$. In the first

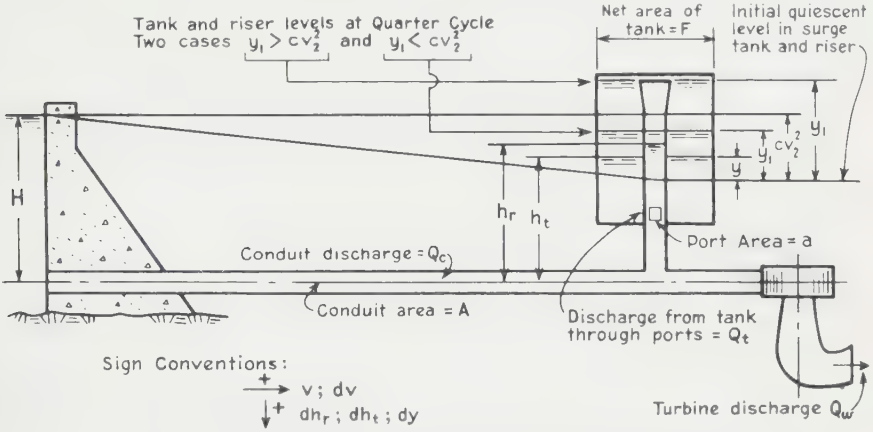

FIG. 3. Differential surge tank, two cases, load-rejection condition.

instance, if $y_1 < cv_2^2$, the equation for F, upon integration of Eqs. (15) and (16), will lead to the formula

$$F = \frac{AL}{2gcy_{1r}}\left[\log_e \frac{v_2^2 - Z_1^2}{v_1^2 - Z_1^2} - \frac{v_1}{Z_1}\log_e \frac{(v_2 - Z_1)(v_1 + Z_1)}{(v_2 + Z_1)(v_1 - Z_1)}\right] \tag{17}$$

On the other hand, when the surge rises above the reservoir level and $y_1 > cv_2^2$, we have

$$F = \frac{AL}{2gcy_1}\left[\log_e \frac{v_2^2 + Z_0^2}{v_1^2 + Z_0^2} - \frac{2v_1}{Z_0}\left(\text{arc tan}\,\frac{v_2}{Z_0} - \text{arc tan}\,\frac{v_1}{Z_0}\right)\right] \tag{18}$$

For the case of greatest interest in practice, that of complete shutdown with $v_1 = 0$, Eq. (18) becomes

$$F = \frac{AL}{2gcy_1}\log_e \frac{v_2^2 + Z_0^2}{Z_0^2} \tag{19}$$

or, since

$$k_r = \frac{y_1}{cv_2^2}, \tag{20}$$

$$F = \frac{AL}{2gc^2v_2^2k_r}\log_e \frac{k_r}{k_r - 1} \tag{21}$$

we may develop a useful graphical chart for the computation of this equation in the same general fashion as for load demand. In this case let

$$100N_r^2 = 100v_2c\sqrt{\frac{2gF}{AL}} \tag{22}$$

For given values of y_1 and v_2, we derive a corresponding value of k_r and may read $100N_r$ from the chart (Fig. 7). F is then easily obtained from Eq. (22).

From Fig. 3 the port area required at the start of the cycle will be

$$a_0 = \frac{A(v_2 - v_1) - \text{discharge over top of riser}}{\sqrt{2gy_1}} \tag{23}$$

The size of port[1] required at the quarter cycle will be

$$a_1 = v_2 \left[\frac{AFc}{L} (k_r - 1) \right]^{1/2} \tag{24}$$

The port area for the rejection condition will be established by Eq. (24) rather than Eq. (23) because of the discharge capacity over the top of the riser as a weir.

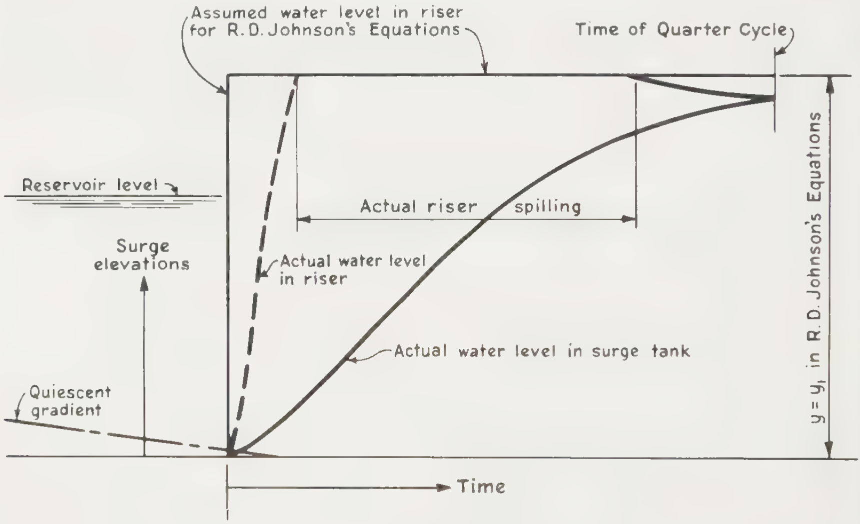

FIG. 4. Difference between actual and assumed rectangular riser level curves for rejection condition.

The effective size of port for the demand condition, Eqs. (13) and (14), must not exceed that prescribed by Eq. (24) for the rejection condition; otherwise, the water level in the riser during rejection will drop down again before the quarter cycle is reached. This would be contrary to our assumption of constant y_1 in Fig. 3 and might introduce appreciable error intc the equations for tank diameter.

JOHNSON'S EQUATIONS FOR THE CRITICAL VELOCITY

There are certain combinations of tank design and conduit for which rejection from the maximum full-load velocity does not give the maximum height of surge. In these cases, some lesser velocity v_c, called the critical velocity, will govern the upper limiting elevation of tank.

Let d equal the required height of surge tank above the reservoir level. Then

$$d = cZ_0^2 = c\left(\frac{y_1}{c} - v_2^2\right) \tag{25}$$

and

$$y_1 = c(Z_0^2 + v_2^2) \tag{26}$$

[1] JOHNSON, *op. cit.*, Eq. (33), p. 778.

Substituting Eq. (26) in Eq. (19), we obtain

$$\frac{2gc^2F}{AL} = \frac{\log_e (v_2^2 + Z_0^2) - 2 \log_e Z_0}{Z_0^2 + v_2^2} \tag{27}$$

To find what value of v_2 makes d a maximum, differentiate Eq. (27) with respect to v_2. Place $\frac{dZ_0}{dv_2} = 0$ and solve for v_2. Then this value of $v_2 = v_c$ or

$$v_c = \frac{1}{c}\left[\frac{AL(e-1)}{2gFe}\right]^{1/2} \tag{28}$$

Solving for $d = cZ_0^2$ in Eq. (25)

$$d_{max} = \frac{AL}{2gceF} \tag{29}$$

Figure 8 affords an interesting summary of the heights of surge resulting from shutdown from conduit velocities other than the critical. The corresponding value of port area for the critical velocity is, from Eqs. (24), (28), and (29),

$$a_1 \text{ (for } v_c) = \frac{A}{\sqrt{2gce}} \tag{30}$$

or

$$a_1 = \sqrt{\frac{AFd}{L}} \tag{31}$$

TEST FOR INCIPIENT STABILITY

It was remarked in Art. 1 that one of the requirements of a satisfactory surge tank is that it have the ability to quench positively and rapidly the pendulations of water surface following load changes of whatever magnitude. During the larger load changes, the velocity of flow through the ports is relatively large; there is a very marked difference in elevation between the water surface levels in the main surge tank and riser, with the natural result that comparatively large conduit accelerating or decelerating forces are mobilized. These in turn act with telling effect to throttle and suppress the transient phenomenon.

In contrast, during fairly small load changes, say in the order of 1,000 kw in 50,000, the difference between the main tank and riser levels is likewise small; the velocity through the ports is comparatively insignificant, and the requisite quick suppression of surge must be effected principally by the friction in the conduit. If the tank diameter is sufficiently large, conduit friction will damp down the surge from any small load change before the water levels in the tank and riser have made any appreciable change from quiescence. On the other hand, it can be readily appreciated that the water levels in a tank of too small diameter would rise with greater rapidity, develop a phase lead ahead of conduit friction, with proportionate overtravel of water levels beyond the second steady-state position, and so tend to aggravate, magnify, and perpetuate each small load variation.

For the above reasons, as well as to obtain expressions that are more readily susceptible to mathematical attack, the basic equation for gaging tank stability is predicated upon small load changes as being more critical, since the throttling effect of the ports is then negligibly small. Because of its importance, we proceed to develop in considerable detail the criterion for stability now in universal use, namely, the formula of Dr. Dieter Thoma. For this purpose we assume that the action of riser and ports of the differential tank is negligible and that they may be entirely removed, giving in effect an old-style simple surge tank.

Referring to Fig. 5, we shall assume in the interest of simplicity that the turbine gates are closed and the water levels in the entire hydraulic system stand at reservoir elevation. We then place a very small load on the turbine and, from the character of the resultant differential equations, deduce what the diameter of surge tank must be to ensure the requisite damping effect.

The notation adopted is in general in conformity with Art. 4, and the meaning of the additional new terms will be apparent from the diagram (Fig. 5).

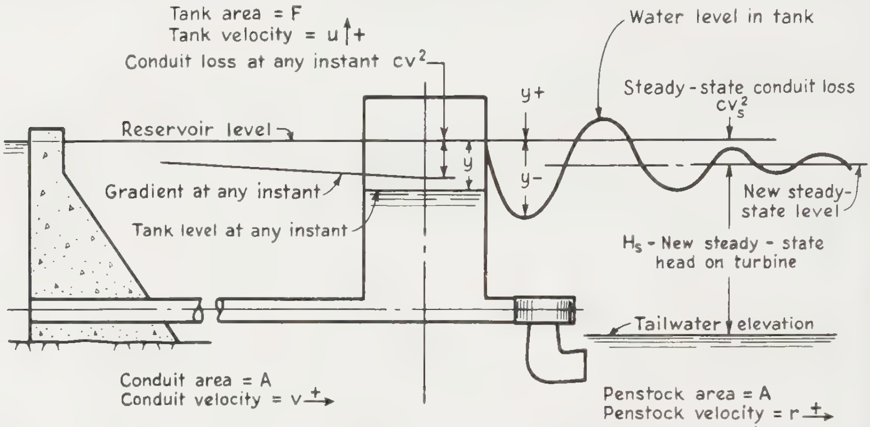

FIG. 5. Analysis of stability showing effect of placing small load on turbine starting from gates closed and entire system at reservoir level.

With the algebraic sign conventions postulated in Fig. 5, the basic differential equations will have the following form:[1]

$$\frac{L}{g}\frac{dv}{dt} + y + cv^2 = 0 \tag{32}$$

$$Av = Fu + Ar = F\frac{dy}{dt} + Ar \tag{33}$$

Now, if we were to proceed to attack the solution of these two equations directly, according to the conventional procedure, we should again encounter the familiar recurrent difficulty, namely, that the resulting differential equation would be of the form

$$\frac{d^2\phi}{dt^2} + \beta\left(\frac{d\phi}{dt}\right)^2 + \theta = 0 \tag{34}$$

for which there is at present no known solution. Accordingly, we shall be required to introduce sufficient permissible simplifications to transform this equation into the type

$$\frac{d^2\phi}{dt^2} + \beta\frac{d\phi}{dt} + \theta = 0 \tag{35}$$

In essence, then, we must find some legitimate means of expressing the friction head loss according to the first rather than the second power of the conduit velocity, and fortunately for the case of small load changes, this requirement is obtainable without any great difficulty or sacrifice in accuracy. Our second approximation relates to turbine discharge under varying net effective head, but again in this case the assumption of small load changes permits the requisite simplification. Under these condi-

[1] CALAME, J., and DANIEL GADEN, "Theorie des chambres d'equilibre," Paris and Lausanne, 1926.

tions the friction head loss in the conduit at any instant will be an insignificant percentage of the net effective head and the variation in turbine efficiency over the range considered will likewise be negligible.

Accordingly, we may express the penstock velocity as follows:

$$r = r_s \left(\frac{H_s}{H_s + cv_s^2 + y} \right) \tag{36}$$

in which r is the penstock velocity at any instant and r_s is the steady-state penstock velocity. Since, in our case, cv_s^2 will be very small in proportion to H_s, we may write

$$r = r_s \left(\frac{1}{1 + \frac{y}{H_s}} \right) \tag{37}$$

We may then expand the parenthesis by means of the well-known infinite series:

$$\frac{1}{1 + x} = 1 - x + x^2 - x^3 + x^4 - x^5 + \cdots \qquad \text{for} \qquad x^2 < 1 \tag{38}$$

Again, because of our assumption of small load change, y will be relatively small and we may drop all terms of this infinite series involving the second and higher powers of y/H_s, giving finally

$$r = r_s \left(1 - \frac{y}{H_s} \right) \tag{39}$$

Substituting this expression in Eq. (33), we obtain

$$v = \frac{F}{A} u + r_s \left(1 - \frac{y}{H_s} \right) \tag{40}$$

and the friction head loss cv^2 becomes

$$c \left(\frac{F}{A} u + r_s - \frac{r_s y}{H_s} \right)^2 = c \left(r_s^2 + \frac{2Fr_s u}{A} - \frac{2r_s^2 y}{H_s} \right) \tag{41}$$

since u^2 and $\left(\frac{r_s y}{H_s} \right)^2$ are very small. With these substitutions, the original differential Eq. (32) will take the form

$$\frac{d^2y}{dt^2} - \left(\frac{Ar_s}{FH_s} - \frac{2cr_s g}{L} \right) \frac{dy}{dt} + \left(\frac{gA}{FL} - \frac{2cr_s^2 gA}{FLH_s} \right) y + \frac{cgAr_s^2}{FL} = 0 \tag{42}$$

From the general theory[1] of ordinary linear differential equations we know that the character of the solution of the above equation will be determined by the complementary function, that is, the solution of the equation

$$\frac{d^2y}{dt^2} - \left(\frac{Ar_s}{FH_s} - \frac{2cr_s g}{L} \right) \frac{dy}{dt} + \left(\frac{gA}{FL} - \frac{2cr_s^2 gA}{FLH_s} \right) = 0 \tag{43}$$

The auxiliary equation for the complementary function will be

$$\omega^2 - \beta\omega + \theta = 0 \tag{44}$$

in which

$$\beta = \frac{Ar_s}{FH_s} - \frac{2cr_s g}{L} \qquad \text{and} \qquad \theta = \frac{gA}{FL} - \frac{2cr_s^2 gA}{FLH_s} \tag{45}$$

[1] Granville, William A., "The Elements of the Differential and Integral Calculus," Chap. 30, p. 431, Ginn and Company, 1911.

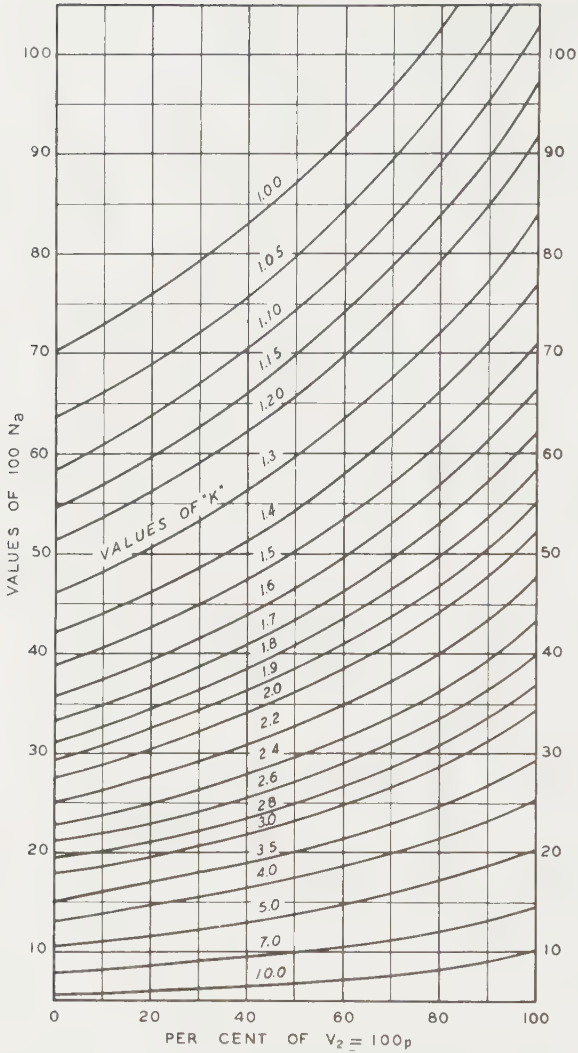

Fig. 6. Johnson chart, load-demand condition.

The complementary function will then have the form:

$$y = C_1e^{\omega_1 t} + C_2e^{\omega_2 t} \tag{46}$$

in which ω_1 and ω_2 are roots of Eq. (44).

We perceive from inspection of β, θ, and Eq. (43) that there is no possibility of repeated roots for the auxiliary equation. Accordingly, we have two remaining possibilities. A pair of complex roots of the auxiliary equation will afford a solution of the type

$$y = C_1e^{\frac{(\beta+\sqrt{\beta^2-4\theta})t}{2}} + C_2e^{\frac{(\beta-\sqrt{\beta^2-4\theta})t}{2}}$$

or letting $\frac{\sqrt{\beta^2 - 4\theta}}{2} = \sqrt{-1}\,\lambda = i\lambda$,

$$y = C_1 e^{\frac{\beta t}{2}} (\cos \lambda t + i \sin \lambda t) + C_2 e^{\frac{\beta t}{2}} (\cos \lambda t - i \sin \lambda t) \tag{47}$$

Real roots will give solution of the form of Eq. (46).

The case which occurs almost invariably and is of greatest interest in practice is that in which the auxiliary equation has a pair of complex roots, Eq. (47). If 4θ is greater than β^2, and we can see by inspection that this is generally the case, the quantity under the radical sign will be negative and our solution will be periodic. The fundamental requirement in which we are particularly interested, the factor that really determines whether our oscillations shall continue to increase indefinitely with the time or decrease progressively with the time, is obviously the algebraic sign of β [Eq. (47)]. The oscillations increase indefinitely with the positive sign and damp down to quiescence for the negative sign of β. In other words, then, β must be negative or

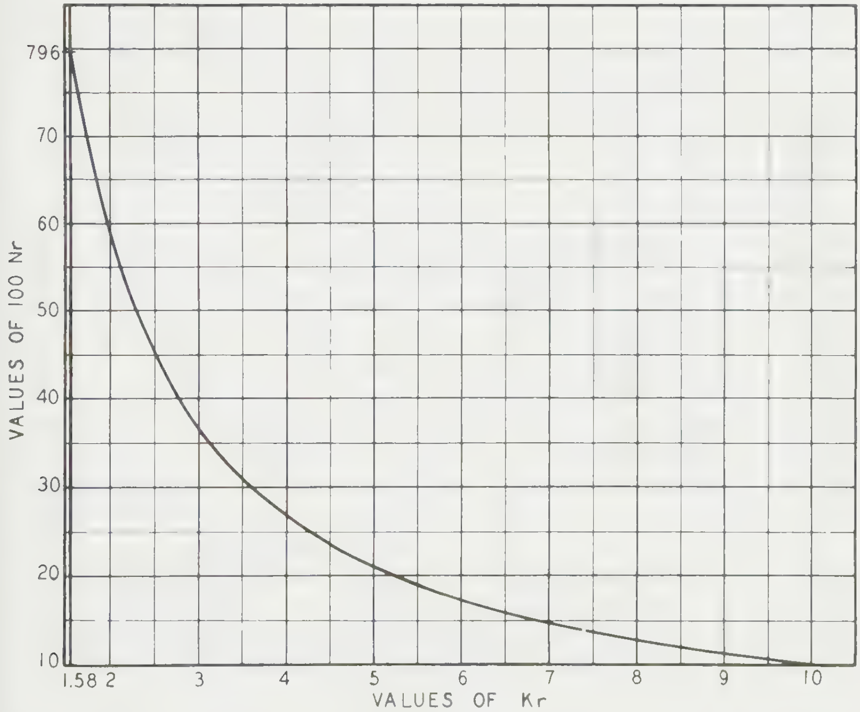

FIG. 7. Johnson chart, load-rejection condition.

$$\frac{Ar_s}{FH_s} - \frac{2cr_sg}{L} < 0 \tag{48}$$

$$\frac{2cr_sg}{L} > \frac{Ar_s}{FH_s} \tag{49}$$

or

$$F = \frac{AL}{2gcH_s} \tag{50}$$

That is, the minimum area of surge tank, just barely on the theoretical boundary line between perpetual and damped oscillations, is given by the formula

$$F = \frac{AL}{2gcH} \tag{51}$$

However, it should again be emphasized, and it should be apparent from the above theoretical derivation, that this size of tank is just sufficient to damp disturbances down to quiescence in a time barely short of eternity. To secure satisfactory rapidity of damping, an appreciable increase over this phantom value must be adopted, and the magnitude of this essential increase is based entirely upon experience and the knowl-

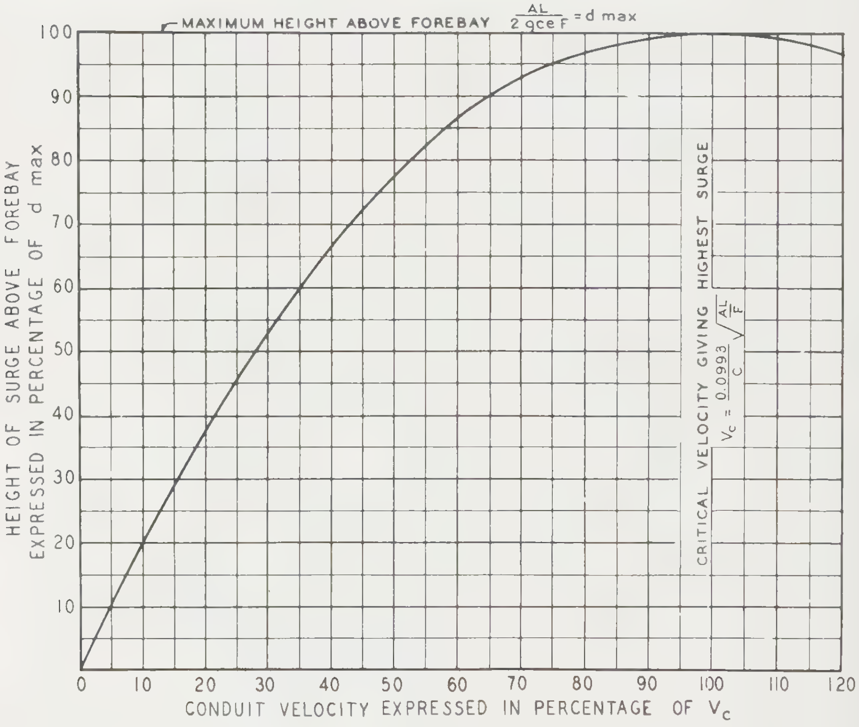

Fig. 8. Johnson chart, height of surge following rejection of full load.

edge derived from actual practice. It has been found from the consideration of a great range of tanks that this theoretical diameter must be increased at least 25 per cent for differential tanks (in which some benefit derives from the throttling action of the ports even at moderately light loads as compared with the almost infinitesimal load assumed to make our theoretical analysis mathematically workable) and 50 per cent in the case of simple tanks. Experience also dictates that this increase of 25 per cent in the Thoma tank diameter be used in conjunction with a value of H resulting from water levels assumed to be near the limiting bottom elevation of the surge tank. A convenient means of estimating this level in advance is to compute H from the maximum demand surge at the quarter cycle. The factor of 25 per cent also assumes that F be taken as the net area of tank with riser area deducted.

It should be clear from the above derivation that the Thoma formula is not an instrument of hairline precision; it is simply the best rough tool we have been able to forge for gaging stability up to the present time; and its derivation has been given in considerable detail principally as a means of counteracting the almost universal tendency of designers to attempt to infringe on the 25 and 50 per cent increases essential to ensure practical rapidity of quiescence.

Although the writer has never had occasion in actual practice to use the stability equation covering the aperiodic case, the derivation will be given for the sake of completeness. The basic requirement for aperiodic action is that the roots of Eq. (44) be real. In other words, if β is negative and β^2 greater numerically than 4θ, we obtain

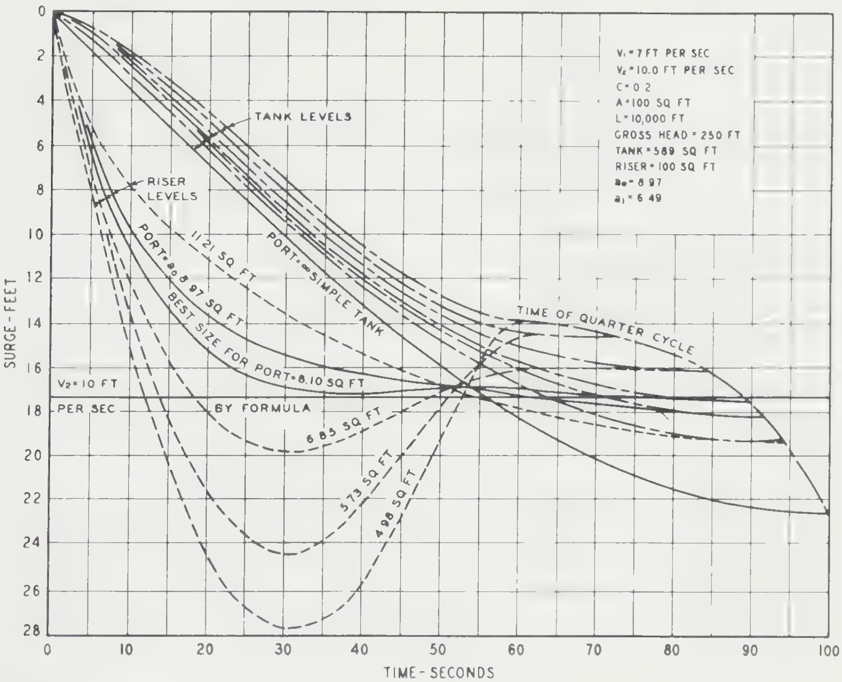

REPRINTED FROM TRANS. ASCE VOL 78 P 803

FIG. 9. Water levels following a load demand with ports of various sizes.

damped aperiodic or deadbeat action; if β is positive and β^2 greater numerically than 4θ, we have aperiodic action with the surge increasing indefinitely with the time.

The basic inequality is

$$\left(\frac{-2cgr_s}{L} + \frac{Ar_s}{FH_s}\right)^2 > 4\left(\frac{gA}{FL} - \frac{2cr_s^2gA}{FL}\right) \tag{52}$$

Solving,

$$F = \frac{AL}{2c^2gH_sr_s^2}\left(H_s - cr_s^2 \pm \sqrt{H_s(H_s - 2cr_s^2)}\right) \tag{53}$$

The positive sign before the radical gives the smallest value of tank diameter to ensure the damped aperiodic or deadbeat condition, while for the negative sign before the radical the surge will be aperiodic and increasing with the time without limit. It will be noted that in Eq. (53) it is necessary to insert the steady-state turbine discharge velocity as well as the steady-state head on the turbine.

DESIGN OF APALACHIA SURGE TANK

As a typical illustration of the commercial application of the foregoing principles, determination of the principal elements of design for the surge tank of the Apalachia project of the Tennessee Valley Authority (Paul F. Kruse, consulting engineer) will be given in detail.

One feature of the design specification, the provision to accommodate practically full-load instantaneous demand, is somewhat unusual. The average specification prescribes full-load rejection corresponding to the short-circuit condition; but the most common specified demand is an instantaneous load increase of 50 per cent from half load to full load.

The reason for the large demand prescribed in the case of Apalachia is that this plant serves an area in which close frequency regulation is important for textile manufacturing and other industries requiring close speed control. The Apalachia plant is essentially a seasonal peaking project, and during the off season, when water is accumulating in the reservoir, the generating units are operated floating on the line as synchronous condensers. The governors, however, are so set that in the event that electrical system disturbances cause disconnection of the area load from the main T.V.A. system transmission line, the Apalachia turbine gates will open and the units will absorb the entire local load.

The effect of specifying large load demand not only depresses the limiting bottom elevation of the surge tank but also has a marked influence upon port design. In the conventional tank design the port area required for the relatively smaller demand load will be found to be somewhat less than the theoretical port area required for rejection, and a single port area determined by rejection requirements is selected.

In the case of large demand loads, however, the required port area for demand is appreciably greater than that for rejection, and if a single port size were selected to fit the demand requirement, the result in the case of rejection would be that the water surface in the riser would start dropping down the riser again before the time of the quarter cycle is reached. This recession would give less efficient deceleration of the conduit velocity and subsequently a relatively higher peak elevation of the rejection surge.

This apparent conflict in port area requirements was resolved by incorporation of the port design shown in Fig. 10 and established on the basis of model tests in the hydraulic laboratory. The port orifices, instead of being uniformly rectangular, as in the conventional case, are given a diverging flare in the upward direction. The action of the port is obvious: For conditions of load demand, when the flow is downward from tank into riser, the flow filaments are compressed, flow conditions are improved, and the discharge coefficient for the conditions encountered will be in the order of 0.94. On the other hand, during rejection conditions, the flow will be from riser to tank in the upward direction through the ports. The comparatively rapid rate of flare introduces additional turbulence near the exit of the orifice. Flow conditions are impaired, with the result that the discharge coefficient for operating conditions will be in the vicinity of 0.71. This discrepancy in discharge coefficients was predetermined to match the particular conditions of the Apalachia installation. By changing the rate of divergence of the orifices, the requisite compensation could be obtained to match the requirements of any particular case. This simple device is obviously a marked improvement over some earlier European installations in which this same type of compensation was effected by the use of rectangular orifices, some of which were provided with flap valves to close during rejection and so reduce the rejection port area. As is pointed out in Johnson's basic article, it will be found in the conventional case for load demands up to 50 per cent that the single area determined for the load-off condition will be entirely satisfactory for load demand. In the following tabulations the principal features of the design will be established, first using Johnson's curves and formulas. Arithmetic integration tabulations will then be given together with the corresponding performance curves, demonstrating the adequacy of the trial design.

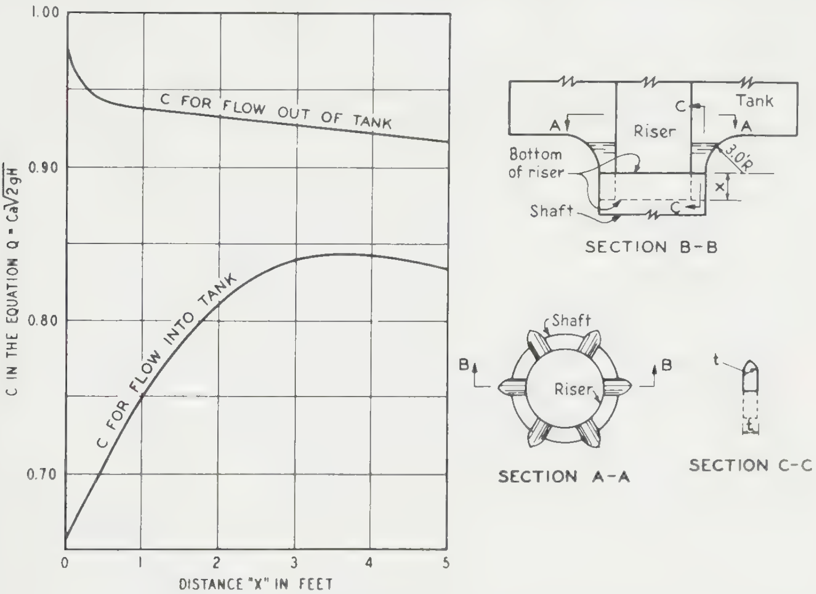

Fig. 10. Differential surge tank, detail of port.

Design Specifications for Apalachia Surge Tank. *General.*

Headwater	max El. 1282.
	normal El. 1265.
	min El. 1240.
Tailwater	normal El. 840.
Tunnel	41,200 ft of 18-ft-diameter concrete-lined tunnel and 2,000 ft of 16-ft-diameter steel-lined tunnel.
Penstock, tunnel and surge tank	for layout see Fig. 11.
Turbines and generators:	
Turbines	Two 50,000 hp at full gate at 286-ft head, 180 rpm. Best efficiency at 375- to 400-ft head.
Generators	Two 40,000 kva at 0.9 power factor and 60C temperature rise. Assume generator can take the full output of the turbine up to 66,000 hp corresponding to generator rating at 80C temperature rise.
Governors	Net traversing time 5 secs.

Incipient Stability. Check the diameter of tank to meet stability requirements by using a value of $n = 0.010$ in the Manning formula. Use the minimum possible net head as determined from analysis to establish economic diameter.

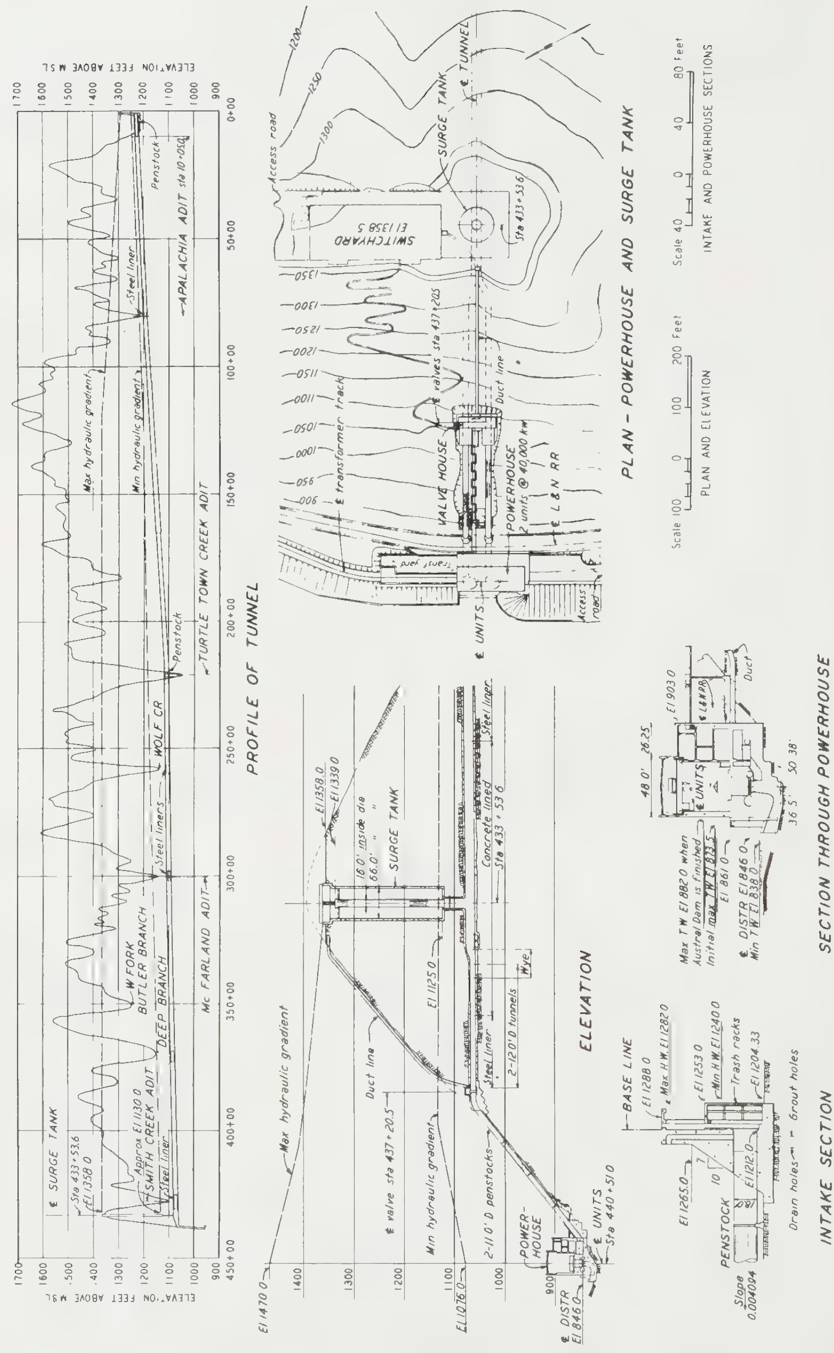

FIG. 11. General arrangement, Apalachia project.

Load-on. Design tank to supply water for an instantaneous and continuous demand load of 100,000 hp, starting from 0 hp, with pool at minimum level, using a value of $n = 0.013$.

Load-off. Design tank to store water from an instantaneous load rejection of 132,000 to 0 hp with pool at maximum level, using a value of $n = 0.0115$.

Conduit. The first step is to determine the hydraulic properties of the supply conduit. Using a basic discharge of 3,000 cfs for two units, the head loss and value of c are computed for the three values of n required. With the value of c established, it is possible to compute the head loss for any discharge by one simple operation.

The tunnel as planned is not a uniform section from forebay to tank, which makes it necessary to determine an equivalent conduit.

$$A = \frac{L}{\dfrac{L_1}{A_1} + \dfrac{L_2}{A_2}}$$
$$= \frac{43{,}200}{\dfrac{2{,}000}{201} + \dfrac{41{,}200}{254.5}} = \frac{43{,}200}{172} = 251 \text{ sq ft}$$

For $Q = 3{,}000$ cfs, we have a velocity of 11.95 fps.

By standard hydraulic computations we establish the following properties:

Tunnel from intake to surge tank:

$n = 0.010$,

$$\text{Head loss} = 43.0 \text{ ft (includes velocity head at riser)}$$
$$c = \frac{43.0}{(11.95)^2} = 0.303$$

$n = 0.0115$,

$$\text{Head loss} = 54.3 \text{ ft (includes velocity head at riser)}$$
$$c = \frac{54.3}{(11.95)^2} = 0.382$$

$n = 0.013$,

$$\text{Head loss} = 69.7 \text{ ft (includes velocity head at riser)}$$
$$c = \frac{69.7}{(11.95)^2} = 0.490$$

Tunnel and penstock from surge tank to unit:

$n = 0.010$,

$$\text{Head loss} = 3.5 \text{ ft}$$
$$c = \frac{3.5}{(11.95)^2} = 0.0245$$

$n = 0.0115$,

$$\text{Head loss} = 4.3 \text{ ft}$$
$$c = \frac{4.3}{(11.95)^2} = 0.030$$

$n = 0.013$,

$$\text{Head loss} = 5.10 \text{ ft}$$
$$c = \frac{5.10}{(11.95)^2} = 0.036$$

Tunnel and penstocks from intake to units:

$n = 0.010$,

$$\text{Head loss} = 44.3 \text{ ft}$$
$$c = 0.312$$

$n = 0.0115$,

$$\text{Head loss} = 56.4 \text{ ft}$$
$$c = 0.396$$

$n = 0.013$,

$$\text{Head loss} = 72.6 \text{ ft}$$
$$c = 0.512$$

Riser Diameter. When deciding upon the riser diameter, it should be kept in mind that the area of the riser should be equal to not less than three-fourths of the

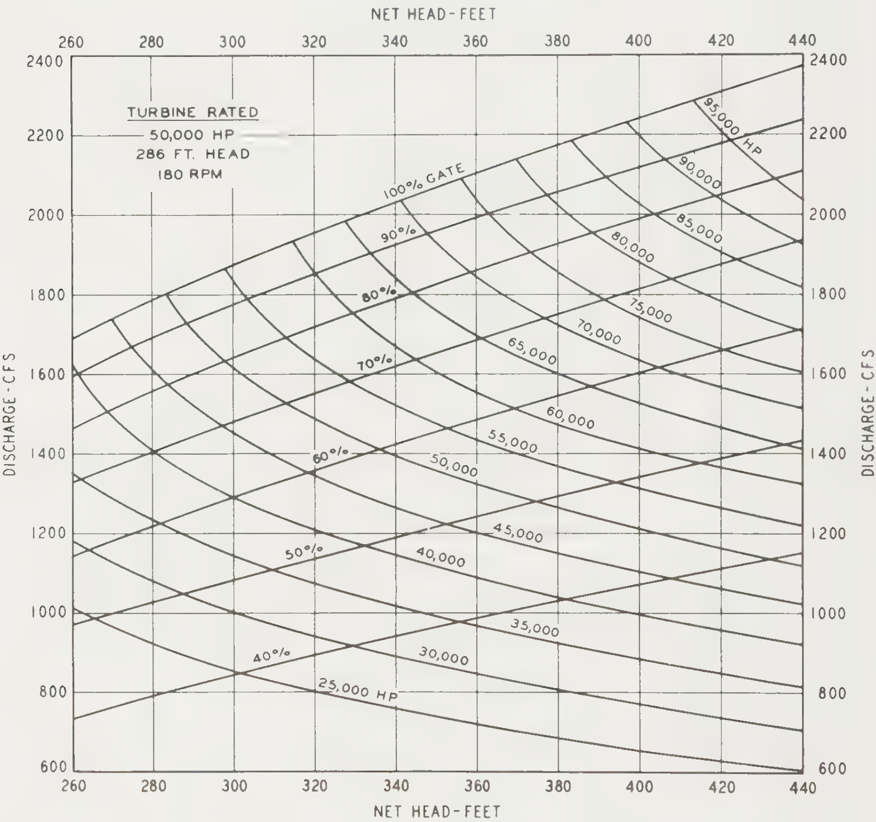

Fig. 12. Turbine performance chart.

area of the conduit. If the riser is too small, the water level changes in it are so rapid that good governing becomes more difficult.

Assume a riser diameter of 16 ft,

$$R = 201 \text{ sq ft}$$
$$^{201}\!/_{251} = 0.80$$

Economic Diameter of Surge Tank. The determination of the economic diameter of the surge tank might well be called the principal element of the design. Contrary to more or less prevalent impression, selection of the most advantageous diameter does not invariably result from simple direct substitution in the Thoma formula, Eq. (51), using the lowest net head that will give the specified power output, but for best return on the investment requires establishing a balance between construction cost, magnitude of surge and consequent limitation of instantaneous power at the lowest point of surge, and satisfactory quenching power or stability.

As an aid to judgment in making this determination, we shall require curves showing the relation between tank diameter and magnitude of surge for the demand and rejection condition for various assumed diameters, the capital cost of the corresponding heights and diameters of tank, and finally an estimate of the minimum diameter required to ensure stability. These data for our particular project are presented in Fig. 13; and as a sample of the method of computation we shall give the calculation in detail for one representative point on the load demand curve and one on the load rejection curve, together with a calculation to establish the diameter to ensure an ample margin of stability.

In our case, in which the tank is excavated from solid rock, the surge curves for load rejection do not have a determining effect on the cost of construction, for the reason that less expensive over-all construction expense results from excavating the tank full-bore from the top of hill, rather than excavating a pilot shaft down to the elevation required to clear the top of surge. Accordingly, the cost curve given in Fig. 13 has been calculated on this basis. However, in a plate-steel tank extending above ground, the construction cost curve would reflect stopping the tank just above the calculated surge for load rejection.

Several striking features are at once apparent from Fig. 13:

1. For the turbine whose performance is given by Fig. 12, a tank diameter of 66 ft is the smallest capable of carrying the prescribed continuous demand load of 100,000 hp through each and every point of the surge. For diameters less than 66 ft, the net head on the turbine at the lower levels of the surge is so reduced that even at full gate the power output falls appreciably short of 100,000 hp.
2. If we assume as large a turbine as necessary to give 100,000 hp at 90 per cent efficiency at the reduced heads near the lower levels of the surge, the curve of surge vs. diameter (heavy dotted line in Fig. 13) breaks sharply upward at about the 66 ft diameter.
3. The curve of construction cost also breaks definitely upward between 60 and 66 ft diameter.
4. For the load rejection condition, the slope of the curve of tank diameter vs. surge steepens noticeably at about the 66 ft diameter.

Even before we make any specific computation with regard to stability, it is evident from the above considerations that the performance of the tank becomes noticeably inferior below the region about 66 ft diameter, so that we are naturally led to suspect a positive reduction in quenching power starting at about this diameter. Our judgment is confirmed by the following analysis.

We have emphasized again and again that the Thoma formula is a rough tool in the application of which all the unavoidable errors in estimating should be made to lie on the side of safety, and the first occasion to exercise this caution is in selecting a liberal value for the minimum steady-state operating head on the turbine H. As a generous but not at all prodigal forecast of the stable steady-state capacity likely to be required at minimum headwater, we are, with the assistance of Fig. 12, able to anticipate the need for developing 100,000 hp at 100 per cent gate with net head between 290 and 300 ft, which calls for a steady-state velocity of about 14.5 fps in the conduit. As a second aid to judgment we readily anticipate from Fig. 13 that the bottom of tank will be in the vicinity of El. 1,125 ft so that steady-state tank levels in the vicinity of El. 1,135 are quite possible. Allowing 5 ft for loss in the penstock, we should have a corresponding steady-state head of about 290 ft. The corresponding computation for stability, following the calculation for representative points on the load-on and load-off surge curves, confirms our tentative selection of a tank diameter of 66 ft.

The important conclusion to be drawn from our investigation is that the Thoma formula is not properly an instrument to predetermine and fix the diameter of tank

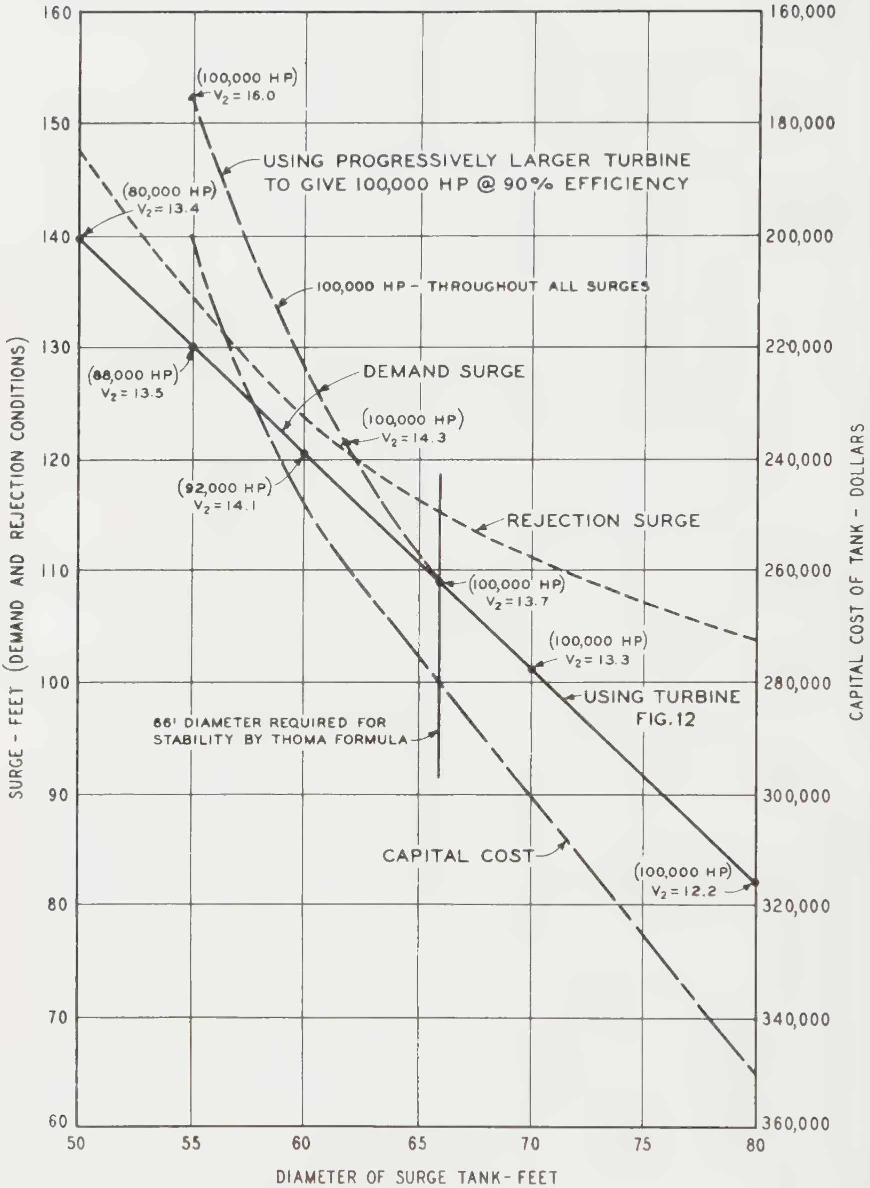

FIG. 13. Economic diameter of surge tank, Apalachia project.

in advance of other steps in the analysis, but rather a device for final confirmation to sustain and reinforce the indications of the economic determination of tank diameter. Plotting of the economic curves is the essential feature, and the tank diameter selected should be substantially on the side of adequacy.

Load Demand. We shall employ the 66 ft diameter to compute a typical point on the surge curve for load demand (Fig. 13). Assume a discharge of 3,450 cfs through the conduit at the low point of the surge; $v_2 = 13.70$ fps; $v_1 = 0$.

$$100N_a = 100v_2c\sqrt{\frac{2gF}{AL}}$$

$$= 100(13.70)(0.490)\sqrt{\frac{64.4}{251 \times 43{,}200}}\sqrt{3{,}220} = 93.5$$

$$p = \frac{v_2 - v_1}{v_2}$$

From the load-on chart, Fig. 6, for $p = 1.0$, $K_a = 1.18$,

$$y_{1_a} = K_ac(v_2^2 - v_1^2)$$
$$= 1.18(0.490)(13.70)^2 = 109 \text{ ft}$$

Gross head = El. 1,240 − El. 840	400.0 ft	
Velocity head at riser = $\frac{(13.70)^2}{64.4}$	2.9	(energy available to unit)
	402.9 ft	
Less surge	109.0	
	293.9 ft	
Head loss in penstock = $(13.70)^2$ (0.036)	6.7	
Net head at low point of surge	287.2 ft	
Water surface in tank prior to load change . . El.	1,240.0	
Surge	109.0	
Water surface at low point of surge . . El.	1,131.0 ft	

From the turbine performance curves, Fig. 12,
For hp = 50,000, Net head = 287.2

Discharge per unit = 1,725 cfs
Conduit discharge = 1,725 × 2 = 3,460 cfs

which checks the assumed discharge.

The arithmetic integration for this case shows the low point of the surge to be at El. 1,130.70 and $v_2 = 13.2 \pm$ fps.

Load Rejection. We shall select the 66 ft diameter to compute a typical point on the surge curve for load rejection (Fig. 13).

First determine the maximum velocity in the tunnel with headwater at its maximum level ($n = 0.0115$).

Try a discharge of 3,300 cfs, $v = 13.15$ fps.

Gross head	442.0 ft
Head loss = $(13.15)^2$ (0.396)	68.5
Net head	373.5 ft

From the turbine performance chart, Fig. 12, the discharge at 66,000 hp for a head of 373.5 ft is 1,650 cfs per unit. This is more than the rated capacity of the generators, but it is less than their assumed capacity at 80C temperature rise.

Use $v_1 = 13.15$ fps, $v_2 = 0$

$$100N_r = 100v_1c\sqrt{\frac{2gF}{AL}}$$

$$= 100(13.15)(0.382)\sqrt{\frac{64.4}{251 \times 43{,}200}}\sqrt{3{,}220} = 69.6$$

From the chart (Fig. 7),

$$K_r = 1.75$$
$$y_{1_r} = K_r c(v_1^2 - v_2^2)$$
$$= 1.75 \times 0.382 \times (13.15)^2 = 115.5 \text{ ft}$$

Headwater elevation	1,282.0 ft
Head loss $= (13.15)^2\ (0.382)$	66.0
Water surface elevation in tank prior to surge	1,216.0 ft
Surge	115.5
Elevation of maximum surge	1,331.5 ft

At this point we should compute the critical velocity.

$$v_c = \frac{1}{c}\left[\frac{AL(e-1)}{2gFe}\right]^{1/2}$$
$$= \frac{0.0993}{0.382}\sqrt{\frac{251 \times 43{,}200}{3{,}220}} = 15.2 \text{ fps}$$

The maximum height of surge above forebay for any discharge can be computed

$$d_{\max} = \frac{AL}{2gceF}$$
$$= \frac{251 \times 43{,}200}{64.40(0.382)(2.718)(3{,}220)} = 50.5 \text{ ft}$$

This is the maximum distance above forebay that the tank need be carried for any discharge.

Forebay	El. 1,282.0 ft
$d_{\max}$	50.5
Max point of highest possible surge	El. 1,332.5 ft

Using the shutdown curve, Fig. 8,

$$\frac{v_2}{v_c} = \frac{13.15}{15.2} = 0.865$$

Height of surge above forebay $= 0.985(50.5) = 49.7$ ft

Forebay	El. 1,282.0 ft
Height above forebay	49.7
Max point of surge	El. 1,331.7 ft

This compares with an elevation of 1,331.5 obtained above. In order to provide ample factor of safety, the top of the riser was placed at El. 1,339 in the tank as constructed.

Stability. Using an assumed conduit velocity of 14.5 fps, we obtain a check on the diameter required to ensure stability as follows:

Min reservoir elevation	1,240.0 ft
Min tailwater elevation	840.0
	400.0 ft
Head loss, reservoir to turbine $(14.5)^2\ (0.512)$	108.0
Steady-state head for Thoma formula	292.0 ft

Net tank area,

$$F = \frac{AL}{2gcH}$$
$$= \frac{251 \times 43{,}200}{64.4 \times 0.303 \times 292} = 1{,}900 \text{ sq ft}$$

Riser area	200
Gross tank area	2,100 sq ft
Corresponding diameter	52 ft
25% increase	13.2
Final diameter	65.2 ft

Use diameter of 66 ft.

Port Area. First determine the port area for load-on. (Port area determined for 50,000-hp continuous output.)

At the start of the demand load cycle,

$$a_0 = \frac{A(v_2 - v_1)}{\sqrt{2gy_1}}$$
$$= \frac{251(13.70)}{\sqrt{64.4 \times 109}} = 40.8 \text{ sq ft}$$
$$k = \frac{y_1}{c(v_2^2 - v_1^2)}$$
$$= \frac{109}{0.490 \times (13.70)^2} = 1.19$$

Near the end of the demand cycle, when $v = v_2$,

$$a_1 = \left[\frac{AFy_1}{L}\left(1 - \frac{1}{k}\right)\right]^{1/2}$$
$$= \left[\frac{251 \times 3{,}220 \times 109}{43{,}200}\left(1 - \frac{1}{1.19}\right)\right]^{1/2} = 18.0 \text{ sq ft}$$

The difference between a_0 and a_1 is large.

Using Taylor's[1] empirical equation,

$$a = a_0 - u(a_0 - a_1), \qquad \text{with} \qquad u = 0.15$$
$$= 40.8 - 0.15(40.8 - 18.0) = 37.4 \text{ sq ft}$$

Check the port area for load-off.

$$k = \frac{y_1}{cv_2^2}$$
$$k_r = \frac{115.5}{0.382(13.15)^2} = 1.75$$
$$a_1 = \left[\frac{AFy_1}{L}\left(1 - \frac{1}{k}\right)\right]^{1/2}$$
$$= \left[\frac{251 \times 3{,}220 \times 115.5}{43{,}200}\left(1 - \frac{1}{1.75}\right)\right]^{1/2} = 30.5 \text{ sq ft}$$

If the port area for load-off exceeds 30.5 sq ft, the water in the riser will recede before the end of the quarter cycle and cause the water ultimately to rise to a higher level than is given by the formula. In order to avoid the use of mechanical devices to close off a portion of the port area during rejection, the port shown on Fig. 10 is used.

[1] JOHNSON, *op. cit.*, p. 801.

From Fig. 10 we find the discharge coefficient to be 0.94 for flow out of the tank. This results in a gross area of $\frac{37.4}{0.94} = 39.8$ sq ft (40 sq ft used). The discharge coefficient of 0.71 applies to the same port for flow into the tank and gives a net area of $0.71(40.0) = 28.4$ sq ft, which is satisfactory.

Time. The time required to complete the quarter cycle for load-on is of interest mainly for estimating the number of time intervals which will be required for the arithmetic integration.

For load-on:

$$Z = \sqrt{\frac{y_1}{c} + v_1^2}$$

$$= \sqrt{\frac{109}{0.490} + 0} = 14.9$$

$$T_a = \frac{L}{2gcZ} \log_e \frac{(Z - v_1)(Z + v_2)}{(Z + v_1)(Z - v_2)}$$

$$= \frac{43{,}200}{64.4(0.490)(14.9)} \log_e \frac{(14.9 - 0)(14.9 + 13.70)}{(14.9 + 0)(14.9 - 13.70)} = 293 \text{ sec}$$

By arithmetic integration we find that $T_a = 300$ sec.

For load-off we get:

$$Z_0 = \sqrt{\frac{y_1}{c} - v_2^2}$$

$$= \sqrt{\frac{115.5}{0.382} - (13.15)^2} = 11.4$$

$$T_r = \frac{L}{gcZ_0}\left(\text{arc tan } \frac{v_2}{Z_0} - \text{arc tan } \frac{v_1}{Z_0}\right)$$

$$= \frac{43{,}200}{32.2(0.382)(11.4)}\left(\tan^{-1}\frac{13.15}{11.4} - \tan^{-1}\frac{0}{11.4}\right) = 264 \text{ sec}$$

From the integration we find that $T_r = 260$ sec.

Check by Arithmetic Integration (Tables 1 and 2, curves Fig. 14). The procedure consists of two basic operations: (1) A change in position of the turbine gates immediately changes flow through the turbine. The riser level starts to change, and this develops a head on the port area so water begins to flow in or out of the tank. For a known gate action and an assumed change in riser level, the flow to turbine, riser, and tank can be computed and the total must be the flow in the conduit. (2) The change in riser level results in an accelerating head on the conduit. The change in conduit velocity can be computed for this head and the total flow determined. If this flow checks that from (1), one step of the integration is completed.

Step 1: Fix the time interval as conditions dictate [column (1)].

Step 2: Assume the rise or fall of the water level in the riser during the time interval [column (6)]. This figure is positive when the water is ascending and negative when descending.

Step 3: Determine the discharge through turbines [column (3)] as follows: Estimate discharge through units and compute the head loss in penstock ($h = cv^2$). Compute the net head on the units [column (2)] by deducting from the gross head [column (6) minus tailwater elevation] the head loss in the penstock and adding the velocity head at the riser. Using the net head on the units and the proper gate position, determine the discharge through the units [column (3)] from the performance chart. Average the discharge through the units at the beginning and end of the interval to obtain the volume passed through the units during the interval [column (4)]. If column (6) has been estimated reasonably close, no further changes will be necessary in this step, except to correct the net head on the unit, since the discharges cannot be read with accuracy for small changes of head on the unit.

Step 4: Assume the change in water level in the tank [column (5)] and compute the rate of flow through the ports into the tank by means of $Q = a\sqrt{2gh}$ [column (7)]. The volume of water stored in the tank can then be computed from the average rate of flow through the ports for the interval [column (8)]. We can then check the assumed change in water level in the tank [column (5)] by dividing the volume flowing into the tank [column (8)] by the value of F. Some cutting and trying are necessary in this step to obtain a balance between the various variables, but it is not troublesome since the water level changes in the tank are relatively sluggish. Columns (5), (7), and (8) are positive for flows into the tank and negative for flows out of the tank.

Step 5: Compute the volume stored in the riser [column (9)] by multiplying the change in water level [column (6)] by the area of the riser. This figure is positive when the riser is filling and negative when it is emptying.

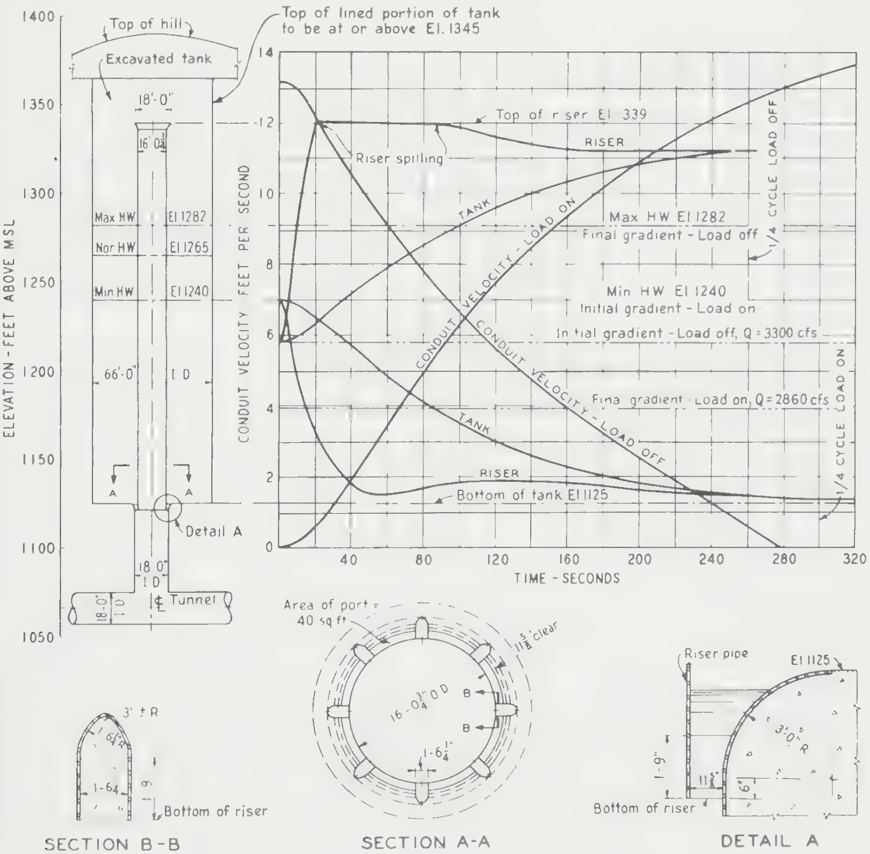

FIG. 14. Differential surge tank, design data.

Step 6: The head on the conduit [column (10)] is computed by taking the difference between the elevation of the riser water surface and the forebay. This result is positive when the water level in the riser is below the forebay and negative when above.

Step 7: Compute the acceleration head at the end of the interval [column (12)] by adding algebraically the value of the head lost in the conduit [column (11)] to the head on the conduit [column (10)]. Column (11) is obtained by assuming the conduit velocity [column (15)] and computing the head loss from $h = cv^2$. This figure will have to be corrected after the velocity is determined, but again the change in discharge is not sensitive to small head changes so that no serious trouble results if the first guess is close. Column (11) is negative for flows toward the surge tank and positive for flows toward the forebay. Column (12) is positive when the velocity is increasing toward the tank and negative when increasing toward the forebay.

Step 8: Average the acceleration heads at the beginning and end of the interval [column (12)] and obtain the average acceleration head during the interval [column (13)].

TABLE 1. ARITHMETIC INTEGRATION—DIFFERENTIAL SURGE TANK—APALACHIA PROJECT (132,000-HP LOAD REJECTION)

Headwater elevation = 1282 ft
Tailwater elevation = 840 ft
Port area 40 (0.71) = 28.4 sq ft for flow into tank
Port area 40 (0.94) = 37.6 sq ft for flow out of tank

C = 0.382 from intake to tank
C = 0.030 from tank to turbine
Tank diameter = 66 ft
Riser diameter = 16 ft

Gross area of tank = 3,421 sq ft
Riser area = 201 sq ft
Net area of tank F = 3,220 sq ft

Conduit L = 43,200 ft
Conduit area = 251 sq ft
Governor time = 5 sec

(1) Time, sec	(2) Net head on turbines, ft	(3) Flow through turbines, cfs	(4) Volume through turbines in Δt, cu ft	(5) W.S. elev tank, ft	(6) W.S. elev riser, ft	(7) Flow to tank and riser, cfs	(8) Volume to tank in Δt, cu ft	(9) Volume to riser in Δt, cu ft	(10) Head on conduit, ft	(11) Head lost in conduit, ft	(12) Acceleration head, ft	(13) Avg acceleration head, ft	(14) Flow through conduit, cfs	(15) Conduit velocity, fps	(16) Volume through conduit in Δt, cu ft	(17) Col (4) + col. (8) + col. (9), cu ft	Remarks
0	373.5	3300	0	1,216.00	1,216.00	0	0	0	66.00	66.00	0.00	0.00	3,300	13.15	0	0	132,000 hp, 66% gate
t = 1 1	375 13	2320	2810	1,216.05	1,217.69	970	145	340	64 31	66.00	− 1.69	− 0.85	3,300	13 15	3,300	3,295	90,000 hp, 46% gate
t = 1 2	383.00	1028	1674	1,216 19	1,223 50	2,272	453	1,168	58.50	66 00	− 7.50	− 4.60	3,300	13.15	3,300	3,295	40,000 hp, 20% gate
t = 1 3 3.3	..	...	670	1,216.52	1,236.25	3,300	1,055	2,560	45 75	65.70	9.95	− 8.73	3,300	13.14	4,290	4,283	0 hp, 0% gate
t = 1.7 5	......	....	....	1,217.15	1,254.00	3,300	2,040	3,580	38.00	65.70	− 27.70	− 18.83	3,300	13.12	5,600	5,620	
t = 2.0 7	......	....	....	1,218.10	1,271.50	3,270	3,050	3,520	10.50	65.20	− 54.70	− 41.20	3,270	13.06	6,530	6,570	
t = 2.0 9	......	....	....	1,219.20	1,286.50	3,270	3,530	3,020	− 4.50	64.40	− 68.90	− 61.80	3,260	12.97	9,720	6,550	
t = 3.0 12	......	....	....	1,221.05	1,305.50	3,220	5,930	3,820	−23.50	62.60	− 86.10	− 77.50	3,220	12.80	8,720	9,750	
t = 3.0 15	.....	....	....	1,223 08	1,320 70	3,170	6,520	3,060	−38.70	61.10	− 99.80	− 92.95	3,170	12 66	9,585	9,580	
t = 3.0 18	......	....	....	1,225.23	1,333.30	3,130	6,920	2,530	−51.30	58.90	−110.20	−105.00	3,130	12.43	9,450	9,450	
t = 2.0 20	......	....	...	1,226.71	1,340.30	3,080	4,800	1,410	−58 30	56.40	−114.70	−112.45	3,060	12.18	6,190	6,210	
t = 20 40	.....	....	....	1,244.41	1,341.60	2,646	Weir 10,300 Tank 46,700	262	−59.60	42.90	−101.90	−108.30	2,650	10.56	57,100	57,262	Weir crest- 18 × 3.1416 = 56.6
t = 20 60	......	...	..	1,259.71	1,339.42	2,290	Weir 7,030 Tank 42,750	− 435	−57 42	31.80	− 89.22	− 95.56	2,290	9.13	49,400	49,358	
t = 20 80	......	....	....	1,273.16	1,340.35	1,960	Weir 3,170 Tank 39,100	187	−58.35	23.30	− 81.65	− 85.43	1,970	7.85	42,600	42,457	
t = 8.0 88	......	....	....	1,274.98	1,339.00	1,835	Weir 845 Tank 14,600	− 270	−57.00	20.80	− 77.80	− 79.73	1,840	7.37	15,240	15,175	Spilling stops
t = 12 100	......	....	....	1,281 56	1,338.00	1,670	21,200	− 201	−56.00	17.20	− 73.20	− 75 50	1,680	6.70	21,120	21,000	
t = 20 120	......	....	....	1,291.46	1,333.00	1,410	31,800	−1,005	−51.00	11.95	−62.95	− 68.08	1,420	5 68	31,000	30,795	
t = 20 140	...	.	....	1,299 86	1,329 00	1,210	27,000	− 804	−47.00	8.44	− 55 44	− 59 20	1,210	4 80	26,200	26,200	

TABLE 2. ARITHMETIC INTEGRATION—DIFFERENTIAL SURGE TANK—APALACHIA PROJECT

(100,000-hp Load Demand—(Continuous)

Headwater elevation = 1,240 ft
Tailwater elevation = 840 ft
Port area 40 (0.71) = 28.4 sq ft for flow into tank
Port area 40 (0.94) = 37.6 sq ft for flow out of tank
C = 0.490 from intake to tank
C = 0.036 from tank to turbine

Tank diameter = 66 ft
Riser diameter = 6 ft
Gross area of tank = 3,421 sq ft
Riser area = 201 sq ft
Net area of tank F = 3,220 sq ft

Conduit L = 43,200 ft
Conduit area = 251 sq ft
Governor time = 5 sec

(1) Time, sec	(2) Net head on turbines, ft	(3) Flow through turbines, cfs	(4) Volume through turbines in Δt, cu ft	(5) W.S. elev tank, ft	(6) W.S. elev riser, ft	(7) Flow to tank and riser, cfs	(8) Volume to tank in Δt, cu ft	(9) Volume to riser in Δt, cu ft	(10) Head on conduit, ft	(11) Head lost in conduit, ft	(12) Acceleration head, ft	(13) Avg acceleration head, ft	(14) Flow through conduit, cfs	(15) Conduit velocity, fps	(16) Volume through conduit in Δt, cu ft	(17) Col. (4) + col. (8) + col. (9), cu ft	Remarks
0	400.00	0	0	1,240.00	1,240.00	0	0	0	0	0	0	0	0	0	0	0	0 hp. 0% gate
t = 2 2	390 69	2,120	2,120	1,239 76	1,233 25	−2,120	−770	−1,352	6.75	0.00	6.75	3.37	1	0.005	1	−4	84,000 hp, 40% gate
t = 3 5	371 10	2,580	7,050	1,238 72	1,214 90	−2,570	−3,351	−3,690	25.25	0 00	25 25	16.00	10	0.041	18	9	100,000 hp, 51% gate
t = 5 10	348 30	2,720	13,250	1,236 04	1,192 50	−2,680	−8,640	−4,500	47 50	0 00	47.50	36.38	43	0.173	135	110	100,000 hp, 56% gate
t = 5 15	332 80	2,855	13,940	1,232 75	1,177.50	−2,760	−10,575	−3,020	62 50	0 00	62.50	55.00	95	0.378	345	347.5	100,000 hp, 61% gate
t = 5 20	321.00	2,959	14,535	1,229.15	1,166 00	2,800	11,575	−2,310	74 00	0 18	73 82	68.16	158	0 632	650	634	100,000 hp, 66% gate
t = 10 30	304 20	3,162	30,650	1,221 45	1,149 00	−2,850	−24,800	−3,420	91 00	0 75	90 25	82.04	312	1.244	2,353	2,430	100,000 hp, 75% gate
t = 10 40	290 60	3,342	33,420	1,213 35	1,137.00	−2,850	−26,100	−2,410	103 00	1 88	101 12	95 68	492	1 961	4,020	4,010	99,000 hp, 85% gate (blocked)
t = 10 50	284 40	3,310	33,100	1,205 24	1,130 70	−2,630	−26,130	−1,265	109 30	3 66	105 64	103 38	686	2 732	5,890	5,865	95,000 hp, 85% gate (blocked)
t = 10 60	284 50	3,300	33,100	1,197.39	1,130.70	−2,420	−25,300	0	109 30	6 02	103 28	104 46	880	3.512	7,830	7,800	95,000 hp, 85% gate (blocked)
t = 20 80	287 40	3,335	66,340	1,183.19	1,134.00	−2,090	−45,800	665	106 00	12 30	93 70	98 49	1245	4.970	21,250	21,205	96,000 hp, 85% gate (blocked)
= 20 100	289 60	3,348	66,830	1,171 09	1,136.00	−1,770	−39,000	402	104 00	19 45	84 55	89.13	1578	6.300	28,230	28,332	98,000 hp, 85% gate (blocked)
= 20 120	290 60	3,340	66,880	1,160 99	1,137 00	−1,460	−32,500	201	103 00	27.60	75 40	79 98	1880	7.490	34,580	34,580	99,000 hp, 85% gate (blocked)
= 20 140	290 60	3,340	66,800	1,152.64	1,137 00	−1,210	−26,700	0	103 00	35.70	67.30	71 35	2130	8.550	40,100	40,100	99,000 hp, 85% gate (blocked)

Turbine gates are blocked at 85% to avoid operation on the rapidly falling portion of the turbine efficiency curve. If the turbine were allowed to open to 100% gate, the result would be a lower required bottom elevation of tank and a reduction of power output at the heel of riser curve with no compensating advantages.

Step 9: Compute the change in discharge in the conduit [column (14)] from the equation $dQ = \frac{H_a g A\, dt}{L}$ and the resulting discharge at the end of the time interval. Check the assumed conduit velocity [column (15)] and make the necessary corrections.

Step 10: Compute the volume of flow through the conduit [column (16)]. Then add the volume of flow through the units to that going into the tank and riser [column (17)]. If columns (16) and (17) are equal or reasonably close, the integration for that time interval is complete. If they are at variance, the necessary corrections must be made.

When the riser is spilling, an additional complication is introduced. In order to determine the exact retarding head which is being applied to the tunnel, it is necessary to compute the height at which the water stands above the top of the riser by use of a weir formula.

The practice of blocking the turbine gates at about 85 per cent as indicated in Table 2 may be considered typical standard practice. If the gates were not so blocked but allowed to open to the 100 per cent position, the surge would be increased quite appreciably owing to the rapid falling away of turbine efficiency after about 85 per cent gate. This would necessitate placing the tank bottom at lower elevation and in addition would result in appreciably lower power output at the heel of the riser drop curve, with no compensating advantages. The output of 95,000 hp at the heel given by Table 2 is usually considered sufficiently close to the specified value of 100,000 hp.

9. OPERATING TESTS

Figure 15 shows the results of applying an instantaneous load demand of 80,000 kw and later, after reasonably quiescent conditions have been established, an instantaneous load rejection of 80,000 kw. These load changes were applied with the

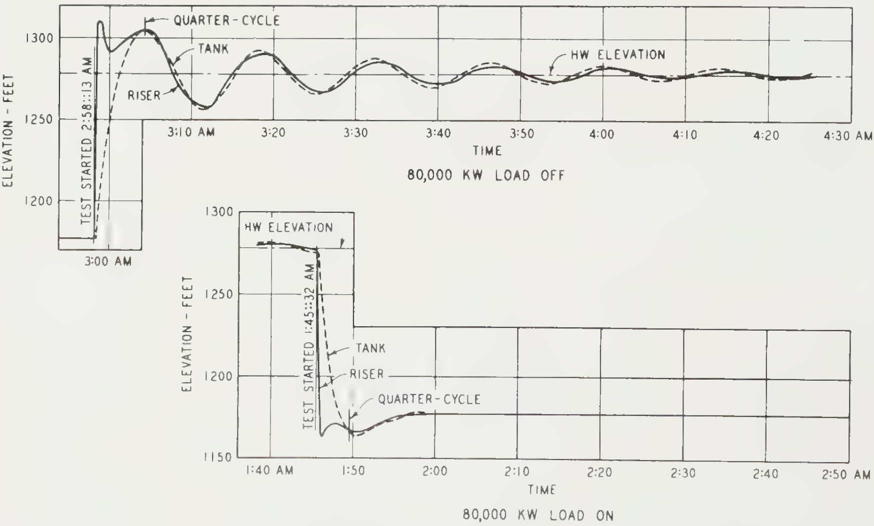

FIG. 15. Surge tank testing with both units operating, Apalachia project.

Apalachia units synchronized and operating in conjunction with the entire T.V.A. system. The large block of load required for making the test was obtained by prearrangement and interconnection with the Louisville Gas and Electric Company.

There are of course several important differences to be emphasized in comparing these actual performance curves with the demand and rejection conditions for which the surge tank was designed. In the first place, the headwater elevation available was about El. 1,280 as compared with El. 1,282 for the design rejection condition and 1,240 for the design demand condition; but the demand test load is about 107,000 hp as compared to the design demand load of 100,000 hp. For the demand condition the value of V_2 is about the same so that the demand surge is practically the same in both cases. As would naturally be expected, the final quiescent gradient for demand is about 1,180 for both the arithmetic integration and the operating test. All factors considered, the test does yield substantial assurance that if both units were given an instantaneous load demand aggregating 100,000 hp starting with headwater at El. 1,240, there would be a margin of at least 5 ft between the bottom of tank and the extreme low elevation of water levels.

The load rejection test starts with the tank levels at about El. 1,180 as compared with the design assumption of El. 1,216, a difference of 36 ft. The design case assumed a load rejection of 132,000 hp as compared with 107,000 hp for the test; but this greater demand is compensated to some extent by the fact that in the design case the units were operating at a head about 40 ft greater than that which obtained during test conditions. There was an adverse factor during test conditions caused by the fact that the riser was unable to spill, giving a characteristic recession and subsequent rise in riser levels during the quarter cycle. These considerations will explain why the rejection surge was about 130 ft under test conditions as compared with 120 ft under design conditions. Again, however, the result of the rejection test was a confirmation of the original design and indicated that, if rejection were started with tank levels at El. 1,216, performance would be in accordance with the design curves.

It is interesting to note that in the case of load rejection a very appreciable time interval is required to damp out the major pendulations of water surface in the tank, about one-half hour being necessary for fairly steady conditions while some unimportant pendulations were still observable for an hour after the completion of the test. This is, however, what might reasonably be expected for the case of a 9-mile tunnel of such large dimensions. It will also be observed that, while a periodic disturbance persisted for a comparatively long period of time in the case of load rejection, damping to the quiescent condition required but a brief interval for load demand. This is, of course, due to the fact that under the demand condition the load itself is a means of absorbing excess energy while, in the rejection condition, conduit friction is the only agency affecting the ultimate dissipation. This case parallels to some degree a similar phenomenon observable in the Angus diagrams for water-hammer pressures in the cases of valve closure as compared with valve opening. After the valve has closed, water-hammer pendulations continue for an appreciable time at relatively high intensity; but in the case of opening, the pendulations subsequent to the fully open condition are of small magnitude and commensurate duration.

OTHER TYPES OF TANK

It is believed that with the foregoing material on the analysis of differential surge tanks as background, the engineer will have no difficulty in preparing any desired investigation of other types of regulator.

Computation of the simple surge tank by arithmetic integration will be found comparatively easy and similar but shorter than the tabulation given in Art. 8. Because of the aforementioned difficulty with the form of its differential equation, no equations similar to Johnson's expression are available for predetermination of the tank size in relation to the surge, so that for preliminary proportions we have only the judgment gained from experience and the Thoma formula for the diameter required for stability. Before the advent of the modern quick-response governor, proponents of the simple tank claimed as one of its advantages a very gradual drop in the water surface curve, which the turbine governor could follow with comparative ease. With the availability of modern high-speed governors, however, this advantage is no longer of any great weight in determining selection of types. With respect to synchronous load changes, the simple tank is at a definite disadvantage in comparison with the differential regulator, in which the water supply and conduit acceleration functions are separated. For given performance, the simple tank design is generally a more expensive solution.

The restricted orifice type of tank (Fig. 16) is somewhat similar in action to the differential surge tank, the principal difference being that no riser is provided, and the entrance orifice into the bottom of the tank is relatively smaller than the corresponding

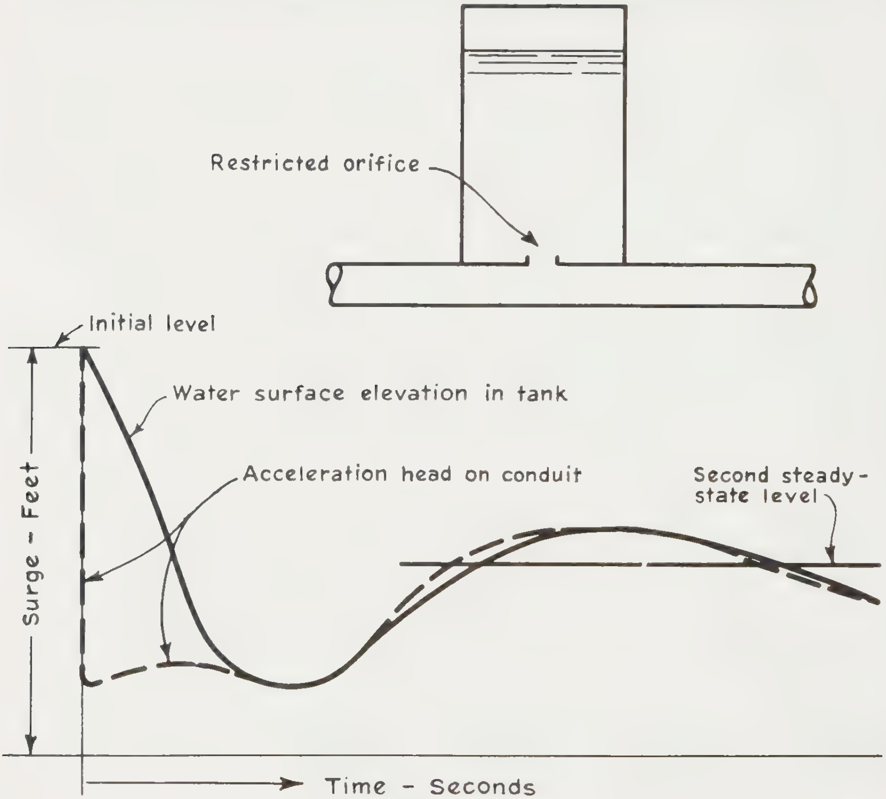

Fig. 16. Load demand. Restricted orifice surge tank with typical performance curves.

riser diameter of the differential regulator. This means that with respect to the mass-acceleration action the retarding or accelerating head is created at the instant of gate movement—in magnitude just sufficient to store in or supply from the tank the requisite decrement or increment of water corresponding to the load change. This accelerating or retarding head on the restricted orifice then varies from instant to instant as required to give hydraulic continuity. In comparison with the differential tank, the adverse effects of water hammer are increased owing to the reduction in size of the opening into the surge tank and the consequent reduction in discharge relief afforded the conduit.

For very high head plants (those having heads in the order of 1,000 ft or higher), the type of tank shown in Fig. 17 has found favor in some installations both in this country and in Europe. This type of design finds application in mountainous terrain, in which the various component sections of the regulator may be excavated from solid rock. The design consists basically of comparatively large upper and lower storage chambers connected by an intermediate vertical shaft of relatively small diameter. Upon the application of a load change of any considerable magnitude the water surface moves promptly to either the upper or the lower chamber, as required, creating a large decelerating or accelerating head on the conduit; and it is a comparatively inexpensive matter to excavate the upper and lower chambers of size sufficient to store or supply the volume of water required for the load change. During normal

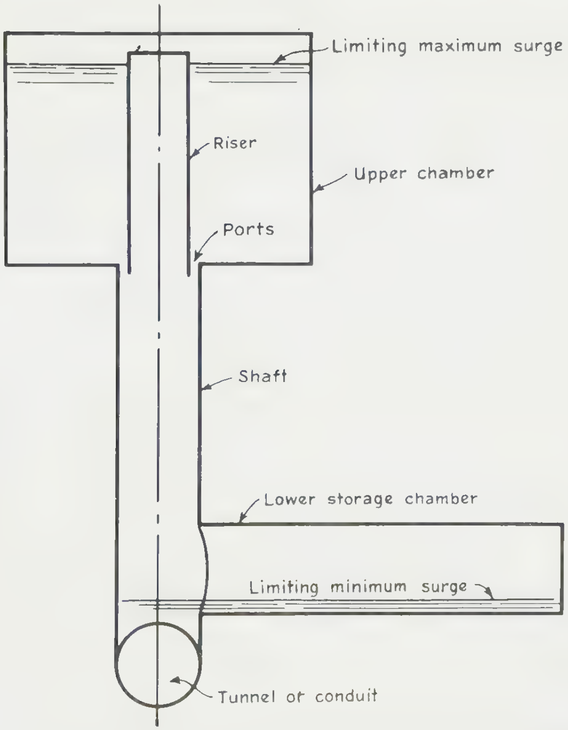

Fig. 17. Compound surge tank applicable to high head installations.

operation and light load changes, the water surface elevation is in the intermediate shaft; and in view of the very high head, it will be seen from the Thoma formula that the area required for stability in the central shaft is comparatively small. It should be emphasized, however, that, because of stability considerations, this small central shaft can be employed only on the higher head installations, and the whole arrangement is, as a general rule, economical only in cases where it is possible to excavate the regulator from the solid rock.

With the development of large modern hydroelectric generating units of great capacity, the field of applicability of the closed-top tank, in which the surge of water is accompanied by the compression or expansion of a superimposed volume of air, appears to be restricted to a few isolated units in remote locations, in which the difficulty of hauling materials or the lack of headroom is a dominant consideration. In view of the reduced likelihood that the engineer will be called upon to design such equipment for hydroelectric installations, and the additional fact that they constitute such a specialty, no further discussion of their design will be given in this chapter other than to refer the reader to the literature on the subject.[1]

As would naturally be expected, surge regulators, particularly those of the differential type, not only are employed for hydraulic turbine installations but are equally applicable to the companion reverse case of centrifugal or other pumps feeding long pipe lines employing moderate to high velocities. The only difference in the application is that, upon stoppage of the pump motor by interruption of the electric power supply, there is a reduction in water supply and a diminution of velocity, and hence the initial impulse propagated along the pipe line is a negative instead of a positive pressure wave. Just as in the case of the turbine plants, water-hammer effects are alleviated by providing by means of a surge tank an open reservoir close to the terminal mechanism, capable of propagating back compensating pressure reflections of opposite sign. Again, as in the case of the turbine, it is feasible and advantageous to separate the water hammer and the mass acceleration computations which may be carried out in fashion exactly similar to the material given in Art. 8. In some installations, optimum over-all economy may be secured by eliminating the check valve in the line ahead of the pump and providing for comparatively slow closure of the main valves. In such cases the centrifugal pump not only may slow down upon loss of power supply but, owing to the slow closure of the valve, may run backward as a turbine for a short interval until valve closure is completed. For the solution of such cases, both for water-hammer and mass-acceleration effects, a complete set of performance curves for the pump acting either as a pump or in reverse as a turbine is an essential prerequisite to the calculation

Bibliography

Johnson, Raymond D., The Differential Surge Tank, *Trans. ASCE, Paper* 1324, vol. 88, 1915.

Johnson, Raymond D., The Surge Tank in Water Power Plants, *Trans. ASME, Paper* 1204, vol. 30, 1908, pp. 443–474; discussion, pp. 474–501.

Warren, Minton M., Air Tanks on Pipe Lines, *Trans. ASCE, Paper* 1407, vol. 82, 1918; discussion by P. Wahlman, pp. 270–275.

Jules, Calame, and Daniel Gaden, "Theorie des chambres d'equilibre," Paris and Lausanne, 1926. An excellent treatment of the subject in French, including charts for rapid calculation and a comprehensive discussion of stability.

Schoklitsch, Armin, "Hydraulic Structures," vol. II. Translation published by The American Society of Mechanical Engineers, New York, 1937, pp. 867–883. Contains a graphical method of solution, numerous examples of European practice, and a long bibliography of German articles.

Rich, George R., "Hydraulic Transients," McGraw-Hill Book Company, Inc., New York, 1951.

[1] Warren, M. W., Air Tanks on Pipe Lines, *Trans. ASCE, Paper* 1407, vol. 82, 1918, discussion by P. Wahlman, pp. 270–275.

SECTION 29

SPEED REGULATION AND GOVERNING STABILITY

By George R. Rich

INTRODUCTION AND SCOPE

The purpose of this section is to furnish background for the calculation and correlation of governor time, generator WR^2, and transient characteristics of the pressure conduit, so as to ensure the degree of speed regulation warranted for the particular project. It is assumed at the outset that the engineer has access to the literature of the governor manufacturers, which gives a very clear and complete account of mechanical construction and accessories.

To meet the increasing demand upon the modern hydraulic engineer for governing stability computations, it was originally intended to present (with the kind authorization of the author and his publishers) simply a translation and abstract of the classic treatise, "Considérations sur le problème de la stabilité des regulateurs de vitesse," by Daniel Gaden.† But in furnishing valued assistance during the progress of this work, Mr. Gaden has virtually rewritten this entire portion of the chapter expressly for American engineers. For this generous cooperation, it is desired to make acknowledgment.

Before proceeding with the analytical work, it appears pertinent to caution against providing refinement in regulation in excess of what is justified economically for the particular project. Improvements in regulation may prove relatively expensive and have a tendency to trespass the boundary of diminishing returns. The actual limits to the regulation must as a general rule be established in collaboration with the operating engineers, who are well aware that investments in speed and frequency control must earn their share of dividends.

FLYWHEEL EFFECT FOR THE OPEN-FLUME SETTING

The most logical first step in breaking ground for the development of the working tools for the governing problem is to formulate the basic expression for speed change as a function of load change and flywheel effect, or WR^2.

To reduce the problem to its simplest elements, we shall consider that the turbine is operating in an open-flume setting and that the governor is simply a means of closing or opening the turbine gates uniformly in a prescribed time. We shall employ the following notation:

Δt = time required by governor to move turbine gates to new position, sec.
hp = *instantaneous* change in horsepower delivered *externally* by turbine.
N_0 = speed of rotation of turbine in rpm at instant of external load change.
N = speed of rotation of turbine at end of time Δt, rpm.
WR^2 = polar moment of inertia of rotating masses about axis, pfs.

† Directeur, Ateliers des Charmilles, Geneva. Published by Editions La Concorde, Lausanne, Switzerland.

Then from elementary dynamics,

$$\text{Applied work} = \text{change in kinetic energy}$$

$$\frac{\Delta t \times hp \times 550}{2} = \frac{W}{g}\frac{1}{2}\left[\left(\frac{2\pi RN}{60}\right)^2 - \left(\frac{2\pi RN_0}{60}\right)^2\right]$$

$$N^2 - N_0^2 = \frac{1{,}620{,}000\ \Delta t(hp)}{WR^2} \tag{1}$$

This derivation is fully rigorous and should be employed in all analyses where complete accuracy is essential. However, because of its greater convenience, the following approximation has found almost universal acceptance in the power industry.

Dividing both sides by N_0^2 and factoring,

$$\left(\frac{N + N_0}{N_0}\right)\left(\frac{N - N_0}{N_0}\right) = \frac{1{,}620{,}000\ \Delta t}{C}$$

in which $C = \dfrac{N_0^2(WR^2)}{hp}$ is known as the regulation constant.

If we take $\dfrac{N + N_0}{N_0} = \dfrac{2N_0}{N_0} = 2$ as an approximation, we obtain

$$\omega = \frac{N - N_0}{N_0} = \frac{8.1 \times 10^5\ \Delta t}{C} \tag{2}$$

Equations (1) and (2), particularly (2), find very wide application, but they usually require two additional corrections: the first to compensate for the fact that at any given head there is an upper limit to the speed which the turbine is capable of reaching, namely the so-called runaway speed; the second to make allowance for the effect of water hammer.

To include the effect of turbine runaway limit, let S = the relative speed of the turbine at runaway, referred as a percentage (such as 180) to the normal or synchronous speed.

We next seek an approximate expression that will yield $\omega_{rs} = S - 100$ for the runaway speed as the maximum value, and make commensurate correction for all intermediate values of ω between normal speed and runaway. The following expression will be found to answer the purpose:

$$\omega_{rs} = \frac{\omega}{100 + \dfrac{100\omega}{S - 100}} \tag{3}$$

For example, if the speed rise computed by Eq. (2) is 60 per cent and the runaway speed of the particular turbine is 180 per cent of normal, the corrected speed rise will be

$$\omega_{rs} = \frac{60}{100 + \dfrac{100 \times 60}{180 - 100}} = 34 \text{ per cent}$$

For speed drop for the condition of load on, Eqs. (1) and (2) are usually applied without correction for variation in the slope of the performance curve of the driving couple as a function of the speed of rotation.

Example 1: On the assumption of an open flume setting, and neglecting the effect of the turbine runaway characteristic, compute the percentage speed rise for the following conditions:

Load rejected	91,500 hp
Synchronous speed	150 rpm
Gate closure time	3 sec
Generator WR^2	53,000,000 pfs

$$\text{Regulation constant } C = \frac{N_0^2 WR^2}{hp} = \frac{150^2 \times 53{,}000{,}000}{91{,}500} = 13 \times 10^6$$

$$\frac{N_1 - N_0}{N_0} = \frac{8.1 \times 10^6\,\Delta t}{C} = \frac{8.1 \times 10^6 \times 3}{13 \times 10^6} = 18.5 \text{ per cent}$$

Speed rise = 18.5 per cent

Example 2: Include the effect of turbine runaway speed correction in Example 1, assuming that the runaway speed of the turbine is 180 per cent of normal synchronous speed.

$$\omega_{rs} = \frac{\omega}{100 + \dfrac{100\omega}{S - 100}} = \frac{18.5}{100 + \dfrac{100 \times 18.5}{180 - 100}} = 15 \text{ per cent}$$

Speed rise = 15.0 per cent

INFLUENCE OF WATER HAMMER

For the installations encountered in practice, the turbine setting will not be an open flume as contemplated by Eqs. (1) and (2), but will be served by some form of waterway or penstock. Accordingly, reductions or increases in the penstock velocity will be accompanied by a head rise or head drop resulting from the phenomenon of water hammer.

The water-hammer increment (or decrement, as the case may be) will change the power supplied to the turbine according to the $3/2$ power of the resultant relative value of the increased head in accordance with established principles.

For the condition of load rejection, velocity decrease, and pressure rise, the power input to the turbine will become $hp_{wh} = hp_0(1 + h)^{3/2}$ in which $h = \dfrac{H_{wh} - H_0}{H_0}$ (with $h > 0$), and since the speed rise in Eq. (1) varies directly as the power, we obtain

$$\omega_{wh} = \omega(1 + h)^{3/2} \tag{4}$$

Including the effect of both runaway speed and water hammer, we have

$$\omega_{rs+wh} = \omega_{rs}(1 + h)^{3/2} \tag{5}$$

For the condition of load demand, velocity increase, and pressure drop, we also find, by a similar approach,

$$\omega_{wh} = \frac{\omega}{(1 + h)^{3/2}} \tag{6}$$

but with $h < 0$.

The requisite relative values of pressure rise and fall are determined by the methods of the section on water hammer.

Example 3: Include the effect of water hammer in Example 2, assuming the water-hammer effect to be 65 per cent greater than the normal head.

$$\omega_{rs+wh} = \omega_{rs}(1 + h)^{3/2} = 15.0(1.65)^{3/2} = 32.0 \text{ per cent}$$

Speed rise = 32.0 per cent

Compare with the arithmetic integration method, Example 5, which has the same physical data.

Example 4: Compute the percentage speed drop for the following conditions:

Load increase from 51,500 to 91,500 hp	
Synchronous speed............	150 rpm
Gate opening time.............	1.5 sec
Generator WR^2...............	53,000,000 pfs
Water-hammer drop...........	30 per cent ($h < 0$)

$$\text{Regulation constant } C = \frac{N_0^2(WR^2)}{hp} = \frac{150^2 \times 53{,}000{,}000}{40{,}000} = 30 \times 10^6$$

$$= \frac{N_1 - N_0}{N_0} = \frac{8.1 \times 10^6\,\Delta t}{C} = \frac{8.1 \times 10^6 \times 1.5}{30 \times 10^6} = 4 \text{ per cent}$$

$$\omega_{wh} = \frac{\omega}{(1 + h)^{3/2}} = \frac{4}{(1 - 0.30)^{3/2}} = 7 \text{ per cent}$$

Speed drop = 7 per cent

Table 1. Speed Rise and Water Hammer

150 rpm. 91,500 hp at 330 ft head. Full gate, 135 in. diameter
(Use Appalachia N^2 test curve)
Neglect friction and velocity head

L = 400 ft
Diameter = 14 ft 0 in.
a = 4,660 fps
A = 153.5 sq ft

Closure time = 4 sec
Use uniform equivalent = 3 sec (to allow for dead and cushioning time)
18 intervals at 0.17 = 3.06 sec
WR^2 = 53,000,000 pfs

(1) Interval	(2) Time, sec	(3) Gate, %	(4) ΔV V	(5) ΔH or 145 ΔV	(6) $\Sigma\,\Delta H$	(7) $H_0 + \Sigma\,\Delta H$	(8) Rpm	(9) Rpm$_1$ 12 in.	(10) Q	(11) Efficiency, %	(12) V	(13) Hp_1 12 in.	(14) Hp	(15) Avg hp	(16) Rpm^2	(17) $N_2^2 - N_1^2$	(18) ΔT
0	0	100	18.25	0	0	330	150	92.75	2,810	86.5	18.25	0.120	91,500	......	22,500		
1	0.17	94.5	−0.05 18.20	+7.2	+7.2	337.2	153.2	94.2	2,790	87.0	18.20	0.119	93,000	92,250	23,450	950	0.17
2	0.34	89.0	−0.15 18.05	+21.7	+14.5	344.5	156.3	95.0	2,760	88.0	18.05	0.117	94,600	93,800	24,430	980	0.17
3	0.51	83.5	−0.25 17.80	+36.3	+21.8	351.8	159.43	96.0	2,730	88.0	17.80	0.115	95,700	95,150	25,408	990	0.17
4	0.68	78.0	−0.37 17.42	+53.6	+31.8	361.8	162.5	96.2	2,670	90.0	17.42	0.114	98,200	96,950	26,406	998	0.17
5	0.85	72.0	−0.51 16.91	+74.0	+42.2	372.2	165.7	96.8	2,600	90.7	16.91	0.111	100,600	99,400	27,456	1,050	0.17
6	1.02	67.0	−0.65 16.26	+94.0	+51.8	381.8	168.8	96.0	2,510	90.6	16.26	0.106	99,300	99,950	28,561	1,037	0.17
7	1.19	61.0	−0.70 15.56	+102.0	+50.2	380.2	171.95	99.5	2,390	90.0	15.56	0.100	94,000	96.650	29,567	1,006	0.17

8	1.36	56.0	−0.70 14.86	+102.0	+51.8	381.8	174.7	101.0	2,280	90.3	14.86	0.094	88,700	91,350	30,520	953	0.17
9	1.53	50.0	−0.90 13.96	+130.5	+78.7	408.7	177.3	98.5	2,150	89.3	13.96	0.085	89,000	88,850	31,435	915	0.17
10	1.70	44.0	−1.05 12.91	+152.5	+73.8	403.8	179.75	101.0	1,980	87.5	12.91	0.077	79,200	84,100	32,310	875	0.17
11	1.87	39.0	−1.05 11.86	+152.0	+78.2	408.2	182.0	101.5	1,825	86.7	11.86	0.071	74,000	76,600	33,124	814	0.17
12	2.04	33.0	−1.20 10.66	+174.0	+95.8	425.8	183.96	101.0	1,630	83.3	10.66	0.059	65,600	69,800	33,841	717	0.17
13	2.21	28.0	−1.40 9.26	+203.0	+107.2	437.2	185.65	100.0	1,424	80.0	9.26	0.049	56,900	61,250	34,473	632	0.17
14	2.38	22.0	−1.70 7.56	+246.0	+138.8	468.8	187.0	97.0	1,165	76.0	7.58	0.037	47,300	52,100	35,015	542	0.17
15	2.55	17.0	2.10 5.46	+305.0	+166.2	496.2	188.10	95.0	840	58.8	5.46	0.020	28,000	37,650	35,409	394	0.17
16	2.72	11.0	−2.60 2.86	+377.0	+210.8	540.8	188.3	92.0	440	29.6	2.86	0.005	8,000	18,000	35,596	187	0.17
17	2.89	6.0	−1.88 0.98	+273.0	+62.2	392.2	188.4	107.0	150	0.00	0.98	0.00	0.00	4,000	35,638	42	0.17
18	3.06	0.0	−0.98 0.00	+142.0	+79.8	409.8	188.4	104.5	0.00	0.00	0.00	0.00	0.00	0.00	35,638	0	

$$\text{Interval} = \frac{2L}{a} = \frac{2 \times 400}{4{,}660} = 0.17 \text{ sec}$$

$$\Delta H = \frac{a\,\Delta V}{g} = \frac{4{,}660\,\Delta V}{32.2} = 145\,\Delta V$$

$$\text{Work} = \frac{MV^2}{2}$$

$$\text{Avg hp} \times 550 \times \Delta T = \frac{W}{2g}\left[4\pi^2R^2\frac{(N_2^2 - N_1^2)}{3{,}600}\right]$$

$$\Delta T = \frac{16.33(N_2^2 - N_1^2)}{\text{Avg hp}}$$

TABLE 2. TIME REQUIRED TO PICK UP FULL LOAD
Gate opening time 150 sec
Assume generator synchronized to system at 300 rpm

(1) Interval	(2) Time, sec	(3) Gate opening, %	(4) ΔV / V	(5) ΔH or $145\,\Delta V$	(6) $\Sigma\,\Delta H$	(7) Friction loss	(8) $H_0 + \Sigma\,\Delta H + F$	(9) Q	(10) V	(11) Turbine efficiency, %	(12) Hp
0	0	0	0.00	0	0	0	534	0	0	0	0
			+0.75								
1	11.50	0.077	0.75	−109	−109	−1	424	59	0.75	Speed, no load	0
			+0.88								
2	23.00	0.154	1.63	−127	−18	−2	514	129	1.64	48	3,600
			+0.67								
3	34.50	0.231	2.30	−97	−79	−3	452	182	2.31	68	6,360
			+0.85								
4	46.00	0.308	3.15	−123	−44	−6	484	250	3.18	79	10,800
			+0.75								
5	57.50	0.384	3.90	−109	−65	−10	459	304	3.88	85	13,500
			+0.85								
6	69.00	0.460	4.75	−123	−58	−14	462	372	4.74	87	17,000
			+0.75								
7	80.50	0.537	5.50	−109	−51	−20	463	433	5.50	91	20,800
			+0.72								
8	92.00	0.614	6.22	−104	−53	−25	456	487	6.22	92	23,200
			+0.71								
9	103.50	0.691	6.93	−103	−50	−32	452	544	6.93	92.5	25,800

10	115.00	0.768	+0.70 7.63	−101	−51	−37	446	600	7.63	92.0	28,000
11	126.50	0.845	+0.72 8.35	−104	−53	−45	436	656	8.35	91.0	29,600
12	138.00	0.922	+0.72 9.07	−104	−51	−52	431	712	9.07	89.0	31,000
13	149.50	1.000	+0.72 9.79	−104	−53	−60	421	767	9.79	88.0	32,300
14	161.00	1.00	+0.45 10.24	−65	−12	−60	462	805	10.24	88.0	37,200
15	172.50	1.00	+0.66 10.30	−9	+3	−60	477	810	10.30	88.0	38,600

Tunnel area = 78.5 sq ft
L = 26,850 ft
a = 4,660 fps

$$\Delta H = \frac{a\,\Delta V}{g} = \frac{4{,}660\,\Delta V}{32.2} = 145\,\Delta V$$

$$\frac{2L}{a} = \frac{2 \times 26{,}850}{4{,}660} = 11.50 \text{ sec}$$

USE OF ARITHMETIC INTEGRATION

For the more involved studies of transient phenomena accompanying load change, the step-by-step method of arithmetic integration will be found to have wide applicability, and it is believed that the details of the process will be clear from the following illustrative examples. The turbine performance data were supplied by the manufacturers in the form of model test curves, plotted according to the so-called oak-tree contour arrangement, giving values of unit power as ordinates, unit speed as abscissas, closed contours as efficiency, and transverse curves to show gate opening. It will be an instructive exercise for the reader to plot curves showing the change in the various variables with the time for the three examples given.

Example 5: Table 1 is a typical, fast, load-rejection study which affords an accurate time history of the transient disturbance. The general mode of attack is to guess simultaneously trial values of V and rpm; when the guess is correct, the values of V in column (11) and Δt in column (17) will check the corresponding values of V in column (3) and Δt in column (1), respectively.

Example 6: This was undertaken (Table 2) to show the length of time required to pick up full load for the case of a plant with a long pressure conduit and no surge tank, but provided with a relief valve for load rejection. Regulation was provided by other plants in the system, but the transient problem is closely allied with the general subject of this chapter. The mode of attack is to guess trial values of ΔV in column (4) and, when the trial value is correct, the value of V in column (10) will check the value of V in column (4). V in column (10) is computed from the total head in column (8) and the turbine efficiency and power in columns (11) and (12). The turbine performance is based upon manufacturers' test curves.

Example 7: This is based (Table 3) upon the same plant as given in Example 6. It is assumed that the turbine gates are stuck in the full open position following rejection of full load for short-circuit condition. Owing to the overspeed characteristic of the turbine, the discharge is reduced as the turbine picks up speed. This in turn produces water hammer just as effectively as if the valve were closed too fast. The fact that the transient disturbance damps down to an equilibrium level indicates that the oscillating system is inherently stable. The general mode of attack is to guess trial values of ΔV in column (3) and rpm in column (8), and verify the trial values in column (12) for V and column (18) for ΔT. For the method of arranging this problem the writer is indebted to W. M. Rheingans, assistant manager, Hydraulic Department, Allis-Chalmers Manufacturing Company. The turbine performance characteristics were obtained from the manufacturer's oak-tree model test curves.

BASIC EQUATION OF GOVERNING (Compensation Omitted)

To an increasing degree, the modern hydraulic engineer is called upon to analyze problems in the field of governing stability, by which is meant the selection and correlation of the elements WR^2, governor action, and pressure conduit features so as to ensure rapid damping of the transient disturbance to normal synchronous speed following a load change, the load afterward remaining constant. When due consideration has not been given to stability, there is the possibility of perpetual pendulation of the gate-operating mechanism and of the speed of operation with resultant disruption to power interchange service, electric time keeping, and other related functions of the present-day highly organized electric power industry.

With the ultimate objective of developing a simple, workable test for governing stability, we shall start by formulating the operating equation for a crude rudimentary governor, consisting merely of a speed-responsive element or flyball, a relay valve with suitable ports, and an oil-pressure-operated servomotor for moving the turbine gates. We shall note the defects inherent in such a rudimentary system, and then in succeeding articles we shall add the necessary corrective elements and incorporate their respective functions in the governor-operating equation. For the material presented in the next four articles, the writer is indebted to the classic treatise† of the French engineer, Daniel Gaden.

As the first step, let us rewrite the fundamental flywheel equation [Eq. (1) Art. 2] in

† GADEN, DANIEL, "Considérations sur le problème de la stabilité des regulateurs de vitesse," Editions La Concorde, Lausanne, Switzerland.

TABLE 3. PRESSURE AND SPEED RISE COMPUTATION

Turbine gates stuck in full gate position[1]

Tunnel area = 78.5 sq ft
L = 26,850 ft
a = 4,660 fps
WR^2 = 4,000,000 pfs

(1) Interval	(2) Time, sec	(3) ΔV / V	(4) ΔH or $145\,\Delta V$	(5) $\Sigma\,\Delta H$	(6) Friction head regained, ft	(7) $H_0 + \Sigma\,\Delta H + F$	(8) Rpm	(9) Rpm_1	(10) Q_1	(11) Q	(12) V	(13) Hp_1	(14) Hp	(15) Avg hp	(16) Rpm^2	(17) $N_1^2 - N_2^2$	(18) ΔT
	0	10.31	0.00	0.00	0	474	300	13.8	37.2	810	....	3.68	38,000	....	90,000		
1	11.50	−1.61 / 8.70	+233	+233	13	720	582	21.7	25.4	683	8.70	+0.80	+15,500	+26,750	339,000	249,000	11.50
2	23.00	−2.30 / 6.40	+334	+101	35	610	608	24.6	20.4	504	6.42	−0.56	−8,440	+3,530	369,000	33,000	11.50
3	34.50	−0.57 / 5.83	+83	−18	39	495	548	24.6	20.4	467	5.81	−0.57	−6,280	−7,360	300,000	69,000	11.50
4	46.00	+0.31 / 6.14	−45	−27	36	483	518	23.6	22.2	488	6.19	−0.05	−530	−3,405	268,200	31,800	11.50
5	57.50	+0.33 / 6.47	−48	−21	34	487	516	23.4	22.55	499	6.36	0.00	0.00	−265	265,725	2,475	11.50
6	69.00	+0.10 / 6.57	−15	+6	32	512	523	23.10	22.95	518	6.60	+0.15	+1,730	+865	273,800	8,100	11.50
7	80.50	−0.10 / 6.47	+15	+9	33	516	532	23.40	22.50	510	6.49	0.00	0.00	+865	281,900	8,100	11.50
8	92.00	−0.05 / 6.52	+7	−2	33	505	529	23.50	22.30	502	6.44	−0.05	−568	−284	279,250	2,650	11.50

$$\text{Interval } \frac{2L}{a} = \frac{2 \times 26{,}850}{4{,}660} = 11.50 \text{ sec} \qquad \Delta H = \frac{a\,\Delta V}{g} = \frac{4{,}660\,\Delta V}{322} = 145\,\Delta V \qquad \text{Work} = \frac{MV^2}{2}$$

$$\text{Avg hp} \times 550 \times \Delta T = \frac{W}{2g}\left[4\pi^2 R^2 \frac{(N_1^2 - N_2^2)}{3{,}600}\right] \qquad \Delta T = 1.235\,\frac{(N_1^2 - N_2^2)}{\text{Avg hp}}$$

[1] For the arrangement used in this computation, the writer is indebted to W. J. Rheingans, assistant manager, Hydraulic Department, the Allis-Chalmers Manufacturing Co., Milwaukee, Wis.

differential form; and in order to give complete generality to the results and thus permit the use of tables applicable to all subsequent numerical cases, we shall use relative values for the principal variables such as $\omega = \dfrac{N - N_0}{N_0}$; $p_0 = \dfrac{P - P_0}{P_0}$, $h = \dfrac{H - H_0}{H_0}$, $x = \dfrac{X - X_0}{X_0}$, and so on.

Symbols for Stability Analysis (Arts. 5 to 8)

Time.

t = general time variable, sec.
t_g = minimum value of time required for governor to move turbine gates from opening at which stability is being investigated, to zero, sec.
T_g = $k\beta t_g$, characteristic time of promptness of governor response, sec.
T_g' = $T_g + k_r\delta' T_d$, modified value of characteristic time of promptness of governor response for a speed-responsive governor with secondary compensation including a dashpot.
$T = \dfrac{C}{16.2 \times 10^6}$, mechanical inertia parameter which characterizes the effect of rotating masses. The dimension of T is in seconds of time.
$T_r = \dfrac{j}{j - 3r} T$ = mechanical inertia parameter corrected for effect of first component of water hammer, taking account of turbine efficiency change. The dimension is in seconds of time.
T'' = period of oscillation of governing, sec.
T' = period of free oscillation of water-hammer wave $= 2\mu = \dfrac{4L}{a}$, sec. (Equal to twice the duration of the phase μ, *i.e.*, twice the duration of a direct and reflected transit of the water-hammer wave.)
T_d = characteristic time of dashpot rigidity (or of dashpot throttling action), sec. This time is defined by the equation

$$\omega_r - \omega_p = T_d \frac{d}{dt}(\omega_p - \omega_c)$$

T_{g1} = value of T_g for the first of two generating units operating in conjunction, sec.
T_1 = value of T for the first of two generating units operating in conjunction, sec.
T_{g2} = value of T_g for the second of two generating units operating in conjunction.
T_2 = value of T for the second of two generating units operating in conjunction.

Water Hammer.

a = velocity of water-hammer wave, fps.
g = acceleration of gravity, ft/sec².
$\Theta = \dfrac{LV_0}{gH_0} = \rho\mu$, hydraulic inertia parameter having the dimension of time, sec. This differs from Allievi's notation, in which he uses $\theta = \dfrac{a(\Delta t)}{2L}$.
$\mu = \dfrac{2L}{a}$ = duration of one phase of the water hammer (one direct and reflected transit of the wave). μ has the dimension of time in seconds.
L = length of pressure conduit, ft.
ϕ = time interval, measured in phase angle, between $t = 0$ instant at which gate opening change is a maximum $q_0 = q_{0\,max}$ and $t = t$ instant at which the head change h is equal to h_0, *i.e.*, beginning of first water-hammer phase in Allievi's interlocked series. The dimension of ϕ is in radians or degrees according to the sense.
ϕ_m = phase displacement between gate opening oscillation and head oscillation (water hammer).
$\chi = \dfrac{T''}{T'}$ = ratio between period of governing oscillation in seconds and period of free water-hammer oscillation in seconds. χ is dimensionless.
ρ = Allievi dimensionless water-hammer parameter $= \dfrac{aV_0}{2gH_0}$.

Head.

H = general head variable, ft.
H_0 = initial or steady-state head, ft.
h = relative head change $= \dfrac{H - H_0}{H_0}$, dimensionless.

h_0 = value of h at beginning of first water-hammer phase, $\frac{2L}{a}$ in Allievi interlocked series, dimensionless.

h_n = value of h at beginning of nth water-hammer phase, $\frac{2nL}{a}$ in Allievi interlocked series, dimensionless.

$h_{0\,max}$ = peak value of h_0.

h_r = $h_{0\,max} \cos \phi_m$ = amplitude of (first) head change (water-hammer) component in opposition (180-deg phase difference) to gate opening oscillation q_0; h_r is dimensionless.

h_s = $h_{0\,max} \sin \phi_m$ = amplitude of the (second) head change (water-hammer) component in quadrature (90-deg phase difference) with gate opening oscillation q_0, h_s is dimensionless.

r = dimensionless coefficient denoting first head change component.

s = dimensionless coefficient denoting second head change component.

Velocity.

V = general velocity variable, fps.

V_0 = initial or steady-state velocity, fps.

v = relative velocity change = $\frac{V - V_0}{V_0}$ dimensionless.

v_0 = value of v at beginning of the first water-hammer phase $\frac{2L}{a}$, in the Allievi interlocked series.

v_n = value of v at beginning of nth water-hammer phase $\frac{2nL}{a}$ in Allievi interlocked series.

Power.

P = general term for power, hp (550 ft-lb per sec).

P_0 = initial or steady-state power.

p = relative power change $\frac{P - P_0}{P_0}$ (dimensionless) in absence of, or neglecting, the speed change effect. This power change p is equal to the power change p_0 plus the effect of $\frac{3}{2}h$ of the head change h.

p_0 = relative power change due to the servomotor piston displacement (gate opening change) in absence of, or neglecting, water-hammer and speed change effects; also the relative driving couple change under constant head and at constant speed.

Discharge.

Q = general discharge variable, cfs.

Q_0 = initial or steady-state discharge, cfs.

q = relative discharge change $\frac{Q - Q_0}{Q}$, dimensionless.

q_0 = relative discharge change in the absence of, or neglecting, the water-hammer effect. q_0 is then a measure of gate opening change.

q_{00} = value of q_0 at beginning of first water-hammer phase $\frac{2L}{a}$ in Allievi interlocked series, dimensionless.

$q_{0\,max}$ = peak value of q_0, dimensionless.

q_n = value of q at beginning of nth water-hammer phase $\frac{2nL}{a}$ in Allievi interlocked series.

q_{0n} = value of q_0 at beginning of nth water-hammer phase $\frac{2nL}{a}$ in Allievi interlocked series.

Speed.

N = general speed of rotation, rpm.

N_0 = initial or steady-state speed, rpm.

$\omega = \frac{N - N_0}{N_0}$ = relative speed change, dimensionless.

δ = permanent speed droop = $\frac{N_{max} - N_{min}}{N_0}$ produced by the process of primary compensation and defined by the equation $\omega + \delta p_0 = 0$ for neutral position of relay valve. For full load on $p_0 = +1$, $\omega = -\delta$.

$k_r\delta'$ = temporary speed droop produced by the process of secondary compensation with dashpot.

ω_r = displacement of flyball collar measured to scale of relative speed change ω.

ω_p = displacement of dashpot piston measured to scale of relative speed change ω.

ω_s = displacement of dashpot cylinder measured to scale of relative speed change ω.

General Constants or Parameters.

WR^2 = parameter characterizing inertia of rotating masses; equal to the weight W multiplied by the square of the radius of gyration.

C = regulation constant = $\dfrac{N_0{}^2(WR^2)}{hp}$.
X = servomotor piston displacement, ft.
X_0 = servomotor piston displacement during the steady-state condition, ft.
$x = \dfrac{X - X_0}{X_0}$ = relative servomotor piston displacement, dimensionless.
m = acceleration constant in the speed-acceleration responsive type of governor, used to denote effect of acceleration-responsive elements, relative to effect of speed-responsive flyball, sec.
k = inverse value of the slope $1/k$ of the turbine performance curve of relative power vs. relative servomotor piston displacement. $k = \cot \gamma = \dfrac{dx}{dp_0}$, dimensionless.
k_r = factor defining effect of stiffness of dashpot spring on the law of the flyball collar displacement ω_r, in terms of the relative speed change ω. $\omega_r = \omega - k_r(\omega_r - \omega_p)$, dimensionless.
β = on experimental test curve of $\dfrac{dx}{dt}$ vs. ω, β is value of ω, for which the servomotor piston speed reaches its maximum rate: $\left(\dfrac{dx}{dt}\right)_{\max} = \dfrac{1}{t_g}$.
j = coefficient denoting effect of turbine efficiency change: $j = \dfrac{1}{1 - \dfrac{de}{dp_0}}$, $\dfrac{de}{dp_0}$ being the slope of turbine performance curve: relative efficiency vs. relative power.
g = acceleration of gravity, ft/sec².
$u = \dfrac{1 + \rho}{1 - \rho}$, a constant in Allievi series.
n = number of nth successive phase in Allievi interlocked series, such as 0, $\dfrac{2L}{a}$, $\dfrac{4L}{a}$, $\dfrac{2nL}{a}$.
D_e = relative value of difference between turbine driving couple and generator resisting couple.
$c_d = \dfrac{C_d}{C_{0d}}$, ratio between turbine driving couple at any speed, for steady-state gate opening, and the corresponding turbine driving couple at synchronous speed.
$c_r = \dfrac{C_r}{C_{0r}}$, ratio between generator resisting couple at any speed, for steady-state value of absorbed load, and the corresponding generator resisting couple at synchronous speed: $C_{0r} = C_{0d}$.
α_d = value of tangent to c_d performance curve (drawn with relative values).
α_r = value of tangent to c_r performance curve (drawn with relative values).
$\alpha = \alpha_r - \alpha_d$.
δ_* = logarithmic decrement of governing oscillation (gate opening, or speed, or head, etc.).
λ_m, λ_t, = damping coefficients used in formulating the Tables 4 to 6.
m_Θ; $(T_g'T_r)_\Theta$ = special values used in formulating the Tables 4 to 6.
Variables used in considering stability of combined operation of two generating units:

$$w_1 = \frac{j_1 - 3r}{j_1}.$$
$$l_1 = \frac{3s\Theta_1}{2j_1}$$
$$w_2 = \frac{j_2 - 3r}{j_2}.$$
$$l_2 = \frac{3s\Theta_2}{2j_2}.$$

$$\left(\frac{N + N_0}{N_0}\right)\left(\frac{N - N_0}{N_0}\right) = \frac{1{,}620{,}000(P - P_0)\,\Delta t}{(WR^2)N_0{}^2} \tag{1}$$

Now let us assume $\dfrac{N + N_0}{N_0} = 2$, giving

$$\omega = \frac{810{,}000P_0p_0\,\Delta t}{(WR^2)N_0{}^2}$$

This is the expression of the relative speed change which occurs at the end of the time interval Δt during which the relative value of the difference between driving couple and resisting couple varies uniformly from the initial value p_0 to zero, with an average value $p_0/2$. The differential $d\omega$ of the relative speed change, when the instantaneous value (relative) of the difference between driving couple and resisting couple is equal to p_0, must then be written:

$$d\omega = \frac{16.2 \times 10^5P_0p_0}{(WR^2)N_0{}^2}\,dt$$

or
$$\frac{d\omega}{dt} = \frac{p_0}{T} \tag{7}$$

in which
$$T = \frac{1}{16.2 \times 10^5} \frac{(WR^2)N_0^2}{P_0}$$

or
$$T = \frac{C}{16.2 \times 10^5}$$

This is the differential form of the standard flywheel equation in the absence of, or neglecting, water hammer and speed change effect on both of the couples.

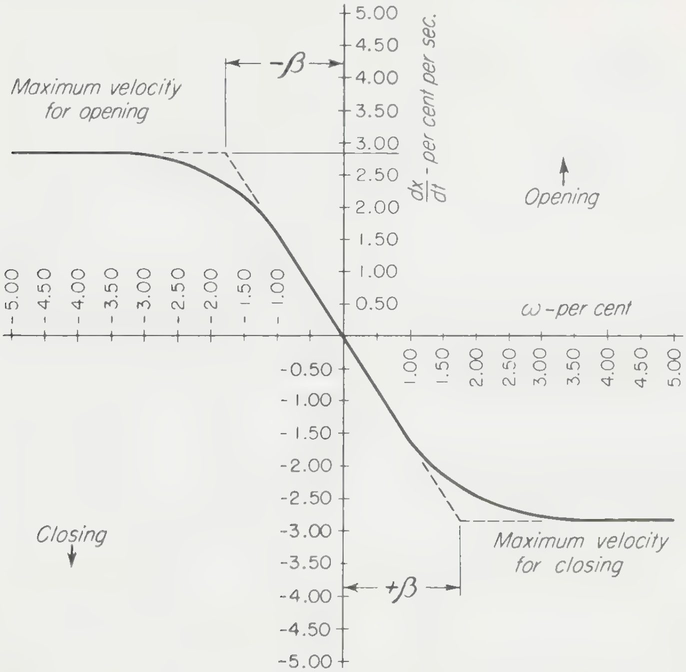

FIG. 1. Experimental test curve. Relative speed ω versus servomotor piston speed dx/dt.

The mechanical inertia parameter T has the dimension of time in seconds. It is the time which is necessary to bring up the rotating masses of the turbine alternator from rest to the normal synchronous speed, by applying to them the normal rated couple. The value of T depends then upon that of the steady-state power P_0 considered.

Second, in Eq. (8), (*remembering that we are dealing with small oscillations* $\omega < \beta$), let us assume that the speed of travel dx/dt of the servomotor piston varies directly in proportion to the speed change in the generating unit as communicated to the flyball element, inversely proportional to the governor time t_g, for a full opening or closing stroke, and inversely proportional to β, the value of ω on the dx/dt vs. ω test curve, for which the speed dx/dt reaches its maximum rate (Fig. 1). In other words, the velocity of servomotor piston attains its maximum value $1/t_g$ when the speed change ω is equal to β, the relay valve being then wide open. The negative sign has been taken to give positive velocity for an opening stroke.

$$-\frac{dx}{dt} = \frac{\omega}{\beta t_g} \tag{8}$$

Next, construct a curve showing the relation between power p_0 and servomotor piston travel x (relative values) at synchronous speed and under constant head.

From Fig. 2,
$$k = \cot \gamma = \frac{dx}{dp_0}$$
or
$$dx = k\,dp_0 \text{ (in the absence of water hammer)}$$

Substituting in Eq. (8),
$$-\frac{dp_0}{dt} = \frac{\omega}{k\beta t_g}$$

Now let $k\beta t_g = T_g$, the characteristic time of promptness of the governor response, and the above equation becomes
$$-\frac{dp_0}{dt} = \frac{\omega}{T_g} \tag{9}$$

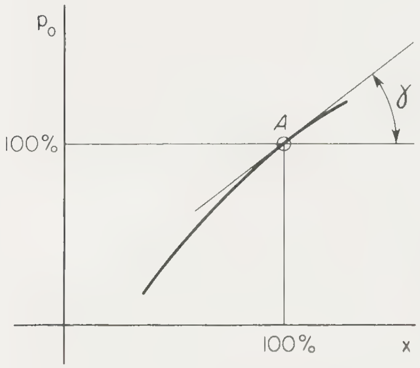

FIG. 2. Power output versus servomotor piston travel at synchronous speed and in the absence of water hammer.

Example 8: Suppose that we wish to investigate stability at the point of full-gate opening and that at this position the test curve of p_0 vs. x shows the value of k to be 6.00. In addition, the test curve of dx/dt vs. ω shows that the servomotor stroke reaches full velocity when the relative speed change ω becomes 5 per cent; in other words, $\beta = 0.05$. The time for a full opening or full closing stroke of the servomotor is 8 sec. Compute the characteristic time of promptness of the governor response.

$$T_g = k\beta t_g$$
$$k = 6.00 \qquad t_g = 8 \text{ sec} \qquad \beta = 0.05$$
$$T_g = 6.00 \times 8 \times 0.05 = 2.40 \text{ sec}$$

Example 9: Compute T_g for the same conditions as for Example 8 except that the turbine is operating at 0.80 gate at which $k = 3.00$.

$$T_g = 3.00 \times (8 \times 0.80) \times 0.05 = 0.96 \text{ sec}$$

The above definition of the time of promptness T_g is only a schematic one, corresponding to the simplified arrangement of Fig. 3. It is then also the case for Examples 8 and 9. The time of promptness is really defined by the Eq. (9) itself:

$$T_g = -\frac{\omega}{\dfrac{dp_0}{dt}} = -\frac{k\omega}{\dfrac{dx}{dt}} \tag{9}$$

in which, for practical calculation purposes, the ratio $\left(\omega : \dfrac{dx}{dt}\right)$ is to be taken on a *test curve*, as shown on Fig. 1. In practice, the time of promptness T_g can be established *independently* from the governor time t_g, by adjusting the dashpot of the compensating device, as it will be explained subsequently.

Next eliminate p_0 between Eqs. (7) and (9).

$$\frac{d\omega}{dt} = \frac{p_0}{T} \tag{7}$$
$$-\frac{dp_0}{dt} = \frac{\omega}{T_g} \tag{9}$$
$$\frac{d^2\omega}{dt^2} + \frac{\omega}{T_g T} = 0 \tag{10}$$

This is the form of the governing equation for the crude mechanism depicted in Fig. 3. Let us now proceed with the assistance of this equation to analyze the effectiveness of such a governor in maintaining constant speed subsequent to a small load change on the generating unit. The boundary condition ($\omega = 0$ when $t = 0$) in this case is satisfied by the solution:

$$\omega = \omega_{\max} \sin \frac{t}{\sqrt{T_g T}} \qquad (11)$$

Consequently the speed will continue to pendulate forever like the trigonometric sine function, or in engineering terms the mechanism is unstable.

It will be useful in our subsequent discussion of stability to employ vector diagrams of the type used by electrical engineers to represent a-c phenomena, and for the applications of this method to governing problems we are again indebted to Daniel Gaden.

For perpetual pendulations representable by the trigonometric functions, the function and its derivative will always differ by a phase angle of 90 deg and the amplitude of the derivative will be that of the function multiplied by ($2\pi : T''$), T'' being the period of the governor oscillations. If this condition is realized in the vector diagram, we know at once that the governing is not stable. On the contrary for *damped* periodic oscillations, the phase angle between the function and its derivative will be greater than 90 deg.

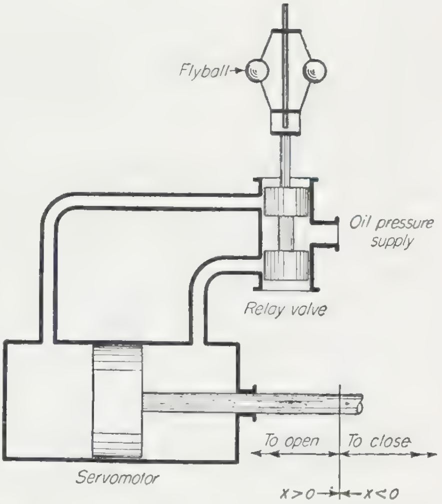

Fig. 3. Schematic arrangement—speed-responsive governor without compensation.

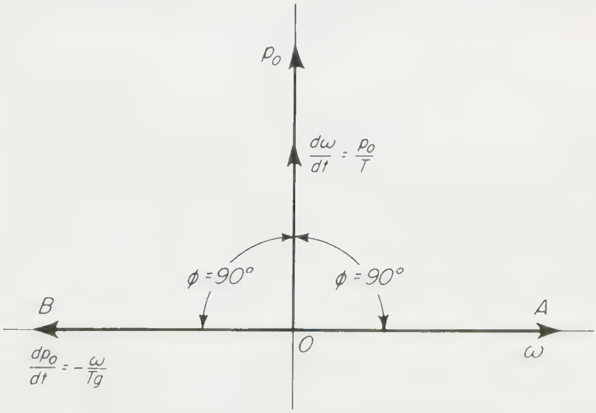

Fig. 4. Vector diagram—speed-responsive-type governor without compensation and water hammer.

The orientation and amplitude (length) of the vectors shown in the diagram Fig. 4 can be verified directly by inserting

$$\omega = \omega_{\max} \sin \frac{t}{\sqrt{T_g T}} = \omega_{\max} \sin \frac{2\pi t}{T''} \qquad (11)$$

in which $T'' = 2\pi\sqrt{T_gT}$ in the differential Eqs. (7) and (9). The diagram shows that the oscillations are perpetual (ϕ = 90 deg) and the governing is unstable.

BASIC EQUATION OF GOVERNING INCLUDING PRIMARY COMPENSATION

We have seen that the fundamental difficulty with the mechanism analyzed in Art. 5 was due to *overtravel* on the part of the servomotor piston, causing the turbine gates to move too far for the given load change. This in turn caused the speed to change too far in the reverse direction and gave rise to a perpetual condition of hunting or instability. Evidently what is needed is some mechanical means of anticipating where the correct position of servomotor piston should be for a particular load change, and then of starting to close the oil supply ports in the relay valve before the piston

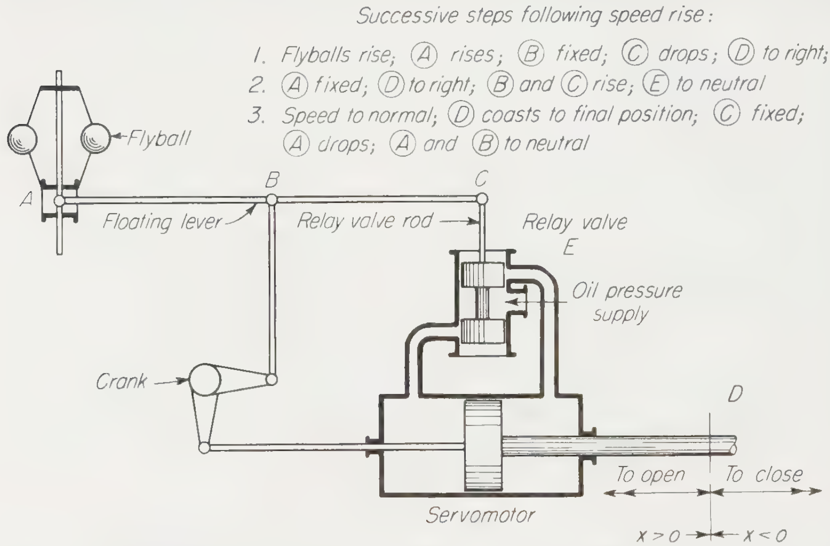

FIG. 5. Schematic arrangement—speed-responsive governor with primary compensation.

reaches this desired position. The device for accomplishing this result is known as the *primary compensation*, and its basic principles are indicated schematically in Fig. 5.

The important feature to note is that the relay rod connection starts to return the relay valve to the neutral position as soon as the servomotor piston starts to move, thus effecting the requisite anticipation or compensation.

Having devised the mechanical means of anticipating the correct position of the servomotor piston, we proceed to incorporate this primary compensation in the basic equation of governing.

The displacement of the oil-pressure relay valve is now due not only to the speed change as reflected in the flyball movement, but also to the relative gate movement change owing to the action of the primary compensation. As a means of calibrating the effect of this primary compensation, we introduce the notation:

$$\delta = \frac{N_{\max} - N_{\min}}{N_0} \tag{12}$$

and since the position of the relay valve is now a function of the speed change and of the gate movement change x, or in other words, the relative power change p_0, we may further define the term δ by the equation $\omega + \delta p_0 = 0$ for the neutral position of the oil-pressure relay valve. With this understanding, the expression $(\omega + \delta p_0)$ may be used to replace ω in Eq. 9 as the displacement of the relay valve for small oscillations. For full load on or $p_0 = +1$, $\omega = -\delta$. This term δ is designated as the speed droop of the governor, and its effect is to displace the relay valve farther and farther from the central position as the gate opening increases. This in turn requires the flyball element to draw in progressively more and more to restore the relay valve to the neutral position. In order that the flyball element draw in, the speed level must progressively decrease or droop as the turbine gates move from the closed to the open position.†

Example 10: When the turbine gates are opened from the speed no-load position to the full-gate position, the speed of operation drops from 150 to 143 rpm. The rated speed is 150 rpm. What is the speed droop?

$$\delta = \frac{N_{\max} - N_{\min}}{N_0} = \frac{150 - 143}{150} = 4.7 \text{ per cent}$$

To include the effect of primary compensation, we replace ω in Eq. (9) by $(\omega + \delta p_0)$ giving

$$-\frac{dp_0}{dt} = \frac{1}{T_g}(\omega + \delta p_0) \tag{13}$$

$$\frac{d\omega}{dt} = \frac{p_0}{T} \tag{7}$$

$$\frac{d^2\omega}{dt^2} + \frac{\delta}{T_g}\frac{d\omega}{dt} + \frac{\omega}{T_g T} = 0 \tag{14}$$

This equation has the well-known form:

$$\frac{d^2\Omega}{dt^2} + C_1\frac{d\Omega}{dt} + C_2\Omega = 0$$

in which $\Omega = \omega$, $C_1 = \dfrac{\delta}{T_g}$, and $C_2 = \dfrac{1}{T_g T}$.

The solution depends upon the roots of the auxiliary equation:‡

$$r^2 + C_1 r + C_2 = 0$$

$$r = \frac{-C_1 \pm \sqrt{C_1^2 - 4C_2}}{2}$$

In order that the relative speed change ω have the form of a damped *periodic* function, it suffices that $C_1 > 0$; which means that the speed droop must be positive $\delta > 0$.

In order that the relative speed change ω have the form of a damped *aperiodic* function of the form $\omega = \omega_{\max} e^{-rt}$, it is necessary that $C_1 > 0$ and $C_1^2 > 4C_2$.

$$C_1^2 \geq 4C_2$$

$$\frac{\delta^2}{T_g^2} \geq \frac{4}{T_g T}$$

$$\delta \geq 2\sqrt{\frac{T_g}{T}} \tag{15}$$

This means that for the small values of speed droop δ, desired in commercial operation, either the inertia characteristic T must be very large (involving proportionate

† See Cabinet Actuator Governing Equipment for Water Prime Movers, *Bull.* W-100, p. 27, Woodward Governor Company, Rockford, Ill.

‡ GRANVILLE, WILLIAM A., "Elements of the Differential and Integral Calculus," Ginn & Company, 1911, p. 432.

expense) or the promptness of governor response T_g must be very short, which in turn aggravates the effect of water hammer.

Example 11: Assuming that the prescribed value of speed droop is 5 per cent and that T_g the characteristic time of promptness of the governor response $T_g = 0.50$ sec, what must be the value of the regulation constant $C = \dfrac{N_0{}^2WR^2}{hp}$, in order that the relative speed change function, ω, have the form of a damped aperiodic?

$$\delta = 2\sqrt{\frac{T_g}{T}}$$

$$0.05 = 2\sqrt{\frac{0.50}{\dfrac{C}{16.2 \times 10^5}}}$$

$$0.0025 = \frac{32.4 \times 10^5}{C} \qquad C = 1.30 \times 10^9 \qquad T = 800 \text{ sec}$$

which is about 100 times the available commercial value.

In practice the method of coping with the situation is to accept a damped periodic instead of an aperiodic speed regulation. The requisite rapidity of damping must be secured by an adequate value

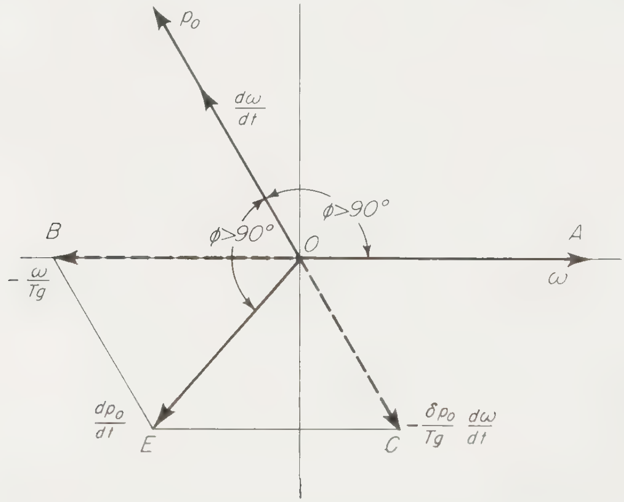

FIG. 6. Vector diagram—speed-responsive-type governor with primary compensation without water hammer.

of the speed droop. If not sufficient, owing to the small value of the allowable speed droop for commercial operation, it will be necessary to have recourse to a secondary compensation with dashpot or to an acceleration responsive element beside the speed responsive flyball. The effect of these devices upon the basic governing equation will be incorporated in succeeding paragraphs.

But first let us proceed to incorporate the action of the speed droop (resulting from the primary compensation) in the vector diagram, Fig. 6.

The basic equations are (13) and (7). From Eq. (13), we deduce that the vector dp_0/dt is equal to the vector sum of the two vector components $-\omega/T_g$ and $-\delta p_0/T_g$. The first component $-\omega/T_g$, because of the fact that it differs from vector ω, or OA, only in algebraic sign and by a multiplying constant, will lie along OB in opposition to OA and of length equal to $1/T_g\ (OA)$. The orientation of vector OC representing the second component—$\delta p_0/T_g$ is at first unknown; but since it differs from p_0 only by algebraic sign and a multiplying constant δ/T_g, it must be in opposition to p_0. By Eq. (7) since the algebraic sign is the same on both sides and $d\omega/dt$ is equal to p_0 multiplied by a constant $1/T$, p_0, and $d\omega/dt$ must be in phase and differ only in magnitude. Furthermore, the various variables ω, p_0, and so on will have the same period of oscillation T''. Moreover, the phase angle between any two variables will remain fixed throughout the oscillation, and the phase angle between their two corresponding derivatives will remain fixed at the same angle as between their parent variables.

Consequently the only position of vector OP_0 capable of maintaining the prescribed identical phase displacement between the vectors ω and p_0, the same as between vectors $d\omega/dt$ and dp_0/dt is at mid-angular position halfway between vectors OA and OE with $\phi > 90$ deg.

Since $\phi > 90$ deg, the oscillation will be damped and the governing will be stable.

BASIC EQUATION OF THE SPEED-ACCELERATION RESPONSIVE-TYPE GOVERNOR

Before proceeding to analyze the effect of a secondary compensation including a dashpot, it will be more logical for reasons that will become apparent during the course of our discussion first to study the effect of adding an acceleration-responsive element to the speed-responsive flyball.

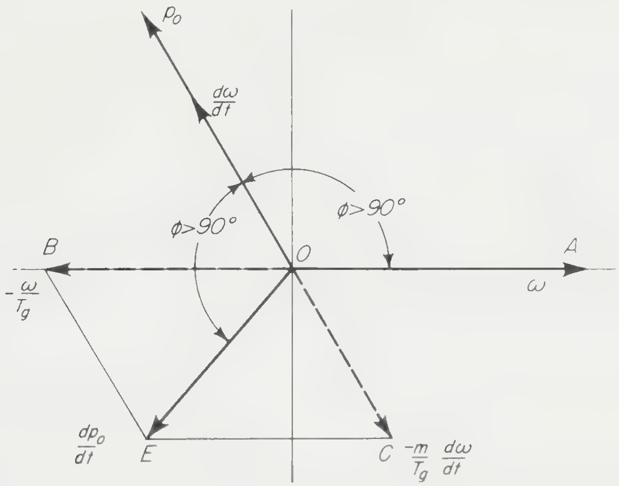

FIG. 7. Vector diagram—speed-acceleration-responsive-type governor without water hammer.

Equation (9) will then change to the following:

$$-\frac{dp_0}{dt} = \frac{1}{T_g}\left(\omega + m\frac{d\omega}{dt}\right) \tag{16}$$

in which the constant m has the dimension of time in seconds and denotes the effect of the acceleration-responsive element in relation to the speed-responsive flyball effect. Combining Eq. (16) with Eq. (7),

$$\frac{d\omega}{dt} = \frac{p_0}{T} \tag{7}$$

we obtain

$$\frac{d^2\omega}{dt^2} + \frac{m}{T_gT}\frac{d\omega}{dt} + \frac{\omega}{T_gT} = 0 \tag{17}$$

In order that ω be a damped *periodic* function, it is required that $m > 0$. In order that ω be a damped *aperiodic* function, it is required that

$$m > 2\sqrt{T_gT}$$

It will be noted at once that Eq. (17) is identical in form with Eq. (14) except that the term $\frac{m}{T_gT}\frac{d\omega}{dt}$ replaces the term $\frac{\delta}{T_g}\frac{d\omega}{dt}$. The vector diagram Fig. (7) will accordingly be identical with Fig. (6) except that the vector $\frac{\delta p_0}{T_G}$ is replaced by $\frac{m}{T_g}\frac{d\omega}{dt}$, and since as before $\phi > 90$ deg, the effect of including the acceleration-responsive element is to ensure stability even *without* the primary compensation.

BASIC EQUATION OF THE SPEED-RESPONSIVE-TYPE GOVERNOR WITH SECONDARY COMPENSATION (DASHPOT)

Now instead of incorporating an acceleration-responsive element beside the flyball or speed-responsive element, let us interpose a secondary compensation including a spring-loaded, oil-filled dashpot as shown schematically by Fig. 8. A primary com-

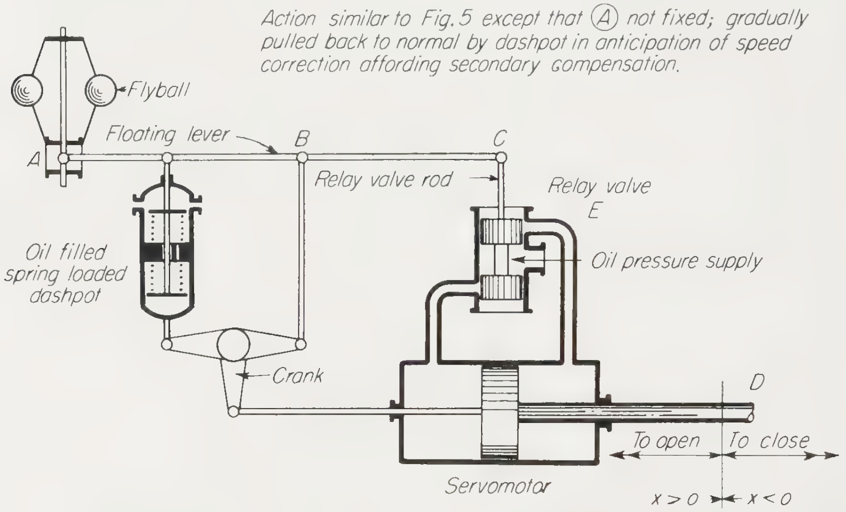

FIG. 8. Schematic arrangement—speed-responsive governor with primary compensation and secondary compensation in the form of a spring-loaded oil-filled dashpot

pensation is also indicated on the said figure; but for this immediate discussion we shall neglect it and suppose that the point B remains fixed ($\delta = 0$). Then let

ω_r = displacement of the flyball collar at A.
ω_p = displacement of the piston of dashpot.
ω_c = displacement of the cylinder of dashpot.

All these displacements being measured to the scale of the relative speed change ω. According to Eq. (9),

$$-\frac{dp_0}{dt} = \frac{\omega_r}{T_g}$$

The displacement of the flyball collar ω_r will depend upon the difference between the uplift force of the flyball which in turn depends upon the relative speed change ω, and the dashpot reaction which is equal to the deflection of its spring $(\omega_r - \omega_p)$, in other words to the differential movement between the flyball collar A and the dashpot piston, multiplied by a factor k_r. This factor k_r characterizes the effect of the stiffness of the said spring on the law of the flyball collar displacement, in terms of the relative speed change ω:

$$\omega_r = \omega - k_r(\omega_r - \omega_p) \tag{20}$$

On the other hand $(\omega_r - \omega_p)$ depends upon the speed of the differential movement between piston and cylinder of the dashpot, and the time required for the oil to move through the ports from one side of the piston to the other, that is,

$$\omega_r - \omega_p = T_d \frac{d}{dt} (\omega_p - \omega_c) \tag{21}$$

in which T_d is the dashpot constant having the dimension of time in seconds; it characterizes the dashpot rigidity or the dashpot throttling action.

Finally the displacement of the dashpot cylinder, which is attached to the gate motion, must be proportional to the relative power change p_0.

$$\omega_c = \delta' p_0 \qquad \text{or} \qquad \frac{d\omega_c}{dt} = \delta' \frac{dp_0}{dt} \tag{22}$$

On combining these equations and inserting them in the fundamental relationships there results the following:

$$-\frac{dp_0}{dt} - T_d \frac{T_g(1 + k_r)}{T_g'} \frac{d^2p_0}{dt^2} = \frac{1}{T_g'} \left(\omega + T_d \frac{d\omega}{dt}\right) \tag{23}$$

in which
$$T_g' = T_g \left(1 + \frac{k_r \delta' T_d}{T_g}\right) = T_g + k_r \delta' T_d \tag{24}$$

Notice that if the dashpot were entirely rigid,

$$T_d = \infty \qquad \omega_p = \omega_c$$

and in order to restore the neutral position of the flyball collar A and of the oil pressure relay valve $E(\omega_r = 0)$, the following condition ought to obtain according to Eq. (20),

$$\omega + k_r \delta' p_0 = 0$$

$k_r\delta'$ is therefore the speed droop produced by the process of the secondary compensation. However, as the dashpot is never an entirely rigid device, but a sliding one, $k_r\delta'$ corresponds to a temporary speed droop or transient speed droop.

Example 12: Given a governor having secondary compensation in the form of a spring-loaded oil-filled dashpot. The characteristic time of promptness of the governor response without the dashpot is $T_g = 0.50$ sec. The dashpot spring factor k_r is equal to 1.00. The constant δ' is equal to 0.25 (transient speed droop $k_r\delta' = 25$ per cent). The dashpot constant T_d is 2.00 sec. Compute the *modified* time of promptness of the governor response T_g'.

$$T_g' = 0.50 + 1.00 \times 0.25 \times 2 = 1.00 \text{ sec}$$

Equation (23) may then be compared with Eq. (16).

$$-\frac{dp_0}{dt} = \frac{1}{T_g} \left(\omega + m \frac{d\omega}{dt}\right) \tag{16}$$

We have already shown by means of Fig. 7 that the governing according to Eq. (16) is stable. To approach the same result with the secondary compensation, we must consequently seek to render the term in $\frac{d^2p_0}{dt^2}$ in Eq. (23) as small as possible. Obviously this is accomplished by making $T_g(1 + k_r)$ as small as possible, in regard to T_g', that, is by making

$$\delta' T_d \gg T_g \tag{25}$$

Our basic equation then becomes

$$\frac{dp_0}{dt} = -\frac{1}{T_g'} \left(\omega + T_d \frac{d\omega}{dt}\right) \tag{23'}$$

This equation has exactly the same form as Eq. (16) with the constant m replaced by the characteristic time T_d of the dashpot rigidity or dashpot throttling action, and the vector diagram would be similar to Fig. 7, indicating stable governing.

However, the condition (25) can practically never be fully realized, and this is one of the reasons why the speed-responsive type of governor with secondary compensation cannot attain, according to Daniel Gaden, the same performance as the speed-acceleration type of governor, all things being equal. But we shall for our present purpose waive this difference and concede the identity of Eq. (16) and Eq. (23) or (23′).

We must also not forget that the time of promptness is no longer T_g, but

$$T_g' = T_g + k_r\delta' T_d$$

depending upon the secondary compensation characteristics: $k_r\delta'$, the transient speed droop, and T_d, the time of dashpot throttling action.

9. BASIC EQUATIONS INCLUDING WATER HAMMER

With respect to the governing problem, the essential effect of water hammer is to modify the power output of the turbine according to the $\frac{3}{2}$ power of the head. For small values of the relative power change and of the relative head change, we may then write with sufficient accuracy

$$p = p_0 + \tfrac{3}{2}h \qquad (26)$$

where p_0 = relative power change due to the gate opening change in the absence of water hammer.

h = relative head change due to water hammer.

p = relative power change due to gate opening change and head change.

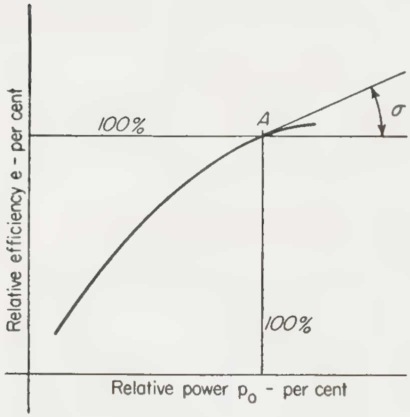

FIG. 9. Turbine performance curve. Relative efficiency versus relative power.

Moreover, *under constant head*, the gate opening change, which produces the relative power change p_0, leads to a relative discharge change q_0, bound to p_0 by the equation

$$p_0 = q_0 + \Delta e$$

in which Δe is the relative efficiency change. Using the relative efficiency vs. relative power curve of the turbine† (Fig. 9),

$$\Delta e = \frac{de}{dp_0}\,p_0$$

$$p_0\left(1 - \frac{de}{dp_0}\right) = q_0 \qquad p_0 = jq_0$$

$$j = \frac{1}{1 - \dfrac{de}{dp_0}} = \frac{1}{1 - \tan\sigma}$$

If at the point of steady-state conditions the efficiency curve is ascending, $j > 1$, and if at the said point this curve is descending, $j < 1$.

In analysing the amplitude ratio and the phase displacement between the gate opening oscillation function q_0, and the head oscillation function h, we shall assume

1. That the pendulation is perpetually sustained or undamped. This simplification is permissible because as will be further shown, the amplitude ratio and the phase displacement between the two oscillations remain constant whatever the amplitudes may be (in the limit of small relative amplitudes),

† And of its penstock, scroll case, and draft tube.

especially when these amplitudes decrease progressively as is the case for a damped periodic oscillation.†

2. That the period T'' of the gate oscillation which is also the period of the forced head oscillation, is exactly χ times the period T' of the free water-hammer oscillation, that is to say, 2χ times the water-hammer phase $\mu = \frac{2L}{a}$. It can be proved that the results so obtained have perfect generality even if χ is not an integer† and also whether χ is relatively small or relatively large.‡

3. That the phenomenon has reached the limit of its final form after several cycles during which this final form is progressively established.

In developing the analysis we shall employ the well-known interlocked series of Allievi, in which the subscripts denote conditions at the control gates at successive phase intervals $\frac{2L}{a}, \frac{4L}{a}, \frac{6L}{a}, \dots \frac{2nL}{a}$, or $\mu, 2\mu, 3\mu, \cdots, n\mu$. We shall accordingly divide the gate-motion period T'' sec into 2χ equal intervals, each corresponding to one water-hammer phase $2L/a$. We shall designate the intervals $0, 1, 2, 3, \dots n, \dots, 2\chi$.

According to the interlocked series,

$$h_n + h_{n+1} = 2\rho(v_n - v_{n+1})$$

or using relative discharges,

$$h_n + h_{n+1} = 2\rho(q_n - q_{n+1})$$

Now since the effect of water hammer is to increase the discharge according to the ½ power of the head, we may write (using relative values) with sufficient accuracy,

$$q_n = q_{0n} + \tfrac{1}{2}h_n$$

According to the first above-mentioned hypotheses, we shall write that the gate-opening change which is defined by the relative value q_0 of the discharge change in the absence of water hammer, varies like a cosine function, with a period $T'' = 2\chi\mu$:

$$q_{0n} = q_{0\,\max} \cos \frac{2\pi n}{2\chi} + \phi$$

n being the measure of the time calculated in phase intervals μ.

We proceed to write the entire interlocked series:

$$\begin{aligned} h_0 + h_1 &= 2\rho[(q_{00} + \tfrac{1}{2}h_0) - (q_{01} + \tfrac{1}{2}h_1)] \\ h_1 + h_2 &= 2\rho[(q_{01} + \tfrac{1}{2}h_1) - (q_{02} + \tfrac{1}{2}h_2)] \\ h_n + h_{n+1} &= 2\rho[(q_{0n} + \tfrac{1}{2}h_n) - (q_{0n+1} + \tfrac{1}{2}h_{n+1})] \end{aligned}$$

and finally,

$$h_{2\chi-1} + h_{2\chi} = 2\rho[(q_{02\chi-1} + \tfrac{1}{2}h_{2\chi-1}) - (q_{02\chi} + \tfrac{1}{2}h_{2\chi})]$$

according to the third above-mentioned hypothesis and since $h_{2\chi} = h_0$ and $q_{02\chi} = q_{00}$,

$$h_{2\chi-1} + h_0 = 2\rho[(q_{02\chi-1} + \tfrac{1}{2}h_{2\chi-1}) - (q_{00} + \tfrac{1}{2}h_0)]$$

Substituting $q_{0n} = q_{0\,\max} \cos \left(\frac{2\pi n}{2\chi} + \phi\right)$,§ and rearranging,

$$\begin{aligned} h_0(1-\rho) + h_1(1+\rho) &= 2\rho\left[q_{0\,\max}\cos(0+\phi) - q_{0\,\max}\cos\left(\frac{2\pi}{2\chi}+\phi\right)\right] \\ h_1(1-\rho) + h_2(1+\rho) &= 2\rho\left[q_{0\,\max}\cos\left(\frac{2\pi}{2\chi}+\phi\right) - q_{0\,\max}\cos\left(\frac{4\pi}{2\chi}+\phi\right)\right] \\ h_n(1-\rho) + h_{n+1}(1+\rho) &= 2\rho\left[q_{0\,\max}\cos\left(\frac{2\pi n}{2\chi}+\phi\right) - q_{0\,\max}\cos\left(\frac{2\pi(n+1)}{2\chi}+\phi\right)\right] \\ h_{2\chi-1}(1-\rho) + h_0(1+\rho) &= 2\rho\left[q_{0\,\max}\cos\left(\frac{2\pi}{2\chi}(2\chi-1)+\phi\right) - q_{0\,\max}\cos\left(\frac{2\pi}{2\chi}(2\chi)+\phi\right)\right] \end{aligned}$$

† GADEN, *op. cit.*, pp. 127, 129.

‡ *Ibid.*, p. 101.

§ ϕ is the time interval, measured in phase angle, between $t = 0$, when the gate-opening oscillation is maximum ($q_0 = q_{0\max}$), and $t = t$, when the head change $h = h_0$, *i.e.*, the beginning of the first water-hammer phase of the interlocked series.

Now operate on these to determine what value of ϕ makes h_0 a maximum. This will then establish ϕ_m, the phase displacement between the gate opening oscillation and the head oscillation (water hammer). First, divide the above array of interlocked equations by $(1 - \rho)$ and let $\frac{1 + \rho}{1 - \rho} = u$.

$$h_0 = -uh_1 + \frac{2\rho}{1-\rho} q_{0\,\max} \left[\cos\phi - \cos\left(\frac{\pi}{\chi} + \phi\right)\right]$$

$$h_1 = -uh_2 + \frac{2\rho}{1-\rho} q_{0\,\max} \left[\cos\left(\frac{\pi}{\chi} + \phi\right) - \cos\left(\frac{2\pi}{\chi} + \phi\right)\right]$$

$$h_n = -uh_{n+1} + \frac{2\rho}{1-\rho} q_{0\,\max} \left[\cos\left(\frac{n\pi}{\chi} + \phi\right) - \cos\left(\frac{[n+1]\pi}{\chi} + \phi\right)\right]$$

$$h_{2\chi-1} = -uh_0 + \frac{2\rho}{1-\rho} q_{0\,\max} \left[\cos\left(\frac{\pi}{\chi}(2\chi - 1) + \phi\right) - \cos\left(\frac{2\pi\chi}{\chi} + \phi\right)\right]$$

Next multiply the equation for h_0 by u^0 or 1; the equation for h_1 by $-u^1$; the equation for h_2 by $+u^2$; the equation for h_n by $\pm u^n$ according as n is even or odd; and finally the equation in $h_{2\chi-1}$ by $-u^{2\chi-1}$. Then add the entire array of equations giving

$$h_0 = \frac{2\rho}{1-\rho} \frac{q_{0\,\max}}{1 - u^{2\chi}} \sum_{n=0}^{n=2\chi-1} (-1)^n u^n \left[\cos\left(\frac{n\pi}{\chi} + \phi\right) - \cos\left(\frac{[n+1]\pi}{\chi} + \phi\right)\right]$$

and
$$\frac{dh_0}{d\phi} = 0 = \sum_{n=0}^{n=2\chi-1} (-1)^n u^n \left[\sin\left(\frac{[n+1]\pi}{\chi} + \phi\right) - \sin\left(\frac{n\pi}{\chi} + \phi\right)\right]$$

or
$$\sum_{n=0}^{n=2\chi-1} (-1)^n u^n \left[\sin\frac{(n+1)\pi}{\chi}\cos\phi + \cos\frac{(n+1)\pi}{\chi}\sin\phi - \sin\frac{n\pi}{\chi}\cos\phi - \cos\frac{n\pi}{\chi}\sin\phi \right] = 0$$

giving

$$\tan\phi_m = \frac{\displaystyle\sum_{n=0}^{n=2\chi-1} (-1)^n u^n \left[\sin\frac{n\pi}{\chi} - \sin\frac{(n+1)\pi}{\chi}\right]}{\displaystyle\sum_{n=0}^{n=2\chi-1} (-1)^n u^n \left[\cos\frac{(n+1)\pi}{\chi} - \cos\frac{n\pi}{\chi}\right]}$$

or by simplifying,

$$\tan\phi_m = -\frac{1}{\rho}\cot\frac{\pi}{2\chi} \tag{27}$$

and

$$h_{\max} = \frac{2\rho}{1-\rho} \frac{q_{0\,\max}}{1 - u^{2\chi}} \sum_{n=0}^{n=2\chi-1} (-1)^n u^n \left[\cos\left(\frac{n\pi}{\chi} + \phi_m\right) - \cos\left(\frac{(n+1)\pi}{\chi} + \phi_m\right)\right]$$

or by simplifying,

$$h_{\max} = 2q_{0\,\max}\cos\phi_m \tag{28}$$

It appears from Eqs. (27) and (28) that the phase displacement ϕ_m and the amplitude ratio ($h_{\max}: q_{0\,\max}$) are independent of the value of the amplitude as mentioned before.

Equation (27) expressing the phase difference ϕ_m between the gate opening oscillation and the head oscillation (water hammer) has been calculated for several representative values of χ and ρ and summarized for convenient reference in the charts Figs. 11 and 12. Figures 13 and 14 calculated on a similar basis summarize Eq. (28) by giving the ratio of $\frac{h_{\max}}{q_{0\ \max}}$ for various combination of χ and ρ.

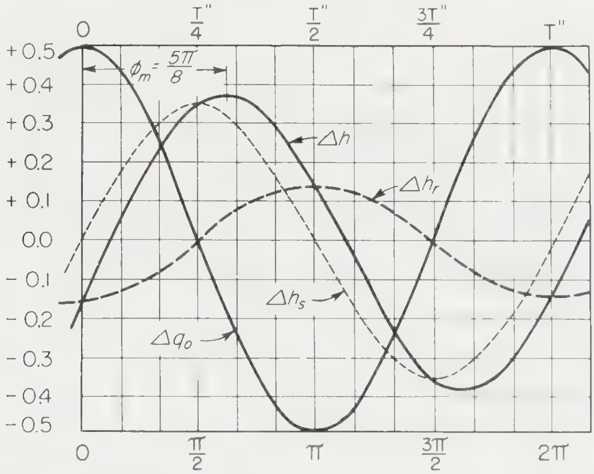

FIG. 10. Forced head oscillation h caused by a gate oscillation of 5 per cent for $\rho = 1$ and $\chi = 4$.

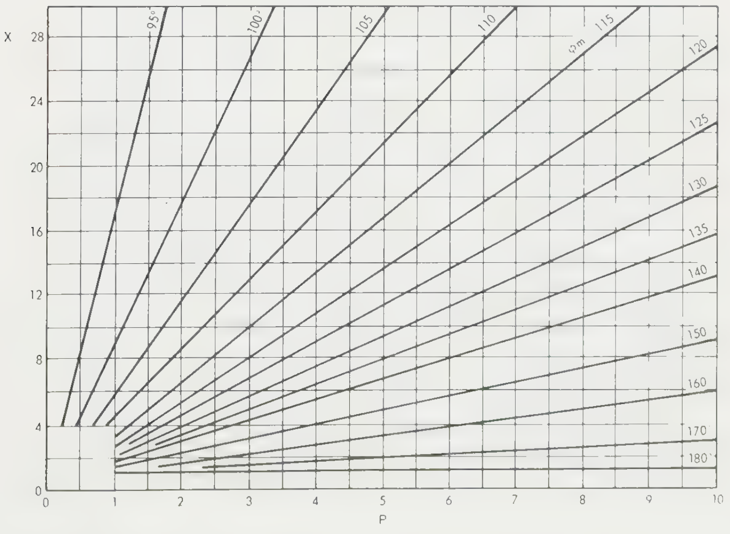

FIG. 11. Values of phase displacement ϕ_m between gate opening oscillation and head oscillation (water hammer) for larger values of χ and ρ.

For reasons that will develop as the discussion proceeds, we shall find it advantageous to resolve the relative head change h (which is a trigonometric sine function) into two components (which are also trigonometric sine functions) as indicated in Fig. 15.

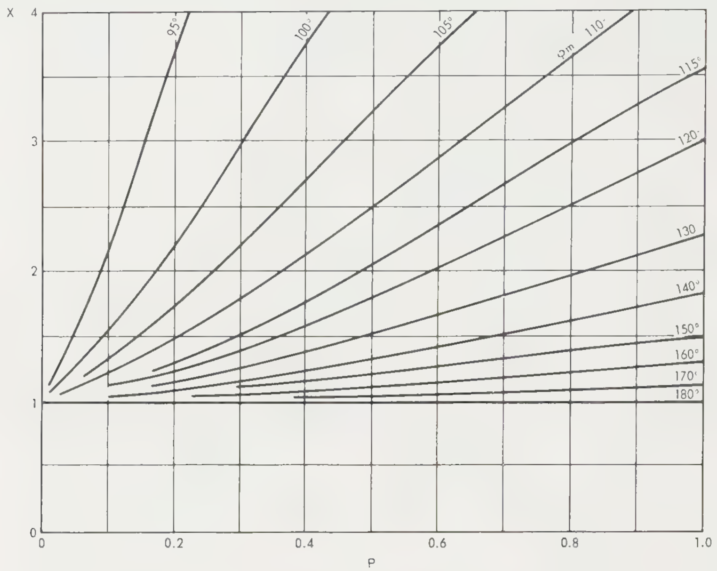

FIG. 12. Values of phase displacement ϕ_m between gate-opening oscillation and head oscillation (water hammer) for smaller values of χ and ρ.

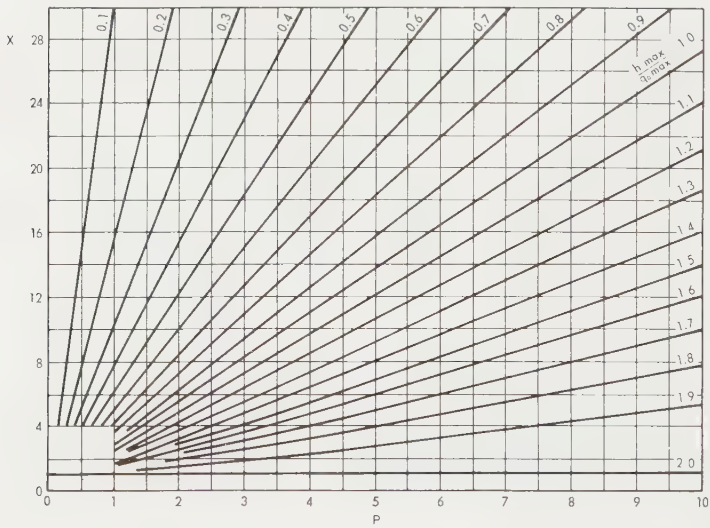

FIG. 13. Values of amplitude ratio $h_{\max}/q_{0\ \max}$ between head oscillation (water hammer) and gate opening oscillation for larger values of χ and ρ.

The first component h_r is in opposition with the gate oscillation q_0, that is to say, in phase with $-q_0$; its amplitude is equal to $h_{\max} \cos \phi_m$. The second component h_s is in quadrature with and backward, that is to say, in phase with $-\dfrac{dq_0}{dt}$; its amplitude is equal to $h_{\max} \sin \phi_m$.

Using for further convenience the coefficients r and s, we shall express these two components as follows:

	Instantaneous Value	Maximum Value (Amplitude)
First component	$h_r = -r(2q_0)$	$h_{r\,\max} = 2rq_{0\,\max}$
Second component	$h_s = -s\Theta \dfrac{dq_0}{dt}$	$h_{s\,\max} = s\Theta \dfrac{2\pi}{T''} q_{0\,\max} = s\dfrac{\pi\rho}{\chi} q_{0\,\max}$

in which $\Theta = \rho\mu = \rho \dfrac{T''}{2}$ is a hydraulic inertia parameter having the dimension of time

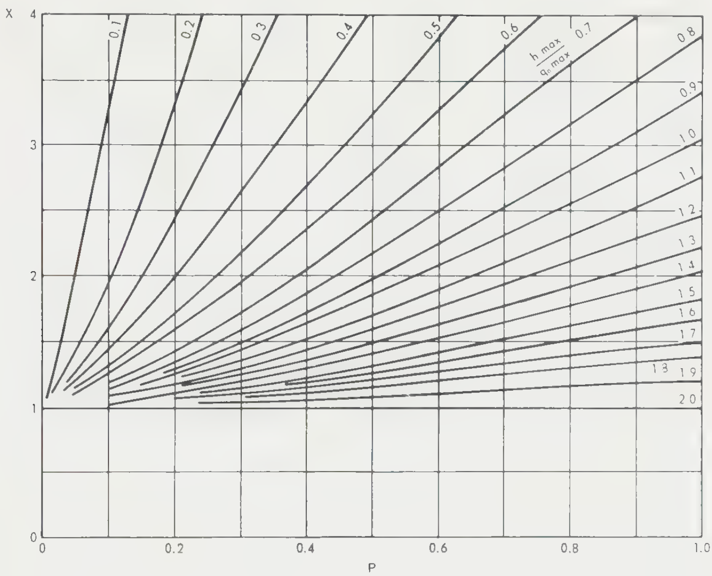

FIG. 14. Values of amplitude ratio $h_{\max}/q_{0\,\max}$ between head oscillation (water hammer) and gate opening oscillation for smaller values of χ and ρ.

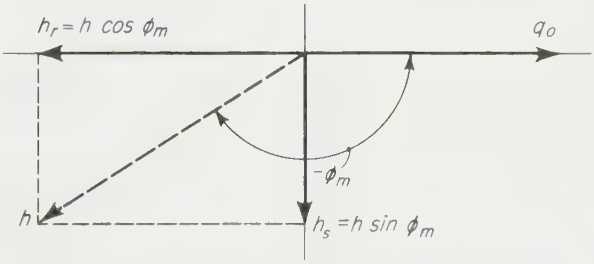

FIG. 15. Vector diagram showing decomposition of relative head oscillation h into components $h_r = h \cos \phi_m$ and $h_s = h \sin \phi_m$.

in seconds. Θ is the time necessary to bring up the water masses contained in the pressure conduit from the rest to the flowing velocity V_0, under the impulse of a pressure difference equal to the head H_0:

$$\Theta = \frac{LV_0}{gH_0}$$

According to Eq. (28),

$$r = \frac{1}{2}\frac{h_{r\,\max}}{q_{0\,\max}} = \frac{1}{2}\frac{h_{\max}}{q_{0\,\max}} \cos \phi_m = \cos^2 \phi_m \tag{29}$$

$$s = \frac{\chi}{\pi\rho}\frac{h_{s\,\max}}{q_{0\,\max}} = \frac{\chi}{\pi\rho}\frac{h_{\max}}{q_{0\,\max}} \sin \phi_m = \frac{2\chi}{\pi\rho} \sin \phi_m \cos \phi_m \tag{30}$$

The values of the coefficients r and s for any combination of χ and ρ may be selected directly from Figs. 16 to 19.

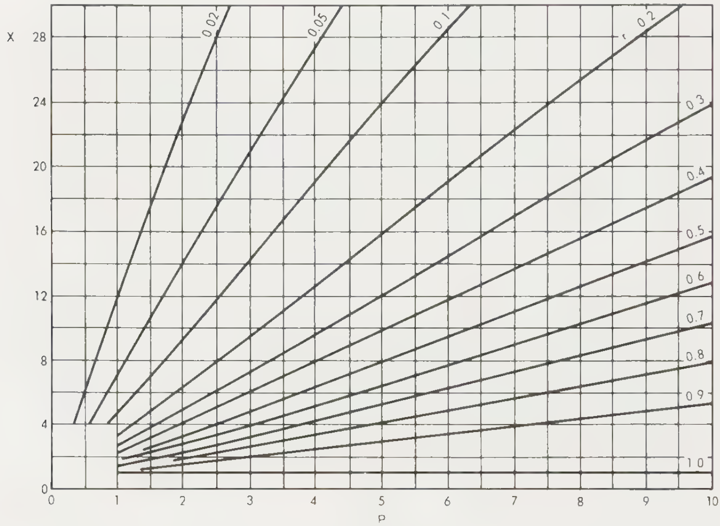

FIG. 16. Coefficient r—denoting the first component h_r of the head oscillation for larger values of χ and ρ.

Example 13: χ is the ratio between period T'' of the governor oscillation in seconds and the period T' of the free water-hammer oscillation in seconds. χ is dimensionless. $\rho = \frac{aV_0}{2gH_0}$, the Allievi, dimensionless water-hammer parameter. Suppose $\chi = 20$ and $\rho = 5$. What is the phase displacement ϕ_m between the governor or gate opening oscillation and the head oscillation?

From Fig. 11, for $\chi = 20$, $\rho = 5$,

$$\phi_m = 112°$$

Example 14: For the condition of Example 13, what is the value of the ratio $\frac{h_{\max}}{q_{0\,\max}}$? From Fig. 13, for $\chi = 20$, $\rho = 5$,

$$\frac{h_{\max}}{q_{0\,\max}} = 0.74$$

Example 15: For $\chi = 3.5$ and $\rho = 0.8$, what is the value of the phase displacement ϕ_m and the value of the ratio $\frac{h_{\max}}{q_{0\,\max}}$?

From Fig. 12, for $\chi = 3.5$, $\rho = 0.8$,

$$\phi_m = 111°$$

From Fig. 14, for $\chi = 3.5$, $\rho = 0.8$,

$$\frac{h_{\max}}{q_{0\,\max}} = 0.72$$

Example 16: Determine the values of r and s for the condition $\chi = 16$, $\rho = 7$.

From Fig. 16, for $\chi = 16$, $\rho = 7$,

$$r = 0.33$$

From Fig. 18, for $\chi = 16$, $\rho = 7$,

$$s = 0.68$$

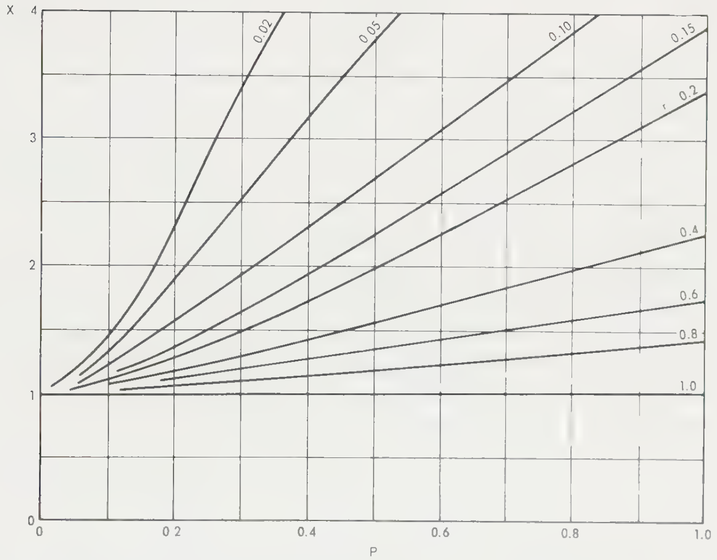

FIG. 17. Coefficient r—denoting the first component h_r of the head oscillation for smaller values of χ and ρ.

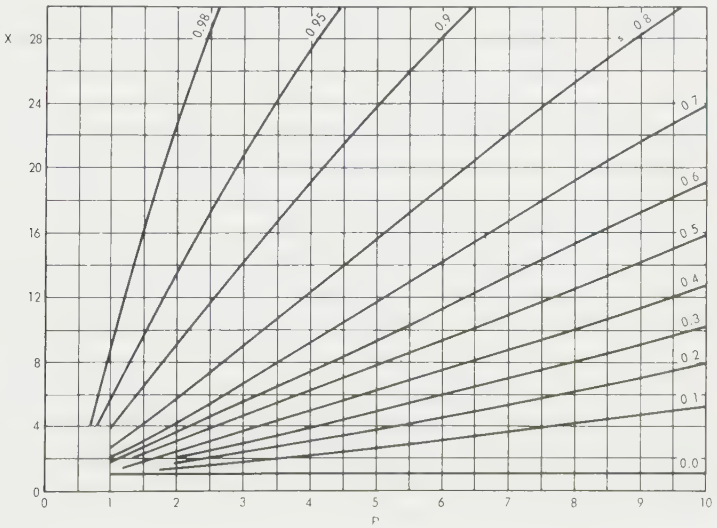

FIG. 18. Coefficient s—denoting the second component h_s of the head oscillation for larger values of χ and ρ.

Example 17: Determine the values of r and s for the condition $\chi = 2.5$, $\rho = 0.4$.
From Fig. 17, for $\chi = 2.5$, $\rho = 0.4$,

$$r = 0.078$$

From Fig. 19, for $\chi = 2.5$, $\rho = 0.4$,

$$s = 1.066$$

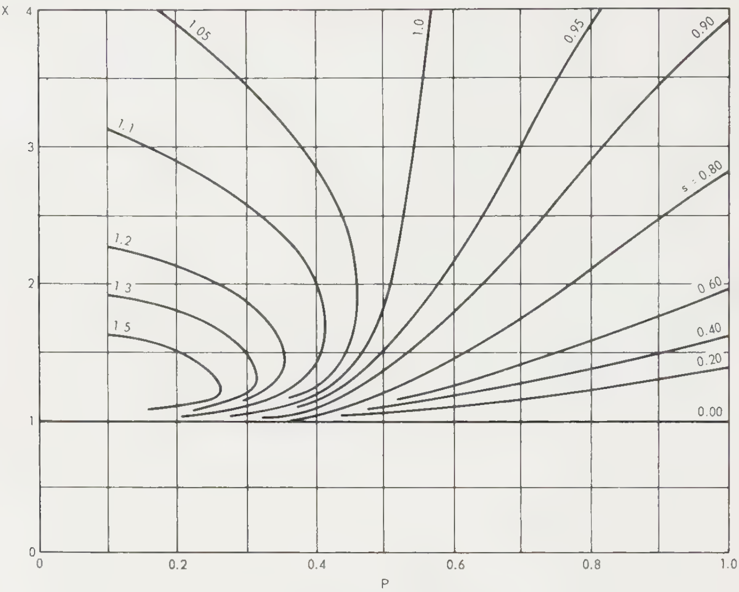

FIG. 19. Coefficient s—denoting the second component h_s of the head oscillation for smaller values of χ and ρ.

In the presence of water hammer, the standard flywheel equation (7) must now be written:

$$\frac{d\omega}{dt} = \frac{p}{T} \tag{7}$$

in which, according to Eq. (26),

$$p = p_0 + \tfrac{3}{2}h = p_0 + \tfrac{3}{2}h_r + \tfrac{3}{2}h_s \tag{31}$$

Effect of the First Component h_r. Taking account of this single component, Eq. (26) becomes

$$p = p_0 + \frac{3}{2}h_r = p_0 - \frac{3}{2}(2rq_0) = p_0\left(1 - \frac{3r}{j}\right)$$

and Eq. (7),

$$\frac{d\omega}{dt} = \frac{p_0}{T}\left(1 - \frac{3r}{j}\right) \tag{32}$$

The effect of the water-hammer component h_r is accordingly to change the mechanical inertia parameter T in the ratio $\frac{j}{j - 3r}$, in other words to increase the inertia parameter T (since $r > 0$) to the effective value $T_r = T\frac{j}{j - 3r}$. This is manifestly a benefit from the standpoint of stability.

Effect of the Second Component h_s Added to That of the First One. Taking account of both of the components, Eq. (26) becomes

$$p = p_0\left(1 - \frac{3r}{j}\right) + \frac{3}{2}h_s = p_0\left(1 - \frac{3r}{j}\right) - \frac{3}{2}s\,\Theta\frac{dq_0}{dt}$$

or

$$p = p_0\left(1 - \frac{3r}{j}\right) - \frac{3}{2}\frac{s}{j}\Theta\frac{dp_0}{dt} \tag{33}$$

and Eq. (7),

$$\frac{d\omega}{dt} = \frac{p_0}{Tr} - \frac{3}{2}\frac{s}{j}\frac{\Theta}{T}\frac{dp_0}{dt} \tag{34}$$

in which

$$T_r = T\frac{j}{j - 3r}$$

is the fictitious value of the mechanical inertia parameter due to the influence of the first component h_r.

We now proceed to combine the flywheel equation (34) with the equations of governor movement comprising three cases: a speed-responsive governor with primary compensation; a speed- and acceleration-responsive governor without primary compensation; a speed-responsive governor with secondary compensation in the form of a dashpot or, in other words, with temporary compensation.

Case I. The basic equation of governor movement is

$$\frac{dp_0}{dt} = -\frac{\omega + \delta p_0}{T_g} \tag{13}$$

Combining Eqs. (34) and (13),

$$\frac{d^2\omega}{dt^2} + \frac{1}{T_g}\left(\delta - \frac{3s}{2j}\frac{\Theta}{T}\right)\frac{d\omega}{dt} + \frac{\omega}{T_gT_r} = 0 \tag{35}$$

In order that this equation represent a *damped* periodic speed oscillation, it is required that†

$$\delta T > \frac{3s}{2j}\Theta \tag{36}$$

Case II. The basic equation of governor movement is

$$\frac{dp_0}{dt} = -\frac{1}{T_g}\left(\omega + m\frac{d\omega}{dt}\right) \tag{16}$$

Combining Eqs. (16) and (34),

$$\frac{d^2\omega}{dt^2} + \frac{m}{T_gT_r}\frac{1 - \frac{3s}{2j}\frac{\Theta}{m}\frac{T_r}{T}}{1 - \frac{3s}{2j}\frac{m}{T_g}\frac{\Theta}{T}}\frac{d\omega}{dt} + \frac{1}{T_gT_r}\left(\frac{1}{1 - \frac{3sm\Theta}{2jT_gT}}\right)\omega = 0 \tag{37}$$

In order that this equation represent a *damped* periodic speed oscillation,† it is required that the factors of $d\omega/dt$ and ω be both positive, that is,

$$m > \frac{3s}{2j}\Theta\frac{T_r}{T}$$

or

$$m > \frac{3s}{2j}\left(\frac{j}{j - 3r}\right)\Theta \qquad \text{and} \qquad T_gT > \frac{3s}{2j}m\Theta$$

When the oscillation is just barely suppressed in time equal to infinity

$$m = \frac{3s}{2j}\left(\frac{j}{j - 3r}\right)\Theta \tag{38}$$

Substituting this value of m in the inequality

$$T_gT > \frac{3s}{2j}m\Theta$$

† Granville, *op. cit.*, p. 434.

there results

$$T_g T > \left(\frac{3s}{2j}\right)^2 \left(\frac{j}{j - 3r}\right) \Theta^2 \tag{39}$$

Case III. As previously indicated, this case is *approximately* the same as Case II, except that the acceleration constant m is replaced by the characteristic time T_d of dashpot rigidity or dashpot throttling action.

According to Eqs. (38) and (39) the value of the characteristic time T_d must then be

$$T_d > \frac{3s}{2j} \left(\frac{j}{j - 3r}\right) \Theta \tag{40}$$

and the criterion of stability becomes

$$T_g' T > \left(\frac{3s}{2j}\right)^2 \frac{j}{j - 3r} \Theta^2 \tag{41}$$

with the understanding that T_g' is very much greater than T_g.

Effect of the Speed Change upon the Difference between the Resisting and the Driving Couples. Before proceeding with the construction of vector diagrams confirming the criteria for incipient instability in cases involving water hammer, it is desirable to mention here one of the most important stabilizing factors, namely, the effect of the speed change upon the difference between the resisting couple of the electric generator and the hydraulic couple driving the turbine.

Writing the standard flywheel equation in the form

$$\frac{d\omega}{dt} = \frac{p}{T} \tag{7}$$

in which

$$p = p_0 + \tfrac{3}{2}h \tag{26}$$

We have assumed that the difference D_c between these two couples corresponds only to the power change p, due to the gate opening change ($p_0 = x:k$) and to the effect $\tfrac{3}{2}h$ of the head change h (water hammer). In other words, we have neglected the effect of the speed change ω upon both of the couples. But this last effect is often very important.

Using again the notation of relative values, let $c_d = \dfrac{C_d}{C_{0d}}$ in which C_d is the turbine driving couple at any speed for the gate opening steady state and C_{0d} is the turbine driving couple at normal synchronous speed for the said gate opening. $c_r = \dfrac{C_r}{C_{0r}}$ in which C_r is the generator resisting couple at any speed for the steady-state value of the absorbed load and C_{0r} is the generator resisting couple at normal synchronous speed for the said load.

By definition $C_{0d} = C_{0r} = C_0$, and both couples are then measured with the same unit C_0. On the diagram of Fig. 20 are represented the curves c_d and c_r in terms of ω; the coefficients α_d and α_r are the slopes of those curves at point A corresponding to the steady-state condition.

For the small oscillations assumed in our investigations of stability, we may write with sufficient accuracy

$$c_d = (1 + p)(1 + \alpha_d \omega)$$

or, neglecting terms of second order,

$$c_d = 1 + p + \alpha_d \omega$$

The value of the coefficient α_d depends upon the specific speed of the turbine. It may vary from $\alpha_d = -1.1$ (low specific speed) to $\alpha_d = -0.6$ (high specific speed).

Similarly, we can write for the resisting couple

$$c_r = 1 + \alpha_r \omega$$

The value of the coefficient α_r depends upon the nature of the load.

If the load is composed of a-c electric motors (load depending upon frequency), the value of the coefficient α_r depends upon the torque-speed characteristic of the driven machines:

$\alpha_r = 0$ for constant torque machines;

$\alpha_r = +2$ for turbomachines such as centrifugal pumps, fans, turbocompressors.

If load is composed of ohmic resistance (load independent of frequency), such as electric boilers, arc ovens, electrolyzers, and lamps, or, of d-c circuits fed by means of rectifiers, the value of the coefficient α_r depends solely upon the voltage-frequency characteristic of the voltage regulation. If the voltage constant, independent of frequency (speed), $\alpha_r = -1$ and that is the only case in which α_r may be equal to α_d:

$$\alpha = \alpha_r - \alpha_d = 0$$

In the other cases $\alpha = \alpha_r - \alpha_d$ is generally positive. The expression of the difference between the resisting and the driving couples must then be written

$$D_c = p - \alpha\omega = p_0 + \tfrac{3}{2}h - \alpha\omega$$

and the flywheel equation (34)

$$\frac{d\omega}{dt} = \frac{p_0}{T_r} - \frac{3s}{2j}\frac{\Theta}{T}\frac{dp_0}{dt} - \frac{\alpha\omega}{T} \qquad (42)$$

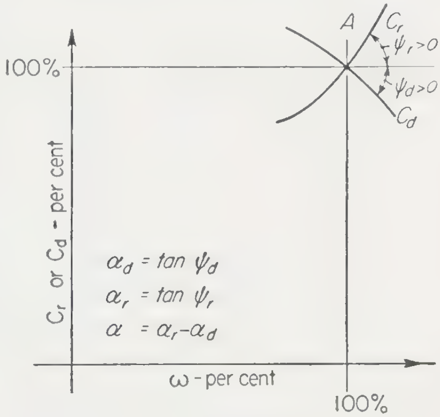

FIG. 20. Turbine-generator performance curve—showing relative values of driving couple and resisting couple in terms of relative speed.

Following the type of analysis previously employed, the criterion for incipient stability in Case II (speed-acceleration responsive governor) becomes

$$T_g T > \frac{\left(\frac{3s}{2j}\right)^2 \frac{T_r}{T}\Theta^2}{1 + \frac{\alpha 3s}{2j}\frac{\Theta}{T}\frac{T_r}{T}} \qquad (43)$$

in which

$$\frac{T_r}{T} = \frac{j}{j - 3r}$$

In other words, the minimum value of the product T_gT given by Eq. (39) assuming $\alpha = 0$ is to be divided by

$$1 + \alpha\frac{3s}{2j}\frac{\Theta}{T}\frac{T_r}{T}$$

It is then evident that for positive values of α† the effect of the speed change upon the difference between the resisting and the driving couples greatly favors the stability.

On the other hand, experimental checking of the speed regulation stability, by loading the generator on a hydraulic resistance, appears to be a very severe test, when

† This means that the resisting couple curve cuts the driving couple curve at the point of steady-state conditions, by passing *over* in direction of increasing speed (Fig. 20).

the voltage is maintained constant independently of the frequency, by quick-acting voltage regulation ($\alpha_r = -1$, $\alpha \cong 0$). In fact, except for some special cases this test is valueless; since at least a part of the load is in practice generally composed of a-c electric motors ($\alpha_r \geq 0$) and for the other part of the load which is independent of frequency, it is always possible to have recourse to a judicious adjustment of the voltage-frequency characteristic of the voltage regulation, in order to secure $\alpha_r > -1$ and $\alpha > 0$. If the voltage change is $\pm n$ per cent for a frequency change of ± 1 per cent, the change of the ohmic load reaches $\pm 2n$ per cent and the change of the resisting couple $\pm(2n - 1)$ per cent so that $\alpha_r = 2n - 1$.

Vector Diagrams. We are now in position to confirm the criteria for incipient stability by means of appropriate vector diagrams, and we shall start (Fig. 21) with the

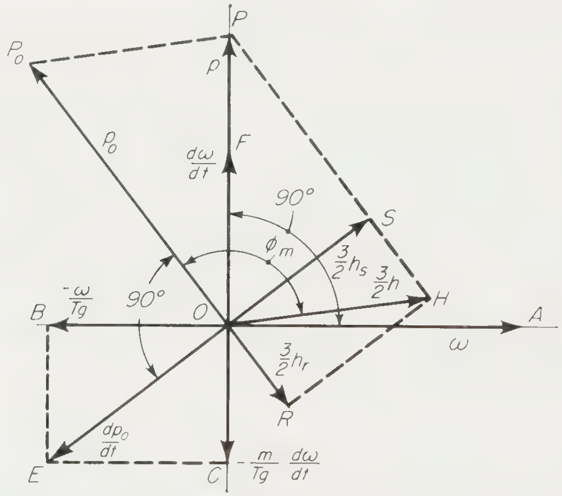

FIG. 21. Vector diagram—speed-acceleration-responsive governor including water hammer.

diagram for Case II, the speed-acceleration responsive governor when water hammer is present. The diagrams will be drawn to indicate that the system is just on the brink of instability, and the corresponding criteria deduced from the geometry of the diagrams:

Vector $\overline{OA}$ represents the speed-change oscillation.
Vector $\overline{OB}$ represents the tachymetric effect upon the relay valve.
Vector $\overline{OC}$ represents the accelerometric effect upon the relay valve.
Vector $\overline{OE}$ represents the oscillation of the relay valve displacement.
Vector $\overline{OP_0}$ represents the power-change oscillation due to the gate opening oscillation.
Vector $\overline{OH}$ represents the power-change oscillation due to the head-change oscillation (water hammer).
Vector $\overline{OP}$ represents the total power-change oscillation.
Vector $\overline{OF}$ represents the acceleration (derivative of speed).

As in the previous simpler cases, the length and orientation of the vectors follow from the basic differential equations for the particular case under investigation. The fundamental assumption of incipient instability is responsible for locating ω and $d\omega/dt$, and p_0 and dp_0/dt at 90 deg phase difference.

To Eq. (16) corresponds the vectorial operation:

$$\overline{OE} = \overline{OB} + \overline{OC}$$

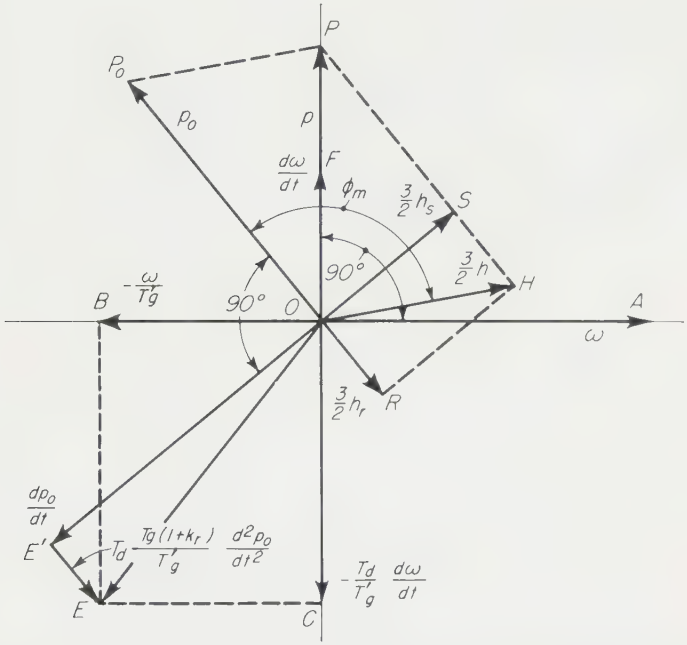

FIG. 22. Vector diagram—speed-responsive governor with secondary compensation (dashpot) including water hammer.

and the manner of passing from vector OE to vector $\overline{OP}_0$:

$$\overline{OP}_0 = \frac{T''}{2\pi}\,\overline{OE}\dagger$$

To Eq. (26) corresponds the vectorial operation:

$$\overline{OP} = \overline{OP}_0 + \overline{OH}$$

and to Eq. (7) (page 736) the manner of passing from vector $\overline{OP}$ to vector $\overline{OA}$:

$$\overline{OF} = \frac{1}{T}\,\overline{OP} \qquad \overline{OA} = \frac{T''}{2\pi}\,\overline{OF}\dagger$$

From elementary geometry,

$$\frac{OP_0 - OR}{OP} = \frac{OB}{OE}$$
$$\overline{OE}^2 = \overline{OB}^2 + \overline{OC}^2$$
$$\overline{OP}^2 = (OP_0 - OR)^2 + \overline{OS}^2$$

By appropriate substitutions and simple calculations, we obtain

$$m = \frac{3s}{2j}\,\Theta\,\frac{T_r}{T} \qquad \text{and} \qquad T_gT = \left(\frac{3s}{2j}\right)^2 \frac{T_r}{T}\,\Theta^2$$

which confirms the criterion for incipient stability according to Eq. (39).

The diagram in Fig. 22, corresponding to Case III, differs from the diagram of Fig.

† Relation between the amplitude of the sine function and the amplitude of its derivative.

21 in a single feature. The relay valve displacement is no longer represented by vector $\overline{OE}$ but by vector $\overline{OE}'$, which is obtained by the vectorial operation:

$$\overline{OE}' + \overline{E'E} = \overline{OB} + \overline{OC}$$

corresponding to Eq. (23). Owing to the effect of vector $\overline{E'E}$, vector $\overline{OE}'$ is displaced backward with respect to vector $\overline{OE}$, which is an adverse effect as regards stability. With a view to reducing this disadvantage to a minimum, we must seek to render the length of vector $\overline{E'E}$ as short as possible and therefore make T_g' very much greater than $T_g(1 + k_r)$, that is to say, $\delta' T_d$ very much greater than T_g, which confirms the condition (25).

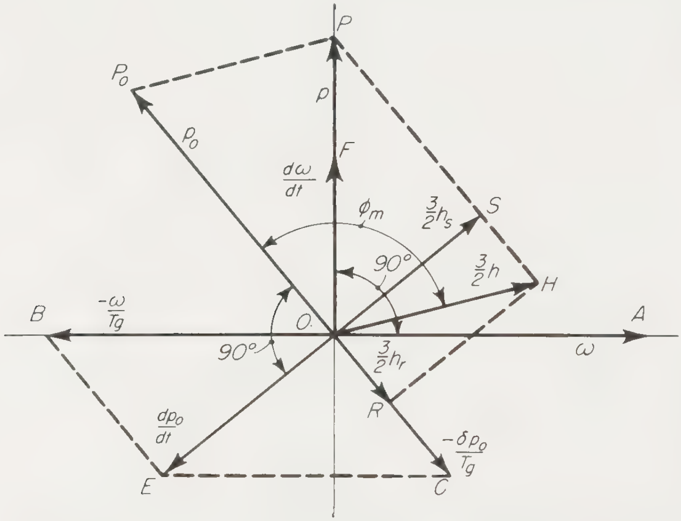

FIG. 23. Vector diagram—speed-responsive governor with primary compensation only including water hammer.

For Case I and the diagram of Fig. 23, in which vector $\overline{OC}$ represents the compensation effect upon the relay valve, we deduce from the geometry of the figure

$$\frac{\overline{OP}_0 - \overline{OR}}{OP} = \frac{OE}{OB}$$

$$\overline{OB}^2 = \overline{OE}^2 + \overline{OC}^2$$

$$\overline{OP}^2 = (\overline{OP}_0 - \overline{OR})^2 + \overline{OS}^2$$

Substituting the appropriate vectors, we confirm the criterion for incipient stability according to Eq. (36):

$$\delta = \frac{3s}{2j}\frac{\Theta}{T}$$

Finally, we draw Fig. 24, the vector diagram for the case of a speed-acceleration responsive governor (Case II) including the effect of speed change upon the difference between the resisting and driving couples, and the influence of water hammer.

Examination of the different diagrams shows clearly that every effect leading to an advance of vector $\overline{OP}$ (total power change oscillation) or of vector $\overline{OD}$ (oscillation of the difference between resisting and driving couples), with respect to vector $\overline{OA}$ (speed-change oscillation), in the trigonometric direction of increasing phase angles, improves stability, *i.e.*, the accelerometric effect upon the relay valve, the compensation effect upon the relay valve, and the effect of the speed change upon the difference between resisting and driving couples, with the understanding that $\alpha > 0$.

On the contrary, every effect leading to a backward rotation of the above vectors imperils stability, the most important influence of this kind being the water-hammer effect.

Experimental Statistics. From the foregoing analyses of Cases II and III, which comprise the important practical applications, we may conclude that for given values of the coefficient j (effect of the efficiency change) and α effect of the speed change upon

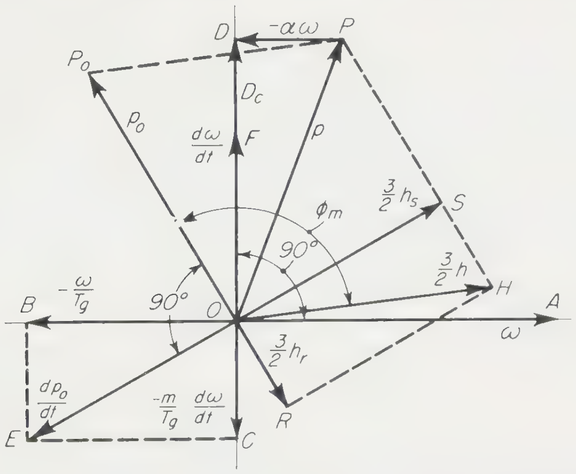

FIG. 24. Vector diagram—speed-acceleration-responsive governor including water hammer and the effect of speed change upon the difference between resisting and driving couples.

the difference between resisting and driving couples) governing stability depends upon five parameters, each having the dimensions of time in seconds:

For the rotating masses:

1. The time T, representing the specific inertia of the rotating masses. The value of T is normally between 2 and 8 sec, except in cases where a separate flywheel is provided in addition to the generator rotor.

For the pressure conduit:

2. The time Θ, representing the effect of water hammer. The value of Θ in practice is usually between 0.5 and 3 sec.

3. The time $T' = 2\mu$, representing the period of the free water-hammer oscillations, *i.e.*, two complete forward and backward transits of the water-hammer wave along the conduit or $4L/a$. The value of T' in practice lies usually between a few hundredths of a second and about 10 sec, seldom more.

For the governor:

4. The time m, measuring the importance of the acceleration factor in a speed-acceleration responsive governor. For a speed-responsive governor with secondary compensation in the form of a spring-loaded oil-filled dashpot, the time m is replaced by the time T_d defining the rigidity of the dashpot or its throttling action.

5. The time T_g measuring the promptness of the governor response. For the speed-acceleration responsive type, T_g depends essentially upon the dimensions of the oil-pressure relay valve. For the speed-responsive type with secondary compensation by dashpot, the value of T_g' depends primarily upon the dashpot rigidity T_d and the temporary speed droop $k_r\delta'$.

Since all installations having the same values for these five parameters will exhibit the same degree of stability, for the same turbine and load characteristics (values of j and α), it will be possible eventually as sufficient statistical data become available to prepare a chart (similar to the specific speed vs. head charts now employed so advantageously in turbine selection) permitting experimental determination of the value of the coefficient K in the general criterion of stability:†

$$T_gT > K(\tfrac{3}{2}\Theta)^2$$

directly deduced from inequality (39) or (41)

$$T_gT > \frac{s^2}{j(j-3r)}\left(\frac{3}{2}\Theta\right)^2$$

This criterion can then be used to check governing stability with the same ease that the Thoma formula is employed to check surge-tank stability.

Until such experimental results can be collected in sufficient volume and without neglecting their importance *in order to verify the analytic calculation,* fairly dependable values of the coefficient K can be computed on the basis of Eq. (37), which is rigorously valid for Case II (speed- and acceleration-responsive governor) and approximately for Case III (speed-responsive governor with secondary compensation).

Calculation of the Coefficient K of the General Criterion of Stability. The differential Eqs. (37) and (17) are of familiar form from vibration theory:‡

$$\frac{d^2\omega}{dt^2} + C_1\frac{d\omega}{dt} + C_2\omega = 0$$

in which, for Eq. (17),

$$C_1 = \frac{m}{T_gT} \qquad \text{and} \qquad C_2 = \frac{1}{T_gT}$$

and for Eq. (37),

$$C_1 = \frac{m}{T_gT_r}\,\frac{1 - \dfrac{3s}{2j}\dfrac{\Theta}{m}\dfrac{T_r}{T}}{1 - \dfrac{3s}{2j}\dfrac{m\Theta}{T_gT}} \qquad \text{and} \qquad C_2 = \frac{1}{T_gT_r}\,\frac{1}{1 - \dfrac{3s}{2j}\dfrac{m\Theta}{T_gT}}$$

Both equations were established neglecting the effect of speed change upon the difference between resisting and driving couples ($\alpha = 0$), the first one (17) in absence of and the second one (37) in presence of water hammer.

Their general solution is

$$\omega = Ce^{-\delta_*\frac{t}{T''}}\cos\left(\frac{2\pi}{T''} - \psi\right)$$

in which C and ψ are constants of integration.

$$T'' = \frac{4\pi}{\sqrt{4C_2 - C_1^2}}, \text{ the period of the oscillations.}$$

$$\delta_* = \frac{2\pi C_1}{\sqrt{4C_2 - C_1^2}}, \text{ their logarithmic decrement.}$$

In the case of Eq. (17), the values of this period and of this decrement are then

$$T'' = 2\pi\sqrt{T_gT}\,\frac{1}{\sqrt{1 - \frac{1}{4}\left(\dfrac{m}{\sqrt{T_gT}}\right)^2}}$$

† The fraction $\frac{3}{2}$ remaining in this expression of the criterion of stability reflects the assumption that at constant speed, the driving couple varies with the power $\frac{3}{2}$ of the head.

‡ Page, Leigh, "Introduction to Theoretical Physics," D. Van Nostrand Company, Inc., 1941, pp. 74–82.

$$\delta_* = \pi \frac{\dfrac{m}{\sqrt{T_g T}}}{\sqrt{1 - \dfrac{1}{4}\left(\dfrac{m}{\sqrt{T_g T}}\right)^2}}$$

In the case of Eq. (37) we have already shown that in order to damp the oscillations, it is required that

$$m > \frac{3s}{2j} \frac{j}{j - 3r} \Theta \tag{38}$$

that is,

$$m = \lambda_m \frac{s}{j - 3r} \left(\frac{3}{2} \Theta\right) \tag{44}$$

with $\lambda_m > 1$ and

$$T_g T > \left(\frac{3s}{2j}\right)^2 \left(\frac{j}{j - 3r}\right) \Theta^2 \tag{39}$$

that is,

$$T_g T = \lambda_t \frac{s^2}{j(j - 3r)} \left(\frac{3}{2} \Theta\right)^2 \tag{45}$$

or

$$T_g T_r = \lambda_t \frac{s^2}{(j - 3r)^2} \left(\frac{3}{2} \Theta\right)^2 \tag{45'}$$

with

$$\lambda_t > 1.\dagger$$

According to Eq. (45) the coefficient K of the criterion of stability is equal to

$$K = \lambda_t \frac{s^2}{j(j - 3_r)} \tag{46}$$

Now using the above defined coefficients λ_m and λ_t, we can express the factors C_1 and C_2 as follows:

$$C_1 = \frac{m}{T_g T_r} \frac{\lambda_t(\lambda_m - 1)}{\lambda_m(\lambda_t - \lambda_m)} \qquad C_2 = \frac{1}{T_g T_r} \frac{\lambda_t}{\lambda_t - \lambda_m}$$

or

$$C_1 = \frac{m_\Theta}{(T_g T_r)_\Theta} \qquad C_2 = \frac{1}{(T_g T_r)_\Theta}$$

in which,

$$m_\Theta = m \frac{\lambda_m - 1}{\lambda_m} \qquad (T_g T_r)_\Theta = T_g T_r \frac{\lambda_t - \lambda_m}{\lambda_t} \tag{47}$$

The effect of water hammer then operates:

1. To reduce the real value of the characteristic time m of the acceleration factor to the fictitious value m_Θ.

2. To reduce the real value of the product $T_g T$ (time of promptness multiplied by time of mechanical inertia) to the fictitious value $(T_g T_r)_\Theta$, in Eq. (47) in which $T_r = \dfrac{j}{j - 3r} T$.

Operating in similar fashion on Eq. (17), we easily obtain the following expressions of the period and of the decrement:

$$T'' = 2\pi \sqrt{(T_g T_r)_\Theta} \frac{1}{\sqrt{1 - \dfrac{1}{4}\left[\dfrac{m_\Theta}{\sqrt{(T_g T_r)_\Theta}}\right]^2}}$$

$$\delta_* = \pi \frac{\dfrac{m_\Theta}{\sqrt{(T_g T_r)_\Theta}}}{\sqrt{1 - \dfrac{1}{4}\left[\dfrac{m_\Theta}{\sqrt{(T_g T_r)_\Theta}}\right]^2}}$$

† Hence for $T_g T$ to be $> \dfrac{3s}{2j} m_\Theta$ (see Case II). It is also required that $\lambda_t > \lambda_m$.

But according to Eq. (47),

$$\frac{m_\Theta}{\sqrt{(T_gT_r)_\Theta}} = \frac{m}{\sqrt{T_gT_r}}\,\frac{\lambda_m - 1}{\lambda_m}\sqrt{\frac{\lambda_t}{\lambda_t - \lambda_m}}$$

and according to Eqs. (44) and (45′),

$$\frac{m}{\sqrt{T_gT_r}} = \frac{\lambda_m}{\sqrt{\lambda_t}}$$

so that

$$\frac{m_\Theta}{\sqrt{(T_gT_r)_\Theta}} = \frac{\lambda_m - 1}{\sqrt{\lambda_t - \lambda_m}}$$

In consequence of

$$R = \sqrt{1 - \frac{1}{4}\left[\frac{m_\Theta}{\sqrt{(T_gT_r)_\Theta}}\right]^2} = \sqrt{1 - \frac{1}{4}\left(\frac{\lambda_m - 1}{\sqrt{\lambda_t - \lambda_m}}\right)^2} \tag{48}$$

and

$$T'' = \frac{2\pi}{R}\sqrt{(T_gT_r)_\Theta} \qquad \delta_* = \frac{\pi}{R}\,\frac{\lambda_m - 1}{\sqrt{\lambda_t - \lambda_m}} \tag{49}$$

Using Eqs. (47) and (45′),

$$(T_gT_r)_\Theta = (\lambda_t - \lambda_m)\,\frac{s^2}{(j - 3r)^2}\left(\frac{3}{2}\Theta\right)^2$$

so that

$$T'' = \frac{3\pi}{R}\,\frac{s}{j - 3r}\sqrt{\lambda_t - \lambda_m}\,\Theta \tag{50}$$

and

$$\chi = \frac{3\pi}{2R}\,\frac{s}{j - 3r}\sqrt{\lambda_t - \lambda_m}\,\rho\dagger \tag{51}$$

(*a*) Let us assume (1) that $j = 1$, that is to say, the typical point of the steady-state condition is on the flat portion of the turbine efficiency curve, and (2) that the system is just on the brink of instability; in other words that the oscillations of gate opening change, head change, driving couple change, speed change, and so on are all sustained or undamped, so that

$$\delta_* = 0 \qquad \lambda_m = 1 \qquad R = 1$$

$$\chi = \frac{3\pi}{2}\,\frac{s}{1 - 3r}\sqrt{\lambda_t - 1}\,\rho \tag{52}$$

Considering a given value of ρ, we can now compute by trial, for different values of λ_t and by means of Eqs. (27), (29), (30), or of Figs. 16 to 19,

1. The values of χ, r and s satisfying Eq. (52).
2. The values of the coefficient K of the criterion of stability.

$$K = \lambda_t\,\frac{s^2}{1 - 3r} \tag{46′}$$

Choosing for each value of ρ, the particular value of λ_t corresponding to the minimum value of the coefficient K, we finally arrive at the results condensed in Table 4. According to the figures of this table, the curve of the diagram Fig. 25 has been drawn, taking as ordinates, the ratio $(K_{\rho=\rho}:K_{\rho=10})$ between the value of K for the considered value of ρ, and the value $K = 1.66$, for $\rho > 10$; as abcissas, at a logarithmic scale, the values of $1/\rho$ and of ρ. Underneath are also indicated the approximate values of the head corresponding to the said values of ρ.

The curve of Fig. 25 shows that the value of the coefficient K varies very little

† For $\chi = \dfrac{T''}{2\mu}$ and $\dfrac{\Theta}{2\mu} = \dfrac{1}{2}\dfrac{LV_0}{gH}, \dfrac{a}{2L} = \dfrac{1}{2}\dfrac{aV_0}{2gH} = \dfrac{1}{2}\rho$.

TABLE 4

ρ	10	2.5	1.5	1.0	0.5	0.3
λ_t	1.255	1.255	1.27	1.30	1.45	1.58
χ	37.3	9.33	5.78	4.08	2.53	1.86
s	0.848	0.857	0.876	0.905	1.021	1.195
r	0.153	0.150	0.148	0.142	0.121	0.102
$\frac{s}{1-3r}$	1.56	1.56	1.57	1.58	1.60	1.72
$K\delta_{*-0}$	1.66	1.68	1.75	1.86	2.37	3.25
$\frac{K_{\rho-\rho}}{K_{\rho-10}}$	100%	101%	105%	112%	143%	196%

in the scale of the low heads, which is an important statement. This value being $K = 1.66$ for a head in the vicinity of 30 ft, its variation is only 5 per cent up to a head of about 330 ft and 10 per cent up to a head of about 550 ft.

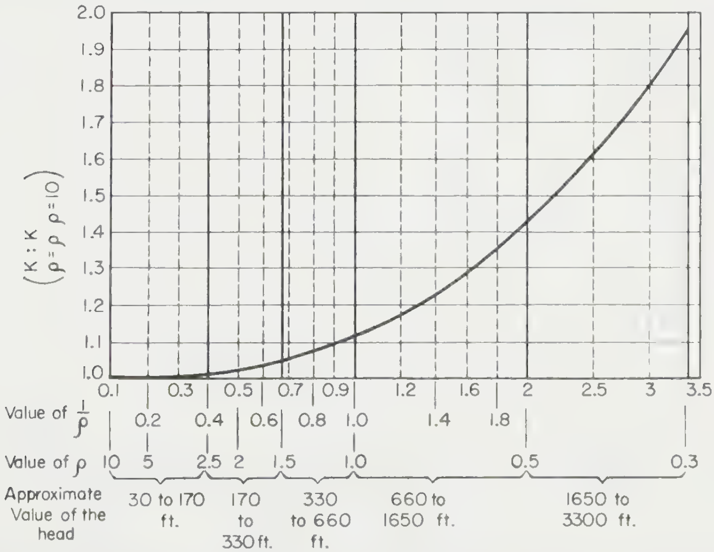

FIG. 25. Relative value (in comparison with the value for $\rho \geq 10$) of the coefficient K of the criterion of stability in terms of ρ — the Allievi water-hammer parameter (that is to say, particularly in terms of the head).

The value of the fraction $\frac{s}{1-3r}$ mentioned in the sixth line of Table 4 is to be used to compute the most convenient value of the characteristic time m(or T_d) of the acceleration factor, by means of Eq. (44), with $\lambda_m = 1$ and $j = 1$,

$$m = \frac{s}{1-3r}\left(\frac{3}{2}\Theta\right)$$

This value of m corresponds fortunately to the minimum value of the coefficient K.

(*b*) If the oscillations should be damped, *i.e.*, with a logarithmic decrement $\delta_* = 1.38$ (such amplitude being then the quarter of the former $e^{1.38} \cong 4$), j being still equal to 1, the calculation of the value of K will be carried on as follows:

1. By means of Eqs. (48) and (49), compute a series of couples of values of λ_m and λ_t, corresponding to $\delta_* = 1.38$.
2. Considering a given value of ρ, compute by trial for different couples λ_m, λ_t, the values of χ, r, and s satisfying Eq. (51),† using for this purpose Eqs. (27), (29), (30) or Figs. 16 to 19.
3. Compute the values of the coefficient K, by means of Eq. (46′).
4. Choose, for each value of ρ, the minimum of the calculated values of K.

The results of these operations are given by Table 5. The value of the expression

TABLE 5

ρ	10	2.5	1.5	1.0	0.5	0.3
λ_t	1.405	1.41	1.425	1.465	1.66	1.80
λ_m	1.196	1.198	1.204	1.215	1.268	1.303
χ	35.9	9.03	5.575	3.965	2.48	1.822
r	0.162	0.159	0.157	0.150	0.1265	0.109
s	0.838	0.849	0.867	0.900	1.022	1.205
$\lambda_m \dfrac{s}{1-3r}$	1.95	1.95	1.97	1.99	2.085	2.30
In % of Table 4 $\dfrac{s}{1-3r}$	125%	125%	125%	125%	130%	134%
$K\delta_{*=1.38}$	1.92	1.945	2.025	2.16	2.78	3.87
$\dfrac{K\delta_{*=1.38}}{K\delta_{*=0}}$	115.8%	115.8%	115.8%	116.2%	117%	119%

$\lambda_m \dfrac{s}{1-3r}$ given in the seventh line of Table 5 is to be used to compute the most convenient value of the time m (or T_d), by means of Eq. (44), with $j = 1$,

$$m = \lambda_m \frac{s}{1-3r}\left(\frac{3}{2}\Theta\right)$$

The figures of Table 6 were established in the same way, for the case in which the value of the logarithmic decrement is equal to $\delta_* = 0.69$ (such amplitude being then half of the former $e^{0.69} = 2$).

The comparison between Tables 5 and 6 and Table 4 leads us to conclude that in order to damp the oscillations with a logarithmic decrement equal to $\delta_* = 0.69$ or to $\delta_* = 1.38$, the values of the coefficient K of the criterion of stability, computed on the basis of the assumption of sustained oscillations, should be increased in an approximately constant proportion of 8 to 10 per cent and 16 to 19 per cent, respectively. This statement is valid over the entire range of head values from 30 ft ($\rho \cong 10$) to 3,000 ft ($\rho \cong 0.3$). Concerning the characteristic time m of the acceleration factor, it should be increased according to the indication of the eighth lines of Tables 5 and 6, in a proportion which is also nearly constant and respectively equal to 13 to 17 per cent or to 25 to 34 per cent.

† But with $j = 1$.

TABLE 6

ρ	10	2.5	1.5	1.0	0.5	0.3
λ_t	1.34	1.35	1.36	1.39	1.575	1.735
λ_m	1.105	1.108	1.109	1.115	1.143	1.165
χ	36.5	9.23	5.70	4.01	2.515	1.856
r	0.157	0.154	0.152	0.146	0.123	0.1025
s	0.842	0.854	0.872	0.903	1.022	1.194
$\lambda_m \dfrac{s}{1-3r}$	1.76	1.76	1.78	1.79	1.85	2.01
In % of Table 4 $\dfrac{s}{1-3r}$	113%	113%	113%	113%	115%	117%
$K\delta_{*=0.69}$	1.80	1.82	1.90	2.02	2.59	3.58
$\dfrac{M\delta_{*=0.69}}{M\delta_{*=\theta}}$	108%	108%	108%	108.5%	109%	110%

(*c*) Let us now return to the case of sustained oscillations, corresponding to the limit of stability $\delta_* = 0$, with the purpose of studying the effect of efficiency change $j \neq 1$.

The procedure is the same as that explained in paragraph (*a*), except that Eq. (51) with $\lambda_m = 1$ and $R = 1$,

$$\chi = \frac{3\pi}{2} \frac{s}{j - 3r} \sqrt{\lambda_t - 1}\, \rho \tag{53}$$

is to be used instead of Eq. (52) and that Eq. (46),

$$K = \lambda_t \frac{s^2}{j(j - 3r)} \tag{46}$$

is to be used instead of Eq. (46′).

The results of the calculation are illustrated by the curves of Fig. 26 having as abcissas, the value of the coefficient j defining the rate of efficiency change at the representative point of steady-state conditions, in other words, the slope of the turbine efficiency curve; as ordinates, the ratio $(K_{j=j}:K_{j=1})$ between the values of K computed taking account of the effect of the efficiency change ($j \neq 1$) and the values of K computed in paragraph (*a*), Fig. 25, neglecting the said effect ($j = 1$).

The three curves of Fig. 26, which are not far apart, have been drawn for $\rho = 10$ (case of low head), $\rho = 1.5$ (case of medium head) and $\rho = 0.3$ (case of high head). Their examination leads to the following comments.

When the turbine efficiency curve is ascending, *i.e.*, when $j > 1$, the value of the coefficient K of the criterion of stability becomes smaller than for $j = 1$. This statement is logical because in this case the discharge change is smaller than the output change, so that the water hammer effect is less important. This evidently improves stability.

On the contrary, when the turbine efficiency curve is descending ($j < 1$), the value of the coefficient K becomes greater than for $j = 1$. In this case the discharge change is in fact greater than the output change, so that the water-hammer effect is more important. The conditions for stability are then more severe.

Moreover, the effect of efficiency change is a little less marked in case of high heads than in case of low and medium heads, the slope of the curves $\rho = 10$ or $\rho = 1.5$ being greater than that of the curve $\rho = 0.3$.

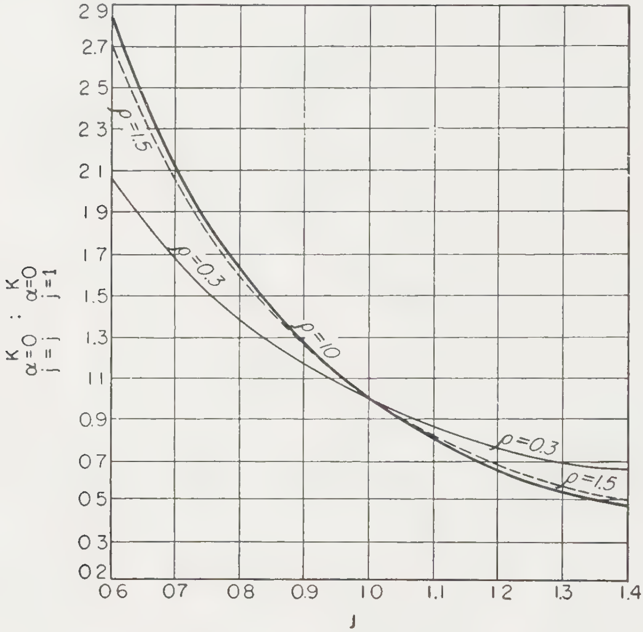

FIG. 26. Relative value (in comparison with the value for $j = 1$) of the coefficient K of the criterion of stability in terms of j — the parameter defining the effect of efficiency change, for different values of the water-hammer parameter.

(*d*) To take account of the effect of speed change upon the difference between resisting and driving couples, we have to use the basic equation of governor movement (Case II):

$$\frac{dp_0}{dt} = -\frac{1}{T_g}\left(\omega + m\frac{d\omega}{dt}\right) \tag{16}$$

The flywheel equation which as seen before must be then written

$$\frac{d\omega}{dt} = \frac{p_0}{T_r} - \frac{3s}{2j}\frac{\Theta}{T}\frac{dp_0}{dt} - \frac{\alpha\omega}{T} \tag{42}$$

Combining these two equations, we easily obtain a single equation of the same form as Eq. (37):

$$\frac{d^2\omega}{dt^2} + C_1\frac{d\omega}{dt} + C_2 = 0$$

in which C_2 has the same value as in the said equation, but

$$C_1 = \frac{m}{T_gT_r}\,\frac{1 - \dfrac{3s}{2j}\dfrac{\Theta}{m}\dfrac{T_r}{T} + \alpha\dfrac{T_gT_r}{mT}}{1 - \dfrac{3s}{2j}\dfrac{m\Theta}{T_gT}}$$

Operating as explained for Eq. (37), the following expressions can be computed for the case of sustained oscillations ($\lambda_m = 1$, $\delta_* = 0$):

1. For the characteristic time m (or T_d) of the acceleration factor, instead of Eq. (38) for Eq. (37):

$$m = \left(\frac{3s}{2j}\Theta - \alpha T_g\right)\frac{j}{j - 3r} \tag{54}$$

2. For the coefficient K of the criterion of stability, instead of Eq. (46) for Eq. (37):

$$K = \lambda_t \frac{s^2}{j(j - 3r)} \frac{1}{1 + \dfrac{3s}{2(j - 3r)} \lambda_t \alpha \dfrac{\Theta}{T}} \tag{55}$$

3. For the period of the oscillations, instead of Eq. (50) with $R = 1$, for Eq. (37):

$$T'' = 3\pi \frac{s}{j - 3r} \sqrt{\lambda_t - 1} \frac{\Theta}{\sqrt{1 + \dfrac{3s}{2(j - 3r)} \lambda_t \alpha \dfrac{\Theta}{T}}} \tag{56}$$

4. For the ratio $\chi = (T'':T') = (T'':2\mu)$, instead of Eq. (51) with $R = 1$, for Eq. (37):

$$\chi = \frac{3\pi}{2} \frac{s}{j - 3r} \sqrt{\lambda_t - 1} \frac{\rho}{\sqrt{1 + \dfrac{3s}{2(j - 3r)} \lambda_t \alpha \dfrac{\Theta}{T}}} \tag{57}$$

As we have already studied the effect of efficiency change in paragraph (c), let us now neglect the said effect and assume that $j = 1$. It appears from Eq. (55), (56), and (57) that the parameter to be used for the present study is $\alpha \dfrac{\Theta}{T}$ composed of the coefficient α defining the effect of speed change upon the difference between resisting and driving couples; the ratio $\dfrac{\Theta}{T}$ between characteristic times of hydraulic and mechanical inertias.

The results of the calculation are illustrated by the curves of Fig. 27, having as abscissas, the values of the parameter $\alpha \dfrac{\Theta}{T}$; as ordinates, the ratio $(K_{\alpha=\alpha}:K_{\alpha=0})$ between the values of K computed taking account of the effect of speed change upon the difference between resisting and driving couples $\alpha \neq \Theta$, and the values of K computed in paragraph (a) (Fig. 25) neglecting the said effect $\alpha = 0$.

These curves were computed for severe values of ρ, but down to $\rho = 1.5$ they all overlap and diverge slightly only for $\rho < 1.5$, as shown in dotted line for $\rho = 0.3$.

Figure 27 confirms the statement already established. The effect of speed change upon the difference between resisting and driving couples favors stability when $\alpha > 0$ (the value of the coefficient K becoming smaller), that is to say, when the resisting couple curve cuts the driving couple curve, at the point of steady-state conditions, by passing *over* in the direction of increasing speed (Fig. 20). We may now add that this advantageous influence, being defined by the value of the parameter $\alpha \dfrac{\Theta}{T}$, is of increasing importance according as the value of the hydraulic inertia parameter Θ becomes large, and the value of the mechanic inertia parameter T becomes small.

Example 18: Compute, for the conditions of Example 5, the minimum value of the time of promptness (maximum governing rapidity), which assures governing stability in the case of a speed-acceleration responsive governor and in the case of a speed-responsive governor with secondary compensation, in absence of or neglecting (1) the effect of the primary compensation $\delta = 0$ and (2) the effect of the speed change upon the difference between the resisting and the driving couples $\alpha = 0$.

The calculation is based on the following values:

$P = 91{,}500$ hp	$N = 150$ rpm	$H = 330$ ft
$L = 400$ ft	$V_0 = 18.25$ fps	$WR^2 = 53 \times 10^6$ pfs
$a = 4{,}660$ fps	$\rho = 4$†	$\mu = 0.172$ sec
$\Theta = 0.688$ sec	$T = 8$ sec	

The diagram of Fig. 28 shows the turbine output curve established as for Fig. 2; the slope of this curve at its upper end corresponds to $k = 3$. The diagram of Fig. 29 shows the turbine efficiency curve established as for Fig. 9; the slope of this curve at its upper end corresponds to $j = 0.77$.

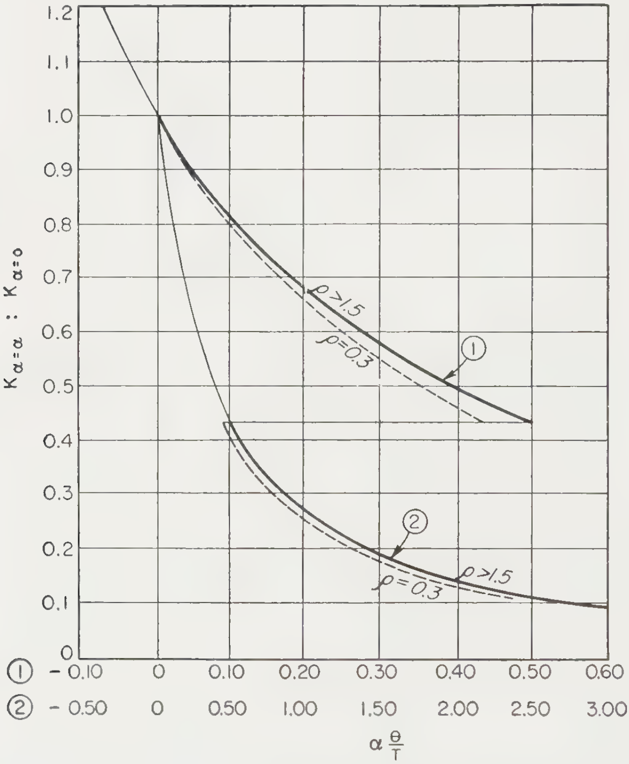

FIG. 27. Relative value (in comparison with the value for $\alpha = 0$) of the coefficient K of the criterion of stability in terms of $\alpha \dfrac{\Theta}{T}$ parameter in which the coefficient $\alpha = \alpha_r - \alpha_d$ measures the effect of the speed change upon the difference between the resisting and the driving couples.

According to Fig. 25, $K\rho_{-4} : K\rho_{-10} = 1$. In the case of sustained oscillations and neglecting first the effect of efficiency change, we may then write, for a speed-acceleration responsive governor:

$$T_gT = 1.66(\tfrac{3}{2}\Theta)^2 = 1.78 \text{ sec}^2$$

$$T_g = \frac{1.78}{8} = 0.223 \text{ sec} \qquad \text{time of promptness}$$

$$m = \frac{3}{2}\Theta \frac{s}{1 - 3r}$$

$$m = \tfrac{3}{2} \times 0.688 \times 1.56‡ = 1.61 \text{ sec} \qquad \text{acceleration constant}$$

† The value of ρ is higher than these normally computed for a head of 330 ft. because, with the very short penstock in proportion to the head, it was possible to adopt a high velocity V_0.

‡ According to Table 4, for $\rho = 4$, $\dfrac{s}{1 - 3r} = 1.56$.

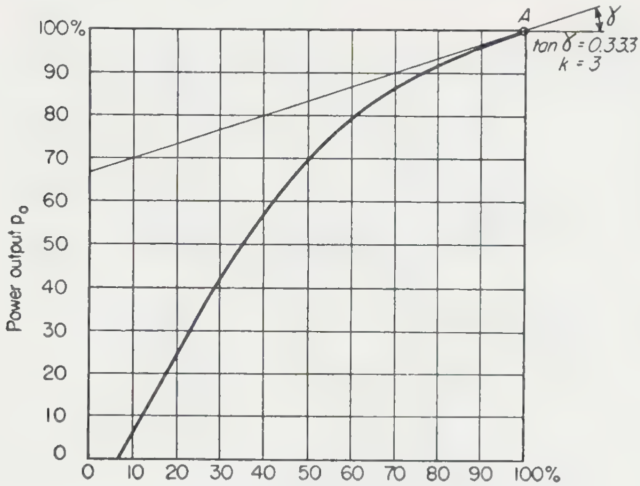

FIG. 28. Servomotor piston travel x.

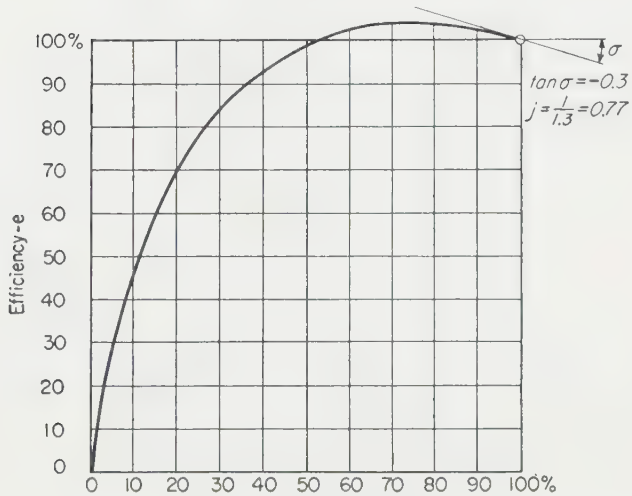

FIG. 29. Power output p_0.

Assuming that condition (25) is fully reached, we may also compute for a speed-responsive governor with secondary compensation:

$T_0' = 0.223$ sec time of promptness
$T_d = 1.61$ sec time of dashpot rigidity
$k_r\delta' = \dfrac{0.223}{1.61} = 13.9$ per cent transient speed droop

In both cases the period of the governor oscillations is about the same and equal to

$$T'' = 3\pi \frac{s}{1-3r} \Theta \sqrt{\lambda_{t-1}} \qquad \frac{s}{1-3r} = 1.56 \qquad \lambda_t = 1.255\dagger$$
$$T'' = 5.10 \text{ sec}$$

Introducing now the effect of efficiency change, we can read on Fig. 26, for $\rho = 4$ and $j = 0.77$,

$$K_{j=0.77} : K_{j=1} = 1.7$$

† See Table 4.

Consequently,

$$T_g = 0.223 \times 1.7 = 0.38 \text{ sec}\dagger$$

Adding a margin of 8 per cent in order to damp the oscillations, with a logarithmic decrement of $\delta_* = 0.69$,

$$T_g = 0.41 \text{ sec}\ddagger$$

This means that, in the presence of a frequency change of ± 0.1 cycles/sec (0.166 per cent of 60 cycles/sec), the governor will be able to decrease or to increase the turbine output at the rate of 0.166 per cent in 0.41 sec, or 0.405 per cent in 1 sec, or 370 hp in 1 sec.

This governing rapidity (promptness) is quite favorable, owing to the small length of the penstock (in proportion to the head) and to the sufficiently large value of the mechanical inertia WR^2 defined by $T = 8$ sec.

Example 19: Compute for the conditions of Example 18, the minimum value of the permanent speed droop which assures governing stability, in case of a speed-responsive governor with primary compensation, assuming that the time of promptness should be the same as calculated for Example 18.

Neglecting first the effect of efficiency change ($j = 1$), we compute by trial for $T_g = 0.223$ sec (see Example 18), according to Eq. (35) and Fig. 16:

$$T'' = 2\pi \sqrt{T_g T_r} \qquad T_r = \frac{j}{j - 3r} T$$

$$T' = 0.344 \text{ sec} \qquad T'' = 9.15 \text{ sec} \qquad \chi \cong 27 \qquad \rho = 4 \qquad r = 0.05 \qquad T_r = 9.4 \text{ sec}$$

$$9.15 = 2\pi \sqrt{0.223 \times 9.4} = 9.15$$

in consequence of which, according to Fig. 18,

$$s = 0.95 \qquad \delta = \frac{3s}{2}\frac{\Theta}{T} = \frac{3 \times 0.95 \times 0.688}{2 \times 8}$$

$$\delta = 12.2 \text{ per cent}$$

Now taking account of the effect of efficiency change ($j = 0.77$), we compute in the same fashion for $T_g = 0.38$ sec (see Example 18):

$$T'' = 2\pi \sqrt{T_g T_r} \qquad T_r = \frac{j}{j - 3r} T$$

$$T' = 0.344 \text{ sec} \qquad T'' = 11.6 \text{ sec} \qquad \chi \cong 34 \qquad \rho = 4 \qquad r = 0.035 \qquad T_r = 9 \text{ sec}$$

$$11.6 = 2\pi \sqrt{0.38 \times 9} = 11.6$$

$$s = 0.975 \qquad \delta = \frac{3s}{2j}\frac{\Theta}{T} = \frac{3 \times 0.975 \times 0.688}{2 \times 0.77 \times 8}$$

$$\delta = 16.4 \text{ per cent}$$

In spite of the favorable conditions of Example 18, as mentioned before, these values of permanent speed droop are much too high and cannot be accepted in practice. Consequently it is not possible in this case to assure governing stability, by means of primary compensation alone.

† We may also compute by trial for $\rho = 4$, $j = 0.77$:

$$\chi = \frac{3\pi}{2}\frac{s}{j - 3r}\rho\sqrt{\lambda_t - 1} \qquad s = 0.9 \qquad r = 0.1 \qquad \lambda_t = 1.26$$

$$K = \lambda_t \frac{s^2}{j(j - 3r)} \qquad \chi = 18.5 \qquad T'' = 6.35 \text{ sec} \qquad K = 2.82$$

$$T_g \text{ or } T_g' = \frac{K}{T}\left(\frac{3}{2}\Theta\right)^2 = 0.38 \text{ sec} \qquad \text{time of promptness}$$

$$m \text{ or } T_d = \frac{3}{2}\Theta\frac{s}{j - 3r} = 1.98 \text{ sec} \qquad \text{acceleration constant or time of dashpot rigidity}$$

$$k_r\delta' \frac{T_g'}{T_d} = \frac{0.38}{1.98} = 19 \text{ per cent} \qquad \text{transient speed droop}$$

‡ The characteristic time m of the acceleration factor or T_d of the dashpot rigidity should be simultaneously increased to

$$m \text{ or } T_d = 1.98 \times 1.13 = 2.24 \text{ sec}$$

so that in the case of a speed-responsive governor with secondary compensation, the transient speed droop should reach

$$k_r\delta' = \frac{0.41}{2.24} = 18.5 \text{ per cent}$$

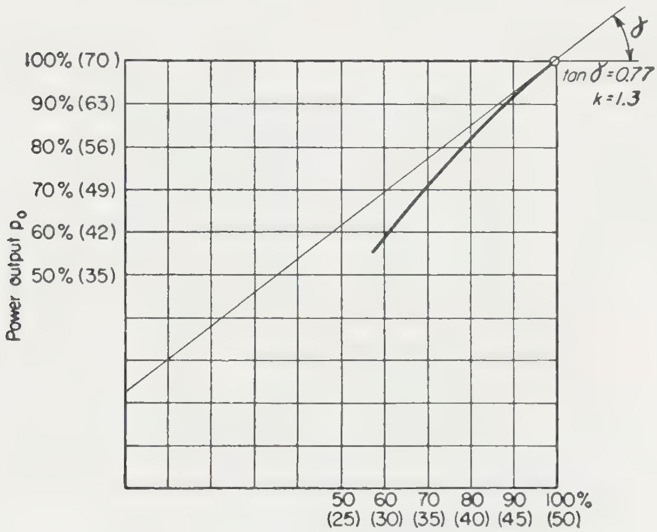

FIG. 30 Servomotor piston travel x.

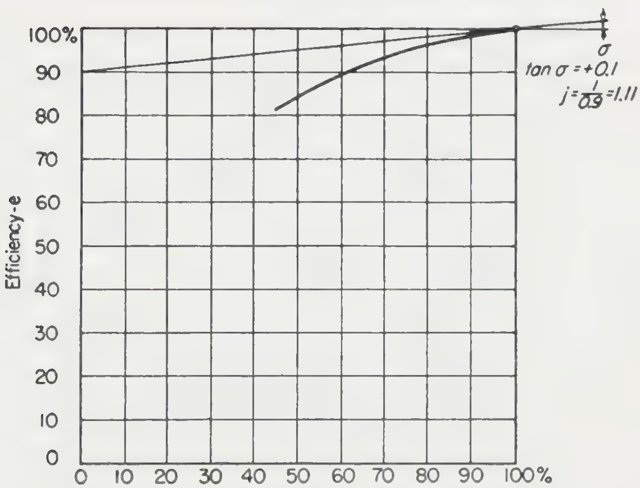

FIG. 31. Power output p_0.

Example 20: Check the stability of governing for the conditions of Example 18, but at 70 per cent of full load (50 per cent of full servomotor piston travel, see Fig. 28), the adjustment of the governor remaining *the same* as calculated for Example 18.

The diagram of Fig. 30 shows the turbine output curve established as for Fig. 2; the slope of this curve at its upper end corresponds to $k = 1.3$. The diagram of Fig. 31 shows the turbine efficiency curve established as for Fig. 9; the slope of this curve at its upper end corresponds to $j = 1.11$.

Neglecting first the effect of efficiency change, we have computed for Example 18: $T_g = 0.223$ sec at full load. To compute the time of promptness for 70 per cent load with the same governor adjustment, we shall reduce the aforesaid value: (1) in the proportion 50/100, the piston stroke for the new steady conditions being 50 per cent, (2) in the proportion of the values of the coefficient $K = \frac{1.3}{3}$ depending upon the slope of the output curve.

$$T_g = 0.223 \times \frac{50}{100} \times \frac{1.3}{3} = 0.0482 \text{ sec}$$

To compute the mechanical inertia parameter T, we shall increase the former value $T = 8$ sec in the proportion 100/70 of the loads:

$$T = 8\,{}^{100}\!/_{70} = 11.4 \text{ sec}$$

To compute the hydraulic inertia parameter Θ, we shall modify the former value $\Theta = 0.688$ sec (1) in the proportion 70/100 of the loads, (2) in the proportion 100/104 of the efficiencies (see Fig. 29).

$$\Theta = 0.688 \times {}^{70}\!/_{100} \times {}^{100}\!/_{104} = 0.462 \text{ sec}$$

In the same way,

$$\rho = 4 \times {}^{70}\!/_{100} \times {}^{100}\!/_{104} = 2.7$$

According to Fig. 25, the value of the coefficient K of the criterion of stability

$$T_gT > K({}^3\!/_2\Theta)^2$$

is equal to $K = 1.66 \times 1.01 = 1.68$. As

$$0.0482 \times 11.4 < 1.68 \times {}^3\!/_2(0.462)^2$$
$$0.55 < 0.805$$

The criterion of stability is not satisfied owing to the greater value of the slope of the output curve ($k = 1.3$ instead of $k = 3$) and the time of promptness should be increased.

Now taking account of the effect of efficiency change, we have computed for Example 18: $T_g = 0.38$ sec at full load, so that the time of promptness for 70 per cent load, with the same governor adjustment, is equal to

$$T_g = 0.38 \times \frac{50}{100} \times \frac{1.3}{3} = 0.0825 \text{ sec}$$

According to Fig. 25 ($K\rho_{=2.7}:K\rho_{=10} = 1.01$) and Fig. 26 ($j = 1.11$; $\rho = 2.7$; $K_{j=1.11}:K_{j=1} = 0.8$) the value of the coefficient K of the criterion of stability is equal to

$$K = 1.66 \times 1.01 \times 0.8 = 1.34$$

As

$$0.0825 \times 11.4 > 1.34({}^3\!/_2 0.462)^2$$
$$0.94 > 0.645$$

The criterion of stability is satisfied, owing to the effect of the efficiency change ($j = 1.11$ instead of $j = 0.77$) and in spite of the greater value of the slope of the output curve ($k = 1.3$ instead of $k = 3$).

Example 21: Check the stability of governing for the conditions of Example 18, but with the following modifications: (1) The length of the penstock is increased to $L = 2{,}000$ ft. (2) In order to reduce the head losses, in spite of this penstock length, the velocity is reduced to $V_0 = 11.1$ fps. (3) The penstock being of metallic construction, the velocity of the water-hammer waves is equal to $a = 2{,}960$ fps. (4) To correspond to the most economical construction, the inertia of the rotor of the generator is reduced to $WR^2 = 36.5 \times 10^6$ pfs.

Consequently,

$$\rho = 1.55 \qquad \Theta = 2.1 \text{ sec} \qquad T = 5.5 \text{ sec}$$

According to Fig. 25 ($K\rho_{=1.55}:K\rho_{=10} = 1.05$) and Fig. 26 ($K_{j=0.77}:K_{j=1} = 1.7$):

$$T_gT = 1.66 \times 1.05 \times 1.7({}^3\!/_2\Theta)^2$$
$$T_g = \frac{1.66 \times 1.05 \times 1.7}{5.5}\left(\frac{3}{2}\,2.1\right)^2$$
$$T_g = 5.4 \text{ sec}\dagger$$

† We may also compute by trial for $\rho = 1.55$ and $j = 0.77$:

$$\chi = \frac{3\pi}{2}\frac{s}{j - 3r}\rho\sqrt{\lambda_t - 1} \qquad s = 0.92 \qquad r = 0.098 \qquad \lambda_t = 1.27$$

$$K = \lambda_t\frac{s^2}{j(j - 3r)} \qquad \chi = 7.5 \qquad T'' = 20 \text{ sec} \qquad K = 2.98$$

$$T_g \text{ or } T_g' = \frac{K}{T}\left(\frac{3}{2}\Theta\right)^2 = 5.4 \text{ sec} \qquad \text{time of promptness}$$

$$m \text{ or } T_d = \frac{3}{2}\Theta\frac{s}{j - 3r} = 6.1 \text{ sec} \qquad \text{acceleration constant or time of dashpot rigidity}$$

$$k_r\delta' = \frac{T_g'}{T_d} = 89 \text{ per cent} \qquad \text{transient speed droop}$$

Notice the high value of the transient speed droop, which would cause prohibitively large frequency deviations.

Adding a margin of 8 per cent in order to damp the oscillations with a logarithmic decrement of $\delta_* = 0.69$,

$$T_g = 5.85 \text{ sec}$$

This means that, in the presence of a frequency deviation of ± 0.1 cycle/sec (0.166 per cent of 60 cycles/sec), the governor will be able to decrease or to increase the turbine output at the rate of $\frac{0.166}{5.85} = 0.0284$ per cent in 1 sec or 26 hp in 1 sec.

This governing rapidity (promptness) is quite unfavorable. For a large hydroelectric unit of 91.500 hp, the poor regulation capacity corresponding to an output change of only 26 hp/sec is not practically acceptable, except when the unit is not required to accomplish frequency control. For this purpose its action must be much quicker, considering the rate of change of load demand on the distribution system.

This calculation was made neglecting the effect of speed change upon the difference between resisting and driving couples $\alpha = 0$. Let us now assume that the load is essentially ohmic and that the voltage regulation is accomplished according to the following law:

$$\frac{u \text{ (voltage change in per cent)}}{\omega \text{ (frequency change in per cent)}} = 1$$

that is,

$$\frac{p}{\omega} = 2 \qquad \frac{C_r}{\omega} = 1 \qquad \alpha_r = +1$$

Moreover taking account of the specific speed of the turbine,

$$\alpha_d = -1, \qquad \text{so that} \qquad \alpha = +2$$

We can then read on the diagram Fig. 27, for $\alpha \frac{\Theta}{T} = 2 \frac{2.1}{5.5} = 0.765$:

$$K\alpha_{=2} : K\alpha_{=0} = 0.31$$

Consequently, the approximate value of the time of promptness is equal to

$$T_g = 5.85 \times 0.31 = 1.81 \text{ sec}$$

In the presence of a frequency deviation of ± 0.1 cycle/sec, the rate of change of the turbine output becomes 0.0925 per cent in 1 sec, or 84 hp in 1 sec.

The effect of the speed change upon the difference between resisting and driving couples allows an increase in the governing rapidity to a higher value which may be acceptable in this particular case. The actual rate of change of the consumer's load is the essential basis for judgment.

Governing Stability of Two (or Several) Generating Units. As the final topic in our abridged summary of the essentials of governing stability, we shall consider the case of two generating units coupled in parallel, so that their relative speed changes ω are necessarily the same. We shall try to discuss, at least approximately, the criterion of stability which is to be satisfied in order to prevent the gate opening changes of both units to oscillate *in phase*, in the undamped condition. For this purpose we shall select the speed-acceleration responsive type of governor, although the method of attack applies equally well to all types. The following method can easily be extended to the case of several generating units.

Using the subscript 1 for the terms corresponding to the first unit and subscript 2 for the terms corresponding to the second, we may write their respective equations (16) of governor movement as follows:

$$\frac{dp_{01}}{dt} = -\frac{1}{T_{g1}}\left(\omega + m_1 \frac{d\omega}{dt}\right) \tag{58}$$

$$\frac{dp_{02}}{dt} = -\frac{1}{T_{g2}}\left(\omega + m_2 \frac{d\omega}{dt}\right) \tag{59}$$

We notice here that, if the total power output at the steady-state condition is

$$P_0 = P_{01} + P_{02}$$

with

$$P_{01} = k_1 P_0 \qquad P_{02} = k_2 P_0 \qquad k_1 + k_2 = 1$$

the relative value p_0 (in regard to the total power output P_0) of the total output change, due to the governor movements (neglecting water-hammer and speed change effects upon driving and resisting couples) of both units, is equal to

$$\begin{aligned} p_0 &= \frac{(P_1 + P_2) - (P_{01} + P_{02})}{P_{01} + P_{02}} \\ &= k_1 \frac{P_1 - P_{01}}{P_{01}} + k_2 \frac{P_2 - P_{02}}{P_{02}} \\ &= k_1 p_{01} + k_2 p_{02} \end{aligned} \tag{60}$$

Considering only the speed change effect upon the governor movements, we may then write:

$$\begin{aligned} \frac{dp_0}{dt} &= k_1 \frac{dp_{01}}{dt} + k_2 \frac{dp_{02}}{dt} \\ &= -\frac{k_1}{T_{g1}}\omega - \frac{k_2}{T_{g2}}\omega \\ &= -\frac{1}{T_g}\omega \end{aligned} \tag{61}$$

in which T_g is the resulting time of promptness of response of both governors acting in concert. It can be calculated by the following formula deduced from the above equations:

$$\frac{1}{T_g} = \frac{k_1}{T_{g1}} + \frac{k_2}{T_{g2}} \tag{62}$$

The flywheel equations (34) of both units, considered independently one from the other, may be written (neglecting the speed change effect upon the couples):

$$\frac{d\omega}{dt} = \frac{1}{T_1}\left(w_1 p_{01} - l_1 \frac{dp_{01}}{dt}\right) \tag{63}$$

$$\frac{d\omega}{dt} = \frac{1}{T_2}\left(w_2 p_{02} - l_2 \frac{dp_{02}}{dt}\right) \tag{64}$$

in which (1) $w = \dfrac{j - 3r}{j} = \dfrac{T}{T_r}$ (dimensionless) measures the importance of the relative power output change component *in phase* with the gate opening change. The value of w depends upon the first component of the water hammer, characterized by the coefficient r, and upon the rate of change of the turbine efficiency, characterized by the coefficient j; (2) $l = \dfrac{3s}{2j}\Theta$ (having the dimension of time) measures the importance of the relative power output change component, in quadrature with the gate opening change. The value of l depends upon the second component of the water hammer, characterized by the coefficient s, upon the hydraulic inertia parameter Θ, and also upon the rate of change of turbine efficiency, characterized by the coefficient j.

We have already shown that the criterion of stability of each unit separately considered, is

$$T_{g1}T_1 > \frac{l_1^2}{w_1} \qquad T_{g2}T_2 > \frac{l_2^2}{w_2} \tag{39}$$

But when both units are coupled together, the flywheel equation must be written

$$\frac{d\omega}{dt} = \frac{1}{T}(k_1 p_1 + k_2 p_2) \tag{65}$$

in which T is the resulting value of the inertia parameter, which characterizes the effect of the rotating masses of both units. In order to calculate this resulting value T, we shall for the time being neglect the water-hammer effect and return to the defining formula of the inertia parameter, given when establishing Eq. (7):

$$T = \frac{1}{16.2 \times 10^5} \frac{(WR^2)_1 N_{01}^2 + (WR^2)_2 N_{02}^2}{P_{01} + P_{02}}$$

$$= \frac{1}{16.2 \times 10^5} \left[\frac{(WR^2)_1 N_{01}^2}{\frac{P_{01}}{k_1}} + \frac{(WR^2)_2 N_{02}^2}{\frac{P_{02}}{k_2}} \right]$$

$$T = k_1 T_1 + k_2 T_2 \tag{66}$$

Now taking account of the water-hammer effect, the flywheel equation (65) becomes

$$\frac{d\omega}{dt} = \frac{k_1}{T}\left(w_1 p_{01} - l_1 \frac{dp_{01}}{dt}\right) + \frac{k_2}{T}\left(w_2 p_{02} - l_2 \frac{dp_{02}}{dt}\right) \tag{67}$$

Combining Eqs. (58), (59), and (67) and operating as explained for Case II, page 735, we arrive at the following criterion of stability:

$$1 - \frac{k_1}{T_{g1}T}\frac{l_1^2}{w_1} - \frac{k_2}{T_{g2}T}\frac{l_2^2}{w_2} > 0 \tag{68}$$

$$T_{g1}T_{g2}T > T_{g2}k_1 \frac{l_1^2}{w_1} + T_{g1}k_2 \frac{l_2^2}{w_2} \tag{69}$$

$$T_{g1}T_{g2}k_1T_1 + T_{g1}T_{g2}k_2T_2 > T_{g2}k_1 \frac{l_1^2}{w_1} + T_{g1}k_2 \frac{l_2^2}{w_2} \tag{70}$$

or

$$T_gT > k_1 \frac{T_g}{T_{g1}}\frac{l_1^2}{w_1} + k_2 \frac{T_g}{T_{g2}}\frac{l_2^2}{w_2}$$

This criterion of stability (70) of both units coupled together will be surely satisfied if

$$T_{g1}T_{g2}k_1T_1 > T_{g2}k_1 \frac{l_1^2}{w_1} \qquad \text{or} \qquad T_{g1}T_1 > \frac{l_1^2}{w_1}$$

and

$$T_{g2}T_{g1}k_2T_2 > T_{g1}k_2 \frac{l_2^2}{w_2} \qquad \text{or} \qquad T_{g2}T_2 > \frac{l_2^2}{w_2}$$

that is, if the individual criteria of stability of the two units separately considered are both satisfied.

On the contrary, the criterion of stability (70) of both units coupled together will certainly never be satisfied, if the individual criteria of stability of the two units separately considered are both unsatisfied.

In summary, if the individual criterion of stability of one unit (unit No. 1) separately considered is not satisfied, the criterion of stability (70) of both units coupled together may, however, be satisfied, when the individual criterion of stability of the other unit (unit No. 2) separately considered is substantially satisfied: $T_{g2}T_2 \gg \frac{l_2^2}{w_2}$. This is especially the case when the instability of the first unit is not too pronounced ($T_{g1}T_1$ not very much smaller than $\frac{l_1^2}{w_1}$ and when its contribution to the total power output is not too great (k_1 not too large).

From further detailed study we may finally reach three very important generalizations, concerning the governing stability of several units operating in parallel:

1. If the governing of each of the units is individually stable, the governing of all of them operating in parallel (their governors acting then in concert) will certainly be also stable.
2. If the governing of each of the units is individually unstable, the governing of all of them operating in parallel will certainly be also unstable.

3. If the governing of an important fraction of units operating in parallel (above all when this fraction corresponds to the major part of the total power output) presents a liberal margin of stability, coupling to them one or several units which are individually unstable may not disturb the governing stability of the whole. This is especially the case when the instability of these last units is not too pronounced and when their contribution to the total power output is not too great.

Example 22: Let us first consider a hydroelectric unit No. 1 and its speed-acceleration responsive governor (without primary compensation), the whole corresponding to the following characteristics:

The Allievi dimensionless parameter	$\rho_1 = 10$
The hydraulic inertia parameter having the dimension of time	$\Theta_1 = 1$ sec
The period of the free oscillations of the water-hammer waves, $T' = 2\mu = 2\dfrac{\Theta}{\rho}$	$T_1' = 0.2$ sec
The characteristic time of promptness of governor response	$T_{g1} = 0.72$ sec
The mechanical inertia parameter having the dimension of time	$T_1 = 6$ sec
The acceleration constant of the governor	$m_1 = 2.93$ sec

We shall assume that $j = 1$ (no efficiency change) and $\alpha = 0$ (no speed change effect upon the difference between the couples). In order to solve Eq. (37), we shall also assume for the period of the governor oscillations:

$$T_1'' = 7.18 \text{ sec}\dagger$$

that is,

$$\chi_1 = 35.9$$

We may then compute:

For the water-hammer coefficients r and s:

$$r_1 = 0.162 \qquad s_1 = 0.838$$

For the coefficient w and the time l:

$$w_1 = 1 - 3r_1 = 0.514 \qquad l_1 = \tfrac{3}{2}s_1\Theta_1 = 1.257 \text{ sec}$$

For the factors C_1 and C_2 of Eq. (37):

$$C_{11} = \frac{w_1}{T_{g1}T_1}\,\frac{m_1 - \dfrac{l_1}{w_1}}{1 - \dfrac{m_1 l_1}{T_{g1}T_1}} = 0.385$$

$$C_{21} = \frac{w_1}{T_{g1}T_1}\,\frac{1}{1 - \dfrac{m_1 l_1}{T_{g1}T_1}} = 0.803$$

For the period of the governor oscillations T'':

$$T_1'' = \frac{4\pi}{\sqrt{4C_{21} - C_{11}^2}} = 7.18 \text{ sec}$$

This result confirms the above-mentioned values ($T_1' = 7.18$ sec, $\chi_1 = 35.9$) which can be now accepted as rigorously correct.

For the logarithmic decrement of governor oscillations, δ_{*1}:

$$\delta_{*1} = \frac{2\pi C_{11}}{\sqrt{4C_{21} - C_{11}^2}} = 1.38$$

Consequently the governing of unit No. 1, independently considered, affords a liberal margin of stability.

Let us then consider a second unit No. 2, with the following characteristics: $\rho_2 = 1.5$; $\Theta_2 = 1.5$ sec; $T_2' = 2$ sec; $T_{g2} = 1.18$ sec; $T_2 = 7.5$ sec; and $m_2 = 3.54$ sec.

In a similar way, we can compute on the basis of

$$\begin{aligned} T_2'' &= 11.56 \text{ sec} & \chi_2 &= 5.78 \\ r_2 &= 0.148 & s_2 &= 0.876 \\ w_2 &= 0.556 & l_2 &= 1.97 \text{ sec} \\ C_{12} &= 0 & C_{22} &= 0.294 \end{aligned}$$

from which we confirm

$$T_2'' = 11.58 \text{ sec}$$

and calculate

$$\delta_{*2} = 0$$

† This value is to be chosen and then verified by further calculation (successive approximations).

The governing of unit No. 2 is consequently just on the brink of instability.

Let us now put both units in parallel, assuming that No. 1 produces 75 per cent ($k_1 = 0.75$) of the total power output and No. 2 produce 25 per cent ($k_2 = 0.25$), so that the resulting value of the mechanical inertia parameter reaches:

$$T = (0.75 \times 6) + (0.25 \times 7.5) = 6.375 \text{ sec}$$

In order to solve Eq. (37), we shall assume for the time being, for the oscillations in phase of both governors, the period:

$$T'' = 8.16 \text{ sec}; \qquad \text{that is to say,} \qquad \chi_1 = 40.8; \qquad \chi_2 = 4.08$$

We can then compute:

$$\begin{array}{llll} r_1 = 0.130 & s_1 = 0.869 & r_2 = 0.272 & s_2 = 0.770 \\ w_1 = 0.610 & l_1 = 1.303 & w_2 = 0.184 & l_2 = 1.730 \end{array}$$

$$C_1 = \frac{\dfrac{k_1 w_1}{T_{g1}T_1}\left(m_1 - \dfrac{l_1}{w_1}\right) + \dfrac{k_2 w_2}{T_{g2}T_2}\left(m_2 - \dfrac{l_2}{w_2}\right)}{1 - \dfrac{k_1 m_1 l_1}{T_{g1}T_1} - k_2\dfrac{m_2 l_2}{T_{g2}T_2}} = 0.249$$

$$C_2 = \frac{\dfrac{k_1 w_1}{T_{g1}T_1} + \dfrac{k_2 w_2}{T_{g2}T_2}}{1 - k_1\dfrac{m_1 l_1}{T_{g1}T_1} - k_2\dfrac{m_2 l_2}{T_{g2}T_2}} = 0.620$$

$$T'' = \frac{4\pi}{\sqrt{4C_2 - C_1^2}} = 8.13 \text{ sec}$$

This result is sufficient confirmation of the above-mentioned value ($T'' = 8.16$ sec) and we can now accept as rigorously correct $T'' \cong 8.15$ sec.

$$\delta_* = \tfrac{1}{2}T''C_1 = 1.01$$

Conclusion. The governing of both units coupled together is stable. The period of the oscillations $T'' = 8.15$ sec is greater than the period $T_1'' = 7.18$ sec of unit No. 1, independently considered, but smaller than the period $T_2'' = 11.58$ sec of unit No. 2, independently considered. Whereas the governing of unit No. 2 is just on the brink of instability, $\delta_{*2} = 0$, and thanks to the margin afforded by the governing of unit No. 1, $\delta_{*1} = 1.38$, the logarithmic decrement of the governor oscillations, when both units operate in parallel, reaches $\delta_* = 1.01$, that is to say, the amplitude is 2.75 ($e^{1.01} = 2.75$) times smaller.

Bibliography

Strowger, Earl B., and S. Logan Kerr, Speed Changes of Hydraulic Turbines for Sudden Changes of Load, *Trans. ASME, Paper* 2009, 1926. Contains discussion of the effect of draft-tube water hammer on speed, by P. F. Kruse.

Gaden, Daniel, "Considérations sur le problème de la stabilité des regulateurs de vitesse," Editions La Concorde, Lausanne, Switzerland, 1945.

Sutherland, R. A., A Better Method of Representing and Studying Water-Turbine Performance, *Trans. ASME*, vol. 68, 1946.

Gaden, Daniel, A. Germond, H. Bovet, T. Desbaillets, "Etude de la stabilité d'un réglage automatique de vitesse par des diagrammes vectorials," Information Techniques Charmilles No. 2, Geneva, Switzerland.

SECTION 30

FLOOD CONTROL

By James H. Stratton, A. L. Cochran, and Wendell E. Johnson

FLOOD PROBLEMS

1. Introduction. A "flood" is any abnormally high water stage or flow over land, in a stream, floodway, lake, or coastal area, that results in significant detrimental effects. The term "flood control" embraces all measures intended to reduce or eliminate detrimental flood effects.

Flood problems are diverse in nature. Rapid runoff results in erosion of lands and contributes to sediment-deposition problems downstream. Floods inundate property and endanger lives. High-velocity currents accentuate damaging effects, and prolonged high flood stages delay rail and highway traffic and interfere with efficient drainage and economic use of lands for agricultural and urban purposes. Floods damage drainage channels, bridge abutments, bank lines, sewer outfalls, and other structures within floodways, and interfere with navigation and hydroelectric power generation. Figure 1 illustrates the intense industrial development which is attracted by a major navigable waterway. Flood risks inhibit optimum utilization of floodplain areas. Economic losses associated with these combined effects average billions of dollars annually. Flood control is, and promises to remain, one of the major requirements of comprehensive water-resources developments. It can be achieved by a

Fig. 1. Downstream view, Mississippi River, New Orleans Harbor.

variety of structures and measures. Knowledge of the capabilities, limitations, and relative advantages of each such measure singly and in combination is necessary for optimum plans.

2. Zoning Regulations and Building Codes. Systematically controlled use of floodplains constitutes one means of limiting flood damages. Zoning plans should include specific provisions for preserving adequate rights of way for future drainage channels, including vertical and horizontal clearances that would be needed when economic development ultimately warrants construction of flood-control improvements. In addition, appropriate limitations should be included regarding types of development permissible in restricted areas, and construction criteria for features such as minimum floor levels, basements, and drainage facilities. Zoning regulations and building codes should be carefully designed to accomplish proper flood-control objectives within limits imposed by economics and other considerations, without retarding optimum development of valuable floodplain areas.[1,*]

3. Reduction of Flood Runoff. Land-treatment measures, including use of vegetative covers, terracing and contour plowing, the construction of numerous small ponds, and erosion-control structures, serve to reduce the quantity and rate of runoff. The effects are limited by the rate and quantity of precipitation that can be absorbed by the ground. The reduction of land erosion is an important benefit. Measures that are effective in reducing runoff from land areas during floods usually act also to reduce streamflow during critical low-flow periods.

4. Reservoirs. Reservoirs range in size from small temporary ponding areas to basins capable of storing more than 30 million acre-ft of water. Their function is to store water during periods of excess runoff and to release it at nondamaging rates. Flood-control reservoirs may be constructed on main streams or tributaries, or located to provide "off-channel" storage of floodwaters diverted from the main stream by diversion control structures. Storage space for flood control may be provided in reservoirs designed primarily for these purposes, or incorporated in "multiple-purpose" reservoirs that serve other purposes also (see Sec. 4).

5. Channel Improvements. Increasing a stream's conveyance capacity by widening, deepening, straightening, removing obstructions to flow, and otherwise improving the hydraulic capacity may effectively reduce overbank flooding in local areas. Channel-stabilization works are used to reduce flood damages resulting from the erosion of banks. Channel improvements have application to both urban and agricultural areas. In most large river basins, reservoirs, levees, and other measures supplementing such channel improvements may be required to obtain the degree of protection desired and economically justified. Channel improvements serve to accelerate flows in the channel reaches involved, with resulting increase in the discharge peaks downstream, which in turn may require remedial measures in the downstream reaches.

6. Levees and Floodwalls. Barriers generally parallel to the stream course in the form of levees, floodwalls, or highway or railroad embankments are widely used for the protection of floodplains associated with a particular stream. Usually the levees or embankments either tie into high ground at both ends or completely encircle the area to be protected. Figure 2 shows a Mississippi River levee designed to protect agricultural development. Interior drainage problems thus created require gated structures in the barrier structures to permit water to drain from the protected area during nonflood periods, and either pumping installations or temporary ponding areas to limit adverse effects when drainage by gravity is prevented by flood stages in the main stream.[2]

In some circumstances, the downstream end of a levee is terminated without tying

* Superior numbers refer to items in the Bibliography at the end of this section.

FIG. 2. Mississippi River levee which provides protection for agricultural development.

into high ground in order to permit gravity drainage of the interior area without structures through the levee embankment. These levees serve primarily to divert high-velocity flows from the protected areas, thereby reducing erosion and dynamic effects on structures and preventing the deposition of sand and debris on the protected lands as floods recede. Under such an arrangement some or all of the lands may be subject to inundation from the downstream open end; however, stages would be lower than would otherwise be the case. Both closed and open-end levees have been used along the Mississippi River and major tributaries. The degree of protection afforded by levees relates to their heights in relation to flood-crest elevations and to their stability under flood conditions, and may vary from very low to complete protection, depending upon the objectives, economic factors, and the physical conditions in the project areas considered in their design.

7. Emergency Floodways. The flood-carrying capacity of a stream sometimes can be increased by providing auxiliary floodways for use during unusually large and relatively infrequent flood events. Examples are Old River diversion (Fig. 3) and the Morganza spillway (Fig. 4) designed to divert up to 1,220,000 cfs from the main stem of the Mississippi River into the Atchafalaya floodway during extreme floods. The Bonnet Carre spillway (Fig. 5) on the Mississippi River will divert up to 250,000 cfs flow into Lake Pontchartrain, leaving only 1,250,000 cfs for the Mississippi River channel to convey through the New Orleans reach of the Mississippi River during the project design flood. The locations of these structures are shown by Figs. 6 and 7.

FIG. 3. Old River control structures.

The lands within emergency floodways are generally susceptible of use for agricultural purposes and other purposes during flood-free periods. Flowage rights, or other suitable arrangements to permit use of these floodways when needed, are essential in an effective flood-control plan involving diversion.

8. Spreading Grounds. Flood flows are sometimes diverted into large flat land areas that are capable of absorbing water at relatively high rates. Such measures are used extensively in the central valley of California. "Spreading grounds" serve to reduce downstream flood peaks and replenish "underground reservoirs" which provide water by pumping for irrigation purposes or other water-supply uses. Similar arrangements are used to raise groundwater levels along coastal areas for general water-supply purposes and to suppress salinity intrusion from the sea.

FIG. 4. The Morganza control structure.

FIG. 5. Bonnet Carre spillway.

9. Pumping Facilities. The control of floods in very flat lands and areas near or below sea level requires pumping stations to discharge excess runoff from within barrier-protected regions. A striking example is that of the Netherlands, where large areas of valuable agricultural lands were reclaimed from the sea. In central and southern Florida, large areas of agricultural lands are substantially protected against flooding from rainfall by a system of canals and pumping stations. Interior drainage systems associated with leveed areas of urban centers usually include pumping facilities.

CHARACTER OF FLOOD-CONTROL BENEFITS

10. Classification. The elimination or reduction of any adverse effect of floods constitutes a "benefit." Those which can be readily estimated in terms of average monetary values are commonly referred to as "tangible" benefits, and others not susceptible to such form of evaluation are classed as "intangible."

In general, tangible benefits associated with flood control include the value of physical damages prevented, emergency costs avoided, the cost of disaster relief, and other financial losses prevented. The creation of conditions conducive to more productive use of lands for agricultural, industrial, or domestic purposes results in tangible benefits of major importance. In many cases these are commonly expressed in terms of "enhancement" benefits, but they can also be estimated in terms of potential increased earnings.

Intangible benefits include such items as reductions in hazards to human life and health during floods, and the elimination of other detrimental effects of floods that cannot be given monetary values. The improvement of aesthetic appearances by alleviating flood effects is a significant intangible benefit in certain areas.

11. Economic Factors. Projects that provide a high degree of security against concentrated flood damages can be credited with substantial intangible benefits, aside

Fig. 6. Control structures and floodways.

from the tangible benefits normally associated with prevention of actual flood losses during the life of the project. Inasmuch as the costs of a flood-protection project are paid out over a long period of years, the charges are borne equitably by successive generations of those who benefit, whereas without the project, those occupying the area at the time of major floods would be required to bear the concentrated flood losses, including probably depressions in real estate values and disruptions in local economy. If, for example, the average annual tangible benefits during the life of a project should exactly equal the average annual project costs estimated on a comparable basis, the project would still afford the advantages inherent in substituting an equitable sharing of project costs by many benefactors for concentrated flood damages and attendant

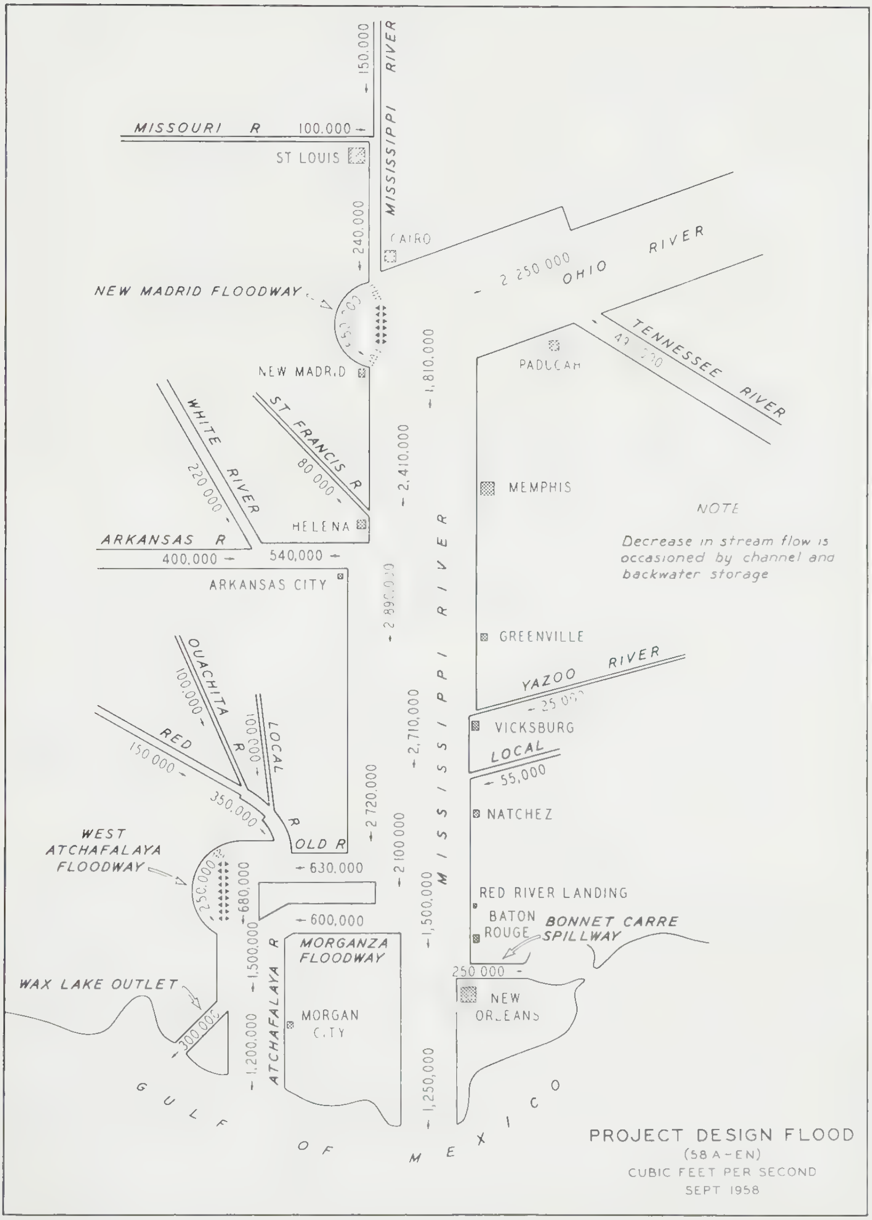

Fig. 7. Project design flood.

hardships otherwise borne by a few. In addition, the assurance of security against flood disasters in adequately protected areas creates conditions more favorable for development of improved living and community stability.

The reservation of rights of way to facilitate future improvements of flood-control measures ordinarily is not treated as a project benefit in computing benefit-to-cost (B/C) ratios for a flood-control project. However, in comparing the overall merits of alternative flood-control plans, including possible stage-construction schemes, the relative advantages that would be afforded by each plan in reservation or dedication of rights of way likely to be needed for future improvements in flood-protection facilities should be given appropriate consideration. Projects that are planned and designed to facilitate future improvements at minimum costs should be credited with all pertinent economic advantages. For example, in planning a channel and levee project intended for interim protection of an urban area, the acquisition of sufficient rights-of-way lands to facilitate future enlargement of the protection is often economically advantageous when considered from a long-range viewpoint, even though initial costs of the interim plan would be increased. The economic advantage gained from probable lower land costs initially is greatly enhanced by preventing the encroachments of buildings, bridges, sewers, water-line, and other utilities on the rights of way required for future improvements of the flood protection.

FORMULATION OF FLOOD-CONTROL PLANS

12. Elements of Plan. In a perfectly formulated comprehensive basin plan for water-resources development, the scale of individual projects and each element of multiple-purpose systems would, insofar as practicable, meet all the following specifications:

1. Provide a practicable and economic means of fulfilling prospective needs
2. Be more efficient in the use, protection, or production of economic resources than any other actual or potential means, public or private, of meeting specific objectives
3. Reflect evaluations of all determinate economic influences, tangible or intangible, beneficial or detrimental
4. Provide for a maximum excess of benefits over costs, insofar as these can be evaluated in monetary terms with a reasonable degree of reliability
5. Conform with standards of safety and functional effectiveness consistent with anticipated uses and standards of development in areas affected by the projects

Expenditures of resources for flood-control projects included in public works programs must be "justified" by the advantages likely to be gained during the life of the project involved, usually assumed to be 50 to 100 years in economic studies. A project is said to be "economically justified" if the estimated B/C ratio exceeds unity, assuming that all benefit and cost values have been adequately expressed in monetary terms. To conform strictly with the principle of maximization of net benefits, a project is scaled to yield the maximum excess of benefits over cost, and the "optimum" B/C ratio is related to this determination. A B/C ratio related to the "optimum" economic justification may be substantially higher than unity, but the degree of protection against floods is then usually less than could be provided at greater cost, at a B/C closer to unity. The application of the economic-efficiency criterion to the benefit-cost relationship for a single project is shown by Fig. 8.

In estimating B/C ratios referred to above, generally only "tangible" benefits are usually included in the benefit equation. However, in situations where "intangible" benefits are particularly important, the degree of protection based on the optimum B/C ratio is likely to be less than warranted. Such deficiency in the economic evalua-

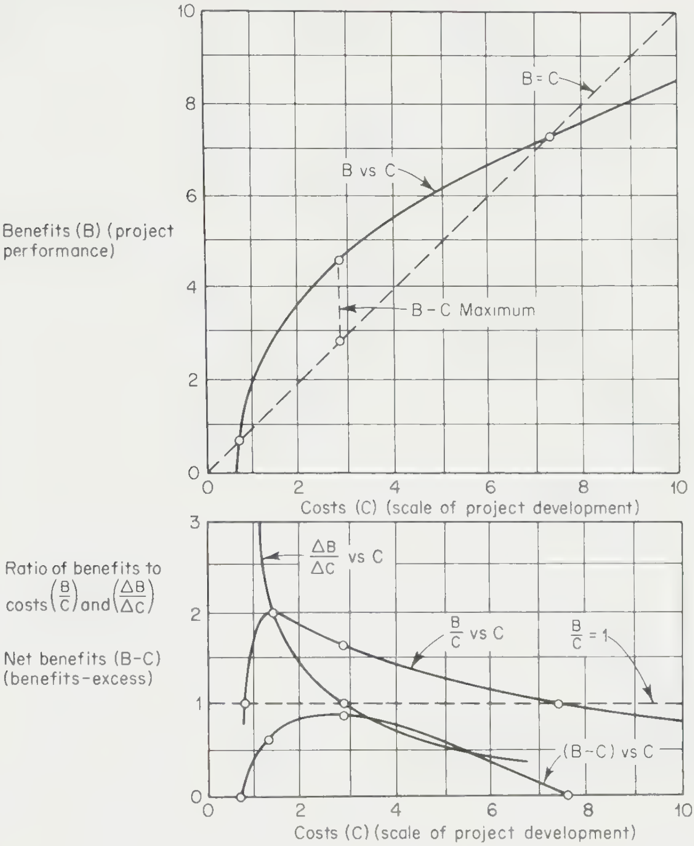

FIG. 8. Application of economic-efficiency criterion in selection for single improvement measure.

tion can be offset by relating intangible benefits to appraised "insurance" values to obtain monetary allowances for inclusion in B/C estimates.

13. Forecasts. In project-formulation studies, "forecasts" of future conditions are necessary as a base for evaluating functional adequacy and economic justification of flood-control measures. Forecast periods have ranged from 10 to 100 years, the longer being favored in the planning of major public works programs. "Economic base studies," developed for regions with pertinent projections to the future, serve as a framework for establishing general program needs and justifications. Supplemental information and analyses are required to establish economic justifications associated with the planning of specific projects.

14. Preproject Conditions. The term "preproject" (or "without projects") identifies conditions that would prevail at any specified time if the projects under consideration were not constructed. Hence "preproject" conditions constitute the reference base for comparing potential benefits of new projects. In project-formulation studies, the term "preproject" normally applies to future conditions during the period selected for benefit analyses. Inasmuch as conditions in a drainage basin are likely to be changed by influences other than the particular project under investigation, "preproject" conditions usually are not the same as "natural" or "present" conditions.

Comparisons of many alternative plans of water-resources development, including various flood-control measures, are required to assure formulation of the best comprehensive plan for a region. Modern concepts of systems analyses and electronic computer techniques have many applications in these studies.

RELATION OF DEGREE OF PROTECTION TO DESIGN FLOOD CRITERIA

15. Degree of Protection. The "degree of protection" afforded by a particular flood-control project represents the extent to which the ultimate objective of complete elimination of all detrimental flood effects within the influence limits of the project is attained.

Complete elimination of adverse flood effects is seldom feasible or economically justified. Hence, engineering and economic analyses are required to determine the "degree" of protection appropriate under specific circumstances. Results of the studies are commonly reflected in the selection of definite "design-flood" criteria to serve as a basis for functional design of a particular project or combination of projects.

Design floods selected to conform with specific project objectives may correspond to the probable maximum flood (PMF), the standard project flood (SPF), a major flood of record, or any other actual or hypothetical flood event. Design-flood characteristics considered in actual design of a project may be the peak discharge, volume of runoff, critical velocity, flood duration above a controlling stage, or any combination of characteristics that significantly affect the design.

16. Probable Maximum Flood. The term "probable maximum flood" refers to the hypothetical flood hydrograph that would result from the most critical combination of precipitation, ground wetness, and other runoff factors considered "reasonably possible" in a particular drainage basin. Because of the high costs usually involved in protecting against the probable maximum flood and its extremely small chance of occurrence, its applications are normally limited to design of spillways for high dams, sudden failure of which would result in extraordinary hazards to human life or disastrous property damages.

17. Standard Project Flood. The standard-project-flood hydrograph represents runoff from the most severe combination of precipitation and snowmelt (if pertinent) that is considered reasonably "characteristic" of the drainage basin under study, based on hydrometeorological analyses applicable to the general region. A relatively small number of maximum floods of record in the United States have exceeded standard-project-flood estimates prepared by the U.S. Army Corps of Engineers. In a large number of studies pertaining to drainage basins less than 5,000 sq miles in size, estimates of standard-project-flood hydrograph peaks and runoff volumes have equaled 40 to 60 percent of probable-maximum-flood hydrographs for corresponding basins, or an average of about 50 percent. These comparisons show that floods equal to standard-project-flood estimates are very infrequent at any one location but are well within the flood-producing capabilities of storms of record in the general vicinity of a particular study area.

18. Design Flood. Design-flood hydrographs corresponding to relatively frequent events are usually expressed in "probability" terms. Several forms of expressions have virtually equivalent meanings. For example, the "1 percent chance" flood may also be referred to in terms of an average recurrence interval of 100 years. Similarly, references to a "10-year frequency" or "100-year frequency" flood event have the same meaning as average recurrence intervals of 10 and 100 years, respectively.

Identification of the degree of protection afforded by a particular project in terms of average frequency of the design flood (or its percent chance of occurrence) is appropriate only within reasonable limits of accuracy in flood-probability estimates. The reliability of flood-frequency estimates is limited by the length and quality of hydrologic records available for the project drainage basin, representativeness of such records with respect to long-period characteristics, probability of future changes in factors influencing flood characteristics, adequacy of analytical methods used, and other considerations. Experience and analyses have shown that estimates of flood-discharge values corresponding to events as rare as a 1 percent chance of occurrence are usually subject to a relatively large margin of error, and that extrapolations to events substantially less frequent are of questionable value in selecting design-flood criteria for a particular project. When an unusually high degree of security is required in the design of a flood-protection project, consideration should be given to potential floods of "standard project flood" or "probable maximum flood" magnitude, to supplement flood-frequency estimates based on statistical analyses of recorded events.

Flood-frequency estimates referred to above are intended to reflect long-term average probabilities but are not likely to reflect accurately the distribution and relative magnitudes of events that may actually occur within, say, the next 100 years, particularly with respect to the flood events of large magnitude and infrequent average occurrence.

DESIGN-FLOOD CRITERIA RELATED TO VARIOUS TYPES OF PROJECTS

19. Relative Merits of Alternatives. Each type of flood-control measure has advantages and disadvantages that must be taken into account in formulating flood-control plans and in selecting design-flood criteria. The functional characteristics of each type of measure under normal operating conditions, and the magnitude of residual damages and hazards likely to occur when design-flood capacities are exceeded, require special consideration in choosing between competitive measures and the proper scale of development with each type. For example, a channel improvement that affords full protection against floods of 10-year frequency and substantial reductions in effects of larger events may be preferable under some circumstances to a levee affording full protection against, say a 25-year frequency flood, if overtopping of the levee would cause severe residual damages or hazards to life. A comparison of B/C ratios would not afford a conclusive basis for choosing either the type of project or design-flood criteria. In the following paragraphs, principles pertaining to the selection of design-flood criteria are discussed and illustrated by reference to applications in actual practice.

Design-flood criteria for a particular flood-control measure may be based on "economic-probability" analyses or on a functional "standard of performance."

20. Economic-probability Benefit-Cost Basis of Selecting Design-flood Criteria. Under this procedure tangible benefits and related project costs, expressed as annual monetary values averaged over the assumed life of the project, are computed for several alternative degrees of protection. Results are plotted graphically to facilitate comparisons and interpolations (Fig. 8). Design-flood criteria are then selected to correspond to some acceptable B/C ratio, which may be the "optimum" or any B/C ratio deemed appropriate under individual circumstances.

In principle, a flood-control project that assures the highest excess of tangible benefits over costs affords the "optimum" degree of protection from an economic viewpoint. This basic principle affords a useful guide in selecting design-flood criteria for projects, provided limitations in the accuracy of computational methods are recognized and adequate adjustments are included in design criteria finally adopted to assure that potential intangible benefits are also guaranteed to an appropriate degree.

The reliability of B/C estimates is influenced by many factors, such as

1. Technical training and experience of staffs responsible for the estimates, and thoroughness of studies
2. Policies and procedures applied in preparing estimates
3. Accuracy of forecasts of economic development and floodplain use
4. Accuracy of forecasts of watershed and floodway characteristics affecting future runoff
5. Accuracy and stability of stage-discharge rating curves
6. Areal extent of overflow vs. flood discharge
7. Accuracy of monetary-damage estimates vs. flood discharges
8. Reliability of flood-frequency estimates based on available data
9. Probable deviations of flood occurrence from most probable relations during assumed 100-year project life
10. Possibility of extraordinary floods (e.g., exceeding 1 percent chance event) during assumed 100-year project life
11. Efficiency of project operations under normal conditions and effectiveness of emergency operations during future floods
12. Adequacy of project cost estimates

Substantial errors in any of the component estimates listed above would be reflected in design-flood criteria selected under the economic-probability procedure to govern the "scale of project development," inasmuch as the criteria are correlated directly with the estimated B/C ratio.

The economic-probability (B/C) method, if properly applied, affords a rational basis for selecting design-flood criteria for flood-control measures that have as a primary objective the reduction of detrimental effects associated with relatively frequent minor or moderate floods, and where a high degree of security against effects of major floods is not a requirement. Inasmuch as the method usually does not include monetary allowances for intangible benefits, its application is most appropriate when potential intangible values are relatively small. If monetary allowances in the form of "insurance" values are included in benefit computations to account for certain intangibles, somewhat higher B/C ratios and correspondingly higher degree of protection could be obtained by the method.

When the economic-probability method is applied to flood-control projects required to provide a high degree of protection against infrequent major floods, design-flood criteria based on B/C estimates must be adjusted upward to assure a reasonable margin of functional safety, particularly when failure of the protection would result in hazards to life and risks of unusually severe property damage. Average annual tangible benefit estimates used in computing B/C ratios are based on long-term flood-probability relations and do not account for abnormal flood sequences within the life of the project or for full damages that would be associated with floods greater than the 1 percent chance event. Supplemental studies involving application of "performance standards" afford one basis for determining the extent of the adjustments needed in design-flood criteria derived from economic-probability analyses.

21. Performance-standards Basis of Selecting Design-flood Criteria. Under this procedure, design-flood criteria are related to general "performance standards" that are deemed appropriate to meet specified primary objectives of a project. The standards are usually expressed in terms of the magnitude of flood against which protection is afforded by the project, and may correspond to any degree of protection applicable under specific circumstances.

The standard project flood corresponds to a high degree of protection that should be equaled, or approached as nearly as practicable, in the design of flood-control projects in which the reduction in hazards to life and prevention of disastrous property damages are major objectives. In unusual circumstances, performance standards higher than the standard project flood are warranted by protection needs and economic considerations. In others, full protection against the standard project flood may be precluded by rights-of-way limitations, prohibitive costs, problems of financing, or other constraints, notwithstanding the need for full protection.

Performance standards corresponding to major floods of record have been adopted as a basis for planning and design of flood-control projects or systems of projects. Practical advantages of this approach in some cases lie in the availability of actual flood records and related data for use in analyses, and the better understanding that the public has of the impact and significance of an actual flood. Adjustments in flood records are usually necessary to develop criteria that are representative of comparable flood potentialities in various parts of a basin, and to account for probable future changes in factors affecting runoff. The relative magnitude of the flood of record, in comparison with the standard project flood or some appropriate probability relation, must be determined at representative locations in the drainage basin in order to evaluate the general degree of protection represented.

A performance standard may be related to some generalized flood-probability value. For example, grades for 12 levee units along the Mississippi River between St. Louis and Cape Girardeau, Missouri, were designed originally to protect 225,000 acres of agricultural lands and improvements against a 50-year-frequency flood.

Performance standards are widely used in the design of drainage projects to afford protection against relatively frequent rainfall-runoff events. For example, design capacities of storm drains for urban communities and interior drainage facilities associated with leveed areas are usually based on runoff frequency relations, without detailed B/C computations.[2]

The "performance-standards" method provides the most reliable basis for establishing safe design-flood criteria for a project required to assure a high degree of protection against major floods. Under this method, the degree of protection afforded by the project is judged by comparison of the design-flood criteria with the magnitude of floods considered reasonably characteristic of the particular drainage basin. Although the evaluations of major flood characteristics of a basin are complex, such analyses do not involve the many additional uncertainties associated with economic forecasts and benefit-cost estimates used in selecting design-flood criteria under the economic-probability method. Supplemental studies involving flood probability and economic analyses are required to estimate tangible benefits likely to be obtained from the proposed project; these may influence selection of a performance standard but would not constitute the primary criteria. Final judgment regarding justification of a project based on performance standards rests on consideration of probable tangible and intangible benefits, giving due consideration to the importance of assuring a high degree of security against floods of extraordinary magnitude.

22. Criteria for Major Drainage Improvements. The term "major drainage" is commonly used to identify improvements in principal drainage channels designed primarily to prevent overflow of lands during relatively minor floods and accelerate removal of overbank storage accumulated during larger floods. Large canals and pumping stations are involved in some projects. Features of major drainage projects do not include "on-the-farm" drainage facilities normally considered to be the responsibility of individual farmers. The depth of inundation during floods of intermediate or large magnitude may not be significantly reduced by major drainage improvements, but the duration of flooding is shortened.

The selection of design-flood criteria for major drainage improvements can be based on economic-probability analyses, with the purpose of establishing the optimum ratio of benefits to cost. However, because of the complications involved in rational analyses, criteria for such projects are usually based on empirical formulas or performance standards derived from experience in the region. These criteria establish the rate of drainage in inches of runoff per day or equivalent average flow rates. Information regarding drainage criteria applicable to various classes of agricultural lands is available from the U.S. Department of Agriculture and from state agencies in many areas.

The Central and Southern Florida Flood Control and Drainage Project includes major drainage facilities of unusual scope. An elaborate network of large canals serves as primary outlets for drainage of more than 1,000,000 acres of highly productive agricultural lands during floods, and for distribution of irrigation waters from Lake Okeechobee when needed. Several large pumping stations at terminal ends of the canals regulate water levels as required. The canals and pumping stations are designed to remove 0.75 in. of runoff per day from the agricultural area. The design-flood value was selected on the performance-standard principle.[3]

23. Criteria for Channel Improvements. Design-flood criteria for channel improvements may correspond to low, medium, or high degrees of protection, depending upon the character and objectives of the particular project. Elementary flood-control measures often involve the removal of miscellaneous obstructions from stream channels and overbank areas, such as dumped materials, old logs, snags, and excessive vegetation; minor improvements in alignment and reshaping of channels; moderate streamlining of existing bridge piers; and modifications of pipelines and sewer crossings to reduce interference with flows. In many instances, these improvements are accomplished without establishing specific design-flood criteria, the objective being simply to remove obvious obstructions to flow, improve general appearances, and correct local erosion problems. However, when these improvements assume substantial proportions, it is common practice to select design-flood criteria corresponding to some relatively low performance standard, such as a 2- to 5-year-frequency flood, to serve as a basis for pertinent hydraulic computations.

The improvement of channels to pass moderate or major floods often requires substantial modifications in utility crossings, bridge pier alterations or complete reconstruction of bridges, channel realignments and enlargements, protection of bank lines against erosion, provision of drop structures for side drainage, and possibly debris and drop structures to simplify maintenance of the project's design capacity. Economic-probability analyses are particularly useful in selecting design-flood criteria for channel-improvement projects required for protection against relatively moderate floods. If a high degree of protection against extraordinary floods is a project requirement, supplemental studies based on performance standards are needed to verify the adequacy of the proposed design capacity. For example, major flood-control channels in metropolitan Los Angeles, Calif., are designed to pass the standard project flood because of the exceptionally high values of properties protected. Velocities in some of these channels range from 20 to 60 fps, requiring extreme care in the hydraulic design of lined channels to assure safe performance.

24. Criteria for Levees Protecting Agricultural Crop and Pasture Lands. In selecting design-flood criteria for low-protection levees for agricultural areas, projects affording a relatively high B/C ratio based on tangible benefits would be favored in planning studies. Economic-probability studies have shown that protection against floods of 5- to 15-year frequencies is usually adequate to yield favorable net benefits under current farming practices, assuming that land use is confined primarily to annual agricultural crops or pastures.

Future changes in agricultural practices and project construction costs are likely to change the level of protection needed for agricultural crop lands. The economic-probability method of selecting design-flood criteria permits rational consideration of these probable changes and accordingly is ideally adapted to such project studies.

25. Criteria for Levees in Large Rural Areas. Design-flood criteria for levees protecting large rural areas that include agricultural lands, farm improvements and buildings, residential facilities, roads, railroads, utilities, and other developments must be of a higher standard than those for agricultural lands only. Economic-probability analyses, including forecasts of economic trends and future developments within the protected area, are needed to estimate tangible benefits likely to be gained with various degrees of flood protection. Final selections of design-flood criteria are usually based on performance standards that represent the degree of protection considered appropriate and practicable under circumstances related to specific projects. A performance standard appreciably higher than the discharge corresponding to an optimum B/C ratio (based on tangible benefits) is required to attain optimum intangible benefits and assure safe protection against major floods.

It is not always practicable to select performance standards adequate to obtain the most desirable degree of protection for safety or long-range economic advantages, particularly when protection of large rural areas by long lines of levees is involved. More limited objectives may be dictated by uncertainties regarding foundation conditions, limitations in funds available for financing, and difficulties in obtaining local sponsorship. The following examples of levee projects protecting large rural areas illustrate a range of conditions.

The 2,300 miles of main-line levees along the lower Mississippi River below Cairo, Ill., afford a high degree of protection to more than 15,000,000 acres of land, including large rural areas, several urban centers (Fig. 1), and extensive communications facilities of great national importance. The plan of protection has been developed in stages since 1882, and the degree of protection and safety of levee designs has been increased progressively. Comprehensive review studies completed by the Mississippi River Commission in 1959[4] established design-flood criteria comparable with or exceeding those of a standard project flood, giving due consideration to the effects of reservoirs located in major tributary basins. A large number of alternative combinations of flood-producing storms were analyzed in detail in developing these criteria.[5,6] The project-flood peak discharge varies from 2,360,000 cfs at Cairo to 3,000,000 cfs near the latitude of Old River, just below Natchez, Miss., after reductions by reservoirs.

Design-flood criteria for authorized main-line Missouri River agricultural levees involving protection of approximately 1,500,000 acres by 1,500 miles of levees are based on a performance standard corresponding to a 100-year-frequency flood with a specified system of reservoirs in operation. This standard was selected to assure reasonable comparability in the degree of protection afforded generally similar classes of lands and developments in 150 separate levee units. This standard was selected after general appraisal of probable future protection needs, foundation and rights-of-way problems that tend to limit levee safety and costs, preliminary benefit-cost relations for representative areas, and the interdependence of adjacent levee systems from the standpoint of safety and general community welfare. The economic justification of individual levee units has been confirmed by B/C estimates applicable to individual units and has been found to vary appreciably, but not sufficiently to warrant departure from the generalized performance standard adopted for the system.

Levee units protecting a total of 103,000 acres of rural lands downstream from Portland, Ore., have grades high enough to pass floods of approximately 50-year frequency with existing and currently authorized upstream reservoirs operating. Consideration has been given to increasing the degree of protection for these developing areas by raising grades of existing levees. However, unfavorable foundation conditions and attendant uncertainties regarding the safety of substantial raises in levee grades have resulted in adherence to the current performance standard, notwithstanding the apparent need for higher protection.

A system of 40 levee units on the Wabash River in Illinois and Indiana authorized in 1946 would protect 207,000 acres of rural lands and substantial developments against a 15-year-frequency flood. This uniform performance standard was selected to assure reasonable comparability in the degree of protection to be afforded to generally similar classes of lands and developments, with an overall economic justification exceeding unity.

26. Criteria for Levees and Floodwalls in Urban Areas. Design-flood criteria for urban-protection projects involving high levees should conform with unusually high performance standards, in view of hazards to life and severe property damages associated with levee overtopping. The standard project flood represents the degree of protection that should be equaled, or approached as nearly as practicable, in order to assure project safety during extraordinary floods. Such performance standards may exceed flood values corresponding to estimated optimum B/C ratios based on evaluation of tangible benefits and normal flood-frequency relations.

Following is a partial list of major urban communities that have high-levee projects capable of providing a degree of protection equal to or approaching standard project flood criteria, including allowances for reservoir systems upstream: (1) Omaha, Neb. (Missouri River); (2) Kansas City (Missouri and Kansas rivers); (3) Huntington, Louisville, Cincinnati, and Paducah (Ohio River); (4) Cairo, Illinois, and New Orleans, La. (Mississippi River); (5) Fort Worth, Tex. (Trinity River); (6) Los Angeles, Calif. (Lower Los Angeles River).

Levees and floodwalls of substantial heights have been used extensively with varying degrees of success in protecting urban communities against floods substantially less severe than the standard project flood. Although compromises in degree of protection are sometimes necessary for compelling reasons, the risks of possible overtopping of the protection under initial and future conditions of development should be carefully appraised before a partial-protection plan is accepted.

Relatively low levees have been used successfully as supplements to channel improvements to increase protection of urban areas without creating unduly hazardous conditions when the levee is overtopped. Low levees (or broad embankments) are also utilized to reduce the frequency of flooding of parks, streets, and other properties located at low elevations, without necessarily providing a high degree of protection. Some interior-drainage problems within leveed areas can be reduced by this means.

27. Reservior Capacities for Flood Control. The purpose of flood storage in a reservoir is to regulate streamflow to attain flood-control objectives associated with specific areas, insofar as practicable and justified by tangible and intangible benefits. The degree of protection afforded may be high, moderate, or low, depending upon objectives. Storage required during a particular flood is equal to the volume of inflow into the reservoir, minus the volume of outflow during a corresponding period. The rate and scheduling of releases must correspond to an appropriate "reservoir-regulation plan" to assure attainment of flood-control objectives. Reference should be made to Sec. 4 for a more detailed discussion of reservoir operations.

The primary objective of a flood-control reservoir (or storage-space allocation) may be to minimize flood damages immediately below the damsite. The Bear Creek Reservoir, located on a small tributary of the Mississippi River near Hannibal, Mo., was constructed solely to eliminate the need for more expensive and less desirable channel improvements through the city. The reservoir exerts no significant effects on Mississippi River flows and was justified entirely by benefits accruing locally. There are hundreds of similar examples associated with protection of urban areas, and thousands of small dams on minor streams are used to reduce flood damages in agricultural areas close to the dams.

If a reservoir is designed primarily for prevention of flood damages near the damsite, the peak rate of reservoir release will usually equal the maximum safe channel capacity through the protected area, minus a small allowance for local inflow and margin of safety. Assuming the maximum rate of outflow thus established, floods of various magnitudes are routed through the reservoir to determine the storage space required for effective regulation. The costs of providing various amounts of storage space are compared with average annual flood-control benefits to be expected, in order to determine B/C ratios. Final selection of the flood-control capacity is based either upon economic-probability analyses or upon performance standards, following essentially the same principles applied in selecting design-flood criteria for local protection projects. The degree of protection afforded by reservoirs located near primary benefit areas usually ranges from moderate to standard project flood proportions.

Some reservoirs serve the objective of reducing flood peaks at several damage centers downstream, possibly including important urban centers and long reaches of floodplains in rural areas. The degree of protection and reliability of protection that can be assured by a single reservoir tends to decrease progressively as the distance from the reservoir to potential benefit areas increases, because of flood runoff from intermediate drainage basins. Accordingly, fully effective flood protection in a large drainage basin usually requires a system of reservoirs and supplemental channel and levee improvements.

Under some circumstances, networks of reservoirs designed primarily for flood control are practicable and desirable for meeting regional needs for flood protection. The Miami Conservancy District and Muskingum networks in Ohio, involving, respectively, 5 and 14 flood-control reservoirs, are good examples. In comprehensive plans for major drainage basins, large multiple-purpose reservoirs play a major role in flood control while providing many other services associated with water-resources developments. The integrated system of reservoirs constructed by the U.S. Army Corps of Engineers and U.S. Bureau of Reclamation in the 500,000-square-mile-Missouri River basin reflects many of the advantages that can be gained from coordinated comprehensive planning. The system, when completed, will include many local protection plans for flood control, 1,500 miles of main-line levees, and a network of reservoirs that will provide irrigation water to millions of acres of land, reduce flood damages in 1,500,000 acres of agricultural lands, augment low flows for the benefit of navigation and pollution abatement, generate huge quantities of hydroelectric power, and afford recreational facilities and many other services to the public.[7]

If the objective of storage in a reservoir is to reduce flood stages at remote locations downstream, several possible variations in flood-producing storm distributions above principal damage centers must be analyzed during design studies to determine the flood-peak reductions that could be effected by the particular reservoir under a range of flood conditions. In many cases, these studies will show that an individual reservoir would reduce the average frequency of damaging floods at key locations but would not assure adequate reduction of severe floods which might result from critical concentrations of rainfall over uncontrolled drainage areas between the damsite and the principal damage centers.

Design-flood criteria finally selected for individual reservoirs or systems on the basis of economic analyses or performance standards may correspond to several alternative hypothetical flood situations or combinations. The "design storage capacities" for flood control are fixed at volumes required to conform with these design-flood criteria, assuming the limiting reservoir release rates and schedules specified in a "reservoir-regulation plan." If major changes in the regulation plan established in design

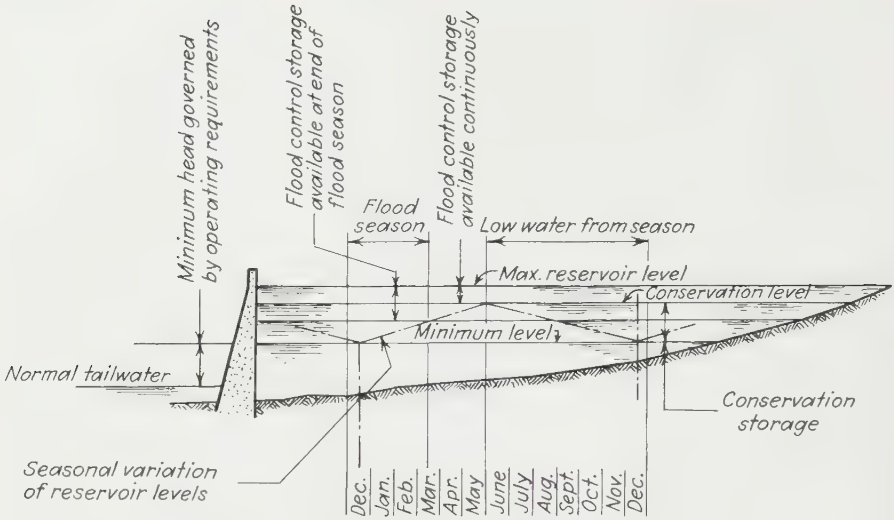

FIG. 9. Diagram illustrating multiple-purpose-reservoir operation.

studies become necessary after the reservoirs are constructed, the degree of protection afforded by the reservoirs will not conform with design objectives. Accordingly, extreme care must be used in evaluating factors that are likely to limit the rate of permissible reservoir releases under forecast future conditions of development, giving due consideration to seasonal variations in flood-control requirements.

The relationship of reservoir capacity to downstream channel conditions is an important one and involves consideration not only of the effects of sudden changes in releases which may cause bank caving and other deleterious effects, but also of the consequences of long-sustained flows. In the case of the latter the sustained flows, even though well within banks, may result in holding the groundwater adjacent to the stream at such levels as to result in severe agricultural losses. The fact that floodplain utilization is generally increased after flood-control reservoirs are built often precludes the full use of the theoretical channel capacities as a basis for reservoir outflow determinations. Hence larger storage capacities than otherwise required may be necessary where this is a consideration.

28. Multipurpose Reservoirs. Multipurpose reservoirs are designed for two or more uses. For example, a reservoir located on the tributary of a major river might be designed to protect the downstream river towns and cities against disastrous floods, increase the dependable water supply, and generate hydroelectric energy. The principles of multipurpose-reservoir planning may best be understood by referring to Fig. 9, which illustrates a typical schedule of operations. Assume that the reservoir shown by Fig. 9 is located on the tributary of a river that is subject to severe floods between December and March. Assume further that this reservoir will be designed to lower the flood stages on the main river and to generate hydroelectric energy. Owing to the seasonal pattern of maximum flood distribution, it would be necessary to keep empty, during the flood season, the storage volume between the maximum and the Mar. 15 reservoir levels.

It would be permissible to fill, during the season of high flow, the space between the minimum and the Mar. 15 levels. This storage would be held for later release, during the low-water season, to increase the dependable energy output of the hydroelectric plant at the dam and possibly the energy output of other plants located downstream.

It would also be permissible to conserve water above the Mar. 15 level, provided sufficient storage space were reserved above the maximum level to control spring and summer floods.

The minimum level would be governed by operating requirements and by the economic balance between the values of the developed head at the site and at the downstream plants. The relation between drawdown and minimum heads should be such that a reasonable turbine efficiency will be maintained throughout the range of operating reservoir levels. Usually only a small part of the reservoir capacity is below the minimum reservoir level.

The dual-purpose use of the flood storage space above the Mar. 15 level should be permitted only if the pattern of flood distribution is distinctly seasonal. Streamflow records taken over a long period of time are required to demonstrate the feasibility of this type of operation. If maximum floods have been known to occur during all the seasons or if the streamflow records are of short duration, safety demands that sufficient storage space to meet flood-control requirements be held available continuously.

Two distinct patterns of seasonal flood distribution that would require different types of operation are shown by Figs. 10 and 11. Figure 10 shows the record of the floods that have occurred on the main stem of a large river; Fig. 11 shows similar data for an upper tributary of this same river. These graphs illustrate that the maximum flood occurrences on the main river are distinctly seasonal and that floods on the upper

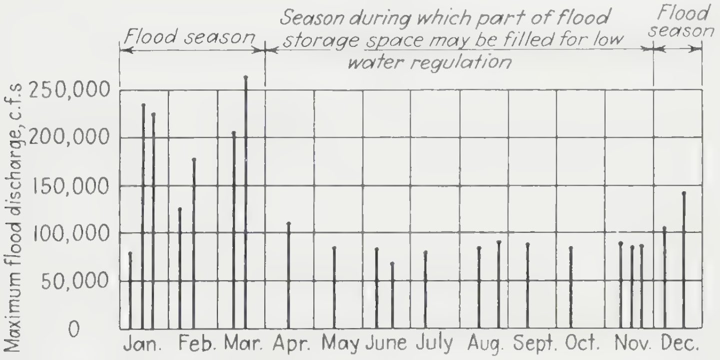

FIG. 10. Distribution of floods over 50,000 cfs, occurring during 50-year period, at point on main stem of large river system.

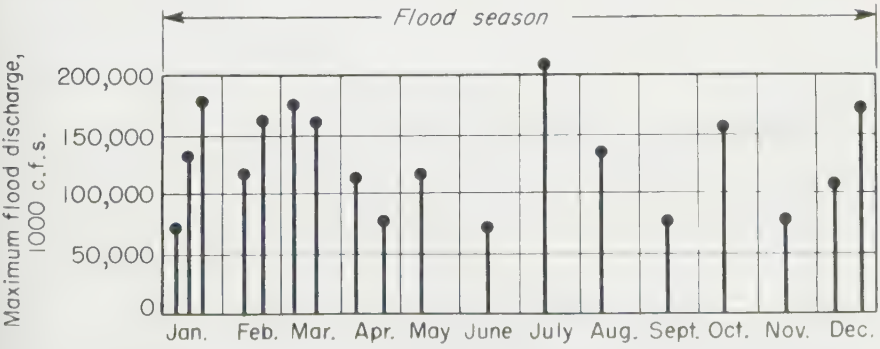

FIG. 11. Distribution of floods over 50,000 cfs occurring during 50-year period at point on upper tributary of large river system.

tributary have occurred in the summer as well as the winter and therefore have no seasonal pattern. If a reasonable reserve of flood-control storage space were held throughout the year for contingencies, it would be possible to operate a multipurpose reservoir designed to control the main river in such a way that flood control and power usage would overlap. In the case shown by Fig. 11 the reservoir would not be filled above the Mar. 15 level. The same principles of planning would govern the design of storage space required for each of the several purposes as would be applied to the design of single-purpose reservoirs.

FIG. 12. Typical example of flood protection by reservoir and levees for a city.

RESERVOIR ECONOMICS

29. Basic Principles. The principal measures of reservoir economy are (1) the cost of attaining a given objective and (2) the return on the investment. Construction costs offer a basis of comparison for alternate schemes for a single reservoir or for a reservoir system designed to accomplish objectives from which the economic benefits may be constant and to some extent independent of the system design. Equivalent navigation benefits, for example, might result from either a high-dam or a low-dam system, provided that proper adjustments were made for the value of the lost time in making the additional lockages required by the shorter reservoirs. Likewise, if a system were designed for the single purpose of providing complete protection against floods to a city, the economic benefits would be constant. In this case, the most economic system would be the lowest-cost combination of reservoirs and local protection works that would adequately serve the purpose. Economic justification would depend upon the ratio of benefits to cost.

If, however, either a flood-control or a power-reservoir system served an extensive area and, furthermore, if increases in flood storage gave corresponding increased benefits, there would be some economic limit to the extent of reservoir development. In this case, the most economic scheme would be that which would yield the maximum return in benefits per dollar of investment. In some cases, it might be desirable to extend the system beyond the most economic stage of development to a point where the return on the additional investment would be satisfactory, even though somewhat less than the maximum obtainable.

Although the principles of reservoir economics are relatively simple, their application to actual problems is complicated by the obstacles experienced in evaluating the various benefits. It is extremely difficult, for example, to obtain a satisfactory estimate of flood-control benefits. These principles will be demonstrated by two typical cases.

CASE I. FLOOD PROTECTION FOR A CITY BY LEVEES AND SINGLE-PURPOSE FLOOD-CONTROL RESERVOIR

Let it be assumed that city *A*, shown by Fig. 12, will be protected from floods by local levees *B* and an upstream reservoir *C*. It is desired to obtain the most economic combination of reservoir and levees that will protect the city.

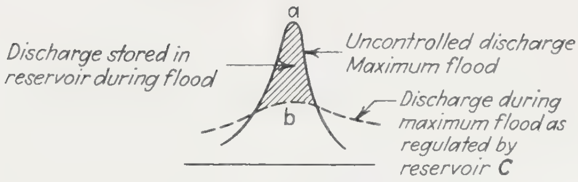

FIG. 13. Flood hydrographs for use in typical example.

In designing this flood-control system, it would be convenient to express both reservoir and levee costs in terms of either channel capacities or their corresponding flood stages at the city. If, for example, the maximum flood expected at the city (Fig. 13) were reduced from a peak flow *a* to a regulated flow *b*, it would be necessary to provide levees higher than the river stage corresponding to discharge *b* and in addition to provide sufficient storage capacity to impound at least the shaded area of the hydrograph of uncontrolled discharge. Increasing the regulated discharge *b* would increase the cost of levee protection and decrease the cost of the reservoir, as shown by Fig. 14. Likewise, decreasing the regulated flow would decrease levee costs and increase the cost of the reservoir. At some stage corresponding to discharge, say *b*, combined costs of the levees and the reservoir would be a minimum. The most economic reservoir in this case would be that which would result in a minimum combined levee and reservoir cost *ab* (Fig. 14). If regulated flow is plotted against height of reservoir, it is also possible to establish, by this procedure, the most economic reservoir level.

CASE II. FLOOD-CONTROL RESERVOIR SERVING LARGE AREA

If reservoir *C* (Fig. 12) would afford general flood-control benefits to a large region, it is possible that increases in storage capacity would result in corresponding increases in benefit values. In this case, the most economic reservoir would be that which would result in the maximum net yield in annual benefits value per dollar of annual costs. Reference to Fig. 15 will make this principle clear. Curve *D* indicates that the most economic height of dam would be that for which the ratio of annual charges to annual benefits would be a maximum with a reservoir capacity corresponding to 3 in. of runoff from the drainage area. From curve *C* it is seen that a reservoir having a 5-in. capacity would still yield a satisfactory rate of return on the additional investment over that required for the 3-in. reservoir, and it might be desirable to construct the dam to the height that would give this capacity.

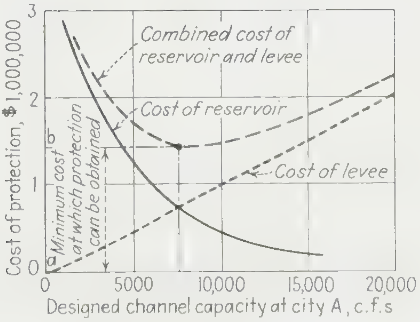

FIG. 14. Economic analysis for typical example.

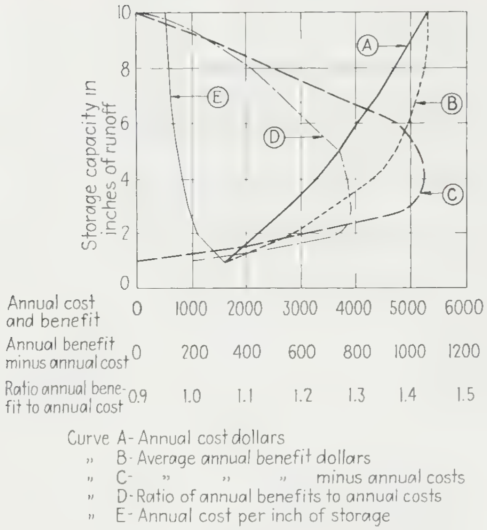

Fig. 15. Economic analysis of reservoir costs.

These principles apply also to multipurpose reservoirs designed for both flood control and the generation of electric energy. In this case, the combined benefits and charges would replace the single-purpose benefits described in the preceding paragraph.

Bibliography

1. Goddard, James E., Flood Plain Management Improves Man's Environment, *Proc. ASCE*, *J. Waterways Harbors Div.*, November, 1963.
2. U.S. Army Corps of Engineers, "Interior Drainage of Leveed Urban Areas: Hydrology," EM 1110-2-1410, Office of the Chief of Engineers, Washington, D.C.
3. Eden, Edwin W., Jr., Resume of Flood Control and Drainage Aspects of the Central and Southern Florida Project, International Commission on Irrigation and Drainage, *Ann. Bull.*, 1965.
4. U.S. Army Corps of Engineers, "Comprehensive Review of the Mississippi River and Tributaries Project," Mississippi River Commission, December, 1959.
5. "Meteorology of Flood Producing Storms in the Mississippi River Basin," HM Report 34, U.S. Weather Bureau, Hydrologic Services Division, Hydrometeorological Section, 1956.
6. "Meteorology of Hypothetical Flood Sequences in the Mississippi River Basin," HM Report 35, U.S. Weather Bureau, Hydrologic Services Division, Hydrometeorological Section, 1959.
7. Johnson, Wendell E., Missouri River Basin Plan in Operation, *Trans. ASCE*, vol. 122, p. 654, 1957.

SECTION 31

NAVIGATION SYSTEMS

By James H. Stratton, Jacob H. Douma, and John P. Davis

1. General. In this text, navigation improvements will be discussed for inland rivers, involving both open-river regulations and canalization of rivers, sea-level canals, delta channels and estuaries, and natural and artificial harbors.

Navigation systems may be classified as (1) *restricted* in the sense that cargo movements are bound to definite patterns established by the limitations of the channel of a river or inland waterway on which the carrier vessels suitable to the purpose operate, and (2) *unrestricted* in the sense that the movements of the appropriate types of carrier vessels are not circumscribed except as to conditions at the cargo terminals by the lakes, seas, or oceans on which they are designed to operate. A further distinction is that of type of vessel employed: in restricted waterways the tolerable draft of the barges, tugs, towboats, and other operating craft generally has a range from 3 to 15 ft, whereas vessels engaged in commerce on unrestricted waters range in draft up to 45 ft. Most of the waterways in the United States may be classified in one of the following four different types, of which only two are affected by tidal action:

Type 1. A deep river channel through a delta, a tidal estuary, a coastal inlet, a sound, or through a man-made sea-level canal which has protection from the wave action of the open sea is one distinct type. This type of waterway can be used by deep-draft ocean vessels, shallow-draft towboats and barges, and pleasure craft. Examples are Mississippi River downstream from New Orleans, La., Columbia River estuary below Portland, Ore., and the Houston Ship Channel. This type of waterway, although not affected by ocean waves, is subject to tidal action.

Type 2. A waterway consisting of a channel in a river, a bay, an estuary, or in a man-made canal that is protected from the open sea and which can be used only by shallow-draft towboats with barges and by pleasure craft is another distinctive type. This type of waterway is also affected by tidal action but is not exposed to direct ocean-wave action. The Intracoastal Waterway and the lower reaches of the Mobile and Apalachicola rivers are examples of this second type.

Type 3. Channels in inland rivers and canals that are not affected in any way by tides and that can be used only by shallow-draft towboats with barges and by pleasure craft are a third type. Examples are the Missouri, the Ohio, and the middle and upper reaches of the Mississippi River.

Type 4. Inland seas or lakes having unrestricted depths with deep connecting channels are a fourth type of waterway. Such waterways are not generally used by the towboats and barges used on the other types of waterways because of wave action on the lakes. The craft used on type 4 waterways are generally large, with drafts up to 26 ft on the Great Lakes. These craft are not built to withstand the open sea and are too large and have too great a draft to use on the channels of types 2 and 3 waterways. The waterway system formed by the Great Lakes, their connecting channels, and the St. Lawrence Seaway is a type 4 waterway. This system is used by large lake vessels and, since there is access to the sea, by oceangoing craft of limited size.

In the United States, the inland-waterway system comprises a vast network of

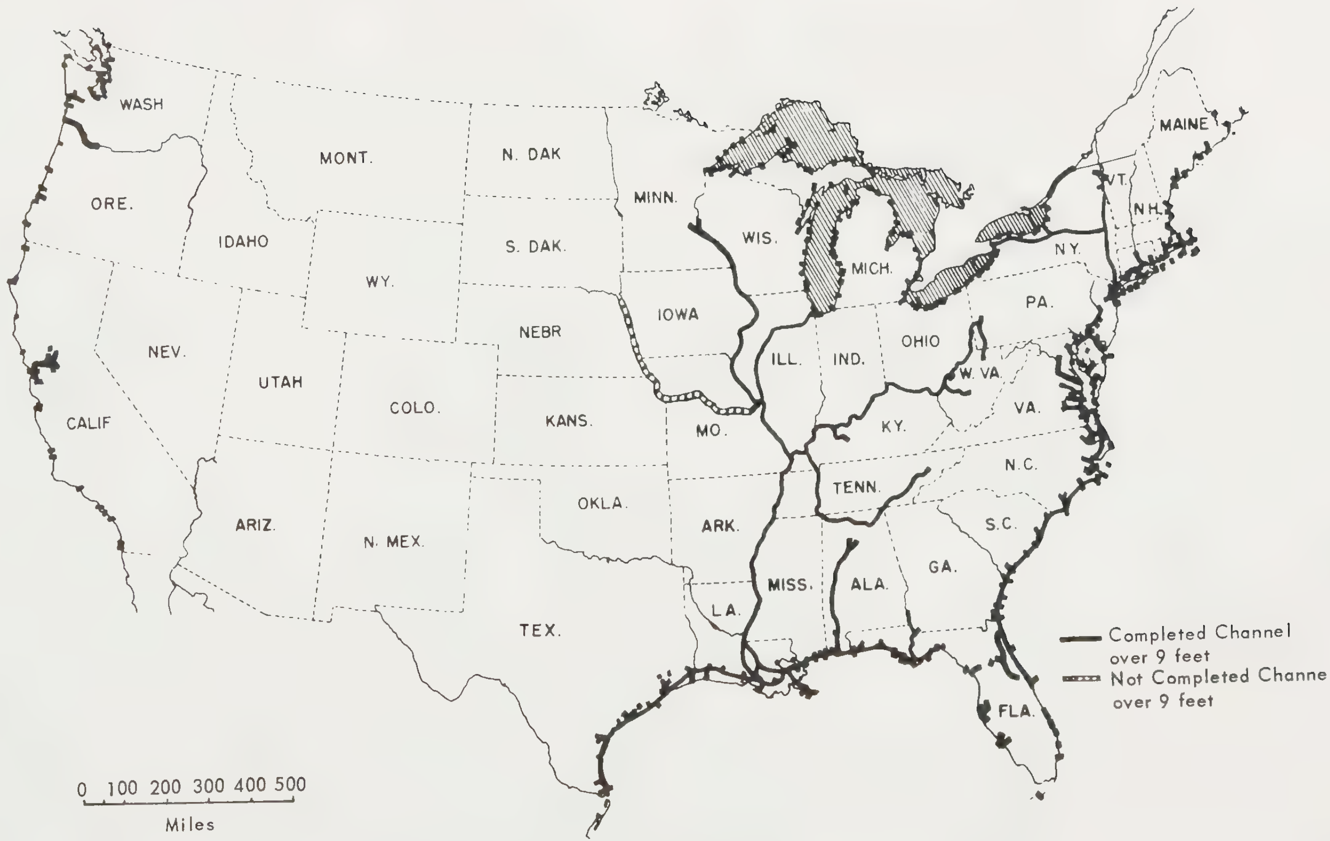

FIG. 1. Principal inland waterways in the United States.

deep channels in coastal areas (type 1) interconnected with river channels and canals (types 2 and 3) and the Great Lakes and St. Lawrence Seaway (type 4). Figure 1 shows the principal navigable waterways in the United States.

All four types of waterways require engineering works of some kind to provide suitable conditions for present-day navigation needs. The improvements and engineering works required for waterways affected by tides differ in many respects from the works required on nontidal rivers and canals.

OPEN-RIVER REGULATION

2. General Considerations. Open-river regulation or channel regulation is the term used to designate the methods used in forcing a stream with erodible characteristics to develop and maintain a navigable channel by its own scouring action. Early attempts at securing navigable depths by open-river-regulation methods included closing of back channels and constriction of the main channel of a stream to force the flow to form a single narrower and deeper channel section. Concentrating the flow into a narrow cross section increases the water-surface slope through the constricted reach. This causes higher velocities that scour the cross section and thus create a navigable channel. Pile dikes, rock dikes, revetment, and dredging are used to constrict, realign, and deepen channels in open-river-regulation work.

Certain conditions must exist for open-river regulation to be successful as a means of providing a navigable channel on a river. The low-water flow must be great enough to sustain the desired channel width and depth. The stream gradient must be no greater than 1 ft/mile and preferably no more than half this amount. Slopes steeper than 1 ft/mile produce velocities that are too great to permit safe navigation by commercial craft. The stream bed must be situated in easily erodible alluvium so that its banks can be controlled and aligned to produce a channel that will maintain a satisfactory cross section under various conditions of flow.

Rivers in alluvial valleys in their natural state develop channel configurations consisting of bends or curves and reverse curves connected by relatively wide shallow sections known as crossings. At low flows, the crossings serve as control sections for flow from the pool of one bend to the pool of the next bend. The bends in the channel have much greater depths than the crossings and the water-surface slopes are much flatter in the bends than on the crossings. An increase in stage tends to submerge the crossings, and the stream slope then becomes more uniform. As the stage increases, depths on the crossings increase, and the entire regimen of flow will change. Such changes have to be considered in planning open-river-regulation works.

Alluvial streams undergo a continuous process of channel shifting and migration of bends that is known as meandering. The meandering of a channel in an alluvial valley is a natural phenomenon involving the runoff characteristics of the watershed, the material composing the alluvium, the valley slope, climatic conditions, suspended sediment load, and effects of man-made changes. In the meandering process, bank caving on the outside of bends and bar formation on the inside of bends and on crossings eventually cause the bends to become channel loops that gradually migrate downstream. As the loop formation and migration proceed, many of the loops are cut off by flood flows which break across the neck or base of the loop. When this occurs, changes in slope and regimen of flow occur that immediately induce the forming of a new system of bends and crossings. When a meandering stream encounters erosion-resistant material, such as the rock bluff of a valley wall or some man-made improvement, the migration may be retarded or stopped. The construction of reservoirs which alter the sediment load of a stream can also have appreciable effects on the natural meandering characteristics of an alluvial stream.

The formation of loops and bends on an alluvial stream is a continuous process, and no channel will remain straight, even when straightened, unless it is restrained from lateral movement by training works of some kind. The most troublesome problems encountered in open-river regulation result from the natural tendency of alluvial streams to meander and form deposition of sediment during and after periods of high flow. Meandering often results in movement of the channel away from completed regulation works.

Experience has demonstrated that the most effective way to stabilize an alluvial stream and develop channels suitable for navigation is to shape the stream in accordance with its natural tendencies toward curve formation. By observation of a stream for several years, the reaches that are the most stable can be determined. Through study of these stable reaches, estimates can be made of the optimum radius of curvature of the channel bends, their widths, depths, and the widths and depths of crossings between the bends. These data can be used as guides in reshaping and stabilizing other reaches. Much of the stabilization and regulation work done on the Missouri and Mississippi rivers has been based largely on "cut-and-try" methods. Increased knowledge of the mechanics of sediment transport, better and more complete hydrologic data, and use of models have all contributed to a better understanding of channel stabilization and to the development of analytical methods of channel design.

Relationships between radius of curvature and depths in bends and widths and depths at crossings are illustrated by the curves shown in Fig. 2, which are based on data for the Arkansas River. The depth increases as the radius of the bend decreases, and, of course, the depths on the crossings increase as the width is decreased. The

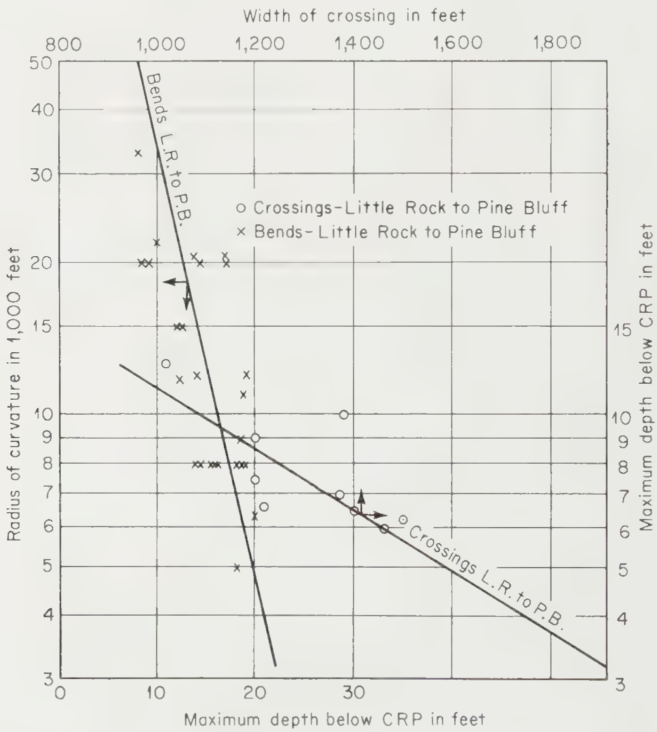

FIG. 2. Radius of curvature of bends vs. depths in bends and widths of crossings vs. depths. CRP = construction reference plane.

FIG. 3. Regulated and stabilized channel - Arkansas River.

proper length of a crossing section, or the length between two reverse curves, is of great importance in making a channel layout. Where natural alignments are favorable, adjacent reverse curves should be directly connected. Connections between two reverse curves should be short and straight. The straight reach should be no longer than two to three times the channel width.

Knowledge of the sediment load carried by a stream is most important in planning regulation works. The accretion of material behind dike structures to form new channel banks is dependent almost entirely on the supply of sediment. However, streams with a heavy sediment load require greater channel velocities to maintain a navigable cross section, which in turn may require additional training works to create optimum velocities.

A reservoir that traps sediment and radically alters the natural sediment load of a stream adds to the complexity of open-channel regulation immediately below the reservoir. Sediment-free outflow from the reservoir, in picking up a load of sediment from the channel bed and banks in the reach immediately downstream from the reservoir, degrades the channel and lowers the water-surface profiles. Canalization of the Arkansas River entails the construction of multipurpose reservoirs which will trap a considerable amount.

Channel regulation is accomplished by realignment to eliminate sharp curves and wide bar crossings and stabilizing the desired channel alignment by constructing dikes or other structures and sometimes dredging cutoffs. Insofar as possible, realignment and stabilization of a channel reach should begin at a location where the banks are erosion-resistant and proceed upstream. A typical reach of channel undergoing realignment and stabilization is shown in Fig. 3. Structures commonly used in channel regulation are the following.

3. Dikes. Dikes are built to (1) guide or deflect the current, (2) slow the current either to prevent scour or to cause the stream to deposit some of its suspended load, or (3) constrict a channel and cause it to scour to a greater depth. Dikes can be either permeable or impermeable. They are generally built normal or nearly normal to the current to move the river channel laterally. When built parallel to the path of the current they help form a desired rectified channel line. Channel-contraction works constructed of dikes at bar crossings to effect scour should function at both low-water and mean-water stages.

Figures 4 through 6 show various types of dike structures used by the U.S. Army Corps of Engineers on the Arkansas River. Figure 7 shows a general layout of permeable dike structures used to develop a new channel alignment. The riverward ends of the pile spur dikes on the left bank are connected by a curving longitudinal pile dike placed on the rectified channel line. Dumped stone placed along the base of the piles serves to prevent loss by scour during high-flow periods. Flows that pass through the permeable dikes are slowed down and drop most of their sediment load. Such accretions eventually build a new channel bank along the longitudinal dike.

Dike structures may be built by (1) driving clumps of piling and connecting the clumps with pile stringers, (2) dumping stone to form a barrier to the current, or (3) combining pile clumps and stringers with dumped stone. The choice of type of dike to use at a specific location depends on the stream conditions and on the availability of materials. Pile dikes are usually preferred where depths are moderate and where adequate penetration for piles can be attained. However, where depths are great and the current swift, the choice may be limited to pile dikes with dumped stone around the base. Where the depths are relatively shallow and stone is not too costly, dumped-stone dikes are used.

4. Revetment. This term is applied to structures placed parallel to the current to prevent bank erosion. Lumber mattresses, weighted down with stone, were used

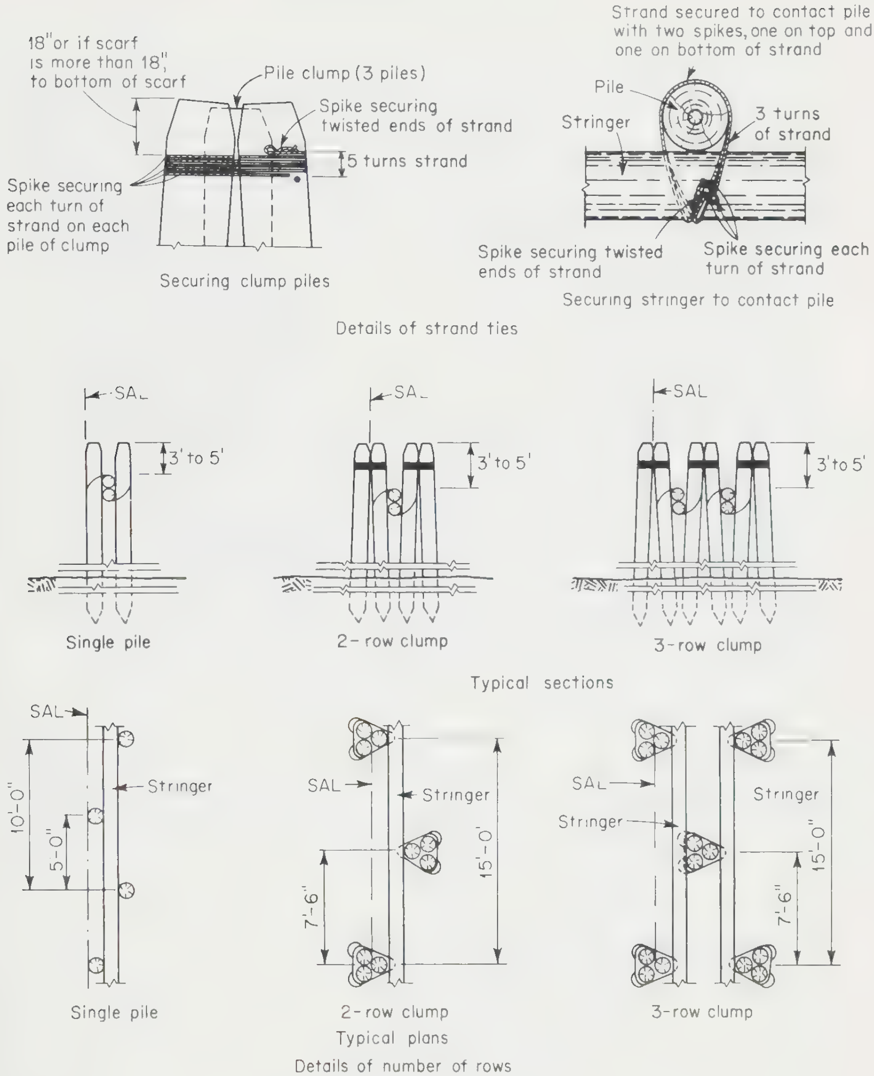

FIG. 4. Pile dike.

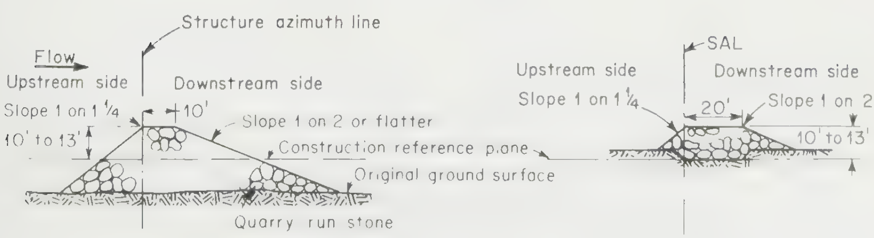

FIG. 5. Stone-fill dike.

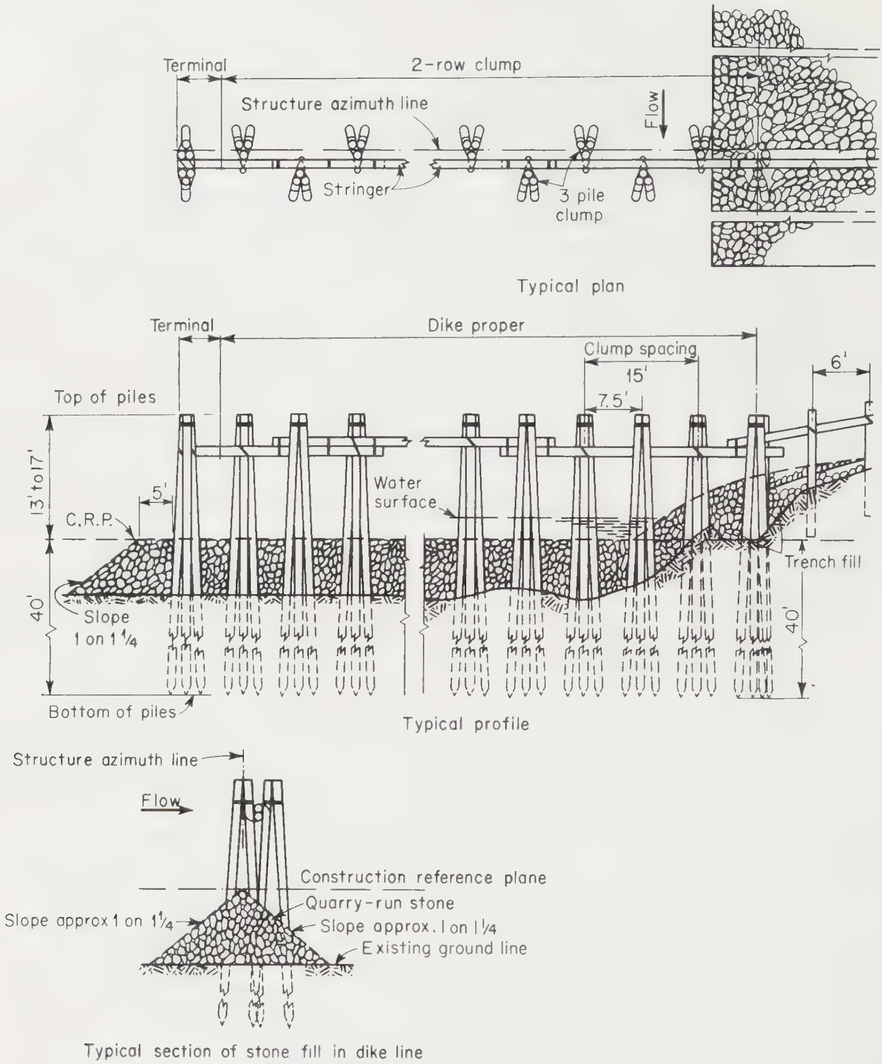

FIG. 6. Pile dike with stone fill.

extensively for many years, but experience has shown that dumped stone is less costly and more durable. Figure 8 illustrates two different types of revetment construction. Bank revetment mattresses made of concrete slabs articulated by use of wire rope developed on the lower Mississippi River are sufficiently flexible to rest on an uneven bottom and bank surface.

5. Pilot Cuts and Cutoffs. When it becomes necessary to depart from the alignment of an existing channel in order to improve it, a pilot cut along the desired alignment is made and the river is induced to complete the excavation by its own scouring action. For success, flow conditions must be developed so that the tractive force will

Fig. 7. Realigned channel before accretion.

be greater in the pilot cut than in the existing channel. Based on satisfactory enlargement of pilot-channel cutoffs on the Missouri and Arkansas rivers, the tractive force in the pilot channel should be at least 1 to 1½ times the tractive force in the existing channel. The pilot-channel entrance should be located on the concave side of the bend upstream from the point of inflection of the existing channel.

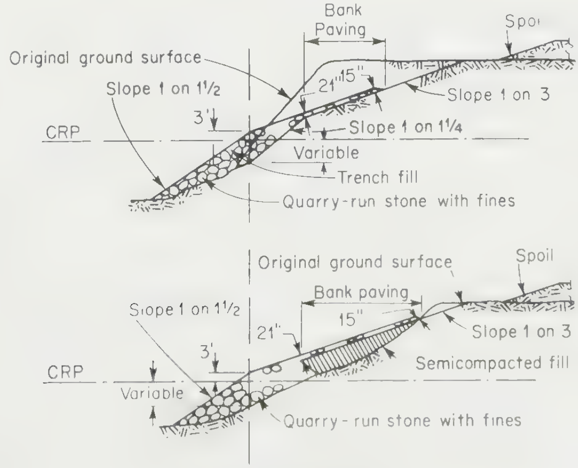

Fig. 8. Bank revetments.

CANALIZATION OF RIVERS

6. General Considerations. Canalization of a free-flowing river is accomplished by its conversion by means of dams into a series of pools of sufficient depth for navigation. Locks are constructed at the dams to transfer vessels from one pool to the other. Where the river slope permits, a combination of land-cut canals and river canalization is sometimes used to improve a waterway for navigation. An example is the New York State Barge Canal with a canalized section of the Mohawk River and land-cut canals generally from Little Falls, N.Y., to the Niagara River. The Welland Canal from Lake Erie to Lake Ontario is a land cut for its entire length. The Ohio River is canalized throughout its entire length except for a 2-mile stretch of canal which bypasses the falls at Louisville, Ky.

Canalization of a river is a very complex and expensive undertaking and can be justified economically only if movement of large tonnages will result in worthwhile savings in shipping costs. From a physical standpoint, the minimum streamflow, sediment load, and stream slope are the major factors which determine whether a navigable channel should be provided by open-river regulation or by canalization. Rivers with heavy sediment loads, such as the Missouri, Arkansas, and middle Mississippi, are the most difficult to canalize. On the Arkansas River, regulation works are being combined with locks and dams, and no serious sediment deposition in the navigable channels of the pools is anticipated. A stream that has wide fluctuations in rate of flow and low discharges during dry periods is not susceptible to open-river regulation. Such a stream must be canalized if a navigable channel is to be assured. Velocities in streams with gradients over 1 ft/mile will be excessive and hazardous to navigation and will preclude open-river regulation even though streamflow is adequate and other factors favor this type of development.

The number and locations of dams required to canalize a stream depend on the minimum depths desired, the slope of the stream, topography of the floodplain, and developments that already occupy the floodplain. The pools should be made as long as possible to minimize the number of dams and locks, but at the same time the inundation of valuable land and existing developments must be held to a minimum. The dams on a canalized waterway must be designed and operated so that during floods and periods of high flow there will be no material increase in natural flood heights.

Costs of land, relocations, and construction must be balanced against transportation savings that will result from plans with different numbers of dams and pool lengths to determine which plan will provide the maximum benefit. The transit time through a waterway and the capacity of the waterway have a direct bearing on the amount and type of freight that will move and thus affect transportation savings. Since the number of locks to be traversed is a major factor in determining transit time and the waterway's capacity, their number must be kept as low as possible, consistent with other requirements. Straight approach channels to the locks, free of adverse currents at all stages of the river, must be provided. Within a given reach that is satisfactory from the standpoint of navigation conditions and relocations, the final selection of the lock and dam site may be governed by foundation conditions.

Water for lockages usually poses the most serious problems for canals that cross divides between two drainage basins. Some means, such as reservoirs and feeder canals, are then required to store and provide lockage water at the canal summit level. Engineering works on streams entering a land-cut canal are generally necessary for the interception of flood inflows to prevent erosion or sediment deposits.

There are no fixed criteria for establishing channel dimensions on canalized waterways except those for deep-draft vessels. Channel-dimension criteria for deep-draft vessels are presented elsewhere. Virtually all the waterways used for barge tows in the United States have minimum depths of at least 9 ft, and the present trend is toward greater depths. Minimum horizontal dimensions of canalized inland waterways used for barge traffic vary from slightly less than 100 ft on a few sections of the Intracoastal Waterway to 300 ft on the Ohio River.

In establishing the width of a canalized waterway for barge traffic, the type, size, and number of tows that are to use the waterway must be considered. Present-day conditions are such that a waterway should be at least wide enough to permit tows of about 70 ft minimum width to pass without delay or hazard. A 70-ft-wide tow normally consists of four or more 35-ft-wide barges arranged two abreast. For two 70-ft-wide tows to pass without interference, a channel width of 225 ft is a desirable minimum. This width of channel provides a clearance space between tows of 35 ft and a bank clearance on each side of 25 ft. If larger and wider tows are to be used, greater channel widths must be provided. If channels of less than 200 ft in width are considered for a canalization project, it must be assumed that most of the traffic will move in tows that do not exceed 55 ft in width.

On a canalized waterway where sediment transport is not a problem, channel curves should have minimum radii of 5,000 to 8,000 ft depending on other factors, such as bank lines, visibility, and speed and direction of currents during periods of high flows. Several attempts have been made to develop minimum channel widths and radii of curvature mathematically; however, the practical value of such determinations is subject to question.

Vertical clearances for bridges and other structures that cross a canalized waterway depend on the heights of vessels that will use the channel. A barge tow that is pushed instead of pulled must have a pilothouse that is high enough for unobstructed pilot vision to the head of the tow. Thus, the length of tow affects the height of the towboat pilothouse, which, in turn, usually controls the required vertical clearance. Criteria in use on the Arkansas River, for instance, specify that bridges must have a minimum vertical clearance of 52 ft above the surface of a flow that will have a duration no greater than 2 percent of the time.

7. Navigation Dams. Navigation dams, as contrasted with other types, are built specifically to create pools in a river of predetermined depth for purposes of navigation only. Navigation dams are of two distinct types: navigable and nonnavigable. A navigable dam is designed for lowering to permit the unobstructed passage of high river flows. When the dam is lowered the open-river condition obtains and vessels can then proceed in either direction without passing through a lock. As the name implies, the nonnavigable dam forms a permanent barrier to vessel passage so that all navigation has to pass through a lock.

Navigable-type dams were adopted for the initial Ohio River canalization project because most of the heavy cargo movements were downriver and loaded tows were accelerated during high-stage periods when the dams could be lowered to make open-river navigation possible. Since most of the barges on upbound tows were empty, no serious difficulties were encountered in overcoming river currents. High maintenance and operation costs and difficulties in designing navigable dams for heads greater than 10 to 12 ft are the principal disadvantages to canalization by movable-barrier structures. Because of the limitation on head with this type of dam, more dams and locks are required, which in turn makes for higher costs and longer trip time for tows when the dams are raised.

On the Ohio River, between the time of inception of the first canalization project and the close of World War II, the character of river traffic changed and freight movement is no longer predominantly downbound. With this change in traffic it has become more economical for heavily loaded upbound tows to move in slack water and transit locks than to contend with the currents encountered under open-river conditions. Accordingly, the navigable-type dam is being abandoned in the United States in favor of the nonnavigable higher-head structures which create longer pools, thus requiring fewer lockages as well as offering other advantages.

Nonnavigable dams can have either movable or fixed crests. The fixed-crest-type dam can be used at locations where increased stages during periods of high flow can be tolerated, *i.e.*, where the increased stage caused by the dam does not cause damage or produce other adverse effects. This type of dam is usually a simple concrete structure with an ogee crest shape and a horizontal stilling basin or apron at the toe of the ogee section. Under present-day conditions of development in the stream valleys in the United States, there are very few, if any, locations where fixed-crest navigation dams are feasible. Consequently, most of the navigation dams constructed since 1930 are of the nonnavigable movable-crest type.

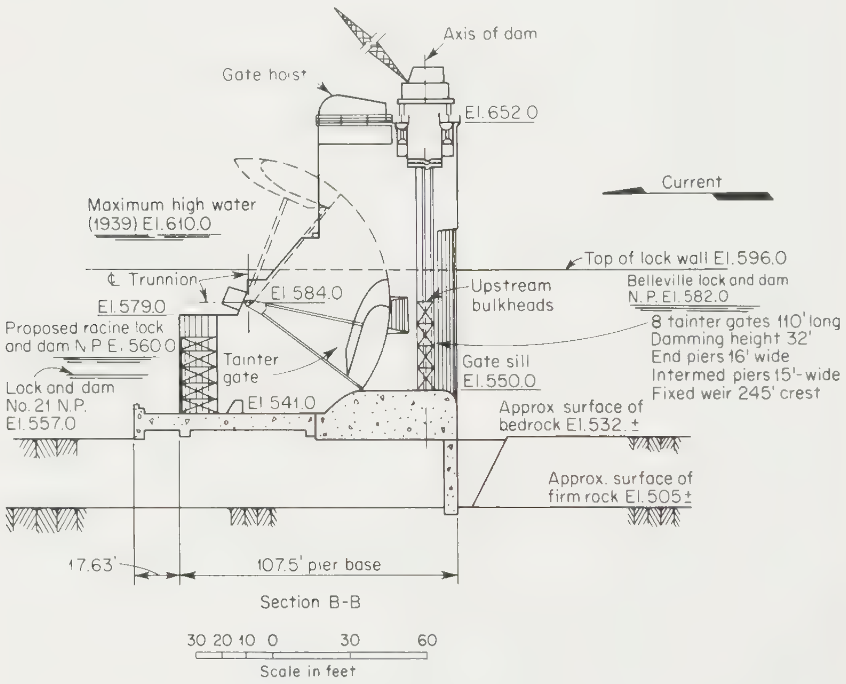

Fig. 9. Belleville Dam, Ohio River.

The types of movable elements or gates used are the vertical lift, Tainter, roller, and Sidney. Various combinations of these gates may be used in a single dam structure. Since 1940, Tainter gates have come into almost exclusive use in the United States for navigation dams. Figure 9 shows a section of a typical navigation dam with Tainter gates used on the Ohio River at the Belleville project.

When the required cross-sectional area or flow space for a dam has been determined, the size of the gates is developed by consideration of the damming height and the optimum gate length for the location under consideration. The elevation of the crest of the sill is usually governed by natural stream-bed elevations and the damming height, and hence the height of the gates is then the difference between the adopted pool level and the elevation of the crest of the sill. The required net length for the gated section is the area divided by the damming height. Model tests are usually made to check the adequacy of the gated section and to investigate swell-head effects at several different flows less than the maximum.

The length of the individual gates in a navigation dam is normally determined by an economic study of span lengths and required sizes of supporting piers. Foundation conditions also influence selection of gate lengths and pier design. Another consideration that may affect the choice of gate length is the need for space to pass large ice flows and accumulation of drift. The span lengths of the Tainter gates on the new Ohio River dams are 100 to 110 ft in length, and on the Arkansas River the Tainter

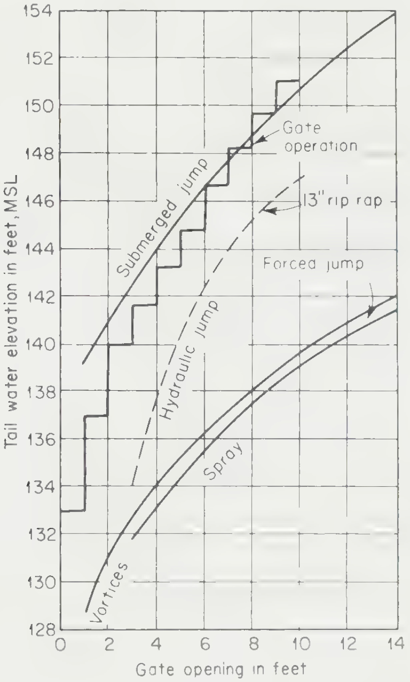

FIG. 10. Typical gate-operating schedule. Gate-sill elevation 134 ft. Apron elevation 119 ft. Apron length 40 ft. End-sill height 4 ft. Upper-pool elevation 162 ft.

gates are 60 ft in length. The gate-hoisting machinery is placed on the tops of piers, and each individual gate has its own hoisting equipment. Stop-log slots are provided both upstream and downstream of the Tainter gates so that the gate bays can be unwatered for maintenance. The new Ohio River dams have gantry cranes on the bridges across the piers to place and remove the stop logs.

Insofar as possible, the gates in a navigation dam are operated so that the upper pool level will not vary more than about 1 ft. Generally, as river flow begins to increase, gates will be raised successively in 1-ft increments until all gates are fully open. At this point, all control of the upper pool level is lost, and if flow continues to increase, the upper pool will then rise at the same rate as the lower pool. The difference in pool levels then represents only the swell-head effects caused by the piers, the lock, and any other fixed portions of the dam. In general, the depth of tail water in the stilling basin must be great enough to produce either a jump or a submerged jump

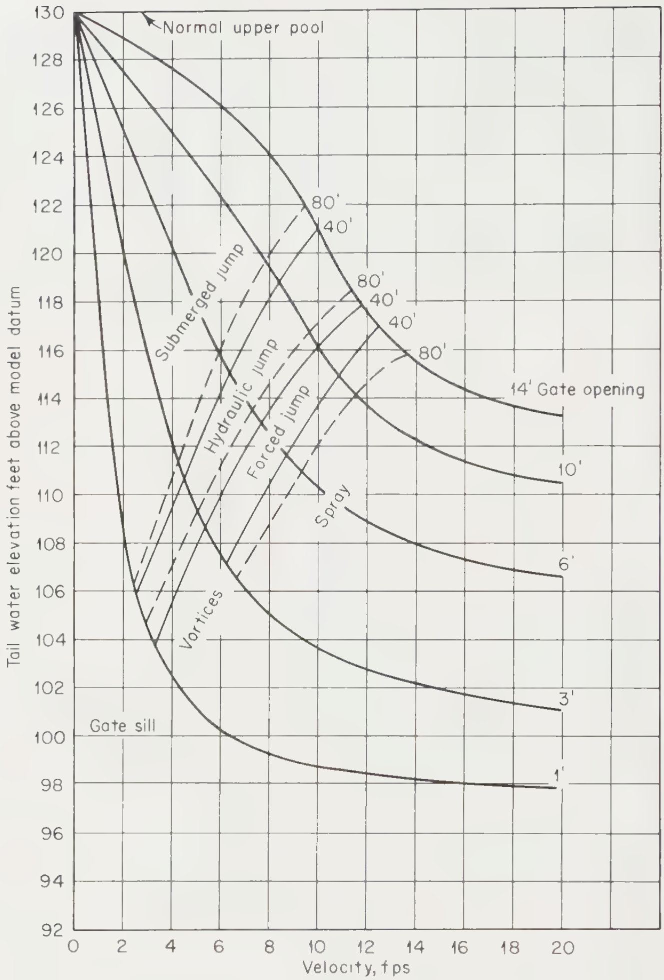

FIG. 11. Stilling-basin performance curves. (1) Approach elevation 95 ft. (2) Exit elevation 95 ft. (3) Pool elevation 130 ft. (4) Height of end sill 4 ft.

that does not create excessive velocities on the stream bed downstream from the end sill.

The selected gate-operating schedule has an important influence on stilling-basin design. Normally, it is not necessary to design a stilling basin for only one gate or a few of the total number of gates operating completely open under a full head. There is little likelihood that an unbalanced operation of the gates would ever be needed. If it were, a very costly stilling basin would be required unless the entire dam structure could be founded on good rock. Figure 10 shows a gate-operating schedule and various tail-water conditions for a typical stilling basin. The opening of all gates by successive small increments permits the tail water to rise sufficiently to maintain an adequate depth in the stilling basin, and the rate of opening of the gates depends on the rate of rise of the tail water.

The curves shown in Fig. 11 delineate the range of operating conditions of a stilling basin for the Arkansas River dams that were developed by model studies at the U.S. Army Engineer Waterways Experiment Station. The bottom velocities shown are used to determine the thickness, gradation, and length of stone protection placed at the downstream end of the stilling basin.

8. Navigation Locks. A navigation lock is a rectangular boxlike structure without a top and with gates in each end so that vessels can move into or out of it from either direction. The water level in the box, or lock chamber as it is called, can be raised or lowered to coincide with the levels in the upper or lower channel by means of valves and conduits. The sequence of events in "locking" a vessel through a navigation lock is as follows: Assume a vessel is moving downstream and that the water surface in the lock chamber is at the same level as the upper pool. With this condition, the lower gates in the lock chamber would be closed and the upper gates could be either open or closed. If closed, the upper gates must be opened to permit the vessel entry into the lock chamber. After the vessel is positioned and moored in the lock chamber and the upper gates are closed, the water in the lock chamber is allowed to flow by gravity into the lower pool by means of valved ports or conduits, until the level in the lock chamber has fallen to the same level as the level in the lower pool. The lower gates are then opened and the vessel is free to move out of the lock chamber into the lower pool and proceed down the channel. Lockage of an upbound vessel involves a similar sequence of operations but in reverse order.

The location of a lock with respect to channel alignment and river currents is very important. If a lock and dam can be placed in a relatively straight reach of channel, free of appreciable natural cross currents, then the lock can probably be placed on either side of the channel. Foundation or other conditions may then control. However, if the lock and dam must be located in a curve, then the lock should be placed on its concave side in order to take advantage of the thread of the current, which generally adheres to the concave side of the curve. This location reduces the tendency for a downbound vessel to be drawn by the currents toward the gated portion of the dam during periods of high flow. A study of river currents and flow conditions on a general hydraulic model is invaluable to determine the best orientation and site for a lock within a given reach of channel.

Approach channels to a lock should, where possible, be straight for a length of three to four times the length of maximum tow that will use the lock. Guide walls, in both the upper and lower pool, should have lengths equal to the length of the lock chamber. In most of the early river canalization projects in the United States, where only one lock was provided, the guide walls were placed on the landward side of the lock in continuation of the landward lock wall. On the newer canalization projects, guide walls have been built in line with and as continuations of the riverward lock wall.

Locks for shallow-draft vessels that are currently being planned, designed, or constructed generally are of the following sizes: 84 by 400, 600, or 720 ft; 86 by 675 ft; and 110 by 600, 800, or 1,200 ft. Depths on the sills for all the above sizes are usually 12 to 15 ft, depending on location of the waterway. The New Second Lock in the St. Marys Canal at Sault Sainte Marie, Mich., has a lock chamber with a usable length of 1,200 ft, a width of 110 ft, and depths on the sills of 31 ft. The maximum size of lock that can be advantageously used on a waterway is ordinarily governed by the maximum size of tow that can efficiently operate in the channels of the waterway. While there are no fixed criteria governing general design of locks, certain guides have been evolved that cover the filling time, emptying time, hawser stress, turbulence in lock chamber, water-surface conditions over intakes, and turbulence conditions at culvert outlets. A discussion of the hydraulics of locks will be found in Sec. 32.

The operation time of a lock is dependent on its size and lift, the size of the culverts, and the hydraulic efficiency of the entire filling and emptying system. Selection of the operation time for a specific lock is essentially an economic problem in that costs of providing various rates of filling should be compared with savings gained in transportation costs. Experience shows that the cost of a system that would fill a large high-lift lock in 2 or 3 min without violating safety requirements would be prohibitive. On the other hand, the increased cost of providing a 10-min instead of a 15-min filling time may be insignificant in relation to a total project cost. Locks with lifts of 30 to 50 ft built in the United States in the past decade have had filling times ranging from 8 to 12 min. The emptying time, in most cases, is about the same as the filling time. For higher lifts, such as those of the Columbia River locks, where lifts are on the order of 100 ft, filling times of 11 to 15 min have been achieved without excessive cost.

The maximum mooring-line stress usually permitted on barge tows and shallow-draft vessels during lockage is 5 tons. A stress of 10 tons is permitted for Great Lakes vessels and oceangoing ships that ply the Great Lakes and the St. Lawrence Seaway. The water in a lock chamber overlying the filling-system intakes must be free of air-entraining vortices and of currents that are hazardous to moored vessels. Experience has shown that where intake ports are spread over a large horizontal area in the vertical face of lock approach walls, conditions will not be conducive to vortex formation. Surface turbulence in a lock chamber must not be so violent as to swamp a small boat or cause excessive mooring-line stresses.

The outlets from the emptying culverts should be arranged to discharge riverward of the lower lock entrance if possible. If this is not possible, then a system of transverse bottom laterals in the lower ends of the lock walls with ports in their sides should be provided. If the lift is not too great, discharge manifolds in the lower approach walls with horizontal ports and baffle blocks in front of the ports may be used for energy dissipation.

The principal components of lock-filling systems are intakes, valves, lock-chamber manifold or bottom culverts, and discharge outlets. Lock-filling systems currently in use in the United States are characterized as follows: (1) end filling, utilizing loop culverts and valves, sector gates, vertical-lift gates, valved ports in miter gates, or combinations of loop culverts and sector gates; (2) wall culverts and side ports; (3) wall culverts and bottom transverse lateral culverts; (4) wall culverts with numerous very small ports; and (5) wall culverts with bottom longitudinal culverts.

The end-filling system is the oldest known type and is still used where lifts are very low (less than 10 ft). Wall culverts and side ports are generally the most economical for lifts under 30 ft. For higher lifts, transverse lateral or longitudinal bottom culverts are usually necessary to obtain satisfactory lock-chamber conditions and reasonable operation time. The bottom longitudinal system developed recently for the Millers Ferry project in Alabama is one of the most efficient developed thus far from the standpoint of hydraulics. With this system, there is an essentially balanced flow condition in each longitudinal half of the lock chamber at all times during the filling cycle. The main features of this system are shown in Fig. 12.

The main types of lock closure gates used in the United States are sector, miter, vertical lift, and Tainter. Sector gates are usually used where reversals of head may occur. Since they can be opened and closed under head, loop culverts are unnecessary. The lock can be filled and emptied by a gradual opening of the gates and letting water spill into or empty out of the lock chamber. The disadvantages of the sector gate are high initial cost and slow opening and closing times. Since sector gates can be closed under head, they are sometimes used as guard gates to close off flow in an emergency.

Over 90 percent of the locks in the United States are equipped with miter gates which in the open position fit into wall recesses. These gates are fairly simple in construction and operation, have low maintenance cost, and can be opened or closed

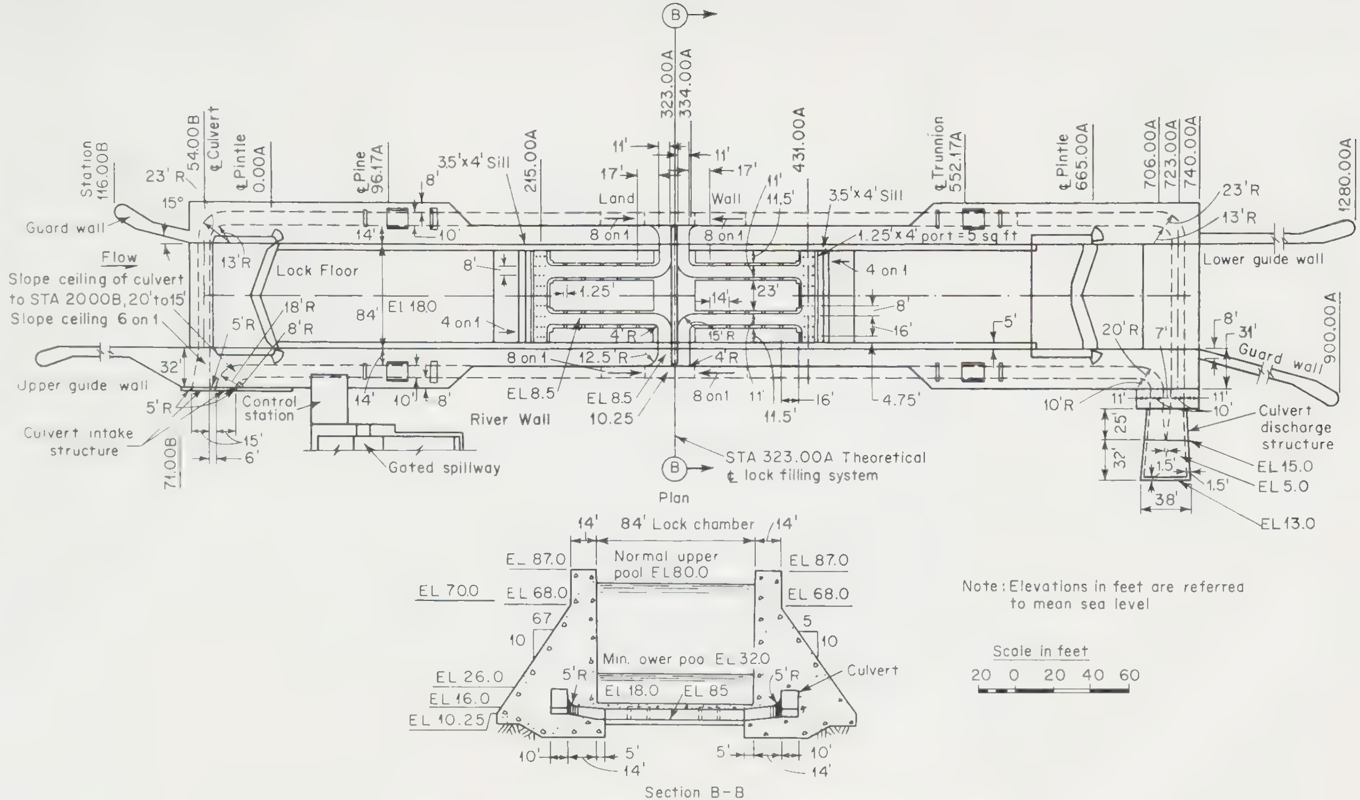

Fig. 12. Filling and emptying culverts—Millers Ferry project.

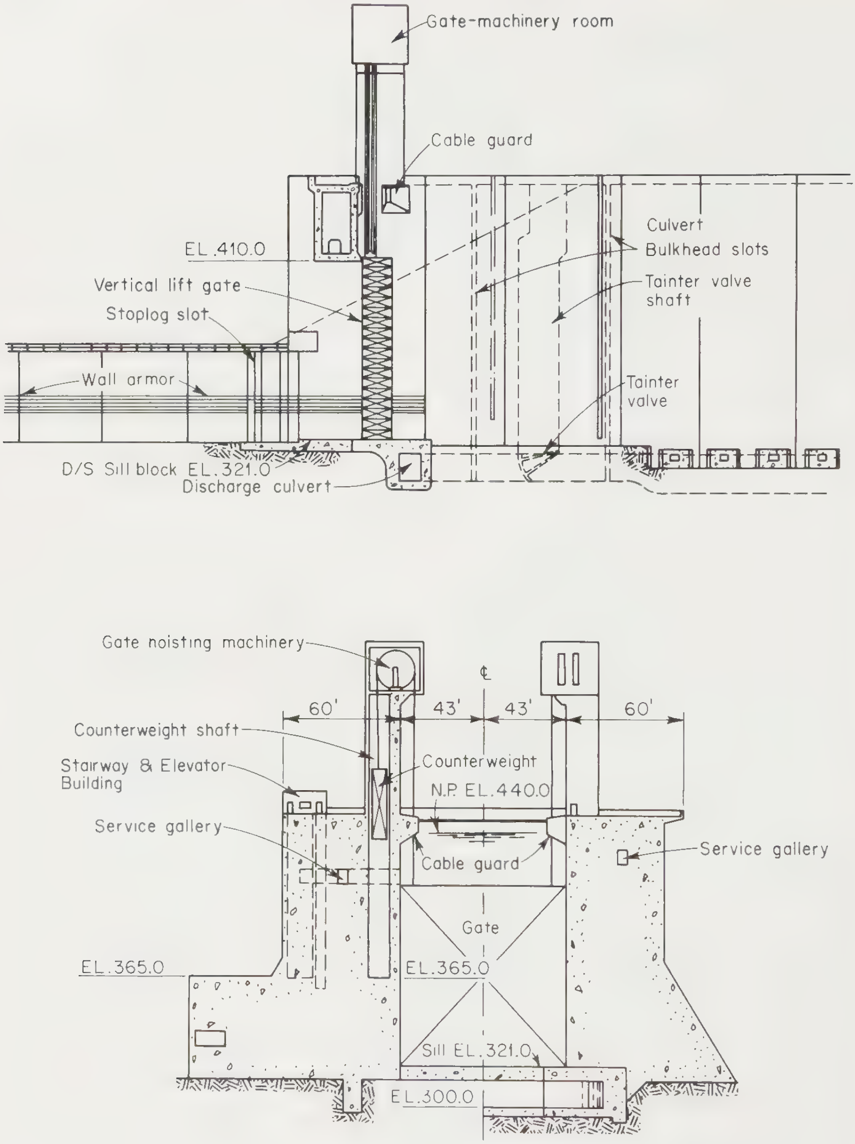

FIG. 13. Vertical-lift gate, Ice Harbor lock.

more rapidly than any other type. The disadvantage of the miter gate is that it cannot be closed under a head and hence cannot be used to close off flow in an emergency situation.

Vertical-lift gates when used to close the ends of a lock chamber possess some of the same advantages and disadvantages as sector gates. They can be raised or lowered under low to moderate heads but are normally not designed for reversal of head. Their operation time is much slower than that of miter gates and their initial maintenance costs are higher than for miter gates. A vertical-lift-gate installation at the upstream end of a lock consists of a vertical rising gate leaf which serves to close off the lock chamber from the upper pool. When the water in the lock is level with the pool, the lock is opened by sliding the gate leaf vertically downward until the top of the leaf is at or below the top of the upper sill. The vertical-lift gate at the downstream end of a lock is designed to be raised vertically to a height above the lower pool level sufficient so that vessels can pass underneath when entering or leaving the lock chamber. To accomplish this, the gate leaf is suspended from towers on the lock walls and equipped with counterweights to reduce the power-hoist size. The vertical-lift gate at the downstream end of Ice Harbor lock on the Snake River is shown in Fig. 13.

Tainter gates have been used at the upstream end of several locks. This gate is designed to be lowered into the upper end of the lock chamber when it is desired to open the lock to the upper pool. A Tainter gate can be raised or lowered under heads and the operation time is fairly rapid, but it is more vulnerable to damage than miter gates.

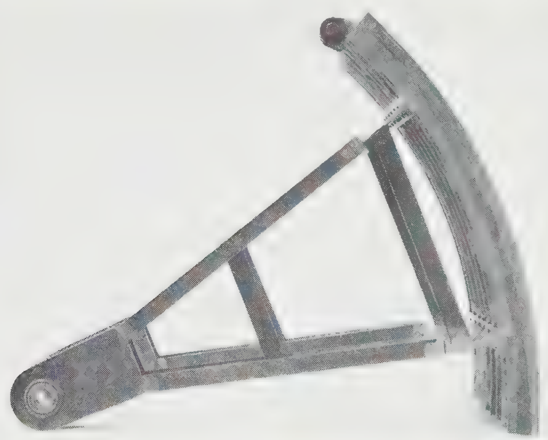

FIG. 14. Reverse Tainter valve.

Valves used in filling and emptying systems of United States locks have been either vertical-lift, butterfly, or reverse Tainter type. Virtually all the locks built since 1940 have used reverse Tainter valves as they require less maintenance and are more reliable than any other type. The latest design of reversed Tainter valve used by the Corps of Engineers, which is shown in Fig. 14, has curved vertical beams with a single skin plate. Spaces between the curved beams permit free circulation of turbulent water in the valve pit, thereby reducing the magnitude and fluctuation of dynamic loads to a minimum. Hydraulic cylinders with mechanical-linkage connections are used to open and close Tainter valves at most installations.

Types of lock guide walls commonly used are concrete gravity, concrete supported on sheet-steel pile cells, floating concrete caissons, and simple timber pile structures with wooden walers. On streams where depths are moderate and heavy traffic is expected, either the concrete gravity wall or the concrete wall on pile cells is preferred. Where the upper pool depth is great, the concrete floating-caisson type may be more economical than other types. On waterways where there is only moderate traffic and where mild climate prevents ice formation, timber-pile guide walls can be used.

SEA-LEVEL CANALS

9. General Requirements. Sea-level canals differ from channels in rivers, estuaries, and inland canals in that fluctuations in water levels primarily due to tidal action are but rarely affected by runoff from adjacent drainage areas. However, if such a canal crosses or intercepts a natural stream of any size, problems from adverse currents may be encountered. From the standpoint of design and construction, a sea-level canal presents no special problems other than those induced by the nature of the formations to be excavated, natural streams that cross or enter the canal, and tidal currents that may create hazards at certain times.

Characteristics of some of the more important sea-level canals are shown in Table 1.

TABLE 1. CHARACTERISTICS OF EXISTING SEA-LEVEL CANALS

Feature	Chesapeake & Delaware Canal	Suez Canal	Cape Cod Canal	Houston Ship Channel
Length, miles	46	100	17	50
Min width, ft	450	137	450	300
Min depth, ft	35	42	32	40
Max current, knots	2.5	3.5	5.2	1.0

TABLE 2. COMPARISON OF RESTRICTED CHANNEL SECTION AND ALIGNMENT

	Proposed Sea-level Canal	Panama Canal (Gaillard Cut)	Suez Canal	Cape Cod Canal	Houston Ship Channel
Section:					
Min depth, ft	60	42	42	32	40
Controlling width, ft (at depth shown in parentheses)	600 (40)	300 (42)	196 (32.75)	480 (32)	300 (34)
Length of restricted section, miles*	30	8	75	8	25
Min cross-sectional area of waterway, sq ft	36,800	13,860	11,440	17,920	8,640
Alignment:					
Total number of curves	8	8	12	5	33
Angularity per mile of restricted section, deg	3.9	17.1	3.4	24.0	55.6
Max curve, deg	26	30	44	75	109
% of channel in curve	15	35	13	72	67

* Restricted section defined as the part of the channel in which the displacement of water is limited by the channel banks.

Table 2 compares the "restricted" sections of three of the waterways listed in Table 1 with those of the proposed Panama Sea-Level Canal.

The proposed Panama Sea-Level Canal was the subject of exhaustive studies and model tests, and much information valuable in its application to design and construction of restricted deep-draft waterways and channels was developed. For comparison, it should be noted that the maximum tidal current in the proposed Panama Sea-Level Canal would be 4.2 knots as compared with 3.5 knots in the Suez Canal and 5.2 knots in the Cape Cod Canal. Although the Sea-Level Canal studies provided for tidal-control structures in the estimates, it was the conclusion that final decision with respect to tidal control should be deferred until such time as detailed design studies are undertaken.

Extensive tests made in the U.S. Naval David Taylor Model Basin, Carderock, Md., developed the following general criteria for establishing the cross section: (1) maximum rudder angle of 5 deg to control a ship with a speed of 9 knots with a

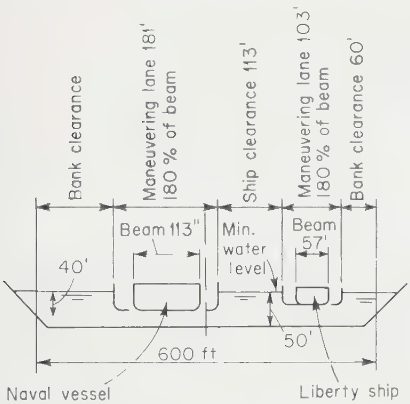

FIG. 15. Elements of channel design, Sea-Level Canal.

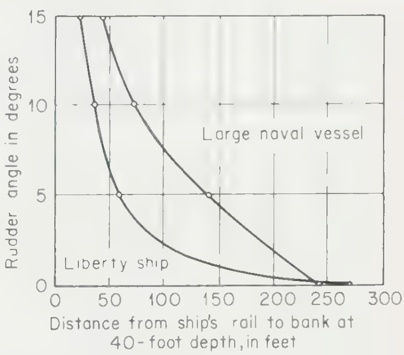

FIG. 16. Bank clearance vs. rudder angle.

following current of 5 knots (land speed 14 knots); (2) width of ship lane 170 percent of the beam of the vessel(s); (3) clearance between ships in passing equal to beam of the largest vessel; and (4) bank clearance established by a rudder angle of 5 deg using test data developed at the David Taylor Model Basin. The section of canal proposed is shown in Fig. 15.

In a restricted waterway which will have a large volume of traffic, the ideal ratio of channel depth to draft of vessel should be of the order of 1.5. The acceptance of a lower ratio for the larger vessels which occasionally transit the waterway may call for special precautions because of reduced controllability. The actual ratio in the Gaillard Cut section of the Panama for the largest vessel transiting the canal is about 1.2; for vessels of this size all traffic in the opposing direction is held up during their transit of the cut, and for notoriously bad handlers tug assistance is also provided.

The Sea-Level tests developed ratios of the cross-sectional area of the channel to the combined mid-section areas of several combinations of passing vessels. For the Gaillard Cut section, where currents are insignificant, the ratios range from 5 to 7. For the proposed Sea-Level Canal with its larger cross section and a current of 4.2 knots, the ratios for good controllability of vessels ranged from 6.5 to 8.6.

Figure 16 depicts the criteria used in establishing bank clearances required for two classes of ships selected for simultaneous transit in opposing directions. This selection of vessels was quite arbitrary but nevertheless was believed to be sufficiently realistic for the purposes of the study and no great handicap in the canal operation. On the very rare occasions when ships of significantly larger combined beam width arrive at the opposing ends of this canal at times of critical tidal flow, it will be entirely feasible to delay the transit of one of them pending the transit of the others. To provide sufficient cross section to meet such contingency in ship transits would be extremely costly, particularly in light of the rarity (2 percent) of the time that the critical tidal flow conditions would obtain.

At the higher speeds required to maintain headway, vessels tend to "squat"; the degree of squat is a factor of vessel dimension, the channel dimensions, and vessel speed. The adopted depth of channel should be based on the sum of the draft of the maximum vessel plus its squat at the speed which can be safely tolerated plus an adequate bottom clearance of not less than 2 ft. Fast-moving vessels moving singly in a channel designed for two-way traffic would not necessarily require greater channel

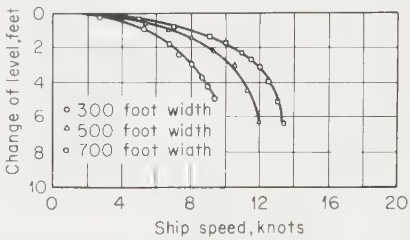

Fig. 17. Ship speed, knots. Effect of channel width on change of level of a ship on center line of a restricted channel. The curves shown are for the stern only. The bow curves are similar. Channel depth = 45 ft.

width because of the speed factor; however, when two vessels are about to pass they should, at the proper point in the approach, lower speed sufficient for safe passing. The change of level (squat) of a vessel at different speeds in channels of various widths determined by tests for the Panama Canal is shown in Fig. 17.

The increasing trend toward larger vessels, particularly increase in length, requires channel alignments free of sharp-angle curves and bends to avoid yawing or crabbing which, with loss of vessel control, risks grounding or bank striking. The passing of vessels at bends, where permitted, further dictates conservative transitions at changes of direction. Figure 18 depicts typical designs of bends employed in improving navigation channels in the United States.

The control of tidal currents in a sea-level canal or restriction of traffic to one-way operation may be necessary during times when tidal currents exceed about 5 or 6 knots. A tidal-control structure would, of course, involve some type of lock-type gate to permit vessels to enter and leave a canal at any time. The Sea-Level Canal control structures could be omitted if delays in transit of notoriously unwiedly ships or limiting traffic movements to a single direction at time of their transit is acceptable. Tug assistance to such ships during transit would assist in the prevention of accidents.

The criteria presented in this section have general application to the planning of waterways if proper cognizance is taken of the characteristics of transiting vessels, tidal influences, vessel speeds, the nature of banks and bottom (the damage to a vessel striking a rock bank or the possibility of its sinking may be a critical factor), wind conditions affecting ship handling, the presence of shore facilities which may limit ship speed in order to reduce wave wash and surges, and whether pilots will be used on ships when transiting the waterway. The David Taylor Model Basin studies indicate that the bank-clearance factor is related significantly to the ship type and may range from 105 to 125 percent of a ship's beam.

The exercise of judgment in the use of the Panama Sea-Level Canal test data combined with the results of observations and experience in actual waterways should be employed in the planning for the development or improvement of a waterway. If, as would be the case in the proposed Panama Sea-Level Canal, there is stream inflow

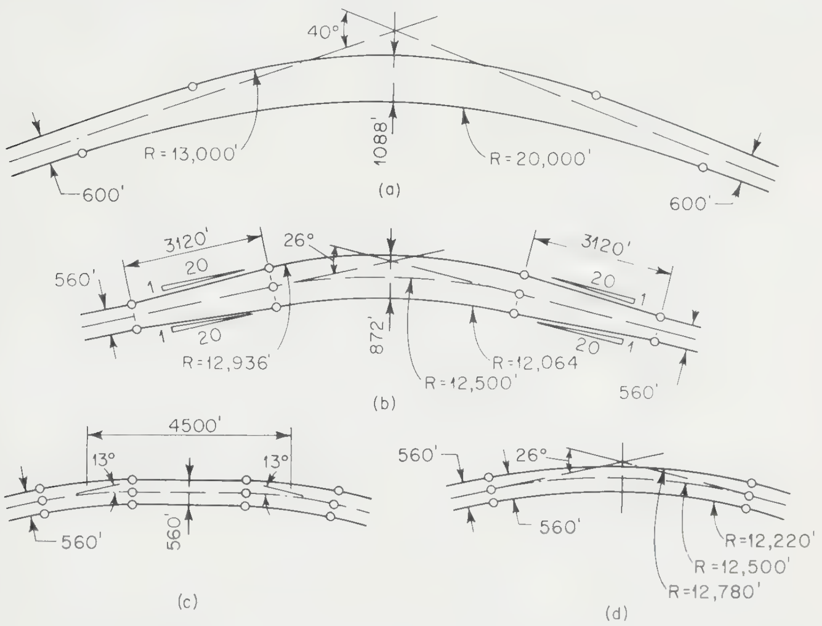

FIG. 18. Typical treatment of bends in channels. (*a*) Unsymmetrical widened 40-deg curve. (*b*) Symmetrical widened 26-deg curve. (*c*) Double 13-deg curve with no widening. (*d*) 26-deg curve with no widening.

into the waterway prism that may adversely affect vessel handling, then special measures may be necessary. Control of inflows by storage regulation is expensive but may be inescapable.

DELTA CHANNELS

10. Problems. Delta channels are the river-flow passageways through the fanlike deposits which characterize the mouths of sediment-bearing rivers emptying into relatively quiet waters. The flow passages or channels are sometimes called distributaries since each in a particular river mouth will carry within its capacity a part of the river flow. Delta channels are notoriously impermanent. Delta building is one of constant action as evidenced by the filling and closing of minor distributaries and the action of river currents in creating new channels as replacements. The combined action of tides, littoral currents, and storms influences the delta building and the development and retrogression of the distributaries. Further influences in the delta formation are the volumes of bed load and suspended materials brought down by the river and the depth of water into which the river flows. The accumulation of sediments in certain cases, as at the mouth of the Mississippi River, causes subsidences of the highly compressible underlying earlier deposits, with the result that the delta growth is retarded. Where this phenomenon does not exist, delta extensions progress at rapid rates. It is estimated that the combined delta of the Tigris and Euphrates rivers has extended into the Arabian Sea at an average rate of 160 ft/year over the past 50 centuries.

Delta channels are in no sense self-maintaining. The effects of tides and littoral currents carrying littoral drift are often sufficient of themselves to form bars at a delta mouth. The combined effect of deposition of river-borne sediments aggravates considerably the problem of sustaining navigation depths. Jetties and breakwaters as training works and dredging may all be required to maintain an opening across an outer bar and to protect shipping against possible groundings.

11. Methods of Control. It is rarely possible in a delta channel to put the river flow to work in developing and maintaining a navigable passageway. Improvements

Fig. 19. Mississippi River—Cupits Gap to Gulf of Mexico.

limited to the closing of certain minor distributaries for the benefit of a single channelway will often result in the opening of new distributaries or in the enlargement of an existing minor distributary. Dredging alone cannot achieve the desired result, and resort must be had to training works. If the delta gradients are too flat, the training works will be ineffective in preventing silt depositions in the navigation channel. As in the case of open-river regulation, the objective should be to direct bed-load movements into the side channels by the use of training works. Training works should be used to prevent excessive widening and filling of the navigation channel, particularly in the lower reaches where the influences of incoming tides and the battering of tidal waves are destructive to the maintenance of navigation depths. Where there are heavy movements of sediments in the navigation channel, the training works must be planned to avoid the possibility of flattening of the river slope. This may require the progressive or stage installation of the training works with fairly long periods of observation between the planned phases of construction.

The Mississippi River at its mouth, shown in Fig. 19, is a classical example of the improvement of delta channels for navigation. Three navigation channels have been authorized for this waterway: Southwest Pass, South Pass, and the Mississippi River from Head of Passes to New Orleans. The plan considered most feasible for carrying out the adopted improvement consists of the following steps: (1) dredging in the Mississippi River proper, in the two passes, and through the bars at the foot of each pass; (2) constructing, regulating, and controlling the distributaries between the Head of Passes and New Orleans. Discussion of the problems involved is limited to those encountered in Southwest Pass, which is the main delta channel.

The combination of poor alignment and hydraulic inefficiency of the channels at the Head of Passes causes a decrease in velocity accompanied by shoaling at the entrance to Southwest Pass. One solution to this problem would involve realignment of the banks of all three passes at their juncture and contraction of the entrance to Southwest Pass to approximately 1,400 ft, which has proved to be the most efficient width throughout the remainder of the pass. The contraction could be obtained by a system of timber-pile training dikes. An alternative solution is dredging of the shoal material to maintain the authorized channel depth. As the annual cost of dredging is less than that of constructing the dikes, the channel at the entrance to Southwest Pass is being maintained by dredging only.

Approximately 3 miles downstream of the Head of Passes the channel width decreases from an average of 1,750 to 1,450 ft, which is the governing width established by pile dikes in the lower reaches of the pass. Sediment moved from the shoal at the head of Southwest Pass tends to be deposited in the wider reach, because of the lower velocities, and forms a shoal along the west bank of the pass. Here the elimination of shoaling by contraction works in the form of permeable dikes was found to be economically justified.

The reach of Southwest Pass from mile 10.5 to 19.5 was contracted to a width of 1,450 ft by permeable pile dikes which were completed in 1939, and dredging for channel alignment and depths was completed in 1943. Shoaling has occurred in this reach, particularly during and after floods of greater than average magnitude, which has required maintenance dredging to restore authorized channel dimensions. The regimen of the channel remains fairly stable during low and normal river flows, and the contraction works effectively reduce the maintenance dredging in this reach of the pass.

In the lower 3 miles of Southwest Pass, which is confined by earth jetties, pile training works, and permeable dikes, high-water shoaling is caused by the sudden reduction in velocity at the end of the jetty channel. Because of unstable foundations and lack of maintenance during the years of World War II, subsidence of the jetties occurred considerably below project grade, permitting large flows to pass over the jetties and thereby reducing the velocity in the jetty channel to the point that additional shoaling resulted. The jetties are now being kept to grade and permeable dikes are being made partially impermeable to increase channel velocities and to reduce shoaling. As the shoal area at the mouth of the jetties progresses into deep water, the jetties will need to be lengthened to maintain nonshoaling velocities.

Shoaling in the entrance to the jetty channel is caused also by the littoral currents which flow around the end of the east jetty. The most serious shoaling occurs in a critical area where the river and littoral currents meet to form a large eddy accompanied by reductions in velocity. Construction of a semipermeable dike, about 800 ft in length, outward from the end of the east jetty, has been considered to deflect the littoral current away from the jetty entrance. While it is probable that shoaling would occur along the channel side of this dike, it would be far enough removed from the channel to prevent any injurious effects.

ESTUARY CHANNELS

12. Problems. Estuaries have higher relative stability than do the delta mouths of alluvial rivers, and when satisfactorily improved to meet the needs of navigation, they usually provide excellent harbors. As the ever-increasing draft of vessels has imposed a need for greater depths, dredging and other works are often required to provide channel access to the inner harbors within an estuary system. Also, dredging may be required to provide passing areas, turning basins, anchorage areas, slips between piers, and other special-purpose requirements.

Channels constructed in estuaries and tidal rivers are affected by considerations other than those found in fluvial streams. As tidal phenomena occurring in an estuary usually result from a complex interaction of a number of factors, the change in each contributing factor and in the resulting interaction must be determined for any proposed estuary improvement. The principal factors to be considered are tides and currents, fresh-water discharge, upland sediment, character of beds and banks, wave action, littoral processes, salinity intrusion, and dispersal and flushing of pollutants.

13. Tides and Currents. The range of tide may have a pronounced effect upon both the improvement works and shoreline properties. Higher tides resulting from an improvement may injure shoreline properties and cause claims for damages. Lower tides result in decreased channel depths. An increase in tidal prism may be an important asset in maintaining navigation channels and bar crossings if construction is properly adapted to the tidal forces. Excessive tidal currents complicate vessel handling, as well as increasing salinity intrusion and the transport of sediments. Tidal formulas have been developed to determine the rise and fall of ocean tides, and several methods have been developed for computing tidal heights and currents in an improved estuary. Among these are the "reflected wave method," described by Colonel Earl I. Brown,[16,*] the methods proposed by General G. B. Pillsbury,[17] and the "method of characteristics" used by Netherlands engineers.[18]

14. Wave Action. Ocean waves may make navigation difficult if not impossible during storms at the entrance to a waterway, and if severe may affect the configuration of sand bars at channel openings. Natural wave action and waves created by passing vessels in narrow waterways cause considerable bank erosion where banks are composed of unconsolidated materials; sediment from bank erosion may contribute materially to channel shoaling. Information on wave characteristics, such as direction of approach, height, period, and length, are needed for the design of bar channels and jetties or breakwaters at the entrance of a waterway.

15. Fresh-water Discharge. Fresh-water discharges into an estuary may modify the tidal regimen by lengthening the ebb and shortening the flood tides and by interaction with salinity-intrusion forces may produce a complicated modification of tidal currents. Fresh-water flows transport upland sediment which deposits in the tidal waterway; however, they also tend to flush pollutants out of the waterway. Reservoirs on stream tributaries of an estuary may either increase or decrease shoaling, depending on the method of reservoir operation as it affects fresh-water flows into the estuary.

16. Upland Sediment. Sediments brought down from the watershed upstream of the estuary flocculate and deposit upon contact with salt water, forming shoals which must be removed from the waterway by dredging if not carried out to sea by currents to preserve navigable depths. The volume of required maintenance dredging may roughly equal the sediment inflow into a navigable estuary.

17. Character of Bed and Banks. A proper waterway study requires the investigation of the characteristics of the bed and banks, particularly where currents are unusually strong because of some peculiarity of the regimen, or where an increase in current will result from the channel improvement. Sandy and silty bottoms and banks, while easily dredged, are also subject to scour with possible deposition of sediment in areas which will require maintenance dredging. Rock banks and bottom and the presence of large boulders will add to the cost of development.

* Superior numbers refer to items in the Bibliography at the end of this section.

18. Littoral Processes. "Littoral processes" is the generic term applied to the methods employed by nature for molding and remolding shorelines. The quantity of sediment moving along a shore is significant in the design of a tidal-waterway entrance. The extent of erosion and accretion occurring along a shoreline subject to a fairly uniform exposure to waves depends on its configuration. Inlets, deeps, and headlands impede the passage of littoral drift. Littoral processes of the shoreline must be investigated to establish whether eroded materials will move into navigable channels or block the entrance of a tidal waterway. Bar formations at channel entrances from the sea are especially feared by navigators because of their migrating tendencies. A channel threading through a bar formation is especially difficult to navigate and is costly to maintain.

19. Salinity Intrusion. Salinity intrusions in a waterway are caused by the difference in densities of the ocean salt water and fresh-water inflows. The dissolved salts in the ocean water have several effects on the sediment-deposition characteristics of a waterway. Upstream density currents at the bottom may cause sediment to deposit to form a shoal at a location not anticipated from the waterway geometry, whereas salt-water flocculation of suspended sediments may induce shoaling in areas some distance downstream of the point of salinity intrusion. As a consequence of waterway improvements, changed tidal currents and the introduction of more salt water may disturb delicate balances of salinity which affect valuable marine fisheries and may cause contamination of fresh-water supplies. The intrusion of salt water into fresh-water areas may permit access of marine borers to waterfront structures. The factors bearing on salinity intrusions are the tidal characteristics of the waterway, its geometry, and the fresh-water runoff entering the tidal estuary. Major channel enlargements may change vertical density gradients or the tidal regimen to increase salinity intrusion. Alteration in the fresh-water inflow, as, for example, by storage or diversion from or to a waterway, may significantly alter the salinity regimen with resultant modification of the pattern and volume of shoaling.

20. Dispersal and Flushing of Pollutants. In recent years the possibilities of dispersing and flushing pollutants have gained recognition in studies to improve tidal waterways for navigation. It is conceivable that, under certain set conditions, there is a balance between the total load of pollutants and the regimen of a waterway such that serious objectionable conditions cannot develop but which, when altered by changes in the waterway or by modification of the fresh-water inflow, may increase or reduce concentrations of pollutants. For this reason, the characteristics of a waterway in relation to its ability to disperse and flush pollutants should be considered in planning waterway developments.

The extent to which each of the various technical factors discussed is likely to influence the plan of navigation improvement and channel maintenance must be evaluated using as a basis the results of hydrographic surveys, current observations, and sediment sampling adequate for the purpose. Studies should be made of the changes which have occurred over the years of record, particularly in the vicinity of the entrance. A comparison of available hydrographic maps covering an extended period of time may reveal natural progressive or cyclic changes which may bear on the plan of improvement. Consideration must be given as well to the public interests, construction methods, and availability of materials. Preliminary alternative plans should be prepared and compared economically.

A diversion channel may be practicable in some cases to divert upland sediment from a navigation channel or estuary. Diversion flows either may be carried around an important reach of the waterway or may be directed completely out of the waterway by providing a separate outlet to the sea. Such diversions may create undesirable conditions. For example, current velocities may be lowered in the estuary to the point of reducing its sediment-transporting capacity and transportation of sediment into the sea. Moreover, the lowering of ebb discharges due to the diversion of river flows may result in either a decrease or increase in the movement of material into the estuary from the sea, depending on the net change in bottom currents at the estuary entrance, causing corresponding changes in shoaling.

The improvement of an estuary entrance may be required to provide an enlarged or more stable entrance channel or to protect against wave action. New openings for estuaries and bays into the ocean may require jetties, sills, and sand-transfer plants to maintain the openings and preserve the adjacent shores. An investigation should be made of historical locations of the entrance and adjacent shorelines. Analyses are necessary to determine existing relations between estuary and entrance characteristics, river and tidal flows, wave action, littoral drift, and river sediment. The effects associated with modification of the natural entrance by stabilization, changes in cross section and alignment, or provision of jetties must be evaluated from these analyses. Jetties may be required to improve the natural depth and alignment of the entrance, to regulate the currents for the benefit of navigation, or to protect against wave action or shoaling by littoral drift. Jetties may be unnecessary if the optimum relations between the desired entrance channel and the tidal regime will assure a relatively stable channel which can be obtained economically by dredging.

Hydraulic-model tests are often required to evaluate the beneficial and detrimental effects of physical changes in a tidal estuary. Computation methods are sufficiently developed. Estuary models successfully integrate prototype tidal hydraulic variables and provide an understanding of phenomena not otherwise identifiable or solvable.

If model tests are necessary, extensive prototype data are needed for construction and verification of the model. Prototype observations should be made over a sufficient period to span a representative range of conditions.

21. Design of Navigation Channels. The objective in designing a navigation channel in an estuary is to meet the needs of the anticipated traffic. A ship forfeits open-water maneuverability when it enters a channel, and the navigator must be ever alert to the restrictions placed on his ship. Maneuverability is affected by configuration of the waterway, alignment and dimensions of channel, depth under keel, tidal fluctuations, currents, wave and meteorological conditions, buoyancy, steerage, and interference from other traffic. These problems have always confronted ship captains and pilots but they have been magnified by the trend toward larger and faster ships.

An improved navigation channel may significantly modify the regimen of a waterway, as in the case of a tidal river, or, in the case of a large estuary, induce very little change in existing tidal hydraulic conditions. If a channel is enlarged, sediment may deposit in the enlarged section and contraction works may be needed to prevent such deposits. Channel deepening modifies density current effects and thus affects shoaling in the saline region of the estuary, even though cross-sectional areas may be held constant by construction of contraction works. If practicable, the channel should be located to avoid areas which are most conducive to shoaling. In a relatively narrow waterway, widths between banks at natural cross sections where project depth exists will furnish a guide in estimating the widths required in reaches of deficient width to minimize shoaling.

22. Channel Depth. Channel depths several feet greater than the loaded static drafts of vessels using the waterway are required in order to ensure safe and economic navigation. On entering an estuary, a vessel will sink from 2 to 3 percent of its draft; depending upon the hull design and difference in sea and estuary water densities. A ship in motion will "squat," or lower, with respect to the bottom an amount depending on (1) the speed of the vessel through the water, (2) the distance between the keel and the bottom, (3) the trim of the vessel, (4) the cross-sectional area of the channel,

(5) whether the channel is located in a wide or narrow waterway, (6) whether the vessel is passing or overtaking another vessel, (7) the location of the vessel relative to the center line of the channel, and (8) the characteristics of the ship itself.

Current practice in designing channel depths requires a 2- to 4-ft allowance for sinkage, depending upon the relationship between the draft and width of the ship, project depth and width, speed and horsepower of the vessel, and restricted character of the waterway. Abnormally low tides may be 2 to 5 ft below mean low water datum but must occur with substantial frequency to require consideration in establishing the channel bottom. An allowance of 1 ft is usually made for vessel trim, and a nominal 2 ft for clearance under the keel will provide for maneuverability and reduce power demands. All these allowances are cumulative and are measured from mean low tide on the East and Gulf coasts, and mean lower low water on the West Coast. Additional depths of up to 8 ft have been provided across ocean bars to allow for wave-induced pitch, heave, and list or roll.

23. Channel Width. Some of the factors that must be considered in determining the proper width of a navigable channel are whether the design vessel must pass a similar or smaller vessel, the normal speed, current velocities and directions, wave action, wind, the depth of water under the keels, the dimensions available, and the composition of the bed and banks. In a restricted waterway, flow patterns created by vessel movement may result in strong reverse-flow currents, high value of squat, and severe scour and shoaling action, making steering difficult. The design width should be sufficient to ensure adequate control of ships that will use the waterway under expected conditions of ship speed, currents, and traffic.

When a vessel enters a navigation channel, not only is sea room sacrificed, but movements and controllability are affected to the extent that a vessel will frequently be moved from its course, particularly when ships pass each other. The effect of a passing vessel is to form an obstruction that accentuates the effects of a constricted channel. As two ships approach and meet, a high-pressure area between the bows tends to cause the ships to yaw away from each other. This action is followed by strong suction, which tends to draw the ships together. The maximum safe speed for two-way traffic is usually 30 to 40 percent less than for one-way traffic in the same waterway.

There is no formula that takes into account all the preceding diverse factors. However, the procedures for the determination of widths for the proposed Panama Sea-Level Canal are useful for making a first approximation of the channel width required for any given waterway.

The first step is the determination of the width of the maneuvering lane. This is defined as that portion of the channel within which the ship may deviate from a straight line without encroaching on the safe bank clearance or without approaching another ship so closely that dangerous interference between ships will occur. On the basis of the Sea-Level Canal tests, it was determined that the width of the maneuvering lane should be 160, 180, and 200 percent of the beam for vessels of very good, good, and poor controllability, respectively. In waters where the currents are at an angle to the channel, or where wave action and strong winds tend to cause the vessel to yaw, the maneuvering-lane width may need to be increased to accommodate the oscillations of the vessel. The width of maneuvering lane for yaw is determined by the length of the vessel and the angle of yaw.

In channels having two-way large-vessel traffic, a ship clearance lane must be provided between the two maneuvering lanes. It is taken to be the distance between the inner boundaries of the maneuvering lanes, as the ships could be in this position during the passing operation. Both vessels are subjected to bank suction and the interaction between the vessels. Model tests made during the Sea-Level Canal investigations revealed that the clearance lane should be equal to the beam of the larger vessel. A minimal clearance lane amounting to 80 percent of the beam of the larger vessel might be provided when the navigation channel is located in a wide estuary, well buoyed, and not subject to strong currents or yawing forces.

The width of the bank clearance line depends on the equilibrium rudder angle; width and depth of the channel; speed of the vessel; strength and direction of currents,

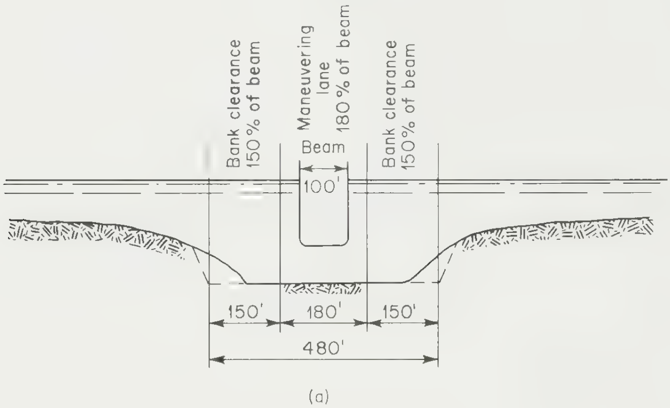

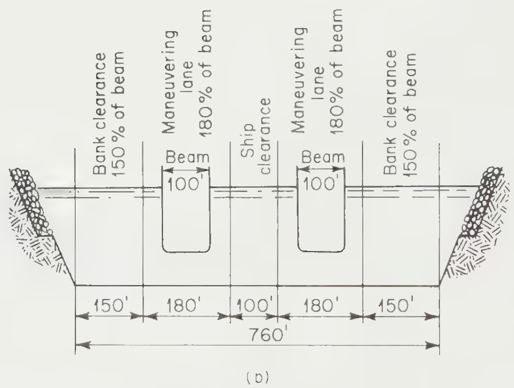

Fig. 20. Elements of channel width. (*a*) Vessel handles satisfactorily. Normal cruising speed in this channel is 8 knots, relative to bottom. Partially restricted channel. Frequent shoaling along edges. Material beyond channel limits is silty. Strength of current 2 knots. Current flows parallel with channel. Moderate to strong winds at an angle to channel occur frequently. (*b*) Vessel handles satisfactorily. Normal cruising speed in this channel is 5 knots, relative to bottom. Fully restricted channel. Revetted banks. Strength of current 4 knots. Current flows parallel with channel. Strong winds rare.

winds, and waves; character of banks; and difficulty in determining the exact limits of the channel. A bank clearance, varying from 60 to 150 percent of the beam of the design vessel, is adopted, depending upon the severity of the controlling factors and the past experience of handling vessels close to banks under various conditions.

Bends are more difficult to navigate than straight reaches, primarily because the ship forms a tangent or secant to the curve and is positioned off center. The rudder and centrifugal force on a vessel making a sharp turn tend to displace the stern to a path well outside of the bow. The width of the ship's path around a curve is a function of the deflection angle that the ship makes with the curve.

The total width of the channel is measured at the bottom of the bank slope at the design depth. Applying the criteria presented here to a tanker 733 ft long and with a beam of 100 ft under the conditions shown in Fig. 20 results in the channel widths shown in Table 3.

TABLE 3. CHANNEL WIDTHS IN STRAIGHT REACHES AND TURNS
Design vessel is 100- by 733-ft tanker

Channel element	Channel width, ft					
	One-way traffic			Two-way traffic		
	Straight channel	26-deg turn	40-deg turn	Straight channel	20-deg turn	40-deg turn
Bank clearance	150	150	150	150	150	150
Maneuvering lane	180	370	440	180	370	440
Ship clearance	...	...	...	100	100	100
Maneuvering lane	...	...	...	180	370	440
Bank clearance	150	150	150	150	150	150
Total	480	670	740	760	1,140	1,280
Increase for turn	...	190	260	...	380	520

24. Channel Alignment. The overriding requirement for channel alignment is that all vessels expected to use the channel be able to navigate it with reasonable safety under adverse conditions of tide, current, and wave and wind action. The alignment should be as straight as practicable, have easy curves, and be aligned to conform approximately with dominant current movements. The minimum permissible radius of curvature at bends is governed by the turning characteristics of the least maneuverable ship.

The maximum practical radius of curvature consistent with the natural channel alignment should be adopted, but in no case should the minimum radius of curvature of a deep-draft channel be less than approximately 5,000 ft. The Houston Ship Channel was constructed originally with a minimum radius of curvature of 3,000 ft, but because of the difficulty experienced by large vessels in the sharp bends, the minimum radius of curvature has been increased to 5,730 ft. Although a straight channel has the advantage of being the shortest route, experience has shown that man-made straight channels often prove difficult and expensive to maintain. Incorporation of the natural alignment of a waterway to a practical degree can reduce or concentrate shoaling areas with resulting minimum maintenance costs.

Critical locations for a ship navigating a channel are at the ocean entrance, bridges, approaches to locks, barriers, and control structures. Here straight approaches, long enough for vessels to become properly aligned, are generally the safest for navigation. While a straight entrance channel parallel to the resultant of current and wave forces is safest, shoaling influences frequently require an adjusted alignment to obtain the most economic maintenance.

25. Channel Currents. Current velocities not only affect shoaling but also are a major consideration in safety of navigation and channel design. The maximum current velocities in deep-draft restricted channels are generally under 6 knots but never more than 10 knots because of the reduced maneuverability of oceangoing vessels in constricted channels at reduced speeds.

26. Training Walls and Contraction Dikes. Training walls and contraction dikes are structures which sometimes can be constructed economically to produce or assist in establishing self-maintaining sections of desired depth in navigation channels. Training walls are constructed approximately parallel to the channel, with the wall becoming the new shoreline, whereas contraction dikes are located nearly perpendicular to the existing shoreline.

The principal consideration in designing a training wall is to ensure its stability against wave attack, foundation erosion by tidal or river currents, and any possible loading behind the wall. Contraction should be used when the reduction in waterway width is relatively large, the shoal area is quite long, and foundations are not favorable to wall construction. The dikes, which usually are constructed of stone or wood or steel piling, should be permeable in some cases to produce a milder overall effect on the natural regimen of the waterway in which the harbor is located. As reliable design criteria are not available for determination of the most effective and economic system of contraction dikes, model tests should be conducted for major projects to establish the best plan of contraction works.

BREAKWATERS AND JETTIES

27. Definitions. A breakwater is defined as a structure employed to reflect and dissipate the energy of the approaching waves, thereby preventing or reducing wave action shoreward. Breakwaters for navigation purposes are constructed to create sufficiently calm waters for safe mooring, operating and handling of ships, and the protection of shipping facilities. A jetty is a structure extending into a body of water to direct or confine stream or tidal flow through selected channel limits to prevent or reduce shoaling within the channel, or to interrupt alongshore littoral drift to prevent its shoaling the channel.

28. Types. Some of the commoner types are:

Rubble Mound. This type, shown in Fig. 21, consists of an interior section, or core, of assorted sizes of stone, gravel, or other durable material, protected by one or more courses of larger, angular-shaped stone or manufactured concrete components. In areas where larger stone for the primary cover layer is not available economically, concrete tetrapods or tribars may be used, as shown in Figs. 22 and 23, respectively.

Composite. A composite structure is a combination of two or more specific types. The commonest consist of monolithic walls placed on underwater rubble mounds. The

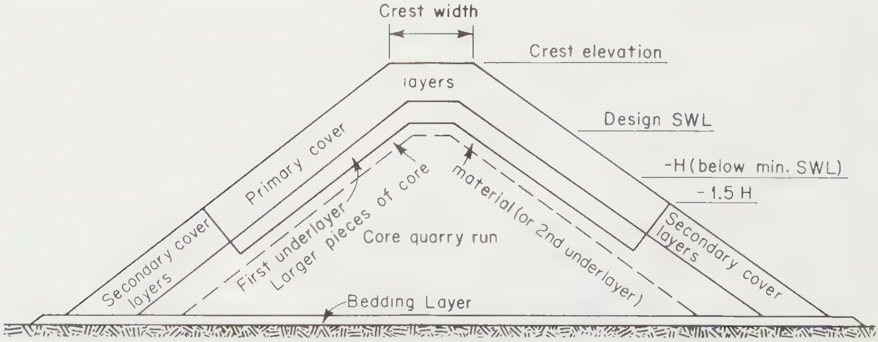

Fig. 21. Typical rubble-mound breakwater section.

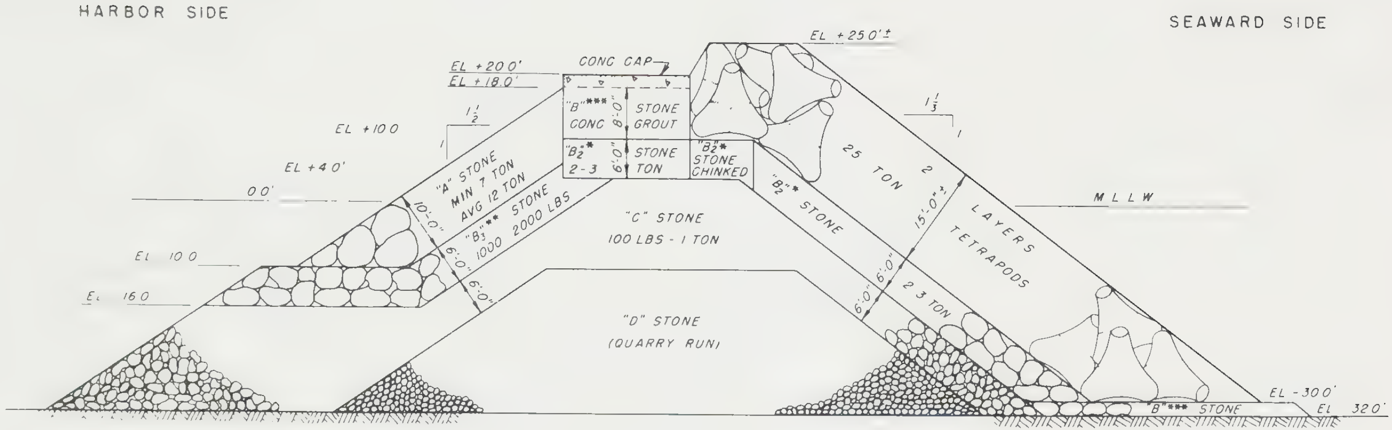

* "B_2" - ONE TON VARIATION TO 7 TON MAXIMUM

** "B_3" - ½ TON TO 1 TON MINIMUM - 7 TON MAXIMUM AS AVAILABLE

*** "B" TON TO 7 TONS OR TO SUIT DEPTH CONDITIONS AT SEAWARD TOE

FIG. 22. Typical tetrapod cross section of outer breakwater.

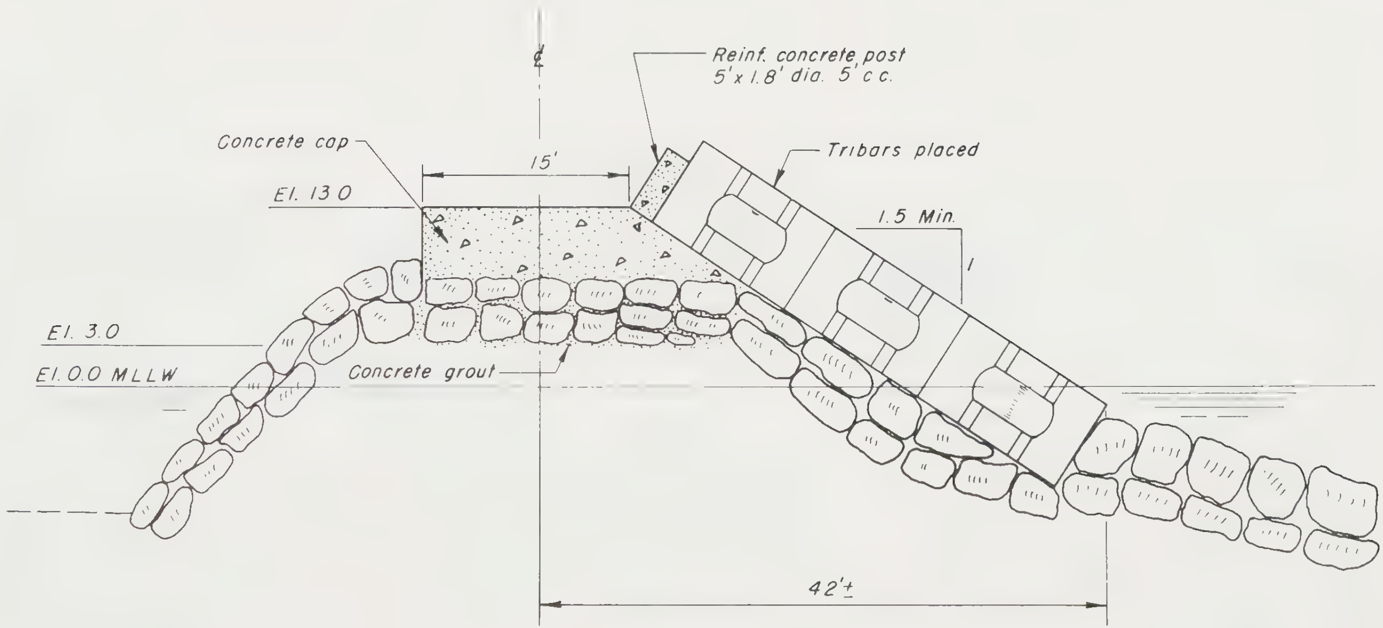

Fig. 23. Typical section, breakwater trunk using tribars.

rubble mound may be used as a foundation for the wall or as a main structure surmounted by a wall superstructure with a vertical or inclined face.

Concrete Caisson. A caisson structure is one of reinforced-concrete shells which are floated into position, settled upon a prepared foundation, filled with stone or sand to provide stability, and then capped with concrete slabs or stone. Generally, it is necessary to place riprap along the toe of the structure to prevent tilting or overturning due to scour.

Steel Sheetpiling. Steel sheetpiling is used to a great extent on the Great Lakes. In saline water it is subject to a high rate of corrosion. In deeper water, where the waves are high, the piling is used to form cells which may be filled with stone or sand. In shallow water and for shore connections to cellular construction, it is often used as a cantilever wall.

Mobile. A mobile breakwater is one which can be readily transported to the site, can be rapidly installed, and is capable of ready removal and transportation to another location for further use. Various types of mobile breakwaters, such as floating bulkheads, floating logs, pneumatic and hydraulic jets, have been tested in laboratories. The tests indicated significant attenuation for very short-period waves, but not for long- or medium-period waves. There are severe anchoring problems with floating breakwaters, and the pneumatic and hydraulic types have large power requirements.

29. Design of Breakwaters and Jetties. In laying out breakwaters and jetties, careful study must be given to the direction and strength of tidal currents and the proper siting and spacing to provide the channel section needed for navigation. Breakwaters must be aligned to restrict energy propagation into the harbor to the maximum degree. Jetties should be aligned so that the channel will be controlled in the position and direction corresponding with the natural tidal flow. The spacing should be great enough to give sufficient entrance width to minimize undermining and admit the flood tides so that the tidal prism will not be materially reduced. Care should be taken in locating the entrance so that areas of peak wave height will be avoided. Wave refraction and diffraction studies should be utilized in locating a harbor entrance and aligning the structures. Wind-generated waves produce critical forces for which breakwaters and jetties are designed.

In the analysis of the forces exerted on structures by waves, a distinction is made between the action of nonbreaking waves, breaking waves, and broken waves. Structures located in an area or zone in which waves will break directly on the structure are designed to withstand greater forces and moments than those which will be subjected only to broken waves. Wave characteristics are determined, first, for deep water, and then extended by computations shoreward to the structure. The stability and height of a computed wave at the structure will be dependent on the controlling water depth at the structure. Wave computations are generally made for the significant wave height; which is a statistical value equal to the average height of the one-third highest waves of a deep-water train. This value is used for rubble-mound design. For structures which may withstand some racking without damage, the 10 percent highest wave of the train is used. For rigid structures, the 1 percent highest is used.

To determine the wave force of a nonbreaking wave attacking a vertical wall, the Sainflou theory is used. This is a diagrammatic method of determining wall pressure based on the hydrostatic pressure occurring from the formation of a clapotis (standing wave) twice the height of the impinging wave.

Pressure caused by a breaking wave varies widely with the shape of the wave as it breaks upon the structure. The Minikin theory assumes breaking with an entrapment of air beneath the forward-bending crest of the wave. While there are limitations on the accuracy of the computations, this method is generally used to determine breaking-wave pressures. According to Minikin, the maximum dynamic pressure is concentrated at still-water level and is given by

$$P_m = \frac{101 H_b w}{L_D} \frac{d}{D} (D + d)$$

where P_m = maximum pressure; H_b = height, ft, of wave breaking on the structure; w = unit weight of water, lb/cu ft; d = depth of water, ft, at the structure; and D and L_D = deeper water depth and wave length, ft, respectively.

As studies have not been made to relate forces due to broken waves to the various wave parameters, pressures caused by broken waves are quite difficult to determine. For example, if a wave breaks close enough to a structure, some dynamic energy may be transmitted to the structure and the pressure would be related to the incident velocity and the run-up on the structure. In most cases, greater force would be caused by a smaller wave breaking at the structure than by a larger wave breaking seaward thereof. A rubble-mound breakwater is composed of random-shaped and random-placed stones, protected by cover layers of selected stones. To obtain sufficient porosity and protect against piping, stone sizes should be reduced about 10 percent by weight in succeeding layers.

When short-period waves impinge upon rubble-mound structures, they may break completely, projecting a jet of water approximately perpendicular to the slope, break partially with a poorly defined jet, or establish an oscillatory motion of the water particles up and down the structure slope, similar to the motion of a clapotis at a vertical wall. Thus, it can be seen that, when waves attack a rubble-mound structure, the resulting interplay of forces developed by the wave-induced water motion and the resisting action of the armor units is extremely complex. Attempts to determine by theoretical analysis the stability characteristics of these structures, when under attack by storm waves, have not been successful. Empirical methods have been developed, however, which give satisfactory results if properly employed.

The weight or size of the armor units, side slopes, density of armor material, and degree of interlocking between units are all interrelated and comprise the principal factors to be considered in the design of a rubble-mound structure. The following equation used in determining the weight of the armor units for a rubble-mound structure was developed by Robert Y. Hudson of the U.S. Army Waterways Experiment Station:

$$W_r = \frac{\gamma_r H^3}{K_\Delta (S_r - 1)^3 \cot \alpha}$$

where W_r = weight of armor unit, lb; γ_r = unit weight of armor unit, lb/cu ft; H = design wave height, ft; S_r = specific gravity of armor unit relative to water in which unit is situated, $S_r = \gamma_r/\gamma_w$; γ_w = unit weight of water; α = angle of breakwater slope, deg from horizontal; and K_Δ = coefficient that varies primarily with shape of units, roughness of surface, sharpness of edges, and degrees of interlocking.

The slope of the cover layer will partly be determined on the basis of the sizes of stone economically available. Generally, a cover-layer slope steeper than 1 vertical to 1.5 horizontal is not suitable as this slope approaches the angle of repose of the stone. Recommended average values of K_Δ, based on model tests and limited prototype verification, are given in Table 4.

The core of the rubble-mound breakwater or jetty should be highly impervious, which is accomplished by using a well-graded mixture of quarry-run stone. The stone sizes of the core and underlayers may be varied to use a greater percentage of the quarry production, thereby reducing costs.

The core height is an important feature in breakwater design. If the core is too low, excessive energy may be transmitted through the breakwater, causing damaging

TABLE 4. AVERAGE K_Δ VALUES

Armor	Breakwater location and type of wave attack*			
	1	2	3	4
Rounded stone, 2 layers, pellmell	2.6	2.5	2.4	2.0
Rough stone, 2 layers pellmell	3.5	3.0	2.9	2.5
Rough stone, 2 layers, placed†	5.5	5.0	4.5	3.5
Tribars, 2 layers, pellmell	10.0	8.5	7.5	5.0
Tribars, 1 layer, uniform	15.0	12.0	9.5	7.5
Tetrapods, 2 layers, pellmell	8.5	7.5	6.5	4.5
Quadripods, 2 layers, pellmell	8.5	7.5	6.5	4.5

* 1. Trunk, nonbreaking waves. 2. Trunk, breaking waves. 3. Conical head, nonbreaking waves. 4. Conical head, breaking waves.

† Good placement with long axis of stone placed normal to the structure face.

waves to be re-formed within the harbor. At Redondo Beach–King Harbor, California, 16 to 21 percent of the incident wave energy passed through and over the breakwater, which has a top-of-core elevation of -10 ft MLW, with a still-water elevation of $+7$ ft MLW. In areas of severe wave action, the construction of the core to excessive height may cause a weakness in the cover layer on the sheltered side. This is caused by concentration of transmitted energy across the top of the core, placing back pressure on the cover stone. In such cases, the cover layers may slide en masse down the back slope. Proper core elevation may be determined by small-scale investigation in a wave flume.

The breakwater crest height is a function of the incident wave-height run-up and allowable overtopping. Wave run-up can be computed by methods described in Ref. 10. The crest width is a function of stability, stone size, amount of overtopping, and method of construction. If the construction equipment must operate from the crest, the crest must be of sufficient height and width for safety of the equipment. For stability in areas of severe wave action, the crest width should generally be sufficient to contain three capstones, but never fewer than two.

The foundations for breakwaters and jetties may require special treatment as wave forces acting against these structures may attack the natural bottom. Unless the structure is sited on rock, a bedding layer of small stone should be used. The gradation of this layer depends on the natural bottom material, but usually quarry spalls will suffice. The bedding layer should extend at least 5 ft beyond the toe of the structure and should not be thinner than about 2 ft in exposed areas.

Breakwater stone should be durable and preferably have a high specific gravity. Characteristics that affect durability are mineral composition, texture, structure, hardness, toughness, and resistance to disintegration on exposure to wetting and drying and to freezing and thawing. Where local stone is markedly inferior, the greater cost of bringing in durable, high-quality stone from outside the immediate area may be justified and advisable. Because of the wide range in climatic conditions in different regions of the United States, acceptable standards of durability for the regions will vary widely.

Bibliography

1. *Trans. ASCE*, **114**, 53, 1949.
2. WILSON, LT. GEN. W. K., JR., LT. COL. IRA HUNT, CHARLES E. LEE, and J. PORTER TAYLOR, "Recreational Craft—A Burgeoning Problem," 21st PIANC Conference.

3. Lee, C. E., Recent Advances in Coastal Structure Design, *Proc. 8th Conf. Coastal Eng.*
4. Sainflou, M., "Essay on Vertical Breakwaters," translated by C. R. Hatch.
5. Minikin, Robert C., "Wind, Waves and Maritime Structures," Charles Griffin & Company, Ltd., London, 1950.
6. Lee, C. E., On the Design of Small Craft Harbors, *Proc. 9th Conf. Coastal Eng.*
7. "Evaluation of Present State of Knowledge of Factors Affecting Tidal Hydraulics and Related Phenomena," Corps of Engineers, Committee on Tidal Hydraulics *Report* 3.
8. Crook, L. T., and A. J. Moors, Criteria Used in the United States in Planning New Inland Waterways and in Reconstructing Existing Waterways, 21st PIANC Conference.
9. Douma, J. H., Engineering Problems in U.S. Tidal Waterways, *Proc. ASCE*, **81,** paper 789.
10. "Shore Protection Planning and Design," Beach Erosion Board (now U.S. Coastal Engineering Research Center) *Technical Report* 4.
11. "Design of Breakwaters and Jetties," Engineering Manual, U.S. Corps of Engineers.
12. Abbett, R. W., "American Civil Engineering Practice."
13. "Symposium on Channel Stabilization Problems," *Technical Report* 1, Corps of Engineers, Committee on Channel Stabilization.
14. Davis, J. P., M. E. Nelson, and R. E. Patton, "United States Development of Hydraulic and Structural Designs for Locks," 21st PIANC Conference.
15. "Navigation Locks," Engineering Manual, Corps of Engineers.
16. Brown, E. I., Flow of Water in Tidal Canals, *Trans. ASCE*, **96,** 1932.
17. Pillsbury, G. B., "Tidal Hydraulics," rev. ed., Corps of Engineers, May, 1956.
18. Dronkers, J. J., and J. C. Schonfeld, Computation of Tides and Currents, *Proc. ASCE*, **81,** 1955.

SECTION 32

NAVIGATION LOCKS

BY GEORGE R. RICH

INTRODUCTION

From the standpoint of the hydraulic engineer determination of proportions for filling and emptying systems is the principal problem in the design of navigation locks. The fundamental difficulty is to reconcile two conflicting requirements: (1), that the lock fill quickly, in the order of 12 to 15 min, to avoid penalizing traffic and (2), that the resultant disturbance in the lock chamber not be sufficient to cause dangerously high hawser stresses with the attendant possibility of breaking a ship from its moorings so as to collide with and wreck the main lock gates.

Owing principally to the effect of the ship in lockage upon the subdivision and partial reflection of the regimen of translatory waves, by means of which filling of the chamber is effected, the practical problem of filling system design is not susceptible to complete and final determination by analytical methods alone, but confirmation must be obtained by the familiar process of reduced-scale model tests in the hydraulic laboratory. However, it would certainly be a mistake to infer that analytical methods have no place in lock design. By isolating certain of the major controlling elements and studying them separately, we establish a more rational and effective basis for trial designs and obtain incisive tools for the planning and interpretation of model tests.

The fundamental physical action in lock-filling systems affords still another instance of wave motion with respect to both water hammer in the conduits and waves of translation, which, as previously noted, constitute the mechanism by which filling of the chamber is accomplished.

For reasons that will appear during the course of our discussion, slow opening or closing of the lock valves is essential to ensure quiet lockage. Accordingly, the hydraulic design of the filling conduits may be treated as a mass-acceleration problem, *i.e.*, stretching of the conduit walls and compression of the water may be disregarded without appreciable error because the magnitude of the sub and superpressures due to water hammer is not significant. The objective in conduit design is primarily to ensure that the filling time is satisfactorily short.

The translatory action in the chamber, while not affecting to any perceptible extent the hydraulic action of the filling conduits, will be found to measure the degree of disturbance to the vessel in lockage; and although the presence of this vessel does complicate all but the initial stages of the wave regimen, the analytical approach is valuable in affording us improved insight into the causes of excessive hawser stress. This second coordinate part of the basic problem has as its objective the insurance that disturbance to the vessel in lockage, as measured in the hydraulic laboratory by model hawser stresses, will not be objectionably great.

We have solved the entire problem completely when an economic and physical balance is effected between these two fundamental but somewhat conflicting tendencies.

BASIC MECHANISM OF LOCK CHAMBER FILLING

When water is admitted to or released from the lock chamber by any of the generally accepted filling systems, the mechanism immediately responsible for the actual change in water surface elevation is a procession of translatory waves traversing the length of the chamber. Before proceeding to the analytical expression of the pertinent physical laws, we may find it helpful to obtain in advance some intuitional introduction from the simplified apparatus depicted in Fig. 1.[1] The lock chamber is rectangular in form and the filling device consists simply of an orifice controlled by a rectangular valve. For the initial case it will be assumed that there is no ship in the chamber and that the lock valve is opened instantaneously.

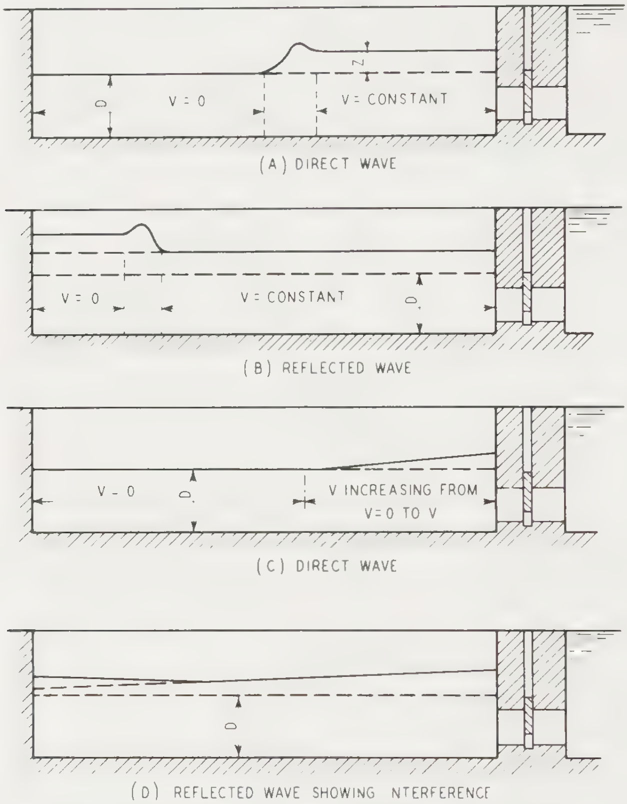

Fig. 1. Action of translatory waves in filling lock chamber.

We should then observe a definite intumescence on the water surface propagated with comparatively slow, readily followed velocity in the direction of the lock gates. As shown by the diagram, the velocity in the chamber behind the wave would be converted from zero to the value V. Upon reaching the lower gate the wave would be reflected in the opposite direction, increasing the depth in the chamber by a second increment and reconverting the chamber velocity behind the wave from V to zero. In other words, the head increments are reflected at the ends of the chamber with positive algebraic sign, and the velocity increments with negative algebraic sign.

[1] Rich, George R., Basic Hydraulics of Water Storage Projects, *Civil Eng.*, August, 1944, p. 352.

Now it is readily apparent that, if a ship were placed in lockage under such conditions, it would be driven with considerable violence first in the direction of the lower and then in the direction of the upper lock gates by an unbalanced force proportional to the crest height Z.

Our natural impulse is to alleviate such adverse conditions by substituting a slow uniform valve motion for the sudden opening employed initially, and we should then observe the marked improvement indicated by Fig. 1(C) and 1(D). In the first place the water surface exhibits, instead of the vertical-faced bore wave, a relatively flat slope with very beneficial interference effects subsequent to the first reflection. The unbalanced force now acting upon the vessel is greatly reduced in magnitude and the

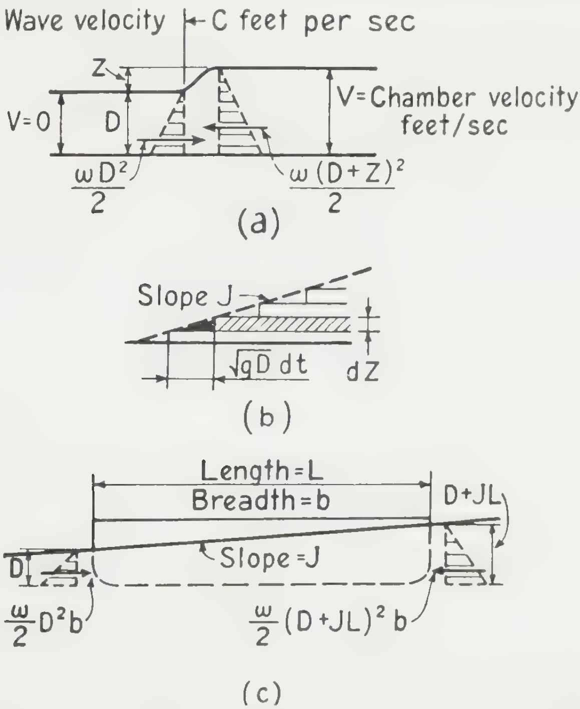

FIG. 2. Development of unbalanced force on ship in lockage.

ship motion, although still in the nature of a characteristic longitudinal shuttling, is markedly decreased in frequency. Obviously slow uniform valve motion is one of the prerequisites of quiet lockage.

But, by means of Fig. 2, we can place this entire matter upon a much firmer foundation than mere intuition. We first obtain the familiar equation for wave velocity C by means of the momentum equation: In every second the passage of the wave changes the velocity of a mass of water $\frac{w}{g} C(D + Z)$ from zero to V, through the action of the unbalanced force $\frac{w}{2} [(D + Z)^2 - D^2]$, or

$$Ft = M(V - 0) \tag{1}$$

$$\frac{w}{2} [(D + Z)^2 - D^2] \times 1 = \frac{w}{g} CV(D + Z) \tag{2}$$

In addition, from considerations of hydraulic continuity, the quantity of water per unit width of chamber and above the dotted line, Fig. 1(*a*), is CZ. But this must be continuously supplied by flow over the entire chamber cross section behind the wave in amount $(D + Z)V$, or

$$CZ = (D + Z)V \qquad \text{or} \qquad Z = \frac{DV}{C} \tag{3}$$

Combining Eqs. (2) and (3) and noting that in the cases we shall encounter Z is very small in proportion to D, we obtain

$$C = \sqrt{gD} \tag{4}$$

Figure 2(*b*) will enable us to express the relationship between the surface slope and the chamber velocity and acceleration.

For a vertical front wave,

$$Z = \frac{(D + Z)V}{\sqrt{gD}} = \frac{DV}{\sqrt{gD}} \tag{5}$$

In addition, we may reason that the sloping surface in the chamber is in reality the envelope curve of a series of differential vertical-front waves each of height dZ, and that in time dt each differential wave travels a distance $\sqrt{gD}\,dt$, since the velocity of propagation is $\sqrt{gD}$. From the geometry of the figure, the slope at any instant is

$$J = \frac{dZ}{\sqrt{gD}\,dt} \tag{6}$$

But from Eq. (5)

$$dZ = \frac{D\,dV}{\sqrt{gD}}$$

Substituting in (6),

$$J = \frac{1}{g}\frac{dV}{dt} \tag{7}$$

For the slope in terms of the chamber flow Q we write

$$Q = bDV, \qquad dV = \frac{dQ}{bD}, \qquad \text{and} \qquad J = \frac{1}{gbD}\frac{dQ}{dt} \tag{8}$$

Finally, by means of Fig. 2(*c*) let us determine the quantitative relationship between the unbalanced force on the ship and the slope of the water surface in the chamber:

$$\text{Unbalanced force on the ship} = \frac{wb}{2}(D^2 + 2DJL + J^2L^2 - D^2)$$

or, since J^2L^2 is a small quantity of secondary order,

$$\text{Unbalanced force} = wLbDJ \tag{9}$$

But the ship displacement is with sufficient accuracy for small values of slope,

$$wLbD = K \tag{10}$$

or

$$\text{Unbalanced force} = KJ \tag{11}$$

and substituting J from Eq. (8),

$$\text{Unbalanced force} = \left(\frac{K}{gbD}\right)\frac{dQ}{dt} \tag{12}$$

The presence of a vessel in the lock will naturally effect a subdivision and reflection of the elementary wave motion upon which these simple equations are predicated, and engineers who are sufficiently interested can pursue the details further in the literature.[1] However, upon detailed examination we should find that these additional refinements introduce no point of conflict with the deductions we shall now make solely upon the basis of the simple parent equations. The implications of Eqs. (7), (8), (11), and (12) really constitute the fundamental principle of ship lockage: To secure the flat slope of chamber surface essential for quiet filling, the initial opening of the lock valves should be very small, and the discharge into the chamber should increase during the earlier stages of filling and decrease during the later stages of filling at a slow uniform rate.

From Eqs. (7) and (8) we also derive a second conclusion of far-reaching importance: The filling conduits may be made of large cross-sectional area since no limitation from the standpoint of quiet lockage is imposed upon the magnitude of the chamber velocity or flow. Only the acceleration dV/dt or dQ/dt need be kept small to ensure flat surface slopes. For the very high lifts in which impulse effects of the inflow are of important magnitude, the larger conduits also tend in the direction of reduced velocities and reduced impulse forces. Aside from this consideration of provision for baffling to avoid excessive impulse forces at the very high lifts, there is no valid objection to designing filling conduits to function as short loops of large cross-sectional area located entirely in the gate blocks, and dispensing with the port and lateral systems frequently installed in the side walls.

Our first natural objection to a slow valve opening rate is that the increased time required for filling and emptying the chamber would penalize traffic. However, owing to the fact that we use conduits of relatively great cross section in conjunction with slow valve motion, we are able to regain practically all of this time. During the later stages of filling, when the available head difference is comparatively small, conduits of large cross section enable us to carry large discharges even at the lower velocities.

Finally, we draw a very important general deduction from Eq. (3) which states the wave increment height:

$$Z = \frac{DV}{C} \tag{3}$$

But

$$V = \frac{\beta\sqrt{2gh}}{bD}$$

in which h is the head difference at any instant.

Substituting in (3) we obtain

$$Z = \frac{D\beta\sqrt{2gh}}{bD\sqrt{gD}} = \frac{\beta}{b}\sqrt{\frac{2h}{D}} \tag{13}$$

From Eq. (13), we conclude that the filling operation rather than the emptying process imposes the heavier burden upon the lock design, for the reason that at the start of filling the chamber depth is much lower than at the start of emptying.

The chief value of the foregoing equations and discussions is to afford us an insight into the basic hydromechanics of lockage, so that we may select the type of filling system best adapted to the exigencies of each particular lock. We shall probably never have occasion to employ the formulas given for the numerical computation of hawser stress, as these are determined with comparative ease and greater dependability as a part of the laboratory model tests to confirm the hydraulic design of the filling

[1] Rich, George R., The Hydromechanics of Ship Lockage, *Military Engr.*, July–August, 1932, pp. 364–369.

conduits. With a clear understanding of the mechanism of filling in the chambers, we may now proceed to develop the basic principles of design of the various forms of filling conduits for admitting water to the chamber.

TYPES OF LOCK-FILLING SYSTEMS

From the many arrangements that have been used as a means of controlling the admission of water to the lock chamber, three types have been selected to illustrate

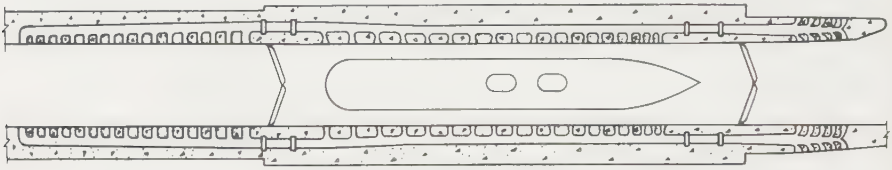

Fig. 3. Longitudinal filling conduits with lateral ports, Kentucky project, TVA.

the fundamental principles of design: The first type, which has found outstanding favor in American practice, is illustrated by Fig. 3 and consists basically of main longitudinal header conduits in the side walls of the lock with numerous short lateral ports delivering discharge to the chamber. No doubt the aim of the originators of that scheme was to distribute the inflow uniformly over the entire chamber and thus

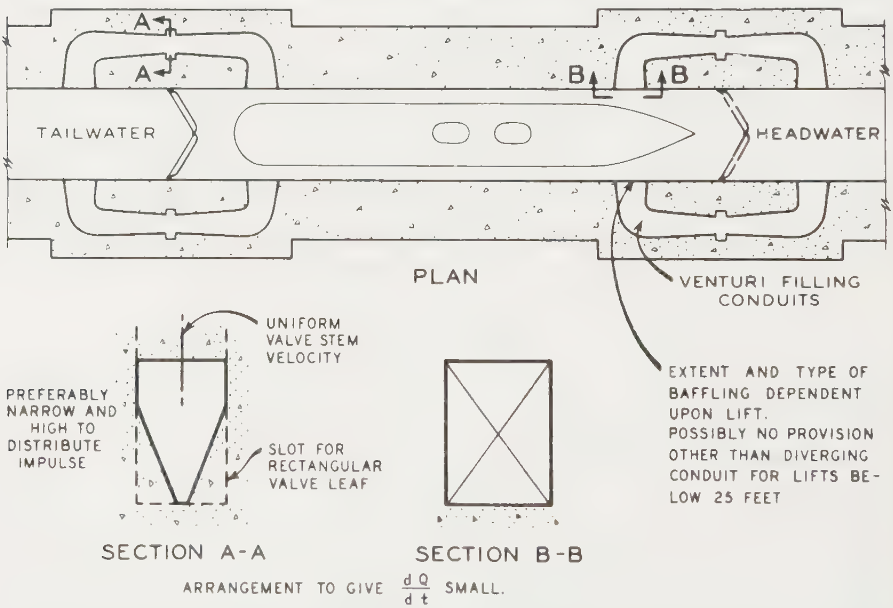

Fig. 4. Venturi-loop conduit filling system.

eliminate what they believed to be the principal source of disturbance to the vessels in lockage. But as will be shown analytically in the course of our subsequent discussion, owing to the influence of the inertia of water in the conduits and the effect of contraction at the port connections, uniform port spacing does not afford anything like uniform discharge. In fact, in the latest examples of this type of design we have the rather anomalous incorporation of marked variation in port spacing to effect the requisite degree of freedom from turbulence. In the light of the best modern theory,

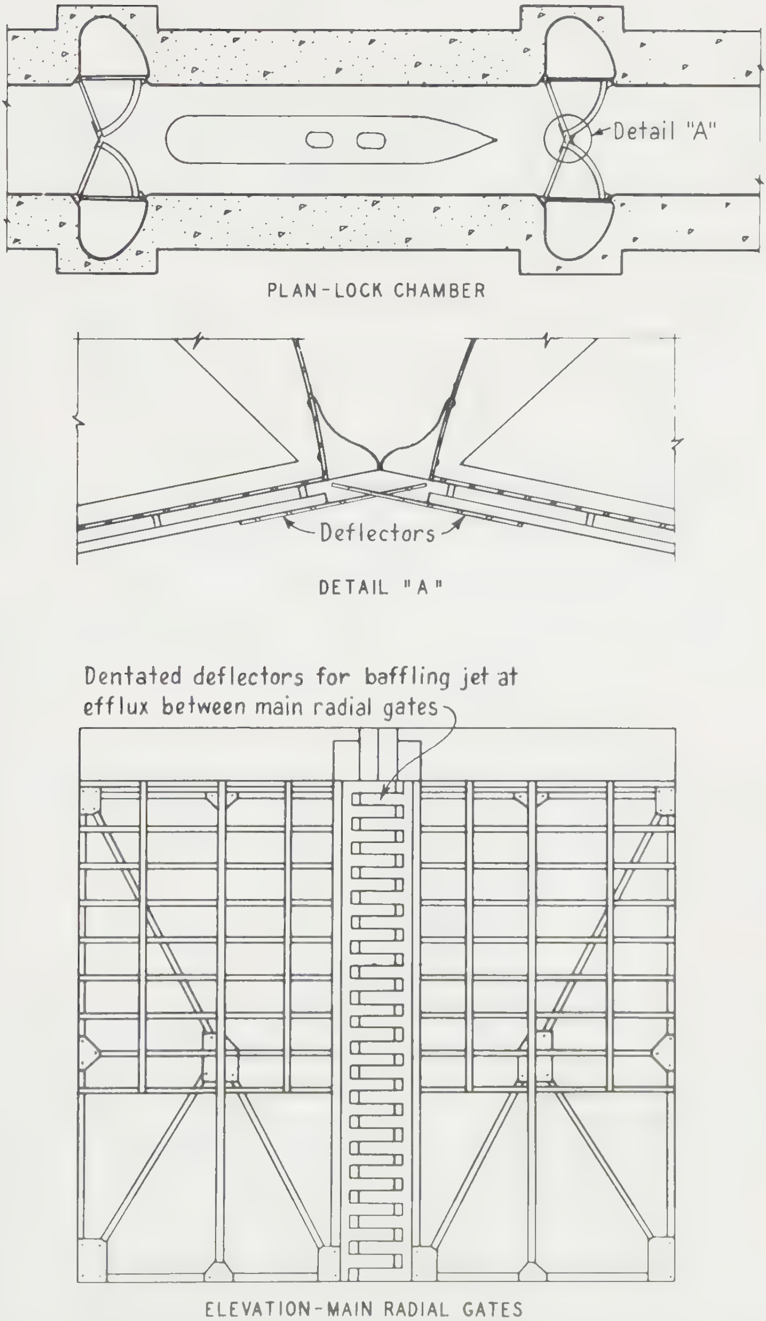

FIG. 5. Filling chamber by cracking main radial lock gates, Passamaquoddy project.

the longitudinal culvert and lateral port arrangement finds its principal justification as a device for baffling the impulse effects of the inflowing discharge, which reach serious proportions in high-lift installations.

For lifts of moderate height (15 to 35 ft), European practice favors the selection of the so-called Venturi-loop filling system (Fig. 4) located entirely in the terminal masonry sections of the lock structure. In the opinion of the author, this type represents the best utilization of scientific principles and deserves more widespread adoption in America. It may be the means of effecting sizable economies in side-wall construction, particularly in the lower medium head range, where it permits the use of sheet piling for side walls, eliminating the necessity for a cofferdam during construction.

The loop principle also permits ready incorporation of the basic requirements for quiet lockage. By employing a trapezoidal cross section at the valves, we obtain the desired small initial valve opening, and by using flared conduits of large cross-sectional area we materially reduce the impulse forces resulting from the velocity of inflow into the chamber. A second advantage of the Venturi construction is that it operates to reduce the size and expense of lock valves.

For lifts in the low-head range, 15 ft or lower, the most advantageous method of admitting water is by cracking the main lock gates (Fig. 5). This is accomplished by imparting a very slow steady initial opening rate to the main gate drive, and after filling is accomplished the mechanism automatically increases the gate opening speed to normal. Some rudimentary form of baffling device, such as indicated, will be found advantageous in reducing disturbances to the vessel in lockage.

The literature abounds with many intermediate variations of the three foregoing fundamental types, but all the principles necessary for their execution will be found embodied in the material to be presented in subsequent paragraphs.

FILLING SYSTEM AS AN ORIFICE

In making comparisons of trial designs, it is of the greatest usefulness to have a simple rapid means of arriving at reasonably close proportions of the various competing types. In practice this is accomplished by means of assigning representative discharge coefficients to various classes of filling systems and then making the computation on the basis of the simple orifice law. The following coefficients are a fairly representative average:

System	Discharge Coefficient[1]
Longitudinal conduit and lateral ports	0.85–0.95
Short Venturi loops	0.75–0.85
Cracking main lock gates	0.80[2]
Simple rectangular orifices	0.60–0.80

[1] RICH, GEORGE R., Hydraulics of Lock-filling Systems, *Military Engs.*, January–February, 1933, pp. 60–64.

[2] Based upon the area of water between the main lock gates at equalization of levels.

The analytical background for applying these discharge coefficients is simply the old school exercise of filling a rectangular tank under a diminishing head. We shall employ the following notation:

t = filling (or emptying) time, sec.
A = horizontal area of lock chamber, sq ft.
F = cross-sectional area of filling conduits taken at the valves.
h = head difference between lock chamber and upper pool at any instant, ft.
h_1 = lift, ft.
g = acceleration of gravity, ft/sec^2.
C = discharge coefficient summarizing all conduit and valve losses.
T_1 = time required to open lock valves, sec.

For any short interval of time dt we may write

$$-A\,dh = CF\sqrt{2gh}\,dt \tag{14}$$

h being taken positive in the increasing direction.

In the first case let us suppose that the lock valves are opened instantaneously. Then, integrating Eq. (14), we obtain for the total time of filling:

$$t = \frac{-A}{CF\sqrt{2g}}\int_0^{h_1}\frac{dh}{\sqrt{h}} = \frac{2A\sqrt{h_1}}{CF\sqrt{2g}} \tag{15}$$

In the second case, assume that the valves are so operated as to reduce the valve area linearly with respect to the time, and that the valve is fully opened before equalization of levels is effected. We then have

$$-A\,dh = \frac{t}{T_1}CF\sqrt{2gh}\,dt \tag{16}$$

or

$$t\,dt = -\frac{AT_1}{CF\sqrt{2g}}\frac{dh}{\sqrt{h}} \tag{17}$$

If h_2 is the head difference remaining to be equalized after the valve is completely opened,

$$\int_0^{T_1} t\,dt = \frac{-AT_1}{CF\sqrt{2g}}\int_{h_2}^{h_1}\frac{dh}{\sqrt{h}} \tag{18}$$

or

$$T_1 = \frac{4A(\sqrt{h_1}-\sqrt{h_2})}{CF\sqrt{2g}} \tag{19}$$

By Eq. (15) the time required to fill the head difference h_1

$$T_2 = \frac{2A\sqrt{h_2}}{CF\sqrt{2g}} \tag{20}$$

The total filling time then becomes

$$\begin{aligned} T_1 + T_2 &= T_1 + \frac{2A\sqrt{h_2}}{CF\sqrt{2g}} = \frac{T_1}{2} + \frac{2A(\sqrt{h_1}-\sqrt{h_2})}{CF\sqrt{2g}} + \frac{2A\sqrt{h_2}}{CF\sqrt{2g}} \\ &= \frac{T_1}{2} + \frac{2A\sqrt{h_1}}{CF\sqrt{2g}} \end{aligned} \tag{21}$$

Equation (21) states that the total filling time is equal to the sum of one-half the time necessary to open the lock valves plus the time that would be required for filling under instantaneous valve opening.

There still remains a third case of fairly frequent occurrence in Venturi-loop designs, namely, that in which equalization of levels is effected before the valves are completely opened. In this case let T_2 be the time at which the levels are equalized. We then write Eq. (18)

$$\int_0^{T_2} t\,dt = \frac{-AT_1}{CF\sqrt{2g}}\int_0^{h_1}\frac{dh}{\sqrt{h}} \tag{22}$$

$$\frac{T_2^2}{2} = \frac{AT_1}{CF\sqrt{2g}}\Big[2\sqrt{h}\Big]_0^{h_1}$$

$$T_2^2 = \frac{4AT_1}{CF\sqrt{2g}}\sqrt{h}$$

$$T_2 = 2\sqrt{\frac{AT_1\sqrt{h}}{CF\sqrt{2g}}} \tag{23}$$

These equations represent the limit of refinement usually found practical for the advance calculation of the longitudinal culvert and port system. Reliance for final performance is placed almost entirely on laboratory model tests. However, in the case of Venturi-loop systems, it is entirely practical to make a more refined calculation, taking full account of acceleration head and a more accurate evaluation of friction and related losses in the tubes. Accordingly, we shall devote the next article to the detailed analysis of the Venturi system. Then, in order to provide a more accurate understanding of what takes place in the longitudinal culvert and port type, we shall present the analytical approach and performance curves for a simplified system. Computation for a practical installation of 10 or more laterals would be hopelessly laborious, out of all proportion to the benefit received.

VENTURI-LOOP SYSTEM

Because relatively slow valve motion is prerequisite to quiet lockage, the analysis of the Venturi-loop lock-filling system may, like the surge-tank problem, be reduced to the consideration of friction and acceleration head effects, neglecting water hammer. It is then essentially a mass-acceleration exercise in which compression of the water and stretching of the conduit walls may be neglected without significant error. The basic principle is that at any instant of time the total instantaneous head difference between the upper pool and the lock chamber is expended in overcoming frictional and other allied losses that are finally dissipated in the form of heat, and in accelerating water in the conduit which is manifested as a change in velocity.

Losses of the frictional type may be calculated by conventional methods and include the following components: head loss at entrance, conduit friction loss in the flared and straight portions of the tube, head loss due to enlargement of sections in the flared section following the straight portion of tube, head loss at exit, and varying head loss due to obstruction at the partially open valve. All the foregoing losses may be conveniently summarized as a constant factor applied to the instantaneous velocity at the cross section of the straight portion of the conduit.

Acceleration head losses are of the familiar form readily obtained from the momentum equation:

$$F = M\frac{dV}{dt}$$

$$F\,dt = M\,dV$$

For a length of conduit dx:

$$wAh\,dt = \frac{wA\,dx}{g}\,dV$$

$$h = \frac{dx}{g}\frac{dV}{dt} \tag{24}$$

In the flared portion of the tube the velocity is expressed as a ratio of the velocity in the straight portion; for example (Fig. 6),

$$V_x = \frac{AV}{A_x} = \frac{AV}{A + \dfrac{(A_1 - A)x}{L_1}} = \frac{AL_1V}{AL_1 + (A_1 - A)x}$$

$$h_1 = \int_0^{L_1} \frac{AL_1\,dV\,dx}{[AL_1 + (A_1 - A)x]\,dtg} = \frac{AL_1\,dV}{g\,dt}\int_0^{L_1}\frac{dx}{AL_1 + (A_1 - A)x} \tag{25}$$

Now, integrating with respect to x, we obtain the instantaneous loss of head due to giving the water in the flared tube L_1 an acceleration increment corresponding to the increment dV in the straight portion of the tube:

$$h_1 = \frac{AL_1\, dV}{(A_1 - A)\, dtg} \log_e \frac{A_1}{A} \tag{26}$$

Similarly, for the flared portion L_2,

$$h_2 = \frac{AL_2\, dV}{(A_2 - A)\, dtg} \log_e \frac{A_2}{A} \tag{27}$$

And finally for the straight portion L,

$$h = \frac{L}{g} \frac{dV}{dt} \tag{28}$$

Adding Eqs. (26) to (28), we obtain an expression of the form

$$h_a = \phi \frac{dV}{dt} \tag{29}$$

and the total head

$$h = \phi \frac{dV}{dt} + \beta V^2 \tag{30}$$

Also, by hydraulic continuity,

$$A_c\, dh = AV\, dt \tag{31}$$

where A_c is the area of lock chamber.

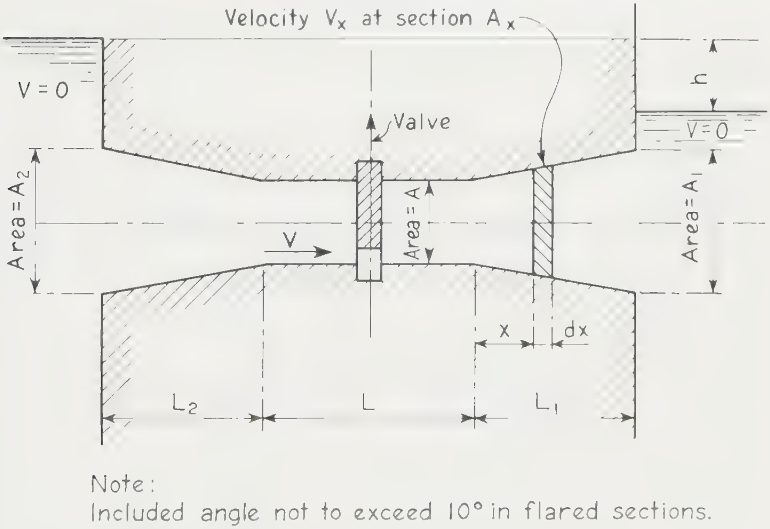

Fig. 6. Analysis of Venturi-loop filling system.

We seek a simultaneous solution of Eqs. (30) and (31) to give the time t. Since the resulting differential equation

$$\frac{d^2h}{dt^2} + \frac{\beta A_c}{\phi A}\left(\frac{dh}{dt}\right)^2 - \frac{hA}{\phi A_c} = 0$$

is not solvable by any means known at present, we resort to the familiar device of arithmetic integration. In Eq. (31) for a small assumed value of Δh for a given time interval Δt, we compute the average value of velocity during the interval V. We next

Table 1. Arithmetic Integration–Venturi-loop Conduits—Kentucky Project (System E)

Headwater elevation = 370 ft
Tailwater elevation = 305 ft
Valve opening rate = 2.4 fpm
V = velocity in conduit near valve
Area of lock chamber = 110 × 675 = 74,250 sq ft

Column (4): $202 V_a \, \Delta t = \dfrac{74{,}250 \Delta h}{2}$

$$\Delta h = \frac{404 \times 50 \times V_a}{74{,}250}$$

$$\Delta h = \frac{V_a}{3.67}$$

Area of conduit at valve = 202 sq ft
V_a = average velocity in conduit near valve
Length of straight portion of tube L = 19.83 ft
Length of flared portion of tube L_1 = 93.33 ft
Length of flared portion of tube L_2 = 101.08 ft

Column (10): $\Delta h = \dfrac{5.45 \Delta V}{\Delta t}$

$$\Delta V = \frac{50 \Delta h}{5.45}$$

$$\Delta V = 9.18 \Delta h$$

(1) Time, sec	(2) Velocity V, fps	(3) Average velocity V_a, fps	(4) $\Delta h = V_a/3.67$, ft	(5) *W.s.* elev in chamber, ft	(6) Head on conduit, ft	(7) Valve and friction loss, ft	(8) Acceleration head, ft	(9) Avg acceleration head, ft	(10) $\Delta V = 9.18 \Delta h$, fps	(11) V, fps
0	0	0	0	305.00	65.00	0	0	0	0	0
t = 50 50	10.03	5.015	1.36	306.36	63.64	61.45	2.19	1.095	10.03	10.03
t = 50 100	15.53	12.78	3.48	309.84	60.16	61.13	−0.97	0.61	5.58	15.61
t = 50 150	18.38	16.96	4.62	314.46	55.54	53.97	1.57	0.30	2.77	18.38
t = 50 200	20.00	19.19	5.22	319.68	50.32	51.536	−1.216	0.177	1.62	20.00
t = 50 250	21.75	20.88	5.70	325.38	44.62	43.04	1.58	0.185	1.70	21.70
t = 50 300	25.08	23.42	6.39	331.77	38.23	39.07	−0.844	0.368	3.38	25.08
t = 50 350	26.45	25.77	7.02	338.79	31.21	30.08	1.13	0.145	1.34	26.42
t = 50 400	28.10	27.28	7.45	346.24	23.76	24.52	−0.764	0.183	1.68	28.10
t = 50 450	25.50	26.80	7.30	353.54	16.46	16.25	0.210	−0.277	−2.54	25.56
t = 50 500	21.20	23.35	6.37	359.91	10.09	11.26	−1.17	−0.48	−4.38	21.18
t = 50 550	15.35	18.28	4.99	364.90	5.10	5.90	−0.80	−0.64	−5.87	15.31
t = 50 600	9.50	12.43	3.39	368.29	1.71	2.26	−0.55	−0.63	−5.79	9.52
t = 50 650	4.22	6.86	1.87	370.16	−0.16	−0.45	−0.61	−0.58	−5.32	4.20
t = 50 700	−1.35	1.43	0.39	370.55	−0.55	−0.046	−0.60	−0.605	−5.55	−1.35
t = 50 750	−2.95	−2.15	−0.59	369.96	0.04	0.22	0.26	−0.17	−1.56	−2.91
t = 50 800	0.20	−1.38	−0.38	369.58	0.42	0.00	0.42	0.34	3.11	0.20
t = 50 850	2.10	1.15	0.31	369.89	0.11	0.11	0	0.21	1.93	2.13
t = 50 900	0.80	1.45	0.40	370.29	−0.29	0.01	−0.30	−0.15	−1.38	0.75

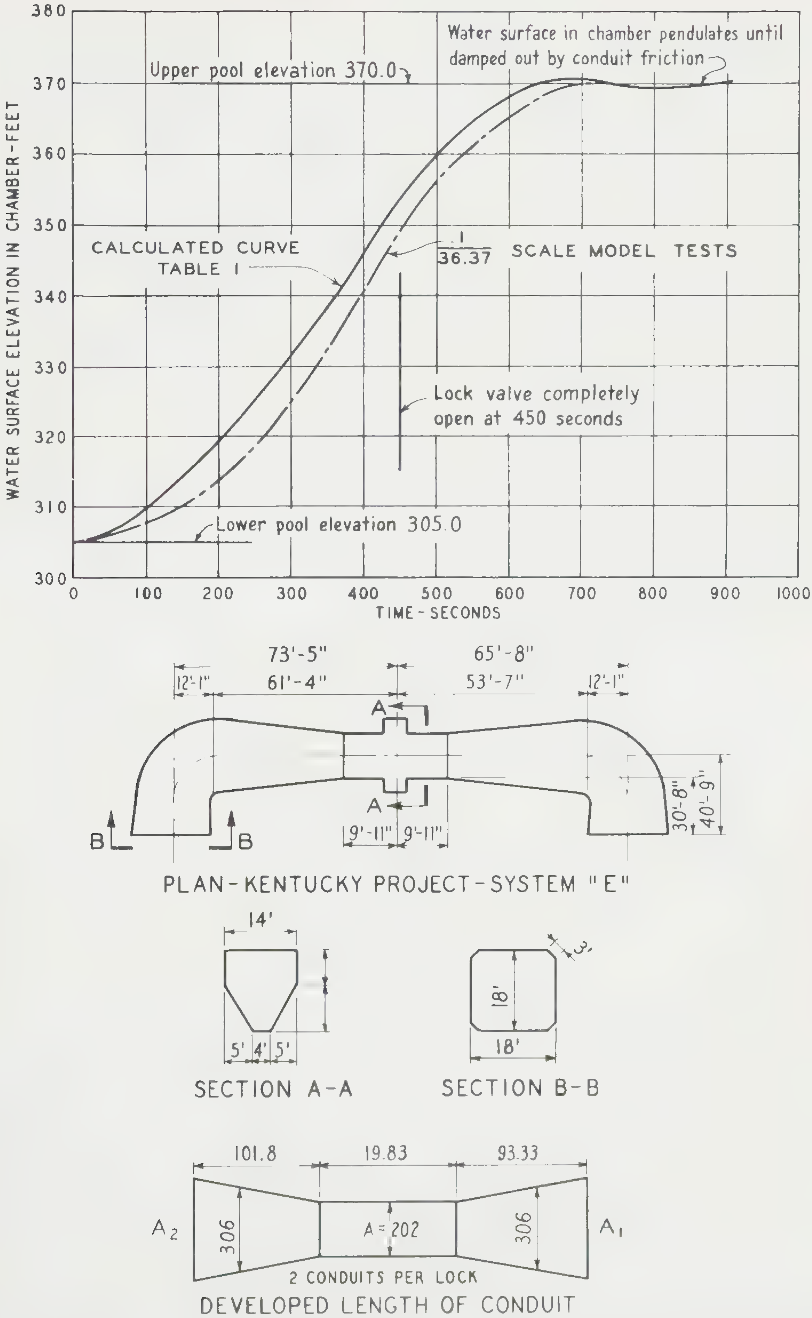

FIG. 7. Lock-filling curve for Venturi-loop system by arithmetic integration and by model test (see Table 1).

calculate ΔV from the expression $\frac{V_1 + \Delta V}{2} = V$, V_1 being the velocity at the end of the preceding interval.

Equation (31) is then applied as a test at the end of the interval: h being equal to $h_1 + \Delta h$; V to $V_1 + \Delta V$, where the subscript 1 denotes values at the end of the preceding interval. Table 1 is a typical example of such calculation.

This tabulation affords a ready answer to a question frequently raised by hydraulic engineers in connection with all lock-filling systems, namely, why filling always continues some distance beyond upper pool level. Referring to the line of integration at time $t = 650$ sec, it will be noted that, when the water surface elevation in the chamber reaches 370.16 ft, the velocity in the filling conduits is still quite appreciable, 4.22 fps. Accordingly, owing to the inertia of water in the conduits, the chamber level continues to rise until this velocity is decelerated. Because of the superelevation of water in the chamber, the flow then reverses in direction until the water surface elevation in the chamber drops sufficiently to decelerate this reversed flow and initiate flow in the normal direction from the pool to the chamber. As shown by the computation, this pendulation of chamber levels continues until damped down by conduit friction.

LONGITUDINAL CONDUIT AND LATERAL PORT SYSTEM

Because of the exceedingly great labor involved, and in view of the fact that laboratory model tests must be conducted in any event to determine hawser stresses, it would be impractical to undertake the analytical determination of design for a longi-

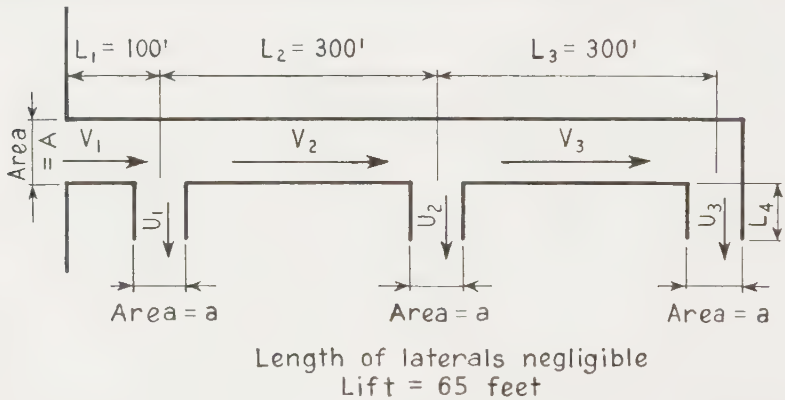

FIG. 8. Elementary filling system. Longitudinal conduit with short laterals.

tudinal conduit system with the usual great number of laterals. The chief value of the analytical approach in this case is that it affords a rational explanation why uniformly spaced ports do not give uniform distribution of water inflow along the longitudinal axis of the chamber, and why the laterals adjacent to the lower lock gates frequently come into action more quickly than laterals adjacent to the valves or upper lock gates. Analytical methods enable us to understand why differential port spacing with the closer spacing at the upper gates is the optimum arrangement for quiet lockage.

For the above purpose it will be entirely sufficient to employ the vastly simplified manifold system indicated in Fig. 8, consisting of a longitudinal main conduit with but three laterals. Our plan of attack is (1) to develop pertinent equations, neglecting the effect of contractions which cause head loss at the entrance to the laterals, (2) to incorporate the effect of such contractions in a second system of equations, (3) to calculate a numerical example by each of these two methods and thus throw into bold relief the profound effect of what might, at first inspection, appear to be a mere trivial refinement.

Just as in the case of the Venturi-loop system, we are again dealing essentially with a mass-acceleration problem in which the head difference is expended in overcoming friction and allied losses and in accelerating the conduit velocity. The valve opening rate is necessarily slow to ensure quiet lockage, so that compression of the water and stretching of the conduit wall may, without significant error, be neglected, *i.e.*, we ignore water-hammer effect.

As in the case of the Venturi-loop system, we shall denote by βV^2 and θU^2 all losses of head manifested eventually as lost energy in the form of heat and by ϕV the summation of all acceleration head losses. We shall employ the symbol V for the main conduit, U for the laterals, and appropriate subscripts will identify the particular branch under consideration.

In the analysis we assume that the water surface in the chamber is a horizontal plane at all times, so that the head difference from upper pool to chamber is the same by paths through each lateral successively. We proceed to write equations for head difference and relationships dictated by hydraulic continuity.

$$h = \beta_1 V_1^2 + \theta_1 U_1^2 + \frac{L_1}{g}\frac{dV_1}{dt} + \frac{L_4}{g}\frac{dU_1}{dt} \tag{32}$$

$$h = \beta_1 V_1^2 + \beta_2 V_2^2 + \theta_2 U_2^2 + \frac{L_1}{g}\frac{dV_1}{dt} + \frac{L_2}{g}\frac{dV_2}{dt} + \frac{L_4}{g}\frac{dU_2}{dt} \tag{33}$$

$$h = \beta_1 V_1^2 + \beta_2 V_2^2 + \beta_3 V_3^2 + \theta_3 U_3^2 + \frac{L_1}{g}\frac{dV_1}{dt} + \frac{L_2}{g}\frac{dV_2}{dt} + \frac{L_3}{g}\frac{dV_3}{dt} + \frac{L_4}{g}\frac{dU_3}{dt} \tag{34}$$

$$AV_1 - AV_2 = aU_1 \tag{35}$$

$$AV_2 - AV_3 = aU_2 \tag{36}$$

$$AV_3 = aU_3 \tag{37}$$

$$\frac{A_c}{2}\,dh = AV_1\,dt \tag{38}$$

If we proceed to solve these seven equations for the seven unknown variables in the conventional manner, we once again encounter the familiar differential equation of type

$$\frac{d^2h}{dt^2} + C_1\left(\frac{dh}{dt}\right)^2 + C_2 h = 0$$

for which no solution is yet known. Accordingly, we employ the device of arithmetic integration with the arrangement given in Table 2. The method of attack is to work with Eqs. (32), (35), and (38) until V_2 in Eq. (35) reaches a significant magnitude. We then add to the calculation Eqs. (33) and (36) and continue until V_3 reaches a significant magnitude in Eq. (36). From then on, we employ all seven equations.

The results of the example of Table 2 are given in Fig. 9, from which it will be noted that the laterals do not all come into action at once, but that there is quite an appreciable time lag between the initial functioning of the successive ports and that they come into play in the order of their distance from the upper lock gates.

In the analysis thus far, we have assumed that the flow in all portions of the system is axial, *i.e.*, we have made no allowance for the effect of contractions at the entrance to the laterals. We shall now incorporate this feature in Eqs. (32) to (38).

In this connection there are two possibilities depending upon whether the lateral is long or short. In either case the cross-sectional area of the discharge will be the same at the plane of intersection of the two tubes and will be equal to $a \cos \alpha$.

In the first case, that of the short lateral, the V component will be expended on

TABLE 2. ARITHMETIC INTEGRATION–LONGITUDINAL CONDUIT WITH LATERALS

Headwater elevation = 370 ft
Tailwater elevation = 305 ft
Valve opening time = 450 sec
Lock chamber area = 74,250 sq ft
Friction loss L_1 (including entrance loss) = $0.010V_1^2$
Friction loss L_2 = $0.005V_2^2$
Friction loss L_3 = $0.005V_3^2$

Discharge at U_1, U_2, and U_3 assumed axial, with orifice discharge coefficients all equal to 0.80.

	Time, sec		
	30	60	90
Time, sec	30	60	90
Velocity V_1, fps	13.613	18.32	19.78
Average velocity V_{1a}, fps	6.807	15.97	19.05
$\frac{400V_{1a}\,\Delta t}{74{,}250} = \Delta h$, ft	1.098	2.58	3.08
W.S. elevation in chamber, ft	306.098	308.68	311.76
Friction loss in L_1 includes valve obstruction head loss, ft	56.72	59.80	52.50
Average acceleration head $= \frac{L_1}{g}\frac{\Delta V_1}{\Delta t}$, ft	1.412	0.488	0.151
Acceleration head for L_1, ft	2.82	−1.84	2.14
Head on port U_1, ft	4.36	3.36	3.60
Velocity through U_1, fps	16.73	14.70	15.22
Velocity $V_2 = \frac{AV_1 - aU_1}{A}$, fps	5.248	10.97	12.17
Friction loss L_2, ft	0.14	0.60	0.74
Average acceleration head $= \frac{L_2}{g}\frac{\Delta V_2}{\Delta t}$, ft	1.627	1.776	0.37
Acceleration head for L_2, ft	3.25	0.30	0.44
Head on port U_2, ft	0.97	2.46	2.42
Velocity through U_2, fps	7.89	12.56	12.48
Velocity $V_3 = \frac{AV_2 - aU_2}{A}$, fps	1.303	4.69	5.93
Friction loss L_3, ft	0.01	0.11	0.18
Average acceleration head $= \frac{L_3}{g}\frac{\Delta V_3}{\Delta t}$, ft	0.41	1.052	0.38
Acceleration head for L_3, ft	0.82	1.28	−0.52
Head on port U_3, ft	0.14	1.07	2.76
Velocity through U_3, fps	3.00	8.30	13.30
Volume $U_1 + U_2 + U_3$ in Δt, cu ft	41,400	94,800	114,800
Volume to chamber in $\Delta t = \frac{74{,}250}{2}\,\Delta h$, cu ft	40,900	95,600	114,200

producing pressure upon the side wall of the lateral, and the discharge into the chamber will be at efflux velocity U_1 and cross-sectional area $a \cos \alpha = \dfrac{aU_1}{\sqrt{U_1^2 + V_1^2}}$. In other words, in Eq. (35) we replace a by $\dfrac{aU_1}{\sqrt{U_1^2 + V_1^2}}$; in Eq. (36) we replace a by $\dfrac{aU_2}{\sqrt{U_1^2 + V_2^2}}$; and in Eq. (37) we replace a by $\dfrac{aU_3}{\sqrt{U_3^2 + V_3^2}}$. In performing the arithmetic integration, we employ values of U_n and V_n from the previous time interval as a first trial and then refine the procedure to effect the requisite balance. For the very first interval, the first trial will naturally be made with the values a and A. In the second case, that of long laterals, the discharge will, after passing the contraction, expand and fill the tube so that the head loss is properly computed for the standard case of a

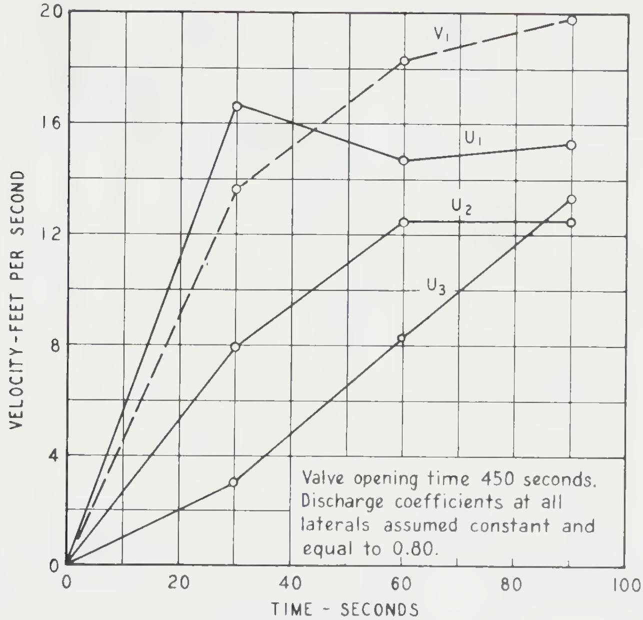

FIG. 9. Showing contraction at laterals.

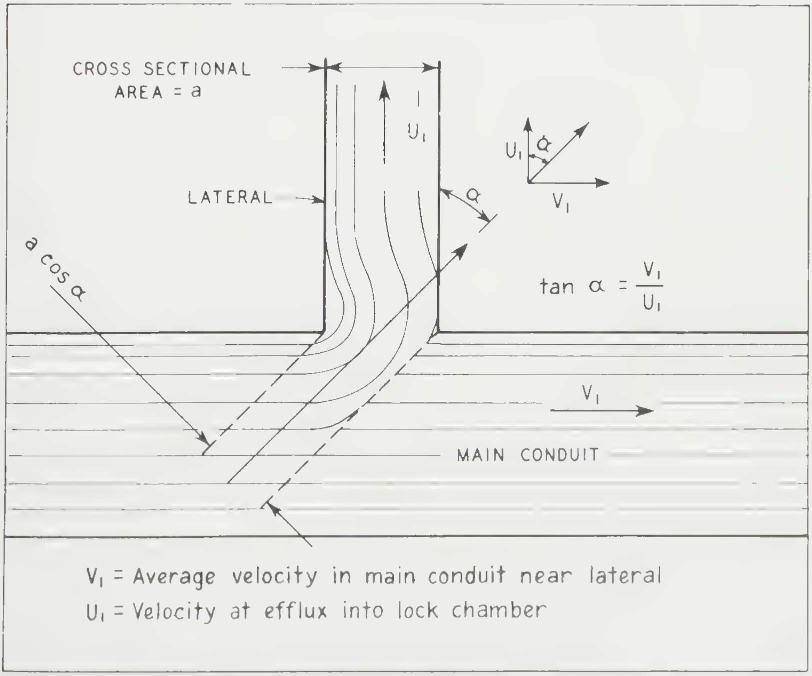

FIG. 10. Performance chart. Elementary filling system. Longitudinal conduit for three short laterals.

sudden increase in cross section of conduit from $a \cos \alpha$ to a. If the velocity is U_1 at efflux into the chamber, it will be $\frac{U_1}{\cos \alpha}$ just after making the right-angle turn, and the component V_1 will, as before, be expended in producing pressure upon the side wall of the lateral. The head loss in the lateral chargeable to effecting the turn will be

$$\frac{\left(\frac{U_1}{\cos \alpha} - U_1\right)^2}{2g} = \frac{U_1^2}{2g}\left(\frac{1}{\cos \alpha} - 1\right)^2$$

in which, as before, $\cos \alpha = \frac{U_1}{\sqrt{U_1^2 + V_1^2}}$. The head loss is, accordingly,

$$\frac{U_1^2}{2g}\left(\frac{\sqrt{U_1^2 + V_1^2}}{U_1} - 1\right)^2 \qquad \text{for the first lateral}$$

$$\frac{U_2^2}{2g}\left(\frac{\sqrt{U_2^2 + V_2^2}}{U_2} - 1\right)^2 \qquad \text{for the second lateral}$$

$$\frac{U_3^2}{2g}\left(\frac{\sqrt{U_3^2 + V_3^2}}{U_3} - 1\right)^2 \qquad \text{for the third lateral}$$

These values are incorporated in the coefficients θ_1, θ_2, and θ_3 in Eqs. (32) to (34). In making the first trials of the arithmetic integration, values of U_n and V_n from the preceding interval may be employed and then refined for the second and succeeding trials.

It will be evident from this derivation that the contraction losses for the first ports may be so large relatively that the ports farthest removed from the lock valves come into action first. This has frequently been observed in actual prototype operation. Table 3 gives a sample of the arithmetic integration process for the case of short laterals. The corresponding operations for long laterals follow directly from the derivation. The chief value of the foregoing analysis is to demonstrate that uniform port spacing for the system of main longitudinal conduits with lateral branches cannot be expected to give uniform discharge into the lock chamber.

From a study of Tables 2 and 3 it will be apparent that the degree of contraction at the entrance to each lateral port depends upon the relative magnitude of conduit and port velocities at the successive laterals. Although there is quite a marked difference in the valve opening rates for the two cases shown in this table, this does not result in any relative difference in the distribution of flow through the various laterals. However, let us consider for a moment the common case of a long main conduit with 10 or 15 laterals. When many laterals are used in this fashion, the cross-sectional area of each will be small in proportion to the main conduit area. Consequently, the major portion of the discharge will still be undelivered to the chamber after passing the first and second laterals. In addition, this velocity will cause a proportionately great drop in pressure head at the first two orifice outlets so that the head on these orifices will be small and the efflux velocity through the first two ports will be very small. Our formula for contraction coefficient for this case of a large conduit velocity and small port velocity will then give a very large contraction at the first few ports, so that the major initial flow will be delivered by the downstream ports. It has been observed in some model tests for high lifts and during early stages of filling that the flow in the first two laterals would actually reverse and be in the direction from the chamber to the main conduit. To carry out this demonstration by arithmetic integration for 15 ports would obviously be a task of prohibitive proportions; but that the mechanism of filling under such conditions would proceed substantially as just indicated above will be evident from the behavior of the integration process in Table 3.

TABLE 3. ARITHMETIC INTEGRATION–LONGITUDINAL CONDUIT WITH LATERAL PORTS, VARIATION IN CONTRACTION AT PORTS CONSIDERED

Headwater elevation = 370 ft — Friction loss L_1 (including entrance loss) = $0.010V_1^2$
Tailwater elevation = 305 ft — Friction loss $L_2 = 0.005V_2^2$
Lock chamber area = 74,250 sq ft — Friction loss $L_3 = 0.005V_3^2$
Effect of difference in contraction at port entrance included in computation.

	Valve opening time, 450 sec	Valve opening time, 90 sec
Time, sec	30	30
Velocity V_1, fps	13.604	23.15
Average velocity V_{1a}, fps	6.81	11.58
$\frac{400V_{1a}\,\Delta t}{74{,}250} = \Delta h$, ft	1.10	1.87
W. S. elevation in chamber, ft	306.10	306.87
Friction loss in L_1 includes valve obstruction head loss, ft	56.64	47.75
Average acceleration head $= \frac{L_1}{g}\frac{\Delta V_1}{\Delta t}$, ft	1.408	2.398
Acceleration head for L_1, ft	2.82	4.79
Head on port U_1, ft	4.44	10.59
Velocity through U_1, fps	16.92	26.10
Discharge coefficient $\frac{U_1}{\sqrt{U_1^2 + V_1^2}}$	0.777	0.748
Velocity $V_2 = \frac{AV_1 - aU_1}{A}$, fps	5.38	10.93
Friction loss L_2, ft	0.15	0.60
Average acceleration head $= \frac{L_2}{g}\frac{\Delta V_2}{\Delta t}$, ft	1.670	3.40
Acceleration head for L_2, ft	3.34	6.80
Head on port U_2, ft	0.95	3.19
Velocity through U_2, fps	7.82	14.32
Discharge coefficient $\frac{U_2}{\sqrt{U_2^2 + V_2^2}}$	0.823	0.795
Velocity $V_3 = \frac{AV_2 - aU_2}{A}$, fps	1.36	3.82
Friction loss L_3, ft	0.01	0.07
Average acceleration head $= \frac{L_3}{g}\frac{\Delta V_3}{\Delta t}$, ft	0.42	1.185
Acceleration head for L_3, ft	0.84	2.37
Head on port U_3, ft	0.10	0.75
Velocity through U_3, fps	2.54	6.95
Discharge coefficient $\frac{U_3}{\sqrt{U_3^2 + V_3^2}}$	0.880	0.878
Volume $U_1 + U_2 + U_3$ in Δt, cu ft	40,900	69,500
Volume to chamber in $\Delta t = \frac{74{,}250}{2}\,\Delta h$, cu ft	40,900	69,500

Bibliography

KREY, H., Neuere Versuche fur Schiffsschleusen, *Zentr. Bauverwaltung*, Nos. 45, 46, and 47, Berlin, 1914.
RICH, GEORGE R., "Hydraulic Transients," McGraw-Hill Book Company, Inc., New York, 1951.
RICH, GEORGE R., The Hydromechanics of Ship Lockage, *Military Engr.*, July–August, 1932, p. 364.
RICH, GEORGE R., Hydraulics of Lock-filling Systems, *Military Engr.*, January–February, 1933, p. 60.
RICH, GEORGE R., Basic Hydraulics of Water Storage Projects, I—Project Layout and Lock-filling Systems, *Civil Eng.*, August, 1944, p. 351.
RINGERS, J. A., and JOSEPHUS JITTA, Rapporten en Mededeelingen van den Rijkswaterstaat, *Dutch Government Report* 23, 1927.

Winkel, Dr. R., Die Hydromechanischen Vorgänge beim Schleusen eines Schiffes, R., *Die Bautechnik*, No. 33, Berlin, August, 1923.
Winkel, Dr. R., Die Wasser und Schiffsbewegungen beim Schleusenbetrieb mit langen und mit kurzen Umlaufen, *Zentr. Bauverwaltung*, Nos. 39 and 45, Berlin, 1924.
Winkel, Dr. R., Besondere Schutzausbildungen gemäss Hydromechanischen Forderungen, *Die Bautechnik*, Berlin, April, 1925.
Winkel, Dr. R., Verminderung der Schiffsbewegungen beim Schleusen durch besondere Schutzegestaltung, *Zentr. Bauverwaltung*, Berlin, October, 1923.
Winkel, Dr. R., Die Schleusungsdauer bei langsam zunehmenden Zuflusse, *Zentr. Bauverwaltung*, No. 38, Berlin, September, 1925.

SECTION 33

IRRIGATION

By Rolland F. Kaser

In determining the feasibility of a contemplated irrigation project, three fundamental questions must be carefully considered: (1) Are the project lands suited to agricultural use from topographic and soil-structure viewpoints? (2) Are available water supplies sufficient in quantity and suitable in quality to meet the irrigation requirements? (3) Will the cost of the necessary engineering works per acre of irrigable land be low enough to justify construction?

The greater part of this section is devoted to the physical aspects of irrigation work, such as water supply, water requirements, water losses, consumptive use, and irrigation methods. The principles governing the design and construction of irrigation works are discussed elsewhere.

LAND CLASSIFICATION

Land classification must be carefully considered in planning new projects. Such classifications must be made by agricultural and soil experts working in cooperation with engineers. Some lands, which may be easily and economically watered, may not merit inclusion in the irrigable acreage because of unproductive soil composition, undesirable soil texture, difficult drainage possibilities, presence of undesirable soluble salts, or danger of developing alkali surfaces under continued irrigation. Other lands, which may cost more to irrigate, may deserve inclusion because of ideal soil characteristics, easy drainage, and high prospects of developing into permanent and prosperous productive areas.

1. Purposes of Classification. Land classification is undertaken to provide an inventory of the relative suitability of available lands for sustained production under irrigation. This primary purpose usually can be served by a survey of reconnaissance scope. Following the selection of the outlines of the project area on the basis of the reconnaissance survey, a semidetailed survey is undertaken to provide the basis for selection of the lands to be served with irrigation water, for determination of the probable productivity of those lands and the crops for which they are suitable, and for determination of the criteria for design of irrigation and drainage works. The semidetailed survey also provides information on the need for soil reclamation to remove deleterious salts and on the characteristics and location of the lands requiring such treatment prior to successful cropping. In some cases, a detailed land-classification survey will be necessary in specific locations where critical problems such as soil-reclamation needs, farm-drainage requirements, or other considerations require more precise definition than that furnished by the semidetailed survey.

2. Physical Properties. Physical properties which are important to the irrigability and drainability of land include (1) topographic relief and slope, which influence the cost and type of water-distribution facilities and the labor requirements for water applications to the fields; (2) texture, grading, and depth of the surface soil and subsoil, which determine the water-holding capacity and drainability of the soil; and (3) natural drainage characteristics, such as surface drainage channels, drainage outlets, and subsurface materials—gravel layers, hardpan formations, impervious soil or rock strata—which influence the drainability and reclaimability of the soil. The land classification must locate and identify changes in each of these characteristics with an accuracy commensurate with the scope of the survey needed.

Air drainage should be studied in classifying lands where appreciable areas may be adapted to fruit or winter vegetable culture. Experience has shown that crops of such nature, grown on low-lying lands where wind movements are obstructed by surrounding hills and consequently are not adequate to provide satisfactory air drainage, may suffer severe damage from frost at times when similar crops, grown on nearby sloping topography where wind movements provide ample air drainage, may suffer no damage at all. For example, orchards on the sloping hillsides of the Roza and Tieton divisions, Yakima project, Washington, frequently are undamaged by frost when similar orchards on low-lying lands near the town of Yakima are severely damaged. Many comparable examples occur in the citrus-fruit sections of Arizona and California, as well as in other sections of the West. Consequently, it may sometimes be desirable to include sloping hillside regions in the irrigable areas, even though the preparation of land and conveyance of water may cost considerably more per acre than in the low-lying, more level divisions of the projects.

3. Chemical Properties. Chemical properties of the soil determine the need for reclamation treatment, the reactions to be expected when irrigation waters having certain chemical characteristics are applied, and the fertilizers and other treatments required to obtain optimum crop yields. In irrigation work, the term *alkali* is used to mean soluble salts that may be brought to the surface by capillary soil-moisture movements and precipitated as the moisture evaporates. The commonest alkali compounds are the sodium sulfates, chlorides, and carbonates. Other alkali compounds are the potassium and magnesium carbonates, chlorides, and sulfates, and the calcium chlorides and nitrates. Sodium carbonates, which cause the decomposition of organic matter and the formation of a dark-colored crust at the surface of the ground, are called *black alkali*. Sodium carbonate (sal soda), sodium bicarbonate (baking soda), and sodium chloride (table salt) are especially detrimental to plant growth, the first two being the more objectionable and more difficult to remove from the soil. Noncaustic compounds that do not deflocculate the soil, such as sodium chloride and sulfate, are often called *white alkali*.

The proportions of alkali salts that the soil may contain and still be irrigated profitably vary with the character of the soil, fertility, drainage, methods of irrigating, and crops grown, as well as with the kinds of salts present. The danger of nonalkali lands developing alkali surfaces under continued irrigation depends on the permeability of the soil, quantity of water applied, drainage facilities, and saline content of the irrigation water. Persons classifying alkali lands, or areas that may develop alkali surfaces, should consult agricultural references which present the findings of the latest research activities applied to similar problems.[1] With a few exceptions, grasses, small grains, alfalfa, and root crops are more resistant to alkali than are corn, beans, peas, melons, and fruits.

The presence of noticeable quantities of alkali on the ground surface or considerable proportions of salts in the soil may not be serious if the ground is permeable and can be economically drained, and if sufficient water can be applied to maintain percolation toward drainage outlets. If the lands are properly drained, objectionable quantities of alkali sometimes can be leached out of the soil by flooding the surface during the winter months, by growing crops such as rice which require or can tolerate the application of

[1] "Diagnosis and Improvement of Saline and Alkaline Soils," U.S. Department of Agriculture Handbook 60, 1954.

large amounts of water, or by other special applications of water for the purpose of leaching out the salts to achieve reclamation.

4. Drainability. One of the principal purposes of a land-classification survey is to assess the properties of the land which influence surface and subsurface drainage. Physical properties concerned with drainage are listed in Art. 2. Chemical properties of the soil may also influence drainability. Excessive concentrations of sodium or sodium salts in the soil or in the irrigation water applied can cause a soil which would otherwise have adequate permeability to "tighten up." The resulting reduction in permeability can, under extreme conditions, render the soil unproductive, and reclamation of that soil may not be economical.

Drainage is important in the suitability of land for permanent productivity under irrigation. Excessive and prolonged inundation resulting from heavy rainfall on the land itself can be destructive to growing crops and also can affect adversely the soil structure and permeability. High water tables affect adversely most irrigated crops by reducing the thickness of the root zone which the plants can utilize for essential nutrients (see Sec. 39, Drainage).

Reclamation of saline and alkaline soils usually can be accomplished by the passage of large amounts of water through the soil profile, and this cannot be done efficiently if the soil permeability is low. A gradual buildup of salts will occur in the soils under continuing irrigation unless natural drainage processes or constructed drainage facilities are effective in removing from the soil, on an annual basis, a volume of salt equal to that brought in by the irrigation water. Accordingly, the soil permeability must be adequate for the accomplishment of routine leaching—application of sufficient irrigation water to the fields to meet the evapotranspiration needs plus the water required to convey excess salts to the water table—and subsurface drainage must be adequate to carry away enough groundwater to prevent the water table from entering the plant root zone.

5. Sampling and Testing. Land-classification surveys include observation of the land and soil in the field, collection and laboratory analyses of samples of the soil and groundwater, field testing of the soil permeability, and examination of aerial photographs. The field observations and collection of soil samples are facilitated by the use of auger holes, test pits, and occasional deep drilling. The density of the sampling, that is, number of auger holes and test pits of various depths per square mile, depends upon the purpose and scope of the survey and the variability of conditions within the area being surveyed. General criteria established by the Bureau of Reclamation for these surveys are summarized in Table 1.

Auger sampling of agricultural soils is usually done by manually operated augers, although modern equipment includes power-operated augers mounted on vehicles of various types. Vehicular-mounted augers take much less time per hole and permit a land classifier to cover more acres per day than would be possible with a manual auger. This advantage is somewhat offset by the fact that better identification of thin soil layers can be obtained with the manual auger. Test pits permit the classifier to inspect the various soil layers down to a considerable depth to identify the soil structure and to obtain undisturbed and other samples of the several layers. These test pits are usually dug manually, although truck-mounted large-diameter power augers can be used to expedite the work.

Field permeability tests are usually necessary where there are clay soils or other indications of low permeability. This is because experience has shown that laboratory tests on disturbed soil samples often result in misleading permeability values and because of difficulties in collecting, transporting, and testing an "undisturbed" sample. Up-to-date reference sources should be consulted for details of equipment

TABLE 1. MINIMUM REQUIREMENTS BY TYPES OF CLASSIFICATION*

	Reconnaissance	Semidetailed	Detailed	
			New lands	Fully developed or highly uniform new land areas
Land classes recognized†	1, 2, 3, 6	1, 2, 3, 6	1, 2, 3, 4, 5, 6	1, 2, 3, 4, 5, 6
Scale of base maps	1:24,000	1:12,000	1:4,800	1:12,000
Max distances between traverse, miles	1	0.5	0.25	0.5
Accuracy, %	75	90	97	97
Field progress per day (one land classifier and crew), sq miles	3–5	1–3	0.25–1	1–3
Min area of class 6 to be segregated from larger arable areas, acres	4	0.5	0.2	0.2
Min area for change to lower class of arable land, acres	40	10	2	10
Min area for change to higher class of arable land, acres	40	20	10	20
Min soil and substrata examination:				
Borings or pits (5 ft deep) per sq mile	1	4	16	4
Deep holes (10 ft or more) per township	1	2	4	2

* From "Irrigated Land Use," Bureau of Reclamation Manual, Vol. 5.
† See Table 2 for a description of these land classes.

and procedures which may be employed under various field conditions and in field laboratories.[1]

Soil samples collected for land-classification purposes must be properly tagged and identified by number, location of hole, depth below surface, and any other pertinent information. The samples should be tagged also to indicate the tests which should be made on the contents. It may be feasible on large projects to construct and equip a special laboratory for the purpose of testing the soil and water samples collected for that project; however, on most projects it probably will be desirable to have the samples tested by a commercial laboratory or by a public-owned laboratory which is authorized to do commercial work. Because many of the details of project formulation and design depend upon results of the land-classification survey—the conclusions of which are based on the field observations and laboratory analyses—it is essential that that survey be scheduled to begin early in the project investigation and that time be allowed for the collection and analysis of soil samples and interpretation of results.

6. Classification Standards. Land-classification surveys must be conducted and the results interpreted in accordance with standard specifications in order that data within and between areas and regions may be compared for purposes of resource appraisal and development. Generalized land-classification specifications used by the Bureau of Reclamation, and developed from the extensive experience of that agency in project development and operation, are summarized in Table 2. The generalized specifications are broad in scope and apply to gravity irrigation in potential and existing project areas. These specifications must be reviewed and refined as necessary to meet the needs of each land-classification survey to be undertaken. The amount of

[1] "Diagnosis and Improvement of Saline and Alkali Soils," U.S. Department of Agriculture Handbook 60, 1954.

TABLE 2. LAND-CLASSIFICATION SPECIFICATIONS—GENERAL*

Land characteristics	Class 1—Arable	Class 2—Arable	Class 3—Arable
		Soils	
Texture	Sandy loam to friable clay loam	Loamy sand to very permeable clay	Loamy sand to permeable clay
Depth:			
To sand, gravel, or cobble	36 in. plus—good free-working soil of fine sandy loam or finer; or 42 in. of sandy loam	24 in. plus—good free-working soil of fine sandy loam or finer; or 30–36 in. of sandy loam to loamy sand	18 in. plus—good free-working soil of fine sandy loam or finer; or 24–30 in. of coarser-textured soil
To shale, raw soil from shale or similar material (6 in. less in each instance to rock and similar material)	60 in. plus; or 54 in. with minimum of 6 in. of gravel overlying impervious material or sandy loam throughout	48 in. plus; or 42 in. with minimum of 6 in. of gravel overlying impervious material or loamy sand throughout	42 in. plus; or 36 in. with minimum of 6 in. of gravel overlying impervious material or loamy sand throughout
To penetrable lime zone	18 in. with 60 in. penetrable	14 in. with 48 in. penetrable	10 in. with 36 in. penetrable
Alkalinity	pH less than 9.0 unless soil is calcareous, total salts are low, and evidence of black alkali is absent	pH 9.0 or less, unless soil is calcareous, total salts are low, and evidence of black alkali is absent	pH 9.0 or less, unless soil is calcareous, total salts are low, and evidence of black alkali is absent
Salinity	Total salts not to exceed 0.2 %. May be higher in open permeable soils and under good drainage conditions	Total salts not to exceed 0.5 %. May be higher in open permeable soils and under good drainage conditions	Total salts not to exceed 0.5 %. May be higher in open permeable soils and under good drainage conditions
		Topography	
Slopes	Smooth slopes up to 4 % in general gradient in reasonably large-sized bodies sloping in the same plane	Smooth slopes up to 8 % in general gradient in reasonably large-sized bodies sloping in the same plane; or rougher slopes which are less than 4 % in general gradient	Smooth slopes up to 12 % in general gradient in reasonably large-sized bodies sloping in the same plane; or rougher slopes which are less than 8 % in general gradient
Surface	Even enough to require only small amount of leveling and no heavy grading	Moderate grading required but in amounts found feasible at reasonable cost in comparable irrigated areas	Heavy and expensive grading required in spots but in amounts found feasible in comparable irrigated areas
Cover (loose rocks and vegetation)	Insufficient to modify productivity or cultural practices, or clearing cost small	Sufficient to reduce productivity and interfere with cultural practices. Clearing required but at moderate cost	Present in sufficient amounts to require expensive but feasible clearing
		Drainage	
Soil and topography	Soil and topographic conditions such that no specific farm-drainage requirement is anticipated	Soil and topographic conditions such that some farm drainage will probably be required but with reclamation by artificial means appearing feasible at reasonable cost	Soil and topographic conditions such that significant farm drainage will probably be required but with reclamation by artificial means appearing expensive but feasible

TABLE 2. LAND-CLASSIFICATION SPECIFICATIONS—GENERAL* (*Continued*)

Class 4—Limited Arable
Includes lands having excessive deficiencies and restricted utility but which special economic and engineering studies have shown to be irrigable
Class 5—Nonarable
Includes lands which will require additional economic and engineering studies to determine their irrigability and lands classified as temporarily nonproductive pending construction of corrective works and reclamation
Class 6—Nonarable
Includes lands which do not meet the minimum requirements of the next higher class mapped in a particular survey and small areas of arable land lying within larger bodies of nonarable land

* From "Irrigated Land Use," Bureau of Reclamation Manual, Vol. 5.

refinement necessary will increase with the detail of the classification. The project specifications must result in significant differences in productivity and payment capacity between land classes and must assure that subclasses within land classes will have comparable payment capacity. In preparing for land-classification surveys, reference should be made to up-to-date bulletins and manuals presenting detailed descriptions of procedures and methods.[1]

CROP EVAPOTRANSPIRATION

7. Principles of Evapotranspiration. In the process of applying irrigation water to the crops, certain losses of water through evaporation occur and these losses are somewhat characteristic of the particular crop—even though they are influenced, of course, by the methods employed in applying the water. For this reason, the term *consumptive use* came to be used to denote the minimum amount of water—usually expressed in inches or feet of water depth or in acre-feet per acre of crops—required from all sources to support optimum growth of a particular crop under field conditions. The consumptive-use requirement of a crop thus includes water evaporated from the fields as well as that transpired by the plants or used by the plants in building plant tissue. The term crop evapotranspiration has been used as synonymous with and in lieu of consumptive use in most recent literature because it is a more descriptive term for the processes involved.

8. Methods of Estimating. Several methods have been developed for estimating the evapotranspiration requirements of crops. The method which will yield the best estimate for a given situation depends upon the basic data available and the nature of the estimate required. Brief discussions of some of the methods now in use, and the circumstances under which each of them is usable, are described in the following paragraphs.

General Methods. These methods are primarily useful for reconnaissance or appraisal studies which do not require consideration of specific crops or cropping patterns. Most of them are usable with climatological data which are ordinarily

[1] "Irrigated Land Use," Bureau of Reclamation Manual, Vol. 5, Part 2, Land Classification; and "Soil Survey Manual," U.S. Department of Agriculture Handbook 18, 1951.

available and produce results in terms of annual or seasonal requirements rather than for periods of 1 month or less.

Lowry-Johnson. This method was developed in 1941[1] for use in the Western United States and is applicable to a variety of climatological conditions and lengths of growing season. It involves use of a graphical relationship between evapotranspiration (consumptive use) of water in feet of depth during the growing season and an index computed as the sum of the daily amounts, during the frost-free season, by which the maximum temperature in degrees Fahrenheit exceeds 32 degrees. The relationship is based on experimental data determined by inflow-outflow studies for several irrigated areas. It is not applicable for short periods representing parts of the frost-free season or for cropping patterns which differ from those generally in use in areas having the indicated "effective heat." Likewise, it is not applicable for areas which have unusual conditions with respect to wind, humidity, or insolation.

Thornthwaite. This method was developed in 1948[2] and involves use of an empirical equation to estimate the "potential evapotranspiration" in a given area by a stand of perennial grass. This method has been used for the preparation of maps showing the estimated annual potential evapotranspiration in many countries of the world. Research studies[3] have demonstrated that monthly evapotranspiration of perennial rye grass at Davis, Calif., varies during the year between limits of 1.3 and 2.0 times the estimated potential evapotranspiration computed by the Thornthwaite method. Estimates of potential evapotranspiration produced by the Thornthwaite method can be used as indexes for crop requirements where monthly adjustment factors have been established to reflect local climatological conditions and growing conditions of specific crops. The Thornthwaite equation is as follows:

$$\text{P.E.T.} = ct^a$$

where P.E.T. = potential evapotranspiration, cm/month
t = mean monthly temperature, degrees centigrade
c and a = constants selected to represent the climatological conditions at the station or area, the latitude of the area, and the month of the year

Penman. This method involves use of an equation developed in 1948[4] for estimating evaporation on the basis of data for wind velocity, vapor pressures for saturated vapor and air, and estimation of crop evapotranspiration by multiplying the evaporation values by empirical constants depending on latitude and length of daylight.[5] This method has been widely used throughout the world and has been found to give good results in comparison with experimental determinations of actual crop evapotranspiration. The Penman equations and relationships are as follows:

$$E_0 = 0.35(e_a - e_d)(1 + 0.01U)$$

$$E_T = \frac{HT + 0.27e_0}{T + 0.27}$$

$$H = R_A(1 - r)\left(0.18 + 0.55\frac{n}{N}\right) - \sigma T_a{}^4(0.56 - 0.092\sqrt{e_d})\left(0.10 + 0.90\frac{n}{N}\right)$$

[1] Lowry, Robert L., Jr., and Arthur F. Johnson, Consumptive Use of Water for Agriculture, *Trans. ASCE*, paper 2158, 1942.

[2] Thornthwaite, C. W., An Approach toward a Rational Classification of Climate, *Geog. Rev.*, **33**, 55–94.

[3] Pruitt, W. O., "Procedures for Estimating Crop Water Requirements for Use in Water Allocations and for Improvement of Irrigation Efficiency," Department of Irrigation, University of California, February, 1964.

[4] Penman, H. L., Natural Evaporation from Open Water, Bare Soil and Grass, *Proc. Roy. Soc. London*, April, 1948.

[5] Penman, H. L., Meteorology and Agriculture. General Survey of Meteorology and Agriculture and an Account of the Physics of Irrigation Control, *Quart. J. Roy. Meteorol. Soc.*, July, 1949.

where H = daily heat budget at the surface, mm of water/day
R_A = mean monthly extraterrestrial radiation, mm of water/day
r = reflection coefficient (about 0.25)
n = actual duration of bright sunshine, hr/day
N = maximum possible duration of bright sunshine, hr/day
σ = Boltzmann constant (2.01×10^{-9} mm/day)
T_a = mean daily air temperature (absolute)
e_d = saturation vapor pressure at mean dew point, mm of mercury
E_0 = evaporation, mm/day
e_a = saturation vapor pressure at mean air temperature, mm of mercury
U = mean wind speed at 2 m above the ground, miles/day
E_T = evapotranspiration of water, mm/day
T = ratio $(d)e_a/(d)T_a$

P/E Index. This method is based on the following formula developed by C. W. Thornthwaite for the computation of a ratio between monthly precipitation in inches and temperature in degrees Fahrenheit:

$$\log \frac{P}{E} = \log 115 + \frac{10}{9} \log P - \frac{10}{9} \log (T - 10)$$

where P = average monthly precipitation, in.
T = average monthly temperature, degrees F

P/E ratios of 1.0, 1.8, 3.2, 4.4, 5.8, 6.0, 6.8, 6.1, 4.6, 3.5, 2.3, and 1.5 for the months of January through December, respectively, were found by Munson[1] to represent adequate conditions for normal plant growth in the Western United States. The sum of the 12 monthly P/E ratios is the P/E index, and a value of 47 for that index corresponds to conditions for normal plant growth. By entering the formula with the average monthly temperature and the desired P/E ratio, the required consumptive use—assumed equal to the precipitation value—is determined. The method checks well with other general methods.

Methods for Specific Crops. These methods provide results for a single crop. Accordingly, they are most useful in determining water requirements for actual or assumed future cropping patterns, as distinguished from water requirements for generalized or typical cropping patterns. Water requirements for entire farms or projects are computed as the sums of requirements for the areas of land devoted to each of the several crops involved. Because these methods permit evaluation of the characteristics of each of the several crops—and usually for monthly or shorter periods during the growing season—they produce results which are generally more reliable for use in design of irrigation structures and in water dispatching for project operation than can be obtained by use of the general methods.

Blaney-Criddle. This method was developed in 1945[2] for use in estimating crop evapotranspiration requirements by use of the limited climatological data usually available. The empirical formula employed is

$$u = kf \qquad \text{and} \qquad U = KF = \text{sum of } kf$$

where $f = tp/100$
t = mean monthly temperature, degrees Fahrenheit
p = monthly percentage of daytime hours of the year (Table 3)

[1] Munson, Wendell C., Method for Estimating Consumptive Use of Water for Agriculture, *Proc. ASCE, J. Irrigation Drainage Div.*, December, 1960.

[2] Blaney, Harry F., and Wayne D. Criddle, "A Method of Estimating Water Requirements in Irrigated Areas from Climatological Data," Soil Conservation Service, U.S. Department of Agriculture, 1945.

TABLE 3. MONTHLY PERCENTAGE OF DAYTIME HOURS OF THE YEAR*
For Latitudes 0 to 65° North of the Equator

Latitude north, deg	Jan.	Feb.	Mar.	Apr.	May	June	July	Aug.	Sept.	Oct.	Nov.	Dec.
65	3.52	5.13	7.96	9.97	12.72	14.15	13.59	11.18	8.55	6.53	4.08	2.62
64	3.81	5.27	8.00	9.92	12.50	13.63	13.26	11.08	8.56	6.63	4.32	3.02
63	4.07	5.39	8.04	9.86	12.29	13.24	12.97	10.97	8.56	6.73	4.52	3.36
62	4.31	5.49	8.07	9.80	12.11	12.92	12.73	10.87	8.55	6.80	4.70	3.65
61	4.51	5.58	8.09	9.74	11.94	12.66	12.51	10.77	8.55	6.88	4.86	3.91
60	4.70	5.67	8.11	9.69	11.78	12.41	12.31	10.68	8.54	6.95	5.02	4.14
59	4.86	5.76	8.13	9.64	11.64	12.19	12.13	10.60	8.53	7.00	5.17	4.35
58	5.02	5.84	8.14	9.59	11.50	12.00	11.96	10.52	8.53	7.06	5.30	4.54
57	5.17	5.91	8.15	9.53	11.38	11.83	11.81	10.44	8.52	7.13	5.42	4.71
56	5.31	5.98	8.17	9.48	11.26	11.68	11.67	10.36	8.52	7.18	5.52	4.87
55	5.44	6.04	8.18	9.44	11.15	11.53	11.54	10.29	8.51	7.23	5.63	5.02
54	5.56	6.10	8.19	9.40	11.04	11.39	11.42	10.22	8.50	7.28	5.74	5.16
53	5.68	6.16	8.20	9.36	10.94	11.26	11.30	10.16	8.49	7.32	5.83	5.30
52	5.79	6.22	8.21	9.32	10.85	11.14	11.19	10.10	8.48	7.36	5.92	5.42
51	5.89	6.27	8.23	9.28	10.76	11.02	11.09	10.05	8.47	7.40	6.00	5.54
50	5.99	6.32	8.24	9.24	10.68	10.92	10.99	9.99	8.46	7.44	6.08	5.65
48	6.17	6.41	8.26	9.17	10.52	10.72	10.81	9.89	8.45	7.51	6.24	5.85
46	6.33	6.50	8.28	9.11	10.38	10.53	10.65	9.79	8.43	7.58	6.37	6.05
44	6.48	6.57	8.29	9.05	10.25	10.39	10.49	9.71	8.41	7.64	6.50	6.22
42	6.61	6.65	8.30	8.99	10.13	10.24	10.35	9.62	8.40	7.70	6.62	6.39
40	6.75	6.72	8.32	8.93	10.01	10.09	10.22	9.55	8.39	7.75	6.73	6.54
38	6.87	6.79	8.33	8.89	9.90	9.96	10.11	9.47	8.37	7.80	6.83	6.68
36	6.98	6.85	8.35	8.85	9.80	9.82	9.99	9.41	8.36	7.85	6.93	6.81
34	7.10	6.91	8.35	8.80	9.71	9.71	9.88	9.34	8.35	7.90	7.02	6.93
32	7.20	6.97	8.36	8.75	9.62	9.60	9.77	9.28	8.34	7.95	7.11	7.05
30	7.31	7.02	8.37	8.71	9.54	9.49	9.67	9.21	8.33	7.99	7.20	7.16
28	7.40	7.07	8.37	8.67	9.46	9.39	9.58	9.17	8.32	8.02	7.28	7.27
26	7.49	7.12	8.38	8.64	9.37	9.29	9.49	9.11	8.32	8.06	7.36	7.37
24	7.58	7.16	8.39	8.60	9.30	9.19	9.40	9.06	8.31	8.10	7.44	7.47
22	7.67	7.21	8.40	8.56	9.22	9.11	9.32	9.01	8.30	8.13	7.51	7.56
20	7.75	7.26	8.41	8.53	9.15	9.02	9.24	8.95	8.29	8.17	7.58	7.65
18	7.83	7.31	8.41	8.50	9.08	8.93	9.16	8.90	8.29	8.20	7.65	7.74
16	7.91	7.35	8.42	8.47	9.01	8.85	9.08	8.85	8.28	8.23	7.72	7.83
14	7.98	7.39	8.43	8.43	8.94	8.77	9.00	8.80	8.27	8.27	7.79	7.93
12	8.06	7.43	8.44	8.40	8.87	8.69	8.92	8.76	8.26	8.31	7.85	8.01
10	8.14	7.47	8.45	8.37	8.81	8.61	8.85	8.71	8.25	8.34	7.91	8.09
8	8.21	7.51	8.45	8.34	8.74	8.53	8.78	8.66	8.25	8.37	7.98	8.18
6	8.28	7.55	8.46	8.31	8.68	8.45	8.71	8.62	8.24	8.40	8.04	8.26
4	8.36	7.59	8.47	8.28	8.62	8.37	8.64	8.57	8.23	8.43	8.10	8.34
2	8.43	7.63	8.49	8.25	8.55	8.29	8.57	8.53	8.22	8.46	8.16	8.42
0	8.50	7.67	8.49	8.22	8.49	8.22	8.50	8.49	8.21	8.49	8.22	8.50

* From *Tech. Bull.* 1275, Agricultural Research Service, U.S. Department of Agriculture, in cooperation with the office of Utah State Engineer, as revised by Wayne D. Criddle.

TABLE 3. MONTHLY PERCENTAGE OF DAYTIME HOURS OF THE YEAR (*Continued*)
For Latitudes 0 to 50° South of the Equator

Latitude south, deg	Jan.	Feb.	Mar.	Apr.	May	June	July	Aug.	Sept.	Oct.	Nov.	Dec.
0	8.50	7.67	8.49	8.22	8.49	8.22	8.50	8.49	8.21	8.49	8.22	8.50
2	8.55	7.71	8.49	8.19	8.44	8.17	8.43	8.44	8.20	8.52	8.27	8.55
4	8.64	7.76	8.50	8.17	8.39	8.08	8.20	8.41	8.19	8.56	8.33	8.65
6	8.71	7.81	8.50	8.12	8.30	8.00	8.19	8.37	8.18	8.59	8.38	8.74
8	8.79	7.84	8.51	8.11	8.24	7.91	8.13	8.32	8.18	8.62	8.47	8.84
10	8.85	7.86	8.52	8.09	8.18	7.84	8.11	8.28	8.18	8.65	8.52	8.90
12	8.91	7.91	8.53	8.06	8.15	7.79	8.08	8.23	8.17	8.67	8.58	8.95
14	8.97	7.97	8.54	8.03	8.07	7.70	7.08	8.19	8.16	8.69	8.65	9.01
16	9.09	8.02	8.56	7.98	7.96	7.57	7.94	8.14	8.14	8.76	8.72	9.17
18	9.18	8.06	8.57	7.93	7.89	7.50	7.88	8.10	8.14	8.80	8.80	9.24
20	9.25	8.09	8.58	7.92	7.83	7.41	7.73	8.05	8.13	8.83	8.85	9.32
22	9.36	8.12	8.58	7.89	7.74	7.30	7.76	8.00	8.13	8.86	8.90	9.38
24	9.44	8.17	8.59	7.87	7.65	7.24	7.58	7.95	8.12	8.89	8.96	9.47
26	9.52	8.28	8.60	7.81	7.56	7.07	7.49	7.90	8.11	8.94	9.10	9.61
28	9.61	8.31	8.61	7.79	7.49	6.99	7.40	7.85	8.10	8.97	9.19	9.74
30	9.69	8.33	8.63	7.75	7.43	6.94	7.30	7.80	8.09	9.00	9.24	9.80
32	9.76	8.36	8.64	7.70	7.34	6.85	7.20	7.73	8.08	9.04	9.31	9.87
34	9.88	8.41	8.65	7.68	7.25	6.73	7.10	7.69	8.06	9.07	9.38	9.99
36	10.06	8.53	8.67	7.61	7.16	6.59	6.99	7.59	8.06	9.15	9.51	10.21
38	10.14	8.61	8.68	7.59	7.07	6.46	6.87	7.51	8.05	9.19	9.60	10.34
40	10.24	8.65	8.70	7.54	6.96	6.33	6.73	7.46	8.04	9.23	9.69	10.42
42	10.39	8.72	8.71	7.49	6.85	6.20	6.60	7.39	8.01	9.27	9.79	10.57
44	10.52	8.81	8.72	7.44	6.73	6.04	6.45	7.30	8.00	9.34	9.91	10.72
46	10.68	8.88	8.73	7.39	6.61	5.87	6.30	7.21	7.98	9.41	10.03	10.90
48	10.85	8.98	8.76	7.32	6.45	5.69	6.13	7.12	7.96	9.47	10.17	11.09
50	11.03	9.06	8.77	7.25	6.31	5.48	5.98	7.03	7.95	9.53	10.32	11.30

f = monthly consumptive-use factor or index
k = monthly coefficient determined from experimental data
u = monthly evapotranspiration by the crop, in.
U = seasonal evapotranspiration, in.
F = sum of the monthly consumptive-use factors for the growing season of the particular crop
K = seasonal crop coefficient

In metric units,

$$u = kp\,\frac{(45.7t + 813)}{100} = \text{monthly evapotranspiration, mm}$$

t = mean monthly temperature, degrees centigrade

Because of its simplicity and adaptability to readily available data, the Blaney-Criddle method has been widely used in the United States and throughout the world for the planning and operation of irrigation projects. The method was first developed to estimate the seasonal requirements of crops for irrigation water, and the crop coefficients presented in the early literature on the method were seasonal values, also. Because of the need for monthly determinations of water requirements for canal and structure design, these seasonal coefficients have often been applied erroneously to

Table 4. Typical Monthly Coefficients k for Use in Blaney-Criddle Method*

Crop	Location	Jan.	Feb.	Mar.	Apr.	May	June	July	Aug.	Sept.	Oct.	Nov.	Dec.
Alfalfa	Mesa, Ariz.	0.35	0.55	0.75	0.90	1.05	1.15	1.15	1.10	1.00	0.85	0.65	0.45
Alfalfa	Logan, Utah					0.50	0.65	0.75	0.80	0.70			
Grass pasture	Merced, Calif.			0.16	0.45	0.65	0.75	0.78	0.74	0.55	0.20		
Oranges	Phoenix, Ariz.	0.26	0.33	0.39	0.45	0.50	0.54	0.58	0.60	0.60	0.56	0.49	0.36
Deciduous fruit	San Joaquin Delta, Calif.			0.23	0.45	0.70	0.85	0.88	0.85	0.47	0.20		
Avocados	Fallbrook, Calif.	0.15	0.25	0.35	0.45	0.54	0.60	0.64	0.63	0.57	0.46	0.39	0.21
Walnuts	Davis, Calif.			0.13	0.30	0.55	0.84	0.98	0.88	0.60	0.37	0.20	
Field corn	Davis, Calif.					0.12	0.40	0.60	0.62	0.45			
Field corn	Mandan, N. Dak.					0.50	0.65	0.75	0.80	0.70			
Grain sorghum	Phoenix, Ariz.						0.40	1.00	0.85	0.70			
Grain sorghum	Great Plains Sta., Tex.						0.30	0.75	1.10	0.85	0.50		
Wheat	Garden City, Kans.	0.40	0.72	0.97	1.05	0.82							
Wheat	Great Plains Sta., Tex.	0.63	0.82	0.93	1.02	1.03						0.38	0.45
Oats	Salt River Valley, Ariz.		0.30	0.80	1.10	1.22	0.92	0.40					
Cotton	Bakersfield, Calif.					0.30	0.45	0.90	1.00	1.00			
Cotton	Weslaco, Tex.			0.20	0.45	0.70	0.85	0.85	0.80	0.55			
White beans	Santa Barbara, Calif.						0.60	0.70	0.70	0.60			
Soybeans	Phoenix, Ariz.						0.30	0.64	0.91	0.50			
Sugar beets	Scottsbluff, Nebr.					0.27	0.50	0.80	1.08	1.00	0.69		
Potatoes	Phoenix, Ariz.		0.20	0.50	1.00	1.20	1.05						
Potatoes	Mandan, N. Dak.					0.45	0.75	0.90	0.80	0.40			
Tomatoes	Sacramento, Calif.					0.41	0.74	0.93	0.98	0.89			
Melons	Murrieta, Calif.						0.45	0.70	0.74	0.64			
Small vegetables	Delta, Calif.				0.23	0.49	0.67	0.78	0.78	0.64	0.40		

* From *U.S. Dept. Agr. Tech. Bull.* 1275.

monthly consumptive-use factors to estimate monthly water requirements. Experimental data which have been available since about 1959 have demonstrated that the monthly coefficients for annual crops are only about half of the seasonal value during the first month of the growing season and may be 1.5 times the seasonal value during the month of maximum requirement. Most of these variations are due to the stage of the root and vegetative growth of the plants. It is most important, therefore, that appropriate crop coefficients are used for monthly—or other short-period—computations of irrigation-water requirements. Typical monthly coefficients for some irrigated crops at various locations in the Western United States are given in Table 4.

Recent research[1] has demonstrated that the monthly relationship between evapotranspiration for a perennial crop in an area with a year-round growing season and the monthly consumptive-use coefficients varies from a low of about 0.3 in winter to a high of 1.15 in summer. This illustrates the fact that monthly values used for the crop coefficient k in the Blaney-Criddle method must account for a seasonal variation in the relationship between evapotranspiration and the consumptive-use factor f. The monthly crop coefficients also must vary between areas because of differences in wind movement, humidity, and other climatological factors which are not represented by

TABLE 5. VALUES OF THE CLIMATIC COEFFICIENT k_t* FOR VARIOUS MEAN AIR TEMPERATURES t†

t, °F	k_t	t, °F	k_t	t, °F	k_t
36	0.31	61	0.74	86	1.17
37	0.33	62	0.76	87	1.19
38	0.34	63	0.78	88	1.21
39	0.36	64	0.79	89	1.23
40	0.38	65	0.81	90	1.24
41	0.40	66	0.83	91	1.26
42	0.41	67	0.84	92	1.28
43	0.43	68	0.86	93	1.30
44	0.45	69	0.88	94	1.31
45	0.46	70	0.90	95	1.33
46	0.48	71	0.91	96	1.35
47	0.50	72	0.93	97	1.36
48	0.52	73	0.95	98	1.38
49	0.53	74	0.97	99	1.40
50	0.55	75	0.98	100	1.42
51	0.57	76	1.00		
52	0.59	77	1.02		
53	0.60	78	1.04		
54	0.62	79	1.05		
55	0.64	80	1.07		
56	0.66	81	1.09		
57	0.67	82	1.10		
58	0.69	83	1.12		
59	0.71	84	1.14		
60	0.72	85	1.16		

* Values of k_t are based on the formula $k_t = 0.0173t - 0.314$. For mean temperatures less than 36°, use $k_t = 0.300$.

† From U.S. Department of Agriculture Soil Conservation Service Technical Release 21.

[1] PRUITT, W. O., "Procedures for Estimating Crop Water Requirements for Use in Water Allocations and for Improvement of Irrigation Efficiency," Department of Irrigation, University of California, Davis, Calif., February, 1964.

air temperature and duration of daylight hours. Experience and judgment are necessary for the selection of appropriate crop coefficients for use in the Blaney-Criddle method for areas where experimental results are not available as a guide for the extrapolation of data from other areas and other climatological conditions.

Modified Blaney-Criddle. This method[1] involves some improvements in the Blaney-Criddle method. The following modifications are made in the original Blaney-Criddle formula:

$$k = k_t k_c$$

where k_t = climatic coefficient related to the mean air temperature t as shown in Table 5

TABLE 6. CROP-GROWTH-STAGE COEFFICIENTS K_c (MODIFIED BLANEY-CRIDDLE METHOD)

Perennial Crops (Northern Hemisphere)

Crop	Average k_c values by months											
	Jan.	Feb.	Mar.	Apr.	May	June	July	Aug.	Sept.	Oct.	Nov.	Dec.
Alfalfa	0.63	0.74	0.86	0.99	1.09	1.13	1.11	1.06	0.99	0.90	0.78	0.65
Grass pasture	0.48	0.58	0.74	0.85	0.90	0.92	0.92	0.91	0.87	0.79	0.67	0.55
Grapes	0.20	0.23	0.32	0.49	0.70	0.80	0.81	0.76	0.66	0.50	0.35	0.25
Citrus orchards	0.64	0.66	0.68	0.70	0.71	0.72	0.72	0.71	0.70	0.68	0.66	0.64
Deciduous, with cover	0.63	0.74	0.86	0.98	1.09	1.13	1.12	1.06	0.99	0.90	0.78	0.65
Deciduous, no cover	0.17	0.25	0.39	0.63	0.87	0.96	0.95	0.82	0.53	0.30	0.20	0.16
Avocados	0.27	0.42	0.58	0.71	0.78	0.81	0.78	0.71	0.63	0.54	0.43	0.36
Walnuts	0.10	0.14	0.23	0.43	0.68	0.92	0.98	0.88	0.69	0.49	0.31	0.15

Annual Crops

Crop	K_c values at listed % of growing season										
	0	10	20	30	40	50	60	70	80	90	100
Field corn (grain)	0.44	0.49	0.58	0.71	0.93	1.05	1.08	1.06	1.01	0.93	0.85
Field corn (silage)	0.44	0.48	0.55	0.65	0.80	0.97	1.06	1.08	1.06	1.02	0.96
Grain sorghum	0.30	0.38	0.60	0.83	1.01	1.07	0.99	0.88	0.76	0.65	0.56
Winter wheat*	1.46	1.44	1.42	1.39	1.35	1.30	1.23	1.15	1.03	0.86	0.78
Spring grains	0.29	0.45	0.67	0.89	1.09	1.28	1.31	1.17	0.90	0.55	0.20
Cotton	0.20	0.25	0.33	0.50	0.79	0.97	1.02	0.95	0.81	0.65	0.29
Dry beans	0.50	0.59	0.71	0.87	1.02	1.10	1.12	1.06	0.94	0.81	0.67
Sugar beets	0.45	0.50	0.61	0.79	0.95	1.10	1.20	1.25	1.21	1.13	1.04
Potatoes	0.33	0.40	0.51	0.72	0.98	1.17	1.31	1.37	1.36	1.31	1.23
Tomatoes	0.45	0.45	0.47	0.56	0.75	0.95	1.03	0.99	0.90	0.80	0.70
Melons and cantaloupe	0.44	0.48	0.56	0.65	0.76	0.81	0.81	0.78	0.75	0.71	0.67
Small vegetables	0.29	0.40	0.57	0.69	0.77	0.81	0.82	0.79	0.72	0.58	0.38

* Data given only for springtime season of 70 days prior to harvest (after last frost). K_c increases from 0.50 at seeding to 1.46 during period with average temperature below 32 F.

[1] Described in "Irrigation Water Requirements," U.S. Department of Agriculture Soil Conservation Service Technical Release 21, Apr. 29, 1964.

k_c = coefficient reflecting growth stage of crop. Values for principal crops are listed in Table 6

The climatic coefficient k_t was introduced as an empirical adjustment to minimize the variations in the resulting k between seasons. Within the limits of experimental data in areas in which irrigation is normally employed, this adjustment appears to overcome the criticism that the Blaney-Criddle formula does not take humidity and wind movement into account. The crop-growth-stage coefficient k_c values have been calculated from reliable research data.

The modified Blaney-Criddle method is recommended for use in estimating crop evapotranspiration requirements whenever reliable information is not available on pan evaporation or climatological factors (air temperature, dew point, wind movement, and solar radiation) necessary for computation of shallow-lake evaporation.

Evaporation-index Method. This method of estimating crop evapotranspiration uses shallow-lake evaporation as the index to which crop-use coefficients are applied. The method is fully described in *Bull.* 6019 of the Texas Water Development Board[1]

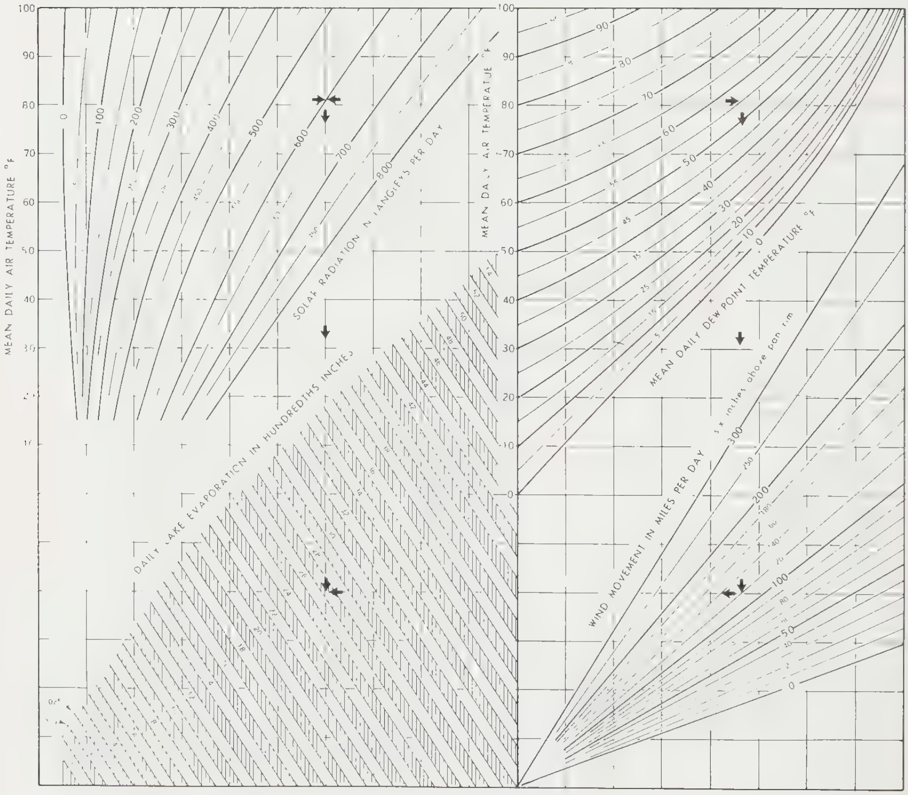

FIG. 1. Lake evaporation relation. NOTE: The International Pyrheliometric Scale which became effective in United States on July 1, 1957, provides values which are 2.0 percent less than those previously obtained. This evaporation relation is based on radiation values obtained prior to that date. For computations based on data subsequent to July 1, 1957, increase radiation values by 2 percent. (*"Evaporation Maps for the United States," Technical Paper No.* 37, *Hydrologic Services Division, U.S. Weather Bureau, August,* 1959.)

[1] McDaniels, Louis L., Consumptive Use of Water by Major Crops in Texas, Texas Board of Water Engineers (now Texas Water Development Board), *Bull.* 6019, Austin, Tex., November, 1960.

and is briefly summarized as follows:

$$UC = IC \times KU$$

where UC = crop evapotranspiration requirement (consumptive use) on a monthly or shorter period basis

IC = climatic index, which is the same as the evaporation from a hypothetical shallow lake situated at the locality under consideration

KU = crop-use coefficient, which reflects the stage of growth of the crop

Values for shallow-lake evaporation to be used in this method should be computed by the graphical solution presented in U.S. Weather Bureau Technical Paper 37[1] if available data on air temperature, dew point, wind movement, and solar radiation are adequate. Otherwise, it may be possible to estimate shallow-lake evaporation by applying appropriate conversion factors to evaporation data collected from pans, Piche evaporimeters, or other instruments. Values for shallow-lake evaporation can be computed by use of the graphs presented in Fig. 1. Average values for crop-use coefficients to be used in this method are presented in Table 7 for a variety of crops.

TABLE 7. CROP-USE COEFFICIENTS FOR USE IN EVAPORATION-INDEX METHOD

Perennial Crops (Northern Hemisphere)

Crop	Average KU values by months											
	Jan.	Feb.	Mar.	Apr.	May	June	July	Aug.	Sept.	Oct.	Nov.	Dec.
Alfalfa	0.83	0.90	0.96	1.02	1.08	1.14	1.20	1.25	1.22	1.18	1.12	0.86
Grass pasture	1.16	1.23	1.19	1.09	0.95	0.83	0.79	0.80	0.91	0.91	0.83	0.69
Grapes			0.15	0.50	0.80	0.70	0.45					
Citrus orchards	0.58	0.53	0.65	0.74	0.73	0.70	0.81	0.96	1.08	1.03	0.82	0.65
Deciduous orchards				0.60	0.80	0.90	0.90	0.80	0.50	0.20	0.20	
Sugarcane	0.65	0.50	0.80	1.17	1.21	1.22	1.23	1.24	1.26	1.27	1.28	0.80

Annual Crops

Crop	KU values at listed % of growing season										
	0	10	20	30	40	50	60	70	80	90	100
Field corn	0.45	0.51	0.58	0.66	0.75	0.85	0.96	1.08	1.20	1.08	0.70
Grain sorghum	0.30	0.40	0.65	0.90	1.10	1.20	1.10	0.95	0.80	0.65	0.50
Winter wheat*	1.08	1.19	1.29	1.35	1.40	1.38	1.36	1.23	1.10	0.75	0.40
Cotton	0.40	0.45	0.56	0.76	1.00	1.14	1.19	1.11	0.83	0.58	0.40
Sugar beets	0.30	0.35	0.41	0.56	0.73	0.90	1.08	1.26	1.41	1.30	1.10
Cantaloupes	0.30	0.30	0.32	0.35	0.46	0.70	1.05	1.22	1.13	0.82	0.44
Potatoes (Irish)	0.30	0.40	0.62	0.87	1.06	1.24	1.40	1.50	1.50	1.40	1.26
Papago peas	0.30	0.40	0.66	0.89	1.04	1.16	1.26	1.25	0.63	0.28	0.16
Beans	0.30	0.35	0.58	1.05	1.07	0.94	0.80	0.66	0.53	0.43	0.36
Rice†	1.00	1.06	1.13	1.24	1.38	1.55	1.58	1.57	1.47	1.27	1.00

* Data given only for springtime season of 70 days prior to harvest (after last frost).

† Evapotranspiration only.

[1] KOHLER, M. A., T. J. NORDENSON, and W. E. FOX, "Evaporation Maps for the United States," U.S. Weather Bureau Technical Paper 37, 1959.

The evaporation-index method is recommended for use in estimating crop evapotranspiration requirements whenever unusual humidity or wind movements prevail in the locality under consideration, or when data are available for the preparation of reliable values of shallow-lake evaporation. When data are insufficient for the estimate of evaporation, or when doubtful approximations must be made to develop data for use in such estimation, it will be preferable to use the modified Blaney-Criddle method. The advantage of the evaporation-index method is that it includes consideration of humidity and wind movement. The disadvantages of the method are that it is time-consuming, particularly if estimates must be made of solar radiation by use of standard tables and adjustments for percent of sunshine or estimates of cloud cover, and may require use of adjusted data of questionable value for solar radiation and wind movement at the proper level above ground.

Methods which are in many respects similar to the evaporation-index method have been developed by Hargreaves,[1] Olivier,[2] and Hansen.[3] Crop-use coefficients given by Hargreaves and Hansen, however, are to be applied to evaporation from a U.S. Weather Bureau class *A* pan instead of evaporation from a shallow lake. A coefficient of 1.00 to be used with pan evaporation would be equivalent to a value of about 1.45 with shallow-lake evaporation.

9. Free-water Evaporation. Although some writers refer to evaporation from pans as "free-water evaporation," the term is generally applied to evaporation from larger bodies of water such as lakes and reservoirs whose surface area is of appreciable size. Furthermore, the term is usually applied to evaporation from shallow lakes and reservoirs, in which advection or change in water temperature would not have a major effect on monthly loss by evaporation.

Evaporation Pans. Losses of water from pans are influenced by the diameter of the pan, the depth of the pan, the color of the pan, the height of the pan rim above water surface, coverings of the pan such as screens, the exposure of the pan (on land or floating in a large body of water), and the material surrounding the pan (air or earth—as in sunken pans). These characteristics of a particular pan and its mounting and environment influence, also, the ratio of the losses from that pan by evaporation to the evaporation losses from a hypothetical lake or reservoir at the same location. That ratio is affected, too, by heat transfer through the pan due to differences between the temperature of the air and that of the water in the pan.

The most widely used pan in the United States for measurements of evaporation is designated the Weather Bureau class *A* pan. It is of cylindrical design—10 in. deep and 47½ in. in diameter (inside dimensions).[4] It is constructed of galvanized iron or an alloy similar to monel metal. The pan should be installed above the ground level and should rest on 2- by 4-in. boards placed flat and spaced at 7.33-in. centers on compacted earth fill high enough to keep the bottom of the pan above the level of surface water in rainy weather. The boards should be leveled carefully so as to extend at least 1 in. above the earth fill to provide air space under the pan. The level of water in the pan should be kept between 2 and 3 in. below the rim of the pan. The pan coefficient for the class *A* pan (shallow-lake evaporation divided by the pan evaporation) averages 0.70 on an annual basis. As shown in Fig. 2, the annual class *A* pan coefficient at various places in the continental United States varies between 0.60 and 0.80. Monthly pan coefficients vary at a particular location or for a

[1] Hargreaves, George H., Irrigation Requirements Based on Climatic Data, *Proc. ASCE, J, Irrigation Drainage Div.*, November, 1956.

[2] Olivier, Henry, "Irrigation and Climate," Edward Arnold (Publishers) Ltd., London, 1961.

[3] Israelsen, O. W., and V. E. Hansen, "Irrigation Principles and Practices," John Wiley & Sons, Inc., New York, 1962.

[4] "Instructions for Climatological Observers," U.S. Weather Bureau Circular B, 10th ed.

FIG. 2. Average annual class *A* pan coefficients. ("*Evaporation Maps for the United States,*" *Technical Paper No.* 37, *Hydrologic Services Division, U.S. Weather Bureau, August,* 1959.)

TABLE 8. ANNUAL EVAPORATION-PAN COEFFICIENTS

Name	Diam, ft	Depth, in.	Other factors	Pan-to-lake coefficient
Class *A*	4	10	Galvanized metal	0.69*
BPI	6	24	Sunken	0.91*
Colorado	3	18	Sunken, square	0.83*
Young	2	36	Sunken, screened	0.91*
	12	36	Sunken	1.00†
	9	36	Sunken	0.99†
	4	36	Sunken	0.85†
	2	36	Sunken	0.78†
	1	36	Sunken	0.63†

* "Water Loss Investigations," Vol. 1, Lake Hefner Studies, Geological Survey Circular 229, 1952.
† SLEIGHT, R. B., Discussion of Paper, "Evaporation on U.S. Reclamation Projects," *Trans. ASCE*, 1927.

particular body of water, depending upon the thermal characteristics of the body of water (temperature of inflowing and outflowing water and change in stored heat).

Pan coefficients for several sizes and types of pans are listed in Table 8. The annual values listed represent average values over a consecutive 12-month period. Monthly values, according to the experiments at Lake Hefner,[1] were found to vary between about 20 and 180 percent of the average annual values. The variations in average annual lake-evaporation values throughout the continental United States are shown in Fig. 3.

Experiments performed with pans having different colored and treated surfaces[2] yielded evaporation results having the following ratios to results from pans having untreated galvanized surfaces:

White enamel	0.83
Orange enamel	0.92
Light yellow enamel	0.93
Aluminum paint	0.98
Dark blue enamel	1.02
Dark green enamel	1.02
Black enamel	1.06
Untreated copper	1.07

Piche Evaporimeters. In many parts of the world the only evaporation data available are those observed with Piche evaporimeters. These instruments are graduated glass tubes, inverted and with a circular blotter held over the lower end by a clamp. They are usually installed in a conventionally louvered shelter with other weather instruments. While the Piche instruments are cheap and convenient to use, the readings obtained therefrom are often more erratic than those from standard pans. In arid areas with high temperatures and low humidities, evaporation from the Piche blotter pad is so rapid that the edges of the pad may become dry and curl, resulting in erroneously low values. Experiments by Keeling[3] have indicated that evaporation values from a class *A* pan are about 70 percent of those from a Piche instrument installed in a double-louvered shelter. A comparison of monthly data for stations in Ecuador and Uruguay where both instruments are in operation under identical con-

[1] "Water Loss Investigations," Vol. 1, Lake Hefner Studies, Geological Survey Circular 229, 1952.
[2] YOUNG, A. A., Discussion on Paper 2262, "Evaporation from a Free Water Surface," by G. H. Hickox, *Trans. ASCE*, 1946.
[3] KEELING, B. F. E., "Evaporation in Egypt and the Sudan," Survey Department Paper 15, Ministry of Finance, Cairo, 1909.

FIG. 3. Average annual lake evaporation (1946 1955). ("*Evaporation Maps for the United States*," *Technical Paper No.* 37, *Hydrologic Services Division, U.S. Weather Bureau, August*, 1959.)

ditions indicates that the correlation is poor and that the average relationship checks that given by Keeling for monthly values less than about 150 mm, but the average ratio may be unity for monthly values of 250 mm or more.

Estimates from Climatological Data. Estimates of evaporation from water surfaces can be made from climatological data by means of the Penman equations[1] presented in Art. 8 or by the graphical solution developed by the U.S. Weather Bureau[2] presented in Fig. 1. Climatological data employed in these solutions include wind movement (adjusted to the proper level above ground), mean daily dew-point temperature, solar radiation, and mean daily air temperature. Wind measurements taken at other heights can be corrected to the desired elevation by use of the following formula:

$$U_x = U_h \frac{\log x}{\log h}$$

where U_h = wind movement, miles/day at the observation level h, ft

U_x = wind movement, miles/day at a height x ft above the ground

While estimates of evaporation computed from climatological data may be preferable to pan data for use in computations of evapotranspiration requirements—because the latter may be biased by the pan location with respect to buildings, trees, or irrigated fields—this advantage may be nullified by the need for estimating solar radiation from standard values adjusted for cloud cover or percent of possible sunshine.

10. Crop Coefficients. Coefficients which reflect the water-using characteristics of each crop are necessary for each method for estimating evapotranspiration requirements, except for those methods which do not consider particular crops or cropping patterns. The latter methods are generally used only for reconnaissance or appraisal studies. Discussions of the several methods presented in Art. 8 cover the crop coefficients which apply to each method, and those coefficients are listed in Tables 4, 6, and 7.

Since the actual crop evapotranspiration is difficult to measure accurately under field conditions, and requires expensive and complex instrumentation, basic data for the determination of crop coefficients are available for only a few experimental sites. In the United States, most of these data result from the cooperative investigations of the Agricultural Research Service of the Department of Agriculture and colleges or universities in states in which irrigation is practiced extensively. Only a few, including the Agricultural Research Station of the University of California at Davis, Calif., are equipped with large-scale lysimeters capable of measuring evapotranspiration under field conditions. Consequently, it is necessary to extrapolate laboratory-type data for a relatively few locations to field conditions throughout the world where irrigation is practiced or may be beneficial.

Much of the published literature on crop coefficients, particularly for the Blaney-Criddle method, includes values applicable only to entire growing seasons. While these seasonal coefficients are useful for general studies, such as those for determining storage-capacity requirements, they do not permit determination of short-period requirements for irrigation water, which are needed for design of adequate canals and irrigation structures. Many erroneous studies have been made using seasonal crop coefficients applied to monthly index data. This results in irrigation-requirement estimates that are too great at the beginning and end of growing seasons and are too low during the months of peak requirements.

Crop coefficients for periods of a month or less throughout the growing season of a crop reflect the characteristics of that crop at the several stages of growth. Since

[1] Penman, H. L., Natural Evaporation from Open Water, Bare Soil and Grass, *Proc. Roy. Soc. London*, April, 1948.

[2] "Evaporation Maps for the United States," U.S. Weather Bureau Technical Paper 37, 1959.

evapotranspiration includes evaporation from the soil surface in the fields, the crop coefficients should also reflect the method used in applying the irrigation water and the frequency of irrigations. The coefficients listed in Tables 4, 6, and 7 are average values, and adjustments of those values may be desirable for application in unusual situations. For example, the coefficients should be increased for fields with shallow or sandy soils where frequent, light applications of irrigation water would be necessary and there would be greater opportunity for evaporation losses from wet soil.

Because actual evapotranspiration has been measured at only a relatively few locations and studies for other areas require extrapolation of those data, the Blaney-Criddle method must be used with caution in areas where humidity and wind conditions are different from those at the experimental sites. The evaporation-index method and the modified Blaney-Criddle method are generally preferable because crop coefficients for those methods have less variation between areas. This situation is to be expected because the latter two methods listed take into account more climatological factors.

FARM-IRRIGATION REQUIREMENTS

Requirements for deliveries of irrigation water to farms depend upon numerous factors including (1) the acreages devoted to each of the several crops grown, (2) the evapotranspiration requirements of those crops under the climatic conditions prevailing in the area, (3) the effective rainfall in the area, (4) the need, if any, for irrigation prior to planting, (5) the farm-irrigation efficiency, and (6) other factors such as the quality of the irrigation water or the need for leaching of previous accumulations of salts from the soil. The farm-irrigation efficiency is the percentage of water delivered that is utilized in crop evapotranspiration, and it is influenced by the size of the farms because of the effect of conveyance losses between the point of delivery to the farm and the several fields. Farm conveyance losses are influenced by the same factors which affect losses from the larger conveyance facilities of an irrigation project, as discussed elsewhere under Conveyance Losses and Waste.

11. Cropping Pattern. The term "cropping pattern" as used here means the percentage of the total field areas actually available and suitable for cropping which are devoted to each crop during each of the two principal growing seasons of a year. Under this definition, the summation of percentages for all crops grown in an area suitable for the year-round cropping could be 200 percent. This would represent complete utilization of the land in each of the two seasons and would involve double counting of crops such as alfalfa, sugarcane, or citrus orchards, which use water in all 12 months of the year.

Cropping patterns for single farms are different from those for a large project, even when the particular farm might be included in the project. This is because the growing seasons of crops grown on a single farm must be compatible, thereby avoiding interference in use of the fields and providing time for harvesting of one crop and for seedbed preparation before planting of the next crop. This is not required in cropping patterns for large project areas because of diversity between the cropping patterns of the several farms. It is quite possible that no single farm would utilize the cropping pattern that would apply for the project.

The distribution of crops in a cropping pattern is influenced by many factors including (1) suitability of the soil for various crops, (2) suitability of the climatic characteristics for various crops, (3) economic conditions which influence the return the farmer may expect to receive for his labor and investment from various crops, (4) governmental controls on acreages devoted to crops in which surplus production has been experienced, (5) limitations imposed by project regulations (generally to avoid having a large percentage of the project land in a single crop which would result in a high peak water requirement, possibly exceeding delivery capabilities or seasonal water supplies), and (6) the preferences and experience of the farmers in growing certain crops. In the United States it can be assumed that a high technical level of farm management will be employed in irrigation enterprises. This will assure the use of rotations of crops to improve or preserve the soil fertility and crop distributions which will make possible efficient employment of labor and equipment. Under such a level of management, it can be assumed that project cropping patterns will change over a period of years as market and economic conditions change. These assumptions may not be warranted or realistic in the planning of irrigation developments in many of the developing nations of the world. In any event, agricultural economic studies are required in order to establish cropping patterns for projects which may be expected to be representative of future conditions with respect to water requirements, agricultural production, and farmers' incomes during the economic life of the project works.

Table 9 presents several typical cropping patterns for project-sized areas. These

TABLE 9. TYPICAL PROJECT CROPPING PATTERNS

	Percentage of irrigable area			
	California	Texas	Argentina	Pakistan
Wheat and other grains	30.7	0.5	10.0	60.0
Rice	....	....	....	8.0
Oil seeds	....	....	....	7.0
Corn (maize)	0.1	4.8	7.5	10.0
Grain sorghum	0.2	14.4		
Sugarcane	....	...	....	10.0
Cotton	0.8	53.3	20.0	17.0
Sugar beets	10.0			
Deciduous fruits	0.1	0.1		
Citrus	0.5	17.2	10.0	2.0
Vegetables	16.2	49.2	32.5	3.0
Hay and pasture	44.2	23.3	35.0	18.0

patterns illustrate the distributions of crops in irrigated areas in the United States and some foreign countries where irrigation is practiced.

12. Effective Rainfall. Part of the rainfall which occurs during the growing season of a crop is lost through surface runoff or deep percolation below the root zone of the soil profile. The portion of the growing-season rainfall which is assumed to be utilized in meeting evapotranspiration requirements of crops is termed "effective rainfall" in irrigation studies. In arid areas effective rainfall may be so small as to be of little consequence, while in humid areas it may provide a major portion of the evapotranspiration requirements for optimum growth of many crops. Growth of irrigation in humid areas in the United States in recent years is evidence of the economic significance of irrigation as an aspect of efficient farm management. This is because the time distribution of rainfall rarely suffices to maintain the soil moisture in the root zone within the range necessary for optimum growth during all parts of a growing season. Information in Fig. 4 is presented to illustrate this point. Curve 3 shows that at Corsicana, Tex., there were 10 periods of 24 days or longer in which no rain occurred during the growing seasons of 10 consecutive years. This means an average of one such period each year. Since moisture stored in the soil root zone could supply crop needs for only about 10 days during the time of greatest water use, such a rainless period would result in some yield reduction, if not a complete failure. Curves 1 and 2 represent more favorable rainfall distributions for crop production.

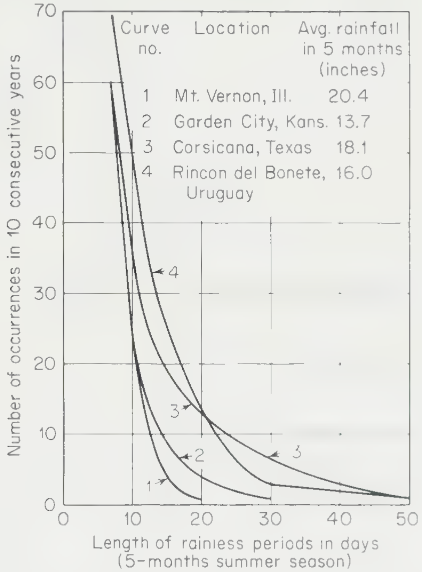

Fig. 4. Duration and frequency of rainless periods.

In estimating irrigation-water requirements, the engineer must estimate the effective rainfall from records of experienced rainfall in the area of the farm or project. In making these estimates, the average moisture level of the soil root zone at the beginning of rainfall is important. This moisture level is influenced by (1) the consumptive use rate of the crop, (2) the moisture-holding capacity of the soil root zone, and (3) the frequency and depth of applications of irrigation water or periods of rainfall. It may be assumed that through infiltration from rainfall or irrigation applications, the moisture level at the soil root zone will be maintained between field capacity and a level somewhat above that at which crop growth would be retarded. This means that even in arid climates some of the rainfall will occur on soil that is at or near field moisture capacity and will not be effective in supplying evapotranspiration. The chance of such a situation is reduced if the rate of evapotranspiration of the crop is high and if the soil root zone has a large range of usable moisture capacity.

Studies by the Soil Conservation Service for 50 years of record at 22 Weather Bureau stations throughout the continental United States[1] have resulted in the relationship between monthly mean rainfall, monthly effective rainfall, and average monthly consumptive use (evapotranspiration) shown in Table 10. Values in that table may not be applicable to areas where soil intake rates are low or rainfall intensities are consistently high. In such cases, the engineer must make adjustments to reflect the local conditions.

The engineer must consider, also, the frequency distribution of effective rainfall. While the crop evapotranspiration requirement will usually vary from year to year by a relatively small amount, there may be a large variation from year to year in rainfall. It may be desirable, for example, to plan for an irrigation supply that will be fully adequate for evapotranspiration requirements in 8 out of 10 years. In such a case it could be assumed that the ratio of the desired effective rainfall to the effective rainfall determined by use of Table 10 would be the same as the ratio of the growing-season rainfall that would be equaled or exceeded in 8 years out of 10 to the sum of the

[1] "Irrigation Water Requirements," U.S. Department of Agriculture Soil Conservation Service Technical Release 21, Apr. 29, 1964.

TABLE 10. AVERAGE MONTHLY EFFECTIVE RAINFALL*,† AS RELATED TO MEAN MONTHLY RAINFALL AND AVERAGE MONTHLY CONSUMPTIVE USE

Monthly mean rainfall rt, in.	Average monthly consumptive use u, in.									
	1.0	2.0	3.0	4.0	5.0	6.0	7.0	8.0	9.0	10.0
	Average monthly effective rainfall re, in.									
0.5	0.20	0.25	0.30	0.30	0.30	0.35	0.40	0.45	0.50	0.50
1.0	0.55	0.60	0.65	0.70	0.70	0 75	0.80	0.85	0.95	1.00
2.0	1.00	1.25	1.35	1.55	1.55	1.55	1.60	1.70	1.85	2.00
3.0	1.00	1.85	1.95	2.10	2.20	2.30	2.40	2.55	2.70	2.90
4.0	1.00	2.00	2.55	2.70	2.90	2.95	3.15	3.30	3.50	3.80
5.0	1.00	2.00	3.00	3.25	3.50	3.60	3.85	4.05	4.30	4.60
6.0	1.00	2.00	3.00	3.80	4.10	4.25	4.50	4.80	5.10	5.40
7.0	1.00	2.00	3.00	4.00	4.60	4.80	5.05	5.40	5.70	6.05
8.0	1.00	2.00	3.00	4.00	5.00	5.30	5.60	5.90	6.20	
9.0	1.00	2.00	3.00	4.00	5.00	5.75	6.05	6.35		

* From U.S. Department of Agriculture Soil Conservation Service Technical Release 21.

† Based on 3-in. net depth of application. For other net depths of application, multiply by the factors shown below.

Net depth of application	0.75	1.0	1.5	2.0	2.5	3.0	4.0	5.0	6.0	7.0
Factor......	0.72	0.77	0.86	0.93	0.97	1.00	1.02	1.04	1.06	1.07

NOTE: Average monthly effective rainfall cannot exceed average monthly rainfall or average monthly consumptive use. When the application of the above factors results in a value of effective rainfall exceeding either, this value must be reduced to a value equal to the lesser of the two.

monthly mean rainfall values in the growing season. This will require the collection and analysis of rainfall records in the project area for the full period of available records. The adequacy of the irrigation supply to be provided is a matter of economics, and it may be desirable for high-value crops to provide a water supply that will be fully adequate except in very rare circumstances.

13. Irrigation Applications. Irrigation involves the application of surface or groundwater to fields to supplement the soil moisture supply provided by natural rainfall as required for increased growth and production of crops. Accordingly, the frequency of irrigation-water applications will vary during the growing season of each crop depending upon (1) the evapotranspiration rate, (2) the distribution and amount of rainfall, (3) the capacity of the usable soil moisture reservoir, and (4) the design capacities and method of operation of the irrigation-distribution facilities. The depth of water applied at each irrigation varies from about 2 to 6 in., with frequent, light applications being required on sandy soils or during the early part of the growing season and less frequent, heavier applications being permissible later in the growing season or on soils with greater water-holding capacity.

Effect of Root Depth. At the beginning of the growing season the emerging roots can obtain moisture and plant nutrients from the zone of soil at the depth the seeds were planted. As the vegetative growth develops above the ground, the root system develops in the upper soil layers as required to furnish the moisture and plant foods needed to sustain that growth. Each crop has characteristic rooting habits which it will tend to follow if the soil is deep and uniform and equally moist throughout. The depth of rooting increases during the entire growing period. Crops which mature in 2 months usually penetrate only 2 to 3 ft, while crops requiring 6 months to mature may penetrate 6 to 10 ft or more.

Normally the greatest concentration of plant roots is in the upper layers of soil, and this concentration may be accentuated if the root zone is restricted by a high water table, shallow soil, or compacted layers (plow pan). When the upper portion of the soil is kept moist, plants will obtain most of their moisture supply from near the surface. As the moisture content of the upper layers decreases the plants withdraw more water from the lower layers. While this may tend to encourage more root development in the lower levels, fewer roots exist in the lower portion of the root zone, and wilting may result, even though moisture is available, because of the inability of the root system to extract enough moisture from the lower levels. Irrigation practice in arid regions usually results in the extraction of 40, 30, 20, and 10 percent of the moisture supply, respectively, from succeeding quarters of the root zone (from the surface downward).

Average root-zone depths for many of the crops grown under irrigation are listed in Table 11. Generally, these depths are reached by the time the foliage of the plant has

TABLE 11. NORMAL ROOT-ZONE DEPTHS OF MATURE IRRIGATED CROPS GROWN IN A DEEP, PERMEABLE, WELL-DRAINED SOIL*

Crop	Ft	Crop	Ft	Crop	Ft
Alfalfa	5–10	Corn (sweet)	3	Peas	3–4
Artichokes	4	Corn (field)	4–5	Potatoes (Irish)	3–4
Asparagus	6–10	Cotton	4–6	Potatoes (sweet)	4–6
Beans	3–4	Cranberries	1–2	Pumpkins	6
Beets (sugar)	4–6	Deciduous orchards	6–8	Radishes	1
Beets (table)	2–3	Grain	4	Spinach	2
Broccoli	2	Grapes	4–6	Squash	3
Cabbage	2	Grass pasture	3–4	Strawberries	3–4
Cantaloupes	4–6	Hops	5–8	Tomatoes	6–10
Cane berries	3–4	Ladino clover	2	Turnips	3
Carrots	2–3	Lettuce	1–1½	Walnuts	12
Cauliflower	2	Mint	3–4	Watermelons	6
Celery	3	Onions	1		
Citrus	4–6	Parsnips	3		

* From "Engineering Handbook, Far Western States and Territories," U.S. Department of Agriculture, Soil Conservation Service, Sec. 15, Part I, May, 1957.

reached its maximum size. Root-zone depths are limited to the soil depth above the water table.

The moisture reservoir available to the plants is determined by the depth of the plant roots at the stage of growth under consideration and by the moisture-retention characteristics of the soil. The variable factor is the root depth, for a particular field, which has a major influence on the depth and frequency of irrigation-water applications and on the changes in those applications during the growing season.

Soil Moisture Capacity. The volume of soil moisture available to the plant is a function of root depth and the moisture-holding capacity of the soil between field moisture capacity and the minimum moisture content at which optimum plant growth can be sustained. Field moisture capacity is defined as the maximum moisture which can be retained in the soil against the forces of gravity. It does not include water which might be in the soil under saturated conditions and which, in time, will percolate downward through the soil profile. Usually, determinations of field moisture capacity are made 2 days after irrigation.

The moisture content of the soil which results in permanent wilting of plants is called the "wilting point." The wilting point varies with temperature and stage of growth of the plant—higher values apply as rates of evapotranspiration increase. Generally, the wilting point is from 40 to 50 percent of field moisture capacity. The "available moisture capacity" of a soil is the amount of water per unit of soil depth between field moisture capacity and the wilting point. This amounts to 50 to 60 percent of the field moisture capacity and represents the amount of water that can be stored in the soil and used to sustain optimum plant growth. Consequently, it represents the maximum range of fluctuation of soil moisture content that can be tolerated between rains or irrigation-water applications without depression of crop yields.

The available moisture capacity of soils is primarily a function of soil texture. Coarse sands have the least moisture capacity and heavy clays the most. Common ranges of available moisture capacities for soils of different textures are as follows:[1]

Soil Texture	In. of Water per Ft of Soil
Very coarse sands	0.40 0.75
Coarse to loamy sands	0.75–1.00
Sandy loams and fine sandy loams	1.00–1.50
Loams and silt loams	1.50–2.30
Sandy clay loams, silty clay loams, clay loams	1.75–2.50
Sandy clays, silty clays, and clays	1.60–2.50
Peats and mucks	2.00–3.00

Soil Moisture Reservoir. Irrigation studies which involve water conveyance and short-period delivery requirements (generally on a monthly basis) must consider the operation of the soil moisture reservoir. The usable capacity of that reservoir increases as the root system develops. The reservoir content diminishes as moisture is withdrawn by evapotranspiration and it increases as moisture is added by rainfall or applications of irrigation water.

In arid regions it is often necessary to irrigate the fields in advance of planting. This "preplanting" irrigation is required when the soil moisture reservoir is depleted and the soil is too dry for preparation of an efficient seedbed, for germination of the seeds, and for initial growth of the plants. The preplanting irrigation application is additional to the irrigation water necessary to supply the crop evapotranspiration requirements, since it makes up for deficient antecedent rainfall (during a period of months prior to the crop growing season under consideration). The amount of water to be applied depends upon the length of time following irrigation applications on the same land for the previous crop, the condition and covering of the soil surface, and the climatic conditions (especially rainfall). Generally, irrigation studies provide for sufficient preplanting irrigation to bring the soil to field capacity throughout the depth of soil to be used by the roots of the crop to be grown. This will supply moisture needed for seed germination and for growth of the young plants until they are able to withstand mechanical operations required for application of irrigation water and the irrigation water itself.

Irrigation-water applications will be relatively light and frequent during the early parts of the growing season—while the root zone is shallow. Later the applications can provide greater depths of water and the frequency will depend upon the rate of evapotranspiration by the crop. Often irrigation applications must be made at

[1] "Conservation Irrigation in Humid Areas," U.S. Department of Agriculture, Agricultural Handbook 107, 1957.

intervals of a week or less during the period of peak water use, particularly if the soil is sandy or shallow.

It is generally desirable to discontinue irrigation-water applications several weeks before the crop is harvested. This practice provides a dry soil surface for harvesting operations, reduces the moisture content of the vegetative growth, and conserves irrigation water. During this period of maturing of the crop, the moisture needed can be drawn from the soil moisture reservoir. The engineer making irrigation studies should recognize that the use of the soil moisture reservoir is an essential feature of irrigation agriculture and that it results in requirements for irrigation-water applications which are phased earlier in time, and adjusted in amount, from the actual crop evapotranspiration.

Computation Procedure. In estimating requirements for application of irrigation water for a project area, the engineer must adapt the information given in the preceding paragraphs of this section to the local conditions expected to prevail at the time to be represented by the estimate. The cropping pattern should represent the distribution of crops to be grown in the entire project area, and the planting and harvesting seasons selected for those crops should reflect the fact that those operations take considerable time and that they are not done simultaneously on all the farms in the project. This can be handled in the computations by assuming, for example, that one-fourth of the area in a crop would be planted at the beginning and at the end of the planting season and that half the area would be planted on the median date of that season. Crop-use factors would then be weighted to account for the three planting dates to obtain weighted use factors for that crop which would be applicable to the entire project area.

The depth of water to be applied in preplanting irrigations must be estimated for each crop from an analysis of the factors influencing the probable average moisture condition in the soil at the time of seedbed preparation. Usually the engineer will select a depth of water in inches of depth over the area to be planted to the crop as the amount of soil moisture to be added by preplanting irrigations to bring the moisture level to field capacity. In some cases it may facilitate the computations to express that depth as a crop-use factor to be applied for the appropriate month to the shallow-lake evaporation or other index used in the estimating method selected. Such factors can be added to the normal crop-use factors and included in the weighting computation to obtain project crop factors.

Another adjustment may be made to the crop-use factors to account for the withdrawal of moisture from the soil at the end of the growing season. The engineer must select an appropriate depth of water which can be withdrawn from the soil after the last irrigation to meet the needs of the maturing crop. That amount of water can be expressed as crop factors to be applied to the selected estimating index for the appropriate month or months. Incorporation of this adjustment in the project crop factors will involve reduction of the normal crop factors by the appropriate amounts and weighting the reduced factors for the selected planting dates to obtain the project factors.

The method of handling the estimated effective rainfall is important if that rainfall is sufficient to supply more than the needs of one of the crops in one or more months. In such cases it is necessary to consider the effective rainfall separately for each crop, rather than lumping it all together as an adjustment to the total project water requirement to determine the amount to be supplied by irrigation water. Otherwise, excess rainfall on one field would be assumed (erroneously) to be utilized on another field or crop requiring a greater amount of water.

A typical computation, by the method described above, for the amount of soil moisture to be supplied by irrigation water for an irrigation project is presented in Table 12. It should be understood that this is an approximate method which is

Table 12. Sample Computation of Monthly Irrigation Requirements

Item	Jan.	Feb.	Mar.	Apr.	May	June	July	Aug.	Sept.	Oct.	Nov.	Dec.	Annual
Climatic index (IC)	2.4	3.0	4.2	5.4	6.0	7.2	8.4	7.8	5.4	4.8	3.0	2.4	60.0
Effective rain R, in.	0.7	0.9	1.7	1.8	1.6	2.1	4.3	2.6	1.6	1.1	0.8	0.7	19.9
Wheat (40 % of irrigable area):													
KU	0.80	1.04	1.36	1.10	......	......	......	......	......	0.30	0.57	0.60	
UC, in.	1.92	3.12	5.72	5.94	......	......	......	......	......	1.44	1.71	1.44	21.29
PP, in.	......	......	......	......	......	......	......	......	2.00	......	......	......	2.00
SM, in.	......	......	......	2.00	......	......	......	......	......	......	......	......	2.00
IR, gross	1.92	3.12	5.72	3.94	......	......	......	......	2.00	1.44	1.71	1.44	21.29
IR, net	1.22	2.22	4.02	2.12	......	......	......	......	0.40	0.34	0.91	0.74	11.97
IR, weighted	0.49	0.89	1.61	0.85	......	......	......	......	0.16	0.14	0.36	0.30	4.80
Cotton (35 % of irrigable area):													
KU	......	......	0.46	0.70	1.06	1.15	0.80	0.24					
UC	......	......	1.93	3.78	6.36	8.28	6.72	1.77	......	......	......	......	28.84
PP	......	3.00	......	......	......	......	......	......	......	......	......	......	3.00
SM	......	......	......	......	......	......	1.50	0.50	......	......	......	......	2.00
IR, gross	......	3.00	1.93	3.78	6.36	8.28	5.22	1.27	......	......	......	......	29.84
IR, net	......	2.10	0.23	1.98	4.76	6.18	0.92	0	......	......	......	......	16.17
IR, weighted	......	0.73	0.08	0.69	1.67	2.16	0.32	0	......	......	......	......	5.65
Rice (25 % of irrigable area):													
KU	......	......	......	......	1.08	1.38	1.57	1.28					
UC	......	......	......	......	6.48	9.92	13.19	9.98	......	......	......	......	39.57
PP	......	......	......	12.00	2.00	......	......	......	......	......	......	......	14.00
SM	......	......	......	......	......	......	......	2.00	......	......	......	......	2.00
IR, gross	......	......	......	12.00	8.48	9.92	13.19	7.98	......	......	......	......	51.57
IR, net	......	......	......	10.20	6.88	7.82	8.89	5.38	......	......	......	......	39.17
IR, weighted	......	......	......	2.55	1.72	1.96	2.22	1.34	......	......	......	......	9.79
Citrus (25 % of irrigable area):													
KU	0.58	0.59	0.65	0.74	0.73	0.70	0.81	0.96	1.08	1.05	0.82	0.65	
UC	1.39	1.77	2.73	4.00	4.38	5.04	6.80	7.49	5.83	4.94	2.46	1.56	48.39
PP	......	......	......	......	......	......	......	......	......	......	......	......	0
SM	......	......	......	......	......	......	......	......	......	......	......	......	0
IR, gross	1.39	1.77	2.73	4.00	4.38	5.04	6.80	7.49	5.83	4.94	2.46	1.56	48.39
IR, net	0.69	0.87	1.03	2.20	2.78	2.94	2.50	4.89	4.23	3.84	1.66	0.86	28.49
IR, weighted	0.17	0.22	0.26	0.55	0.70	0.74	0.62	1.22	1.06	0.96	0.42	0.22	7.14

Table 12. Sample Computation of Monthly Irrigation Requirements (*Continued*)

Item	Jan.	Feb.	Mar.	Apr.	May	June	July	Aug.	Sept.	Oct.	Nov.	Dec.	Annual
Total IR for irrigable area of 100,000 acres:													
In.	0.66	1.84	1.95	4.64	4.09	4.86	3.16	2.56	1.22	1.10	0.78	0.52	27.38
maf	0.0055	0.0153	0.0162	0.0387	0.0341	0.0405	0.0263	0.0213	0.0102	0.0092	0.0065	0.0043	0.2281
Farm delivery (assumed efficiency 65 %) maf	0.0085	0.0236	0.0249	0.0597	0.0525	0.0624	0.0405	0.0328	0.0157	0.0142	0.0100	0.0066	0.3514
Diversion requirement for project, maf:													
Conveyance loss	0.0034	0.0094	0.0100	0.0125	0.0125	0.0125	0.0125	0.0125	0.0063	0.0057	0.0040	0.0026	0.1039
Requirement	0.0119	0.0330	0.0349	0.0722	0.0650	0.0749	0.0530	0.0453	0.0220	0.0199	0.0140	0.0092	0.4553

Abbreviations:
IC = climatic index = lake evaporation
R = effective rainfall
KU = crop coefficient (evaporation-index method)
UC = evapotranspiration requirement = IC × KU
PP = irrigation applied prior to crop growth
SM = soil moisture withdrawn to meet evapotranspiration
IR (gross) = UC + PP − SM
IR (net) = IR (gross) − *R*
IR (weighted) = IR (net) × percent of irrigable area
maf = million acre-feet

usually sufficiently precise for the determination of monthly water requirements for a project, but more detailed analyses may be necessary for special circumstances such as the detailed water operations on a large commercial irrigation enterprise. Detailed analyses may require a daily analysis of the evapotranspiration requirements, rainfall, and soil moisture reservoir operation.

14. Deep Percolation and Leaching. The principal factors which affect the field irrigation efficiency are those which influence the passage of water through the root zone. These include the method of applying the water (row irrigation, wild flooding, borders, or sprinkler systems); the texture and condition of the soil; the slope of the land and the care with which it has been leveled, ditched, or bordered; the rate of flow available to the irrigator in relation to the size of field to be irrigated; and the skill of the irrigator. Experience has shown that field efficiencies under management levels which prevail in the United States generally fall between 60 and 75 percent, with the higher value being achieved with sprinkler systems and/or a very high level of management. In general, the minimum allowance for deep percolation is about 20 percent if adequate irrigation is to be accomplished. It may be permissible to use a higher field efficiency for a project computation than would be appropriate for a single farm, if it can be assumed that the surface waste which would escape the farm would be captured and used elsewhere in the project.

If the irrigation water applied is saline, or if the soil is saline or alkaline and requires reclamation, it may be necessary to pass additional water through the root zone to achieve and maintain a permanent irrigation agriculture. Many areas of the world have gone out of agricultural production because inadequate attention was given to these requirements, and reclamation of those lands to restore their productivity may be uneconomical. The use of saline waters for irrigation supplies should be under the guidance of an experienced soil and water chemist, since the relationships are so complex as to require the services of a specialist. The considerations are (1) that the flow of water through the soil must be sufficient to keep the concentration of salts in the soil solution below levels harmful to the plants being grown and (2) that a salt inflow–

TABLE 13. LEACHING REQUIREMENT RELATED TO QUALITY OF DRAINAGE AND IRRIGATION WATER FOR AN EQUILIBRIUM CONDITION, IGNORING INFLUENCE OF RAINFALL*

Quality of irrigation water				% leaching requirement for given qualities of drainage water			
Micromhos/cm† $EC \times 10^6$	Ppm	*MEQ/L*	Tons/acre-ft	5 millimhos/cm† $EC \times 10^3$	10 millimhos/cm† $EC \times 10^3$	15 millimhos/cm† $EC \times 10^3$	20 millimhos/cm† $EC \times 10^3$
100	63	1	0.09	2	1	0.7	0.5
200	125	2	0.17	4	2	1	1
400	250	4	0.34	8	4	3	2
800	600	8	0.82	16	8	5	4
1,600	1,000	16	1.36	32	16	11	8
3,200	2,000	32	2.72	64	32	21	16
6,400	4,000	64	5.44	128	64	43	32

* ISRAELSEN, ORSON W., and VAUGHN E. HANSEN, "Irrigation Principles and Practices," 3d ed., John Wiley & Sons, Inc., New York, 1962.

† Electrical conductance, which is the reciprocal of resistance, is expressed in "reciprocal ohms" or "mhos," and electrical conductivity is expressed in mhos per centimeter of distance between contact points. Since most soil solutions have a conductivity of less than 1 mho/cm, smaller units have been designated as follows:

1 mho/cm = 1,000 millimhos/cm = 1,000,000 micromhos/cm

salt outflow balance must be maintained, preferably with the level of salinity in the drainage water such that reuse of the water at downstream points will be possible.

Extra water applications made for the purpose of permitting the use of saline irrigation waters or of leaching harmful accumulations of chemicals from the soil root zone are designated "leaching requirements." Some indication of the magnitude of these requirements is given by data in Table 13, in which the leaching requirement (in percent of the applied water) is related to the quality of the irrigation and drainage waters. As shown in that table by interpolation, a normal deep percolation allowance of 20 percent—about the minimum to assure adequate irrigation in all parts of the fields—provides adequate leaching if the quality of the irrigation water does not exceed about 1,300 ppm of dissolved salts and if the quality of the drainage water can be about 6,000 ppm of dissolved salts. While maintenance of a salt balance is important for a permanent agriculture, it is not the sole criterion, since damaging concentrations in the soil solution could occur. The engineer should consult recent published literature on this subject[1] and obtain the advice of a specialist if preliminary studies indicate water quality may be a problem.

15. Surface Waste and Farm Conveyance Losses. Conveyance losses on the farm vary from near zero to about 15 percent of the water delivered to the farm. The lower loss rates are associated with the use of pipelines or lined channels, while the higher values are associated with unlined ditches and coarse soil texture.

Surface waste from individual fields varies with the nature of the soil, slope of ground surface, method of preparing the land, and depth of irrigation. Naturally, larger quantities of water run off the fields during the greater depths of irrigation. Waste is more difficult to control on steep slopes than on flat slopes and more important on clay soils than on sandy soils, since either a flat slope or a sandy soil is more conducive to a higher rate of soil absorption. Waste from individual fields should be kept as low as possible, although some surface runoff is not serious if collected and used on lower areas. Surface waste can be practically eliminated, or effectively recovered, by constructing adequate levees, or drainage ditches, along the lower edges of fields. Charges for irrigation water based on actual deliveries and limitations on water supplies

TABLE 14. AVERAGE SURFACE WASTE FROM FIELDS
PERCENTAGE OF APPLIED QUANTITIES

Crop	Southern Idaho 1910–1913,* avg waste		Coal Creek Valley, Utah, 1917–1919† yearly avg waste, different soils	Sevier Valley, Utah, 1915–1920‡ yearly avg waste		
	Clay loam	Gravelly soil		Shallow irrigation	Medium irrigation	Heavy irrigation
Alfalfa	19.1	1.8	13–16	6–28	6–24	11–25
Grain	25.3	2.3	6–21			
Potatoes	....	...	12–25	1–17	9 29	12–28
Sugar beets	....	...	.....	3–26	17–33	20–35

* BARK, DON H., Experiments on the Economical Use of Irrigation Water in Idaho, *U.S. Dept. Agr. Bull.* 339, 1916.

† FIFE, ARTHUR, Duty of Water Investigations on Coal Creek, Utah, *Utah Agr. Expt. Sta. Bull.* 181, 1922.

‡ ISRAELSEN and WINSOR, The Net Duty of Water in Sevier Valley, *Utah Agr. Expt. Sta. Bull.* 182, 1922.

[1] EATON, FRANK M., "Formulas for Estimating Leaching and Gypsum Requirements of Irrigation Waters," Texas Agricultural Experiment Station Miscellaneous Publication, **111**, 1954.

or canal deliveries encourage or force the use of practices which reduce wastage of irrigation water to a minimum.

Table 14 shows some average values of surface waste on typical irrigated fields in Idaho and Utah. The shallow, medium, and heavy irrigations in the Sevier Valley investigations were 2-, 3½-, and 5-in. depths in the case of potato crops; and 3- to 4½-in., 6-in., and 8- to 10-in. depths, respectively, in the case of the alfalfa and sugar-beet crops.

Average quantities of water actually lost to beneficial use by surface waste on large irrigation projects are considerably smaller than the quantities lost on individual fields. Investigations in the Cache La Poudre Valley, northern Colorado, showed an average surface runoff equal to 6 percent of the quantity applied.[1] An allowance of 10 percent of the quantity delivered to the fields will usually be an ample provision for surface waste in considering a large irrigation project as a whole.

16. Effect of Irrigation Methods. The method of applying irrigation water to the fields to obtain the most efficient water distribution and the best use of labor and equipment will vary according to the crops grown, the soil texture, the land slope, the levelness of the field surface, the frequency of required irrigations, and the rate of flow available to the irrigator. The adaptations and limitations of the common irrigation methods are summarized in Table 15. These methods are described in detail in standard texts and reference books.[2]

TABLE 15. ADAPTATION AND LIMITATIONS FOR COMMON IRRIGATION METHODS*

Furrow	Light-, medium-, and fine-textured soils; row crops; small stream	Slopes up to 3 % in direction of irrigation; row crops; 10 % cross slope
Corrugation	Light-, medium-, and fine-textured soils; close-growing field crops; small stream flows	Slopes up to 12 % with semipermanent crops; 8 % with annual crops; 5 % cross slope; rough for equipment
Border	All soils; close-growing field crops; large streams	Slopes up to 3 % for annual crops; slopes to 8 % for sodded pastures; good leveling required; 0.3 % cross slope; uniform grade; problem of starting crops in soils which puddle readily
Sprinklers	All slopes; soils; crops; and stream size	High initial equipment cost; lowered efficiency in windy and hot climate
Check (or ponding)	Light, medium, and heavy soils; large streams	Deep soils; high cost of land preparation; slopes less than 2 %
Subirrigation	Free lateral movement of water in soils, rapid capillary rise, underlain by low-permeability layer; all crops; large quantities of water	Special soil and annual precipitation conditions; usually causes drainage problems elsewhere

* Prepared by Max Jensen and Claude H. Pair, "Water," Yearbook of Agriculture, 1955, 84th Congress, 1st Session, House Document 32.

Irrigation efficiencies vary with the methods of application used and with the experience of the irrigator. If the method is suited to the crops and local conditions, the irrigation structures are properly designed and constructed, and the irrigator is experienced and efficient, field efficiencies in the range of 50 to 70 percent can be achieved. The higher efficiencies are generally associated with sprinkler systems which generally have pipe conveyance systems, apply the water uniformly, and can be controlled readily to apply the exact amount of water desired. Lower efficiencies generally result from application by wild flooding, improperly designed systems, inade-

[1] HEMPHILL, ROBERT G., Irrigation in Northern Colorado, *U.S. Dept. Agr. Bull.* 1026.

[2] ISRAELSEN, ORSON W., and VAUGHN E. HANSEN, "Irrigation Principles and Practices," 3d ed., John Wiley & Sons, Inc., New York, 1962.

quate land leveling, or overwatering because of inexperience or lack of restraints on use of water.

CONVEYANCE LOSSES AND WASTE

This section is concerned with that portion of the project water supply which is lost (so far as local use is concerned) between the point of diversion from a stream or reservoir and the points where deliveries are made to the farms. Part of the water lost finds its way to the groundwater and another part represents operational waste which is discharged into drainage channels or streams. Those waters may be recaptured and used downstream within the same project or elsewhere. The remainder of the water lost in conveyance is nonbeneficial evapotranspiration.

17. Evaporation Losses. A part of the water diverted into the canal system is lost by evaporation from the water surfaces of the flowing canals and laterals. Evaporation losses vary with the area of the canal water surface and the prevailing rate of evaporation. They may be practically eliminated by constructing closed conduits. However, such losses usually are not great enough or of sufficient value to warrant the expense of such construction. For example, a canal surface 20 ft wide, evaporating water at a rate of ½ in. a day, would lose about 2 acre-ft a day in a length of 20

TABLE 16. CANAL LOSSES AND WASTE ON BUREAU OF RECLAMATION PROJECTS*

State	Project	Length of canals and laterals		Gross diversions, acre-ft/acre	Per cent of diversions		
		Total miles	Lined or enclosed, miles		Canal and lateral losses	Waste	Delivered to farms†
Ariz.-Calif.	Yuma	336	...	10.75	14	58	28
California	Orland	135	89	4.95	27	9	64
Colorado	Grand Valley	180	7	10.31	43	22	35
Colorado	Uncompahgre	470	11	7.48	13	10	77
Idaho	Boise	1,004	37	5.15	28	2	70
Idaho	King Hill	96	43	13.21	..	..	53
Idaho	Minidoka, South Side Pumping	275	...	4.38	39	3	58
Montana	Huntley	232	...	4.09	36	30	34
Montana	Lower Yellowstone	202	...	3.83	44	21	35
Montana	Milk River	275	...	1.44	36	19	45
Montana	Sun River, Fort Shaw	99	...	4.05	36	26	38
Montana	Sun River, Greenfields	190	...	2.72	31	22	47
Nevada	Newlands	319	...	6.40	41	14	45
New Mexico	Carlsbad	45	11	5.11	48	6	46
N. M.-Tex.	Rio Grande	485	10	9.96	32	39	29
Oregon	Klamath	240	2	2.75	39	9	52
Oregon	Umatilla	173	157	10.04	32	18	50
South Dakota	Belle Fourche	547	58	2.35	33	15	52
Washington	Okanogan	68	39	3.66	29	..	71
Washington	Yakima, Sunnyside	602	125	4.70	23	7	70
Washington	Yakima, Tieton	335	86	3.39	24	2	74
Wyoming	Shoshone, Frannie	166	...	5.92	42	21	37
Wyoming	Shoshone, Garland	279	4	4.33	38	7	55
Wyo.-Neb.	North Platte	1,154	...	4.55	43	8	49

* Abstracted from E. B. Debler, Use of Water on Federal Irrigation Projects, *Trans. ASCE*, **94**, 1223–1224, 1930.

† See Table 17 for deliveries in acre-feet per acre and additional pertinent data.

Table 17. Average Use of Water on Federal Irrigation Projects[1]

State	Project	Average elevation	Years considered	Area irrigated, acres	Predominating character of soils	Crops grown, % of total area: Alfalfa, hay, and pasture	Crops grown, % of total area: Small grain	Crops grown, % of total area: Furrow crops	Crops grown, % of total area: Trees	Irrigation season	Precipitation, ft: Before growing season	Precipitation, ft: During growing season	Water delivered to farms, acre-ft/acre	Water delivered plus growing season prec., ft
Ariz.-Calif.	Yuma	120	1917–1926	51,950	Medium	39	3	58	..	Jan.–Dec.	0.33	0.33	3.01	3.34
California	Orland	250	1917–1926[2]	14,554	Light	53	5	19	23	Jan.–Nov.	1.02	0.37	3.17	3.55
Colorado	Grand Valley	4,700	1916–1925	10,139	Heavy	36	24	33	7	Apr.–Nov.	0.27	0.48	3.61	4.09
	Uncompahgre	5,500	1917–1926	61,178	Medium	47	25	25	3	Apr.–Oct.	0.26	0.55	5.76	6.31
Idaho	Boise	2,500	1917–1925[3]	145,616	Light	53	31	13	3	Apr.–Oct.	0.43	0.38	3.60	3.98
	King Hill	2,750	1921–1927	6,460	Very light	75	7	11	6	Apr.–Nov.	0.41	0.35	7.01	7.36
	Minidoka, S. Side Pumping	4,200	1917–1926	44,945	Medium	50	28	22	..	Apr.–Oct.	0.32	0.53	2.54	3.07
Montana	Huntley	3,000	1917–1926	19,406	Heavy	42	34	24	..	May–Sept.	0.37	0.63	1.39	2.02
	Lower Yellowstone	1,900	1917–1926	17,540	Heavy	45	33	22	..	May–Sept.	0.33	0.71	1.34	2.05
	Milk River	2,200	1917–1926	16,793	Heavy	73	22	5	..	Apr.–Oct.	0.18	0.91	0.65	1.56
	Sun River, Fort Shaw	3,700	1917–1926	7,650	Heavy	75	20	5	..	May–Oct.	0.23	0.60	1.54	2.14
	Sun River, Greenfields	3,700	1919–1926	9,867	Medium	23	75	2	..	May–Oct.	0.28	0.65	1.28	1.93
Nevada	Newlands	4,000	1917–1926	38,808	Medium	85	11	4	..	Mar.–Nov.	0.15	0.25	2.88	3.13
New Mexico	Carlsbad	3,100	1917–1926	22,535	Medium	33	4	63	..	Jan.–Nov.	0.06	0.86	2.36	3.22
N. M.-Tex.	Rio Grande	3,700	1919–1926	96,847	Medium	37	8	53	2	Feb.–Dec.	0.06	0.60	2.89	3.49
Oregon	Klamath	4,100	1917–1926	43,325	Medium	77	21	2	..	Apr.–Sept.	0.68	0.18	1.43	1.61
	Umatilla	470	1916–1925	10,970	Light	85	1	6	8	Mar.–Nov.	0.40	0.35	5.02	5.37
South Dakota	Belle Fourche	2,800	1917–1926	45,164	Heavy	62	22	16	..	May–Sept.	0.48	0.86	1.22	2.08
Washington	Okanogan	1,000	1921, 1923, 1925	5,260	Light	9	..	3	88	May–Sept.	0.51	0.42	2.60	3.02
	Yakima, Sunnyside	800	1917–1926	91,726	Medium	57	7	21	15	Mar.–Oct.	0.27	0.21	3.29	3.50
	Yakima, Tieton	1,500	1917–1926	27,607	Light	44	12	11	33	Apr.–Sept.	0.44	0.16	2.51	2.67
Wyoming	Shoshone, Frannie	4,150	1922–1926	7,963	Heavy	72	17	11	..	Apr.–Oct.	0.11	0.39	2.19	2.58
	Shoshone, Garland	4,400	1917–1926	32,380	Medium	59	28	13	..	Apr.–Nov.	0.09	0.33	2.38	2.71
Wyo.-Neb.	North Platte	4,100	1919–1926	107,694	Medium	36	26	38	..	May–Sept.	0.47	0.81	2.23	3.04

[1] Abstracted from E. B. Debler, Use of Water on Federal Irrigation Projects, *Trans. ASCE*, **94**, 1223–1224, 1930.

[2] 1918, 1920, and 1924 omitted because of heavy water shortage.

[3] 1924 omitted because of water shortage.

miles, a quantity equivalent to a continuous flow of about 1 sec-ft—on the order of one-half of 1 percent of the canal flow.

18. Seepage Losses. Seepage losses from canals depend upon (1) the wetted area of the bed and banks, (2) the permeability of the canal bed and the underlying soil, and (3) the difference in level of the water in the canal and the adjacent groundwater table. Such losses are greatest where sandy or other permeable soils predominate and where the groundwater table is low. Sometimes the losses are materially reduced with time through sealing of the canal bed by the deposition of fine sediments brought into the canal in suspension with the diverted water during periods of high concentrations of suspended sediment in the streams. The most efficient method of reducing seepage is the lining of the canals with concrete or other materials. The Bureau of Reclamation has carried on extensive research in low-cost canal linings of various types.[1]

Careful measurements, made on irrigation projects in Idaho, showed that small farm ditches, carrying less than 1 sec-ft, may lose half their flow in a length of 1 mile. The measurements made on canals carrying 10 to 3,000 sec-ft, through sections of different soil texture, showed seepage losses per mile varying from less than 0.1 to 10.8 percent of the flow.[2] Measurements made on canals in the Salt River Valley, Arizona, showed an average seepage rate of approximately 0.34 acre-ft/acre of wetted area/day.[3]

Table 16 shows the average conveyance losses and waste on Bureau of Reclamation projects in Western United States, expressed as percentages of total diversions. Total lengths of canals and laterals and lengths of lined or enclosed sections are also included in the tabulation. Data on predominating soil characteristics and other characteristics of those projects are given in Table 17. The canal and lateral losses are seen to vary from a minimum of 13 percent of the diversions on the Uncompahgre project in western Colorado to a maximum of 48 percent on the Carlsbad project in southeastern New Mexico.

In making detailed studies of irrigation requirements and canal operations, it must be recognized that higher than average conveyance losses (in terms of percent of the diverted flow) occur when relatively small diversions are being made and the percent lost is least when the canal system is operating at capacity. The practice of rotating flows between the smaller laterals during periods of small diversions, with each of those laterals being dry during a considerable portion of those periods, tends to make the conveyance losses therein more of a function of the flow carried. On the other hand, check structures must be used to a greater extent during canal operations with small rates of flow in order to serve the several offtakes adequately, and the backwater thus created increases the wetted area of the canals and tends to increase the seepage losses.

19. Operational Wastes. Operational wastes of water are practically unavoidable if optimum service is to be given to all farms. These wastes result from more water arriving at critical points in the canal system than can be carried. This situation results from rainfall or other factors which produce unexpected canal flows or reduce the irrigation requirements below that which has been scheduled, and from unavoidable inabilities to dispatch and to measure diversions and deliveries to achieve a perfect balance between diversions, conveyance losses, channel storage, and irrigation delivery requirements.

Waste on Bureau of Reclamation projects varies from a minimum of 2 percent on the Boise project in southwestern Idaho to a maximum of 58 percent on the Yuma project in southeastern California and southwestern Arizona. The relatively high

[1] "Linings for Irrigation Canals," U.S. Bureau of Reclamation, 1963.

[2] Bark, Don H., Experiments on the Economic Use of Irrigation Water in Idaho, *U.S. Dept. Agr. Bull.* 339.

[3] Smith, G. E. P., The Use and Duty of Water in the Salt River Valley, *Arizona Agr. Expt. Sta. Bull.* 120, 1927.

waste on the Yuma project is due partly to the use of water for power development and partly to the operation of the canals at high levels in order to reduce silt deposition. Wastage on some of the other projects is high because ample supplies are available and the excess diversions can be returned to the streams for rediversion to lower areas. Quantities given as waste do not include water used in sluicing sand and silt deposits at points of diversion.

20. Project and Experimental Data. Data on canal losses and waste which have been experienced on several Bureau of Reclamation projects are listed in Table 16. Table 14 presents typical data on surface waste from fields. Typical irrigation efficiencies for three general soil types are listed in Table 18.

TABLE 18. TYPICAL WATER-APPLICATION LOSSES AND IRRIGATION EFFICIENCIES FOR DIFFERENT SOIL CONDITIONS*

Item	General soil type		
	Open porous, %	Medium loam, %	Heavy clay, %
Farm lateral loss†	15	10	5
Surface-runoff loss	5	10	25
Deep-percolation loss	35	15	10
Field irrigation efficiency	60	75	65
Farm irrigation efficiency	45	65	60

* BLANEY, H. F., and W. D. CRIDDLE, Determining Consumption Use and Irrigation Water Requirements, *U.S. Dept. Agr. Tech. Bull.* 1275, 1962.

† Unlined ditches (loss in new-lined ditches and pipelines is usually about 1 percent).

REUSE OF DRAINAGE WATER

When fields are irrigated adequately to sustain optimum crop production and to prevent gradual soil salinization, it is inevitable that some deep percolation to drains or underlying aquifers will take place. Additional deep percolation results from seepage from canals and laterals. Drainage flows include also water wasted at the lower ends of fields and excess water discharges from canals through wasteways to avoid overflows or breaches of the canal banks. Such excess canal flows are normal occurrences in irrigation-project operation and result from errors in measuring or controlling diversions or deliveries, unanticipated reductions in farm requirements caused by rainfall after water orders had been placed, or smaller conveyance losses than had been provided for in the water-scheduling computations. Failure to use or to remove these drainage waters can impair land productivity through waterlogging and soil salinization. In many areas drainage waters provide a bonus value of additional water supplies which augment the original surface-water source and provide for the most efficient development and use of the water resource.

21. Integration of Ground- and Surface-water Use. Many areas irrigated from a surface-water source are underlain by aquifers which are recharged by the irrigation operations or by lateral groundwater movement from external recharge areas. When the groundwater level is near the zone of soil penetrated by crop roots the ideal irrigation development involves coordinated and integrated use of groundwater and surface water to maintain a balance between groundwater pumping and recharge. The amount of water pumped must include the volume used for irrigation on the overlying lands and an amount to be exported from the area to carry away an annual volume of salts equal to the salts brought to the area in the imported surface water. Because the salt concentration in the groundwater is usually considerably higher than that in the surface water, the amount of water to be exported for salt-balance purposes is usually comparatively small.

The discussion in the preceding paragraph is predicated on pumping of the groundwater, and that pumping is usually accomplished by the use of turbine pumps sized to comply with irrigation needs, aquifer characteristics, and the designs of the wells and screens. In many areas the aquifer is deep enough to provide a groundwater reservoir of large capacity which can be used to compensate for year-by-year variations in surface-water supplies. This will require deep-well pumps to be operable over a wide range of water-table fluctuations.

Coordinated use of ground and surface waters requires controlled use of those groundwaters which contain potentially damaging concentrations of salts, sodium, or bicarbonates. This may require that the groundwater be pumped into large-capacity canals so that it will be diluted prior to irrigation use. In other cases it may suffice to alternate irrigation applications between ground and surface supplies so that adequate dilution is accomplished in the soil. The practice to be followed in a particular case will depend upon the chemical qualities of the ground and surface waters and upon the chemical properties of the soil and should be determined by a qualified, experienced soil and water chemist or soil scientist.

Irrigated areas that are not underlain by a usable aquifer, or which have an impermeable stratum near the crop root zone, must be drained by open or tile drains. The drainage water collected will usually be of adequate quality to be reused for irrigation, either directly or diluted with surface water of better quality. This reuse can be accomplished within the project area by discharging the drains into canals by gravity or by pumping, or the drainage waters can be delivered into the stream channels for diversion at a point some distance downstream.

22. Quality of Irrigation Water. The usability of water for irrigation of crops, or the conditions under which a particular water may be used, is determined by the chemical quality of the water, the sensitivity of the crops to salts and water-soluble elements, and the chemical characteristics of the soil to which the water will be applied. The most important quality consideration of irrigation water is the total salt content, which is usually expressed in terms of electrical conductivity—micromhos per centimeter—or in parts per million of total dissolved solids. A value of 1,000 micromhos/cm is equivalent to about 640 ppm of total dissolved solids.

Irrigation waters are classified into four salinity groups: low salinity, less than 250 micromhos/cm; medium salinity, 250 to 750; high salinity, 750 to 2,250; and very high salinity, greater than 2,250 micromhos/cm. About half the irrigation waters now in use in the Western United States fall in the medium-salinity classification.[1]

The second most important factor in irrigation-water quality is the relationship of the cations of sodium to those of calcium and magnesium. The most satisfactory expression of that relationship is the sodium adsorption ratio (SAR), defined as

$$\mathrm{SAR} = \frac{\mathrm{Na}^{++}}{\sqrt{\dfrac{\mathrm{Ca}^{++} + \mathrm{Mg}^{++}}{2}}}$$

Because of the highly significant relationship between the SAR of an irrigation water and the exchangeable sodium percentage of the soil irrigated with that water, it is possible to anticipate the effect of a water on the soil. Irrigation waters with SAR values of 8 or less are probably safe, those with values of 12 to 15 are marginal, and

[1] Wilcox, Lloyd V., Water Quality from the Standpoint of Irrigation, *J. AWWA*, **50**(5), 1958

continued use of waters with values greater than 20 could lead to serious sodium problems. Sodium soils are relatively impermeable to air and water, are hard when dry, are difficult to till, and are plastic and sticky when wet. These conditions retard or prevent germination and are unfavorable for plant growth. The sodium ion is toxic to many plants.

Boron is an essential element to normal plant growth, but concentrations only slightly above optimum are toxic to many plants. Only a few surface waters contain harmful concentrations of boron but many groundwaters and many saline soils are contaminated. Permissible limits of boron in irrigation water are 0.3 to 1.0 ppm for sensitive crops, 1.0 to 2.0 ppm for semitolerant crops, and 2.0 to 4.0 ppm for tolerant crops. The sensitive crops are citrus fruits, nuts, and beans; the semitolerant include cereals, some vegetables, and cotton; and the tolerant group includes alfalfa, sugar beets, and asparagus.

The concentration of bicarbonate is another major consideration in the quality of irrigation water. The use of waters that are low in total salts but high in bicarbonate may aggravate the sodium problem if the amount of bicarbonate is considerably in excess of the calcium and magnesium present. This excess bicarbonate is referred to as residual sodium carbonate. When an irrigation water containing residual sodium carbonate evaporates in the soil, calcium and magnesium carbonates precipitate, and the sodium percentage of the soil solution increases. Then sodium replaces calcium on the soil particles, the exchangeable-sodium percentage of the soil increases, and the physical condition of the soil, especially the permeability, may be impaired. In addition, the pH may increase and organic matter may be dissolved, giving the dark color typical of a so-called black alkali soil.[1]

Crops should be selected on the basis of their salt tolerance and the salt content of the irrigation water and the soil. The relative salt tolerance of the more important crops follows.

Salt-sensitive	
Avocado	Prune
Citrus	Apple
Strawberries	Pear
Peach	Beans
Apricot	Celery
Almond	Radish
Plum	Clover
Medium Tolerance	
Grape	Olive
Cantaloupe	Fig
Cucumber	Pomegranate
Squash	Cauliflower
Peas	Cabbage
Onion	Broccoli
Carrot	Tomato
Peppers	Oats
Potato	Wheat
Sweet corn	Rye
Lettuce	Alfalfa
High Tolerance	
Asparagus	Cotton
Garden beets	Barley
Sugar beets	

Water-quality considerations are most important when groundwaters or drainage flows are being used. This is because those waters characteristically contain concen-

[1] Fireman, Milton, and H. E. Hayward, "Irrigation Water and Saline and Alkali Soils," Water, The Yearbook of Agriculture 1955, U.S. Department of Agriculture.

trations of salts and other potentially harmful elements, since they result from the passage of water through the soil and the chemical concentrations are increased by the removal of pure water through evapotranspiration.

Brackish water may be used safely for irrigation of crops in some cases when such waters are available and supplies of more suitable water are temporarily deficient. The amount of brackish water that can be used depends on the salt concentration of the water, the number of irrigations between leaching rains or irrigations with fresh water, the salt tolerance of the crop, and the salt content of the soil before irrigation. A guide for the use of brackish waters for irrigation is provided in Table 19.

TABLE 19. PERMISSIBLE NUMBER OF IRRIGATIONS WITH BRACKISH WATER BETWEEN LEACHING RAINS FOR CROPS OF DIFFERENT SALT TOLERANCE*

Irrigation water		No. of irrigations for crops having		
Total salts, ppm	Electrical conductivity, millimhos/cm at 25 C	Good salt tolerance	Moderate salt tolerance	Poor salt tolerance
640	1	...	15	7
1,280	2	11	7	4
1,920	3	7	5	2
2,560	4	5	3	2
3,200	5	4	2–3	1
3,840	6	3	2	1
4,480	7	2–3	1–2	
5,120	8	2	1	

* LUNIN, GALLATIN, BOWER, and WILCOX, Use of Brackish Water for Irrigation in Humid Regions, *U.S. Dept. Agr. Inform. Bull.* 213, 1960.

RESULTS FROM IRRIGATION

Irrigation is a management practice which has been utilized for centuries for the purpose of increasing agricultural production and income. Feasibility studies of potential irrigation developments, whether for individual farms or for projects covering thousands of acres, must include determinations of the agricultural production volumes and values, the production costs, and the gross and net farm and project incomes for conditions with and without irrigation.

23. Crop-yield Responses. The direct result which irrigation must achieve if the effort and expense involved are to be justified is an increase in crop yields over those which can be obtained without irrigation. The contribution of irrigation ranges from 15 to 20 percent of yield without irrigation in the more humid regions to the entire yield achieved under irrigation in areas which have little or no rainfall. Yield responses for a particular crop in a specific location can usually be estimated from yields realized in the area under irrigated and unirrigated conditions. Such evaluations should be made by experienced agriculturists who can interpret the effects of differences in management levels, use of fertilizers and plant-protection measures, and other inputs which influence crop yields.

Production responses from irrigation include not only increases in yields of particular crops but those resulting from the situations where irrigation makes possible the growth of high-value or high-yielding crops which could not be justified without irrigation. Irrigation also may make it possible to obtain highly beneficial results from the application of fertilizers. In those cases part of the total yield response is attributable to the irrigation water alone and part is due to the integrated action of the water and the fertilizers, plant-protection measures, special seeds, and any other aspects of modern, efficient farm management made possible by a dependable supply of soil moisture. The services of a skilled agronomist are required to apportion the total production increase between water and other agricultural input factors if each of those factors is to be justified independently. Frequently it will suffice to make a collective evaluation of the entire irrigation enterprise, and in that case it is not necessary to identify the contribution of each factor to the total production increase.

24. Effect of Water Shortages. Since irrigation involves the application of developed surface or groundwater supplies to supplement those provided by natural rainfall, the engineering of the irrigation development requires the determination of the increase in the water supply which can be supported economically. Experience has shown that it is rarely justifiable to provide an irrigation water supply of a size that will support optimum plant growth under all possible conditions of natural rainfall. Ideally several alternative levels of irrigation-water supplies should be evaluated economically to determine the net farm or project income which could be realized. The crop production estimated in each case should reflect the yield depressions which might be expected to result from shortages in irrigation-water supplies over 50 years or other periods selected for analysis. The level of irrigation-water supply to be provided could then be selected as that offering the optimum benefits. As a general rule, one 100 percent shortage in irrigation-water supply might be tolerated in a 50-year period, and the maximum tolerable average annual shortage would be about 5 percent.

25. Economic Analyses. Decisions and support for the undertaking of irrigation developments or projects are based primarily on economic findings concerning the soundness of the enterprise, although frequently social and political aspects, which are not susceptible to expression in monetary terms, are also important considerations. The economic analyses must cover conditions with and without the irrigation development, thereby determining by differences the economic values which will result from the investment in initial and annual costs. The end results to be provided by these analyses include determinations of the production increases to be realized; the direct economic benefit on the investment expressed in terms of the ratio of benefits to costs and in percentage of annual return on the investment; the economic benefits to the farmers in terms of increased profit from their investments and returns for their labor; and the benefits to the community and the nation in terms of employment opportunities, business opportunities, reductions in welfare costs, foreign-exchange earnings or reductions in foreign purchases, and increased tax revenues.

The economic analysis usually begins with the preparation of farm budgets for typical or representative farms in the project area under conditions with and without the project. Those budgets include estimates of the gross income from the area devoted to each crop in terms of production sold and production used on the farm; production costs including land leveling, farm ditches and drains, seeds, seedbed preparation and tillage, fertilizers, plant-protection measures including insecticides and fungicides, harvesting, storage, and delivery to market, hired labor, and investment in work animals, breeding stock, mechanical equipment, and storage facilities; an appropriate allowance for family labor and return on investment; and the net amount available annually to the farmer for profit, payments for irrigation water delivered, and repayment of the capital and operation and maintenance costs of the irrigation project. In addition to providing an evaluation of the capability of the farmers to repay costs of building and operating the irrigation facilities, the farm budgets provide information which can be combined to develop the direct economic benefits from the project.

Project costs include the capital costs involved in formulating the project and bringing the physical works into being and the costs of operating those works and maintaining them or replacing them as required for continuing service. The project works include storage facilities, diversion dams, canals and laterals to deliver water to each farm, drainage facilities as needed to collect drainage waters from the on-farm drainage ditches or tile drains and to reuse or dispose of those waters, and any special works required such as desilting works, dredges, pumping plants, or wells. The capital costs include engineering services for appraisal and feasibility studies, designs and tender documents, and supervision of construction; construction costs; administrative costs by the owner or owning agency; and financing costs including interest during construction and debt service. Operation and maintenance costs include costs of administration, water scheduling and control of deliveries, and the maintenance and repair of the project facilities.

The benefit/cost ratio and the percentage return on investment are two measures used in expressing the economic viability of an irrigation development. The benefit/cost ratio will vary with the rate of interest charged on borrowed capital; hence the analyses must cover the range of interest rates which apply to the available sources of financial assistance at the time the study is being made. A benefit/cost ratio may be determined by using primary benefits, and a value greater than unity on that basis will be recognized as indicating justifiability from an economic standpoint. Primary benefits in this case mean the increase in the net income of agricultural production resulting from the project. Usually these benefits are determined as the annual average over a 50-year period of analysis, discounted to allow for a reasonable development after completion of the works before realization of full production from the entire project area. Costs for comparison with average annual benefits would be annual values including the amount necessary to amortize the capital investment over the repayment period and the costs of operation, maintenance, and replacements. A benefit/cost ratio may be determined also from "present worth" values computed for both benefits and costs to the date when the decision to undertake the project is to be taken, using an appropriate discount rate. The discount rate which will result in a benefit/cost ratio of unity when the benefits include all values which can be expressed in monetary terms is the percentage return on the investment. That percentage return is a value frequently used in comparing the relative desirability of undertaking or financing alternative schemes or projects. The percentage return or benefit/cost ratio will be considered along with intangible social and political factors in the legislative process involved in authorization of irrigation projects by governmental agencies.

Economic analyses of irrigation developments are complex undertakings which should be performed by experienced agricultural economists, particularly where the irrigation enterprise is a part of a multiple-purpose project for utilization of land and water resources. The information to be developed by the analyses and the methods of presentation will be influenced to some extent by the requirements of the lending agency or agencies which will be approached for financial assistance.

SECTION 34

IRRIGATION STRUCTURES

By Nicholas M. Hernandez[1]

Structures on irrigation projects include dams, spillways, desilting works, intakes, pumping stations, canals, tunnels, pipelines, flumes, inverted siphons, chutes, drops, checks, turnouts, measuring devices, wasteways, culverts, overchutes, drainage systems, and other features peculiar to the project.

Dams vary from low diversion weirs to high storage structures. Distribution channels vary from small farm ditches, where the flow can be controlled by movable canvas barriers, to huge supply canals carrying several thousand cfs.

The Marala-Ravi Canal in West Pakistan has a maximum capacity of 22,000 cfs. Here in the United States, some sections of the All-American Canal, built to carry water to Imperial Valley, southern California, have a bottom width of 160 ft, a permissible flow depth of 22 ft, and a capacity of 15,000 cfs. Other irrigation structures vary almost as widely.

Hydraulic features of reservoirs, dams, spillways, tunnels, canals, and other major structures are described in other sections. The following discussions are confined to irrigation structures not treated elsewhere and to such special considerations as may be necessary from the viewpoint of irrigation. Except as otherwise noted, designs included as illustrations are presented through the courtesy of the Bureau of Reclamation.

DIVERSION WEIRS

Irrigation projects supplied by gravity diversions from natural streams usually require the construction of weirs near the upper limits of irrigable lands, the purpose being to raise river surfaces high enough to permit controlled diversion of irrigation-water requirements. When two or more feasible sites are available, the weir location should be determined on the basis of economic considerations. Ordinarily, adoption of a site farther upstream permits a reduction in height of weir, since the canal can usually be built on a grade somewhat flatter than the river slope. However, savings resulting from a reduced height may be offset by costs of extending the canal upstream. When weir-height minimization is under consideration, care also should be taken to ensure that flood tail water will not exceed the elevation of the canal system, thereby subjecting it to damage during flood flows.

1. Types of Diversion Weirs. Since canal flows are relatively small proportions of total stream discharges during flood periods, diversion weirs must be of overflow or open-dam types or provided with bypass channels capable of carrying flood discharges. If bypass channels are not feasible, the dams must either be capable of carrying flood flows over their crests or be provided with enough gates or collapsible elements to pass flood discharges without damage. Weirs designed with gates to pass flood flows are sometimes called *barrages*. They are usually built in bays, sepa-

[1] Acknowledgment is made to Mr. Ivan E. Houk for the illustrations, tables, and other material in this section which also appear in Section 18, Irrigation Structures, in "Handbook of Applied Hydraulics," 2d ed., McGraw-Hill Book Company, 1952.

rated by piers and surmounted by operating bridges. Flow between piers may be controlled by collapsible shutters; by Stoney, radial, roller, or drum gates; or, in comparatively low weirs of inexpensive design, by horizontal removable flashboards.

Overflow weirs may vary from low temporary cobble and brush barriers, resembling beaver dams, to costly concrete arch or gravity structures. Intermediate designs may be built of logs, piles, cribs, rock, timber, steel, masonry, or reinforced concrete. Overflow weirs of permanent construction are usually provided with gate-controlled sluiceways, so that detritus may be flushed out periodically. Fish ladders or other provisions for passing fish over the dam may be required on streams where fishing is important, as in northwestern United States (see Sec. 23). Earth or earth and rock embankments extending to high ground are often built at the ends of weirs, in both overflow and open-dam types.

The most desirable type of diversion weir for a given site depends on height of weir, foundation conditions, streamflow, permissible upstream flooding, available construction materials, and amount of expense justified. Overflow types are desirable from the viewpoint of floating material, since they offer less obstruction to passage of ice, logs, brush, and miscellaneous debris. Gate installations are advantageous from the viewpoint of detritus problems, since deposits above the weir are scoured downstream during flood periods. Gate installations are also advantageous from the viewpoint of canal operation, since they permit some regulation of river surfaces at intake structures.

2. Design of Diversion Weirs. Diversion weirs should be designed as dams. Concrete weirs on rock foundations should be made safe against failure by sliding, along any plane in the structure or its foundation, overturning, crushing, or rupture by tension. Analysis should include adequate allowances for wind, wave action, hydrostatic uplift along the foundation, horizontal and vertical water loads, and the structure dead load. Where conditions dictate, silt and ice, and dynamic loads due to the seismic acceleration of the structure and the mass being retained, that is, water, silt, or ice, are also considered. Weirs on sand, gravel, and other earth foundations should be made safe against the same forces and should also provide ample bearing resistance, percolation distance, and protection against erosion. An analysis of piping and percolation movements with the investigation of over 200 masonry dams on earth foundations has been published.[1] Detailed methods of design are discussed in Secs. 8 and 19.

Figure 1 shows some condensed cross sections of diversion weirs built on earth foundations. Figure 2 shows some cross sections of weirs built on rock foundations.

RIVER INTAKES

In rivers having stable beds and low-water discharges considerably greater than diversion requirements, intake structures sometimes may be built without constructing diversion dams. However, such cases are rare. Ordinarily, intake structures are appurtenant parts of diversion weirs and are built at one or both ends of the weirs. Sometimes they are constructed short distances upstream, as when water is diverted into tunnel sections instead of open channels. When the intake is to be placed on one side of the river, it is advantageous from the standpoint of reducing the amount of detritus entering the intake to locate it just downstream of a bend in the river on the concave side. Figure 3[2] indicates results of model tests on bed-load distribution between the main course and branch watercourses. If intakes are to be on both sides of the river, the diversion should take place in a straight reach of the river. Figure 4 indicates a diversion scheme in a straight reach. Since obstruction of river flow causes

[1] Lane, E. W., Security from Under-seepage, Masonry Dams on Earth Foundations, *Trans. ASCE*, **100**, 1235–1351, 1935.

[2] From experiments conducted by F. Habermaas; figure from Emil Mosonyi, "Water Power Development," Vol. 1, Hungarian Academy of Sciences, 1963.

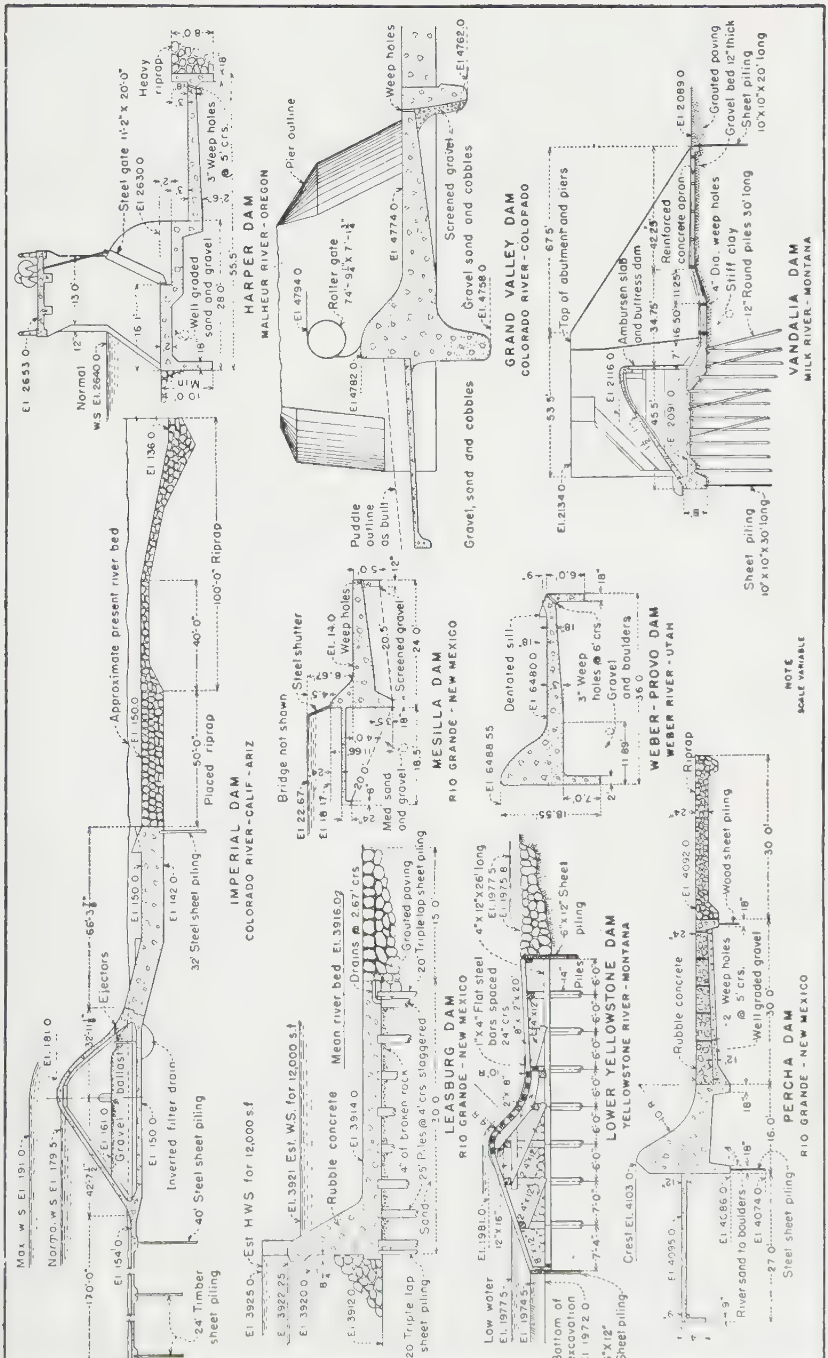

FIG. 1. Diversion weirs on earth foundations.

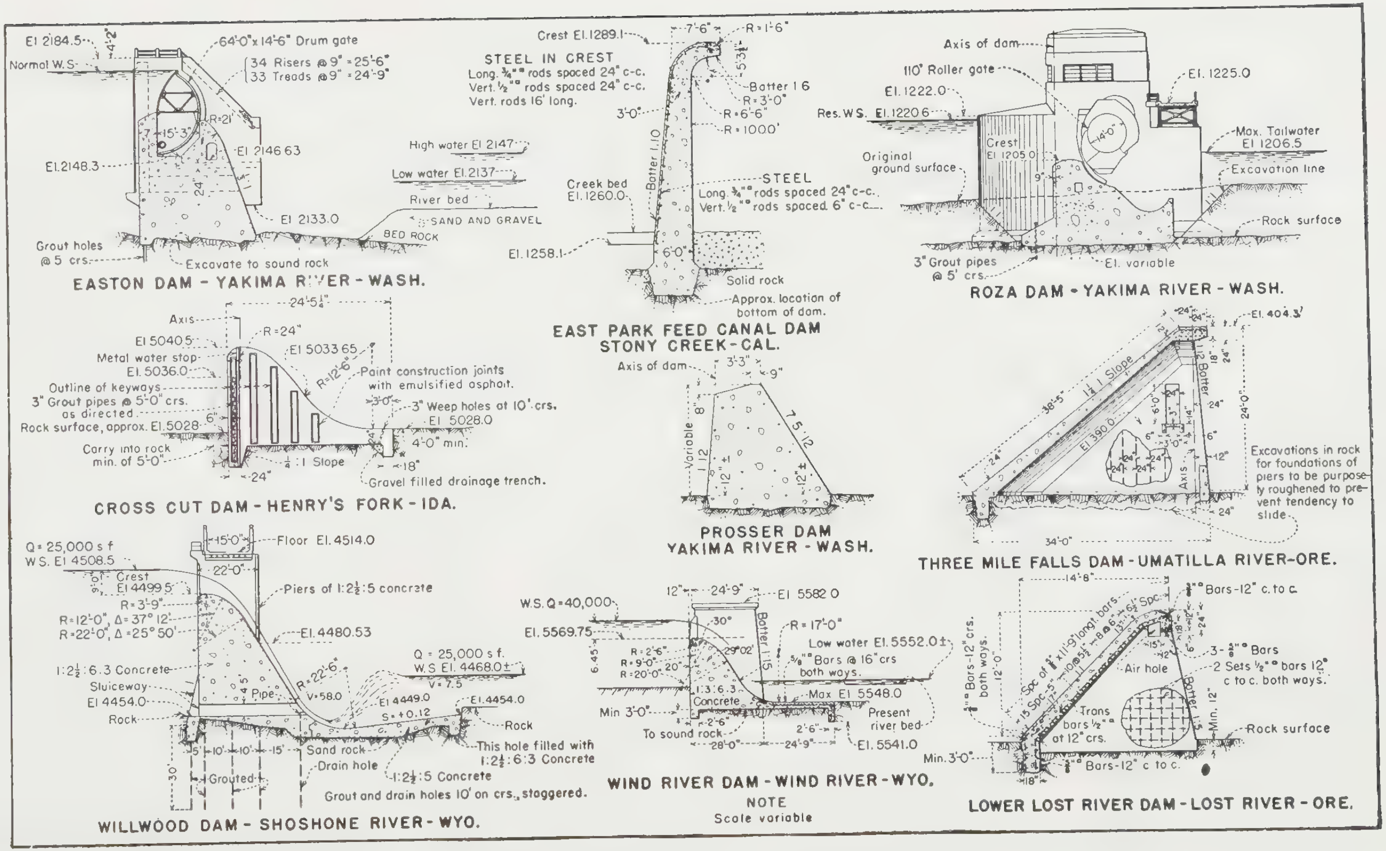

FIG. 2. Diversion weirs on rock foundations.

detritus deposition above the weir, sluices often must be constructed. This is especially true when weirs are of the overflow type.

Depending upon the habits of the river's aquatic life, a means for excluding same from the distribution system may be required at the intake. A discussion of the various devices to effect this is covered in Sec. 23.

3. Design of Intakes. Intakes should be designed to control and regulate water drawn from river channels with minimum entrance losses and as little disturbance as possible. Temporary timber structures may be built on small projects, but permanent concrete or masonry construction usually is desirable. Ordinarily, a permanent structure consists of one or more bays, controlled by radial or vertical slide gates, the bays being separated by piers and surmounted by an operating platform. Vertical slide gates are suitable for small intakes; but radial gates are usually more economical and easier to operate. Stoney or roller gates may be used at large diversion structures. Overpour types have the advantage of drawing water from river surfaces, but undershot types are less likely to become clogged by sediment.

In diversions to concrete-lined conduits, where water is carried at relatively high velocities, total areas of gate openings are usually made about the same as conduit areas. In diversions to earth canals, where water is carried at relatively low velocities, total gate areas are usually based on velocities of about 5 fps. However, full gate openings can be utilized only during periods of low river flow and high irrigation demand. At other times, water is diverted through partial gate openings, and gate velocities may be considerably higher than 5 fps.

A transition structure, consisting of a concrete floor and diverging curved or warped side walls, should connect the gate section with the head of the canal. The length of the transition should be great enough to quiet entrance disturbances and permit the gradual adjustment of flow to canal dimensions. Transition design will be discussed in Art. 12. The gate sill, with connecting transition floor, is usually placed at the same elevation as the canal bed. Portions of the abutment walls and piers upstream from the gates should be rounded to reduce entrance losses. Figure 5 shows an intake structure built on the Salt Lake Basin project, northern Utah.

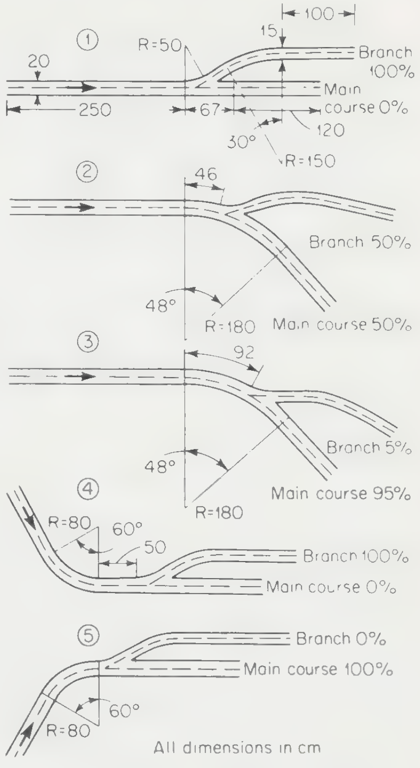

FIG. 3. Typical shapes of diversion. Scale-model tests.

4. Sluices. Sluices are usually located at ends of diversion weirs, just below or adjacent to intake structures (see Fig. 4), so as to draw water from the front of the intake gates. Sluiceway sills should be placed somewhat lower than intake sills, but above the river bed. The size and number of sluice gates required depend on the detritus-carrying characteristics of the stream.

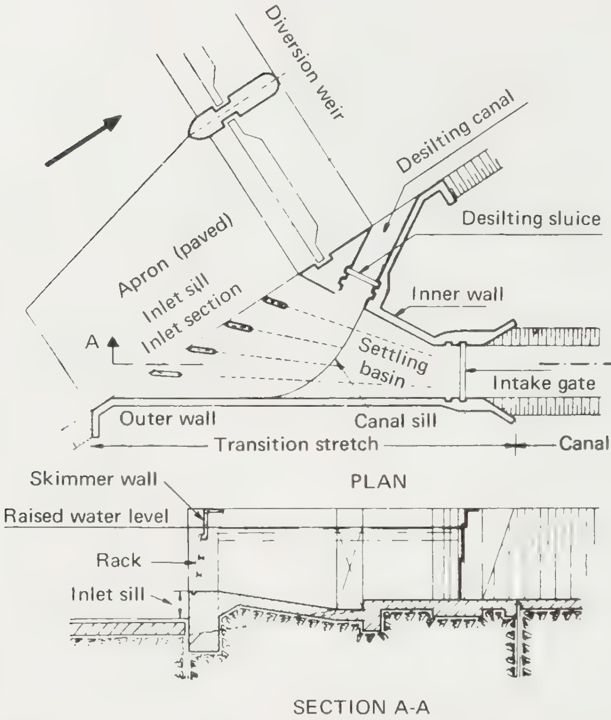

FIG. 4. Canal intake on rivers carrying heavy bed load.

DISTRIBUTION SYSTEM

5. General Discussion. The distribution system includes conduits, conveyance structures, regulating works measuring devices, protective elements, and miscellaneous features needed to deliver water to all parts of the irrigable area. On projects where irrigable lands are located on both sides of the river, or where water is diverted at more than one point, the distribution system may include two or more separate units. When parts of the irrigable area cannot be supplied by gravity flow, the system may also include pumping units, consisting of pumping plants, pressure pipelines, and various incidental structures required by such methods of distribution.

On some gravity projects, as where water supplies are limited and where seepage and evaporation losses are to be minimized, distribution systems may consist principally of pipelines, or closed conduits, with their necessary appurtenant works. However, distribution systems on most gravity projects consist, primarily, of open canals and appurtenant canal structures.

Conduits on a gravity project usually include main canals, branch canals, laterals, sublaterals, such additional ditches as may be necessary to convey water to individual farm units, and such waste canals as may be needed to carry surplus delivered and undelivered water back to natural channels. Conveyance structures may include chutes, drops, transition sections, inverted siphons, lined or unlined tunnels, flumes, aqueducts, closed conduits, or other crossings at railways, highways, or drainage courses. Regulating works usually consist of canal checks and major gate structures

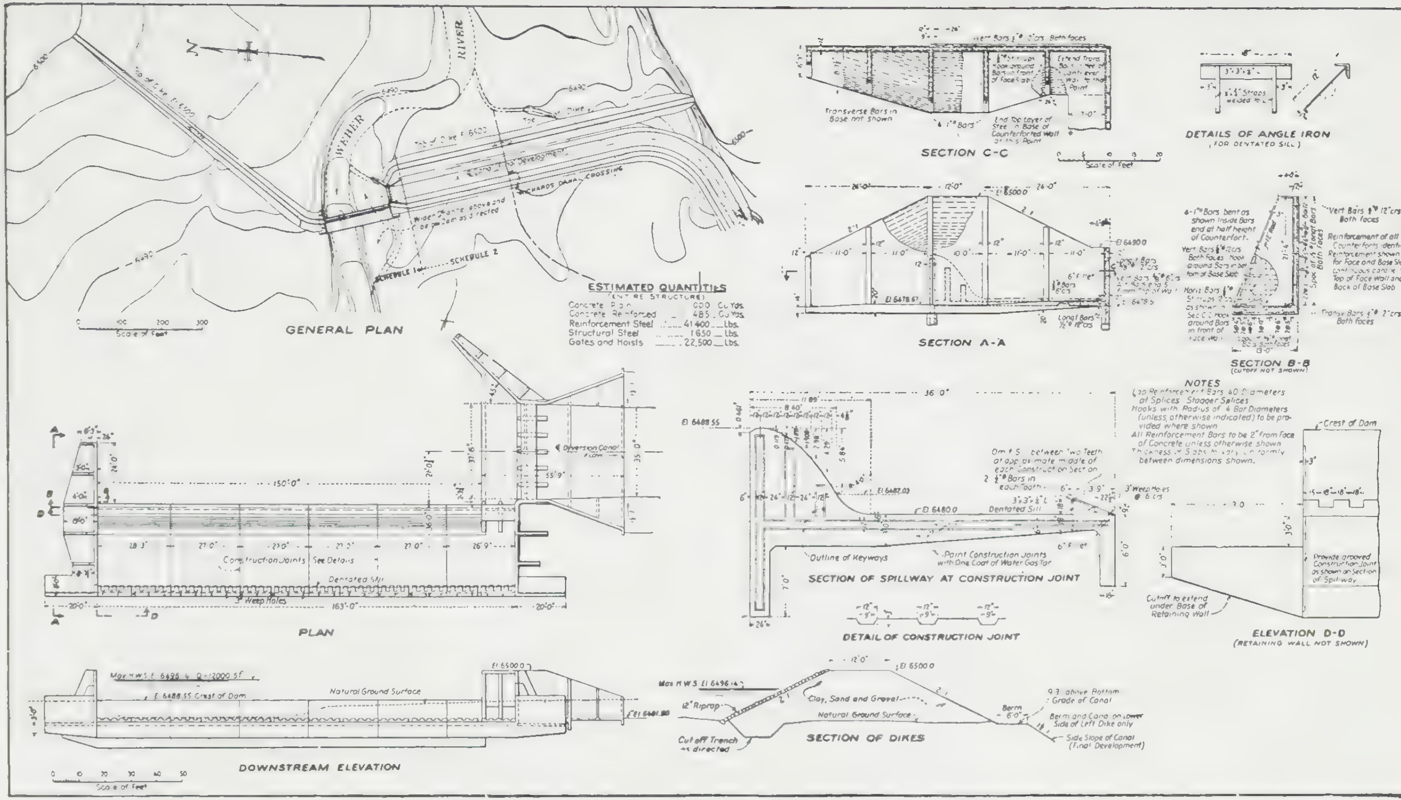

FIG. 5. Intake structure at Weber-Provo Diversion Canal, Salt Lake Basin project, Utah.

such as division works, large lateral intakes, and wasteways. Protective elements include automatic spillways, tributary flood overchutes, settling basins, and sediment traps. Miscellaneous features include drainage inlets, drainage culverts, farm and highway bridges, measuring structures, and other incidental construction.

Naturally, features for two or more purposes are often combined in one structure. For instance, box culverts, checks, radial gate wasteways, and siphon spillways were combined in one structure at two locations on the Casper Canal, Kendrick project, Wyoming. Furthermore, a single feature may serve dual purposes. Wasteways, although essentially of a regulating nature, may also constitute protective structures, since they may be used to sluice sand and silt deposits off canal beds, to divert canal flow during emergencies, or to discharge excess drainage waters which enter canal sections during storm periods. Various elements of the distribution system are discussed on the following pages.

CANALS

In general on gravity-flow irrigation projects, canals are used as the primary water-transporting medium. Canals in the majority of cases are excavated in earth or man-placed embankments. Occasionally rock may be encountered along the proposed alignment, and this may require the use of other types of conveyance structures.

6. The Need for Canal Lining. The decision whether to have a lined canal or to have no lining is an economic one. The relevant factors in making this decision are (1) permeability of the native soil, (2) its resistance to erosion, (3) the capitalized cost of water diversion, and (4) the amount of water available for diversion.

When canals are excavated in permeable soils and it is evident that the seepage losses through the soil will not substantially change with aging of the canal, some type of lining or surface treatment should be used because (1) the area below the canal can become waterlogged and nonproductive, (2) the diversion structure, canal section, and conveyance structures will require a greater capacity to compensate for the water lost. Canals excavated in erodible material will require lower operational velocities; consequently larger canal sections and larger maintenance costs can also be expected. The capitalized cost of water diversion is influenced by the size of the intake and its appurtenant features. If the available water for irrigation diversion is exceeded by the diversion demand, then a more impermeable canal section is required to maximize the area that can be served.

7. Canal Linings. The term canal lining implies a treatment applied to an excavated canal prism to increase the impermeability of the canal section. This treatment can be as simple as filling the canal section with silty water and allowing it to percolate through the foundation where the silt can fill the voids. Or it can be as sophisticated as precast-concrete elements placed on the foundation.

For the most part, linings can be classified as (1) exposed linings, (2) buried linings, (3) earth linings, and (4) soil sealants. Exposed linings are placed upon the prepared earth foundation. The commonest linings are constructed from Portland-cement concrete (unreinforced and reinforced), pneumatically applied Portland-cement mortar, asphaltic concrete, asphalt macadams, soil-cement mixtures, precast units of Portland-cement concrete or asphaltic mixtures, and stone and brick masonry.

Buried linings are impervious membranes that are placed against the excavated earth prism and backfilled with a layer of earth. This layer of earth forms a protective cover for the membrane, since the membranes are fragile, have little structural value, and rely upon the foundation for full support. Sprayed asphalt, prefabricated asphalt, rubber sheet, polyvinyl and polyethylene film, butyl-coated fabrics, and montmorillonite clay blankets are examples of buried linings.

Earth linings are blankets of earth placed on the excavated earth prism. The blankets may be compacted to a true thickness of 18 to 24 in. along the invert and 18 to 54 in. along the sides for medium- to large-sized canals. Thin earth linings composed of a 6- to 12-in. layer of compacted cohesive soil protected by a blanket of coarser soil also have been used. Loose blankets composed of selected fine-grain soils can be used where suitable equipment for compaction is not available. The latter two linings require the use of selected materials and will require excavation and haul from borrow areas.

Soil sealants for increasing the impermeability of the canal are a solution offering the least initial cost. Sealants used are silt, diversion water sediments, and chemical sealants. Three types of chemical sealants have been used by the U.S. Bureau of Reclamation,[1] (1) a resinous polymer, (2) a petroleum-based emulsion, and (3) a cationic asphalt emulsion. These and the earth sealants are applied to the canal by introducing the sealant either into the canal flow or into the stagnant water caused by damming the canal at intervals. The latter method has proved more effective, with reductions in seepage from 25 to 99 percent having been recorded.

The preceding discussion justifies a canal lining on the basis of reducing water losses. Exposed linings may be required where steep slopes require conveyance of water at relatively high velocities or in deep cuts where savings in excavation costs, resulting from carrying water at high velocity, overbalance lining costs. Lined canals are usually preferable from operation and maintenance viewpoints, except that maintenance costs may be relatively high for concrete-lined canals in cold climates. For a more detailed discussion of canal linings see Sec. 7.

8. Canal Location. Main canals are usually located along higher edges of irrigable areas but may follow interior ridges, depending on local topographic conditions. Branch and lateral canals may follow interior ridges or may be located at approximately right angles to general ground slopes. Canal locations should follow roads or property lines whenever possible. On the Garland Division, Shoshone project, northern Wyoming, the main canal parallels a railroad right of way which runs diagonally across the irrigable area, lateral canals branching off on each side at 1.5- to 3.0-mile intervals and running approximately parallel around the comparatively uniform basin slopes. The basic criterion for canal location is that maximum water surfaces in laterals and sublaterals must be high enough to permit deliveries to farm units.

In planning a canal system for a proposed irrigation project, approximate office locations of principal canals are made on topographic maps. Final locations are then made in the field, where the engineer can give more adequate consideration to local requirements.

9. Canal Capacities. Capacities for which canals must be designed should be based upon the consumptive-use requirements of the crops anticipated after implementation of irrigation in the area.

This quantity of water should then be increased because of inefficiencies in the conveyance system and the application of the water to the land. Conveyance losses can be attributed to seepage, operational losses, and evaporation. The losses in this category represent losses in the distribution system up to farm delivery. Farm application efficiency is a measure of the ability to store in the root zone the crop's water demand. The shape and slope of the farm unit, method of application, and type of soil are all factors which affect this efficiency.

The period between irrigations and the selection of the period with the least rainfall are then used to determine the canal capacity

$$Q = \frac{\Sigma(W_c A) - R}{12 E_c E_a}$$

[1] "Linings for Irrigation Canals," U.S. Bureau of Reclamation, 1963.

where Q = cu ft of water required during an irrigation period
W_c = consumptive use of each crop, in. of water
A = area under each crop, sq ft
R = estimated effective rainfall, in., during dry period
E_c = conveyance efficiency
E_a = application efficiency

Capacities for laterals and sublaterals should be determined in a similar method but should be increased by 25 percent because of a greater sensitivity to changes in crops and water demands.

10. Canal Cross Sections. Unlined earth sections should ordinarily be provided with side slopes of 1½:1 to 2:1, depending on earth materials. Extremes of 1:1 and 2½:1 have been used. Side slopes of 1¾:1 and 2:1 have been used on the All-American Canal. Rock sections and lined earth sections may be provided with steeper side slopes. Relatively large canals are often designed with berms between excavated sections and waste banks. When canal sides are in fill and the excavated earth is not uniformly satisfactory, core banks of selected fine materials should be specified along the inner slopes, extending from natural ground levels to a minimum height of 12 in. above maximum canal water surfaces. In certain cases, it may be desirable to compact the core material by sprinkling and rolling. Freeboard provisions should vary with size of canal, nature of canal banks, possible variation in water surface during full operation, and extent of damages that may result from breaks in canal banks. Concrete linings usually should be carried 9 to 24 in. above maximum canal water surfaces.

Canal cross sections may be designed by Kutter's formula, using roughness factors n selected from Table 1. All-American Canal sections were designed for roughness

TABLE 1. VALUES OF KUTTER'S ROUGHNESS FACTOR FOR USE IN DESIGNING IRRIGATION CANALS

Wetted perimeter	Canal description	Roughness factor, range
Concrete	Sections free from curvature	0.013–0.014
Concrete	Sections containing curvature	0.015–0.017
Concrete and gunite	Lined bottom with gunited rock side slopes	0.020–0.025
Concrete and rock	Retaining wall and lined bottom, one rock side	0.020–0.025
Concrete and rock	Retaining wall, unlined bottom and one rock side	0.025–0.030
Rock	Main, branch, and large lateral canals	0.030–0.035
Rock	Small canals, rough excavation	0.035–0.040
Earth	Main, branch, and large lateral canals	0.020–0.025
Earth	Small laterals and farm ditches	0.025–0.030

factors of 0.020 to 0.025 in unlined earth sections, 0.014 in concrete-lined sections, and 0.035 in unlined rock sections. Proper factors for unlined or partly lined rock sections depend on size of canal, smoothness of excavation, and proportion of wetted perimeter lined with concrete. Sometimes flow in rock canals can be economically improved by lining the bottom with concrete and guniting the side slopes. Gunite may also be used in repairing damaged linings.[1] Many comprehensive tables for use in designing canal cross sections have been published.[2]

[1] REEVES, A. B., Concrete Rehabilitation Work on the Uncompahgre Project, *J. Am. Concrete Inst.*, January–February, 1937, pp. 303–310.

[2] "Hydraulic and Excavation Tables," 11th ed., U.S. Bureau of Reclamation, 1957.

CONVEYANCE STRUCTURES

11. General. Conveyance structures, as the name implies, are the structures necessary to maintain the flow of water when the use of the canal section is no longer feasible. Examples where conveyance structures may be required are

1. Changes in grade caused in crossing existing highways or railways
2. Topography causing limitations on the breadth of the water conductor
3. Abrupt changes in grade due to topography
4. River- or drainage-course crossings
5. The need for maintaining the water surface over low-lying areas
6. Where topography greatly exceeds in elevation the canal water surface

Flumes, inverted siphons, and tunnels are examples of conveyance structures.

Conveyance-structure design differs from that of canals in that, although they rely upon the earth foundation for support, they are designed for either or both earth pressures and water loads. Because of this, they are generally built of reinforced concrete and in some instances pneumatically applied mortar, steel, or timber. The use of timber for the water-carrying part of the conveyance structure should be limited to small structures and those which operate more or less continually. Cyclic operation may cause warping of the timber, and leaking.

12. Transitions. The change from a canal section to a conveyance structure requires the use of a transition. Transition sections are built to conserve head. Their purpose is to minimize losses where the velocity is increasing and to recover as much head as possible where the velocity is decreasing. They are used at inlets and outlets of flumes, inverted siphons, and closed conduits, as well as at places where the shape of the canal cross section suddenly changes. In open conduits, they are usually concrete sections with gradually converging or diverging side walls, but may also include gradually changing bottom grades. In closed conduits, gradual transformations are made at tops and bottoms of sections as well as at sides. Sharp angles should be avoided in all major transition structures. Transitions in small lined ditches and at ends of small flumes and turnouts may include straight bottom grades and straight converging or diverging side walls; but all large transitions should be designed with curved or warped section transformations.

The proper length of a transition depends on the relative change in shape of section, initial velocity, and velocity change, the longer transitions being required for the higher velocities and greater velocity changes. Outlet transitions, where velocities are decreasing and flow conditions relatively unstable, should be 10 to 20 percent longer than inlet transitions, where velocities are increasing and flow conditions relatively stable. Curves in alignment, either within or close to transition sections, have disturbing effects that tend to increase hydraulic losses. Laboratory measurements in small rectangular channels, containing 180-deg curves with inner radii equal to channel widths, have shown curve losses as great as two-tenths the velocity head.[1] However, irrigation conduits seldom, if ever, contain such pronounced curvature.

In carefully designed, warped, transition structures, free from curves in alignment, hydraulic losses are probably less than 0.1 the difference in velocity head at the inlet and less than 0.2 the difference in velocity head at the outlet.

As a general rule, designs for transition structures should include the following allowances for hydraulic losses, including friction, the exact allowance to be made in a given case depending on the size of the transition and the care exercised in design.

[1] Yarnell and Woodward, Flow of Water around 180-degree Bends, *U.S. Dept. Agr. Tech. Bull.* 526, 1936.

1. Inlet transitions, free from curves in alignment, 0.1 to 0.3 the velocity head of the smaller cross section.

2. Outlet transitions, free from curves in alignment, 0.2 to 0.5 the velocity head of the smaller cross section.

3. Inlet and outlet transitions, curved alignments, and 0.05 to 0.1 the head to values considered applicable for straight alignments.

Careful hydraulic calculations should be made in planning all important transition structures, in order to secure efficient designs and avoid complications that may be experienced if flow occurs at or near critical depths.[1] Ample freeboard should be provided at the outlet, so that the water surface will not rise above any part of the structure in case the velocity head recovered should be greater than assumed.

Figure 6 shows well-designed, warped transitions constructed between lined earth and rock sections on the Kittitas Main Canal, Yakima project, Washington. Figure 14 shows warped inlet and outlet transitions at a monolithic reinforced-concrete siphon built on the Heart Mountain Canal, Shoshone project, Wyoming. Figure 7 shows the table and sample computations necessary for the design of the lined-earth to lined-rock transition shown in Fig. 6. The outlet transition-design method would be similar, except that a recovery of an 0.8 change in velocity head would determine the change in water surface (ΔW.S.).

13. Chutes. Chutes may be pipes, closed box sections, flumes, or open lined channels. A typical chute includes an inlet structure downstream of the transition, to control upstream water surfaces and regulate inflow; a relatively long inclined section in which the greater portion of the drop takes place; and an outlet structure designed to destroy the excessive energy developed in the inclined section. Chutes are often used on relatively steep slopes where a single drop or series of drops would be more expensive or less desirable from other viewpoints. Open, concrete-lined rectangular sections are preferable for the larger discharges though concrete trapezoidal sections have been used for smaller discharges.

Velocities in long inclined portions of open chutes are generally greater than critical; the drop through critical stage occurs in the transition if the inlet has no obstruction to flow such as a gate or stop planks.

Water-surface curves in inclined portions usually belong in the class where neutral depths are less than critical depths and actual depths are intermediate between critical depths and neutral depths, the neutral depth being the depth at which the water-surface slope parallels the bottom slope.[2] Water surfaces along inclined portions of chutes can be determined by backwater calculations, proper allowance being made for changes in velocity head as well as friction losses. Friction losses in concrete-lined chutes may be computed by Manning's or Kutter's formula, using roughness factors of 0.012 to 0.014, depending on smoothness. A sample backwater calculation for a chute follows.

Given: a rectangular chute 10 ft wide discharging 64 cfs per ft of width $n = 0.014$, slope of chute $S_0 = 0.10$.

$$\text{Critical depth } d_c = \sqrt[3]{\frac{q^2}{g}} = \sqrt[3]{\frac{64.0^2}{32.2}}$$
$$= 5.02 \text{ ft}$$
$$V = \frac{640}{50.2} = 12.75 \text{ fps}$$

[1] Scobey, Fred C., The Flow of Water in Flumes, *U.S. Dept. Agr. Tech. Bull.* 393, 1933.

[2] Woodward, Sherman M., Theory of the Hydraulic Jump and Backwater Curves, Part III, *Tech. Rept.*, The Miami Conservancy District, Dayton, Ohio, 1917.

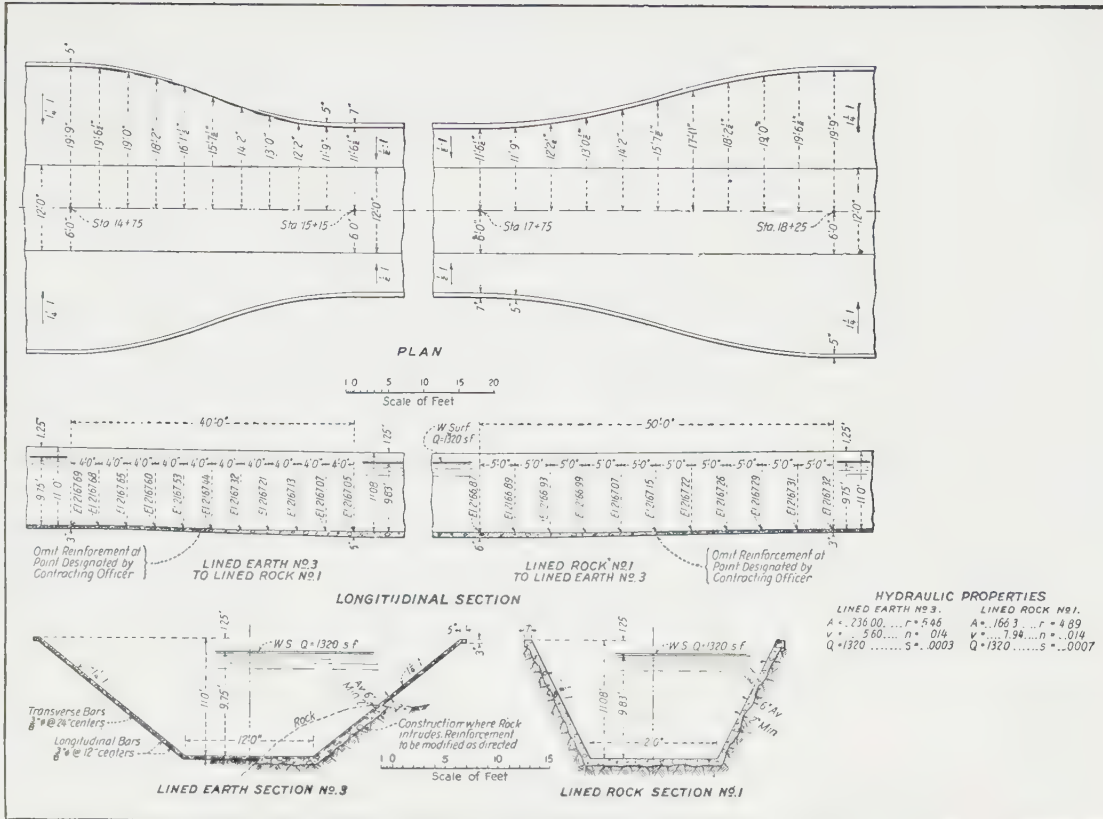

FIG. 6. Warped transition sections, Kittitas Main Canal, Yakima project, Washington.

Rock lining $V = 7.94$ fps $h_v = 0.980$ El. W.S. at beginning of transition = 2,177.44, *i.e.*, 77.44
Earth lining $V = 5.60$ fps $h_v = 0.489$ with El. 2,100 as base. Entrance loss = $1.1h_v$

Assume a water-surface profile of reversed parabolas.

$\Delta h_v + 1.1\Delta h_v = 0.541$ Transition length = 40′-9″

	Station, ft										
	0	4	8	12	16	20	24	28	32	36	40
ΔW.S. (neglects friction), drop in W.S.	0	0.011	0.043	0.094	0.173	0.27	0.367	0.446	0.497	0.529	0.541
Δh_v = ΔW.S. ÷ 1.1	....	0.01	0.039	0.086	0.157	0.246	0.334	0.405	0.451	0.481	0.491
$h_v = 0.489 + \Delta h_v$	0.489	0.490	0.528	0.575	0.646	0.735	0.823	0.894	0.940	0.970	0.980
$V = \sqrt{2gh_v}$	5.60	5.62	5.83	6.08	6.44	6.88	7.28	7.59	7.78	7.90	7.94
Area = $Q \div V$	236.0	234.9	226.4	217.1	205.0	191.9	181.3	173.9	169.7	167.1	166.3
$\frac{1}{2}T$ = ½ width at W.S.	18.19	18.05	17.55	16.87	15.76	14.54	13.22	12.18	11.45	11.09	10.92
$\frac{1}{2}B$ = ½ bottom width	6.0	6.0	6.0	6.0	6.0	6.0	6.0	6.0	6.0	6.0	6.0
Average width	24.19	24.05	23.60	22.87	21.76	20.54	19.22	18.18	17.45	17.09	16.92
d = area ÷ avg width	9.75	9.76	9.60	9.49	9.43	9.34	9.43	9.57	9.73	9.79	9.83
S_f − friction slope	0.00029	0.00029	0.00033	0.00035	0.00040	0.00047	0.00053	0.00060	0.00063	0.00066	0.00068
h_f (each station)	......	0.0012	0.0012	0.0014	0.0015	0.0017	0.0020	0.0023	0.0025	0.0026	0.0026
h_f (cumulative)	......	0.0012	0.0024	0.0038	0.0053	0.0070	0.0090	0.0113	0.0138	0.0164	0.0190
W.S. El. = 77.04 − ΔW.S. − h_f	77.44	77.428	77.395	77.342	77.262	77.163	77.064	76.983	76.929	76.895	76.881
Grade = W.S. El. − d	67.69	67.668	67.795	67.852	67.832	67.823	67.634	67.413	67.199	67.105	67.051
$\frac{1}{2}T - \frac{1}{2}B$	12.19	12.05	11.60	10.87	9.76	8.54	7.22	6.18	5.45	5.09	4.92
Side slopes	1.25	1.24	1.19	1.11	1.00	0.877	0.741	0.631	0.555	0.517	0.500
H = top lining El. − grade El.	11.00	10.966	10.783	10.670	10.614	10.587	10.720	10.885	11.043	11.081	11.079
Side slope × $H = \frac{1}{2}W - \frac{1}{2}B$	13.75	13.58	12.83	11.83	10.614	9.27	7.95	6.86	6.13	5.73	5.54
$\frac{1}{2}W$ = ½ top lining width	19.75	19.58	18.83	17.83	16.614	15.27	13.95	12.86	12.13	11.73	11.54
$\frac{1}{2}W$ (to nearest ½ in.)	19′-9″	19′-7″	18′-10″	17′-10″	16′-7½″	15′-3″	13′-11½″	12′-10½″	12′-1½″	11′-9″	11′-6½″

NOTES:

1. Values for $\frac{1}{2}T$ are scaled from a trial plan showing water intersection with transition walls.
2. A tangent to this water-surface boundary should have an included angle between it and the transition center line of not more than 22°30′.
3. The term $\frac{1}{2}B$ is also varied when the transition requires a change in base widths.
4. Differences between the above and dimensions shown on Fig. 6 can be attributed to differences in water-surface profile assumptions and numerical rounding off.

FIG. 7. Comparative computations for inlet transition (Fig. 6).

Assuming that the depth of flow at the inlet passes through critical, what will be the depth of flow 45 ft down the chute?

Check neutral depth d. Manning's equation

$$Q = \frac{1.486}{n} AR^{2/3}S^{1/2}$$

$$AR^{2/3} = \frac{Qn}{1.486} S^{1/2}$$

$$10d\left(\frac{10d}{10 + 2d}\right)^{2/3} = \frac{640(0.014)}{1.486} (0.1)^{1/2}$$

A trial-and-error solution gives a neutral depth of 0.38 ft.

For nonuniform flow the length L between two sections designated 1 and 2 can be determined by the following equation:

$$L = \frac{(V_2^2/2g + d_2) - (V_1^2/2g + d_1)}{S_0 - (nV/1.486R^{2/3})^2}$$

where $V_{1,2}$ = velocity at the particular section
$d_{1,2}$ = depth at the particular section
S_0 = channel slope
V = mean velocity between sections
R = mean hydraulic radius between sections

Assume a change in depth of 1 ft; then $d_2 = 4.02$ ft; therefore,

$$V_2 = \frac{640}{4.02(10)} = 15.92$$

$$V = \frac{640}{4.52(10)} = 14.17 \qquad \text{and} \qquad R = \frac{4.52 \times 10}{10 + 2(4.52)} = 2.37$$

$$L = \frac{(15.92^2/64.4 + 4.02) - (12.75^2/64.4 + 5.02)}{0.10 - [0.014(14.17)/1.486(2.37)^{2/3}]^2}$$

$L = 43.8$ ft; therefore, the depth of flow at the required section will be approximately 4 ft.

Open chutes, carrying water at high velocities, often contain waves and agitated water surfaces, even though hydraulic jumps occur at the outlets. Consequently, ample freeboard must be provided in inclined sections. The U.S. Bureau of Reclamation[1] has recommended that the freeboard be not less than $0.4d_c$ (critical depth) or the following:

Capacity Q, cfs	Freeboard, in.
100 or less	12
101–500	15
501–1,000	18
Over 1,000	24

The above freeboard should be added to the depth of flow in the chute section computed using a roughness factor of 0.014. In long chutes the width of the chute section can be narrowed a short distance below the intake to effect an economy. A spreading transition will then be required between the narrow chute section and the stilling pool. The angle of flare on each side of the spreading transition should not exceed arctan $(\sqrt{gd}/3V)$, where V = velocity at beginning of transition with $n = 0.010$, d = corresponding depth of flow.

The longitudinal profile of the spreading transition is usually to a curve defined by the chute slope ($\tan \phi$) and the desired slope of the transition at the intersection with

[1] "Canals and Related Structures," U.S. Bureau of Reclamation, Design Standards No. 3.

the stilling pool ($\tan \alpha$). A slope of 2 horizontal to 1 vertical for the latter is preferred, with upper and lower limits being 1½ horizontal to 1 vertical and 3 horizontal to 1 vertical.

The curved profile of the transition reduces the hydrostatic pressures on the transition floor. To ensure positive pressures on the floor a K value of 0.5 or less is desirable:

$$K = \frac{(\tan \alpha - \tan \phi)2h_v \cos^2 \phi}{L_T}$$

where L_T = horizontal length of the curved profile
h_v = velocity head at beginning of transition using $n = 0.010$
The curved profile is defined by the equation

$$Y = X \tan \phi + \frac{(\tan \alpha - \tan \phi)X^2}{2L_T}$$

where X = horizontal length from origin of curve
Y = vertical drop from origin of curve to point X on curve

The outlet structure is some form of stilling pool to dissipate energy to a level that will not cause damage by erosion, and also will allow a steady state of flow in the canal. The length of the stilling pool, excluding the outlet transition, should be four times the depth of flow after the hydraulic jump for structures in use for long duration and three times this depth for intermittent or short-duration use. The stilling-pool invert should have no longitudinal slope; thus, using the computed depth of flow at the end of the chute section d_1, the depth of flow d_2 after the hydraulic jump will be

$$d_2 = -\frac{d_1}{2} + \sqrt{\frac{2V_1^2\, d_1}{g} + \frac{d_1^2}{4}}$$

Hydraulic-energy losses in the outlet transition are ignored; consequently, the difference between d_2 and the normal depth of flow plus velocity head in the canal below the outlet will determine the difference between canal and stilling-pool inverts. A chute embodying the design features discussed is shown in Fig. 8.

Model studies are often desirable in designing outlet sections for chutes carrying large discharges.[1]

14. Drops. Drops fulfill essentially the same purpose as chutes but are used when the required lowering of water surfaces is small. Drops can be either vertical or inclined; of the latter there are two types: the open channel, as in the chute, and the pipe drop.

The vertical drop, as the name implies, causes an abrupt change in elevation of the canal inverts. For a concrete drop structure in an earth canal, the change in water-surface elevation should not exceed 3 ft. A structure typical of this type is shown in Fig. 9. In concrete or hard-surfaced canals, the drop can be as high as 8 ft. The length L of the stilling pool can be determined by

$$L = \left[2.5 + 1.1\frac{d_c}{h} + 0.7\left(\frac{d_c}{h}\right)^3\right]\sqrt{hd_c}$$

where d_c = critical depth
h = drop in canal inverts

The pool invert should be a distance of $d_c/2$ below the invert of the downstream canal section. To effect relatively tranquil flow, the downstream water surface should be at least $0.4d_c$ below the upstream water surface. This allows some plunge to the

[1] Elevatorski, Edward A., "Hydraulic Energy Dissipators," McGraw-Hill Book Company, New York, 1959.

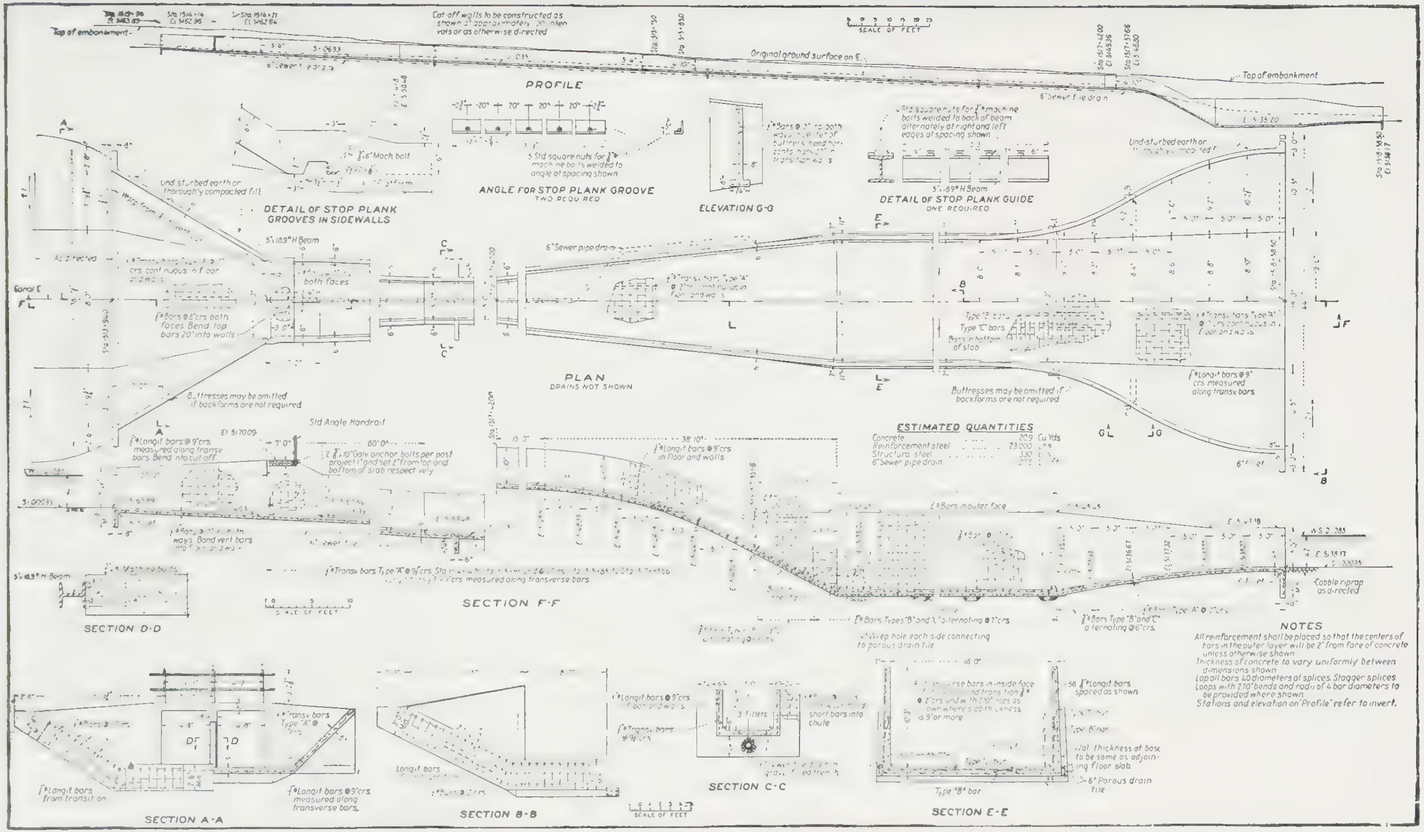

FIG. 8. Open lined chute on Pilot Canal, Riverton project, Wyoming.

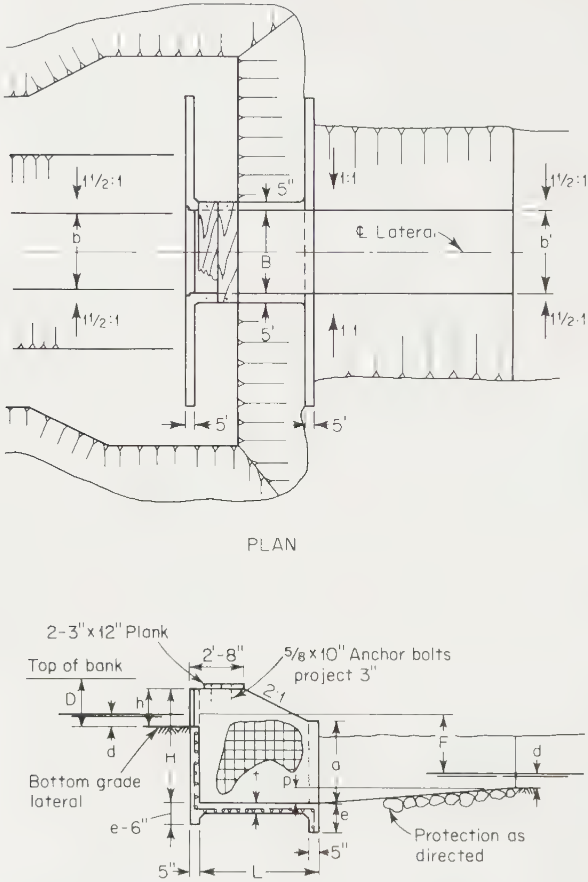

LONGITUDINAL SECTION

Fig. 9. Vertical concrete drop.

jet and reduces waves. The use of vertical drops is dictated by a severe change in ground-surface elevation and the need to maintain tranquil flow in canal sections close to each other, but when water surfaces differ by several feet in elevation.

Inclined drops are used where the drop in water surface is greater than that allowed in a vertical drop and the distance between sections having tranquil flow is not limited. Figures 10 and 11 show typical rectangular and trapezoidal inclined drops. The hydraulic design of the inclined open-channel drop parallels that discussed in the section on chutes.

Pipe drops accomplish the desired change in water-surface elevations by introducing the canal flow into a steeply sloping closed conduit. The sloping conduit effects the elevation change, and an outlet structure dissipates the energy. The outlet structure may be of the stilling-pool type, but more often an impact stilling basin is used (Fig. 12, Table 2). This stilling basin relies upon the impact with the vertical baffle for energy dissipation. A downstream water surface is not required.[1]

[1] "Hydraulic Design of Stilling Basins and Energy Dissipators," U.S Bureau of Reclamation, Engineering Monograph No. 25, July, 1963.

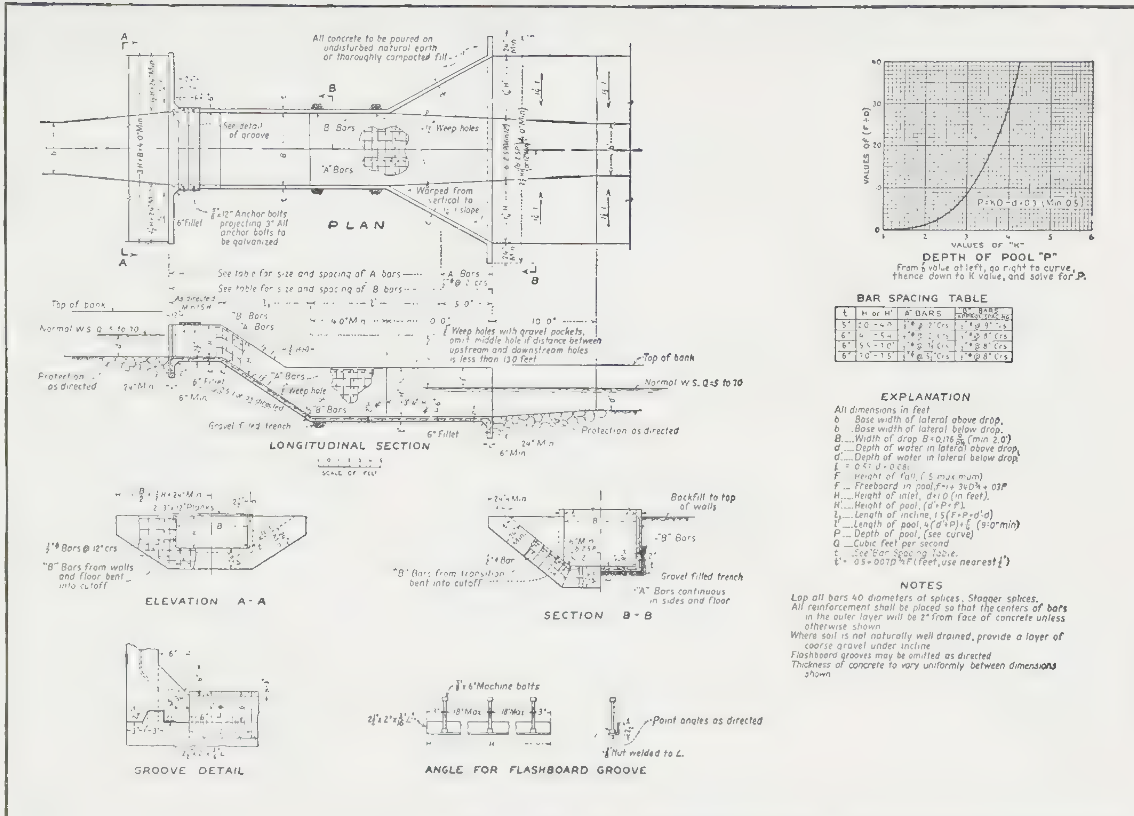

FIG. 10. Rectangular inclined drop for capacities of 5 to 70 cfs.

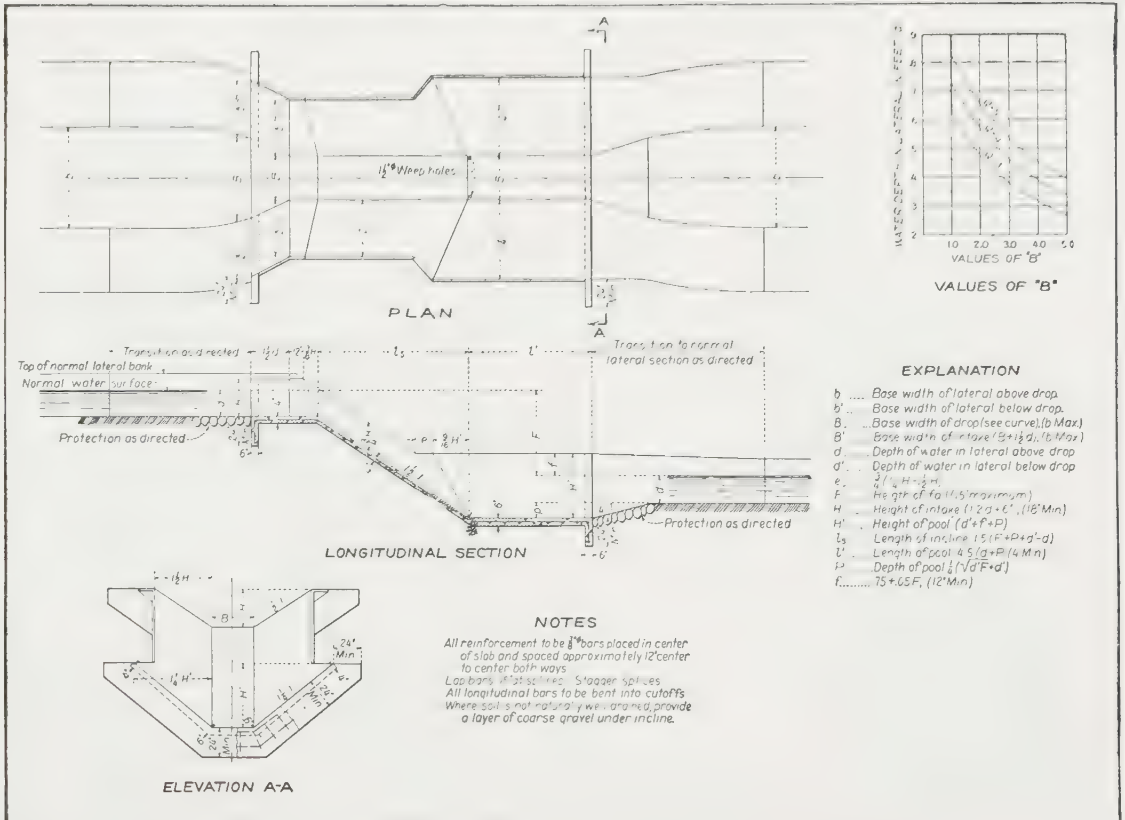

FIG. 11. Trapezoidal inclined control-section drop, maximum capacity 5 cfs.

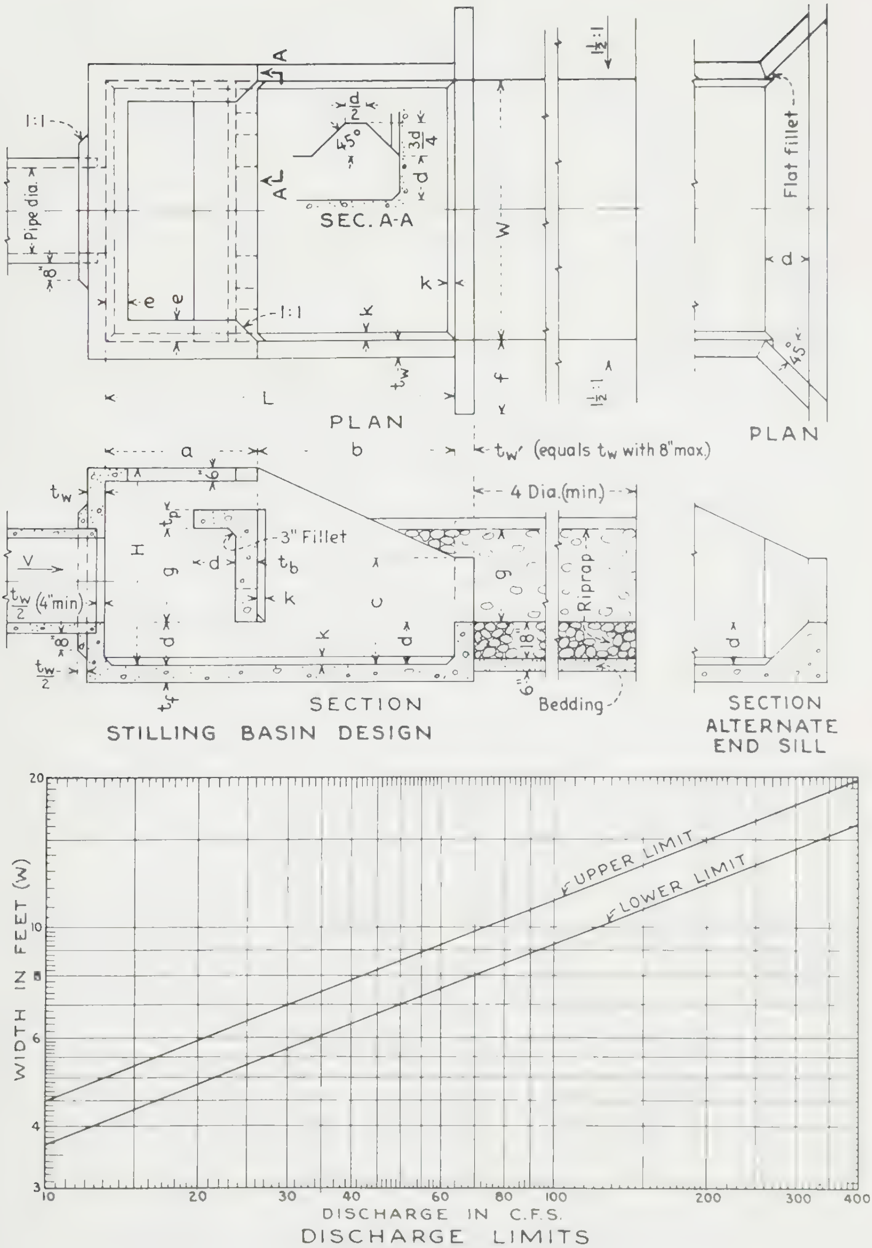

Fig. 12. Impact-type energy dissipator.

TABLE 2. STILLING-BASIN DIMENSIONS. IMPACT-TYPE ENERGY DISSIPATOR

Suggested pipe size*		Max discharge Q	Feet and inches										Inches					
Diam, in.	Area, sq ft		W	H	L	a	b	c	d	e	f	g	t_w	t_f	t_b	t_p	K	Suggested riprap size
(1)	(2)	(3)	(4)	(5)	(6)	(7)	(8)	(9)	(10)	(11)	(12)	(13)	(14)	(15)	(16)	(17)	(18)	(19)
18	1.77	21†	5-6	4-3	7-4	3-3	4-1	2-4	0-11	0-6	1-6	2-1	6	6½	6	6	3	4.0
24	3.14	38	6-9	5-3	9-0	3-11	5-1	2-10	1-2	0-6	2-0	2-6	6	6½	6	6	3	7.0
30	4.91	59	8-0	6-3	10-8	4-7	6-1	3-4	1-4	0-8	2-6	3-0	6	6½	7	7	3	8.5
36	7.07	85	9-3	7-3	12-4	5-3	7-1	3-10	1-7	0-8	3-0	3-6	7	7½	8	8	3	9.0
42	9.62	115	10-6	8-0	14-0	6-0	8-0	4-5	1-9	0-10	3-0	3-11	8	8½	9	8	4	9.5
48	12.57	151	11-9	9-0	15-8	6-9	8-11	4-11	2-0	0-10	3-0	4-5	9	9½	10	8	4	10.5
54	15.90	191	13-0	9-9	17-4	7-4	10-0	5-5	2-2	1-0	3-0	4-11	10	10½	10	8	4	12.0
60	19.63	236	14-3	10-9	19-0	8-0	11-0	5-11	2-5	1-0	3-0	5-4	11	11½	11	8	6	13.0
72	28.27	339	16-6	12-3	22-0	9-3	12-9	6-11	2-9	1-3	3-0	6-2	12	12½	12	8	6	14.0

* Suggested pipe will run full when velocity is 12 fps or half full when velocity is 24 fps. Size may be modified for other velocities by $Q = AV$, but relation between Q and basin dimensions shown must be maintained.

† For discharges less than 21 sec-ft, obtain basin width from curve of Fig. 12. Other dimensions proportional to W; $H = 3W/4$, $L = 4W/3$, $d = W/6$, etc.

The design of the inlet to the drop structure should ensure water-surface control. If the structure is adjacent to a farm delivery or a division in canal flows, the design canal water surface should be maintained in the canal section; otherwise the depth of flow at the control could be at critical depth or above. Methods by which the water surface may be controlled are weirs, flashboards, slide gates, or, on larger structures, radial gates.

15. Inverted Siphons. Inverted siphons are used to carry canal discharges under highways, railways, streams, or across relatively long and deep drainage courses where construction of flumes or other aqueducts at or near canal grades would not be feasible. They usually consist of reinforced-concrete inlet and outlet transitions with connecting barrels of reinforced concrete, wood staves, or steel. Rectangular or square reinforced-concrete sections are used when the head is less than 30 ft. Reinforced-concrete precast and monolithic circular sections have been used for heads in excess of 100 ft. Prestressed-concrete pipe and steel plate can be used for higher heads. Steel plate and reinforced concrete were combined in certain sections of the Soap Lake Siphon in the state of Washington.[1]

In some cases the siphon barrel may be lowered to an elevation where it may cross the depressed ground surface on a trestle. Conduit weight then becomes a factor in the design of the trestle, and wood staves in smaller siphons, or steel plate, are most generally used. The use of steel plate in water conduits has greatly advanced in recent years with the use of phenolic, vinyl, and, more recently, coal-tar epoxy paints to deter corrosion.

The structural design of circular barrel siphons is based upon a hoop stress due to the hydrostatic head on the crown of the section, a moment due to the weight of the water contained in the section, and the reaction of the foundation assumed in contact with the pipe.[2]

In reinforced-concrete siphons, the allowable stresses in the reinforcement are reduced as the head increases.[3] Cognizance of the fact that Hooke's law is not appropriate in curved members is also necessary. Design for an external loading when the conduit is empty should also be considered.

Provision for draining the siphon should be made either by connecting a valved pipe at the low point of the siphon or by pumping the water out. If the siphon is beneath a watercourse, it must be capable of resisting the buoyant forces exerted by the watercourse and the undermining of its foundation by scour.

Siphons should be inspected and cleaned occasionally. The use of sand and gravel traps upstream of the inlet will reduce the amount of cleaning required. Sand traps are discussed under Protective Structures.

The velocity of flow in the siphon is dependent upon the available head and economic considerations. Siphons with water containing abrasive suspended material should have a velocity less than 10 fps.

The hydraulic design of siphons should consider the hydraulic losses in the inlet transition, closed transition to pipe section (circular-section siphons only), friction and bend losses in the siphon barrel, and the hydraulic losses in the outlets of closed and open transitions. Friction losses in the transition are usually discounted, but a safety factor of 10 percent is added to the losses computed.

Figures 13 and 14, respectively, show a sample computation of siphon head losses, and the siphon on the Heart Mountain Canal of the Shoshone project in Wyoming. Siphons designed to have a water surface subject to atmosphere within the closed sections of the siphon may entrain air with serious consequences.[4]

[1] "Soap Lake Siphon," U.S. Bureau of Reclamation, Engineering Monograph No. 5.
[2] "Stress Analysis of Concrete Pipe," U.S. Bureau of Reclamation, Engineering Monograph No. 6.
[3] "Soap Lake Siphon," U.S. Bureau of Reclamation, Engineering Monograph No. 5.
[4] Entrainment of Air in Flowing Water—Closed Conduits, *Trans. ASCE*, **108**, 1435, 1943.

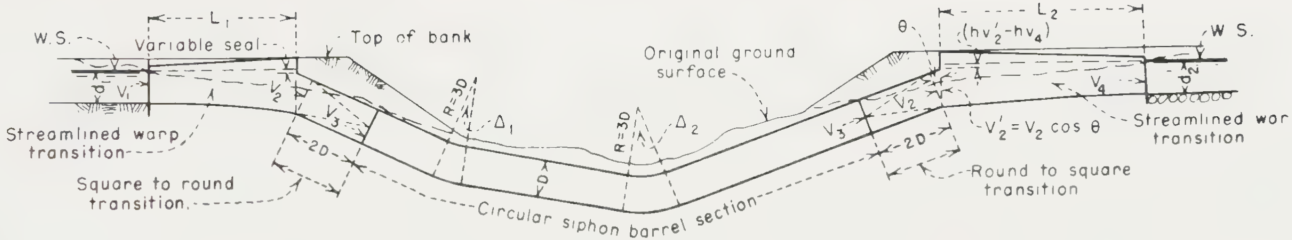

PROFILE-TYPICAL SIPHON

EXAMPLE:

DIMENSIONS AND HYDRAULIC PROPERTIES

CANAL END OF INLET AND OUTLET TRANSITIONS

Base Width = 25.0'
Side slopes = $1\frac{1}{2}$ 1
$d_1 = d_2 = 10.00'$
Q = 1000
A = 400.00
$V_1 = V_4 = 2.50$, $hv_1 = hv_4 = .097$
r = 6 55
n = .014
s = 00005-

SQUARE OPENING OF CLOSED TRANSITIONS

Size = 11 0' x 11.0'
Q = 1000
A = 121 00
$V_2 = 8\ 26$, $hv_2 = 1.061$
r = 2 75
n = .014
s = .00157

CIRCULAR SIPHON BARREL

Dia. = 11.0'
Q = 1000
A = 95.03
$V_3 = 10.52$, $hv_3 = 1.721'$
r = 2.75
n = .013 (Steel form finish or equal)
s = .00220
n = .014
s = 00255

COMPUTATION OF HEAD LOSSES

Inlet Open Transition (Friction)	$= 45'(L_1)\left(\frac{.00005+.00157}{2}\right)$	= 036'
Inlet Open Transition (Convergence)	$=^{*}.1\,[1.061\,(hv_2)-.097\,(hv_1)]$	= .096'
Inlet Closed Transition (Convergence)	$= .1\,[1.721\,(hv_3)-1.061(hv_2)]$	= .066'
Closed Transitions (Friction)	$= 2 \times 22'\left(\frac{.00157+.00255}{2}\right)$	= .091'
Circular Barrel (Friction)	$= 160' \times .00220$	= .352'
Barrel Bend $\Delta_1 = 15°$	$=^{**}\ 027 \times 1\ 721\ (hv_3)$	= .046'
Barrel Bend $\Delta_2 = 30°$	$=^{**}\ 058 \times 1\ 721\ (hv_3)$	= .100'
Outlet Closed Transition (Divergence)	$= \ 2\,[1\ 721(hv_3)-1\ 061(hv_2)]$	= 132'
Outlet Open Transition (Divergence)	$=^{*}2\,[1\ 061\,(hv_2)\ \ 097\,(hv_4)]$	= 193'
Outlet Open Transition (Friction)	$= 60'(L_2)\left(\frac{00005+00157}{2}\right)$	= .049'
Total Loss (Energy Gradient)		= 1 161'
Add 10% ± for excess capacity		= 116'
Total Head required		= 1.277'

*Coefficient used for computation of head loss in open transition should conform with type of transition selected.

** See Figure 13A

HEAD LOSS DETERMINATION FOR MONOLITHIC CONCRETE SIPHONS

Fig. 13. Head-loss determination for monolithic concrete siphons.

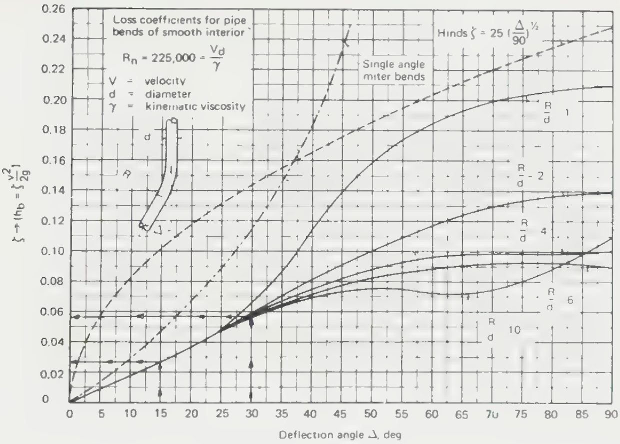

FIG. 13*A*. Head losses in pipe bends.

16. Flume Crossings. Flume crossings at canal grades may include timber, wood-stave, metal, or reinforced-concrete aqueducts of either monolithic or precast construction. They may be supported on piles, pile bents, structural-steel bents on concrete pedestals, concrete piers, structural-steel trusses, or other construction. Timber-box flumes, supported on piles or pile bents, are often used to carry farm deliveries; metal flumes supported on pile or structural-steel bents are frequently used to carry lateral discharges; and large metal or reinforced-concrete flumes, supported on concrete piers, steel trusses, or other construction, are used to carry main-canal, branch-canal, and large lateral discharges.

Practically all flumes connecting canal sections should be provided with inlet and outlet structures (see discussion of transitions). In relatively small flumes, such as those required for farm deliveries, outlet losses need no special consideration, except that ample freeboard should be provided to prevent overlapping of the banks or outlets. Riprap or other protection against scour may be needed for short distances beyond outlet transitions, depending on flume velocities and composition of canal beds. The flume sections are designed in the same manner as canals, except that economic considerations dictate that the flume section be optimized consistent with allowable head losses. The freeboard on the flume should match in elevation that of the canal section or be greater if water splashed from the flume is to be avoided.

Semicircular flumes, free from curves in alignment, are usually provided with freeboards varying from 6 to 10 percent of the diameter, the larger percentages being used for the smaller flumes, and no freeboards of less than 3 in. being used in any installations. Curved flumes require greater freeboards, especially along outer edges of curves.

Figure 15 shows a reinforced-concrete aqueduct, built to carry the Milner-Gooding Canal over the Big Wood River, Minidoka project, southern Idaho.

The structural design of the box flume section considers the vertical walls as beams spanning between supports carrying half the flume and water weight.

When the supporting structure is founded on rock or other firm foundation, not subject to appreciable settlement, the flume can be monolithically continuous over several supports; otherwise the flume spans should be simply supported. The flume walls should also be designed as vertical cantilevers fixed at the flume floor. In some

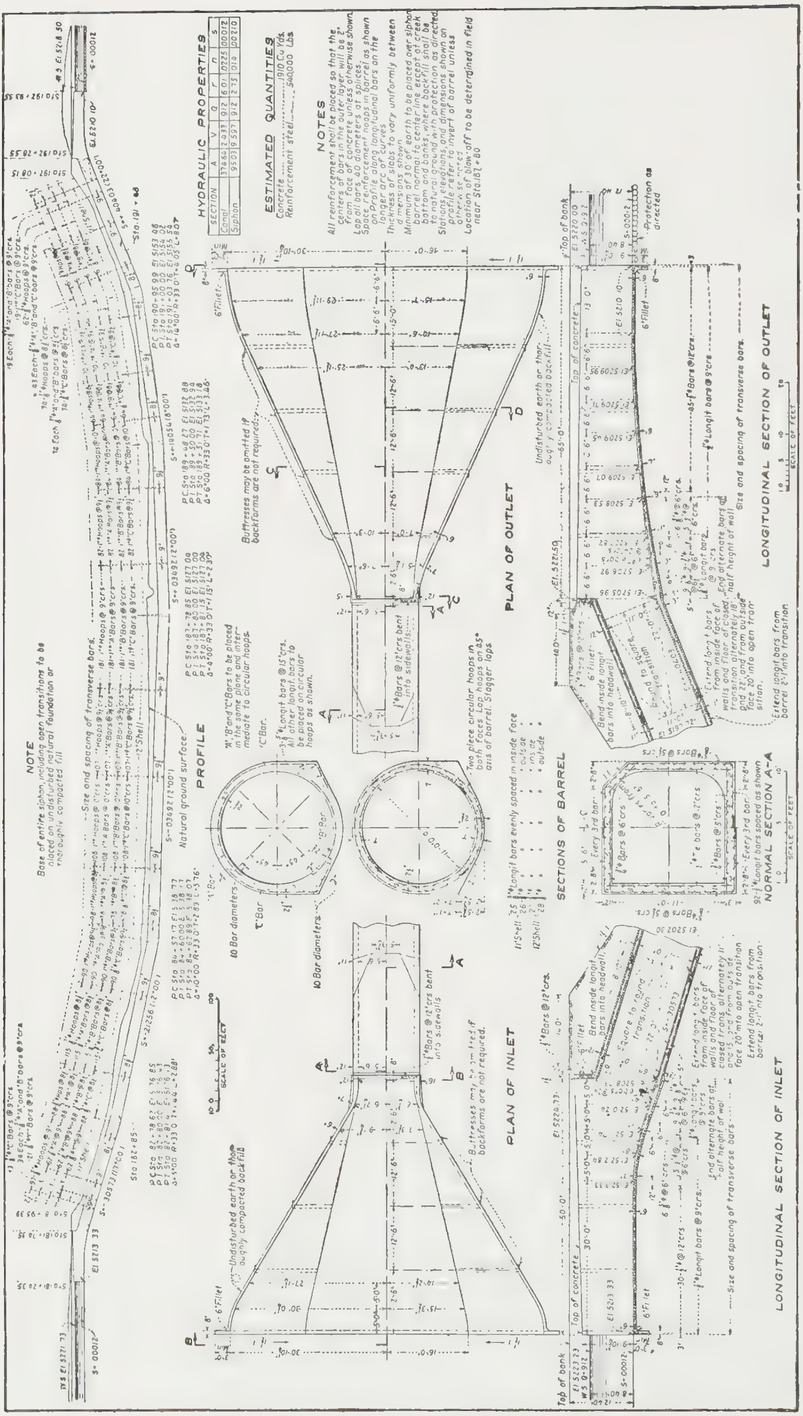

Fig. 14. Reinforced-concrete siphon, Heart Mountain Canal, Shoshone project, Wyoming.

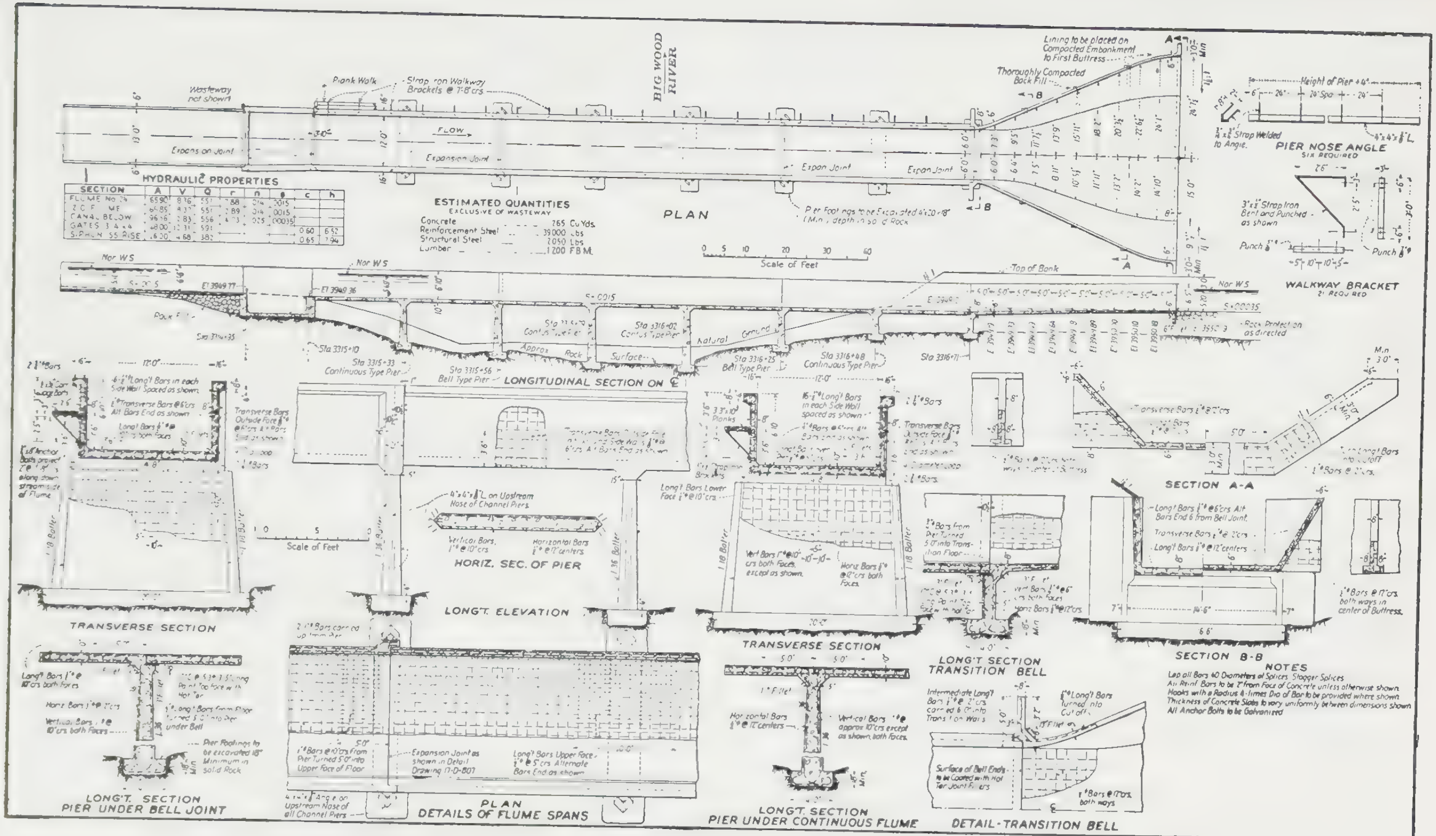

FIG. 15. Reinforced-concrete aqueduct over Big Wood River, Minidoka project, Idaho.

instances struts across the top of the flume are used. These struts are either tension ties or compression struts, depending upon the proportion of flume width to water height. This scheme reduces the amount of cantilever reinforcement required and offers lateral support to the compression zone of the wall, but also reduces the effective freeboard. Another means of obtaining restraint at the top of the wall, without the above drawback, may be achieved by adding a corbel to the top of the wall and vertical buttresses on the outside of the wall at the flume supports. The corbel would act as a beam spanning between the vertical buttresses and subject to deflection in a horizontal plane. The flume floor should be designed for a moment due to the water weight minus the cantilever end moments. Axial thrust on the slab caused by hydrostatic pressure on the wall should also be considered.

REGULATING STRUCTURES

Regulating structures are built where canal water surfaces or discharges must be controlled. Checks are built to raise canal water surfaces so that deliveries can be made to relatively high lands. Major gate structures are built where main canals divide into branch canals, usually called *division works*, at large lateral intakes and at wasteways. Wasteway structures often include automatic spillway elements.

Temporary regulating works and minor control structures may be constructed of timber, but permanent works of major dimensions are usually built of reinforced concrete. Water surfaces and discharges are regulated by timber flashboards or various types of steel gates.

17. Checks. Most check structures on irrigation canals with depth of flows generally less than 5 ft are designed for flashboard regulation, although checks of this size and larger have been designed for a combination of flashboards and a radial gate. Check structures on laterals control water surface by use of either flashboards or slide-leaf gates.

Since a check structure has the possibility of having a design water surface on its upstream side, and being unwatered on the downstream side, it must be designed against sliding and overturning. In analyzing this, hydrostatic uplift on the structure's base should also be considered. Seepage calculations[1] along the base will give values for this force.

The velocity of flow through check structures with flashboards should not exceed 3.5 fps, because of the difficulty of placing and removing the flashboards. Checks with gates can tolerate velocities greater than 5 fps. Naturally, this must be tempered to meet acceptable head losses. The total head loss through a check structure can be estimated at 0.5 times the difference in the velocity heads of the upstream canal section and the check opening.

Some riprap protection may be required downstream of the check structure in earth canals because of the turbulence caused by partial flows over the flashboards, or the jet coming from underneath the gate. Figure 16 shows a concrete check constructed on the South Canal, Succor Creek division, Owyhee project.

18. Division Works and Intakes. Division works and large lateral intakes are similar to river intakes but are subjected to less uncontrolled variation in water surfaces at upstream ends. They usually consist of one or more bays where flow is controlled by gates. Radial or roller gates may be used in structures of unusual size; but radial or vertical slide gates are commonly installed in structures of ordinary dimensions.

In division structures, gates are usually installed at the head of each branch canal, so that the division of flow can be regulated at all times and so that flow in any branch

[1] Lane, E. W., Security from Under-seepage, Masonry Dams on Earth Foundations, *Trans. ASCE*, **100,** 1235, 1351, 1935.

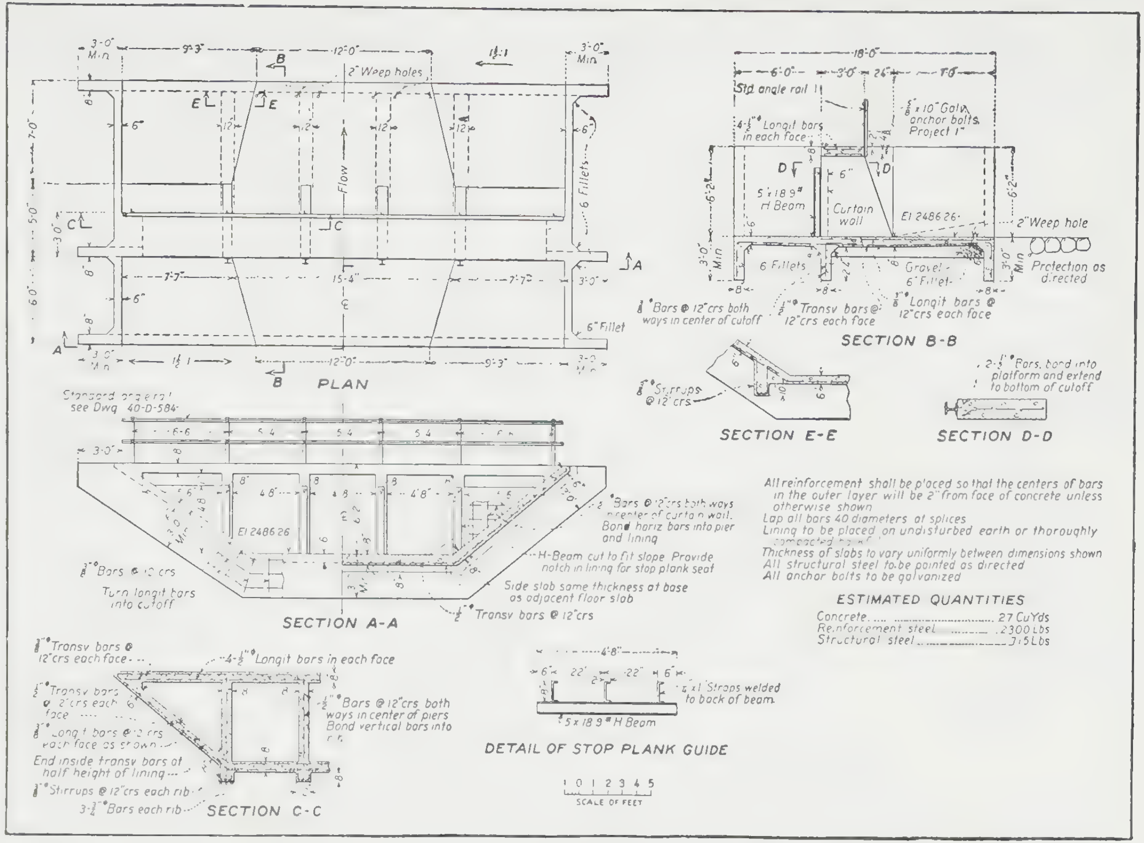

FIG. 16. Concrete check on South Canal, Succor Creek Division, Owyhee project, Idaho.

can be shut off when desired. At lateral intakes, main canal water surfaces may be controlled by checks.

Total gate openings at lined canal intakes are made approximately the same area as canal flow sections, since the canals are designed to carry water at relatively high velocities. At earth canal intakes, total gate openings are usually based on a velocity of about 5 fps. However, actual gate velocities are often higher, owing to operation at partial openings. Reinforced-concrete transition structures are provided below the gates, so that velocities can become adjusted to canal requirements before leaving transition sections. Transition side walls and floors may also be needed above the gates, depending on the design of canal sections and layout of gate structures.

Hydraulic losses through gate openings are seldom controlling factors in designing large gate structures. When gates are operated at full openings, entrance losses are simply transition losses. When operated at partial openings, available heads are not being fully utilized, so that increased losses due to gate contractions are not important. Figure 17 shows the South Branch Canal headworks, Kittitas Main Canal, Yakima project, Washington.

19. Wasteways. Wasteways serve two basic functions: (1) to empty the canal section and (2) to remove uncontrolled excess canal flows. The wasteways for these functions are respectively manually and automatically operated.

The manual-operated wasteway is designed to discharge the canal design flow at a water surface equal to or lower than canal design water surface. The wasteway should be located so it may discharge into a natural watercourse capable of accommodating the wasteway discharge, plus the flow of the watercourse. For this type of wasteway to operate effectively, it must be located upstream of a check structure or division works, which must be closed to keep water from going farther down the canal.

Wasteway discharge is usually controlled by radial gates on larger canals. The use of flashboards on medium canals has the drawback of leakage. On smaller canals, wasteways may have slide-gate controls.

The hydraulic design of a wasteway is generally not concerned with conservation of head; therefore, velocities may be high.

The operation of a wasteway usually produces nonuniform flow conditions in the canal, with velocities approaching critical velocity, which results in increased scour. Earth canals should be paved for adequate distances adjacent to the wasteway, or a control section should be used in the wasteway to keep the canal velocities low.

If the difference in invert elevations of the canal and the wasteway discharge channel is great, chute and stilling-pool elements will be required, design of which is the same as discussed in Art. 13.

The automatic wasteway may be either a side-channel spillway or a siphon spillway. The former is a long weir, either forming a part of the canal lining or adjacent to the canal section, with its crest above the normal operating water surface. When excess canal flows raise the water surface in the canal, the water will flow over the weir into a collector which discharges into a drainage course. The efficiency of this weir is reduced by the fact that the weir is parallel to canal flow. Standard weir coefficients will have to be modified to reflect this condition. The velocity of flow in the main canal should be low for more efficient operation. Weir formulas are approximately correct for canal velocities less than 2½ fps. For canals with high velocities, the momentum of the water flowing parallel to the weir will cause the upstream end of the weir to be less efficient than the remainder of the weir because change of flow direction cannot be effected immediately. The use of side-channel spillways requires increased freeboard requirements unless small discharges over the weir, due to waves or higher water-surface elevations caused by operational errors, can be tolerated.

The siphon spillway represents a more sophisticated approach to an automatic

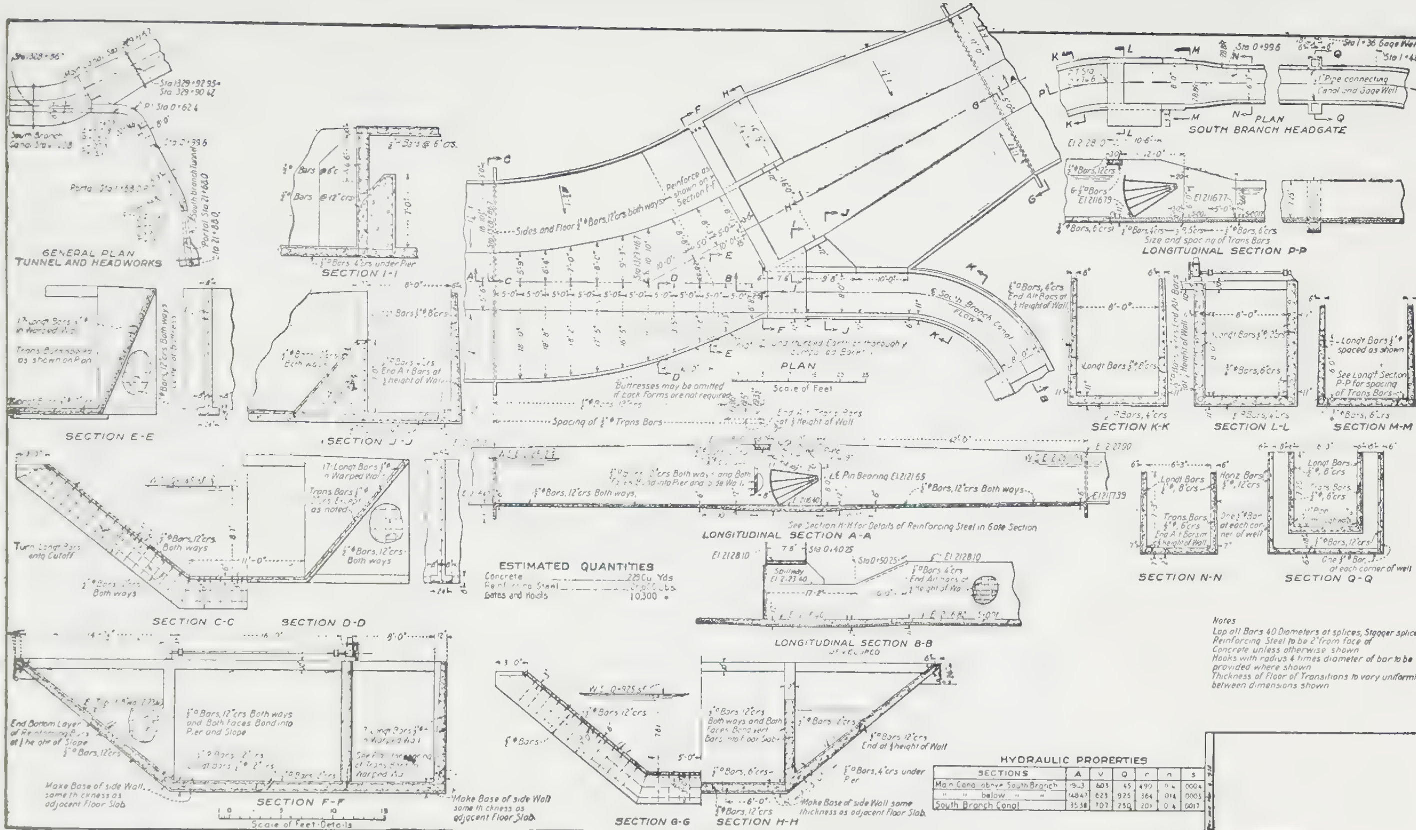

Fig. 17. South Branch Canal headworks, Kittitas Main Canal, Yakima project, Washington.

wasteway. By developing a head approximately equal to the change in water surface between canal and wasted water, but not in excess of the atmospheric pressure in feet of water, the discharge obeys the orifice equation

$$Q = CA\sqrt{2GH}$$

Figures 18 and 19[1] offer a design guide for low-head siphon spillways with various outlet conditions.

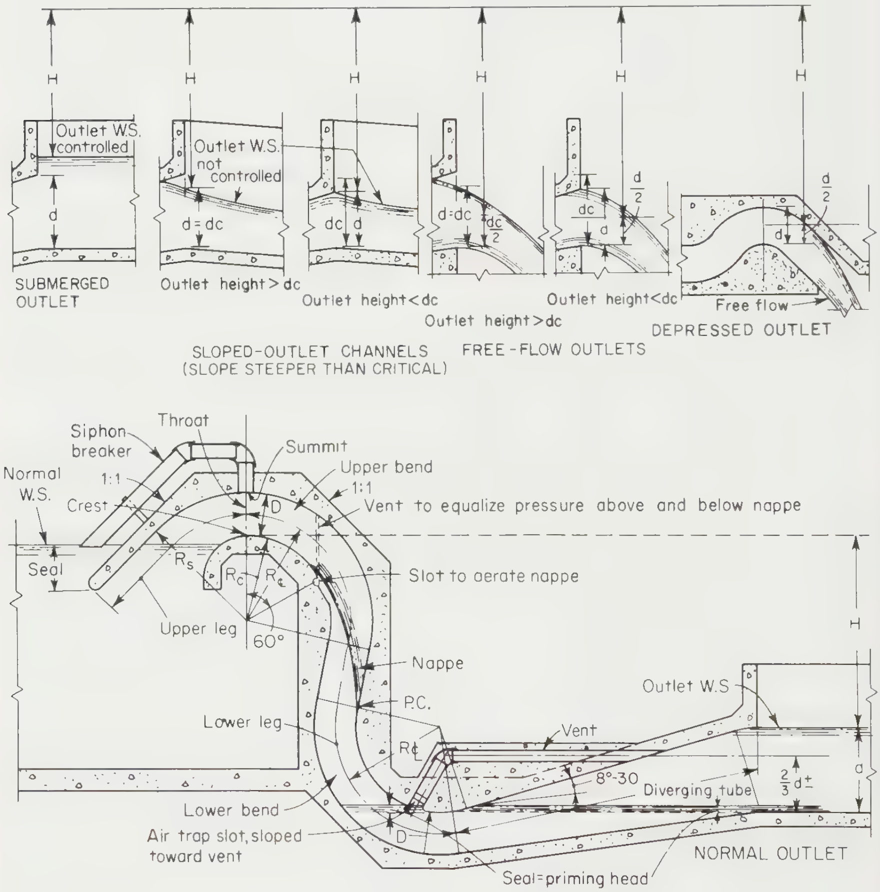

Fig. 18. Typical low-head siphon spillway.

Flexibility may be obtained by using an adjustable crest made of steel. The siphon breaker and seal portion of the upper leg then should also be adjustable.

Both types of spillways can be incorporated with other canal structures to effect an economy. It is not necessary that the adjoining structure be a wasteway since the requirements for the location of a manual-operated wasteway are not necessarily the same as those for an automatic wasteway. Culverts passing beneath the canal and

[1] "Canals and Related Structures," U.S. Bureau of Reclamation, Design Standards No. 3.

overchutes are typical of other structures that may be used to accept wasted canal discharges.

PROTECTIVE STRUCTURES

Protective structures are built to prevent damage to the distribution system by flooding or silt deposition. Automatic spillways discussed under Regulating Structures may also be considered a protective structure. Overchutes are sometimes built to carry drainage course flows across canals at places where aqueducts, flume crossings, or inverted siphons are impracticable, to keep flood flows from entering canal sections. Culverts are used to carry drainage-course flows beneath the canal prism. Settling basins are built to remove the heavier sand and silt loads in river diversions, which otherwise would settle to the canal beds and impair the efficiency of the system. Sand traps are built at places where local sand troubles are pronounced.

20. Overchutes. An overchute is usually some type of flume running transversely over the canal. It is provided with inlet and outlet sections, consisting of erosion-protected floors and training walls of masonry or riprapped embankments, designed to prevent drainage-course flows from overtopping canal banks and discharging into the canal section. It may or may not be provided with a stilling basin at the outlet end, depending on local soil and topographic conditions. Overchutes are used where ordinary types of canal crossings are impractical and where heavy loads of sand, gravel, and debris carried by drainage courses would soon clog culverts under canal sections.

Adjacent to, and in crossing the canal, the flow should have a high velocity to ensure that the drainage-course bed load is carried over the canal. The use of an overchute requires the drainage-course bed to be above the canal water prism. This requirement usually places the canal in a relatively deep cut, and unless the drainage course has a steep slope, it will have to be deepened below the canal. Figure 20 shows an installation near Yuma, Ariz.

21. Culverts. Culverts are structures that carry drainage-course flows beneath canal sections. Principally they are composed of a closed conduit, or multiple conduits, which may or may not have inlet and outlet transitions. Figure 21 shows a single-barrel box culvert, built on the South Canal of the Succor Creek division, Owyhee project, Idaho.

The flow condition in the culvert can be categorized as being controlled by either the inlet or the outlet. If the former, the discharge will be dependent upon the headwater elevation, entrance shape, and conduit size. This condition occurs when the conduit has the capability of transporting the water faster than it can enter the conduit. Outlet control will exist when the discharge is limited by the capability of the conduit and not the inlet. The condition where the tail water submerges the outlet is indicative of an outlet controlling discharge.

Recent publications[1] and texts[2] cover culvert hydraulic design for the flow conditions mentioned.

22. Settling Basins. Settling basins, properly planned and constructed, are effective means of removing suspended sand loads and some of the heavier silt loads. However, only relatively small proportions of the finer silt particles carried in suspension can be removed by settling-basin operation. Such particles are usually carried through the basins and later deposited on canal beds or farmlands. Ordinarily, settling basins should be built just below diversion structures, where deposited materials can be sluiced back to river channels. When properly designed basins are

[1] Bossy, H. G., "Hydraulics of Conventional Highway Culverts," Division of Hydraulic Research, Bureau of Public Roads, Washington, D.C. "Culvert Design Aids: An Application of the U.S. Bureau of Public Roads Culvert Capacity Charts," Portland Cement Association, 1962.

[2] "Design of Small Dams," U.S. Bureau of Reclamation, 1960. "Handbook of Concrete Culvert Pipe Hydraulics," Portland Cement Association, 1964.

Design Data

$$q = CD\sqrt{2gH} \leqq R_c\sqrt{0.7h(2g)} \times \log_e \frac{R_s}{R_c} = (\text{vortex flow} \sim \max q)$$

q = cu ft per sec per ft of crest width
R_c = radius of crest at throat, ft
R_s = radius of summit at throat, ft
D = throat size, ft
d = depth of water at outlet, ft
h = atmospheric pressure at site, ft of water
H = available head = (see outlet details)
C = discharge coefficient based on d/D and $R ℄/D$
g = 32.16

Section	Design	Reasons	Remarks
Upper leg	A well-proportioned transition providing a gradually contracting area. Inlet area should be 2 or 3 times the area of the throat	Provides accelerating velocity. Reduces entrance losses	Entrance loss for form shown suggested as 0.2 Δhv
Throat	Size depends upon required capacity. Recommended ratio of $R ℄$ to D is 2.5. For forming with timber, D is 2′-0″ min; metal forms left in place may be used for less than 2′-0″. Recommended width of throat = $2D$	Keeps bend losses low	Wide crests and shallow depths reduce priming time
Upper bend	Recommended ratio of $R ℄$ to D is 2.5. Aerating slot is set at 60° from crest. Pipe vent, set in sidewalls, connects slot to summit area	Keeps bend losses low. Slot prevents nappe from clinging to crest Vent insures nappe trajectory	Area in upper and lower bend is same as area at throat
Lower bend	P.C. is set to contact nappe. P.C. is a point on trajectory of nappe as determined from desired priming head at crest Recommended ratio of $R ℄$ to D is 2.5. Top of siphon at vertical section is set at elevation of outlet bottom Air-trap elevation is elevation of outlet bottom plus desired priming head. Vent area = throat area ÷ 48 (approx)	Provides seal and exhausts air from upper bend. Provides seal of lower bend and ensures creation of partial vacuum. Vent exhausts entrained air with negligible loss of discharge	Vent decreases priming time, increases priming head slightly
Diverging tube	Outlet end set at desired elevation. Length of tube is set by 8°30′ angle of divergence. Vent outlet set at ⅔ depth (±) of outlet at max capacity	Provides transition. Increases discharge	Discharge loss for form shown suggested as 0.2 Δhv
Siphon breaker	A pipe vent set at summit with inlet end set at or slightly below normal water surface Area = throat area ÷ 24 (min)	To break siphonic action slowly; prevents severe vibration	If practicable, adjustable inlet on siphon breaker is desirable
Seal at intake	Lip of upper leg is submerged an arbitrary distance, but should be set deep enough to prevent excessive drawdown	Prevents "gulping" of air, and provides more normal action of siphon breaker	

NOTE: Design recommendations given above are presumed to give minimum losses according to experiments. Deviation therefrom should include consideration of additional losses.

Recommended Design Procedure

1. Determine crest El. (canal W.S. El. + freeboard desired).
2. Determine head available (crest El. − W.S. El. at outlet).
3. Select preliminary values for D and $R ℄$ and solve for max q using vortex flow formula

$$q = R_c\sqrt{0.7h(2g)}\,\log_e (R_s/R_c)$$

(Recommend D = 2′-0″ min and $R ℄/D = 2.5$.)

4. Select values of d and H and obtain value of C from graph. Solve equation $q = CD\sqrt{2gH}$. (q must not be greater than value obtained in 3.)

5. Solve for required crest width = Q/q. Select crest width and number of siphons to be used for total Q, and determine q for this crest width.
6. Repeat 3 and 4 until $q = CD\sqrt{2gH} \gtreqless R_c\sqrt{0.7h(2g)}\,\log_e(R_s/R_c)$.
7. Select priming head by determining the canal W.S. El. at which operation is desired. If priming head is less than D/s, locate P.C. of lower bend on trajectory of nappe.
8. Determine size and inlet El. of siphon breaker. (Area of siphon breaker = area of throat ÷ 24.)
9. Select and design priming aids to be used. (Slot to aerate nappe; vent to equalize pressure above and below nappe, and vent at lower bend.)

References

Rock, E., Design of a High-head Siphon Spillway, *Trans. ASCE*, **105**, 1050.
Owen, T. G., "A Study of Low-head Siphons," 1939.
USBR Data on Model Tests, Wasteway No. 2 (Yakima Project), 1942.
Trans. ASCE, 986, 1934.
Trans. ASCE, 1789, 1939.
Naylor, A. H., "Siphon Spillways," 1935.

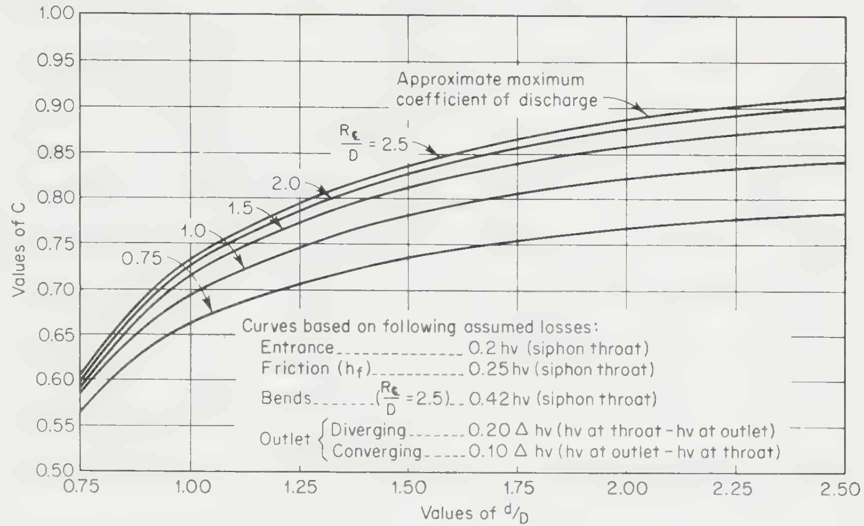

FIG. 19. Siphon spillway coefficients of discharge.

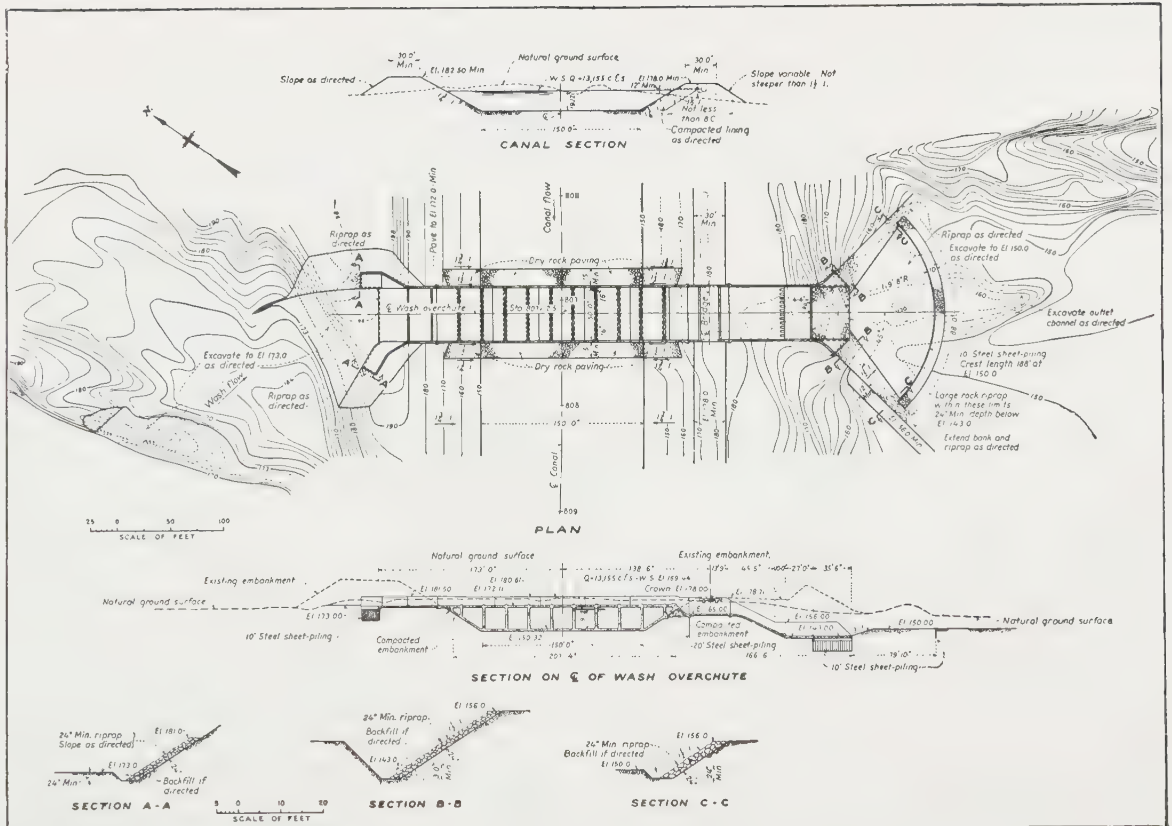

Fig. 20. Overchute on All-American Canal near Yuma, Ariz.

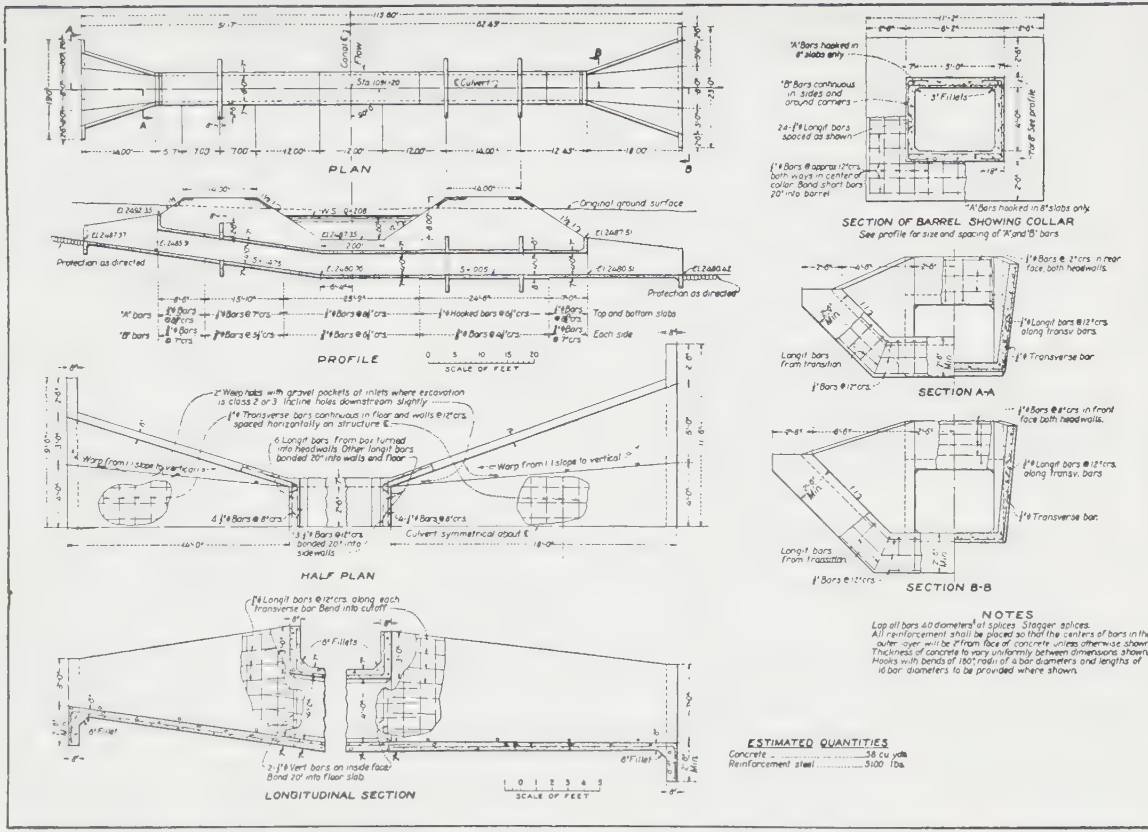

FIG. 21. Box culvert on South Canal, Succor Creek division, Owyhee project, Idaho.

built at such locations, major sand-removal structures are seldom required at other places along the canal system.

A typical settling basin usually has a skimming weir at the downstream end, over which canal flow is withdrawn; a gate-controlled sluiceway at one end of the weir, for sluicing deposited material off the floor of the basin; and a sluiceway channel, to carry the sluicing discharge back to the river at relatively high velocities. The skimming weir should be provided with gates or flashboards, so that canal flow can be shut off during sluicing operations. The sides and floor of the basin should be riprapped, or lined with concrete, to prevent excessive erosion during sluicing operations. In order to minimize interference with canal operation, it usually is desirable to design the sluiceway gates and wasteway channel so that velocities developed are capable of removing the deposited material from the basin.

The size of the settling basin is determined by the canal discharge and the maximum velocity that can be maintained through the basin with the sluice gates closed, without carrying sediment over the skimming weir. Since it is seldom practicable to remove all deposited material during a sluicing period, the presence of some sediment on the basin floor must be considered in calculating basin velocities during normal canal operation. In most cases, it probably is desirable to proportion basin dimensions so that mean velocities do not exceed 1 fps during normal full canal discharge. However, effective results were secured at the Fort Laramie Canal basin, North Platte project, Wyoming, where the sediment was mostly sand and the basin was designed for a maximum velocity of 1.25 fps.[1] Figure 22 shows the Fort Laramie installation.

23. Sand Traps. Sand traps are built to trap and remove bed load moving along or suspended near the canal invert. Sand traps may be located in the headworks, preceding a settling basin, at siphons or drainage inlets, and in canal sections where the canal capacity is reduced by sediment deposition. For effective removal of sediment, the sand trap should be located near a drainage course so the sediment can be sluiced from the canal.

A sand trap may consist of a short depressed length of canal section provided with a sluice to remove sediment. In current favor is the vortex-tube sand trap, which had its beginning in the early 1930s.[2]

The vortex-tube sand trap consists of a slot in the canal invert, usually circular in cross section, with the center located a distance less than the radius below the invert.

The tube crosses the canal invert at an acute angle with the direction of flow exiting the conveyance channel. The outlet should be provided with a gate which can be adjusted to correspond to sediment concentrations. Sections other than circular have been tested[3] but presented no overall material advantage. The vortex-tube discharge varies from 5 to 15 percent of the conveyance-channel discharge.[3] The spiral flow developed in the tube will remove small cobbles, and a properly designed tube will remove over 90 percent of material 1 mm in diameter and about 35 percent of material 0.3 mm in diameter.

Laboratory tests and a survey of literature[4] on vortex sand traps produced the following design criteria for effective operation:

1. The Froude number of the conveyance channel at the vortex tube should be approximately 0.8.

[1] Houk, Ivan E., Sand Control Works at Fort Laramie Canal Intake, *Eng. News-Record*, **100**, 922–926, 1928.

[2] Parshall, R. L., Control of Sand and Sediment in Irrigation, Power and Municipal Water Supplies, Water Works Association Annual Meeting, Denver, Colo., October, 1933, p. 18.

[3] Rowher, Carl, "Effect of Shape of Tube Efficiency of Vortex Tube Sand Traps for Various Sizes of Sand," Ft. Collins, Colo., 1935.

[4] Robinson, A. R., Vortex Tube and Sand Trap, *Proc. ASCE, J. Irrigation Drainage Div.*, December, 1960.

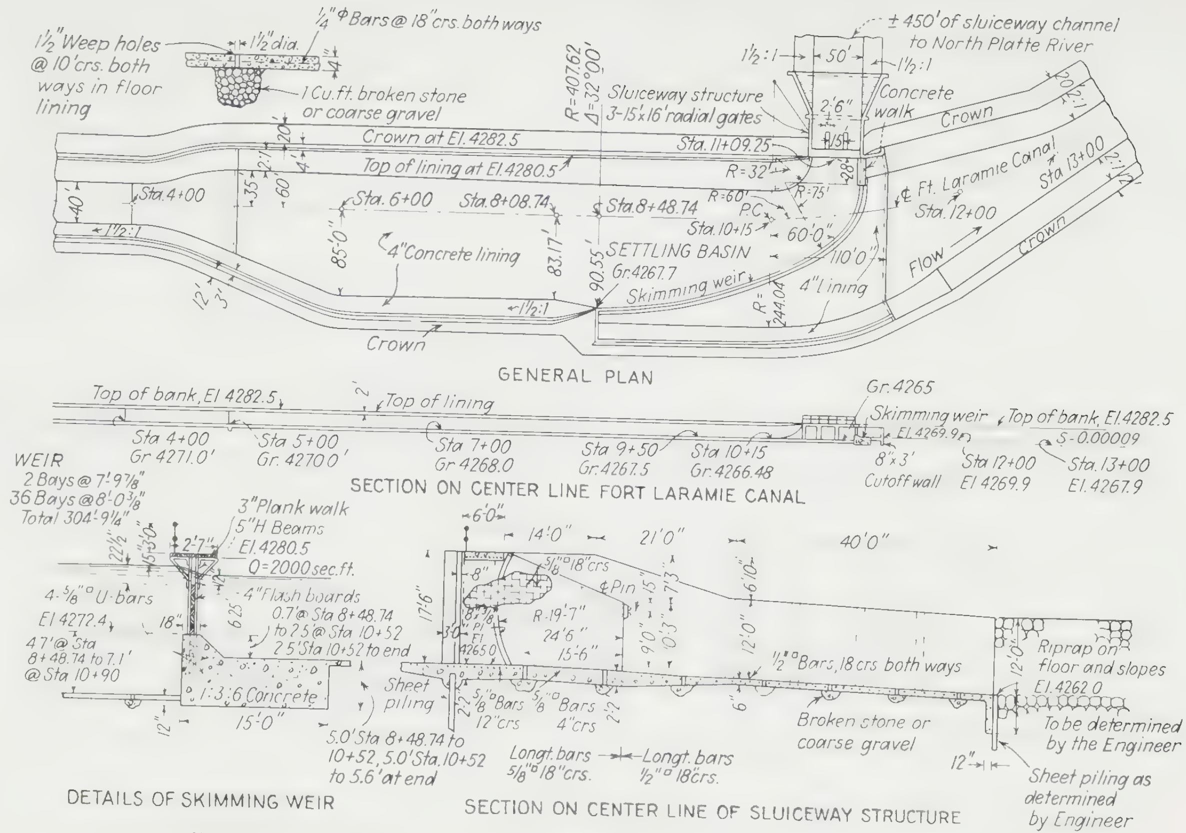

FIG. 22. Desilting works on Fort Laramie Canal, North Platte project, Wyoming.

2. The width of the slot should be between 0.5 and 1.0 ft.

3. The ratio of tube length to opening width L/D should not exceed 20, with the maximum length being about 15 ft.

4. The tube angle should be about 45 deg.

5. The elevation of the upstream and downstream lips of the tube should be set at the same elevation; raising the downstream lip has little effect on operational efficiency.

6. Tubes of constant cross section operate as well as tubes with varying cross sections (tapered).

7. The required area of the tube can be approximated by the relationship $A_T = 0.06DL \sin \theta$, where D = slot width, L = tube length, and θ = tube angle with flow.

The discharge of the tube can be approximated by the equation for orifice discharge. The coefficient of discharge should be modified for the velocity of approach and the tube geometry.

DELIVERY STRUCTURES

24. General. Delivery structure, measuring device, or farm turnout, regardless of what it is called, performs the final function of the irrigation system. The design and construction skill that went into the diversion, canals, conveyance structures, regulating structures, and protective structures will be judged predominantly on the operation of the delivery structure. It is here that nature's life-giving substance is turned over to the irrigator. Any inadequacy in the delivery structure's operation will most likely produce condemnation of the entire irrigation system. Therefore, it cannot be overstressed that considerable thought should be given to this structure in the planning and design stages.

The perfect delivery structure should incorporate the following: (1) be capable of delivering the water an irrigator may need to meet the consumptive use of any conceivable cropping pattern, (2) accurately deliver the rate prescribed (within 5 percent is acceptable), (3) have minimal loss in hydraulic head to effect the delivery, (4) have a discharge rate of water delivered that is oblivious to fluctuation in the canal water surface, (5) have a rate of water delivered that is also oblivious to fluctuations in the water surface of the irrigator's head ditch, (6) have practical and economical construction, (7) have a structure that is easy to adjust for varied discharges, and (8) be tamperproof; that is to say, it should not be possible to adjust it illegally. Needless to say, no one delivery structure embodies all the above requirements.

The key to which of the above items may be dismissed is in the distribution system's method of operation. The distribution-system methods are (1) rotation method—a fixed quantity of water is delivered to each irrigator at predetermined intervals; (2) demand method—each irrigator specifies the quantity of water and time of each delivery; and (3) continuous method—the delivery structure is operating continually. Distribution may also be accomplished by a combination of the above methods.

The rotation method, with water being available at intervals for a specified length of time, requires a delivery structure with an adjustable discharge. As an example, if an irrigator who is delivered water for 12 hr every 10 days decides to put in crops that require a 50 percent increase in delivered water, his only recourse with a fixed delivery time is to increase the delivery rate.

The demand method, by virtue of not having any limitation on the length of time the water is delivered, allows the use of a delivery structure with a constant or limited range of discharge.

The continuous method would require an adjustable delivery to allow for any increase or decrease in water demand.

25. Classification of Delivery Structures. Delivery structures can be categorized into three classifications. Structures in which fluctuations in the water surface of either the canal or the head ditch have relatively no effect on the discharge rate will be called invariant delivery structures.

Structures in which the rate of discharge remains relatively constant, that is, (1) fluctuations in the head-ditch water surface as long as the canal water surface remains constant and (2) fluctuations in the canal water surface as long as the head-ditch water surface remains constant, will be called semivariant delivery structures.

Structures where the rate of discharge is affected by changes in canal and head-ditch water surface and which therefore require water-surface control structures in the canal will be called variant delivery structures.

26. Invariant Delivery Structures. A most interesting delivery structure of this type is the autoregulator[1] of Italian design (see Fig. 23).

This device is a cylindrical sleeve with circumferential apertures which act as weirs.

[1] ANONYMOUS, New Automatic Channel Flow Regulator, *Water and Water Eng.*, 1956, pp. 250–251.

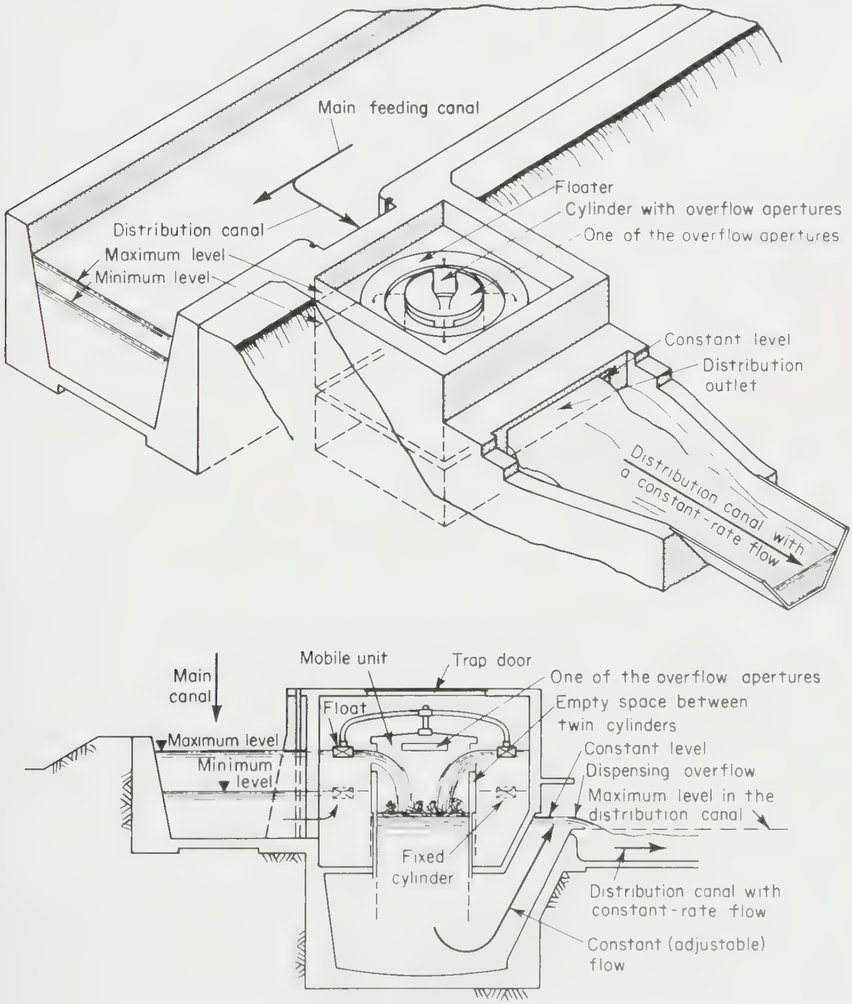

FIG. 23. Autoregulator.

The cylinder is supported by floats or pontoons at the canal water-surface level. Thereby, regardless of fluctuations in the canal water surface, the weir crest remains at the original preset distance below the canal water surface. The originator of this device claims an accuracy of delivery of over 99 percent.

A delivery structure of somewhat less accuracy for a fluctuating canal water surface is the single-baffle distributor.[1]

This device consists of a battery of slide leaves, each of a different rated discharge. Altering discharge rates may be achieved by raising the leaves in combination or singly. The distributor discharge remains unaffected by variations in the downstream level because it is designed to pass water through critical depth. So long as the downstream water level does not drown out the hydraulic jump, it will exert no influence on the discharge rate. This principle has been used on many delivery structures in the semivariant classification. The single-baffle distributor, being sensitive to changes in the canal water surface, has been improved upon by the advent of the double-baffle distributor. See Fig. 24 for operation curves for the two distributor types. The second baffle presents a smaller orifice for discharge with the increased head, and at the lower water surface, the contraction of the vena is sufficient to pass unrestricted through the orifice caused by the second baffle. The maximum change in water surface for comparable single- and double-baffle distributors to maintain discharge within ± 5 percent of the nominal discharge would be $3\frac{1}{8}$ and 9 in., respectively. See Thomas[2] for descriptions of other invariant delivery structures.

27. Semivariant Delivery Structures. Critical-flow flumes,[3] of which the commonest in the United States is the Parshall measuring flume,[4] form the major type under this classification.

Figure 25 shows a Parshall measuring flume with a 30-ft throat. Measurement of discharge is based on coefficients determined through experiments on prototype flumes.[5]

The discharge Q, in cubic feet per second, may be estimated as

$$Q = K_e b Y_1^n$$

where K_e = discharge coefficient ≈ 4.0
b = channel width, ft
Y_1 = depth at measuring section, ft
$n \approx 1.55$

The exact values of K_e and n for the particular flume sizes are given in the Parshall references cited above.

Weirs are a most common semivariant delivery structure. The discharge is quite sensitive to changes in water-surface heights above the weir crest because the discharge is proportional to the water height raised to a power. Criteria for design and construction and tables for discharge computations are available.[6]

28. Variant Delivery Structures. There are many delivery structures that come under this classification, but the two commonest in the United States will be covered here. The metergate is a gated-orifice-type delivery (Fig. 26)[7] where the head loss

[1] "Irrigation," Laboratoire Dauphinois d'Hydraulique Neyrpic, July, 1951.

[2] Thomas, C. W., World Practices in Water Measurement at Turnouts, *Trans. ASCE*, **126**(III), 715–741, 1961.

[3] Parshall, R. L., The Improved Venturi Flume, *Trans. ASCE*, **89**, 841–880, 1926.

[4] Parshall, R. L., Parshall Flumes of Large Size, *Colo. Agr. Expt. Sta. Bull.* 386, May, 1932.

[5] Parshall, R. L., Parshall Flumes of Large Size, *Colo. Agr. Expt. Sta. Bull.* 386, May, 1932. Parshall, R. L., Parshall Measuring Flumes of Small Sizes, *Colo. Agr. Expt. Sta. Bull.* 423, March, 1936.

[6] "Water Measurement Manual," U.S. Bureau of Reclamation, May, 1953.

[7] Ball, J. W., Limitations of Metergates, *Proc. ASCE, J. Irrigation Drainage Div.*, **88** (IR4), Part 1, December, 1962.

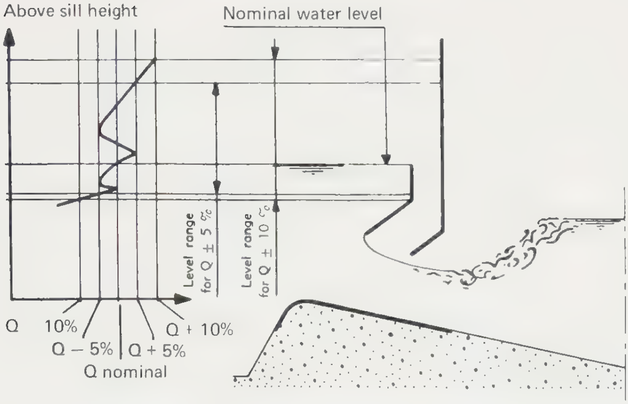

(a) Diagrammatic layout and operating curve for double-baffle distributors

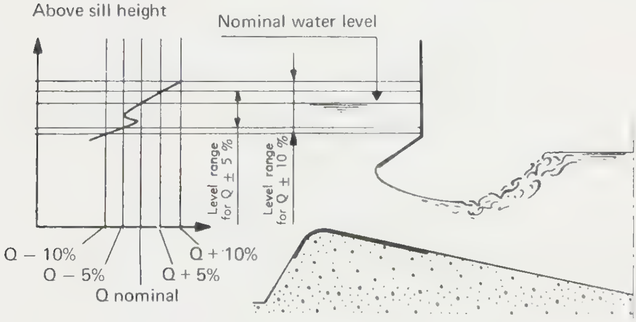

(b) Diagrammatic layout and operating curve for single-baffle distributors

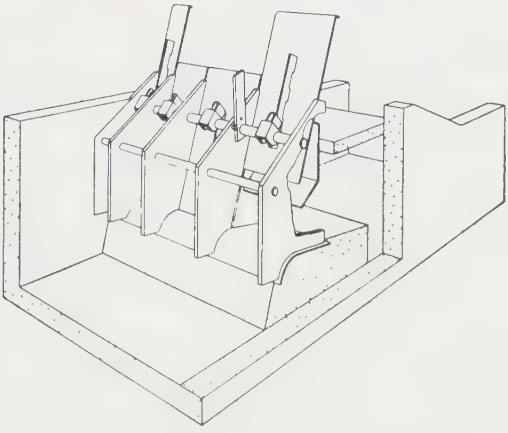

(c) Single-baffle distributor

FIG. 24. Operation curves for the two distributor types.

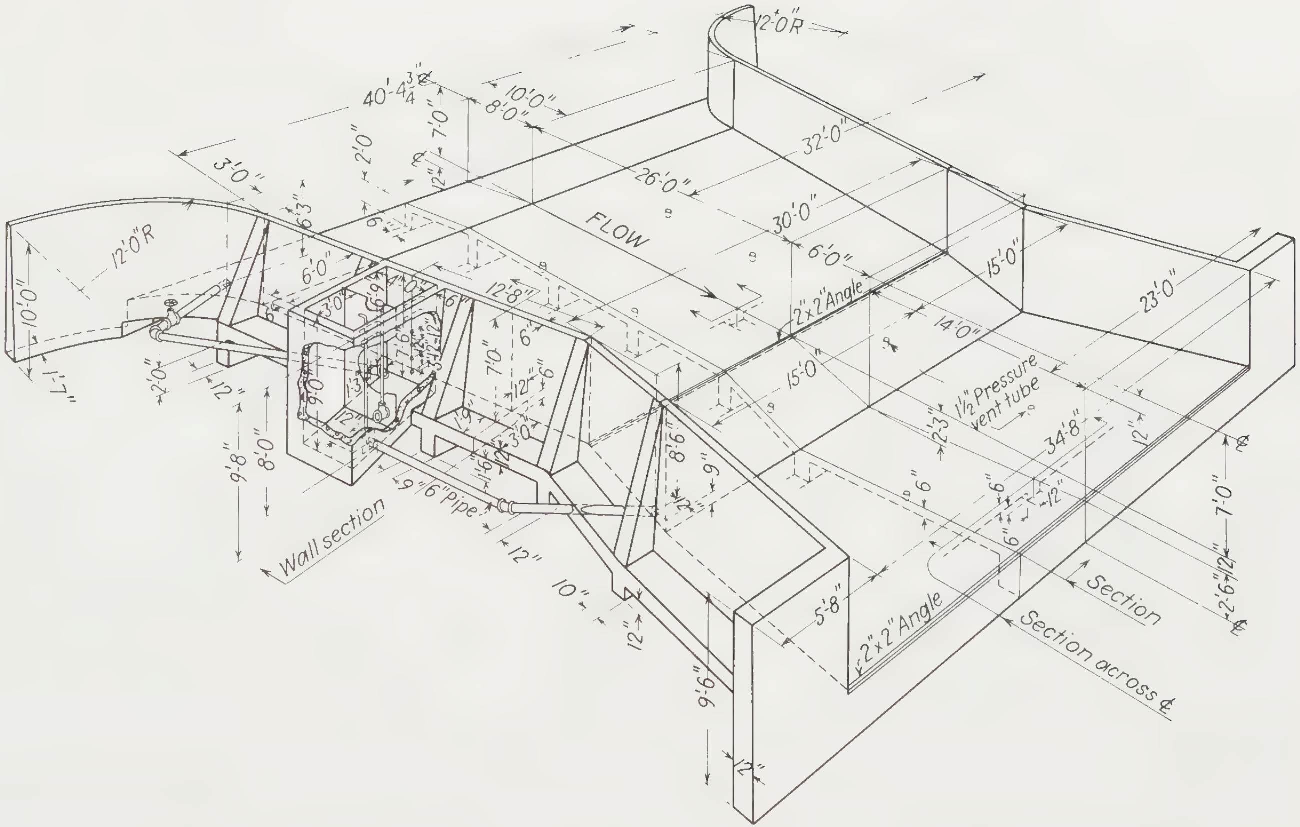

Fig. 25. Reinforced-concrete Parshall measuring flume, 30-ft throat.

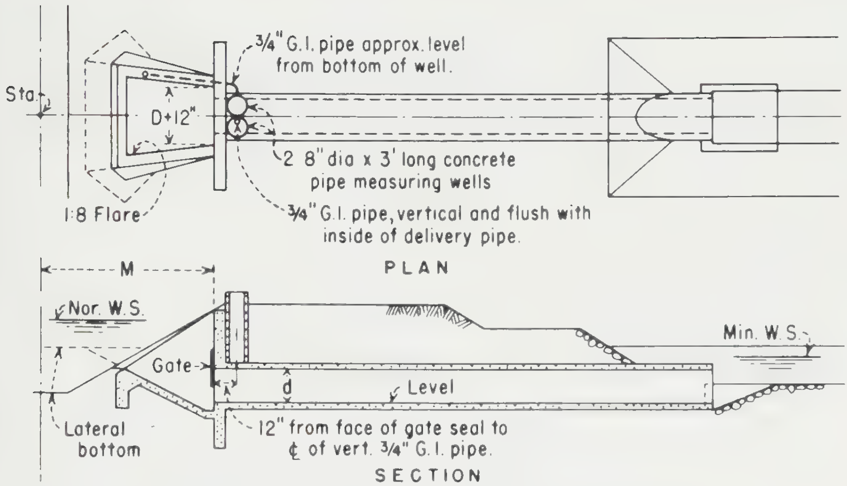

(a)-Typical field installation of metergate

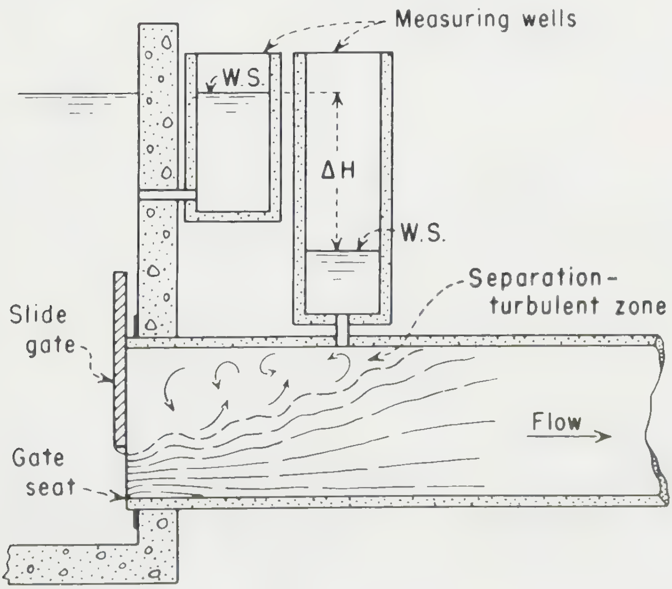

(b)-Metergate flow-measuring principle

FIG. 26. Installation of metergate and metergate flow—measuring principle

through the gate is measured and, with the known gate opening, the discharge may be determined from tables.[1]

For accurate water measurement the following should be noted: (1) the metergate should be submerged by one diameter, (2) the outlet should be sufficiently submerged so as to establish a pressure gradient on the crown of the pipe, and (3) the length of pipe downstream of the gate should be long enough to allow a uniform velocity distribution in the pipe at the outlet.

The constant-head-orifice delivery structure is a two-gated structure. The first gate is calibrated for discharges due to a head differential of 0.2 ft; the second gate is adjusted so that this differential is obtained. If calibration tables are not available, the discharge can be computed using the orifice equation and discharge coefficients of 0.70 and 0.75 for the first and second gates, respectively. Figure 27[2] lists the dimensional criteria for a constant-head-orifice delivery structure.

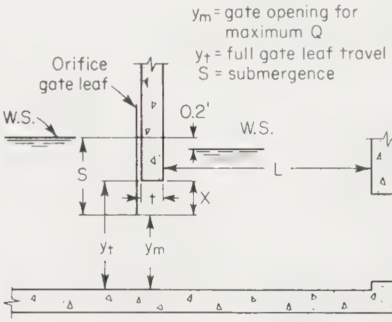

X must be equal to or greater than "t" for maximum Q.
S is equal to or greater than "y_m" for good accuracy.
For Q up to 10 cfs, L must be at least 2¼ y_m or 1¾ y_t, whichever is greater (3'–6" minimum).
For Q above 10 cfs, L = 2¾ y_m minimum.

FIG. 27. Dimensions for a constant-head orifice.

MISCELLANEOUS STRUCTURES

Miscellaneous structures not discussed on the preceding pages may include drainage inlets, farm bridges, highway bridges, fish-control structures, and other construction incidental to irrigation developments. Drainage inlets are provided to supplement the canal flow and are located to intercept flows from springs or drainage courses. Farm and highway bridges are built where needed for crop and rural population transportation. Fish-control structures are required by law in many states on hydroelectric and irrigation developments. Whether the interests are commercial or sporting, considerable expenditures have been made for the protection of fish.

29. Drainage Inlets. Drainage inlets may be pipes or open channels running through canal banks. Riprap or concrete protection against erosion should be pro-

[1] "Water Measurement Tables for the Armco Metergate," Armco Metal Products, Denver, Colo., 1951.

[2] "Canals and Related Structures," Chapter 6, Water Measurement Structures, U.S. Bureau of Reclamation.

vided at both ends. Automatic flap gates should be provided at outlet ends when pipes are placed below canal water surfaces. However, the use of flap gates requires a water surface or head in the inlet greater than the water surface in the canal. If the bed of the drainage course is higher than the canal water surface, a gate is not required. In this case an open-channel inlet can be used.

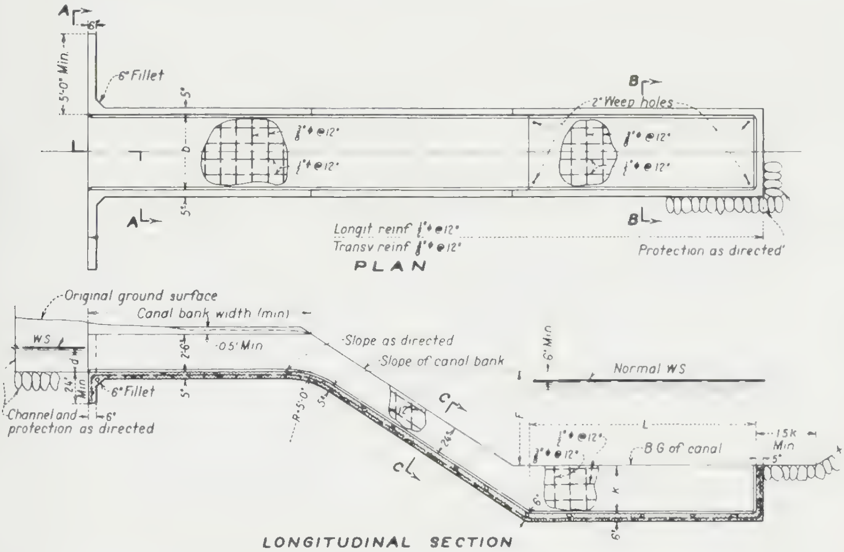

			DISCHARGE IN SECOND FEET									
			10	20	30	40	50	60	70	80	90	100
		d	1 50'	1 56'	1 61'	1 67'	1 72'	1 78'	83'	1 89'	1 94'	2 00'
		b	2 3"	4' 3"	6'-0"	7'-7"	9'-0"	10'-4"	11'-6"	12'-7"	13'-7"	14'-5"
F IN FEET	6	k	2' 9"	2' 10"	2'-11"	3'-0"	3'-1"	3'-2"	3'-3"	3'-4"	3'-5"	3'-6"
		L	12 0"	12' 4"	12' 8"	13' 0"	13' 4"	13'-8"	14' 0"	14' 4"	14 8"	14 11"
	8	k	2' 11"	3 0"	3' 1"	3 2"	3' 3"	3' 4"	3 5"	3' 6"	3' 7"	3' 8"
		L	12' 9"	13 2"	13 7"	13 11"	14 3"	14 7"	14' 11"	15' 4"	15' 8"	16' 0"
	10	k	3 1"	3 2"	3 3"	3' 4"	3' 5"	3 6"	3' 7"	3' 8"	3' 9"	3' 10"
		L	13 6"	13 10"	14'-3"	14'-8"	15'-0"	15'-4"	15'-8"	16'-1"	16'-5"	16'-10"
	12	k	3 2"	3' 3"	3 4"	3'-5"	3' 6"	3 7"	3 8"	3' 9"	3' 10"	3' 11"
		L	14 1"	14 5"	14'-10"	15'-3"	15'-8"	16'-0"	16'-5"	16'-9"	17'-2"	17'-6"
	14	k	3' 3"	3' 4"	3' 5"	3' 6"	3' 7"	3 8"	3' 9"	3'-10"	3' 11"	4 0"
		L	14 7"	15 0"	15 5"	15 10"	16 3"	16 7"	17' 0"	17 -4"	17' 9"	18 2"
	16	k	3 4"	3' 5"	3'-6"	3 7"	3' 8"	3' 10"	3 11"	4 0"	4' 1"	4' 2"
		L	15' 1"	15 6"	15-11"	16' 4"	16' 9"	17 2"	17' 7"	17' 11"	18' 4"	18' 9"

NOTES

All reinforcement shall be placed so that the centers of bars in the outer layer will be 2" from face of concrete unless otherwise shown.
Lap all bars 34 diameters at splices
Thickness of concrete to vary uniformly between dimensions shown.
Base of entire structure to be placed on undisturbed natural foundation or thoroughly compacted fill
Backfill around structure to be compacted as directed.
If L + 1.5k exceeds normal base of canal, inlet shall be set back in canal bank as directed

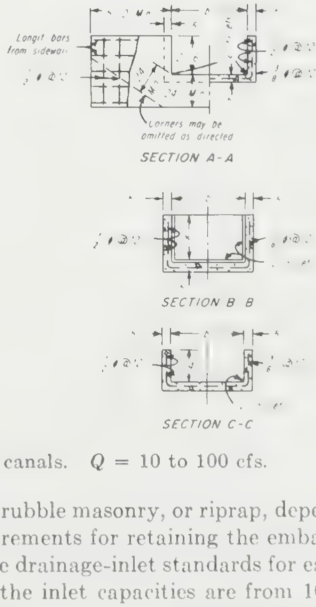

FIG. 28. Drainage-inlet standards for earth canals. Q = 10 to 100 cfs.

Open-channel inlets can be lined with concrete, rubble masonry, or riprap, depending upon the inlet section and the structural requirements for retaining the embankment through which it passes. Figure 28 shows the drainage-inlet standards for earth canals used on the Deschutes project in Oregon; the inlet capacities are from 10 to 100 cfs. Inlets may terminate at the upper edge of the canal lining when discharging into lined canals but should be carried down the side slope to the bottom of the canal when discharging into earth canals.

Design discharge capacities for inlet structures should be based upon streamflow data if they are available, or determined by gathering maximum rainfall and frequency data, watershed area, and runoff conditions, using methods described in Sec. 39. The flow intercepted should not carry appreciable sediment nor should the discharge exceed that which can safely be admitted into the canal. The U.S. Weather Bureau has available many technical papers and reports prepared in cooperation with other Federal agencies relating precipitation rates to frequency of occurrence.

30. Farm and Highway Bridges. Farm bridges are usually timber-trestle structures. Highway bridges may be of steel or reinforced concrete. Bridges on state or interstate thoroughfares are designed in accordance with state or Federal specifications. Bridge members spanning the canal should not encroach upon the prescribed canal freeboard. Bridge piers located in the canal flow section require no special consideration, although the canal may be widened to compensate for their obstruction. Piers in unstable earth canals may require the canal bed to be stabilized around them.

31. Fish-control Structures. Fish screens may be needed at canal intakes, and fish ladders or other means of facilitating fish migrations may be needed at diversion weirs; the latter is covered in Sec. 23. Screens may be classified in three categories, stationary, moving, and electric. Stationary and moving screens usually are preceded by a trash rack to protect them from becoming clogged by debris.

Stationary screens are supported on a frame or series of frames covering the entire water prism. The screens are inclined from the vertical in an upstream direction and can be supported by the same overhead member that supports the trash rack, which has an opposite inclination.

Moving screens are of the rotating-drum or traveling-screen type. The rotating-drum screen is a cylinder with screening material forming its curved surface, the length of the cylinder being equal to the water-prism width and the diameter being $1\frac{1}{3}$ to $1\frac{1}{2}$ times the depth of the water prism passing through the screen. The screen has a rotation that is directed upward from the approaching water side. Any trash sticking to the screen will be removed by the flowing water when it is immersed on the downstream side. The amount of trash passing the screen in this manner is inconsequential; the important feature is that the screens are self-cleaning and not prone to clogging. The screen diameter is considerably greater than the water depth so that the screen velocity when leaving the water surface will have a near vertical direction and fish will not be carried over the screen.

The traveling screen has its primary use in domestic water supply and sewage treatment, but it has been adapted for use in screening fish. This screen can be described as an endless belt of screening material around two pulleys whose axes are horizontal and determine a vertical plane. Since the screen is vertical when it leaves the water, there is little likelihood that fish will be carried over the screen. The screen need only extend a little more than a pulley diameter above the water surface if the flow is tranquil. If the approach to the screen is susceptible to waves, a further allowance should be made. There are many innovations on the basic moving screen.[1]

Both types of moving screens mentioned are subject to damage from silt and sand; therefore, sand traps and settling basins should precede the screens when the water contains appreciable amounts of sand and silt. Screen movement may be supplied by a motor drive or a chain drive from a paddle wheel in the conveyance channel.

Electric screens are composed of a series of immersed conductors suspended from a structure crossing the conveyance channel, and another series of conductors placed on

[1] Leitritz, Earl, Stopping Them: The Development of Fish Screens in California, *California Fish and Game*, **38**(1), 53–62.

the bed of the channel. A voltage drop across the conductors affords the deterrent to fish passage. A large-scale installation of electric screens after promising extensive laboratory investigations proved disappointing at the Baker Dam.[1]

The use of any of the screens mentioned requires (1) that the velocity of the water approaching the screen will allow the fish to extricate themselves from the screen, and (2) because of the persistence exhibited by fish, a fish bypass flow back to the body of water being diverted from should be provided adjacent to the screen. It has been observed that fish die of exhaustion in trying to get through the fish screen. The velocity of flow is dependent upon the minimum size, type of fish expected, and minimum water temperature in which the screen will operate.[2] For fish a year and under velocities between 0.5 and 1.5 fps have been used. Colder temperatures decrease the swimming efficiency of fish.

Although it could be classified as a stationary screen, a louvered system was used on the Tracy Pumping Plant and the Delta Mendota Intake Canal.[3] This system consisted of a set of vertical bars or louvers normal to flow crossing the channel at an acute angle. The fish make no attempt to pass through the louver but swim parallel to the set of louvers. A fish bypass at the acute intersection of the set of louvers and the channel wall is necessary to return the fish. The design criteria[4] may be summarized as follows:

1. The angle of the louver system in the channel may vary between 10 and 15 deg with the direction of flow.
2. Louver slats should be placed at 90 deg to the direction of flow.
3. Average maximum velocity of water in the channel as it approaches the louver system should not exceed 5.3 fps.
4. A trash rack should be built ahead of the louver system, and there should be a minimum of 25 ft of nonturbulent flow.
5. Bypasses for entry of fish diverted by the louvers should be about 75 ft apart.
6. Bypass openings should be 6 in. wide.
7. Trash-rack bars should have a clear opening of 2 in.
8. Provision should be made for installation of a saline-bath arrangement in the event that young striped bass suffer shock.

PUMPING INSTALLATIONS

32. General. Pumping installations are used in delivering water to irrigable areas that cannot be reached economically, or otherwise, by gravity systems. Large areas are usually supplied from control pumping plants, which are generally cooperatively installed and operated. Most large plants pump water from surface sources, i.e., from canals, rivers, or lakes. Farm plants are usually installed and operated by individual landowners. They generally pump from underground sources but sometimes draw water from surface supplies. In all cases, pumped water is delivered to the highest part of the irrigable area, so that further distribution can be made by gravity.

[1] Andrew, F. J., L. R. Kersey, and P. C. Johnson, An Investigation of the Problems of Guiding Downstream Migrant Salmon at Dams, *Intern. Pacific Salmon Fish Comm. Buli.* VII, 1955.

[2] Brett, J. R., and D. F. Alderdice, Research on Guiding Young Salmon at Two British Columbia Field Stations, *Bull.* 117, Fish Research Board, Canada, 1958. Brett, J. R., D. F. Alderdice, and M. Hollands, The Effect of Temperature on the Cruising Speed of Young Sockeye and Coho Salmon, *J. Fish Res. Board, Canada*, **15**(4), 587-605. Kerr, J. E., Studies on Fish Preservation at the Contra Costa Steam Plant of the Pacific Gas and Electric Co., California Fish and Game, *Fishery Bull.* 92, 1953.

[3] Hydraulic Studies of Fish Collecting Facilities—Delta Mendota Intake Canal, Central Valley Project, Calif., U.S. Bureau of Reclamation, Division Engineer Laboratories, *Hydraulic Lab. Rept.* Hyd-410, 1956. "Fish Protection at the Tracy Pumping Plant," U.S. Bureau of Reclamation, Region 2, and U.S. Fish and Wildlife Service, Region 1, 1957.

[4] "Fish Protection at the Tracy Pumping Plant," U.S. Bureau of Reclamation, Region 2, and U.S. Fish and Wildlife Service, Region 1, 1957.

33. Pumps. In irrigation projects where water is pumped the types of pumps encountered fall in one of four broad categories:

1. Reciprocating pumps, where water is moved by the displacing action of pistons or plungers.
2. Propeller pumps; develop head by the propelling or lifting action of the propeller on the water. The mixed-flow pump, which may be considered in this category, develops its head in part as above and in part by centrifugal force.
3. Centrifugal pumps develop head by the impeller accelerating the water from the center of rotation.
4. Turbine pumps develop head by a rotation in a radial plane between the impeller vanes as the impeller rotates, the pressure increasing in the water between each vane as it rotates from the suction inlet to the discharge outlet.

The reciprocating pump is used in small installations such as a single farm, because its capacity is limited. Turbine pumps are prone to wear if the water has a silt or sand content. The capacity is somewhat limited, but heads over 2,500 ft can be developed in the smaller pumps. Figure 29[1] shows three of the pumps discussed. Figure 30[1] is a diagrammatic aid in pump selection, based upon the parameter head vs. capacity. This figure gives a conservative estimate of the range for each type of pump. It must be remembered that pumps not consistent with the range defined in this diagram have been used in some instances. In such cases other conditions would dictate the pump selection, and the pump manufacturer would have to guarantee the operation of the pump for these conditions.

Pump selection is generally based on the specific speed N_s, which is expressed by the following equation:

$$N_s = \frac{\text{rpm}}{H^{3/4}} \sqrt{Q}$$

where rpm = pump revolutions per minute
Q = pump discharge, gal/min
H = head, ft

For maximum pump efficiency, the N_s should be in a range between 1,500 and 5,000 for pumps with capacities in excess of 100 gal/min.

Pump impeller types with their mean specific speeds are as follows:

Radial flow	800
Francis type	3,000
Mixed flow	5,000
Propeller	10,000

34. Pump Setting. For pumps that are not submerged the suction head should not exceed 22 ft. The amount of submergence at the pump inlet is a requirement determined by the pump manufacturer, although the Hydraulic Institute has developed a graph (Fig. 31) that sets this and other sump requirements in relation to pump capacity. The values obtained should be used for preliminary design only. The pump manufacturer should be consulted for the sump dimensions that allow the pump to meet its guaranteed efficiency.

35. Pumping Equipment. The equipment needed for an irrigation pumping plant, exclusive of the pumps, are the prime mover, suction and discharge line, discharge-line valves, and, depending on the water source, trash racks and fish screens. If the prime mover is an electric motor, transformer and electrical breakers may be required. Other prime movers are gasoline and diesel engines.

[1] "Turbines and Pumps," U.S. Bureau of Reclamation, Design Standards No. 6, 1960.

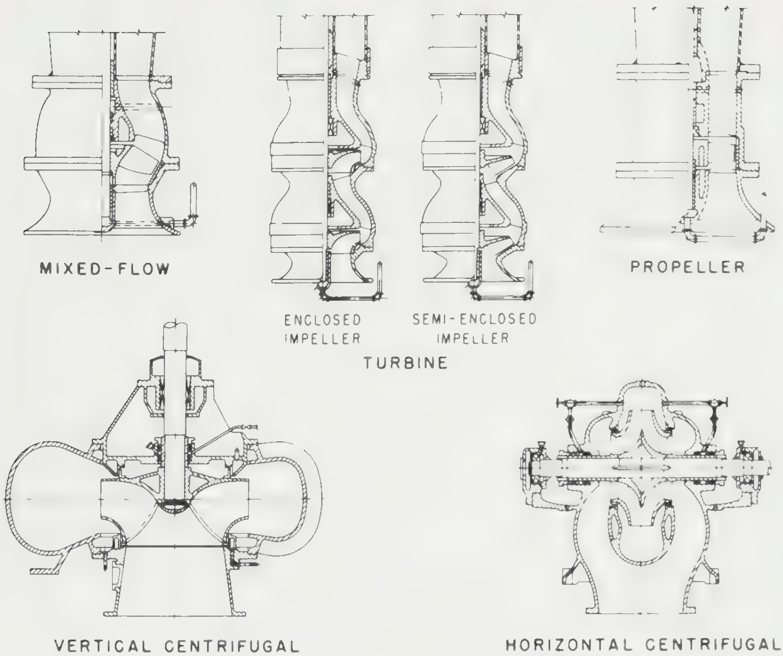

FIG. 29. Types of pumps.

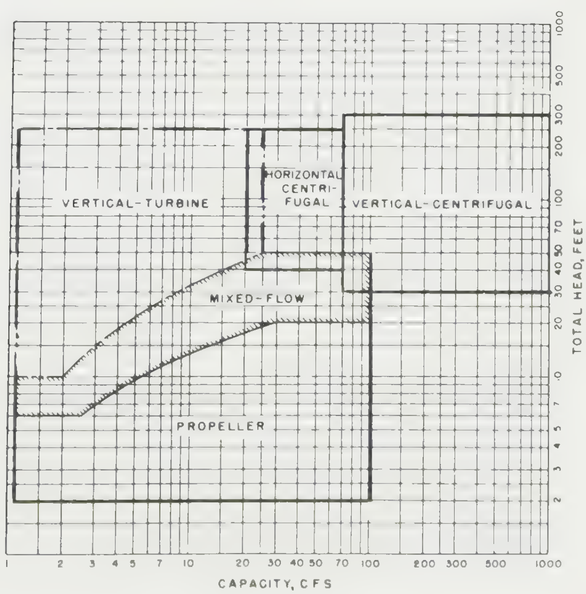

FIG. 30. Pump-selection diagram.

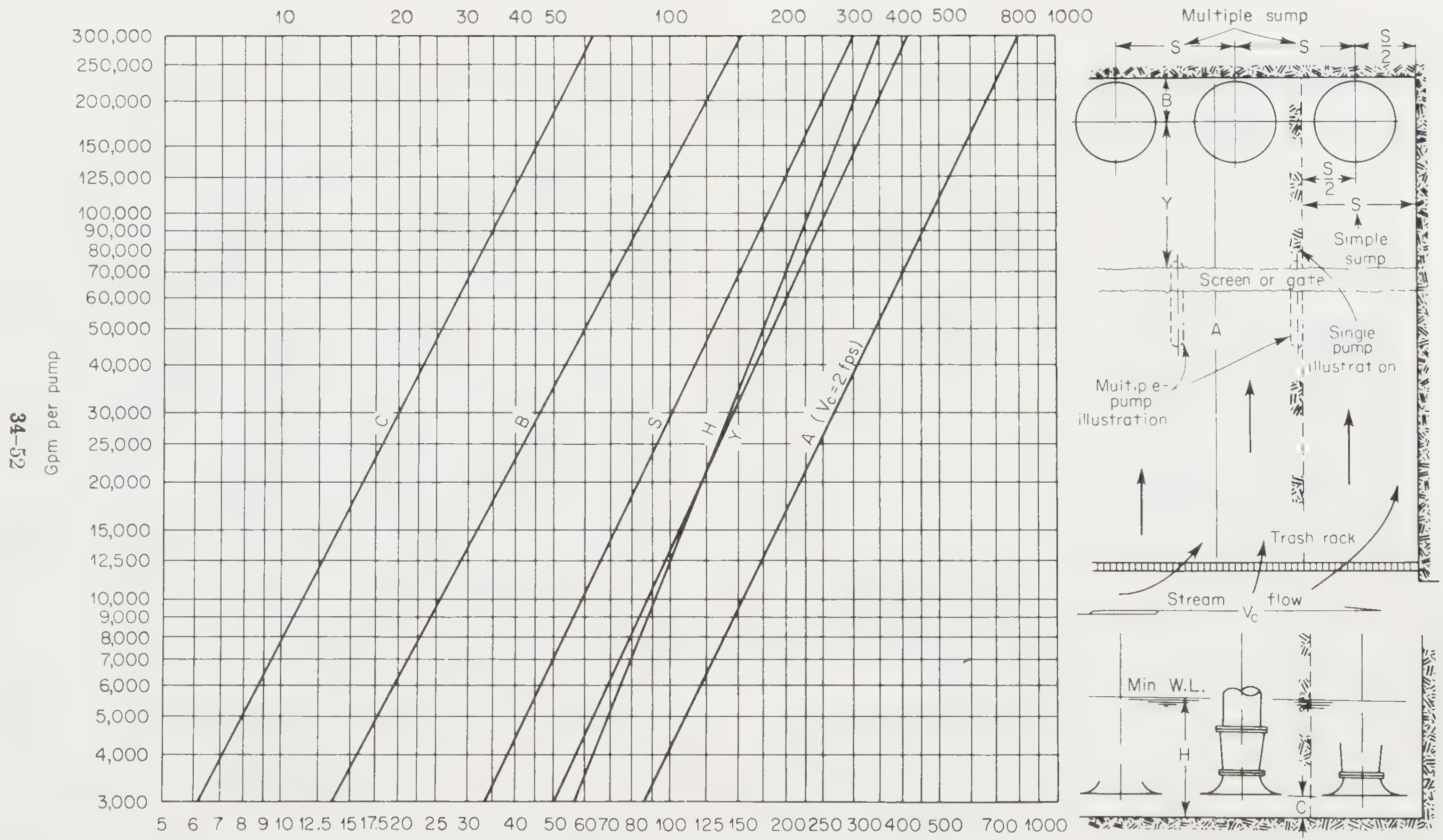

FIG. 31. Recommended sump dimensions in inches.

A valve in the discharge line can be used to throttle or curtail flow of water. In mixed-flow or propeller pumps, adjustment of flow by operation of the valve may overload the prime mover. Therefore, valves used with these pumps are for closure and their operation should be mechanically limited to this; otherwise operation procedures should specify no discharge control by valve operation. Valves used for discharge regulation are gate, plug, ball, spherical, or butterfly valves. To prevent a critical amount of reverse flow in the discharge line and pump, in the event of power failure, a cylinder-operated butterfly valve or a check valve should be used. The discharge line should then be designed for the pressure rise due to this condition.[1] The use of a cylinder-operated butterfly valve would require an air compressor and accumulator tank, whereas a controlled closing check valve would need no ancillary facilities. It must be pointed out that head loss through a check valve is considerable.

36. Plant Efficiencies. Plant efficiencies depend on pumping units, power equipment, and load conditions. Large, electrically operated, pumping plants, properly designed for use in cooperative irrigation enterprises, should have plant efficiencies of 70 to 75 percent. However, small farm plants seldom have efficiencies higher than about 60 percent, even when operating under the most favorable conditions. Tests of about 90 small plants in California showed average efficiencies of 49.8 percent for plants equipped with centrifugal pumps, 40.5 percent for plants equipped with deep-well turbine pumps, and 44.5 percent for plants equipped with deep-well screw pumps.[2]

37. Power Requirements. The power requirement for an irrigation pumping plant varies with the plant efficiency, discharge pumped, and total pumping head. The total pumping head includes static head, pipe friction, loss at pipe bends, and such other losses as may be included in the piping system. In a plant pumping from a surface supply, static head is the difference between water-surface elevations at intake and discharge ends. In a plant pumping from an underground supply, the depth of drawdown required to bring water through the soil to the suction pipe must be added to the difference in water-surface elevations. The discharge required varies with the size of area irrigated and depth of application needed.

[1] PARMAKIAN, JOHN, "Waterhammer Analysis," Chap. XI, Dover Publications, Inc., New York, 1963.

[2] JOHNSTON, C. N., Principles Governing the Choice of, Operation, and Care of Small Irrigating Pumping Plants, *Calif. Agr. Expt. Sta. Circ.* 312, 1928; also see Cost of Irrigation Water in California, *Calif. Dept. Public Works Bull.* 36, 1930.

SECTION 35

GROUNDWATER

By Thomas R. Camp and Joseph C. Lawler

INTRODUCTION

1. Role of Groundwater.[1] That portion of the world's total water resources which, in the hydrologic cycle, finds its way back to surface sources and to the oceans *beneath* the land surface comprises the earth's groundwater resources. These vast resources are closely interrelated with surface water and, of course, know no political boundaries. Groundwater exists wherever water can penetrate beneath the land surface in permeable material and be transmitted through such material. These conditions prevail so universally that groundwater has been an important factor in past ages in enabling human occupation of many large regions that otherwise could not have been settled. Although many groundwater regions have been defined, much more reconnaissance and exploration are necessary to evaluate fully the extent of groundwater storage. Large groundwater-storage basins serve to equalize the flow of water and, because they are underground, are not subject to so high evaporation losses as surface-water reservoirs, nor are they subject to so much contamination. In regions where there are large groundwater-storage basins, such basins provide means of managing total water resources, whereby water may be stored during times of surplus and utilized during periods of drought.

2. Types of Collecting Works. Rainwater which percolates into the soil beyond the reach of vegetation collects in the pores and fissures, and flows, usually in the general direction of the slope of the ground surface, toward outlet points. The water-bearing strata, called *aquifers,* include formations of soil and sand, porous sandstone, alluvial deposits of sand and gravel, porous lava flows, glacial drift, and limestone containing fissures.

Groundwater occurs in both unconfined and confined aquifers. The upper surface of unconfined groundwater is called the *groundwater table.* Flow through the soil is in the direction of the slope of the groundwater table. The water table rises during rainy seasons and falls during droughts. Excessive draft of groundwater from wells also lowers the water table. Figure 1 illustrates the position of the groundwater and shows several different types of collection works.

A *filter gallery* is an elongated basin constructed in an unconfined aquifer along the shore of a river or lake. As the draft from a filter gallery lowers the water table at the gallery below the water surface in the adjoining body of water, flow is induced from the river or lake to the gallery. Filter galleries, formerly an important source of water supply, are now generally obsolete. Groundwater-collecting systems are a form of filter gallery; they consist of open-joint conduits, laid in an unconfined aquifer, through which the water flows by gravity to a collecting basin or pump well. A *collector well*[2] is a caisson from which perforated or slotted well pipes are jacked horizontally into an aquifer, sometimes to lengths of several hundred feet and often under the bed of a river or lake.

[1] McGuinness, C. L., The Role of Ground Water in the National Water Situation, *U.S. Geol. Surv. Water Supply Paper* 1800, 1963.

[2] Kazmann, *Trans. ASCE,* **113,** 404–424, 1948.

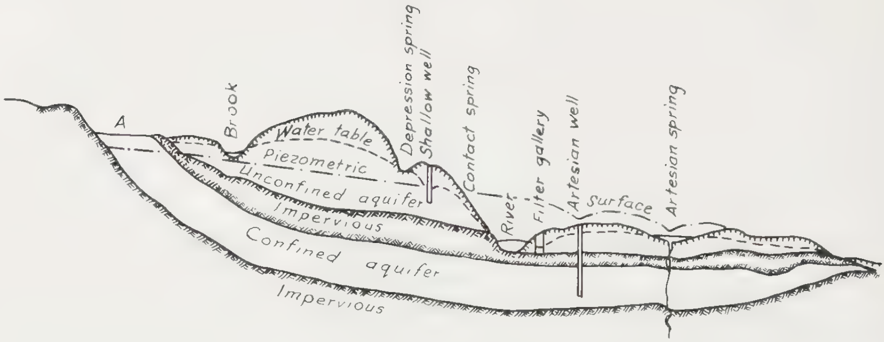

FIG. 1. Hypothetical section showing relation of groundwater to topography.

Groundwater in a confined aquifer is under pressure because of the presence of an impervious stratum above the aquifer. A well which penetrates the impervious stratum to a confined aquifer is called an *artesian well.* The surface to which water would rise because of the pressure in a confined aquifer is called the *piezometric surface.* If the piezometric surface is above the ground surface at an artesian well, the well is called a *flowing well.*

A number of different types[1] of springs are encountered in nature. An *artesian spring* is one in which the water issues under artesian pressure through a fissure in the impervious rock overlying the aquifer. Springs formed at points where the groundwater table outcrops are called *gravity springs.* A gravity spring in which the water flows to the surface from permeable material over an outcrop of impermeable material is called a *contact spring.* A *fracture* or *fissure spring* is a gravity spring in which the water issues from relatively large openings in rock. A *depression spring* is a gravity spring due to a depression of the ground surface below the water table. During the dry seasons of the year, depression and contact springs may go dry owing to the lowering of the water table.

Works for the collection of water from springs consist mainly of collecting basins, from which the water may be pumped to the distribution system, and safeguards against the contamination of the springwater.

HYDRAULICS OF GROUNDWATER

3. Darcy's Law and Groundwater Flow. The basic principle for describing the flow of groundwater dates from the middle of the nineteenth century and the work of Henri Darcy with flows through filter sand. Darcy's law and the law of continuity are the two basic concepts for describing the flow of groundwater. Darcy's law can be expressed as

$$v = k\frac{dh}{dl} \tag{1}$$

where v = filtration velocity of the discharge per unit cross-sectional area of the porous media through which the water is flowing

k = coefficient of permeability, also termed the hydraulic conductivity

$\frac{dh}{dl}$ = hydraulic gradient, *i.e.*, the loss of head divided by the unit length in the direction of flow

[1] MEINZER, *U.S. Geol. Surv. Water Supply Paper* 494.

Darcy's law is considered valid for groundwater velocities resulting in a Reynolds number below a range of 1 to 10. Grain shapes, packing, and distribution of grain sizes in a natural formation are not definitive, and consequently a range of numbers is appropriate rather than a definite limiting number. The concept of a Reynolds number originated with the flow of liquids through pipes and is generally expressed as follows:

$$N_r = \frac{\nu v d}{\mu} \tag{2}$$

where N_r = Reynolds number
ν = liquid density
v = flow velocity
d = diameter of pipe
μ = viscosity of liquid

When a Reynolds number is used in connection with the flow of liquids through porous media, d is usually taken as a representative grain-size diameter.

Dupuit applied Darcy's law to well hydraulics, and Theim, Slichter, and others modified the earlier work into equations describing a steady flow condition, generally referred to as "equilibrium formulas," where the flow to the well equals the pumped discharge.

Theis is credited with the development of the nonequilibrium theory and the introduction of the factor of time to the field of well hydraulics. The application of this theory and the related formulas presented problems in mathematics which have been circumvented by utilizing graphical solutions.

For a review of the theory of groundwater flow, the reader is referred to recent texts.[1,2,3]

Hydraulics of Wells under Equilibrium Conditions. In a *confined aquifer*, well-discharge formulas have been employed for a great many years based on the work of early investigators.[4,5,6] These early investigators demonstrated that laminar flow to a well under equilibrium conditions could be described mathematically. The development of the equilibrium formulas was based on the assumptions that flow in a medium was taking place under conditions described as follows:

1. That equilibrium of the water level or piezometric surface throughout the area of influence of the well has been attained (drawdown stabilized) and that this surface is horizontal (no slope)
2. That the aquifer is of a constant thickness and constant permeability (isotropic) throughout the area of influence
3. That the pumping well penetrates to the bottom of the aquifer and is 100 percent efficient and that flow to the well is strictly radial

The *equilibrium formula for nonleaky-artesian conditions* also assumes that the aquifer is confined between two confining layers through which no water is entering or leaving the aquifer. It is written as

$$s_w = h_e - h_w = \frac{Q}{2\pi k m} \ln \frac{r_e}{r_w} \tag{3}$$

[1] Todd, D. K., "Ground-water Hydrology," p. 336, New York, John Wiley & Sons, Inc., New York, 1959.

[2] Hantush, M. S., Hydraulics of Wells, in "Advances in Hydrosciences," vol. 1, pp. 281–432, edited by Ven te Chow, Academic Press Inc., New York, 1964.

[3] De Wiest, R. J. M., "Geohydrology," p. 366, John Wiley & Sons, Inc., New York, 1965.

[4] Slichter, C. S., Theoretical Investigation of the Motion of Ground Water, *U.S. Geol. Surv. 19th Ann. Rept.*, p. 359, Washington, D.C., 1899.

[5] Turneaure, F. E., and H. L. Russell, "Public Water Supplies," p. 269, John Wiley & Sons, Inc., New York, 1901.

[6] Theim, G., "Hydrologische Methoden," p. 56, J. M. Gebhardt, Leipzig, 1906.

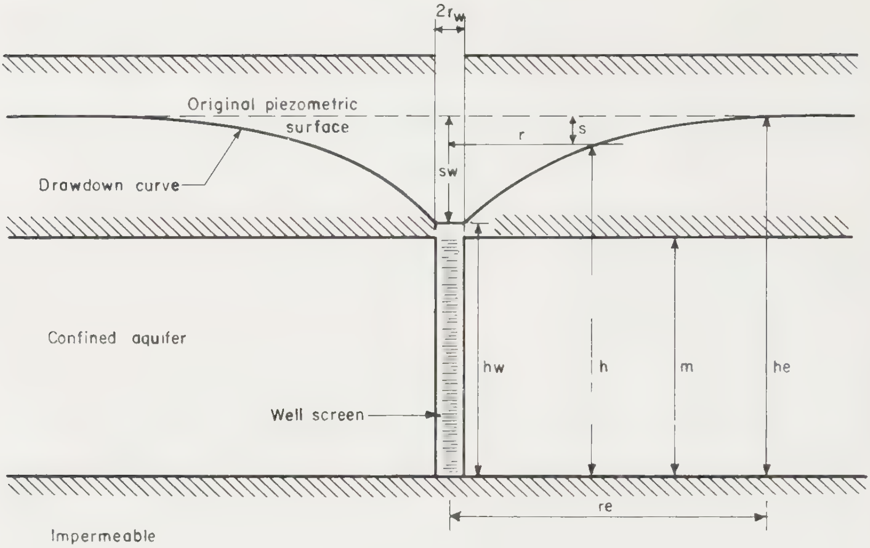

FIG. 2. Equilibrium conditions for steady-state confined flow.

where Q is discharge or pumping rate and all other terms are as previously defined or as shown in Fig. 2. Equation (3) may be rewritten as

$$h_e - h_w = \frac{2.3Q}{2\pi km} \log \frac{r_e}{r_w} \tag{4}$$

or

$$Q = \frac{T(h_e - h_w)}{528 \log (r_e/r_w)} \tag{5}$$

where Q = discharge, gpm, and the symbol T is introduced
T = coefficient of transmissibility; rate of flow of water, gpd, which will flow through a 1-ft-wide section of an aquifer for the fully saturated depth under a hydraulic gradient of 1 ft/ft; T = average $k \times m$, gpd/ft

Drawdown in a well includes well losses and should not be used to compute permeability. Generally, a field investigation involves two or more observation wells. When records from such observation wells are available, simultaneous readings of the piezometric surface can be used to find the permeability. With Q in gallons per minute, Eq. (5) is rewritten as

$$k = \frac{528Q \log (r_2/r_1)}{m(h_2 - h_1)} \tag{6}$$

where all terms are as previously defined except
r_1 = distance to nearest observation well, ft
r_2 = distance to the farthest observation well, ft
$h_2 - h_1$ = difference in piezometric head in the respective observation wells

The *equilibrium formula for unconfined conditions* is written as

$$h_e^2 - h_w^2 = \frac{Q}{\pi k} \ln \frac{r_e}{r_w} \tag{7}$$

where Q is the pumping rate and all other terms are as previously described.

Equation (7) can also be written as

$$h_e^2 - h_w^2 = \frac{2.3Q}{\pi k} \log \frac{r_e}{r_w} \tag{8}$$

or

$$h_2^2 - h_1^2 = \frac{2.3Q}{\pi k} \log \frac{r_2}{r_1} \tag{9}$$

where h_1 and h_2 are the heights of the water surface above the impermeable base at

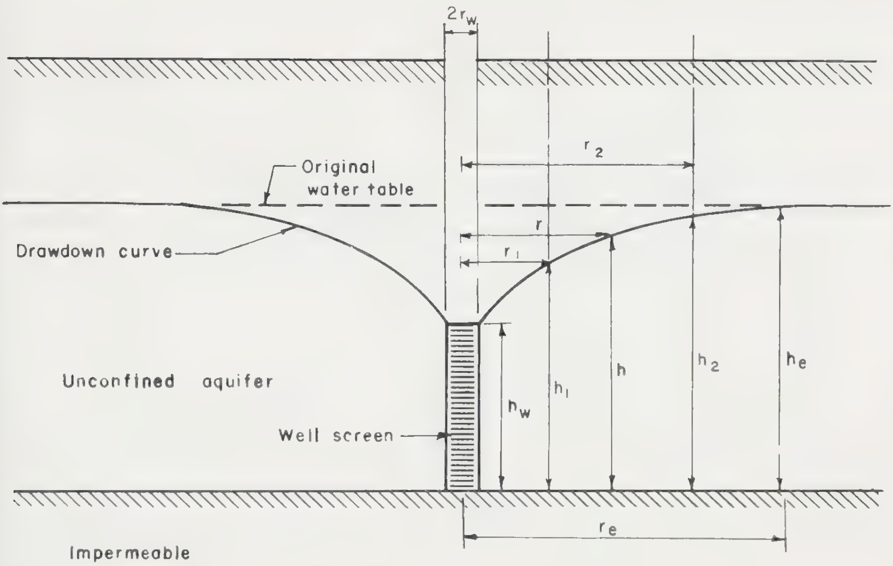

FIG. 3. Equilibrium conditions for steady-state unconfined flow.

radial distances r_1 and r_2, respectively (see Fig. 3).

$$Q = \frac{k(h_e^2 - h_w^2)}{1{,}055 \log (r_e/r_w)} \tag{10}$$

where Q is represented in gallons per minute.

As noted previously, it is not advisable to use records from the pumping well to find permeability. Where records from two observation wells are available, Eq. (7) can be rewritten with Q in gallons per minute as

$$k = \frac{1{,}055Q \log (r_2/r_1)}{h_2^2 - h_1^2} \tag{11}$$

where all terms are as previously defined except

r_1 = distance to the nearest observation well, ft
r_2 = distance to the farthest observation well, ft
h_2 = saturated thickness, ft, at the site of the farthest observation well
h_1 = saturated thickness, ft, at the site of the nearest observation well

4. Hydraulics of Wells—Nonequilibrium Conditions. In 1935, Theis[1] introduced

[1] THEIS, C. V., The Relation between the Lowering of the Piezometric Surface and the Rate and Duration of Discharge of a Well Using Ground Water Storage, *Trans. Am. Geophys. Union*, 1935, pp. 519–524.

a formula describing radial flow to a well completely penetrating an isotropic aquifer of uniform thickness and infinite areal extent. The formula is sometimes referred to as the *nonleaky-artesian formula* after two additional assumptions made in its derivation. It is more commonly known as the Theis formula and is written

$$s = \left(114.6 \frac{Q}{T}\right) W(u) \tag{12}$$

where $W(u)$ = well function for nonleaky aquifers, values of which are extensively tabulated in many texts[1,2] crediting Wenzel,[3] and is dimensionless

and
$$u = 2{,}693 \frac{r^2 S}{Tt} \tag{13}$$

where S = storage coefficient, which is dimensionless
t = time after pumping started, min
s = drawdown at radius r, ft
r = distance from observation well to pumping well, ft

The formula is based on the assumption that the pumped well is 100 percent efficient; therefore, when it is employed in connection with field results from a pumping test, measurements from an observation well should be used. A calculated solution

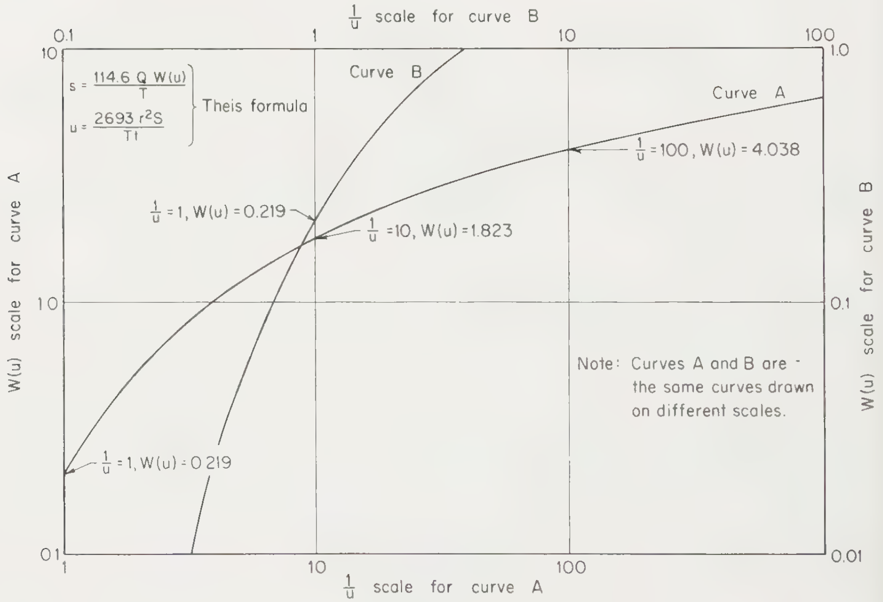

FIG. 4. Theis nonleaky-type curve.

of Eqs. (12) and (13) for values of T and S is not possible, and a graphical solution is used instead. The Theis-type curve by which a solution of the nonleaky formula is possible is prepared on standard log paper, as shown in Fig. 4, from available tables of

[1] WALTON, W. C., Selected Analytical Methods for Well and Aquifer Evalution, *Illinois State Water Survey Bull.* 49, 1962.
[2] "Ground Water and Wells," Edward E. Johnson, Inc., 1966.
[3] WENZEL, L. K., Methods for Determining Permeability of Water-bearing Material, *U.S. Geol. Surv. Water Supply Paper* 887, 1942.

$W(u)$ and u. This curve is matched against a curve plotted from the test data so that the vertical and horizontal axis of both the Theis-type and test curves are parallel when the two curves are superimposed. Both the horizontal and vertical scales against which the test data are plotted must be the same as used for the Theis-type curve. The vertical scale of the test-data curve is plotted as s (drawdown) and the horizontal scale as t (time) where s and t are analogous to $W(u)$ and $1/u$, respectively, as shown in Fig. 5. As long as the units of the plotted test data are the same as the

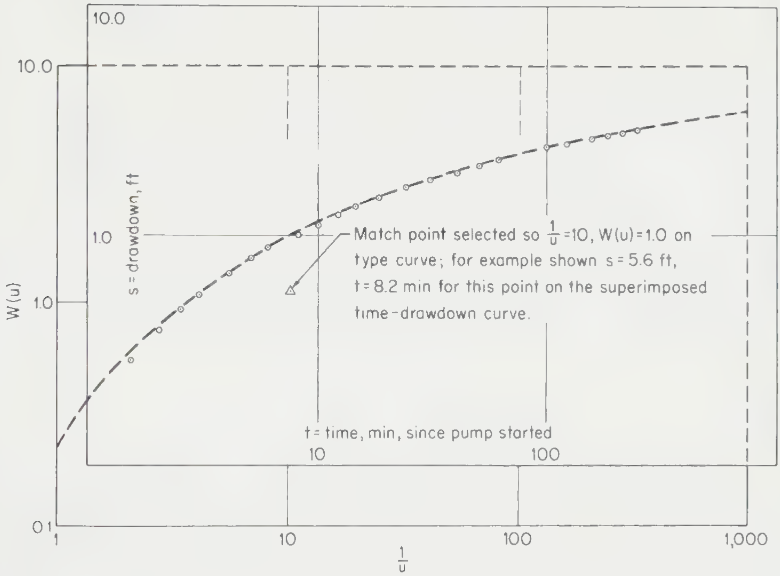

FIG. 5. Example of matching field data with Theis nonleaky-type curve.

units in which Eqs. (12) and (13) are represented the values obtained from the test-data curve and the Theis-type curve will be comparable. The field-data curve is fitted to the Theis-type curve, trying to achieve a good fit between the two curves. A deviation in some portion of the field-data curve from the Theis-type curve provides information relative to deviation of actual conditions from those as assumed for the derivation of the basic formulation. After the best match of the two curves is achieved, a match point is selected. It is advantageous to select a point where the coordinates of the Theis-type curve are known such as $W(u) = 1$, $1/u = 10$, so that calculations are kept simple. The corresponding values for s and t are then substituted along with $W(u)$ and u in Eqs. (12) and (13), to solve for T and S. Figure 5 provides an example of a time-drawdown curve matched with a Theis-type curve and shows that a match point can be selected anywhere within the overlap of the curves.

It should be noted that the above technique to determine T and S is based on a time variation of drawdown for a single observation well. If at least three observation wells are available, further verification of the estimated values of T and S can be obtained by plotting drawdown for each well on the vertical scale vs. $1/r^2$ of each respective observation well on the horizontal scale. This is done for the same instant of time for each well. A match between the Theis-type curve and test-data curve is then attempted with the match point giving a value of r rather than t, as in the prior procedure.

The flow of groundwater in *unconfined aquifers* may also be studied by the Theis nonequilibrium formula under certain conditions. In unconfined aquifers, water is obtained by gravity drainage, which is not instantaneous. As a result, a varying coefficient of storage occurs but changes at a diminishing rate with the time of pumping. Bolton[1] suggests that reasonably reliable results may be obtained where field data from observation wells located between 0.2 to 0.6 times aquifer thickness are available from the pumping well. Bolton's considerations provide a formula for the determination of the time interval after the start of pumping, before which use of the nonequilibrium formula is not justified. This formula is represented as follows:

$$t_{wt} = 37.4 \frac{Sm}{k} \tag{14}$$

where t_{wt} = time after pumping began, days, and S, m, and k have been previously defined. Walton[2] presents the formula with the specific yield Sy in place of the storage coefficient. In an unconfined aquifer, the specific yield (amount of water that can be drained by gravity) and the coefficient of storage will be represented by the same value only after the initial drainage effect has been largely minimized.

The *modified nonequilibrium formula*, and the graphical solution for it, was published in 1946 by Cooper and Jacob.[3] The formula is essentially a simplification of the Theis equation and is based on the same assumptions, so that when u is small, Eq. (12) can be expressed as

$$s = \left(114.6 \frac{Q}{T}\right)(-0.5772 - \ln u) \tag{15}$$

Equation (15) is generally considered valid for values of u less than 0.02.

"Ground Water and Wells"[4] provides a good review of the semilog graphical solutions involved with the indirect solution of the modified nonequilibrium formula and states that for all practical purposes utilization of the graphical solution of the modified formula will provide essentially the same results as the Theis formula for values of u less than 0.05. In application, drawdowns in pumping or observation wells are plotted against an arithmetic scale, while time or distance from the pumped well is plotted against a logarithmic scale to produce semilog plots termed time-drawdown and distance-drawdown graphs. Prior to plotting, values should be adjusted for partial penetration or other factors which would significantly affect the results. The plotted value should produce a straight-line plot, and any variation reflects a condition where actual conditions differ from the basic assumptions made in the derivation of the formula.

Application of the plots utilizes the following equations, developed from Eq. (15), for the determination of aquifer coefficients:

$$T = 264 \frac{Q}{\Delta s} \tag{16}$$

$$S = \frac{Tt_0}{4{,}790r^2} \tag{17}$$

Equations (16) and (17) are applicable to use with time-drawdown plots where

[1] Bolton, N. S., The Drawdown of the Water Table under Nonsteady Conditions Near a Pumped Well in an Unconfined Formation, *Proc. Inst. Civil Engrs. (London)*, **3** (III), 564–579, 1954.

[2] *Op. cit.*

[3] Cooper, H. H., Jr., and C. E. Jacob, A Generalized Graphical Method for Evaluating Formation Constants and Summarizing Well Field History, *Trans. Am. Geophys. Union*, **27**, 524–526.

[4] "Ground Water and Wells," Edward E. Johnson, Inc., 1966.

Δs = drawdown difference per log cycle, ft
t_0 = value indicated by extending straight-line slope to zero drawdown, min

$$T = 528 \frac{Q}{\Delta s} \tag{18}$$

$$S = \frac{Tt}{4{,}790 r_0^2} \tag{19}$$

Equations (18) and (19) are applicable to use with distance-drawdown plots where
r_0 = value indicated by extending straight-line slope to zero drawdown, ft

The effective radius of a well cannot generally be determined with a sufficient degree of accuracy to allow use of the above method for the determination of the coefficient of storage from field data of the pumped well only. Cooper and Jacob[1] pointed out that the modified method supplemented rather than superseded the type-curve solutions, and that under certain circumstances it was usable with nonartesian aquifers.

The *leaky-artesian formula* was developed by Hantush and Jacob[2] and is written

$$s = \left(114.6 \frac{Q}{T}\right) W\left(u, \frac{r}{B}\right) \tag{20}$$

where $W(u,r/B)$ = well function for leaky aquifers which is defined by an integral equation given in Hantush[3] along with values for $W(u,r/B)$

and
$$u = 2{,}693 \frac{r^2 S}{Tt} \tag{21}$$

and
$$\frac{r}{B} = \frac{r}{\sqrt{T/(k'/m')}} \tag{22}$$

where k' = coefficient of vertical permeability of the confining layer, gpd/sq ft
m' = thickness of confining layer

Assumptions on which the formula is based are as made for the *nonleaky-artesian formula*, except that the aquifer is confined by a semipermeable stratum through which leakage takes place vertically and is proportional to drawdown without change in the water level of the layer supplying the leakage. A modification of the graphical method used for solving the Theis formula is employed to achieve solutions for the leaky-artesian formula. Figure 6 is taken from Walton[4] and shows a family of type curves where $W(u,r/B)$ is plotted against $1/u$. In utilizing the type curves, a time-drawdown graph is prepared from field data on logarithmic paper of the same scale. The time-drawdown plot is superimposed on the type curves with the respective axis parallel and a match point is selected after the field-data curve has been matched with one of the curves of Fig. 6. The values of $W(u,r/B)$, $1/u$, s, and t at the match point are then used with the appropriate formulas along with the r/B value for the curve matched with the field-data curve to give values for the hydraulic properties of the aquifer and confining layer. When the confining layer is impermeable, $r/B = 0$ and Eq. (20) becomes the same as Eq. (12), and the limiting curve of the family of leaky-artesian curves is the Theis nonleaky curve of Fig. 6. It is not good practice to place full reliance on the values obtained from matching a time-drawdown curve to the leaky-type curves, and it is suggested that such values be compared with values obtained by

[1] *Op. cit.*
[2] Hantush, M. S., and C. E. Jacob, Nonsteady Radial Flow in an Infinite Leaky Aquifer, *Trans. Am. Geophys. Union*, **36,** 1955.
[3] Hantush, M. S., Analysis of Data from Pumping Tests in Leaky Aquifers, *Trans. Am. Geophys. Union*, **37,** 1956.
[4] *Op. cit.*

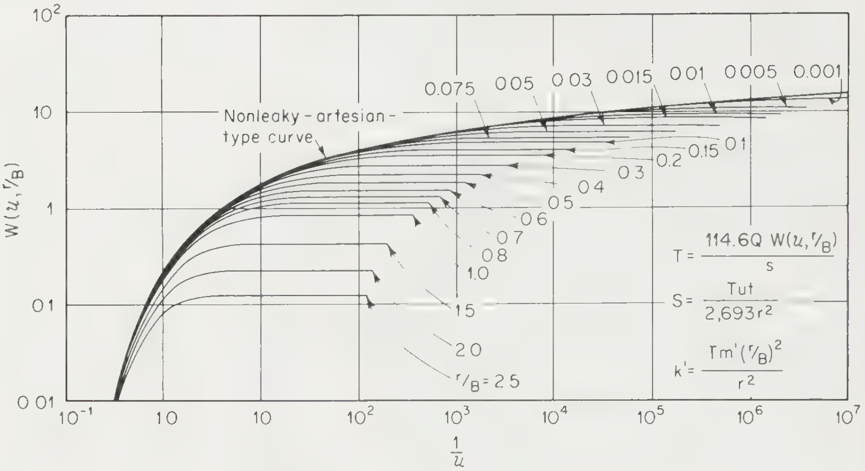

FIG. 6. Non-steady-state leaky-artesian-type curves.

repeating the process with a time-distance, s against r, plot matched against a family of type curves where values of $W(u,r/B)$ are plotted against r/B with each curve of the family representing a different value for u/r^2.

Wells Partially Penetrating an Aquifer. Many artesian wells do not penetrate through the full thickness of the aquifer, and many wells are provided with casings which are perforated or provided with screens for only a portion of the thickness of the aquifer. In such cases, the streamlines are not horizontal in the vicinity of the well. They converge vertically and thus increase the velocity in the vicinity of the well. The drawdown at the well is greater than for an ideal well. Muskat[1] gives a solution for the case of a well that partly penetrates an artesian aquifer. Kozeny[2] developed a formula for determining the capacity of wells partially penetrating an aquifer of known thickness. From the Kozeny formula, Edward E. Johnson, Inc.,[3] has developed a set of curves by which the specific capacity of partially penetrating wells in reasonably homogeneous artesian aquifers can be estimated.

5. Specific Capacity and Safe Yield. The specific capacity of a well is the discharge per foot of drawdown at the well. In determining the well yield by test, it is assumed that the potential in the well is the same from the water surface to the bottom. If the well is small in diameter and being pumped at a high rate, it is necessary to correct for friction loss and velocity head in the casing in determinations of the drawdown.

For artesian wells, it may be noted from Eq. (3) that the yield is not directly proportional to the drawdown. If r_e is assumed constant, h_w will increase as h_e is increased, but not at the same rate. If the value of r_e is taken such that h_w is very small compared with h_e, the capacity is very nearly directly proportional to the drawdown. For artesian wells, therefore, it is usually assumed that the specific capacity is constant within the working limits of the drawdown.

The specific capacity for wells in unconfined aquifers decreases as the drawdown is increased. In Eq. (7), $h_e^2 - h_w^2$ may be written $(h_e - h_w)(h_e + h_w)$. The first term

[1] MUSKAT, M., "The Flow of Homogeneous Fluids through Porous Media," chap. V, McGraw-Hill Book Company, New York, 1937.

[2] KOZENY, J., Theorie und Berechnung der Brunnen, *Wasserkraft u. Wasserwirtschaft*, **28**, 101, 1933.

[3] "Groundwater and Wells," p. 134, Edward E. Johnson, Inc., 1966.

$h_e - h_w$ approximates the drawdown at the well if r_w is small and r_e large. With increase in the drawdown, the term $h_e + h_w$ is decreased, the result being a decreased specific capacity with increased drawdown.

The *maximum safe yield* of a well or well field is limited by the capacity of the aquifer to supply water without suffering a continuous lowering of the water table or piezometric surface. The maximum safe yield is limited, therefore, by the rate at which the groundwater is replenished by rainfall. The seasonal fluctuation in safe yield from shallow-well supplies is more marked than for artesian supplies.

If a well or well field is not developed to the full capacity of the aquifer, the maximum yield is limited by the maximum permissible drawdown at the well and by the size and method of construction of the well. For fields of shallow tubular wells, the maximum permissible drawdown may be limited by the suction head on the pumps or by the depth of the wells. For economy of pumping, the drawdown should be kept to a minimum. For greatest overall economy, the cost of pumping against the additional head due to drawdown should be balanced against the cost of securing additional yield by improving the method of construction of the well. In practice, such an economic balance is difficult to obtain because it is not possible to predict accurately the yield of a well before it is constructed.

For a given drawdown, the yield increases slightly with increase in diameter. To secure the greatest yield, it is also desirable for the well to penetrate the full thickness of the aquifer and thus reduce vertical convergence of the streamlines near the well.

The specific capacity of wells ranges from about 5 gpm for small shallow driven wells to over 100 gpm for large-diameter gravel-wall deep wells.

Special Studies of Groundwater Flow and Flow to Wells. Walton[1] presents discussions of various special formulas for special studies of flow such as partial penetration, flow-net studies, constant-drawdown conditions, estimating the time to reach equilibrium, multiple boundaries, multiple wells, and estimating economical spacing of wells. Lang[2] authored a paper detailing spacing of wells in artesian aquifers under various conditions. Other authors such as Todd[3] have detailed special studies of groundwater flow and flow to wells under considerations not mentioned above.

Hantush[4] presents tables of various functions of common occurrence in problems of groundwater flow such as

Flowing-well function for nonleaky aquifers
Flowing-well discharge function for nonleaky aquifers
Gravity-well function
Well function for leaky aquifers

The above functions permit special type curves to be drawn.

Application of Formulas Describing Flow to Wells. When data from actual conditions vary from predictions made by standard formulation, it shows that conditions differ from the basic assumptions on which the formulation was based. If a field-data plot on logarithmic paper does not coincide with a nonleaky-type curve, it indicates that possibly recharge or leakage was taking place if displaced in one direction, while displacement in the opposite direction would indicate boundary conditions which are affecting the assumption of constant permeability or constant thickness of an aquifer. These variations are not always readily evident, and interpretation in many cases is not clear until various approaches are tried and compared, such as the preparation of

[1] *Op. cit.*
[2] LANG, S. M., Methods for Determining the Proper Spacing of Wells in Artesian Aquifers, *U.S. Geol. Surv. Water Supply Paper* 1545-B, 1961.
[3] *Op. cit.*
[4] *Op. cit.*

time-drawdown plots in accordance with the nonleaky Theis method and the modified nonleaky semilogarithmic plot. Calculations and interpretation are simpler when the semilogarithmic plot is used, and the variation from assumed conditions is more easily seen than on the curves of other graphical solutions. As previously noted in the discussion of this method, its application is useful only when the value of u is small.

In all analyses, it is important that sufficient information is available. Water-table data, for example, might present a problem involving interpretation of distorted curves where the effects of gravity drainage might be confused with barrier boundaries. This problem can be simply resolved if it is known that the cone of depression is or is not distorted. The possibility of boundary effects can be eliminated if data from observation wells are available to indicate that no distortion of the cone of depression has taken place.

6. Testing for Groundwater. In a search for underground sources of water supply, it is often advisable to make various preliminary investigations prior to installing test wells so that the more promising sites may be located. These preliminary investigations may include tests for electrical resistivity and tests for seismic refraction.

In the electrical-resistivity method,[1] the electrical resistance determined by applying an electric current to metal stakes driven into the ground and measuring the apparent potential difference between two other points gives an indication of the type and depth of subsurface material. This method also is useful in locating salt-water boundaries because of the decrease in resistance when salt water is encountered. Changing the spacing of the electrodes at a given site is an aid in interpreting the resistivity data.

The seismic-refraction method[1] is based on the time required for a sound or shock wave to travel known distances. The sound or shock wave is created by exploding a small charge of dynamite (usually less than 1 lb) just below the ground surface. The velocity of a shock wave depends upon the media through which it passes and is greater in solid rock and less in unconsolidated formations. In saturated strata, the velocities are somewhat greater than in unsaturated strata, while in solid rock they are substantially greater. Proper interpretation of the data, therefore, will indicate the depth to solid rock and whether or not the unconsolidated deposits are likely to contain groundwater. This may eliminate needless drilling in search of groundwater deposits.

The development of groundwater supplies is an engineering project and requires knowledge of hydraulics, hydrology, and geology. In spite of popular belief in water dowsing, groundwater sources cannot be located by divining rods, nor can any estimate be made of the amount of groundwater available at any location by the so-called "pull" of the divining rod or forked twig.

Groundwater storage and the watershed tributary to a well are major factors affecting its safe yield, particularly where the pumping rate of the well approaches the safe yield of the aquifer. A typical graph of the relationship of yield to storage and watershed area is shown in Fig. 4, Sec. 36, under yield of surface-water supplies.

Figure 4 is based on data from surface supplies, and strictly speaking is applicable only to surface supplies in New England. However, the graph can also be used to approximate the safe yield of groundwater supplies in New England. The greatest difficulty in applying the graph to groundwater supplies is in estimating the available groundwater storage. In spite of the difficulty of making a reliable estimate of the available groundwater storage, this method of estimating the safe yield of groundwater supplies is a valuable tool and, together with pumping tests, increases the reliability of estimates of the safe yield.

[1] Todd, "Ground Water Hydrology," John Wiley & Sons, Inc., New York, 1959.

Pumping Tests. In areas where information relative to the safe yield of an aquifer is not available, continuous-pumping tests of proposed wells are considered necessary. The wells to be pumped during the continuous-pumping test are usually temporary test wells. It may be inadvisable to install permanent wells prior to making a continuous-pumping test because of the danger that the investment may be wasted if subsequent pumping reveals the quantity or quality of water to be unsatisfactory.

The water being pumped should be discharged through a temporary pipeline a sufficient distance from the test wells to eliminate any appreciable "recharge" of the aquifer being pumped. Extensive flooding of the immediate area especially is to be avoided. In addition to the test wells being pumped, it is desirable to have a number of observation wells. One or two should be close to the test wells, and additional observation wells should be provided in various directions up to several hundred feet in distance, so that the drawdown effect over the entire area can be determined. If the test well being pumped is near an existing watercourse, it is desirable to have an observation well on both sides of the river or stream to determine whether the drawdown effect extends to or beyond the watercourse.

Prior to starting pumping, "static" water-level readings should be taken at all wells and converted to elevations referred to a common base. After the start of pumping, readings are usually taken at close intervals at the beginning of the test, and these intervals are gradually lengthened to 1- or 2-hr intervals as the test continues. Rainfall records should be kept or obtained from some nearby official source. Records of water levels in adjacent streams, rivers, or ponds should be kept and plotted along with the water level in the various wells. If, for example, the water level in the test wells rises and falls in unison with the water level in a nearby river, it is evidence of a hydraulic connection between the two.

Once started, pumping should be continuous without interruption, except for brief shutdowns for engine maintenance, until the water levels in the various test wells stabilize. After stabilization, the pumping test should continue for a minimum of 24 hr, and preferably for 2 or 3 days. The time required for stabilization may vary from hours to weeks or more. Most typical groundwater supplies stabilize in less than a week.

After pumping has ceased, observations of the rate of recovery of the water level in the various observation wells should be made similar to those made at the start of the pumping test, except that after the first few hours, it is not usually necessary to take hourly readings. Readings once or twice per day usually will suffice until such time as the wells have recovered to static levels. The time required for complete recovery may range from hours to several weeks or more, but most typical groundwater supplies recover completely within a week or two.

If the continuous-pumping test is conducted during a period of severe drought, the natural groundwater table may be dropping gradually aside from the effects of pumping. Accordingly, recovery of the wells following completion of the continuous-pumping test will not be complete, except over a long period of time. During such a drought period, water-level measurements should be taken at the various observation wells for several days *prior* to the start of the continuous-pumping test to determine the rate of lowering of the groundwater table caused by drought conditions. This information may then be compared with the amount by which the wells fail to recover, following the continuous-pumping test.

Continuous drafts of water from an underground source which exceed the long-term mean annual inflow deplete the groundwater storage, and are often referred to as "mining" of groundwater because it will eventually exhaust the resource in a similar manner to the mining of minerals. Although the draft can exceed the inflow in any one year without causing permanent depletion, it should not exceed the inflow averaged over a series of wet and dry years. Proper interpretation of pumping tests will avoid overdrafts or "mining" of groundwater.

7. Groundwater Management. The interrelationship of groundwater and surface water is basic in solving the problems of groundwater management. Watershed areas of surface sources can be readily defined, while groundwater watershed areas may extend far beyond their surface indications. All groundwater not returned to the atmosphere via transpiration or reaching the ocean beneath the ground eventually contributes to surface sources. The use of surface waters integrated with the use of groundwaters can improve the efficiency of use of the total water resource to minimize cost of development or to maximize yield. This can be accomplished by groundwater recharge from surface sources during periods of high surface runoff, and by making full use of groundwater during periods of deficient surface flow. In arid climates, the conjunctive use of surface and groundwater minimizes overall losses, and pumping from basin outlets prevents losses to the ocean. The U.S. Geological Survey, by the use of an infrared scanner, has published an atlas of Hawaii's coastal areas, pinpointing the location of underground fresh-water flows. It is possible that infrared detection of underground fresh-water flows may in the future be of great value in groundwater management.

GROUNDWATER WELLS

8. Methods of Construction of Wells.[1,2,3] Wells are classified as *dug, driven, jetted, and drilled* wells, depending upon the method of construction. Shallow wells are sometimes constructed as dug wells, the methods used being similar to methods used in excavating any open shaft. Driven wells are constructed by driving a pipe of small diameter into the water-bearing formation. The pipe is generally $2\frac{1}{2}$ in. or less in diameter and equipped with a well point or strainer at the bottom. In its simplest form, a jetted well is installed by the washing action of a jet of water washing an open or uncased borehole into the ground as the jetting pipe is lowered. In this type of construction, a screen may be set inside the original wash pipe, or where the formation is stable enough or has been stabilized by artificial means, the wash pipe can be removed, a screen attached to a permanent casing pipe, and relowered to the desired depth. Through the use of a special screen incorporating a check valve, the screen and casing may be washed into place with one operation. This is common practice with the installation of a well-point system used for dewatering construction sites. In this procedure, the wash pipe is installed through the casing and attached to the check valve at the bottom of the screen. Upon reaching the desired depth, the wash pipe is unscrewed from the screen and removed. While both small and large wells have been constructed in the past to relatively large depths by some form of jetting action, other methods of construction have superseded this form to a large extent except for the smaller diameters. A combination of driving and jetting is often used in connection with test-well exploratory programs. This method, sometimes referred to as the *jet-percussion* method, employs a chisel-shaped bit attached to a wash pipe to loosen and wash to the surface native material from a casing with an open bottom. While the fine material is almost entirely washed out of formation samples collected by the jet-percussion method, it does provide a more reliable sample than a straight jetted well where the formation material that is washed to the surface is not contained by a casing. Multiple small-diameter wells installed by either driving or jetting have been developed into well fields for many purposes, including municipal supplies. Such development can supply large quantities of water where there is a shallow aquifer with

[1] Anon., "Wells," U.S. Army Technical Manual TM-5-297, 1957.
[2] Gordan, Raymond W., "Water Well Drilling with Cable Tools," Bucyrus Erie Co., 1958.
[3] "Ground Water and Wells," Edward E. Johnson, Inc., 1966.

an extensive watershed area and a water table within a few feet of the surface of the ground. The wells are usually connected to a common suction header. Pumping from a well field through a suction header depends upon the amount of vacuum maintained in the system. Such an installation is practical only where the water surface is within 15 to 20 ft of the ground surface. Pumping units may be placed at a lower elevation within reasonable limitations to compensate for a deeper water surface.

Deep wells and high-capacity wells for municipal, irrigation, or industrial use are installed by several different methods, depending upon the character of the material penetrated and the locality. Some of the important methods for installing such wells are described below.

The *standard or cable-tool method* is used for wells 4 to 12 in. in diameter through both earth and rock to depths sometimes exceeding 5,000 ft, and under certain circumstances larger-diameter wells have been installed by this method. Drilling by the cable-tool percussion method is accomplished by utilizing a four-part string of drill tools consisting of a drill bit, drill stem, drilling jars, and a rope socket. The string of tools is suspended in the hole from a cable which is attached at the upper end to a walking beam which is the principal distinguishing feature of a cable-tool drilling rig. The action of the walking beam alternately lifts and drops the string of tools, breaking and mixing the material in the drill hole into small fragments for subsequent bailing. Various designs of bailers are employed according to driller preference and the character of the material to be removed from the drill hole. When the well is to be completed in consolidated rock, the drill hole is carried into the rock a few feet, at which point a casing is installed and sealed or cemented to the rock. After the installation of the casing, the drilling is continued to the depth desired. Regardless of the drilling method employed, it is desirable to grout or otherwise seal off water-bearing strata containing water of unsatisfactory quality. Water-bearing strata encountered in a consolidated rock well may be either cased, sealed, or screened, depending upon the quality and quantity of water available from the particular stratum.

If the aquifer is of loose granular materials, drilling and bailing are done through a casing which is installed in the borehole as the work progresses. In the case of municipal wells where sanitary precautions are important, a larger-diameter outside casing is installed to a depth of at least 20 ft. The space between this outside casing and the well casing is grouted as a sanitary seal and the outside casing is removed during the grouting process. Well construction may include an artificial gravel packing between the screen and native material, or the screen may be in direct contact with the native material of the aquifer. Gravel-packing techniques and design are further discussed later in this section. When gravel packing is not used, normal well completion is accomplished by lowering the screen to the bottom of the casing, which is then withdrawn sufficiently to expose the screen. The fines in the native material surrounding the screen are then removed by a surging and pumping action, termed well development, to produce a sand-free well and reduce hydraulic-head losses in the native material adjacent to the screen.

The California or stovepipe method is used for wells 6 to 38 in. in diameter through earth or alluvial deposits. The casing consists of two sizes of lap-riveted or welded steel cylinders, one of which just fits over the other, the joints of the outer cylinders butting at the mid-points of the inner cylinders. The cylinders are usually made 4 ft long and of 12- to 8-gage steel, 8-gage being used for diameters greater than 20 in. The casing is forced down by means of hydraulic jacks, the casing being fitted with a drive pipe and starter shoe at the bottom. As the casing is forced down, the material within is excavated by standard methods or by means of a mud scow alternately raised and dropped.

When the well has been driven through the aquifer to impervious material, the casing is perforated for the depth of the aquifer by a specially designed tool. Stovepipe casing cannot be pulled back for setting screens. If it is desired to set a screen at the bottom, the stovepipe casing must be stopped at the level proposed for the top of the screen. The screen is then lowered through the casing to the bottom and is sunk into position by bailing the material from within the screen.

The *hydraulic rotary method* is now in general use in areas where the formations are of unconsolidated sand and clay. A hollow drill rod driving a hollow drill is rotated and lowered into the hole, while a slurry composed of water and native or commercial clay (driller's mud) is pumped through the drill rod into the hole. The mud plasters the side of the hole and seals the pores, preventing the leakage of the pumped water out into the formation. The velocity of the rising slurry is kept high enough to lift the cuttings to the surface, while the mud which is plastered into the sides of the hole combined with the lateral pressure of the slurry in the hole prevents caving of the walls while the casing is being placed.

It is possible with this method to set 2,000 or 3,000 ft of casing without the necessity of reducing the diameter. Bores 10 to 60 in. in diameter have been constructed. The larger diameters are sometimes drilled by first sinking a small hole and then reaming to large size.

The small rotary hole may be a part of a test program in which 6- or 8-in.-diameter uncased holes are initially installed and electrically logged to provide information on underground stratification. Samples of the native material may be taken through the drill rod. The small-diameter holes may be cased and screened for observation wells or for other test purposes. During the process of boring, samples of the native material may be collected. Samples collected in this manner are suspect, since the drilling mud is mixed with the sample and may mask the presence of thin clay layers in the underground formation.

It is generally advisable to provide a separate screen of appropriate design for the aquifer formation. While well development is an important part of construction regardless of the method employed, it is especially important with the hydraulic rotary method. The driller's mud used to seal the face of the borehole during construction must be effectively removed to provide an efficient well. Different development procedures are necessitated by the design incorporated into the construction of different well screens. Well-screen manufacturers generally publish detailed development procedures applicable to the type of screen that they manufacture.

The *reverse rotary method* of well drilling is generally considered to be the fastest and most practical means of drilling large-diameter holes in unconsolidated formations. The flow of drilling fluid, as the name implies, is in the reverse direction when compared with the conventional rotary method. The subsurface material loosened by the bit is carried to the surface through a drill pipe which is generally 6 in. in diameter. The circulation of the drilling fluid is normally maintained between 500 and 1,000 gpm by the use of a large-capacity suction pump or by an air lift. The relatively high velocity of the fluid in the drill pipe enables the cuttings to be carried to the surface without the deliberate use of clay or other additives to increase viscosity. The boring is done without a casing and hydrostatic pressure is used to support the walls of the borehole during construction. This hydrostatic pressure is provided by maintaining a water level in the borehole at least 6 ft above the natural level. A greater differential is desirable. Before the drilling fluid is returned to the well, it is passed through a settling pit which is normally constructed three times the volume of the material expected to be removed from the borehole. While the settling pit does not remove all the fine excavated material, the recirculated water does not seal the sides of the borehole with a mud cake as is done when the hydraulic rotary method is used. While a relatively clean borehole may necessitate a large volume of make-up water to maintain the required hydrostatic pressure, it does allow the well to be completed with only a minimum of development work.

Caisson wells are relatively shallow large-diameter wells, sometimes installed where it is desired to obtain water from a rather thin water-bearing stratum probably less than 35 ft below ground surface. As the caisson is sunk, material within it is removed mechanically rather than hydraulically. Openings to allow the entrance of water are generally sized according to information obtained from previously installed test wells.

A common method of installing wells and boreholes is through the use of an *earth auger*. A continuous-flight spiral auger 4 to 6 in. in diameter is often used for exploratory work. In general, auger holes are practical only where fairly stable soil material, not subject to caving, is present. When saturated sand is encountered, the continuous-spiral auger is unable to carry the material to the surface, and if it is desired to complete a well in such a material, it is necessary to jet the screens into place. Where an auger is used for large-well installations, the boring is accomplished by a bucket-like device with auger-type cutting blades on the bottom. Difficulties with this are also experienced when saturated sands are encountered. Some success in completing wells with the bucket auger has been achieved by keeping the borehole full of water. A casing is often installed where difficulties are encountered and the well is completed, utilizing other methods. This method is not normally used in areas where cobbles or boulders would be expected. Auger boring is one of the cheapest and fastest methods of boring where favorable conditions prevail.

9. Gravel-packed Wells.[1] The gravel-packed well is a popular and very important facility for obtaining groundwater, usually from unconfined aquifers. Gravel-developed wells are sometimes erroneously referred to as gravel-packed wells. Gravel-developed wells do not have an artificially graded and placed gravel packing, but utilize the natural gravel deposits from which the fine materials are removed by intermittent pumping, surging, and backwashing so that an envelope of natural gravel surrounds the well screen. A variation of the gravel-developed well is sometimes constructed by feeding graded gravel to the aquifer through feed pipes alongside the casing while the well is being pumped and surged. This method provides little control over the thickness, depth, or shape of the so-called gravel packing.

Large important wells in unconsolidated sand and gravel are now frequently of the gravel-wall type. They may be constructed by the California, the cable-tool, the hydraulic rotary, or the reverse rotary method. If the California or cable-tool method is used, a large conductor pipe or caisson 6 to 12 in. larger than the well casing is first sunk down to the full depth of the well. Gravel, which must be selected on the basis of the size and grading of the material in the aquifer,[2] is then fed into the annular space between the inner and outer casing, usually by the use of a tremie. See Fig. 7 for grading of gravel pack, as developed by Mogg.

As the depth of gravel is increased, the outer casing is pulled back to expose the gravel wall to the native formation. The steps of feeding more gravel and pulling back the outer casing are repeated until the gravel is well above the elevation selected for the top of the screen. The addition of gravel is sometimes continued until the surface of the ground is reached and sometimes to a point about 20 ft below the ground surface. Whichever method is followed, provision must be made for adding additional gravel, since some settlement of the gravel will occur as the well is being developed. A concrete seal should be placed around the outer casing to a depth of about 20 ft to seal off the well from the entrance of surface drainage.

The well screen is telescoped into the inner casing and the casing is withdrawn to expose the screen to the gravel wall. The top of the screen is usually swaged to the

[1] AWWA Standards for Deep Wells, 1958.
[2] Mogg, Technical Aspects of Gravel Well Construction, *J. NEWWA*, **77**, 1963.

casing by means of a lead packer. Development of the well is carried out by pumping and surging until the contact surface between the gravel wall and the native formation is thoroughly cleansed and the fines removed.

The well-screen opening is selected as the size which will retain 90 percent of the gravel pack. The grading of the gravel shown in Fig. 7 would call for a screen slot size of 0.020 in.

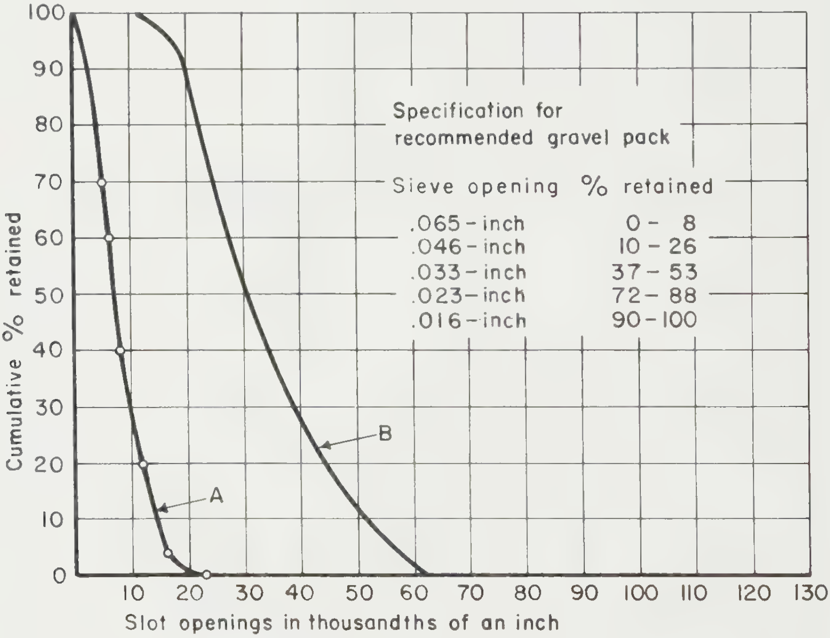

FIG. 7. The steps in the design of a gravel-packed well.

Gravel-developed Wells. When the natural gravel is in contact with the well screen, it is desirable to develop the well by various means to remove the finer particles from the formation. When a well is constructed in this manner, the well-screen opening is selected as the 40 percent retained size of the aquifer material. The development of the well will bring the finer portion of the material through the screen to be pumped out, leaving a more desirable coarser packing around the well screen.

The literature on well design exhibits a diversity of opinion on the importance of the open area and the entrance velocity of water entering the well screen.

Walton[1] suggests that well design should take into account the coefficient of permeability of the aquifer for establishing optimum screen entrance velocities.

10. Groundwater Recharge.[2] The natural supply of groundwater is sometimes increased by artificial recharging by means of spreading the water on the surface of the ground, oftentimes in diked areas; storing the water in reservoirs, basins, and pits; or discharging it into recharge wells. In some areas, notably Long Island, New York, it is common practice to collect storm-water runoff in seepage pits in an attempt to prevent too great a depletion of groundwater resources. Furthermore, many states

[1] *Op. cit.*

[2] BAUMANN, *Proc. ASCE, J. Hydraulics Div.*, **155,** November, 1961.

require that well water used for cooling and air conditioning be returned to the ground.[1]

The hydraulics of recharge wells are much different and more complex than the hydraulics of water wells. In a horizontal aquifer, the shape of the cone of depression of a water well remains unchanged under conditions of a constant rate of withdrawal and stabilization of the water level. On the other hand, the cone of impression of a recharge well, which is concave upward, continues to become flatter, even at a constant rate of recharge, because of the displacement of the native water as the recharge water enters the aquifer. Accepting the hypothesis that the recharge water moves radially from the recharge well in the form of a wave, its movement may cause the water level in an observation well remote from the recharge well to rise long before the recharge water itself reaches the observation well. The wave effect is an aid in reducing the ill effects of saline or other undesirable waters in areas where recharge is necessary.

In an inclined aquifer, a recharge well can reach an equilibrium, theoretically, in infinite time. A point of stagnation is reached upstream of the well, while the boundaries on the downstream side approach two asymptotes, as shown in Fig. 8. Spacing of the recharge wells is important where the prevention of saline-water intrusion is a factor, because the saline water could flow between the cones of impression, if the spacing is greater than W, as shown in Fig. 8.

Considerable study has been made of the creation of fresh-water barriers, particularly along the southern California coast. The relationship of the elevation of salt water along the coast to the elevation of fresh water above sea level was discovered prior to 1900 by Ghyben and Herzberg working independently along the European coast. The hydrostatic equilibrium between the two fluids of different densities led to the development of the equation

$$h_s = \frac{p_f}{p_s - p_f} h_f$$

where h_s is the depth below sea level to the salt-water interface, h_f is the head of fresh water above sea level, p_s is the density of salt water, and p_f the fresh-water density. This is known as the *Ghyben-Herzberg principle.* If the density of salt water is 1.025 and the fresh-water density is 1.000,

$$h_s = \frac{1.000}{1.025 - 1.000} h_f = 40h_f$$

The salt-water interface, therefore, will be at a depth below sea level of forty times the elevation of the fresh water above sea level.

Rates of infiltration in groundwater recharge vary widely. A Task Group of the American Water Works Association[2] reported in 1963 that in seven states, basin infiltration ranged from 0.1 to 170 ft per day, while injection wells varied from 58 to 660 gpm. The presence of salt, microscopic organisms, or other foreign material may cause clogging and reduce the rate of infiltration; the formation of air bubbles may also reduce infiltration by air binding.

The use of fresh-water barriers, created by groundwater recharge to prevent sea-water intrusion, is practiced extensively on the seacoast in southern California. It has been found there that the sea water intrudes inland in the form of a wedge. The fresh-water barrier, therefore, should be far enough inland to force all the wedge back seaward. Otherwise, the fresh water will separate the wedge and force the landward edge still farther inland, creating a saline wave.

A dispersion zone and the dynamics of groundwater flow in coastal areas cause a

[1] Task Group Report, *J. AWWA*, **48**, 493, 1956.
[2] Artificial Ground-water Recharge, Task Group Report, *J. AWWA*, **55**, 707, 1963.

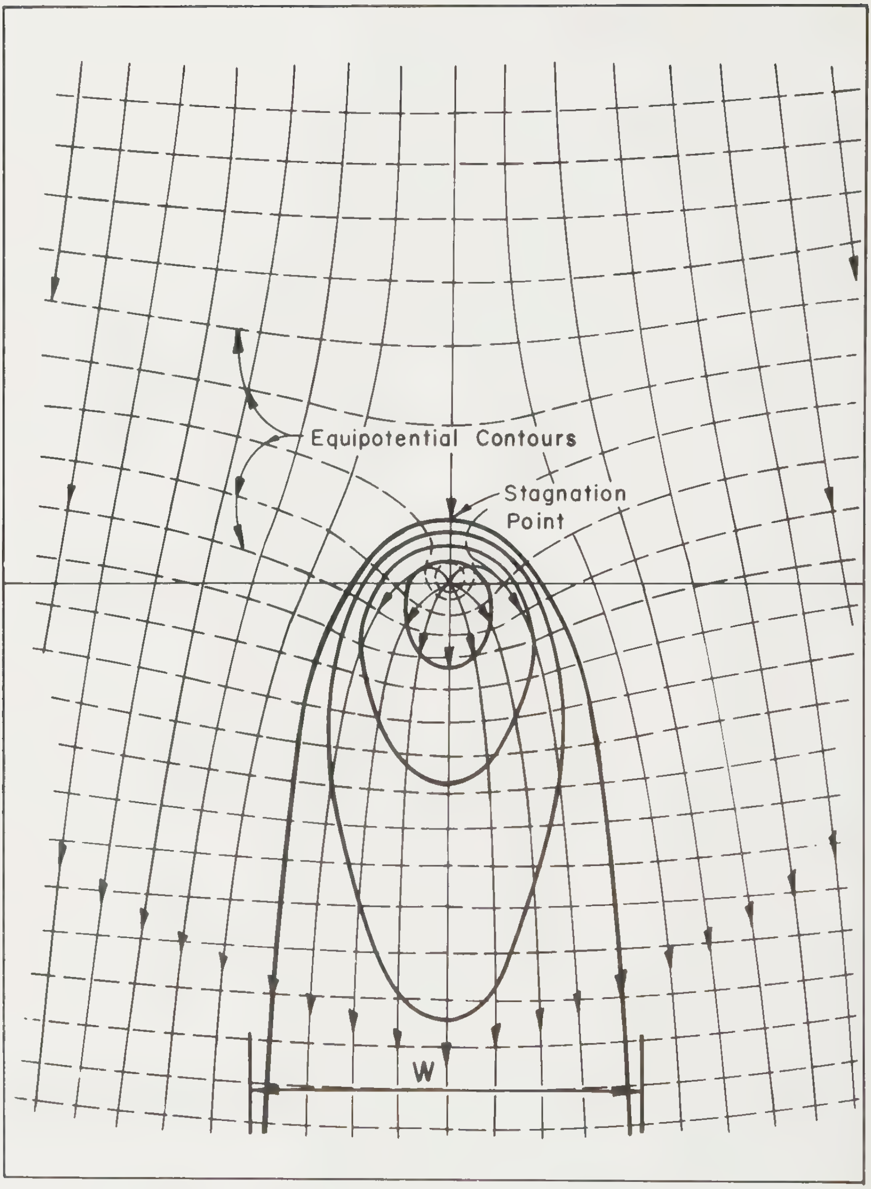

Fig. 8. Recharge through well in open, inclined aquifer.

variance for the location of the interface between fresh and salt water from what would be expected by a strict application of Ghyben-Herzberg. De Wiest[1] and others discuss various approaches by which these aspects are involved in coastal areas.

11. Sanitary Precautions. Wells should be so located as not to be subject to sur-

[1] De Wiest, "Geohydrology," John Wiley & Sons, Inc., New York, 1965.

face drainage of floodwater and seepage from cesspools, privies, and sewers. A minimum distance from sources of pollution of 50 to 100 ft or more is sometimes specified, but it must be kept in mind that the effectiveness of removal of polluting matter from seeping water depends upon the character of the formation through which the water percolates as well as the length of the path. The importance of safeguards against contamination cannot be overemphasized. Many cases of typhoid and other intestinal diseases have been traced to polluted well supplies. No toxic materials, chemical compounds, or petroleum products should be stored in or on the ground in the vicinity of the well, unless all precautions are taken to prevent seepage into the ground. All sewers in the vicinity should be of watertight construction. Garbage and refuse-disposal areas should not be located on the watershed of a well. Salt-storage piles for highway-maintenance purposes should also be kept off the watershed, and a highway drainage system which may contain salt and other objectionable materials should discharge at locations where the well-water quality will not be impaired.

In order to minimize the possibility of pollution and to protect the well casing against exterior corrosion, at least a portion of the casing should be sealed with concrete or cement grout. Materials, methods, and procedures in grouting and sealing wells are covered in the 1958 revision of the Standard for Deep Wells[1] prepared by the Water Works Practice Committee of the American Water Works Association. The top of a well should be sealed against the possibility of contamination from the surface, and the top of the well or pump-house floor should be drained away from the well. Before a well is placed in service, it is desirable to disinfect it by chlorination. Procedures and methods of disinfection of wells are also covered in the Standard for Deep Wells.[1]

12. Well Pumps. Driven-well fields are usually pumped by horizontal centrifugal pumps, equipped with a sand catcher on the main suction pipe. The maximum total suction lift of these pumps, which includes elevation and friction losses, should not exceed 25 ft. Pumps of this type should be self-priming or primed by the installation of air aspirators, auxiliary vacuum pumps, or foot valves.

Deep-well pumps suitable for varying uses are (1) air-lift pumps, (2) reciprocating pumps, (3) jet pumps, and (4) vertical centrifugal pumps. Small-bore deep wells are pumped by air lifts or by reciprocating deep-well pumps. Large deep wells are usually pumped by deep-well turbine pumps.

Because of the expense of maintenance and limited capacity, reciprocating pumps are not used widely. Overall efficiency from motor input to water delivered is about 65 percent. The plunger pump with a given size cylinder will pump at a constant rate regardless of variation in total head. Pumps of this type are normally made for capacities up to 300 gpm and operate at heads up to 800 ft.

The efficiency for air-lift pumps ranges from 20 to 35 percent. These pumps have the advantage of having no moving parts below ground. However, the disadvantage of low efficiency coupled with the pump's inability to pump against high-head requirements has limited its use. Air lifts are adapted to crooked wells, to wells discharging large amounts of sand, and to installations where reliability is of more importance than efficiency. Capacities for well pumping range from 20 to 2,000 gpm.

Jet pumps are limited in capacity with an average range from 5 to 70 gpm and a maximum lift of approximately 150 ft.[2] These pumps can be used in deep wells when the depth of water to be raised, by suction lift, exceeds the absolute vapor pressure of the liquid. A jet pump consists of a pump and a jet. Water is recirculated from the discharge pipe of the pump to the bottom of the suction pipe and discharged through a

[1] AWWA Standard 100.
[2] Hubbell, *J. AWWA*, **43**, 455, 1951.

jet-type nozzle. The water from the nozzle creates a partial vacuum at this point. Additional water is pulled in from the well by this vacuum and is then pushed up the pipe leading to the intake of the pump. The advantage of the jet pump over most other types of deep-well pumps is that the pump and motor may be set away from the well. A jet pump, used in conjunction with a centrifugal pump at ground level, can be lowered into the well shaft. These jet pumps can be used in multistage where the suction lift becomes very large. This combination will lift water 200 ft, compared with 15 to 25 ft for the centrifugal pump alone.

The vertical turbine pump is most widely used for well pumping. For large-diameter wells, these pumps have been used to capacities exceeding 7,000 gpm and pumping heads of 1,000 ft. Overall efficiencies for turbine pumps range from about 50 percent for the small installations to above 80 percent for large pumps. This type of pump has the advantages of high efficiency, high-head pumping capability, and excellent serviceability. The pump when running at constant speed requires less horsepower to operate as the head increases and the flow decreases. The impellers are always submerged, and no special priming equipment is required as with horizontal pumps. The impellers can be obtained semiopen or fully enclosed. Open impellers can be adjusted from the top of the line shaft. This will prevent sand clogging and permits about a 25 percent variation of the pump capacity. Enclosed impellers usually provide higher sustained efficiencies and general stability but no variation in pump capacity. A multistage, deep-well turbine pump is simply a special arrangement of pump bowls or casings in series, usually with a radial-type runner.

The submersible vertical turbine pump is a type of construction that has the motor as well as the pump submerged. A waterproof cable supplies power to the motor. This type of pump has advantages in (1) extremely deep wells which may present problems with shafting, especially if the well is crooked; (2) installations subject to surface flooding which may be damaging to electric motors; (3) applications such as booster pumps that are in locations that require quiet operation; and (4) installations where there is little or no floor space to install the unit.

13. Groundwater Models and Computers. Both analog and digital computers are now being used in groundwater studies. One of the major problems in management of groundwater is the prediction of future changes in water level in the aquifer as water continues to be pumped. Various patterns of pumping can be analyzed. Determinations as to the economic safe yield of a basin being pumped over a period of years can be made. The maximum safe yield of a single well pumped over an extended period can also be computed. The most economical spacing of wells to provide a maximum amount of water at the lowest pumping cost can be estimated. Also, an estimate can be made of how long the water stored in the basin can last if sustained large-scale pumping is undertaken.[1] The accuracy of the results obtained from these studies depends mainly upon the quantity and quality of data collected to define the aquifer. The three major characteristics which must be defined are first, the size and shape of the drainage basin; second, the storage coefficient of the basin; and third, the coefficient of transmissibility of the aquifer.

Models for simulating the aquifer system are designed for the analog computer, by utilizing the basic laws and continuity relationships of laminar flow and electrical flow. The flow of electric current is expressed by Ohm's law. Electric networks can be set up to simulate three-dimensional flow which will satisfy Laplace's equation. Analog computers have been used to study groundwater basins, in both steady and unsteady flow. Most of the formations and flow conditions can be represented by appropriate circuits.

The electrical model is constructed in a shape similar to that of the actual aquifer

[1] *U.S. Geol. Surv. Circ.* 468.

system. The thickness of the aquifer and the properties of water storage and transmittal are represented by electrical properties. By the use of oscilloscopes, drawdown curves can be plotted during the period of pumping. The scales of the graph on the oscilloscope screen can be read directly in feet of change of the water level and in days, months, years, or any unit of time that is desired. Various patterns and rates of pumping are tried and their effects are measured. With this model, it is possible to analyze quickly the effects of pumping over a long period of time. From this information, the best patterns of water development for a particular aquifer can be determined.

Large quantities of data for a drainage basin may be compiled through numerous groundwater investigations. These data can be stored easily on punch cards and magnetic tapes. With the aid of these data mathematical models can be set up to represent a given basin. The aquifer data may be identified by a two-dimension grid system. A mathematical groundwater model is an expression that describes the aquifer functioning. Finite-difference equations describing these functions may be solved by the digital computer.

Variability in the aquifer creates no problem provided the data distribution represents continuous smooth functions. This approach allows great flexibility for changes in the coefficients of transmissibility and storage; recharging and discharging of various areas; gains and losses of water due to interaquifer leakage; and confined and unconfined aquifers.

SECTION 36

WATER SUPPLIES

By Thomas R. Camp and Joseph C. Lawler

The treatment of the subject of water supplies in Secs. 35 to 38 is limited to the material that is not dealt with elsewhere in this book in detail. Such duplication as does appear is due to the desirability of emphasizing differences in practice and differences in factors controlling the methods of design.

WATER CONSUMPTION

1. Uses of Water. The uses of water are generally classified as domestic, commercial, industrial, public, and agricultural. Domestic use includes all water used in and around residences. The amount of domestic consumption varies with the standard of living but is proportional to the resident population. Commercial use includes water used in business or commercial districts by persons who are not residents of the district. Commercial use is itinerant domestic and light manufacturing use and cannot be stated conveniently in terms of the population of a business district. Such use is often best estimated in terms of the floor area of the buildings in the district. Industrial use is for manufacturing purposes, and the amount of such use bears no relation to the population of an industrial district. Public use of water is for fire fighting, street and sewer flushing, and for unmetered public buildings. Waste due to leakage and other causes, frequently a substantial portion of the total supply, is sometimes classed as public use. Agricultural use is for irrigation purposes. Such use is very important for municipal supplies when great quantities of water are used for lawn sprinkling.

A research project on residential water use conducted by the Johns Hopkins University, Baltimore, Md., from 1959 to 1963 showed the tremendous impact that lawn sprinkling has on water-supply systems. Table 1 demonstrates that lot size is the predominant factor in sprinkling demands.

2. Per Capita Consumption. The average per capita consumption for a waterworks is the total consumption for a year divided by the population and the number of days in the year. Sometimes the average per capita consumption is based upon the population of the community and sometimes upon the number of consumers. The population and number of consumers may differ greatly in some cities.

The average consumption in the United States varies from about 50 to as high as 500 or more U.S. gal per capita per day (gpcpd) with a mean value for the whole country of about 150. In strictly residential communities, the consumption is usually less than 100 gpcpd; but it is higher, the higher the standard of living. Some of the factors affecting the amount of consumption are climate, class of consumer, industrial use, quality of water, pressure in the distribution system, cost of water, sewer facilities, and extent of metering of consumers' services. For a given city, the per capita consumption usually increases as the population increases.

The quantity of water required for strictly domestic use in residential communities of the United States ranges from about 30 gpcpd for lower-class districts to about 115 gpcpd for high-class districts. These figures do not take into account necessary

Table 1. Residential Water-use Data*

Net lot size	Consumption for given period, gal/day/dwelling unit			Ratios	
	Avg annual	Max day	Peak hr	Max day to avg annual	Peak hr to avg annual
Domestic Water-use Data (Sprinkling Use Not Included)					
1,100	144	183	490	1.2	3.40
7,000	187	213	414	1.14	2.21
7,600	214	250	565	1.17	2.64
28,000	202	290	860	1.44	4.26
Sprinkling-use Data (Domestic Use Not Included)					
1,100	12	67	303	5.58	25.2
7,000	40	470	1,120	11.8	28.0
7,600	49	880	2,080	18.0	42.5
28,000	130	1,180	3,900	9.08	30.0

* Geyer, J. C., J. B. Wolff, and L. P. Linaweaver, "Report on Phase One of the Residential Water Use Research Project," Department of Sanitary Engineering and Water Resources, The Johns Hopkins University, Baltimore, October, 1963.

public use of water in residential areas which amounts to 5 to 10 gpcpd and leakage or water unaccounted for which amounts to 20 to 30 percent of the quantity delivered to the system.

The quantity of water required for commercial and industrial use bears no relation to the population. In large American cities, the amount of commercial and industrial consumption has been estimated at 15 to 65 percent of the total consumption.

A study by the Senate Select Committee on National Water Resources of the 86th Congress, 2d Session (1960) estimated that the water requirements of the municipal water systems in the United States would be 28,588 million gal daily by 1980 and 42,543 mgd by the year 2000. Tables 2 and 3 prepared by that committee compare the municipal water requirements with the estimated requirements of other major water users.

Table 2. Requirements of Principal Water Users in the United States

	Millions gal daily	
	1980	2000
Agriculture	167,166	184,230
Mining	2,672	3,391
Manufacture	101,556	229,207
Steam-electric generation	258,895	429,408
Municipal	28,588	42,543
Total	558,877	888,779

TABLE 3. ESTIMATED REQUIREMENTS OF PRINCIPAL WATER-USING INDUSTRIES

	Millions gal daily		
	1959	1980	2000
Iron and steel	9,600	18,750	22,300
Chemical	8,800	22,000	52,900
Pulp and paper	5,870	14,400	28,700
Food	1,728	2,325	2,740
Aluminum	764	1,810	3,120
Copper	134	214	268

3. Fluctuations in Demand. Fluctuations in per capita consumption from day to day and throughout any one day are of great importance in design.

The average consumption per day based upon a year's record is referred to as the average daily consumption. The maximum consumption during any one day in the year is called the maximum daily or the maximum 24-hr consumption. The peak consumption during any moment of the year, excluding fire drafts, is called the peak

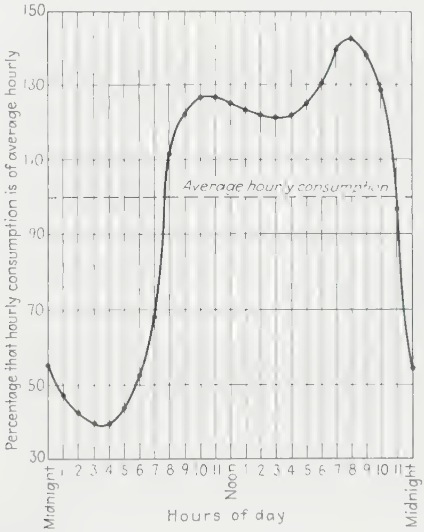

FIG. 1. Typical hourly variations on days of large consumption.

or maximum hourly consumption. Similarly, the minimum consumption during any one day is called the minimum daily or minimum 24-hr consumption; and the lowest momentary rate of consumption during the year is called the extreme minimum or minimum hourly consumption.

The use of water during summer months for sprinkling lawns and gardens and for air conditioning causes demands for water which are of considerable magnitude. It was reported[1] in 1958 that in five large water systems in the United States, special

[1] Task Group Report: Study of Domestic Water Use, *J. AWWA*, **50**, 1408-1418, 1958.

summer loads attributed to lawn sprinkling, air conditioning, and refrigeration caused demands on peak days to be 39 to 77 percent above corresponding days when those loads did not occur. Those percentages corresponded to additional demand rates of 140 to 277 gpcd. In that same study, the maximum hourly draft rates in those five systems were from 37 to 70 percent of the maximum day rate for lawn sprinkling and 22 to 32 percent of the maximum day rate for air conditioning.

The maximum daily consumption ranges from 125 to 250 percent of the average daily consumption, with an average ratio for the whole country of 175 percent. For cities of more than 100,000 population, the average ratio is 150 percent (Table 4).

In general, it may be said that fluctuations are greatest in smaller cities, but the local factors affecting the demand are much more important than size of community. In estimating future demands for a city, it is not safe to neglect local factors.

Fluctuations in demand below the average are in general much less than fluctuations above the average. The extreme minimum draft is never zero even for the smallest system, as there is always some leakage or waste.

TABLE 4. VARIATIONS IN RATES AND DEMAND*
Percent of annual average

	Less than 100,000 population	More than 100,000 population
Max:		
Month	120–150	110–130
Day	150–250	125–175
Hour	300 400	200–300

* BABBITT, H. E., J. J. DOLAND, and J. L. CLEASBY, "Water Supply Engineering," 6th ed., p. 10, McGraw-Hill Book Company, New York, 1962.

The hourly variations of consumption on the days of large demand are of importance in design inasmuch as these variations affect the storage requirements in distribution and filtered water reservoirs. A typical curve of hourly fluctuations is shown in Fig. 1. The fluctuations will be greater than shown in Fig. 1 for small communities and less for larger municipalities.

4. Fire Demand. The quantity of water used for fire fighting in relation to the total consumption for the year is negligible, but the heavy demands for brief periods of time during fires greatly influence the design of distribution systems and storage reservoirs. The rate of fire flow for the entire system indicated by the American Insurance Association (formerly the National Board of Fire Underwriters[1]) is given by the following empirical formula:

$$Q = 1{,}020\sqrt{P}\,(1 - 0.01\sqrt{P}) \tag{1}$$

in which Q is the rate of fire flow in U.S. gpm, and P the population in thousands. The formula is applicable to populations up to 200,000, in which case 12,000 gpm is required. For populations greater than 200,000, an additional flow of 2,000 to 8,000 gpm is required for a second fire.

The Association recommends that sufficient water be available to sustain the fire flow and the maximum daily flow for at least 4 hr for a population of 1,000, 5 hr for 1,500, 6 hr for 2,000, 7 hr for 3,000, 8 hr for 4,000, 9 hr for 5,000, and 10 hr for a population of 6,000 or more.

Usual practice in determining fire flows for municipalities is to use the above

[1] "Standard Schedule for Grading Cities and Towns of the United States with Reference to Their Fire Defenses and Physical Conditions," National Board of Fire Underwriters, 1956.

formula as a guide but to make the actual determination of required fire flow on the basis of character and congestion of buildings. In some cases the required flows so determined will differ materially from that computed by Eq. (1).

Distribution systems should be so designed as to make it possible to concentrate the fire flow given by the preceding equation at any point in the high-value commercial or industrial areas of the city at a time when the normal draft is equal to the maximum daily consumption. In residential districts, according to the Underwriters:

"The required fire flow depends upon the character and congestion of the buildings. Sections where buildings are small and of low height and with about one-third of the lots in a block built upon require not less than 500 gpm; with larger or higher buildings, up to 1,000 gpm is required, and where the district is closely built, or buildings approach the dimensions of hotels or high-value residences, 1,500 to 3,000 gpm is required with up to 6,000 gpm in densely built sections of 3-story buildings."

Table 5. Water Consumption for Typical Large Fires

City, date	Population nearest U.S. census	NBFU requirements			Actual use		
		Fire flow, gpm	Duration, hr	Extra water, million gal	Fire flow, gpm	Duration, hr	Extra water, million gal
Salem, Mass.,* June 25–26, 1914	43,697	6,000	10	3.6	15,000	13	16
Fall River, Mass.,* Feb. 2–3, 1928	115,274	10,000	10	6	18,000	12	20
Nashua, N.H.,* May 4–5, 1930	31,463	5,000	10	3	6,500	19	5
Norfolk, Va.,* June 7, 1931	129,710	10,000	10	6	8,500	14	3.6
Chicago, Ill.,† May 19–21, 1934	3,376,438	20,000	10	12	70,000	56	69.5
Cambridge, Mass., 1965	107,716	10,000	10	6	8,000		

* Mowry, Water Consumption during Fires, *J. NEWWA*, **46,** 93, 1932.
† Gayton, The Chicago Stock Yards Fire, May 19, 1934, *J. AWWA*, **27,** 803, 1935.

The water used for fighting several typical conflagrations is shown in Table 5 with the duration of each fire and the maximum fire flow. For comparison, the requirements of the National Board of Fire Underwriters are also given. In all but one of the examples, the maximum fire flow and quantity of water used exceeded the Underwriters' standards.

5. Forecasting Demand. As a preliminary to the design of waterworks or extensions to an existing plant, it is necessary to estimate future demands and agree upon one or more suitable *design periods*. The design period for a large water supply which requires many years to complete may be more than 50 years. The design period may be only 10 years for pumps, filter units, and other items that may be added with facility in a short time or that have short lives or high rates of obsolescence.

Demands are estimated from the per capita consumption and the population, due account being taken of industrial and commercial use and fire demand. For extensions to distribution systems, population density is an important factor. Zoning regulations tend to stabilize population densities and hence to increase the reliability of estimates of future population density.

Table 6 contains the rates of flow, exclusive of fire flow, which may be of importance in the design of water facilities.

Table 6. Discharge Table for Waterworks Design

	Extreme min consumption	Min daily consumption	Average daily consumption	Max daily consumption	Peak consumption
Beginning of design period	*A*	*B*	*C*		
End of design period	. .	. .	*D*	*E*	*F*

For a system provided with no storage, facilities must be provided for all rates of flow from *A* to *F* in the table and in addition thereto for the fire flow. If elevated storage is provided for hourly fluctuations in demand, pumps and filters may operate at constant rates during any one day. In this case, items *B* to *E* are significant for design. The average daily consumption is of importance in estimating costs of operation.

6. Population Estimates. The prediction of future population is at best only a guess. The accuracy of the prediction if done intelligently is greatest with large populations and small periods of forecast. The normal growth curve of cities of large population is one of increasing rate of growth for a time followed by a decreasing rate of growth.

Table 7 shows estimates which have been made of the ranges of population which might be expected in the United States up to the year 2000.[1]

Table 7. Population Estimates
Population in millions

	1970	1980	2000
Low	201	224.9	266.7
Middle	207	243.8	329.3
High	221.9	277.6	430.8

The best basis upon which to estimate future population trends of a community is its past development. If the curve of population up to the present time is comparatively smooth and no major changes in the factors affecting population growth are anticipated, the curve may be projected into the future. If the city is free to extend its boundaries, there is no way of knowing whether the rate of growth during the design period will continue at approximately the present rate, will decrease, or will increase. In a particular case, the probability of boundary extensions and the effect of such extensions on the population may be taken into account in projecting the curve. The extent to which a given area is built up should be considered in estimating the future population growth of that area. Curve *A* of Fig. 2 is a straight-line projection of the growth curve of Milwaukee from 1910. The actual population of the city in 1920, 1930, 1940, 1950, and 1960 is shown by crosses.

The projected growth curve of a community may be estimated by comparison with the past growth of other cities. The past growth curves of the cities selected for the comparison should be somewhat similar to the growth curve of the community prior to the time when their populations were the same as the present population of the community. This similarity being the case, it is assumed that their growths subsequent

[1] Senate Select Committee on Water Resources Activities in the United States, 86th Congress, 2d Session, Committee Print No. 5.

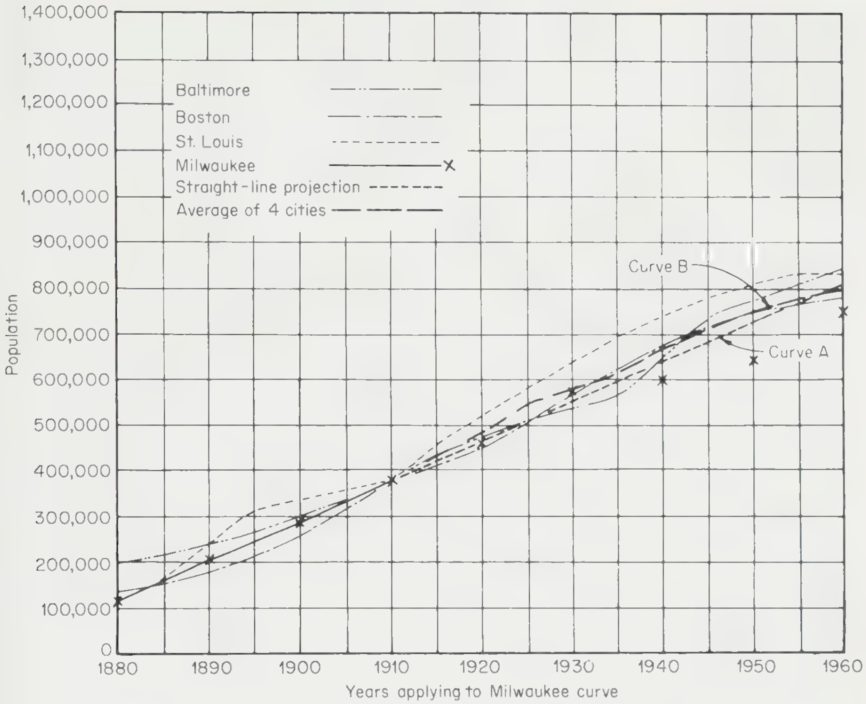

Fig. 2. Forecast of population for Milwaukee.

to this time will be an indication of the trends to be expected in the future growth of the community. Curve *B* of Fig. 2 is a projected growth curve of Milwaukee from 1910 determined by this method.

The density of population for whole cities varies in the United States from less than 10 to about 80 persons per acre.[1] The density of population varies widely, however, from district to district within a city. The density in a high-class residential district fully built up may be less than five persons per acre, depending upon the size of the lots. In a middle-class residential district, fully built up with single-family houses, the density will be 15 to 30 persons per acre. In a densely built-up residential area consisting of two-family houses and six-family apartment buildings, the density will be 30 to 100 persons per acre.[2] In districts built up with five- and six-story apartment buildings, the density will run from about 300 persons per acre for high-class apartments to 1,000 persons per acre for tenements. The population density in industrial and mercantile districts will usually be 10 to 30 persons per acre. The preceding figures are for fully built-up districts. They take into account the area occupied by streets and alleys but do not account for parks, lakes, and cemeteries.

In order to estimate the future population of a portion of a city or district, the character of occupancy and degree of population saturation must be taken into account. Such estimates are essential to the design of distribution works. For very small areas, say 25 acres or less, it is unsafe to estimate future populations at less than

[1] Metcalf and Eddy, "American Sewerage Practice," Vol. I, p. 186, McGraw-Hill Book Company, New York, 1928.

[2] Babbitt, "Sewerage and Sewage Treatment," p. 29, John Wiley & Sons, Inc., New York, 1940.

the saturation values even for short design periods. For larger areas, the degree of population saturation will decrease as the size of the area increases. If the character of the various districts in a city is controlled by zoning regulations, estimates of future population density will be much more reliable than if no such regulations exist. Even for a city with a zoning ordinance, the growth rate of small areas within the city is so difficult to predict that for design purposes higher growth rates should usually be assumed than for the city as a whole. The smaller the area of the district, the higher should be the assumed growth rate.

SOURCES OF WATER SUPPLY

7. Classification. Water supplies are classified as *surface* and *groundwater supplies.* Surface supplies may be divided into two groups: class *a*, those from large rivers or lakes which must be pumped into the distribution systems, and class *b*, those from smaller upland streams which require storage reservoirs and aqueducts or pipelines for delivery, usually by gravity, to the distribution systems. *Groundwater supplies* are obtained from wells, springs, and filter galleries.

In 1963, there were about 17,000 public water-supply systems in the United States serving 146 million people. About three-fourths of these people are served by surface supplies and the remainder by public groundwater supplies. Some 50 million persons, or approximately 26 percent of the total population, use private well supplies.

8. Reliability of Source of Supply. An important consideration in the selection of a new source of water supply is its reliability. A new supply should be capable of furnishing an adequate quantity of water continuously with a minimum danger of interruption due to breakdown or other causes.

The relative order of reliability[1] from the standpoint of quantity of water is substantially as follows:

1. A supply from a practically inexhaustible source distributed to and throughout the city by gravity
2. A gravity source of supply that is inadequate at times and therefore requires storage reservoirs
3. A never-failing source that requires pumping
4. A source of supply that requires both storage reservoirs and pumping

9. Effects of Source of Supply upon Water Quality. The quality of water is determined by its content of living organisms and by its content of mineral and organic matter. Living organisms may be present in suspension and in colloidal dispersion. Mineral and organic matter may be in solution, in colloidal dispersion, and in suspension. Practically all the foreign matter in water is collected as the water flows over the surface of the ground or through the soil and rocks. Rainwater is saturated with the gases of the atmosphere, but it contains few other impurities except in areas where the atmosphere is charged with smoke, industrial fumes, or dust.

Water that flows over the surface of the ground collects silt and particles of organic matter in suspension. A small portion of these materials will go into solution. Surface waters also contain bacteria from the topsoil and other microorganisms and aquatic life which feeds upon the organic matter in the water. If pesticides are used on the watershed, toxic material may also be present. If the watershed is inhabited, the water may contain industrial wastes and sewage together with the living organisms and disease germs which are associated with such wastes.

Water that percolates through the soil or rocks dissolves the more soluble of the

[1] Babbitt, H. E., J. J. Doland, and J. L. Cleasby, "Water Supply Engineering," 6th ed., p. 581, McGraw-Hill Book Company, New York, 1962. National Board of Fire Underwriters, Standard Schedule for Grading Cities and Towns, 1930.

minerals with which it comes in contact. The quantity of such minerals held in solution depends upon their abundance in the soil and the amount of carbon dioxide dissolved in the water. Most of the carbon dioxide in groundwaters is obtained from the topsoils in which this gas is continuously being generated by bacterial action. Groundwater is practically free from suspended matter, for such material is effectively strained out in the pores of the soil. Groundwater is usually free from sewage and industrial wastes but may contain traces of wastes and some bacteria if they are free to percolate through crevices or large soil pores to the groundwater near wells or springs.

Water from surface supplies is a mixture of surface runoff and groundwater. The quantity of dissolved substances in surface waters depends upon the relative content of groundwater as well as the solubility of the substances with which the water has come in contact. River waters of the class *a* group tend to be turbid, sometimes colored, and are usually polluted with sewage and industrial wastes. Lake waters of the class *a* group are usually clearer than river waters but are also subject to pollution. Waters of the class *b* group are usually quite clear and pure and are suitable in their natural state for human consumption. They are, however, subject to pollution from transient population and cannot be considered safe without protective measures. The protection may be by regulation of the watershed by patrolling and placarding, by closing it entirely to public trespass, or by treating the water.

When surface waters are stored in impounding reservoirs, their quality is usually changed considerably. The first and most noticeable effect is the clarification of the water due to the settling of suspended particles. Color is also reduced owing to bleaching by sunlight and the coagulation and settling of colloidal color particles. From the standpoint of safety of the water for drinking purposes, storage results in a reduction of the bacteria, particularly pathogenic organisms. Storage of 1 to 2 months will render a water practically free from typhoid bacilli if they are present in the inflowing water. The extent to which these improvements in quality take place is dependent principally upon the length of the storage period.

The impounding of surface waters also results in impairments to their quality which are particularly troublesome in new reservoirs. Bacterial decomposition of the organic matter on the floor of the reservoir is accompanied by a depletion of the dissolved oxygen in the water and the formation of carbon dioxide. The corrosiveness of the water is increased by the carbon dioxide, and it also causes the solution of deleterious minerals such as iron and manganese and the hardness-producing minerals calcium and magnesium from the soil of the reservoir floor. The extent to which these changes take place depends upon the amount of organic matter available for decomposition on the reservoir floor and the character of the mineral matter in the soil and rocks.

If the reservoir is deep enough so that wave action is insufficient to destroy the stratification of the water because of temperature and consequent density variations, the carbon dioxide content will be greatest at the bottom and the oxygen content least. The variation in chemical composition with depth is accompanied by a variation in the character and numbers of microorganisms. In regions where the water temperature passes through that of maximum water density (4 C) in the spring and fall, turnovers occur in deep reservoirs which mix the water from top to bottom and stir up the bottom sediment. During these turnover periods, which last from a few days to several weeks, the water is of poor quality.

During periods of high rainfall, the total amount of suspended matter in surface waters increases because of soil erosion. The concentration of suspended matter in runoff from heavily wooded watersheds may decrease with increase in runoff, but both concentration and total amount of suspended matter will increase with the runoff from cultivated and deforested watersheds. During periods of drought, the concentration of dissolved minerals in surface waters increases. Powell[1] shows an increase in the hardness of the Delaware River water due to low runoff at one point of as much as fivefold.

The quality of groundwater from a given source is not affected greatly by rainfall, and the mineral content changes only slightly from season to season. This is particularly true of deep-well supplies. The quality of groundwater is affected by its abundance. Where the water is plentiful, it is usually not excessively hard; where it is sparse, it is likely to be highly mineralized. Most deep-well and artesian supplies are quite hard. Most shallow-well waters are relatively soft. They are also more subject to dilution and interchange with surface runoff and are therefore more likely to be polluted and infected than are deep-well waters.

Dissolved mineral matter has little effect upon the potability of water. It is a serious economic factor, however, for other domestic and many industrial uses. The average hardness of surface- and groundwater supplies and the iron content of groundwaters of the United States are given by Powell in the 1934 Report of the National Resources Board. Figures 3*a*, *b*, and *c* summarize more recent information on the hardness, dissolved solids, and iron content of finished waters in the United States.[2]

SURFACE-WATER SUPPLIES

10. Yield. The quantity of water that may be drawn continuously from a stream or lake depends upon the area of the watershed, the topography, vegetation, rainfall, climate, and amount of storage. The maximum quantity of water that may be drawn continuously after deducting losses due to evaporation from the proposed reservoir surface, leakage through and under dams, and necessary withdrawals for riparian owners downstream is called the *safe yield.* The estimated safe yield must exceed the estimated future demand if a proposed water supply is to be adequate.

The safe yield of a source of supply can be estimated only from records of the past. The most reliable information from which to predict yield is a hydrograph of the stream for a long period of years at the location of the proposed intake or dam. The hydrograph should be of sufficient duration to include a period of extreme drought. If no such hydrograph exists, it is necessary to supply equivalent data by adjusting hydrographs made at other points nearby or by computing runoff from rainfall records. The methods that may be used for estimating runoff are described in Sec. 1. Surface supplies are more frequently taken from small upland streams than from large rivers both because of the superior quality of the water and because of the savings to be had in pumping costs. Hydrographs are seldom available for the smaller streams, although rainfall records are usually available at nearby stations. Hence, the computation of runoff from watersheds by means of the rainfall-loss method is more commonly desirable for water supplies than for water-power projects.

If the minimum runoff from a watershed is insufficient to satisfy the estimated demand but the average runoff over a period including the driest period of record is more than sufficient, the demand can be met by the construction of one or more impounding reservoirs. The methods of estimating the amount of storage necessary to provide or, conversely, the safe yield from a watershed having a given reservoir capacity are described in Sec. 4.

A mass curve showing accumulated net runoff throughout a period of extreme drought may be constructed from the hydrograph and studied to determine the relation of storage volume to safe yield. A comprehensive report[3] of the yield of drainage areas in New England was made by the Committee on Yield of Drainage

[1] Report of National Resources Board, Dec. 1, 1934, p. 313.
[2] Quality of Water Furnished Cities in the United States, U.S. Geological Survey, February, 1959.
[3] *J. NEWWA*, December, 1914.

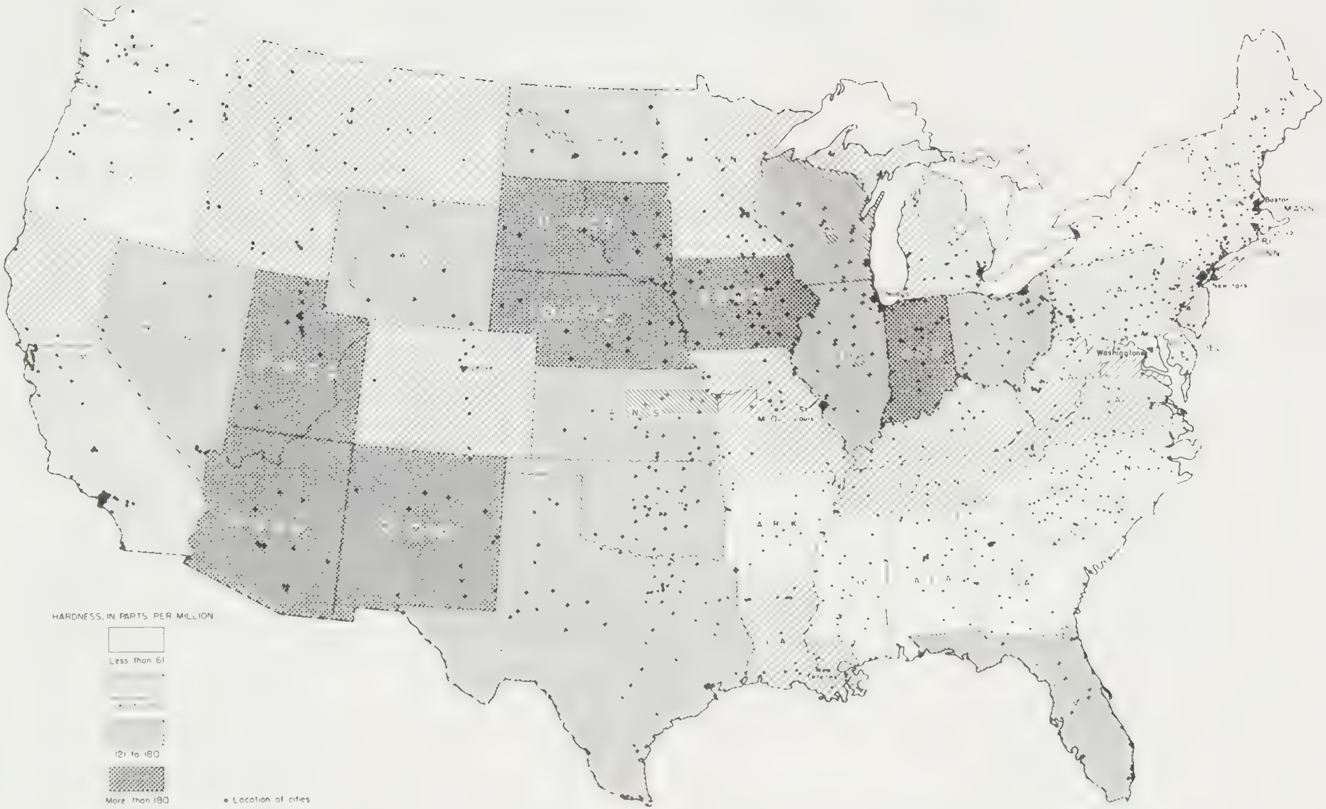

FIG. 3a. Weighted average hardness, by states, of finished water from public supplies.

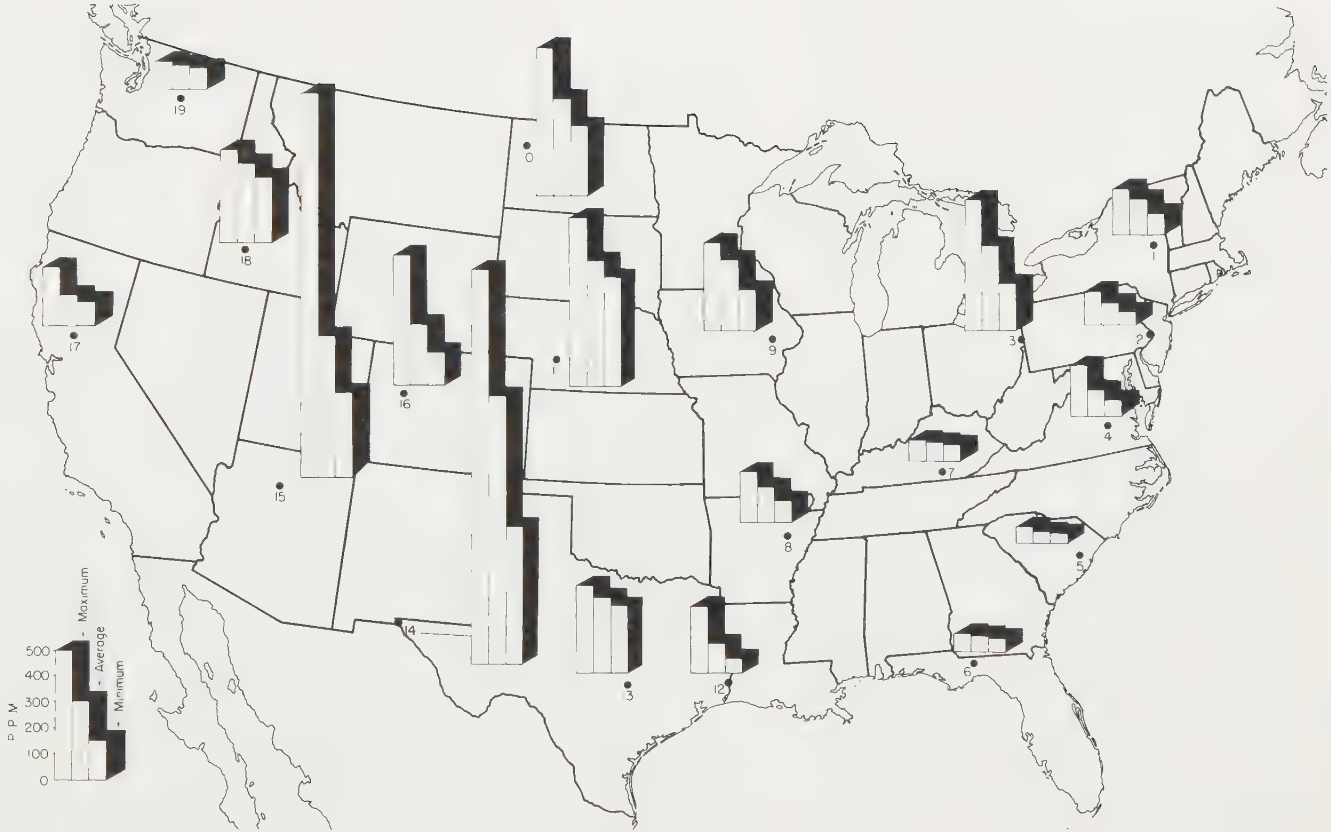

FIG. 3b. Range in dissolved solids in surface waters in the United States.

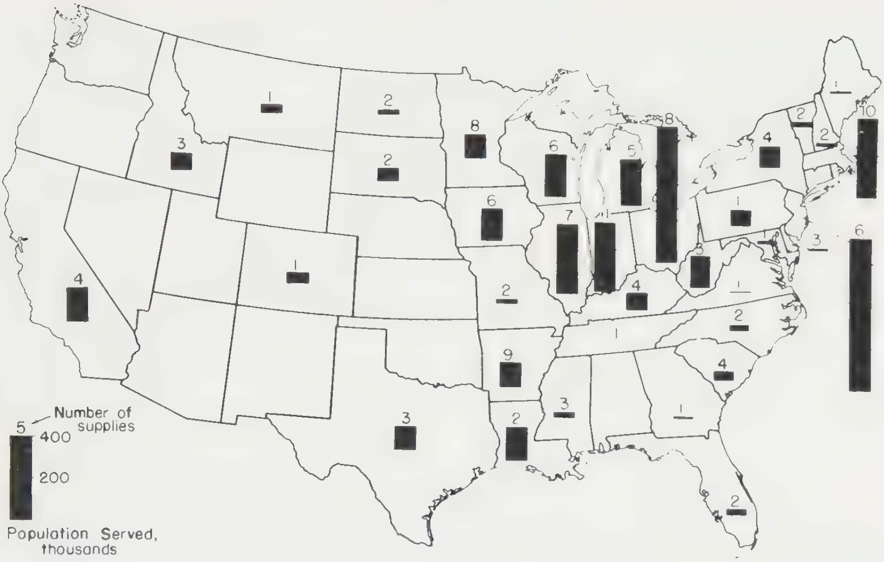

FIG. 3c. Iron in excess of 0.30 ppm in 1,157 public water supplies of the United States, 1952.

Areas of the New England Water Works Association for the extreme drought which started in June, 1908. The Committee on Rainfall and Yield of Watersheds in New England in its second[1] (1940) and third[1] (1941) progress reports studied the yields in the light of subsequent records and presented curves of safe yield for various amounts of storage and water surface area. Figure 4 shows average curves based on the 1941 composite curve of the NEWWA Committee.

11. Selection of Sites for Impounding Reservoirs. The proper location of an impounding reservoir for a water supply is determined primarily by the existence of

[1] *J. NEWWA*, September, 1945, pp. 285 and 310.

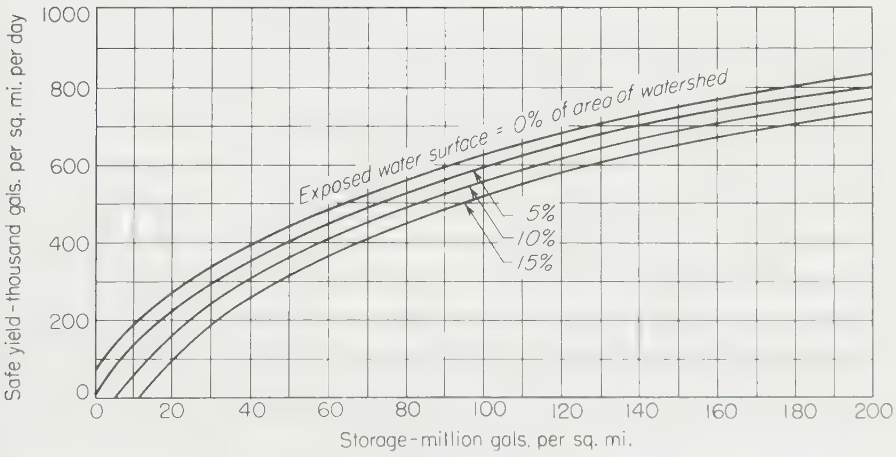

FIG. 4. Safe yield of watersheds in New England.

suitable damsites. It is also influenced by the quality of the water that may be had from the reservoir, the size of the watershed, and the distance of the reservoir from and its elevation with relation to the point of distribution. To be acceptable, a proposed reservoir site should have a tributary drainage area which, with the storage capacity it is possible to impound, will produce a satisfactory yield. Moreover, it should be possible to construct the works and supply water of acceptable quality to the city at less cost than from another available site.

A reservoir site that is capable of supplying pure water that may be distributed with little or no treatment is ordinarily preferable to a proposed supply that will require continuous treatment, other factors being equal. It should be noted, however, that water-quality requirements are becoming so exacting and the difficulties in the prevention of pollution are so great that few supplies will be both safe and satisfactory for future American communities without some kind of treatment. Many supplies that have been selected because no treatment was thought necessary will in the future require treatment plants. Such problems as taste and odor control, correction of corrosiveness, reduction of iron and manganese content, and reduction of color, which arise occasionally in the operation of nearly all waterworks reservoirs, are difficult to meet without filtration plants.

The density and distribution of population upon a watershed are important factors with regard to pollution and possible infection of the supply. A watershed containing scattered dwellings located at some distance from the main streams is obviously preferable to one upon which there are sewered municipalities and industries. Regional planning of water resources resulting in the early selection of future reservoir sites is desirable. Population and industrial development on the watersheds can thus be better controlled.

Waters from streams in limestone regions are not so desirable as water from a catchment area in a noncalcareous region because of hardness. It is desirable that a watershed should be free from considerable amounts of swampland. Swamps contribute to high color in the water and also produce extensive growths of microorganisms which may occasionally seed the reservoir. Hilly drainage areas with considerable farmland are undesirable because they produce water high in turbidity during heavy rainfall.

The shape of a proposed reservoir should not be favorable to short-circuiting of runoff to the intake. Narrow reservoirs with their major axes in the direction of the prevailing winds are subject to this danger. Large reservoirs with storage capacity for a year or more are not so subject to troubles from microorganisms as small ones. If the banks of the reservoir are steep and the water is deep around the edge, fluctuations in water level will have little effect upon the water quality. If large portions of the reservoir are so shallow, however, that they are uncovered by the lowering of the water surface and are subsequently submerged, difficulties are likely to ensue from decaying vegetable matter, color, and microorganisms.

The amount of storage to provide at a given reservoir site depends upon the height to which the dam can be built economically, the storage required for the desired yield, the capacity of the watershed to replenish the reservoir following droughts, and sometimes the effect of volume of storage and fluctuations in reservoir level on the water quality. It is frequently cheaper to build more than one reservoir on a watershed than to store the required volume of water behind a single dam. In this case, the intake is usually located at the lower reservoir, and only during dry periods is this reservoir replenished by opening gates in the upper dams.

If a reservoir is constructed with too much capacity, the watershed may be incapable of filling it and of delivering water to the city at the same time. It is desirable, however, to have sufficient capacity so that it will never be necessary to draw the water level too low during a drought. The water remaining in a reservoir after the level has been drawn down severely is usually high in color, microorganisms, and carbon dioxide. Moreover, the actual time of storage is so low that short-circuiting may occur during freshets.

12. Preparation of Reservoir Sites. The site of a proposed reservoir should be cleared of all trees and brush, and a marginal strip around the water's edge should be grubbed. This marginal strip should extend above the high water level and to some depth below the average water level. If funds are available, it may be desirable to riprap the steeper banks in order to prevent the growth of weeds and water plants and to protect the banks from erosion due to wave action.

Plants that grow around the water's edge with their roots submerged, sometimes to depths of 20 ft below the water surface, may impart tastes and odors[1] to the water. It is usually too expensive to riprap all the areas upon which such growths will develop. Areas that are too shallow and are subject to exposure when the water level is lowered should be filled in or stripped of fertile topsoil to prevent growths. Sand or gravel is best for filling as clay will impart turbidity to the water. If the expense of preventing weed growths is too great, weeds that cause trouble may be killed after the reservoir is in operation by lowering the water level to expose the roots. The dead weeds may then be burned off and removed.

Swampy areas on the reservoir site should be excavated and the muck removed. If this is too expensive, the deposits may be covered with gravel or sand. All habitations on the site should be destroyed and removed. Barnyards, privies, and cesspools should be cleaned and manure piles removed.

It was formerly considered good practice to strip or remove the top layer of soil from the entire reservoir area in order to eliminate organic matter subject to bacterial decomposition. This policy was inaugurated by the late Desmond FitzGerald for the Boston water supply after exhaustive studies. The Wachusett Reservoir, constructed about 1900, was thoroughly stripped. The advantage of stripping is that a clean basin for storing water is provided immediately. Experience indicates that after 10 or 15 years the quality of the water is about the same whether the reservoir was stripped or not. The great expense for stripping is not usually justified today, since the money can better be spent for adequate purification works which will usually be required in the future in any event.

For other details with regard to the construction and operation of reservoirs, see Sec. 4.

13. Watershed Control. In addition to the cleaning up of the reservoir site itself, it is desirable to remove possible sources of pollution and contamination on the watershed. In order to accomplish this, it is frequently necessary to purchase the property upon which such sources of contamination exist. Future control of the watershed is best effected by ownership of the entire area. When complete ownership is too expensive or otherwise impractical, marginal strips around the reservoir and other strategic areas including principal tributary streams may be acquired.

All habitations upon these marginal areas should be removed, and farmlands and other deforested lands should be planted to trees. Evergreens are superior to deciduous trees for this purpose, because they contribute less color to the water, because leaves from deciduous trees frequently blow into the water, and because there is less transpiration from evergreen trees than from deciduous trees. Reforestation of the areas contiguous to reservoirs is advantageous in several respects. It reduces the amount of silt and clay that would otherwise be washed into the reservoir, and it also results in retarding runoff and thus reduces flood flows. The shading provided by evergreen trees during the winter months also retards the snowmelt and slows the

[1] Arnold, Weed Growths in Reservoirs, *J. AWWA*, **27**, 1684, 1935.

rapidity of runoff without excessive evaporation losses. Many water-supply agencies have established a forest-management program on their watersheds and realize a substantial income by selected cutting of mature evergreen trees.

A water-supply agency must supply its consumers with a safe and palatable water. To this end, the American Water Works Association adopted the following statement of policy on the recreational use of domestic water-supply reservoirs (a statement adopted by the Board of Directors on Jan. 26, 1958, and revised Jan. 25, 1965):

"Reservoirs may be classified as:

"1. Equalizing reservoirs—reservoirs within the area served and delivering finished water ready for consumption to the distribution system.

"2. Terminal reservoirs—areas providing end storage of water prior to treatment.

"3. Upstream reservoirs—reservoirs providing storage of untreated water at various points in the watershed to provide or supplement the supply at the terminal.

"4. Multipurpose reservoirs—reservoirs constructed for purposes in addition to the supply of domestic water, over which the water purveyor does not have complete control.

"*Equalizing and Terminal Reservoirs.* Policy: It is considered generally that recreational use of equalizing and terminal reservoirs and the adjacent marginal lands is inimical to the basic function of furnishing a safe and potable water supply to the system's customers and should be prohibited.

"*Upstream Reservoirs.* Impounded or stored water in upstream reservoirs can be classed in three categories:

"Class A: Water derived from an uninhabited or sparsely inhabited area, at or near the point of rainfall or snow melt collected in a storage reservoir, clean and clear enough to be distributed to the consumers with disinfection only.

"Policy: Safe practice in the water works field recognizes the necessity of permitting no recreational activity on the water and watershed lands in and about such storage reservoirs.

"Class B: Water impounded from an area not heavily inhabited and allowed to flow from storage in a natural stream to the point of withdrawal and requiring treatment in varying degree in addition to disinfection.

"Policy: Limited recreational activities on such reservoirs and adjacent lands are considered permissible under appropriate sanitary regulations.

"Class C: Water which has flowed in a natural stream before storage for a considerable distance, having received polluting materials from municipalities, industries, or agricultural areas; confined in a reservoir primarily for purposes of storage until such time as low stream flow makes the stored water necessary for the use of the downstream city; and later allowed to flow from the reservoir to the tributary water works in an open stream accessible to the public; and requiring complete treatment.

"Policy: Recreation is considered permissible under appropriate sanitary regulations. The determination of the kind and extent of recreational use shall be the sole responsibility of the water works executive of the system involved, whose primary obligation it is to provide a safe and potable water, and subject only to existing police powers.

"*Multipurpose Reservoirs.*

"Policy: Recreation normally will be permitted. Water withdrawn from multipurpose reservoirs for domestic water supply purposes shall be given the same complete treatment as those waters derived from polluted sources.

"*Summary.* The American Water Works Association registers its opposition to legislation permitting or requiring the opening of domestic water supply reservoirs and adjacent lands to recreational use. Control of water supply reservoirs must remain the prerogative of the water purveyor."

Inasmuch as the most desirable watersheds have in general already been developed and controlled for public water-supply purposes and since demands for recreational uses are increasing, it is quite apparent that there will be more and more multiple use of water-supply reservoirs. With the exception of equalizing and terminal reservoirs, recreational activities can be permitted on public water-supply reservoir watersheds without hazard to public health if adequate water-treatment facilities are provided and particularly so if waters used for recreational activities can be diverted from equalizing or terminal reservoirs during the recreational seasons. Flood-control reservoirs, when designed for the specific purpose, can be used for water-supply purposes. Hydroelectric plants can be built at dams on water-supply reservoirs for another multiple use with no health hazard.

The use of pesticides on public water-supply watersheds to control the growth of undesirable animals, insects, or plants is a real health hazard to water consumers. The major pesticide compounds used most extensively on watersheds are aldrin-toxaphene and DDT, both chlorinated hydrocarbons, and parathion and methyl parathion, which are organic phosphorus compounds. The evaluation of the hazard of using any pesticide on a public water-supply watershed must be based on toxicity persistence and exposure;[1] toxicity being the amount that can be tolerated by a human being over a specific time period, persistence being the length of time the compound remains in its basic state, and exposure the dosage per unit area with relation to runoff.

The sanitary quality of the water can be protected to some extent by the enforcement of the regulations established by health departments. These regulations usually prohibit direct acts of pollution and set distances limiting the proximity of sources of pollution to the streams and reservoirs. Methods of enforcement include the posting of the regulations at points on the watershed and patrolling and policing the watershed.

14. Dams. Descriptions of types of dams, spillways, and other appurtenances and methods of design are given in Secs. 8 to 23. Certain features of intakes and outlet works that are peculiar to waterworks are discussed in the following article.

In the design of spillways for water-supply dams, the flood flow per square mile of drainage area desirable to provide for is usually greater than for water-power projects because so many water supplies are taken from small mountain streams. The records of floods in many parts of the world indicate the possibility in almost any location of runoffs in excess of 2,000 cfs/sq mile for catchment areas less than 10 sq miles. Some excessive floods have exceeded 4,000 cfs/sq mile on even larger catchment areas. Corrections for storage above the spillway crest during flood flows will reduce the discharge passing over the spillway. In the selection of the maximum spillway head and the length of the spillway, consideration should be given to the effect of fluctuations in water level upon the quality of the water.

15. Intakes. Intake structures for surface supplies consist of some form of conduit with protective works and screens at the open end and gates or valves for regulating the flow. In the location and design of intake works, both reliability of operation and water quality are important considerations. The factors that influence reliability and the quality of the water at the intake differ with the character of the body of water from which the supply is taken. Four general classes of intakes may be differentiated as follows:

1. Intakes in large rivers
2. Intakes in small streams requiring diversion dams
3. Intakes in large shallow lakes or reservoirs
4. Intakes in large deep lakes or reservoirs

Intakes in large rivers should be so located that the ports are submerged at all stages of the river to a sufficient depth to avoid trouble with ice cakes or floating

[1] Taylor, Watershed Sanitation, *J. NEWWA*, **78**, 1964.

debris and to preclude the entraining of air. The ports should also be several feet above the bottom of the stream so that sand and gravel being transported on the bottom will not be drawn into the intake. In order to meet these requirements, it is often necessary to locate the intake in the deepest part of the stream and away from the shore, particularly if the river is subject to large fluctuations in stage. Under these conditions, the water must be conveyed from the intake to the shore through a pipe laid in the river bottom or through a tunnel constructed under the bottom. Pipes laid in or on the river bottom should be securely anchored.

For small water supplies, submerged pipelines are usually used with some type of submerged crib or a screened bellmouth at the open end. For large supplies, tunnels are often required; and in this case, the intake itself must be of the exposed type in order that the intake shaft may be used in constructing the tunnel. Intake towers are usually constructed of masonry circular in plan or similar in shape to a bridge pier. The top of the masonry structure must be above the maximum high water, and the structure must be designed to withstand impact due to floating debris in times of flood. One or more chambers consisting of vertical shafts open at the top are provided in the interior of the structure which connect with the tunnel below. The intake ports are constructed through the walls of the structure to the interior chamber. The masonry structure is usually surmounted by an operating house. The intake ports should be provided with gates which are preferably mounted within the interior chamber. Screens may also be provided in the chamber, so that cleaning of the screens and operation of the gates may be performed by attendants within the operating house. At least one port and gate should be provided at the bottom of the interior chamber to be used for flushing sediment out of the chamber. If the intake is not too far out in the river, access to the tower from the shore should be provided by means of a bridge.

If the river stage does not fluctuate too much, it is sometimes possible to construct the intake on the shore of the river. The necessity for a tunnel or subaqueous pipeline is thus avoided, and the design of the intake structure is much simplified.

Most intakes in large rivers are so low with relation to the distribution system that pumping is required. The pumping stations are usually constructed on the river bank adjacent to the intake. The site should be on high ground which is accessible during flood stage for the bringing in of fuel and other supplies. The pumps must be placed so that the suction lift, including friction, is not more than 15 or 20 ft when the river is at its lowest stage. This requirement frequently necessitates the construction of very deep pump wells with the pumps located many feet below high water level. If the pumps are located in a dry well, as is usually the case with larger stations, the walls of the building must be made watertight to an elevation above the maximum flood stage. The walls and floor of the pump well must be designed to withstand the water pressure during flood stages, and the whole structure must be designed against flotation. In cases where the intake can be built at the bank of the river, it is sometimes economical and otherwise desirable to combine the intake and pump station in a single structure.

Intakes in small streams frequently require the construction of small diversion dams for the double purpose of providing a sufficient depth of water at all flows to divert water into the intake port and a settling period in order to reduce the turbidity of the water. A small period of quiescent flow will also permit suspended leaves and wood either to rise to the surface or to sink if they have become waterlogged; and it will also favor the formation of sheet ice in cold weather and thus reduce the difficulties from anchor and frazil ice. Supplies of this type are usually small gravity supplies located at some distance from the distribution systems. It is not usually feasible to keep an attendant at the intake or even to make daily inspections. It is therefore desirable to design the intake so that it will function reliably with a minimum of attention. Water from this class of supplies contains a great deal more suspended vegetable matter such as leaves, pine needles, moss, and twigs than does water from large rivers. The problem of screening is particularly important, therefore, especially in the autumn.

Both bar racks and mesh screens are frequently necessary with this type of intake, the former to protect the latter from heavy floating objects. The opening in bar racks when used alone cannot be made small enough for effective removal of small suspended particles. If hand raking is required, the racks should have a slope of 2 to 4 in. horizontal to 12 in. vertical, and a suitable raking platform should be provided above high water. The bars of the rack should be supported top and bottom at the downstream edge of the bars so that the tines of the rake may penetrate between the bars to the full depth of the bars.

Screens should have not less than two and sometimes as many as eight meshes to the inch, depending upon the character of the floating matter in the water. Screens

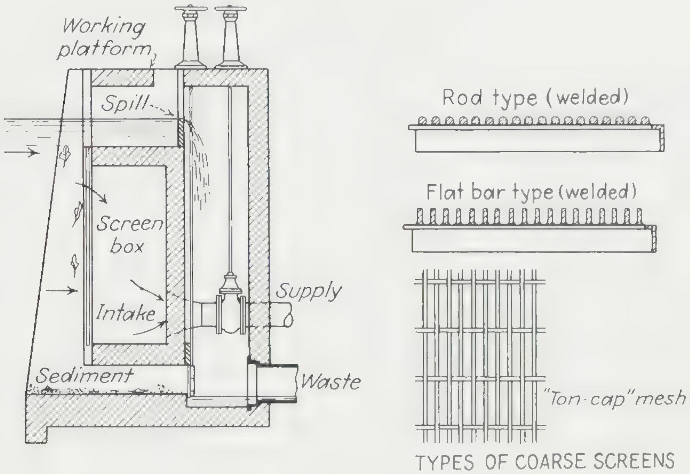

FIG. 5a. A small intake structure.

should be of corrosion-resistant metal, easily removable, and, if hand cleaning is necessary, provisions should be made for washing them with a hose stream. Manually operated screens should be installed in duplicate so that screening of the water may be continuous while a screen is being cleaned. Provision should also be made for sanitary disposal of the screenings and waste wash water. Low velocities and small openings are necessary to prevent the entrance of fish. Figure 5 shows some screen arrangements for small supplies proposed by Cunningham.[1] In Fig. 5*a*, the screen is placed vertically so that leaves drifting against the screen will tend to slide vertically upward or downward off the screen, the direction depending upon their density. In order to encourage this tendency toward self-cleansing, the velocity through the screen must be very low. In Fig. 5*b*, the drum screen revolves because of the water impinging upon the vanes and thereby throws the screenings off into the waste. A constant water level is necessary for the satisfactory operation of this screen. In Fig. 5*c*, the screen is ordinarily cleaned by washing it down with a hose stream, but if brushing is necessary the screen may be tilted as shown.

[1] CUNNINGHAM, Waterworks Intakes and the Screening of Water, *J. AWWA*, **23**, 258, 1931.

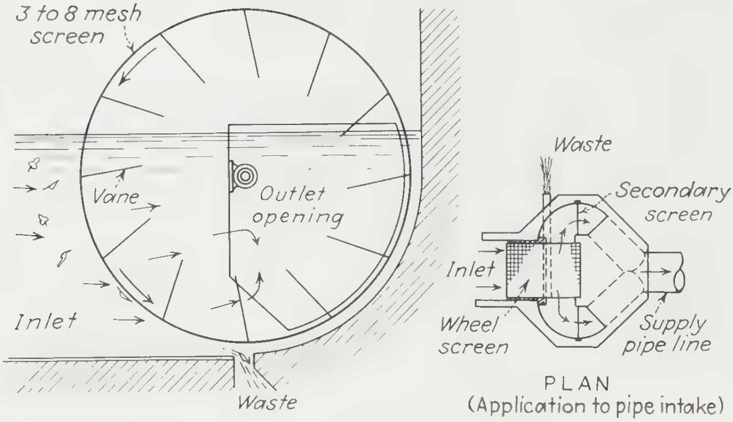

Fig. 5b. Self-cleaning leaf screen.

An unusual type of intake on a small stream is the Ware River intake[1] of the Boston Metropolitan Water Supply. Water is delivered from this intake through a vertical shaft 18 ft 8 in. in diameter to the Quabbin Aqueduct tunnel about 250 ft below. Water is taken into the shaft by means of nine automatic siphons having a maximum capacity of 3,100 cfs. The flow in the Ware River is allowed to pass downstream up to a maximum of 131 cfs, everything in excess of this amount up to the capacity of the intake being diverted during normal operation. The water level in the small reservoir is kept practically constant at 1.0 ft below the crest of the diversion dam, except when the streamflow exceeds the capacity of the works at which time water flows over the dam. Operation is entirely automatic.

Intakes in large lakes or reservoirs should be located in the deepest water economically available. In the case of large natural lakes, such as the Great Lakes, it is seldom feasible to locate an intake in water that is more than 30 or 40 ft deep because of the excessive distance of deep water from the shore. In large lakes, wind and convection

[1] Kennison, Boston Metropolitan Water Supply Extension, *J. NEWWA*, **48**, 147, 1934. Kennison, Ware River Intake Shaft and Diversion Works, *Civil Eng.*, August, 1934, p. 388.

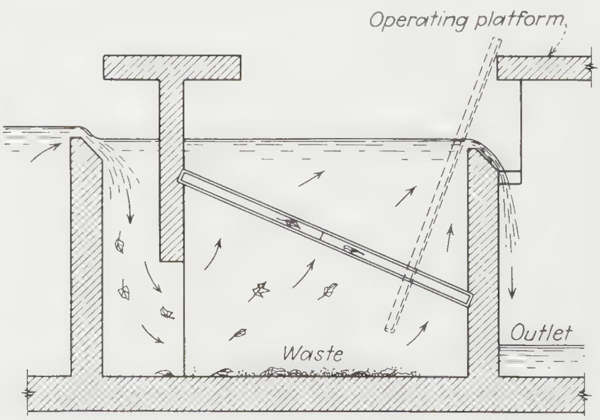

Fig. 5c. Upward flow screen for fine screening.

currents will keep the water circulated and mixed to depths as great as this. In large impounding reservoirs, however, the most desirable location for an intake is usually at or near the dam where greater depths can frequently be had. Moreover, impounding reservoirs are usually not so exposed to wind action as are large natural lakes, and the zone of circulation is therefore of less depth. Below the zone of circulation in a deep reservoir or lake is a small region of transition in which the temperature changes rapidly with depth, and below this region is a zone of stagnation in which there is very little circulation of water. In the bottom zone, the chemical and biological character of the water may vary considerably with depth.

Intakes in large shallow lakes are comparatively simple in design. If the supply is a small one, a subaqueous pipeline with a submerged crib or bellmouth at the open end may be used. Where ice is a major difficulty, the ports should be kept about 25 ft under the surface.

For large supplies such as for Chicago and Cleveland, exposed cribs several miles from shore are used. The location of the cribs is determined by the desired depth of the ports and the proximity of pollution.

The tunnel shaft is usually extended up into the interior chamber of the crib and equipped with screens at the top. The intake ports should be submerged about 25 ft and may be equipped on the inside, as at Buffalo, with gates. The crib should be surmounted with an operating house which should be provided with living quarters for the attendants and a boat landing. In Chicago, the crew consists of four men normally on each crib with two additional men in winter because of ice difficulties.

The design of Great Lakes cribs is controlled largely by the requirements of protection against storms and waves by ice difficulties. The large diameters are dictated by the necessity of stability during storms. Ice difficulties are minimized by placing the ports deep and keeping entrance velocities down to 3 or 4 in./sec. Vortices in the ports should be avoided if possible. Screens may have to be raised in winter to prevent clogging with frazil. Steam or compressed air may also be used to blow the ice from the screens. Dynamite charges of one-fourth to one-half stick have been used to dislodge ice from the crib ports. For some intakes, breakwaters have been constructed for protection.

Deep reservoirs should be provided with intakes or gate houses designed so that water may be taken at several different depths. The advantages of this provision are

1. Avoidance of microorganisms which live near the surface and require sunlight, many of which produce objectionable odors in water
2. Avoidance of surface water at too warm a temperature during the summer
3. Avoidance of too much turbidity during windstorms by drawing from the surface
4. Avoidance of troublesome plankton by drawing from a depth at which they are not prevalent
5. Avoidance of too much carbon dioxide by drawing near the surface
6. Reduction in the quantity of coagulant required by drawing bottom water high in iron
7. Avoidance of too much iron, manganese, color, and hardness by drawing near the surface

A common type of deep reservoir intake is in the form of a masonry tower exposed above the water surface and housed for the gate and screen hoisting machinery. In order that the tower may be in deep water, it is frequently necessary that it be some distance from the shore. Sometimes bridges are built from the shore or the dam to the intake, but if it is too far out boats are used by the operators. In order to make the tower accessible during all weather, it is sometimes built into the dam. If the dam is of earth, this procedure may require expensive retaining walls in order to provide a vertical face for the intake ports. Ports should be at two or three different levels, depending upon the water depth. Gates and screens should be inside the tower for protection. In important works, emergency gates or stop plank grooves should be provided in front of the sluice gates to permit the unwatering of the intake well for repair to service gates. It is also desirable, in order to increase reliability, that the intake well be divided into two parts equipped with duplicate gates, screens, and outlet pipe. The screens are commonly placed in an interior wall across the direction of flow. Blowoff gates and pipes should be provided at the bottom of the tower for flushing sediment out of the tower and silt from the reservoir around the base of the tower. Intakes of this type can usually be constructed in the dry, but the walls and gates must sometimes be designed to withstand very high pressures.

The use of large-diameter well screens installed so as to backwash them hydraulically has been successful for screening surface water in a number of installations.[1] Where ample headroom conditions are available, the screens are placed vertically because of the smaller horizontal area required; however, horizontal installations have been made where there are low overhead conditions.

16. Pipelines and Aqueducts. Descriptions of types of pipelines and aqueducts and methods of design are given in Secs. 5 to 7. For pipelines in distribution systems, see Sec. 37.

[1] *J. AWWA*, **50**, 1337, October, 1958.

SECTION 37

WATER DISTRIBUTION

By Thomas R. Camp and Joseph C. Lawler

The distribution system of a waterworks consists of the pipes, valves, hydrants, and appurtenances used for distributing the water; the elevated tanks and reservoirs used for fire protection and for equalizing pressures and pump discharges; and the consumer service pipes and meters. For administrative purposes, booster pump stations and treatment works located within the bounds of the distribution system are sometimes classed as distributing works.

A distribution system should be so designed that an adequate supply of water is available to the consumers and for fire protection at all times at a minimum of cost. It should also be so constructed and operated that the chances for contamination of the water after it has entered the system are reduced to a minimum. Since most distribution systems have developed with the growth of the community served, the problem of designing a complete new system seldom arises in the United States except for small towns. The principles involved in the design of a complete system may be employed in the design of extensions and reinforcing mains with modifications to suit each individual case.

The twofold function of distribution systems as designed in America requires (1) the relatively uniform distribution of water throughout the system for ordinary use, and (2) the concentration at any point in the system of high rates of flow for fire extinction. The investment[1] in the distributing system varies from over 90 percent of the total waterworks investment for small communities supplied from wells to about 40 percent for large cities; whereas the percentage of the cost of the distribution system chargeable to fire protection varies from about 60 for small towns to about 4 or less for large cities.

DESIGN OF PIPE DISTRIBUTION SYSTEMS

1. Pressure and Flow Requirements for Normal Consumption. The pressure required in the mains for normal domestic consumption depends upon the height of the buildings served directly without pumping within the building, the maximum instantaneous rate of flow through the house service pipes, and the friction losses in meters, house services, plumbing, and fixture outlets.

The maximum rate of flow through a house or building service pipe depends on the number and character of plumbing fixtures in simultaneous use. In a system containing many fixtures the load depends on the flow capacity of each fixture, the frequency of use, and the length of time involved in a single use of the fixture. The maximum flow required for adequate supply to a building by the theory of probability using "fixture units" is a basis for evaluation. A fixture unit is defined by Dr. Roy B. Hunter as "a factor so chosen that the load producing values of the different plumbing fixtures can be expressed approximately as multiples of that factor."

Fixture-unit ratings for estimating water-supply demands are shown in Table 1.[2]

[1] See "Water Works Practice," p. 297, American Water Works Association, 1929.

[2] Hunter, R. B., National Bureau of Standards—Building Materials and Structures Report BMS65, 1940.

Table 1. Fixture-unit Ratings for Estimating Water-supply Demands*

Fixture and Type of Installation†	No. of Fixture Units‡
Lavatory or washbasin:	
Public or office toilet	2
Private	1
Water-closet flush valve:	
Public or office toilet	10
Private	6
Water-closet flush tank:	
Public or office toilet	5
Private	3
Urinals, public or office toilets:	
Pedestal-urinal flush valve	10
Wall- or stall-urinal flush valve	5
Wall- or stall-urinal flush tank	3
Bathtub or separate shower head:	
Public or office	4
Private	2
Bathroom group, private:	
With flush-valve supply	8
With flush-tank supply	6
Separate shower head	2
Kitchen sink:	
Public, hotel, or restaurant	4
Private	2
Service sink§	3
Laundry trays (1 to 3) or combination fixture	3

* For supply outlets likely to impose a continuous demand when other fixtures are in extensive use, add the estimated continuous demand to the total demand for fixtures. For example, 5 gpm for a sill cock or hose connection is a liberal but not excessive allowance.

† Fixtures not listed in the table, if installed in relatively small numbers compared to the rated fixtures, may usually be safely ignored in estimating for the building main and large distributing branches. If installed in sufficiently large numbers to justify their consideration, they may be assigned fixture-unit ratings on the basis of a comparison with a rated fixture that uses water in similar quantities and at similar rates. For example, if washsinks or washtroughs with multiple supply outlets are to be installed, each supply outlet may be considered as comparable in demand to that of a washbasin in public service.

‡ The ratings given in the table are for the total hot- and cold-water demand. The engineer will need to exercise judgment in estimating separately for hot- and cold-water demands, depending to a large extent on conditions. The following are suggested as ample allowances under favorable conditions: For main hot-water branches allow three-fourths of the total fixture units as given by the table for all fixtures using hot water; for main cold-water branches compute the total fixture units separately for fixtures that are and are not supplied with hot water and add three-fourths of the total for fixtures that are supplied with hot water to the total for fixtures that are supplied with cold water only. If the character of the water is such as to produce corrosion and caking in the hot-water lines, it may be advisable either to allow the full table rating in estimating the demand for hot-water branches or to allow for a decrease in diameter by selecting the next larger size of pipe than that indicated by the computed estimate.

§ Ignore demands for service sinks except for hot-water supply and that for the cold-water branch to the fixture itself. Other fixtures, similarly used out of hours, may be treated similarly.

Flows which will not be exceeded more than 1 percent of the time may be determined from Fig. 1.[1] If plumbing fixtures, such as lawn sprinklers and air-conditioning units, are likely to impose a continuous demand when other fixtures are in extensive use, the continuous demand should be added to the estimated flow obtained from Fig. 1. The approximate flow and pressure requirements for some common domestic-fixture outlets are shown in Table 2.

[1] National Bureau of Standards Building Materials and Structures Report BMS66.

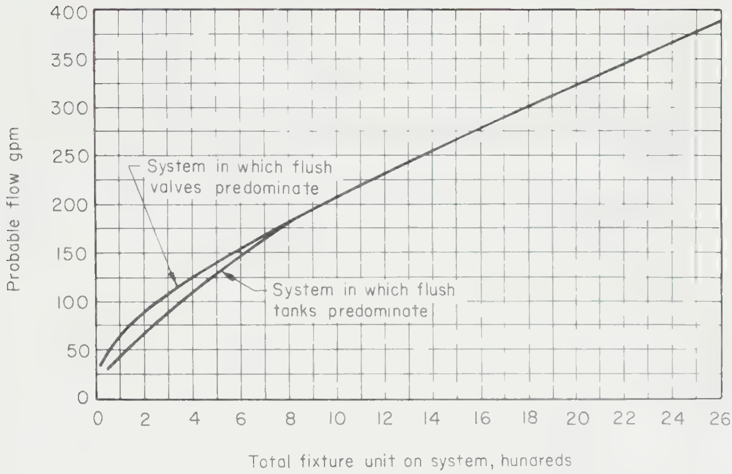

FIG. 1. Curve showing relation of discharge to fixture units.

A substantial loss of pressure is required at high flows through house meters, and the pressure loss varies considerably with different makes of meters. The Standard Specifications for Cold-Water Meters adopted in 1941 and 1964 by the American Water Works Association and the New England Water Works Association limits the pressure loss to 15 psi for meters 1 in. and smaller and to 20 psi for larger meters at the maximum flow capacity (see Table 10). The limiting pressure losses at other rates of flow may be estimated by assuming that the pressure loss varies as the square of the discharge. The estimated maximum loss of head through meters for residences equipped with tank toilets is thus 3.6 psi, and for residences equipped with flushometer toilets is 12 psi, unless the flushometers are fed from tank storage within the building.

If the pressure loss in the house service pipe and water lines within the building is assumed at 20 psi, the total pressure loss from the main to a residence with tank toilets at peak flow of 10 gpm is about 28 psi. The pressure required at the street level for excellent flow to a three-story building is therefore about 42 psi. Experience indicates that flow is adequate for residential areas if the pressure is not reduced below 35 psi.

TABLE 2. FLOW REQUIREMENTS TO HOUSE PLUMBING FIXTURES

Fixture	Excellent flow, gpm	Pressure at outlet (faucets wide open), psi
Lavatory faucets, single	4	4
Bathtub faucets, single	6	5
Combination bathtub faucets	8	5
Sink faucets	6	5
Shower heads	6	3
Shower mixing valves	6	30
Water closets, tank type	5	5
Water closets with flush valves	30	25
Garden hose and nozzle	6	30 at hydrant

Flushometers and shower mixing valves cannot be used satisfactorily with such low pressures.

In business districts, the required pressure for normal use depends directly upon the height of the buildings. Buildings up to about 20 stories in height may be conveniently served directly from the pressure in the street main in many cases. The pressure required at the street for a 20-story building will be about 120 psi. Such high pressures are not ordinarily desirable in the mains or in plumbing systems because of leakage and waste, but they frequently exist in the lower sections of a district in which there are marked differences in ground elevation. Very tall buildings are usually served with their own pumping equipment, and the building water piping may be divided into several pressure zones.

The capacity of the pipes in a distribution system should be sufficient to deliver the maximum domestic flow together with the fire flow. In the absence of maximum daily consumption figures the Underwriters estimate the flow on the basis of consumption in other cities of similar character and climate, but such estimates should be at least 50 percent greater than the average daily consumption. The maximum daily consumption is defined as the maximum total amount of water used during any 24-hr period in the past 3 years. High consumption that will not occur again, such as water-main breaks, should not be included.

For design purposes, the estimated maximum daily consumption at the end of the design period should be used. The domestic-consumption loads for each district in the distribution system may be computed from the estimated population and the per capita consumption for the maximum day. A study undertaken by Jerome B. Wolff, of Johns Hopkins University, reports that consumption in residential areas is related to lot sizes, the ratio of peak hour to average day varying from slightly less than 4:1 for group houses to more than 40:1. The results of the Johns Hopkins study for residential areas of Baltimore County, Maryland, are tabulated in Table 1, Sec. 36. Forecasting future use for industrial consumption depends upon the nature of the industries involved. It is difficult to predict future industrial consumption for undeveloped areas; established industries, on the other hand, may have planned future growth and water-consumption needs.

2. Flow and Pressure Requirements for Fire Protection. The fire flow for the whole system and for each district within the system, as required by the Underwriters,[1] is given by Eq. (1) and the paragraphs that follow it in Sec. 36. The Underwriters recommend that when pumping engines are used a residual pressure at the hydrants of not less than 10 to 20 psi should be maintained with fire flow plus domestic flow, 10 psi being allowed only where hydrant spacing and sizes are adequate.

If hose streams are to be used direct from hydrants a higher residual pressure is required. For communities of not more than 6,000 people and having not more than 10 buildings exceeding 3 stories in height, a residual pressure of 60 psi is required. For other places, a residual pressure of 75 psi is required if hydrant spacing is such as to allow short hose lines; and in thinly built residential sections or in small villages having buildings of small floor area, not over two stories in height, a residual pressure of 50 psi may be satisfactory. Most communities now have mobile pumping equipment, and direct hose connections are not commonly used, except where high pressures exist. The criterion for design for systems having mobile pumping equipment available is therefore usually 20 psi.

In districts in which the mains are designed for a normal pressure just sufficient to give adequate domestic flow to homes, it is evident that there will be an insufficient pressure for fire fighting without mobile pumpers. According to the American Water Works Association,[2] it is desirable that a normal pressure of 60 to 75 psi be maintained

[1] "Fire Engine Tests and Fire Stream Tables," National Board of Fire Underwriters, 5th ed., 1959.
[2] "Water Works Practice," p. 298, American Water Works Association, 1929.

on a distribution system for the following reasons:

"*a.* It will supply ordinary consumption for buildings up to 10 stories in height.

"*b.* Gives effective sprinkler service in buildings of 4 or 5 stories.

"*c.* Permits direct hydrant-service for a few hose streams, insuring quicker operation by the fire department.

"*d.* Allows a larger margin of fluctuation in local pressures in meeting sudden drafts, and offsets losses due to partial clogging or excessive length of service pipes."

An additional advantage of such a high pressure is that it will permit the wider use of flushometers and shower mixing valves. The advantages of higher pressures, however, should in every case be weighed against the additional pumping cost, for all the water pumped must be against the additional head.

Four methods are in use for supplying pressure for fire streams, as follows:

1. The maintenance of sufficient pressure on the mains at all times for direct hydrant service for hose streams
2. The use of emergency fire pumps to boost the pressure in the distribution system during fires
3. The use of mobile pumping engines which take suction from the hydrants
4. The use of a separate high-pressure distribution system for fire protection only

The first method is not ordinarily economical for large communities but is usually the best method for villages not provided with full-time fire departments and mobile pumpers. The second method is applicable to villages requiring higher pressures for fire fighting than are desirable for normal consumption and in which there are no mobile pumpers. It is more economical but less reliable than the first method. The third method is preferable for all communities large enough to maintain modern and well-trained fire departments. The fourth method is in use only in portions of some of the large cities. Separate high-pressure systems are usually supplementary to the main distribution system and thus give added fire protection in high-value districts. Pressures of 150 to 300 psi are used in high-pressure systems.

The effective reach of fire streams for smooth nozzles and for various nozzle pressures, as determined by Freeman,[1] is shown in Table 3. The corresponding values of the discharge and pressure loss in 2½- and 3-in. best-quality rubber-lined fire hose, as given by the National Board of Fire Underwriters,[2] are also shown. Nozzle pressures are velocity heads in pounds per square inch at the nozzle tips, measured by means of Pitot tubes. The effective reach is the distance in feet from the nozzle at which streams will do effective work with a moderate wind blowing. It will be noted that the vertical reach ranges from about 78 percent of the nozzle velocity head at 20 psi to only 46 percent at 90 psi. The maximum practical vertical reach is therefore about 100 ft, and the streams are more effective if the nozzles are elevated.

For inside hand lines a 1½-in. hose with a ½-in. nozzle is run in initially. The small hose is then backed up by 2½-in. hoses with 1⅛-in. or larger nozzles. Shutoff nozzles are usually used. Cellar, foam, or fog nozzles are commonly used. When the nozzle pressure exceeds about 50 psi, the jet reaction is too great for the nozzle to be held by hand. For fighting large fires from the outside, 1½-in. or larger nozzles should be used with siamesed 2½-in. lines using a deluge set, or a deck nozzle or turret type. Such nozzles are usually fixed in position and require pressures of 65 to 80 psi.

For direct hydrant service in business areas with 250-gpm standard streams and 300-ft lines, it may be noted from Table 3 that hydrant pressures of about 95 psi are required. Since such high pressures on the system are not normally advisable, mobile

[1] FREEMAN, *Trans. ASCE*, **21**, 303, 1889.

[2] "Fire Engine Tests and Fire Stream Tables," National Board of Fire Underwriters, 6th ed., 1959.

TABLE 3. FIRE-STREAM AND HOSE DATA

Nozzle pressures by Pitot, psi	Size of nozzle, in.: 1 — Discharge, gpm	1 — Pressure loss 100 ft 2½-in. hose, psi	1 — Vertical reach, ft	1 — Horizontal reach, ft	1⅛ — Discharge, gpm	1⅛ — Pressure loss 100 ft 2½-in. hose, psi	1⅛ — Vertical reach, ft	1⅛ — Horizontal reach, ft	1¼ — Discharge, gpm	1¼ — Pressure loss 100 ft 2½-in. hose, psi	1¼ — Vertical reach, ft	1¼ — Horizontal reach, ft	1⅜ — Discharge, gpm	1⅜ — Pressure loss 100 ft 3-in. hose, psi	1⅜ — Vertical reach, ft	1⅜ — Horizontal reach, ft	1½ — Discharge, gpm	1½ — Pressure loss 100 ft 3-in. hose, psi	1½ — Vertical reach, ft	1½ — Horizontal reach, ft
20	132	4.8	35	37	167	7.3	36	38	206	10.6	36	39	250	5.8	36	40	298	8.1	37	42
25	148	5.8	43	42	187	8.9	44	44	230	13.1	45	46	280	7.2	45	47	333	10.1	46	49
30	162	6.8	51	47	205	10.5	52	50	253	15.5	52	52	307	8.6	53	54	365	11.9	54	56
35	175	7.9	58	51	221	12.1	59	54	273	17.8	59	58	331	9.9	60	59	394	13.7	62	62
40	187	8.9	64	55	237	13.8	65	59	292	20.0	65	62	354	11.2	66	64	422	15.5	69	66
45	198	9.9	69	58	251	15.3	70	63	309	22.2	70	66	376	12.5	72	68	447	17.3	74	71
50	209	10.9	73	61	265	16.8	75	66	326	24.7	75	69	396	13.8	77	72	472	19.1	79	75
55	219	11.9	76	64	277	18.3	79	69	342	27.2	80	72	415	15.1	81	75	494	20.8	83	78
60	229	12.8	79	67	290	19.8	83	72	357	29.6	84	75	434	16.4	85	77	517	22.6	87	80
65	238	13.8	82	70	301	21.3	86	75	372	31.7	87	78	451	17.6	88	79	537	24.3	90	82
70	247	14.8	85	72	313	22.9	88	77	386	33.9	90	80	469	18.8	91	82	558	26.0	92	84
75	256	15.8	87	74	324	24.5	90	79	399	36.1	92	82	485	20.0	93	84	578	27.8	94	86
80	264	16.7	89	76	335	26.1	92	81	413	38.6	94	84	500	21.2	95	86	596	29.5	96	88
85	272	17.7	91	78	345	27.7	94	83	425	40.8	96	87	516	22.5	97	88	614	31.2	98	90
90	280	18.7	92	80	355	29.3	96	85	438	43.1	98	89	531	23.8	99	90	633	32.9	100	91

pumping engines are usually employed for important fires. The ordinary capacities of pumpers range from 500 to 1,000 gpm with some of the larger cities having pumpers with capacities of 1,250 to 1,500 gpm.

3. General Arrangement of Pipe System. The location of the small distributor pipes in a distribution system is controlled by the location of the consumers and by the location of property requiring fire protection. The pipes are usually laid in the streets at some standardized position between curbs. In the case of very wide streets, however, it is sometimes cheaper to install a main behind the curb on each side of the street because of the saving in service pipes. The system should be gridironed with connecting pipes laid on the cross streets at intervals not exceeding about 600 ft whether or not there are consumers on the cross streets. Dead ends should be avoided in order to minimize troubles from corrosion and from organic growths. Moreover, a pipe fed from both ends has a capacity equivalent to that of two pipes.

A large system will consist of supply mains, arteries, and secondary feeders spaced at intervals of about 3,000 ft in the grid system and preferably looped. The approximate location of the feeders will be determined largely by the distribution of the consumers and high-value property.

For fire protection, the Underwriters[1] specify a minimum size of main of 6 in. for residential areas and 8 in. for high-value districts if cross-connecting mains are not more than 600 ft apart. On principal streets and for all long lines not cross-connected at frequent intervals, 12-in. and larger mains are required by the Underwriters.

Gate valves should be so located that no single case of breakage in the pipe system, exclusive of arteries, shall require more than 500 ft of pipe to be shut from service in high-value districts, or more than 800 ft in other sections, or shall require the shutting down of an artery. The valves should be located at street intersections in standardized positions so that they can be readily found in case of pipe breakage. All small distributors branching from larger pipes should be equipped with valves, although the larger pipes need not have valves at each such branch. At intersections of large pipes, a valve in each branch is desirable. Large supply mains should be gated about once a mile and should be provided with air valves at high points and blowoffs at low points. Arteries should be gated so that not more than ¼ mile within the system will be affected by a break.

Hydrants should be located at street intersections where they are accessible from four directions, with one or two hydrants at each intersection. They should be so spaced that no hose line need exceed 500 to 600 ft. The spacing will vary from about 150 ft in high-value districts of large cities to about 600 ft in suburban residential districts, the usual spacing being about 300 ft. The requirements[1] of the Underwriters for hydrant distribution are given in Table 4.

Hydrants are required to have not less than two 2½-in. hose outlets, standard 4½-in. suction outlets where necessary, and to be connected to the main with pipe not smaller than 6 in. and gated. Hydrants should be able to deliver 600 gpm with a loss of not more than 2.5 psi in the hydrant and a total loss of not more than 5 psi between the street main and the outlet.

The depth to which pipes should be laid is controlled by the cover required for protection against structural failure due to street traffic loads and for protection against freezing. Where there is little or no frost penetration into the ground, a minimum cover of 18 to 24 in. has been used. For protection against wheel loads of heavy trucks, the amount of cover required increases with the size of pipe and is greater for steel than for cast-iron mains. For important mains, the amount of cover to be used

[1] "Standard Schedule for Grading Cities and Towns of the United States with Reference to Their Fire Defenses and Physical Conditions," National Board of Fire Underwriters, 1956.

Table 4

Required Fire Flow, gpm	Average Area per Hydrant, sq ft
1,000	120,000
2,000	110,000
3,000	100,000
4,000	90,000
5,000	85,000
6,000	80,000
7,000	70,000
8,000	60,000
9,000	55,000
10,000	48,000
11,000	43,000
12,000	40,000

should be determined after an investigation of the stresses produced by wheel loads. Less cover is required for pipes under concrete pavements than for pipes under more resilient pavements and dirt roads. The depth of cover required for protection against freezing may be estimated from Table 5, which shows the frost penetration and the depth of cover used in cities with widely divergent climatic conditions.

4. The Pressure Table and Pressure Districts. The pressure table, or piezometric surface, of a distribution system is the imaginary surface above the ground to which the water would rise in piezometers connected into the pipes. The pressure at any point in the system corresponds to the height of the pressure table above the ground. If the pressure table is controlled by elevated tanks or reservoirs within the system, it may be called a *fixed* pressure table. If there are no open surface tanks within the system, the elevation of the pressure table may be varied at will by varying the rate of inflow to the

Table 5

	Charleston,[1] S. C.	Washington[2] Suburban Sanitary District	Wilmington,[2] Del.	Portland,[3] Me.	Chicago,[2] Ill.	Peterborough,[4] Ont.	Sudbury,[4] Ont.	Ottawa,[4] Canada
Frost penetration, ft	....	2½	3	4	Clay, 5–5½ Sand, 5–6	Gravel with pavement, 6–7 Gravel no pavement, 5–6 Clay or sand, 5	7	Paved streets, 7½
Depth of cover, ft	2 to 2½	4	4	5-ft trench	Pipes 12 in. and smaller, 5½ large feeders, 2	....	7-ft trench	7

[1] Gibson, *J. AWWA*, **22,** 1315, 1930.
[2] Hechmer, Wills, and Gayton, *J. AWWA*, **28,** 841, 837, 849, 1936.
[3] Fuller, *J. NEWWA*, **50,** 300, 1936.
[4] Dobbin, Martindale, and MacDonald, *J. AWWA*, **26,** 1160, 1159, 1166, 1934.

system above or below the rate of consumption. Such a system has a *variable* pressure table.

The pressure table slopes in the general direction of the flow of the water because of head losses in the pipes, and the slopes are greatest where friction losses are greatest. The slopes increase with the consumption and are greatest during fire flows, particularly in the immediate vicinity of a fire. The fluctuation in the elevation of the pressure table is greatest at points most remote from the source of supply to the system or from equalizing tanks. The shape of the pressure table for any particular condition of flow may be illustrated by a contour map.

When the flow approaches zero, the pressure table approaches a horizontal plane, which may be conveniently referred to as the static pressure table. A fixed static pressure table is a horizontal plane at the water surface of the equalizing reservoir. Actually a fixed static pressure table varies somewhat owing to the fluctuation in the elevation of the water level in the equalizing tank. In order to minimize this fluctuation, equalizing reservoirs should be shallow. A variable static pressure table is a horizontal plane at the elevation corresponding to the pressure at the pumps. The elevation of this plane may be raised or lowered by increasing the rate of inflow above

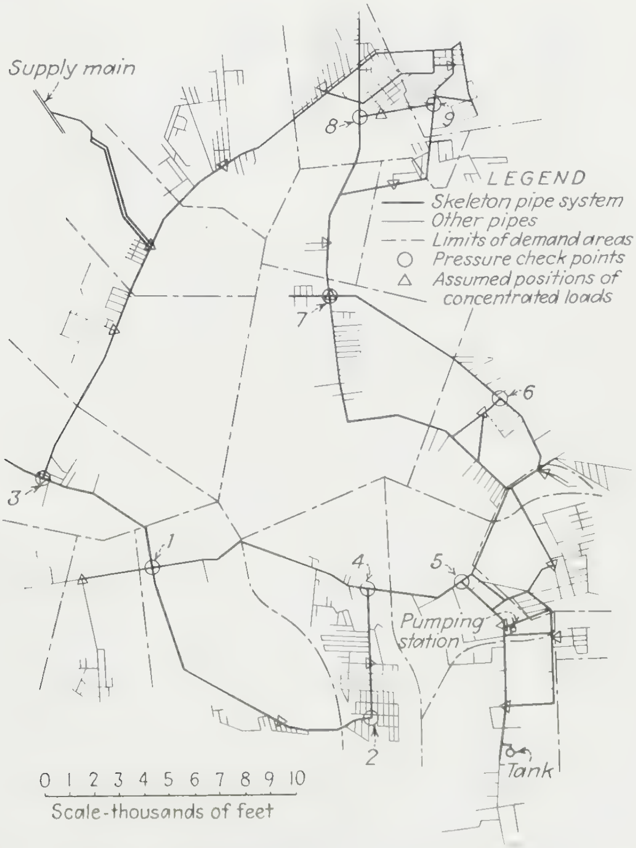

FIG. 2. Water-distribution system, Warwick, R.I.

or reducing it below the rate of consumption. It may be held constant by continuously varying the rate of inflow to correspond to the demand. Because of the difficulty of controlling pressures by changes in the pumping rate, most modern systems have equalizing reservoirs. Such reservoirs, when provided with sufficient capacity, permit the pumps to operate at a constant rate throughout the daily pumping period and provide fire storage. In large systems, better equalization of pressures is obtained by having several reservoirs or elevated tanks distributed at strategic points in the system. However, some distribution systems are supplied by direct pumping without equalizing reservoirs.

In communities located in hilly country with large differences in ground elevation and for very large systems, two or more pressure districts may be required. Each pressure district has its own pressure table, and the distribution system in each district operates independently. Connections may be made between the districts by means of mains equipped with gate valves normally closed or equipped with automatic pressure-reducing valves. High-pressure fire systems are usually not connected with the distribution system carrying the domestic supply. Complete separation of the two systems makes it possible to use a cheap, nonpotable water or salt water in the high-pressure fire system. However, cross connections to a potable water system constitute a serious hazard.[1]

5. General Procedure in Design. In the design of a distribution system, the following general procedure may be used.

1. *Preliminary Layout.* A preliminary layout of all the pipes is prepared on a suitable map of the community. A contour map showing all street and lot lines is preferable. The location of all existing buildings, with heights shown, is helpful. The layout should include the distributing reservoirs and elevated tanks, with their water surface elevations indicated if they are fixed arbitrarily or by the topography. The desired residual pressures for peak flows at critical points in the system stated in terms of the elevation of the pressure table at these points should be shown. A tentative division of the system into two or more pressure zones may be made if required. Pipe sizes may next be assumed in accordance with the Underwriters' requirements or the designer's judgment. These sizes are checked or corrected as a result of the hydraulic computations and economic analyses that follow.

2. *Skeleton Systems.* If practicable, the system is skeletonized for the hydraulic computations by eliminating all the smaller pipes in which the flow is negligible for a particular assumed position of the fire load. Figure 3 shows the skeleton framework for a small system. The system must be examined for several positions of the fire load. Hence several skeleton frameworks may be required. These systems will be similar with regard to the larger mains but may differ in the inclusion of smaller pipes immediately surrounding the fire. The purpose of the simplified framework is to reduce the number of variables in order to make the hydraulic computations practicable. In skeletonizing the system, it is desirable to examine the magnitude of the errors caused by the neglect of smaller pipes. When the error is too great for a particular element in the skeleton framework, it is desirable to use an equivalent pipe for this element which is of sufficient size to take account of the smaller pipes. In some cases, also, the skeleton system may be simplified by substituting a single equivalent pipe for several elements.

For many systems, the small differences in the size of the pipes or the difficulty of evaluating the errors due to the neglect of the smaller pipes may make skeletonizing impractical. In such cases, approximate hydraulic analyses or the use of electronic

[1] Devendorf, The Pollution and Emergency Disinfection of Rochester's Water Supply, *J. AWWA*, **33**, 1334, 1941.

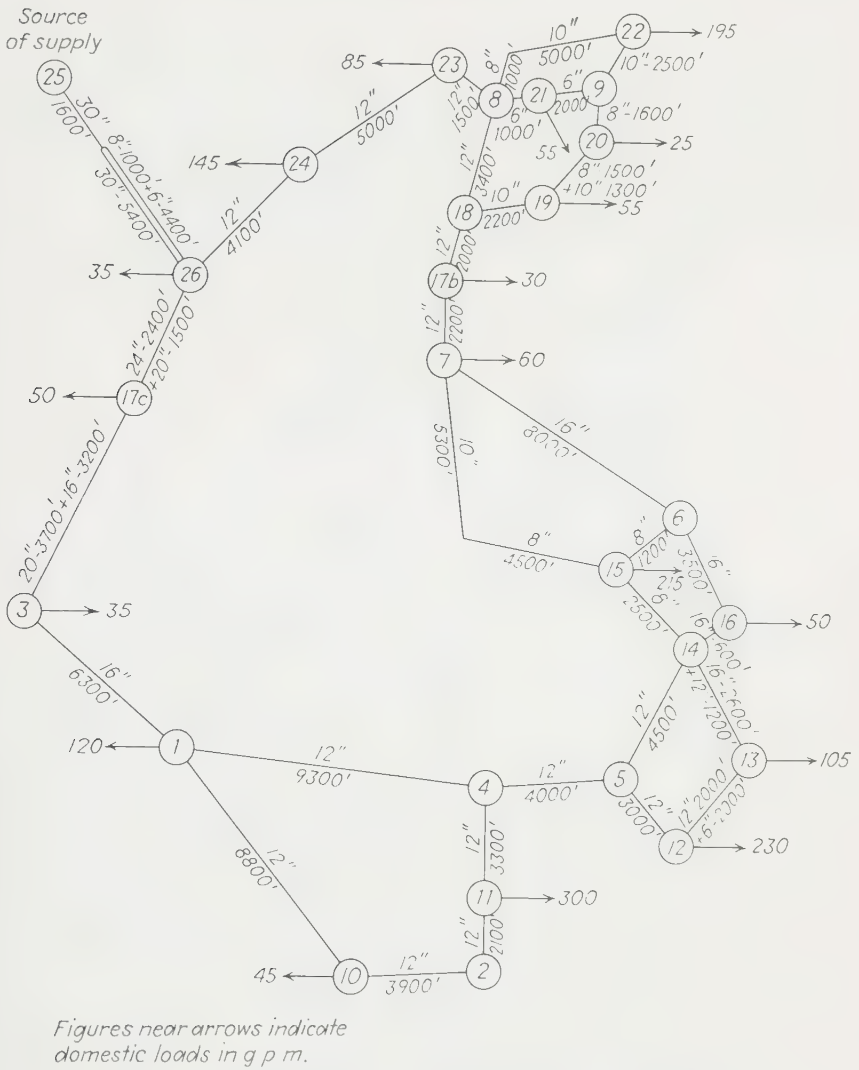

Fig. 3. Simplified skeleton distribution system at Warwick, R.I.

computers may be required since the accurate methods available are too laborious to be carried out by hand.

3. *Computation of Loads.* In order to simplify the computations the draft from the system for ordinary use is assumed to be concentrated at relatively few take-off points on the network. The loading points are taken at pipe junctions where feasible in order not to increase the number of elements in the system. Fire loads are applied at junctions also. The elevation of the pressure table corresponding to the minimum desired residual pressure for each loading point should be determined. When the loading points are selected it is necessary to divide the system into districts, one to

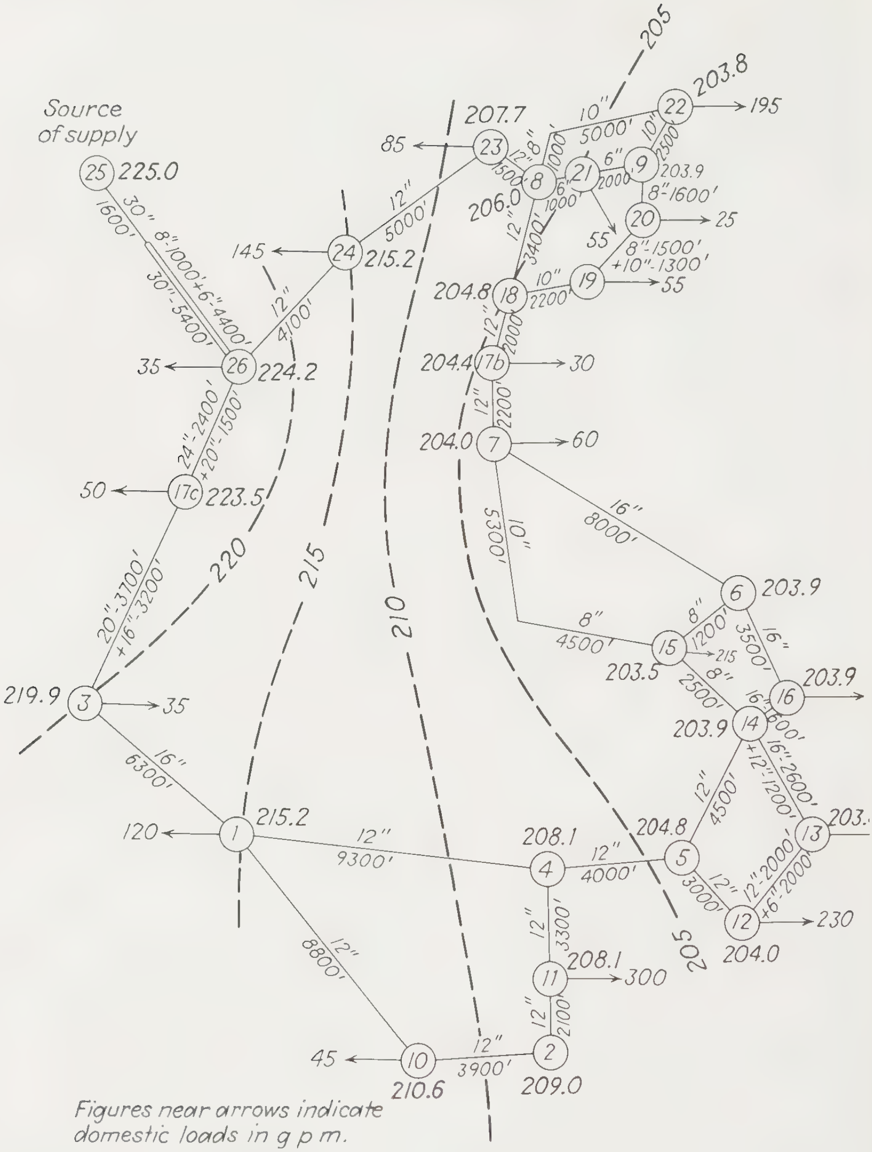

Fig. 4. Pressure contours for domestic consumption. (Hazen-Williams $C = 110$.)

each loading point, in order to compute the loads. The district boundaries are arbitrarily selected, but some of the bounds may be conveniently located on natural bounds between districts of different types or on natural fire breaks. The number of loading points used is also arbitrarily selected, but the accuracy of the hydraulic computations increases with the number of districts selected. Figure 2[1] shows the assumed loading points and district boundaries for a small distribution system.

[1] Collins and Jones, Bachelor's Thesis, M.I.T., 1933. Camp and Hazen, Hydraulic Analysis by Electric Analyzer, *J. NEWWA*, **48**, 383, 1934.

Figure 3[1] shows the simplified skeleton system with pipe sizes and lengths and domestic loads indicated.

4. *Hydraulic Analysis.* Hydraulic computations are made to determine the discharge and head loss in each pipe element of the system for the domestic loads only and for the combined domestic and fire loads for each position of the fire load to be investigated. From these computations, the shape of the pressure table may be determined for each loading condition. Figure 4 shows the pressure contours for the Warwick system in feet above sea level for domestic loads only. Figure 5[1] shows the contours for the fire load at point 6. Methods for making the hydraulic analysis are described in the following articles.

[1] Collins and Jones, Bachelor's Thesis, M.I.T., 1933. Camp and Hazen, Hydraulic Analysis by Electric Analyzer, *J. NEWWA*, **48**, 383, 1934.

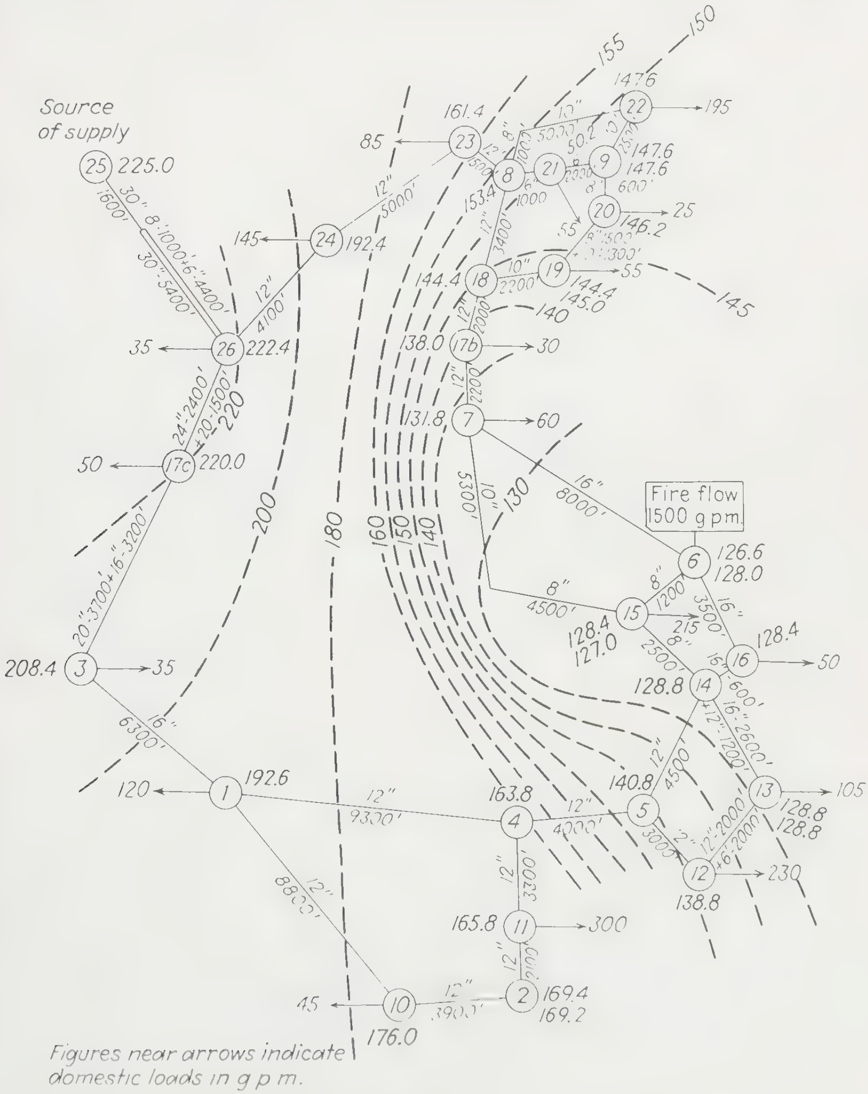

Fig. 5. Pressure contours for fire at point 6. (Hazen-Williams $C = 110$.)

5. *Correction of Pipe Sizes.* The adjustment of pipe sizes to secure the desired pressures at critical points and best economy is a trial-and-error process requiring the alternate use of economic and hydraulic analyses. Several adjustments may be required before the best sizes are found. Methods for determining economic pipe sizes are described below.

6. Hydraulic Analysis of Pipe Networks. The relation between the head loss and discharge for any pipe or system of pipes in which there is turbulent flow may be expressed as follows:

$$h = kQ^x \tag{1}$$

in which h is the head loss and Q the corresponding discharge. The coefficient k is a constant for the pipe or system and may be computed for a single pipe directly from the friction formula used. For the Hazen-Williams formula which is widely used in America, the value of the constant k if h is in feet and Q in cubic feet per second is

$$k = \left(\frac{1{,}594}{C}\right)^{1.85} \frac{l}{d^{4.87}} \tag{2}$$

in which C = Hazen-Williams coefficient
l = pipe length, ft
d = diameter, in.

For the Chézy formula, also widely used, with Manning's value of the Chézy coefficient,

$$k = 2.65(1{,}000n)^2 \frac{l}{d^{5.33}} \tag{3}$$

in which n is the Manning coefficient of roughness and the other symbols are the same as above. The value of the exponent x is equal to the reciprocal of the exponent of the hydraulic slope in the friction formula used. For the Hazen-Williams formula, x is 1.85; for the Chézy formula, x is 2.00. If Q is expressed in gallons per minute, the value of k from Eqs. (2) and (3) must be divided by 450^x.

The value of k for the Hazen-Williams formula may be obtained quickly for each element from Fig. 6 by finding the head loss corresponding to any discharge and dividing it by Q^x. The same procedure may be used with charts for other friction formulas.

1. *Analytical Relations for Compound Pipes.* The hydraulic problem in connection with pipe networks consists of solving for the distribution of flow and head loss in the individual elements for a given total discharge or for a given total head loss. For each element, there are two unknowns, the discharge and head loss, and for the system as a whole one unknown, the head loss or the discharge. Hence the number of unknowns equals twice the number of elements plus one.

The equations required for the solution of the unknowns are of three types and arise from three laws[1] as follows:

1. The head loss varies as some power of the discharge, Eq. (1).
2. The algebraic sum of the discharge rates toward any junction point is zero.
3. The total head loss between any two points in the system is the algebraic sum of the head loss of all the elements along any route between the points, and the total head loss is the same by all routes.

Figure 7 shows three simple compound pipe systems and the equations required for their analysis. It will be noted that only two types of equations are actually required for the solution of series and parallel systems since the other equations are identities but that all three types of equations are required for the analysis of a complex system. For any network, the number of equations available is sufficient for a solution. To solve for the unknowns, the equations must be solved simultaneously, but the direct

[1] Camp and Hazen, Hydraulic Analysis by Electric Analyzer, *J. NEWWA*, **48,** 383, 1934.

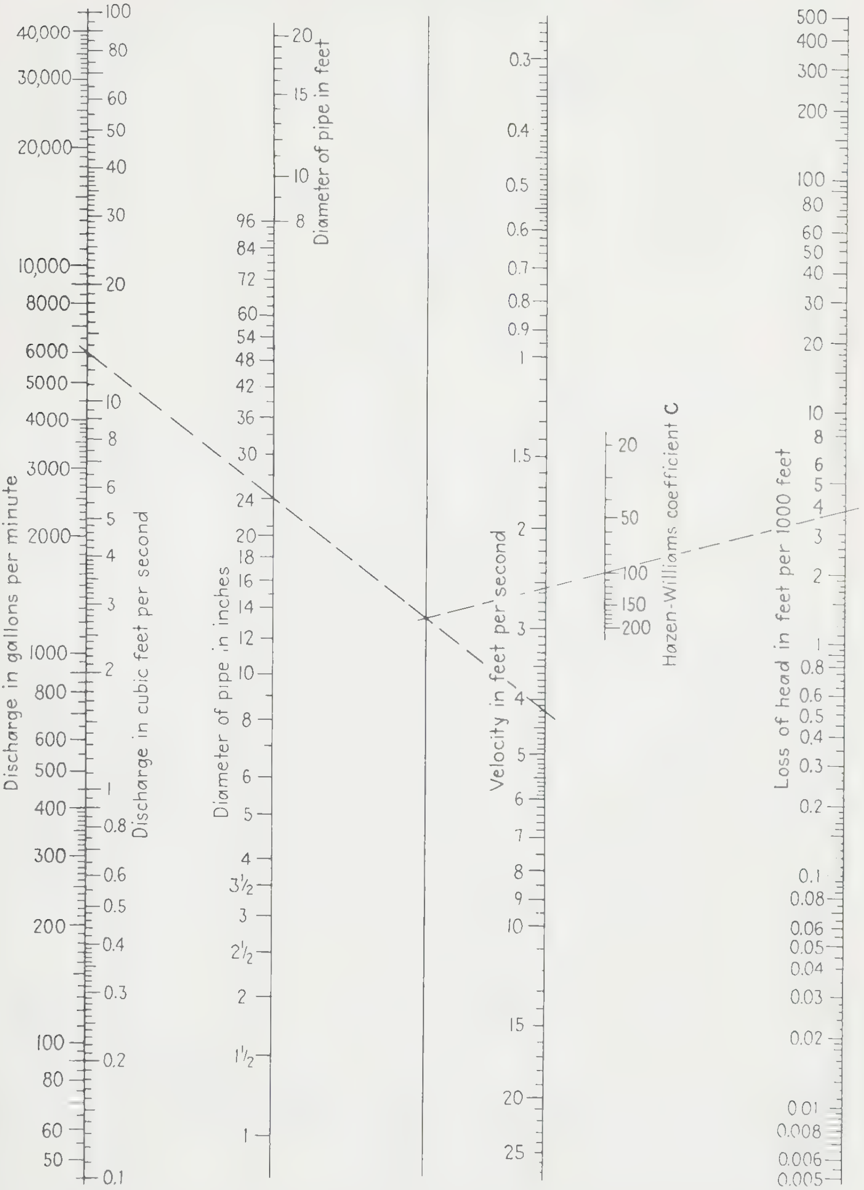

FIG. 6. Alignment chart for flow in pipes. Hazen-Williams formula: $V = 1.318CR^{0.63}S^{0.54}$.

solution of the large number of simultaneous equations involved in distribution systems is impractical for all but the simplest systems. Trial-and-error methods are used in practice.

2. *Equivalent Pipes.* A simple system consisting of two or more elements and having one inlet and one outlet point may be replaced by an equivalent pipe. The head

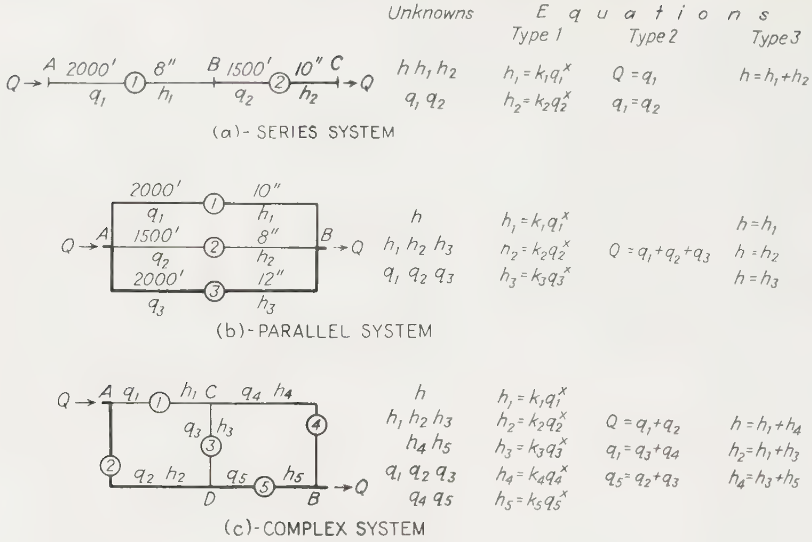

FIG. 7. Simple compound pipes.

loss through an equivalent pipe for any given flow is the same as for the replaced system. Equivalent pipes may be found readily by means of flow charts such as Fig. 6 for simple series and parallel systems such as Fig. 7*a* and *b*.

To find an equivalent pipe for a simple series, assume a discharge rate and find the head loss for each element. Any pipe which has for the assumed discharge a head loss equal to the sum of the losses in all the elements is an equivalent pipe. Any size of pipe may be selected provided the proper length is chosen to give the desired head loss. For example, in Fig. 7*a*, for $C = 100$, and an assumed discharge rate of 800 gpm, $h_1 = 39$ and $h_2 = 10$ from Fig. 6. Hence $h = 49$, and 7,350 ft of 10 in. and 2,510 ft of 8 in. are equivalent pipes. It will be noted that if the discharge is given, a simple series may be solved directly from a chart; but if the total head loss is given, an equivalent pipe must first be found before the discharge can be solved for by means of the chart.

To find an equivalent pipe for a simple parallel system, assume a total head loss and find the corresponding discharge for each element. Any pipe that has for the assumed head loss a discharge equal to the sum of the discharge rates for all the elements is an equivalent pipe. For example, in Fig. 7*b*, for $C = 100$, and an assumed head loss of 30 ft, $q_1 = 1{,}250$, $q_2 = 810$, and $q_3 = 2{,}010$ gpm from Fig. 6. Hence $Q = 4{,}070$ gpm, and 2,190 ft of 16-in. pipe is an equivalent pipe. It will be noted that if the head loss is given a simple parallel system may be solved directly from a chart, but if the total discharge is given an equivalent pipe is first required.

An equivalent pipe for a complex system such as Fig. 7*c* cannot be found directly by the foregoing methods, for neither the head nor the discharge for any element is known when either the head or discharge for the whole system is known. Howland and Aldrich[1] have developed a trial-and-error method for solving complex systems using Freeman's[2] graphical method.

[1] HOWLAND, Expansion of the Freeman Method for the Solution of Pipe Flow Problems, *J. NEWWA*, **48**, 408, 1934. ALDRICH, Solution of Transmission Problems of a Water System, *Trans. ASCE*, **103**, 1579, 1938.

[2] FREEMAN, *J. NEWWA*, **7**, 1892.

The equivalent-pipe method is a convenient device for reducing the number of elements and thereby simplifying the framework of a distribution system. When used for this purpose, it is not necessary to find an equivalent pipe for the replaced elements but only to find the value of the constant k of Eq. (1) which corresponds to the equivalent pipe. For example, the equivalent pipes of the series in Fig. 7*a* all have the same value of k as follows: $k = (49/800^{1.85}) = 20.9 \times 10^{-5}$ for the discharge in gallons per minute. Similarly, the value of k for all equivalent pipes of the parallel system (Fig. 7*b*) is 0.625×10^{-5}.

3. *Hydraulic Network Solutions.* Six methods are available for making solutions of the simultaneous equations involved in the hydraulic analysis of distribution systems:

1. Uncontrolled trial-and-error method
2. Freeman graphical method[1]
3. Hardy Cross method[2]
4. Newton's method[3]
5. Electric-network analyzer method[4]
6. Hydraulic-model method[5]

In the first four methods, a trial distribution of either the flow or the head loss is made throughout the system, the corresponding head or discharge is computed or measured for each of the elements, and adjustments are then made in the distribution of values. The process is repeated until a set of values is obtained which approximately satisfy all three laws described above under Analytical Relations.

In the uncontrolled method, the adjustments in the assumed values are made arbitrarily. The convergence of errors by this method is therefore slow and uncertain, and it is impractical for most systems. The same may be said of the Freeman method.

The fifth method consists of the use of an electric-network analyzer in which electric resistors are connected together in such a manner that each element of the hydraulic system is represented by a resistor in proper position. The analyzer is an electric model of the distribution system in which voltage represents head loss and current the discharge, with a suitable scale ratio selected for each. When the method was first developed, ordinary resistors were used with which the voltage drop is proportional to the first power of the current instead of the x power as required by the hydraulic system. Because of this defect, it was not possible to represent each element of the hydraulic system by a constant electrical resistance; and trial-and-error solutions were obtained by adjusting the resistance in all the resistors so that the relation of voltage to current in each resistor satisfied the analogous head-discharge relation as indicated by Eq. (1). Satisfactory solutions could usually be obtained with three adjustments of the resistors. Lamps have now been developed with suitable filaments for use as resistors such that upon heating the filaments the resistance changes automatically to represent a hydraulic element without subsequent adjustment and results can be read as soon as the loads are applied. Figure 5 represents a hydraulic analysis of a distribution system by means of an electric-network analyzer.

[1] Aldrich, Solution of Transmission Problems of a Water System, *Trans. ASCE*, **103,** 1579, 1938.

[2] Cross, Analysis of Flow in Networks of Conduits or Conductors, *Univ. Illinois Eng. Expt. Sta. Bull.* 286, November, 1936. Doland, *Eng. News-Record*, **117,** 475, 1936.

[3] Martin and Peters, The Application of Newton's Method to Network Analysis by Digital Computer, *Inst. Water Engs.*, **17,** 115, 1963.

[4] Collins and Jones, Bachelor's Thesis, M.I.T., 1933. Camp and Hazen, Hydraulic Analysis by Electric Analyzer, *J. NEWWA*, **48,** 383, 1934. McIlroy, Direct Reading Electric Analyzer for Pipeline Networks, *J. AWWA*, **42,** 347, 1950.

[5] Camp, Hydraulics of Distribution Systems—Some Recent Developments in Methods of Analysis, *J. NEWWA*, **57,** 334, 1943.

The hydraulic-model method consists of representing the distribution system by means of a small-scale hydraulic model. The elements may be represented by constrictions in rubber tubes produced by means of pinch cocks, in which case the value of x in Eq. (1) will be about 1.75 but may be higher or lower depending upon the amount of throttling. The elements may also be represented by orifices inserted in pipe or rubber tubing, in which case x will have a value of nearly 2.0; or they may be represented by short tubes inserted in rubber tubing, the ratio of length to diameter of short tube being selected to produce the required value of x. Results may be read directly on hydraulic models as soon as the loads are applied.

The Hardy Cross method is a trial-and-error method in which the adjustments to be made in the assumed values are computed and are therefore controlled. Convergence of errors is often rapid, and sufficient precision in the results can ordinarily be had by three adjustments. Two methods may be used: the method of balancing heads or the method of balancing flows. The method of balancing heads is as follows:

1. Assume any distribution of discharge.
2. Compute the head loss in each element by means of Eq. (1): $h = kq_0^x$.
3. With due attention to sign, compute the total head loss around each elementary closed circuit: $\Sigma h = \Sigma kq_0^x$.
4. Compute also for each elementary circuit without reference to sign the sum: $\Sigma xkq_0^{(x-1)}$.
5. To balance the head in each circuit (so that $\Sigma k\mathrm{q}^x = 0$), set up a counterbalancing flow equal to

$$\Delta = \frac{\Sigma kq_0^x(\text{with due attention to direction of flow})}{\Sigma xkq_0^{(x-1)}(\text{without reference to direction of flow})} \tag{4}$$

6. Compute the revised flows, and repeat the process until the desired accuracy is obtained.

The flow correction Δ for each circuit places the heads for that circuit substantially in balance if Δ is small. Since some elements of each circuit are common to other circuits, however, the balance of heads in each circuit is disturbed by subsequent adjustments in other circuits. Hence several traverses of the system are required before satisfactory precision is obtained. The proof of the method is as follows:

$$q = q_0 + \Delta$$

in which q = actual discharge for any element
q_0 = assumed discharge
Δ = required flow correction

Then

$$kq^x = k(q_0 + \Delta)^x = k(q_0^x + xq_0^{(x-1)}\Delta + \cdot \cdot \cdot)$$

The remaining terms in the preceding expansion may be neglected if Δ is small as compared with q_0. For a single circuit,

$$\Sigma kq^x = 0$$

and from above,

$$\Sigma kq^x = \Sigma kq_0^x + \Delta\Sigma xkq_0^{(x-1)}$$

Therefore,

$$\Delta = -\frac{\Sigma kq_0^x}{\Sigma xkq_0^{(x-1)}} \tag{4}$$

If Δ is large compared with q_0, Eq. (4) does not give a close approximation of the value of Δ because of the neglect of the terms beyond the second term in the expansion. This neglect is not usually important, however, particularly if subsequent adjustments bring rapid convergence.

High-speed electronic digital computers make it possible to carry out computations for distribution systems by the Hardy Cross method, or by Newton's method with great speed and accuracy. Programs have been developed and computers are located in most large cities throughout the country. Numerous problems having many unknowns, for which complete solutions were not practical, may now be analyzed. Figure 4 represents a hydraulic analysis of the Warwick system by means of the Hardy Cross method. Figure 8 shows the skeleton framework with the value of the constant $k \times 10^5$ for each element indicated on the line representing the element. The figures nearest each element represent the flow in the element corresponding to the assumed distribution of discharge. The underlined figures near each element represent the adjusted discharge. The computations are shown in Table 6.

There appears to be nothing inherent in either the electric analyzer with ordinary resistors or the Hardy Cross method which will consistently produce convergence of the

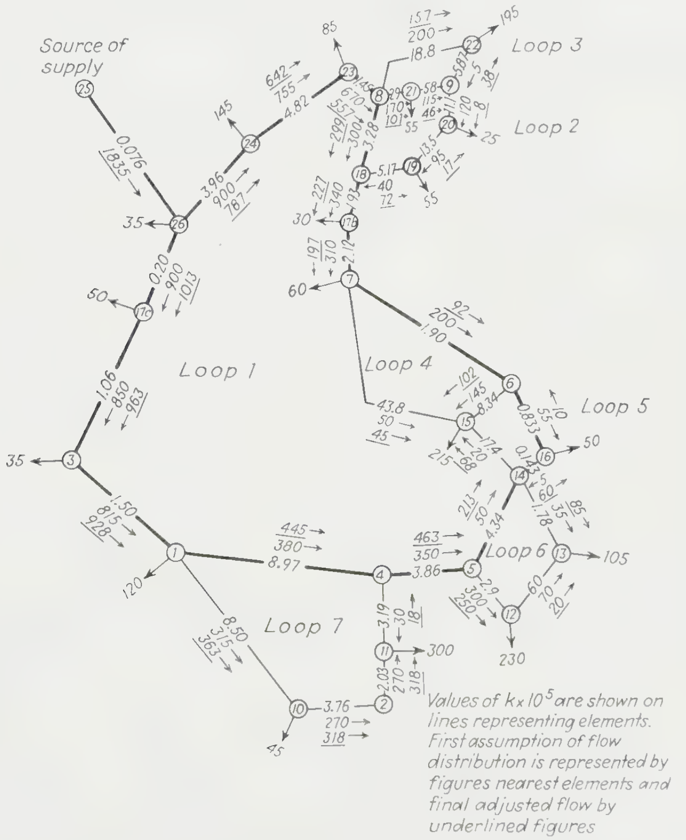

FIG. 8. Computation of domestic flow distribution by Hardy Cross method. (Hazen-Williams $C = 110$.)

Table 6. Computation of Domestic Flow Distribution in Warwick, R.I., Distribution System by Hardy Cross Method (Hazen-Williams $C = 110$)

Element	10^5k	First adjustment				Second adjustment				Third adjustment				Final values			
		$q_0^{0.85}$	$10^5kq_0^{0.85}$	q_0' gpm	h' ft	$q_0^{0.85}$	$10^5kq_0^{0.85}$	q_0'' gpm	h'' ft	$q_0^{0.85}$	$10^5kq_0^{0.85}$	q_0''' gpm	h''' ft	$q^{0.85}$	$10^5kq^{0.85}$	q gpm	h ft
Loop 1																	
26-24	3.96	324	1,284	+900	+11.55	292	1,157	+ 799	+9.25	288	1,141	+ 788	+9.00	288	1,141	+ 787	+8.98
24-23	4.82	278	1,340	+755	+10.12	248	1,195	+ 654	+7.82	243	1,171	+ 643	+7.53	242	1,166	+ 642	+7.49
23-8	1.45	252	365	+670	+ 2.45	220	319	+ 569	+1.82	216	313	+ 558	+1.75	215	312	+ 557	+1.74
8-18	3.28	128	420	+300	+ 1.26	113	371	+ 262	+0.97	120	394	+ 280	+1.10	127	416	+ 299	+1.24
18-17*b*	1.93	142	274	+340	+ 0.93	105	203	+ 239	+0.49	101	195	+ 228	+0.44	101	195	+ 227	+0.44
17*b*-7	2.12	131	278	+310	+ 0.86	94	199	+ 209	+0.42	89	189	+ 198	+0.37	89	189	+ 197	+0.37
7-6	1.90	90	171	+200	+ 0.34	45.6	87	+ 90	+0.08	46.6	89	+ 92	+0.08	46.6	89	+ 92	+0.08
6-16	0.833	30.1	25	+ 55	+ 0.01	2.5	2	+ 3	+	6.5	5	− 9	−	7.1	5.9	− 10	−0.
16-14	0.143	3.9	1	+ 5	+	26.3	4	− 47	−	32	5	− 59	−0.003	32.5	4.6	− 60	−0.003
14-5	4.34	27.8	121	− 50	− 0.06	87	378	− 191	−0.72	94	408	− 211	−0.86	95.1	413	− 213	−0.88
5-4	3.86	145	560	−350	− 1.96	180	695	− 451	−3.14	184	710	− 462	−3.28	184	710	− 463	−3.29
4-1	8.97	156	1,399	−380	− 5.32	176	1,578	− 438	−6.91	178	1,596	− 444	−7.10	178	1,596	− 445	−7.11
1-3	1.50	294	441	−815	− 3.59	330	495	− 916	−4.53	333	500	− 927	−4.64	334	501	− 928	−4.65
3-17*c*	1.06	309	328	−850	− 2.79	340	360	− 951	−3.42	343	364	− 962	−3.50	345	366	− 963	−3.53
17*c*-26	0.20	324	65	−900	− 0.58	355	71	−1,001	−0.71	357	72	−1,012	−0.73	357	72	−1,013	−0.73
			7,072		+13.22		7,114		+1.42		7,152		+0.16		7,176		+0.15
		$\Delta = \frac{-13.22 \times 10^5}{1.85 \times 7{,}072} = -101$				$\Delta = \frac{-1.42 \times 10^5}{1.85 \times 7{,}114} = -11$				$\Delta = \frac{-0.16 \times 10^5}{1.85 \times 7{,}152} = -1$				$\text{Error} = \frac{+0.15 \times 10^5}{1.85 \times 7{,}176} = +1.1$ gpm			
Loop 2																	
8-21	29.0	78.7	2,281	+170	+ 3.88	57.0	1,653	+ 117	+1.93	52.8	1,531	+ 109	+1.67	50.2	1,456	+ 101	+1.47
21-9	58.0	56.4	3,272	+115	+ 3.76	33.4	1,937	+ 62	+1.20	29.7	1,723	+ 54	+0.93	25.9	1,503	+ 46	+0.69
9-20	11.1	58.6	650	+120	+ 0.78	31.1	345	+ 57	+0.20	17.0	189	+ 28	+0.05	5.9	65	+ 8	+0.005
20-19	13.5	48.0	648	+ 95	+ 0.61	19.0	256	+ 32	+0.08	2.5	34	+ 3	+0.001	11.1	150	− 17	−0.025
19-18	5.17	23.0	119	+ 40	+ 0.05	14.4	75	− 23	−0.02	28.7	148	− 52	−0.08	37.9	196	− 72	−0.14
18-8	3.28	90.0	295	−199	− 0.59	109.0	357	− 251	−0.90	120.0	394	− 279	−1.10	127.0	416	− 299	−1.24
			7,265		+ 8.49		4,623		+2.49		4,019		+1.47		3,786		+0.76
		$\Delta = \frac{-8.49 \times 10^5}{1.85 \times 7{,}265} = -63$				$\Delta = \frac{-2.49 \times 10^5}{1.85 \times 4{,}623} = -29$				$\Delta = \frac{-1.47 \times 10^5}{1.85 \times 4{,}019} = -20$				$\text{Error} = \frac{+0.76 \times 10^5}{1.85 \times 3{,}786} = +11$ gpm			
Loop 3																	
8-22	18.8	90.0	1,693	+200	+ 3.39	86.3	1,623	+ 190	+3.08	78.2	1,468	+ 169	+2.48	73.3	1,378	+ 157	+2.16
22-9	5.87	3.9	23	+ 5	+	3.9	23	− 5	−	15.9	93	− 26	−0.02	22.0	129	− 38	−0.05
9-21	58.0	28.7	1,665	− 52	− 0.87	19.5	1,131	− 33	−0.37	20.0	1,160	− 34	−0.39	25.9	1,503	− 46	−0.69
21-8	29.0	53.0	1,536	−107	− 1.64	45.0	1,305	− 88	−1.15	45.4	1,317	− 89	−1.17	50.2	1,456	− 101	−1.47
			4,917		+ 0.88		4,082		+1.56		4,038		+0.90		4,466		−0.05
		$\Delta = \frac{-0.88 \times 10^5}{1.85 \times 4{,}917} = -10$				$\Delta = \frac{-1.56 \times 10^5}{1.85 \times 4{,}082} = -21$				$\Delta = \frac{-0.90 \times 10^5}{1.85 \times 4{,}038} = -12$				$\text{Error} = \frac{-0.05 \times 10^5}{1.85 \times 4{,}466} = -0.6$ gpm			

Loop 4

7-6	1.90	49.7	95	+ 99	+ 0.09	41.0	78	+ 79	+0.06	46.3	88	+ 91	+0.08	46.3	89	+ 92	+0.08
6-15	8.34	69.0	576	+145	+ 0.83	44.5	371	+ 87	+0.32	50.2	419	+ 101	+0.42	50.9	424	+ 102	+0.43
15-7	43.8	27.8	1,217	− 50	− 0.61	32.0	1,403	− 59	−0.83	25.9	1,134	− 46	−0.52	25.4	1,113	− 45	−0.51
			1,888		+ 0.31		1,852		−0.45		1,641		−0.02				0
			$\Delta = \frac{-0.31 \times 10^5}{1.85 \times 1{,}888} = -9$				$\Delta = \frac{+0.45 \times 10^5}{1.85 \times 1{,}852} = +13$				$\Delta = \frac{+0.02 \times 10^5}{1.85 \times 1{,}641} = +1$				Error = 0		

Loop 5

6-16	0.833	25.9	21	− 46	− 0.010	5.9	5	− 8	....	7.1	6	− 10	....	7.1	5.9	− 10	−0.
16-14	0.143	48.3	7	− 96	− 0.007	31.5	5	− 58	−0.003	32.5	5	− 60	−0.003	32.5	4.6	− 60	−0.003
14-15	17.4	12.7	221	+ 20	+ 0.044	36.5	635	+ 69	+0.438	36.2	627	+ 68	+0.427	36.2	630	+ 68	+0.43
15-6	8.34	65.0	542	−136	− 0.738	50.0	417	− 100	−0.417	50.9	426	− 102	−0.435	50.9	424	− 102	−0.43
			791		− 0.711		1,062		+0.018		1,064		−0.005				0
			$\Delta = \frac{+0.711 \times 10^5}{1.85 \times 791} = +49$				$\Delta = \frac{-0.018 \times 10^5}{1.85 \times 1{,}062} = -1$				$\Delta = \frac{-0.005 \times 10^5}{1.85 \times 1{,}064} = 0$				Error = 0		

Loop 6

5-14	4.34	71.0	308	+151	+ 0.465	91.0	395	+ 202	+0.798	95.0	412	+ 212	+0.875	95.1	413	+ 213	+0.88
14-13	1.78	20.5	37	+ 35	+ 0.013	39.2	70	+ 75	+0.052	43.2	77	+ 84	+0.065	43.6	78	+ 85	+0.066
13-12	60.0	37.0	2,220	− 70	− 1.554	18.0	1,080	− 30	−0.324	13.3	798	− 21	−0.168	12.8	768	− 20	−0.154
12-5	2.9	128.0	371	−300	− 1.113	113.0	328	− 260	−0.852	110.0	319	− 251	−0.802	109.0	316	− 250	−0.790
			2,936		−2.189		1,873		−0.326		1,606		−0.03				0
			$\Delta = \frac{+2.189 \times 10^5}{1.85 \times 2{,}936} = +40$				$\Delta = \frac{+0.326 \times 10^5}{1.85 \times 1{,}873} = +9$				$\Delta = \frac{+0.03 \times 10^5}{1.85 \times 1{,}606} = +1$				Error = 0		

Loop 7

1-4	8.97	190.0	1,704	+481	+ 8.200	180.0	1,614	+ 449	+7.250	178.0	1,596	+ 445	+7.100	178.0	1,596	+ 445	+7.11
4-11	3.19	18.0	57	+ 30	+ 0.017	8.8	28	− 13	−0.004	11.7	37	− 18	−0.007	11.7	37.3	− 18	−0.007
11-2	2.03	116.0	235	−270	− 0.635	132.0	268	− 313	−0.839	134.0	272	− 318	−0.866	134.0	272	− 318	−0.866
2-10	3.76	116.0	436	−270	− 1.176	132.0	496	− 313	−1.553	134.0	504	− 318	−1.605	134.0	504	− 318	−1.605
10-1	8.50	133.0	1,130	−315	− 3.560	148.0	1,258	− 358	−4.51	150.0	1,275	− 363	−4.63	150.0	1,275	− 363	−4.63
			3,562		+ 2.846		3,664		+0.34		3,684		0				0
			$\Delta = \frac{-2.846 \times 10^5}{1.85 \times 3{,}562} = -43$				$\Delta = \frac{-0.34 \times 10^5}{1.85 \times 3{,}664} = -5$				$\Delta = 0$				Error = 0		

errors toward zero with subsequent adjustments. Some networks have been studied by the Hardy Cross method with which convergence in many of the loops does not occur. In such a case, the designer may have to be content with an approximate hydraulic analysis such as the contour and circle methods.[1]

PIPES AND MATERIALS[2]

Cast iron is the most widely used material for the mains of distribution systems for sizes up to about 30 in. In sizes above 30 in., steel pipe and prestressed reinforced-concrete pipe compete favorably with cast iron, and in smaller sizes cement-asbestos pipe competes favorably.

7. Cast-iron Pipe and Fittings. There are two methods of manufacturing cast-iron pipe, (1) cast-iron pit-cast pipe, and (2) cast-iron pipe centrifugally cast. Pit-cast pipe is manufactured by pouring molten iron into a vertical sand mold. Centrifugally cast pipe is manufactured by pouring molten iron into a mold rotating at a comparatively high speed on rollers. Centrifugally cast pipe may be manufactured in metal molds or in sand-lined molds. After the pipe is cast and the mold stripped, rough places are ground off, the pipe is cleaned, and slag is removed. The pipe is then hydrostatically tested, inspected, and coated. Lighter and stronger pipe may be obtained by the centrifugal method of casting, whereas pit-casting methods are required for pipe of large diameter. The sizes, weights, and thickness of cast-iron pipe may be obtained from the Handbook of the Cast-Iron Pipe Research Association, Chicago, Ill., or from the pipe manufacturers.

Cast-iron pipe may be designed by a method developed by the United States of America Standards Institute Committee A 21, sponsored by the American Water Works Association, the New England Water Works Association, the American Gas Association, and the American Society for Testing and Materials. The USASI method of design takes into account a number of factors. The wall thickness is based on the combined loads caused by internal pressures, including water-hammer allowance; the external load from the weight of backfill; the weight of traffic plus impact; and the trench bedding condition. Tables have been prepared from which the pipe thickness may be determined for pit-cast pipe 3 through 60 in. in diameter, and for centrifugally cast pipe 3 through 48 in. in diameter for various loading conditions. The standard thicknesses of pipe centrifugally cast for the diameters in common use are shown in Table 7*a*. For convenience, these thicknesses may be referred to by standard thickness class numbers, each class being 8 percent heavier than the preceding class as shown in Table 7*b*.

Small-diameter cast-iron pipe in sizes 1¼, 1½, 2, and 3 in. and larger may be had from several manufacturers with several different types of joints. Small pipes are useful in filter plants and pumping stations and for service pipes.

There are a number of types of joints available for connecting cast-iron pipe as shown in Fig. 11. Bell-and-spigot was once the commonest type of joint, but it is now being replaced by joints requiring less skill for installation. Bell-and-spigot joints are, however, used extensively for fittings. The commonest materials used for making bell-and-spigot joints are lead or cement. Sulfur compounds, formerly used quite extensively, are no longer included in AWWA Specifications. When bell-and-spigot joints are made, the yarn used to prevent the joint material from running into the pipe should consist of one of the following: (1) molded or tubular rubber rings, (2) asbestos rope, or (3) treated paper rope. The older practice of using a yarn made

[1] Turneaure and Russell, "Public Water Supplies," pp. 721–725, John Wiley & Sons, Inc., New York, 1924. Bardoe, *Eng. News-Record*, **93**, 517, 1924. Tyler, *Water Works Sewerage*, August, 1939, p. 285.

[2] For further discussion of pipelines, see Sec. 3.

TABLE 7a. STANDARD THICKNESS* OF PIPE CENTRIFUGALLY CAST IN METAL MOLDS

Size, in.	Working pressure, psi	3½ ft of cover				5 ft of cover				8 ft of cover			
		Laying condition†				Laying condition†				Laying condition†			
		A	B	C	D	A	B	C	D	A	B	C	D
		Thickness, in.											
3	50	0.32	0.32	0.32	0.32	0.32	0.32	0.32	0.32	0.32	0.32	0.38	0.32
	100	0.32	0.32	0.32	0.32	0.32	0.32	0.32	0.32	0.32	0.32	0.38	0.32
	150	0.32	0.32	0.32	0.32	0.32	0.32	0.32	0.32	0.32	0.32	0.38	0.32
	200	0.32	0.32	0.32	0.32	0.32	0.32	0.32	0.32	0.32	0.32	0.38	0.32
	250	0.32	0.32	0.32	0.32	0.32	0.32	0.35	0.32	0.32	0.32	0.38	0.32
	300	0.32	0.32	0.32	0.32	0.32	0.32	0.35	0.32	0.32	0.32	0.38	0.32
	350	0.32	0.32	0.32	0.32	0.32	0.32	0.35	0.32	0.32	0.32	0.38	0.32
4	50	0.35	0.35	0.35	0.35	0.35	0.35	0.35	0.35	0.35	0.34	0.41	0.35
	100	0.35	0.35	0.35	0.35	0.35	0.35	0.35	0.35	0.35	0.35	0.41	0.35
	150	0.35	0.35	0.35	0.35	0.35	0.35	0.38	0.35	0.35	0.35	0.41	0.35
	200	0.35	0.35	0.35	0.35	0.35	0.35	0.38	0.35	0.35	0.35	0.44	0.35
	250	0.35	0.35	0.35	0.35	0.35	0.35	0.38	0.35	0.35	0.35	0.44	0.35
	300	0.35	0.35	0.35	0.35	0.35	0.35	0.38	0.35	0.35	0.35	0.44	0.35
	350	0.35	0.35	0.38	0.35	0.35	0.35	0.38	0.35	0.35	0.35	0.44	0.35
6	50	0.38	0.38	0.41	0.38	0.38	0.38	0.44	0.38	0.38	0.38	0.48	0.38
	100	0.38	0.38	0.41	0.38	0.38	0.38	0.44	0.38	0.38	0.38	0.48	0.38
	150	0.38	0.38	0.41	0.38	0.38	0.38	0.44	0.38	0.38	0.38	0.48	0.38
	200	0.38	0.38	0.41	0.38	0.38	0.38	0.44	0.38	0.38	0.38	0.52	0.38
	250	0.38	0.38	0.44	0.38	0.38	0.38	0.44	0.38	0.38	0.38	0.52	0.38
	300	0.38	0.38	0.44	0.38	0.38	0.38	0.44	0.38	0.38	0.38	0.52	0.38
	350	0.38	0.38	0.44	0.38	0.38	0.38	0.48	0.38	0.38	0.38	0.52	0.38
8	50	0.41	0.41	0.44	0.41	0.41	0.41	0.48	0.41	0.41	0.41	0.52	0.41
	100	0.41	0.41	0.48	0.41	0.41	0.41	0.48	0.41	0.41	0.41	0.56	0.41
	150	0.41	0.41	0.48	0.41	0.41	0.41	0.48	0.41	0.41	0.41	0.56	0.41
	200	0.41	0.41	0.48	0.41	0.41	0.41	0.52	0.41	0.41	0.41	0.56	0.44
	250	0.41	0.41	0.48	0.41	0.41	0.41	0.52	0.41	0.44	0.41	0.56	0.44
	300	0.41	0.41	0.48	0.41	0.41	0.41	0.52	0.41	0.44	0.44	0.60	0.44
	350	0.41	0.41	0.52	0.41	0.44	0.41	0.52	0.44	0.48	0.44	0.60	0.48
10	50	0.44	0.44	0.48	0.44	0.44	0.44	0.52	0.44	0.44	0.44	0.60	0.48
	100	0.44	0.44	0.52	0.44	0.44	0.44	0.52	0.44	0.48	0.44	0.60	0.48
	150	0.44	0.44	0.52	0.44	0.44	0.44	0.56	0.44	0.48	0.44	0.60	0.48
	200	0.44	0.44	0.52	0.44	0.44	0.44	0.56	0.44	0.48	0.48	0.60	0.52
	250	0.44	0.44	0.56	0.44	0.48	0.44	0.56	0.48	0.52	0.48	0.65	0.52
	300	0.48	0.44	0.56	0.48	0.48	0.48	0.56	0.48	0.52	0.52	0.65	0.56
	350	0.48	0.48	0.56	0.48	0.52	0.52	0.60	0.52	0.56	0.52	0.65	0.56
12	50	0.48	0.48	0.52	0.48	0.48	0.48	0.56	0.48	0.52	0.48	0.65	0.52
	100	0.48	0.48	0.56	0.48	0.48	0.48	0.56	0.48	0.52	0.48	0.65	0.52
	150	0.48	0.48	0.56	0.48	0.48	0.48	0.56	0.48	0.52	0.52	0.65	0.56
	200	0.48	0.48	0.56	0.48	0.48	0.48	0.60	0.52	0.56	0.52	0.65	0.56
	250	0.52	0.48	0.60	0.52	0.52	0.52	0.60	0.52	0.56	0.56	0.70	0.60
	300	0.52	0.52	0.60	0.52	0.56	0.52	0.60	0.56	0.60	0.56	0.70	0.60
	350	0.56	0.56	0.60	0.56	0.56	0.56	0.65	0.60	0.60	0.60	0.76	0.65

TABLE 7*a*. STANDARD THICKNESS* OF PIPE CENTRIFUGALLY CAST IN METAL MOLDS (*Continued*)

Size, in.	Working pressure, psi	3½ ft of cover				5 ft of cover				8 ft of cover			
		Laying condition†				Laying condition†				Laying condition†			
		A	B	C	D	A	B	C	D	A	B	C	D
		Thickness, in.											
14	50	0.51	0.48	0.59	0.51	0.51	0.48	0.59	0.55	0.59	0.55	0.69	0.59
	100	0.51	0.48	0.59	0.55	0.55	0.51	0.64	0.55	0.59	0.55	0.69	0.64
	150	0.55	0.51	0.59	0.55	0.55	0.51	0.64	0.59	0.64	0.59	0.75	0.64
	200	0.55	0.51	0.64	0.59	0.55	0.55	0.64	0.59	0.64	0.59	0.75	0.69
	250	0 59	0.55	0.64	0.59	0.59	0.59	0.69	0.59	0.64	0.64	0.75	0.69
	300	0.59	0.59	0.69	0.59	0.64	0.59	0.69	0.64	0.69	0.64	0.81	0.69
	350	0.64	0.64	0.69	0.64	0.64	0.64	0.75	0.69	0.75	0.69	0.81	0.75
16	50	0.54	0.50	0.63	0.58	0.58	0.54	0.63	0.58	0.63	0.58	0.73	0.63
	100	0.54	0.54	0.63	0.58	0.58	0.54	0.68	0.58	0.63	0.58	0.73	0.68
	150	0 58	0.54	0.63	0.58	0.58	0.54	0.68	0.63	0.68	0.63	0.79	0.68
	200	0.58	0.58	0.68	0.63	0.63	0.58	0.68	0.63	0.68	0.63	0.79	0.73
	250	0.63	0.58	0.68	0.63	0.63	0.63	0.73	0.68	0.73	0.68	0.79	0.73
	300	0.63	0.63	0.73	0.68	0.68	0.68	0.73	0.68	0.73	0.73	0.85	0.79
	350	0.68	0.68	0.73	0.68	0.73	0.68	0.79	0.73	0.79	0.73	0.85	0.79
18	50	0.58	0.54	0.63	0.58	0.58	0.54	0.68	0.63	0.68	0.63	0.79	0.68
	100	0.58	0.54	0.68	0.63	0.63	0.58	0.73	0.63	0.68	0.63	0.79	0.73
	150	0 63	0.58	0.68	0.63	0.63	0.58	0.73	0.68	0.73	0.68	0.79	0 73
	200	0.63	0.58	0.73	0.68	0.68	0.63	0.73	0.68	0.73	0.68	0.85	0.79
	250	0.68	0.63	0.73	0.68	0.68	0.68	0.79	0.73	0.79	0.73	0.85	0.79
	300	0.68	0.68	0.79	0 73	0.73	0.73	0.79	0.79	0.79	0.79	0.92	0.85
	350	0.79	0.73	0.79	0.79	0.79	0.79	0.85	0.79	0.85	0.85	0.92	0.85
20	50	0.62	0.57	0.72	0.62	0.67	0.57	0.72	0.67	0.72	0.67	0.78	0.72
	100	0.62	0.57	0.72	0.67	0.67	0.62	0.78	0.67	0.72	0.67	0.84	0.78
	150	0.67	0.62	0.72	0 67	0.67	0.62	0.78	0.72	0.78	0.72	0.84	0.78
	200	0.67	0.62	0.78	0.72	0.72	0.67	0.78	0.72	0.78	0.72	0.91	0 84
	250	0.72	0.67	0.78	0 72	0.78	0.72	0.84	0.78	0.84	0.78	0.91	0.84
	300	0.78	0.72	0.84	0.78	0.78	0.78	0.84	0.84	0.84	0.84	0.98	0.91
	350	0.84	0.78	0.84	0.84	0.84	0.84	0.91	0.84	0.91	0.84	0.98	0.91
24	50	0.68	0.63	0.79	0.68	0.73	0.63	0.79	0.73	0.79	0.73	0.85	0.79
	100	0.73	0.63	0.79	0.73	0.73	0.68	0.85	0.79	0.85	0.73	0.92	0.85
	150	0.73	0.68	0.79	0.79	0.79	0.73	0.85	0.79	0.85	0.79	0.92	0.85
	200	0.79	0.73	0.85	0.79	0.79	0.79	0.92	0.85	0.92	0.85	0.99	0.92
	250	0.79	0.79	0.85	0.85	0.85	0.79	0.92	0.85	0.92	0.85	0.99	0.99
	300	0.85	0.85	0.92	0.85	0.92	0.85	0.99	0.92	0.99	0.92	1.07	0.99
	350	0.92	0.92	0.99	0.92	0.99	0.92	0.99	0.99	1.07	0.99	1.07	1.07

* Thicknesses include allowances for foundry practice, corrosion, and either water-hammer or truck load.

† Laying conditions: A – flat-bottom trench, without blocks, untamped backfill. B = flat-bottom trench, without blocks, tamped backfill. C = pipe laid on blocks, untamped backfill. D = pipe laid on blocks, tamped backfill.

TABLE 7b. STANDARD THICKNESS CLASSES FOR CENTRIFUGALLY CAST PIPE*

Pipe size, in.	Pipe wall thickness, in., for standard thickness class No.									
	21	22	23	24	25	26	27	28	29	30
3	....	0.32	0.35	0.38	0.41	0.44	0.48	0.52	0.56	0.60
4	....	0.35	0.38	0.41	0.44	0.48	0.52	0.56	0.60	0.65
6	....	0.38	0.41	0.44	0.48	0.52	0.56	0.60	0.65	0.70
8	....	0.41	0.44	0.48	0.52	0.56	0.60	0.65	0.70	0.76
10	....	0.44	0.48	0.52	0.56	0.60	0.65	0.70	0.76	0.82
12	....	0.48	0.52	0.56	0.60	0.65	0.70	0.76	0.82	0.89
14	0.48	0.51	0.55	0.59	0.64	0.69	0.75	0.81	0.87	0.94
16	0.50	0.54	0.58	0.63	0.68	0.73	0.79	0.85	0.92	0.99
18	0.54	0.58	0.63	0.68	0.73	0.79	0.85	0.92	0.99	1.07
20	0.57	0.62	0.67	0.72	0.78	0.84	0.91	0.98	1.06	1.14
24	0.63	0.68	0.73	0.79	0.85	0.92	0.99	1.07	1.16	1.25
30	0.73	0.79	0.85	0.92	0.99	1.07	1.16	1.25	1.35	1.46
36	0.81	0.87	0.94	1.02	1.10	1.19	1.29	1.39	1.50	1.62
42	0.90	0.97	1.05	1.13	1.22	1.32	1.43	1.54	1.66	1.79
48	0.98	1.06	1.14	1.23	1.33	1.44	1.56	1.68	1.81	1.95

* Each class is made 8 percent heavier than the preceding class, starting with the thinnest, *i.e.*, minimum thickness, as the base class.

from jute or hemp (oakum) is not currently recommended, inasmuch as it was found that its use promoted the growth of bacteria. Neat Portland-cement mortar, also a nonconductor, has been used successfully as a jointing material. Mechanical-joint pipe, or pipe with push-on joints, is commonly used for new installations. The method of laying and jointing cast-iron pipe is covered in the AWWA Standard Specifications for Installation of Cast-iron Water Mains, C 600.

The standard types of bell-and-spigot fittings are shown in Fig. 9. USA Standard flanged fittings are shown in Fig. 10. Cast-iron pipe fittings with some of the special types of joints may be had from the manufacturers. For dimensions and weights of fittings see "Cast-iron Pipe Handbook" or manufacturers' catalogues.

8. Reinforced-concrete Pipe. Reinforced-concrete pipe is commonly used in sizes from 16 in. and up. In larger diameters, the cost compares favorably with that of cast-iron pipe.

Four types of reinforced-concrete pressure pipe are manufactured: (1) reinforced concrete; (2) prestressed reinforced concrete; (3) reinforced concrete with a steel membrane or cylinder; and (4) prestressed reinforced-concrete cylinder pipe. The AWWA Standards for the design and manufacture of reinforced-concrete water pipe are respectively: C 300, Reinforced-concrete Water Pipe—Steel Cylinder Type, Not Prestressed; C 301, Reinforced-concrete Water Pipe—Steel Cylinder Type, Prestressed; and C 302, Reinforced-concrete Water Pipe—Noncylinder Type, Not Prestressed.

Beveled pipe suitable for laying long-radius curves is available, as well as numerous standard fittings and adapters. Reinforced-concrete pipe may be tapped under pressure for large- and small-diameter connections by means of special techniques which are described in the manufacturers' literature.

Pipes and fittings are connected by means of a bell-and-spigot-type joint sealed by

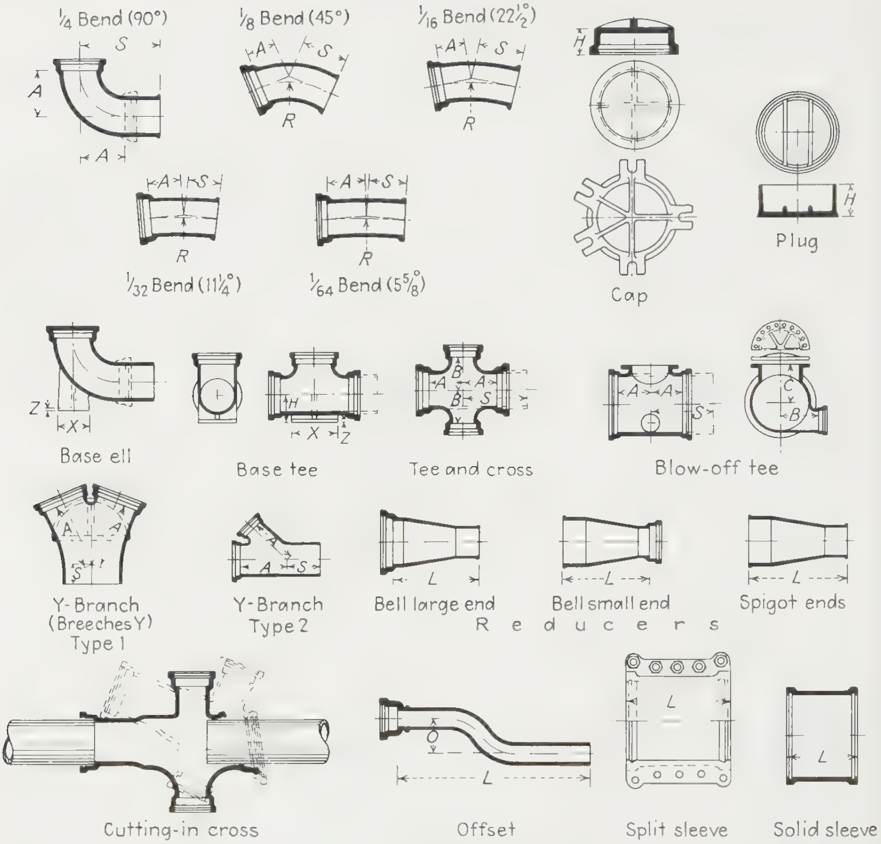

FIG. 9. AWWA standard cast-iron bell-and-spigot fittings. (*The Cast Iron Pipe Research Association.*)

a rubber gasket. Cement mortar, or other plastic material, is used to fill the space between the ends of adjacent pipes or fittings. Several typical joints are shown in Fig. 12.

9. Other Pipe Materials. Steel is widely used for pipelines larger than 30 in., particularly for supply lines and other lines in distribution systems that are not too frequently interconnected with smaller distributors. Both riveted and welded pipe are used. Because of the thinness of the plate used, it is particularly important to protect steel pipe against corrosion with interior lining and covering. Galvanized steel and wrought-iron pipes with screw joints are widely used for small distributors (less than 4 in.) upon which there are no hydrants. Galvanized pipe stands up well until the zinc coating is perforated, after which corrosion is very rapid.

10. Asbestos-cement Pipe. Asbestos-cement pipe is made from a mixture of asbestos fiber and Portland cement in the approximate proportions of 15 and 85 percent by weight, with silica added. The American product is made in three classes. Figure 13 shows the type of coupling used. The thickness of the pipe is 1.5 to 3 times that of the corresponding class of centrifugal cast-iron pipe. Cast-iron fittings and gate valves are used, but because of the extra thickness of asbestos-cement pipe, special bells are required for use with the larger sizes of class 150 and heavier pipe. Fittings with rubber ring joints for use with asbestos-cement pipe are available from several manufacturers.

Asbestos-cement pipe for pressure below 200 psi is lighter than cast-iron, class 150 asbestos cement weighing 60 to 85 percent of the weight of the corresponding class and size of cast-iron pipe (the percentage increasing with pipe size). The material is a nonconductor of electricity and is not subject to tuberculation but may collect iron

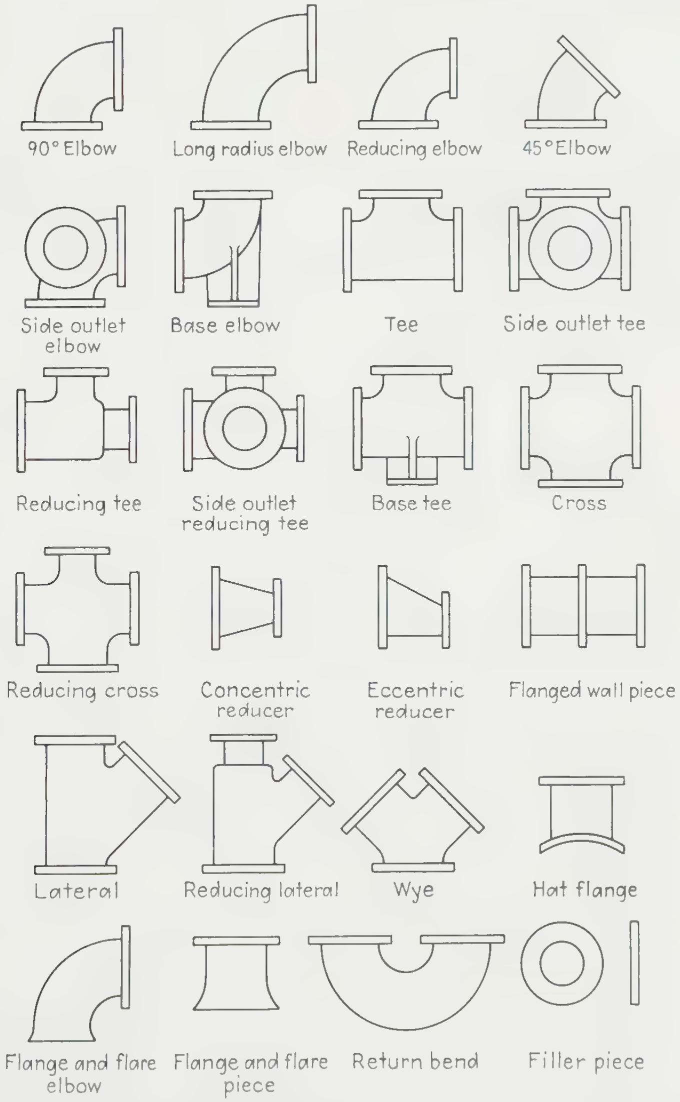

FIG. 10. American standard flanged fittings for cast-iron pipe. (*The Cast Iron Pipe Research Association.*)

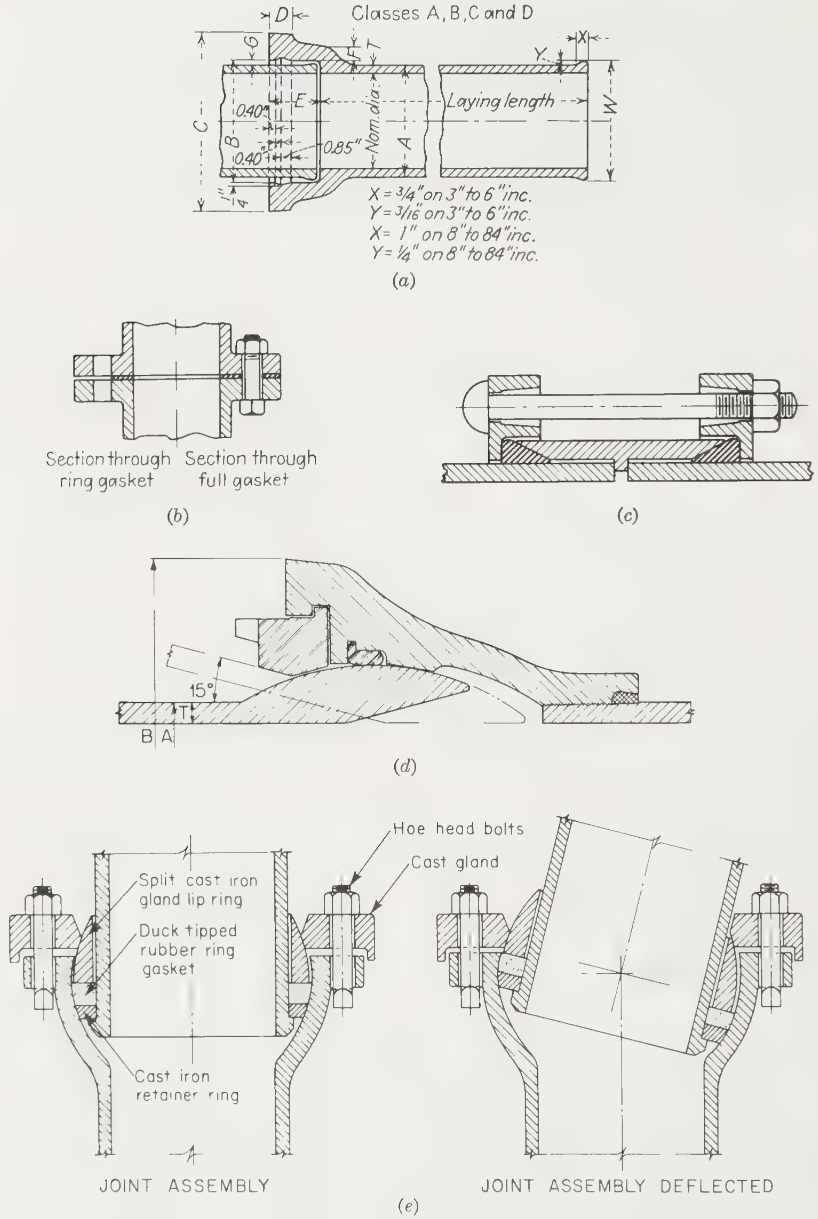

Fig. 11. Typical joints for cast-iron pipe. (*a*) AWWA standard bell-and-spigot pipe. (*b*) American standard flanged joint. (*c*) Dresser or sleeve-type coupling for plain-end pipe. (*d*) Usiflex boltless flexible joint. (*U.S. Pipe and Foundry Co.*) (*e*) Molox bolted flexible joint. (*American Cast Iron Pipe Co.*) (*f*) Tyton joint. (*U.S. Pipe and Foundry Co.*) (*g*) Victaulic joint. (*American Cast Iron Pipe Company.*) (*h*) Standardized mechanical joint pipe. (*i*) Threaded joint for small cast-iron pipe. (*American Cast Iron Pipe Company.*)

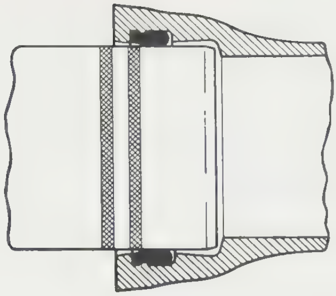

(f)

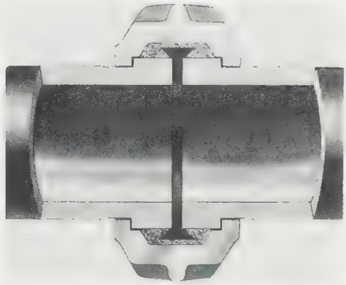

(g)

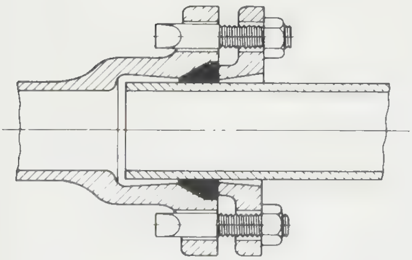

(h)

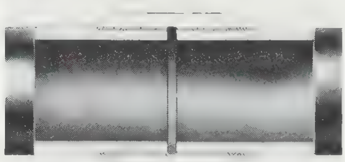

(i)

FIG. 11. *(Continued)*

and manganese oxides from waters heavily charged with iron or manganese. The material can be cut with a saw and other woodworking tools. Drilling and tapping for house services are readily accomplished. Tar coating of asbestos-cement pipe is desirable to retard the leaching of free lime from the cement.

11. Valves and Hydrants. Gate valves for distribution mains are usually of the inside-screw or nonrising-stem type illustrated in Fig. 14*a* and *c*. The outside screw and yolk or rising-stem-type valve, illustrated in Fig. 14*b*, is advantageous in that the position of the stem indicates how wide the valve is open; but this type cannot ordinarily be used on mains because of the depth of trench required for the rising stem. Valves for underground mains are usually provided with bell ends; but spigot ends, flanges, and special types of joints are available.

The standard specifications[1] for gate valves of the AWWA embrace hand-operated inside-screw, iron-body, bronze-mounted gate valves of both the solid-wedge and double-disk (either parallel seat or inclined seat) type, ranging in size from 3 to 48 in., for ordinary water service in approximately level setting under operating pressures not exceeding 150 psi. Valves are required to withstand an internal test pressure of 300 psi and to operate satisfactorily with 150 psi pressure on one side of the gate. The diameter of the waterway must be not less than the pipe diameter. In valves 3 in. in size and smaller, gates are of solid bronze. In larger valves, disks may be of cast iron with bronze rings. Valve seat rings, thrust bearings, packing glands, gear spindles, wedging devices, guides, rollers and tracks, and indicator mechanisms are made of bronze or are bushed or faced with bronze. Valve stems, stem collars, and nuts are made of manganese bronze having a tensile strength of not less than 60,000 psi for valve sizes 24 in. and smaller and 80,000 psi for valve sizes 30 in. and larger. Bell-end

[1] AWWA C 500.

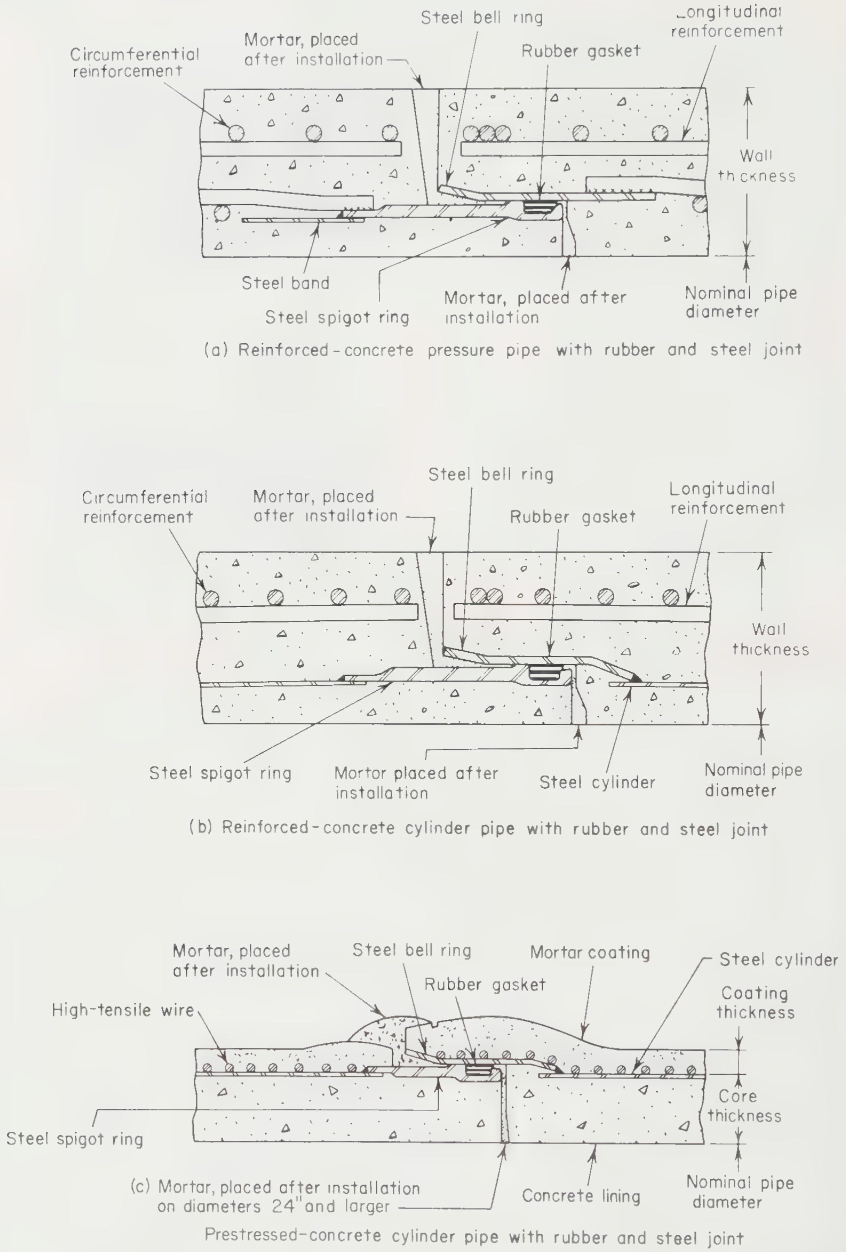

FIG. 12. Typical joints for reinforced-concrete pipe. (*International Pipe and Ceramics Corp.*)

valves up to and including 24 in. are made with sockets for class D pipe. Valves 16 in. in size and larger, designed to lie on their sides with horizontal stems, are required to have tracks and rollers to carry the weight of the gate as it moves into the bonnet. Stuffing boxes are packed with graphited hydraulic packing made of flax or properly lubricated braided asbestos or provided with O-ring seals. Wrench nuts are of cast iron, 2 in. square at the base, and provided with an arrow to mark the direction of turn for opening the valve. Gears for larger valves may be of cast iron or of steel if enclosed in an oiltight cast-iron gear case. All ferrous parts of the valve, except finished or bearing surfaces, are required to have two coats of pipe dip or varnish on the interior and three coats outside.

Large valves are usually provided with gears to facilitate hand operation. Vertical-stem valves are provided with spur gears (Fig. 14*b*) and horizontal-stem valves with bevel gears (Fig. 14*d*). Such valves may also be provided with bypasses (Fig. 14*b*) to facilitate opening. Smaller valves are usually provided with valve boxes (Fig. 14*c*), and for such valves it is necessary to remove the box and excavate down to the valve in order to repack the stuffing box. It is advisable to install large valves (16 in. and larger) in vaults or manholes in order to facilitate repacking and repairs.

Gate valves are sometimes used on lines between low-pressure and high-pressure districts, and in order to obviate the effects of dead ends in the pipe on both sides of the gate they are sometimes kept partly open. The gates thus act as throttling valves. Ordinary gate valves are unsatisfactory when used for this purpose owing to the chatter of the disks and their deflection downstream, which causes vibration and wear on the seats. Square-bottom valves designed especially for this purpose are now available.

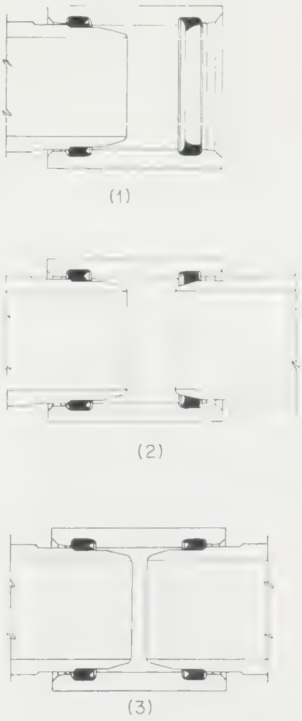

FIG. 13. Simplex joint for Transite pressure pipe. (1) Starting position. (2) Second position—one rubber ring compressed. (3) Final position—both rubber rings compressed.

Gate valves may be inserted in a water main under pressure by the use of special equipment. Figure 14*f* shows a machine which is sealed to the pipe in which the valve is to be inserted. A special cutter removes a short section of pipe which is then pulled into the bonnet with the cutter and a slide valve is closed. The bonnet is removed and the cutter is replaced with the gate valve to be inserted. The bonnet is replaced, the slide valve is opened, and the valve is positioned in the opening in the pipe. A special sleeve is then jacked against the valve, making watertight joints at the pipe, valve, and sleeve. The inserting machine is then removed and permanent joints made at the sleeve and valve.

When a distribution system receives its supply by gravity from a distant reservoir at a much higher elevation or through pipes from a high-pressure district, pressure-reducing valves are required in order to limit the pressure in the system at times of minimum draft. Automatic pressure-reducing valves which maintain the pressure constant on the downstream side of the valve are available for this purpose. Figure 15 illustrates a typical pressure-reducing valve, shown in the closed position. The pilot control valve is adjusted by hand for any desired pressure on the delivery side of the main valve. Whenever the delivery pressure lowers below the adjusted value, the spring against the pilot diaphragm causes the pilot valve to open and permit water above piston B to escape through M and N to the delivery side. The valve thus opens owing to the higher pressure under piston B. While the valve is open, water flows through the main valve and also through port L and needle valve S into the chamber above B. When the flow through the main valve becomes sufficient to raise the delivery pressure to the adjusted value, the pilot valve closes and the piston is held in position at the proper opening.

Altitude-control valves are used on the inlet pipes to distribution reservoirs and elevated tanks to shut off the inflow and prevent overflow when the water level gets too high. Figure 16 shows a typical altitude valve in the closed position. When the valve is open, water may flow in either direction. During inflow when the reservoir water level reaches the value sufficient to overcome the adjustment of the spring W by exerting pressure above diaphragm R, the pilot exhaust valve I is closed and pilot valve H is opened. Water is thus permitted to flow through L and M into the chamber above B and close the valve. In the type of valve shown in the figure, the valve will

Fig. 14*a*. Inside-screw-type cast-iron gate valve. (*Ludlow.*)

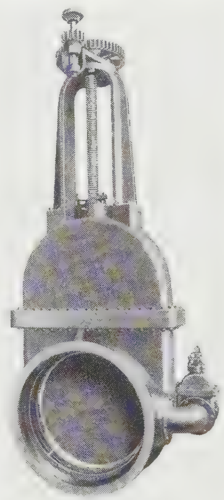

Fig. 14*b*. Outside-screw-and-yoke-type cast-iron gate valve with spur gears and bypass. (*Rensselaer.*)

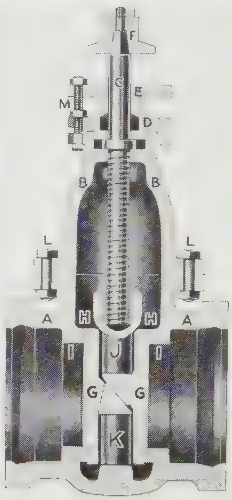

Fig. 14*c*. Details of inside-screw-type gate valve. (*Ludlow.*)

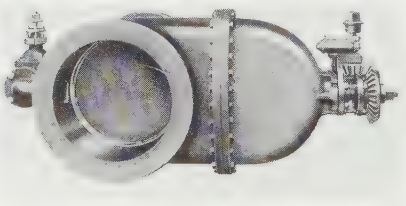

Fig. 14*d*. Inside-screw-type cast-iron gate valve with horizontal stem, cast-iron bevel gears, and bypass. (*Rensselaer.*)

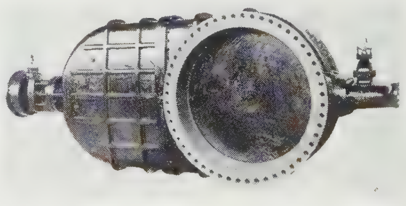

Fig. 14*e*. Inside-screw-type cast-iron gate valve with horizontal stem and oil-encased steel bevel gears and bypass. (*Darling.*)

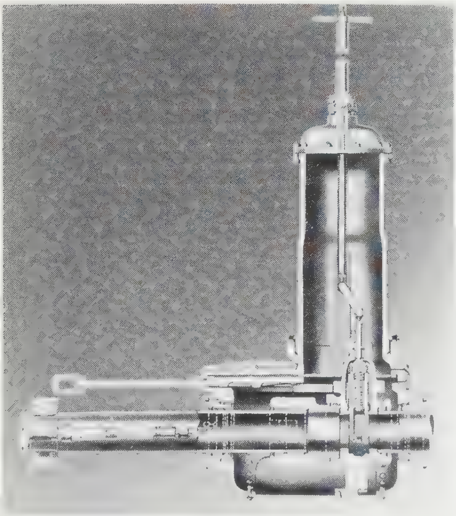

FIG. 14*f*. Valve-inserting machine showing gate valve in place. (*A. P. Smith.*)

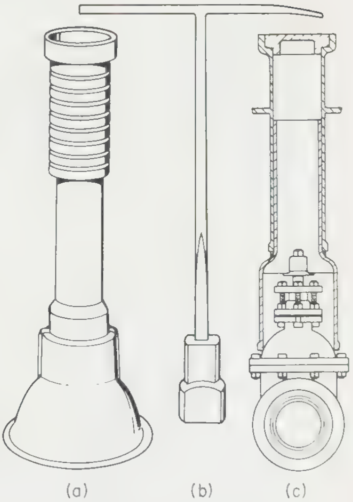

FIG. 14*g*. Extension valve boxes and valve wrench. (*Kennedy.*)

not open until the reservoir water level is lowered. Hence for removing storage water for distribution when the altitude valve is closed, a separate discharge line from the reservoir or a bypass around the altitude valve is required, as shown in Fig. 17. Other styles of valves are available, some of which are double-acting and will open when the pressure on the inlet side of the valve lowers below the pressure corresponding to

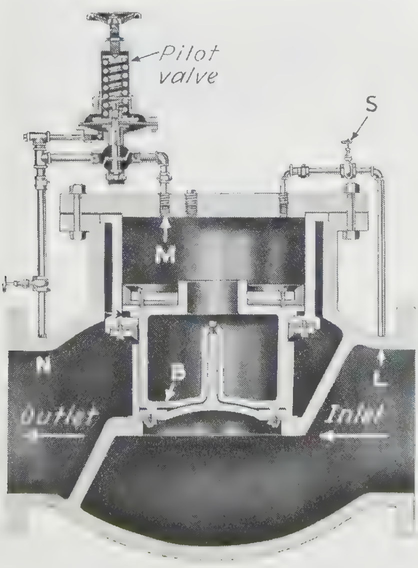

FIG. 15. Automatic pressure-reducing valve. (*Golden-Anderson.*)

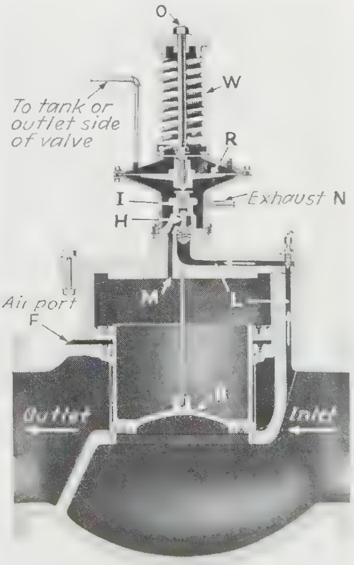

FIG. 16. Single-acting altitude-control valve. (*Golden-Anderson.*)

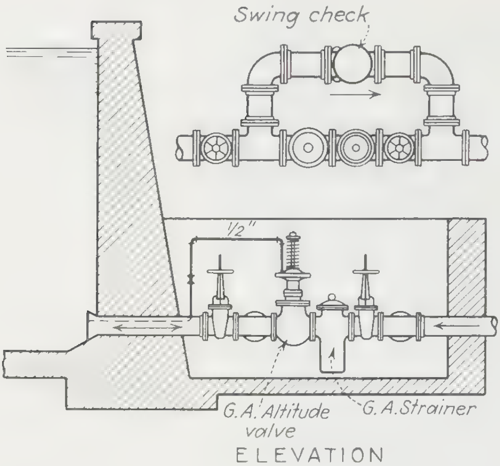

FIG. 17. Installation of single-acting altitude valve. (*Golden-Anderson.*)

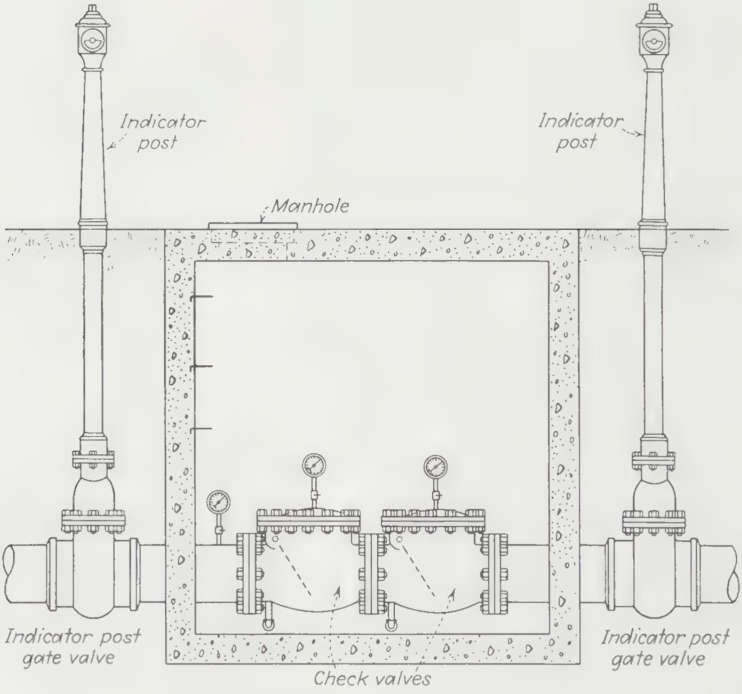

FIG. 18. Fire-service connection using two Factory Mutual check valves. (*Ludlow.*)

the reservoir level. Other valves are designed to close when a high-pressure fire pump is discharging into the system regardless of the reservoir water level.

Pressure-reducing and altitude valves are particularly susceptible to trouble from freezing in cold weather because of the presence of the small-size control water pipes and passages in which water is often still. For this reason, such valves should be adequately housed where they are readily accessible, and provisions should be made for heating the interior of the housing in extremely cold weather.

Check valves, which permit flow through a pipe in only one direction, have their principal use in the suction and discharge lines of pumps. They are sometimes used in distribution systems, however, one use being in connection with altitude valves as shown in Fig. 16. One important use in distribution systems is for the prevention of backflow of a separate contaminated industrial fire supply into the municipal distribution system. Any such cross connection between an impure and a potable water is a potential health hazard, because of the possibility that the valves may not seat tightly. An installation consisting of two swing check valves in series (Fig. 18) is recommended by the Associated Factory Mutual Laboratories and is accepted by some health departments. Figure 19 illustrates a typical horizontal swing or flap check valve. There is considerable friction loss through this type of check valve. In cases where it is necessary to minimize the friction loss, automatic power-operated check valves of various types which provide openings the full area of the pipe may be had. Motor- or hydraulic-operated gate valves may be used, but the recently developed revolving cone or butterfly valves are superior. Cone or butterfly valves may also be used as gate, altitude, and pressure-reducing valves with suitable controls. Tilting-disk check valves are also much superior to swing checks with regard to head loss and to chatter.

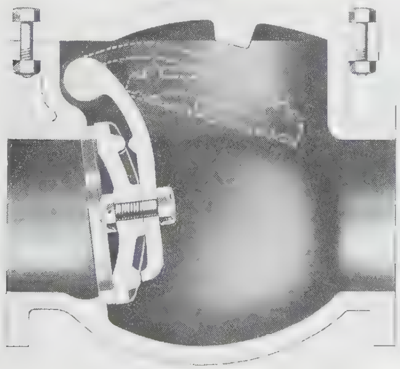

FIG. 19. Typical horizontal swing check valve. (*Ludlow.*)

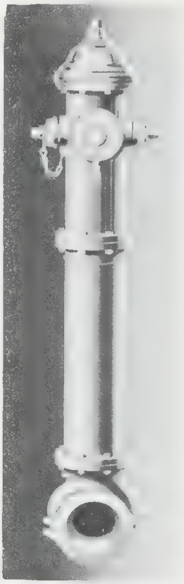

FIG. 20*a*. Compression-type post fire hydrant. (*A. P. Smith.*)

Fire hydrants are made in three general types: (1) the post hydrant with a vertical barrel extending 2 or 3 ft above the ground surface; (2) the flush hydrant in which the top of the barrel and the nozzle are underground in a box whose cast-iron cover is flush with the ground surface; and (3) the wall hydrant which is set back in the wall of a building. Post hydrants are usually just in back of the curb line, and because of this exposed position they are frequently damaged by motor vehicles. The other two types of hydrants are not thus subject to damage, but they are not so satisfactory as post hydrants because of their limited capacity and because they are more difficult to find quickly. Flush hydrants are not satisfactory in northern climates because of the difficulty of keeping the covers clear of snow.

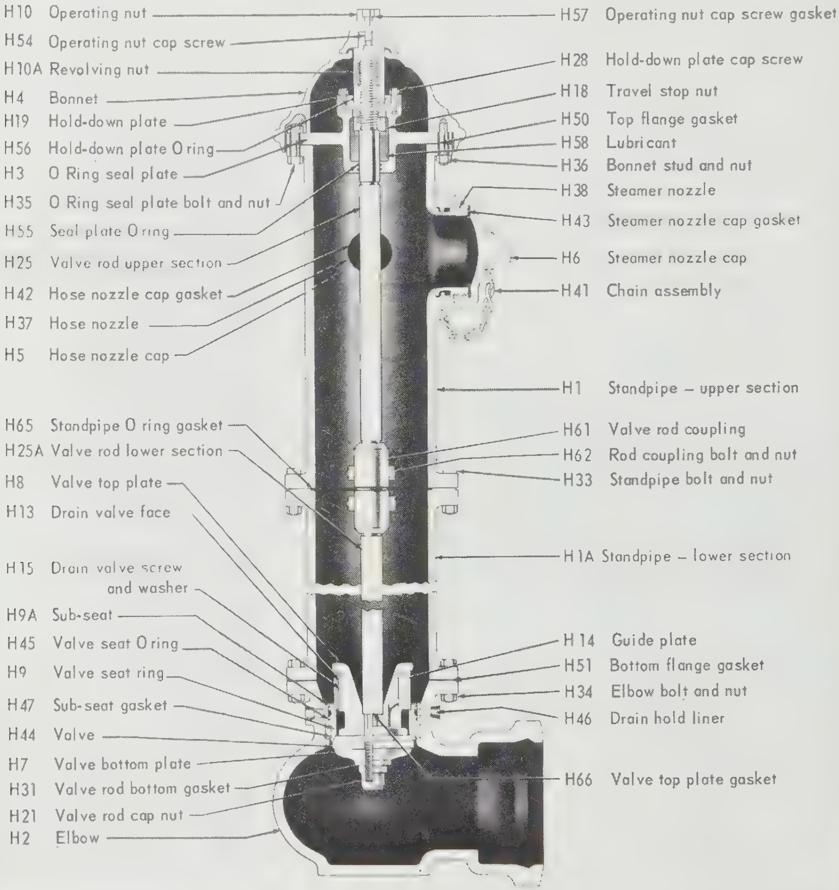

FIG. 20*b*. Details of compression-type post fire hydrant. (*A. P. Smith.*)

The standard specifications[1] (1964) of the AWWA and the NEWWA are for post hydrants of the compression-valve (Fig. 20*a*) and gate-valve (Fig. 21) type. The design should permit the ready removal of the valve without excavation and should be such that the valve will remain closed in case of damage to the top of the barrel. Hydrants are classed as single-hose, two-hose, and two-hose and pumper, according to the arrangement of hose and pumper nozzles. The size of the hydrant is designated by the diameter of the valve opening, which should be at least 4 in. for two-hose, 5 in. for three-hose, and 6 in. for four-hose hydrants. The length of the hydrant is defined

[1] AWWA C 502.

as the vertical distance from the ground surface to the bottom of the connecting pipe. Friction losses should be under 1 psi for each 250-gpm fire stream. When the barrel is made in sections, the flanges or connection should be at least 2 in. above the ground surface. Positive-operating drain valves are required to drain the hydrant completely and quickly when the main valve is closed in order to prevent freezing and to close tightly when the main valve is opened. The hydrant top should be designed to prevent interference with operation due to freezing, and provision should be made for convenient lubrication. Barrels, hydrant heads, valve gates, and nozzle caps may be made of cast iron. Outlet nozzles, valve seats or seat rings, drain valves, stuffing-box glands and gland-bolt nuts, and either the operating stem or the operating nut should be made of bronze or other noncorrodible material. The main valve should be faced with rubber, leather, or balata or, in case of slide-gate type valves, with a bronze ring. All iron parts inside and out, except the outside surface above the ground which should be painted, are required to have a hot bituminous dip coat or two bituminous paint coats. The outside surface above the ground should be painted a color[1] to distinguish between private and public hydrants, and the hydrant tops and nozzle caps should be given a proper color to indicate the hydrant capacity.

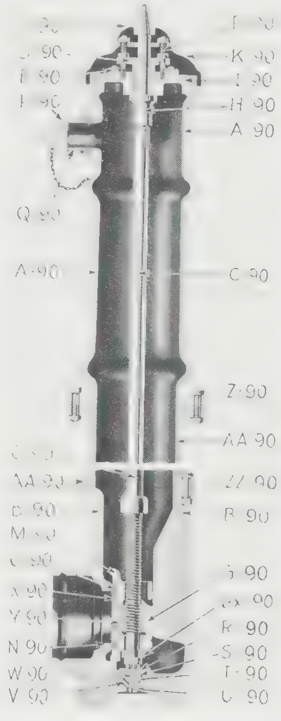

Fig. 21. Slide-gate-type post fire hydrant. (*Ludlow.*)

A post hydrant constructed with a safety joint above the ground surface permits the top of the hydrant to be knocked off by motor vehicles with a minimum of damage (see Fig. 20*b*). In installing a hydrant, it is desirable that the drain valve be below the frost line and be provided with a reliable outlet to ensure proper emptying of the barrel in cold weather. A usual provision is to surround the bottom of the barrel with gravel, but this is inadequate if the groundwater table is above the drain valve or if the earth surrounding the gravel is impervious. It is good practice to provide hydrants with gate valves on the supply pipes in order to make repairs to a hydrant without the necessity of shutting off a section of main. In order to prevent strains on hydrant barrels when the surrounding ground heaves owing to frost action, the barrel should be surrounded with gravel to the ground surface and flanges placed above the ground as provided by the standard specifications of the AWWA and the NEWWA. Some manufacturers provide sliding frost cases of cast iron for protection against heaving ground.

Both hydrants and gate valves in distribution systems are so infrequently used that they are subject to jamming due to corrosion and injury from other causes which may make them useless when needed. Complete inspections of all valves should be made annually and hydrants should be inspected semiannually and after each use, during which each valve and hydrant is opened and closed, lubricated, repacked, and repaired if necessary. Records of all inspections and repairs should be kept. Such inspections frequently result in the discovery of closed gate valves which should be open.

[1] AWWA C 502.

12. Corrosion and Electrolysis.[1] Corrosion may be broadly defined as the chemical action of certain external agencies on metals which causes their deterioration or destruction. Metals tend to revert to more stable compounds, of which the metal ores, as found in nature, are familiar examples. Corrosion is of great economic importance in water distribution, for the deterioration of pipelines and their loss of capacity with age are due primarily to corrosion and its products, scale and rust tubercles. It is also of great importance in water treatment, for the protection of the piping against corrosion and the prevention of red-water troubles are now recognized as a major function of water treatment.

The electrochemical theory of corrosion is presented briefly below in terms of the corrosion of iron, lead, copper, and zinc, the principal metals used for water distribution.

Water is corrosive to a solid metal when it tends to dissolve the metal as positive ions or to furnish negative ions to react with the metal at the interface. Corrosion proceeds by a transfer of negative electrons at *anodic* areas from the water to the metal. These electrons flow through the metal to *cathodic* areas where they are given up to constituents in the water. This flow of electrons constitutes a flow of electric current, and the circuit is completed through the water by the motion of ions between the two electrodes of the cell. In order that the current may flow, there must be an electrochemical or *half-cell* reaction at the anode and an equivalent half-cell reaction at the cathode. The two reactions which take place in a particular case are those which produce the greatest potential between the electrodes. The actual potential is determined by the difference ΔE of the oxidation potentials of the half-cell reactions.

The potential E of a half-cell reaction is a function of the water temperature and the concentrations of the ions and dissolved substances which take part in the reaction. At 25 C, the potential is

$$E_{25} = E_{25}^{\circ} - \frac{0.05916}{n} \log Q \tag{5}$$

where E_{25}° is the *standard oxidation potential* of the half-cell reaction at 25 C, n is the number of electrons transferred, and Q is the product of the activities of the reaction products divided by the product of the activities of the reactants. For details see Camp.[1]

In the presence of dissolved oxygen, an oxide film will form in the anode. If this film stays intact, as it probably does over most of the metal surface, the metal which took part in the formation of the film becomes *passive* and can no longer take part in an anodic half-cell reaction. The film probably does take part in the cathodic reactions with further buildup of the film with precipitates. For corrosion to proceed, other anodic reactions must take place beneath the film where they are protected from dissolved oxygen or other *passivators* such as NO_2^-, NO_3^-, and $Cr_2O_7^{--}$, which form similar oxide films at the anode. Since $Zn(OH)_2$ is quite soluble below pH 8.8, any film formed gives no protection below this pH. At higher pH values, the reaction may become so violent that the precipitate is pulled out of the metal surface in a fluffy white deposit of considerable thickness.

At low pH values, the metals enter solution at the anode as positive ions, and at high pH values solid precipitates are formed at the anode. It is evident, therefore, that except in the case of Zn, corrosion may be retarded by anodic protection through a rise in pH value to plate out hydroxide, carbonate, or phosphate at the anode. The

[1] Camp, T. R., "Water and Its Impurities," p. 145, Reinhold Publishing Corporation, New York, 1963.

degree of protection furnished depends upon the effectiveness of the coating produced. Ferrous hydroxide formed on iron will probably oxidize in the presence of dissolved oxygen to form ferric hydroxide, or ordinary iron rust, which is known to be a relatively poor coating. For all the metals, the most important cathodic reactions depend upon the presence of dissolved oxygen which enters into the reactions. In natural waters, the corrosion rate is almost directly proportional to the concentration of dissolved oxygen.

In the corrosion of iron, it will be noted that ferric hydroxide (hydrous ferric oxide), or red iron rust, is usually formed at the cathode and it may be formed at the anode by oxidation of the hydrous ferrous oxide. Magnetic iron oxide, Fe_3O_4, sometimes found in rust deposits, is a mixture of ferric and ferrous oxides. Iron rust is a loosely formed crystalline structure which in water pipes sometimes contains organic deposits all of which are easily scoured from the metal surface during heavy drafts to produce red water. If permitted to grow unrestricted, rust may be built up into tubercles or blisters which restrict the area of the pipe and reduce its capacity. One of the principal objects of corrosion abatement, therefore, is to inhibit the formation of iron rust.

Bronze is a copper-tin alloy. Cast bronze contains about 85 percent copper, 5 to 10 percent tin, and the remainder zinc and sometimes lead. Silicon-manganese bronze, which is quite strong, contains 96 percent copper, 3 percent silicon, and 1 percent manganese. Brass is a copper-zinc alloy containing 60 to about 90 percent copper. Red brass with an 85:15 ratio is comparatively immune from dezincification. Manganese bronze is a 60:40 brass modified in casting form with small amounts of iron, manganese, aluminum, and nickel for strength and hardness. Copper-nickel alloys, cupronickels with more than 50 percent Cu, and monels with less than 50 percent Cu are very resistant to corrosion in both fresh and salt water. Stainless steel is an alloy of steel with Cr and Ni. It is highly resistant to corrosion over a wide pH range but should not be used in brackish or salt water because Cr forms a complex ion with Cl^-. Ferrous chromite formed at the cathode in the corrosion of stainless steel is practically insoluble.

When any metal, such as iron, is placed in contact with a more cathodic material, such as copper, the corrosion potential is greater than for a single metal. A galvanic cell is thus set up, and a form of corrosion known as *electrolysis* is produced. With steel in contact with brass, the corrosion rate of steel is approximately doubled and that of brass greatly reduced. If iron is in contact with a more anodic metal such as zinc, the zinc tends to dissolve. Zinc coatings (galvanizing) on iron thus protect iron from corrosion until the coating is destroyed. Although zinc tends to dissolve faster than iron, protective coatings are produced by zinc in neutral waters which are more effective in retarding the corrosion of zinc than the analogous compounds are in retarding iron corrosion. In the acid range, however, and in the presence of free CO_2, zinc galvanizing is not a very effective protection.

Another form of electrolysis known as *stray-current electrolysis* is best exemplified by the corrosion of iron pipes laid in the soil near electric railway tracks. Direct current escapes from the rails, or is returned through both the rails and the soil, and flows from soil to pipe where the potential is in the proper direction and from pipe to soil where the potential is reversed. Where the positive current leaves the pipes, the iron goes into solution and pitting of the pipe results. With alternating current, the corrosive effect is usually less than 1 percent of that with direct current because of the counteracting effect of the reverse in potential. The effects of stray-current electrolysis on piping may be mitigated by (1) better bonding of rails, (2) track insulation, (3) reinforcement of rail conductivity, (4) increasing the number of power substations, (5) interconnection of tracks, (6) insulated negative feeders, (7) three-wire system, (8) reversed polarity trolley system, (9) double-contact conductor system, (10) a-c system, (11) safe location of pipes with respect to rails, (12) insulation of pipes and cables, (13) insulating joints in pipes, and other methods.

The grounding of electric circuits in buildings on water pipes for the safety of persons using the electrical equipment is widely practiced. No deleterious effects seem to result from this practice provided the connections do not result in the continuous or intermittent flow of stray currents through the pipes under normal operating conditions.

There are two general methods for minimizing or preventing the corrosion of metals in contact with water or moisture: (1) the protection of the metal itself by the application of a protective lining or covering, and (2) the treatment of the water to remove the agents contributing to corrosion or to form precipitates that act as protective films. Plastics, such as polyvinyl chloride, are highly resistant to disintegration over a wide pH range and are coming into use for plumbing systems. For metal tanks, pipe, and structures in contact with the air, water, or soil, protective coatings are used. They may be in the form of paints, bituminous coatings, enamels, alloys, zinc coatings, rubber and plastic linings, cement linings, and concrete encasement. The corrective treatment of water is discussed in Sec. 38.

Cathodic protection[1] is sometimes used for the interior wetted surface of steel water tanks. In this process, a direct current is passed continuously from anodes immersed in the water to the tank plates as cathodes.

Rust tubercles in iron pipelines may be partly removed by pulling cleaners through the pipes or by water-driven turbine cleaners. A portion or all of the pipeline to be cleaned must be taken out of service during the cleaning operation. Pipelines have been restored to almost their original capacity by cleaning, but corrosion proceeds more rapidly after cleaning owing to the fact that the surface of the metal is exposed unevenly. Loose rust, growths, and sediment in pipes may be partly removed by flushing through fire hydrants or blowoffs.

13. Pipe Linings and Protective Coatings. The AWWA Specifications (1964) for cast-iron pipe and fittings require a bituminous coating inside and out of either asphalt or coal-tar base. Coal-tar coatings are more durable than asphalt coatings for underground water pipes after the pipes are in service, but they are more subject to damage in shipping and handling the pipes because the temperature range between the brittle and softening points of coal-tar pitch usually does not exceed 45 F, whereas asphalts have a range of 120 to 130 F. Nearly all cast-iron water pipe is furnished with dip coatings unless more effective coatings are specified. Flanged pipe is commonly furnished without coating.

The USA Standard Specifications (1953) for cement lining for cast-iron pipe call for minimum thicknesses of $\frac{1}{8}$ in. for pipes to 12 in. in diameter, $\frac{3}{16}$ in. for pipes 14 to 24 in. in size, and $\frac{1}{4}$ in. for pipes 30 to 48 in. in size. A satisfactory mortar may be obtained with 1 part Portland cement to 1 part sand by volume. Pipe to be lined with cement should not be precoated on the inside with tar or asphalt and should be cleaned thoroughly. New pipe is cement-lined at the foundry by the centrifugal process, the method being similar to that used in applying bitumastic lining. Fittings are lined by hand brushing. When water is first applied to cement-lined pipe, some free lime and other materials are leached out of the cement and cause hardness and alkalinity in the water. This effect usually lasts for only a few days but may continue if the water is soft and corrosive and result in the slow disintegration of the lining. Smaller pipes may be given hot-tar dip coatings after the cement lining has set, but for larger pipes the expansion due to the heat may result in breaking the bond between pipe and cement. Bituminous paint may be used with larger pipes. Cement lining of pipes in place may be accomplished by special machines.

[1] Hamilton, *Water Works Sewerage*, November, 1939, p. 433.

14. Capacity of Mains. The capacity of water mains is generally expressed in the United States in terms of the Hazen-Williams coefficient C. The 1935 Report[1] of the Committee on Pipe Line Friction Coefficients of the NEWWA contains a comprehensive summary of existing information on this subject.

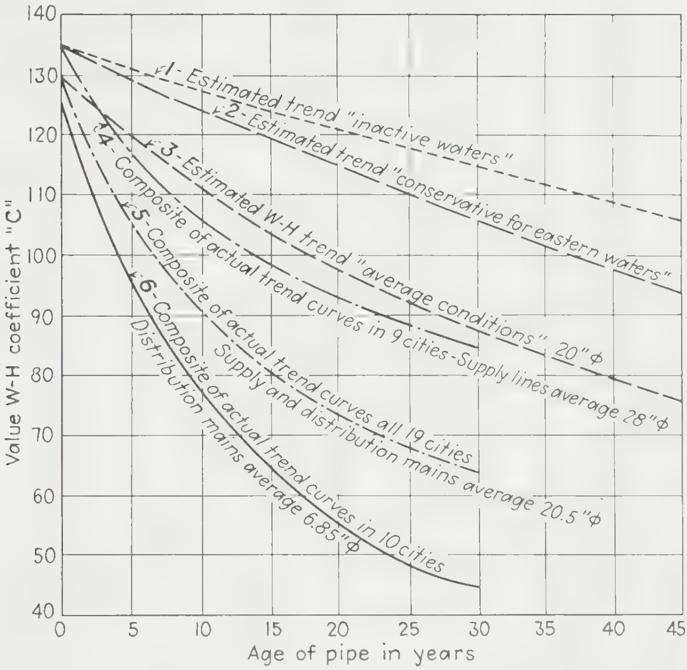

Fig. 22. Summary of estimated and actual trends of age-coefficient relations for tar-coated cast-iron pipe.

The average capacity of tar-coated cast-iron pipes of all sizes and their loss of capacity with age are shown in a general way in Fig. 22, taken from the Report. The effect of the pH value of the water upon the loss of capacity of tar-coated pipe is indicated by Table 8. The value of C adopted for the design of new tar-coated cast-

Table 8*

pH Value of Water	Average Capacity Loss in Tar-coated Cast-iron Pipe in 30 Years, %
8.0	30
7.5	35
7.0	45
6.5	60
6.0	85

* *J. NEWWA*, **49**, 235, 1935.

iron pipelines is 135 for mains 16 in. and larger and 125 for smaller mains, which includes an allowance for friction due to tees, valves, bends, etc.

For cement lining applied centrifugally to cast-iron pipe 4 to 24 in. in diameter, the data[1] indicate an average value of C of 134 based on nominal diameter and 150 based on actual net diameter. Service tests indicate very little loss of capacity with age.

[1] *J. NEWWA*, **49**, 235, 1935.

The data[1] on new bitumastic enamel, centrifugally applied, indicate values of C from 145 to 160 for supply lines 16 in. and larger and from 140 to 150 for distribution mains less than 16 in. in diameter. Bitumastic lining if properly applied is effective in sustaining hydraulic capacity, but experience indicates that it adheres better to steel than to cast-iron pipe, and for satisfactory adherence the metal surface must be thoroughly clean. Tests on Transite[2] and other asbestos-cement pipe indicate values of C from 145 to 165. For design purposes, a value of C of 140 is recommended for Transite pressure pipe. The capacity of asbestos-cement pipe is expected to remain constant, for no deterioration was observed in some lines which had been in service for 16 years.

FIG. 23*a*. Corporation tapping machine. (*Mueller.*)

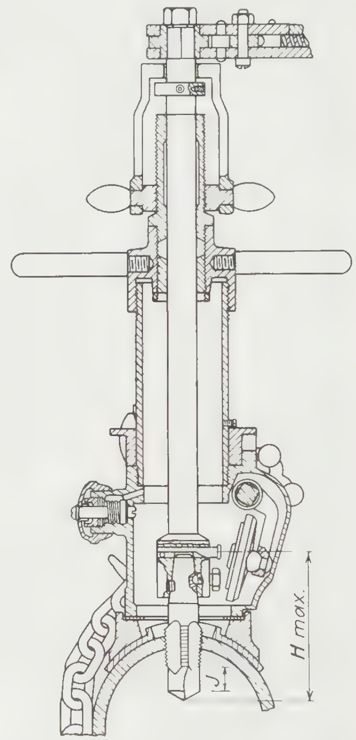

FIG. 23*b*. Corporation tapping machine with tapping tool in use. (*Mueller.*)

Measurements of head losses due to 6- and 12-in. bends, tees, and crosses in distribution systems by Schoder and Vanderlip[3] indicate that the additional loss in excess of that due to straight pipe is less than the velocity head for a single fitting even for the worst case of flow division. The average loss for 90-deg bends is about 0.1 the velocity head for AWWA standard long-turn bends and about 0.27 for short-turn bends. The average loss for crosses and tees with deviated flow is about 0.51 times the entry velocity head for AWWA standard long-turn fillets and about 0.57 for short-turn fillets. An investigation by Ricketts[3] of the head losses between two points in a typical distribution system for both average and fire flows, in which the Schoder-

[1] *J. NEWWA*, **49**, 235, 1935.
[2] McGINNIS, *J. AWWA*, **26**, 596, 1934.
[3] *Cornell Univ. Eng. Expt. Sta. Bull.* 20, September, 1935.

Vanderlip head-loss values for tees and crosses were used, indicated that the loss due to fittings was about 1.3 percent of the total loss and was about the same for both long and short types. A saving of 3 to 10 percent of the cost of fittings was indicated by the use of short instead of standard AWWA tees and crosses. From a study by Wiggin[1] of the economics of bends, the long-turn bends were shown to be more economical because of the reduced friction loss.

15. Customers' Services. Service taps ½ to 2 in. in size may be made to mains under pressure by means of corporation tapping machines (Fig. 23*a*). With such a machine held tight against the main, the pipe is drilled and tapped with a special tool (Fig. 23*b*). The tool is then withdrawn above the flap valve, which is closed to prevent the escape of water, after which the tool is removed from the cylinder by unscrewing the cap. A corporation cock is then substituted for the tool in the boring bar, which is inserted in the cylinder, and the cap is screwed on. The flap valve is opened and the corporation stop is screwed into the pipe, after which the machine is removed.

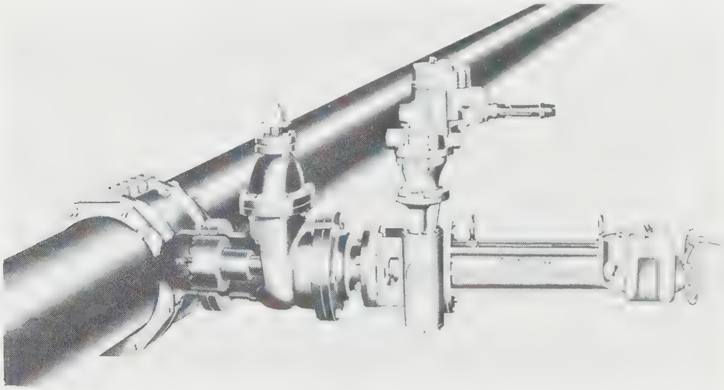

FIG. 24. Mechanical joint-tapping sleeve and valve and power-operated tapping machine. (*A. P. Smith.*)

Taps 2 to 8 in. in size may be made to mains under pressure with the tapping machine shown in Fig. 24. This machine operates through a tapping valve which is held to the pipe permanently by means of a tapping sleeve, the service pipe being attached to the flanged end of the valve. Similar machines are available for making larger taps up to 42 in., the larger machines being power-operated. Most service taps are made with corporation tapping machines. The larger taps are useful for large consumers, for fire-protection services, or for connecting new mains or hydrants into the system.

Small service lines consist of corporation cocks with or without lead goosenecks, the service pipe to the curb at which point an accessible curb cock is usually placed, the service pipe into the building, the meter, and a stop-waste valve. The meter is preferably placed at the curb (Fig. 25*a*), except in very cold climates or where cellars are available. Goosenecks are for the purpose of providing flexibility to relieve strains due to unequal settlement. They are omitted with lead pipe and sometimes with copper tubing. Services should be deep enough to avoid freezing in winter.

Small service pipes,[2] ⅝ to 1¼ in., may be made of copper tubing, galvanized steel, wrought iron, and iron-pipe-size brass or copper, the preference[3] in America being in the order named. For sizes 1¼ in. and larger, cast iron is also available, with and

[1] *Cornell Univ. Eng. Expt. Sta. Bull.* 20, September, 1935.
[2] AWWA C 800.
[3] *J. AWWA*, **44**, 1021, 1952.

without lining. The use of plastics for service pipes is also coming into more prominent use. The use of lead pipe is not recommended as advisable for use in underground service lines. Service pipes may be laid by excavation for the full length of the pipe, by boring under the pavement, and by jacking or driving the pipe under the pavement. Lead and copper tubing cannot be jacked. According to Pracy,[1] the relative costs of services installed in San Francisco under pavements where driving was used for iron-size pipes were as follows for several different materials in the order of increasing cost:

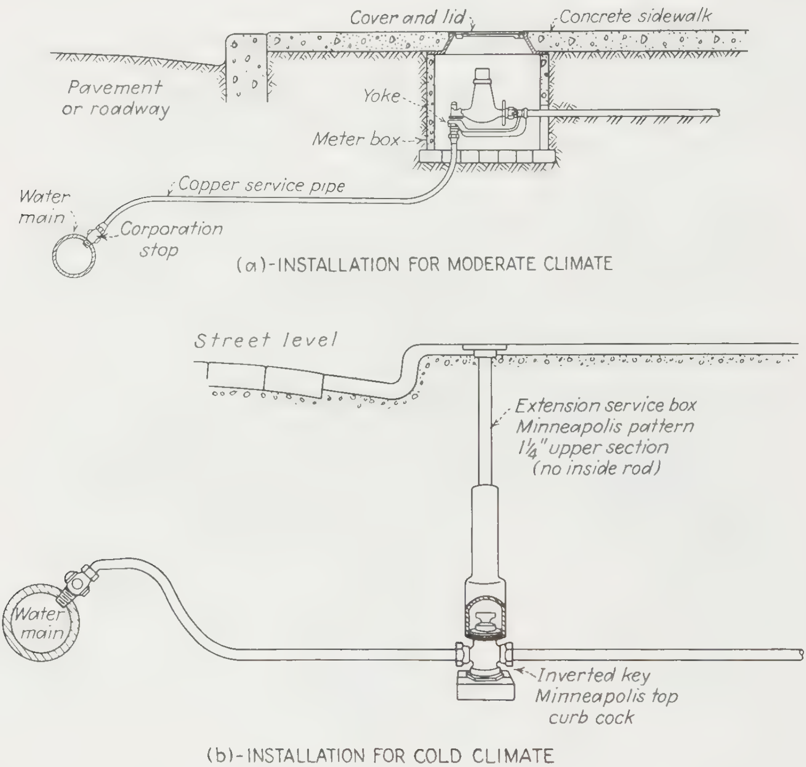

FIG. 25. Typical customers' services. (*Mueller.*)

(1) galvanized steel, (2) I.P.S. brass, (3) I.P.S. copper, (4) copper tubing, and (5) AA lead. Where no pavement was encountered, the relative costs were as follows: (1) copper tubing, (2) galvanized steel, (3) I.P.S. brass, (4) I.P.S. copper, and (5) AA lead. The type of material best suited for a given case depends not only on first cost but also on the corrosive qualities of the water and the soil.

The size of services should be determined from the customers' demand, the available pressure, and the friction losses, but should preferably be not less than ¾ in. Corporation cocks and meters[2] should preferably be the same size as the service, except that meters must also be selected for accurate registration at low flows and this provision may call for a smaller meter. Friction losses in new services may be estimated by means of Table 9.

[1] *J. AWWA*, **46**, 775, 1954.
[2] *J. AWWA*, **23**, 1435, 1931.

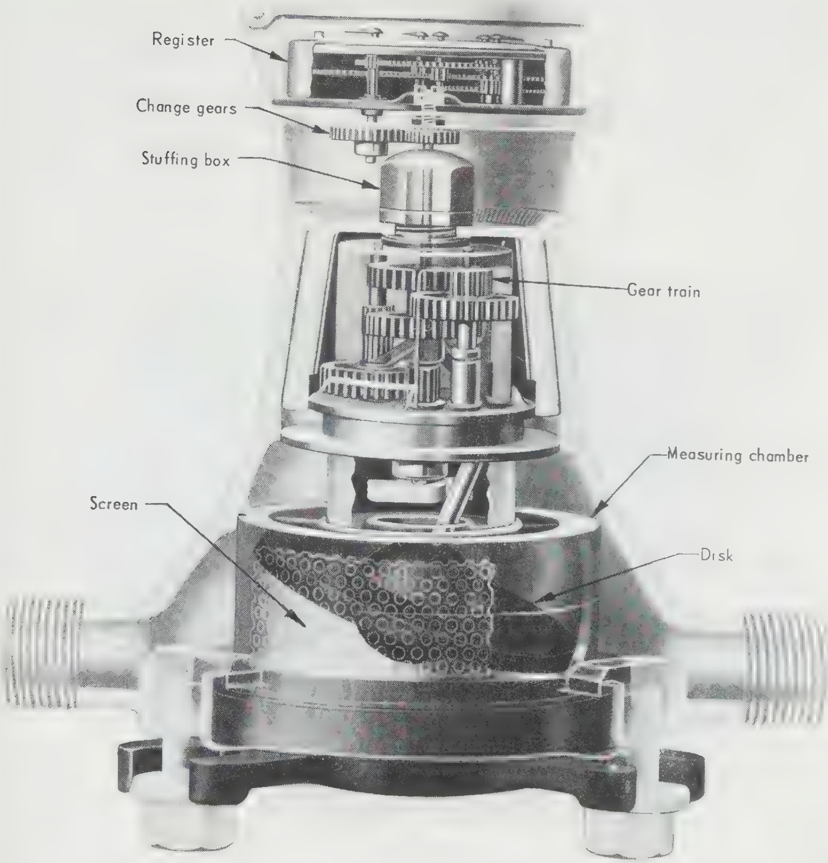

FIG. 26. Disk meter with open gear train and frostproof housing. (*Neptune.*)

TABLE 9. PRESSURE LOSSES IN NEW SERVICES*
Values of k in $p = kQ^2$
p = pressure loss, psi for Q gpm

Size, in.	Corp. cocks	100 ft of service pipe				Curb cocks	Meter yokes		Compression stop-waste valves
		Copper	Lead	G.W. iron	Cast iron		Straight	Ram's-horn	
⅝	0.0166	......	0.40	....	.....	......	0.011	0.036	0.031
¾	0.0095	0.15	0.16	0.11	.....	0.0082	.....	0.013	0.020
1	0.0029	0.04	0.045	0.03	.....	0.0010	.....	.....	0.013
1¼	......	0.0085	0.0085	.....	0.01				
1½	......	0.0035	0.0035	.....	0.004				
2	......	0.0008	0.0008	.....	0.001				

* Compiled from data from Niemeyer and Bruhn, *J. AWWA*, **24**, 631, 1932, and other sources.

16. Service Meters. Cold-water service meters serve two main purposes, to give a basis for charging for water used and to restrain waste. For the second purpose, it is highly desirable that all services be metered, both to restrain all customers from wasting water and to furnish a basis for detecting waste due to leakage from mains by balancing meter readings against total inflow. Service meters register continuously the total flow that passes through. The important characteristics of meters are accuracy and sensitiveness, durability, low pressure loss, cost, and ease and economy of maintenance.

Meters are classified as displacement, current or velocity, compound and fire-service meters. Displacement meters are of the piston, rotary, and nutating-disk types and displace a fixed quantity of water with each stroke or revolution. They are made in sizes from ⅝ to 6 in. Displacement meters of the disk type (Fig. 26) are almost universally used on supply lines to dwellings. Current meters, operated

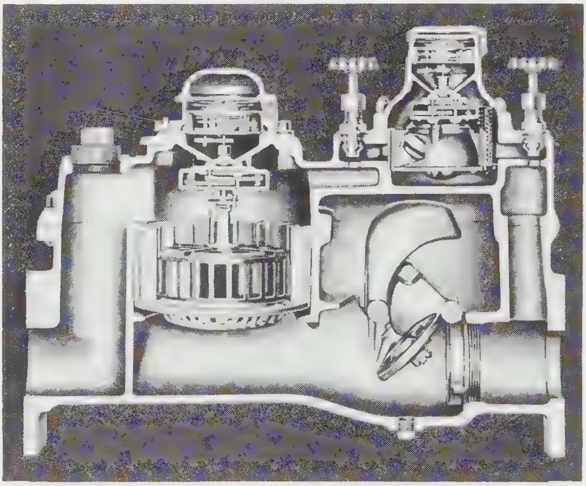

FIG. 27. Compound meter. Disk meter above lever valve, current meter at left. (*Hersey.*)

by the flow of water through a propeller or water wheel, are made in sizes from 1½ to 72 in. When a low friction loss is required, current meters of the proportional type may be used. In this type, only a portion of the water passes through the propeller, which is on a bypass, the remainder flowing through the main waterway, which contains a friction ring between the bypass connections. Current meters are not sensitive to small flows. Compound meters (Fig. 27) consist of a combination of a main-line meter of the current or displacement type for measuring large flows and a small bypass meter of the displacement type for measuring small flows, together with an automatic valve mechanism for diverting the small flows through the bypass meter. This valve remains closed for low flows. Compound meters are made in sizes from 1½ to 12 in. Fire-service meters (Fig. 28) are compound meters having the main-line meter of the proportional type. They are the type required by the Fire Underwriters on private sprinkler and fire-hydrant connections and are made in sizes from 3 to 12 in.

In the disk-type meter, a disk (Fig. 26) moves in a circular chamber owing to the passage of water through the chamber on both sides of the disk. The motion of the disk is described as nutating or similar to that of a spinning top in dying except that the disk as a whole does not revolve. It is kept from revolving by a vertical diaphragm fastened to the chamber which passes through a slot in the disk. Water enters the chamber on one side of the diaphragm and passes around the disk ball and out on the other side of the diaphragm. Disks are made of hard rubber, usually in three pieces which are held together by a threaded spindle. The top of the spindle, revolving around a pivot, drives the gear train (which may be either open or of the oil-enclosed type), which in turn drives the register in the top of the meter. Magnetic couplings to the gear train are coming into more prominent use, eliminating packing problems at the connection. Two types of meter housings are furnished, split casing and frostproof. The bottom of a frostproof housing consists of a separate plate so bolted on that should the contents of the meter freeze the bottom will fail, with a minimum of damage to the working parts of the meter.

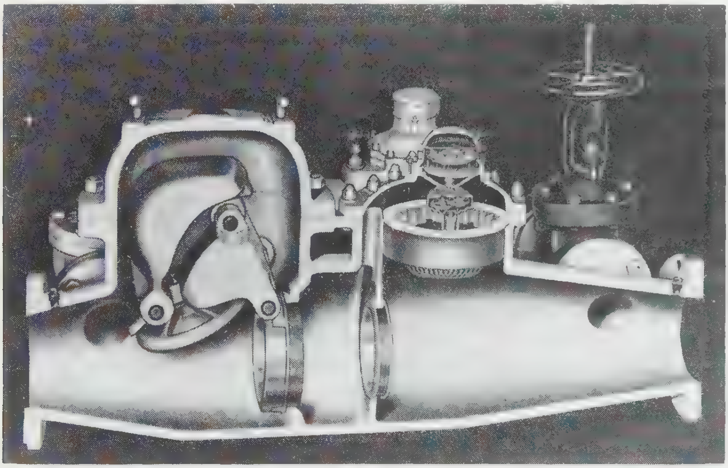

FIG. 28. Fire-service meter. Disk meter on bypass, proportional meter and automatic valve on main line. (*Hersey.*)

The specifications for cold-water service meters of the AWWA and NEWWA (1964) require meters of all types to be designed for an operating pressure of 150 psi. Bronze or nonferrous material is required for measuring chambers and cages of all meters and for outer cases of disk meters 2 in. and smaller. Larger meters may have cases of cast iron with suitable protective coating. Gear trains and strainers are to be of nonferrous metal and measuring disks and wheels of vulcanized rubber. Registration of new meters is required to be accurate within the normal test flow limits given in Table 10 to 1.5 percent for disk meters and to 3 percent for other types. The registered flow at minimum test flow must be not less than 95 percent of the actual flow for all types. The pressure loss at the upper normal test flow limit should not exceed 15 psi for disk meters 1 in. and less in size, 20 psi for larger disk meters, current and compound meters, and 4 psi for fire-service meters.

The sensitiveness and accuracy of meters at low flows are very important. Most well-made modern disk meters will retain their accuracy fairly well within the normal test flow limits for 15 to 20 years, but their sensitiveness to low flows falls off with age. Even new meters which conform to the preceding specifications for accuracy will fail to account for about 2 to 3 percent of the total water passed because of underregistration at low flows. Periodic testing of meters and repair of those which need

TABLE 10. TEST FLOW LIMITS FOR COLD-WATER SERVICE METERS
(In gallons per minute)

Size	Disk meters		Current meters		Compound meters		Fire-service meters	
	Normal test flow limits	Minimum test flow	Normal test flow limits	Minimum test flow	Normal test flow limits	Minimum test flow	Normal test flow limits	Minimum test flow
5/8	1 to 20	1/4						
3/4	2 to 30	1/2						
1	3 to 50	3/4						
1 1/2	5 to 100	1 1/2	12 to 100	7	2 to 100	1/2		
2	8 to 160	2	16 to 160	10	2 to 160	1/2		
3	16 to 300	4	24 to 350	15	4 to 320	1	8 to 400	2
4	28 to 500	7	40 to 600	20	6 to 500	1 1/2	8 to 700	2
6	48 to 1,000	12	80 to 1,400	30	10 to 1,000	3	16 to 1,600	4
8	....	....	144 to 2,500	50	16 to 1,600	4	28 to 2,800	7
10	....	....	224 to 3,800	75	32 to 2,300	8	48 to 4,400	12
12	....	....	320 to 5,800	100	32 to 3,100	14	48 to 6,400	12
16			400 to 11,500	150				

it are essential to minimize loss of revenue. The waterworks associations[1] recommend testing at intervals not exceeding 5 years for small meters and more frequently for meters larger than 1 in. Registers are available which may be read from outside of customers' premises. These registers have a remote connection to a meter located within the building.

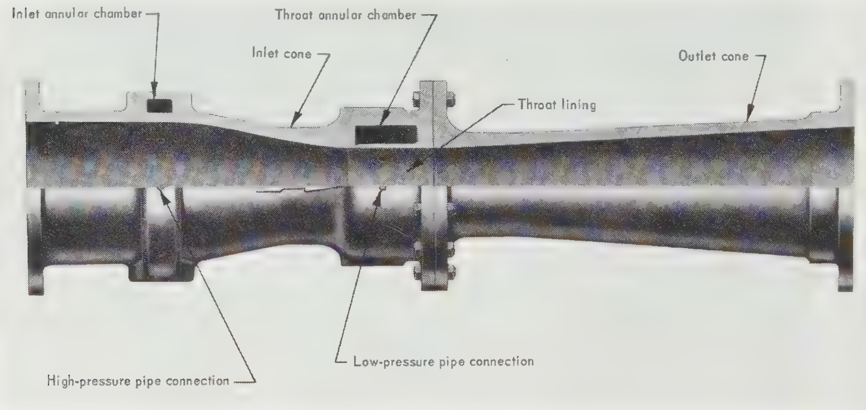

FIG. 29. Cross section of typical Venturi meter. (*B.I.F. Industries.*)

Tests of 824 5/8-in. meters of the open-gear type which had been in continuous service in Indianapolis[2] for periods up to about 20 years showed that the oldest group conformed to about 2 percent accuracy within the normal test-flow limits. At 0.17 gpm, however, the registration varied from about 80 percent of the total flow for the 5-year-old group to only 41 percent for the 20-year-old group. The calculated unrecorded flow at the time these meters were removed was estimated at 5.4 percent

[1] See "Water Works Practice," pp. 700, 707, American Water Works Association, 1929.
[2] NIEMEYER, LEBO, and HORSTMAN, *J. AWWA*, **26**, 819, 1934.

for the 5-year-old group to 17.3 percent for the oldest group. Comparative tests indicated the superiority of oil-enclosed gear trains over open gear trains in sustained sensitiveness to low flows. The Indianapolis system is fully metered, 96.9 percent of the meters (in 1933) being ⅝-in. disk meters. It was estimated that about 6 percent of the unaccounted-for water was due to underregistration of meters.

At Hartford,[1] where (in 1932) 87 percent of the meters are ⅝- and ½-in. disk type and account for about 53 percent of the water revenue, studies of the rate of flow to a number of one-, two-, and three-family houses indicated that 27 to 50 percent of the total water was used at rates less than 1 gpm in houses with tank-type water

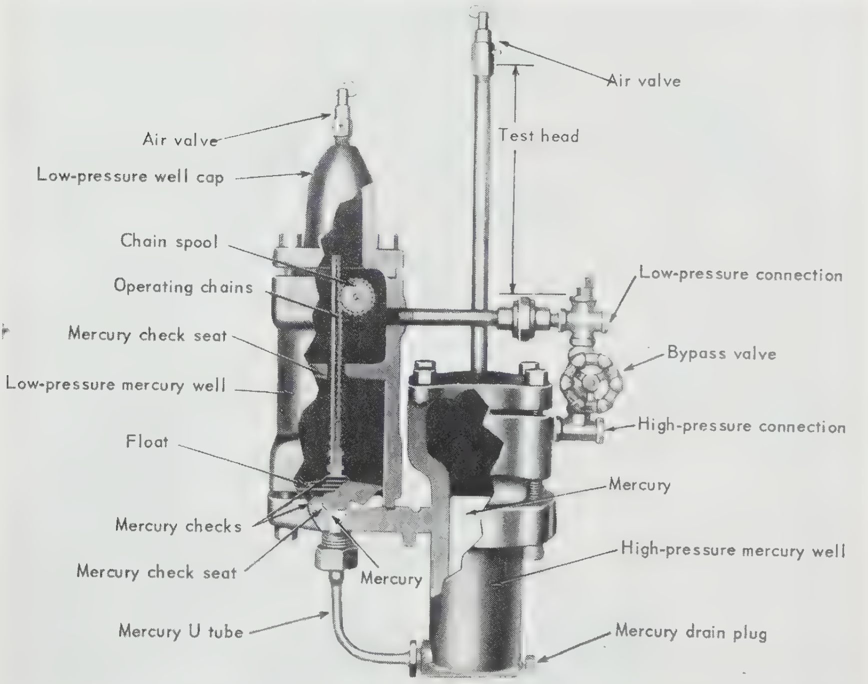

FIG. 30. Instrument for converting differential static pressure to rate of flow reading (*B.I.F. Industries.*)

closets. At rates less than 2 gpm, 38 to 78 percent was used. In houses with flushometer closets, 10 to 33 percent was used at rates less than 1 gpm and 20 to 55 percent at rates less than 2 gpm. In tests of the accuracy of the meters in these houses both before and after repairing them, it was found that about 7 percent of the water was unrecorded before repair and about 2.3 percent after repair.

Two types of meters in common use, in addition to the displacement meters described above, are (1) pressure-differential and (2) magnetic flowmeters. These meters are used extensively in larger water-supply mains or for applications where the rate of flow is to be determined. Pressure-differential meters include orifice plates and Venturi meters with numerous modifications. In a pressure-differential-type meter, the difference in static pressure between two cross sections of the meter is used to

[1] GRISWOLD and GENTNER, *J. NEWWA*, **46**, 288, 1932.

determine the rate of flow, which is indicated by means of a pointer or recorder or is totalized through appropriate instrumentation. With an orifice plate, the differential static pressure between taps upstream and downstream of the orifice is used to ascertain the rate of flow.

A Venturi meter provides a more stable differential producer under a variety of approach conditions and produces a lower head loss than does an orifice plate. For these reasons, it is more commonly used in waterworks application than the orifice-type meter. The construction of a Venturi meter is shown in Fig. 29.

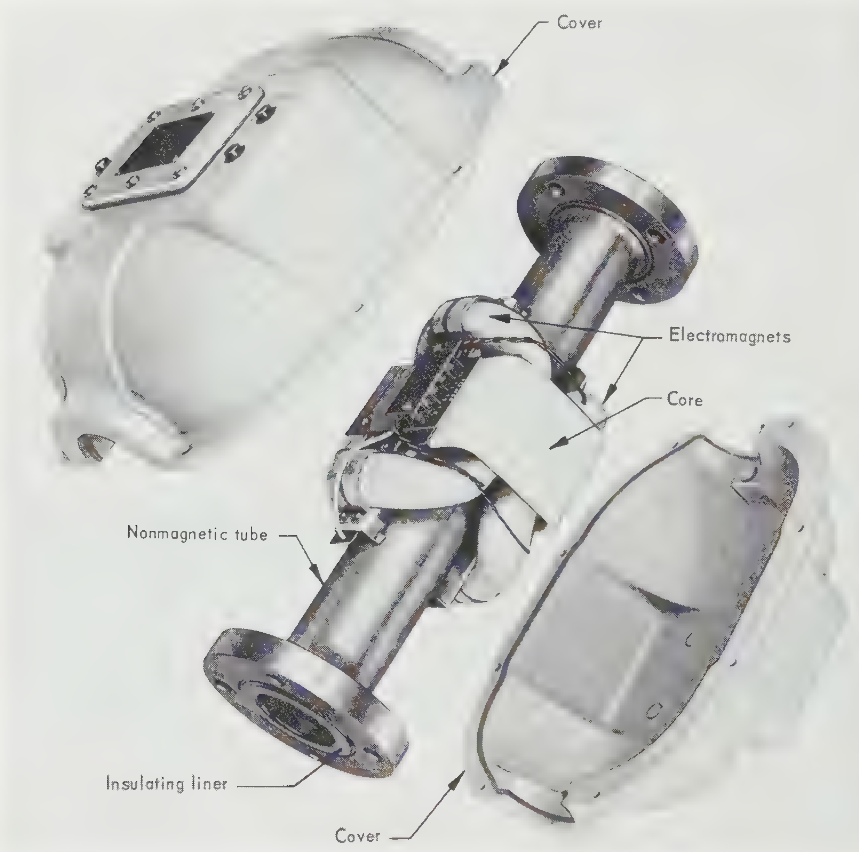

FIG. 31. Magnetic flow transmitter. (*The Foxboro Company.*)

The differential static pressure produced by either a Venturi meter or an orifice plate is applied to a manometer to indicate the rate of flow. Figure 30 shows a mercury manometer adapted to convert a pressure differential to an indication of flow. The position of the float causes the chain to rotate the chain spool, thereby positioning a pointer or activating a totalizer.

A magnetic flowmeter has an advantage in that there is no constriction in flow and the friction loss is no more than that of an equivalent length of pipe. A magnetic flowmeter is very sensitive and is capable of measuring rapidly fluctuating rates of flow, as well as flow reversals.

A magnetic flowmeter is shown in Fig. 31. Electromagnets create a uniform field in the meter. A voltage generated by the movement of water, a conductor, through the magnetic field is determined from diametrically opposed electrodes mounted flush with the sides of the meter. The voltage thus measured is translated directly to the rate of flow.

DISTRIBUTING RESERVOIRS

17. Classification and Purpose. Distributing reservoirs are used for storing water within or contiguous to the distribution area. Such storage may be designated as *elevated storage* if it serves to control the pressure table and *ground storage* if the water must be pumped into the mains. Distributing reservoirs are of two general types: (1) surface reservoirs which have little or no elevation above the ground and which are usually constructed of earth or masonry or a combination of earth and masonry; and (2) elevated reservoirs built entirely above the ground such as standpipes and elevated tanks which are usually of steel, reinforced concrete, or wood. Many surface reservoirs are built on hills and thus comprise elevated storage. Reservoirs are said to be "floating on the system" when the water enters and leaves by the same pipe.

Distribution reservoirs serve a variety of purposes as described below.

With regard to water quantity:

1. *Fire Storage.* The immediate availability of large quantities of water within the system for fire fighting safeguards the community and results in lower fire insurance rates. Elevated storage is a more effective protection and results in lower insurance rates than ground storage.

2. *Storage for Fluctuating Demand.* Reservoirs are filling when the rate of pumping or filtration exceeds the demand rate and are emptying when the reverse occurs. This action permits pumps and treatment plants to operate at constant rates throughout any one day and thereby allows the use of pumps and treatment plants of less capacity. Filtered water reservoirs come within this classification if the discharge from them fluctuates with the demand.

3. *Emergency Storage.* The storage of sufficient water within the system gives protection against the failure of a supply conduit or intake delivering water to the system from a distant source.

With regard to pressures:

4. *Equalizing Pressures in Distribution System.* Reduction of the amount of fluctuation in pressure at points in the system due to fluctuating demand results in improved service to consumers and better pressures to fire hydrants.

5. *Raising Pressures at Remote Points.* Location of elevated storage near points distant from pumping stations or main supply results in improved pressures during periods of peak demand. The same improvement may be accomplished with ground storage and booster pumps.

6. *Equalizing Heads on Pumps.* Location of elevated storage near pumping plants results in more uniform pumping heads and permits the selection of pumps for and their operation at highest efficiency.

Distributing reservoirs are built with and without covers. In order to prevent the contamination of the water from dust, fumes, bird droppings, algae growth, and other causes, it is highly desirable that distribution reservoirs be covered. This precaution seems particularly appropriate for waters that have already been purified at considerable expense. Elevated tanks and standpipes are usually covered. Many small surface reservoirs are provided with concrete or wood covers, but many large surface reservoirs built in natural depressions at comparatively small expense are too large to be covered economically. Water from uncovered distribution reservoirs should be chlorinated from a public health standpoint.

18. Capacity and Location. The capacity required for distribution reservoirs is determined from their functions, 1, 2, and 3, above. The fire storage may be estimated from the population in accordance with the Underwriters' requirements (Sec. 36). The storage required for fluctuating demand should be determined from the fluctuations on the maximum day and the proposed period of pumping or filtration. Wherever possible, filter plants should be operated throughout the 24 hr in order to secure uniformity of results, but since this requires several shifts it is not economically feasible in small towns.

The storage required for hourly demand fluctuations is the maximum cumulative difference between the amount of water pumped or filtered and the water used. It may be computed or determined graphically from either a mass or rate curve. For example, in the rate curve illustrated by Fig. 32, the shaded area corresponds to the storage required for a constant 24-hr rate of pumping. In this case, the storage is 17.5 percent of the daily demand. Either area between the two rate curves, *i.e.*, above or below the pumping rate curve, may be used. Figure 32*a* shows the same demand curve and the storage required for one pumping shift from 8 A.M. to 6 P.M., the storage being 48 percent of the daily demand for this case.

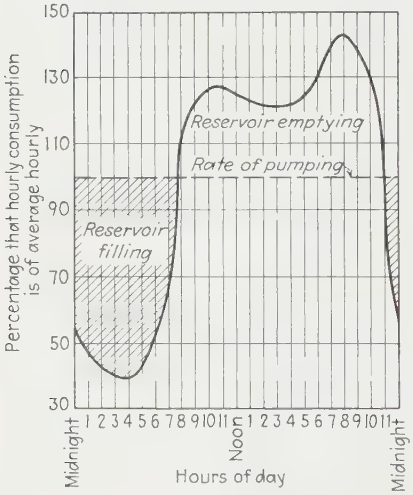

FIG. 32. Storage for fluctuating demand. Constant pumping rate throughout the 24 hr.

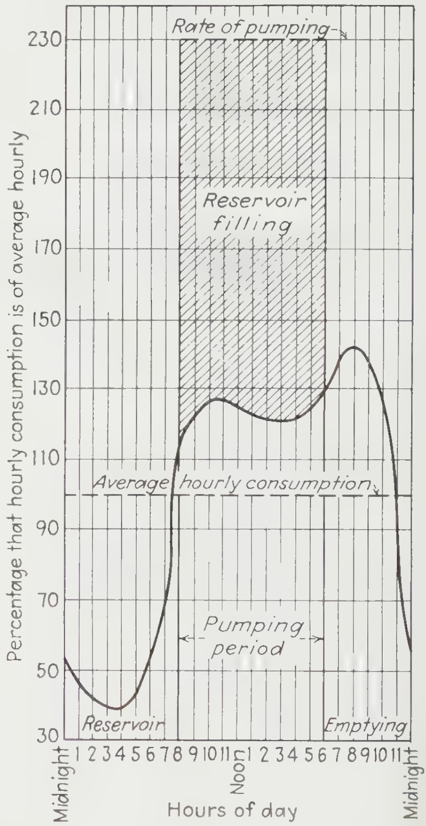

FIG. 32*a*. Storage for fluctuating demand. One-shift pumping at constant rate from 8 A.M. to 6 P.M.

The emergency storage should be determined from the estimated time required to repair the supply works that have been damaged and to place them back into service. The amount will vary greatly with the length and size of the conduit and the means by which and the extent to which the works are subject to damage. Such storage may vary from a few hours' supply to several weeks' supply.

The total amount of distribution storage required may be estimated from a reasonable combination of the three classes of storage, *viz.*, fire, fluctuating demand, and emergency. A major fire may readily occur on a day of large demand, but it is quite unlikely that emergency storage will be required at the same time. If the conditions are such that the required emergency storage is very large in comparison to the sum of the other two classes, the latter may be neglected safely.

The location of storage may be determined by the function of the reservoirs, the available sites, or both. Storage for the control of pressures should be elevated, and the location of reservoirs for this function should be within or near the regions where pressure improvement is desired. If there are hills in the proper location, surface reservoirs may be used; otherwise elevated tanks are required. Elevated storage is more effective if distributed strategically among a number of reservoirs, but the cost usually is greater than for a single reservoir. When a number of reservoirs are used, the capacity of each should be determined by the demand of the district it is intended to serve.

19. Surface Reservoirs. Surface reservoirs are usually constructed partly by excavation and partly by building up of embankment. The most economical sites are usually those which require a minimum of excavation and embankment, such as the Eden Park Reservoir site at Cincinnati, which is a natural valley with a dam across it, or the Loudonville Reservoir at Albany, which consists of three basins built in natural depressions of glacial origin. An economical design for a given site is usually one in which the volume of excavated material suitable for embankment balances the volume of embankment. The bottom of a reservoir should be on firm virgin soil or in cut. The sides of a reservoir may be of earth or of masonry walls usually surrounded by embankment. In the former case, as much of the sides as feasible should be in cut. Slopes of cuts depend upon the material but should generally be not steeper than 1 to 1½. Sides constructed of earth embankment should be well compacted to minimize settlement which is particularly important if the basin is to be lined. A satisfactory method is to place the fill in 6- to 12-in. layers, each wetted and compacted by rolling. Interior slopes of embankments should preferably be 1 to 2 or flatter. Embankment placed around structurally independent masonry walls does not require careful compacting for settlement is of less importance. For more detail on methods of construction of earth embankment, see Sec. 14.

If it is economically feasible, surface reservoirs should be lined to protect the quality of the water and to prevent leakage or inflow of groundwater. Reinforced concrete is invariably used for lining in new construction. Bottom linings consist of reinforced-concrete slabs 1½ to 12 in. thick, usually provided with contraction joints to care for shrinkage and expansion of the concrete. If the side walls of the basin are of earth, the interior slopes may be lined in the same manner; but particular care should be taken with the joints on embankment slopes.

Concrete side walls may be designed as cantilever retaining walls, counterforted walls, vertical slabs supported top and bottom when a concrete roof is used, and as ring-tension cylindrical walls for small circular reservoirs. Figure 33[1] is an example of a circular covered reservoir in which the wall is designed as a vertical cantilever retaining wall. In ring-tension reservoirs, sufficient horizontal steel is placed in the circular wall to take the entire water load in tension. Since the concrete cannot take tension, it tends to crack and is thus subject to leakage. There is some cantilever action[2] in ring-tension walls because of the restraint at the bottom. In some cases where embankment is placed against concrete reservoir walls, the passive earth pressure is relied upon to assist the wall in carrying the water load. This practice may be

[1] Ullrich, *Eng. News-Record*, **109**, 63, 1932.
[2] See Crist, *J. AWWA*, **26**, 39, 1934.

unsafe owing to the possibility of shrinkage of the embankment away from the wall or of its subsequent removal for placing pipelines or for other causes. Walls should be designed strong enough to withstand full water pressure without supporting embankment and full embankment pressure with the reservoir empty.

Provisions should be made to drain off water that leaks through linings and to prevent the groundwater table from rising above the reservoir bottom; otherwise the lining may be ruptured by the upward water pressure when the basin is emptied. To accomplish this purpose, open drains are usually placed under the lining at the bottom of side slopes and at intervals under the bottom lining, preferably near and

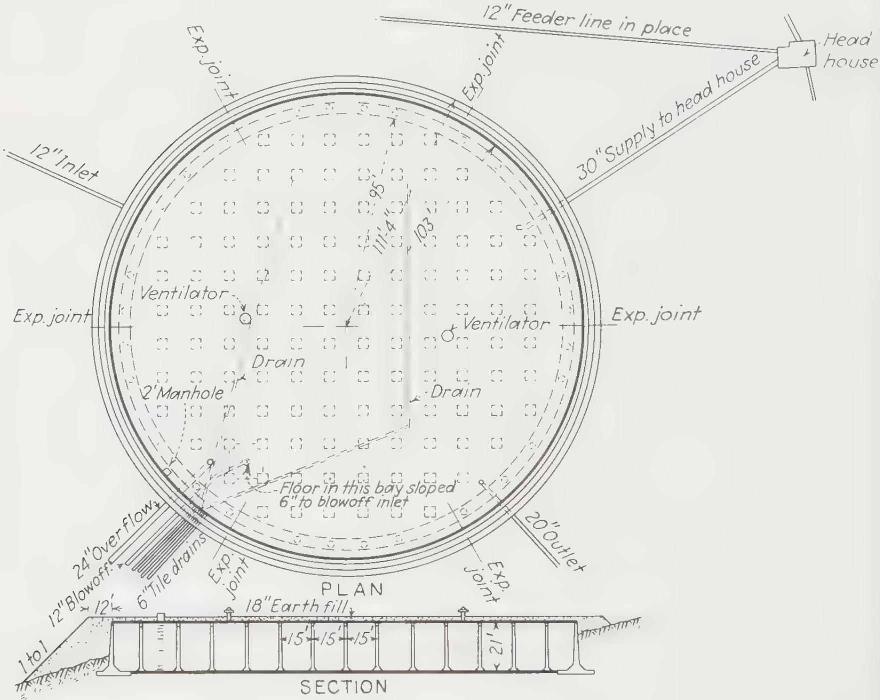

Fig. 33. Equalizing reservoir at Provo, Utah. (*Ullrich.*)

parallel to joints. Drain pipes should be surrounded by gravel or crushed stone, and in some cases it is desirable to place the side slope lining upon a layer of well-compacted gravel.

Surface-reservoir covers are now generally made of reinforced concrete except that wood roofs are sometimes used where funds are scarce. Flat-slab construction such as is shown in Fig. 33 is widely used and is economical. It is desirable that concrete roofs be covered with a layer of earth for the protection of the concrete and to equalize the temperature of the water in the basin. It is also desirable that reservoirs be constructed in two or more parts so that repairs may be made to one part without taking the entire reservoir out of service. Inlet and outlet pipes should be so arranged that the water circulates through the reservoir, particularly if the basin is large.

The proper depth for a reservoir depends upon its function, the site, and the cost. Reservoirs for pressure control should be shallow in order to minimize fluctuations in

Fig. 34. A 3-million-gal standpipe with ornamental cupola and pilasters in Madison, Wis., 73 ft in diameter by 90 ft high. (*Chicago Bridge and Iron Co.*)

Fig. 35. Prestressed-concrete water-storage tank. (*Natgun.*)

pressure. According to Turneaure and Russell,[1] the economic depth of a surface reservoir based upon first cost varies approximately as the fourth root of the capacity. In practice, depths vary from 10 to about 35 ft, usually increasing with the capacity.

20. Standpipes and Elevated Tanks. Circular reservoirs built above the ground surface for which the height exceeds the diameter are called standpipes (Fig. 34).

[1] "Public Water Supplies," p. 619, John Wiley & Sons, Inc., New York, 1940.

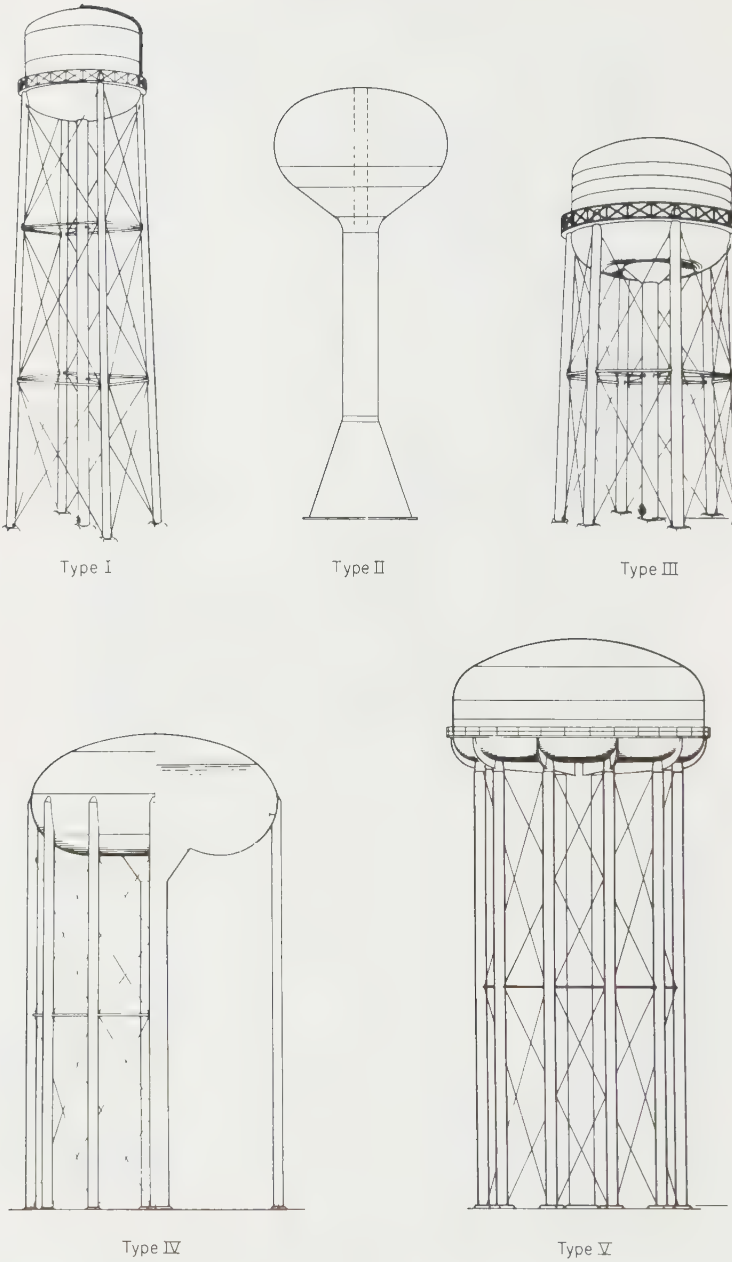

Fig. 36. Types of elevated steel tanks.

They are built of either steel or reinforced concrete, steel being more generally used because of the difficulty of securing watertightness in concrete shells with relatively high heads. Except for emergency use the water in the bottom of a standpipe used for elevated storage is usually not available as storage because distribution-system pressure requirements limit the allowable fluctuations in water level to 25 or 30 ft. The bottom part of the standpipe shell therefore serves mainly to support the upper useful portion of the standpipe; and standpipes become uneconomical when their height is such that the tower structure of an elevated tank becomes cheaper than the supporting part of the standpipe shell.

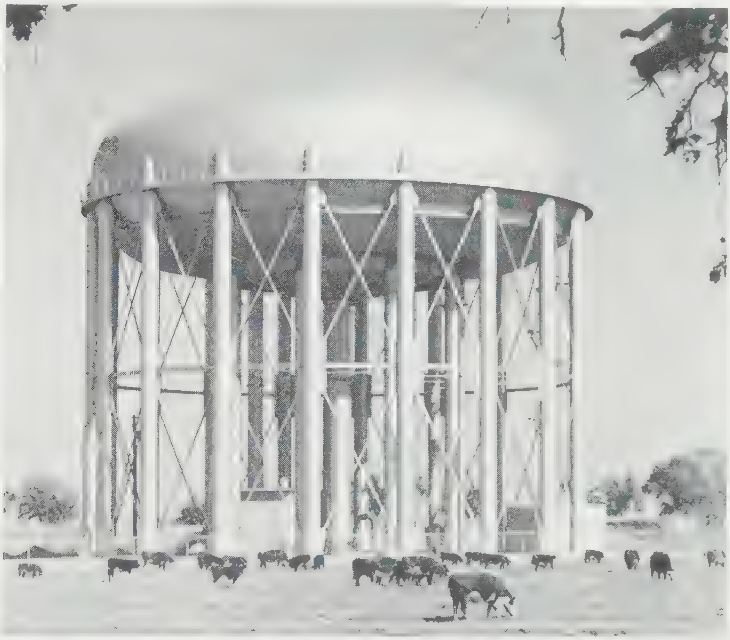

FIG. 37. A 3-million-gal spheroidal tank at Sacramento, Calif., 77 ft to bottom. It is designed for a 6 percent earthquake factor. (*Chicago Bridge and Iron Co.*)

Prestressed-concrete water-storage tanks, shown in Fig. 35, are usually constructed of either a concrete core wall on which circumferential, and possibly vertical, prestressing steel is placed, or a concrete core wall with a sheet-steel diaphragm and circumferential prestressing steel. Criteria for the design of these tanks have been proposed.[1] It is recommended that the tank incorporate the sheet-steel diaphragm, which should be interlocked and sealed by a suitable plastic material.

After the concrete core wall has been completely formed, the steel wire, initially stressed to 140,000 psi, is wrapped circumferentially around the tank. Subsequent physical changes reduce this stress to about 105,000 psi. The spacing of the wire is determined by the expected depth of water and is increased with depth. A final coat of mortar is applied to the prestressed wire to prevent corrosion.

The design of prestressed-concrete tanks is based on the desirability of having the concrete wall of the tank always in compression. By keeping the concrete wall in compression, cracking and the subsequent leakage are reduced. High-strength steel

[1] Suggested Specifications for Prestressed Concrete Water Storage Tanks, *J. NEWWA*, **76**, 363. 962.

wire is used to introduce a compressive force to the concrete which is greater than the maximum tensile force due to water pressure when the tank is filled. The use of pneumatically placed mortar, precast-concrete panels, and sliding joints has been developed in recent years to improve the design of these tanks.

Steel is the most satisfactory material for elevated tanks. Elevated tanks are widely used for elevated storage with capacities up to 4,000,000 gal.

The commonest design for elevated steel tanks is illustrated in Fig. 36. Type I illustrates a tank with both an ellipsoidal bottom and top, and is available in capacities up to 500,000 gal. The design utilizes a relatively large diameter for the depth, which tends to minimize the variation in water pressure as water is consumed.

Available in the same capacity range is the Type II tank. This tank consists of a sphere for capacities up to about 250,000 gal, or a spheroid for capacities up to 500,000 gal. Access to the top is by means of a ladder within the column. Accessories such as level controls or pumps are often housed in the tank house.

Type III and Type IV tanks are quite similar in design and range in capacity from about 200,000 to 4,000,000 gal. The Type III tank has a spheroidal or torus bottom and a cylindrical section between the bottom and the roof. The Type IV tank, shown in Fig. 37, has a spheroid or torospherical shape. Both types are supported by a circle of cylindrical columns with a central riser pipe.

The Type V tank is of a radial-cone design. The tank is supported by radial girders which are in turn supported by cylindrical columns and the central riser. The capacity range for Type V tanks is similar to that of Type III or IV.

21. Appurtenances and Regulating Devices. Distributing reservoirs are usually provided with automatic altitude valves which shut when the water level reaches a predetermined maximum. In case of failure of the altitude valve, an overflow should be provided which leads to a drain or other suitable outlet. The capacity of the overflow should be equal to the maximum rate of inflow to the reservoir. Suitable valves should be provided on inlet and drain pipes so that reservoirs and tanks may be emptied for repairs or painting.

Many types of water-level indicators are available for reservoirs and tanks. The simplest type for elevated tanks consists of a float attached by wire or chain over a pulley to a telltale on the outside. Float gages are very accurate, except in very cold weather when ice on the water surface may interfere with their operation. Both float and hydrostatic water-level gages may be equipped for remote recording, so that pumping-station operators may follow the performance of the reservoir. Telephone-company wires are often used for transmitting signals indicating the liquid level in a reservoir. It is sometimes desirable that altitude valves be wired for remote control so that they may be operated either automatically or from the pump station. Remote recording of the position of the altitude valve in automatic operation is also helpful to pump-station operators.

SECTION 38

WATER TREATMENT

By Thomas R. Camp

The treatment of water to improve its sanitary quality is called water purification. Purification consists primarily of the removal or destruction of bacteria and the removal of turbidity and color. It is accomplished by sedimentation, filtration, and disinfection; with or without pretreatment of the water by chemical coagulation. A complete plant for this purpose is known as a purification or filtration plant or, more broadly, a treatment plant. In modern treatment plants, many other processes not related to sanitation are applied to the improvement of water quality to meet the exacting requirements of the consumers. These processes include corrective treatment to retard corrosion, removal of iron and manganese, removal of odors, softening, and demineralization.

QUALITY OF WATER

1. Composition. The quality of natural water depends upon its content of impurities. Water itself is an associated liquid consisting of single molecules of H_2O, groups of such molecules, and hydrogen and hydroxyl ions H^+ and OH^-. The impurities in water occur in three progressively finer states of subdivision, suspended, colloidal, and dissolved, which are of significance in that they influence the methods required for the removal of the impurities. The total amount of solid impurities in a water is obtained by the total-solids[1] test, in which a sample of unfiltered water is evaporated and the residue weighed. The result is expressed in parts per million by weight, or milligrams per liter, and it includes suspended, colloidal, and dissolved solids.

A suspension is a dispersion of solid particles that are large enough to be removed by filtration or settling. Such particles are macroscopic and contribute turbidity to the water. The concentration of suspended matter in water is measured by its turbidity or by the suspended-solids analysis. The turbidity of a water is its capacity for absorbing or scattering light and is measured by the concentration of fine silica in ppm which produces an equivalent effect. The suspended-solids content of a water is the concentration in ppm by weight of solid matter removed from the water by filtration through a Gooch crucible or filter paper. There is no definite relation between suspended solids and turbidity inasmuch as the latter is influenced by the size and character of suspended particles as well as their concentration by weight. The ratio of the suspended solids to the turbidity, called the *coefficient of fineness*, is a measure of the size of particles causing turbidity, the particle size increasing with the coefficient of fineness. The suspended-solids determination is widely used for concentrated suspensions such as sewage but is difficult to apply to relatively clear water and therefore is not commonly used in routine water analysis.

A colloid, or sol,[2] is a finely divided dispersion of one material called the *dispersed phase* in another called the *dispersion medium.* An aqueous suspensoid colloid is a

[1] For analytical methods, see "Standard Methods for the Examination of Water and Wastewater," American Public Health Association, 1965.

[2] See Kruyt and Van Klooster, "Colloids," John Wiley & Sons, Inc., New York, 1930; and Weiser, "Inorganic Colloid Chemistry," John Wiley & Sons, Inc., New York, 1935.

water sol of solid particles that are too small to be removed effectively by ordinary filters and which are so small that they exhibit Brownian motion (*i.e.*, they diffuse) and that the electric charges on their surfaces are large enough in comparison with their mass to cause the particles to repel one another when they move within the sphere of action of each other's charges. The electric charge is due to the presence of adsorbed ions on the surface of the solid, and the sign of the charge is determined by the material of the particle and the pH value and ion content of the liquid. Neutral or acid materials such as silica, glass, and most organic particles tend to acquire negative charges in neutral water; whereas basic materials such as the metallic oxides Al_2O_3 and Fe_2O_3 tend to be positively charged. Many colloidal particles also adsorb water, and when the amount of adsorbed water is large as compared with the solid matter in the particle the colloid is called an *emulsoid*. Most of the properties of colloidal particles are due to their size. The upper limit of the size of colloidal particles varies widely with the character of the particle but is approximately 1μ (1μ = 1 micron = 0.001 mm). The lower limit of size is approximately that of single molecules of the substance, or about 1 mμ (1 mμ = 1 millimicron = 0.001μ).

Colloidal particles cannot be seen with the naked eye except with the aid of a Tyndall cone of light. In ordinary light, a suspensoid appears clear but is usually colored. Most of the color of water is due to the presence of colloidal particles, but some colloids such as silica are colorless. There is no convenient means in routine laboratory technique for measuring the amount of colloidal matter in water, but the color test is an indication of the concentration of certain types of colloidal matter. The color of a water is the amount of platinum in platinum-cobalt color standards expressed in ppm required to match the strength of color of the water. In order to remove colloidal particles from water, they must first be combined into larger particles by coagulation, after which settling and filtration are effective. Some color may also be removed by adsorbents or by chlorination.

A solution is a molecular or ionic dispersion. Solids, liquids, and gases are dissolved in natural waters. Some substances, particularly organic compounds, remain in solution largely as molecular dispersions. Other substances, the strong electrolytes, ionize completely when they are dissolved in natural water. Practically all inorganic rocks or salts found in true solution in natural waters are fully ionized in the concentrations in which they normally occur. The concentration of total dissolved solids,[1] usually expressed in ppm, is obtained by weighing the residue after evaporation of the water from a filtered sample. The determination will include colloidal matter if present. Substances in true solution may be removed from water in a variety of ways. Some dissolved solids may be removed by adding a chemical that reacts with the soluble substance to form a precipitate, the precipitate being subsequently coagulated and removed by sedimentation and filtration. Some dissolved substances may be removed by an exchange process with zeolites or ion-exchange resins and some by adsorption on activated carbon or other adsorbents. Still another method is aeration for the liberation of gases and volatile and odoriferous substances and to capture atmospheric oxygen for the precipitation of iron.

Most of the substances that occur in natural waters are shown in Table 1. These substances do not all occur in a single water, and their concentration varies widely for different waters. Some substances of sanitary significance occurring in water because of artificial contamination, such as detergents, radioactive impurities, pesticides, phenols, and cyanides, are not specifically included in the table. Other substances, such as the secretions of certain microorganisms which cause odors but which occur in such minute amounts that they cannot be detected by chemical analysis, are

[1] "Standard Methods for the Examination of Water and Wastewater," American Public Health Association, 1965.

TABLE 1. SUBSTANCES OCCURRING IN NATURAL WATERS

Substance	Suspended	Colloidal	Dissolved: Not ionized	Dissolved: Positive ions	Dissolved: Negative ions
Of mineral origin	Clay Sand Other inorganic soils	Clay Silica, SiO_2 Iron Oxide, Fe_2O_3 Alumina, Al_2O_3 Manganic oxide MnO_2		Calcium, Ca^{++} (40) Magnesium, Mg^{++} (24.3) Sodium, Na^{+} (23) Potassium, K^{+} (39.1) Iron, Fe^{++} (55.8) Manganese, Mn^{++} (54.9) Hydrogen, H^{+} (1)	Bicarbonate, HCO_3^{-} (61) Sulphate, SO_4^{--} (96) Chloride, Cl^{-} (35.5) Nitrate, NO_3^{-} (62) Carbonate, CO_3^{--} (60) Hydroxyl, OH^{-} (17) Silicate $HSiO_3^{-}$ (77.1) Borate, $H_2BO_3^{-}$ (60.8) Phosphate, HPO_4^{--} (96) $H_2PO_4^{-}$ (97) Iodide, I^{-} (126.9) Fluoride, F^{-} (19)
Of organic origin	Organic soil (topsoil) Decomposing organic wastes	Vegetable coloring matter Organic wastes	Vegetable coloring matter Organic wastes Ammonia, NH_4OH Carbonic acid, H_2CO_3 Other organic acids	Ammonium, NH_4^{+} Hydrogen, H^{+} Other organic acids	Nitrate, NO_3^{-} Nitrite, NO_2^{-} Hydroxyl, OH^{-} Bicarbonate, HCO_3^{-}
Gases			Free carbon dioxide, CO_2 Oxygen, O_2 Nitrogen, N_2 Hydrogen, H_2 Hydrogen sulphide, H_2S Methane, CH_4 Sulphur dioxide, SO_2 Ammonia, NH_3 Odorivectors		
Living organisms	Fish life Algae, diatoms Minute animals	Bacteria, viruses Algae, diatoms Minute animals			

Figures in parentheses after the ions are the ionic weights.

not shown. Their presence and concentration are indicated by odor[1] measurements. Several other substances of some sanitary significance, such as lead, copper, zinc, and chlorine, Cl_2, which enter water because of treatment or from the pipes of the distribution system, are not shown since they do not usually occur in natural waters.

For methods of identification and measurement of concentration of the various impurities in water, see "Standard Methods for the Examination of Water and Wastewater."[1] Living microorganisms are identified and counted in accordance with the microscopic and bacteriological examinations. Chemical substances are determined from the sanitary chemical and mineral examinations. A mineral analysis is preferably stated in terms of the concentration of the ions. The sum of the milliequivalents of basic radicals (positive ions) equals the sum of the milliequivalents of acid radicals (negative ions) in an accurate analysis. The milliequivalent of an ion is equal to its concentration in ppm divided by its combining weight. The combining weight is the molecular or ionic weight divided by the valence. The valence of an ion is indicated by the number of charges. The molal concentration of a substance (designated [A] for substance A) is its concentration in ppm divided by its molecular or ionic weight and multiplied by 10^{-3}.

2. Ionization and pH Value. Water ionizes in accordance with the following reaction:

$$H_2O \rightleftarrows H^+ + OH^- \tag{1}$$

The reaction goes to the right very slightly, only one out of every 555 million H_2O molecules being dissociated in pure water. The law of mass action applied to the dissociation of water is approximately

$$[H^+][OH^-] = K_w \tag{2}$$

K_w is called the ion product of water, and its value is $10^{-14.0}$ at 25 C. In pure water at 25 C, both the hydrogen-ion concentration $[H^+]$ and the hydroxyl-ion concentration $[OH^-]$ are equal to 10^{-7}. Experimental values[2] of K_w for various water temperatures are shown in Table 2.

Table 2. Ion Product of Water

Temp, °C	0	10	20	25	30	40	50	60	80	100
$K_w \times 10^{14}$	0.11	0.29	0.68	1.00	1.47	2.91	5.48	9.65	23	52

A substance that dissolves in water to yield H^+ or to add to itself OH^- is called an *acid*. Both these reactions, examples of which are shown below, increase the $[H^+]$ and decrease the $[OH^-]$.

$$HCl \rightleftarrows H^+ + Cl^- \tag{3}$$
$$CO_2 + OH^- \rightleftarrows HCO_3^- \tag{4}$$

Note: Reaction (4) may also be written $CO_2 + H_2O \rightleftarrows H_2CO_3 \rightleftarrows H^+ + HCO_3^-$.

Conversely, a substance that dissolves in water to yield OH^- or to add to itself H^+ is called a *base*, or *alkali*. Typical reactions are as follows:

$$NaOH \rightleftarrows Na^+ + OH^- \tag{5}$$
$$Na_2CO_3 \leftrightarrows 2Na^+ + CO_3^{--} \tag{6}$$

and $$CO_3^{--} + H^+ \rightleftarrows HCO_3^-$$

[1] American Public Health Association, 1965.
[2] Camp, T. R., "Water and Its Impurities," p. 56, Reinhold Publishing Corporation, New York, 1963.

A substance that ionizes in a manner which does not affect the $[H^+]$ is called a *salt*. An example of such a reaction is

$$NaCl \rightleftarrows Na^+ + Cl^- \tag{7}$$

It follows that at 25 C a solution is acid when $[H^+]$ is greater than 10^{-7} and basic when $[H^+]$ is less than 10^{-7}. For convenience, the exponent of 10 without sign, *i.e.*, the logarithm of the reciprocal of the hydrogen-ion concentration, is used to express the acidity or alkalinity of a solution. This figure is known as the *pH value*. A solution with a pH of 7.0 is neutral. Solutions with a pH value less than 7 are acid and greater than 7 are alkaline. Most natural waters have pH values between 6 and 8. Note from Table 2 that the neutral $[H^+]$ changes with the water temperature, being 1.21×10^{-7} at 30 C, for example.

The pH value of dilute solutions of strong acids and bases in pure water may be computed from the amount of the material in solution, as strong electrolytes ionize completely in dilute solutions. For example, a $0.001N$ solution of HCl or any other strong acid in pure water at 25 C has a $[H^+]$ of 10^{-3} and the pH is 3. The pH value of solutions of weak acids and bases in pure water cannot be computed directly from the amount of material in solution, for the compounds are not fully ionized. In this case, it is necessary to take account of the ionization constants of the material and water. If a strong acid is added to water containing HCO_3^-, the change in $[H^+]$ is not proportional to the amount of acid added. As the acid is added, the bicarbonate ionizes in accordance with reaction (4) and the OH^- liberated reacts with the H^+ from the acid to form water. A similar phenomenon occurs when a strong base is added to water containing HCO_3^-. In this case, as the OH^- is increased by the base, the bicarbonate ionizes as follows:

$$HCO_3^- \rightleftarrows H^+ + CO_3^{--} \tag{8}$$

The H^+ liberated in reaction (8) combines with the OH^- of the base to form water. This phenomenon is called *buffer action*, and a buffer solution is one in which the change in $[H^+]$ upon the addition of an acid or base is less than would be expected from the ionizing characteristics of the substance added. The buffer acts as a reservoir of acidity or alkalinity to oppose changes in the pH value. Weak acids or bases exhibit buffer action. The pH value of a buffered solution may be computed by the simultaneous solution of equations involving the concentrations of all the substances in the water, including the ions, and the ionization constants.

The pH of a solution may be determined by test[1] electrometrically or colorimetrically.

3. Alkalinity and Hardness. The alkalinity[1] of a water represents its content of OH^- or of other ions that combine with H^+ upon the addition of acid. The most important of these other ions is HCO_3^-, which is usually present in considerable quantity. In alkaline waters, normal carbonate, CO_3^{--}, is a source of alkalinity since it forms HCO_3^{--} upon the addition of acid. Borates, silicates, and phosphates also cause alkalinity, but they are usually not present in natural waters in appreciable quantities. Alkalinity is measured by titration with acid. The amount of acid required to bring the water to pH 4 expressed in ppm of equivalent $CaCO_3$ is called the *total*, or *methyl orange, alkalinity*. If the water is alkaline, the amount of acid required to bring the pH down to 8 expressed in ppm of equivalent $CaCO_3$ is called the *phenolphthalein alkalinity*. Methyl orange and phenolphthalein are indicators that have significant color changes at about pH 4 and pH 8, respectively.

[1] "Standard Methods for the Examination of Water and Wastewater," American Public Health Association.

Alkalinity is commonly differentiated into three kinds: hydroxide or caustic alkalinity, carbonate alkalinity, and bicarbonate alkalinity. Caustic alkalinity is caused by OH^-, and it is negligible ($[OH^-]$ = 0.34 ppm or 1 ppm as $CaCO_3$ at pH 9.3) at pH values less than 9.3. The relation between the carbonate and bicarbonate alkalinity and the relation between the bicarbonate and the free CO_2 are functions of the pH value. The mass-action relation for Eq. (8) is

$$\frac{[H^+][CO_3^{--}]}{[HCO_3^-]} = 4.69 \times 10^{-11} \text{ or } 10^{-10.32} \text{ at 25 C} \tag{9}$$

and for Eq. (4) with the OH^- expressed in terms of H^+ it is

$$\frac{[H^+][HCO_3^-]}{[CO_2]} = 4.31 \times 10^{-7} \text{ or } 10^{-6.37} \text{ at 25 C} \tag{10}$$

The numerical value of the exponent of 10 in the preceding ionization constants[1] is increased by about 0.01 for each degree centigrade decrease in temperature and

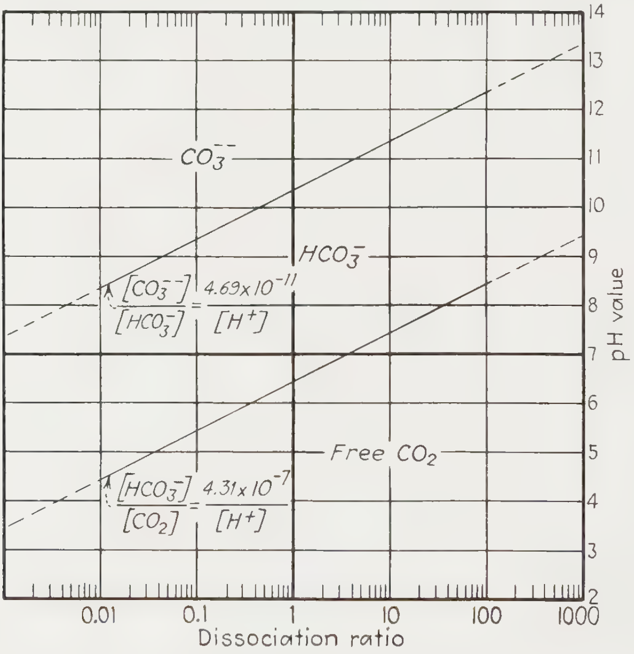

FIG. 1. Bicarbonate ionization at 25 C.

appears to be decreased slightly by increase in concentration of total dissolved solids. Langelier notes a decrease of about 0.01 in the exponent of the constant of Eq. (9) for each 100 ppm of total solids.

The significance of these equations is shown graphically in Fig. 1. The ratio of the CO_3^{--} alkalinity to the HCO_3^- alkalinity is twice the corresponding dissociation ratio, as shown on the figure, and the ratio of the HCO_3^- alkalinity to the free CO_2

[1] See LANDOLT-BORNSTEIN, "Physikalischchemische Tabellen," Springer-Verlag OHG, Berlin, 1923. Also MACINNES and BELCHER, *J. Am. Chem. Soc.*, **55**, 2630, 1933; and LANGELIER, *J. AWWA*, **28**, 1500, 1936.

expressed as $CaCO_3$ is one-half the corresponding dissociation ratio. It will be noted from the figure that, in titrating an alkaline water with acid, at pH 8 practically all the CO_3^{--} has been converted to HCO_3^- and at pH 4 practically all the HCO_3^- has been converted to free CO_2. A water must be caustic with a pH above 12 in order to convert practically all the HCO_3^- to CO_3^{--}.

The hardness[1] of a water represents its content of metals which form precipitates under the normal conditions of use of the water. These include all the metals of Table 1 except Na^+ and K^+ whose salts are all soluble. Most of the hardness of a water is due to the presence of Ca^{++} and Mg^{++}, for these elements occur in substantial amounts. Hardness, like alkalinity, is expressed in ppm as $CaCO_3$. It is objectionable principally because of soap waste and boiler scale. The hardness metals form insoluble precipitates with soap, and a lather cannot be obtained until all the hardness has been so precipitated. The precipitated hard soap, moreover, may form stains upon fabrics being laundered, particularly if Fe and Mn are present. Precipitated hard soap is no longer an important problem because of the widespread use of synthetic detergents which cannot be precipitated by the polyvalent metals. Boiler scale is obtained by the precipitation of the metals as salts (principally carbonates, sulfates, chlorides, and nitrates) owing to their increased concentration upon the evaporation of the water. If the hardness is less than 100 ppm, a water is generally considered soft, but for efficient boiler use and for certain industrial processing purposes demineralized waters of zero hardness are desirable. The hardness of many waters of the Middle West in the United States exceeds 500 ppm, whereas the hardness of many waters on the Eastern seaboard is less than 50 ppm.

4. Sanitary Significance of Impurities. The impurities of greatest sanitary significance in water to be used for drinking purposes are the pathogenic bacteria and other pathogenic microorganisms. The most serious water-borne diseases are cholera in the Old World and typhoid fever in America, but other important human diseases, such as infectious hepatitis, dysentery, and diarrhea, are known to be water-borne, and still others may be. The isolation of the causative organism of these diseases from water is impractical in routine water examination. Because these diseases are of intestinal origin and the source of the germs in water is human excreta, the presence of sewage in water is evidence of the possibility of the presence of infectious organisms. The presence of coliform bacteria whose normal habitat is the intestinal tract of man and other mammals is the best evidence of sewage pollution.

The 1962 U.S. Public Health Service Drinking Water Standards[2] for water used for drinking and culinary purposes on interstate carriers, which standards have been adopted by many public health authorities and are widely used, require an arithmetic mean coliform density not exceeding 1 per 100 ml of water for all samples collected in any one month. Other requirements of the U.S. Public Health Service Standards are as follows:

Physical characteristics:

1. Turbidity should not exceed 5 units.
2. Color should not exceed 15 units.
3. Threshold odor number should not exceed 3.

Chemical substances:

1. Alkyl benzene sulfonate (ABS) should not exceed 0.5 mg/l.
2. Arsenic (As) should not exceed 0.01 mg/l and shall not exceed 0.05 mg/l.

[1] "Standard Methods for the Examination of Water and Wastewater," American Public Health Association.

[2] *U.S. Public Health Serv. Publ.* 956, 1962.

3. Barium (Ba) shall not exceed 1.0 mg/l.
4. Carbon chloroform extract (CCE) should not exceed 0.2 mg/l.
5. Cadmium (Cd) shall not exceed 0.01 mg/l.
6. Chloride (Cl) should not exceed 250 mg/l.
7. Chromium, hexavalent (Cr^{+6}), shall not exceed 0.05 mg/l.
8. Copper (Cu) should not exceed 1.0 mg/l.
9. Cyanide (CN) should not exceed 0.01 mg/l and shall not exceed 0.2 mg/l.
10. Fluoride (F), when naturally present, should not average more than 0.8 mg/l and shall not average more than 1.4 mg/l where the annual average of maximum daily air temperatures range from 79.3 to 90.5 F, with increases in recommended and allowable average fluoride contents for colder climates up to 1.7 mg/l and 2.4 mg/l for air temperatures from 50.0 to 53.7 F. Where fluoridation is practiced, the fluoride concentration shall be controlled between 0.6 and 0.8 mg/l for air temperatures from 79.3 to 90.5 F up to between 0.9 and 1.7 mg/l for air temperatures from 50.0 to 53.7 F.
11. Iron (Fe) should not exceed 0.3 mg/l.
12. Lead (Pb) shall not exceed 0.05 mg/l.
13. Manganese (Mn) should not exceed 0.05 mg/l.
14. Nitrates (NO_3) should not exceed 45 mg/l.
15. Phenols should not exceed 0.001 mg/l.
16. Selenium (Se) shall not exceed 0.01 mg/l.
17. Silver (Ag) shall not exceed 0.05 mg/l.
18. Sulfate (SO_4) should not exceed 250 mg/l.
19. Total dissolved solids should not exceed 500 mg/l.
20. Zinc (Zn) should not exceed 5 mg/l.
21. Radium 226 and strontium 90 should not exceed 3 and 10 micromicrocuries/l, respectively.
22. Gross beta concentrations, in the absence of strontium 90 and alpha emitters, should not exceed 1,000 micromicrocuries/l.

NOTE: Concentrations of substances in excess of the above specified limits constitute grounds for the rejection of the water supply if the limits are prefaced by the words "shall not exceed."

Many of the requirements of the U.S. Public Health Service Standards have no health significance, although they are of aesthetic importance. The presence of too much Pb may result in lead poisoning. Lead is not present in natural waters but may enter the water in wastewaters and by solution from lead services and plumbing systems if the water is corrosive to lead. Arsenic, barium, cadmium, selenium, and hexavalent chromium are all toxic, and their concentrations must be limited. The toxicity[1] of copper to man has been the subject of much discussion, but it appears that Cu in solution is not injurious to man up to concentrations of about 20 ppm, although much lower concentrations are toxic to microorganisms and fish. The taste of water becomes disagreeable when the Cu content exceeds about 1 ppm, and blue-green stains will appear on plumbing fixtures.

Zinc[2] appears to be safe in drinking water up to concentrations of about 40 ppm but at concentrations exceeding about 5 ppm may impart a milky appearance and an astringent taste to the water. Too much $MgSO_4$ (Epsom salt)[3] and Na_2SO_4 (Glauber's salt) in water produces laxative effects, NaCl and $NaNO_3$ tend to produce thirst, and carbonates and hydroxides tend to neutralize the acid of the stomach. Iron is beneficial to the health, but it is objectionable because of red water and stains. Manganese is more objectionable than Fe because of stains and brownish water. Water with pH

[1] See SCHNEIDER, *J. NEWWA*, **44**, 485, 1930.
[2] See ANDERSON, REINHARD, and HAMMEL, *J. AWWA*, **26**, 49, 1934.
[3] See POLLARD, *J. AWWA*, **28**, 1038, 1936.

values from 3.5 to 10.5 has been used continuously for municipal supplies without reported harm to drinkers at the extreme pH values, but pH values less than about 8.0 are usually corrosive to metal pipes.

The presence of fluoride[1] in concentrations exceeding 0.5 ppm may result in mild endemic dental fluorosis (mottled enamel) in children, although about 1.5 or more ppm of F is required for severe cases. It has been found that fluoride in drinking water is accompanied by low incidence of dental caries (tooth decay) in children, and many health agencies are now advocating the addition of fluorides to drinking water up to about 1.0 ppm in regions where caries is prevalent. Because simple goiter has been shown to be due to a deficiency of iodine[2] in the thyroid gland, attempts have been made to supply the deficiency in regions where this condition is endemic by adding NaI to the water supplies. Studies of the relationship of the incidence of goiter to the I content of drinking waters have given conflicting results, however, and it is probable that I in organic combination in foods where it is also more concentrated is more readily assimilated than I in water. An excess of iodides in drinking water may cause hyperactivity of the thyroid in some individuals. Disinfection by means of iodine or ionic silver[3] has been used for swimming-pool waters, but these disinfectants should not be used for drinking water because of the danger of excess iodides with I and the skin disease argyria with excess Ag in the human body.

The synthetic detergents now used so widely in place of soap are objectionable in drinking water because of foaming and taste. Detergents containing ABS will produce a noticeable taste in drinking water and also will foam when the ABS concentration is 1.0 to 1.5 ppm. The detergents containing ABS with a branched-chain molecular structure are very difficult to remove from water or wastewater (except by activated carbon) because they cannot be precipitated chemically and are broken down very slowly by bacteria. For this reason, the producers are now marketing detergents with a straight-chain molecule, linear alkylate sulfonate (LAS), which is readily decomposed by bacteria.

Numerous new organic chemicals are finding their way into our watercourses, including agricultural pesticides of many kinds which are toxic to all life. These substances are so numerous and varied as to defy detection and identification by practical means. The CCE method has been developed as a means for determining the gross concentration of some of these organics.

The limit suggested in the Standards for phenolic compounds (including cresols and xylenols) is to minimize odors. It has no health significance. The limit for cyanide is based primarily on its toxicity to fish rather than to man. The nitrate limit is to prevent methemoglobinemia in infants.

TYPE AND CAPACITY OF PLANT

5. Slow and Rapid Sand Filtration. Slow sand filters, also known as English-type filters, are beds of sand 30 to 40 in. deep in concrete basins, each about 1 acre in area. They were first used about 1830. Slow sand filters are usually preceded by plain settling basins with no chemical coagulation. The water passes downward through the sand at rates of 2 to 8 mgd/acre. Filter runs are from 2 to 8 weeks, and in order to clean the sand the beds are usually taken out of service. Cleaning is accomplished by the removal of the top layer of sand to a depth of about an inch or by washing it in place by means of special machines. Slow sand filtration is adapted to waters low in color and with turbidities less than about 30 ppm. Because this type of plant is not suitable for many treatment processes now required, its use for new plants has been

[1] Dean and Elvove, *Am. J. Public Health*, June, 1936, p. 567.
[2] Weston, *Am. J. Public Health*, July, 1931, p. 715.
[3] Camp, "Water and Its Impurities," pp. 91, 99, Reinhold Publishing Corporation, New York, 1963.

superseded by the rapid or mechanical type of filter plant which first came into use about 1890.

An essential feature of rapid filtration is the use of chemical coagulants applied to the water preceding filtration and usually preceding settling. Because of this feature, colloidal impurities are flocculated and effectively removed by the filters at rates of filtration from 2 to 8 U.S. gpm/sq ft (125 mgd/acre is about 2 gpm/sq ft). Very much less bed area is required than for slow filters, and the length of filter runs is correspondingly reduced, ranging from about 3 hr to a week. Cleaning is accomplished by upward flow of clean water through the bed at rates sufficient to fluidize the bed. The washing process tends to stratify the medium according to grain size with the small grains at the top. The underdrainage system is designed especially for the washing function, which is accomplished in 5 to 10 min. The depth of filter medium commonly used varies from 2 to 4 ft.

Both slow and rapid filters for municipal use are usually of the gravity type; that is, the filters are open at the top with the water level 3 to 8 ft over the top of the filter medium. Rapid filters are also constructed in enclosed steel tanks so that the water may be pumped direct to the distribution system through the filter. Such filters, called pressure filters, are extensively used in industry.

6. Types of Rapid-filter Plants. Rapid-filter plants are employed both for purification and for softening by the lime-soda process. The essential features are chemical coagulation (including the softening reactions of the lime-soda process) accomplished in flocculation basins, clarification accomplished in settling basins, and filtration. Other processes may also be employed such as disinfection, carbonation (addition of CO_2), aeration, zeolite softening, demineralization, iron and manganese removal, and activated-carbon treatment, some of which require separate treatment units. The number, size, and arrangement of the units depend upon the character of the treatment process as a whole and the plant size.

Figure 2 is a typical flow diagram showing places of application of chemicals and the unit processes in a rapid-filtration plant. The unit processes and the chemicals will vary from plant to plant depending upon the quality of the raw water and the required quality of the filter effluent. The heavy lines of Fig. 2 show the usual or preferred points of application of chemicals and the lighter lines show other points of application.

Powdered activated carbon is used either continuously or intermittently for removal of odors, detergents, pesticides, and other organics. Since removal is accomplished by adsorption on the surfaces of the carbon particles, the carbon should preferably be added ahead of the coagulants which will flocculate with the carbon particles and reduce their capacity for adsorption, and ahead of the chlorine which reacts with the carbon to reduce the effectiveness of both the carbon and chlorine. It should be added to the influent of a contact chamber designed to keep the carbon in suspension for a period long enough for effective removal, about 5 min. Carbon which is sometimes added to the filter influent in small doses may contribute to the formation of filter mud balls.

Chlorine is widely used as a disinfectant and is effective against both bacteria and viruses if applied in adequate doses for sufficient contact periods. Disinfection is the most important single process for the treatment of drinking water. *Prechlorination* ahead of flocculation, as shown in Fig. 2, is preferable because the long contact periods in flocculation and clarification are made available for disinfection and, in some cases, for oxidation of hydrogen sulfide, iron, and manganese. *Postchlorination,* following filtration, with a contact period of not less than 30 min in the clear well, is also desirable in order to control the chlorine residual entering the distribution system. Ammonia is sometimes added with chlorine to produce chloramines in order to reduce the odor of free chlorine and to sustain the chlorine residual for longer periods. Chlorine dioxide is also used instead of chlorine in some plants. Free chlorine is a more effective disinfectant than chloramines, and the effectiveness of both is greatly decreased as the pH value is increased into the alkaline range. Prechlorination is therefore not very effective in plants where the pH is high during flocculation and clarification (that is, lime-soda softening plants and plants using ferric sulfate at high pH for manganese removal), unless the chlorine is applied at a contact chamber preceding flocculation as shown by the lighter line of Fig. 2. In this case the chlorine contact chamber should

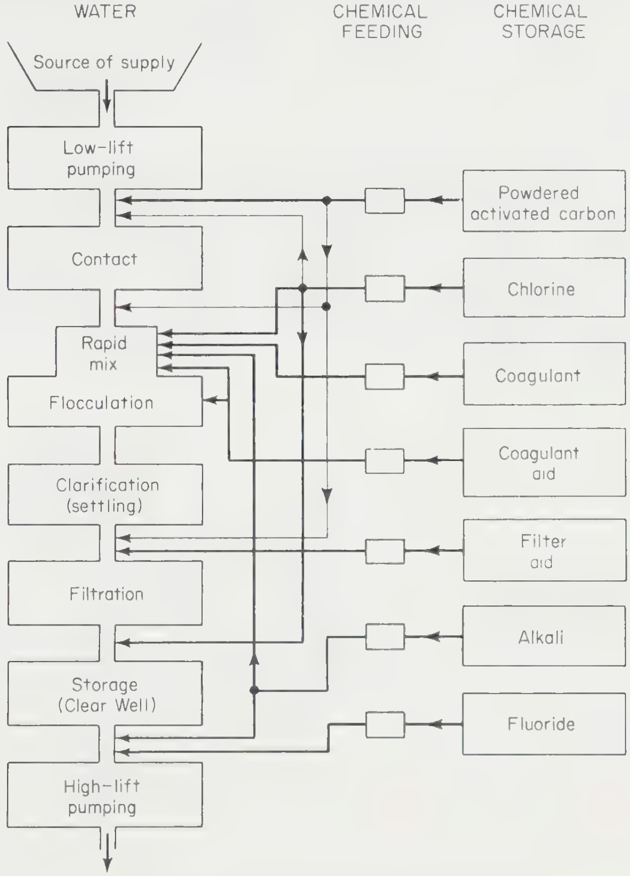

Fig. 2. Flow diagram for rapid-filter plant.

have a detention period of 30 min or more, and the activated carbon should be added to the flocculators or to a separate carbon contact chamber ahead of the chlorine contact chamber. Figure 3 illustrates a modern rapid-filter plant at Troy, N.Y.

The coagulant most widely used is filter alum, which flocculates best at pH values of 5.5 to 7.5. Ferric sulfate, ferric chloride, and chlorinated copperas (ferrous sulfate) are also used and may be flocculated over a much wider pH range. Copperas has been used with lime at pH values above 8.5. In a lime-soda softening plant, the lime and soda ash, together with a coagulant, are applied at the flocculation basins, as shown for the coagulant in Fig. 2. The pH of the water during flocculation and clarification will be 10 to 11. Carbonation with carbon dioxide gas in a carbonation chamber is necessary following clarification to lower the pH and prevent afterprecipitation of $CaCO_3$ on the filter medium and in the distribution system. If it is required to remove magnesium as well as calcium, two-stage flocculation and settling may be used with

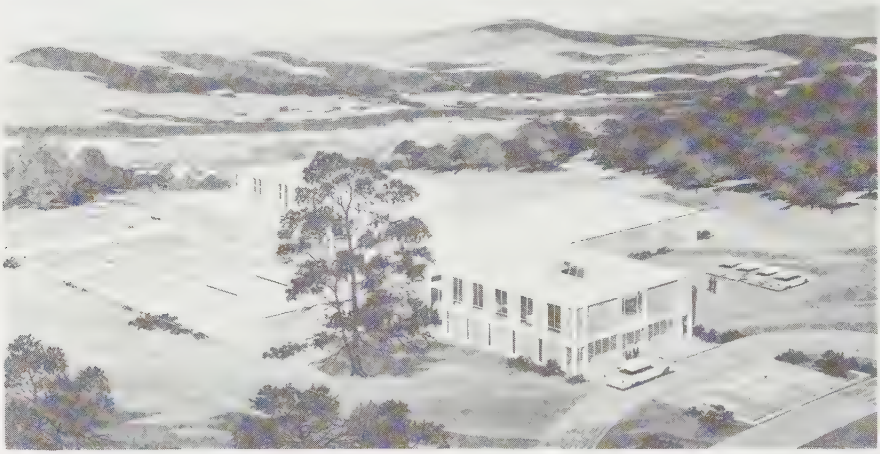

FIG. 3. Modern rapid-filter plant at Troy, N.Y.

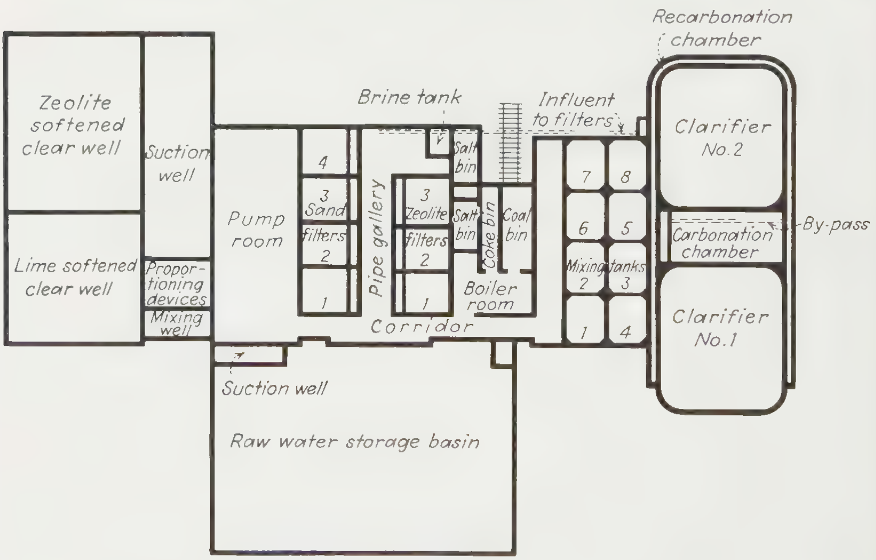

FIG. 4. Plan of 4-mgd water-softening plant at Findlay, Ohio.

carbonation between stages. Two-stage flocculation and settling are sometimes required for purification plants treating highly polluted or very turbid water.

Softening plants and demineralization plants for clear colorless water may consist entirely of zeolite units or ion-exchange units constructed like rapid filters. Some lime-softening plants employ ion-exchange units following filtration to remove part of the hardness. Figure 4[1] is the plan of a lime-softening plant with two-stage mixing and

[1] ROBERTS, Ohio Conference on Water Purification, *11th Ann. Rept.*, 1931, p. 52.

clarification and zeolite beds following the filters. The settling tanks are equipped with sludge-removal equipment, which is usually desirable for softening plants because of the large amount of sludge produced. Both carbonation and recarbonation are practiced at this plant. The plant is so arranged that any portion of the lime-softened water may be passed through the zeolite beds.

7. Plant Capacity. It is good practice to operate filters and basins continuously and at constant rates during any one day, except for the smallest plants where the expense of more than one shift is prohibitive. Hourly fluctuations in demand are cared for by elevated and filtered water storage. The capacity of a plant is therefore determined by the maximum daily demand at the end of the design period (E of Table 6, Sec. 36). The capacity should be adequate for the day of maximum demand at the end of the design period. The design period for units that are readily duplicated, such as flocculation basins, clarifiers, and filters, is usually limited to 10 to 20 years, but the design period selected for the pump rooms, office, laboratory, and chemical rooms may be 25 to 50 years.

The number of filter units and basins in parallel is established from the minimum daily demand (B of Table 6, Sec. 36) and economic considerations. There should be a sufficient number of units of any type in order that one may be taken out of operation without disturbing the process and without dangerous loss of capacity. Filter units are built with capacities up to about 5 mgd. Each basin should preferably serve one filter but may serve two or more filters. Where feasible, it is desirable to arrange the plant so that flow may be divided throughout the plant. This makes it possible to treat two portions of the flow differently and to compare the results on the same raw water.

8. Plant Requirements for Purification. A study by Walton[1] (1954–1956) of data from about 60 plants indicates that simple chlorination may be used effectively with somewhat higher raw-water counts than 50 coliforms per 100 ml; that coagulation, settling, and filtration without chlorination are less effective than simple chlorination; and that conventional rapid-filter plants with adequate pre- and postchlorination can meet the Public Health Service Drinking Water Standards with raw-water coliform counts greatly in excess of 20,000 per 100 ml (up to 1,000,000 or more).

Chlorination as an adjunct to filtration for bacterial removal from polluted waters is of such importance that it always should be used in ordinary purification plants. With chlorination, bacterial efficiency of the filters is of less importance, and their effectiveness, along with coagulation and settling, in the removal of turbidity and color can be promoted. Modern rapid-filter plants should produce effluents with an average turbidity of less than 0.5 unit. In order to accomplish this, the pretreatment should be such that the water going to the filters has a turbidity of not more than about 5 units. The overflow rates usually used in the clarifiers of ordinary purification plants for comparatively clear waters range from 600 to 1,500 U.S. gpd/sq ft of floor area at the plant capacity. For highly turbid waters, the required overflow rate may be as low as 100 gpd/sq ft. The overflow rate in U.S. gallons per day per square foot equals 180 times the depth in feet divided by the settling period in hours.

According to Fleming,[2] the treatment of waters with turbidities in excess of 1,000 ppm, such as that of the Mississippi River, requires double coagulation and sedimentation with 8 to 12 and 4 to 6 hr for the first and second settling periods, respectively. If the turbidity is 1,200 to 2,000 with the fineness coefficient greater than 1.1, or is greater than 2,000 with the fineness coefficient greater than 0.7, the double coagulation-sedimentation process should be preceded by 3 to 5 hr of plain

[1] WALTON, GRAHAM, Effectiveness of Water Treatment Processes as Measured by Coliform Reduction, *U.S. Public Health Serv. Publ.* 898, Washington, D.C., 1961.

[2] *J. AWWA*, **22**, 1559, 1930.

settling. A considerable amount of fine sand is present when the fineness coefficient exceeds 0.7, and plain settling to reduce the turbidity to 1,200 or less results in the saving of chemicals. Grit chambers are effective if the fineness coefficient exceeds 1.1. For turbidities in excess of 2,000 with the fineness coefficient less than 0.7, triple coagulation and settling are required with settling periods of 10 to 12, 4 to 6, and 4 to 6 hr, respectively.

CLARIFICATION

9. Settling Velocities of Individual Particles. When a particle is permitted to move without interference through a fluid owing to the difference between its density and that of the fluid, the settling or rising velocity with respect to the fluid quickly

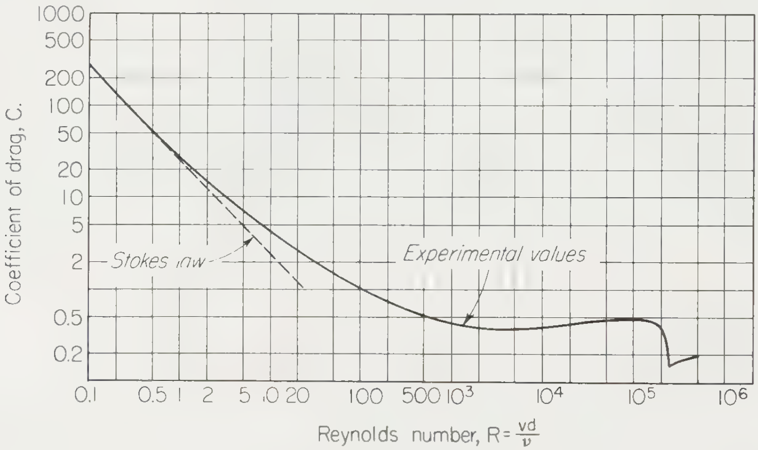

FIG. 5. Drag coefficients of spheres in fluids as a function of Reynolds number.

becomes constant, the resistance becoming equal to the weight of the particle in the fluid. The general equation for the settling velocity[1] of a sphere, obtained by equating Newton's value of the resistance, or drag, to the weight of the sphere in the fluid, is as follows:

$$v = \sqrt{\frac{4}{3}\frac{g}{C}\frac{\rho_1 - \rho}{\rho}d} \tag{11}$$

in which v = settling velocity
g = acceleration of gravity
C = drag coefficient
ρ = density of the fluid
ρ_1 = density of the particle
d = diameter of the particle

Experimental values of the drag coefficient of spheres in terms of Reynolds number are shown in Fig. 5.[2] For Reynolds numbers up to about 0.5 to 1, the drag is entirely streamline, and for larger Reynolds numbers, eddying resistance comes into play.

The viscous drag,[3] as developed by Stokes, may be equated to the weight of the

[1] See CAMP, Sedimentation and the Design of Settling Tanks, *Trans. ASCE*, 1946, p. 895.
[2] CAMP, *Sewage Works J.*, September, 1936, p. 742.
[3] CAMP, *Trans. ASCE*, 1946, p. 895.

sphere to obtain Stokes' law, which is given below:

$$v = \frac{1}{18}\frac{g}{\mu}(\rho_1 - \rho)d^2 \tag{12}$$

in which μ is the absolute viscosity of the fluid.

Values of μ for pure water at various temperatures are given in Fig. 6. The impurities in natural fresh water and in municipal sewage usually occur in such low concentrations as to have a negligible effect on the density and viscosity. The

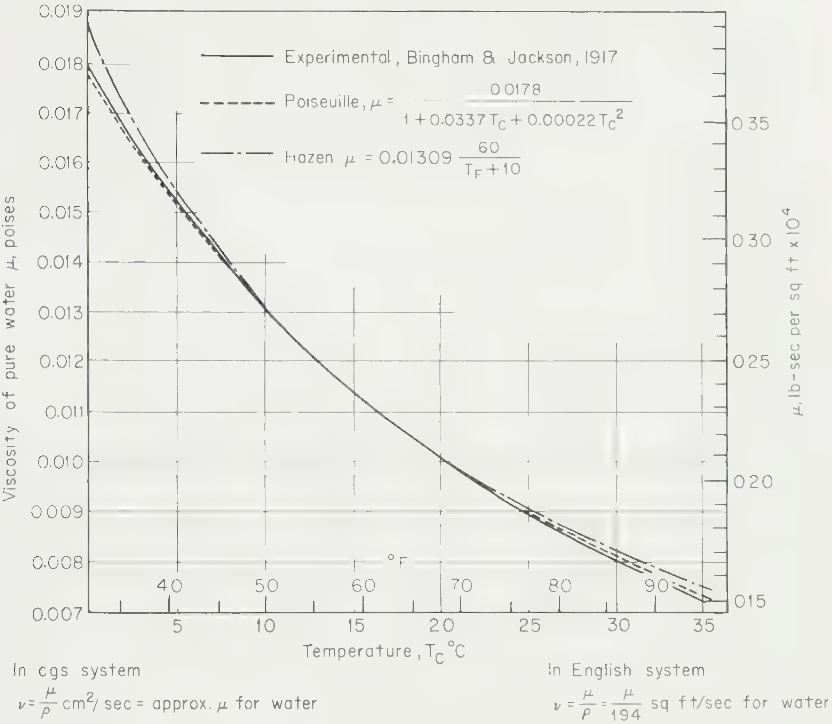

Fig. 6. Viscosity of pure water as a function of temperature.

impurities in natural sea water, which contains about 3.5 percent by weight of salts, increase the density about 2.5 percent but have a negligible effect on the viscosity. The change in water temperature between summer and winter has an enormous effect on the viscosity and hence on the settling velocity. The viscosity at 0 C is about 2.2 times the viscosity at 30 C from Fig. 6. Sand grains and heavy floc particles settle in the transition region, but most of the particles significant in forecasting removal by settling in water-treatment plants settle well within the Stokes' law region. Particles with irregular shapes settle somewhat more slowly than spheres of equivalent volume.

When the volumetric concentration of suspended particles exceeds about 1 percent (10,000 ppm), settling is appreciably hindered and the settling velocities are reduced by 10 percent or more.

10. Clarification Theory.[1] **Ideal Basin and Discrete Particles.** The following simplifying assumptions are made to develop the theory for the ideal rectangular basin:

1. The direction of flow is horizontal, and the velocity is the same in all parts of the settling zone. Hence each particle of water is assumed to remain in the settling zone for a period equal to the retention period, which is the volume of the settling zone divided by the rate of discharge.
2. The concentration of suspended particles of each size is the same at all points in the vertical plane perpendicular to the direction of flow at the inlet of the settling zone.
3. All suspended particles maintain their shape, size, and individuality during settling and settle without interference. Hence each particle is assumed to settle at constant velocity for a given temperature.
4. A particle is removed when it strikes the bottom of the settling zone.

The settling path of a particle is determined by the vector sum of its settling velocity and the velocity of the liquid. Hence, in the ideal basin, particles having

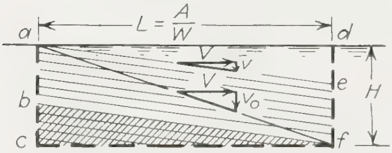

FIG. 7

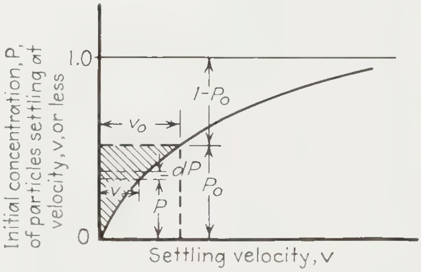

FIG. 8. Typical settling-velocity analysis curve of suspension of discrete particles.

settling velocities equal to or greater than v_0, as shown in Fig. 7, will all settle out; and the removal of particles with any settling velocity v less than v_0 will be

$$r = \frac{v}{v_0} = \frac{Av}{Q} \tag{13}$$

in which r is the removal ratio, and v_0 the overflow rate, or the discharge per unit of tank floor area $= Q/A$. An overflow rate of 1,000 U.S. gpd/sq ft corresponds with a settling velocity of 0.0471 cm/sec.

If the settling-velocity analysis of the original suspension is represented by a curve, such as Fig. 8, the total removal ratio for the entire suspension is

$$r = 1 - P_0 + \frac{1}{v_0}\int_0^{P_0} v\, dP \tag{14}$$

The value of the last term in Eq. (14) is the average vertical distance from the curve (Fig. 8) to the horizontal line for $P = P_0$. The concentration of suspended matter at any point in the basin, such as at e (Fig. 9), is

$$x = \int_0^{P_1} dP = P_1 \tag{15}$$

where P_1 is the value of P from Fig. 8 for $v = (h/H)v_0'$ from Fig. 9.

[1] CAMP, *Trans. ASCE*, 1946, p. 895.

The above theory, Eqs. (13), (14), and (15), also applies to ideal radial-flow basins in which the velocity is horizontal in a radial direction from the center and varies inversely as the distance from the center.

As a consequence of this theory, the following conclusions may be drawn with respect to settling of discrete particles in an ideal basin:

1. For any given discharge, the removal is a function of the surface area and independent of the depth of the basin; or the removal is a function of the overflow rate and not the retention period.

2. The concentration of suspended matter at any cross section in the settling zone increases with the depth below the surface and decreases with the proximity of the cross section to the outlet end of the basin.

The settling-velocity analysis curve of a suspension of discrete particles may be determined experimentally by quiescent settling in a container such as Fig. 10. At various time intervals after the start of the test, samples are withdrawn from a given point, such as D, and the concentration is determined for each sample. The concentration may be measured in terms of suspended solids, turbidity, iron, alumina, color, or any other quantity that is reduced by settling. The corresponding settling velocity is obtained by dividing the depth of water above the sampling point by the period of settling. Extreme care must be exercised to maintain a constant temperature and to reduce eddy and convection currents to a minimum. If the test is satisfactory and no flocculation of the particles is taking place, the same analysis curve should be produced by samples taken from any depth. On the other hand, if the velocity analysis curve from deep samples lies below the analysis curve for shallow samples, coagulation is taking place and the velocities obtained are meaningless. If the particles coalesce, the preceding theory is not applicable.

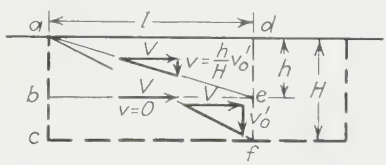

Fig. 9

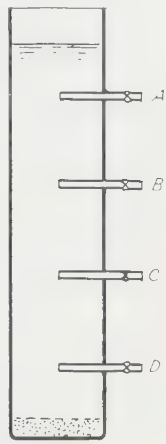

Fig. 10

11. Clarification Theory.[1] **Ideal Basin and Coalescing Particles.** An analysis of a suspension which includes the effect of flocculation and is satisfactory for forecasting settling-basin removal may be made by determining concentrations in samples from each sampling point of the container (Fig. 10) at the end of various time intervals. The effects of turbulent mixing[2] may be approximated by means of a mixing grid moving up and down in the sample. Table 3 shows a typical analysis of this type. The depth of the container should be as great as that of the settling basin for best results, and the capacity of the container should be large enough so that the depth is not appreciably changed by the withdrawal of samples.

The removal may be estimated for any settling period by subtracting from unity the average of the concentration ratios. For example, the removal ratio for a basin the same depth as the container for a 160-min retention, from Table 3, is 0.645. For a

[1] Camp, *Trans. ASCE*, 1946, p. 895.

[2] Camp and Stein, Velocity Gradients and Internal Work in Fluid Motion, *J. Boston Soc. Civil Engrs.*, October, 1943, p. 219.

TABLE 3

Sampling point	Concentration ratio					
A	1.0	0.82	0.66	0.47	0.28	0.21
B	1.0	0.83	0.69	0.50	0.33	0.25
C	1.0	0.85	0.72	0.54	0.38	0.30
D	1.0	0.87	0.75	0.59	0.43	0.36
Time, min	0	20	40	80	160	300

basin half the depth of the container, the removal is 0.695 for the same period and 0.515 for half the period. It may be seen, therefore, that the removal for this suspension is not independent of the depth and is influenced by both overflow rate and retention period.

The particles in most of the suspensions dealt with in water-treatment plants flocculate during settling. This is notably true of particles of floc formed by chemical coagulation, but it has also been observed with clay suspensions.

12. Velocity and Basin Dimensions.[1] The velocity in an actual rectangular basin is not uniform over the cross section even though uniform dispersion at the inlet end and uniform collection at the outlet end of the settling zone are effected. Because of the drag on the walls and floor the velocity at these boundaries is zero, and it is greater than the average at some points out from the boundaries. The velocity distribution over the cross section of most settling basins is not stable, moreover, owing to the disturbing influences of masses of water of varying density. This variation in density, which is due to temperature differences and differences in concentration of solids and entrained gases, though slight is nevertheless sufficient to cause vertical movements of water masses, dead spaces, and reversals in the direction of flow. As a result of these disturbing influences, the probable time of passage of all the particles in a given volume of water will be less than the retention period, and the volume will disperse itself while passing through the basin so that the time interval between the passing of the first and last particles at the basin outlet will be much greater than at the inlet. This phenomenon is called *short-circuiting.* If two or more succeeding volumes of water passing through the basin at the same rate of flow require markedly different times for passage, the basin lacks stability of flow.

A particular type of short-circuiting common to many settling basins is caused by *density currents.* If the incoming suspension is heavier than the basin contents, and the basin velocity is insufficient to cause mixing, the heavy suspension will flow along the bottom as a density current. Similarly, light suspensions will flow along the surface. Since the incoming suspension contains more solids than the clarified water in the basin and is therefore likely to be heavier, it is better to introduce it near the bottom and to make the basin shallow.

Short-circuiting may be measured by inserting a charge of dye or other tracer into the basin influent and observing its concentration in the effluent after various time intervals as the slug of water containing the charge passes out of the basin. Short-circuiting studies are usually made on model tanks operating in accordance with Froude's law. Figure 11 shows the results of several such studies plotted in dimensionless terms; with the relative concentration c/c_0 as ordinates and the relative time t/T as abscissas, where c is the concentration of the tracer in the effluent after time t, c_0 is the concentration at $t = 0$ which would result with instantaneous dispersion of the tracer throughout the tank, and T is the retention period, volume of basin/Q. If all

[1] CAMP, *Trans. ASCE*, 1946, p. 895.

the tracer charge is accounted for in the effluent, the area under the curve will be 1.0. If the flow pattern is stable and there are no dead spaces, the value of t/T to the center of gravity of the curve will also be 1.0. A stable flow pattern is indicated when the same curve can be reproduced with repeated runs under the same conditions.

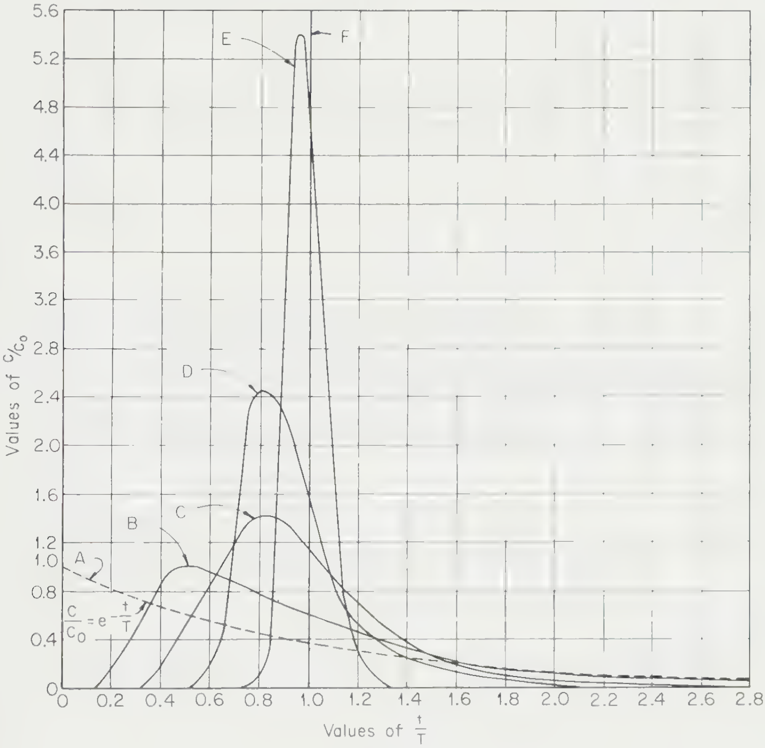

FIG. 11. Typical dispersion curves for tanks.

The relative time to the center of area t_A/T is usually less than 1.0 and is smaller the worse the short-circuiting. Since half the particles of water pass in less time, t_A is the *probable flowing through time.* The dispersion of the water is measured approximately by the time of initial appearance t_i of the tracer in the settling-tank effluent. Small values of t_i/T and t_A/T indicate serious short-circuiting; and small values of Froude's number F indicate unstable flow patterns. Table 4 shows the hydraulic characteristics of the curves of Fig. 11.

TABLE 4. HYDRAULIC CHARACTERISTICS OF TYPICAL TANKS

Curve (see Fig. 11)	Type of tank	b, ft	H, ft	L, ft	V, fpm	$F = \frac{V^2}{Rg}$	t_i/T	t_A/T
A	Ideal dispersion	.....	....	.....	.....	....	0.0	0.693
B	Radial-flow circular	.....	14.2	.....	1.11	7.5×10^{-7}	0.14	0.831
C	Wide rectangular	135	18.5	330	3.12	5.8×10^{-6}	0.30	0.925
D	Narrow rectangular	16	14	273	5.17	4.53×10^{-5}	0.52	0.903
E	Baffled mixing	2	22.3	1,056	66.6	4×10^{-2}	0.74	0.988
F	Ideal settling	.....	....	.....	.....	....	1.0	1.0

Curves *B*, *C*, *D*, and *E* of Fig. 11 are characteristic of progressively better types of settling tanks under stable flow conditions. The ideal dispersion tank, the baffled mixing chamber, and the ideal settling tank have been added for the purpose of comparison. A rough estimate of the effect of short-circuiting on removal may be had if it is assumed that the suspension is subjected to varying settling times distributed as indicated by the dispersion curves.

Since, from the clarification theory with discrete particles in an ideal basin, removal is independent of depth for a given rate of discharge, it is evident that the most economical basin will be that with the least practicable depth. Camp[1] has shown that this is also true for actual basins, even with flocculation and turbulence during settling, and that the least practicable depth is that for impending scour of sludge at the peak rate of flow. For a particular type of sludge deposit, scour depends primarily upon the magnitude of the basin velocity. Experience indicates that the velocity of impending scour of settled alum floc is greater than 4 fpm. Reductions in short-circuiting and improvements in settling efficiency of existing basins have been reported following the judicious use of baffles in the basins normal to the direction of flow. This procedure has the effect of increasing *F*, but it also may introduce dead spaces and eddy currents and cause disturbance to the deposited solids. A more satisfactory procedure for existing basins is the use of longitudinal baffles or of trays.

The design of new settling basins should be based upon the overflow rates required to obtain the desired removal of suspended matter at the expected rates of discharge. The basin floor area will thus be established. The required floor area may be provided in single-story basins or in multiple-story basins, the choice depending largely upon the amount of sludge to be produced and the methods available for sludge removal. Multistory basins will generally prove to be the more economical to construct, since the required floor area may be provided in the least basin volume the greater the number of trays. The depth of a single-story basin to the top of the sludge blanket or the clear depth of a single pass of a multistory basin from ceiling to the top of the sludge should be the minimum consistent with no scour for best economy except as limited by the method of removal of the sludge.

Figure 12 illustrates in plan two complete bays of a rapid water-filtration plant and a longitudinal section through one bay. The settling basin illustrated has three floors with two sludge collectors, one for the top floor and the other for both middle and bottom floors. The collector blades travel in the direction of flow at a velocity of 1 to 3 fpm depending upon the rate of accumulation of sludge. The clear height from floor to ceiling in each pass should be about 6.5 ft so as to provide headroom for workmen during maintenance operations. The width of each bay is limited to about 20 ft, the practical limit to the length of collector blades. The spaces occupied by inlet and outlet zones and by return bends should not be counted as effective floor area for settling purposes because of excessive turbulence and upward components of velocity within these zones.

If the rate of accumulation of sludge is small, the sludge collectors may be omitted. In this case, sludge is removed intermittently at intervals of several weeks by withdrawing a basin from service, draining it, and flushing the walls and floors with hose streams. With this type of basin, additional depth must be provided for the accumulated sludge so that scouring velocities will not be developed in the depth remaining above the top of the sludge blanket.

Experiments indicate that, with well-designed inlets and outlets, both the inlet and the outlet zone will extend out into the basin for a distance about equal to the basin depth. Since the floor area in these zones is ineffective for settling, it is obvious that the length of a basin should be great as compared to its depth. Since single-

[1] *Trans. ASCE*, 1946, p. 895.

story radial-flow circular tanks and single-story square tanks are quite inefficient for this reason, the design of the inlets and outlets for such tanks is a critical problem. In order to effect good distribution at the inlet of such a tank and good flow distribution over the cross section at the outlet end, with a minimum length for both inlet and

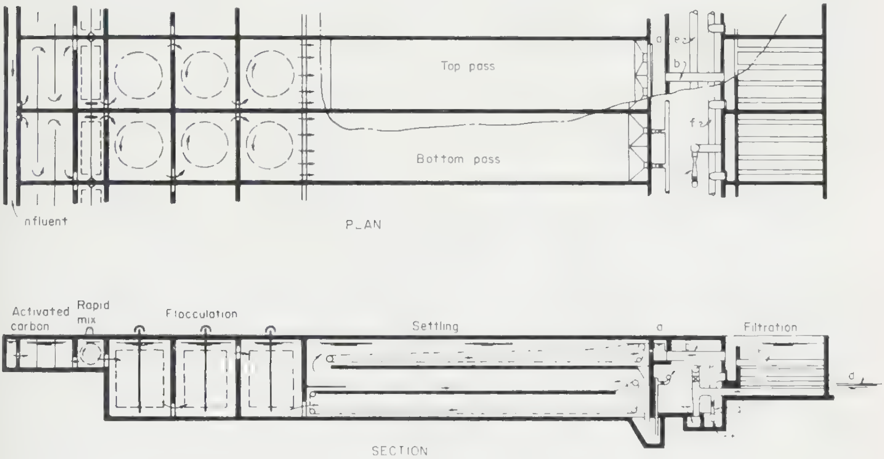

FIG. 12. Water-filtration plant showing two complete bays in plan. (*a*) Equalizing channel. (*b*) Filter influent. (*c*) Filter effluent. (*d*) Effluent overflow. (*e*) Wash water. (*f*) Waste water. (*g*) Filter to waste. (*h*) Wash-water gutter. (*j*) Sludge.

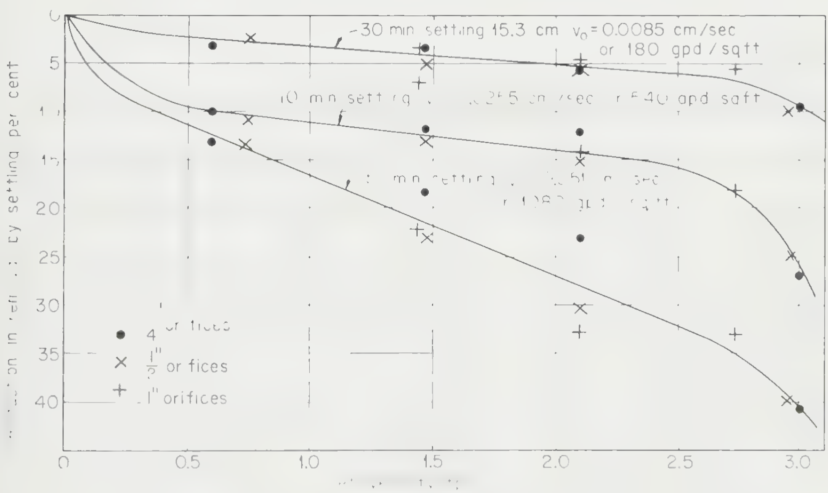

FIG. 13. Effect of dispersion wall jets on destruction of ferric hydrate floc.

outlet zones, it is essential to use orifice walls to the full depth and to have a relatively high velocity through the orifices. Unfortunately, such a wall is detrimental at the inlet end since the high velocity through the orifices may destroy floc. Figure 13 shows the effect of the velocity of submerged jets on the destruction of ferric hydrate floc, based on experiments by Dennis.[1] Water containing the floc was allowed to flow

[1] DENNIS, A. P., JR., Master's Thesis, M.I.T., Cambridge, Mass., 1939.

through an orifice wall from the chamber in which it was formed, and settling tests were then made by collecting samples for iron analysis at a depth of 15.3 cm on both sides of the orifice wall. The plotted points in Fig. 13 show the reduction in removal by settling for various jet velocities. The top curve shows that removal by settling is little affected by inlet jet velocities up to about 2 fps if the overflow rate is very low. The bottom curve shows that with high overflow rates inlet jet velocities in excess of about 0.1 fps will substantially reduce removal by settling.

The problem of inlet and outlet design is much simplified if the length of the basin is made so great as compared to its depth that the inlet and outlet zones are a negligible part of the gross length. For example, the effective settling area in a basin with a 20:1 ratio of length to depth is about 90 percent of the total floor area. Orifice walls are of no benefit in such a tank.

Settling basins should be covered in order to minimize convection and eddy currents due to temperature changes and wind action and to obviate ice difficulties. The covering of basins is becoming common practice in design unless the basins are so large that the cost is too great. Occasionally natural sites are available, as at the Providence, R.I., purification plant, which permit the construction of very large settling basins with much more capacity than is needed at a minimum of cost. Under such conditions, short-circuiting is of little importance and roofs are not needed.

13. Inlet and Outlet Devices. The purpose of properly designed inlets and outlets is to distribute the water uniformly among the basins and uniformly over the cross section of each settling basin at the inlet end and to collect the effluent uniformly at the outlet end. Properly designed inlets and outlets assist in the reduction of short-circuiting and are very important for short basins with low velocities. The velocity in the basin must be reduced to less than 1 percent of the velocity in the influent conduit in some cases.

The water may be distributed across the width of the plant by bringing it in through several pipes at intervals across the width, as shown in Fig. 14*a*, or by bringing it in through a single conduit to a transverse influent flume, as shown in Fig. 14*b*, which in turn distributes water across the width through orifices or sluice gates. An equal division of flow to all the basins is most readily approached if the water level is nearly the same in all; this may be accomplished by means of freely discharging effluent weirs all at the same level, or by means of an effluent equalizing channel with a substantially level water surface together with submerged effluent slots having the same capacity for all tanks.

A uniform distribution of flow through inlet pipes or orifices, all of the same size, may be approached by making the head loss at the inlet pipes or orifices large as compared with the maximum difference in energy head available at the inlets. The maximum difference in available energy head in Fig. 14 will be between inlets A and B owing to the change in energy head through the pipe CD or the flume. The head loss at one of the two inlets considered is $h_o = kq^2$, where q is the discharge through the inlet. If h_f is the difference in energy head available at A and B and m is the ratio of the rates of discharge at the two inlets, the head loss at the other inlet is $h_o - h_f = k(mq)^2$. Then the *distribution formula* is

$$\frac{h_o}{h_o - h_f} = \frac{1}{m^2} \tag{16}$$

This equation may be used to compute the required inlet head loss h_o for any desired variation in discharge between the inlets. For example, if it is desired that the discharge at A vary by not more than 5 percent from the discharge at B, $m \gtreqless 0.95$ and $h_o \gtreqless 10h_f$. The value of h_f may be estimated from friction losses and velocity-head changes.[1] The size of orifices or gates may be determined by introducing the required value of h_o in the orifice formula with the proper discharge coefficient. The leading edges of all ports should be rounded to approach 1.0 for the coefficient of contraction and thus reduce the required port area. The proper size of inlet pipes may be determined by making the velocity head in the pipes equal to the required value of h_o. The design should be based upon the peak flow and should be checked for minimum-flow conditions.

For settling basins treating water with very fragile floc, high velocities at inlets and through dispersion walls are not permissible. Very low velocities in the inlets and less satisfactory distribution may be required. Permissible velocities for any particular floc can be determined only by test. The best solution for fragile floc and also the

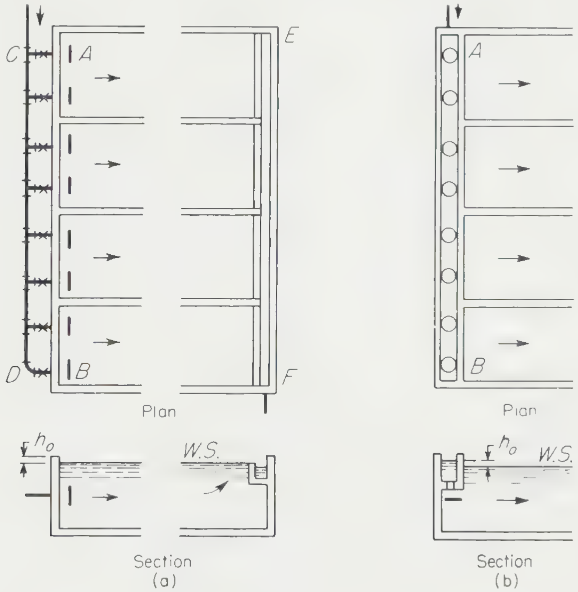

Fig. 14

simplest from the standpoint of inlet design is the use of flocculation tanks just preceding each settling tank as shown in Fig. 12. With this design the inlets are transferred to the inlet end of the flocculation tanks where the velocity may be made as high as is required for good distribution of flow among parallel bays. The wall openings between flocculation tanks and settling basins may be made quite large, the size being limited only by the desirability of minimizing short-circuiting.

The effluent from settling tanks may be collected uniformly across the width of each basin, and the basin water levels may be kept nearly the same by means of freely discharging weirs at the same level across the width of all basins at the effluent end. Such weirs discharge into effluent flumes, such as *EF* (Fig. 14*a*), which, hydraulically, are lateral spillway channels. Where freely discharging weirs are used, the operator is free to increase the free fall by lowering the water level on the filters. A free fall of 1.0 ft is equivalent to a jet velocity of 8 fps, which may be destructive to fragile floc. In some plants, the effluent weirs are submerged in operation in order to eliminate the

[1] Camp, T. R., and S. D. Graber, Dispersion Conduits, *J. Sanit. Eng. Div.*, *ASCE*, February, 1968, p. 31.

high velocity of a freely discharging weir and thus prevent the destruction of small floc particles going to the filters. Since the surface profile in lateral spillway channels drops in the direction of flow, the use of submerged weirs promotes short-circuiting toward the downstream end of the flume. Both hazards accompanying effluent weirs may be eliminated by using submerged effluent slots and equalizing channels, as shown in Fig. 12.

The drawdown of the water-surface curve, the effect of friction being excluded, in a lateral spillway channel of rectangular cross section and with a level invert (see Fig. 15) may be estimated by means of the following equation:[1]

$$H = \sqrt{h^2 + \frac{2q^2x^2}{gb^2h}} \tag{17}$$

where H = depth at the upstream end
h = depth at distance x
q = discharge per unit length of weir
g = gravity constant
b = width of the channel

This equation results from the integration for the special case of the general differential equation developed by Hinds from the momentum theory. It is based upon the assumption of hydrostatic-pressure distribution, which is nearly correct in treatment plant applications. Equation (17) is correct for parallel-wall flumes of other than rectangular cross section provided the invert is level; and the effects of sloping invert and friction may also be taken into account with additional terms. Experimental studies indicate that the friction loss in the flume may be estimated with values of Darcy's f varying from about 0.03 to 0.12, depending upon the turbulence in the channel, and the friction will account for 6 to 16 percent of the water-surface drawdown.

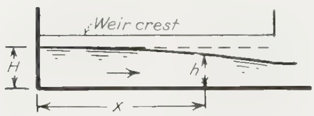

FIG. 15

The *distribution formula* (16) may also be used for the design of *equalizing* channels and effluent slots such as shown in Fig. 12. In this case, h_f may be computed by means of Eq. (17) assuming that h_f is $H - h$ plus an allowance for friction. Where one end filter is taken out of service for washing, the discharge from the settling tank serving that filter must flow laterally to the adjacent filter influent, together with one-half the discharge of the adjacent tank. For this case, the value of qx to use in Eq. (17) is 1.5 times the discharge per bay. The velocity through the slot should be limited to about 2 fps ($h_0 \leqq 0.062$) in order to minimize floc destruction in the filter influent and so that the variation in water level between settling tanks will be negligible as compared with the value of h_0 selected for the inlet ports to the plant.

The *distribution formula* (16) has a variety of other uses, including the design of orifice walls, the design of filter underdrains for uniform distribution of washwater, and the design of manifold systems for feeding of chemical solutions, air, and carbon dioxide.

14. Sludge Removal. For ordinary purification plants treating comparatively clear water, the settling basins may be designed without mechanical equipment for sludge removal. Such basins are usually designed with bottoms sloping gently to one or more sludge drainpipes; the sludge is removed by taking a basin out of service, draining it, and hosing the sludge to the drains. The period of accumulation of sludge between cleanings may vary from a few weeks to several months. The moisture content of the deposited sludge varies from about 90 percent for very turbid

[1] CAMP, *Trans. ASCE*, **105**, 606, 1940.

water and for some softening plants to more than 99.5 percent for ordinary coagulation of clear waters, and it decreases with time as the sludge compacts.

Two general types of mechanical sludge-removal equipment are in common use in water-treatment plants: the straight-line type of equipment suitable for rectangular tanks, and rotary equipment suitable for square tanks and for radial-flow circular or square tanks. In the first type, the sludge is scraped in a straight line to sludge hoppers at one end of the basin from which it is removed through a sludge pipe, as shown in Fig. 12. In the second type, the sludge is scraped to the center of the basin where it is removed.

The velocity of the sludge-removal equipment should not be sufficient to throw the sludge back into suspension. Lower velocities are required for flocculent sludge of high moisture content than for granular solids. On the other hand, the velocity of the mechanism must be high enough to remove the sludge as fast as it deposits.

This consideration is of little importance for most water plants but may become of consequence with long narrow basins and for very turbid water. The sludge-removal mechanism may be operated intermittently with waters of low suspended content, but continuous operation is necessary for highly turbid waters and for lime-softening plants.

15. Upflow Sludge-blanket Clarifiers. Upward-flow sludge-blanket clarifiers have been under development in the United States since about 1940, starting with the Spaulding precipitator. They are widely used by industry, particularly for softening; and their use is growing for municipal supplies. The sludge blanket or slurry pool is a fluidized bed functioning as a filter. The upward velocity of the water at any horizontal layer in a stable pool is v_0/p where v_0 is the overflow rate at that layer and p is the corresponding porosity between the floc particles. This upward velocity is the hindered settling velocity of the floc particles, which for small light particles is inversely proportional to the viscosity of the water, following Stokes' law. The volumetric concentration of the floc particles is $1 - p$. Following Stokes' law, the value of v_0/p will increase with the net density of the floc particles.

The overflow rate v_0 at a selected level increases directly with the discharge so that with increase in flow the top of the pool will rise to increase the porosity p proportionately. In order to minimize the range within which the top of the pool will fluctuate with changes in flow or water viscosity, the side walls of the tank may be constructed to slope vertically to provide an increase in horizontal area with increase in depth above the bottom.

Figure 16 shows the suspended solids content at the top of the slurry pool for various overflow rates at the same level, computed by the authors from the results of experiments by Bond[1] at a water temperature of about 15 C.

The hindered settling velocity v_0/p, the porosity p, the volumetric concentration of the floc particles $1 - p$, and the water content of the floc particles for any overflow rate v_0 may be computed from an experimental curve, such as those shown in Fig. 16, if it is assumed that the hindered settling velocity does not change substantially with small changes in floc concentration and that the volumetric concentration is directly proportional to the concentration of dry suspended solids by weight. If the value of v_0/p for the selected overflow rate is equated to the value for a slightly higher overflow rate $v_0 + dv_0$ from the same curve, the following equations result:

$$p = \frac{v_0(dc_s/dv_0)}{v_0(dc_s/dv_0) - c_s} \tag{18}$$

$$w = 1 - \frac{\rho c_s}{\rho_s(1 - p)} \tag{19}$$

$$\frac{\rho_f}{\rho} = \frac{c_s}{1 - p} + w \tag{20}$$

[1] Bond, A. W., Behavior of Suspensions, *Proc. ASCE, J. Sanit. Eng. Div.*, May, 1960, p. 57.

where p is the porosity at overflow rate v_0, c_s is the corresponding concentration of dry suspended solids by weight expressed as a decimal fraction, w is the water content of the floc expressed as a fraction of the floc volume, ρ_s/ρ is the specific gravity of the dry suspended solids, and ρ_f/ρ is the specific gravity of the floc.

Bond's experiments were undertaken in a tank with vertical glass end walls and wooden side walls diverging upward at 30 deg from the vertical. It was found that the floc settled on the sloping walls at all levels and rolled down to the bottom of the upflow zone, where it was again lifted into suspension nearer the center and rose at gradually decreasing velocity. There was little movement of the floc at the top of the

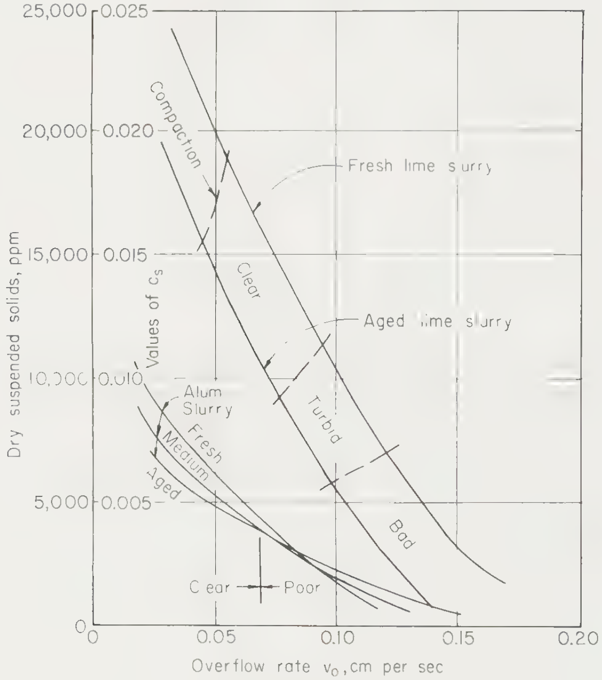

FIG. 16. Overflow rates for sludge-blanket clarifiers at 15 C.

slurry pool and the concentration was about the same throughout the pool. The presence of the rollers on the sloping walls indicates that most of the water escaped through the top of the slurry pool near the middle at somewhat higher overflow rates than the averages reported by Bond. The average overflow rate may, however, be used for v_0 to estimate the porosity by means of Eq. (18); because if the curve (Fig. 16) is shifted to the right to reflect the higher overflow rates in the middle, dv_0 will increase proportionately. Nevertheless, higher overflow rates are obtainable if the rollers are eliminated by using vertical side walls throughout.

A study of the curve for fresh alum slurry (Fig. 16) shows that good results were produced at concentrations between 4,400 and 7,100 ppm with porosities between 0.582 and 0.374, floc water contents between 0.9953 and 0.9949, and floc specific gravities between 1.0058 and 1.0062. At a concentration of 10,000 ppm, the estimated porosity was 0.27, the floc water content was 0.9939, and the specific gravity was 1.0076. At a concentration of 710 ppm, the estimated porosity was 0.908, water content 0.9966, and specific gravity 1.0043. The values of v_0/p ranged from 0.074 cm/sec for p of 0.27 to 0.129 for p of 0.908.

A study of the curve for fresh lime slurry (Fig. 16) indicates good results at concentrations between 11,500 and 18,000 ppm with porosities between 0.60 and 0.406, floc water contents between 0.9781 and 0.9769, and floc specific gravities between 1.0068 and 1.0072. At a concentration of 22,600 ppm, the estimated porosity was 0.307, the floc water content was 0.9752, and the specific gravity was 1.0078. At a concentration of 1,800 ppm, the estimated porosity was 0.861, the floc water content was 0.9901, and the specific gravity was 1.00305. The values of v_0/p ranged from 0.13 cm/sec for p of 0.307 to 0.196 for p of 0.861.

To maintain a stable pool, sludge must be withdrawn as fast as floc is added to the pool. For vertical side walls, the addition in time t is $v_0\ (\Delta c_s/l)\ t$, where l is the pool depth and Δc_s is the floc concentration added to the pool. For example, the time to build up a pool 150 cm deep to a suspended solids concentration of 6,000 ppm at an overflow rate of 0.05 cm/sec when floc is added at 100 ppm is $6{,}000 \times 150/0.05 \times 100 = 180{,}000$ sec or 2.08 days.

Changes in overflow rate or water temperature will cause the top of the slurry pool to rise or fall. If the water surface is not set high enough, slurry may be discharged to the filters in high concentrations. To avoid this and to facilitate withdrawal of excess slurry, submerged weirs are provided for overflow of slurry to sludge hoppers. A maximum slurry level may thus be maintained, but control of the weight of solids in the pool is made more difficult.

The velocity gradients and times used for formation of floc entering the bottom of the pool will affect the volume and density of the floc in the slurry pool. Pilot-plant studies are sometimes essential for the determination of design factors.

The velocity gradients and times used by Bond for the data shown in Fig. 16 are not available. The velocity gradient at the top of a stable slurry pool may be estimated by means of Eq. (38). For the case of fresh alum slurry in Fig. 16, at v_0 of 0.041 ρ_f/ρ is 1.0062 for the floc particles including their water content. The porosity p is 0.374, ν is 0.0114 at 15 C, and from Eq. (41), i is 0.0039. From Eq. (38), G is 6.07 sec^{-1}.

Laboratory studies indicate a tendency of slurry blankets to gel into large impermeable masses with channeling of the water through large passes when treating water with low turbidities using alum slurries. For satisfactory results, the slurry pool must consist of separate floc particles. Adequate preflocculation is required.

FLOCCULATION

16. Purpose of Coagulants. Coagulation in its strictest sense means the agglomeration or flocculation of smaller particles to form larger ones. Coagulants are added to water to assist in the removal of finely divided or colloidal impurities that require agglomeration before they can be effectively removed by settling and filtration. In water treatment, the term is generally used to include all the processes that take place from the addition of the chemicals to the formation of the floc.

The most important of these processes are the formation of colloidal precipitates, the neutralization of charges on the colloidal particles, the flocculation of the particles by Brownian motion followed by mechanical stirring, and the adsorption by the floc of impurities in the water. In most cases, the floc is formed from the precipitation of the chemicals added to the water by interreactions or by reaction with soluble constituents of the water. In some cases, however, the floc is produced by coagulation of colloidal particles, such as vegetable coloring matter, already present in the water. A part of the lime-softening process consists of coagulation, inasmuch as the precipitates formed in the removal of hardness must be flocculated before they can be removed from the water.

17. Chemistry of Coagulation. The most commonly used coagulant is filter alum [sulfate of alumina, $Al_2(SO_4)_3 \cdot 14H_2O$], which is available commercially in both lump and powdered form, and in solutions of about 50 percent. Another chemical in common use is copperas (ferrous sulfate, $FeSO_4 \cdot 7H_2O$), also available in solid form; and other coagulants are ferric chloride, $FeCl_3$, available as an amorphous solid or in concentrated aqueous solution; ferric sulfate, $Fe_2(SO_4)_3$, available in solid form; and chlorinated copperas made at the plant by combining Cl_2 with copperas.

The reactions are much the same with all the coagulants, with some variations that will be pointed out below. In the case of sulfate of alumina, for example, the first reaction upon the addition of the chemical to the water is its solution, as follows, which with the small concentrations used goes to completion to the right:

$$\underline{Al_2(SO_4)_3 \cdot 14H_2O} \rightleftarrows 2Al^{3+} + 3SO_4^{--} + 14H_2O \tag{21}$$

The Al^{3+} ions combine with OH^-, which is liberated from the alkalinity of the water in accordance with reaction (4), as follows:

$$2Al^{3+} + 6OH^- \rightleftarrows \underline{Al_2O_3 \cdot xH_2O} \tag{22}$$

The extent to which this reaction goes to the right to form the hydrous aluminum oxide precipitate depends upon the available alkalinity and the equilibrium constant for reaction (22). It will be noted that three OH^- ions are required for each Al^{3+} ion. If sufficient alkalinity is not available, it must be added to precipitate the Al as hydrous oxide. For this purpose, hydrated lime, $Ca(OH)_2$, is usually added, or to avoid increase in hardness, soda ash (sodium carbonate, Na_2CO_3) or lye (sodium hydroxide, NaOH) may be used. Ferric coagulants produce hydrous ferric oxide, $Fe_2O_3 \cdot xH_2O$, as a precipitate in reactions analogous to (22). Ferrous sulfate cannot be used without lime or alkali, as will be explained below.

When a relatively insoluble compound, such as Al_2O_3 or Fe_2O_3, is in equilibrium with a solution of its ions, the mass action expression may be written by omitting the solid term. The equilibrium constant is called a *solubility product*. The solubility product for reaction (22) is

$$[Al^{3+}][OH^-]^3 = 5 \times 10^{-33} \text{ at } 25\text{ C}^1 \tag{23}$$

and for Fe_2O_3 it is

$$[Fe^{3+}][OH^-]^3 = 6 \times 10^{-38} \text{ at } 25\text{ C}^1 \tag{24}$$

The value of the solubility product for these equations is influenced by both temperature and concentration of dissolved solids.

In the presence of caustic alkalinity, Al_2O_3 dissolves as an aluminate as follows:

$$\underline{Al_2O_3} + 2OH^- \rightleftarrows 2AlO_2^- + H_2O \tag{25}$$

The solubility product for this reaction is

$$[AlO_2^-][H^+] = 4 \times 10^{-13} \text{ at } 25\text{ C}^1 \tag{26}$$

Reaction (25) is peculiar to Al. It does not take place with the iron salts.

[1] LATIMER, "Oxidation Potentials," 2d ed., Prentice-Hall, Inc., Englewood Cliffs, N.J., 1952.

When copperas is dissolved in water, Fe^{++} and SO_4^{--} ions are liberated in a reaction analogous to (21), and the ferrous ions react with the CO_3^{--} ions and the OH^- ions in the solution to produce ferrous carbonate, $FeCO_3$, and the hydrous ferrous oxide, $FeO{\cdot}xH_2O$. The solubility products are

$$[Fe^{++}][CO_3^{--}] = 2.11 \times 10^{-11} \text{ at } 25\ C^1 \tag{27}$$

and

$$[Fe^{++}][OH^-]^2 = 1.8 \times 10^{-15} \text{ at } 25\ C^1 \tag{28}$$

which indicate that hydrous ferrous oxide does not begin to precipitate until the pH exceeds 8.5, although ferrous carbonate starts precipitating at lower pH values. For this reason lime is always used in conjunction with copperas, and enough lime is used to raise the pH to 8.5 to 10.0. The process is sometimes called the iron and lime process. Ferrous oxide is unstable in the presence of dissolved oxygen and is rapidly oxidized to hydrous ferric oxide as follows:

$$\underline{4FeO} + O_2 \rightleftarrows 2\underline{Fe_2O_3} \tag{29}$$

Aeration is helpful in this process as a first step before lime is added in order to furnish dissolved oxygen and to save lime by the liberation of free CO_2.

The significance of the foregoing solubility products is indicated in Fig. 17, which shows the approximate solubility of aluminum and iron oxide floc and of ferrous carbonate at various pH values. The best precipitate is obtained at points of least solubility, which for alum is pH 5.0 to 7.5 and for ferric coagulants for all pH values above about 4.0, the solubility decreasing greatly as the pH is increased. The least solubility for hydrous ferrous oxide is at pH values above 9.5.

Copperas may be used successfully as a coagulant at low pH values if the ferrous iron is first oxidized to ferric by the introduction of chlorine into a copperas solution to form chlorinated copperas as follows:

$$6FeSO_4{\cdot}7H_2O + 3Cl_2 \rightleftarrows 6Fe^{3+} + 6SO_4^{--} + 6Cl^- + 7H_2O \tag{30}$$

This reaction requires about 1 lb of chlorine to 8 of copperas. Organic-bound iron in waters of high color has been effectively oxidized and precipitated by $KMnO_4$ at a pH of 8.8 to 9.8.

The hydrous aluminum or ferric oxide when first formed is a positively charged colloid in the acid region up to a pH of about 6 to 7.5, adsorbing H^+ and probably some Al^{3+} or Fe^{3+} from solution. In order to flocculate a colloid, a sufficient concentration of flocculating ions of opposite charge must be present. The flocculating value of an ion is measured by the concentration required to completely flocculate a sol in a given time. The flocculating value[2] increases enormously with the valence of the ion, the relative flocculating values of trivalent, bivalent, and monovalent ions being roughly in the order of 500 to 7 to 1. In the case of coagulation with alum or ferric sulfate in the acid region, bivalent SO_4^{--} is automatically present to flocculate the hydrous oxides effectively. If $FeCl_3$ is used, however, flocculation is not so effective because only the monovalent Cl^- is present. Investigators[3] have shown that additional negative ions extend the range of pH in the acid region over which rapid

[1] Latimer, "Oxidation Potentials," 2d ed., Prentice-Hall, Inc., Englewood Cliffs, N.J., 1952.

[2] Kruyt and Van Klooster, "Colloids," John Wiley & Sons, Inc., New York, 1930; Weiser, "Inorganic Colloid Chemistry," John Wiley & Sons, Inc., New York, 1935.

[3] Peterson and Bartow; Black, Rice, and Bartow; Bartow, Black, and Sansbury: *Ind. Eng. Chem.*, January, 1928, p. 51; July, 1933, p. 311; and August, 1933, p. 898.

flocculation of alum and ferric salts takes place (see Fig. 18) and that, as expected, SO_4^{--} is much more effective than Cl^-. These investigators have also shown that the colloidal oxides of Fe and Al are negatively charged in the alkaline region, for additional positive ions promote more rapid flocculation. This effect is not appreciable in the case of alum floc because of reaction (25); but it is quite evident for ferric oxide floc, and as expected, Ca^{++} is much more effective than Na^+.

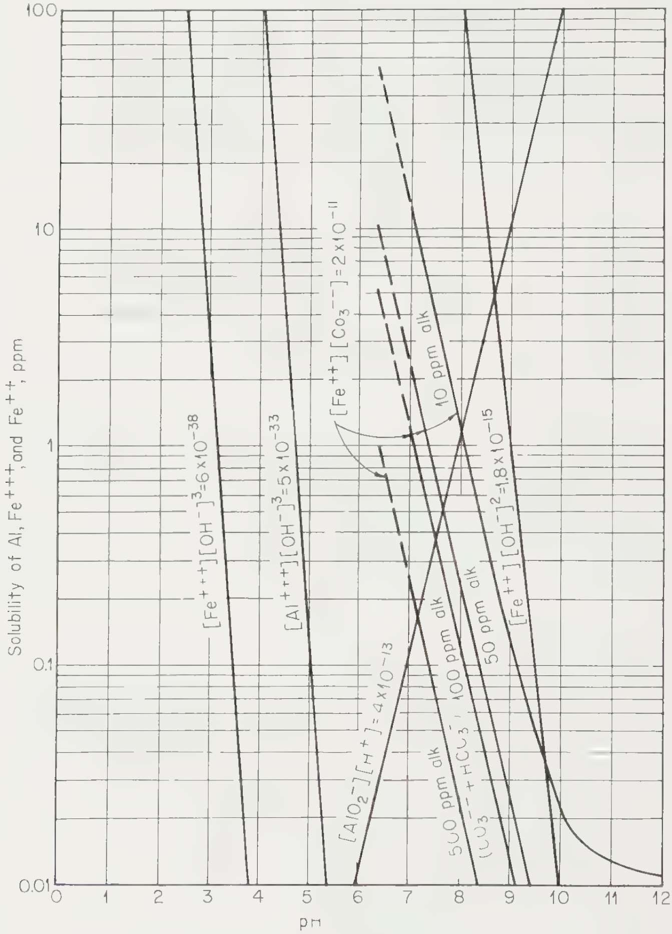

FIG. 17. Solubility of hydrous oxides of aluminum and iron at 25 C.

The curves in Fig. 18 are for coagulation in distilled water containing only the added salts. SO_4^{--} and Cl^- were added as sodium salts and Na^+ and Ca^{++} as chlorides. The presence of other salts and the concentration of dissolved solids may be expected to affect the position of the curves. The position of the curves is also shifted by changes in temperature, and the shift is greatest for smaller doses.

In the case of highly colored waters, best removal of color may be obtained by flocculating at low pH values, 4 or less, in which case very little oxide is formed and Al^{3+} or Fe^{3+} becomes an effective flocculating agent for the negatively charged color particles. Double coagulation is often required with an alkali added in the second stage in order to remove the residual Al or Fe as hydrous oxide.

The amount of coagulant required varies from about 0.3 gpg (1 grain per U.S. gal, gpg = 17.1 ppm) for clear waters to more than 6 gpg for some waters of high turbidity. The proper coagulant to use for a given water, the amount required, and the optimum pH value and velocity gradients for effective flocculation can best be determined by jar tests on a laboratory stirring device (Fig. 19). Flocculation is initiated by the Brownian motion of the colloidal particles which brings them in contact with one another. When the particles become too large to be influenced by Brownian motion, they are still too small for effective settling and filtration. Hence, in order to continue the flocculation process, mechanical stirring is required. The stirring must be sufficiently violent to prevent settling but not violent enough to destroy the floc particles after they are formed. The laboratory stirring device performs in the laboratory the function of the flocculator, and for comparable results

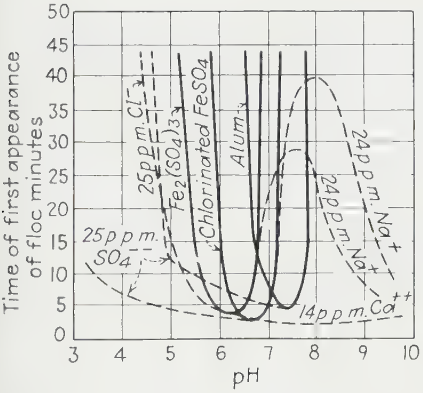

FIG. 18. Time of flocculation as a function of pH value. (Concentration of Al and Fe equivalent to about 2 gpg of alum. Temperature not reported.)

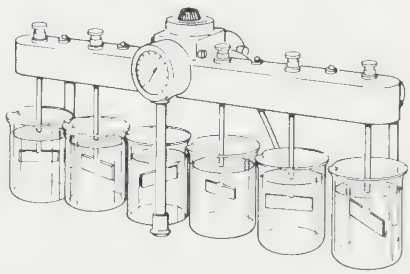

FIG. 19. Laboratory stirring device. (*Phipps & Bird.*)

the velocity gradients and temperature should be the same in the jars as in the flocculation chambers.

Laboratory tests to determine the optimum pH value in terms of the time of first appearance of floc, such as illustrated in Fig. 18, should be made at the temperature of the raw water in the plant with the same coagulant dose and the same velocity gradient in all six jars. The pH in the jars should be varied by the addition of HCl or NaOH. To facilitate the tests the water temperature in the jars should be controlled by insulating the jars or by a constant-temperature water bath. The temperature of raw water samples at 5 C placed in uninsulated jars in the laboratory will rise to about 9 C in 1 hr and to 12.5 C in 2 hr. The first appearance of floc is best observed in a Tyndall light beam with a dark background. In order to study the effect of velocity gradient, various coagulant doses, and coagulant aids, settling tests must be made in the jars following flocculation. The laboratory stirring device should therefore be equipped with pipettes for sampling after various periods of settling; and the device should be calibrated at various water temperatures for velocity gradient vs. rpm. Figure 20 shows such a calibration using 2.0-l samples in 2.0-l beakers. The calibration is made by supporting the beaker on a platform suspended from a piano wire and measuring the torque required to prevent angular deflection from the still position for selected speeds and water temperatures. The velocity gradient G is computed by means of Eq. (31).

It has been shown by Hudson[1] that the volume of floc formed is proportional to the coagulant dose and varies approximately inversely with the velocity gradient G. Inasmuch as 95 percent or more of the floc volume is bound water, it follows that destruction of floc consists of loss of bound water. It has been shown that an alum dose of 16 ppm will produce a good floc after 45 min flocculation at a G of 16 preceded by a 2-min rapid mix at a G of about 80, but that no floc will result if a Waring blender

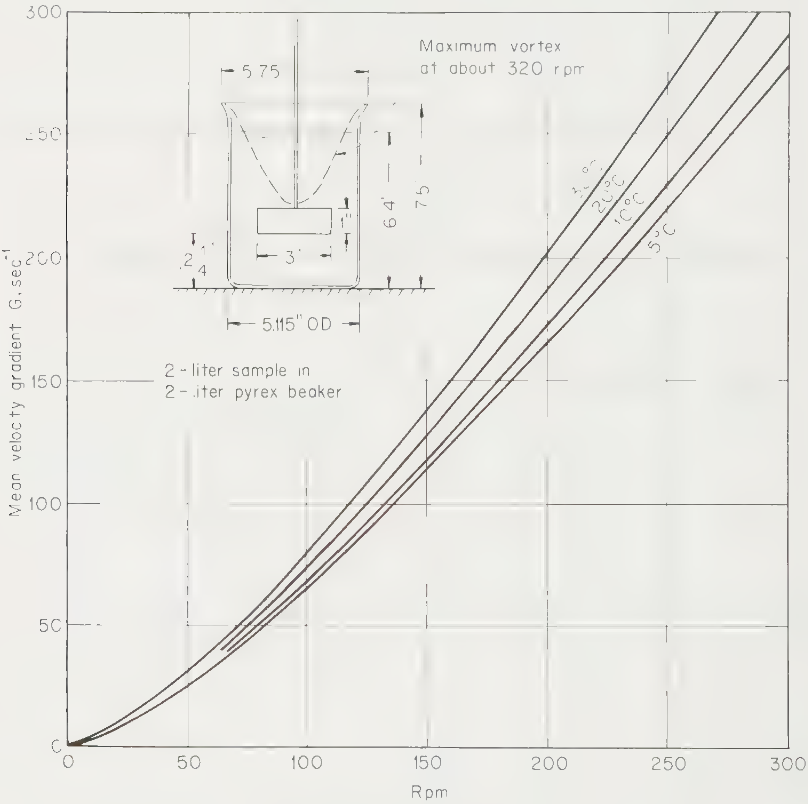

Fig. 20. Velocity gradient calibration for 2-l samples in 2-l Pyrex beakers.

(10,000 rpm) is used for the initial mix. The velocity gradient and time used for the rapid initial mix are therefore very important factors in plant performance and economy.

In coagulation of very clear waters, it is sometimes difficult to produce a good floc because of the absence of nuclei in the water about which the precipitates may collect. Finely divided clay in small amounts (1 to 7 gpg) has been successfully used in some cases to promote floc formation and hasten settling. Activated silica and a number of organic polyelectrolytes are available for use as coagulant and filter aids.

18. Feeding and Solution of Chemicals. Chemicals are proportioned to the water by dry feeding or by solution or slurry feeding. In the former method, the dry granu-

[1] Hudson, H. E., Jr., Physical Aspects of Flocculation, *J. AWWA*, **57**, 885, 1965.

lated chemical is fed volumetrically or gravimetrically from a dry-feed machine of which there are several types commercially available. Alum, ferric sulfate, and powdered activated carbon can be proportioned without difficulty with dry feeders. Hydrated lime and soda ash may be fed successfully if sufficient agitation is provided in the hoppers to prevent arching. It is difficult to feed copperas dry because of its tendency to cake. Dry feeders for dusty chemicals such as hydrated lime should be wholly enclosed. Feed machines are most conveniently fed from storage bins above.

The chemicals are usually raised to the storage rooms or bins by means of elevators, but where large quantities of chemicals are used, pneumatic conveyors are economical. Dry feeders usually dose the chemicals into a small stream of water which is discharged through a solution pot and a pipe or hose into the water at the desired point. Coagulants and alkalies should be dissolved before they reach the point of mixing with the water. Otherwise a portion of the flocculation time will be used for dissolving the chemicals. The solutions of alum, copperas, and soda ash from the dry feeders are usually prepared with a strength of less than 6 percent. Hydrated lime, which is soluble to only about 0.08 percent at 25 C (not enough to be prepared as a clear solution in small water streams), is prepared as milk of lime with about the same strength. Activated-carbon slurries may be transported at strengths of about 12 percent. Solid ferric sulfate may be proportioned by dry feeders but should be mixed for not less than 20 min with water heated to above 25 C to produce a 35 percent colloidal solution.

The time required to dissolve solid chemicals is directly proportional to the size of the particles in dilute solutions. The rate of solution of alum, ferric sulfate, and ferric chloride increases two- to threefold for each 10 C increase in temperature and appears to be independent of the concentration of the solute up to about 8 percent. Alum and ferric sulfate require about 10 min for each 1.0 mm of size of particle to dissolve at 10 C in dilute solutions. Ferric chloride dissolves at nearly a hundred times this rate, but lime dissolves at very much slower rates than alum. Solutions should be kept stirred during preparation in order to procure uniform concentrations and to speed up the process.

In solution feeding, the solution or slurry of known strength is proportioned by means of orifices, V-notch weirs, chemical feed pumps, or rotary dip buckets. Liquid alum is available from some suppliers as a 50 percent water solution containing about 8.3 percent Al_2O_3 and is delivered in tank trucks or tank cars. Liquid alum crystallizes at temperatures lower than about -15 C, and the crystallization temperature remains below the freezing point of water with all dilutions. Ferrous sulfate is available in some areas (principally from pickling liquors in the steel industry) as a water solution containing about 7 percent available iron or about 35 percent copperas. Liquid caustic soda (sodium hydroxide) is available in tank-truck and tank-car lots as water solutions containing 50 percent and 70 to 74 percent sodium hydroxide. Since the 70 to 74 percent solution crystallizes at temperatures below 64 C and the 50 percent solution crystallizes at temperatures below 15 C, the solutions should be diluted to 25 percent as soon as received. The crystallization temperature of all caustic soda solutions weaker than 30 percent is below the freezing point of water. Liquid ferric chloride may be obtained as a water solution containing 39 to 45 percent ferric chloride; and it is usually diluted to 2 to 3 percent for feeding.

The strong solutions and slurries should be applied to each bay of the treatment plant to ensure control of the chemical dose and to permit variation of the dose from bay to bay when desired. In Fig. 12, the carbon slurry should be applied at the entrance gate of each contact chamber; and the coagulant, chlorine, and alkali at the entrance port of each rapid mix. The postchlorine dose should be applied to the main filter-effluent conduit between the filters and the filtered water reservoir.

Solutions of alum and iron scales are quite corrosive. Glazed tile, polyvinyl chloride, hard rubber, and neoprene-lined pipe are satisfactory for conveying the solutions. Solution tanks should be lined with rubber, neoprene, acidproof brick, or other acid-proof lining. Iron pipe may be used for sodium hydroxide and lime and soda solutions, but with milk of lime, flexible rubber hose is better in order that deposits may be readily removed. Milk of lime, when cold, may be stored in concrete tanks. Soda ash and sodium hydroxide, however, should be dissolved and stored in steel tanks.

19. Mixing and Flocculation. When strong chemical solutions or slurries are added to the water, they should be quickly and uniformly dispersed throughout in order to hasten the chemical reactions. The chemical reactions after the chemicals are dissolved are almost instantaneous, but the formation of the floc is a time-consuming process. The principal function of flocculation basins is to form the floc, and their capacity is determined from the time required for this function. Another function of mixing, however, is the dispersion of the chemicals in the water. This function is automatically performed by all flocculation chambers, but dispersion and flocculation may be improved by rapid initial mixing at optimum velocity gradients and times as determined by jar tests.

The agglomeration of small dispersed particles to form larger ones is brought about first by true diffusion or Brownian motion and thereafter by the relative motion of the suspension, usually by turbulent mixing. It has been shown by Camp, Root, and Bhoota[1] that the Brownian-motion phase of coagulation is completed in a few seconds and is therefore of negligible importance in fixing tank dimensions as compared to the turbulent mixing phase.

Camp and Stein[2] have shown that the speed of flocculation at a point in a moving suspension is directly proportional to the concentration of suspended particles and to the space rate of change of velocity or *velocity gradient* at the point. For efficient coagulation, therefore, the motion of the suspension should be great enough to prevent settling of the floc particles and to produce velocity gradients of sufficient magnitude to promote rapid coalescence. The velocity gradients should not be great enough, however, to shear apart floc particles already formed. For best results, flocculation should be carried out in several stages in a series of tanks, such as shown in Fig. 12, with the velocity gradients progressively decreased as the floc particles grow in size. This procedure was first developed by Langelier and is known as the Langelier process.

The velocity gradients throughout a flocculation tank vary considerably, but the speed of flocculation may be taken as proportional to the *mean velocity gradient* G, which is given by the relation[2]

$$G = \sqrt{\frac{W}{\mu}} \tag{31}$$

in which W is the work done on the water by shear per unit of volume per unit of time and μ is the absolute viscosity.

The value of W for a tank equipped with mechanical mixers is the difference between the power input to the shaft per unit of tank volume with the tank full and in operation and with the tank unwatered. For tanks in which mixing is produced by an inlet jet, W may be computed from the kinetic energy of the jet. For baffled mixing channels, W may be computed from the discharge and head loss as follows:

$$W = \frac{Qg\rho h_f}{V} = \frac{g\rho h_f}{T} \tag{32}$$

[1] *J. AWWA*, **32**, 1913, 1940.

[2] Camp and Stein, Velocity Gradients and Internal Work in Fluid Motion, *J. Boston Soc. Civil Engrs.*, October, 1943, p. 219.

where Q = discharge
g = gravity constant
ρ = mass density
h_f = head loss
V = volume of the channel or conduit
T = retention period, sec

The maximum values of the mean velocity gradient G provided in existing flocculation basins[1] for water-purification plants built from 1909 to 1932 throughout the United States vary from about 20 to 75 fps/ft (sec^{-1}). Where the Langelier process is used, it is probable that the initial value of G should be from 30 to 100 with even higher values (up to 500) for flash mixing and the final value before settling should be between 5 and 15 sec^{-1}. Optimum values for G vary widely for different types of floc, and jar tests are required for their evaluation.

Since the speed of flocculation varies directly with the magnitude of the mean velocity gradient G, it follows that satisfactory coagulation should be produced with particular values of the product GT for each stage, where T is the flocculation period. If G and T are expressed in seconds, GT is a dimensionless number. The overall

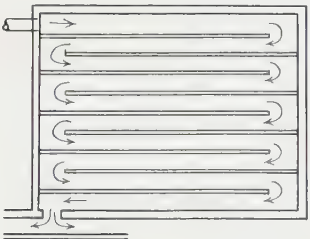

Fig. 21. Plan of round-the-end baffled mixing basin.

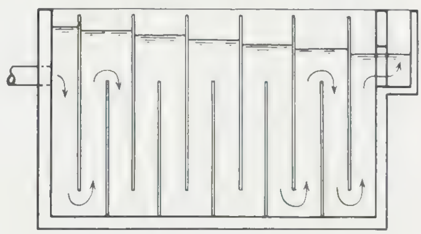

Fig. 22. Section through over-and-under baffled mixing chamber.

values of GT for American flocculation basins[1] of all types built from 1909 to 1932 ranged from 23,000 to 210,000 and correspond to floc periods ranging from 10 to 100 min. The velocities used for channel mixing chambers range from about 0.3 to 3 fps, and the same range of velocities is generally employed for paddle-tip speeds in mechanical mixers.

Two general types of flocculation basins are in common use, baffled basins and tanks with mechanical stirring devices or tangential flow. Baffled basins are of two types: with round-the-end baffles as illustrated in Fig. 21 and with over-and-under baffles as illustrated in Fig. 22. One of the important considerations in the use of baffled mixing chambers is the head loss, which ranges from about 0.5 to nearly 3 ft, depending upon the number of 180-deg bends. The head loss per 180-deg bend is approximately 3.5 times the velocity head in the adjacent channels. The head lost in the bends is about 80 percent of the total loss in round-the-end chambers and constitutes nearly all the loss in over-and-under chambers. An advantage of baffled chambers is the elimination of power-driven mechanical equipment.

A major defect in fixed-dimension baffled chambers, as illustrated in Figs. 21 and 22, is that they must be designed for a particular discharge and water temperature to obtain the selected value of G. Since the value of G varies as $\sqrt{Q^3/\mu}$ in an existing chamber, it will increase about 50 percent with a change in water temperature from near freezing to 30 C and it will increase about fivefold for a threefold increase in

[1] Camp, T. R., Flocculation and Flocculation Basins, *Trans. ASCE*, 1955, p. 1.

discharge. This defect may be compensated for with round-the-end baffled chambers by means of a series of gates, illustrated by Fig. 23, which may be adjusted to provide a series of slots, each with a selected width. If the chamber is designed with a velocity ranging from 0.15 fps at minimum flow to 0.45 fps at maximum design flow, with all gates open, G will range from about 2.2 to 11 sec^{-1} at 10 C. The lower velocity, 9 fpm, should be adequate to transport most of the floc. The volume of the chamber should be adequate to provide at least 30-min flocculation at the maximum flow. The gates should be spaced about 12 ft apart for the first 60 ft at the upstream end of the chamber and about 24 ft apart thereafter. The head loss re-

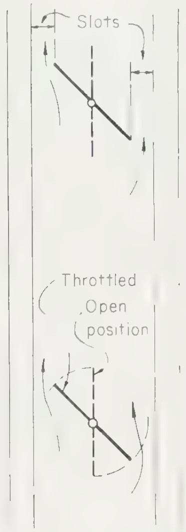

Fig. 23

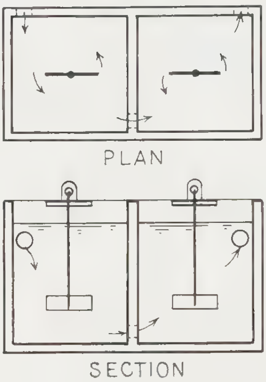

Fig. 24. Flocculation chambers with mechanical agitation.

quired to produce any value of G in the section of channel between two gates may be computed by means of Eqs. (31) and (32), and the gate at the upstream end of the section may then be adjusted to produce this head loss.

Flocculation basins with mechanical agitators are usually made with two or more basins in series, as shown in Figs. 12 and 24. In some plants, the mechanical stirrers have been omitted, and sufficient velocity is provided at inlets to impart a whirling motion to the basin contents. This port velocity is permissible at the inlet to the first tank, but it will inhibit floc growth if applied at the inlets of the other tanks in a series. For example, for a 15-min retention period per tank at 10 C, the required port velocities are 0.79, 1.59, and 3.18 fps for G values of 5, 10, and 20 sec^{-1}, respectively. The great advantage of mechanical mixers is the provision for varying the velocity of stirring independently of the discharge. This advantage is lost in basins without stirring devices. In them, the velocity is proportional to the discharge as it is with baffled basins. Another advantage in basins of this type, with or without stirrers, is the negligible head loss.

A serious drawback to mechanical and tangential flow tanks is short-circuiting. Hydraulic studies at the Massachusetts Institute of Technology[1] on miniature mixing basins indicate that the minimum time is almost zero, as shown by the experimental curve for a cubical tank in Fig. 25. The stirring process short-circuits some of the water quickly from inlet to outlet of each chamber. If a charge of tracer is assumed to be mixed instantaneously throughout the contents of the first chamber in a series of equal size, and the influent to each chamber is assumed to be mixed instantaneously with its contents, the relative concentration of the tracer in the effluent of the last

[1] Stein, P. C., unpublished paper, October, 1941.

chamber after various periods of time will be as shown by the curves in Fig. 25. It will be noted that the experimental curve for one tank closely approximates the theoretical curve. The equation for the theoretical curves for n tanks of equal size in series was developed by Stein[1] as follows:

$$\frac{c}{c_0} = \frac{n^n}{(n-1)!}\left(\frac{t}{T}\right)^{n-1} e^{-n(t/T)} \tag{33}$$

where c is the concentration of the tracer in the effluent of the last tank after time t, c_0 is the initial concentration if the tracer is instantaneously dispersed throughout the

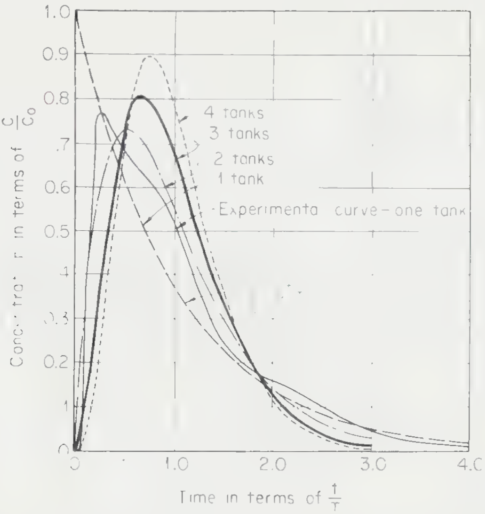

FIG. 25. Experimental curve for cubical tank.

contents of the n tanks, T is the total retention period in the n tanks, and e is the base of Napierian logarithms. For a single tank ($n = 1$), Eq. (33) reduces to

$$\frac{c}{c_0} = e^{-t/T} \tag{34}$$

The fraction of the tracer charge F_t which will pass out of the tanks in time t is

$$F_t = \int_0^t \frac{c}{c_0}\, dt \tag{35}$$

where c/c_0 is obtained from Eq. (33). Figure 26 shows the fraction of the tracer discharged out of the chambers after various fractions of the retention period. It will be noted that after one-fourth the retention period, about 22 percent will be discharged from a single tank but 4 percent from three tanks in series; and that after one-half the retention period, about 39 percent will be lost from a single tank but only 19 percent from three tanks in series.

Most of the apparatus used for flocculation is of the revolving-paddle type with either horizontal or vertical shafts. In most installations only rotor paddles are provided and the only resistance to rotation of the water with the paddles is the drag on the walls of the tank. This drag may be supplemented with stators to increase the

[1] STEIN, P. C., unpublished paper, October, 1941.

stability of the flow pattern. A number of rotor paddles are usually required with varying paddle areas and varying distances from the shaft. The value of the power input per unit of tank volume is as follows:

$$W = \frac{\Sigma F v}{V} = \frac{4\pi^3 \rho C_D \left[(1-k)^3 \left(\Sigma A_p r_p{}^3 + \Sigma A_r \frac{r_r{}^3}{4} \right) + k^3 \left(\Sigma A_s r_s{}^3 + \frac{f}{C_D} A_w \frac{r_s{}^3}{4} \right) \right] S^3}{V} \tag{36}$$

where v is the velocity of the blade with respect to the water, F is the drag force, V is the tank volume, C_D is the drag coefficient, ρ is the mass density of the water, S is the shaft speed in rps, kS is the water speed in rps, A_p is the area of a rotor paddle parallel to the shaft, r_p is the distance from the center of the shaft to the middle of the parallel

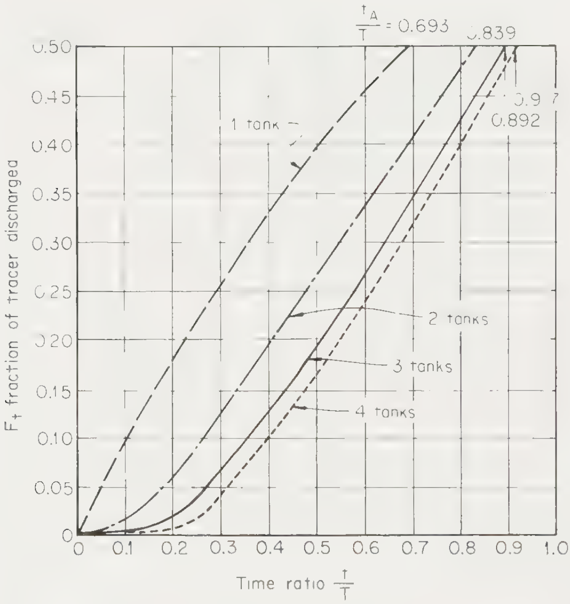

Fig. 26

rotor paddle, A_r is the area of a radial rotor arm or paddle of constant width, r_r is the length of this radial rotor paddle from the center of the shaft to its tip, A_s is the area of a stator blade, r_s is the radial distance from the center of the shaft beyond which the tangential velocity of the water is assumed to be constant at any value of S ($r_s = r_p$ or r_r, whichever is the greater), f is the Weisbach-Darcy wall friction factor, and A_w is the wetted area of the tank walls and floor. The tangential velocity of the water is assumed to be directly proportional to r out to r_s and constant for greater values of r.

Equation (36) may be used to design the flocculator mechanism. The outside width of the paddle reel should not exceed about 70 percent of the tank width or depth, and the paddle area in one plane should not exceed about 25 percent of the cross-sectional area of the tank. The drag is proportional to v^2 at high values of S, as shown by Eq. (36), and is proportional to v at low values of S. Another equation, similar to Eq. (36) but with different terms for the geometric parameters, may be derived for the region of streamline drag. The values of k and the drag coefficient for each region may be estimated[1] from the geometric parameters if it is assumed that W is a minimum at the correct value of k. Variable-speed drives are essential to produce the required values of the velocity gradient with changes in the coagulant dose and water temperature.

The velocity gradient in a straight pipe or channel of uniform cross section may be estimated by substituting the value of h_f from the Weisbach-Darcy friction formula in Eq. (32). The following results:

$$G = \sqrt{\frac{f}{8\nu R} v^3} \tag{37}$$

where f is the Weisbach-Darcy friction factor, R is the hydraulic radius, ν is the kinematic viscosity of the water, and v is the mean velocity in the conduit.

The velocity gradient at any level in a filter bed or upflow sludge-blanket clarifier may be derived from Eqs. (31) and (32) by noting that $T = (p/v_0)l$, where v_0 is the overflow rate or rate of filtration as a velocity, p is the porosity, v_0/p is the pore velocity, and T is the time of flow through the vertical distance l. The resulting value of G is as follows:

$$G = \sqrt{\frac{g}{\nu} i \frac{v_0}{p}} \tag{38}$$

where i is the hydraulic gradient. In a fluidized filter bed or upflow sludge blanket, $i = [(\rho_1 - \rho)/\rho](1 - p)$, as shown by Eq. (41), where ρ_1/ρ is the specific gravity of the filter grains or the floc particles in the sludge blanket (including their water content).

FILTRATION

20. Operation of Rapid Filters. The essential features of a rapid sand filter are illustrated in Fig. 12. Each filter is equipped with four valves: influent, effluent, wash, and waste. Sometimes a connection is provided from the manifold to the drain and equipped with a filter-to-waste valve. The effluent pipe is provided with a rate controller which keeps the discharge constant.

During filtration, the influent and effluent valves are open and the others are closed. The water enters from the settling tanks, passes up through and over the wash gutters and thence downward through the filter and into the underdrainage system and out through the effluent valve.

When a filter needs to be washed, it is taken out of service by first closing the influent valve. When the water has drained down below the level of the gutters, the effluent valve is closed and the drain is opened. The wash-water valve is then opened slowly, which permits filtered water to enter the manifold from the wash-water pump or tank and pass up through the bed over the gutter weirs and out through the gutters and drain. When the rate of wash reaches a maximum after about 1½ min, the filter medium should be fluidized (suspended) with the bed expanded 10 percent or more above its normal depth. This rate of wash is maintained until the water above the sand begins to clear, usually 2 to 4 min, and then the wash valve is closed. To place the bed back into service, the drain is closed and the influent and effluent valves are reopened. When the filter is provided with a filter-to-waste connection, the filtered water is sometimes discharged to the drain for a few minutes after washing. This practice, which is seldom necessary, is to prevent sediment that may possibly be near the bottom of the bed from passing into the filtered water reservoir.

[1] Camp, T. R., "Hydraulics of Mixing Tanks," 1969, John R. Freeman Memorial Lecture, Boston Society of Civil Engineers.

The permissible length of a filter run between washes is fixed by the head lost through the bed or the character of the filter effluent. Usually 7 to 10 ft of the operating head is available for loss through the bed and rate controller. When a clean bed is put back into service, the head loss through the bed is about 1 ft, the remainder of the 7 to 10 ft being taken by the controller, which is nearly closed. As the bed clogs and the head loss through it builds up, the controller opens so that the total loss through bed and controller remains constant until the controller is wide open. At this point, the rate will change; hence washing becomes necessary before this point is reached. In many cases, however, a filter will begin to pass abnormal turbidity before all the available head is used up. Some filters are designed without rate controllers so that the rate of flow decreases as the head loss builds up or so that the rate of flow varies with the demand.

The length of filter run is an important factor in the economy of filtration. If filter runs are very short, the capacity of the plant is reduced because of the time filters are out of service for cleaning. Moreover, the portion of filtered water required for washing, which is subsequently wasted, becomes abnormally high and results in higher costs of plant operation. Generally, the water required for washing should be less than 2 percent of the total water filtered. The length of filter runs is determined principally by the efficiency of pretreatment, the rate of filtration, and the character of the filtering materials.

21. Hydraulics of Flow through Granular Media.[1] Viscous flow of clean water through clean sand and other loose granular media, which has been studied by many investigators, appears to be represented very well by an equation developed rationally by Kozeny[2] from Poiseuille's law of flow through capillary tubes. The same equation was later developed independently by Fair and Hatch.[3] This equation states that the hydraulic slope is

$$i = \frac{dh}{dl} = \frac{\beta\mu}{g\rho}\frac{(1-p)^2}{p^3}\frac{v}{d^2} \tag{39}$$

in which dh = head loss through bed thickness dl
p = porosity ratio
d = diameter of the grains
v = rate of filtration as a velocity
β = dimensional friction factor

μ, g, and ρ are the same as for Eqs. (11) and (12). It will be noted that the value of the permeability coefficient k of Eq. (1), Sec. 35, is, from Eq. (39),

$$k = \frac{g\rho}{\beta\mu}\frac{p^3}{(1-p)^2}d^2 \tag{40}$$

Silica sand, with a specific gravity of about 2.65, and anthracite coal, with a specific gravity of 1.4 to 1.7, are widely used for filter materials. With repeated backwashing, any material tends to become stratified with the smaller and lighter grains at the top and larger grains below. With filtration downward, most of the floc is removed near the top of the bed where, as a result of stratification, the pores are smallest. When sand is used alone, this effect shortens filter runs and limits the rate of filtration to about 4 gpm/sq ft. Much higher filter rates may be used, up to about

[1] CAMP, T. R., Theory of Water Filtration, *Proc. ASCE, J. Sanit. Eng. Div.*, August, 1964, February, April, and October, 1965.

[2] KOZENY, J., *Wasserkraft und Wasserwirtschaft*, **22**, 67, 1927. See also DONAT, *Wasserkraft und Wasserwirtschaft*, **24**, 228, 1929.

[3] *J. AWWA*, **25**, 1551, 1933.

8 gpm/sq ft, if a bed of anthracite with coarse grains is superimposed on the sand bed. If the average grain size of the anthracite is about 60 percent larger than the average sand size there will be little intermixing at the interface during backwashing.

The rate of wash required to fluidize the bed is determined by the density and size of the largest grains and the highest temperature of the wash water. To minimize the cost of washing facilities, the filter grains should not vary greatly in size. The materials must be prepared by the supplier between certain limiting sieve sizes, as specified by the user. If sand alone is used, the authors suggest that all should pass a U.S. No. 18 or No. 16 sieve (1.00 or 1.19 mm) and be retained on a U.S. No. 40 or No. 35 sieve (0.42 or 0.50 mm). If anthracite is used on top of the sand, the sand should be retained on a U.S. No. 30 sieve (0.59 mm); and the anthracite should all pass a U.S. No. 14 or No. 12 sieve (1.41 or 1.68 mm) and be retained on a U.S. No. 18 or No. 16 sieve (1.00 or 1.19 mm).

The stratification resulting from backwashing is far from perfect, and a sample of a filter medium collected at any level may contain grains of almost all sizes. In order to use Eq. (39) for filtration studies, therefore, it is necessary to use an *average grain size* at each filter level. The average grain size may be estimated by collecting samples after prolonged backwashing from the top, mid-depth, bottom, and intermediate points (if necessary) of each filter medium for density and grain-size determinations. Grain-size determinations are made on each sample by counting and weighing several groups of 100 grains each and computing the diameter of the sphere whose volume equals the average volume of the counted grains. For other bed levels, the grain size is estimated by interpolation.

Equation (39) may be used for studies of filtration in both the viscous range and the transition range between viscous and turbulent flow, and it also may be used for fluidized beds, provided β is evaluated experimentally. The hydraulic gradient i may be measured in a bed by means of a piezometer column with piezometers at small intervals of depth (about 0.1 ft). Figures 27 and 28 show the results of backwashing experiments on sand and coal conducted in a 5-in. plastic tube with piezometers at 0.1-ft intervals of depth.

The weight of a bed in water per unit of bed area is $g(\rho_1 - \rho)(1 - p)l$, where ρ_1 is the mass density of the material and l is the depth of the bed. Since filter beds are usually constructed to specified depths, the weight per unit area is seldom known and the porosity cannot be computed. If the bed is fluidized, however, the weight in water per unit area may be readily computed because it equals the friction loss past the grains $g\rho h$, where h is the lost head. The weight of a bed being constant, the head loss is also constant if the bed is fully fluidized, regardless of increase in wash rate or changes in water temperature (neglecting the small change in ρ with temperature). If the bed is fluidized in a small container, the measured head is somewhat greater than that corresponding to the actual weight because of arching against the walls; and corrections must be made to the measured head and hydraulic gradients as shown for the head in Figs. 27 and 28. The average porosity of the unexpanded sand bed of Fig. 27 is $1 - 1.752/1.64 \times 2.09 = 0.49$, from the above relation.

From the above relation, it follows that at any level in a fluidized bed the hydraulic gradient is

$$i = \frac{\rho_1 - \rho}{\rho} (1 - p_e) \tag{41}$$

where p_e is the expanded porosity at that level. The porosity at any level in a fluidized bed, therefore, depends only on the measured hydraulic gradient and the specific gravity of the filter medium. If the values of i in Eqs. (39) and (41) are

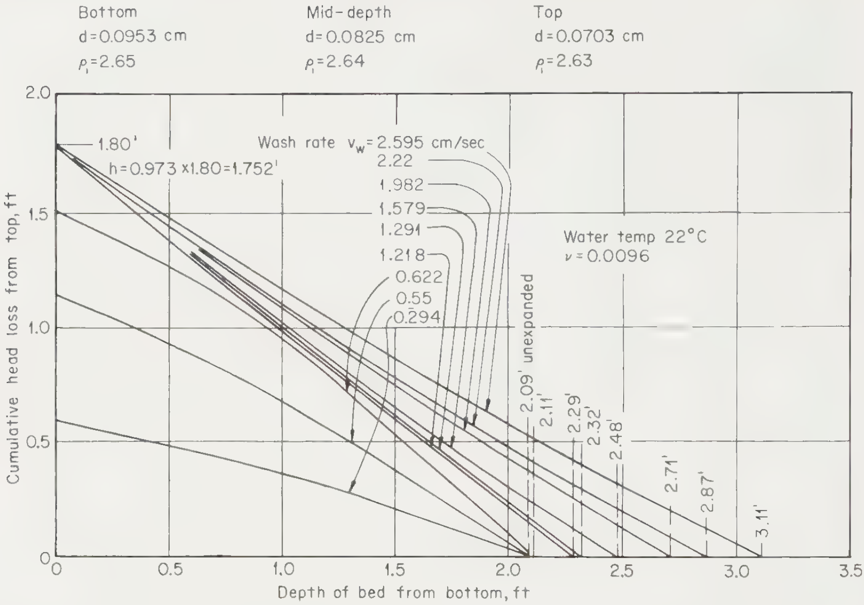

FIG. 27. Results of backwashing experiments with sand grains sized between U.S. sieves 18 and 30.

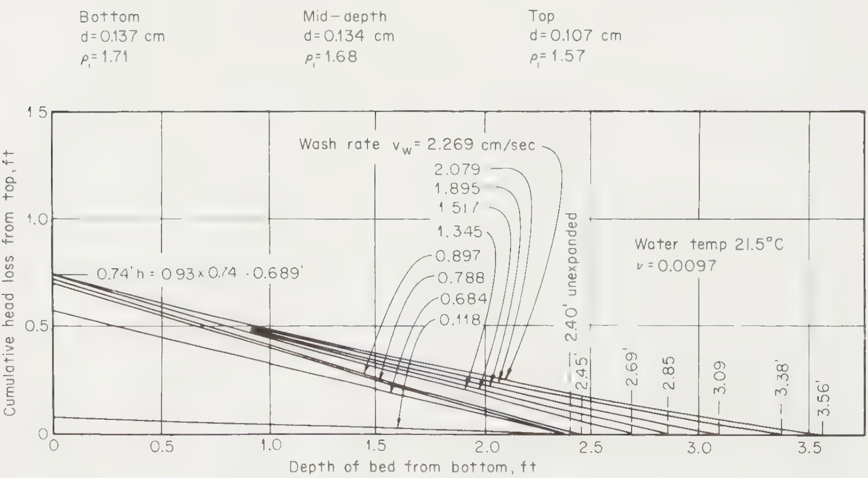

FIG. 28. Results of backwashing experiments with anthracite grains sized between U.S. sieves 14 and 18.

equated, the following results:

$$v_w = \frac{g(\rho_1 - \rho)}{\beta \nu \rho} \frac{p_e^3}{1 - p_e} d^2 \tag{42}$$

where v_w is the wash rate as a velocity, ν is the kinematic viscosity of the water, and p_e is the expanded porosity in the layer where d is the average grain size. From the results of backwashing experiments, such as illustrated in Figs. 27 and 28, p_e may be calculated for any level by means of Eq. (41) from measured values of i; and β may then be computed by means of Eq. (39) or (42).

The average porosity of a bed at rest may be computed from the weight, volume, and average density of the material, as illustrated above; but no means are available for determining the porosity variation throughout the depth of the bed. Equation (39) may be used to evaluate the product of β and the porosity term at any level from the results of downflow experiments. If β is assumed constant throughout the depth, it may be computed by averaging the products of β and the porosity term for the sampling points and dividing this average by the porosity term for the average porosity. The porosity for each of the sampling points may then be computed. Values of β

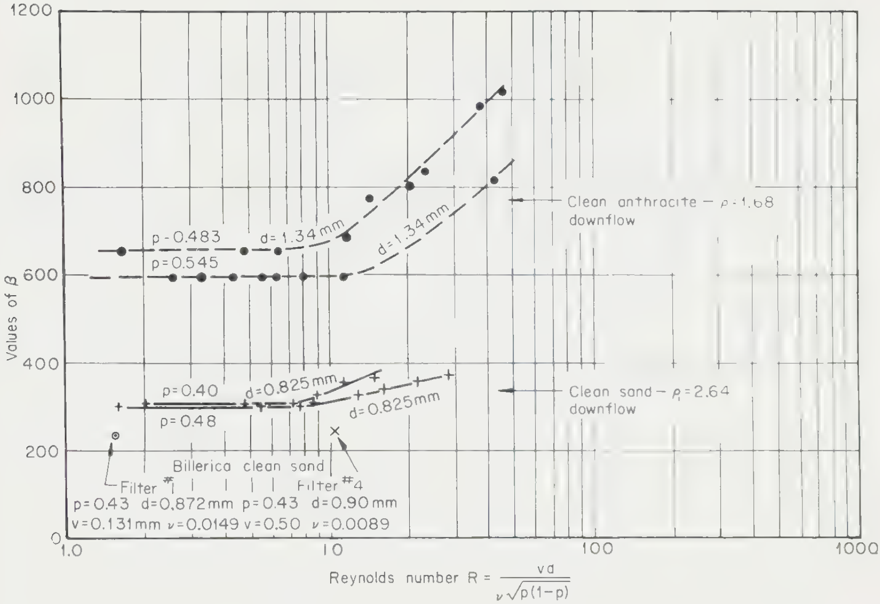

FIG. 29. Effect of Reynolds number on β for beds at rest.

determined in this manner for the sand and coal of Figs. 27 and 28 at mid-depth are shown in Fig. 29. The computed porosities for the other sampling points were within 3.0 percent of the average for the sand and within 5.0 percent for the coal.

The pore size for the Reynolds number has been taken as the diameter of a circle with area approximately equal to the average pore area $d\sqrt{p/(1-p)}$, in order to remove from the Reynolds number the effects of pore shape. Figure 29 shows that, for downward flow, the flow is viscous with β constant for Reynolds numbers up to 8 to 12. The value of β increases at higher Reynolds numbers with increase in Reynolds number. The upper curves of Fig. 29 are for the beds compacted by tapping the wall of the plastic tube. It is evident that, in the viscous-flow regime, β changes little with wide changes in porosity for sand (rounded grains), but the change is substantial (about 10 percent) for coal with angular grains. The porosity at which a bed comes to rest after backwashing depends upon the rate of closing the wash-water valve, which, if too slow, will result in excessive compacting. Loose filter beds result in longer filter runs. The two points in Fig. 29 for the Billerica, Mass., filter plant show that, with viscous flow, β is approximately the same for water temperatures from 6 to 25.5 C and filter rates from 1.93 to 7.35 gpm/sq ft.

Figure 30 shows the values of β in upflow experiments on the sand and coal of Figs. 27 and 28. Since each layer contains grains of many sizes, the smaller grains will be lifted at flow rates which are inadequate to lift the surrounding larger grains. The motion of these smaller grains will increase the value of β before the bed expands; and if this motion is sustained long enough, the positions of the larger grains will be rearranged to compact the bed. Figure 30 shows that at upflow rates too low to lift the smaller grains, the value of β for sand is approximately the same as for downflow.

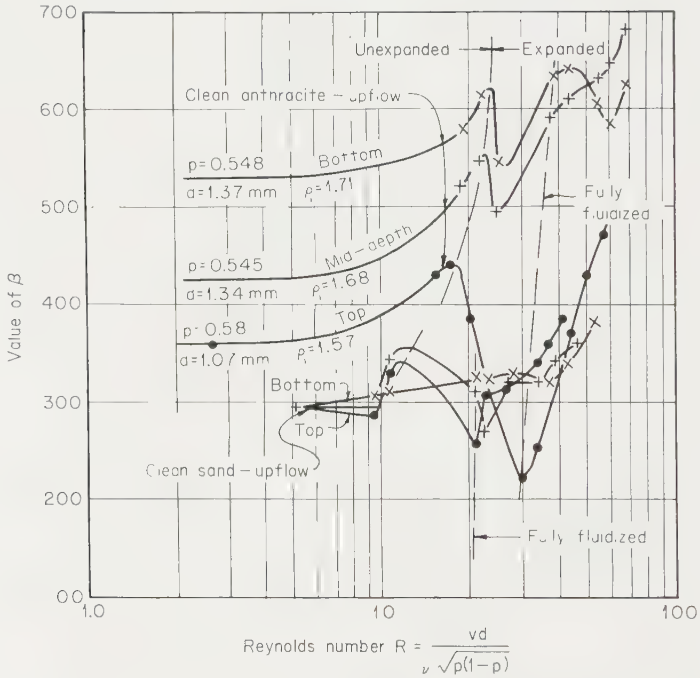

FIG. 30. Effect of Reynolds number on β for fluidized beds.

For the coal, however, the value of β at low upflow rates is substantially less than for downflow and it varies widely from top to bottom. This may be explained by the fact that the angular-shaped grains tend to orient themselves to develop the least drag when the bed is fluidized, and these attitudes tend to be maintained when the bed settles back after washing. When the flow direction is reversed, the drag tends to be a maximum. After a bed starts to expand, β decreases to a minimum value with further increases in wash rate and then increases again. Figure 30 shows at what points expansion starts and fluidization is complete.

22. Mechanism of Filtration. Suspended matter is removed from water by sand filters through the adhesion of small particles to the surfaces of the grains. The small particles are brought into contact with the surfaces of the grains by the convergence of the streamlines. In slow sand filters, removal by adhesion and straining may be expedited to some extent by flocculation of suspended particles within the pores; but experiments by Stein[1] indicate that the velocity gradients (being of the order of 200 sec^{-1}) are too high in rapid sand filters to permit much flocculation.

As the filter passageways become reduced in cross-sectional area owing to the accumulation of adhering material, the velocities in the pores and hence the shear will increase. When the shear forces become large enough, the rate of adhesion is decreased and suspended matter will be carried more deeply into the filter.

If the floc particles are larger than the pore constrictions, they will deposit right at the top of the bed and filter runs will be very short; if very much smaller, they will penetrate deeply into the bed and filter runs will be longer. As the top pores become clogged, some of the suspended particles may settle on top of the bed above these pores and thus will be removed by sedimentation. The mud blanket thus formed, called the *schmutzdecke*, was once thought to be essential to proper filter performance. It is now known, however, that it bears no relation to the removal effected and is a positive detriment to rapid filters as it is the main source of formation of mud balls during the washing process. Many filters perform efficiently without a mud blanket.

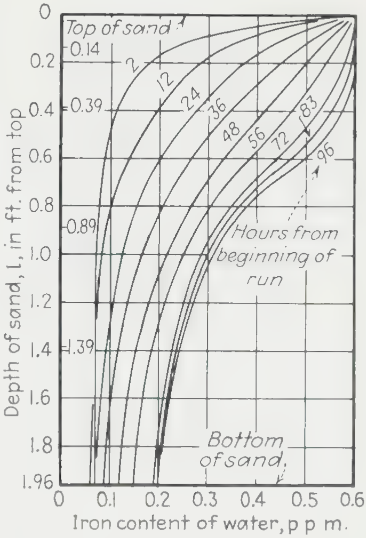

Fig. 31. Iron content of water, ppm.

A certain ripening process of a filter after it is first put into service, during which the sand grains become partly coated, is known to improve the efficiency of the filter. This improvement is probably due to an increase in effective surface area of the grains. Slow sand filters are known to be poor removers of negative color colloids. Rapid-filter sand becomes coated with alumina or ferric oxide which is adsorbed from the floc. This adsorption process is so slow, however, as to be a negligible factor in the removal accomplished in a single filter run.

The mechanism of filtration is illustrated well by the data from a filter run taken by Eliassen[2] during studies made with an experimental rapid filter at the Providence, R.I., water-treatment plant. The finer sand grains were screened out to ensure penetration of all the floc into the bed, and the performance of the filter as regards removal and length of run before too much floc was passed was correspondingly impaired. Eliassen demonstrated that less than 5 percent of the floc volume was solid with the remainder water. This is doubtless true of other floc. The average size of the visible portion of the iron floc particles in water samples taken from the filter varied from about 11μ above the filter to about 8μ at a depth of 0.89 ft. The size of the pore constrictions was about ten to twenty times the floc size. The sand for this bed was contained between sieves with openings of 0.42 and 0.83 mm. The penetration of floc into the bed during a run at 2 gpm/sq ft is illustrated in Fig. 31. It will be noted that at the start of the run about 90 percent removal was accomplished, nearly all the deposit being in the top 6 in. of the bed. As the top sand became clogged, its effectiveness grew less and the floc penetrated deeper, the total removal decreasing after about a fourth the length of the run. During the clogging process, the burden of removal was gradually transferred to sand deeper in the bed.

[1] Stein, Doctor's Thesis, M.I.T., 1940.
[2] Eliassen, Doctor's Thesis, M.I.T., 1935.

The time rate of clogging and the depth of penetration of suspended matter depend upon the grain size and the quantity and size of floc in the applied water. The time rate of clogging as measured by lost head dh/dt appears from many observations to be approximately constant or to increase slightly with time, if the size and amount of suspended matter applied to the filter, the rate of filtration, and the temperature of the water remain constant during a run. The time rate of clogging for a given water, according to experiments by Baylis[1] and others,[2] varies inversely with some power between 1 and 2.15 of the sand size; and according to Stein[3] varies inversely with the square of the sand size.

Numerous experiments under the author's direction appear to indicate that dh/dt is about directly proportional to the volume of suspended matter in the water applied to the filter, other factors remaining constant. Inasmuch as the head loss and the rate of application of suspended matter to a filter are both directly proportional to the rate of filtration, it might be expected that dh/dt should vary as the square of the rate of filtration. This is not the case, however, for the solids penetrate deeper into the bed with increasing velocities. Experiments indicate that dh/dt increases approximately with some power of the rate of filtration less than 1.

The head at any point in a filter during filtration is equal to the static head at the point less the lost head in the sand layer above the point. When the lost head exceeds the static head, a partial vacuum called a *negative head* is produced at the point. Negative heads should be avoided in filter effluent pipes, valves, and rate controllers because they cause pressure pulsations which travel back to the filters and dislodge floc; and they should be avoided in filters because they accentuate the pulsations and cause the evolution of dissolved air from the water. Negative heads may be prevented in design by providing an effluent overflow (d of Fig. 12) at least 5 ft above the rate controller and valve, and a water depth of 7 ft or more above the filter.

The pressure corresponding to the head loss in the top layer of a filter, which becomes very high because of clogging, tends to compact the bed and results in shrinkage. Shrinkage is greater for high porosities and for dirty beds. The path of flow adjacent to the filter walls is less tortuous and the head loss correspondingly less than through the bed proper. Therefore, the head at any depth is greater at the wall than at a small distance from it. This difference in head results in flow inward from the wall and a corresponding shrinkage of the bed away from the wall. As the shrinkage cracks open, short-circuiting of more water and sediment to these cracks results. Mud sometimes penetrates through the bed because of shrinkage, and caking of the bed near the wall results. Shrinkage cracks also occur in the interior of some beds owing to inequalities in flow and shrinkage. Shrinkage can be minimized by using coarse grains and washing the beds clean.

Stein[3] demonstrated by photomicrographs that floc particles accumulate on the grains of a filter to form sheaths around the grains, thus to increase the size of the grains and decrease the porosity. He adapted the Kozeny equation for use during filtration, as follows:

$$g\rho \frac{id_0^2}{v\beta\mu} = \frac{(1 - p_0 + \sigma)^2}{(p_0 - \sigma)^3} \frac{1}{\sqrt{\sigma/3(1 - p_0) + 0.25} + \sigma/3(1 - p_0) + 0.50} \qquad (43)$$

where d_0 and p_0 are the grain size and porosity at any depth l at the beginning of a filter run; and where, at depth l and any time t during a run, i is the hydraulic gradient, v is the filter rate, β is the friction factor, μ is the viscosity, and σ is the deposit ratio. Stein[3] demonstrated in a study of Eliassen's experiments that Eq. (43) can be used to

[1] *Water Works Sewerage*, October, 1934, p. 352.
[2] *Proc. ASCE*, December, 1936, p. 1543.
[3] STEIN, Doctor's Thesis, M.I.T., 1940.

compute values of σ during a filter run, assuming β remains constant. Camp[1] has shown that Eliassen's experiments can be approximated more closely if β is assumed to decrease during a run. Figure 32 is a graph to facilitate calculations for σ. Camp's correction factors for decreasing β are also shown in Fig. 32.

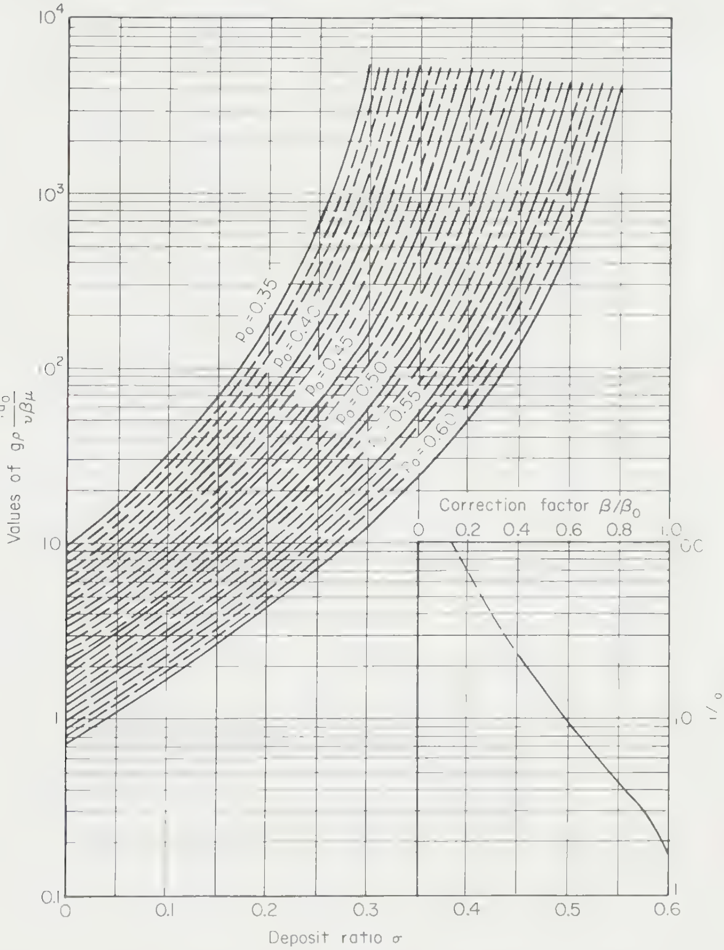

FIG. 32. Deposit ratio as a function of hydraulic gradient.

Iwasaki[2] has shown that the rate of removal of floc from the water at any depth l in the bed and at any time t during a filter run is

$$-\frac{dc}{dl} = \frac{1}{v}\frac{d\sigma}{dt} \tag{44}$$

where c is the volumetric concentration of floc in the water at depth l and time t and v is the rate of filtration at time t. The validity of Eq. (44) is restricted to cases where the

[1] Theory of Water Filtration, *Proc. ASCE, J. Sanit. Eng. Div.*, August, 1964, February, April, and October, 1965.
[2] IWASAKI, T., Some Notes on Sand Filtration, *J. AWWA*, **29**, 1591, 1937.

volume of floc already deposited is not reduced by loss of water during a run. In a study of Stein's data from Eliassen's experiments, Camp[1] has shown that there was no significant decrease in water content of the deposited floc during the runs. The average volumetric concentration c in Eliassen's experiments was about 2.5×10^{-4} (250 ppm) per ppm of iron.

The rate of removal of floc may be computed from measurements of hydraulic gradient within the bed without analyses of water samples collected from the bed.

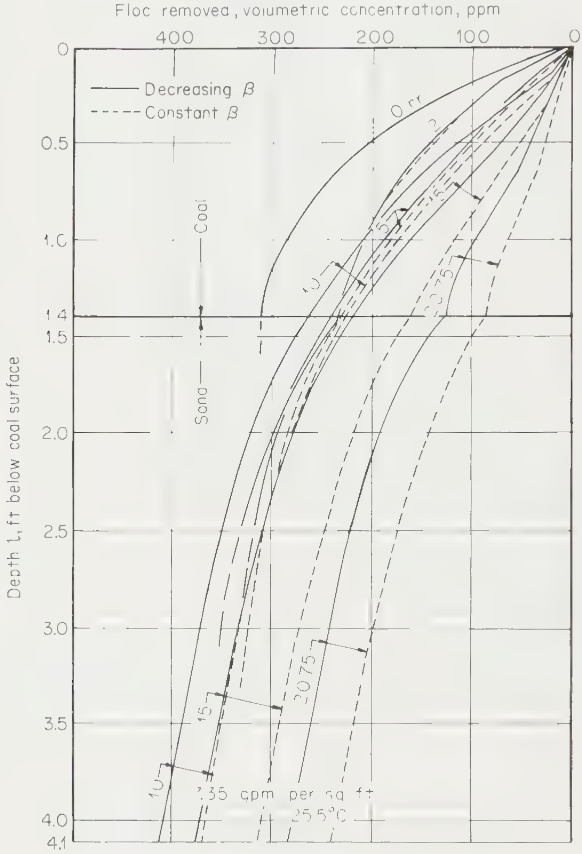

FIG. 33. Run 1, filter 4, June 29–30, 1964, Billerica, Mass.

The cumulative head losses at small intervals throughout the depth of the bed are read and plotted for the beginning of a run and for the end of selected time intervals throughout the run. Values of i at small intervals of depth are read from the plotted curves, and the corresponding values of σ are computed from Eq. (43) or Fig. 32. Plots are then made of values of σ against time during the run for each small interval of depth; and values of $d\sigma/dt$ are read from the plots at selected time intervals throughout the run. Rates of removal are then computed by means of Eq. (44). The cumulative removal for each time is then plotted by adding the removals for the small intervals of depth starting at the top of the bed, as illustrated by Fig. 33 for alum floc. The solid

[1] Theory of Water Filtration, *Proc. ASCE, J. Sanit. Eng. Div.*, August, 1964, February, April, and October, 1965.

lines in Fig. 33 were computed using the correction factors of Fig. 32 for reducing β during the run; and the light broken lines are based on β remaining constant during the run.

23. Washing of Rapid Filters. The effective washing of a rapid filter requires (1) a sufficient velocity of water (or air) past each grain to dislodge the sediment, (2) a sufficient expansion of the bed to permit the sediment to pass upward between the grains, (3) a sufficient wash rate to carry the sediment upward above the bed, and (4) a length of wash great enough to allow the sediment to pass out of the filter.

Early rapid filters were washed at rates of about 18-in. vertical rise per minute (12-in. rise per minute corresponds to a filtration rate of 7.5 U.S. gpm/sq ft) when water alone was used and at lesser water rates when air or mechanical raking of the surface of the beds was also used. Air is usually distributed to the underside of the sand through the water underdrainage system or through a separate perforated-pipe system just above the underdrainage system. The difficulty of distributing air uniformly, the extra cost of using air, and the danger of air-binding have led to the general abandonment of the air-wash method in the United States in favor of higher velocity of wash with water. It is general practice to provide rates of wash from 24 to 42 in., depending upon the size and density of the filtering material.

In order to wash a bed properly, all the grains should be suspended, and a sufficient rate of wash should be available to suspend the entire bed at the highest temperature of the wash water. Figures 27 and 28 show the expanded depths and wash rates required at a particular water temperature for particular beds of sand and coal. If the expansion E is expressed as the fractional increase in depth by expansion, the data of Figs. 27 and 28 may be used for beds of any depth; provided the materials and the average porosity of the unexpanded beds are the same. Figure 34, with the expansion E for these materials plotted against the required wash rates, shows that the beds are fully fluidized at an expansion of about 9 percent. For a particular expansion E in excess of the minimum required for full suspension, the values of p_e throughout the depth of the bed will be the same for any water temperature. From Eq. (42), it is evident that the required wash rate for other water temperatures is inversely proportional to the viscosity, assuming no change in β. The light lines in Fig. 34 show the wash rates required at the extreme temperatures of 2 and 30 C, computed from the viscosity ratios. If a 16 percent expansion is selected as desirable for the coal, the corresponding sand expansion will be 15 percent, requiring a wash rate of about 42 in./min. If the maximum available rate is made 36 in., the desired expansion will be available at all water temperatures below 23.5 C and the coal will be barely fluidized at 30 C.

As shown by Eq. (42), the rate of wash for a given expanded porosity, and therefore the cleansing efficiency, varies directly as the weight of the material in water. Light materials such as coal require large grain sizes for efficient cleansing. The amount of expansion required to get all the grains in suspension depends upon the size and grading of the material. Expansions used in practice vary from about 10 to 50 percent. The freeboard between the top of the sand during filtration and the bottom of the wash troughs (see Fig. 12) should be great enough for the maximum expansion required. In many sand filters, the surface sand is too small to be washed effectively by suspension alone. Baylis[1] recommends a supplementary surface wash of 2 to 8 gpm/sq ft applied through perforated pipes immediately above the sand surface at a pressure of about 10 lb in the pipes in order to break up the clogged masses at the surface before the bed is fully expanded. Mechanical raking is also of value.

24. Hydraulic Design of Filters. The sizes of pipes and conduits in the pipe gallery should be kept small for economy, but in general the velocities at the nominal

[1] *Water Works Sewerage*, January, 1935, p. 20.

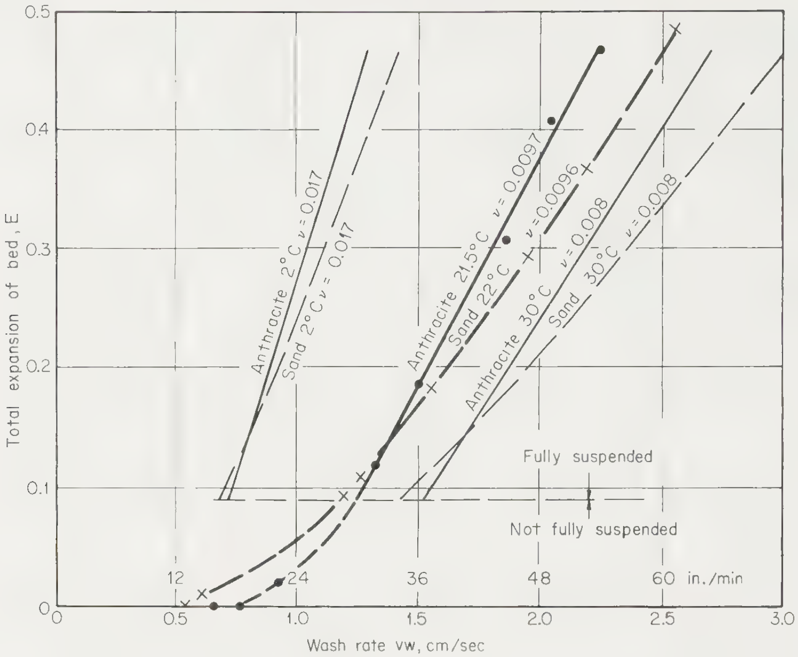

FIG. 34. Wash rates required for sand of Fig. 27 and coal of Fig. 28.

capacity of the plant and at the maximum wash rate should not exceed the following:

Pipe	Fps
Filter influent	2
Filter effluent	5
Wash water	12
Waste water	8
Filter to waste	15

For fragile floc, limiting influent velocities should be estimated from limiting velocity gradients which will not rupture the floc. Local considerations, such as inadequate head, may require lower velocities than given above for the other lines.

The principal function of a filter bottom or underdrainage system is to distribute the wash water uniformly to the underside of the sand bed. The most commonly used type of filter bottom is one composed of perforated pipes surrounded by gravel. The perforations are usually circular orifices drilled in the underside of the laterals at uniform intervals preferably not greater than 12 in. The velocity of the wash water issuing from the orifices is largely dissipated against the floor and in the gravel around the laterals.

The function of the gravel is to support the sand and to spread the wash water over the covering area of each orifice before it reaches the sand and thus to prevent jetting through the sand. This can usually be accomplished with about 18 in. of gravel, which should be graded from about 12 mesh at the top to about 1 in. at the bottom. The grading should be such that the particles of gravel are large enough at all depths to remain undisturbed by the velocity of the wash water past them, and it should be such that particles above cannot fall through the interstices of the lower gravel. The head lost through graded gravel during washing is approximately 0.1 ft for each 12 in. depth at a wash rate of 12 in./min with the water at about 0 C and is about 0.06 ft at 30 C. Most of the head is lost through the top 3 in. of finer material which is the effective agent for the final distribution of the water to the sand.

A uniform distribution of the wash water to the orifices may be approximated by making the orifice head loss great as compared with the maximum difference in energy head available for flow through the orifices. Equation (16) may be used to determine the required orifice head loss. It is good practice to make the orifice ratio (ratio of orifice area to total bed area) 0.3 to 0.5 percent, which, for a 36-in. wash rate and an orifice discharge coefficient of 0.6, corresponds to an orifice velocity of 27.8 to 16.7 fps and a head loss of 12 to 4.3 ft. The velocity head at the entrance to each lateral should generally be less than one-tenth the orifice head loss for good distribution. The velocity for a 36-in. wash rate should preferably be less than 6 fps for the laterals and 8 fps for the manifolds.

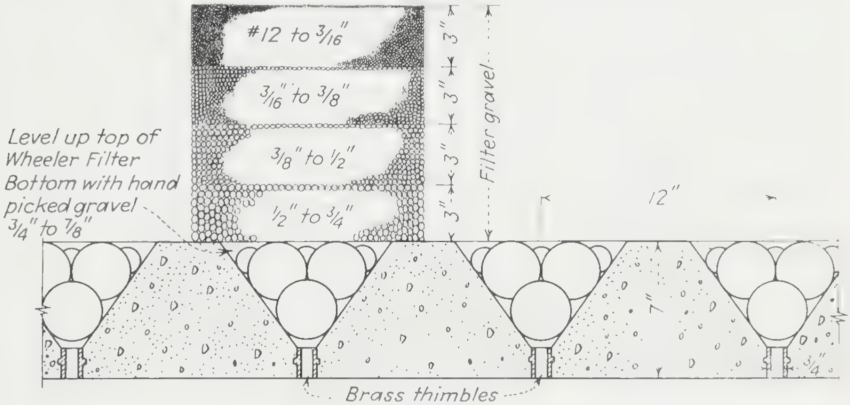

Fig. 35. Wheeler filter bottom.

Inasmuch as the fine gravel supporting the filter sand is the effective agent for distribution of the wash water to the sand and since the coarse gravel surrounding the orifices functions as an equalizing chamber, uniform distribution of wash water to the orifices is not so important as is commonly supposed.

The use of umbrella-type strainer heads fastened into the tops of the laterals was formerly widespread in the United States but has now been largely abandoned because of the superiority and economy of perforated pipes. Laterals should be made of corrosion-resistant materials. Numerous other types of filter bottoms have been developed. Among the most satisfactory are the Leopold bottom and the Wheeler bottom. The wash water is delivered to the underside of a Wheeler bottom through concrete channels or from an equalizing chamber below the Wheeler slab, in which latter case the slab is supported above the filter floor on columns (Fig. 35).

All filter bottoms which require graded gravel to support the sand depend upon the top layer of loose fine gravel to effect uniform distribution of wash water to the underside of the sand bed. In order to function properly, the top layer of fine gravel must be carefully sized and placed and must not be displaced by the washing process. Unfortunately, some sediment will always pass through the sand during filtration, and some of this will accumulate in the pores of the fine gravel so as to increase the velocity through this gravel during washing until ultimately the velocity is sufficient to displace the gravel and allow the sand to fall through it. This is a defect inherent with the use of loose gravel. The fine gravel may be held in position by means of a perforated stainless-steel plate on top of it and tied to the concrete bottom of the filter by means of stainless-steel bolts at intervals of about 12 in. Each filter should be equipped with a manometer to monitor the increase in head loss through the gravel with clogging. At intervals of 2 to 10 years, the gravel should be removed, washed, and replaced.

Another type of filter bottom is the porous-plate bottom first developed by Camp[1] in which the filtering material is supported directly upon a false bottom of porous plates. The plates are constructed of granular material cemented rigidly together, and they are supported above the floor as shown in Fig. 36 to produce an equalizing chamber under the plates. The porous plates perform the same function as the top layer of gravel in other types of bottoms, but the grains in the plates are not subject to

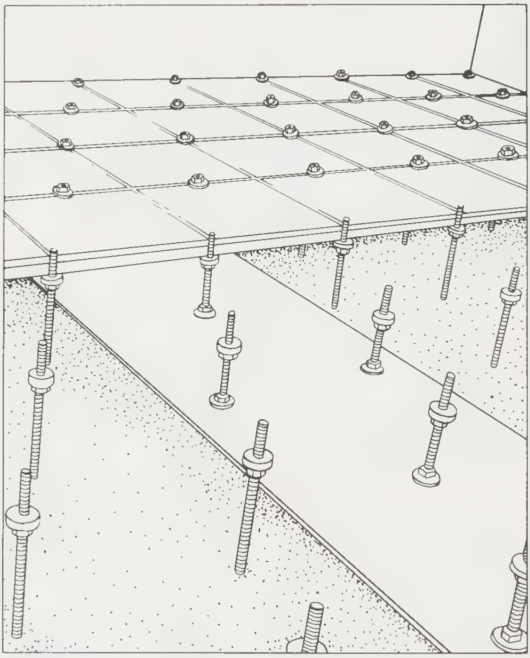

Fig. 36. Porous-plate filter bottom.

displacement by the washing process. The pores of the plates gradually clog with sediment, and the eventual replacement of the plates or periodic cleaning with acid or alkali is indicated. Experience indicates that porous ceramic plates will gradually lose strength if cleaned too frequently with acid or alkali, particularly with acid.

Wash-water gutters with level bottoms may be designed by means of Eq. (17), due account being taken of the additional drawdown of the water surface due to friction. Usually, gutters discharge freely into the gullets, in which case the depth h at the discharge end may be assumed at the hydrostatic critical depth without serious error. Equation (17) then becomes

$$H = \sqrt{3}\, h_c \tag{45}$$

in which h_c = the hydrostatic critical depth = $\sqrt[3]{q^2x^2/gb^2}$. In practice, gutters are spaced with clear distances between the weirs 3 to 6 ft. The distance of travel of

[1] Camp, *J. NEWWA*, **49**, 1, 1935.

waste wash water from the top of the bed to the gutter weirs should be kept small to minimize the length of wash. Gutters are made of steel, cast iron, fiber glass, and reinforced concrete. Metal gutters should be adequately coated to reduce corrosion. Gullets also may be designed by means of Eq. (17) except that the inflow is at intervals and not continuous along the length of the gullet. Gullets should be wide enough for the access of workmen.

Filtered water for washing filters should preferably be stored underground so that it will not be subjected to rapid temperature changes by the sun or building heating system. As indicated by Fig. 34, the rate of wash for the desired bed expansion changes greatly with the temperature of the wash water. For best results, the rate and length of wash should be controlled automatically from the temperature of the water to be used for washing. Control is facilitated by pumping directly from the clear well through a wash-water rate controller, partially throttled at the highest required wash rate. Duplicate pumps should be provided, each with a capacity slightly in excess of the required maximum. Very large filters may have to be divided into two or more parts for washing purposes in order to reduce the cost of washing facilities and stay within the capacities of commercially available centrifugal pumps.

25. Filter Accessories. Butterfly valves are used in most modern rapid-filter plants and are usually power-operated. Since they are operated very frequently, they should be well constructed and corrosionproof. The valves are controlled from operating tables at the filters or from a central console, and automatic control may be used. Continuous recording of rate of flow and loss of head gages is desirable. Filter runs should be terminated when the loss of head reaches a preselected maximum or when the turbidity of the effluent from each filter reaches a preselected maximum, whichever comes first. This is facilitated with continuous recording of the turbidity of each filter effluent, and the turbidity of the filter influent is similarly monitored.

The discharge line from each filter should be equipped with a rate controller as shown in Fig. 12, and for large plants master rate controllers are sometimes desirable. All rate controllers consist of two essential parts, a measuring device and a valve actuated by the measuring device. Venturi tubes are commonly used as the measuring device and are superior to orifices because of the lower head loss and more constant discharge coefficient. Many other accessories such as sampling devices and automatic-control equipment for wash-water pumps are desirable for modern plants.

SOFTENING AND DEMINERALIZATION

26. Lime-Soda Process. The purpose of adding lime in softening is to convert free CO_2 and HCO_3^- to normal CO_3^{--}, which reacts with Ca^{++} to form the precipitate $CaCO_3$, and to add sufficient OH^- to remove Mg^{++} as the insoluble $Mg(OH)_2$. Ca^{++} and Mg^{++} will be removed to the extent that there are CO_3^{--} and OH^- available to form the precipitates. If the water contains SO_4^{--}, NO_3^-, or Cl^-, the so-called incrustants that contribute to noncarbonate hardness, the conversion of CO_2 and HCO_3^- to CO_3^{--} does not furnish sufficient CO_3^{--} to remove the Ca^{++}. Additional CO_3^{--} must therefore be furnished, and the usual method is to add soda ash, Na_2CO_3. The reactions with lime are as follows:

$$Ca(OH)_2 \rightleftarrows Ca^{++} + 2OH^- \tag{46}$$

$$CO_2 + OH^- \rightleftarrows HCO_3^- \tag{47}$$

$$HCO_3^- + OH^- \rightleftarrows CO_3^{--} + H_2O \tag{48}$$

$$Ca^{++} + CO_3^{--} \rightleftarrows CaCO_3 \tag{49}$$

$$Mg^{++} + 2OH^- \rightleftarrows Mg(OH)_2 \tag{50}$$

Reaction (46) may go to completion to the right, but the others do not. The ionization constants for reactions (47) and (48) are given, respectively, by Eqs. (10) and (9). The solubility product for reaction (49) is

$$[Ca^{++}][CO_3^{--}] = 4.7 \times 10^{-9} \text{ or } 10^{-8.32} \text{ at } 25 \text{ C} \tag{51}$$

The numerical value[1] of the exponent of 10 in the foregoing solubility product increases about 0.01 for each degree centigrade increase in temperature and appears to decrease with increase in dissolved solids by an amount approximately equal to 0.02 times the square root of the concentration of dissolved solids in ppm. The solubility product[2] for reaction (50) is

$$[Mg^{++}][OH^-]^2 = 8.9 \times 10^{-12} \text{ at } 25 \text{ C} \tag{52}$$

The amount of chemicals required is usually estimated on the assumption that reactions (46) to (50) go to completion. Sufficient lime is added in the ordinary process to change all the free CO_2 and HCO_3^- to CO_3^{--}, and sufficient soda is added to balance the incrustants with carbonates. In order to remove the Mg^{++}, sufficient additional lime is required to produce $Mg(OH)_2$ and to leave an excess caustic alkalinity of 25 to 50 ppm. This process is called the *excess lime* process, and it should be followed after precipitation of the Mg^{++} by recarbonation with CO_2 gas to neutralize the causticity and to precipitate the excess Ca^{++} added. Carbonation is used in many lime-softening plants just before the water reaches the filters in order to minimize the incrustation of the sand with $CaCO_3$.

The residual hardness and the analysis of the water after softening may be estimated by the solution of simultaneous equations involving concentrations and equilibrium constants. The results of such a computation are based upon the assumptions that the reactions have reached equilibrium and that all precipitates have been removed from the water. The $CaCO_3$ precipitate is difficult to flocculate and hence may not all be removed by settling and filtration. $Mg(OH)_2$ floc is similar to alum floc and settles readily, although more slowly than $CaCO_3$.

Alum improves the flocculation and settling of $CaCO_3$, although, at the high pH values (10.2 to 11), AlO_2^- tends to form instead of the hydrous Al_2O_3. Homack[3] has shown that 250 ppm of $CaCO_3$ flocculates well with the addition of 37 ppm of alum (3.36 ppm of Al) or 5.17 ppm of Al added as $AlCl_3$, but not at all with 18 ppm of Al added as $NaAlO_2$. This indicates that Al^{3+} acts as a flocculating ion for the $CaCO_3$ precipitate. Homack[3] found that the solubility product of $Ca(AlO_2)_2$ was about 2.5×10^{-10} at 25 C. In the presence of $CaCO_3$ precipitate, the minimum concentration of AlO_2^- required to start precipitation of $Ca(AlO_2)_2$ is

$$[AlO_2^-] = \sqrt{\frac{K_4}{K_2}[CO_3^{--}]} \tag{53}$$

where K_4 and K_2 are the solubility products of calcium aluminate and calcium carbonate, respectively. Equation (53) indicates that, at 25 C, an alum dose of 216 ppm (19.6 ppm Al) is required to start precipitation of $Ca(AlO_2)_2$ when the CO_3^{--} concentration is as low as 0.6 ppm, and more alum is required at higher concentrations of CO_3^{--}. Calcium aluminate precipitate is therefore not normally present in softening slurries.

The computations for the amounts of chemicals required and for the residual hardness are illustrated in the following example for a water having a hardness of 221.6 ppm, the analysis of which is given in Tables 5 to 7.

[1] Langelier, *J. AWWA*, **28**, 1500, 1936.
[2] Latimer, "Oxidation Potentials," 2d ed., Prentice-Hall, Inc., Englewood Cliffs, N.J., 1952.
[3] Homack, Peter, Master's Thesis, M.I.T., 1941.

TABLE 5. ANALYSIS OF RAW WATER

Ion	ppm	Mol. wt.	ppm as $CaCO_3$ Positive	ppm as $CaCO_3$ Negative
Ca^{++}	59	40	147.6	
Mg^{++}	18	24.3	74.0	
Na^{+}	10	23	21.7	
HCO_3^{-}	222	61	.....	182.0
CO_3^{--}	0.6	60	.....	1.0
SO_4^{--}	38.6	96	.....	40.2
Cl^{-}	12	35.5	.....	16.9
NO_3^{-}	4	62	.....	3.2
			243.3	243.3
Free CO_2	8	44	18.2 ppm as $CaCO_3$	
pH	7.82			

Chemicals required:

Lime, for	CO_2	18.2 ppm as $CaCO_3$
	HCO_3^-	182.0 ppm as $CaCO_3$
	Mg^{++}	74.0 ppm as $CaCO_3$
	Excess	40.0 ppm as $CaCO_3$
	Total =	314.2 ppm as $CaCO_3$
		or 233 ppm as pure $Ca(OH)_2$
Soda ash, for	SO_4^{--}	40.2 ppm as $CaCO_3$
	Cl^-	16.9 ppm as $CaCO_3$
	NO_3^-	3.2 ppm as $CaCO_3$
	Total =	60.3 ppm as $CaCO_3$
		or 64 ppm as pure Na_2CO_3

TABLE 6. BALANCE OF RADICALS AFTER ADDITION OF CHEMICALS

	ppm as $CaCO_3$							
	Positive			Negative				
	Ca	Mg	Na	SO_4	Cl + NO_3	CO_3	HCO_3	OH
Original	147.6	74.0	21.7	40.2	20.1	1.0	182.0	
Added	314.2	....	60.3	....	....	60.3	.....	314.2
From CO_2	.....	....	....	....	....	+18.2	.....	−18.2
Total	461.8	74.0	82.0	40.2	20.1	79.5	182.0	296.0
		= 617.8				= 617.8		

TABLE 7. TOTAL MOLAL CONCENTRATION OF RADICALS

$[Ca] = 4.618 \times 10^{-3}$ $\quad [Cl + NO_3] = 0.402 \times 10^{-3}$

$[Mg] = 0.74 \times 10^{-3}$ $\quad [CO_3] = 0.795 \times 10^{-3}$

$[Na] = 1.64 \times 10^{-3}$ $\quad [HCO_3] = 3.64 \times 10^{-3}$

$[SO_4] = 0.402 \times 10^{-3}$ $\quad [OH] = 5.92 \times 10^{-3}$

When the reactions have reached equilibrium, the Ca, Mg, CO_3, and OH appear both as solid and as ions. The concentration of all constituents is determined by the solution of the simultaneous equations shown in Table 8.

The results obtained by the solution of the equations in Table 8 are shown in Table 9. The residual hardness is 22.09 ppm, nearly all due to the Ca^{++} in the excess lime, and the caustic alkalinity is 41.58 ppm, which corresponds to a pH value of 10.92.

If the free CO_2 content of the raw water is high, it may be economical to remove a portion of it by aeration before the chemicals are added. Spray nozzles are most effective for aeration and will sometimes accomplish the removal of as much as 75 percent of the free CO_2. As the free CO_2 gas is liberated, the HCO_3^- breaks down in accordance with reaction (47) to furnish OH^- and thus raise the pH value. Since some of the OH^- reacts with H^+ to form water, the alkalinity is very slightly reduced by aeration.

Recarbonation is required after settling in order to eliminate the caustic alkalinity added in the excess lime. The reactions that take place upon the addition of CO_2 are shown in Eqs. (47) and (48). If sufficient CO_2 is added to barely remove the

Table 8

Unknowns	Equations	
(1) $[Ca^{++}]$	$[H^+][OH^-] = k_w$	(1)
(2) $[OH^-]$	$\dfrac{[H^+][CO_3^{--}]}{[HCO_3^-]} = K_1$	(2)
(3) $[CO_3^{--}]$	$[Ca^{++}][CO_3^{--}] = K_2$	(3)
(4) $[HCO_3^-]$	$[Mg^{++}][OH^-]^2 = K_3$	(4)
(5) $[H^+]$	$[Ca^{++}] + [Ca_s] = A = 4.618 \times 10^{-3}$	(5)
(6) $[Mg^{++}]$	$[Mg^{++}] + [Mg_s] = B = 0.74 \times 10^{-3}$	(6)
(7) $[Ca_s]$	$[Ca_s] = [CO_{3s}]$	(7)
(8) $[Mg_s]$	$2[Mg_s] = [OH_s]$	(8)
(9) $[CO_{3s}]$	$[CO_3^{--}] + [HCO_3^-] + [CO_{3s}] = C = (3.64 + 0.795)10^{-3}$	(9)
(10) $[OH_s]$	$[OH^-] + [OH_s] - [HCO_3^-] = D = (5.92 - 3.64)10^{-3}$	(10)

OH^-, much of the remaining Ca^{++} will be precipitated and the water will be further softened. If this is desired, carbonation should be followed by secondary flocculation with a coagulant or returned sludge and settling before the water goes to the filters; this process may be followed by secondary carbonation just prior to filtration to minimize afterprecipitation of $CaCO_3$ on the sand grains. The Ca^{++} may also be precipitated by secondary treatment with Na_2CO_3, but the causticity will remain and must be removed later by recarbonation. The final carbonation may be so adjusted

Table 9. Balance of Ions after Completion of Reactions

	ppm as $CaCO_3$							
	Positive			Negative				
	Ca^{++}	Mg^{++}	Na^+	SO_4^{--}	$Cl^- + NO_3^-$	CO_3^{--}	HCO_3^-	OH^-
Ions	20.8	1.29	82.0	40.2	20.1	2.26	0.29	41.58
Total	104.09			104.43				

as to constitute corrective treatment of the water for protection against corrosion. If carbonation is carried far enough to throw the residual Ca back into solution, incrustation of filter sand will be lessened but further corrective treatment after filtration with sodium hydroxide or lime will usually be required. A small dose of sodium hexametaphosphate[1] may be used instead of secondary carbonation to prevent incrustation of the filter sand.

CO_2 gas for carbonation may be produced by the following types of plants: (1) gas burning, (2) combined gas and coke burning, (3) oil burning, (4) combined oil and coke burning, (5) coke burning, (6) utilization of stack gas, and (7) generation and use of producer gas. A carbonation plant consists principally of (1) a combustion chamber so designed as to permit proper admixture of air and fuel, (2) a washer or scrubber where the products of combustion are cleaned and cooled, (3) a drier for removing the water that may come over with the gas, (4) a compressor or blower for forcing the gas into the carbonation chamber, (5) a gas flowmeter, and (6) a carbonation chamber in which the gas is diffused into the water.

For small treatment plants, gas- or oil-burning carbonation plants are most satisfactory because of the ease with which the rate of combustion may be controlled. Fuel oil yields about 2.3 lb of CO_2 per pound; kerosene about 3.1 lb of CO_2 per pound; and gas 82 to 115 lb of CO_2 per 1,000 cu ft of gas. For large softening plants, gas-producer carbonators are economical. Gas is produced from coke and burned under a boiler, the steam from the boiler being used to drive the compressor or for other power or heating purposes. Coke produces about 3 lb of CO_2 per pound of coke. The burned gas from this type of plant contains up to 19 percent CO_2; whereas, from the ordinary burning of coke and other types of carbonators, the gas contains only about 10 to 12 percent CO_2. One cubic foot of CO_2 weighs 0.1145 lb at atmospheric pressure and 70 F.

The gas from the compressor is diffused into the water through perforated pipes or diffuser plates in the bottom of the carbonation chamber. The depth of the chamber may be made the same as the adjacent basins for structural convenience. The retention period for the water in the chamber is of no significance, and the size may be made just sufficient to accommodate the diffuser system. Perforated-pipe diffusers may be designed according to the same principles used for filter underdrains. Corrosion-resistant pipe should be used.

27. Ion Exchangers. Ion-exchange materials[2] are solid compounds which contain loosely bound ions. The ions bound to the ion-exchange material depend upon the concentrations of the various ions in the solution in contact with the ion-exchange material and upon the relative attraction between the ion-exchange material and the various ions present. Thus a cation-exchange material immersed in a strong salt (sodium chloride) solution will bind the Na^+; however, when immersed in a dilute solution of Ca^{++} and Mg^{++} the ion-exchange material will give up the Na^+ and bind the Ca^{++} and Mg^{++}. Furthermore in the presence of a strong salt solution the ion-exchange material will again revert to the Na form, giving up the Ca^{++} and Mg^{++}. This ability of ion-exchange materials to exchange one ion for another is used to remove unwanted ions from solutions and replace them with more desirable ions. Water may be softened by exchanging the Ca^{++} and Mg^{++} in the water for Na as long as Na is available in the ion-exchange material. By the use of appropriate ion-exchange materials all the mineral and nonmineral ions found in natural waters may be exchanged for H^+ and OH^-, thereby demineralizing the water.

The following reactions to the right represent ion removal and to the left regeneration of the exchange material:

[1] Rice and Hatch, *J. AWWA*, **31**, 1171, 1939.

[2] See Nachod, F. C., and Jack Schubert, "Ion Exchange Technology," Academic Press Inc., New York, 1956.

Sodium cation exchanger

$$2NaZ + Ca^{++} \rightleftarrows CaZ + 2Na^{+} \tag{54}$$

Hydrogen cation exchanger

$$2HZ + Ca^{++} \rightleftarrows CaZ + 2H^{+} \tag{55}$$

Anion exchanger (strongly basic)

$$2R_4NOH + SO_4^{--} \rightleftarrows (R_4N)_2SO_4 + 2OH^{-} \tag{56}$$

In the above reactions Z represents the cation exchanger and R_4N the anion exchanger.

The first ion-exchange materials, "called" zeolites, were natural and synthetic siliceous minerals which contained aluminum and alkali or alkali earth. They were used principally to soften water. Many nonmineral cation materials have been developed

TABLE 10. CATION-EXCHANGE MATERIALS

Description	Physical form	Mesh size range	Color	Approx. shipping weight, lb/cu ft	Salt consumption		Exchange capacity, kgr*/cu ft (as $CaCO_3$)
					lb/kgr*	lbs/cu ft	
Greensand	Grains	16 50	Green	85	0.4–0.5	1.0–1.5	2.4–3.0
Processed greensand	Grains	16 -50	Black	80	0.4–0.5	1.8–2.8	4.4–5.5
Synthetic alumino-silicate	Grains	16 50	Yellowish	54	0.4–0.5	3.2–5.0	8.0–10.0
Sulfonated coal	Grains	16–50	Black	30	0.4–0.5	2.1–3.1	6.0 -8.0
Sulfonated polystyrene	Beads	16–50	Amber	54	0.3–0.5	6.6–13.5	20.0 30.0

* Kilograins as $CaCO_3$.

which are referred to as zeolites or resins. Table 10 lists by type the available cation-exchange materials used for water softening together with their properties and softening capacities. A 5 to 20 percent NaCl solution is usually used for regeneration. The greensands are natural sands which are processed to enhance their ion-exchange properties. The synthetic aluminosilicate zeolite is made from mixtures of sodium silicate, aluminum sulfate, and sodium aluminate. The resulting gel is dried, crushed, and screened. The carbonaceous type is made by the sulfonation of crushed and screened coal. The sulfonated polystyrene ion exchangers are made by the copolymerization of styrene and divinylbenzene. The synthetic resin thus formed is then sulfonated. The resulting product is small balls 0.3 to 1.0 mm in diameter. As may be seen from Table 10 these synthetic resins have about ten times the exchange capacity of greensand. Another advantage of the carbonaceous and synthetic resin types of ion exchangers for boiler-water treatment is that they do not contribute silica to the treated water, a fault of the natural zeolites. The carbonaceous and polystyrene resins are also used as hydrogen cation exchangers, which is not possible with the mineral zeolites because they would be destroyed by the strong acid used for regeneration—2 to 15 percent H_2SO_4.

The anion exchangers may be classified as strong-base, intermediate-base, or weak-base. The weak-base and intermediate-base exchangers are cheaper than the strong-base type but will remove only strongly ionized acids from solution while strong-base exchangers will remove both strongly and weakly ionized acids. The strong-base anion exchangers are synthetic resins made from polystyrene with alkyl, alkanol, or a pyridinium quaternary ammonium or amine group at the active ion-exchange sites. These ion-exchange resins are regenerated with a 3 to 6 percent NaOH solution.

Cation softeners are built in units similar to both pressure- and open-type rapid filters. In addition to the piping and valves provided for rapid filters, cation units are provided with salt-solution inlets and outlets. The brine may be introduced by a perforated-pipe system at the surface of the bed, in which case the brine flows downward; or through the underdrainage system, in which case the brine flows upward through the bed. Cation beds are made 24 to 75 in. deep and are operated as either downflow or upflow units at rates up to 4 to 8 gpm/sq ft. Wash-water requirements range up to 5 to 10 percent for synthetic zeolites and up to 20 to 25 percent for greensands, the requirements for a single wash and rinse being about 100 gal/sq ft.

Brine is prepared in a salt storage bin, usually made of concrete with duplicate compartments, as a saturated solution containing about 25 percent salt. The bottom of the bins is usually made hopper-shaped and provided with a screen and about a foot of graded gravel to support the salt. The salt is covered with water which dissolves it, the solution being withdrawn from below to a collecting reservoir of sufficient capacity to regenerate one softening unit. From the collecting reservoir, the brine is withdrawn, diluted to the proper strength, and applied to the unit. The brine solution is passed slowly and continuously through greensand, but it is customary to hold the brine in synthetic zeolite or resin beds 5 to 15 min.

It is usually not economical to operate ion-exchange units as filters, as the sediment that deposits on the grains reduces the softening capacity of the material. Ion-exchange units may be used alone with clear well waters not too high in iron, but they should follow filters with turbid waters. Cation-exchange units will remove Fe and Mn in true solution by base exchange, but with dissolved O_2 present some of the iron nearly always takes the form of Fe_2O_3 and as such coats the grains and reduces their softening capacity. Mineral zeolite disintegrates in acid waters and in waters having appreciable free CO_2 content, but this is not true of resinous exchangers.

Although cation-exchange units produce water of zero hardness, the total dissolved solids in the softened water are nevertheless greater than in the raw water and the water is high in Na. In contrast with the lime-soda process, which may produce 200 cu ft or more of sludge per million gallons of water, there is no sludge-disposal problem with the cation-exchange process. As regards softening economy, lime costs only about 25 percent as much as salt for removing bicarbonate hardness, whereas soda ash costs about 25 percent more than salt for removing noncarbonate hardness. Hence cation exchange is sometimes used following lime-softening to remove noncarbonate hardness.

Ion-exchange processes have been used since World War II for demineralization of sea water for emergency purposes such as water-supply kits on life rafts. In comparison with other methods which are available, they are not economical for the large-scale conversion of brackish water or sea water to fresh water.

At the present time the most economical commercially available processes for desalting brackish waters on a large scale are distillation and electrodialysis. The only economically feasible process for desalting sea water is distillation. A number of other processes are under investigation, and many improvements are being made in the application of the existing processes. A few of the newer processes worthy of mention are (1) freeze-thawing, (2) reverse osmosis, (3) the hydrate process, and (4) the solvent-extraction process. Some of the methods being investigated to improve the efficiency of distillation and reduce the operating problems are (1) multistage flash distillation,

(2) thin-film evaporation, (3) vapor-compression stills, (4) fluidized-bed evaporation, and (5) liquid-liquid heat-transfer stills.

In the electrodialysis process use is made of the property of certain plastic membranes to pass only cations, and of other membranes to pass only anions. An electrodialysis cell consists of ultimate cation and anion permeable membranes between which water flows and electrodes at the end of the cell for applying an electromotive force across the membranes. When the electromotive force is applied the cations pass through the cation-permeable membrane and the anions pass through the anion-permeable membrane. Thus the water passing between alternate membrane pairs is depleted of salts, while that passing through the intervening pairs is enriched. The amount of electric current required is proportional to the amount of salt to be removed. Scaling of the membranes and polarization of the electrodes are among the common operating problems encountered. Adjustment of the pH of the feed water is one means of control of scaling. Polarization is related to the current density and the feed-water composition.

The most widely used method of desalting brackish water and sea water is distillation. Distillation plants having capacities up to 1.7 mgd are in use. The larger plants, other than United States government demonstration plants, employ submerged tube heaters or multistage flash evaporation. The commonest operating problems are scaling, corrosion, and biological fouling. These are overcome with various types of feed-water treatment which may consist of one or more of the following processes: screening, softening, pH adjustment, flocculation, filtration, disinfection, and degasification. During 1963, large distillation units produced desalted water from sea water at a cost of about $1.50 per 1,000 gal, not including the cost of distribution. This is ten to twenty times the cost of purification of fresh water.

28. Iron and Manganese Removal.[1] Iron and manganese in hard water are effectively removed by the lime-softening process. Fe precipitates as ferrous oxide or carbonate which is rapidly oxidized to Fe_2O_3 [reaction (29)] by the dissolved O_2. Mn precipitates by a similar reaction as white hydrous manganous oxide, $MnO \cdot H_2O$, which is similarly oxidized quite rapidly to hydrous manganic oxide, $Mn_2O_3 \cdot xH_2O$, and hydrous manganese dioxide, $MnO_2 \cdot xH_2O$, brownish-black precipitates.

The solubility product for hydrous ferrous oxide is given by Eq. (28) and for hydrous manganous oxide is as follows:[2]

$$[Mn^{++}][OH^-]^2 = 2 \times 10^{-13} \text{ at } 25 \text{ C} \tag{57}$$

The solubilities of ferrous iron and manganous manganese corresponding to these solubility-product constants are shown in Fig. 37, which also shows the solubilities of Fe^{3+} and Mn^{3+}. The solubility product for hydrous ferric oxide is given by Eq. (24) and for hydrous manganic oxide is as follows:[3]

$$[Mn^{3+}][OH^-]^3 = 2 \times 10^{-36} \text{ at } 25 \text{ C} \tag{58}$$

Figure 37 shows that to remove Fe^{++} and Mn^{++} without an oxidizing agent the pH must be raised to about 9.6 and 10.6, respectively; whereas Fe^{3+} and Mn^{3+} may be removed effectively at all pH values above about 4.5. Unless lime softening is required, the pH should be low in the flocculation and settling basins so that the contact period in these units will be available for disinfection by chlorine. Chlorine is an ineffective germicide at high pH. It is therefore desirable to use an oxidizing agent for removal of iron and manganese.

[1] Zapffe, *J. AWWA*, **25**, 665, 1933; Weston, *J. NEWWA*, **50**, 231, 1936.
[2] Latimer, "Oxidation Potentials," 2d ed., Prentice-Hall, Inc., Englewood Cliffs, N.J., 1952.
[3] Computed from data given by Latimer.

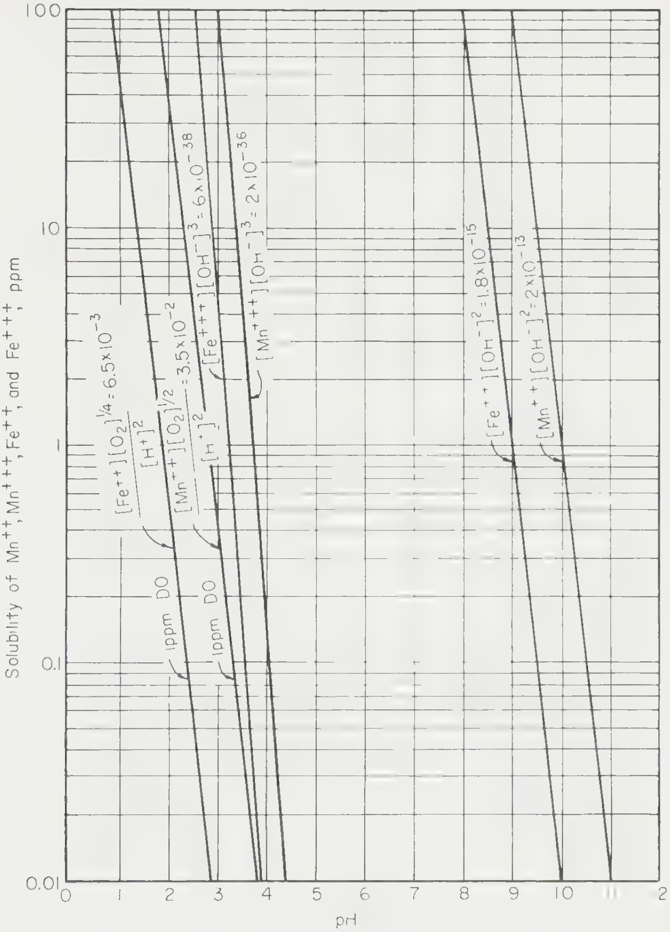

FIG. 37. Solubility of iron and manganese at 25 C.

The complete reactions and solubility products for removal of Fe^{++} and Mn^{++} as $Fe(OH)_3$ and MnO_2, respectively, with various oxidizing agents, are presented below.[1] With dissolved oxygen,

$$Fe^{++} + \tfrac{5}{2}H_2O + \tfrac{1}{4}O_2 \rightleftarrows \underline{Fe(OH)_3} + 2H^+ \tag{59}$$

$$\frac{[Fe^{++}][O_2]^{1/4}}{[H^+]^2} = 6.5 \times 10^{-3} \text{ at } 25 \text{ C} \tag{60}$$

$$Mn^{++} + H_2O + \tfrac{1}{2}O_2 \rightleftarrows \underline{MnO_2} + 2H^+ \tag{61}$$

$$\frac{[Mn^{++}][O_2]^{1/2}}{[H^+]^2} = 3.5 \times 10^{-2} \text{ at } 25 \text{ C} \tag{62}$$

These reactions require 0.143 ppm O_2 per ppm Fe^{++} and 0.29 ppm O_2 per ppm Mn^{++}. With chlorine,[1]

[1] Computed from data given by Latimer.

$$Fe^{++} + \tfrac{5}{2}H_2O + \tfrac{1}{2}HOCl \rightleftarrows \underline{Fe(OH)_3} + \tfrac{1}{2}Cl^- + \tfrac{5}{2}H^+ \tag{63}$$

$$\frac{[Fe^{++}][HOCl]^{1/2}}{[Cl^-]^{1/2}[H^+]^{5/2}} = 4 \times 10^{-8} \text{ at 25 C} \tag{64}$$

$$Mn^{++} + H_2O + HOCl \rightleftarrows \underline{MnO_2} + Cl^- + 3H^+ \tag{65}$$

$$\frac{[Mn^{++}][HOCl]}{[Cl^-][H^+]^3} = 1.05 \times 10^{-9} \text{ at 25 C} \tag{66}$$

These reactions require 0.636 ppm Cl_2 per ppm Fe^{++} and 1.29 ppm Cl_2 per ppm Mn^{++}. With potassium permanganate,[1]

$$Fe^{++} + \tfrac{7}{3}H_2O + \tfrac{1}{3}MnO_4^- \rightleftarrows \underline{Fe(OH)_3} + \underline{\tfrac{1}{3}MnO_2} + \tfrac{5}{3}H^+ \tag{67}$$

$$\frac{[Fe^{++}][MnO_4^-]^{1/3}}{[H^+]^{5/3}} = 1.78 \times 10^{-11} \text{ at 25 C} \tag{68}$$

$$Mn^{++} + \tfrac{2}{3}H_2O + \tfrac{2}{3}MnO_4^- \rightleftarrows \underline{\tfrac{5}{3}MnO_2} + \tfrac{4}{3}H^+ \tag{69}$$

$$\frac{[Mn^{++}][MnO_4^-]^{2/3}}{[H^+]^{4/3}} = 2.15 \times 10^{-16} \text{ at 25 C} \tag{70}$$

These reactions require 0.944 ppm $KMnO_4$ per ppm of Fe^{++} and 1.92 ppm $KMnO_4$ per ppm of Mn^{++}.

The solubility of Fe^{++} and Mn^{++} corresponding to the solubility products of Eqs. (60) and (62), with 1 ppm dissolved oxygen, are shown in Fig. 37. The solubilities with Cl_2 and $KMnO_4$ are too low to show in Fig. 37. With 0.1 ppm residual Cl_2 and 10 ppm Cl^-, the solubility of Fe^{++} is about 0.03 ppm and of Mn^{++} is about 0.01 ppm at pH zero. With 0.01 ppm Mn in residual MnO_4^-, the solubility of Fe^{++} is about 2×10^{-4} ppm and of Mn^{++} is about 3.7×10^{-7} ppm at pH zero. The actual quantities of Cl_2 and $KMnO_4$ required for most waters are less than indicated by the reactions because dissolved oxygen is also present. The solubility of Fe^{++} and Mn^{++} for all the above reactions decreases with increase in pH.

The rate of the above reactions for oxidizing Fe^{++} and Mn^{++} is comparatively slow because the concentration of the reactants is usually low, and with surface waters the Fe and Mn may be protected within organic colloidal particles. Moreover, to remove the precipitates they must be adsorbed on a solid surface or be flocculated for removal by settling and filtration. Copper ion, Cu^{++}, is known to enhance air oxidation. The presence of large concentrations of MnO_2 in the floc or on solid surfaces greatly improves the removal of both Fe^{++} and Mn^{++}. Deferrization or demanganization plants, which involve the use of aeration and contact beds of coke or crushed stone followed by settling and filtration, have long been used. Aeration is for the double purpose of raising the pH value by CO_2 reduction and of increasing the dissolved O_2 content. The surfaces of the contact material after usage collect deposits of MnO_2 and hydrous Fe_2O_3. MnO_2 ore, pyrolusite, has been used as a contact medium because of its high catalytic power. Limestone has also been used because of its basic reaction. In cases with high content of organic matter, chlorination or $KMnO_4$ or both are effective in oxidizing the organic matter and assisting in the precipitation of the oxides.

Trickling or downflow contact beds should be made 6 to 10 ft deep in order to ensure an ample period of contact. The water is sprayed on the surface and allowed to trickle downward at rates of 50 to 80 mgd/acre. Upflow contact beds are more effective than downflow beds because of the longer period of contact, provided the water is previously aerated. Such beds are apt to unload and are more easily cleaned

[1] Computed from data given by Latimer.

than tricklers. Aeration is best effected by spray nozzles or superimposed trays filled with coke. Filters for deferrization plants may be either rapid or slow sand filters. If coagulants are used, rapid filters are essential.

Manganese zeolite, sodium zeolite treated with manganous chloride and subsequently with sodium permanganate, is effective in the removal of Fe and Mn from water. The superior effectiveness of this material results from the catalytic action of the MnO_2 on the zeolite grains. The precipitates are removed by filtration in the zeolite bed. The bed is regenerated intermittently or continuously with permanganate. Precipitates are removed from the bed by backwashing.

CORRECTIVE TREATMENT OF CORROSIVE WATERS

Two general methods of attack are available for reducing the corrosiveness of water: (1) the removal of the dissolved oxygen and (2) the adjustment of the pH value.

29. Dissolved-oxygen Removal. Two methods of removal of dissolved oxygen on a small scale have been used in industrial plants for some time. One of these methods, called *deactivation,* consists of heating the water to reduce the solubility of O_2 and then passing it over steel scrap which unites with the oxygen to form rust. In the other method, called *deaeration,* the water is heated to just below boiling to free the O_2 and is then allowed to trickle over a series of copper trays to liberate the gas. Both these methods require heat and are expensive.

Powell and Bacon[1] describe a method in which deaeration is accomplished by vacuum. The water is introduced into the top of an enclosed steel tower and allowed to trickle downward over bundles of wood laths, while a vacuum of about 28.5 in. is maintained inside the tower by means of a vacuum pump taking suction at the top of the tower. A 95 percent removal of O_2 is obtained by means of the vacuum. The remaining dissolved oxygen is removed after the water flows from the bottom of the tower by means of a dose of sodium sulfite, a reducing agent.

In once-through systems, oxygen removal is more expensive generally than adjustment of the pH with alkali and is used only where additional chemicals, particularly Ca^{++}, are objectionable in the water. In closed systems for heating or cooling, where little makeup water is required, oxygen removal with sulfite is simple, effective, and economical.

30. Adjustment of the pH Value. The chemical adjustment of water to reduce corrosiveness is for the double purpose of raising the pH value and of stabilizing protective coatings on the interior surfaces of metal pipes. As has been shown in Sec. 37, the metals tend to enter solution as metallic ions at low pH values but are protected by the plating out of OH^- and CO_3^{--} at the anode in the alkaline range. A pH of 9.5 to 10.0 is required to ensure plating out of OH^- and CO_3^{--} on iron.

The most commonly used method of chemical treatment for corrosion abatement in iron pipes is to lay down a coating of $CaCO_3$ on the interior surfaces of the pipes. Except for very soft waters, this may be done at pH values lower than 9.5 to 10.0. If a water is undersaturated with $CaCO_3$, it will dissolve $CaCO_3$ coatings and iron from the surface of iron pipes to which it is exposed. If supersaturated, $CaCO_3$ will be precipitated upon the surface of the pipe and thus form a protective coating. If the water is just saturated, coatings of $CaCO_3$ will be stable and will protect the iron against corrosion. Two methods are available for determining whether a water is in equilibrium with $CaCO_3$: (1) by chemical test using powdered $CaCO_3$ and (2) by computation from the analysis of the water.

The chemical test as described by Baylis[2] requires several days for completion, in order that the water may come to equilibrium with the powdered $CaCO_3$ with which

[1] *Water Works Sewerage,* April, 1937, p. 109.
[2] Baylis, *J. AWWA,* **27,** 220, 1935.

it is placed in contact. If after the contact the pH and alkalinity of the water are unchanged, the water is in equilibrium with $CaCO_3$. If the pH and alkalinity are increased, the water is corrosive to $CaCO_3$, and if decreased, the water is supersaturated with $CaCO_3$. Baylis presents a graph showing the relation of pH to alkalinity where a water is in equilibrium with $CaCO_3$. Since the concentrations of Ca^{++} and total dissolved salts are influencing factors, as has been shown by Langelier,[1] the graph is not the same for all waters even at the same temperature.

Langelier has developed a method for computing the equilibrium values of a water from the analysis and equilibrium constants. If the water is just saturated with $CaCO_3$, Eq. (51) holds, and the solution of this equation simultaneously with Eq. (9) gives the following:

$$[H^+]_s = \frac{K_1}{K_2}[HCO_3^-][Ca^{++}] \tag{71}$$

in which $[H^+]_s$ is the hydrogen-ion concentration at saturation and K_1 and K_2 the equilibrium constants of Eqs. (9) and (51), respectively. $[H^+]_s$ is computed by means of this equation from the values of $[HCO_3^-]$ and $[Ca^{++}]$ as determined by chemical analysis. The influence of temperature and total solids makes itself felt in the values of K_1 and K_2. If the computed value of $[H^+]_s$ is less than the $[H^+]$ as determined by analysis (pH_s greater than pH), the water is corrosive to $CaCO_3$; and if $[H^+]_s$ is greater than $[H^+]$ (pH_s less than pH), the water is supersaturated with $CaCO_3$. pH_s may vary from about 7.5 for hard waters to 10 for very soft waters.

The chemical adjustment of a corrosive water is usually done by adding lime, or by adding soda ash or caustic soda if it is desired not to increase the hardness. Adjustment may be made with CO_2 if the water is oversaturated with $CaCO_3$. Aeration and contact treatment through beds of marble or limestone are also used for corrosive waters. Equation (71) cannot be used to compute the amount of treatment or chemicals required. These are determined by trial and error, the equation being used to check the results. The addition of lime and contact treatment with marble, it will be noted, changes all three variables in Eq. (71). Soda ash, caustic soda, and CO_2 affect two of the variables. Aeration affects only the $[H^+]$, the influence on alkalinity being very slight. Aeration alone is usually not sufficient treatment for a corrosive water, for only about 75 percent of the free CO_2 can be removed; but it may suffice, according to Cox,[2] if the alkalinity exceeds about 100 ppm. Contact treatment with limestone or marble, on the other hand, is not economical if the alkalinity exceeds about 50 ppm and the free CO_2 about 30 ppm. The hardness is increased too much by the treatment, and the contact period is too long. For waters amenable to treatment by the contact method, Cox recommends stone about 2 mm in size and contact periods of 10 to 20 min. Beds should be equipped for washing.

When corrective treatment is started with a corrosive water, the water should be slightly overtreated in order to lay down a $CaCO_3$ coating on the interior surface of pipes. If water is slightly supersaturated, several hours are required for precipitation of the excess $CaCO_3$ and distant pipes will thus be coated. A coating of 1/64 to 1/32 in. is satisfactory and does not reduce the carrying capacity of pipes greatly. When a satisfactory coating is produced, the water should be brought to equilibrium with $CaCO_3$ and maintained there. When repairs and extensions are made to the distribution system, the coatings in the uncovered pipes should be examined where possible as a guide to corrective treatment. Experience indicates that it is very difficult to produce a satisfactory protective coating uniformly throughout a dis-

[1] LANGELIER, *J. AWWA*, **28**, 1550, 1936.
[2] COX, *J. AWWA*, **25**, 1505, 1933.

tribution system, and that flushometer screens and small meters may be clogged in the attempt.

Sodium hexametaphosphate (Calgon) is being widely used to prevent the formation of *red water* where considerable iron is present in a water. Its action in this connection is as a peptizing agent to prevent the growth of iron-rust crystals. It is also effective following lime softening to prevent *afterprecipitation* of $CaCO_3$. It is claimed that this chemical is also effective in corrosion abatement by inhibiting the solution of iron, but conflicting results have been obtained in practice.

DISINFECTION

31. Methods. Disinfection may be effected by the use of (1) chemical disinfectants, (2) ultraviolet light, and (3) heat. The application of heat is a very satisfactory method of disinfection on a small scale for laboratory or emergency purposes, but it is too expensive for plant-scale disinfection. Complete sterilization may be obtained by boiling water 30 min, and disinfection (*i.e.*, destruction of pathogenic bacteria) may be obtained by heating to 60 C for 15 min or by boiling for a shorter period. Chemical disinfectants are the more generally used in treatment plants. The following chemicals have found practical application: (1) chlorine gas, (2) hypochlorites, (3) chloramine, (4) excess lime, (5) ozone, (6) silver, (7) permanganate, (8) bromine, (9) iodine, and (10) chlorine dioxide. Some of these chemicals are strong oxidizing agents. The first three chemicals are the most widely used and will be considered together.

32. Chlorine and Chloramines. Calcium hypochlorite is available commercially in the United States in powdered form as $Ca(OCl)_2 \cdot 4H_2O$ containing the equivalent of about ⅔ lb of Cl_2 per lb. Sodium hypochlorite, NaOCl, is available in water solution containing the equivalent of about 1 lb of Cl_2 per gal. Chlorine gas, furnished in liquid form in pressure containers, is most widely used because of its lower cost. Hypochlorites dissolve in water to form hypochlorous acid, HOCl. Chlorine gas also reacts with water to produce hypochlorous acid and Cl^- as follows:

$$Cl_2 + H_2O \rightleftarrows HOCl + H^+ + Cl^- \tag{72}$$

The reaction goes almost to completion to the right in dilute solutions but is said to require several hours for equilibrium.

Hypochlorous acid ionizes as follows:

$$HOCl \rightleftarrows H^+ + OCl^- \tag{73}$$

The dissociation constant is

$$\frac{[H^+][OCl^-]}{[HOCl]} = 3.2 \times 10^{-8} \text{ at } 25 \text{ C}^{1} \tag{74}$$

Equation (74) indicates that a hypochlorous acid solution is about 97 percent HOCl at pH 6 and about 3 percent HOCl at pH 9. Cl_2, HOCl, and OCl^- are known as free available chlorine.

Chloramine is produced by combining chlorine with ammonia or amino compounds in the water. Free ammonia and amino compounds are present in many natural waters containing dissolved organic matter. If added artificially, aqua ammonia (NH_4OH) solutions or anhydrous gaseous ammonia, NH_3, are used. NH_3 is applied by means of ammoniators similar in type to chlorinators. The chemical reactions of

[1] Latimer, "Oxidation Potentials," 2d ed., Prentice-Hall, Inc., Englewood Cliffs, N.J., 1952.

NH_3 with Cl_2 in water treatment are varied and not well understood. The most important reactions are as follows:[1]

$$NH_4^+ + HOCl \rightarrow \underset{\text{Monochloramine}}{NH_2Cl} + H^+ + H_2O \tag{75}$$

$$NH_2Cl + HOCl \rightleftarrows \underset{\text{Dichloramine}}{NHCl_2} + H_2O \tag{76}$$

$$NHCl_2 + HOCl \rightarrow \underset{\text{Nitrogen trichloride}}{NCl_3} + H_2O \tag{77}$$

NH_2Cl, $NHCl_2$, and NCl_3 are known as *combined available chlorine.* The concentration in water of the available *oxidizing* chlorine, *free* and *combined,* may be determined by the ortho-tolidine-arsenite (OTA)[1] test and the distribution of the components Cl_2, NH_2Cl, $NHCl_2$, and NCl_3 by the Palin[2] test. The distribution of the components depends upon the molar ratio of Cl_2 dose to NH_3, the pH of the water, the contact time, and the temperature.

Experiments by Palin[2] in chlorinating water at 18 C containing 0.5 ppm of NH_3-N indicate that, when the molar ratio of Cl_2 dose to NH_3 is less than 1, $NHCl_2$ predominates at pH 4 to 5.5 with considerable free chlorine and NCl_3 at 10 min, most of which is converted to $NHCl_2$ at 2 hr. At pH 6 to 10, nearly all the residual is NH_2Cl with a small amount of $NHCl_2$ at pH 5 to 7. With molar ratios of 1 to 3, free chlorine is present at 10 min from pH 4 to 10 with minimum concentrations at pH 5 to 7; NCl_3 is present and more stable at low pH values, the upper pH limit increasing with molar ratio to 8.5 at 3.12 molar ratio; and $NHCl_2$ predominates in the acid pH range with NH_2Cl in the alkaline pH range.

With a molar ratio of Cl_2 dose to NH_3 greater than 1 and pH exceeding 5, the total residual chlorine decreases with increase in dose to a minimum called the *breakpoint* at a molar ratio of 1.5 to 3, and then increases directly with increase in Cl_2 dose. Chlorination past the breakpoint is called *breakpoint chlorination.* The reduction in residual to the breakpoint results primarily from the decomposition of $NHCl_2$. According to Palin, if the initial residual is almost entirely $NHCl_2$, it will break down to N_2, HOCl, H^+, and Cl^- with a loss of about 75 percent available chlorine; and if both $NHCl_2$ and NH_2Cl are initially present they may react together to produce N_2, H^+, and Cl^-.

Both free and combined chlorine react with reducing substances in water to form products which are not germicides. These substances include Fe^{++}, Mn^{++}, sulfides, and organic matter. The amount of oxidizing chlorine for a particular dose and contact time which is lost by reaction with reducing substances, to the atmosphere as Cl_2 or NCl_3 gas and by breakdown of combined chlorine, is called the *chlorine demand.* The corresponding *chlorine residual* is the dose less the demand, as shown in Fig. 38.

The residual may include any of the six forms of oxidizing chlorine, Cl_2, HOCl, OCl^-, NH_2Cl, $NHCl_2$, and NCl_3, because the valence of the oxidizing chlorine atom is +1 in each; and it may include other compounds of chlorine with organic matter. The reduction of the chlorine atom to −1 is accompanied by the oxidation of the N in the chloramines from −3 to zero in N_2. NCl_3 is not considered an appropriate constituent of combined available chlorine, because it is a volatile toxic gas to be avoided by avoiding the conditions favorable to its formation. Palin's experiments on chlorination of amino acids show that in no case was NCl_3 found. It appears to be a problem only when NH_3 or urea is present. Figure 39, based on Palin's experiments using

[1] See "Standard Methods for the Examination of Water and Wastewater," American Public Health Association, 1965.

[2] Palin, A. T., "Chloro Derivatives of Ammonia and Related Compounds," British Waterworks Association, November, 1950.

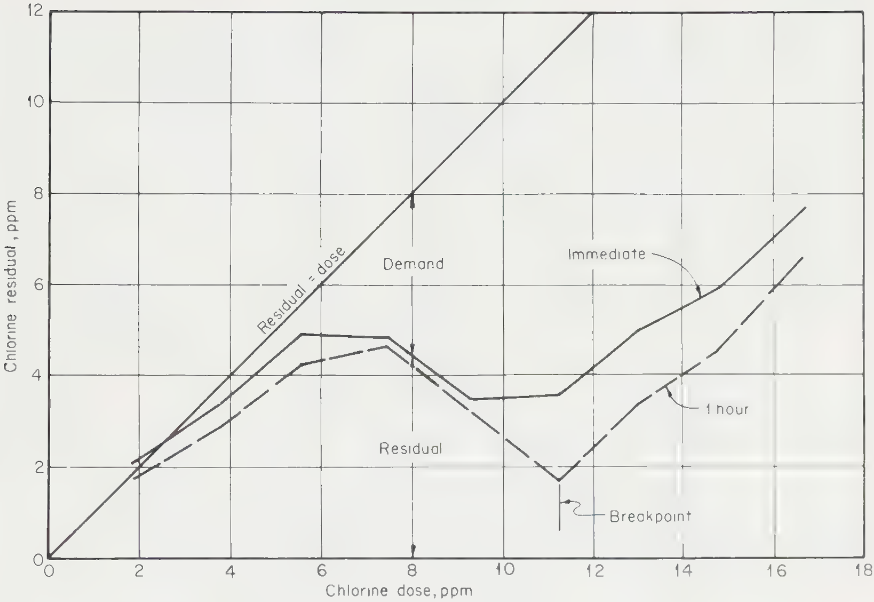

FIG. 38. Breakpoint test, Concord River, Sept. 24, 1956, pH 6.8.

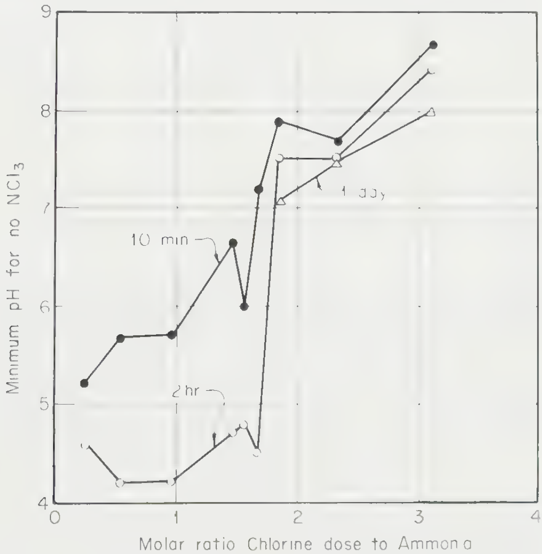

FIG. 39. Minimum pH for avoidance of nitrogen trichloride.

NH_3, shows the pH values above which NCl_3 will not be present. The 2-hr chlorine residual with breakpoint chlorination will contain about one-fourth NCl_3 and the remainder Cl_2 at pH values between 6 and 7.5; and a pH above 8 is required to avoid NCl_3. Figures 40, 41, and 42, which show the chlorine residuals at pH 5, 6, and 7, respectively, based on Palin's experiments with NH_3, indicate that in this pH range NCl_3

cannot be avoided in chloramine treatment unless the molar ratio of Cl_2 dose to NH_3 is less than 1.6 and a contact period of about 2 hr is used.

The purpose of disinfection is to destroy pathogenic microorganisms including bacteria, viruses, and protozoa. Since pathogens are not usually present in water or waste water in sufficient numbers to use their counts as a measure of the effectiveness

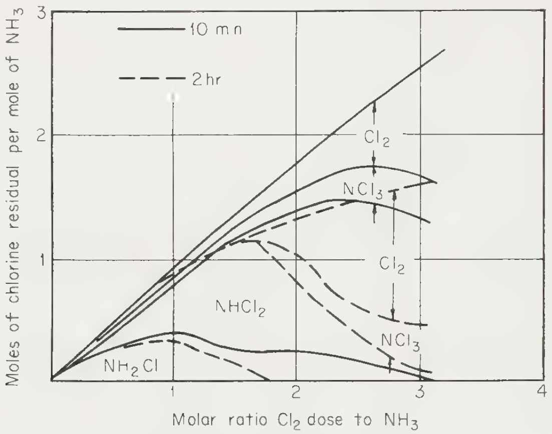

FIG. 40. Chlorine residuals at pH 5, 0.5 ppm NH_3–N.

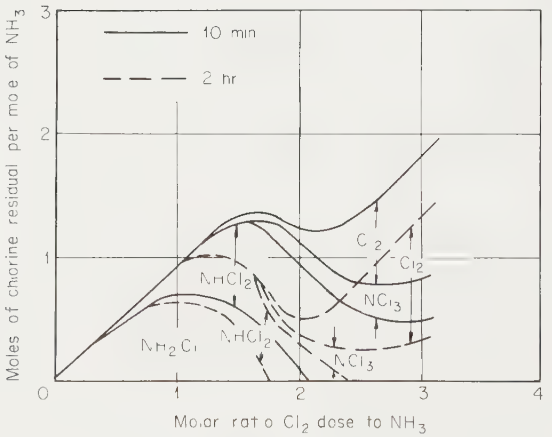

FIG. 41. Chlorine residuals at pH 6, 0.5 ppm NH_3–N.

of a disinfectant, the count of coliform bacteria is commonly used. Coliform bacteria are excreted from the human intestine at an average rate per person of about 200 billion per day and they are present in raw municipal sewage during dry weather in concentrations of 50 to 300 million/100 ml. The resistance of coliform bacteria to chlorine is about the same as the resistance of the common pathogenic bacteria but is considerably less than the resistance of pathogenic viruses and some protozoa.

According to Fair and Geyer,[1] an effective kill of coliforms requires a contact period about eighty times as long with OCl^- as with HOCl with the same chlorine residual; or with the same contact period a residual about forty times as great with OCl^- as with HOCl. It is evident, therefore, that for economy disinfection with free chlorine should be undertaken at pH values below 7 where more than 80 percent of the residual is HOCl. Combined chlorine is a slower bacteriocide than HOCl. Kelly and Sanderson[2] have found in chlorination of five strains of polio and two strains of coxsackie viruses that 0.3 ppm of free residual chlorine for at least 30 min contact is required for 99.9 percent inactivation, and that about 10 ppm of combined residual chlorine for about 60 min is required. For adequate virus kills, prechlorination appears essential in order to take advantage of the long contact periods available during flocculation and settling. Postchlorination also may be used with a short contact period in the filtered-water reservoir.

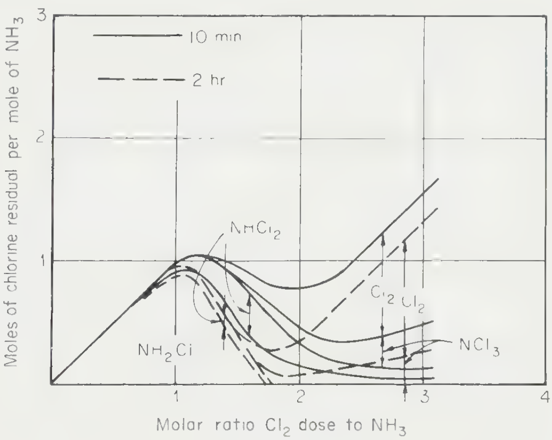

FIG. 42. Chlorine residuals at pH 7, 0.5 ppm NH_3–N.

McKee[3] has shown that chlorination of settled sewage with high doses, 20 to 40 ppm, for 15 min is capable of reducing the coliform count to less than 100 per 100 ml, and that chlorine penetrates into the suspended particles. Camp[4] has shown that chlorination of comminuted raw or settled sewage with a dose sufficient to produce a combined chlorine residual of 10 ppm after 1 hr, about 20 to 40 ppm, will effect a coliform kill in 10 min exceeding 99.99 percent with a survival of about 1,000 per 100 ml. Camp[4] has also shown that blending of a portion of each sample in a Waring blender for 1 min following chlorination increases the coliform count by only 5 to 10-fold, thus confirming McKee's finding that chlorine penetrates suspended matter. The residual in sewage chlorination is nearly all NH_2Cl.

There are two purposes in the use of ammonia with chlorine: (1) to prevent odors produced by overchlorination or the combination of the Cl_2 with substances in the water and (2) to create a persistent chlorine residual that is effective in preventing aftergrowths of bacteria in the distribution system. If the ammonia is used to

[1] FAIR, G. M., and J. C. GEYER, "Water Supply and Wastewater Disposal," John Wiley & Sons, Inc., New York, 1954.

[2] KELLY, SALLY, and W. W. SANDERSON, *Am. J. Public Health*, **48**, 1323, 1958; and **50**, 14, 1960.

[3] MCKEE, J. E., "The Disinfection of Settled Sewage," California Institute of Technology, April, 1957.

[4] CAMP, T. R., Chlorination of Mixed Sewage and Storm Water, *Trans. ASCE*, **127**(III), 452, 1962.

prevent odors, it is more effective if applied before the chlorine. The chlorine should follow within 10 min or some of the NH_3 may be lost. Passage of ammoniated water through filters prior to the application of chlorine sometimes results in the absorption of much of the NH_3 by the filter sand. If rapid germicidal action together with a persistent residual is desired, it may sometimes be accomplished by applying the chlorine first, followed in a few minutes by the ammonia. This process also results in a saving of ammonia, but it may result in odors with some waters. Breakpoint chlorination may be used to control odors if the conditions are such as to avoid NCl_3.

Hypochlorites are prepared as solutions with a strength of 0.5 to 5 percent available Cl_2. Solutions should be protected from light and if stored for more than 2 weeks before use should be stabilized with alkali in order to prevent loss of Cl_2. Commercial feed apparatus is available for both manual and automatic control of the dose.

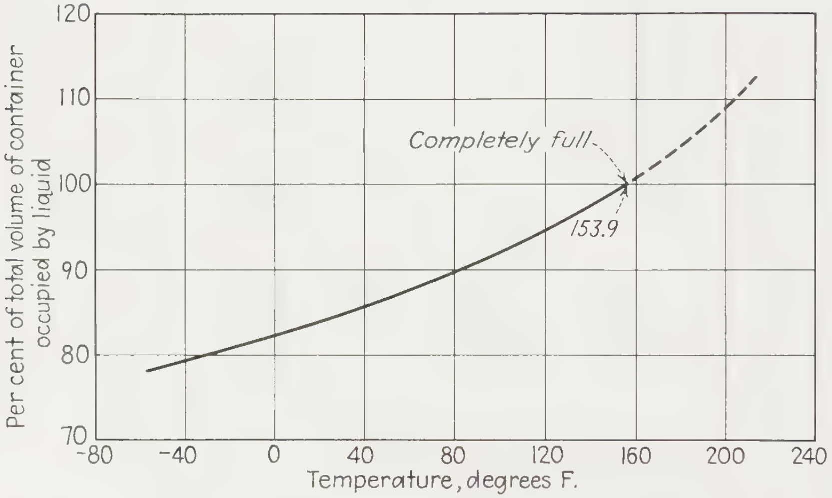

FIG. 43. Volume-temperature relations of liquid chlorine in closed containers.

Liquid chlorine is commercially available in the United States in closed drums of 100 lb, 150 lb, and 1 ton capacity and in tank cars of 16, 30, and 55 tons capacity. The weight of liquid chlorine varies inversely with the temperature, being 91.8 lb/cu ft at 32 F and 78 lb at 153.9 F. When shipped under Interstate Commerce Commission regulations, the volume-temperature relations in the containers are as shown in Fig. 43. It is obvious from the figure that to avoid explosion containers should not be heated to above 153.9 F or be filled at lower temperatures with more liquid than is indicated by the curve. The vapor pressure of liquid chlorine for various temperatures is shown in Fig. 44, from which it may be seen that the gage pressure of a container is about 85 psi at room temperature and about 39 psi at 0 C. When the pressure on the cylinder is released, the liquid boils away as a gas.

Liquid chlorine is withdrawn from the container as a gas and fed through a chlorinator into the water. Several types and makes of chlorinators are available, of which some proportion the chlorine as a water solution and others proportion the gas directly to a water stream. The solubility of Cl_2 in water as affected by the temperature is shown in Fig. 45. Below 49.2 F, solid chlorine hydrate[1] is formed. It is therefore

[1] HAMMER, JACKSON, and THURSTON, "Industrial Water Treatment Practice," p. 412, Butterworth & Co. (Publishers), Ltd., London, 1961.

desirable that chlorine solutions be kept at temperatures above 50 F or that the solution should be sufficiently dilute to assure a negligible formation of chlorine hydrate.

In the presence of moisture, chlorine gas is exceedingly corrosive. It seriously affects the linings of the throat, nose, and lungs, and if inhaled in sufficiently large quantities will produce death. The dry gas or liquid may be conveyed from the

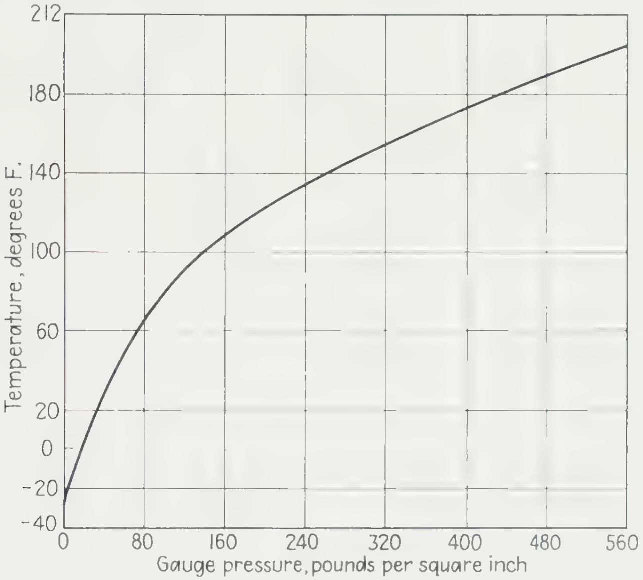

Fig. 44. Vapor pressure of liquid chlorine.

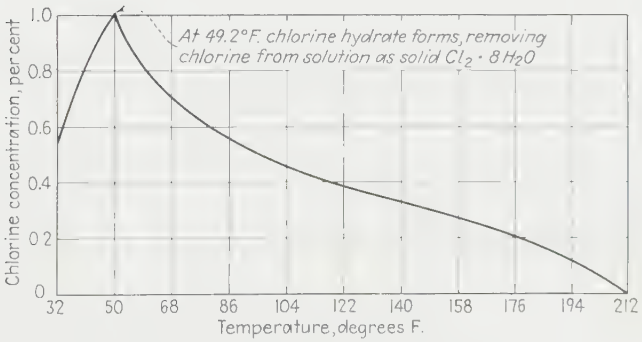

Fig. 45. Solubility of chlorine in water.

cylinders to the chlorinator by high-pressure iron or copper pipe, but wet gas and chlorine solutions should be conveyed in pipes made of glass, chemical rubber, silver, or special alloy, or PVC and other suitable plastics. Rubber should not be used with liquid chlorine. Chlorine is about 2.5 times as heavy as air, and it therefore sinks to low places when it escapes owing to accidents or leaks. Chlorinator rooms should be provided with forced-draft ventilation exhausting at the floor, and the exhaust pipe should discharge at sufficient height to secure adequate diffusion of the gas before it reaches the ground. Sprinkler systems handling NaOH solutions are an added precaution, for alkaline solutions will absorb some of the gas on the floor. All chlorinating plants should be equipped with gas masks and other approved safety devices.

Ammoniators are designed similar to chlorinators, except that different materials are used for the conduits in order to avoid corrosion. Ammonia gas is also an irritant to the nose and throat and in the presence of moisture is corrosive to copper. Steel pipe and valves may be used for conduits. Ammonia is only about half as heavy as air and hence rises. Where ammonia is used, ventilation exhausts should be at both floor and ceiling. Anhydrous ammonia is sold commercially in steel drums as a liquid under pressure. At room temperature, the gage pressure is about 115 psi and at 0 C about 50 psi. Precaution should be taken never to mix chlorine and ammonia gases, or concentrated solutions of the gases, before they are applied to the water, for under certain conditions they may combine to form the highly explosive nitrogen trichloride. Sprays of water are effective in removing gaseous ammonia from a room since it is highly soluble. Chlorine and ammonia apparatus should be housed in a special room provided for that purpose, and in large plants the apparatus and containers are preferably housed in separate rooms.

Experience indicates that a maximum continuous rate of evaporation at room temperature may be maintained for liquid chlorine of about 35 lb/day from 100- and 150-lb cylinders and 400 lb/day from ton containers. Higher rates may be maintained by immersing the containers in warm water or passing the liquid Cl_2 through evaporators. Ammonia may be evaporated at a rate of about 30 lb/day from 100- and 150-lb cylinders, and at higher rates with evaporators.

In dosing chlorine and ammonia into water, it is important that the solutions be well mixed with the water to ensure uniform diffusion. Violent mixing is desirable and if obtained will usually result in a saving of chemicals.

In view of the many hazards involved in the handling of gaseous Cl_2 and NH_3, it is desirable to use NaOCl and aqua ammonia solutions in their stead even though their cost may be greater.

Chlorine dioxide has recently been adapted to use for disinfection and odor control. Chlorine dioxide, ClO_2, is a powerful oxidizing agent produced by the reaction of chlorine with a solution of sodium chlorite, $NaClO_2$. It has been found effective for taste and odor control with some waters, and it is a germicide at pH values up to and above 10.

33. Other Disinfectants. Mallman[1] showed that germicidal action begins with *E. coli* when sufficient alkali is present for a pH of 11 and that sterilization is complete in less than 1 min at pH 13. According to Hoover,[2] in softening the Columbus, Ohio, water, when enough lime is added to precipitate Mg, *E. coli* and *B. typhosus* are killed in 48 hr, provided the water does not have a large organic content. Disinfection is complete in 5 to 24 hr when an excess of ½ to 1 gpg of lime is added. Disinfection by excess-lime treatment is practical only in lime-softening plants.

Ozone, O_3, is a powerful oxidizing agent and a very effective germicide. It is usually produced by the electrolysis of air at 7,000 to 20,000 volts. At 25 C, about 10 g of ozone are produced per cubic meter of air. For disinfection, a dose of 1 to 3 ppm of ozone is required. The water should be clear and low in organic matter in order to avoid waste of ozone due to oxidation of organic matter. Ozonization of the water is usually accomplished by allowing the O_3 gas to pass upward through a bed of coke or gravel through which the water is trickling downward. Ozonized water is very corrosive, but the residual dissipates rapidly. Ozone is effective in odor control

[1] Mallman, *J. AWWA*, **24**, 1054, 1932.
[2] Hoover, *J. AWWA*, **23**, 1196, 1931.

because it oxidizes odor-producing organic compounds. Ozonization has been extensively used in Europe, but it has been found costly in the United States.

Ultraviolet light rays with a wave length of 0.3μ or less are effective germicides in clear water. The light is usually produced by mercury-vapor quartz lamps, but carbon arcs are also applicable. According to Perkins and Welch,[1] ultraviolet rays are effective to a depth of 20 in. in clear colorless water, and the killing action is instantaneous on all save certain resistant forms of bacteria. The resistant forms comprise less than 10 percent of the bacteria. The usual method of application of ultraviolet light is to pass the clarified water in thin layers much less than 20 in. past a series of lamps, but, according to Perkins and Welch, this practice is not necessary since the resistant forms will survive the whole series. Thoroughly clarified and colorless water is essential for the success of this method. The advantages of the method are (1) no change in the chemistry of the water and (2) no possibility of an overdose. The method is more expensive than the use of chlorine or chloramines.

Ionized silver[2] in concentrations of 0.05 to 0.3 ppm effects sterilization of water after 2 to 8 hr. Much larger doses are required for rapid bacterial kill, and according to Morris,[3] concentrations as high as 20 ppm appear to have no effect on waterborne viruses. Inasmuch as the allowable limit in the U.S. Public Health Service Drinking Water Standards is only 0.05 ppm, silver should not be used for disinfection of drinking water. It is less effective and much more expensive than chlorine.

34. Algaecides. Plankton which grow in open reservoirs are troublesome owing to the production of odors and because they cause rapid clogging of filters. The most widely used method of destruction of plankton is by the use of copper sulfate distributed evenly over the water surface. The chemical is customarily distributed by dragging a sack of the crystals systematically through the water by boat until the desired dose is obtained. Treatment is required only at times when the algae growth is heavy enough to cause trouble. The killing action of dissolved copper is similar to that of silver. A list of the names of common troublesome microorganisms together with characteristic odors produced and the required copper sulfate dose to kill each is given in "Water Works Practice."[4] The required dose ranges from 0.05 to 10 ppm, depending upon the organism. Methods of identification and counting plankton are given in "The Microscopy of Drinking Water"[5] and "Standard Methods." If copper sulfate is applied in sufficient concentration, it may result in the destruction of fish life. The safe dose ranges from about 0.14 ppm for trout to 2.1 ppm for black bass.

Chlorine is also used as an algaecide, both in liquid form and as hypochlorite. It is usually applied at treatment plants, but portable chlorinators are available for distributing chlorine over the surface of reservoirs. The dose required varies from about 0.3 to 3 ppm. If the organisms are causing odors, chlorine may accentuate them at the time of application.

TASTES AND ODORS

35. Sources and Measurement. The term *tastes and odors*[6] as applied to drinking water usually refers to cases where only odors are present. Only four true taste sensations are recognized: (1) sour or acid, associated with hydrogen ions; (2) sweet, found in sugars and associated with hydroxyl; (3) salty, produced by chlorides, nitrates, and sulfates; and (4) bitter, associated with alkaloids. Most other so-called

[1] *J. AWWA*, **22,** 959, 1930.

[2] See Just and Szniolis, *J. AWWA*, **23,** 492, 1936; and Gibbard, *Am. J. Public Health*, September, 1933, p. 910.

[3] Morris, J. C., Disinfection of Water, *The Sanitarian*, **16,** 221, 1954.

[4] AWWA, 1929, p. 168.

[5] Whipple, Fair, and Whipple, John Wiley & Sons, Inc., New York, 1927.

[6] See Fair, *J. NEWWA*, **47,** 248, 1933.

tastes are due to odors that reach the olfactory organs at the time the material is tasted.

The sources of odors in water may be classified[1] as follows:

1. Essential oils from plankton
2. Decaying vegetation
3. Sulfur gases in groundwater
4. Chlorine
5. Phenolic wastes from
   - Dye plants
   - Phenol-manufacturing plants
   - Coke-oven plants
   - Gas plants
   - Wood-distillation plants
   - Tar and oil refineries
6. Nonphenolic wastes from
   - Paper mills
   - Tanneries
   - Beet-sugar mills
   - Canneries
   - Starch plants
   - Sewage-treatment plants
7. Chlorine combined with substances listed in 2, 5, and 6.

Odor-producing substances are volatile, and it is the gaseous molecules that produce the sensation of smell in the olfactory region of the nose. The concentration in solution which is required to produce an odor is so extremely small for many odor-producing substances that relatively few of them have been identified chemically. The only means of measuring the concentration of such substances is through the strength of the odor produced, and the human nose is the measuring instrument. Consequently, the measurement of odors is not yet on a very satisfactory basis. The smallest amount of a substance required to produce an odor, usually measured in terms of its concentration in air, is called the *threshold value* of the odor. An odor in water is measured by sniffing the air in contact with the water when the air and water have come to equilibrium with reference to the odor-producing substance. The threshold point may be reached by diluting either the water with odor-free water or the air with odor-free air until the odor is just discernible. The ratio of the volume of the diluted sample to the undiluted sample is called the *threshold number*,[2] or *odor intensity*.

36. Methods of Control. The following methods[3] of treatment for control of odors have found practical application:

1. Ammonia, chlorine, chlorine dioxide
2. Powdered activated carbon
3. Prechlorination
4. Aeration
5. Copper sulfate treatment of reservoirs

[1] See Buswell, "Chemistry of Water and Sewage Treatment," p. 195, Reinhold Publishing Corporation, New York, 1928.

[2] For methods, see "Standard Methods for the Examination of Water and Wastewater," American Public Health Association, 1965; Spaulding, *Am. J. Public Health*, 1931, p. 1038; Fair, *J. NEWWA*, **47**, 248, 1933; Fair and Wells, *J. AWWA*, **26**, 1670, 1934; and Baylis and Gullans, *J. AWWA*, **28**, 507, 1936.

[3] For extended discussion, see Baylis, J. R., "Elimination of Taste and Odor in Water," McGraw-Hill Book Company, New York, 1935.

6. Superchlorination followed by dechlorination
7. Potassium permanganate
8. Granular activated carbon
9. Bleaching clay
10. Chlorine for hydrogen sulfide
11. Ozone

The first five methods are widely used. The best method for any particular case depends upon the circumstances and sometimes can be determined only by trial. Many of the processes have treatment value in other respects, and they therefore cannot be evaluated solely on the basis of odor control. Ammonia-chlorine treatment, for example, has considerable value in the long-sustained chlorine residual; and all the methods involving the use of chlorine, ozone, and permanganate may be primarily for disinfection purposes. Aeration has value in iron removal, softening, and corrosion control due to carbon dioxide removal. For odor removal, aeration is effective in the case of H_2S and for very volatile odorous substances from certain of the microorganisms. The destruction of plankton by copper sulfate is of value in increasing filter runs as well as for odor control.

Prechlorination may be used when chlorine successfully oxidizes the odor-producing compound or destroys the causative microorganisms and is not itself required in sufficient concentration to produce an odor. When the usual dose of chlorine combines with odor-producing substances to accentuate the odor, it has sometimes been found that an overdose of chlorine will destroy the odor provided the residual chlorine is later removed by an antichlor. The earliest dechlorinating methods involved the use of reducing agents, among which are sulfur dioxide gas, sodium thiosulfate, sodium sulfate, sodium bisulfate, and sodium metabisulfate. The reaction of Cl_2 with all these agents produces Cl^- ions. Activated carbon may also be used for dechlorination, the reaction producing CO_2 and Cl^-.

Activated carbon effectively destroys most odors by adsorbing the compounds from solution onto the surface of the solid carbon. The adsorption process is not well understood, and the mechanism probably varies with the character of the compound adsorbed. Adsorption is a surface phenomenon, and the rate of adsorption is a function of the amount of unsaturated surface area on the adsorbent. Activated carbon is prepared from both vegetable and animal (bone) chars which are very porous and hence have immense surface areas. The carbons most widely used in water treatment are prepared from lignite, a paper-mill wood pulp, and birch and maple wood. The process of activation consists of heating the char in steam or air to a temperature somewhat less than 600 C. Activation apparently results in the volatilization of adsorbed compounds, such as hydrocarbons, leaving the primary carbon surface free.

Carbon is widely used in the powdered form and is dosed into the water by means of either dry or slurry feed machines. It may be applied in a carbon contact chamber preceding flocculation (see Fig. 12), with the coagulating chemicals into the rapid mixing chamber, during flocculation or just prior to filtration. It is usually better to provide separate carbon contact chambers with about 5 min mixing as the first step in treatment so that adsorption of odor-producing substances may be substantially completed without interference of floc and chlorine. The used carbon will combine with the floc in the flocculation chambers and most of it will be removed from the water by settling. Provision should be made to add a small amount of carbon to the filters if needed, but the practice should be avoided unless needed because it may result in mud balls in the filters. The amount of powdered carbon required varies from about 2 to 100 ppm depending upon the strength and type of odor. Powdered carbon is wasted after use with the sludge of the settling tanks and with waste wash water.

A more economical use of the carbon may be obtained with granular carbon beds, but additional units similar to rapid filters are required at considerable expense. The additional capital cost is not justified in most cases. Carbon beds are made 2 to 4 ft deep and are operated at rates of 1 to 6 or more gpm/sq ft. The required rate of application of water depends upon the concentration and type of odor-producing substances to be adsorbed. Carbon beds are usually used after filtration, but the beds nevertheless require washing occasionally and should be designed for washing. Relatively low wash rates are required for expansion, owing to the lightness of the material. The activity of granular carbon is gradually exhausted in service because of adsorption of many substances in addition to odor-producing compounds. The life of granular carbon may be several years, in which case it may be more economical to replace the carbon with new material than to reactivate it.

SECTION 39

DRAINAGE

By William W. Donnan

INTRODUCTION

1. Scope of the Section. This section will not deal with removal of storm water from city streets or with any matters dealing with urban and suburban drainage. It will be confined to principles and practices applicable to agricultural drainage. In treating this subject, more emphasis has been placed on the solution of man-made drainage problems, although the principles apply equally to natural drainage problems. A very detailed and complete discussion of this subject can be found in "Engineering for Agricultural Drainage" (Roe and Ayres, McGraw-Hill Book Company, New York, 1954).

2. Drainage Needs. Drainage problems are both natural and man-made. For the most part, natural drainage problems occur in the humid areas of the world and man-made problems occur in the arid areas. A UNESCO[1] study in 1961 revealed there are over 5.4 million sq miles of arable land and nearly 10 million sq miles of meadows and pastures in the world. Perhaps one-fourth of this land would benefit materially by the application of drainage engineering.

Man-made drainage problems usually develop as a consequence of irrigation. Historic evidence of this can be found on every continent of the world. A major contribution to the decline and disappearance of some ancient civilizations can be attributed to their failure to heed the drainage problem. A conservative estimate would be that 150 to 200 million acres of cropland are affected to some degree by man-made drainage problems around the world. This figure is obtained by taking the world acreage of irrigated land,[2] 300 million acres, and assuming that about one-half to two-thirds of this land has potential drainage problems.

3. Drainage Principles. A properly designed drainage system removes excess surface water and/or lowers the groundwater level to prevent waterlogging. Ordinary farm crops cannot grow in soil that is saturated with water. Where subsoil waters contain salts, these mineral elements migrate to the ground surface because of evaporation. This concentration in the root zone greatly retards plant growth and prevents seed germination.

Surface drainage is accomplished by the construction of lateral ditches and open drains. Subsurface drainage and lowering of the water table are accomplished by a system of open drains or buried tile lines into which the gravity water seeps. Water collected in drains is conveyed to a suitable outlet. Subsurface drainage can also be accomplished by pumping from wells to lower the water table.

[1] "Production Yearbook 1962," Vol. 16, Food and Agricultural Organization of the United Nations, Rome.

[2] Gulhati, N. D., "Irrigation in the World, a Global View," International Commission on Irrigation and Drainage, New Delhi, India, 1955; Worldwide View of Irrigation Developments, *Proc. ASCE, J. Irrigation Drainage Div.*, **84**(IR3), 1958.

DRAINAGE SURVEYS AND INVESTIGATIONS

Drainage problems differ widely because of the varied nature of the physical land and hydrologic conditions. There are no fixed short-cut methods of investigation that are uniformly applicable.[1] Some problems are fairly simple and their solution is quickly apparent. Others require only limited investigation. Generally, however, the topography, hydrology, soils, and crop-management practices vary so greatly, both individually and in their total effect, that a complete and thorough evaluation is needed to determine the specific causes of undesirable drainage conditions and their correction. Holes must be bored, observation wells installed, soils examined, and hydrologic measurements taken. Every source of information relating to the problem must be explored and the information analyzed.

The basic information important in any drainage investigation deals with the following factors: (1) topography, (2) sources of water, (3) soils, (4) salinity, and (5) water tables.

4. Topography. Good topographic maps are necessary in order to plan an adequate drainage system. The topographic survey is the basis for all subsequent investigations since it is the framework upon which are built the soil survey, water-level survey, drain location, and depth and outlet feasibility. A topographic survey should determine the surface configuration, including the surface slopes, the direction of natural drainage, and potential drainage outlets. This survey gives a clue to the type of drainage needed. It gives positive information upon which to base specific drainage plans.

If suitable topographic maps are not available, it is recommended that they be made by photogrammetric methods. Aerial coverage at an elevation compatible with the preparation of photogrammetric contour maps on a scale of 1:5,000 with 1-m contour intervals and machine interpolated to ½-m contours is advisable.[2]

All survey information should be plotted on plan and profile sheets. Although topographic maps provide the primary basis for drainage layouts, profile drawings are necessary for planning such details as the depth, slope, and alignment of drains. Breaks in slope, benches, alluvial fans, canals, old creek channels, and other natural drainageways are important land features.

For example, analysis of the topography may reveal the lack of natural outlets for drainage water. Irrigation systems are usually developed on broad, flat expanses of land which are often devoid of natural drainage channels. Therefore, drainage systems in irrigated areas usually require a trunk outlet system. Broad, flat fields are ideal for tiling in a grid pattern, while benches and swales call for interceptor patterns. A basin type of topography often lends itself to pumping for drainage. The objective is to key the drainage system to the topography.

SOURCES OF WATER

The source of all waters coming into the area must be determined. The water-source survey provides a key to the measures needed to remedy undesirable drainage conditions. More specifically, the water source often governs the type of drainage to be installed. Thus, if excess water is due to precipitation, the remedial measure would probably be better surface drainage; if due to canal seepage, an interception drain may be indicated; and if due to artesian pressure, pumped wells may provide the most practicable remedy. In some problem areas the source of water is obvious. In others the sources of water may be both numerous and complex, making specific

[1] Donnan, W. W., and G. B. Bradshaw, Drainage Investigation Methods for Irrigated Areas of Western United States, *U.S. Dept. Agr. Tech. Bull.* 1065, 1952.

[2] Drainage Surveys, Investigations, and Reports, Chap. 2, Sec. 16, "Soil Conservation Service National Engineering Handbook," U.S. Department of Agriculture.

origins difficult to discern. A consideration of all the pertinent information on geology, topography, soil strata, and water table is needed to determine the source of the water.

The common sources of water of major importance in drainage problems are precipitation, irrigation, seepage, and hydrostatic pressure.

5. Precipitation (refer to Sec. 1 for a detailed discussion on precipitation). A positive correlation between the distribution of precipitation during the year and the fluctuations in water-table elevations may be evidence that seasonal precipitation is one of the chief sources of water. Lack of such correlation indicates that precipitation probably has little effect on the water table.

An attempt should be made to determine whether long-term cycles of precipitation are related to long-term hydrographs of water levels. For example, wet cycles may be followed by rising water tables. Deep seepage to artesian or other aquifers, though slow, may often be manifested by a rise in water levels, sometimes years after the peak of a precipitation cycle has passed.

Precipitation affects artesian wells, deep static wells, and shallow piezometer wells differently. The response of water-surface levels in these wells provides indications of the degree, mode, and duration of influence of precipitation on the water table.

6. Irrigation (refer to Art. 14, Sec. 33). Many drainage problems in irrigated areas are caused by the application of too much irrigation water. Studies should be made of (1) the effect on the water table of single irrigations, (2) water-table fluctuations throughout the irrigation season, and (3) long-time changes in water-table elevation over a period of years subsequent to the beginning of irrigation.

Poor methods of water application and inefficient use of irrigation water are likely to result in the loss of large amounts of water by deep percolation and surface runoff. Methods of applying water vary widely, depending on such factors as soil, slope, crops, size of field, delivery schedule of water, and availability of water.

7. Seepage. Seepage is a major source of water in many drainage problem areas. A study should be made to determine the locations and amounts of excessive seepage from canals. A comparison should be made of water-table hydrographs when canals are full of water and when they are empty to show any correlative relationship.

8. Hydrostatic Pressure. Water originating from precipitation, irrigation, or seepage may cause drainage problems in areas far removed from the water source. The locations of springs, seeps, and abandoned wells may be important clues to the source of water.

SOILS

The soil-stratum survey, which gives the location, extent, and physical characteristics of the various underlying soil layers, is probably the most important single technical phase of the drainage investigation.[1]

No drainage system can be adequately designed without a knowledge of the soil profile and the characteristics of the subsurface strata. Points which should be considered are (1) kinds of soils, (2) thickness of the various strata, (3) continuity of strata, and (4) position of the various strata with respect to the ground surface and to each other.

Some soils drain easily; others are extremely difficult to drain. Generally speaking, the coarse-textured soils drain better than the fine-textured soils. In many irrigated areas the soils are formed into complex profile patterns. Stratified sands, silts, and clays are commonly found. Fine-textured clay layers are often underlain or overlain by coarse-textured sands. The sequence of permeable and impermeable soils and

[1] Donnan, W. W., G. B. Bradshaw, and H. F. Blaney, Drainage Investigation in Imperial Valley, California, *Soil Conservation Serv. Tech. Publ.* 120, U.S. Department of Agriculture, 1954.

their ability to transmit water determine both the type of system that should be installed and the design. For example, open drains at intervals of 1 mile may be adequate for drainage of coarse-gravel subsoils, whereas a fine-textured clay soil to a depth of 10 or 12 ft might require mole drains spaced at 30 ft. Lack of drainable aquifers at the 3- to 5-ft level may make drainage by tile lines unfeasible. Deep underground sand and gravel layers are usually easy to drain with pumps.

9. Borings. The soil borings should be made in a grid over the project area. A minimum of one hole per square mile to a depth of 12 ft should be used to characterize the soils in the project. In addition to this reconnaissance grid there should be a series of detailed spot boring grids. These surveys should consist of a very detailed soil investigation of a 1,000-acre parcel in each 20,000-acre block of the project. On these smaller parcels the borings would be spaced at about 400-ft intervals or at such spacing as to map carefully individual soil types and series.

10. Permeability. An estimate of the permeability of the strata underlying the soil surface is essential in developing sound techniques of land drainage. Water-transmission rates should be determined in quantitative terms to be of practical use in this connection.

Coefficient of permeability may be defined as the rate of flow of water through a unit cross-sectional area under a unit head during a unit period of time.[1] For convenience in making comparisons, coefficient values are stated in terms of flows of water through saturated soil.

Methods of accurately determining the coefficient of permeability may be grouped in three broad classes, as follows:

1. Field measurements.[2]
   a. Direct measurement of the permeability of an entire soil profile, based on pumped-well data. A drawdown curve and data on quantity of water pumped are used to compute the coefficient.
   b. Direct measurement of the permeability of individual strata by means of small tubes, piezometers, or auger holes.[3]
2. Laboratory measurements utilizing a permeameter device and either in-place undisturbed specimens taken in the field by means of one of the various sampling devices, or samples of disturbed soil prepared for laboratory examination by drying the soil and packing it into the permeameter.
3. Indirect evaluations of permeability based on physical and chemical soil properties.

Each of these methods has its merits and drawbacks. The particular method selected will depend upon the requirements of the drainage survey, the availability of appropriate measuring devices, and the degree of accuracy desired.

11. Indirect Evaluations of Permeability. Some of the soil characteristics that control the movement of water through the soil are type of structure, arrangement of aggregates, grain size, texture, pore space, dispersion, swelling, and type of clay mineral. In many sections of the country, including Western United States, visible soil characteristics have been correlated with measured percolation rates, and the soil permeability is graded in accordance with a classification which has been used extensively by the Soil Conservation Service[4] in describing mapping units of soil-conservation surveys. This classification follows:

[1] Wenzel, L. K., Methods for Determining Permeability of Water-bearing Materials, *Water Supply Paper* 887.

[2] Donnan, W. W., Field Experiences in Measuring Hydraulic Conductivity for Drainage Design, *J. Am. Soc. Agr. Engrs.*, **40**(5), 270–273, 1959.

[3] Frevert, R. K., and D. Kirkham, A Field Method for Measuring the Permeability of Soil below the Water Table, *Highway Res. Board Proc.*, **28**, 433, 442, 1948.

[4] Soil Survey Manual, "Soil Conservation Service Agricultural Handbook" 18, U.S. Department of Agriculture.

Permeability class	Permeability	Percolation rate, in./hr, through saturated undisturbed cores under ½-in. head of water
Very slow	1	Less than 0.05
Slow	2	0.05–0.2
Moderately slow	3	0.2 –0.8
Moderate	4	0.8 –2.5
Moderately rapid	5	2.5 –5.0
Rapid	6	5.0 –10.0
Very rapid	7	More than 10.0

12. Texture Index. One mappable characteristic which can be used to describe permeability is texture. The following arbitrary relationship between texture and permeability is used in the determination of soil drainability.

EMPIRICAL RATIO BETWEEN TEXTURE AND PERMEABILITY OF SOILS

Textures	Avg permeability		
	gal/day	cc/hr	m/day
Coarse sand	2,500	500	120
Sand	250	50	12
Fine sand	100	20	4.8
Very fine sand	50	10	2.4
Loamy sand	25	5	1.2
Sandy loam	5	1	0.24
Very fine sandy loam	2.5	0.5	0.12
Loam	1.0	0.2	0.048
Silt loam	0.5	0.1	0.024
Silty clay loam	0.25	0.05	0.012
Silty clay	0.05	0.01	0.0024
Clay	0.025	0.005	0.0012

SALINITY

The diagnosis and treatment of saline and alkali soils is a problem in soil chemistry, but because it is so frequently associated with areas needing drainage, especially in arid and semiarid regions, it is necessary for the drainage engineer to become familiar with this problem.

There must be a thorough and detailed study of the salinity problem of the drainage area. This should include a study of the salinity of the surface soils and of the groundwater.

Soil samples taken from boreholes made on the soil-survey grid should be analyzed for mineral content. A minimum of one sample for each square mile of the project area is suggested. In addition, spot checks should be made at intervals so as to be able to draw a map showing the location and degree of severity of saline and alkaline deposits.

Excessive quantities of mineral elements in the root zone of the soil inhibit plant growth. They must be leached downward and disposed of by the drain system.

Saline and alkaline soils have been separated into three groups, namely, (1) saline,

(2) saline-alkali, and (3) nonsaline-alkali. The following discussion is taken largely from U.S. Department of Agriculture Handbook 60, "Diagnosis and Treatment of Saline and Alkali Soils," 1954.

13. Saline Soils. The term saline is used in connection with soils for which the conductivity of the saturation extract is more than 4 mmhos/cm at 25 C and the exchangeable-sodium percentage is less than 15. Ordinarily the pH is less than 8.5.

Saline soils can usually be improved through leaching, as the soluble salts present will go into solution and be removed with the drain water. Leaching in areas of high precipitation is usually a natural process after subsurface drainage is established. In arid and semiarid regions it is necessary to supply irrigation water to accomplish this leaching. In summary, the reclamation of saline soils can usually be accomplished through some type of leaching without the addition of chemical amendments. Adequate subsurface drains are, of course, a prerequisite.

14. Saline-alkali Soils. The term saline-alkali is applied to soils for which the conductivity of the saturation extract is greater than 4 mmhos/cm at 25 C and the exchangeable-sodium percentage is greater than 15. These soils form as a result of the combined processes of salinization and alkalization. As long as excess salts are present, the appearance and properties of these soils are generally similar to those of saline soils. Under conditions of excess salts, the pH readings are seldom higher than 8.5 and the particles remain flocculated. If the excess soluble salts are leached downward, the properties of these soils may change markedly and become similar to those of nonsaline-alkali soils.

Drainage of these soils may require certain chemical amendments based on laboratory analysis of soil samples. Insofar as the engineer is concerned, the difficult problem with saline-alkali soils is their identification, as they may exhibit characteristics of both saline and nonsaline-alkali soils. As pointed out in the definition of saline-alkali soils, they may be flocculated because of the presence of excess salts and may have a permeability equal to or higher than nonsaline soils. This is often misleading and may give the impression that soils can be reclaimed through simple leaching. Actually this may not be the case because leaching will remove the soluble salts, thereby causing the soils to become strongly alkaline, and the permeability will be materially reduced.

15. Nonsaline-alkali Soils. The term nonsaline-alkali is applied to soils for which the exchangeable-sodium percentage is greater than 15 and the conductivity of the saturation extract is less than 4 mmhos/cm at 25 C. The pH readings usually range between 8.5 and 10. These soils frequently occur in semiarid and arid regions in small irregular areas, which are often referred to as "slick spots."

The treatment of nonsaline-alkali soils is different from that for saline soils as it may be impossible to leach the soil until after certain chemical amendments are added. Through alkalization, soil particles undergo certain physical changes. These changes tend to destroy the original soil structure and leave the soil as a deflocculated mass. Nonsaline-alkali soils have the consistency of tar or heavy machine grease, which is smooth and without texture. As alkalization progresses, the soil becomes less and less permeable. Strongly alkaline soils become virtually impermeable and impracticable to drain under most conditions.

It is highly important that nonsaline-alkali soils be recognized as such before attempting to establish subsurface drainage. This is important because these soils have lost some of their internal drainage characteristics and may not drain properly regardless of the type of drainage system installed. Where it is economically feasible to reclaim these soils, chemical treatment may be necessary to flocculate the soil particles and restore soil permeability before leaching and drainage. Some of the chemical amendments commonly used are calcium chloride, gypsum (calcium sulfate), sulfur, and sulfuric acid. The kind and amount of amendment applied must be based on recommendations following an analysis of representative soil samples.

16. Water Quality. A knowledge of the salinity of the groundwater in the drainage problem area is important because of the adverse effect of saline water on the growth and production of beneficial plants. In areas of good-quality groundwater, the solution to the drainage problem is largely a matter of lowering the water table below the root zone of the plants to keep excess water from interfering with normal plant-growth processes. Some latitude in the fluctuation of the water-table elevations is permissible.

In areas of saline groundwater, however, the water table not only must be lowered to a point well below the feeding zone of the plant roots but must also be kept from rising above that level so that evaporation and capillary forces will not concentrate the salts in the root zone. The presence of large amounts of harmful mineral elements in the root zone of the soil intensifies the drainage problem since steps must then be taken to drain not only the excess water initially present but also any additional quantities that must be applied to leach the salts out of the soil. The danger of losing essential plant nutrients in the leaching process further complicates the problem of devising effective drainage systems and measures.

WATER TABLES

The water-table survey will indicate the height, movement, and cyclic trend of groundwater levels. These data can be further analyzed to pinpoint the sources of excess water, the quantity, and the direction of the underground flow. If observations indicate artesian pressure from deep aquifers, relief wells and pumpage are usually necessary. Where rainfall contributes to the rise in water table some type of surface drain may be indicated. If seepage from an adjacent canal or reservoir can be detected but not controlled, an interceptor drain may solve the problem.

Records of water levels, maps of depths to water table, and other hydrologic data for past years are often available for many drainage problem areas. Such data, when correlated with current conditions, furnish clues to the cause of fluctuations in the water table. The plotting of water-table hydrographs in conjunction with data on precipitation, irrigation, runoff, effect of pumping, and other hydrologic phenomena provides a useful basis of analysis.

17. Observation Wells. There should be a grid of observation wells established at the beginning of any project study. This grid should consist of cased holes to a depth of 15 to 20 ft spaced at about one per square mile. Water-table observations should be carried on periodically, at sufficient frequency to obtain an adequate seasonal and annual hydrograph. The records for any given project area should be related and compared with hydrographs from other observation wells having long-term hydrographs.

18. Piezometers. A useful drainage-investigation tool is the groundwater piezometer, an unperforated small-diameter pipe so designed and installed that after it is driven or jetted into the ground, water can enter only at the bottom end.[1] The piezometer registers the hydrostatic pressure of the underground water at whatever level it is terminated. Since underground water moves from a point of high pressure to one of low pressure, the piezometer opens up a wide range of possibilities for investigating groundwater movement. With sets of piezometers installed at different depths and spaced at intervals the hydrostatic pressures of an entire soil profile may be determined, and seepage movement detected.

[1] Christiansen, J. R., Ground-water Studies in Relation to Drainage, *J. Am. Soc. Agr. Engrs.*, **24**, 339-342, 1943. Donnan, W. W., and J. E. Christiansen, Piezometers for Ground Water Investigation, *Western Construct. News*, **19**, 77-79, 1944.

SURFACE DRAINS

19. Design Criteria. All the data developed from the drainage surveys and investigations should be utilized in the design of both surface drains and subsurface drains. Surface drains are usually constructed as open ditches. The main outlet drain and its principal branches or laterals form the backbone of the drain system and they are usually installed as open unlined channels.

20. Location. The topography of the area is generally the controlling factor in the location of the main and lateral drains. Topography also influences the spacing of the laterals. For very flat areas, the laterals should be not more than ½ mile apart. In no case should the laterals be more than 1 mile apart. The open lateral thus provides an outlet for both surface and subsurface drain water. Property lines or government subdivision lines should be considered in determining the locations of the laterals. Drainage ditches in irrigated areas usually serve primarily to control surface and subsurface irrigation waste and seepage waters. Their location is often dictated by the location of the irrigation-canal system. Main outlet ditches may follow natural streams and provide channel capacity to handle flood runoff in addition to the drainage waters from irrigated lands.

21. Rate of Discharge. The rate of discharge is generally expressed in cubic feet per second per square mile of drainage area. Various empirical formulas have been developed for determining runoff into drainage channels (see Sec. 1, Art. 1).

22. Rational Formula. A formula developed by Ramser[1] for estimating storm-water runoff from agricultural areas is as follows:

$$Q = CIA$$

where Q = maximum rate of runoff, cfs
C = runoff coefficient dependent on topography, vegetation, etc.
I = rainfall intensity, cfs/acre, which corresponds to intensity, in./hr
A = watershed area, acres

General values of C runoff coefficient are as follows:

Kind of watershed	Slope %	Value of C
Cultivated gentle	0–5	0.40
Cultivated rolling	5–10	0.60
Cultivated hilly	10–30	0.72
Pasture gentle	0–5	0.25
Pasture rolling	5–10	0.36
Pasture hilly	10–30	0.42
Timber gentle	0–5	0.15
Timber rolling	5–10	0.18
Timber hilly	10–30	0.21

23. Southwestern Drainage Formula. A formula developed for conditions in the Southwestern United States[2] but which has been used in many other areas is as follows:

$$Q = CM^{5/6}$$

where Q = runoff, cfs
C = coefficient dependent upon the topography, soils, and land use
M = watershed area, sq miles

[1] Ramser, C. E., Runoff from Small Agricultural Areas, *J. Agr. Res.*, **34**(9), 1927.

[2] Open Ditches for Agricultural Drainage, Chap. 6, Sec. 16, "Soil Conservation Service National Engineering Handbook," U.S. Department of Agriculture.

Some examples of coefficients, which have been developed for specific areas, are as follows:

C = 125 for hill areas (maximum)
C = 75 for hill areas (minimum)
C = 45 for coastal area, cultivated land
C = 40 for delta area, cultivated land
C = 35 for western plains, cultivated land
C = 30 for improved pasture
C = 22 for rice land
C = 15 for range land

In irrigated areas the mains and laterals must have a capacity to remove rainfall runoff as well as excess irrigation water and inflow from tile drains. Where appreciable rainfall occurs, one of the above empirical formulas should be used to develop runoff design capacities. Where little or no appreciable rainfall occurs, capacities of 6-ft-depth open drains are seldom if ever exceeded. Studies made by the U.S. Bureau of Reclamation and others indicate that the overall yield of seepage into an open drain system aggregates about 0.10 to 0.15 cfs/sq mile of irrigated land.[1]

HYDRAULIC DESIGN

The actual hydraulic design of open drains with respect to capacity, permissible velocity, roughness factors, grade, side slopes, and bottom width is all adequately covered in Secs. 7 and 34. For the most part, open drainage channels are designed in the same manner as open irrigation canals. Some additional pertinent factors are as follows:

24. Grade.[2] The longitudinal slope or grade of a ditch is determined almost entirely by local topographic and soil conditions. The grade of a ditch must follow more or less closely the slope of the ground surface along the center line of the ditch, and its value is fixed within narrow limits by topographic conditions. Because of this fact, the grade is the first of the hydraulic elements entering into the design of a ditch which is considered.

It is impracticable to distinguish between the grades of mains, submains, and laterals, since these terms are relative, and the lateral ditches in a large drainage system may be larger than the main ditch of a small system. In any one system, however, the grade of the main ditch will usually be flatter than those of the laterals.

The elevation of the bed of the outlet stream gives a starting point for the grade line of the main ditch. A tentative grade is then assumed for the main which establishes tentative starting elevations for the submains. Tentative grades are then chosen for the submains, which in turn establish the elevations of the ends of the laterals. As the study progresses, the tentative grades will have to be modified somewhat in order to meet more satisfactorily the requirements of the other ditches. Even after these changes have been made, further adjustments may be necessary later when the size of channels and velocity of flow are considered. The nature of the soil through which a ditch is to be constructed also has a bearing on the grade line, since it may affect the depth of the ditch.

25. Depth. Ditches for agricultural drainage are usually 6 to 12 ft in depth. The depth of each lateral is first determined. The criterion is that each lateral must be of sufficient depth to serve as an outlet for the tile underdrains that are to discharge into it. The flatter the topography and the greater the spacing of laterals, the deeper will the laterals have to be. Thus depth and spacing of laterals are interrelated. The

[1] "Land Drainage Techniques and Standards," Reclamation Institute Series 520, U.S. Bureau of Reclamation.

[2] Discussion taken in part from Sec. 22, Drainage, by George W. Pickels, 1st ed., 1942.

laterals are the most important part of the drainage system. Each submain must be of sufficient depth to receive the discharges of the group of laterals that it serves. The depth of the submain, therefore, will be determined by either the longest lateral or the lateral from the flattest portion of the area.

Likewise, the depth of the main ditch is determined by the elevations of the bottoms of the submains at their ends. In very flat country, this may result in too low a grade for the main ditch. In this case, the best solution is to reduce the area served by a main ditch, *i.e.*, divide the total area to be drained into two or more parts and design an independent system of drainage for each part.

In muck and peat soils, deeper drainage channels are necessary than in other soils to allow for the subsidence that occurs when the soil is drained and cultivated. In the virgin muck soils of the Florida Everglades, it has been found necessary to make the laterals 8 ft deep in order to have a depth of 5½ ft 3 or 4 years after construction.

26. Spacing. It will rarely be necessary in agricultural drainage to place the lateral ditches closer than ½ mile. With this spacing no portion of the area will be more than ¼ mile from an outlet, and even if the ground is very flat a satisfactory underdrainage system can be designed. Where the natural surface slopes 5 to 10 ft/mile, a spacing of laterals of 1 mile is satisfactory. The mile has been used as the unit of spacing, since ditches are usually located on government section or quarter-section lines.

In situations where open lateral drains are designed to accomplish the entire dewatering of the problem area the spacing criteria should follow that prescribed for tile spacing (see Art. 39). In other words, one 6-ft-depth open drain is analogous to one 6-ft-depth tile line. It is equally effective but no more effective in drawdown of subsurface water than a tile line.

Generally speaking, open drains are not designed for this purpose except in coarse-textured soils since their installation at close spacings removes a considerable portion of the crop land from cultivation and their maintenance becomes a problem.

DRAINAGE STRUCTURES

See Sec. 34 for design criteria on chutes, drops, transitions, inverted siphons, flume crossings, and/or other types of structures employed in the development of a drainage system.

SUBSURFACE DRAINS

The various materials used for subsurface drains are clay and concrete tile, corrugated metal pipe, bituminous-fiber pipe, and plastic tubing. Clay and concrete tile come in 1-, 2-, or 3-ft lengths. Metal and fiber pipe, and plastic tubing are usually manufactured in 8-ft or longer lengths and must be perforated to permit entry of water to them. The following general design criteria for tile drains usually apply to all types of underdrainage.

27. Types of Tile Drainage Systems. The commonest type of tile drainage systems is shown in Fig. 1.[1]

The herringbone system consists of parallel laterals that enter the main at an angle usually from both sides. This system is adapted to fields where the main or submain lies in a slight depression. It may also be used where the main is located in the direction of greatest slope and better grades for laterals are obtained by angling the laterals upslope. The gridiron-tile system consists of parallel laterals located perpendicular to the main tile. It is used on flat, regularly shaped fields and on uniform soil.

The double-main system is a modification of the gridiron or herringbone systems

[1] Subsurface Drainage in Humid Areas, Chap. 4, Sec. 16, "Soil Conservation Service National Engineering Handbook," U.S. Department of Agriculture.

and is applicable where a depression, which is frequently a natural watercourse, divides the field where tile is to be installed. Placing a main on each side of the depression may serve to drain the waterway and provides an outlet for the laterals. Parallel mains are also used to reduce the size of the main.

A random system of tile is used where the topography is undulating or soils vary and fields contain isolated wet areas.

The interception system intercepts seepage moving down a slope.[1] The interceptor usually should be placed at about the upper boundary of the wet area as determined by drainage investigations.

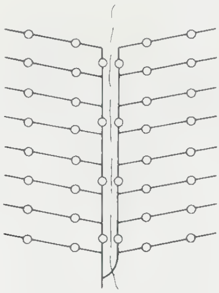

Fig. 1. A type of tile drainage system.

DESIGN CRITERIA

The design of a closed subsurface drainage system involves the determination of depth, spacing, and size of drain, together with an adequate outlet and appurtenant works. Depth and spacing are roughly proportional, depending on the permeability of subsurface materials. Generally, the greater the depth of drain the wider the spacing between drains; the choice of depth and spacing is often an economic consideration.

28. Depth. The depth of tile drains is often controlled by depth of the outlet system. Where this circumstance does not prevail, depth is determined by a combination of such factors as crop type, soils, drainable strata, and spacing. For best growth of ordinary crops in humid regions, the water table should be drained to at least $2\frac{1}{2}$ ft below ground surface. This would require a depth of drain of from 3 to 4 ft.

In arid areas of general high water table or where salts occur in the water and soil, drains should be relatively deep. It is necessary to maintain a water table at such a depth that water rising by capillarity from the water table will not reach the ground surface from which it can evaporate and deposit the dissolved salts. For medium-textured soils, the water table should be a minimum of about 4 ft, and for fine-textured soils about 5 ft. This means that for salt control, drains should be placed at least 6 ft in depth.

There is opportunity for crop diversification on many of the irrigated farms. Different crops have different rooting characteristics, with some rooting to shallow depths and some deeper, and ranging from 1 to 10 ft. Any curtailment of natural rooting will have an adverse effect on production. Since tile drains are relatively permanent they should be installed as deeply as possible to develop the deepest root area for any crop that may be grown. A drain cannot lower the water table below the depth to which the tile is laid. Tile laid above the water table will not intercept

[1] Donnan, W. W., Drainage of Agricultural Lands Using Interceptor Lines, *Proc. ASCE, J. Irrigation Drainage Div.*, **85**(IR1), 1959.

downward percolating water and no water will be collected until the water table has risen to the tile. Except in the immediate vicinity of the tile line the water table will always stand higher than in the tile.

The deeper the tile, the greater the tile spacing can be to obtain the same minimum depth of water table. In stratified soils it is advisable to place tile in the most permeable layer—provided, of course, this is below the depth to which the water table should be lowered, and within a depth that can be economically reached. Where stratifications are undulating or discontinuous, it may not be possible to place the tile in the more permeable layer since the tile must be on grade and continue to a point of discharge. In summary, it may be said that considering cost and soil conditions, tile should be placed as deeply as possible.

29. Spacing. Spacing between tile lines depends upon the texture of the soil and the depth of tile below the ground surface. Since water usually stands nearer the ground surface midway between drains, the depth at this point determines whether or not the drains are lowering the water table satisfactorily. Water usually moves through a coarse-textured soil more rapidly than it does through fine-textured ones. Therefore, drains can be spaced greater distances apart in coarse-textured than in fine-textured soils. Soil texture is generally used as a guide to the rate of water conductivity. In most cases it is a satisfactory guide but in others, where such things as the method of soil deposition may alter the conductivity, soil texture may be misleading. Differences may be detected by reliable investigations, as previously discussed.

In an irrigated area over a general high-water-table condition, with tile installed at 6- to 8-ft depths, drains may be placed 300 to 600 ft apart in sandy soils and 100 to 300 ft apart in clay soils.

30. Donnan Spacing Formula. Several theories covering the flow of water to tile drains have been proposed in recent years.[1] These theories have modified the approach of the drainage engineer toward the solution of many tile drainage problems. Considerable progress has been made toward the rational design of drainage systems using such theories.

Among these formulas is the one commonly known as the Donnan formula,[2] which is typical. The formula was developed for relief drains and is based upon certain barrier conditions. This is illustrated by the following expression:

$$S = \frac{4P(b^2 - a^2)}{Q_d}$$

where S = spacing of tile lines, ft
P = hydraulic conductivity or coefficient of permeability, gal/sq ft/day
b = distance from the average tile depth to barrier stratum at the mid-point between the tile lines, ft
a = distance from the average tile depth to barrier stratum, ft
Q_d = quantity of water to be drained, gal/ft/day

Where no barrier straum is present, a barrier should be assumed at a depth equal to twice the drain depth. Figure 2 is a sketch showing the above relationship.

The units for hydraulic conductivity or the coefficient of permeability P and Q_d can both be expressed in gallons per square foot per day or in cubic inches per square inch per hour in this formula without changing its validity.

The Donnan and other formulas require that the average effective permeability and barrier conditions be established by field investigations. The quantity of water to be drained Q_d is dependent upon a multitude of complex interrelationships of soil-

[1] van Schilfgaarde, Jan, D. Kirkham, and R. K. Frevert, Physical and Mathematical Theories of Tile and Ditch Drainage and Their Usefulness in Design, *Iowa State Univ. Res. Bull.* 436, 1956.

[2] Donnan, W. W., Model Tests of a Tile-spacing Formula, *Soil Sci. Soc. Am. Proc.*, **11**, 131–136, 1946.

water hydrology. All the various factors, such as rainfall, irrigation, slope, soil type, ponding time, waste disposal, crop, infiltration rate, evapotranspiration, and seepage in and out of the problem area, enter into the final determination of the amount of water which must be drained by the drainage facility. It is essential that a reasonable determination of this amount be made since it is a factor in the design of the facility.

Where precise criteria are lacking, the designer can arbitrarily take a percentage of the irrigation water applied for estimating Q_d. In humid areas the "drainage modulus" can be used to determine Q_d, quantity of water to be drained. The drainage modulus, or drainage coefficient, is the discharge of an underdrainage system, expressed in inches of depth of water which must be removed from the area in 24 hr. The drainage modulus is a measure of the maximum rate at which the water will move through the soil to the laterals. The proper drainage modulus for a specific section of

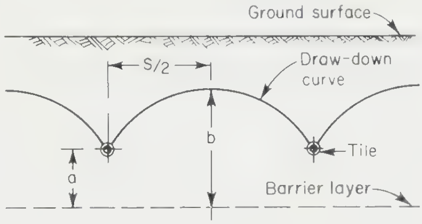

Fig. 2. Development of the Donnan spacing formula.

the country can be stated in general terms only, since it varies not only with the rainfall intensity but also with the soil texture, topography, and depth and spacing of laterals. The following general values, based on annual rainfall, will aid in the choice: for 30 in. of annual rainfall, a modulus of $\frac{1}{4}$ in.; for each additional 5 in. of annual rainfall, an additional $\frac{1}{16}$ in. in the modulus.

Where salt is a problem, research has indicated that at least 8 to 10 percent of the water applied must drain down and out of the root zone in order to maintain a favorable salt balance in the soil. Therefore, under these conditions, not less than 10 percent of the water applied would be considered as the amount to be drained.

31. Grade. Tile lines laid in most soils with little or no grade tend to silt up. On flat lands a minimum grade for tile lines should be established based on site conditions. These should be not less than the following limits, with a specific limitation on length, depending on soil conditions:[1]

Minimum Grades for Clay-Loam Soils

	%	Suggested max length for min grade, ft
4-in. tile	0.10	1,500
5-in. tile	0.07	2,000
6-in. tile	0.05	3,000

Under exceptional conditions, grades less than those recommended have been justified where the soil was cohesive and where the quality of installation and local experience indicated that lesser grades would give satisfactory performance.

[1] Subsurface Drainage in Humid Areas, Chap. 4, Sec. 16, "Soil Conservation Service National Engineering Handbook," U.S. Department of Agriculture.

Under many site conditions where, as an example, sandy or other noncohesive soils are present, the minimum allowable tile grade of laterals should be 0.30 percent or greater. However, for these situations, the permissible grade of mains may need to be set at a lower value and sediment traps installed so that the system design is feasible.

Although the maximum permissible grade for tile mains constructed with clay or concrete varies with different soils, special precautions should be considered if the

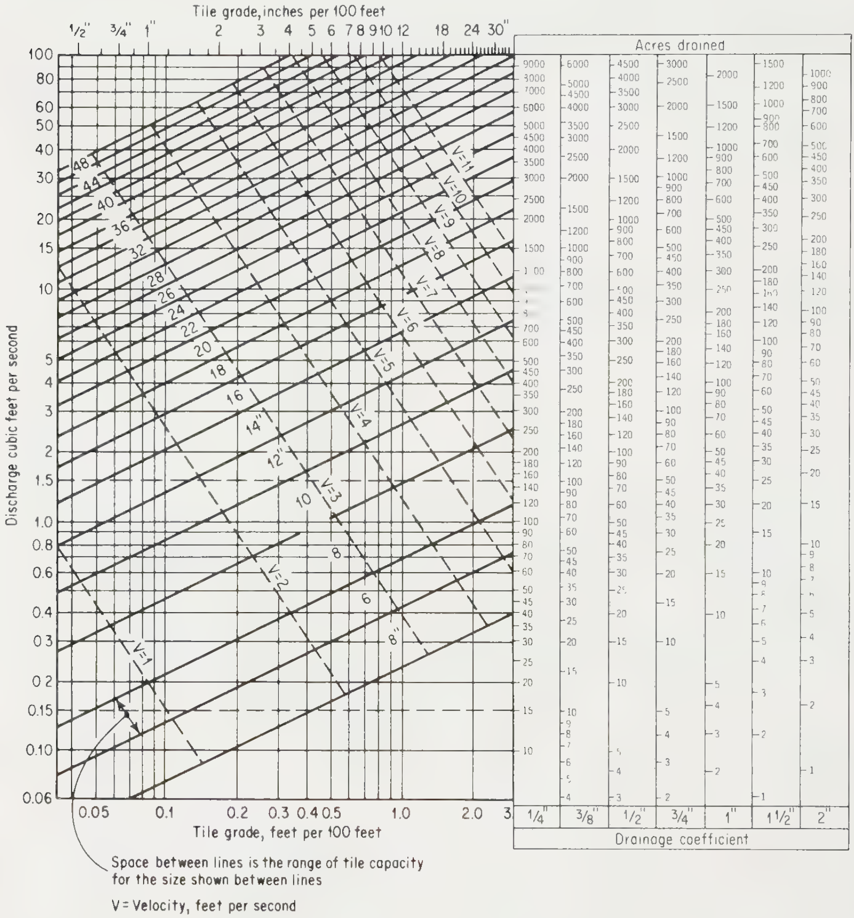

FIG. 3. Discharge diagram for tile drains based on U.S. Department of Agriculture formula.

grades exceed 2 percent. Tile laid in sand and in sandy-loam soil on grades more than 1 percent may cause trouble.

32. Yield from Tile Drains. The average "runoff" from tile-drain systems will vary depending on spacing, soil type, irrigation practice, rainfall intensity, and many other interrelated factors. For humid regions the tile-drainage chart (Fig. 3) may be used to compute flow in drain tile and required tile sizes.

For irrigated regions, yield from tile-drain systems can be estimated from the following criteria:[1]

Size of Area Drained, Acres	Average Yield from Area, cfs
0–40	0.4
41–80	0.7
81–999	0.7 plus 0.2 cfs for each 40 acres over 80 acres
1,000–3,000	5.0 plus 0.1 cfs for each 40 acres over 1,000 acres

DRAIN SIZE

Four-inch tile is the smallest tile in general use in the United States. The problems of maintaining an accurate grade and alignment and the possibility of some settlement encourage the use of a minimum size of tile to obtain a longer useful life of tile systems even though not required by capacity needs. High labor costs generally make it impractical to clean out small tile.

In designing tile systems for capacity, the size of the drain conduit is determined from its design flow, slope, and roughness. Manning's formula, $Q = 1.486R^{2/3}S^{1/2}A/n$, is commonly used to determine required size. In so determining size, R and A are those values for the design flow Q in the conduit at a depth not greater than 70 percent of the inside diameter or height of the conduit. Minimum recommended values of n for various conduit materials are

Conduit Material	Min Manning's n
Clay tile	0.011
Concrete tile and pipe	0.011
Vitrified clay pipe	0.011
Perforated plastic and bituminous fiber pipe	0.011
Lumber box drains	0.012
Perforated corrugated-metal pipe	0.021

MATERIALS USED

33. Clay Tile. ASTM Specification C4-62 currently provides for three grades of clay drain tile having average strengths per foot of length by three-edge bearing test for 4-, 5-, and 6-in. sizes: for "standard" clay drain tile, 800 lb; "extra-quality" clay drain tile, 1,100 lb; and for "heavy-duty" clay drain tile, 1,400 lb.

Perforated clay drain tile is covered by ASTM Specification C498-62T. In addition to the grades of tile given above, it includes the "extra-strength" drain tile having a minimum crushing strength of 2,000 lb/ft average for three-edge bearing test.

A hazard to clay drain tile is freezing and thawing action where frost penetrates the ground to depth of tile or where tile are exposed on the ground during the winter before installation. The absorption of water by tile is a valuable index of the resistance to freezing and thawing.

34. Concrete Tile. ASTM Specification C412-60 provides for three classes of concrete drain tile: standard quality (800 lb/ft average minimum strength), extra quality, and special quality (both 1,100 lb/ft). Special-quality concrete drain tile are dense tile designed for use in soils that are subject to corrosive acids or sulfates in the soil or soil water. These tiles are manufactured on special order to meet the requirements based on site conditions, and sulfate-resistant cement may be needed.

In Western irrigated areas where deeper drains are used, ASTM C118-60, Concrete Pipe for Irrigation or Drainage, is used to obtain a stronger tongue-and-groove pipe. Under this class of specification, pipes of 4, 5, and 6 in. diameter have average minimum

[1] Weeks, L. O., Drainage in the Coachella Valley of California, *Proc. ASCE, J. Irrigation Drainage Div.*, **85**(IR3), 1959.

supporting strengths of 1,200, 1,250, and 1,300 lb/ft, respectively. The tongue-and-groove construction protects pipe from settling out of line.

If concrete pipe may be used under acid or sulfate exposure conditions, samples for determining acid or sulfate concentration of the soil and soil water should be obtained.

35. Bituminized Fiber Pipe. Bituminized fiber pipe usually comes in 8-ft or longer lengths with the size and spacing of perforations optional to the purchaser. In laying, adjoining sections are joined by collars. One or more lengths of this pipe are used in many locations to protect the outlets of tile lines of short lengths.

ASTM Tentative Specifications D1861-61T and D1862-61T cover homogeneous and laminated-wall bituminized fiber drain and sewer pipe. These specifications may be modified if 800 lb crushing strength is adequate.

36. Metal Pipe. In the United States, metal pipe is used chiefly (1) for outlets for tile drains, (2) as a substitute for concrete or clay tile where minimum cover of soil is not available, (3) at road crossings where additional load-bearing capacity is required, (4) for use in auxiliary structures, and (5) for installation through pockets of quicksand or other unstable soils where a continuous pipe of high strength is required. Metal pipe is also used in other situations where strength, economy, and reliability justify use.

37. Sewer and Culvert Pipe. Sewer or culvert pipe may be specified for unusual load conditions occurring in deep wide trenches or where bell-and-spigot or tongue-and-groove pipes are needed to provide greater resistance to misalignment.

Imperfect sewer or culvert pipe classed as seconds in the trade may often be obtained at considerable saving in cost and may be satisfactory for drainage work. The use of such pipe should be limited to cases where the damage to the pipe is of a nature such as breaks in the bell end or minor cracks at the spigot end and where strength and soundness are ample for site conditions.

38. Plastic Pipe. Small-sized plastic pipe about 8 to 10 cm in diameter, laid with standard tile trenches to depths of about 1 m, is used extensively in the Netherlands and other areas. With in the past two years the use of 3-in.- and 4-in.-diameter, thick-walled, corrugated polyethylene drain pipe has come into use in the United States. This material is lightweight and durable and can be coiled into 400-ft lengths for transportation to the field. It is laid with an ordinary tile trenching machine to depths of 6 or 7 ft. Costs are competitive with clay or concrete tile.

The use of plastic liners for mole drains is in the process of development.[1]

39. Filter Materials. Closed subsurface drains should be installed with suitable filter material around the conduit. The purposes of placing filter material around the tile are to prevent sediment from entering the tile and to allow water to flow more freely into the tile. In most tile installations in the humid area of the United States, only the topsoil or selected permeable soils from the sides of the trench are placed around the tile, and tile are covered. This is called "blinding." However, before "blinding," the joints are covered, if required, with tar-impregnated roofing paper, glass-fiber filter, plastic guards, burlap, or other materials. This joint covering is usually laid around the upper two-thirds of the tile to prevent sediment from entering the lines.

Materials such as hay, straw, sawdust, wood chips, and corncobs are used on many installations. These are generally effective but for an indeterminate period. Observations of systems installed in western Washington, in organic soil, indicated that straw remained effective 6 to 11 years. At one site wood chips were only slightly decayed after 9 years in the ground. The availability of filter material, its cost, and extent of local successful experience usually determine the type used. In irrigated areas of the United States sand and gravel filters are generally used. The minimum thickness of filter material placed around the conduit is 3 in. Design criteria are

[1] Fouss, J. L., and W. W. Donnan, Plastic Lined Mole Drains, *J. Am. Soc. Agr. Engrs.*, **43**(9), 512–515, 1962.

available for filter material based on research by the U.S. Bureau of Reclamation and the Corps of Engineers, U.S. Army.

INSTALLATION OF SUBSURFACE DRAINS

Digging of the trench should start at the outlet end and proceed upgrade. The alignment of the trench should be such that the tile can be laid in straight lines or smooth curves. The trench width is often fixed by the width of available trenching machines. The trench width measured at the top of the tile may be equal to the outside diameter of the tile, plus about 0.5 ft. This clearance between the tile and the sides of the trench is necessary for proper bedding and blinding of the tile. It is very important that the bottom of the trench be cut accurately to grade and shape, and then the tile set to grade. If the trench is overcut, the depth should be sufficient to place gravel filter material at any place. It should be backfilled either with graded gravel or with pulverized soil and tamped sufficiently to provide a firm foundation. The bottom of the trench is then recut to grade and shape.

The bottom of the trench should be rounded so that the tile will be embedded in undisturbed soil for at least 60 deg of its circumference. Some tile-trenching machines shape the bottom of the trench as a part of trenching operations.

40. Joint Spacing. Laying the tile should begin at the lower end of the line and progress upgrade. Each tile should be turned until it fits correctly. A tight fit is required in noncohesive soils having a high percent of silt or sand. The gap may be about $\frac{1}{16}$ to $\frac{1}{8}$ in. for clay and clay-loam soils. However, local experience may indicate a wider spacing for peat and muck soils up to $\frac{1}{4}$- to $\frac{3}{8}$-in. spacing. Where large gaps occur between tile, as on the outer side of a curve, the joints should be covered by broken tile, plastic, etc.

Perforated pipe should be laid with the perforations on the underside of the line.

41. Laying Tile in Unstable Soil. Special construction methods should be used when tile are laid through unstable pockets of soil such as saturated fine sand. One method is to place stable soil, coarse hay or straw, tough sod, crushed limestone, or gravel in the bottom of the trench before laying the tile. Another method is use of a broad cradle to support the pipe. A third method is use of a tightly sealed sewer pipe, continuous pipe, including corrugated-metal pipe, or nonperforated bituminized fiber or plastic pipe.

PUMPING FOR DRAINAGE

Pumping for drainage falls into two categories. Low-lift drainage pumps are used to pump surface water to lower the water level behind a levee or to lift water out of a shallow sump. High-lift drainage pumps are installed in deep wells in a grid pattern for the purpose of dewatering a large contiguous area to effect a general lowering of the water table.

42. Low-lift Pumping.[1] The factors that determine the location of a pumping plant for a levee district are topography, nature of foundation, and proximity to towns. Generally, the ditch system is first designed in conformity with the topography and the pumping plant is located at the lower end of the main ditch. An exceptionally poor foundation for the building and pumping machinery at this point, however, may make a change of location necessary. The other factors may at times be the controlling ones.

43. Pumping Capacity. The rate at which the drainage water will have to be removed by the pumps depends upon the amount and distribution of rainfall, the size of the district, the nature of the soil, the quantity of water contributed by the higher lands outside the district, the storage capacity of the ditches, the amount of seepage under the levee, and the completeness of drainage desired.

[1] This discussion was taken primarily from Sec. 22, 1st ed.

The pumping capacity required is expressed in inches of depth of water over the entire drainage area which must be removed in 24 hr. The capacities of pumping plants in successful operation vary from 0.25 to 1.50 in. The average capacity of a number of plants on the Illinois River is 0.36 in. The rate of removal in terms of inches of depth in 24 hr is then converted into discharge in cubic feet per second. Most pump manufacturers rate their pumps for a discharge velocity of 10 fps, but as operated in practice this velocity is about 8 fps. With these data, the size of pump can be determined.

44. Types of Pumps. Centrifugal, rotary displacement, plunger, and sewer pumps have all been used, but the centrifugal pump is generally better adapted to drainage district pumping and is used almost exclusively at present.

Drainage pumping plants are operated only a small part of the time and rather intermittently. For a large part of the time, the pumps will operate at about one-third capacity. For this reason, it is desirable to have two or more small pumps rather than one large one. Where two pumps are used, one should have about twice the capacity of the other. Where three or more are required, they should be of the same size.

45. Inlet and Outlet Pipe. The suction lift of the pump should be as low as possible. Generally, the elevation of the floor of the pumping plant is about 1 ft above the highest elevation to which the water in the suction bay can rise during periods of excessive rainfall with the pumps not operating.

Suction pipes are generally of riveted steel, although reinforced concrete has also been used. They must be airtight, smooth on the inside, and as straight as possible. The lower end should be expanded so that the entrance velocity will be not more than 2 fps.

The discharge pipe should be gradually enlarged immediately after leaving the pump to about twice the area of the pump discharge opening, so that the discharge velocity will be not more than 5 fps. The end of the discharge pipe should be submerged.

The discharge pipe may pass either through the levee or over its top. The latter arrangement is preferable, since it eliminates danger of seepage through the levee along the pipe and prevents the water in the river from flowing back through the pump when it is not operating.

46. Power. Steam engines, electric motors, and internal-combustion engines are all used to operate pumps. Steam engines are found in all the older plants, but the newer ones use either electric motors or diesel engines. Each type has its advantages and disadvantages.

The water, or theoretical, horsepower developed by a pump at maximum head and rate of discharge can be computed from the equation

$$\text{Water hp} = \frac{62.5hQ}{550} = 0.1136hQ$$

in which h is the dynamic head in feet and Q the maximum discharge in cubic feet per second.

The brake horsepower required will be greater than the water horsepower and depends upon the efficiency of the pump. With a pump efficiency of 70 percent, the brake horsepower will be 1.43 times the water horsepower.

47. Operation. Drainage pumping plants are run only a small part of the time, generally 60 to 90 days a year. During the fall months, after the crops are harvested, the pumps are not used. During the winter, the pumps are operated occasionally to remove the water that accumulates during winter storms. In the late winter and early spring, the pumps are operated continuously, not necessarily at full capacity, to remove the water from the saturated soil and to place the soil in condition for early plowing and planting. During the latter part of this period, the pumps will be run more or less intermittently, and it is at this time that the advantage of gasoline engines or electric motors is most apparent. During the growing season, pumping will be required after each storm period to keep the groundwater at the desired elevation. At this time, the full capacity of the plant may be needed.

48. Pumping from Wells for Drainage. Drainage by pumping from wells is usually practiced in irrigated areas. Under some conditions, pumping groundwater to provide land drainage is an effective method of lowering a high groundwater table and reducing salinity hazards. Careful engineering investigations should precede the installation of wells to ensure the success and economy of the project. The following conditions singly or conjunctively contribute to the use of wells for drainage:

1. Large areas of flat lands with extensive high water table and salinity problems
2. Well-defined contiguous permeable aquifers underlying the wet areas
3. Aquifer deep enough to permit an efficient well
4. Groundwater under artesian pressure
5. Groundwater having good quality suitable for irrigation use with or without mixing with other irrigation waters
6. Electric power available at reasonable cost

It is desirable to investigate the feasibility of drainage by pumping from one or more test wells if there is a possibility that the method will succeed. In areas where the method has proved successful it has solved the drainage problems effectively and eliminated the need for open and closed subsurface drains to control the water table. In most instances the drain water is used to supplement the supply of irrigation water.

In some areas it is possible to determine subsurface conditions from logs of existing wells. In other areas deep borings, often to depths of 100 to 200 ft, are necessary to explore underground aquifers. Nearly always it is advisable to operate one or more test wells at capacity and make observations of the rates of pumping and the drawdown by lines of observation wells radiating from the test well. If the well produces a significant drawdown at distances from 300 ft to ½ mile from the well, the method of drainage by pumping deserves additional study, especially if there is a use for the pumped water.

The actual design and construction of wells, including well screens, gravel treatment, and other related items, has the same criteria as for an irrigation water-supply well (see Sec. 35).

49. Spacing. The radius of influence of a drainage well will depend on the soil strata, rate of pumping, and other related factors. It is not unusual to find radii of 1,000 to 4,000 ft around a pumped well. The well spacing should be less than twice the radius of influence or drawdown cone of depression around the well. Drainage wells should be placed in a grid, and there should be a sufficient number of wells in the grid so as to command an extensive contiguous area. The spacing and location might be dictated by location of power supply or the location of disposal facilities for the pumped water. A grid of 1-mile spacing for 200-ft-depth gravel-packed wells having a 3-cfs pumping capacity has been used with success.

Bibliography

Roe, Harry B., and Q. C. Ayres, "Engineering for Agricultural Drainage," McGraw-Hill Book Company, New York, 1954.

Israelson, O. W., and Vaughn E. Hanson, "Irrigation Principles and Practices," John Wiley & Sons, Inc., New York, 1962.

White, Gilbert F., Editor, "The Future of Arid Lands," American Association for the Advancement of Science, Publication 43, 1956.

Luthin, James N., Editor, "Drainage of Agricultural Lands," American Society of Agronomy, 1957.

SECTION 40

SEWAGE QUANTITIES, SEWERS, AND PUMPING STATIONS

By Samuel A. Greeley,* William E. Stanley, and Donald Newton

INTRODUCTION

This section covers the hydraulic aspects of the design of sanitary and storm-water sewers. The engineer, in determining the best sewer design for a specific project, must also consider other factors. An early decision must be reached between a combined system of sewers, which would carry both sewage and storm water, and two separate systems of sewers in which sewage and storm water would be carried in separate conduits, designated as *sanitary sewers* and *storm sewers*, respectively.[1,†] Engineering practice and state regulatory codes tend toward separate sewer systems. In some cases, local considerations and costs require that combined sewers be designed or continued in use. Two major factors favoring separate sewer systems are the effect of sewage overflows, during heavy rains, and the lesser costs of sewage-treatment works. Conclusions as to the type of sewer system to be installed are properly based on the extent and character of existing sewers, the topography, the geographic location, the relative elevations of sewers and waterways, the extent of sewage treatment, and costs, both present and future.

SEWAGE QUANTITIES

1. General. Domestic sewage comprises the soiled water of a community and such groundwater as infiltrates into the sewers. It is important, therefore, to determine the tributary population, the portion of the water consumption that is discharged into the sewers, and a reasonable estimate of the infiltration. Also sewers generally carry some commercial and industrial waste waters, which amounts must also be determined.

2. Design Period. Sewers should be designed with a capacity sufficient to provide for some future development, the extent of which depends upon local considerations and the character and use of the sewers.

Generally, lateral and submain sewers should be designed for the anticipated ultimate development of the area; whereas the capacity of main sewers, outfalls, and intercepting sewers should be based upon estimates of developments 40 or 50 years in the future. Another procedure, sometimes useful, is to consider what capacity the present population might reasonably undertake to provide for future growth. Some typical data (Table 1) from trunk-line sewer-design experience indicate ratios of future to present population ranging from 1.4 to 3.7, with an average of about 2.3. Similar data for capacity of sewage-treatment works are given in Table 2.

3. Area Development. Sewer design should include a consideration of the present needs and probable future expansion of the study area. Older portions of

* Deceased.

† Superior numbers refer to items in the Bibliography at the end of this section.

existing cities are experiencing population and sewage-quantity changes as residential areas are redeveloped with apartment-type dwelling units or are replaced by expanding commercial and industrial areas.

Large land areas near population centers may be developed as complete community units with readily predictable future expansion plans. Studies for sewerage development of larger metropolitan areas may include several areas of these community types of development with many intermediate variations. A reasonable amount of capacity should be provided in the main sewer lines to take sewage from the likely

TABLE 1. POPULATION INCREASES FOR WHICH TRUNK-LINE SEWER CAPACITY HAS BEEN PROVIDED AT VARIOUS PLACES

City	At time of design	Design basis	Ratio, population basis of design to population at time of design
Appleton, Wis	27,000	58,000	2.15
Baton Rouge, La	43,700	89,125	2.04
Buffalo, N.Y	600,000	1,100,000	1.83
Cranston, R.I	53,000	90,000	1.70
Decatur, Ill	43,818	120,000	2.74
District of Columbia	1,406,000	1,925,000	1.37
East Bay Municipal Utility District, Calif	574,000	884,900	1.54
Eau Claire, Wis	30,000	90,000	2.33
Elgin, Ill	28,260	70,000	2.48
Evansville, Ind	105,000	225,000	2.14
Knoxville, Tenn	160,000	350,000	2.18
Lexington, Ky	60,000	156,000	2.60
Madison, Wis	137,600	500,000	3.64
Milwaukee, Wis	414,000	862,000	2.08
Oshkosh, Wis	40,000	70,000	1.75
Greater Peoria Sanitary District, Ill	133,000	335,000	2.52
Richmond, Va	248,900	667,000	2.68
Rockford Sanitary District, Ill	185,000	404,700	2.18
Spokane, Wash	134,800	223,000	1.65
Springfield, Ill	62,000	193,000	3.12
Tampa, Fla	164,696	335,000	2.04
Tullahoma, Tenn	6,700	25,000	3.73
Westchester County, N.Y., Mamaroneck District	73,000	130,000	1.78
Westchester County, N.Y., Yonkers District	359,700	708,000	1.97

extensions of sewered areas. Table 3 shows illustrative data on the extensions of area for which provisions were made in a number of comprehensive sewerage projects.

The areas within a city may be classified with regard to their effect upon sewage quantities as follows:

1. Residential
   a. Light residential, single houses
   b. Heavy residential, multiple dwellings and apartment houses
2. Commercial
3. Industrial
4. Public use: parks, playgrounds, cemeteries, etc.

Zoning regulations aid materially in anticipating future developments, but they are sometimes modified, generally at the expense of the single-home residential areas,

TABLE 2. POPULATION INCREASES FOR WHICH SEWAGE-TREATMENT PLANTS HAVE BEEN DESIGNED AT VARIOUS PLACES

City	Population		Ratio, population basis of design to population at time of design
	At time of design	Design basis	
Albany, N.Y.	101,000	150,000	1.49
Appleton, Wis.	46,300	71,000	1.54
Austin, Minn.	26,000	43,000	1.65
Boston, Mass.	1,447,000	1,701,500	1.17
Decatur, Ill.	62,500	72,500	1.16
District of Columbia	1,406,000	1,791,000	1.27
East Bay Municipal Utility District, Calif.	574,000	716,900	1.25
Fitchburg, Mass.	42,000	55,000	1.31
Houston, Tex.	434,000	776,000	1.79
Indianapolis, Ind.	350,000	500,000	1.43
Knoxville, Tenn.	160,000	269,500	1.68
Lexington, Ky.	60,000	114,000	1.90
Madison, Wis.	137,600	210,000	1.58
Miami, Fla.	230,000	330,000	1.43
Nassau County, N.Y.	470,000	570,000	1.21
Greater Peoria Sanitary District, Ill.	133,000	258,000	1.94
Richmond, Va.	248,900	330,000	1.33
Rochester, N.Y.	250,000	438,000	1.75
Rockford Sanitary District, Ill.	185,100	308,600	1.67
Spokane, Wash.	150,000	176,000	1.18
Springfield, Ill.	58,300	90,000	1.55
Syracuse, N.Y.	269,000	336,000	1.25
Tampa, Fla.	164,700	260,000	1.58
Westchester County, N.Y., Mamaroneck District	73,000	105,000	1.44
Westchester County, N.Y., Yonkers District	359,700	505,000	1.40
Worcester, Mass.	175,000	200,000	1.14

TABLE 3. EXTENSION OF AREA FOR COMPREHENSIVE SEWERAGE DEVELOPMENTS (AREAS IN ACRES)

City	Incorporated	With future extensions	Ratio
Appleton, Wis.	13,800	23,500	1.70
Boston Metropolitan District Commission, Mass.	62,165	89,800	1.44
East Bay Municipal Utility District, Calif.	35,569	46,221	1.30
Knoxville, Tenn.	22,000	55,000	2.50
Madison, Wis.	40,800	93,000	2.28
Metropolitan Dade County, Fla.	69,000*	297,000	4.20
Greater Peoria Sanitary District, Ill.	18,459	33,198	1.80
Richmond, Va.	17,483	46,606	2.68
Rockford Sanitary District, Ill.	27,000	70,000	2.60
Spokane, Wash.	8,990	18,237	2.02
Tampa, Fla.	29,591	47,387	1.60

* Estimated sewered area by 1970.

when there is a need for more extensive commercial, industrial, or apartment-house districts.

Some indication of the relative proportions of urban areas likely to be devoted to various uses is furnished by the typical data in Table 4.

4. Population Forecasts. The *present* population is necessary as a basis for forecasts and for determinations of the present population distribution and density of development. When the studies are undertaken sometime after a census year, it may be desirable to make an estimate of *present* population using locally available indexes of growth. School enrollments, school censuses, and utility customer information are frequently available and useful in making such population estimates for noncensus years. Table 5 illustrates the use of various indicators in estimating population.

TABLE 4. PERCENTAGE OF TOTAL LAND AREAS ALLOCATED TO VARIOUS USES

City	Residential	Industrial	Commercial	Parks and others	Undeveloped
Appleton, Wis	54.4	6.9	5.8	18.7	14.2
Austin, Minn	65.7	4.8	5.0	8.5	16.0
Chicago, Ill	29.9	15.4	5.6	35.0[a]	14.1
Knoxville, Tenn	87.7	10.7	1.6	[b]	[b]
Los Angeles, Calif	49.5	5.3	5.5	39.7[c]	
Madison, Wis	24.3	4.1	3.7	41.9[d]	26.0
Nassau County, N.Y	42.6	2.7	2.2	26.7[e]	25.8
Greater Peoria Sanitary District, Ill	62.5	11.7	5.3	13.5	7.0
Richmond, Va	83.5	7.9	4.6	4.0	[b]
Spokane, Wash	82.1	12.0	4.9	[b]	[b]
Tampa, Fla	34.0	3.8	3.0	25.0[f]	34.2
Medellín, Colombia	25.2	2.4	1.5	6.7	64.2
Panama City, Republic of Panama	11.7	0.1	0.9	10.1	77.2
São Paulo, Brazil	29.8	1.9	2.2	3.1	63.0

[a] Includes streets and parkways, 25.1 percent.
[b] Included in other categories.
[c] Includes vacant.
[d] Includes streets and parkways, 15.4 percent.
[e] Includes streets and parkways, 11.9 percent.
[f] Includes streets and parkways, 19.9 percent.

Several bases have been used to forecast the future growth of cities from past population records. Some are as follows:

1. A uniform percentage rate of increase per decade for future growth based upon the rate of growth between recent census periods.
2. An arithmetical increase in population per decade or per year.
3. A graphical extension of the curve of past growth into the future.
4. A graphical comparison with the growth of other similar but larger cities after the date at which their population was the same as that of the city under consideration.
5. A decreasing percentage rate of increase for each decade in the future. This is particularly applicable to larger cities.

The method of graphical comparison has been, perhaps, the most generally used, but it is frequently advisable to compare the results obtained by several procedures. A number of procedures are described in the literature.[2,3,4,5]

Local conditions that may have been responsible for peculiar changes in past growth or that are likely to affect future growth in any unusual way should be given careful study. Consideration should also be given to the relative growth of other nearby cities and to the current trend of birth and mortality rates. It is sometimes useful to represent the probable future growth by two limiting lines on the population curve, as illustrated in Fig. 1.

5. Metropolitan Areas. The metropolitan area around and including larger cities is being more generally considered as the municipal unit for study and design of sewers and sewage disposal. The 1960 Federal Census report and statistical supplements include population distribution and area data for a number of metropolitan areas. The probable future areal expansion is a factor to consider in the design of major sewer systems. Limited data, obtained from a number of regional-plan studies, are shown in Table 3.

The ratio of the central-city population to the metropolitan-area population has been declining (Fig. 2). Extension of the rate of decline provides a useful basis for

TABLE 5. VARIOUS ESTIMATES OF POPULATION AT TIME OF SEWERAGE STUDY FOR SHEBOYGAN, WIS.

Basis	Index No.	Population estimate factor	Estimated population
School census	11.788	3.33	39,200
School enrollment	7.443	5.10	37,900
Water services	11.173	3.54	39,600
Gas services	12.872	3.14	40,400
Power and light services	11.797	3.28	38,700
Telephones	9.015	4.35	39,300
Chamber of Commerce estimate	......	....	42,408
Telephone Company commercial survey (based on past growth)	......	....	37,400
Adopted estimate	......	...	40,000
U.S. Census (made 1 year later)	......	....	39,251

predicting the future population of the metropolitan area. Population forecasts may be made for the individual communities by the foregoing listed procedures.

6. Population Distribution. As a basis for estimating sewage quantities for various sewers, the area under study should be subdivided into sewer districts and subdistricts, with boundaries determined largely by topography and by artificial developments of the city, and the present and estimated future populations should be distributed into the several districts. Distribution of the present population may be estimated by obtaining the number of residences in the several districts from fire insurance maps, aerial photographs, and actual field counts of houses, by the registration of voters by precincts, or by recent census counts by enumeration districts. Large community units, developed from raw land, are generally planned to such a degree that future population distribution is not difficult to predict, though property sales and hence the rate of growth may be.

Based upon a study of such factors as present population densities, type of development, zoning regulations, and any indicated migration of population from one district to another, the future density can be estimated for each district.

The population of various types of districts tends to approach maximum densities, approximating 15 to 20 persons per acre for light residential (single-residence) areas, 50 per acre for small-apartment-house districts to more than 100 per acre for multistoried developments, and ranging from 10 to 30 per acre for large commercial and industrial districts. Average population densities for a number of large cities are given in Table 6.

7. Capacity Factors. The distribution of future population into sewer districts is less certain than the population estimate for the entire city. This uncertainty is less (1) for larger districts than for smaller districts and (2) for densely populated

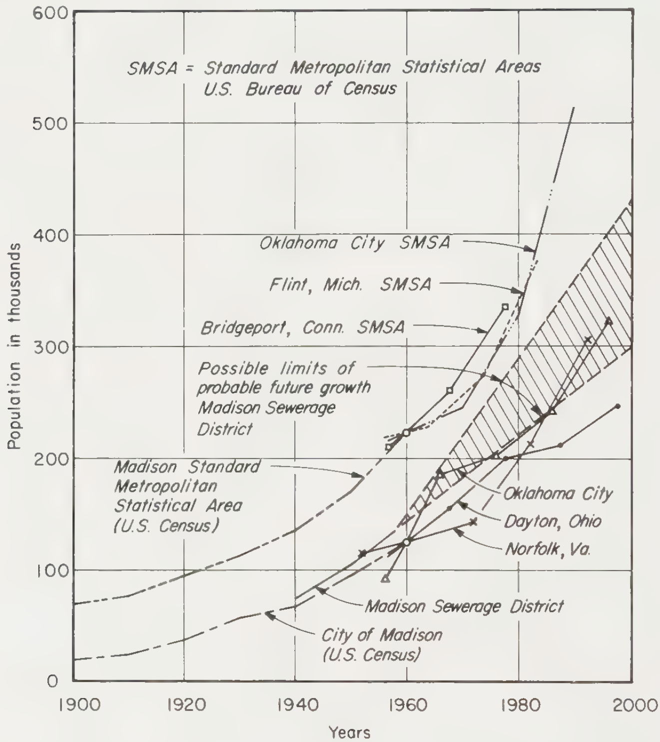

FIG. 1. Estimated population for sewerage district, Madison, Wis.

districts than for sparsely developed districts. Some allowance should be provided in the computed capacity of main and submain sewers to cover such uncertainties of population distribution. In practice, this may be done by multiplying the estimated future population for a given area by a capacity factor, ranging from 1.0 to 2.0 (Fig. 3), to obtain a figure that may be designated as the basis of design population, which is then multiplied by the selected per capita flow to obtain the rate of sewage flow for which sewer capacity should be provided.

8. Designation of Sewage-flow Rates. Unit domestic sewage quantities are frequently stated in terms of gallons per capita per 24 hr (gcd). Thus it is convenient to state total flow rates in terms of million gallons per 24 hr (mgd). However, it is rather a general practice to state capacities of pumps in gallons per minute (gpm) and to express storm-sewage flows in cubic feet per second (cfs). These terms

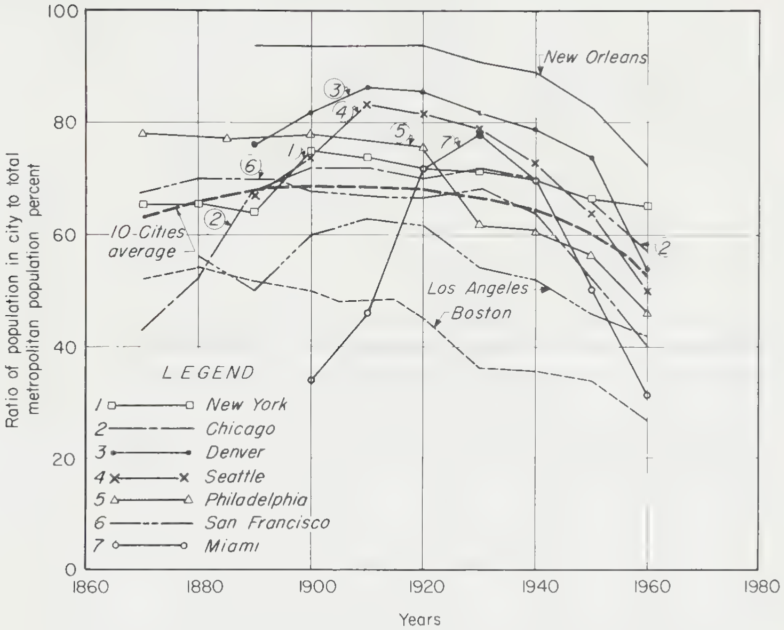

FIG. 2. Population data, ratio of city to metropolitan population.

TABLE 6. POPULATION-DENSITY COMPARISON*

Municipality	Population	Area, acres	Population density, persons per acre
New York, N.Y.	7,781,984	201,660	38.6
Chicago, Ill.	3,550,404	143,490	24.8
Los Angeles, Calif.	2,479,015	291,070	8.5
St. Louis, Mo.	750,026	39,040	19.2
New Orleans, La.	627,525	127,230	4.9
Minneapolis, Minn.	482,872	36,160	13.4
Seattle, Wash.	557,087	56,640	9.8
Denver, Colo.	493,887	45,440	11.9
Atlanta, Ga.	487,455	82,050	5.9
Portland, Ore.	372,676	43,010	8.7
Miami, Fla.	291,688	21,880	13.3
Tulsa, Okla.	261,685	30,590	8.6
Richmond, Va.	219,958	23,680	9.3
Albuquerque, N.M.	201,189	35,970	5.6
Salt Lake City, Utah	189,454	35,900	5.3
Nashville, Tenn.	170,874	18,560	9.2
Lincoln, Nebr.	128,521	16,260	7.9
Canton, Ohio	113,631	9,150	12.4
Peoria, Ill.	103,162	9,730	10.6

* 1960 Census data.

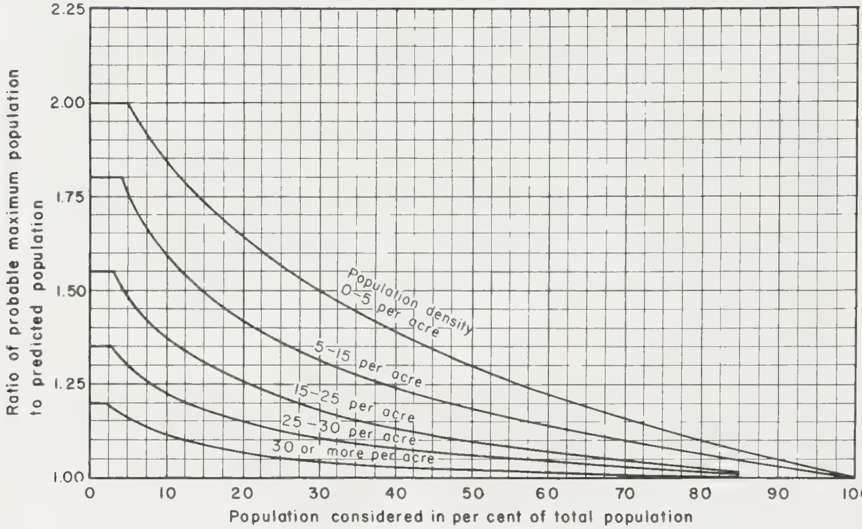

FIG. 3. Capacity factors for unequal population development.

may be converted from one to another by the following factors:

To change from	Multiply by	Or divide by
gpm to mgd	0.00144	694
gpm to cfs	0.00223	449
mgd to gpm	694	0.00144
mgd to cfs	1.55	0.646
cfs to gpm	449	0.00223
cfs to mgd	0.646	1.55

9. Computation of Sewage Quantities. Estimates of probable future sewage flows may be based upon one or more of the following items:

1. Water consumption from public and private sources with a deduction for water that does not reach the sewers and an addition for probable infiltration
2. Short-term records of sewer gagings
3. Long-term records of sewer gagings
4. Arbitrarily selected per capita sewage-flow rates based upon experience elsewhere
5. The tributary area and a unit per acre allowance for the sewage flow based upon experience elsewhere

The first method is perhaps the most commonly used. Long-term gagings give the most reliable results but are frequently not available. In estimating future sewage flows, the available records of water or sewage quantities should be related to the actual present or past population to which the quantities apply in order to obtain per capita quantities for use with the future population. Total water consumption as routinely reported often includes only the public water supply. Localities with private unreported water supplies or large infiltrations of groundwater into

TABLE 7. RATIO OF SEWAGE FLOW TO WATER PUMPAGE IN VARIOUS CITIES

Place	Avg Sewage Flow, % of Avg Water Pumpage*
Appleton, Wis	178
Knoxville, Tenn	189
Sioux Falls, S.D	205
Carol City, Fla	75
Honolulu, Hawaii	80
Nassau County, N.Y	102
Westchester County, N.Y., Yonkers District	95
Tullahoma, Tenn	222
Richmond, Va	128
District of Columbia	89
Syracuse, N.Y	131
Lexington, Ky	114

* Data at time of studies, various years, 1948 through 1959.

the sewers may have a total sewage flow greater than the recorded total water consumption. The nonuniformity of relative average sewage flow and water consumption is illustrated for representative cities by Table 7 and by variance in per capita data for a large city in Fig. 4.

In a study of water-supply quantities as related to sewage flows, consideration should be given to the seasonal, daily, and hourly variations as well as the yearly average rate in gallons per capita per day. All water supplied to a community may not be returned to a sewer. The yearly average per capita water-consumption rates differ widely for various cities (see Table 8).

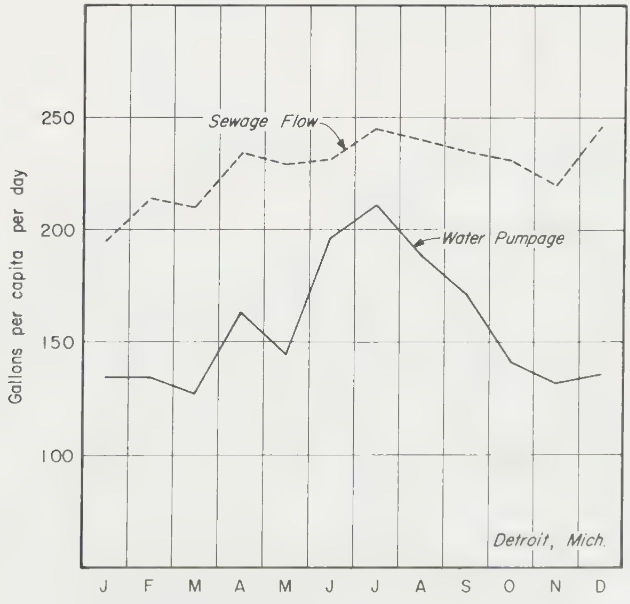

FIG. 4. Monthly variation in water pumpage and sewage flow rates.

TABLE 8. AVERAGE YEARLY TOTAL WATER-CONSUMPTION DATA

City	Population supplied	Water supply, gcd*
Chicago, Ill. (city)	3,550,000	255
Chicago, Ill. (suburbs)	873,000	141
Detroit, Mich	3,138,850	154
East Bay Municipal Utility District, Calif	1,000,000	157
Denver, Colo	612,000	215
Honolulu, Hawaii	422,000	154
Long Beach, Calif	326,000	144
Tulsa, Okla	292,000	149
Miami, Fla	312,000	148
Little Rock, Ark	199,900	106
Flint, Mich	196,000	162
Erie, Pa	160,000	230
Pasadena, Calif	137,100	201
Dubuque, Iowa	57,000	73
North Miami, Fla	47,000	111
Holland, Mich	18,360	172
South Haven, Mich	7,000	183

* Data for 1960 (about) including total supply to municipal users—domestic, commercial, and industrial.

The hourly and daily variations of the flows in sewers are so affected by infiltration and other factors that frequently during wet seasons there is little relation between the sewage flow and the water consumption. This is illustrated by a series of careful gagings of sewers at Springfield, Ill. (Fig. 5).

There is a tendency for per capita average daily water consumption to increase. The following data for 16 cities in Massachusetts, ranging in present population

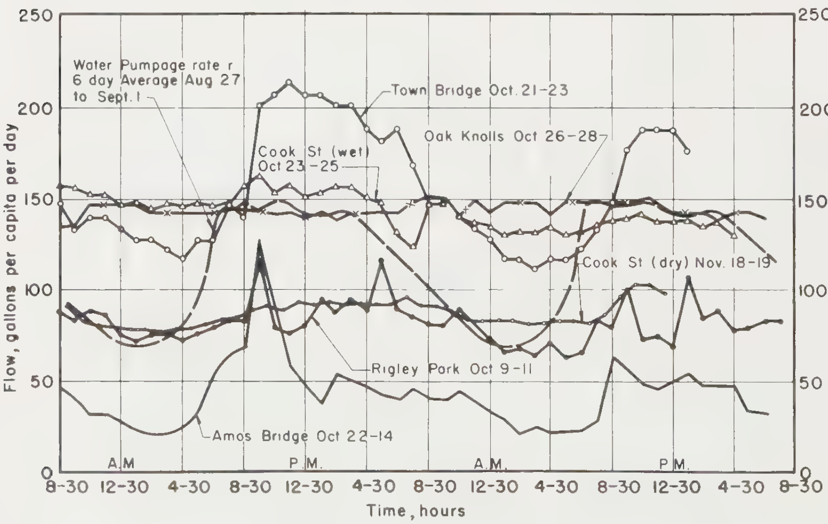

FIG. 5. Sewage gaging, Springfield, Ill.

from 3,000 to 150,000, illustrate the increase in water use and the wide variation in per capita usage between cities.

Period	Avg daily consumption, gcd (data from 16 cities)		
	Avg	Max	Min
1875–1910	46.6	129	16
1956–1958	127.4	242	55

10. Sewer Gaging and Sewage-flow Records. In the absence of the more reliable long-term records of measured sewage flows, it is sometimes desirable to secure approximate flow data from short-term gagings. These gagings may be made by installing weirs in selected manholes and making measurements at intervals of 1 hr or less over a period of a few days. Less accurate methods make use of floats or dye to indicate the time of travel between manholes, the flow being computed from the velocity thus obtained and the depth of flow found by careful measurement.

Such short-term records must be used judiciously and with due regard to groundwater elevations and rainfall and runoff conditions just preceding and during the period of measurement. Frequently the flows during a wet season have been as much as twice the dry-weather flow, as indicated by the following typical results of sewer gagings.

City	Ratio Wet-season to Dry-season Sewage Flow
Bloomington, Ill	2.0
Decatur, Ill	1.5
Oklahoma City, Okla	1.7
Toledo, Ohio	1.4
Urbana-Champaign, Ill	2.0

Tables 9 and 10 show some data on average domestic sewage-flow rates for various cities. In general, the yearly average sewage flows range from 125 to 250 gcd for larger cities to as low as 50 to 80 gcd for smaller cities or for the less congested residential areas in larger cities.

11. Sewage-flow Variations. The seasonal, daily, and hourly variations in sewage flow for typical locations are illustrated by Figs. 6 to 8. Also, Fig. 9, based on studies of sewage flows at Urbana-Champaign and Decatur, Ill., indicates the number of times each year the sewage flow equals, or remains above, a given flow rate. In Fig. 10, data are given on the percentage of time various sewage-flow rates are equaled or exceeded. The latter curves may be based on hourly or daily flow records, preferably hourly, expressed in terms of the yearly average rate of flow, and are frequently designated as flow-duration curves.

Data from extensive sewer gagings at Minneapolis–St. Paul, Minn., relating to the hourly variations in sewage flows are given in Fig. 11 for domestic or residential areas, industrial areas, and a composite curve for all areas. It will be noted that the general effect of industrial sewage and infiltration is to reduce the hourly variations somewhat.

The hourly variations of domestic-sewage flow in terms of the yearly average daily rates are indicated by Fig. 12 for flows in the Pasadena main outlet sewer.

TABLE 9. ACTUAL YEARLY AVERAGE SEWAGE-FLOW RATES IN VARIOUS CITIES

City	Tributary population	Avg sewage flow	
		mgd	gcd
Detroit, Mich	2,634,000	619.4	235
Philadelphia, Pa	1,089,000	150.0	138
Minneapolis–St. Paul, Minn	1,061,000	158.2	149
San Francisco, Calif	770,000	71.4	101
East Bay Municipal Utility District, Calif	635,000	60.8	96
Buffalo, N.Y	615,000	126.0	205
Cincinnati, Ohio	500,000	72.5	145
Winnipeg, Man	432,900	39.8	92
Tampa, Fla	196,200	21.1	107
Gary, Ind	170,000	30.09	177
Madison, Wis	137,600	19.07	138
Alexandria, Va	101,700	9.27	91
Fitchburg, Mass	42,000	3.87	92
Eau Claire, Wis	37,990	3.98	105
North Miami, Fla	30,030	5.55	178
Boise, Idaho	29,700	6.1	205
Walla Walla, Wash	26,000	6.1	234
Painesville, Ohio	16,000	1.9	119
Lexington, N.C	15,700	1.0	64
Coral Gables, Fla	15,500	3.0	130

TABLE 10. ESTIMATED QUANTITIES OF DOMESTIC SEWAGE IN VARIOUS CITIES

City	Year estimated for	Tributary population	Quantity, gcd (design)
Tampa, Fla	2000	300,000	50–80
Westchester County, N.Y	1985	105,000	103
	2000	130,000	110
Houston, Tex	1970	776,000	88
Minneapolis–St. Paul, Minn	1980	1,454,000	65
	2000	1,557,000	75
Dade County, Fla	2000	3,692,000	80
Richmond, Va	2000	660,000	60
North Va. metropolitan area	1970	2,432,000	70
Washington Suburban Sanitary District	2000	1,925,000	65
Honolulu, Hawaii	1975	400,000	70
Baltimore, Md., Design Manual	....	....	75

These data include very little industrial sewage but reflect the effect of occasional rains, although, in general, the normal amount of groundwater infiltration into the Pasadena sewers was quite small because of the low rainfall.

12. Maximum Rates of Flow. Sewers must be designed for maximum rates of flow, which usually are obtained most conveniently by applying suitable ratio factors to the average sewage quantities. Frequently the term "peak rates" is used instead

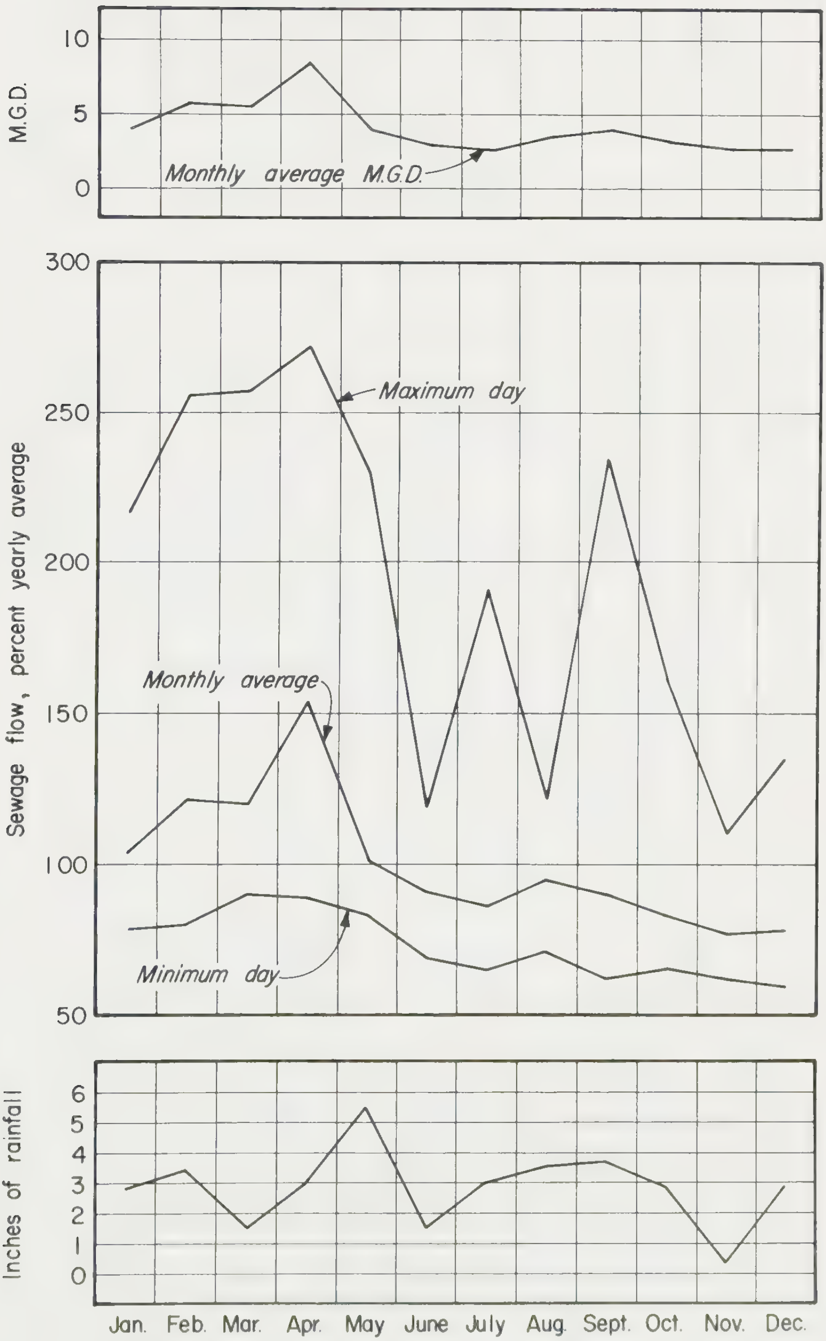

FIG. 6. Monthly sewage-flow variations, Alexandria, Va.

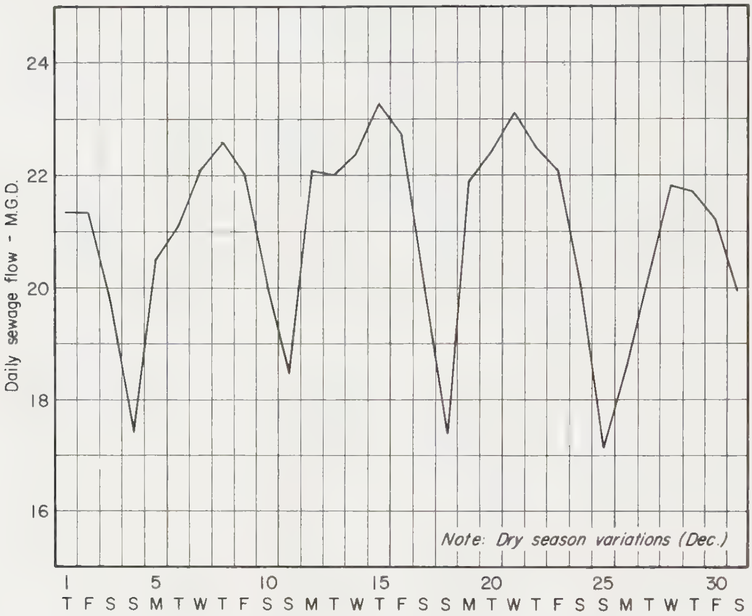

FIG. 7. Daily variations in sewage flow, Tampa, Fla.

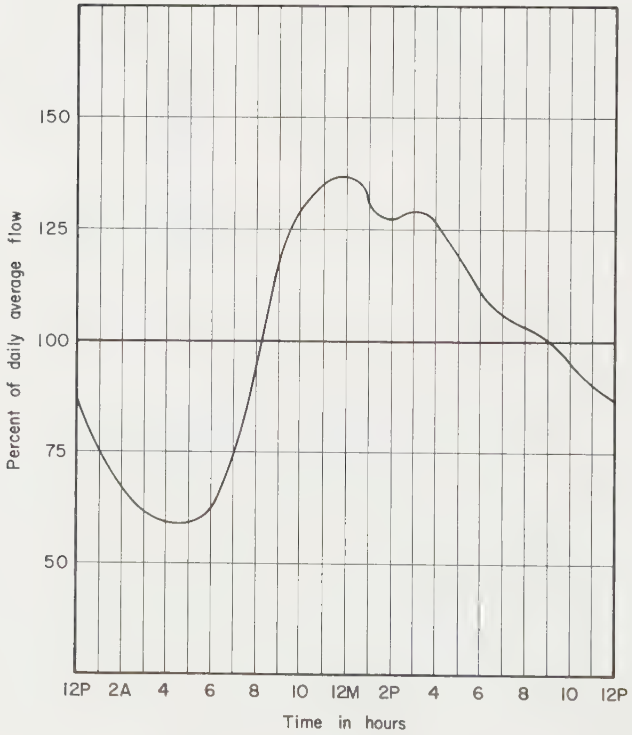

Fig. 8. Hourly variations in dry-weather sewage flow, Shockoe Creek Sewer, Richmond, Va.

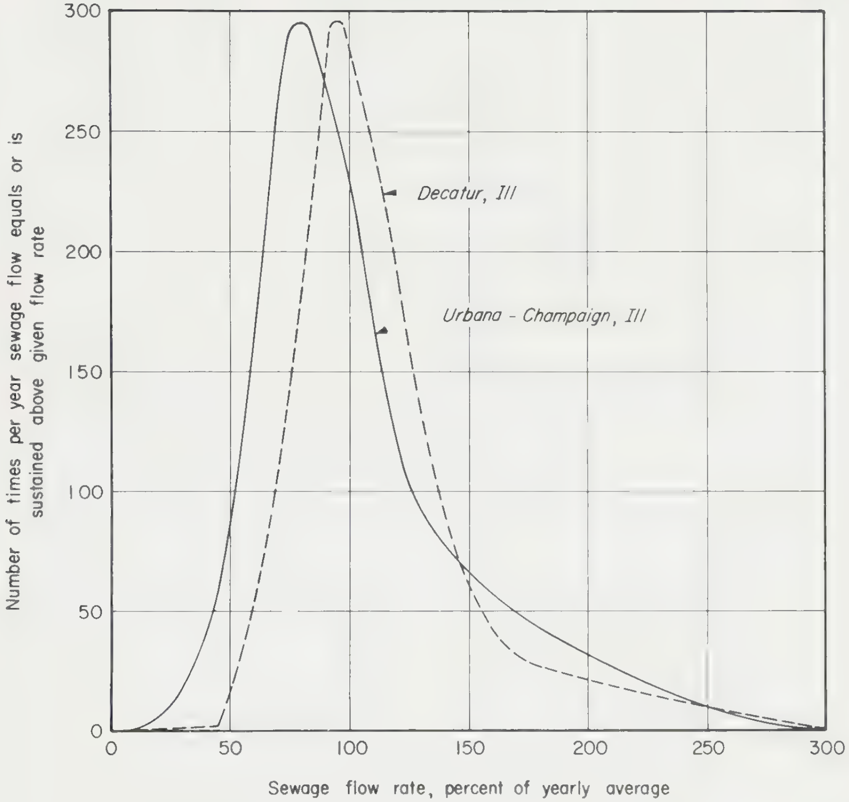

FIG. 9. Occurrence of various rates of sewage flow.

of, or interchangeably with, the term "maximum rates." Long-term records of sewage flow, available for many cities, furnish helpful information regarding the relation of maximum sewage-flow rates to the yearly average daily rates.

Figure 10, based upon sewage-flow records, is helpful in evaluating the proportion of time for various rates of sewage flow. Thus the curve for hourly flow data at Urbana-Champaign indicates the following:

Ratio of max rate to yearly avg	Proportion of time flow occurs	
	% of time	Hr/year
2.3	0.6	52
2.0	3.0	263
1.8	5.2	455
1.5	11.0	964

It seems reasonable to expect higher maximum rates of flow, as compared with average rates, for smaller areas or smaller numbers of people. This principle is

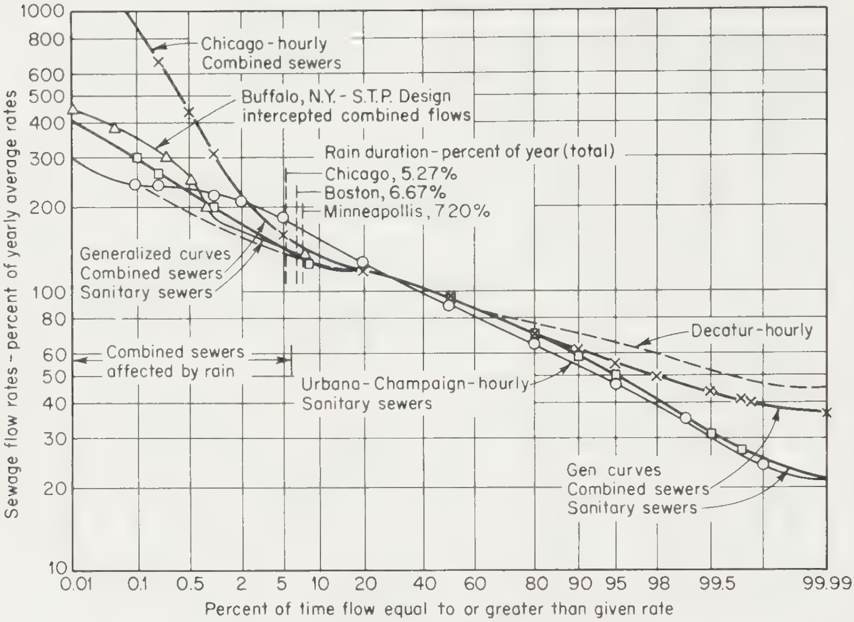

FIG. 10. Probable variations of flow in sewers.

reflected in many of the empirical procedures that have been proposed for arriving at maximum rates of domestic-sewage flow for which sewers should be designed.

Examples of these are (1) the formula given by Babbitt,[6] for use between the limits of 1,000 and 1,000,000 population, $M = 5/P^{1/5}$; (2) a similar relationship proposed by Gifft[7], $M = 5/P^{1/6}$; and (3) the relation offered by Harmon[8], $M = 1 + 14/(4 + P^{1/2})$, in which P is the tributary population in thousands and M the ratio of maximum sewage-flow rate to average rate to obtain the sewer design capacity.

These formulas relate to the sewer design capacity to be provided for domestic-sewage flows. The fluctuations in total sewage-flow rates may be less owing to the leveling influence of groundwater infiltration and industrial and commercial sewages.

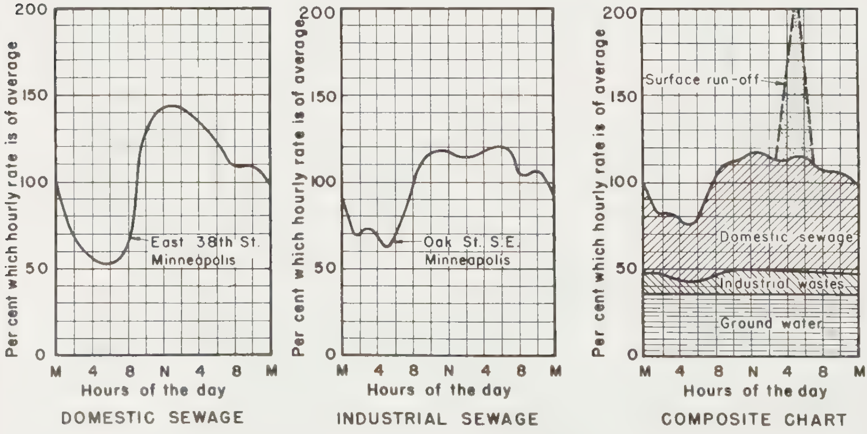

FIG. 11. Hourly variations in sewage flows.

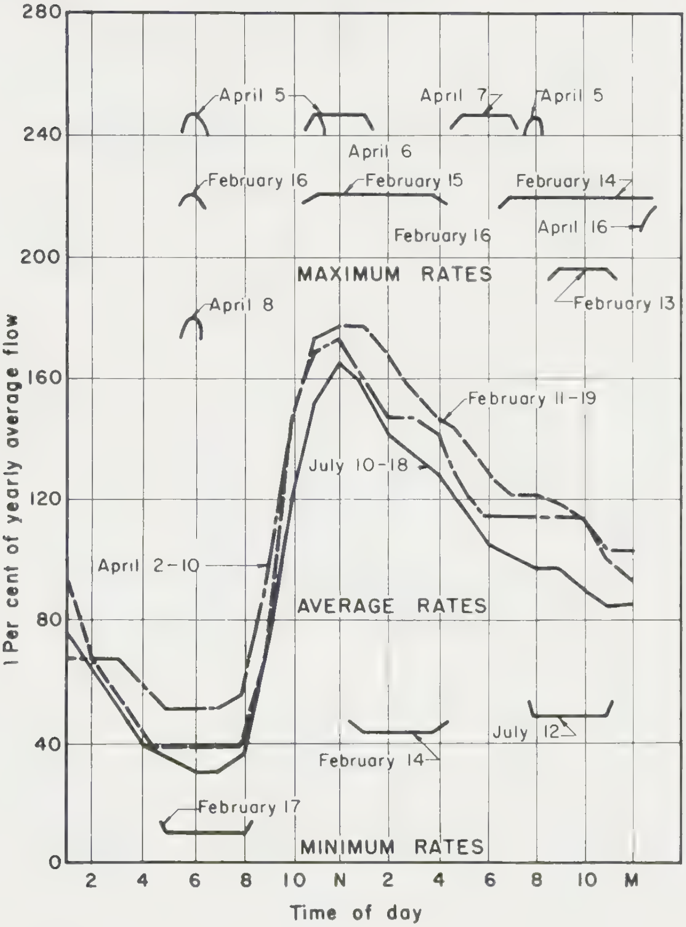

FIG. 12. Hourly variation in sewage flow, Pasadena, Calif.

The Maryland State Department of Health has proposed that the basis of design of sanitary sewers should be related to the average sewage flow according to a certain chart, from which the following ratios have been computed (similar charts have been in use by the Washington Suburban Sanitary District and in New York City):

Sewage flows, mgd		Ratio design flow avg
Avg sewage flow	Basis of sewer design	
0.2	0.8	4.0
0.5	1.7	3.4
1.0	3.2	3.2
2.0	5.6	2.8
4.0	9.9	2.5
6.0	13.7	2.3
10.0	21.2	2.1
16.0	32.0	2.0*

* This factor applies to all flows greater than 16 mgd.

On the basis of 100 gcd for the yearly average daily domestic-sewage flow, the procedures of Babbitt, Gifft, Harmon, and the Maryland State Department of Health yield the following comparative results:

Population	Avg domestic-sewage flow, at 100 gcd, mgd	Ratios of max to avg sewage-flow rates as computed by various methods			
		$M = \frac{5}{P^{1/5}}$	$M = \frac{5}{P^{1/6}}$	$M = 1 + \frac{14}{4 + P^{1/2}}$	Maryland State Dept. of Health diagram
10,000	1.0	3.1	3.4	3.0	3.2
25,000	2.5	2.6	2.9	2.6	2.7
50,000	5.0	2.3	2.6	2.3	2.4
100,000	10.0	2.0	2.3	2.0	2.1
200,000	20.0	1.7	2.1	1.8	2.0
500,000	50.0	1.4	1.8	1.5	2.0
1,000,000	100.0	1.3	1.6	1.4	2.0

The following tabulation shows the ratio of the maximum hourly to the average flow, as indicated by measured sewage-flow records for several cities.

City	Population (approx)	Ratio of peak hourly to yearly avg flow	
		Equaled or exceeded 0.1 % of time	Equaled or exceeded 1 % of time
Long Beach, Calif.	125,000	2.2	1.8
Los Angeles, Calif.	1,060,000	1.8	1.5
Pasadena, Calif.	70,000	2.4	2.0
Urbana-Champaign, Ill.	40,000	2.8	2.5

On the basis of a number of gagings at Buffalo, where the sewage flow in combined sewers is intercepted for treatment, ratios of peak flows to the average flow at the treatment plant were estimated as follows (Fig. 10):

Period	% of time per year	Ratio of flow to yearly avg
Peak rate	0.01	4.44
4-hr max	0.046	3.80
24-hr max	0.274	3.00
2-day max	0.55	2.50
3-day max	0.82	2.00
Max month	8.2	1.33
Min	.....	0.50

13. Industrial and Commercial Waste-water Flows. Careful consideration must be given to the quantities of industrial and commercial waste waters for which sewer capacity should be provided. In smaller communities with no large volumes of industrial wastes, the allowance for such wastes can generally be included in the per capita flow of domestic sewage; but in the larger cities having numerous industries and commercial establishments, the quantities of these wastes are preferably estimated as separate items and added to the estimated domestic-sewage quantity. The proportion of the city area used for industrial and commercial purposes is usually small (see Table 4). The probable future extension of these areas should be carefully estimated.

A usual practice is to estimate future flows of industrial and commercial waste water in terms of gallons per acre per day based upon a study of the quantities

TABLE 11. COMMERCIAL AND INDUSTRIAL SEWAGE FLOWS BASIS OF SEWER DESIGN*

Municipality	Population	Total commercial and industrial acreage	Industrial waste-water flows		
			Total million gal/day	Gal/acre/day	gcd
Tampa, Fla.	335,000	2,629	13.69	5,200	41.0
Spokane, Wash.	223,000	3,155	19.13	6,330	89.5
Knoxville, Tenn.	350,000	3,835	20.16	5,260	57.6
Richmond, Va.	666,800	6,570	50.13	7,640	75.2
Minneapolis–St. Paul	1,453,530	21,390	52.2	2,440	35.9
Metropolitan area	1,557,390	23,655	56.7	2,440	36.5
Dade County, Fla. Metropolitan area	3,692,000	18,680	41.2	2,200	11.2
São Paulo, Brazil	5,000,000	15,300	159.1	10,400	31.8

* Estimated flows used as basis of design of main sewers serving the total commercial and industrial areas.

discharged from presently developed areas and comparative data from other cities. Special consideration should be given to existing industries that produce exceptionally large quantities of wastes. Table 1 (Sec. 41) gives illustrative data on the volumes of wastes produced in various types of industries. Sewer-capacity allowances for industrial and commercial areas based on careful analyses of existing conditions are given in Table 11 for several cities.

14. Infiltration. The flow in sewers is increased by surface water and groundwater from two sources: (1) the entrance of runoff from rains directly through inlets such as downspouts, street inlets, and other openings; (2) the entrance of water from the ground into the sewers through leaky joints and other structural defects and foundation drains. Improperly constructed or defective house-connection sewers frequently are sources of large infiltration rates, estimated by one authority[9] at 90 percent of the total infiltration, and are impractical to remove. This possibility must be considered in providing new or relief sewers for any areas with old sewers. Drains might be improperly connected to sanitary sewers, a condition which, if universal in a subdivision, may produce maximum rates of flow more than twice as large as normally expected.

In spite of the fact that most modern plumbing codes and sewer regulations properly prohibit the discharge of rainwater or other surface water into sanitary sewers, it is generally necessary to provide capacity for a limited amount of surface runoff. Figure 13 shows the influence of rain on domestic-sewage flows in one specific case.

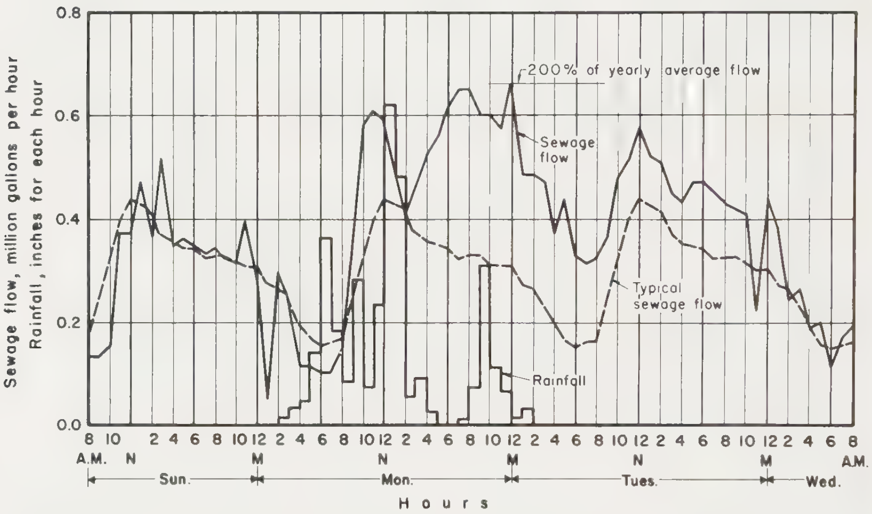

FIG. 13. Effect of rain on the hourly sewage flows at Long Beach.

The infiltration of groundwater into sanitary sewers depends upon a number of major factors, including the following:

1. The level of the groundwater with reference to the sewer.
2. The character of the subsoil. Sand and gravel will permit more water to leak into a sewer than will clay.
3. The watertightness of joints and the provisions to prevent cracking of the sewer pipes.
4. The character of the construction of the house connections. This usually relates to the extent and care with which the construction of the house connections is supervised.
5. Foundation drains connected to sanitary sewers.

Reduction of the amount of surface water entering existing sewers is sometimes possible, but it is difficult, costly, and impracticable to reduce the groundwater infiltration after a sewer system and the house connections have been built. Therefore, every effort should be made during the period of construction to assure watertight sewers.

In some Western cities, the elevation of groundwater is raised several feet during the irrigation season and the infiltration is greatly increased (about 2.5 times), as indicated by the following rates of seasonal per capita sewage flow at Yakima, Wash.:

Nonirrigation		Irrigation	
Month	gcd	Month	gcd
January	181		
February	189		
March	205		
April	315		
		May	448
		June	567
		July	595
		August	667
		September	571
		October	436
November	238		
December	215		

Several units of measurement of infiltration have been suggested, such as gallons per 24 hr per capita, per acre, per foot of joint, per square yard of interior surface, and per mile of sewer. The rather extensive available data on measured leakage into sewers show quite a wide range in amounts even for new sewers built under careful supervision. Also a large proportion of infiltration is an indeterminate flow into house-connection sewers.

Accordingly, there appears no justification for any refinement of the units of measurement. The units of gallons per 24 hr per mile of sewer or gallons per day per acre (gad) of sewered area are easily applied and are most commonly used.

The approximate lengths of sewer lines per acre of sewered area provide a basis for changing the infiltration rate from one to the other of the latter two terms. This will vary, depending on the size of lots, and may range from 132 ft per acre for a rectangular street pattern with lots 135 ft deep to 218 ft per acre for lots 100 ft deep.

The following data are typical of measured quantities of infiltration for newly constructed sewers and may be useful in determining reasonable allowances for design purposes:

Locality	Size of sewers included in measurements, in.	Groundwater infiltration, gal/mile of sewer/24 hr*
North Shore Sanitary District, Ill	30–42	2,300
Richmond, Va	30–36	3,250
Tampa, Fla	30–60	4,800
Tampa, Fla	6–21	2,200
Portsmouth, Va	6–18	3,850

* These rates relate to the main sewer—not to tributary laterals or house sewers.

Some increase in infiltration rates is likely to occur as a sewer system becomes older. The infiltration provided for in the planning and design of a number of well-considered sewerage projects, given in Table 12, may be helpful as a guide to judgment. If the average domestic-sewage flow per capita is based upon gagings or flow records the average infiltration is included and the allowance for infiltration for sewer design should be considered as an additional maximum flow rate above the average. If the average domestic-sewage flow does not include any infiltration, a larger allowance should be used.

15. Summary –Sewage-quantity Computations, Sanitary-sewer Design. Sanitary-sewer design requires determination of sewage quantities considering the following:

1. The area for which capacity is to be provided, including appropriate subdistricts.
2. The design period, usually 40 or 50 years in the future; or population increases ranging from 1.3 to 3.8 times the population at the time of design.
3. The population forecast and distribution of population.
4. An estimate of average per capita domestic-sewage contributions based on water supply entering the sewers plus average infiltration, or sewage-flow records (or gagings) including average infiltration.
5. The maximum domestic-sewage flow rate (sometimes improperly called the peak rate) based on average sewage flow multiplied by a maximum-flow factor, to which should be added allowances for maximum infiltration and industrial and commercial waste-water flows.
6. Infiltration allowances should be made to provide for some reasonable maximum infiltration rate per 24 hr per acre of tributary sewered area.
7. Estimates of the probable future waste-water contributions from industries and commercial establishments, based on areas expected to be developed within the design period at a general allowance in gallons per acre per 24 hr, plus any special flow rates determined by a study of existing industries producing large waste-water flows. The industrial and commercial contributions generally relate to relatively small areas tributary at specific locations on a few sewers. These flow rates must be included in the design capacity for sewers downstream of the points of contribution.

Table 12. Typical Allowances for Groundwater Infiltration Basis of Design

Locality	Groundwater infiltration per 24 hr	
	Gal/mile of sewer*	Gal/acre
Mamaroneck District, Westchester County, N.Y.	36,900 existing	1,050
	12,000 future	340
Washington, D.C.	24,000	700 older lines in city
	14,000	400 newer lines in suburbs
Richmond, Va.	10,500–52,500	300–1,500 depending on age of sewer and location
Metropolitan area of North Va.	10,500–17,500	300–500
Minneapolis–St. Paul Sanitary District	14,000	400 central city
	7,000	200 suburbs
Metropolitan area of Seattle, Wash.	10,500	300 summer
	21,000	600 winter
Tampa, Fla.	8,800	250 high, dry areas
	16,000	450 low, wet areas

* Estimate based on 150 ft of sewer per acre except Mamaroneck District, which was based on 35 acres/mile of sewer (150.1 ft/acre).

8. Contributions from institutions, colleges, and schools which sometimes are sufficiently large to justify special allowances may be handled in a manner similar to industrial or commercial waste waters but usually are computed on the basis of concentrated populations. Generally sewage flows from schools are not included in major sewers or sewage-treatment works, as the school population is included in the community population.

9. The summation of computed sewage flows, as described below under Capacity Design.

Each sewer system has special conditions and factors which require adjustments in the application of the foregoing basic considerations to the capacity design of sanitary sewers.

STORM-RUNOFF QUANTITIES

16. Introductory. The design of storm sewers or combined sewers involves a decision as to the degree of protection to be provided against property damage, nuisance, and inconvenience from surcharged sewers. It is not economically feasible to construct sewers of sufficient size to take the runoff from the extreme storms likely to occur at infrequent intervals. Surcharging of combined sewers is more objectionable than surcharging of storm sewers, because of the nuisances and health hazards that result from the flooding of basements and the overflowing of domestic sewage.

Thus, the quantity of storm water for which sewer capacity should be provided is a balance among the first cost and the capitalized damage to private property, the hazard to health, and the curtailed convenience to the public.[10] These factors, therefore, should be given consideration as well as the technical hydraulic factors.

An exact determination of the permissible frequency of surcharging is impossible in present practice, and the conclusion as to the basis of design depends, finally, upon the judgment and experience of the designing engineer. Data with reference to sewer costs, sewer capacities for storm water, and the results of operating experience in a number of cities are helpful guides to judgment.

A study[11] of new and relief sewers at Decatur for a residential area, including consideration of sewer assessments (costs per foot of assessed frontage) and sewer capacities, resulted in the data in Table 13 for a proposed sewer district of about 525 acres, approximately 9,000 ft long by 2,500 ft wide. Comparative data from a number of cities are given in Table 14. The Decatur estimates indicated that a storm sewer for a 3-year storm must have a capacity 2.2 to 2.7 times as great, and would cost 1.43 times as much to build, as one for a storm frequency of four times per year.

17. Bases of Storm-sewer Design—General. In past computations of storm-water quantities, engineers have used two general procedures: (1) the empirical-formula method and (2) the "rational method."

In either of these procedures, the computed quantity of storm water for sewer-capacity design is a function of (1) the area to be drained, in acres, as determined by field surveys or by scaling from a map; (2) the rainfall intensity, which results from an analysis of rainfall records and storm frequencies; and (3) the maximum rate, or coefficient, of runoff. The latter factor depends upon the surface slope and the anticipated future condition of the drainage area with reference to the proportion of the rainfall that may run off.

In the empirical-formula method, experience in the design and operation of storm sewers, in one or more localities, has been expressed in formulas proposed for application to other localities. Because such empirical formulas were expressions of the judgment of others, based on conditions for limited localities, they are no longer in general use. They may, however, be useful sometimes as rough checks, and particularly in large cities where the results of sewer-design practice are known and the sewer-department engineers are experienced in expressing their judgment through the formula, but this practice is also losing favor.

The so-called *rational method,* which has been widely used, relates the storm-water runoff directly to the tributary area, the rainfall intensity, and an estimated proportion of the rainfall reaching the sewer as direct runoff.

More recently, procedures have been developed for estimating rainfall runoff by the *hydrograph method.* These procedures recognize a number of separate factors

Table 13. Relative Cost of Sewers per Front Foot as Estimated for the Proposed North Side Sewer District, Decatur, Ill.

Projects	Relative cost of sewers per foot of assessed frontage*			Approx capacity of sewers, cfs/acre storm water	
	Main sewers	Lateral	Total	400 acres	100 acres
Combined sewers:					
Rainfall frequency					
10 years	1.44	1.96	3.40	0.73	1.06
3 years	1.21	1.78	2.99	0.42	0.76
1 year	1.14	1.61	2.75	0.38	0.57
Storm sewers:					
Rainfall frequency					
3 years	1.21	1.67	2.88		
1 year	1.14	1.51	2.65		
4 times per year	0.88	1.22	2.10	0.19	0.28
Sanitary sewers	0.18	0.82	1.00†		
Separate sewers (storm and sanitary):					
Rainfall frequency					
3 years	1.39	2.49	3.88		
1 year	1.31	2.34	3.65		
4 times per year	1.06	2.05	3.11		

* Referred to total cost of sanitary sewers = 1.00.

† Capacity 300 gal per capita and 19 people per acre, sewers flowing full = 5,700 gad.

which affect the quantity of runoff which may result from rainfall and also the relative time of occurrence of the peak rates of runoff from various future types of surfaces in each tributary area and from several separate tributary areas. Unlike the "rational method," in which, generally, all factors are combined into one coefficient C expressing the judgment of the sewer designer, the principal factors considered in the hydrograph method include

1. The time occurrence of the peak rate of rainfall in a selected typical storm with respect to the start of precipitation
2. The diminution and delay in runoff due to depression storage and infiltration
3. The relative time of appearance of runoff at the sewer inlet from different types of surfaces
4. The time of flow in the sewers, including the house and lot drains, and the storage effect of sewers and catch basins

The *hydrograph method* appears to be most applicable to large sewer systems where considerable similarity in drainage areas exists and a computer can be used to determine unit runoff quantities from typical areas for repetitive use in design studies. The procedure has received attention from a number of investigators, culminating in a full development of methodology by Tholin and Keifer for the city of Chicago, which is presented in the ASCE Manual of Engineering Practice No. 37.[12] The "hydrograph method" is not yet in general use and will not be discussed further here.

TABLE 14. RELATIVE SEWER CAPACITIES AND ASSESSMENTS SUMMARY OF APPROXIMATE DATA FOR VARIOUS CITIES

City	Kind of sewer system	Sewer capacity, cfs/acre		Relative cost of equivalent combined sewer service per front foot			
		100 acres	500 acres	As reported	On basis of 200 ft frontage per acre	On basis of 250 ft frontage per acre	Trend
Louisville	C	1.46	1.16	.....	1.24	0.99	1.02
St. Louis	C	2.55	2.44	.....	1.05	0.92	1.02
Chicago	C	0.26	0.16	.....	.....	.....	0.83
Indianapolis	C	0.60*	0.43	.....	.....	.....	0.56
Buffalo	C	0.82	....	1.55	.....	.....	1.55
Milwaukee	S	0.80	0.65	0.74†	.....	.....	1.02
Detroit	C	....	....	.....	0.60‡	0.48‡	1.02
Syracuse	C	0.50	0.75	0.55§			
New Bedford	C	1.0	....	0.37§			
Los Angeles	S	.....	....	0.74†	.....	.....	1.02
Avg.	...	.....	....	.....	.....	.....	1.00¶

C = combined.
S = separate.
* Based on $C = 0.4$ and slope of 0.002.
† Storm sewers only.
‡ Laterals only.
§ Assessment fixed by law.
¶ Relative costs are related to an adjusted average cost of \$24 per front foot, at *Engineering News-Record* Construction Cost Index of 950.

18. Rational Method. Here the so-called "rational-method" computation procedure will be represented by the formula

$$Q = ciA$$

in which Q = storm-water runoff entering the sewer, cfs
c = a coefficient representing the ratio of runoff to rainfall, commonly called the runoff coefficient
i = rainfall rate, cfs/acre, or (close enough for all practical computations) intensity of rainfall, in./hr (1.00 in./hr = 1.008 cfs/acre)
A = tributary drainage area, acres

The application of the *rational method* requires the exercise of sound judgment in the selection of the coefficient c and the rainfall intensity i. The tributary area A can be more definitely determined.

In practice, the *first step* is a tentative arrangement of proposed sewer lines on a plan of the sewer district for which the sizes of sewers are to be computed; a division of the district into subdistricts tributary to several concentration points along the proposed sewer lines; and the successive summation of the areas tributary at or above the various concentration points, related to the sewer directly below each concentration point.

The *second step* is the selection of a future storm frequency for which sewer capacity is to be provided and the determination of the rainfall intensity of this frequency for a storm duration equal to the computed "time of concentration," which includes two factors: an "inlet time," *i.e.*, the time required for rain falling on the most remote point of the tributary area to flow across the ground surface, along pavement gutters to the street inlet, and through the inlet into the sewer; and a "time of travel" within the sewer from the uppermost inlet to the concentration point under consideration.

The *third step* is a determination of the proportion of the rainfall which may enter the proposed sewer as runoff, expressed as a rate, based on the anticipated future conditions in the tributary areas.

19. Area to Be Served. The area to be served by the proposed storm sewers will be determined primarily by topography, though the arrangement of streets will affect the arrangement of the sewers and must be considered in determining the subdistricts tributary at various concentration points.

Initial layout of the proposed sewers and anticipated future tributary drainage areas can be accomplished best on moderate-scale topographic maps. U.S. Geological Survey maps, where available at the scale of 1 in. = 2,000 ft, are useful, though this scale is often too small for the area to be served. Topographic maps prepared at scales in the range of 1 in. = 200 to 500 ft, prepared by aerial photographic methods, are most suitable. The present development of the tributary areas is a useful guide to judgment as to the probable future character of areas.

Careful analysis of the present development of an area to be sewered is particularly necessary where relief storm sewers are being planned. Such development analyses should determine the percentages of the area covered by various types of impervious surfaces and the average ground slope, both of which affect the proportion of rainfall likely to appear as direct runoff.

The estimated future development to be used as the basis of design is a matter of engineering judgment, based on experience and extensive study. The present development will serve as a guide, but such factors as zoning ordinances, susceptibility to total change in character of the tributary areas, such as development of apartments or urban-renewal projects replacing residences, must be considered. The effect of large paved parking areas associated with suburban shopping centers must be considered. Determination of the relative amounts of impervious area in present fully developed blocks is helpful and is facilitated by aerial photography.

20. Storm-flow Concentration Time. The time of concentration t in the "rational method" comprises two parts:

1. The *inlet time* is affected materially by the character and slope of the ground surface, and selection of an allowance for this time has a considerable influence upon the rainfall-intensity rate. The selected "inlet time" may be as short as 5 min for closely spaced street inlets of ample size on areas highly developed or with steep slopes, or 10 to 15 min on flatter slopes with greater inlet spacing. Inlet time also can be controlled by size and design of the storm-water inlet structures. Under certain conditions, an inlet time up to 20 or 30 min may be considered for relatively flat residential areas with small-capacity street inlets or with street inlets spaced at relatively long distances, where some surface ponding may be permissible. "Inlet time"

selection practice in several cities has been reported as follows:

City	Min	City	Min
Buffalo	15	Rochester	7
Chicago	10	St. Paul	10
Cincinnati	5*–10†	San Francisco	4
Cleveland	8	Springfield, Mass	20†
Columbus	10	St. Louis	5
Des Moines	5	Toledo	20† and 15*

* Business district.
† Outlying area.

In general, drainage areas in Chicago are quite flat while ground-surface slopes in San Francisco are much steeper, and the inlet times used reflect this difference. The character of the area being sewered is another factor. Thus the 20-min inlet time for Springfield, Mass., applies to outlying fairly flat residential districts.

2. The *time of travel* in sewers, or "flow time," computed from the length of sewer

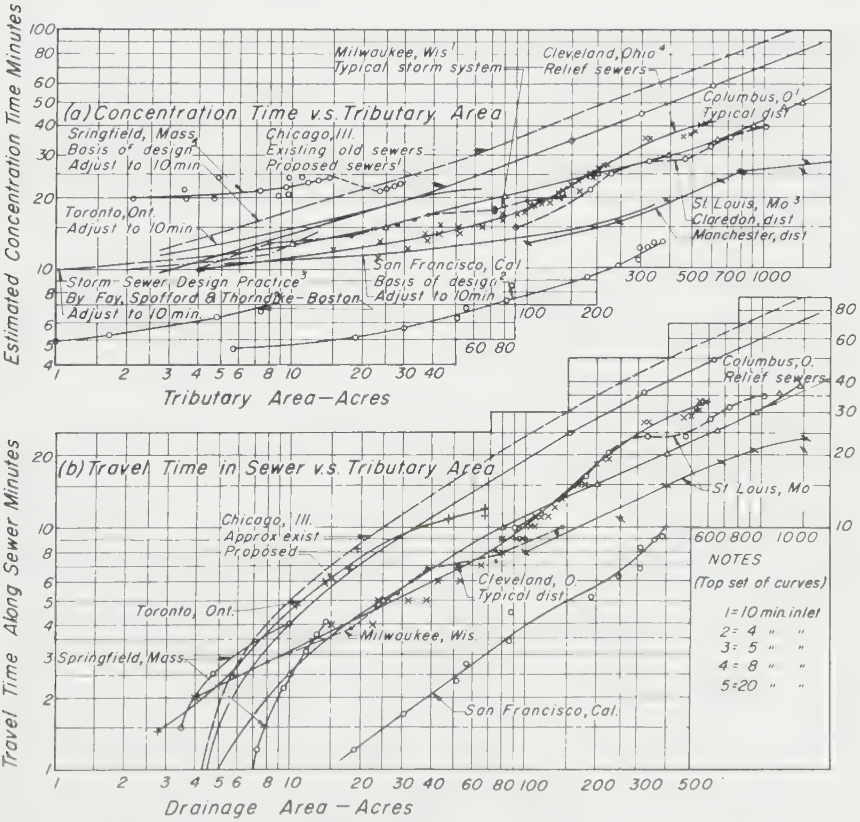

Fig. 14. Storm-sewer design—time of concentration and travel time related to tributary area.

divided by the average velocity of flow, will be shorter for steep slopes. Thus steeper topography results in a shorter "time of concentration" and hence, with a given rainfall-intensity curve, a higher average rainfall intensity and a larger sewer-capacity requirement.

Theoretically, "flow time" in the sewer should be a simple computation (length

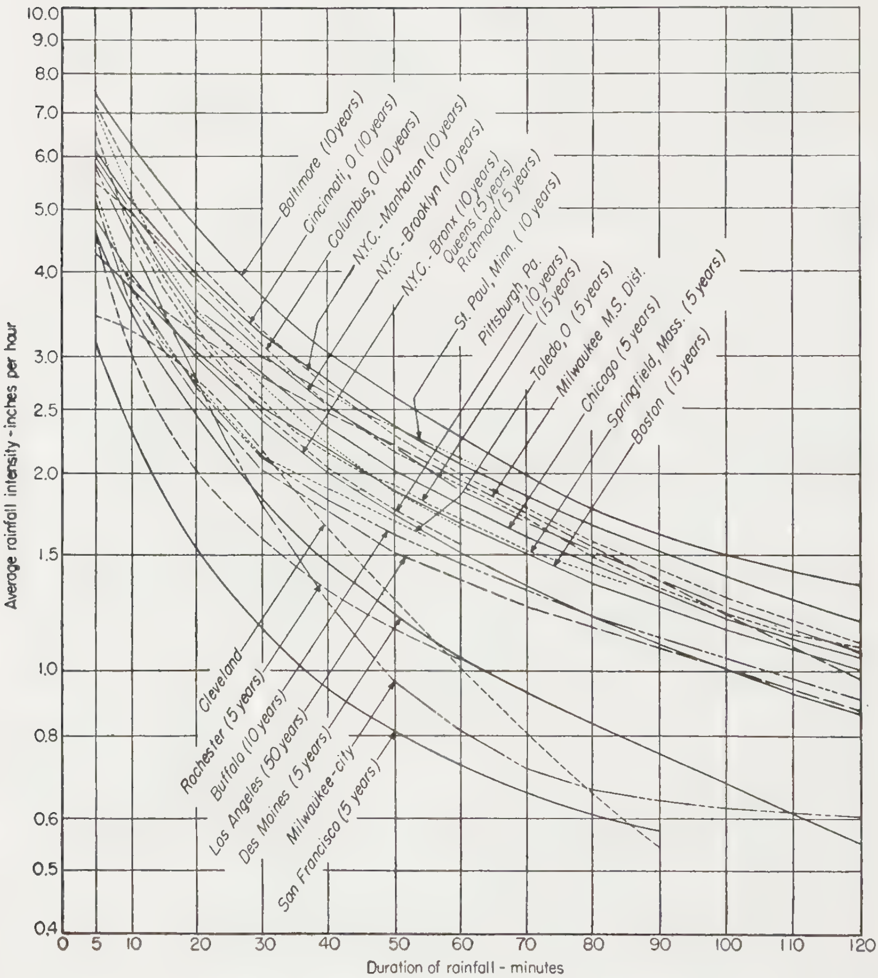

FIG. 15. Rainfall curves used for sewer design.

divided by average velocity). However, there is considerable uncertainty as to the resistance to flow in older sewers, and hence there is uncertainty as to the velocity of flow at the design period of 30 or 40 years in the future.

Accordingly, some sewer designers have attempted to relate the effective time of concentration to the tributary area, as illustrated by Fig. 14, which shows "travel time" vs. tributary area and "concentration time" vs. tributary area, for a number of cities.

21. Rainfall-intensity Data. The basic procedure in studying rainfall data for storm-sewer design is to obtain the records of all excessive rainstorms for as many years as they are available. The greatest average rate of rainfall, in inches per hour for periods of 5, 10, 15 min and up, may be determined throughout the duration of each storm. The intensities are tabulated in order of magnitude for each duration of time and the frequency in years for each intensity is determined by dividing the number of years of record by the number of occurrences. By plotting these data and drawing smooth curves through the plotted points, a series of rainfall-intensity curves can be obtained, representing various frequencies of storm occurrence.

The rainfall curves and storm frequencies which have been used for storm-sewer design in a number of cities are compared graphically in Fig. 15.

Some investigators have combined the records of several rain-gaging stations,

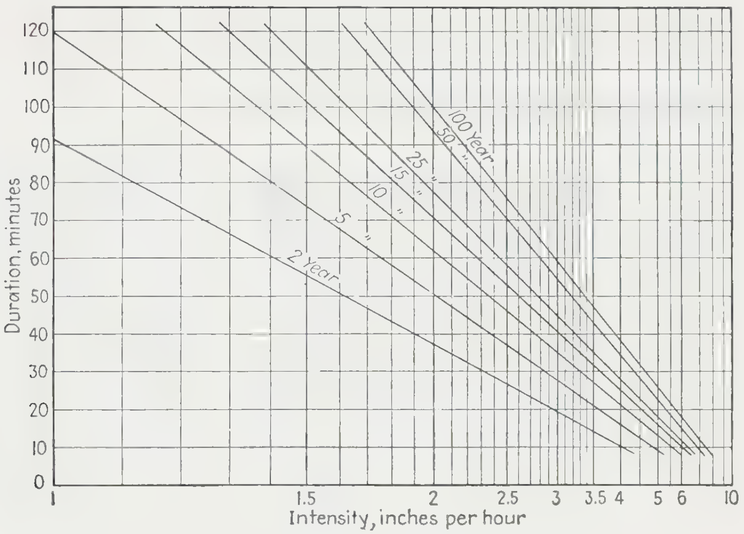

FIG. 16. Intensity and duration of rainfall, Chicago area.

assuming, for example, that the storm records of two stations for 10 years at each station would be equivalent to a 20-year record at one station. There is doubt as to the validity of this procedure.

Figure 16 gives the results of an investigation of the records of 13 recording rain gages within the Chicago area, equivalent to 330 station-years. The semihyperbolic plotting used in Fig. 16 yields straight-line results. About 1944, the Chicago Bureau of Sewers adopted the Eltinge-Towne rainfall-intensity formula for a 5-year storm, $i = 90/(t^{0.9} + 11)$, as the basis for combined sewer design.

Curves for other cities may be developed from an analysis of the available records of local recording rainfall gages. Such recording gages are more in use today than formerly.

22. Rainfall Formulas. Efforts have been made to represent the time-intensity relation for rainfall by a mathematical formula. Many of these follow the form $i = A/(t + b)$, devised by Talbot in 1891, in which i is the rainfall intensity in inches per hour, t is the storm duration in minutes, and A and b are constants. An extensive study by Schafmayer[13] seemed to indicate that this hyperbolic type of formula was as good as any for showing the relation between intensity and duration for storms not exceeding 120 min. Factors A and b for the curves in Fig. 16, as computed by Schafmayer, were as follows:

Storm frequency, years	Factors in $i = \frac{A^*}{c+b}$	
	A	b
2	102	16
5	138	19
10	166	21
15	182	21
20	193	22
25	203	22

* Schafmayer for Chicago area.

Some authorities have considered that an exponential formula such as $i = A/t^b$ or $i = A/\sqrt{t+b}$ would fit the rainfall data better. However, neither the accuracy of the available data nor the reliability of their application in storm-sewer design warrants much complexity in the mathematical formulas representing the relation between duration time and average rainfall intensity.

Formulas proposed by Meyer[14] have been found useful in the absence of any better analysis of a long-term record of local data. These are in the form $i = A/(t + b)$, and he gives values of A and b (Table 15) based upon the rainfall records of various groups of localities (Table 16).

Collection and processing of comprehensive rainfall data can be undertaken only on large extensive projects. For most projects, data published by governmental agencies are available in usable form. Charts prepared by Yarnell[15] have given good

Table 15. Meyer's Constants in Rainfall Formula $i = \frac{A}{t+b}$

Regional group	Constants	Storm frequency, years						
		1	2	5	10	25	50	100
1	A	145	180	220	276	355	450	600
	b	23	24.5	27	32	40	50	65
2	A	100	131	171	214	252	289	325
	b	18	21	23.5	26	28	30	32
3	A	72	96	122	150	181	216	256
	b	13	16	18	19.5	21	23	25
4	A	60	84	108	132	160	186	210
	b	15	16	17.5	19	20	21	22
5	A	60	75	90	105	126	152	180
	b	13	13	13	13	14	16	18

results. More recent analyses of rainfall data are available in U.S. Weather Bureau publications, particularly Technical Papers 24, 25, and 28.

Data from Technical Paper 25 have been used by B. A. Swab to prepare and publish[16] small-scale charts of mass rainfall for various frequencies for the United States east of the Rockies (east of 105th meridian). These may be useful in communities where local rainfall records are insufficient or have not been fully analyzed.

23. Rainfall Distribution. The rainfall-intensity factor i, in the "rational formula," usually represents rainfall measured at a single point, or the average of several single-point measurements. Data are meager on rainfall distribution over large areas but indicate that the rainfall intensity, when averaged over the total area, reduces as the size of the area increases, with the reduction being greatest for storms

TABLE 16. LIST OF RAINFALL STATIONS USED BY MEYER AS BASIS FOR HIS FORMULAS

Cities in various regional-group numbers				
1	2	3	4	5
Galveston	New York	Boston	Duluth	Denver
New Orleans	Philadelphia	Albany	Escanaba	Bismarck
Jacksonville	Washington	Pittsburgh	Buffalo	
	Norfolk	Elkins	Rochester	
	Raleigh	Asheville		
	Savannah	Knoxville		
	Atlanta	Memphis		
	Little Rock	Cairo		
	Fort Worth	Indianapolis		
	Abilene	Cincinnati		
	Bentonville	Cleveland		
	St. Louis	Detroit		
	Kansas City	Grand Haven		
	Lincoln	Chicago		
	Des Moines	Madison		
		St. Paul		
		Moorhead		
		Yankton		
		Dodge		

of shorter duration. Marston called attention to this phenomenon more than 40 years ago.[17]

The sewer departments of Chicago[18] and Pasadena[19] have used reduction factors or coefficients R, which may be useful guides to sewer designers. These R factors, to compensate for the reduced rainfall intensity averaged over large areas, are reported here in Table 17. These coefficients for reduction in average rainfall intensities over large areas may be useful in the plains states and elsewhere on the United States mainland where there is substantial similarity in storm types.

However, in Hawaii, other Pacific islands, and some parts of the mainland, mountain ranges and prevailing winds result in large differences in rainfall intensities and in total annual rainfall for areas only short distances apart. Thus on Oahu the total annual rainfall along the shore near Pearl Harbor is about 20 in. while 10 miles away it is 300 in. On the island of Kauai the total annual rainfall ranges from 20 to 600 in. in less than 10 miles.

TABLE 17. REDUCTION FACTORS R FOR RAINFALL INTENSITIES AVERAGED OVER LARGE AREAS

$$R \text{ values} = \frac{\text{areal avg rainfall intensity}}{\text{areal max point rainfall intensity}}$$

Drain area, acres	30 min*			60 min*			120 min		180 m* Ref. 18†
	Ref. 18†	Ref. 19†	Ref. 17	Ref. 18†	Ref. 19†	Ref. 17	Ref. 18†	Ref. 19†	
0	......	....	1.00	.....	....	1.00			
500	.....	....	0.94	.....	....	0.97			
640	0.934	....	....	0.964	....	....	0.985	....	0.996
1,000	.....	....	0.91	.....	....	0.95			
2,500	0.854	0.91	....	0.922	0.93	....	0.964	0.98	0.985
2,000	.....	....	....	.....	....	0.93			
5,000	0.788	0.87	....	0.885	0.90	0.86	0.94	0.96	0.972
10,000	0.682	0.82	....	0.828	0.86	....	0.906	0.93	0.952
15,000	0.604	....	....	0.784	....	....	0.875	....	0.935
20,000	0.544	0.75	....	0.752	0.80	....	0.85	0.89	0.915

* Time of concentration or rainfall duration, minutes.

† Figures from Ref. 20.

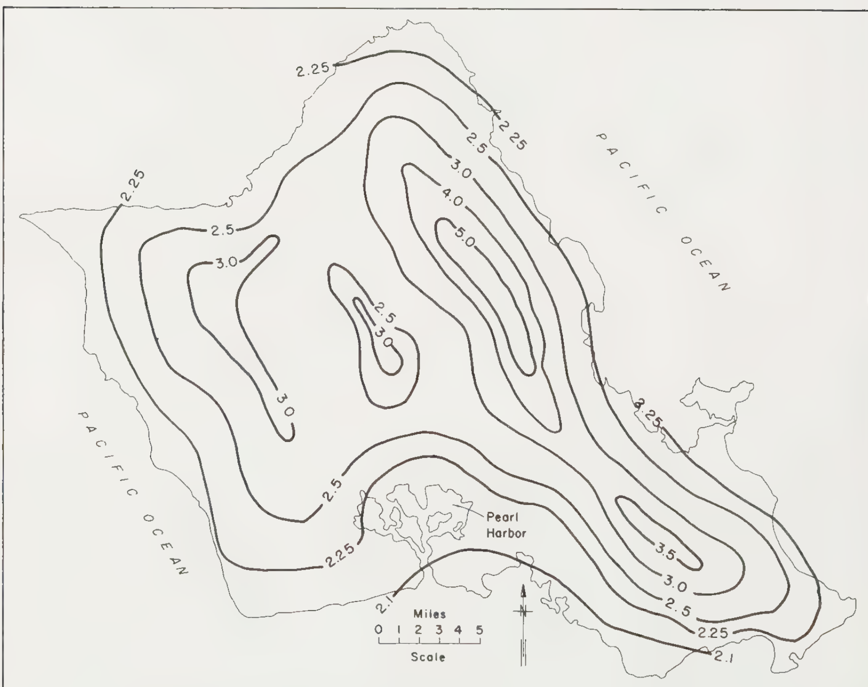

FIG. 17. One-hour rainfall intensity for recurrence interval of 10 years, city and county of Honolulu.

Thus storm-sewer designers for the city and county of Honolulu determine 1-hr rainfall intensities from a chart (Fig. 17 is illustrative for a recurrence interval of 10 years) for the locality to be sewered; then from a second chart (Fig. 18) the selected 1-hr rainfall intensity is used to determine the intensity for a computed time of concentration. For example, near Pearl Harbor the intensity of 1-hr rainfall = 2.2 in.

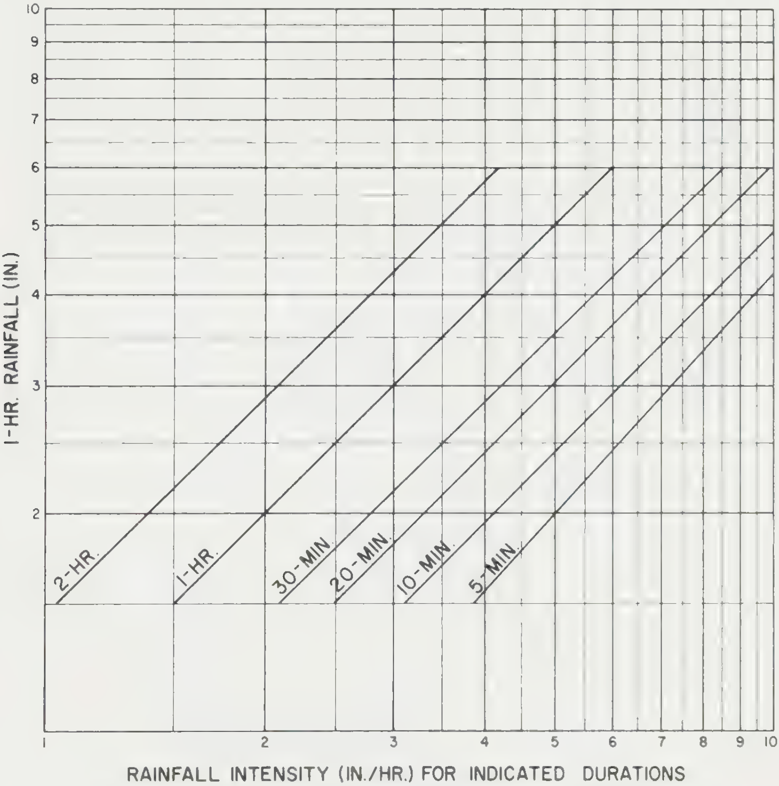

Fig. 18. Intensity for various durations from 1-hr rainfall curves for city and county of Honolulu.

(Fig. 17). From Fig. 18 for a 20-min storm duration (i.e., concentration time), the rainfall intensity to be used would be 3.63 in.

The city and county of Honolulu "Storm Drainage Standards" include a reduction coefficient R, based on the *storm-recurrence interval*, as follows:

Storm-recurrence Interval Tm, Years	Reduction Coefficient R
10	0.79
20	0.85
30	0.89
50	0.93

24. Use of Rainfall Data. A procedure in the use of rainfall data by the "rational method," i.e., to compute storm-water quantities, for which storm-sewer capacity should be provided by the formula $Q = ciA$, would include the following steps, supplemental to the three basic steps outlined in Sec. 18:

1. Plot an average rainfall-intensity vs. rainfall-duration curve (comparable with a curve in Fig. 15) for the selected storm frequency, or occurrence in years, for which storm-sewer capacities are to be provided. [The chart may be replaced by a formula, such as the Eltinge formula, $i = 90/(t^{0.9} + 11)$ in Chicago, and the rainfall intensity computed.]

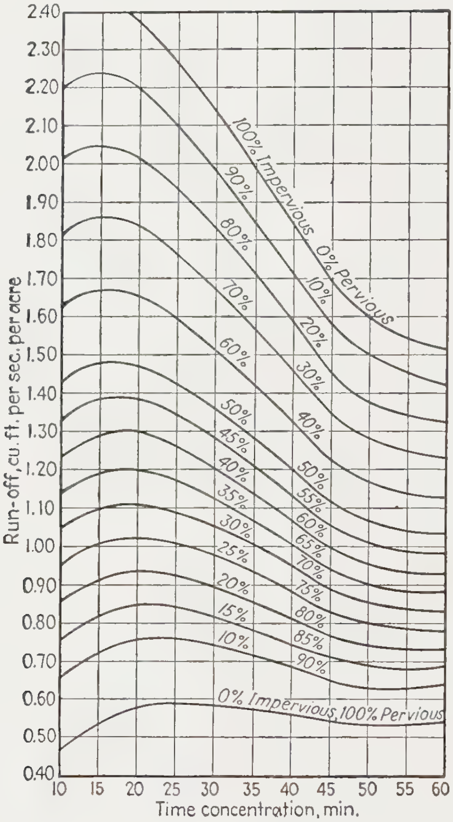

Fig. 19. Runoff from sewered areas computed for rainfall intensities exceeded once in 10 years, Peoria, Ill.

The selection of the rainfall storm frequency for any specific storm-sewer design may be determined by one of a number of procedures: (*a*) by a "manual of design" set up by some controlling or supervisory authority, for example, the "Storm Drainage Standards" of the city and county of Honolulu; (*b*) by judgment based upon a study of the operation of existing sewers over a period of years; (*c*) by judgment based upon operating experience in other communities where good records are available.

2. Determine the time of concentration (= rainfall duration in above) by selecting

an allowance for "inlet time" and computing the "time of travel" in the sewer. The methodology for this is illustrated by Table 24.

3. Determine runoff in cubic feet per second per acre by multiplying the average intensity i for the computed concentration time by a selected "runoff coefficient" (see Art. 25). This resultant is frequently called the ci value. The anticipated runoff, in cubic feet per second per acre, may also be determined from a chart similar to Fig. 19.

4. The total storm-flow quantity for the sewer below any concentration point is then determined by the product of the ci value at the concentration point and the sum total of all tributary areas, i.e., A, in acres tributary above the concentration point.

25. Runoff Coefficients. Pondage in depressions, evaporation, absorption, and other factors reduce the runoff, so that not all the rainfall, even on impervious

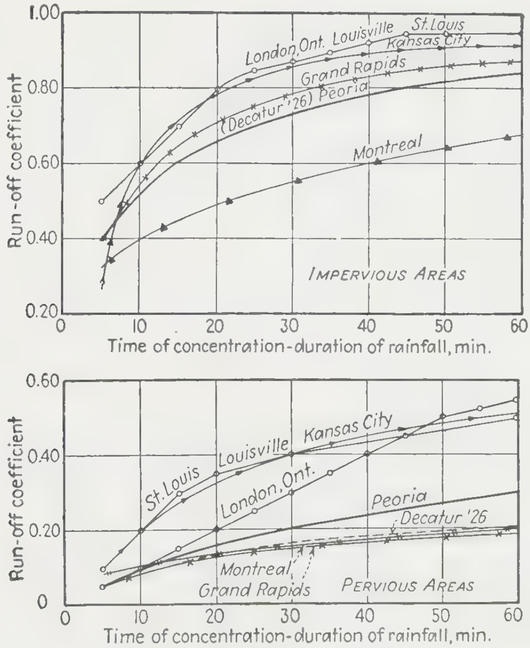

FIG. 20. Runoff coefficients for pervious and impervious areas, Peoria, Ill.

surfaces, reaches the sewer inlets. The longer the storm duration, the larger may be the percentage of rainfall runoff.

The proportion of pervious and impervious areas probably affects the runoff as much as any other factor. In designing storm sewers, a practical procedure includes a reasonable estimate of the probable future percentage of impervious area. The typical curves in Fig. 20 represent the bases for selecting runoff coefficients used for certain projects in various cities.

Estimates of the relative proportion of pervious and impervious areas can be made by considering the present development of a number of typical areas in the more completely developed sections of the city for which sewers are to be designed and comparing these with the anticipated future development of the districts to be sewered.

Certain illustrative data on the percentage of impervious surfaces, used in connection with various storm-sewer projects, are as follows:

Project and Type of Area	Impervious Surfaces, %
Peoria, Ill.:*	
Residential	30-40
Residential with neighborhood commercial areas	45–50
Decatur, Ill.:*	
Mercantile	70
Industrial	60
Commercial	50
Residential (16–30 per acre)	25
Parks and undeveloped	10
New Orleans, La.:†	
Commercial	76–100
Residential	42– 72
Residential, light	40– 45
Residential, suburban	39– 48
Analysis of typical areas in several cities:‡	
Louisville, Ky., residential	32–56
Springfield, Mass., residential	49
Cincinnati, Ohio	
Residential, 20 per acre	35
55 per acre	55
135 per acre	84
Commercial	100

* Greeley and Hansen, engineering reports and designs.

† MacDonald, F. W., and Mehn Adams, Jr., Determination of Runoff Coefficients, *Public Works Mag.*, November, 1963, p. 74.

‡ Metcalf and Eddy, "American Sewerage Practice," vol. 1, 2d ed., p. 286, McGraw-Hill Book Company, New York, 1928.

To apply these coefficients, the area under consideration is divided into zones representing the anticipated future extent of impervious area and a tabulation is made showing the pervious and impervious areas tributary to each concentration point, from which an average coefficient of runoff may be computed corresponding to the computed time concentration.

These computations may be simplified for use in an extended study of several proposed sewer districts by constructing a diagram to give the computed runoff in cubic feet per second per acre for various times of concentration (storm duration) and the proportions of impervious area (Fig. 19).

Another method, sometimes used, includes a fixed coefficient of runoff based upon the anticipated future development of the area. This, in effect, assumes that the uncertainties in forecasting area development and the selection of rainfall intensities make unnecessary the refinements in the foregoing procedure. Table 18 gives the runoff coefficients which have been used in a number of cities.

26. Storm-sewer Computations. The procedures for computing sewer sizes, designated hereafter as "capacity design," are discussed in Arts. 43 to 52, for sanitary sewers, storm sewers, and combined sewers. Other aspects of storm-sewer design are also discussed under Capacity Design.

27. Comparative Capacities per Unit Area. Computed storm-water runoff quantities per unit of tributary area (generally cubic feet per second per acre) are a logical basis for comparing the sewer capacities provided by the sewer-design practice in various communities. Some careful inquiries as to service satisfaction

TABLE 18. RUNOFF COEFFICIENTS FOR VARIOUS CITIES

City	Type of area	Runoff coefficients	
Baltimore County, Md.*	Roofs, pavements, and walls, pervious areas, varies with slope and soil type	0.95	
	Sparse vegetation	0.30–0.55†	
	Lawns	0.12–0.20†	
	Dense vegetation	0.08–0.12†	
Buffalo, N.Y.‡	Residential	0.48–0.58	
	Apartments	0.60–0.65	
	Commercial	0.60–0.70	
	Industrial	0.55–0.60	
Cincinnati, Ohio‡	Suburban (large lots)	0.30	
	Residential	0.35–0.40	
	Apartments	0.50–0.65	
	Retail business and downtown	0.70–0.90	
Milwaukee County Metropolitan Dist., Wis.‡	Most dense community	0.75	
	Adjoining densely built-up	0.65	
	Residential, well built-up	0.53	
	Adjoining built-up residential	0.45	
	Suburban	0.30	
Pittsburgh, Pa.‡	Varies with % impervious and slope		
	0– 10% impervious	0.20–0.30	
	50% impervious	0.50–0.57	
	100% impervious	0.90	
Rochester, N.Y.‡	Residential	0.25–0.40	
	Commercial	0.50–0.90	
	Industrial	0.60	
St. Louis, Mo.‡	Varies with % impervious and storm duration		
		15 min	120 min
	0% impervious	0.30	0.60
	50% impervious	0.50	0.78
	100% impervious	0.70	0.95
San Francisco, Calif.‡	Industrial	0.60–0.90	
	Commercial	0.80–0.70	
	Apartments and flats	0.60–0.75	
	Residential, attached houses	0.45–0.60	
	Residential, detached houses	0.40–0.50	
	Suburban	0.25–0.35	
	Parks	0.10–0.20	

* "Baltimore County Design Manual," Department of Public Works, Baltimore County, Md., 1955.
† For average slopes, 2.1 to 7 percent, and sand to clay, extremes range from 0.03 to 0.70.
‡ Ref. 20.

of existing sewers may provide technical evidence useful as a guide to judgment for communities in regions of similar rainfall characteristics.

Some comparative data are given by Fig. 21. These data in terms of cubic feet per second per acre vs. tributary area for various communities show a wide range of unit capacities. For 500 acres, the overall range (Fig. 21) is from 3.0 down to 0.7 cfs per acre, i.e., 4:1. A considered study by Stanley and Kaufman[20] indicated reasonable unit storm-sewer capacities for the general region of United States mainland and Canada east of the Rocky Mountains might be as follows:

Extent of drainage area, acres	Reasonable sewer capacity, cfs/acre	
	Outlying residential districts	Downtown or thickly populated areas
10	1.0	2.0–3.0
100	0.8	2.0–2.5
1,000	0.6	1.2–1.5

These unit-capacity figures may be used as rough guides to judge the probable adequacy of proposed storm sewers. They should not be used as a basis for storm-sewer design, without careful study of basic factors, as outlined in the foregoing sections.

28. Effect of Storage on Storm-water Quantities. The runoff of storm water, for which sewer capacity may be required, is greatly affected by any storage of storm-water quantities. (This is one factor affecting the application of unit sewer-capacity figures to any particular sewer district.) Storage of storm water may be in these forms:

1. *Infiltration capacity* of soil and land cover. This factor is substantially affected by pavements, roof surfacing, and other impervious coverings which result from urban development. It is an important consideration in application of the "hydrograph method" (ASCE Manual of Engineering Practice No. 37).
2. *Depression storage,* i.e., that portion of rainfall retained in surface depressions.
3. *Detention* of storm-water flow over land, in gutters, and in house drains, catch basins, and lateral drains. This is covered in part by the selected value of "inlet time" in the "rational method."
4. *Lakes, Ponds, or Reservoirs.* Sometime sizes of lower trunk sewers may be reduced by conserving natural lakes or ponds or by constructing storage reservoirs. This generally may be more practical in outlying semiurban areas than in highly developed urban areas. However, any storage lakes, ponds, or reservoirs have a tendency to become a catchall for debris or a source of breeding of mosquitoes, unless developed for some recreation use and properly controlled.

The basic effect of any storage is to retard flow and thus reduce peak runoff flow rates. However, the effect is reduced with time because of filling up of storage and so has less or no effect on runoff from long durations of rainfall. Storage effects are a part of the factors needed in the "hydrograph method." Probable storage effects should be considered in selecting runoff coefficients in the "rational method." In either method, storage effects must be forecast for the future period for which the storm sewers are designed.

29. Summary Statement. The determination of storm-water runoff quantities for which storm-sewer capacities should be provided has been done, in various communities and at different periods, by three methods.

1. *Formulas,* used frequently in early years, but not now used for routine storm-sewer design.
2. The *rational method,* as discussed above.

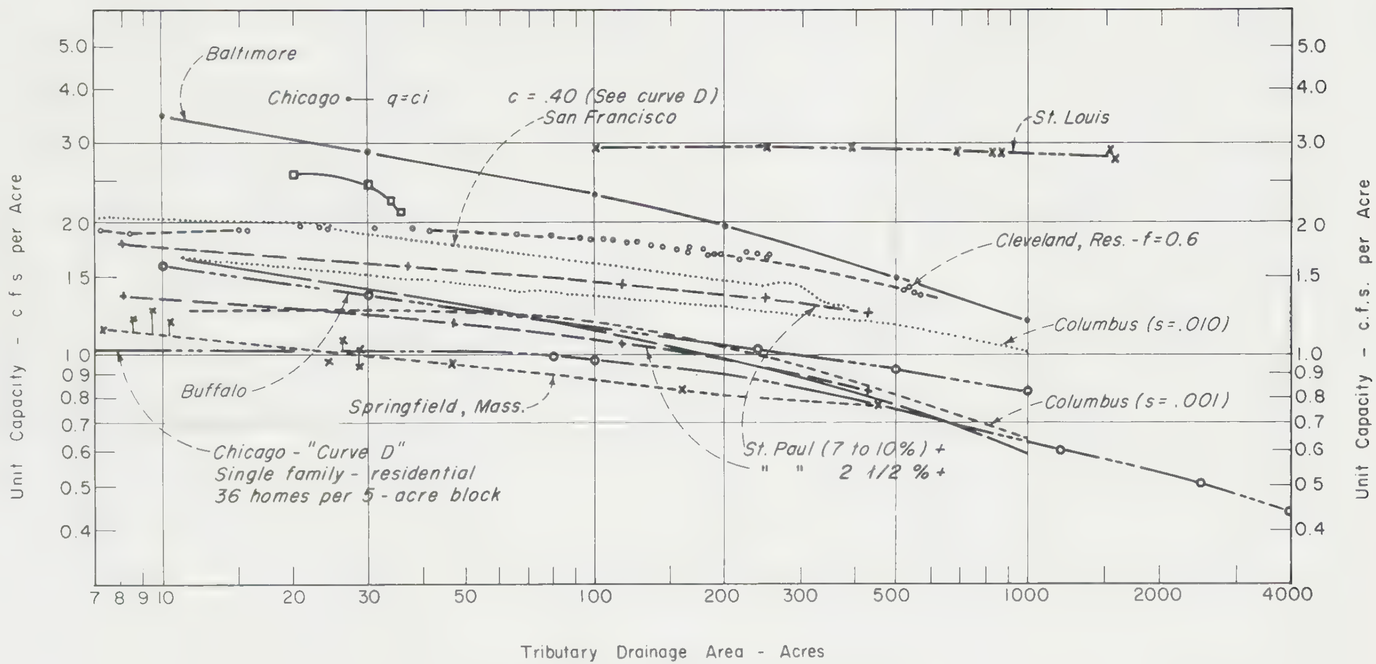

FIG. 21. Comparative capacities provided in storm sewers, various cities.

3. The *hydrograph method;* one version is discussed in detail in ASCE Manual of Engineering Practice No. 37.

The "rational method" represents the most practical present basis, in general, for estimating storm-water runoff quantities for storm-sewer-capacity design, in most communities, when used with mature judgment based upon engineering experience in relating storm-sewer capacity to troubles from sewer surcharge, or to actual measurements of storm-sewer flows serving various types of tributary areas. The "rational method" is not an easy method, nor is it always reliable for an inexperienced engineer to use without guidance.

Recently, the "hydrograph method" has been used in a limited number of large cities. However, it requires a great deal of local data collected over many years. Typical discussions of basic aspects of this method may be found in the following references:

Horton, Robert E., *Trans. Am. Geoph. Union*, **14**, 446, 1933.
Sherman, LeRoy K., *Eng. News-Record*, **108**, 501, 1932.
Horner and Flynt, *Trans. ASCE*, **101**, 140, 1936.
Bernard, M. M., *Trans. ASCE*, **100**, 347, 1935.
Tholin, A. L., and Clint J. Keiffer, *Proc. ASCE*, March, 1959, p. 85.
ASCE Manual of Engineering Practice No. 37, pp. 53 76, 1960.

HYDRAULICS OF SEWERS

30. General. The laws of hydraulics are applied to sewers for three general purposes:

1. To design new sewers to carry the estimated quantities of waste waters, including the proper size and slope and resistance to flow caused by junctions and other appurtenances
2. To estimate the capacity of existing sewers, recognizing the effect of resistance to flow caused by junctions and other appurtenances, to determine the relief capacity which may be needed to prevent surcharge with the anticipated waste-water quantities
3. To determine the flow in a sewer as a means of estimating existing waste-water quantities

A high degree of refinement in hydraulic computations for sewers is unnecessary because of the practical limitations on the accuracy with which the quantities and future physical factors, which affect hydraulic flow, can be anticipated.

Sewage is composed of about 99.9 percent water and about 0.1 percent pollution matter, partly suspended and partly dissolved. Industrial wastes may be, at times, somewhat more concentrated, and storm water may include considerable grit and other debris from street washings. Sewers are considered in hydraulic computations as conduits carrying clear water, with the following exceptions:

1. Velocities of flow must be maintained sufficiently high to prevent deposits of solids.
2. Reduction in the carrying capacity of a sewer may be caused by openings or connections cut in at frequent intervals and by variations in alignment of the short pipe sections.
3. There may be some reduction in the carrying capacity of sewers, with the passage of time, owing to deposits or adhesions of matter from the sewage or to deterioration of the interior of the sewer surface as a result of chemical reactions of sewage substances and the sewer material.

The first exception relates to the minimum slopes at which sewers should be constructed, and the last two relate to the selection of the roughness coefficients, or flow-resistance factors, to be used in the hydraulic formulas for computing the sizes of the sewers.

31. Hydraulic Formulas. Usually sewers are considered as open channels in the selection of hydraulic formulas, except for pressure lines such as depressed sewers or pumping-station discharge lines.

Various hydraulic formulas are discussed in Sec. 2 for flow in open channels and pipes flowing under pressure.

The Kutter and Manning formulas have been widely used in sewage-flow computations for open-channel conditions. The Manning formula has had increased use in recent years because of its simplified form and relative ease of use in slide-rule computations for all channel shapes. The Hazen and Williams formula has been widely applied in connection with pressure pipes carrying sewage. These formulas in their usual general forms are as follows:

Kutter:

$$V = \left[\frac{\dfrac{1.81}{n} + 41.67 + \dfrac{0.0028}{S}}{1 + \dfrac{n}{\sqrt{R}}\left(41.67 + \dfrac{0.0028}{S}\right)} \right] \sqrt{RS}$$

Manning:

$$V = \frac{1.486}{n} R^{2/3} S^{1/2}$$

Hazen and Williams:

$$V = 1.318 C R^{0.63} S^{0.54}$$

32. Roughness Coefficients. Selection of the proper value of the coefficient of roughness n (*i.e.*, flow resistance) to be used in hydraulic computations for sewers is most important. Generally used values of n, which are the same for both the Kutter and the Manning formula, are discussed in Sec. 2.

The results of a number of actual measurements of flows in sewers are available showing values of n ranging from 0.011 to 0.016 for sewers in reasonably clean condition and up to 0.020 for sewers in poor alignment or with deposit on the bottom. Laboratory experiments, without the variables of field conditions and effect of sewage contaminants, have resulted in n values of 0.009 to 0.012 under variable slope and velocity conditions. However, sound design should provide some factor of safety for future deterioration in capacity of the sewers.

A joint committee of the ASCE and WPCF[21] suggested the following values of n for use in the Manning formula. The lower values are suggested for clear water.

For cement-lined cast-iron pipe	0.012–0.015
For dirty or tuberculated cast-iron pipe	0.015–0.035
For concrete pipe	0.012–0.015
For asbestos-cement pipe	0.012–0.015
For vitrified-clay sewer pipe	0.012–0.015
For corrugated steel:	
Uncoated, ½-in. corrugations	0.024–0.026
Asphalt-coated and 25% paved	0.021–0.023
Smooth asphaltic lining	0.012–0.015

It has been the practice of the authors to base preliminary designs of sewerage projects for sewers 8 to 108 in. in size upon $n = 0.015$ to cover all hydraulic losses in the sewers and then in the preparation of final design drawings to use $n = 0.013$ for straight sewer sections with additional fall included to provide for hydraulic losses caused by manholes, curves, junctions, and other factors.

Recently more research data have become available on the absolute roughness of pipe surfaces and the effect on conditions of flow within the conduit. The Kutter and Manning formulas consider the flow to be in the turbulent state, affected only by the roughness of the conduit walls. At the velocities normally encountered in sewers, this condition is not fully developed and the friction loss is affected by the roughness and irregularities of the pipe walls and properties of the fluid. The friction coefficient f in the Weisbach-Darcy formula (Sec. 2) has been shown by experiment to be related to the boundary roughness and Reynolds number and presented in a form for engineering use.[22] If the Manning and Weisbach-Darcy formulas are rearranged, the theoretical relation between friction coefficients can be expressed as follows:

$$n = 1.486R^{1/6}\left(\frac{f}{8g}\right)^{1/2}$$

where R = hydraulic radius

The effect of increasing size and R on the value of n is evident. However, research has indicated the effect of diameter and velocity, as expressed in the Reynolds number, on the value of f for any given magnitude of the roughness of the pipe walls tends to decrease f with increasing size or velocity of flow. The combined effect with an absolute roughness commensurate with the surface character of commercial sewer pipe, and usual sewer velocities, is computed values of n which increase slightly with increasing size. Some engineers have used lower values of n in larger sewers, but this assumption is not supported by the research data.

33. Computation Diagrams. Diagrams for the general solution of the Kutter, Manning, and Hazen and Williams formulas are included in Sec. 2.

Various forms of diagrams, prepared specifically for the design of circular sewers, are available. The large diagrams originally prepared by John H. Gregory,[23] based on the Kutter formula, have had wide acceptance. Figure 22, a somewhat more conveniently sized diagram for $n = 0.013$ and $n = 0.015$, is based on the Manning formula.

Figure 22 permits the use of a straightedge to show the relation of the several factors that determine sewer capacity for $n = 0.013$ or 0.015.

The results obtained with these diagrams are as accurate as warranted by the generally available basic data. Diagrams can be prepared for noncircular sewer sections and may be used where elliptical, horseshoe, or other sections are involved in extensive computations. In general, problems involving noncircular sections can be solved by the general nomographic solution for the Manning formula, given in Sec. 2, or by computations using a loglog slide rule as explained in Sec. 34.

34. Slide-rule Computations. The Manning formula, $V = (1.486/n)R^{2/3}S^{1/2}$, can be readily used for direct computation on a loglog slide rule. Its application to slide-rule computation can, however, be facilitated by some rearrangement and the use of factors computed for the common sewer sizes, as follows:

$$V = K_1S^{1/2} \qquad \text{or} \qquad S = \left(\frac{V}{K_1}\right)^2$$

where $K_1 = \dfrac{1.486}{n} R^{2/3}$

and

$$Q = K_2S^{1/2} \qquad \text{or} \qquad S = \left(\frac{Q}{K_2}\right)^2$$

where $K_2 = \dfrac{1.486}{n} R^{2/3}A$

Table 19 contains values of K_1 and K_2 for $n = 0.013$ and 0.015 for sewers flowing full, up to 144 in. in diameter. Values of these coefficients for other sewer sizes, or values of n, can readily be computed. Coefficients for noncircular sections can similarly be computed, using the appropriate values of hydraulic radius and area of section.

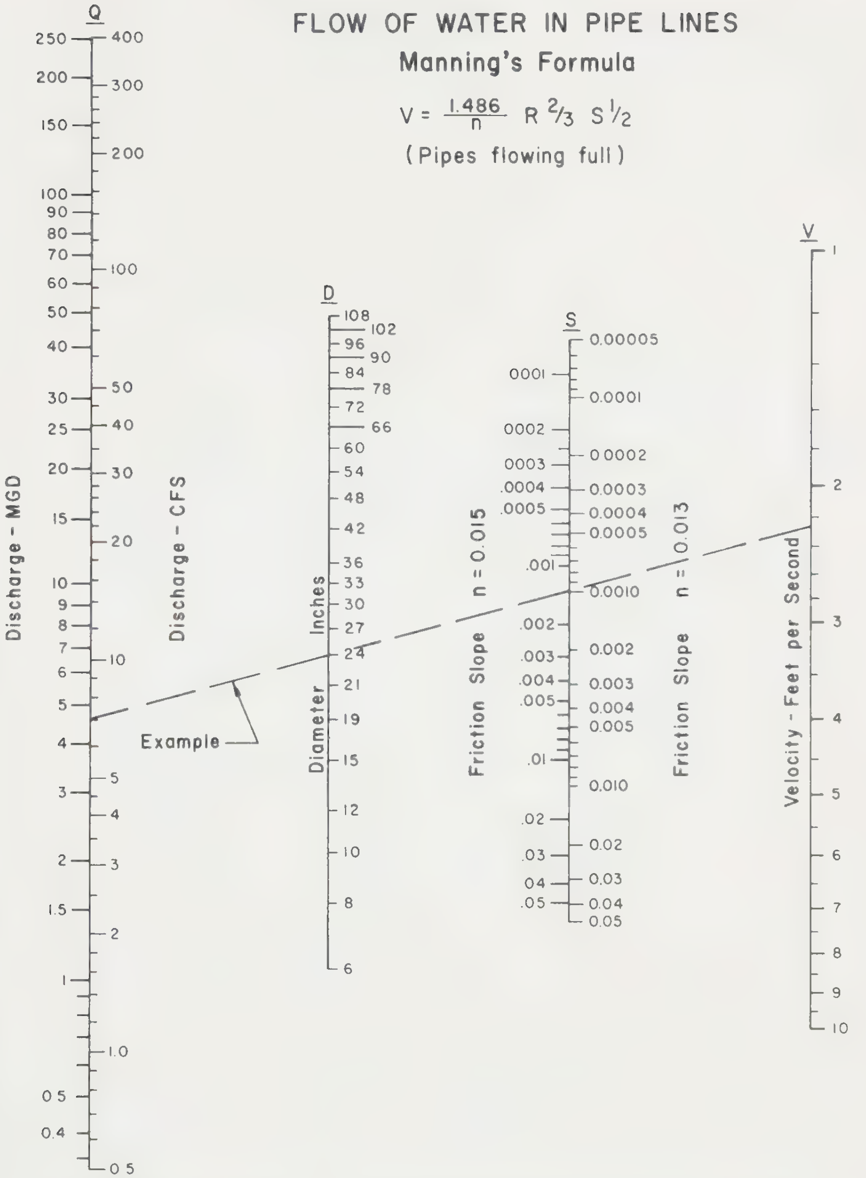

Fig. 22. Nomograph for solution of Manning's formula for circular pipes.

35. Hydraulic-elements Graphs. Hydraulic-elements graphs are used for the solutions of problems involving sewers flowing partly full. Most of the hydraulic-elements graphs in common use to date have been based on the assumption that the coefficient n does not vary with the depth of flow in the conduit. For some time this assumption has been known to be erroneous, but lack of suitable information has delayed its correction. The experiments of Wilcox and Yarnell and Woodward

TABLE 19. SLIDE-RULE COMPUTATIONS BY THE MANNING FORMULA

$$V = \frac{1.486}{n} R^{2/3} S^{1/2}$$

Diam of sewer, in.	Velocity factors K_1*		Capacity factors K_2†	
	n = 0.013	n = 0.015	n = 0.013	n = 0.015
8	32.6	28.2	11.4	10.0
10	40.1	34.8	21.8	19.0
12	45.4	39.4	35.6	30.9
15	52.7	45.6	64.9	54.9
18	59.5	51.5	105.0	91.1
21	65.9	57.1	158.5	137.5
24	72.0	62.5	226.0	196.3
27	77.8	67.5	309.0	269.0
30	83.6	72.5	410.0	356.0
36	94.3	81.8	666.0	577.0
42	105.9	90.6	1,018.0	871.0
48	114.3	99.1	1,425.0	1,247.0
54	123.9	107.3	1,970.0	1,701.0
60	132.7	116.0	2,605.0	2,275.0
66	141.3	122.4	3,360.0	2,910.0
72	149.9	129.9	4,230.0	3,670.0
78	158.0	137.0	5,240.0	4,550.0
84	166.0	144.0	6,390.0	5,540.0
90	174.0	150.6	7,690.0	6,650.0
96	181.5	158.1	9,130.0	7,950.0
102	189.2	164.0	10,750.0	9,300.0
108	196.5	170.1	12,300.0	10,800.0
114	203.5	176.3	14,400.0	12,500.0
120	211.0	182.6	16,580.0	14,330.0
126	217.5	188.5	18,850.0	16,330.0
132	224.5	194.5	21,300.0	18,490.0
138	231.5	200.5	24,050.0	20,850.0
144	238.0	206.0	26,900.0	23,300.0

* Constants for given size and n for velocity computations:
Slope known.......... $V = K_1 S^{1/2}$
Velocity known....... $S = (V/K_1)^2$

† Constants for given size and n for capacity computations:
Slope known.......... $Q = K_2 S^{1/2}$
Capacity known...... $S = (Q/K_2)^2$

have demonstrated that the values of the Weisbach-Darcy friction factor f and n in a partly full pipe are greater than for the same pipe when flowing full. The relation between the two friction factors in partially full pipes is as follows:

$$\frac{n}{n_f} = \left(\frac{R}{R_f}\right)^{1/6} \left(\frac{f}{f_f}\right)^{1/2}$$

Figure 23 is a hydraulic-elements graph, from a similar diagram by Camp, using the principle of varying n and f with depth of flow. The graph includes curves showing the variation of the friction factors with depth from experiments of Wilcox and of Yarnell and Woodward, and certain measurements made by C. Frank Johnson in large sewers in Louisville, Ky. The graph also includes as broken lines the hydraulic elements based on a constant value of n, as commonly assumed in the past.

36. Self-cleansing Velocities. A theoretical development by Shields[24] of the movement of particles in flowing water indicates that the force required to produce particle motion varies approximately proportional to the diameter and the submerged

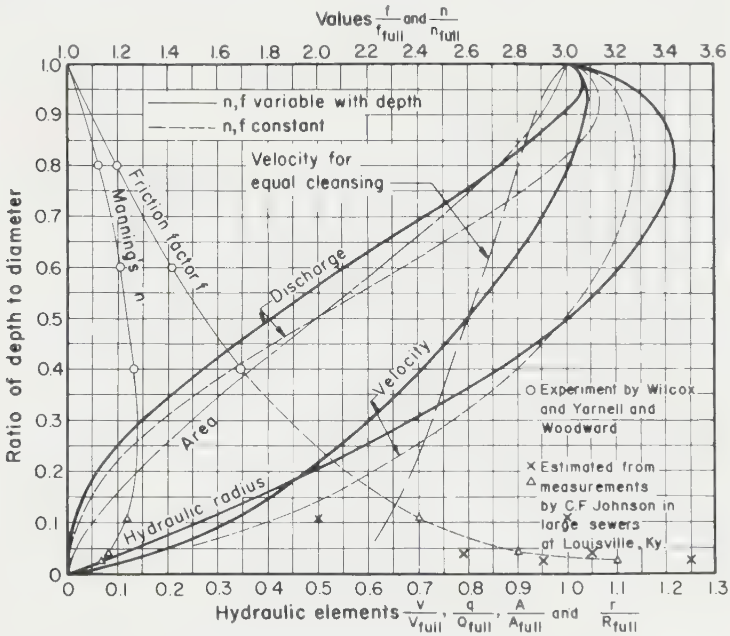

FIG. 23. Hydraulic elements of circular sewers.

weight of the particles. The critical velocity has been expressed by Shields and Camp in the following formula:

$$v = \sqrt{\frac{8\beta}{f} g(s-1)d} = \frac{1.486}{n} R^{1/6} \sqrt{\beta(s-1)d}$$

in which v is the mean velocity of the stream in feet per second, f is the Weisbach-Darcy friction factor, g is the acceleration of gravity in feet per second per second, s is the specific gravity of the particle, n is the roughness coefficient, R is the hydraulic radius, d is the diameter of the particle in millimeters, and β is a dimensionless constant varying from about 0.04 to start motion to about 0.8 for adequate self-cleansing of sewers.

This Camp-Shields equation with a friction factor f of 0.025 for a pipe flowing full indicates that a 2-fps velocity will be capable of barely moving a coarse sand particle with a diameter of 1.8 mm or an organic material (specific gravity of 1.2) with a diameter of about 14.8 mm. For effective scouring at a 2-fps velocity, the maximum size of sand particle would be 0.09 mm, about equal to U.S. Standard 170 sieve openings, and for organic material, 0.75 mm.

Since sewers generally are designed on the basis of their capacity when flowing full, the provision of a velocity adequate for self-cleansing under these conditions does not necessarily ensure prevention of deposits at all conditions of flow, especially during the early years when the tributary sewage quantities may be a small proportion of the design capacity. It may be desirable, therefore, to design sanitary sewers to provide scouring velocities for lower rates of flow, such as the estimated average daily rate of flow in the early years.

The Camp-Shields equation shows that the scouring velocity decreases with increases in the friction coefficient. Since the friction coefficient increases with decreasing depth of flow in a pipe, equal cleansing ability will occur in partially full pipes at somewhat less than the critical velocity when flowing full. Based on these principles, a curve of the proportional velocity required for equal cleansing ability at all depths of flow has been added to the graph of hydraulic elements associated with

Table 20. Minimum Grades for Sanitary Sewers

Diam, in.	Slope, ft/1,000 ft ($n - 0.013$)	
	Ordinary min* for velocity when full = 2.0 fps	Extreme min† for velocity when full = 1.80 fps
8	4.0	3.0
10	2.8	2.0
12	2.2	1.6
15	1.6	1.2
18	1.2	0.95
21	1.0	0.75
24	0.8	0.65
30	0.6	0.47
36	0.44	0.37
42	0.36	0.29
48	0.32	0.25
54	0.26	0.21
60	0.24	0.19

* Usual minimum requirements of state boards of health, ASCE Manual No. 37, 1960, p. 98.

† These grades should be used only where they will make pumping or excessive excavation unnecessary and then with extraordinarily careful construction and operating precautions.

a circular sewer (Fig. 23). This curve indicates that for a sewer expected to flow at all times greater than half full, no change in slope is required, but considerable change in the slope may be required to ensure self-cleansing when the minimum depths of flow are less than half full.

37. Minimum Grades. It has been common practice, and in accordance with most state board of health codes, that the minimum slopes be such as to produce a minimum velocity of 2 fps when flowing full, based on the assumption that this velocity will produce self-cleansing sewers. The assumption is generally borne out by experience, although some municipalities have experienced no serious problems with sewers designed with minimum velocities of about 1.5 fps.

High construction costs sometimes warrant designing sewers with velocities less than 2 fps. The sewer grades normally considered as the desirable minimum and the flat test grades that should be considered in any well-designed sewer system are indicated in Table 20.

38. Maximum Velocities. Maximum velocities in sewers may be important because of the possibilities of excessive erosion on sewer inverts and occasionally because of the piling up of water or sewage at the lower end of a high-velocity section due to the abrupt reduction in velocity. The erosive effect may depend upon the material used in construction or upon irregular surfaces. Evidence is available that velocities in excess of 40 fps have been harmless to smooth, dense concrete and regular vitrified-clay surfaces. Considerable erosion may be caused by gritty particles at much lower velocities. A limiting velocity of about 10 fps is desirable for the usual materials of construction. Special construction may occasionally be required to reduce the velocity at the lower end of a steep sewer section, such as a series of drops or a specially designed hydraulic-jump chamber. These may be particularly desirable at storm-sewer outlets to prevent soil erosion.

TABLE 21. HYDRAULIC FACTORS FOR SEWER SECTIONS OTHER THAN CIRCULAR*

Type of section	Relative to circular section		Hydraulic elements, ratio to height		
	Capacity X	Height Y	Area	Wetted perimeter	Hydraulic radius
1 × ¾ oval	0.96857	1.15783	$0.60488H^2$	$2.80138H$	$0.21592H$
Ovoid	0.95280	1.20782	$0.56505H^2$	$2.72991H$	$0.20698H$
Standard egg	0.91808	1.29456	$0.51046H^2$	$2.64330H$	$0.19311H$
Semielliptical	0.91603	1.02687	$0.81311H^2$	$3.33984H$	$0.24346H$
Horseshoe	0.95554	0.98499	$0.84719H^2$	$3.33789H$	$0.25381H$
Basket handle	0.98535	0.97922	$0.83126H^2$	$3.25597H$	$0.25530H$
Modified horseshoe, type I	0.92717	0.89166	$1.06544H^2$	$3.80006H$	$0.28037H$
Modified horseshoe, type II	0.92522	0.88392	$1.08646H^2$	$3.84140H$	$0.28383H$
Square (4 sides wet)	0.78540	1.00000	$1.00000H^2$	$4.00000H$	$0.25000H$
Square (3 sides wet)	1.39626	0.75000	$1.00000H^2$	$3.00000H$	$0.33333H$

* ROBERTS, BEARD, *Eng. News-Record*, **72**, 608–610, 1915.

39. Sewer Sections Other than Circular. Circular sewers are commonest in modern construction practice. Some large sewers and many older sewers may have shapes other than circular. Certain noncircular sewer sections are shown in Fig. 24, with various hydraulic factors given in Table 21, wherein the factor X, for a particular noncircular sewer section multiplied by the required capacity, gives the capacity of a circular sewer having the same velocity. The factor Y is the ratio of the height of the particular noncircular sewer section to the diameter of a circular section having the same hydraulic radius.

When required by special design problems, hydraulic-element graphs can be developed for these special shapes by computations following the general method, illustrated for circular sections by Fair and Geyer.[25]

40. Critical Flow. The theoretical considerations of critical flow are discussed in Sec. 2. Most sewer designs will involve flow in the "upper alternate stage," at depths in excess of the critical depth, and critical flow is usually not a matter of concern.

Stable flow in the upper alternate stage is assured when $d/H = 0.75$ and $H = d + V^2/2_g$. When the depth of flow is less than critical depth, and $d/H = 0.5$, the flow will also be stable, but it may be characterized as "shooting flow," and there is greater uncertainty as to the estimates of losses of head. Between these ratios it is necessary to compare the ratio d/D with the critical depth itself in order to determine the stage of flow.

It may occasionally be desirable to investigate critical flow, such as in a large steep sewer designed to flow partly full, and reference may then be made to discussions by Camp[26] and Fair and Geyer.[27]

41. Head Losses Other than Friction. At various places in the sewer system there may be head losses other than friction losses. These may be due to turbulence or eddies produced by changes in velocity, direction of flow, or obstructions. The

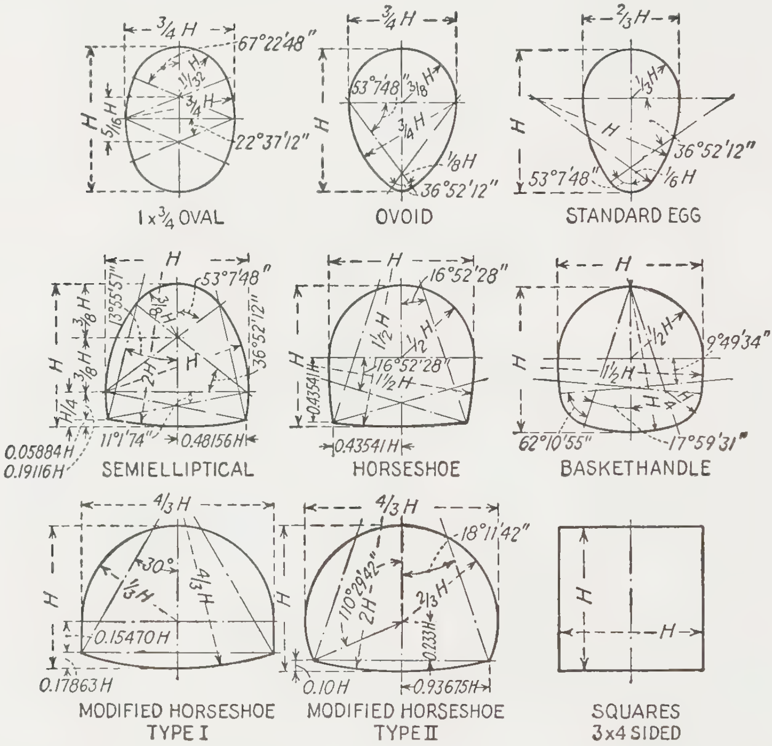

FIG. 24. Typical sewer sections.

commoner locations of special head losses are manholes, curves, changes in sewer size, and junctions of two or more sewers.

Some engineers include allowance for the commoner losses by the use of a larger value of the coefficient n. More commonly a lower value of n is used and allowances are added for the special losses. There are very few data on actual measurements of special losses in sewers. Allowances for special head losses must be based on somewhat arbitrary estimates, drawing largely on data for pressure conduits. The bases for estimating the commoner special losses in sewers are outlined in the following discussions.

Transition and Junction Losses. Head losses at sewer transitions and junctions could be computed theoretically by the application of the momentum principle. In practice this refinement is obscured by the inaccuracies in estimating sewage-flow rates; so resort is generally made to estimates of the head loss using empirical coefficients applied to the change in velocity head. The best data available are given by Hinds,[28] who recommends estimating the head loss in well-designed increasing velocity transitions at as low as

$$0.1\left(\frac{V_L^2}{2g} - \frac{V_u^2}{2g}\right)$$

and double this for decreasing velocity transitions. The magnitude of the loss is affected by the flare of the transition. Where practical, Hinds indicated that the angle of divergence between the center line and each wall be not more than 12.5 deg, especially for expanding transitions (i.e., decreasing velocity transition). Suggested values of the losses for ordinary sewer conditions are as follows:

For increasing velocity transitions:

$$h = 0.2\left(\frac{V_L^2}{2g} - \frac{V_u^2}{2g}\right)$$

For decreasing velocity transitions:

$$h = 0.3\left(\frac{V_u^2}{2g} - \frac{V_L^2}{2g}\right)$$

and V_u and V_L are, respectively, the velocities before and after the transition. Junctions can be treated as two or more transitions, with computations being made separately for each incoming sewer.

The necessary invert drop for all special sewer losses should be determined from the energy grade line using the following general formula:

$$\text{Invert drop} = y = \left(d_u + \frac{V_u^2}{2g}\right) - \left(d_L + \frac{V_L^2}{2g}\right) + h$$

where the subscripts u and L denote, respectively, condition before and after the invert drop. Negative values of y, suggesting invert rises, are to be ignored and inverts matched in such cases.

Manholes. Manholes are the commonest form of transitions, junctions, and changes in direction. Losses at changes in size or slope and for junctions can be estimated as discussed in the preceding paragraphs. Bend losses should be allowed as discussed in the following paragraphs. A minimum loss allowance of 0.02 ft per manhole having these characteristics is desirable, when invert flow channels are constructed in the bottom of the manholes.

Where essentially no change in conditions of flow occurs, as in straight-through manholes, with the formed channel depth at least $3/4D$, the loss in the manhole may be neglected.

Bends. Losses in bends can be expressed as $h = K(V^2/2g)$, where V is the velocity when full and the loss is that in excess of the friction loss in an equal length of straight pipe. Data on the magnitude of the coefficient for open-channel flow are needed. Based largely on data for small pressure pipes, the following values of K appear realistic for 90-deg changes in direction:

Radius to Center Line of Pipe	K
D	0.5
2 to $8D$	0.25

For radii greater than about $10D$ the bend loss may be neglected. For less than 90-deg bends, the coefficients may be reduced by the ratio $\phi/90$, where ϕ is the bend angle.

Increases in Pipe Size. These should be treated as transitions with the necessary invert drop based on computations using the energy grade line. It is not correct to match inverts. The frequent practice of matching the 0.8 depths is based on hydraulic elements determined with n assumed constant at all depths of flow and neglecting the transition loss. A more conservative procedure in small-pipe sewers with low velocities of flow would be to match crowns and neglect the transition loss.

42. Nonuniform Flow. Flow in an open channel is considered uniform when the depth, cross-sectional area, and other elements of flow are substantially constant from section to section along the channel. The foregoing discussion of sewer hydraulics relates to uniform flow, which is the usual condition in sewers.

Whenever the depth and other features of flow, such as the velocity, the cross-sectional area, and slope, vary from section to section, the flow is nonuniform or varied. Steady nonuniform flow exists when a constant quantity of water flows with variable cross-sections, slopes, and velocities. Under these conditions the surface of the water is not parallel with the sewer invert.

The commoner examples of nonuniform flow in sewers include:

1. The *drawdown curve*, which occurs near the free outlet end of a sewer in which the velocity increases toward the outlet.
2. The *backwater curve* caused by an obstruction in the sewer such as a dam or by discharge into a body of water whose surface is above the normal level of flow in the sewer. A flattened grade in the sewer also will produce a backwater curve. In such cases, the velocity and surface slope decrease and the depth increases toward the obstruction or flattened grade.
3. The *hydraulic jump*, which is the rise in the surface of the moving stream of sewage likely to occur when sewage moving at high velocity in a relatively shallow stream strikes a stream having a substantial depth and generally moving at a lower velocity.

The first two types of nonuniform flow are the more common, and of them the backwater curve is perhaps the more important in that it frequently is the cause of surcharging in sewers. The hydraulic jump is not common, but it may be quite important under certain conditions.

A profile of the drawdown or backwater curve can be computed by the application of the general formula for steady nonuniform flow in open channels

$$Q = A_m C \sqrt{R_m{}^5}$$

in which A_m and R_m are the average values of area and hydraulic radius for the two ends of the section of channel or conduit being studied. Consideration must be given to the shape and slope of the conduit, the quantity of flow, the coefficient of roughness, and the depth of flow at some known point.

In the solution of any specific problem, use is made of the following procedure:

1. The depth of flow at the outlet is computed.
2. The depth of flow at a section at some selected distance upstream is assumed.
3. The loss of head between these two sections is computed.
4. The distance between the two sections is related to the difference in total head (depth of flow plus velocity head) at each section. If the computed factors check the assumed factors, they become known.
5. The computation is repeated for the next section until sufficient points have become known to establish the drawdown or backwater curve.

The procedure is general and is applicable to all conditions of steady nonuniform flow. It is limited only by the accuracy of the assumptions on which it is based.

CAPACITY DESIGN

43. General Statement. The capacity design of any system of sewers involves three major steps:

1. The preparation of a general plan showing the sewer lines and the area tributary to each
2. The determination of the anticipated sewage quantities for which capacity is to be provided
3. The determination of proper sewer sizes and grades to carry the anticipated sewage quantities

Procedures for computing sewage quantities have been given in the foregoing articles, and the application of hydraulics to sewer design has been discussed. In the following articles the practical application of sewage quantities and sewer hydraulics to a computation of sewer sizes and grades will be discussed.

44. Sewer Systems. Four general types of sewer systems, each including trunk sewers, submains, and laterals, will be considered as follows:

1. Sanitary sewers
2. Storm sewers
3. Combined sewers
4. Intercepting sewers

Some considerations pertinent to the relative capacities of the several types of sewers are as follows:

1. Sewers required to carry off the domestic sewage and industrial waste waters should be provided with ample capacity at any cost, as they concern public health.
2. There is more leeway in determining the capacity of storm sewers as surcharging of these would back relatively clean storm water onto the streets. Thus there is a factor of convenience vs. cost as distinct from a factor of public health.
3. Combined sewers should have larger capacities than separate storm sewers because of the public-health hazards and inconvenience from basement flooding.
4. The capacity provided in storm or combined sewers to carry off storm water is in the nature of an insurance against inconvenience resulting from flooded streets or flooded basements. Thus the relationship between cost and capacity is pertinent.

45. Maps and Profiles. An early step in sewer design requires an accurate map of the district to be sewered, on which should be given street lines, lot lines, waterways, and contours for surface elevations to outline the ground slopes and to permit the preparation of preliminary profiles. Such a map should be drawn to a reasonably large scale, around 200 to 400 ft to 1 in. Aerial maps are well adapted to preliminary layout work and can be prepared at considerable savings over ground-survey methods where large areas are to be studied. Federal agencies, such as the agricultural stabilization and conservation service, have aerial photographs from which aerial mosaics may be prepared.

Where aerial maps are available at a scale of 200 or 400 ft to 1 in., the original photography may be subsequently used to prepare plan strips along the selected routes on drafting films for the construction plans. In reasonably open terrain these are sufficiently accurate to reduce the surveying to construction layout surveys and easement surveys. In built-up areas a center-line survey and profile may be desirable after the sewer location is determined.

46. Sewer Design. An arrangement of the proposed system should be made with the sewers following the natural slopes by the shortest route toward the outlet of the district. Sometimes, several preliminary arrangements may be required to determine the most suitable and economical plan.

When the sewer arrangement is fixed, the subareas tributary to each lateral sanitary sewer or to each storm-water inlet, or other concentration point, should then be outlined and the areas determined by scaling or by a planimeter. Subarea boundaries must be located in anticipation of the probable future street and lot improvements within the sewer district. Sewerage for each lot must be provided in the layout of separate and combined sewers.

Finally the sewer sizes may be computed by one of the several procedures outlined

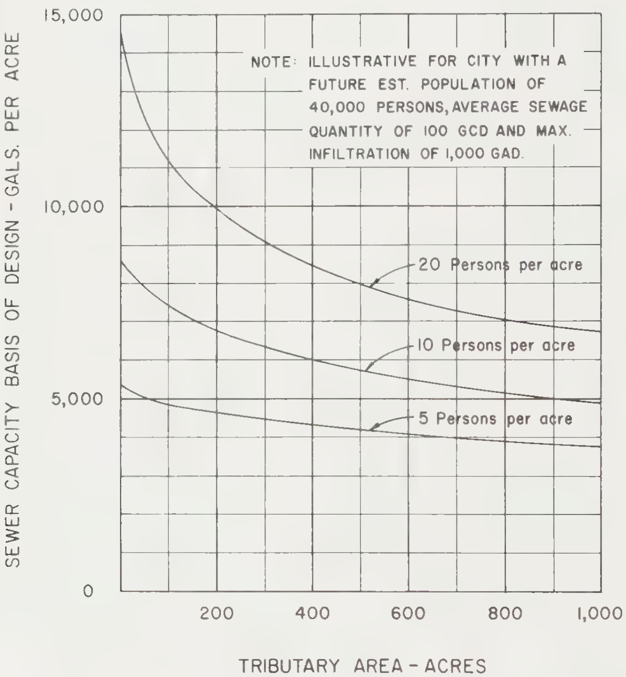

FIG. 25. Typical sewer-capacity curves.

in the following articles. Good engineering practice includes 8- and 12-in. pipe as the minimum sizes for sanitary and storm systems, respectively. Smaller sizes are more likely to become obstructed by debris, tree roots, and the like.

In selecting the proper sewer sizes, it is helpful to determine first a general slope corresponding to the ground-surface slope. The final sewer invert slopes will be somewhat flatter over a long line of sewers than the ground surface, as part of the available fall must be used for the invert drops required to provide for special losses and changes in sewer sizes. The minimum depth of the sewer invert should, in general, be not less than 5 ft, or sufficient to provide a minimum cover of 2 to 3 ft. The depth for storm sewers is governed by the minimum required cover, and the depth for sanitary or combined sewers is determined, in many instances, by the necessity of providing drainage for basement plumbing fixtures, generally requiring a minimum cover of 7 to 8 ft.

47. Computation Procedure for Sanitary Sewers. A procedure for sanitary-sewer design which has been found useful is the adoption of a curve representing the quantity per acre for which capacity is to be provided, as illustrated in Fig. 25. Such a basis-of-design curve is determined from the estimated population densities, the per capita sewage flows, the allowances for groundwater, and the like, as illustrated by the computations shown in Table 22. Obviously, any single curve will apply to only one set of conditions.

TABLE 22. COMPUTATION FOR UNIT PER ACRE CAPACITY—SANITARY SEWERS, ILLUSTRATIVE FOR CITY WITH FUTURE TOTAL POPULATION OF 40,000

Item	Quantities for various areas, acres					
	10	50	100	300	500	1,000
Estimated concentration of future population per acre	20	20	20	20	20	20
Factor for uncertain development (see Fig. 3)	1.6	1.6	1.5	1.3	1.2	1.1
Basis of design population per acre	32	32	30	26	24	22
Estimated average daily per capita sewage flow—future	100	100	100	100	100	100
Factor for peak flows: $M = 1 + \frac{14}{4 + \sqrt{p}^*}$	4.1	3.6	3.4	3.1	2.9	2.6
Per capita peak sewage flows	410	360	340	310	290	260
Total daily sanitary sewage flows, gal/acre (peak flows times basis of design population per acre)	13,000	11,500	10,200	8,100	7,000	5,700
Infiltration at 1,000 gal/acre†	1,000	1,000	1,000	1,000	1,000	1,000
Total sewer basis of design, gal/acre capacity	14,000	12,500	11,200	9,100	8,000	6,700

* p = total population for area in thousands.
† Illustrative figure only—actual to be carefully determined.

It seems logical to use gad for the unit capacity of sanitary sewers, though some engineers prefer cfs per acre or per 100 acres. In certain cities, unit sanitary-sewer capacities considerably lower than those shown in the illustrative computation have been found satisfactory as a basis of design. Among these are the following:

Madison, Wis. The original sewer system was designed in 1885. Data from the city engineer (1937) indicated the original design was reasonably satisfactory, some relief sewers being required only in commercial and more congested districts. All sewage in Madison is pumped two or more times, and determined efforts have been made to prevent downspout and surface-water connections to sanitary sewers and to reduce infiltration.

The design of sewers in 1930 was based upon 100 gcd with population densities of 25 per acre for light residential areas and 50 per acre for apartment districts, plus 25 percent for infiltration and allowance in the design for 100 percent overload.

Thus these two bases for the sewer flowing full become equal to:

Area	gad	cfs/100 acres
Light residential	6,250	0.96
Apartment	12,500	1.9

Later sewer designs for areas of anticipated heavy future development have been checked as to capacity by the engineers in the Madison Metropolitan Sewerage District, on the following basis:

Population to be served	30 per acre
Max hourly rate	300 gcd
Max rate of sewage flow	9,000 gad
Infiltration	2,000 gad
Max rate of flow in sewer	11,000 gad
	or 1.7 cfs/100 acres

Milwaukee, Wis. Engineers of the Sewerage Commission, city of Milwaukee, according to Ray D. Leary, Chief Engineer and General Manager, use the following criteria in designing main and intercepting sewers and in reviewing plans for sanitary sewers:

Description of Area	Quantity of Sewage, gad
1. Residential (10–14/acre)	9,700
(15–20/acre	12,900
Main sewers	19,400
2. Commercial	60,500
3. Industrial*	
5 acres or less	242,300*
10 acres	129,200
50 acres	32,300
100 acres	23,900
500 acres	11,000

* Within 1916 city limits, use double these rates.

Phoenix, Ariz. Bennett published a sanitary-sewer design curve (*Engineering News-Record,* Oct. 14, 1948) ranging from 12,000 gad for 50 acres or less to 4,000 gad for 1,500 acres or more (see Fig. 26, curve 6), based on maximum-flow measurements in existing sewers.

Columbus (Franklin County), Ohio. Curves 5 and 5*a* in Fig. 26 illustrate some experiences frequently found in highly developed urban areas where control of infiltration has been a problem. Bradley (*Proc. ASCE,* September, 1928, p. 2065) published the design basis for sanitary sewers in Franklin County near Columbus, Ohio, with bases of design capacities ranging from 2.0 cfs per 100 acres for areas less than 50 acres to 1.0 cfs per 100 acres for areas over 500 acres (curve 5, Fig. 26). In 1938, an investigation of the Franklin County sewers, then a part of the developed urban area of the city of Columbus, showed that the sewers were overloaded in wet weather because of infiltration from foundation drains, roof drains, and leaky sewers. A new design capacity 50 percent higher than the Bradley basis (curve 5*a*, Fig. 26) was considered desirable. Certain relief sanitary sewers were considered with capacities of 4.0 cfs per 100 acres (25,800 gad).

Los Angeles, Calif. The basis of design for sanitary sewers has been as follows:

Description of area	Sewage quantities per acre per 24 hr		Sewer capacities flowing full, gal/acre	
	cfs	gal	15-in. and smaller*	18-in. and larger†
Residential, R-1 single-family‡	0.004	2,580	5,160	2,800
Residential, R-5 unlimited	0.020	12,920	25,840	14,000
Commercial (all)	0.015	9,690	19,380	10,500
Industrial, M-1 and M-2, light§	0.024	13,570	27,100	14,700

* Sewers 15 in. or smaller design to flow one-half full (*i.e.*, 0.5 full capacity).

† Sewers 18 in. or larger design to flow 0.85 full (*i.e.*, 0.85 full capacity).

‡ Two-, three-, and four-family zones should have unit capacities of two, three, and four times single-family zone.

§ Major industrial districts—determined for each area.

The reported Los Angeles basis-of-design data for sanitary sewers in single-house areas provide the lowest per acre sewer capacity of any major city (curve 7, Fig. 26).

48. Footing Drains. Care should be taken in determining sewer-capacity requirements where footing drains are permitted to be connected to sanitary sewers. In Peoria, Ill., investigation revealed rates of flow in a small sewer system during rains in excess of 25,000 gad, which were attributed to "piping" of surface water rapidly to the footing drains and thence to the sanitary sewer.

49. Storm-water Allowances in Sanitary Sewers. In many cities the discharge of roof water into sanitary sewers occurs; so additional capacity should be provided. At Waukegan, Ill., where a house count in several sewer districts showed that 48 and 92 percent of the houses had downspout connections, capacity was provided for roof water from 90 percent of the existing houses computed for a 15-min storm duration and a runoff of 80 percent. In other cases, allowance in sanitary-sewer capacities is made for runoff from courtyards. The computation of sewer sizes and slopes is, in general, similar to that for combined sewers with resulting unit capacities from 40,000 gad for 500 acres to about 120,000 gad for 20 acres (Fig. 26, curve 3).

50. Computation Forms. Computations for determining the required sewer sizes and slopes may be simplified by using a form similar to that shown in Table 23. The rate per acre, obtained from the curve previously adopted as a basis for the design, is entered in column 6 and is multiplied by the total area (column 5) to obtain the total flow rate (column 7) for which capacity is to be provided. Column 14 is the sum of the losses due to bends, manholes, junctions, and special structures. Where sanitary-sewer flow rates are to be computed from the population, as shown in Table 23, they may be computed directly on the design computation form by appropriate modifications to columns 4 through 7.

51. Computation Procedure for Storm Sewers. Application of the rational method, which is discussed in Arts. 18 to 25, to the selection of sewer sizes and slopes may be simplified by the use of a form similar to that shown in Table 24. Values of the runoff coefficient relating to the total area tributary at a particular point are entered in column 6. The rainfall intensity (column 9) corresponding to the time of concentration (time of flow) (column 7) is obtained from a previously adopted rainfall time-intensity curve. The rate of runoff per acre (column 10) is the product of the runoff coefficient (column 6) and the rainfall intensity (column 9) and is some-

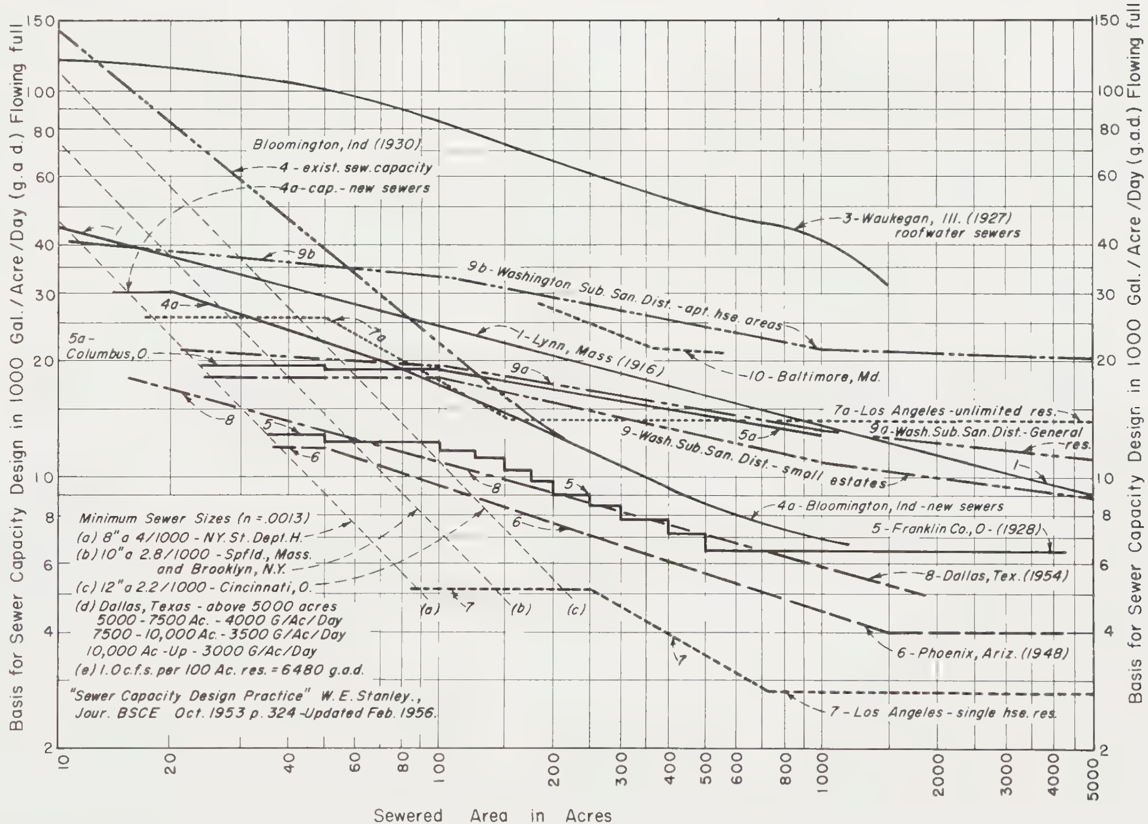

FIG. 26. Basis of sanitary-sewer design, relation of capacity to area, illustrative practice.

TABLE 23. FORM FOR SANITARY-SEWER DESIGN COMPUTATIONS

Sewer location			Tributary area, acres		Max rate of sewage flow		Design				Profile				
Street	From manhole No.	To manhole No.	Increment	Total	Rate per acre, gpd	Total mgd	Diameter, in.	Slope, ft/1,000	Capacity when full, mgd	Vel. when full, fps	Length, ft	Fall, ft	Other losses, ft	Invert elev. upper end	Invert elev. lower end
(1)	(2)	(3)	(4)	(5)	(6)	(7)	(8)	(9)	(10)	(11)	(12)	(13)	(14)	(15)	(16)
Third	10	11	40.0	40.0	13,000	0.52	8	5.3	0.52	2.3	325	1.72	0.00	95.33	93.61
Third	11	12	15.0	55.0	12,500	0.69	8	9.5	0.69	3.1	400	3.60	0.08	93.53	89.93
Chestnut	12	13	12.4	67.4	12,000	0.81	10	3.8	0.82	2.3	350	1.33	0.21	89.72	88.39

TABLE 24. FORM FOR STORM-SEWER DESIGN COMPUTATIONS

Sewer location			Tributary area, acres		Runoff coefficient	Time of flow, min		Rainfall intensity, in./hr	Runoff, cfs		Design				Profile				
Street	From manhole No.	To manhole No.	Increment	Total		To upper end	In section		Rate per acre	Total	Diameter, in.	Slope, ft/1,000	Capacity, cfs	Vel., fps	Length, ft	Fall, ft	Other losses, ft	Invert elev. upper end	Invert elev. lower end
(1)	(2)	(3)	(4)	(5)	(6)	(7)	(8)	(9)	(10)	(11)	(12)	(13)	(14)	(15)	(16)	(17)	(18)	(19)	(20)
Oak	1	2	7.20	7.20	0.47	15.0	1.7	3.2	1.50	10.8	21	5.0	11.1	4.6	470	2.35	0.00	45.00	42.65
Chestnut	2	3	6.40	13.60	0.50	16.7	1.0	3.0	1.50	20.4	24	10.0	22.8	7.3	430	4.30	0.28	42.37	38.07
Maple	3	4	6.68	20.28	0.51	17.17	1.0	2.9	1.48	30.0	30	7.0	34.5	7.0	430	3.01	0.48	37.59	34.58

times designated ci; whereas the total runoff for which capacity is required is the product of the total area (column 5) and the rate of runoff per acre.

Where the hydrograph method is used for computing the capacity, as discussed in Art. 17, the weighted imperviousness is computed, requiring expansion of columns 4, 5, and 6. The runoff rate is determined from standard design curves for various percentage imperviousness and flow times in the sewer and is entered in column 10. The rainfall-intensity column (column 9) is not used.

If the storm-sewer capacity is to be based upon the arbitrary method in which a per acre runoff is selected for future conditions from experience with existing sewers as discussed in Art. 27, a rate per acre may be taken directly from a curve similar to that shown in Fig. 21, prepared especially for the city under consideration. In this case, columns 6, 7, 8, and 9 of Table 24 are not needed. This procedure is useful in the design of new and relief sewers covering substantial portions of a city already provided for storm water with combined sewers. Since this procedure does not include consideration of the time of concentration, care must be taken in the selection of the runoff curve to give due consideration to differences in surface slopes and the characteristics of individual sewer districts.

52. Computation Procedure for Combined Sewers. Sizes and slopes of combined sewers are computed in the same manner as for storm sewers, with the exception that higher runoff values should be used. Also, some engineers add the estimated maximum rate of sewage flow to the computed storm runoff to determine the required sewer capacity. However, this may be a questionable refinement since rainfall runoff is in the magnitude of 100 times the sanitary-sewage flow.

53. Intercepting Sewers. Intercepting sewers are generally used in connection with a sewage-treatment project and serve as the collection system to take such part of the flow from existing sewers as may be necessary to eliminate objectionable waterway pollution. Intercepting sewers may be classed as follows:

1. Sewers to take the flow from existing sanitary sewers
2. Sewers to take the dry-weather flow and a portion of the storm flow from combined sewers

The first class of intercepting sewer is essentially a trunk collecting sewer, directly connected to the existing sewers and designed to take the full flow at the peak rates that may be reasonably expected from the tributary areas within the design period.

The basis of design of the second class of intercepting sewers is less easily determined because of the rapid and large increases in the rate of flow in the tributary combined sewer system during rainstorms. The major problem is to determine how much of the storm runoff should be diverted into the intercepting sewer before the sewage diluted with rainwater is permitted to overflow through the old outlets into the waterway.

Determination of the quantity of storm water to be admitted to the intercepting sewer requires consideration of the following principal factors:

1. The pollutional characteristics of the sewage to be intercepted
2. The quantity of sewage in relation to the minimum flow in the waterway receiving the overflow
3. The use to be made of the waterway or body of water and the water quality desired, or required, in the waterway
4. The extent, frequency, duration, and intensity of rainfall and resulting overflow of sewage
5. Considerations of cost

The design of large intercepting sewers must be based upon an extended investigation including both the capacity of the waterway to take pollution without creating objectionable conditions and experiences elsewhere in actual operation of similar intercepting systems. These questions will become more complex as the need for stream-pollution abatement increases.

Some data on the capacities of intercepting sewers at various places in the past are summarized in Table 25. Generally, intercepting sewer capacities have been

TABLE 25. COMPARATIVE DATA ON INTERCEPTING-SEWER CAPACITIES

	Avg dry-weather sewage flow, gcd	Interceptor capacity at date of ultimate design	
		gcd	gad
Minneapolis–St. Paul Sanitary District			
Main interceptor near plant, original design basis, 1970	151	368	5,650
Revised by 1960 review of existing sewers—2000	173	342	4,260
Wheeling, W. Va.	280	665	9,200
Spokane, Wash.	233	536	6,830
Peoria, Ill., Kickapoo interceptor	145	407	3,859
Buffalo, N.Y.	186	512	18,000
Rochester, N.Y.	120	420	12,200
Detroit, Mich.	155	329	6,620

350 to 500 gcd based on the future population. However, in certain instances a much larger capacity has been considered desirable, as at Springfield, Ill., where the southeast intercepting sewer was designed for a capacity of twenty-five times the dry-weather flow or about 2,200 gcd, as it was anticipated at the time of design that the stream into which the overflow would discharge would flow into the future source of water supply.

SEWER MATERIALS AND JOINTS

54. General. Sewers are usually constructed as underground conduits, and their structural design is discussed in Sec. 7. Structural considerations affect the hydraulic characteristics of sewers principally through the selection of the shape and through roughness, or frictional resistance of the materials used in the construction.

Most of the faults in sewers are traceable to poor construction methods leading to cracked pipes and leaking joints which lead to overloading the sewer system by excessive groundwater infiltration.

55. Materials of Construction. The most commonly used materials for sewers are clay pipe and monolithic and precast-concrete pipe (plain or reinforced). Asbestos-cement pipe is being used in increasing quantities. Cast-iron, steel, corrugated-metal, and plastic pipes are also employed, usually where special conditions can be best met by properties unique to each of these materials.

A more detailed discussion of sewer materials may be found in the ASCE Manual of Engineering Practice No. 37.[21]

56. Sewer-pipe Joints. The design of the joints in sewer pipe is extremely important to the proper installation of a sewerage system. A tight joint becomes a necessity when treatment plants and pumping stations are added to a sewer system, since hydraulic capacity must be provided for infiltration, which usually occurs at pipe joints, including house connections. An acceptable joint must be watertight, resistant to root penetration, resistant to corrosion, and durable and must provide for flexibility.

At one time a simple cement mortar joint was considered adequate; however, the trend in recent years has been toward the use of rubber or neoprene gaskets in all sanitary sewers. Many shapes of gaskets have been developed and used with varying degrees of success. A gasket with a circular cross section retained in a groove on the pipe spigot has been used in almost all pressure pipe for some time, and its use for gravity sewers has been rapidly increasing. This joint is watertight, flexible, and durable and is relatively easy to make up in the field.

A more detailed description of other common and special pipe joints may be found in ASCE Manual of Engineering Practice No. 37.[21]

57. Sewer Sections. The circular sewer section will, in general, be found the most economical, owing largely to its availability in precast pipe up to 10 ft in diameter. Pipes with elliptical cross sections, equivalent to circular pipe up to 10 ft in diameter, are available at a higher cost for use with the long dimension laid either vertical or horizontal, depending on the location.

Larger sewers of reinforced monolithic concrete are frequently of horseshoe or semielliptical section, though in some cases other special sections have been used. The choice of the sewer cross section is governed by relative construction costs, with consideration given to possible operating difficulties where small flows, and hence low velocities, may be expected.

58. Deterioration of Sewer Materials. The principal causes of the deterioration of sewer pipe are acid industrial wastes and hydrogen sulfide. Certain anaerobic bacteria can reduce sulfates, present in the sewage, to form sulfurous acid which accumulates in moisture on the pipe walls above the sewage. The acid attacks the cement and may ultimately destroy the concrete pipe. Deterioration from acid industrial wastes usually occurs in the bottom of the pipe.

Problems with concrete-pipe deterioration are more prevalent where there are high sulfate concentrations in the water supply, or where there is seawater infiltration, where the climate is warm, and where low velocities of flow or stagnant sewage allow solids to settle out. The problem does not occur where pipes flow full, as in sewage force mains.

Some methods of reducing deterioration of sewers are as follows:

1. Provide scouring velocities which will reduce solids deposits and reduce surface-film accumulation
2. Avoid excess turbulence which causes the release of hydrogen sulfide
3. Provide ventilation of the pipe, thus preventing the accumulation of condensate on the pipe walls and reducing the concentration of sulfide gas in the sewer atmosphere
4. Provide internal protection of pipe:
   a. Vitrified-clay liners
   b. Plastic liners
   c. Utilize fly ash in concrete
   d. Provide additional concrete cover on steel to allow for loss due to hydrogen sulfide
   e. Vinyl and epoxy coatings

Discussions of hydrogen sulfide control and protection of pipes have been presented by Pomeroy and Bowlus,[29] by Parker,[30] and by Santry.[31]

59. Pipe Laying and Bedding. Proper laying of sewer pipe is important to attain properly aligned and smooth joints. The hydraulic capacity can be reduced by turbulence and increased friction losses resulting from poor pipe jointing. A detailed discussion of the structural design and bedding requirements for pipe in trenches will be found in Sec. 7.

It should be noted, however, that particular attention should be made to the preparation of the pipe bed, the maximum width of trench at the top of the pipe, and proper compaction of backfill up to the top of the pipe.

SEWER APPURTENANCES AND SPECIAL STRUCTURES

60. General. The commoner sewer appurtenances include manholes, junction chambers, street inlets, and catch basins. Special structures used occasionally for specific purposes include inverted siphons (depressed sewers), sewage-regulating devices, overflows, outfall structures, and tide gates.

61. Manholes. Manholes are constructed to provide ready access into sewers for inspection, cleaning, and repairs. They are generally provided at changes in alignment or grade, at sewer junctions, and at such intermediate points that the distance between manholes will not exceed 300 to 500 ft, with the greater spacing on the larger sewers.

Where one sewer joins another with a difference in invert elevations of 2 to 3 ft or more, a drop manhole is usually constructed to permit the sewage to fall vertically through a pipe placed just outside the manhole barrel and entering the manhole near the bottom, providing a minimum disturbance to flow and inconvenience to workmen who must enter the manhole.

Standard manholes are shown in Figs. 27 and 28. Illustrative drop manholes are shown in Figs. 27 and 29. Details of a special bend manhole design used in recent work at Peoria, Ill., are shown in Fig. 30.

To provide for the head losses resulting from the disturbance to flow caused by manholes, it is considered good practice to allow an additional elevation drop through the manhole. This drop is dependent on the velocities in the sewer and the degree of change in direction of flow and varies from 1 in. to as much as 3 in.

62. Junction Chambers. Junction chambers for small sewers usually are manholes, but special structures are frequently included for the junction of large sewers (42 in. and larger). The major hydraulic problem is the prevention of deposits and head losses incident to the checking of high velocity in one sewer by a lower velocity in another. Insofar as practicable, the velocities of flows should be the same in both sewers at a junction. To prevent backing up of flow in one sewer due to a higher elevation of flow in a larger sewer, it is usually desirable to bring the sewers together so that the 0.8 depths of both sewers will be at the same elevation. Where there is a change in the direction of flow at a junction, the upstream sewer is usually raised to allow for an additional head loss due to turbulence.

As long as reasonable care is exercised to avoid sudden enlargements or contractions, and changes of direction are accomplished by the use of smooth, easy curves, the hydraulic features of junction structures generally present no very complex problem for velocities up to 6 or 8 fps. A typical junction chamber is shown in Fig. 31.

63. Inlets. Street inlets, used to permit entrance of storm water from the street, should usually be located upstream of the crosswalk at each street intersection and at low points between streets.

The time of entrance and hence the required capacity of the storm-water sewer may be controlled to a limited extent in flat areas by restricting the capacity of the inlet or by spacing the inlets at greater intervals. On steep grades the inlets must be designed to catch the storm water as it flows along the gutter and to prevent objectionable accumulation of the water on lower property.

It is frequently necessary, particularly on steep slopes, to depress the gutter at the inlet, but such depressions should be carefully designed to avoid traffic hazards. The maximum height of the inlet opening is limited by the curb height and the per-

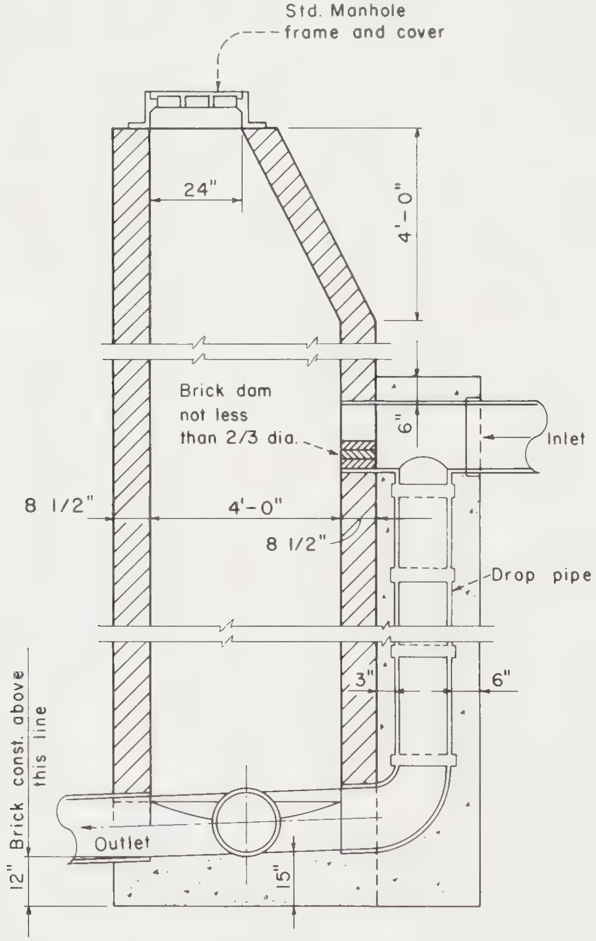

Fig. 27. Drop manhole, Sanitary District of Bloom Township, Chicago Heights, Ill.

missible depth of depression. Experience in many places indicates that heights of 4 to 6 in. are desirable. On steep grades, the inlet openings may be made longer than elsewhere to provide sufficient inlet capacity.

Formerly, bar gratings were provided on the vertical openings of side inlets to prevent entrance of materials of sufficient size to clog sewers. Practice today varies, but with more paved streets there is a tendency to use clear openings with no bars. Data on inlet capacities are few, and quite generally the type and number of inlets

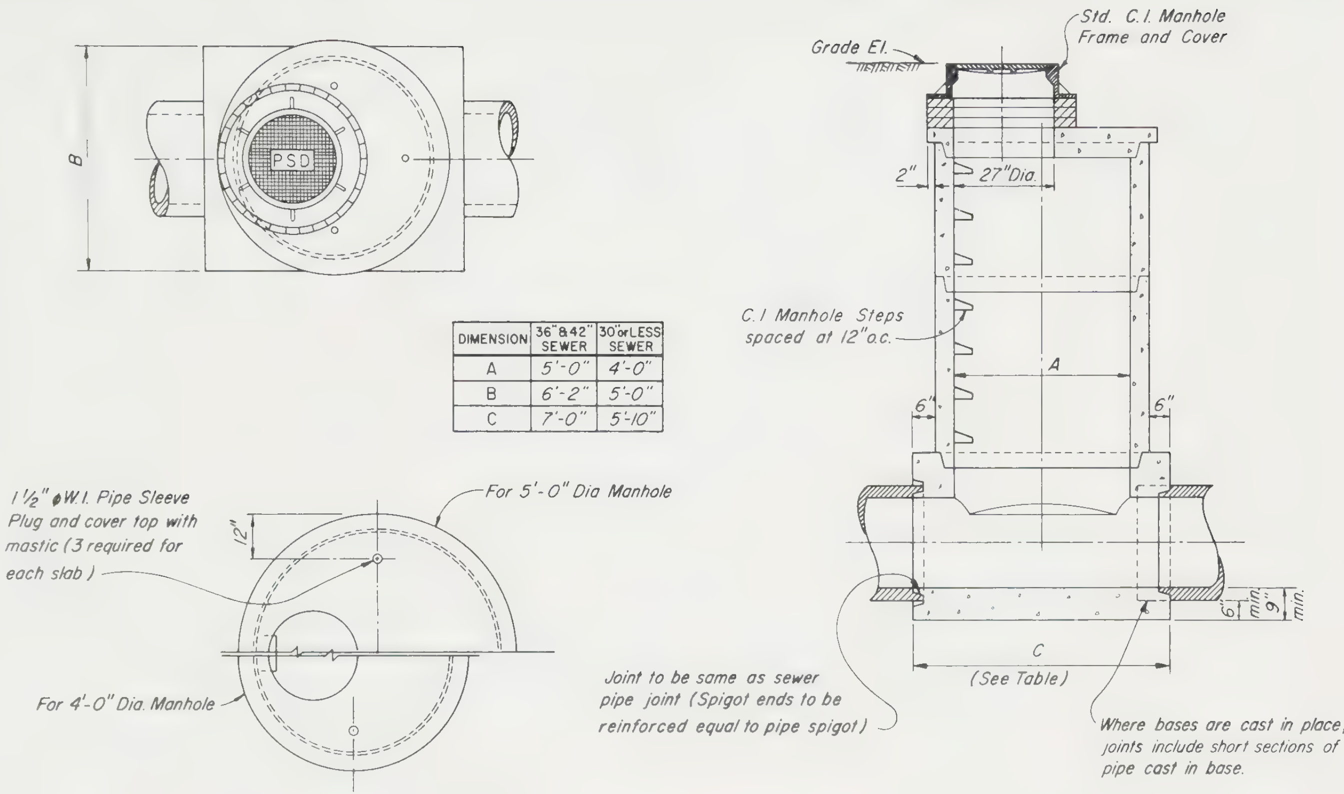

DIMENSION	36" & 42" SEWER	30" or LESS SEWER
A	5'-0"	4'-0"
B	6'-2"	5'-0"
C	7'-0"	5'-10"

FIG. 28. Typical precast standard manhole.

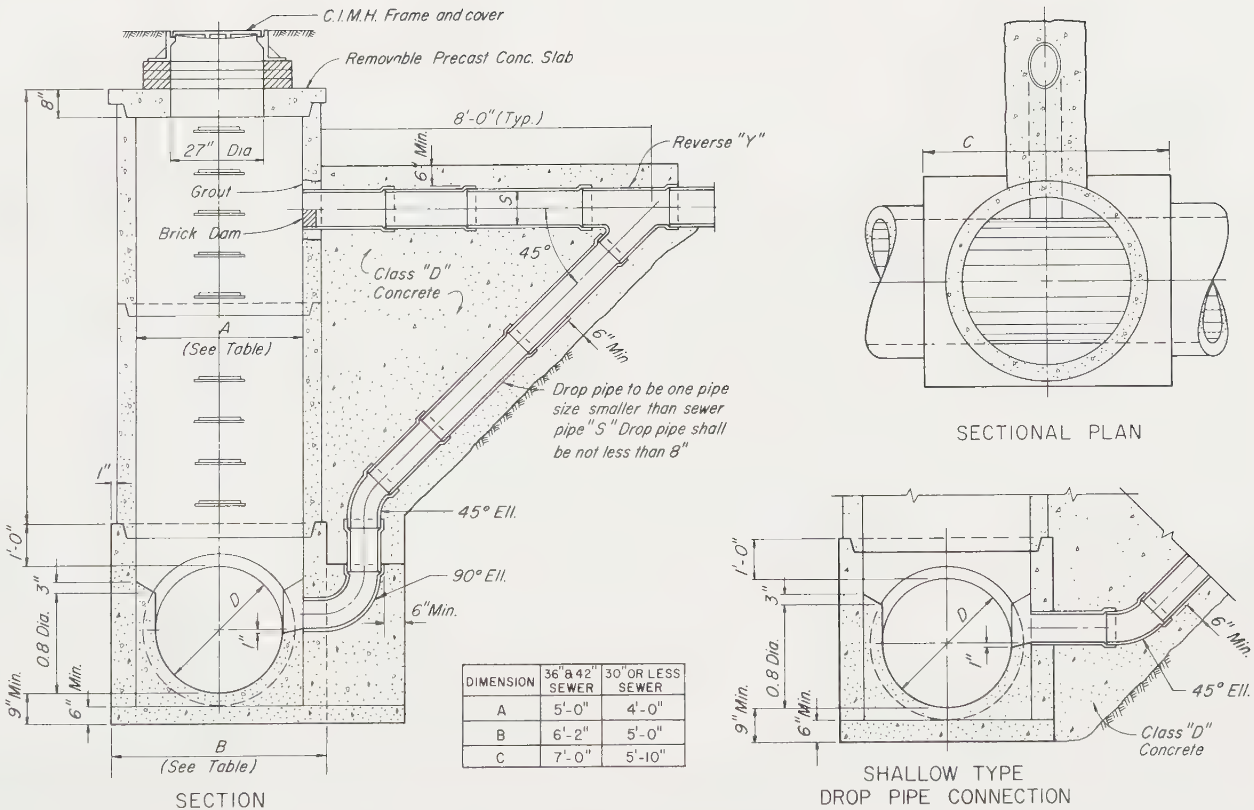

DIMENSION	36" & 42" SEWER	30" OR LESS SEWER
A	5'-0"	4'-0"
B	6'-2"	5'-0"
C	7'-0"	5'-10"

FIG. 29. Typical drop manhole.

are determined by local experience. It is not feasible to check capacities closely by experimental installations, as partial clogging of the inlets by debris is frequent. Capacities of particular inlet designs should be calculated with various depths of flow. An inlet should be designed to pass the required design flow with the inlet 50 percent clogged.

A typical inlet design is shown in Fig. 32 and capacity data are given in Table 26.

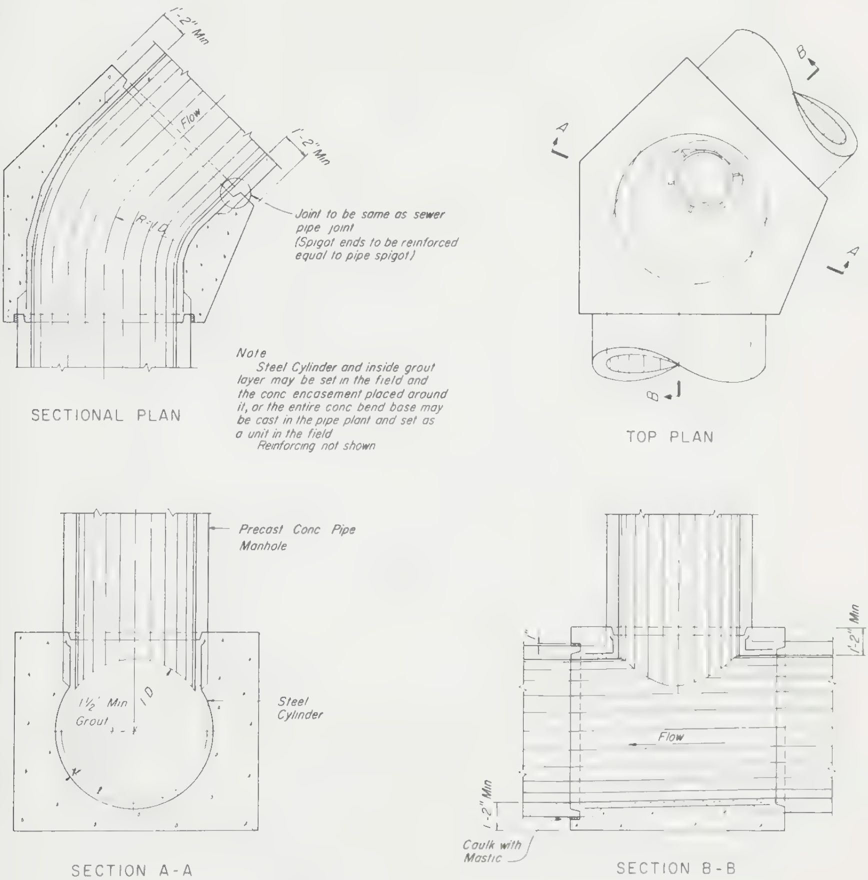

FIG. 30. Typical special bend manhole for sewers 48 in. and larger in diameter.

64. Catch Basins. Catch basins are used to retain solids washed off the street and prevent them from reaching the sewer. With the increasing number of streets being paved, the catch basin is being used less and less.

In new sewer systems, with steep grades, catch basins may be omitted with a considerable reduction in the maintenance required.

65. Inverted Siphons (Depressed Sewers). Sewers normally are constructed to grade and operate with the hydraulic gradient approximately parallel with the sewer invert. Occasionally it is necessary to construct a sewer under some obstacle. In this case, an inverted siphon may be used. A true siphon, carrying the sewage flow above the hydraulic gradient, is rarely used.

An inverted siphon, or depressed sewer, is a sewer constructed below the hydraulic gradient so that the sewer flows under pressure. Usually an inverted siphon includes one or more conduits, an inlet chamber, and an outlet chamber. The inlet chamber includes controlling devices to direct the sewage flow into the several conduits so as to develop self-cleansing velocities in them.

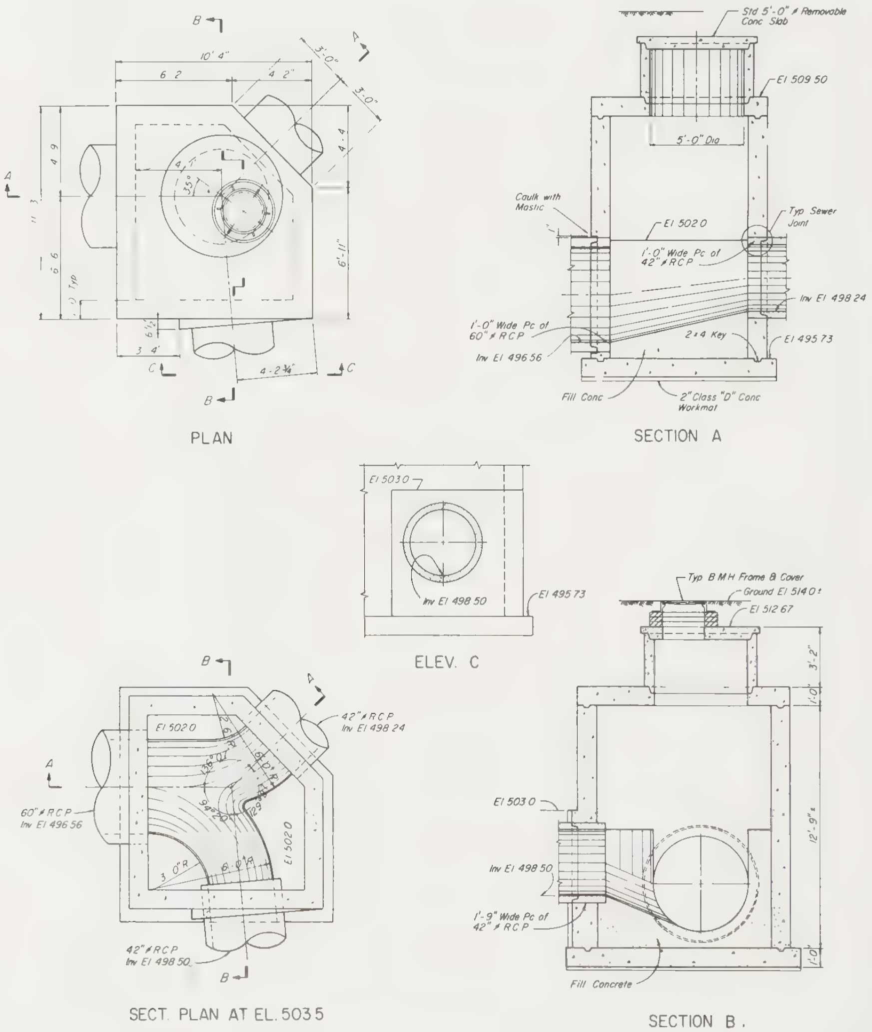

Fig. 31. Typical junction chamber.

The hydraulics of an inverted siphon relate to the velocities required to prevent the depressed sections from filling up with deposits. Either the velocities during minimum flows must be sufficient to prevent deposits, or the velocities during maximum flows must be sufficient to scour out any deposits that may form during periods of low flow. A considerably higher velocity may be required to scour out deposits than is necessary to prevent their formation.

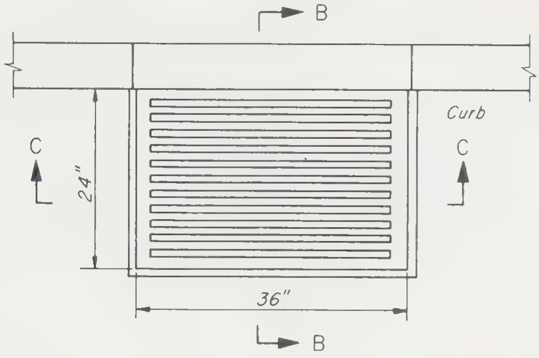

PLAN

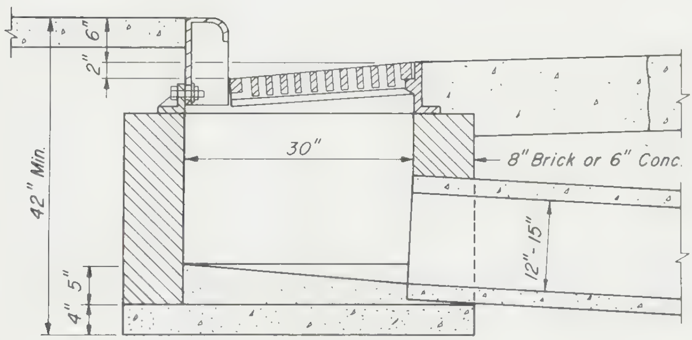

SECTION B-B

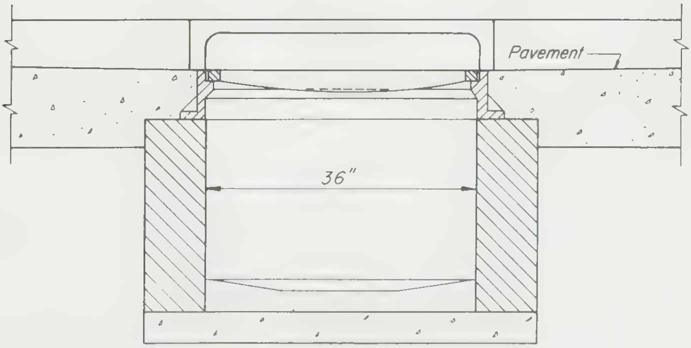

SECTION C-C

Fig. 32. Inlet detail.

Experience in the design and operation of inverted siphons has indicated that velocities for the estimated near-future minimum dry-weather flows of short duration should not be less than 1.0 to 1.5 fps and that velocities during normal flows should not be less than 2 to 3 fps for sanitary sewers and 3 to 4 fps for combined sewers.

When sufficient elevation difference can be obtained between the two ends of the depressed sewer section without undue cost and the sewage quantities are sufficient to create the proper velocities, a single pipeline may be used. However, it is usually uneconomical to use the required head to create velocity, and as the sewage flows vary over quite a range, the more economical design to obtain suitable velocities may

TABLE 26. CAPACITY OF STANDARD GRATING INLETS

Street Grade, %	Capacity of Inlet, cfs
0	3.70
1	3.55
2	3.38
3	3.20
4	3.02
5	2.85
6	2.69
7	2.53
8	2.38
9	2.25
10	2.12
12	1.88
14	1.71
16	1.57
18	1.47
20	1.40

Note: Data are for an inlet 25½ by 36 in. overall in plan, with ½-in. bars and 1-in. clear spaces. Bars placed parallel to curb. Two-inch local depression in pavement. Capacity figures are for no overflow past inlet. With a slight overflow the rated capacity may be increased 50 percent.

include two or more pipes of different sizes. Some typical data for siphons are given in Table 27.

The hydraulic design of an inverted siphon requires the determination of the following and their interrelationship:

1. The present and future maximum and minimum rates of sewage flows to be taken through the depressed sewer.
2. The difference in elevation in feet which is available or may be obtainable across the depressed sewer within reasonable limitations as to construction and operating costs.
3. The head losses across the siphon for various sewer sizes with one, two, or three depressed conduits.
4. The minimum and maximum velocities of flow for several combinations of sewer sizes. (If there is more than one pipe, the minimum flows may be taken by the smaller pipe, in which case the other pipe or pipes will have a minimum velocity of zero.)
5. The pipe materials to be used in construction. This may modify slightly the conduit sizes, as the standard commercial sizes vary for different materials.

The total head available to force sewage through the siphon at desirable velocities is the difference in water-level elevations in the two sewers on either side of the siphon.

The total loss of head in a siphon includes the head loss at entrance and exit, at bends, and at changes in cross section plus the frictional resistance along the length of the depressed conduit between the inlet and outlet chambers.

One typical design of an inverted siphon for a river crossing at Appleton, Wis., is shown in Fig. 33.

A detailed outline of the design of inverted siphons will be found in Ref. 34.

66. Special Sections. Special sections are often used where the interference with the proposed sewer is not of sufficient degree to require an inverted siphon. In

TABLE 27. DATA ON TYPICAL INSTALLATIONS OF INVERTED SIPHONS

Place	Capacity, mgd	Length, ft	Pipe diam, in.	Diff. between invert elev., ft	Max velocity, fps
Appleton, Wis.	17.4	950	1–15	3.71	4.8
			1–30		
Los Angeles, Calif.	36	800	1–30	0.4	4.6
			1–36		
Charlevoix, Mich.	1.55	210	2–8	4.30	3.4
Carlisle, Pa.	0.92	51.5	1–12	0.05	1.8
Urbana, Ill.	5.8	42	1–12		
			1–14	0.44	2.7
			1–16		
Boston, Mass.:	88	890	1–60	3.87	6.9
Chelsea Creek	320	1,000+	2–60	....	12.6
Buffalo, N.Y.:					
Black Rock Harbor	570	545	2–96	1.58	8.8
Buffalo River	90	210	1–36	3.36	5.2
			1–48 × 77 sec. with 23.85 sq ft area		
Peoria, Ill.:					
Siphon A	62.5	185	1–30	0.88	4.7
			1–54		
Siphon B	62.5	180	1–30	1.00	4.6
			1–54		
Siphon C	62.5	318	1–30	1.25	4.6
			1–54		
Siphon D	57.0	197	1–20	1.18	5.2
			1–48		
Siphon E	57.0	228	1–27	1.60	5.2
			1–48		
Siphon F	57.0	183	1–27	1.53	5.2
			1–48		

such cases it is often feasible merely to reduce the vertical height of the sewer by providing a transition from a circular conduit to a rectangular section. Relatively low head loss can be obtained by maintaining a constant cross-section area and velocity throughout such transitions. An example of a special section designed for use in Peoria, Ill., is shown in Fig. 34.

67. Intercepting Devices. Intercepting devices are used to regulate the quantity of mixed storm water and sewage diverted from a combined sewer to an intercepting sewer. On occasion they may also be used to control and regulate overflows into a relief sewer.

With the present emphasis on reduction in discharges from combined sewers to streams, these devices may be required less frequently. However, an understanding of their design is also necessary to facilitate measures to control overflows from existing combined sewers.

In general, an intercepting device will include a dam in the combined sewer, designed to divert all dry-weather flow to the intercepting sewer, and a regulating device to limit the quantity diverted when the combined sewer is also carrying storm runoff. The hydraulics of intercepting devices all include determination of the following:

1. The quantity to be diverted, usually expressed as the average dry-weather flow and, as a maximum, this quantity plus one or more volumes of storm water

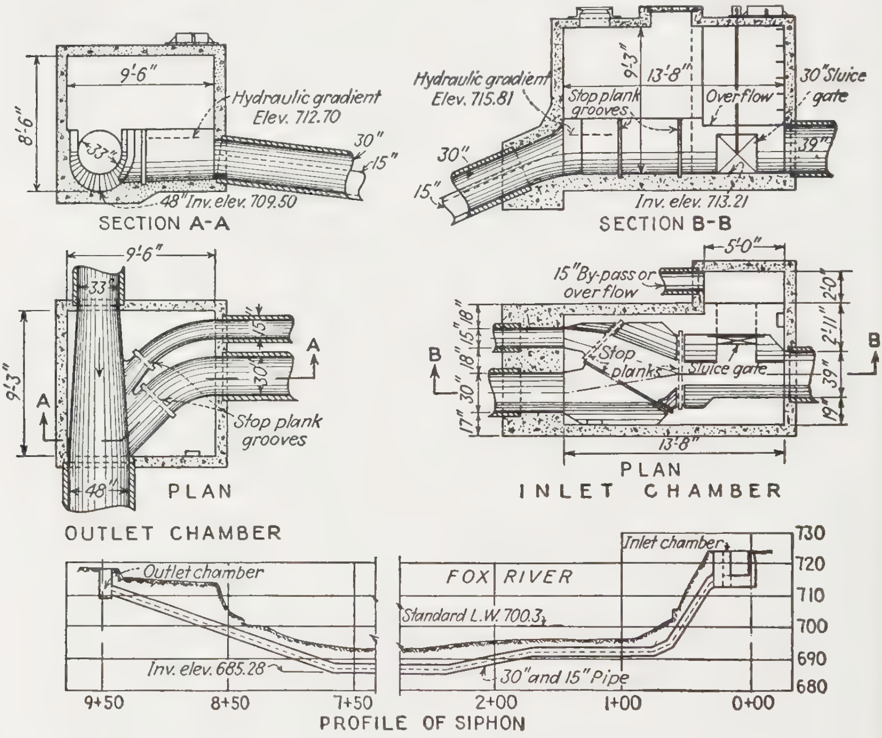

Fig. 33. Profile of crossing, plan of inlet chamber, and plan of outlet chamber.

2. The capacity of the combined sewer and the partial depth of flow corresponding to the quantity to be diverted

3. The size and setting of the control device so that the variation in depths in the combined sewer will not result in excessive variation in the quantity diverted to the intercepting sewer

The design of the intercepting device should have provision for adjustment so that the quantity intercepted can be modified as operating experience may indicate to be desirable. Some of the more commonly used devices are described in the following articles.

68. Overflow Weir. Although commonly referred to as an intercepting device, the overflow weir actually comprises a dam whose purpose is to regulate the water depth in a combined sewer at an interception point. Usually the weir is built on a diagonal in the combined sewer to obtain greater length. Regulation of the diverted flow is accomplished by an orifice or the throttling effect of the pipe connection to the intercepting sewer. All quantities are diverted as the combined sewage flow increases until excess storm water overflows the weir. This type of device is particularly useful where the available head on the control is limited. Since the head on the outlet and hence the rate of diversion increase with the depth of flow over the

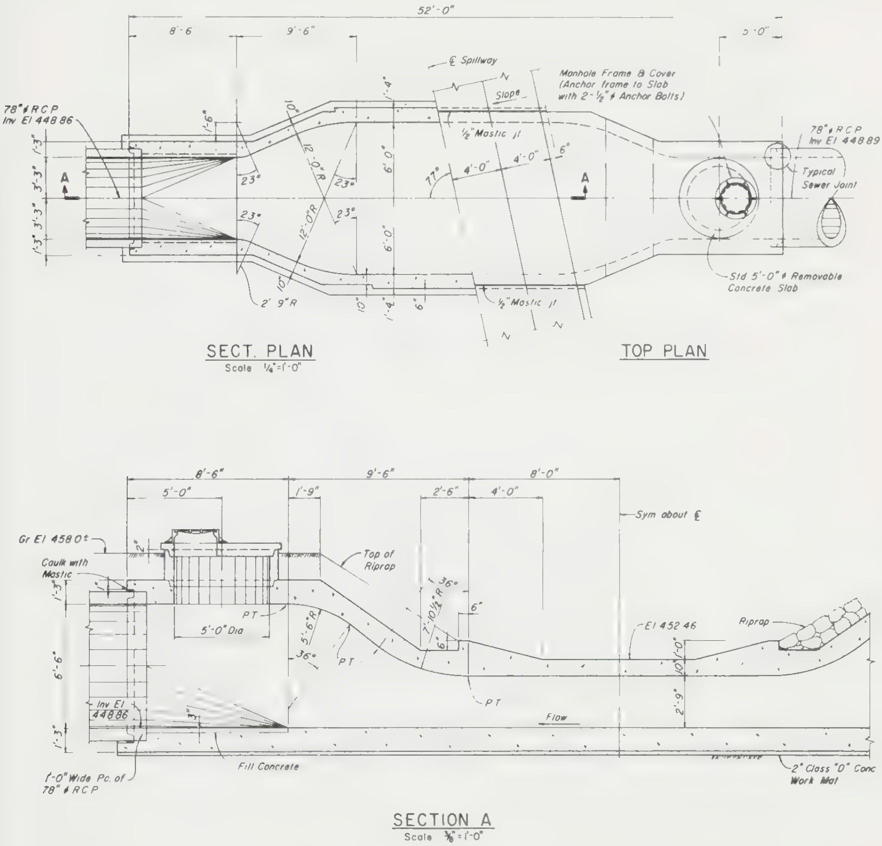

FIG. 34. Special depressed section.

weir, the length of the weir materially affects the amount diverted in excess of the desired quantity.

In addition to the general hydraulic data, the computations require special consideration of the probable increase in diverted flows above the desired quantity and the likely effect on the intercepting sewer capacity for various alternative lengths of overflow weir. The length and elevation of the weir are selected on the basis of these computations. Occasionally the importance of closely regulating the quantity of diverted flow will warrant constructing an overflow weir of considerable length, such as at the Broadway overflow chamber at Decatur, Ill. (see Fig. 35), but the expense of such long structures is not always warranted. The hydraulics

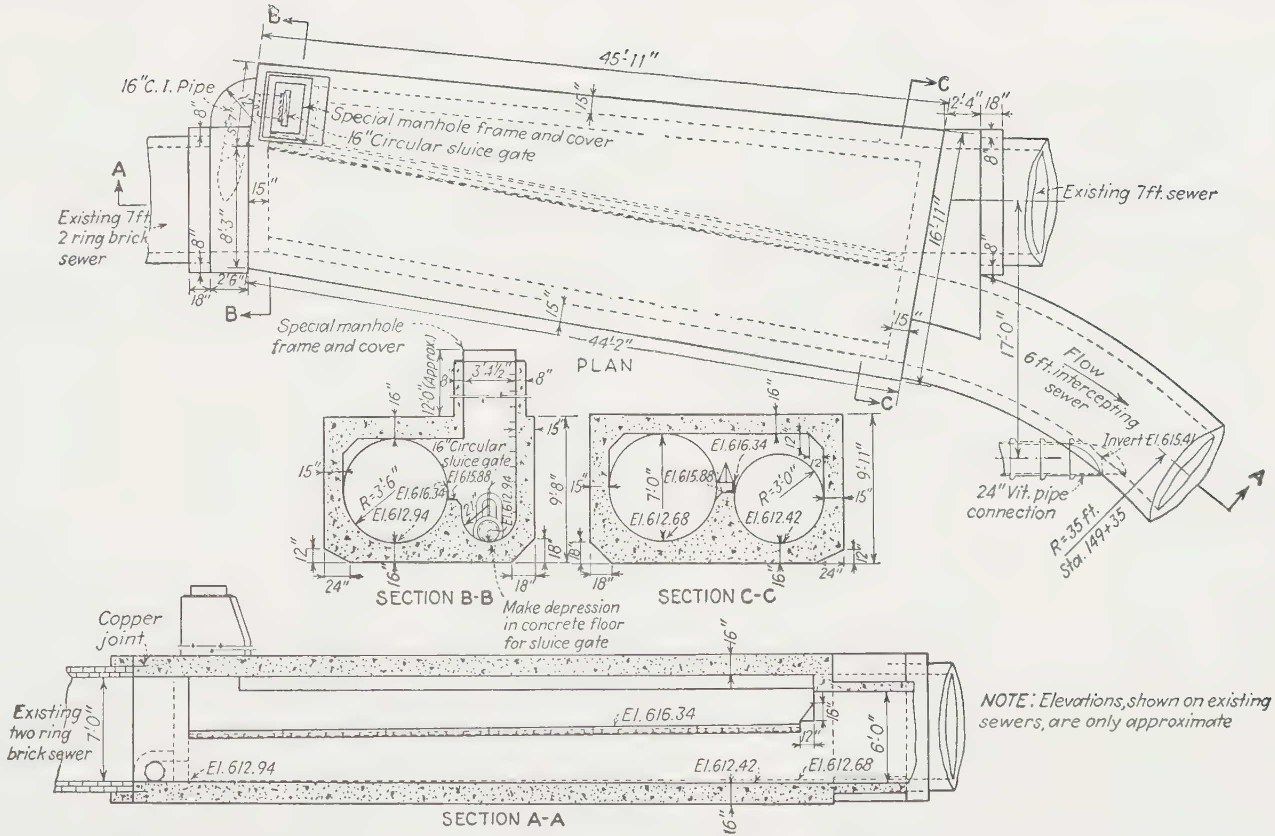

FIG. 35. Sanitary District of Decatur, Ill., intercepting chamber.

of this type of design has been considered on a theoretical basis by various hydraulicians, and several formulas for practical application are given in some detail by Metcalf and Eddy.[32]

For intercepting chambers on small sewers, it has often been feasible to build the diversion weirs in manholes (see Fig. 36). Sometimes the connecting sewer to the intercepting sewer can be used as the control to prevent interception of quantities greatly in excess of the desired diversion. In other cases, additional control has

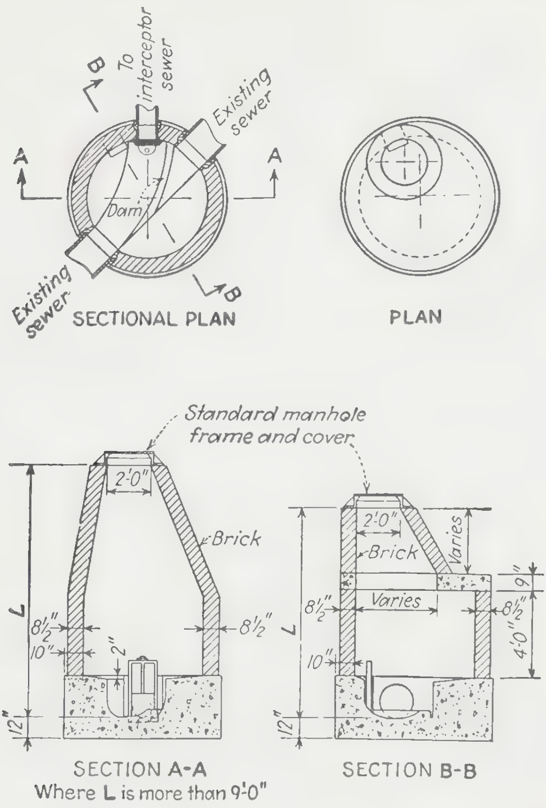

Fig. 36. Standard intercepting chambers.

been provided by using an adjustable gate as illustrated in Fig. 36, an orifice plate, or stop logs to throttle the discharge into the intercepting sewer. A more detailed outline of the design of an overflow-weir device may be found in ASCE Manual of Engineering Practice No. 37.[21]

69. Leaping Weir. The leaping weir comprises an opening in the invert of the sewer of such dimensions as to permit the flow that is to be intercepted to fall through, the increase in velocity and depth at times of storm causing the storm water to pass over or leap the opening and continue along the sewer to the storm-water outlets. Figure 37 shows a typical design with adjustable plates to permit some modifications in the quantity of intercepted flow.

A diversion dam is not used, and this type device is particularly useful in existing

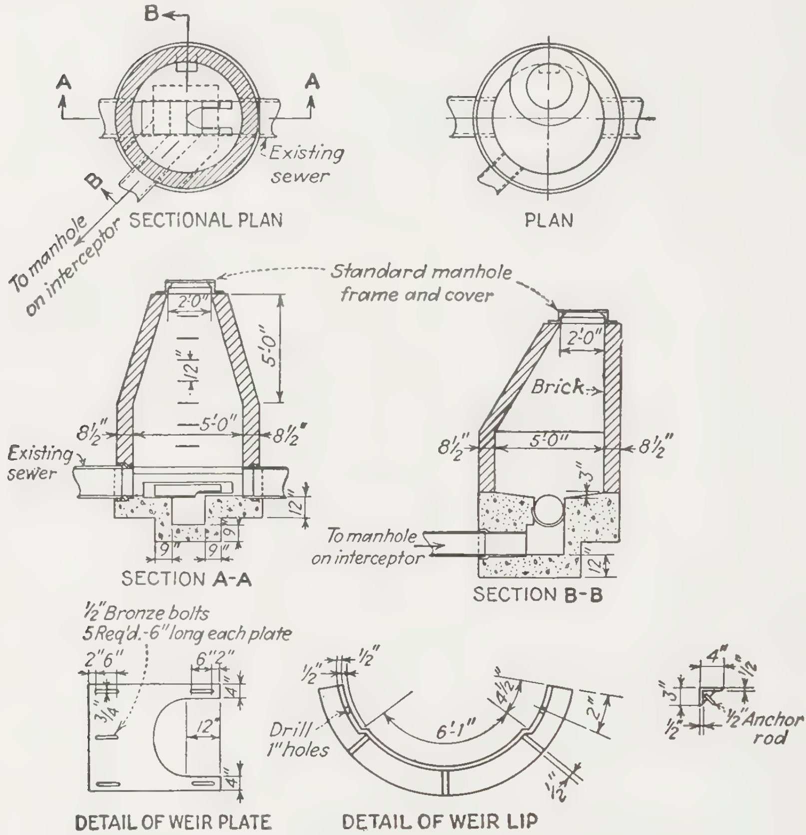

Fig. 37. Leaping-weir intercepting chamber.

sewers with steep grades. Considerable difference of elevation is required between the invert of the combined sewer and the connection to the intercepting sewer.

The form and width of the weir opening will depend upon the depth of flow and the surface velocity at any point across the stream flowing in the sewer. The theory for this has been developed by McClenahan[33] substantially as follows (see Fig. 38):

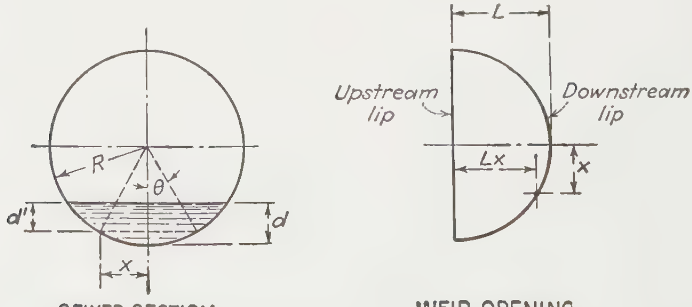

Fig. 38. McClenahan's formula for leaping weirs.

Let d = depth of flow, ft, at center of sewer (computed from Fig. 23 by proportional quantity data)

d' = depth, ft, at any distance X from center line

R = radius of sewer, ft

L = distance across weir opening at center of sewer, ft

L_X = distance across weir opening at any distance X from center, ft

θ = angle whose sine is X/R

V = effective surface velocity, fps

$d' = d - R \text{ vers } \theta$

$$L = V \sqrt{\frac{2d}{g}}\,{}^{*}$$

$$L_X = V \sqrt{\frac{2d}{g} - \frac{2R}{g} \text{ vers } \theta}\,{}^{\dagger}$$

In a given sewer, the effective surface velocity may be somewhat greater than the mean velocity and may vary across the width of the stream. However, the uncertainties as to the exact flows in the sewers and the amounts to be diverted are sufficient to warrant ignoring the refinements relating to the variations in velocity across the section of the flowing stream.

The usual practice is to construct the weir as a movable plate and to provide for adjustments of about 50 percent of the L distance in each direction. Thus, at the Bond Street intercepting chamber in Springfield, Ill., the L distance was computed to be 7 in. and the weir plate was designed to provide an opening adjustable from 5 to 11 in.

To determine the dimensions for cutting the weir plate before it is bent into a circular form, the L_X distances may be taken at a distance X' from the center line, where

$$X' = \frac{\pi}{180} R\theta$$

In larger intercepting chambers, it is desirable to cut the weir plates to the computed forms, but in many cases in small sewers a simple circular cut will be sufficiently accurate.

70. Orifice Control. The orifice control includes an orifice set horizontally (and occasionally vertically) somewhat below the flow line of the combined sewer. A low dam in the combined sewer diverts the normal flow to the orifice. The area of the orifice will depend upon the quantity to be intercepted and upon the distance that the orifice is placed below the crest of the diversion dam and may be computed from the orifice formula

$$q = CA \sqrt{2gh}$$

with C taken at 0.60. Experience in operation has indicated that orifices less than about 6 in. in diameter should not be used as they require excessive attention to prevent clogging. Figure 39 shows a typical installation. The loss due to the obstruction caused by the dam will depend upon the characteristics of any particular installation. The permissible loss is the difference in depth of flow required for the total flow in the combined sewer and that required for the total flow less the maximum amount to be diverted.

* This formula applies for distance across weir opening at center of sewer only.

† This formula applies for distance across weir opening at any distance X from center of sewer.

The following velocity-head coefficients have been used in pumping-station designs with satisfactory results:

Type of fitting	Coefficient K in $hf = K \frac{V^2}{2g}$	Authority
Gate valve (wide open)	0.19	*Univ. Wis. Bull.* 252
Check valve	3.0 –10.0	
Standard 90-deg bend (4 to 18 in.)	0.25–0.40	"Handbook of Hydraulics," King
Long-radius 90-deg bend (4 to 18 in.)	0.20–0.35	"Handbook of Hydraulics," King
Standard 45-deg bend (4 to 18 in.)	0.20–0.30	"Handbook of Hydraulics," King
Standard reducers	0.04*	"Hydraulics," Daugherty

* Based on velocity head at smaller section.

It will be noted that the check-valve loss is the largest and the most uncertain individual loss. Some data on measured check-valve losses are given in Table 28.

TABLE 28. CHECK-VALVE LOSSES
(Loss in terms of velocity head in pipe)

Size of check valve, in.	Velocity in pipe, fps	Velocity head $V^2/2g$	Estimated loss through check valve, ft	K
12	2.84	0.125	0.2	1.6
12	5.67	0.518	0.5	1.0
14	5.8	0.53	4.6	8.7
14	6.1	0.58	2.8	4.9
16	5.0	0.39	3.0	7.7
16	3.2	0.16	0.3	1.9
18	2.52	0.099	0.8	8.1
18	5.05	0.40	1.5	3.8

Data derived from tests in pumping stations at Whiting, Ind., and Urbana, Ill.

Check valves are also undesirable as they sometimes clog and may be quite noisy. Sometimes the hammering, due to the rapid closing of the check valve, sets up undesirable vibrations in the piping. For these several reasons, the usual type of check valve may be replaced by an automatic cone or ball type of valve. Automatic cone or ball check valves in large sizes are relatively expensive. However, they afford good control of the closure speed and are especially desirable where long force mains are involved and water-hammer problems can be anticipated.

In another type of design which has been successfully used in many medium-sized and larger pumping stations, discharge valves are eliminated entirely. The discharge pipe is extended above the sewage level in the outlet conduit and is then turned down so as to be sealed below the sewage surface. During pumping, the gooseneck acts as a true siphon and the static head is measured to the sewage surface in the discharge conduit. To prevent back siphonage from the conduit with the stopping of the pump, an electrically controlled siphon-breaking valve is provided at the top of the gooseneck. A time delay should be incorporated into the pump-starting controls so that the pump cannot be started when backflow from the vertical discharge pipe is turning the pump in reverse rotation.

74. Force Mains. Frequently the discharge from the pumping station will be through a long force main. In this case, two factors must be given consideration, which may, at times, be somewhat opposing. On the one hand, the pipe must be small enough so that unduly low velocities and objectionable deposits will not result during minimum pumpage rates. On the other hand, there should be an economic balance between construction costs and operating costs which may require somewhat larger pipes. Table 29 shows an illustrative computation to determine the size of a force main.

TABLE 29. TYPICAL COMPUTATION TO DETERMINE SIZE OF FORCE MAIN

Sewage quantities:

1. Minimum 1930	0.47 mgd
2. Dry-weather flow (Dwf) 1930	0.82 mgd
3. Yearly average flow	1.10 mgd
Total average monthly pumpage	34 mg
4. Maximum rate, 1940	6.6 mgd
5. Maximum rate, 1970	13.2 mgd
6. Maximum pump capacity, say	7.0 mgd
7. Force main maximum capacity	13.2 mgd

Force main:

Length	21,000 ft
Static lift (wet well to end of force main)	11 ft
Loss through P. sta (assumed constant)	4
Total lift	15 ft

Diam. F.M. (in.)	Pump capacity for V. of 1.0 fps		V. in F.M. fps		% time min. pump. operating		Friction per 1,000 ft			Losses, ft total			Total head, ft.		
	Mgd	Gpm	At max pump.	At 1970 max	Min	Dwf	Min pump.	Max pump.	1970 max	Min pump.	Max pump.	1970 max	Min pump.	Max pump.	F.M. capacity
20	1.4	972	4.96	9.3	0.333	0.58	0.33	6.4	21	7.0	134	440	22.0	149	455
24	2.0	1389	3.45	6.5	0.235	0.41	0.26	2.63	8.5	5.5	55	178	20.5	70	193
30	3.0	2083	2.20	4.2	0.157	0.27	0.18	0.89	2.9	3.8	18.7	61	18.8	33.7	76
36	4.4	3056	1.53	2.9	0.107	0.19	0.17	0.37	1.2	3.6	7.8	25	18.6	22.8	40

Head considerations indicate force main size should be 24 or 30 in., depending on relative costs (see below).

COMPARATIVE COST OF FORCE MAINS

Item	Construction cost	Fixed charge at 7½%	Power cost	Total annual cost
24-in. force main, pipe line only	$133,000	$10,000	$4,040	$14,040
30-in. force main, pipe line only	145,000	10,900	3,700	14,600

Use 30-in. force main.

75. Pump Selection. The head-discharge conditions will not be the same for all pumping units within a given station, but for most situations it is sufficiently accurate to assume that the head conditions will vary with the total station pumpage. Some preliminary assumptions are necessary as to the number of pumping units and their respective capacities in order to compute the hydraulic losses. On the basis of these computations, preliminary head-discharge curves may be prepared representing

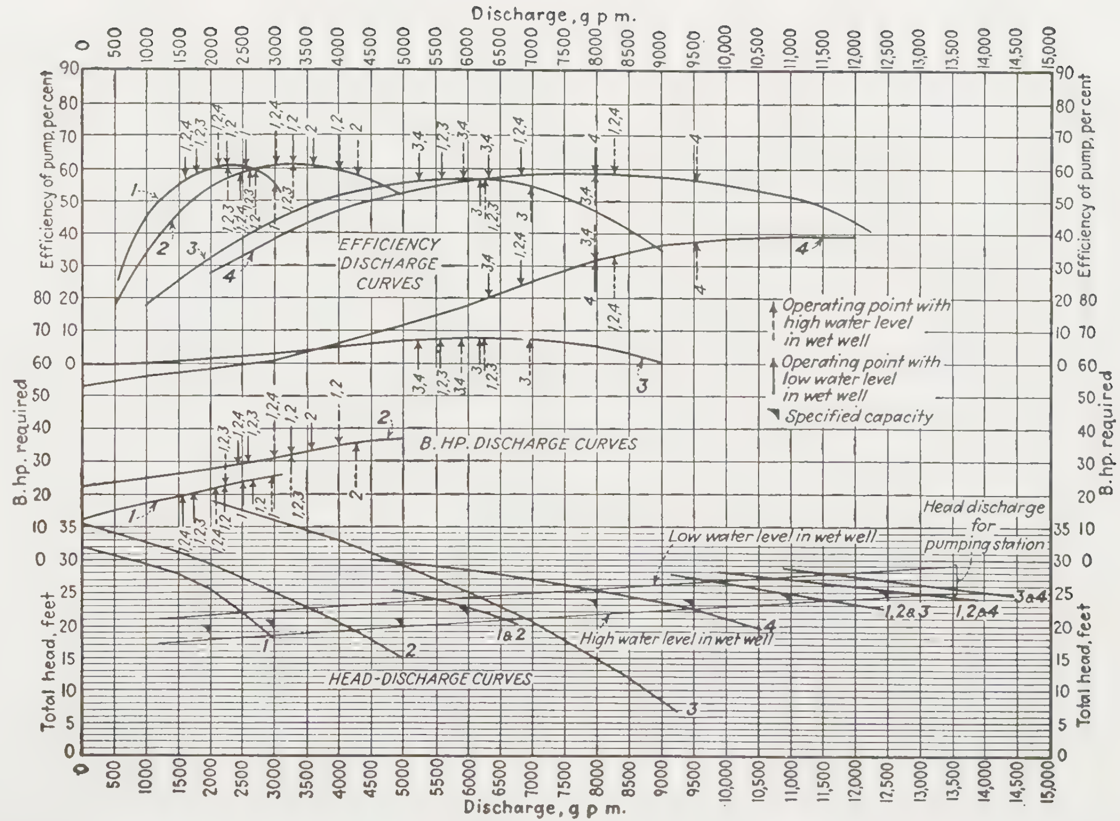

FIG. 42. Performance of pumping units.

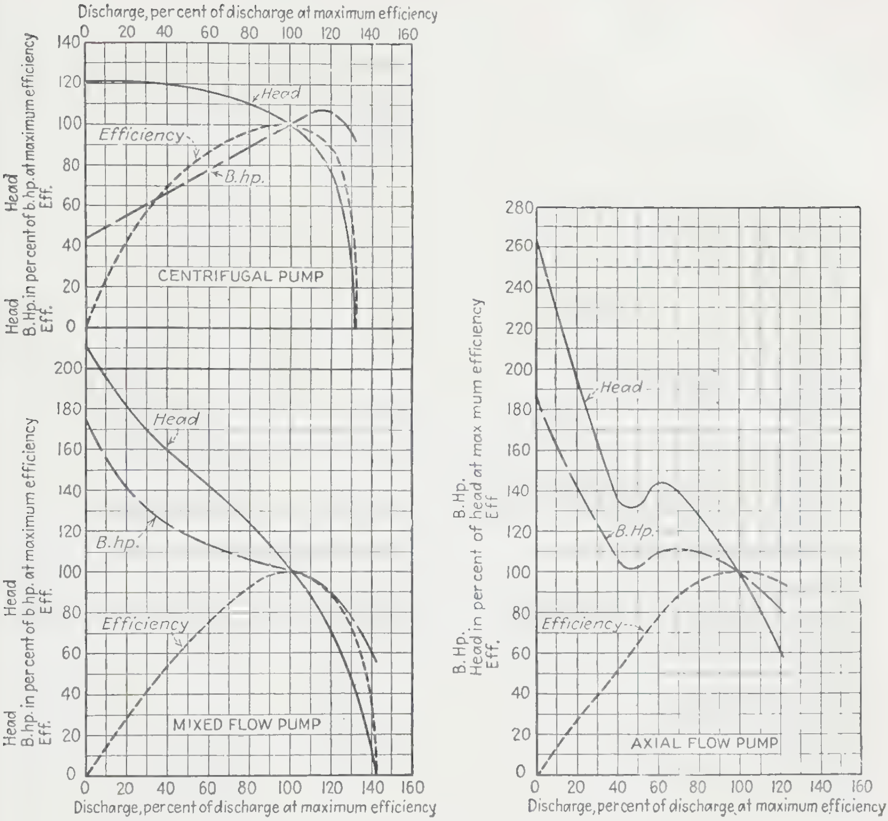

FIG. 43. Pump characteristics.

the anticipated performance of the pumping station. These preliminary head-discharge conditions should then be compared with head-discharge curves for pumps likely to be available. A typical pump selection is shown in Fig. 42. General characteristics of several classes of pumps are shown in Fig. 43.

76. Other Design Considerations. The foregoing brief discussion of pumping-station design touches on matters of hydraulic significance. A complete discussion of all phases of design and sewage-pumping facilities is beyond the scope of this handbook and would cover such additional items as follow:

1. Screens vs. comminutors for protection of pumps
2. Flowmetering
3. Ventilation, particularly as regards the wet well, and odor control for exhausted air
4. Facilities for chlorination
5. Automation of pump operation and variable-speed drives
6. Prefabricated steel pumping stations for smaller capacity requirements
7. Storm-water pumping facilities

For additional discussion of such matters reference should be made to other sources, such as "Design and Construction of Sanitary and Storm Sewers," ASCE Manual of Engineering Practice No. 37.

Bibliography

1. "Glossary, Water and Sewage Control Engineering," March, 1949, APHA, ASCE, AWWA, and FSWA.
2. McLean, J. E., *Civil Eng.*, 1952, p. 35.
3. Stanbery, V. B., "Better Population Forecasts for Areas and Communities," Government Printing Office, Washington, D.C., September, 1952.
4. Barclay, George W., "Techniques of Population Analysis," pp. 231–240, John Wiley & Sons, Inc., New York, 1958.
5. Cox, Peter R., "Demography," pp. 204–235, Cambridge University Press, New York, 1959.
6. "Sewerage and Sewage Treatment," 8th ed., p. 36, John Wiley & Sons, Inc., New York, 1958.
7. *Waterworks and Sewerage*, **92,** 175, 1945.
8. *Eng. News-Record*, **80,** 1234, 1918.
9. "Design and Construction of Sanitary and Storm Sewers," WPCF Manual of Practice No. 9 (ASCE Manual of Practice No. 37).
10. Bernard, M. M., *Trans. ASCE*, **96,** 1150, 1932.
11. Greeley, Samuel A., Some Notes on Relation between the Capacity of Combined and Storm Sewers and the Frontage Assessment, *J. Western Soc. Eng.*, **30** (1), 13–24, 1925.
12. "Design and Construction of Sewers," p. 54, ASCE Manual of Engineering Practice No. 37.
13. Schafmayer, A. J., Rainfall Intensities and Frequencies, *Proc. ASCE*, February, 1937.
14. Meyer, A. F., "Elements of Hydrology," 2d ed., 1928.
15. Yarnell, D. L., Rainfall-intensity Frequency Data, *U.S. Dept. Agr. Misc. Publ.* 204, 1935.
16. "Design and Construction of Sewers," pp. 36–43, ASCE Manual of Engineering Practice No. 37.
17. Marston, Frank A., *Trans. ASCE*, **87,** 535, 1924.
18. Chicago, Ill., Bureau of Sewers, practice reported by Tholin personal letter.
19. Hicks, *Trans. ASCE*, **109,** 1222, 1944.
20. Stanley, W. E., and W. J. Kaufman, Sewer Capacity Design Practice, *Boston Soc. Civil Engrs.*, October, 1953.
21. "Design and Construction of Sanitary and Storm Sewers," ASCE Manual of Engineering Practice No. 37, WPCF Manual of Practice No. 9.
22. Moody, L. F., Friction Factors for Pipe Flow, *Trans. ASME*, November, 1944.
23. "Handbook of Applied Hydraulics," 2d ed., pp. 1043, 1044.
24. Shields, A., Anwendung der Aehnlichkeitsmechanik und der Turbulenzforschung auf die Geschiebebewegung, *Mitteilungen der Preussischen Versuchsanstalt für Wasserbau und Schiffbau*, Heft 26, Berlin, 1936.
25. Fair, G. M., and J. C. Geyer, "Water Supply and Waste Water Disposal," p. 402, John Wiley & Sons, Inc., New York, 1954.
26. Camp, T. R., Hydraulics of Sewers, *Public Works*, **83,** June, 1952.
27. Fair, G. M., and J. C. Geyer, "Water Supply and Waste Water Disposal," p. 409, John Wiley & Sons, Inc., New York, 1954.
28. Hinds, Julian, The Hydraulic Design of Flumes and Siphon Transitions, *Trans. ASCE*, 1928, p. 1423.
29. Pomeroy, Richard, and Fred D. Bowlus, Progress Report on Sulfide Control Research, *Sewage Works J.*, July, 1946.
30. Parker, C. D., Mechanics of Corrosion of Concrete Sewers by Hydrogen Sulfide, *Sewage Ind. Wastes*, **23,** 1477.
31. Santry, I. W., Jr., "Hydrogen Sulfide in Sewers," Water Pollution Control Federation, December, 1963.
32. "American Sewerage Practice," vol. 1, 2d ed., p. 631, McGraw-Hill Book Company, New York, 1928.
33. *Illinois Soc. Eng., Ann. Rept.*, 1922 (prize paper).
34. Steel, E. W., "Water Supply and Sewerage," 4th ed., McGraw-Hill Book Company, New York, 1960.

SECTION 41

SEWAGE AND WASTE-WATERS TREATMENT

By Samuel A. Greeley,* William E. Stanley, and Kenneth V. Hill

INTRODUCTION

This section covers the application of applied hydraulics to a limited number of basic types of treatment processes. The applications of hydraulics, discussed here, are related mainly to treatment plants for municipal sewage and such process waste waters as may enter municipal sewers. Most of the application procedures would also apply to industrial waste-water-treatment plants.

THE SEWAGE AND WASTE-WATERS DISPOSAL PROBLEM

1. Sewage and Waste-waters Disposal. Waste waters from communities (sewage) and from industries (process wastes) have been permitted to flow by gravity or have been pumped into waterways for disposal. This practice was reasonable so long as the pollution introduced by the sewage, or process wastes, did not cause a danger to public health, a nuisance, a water-resource impairment (or recreational use), or uncompensated damage to property.

2. Sewage and Waste-waters Treatment. Treatment of sewage or process wastes constitutes the correction factor between the quantity of pollutional material in the waste waters and the capacity of the waterway to assimilate pollutional material without causing objectionable conditions. The pollutional matter is in part inorganic, in part organic of animal or vegetable origin, and in part living organisms, largely bacteria; it comprises matters in suspension and matters in solution.

Nature provides for the conversion in waterways of the organic matter into inorganic matter. Oxygen, an important requirement in this conversion, is supplied from the water. The water absorbs oxygen from the air through its surface, the amount increasing as the surface becomes turbulent, and the polluted stream also may receive oxygen from tributary streams and from the life processes of algae. If the supply of dissolved oxygen is sufficient, so that the oxygen demand of the organic matter does not eventually exceed or nearly exceed it, the conversion of organic matter proceeds normally, without objectionable conditions.

Many field investigations and analyses have been made of surface waters and of seawater to determine the pollution-assimilation capacities of the natural waters. Increasing numbers of investigations are being made of marine disposal of waste waters into seawater, at bays and estuaries or offshore.

Other pollution factors which determine the need for waste-waters treatment include the visual nuisance of objectionable floating matter; deposits of suspended solids which form sludge banks; poisonous or discolored wastes from industries; and especially the bacterial pollution which is dangerous to water supplies, bathing and recreation, shellfish, and the public health.

The objectives of sewage and waste-waters treatment include (1) the removal of floating and suspended solids; (2) the removal of pollutional matter in colloidal or

* Deceased.

dissolved state, when required by receiving waters; (3) the reduction of bacteria; and (4) the stabilization and disposal of the settled solids removed.

The treatment problem comprises five main parts: (1) a determination of the extent or degree of treatment necessary and the most economical or advantageous treatment process; (2) computations of plant capacities and plant hydraulics; (3) choice of equipment and design of structures; (4) construction of treatment facilities; and (5) operation and maintenance of the plant facilities to produce adequate results.

Commonly used methods, structures, and equipment are described briefly with principal emphasis on the hydraulic design of the various treatment-plant elements.

SEWAGE QUANTITIES AND CHARACTERISTICS

3. Flow Rates for Plant Design. Normal quantities of municipal sewage and rates of flow are given in Sec. 40. The ratio of the maximum to the average yearly rate of flow to be passed through each element of a treatment plant determines the capacities of plant elements and the hydraulic losses. The following ratio figures represent reasonable engineering design practice:

Type of Treatment	Ratios of Max Hydraulic Capacity* to the Basis of Design Rate of Flow
Plain sedimentation tanks	2.5–4.0
Chemical-treatment plants	2.5
Activated-sludge-treatment plants:	
Screens, grit chambers, preliminary settling tanks	2.5–4.0 or more
Aeration units and final tanks	1.5–2.0
Trickling-filter plants	2.5

* Hydraulic capacity provided in pipes, channels, and openings to take maximum rates of flow.

The maximum rates of flow permitted to pass through a treatment plant may be controlled by overflows or bypasses. Computations of these hydraulic losses would be separate from those for the treatment plant. The minimum rates of flow through the treatment plant will be determined by the actual flows from the sewers and cannot be avoided, except in those cases where the flows are pumped to the treatment plant, in which cases the minimum pump capacity determines the minimum flow rate.

Adequate velocities, aeration of channels, or other means must be provided to prevent objectionable deposits in conduits at minimum rates of flow.

4. Sewage Characteristics. Municipal sewage may be considered as soiled water plus limited quantities of industrial-process wastes, the water content comprising over 99.9 percent of the total volume. The pollutional material consists of large floating matters which are usually removed by screening, heavy inert material called "grit" which is removed by a grit chamber, and fine particles in suspension or solution. A portion of suspended matter may be removed by plain sedimentation, and a larger portion including dissolved matter by chemical or biological treatment.

Laboratory analyses include a number of chemical, mineral, and biochemical characteristics. The two most important characteristics are the suspended solids and the biochemical oxygen demand (BOD), with reference to basic capacity factors in treatment-plants design. Typical per capita quantities of these two characteristics may be as shown in the table at the top of the next page.

The use of home garbage grinders is increasing, and their effect on sewage characteristics for any particular community should be determined. In general, it appears that the unit quantities of suspended solids and 5-day BOD in the foregoing table may be expected to increase from 20 to 40 percent and 10 to 40 percent, respectively, because of the presence of home-ground garbage in the municipal sewage.

5. Effect of Industrial Waste Waters. Liquid wastes from industries vary in amount and strength within a given industry and vary in characteristics according

Item	Lb per Capita Daily (Municipal Sewage)
Suspended solids:	
Separate sewers	0.17 (1/6)
Combined sewers	0.33 (1/3)
5-day BOD:	
Residential areas only, with separate sewers	0.12 (1/8)
Residential cities including ordinary commercial establishments, with separate sewers	0.17 (1/6)
Residential cities including ordinary commercial establishments, with combined sewers	0.25 (1/4)
Manufacturing city, with no large special industrial wastes	0.33 (1/3)
Industrial wastes (frequently quite high)	0.33–0.50 (1/2)

to the type of industry. Certain industries have waste waters with characteristics high in suspended solids, dissolved solids, and biochemical oxygen demand. Some industries produce wastes with one or more of the following characteristics requiring specific waste-waters control and treatment: high temperature, flammable matter, toxicity, salinity, acidity, alkalinity, grease and oil, taste, odor, color, and bacteria. Some industries recover material from waste waters for reuse or to process into by-products. Usually, special industrial waste-water surveys are required.

For purposes of indicating the possible effect of industrial waste waters, approximate average quantities per production unit, for a number of selected industries as to volume, the suspended solids, and biochemical oxygen demand, are given in Table 1.

TABLE 1. APPROXIMATE AMOUNTS OF POLLUTIONAL MATTER FOR SELECTED INDUSTRIES

Industry	Production unit	Gal per unit	Lb per unit	
			Suspended solids	BOD
Brewery	bbl	320	1.7	3.2
Cannery:				
Asparagus	Case	70	0.02	0.06
Pumpkin and squash	Case	25	0.38	1.3
Lima beans	Case	250	0.88	0.40
Distillery, grain	Bushel	600	0.45	0.58
Laundry	100 lb dry	400	1.7	4.0
Meat:				
Packinghouse	100 hogs	550	2.8	4.1
Slaughterhouse	100 hogs	160	1.2	3.0
Milk:				
General dairy	1,000 lb	340	1.8	2.7
Cheese factory	1,000 lb	200	1.0	1.7
Oil refining	bbl of crude oil	770	0.24	0.10
Paper, bleached	Ton	47,000	44	6.7
Poultry	1,000 chickens	6,000	25	12
Tannery, vegetable tanning	100 lb of hides	300	16	8

It is outside the scope of this section to discuss industrial wastes in detail. In general, the hydraulic problems for process waste-waters-treatment plants are similar to those for municipal sewage plants.

Industrial waste waters discharged into public sewer systems must not exceed the hydraulic capacities of sewers or treatment-plant limitations, nor should they damage sewers, structures, or equipment. Some waste waters may not be amenable to treatment in the municipal plant.

There have been great increases in the manufacture of synthetic products producing organic chemical waste waters, frequently termed "exotic" wastes. For a great variety of these liquid-process wastes there is limited information as to characteristics and effective treatment processes. Various industries have increased the production of radioactive wastes. These are closely regulated by state and Federal agencies.

6. Sludge Characteristics. Sludge, comprising the solids settled in bottoms of tanks, has a high water content; is putrescible with high concentrations of organic solids, bacteria, and other organisms; and requires special consideration in the design of the sludge-handling elements of treatment plants.

Sludges vary in quantity and characteristics depending on the composition of the waste waters and the type and extent of treatment processes. Typical percentages of solids, by weight in a given volume of settled fresh sludges and digested sludges, from residential cities, for some illustrative sewage-treatment processes are as follows:

Treatment process	% solids by weight	
	Settled sludge	Digested sludge
Plain sedimentation	2.5–5	10–15
Plain sedimentation and trickling filters*	3 –6	10
Activated sludge*	4 –5	6– 8
Chemical precipitation	2 –5	10

* Humus or activated sludge mixed with plain sedimentation sludge.

Sludge thickeners are often used to reduce volumes, and their use results generally in considerable economy in sludge-disposal processes. Thickening of settled sludge reduces the sludge volume by increasing solids concentrations, which generally results in higher solids loadings, per cubic foot of digester capacity, lesser sludge volumes in ocean disposal, and reduced chemical requirements for sludge dewatering. The following percentages are typical results in thickening settled sewage sludge:

Treatment Process	Thickened Sewage Sludges,* % Solids by Weight
Plain sedimentation	8–10
Plain sedimentation and trickling filters	7–9
Activated sludge	5-8
Modified activated sludge	8–12

* Raw primary sludge at 10 percent solids is difficult to pump. The addition of secondary solids or digested solids has the effect of a lubricant making it possible to pump up to 14 percent solids through piping systems with short suction lines.

PLANT ELEMENTS AND TREATMENT PROCESSES

7. Introductory. Treatment-plant hydraulics depend upon the treatment processes, the arrangement of plant elements, and the topography and shape of the treatment-plant site. Brief descriptions of the more commonly used plant elements and treatment processes are included, but no attempt has been made to include all varieties.

Continued increased presence of detergents, radioactive materials, exotic chemicals, and toxic substances in liquid waste waters will require the expansion and modification of many present sewage-treatment processes and the development of new ones, as some waste waters are not amenable to treatment in many present plants or by natural purification processes.

In most states the review and approval of designs of sewage works are influenced largely by "Guides for the Design of Sewage Works" or "Recommended Standards." The "Recommended Standards for Sewage Works" adopted by the Great Lakes–Upper Mississippi River Board of State Sanitary Engineers are used officially or unofficially in many states. Recently, many new state and federal water-quality standards have been promulgated.

8. Dilution. This process comprises the mixing, dispersing, and dilution of sewage or industrial liquid wastes into a body of water. When the quantity of pollutional matter is too great, the self-purification capacity of the body of water is overloaded and artificial treatment becomes necessary. Aerated stabilization ponds are being used in greater numbers in recent years, as a type of dilution.

The Metropolitan Sanitary District of Greater Chicago has experimented with a floating mechanical aerator to add oxygen to the Chicago River to assist the natural purification processes (Fig. 1).

Fig. 1. Experimental river aerator. (*Yeomans.*)

9. Coarse Screens. The relatively large suspended solids in sewage and waste waters are removed to protect the operation of mechanical equipment and to prevent clogging of flow channels in following treatment elements. The materials are removed by manually or mechanically cleaned screens, or racks, made of parallel steel bars spaced ¾ to 2 in. apart (Fig. 2). A combination type of screen and comminutor has a comminuting machine which travels up and down on the screen (Fig. 3).

10. Comminutors. Comminutors may be used instead of coarse screens. There are two commonly used types: (1) bottom outlet with either vertical or horizontal discharge (Fig. 4, horizontal discharge) and (2) straight-through flow (Fig. 5). Com-

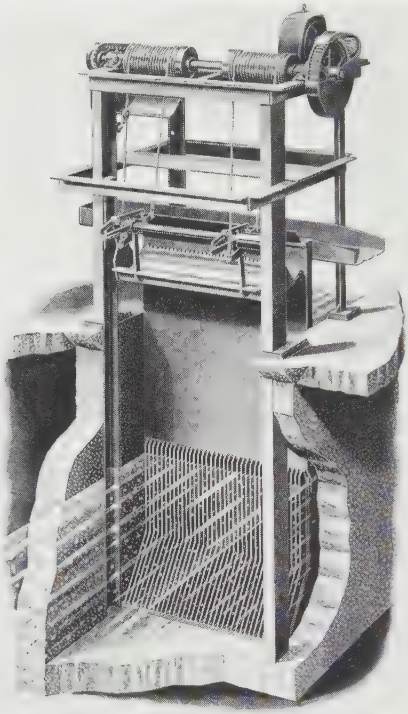

FIG. 2. Mechanically cleaned bar screen. (*Link Belt Co.*)

minutors generally should be placed after grit chambers unless some special conditions make it preferable to place them ahead.

11. Grit Chambers. Grit removal from waste water is essential to prevent abrasion of moving equipment, and especially formation of grit deposits in digestion tanks.

The principal grit-removal devices include long velocity-controlled horizontal-flow grit-collector channels (Fig. 6) (also Art. 36) and gravity separation tanks, rectangular or square. Aerated tanks or channels (Fig. 7) and centrifugal separators or cyclones, such as Dorr-Oliver (Fig. 8), have been used. Grit with less than 10 percent putrescible organic matter may be removed from grit by a washer, such as an inclined-screw conveyor (Fig. 6) or a reciprocating-rake classifier.

12. Fine Screens. There is presently only limited use of fine screens in the form of revolving drums, disks, or traveling bands, or screens with openings $\frac{3}{16}$ in. or less in the treatment of sewage. They have been used, sometimes, for screening settled sewage ahead of trickling filters, or the final effluents from activated-sludge plants. They have been used extensively in the screening of industrial waste waters such as those from canneries, tanneries, poultry processors, packinghouses, and breweries.

13. Grease and Oil Removal. Unemulsified oils and greases tend to rise to the surface of waste waters and may be removed by skimming, usually from the surface of sedimentation tanks. The removal of large quantities of oil and grease of indus-

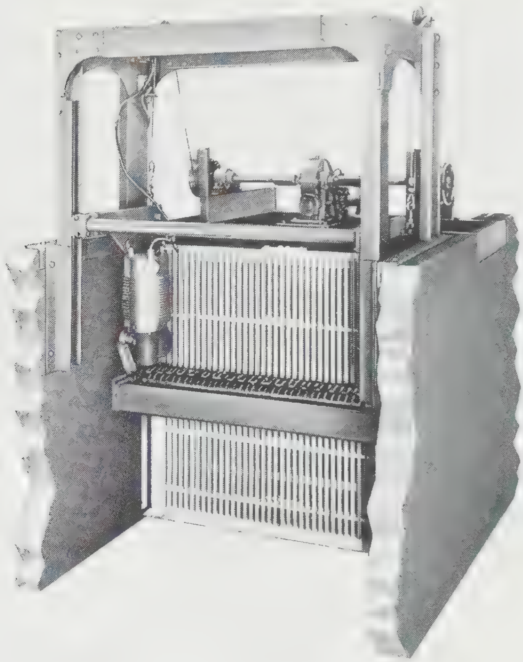

FIG. 3. Bar screen and comminutor. (*Chicago Pump Co.*)

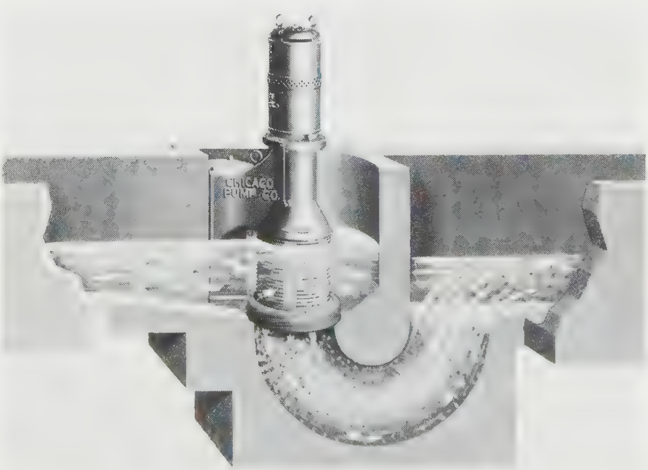

FIG. 4. Comminutor, bottom outlet with horizontal discharge. (*Chicago Pump Co.*)

FIG. 5. Comminutor, straight-through flow. (*Worthington Corp.*)

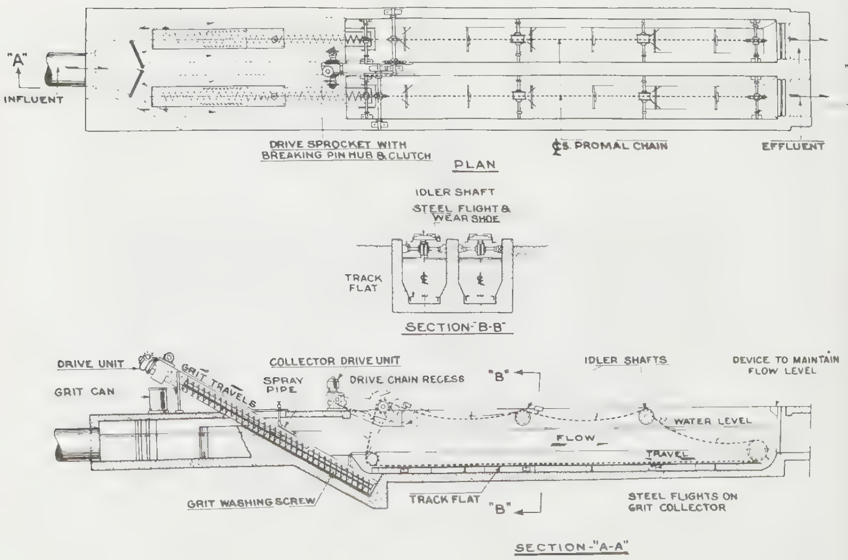

FIG. 6. Mechanically cleaned grit channels and grit washers. (*Link Belt Co.*)

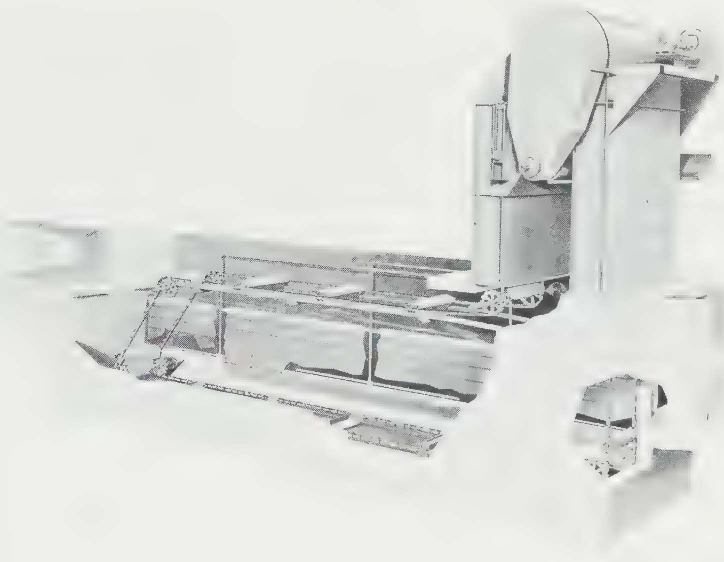

FIG. 7. Aerated mechanically cleaned grit channel. (*Chain Belt Co.*)

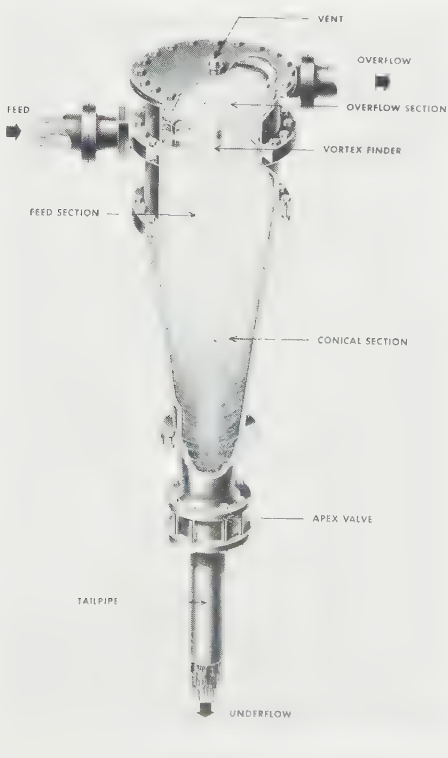

FIG. 8. Centrifugal separator. (*Dorr-Oliver, Inc.*)

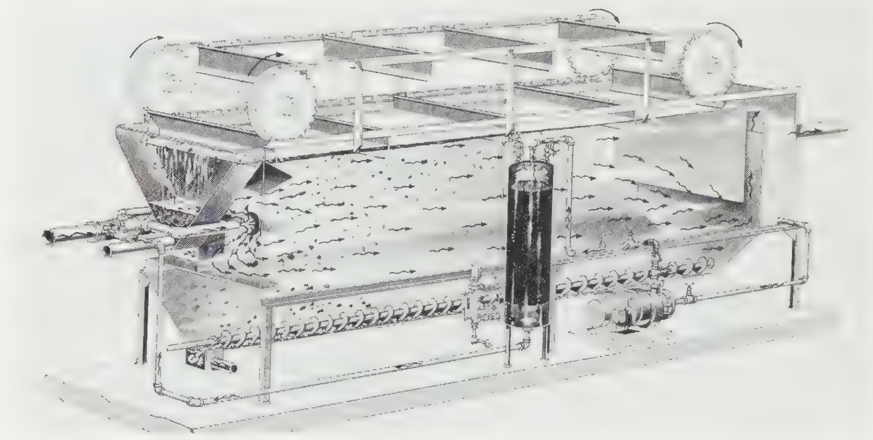

FIG. 9. Grease separator by air flotation. (*Chain Belt Co.*)

trial-waste origin can be increased greatly by a short aeration period with or without chlorination ahead of the sedimentation tanks.

Commercial grease air-flotation units (Fig. 9) may be suitable for particular industrial waste waters, especially in an industrial waste-waters-treatment plant, or for pretreatment at the industry, to meet requirements for waste-waters disposal into combined or sanitary sewers. These units are of three types, operating (1) at atmospheric pressure, (2) under pressure, or (3) under vacuum.

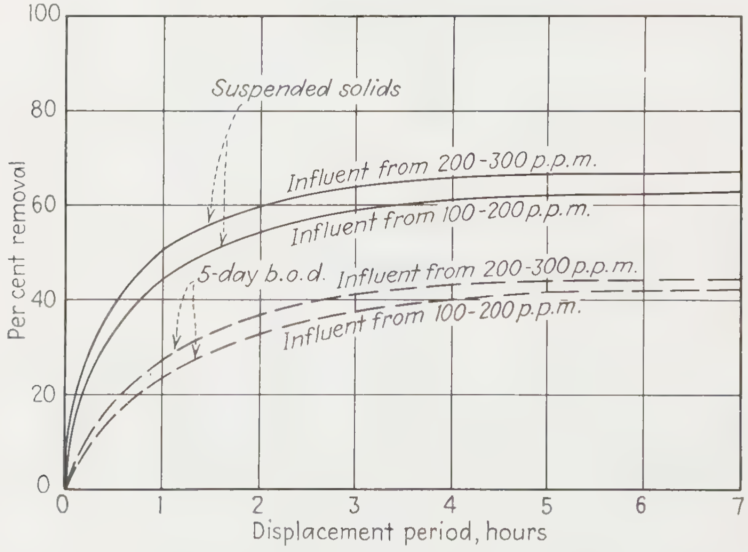

FIG. 10. Suspended-solids and 5-day-BOD removal vs. displacement period, hours. (*After G. J. Schroepfer, Sewage Works Journal, vol. 5, no. 2.*)

14. Plain Sedimentation. The removal of suspended solids in a sedimentation tank depends upon many factors in design including (1) hydraulic distribution of flow and (2) conditions significantly affecting the characteristics of the waste water in the sedimentation process.

Figure 10 indicates the approximate relationship of detention period and the concentration of suspended solids upon the percentage removal of suspended solids and 5-day BOD from sewage.

Current design practice for settling tanks gives more weight to surface loading (sewage flow, in gallons per day, divided by tank surface area in square feet), often designated "overflow rate" or "settling rate." Some experience data on suspended-solids removal from sewage vs. "overflow rate" are shown by Fig. 11.

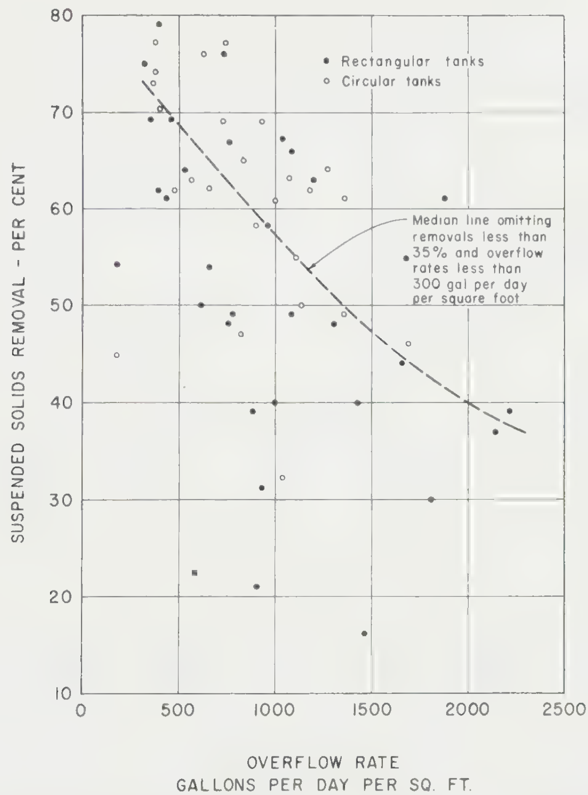

FIG. 11. Suspended-solids removal vs. surface overflow rates. (*ASCE Manual of Engineering Practice no.* 36, *Fig.* 6, *p.* 93.)

Design of primary settling tanks has been generally based on the expected per-cent removal of BOD from sewage, as determined by Fig. 12.

The "Ten-state Standards" do not specify a detention period, except for Imhoff tanks, which should have a detention period of at least 2 hr. Instead of detention a depth is specified. Thus, "the liquid depth of mechanically cleaned settling tanks

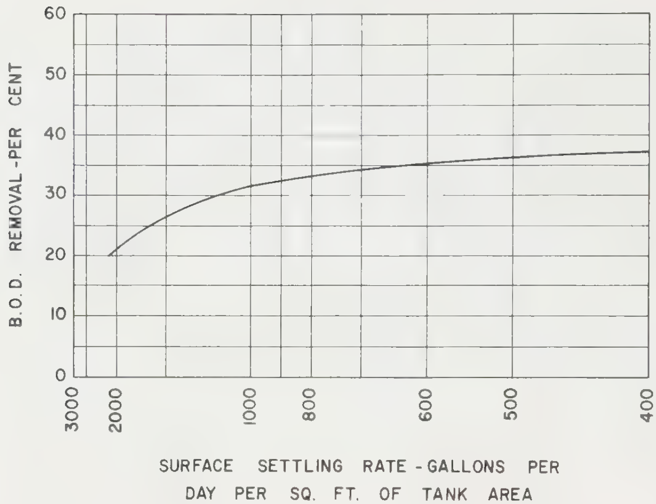

Fig. 12. BOD removal vs. surface settling rates. ("*Ten-state Standards*," *Fig.* 1.)

shall be as shallow as practical, but not less than seven (7) feet. Final clarifiers for activated sludge should not be less than eight (8) feet."

The following table illustrates the detention periods (in hours) corresponding to the "Ten-state Standards" for surface settling rates with settling tanks having liquid depths of 7, 8, and 10 ft:

Type of tank	Settling rate, gal/sq ft/day (sewage)	Detention periods, hr, for a liquid depth of		
		7 ft	8 ft	10 ft
Primary	600	2.1	2.4	3.0
Final	800	1.6	1.8	2.25
Intermediate	1,000	1.25	1.4	1.75

Plain sedimentation, designated "primary treatment," may be the only waste-water treatment required when receiving waters can assimilate the settled effluent satisfactorily. Storm-water tanks may be used for the same purpose in providing partial treatment of overflows from combined sewers or storm sewers. Plain sedimentation tanks are used as a primary step to "secondary-treatment" processes. Sedimentation tanks, in general use, comprise either rectangular (Fig. 13) or round structures with mechanical means of sludge and scum removal.

The same type of tank is used for "final sedimentation" (see Art. 22), except that scum-removal equipment is not usually necessary (see Fig. 14).

15. Chemical Treatment. Chemical coagulation of waste waters to increase effectiveness of sedimentation is used occasionally where greater removal of suspended solids and BOD is required as with seasonally higher concentrations. Chemical treatment of sewage may find increased use with availability of cheaper chemicals or as an aid to other processes in tertiary treatment, for the relief of overloaded trickling-filter or activated-sludge plants, and for many industrial waste waters.

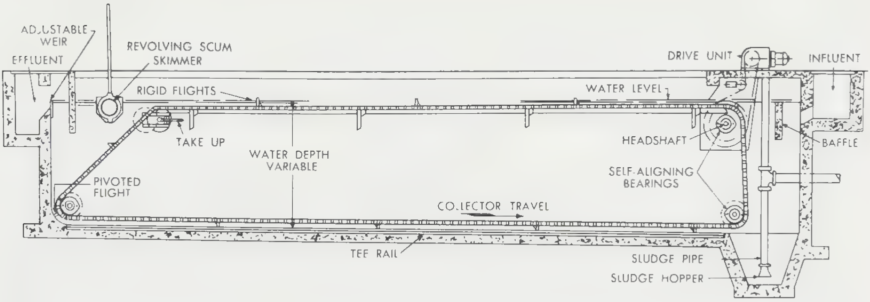

Fig. 13. Primary sedimentation tank, mechanical sludge and scum collector. (*Chain Belt Co.*)

The hydraulic computations for chemical-treatment plants are related closely to plain sedimentation, except that lower plant velocities through inlets are used to avoid breakup of chemical floc and a flocculation tank element is usually included.

16. Flocculation. Air or mechanical flocculation with or without chemicals ahead of or in conjunction with sedimentation is sometimes used to increase sus-

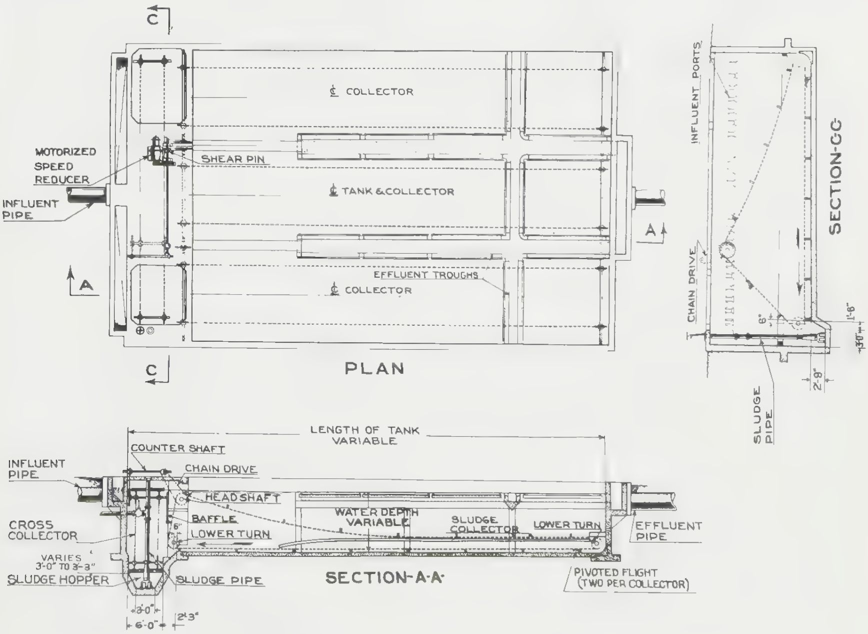

Fig. 14. Final sedimentation tank, mechanical sludge collector. (*Link Belt Co.*)

pended and colloidal solids removal, as much as 10 to 30 percent, depending on characteristics of the sewage or waste waters. In chemical treatment, the chemicals should be well mixed and allowed to flocculate for a detention period of 20 to 90 min depending on the sewage characteristics. Depths of facilities are generally determined by the aeration or the mechanical flocculator equipment. . Hydraulic losses are computed by methods similar to sedimentation tanks, except that the water levels are usually controlled by the following settling tanks so that outlet weir losses are avoided. Outlet weirs are not desirable as they tend to break up chemical floc.

17. More Complete Treatment Methods. Several methods are available for greater reduction of the pollutional components of waste waters, which depend on biological oxidation of the putrescible organic matter, in suspension and in solution, by living organisms. Among the more complete methods of sewage, and some industrial waste waters, treatment are the following:

- Irrigation, broad and spray
- Lagoons and oxidation ponds
- Sewage filters
  - Intermittent sand filters
  - Trickling filters
  - Rotary mechanical fine screens
- Activated sludge systems
  - Conventional
  - Step aeration
  - Modified or high-rate
  - Completely mixed
- Disinfection and chlorination

18. Irrigation. Broad irrigation or spreading of sewage and waste waters over land areas, usually after plain sedimentation, is an old method of sewage disposal not now used extensively in this country. Spray irrigation has been used successfully by some canneries and other industries in a few places for disposal of liquid wastes, and is being proposed for plant effluent disposal.

19. Lagoons and Stabilization Ponds. Lagoons, built of earth dikes, are sometimes used as an adjunct to sewage treatment for sludge digestion, storage, and disposal. Stabilization or oxidation ponds, generally designated "waste-stabilization lagoons," are being used by smaller communities and by some industries for waste-waters treatment, particularly in regions of favorable climate and low land values. Aerobic oxidation is carried on in these artificial ponds of shallow depth by a combination of bacteria and algae. Some states have promulgated design criteria, for example, the state of Missouri, in a "Guide for Design" dated 1962.

No specific or routine procedures can be outlined for application of hydraulics to design of lagoons. Flow in sewers and possibly outlet weirs, generally, would be involved.

20. Sewage Filters. Biological treatment of sewage and some industrial waste waters has been provided by two types of sewage filters:

Intermittent Sand Filtration. This comprises the intermittent application of settled sewage, or waste waters, over natural or artificial sand beds, each dose being oxidized during its passage through the sand. Large sand-bed areas are required; so the size of the community which can be served is limited. Such sand filters have been used sometimes as a finishing treatment after trickling filters.

Trickling Filters. These comprise a bed of crushed stone, or other types of media, a distribution system, and an underdrainage system. A variety of recirculation systems are used in part to dilute a strong sewage, or waste water, and in part to maintain sufficient flow to keep sewage-distributor equipment (Fig. 15) moving, in order to maintain an active biological film growth on the broken stones or other filter media.

Trickling filters, for reduction of BOD in waste waters, may be ". . . designed so

FIG. 15. Rotary distributor for trickling filter. (*Yeomans.*)

as to provide the reduction in BOD required . . ."[1,*] by proper selection of (1) the number of stages, (2) the recirculation ratios, and (3) the proper filter loading rates (hydraulic and organic).

Reasonable design results, for domestic sewage, may be obtained by complex procedures, as published in the ASCE Manual of Engineering Practice No. 36[2] (Sec. 11.4, Design Criteria). Rankin[3] has proposed three methods to compute filter operation results. Computation procedures can be found in detail in Refs. 1, 2, and 3.

The foregoing procedures determine the number, arrangement, and size of filter units. The hydraulic computations are outlined in Art. 39.

21. Activated Sludge. There are many types of activated-sludge processes, in which aerobic biological oxidation is accomplished in aeration tanks where screened or settled organic waste waters, together with bacteria and other microorganisms, are combined in a mixed liquor which develops into a sludge floc that reduces BOD and stabilizes the organic matter. The biochemical process is maintained by the return of microorganisms with settled sludge, designated "activated sludge," to the aeration tanks.

The loading of aeration tanks has been expressed as both (1) BOD loading and (2) solids loading. The BOD loading is determined by dividing the total pounds daily of BOD applied to aeration tanks by total tank volume, in thousands of cubic feet, to get BOD loading in pounds per 1,000 cu ft/day. The solids-loading rate of aeration tanks may be determined by dividing the total dry weight of solids in the tanks by the dry weight of the suspended sewage solids added daily. This figure has been expressed by R. H. Gould as "sludge age" in days required for the sludge floc to be sufficiently oxidized that it will settle readily. Aeration and mixing are accomplished by diffused air or mechanical aeration systems or a combination of both (Figs. 16 to 18).

The activated-sludge process, with many modifications, has become an important

* Superior numbers refer to items in the Bibliography at the end of this section.

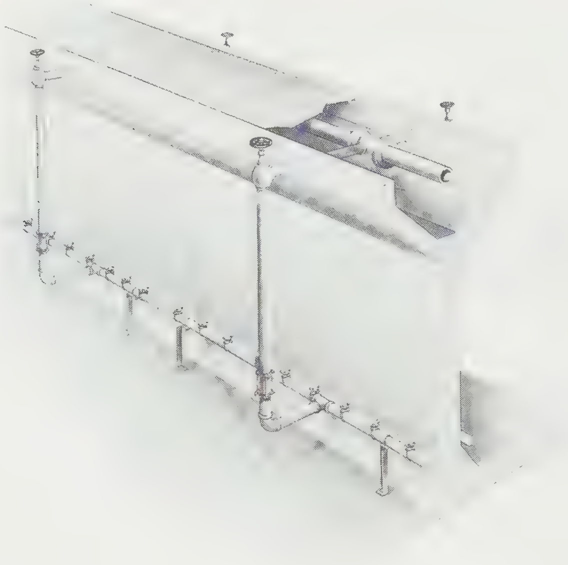

FIG. 16. Diffused-air aerator. (*Walker Process Equipment, Inc.*)

waste-water-treatment method where substantial reduction in the organic pollutional content is required.

Reliable design criteria for domestic sewage have been set up by various authorities, such as the "Ten-state Standards," for the conventional activated-sludge process. Approval of the many modifications of the accepted conventional activated-sludge process by public supervisory authorities may require considerable investigation of

FIG. 17. Mechanical aerator. (*Yeomans.*)

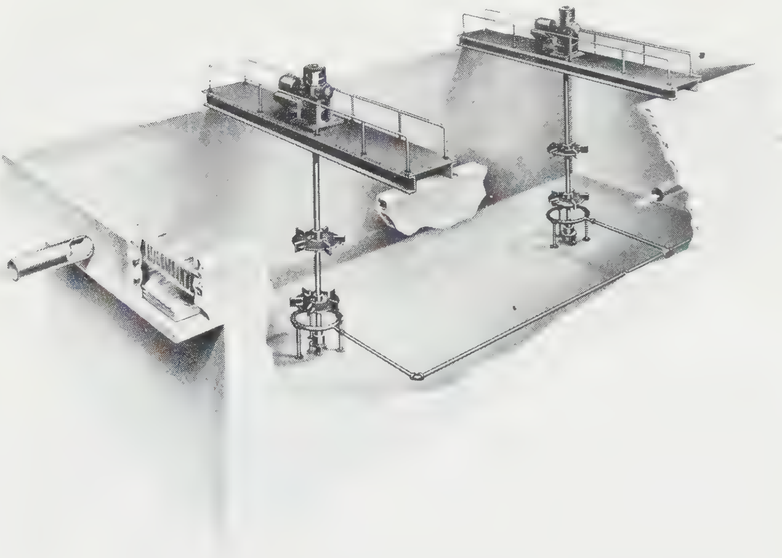

FIG. 18. Combined air and mechanical aerator. (*Dorr-Oliver, Inc.*)

probable results based on basic research, pilot-plant studies, and operation experience from existing plants, particularly for industrial waste waters.

The objective of modifications of the activated-sludge process is to provide a less costly treatment system which will produce substantially equivalent results. Special studies of the process, its application, and the proper design factors must be made for each proposed waste-water-treatment project. Some comparative data are given by Table 2, based on tabulated figures proposed by Chicago Pump Company.

TABLE 2. DESIGN PRACTICE—DIFFUSED-AIR AERATION PROCESSES

Treatment process	BOD loading, lb/1,000 cu ft*	Cu ft air/lb BOD	Sludge age, days†	BOD removed, %†	Ratio plant sizes‡	
					Area†	Volume†
Conventional activated sludge	35	1,000	3.5	90+	1.0	1.0
Step aeration or contact stabilization	50	800-1,000	3.5	90+	0.86	0.67
Modified aeration (high-rate)	100	600-800	0.2 0.5	60 75		
Extended aeration	20	1,500–2,500	1.2–20	80–90+		
Completely mixed "rapid bloc"	150	800–1,000	3–4	90+	0.57	0.28

* Aeration-tank capacity.

† Including aeration and final tanks.

‡ Chicago Pump Co. used "rapid bloc" as 1.0, with other processes requiring larger plant-size ratios. These data have been rearranged to use 1.0 for conventional activated sludge.

22. Final Sedimentation. The effluents from trickling filters and aeration tanks contain large amounts of settleable solids which must be removed in final sedimentation tanks to produce satisfactory treatment-plant results. These tanks must be designed for rapid removal of sludge, as trickling-filter effluent contains putrescible solids, especially at times of "unloading," and activated sludge must be maintained in a fresh condition for that large portion which must be returned quickly to the aeration tanks to avoid loss of dissolved oxygen and deterioration of biological activity. Density currents of activated-sludge mixed liquor along the bottom of a tank have been used in the design to assure short detention of well-conditioned sludge quickly settled from the mixed liquor (Fig. 19). Effluent weirs should be located away from the upturn of the density currents.

FIG. 19. Density currents and flow patterns in final tank. (*Chain Belt Co.*)

The design of final sedimentation tanks should be based on the design flow, or the design flow plus recycled flow related to a proper surface settling rate (sometimes designated "overflow rate").

Earlier issues of "Ten-state Standards" used surface settling rates for "final tanks" as follows:

Type of Treatment	Surface Settling Rate, gpd/sq ft
Low-rate trickling filters	1,000
High-rate trickling filters	800
Activated sludge (over 2 mgd)	1,000
Activated sludge (under 2 mgd)	800

Detention periods are not specified but result from the selected settling rate and a specified minimum water depth.

The quantity of activated sludge returned to aeration tanks and the solids content of the mixed liquor vary, depending on the type of activated-sludge process used and the characteristics of the waste water being treated. Since "mixed liquor" is recycled as underflow, it is not considered in the "surface settling rate" but must be considered in computing detention periods in both aeration and final tank.

23. Disinfection. The primary use of chlorine is the destruction of pathogenic and other bacteria for disinfection of waste-water-treatment-plant effluent before discharge into receiving waters which may be used for water supply, bathing, and shellfish propagation or crop irrigation. A contact period from 15 min at peak flows to 45 min in a contact tank or the plant outfall sewer with a chlorine residual of 0.2

to 1.0 mg/liter usually provides satisfactory disinfection. Chlorine may be used also in waste-water treatment for many other purposes. The application rate will depend upon the chlorine-demanding chemicals in the plant effluent.

24. Outfalls. The present practice is to install a submarine outfall sewer to a series of outlets adequately spaced along the line of a diffuser section to minimize interference of rising effluent columns; the placement of the diffuser on the bottom with horizontal discharge ports to increase initial dilution; orientation of the diffusers, in most cases, being normal to the diluting flow, or current, to provide maximum horizontal diffusion; and the location of the diffusers at a sufficient distance from the shore to provide the required reduction in concentration of coliform bacteria for acceptable shoreline standards.

In a lake the diffuser should be located in an optimum circulation zone. In a stream the diffuser should be located in a reach related most favorably to the dissolved-oxygen consumption-time curve of the stream.

Estuaries, semienclosed bays, and harbors vary widely in their circulation systems which govern the dispersion, dilution, and transport of waste waters. In open coast waters, ocean temperature and salinity gradients and seawater renewal rates have an important effect on the initial effluent mixing with seawater and the dispersion characteristics of the effluent seawater mass. The elements of time and distance are significant in overall bacterial removal.

25. Sludge Treatment. The objectives of sludge treatment include the reduction of volume and the conversion of the putrescible solids into innocuous substances, so that the residual sludge may be disposed of without creating objectionable conditions. Various processes are used in reducing sludge volume, including thickening, centrifuging, chemical conditioning, elutriation, anaerobic digestion, aerobic digestion, biological flotation, vacuum filtration, air drying, heat drying, and incineration. The reduction or destruction of the putrescible solids is accomplished partially by digestion, and completely by incineration.

Two relatively new processes for sludge treatment are "wet combustion" and "atomized suspension."

Disposal of treated sludge from treatment works has included ocean disposal for plants near the coast, as fill on land, as a low-grade fertilizer, in lagoons or in some places discharging into a river at times of flood (the latter procedure is no longer permissible).

26. Summary Plant Elements. Several elements that may be integrated in varied combinations of processes in a waste-water-treatment plant are as follows:

I. Liquid waste elements
   1. Incoming sewer
   2. Preparatory devices
      a. Screening arrangements
      b. Grit-removal devices
      c. Flocculation tanks
   3. Measuring weir, meter, or Parshall flume
   4. Preliminary or primary sedimentation tanks
   5. Biological treatment
      a. Trickling filters
      b. Aeration tanks
      c. Oxidation ponds
   6. Final sedimentation tanks
   7. Effluent screens (if used)
   8. Contact tanks for disinfection

9. Conduits for flows through the plant
10. Plant outfall for effluent disposal

II. Sludge-handling elements
1. Sludge from sedimentation tanks
   a. Sludge collectors, in tanks
   b. Sludge piping
   c. Sludge pumps
2. Sludge treatment
   a. Thickening tanks
   b. Digestion tanks
   c. Wet combustion
   d. Lagooning
   e. Drying beds
   f. Conditioning tanks—chemical treatment
   g. Dewatering by vacuum filters or filter presses
   h. Dewatering by centrifuges
   i. Heat drying
3. Sludge solids disposal
   a. Dumping (wet or dried)
   b. Fertilizing land
   c. Incineration
   d. Barging to sea
   e. Outfall to sea

Certain plant elements for the treatment of waste water or handling of sludge may be alternative items to be used in case others are not.

HYDRAULIC LOSSES—GENERAL

27. Introduction. Waste waters flowing through various treatment-plant elements require a difference in elevation of the water levels between the plant entrance and outlet to overcome various hydraulic losses. These head differences vary with the rate of flow. Successful operation depends in a large measure upon their accurate evaluation.

The hydraulic transportation of wet sludge in piping depends on its temperature, solids concentration, and plasticity as determined by the extent and type of the sludge-treatment process. Special consideration in conveying different types of sludge is given in Art. 42.

The following discussion of hydraulic losses is based largely on sewage-treatment-plant design experience. It would also apply to most waste-waters-treatment plants.

28. Types of Losses. Hydraulic-head losses at various points through treatment-plant elements are:

1. Friction and turbulence losses through conduits
2. Velocity-head losses
3. Heads required for discharge over weirs, through orifices, and other controlling or measuring devices
4. Water-level drops at various points such as a free fall below a weir
5. Head allowances for future plant extensions
6. Head allowance for higher water levels in the receiving waterway

The extent and variation in the several hydraulic losses may be affected by a number of factors, such as:

1. Variations in flow from minimum to maximum rates. The greatest hydraulic loss occurs at the maximum rate of flow for which treatment is to be provided.

2. The type and effectiveness of the devices to measure and control the distribution of flow through various plant elements. Thus close control and accurate measurements may indicate larger hydraulic losses than those obtained by more approximate methods.

3. The tendency for the deposition of solids, particularly in advance of the sedimentation tanks. Thus the use of higher velocities or agitation, by air, or other methods to prevent deposits in conduits generally results in hydraulic losses greater than those with clear water or well-settled waste water. Minimum flow rates and minimum cleansing velocities often control plant elevations.

4. The size and character of openings and the arrangements of flow channels. Thus small openings and abrupt changes in direction of flow increase velocity-head losses.

Hydraulic design and satisfactory operation are related closely. Thus, in sedimentation and aeration tanks, it is advisable to maintain the flow level practically

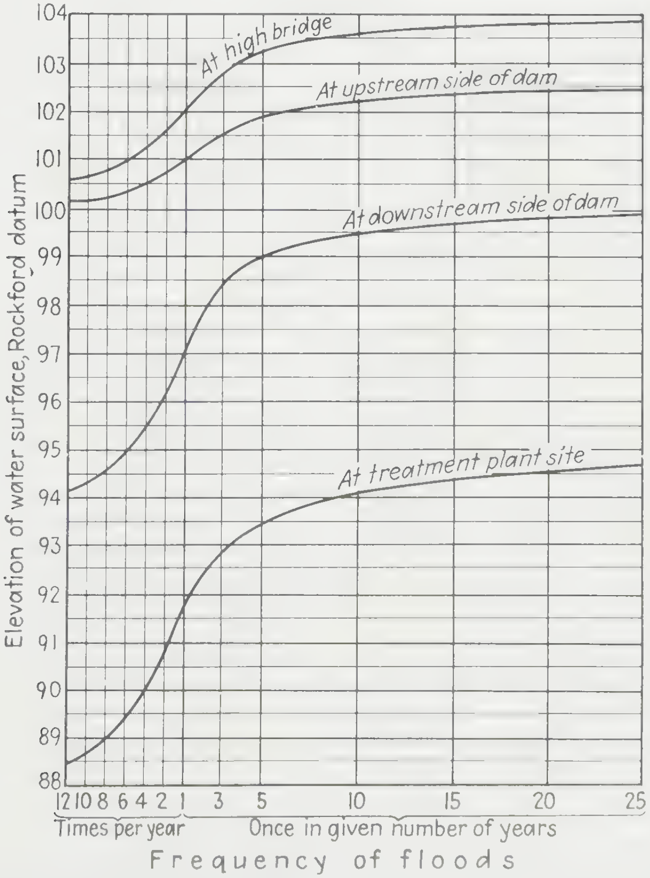

FIG. 20. Frequency of flood heights, Rock River, Rockford Sanitary District, Illinois.

constant. The distribution of flows equally into each of several tanks and the delivery of the flow quietly and gently into the tank cross section determine the effective use of the displacement period.

It is good practice to anticipate future enlargements of various plant elements. Head allowances should be included at various points to provide for such future enlargements. Often a plant extension of 50 to 100 percent of the initial capacity is reasonable to anticipate.

The head available for the operation of a treatment plant is the difference between some elevation of the flow in the inlet sewer and some elevation of high water in the receiving body of water. The frequency of occurrence of these controlling elevations is important (Fig. 20 or 21). Less effective hydraulic operating control may be

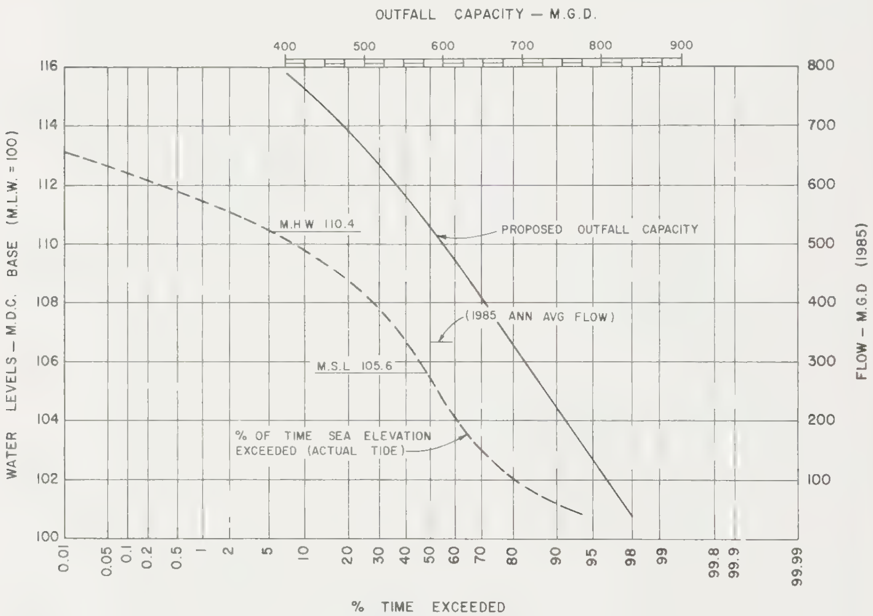

FIG. 21. Frequency of tidewater levels and outfall capacity, Deer Island Outfall, Metropolitan District Commission, Boston, Mass.

permissible at infrequent intervals, if the cost of avoiding this is great and the resulting small pollution is not objectionable. Also, in some cases, a higher inlet elevation may be had by backing up the flow in the inlet sewer, if the resulting lower velocity is infrequent and not too low, say somewhat above 1 fps. The high water in the outlet for the computation of the hydraulic gradient may be somewhat below the maximum and may be taken generally as that water level expected to be exceeded only 1 percent or, occasionally, 10 percent of the time.

HYDRAULIC COMPUTATIONS—MAJOR TREATMENT-PLANT ELEMENTS

29. Introduction. In an actual design project, the hydraulic computations might start with the selected high-water level of the river, or other body of water, into which the plant effluent is to be discharged, and extend upstream through the outfall and treatment plant in reverse direction to the flow through the plant elements.

This is a particularly useful procedure if the plant hydraulics are determined before the incoming sewer is designed.

To determine the proper elevations for various plant elements, the hydraulic gradient through the plant should be computed for the estimated maximum and minimum flows, as well as the basic design rate of flow. Frequently, minimum flows and required velocities control the elevations of certain plant elements.

30. Entrance Losses. At the entrance, two types of major head losses may occur:

1. Loss due to the difference between the high-water level in the incoming sewer and the high-water level in the treatment plant, controlled by elevation of settling-tank weirs. These water-level differences require careful computations, as the changes in water levels from incoming sewer to treatment plant may cause large entrance losses.
2. Friction and velocity-head losses, due to control gates and changes in conduit direction or section.

The variation in water level in the incoming sewer, between maximum and minimum flows, should be used as much as possible to overcome hydraulic losses at the higher flow rates through the various plant elements, such as the bar screens, grit chambers, flow-measuring devices, and conduits.

If a pumping station is required at the entrance, some part of the variation in water level in the incoming sewer may be utilized to reduce the head against which the pumps must operate.

The friction and velocity-head losses at the entrance usually are not large, depending upon the type and design of control gates and the necessary changes in direction of flow.

Losses through inlet gates may be computed by the velocity-head formula $h = k(V^2/2g)$, with the following values of k as reasonable for practical design purposes:

Type of Entrance	Coefficient k
Sluice gate:	
As a submerged port in a 12-in. wall	0.8
As a contraction in a conduit	0.5
Width equal to full conduit width and without top submergence	0.2

31. Conduit Losses. Conduits may flow as open channels or as pressure pipes. They are generally circular but may have other shapes. Aerated channels are usually designed to flow as open channels.

Head losses through conduits include:

1. Friction resistance to flow
2. Velocity-head losses resulting from (*a*) entrance disturbances, (*b*) disturbances along conduits, (*c*) sudden enlargements, (*d*) gradual enlargements, (*e*) sudden contractions, (*f*) obstruction, (*g*) bends

The head losses from resistance to flow in open circular channels may be computed as indicated for sewers (Sec. 40, Art. 30). The friction-head loss in pipes under pressure may be determined by the Hazen and Williams formula (Sec. 40, Art. 31) or by using Fig. 22. The friction-head losses in open channels of rectangular, trapezoidal, or other noncircular forms may be determined by the Manning formula (Sec. 40, Art. 31). This formula may be computed by a loglog slide rule (Sec. 40, Art. 34). Also other diagrams and tables are available for both formulas (Sec. 2, Art. 5). The choice of C or n is dependent on the judgment of the designer assisted by published values determined for types of conduit material and expected roughness condition of interior surface. However, uncertainties due to velocity disturbances

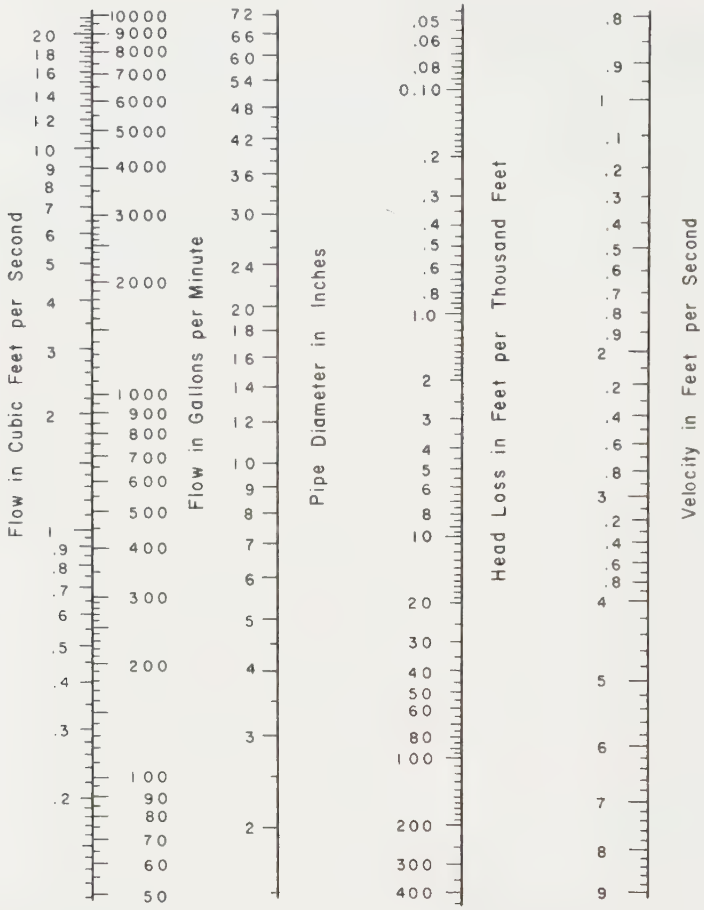

FIG. 22. Flow in pressure in pipes, Hazen and Williams formula, $C = 100$. (*Frederick E. McJunkin, Water and Sewage Works, vol.* 113, *no.* 9.)

usually make close refinements in the selection of coefficients unnecessary. Values of $C = 100$ or $n = 0.015$ are usually reasonable for design computations.

Disturbances at entrances may be covered by the entrance k factor unless there is a waterfall or other disturbance in the following conduit. In this case an allowance for the extra conduit loss may be made as described for aerated conduits (Art. 32), *i.e.*, by using an n factor of 0.035 or 0.040.

Velocity-head losses in pipelines due to changes in direction, section, and obstructions, such as gate valves partly open, may be determined by the velocity-head formula with appropriate values of the coefficient k from the following data compiled by King[4] and King and Brater:[5]

1. Entrance losses	
Type of entrance	k_1
Inward-projecting, square-cornered	0.8-0.9
Square-cornered, flush with wall	0.50
Slightly rounded	0.20
Bellmouth	0.04
2. Sudden enlargements	See Table 3

3. Gradual enlargements.......................... See Table 4
4. Sudden contractions.......................... See Table 5
5. Obstructions: specifically, gate valves partly open . . See Table 6
6. 90-deg bends.................................. See Fig. 23
   For 45-deg bends, use three-fourths of the losses for 90-deg bends
   For 22.5 deg bends, use one-half of the losses for 90-deg bends
7. Tees[5]

Velocity, fps	k_t
2	1.0
5	1.3
9	1.5
15	1.7

For Y branches, use three-fourths of the losses for a tee.

TABLE 3. VALUES OF K_2 FOR DETERMINING LOSS OF HEAD DUE TO SUDDEN ENLARGEMENTS IN PIPES, FROM THE FORMULA

$$H_2 = K_2(v^2/2g)$$

d_2/d_1 = ratio of larger pipe to smaller pipe. v = velocity in smaller pipe

$\frac{d_2}{d_1}$	Velocity v, fps												
	2	3	4	5	6	7	8	10	12	15	20	30	40
1.2	0.11	0.10	0.10	0.10	0.10	0.10	0.09	0.09	0.09	0.09	0.09	0.09	0.08
1.4	0.26	0.26	0.25	0.24	0.24	0.24	0.24	0.23	0.23	0.22	0.22	0.21	0.20
1.6	0.40	0.39	0.38	0.37	0.37	0.36	0.36	0.35	0.35	0.34	0.33	0.32	0.32
1.8	0.51	0.49	0.48	0.47	0.47	0.46	0.46	0.45	0.44	0.43	0.42	0.41	0.40
2.0	0.60	0.58	0.56	0.55	0.55	0.54	0.53	0.52	0.52	0.51	0.50	0.48	0.47
2.5	0.74	0.72	0.70	0.69	0.68	0.67	0.66	0.65	0.64	0.63	0.62	0.60	0.58
3.0	0.83	0.80	0.78	0.77	0.76	0.75	0.74	0.73	0.72	0.70	0.69	0.67	0.65
4.0	0.92	0.89	0.87	0.85	0.84	0.83	0.82	0.80	0.79	0.78	0.76	0.74	0.72
5.0	0.96	0.93	0.91	0.89	0.88	0.87	0.86	0.84	0.83	0.82	0.80	0.77	0.75
10.0	1.00	0.99	0.96	0.95	0.93	0.92	0.91	0.89	0.88	0.86	0.84	0.82	0.80
∞	1.00	1.00	0.98	0.96	0.95	0.94	0.93	0.91	0.90	0.88	0.86	0.83	0.81

TABLE 4. VALUES OF K_2 FOR DETERMINING LOSS OF HEAD DUE TO GRADUAL ENLARGEMENTS IN PIPES, FROM THE FORMULA

$$H_2 = K_2(v^2/2g)$$

d_2/d_1 = ratio of diameter of larger pipe to diameter of smaller pipe. Angle of cone is twice the angle between the axis of the cone and its side

$\frac{d_2}{d_1}$	Angle of cone													
	2°	4°	6°	8°	10°	15°	20°	25°	30°	35°	40°	45°	50°	60°
1.1	0.01	0.01	0.01	0.02	0.03	0.05	0.10	0.13	0.16	0.18	0.19	0.20	0.21	0.23
1.2	0.02	0.02	0.02	0.03	0.04	0.09	0.16	0.21	0.25	0.29	0.31	0.33	0.35	0.37
1.4	0.02	0.03	0.03	0.04	0.06	0.12	0.23	0.30	0.36	0.41	0.44	0.47	0.50	0.53
1.6	0.03	0.03	0.04	0.05	0.07	0.14	0.26	0.35	0.42	0.47	0.51	0.54	0.57	0.61
1.8	0.03	0.04	0.04	0.05	0.07	0.15	0.28	0.37	0.44	0.50	0.54	0.58	0.61	0.65
2.0	0.03	0.04	0.04	0.05	0.07	0.16	0.29	0.38	0.46	0.52	0.56	0.60	0.63	0.68
2.5	0.03	0.04	0.04	0.05	0.08	0.16	0.30	0.39	0.48	0.54	0.58	0.62	0.65	0.70
3.0	0.03	0.04	0.04	0.05	0.08	0.16	0.31	0.40	0.48	0.55	0.59	0.63	0.66	0.71
∞	0.03	0.04	0.05	0.06	0.08	0.16	0.31	0.40	0.49	0.56	0.60	0.64	0.67	0.72

TABLE 5. VALUES OF K_3 FOR DETERMINING LOSS OF HEAD DUE TO SUDDEN CONTRACTION, FROM THE FORMULA $H_3 = K_3(v^2/2g)$

d_2/d_1 = ratio of larger to smaller diameter. v = velocity in smaller pipe

$\frac{d_2}{d_1}$	Velocity v, fps												
	2	3	4	5	6	7	8	10	12	15	20	30	40
1.1	0.03	0.04	0.04	0.04	0.04	0.04	0.04	0.04	0.04	0.04	0.05	0.05	0.06
1.2	0.07	0.07	0.07	0.07	0.07	0.07	0.07	0.08	0.08	0.08	0.09	0.10	0.11
1.4	0.17	0.17	0.17	0.17	0.17	0.17	0.17	0.18	0.18	0.18	0.18	0.19	0.20
1.6	0.26	0.26	0.26	0.26	0.26	0.26	0.26	0.26	0.26	0.25	0.25	0.25	0.24
1.8	0.34	0.34	0.34	0.34	0.34	0.34	0.33	0.33	0.32	0.32	0.31	0.29	0.27
2.0	0.38	0.38	0.37	0.37	0.37	0.37	0.36	0.36	0.35	0.34	0.33	0.31	0.29
2.2	0.40	0.40	0.40	0.39	0.39	0.39	0.39	0.38	0.37	0.37	0.35	0.33	0.30
2.5	0.42	0.42	0.42	0.41	0.41	0.41	0.40	0.40	0.39	0.38	0.37	0.34	0.31
3.0	0.44	0.44	0.44	0.43	0.43	0.43	0.42	0.42	0.41	0.40	0.39	0.36	0.33
4.0	0.47	0.46	0.46	0.46	0.45	0.45	0.45	0.44	0.43	0.42	0.41	0.37	0.34
5.0	0.48	0.48	0.47	0.47	0.47	0.46	0.46	0.45	0.45	0.44	0.42	0.38	0.35
10.0	0.49	0.48	0.48	0.48	0.48	0.47	0.47	0.46	0.46	0.45	0.43	0.40	0.36
∞	0.49	0.49	0.48	0.48	0.48	0.47	0.47	0.47	0.46	0.45	0.44	0.41	0.38

TABLE 6. LOSS OF HEAD DUE TO GATE VALVES

Values of K_g in $H_g = K_g \dfrac{V^2}{2g}$

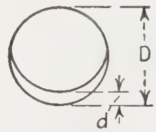

Nominal diam of valve, in.	Ratio of height d of valve opening to diam D of full valve opening					
	⅛	¼	⅜	½	¾	1
½	450	60	22	11	2.2	1.0
¾	310	40	12	5.5	1.1	0.28
1	230	32	9.0	4.2	0.90	0.23
1½	170	23	7.2	3.3	0.75	0.18
2	140	20	6.5	3.0	0.68	0.16
4	91	16	5.6	2.6	0.55	0.14
6	74	14	5.3	2.4	0.49	0.12
8	66	13	5.2	2.3	0.47	0.10
12	56	12	5.1	2.2	0.47	0.07

32. Aerated Conduits. Frequently, diffused air is blown up through the waste water in conduits to prevent deposits of solids with low velocities. Data are meager on the effect of agitation on the head losses in conduits. Some tests at Milwaukee were reported by D. W. Townsend,[6] from which it was concluded that Kutter's

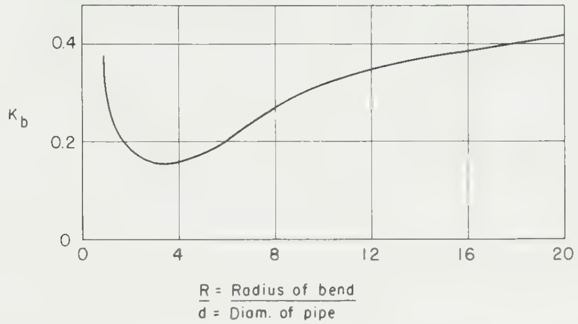

FIG. 23. Head loss at 90° bends, $H_b = K_b(V^2/2g)$. (*K. H. Beij, U.S. National Bureau of Standards, Research Paper* RP110.)

coefficient n might range as follows:

Velocity in Aerated Channel, fps	Value of n in Kutter's Formula
1.3	0.034
1.0	0.039
0.9	0.043

33. Bar-screen Losses. Hydraulic computations for the design of bar screens (see Art. 9) include the determination of the screen area and the head loss to be allowed for the operation of the screen. Bar screens may include iron bars 2 to 3 in. wide and ⅓ to ⅜ in. thick spaced ½ to 2 in. apart. Common spacing is ½ to ¾ in. for mechanically cleaned screens and 1 to 1½ in. for manually cleaned units.

The required area of submerged screen surface may be determined on the basis of a velocity of flow through the openings (when clean) of 2.0 fps for average flows and 3.0 fps for maximum rates of flow. The larger of the two areas thus obtained is the controlling area, but it may be increased for small installations to provide a minimum working width of 18 in. for manually cleaned units and 2 to 3 ft for mechanically cleaned units. In general, the effective screen area should be about twice the cross-sectional area of the incoming sewer.

Head losses through bar screen will vary, depending upon the amount of coarse material caught by the screen and the frequency of cleaning. A computation may be made of the head loss for a clean screen by the formula

$$h_1 = \frac{V^2 - v^2}{2g} \frac{1}{0.7}$$

or

$$h_1 = \frac{0.5V^2}{2g} + \frac{V^2 - v_2}{2g}$$

in which V and v represent, respectively, the velocity between the bars and in the approach channel and h_1 is the head loss due to a clean bar screen (foot and second units).

In practice for large installations, the screen may be kept partially clean by continuous operation of the cleaning mechanism, but for the more usual size of installation, the cleaning mechanism may operate intermittently, in which case some arbitrary allowance is usually included to permit some backing up, due to clogging of the screen, and a high-water overflow is provided. A reasonable amount for this head-loss allowance is about 3 to 6 in.

34. Fine-screen Losses. The hydraulic losses for each type of fine screen are different and are determined experimentally. Results are usually furnished by the manufacturer.

35. Comminutor Losses. Generally, comminutor installations (see Art. 10) are designed to take a maximum waste-water flow rate which may occur infrequently, possibly 1 or 2 percent of the time, with higher flow rates permitted to overflow a weir and bypass through a hand-cleaned bar screen.

Head requirements of comminutors depend upon waste-water flow rates; the machine capacity (*i.e.*, screen diameter, height, and slot widths); machine characteristics; and the upstream and downstream conduit widths and flow depths. A comminutor affects only the upstream flow depth, while the downstream flow depth depends upon hydraulic characteristics of the downstream conduits and settling tanks, particularly the settling-tank-effluent weir elevation.

Computations of head losses for a comminutor installation comprise three principal items:

1. The waste-water level drop required, from upstream to downstream, to force the desired flow rates through the comminutor. This drop varies with depths of flow. These water-level drops may be determined from hydraulic-performance charts, found in engineering manuals[7,8] furnished by comminutor manufacturers.
2. The open-channel friction losses in the approaching and following channels.
3. The waste-water drop in elevation due to the relative elevations of comminutors and the approaching and following conduits. By careful design these drops may be kept to a minimum.

Basic design data, useful for preliminary computations, are given in the following tabulation for two types of comminutors, shown by Figs. 4 and 5 (final design computations should be based on the manufacturer's manual):

Sizes		Max capacity, mgd		Head loss, in.‡		Approach conduit width, in.	
Size	Diam, in.						
I	II	I*	II†	I	II	I	II
4R	4-6-4	0.045	0.06				
7B	7-4	0.35	0.45	2–7	2–5	8 in. diam	
10A	....	1.1	.....	3–10	....	12	
	12 4	......	1.1	....	2 14	....	9
	12-5	......	1.4	....	....	....	12
	12-5	......	2.0	....	....	....	16
15M	15-5	2.3	2.4	4–10	....	15	18
	15-5	......	3.5	....	4–16	....	22½
	20-6	......	4.6	....	....	....	20
	20-6	......	7.5	....	3–24	....	30
25M	....	6.0	.....	4–10	....	24	
25A	25-6	11.0	11.0	4–15	5–28	30	36
36A	36-6	25.0	19.0	4–15	....	42	48
	36-6	......	26.0	....	6–43	....	48
	42-6	......	45.0	....	7–54	....	42
54A	(See engineering department of manufacturer)						

I = Fig. 4 type (Chicago Pump Co.).
II = Fig. 5 type (Worthington Corp.).
* Bottom-outlet type, controlled discharge.
† Straight-through-flow type, controlled discharge.
‡ Maximum head loss, inches, is with screen fully submerged.

Hydraulic-design computations for comminutors should include a conduit width and conduit depth related to a flow velocity sufficient to hold coarse material in suspension and slot widths for a velocity to carry coarse material against the drum face to be shredded by the cutters. The conduit widths and slots indicated (by the letter or second number under sizes) in the foregoing tabulation should be checked during design computations.

The selection of the proper comminutor size and determination of the overall head requirement for any given installation may require a number of trial computations and considerable study. In a general way a comminutor installation may be expected to require a hydraulic drop of 6 to 30 in. depending on plant size. Engineering manuals or selection and application handbooks furnished by comminutor manufacturers give helpful instructions.

36. Grit Chambers—Hydraulic Design. Hydraulic computations for design of grit chambers are affected by three factors: (1) waste-water flow rates; (2) proposed type of grit-removal device; and (3) quality of grit desired (*i.e.*, size of grit and percentage of organic matter). The long-horizontal-flow type of grit chamber is designed normally with a velocity-control device at the grit-chamber outlet (Fig. 24) to maintain a flow-level and flow-rate relationship such that the velocity through the grit channels would be about 1.0 fps (0.75 to 1.25 fps range) for all variations of flow rate. Such a flow velocity generally should keep the organic matter in suspension and remove grit of 65 mesh at a settling velocity of about 3.7 fpm (for quartz).[13]

The settling velocity of the grit size to be removed and the hydraulic characteristics of the outlet-control device determine the depth of flow and the proper length of the grit channels. Maximum flow rates relative to minimum flows determine the number of grit channels. Generally, a number of trial computations may be required.

The two commonest velocity-control devices are the proportional weir (several types) and the Parshall flume. The Parshall flume has become possibly the more frequently used velocity-control and -measuring device.

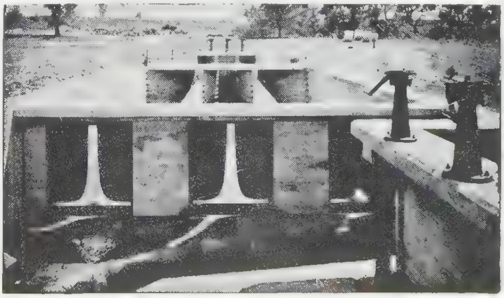

FIG. 24. Outlet end of grit chamber, Springfield, Illinois.

The control of flow depth by the Rettger proportional-flow weir (Figs. 24 and 25) for practical purposes may be computed by the formula

$$Q = 7.82 b_r h^*$$

where Q = flow rate, cfs

h = height of flow, ft, above theoretical weir crest (Fig. 25)

b_r = Rettger weir constant

The weir constant b_r may be computed after maximum values of Q and h are selected.

* Derived from Rettger's formula $Q = (C/2)\sqrt{2g}\, b_r \pi h$, with average $C = 0.62$.

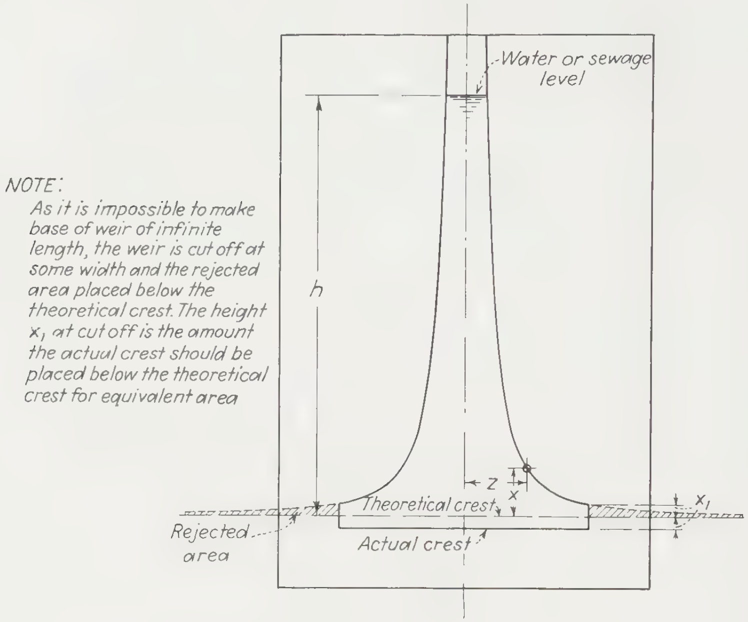

FIG. 25. Rettger proportional-flow weir.

Dimensions of the curves for the sides of the weir opening may be computed by the formula

$$Z = \frac{b_r}{2\sqrt{X}}$$

where Z = distance from center line to sides of openings
X = vertical distance above theoretical weir crest

A Parshall flume (Fig. 26) comprises three principal sections: (1) a converging level-floor upstream section B, (2) a downward-sloping uniform throat section F, and (3) an upward-sloping diverging downstream section G. At each end of the flume there is a converging or diverging transition section to connect to the main-flow conduit. Dimensions of flumes for throat width sized from 3 in. to 10 ft with the range of unrestricted rates of discharge are given in Table 7.

Parshall flumes operate as accurate measurement and flow-control devices as long as the flow depth H_b near the end of the throat does not exceed the upstream converging flow depth H_a by the following ratios according to throat-width size W:

W, Throat Size	H_b/H_a (Fig. 26)
3–9 in.	0.6
1–8 ft	0.7
10–50 ft	0.8

Above the limiting flow-depth ratios or permissible degree of throat submergence, the rate of flow is retarded. In the range below the flow-depth ratios, the rate of discharge is unrestricted or in free-flow discharge according to formulas developed from extensive experimental data.

Tables are available for free-flow discharge rates at various heads H_a for the different sizes of flumes. However, sufficiently close determinations of heads for

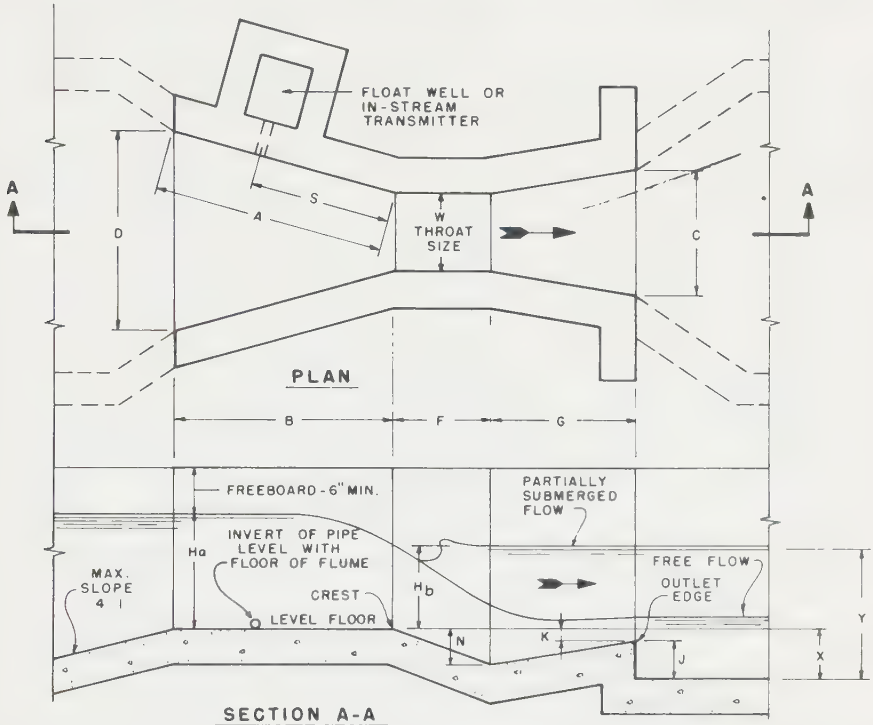

Fig. 26. Parshall flume, plan and section. (*U.S. Dept. of Agriculture, Farmers' Bull.* 1683, *January*, 1932, *revised October*, 1941.)

Table 7. Parshall-flume Dimensions and Capacities

Dimensions in feet and inches

W	*A*	*B*	*C*	*D*	*F*	*G*	*K*	*N*	Free-flow capacity, cfs	
									Max	Min
0-3	1-6 3/8	1-6	0-7	0-10 3/16	0-6	1-0	0-1	0-2 1/4	1.1	0.03
0-6	2-0 7/16	2-0	1-3 1/2	1-3 5/8	1-0	2-0	0-3	0-4 1/2	3.9	0.05
0-9	2-10 5/8	2-10	1-3	1-10 5/8	1-0	1-6	0-3	0-4 1/2	8.8	0.09
1-0	4-6	4-4 7/8	2-0	2-9 1/4	2-0	3-0	0-3	0-9	16.1	0.35
1-6	4-9	4-7 7/8	2-6	3-4 3/8	2-0	3-0	0-3	0-9	24.6	0.51
2-0	5-0	4-10 7/8	3-0	3-11 1/2	2-0	3-0	0-3	0-9	33.1	0.66
3-0	5-6	5-4 3/4	4-0	5-1 7/8	2-0	3-0	0-3	0-9	50.4	0.97
4-0	6-0	5-10 5/8	5-0	6-4 1/4	2-0	3-0	0-3	0-9	67.9	1.26
6-0	7-0	6-10 3/8	7-0	8-9	2-0	3-0	0-3	0-9	103.5	2.63
8-0	8-0	7-10 1/8	9-0	11-1 3/4	2-0	3-0	0-3	0-9	139.5	4.62
10-0	14-3 1/4	10-0	12-0	15-7 1/4	3-0	6-0	0-6	1-1 1/2	200	6

Dimension $S = \frac{2}{3} A$ (Fig. 26), except 6 ft 0 in. for W = 10 ft 0 in.

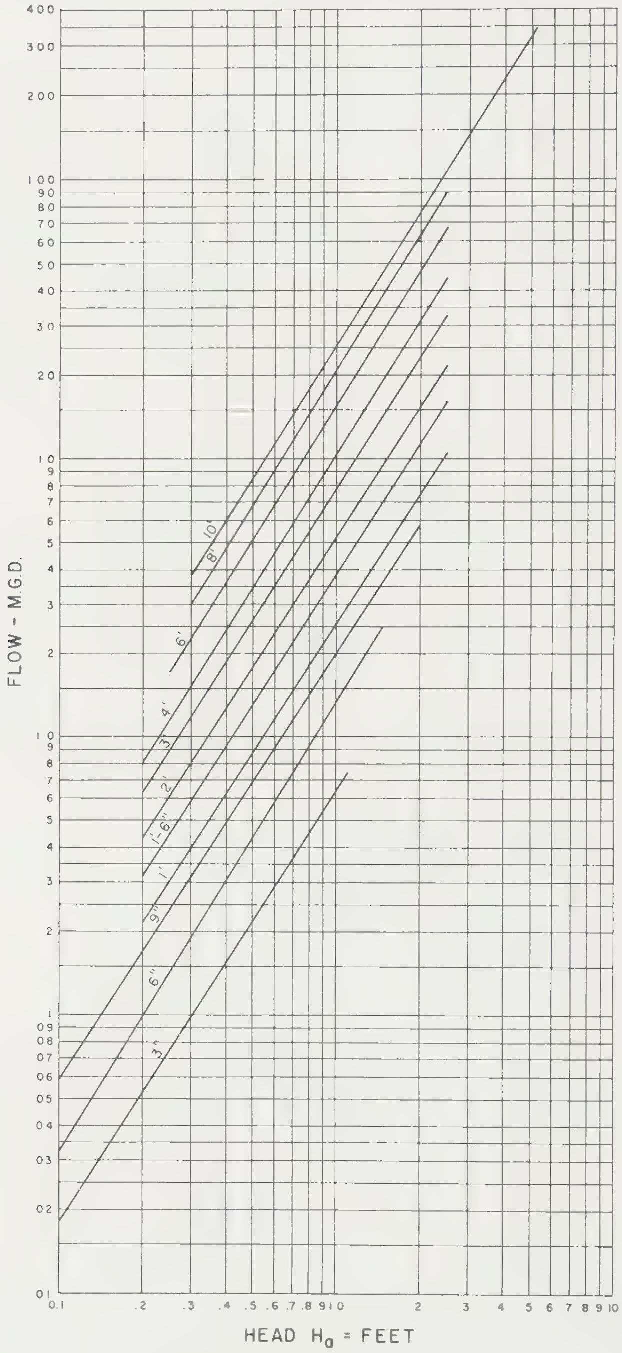

FIG. 27. Parshall flumes—flow rates and heads H_a. (*Chart plot data from U.S. Dept. of Agriculture, Farmers' Bull.* 1683, *and Colorado A&M College, Bull.* 426-A.)

practical hydraulic-design computations may be taken from the log-log chart of Fig. 27.

Investigation of several sizes of flumes carrying the design flow, unrestricted at the H_b/H_a ratio, should resolve the choice of an economical size. This usually falls within a throat-size range of one-third to one-half the width of the main-flow conduit.

Other types of grit chambers, such as short-term settling tanks and aerated grit chambers, require less rigorous hydraulic studies but do require grit washers to obtain a sufficiently clean grit.

Head losses for grit chambers include hydraulic losses through flow-control gates, inlet and outlet conduits, and the necessary head differential for the two sides of the weir or flume used for velocity-control and flow measurements. Generally, the net head losses for grit chambers can be reduced by using part of the variations of flow depths in the incoming sewer, provided that the inlet screen and other structures upstream are properly designed.

37. Flowmeters—Head Requirements. Flow measurements are essential to operation. Such devices require some head or drop in the hydraulic profile. In general, total plant-flow measurements are best made near the upstream part of the plant. However, measurement of untreated flows by weirs may not be satisfactory because of clogging of the weir crest by stringy materials. In smaller plants, flows have been measured by weirs at the outlet of chlorination contact tanks, but these measurements do not record all flow-rate variations.

Proportional weirs and Parshall flumes are used for both flow measurements and velocity control of grit chambers, as discussed in Art. 36.

Venturi meters, especially designed, are frequently used but may require more head loss than Parshall flumes. Such head losses depend upon the meter design and the ratio of the inlet velocity and the throat velocity. Flow measurement, by Venturi meter, is determined by the differential between the inlet and the throat pressure heads. The head loss is often given as a percentage of the pressure-head differential, as illustrated by Fig. 28. This chart shows a lesser percentage of differential, as lost head, for the Dall flow tube, with the long Venturi meter next lowest. Loss of head for Venturi meters may also be computed as a fraction of the throat velocity head, as follows:

Type of Meter Tube	Head Loss, ft
Long-form Venturi	$h_L = 0.108h_v$
Short-form Venturi (based on ratio of throat to inlet diam):	
Ratio 4/12 (*i.e.*, 0.33)	$h_L = 0.27h_v$
Ratio 6/12 (*i.e.*, 0.50)	$h_L = 0.18h_v$
Ratio 7/12 (*i.e.*, 0.583)	$h_L = 0.143h_v$
Ratio 8/12 (*i.e.*, 0.667)	$h_L = 0.14h_v$
Ratio 9/12 (*i.e.*, 0.75)	$h_L = 0.135h_v$

where h_L = head loss, feet
$h_v = V^2/2g$ (throat velocity)

The total head, in feet, required for flows in cubic feet per second over various types of sharp-crested weirs (with clean crests), without corrections for velocity of approach, may be computed by formulas as follows:

1. Rectangular weir, per foot length (no end contractions), by Francis formula, $Q = 3.33H^{3/2}$

2. V-notch weirs, with end contractions, (*a*) 90-deg notch, $Q = 2.48H^{2.48}$; (*b*) 60-deg notch, $Q = 1.44H^{5/2}$

3. Cipolletti weir, per foot length of crest, $Q = 3.367H^{3/2}$

Any velocity of approach toward the weirs would increase the flow capacity for

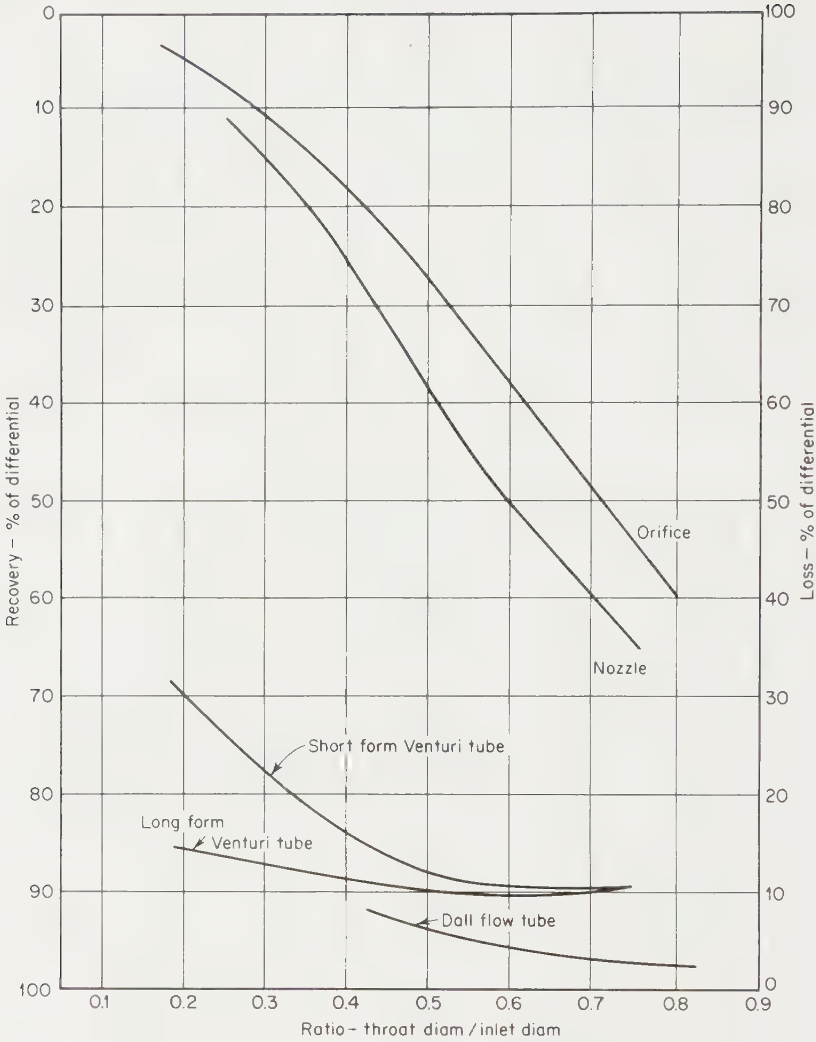

Fig. 28. Characteristics of pressure head losses of differential producers. (*B.I.F. Industries.*)

a given observed head. Any deposits on the weir crest would increase the head required for a given flow. It is common practice to design the downstream structures with hydraulic gradients, to provide some free fall below the measuring or control weir, so as not to submerge the weir. A reasonable allowance for free fall would be 0.2 to 0.5 ft, depending in part on the total head available.

Magnetic flowmeters are being used in waste-water treatment plants, where loss of head becomes an important factor and the larger costs for such meters are justified.

Magnetic flowmeters have no restrictions to flow through the meter tube, except that they may require heaters to prevent grease deposits. However, it is frequent design practice to use smaller pipe-size meters than the connecting pressure conduits. Some head loss is therefore involved in the reducing and enlarging connection sections.

The foregoing data are useful for preliminary computations. However, because measurement meters are always provided with flow recorders, often with transmitters for recording at a distance, it is generally necessary to call in some specialist on instrumentation, who would also be ready to supply head losses for various arrangements of flow-measurement instruments.

Auxiliary devices, or instruments, additional to the main meter, may be needed to measure airflows, sludge flows, recirculation flows, and other flow measurements. Instrumentation for modern waste-water treatment plants has become complicated.

38. Sedimentation Tanks. Hydraulic computations for sedimentation tanks include the following determinations:

1. Control-chamber losses
2. Losses due to distribution devices
3. Inlet-conduit dimensions and losses
4. Velocity-head losses at inlets
5. Head on outlet weir and free fall below weir
6. Outlet channels, dimensions and losses

The control chamber often comprises a small chamber with outlets controlled by sluice gates. The head losses are a portion of the velocity head on entrance to the chamber through a sluice gate, additional proportions of the velocity head if changes in direction of flow are necessary, and further velocity-head losses through chamber-outlet openings.

In any project comprising two or more tank units, the flow should be equally divided among the several tanks. Sometimes measuring devices are included such as Venturi tubes, Pitot tubes, or weirs, by which the flow to each tank is actually measured and the division controlled with considerable accuracy. The hydraulic losses through these devices can be computed from the data given elsewhere. Generally, such accuracy of control and large head losses have not been considered necessary.

Conduit losses may be computed by methods already described. Thus the losses in the inlet conduit might include about one-half the velocity head with a sharp-edged entrance ($0.5V^2/2g$), plus the friction loss along the length of the conduit, plus the full velocity head on discharge into the sedimentation tank.

The head required for an outlet rectangular-type weir will depend upon the flow per unit length of weir and may be computed by the Francis formula (Art. 37).

Thus, at Buffalo, for a maximum flow of 570 mgd (882 cfs) four round sedimentation tanks were included, each having a diameter of 160 ft and 500 lin ft of effluent weir. This amounted to 0.441 cfs (285,000 gpd) per foot of effluent weir and required a head of 0.26 ft.

Current design practice limits the settling tank outlet-weir overflow rate to 15,000 or fewer gallons per day per foot of weir. Thus design approved by "Ten-state Standards" would be as follows:

"Weir loadings should not exceed 10,000 gallons per day per linear foot for plants designed for average flows of 1.0 mgd or less—for plants designed for flows in excess of 1.0 mgd—should preferably not exceed 15,000 gallons per day per linear foot."

This restriction in weir overflow rate requires special outlet-weir design including a total weir length for rectangular tanks, several times the tank width, and for circular tanks often two weirs with an outlet conduit between them, or a series of radial-flow conduits may be used. Also, the outlet-weir plates are quite generally cut into a series of 90- or 60-deg V-notch weirs about 8½ in. center to center for better control of the low overflows. In addition to the head above the bottom line of the V-notches, a reasonable free fall of 0.2 to 0.5 ft should be allowed for maximum flows, if ample head is available for the plant.

The need for long outlet weirs and long outlet conduits with a varying inflow rate along the conduits results in hydraulic computations more complicated than a simple weir discharging into the upper end of an outlet channel. Head on the outlet weir may be determined by dividing the flow by total weir length (or total numbers of V-notches) and applying the appropriate weir formula (Art. 37).

Hydraulics of free-flowing and free-outlet discharging conduits may be computed by the equations set up in Sec. 38, Art. 14, for lateral spillway channels [Eq. (17), Sec. 38, Art. 14] and for the critical depth at ends of wash-water gutters discharging freely [Eq. (42), Sec. 38, Art. 24]. For proper use of these equations to compute conduit head losses, the hydraulic design of conduits and structure downstream should not permit a backwater level above the hydrostatic critical depths at the channel outlets around or across the settling tanks. Friction losses computed as for conduits (Art. 31) should be added to the differences in upper and lower conduit depths (level-bottom types). In general design practice, the effluent conduit often is planned with a sloping bottom, which requires some modifications in application of the wash-water gutter and the conduit formulas.

The computed hydraulic losses for a number of illustrative sedimentation tanks are given in Table 8.

Table 8. Illustrative Hydraulic Losses for Sedimentation Tanks

<table>
<tr><th>Item</th><th>Buffalo, N.Y., 570 mgd</th><th>Yonkers,* N.Y., 230 mgd</th><th>Richmond, Va., 70 mgd</th><th>Alexandria, Va., 40 mgd</th><th>Appleton, Wis., 32 mgd</th></tr>
<tr><td>Inlet chamber</td><td>0.13</td><td rowspan="2">0.14</td><td>0.05</td><td>0.15</td><td>0.10</td></tr>
<tr><td>Inlet conduit</td><td>1.04</td><td>0.05</td><td>0.10</td><td rowspan="2">0.15</td></tr>
<tr><td>Riser pipe†</td><td>0.59</td><td>0.69§</td><td>0.08§</td><td>0.11§</td></tr>
<tr><td>Fall across tank:</td><td></td><td></td><td></td><td></td><td></td></tr>
<tr><td>Head on weir</td><td>0.25</td><td>0.20</td><td>0.08</td><td>0.06</td><td>0.07</td></tr>
<tr><td>Free fall below weir</td><td>1.48</td><td>0.01</td><td>0.50</td><td>0.98</td><td>0.18</td></tr>
<tr><td>Collecting conduit</td><td>0.14</td><td>0.04</td><td rowspan="2">0.04</td><td rowspan="2">0.04</td><td>0.15</td></tr>
<tr><td>Outlet connection‡</td><td>0.49</td><td>0.14</td><td>0.07</td></tr>
<tr><td>Total</td><td>4.12</td><td>1.22</td><td>0.80</td><td>1.44</td><td>0.72</td></tr>
</table>

* Yonkers Joint Plant, Westchester County, N.Y.
† For round center-feed tanks.
‡ Connection from individual tank to main outlet conduit.
§ Head on inlet ports.

39. Rotary Trickling Filters. Hydraulic computations for reaction-type rotary trickling filters involve the following major factors and head requirements:

1. Area and depth of filter
2. Losses through connecting piping and control chambers
3. Head required in center column and through rotating arms
4. Height of arms above filter stone
5. Underdrains and outlet drainage channel

The area and depth of the filter should be computed on the basis of type of filters and concurrent BOD and flow-rate loadings, with or without recirculation, necessary to meet the extent of BOD removal required.

The head losses through the connecting piping from the control structure to the center column of the distributor at the center of the filter include the entrance and exit losses to and from the piping and the friction losses in the pipeline, computed as outlined before.

The head required for flow distribution over a rotary distributor-type filter includes the losses in the center column, the distribution arms, and the orifices, which depend upon specific design factors, such as the special construction required to control the rate of flow into the rotating arms, the number of arms, the design of discharge nozzles or orifices, and the velocity head of discharge required to cause the reaction force of rotation. The heads required in the center column and arms have been based on actual hydraulic tests by the specific equipment manufacturer. In design practice, it is usual to state the maximum, average, and minimum rates of flow, the filter size, the available head, at the center column or at the center of the arms; to provide details of the column base with the surface of the filters; and then to require manufacturers to provide distributors to operate within specified capacities and head limitations. However, the engineer's hydraulic design must be close to the manufacturer's standard designs, so some preliminary consultations may be desirable.

The height from the surface of the filters to the center line of the distributor arms or arm-clearance loss depends upon the diameter of the filter and the details of the distributor. There is a static loss or clearance of approximately 9 in. per 100 ft of filter diameter with a minimum of about 6 in.

Underdrains comprise both a filter-floor collection system and a subfloor supporting the filter media, which may be constructed of vitrified-clay blocks to carry the filter effluent and to provide air for the filter treatment process. The top faces of the blocks have openings of at least 20 percent of the top surface area. The rated discharge through the blocks should be carried in not more than 50 percent of the cross-sectional area. These blocks are laid on the filter floor with a minimum slope of 0.5 percent toward a main drainage channel. The velocity in the main drainage channel is usually 2 to 3 fps with the maximum discharge flow level in the main drainage channel kept below the bottom of the underdrain blocks.

The maximum loss of head within the rotary trickling filter is the distance between the water levels for the maximum flow in the center column of the distributor to the minimum flow in the drainage channel at the outlet, or to the outlet weir level in the final tanks.

Roughly the overall head loss for a rotary trickling filter may be as follows:

Filter element	Approx head, ft	
	Avg	Range
Distributor	2.5	1.0– 4.0
Filter depth	6.0	3.0– 8.0
Underdrainage	2.5	2.0– 4.0
Total	11.0	6.0–16.0

The computed head requirements for a number of illustrative trickling filters are given in Table 9.

TABLE 9. ILLUSTRATIVE HEAD REQUIREMENTS FOR TRICKLING FILTERS

Plant	Filter units		Flow, mgd	Head required, ft			
	No.	Diam, ft		Influent system*	Media depth†	Effluent system‡	Total
Alexandria, Va	3	160	40	3.73	4.33	3.37	11.43
Austin, Minn.:							
First stage	2 2	68 74	7.32	5.78	6.75 6.34	1.11 1.52	13.64
Second stage	1	0.88 acre§	9.30	8.50	8.00	4.20	20.70
Knoxville, Tenn., Loves Creek Plant	2	75	3.32	3.94	6.25	10.91	21.10
Sioux Falls, S. Dak.:							
First stage	4	87	4.9	6.54	6.18	2.86	15.58
Second stage	4	197	9.8	5.29	7.42	18.14	30.85
Rockford, Ill	4	150	30	2.97	5.08	0.65	8.70
Tullahoma, Tenn	2	123	1.5	3.57	5.63	1.29	10.49

High heads required shown for some processing units are due to elevated locations dictated by restrictive sites or topography.

* Water surface in preliminary or intermediate tanks to top of media.

† Media depth at channel.

‡ Bottom of media to water surface in intermediate or final tanks.

§ Fixed-nozzle-type filter.

40. Aeration Tanks. Inlet, outlet, and conduit capacities and head losses are computed as described for sedimentation tanks. Conduits carrying mixed liquor and aeration-tank effluents are usually aerated to prevent the depositing of solids. The relatively small losses through the aeration tank can be neglected. Head variations on the effluent weirs are computed by the Francis weir formula, as described for sedimentation tanks. However, often water levels in aeration tanks may be controlled by the effluent weirs of the final tanks and no effluent weir used in the aeration tank.

The diffused-air-type system for aeration tanks involves the capacity and the head losses of air piping and type of aeration device and the back pressure from the sewage depth to the device. Porous diffusers of all types require air filtering to control clogging. The head losses for the various aeration devices are available from the manufacturers.

One of the functions of an aerator is to mix the solids in the sewage thoroughly and prevent sedimentation, which is considered in the design of the tank and the placement of the aerators. Spiral-flow tanks should have a transverse velocity of 1 to 1½ fps to prevent solids deposition. Numerous factors are involved in the primary function of an aerator, which is the amount of BOD to be removed. Air requirements in the past have been related to volume of sewage, but with increasing performance data, present practice is to relate the volume of air required to the amount of BOD to be removed, which is dependent on the type of activated-sludge process used. The "Ten-state Standards" assume 1,000 cu ft of air/lb of applied primary effluent BOD/day for the average flow. These "standards" require the diffused-air-type system to have 150 percent of the average capacity for piping, diffuser piping, and blowers or compressors, including additional service conditions for the latter. Mechanical aerators are also required to meet the same objectives.

Air-piping losses may be computed by the Fritzsche formula (Fig. 29), which in English units may be written as follows:[9]

$$P = \frac{1.268(t + 460)Q^{1.852}L}{10^6(p + 14.7)d^{4.973}}$$

where P = drop in pressure, psi per foot of piping
p = mean gage pressure, psi
t = mean air temperature, °F
d = pipe diameter, in.
L = length of pipe, ft
Q = cubic feet of free air per minute at 60F and 760 mm pressure

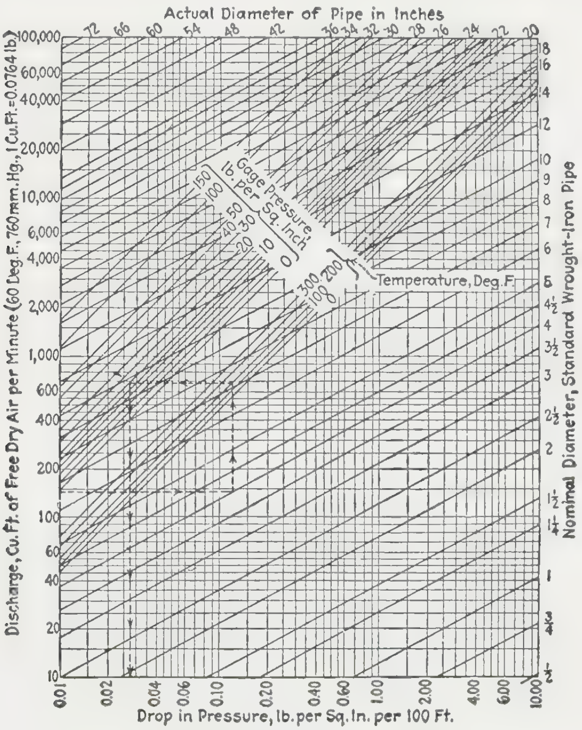

FIG. 29. Flow of air in circular pipes based on Fritzsche formula.

Bushee and Zack have reported[10] the results of early experiments by the Chicago Sanitary District on air-pressure losses through piping, meters, valves, and diffuser-plate connections.

Measurements with 4-in. steel pipe gave losses practically the same as computed by the Fritzsche formula, whereas the measured losses for 10- and 24-in. Brown and Sharpe cast-iron pipe were about 25 percent greater than the computed losses. Some allowance should be included for increased losses with age—possibly 20 percent of computed head losses.

Measurements of air-pressure losses through Venturi meters gave results summarized as follows:

Size of meter, in.	Compressed-air factors		Pressure losses	
	Pressure, psia	Temp, °F	% of meter differential head	psi per 1-ft differential
10 × 5	21.5	86	18	0.078
5 × 2	22.0	80	22	0.095
4 × 2	18.7	86	21	0.091
3 × ¾	21.5	78	24	0.104

Bushee and Zack stated that meters could be obtained to keep the total loss to 0.1 psi.

Tests of air-pressure losses through a 10-in. check valve with an aluminum flap gave results as follows:

Rate of free air, cfm	Loss of pressure, psi	
	Check valve and elbow	Check valve alone*
500	0.042	0.04
1,000	0.066	0.06
1,500	0.074	0.06
2,000	0.078	0.06

* Assuming loss through elbow equal to 30 diameters of straight pipe.

Air-pressure losses through elbows and bends in pipelines in terms of equivalent length of pipe have been given as follows:

Diam, in.	Equivalent length of pipe, ft	
	Elbow	Bend
1	1.5	0.23
2	4.9	0.74
3	9.4	1.41
4	14.5	2.2
6	25.9	3.9
8	38.0	5.7
10	50.7	7.6
12	63.7	9.6
14	76.7	11.5
16	90.1	13.5
18	104	15.5
20	117	17.5
24	144	21.6

Air-pressure losses through globe valves, tees, and elbows in terms of equivalent length of straight pipe have been given as follows:[14]

Nominal pipe diam, in.	Additional length of straight pipe, ft	
	Globe valves	Tees and elbows
1	2	2
1½	4	3
2	7	5
2½	10	7
3	13	9
3½	16	11
4	20	13
5	28	19
6	36	24
7	44	30
8	53	35
10	70	47
12	88	59
15	115	77
18	143	96
20	162	108
22	181	120
24	200	134

41. Outfall Losses. Hydraulic losses for outfalls from treatment plants depend upon the distance to the waterway, the design of the entrance to the outfall conduit and of the outlet chamber, length and size of the outfall conduit, the depth and design details of the diffuser section, the differential density of the plant effluent and the sea or fresh water, and the variations in receiving water levels.

The friction losses in the outfall conduit leading to the waterway are computed as described in Sec. 40, Art. 33, except that for settled sewage a minimum velocity of at least 2 to 3 fps should be used for scouring material settled during low flows. Entrance and outlet-chamber losses are computed as a portion (generally 0.5 to 1.0) of the velocity head.

Usually a free fall at the plant outlet is provided equal to the rise in river or lake level above the normal water level at which the plant is designed to operate. For a sea outfall the high tide for plant operation with full discharge through the submerged outfall requires extended study of tide levels (Fig. 21); sewage-flow durations (Sec. 40, Fig. 10); and effects of closer-in discharge of peak flows, infrequently and for short duration. A gate included in the outlet structure may be opened at high water levels to compensate for submergence of the overflow weir.

A common practice after treatment is to extend the outfall conduit to a series of submerged outlets, so as to distribute the effluent into the water. Figure 30 illustrates such a design. The head losses include (1) $0.5V^2/2g$ at the entrance to the outfall; (2) the pipe-friction losses through the straight pipe sections; (3) the velocity head in the pipeline; and (4) the nozzle head required to force the discharge out through the openings, which may be computed by the formula

$$h_1 = \frac{1}{C^2}\frac{V_1^2}{2g}$$

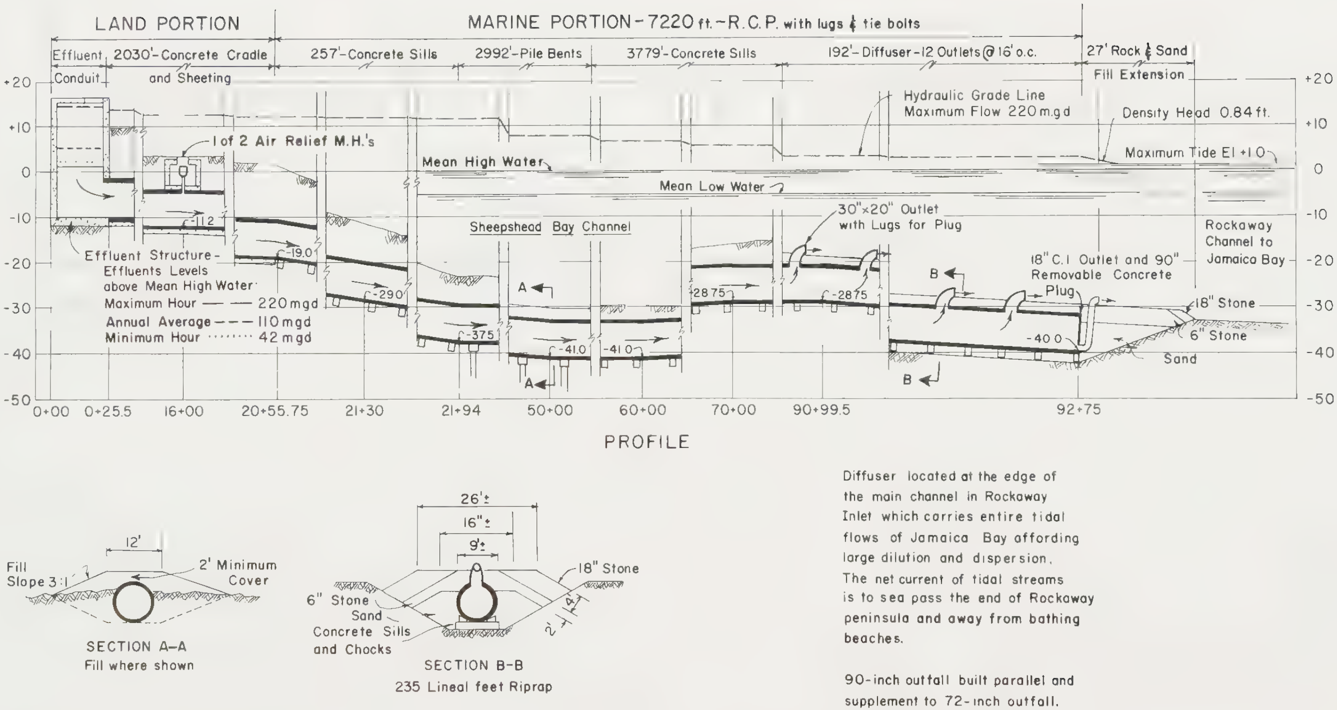

FIG. 30. 90-in. R.C. outfall, Coney Island Sewage-treatment Plant, New York.

where h_1 is the discharge head, which is considered all lost, and V_o the velocity through the openings—for a short-tube type of opening, the discharge coefficient C may be taken at 0.82, and the head loss is 1½ times the velocity head ($h_1 = 1.5V_o^2/2g$)—if the opening is an orifice cut in the pipe, C may be taken as 0.6, and the head loss will be $h_1 = 2.8V_o^2/2g$; and (5) density head = (seawater density) ÷ (fresh-water or effluent density) times depth of seawater over outlet opening.

The height of the overflow weir above normal water level will provide the head to force the effluent through the submerged pipe and outlets. Thus a greater rate of flow can be discharged through the submerged outlets during low-water levels than during high-water levels.

Outfalls designed and built from research and investigations made by the Los Angeles Sanitation District[11] and for the city of Los Angeles[12] are valuable in more detailed consideration of the hydraulic design of outfalls.

42. Sludge Handling. Sludges from processing elements vary in their nature and solids concentration, which, together with temperature, determine flow behavior and hydraulic losses in the handling of sludge. Some processing elements produce sludge low in solids concentration and with characteristics close to the viscosity of water so that hydraulic losses may be computed in turbulent-flow friction losses by common hydraulic formulas. Such hydraulic computations can be applied to systems for returning activated sludge and usually to sludge from intermediate and final sedimentation tanks used in conjunction with trickling filters. Other processing elements produce sludge of increasingly higher sludge concentration and of plastic or pseudoplastic nature with such shear resistance to flow that when overcome the flow is laminar unless the pressure is increased to produce the velocity required for turbulent flow, resulting in greater hydraulic losses. Such process products are raw primary sludge, thickened sludge, concentrated sludge, elutriated sludge, digested sludge, and scum. The characteristics of these sludges will vary further according to the quantity and type of solids added from other processing elements. Raw sludge has been found to give pressure drops greater than a digested sludge of the same solids concentration in the same pipeline.

Reference 15 contains references to many investigators whose papers with those of Behn give an understanding of the complexity of rheological sludge flow behavior and progress in quantitative development of reasonable predictions of pressure drops for laminar flow of non-Newtonian sludges in pipelines. Where long pipelines are to be used for transporting sludges of high concentration and plasticity, they must be designed for laminar flow to keep friction losses to the minimum.

At present, empirical methods with a large safety factor based on experience continue to be generally used. Head losses in piping are computed using the Hazen and Williams formula with a C factor range of 90 to 60, usually $C = 80$. Velocities range from 3 to 5 fps, increasing to the range from 5 to 8 fps for piping carrying heavy sludge and grease. Sludge piping has a minimum size of 6 or 8 in., with suction piping used of the shortest lengths to the pumps, and, if possible, a positive head for self-pump-priming. Provisions should be made for cleanouts, vent pipes, taps for steam cleaning, and access openings for mechanical cleaning.

Clogging of pipelines and pump stoppage have caused major maintenance costs and upset operation of sludge processing. Efficiency of sludge pumps should be subordinated to dependable and trouble-free operation.

Stand-by pumps are generally provided for scum and primary, secondary, and elutriated sludge systems. Stand-by provisions are not required where repair time is permissible in recirculation and sludge-transfer lines.

The handling, treatment, and disposal of sludges from waste waters comprise design problems comparable with the design of waste-waters-treatment plants but with the selections of sludge-handling equipment more dependent on the peculiar characteristics of the sludges at the various stages of the sludge-processing system.

Applied hydraulics for sludge handling may reasonably include the foregoing described hydraulics for pipelines plus head losses for sludge-handling equipment based on experience data obtainable from the manufacture of the equipment anticipated to be selected. When other sludge equipment is used, in actual construction, some minor modifications in applied hydraulics may be necessary.

ILLUSTRATIVE PLANT HEAD LOSSES AND HYDRAULIC PROFILES

43. Summary. The foregoing indicates that some of the hydraulic losses in waste-water-treatment plants are readily computed, whereas others depend on special allowances made by the engineer to provide for satisfactory operation, future additions, and the like, based on judgment. Therefore, the computations should be related to and checked by actual plant-operating experience.

The total head available, for a treatment plant, is the difference in elevation between the high level of the sewage in the inlet sewer and the high level of the water surface in the receiving waterway. Where this difference does not provide sufficient head for the operation of the treatment plant, pumping generally will be required.

TABLE 10. OVERALL HEAD ALLOWANCES FOR VARIOUS TYPES OF WASTE-WATER-TREATMENT PLANTS

Treatment process and plant	Rated plant capacity, mgd		Loss of head through plant, ft*	
	Avg flow	Max flow	At avg flow	At max flow
Plain sedimentation:				
Yonkers Joint Plant, N.Y.	63.0	230.0	15.67	12.75
Richmond, Va.	70.0	200.0	7.92	7.81
Buffalo, N.Y.	150.0	570.0	4.34	6.22
Tampa, Fla.	36.0	86.4	4.92	6.32
Trickling filters:				
Alexandria, Va.	18.0	82.5	14.20	16.73
Austin, Minn.	9.3	12.2	58.29‡	58.30‡
Knoxville, Tenn., Loves Creek	3.32	8.17	28.26‡	28.29‡
Sioux Falls, S. Dak.†	4.9	8.9	46.43‡	46.45‡
Rockford, Ill.†	31.0	39.0	17.63‡	20.03‡
Tullahoma, Tenn.	1.5	4.2	10.53	10.55
Activated sludge:				
Appleton, Wis.	16.0	32.0	4.37	4.43
Sioux Falls, S. Dak.†	17.0	25.6	3.59	3.62
Rockford, Ill.†	39.0	56.0	7.43	7.53
Knoxville, Tenn.:				
Third Creek	31.4	60.0	13.88‡	14.25‡
Fourth Creek	7.72	15.20	38.70‡	34.15‡
North Shore Sanitary District, Lake County, Ill., Clavey Road	4.5	15.0	2.17	2.24
Nassau County, N.Y., Sewage Disposal District No. 2	60.0	140.0	10.94‡	31.11

* Generally the difference in elevation from the water surface in Parshall flume or grit chambers or preliminary sedimentation tanks to weir crest controlling plant effluent or selected receiving water level; plus restored head by pumping in continuing plant flow, if required.

† Integrated trickling-filter and activated-sludge processes.

‡ Head loss includes restored head by pumping.

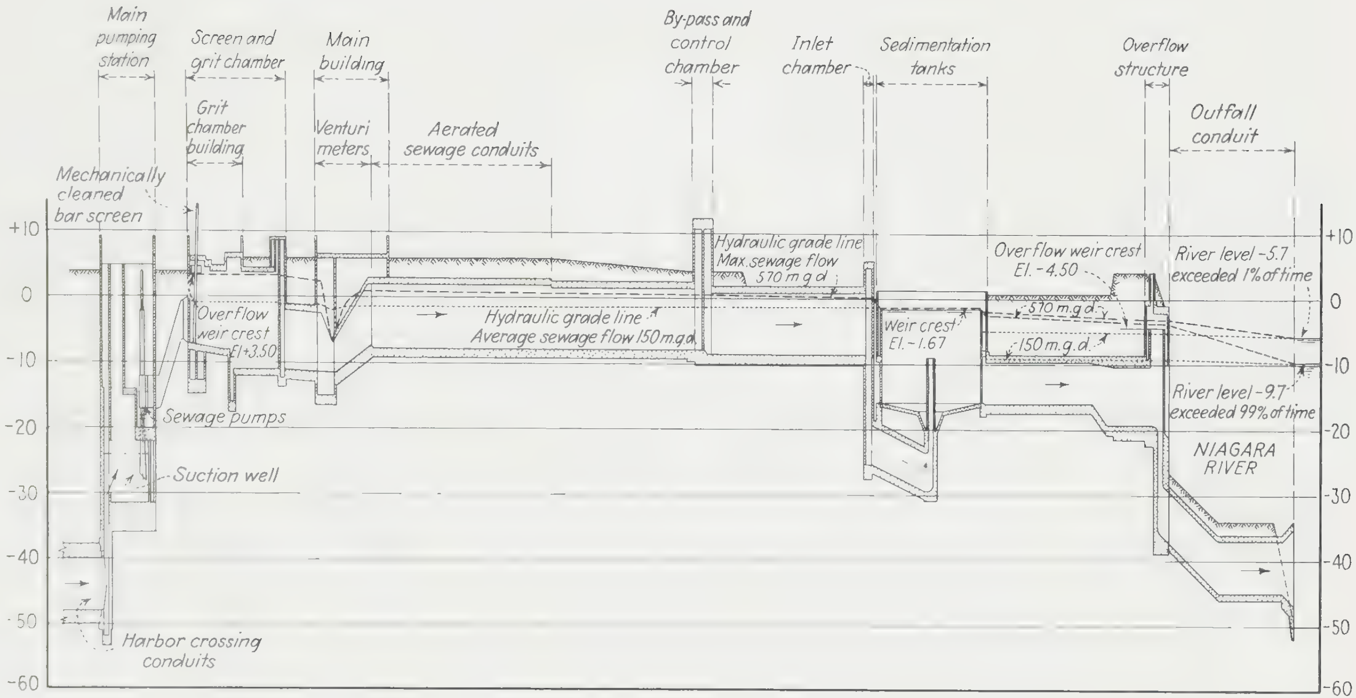

FIG. 31. Sewage-treatment plant, hydraulic profile—Buffalo Sewage Authority, Buffalo, N.Y.

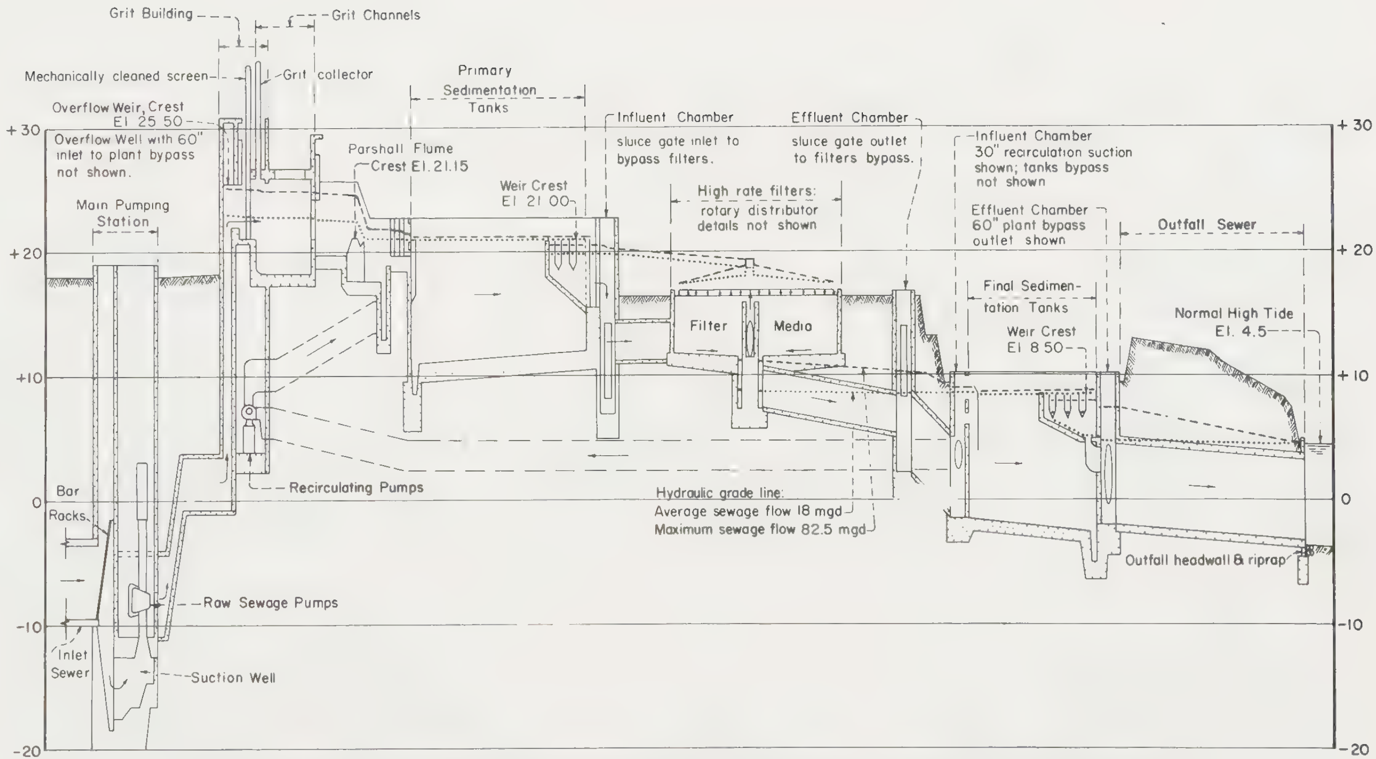

FIG. 32. High-rate trickling-filter plant, hydraulic profile—Sanitation Authority, City of Alexandria, Va.

Hydraulic profiles are computed to determine the head required for the operation of the treatment plant. The overall head requirements will vary for different types of sewage-treatment plants and for different plants of the same type, as illustrated by data in Table 10.

Sewage treatment by plain sedimentation requires the lowest overall head. The greatest losses in this type of treatment occur through the preparatory elements (screens, grit basin, etc.) and the conduits.

Chemical treatment plants usually include a flocculation tank and some extra length of conduit and require some head in addition to that for plain sedimentation.

An effluent filter may be included, constructed either around the sedimentation tanks or as a separate structure. Effluent filters may be operated on a 3-in. normal and about 6-in. maximum head. To provide a factor of safety, 8 or 9 in. is sometimes allowed. A separate structure would require additional head for extra conduits.

Activated-sludge treatment plants will require additional head allowances for conduits, aeration tanks, and final sedimentation tanks.

Trickling-filter treatment plants usually require more head than other types, as head is required to distribute the sewage properly over the filter, to provide for the depth of the filter and for the underdrainage system.

When a plant outfall is too short, a contact tank might be included for chlorination, in which case moderate additional losses will occur.

Hydraulic profiles illustrating head requirements are shown in Fig. 31 for a plain sedimentation plant and in Fig. 32 for a high-rate single-stage filter plant.

Bibliography

1. "Ten-state Standards," Sec. 71.12.
2. "Sewage Treatment Plant Design," WPCF Manual of Practice No. 8 (ASCE Manual of Engineering Practice No. 36).
3. Rankin, R. S., Performance of Biofiltration Plants by Three Methods, *Proc. ASCE*, **79,** Separate No. 336.
4. King, H. W., "Handbook of Hydraulics," 3d ed., pp. 194, 234, McGraw-Hill Book Company, New York.
5. King, H. W., and E. F. Brater, "Handbook of Hydraulics," 5th ed., sec. 6, McGraw-Hill Book Company, New York, 1963.
6. *Trans. ASCE*, **100,** 558.
7. Figure 4 type comminutor, *Eng. Bull.* 185-D, Chicago Pump Co.
8. Figure 5 type comminutors, Application and Engineering Handbooks, Worthington Corp.
9. McMillan, *Eng. News-Record*, **91,** 178.
10. *Eng. News-Record*, **93,** 823.
11. *Proc. ASCE*, **86** (SA2).
12. Hyperion Engineers, Ocean Outfall Design.
13. Kivell, W. A., and N. B. Lund, *Waterworks and Sewerage*, April, 1940, p. 176.
14. Harris, E. G., "Compressed Air," 2d ed., p. 170, McGraw-Hill Book Company, New York.
15. Behn, Vaughn C., Experimental Determination of Sludge Flow Parameters, *Proc. ASCE*, **88** (SA3), 1962.

SECTION 42

TIDAL-ENERGY DEVELOPMENT

By Eric M. Wilson

THE SOURCE OF TIDAL ENERGY

1. The Gravitational Influence of the Sun and Moon. Every particle of matter on the earth is subjected to the gravitational attraction of the rest of the earth, the moon, and the sun. Since the earth is not a point in space but has appreciable size relative to the distances between these bodies, there are slight differences in the attractive forces exerted by both sun and moon on different parts of the earth. These small but significant variations are responsible for the rise and fall of the tides. Figure 1 shows the gravitational attraction that a heavenly body has on an earth

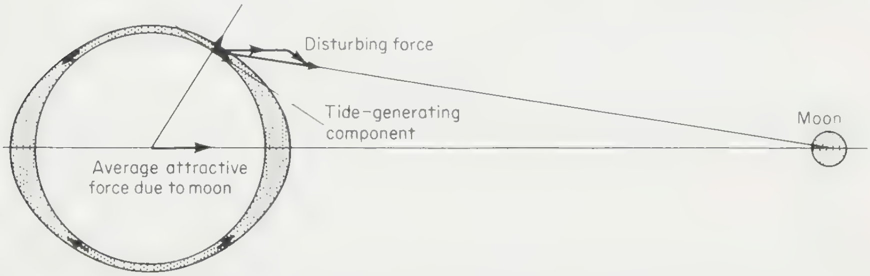

Fig. 1. *Semidiurnal* tides are caused by the difference in the moon's attraction of an average earth particle, acting at the center of the earth, and a particle on its surface, off the earth-moon line. Triangle of forces shows average particle force, the actual force, and the resultant force, which is the difference between them. This force is also divided into components tangential and vertical to the earth's surface—the tangential component is responsible for tide generation. On the other side of the earth, away from the moon, this component acts away from the moon, tending to create a "hump" of water on the earth's far side. The two humps correspond to the high tides which occur twice every 24 hr 50 min—the time of the moon's apparent rotation around the earth. Similar tides are produced by the sun.

particle, at the center of the earth where it is average in value, and at a point on the earth's surface, off the earth-body line. The disturbing force is the vector difference between these two. The disturbing force may be resolved vertically and tangentially to the surface, and it is the latter component which causes those particles which are free to move, *i.e.*, liquids and gases, to do so. On the side of the earth away from the body, this component acts away from it, tending to cause "humps" of water on the earth-body line.

The two bodies responsible for almost all tidal movement on the earth are the moon and the sun. Both of these have an apparent rotation around the earth, with a periodicity of 24 hr 50 min and 24 hr, respectively. Accordingly a tide due to the moon's attraction occurs every 12 hr 25 min and one due to the sun every 12 hr.

Although the sun has 2½ million times the moon's mass, it is 390 times farther away. The attractive force of a body is proportional to the inverse square of its distance away; however, since it is the tangential (to the earth's surface) component of this force which causes the tides, and as this also reduces as a function of distance compared with the vertical component, the net result is to make the tide caused by the sun only 0.46 times that due to the moon. These tides which occur either at, or approximately at, half-day intervals are termed *semidiurnal.*

2. The Effects of Declination and Elliptical Orbits. Since the axis of the earth's rotation is not perpendicular to the plane of the sun's apparent orbit of the earth (except on rare occasions), there is a continual variation in the angle of incidence of the sun's attractive force during the solar day. This variation alters the magnitude of the attractive force, which has a maximum and minimum value once a day. This gives a *diurnal* variation in the tides caused by the sun. The moon's attractive force varies in this way for a similar reason, so that lunar diurnal variation also occurs. The variation is illustrated in Fig. 2. Further tides arise from the elliptical nature of the

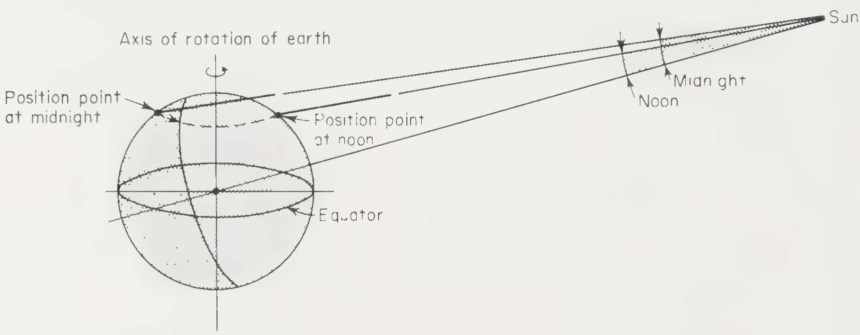

FIG. 2. *Diurnal* tides result from the continually varying angle of the sun in relation to the axis of the earth's rotation as the earth makes a complete revolution. The angle of incidence of the sun's attractive force on a point on the earth's surface at midnight differs from the angle of incidence on the same point at midday. The moon also causes a diurnal tide.

moon's orbit of earth and of earth's orbit of the sun. These tides are semiannual for the sun and fortnightly in the case of the moon.

Phase Difference. The earth revolves on its own axis every 24 hr—the solar day. The moon revolves in an elliptical orbit around the earth every 29½ days, giving it a period of revolution relative to a point on the earth's surface of 24 hr 50 min. If the sun and moon are in line with the earth, or nearly so, the effects of their attractions are additive and give rise to *spring* tides. As each day passes, the time difference between their apparent orbits moves the two tidal attractions apart until they are 90 deg out of phase, resulting in *neap* tides. At this time the moon, earth, and sun are in a right-angled triangle configuration. As the phase difference increases the bodies move into, or nearly into, line again with the moon on the side of the earth remote from the sun, and spring tides occur again at 180-deg phase difference, and so on. This is illustrated in Fig. 3. There is therefore an oscillation in tidal amplitude, with a period of approximately 2 weeks.

The actual tides which occur depend on the combination of all the factors mentioned and others which have not been discussed. Constituents of tidal motion have periodicities ranging from 3.1 hr up to 1,600 years, and by combination of all the harmonic oscillations, the tractive forces can be calculated for any particular time, past or future. The theoretical maximum possible tractive forces have been calculated to occur about every 1,600 years, when phenomenally high tides should result. The next occasion when this will happen is A.D. 3300. By observation of the actual sea levels at particular locations, knowing the concurrent tractive forces, the likely sea levels for different values of tractive force may be deduced and so predicted for future use.

The source of tidal energy is by no means clear. The diminution of the energy in the moon's orbit around the earth and the earth's orbit around the sun is hardly

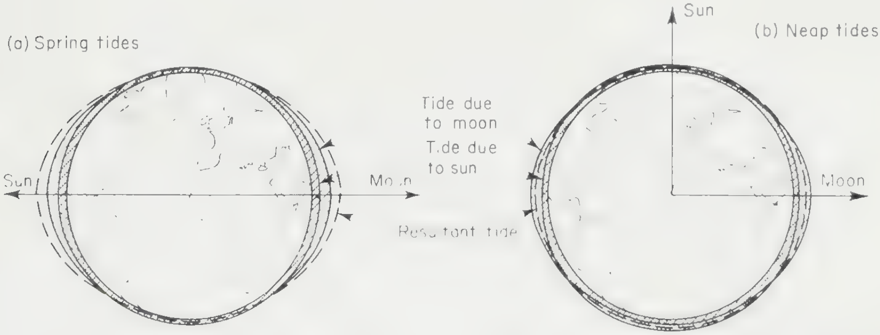

FIG. 3. *Spring* and *neap* tides arise from the interaction of the attractive forces of the sun and moon. When the lines joining the centers of the earth, sun, and moon are in a straight line the sun and moon tide-generating forces are additive, because both bodies tend to produce "humps" of water on both sides of the earth. The resulting maximum tidal range is called a spring tide. When the sun-earth and moon-earth lines are at right angles the forces are subtractive and neap tides occur. Spring tides occur at new and full moon.

perceptible, though it is often assumed that it is being infinitesimally absorbed by the movement of the earth's oceans. Other recent hypotheses have suggested the rotational energy of the earth and the solar energy of the sun as possible sources. The matter is not settled, and we simply do not know.

TIDAL OSCILLATIONS

3. Oceanic Tides. The variation in elevation of sea level in the open ocean is very difficult to measure. Observations at oceanic islands indicate that the range is probably only about 2 ft. As a tidal wave travels across the shallower water of a continental shelf the mid-ocean range is amplified by shoaling effects. By the time the coast is reached this amplification is typically about three or four times the original range.

4. Estuarial Tides. At an estuary mouth there is a cyclical rise and fall of water level with a period, for a semidiurnal tide, of about 12.4 hr. The estuary water content is very small on any absolute scale and is not subject to appreciable tides on its own account. The period of the tidal wave, 12.4 hr, is long enough to make the wave length generally much longer than the physical length of the estuary. Such a long wave tends to move along an estuary with a celerity $C = \sqrt{gh}$, where h = mean depth. For example, if a semidiurnal tide with a period T of 12.4 hr propagates along an estuary of mean depth 100 ft then the wave length L is given by $L = TC$. In this case $C = 57$ fps and $L = 44{,}700 \times 57/5{,}280 = 470$ miles. Most estuaries are shorter than this, but there are many of particular interest whose lengths and depths are such that the length is approximately one-half or one-fourth the wave length. In these cases, it is possible for resonance to occur, and the amplitude of the tidal wave may increase along the estuary by factors of between 2 and 4. Well-known examples where such resonance plays a part in the increased tidal range are the Bay of Fundy on the eastern coast of Canada and the Bristol Channel on the western coast of England. In the case of Fundy, the tides at the mouth of the bay are increased some 2½ times at the head. In the case of the Bristol Channel the maximum range is increased to about three times that of the Irish Sea at its mouth.

There is little doubt that the funneling effect of converging estuary tides also plays a part in increasing the range within an estuary.

5. Coriolis Force. Another influence on the tidal range at a particular location is that of the Coriolis force. This force results from the conservation of angular momentum in a fluid stream moving north or south on the rotating earth. As the stream moves north in the Northern Hemisphere it moves nearer to the earth's axis. In this position its angular momentum is greater than required, producing an increase in angular velocity and so causing the stream to be deflected eastward. Similarly moving south, it moves farther from the axis and so requires additional momentum. It can derive this momentum only from the earth itself and so it tends to swing or slope up to the west until frictional and hydrostatic forces stabilize it. An example of this phenomenon and its effect on tidal range is apparent in the Irish Sea. This is a comparatively small landlocked shallow sea between Great Britain and Ireland, too small to produce appreciable tides on its own account. It is filled and emptied cyclically by tidal waves from the Atlantic, principally through its southern end, so that a flood tide results in a northward-flowing current and an ebb tide in a southward-flowing one. The Coriolis force induces the sea to slope up to the east on the flood and up to the west on the ebb by approximately 4 ft in a width of about 80 miles. The net result is to give a tidal range on the eastern coast about 8 ft greater than on the western, or Irish, coast. This Coriolis amplification is one of the reasons for the high ranges in the Bristol Channel and on the western coast of England and Wales.

6. Barrage Effects. The most important effect that the construction of an obstruction across a sea inlet may have on the tidal oscillation may be through alteration of the resonance of the basin. If the length of a resonating basin is altered by an artificial barrier it is likely the range of the tide outside the barrier will change. A practical example of this is cited in Holland, at the mouth of the old Zuider Zee. When the closing dike was built across this inland sea (now called the Ijsselmeer) in 1932, the tidal range was increased at locations immediately outside the barrier by some 4 ft.

It is essential, in planning a tidal-power barrage, to be sure that the sea levels outside the reservoir will maintain or increase their existing range, or at worst diminish by some relatively small amount, so that the production of energy, on which the economic return of the project depends, will not be found less than estimated before construction. Various analytical methods for carrying out such an investigation have been fully described in the literature.[1,2,3,*] All these methods involve assumptions and simplifications which affect the correspondence with the real estuary, and it would almost certainly be necessary in a particular case to build a large-scale hydraulic model of the sea area affected as a check on the analysis.

THE GENERATION OF MECHANICAL AND ELECTRICAL ENERGY

7. Historical Methods. One of the earliest written references to a useful machine for exploiting the energy of the tides is a description in the Domesday Book, in the British Museum, of a tidal mill which worked in Dover Harbour. Certainly in medieval times tidal mills were common in the estuaries of Britain and France. There

* Superior numbers refer to items in the Bibliography at the end of this section.

is a record of one at Brooklyn, N.Y., built by Dutch colonists in 1617, and in 1734 a Massachusetts mill was developing 50 hp and was used for spice grinding. They worked as simple, undershot water wheels, the sea water being contained at high tide by wooden tidal flaps and released to drive the wheels when the tide fell. Although such wheels were cumbersome and inefficient, they could be relied upon to turn for the millers, even when river mills had ceased to work in periods of drought.

Later inventors had the idea of using the rise and fall of floating weights to do useful work, and many patents were taken out in Europe in the seventeenth and eighteenth centuries for such devices. Another common idea was to use the rising water surface to compress air in large metal or masonry vessels, the compressed air

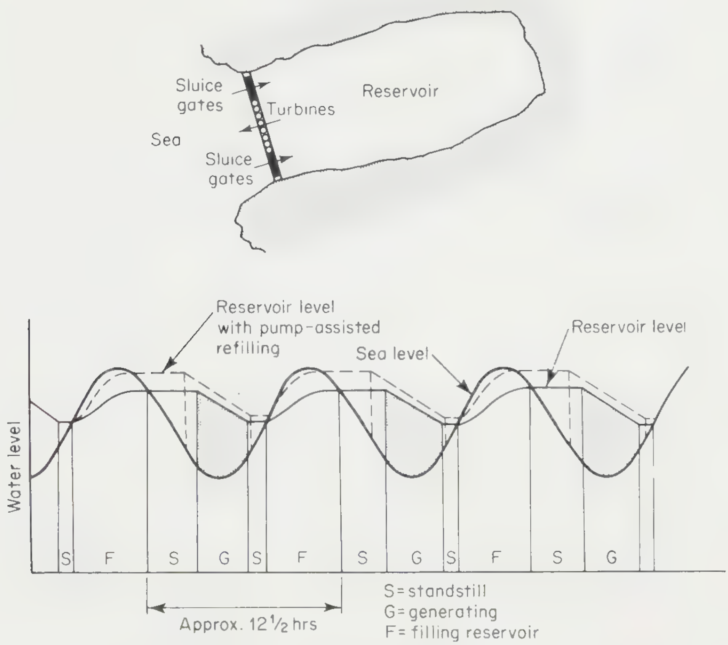

FIG. 4. Typical layout and operating regime for one-way generation.

then to be used to drive air engines. None of these ideas is practicable for using tidal energy on a large scale.

8. Methods Proposed in the Recent Past. With the development of the hydraulic turbine and electrical power systems there was a resurgence of interest in tidal power. The concept of enclosing whole estuaries by dams and building large power stations with many turbogenerators, to generate electricity, became accepted. The earliest schemes proposed simply to impound the rising tide behind a single dam, generating electricity as the impounded water was released through the turbines at low tide. Sluice gates could then be opened to allow the basin to refill. This *one-way* method, of which a typical layout and operation regime are shown in Fig. 4, requires that some 5 hr generation is followed by 6 to 7 hr of refilling and standstill. The power and energy output can be improved by using the turbogenerators as motor pumps to assist the refilling operation. The concept of pumping in this way came much later in the historical development of tidal energy, and in the earlier schemes refilling was by means of large numbers of sluice gates, which increased the capital cost of the works substantially. The pump-assisted regime is shown by the dashed line in Fig. 4.

After the one-way working system, *two-way* working was proposed and various ingenious power-station layouts were devised to enable energy to be generated with water moving either from reservoir to sea or from sea to reservoir. A typical design for such a station and its operating regime is shown in Figs. 5 and 6. It is possible to extract more energy from an estuary by two-way working, but the average head on the turbines is lower than in the one-way method and so they are necessarily larger and

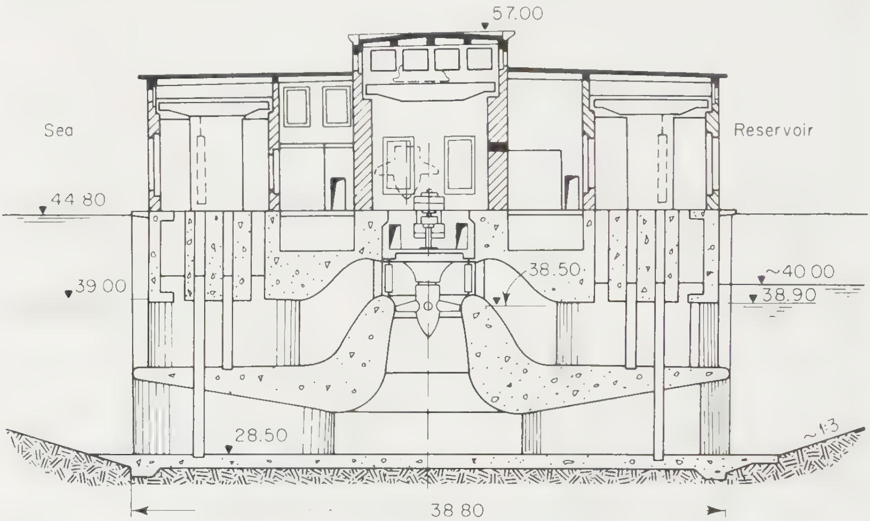

Fig. 5. Cross section through a two-way generation power station for Kislaya Bay, U.S.S.R. (*Based on a 1940 design by L. B. Bernshtein.*)

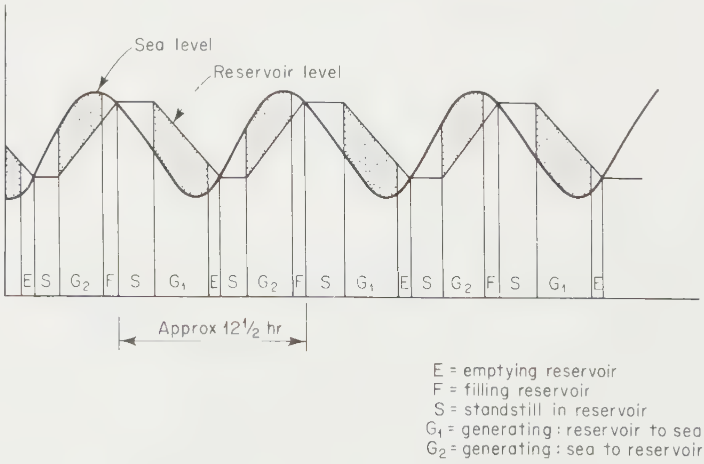

Fig. 6. Two-way generation operation cycle.

more expensive. Neither method overcomes tidal power's principal disadvantage, that is, that power and energy are developed intermittently and to a periodic cycle which is out of phase with the cycle of public demand, which is that of the solar day. Electricity systems are designed to meet foreseeable power demand, on demand, and only secondly to meet overall energy requirements. A power source which does not provide this facility is economically handicapped, since at a time of peak demand on the system it cannot guarantee power.

To overcome the disadvantages of discontinuity in generation the use of *multiple basins* was proposed. For example, in Fig. 7 is shown a possible multiple-basin scheme. Referring to Figs. 7 and 8, it works as follows: The high-level basin A is filled through sluice gates A as the tide rises and for some time after peak high water in the sea has passed. As soon as falling sea level meets rising basin level C, sluice A is closed, preventing outflow. Water is continually passing from high-level basin A to low-level basin B through the power-station turbines; so the level of basin B rises. However, as soon as the falling outside sea level drops below the lower basin level J, sluice B opens and allows basin B to discharge to the sea. This continues until sea level rises again to K when sluice B closes and the lower basin starts to fill again while the upper basin level continues to fall. Soon after, the rising sea level passes the now depressed upper basin A (D) and sluice A opens to refill the upper basin, thus completing the cycle. By these means a continuous power output may be obtained, though it will fluctuate in magnitude throughout the cycle as indicated by the con-

FIG. 7. Typical layout for two-basin scheme for continuous power generation or peaking power.

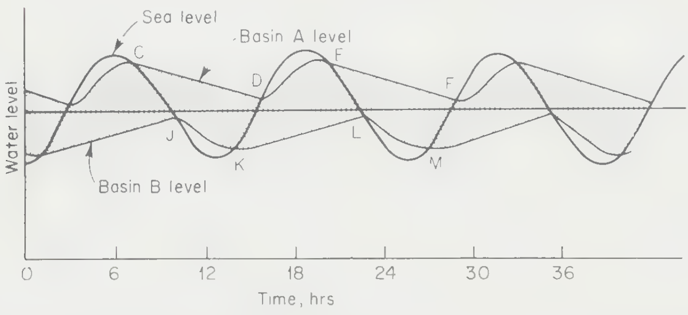

FIG. 8. Operating regime for two-basin scheme with continuous power generation.

tinually varying head on the turbines, shown in Fig. 8. The power-output fluctuation depends on relative basin size and installed capacity and is usually through a factor of about 2 cyclically, and about 5 throughout the lunar month. The firm power generated in this way is therefore low in relation to the installed generating capacity. Multiple basins have the disadvantages of requiring two sets of sluices and greater lengths of embankment dam. On the other hand, the power station is in protected water, the central embankment may be low, and there need be no compromise in the structures' design for best hydraulic performance since all flow passes in one direction only. Nevertheless, the quantity of energy that can be developed in a particular location by multiple basins is only about half that of a one-way ebb scheme and still less than from a two-way generation scheme. A full treatment of the theoretical outputs of an idealized estuary under various modes of operation has been given by Davey.[4]

9. Peaking Operation. At this stage it is useful to consider what a modern electricity system needs that can best be supplied by tidal energy. This approach is more rewarding than simply designing schemes which provide particular quantities of power or energy at inconvenient times or provide continuous but fluctuating output. A modern electricity system doubling in size every 10 years has normally a substantial part of its capacity of recent design standing idle for part of the 24-hr day. The night load is typically about 35 percent of daily peak demand, and so a fluctuating continuous output from the tides is of little interest on most systems. Such output would relegate, even more perfectly, adequate plant to a standby capacity, probably to the detriment of overall system economy. It seems clear that the most valuable contribution that tidal power can make is the provision of guaranteed peak power so that conventional plant load factors may be improved.

There are two ways in which this may be done, and they both involve the storing of potential energy by pumping water. The first method is the pump-turbine system which has been installed at the French tidal-power station on La Rance, in Brittany. The second is the well-proved system of high-head pumped storage.

10. The Pump-Turbine Concept. The essential feature of this method of providing peaking power from tidal plants is the hydroelectric machinery. The turbogenerator is an axial-flow machine mounted horizontally in the water passage with the alternator contained in a submerged steel bulb. The turbine has variable-pitch blades controlled by mechanisms in the nacelle, which is therefore larger than in a fixed-blade propeller. The alternator also serves as a motor, so that the whole unit can be power-driven to pump water. Since the turbine blades are reversible the unit can thus generate electricity with flow in either direction and can pump in either direction. This gives great flexibility in the operation of the machine and enables the reservoir to be filled to a level higher than that to which it would normally fill, by pumping in additional water after gravity flow has ceased. Similarly the reservoir can be lowered below the gravity-flow level by pumping to the sea. Pumping in this way requires the consumption of electrical energy, normally supplied off-peak from the interlinked conventional sources. It may be seen that, provided the time of peak demand is known some hours beforehand, the reservoir level can be regulated to ensure that there is a sufficient difference in level between it and the sea during peaking hours, when power is required. In this way, and for the first time, it has become possible to use a tidal-power station economically as a source of firm power in meeting demand on a public electricity supply system.

Further advantages are inherent in the system. For example, if off-peak network energy is available for pumping when the level difference between sea and reservoir is small, this energy may be recouped several times over by subsequent generation with the extra pumped water, when the level difference is large. The flexibility of operation is shown in Fig. 9, which shows some of the principal ways in which a pump-turbine tidal station can be operated to provide power at any time in the tidal cycle.

There are inevitably disadvantages also in the system which should be understood. These are listed below:

1. The axial pump-turbines are expensive.
2. They require fairly large waterways and hence large containing structures for a given flow. Each end of the waterway must be proportioned to act as a draft tube, which increases the containing-structure cost.

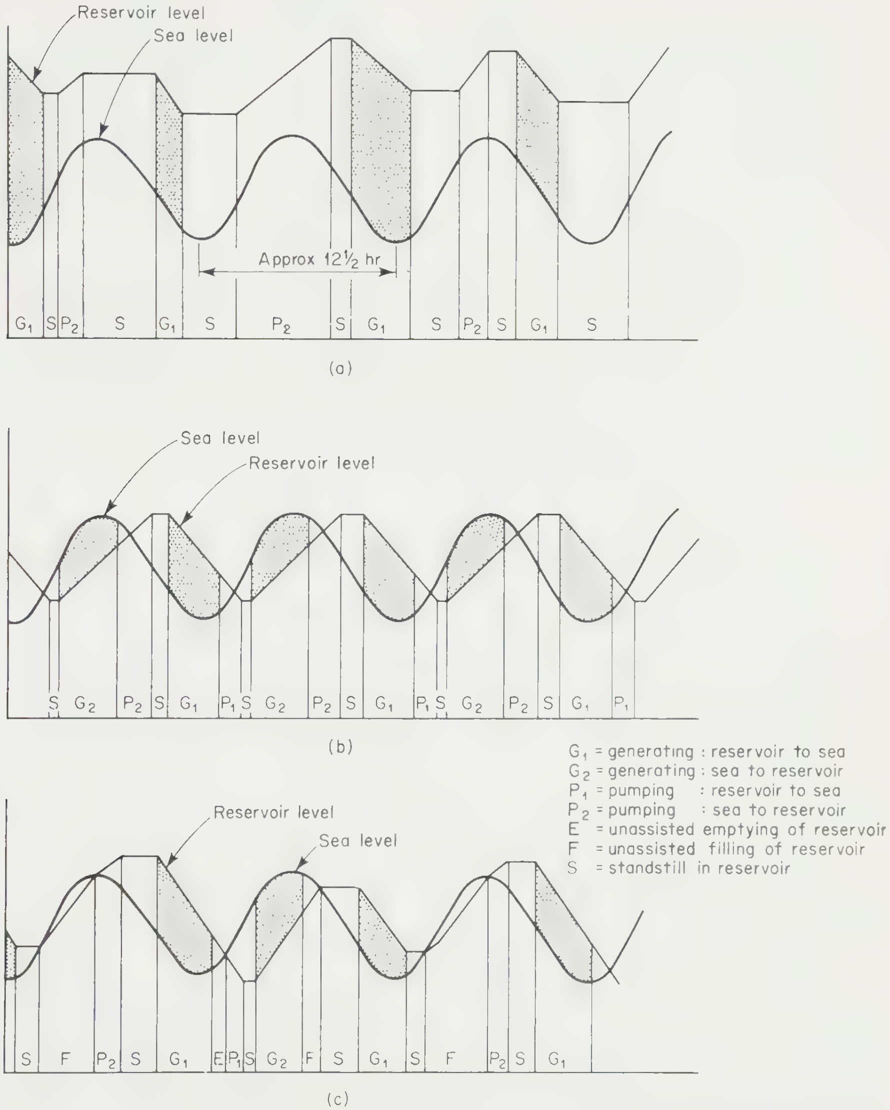

FIG. 9. (*a*) One-way generation with pumped refill. Reservoir level is always above sea level; for exceptionally low tidal ranges. For average neap tides repeated one-way generation with pumping (as Fig. 4) is used. (*b*) Two-way generations with double pumping; for medium tidal ranges. (*c*) "Sesqui" operation; three turbining and two intermediate pumping phases during two average spring tides. For exceptional spring tides, repeated two-way generation is used. NOTE: These diagrams are not to scale in elevation. Each represents a different tidal amplitude. Numerous other cycles are possible.

3. The turbine has a comparatively low pumping efficiency, about 70 percent.

4. The peak period for which power can be guaranteed is of the order of 5 hr, since it depends on sea level, which fluctuates between low and high level every 6 hr approximately.

5. The guaranteed firm power is less than the installed capacity, since the firm power depends largely on the level difference at neap tides, while the installed capacity depends on an economic evaluation of the value of both power and energy, much more of the latter being available at spring tides.

6. Available energy is lost because it is necessary to keep a level difference for peak generation at specific times.

Using the pump-turbine method, the world's first large-scale tidal-power station has been commissioned (in 1966) near Dinard, on the estuary of La Rance, in Brittany, France.

11. La Rance Tidal-power Station. The scheme has been very fully described.[5,6,7,8] Only a brief synopsis of the principal features is given here.

The barrage is about $2\frac{1}{2}$ miles inland from the mouth of the estuary of the Rance, giving it a well-sheltered position. The storage reservoir formed by the barrage

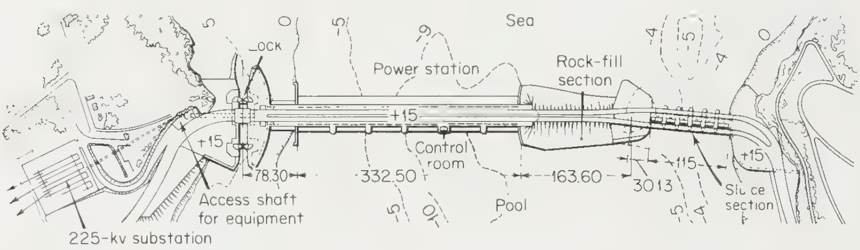

FIG. 10. General plan of La Rance tidal-power station (dimensions in meters). (*Electricitè de France.*)

extends nearly to Dinan some 12 miles upstream and has a surface area of $8\frac{1}{2}$ sq miles. The tidal range at the site varies between extremes of 11 and 44 ft and has a mean value of 28 ft.

Figure 10 shows an overall plan of the development and Fig. 11 a cross section through the power station. The power station is a hollow concrete structure, approximately 390 m long with buttresses at 13.3 m on centers. The roof is arched and carries a two-lane highway. The station contains 24 bulb sets, one of which is illustrated in Fig. 12. Each set consists of a propeller turbine of 5.35 m diameter, with four adjustable-pitch blades, directly coupled to an a-c generator rated at 10 mw, which rotates in the pressurized bulb at a pressure of 2 kg/sq cm at 93.75 rpm. Movable guide vanes are arranged peripherally around the bulb on the estuary side of the turbine and are used also as regulating sluice gates by closing off the flow completely during standstill. A man-access shaft is provided to the interior of each bulb.

Current is generated at 3.5 kv and the output of each of three groups of eight sets is conducted to a 3.5/225 kv transformer rated at 40 mva, three of which are installed in the power station. The crane capacity is 90 tons.

Each turbine waterway is equipped with gates on both sea and reservoir sides to enable dewatering and maintenance to be carried out. Trash racks are not provided on either side.

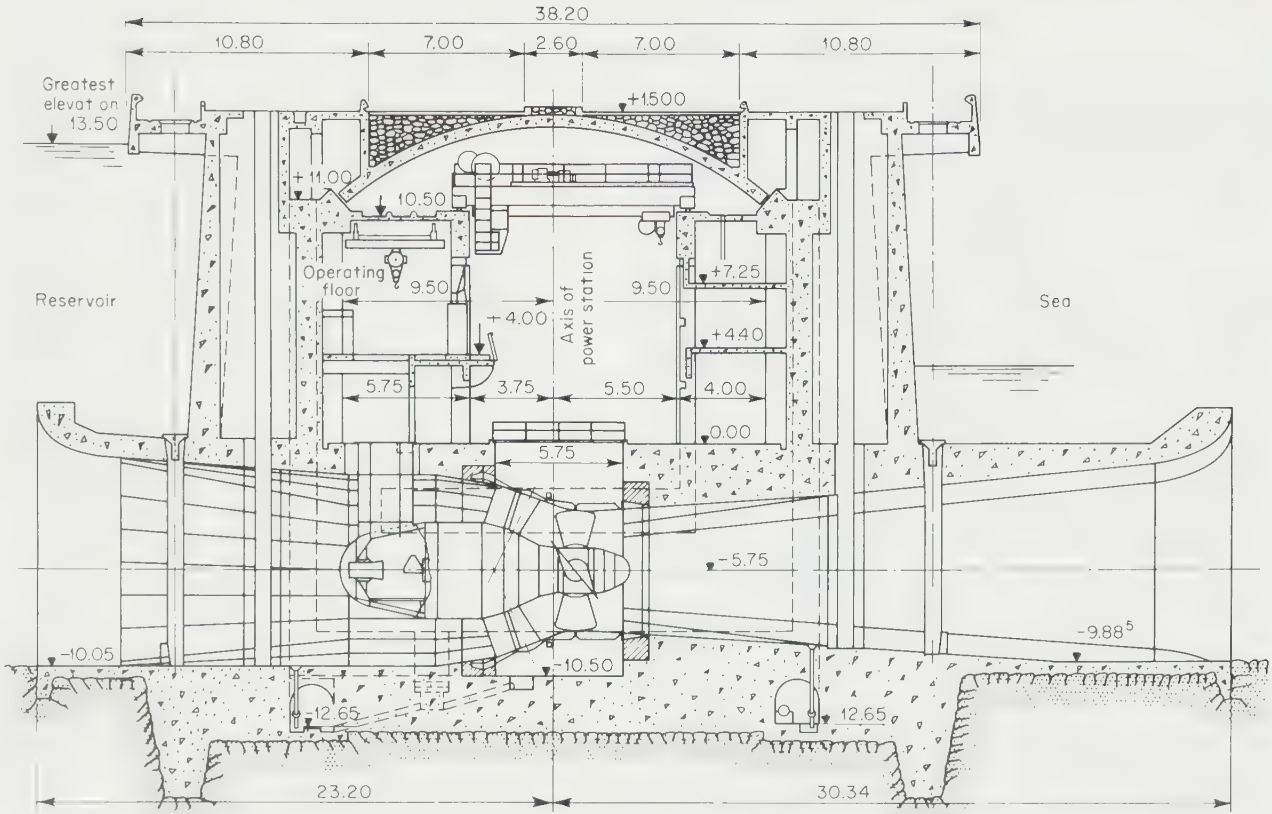

FIG. 11. Section through the Rance power station on a machine centerline (dimensions in meters).

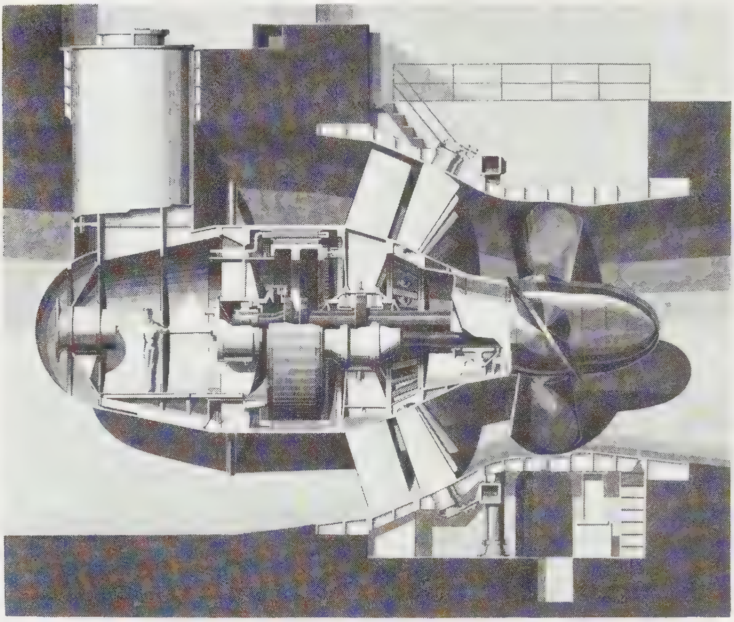

FIG. 12. Cutaway diagram of a Rance "bulb" set. (*Photo Neyrfilm, courtesy of Les Constructeurs des Groupes Marémoteurs de la Rance.*)

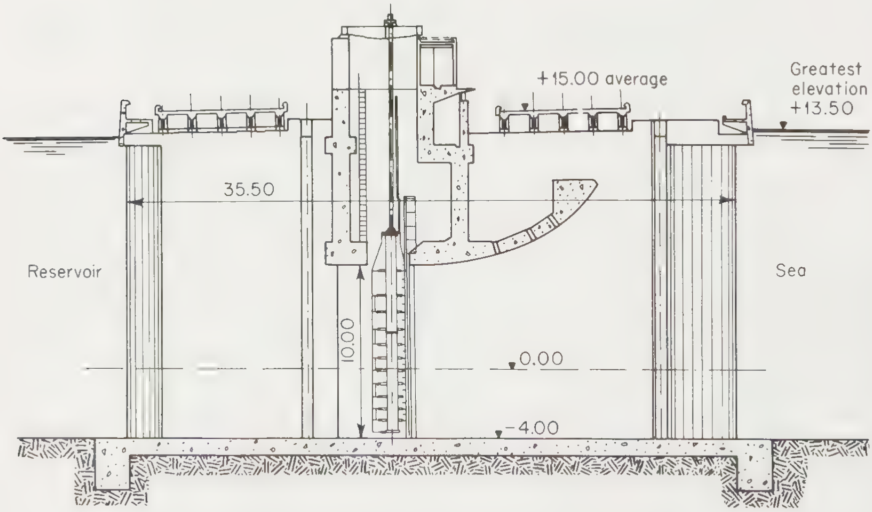

FIG. 13. Section through a sluice gate, La Rance tidal-power station (dimensions in meters).

The sluice-gate section of the barrage has six fixed-roller-type gates, 15 m wide and 10 m deep. A section through the center of one of the gates is shown in Fig. 13.

The net annual output of the station is estimated at 544 Gwh made up as follows:

	Gwh
Basin-to-sea generation	537
Sea-to-basin generation	71.5
	608.5
Energy absorbed by pumping	64.5
	544

The total cost of the Rance project is variously quoted between 420 million and 500 million francs. (The lower value has a 1966 equivalent of £30.6 million and $85.5 million.) At this lower estimate, using an interest rate of 5 percent per annum and conventional amortization, the fixed charges alone would price the energy at 0.86 cent per kilowatthour. About half the energy can be supplied at peak demand periods, but it must be conceded that it is expensive in comparison with alternative means of generation. It should be remembered, however, that the scheme was originally intended as a pilot scheme for the much larger Chausey Islands project which would impound about 200 sq miles of the sea in the corner formed by Brittany and Normandy, and that it has already given substantial benefit in the development of the low-head bulb turbine. The completion of La Rance Tidal Power scheme was a historic achievement and a lasting tribute to the imagination and ingenuity of its designers.

12. Developments in the U.S.S.R. In the last few years there has been considerable work on tidal power in the U.S.S.R., and a pilot scheme is under construction

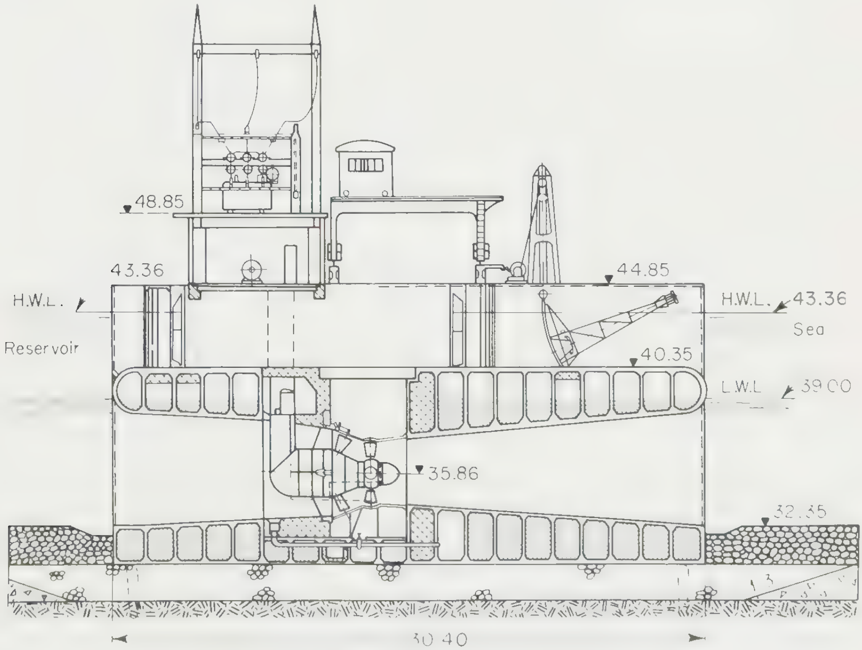

Fig. 14. Section through proposed Kislaya Bay unit. (*Based on the 1960 project design by L. B. Bernshtein.*)

at Kislaya Bay in the White Sea. This scheme is based on the pump-turbine concept using sets similar to the French ones. Methods of precasting the power station and of installing the sets in "floating-dock" sections of the power station have been proposed and are being used by the Russians. This is a development which has been independently considered in Britain and may lead to considerably lower capital costs than appear possible if cofferdamming is employed. The Russian work has apparently concentrated on this method of prefabrication of the power station and on the integration of the tidal energy into the output of existing hydroelectric installations with a view to providing a larger firm power capacity than that obtainable if the two types of installation operated independently. It has been very fully reported by Bernshtein.[9] A cross section of one of the most recent Russian proposals, that for the Kislaya Bay pilot scheme of 1960, using prefabricated units, is shown in Fig. 14.

TIDAL ENERGY WITH PUMPED STORAGE

13. Advantages and Disadvantages. In the preceding section the pump-turbine concept of meeting peak demand was described and the other, alternative method of high-head pumped storage was mentioned. Pumped-storage schemes are discussed in Sec. 25, and here we are concerned only with their application to tidal energy. The advantages of using a high-head pumped-storage scheme with the output from a tidal-power station* are several, and are listed below.

1. Since the generation of the electrical energy is not critical with respect to time, the most suitable tidal conditions may be selected and maximum energy obtained.
2. Operating conditions may be chosen so that the installed turbogenerators always work at or near an optimum condition. The turbines can therefore be fixed-blade, large-diameter, and comparatively cheap.
3. Peaking power is now supplied directly to the network when the time of tidal generation coincides with peak demand and by the pumped-storage plant when it does not. The peak energy may be used with great flexibility to meet all demands above certain load levels.
4. The optimal integration of large quantities of energy through pumped storage can improve the system load factor and the individual plant load factors of the conventional plant in an electrical network.
5. The t.p.p.s. scheme can act as "hot-standby" plant at any time it is not at peak capacity.
6. If there are future unforeseen changes in load characteristics, for example, a flattening of the daytime load by reason of heavy off-peak use of cheaper-priced units, the t.p.p.s. scheme still offers a firm capacity for 12 hr at a time. The pump-turbine concept cannot do this and could become obsolete in these circumstances.

The disadvantages are the necessity of finding a good pumped-storage site with adequate storage capacity in the neighborhood of either the load center or the tidal-power station, or on the transmission-line route between, and the extra costs of the pumped-storage plant. The value of the t.p.p.s. scheme to the network is not immediately calculable and depends on the network characteristics, its demand pattern, and its growth rate. Accordingly, the comparison of a t.p.p.s. scheme with any alternative means of providing for load growth must be made on the basis of overall system economy. No other comparison is valid.

14. The Effect of Tidal Energy on Interconnected Electrical Networks. Pumped-storage schemes are considered only when they form a part of a whole interconnected system, since their viability depends on the effects they have on the other plant, normally fossil-fuel thermal and nuclear-powered stations. This dependence of

* A tidal-power station operating with a pumped-storage scheme is referred to subsequently in this section as a t.p.p.s. scheme.

different power sources within a connected system on each other for smooth working and maximum economy becomes even more important when a tidal-energy source is included. The reason for this may be seen from Figs. 15 and 16. In Fig. 15*a* a typical annual load curve is illustrated with the various plant capacities available shown as working their respective proportions of total time. Only thermal plant (nuclear, oil, or coal) is available on the system. In Fig. 15*b* a pumped-storage plant is introduced, and immediately the peaking and standby duties are taken over by it,

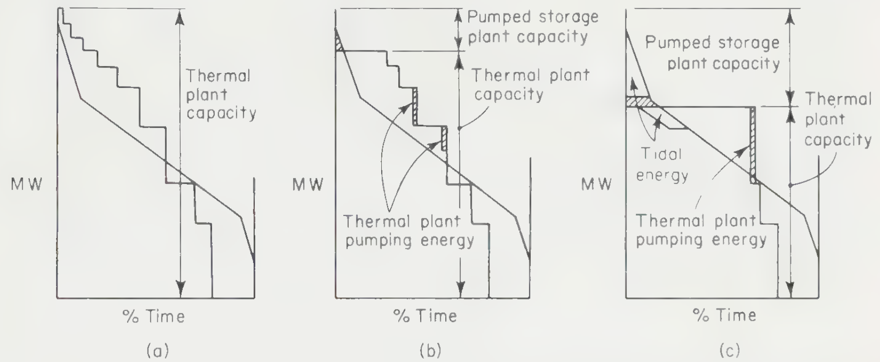

FIG. 15. Typical annual load curves with and without pumped-storage capacity and tidal energy.

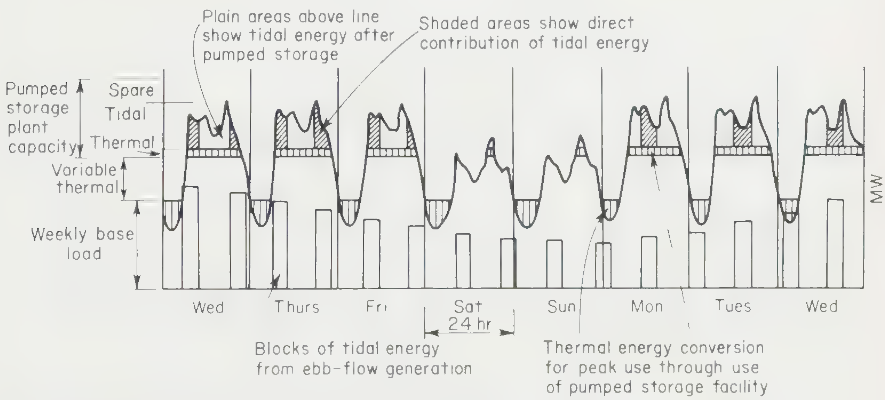

FIG. 16. Possible integration pattern of tidal energy in a predominantly thermal-power electricity system, as applied through pumped storage to a typical weekly demand curve.

with corresponding improvement in thermal load factors. The pumped-storage-plant capacity is limited by the off-peak energy available from the high-merit-order thermal plant, since the farther down the peak the pumped-storage-scheme capacity comes, the more energy, as well as power, is required from it. More energy must therefore be supplied by lower-merit-order plants, and the situation is such that the point is quickly reached where it is uneconomic to increase the pumped-storage-plant capacity.

Figure 15*c* shows what can be done with a large tidal-energy source in the system. All the tidal kilowatthours cost the same. There is therefore no economic disadvantage in providing pumped-storage-plant capacity as far down the load curve as there is tidal energy available. Referring now to Fig. 16, which shows a typical system load curve for a period of a week, the "peak" may by now cover a generation period of 8 to 10 hr depending on the amount of tidal energy available, pumped-storage-plant capacity being available for standby duties for much of this time. The system is now very flexible in operation; for example, in altering from a winter to a summer demand curve, the life load factor of the thermal plant is increased. The pump-turbine method of operation cannot provide the same flexibility, being limited to about 5½ hr continuous generation and having a firm power capacity which is governed by the neap tidal range and thus is unrelated to system requirements.

It should be pointed out that the pumped-storage reservoir capacity must be larger than what would normally be considered adequate, because of the variation in energy output of the tidal station from neap to spring tides. This larger capacity will not always be fully utilized by tidal-energy requirements so that a pumped-storage facility will be made available for part of the time to the network's conventional plant. Here again the tidal scheme cannot be considered in isolation from the demands it will be helping to meet, since the demand-curve shape will influence the storage requirements. An investigation[10] into the integration of the tidal energy of the Solway Firth (between England and Scotland) into the estimated demand of the Scottish electrical

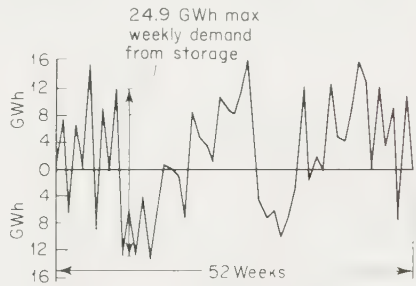

FIG. 17. Fluctuation in weekly storage capacity for the complete integration of Solway Firth tidal energy into the hypothetical 1975 demand of the Scottish electrical system. (*From Water Power.*)

system, as postulated for 1975, yielded the storage fluctuation shown in Fig. 17 and so directed the search for a suitable pumped-storage site.

When comparing the advantages of different types of tidal-energy development and the alternative conventional systems it is therefore necessary to cost the whole system over a future period of years, probably at least 20, before the true relative economic merits emerge.

FUTURE DEVELOPMENTS

15. Simplification of Turbogenerating Machinery. All tidal schemes proposed in the past, including the Rance scheme, are uneconomic when the unit cost of energy is compared with that from alternative power sources. If tidal development is to be continued there must be a considerable cheapening of the plant and construction costs. These costs cannot be considered in isolation. For example, suppose the turbine is made with fixed blades. It will then operate efficiently in only one direction of flow. This means its output will be of the form shown in Fig. 4. This, as has been shown, is feasible only in a t.p.p.s. scheme.

The possible types of generating machinery seem to be as shown in Fig. 18. Machines of all four types have been successfully constructed, and they are shown together here for comparison. The runner diameter is the same in each case. Type *A* is the French bulb unit like the Rance installation, with reversible-pitch blades and a directly coupled generator. Type *B* is similar but has a geared coupling designed to reduce the bulb diameter by speeding up the alternator, thus reducing its size and cost and improving the hydraulic efficiency of the water passage. The French considered the geared unit to be less reliable and opted for the directly coupled machine although

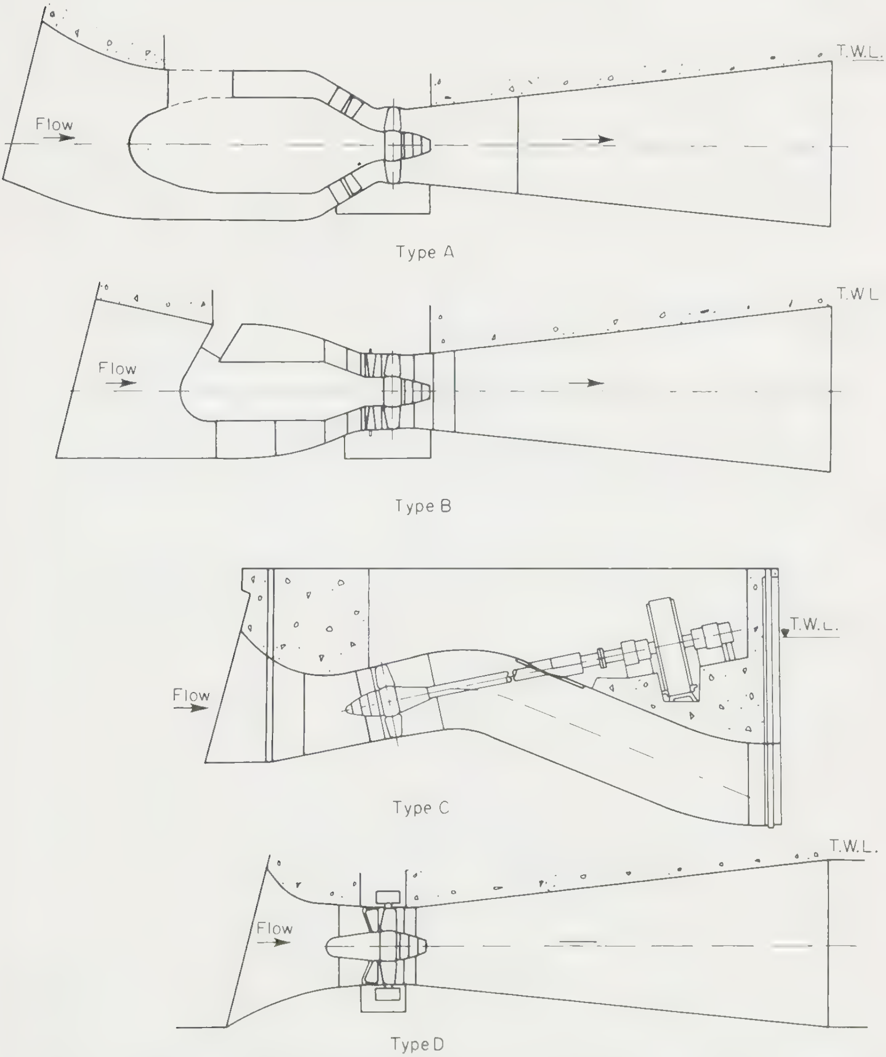

Fig. 18. Comparison of alternative types of tidal-energy generating machinery. [*Courtesy of Institution of Civil Engineers (London).*]

the center-to-center distance between the sets must be larger than with Type *B*. Since the Type *A* bulb is the only one of the machines actually in service in a tidal-power station and is fully developed, it must be regarded as the standard against which the alternatives may be measured.

If future tidal development does not follow the patterns of La Rance and is toward t.p.p.s. schemes, the complexity of Types *A* and *B* would be unnecessary and the balance of economic advantage might then lie with Types *C* and *D*.

Type *C* is the TUBE turbine with the generator directly coupled to a long turbine shaft, thus requiring a curved water passage. Type *D* is the straight-flow turbine

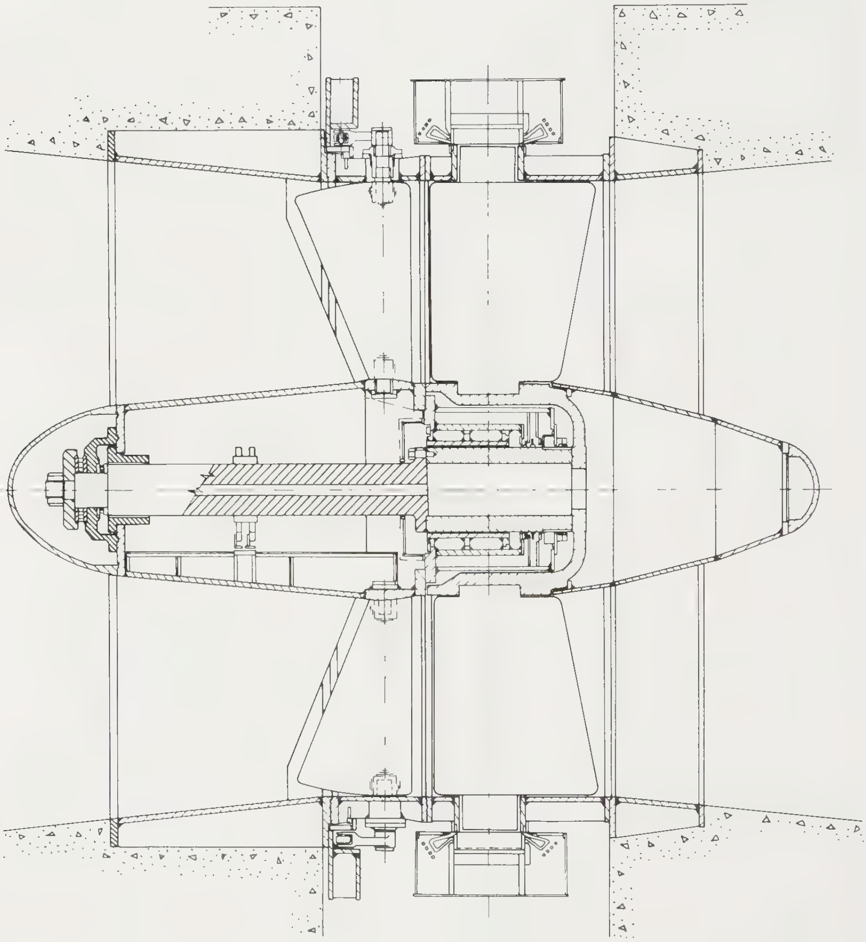

Fig. 19. Proposed design for a straight-flow turbine with rim generator. (*English Electric Co.*)

with rim generator.* The shortest and simplest containing structure is that for Type *D*, and it seems to offer a cost advantage in this respect for t.p.p.s. schemes. It can be designed to operate as a fixed-blade unit capable of being motored in the reverse flow direction, thus providing assisted refill and reducing the need for separate sluices in the barrage. Figure 19 shows a proposed design for such a machine.

Type *C* has a waterway with less desirable hydraulic characteristics. It requires

* Seventy-five machines of this type were built and installed on low-head schemes on the Lech and Iller rivers in Germany in the period 1936–1951. They are all running and in service in 1967. None has yet been built as a pump-turbine.

deeper foundations, though this is not necessarily disadvantageous, as will be seen. It is likely to cost more. On the other hand, it can be readily provided with adjustable turbine blades (much more of a problem on Type D) and has very good accessibility and no cooling problems. Figures 20 and 21 show design proposals for caisson units incorporating machines of each type. Both will probably be further developed, and at present it is not possible to be sure about the economics of one compared with the other. This is so primarily because the *function* of the machine is so important in the design of the power station, and because the relative size and numbers of machines and the way they are operated control the optimum design of the machine itself. It is so secondarily because there is as yet little manufacturing and operating experience with either type. This is true also of the French machines, though they have been operating as prototypes for some years.

16. Cheapening of Civil Construction Work. The construction of a cofferdam in an estuary is a difficult undertaking at any time, because of tidal currents and wave action. When the site is subject to a large tidal range and the cofferdam is required to cut off an appreciable part of the waterway, then the work may become extremely difficult and prohibitively expensive. If large-scale tidal development is to take place in the future, construction methods must avoid very large cofferdams like that of La Rance. The simplest way to do this is to prefabricate the power station in sections, in drydocks or on slipways, and to float the sections, or caissons, to the barrage site and then at slack water sink them onto a dredged, level rock-rubble foundation. This caisson technique is well established and, though not yet executed on the scale suggested here, has been applied to many problems, two notable recent examples being the closure of the Veersche Gat in Holland in 1961[11] and the prefabrication and installation of a complete lighthouse in the Irish Sea.[12] The method has also been used successfully for subway-tunnel construction at Montreal and Rotterdam in the last few years. The Russians have now apparently actually built a tidal-power station at Kislaya Bay in this way[9] (Fig. 14).

Each caisson would consist of a horizontal water duct incorporating an intake, with space for an axial-flow turbine and draft tube. If the scheme is one in which positive-head pumping is necessary to ensure firm capacity the intake may be nearly as long as the draft tube, so that velocity head is recovered. If the scheme is designed for assisted refill pumping only, the intake may remain short. Two or more waterways might be incorporated in a single caisson. Projects considered to date in any detail envisage the installation of large numbers of these cells, using large-diameter runners. For example, a recent proposal for the Bristol Channel in Britain had 220 cells each carrying a 30-ft-diameter axial-flow turbine.[13] Tidal-power projects are likely to be viable only with large tidal ranges, and machine runner diameters as large as conveniently possible. Since water depths required for a 30-ft-diameter runner are of the order of 60 ft at low water springs, the overall height of the units may be as great as 100 ft. For this diameter of runner they would be about 180 ft long by 55 ft wide for each waterway. Smaller units are perfectly possible and water depths will correspondingly decrease if they are used, though the unit cost of energy will increase as size decreases, other things being equal. Where channel-bottom elevations are lower than the required foundation levels for the caisson cells, dumped rock rubble would be used as filling. It might therefore conceivably be cheaper to have a deep rather than a shallow caisson. Necessary protection to the rubble bank against scour from the waterway discharge would be provided by underwater placement of hot asphaltic-concrete mixtures, whose development and use have recently been pioneered by the Dutch on the Ijmuiden harbor moles on the North Sea coast of Holland.[14] Such a rubble bank will inevitably be permeable to some extent at least at first, but this is not a vital matter as it is in normal hydroelectric practice

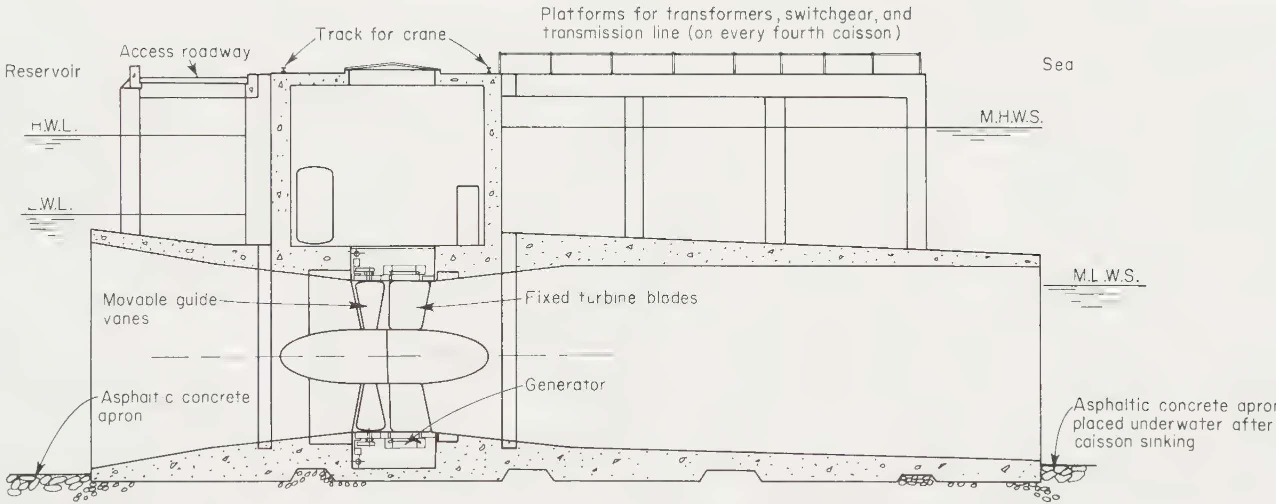

Fig. 20. Longitudinal section through caisson unit with a straight-flow turbine, as proposed for Solway Firth project, 1964.

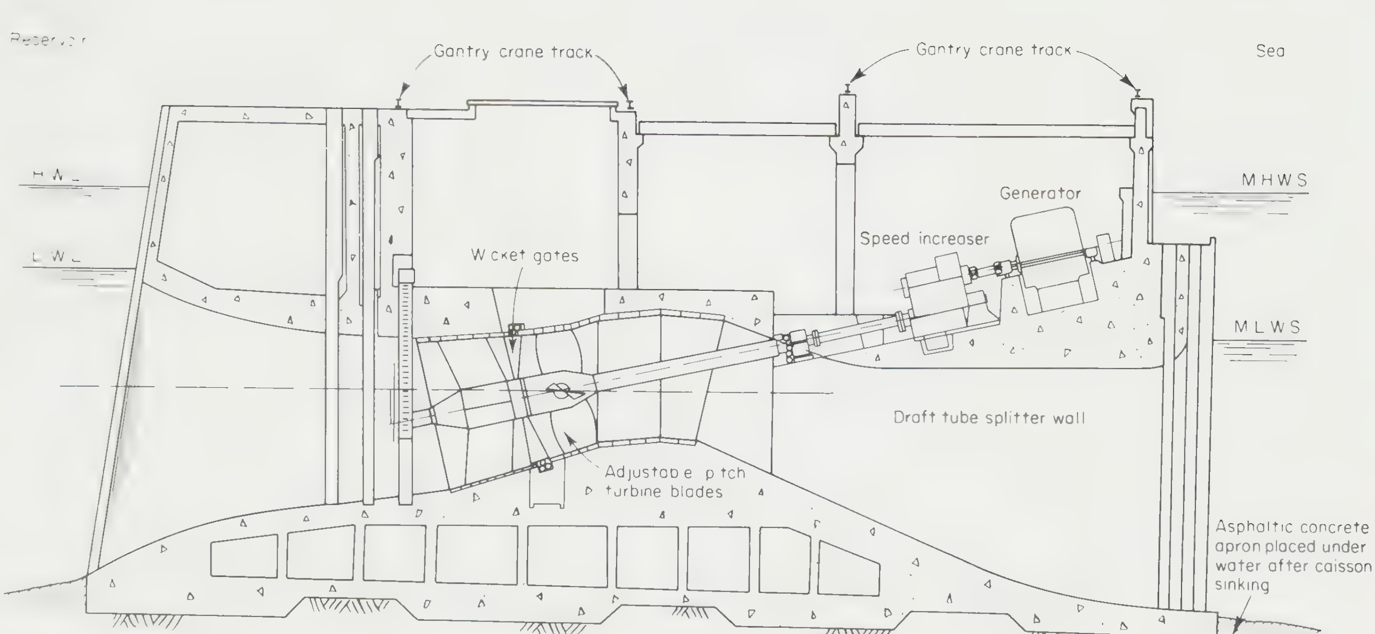

FIG. 21. Longitudinal section through proposed caisson unit with TUBE turbine; cf. Fig. 19 of Chap. 26.

since the water loss is likely to be very small in relation to the vast quantities passing every few hours, and the head is comparatively small. The Bristol Channel scheme referred to above has peak discharges of the order of 3 million cfs.

The elimination of trash racks, isolating valves and gates, and so far as is possible, large sluice gates is also desirable. If the machine size is large enough, incidental trash and surface ice may be safely passed. If the turbines are used also as pumps, then sluices may be largely or completely eliminated. This design decision must be based on the availability of input off-peak energy and the relative economic worth of extra energy obtainable by installing sluices.

Underwater placement of fill material is a well-tried technique and has been used on a large scale in many projects, notably recently at Arrow Dam in British Columbia, and Ijmuiden and Plover Cove, Hong Kong.

THE ECONOMICS OF TIDAL ENERGY

Most tidal projects considered in the past have been shelved because alternative sources could be shown to produce the same power and energy for less cost at the time. As each new development in hydraulic engineering has occurred, corresponding improvements have been made in the comparable technologies. It has been aptly said that every tidal-power proposal ever made would have been an economic success 10 years after it was built. The two factors principally responsible for keeping tidal projects from realization have been capital cost and lack of firm capacity. It will be realized from the foregoing material of this section that recent proposals are aimed at reducing capital cost, (1) by eliminating cofferdams, (2) by shortening the construction period, and (3) by simplifying the hydraulic machinery. At the same time firm capacity is to be provided, either by using the pump-turbine concept or by integrating the tidal energy into system demand by pumped storage; in other words, by selling peak-demand-period power and energy. Since most modern electricity systems contain large low-unit-cost producers in nuclear and thermal plants working at high load factors, tidal energy, like much other hydropower, can best be utilized as peaking energy.

The trend in energy costs in fossil-fuel-fired plants appears to have reached relative stability, and current costs (1968) do not seem likely to fall much further. This may be seen graphically in Fig. 22, which indicates how little further room for improvement

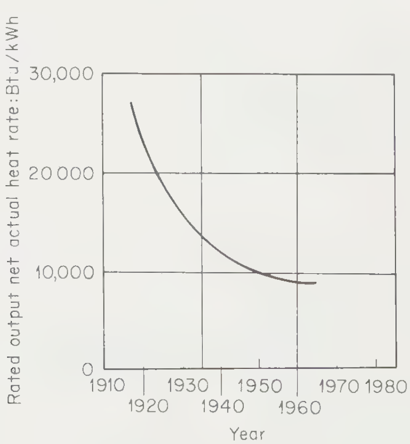

FIG. 22. Historical heat-rate improvement. (*After Baldwin, Houser and Smith.*)

there is. Current prices in the United States are about \$120 per kilowatt installed for large units, and these working at 70 percent load factor give unit costs including all expenses of about 0.6 cent per kilowatthour. European figures are very similar. Latest British plants have corresponding costs of £42 per kilowatt installed and 0.5 pence per kilowatthour. Nuclear-power plants are still being actively developed, and so figures are less definite. Projected capital costs for large stations of the breeder-reactor type are about \$170 per kilowatt installed with total unit costs around 0.3 cent per kilowatthour depending on interest charged. It should be emphasized that these costs by themselves are not figures that tidal energy has to meet. Only overall system cost is a valid basis for comparison since tidal energy used for peaking will be replacing energy generated at much higher costs than those quoted here and in doing so will alter the conventional plant load factors beneficially. These figures are nevertheless useful as standards against which estimates for tidal energy may be judged.

The multipurpose aspect of tidal barrages should also be considered. Economic advantages may accrue from:

1. The use of barrages as bridges
2. The saving of land use by alternatives (apart from capital costs)
3. The prevention of exceptionally high water levels in the estuary with reduction in levee maintenance and improvement in drainage
4. Improved navigation facilities to estuary ports
5. The prevention of air and water pollution and thermal degradation of rivers
6. Aesthetic benefits and opportunities for recreation on sheltered estuaries

Concerning the last of these it is sometimes held that such benefits are largely intangible and have little relevance to the "economic cost" of a project in comparison with alternatives which may offer no such advantages, and may have further disadvantages, such as spoliation through mining operations. Such views take too narrow a look at our use of natural resources. Although side benefits and detriments may be difficult to assess, some attempt should be made in every case.

WORLD POSSIBILITIES

There are comparatively few places in the world where the tidal range is large enough to justify tidal projects. Generally a mean range of about 20 ft is required before economic viability is possible, though this must depend on many factors of differing importance in different locations.

The range is only part of the requirement. A suitable estuary or coastal indentation must be available whose damming will not substantially reduce the range, and finally, if pump-turbines are to be used there should already be an interconnected system with surplus off-peak power available for pumping. The absence of any one of these three prerequisites will generally preclude tidal-energy development. For example, both tidal range and suitable estuaries appear to be available at Frobisher Bay in Baffin Island, Canada, but there is no demand there for power and so no electrical system.

The number of good sites where all three prerequisites seem presently satisfied is soon listed:

1. Bay of Fundy, Canada
2. Bristol Channel, England
3. Baie de St. Michel, France
4. Yang-tse-kiang estuary, China

FIG. 23. World sites for possible tidal-energy development.

5. Gulf of San José, Argentina
6. Solway Firth, England/Scotland
7. Mezen and Penzhina Bay, U.S.S.R.
8. Cook Inlet, Alaska

Future possibilities exist at Ungava Bay and Hudson's Bay, Canada; Magellan Archipelago, Chile; Gulf of Kutch, India/Pakistan; and the northwest coast of Australia. However, it is not beyond possibility that development may make mean ranges of 15 ft economic, and in that case many more possibilities arise. Figure 23 shows on a world map where development is possible now or in the future.

ACKNOWLEDGMENTS

Some of the material in this chapter has been published previously, and the author is indebted to the publishers for their permission to reuse the material. In particular, acknowledgment is made to *Science Journal*, London (Figs. 1, 2, 3, and 23 from the issue of July, 1965); Israel Program for Scientific Translations, Jerusalem (Figs. 5 and 14 from Ref. 9); Institution of Civil Engineers, London (Fig. 18 from *Proc. Inst. Civil Engrs.*, **34,** May, 1966); *Water Power*, London (Fig. 17 from Ref. 10); Électricité de France, Paris (Figs. 9, 10, 11, and 13); Les Constructeurs des Groupes Marémoteurs de la Rance, Grenoble (Fig. 12); The English Electric Co., London (Figs. 18 and 19); The Allis Chalmers Manufacturing Co., York, Pa., for advice and criticism on Fig. 21; Proceedings of the American Power Conference, 1964 (Fig. 22 from Ref. 15).

Bibliography

1. Bonnefille, M., Étude énergétique de la marée dans le golfe de Saint Malo à partir des observations en nature, *Bull. du C.R.E.C.*, No. 5, 1963.
2. Dronkers, J., "Tidal Computations in Rivers and Coastal Waters," North Holland Publishing Company, Amsterdam, 1964.
3. Ippen, A. T., et al., "Estuary and Coastline Hydrodynamics," McGraw-Hill Book Company, New York, 1966.
4. Davey, N., "Studies in Tidal Power," Constable & Co., Ltd., London, 1923.
5. Gibrat, R., "L'Usine marémotrice de la Rance," Revue Française de l'Energie, April, 1956.
6. Duhoux, L., "Fermeture de la Rance—Déroulement des travaux et analyse des observations," La Houille Blanche, No. 4, 1964.
7. Allary, R., "L'Usine marémotrice de la Rance," La Technique des Travaux, January/February, 1966.
8. "The Rance Tidal Power Scheme," Revue Française de l'Energie (special edition), No. 183, September/October, 1966.
9. Bernshtein, L. B., "Tidal Energy for Electric Power Plants," translated from the Russian, Israel Program for Scientific Translations, Jerusalem, 1966.
10. Wilson, E. M., The Solway Firth Tidal Power Project, *Water Power*, **17,** November, 1965.
11. Walker, K. F., and W. C. Bischoff Von Heemskerck, "Some Aspects of the Delta Project," Selected Aspects of Hydraulic Engineering, Technical University of Delft, 1963.
12. Turner, J. S., Design and Construction of the Kish Bank Lighthouse, *Civil Eng. Public Works Rev.*, August, 1965.
13. Wilson, E. M., A Multi-purpose Barrage on the Bristol Channel, *Water Power*, **18,** April, 1966.
14. Kerkhoven, R. E., Hydraulic Applications in the Netherlands, *Shell Marketing Rept.* 110F.
15. Baldwin, C. J., H. G. Houser, and H. L. Smith, Peaking Capacity for Power Pools—Pumped Storage or Gas Turbines, *Proc. Am. Power Conf.*, 1964.

INDEX

(continued from front flap)

in the design of dams, waterways, and regime canals.

Written from the practicing engineer's point of view, the book is organized in the order which is usually followed in making regional plans for water use and control. Conveniently divided into four major parts, it contains comprehensive coverage that ranges from basic hydraulics, reservoir hydraulics, and natural channels . . . through river diversion, the finite-element method of analyzing dams, foundations material, basic principles of concrete dam design, prestressed dams, barrages and dams on soft foundations, and fishways at dams . . . to pumped storage, flood control, groundwater, and navigations systems. You will also find detailed discussions on several advances from Europe, notably dams of the flexible-concrete-block type, the cored-gravity type, and the wide-span multiple-arch type.

ABOUT THE EDITORS

CALVIN VICTOR DAVIS, Consulting Hydraulic Engineer for Harza Engineering Company, has planned and designed numerous large hydraulic projects located both in the United States and abroad. He was formerly chairman and President, Harza Engineering Company; Chief Engineer, Ambursen Engineering Company; Principal Planning Engineer, Tennessee River System, TVA; Project Engineer for the Fontana Project, TVA; and Vice President, Frederic R. Harris Engineering Corporation. Mr. Davis is also the Editor-in-Chief of the first and second editions of the HANDBOOK OF APPLIED HYDRAULICS, as well as author of numerous articles on river development and regional planning.

KENNETH E. SORENSEN is Vice President, Harza Engineering Company. Prior to becoming Vice President he was Head of the Planning Department in charge of feasibility studies for dams, hydroelectric plants, irrigation, and flood control projects. Mr. Sorensen has also worked as a structural engineer with the Kimberly Clark Corp. and in the Panama Canal Zone.

0-07-015538-0